جامعة قطر
QATAR UNIVERSITY

هيئة الأشغال العامة
Public Works Authority

وزارة البلدية
Ministry of Municipality
State of Qatar • دولة قطر

وزارة البيئة والتغير المناخي
Ministry of Environment and Climate Change
State of Qatar • دولة قطر

CIC 2023

Proceedings of the 2nd International Conference on Civil Infrastructure and Construction (CIC 2023)



Print ISSN: 2958-3128
Online ISSN: 2958-3136

دار نشر جامعة قطر
Qatar University Press

Proceedings of the 2nd International Conference on Civil Infrastructure and Construction (CIC 2023)

Proceedings of the 2nd International Conference on Civil Infrastructure and Construction (CIC 2023)

Editor-in-Chief

Wael Alnahhal

Editors

Mohammed Hussein
Ahmad Ali Al-Ansari
Mohammed bin Saif Al-Kuwari
Elalim Ahmed
Murat Gunduz
Vagelis Plevris
Mohd Faris Khamidi
Mohamed Arselene Ayari

Doha, Qatar
2023 AD/ 1445 AH

دار نشر جامعة قطر
Qatar University Press

Proceedings of the 2nd International Conference on
Civil Infrastructure and Construction (CIC 2023).
5-8 February, 2023. Qatar University, Doha, Qatar

Print ISSN: 2958-3128

Online ISSN: 2958-3136

Published by Qatar University Press (© 2023), under the terms of the Creative Commons Attribution-NonCommercial 4.0 International (CC BY-NC 4.0), which permits non-commercial use of the material, appropriate credit, and indication if changes in the material were made. You can copy and redistribute the material in any medium or format as well as remix, transform, and build upon the material, provided the original work is properly cited. The full terms of this license may be seen at https://creativecommons.org/licenses/by-nc/4.0

دار نشر جامعة قطر
Qatar University Press

ص.ب. 2713، الدوحة - قطر

qupress@qu.edu.qa

دار نشر جامعة قطر: نحن دار نشر جامعية غير ربحية، تأسست عام 2018، تعمل على تعزيز ونشر الكتب والبحوث المحكَّمة في العديد من مجالات المعرفة. تسعى الدار إلى أن تصبح رائدة في نشر الكتب والمجلات العلمية، وتهدف إلى دعم رؤية جامعة قطر نحو التميّز في البحث والتعليم في دولة قطر وخارجها.

Qatar University Press (QU Press): We are a non-profit university publishing house established in 2018, dedicated to promoting the dissemination of peer-reviewed and research-based publications in various fields. QU Press aims to be a leading publisher of scholarly books and journals. QU Press endeavors to support QU's vision towards excellence in research and education in Qatar and beyond.

هذا الكتاب لا يعبر بالضرورة عن رأي دار نشر جامعة قطر

This book does not necessarily reflect the opinion of QU Press

Online ISSN: 2958-3136

2958-3136

ABOUT

Welcome to the 2nd International Conference on Civil Infrastructure and Construction (CIC 2023). The aim of the conference is to provide a platform to report and discuss the recent advances and developments in infrastructure and construction besides urban planning and design for society's wellbeing. Furthermore, the conference provides a forum to discuss challenges and developments associated with the Environment and Climate Change.

ORGANIZATION

The conference is organized by Qatar University, the Public Works Authority (Ashghal), the Ministry of Municipality, and the Ministry of Environment and Climate Change. The conference includes a number of professional partners from engineering societies inside and outside Qatar. The conference features world-class keynote speakers from top international engineering organizations and societies. The invitation are also extended to the policymakers and key figures in Qatar in the field of infrastructure and construction to present at the conference.

HIGHLIGHTS

- Research and technological advancements in civil infrastructure and construction
- Case studies – lessons learned
- Best practices in infrastructure development and construction
- Bringing experiences of practitioners, policymakers, and research scholars together

THEMES AND TOPICS

Theme 1: Contemporary issues in Construction Engineering and Management

- Digital construction
- Design management
- Facilities management
- Lean construction
- Applications of Industrial Revolution 4 (IR4) Technologies in Architecture, Engineering, and Construction (AEC)
- Modularization and standardization strategies in the construction industry
- Construction contracts, legal affairs, and dispute resolution
- Construction productivity and performance measurement
- Workforce welfare, occupational health, and safety in construction

- Professional issues in education and practice
- Sustainable construction technologies

Theme 2: Advances in Infrastructure Sustainability, Renovation, and Monitoring

- Use of recycled and innovative materials in infrastructural projects
- Sustainable materials and solutions
- Sinkholes in Karst Environment as Transportation, Infrastructure and Urban Planning Geohazard
- Infrastructure maintenance and rehabilitation
- Resilient civil infrastructure systems
- Structural control and health monitoring
- Computational methods and soft computing in Civil Engineering applications

Theme 3: Sustainable Architecture and Urban Planning for Society's Wellbeing

- Architectural design challenges and solutions for Hot and Arid Climate
- Healthy Building, Indoor Environmental Quality and post-Covid19 building design
- Heritage Building Conservation, Adaptive Reuse, and Circular Design
- Urban Mobility and Transit-oriented Development for Sustainable Transport
- Disaster Risk Reduction and Resilient Cities
- Urban farming, vertical gardening, green roof, and bio-wall
- Contributing to cities that subscribe to equitability rather than simply equality
- Improving access to education, health, affordable housing, and neighborhoods of quality and which provide its users with economic opportunities

Theme 4: Water, Environment, and Climate Change

- Environmental effect of recycling and use of recycled materials
- Waste management and circular economy
- Water sustainability for food security
- Advanced water and wastewater treatment processes
- Integrated water resources management
- Managed aquifer recharge
- Fate and transport of contaminants in subsurface systems
- Carbon management through geological carbon sequestration

- Air pollution and climate change
- Green buildings

CONTACT US

Telephone: +974 4403 4170

Email: cic@qu.edu.qa

Website: www.cic.qa

Organizers



Sponsors

Platinum Sponsor







Research Council Sponsor





Silver Sponsor



Professional Partners



Preface

This book contains the proceedings of the 2nd International Conference on Civil Infrastructure and Construction (CIC 2023), held at Qatar University in Doha, Qatar, from February 5th to 8th, 2023. Organized by Qatar University, along with the Ministry of Municipality, the Ministry of Environment and Climate Change, and the Public Works Authority (Ashghal), CIC 2023 served as a nexus for a diverse array of participants, extending beyond academia to embrace professionals, policymakers, and visionaries.

The primary aim of the CIC 2023 conference was to cultivate an environment conducive to the exchange of knowledge, experiences, and solutions at the forefront of infrastructure and construction. The themes explored within this volume show the wide spectrum of discussions that unfolded during the conference, ranging from challenges in Construction Engineering and Management to the strides made in Infrastructure Sustainability, Renovation, and Monitoring. There was also a strong emphasis on Urban Planning and Design for Society Wellbeing, as well as matters concerning Water, Environment, and Climate Change.

Our gratitude extends to the distinguished keynote speakers, esteemed professionals, and dedicated participants and authors who made this conference vibrant with their ideas. We are very grateful to the strong support received from the conference sponsors and our professional partners. A special note of thanks is reserved for the unwavering commitment of the organizing, technical, and scientific committees, whose unwavering dedication played an instrumental role in the success of this event.

We also would like to express our genuine appreciation to Qatar University Press, and its distinguished team for their efforts in all stages of the book's production; editing, proofreading, designing and publishing, until this work came out to the readers in this distinctive form

As we present these conference proceedings, we do so with the aspiration that the knowledge shared within these pages will continue to inspire and guide researchers, practitioners, and policymakers in their ongoing efforts to build resilient, sustainable, and thriving societies.

Dr. Wael Alnahhal

Editor-in-Chief

Keynote Speakers



Keynote Speaker

Maria Lehman

PhD, P.E.
ASCE 2023 President
American Society of Civil Engineers, USA

Maria Lehman, P.E., ENV SP, F.ASCE, is GHD's infrastructure market leader for the United States since May 2020. Maria was the former vice president for critical infrastructure for Parsons, COO and acting executive director of the New York State Thruway Authority and commissioner of public works for Erie County, New York. She has 40 years of diverse, increasingly responsible, multi-disciplinary technical and leadership experience, both in the private and public sectors, and in traditional and alternative delivery. She received her bachelor's degree in civil engineering at the State University of New York at Buffalo, magna cum laude, and is a licensed professional engineer in several states.

She has served as principal-in-charge, project executive, program and project manager, and project engineer for more than 700 projects, which required everything from scoping, planning, environmental studies, preparation of plans, specifications, estimates, construction management, and operations and maintenance – ranging in size from $10,000 to $3.9 billion. Her strength has been around complex element coordination – well-developed project communications, government, and community relations, including innovative finance and grants – and fast-track implementation on complex projects. She has successfully led alternative delivery projects, such as design-build, best value, and public private partnerships.

Maria has served ASCE since her days at UB, first as a student, then as a younger member. She co-founded the Northeast Region Younger Members Council in 1983 and stayed active in her section, serving all board positions including president in 1990, while her husband Carl was president-elect. She was a delegate to the NYS and District 1 Councils and became a society director in 1993, followed by Zone 1 vice president in 2001. She has continuously served or chaired numerous society-level committees, councils, and institutes since 1993. She returned to the Society's Board of Direction in 2018 as assistant treasurer.

Maria has won numerous national, statewide, and local awards including the ASCE President's Medal, Edmund Friedman Young Engineer Award, UB's School of Engineering Alumna of the Year, and the New York State Society of Professional Engineers Engineering Manager of the Year.

Keynote Presentation Title: Engineering the Future

Abstract: With an expanding global population, we must take care of our aging infrastructure to meet current needs, and at the same time, move it into the future with innovative technologies and capabilities that will enable us to combat the problems of tomorrow. In this presentation, ASCE President Maria C. Lehman will share how we need to prepare future civil engineers to meet these challenges.

As the oldest engineering society in the United States, ASCE represents 150,000 members in 177 countries. ASCE stands at the forefront of a profession that plans, designs, constructs, and operates society's economic and social engine – the built environment – while protecting and restoring the natural environment.

Cite as: Lehman M., "Keynote Speaker", *The 2nd International Conference on Civil Infrastructure and Construction (CIC 2023)*, Doha, Qatar, 5-8 February 2023, DOI: https://doi.org/10.29117/cic.2023.0003



Keynote Speaker

Anil Sawhney

Director of the Infrastructure Sector, Royal Institution of Chartered Surveyors (RICS)

Anil Sawhney is the Global Lead of the Construction and Infrastructure Sector at the Royal Institution of Chartered Surveyors (RICS). Anil is a construction and infrastructure sector expert, an educator, a researcher, and a Construction tech enthusiast. He is involved in producing the construction and infrastructure sector's body of knowledge, standards, guidance, practice statements, education, and training. Dr. Sawhney is also an Adjunct Faculty at Columbia University, Visiting Professor at Liverpool John Moores University in the UK, and an adjunct faculty at the University of Southern California. Anil has a rich mix of academic, research, industry, and consulting experience gathered in the USA, India, Canada, the UK, and Australia. In 2020, he co-authored a book entitled "Construction 4.0-Innovation Platform for the Built Environment." He is currently the co-editor of the Construction Innovation Journal. Dr. Sawhney serves on the international editorial board of the ICE Infrastructure Asset Management journal and the Journal of Information Technology in Construction.

Keynote Presentation Title: Industrialized Construction: Megatrends shaping the future of construction

Abstract: The construction sector faces an uncertain operating environment in 2023 – a trend in all global markets. Components of this uncertainty – a seemingly never-ending health crisis, the war in Europe, supply chain snarls, fixed-price contracts in a hyperinflationary environment, the shifting nature of the workforce, and an emerging response to environmental and social challenges – are complex and require a holistic response from all industry stakeholders. In the last three years, every sector of the economy, irrespective of maturity level, had to embrace changes supported mainly by technology. The construction sector was also swept up by this irreversible change seeing a significant acceleration in technology adoption and reconfiguration of processes and practices. Couple this with the changes driven by the Industry 4.0 framework, and the construction sector can leapfrog to more efficient production processes, business models, and value chains. The past three years have brought the following five technological megatrends to the forefront:

1. Prefabrication and advanced manufacturing
2. Robotics and automation
3. Big data, artificial intelligence, machine learning, and predictive analysis
4. Internet of Things and digital twins
5. Realtime data capture using drones, laser scanners, and other devices

With these megatrends and the progress in building information modelling and common data environment, the construction sector is now at an inflection point. A holistic paradigm that combines these emerging trends into a new operating model is needed. In this session, the speaker provides Industrialized Construction as this new operating system upon which our

sector can continue to innovate. Industrialized Construction promises to reshape how we design, construct and operate our built assets. It is envisioned that the current challenges the industry faces can be overcome using this framework. This talk will discuss the key concepts, opportunities, and challenges of Industrialized Construction.

Cite as: Sawhney A., "Keynote Speaker", *The 2nd International Conference on Civil Infrastructure and Construction (CIC 2023)*, Doha, Qatar, 5-8 February 2023, DOI: https://doi.org/10.29117/cic.2023.0004



Keynote Speaker

Lauri Koskela

Professor of Construction and Project Management at University of Huddersfield

Dr. Lauri Koskela is Professor of Construction and Project Management at the University of Huddersfield. Previously he worked at the University of Salford as Professor of Lean Theory Based Project and Production Management. Prior to that he was involved in applied research at VTT Technical Research Centre of Finland. Since 1991, Lauri has been involved in research on lean construction. His research has focused especially on the theories of production management as well as design management, underlying lean construction. Lauri is a founding and continuously active member of the International Group for Lean Construction. He has been Director, Trustee and Company Secretary at Lean Construction Institute – UK.

Keynote Presentation Title: The continuous evolution of Lean Construction – what next?

***Abstract*:** The presentation first gives an overview on the evolution of Lean Construction hitherto and analyses the drivers for new achievements as well as difficulties encountered. Among the drivers, especially the Toyota Production System, problematic characteristics of construction, digitalisation, and sustainability accentuate; in those characteristics, one-off products, site production and temporary project organisation are especially commented.

The second part of the presentation addresses new practical developments in Lean Construction, occurring currently and in near future. The Toyota Production System continues to evolve, and the newest methods deserve to be adopted in construction. First experiences regarding the new quality method of Ji Koutei Kanketsu (JKK) are discussed. Takt production, as a way to overcome problems usually seen in site production and temporary project organisations, is analysed. The opportunities for mutual support between lean and the digital are illustrated through the cases of Building Information Modelling (BIM) and Digital Whiteboards. Finally, moving to the area of sustainability, the role of lean in circular construction is covered.

Cite as: Koskela L., "Keynote Speaker", *The 2nd International Conference on Civil Infrastructure and Construction (CIC 2023)*, Doha, Qatar, 5-8 February 2023, DOI: https://doi.org/10.29117/cic.2023.0005



Keynote Speaker

Rafat Siddique

Dean of Research and Sponsored Projects & Senior Professor of Civil Engineering at Thapar Institute of Engineering and Technology

Professor Rafat Siddique is Dean, Research and Development & Senior Professor of Civil Engineering at Thapar Institute of Engineering and Technology (Deemed University), India.

He is Editor of the Journal of Construction and Building Materials (Elsevier), Journal of Materials in Civil Engineering (ASCE), and European Journal of Environmental and Civil Engineering (Taylor & Francis).

He is among top 15 academicians in the world with total citations of 20000+ having H Index of 76 in the area of sustainable construction materials. He has published 200+ Q-1 Journal articles and 80+ conference papers. He has been Invited Professor to number of universities in UK, USA, Australia, France, Germany, Thailand, etc.

He has been sought-after speaker, and been to several countries; Australia, Bangkok, Belgium, Botswana, Burkina Faso, Canada, China, Czech Republic, Finland, France, Germany, Hong Kong, Indonesia, Italy, Japan, Malaysia, Mexico, New Zealand, Poland, Portugal, Saudi Arabia, Singapore, Spain, Sri Lanka, Switzerland, Turkey, United Kingdom, UAE, USA

Keynote Presentation Title: Utilization of Waste Materials and Industrial By-Products in the Development of Sustainable Greener Concrete

Abstract: There is exponential growth in the generation of waste materials & industrial by-products from manufacturing processes, service industries and municipal solid wastes. As a result, solid waste management has become one of the major environmental concerns in the world. With increasing awareness about environment, scarcity of space for landfilling and due to its ever-increasing cost, waste materials and by-product utilization has become an attractive alternative to disposal. Utilization of such materials has gained significant importance in the development of sustainable greener cement-based materials. There are several types of waste materials/by-products such as fly ash, bottom ash, foundry sand, scrap-tires, cement kiln dust, waste glass, recycled plastic, dredged materials, MSW ash, etc.

Extensive work has been reported on the influence of such materials on the fresh, strength and durability properties of concrete. Use of such materials in concrete not only makes it economical, but also helps in reducing disposal and environmental related issues. This presentation is about the possible uses of some of these materials in the development of sustainable greener concrete.

Cite as: Siddique R., "Keynote Speaker", *The 2nd International Conference on Civil Infrastructure and Construction (CIC 2023)*, Doha, Qatar, 5-8 February 2023, DOI: https://doi.org/10.29117/cic.2023.0006



Keynote Speaker

Robert Cervero

Professor emeritus of City & Regional Planning, Berkeley University. Director of the University of California Transportation Center & the Institute of Urban and Regional

Robert Cervero has long focused on sustainable transportation policy and planning. He has been consulted on numerous transportation and urban planning projects worldwide, most recently advising long-range planning in Dubai and Singapore. His most recent book, Beyond Mobility, won the 2019 National Urban Design Best Book Award. Dr. Cervero was a member of Berkeley's city and regional planning faculty from 1980 to 2016, where he twice served as Department Chair, held the Carmel P. Friesen Chair in Urban Studies, and directed both the University of California Transportation Center and the Institute of Urban and Regional Development. More recently he has held visiting faculty appointments at Tongji University in Shanghai and NYU-Abu Dhabi. He was a contributing author to the IPCC's Fifth Assessment on Climate Change, UN-Habitat's Global Report on Sustainable Mobility, and recently received the Athena Accolade from KTH University and Distinguished Legacy Award from UC Berkeley's Institute of Transportation Studies.

Keynote Presentation Title: **Transit Oriented Development in Disruptive Times**

Abstract: This talk focuses on the future of transit oriented development (TOD), arguably one of the most sustainable forms of urbanization, in light of mobility disruptors, such as pandemics, automated and electro-mobility, shared economies, mobility as a service, and megatrends (e.g., aging societies; non-nuclear families; remote work). International experiences are drawn upon in recasting TOD in light of forces that are powerfully changing employment, lifestyle, and socio-cultural preferences in both developed and developing urban contexts. Key features of TOD, including walkability and diversity in land uses, affordable housing options, and mobility choices are likely to gain a market foothold, albeit a cardinal feature of TOD – proximity to major transit hubs – could very well wane in importance. Shaped by policies focused on accessibility versus movement (e.g., '15-minute city'), Transit Villages and a panoply of micro-mobility services are likely to become more prominent. Such trends call for new public policy responses, like curb access management and inclusionary housing, to avoid unintended consequences. Innovative financing tools building upon value capture principles should gain favor as well.

Cite as: Cervero R., "Keynote Speaker", *The 2nd International Conference on Civil Infrastructure and Construction (CIC 2023)*, Doha, Qatar, 5-8 February 2023, DOI: https://doi.org/10.29117/cic.2023.0007



Keynote Speaker

Armistead Russel

Howard T. Tellepsen Chair, Regents Professor of Civil and Environmental Engineering, Georgia Tech

Prof. Armistead (Ted) Russell is the Howard T. Tellepsen Chair and Regents' Professor at the Georgia Institute of Technology. At Georgia Tech, his research is aimed at better understanding the dynamics of air pollutants and the resulting health impacts, with an ultimate goal to develop approaches to design effective strategies to improve air quality and health. Before coming to Georgia Tech, he was a professor at Carnegie Mellon University in Pittsburgh, Pennsylvania. He earned his M.S. and PhD degrees in Mechanical Engineering at the California Institute of Technology in 1980 and 1985 and his B.S. from Washington State University. Prof. Russell has served on fifteen National Academy Committees, as well as IARC and EPA Committees, including the Clean Air Scientific Advisory Committee. He is the recipient of the AWMA Frank Chambers, SAE Ralph Teetor, WSU Distinguished Alumni, FHWA Environmental Excellence and Siggraph Visualization Awards

Keynote Presentation Title: Integrating Satellites and Models for Air Quality and Health Analyses

Abstract: A revolution in our ability to observe air pollution and its impacts on health has been rapidly happening largely unobserved to many since it is really occurring up in space. Satellites are constantly characterizing levels of a range of compounds in the air, and what is truly unique and powerful is that we now have information across the globe, even in remote regions. Atmospheric scientists have teamed with health scientists to use this information to better understand how air pollution impacts disease in every country and what can be done to reduce air pollution-related disease.

Cite as: Russel A., "Keynote Speaker", *The 2nd International Conference on Civil Infrastructure and Construction (CIC 2023)*, Doha, Qatar, 5-8 February 2023, DOI: https://doi.org/10.29117/cic.2023.0008

Executive Speakers



Dr. Khalid Naji
Dean of College of Engineering, Qatar University



Eng. Salem Mohd Al-Marri
Manager of Technical Office, Public Works Authority (Ashghal)



Eng. Ibrahim Abbas
Director of Infrastructure Planning Department, Ministry of Municipality



Eng. Jassim Al-Ansari
Chief of Program Delivery, Qatar Rail



Eng. Bodour Almeer
Sustainability Executive Director at the Supreme Committee for Delivery & Legacy



Dr. Eng. Mohammed Saif Al-Kuwari
Assistant Undersecretary, Environmental Expert and Engineering Consultant, Ministry of Environment and Climate Change

Organizing Committee

Prof. Mohammed Hussein (Chair), Qatar University, Qatar

Eng. Salem Mohd S. A. Al-Marri, Public Works Authority (Ashghal), Qatar

Dr. Wael Alnahhal, Qatar University, Qatar

Dr. Raffaello Furlan, Qatar University, Qatar

Ms. Fatima Al-Kubaisi, Public Works Authority (Ashghal), Qatar

Mr. Jabir Ali Alshawi, Ministry of Municipality, Qatar

Ms. Jawaher Albader, Ministry of Municipality, Qatar

Mr. Farhood Al-Hajri, Ministry of Environment and Climate Change, Qatar

Technical Committee

Dr. Wael Alnahhal (Chair), Qatar University, Qatar

Prof. Mohammed Hussein, Qatar University, Qatar

Eng. Ahmad Ali Al-Ansari, Public Works Authority (Ashghal), Qatar

Dr. Mohammed bin Saif Al-Kuwari, Ministry of Environment and Climate Change, Qatar

Eng. Elalim Ahmed, Ministry of Municipality, Qatar

Prof. Murat Gunduz, Qatar University, Qatar

Dr. Vagelis Plevris, Qatar University, Qatar

Dr. M Faris Khamidi, Qatar University, Qatar

Dr. Mohamed Arselene Ayari, Qatar University, Qatar

Scientific Committee

Eng. Ali Kara, Public Works Authority (Ashghal), Qatar

Prof. Ali Alraouf, Ministry of Municipality, Qatar

Prof. Brian R. Sinclair, University of Calgary, Canada

Prof. Nikos D. Lagaros, National Technical University of Athens, Greece

Prof. Caryl Bossman, Griffith University, Australia

Honorary Prof. Neil Sipe, The University of Queensland, Australia

Dr. Wael Alnahhal, Qatar University, Qatar

Prof. Dimitrios Lignos, École polytechnique fédérale de Lausanne, Switzerland

Prof. George Tsiatas, University of Patras, Greece

Dr. Mustafa Mashal, Idaho State University, USA

Dr. Vagelis Plevris, Qatar University, Qatar

Dr. Mohd Faris Khamidi, Qatar University, Qatar

Dr. Francesco Clementi, Università Politecnica delle Marche, Italy

Dr. Muhammad Azzam Ismail, Universiti Malaya, Malaysia

Prof. Murat Gunduz, Qatar University, Qatar

Dr. Mohamed Arselene Ayari, Qatar University, Qatar

Dr. Ungku Norani Sonet Ungku Abdul Rahman, Taylor's University, Malaysia

Dr. Stergios Aristoteles Mitoulis, University of Surrey, UK

Dr. Mohammad Reza Nikoo, Sultan Qaboos University, Oman

Dr. Motasem Alazaiza, A'Sharqiyah University, Oman

Dr. Weiwei Lin, Aalto University, Finland

Dr. Osama Dawoud, Istinye University Istanbul, Turkey

Dr. Paul Vardanega, University of Bristol, UK

Dr. Zili Li, University College Cork, Ireland

Dr. Kasun Kariyawasam, University of Moratuwa, Sir Lanka

Prof. Omar Laghrouche, Heriot-Watt University, UK

Dr. Samir Dirar, University of Sharjah, UAE

Dr. Amged Osman Abdelatif, University of Khartoum, Sudan

Prof. Ashraf Osman, Durham University, UK

Dr. Wenbo Yang, Southwest Jiaotong University, China

Prof. Ahmed Senouci, Univesity of Houston, USA

Prof. Rifat Sonmez, Middle East Technical University, Turkey

Prof. Irem Dikmen, Middle East Technical University, Turkey

Dr. Ying-Yi Chih, Australian National University, Australia

Dr. Osama Abdeljaber, Linnaeus University, Sweden

Dr. Wasim Barham, Jordan University of Science and Technology, Jordan

Prof. Hamid Ronagh, University of New South Wales, Australia

Prof. Mustafa Şahmaran, Hacettepe University, Turkey

Prof. Tarek Ragab, Arkansas State University, USA

Dr. Ahmed El Refai, Laval University, Canada

Dr. Ashraf Ashour, University of Bradford, UK

Prof. Adel Younis, Linnaeus University, Sweden

Dr. Mohammed Hussein, Qatar University, Qatar

Prof. Mohammad Farid Mohamed, Universiti Kebangsaan Malaysia, Malaysia

Dr. Muhammad Waris Ali Khan, The British University in Dubai, UAE

Dr. Adeeb Qaid Al-Ameri, University of Bahrain, Bahrain, UAE

Dr. Izudinshah Abd Wahab, Universiti Teknologi Tun Hussein Onn, Malaysia

Dr. Raffaello Furlan, Qatar University, Qatar

Dr. Yasser Mansour, Prince Sultan University, Saudi Arabia

Prof. Georgios Kapogiannis, Oryx Universal College, Qatar

Dr. Hatem Ibrahim, Qatar University, Qatar

Prof. Djamel Boussa, Qatar University, Qatar

Dr. Guglielmo Minervino, IUAV University of Venice, Italy

Dr. Benno Albrecht Tolentini, IUAV University of Venice, Italy

Prof. Mohammad Hamdan Ahmad, Universiti Teknologi Malaysia, Malaysia

Prof. Djamel Ouhrani, Qatar University, Qatar

Dr. Fodil Fadli, Qatar University, Qatar

Dr. Abd Razak Sapian, International Islamic University of Malaysia, Malaysia

Prof. Yakubu Aminu Dodo, Najran University, Kingdom of Saudi Arabia

Dr. Mohammad Rodzi Ismail, Universiti Sains Malaysia, Malaysia

Dr. Zalina Shari, Universiti Putra Malaysia, Malaysia

Dr. Rashid Al Matwi, Qatar University, Qatar

Dr. Madhavi Indraganti, Qatar University, Qatar

Dr. Mark David Major, Qatar University, Qatar

Dr. Ahmad Mohammad Ahmad, Qatar University, Qatar

Dr. Goze Bayram, Qatar University, Qatar

Dr. Tarryn Pacquet, Qatar University, Qatar

Dr. Amina Al-Kandari, Qatar University, Qatar

Dr. Walaa S. Mogawer, University of Massachusetts Dartmouth, USA

Prof. Adel Elsafty, University of North Florida, USA

Prof. Maged Yousef, Western University, Canada

Prof. Neaz Sheikh, Wollongong University, Australia

Dr. Alaa Alhawari, Qatar University, Qatar

Prof. Hisham Eid, Qatar University, Qatar

Prof. Okan Sirin, Qatar University, Qatar

Prof. Hamdy Mohamed, University of Sherbrooke, Canada

Dr. Jamal Thaheem, Deakin University, Australia

Dr. Abid Hasan, Deakin University, Australia

Dr. Waleed Umer, King Fahd University of Petroleum and Minerals, Saudi Arabia

Dr. Amos Darko, Hong Kong Polytechnic University, Hong Kong

Dr. Muhammad Zeshan Akber, Hong Kong University of Science and Technology, Hong Kong

Dr. Mahdi Kioumarsi, Oslo Metropolitan University, Norway

Dr. Mattias Schevenels, KU Leuven, Belgium

Prof. Izuru Takewaki, Kyoto University, Japan

Dr. Mo'ayyad Shawaqfah, Al Al-Bayt University, Jordan

Dr. Abdallah Shanableh, University of Sharjah, UAE

Prof. Riyadh Al-Raoush, Qatar University, Qatar

Dr. Tayyab Ahmad, Qatar University, Qatar

Prof. Tarek Ragab, Arkansas State University, USA

Dr. Mohamed Laoucet, Ball Corporation, USA

Dr. Latif Onur Ugur, Düzce University, Turkey

Dr. Mürsel Erdal, Gazi University, Turkey

Prof. Adeb Qaid, Kingdom University, Bahrain

Dr. Mohammad Ghanim, Ministry of Transport, Qatar

Dr. Dodo Yakubu Aminu, Najran University, Saudi Arabia

Dr. George Papazafeiropoulos, National Technical University of Athens, Greece

Dr. Nikos Bakas, National Technical University of Athens, Greece

Dr. Alejandro Jimenez Rios, Oslo Metropolitan University, Norway

Dr. Ala Abutaqa, Aqaba University of Technology, Jordan

Dr. Hesham Elsherbeny, Qatar University, Qatar

Dr. Amina Alkandari, Qatar University, Qatar

Dr. Reem Awwaad, Qatar University, Qatar

Dr. Abdelbaki Benamor, Qatar University, Qatar

Dr. Djamel Boussaa, Qatar University, Qatar

Dr. Tarek Elmekkawy, Qatar University, Qatar

Dr. Mohammed Elshafie, Qatar University, Qatar

Dr. Amith Khandakar, Qatar University, Qatar

Dr. Djamel Ouahrani, Qatar University, Qatar

Dr. Tarryn Paquet, Qatar University, Qatar

Dr. Shaligram Pokharel, Qatar University, Qatar

Dr. Probir Probir Das, Qatar University, Qatar

Dr. Faris Tarlochan, Qatar University, Qatar

Dr. Tadesse Wakjira, Qatar University, Qatar

Dr. Ungku Sonet, Taylor's University, Malaysia

Dr. Wardah Yusoff, Universiti Kebangsaan Malaysia, Malaysia

Dr. Dalilah Dahlan, UPM, Malaysia

Table of Contents

About the Conference 5

Organizers, Sponsors and Partners 8

Preface 9

Wael Alnahhal, Editor-in-Chief

Keynote Speakers 11

Maria Lehman 13

Anil Sawhney 15

Lauri Koskela 17

Rafat Siddique 19

Robert Cervero 21

Armistead Russel 23

Executive Speakers 25

Organizing Committee 26

Technical Committee 26

Scientific Committee 26

Theme 1: Contemporary issues in Construction Engineering and Management 47-364

Criteria and Challenges of Inclusive Design In The Built Environment 49

Shimaa Abdelkarim, Ahmad Mohammad Ahmad, Janet Zahrah, Nancy Makhoul, Maryam Al-Nuaimi, Khalid Naji

Focus on Lean Construction at Umm Lekhba (Land Mark) Interchange 59

Nader Halimeh

Duality of Lean Construction and Building Information Modeling into Digital Collaborative Scheduling in Qatar: A Conceptual Framework 67

Murat Gunduz, Khalid Naji, Ayman Fahmi Naser

Practical Implementation of Campus Facility Management Performance Measurement in Qatar 76

Murat Gunduz, Khalid Naji, Omar Maki

Pavement Automated Condition Assessment Model Using Unmanned Aerial Vehicle and Convolutional Neural Network 83

Vinay Chawla, Carol Massarra, Husam Sadek, Mohammed Sadeq, Zhen Zhu

Strategies for Improving Construction Safety Performance in Developing Context 90

Wesam Beitelmal, Wael Alruqi, Mohamed Zoubi

TBM Challenges on Musaimeer outfall tunnel **99**

Gary Peach, Hernan Vigil Fernandez, Saad Zayed Al-Marri

Performance of an Infrastructure Project Following the Deployment of a Customized Lean Strategy **108**

Ramez Alchamaa, Hisham M. S. Abushaqra

Digitalization and usage of QR-code System in Documents Management **117**

Loai Abdrabou

Study on Business Value of Building Information Modelling – Applied in Developing Countries **122**

Amr Sadek

Implementing the Last Planner system in a Design Project **130**

Dawlat Elmosalmi

Investigation and Comparative Study between Research Methods used in the Five Categories of BIM-Based Built Environment Sustainability Studies **138**

Hanane Bouhmoud, Dalila Loudyi, Andrea Giordano, Salman Azhar, Mounia Farah

Enhancement of Workers' Occupational Health, Safety and Welfare in Ashghal **147**

Naji Al-Faridi, Yasser Mohamed Berzan

A Side-by-Side Comparison of Shaft Excavation locally in Qatar **151**

John Brown, Sunit Saurabh, Ahmed Alslakhi, Eisa Al-Mohannadi

Flow of Activities: Utilizing Parade of Trade to Develop Visual Management Tool Tailored for Infrastructure Projects **157**

Yehia Ibrahim, Saoud Ali Al-Tamimi

Enhancing Micro-Tunnelling Activity in Infrastructure Construction Adopting Hybrid Lean Approaches: A Case Study **163**

Asghar Kamal, Jamalelden Hakouz, Yehia Zakaria, Maryam Shalabi, Ayman Naser, Saoud Ali Al-Tamimi

Assessment of Workflow Reliability in Two Infrastructure Projects Considering Efficient Adoption of Lean Leadership Culture and Engagement **172**

Zied Dahmani, Ramez Alchamaa, Saoud Ali Al-Tamimi

Implementation of Building Information Modelling (BIM) on Public Infrastructure and Building Projects in Qatar **180**

Robert Grys

Using Value-Stream Mapping to Enhance the Production Performance in Infrastructure Construction Projects in Qatar: A Case Study **189**

Ayman Naser, Asghar Kamal, Saoud Ali Al-Tamimi, Zied Dahmani

Marketing Strategies for Smart Buildings 197

Ahmed Mahfouz, Ahmad Mohammad Ahmad, Shimaa Abdelkarim, Nada Nabil Hammam, Maryam Adel Almulla, Yongcheol Lee, Khalid Naji

The Impact of COVID-19 on Contracts and Claims for Infrastructure Projects 206

Mona Adam, Amani Mohammed

An Integrated Workflow for Transforming Infrastructure Projects Data into The Metaverse 215

Mohammed Al-Shaheen, Raj Mukta Sundaram, Thirunavukkarsu Ramalingam

Use of Immersive Augmented Reality Technology in Public Works: Myth or Reality? – A Case Study on Implementation Challenges 225

Balamohan Narayanasamy, Suresh Manickam

GIS-Based Solutions for Monitoring and Controlling COVID-19 in ASHGHAL Construction Projects: Improving Construction Sector Resilience 234

Mohammed Al-Shaheen, Amna Mohammed Al-Sayed, Ahmad Yacoub Hasan

Challenges and Perspectives on Resilient Collaboration for Building Information Modelling (BIM) Education in the GCC Context 244

Raya Atour, Ahmad Mohammad Ahmad

Assessment of Contractor's Extension of Time Claim (Eot) 253

Neveen Asaad Saleh Ahmed

Choosing by Advantages (CBA) Used as a Qualitative Assessment Methodology in Lean Construction 262

Zied Dahmani, Juhaina Essa Al-Sulaiti, Ayman Naser

The Implementation of Enterprise Resource Planning Systems for Roads and Infrastructure Construction Companies in Developing Countries 269

Dima Jawad, Marie-Belle Boutros, Sophia Ghanimeh

An Exploration into Delay-Influencing Factors on Healthcare Construction Projects: The Case of Saudi Arabia 278

Bader Almutairi, Abdurahman Bin Mahmoud

Investigating the Potential for Standardization of Glass Reinforced Polymer (GRP) Shutter Molds Designs in Bridge Projects in the UAE 284

Mhd Amer Alzaim, Mariam Alali, Ghassan Abu-Lebdeh

Digital Transformation Readiness in Infrastructure Project 293

Nada Wadi, Mohammad Anabtawi

Leading Technologies Adoption in Construction Safety Management 299

Yash Kumar Mittal, Pooja Tripathi

Blockchain Technology Adoption in the State of Qatar: Qualitative Risk Analysis 308

Awad Alomari, Noora Fetais

Investigating the Barriers Involved in the Sustainable Implementation of LC and BIM Approaches in Qatar's Construction Industry 317

Faheem Memon

Medical Facility Management under BIM Paradigm for Hospital Operations Performance in China During COVID-19 325

Georgios Kapogiannis, Tianlun Yang, Professor Jiequn Guo, Michael Gerges

Advancement in Construction Management 334

Ravish Kumar, Arpita Srivastava, Manoj Kumar Rajak, Fulena Rajak, Bijay Kumar Das

Offsite Construction in the UK: Economic and Environmental Benefits 343

Mohammad Maleki Sadabad

Mitigating Legal Risks in Construction Project Contracts: The Importance and the Applicability of Force Majeure Clauses 350

Dana Ahmad Al Marri

Why Construction Projects are Delayed in PWA: Problems and Solutions 359

Dana Ahmad Al Marri, Noof Mohamed Al Kaabi

Theme 2: Advances in Infrastructure Sustainability, Renovation, and Monitoring 365-912

Modeling Short-Term Deflection of Reinforced Concrete Slabs Using the Layered Approach 367

Abeer Fageer, Shahd Khalid, Anfal Abdelgadir, Amina Elbagir, Mohammed Kabosh, Amged Abdelatif

Early Thermal Cracking Control in Concrete Structures in Qatar 373

Firas Alkadour, Christina Anagnostaki, Theodoros Tzaveas, Anil Kumar Oruganti, Ali Kara

Box Jacking Method Implementation in Rock for Mesaimeer Pedestrian Underpass Structure in Qatar 382

Firas Alkadour, Anbalagan Chelliah, Ali Kara, Theodoros Tzaveas

Self-healing Concrete using Gum Arabic for Immobilizing of Bacterial Spores on Sand 391

Amged Osman Abdelatif, Ahmed A. Ibrahim, Khadija E. Elamin, Adil A. El Hussein, Marmar A. El Siddig

Top-Down Construction Method: A Case Study For Underpass Structure in Qatar 397

Ali Kara, Anbalagan Chelliah, Theodoros Tzaveas

Experimental Investigation on the Flexural Capacity of Reinforced Concrete Beams with Treated Wastewater and Recycled Concrete Aggregates 404

Abdelrahman Abushanab, Wael Alnahhal

Widening of an existing bridge to accommodate two traffic lanes – Al Bustan South Project in Qatar 411

Georgios Sergakis, Yoji Matsuo, Christina Anagnostaki, Theodoros Tzaveas

Influence of Adding Demolition Wastes on the Mechanical Properties of Concrete in Sultanate of Oman 419

Said Almaawali, Samiya Alhamrashdi, Ameera Alsiyabi

RSM Analysis for Optimum Content of Graphene Nanoplatelets for 3D-Printed Clay Strength 426

Mohamed Mohsen, Malak Al-Diseet, Mervat Abu Rumman, Ramzi Taha, Khalid Naji

Static and Free Vibration Analysis of Functionally Graded Beams with Porosities 433

Lazreg Hadji, Vagelis Plevris, Royal Madan

The effect of atrium configuration on inside thermal comfort in buildings in hot arid zones 442

Bencheikh Hamida, Bousebci Khalida

Theoretical Simulation of Thermal Deformations in Concrete Beams Reinforced with Two Overlapped FRP Bars in Cold Regions 449

Ali Zaidi, Hizia Bellakehal, Radhouane Masmoudi, Oumelkhir Terbagou, Naima Nia

ABAQUS Modelling and Experimental Tests Comparison For Certain Classes of Composite Isolated Joints 458

Bashir Saleh

Recycled polypropylene fibers for reinforcing cement mortar under arid conditions 465

Khadra Bendjillali, Mohamed Chemrouk

Alternatives to RQD and FI usage – Corrected Rock Quality Designation RQDC and Corrected Fracture Index FIC applied to Qatari rock masses 474

Hrvoje Vučemilović

Significance of GOs, GNPs and CNTs nanomaterials on the mechanical properties of Cement Paste 482

Malak Al-Diseet, Mervat Abu Rumman, Ramzi Taha, Mohamed Al Ansari, Ala Abutaqa, Mohamed Mohsen, Mu'Tasim Abdel-Jaber

A Comparison between Natural Pozzolana and Fly Ash replacements on the mechanical properties of Concrete 489

Mervat Abu Rumman, Malak Al-Diseet, Mu'Tasim Abdel-Jaber, Ala Abutaqa, Khaled Naji, Mohamed Mohsen

Analysis of factors affecting the performance of Dynamic Compaction technique: A study of coastal area of Eastern province in Saudi Arabia 496

Ahmad Salah, Mahmoud Sodangi, Eyad Dardas, Jawad Alnasser, Ayad Alshehri

Comparison of Geotechnical Investigation Results with Encountered Ground Conditions during Subsea Tunneling in Qatar 505

Saad Zayed Al-Marri, Gary Peach, Furqan Hameed

A Review on the Performance of Pile Foundations in Qatar 514

Muhammad Humza, Mannan Ali, Majid Naeem

Tunnel Surveying Works. A challenge of 10 km long tunnel under the Arabian Gulf - Qatar 523

Gary Peach, Saad Zayed Al-Marri, Hernan Vigil Fernandez, Simbarashe Kazingizi, Pavel Chumakou

Numerical Study on the Pullout Behavior of Steel Fibers in Cement-Based Composites 531

Ammar Babiker, Ebtihaj Abu-Elgasim

Ashghal Guidelines for the Evaluation and Repair of Sinkholes 539

Jamal Al-Ansari, Khaled Hassan, Kantha Kumar, Khaled Helali

Characterisation of Sewage sludge and municipal solid waste for Use as Cementitious Materials 547

Mohammed Al-Kuwari, Khaled Hassan

Parametric Optimization of RC Beams Strengthened with FRCM Using Finite Element Modelling and Response Surface Methodology 555

Qusai Aborahmeh, Mohamed Rabie, Usama Ebead

Modelling Asphalt Pavement Frictional Properties using Different Machine Learning Algorithms 563

Mohammad Ali Khasawneh, Mohammad Ahmad Alsheyab, Haneen Issa Al Akhrass

Modeling Thermal Conductivity, Thermal Diffusivity and Specific Heat of Asphalt Concrete Using Beta Regression and Mixture Volumetrics 572

Mohammad Ali Khasawneh, Mohammad Ahmad Alsheyab

Planning and Implementing of Effective Enabling Works for a Successful TBM Tunnelling Project 580

Saad Zayed Al-Marri, Gary Peach, Hernan Vigil Fernandez

Ashghal Quality Assurance & Quality Control system – QSD Role in Monitoring & Reporting the Quality Performance in Ashghal Projects 588

Aisha Abdulaziz A M Al-Ibrahim, Shiekha Aisha Abdulla N J Al-Thani, Effrosyni Plexousaki, Mounera Ismail R M Al-Ansari

Utilisation of Waste Plastics Admix with Laterite Soil for Production of Road Pavement Interlock Blocks 597

Yamusa Bello Yamusa, Mubarak L. Liman, Bilkisu Danjuma, Abubakar Sani, Yusuf Walliyullah

Utilization of Recycled Materials in Infrastructure Projects: Ashghal Approach 605

Osman Elhussien, Aljazi Al-Mansoori

Launching a 148m-Long Tunnel Boring Machine from a 15m-Inner Diameter Shaft 614
John Brown, Volkan Salepciler, Jacek Stypulkowski, Sheikh Abdulrahman Al-Thani

Backfilling Shaft Surround Using Recycled Concrete Waste Material 623
John Brown, Suvish Valsan, Nand K. Vashisht, Anna Olliver, Eisa Abdulla S A Al-Mohannadi

Impact of the Fiber Distribution Characteristics on the Uniaxial Behaviour of Fiber-Reinforced Composites- An Experimental Study 632
C B Kameswara Rao, S R R Teja Prathipati, Hanuma Kasagani

Influence of Pier Stiffness on Track-Bridge Interaction 640
Ali Mubarack C K, Akhil Upadhyay

The Use of Demolished Concrete Lumps (DCL) in Rectangular CFSTs Under Flexure 647
Salem Khalaf, Farid Abed

Marine Dredging Sediments Valorization in Self-Compacting Concretes 654
Walid Maherzi, Mahfoud Benzerzour, Ahmed Senouci, Nor-Edine Abriak

Self-compacting Backfills using Fly Ash and Dredged Marine Sediments for Public Work Applications 662
Walid Maherzi, Mahfoud Benzerzour, Nor-Edine Abriak, Ahmed Senouci

Sustainability Driven Strategy for Achieving Sustainable Infrastructure: Musaimeer Pumping Station and Outfall Project 669
Dila Ersenkal, Gary Peach, Biliana Paskova

A Markovian-Genetic Algorithm Model for Predicting Pavement Deterioration 677
Ala Sati, Saleh Abu Dabous, Hissam Tawfik

Potential Implementation of Warm Mix Asphalt (WMA) in Pavement Construction in The State of Qatar 686
Mohammad Anshasi, Charles Nunoo

Potential Utilization of Alternative Construction Materials in Qatar, in lieu of Conventional Washed Sand 695
Subrahmanyam Pilaka Venkata, Aisha Zayed M. A. Alkhayareen, Noora Ibrahim Q. S. Al Ansari, Ahmed Ghanim Abdulsalam Abunahia

Experimental Validation of Repair Methods for Earthquake-Damaged Bridges Incorporating Pipe-Socket Precast Pier System 701
Kathryn Hogarth, Arya Ebrahimpour, Mustafa Mashal

Efficacy in developing a Sustainable, Resilient, and Interdependent Infrastructure System in the Gulf Region 709
Mohamed G. Mohamed, Muiruri Kevin

Digital Twins in AEC Infrastructure and Building Management Systems 717
Mohammad Oditallah, Md Morshed Alam, Palaneeswaran Ekambaram

Sustainable Alternatives for Concrete by adding Different Types of Natural and Industrial Waste Materials 727
Rana Ezzdine Lakys, Mohammad Hany Yassin, Adel Jumaah

Exploration of Carbonate Aggregates in Road Construction using Ultrasonic and Artificial Intelligence Approaches 736
Mohamed Abdelhedi, Rateb Jabbar, Chedly Abbes

Identification of Karstic Features with Extensive Geophysical Investigation for Underground Infrastructure - South of Wakrah Pumping Station and Outfall (SWPSO) Project 743
Ali Akbar, Fathelrahman Dafalla, Ilayaraja Kumba Krishnamurthi, Andres Pinto

Robust Geotechnical Hazard Identification and Assessment for Major Underground Projects in Qatar. Case Study: South of Wakrah Pumping Station and Outfall (SWPSO) Project 752
Mohamed Khalil, Fathelrahman Dafalla, Andres Pinto, Atif Galal Ahmed

Influence of Fine Dune Sand on the Modulus of Elasticity of Eco-Self-Compacting-Concrete 762
Makani Abdelkadir, Tafraoui Ahmed, Zaoiai Said, Benmerioul Farid

Upgrading Existing Infrastructures - The Case Study of Industrial IC Bridge 769
Christina Anagnostaki, Theodoros Tzaveas, Georgios Sergakis, Yoji Matsuo

Data Interpretation Framework for Pile Thermal Integrity Testing 776
Qianchen Sun, Mohammed Elshafie, Chris Barker, Anthony Fisher, Andrew Bell

Galvanized Steel as a Sustainable Material-Technology and Failure Analysis 784
Abdulwahab Ibrahim, Scott MacIntyre

Performance of Mild Steel and Corrosion-Resistant Steel Rebars in Chloride-Contaminated Concrete 792
Muazzam Ghous Sohail, Nasser Al Nuaimi, Wael Al-Nahhal, Ramazan Kahraman

Bio-Based Self-Healing Concrete for Sustainable and Durable Concrete Infrastructure 798
Muazzam Ghous Sohail, Nasser Al Nuaimi, Ramazan Kahraman, Zulfa Aldisi, Nabil Zouari, Bora Gencturk, Debora Rodrigues, Yucel Yildirim

Along-Wind Aerodynamic Forces on a Rectangular Plan Building in Vicinity of a Gently Sloped Two-Dimensional Hill 806
Abdul Haseeb Wani, Rajendra Kumar Varma, Ashok Kumar Ahuja

Effect of Chemicals on Compressive Strength of Plastic-Laterite interlock paving Blocks 814
Mubarak L. Liman, Yamusa Bello Yamusa, Bilkisu Danjuma, Abubakar Sani, Yusuf Walliyullah

Hardened Properties of Self-Compacting Concrete Incorporating Recycled Granite Waste as Fine Aggregate 822
Aboubakeur Boukhelkhal

A Comparative Study on Punching Shear Strength Statistics for Ferrocement Slabs 829
Mohammed Ihtesham Hussain, Ahmed Majid Salim Al Aamri, Manjunath Shantharam Amalkar, Chimdi Gadafa Benti

Optimum Design of Plane Trusses Using Mathematical and Metaheuristic Algorithms on a Spreadsheet 836
Vagelis Plevris, Ismail Hafez Mohammed Elias, Aristotelis E. Charalampakis

The Effect of Surface Treatment of Basalt FRP Bars on the Shear Capacity of One way High-Strength Concrete Slabs 846
Abathar Al-Hamrani, Wael Alnahhal

Bond Performance of Near-Surface Mounted BFRP Bars to Concrete 852
Omar Aljidda, Ahmed El Refai, Wael Alnahhal

Blockchain and its Potential in the Digitization of Land and Real Estate Property Records 861
Vagelis Plevris, Hassan Abdallah, Azzam Alnatsheh

Enhancing the Bond Durability of Basalt Fiber Reinforced Polymer Bars Using Basalt-Macro Fiber Reinforced Concrete 871
Alaa Taha, Wael Alnahhal, Nasser Alnuami

Synthesis of Calcium Nitrate Self-Healing Microcapsules Using Aerosol OT-Hexane Solution for Cementitious Materials 879
Ala Abutaqa, Ghassan Suleiman, Ahmed Senouci, Mohamed Mohsen

Assessment of the Current Frequency Calculation Methods Used in the Determination of the Dynamic Modulus Value in Pavement Design and Analysis 887
Mohammed Alfarra, Mohammed Sadeq, Husam Sadek

Preliminary Study on the Use of Reclaimed Asphalt in Public Works Authority Road Projects in the State of Qatar 896
Ezio Santagata, Sadegh Yeganeh, Haissam Sebaaly, Osman Elhussein, Ali Al Marri

Development of a Comprehensive Pavement Design System for Roads in Wind and Solar Farms 905
Ezio Santagata, Haissam Sebaaly, Vittorio Capozzi

Theme 3: Sustainable Architecture and Urban Planning for Society Wellbeing 913-1208

The Urban Morphology of Mshereib, the Heart of Downtown Doha 915
Rozan A.A Amleh, Mark David Major, Heba O. Tannous, Almaha M. Alyafei, Ghada H. Fetais, Mohammad A. Najjar, Reem Y. Awwaad

Social Outcomes and Needs Study for Housing Development 924
Gozde Calim, Morgan Belsher

Multimodal Transport For Smart Mobility in Emerging Cities: Case of Doha 933
Mahnoor Hasan, Fodil Fadli

A Bibliometric Study of Visual Quality Research in the Context of Urban Open Spaces 941
Mohammad Najjar, Madhavi Indraganti, Goze Bayram

Investigation of Indoor Thermal Perceptions and Comfort Temperature in Educational Spaces in Qatar 952
Madhavi Indraganti

The Use of Newly Developed Public Transportation System in Relation to People's Thermal Perception of Outdoor Climate 962
Deema Alattar, Madhavi Indraganti

An Analytical Review of Attempts to Mitigate Visual Pollution in Urban Settings 971
Diala Al Midani, Fodil Fadli

Environmental Sustainability Comparative Assessment of Low-Rise and High-Rise Neighbourhoods based on People's Lifestyle Preferences: The Case of Doha, Qatar 978
Shikha Patel, Hatem Ibrahim

Transit-oriented Development from the View of Traditional City Model 988
Sara Nafi, Djamel Ouahrani

Assessment of Aesthetic Control in Qatar's Urban Design 1000
Nur Alah Abdelzayed Valdeolmillos, Almaha Ahmad E R Al-Malki, Shaligram Pokharel, Mohamed Arselene Ayari

Application of PERS to Evaluate Walkability in State of Qatar 1010
Mohamed Ibrahim Elsayyad, Deepti Muley

Area-Specific Traffic Peak Hour Timing Using Traffic Signal Detectors: A Case Study of Qatar 1023
Almodather Mohamed, Ali Al-Saudi, Mohammed Al-Marri, Mohamed Batran

Exploring Crowd Management and Evacuation Strategies using Microscopic Pedestrian Simulation: A Case Study of Souq Waqif 1032
Shabna Sayedmohammed, Charitha Dias, Wael Alhajyaseen, Mohammed Alqaradawi

Adapting Smart Street Strategy for Post-Covid Built Environment 1042
Ahmad Mohammad Ahmad, Shimaa Abdelkarim, Nasir Mohammad, Ahmed Mahfouz, Yongcheol Lee, Khalid Naji

Nairobi MRTS Conceptualization: Transit-Oriented Development for Sustainable Transport 1053
Bidhan Chandra Roy, Satyaki Bhattacharyya

An Adaptive Tabu Search OptimisationAlgorithm for Solving E-Scooters Battery Swapping Problem 1062
Mahmoud Masoud

Multicriteria Approach in Developing Pedestrian Network Data for Sustainable Urban Mobility 1069
Sagar Sonone, Balamohan Narayanasamy

A Quantitative Evaluation of Urban Green Spaces in Rajshahi, Bangladesh 1077
Md. Asaduzzaman, Nafis Sadat

Post-COVID-19 Ventilation Strategies for Shopping Malls in Hot Humid Climate 1087
Wardah Fatimah Mohammad Yusoff, Zinnirah Wellun, Nur'Aina Farhana Norzelan

Theoretical Framework for Planning Urban Roadside Vegetation to Enhance Air Quality for Roadside Users 1096
Soujanya Mogra, Mohd Faris Khamidi, Fodil Fadli

The Challenges and Future Aspirations of Implementing Global Sustainability Assessment System (GSAS) in the Urban Facilities of Mega Sport Events [MSEs] in Qatar 1104
Raya Atour, Fodil Fadli

Climate-cultural Conscious Design Approach to the Post-COVID-19 Built Environment 1113
Mohd Shahrudin Abd Manan, Nur Dalilah Dahlan

Resilience Urban Planning from Climate Change Point of View: A Case Study for Qatar 1122
Husam Samman, Ruzanna Ahmed Zahir

Megaprojects to Improve Public Transport from the User' Perspective 1134
János Varga, Ágnes Csiszárik-Kocsir

An Inclusive Transportation for Iraya-Mangyan IP in Accessing Social Infrastructure using Scalogram Analysis 1143
Samantha Nicole Regala, Junekaycelle Aubrey Grace Carillo, Frances Dale Danielle Dadiz, Geoffrey Cueto

Revisiting the Building Design Attributes and Indoor Radon: A Survey of 36 Homes in the Commonwealth of Kentucky 1151
Osama E. Mansour, Shahnaz Aly, Peter Hall

Effect of Double Decker Flyover construction on Urban Fabric of Ashok Rajpath, Patna, India 1159
Bijay Kumar Das, Arpita Srivastava, Avi Kush

Built Environment Attributes and Walking Patterns: A Case Study of Abu Dhabi Downtown 1167
Jiin Baek

Ganga Riverfront Development at Patna, India: Urban Rejuvenation Project 1176
Fulena Rajak, Bijay Kumar Das

The Impact of Land Mix-use on Inhabitants' Social Wellbeing in the Qatari Neighbourhoods 1181
Hameda Yousef A Janahi

Building Information Modeling (BIM) for Energy Efficiency Awareness in Gulf Countries 1191
Ali Alhamami, Mohammed Awad Abuhussain, Yakubu Aminu Dodo

Cultural Heritage Tourism as a Catalyst for Urban Regeneration: Case of the Doha Historic Center in Qatar 1199
Djamel Boussaa

Theme 4: Water, Environment, and Climate Change 1209-1530

Efficient Reservoir Operation in an Arid Region with Extreme Hydrologic Flows: A Case Study, Largest Oman's Dam 1211
Akbar Karimi, Banafsheh Nematollahi, Mohammad Reza Nikoo

Numerical Simulation of Climate Changes Impacts on The Coast of Oman Sea 1220
Talal Etri, Ghazi Al-Rawas, Ahmad Sana, Mohammad Reza Nikoo

The Dependent Clogging Dynamics and Its Impact on Porous Media Permeability Reduction 1229
Ahmed Elrahmani, Riyadh Al-Raoush

Environmental, Social and Governance in the Construction Industry 1238
Khalil Roukoz, Francis Porter, Lisa Terry, Dila Ersenkal

Diffuser Bed Construction Challenges on the Musaimeer Pump Station and Outfall Project 1253
Gary Peach, Hernan Vigil Fernandez, Saad Zayed Al-Marri

Assessment of Ablution Water Consumption in Mosques 1260
Aliya Ali Said Al Alawi, Parameswari K, Gopalakrishnan Kumarasamy, Khoula Said Khamis Al Kaabi

Review on Decarbonizing the Building Sector in Oil and Gas Countries: The Case of Qatar 1266
Reem Al-Mohammed, Djamal Ouahrani

Estimation of Blue and Green Water Potentials of Türkiye under Global Climate Change Effects 1272
Ali Erturk, Gokhan Cuceloglu, Alpaslan Ekdal, Mehmet Kalfazade, Salim Yaykiran, Aslı Ozabalı Sabuncugil, Aysegul Tanik, Izzet Ozturk

Efficient Turbidity Removal Using a New Gel Filtration Process 1283
Mohammed Talhami, Wardan Khatib, Obadah Dahdal, Mohamed Hassan, Alaa Al Hawari

How Efficient Would Demand-Based Water Strategies Be for Qatar? 1287
Sophia Ghanimeh

Improvement in Environmental Management Performance in Ashghal Projects 1295

Abdel Rahman Tariq A. Abdel Rahman, Maitha Al-Naimi, Hany Mohamed A. Hussein, Aysegul Korur

Emerging Brine Management Approaches for Sustainable Desalination in the GCC Countries 1300

Syed Javaid Zaidi, Haleema Saleem, Hammadur Rahman Siddiqui

Enhancement of Polysulfone Ultrafiltration Membrane Performance for Produced Water Treatment by Incorporation of Graphene oxide/Chitosan/Silicon dioxide Nanocomposite 1309

Ahmed Yasir, Nadeen Alshaibi, Nchwa Ndame, Alaa Hawari, Abdelbaki Benamor

Adsorption of Congo red dye Using Activated Carbon-Fe_3O_4 Composite 1317

Nafis Mahmud, Ludan Yasser, Rahaf Mahmoud, Abdelbaki Benamor

Implementation of Odour Control Systems for a Nuisance-free and Public Friendly Environment in Qatar 1324

Spyridon Trikis, Vaibhav Sumant, Arshad Muhammed, Anna Olliver, Meshaal Abushereeda, John Brown

Study of Turbulence in Open Channels Using Two-Equation Models 1333

Ahmad Sana, Ghazi Al-Rawas, Talal Etri, Abdullah Al-Mamun

Development of Climate Data Inputs Towards the Implementation of Mechanistic-Empirical Pavement Design in the UAE 1341

Waleed Zeiada, Sham Mirou, Ayat Ashour, Reem Hassan, Muamer Abuzwidah

Impact of Pore Morphology on Colloid Migration and Pore Clogging at Variable Saturation Levels in Microfluidics of Natural Porous Media 1349

Mhd. Taisir Albaba, Jamal Hannun, Riyadh Al-Raoush

A Strategic Design Approach for Implementing Rainwater Management System Using an Integration of GIS and BIM Tool 1358

Deshbhushan Patil, Raghavendra Kumar Raya, Abobakr Al-Sakkaf, Ashutosh Bagchi, Rajiv Gupta

The Influence of Urbanization on Natural Overland Flow Paths 1366

Amna Mohammed Al-Sayed, Mohammed Al-Shaheen

Potential Application of Porous Membrane from Blends of Homopolymer for Industrial Water Treatment 1378

Rayane Akoumeh, Tamara Elzein, Juan Rodriguez-Hernandez, Mohammad K. Hassan

Recycling of Tetra Pak for Space and Water Heating by Blending with Phase Change Materials 1384

Safna Nishad, Igor Krupa

Design Considerations of MPSO Marine Outfall and Diffuser Field 1392

Panagiotis Verros, Saad Zayed Al-Marri, Alexios Kyriakopoulos, Lefteris Alvanitopoulos

Challenging Hydraulic Aspects of MPSO Project, Qatar's Showcase for Storm Water Outfall 1401

Panagiotis Verros, Joao Carlos Henriques Miranda, Nikola Manojlovic, Alexios Kyriakopoulos

Automated Calibration of the EPA-SWMM Model for an Impact of Land Use and Land Cover Changes on Peak Discharge for a Sub-Urban Catchment of Delhi 1410

Ved Prakash, Dhruba Jyoti Sarmah, Rajib Kumar Bhattacharjya

Advanced Block Copolymer Membranes for Oily Industrial Wastewater Treatment 1417

Mohammad Hassan, Shifa Shaikh, Moustafa Zagho, Mustafa Nasser, Xiaodan Gu, Sergei Nazarenko, Alamgir Karim

Rainfall Change Projections under Different Climate Change Scenarios in the UAE 1422

Muamer Abuzwidah, Ahmed Elawady, Waleed Zeiada, Tala Abushukair, Rafeeah Al Ali, Soughah Al Samahi, Habiba Aflatoon

Retention of Hydrophobic Colloids in Unsaturated Porous Media using Microfluidics 1431

Jamal Hannun, Riyadh Al-Raoush

Geotechnical Challenges for Underground Infrastructure in Qatar: Hydrogeological Assessment for Dewatering and Deep Excavation Works: South of Wakrah Pumping Station and Outfall (SWPSO) Project 1437

Enric Vázquez-Suñé, Ignacio Bulboa, Ilayaraja Kumba Krishnamurthi, Andres E. Pinto Candia

UV Induced Photodegradation of Direct Green dye by Tb-doped $La_{10}Si_6O_{27}$ Catalyst 1449

Rajender Boddula, Ramachandra Naik, Naveen Kumar A, Ramyakrishna Pothu, Ahmed Bahgat Radwan, Noora Al-Qahtani

Sustainable Urban Drainage Master Plan for Al Khor Municipality 1456

Hassan Qasem, Mohsin Mahmood

The Importance and Evaluation of Environment-Friendly Megaprojects - As Perceived By Users 1460

Ágnes Csiszárik-Kocsir Ph.D., János Varga Ph.D.

A Multi-Criteria Decision-Making Approach for Selection of Wave Energy Converter Optimal Site 1469

Alireza Shadmani, Mohammad Reza Nikoo, Amir H. Gandomi, Ghazi Al-Rawas

Physico–mechanical Properties of Sustainable Building Material Based Gypsum and Recycled Polyethylene Waste 1478

Djoudi Amina

Biogas Production from Cow Manure Using an Anaerobic Digestion Technique 1484
Abdul Rahim Al Umairi, Hatem Al Amri, Abdullah Al Kalbani, Al Hussain Al Hadidi, Marwan Al Hashami

Statistical Analysis of the Effect of Water Table Fluctuation and Soil Layering on the Distribution of BTEX on Soil and Groundwater Under Anaerobic Condition 1491
Reem Ismail, Riyadh Al Raoush

Eco-friendly Concrete Using Waste Plastic Bottles as Aggregate: A Case Study from Oman 1498
Abdul Rahim Al Umairi, Nawf Al Mahrouqi, Maryam Al Wahaibi, Maryam Al Hooti, Fatma Alnabhani, Hiba Al Mamri

Watermain Breaks in Hong Kong: Identifying Causes and Consequences 1505
Tayyab Ahmad, Ibrahim Shaban, Tarek Zayed

Performance Criteria Priorities in Green Buildings: A Proof-of-Concept Study 1513
Tayyab Ahmad

New Technique for Flood Risk Assessment of Sub-Networks in Large Networks Using InfoWorks ICM: A Case Study of Qatar's Full Storm Water Network 1522
Yahia Alabbasi, Khaled Aboelenen, Mohammed Sadeq

Theme 1:

Contemporary issues in Construction Engineering and Management

Criteria and Challenges of Inclusive Design in the Built Environment

Shimaa Basheir Abdelkarim
College of Engineering, Qatar University, Doha, Qatar
shimaa666@hotmail.com

Ahmad Mohammed Ahmad
College of Engineering, Qatar University, Doha, Qatar
am.ahmad@qu.edu.qa

Janet Zahrah
Lean Construction Institute, Doha, Qatar
janet.zahrah@lci.qa

Nancy Nabil Makhoul
Ministry of Municipality, Doha, Qatar
nancymakhoul.architecture@gmail.com

Maryam Nasser Al-Nuaimi
Qatar University, College of Engineering, Doha, Qatar
m.alnuaimi19@gmail.com

Khalid Naji
College of Engineering, Qatar University, Doha, Qatar
knaji@qu.edu.qa

Abstract

Inclusive design is about designing accessible spaces for individuals with different needs. It beholds the ability to affect people's behaviour in the built environment, especially People With Disability (PWDs). Inclusive design aims to remove the barriers that hinder the accessibility and interaction of PWDs within their surroundings, enabling equal opportunities and expanding the scope of their activities. Ensuring an inclusive environment is the responsibility of architects, planners, engineers and facility managers. It is essential to ensure that buildings' design and operation align with inclusive principles through regular assessments. Many comprehensive assessment tools have been developed by scholars and used in the industry. Still, when issues arise like insufficient funding, the decision-makers should be able to prioritize inclusive design criteria in a defined assessment checklist. Addressing accessibility at the building level is particularly important to provide a suitable environment that facilitates users' interaction with the built environment. This study aims to identify prioritized accessibility assessment criteria for PWDs in higher education facilities through the lens of experts and to provide justifications for selecting the highest and lowest priorities. A targeted sampling methodology was adopted for the semi-structured interviews. Findings include a list of the highest and lowest prioritized criteria, identification of criteria with significant differences, justifications for selections and a close-up look into the influence of experts' experience on the criteria rankings. Furthermore, this paper provides insight into significant inclusive design criteria for improved FM decision-making processes and the strategy for managing the challenges of inclusive design in new and existing facilities.

Keywords: Persons with disability; Accessibility; Inclusiveness; Educational buildings; Facility management

1 Introduction

In 2022, the World Health Organization (WHO) estimated that a number of 1.3 billion people (16% of the population) have some form of significant disability. As an integral part of the natural human experience, disability results from several health conditions and personal and environmental factors. Persons With Disability (PWDs) have a shorter life span and less health and are faced with more functional limitations than others (WHO, 2022). Therefore, it is essential to integrate PWDs with society to offer them ample opportunities to improve their quality of life. It is necessary to show integration through different means, such as education, engagement in social activities and empowerment. As it is the right of both PWDs and People With No Disability (PWNDs), it is claimed by Simonson et al. (2013) that decision-makers must deliver high-quality, accessible educational environments. Accessing the built facility is the most challenging for PWDs compared to other features (Jacklin et al., 2007; Hopkins, 2011; Moriña and Morgado, 2018).

Ensuring an inclusive, accessible environment is the responsibility of architects, planners, engineers and facility managers. It is vital to ensure that buildings' design, construction and operations align with inclusive principles that respond to users' needs through regular assessments. Similar to requirements in engineering practices, building accessibility assessments need analysis and prioritization of the assessment criteria. Prioritization of accessibility assessment criteria is required to give attention to the most important ones and guide professionals in coping with challenges in some cases.

This study aims to identify prioritized accessibility assessment criteria for PWDs in higher education facilities through the lens of experts and to provide justifications for selecting the highest and lowest priorities. The study adopted a mixed-method research methodology; qualitative and quantitative data were acquired through the literature review and the semi-structured interviews with experts within a Facility Management (FM) team. Experts were selected based on targeted sampling. Findings include a list of the highest and lowest prioritized criteria, identification of criteria with significant differences, justifications for selections and a close-up look into the influence of experts' experience on the criteria rankings. Furthermore, challenges of PWDs, user requirements and environmental barriers are aligned with prioritized assessment criteria.

2 Literature review

2.1 Inclusive Design, Accessibility and Challenges in the Built Environment

The development of a universal design that prioritizes user requirements is known as inclusive design (Hadjri et al., 2016). It aims to provide building users with easy movement by removing all barriers in the built environment that hinder their activities and accessibility. Accessibility is derived from the word access, which means the ability to enter a space, giving the freedom of movement in complete safety despite age, gender, or disability, having no challenges or obstacles and providing full independence (Derese, 2020). Accessibility in the built environment, specifically, is the ability of the design of the environment to either support or restrict users' activities and movement, as defined by (Carlsson et al., 2022).

For example, challenges of physical disability in educational built environments include the lack of adequate furniture for PWDs in classes, auditoriums, eating areas, libraries, etc., entry obstacles and absence or inadequacy of design and surface material of ramps, handrails and doors. Moreover, it also includes inaccessible parking areas and insufficient maneuvering space externally and internally

(Mulazadeh and Alharbi (2018); Machado and Olivera (2021); Moriña and Morgado (2018); Muzemil (2018), Seshadhri and Paul (2017); Sholanke et al. (2019), Meyers et al. (2019)). According to Carlsson et al. (2022), steps and stairs are also considered environmental barriers, especially for people using a wheelchair. Movement on slippery or uneven floors, seeing from or reaching a certain height, and restless long travel distances are other challenges, as mentioned by Derese (2020).

The construction industry is essential for the country's development and is measured by improved infrastructure (Derese, 2020). It involves different participants, several phases like design, construction and operations, and different processes. Decision-makers are often faced with challenges within these stages when adopting inclusive design. These include non-complying to laws and policies, finance and complexity of design incorporating PWDs requirements, ignorance and lack of effective coordination and consultation with disability groups. It is beneficial for decision-makers and PWDs to understand information about accessibility and user needs; this reinforces the adoption of inclusive design in the built environment.

2.2 Inclusive Design Practices' Integration with Accessibility

To properly integrate inclusive design practices with accessibility, inclusive design focus should include operations' use, limitations and capabilities and PWDs preferences. According to Hadjri et al. (2016), decision-makers need to be able to select the right set of user requirements and consider the involvement of PWDs to meet their needs, prioritize, design accordingly and assess the final deliverable as per their requirements. Similarly, evaluating accessibility in facilities when faced with challenges requires analysis and prioritization of assessment criteria.

2.3 Accessibility Assessment Criteria

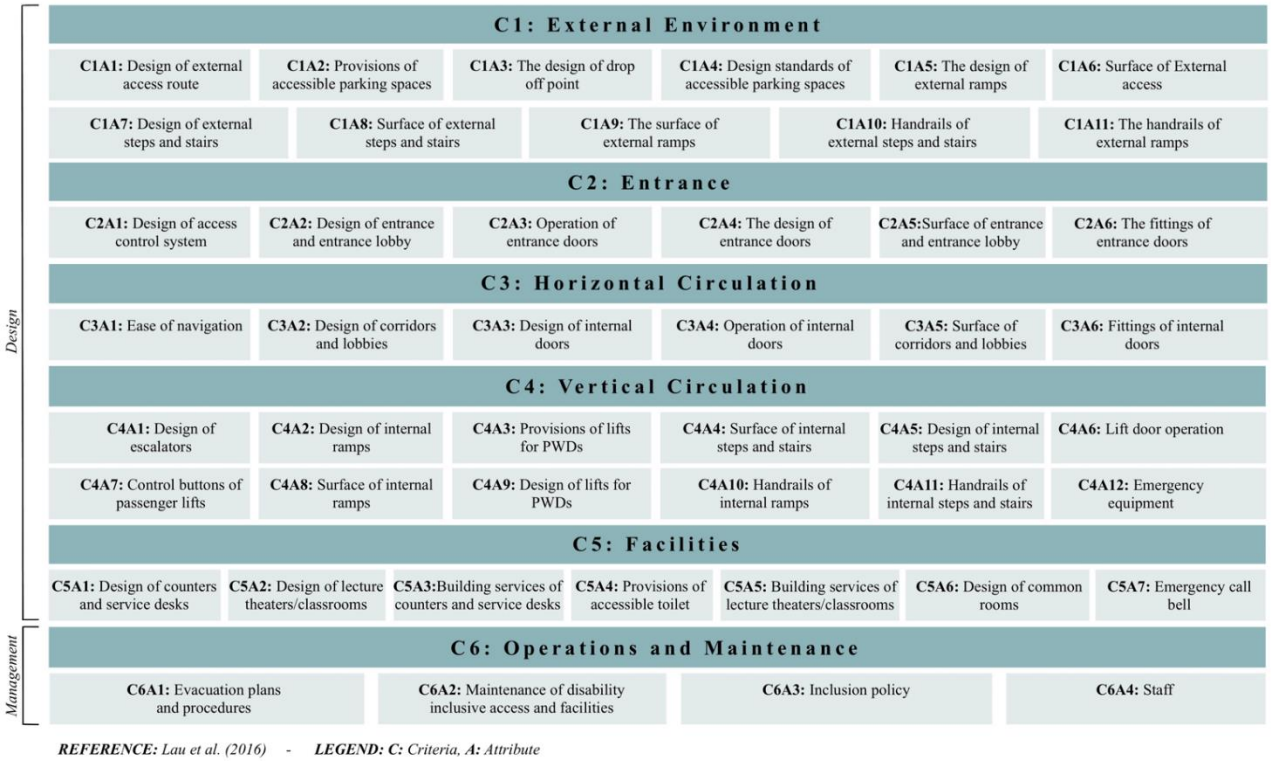


Fig. 1: Accessibility Assessment Criteria and Attributes

Ensuring an inclusive environment is the responsibility of architects, planners, engineers and facility managers. It is essential to ensure that buildings' design and operations align with inclusive design principles through regular assessments. Many comprehensive assessment tools have been developed by scholars and used in the industry. This paper adopted the accessibility assessment checklist developed by (Lau et al., 2016), as illustrated in Figure 1.

3 Methodology

To identify prioritized accessibility assessment criteria, the research methodology adopted a mixed-method approach; qualitative and quantitative data were acquired through a literature review and semi-structured interviews with experts. The study first explored the challenges of physical disability in educational built environments and the environmental barriers through a literature review to understand users' perceptions. Then, it explored experts' perceptions of challenges in the design, implementation and operations phases.

Furthermore, a checklist criteria developed by Lau et al. (2016) was adapted for the conducted interviews with selected industry experts. The sample included eight practitioners complying with the Americans with Disabilities Act (ADA), such as one facility manager, two architects, two interior designers, two implementation engineers and one landscape architects within an FM team between 1-25 years of experience. During the semi-structured interviews, experts were presented with assessment criteria to rank according to their importance and provide justifications for their highest and lowest selections. The session took 30 minutes.

The paper adopted two types of statistical analyses for the data; inferential and descriptive. The inferential analysis conducted a non-parametric test (Friedman's test) to test for the ranking significance of the attributes within each criterion. Furthermore, descriptive analysis was adopted for the overall ranking of the attributes within the six criteria and the ranking of criteria with significant differences according to experts' experience. Figure 2 illustrates the research methodology.

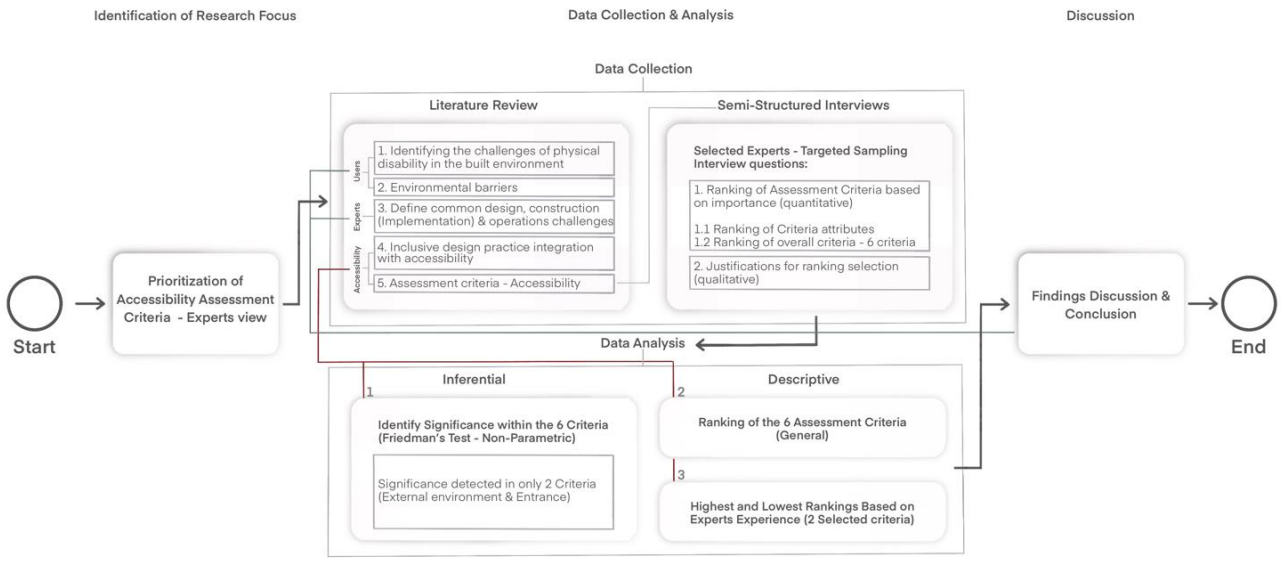


Fig. 2: Research methodology

4 Data Analysis

The data analysis for ranking of accessibility assessment criteria includes inferential analysis to identify significance among the criteria rankings, descriptive analysis for the overall ranking of criteria, and an in-depth analysis of experts' experience in relation to rankings of criteria with significant differences. Decsriptive analysis offers a summary of the data, while the inferential analysis creates a path to conclusions, predictions and estimations.

4.1 Inferential Analysis

As the criteria are ranked, a non-parametric test must be conducted. The test used is Friedman's test, which is the non-parametric equivalent to the two-way ANOVA. Each criterion is tested separately using an alpha (α) of 0.05 to identify significance in attribute rankings. Table 1 shows the test results.

$$H_0: There\ is\ no\ significant\ difference\ between\ the\ attributes$$

$$H_a: There\ is\ at\ least\ one\ difference\ between\ the\ attributes$$

Table 1: Inferential analysis

No.	Criteria	FT	Critical Value (χ^2)	P-Value	Significant/Not Signficant
1	External Environment	20.25	18.30	0.02	Significant
2	Entrance	11.28	11.07	0.04	Significant
3	Horizontal Circulation	7.57	11.07	0.18	Not Significant
4	Vertical Circulation	14.00	19.67	0.23	Not Significant
5	Facilities	0.53	12.59	0.99	Not Significant
6	Operations and Maintenance	2.25	7.81	0.52	Not Significant
Overall		11.67	12.59	0.06	Not Significant

The test results showed significance in ranking within two assessment criteria only; the external environment and the entrance. Furthermore, the test statistic in these two significant criteria is greater than the critical value. At the same time, the P-Value is less than (α). This indicates that the null hypothesis is rejected, and there is at least one difference among the attributes. On the other hand, the horizontal and vertical circulations, facilities and operations and management criteria failed to reject the null hypothesis; hence it is assumed that there is no difference among the attributes.

4.2 Descriptive Analysis

The descriptive analysis in Table 2 presents the rankings of all assessment criteria based on importance. The experts were presented with all criteria and their attributes and were asked to rank them (numerical order) in a 30 minutes long session. The attributes highlighted in green are the highest rankings, and the lowest rankings are highlighted in red.

Table 2: General ranking of all Accessibility Assessment Criteria (Legend: C-Criteria, A-Attribute, R-Ranking)

Accessibility Assessment Criteria Ranking						
C1: External Environment						
A-	C1A1 – *1*	C1A2 – *2*	C1A3 - *2*	C1A4 - *5*	C1A5 - *5*	C1A6 - *7*
R	C1A7 – *8*	C1A8 - *9*	C1A9 - *9*		C1A10 - *10*	C1A11 - *10*
C2: Entrance						
A-	C2A1 – *1*	C2A2 – *2*	C2A3 - *2*	C2A4 - *2*	C2A5 - *4*	C2A6 - *6*
R						
C3: Horizontal Circulation						
A-	C3A1 – *1*	C3A2 – *2*	C3A3 - *4*	C3A4 - *5*	C3A5 - *6*	C3A6 - *6*
R						
C4: Vertical Circulation						
A-	C4A1 – *2*	C4A2 – *4*	C4A3 - *5*	C4A4 - *6*	C4A5 - *7*	C4A6 - *8*
R	C4A7 – *8*	C4A8 – *9*	C4A9 - *10*	C4A10 - *11*	C4A11 - *12*	C4A12 - *N/A*
C5: Facilities						
A-	C5A1 – *1*	C5A2 - *2*	C5A3 - *2*	C5A4 - *3*	C5A5 – *4*	C5A6 - *5*	C5A7 - *6*
R							
C6: Operations and Maintenance						
A-	C6A1 – *1*	C6A2 - *2*	C6A3 – *3*	C6A4 - *4*		
R						

According to the inferential analysis, the external environment and the entrance are the only two criteria with significant differences. Based on the general ranking, the two highest attributes include; the design of the external access route (C1A1) within the external environment and the design of the access control system (C2A1) for the entrance. As for the lowest rankings, the external environment included two attributes with the same score; the handrails of external steps and stairs (C1A10) and the handrails of exterior ramps (C1A11). On the other hand, the entrance presented the fittings of entrance doors (C2A6) as the lowest ranking.

The analysis further investigated the influence of experts' years of experience on selecting the highest and lowest attributes. Figure 3 illustrates the detailed ranking of attributes within external environment criteria based on experts' experience.

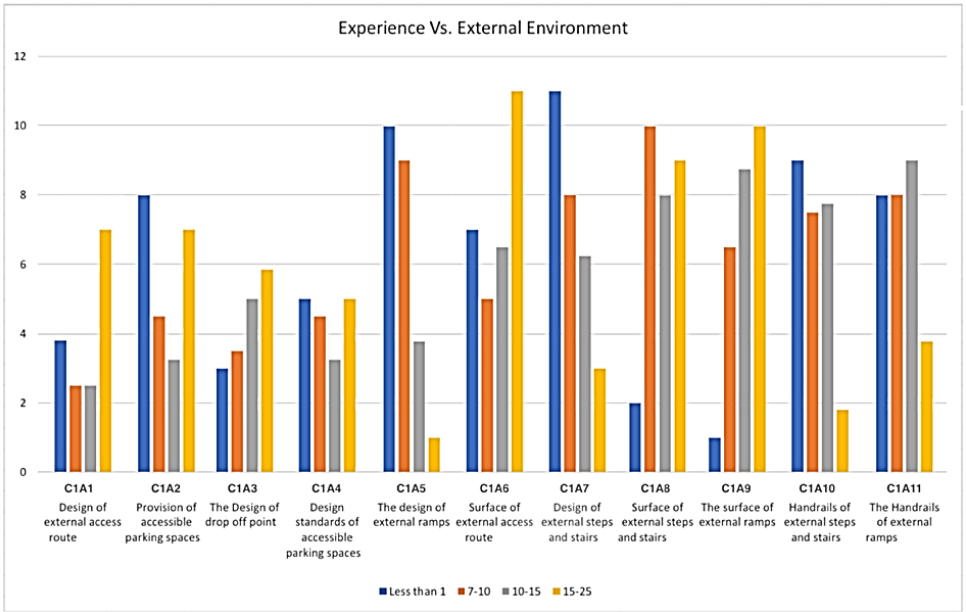


Fig. 3: External environment rankings based on experts' experience

According to Figure 3, the highest ranking was given to the design of external ramps (C1A5) by experts with experience of 15-25 years and the surface of exterior ramps (C1A9) by experts with experience of less than a year, making these two attributes the highest priority from the view of these experts. On the other hand, the lowest ranks are given to the surface of external access routes (C1A6) by experts with experience of 15-20 years and design of external steps and stairs (C1A7) by experts with experience of less than one year, making these two attributes the least priority.

Figure 4 illustrates the detailed ranking of attributes within entrance criteria based on experts' experience.

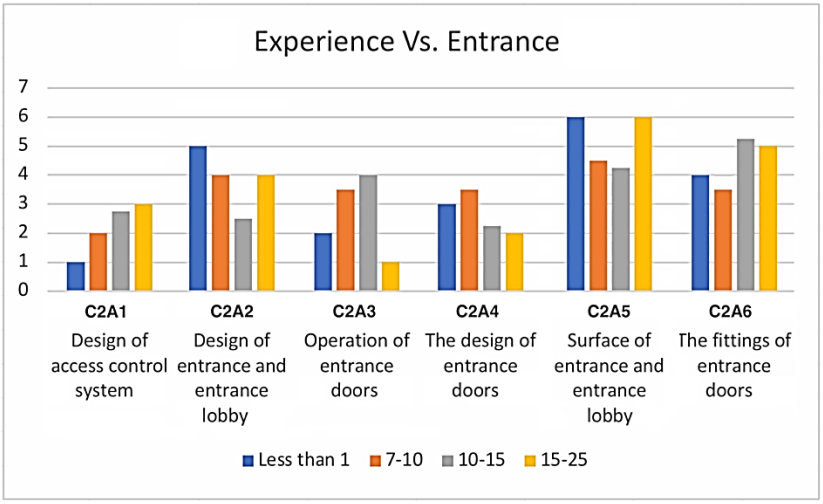


Fig. 4: Entrance based on Experts' Experience

Figure 4 presents that the highest ranking was given to the operation of entrance doors (C2A3) by experts with experience of 15-25 years and the design of access control system (C2A1) by experts with experience of less than a year, making these two attributes the highest priority. Furthermore, experts with experience of 15-20 and less than one year agree that the lowest rank is given to the surface of the entrance and entrance lobby (C2A5) as the least priority.

5 **Discussion**

This section explores the justifications for selecting the highest-ranking criteria attributes based on the view of experts with experiences of less than one year and 15-25 years. To integrate inclusive design practices with accessibility, it is essential to show how the highest-ranked criteria respond to vital challenges of physical disability in the built environment. Furthermore, the highest-ranked criteria should also be responding to decision-makers' challenges. Table 3 presents the physical challenges mentioned earlier, criteria and phases thematically. Also, according to Ahmad et al. (2022), the criteria can be categorized as general or essential requirements. The essential requirements would define the building as entirely inadequate if it failed to comply. On the other hand, the general requirements would cause the building to be partially inadequate.

Table 3: Challenges of physical disability and high ranked assessment criteria

(Legend: D-Design, C/I-Constriction/Implementation, O&M-Operation and Maintenance)

Users Focus	Experts Focus - Accessibility Assessment	Phase			Theme	Priority (General /Essential)
Challenges of physical disability	**Criteria (C) & Attributes (A)**	**D**	**C/I**	**O&M**		
	C1: External Environment					
Entry obstacles	C1A1: Design of external access route	X			Navigation	Essential
Inaccessible parking areas						
Insufficient maneuvering space						
Steps and stairs						
Seeing from or reaching a certain height						
Restless long travel distances						
Entry obstacles	C1A5: Design of external ramps	X			Entry	Essential
Insufficient maneuvering space						
Inadequacy of design and surface Materials of ramps	C1A9: Surface of external ramps		X	X	Movement	General
Slippery or uneven floors						
	C2: Entrance					
- Entry obstacles - Insufficient maneuvering space at the door	C2A1: Design of access control system		X	X	Restriction	General
	C2A3: Operation of entrance doors		X	X	Entry	Essential

The first criterion ranked as highest based on the general view of all experts collectively is C1A1: the design of external access route; it is an essential requirement that responds to vital challenges of physical disability, as displayed in Table 3. Experts ranked it as one of the highest for many reasons, such as; ease of circulation and access to PWDs, comfort and clarity in knowing the entries and exits from the drop-off points or parking. Failing to provide an adequate design for the external access route renders the facility entirely inadequate for PWDs. The second highest criteria attribute is C1A5: design of exterior ramps that is also an essential requirement. One crucial justification provided by the majority of experts with experience of 15-25 years is that PWDs must be provided with means of access to any buildings, lack of ramps imposes entry obstacles. Furthermore, C1A9: the surface of external ramps can affect the movement of PWDs, especially if the finishing material is slippery, as it may lead to accidents that can be avoided if proper rough materials are selected. However, it is considered a general requirement as it causes the building to be partially adequate.

Moreover, the first entrance criteria attribute ranked as highest is C2A1: design of access control system. This attribute leans more towards the facility management side; experts believe that access control systems should operate efficiently, or else it would cause obstruction and restrict movement. Furthermore, C2A3: operation of entrance doors is considered an essential requirement as it obstructs entry if not operating adequately, especially since PWDs would face difficulty trying to use them manually.

6 Conclusion

To sum up, it is an essential responsibility of decision-makers towards PWDs, to ensure that the buildings' design, construction and operations align with inclusive principles that respond to users' needs through regular assessments. There is a need to prioritize accessibility assessment criteria that would render the buildings either partially or fully inadequate to use by PWDs, to tackle physical and decision-makers challenges. This paper highlighted some assessment criteria ranked the highest by a targeted group of experts within an FM team. The general ranking showed a hierarchy of importance among all assessment criteria attributes. Furthermore, the ranking based on experts' experiences provided insight into how the years of experience influence the view of experts in ranking. Ultimately, the design of the external access route, the design and surface of exterior ramps, the design of access control and the operation of entrance doors are considered the highest-ranked accessibility assessment criteria.

Limitations

Project limitations include the small sample size that covered 70% of the ADA practitioners for the semi-structured interviews. In addition, the sample size was limited due to the extended session period and the availability of the practitioners.

Acknowledgment

This study is supported by Qatar National Research Fund, NPRP grant with project number NPRP 12S-0304-190230. Also, supported by Qatar University, College of Engineering (CENG) with project number QUCP-CENG-2020-1. The content of the paper is solely the view of the authors and has not been shared or published elsewhere.

References

Ahmad, A.M. et al (2022), "Inclusiveness Assessment Tool for Disabled Persons in Higher Education Facilities," Journal of Facilities Management, vol. ahead-of-print no. ahead-of-print. https://doi.org/10.1108/JFM-08-2021-0086.

Carlsson, G. et al. (2022). A Scoping Review of Public Building Accessibility. Disability and Health Journal 15 (2022) 101227, pp. 1-11. DOI: https://doi.org/10.1016/j.dhjo.2021.101227

Derese, B. (2020). Assessing the Efficiency and Challenges with Implementing Accessible Building Facilities for Persons with Disabilities in Public Building of Addis Ababa. Addis Ababa Institute of Technology School of Civil and Environmental Engineering (Thesis). Addis Ababa, Ethiopia. Retrieved from: https://bit.ly/3VAmpnK [Accessed 27 November, 2022].

Hadjri, K., Afacan, Y. & Gadakari, T. (2016). Inclusive Design – Chapter 6. M. Noguchi (ed.), ZEMCH: Toward the Delivery of Zero Energy Mass Custom Homes, Springer Tracts in Civil Engineering, pp. 151-173. Springer International Publishing Switzerland 2016. DOI 10.1007/978-3-319-31967-4_6.

Hopkins, L. (2011). The Path of Least Resistance: A Voice-Relational Analysis of Disabled Students' Experiences of Discrimination in English Universities. International Journal of Inclusive Education, vol. 15 no. 7, pp. 711-727. DOI: 10.1080/13603110903317684.

Jacklin, A. et al. (2007). Improving the Experiences of Disabled Students in Higher Education. Available at: www.heacademy.ac.uk/assets/documents/research/jacklin.pdfJones [Accessed 10 December 2022].

Lau, W.K., Ho, W.D.C. and Yau, Y. (2016). Assessing the Disability Inclusiveness of University Buildings in Hong Kong. International Journal of Strategic Property Management, vol. 20 no. 2. pp. 184-197. DOI: 10.3846/1648715X.2015.1107653.

Machado, L. & Oliveira, U. (2021), "Analysis of Failures in the Accessibility of University Buildings", Journal of Building

Engineering, vol. 33 no. 2021, p. 101654, DOI: 10.1016/j.jobe.2020.101654.

Meyers, A. et al. (2002), "Barriers, Facilitators, and Access for Wheelchair Users: Substantive and Methodologic Lessons from a pilot Study of Environmental Effects", Social Science & Medicine, vol. 55 no. 8, pp. 1435-1446, DOI: 10.1016/S0277-9536(01)00269-6.

Moriña, A. & Morgado, B. (2018). University Surroundings and Infrastructures that are Accessible and Inclusive for all: Listening to Students with Disabilities. Journal of Further and Higher Education, vol. 42 no. 1, pp. 13-23. DOI: 10.1080/0309877X.2016.1188900.

Mulazadeh, M. & Alharbi, T. (2018), "Disability Policy and Wheelchair Users' Accessibility in Jordan", Review of Disability Studies: An International Journal, vol. 14 no. 4, pp. 1-2, available at: https://rdsjournal.org/index.php/journal/article/view/770/2078 [Accessed 19 December 2022].

Muzemil, A. (2018), "Campus Physical Environment Accessibility for Person with Disabilities in the Ethiopian Public Universities", International Journal of Multicultural and Multi-religious Understanding, vol. 5 no. 5, p. 286, DOI: 10.18415/ijmmu.v5i5.45.

Sholanke, A., Adeboye, A. and Alagbe, O. (2019), "Design Solutions Creating Barriers to Achieving Universal Design Compliance of Academic Buildings in Universities in Nigeria", International Journal of Civil Engineering and Technology (IJCIET), vol. 10 no. 1, pp. 671-690, available at: www.iaeme.com/ijciet/issues.asp?JType=IJCIET&VType=10&IType=01, ISSN Print: 0976-6308 and ISSN Online: 0976-6316 [Accessed 19 December 2022].

Simonson, S., Glick, S. & Nobe, M. (2013). Accessibility at a Public University: Student's Perceptions. Journal of Facilities Management, vol. 11 no. 3, pp. 198-209. Iss Emerald Group Publishing Limited. DOI: 10.1108/JFM-06-2012-0025.

WHO (2022). Disability. [Online] available at: www.who.int/mediacentre/factsheets/fs352/en/ [Accessed 11 December 2022].

Cite as: Abdelkarim S., Ahmad A.M., Zahrah J., Makhoul N., Al-Nuaimi M. & Naji K., "Criteria and Challenges of Inclusive Design In The Built Environment", *The 2nd International Conference on Civil Infrastructure and Construction (CIC 2023)*, Doha, Qatar, 5-8 February 2023, DOI: https://doi.org/10.29117/cic.2023.0011

Focus on Lean Construction at Umm Lekhba (Landmark) Interchange

Nader Halimeh
Parsons International Limited, Doha, Qatar
naderhalimeh@gmail.com

Abstract

Umm Lekhba (Landmark) Interchange is the largest four level Interchange built in Doha-Qatar, which has 9 flyover bridges with 11 km in total length, constructed partly using 735 heavy precast concrete segments fabricated off-site, transported, and installed using heavy cranes and launching trusses with a minimum impact on the public traffic flow and on the shopping activities at the busiest interchange in Doha. The Lean Construction Institution–Qatar (LCI-Q) was established in October 2019, and the Lean Construction implementation became mandatory for all new projects of Ashghal in Qatar as of 2022, however the construction of Landmark Interchange was started in May 2017, and two of its flyover bridges were opened to traffic at the end of 2019. The contract of the Landmark project did not mandate implementation of Lean Construction but the contractor had implemented part of Lean Construction and BIM techniques at his own cost to overcome the challenges faced in the design and construction of the project, including consideration of using the Last Planner System, Organization/Standardization of the workplace, implementation of Just in Time concept, using a systematic procurement approach, utilization of Multi-layer subcontractors and consultants, etc. This paper will present briefly the construction of Landmark Bridges and discuss Lean implementation during the construction.

Keywords: Lean construction; Precast segments; Landmark

1 Introduction

Lean Construction is a project delivery process that uses lean methods for maximizing stake holder value while reducing waste by emphasizing collaboration between teams on the project, the goal of Lean Construction is to increase Productivity, Profits, and Innovation in the Industry, based on Lean Construction Institution (LCI-US), which funded the research sources, showing that the projects which implemented lean building tools and techniques give much better outcomes across variety of benchmarks. (LCI, 2022). The Lean Construction methods include the Last Planner System, Choosing by Advantages, Target Value Delivery, Integrated Project Delivery, etc. The Lean Principles are the concepts that help us to achieve the Lean Philosophy and can include: Continuous Flow, Single Piece Flow, Pull, Small Batch Size, Fast Switch Over, Visual Management, etc. The Lean Construction tools that allow using the Lean methods within the projects including Software, Analog (aka stickies), Hybrid implementation. (Do, 2022).

The term Lean Construction was born and used for the first time in the year 1993 on the first endeavour of the International Group for Lean Construction, organized by: Glenn Ballard and Lauri Koskela, both worked together with Greg Howell in the late 1980s and early 1990s to improve construction through planning production, and they have developed the Last Planner System and the Target Value Delivery methods for Lean Construction. (Do, 2022).

In addition to the above mentioned Lean Construction methods, there are several methods imported from Toyota Production System (TPS) that have been translated well into the Design and Construction including: 5whys, 5s, A3 Problem Solving, PDCA (Plan, Do, Check, Act), Poka-Yoke (Error Proofing), Single Minute Exchange of Die (SMED), Standardized Work, Value Stream Mapping and Visual Management, however the first book which was published on Lean Construction in 1993 titled **"**The Machine that Changed the World" showed many similarities with Toyota Production System. (Do, 2022).

The Public Works Authority Infrastructure Affairs had engaged the Consolidated Contractor Group and Tayseer (CCC/TCC) to design and build Al-Bustan Street North Project, including the Landmark interchange (Junction B6), which is the last main Junction on the new Sabah Al Ahmad Corridor. The construction of Landmark flyover bridges will be briefly presented and the Lean implementation will be discussed in this paper.

2 Al Bustan Street North Project

Al-Bustan Street North Project is a re-development of the existing Al-Bustan Street North into a length of expressway approximately 3.6 kms., in addition to re-construction of Al-Bustan Street North/Al-Markhiya Street, Al-Ittihad Street, upgrading of approximately 1.7 kms. section from Al-Shamal road and the construction of Al-Ittihad Bridge, Duhail TTM and Duhail Green Belt.

Al-Bustan Street North starts from Al-Luqta roundabout and ends at the Landmark Mall, it includes a section of Al-Ittihad Street and Al-Ittihad bridge connecting Al-Gharafa with Khalifa City North, the scope of works of the project comprises the design and construction of 4 main Junctions with 4 lanes in each direction, including the largest 4 levels interchange in Doha, which have 9 flyover bridges with 11 km in total length (Junction B6), one left turn bridge connecting the project with Al-Ittihad Street (Junction B5), one Cut and Cover Tunnel (Junction K1), and one Viaduct of two twin Bridges (Junction B4), in addition to the micro tunnelling, signs, utilities, retaining walls, pedestrian bridges, pedestrian/cycle paths, traffic signals, gantry signs, landscaping works and street lighting. The location map of Al-Bustan Street North Project is shown in Figure 1 below.

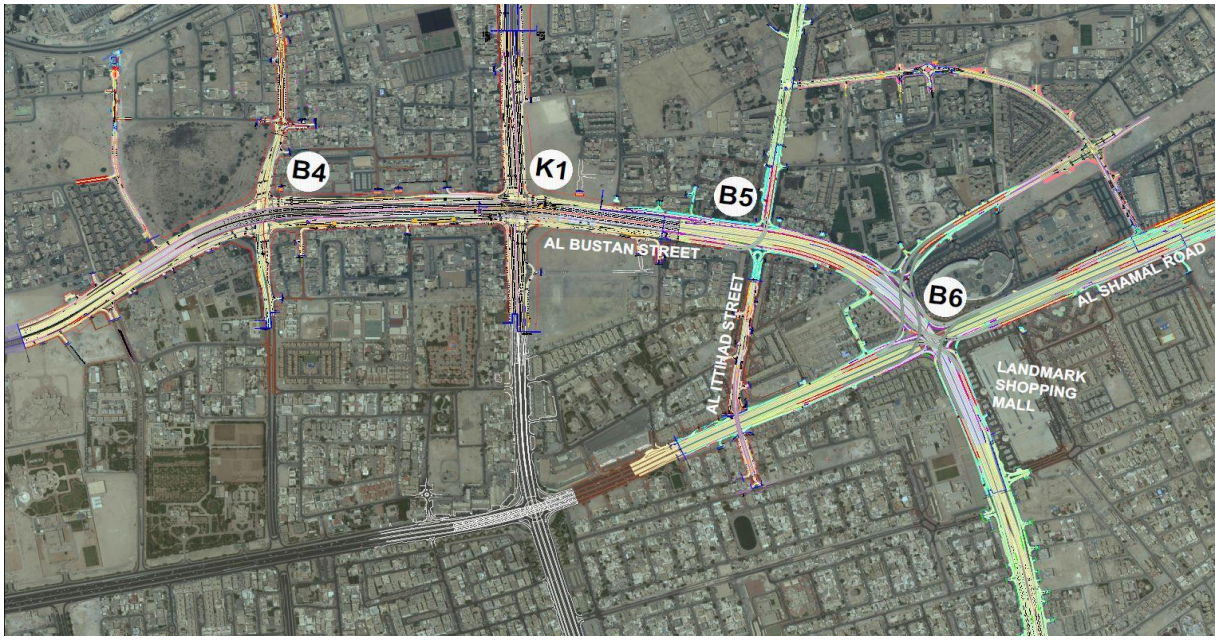


Fig. 1: Location map for Al-Bustan Street North Project

3 Construction of Junction B6 (Landmark) Interchange

Junction B6 Interchange consists of nine flyover bridges, B6-B1 and B6-B2 bridges at grade level, B6-B3, B6-B4, B6-B5 and B6-B9 bridges at level +1, B6-B6, B6-B7 and B6-B8 bridges at level +2. The span arrangements for bridges varies from 36.0m to 90.0m, consisting of simple and continuous superstructure of precast segmental and cast in-situ box girder. The bridge section depths are varying from 2.0 m to 4.5 m. There are in principle two bridge deck widths, wide deck for level +1 and narrow deck for level +2. Figure 2 below shows all flyover bridges of Junction B6.



Fig. 2: Junction B6 (Landmark) with all Flyover Bridges



Fig. 3: Landmark Interchange during the Substructure Construction

3.1 Substructure Construction

Consolidated Contractor Group and Tayseer (CCC/TCC) had divided Junction B6 site into five working zones. Temporary Traffic Management (TTM), Relocation of Existing Utilities and Removal of all Constraints were given top priority to enable the construction of 101 foundation and pier columns required for the flyover bridges, in addition to the retaining wall foundations. Fabrication of 735 heavy precast segments was carried off-site at VSL yard which is located 50kms. south of Doha. The development of the design to satisfy the client and stake holders' requirements was continued during all phases of construction, including new design for Junction B6-B9 and Junction B6-B4 bridges, and design improvement for other bridges. MSE earth wall system was adopted for all bridges of the project. Substructure during construction is shown on Figure 3 above.

3.2 Precast Concrete Segment Construction

The balanced cantilever construction technique was adopted for all bridges which have precast concrete segment as their superstructure. The balanced cantilever construction is an effective method when the access from below is restricted or impossible, the superstructure made of box section–precast segments. The segments were casted, cured, and stored off-site in a controlled manner in a tailored made casting yard. The pier and first pier segments were casted using bulkhead on both faces, next segments were matching cast on one side using the previously completed segment and bulkhead on the other. The segments had shear keys to enhance precision when re-assembled on site as shown in Figure 4 below. The segments were transported to the site for installation using trailers, nominal segment lengths were limited to a maximum of 3.4 meters to fit within one traffic lane width. The largest segment height was limited to 4.5 m to ensure that the trailer plus segment height is clear under the existing bridges on the route from the casting yard to the site. The largest segment weight taken was ninety metric tons. The superstructure installation used was started from the top of the pier, with the pier segment fixed to the top of the column either permanently for monolithic piers or temporarily using U-Ties during the construction as shown in Figure 5. Additional temporary supports at piers, (on one side of the pier used where necessary), stitches between pier segment and the first pair of segments were deployed for alignment adjustment. Next, segments were hoisted by the crane, either directly to the desired position for post-tensioning, or onto the transporter waiting on the top of the pier segment before transported to the cantilever tips and dropped into place by the Lifting Frames (Figure 6). Once the segments are in place, a temporary post-tensioning with the use of Prestressed bars were applied to secure the segment temporarily to the earlier completed section. The segments were equipped with temporary concrete bottom blister with cone opening provisions in the top slab or the temporary steel upper blister, which were designed for the weight of the segment and the temporarily post-tensioning works. Epoxy resin was used to be applied between segments; the segments were installed on alternate sides of the pier columns so that the out-of-balance moment was kept to a minimum. The segment installation sequence was repeated till the completion of the last pair of segments. Closure stitching was applied between the two cantilever tips coming out from consecutive piers. While for the end span segments, and at the expansion pier columns, the segments were installed on traditional falsework and stitched to the cantilever tip. Continuous post-tensioning was subsequently applied to complete the installation works for the superstructure. Street furniture and road surfacing were applied to complete the bridge work.



Fig. 4: Precast Concrete Segment Fabrication in VSL Yard 50 kms. south of Doha



Fig. 5: Precast Concrete Segment Installation for Junction B6 bridge

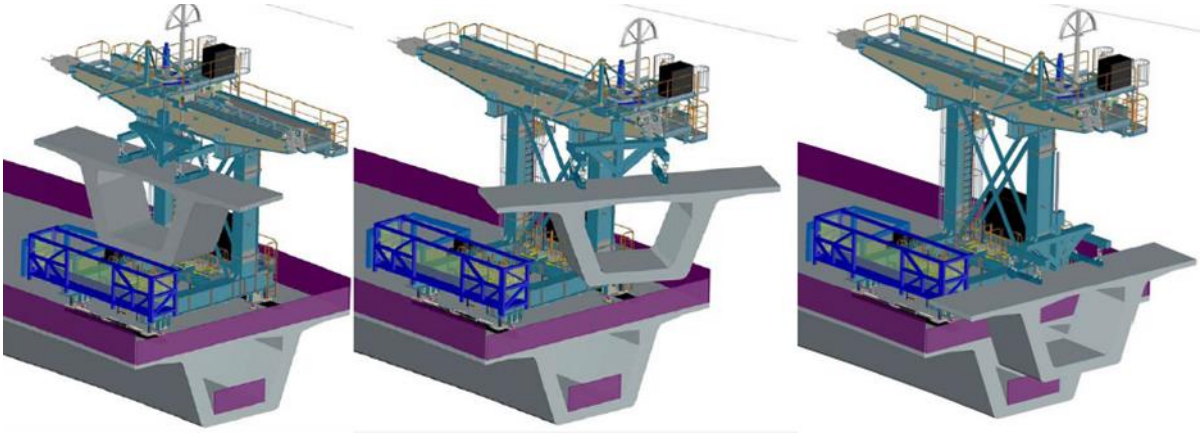


Fig. 6: Installation of Precast concrete Segments using Lifting Frame



Fig. 7: Photo for Shamal Road during Landmark Construction

3.3 Cast in-situ post-tensioning Superstructure Construction

Junction B6-B1, B6-B2 bridges were designed to be cast in-situ concrete post-tensioned voided slabs, the deck superstructure was supported on mechanical bearings over the abutment and the two pier columns, while a traditional formwork support was deployed and considered in the design.

4 Lean Implemantation during Construction

The contract of Landmark project does not mandate the implementation of Lean Construction; however, the Contractor had implemented part of Lean Construction and BIM techniques of the Landmark flyover bridges at his own cost, moreover and during the construction in August 2019, the senior management of the contractor had engaged the Global Management Consulting Firm "McKinsey" to study and provide their feedback about the project management and Lean Construction implementation. Part of the contractor key staff had been previously trained on the Lean Construction implementation under Boston Consulting Group 'BCG" in August 2015.

Based on the contractor planning team, the Lean principles and techniques were implemented to overcome the following changes:1) Design and Build Project, 2) Change in Design Strategy during Construction, 3)Value Engineering Proposals by the Contractor, by Change in the Design (example from underpass to overpass bridge) and Savings to the Client, which resulted in a tight working schedule due to design approval process requirement by the stakeholders, 4) Variation to the Contract, additional scope (from a concept design to detail design), which resulted in changes to the original scope of the work, 5) Procurement of Long Lead Items, 6) Managing Multiple sub-contractors and Suppliers, 7) Complexity in Construction, while maintaining free flow of traffic in the busiest interchange in Qatar.

The Lean Principles and techniques were implemented on Landmark Project as follows; 1) The baseline schedule was established in the beginning of the project, but due to the complexity of the project with unforeseen circumstances on site like existing utilities and design delays, the project started loosing track of meeting intermittent site established deadlines. 2) Pull Planning was established on how to achieve the completion date of each bridge as set in the baseline, the recovery baseline was set by involving all construction teams, the durations of each activity and the sequence was agreed with the construction team, the delivery of the design drawings, and the delivery of every material used to be discussed and considered in the developing of the schedule. 3)Three months look ahead schedules were issued to the construction team for close following-up, the schedules were part of the weekly progress meetings. The planning team compiled the progress of the week, and highlighted the slippage activities and discussed the ways of mitigation, maintaining the same target date. 4) The productivity of the crews was monitored on weekly basis, the reasons for shortage of the productivity were discussed and analysed in the weekly meetings. 5) The procurement of Long Lead Items was a big challenge, mainly due to the huge quantity of bridge bearings, identifying the required date for each bridge bearing on site and accordingly the schedule was provided to the supplier, some were procured by air fright to mitigate the delays. 6) All main sub-contractors of the project were engaged to be in integration with the contractor's main project program on a daily communication and during the weekly progress meetings.

Intermittent milestones of the program, for example, the nine bridges in the Landmark interchange, the target date to complete each bridge and open to traffic was a Milestone, which was strictly implemented in the project to respect the intermittent milestones. Weekly planning meetings with the construction team played a vital role in mitigating the delays by pull planning concepts as shown in

Figures 8, 9, 10 and 11 below.

Last Planner System (LPS) definition is a collaborative, commitment-based planning system that integrates the concept of the 'should-can-will-did' planning. It includes master scheduling and phase planning to define what should be done. Look ahead planning is based on constraints identification and removal (the make-ready process) to establish what can be done, weekly work planning based on reliable promises reflecting what will be done, and learning based upon analysis of the PPC (comparing 'did' against 'will') and the reason for variance. The goal of the Last Planner System is to improve the PPC since the PPC is the measure of the reliability of the work completed versus the work planned, the increase of the PPC will provide better productivity and safety for the construction. (Do, 2022).

Target Value Delivery (TVD) is a management practice that drives the design and construction to deliver customer values within project constraints (Bollard, 2009 and Do, 2022). The goal of TVD is to address Cost Reliability Value Delivery and Continuous Improvement of the projects (Do, 2022).



Fig. 8: Commitment meeting of Section, Construction and Project Managers

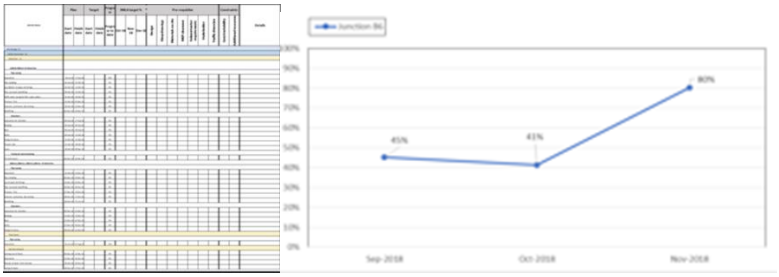


Fig. 9: Commitment to plan Work Sheet & KPI reliability CR%



Fig. 10: Crew Leaders Meeting and Updating the Progress on Daily Basis



Fig. 11: Lean Production Worksheet & KPI Target Percentage completed by Crew

5 Conclusion

Part of Lean principles and techniques were implemented by the contractor during construction of the Landmark bridges, including consideration of Waste Elimination, Organization/Standardization of the Workplace, Implementation of Just-in-Time Concept, implementation of Safety at Work Place, using 5whys for root cause analysis, consideration of total quantity management in the project, considering the use of the Last Planner System, using systematic procurement approach, utilization of multi-layer subcontracting and consultants for the project. It involved off-site construction technique, using digital and fast approval procedure for the critical project decisions. Supply chain management for the project, cost optimization, productivity measurement using Percent of Plan completed PPC, reduced consumption of resources, etc., which contributed to the successful, early and safe completion of the Landmark bridges, based on full collaboration between all parties involved in the construction including the client and the related stakeholders.

Lean Construction methods were not known during construction of Kizlac Motorway Viaduct in Turkey in late 1990s, however, a methodology similar to the "Target Value delivery" TVD of Lean Construction was adopted by the contractor for the design and construction at that time and led to the successful completion of the Viaduct (Halimeh,2000). It is recommended to mandate the use of the Last Planner System and Target Value Delivery methods for all new projects, because the two methodologies which were developed by "Glenn Ballard" and "Greg Howell" are unique and required for the Construction Industry (Do, 2022).

References

Do, Donah (2022). *The Art and Philosophy of Lean Construction*. Lean Construction Blog (Online Book). https://leanconstructionblog.com. San Francisco. California.

Lean Construction Institution, LCI (2022), (learning -search). www.leanconstruction.org

Halimeh, Nader (2000). *Construction of Kizlac Motorway Viaduct*. Bridge Engineering Conference 2000. (Fib Symposium). Egyptian Society of Engineers and Egyptian National Group of IABSE. Sharm Elsheikh- Egypt.

Cite as: Halimeh N., "Focus on Lean Construction at Umm Lekhba (Land Mark) Interchange", *The 2nd International Conference on Civil Infrastructure and Construction (CIC 2023)*, Doha, Qatar, 5-8 February 2023, DOI: https://doi.org/10.29117/cic.2023.0012

Duality of Lean Construction and Building Information Modeling into Digital Collaborative Scheduling in Qatar: A Conceptual Framework

Murat Gunduz
Professor of Civil Engineering, College of Engineering, Doha, Qatar
mgunduz@qu.edu.qa

Khalid Naji
Dean of College of Engineering, College of Engineering, Doha, Qatar
knaji@qu.edu.qa

Ayman Fahmi Naser
PhD Candidate, Engineering Management, College of Engineering, Doha, Qatar
an1401569@student.qu.edu.qa

Abstract

Long has the construction industry been chastised for its low production performance. Building Information Modelling (BIM) and Lean Construction (LC) are two of the most widely adopted concepts in the construction industry for improving project delivery performance. LC is a complex blend of project management principles and tools whose origins can be traced to the automobile manufacturing industry. BIM refers to the technologies and processes that allow for the effective management of project information from inception to deconstruction. There are significant positive synergies when LC and BIM are implemented together. Nonetheless, these two concepts are frequently managed and implemented by separate teams within client, design, and construction organizations. This is largely due to the LC and BIM teams' lack of awareness and incorrect biases. Collaboration between the LC and BIM teams is necessary for BIM to facilitate LC principles/tools and for LC to enhance BIM processes in order to maximize the synergy between these two concepts. Globally, this is also a major concern for the industry.

The objective of this research is to develop a collaborative digital model that facilitates the integration of BIM and LC teams in the construction industry. These objectives will comprise the proposed research on literature-based understanding of the collaboration dynamics between various teams. Document and map the two-way synergy between LC and BIM in design and construction management based on the literature, workshops and interview with expertise. Understanding the requirements for a digital, interactive, collaborative tool that will allow both LC and BIM teams to improve their processes. It is a conceptual and digital tool that may be referred to as a "LC and BIM translator."

Keywords: Lean construction; Building Information Modelling; Integration; BIM and Lean assessment; Visual and design management

1 Introduction

Qatar's efforts to modernise and attract investment in infrastructure projects have increased. The allocation of QAR 53.9 billion (US$ 14.8 billion) in infrastructure projects between 2021 and 2025 in conjunction with Ashghal, Qatar's public works administration, would contribute to the country's continued expansion. These projects consist of QAR 1.58 billion (US$ 440 million) for road and

public area restoration and QAR 5.8 billion (US$ 1.59 billion) for infrastructure maintenance. As a result, a number of capital projects are supported, and the construction industry remains to be an integral part of the national plan. In the next years, Qatar will enhance to invest over $110 billion in infrastructure and mega-projects. Considered one of Qatar's most important industries, construction contributed 13.8, 16.7, and 18.7% of real Gross Domestic Product (GDP) in 2019, 2020, and 2021, respectively, and will continue to be the main contributor to economic growth over the next several years. Production in construction domain is often hampered by poor productivity, high labour turnover, low skill levels, and a lack of innovation. Estimates of building projects totaling billions of dollars over the next quarter-century have spurred the government and business to wonder, ***"Is the construction sector equipped to complete these projects?***"

Site construction teams spend an inordinate amount of time each week planning and monitoring non-systematic schedules, subcontractors do improper and stand-alone planning, absence of cooperation and communication between construction parties, and inefficient information sharing are all problems caused by the fact that traditional planning does not reflect the reality of the activities taking place on the construction site. These problems are usually overcome by assigning a skilled planning team to operate inside the project management structure (Heigermoser et al. 2019). However, the picture is different for the site teams, seldom is the theoretical knowledge provided in schedules digested and adapted to the reality of the site employees, resulting in a gap between theoretical information and worksite planning methods. In reality, having a planning staff as part of management just makes existing communication problems and silos worse. In the setting of a large-scale project with intricate management structures, this statement rings truer than ever (Heigermoser et al. 2019). To prevent the disconnection and meet the problems, an interoperable Lean-BIM model integrating BIM Operations and Lean techniques was designed. The framework is a product of merging action and design science research, which is tailored to service the different project planning stages and stakeholders. Duality with BIM is offered on this digital platform for collaborative planning of targets. The purpose of the article is to simplify the communication of schedules, support the understanding of planning-related challenges, optimise construction sequences, and guarantee that the schedule is updated in a smooth and efficient way for continual progress monitoring. The evaluation stated here is beyond the boundaries of this study and it will be investigated further in the future.

2 Literature Review

Few quantified and published outcomes of such collaboration on-site have been recorded yet, despite the fact that various studies over the previous decade have highlighted the advantages of combining Lean Construction and BIM. Numerous ways in which merging Lean concepts with BIM has improved construction are detailed in the literature (Sack et al. 2017; Maraqa et al. 2021; Evans et al. 2021). Lean construction practises allow for the enhancement of customer value and the maintaining of a steady work flow (Tezel et al. 2018). Planning is much more of a team effort when Lean construction concepts and Lean production processes are used to the building process instead of the more conventional approach of individuals working independently of one another. BIM may mean either "Building Information Modeling" or "Building Information Management." Construction experts such as architects, engineers, real estate developers, builders, manufacturers, and others may all work together in a single 3D model to plan, design, and construct a building or structure. The number of dimensions used by BIM in construction has expanded from 3D to 4D (scheduling), 5D (estimating), and 6D (facilities management) (Terreno et al. 2019; Evans et al. 2021). While one is often used separately, the other may enhance or diminish its benefits. It has been shown that there are

a total of 56 interactions between Lean principles and BIM features (Sacks et al. 2010), with the authors concluding that the full potential of this connection can only be achieved via their completely integrated use. Although there is some evidence that Lean and BIM may enhance construction, no BIM-integrated planning, scheduling, and monitoring framework has been documented as of yet (Sacks et al. 2017). Guerriero et al. (2017) developed an intelligent construction planner as a software tool that promotes cooperative planning in line with the previous planner system. Their study also included a mapping of the planning stages to BIM 4D scheduling and the argument that the two should be used together in a single framework. Recent research into LCM and BIM, say Toledo et al. (2016), has focused too much on the theoretical synergy potential of both methodologies and too little on the creation of really usable methods and tools.

As a result, they suggest planning model, whereby a BIM model is integrated into the last planner system process, and its optimal utilisation across many stages is explained. With the approach suggested by Evans et al. (2021), project key stakeholders may prioritise addressing the critical problems and impediments to widespread use of LC and BIM in construction of megaprojects. The paper's results were limited to some suggested practical strategies for boosting the embracing of LC philosophies and BIM technologies in construction mega-projects, with the goal of encouraging key stakeholders in the construction industry to focus on overcoming the substantial challenges of integrating BIM and LC principles. In particular, Sbiti et al. (2021) performed a thorough literature assessment of the most recent advances on interconnection between BIM and lean construction, identifying key linkages between lean construction practices and BIM functional concerns. As an added bonus, the authors show how the existing BIM-based IT software used to assist Lean Construction has several serious automation flaws. Project management software that does not use BIM data continues to depend on manual operations including planning, evaluating limitations, measuring workloads, and managing site progress. As these two ideas are often led and implemented by different teams at client, design, and construction organizations in silos, these restrictions prevent an operable duality of BIM and Lean at the actual and actuate data level and make current lean IT tools extremely laborious, subjective, and prone to error. To maximise the synergy between LC and BIM, the authors were prompted by the preceding statement to develop a concrete recommendation to direct future researchers in forming a partnership between the two teams and looking into the mechanisms of automating construction schedule generation and progress monitoring.

3 Developing a Conceptual Lean-Bim Duality

In this article, we use a hybrid action research (Azhar et al. 2013; Naji et al. 2022b) strategy, which combines a systematic literature review with the Delphi technique and Design Science Research. The study identifies and builds a conceptual framework for simultaneous implementation of LC and BIM. The research strategy used in this study may be thought of as one in which an issue is tackled via the development of a fresh theoretical framework that adds to the existing body of work. Using a literature study and input from Lean and BIM specialists, we hypothesise a way forward that fills the current vacuum in the literature. As a result, the duality of Lean-BIM framework is at conceptual stage for this study and future research will address the assessment proposed in this publication, which is beyond the scope of the current investigation. The research strategy presented in the study is shown in Figure (1).



Fig. 1: Research methodology

3.1 Interoperable Lean-BIM interactions

Literature study and Delphi Method were used to uncover Lean-BIM Interaction variables based on Naji et al. (2022b) research's methodology. The variables with comprehensive measurements were established, studied, and evaluated using a three-step study approach. Step one is a thorough assessment of the literature on Lean techniques and BIM operations, with an emphasis on Lean-BIM interactions. Step two involves rigorous analysis of relationships between LC and BIM dual adoption. LC techniques and BIM activities that improve Lean-BIM duality are also from literature-review evaluations. Critical review, ten construction expert practitioners, and senior academic researchers were interviewed in face-to-face and semi-structured interviews to verify the Lean-BIM variables and interactions that would be used to construct the LEAN-BIM Duality Framework. As illustrated in Appendix A, ten lean construction practises (LC 1 to 10), ten BIM operations (BIM 1 to 10), and four dual LC-BIM interactions (LC-BIM1 to 4) were selected by literature analysis and conferences with ten construction experts. In the second stage, a two-round Delphi research with 25 construction professionals was undertaken to determine expert consensuses using advanced statistical analysis. Criteria for selection of experts was developed based on Naji et al. (2022a). Inter-rater agreement (IRA) analysis was used in the third phase to assess the strength of agreement, which was 96.8% for Lean practices and BIM operations and 100% for Lean-BIM dual interactions. Thus, a strong agreement was reached, and building specialists acknowledged the relevance of the highlighted parameters.

3.2 Developing a conceptual scheduling platform

Naji et al. (2022a) note that to accomplish construction project objectives often includes the optimization of the interdependent goal variables, time, costs and quality, for which avoiding the planning variabilities and maintaining process stability in execution are critical. Subsequently, approaches aimed toward achieving Lean and BIM aims, such as Collaborative Target Planning (CTP), become anchors for developing scheduling platform system. Four major potential factors were identified according to the interoperable Lean and BIM interaction that have significant room for potential improvement, and as a result, those areas will be added into the integration platform.

LC-BIM01, enhanced multi-dimensional visualization for evaluating design alternatives according to customer value and conformance with predictive analysis of performance and early cost prediction. After investigating, visual management, also known as "control by sight," Gunduz and Naser (2019) has emerged as an essential component of the Lean philosophical framework. Visual management is directed toward visual control in workplace organization, quality, cost, production delivery, people skills, and safety. Therefore, collaborations were realized within different construction life-cycle stages. At the design stage, design alternatives offer an admirable opportunity to the owner and designer to choose the best option to maximize their value. Simulation and modelling of construction sequences utilizing "4D" and "5D" software provides an amazing opportunity to view construction processes throughout the construction phase. This enables the detection of resource conflicts in time and place, as well as the resolution of constructability issues and their related cost implications. In addition, it encourages process improvement, so boosting efficiency and safety assists in identifying bottlenecks. The increased use of mobile devices with cloud databases (such as BIM 360/AutoCAD) adds to the widespread use of BIM visualization. In addition, the utilization of mobile devices and virtual reality improves the process transparency and visualization options accessible throughout the construction stages. Therefore, earned value analysis may be derived using earned value management (EVM) measures, such as Planned Value (PV) and Earned Value (EV). The CTP will outline the required effort and identify the "earning-value" used to determine the task accomplishment or not. Determining the actual costs (AC) and evaluating them to projected costs (EV) can ultimately provide insight into the current situation of overall spending (Gunduz and Fahmi Naser 2017).

LC-BIM02, enhanced collaboration throughout construction project lifecycle via the use of multi-user operating systems to modify and evaluate a single model. In collections of 2D drawings and relevant shop drawings, the exact same objects are depicted in a number of different locations. BIM operators are required to sustain consistency between the multiple illustrations and presentation views as the design process moves forward and modifications are made. By utilizing a singular representation of the information, from which all reports are automatically derived, BIM completely eliminates this problem. Even without producing drawings, sharing models among all team members is an effective way to improve communication during project construction phases.

LC-BIM03, Digital transformation and control with virtual transdisciplinary interaction and actual operating status for project during construction phases. As a 3D model captures all aspects of the design intent and relevant code of practices, BIM visualization features have been used to engage clients and stakeholders, as well as to enhance the collaboration during the construction phase during the CTP meeting sessions. Therefore, BIM based simulations of installation sequences and production can be digitized, which directs supervisors in how to carry out work in certain settings and is an effective tool for ensuring that standardized processes are adhered to. BIM models offer a centralized data repository for the entire life cycle of a project, which helps to decrease variability caused by problems with coordination and the transfer of project data between project phases.

LC-BIM04, Developing an integrated project construction stakeholder databases (i.e., material supply chains and sub-contractors)–Quantities that are automated and connected to BIM models provide more accurate results than those that are performed manually. In addition, modifying the design at a later stage causes corresponding modifications to be made in the connected quantity files. This further helps to guarantee that the amounts are always correct. In addition to this, any modifications that are made to a section or plan are instantly reflected in all of the other sections and plans, which helps to keep the design uniform and eliminate change orders. A BIM database enables construction teams to retrieve construction

drawings as required, hence avoiding the traditional approach. With BIM adoption, the quantity take-offs, resource management, and suppliers' records, just-in-time material and consumable logistics for the construction site can be facilitated via timely coordination with suppliers.

4 The Scheduling Process via Lean-Bim Translator

Developing a master schedule that includes representations of key milestones is a point of commencing when planning out individual phases in accordance with the pull planning. The master schedule, actual material quantities, contractual documents, and the harmonised BIM model in the Issued for Construction (IFC) drawings are taken as input to the framework. Basically, Lean-BIM scheduling process follows the logic steps of pull planning as implemented in infrastructure projects, the State of Qatar as shown in Table (1) and Figure (2). The collaborative/pull planning was introduced as part of contractual enhancements to support project delivery and minimise programme disruption. The Lean-BIM translator is digital process interlinked with relevant BIM objects. During the planning phase and updating production performance, the construction team (last planners) can provide their individual input via cell phone. KANBAN Card application can be downloaded in the cell phone and linked to the Lean-BIM translator. Each kanban card includes a concise description of a work item, as well as its owner, due date, and status. The card may also contain references to source documents or a list of constraints impeding the item's completion.

12-Weeks Collaborative Target Planning (CTP), 4-Week Look Ahead Plan (4WLAP), Weekly Production Review (WPR), and Daily Huddles (DH) were set as an enhancement scheduling and controlling tools to evaluate and assess the performance of production and productivity in enhanced infrastructure projects. 12-week CTP is, master schedule, collaborative pull production planning session and including all relevant stakeholders to define and sequence tasks to manage interfaces, clarify requirements for handovers, and create/improve overall workflow and productivity for the following 12 weeks. In this session, phase planning can be developed collaboratively by construction and stakeholders' team. The CTP sessions are to eliminate waste, identify any missing approvals/key resources or materials etc. that are preventing maintenance of a continuous work flow i.e., design, resources, access, material, plant, permits, safety, and share understanding (DRAMPPSS). A written action plan shall be listed to ensure that the necessary activities to complete the works are correctly identified and required preparations are in place to ensure a successful on time completion. 4WLAP is a detailed work activity plan for the next 4 weeks, and should be aligned to the agreed CTP milestone dates. Relevant project construction team members visualize how best to set-up, organize and carry-out planned works. Then, verify DRAMMPSS –action as appropriate to support 4-WLAP, which is a rolling work plan updated every week as part of WPR. Percentage Planned Complete (PPC) may be calculated and recorded to assess the performance and effectiveness of the plan and study the way for improvement in next week. This can be monitored through DH to ensure continuous daily focus on the delivery of the CTP and weekly plan.

Table 1: Lean-BIM scheduling process

Step	Collaborative Pull Planning	Lean-BIM Translator
1	List of key milestones /activities for upcoming 12 weeks.	Select the BIM objects via IFC viewer to incorporate the milestone date.
2	Define the phase schedule works and relevant pre-requisites.	Select BIM items in IFC Viewer and click *Kanban Card* on mobile device or using digital board.
3	Estimate the time required to complete the phase and any significant intermediate releases from earlier or later phases.	Click on particular milestone and set completion date.

Step	Collaborative Pull Planning	Lean-BIM Translator
4	Conduct collaborative scheduling and post-it notes, construct the logic chain of construction events that are expected to accomplish the phase, and pull planning from the date of the milestone.	Link *Kanban Card* to accomplish the phase, starting from the milestone date via cell phone or using digital board.
5	Estimate time duration for each activity without contingency or float.	Set the duration using *Kanban Card*.
6	Double-check the duration of each activity to reduce the total duration and determine the earliest feasible phase start date.	The duration can be confirmed during 12 Week CTP meeting and 4WLAP.
7	Update the daily production data.	Update the *Kanban Card* via cell phone.
8	Evaluate the production performance via PPC, EV, KPI.	PPC, EV, and KPI values can be displayed in weekly production review meetings in order to evaluate and assess production performance.

4.1 Monitoring and Controlling via Project Performance Indicators

EVM's metrics PV, EV, and AV will enhance pull planning metrics including PPC, average cycle durations (CT), value added, non-value added (NVA), and lead times (LT). As an addition to the systematic CTP, the EV of each accomplished Kanban Card update will be pooled and utilized to assess project success each week. The BIM viewer may preserve each process's state as a query parameter for visual study of building progress, as illustrated in Figure (2).

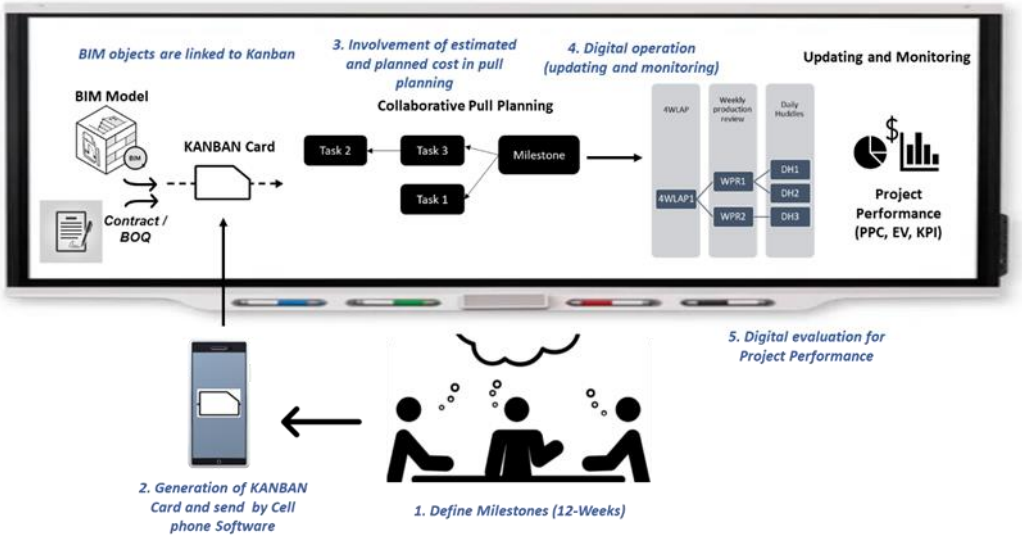


Fig. 2: Lean-BIM Process to develop a digital scheduling platform

5 Conclusion and Future Implementation

The conceptual production planning platform that has been presented integrates several different tried-and-true methods, including the following: EVM gives tools that may be used to assess whether or not a project is working efficiently, while CTP provides the methods to establish when and if value has been generated. In addition to this, it provides a basis for greater process stability as well as increased workflow dependability, which was expected. BIM, which gives the essential information to predict the costs and durations of construction activities, is the gap portion of this jigsaw. In contrast, it provides a more solid foundation for decision-making during 4WLAP, WPR, and DH sessions, in addition to serving as a

platform for effectively depicting the project's current status. These qualities are able to be included into the digital Lean-BIM Translator board that has been developed.

For this reason, this paper proposes a conceptual framework for an operable Lean-BIM duality based on reality of planned activities and actual updating data on daily and weekly basis. This framework will be utilized as a departure point in the current research study to generate an operating system model for Lean-BIM Translator that is applicable for analysis of construction project models and, therefore, for assessment in the logic of the developed research design strategy. Consequently, this paper also assesses the developed research design approach. It was also considered the possible scope of the Lean-BIM Translator, as well as its guiding principles and the new roles that would be formed as a tribute to digital production monitoring system. In this manner, it has been demonstrated that the conceptual platform is a production system that not only fully represents the lean management principles, but also functional areas as a comprehensive construction management system that harmonises the project objectives of accurate planning, excellent deliverables, and minimizing a non-value added cost by imposing a digital planning platform integrating Lean-BIM viewpoint.

References

Azhar, S., Maulik, Y. L, & Ahmad, I. (2013). "An Investigation of Critical Factors and Constraints for Selecting Modular Construction over Conventional Stick-Built Technique." *International Journal of Construction Education and Research* 9, no. 3 (2013): 203-225.

Evans, M. et al. (2021). "Analysis Framework for the Interactions between Building Information Modelling (BIM) and Lean Construction on Construction Mega-Projects." *Journal of Engineering, Design and Technology*.

Guerriero, A. et al. (2017). "BIM-enhanced Collaborative Smart Technologies for LEAN Construction Processes." In *2017 International Conference on Engineering, Technology and Innovation (ICE/ITMC)*, pp. 1023-1030. IEEE.

Gunduz, Murat, & Naser, A. F. (2017). "Cost-based Value Stream Mapping as a Sustainable Construction Tool for Underground Pipeline Construction Projects." *Sustainability* 9, no. 12: 2184.

Gunduz, M., & Naser, A. (2019). Value stream mapping as a lean tool for construction projects. *International Journal of Structural and Civil Engineering Research, Issue, 8*(1), 69-78.

Heigermoser, D. et al. (2019). "BIM-based Last Planner System Tool for Improving Construction Project Management." *Automation in Construction, 104*, 246-254.

Maraqa, M. J., Sacks, R., & Spatari, S. (2021). "Quantitative Assessment of the Impacts of BIM and Lean on Process and Operations Flow in Construction Projects." *Engineering, construction and architectural management*, *28*(8), 2176-2198.

Naji, Khalid K., Gunduz, M., & Naser, A. F. (2022a). "The Effect of Change-Order Management Factors on Construction Project Success: A Structural Equation Modeling Approach." *Journal of Construction Engineering and Management* 148, no. 9: 04022085.

Naji, K. K., Gunduz, M., & Naser, A. F. (2022). Construction change order management project support system utilizing Delphi method. *Journal of Civil Engineering and Management, 28*(7), 564-589.

Sacks et al. (2010). "Interaction of Lean and Building Information Modeling in Construction." *Journal of Construction Engineering and Management* 136, no. 9: 968-980.

Sacks, R., Korb, S., & Barak, R.. (2017). *Building Lean, Building BIM: Improving Construction the Tidhar Way*. Routledge.

Sbiti et al. (2021). "Toward BIM and LPS Data Integration for Lean Site Project Management: A State-of-the-Art Review and Recommendations." *Buildings* 11, no. 5 (2021): 196.

Terreno, S., Asadi, S., & Anumba, C. (2019). "An Exploration of Synergies Between Lean Concepts and BIM in FM: A Review and Directions for Future Research." *Buildings* 9, no. 6: 147.

Tezel, A., Koskela, L., & Aziz, Z. (2018). “Lean Thinking in the Highways Construction Sector: Motivation, Implementation and Barriers.” *Production Planning & Control* 29, no. 3: 247-269.

Toledo, M., Olivares, K., & González, V. (2016). “Exploration of a Lean-BIM planning framework: A Last Planner System and BIM-based Case Study." In *24th Annual Conference of the International Group for Lean Construction*, vol. 7, no. 20, p. 2016.

Appendix A: Lean-Bim Interaction Factors

Lean Construction Practices (LC)	BIM Main Functions (BIM)
LC 1. Reducing project process variability and enhancing upstream flow.	BIM1. Superior visualizations for the assessment of the design's imaginary and functionality
LC 2. Reducing work in progress and cycle time	BIM2. Developing various design alternatives enhancing construction activities and minimizing change-orders
LC 3. Minimizing batch size and pursue single-item flow maintaining continuous output	BIM3. Developing predictive enhancement analysis evaluating the design and construction workflow performance
LC 4. Enhancing adaptability via multiskilling.	BIM4. Systematic cost and time estimate throughout the design and construction phases
LC 5. Standardizing procedures with user-friendly systems to manage production.	BIM5. Reviewing of client value conformity throughout the design and construction phases
LC 6. Improving visualization management controlling production flow.	BIM6. Collaborative modeling techniques based on different design disciplines, and automatic clash management
LC 7. Reliable lean technology enhancing the parallel workflow and line of balance.	BIM7. Collaboratively maintaining a single model throughout the design and construction phases
LC 8. Standardizing value streams via continually validating and verifying.	BIM8. Assessing the potential construction plans utilizing multi-dimensional visualization
LC 9. Collaborative problem-solving opportunities leveraging enhancement strategies.	BIM9. Virtual transdisciplinary collaboration and multi-dimensional visualizations throughout construction phase
LC 10. Enhancing construction stakeholders’ networks to foster collaboration and sustain beneficial long-term connections with supply chains.	BIM10. Collaboration of project construction stakeholders and supply chains database
LC-BIM Translators (LC-BIM)	
LC-BIM1. Enhanced multi-dimensional visualization for evaluating design alternatives according to customer value and conformance with predictive analysis of performance and early cost prediction	
LC-BIM2. Enhanced collaboration throughout design and construction via the use of multi-user platforms to modify and evaluate a single model	
LC-BIM3. Digital transformation and control with virtual transdisciplinary interaction and actual operating status for projects during construction phases	
LC-BIM4. Developing an integrated project construction stakeholder databases (i.e., material supply chains and sub-contractors).	

Cite as: Gunduz M., Naji K. & Naser A.F., “Duality of Lean Construction and Building Information Modeling into Digital Collaborative Scheduling in Qatar: A Conceptual Framework”, *The 2nd International Conference on Civil Infrastructure and Construction (CIC 2023)*, Doha, Qatar, 5-8 February 2023, DOI: https://doi.org/10.29117/cic.2023.0013

Practical Implementation of Campus Facility Management Performance Measurement in Qatar

Murat Gunduz
Department of Civil Engineering, College of Engineering, Qatar University, Doha, Qatar
mgunduz@qu.edu.qa

Khalid Naji
Department of Civil Engineering, College of Engineering, Qatar University, Doha, Qatar
knaji@qu.edu.qa

Omar Maki
Engineering Management Program, College of Engineering, Qatar University, Doha, Qatar
omar.alazzawi@qu.edu.qa

Abstract

Effective facility management is crucial to overall firm performance and is becoming a core competency for organizations seeking to gain a competitive advantage and attain their goals. Recent research on facility management indicates that ineffective management is a leading cause of budget overruns, maintenance delays, reworks, variations, non-compliance events, unnecessary risk, and dissatisfied customers. In Qatar, there is an expansion of educational facilities to achieve the 2030 Qatar National Vision of having an educated population through a well-developed, accountable, and accessible educational system. This expansion is causing a growing demand for effective campus facility management (CFM) in order to effectively manage and accurately monitor the performance of campus facilities. Through a comprehensive literature review, expert interviews, and online questionnaire responses, this paper aims to develop a Campus Facility Management Performance Framework (CFMPF) that consists of tactical and strategic critical campus facility management success factors categorized into process groups. The proposed framework provides an operational foundation for benchmarking the CMF performance to support the identification of underperforming areas. The CFMPF has been used in real-world facility management firms to benchmark their performance and determine which areas of management need to be improved.

Keywords: Facility management; Operation and maintenance; Campus facility management framework; Performance measurement framework

1 Introduction

As reflected in Qatar's National Vision 2030, education is seen as a crucial pillar for the State of Qatar. Qatar, as represented by the Ministry of Education and Higher Education (MOEHE), is committed to collaborating with numerous academic institutions to offer the best educational opportunities both locally and internationally. This is done in an effort to foster a distinctive academic setting that encourages students to develop their imagination and enhance their skills in order to succeed and stand out in various facets of undergraduate and student life. As shown in Table 1, the Ministry of Higher Education has identified 31 universities in Qatar that provide exploration and knowledge generation as well as teaching and research activities in various fields of study (Hukoomi, 2021). These facilities require effective management in order to accomplish their main objectives at the lowest possible cost. According to Matse et al. (2022), poor facility management lowers the value

of existing buildings, raises the cost of unrepaired maintenance issues, raises the price of emergency repairs, and lowers the quality of public services. Additionally, Yasin et al. (2022) highlights facility management of higher education buildings as a crucial element to guarantee the building's sustained peak performance throughout its design life to a workable degree. Therefore, proper facility management is needed for university buildings in order to provide a valuable environment that supports and stimulates teaching, learning, innovation, research, and other diverse academic purposes that all support the government's overall vision for the country. Otherwise, it will hinder the productivity and comfort level in universities, which will ultimately lead to a decline in the quality of its outputs. This paper's goal is to conduct research and make recommendations for a campus facility management framework that can be used in Qatar's higher education facilities.

Table 1: Universities in Qatar as of 2022

University	Sector	University	Sector
Stenden Qatar University of Applied Sciences.	Private	Police College	Public
Doha Institute for Graduate Studies	Private	University of Calgary in Qatar	Public
AFG College with the University of Aberdeen	Private	College of the North Atlantic–Qatar	Public
University Foundation College	Private	Qatar Finance and Business Academy with Northumbria University	Public
City University College	Private	Rule of Law and Anti-Corruption Centre (ROLACC) with University of Sussex	Public
Oryx Universal College with Liverpool John Moores University	Private	Qatar Leadership Center	Public
Lusail University	Private	Ras Laffan College for Emergency and Safety with University of Central Lancashire	Public
Indian State University Savitribai Phule Pune	Private	Georgetown University in Qatar	A
Qatar University	Public	Northwestern University in Qatar	A
Hamad bin Khalifa University	Public	Virginia Commonwealth University School of the Arts in Qatar	A
Community College of Qatar	Public	Texas A&M University in Qatar	A
Qatar Aeronautical Academy	Public	Carnegie Mellon University Qatar	A
Ahmed Bin Mohamad Military College	Public	HEC Paris in Qatar	A
Al Zaeem Mohammed Bin Abdullah Al Attiya Air Academy	Public	Weill Cornell Medicine-Qatar	A
Joaan bin Jassim Joint Command and Staff College	Public	University College London in Qatar	A

A: Higher Educational Institutions affiliated with Qatar Foundation for Education, Science and Community Development

2 Qatar Expansion

Qatar National Vision 2030 was unveiled as a strategy for the country's development. Its goal is to advance Qatar by coordinating the country's human and natural assets in a way that fosters economic growth. To ensure that the next few decades of development in Qatar are inclusive and beneficial for all citizens and residents of the country, this vision will serve as a guide for the country's economic, social, human, and environmental development. Qatar's economy is expanding, and the quarterly GDP at current prices for the third quarter of 2021 is QR 176,225 billion (Authority, 2021). This represents an increase of 40.6% compared to the estimate of QR 125,336 billion for the third quarter of 2020. The construction industry is the second source of growth in non-hydrocarbon activities, with a quarterly GDP at Q3 2021 prices of $22,923 billion, representing a 31.5% increase over 2020. As

a component of human development, Qatar aims to attain a world-class educational system that equips citizens to realize their aspirations and meet the needs of Qatar's society. According to Qatar's Planning and Statistics Authority (2020), out of 222,701 buildings in Qatar, 745 are educational buildings. Campus facility management must be equipped with the most current research and practical experience in order to accommodate the growth of the Qatari construction industry.

3 Campus Facility Management Performance Model

Using a three-step research design, a framework with specific measures is created, investigated, and tested. An extensive literature review and five field expert interviews were used to identify 45 factors classified into seven process groups. In the second step, an online questionnaire was distributed to approximately 1,400 FM experts to rank the CFM key success factors and factor groups; 402 responses were obtained and analyzed. The model has been validated through real-world case studies, and the findings show that the proposed framework can be applied to quantify the performance of a wide variety of campuses.

The proposed framework was built on a 1) extensive review for the relevant literature on effective and successful campus facility management, 2) critical success factors for campus facility management, and 3) strategies to prevent poor campus facility management. As shown in Appendix I, the proposed framework included seven CFM process groups and forty-five key factors affecting the performance of campus facility management. The Group Performance Index and CFMPI were computed using the standard factor loading as weighted scores, similar to the procedure used by Gunduz et al. (2016), and the within-group measure weights are presented in Appendix I. The CFMPI index is computed using Equation 1, where Xj is the within-group weight and Pj is the sum of performance measures in each process group:

$$CFMPIj = \sum XjPj \quad (1)$$

4 Research Methodology

A "case studies" research methodology was used in the study. Six campuses are chosen at random from among Qatar's 31 campuses based on their sector type. Facility management specialists from each of the selected campuses completed performance evaluation forms, which were then input into the CFMPF model to quantify CFM performance. The findings are then discussed, and a conclusion is reached.

5 Framework Implementation

5.1 Selected Campuses

The CFMPF was used to evaluate CFM performance across six campuses in Qatar. CFM experts (minimum of 10 years of facility management experience) completed the assessment forms on a scale of 0 to 100, with a blank assessment for any inapplicable factors. The sizes of the campuses vary, which affects their level of manageability; however, the specific campuses names will not be revealed in order to maintain confidentiality.

5.2 Results

Table 2 demonstrates the results of the campus facility management performance index (CFMPI) for the six campuses and the Group Performance Index (GPI) for the seven process groups. The calculated CFMPI for Campus 1 is 88.42%. Quantifying the levels of performance reveals that PG4 - Organizational Management has the highest performance (GPI = 93%) for campus 1. There are no discernible differences between the different GPIs. CFMPI is calculated to be 81.11% for campus number two. PG1-Workforce

Management and PG2-Assets Management have the highest performance with GPIs of 90%, while PG5-Financial Management has the lowest performance (GPI = 67%). For campus number three, the CFMPI is calculated to be 81.57 percent, and the highest GPIs are for Sustainability and Environmental Management (90 percent). In contrast, PG2-Communications Management and PG3-Systems Management have GPIs of 75% and 76%, respectively, making them the least effective process groups. Only minor significant differences exist between groups. CFMPI is calculated to be 88.49% for campus 4. The process groups with the highest performance are PG5-Financial Management and PG6-Sustainability and Environmental Management. The group with the poorest performance is PG5-Organizational Management (79% GPI). For campus #5, the CFMPI is 86.86, and the top performing process groups are PG6-Sustainability and Environmental Management and PG5-Financial Management, with a GPI of 76% for both PG3-Systems Management and PG4-Organizational Management. The CFMPII for campus number 6 is 88.30%. PG7-Assets Management, PG3-Systems Management, and PG5-Financial Management are the process groups with the highest performance.

Table 2: CFMPI and GPI for Campuses 1 to 6

			GPI of Each Campus						
Process Group	**Factor Loading**	**Relative Weight**	**Campus 1**	**Campus 2**	**Campus 3**	**Campus 4**	**Campus 5**	**Campus 6**	**Average GPI**
PG 1	0.840	0.143	87	90	85	90	86	82	86.8
PG 2	0.840	0.143	85	85	75	91	90	84	85.1
PG 3	0.826	0.141	91	79	76	80	76	98	83.2
PG 4	0.820	0.140	93	69	81	79	76	80	79.5
PG 5	0.870	0.148	91	67	79	95	93	91	86.0
PG 6	0.841	0.143	85	88	90	94	100	90	91.2
PG 7	0.834	0.142	87	90	85	90	87	93	88.7
Sum	5.871	1.00	**CFMPI**						
			88.42	81.11	81.57	88.49	86.86	88.30	85.8

5.3 Discussion of Results

The CFMPI benchmarking value for the six campuses is 85.8%, as depicted in Figure 2. The result indicates that campus #1 has the highest determined CFMPI, at 88.42%, while campus #2 has the lowest, at 81.11 %. The CFMPI values for campuses 1, 4, 5, and 6 are higher than the benchmark value. The CFMPI of campuses 2 and 3 deviates from the benchmark value; consequently, the managements of the last-mentioned campuses are advised to focus on enhancing the weak performing process groups in order to boost the firm's performance. In addition, the significant differences between campuses necessitate the identification of the campus team's performance across the various groups. The model has demonstrated that it can be utilized in practice to evaluate the performance of campus facility management in order to identify pitfalls and strengthen weaknesses.

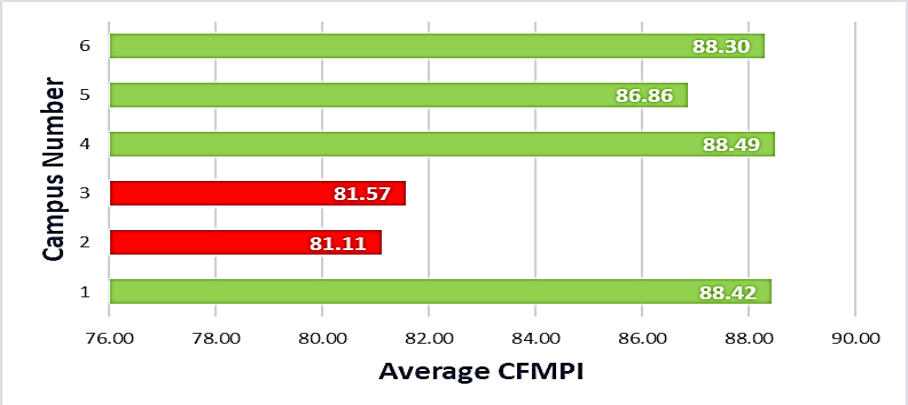


Fig. 1: Calculated CFMPI for campuses # 1 to 6

With respect to the process groups' levels depicted in Figure 3, it is important to note that all process groups, with the exception of PG4, exhibit a higher than average GPI, with PG6 – Sustainability and environmental management being the highest performing group (GPI=91.2%) and PG7–Assets Management being the second highest performing group (GPI=90.9%). This describes Qatar's significant shift toward environmentally friendly and sustainable building facilities. PG3-Organizational management, on the other hand, is slightly below the benchmark but within a 6% range. Therefore, it could be argued that the top management should examine the organizational management factors proposed by the present framework more closely in order to improve the management of campus facilities. According to the performance rating scale, it is possible to conclude that group performance indicators on the studied campuses are in good standing.

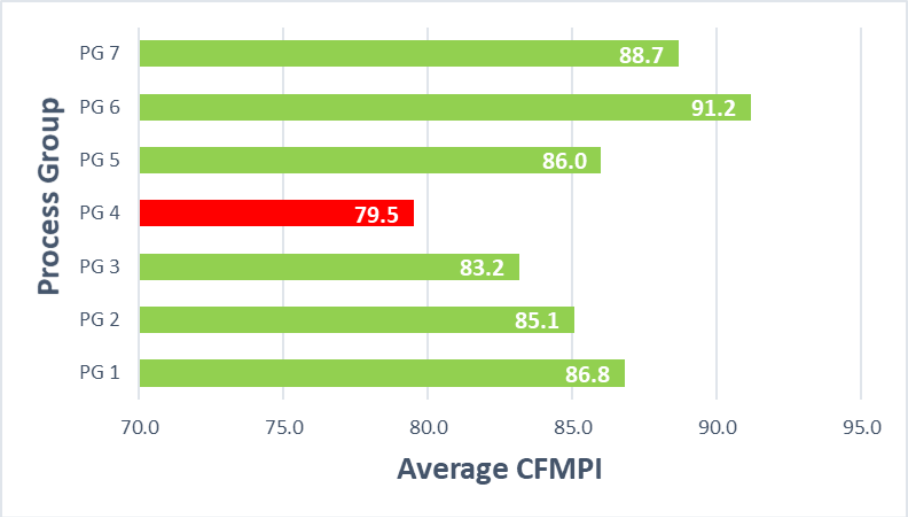


Fig. 2: Performance index for process groups

6 Conclusion

This research shows how the CFMPM can be used by industry experts to determine the overall CFM Performance Index (CFMPI) for campuses of all sizes and sectors. Using data from six campuses in Qatar, the practical application of CFMPM is illustrated. The case study's findings showed how the CFMPM implementation can be used to gauge the actual performance levels of different process groups and how they deviate from the facility management's projected performance. The benchmarking value for the CFMPII (85.8%) indicates that the average CFM performance across the six campuses is satisfactory. Additionally, the performance of CFM process groups is satisfactory with the exception of a few areas that require improvement. The proposed framework of the study can be used by universities of varying sizes by just adjusting the weighting of the factors according to the priorities of different administrations.

References

Authority (2021). "Qatar Economic Outlook 2021-2023". Ministry of Development Planning and Statistics. Doha, 1-50.

Gunduz, M., Birgonul, M. T., & Ozdemir, M. (2017). Fuzzy Structural Equation Model to Assess Construction Site Safety Performance. *Journal of Construction Engineering and Management*, *143*(4), 04016112.

Matse, N. et al. (2022). A Theoretical Assessment of the Impacts of Poor Maintenance of Public Infrastructure. In IOP Conference Series: Materials Science and Engineering (Vol. 1218, No. 1, p. 012018). IOP Publishing.

Yasin, M. N. et al. (2022). A Factor Analysis to Establish a Group of Causes of Deferred Maintenance at Malaysia's Public University Buildings. In IOP Conference Series: Earth and Environmental Science (Vol. 1022, No. 1, p. 012019). IOP Publishing.

Appendix I: Campus Facility Management Framework

Campus Facility Management Framework

PG1 - Campus Facility Work Force Management (0.1431)

PG01.01 - A collaborative and integrated team of professionals on the campus facility (0.1216) (0.1216)
PG01.02 - Recruiting a team of exceptional individuals with extensive qualifications and expertise (0.1119)
PG01.03 - Development and implementation of ongoing training initiatives (0.1126)
PG01.04 - Regular team performance monitoring and assessment (0.1108)
PG01.05 - Allocating appropriate personnel to oversee and maintain campus facilities (0.1101)
PG01.06 - Utilizing the transformational leadership approach to effectively managing the teams (0.1114)
PG01.07 - Timely communication of updates regarding job roles and responsibilities (0.1054)
PG01.08 - Implementing incentive programs to enhance motivation among the campus facility team (0.1096)
PG01.09 - Developing a flexible attendance system for the campus facility team (0.1066)

PG2 - Campus Facility Communication Management (0.1431)

PG02.01 - Formulating an effective communication management strategy inclusive of evaluating communication requirements, selecting appropriate technology, and determining suitable methods and tools. (0.1703)
PG02.02 - Continuous engagement of senior management personnel is essential for effective facility management (0.1541)
PG02.03 - Timely and effective handling of communications from various stakeholders including faculty, staff, students, contractors, and others (0.1731)
PG02.04 - Engaging in scheduled stakeholder meetings to effectively address concerns (0.1671)
PG02.05 - Up to date registers/logs including stakeholders register (the faculty, staff, students, contractors, etc.) , issues log, inventory list, etc. (0.1670)
PG02.06 - Utilizing appropriate software for effective communication management (0.1684)

PG3 - Campus Facility Systems Management (0.1407)

PG03.01 - Establishing an independent quality control and quality assurance system (0.1104)
PG03.02 - Establishing an effective health, safety and security management system (0.1185)
PG03.03 - implementation of an efficient workflow system for campus facility services, aiming to enhance operational effectiveness (0.1093)
PG03.04 - Establishing effective procurement management system (0.1075)
PG03.05 - Implementing decision making techniques for campus facility management (0.1070)
PG03.06 - Executing efficient strategies for operational risk management (0.1151)
PG03.07 - Implementing a proactive maintenance initiative (0.1128)
PG03.08 - Establishing a digital document tracking system (0.1076)
PG03.09 - Formulating and implementing contingency strategies and financial plans to address unexpected events (0.1117)

PG4 - Campus Facility Organizational Management (0.1397)

PG04.01 - Synchronization of facility management objectives and plans with the overall organizational strategy (0.1276)
PG04.02 - Conducting regular external and internal audits to assess the efficiency of campus facility management operational processes (0.1266)
PG04.03 - Possessing an agile management framework capable of seamlessly adjusting to evolving external conditions (0.125)
PG04.04 - Engaging the stakeholders (the faculty, staff, students, visitors, etc.) in decision making process (0.1217)
PG04.05 - Choosing capable facility management contractors for subcontracting purposes (0.1247)
PG04.06 - Analyzing the cost-effectiveness of purchasing or leasing necessary assets (0.1249)
PG04.07 - Implementing protocols to ensure that all stakeholders, including faculty, staff, students, and contractors, are fully dedicated to the sustainable management of the facilities (0.1243)
PG04.08 - Implementing a system for process improvement through the utilization of lessons learned registers (0.1251)

PG5 - Campus Facility Financial Management (0.1482)

PG05.01 - Implementing the value engineering framework as part of service delivery (0.3307)
PG05.02 - Implementing lifecycle cost analysis (LCCA) as a pre-requisite for asset procurement (0.3237)
PG05.03 - Establishing effective financial management system (0.3457)

PG6 - Campus Sustainability & Environment Management (0.1432)

PG06.01 - Implementing sustainable development concepts and principles in establishing the strategic direction, purpose, targets, and aims of the facilities (0.1641)
PG06.02 - Implementation of a waste management strategy integrating sustainable waste collection methods, efficient transportation practices, and the promotion of reuse and recycling initiatives (0.1678)
PG06.03 - Using water saving technologies in serving the campus facilities (0.1705)
PG06.04 - Using noise reduction/control methods during maintenance works (0.171)
PG06.05 - Implementing sustainable energy practices to power the campus facilities, such as utilizing photovoltaic systems and ground source heat pumps. (0.1625)
PG06.06 - Establishing environmental impact management system (0.164)

PG7 - Assets Management (0.142)

PG07.01 - Ensuring the acquisition of materials of superior quality and long-lasting durability (0.2605)
PG07.02 - Utilizing contemporary technologies such as Building Information Modeling (BIM), Computer-Aided Facility Management (CAFM), Computerized Maintenance Management Systems (CMMS) in order to effectively manage the facilities (0.251)
PG07.03 - Implementing a reliability-centered maintenance (RCM) approach to optimize equipment maintenance efficiency (0.2415)
PG07.04 - Establishing a resource management system (0.247)

Appendix II: Survey Sample

Subject: Invitation to Participate in a Research Validation Process - Campus Facility Management.

Dear Madam/Sir,

It is our pleasure to invite you to take part in the validation process of a newly developed Campus Facility Management model as part of a conference paper titled: "**Practical Implementation of Campus Facility Management Performance Model in Qatari Campuses.**" Your responses and information gathered for this study will be kept strictly confidential and used for academic research purposes only.
As a practitioner with extensive experience in the facility management industry, you are the ideal expert to offer us your insightful ratings and assessments for what you think it is the actual performance of your campus facility management firm. Please rate your firm's degree of compliance with each of the below 45 factors and 7 process groups based on your own opinion using the scale provided.

Please scroll down and insert your ratings for the degree of compliance as per the following scale:

1 = Totally noncompliant **2 = Slightly complied** **3 = Moderately complied**
4 = Very complied **5 = 100% complied**

Group 1: Campus Facility Workforce Management

SN	Factor	Degree of Compliance	Comments/Feedback
PG1-01	Building of a multidisciplinary and cohesive campus facility team		
PG1-02	Hiring highly qualified and experienced campus facility team		
PG1-03	Establishing continuous training program with the most updated campus FM practices		
PG1-04	Regular campus facility team performance monitoring and assessment		
PG1-05	Assigning reasonable numbers of workforce to operate and manage campus facilities		
PG1-06	Employing the transformational (open to reform and adapting policies) leadership style for managing the campus facility teams		
PG1-07	Regular update of roles and responsibilities		

Cite as: Gunduz M., Naji K. & Maki O., "Practical Implementation of Campus Facility Management Performance Measurement in Qatar", *The 2nd International Conference on Civil Infrastructure and Construction (CIC 2023)*, Doha, Qatar, 5-8 February 2023, DOI: https://doi.org/10.29117/cic.2023.0014

Pavement Automated Condition Assessment Model Using Unmanned Aerial Vehicle and Convolutional Neural Network

Vinay Chawla
E2 Consulting Engineers, Inc., Los Angeles, CA, USA
vinay.chawla@e2.com

Carol Massarra
East Carolina University, Greenville, USA
massarrac19@ecu.edu

Husam Sadek
SEERO Engineering Consulting LLC., Doha, Qatar
husam.sadek@seeroeng.com

Zhen Zhu
East Carolina University, Greenville, USA
zhuz@ecu.edu

Mohammed Sadeq
SEERO Engineering Consulting LLC., Doha, Qatar
mohammed.sadeq@seeroeng.com

Abstract

Assessing pavement condition is essential in any efforts to reduce future economic losses and improve the pavement performance. The resulting data are used as a record to evaluate pavement performance and assess their functionality and reliability. Traditional pavement condition assessment approaches rely on expert visual inspection and observational information along with testing using specialized equipment. However, these approaches are challenging because of the cost associated with assessment, safety issues, and the accessibility restrictions, especially after natural hazard events. This paper aims to develop an automated classification model to rapidly assess pavement condition by classifying pavement distresses using image classification that is based on Convolutional Neural Network (CNN) model. High-resolution aerial images representing alligator and longitudinal cracks for flexible pavements are collected using Unmanned Aerial Vehicle (UAV) images. The results of the developed model indicate an accuracy of 96.7% in classifying the two categories of pavement distress, while the use of UAV provides flexibility and manoeuvrability to capture the necessary data without risking personal safety and provides operational benefits in relatively lesser time. The methodology behind the developed model will help to reduce the need for on-site presence, increase safety, and assist emergency response managers in deciding the safest route to take after hurricane events. Additionally, application of the model will enable pavement engineers in rapidly assessing the pavement damage, aid in making quick decisions for road rehabilitation and recovery, and devise a restoration or repair plan.

Keywords: Unmanned Aerial Vehicle (UAV); Convolutional Neural Network (CNN); Flexible pavement

1 Introduction

Transportation, more importantly, road networks are significant components of infrastructure, which greatly affect the economic and social well-being of a region as people heavily depend on them for their daily activities. Asphalt (or flexible) pavements are a vital part of the transportation networks. Acquiring critical information on the pavement damage through pavement condition assessment is essential, especially after a hurricane. This information helps gain knowledge about the underlying physical phenomena, examines the impact of a natural hazard on the pavement, assesses and mitigates the damage, determines the need for external assistance (Lindell et al., 2003), aids in rehabilitation and alternative hazard management practices. However, pavement condition assessment is a very challenging process because it is expensive, protracted, and laborious, especially after a hurricane when access to the disaster-struck area is restricted (Morton et al., 2011).

Conventional ground-based approaches for pavement condition assessment mainly rely on expert human visual inspection and observational information along with testing using specialized equipment (Aksamit et al., 2011;Weinmann et al., 2004). These techniques are labor-intensive and time-consuming and require both field and laboratory testing, which may cause further damage to the pavements. Recent technological advancement in the form of Unmanned Aerial Vehicles (UAVs) has proven to aid in rapid data collection through aerial reconnaissance, provide emergency responses and humanitarian relief, facilitate aerial monitoring and damage evaluation (Estrada et al., 2019; Restas, 2015), especially for inaccessible areas (Floreano et al., 2015), and provide operational and economic benefits (Adams et al., 2010; Ezequiel et al., 2014).

Several studies have used image classification approaches to assess pavement conditions. These studies used either images collected from UAVs or from high-resolution cameras. (Ersoz et al., 2017; Gopalakrishnan et al., 2017; Ibragimov et al., 2020; Li et al., 2019; Zakeri et al., 2016). A general deficiency within current pavement condition assessment approaches is twofold: 1) limitation of image classification applications to either specific distress (cracking) or binary distress (crack or no crack), and 2) relying on image pre-processing to extract relevant information for the model. The advancement in technology and computer vision has made several progresses to reduce human effort in various fields, including civil infrastructure, creating possibilities for automatic pavement distress detection and classification. Hence, to rapidly identify and classify pavement distresses, novel non-traditional pavement condition assessment methods that use aerial images based on machine or deep learning classification algorithms are needed to be developed. In this paper, a Convolutional Neural Network (CNN) is developed to classify two distress types of flexible pavements (i.e., alligator and longitudinal cracking) using aerial images collected from UAVs. The aerial images are captured using DJI Mavic Mini UAV and used in their raw form without pre-processing. Model performance is validating using a cross validation, and the model accuracy is expressed in terms of cross-classification rate (CCR).

2 Methodology

2.1 Data

The field data collection consisted of the acquisition of aerial images for pavement distress using Unmanned Aerial Vehicles (UAVs). Streets shown in Figure 1 with flexible pavements at East Carolina University (ECU) campus in Greenville, United States were selected with two types of distress (i.e., alligator and longitudinal cracks). The UAV flight was manually operated, and the recorded videos for the streets were captured in segments of single flights in one direction. Still, images were then extracted from the collected videos and cropped to represent the distresses in post-

processing. The aerial images were manually labeled and classified into two categories before inputting them into the model for training.

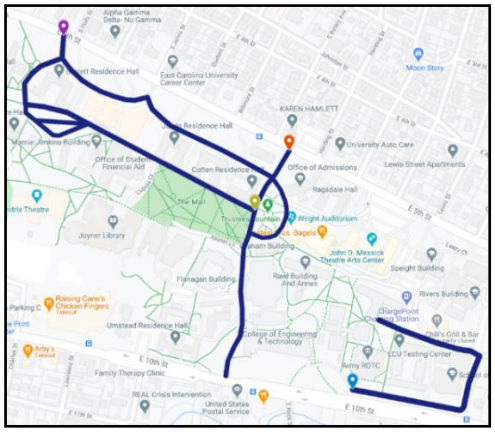


Fig. 1: Locations of Surveyed Streets with Pavement Distresses on ECU campus

The resulting dataset consists of 100 high-resolution aerial images of two types of pavement distress (i.e., alligator and longitudinal cracking) and is randomly divided into training and validation sets. The training set comprises 70% of the original dataset and is used to train the model, and the validation set comprises 30% of the original dataset and is used to validate the model. Table 1 shows the pavement distress categories and number of images for the training and validation sets.

Table 1: Pavement Distress Categories and Frequency of Collected Data for Training and Validation

Categories	Training Set	Validation Set	Total
Alligator Cracks	35	15	50
Longitudinal Cracks	35	15	50
Total	70	30	100

2.2 Model Training

To assess the pavement condition, image classification approach named Convolutional Neural Network (CNN) (Xie et al., 2017) is used. CNN classifies images by perceiving information from the raw input data (i.e., aerial images) and then learning from the features of these data. CNNs are being widely used for structural and road damage detection, pavement crack analysis, and pavement distress detection (Abdeljaber et al., 2018; Nie et al., 2018; Wang et al., 2018; Wang et al., 2017). Two primary operations, named as convolutions and pooling operations, and three secondary operations, named as ReLU activation, normalization, and dropout operations, take place in the feature extraction part. The rationale behind the primary operations is extracting features of the input images, while the rationale behind the secondary operations is enhancing the network performance. For features with two categories, probabilities of being in one of the two categories are calculated using logistic regression. For the two categories of pavement distress, the probabilities of being in one of the two categories are calculated as given in Equation 1:

$$p(\theta) = \frac{1}{1+exp^{\theta_j}} \quad (1)$$

where; p is the probability associated with the class j during the observation n, and θ are the model parameters.

Due to a sample size restriction, a transfer learning approach using AlexNet, pre-trained CNNs, is adopted and modified to match the smaller dataset (Gopalakrishnan et al., 2017). All the feature layers are considered for the modified network except the last two layers of the network (i.e., final fully

connected and the Softmax layers), which are initially configured to classify 1,000 objects. Therefore, to enable detection of the new two categories, the properties of these layers are modified. The fully connected layer is modified with new learning rate factor, and the Softmax layer is customized using a logistic regression model. The input images are resized to 227×227 to fit the network requirements and prevent model overfitting.

The model is then trained using a stochastic descent gradient (SGD) algorithm with momentum. SGD updates the network parameter after each input during the training process to increase accuracy (Li et al., 2019). The mini-batch size is set to 35 images, which is number of images used per update during training. The maximum number of epochs, which is the number of times that the learning algorithm will work through the entire training dataset, is set to 6, which is the number of complete updates of the entire dataset during training. The initial learning rate is set to 0.0001, and the feature layer is specified as drop 7. This layer extracts the distress features for the CNN model.

2.3 Model Validation

After the CNN model is trained, the predictive performance of the model is validated using cross-validation. Cross-validation is a technique to estimate the accuracy at which the model will perform in practice, illustrating the model's ability to predict new or unseen data. The validation set comprising 30% of the original dataset is used to perform the cross-validation. Model performance is assessed by finding the cross-classification rate (CCR), which indicates the percentage of pavement distress where the predicted distress class corresponds to the observed distress. The percentage of the correctly classified distress is calculated as given in Equation 2:

$$CCR = \frac{\sum_{d=1}^{D} F_{dd}}{\sum_{d=1}^{D}\sum_{c=1}^{C} F_{cd}} \quad (2)$$

where F_{dd} are observations along the diagonal of the error matrix, and F_{cd} are all observations in the error matrix.

3 Results

The CNN model was trained using a training set that counts for 70% of the original dataset. A randomly generated array of images for model training is shown in Figure 2.

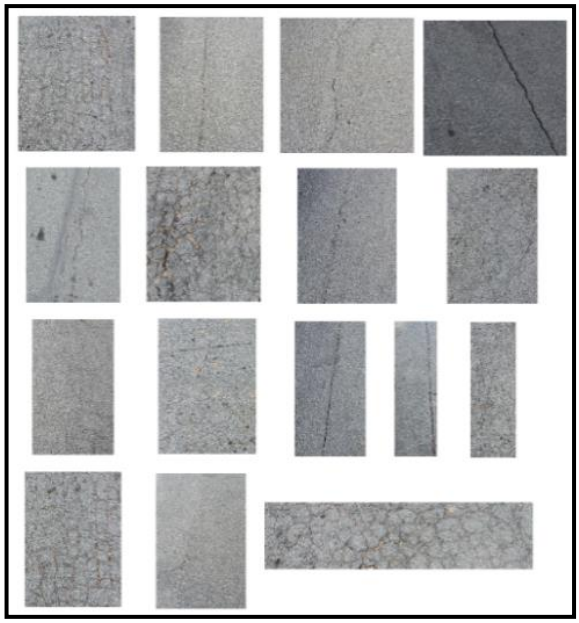


Fig. 2: Array of Random Images of Pavement Distress Used for Model Training

Results of model training are illustrated in Figure 3. The accuracy and loss during training are indicated with the blue and orange lines in the graph, respectively. The training accuracy gradually increases (i.e., from approximately 58% to 97%) as the algorithm passes through the dataset, with each epoch updating the parameters and learned features. Simultaneously, the loss during the training is reduced over the epochs increased (i.e., from approximately 1.1 to 0.18). The dotted line represents the accuracy and loss based on the validation data set for which a similar trend is observed (i.e., an increase in accuracy and decrease in loss) over the subsequent epochs.

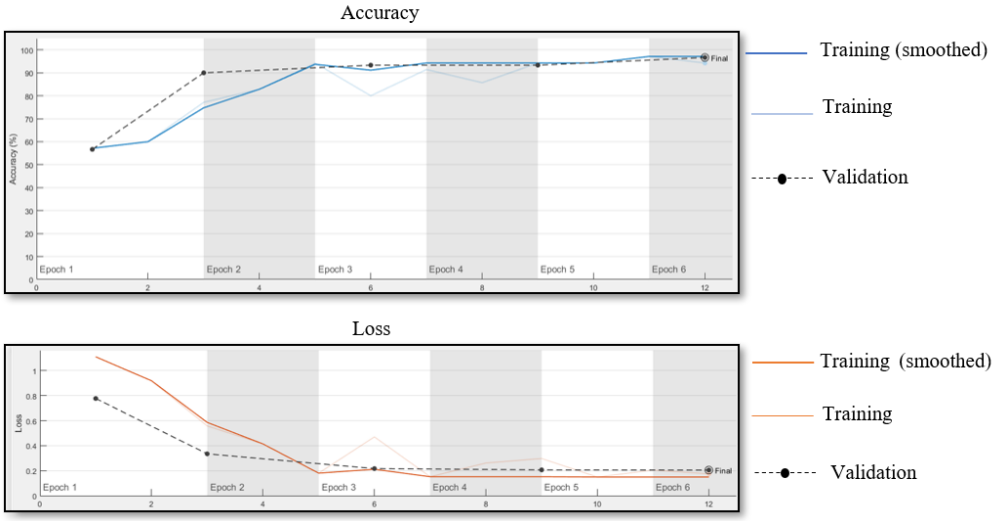


Fig. 3: Traces of Training and Validation Accuracy (Top) and Loss (Bottom) During Model Training

The predictive performance of the CNN model was validated using a validation set that counts for 30% of the original dataset. The validation accuracy was represented every three iterations during the training in Figure 3. The overall model accuracy is represented by the confusion matrix (Table 2) and was found to be 96.7%, misclassifying only one image for a single class during model validation which indicated a satisfactory model performance.

Table 2: Target vs. Output Model Confusion Matrix and CCR for the Pavement Classification Model

	Target Class			
Output Class		Alligator	Longitudinal	CCR 96.7%
	Alligator	14 (46.7%)	0 (0%)	
	Longitudinal	1 (3.3%)	15 (50%)	

The output class refers to the prediction from the model, whereas the target class refers to actual label of the input image. The diagonal from left to right represents the correctly classified quantity (the number on top) and the correctly classified percentage (the percentage on bottom) of the corresponding categories.

4 Conclusion

The major contribution includes the use of advanced technology (Unmanned Aerial Vehicle) to collect aerial imagery for flexible pavement distresses and development of a deep learning classification model (Convolutional Neural Network) for the classification of the two pavement distresses (alligator and longitudinal cracks) in MATLAB.

Based on the overall model accuracy, the developed CNN classification model proved to be a successful approach for automated pavement distress classification. The use of computer vision resulted in a reduction of human effort and time spent in the field for assessing pavement conditions.

The finding from this research will aid transportation engineers in rapidly assessing the damages to pavements and devise a restoration or repair plan for pavements in a quick, effective, and economic manner. Finally, application of the developed model will provide a platform to minimize the damage to the pavements, which is sometimes caused by traditional approaches for pavement assessment and make the examination process efficient and rapid.

Collecting data for various distresses and types of pavements, using techniques such as LIDAR or multispectral camera and creating 3D models for pavement distresses will aid in more realistic and improved evaluation of the pavement distresses. Expanding the methodology to a road network level and geo-referencing the location of pavement distress will provide an exact record of distress locations, which enable emergency responders to locate the safe routes for relief, especially after natural hazards and aid in decision-making regarding immediate repair and maintenance.

References

Abdeljaber, O.et al. (2018). "1-D CNNs for Structural Damage Detection: Verification on a Structural Health Monitoring Benchmark Data". *Neurocomputing, 275*, 1308-1317. doi:https://doi.org/10.1016/j.neucom.2017.09.069

Adams, S., Friedland, C., & Levitan, M. (2010). "*Unmanned aerial vehicle data acquisition for damage assessment in hurricane events"*. Paper presented at the Proceedings of the 8th International Workshop on Remote Sensing for Disaster Management, Tokyo, Japan.

Aksamit, P., & Szmechta, M. (2011). "*Distributed, mobile, social system for road surface defects detection"*. Paper presented at the 2011 5th International Symposium on Computational Intelligence and Intelligent Informatics (ISCIII), Floriana, Malta.

Ersoz, A. B., Pekcan, O., & Teke, T. (2017). "Crack Identification for Rigid Pavements Using Unmanned Aerial Vehicles". *IOP Conference Series: Materials Science and Engineering, 236*(1), 012101. doi:https://doi.org/10.1088/1757-899X/236/1/012101

Estrada, M. A. R., & Ndoma, A. (2019). "The Uses of Unmanned Aerial Vehicles–UAV's-(Or Drones) in Social Logistic: Natural Disasters Response and Humanitarian Relief Aid". *Procedia Computer Science, 149*, 375-383. doi:https://doi.org/10.1016/j.procs.2019.01.151

Ezequiel, C. A. F. et al. (2014). "*UAV aerial imaging applications for post-disaster assessment, environmental management and infrastructure development"*. Paper presented at the 2014 International Conference on Unmanned Aircraft Systems (ICUAS), Orlando, FL, USA.

Floreano, D., & Wood, R. J. (2015). "Science, Technology and the Future of Small Autonomous Drones". *Nature, 521*(7553), 460-466. doi:10.1038/nature14542.

Gopalakrishnan, K. et al. (2017). "Deep Convolutional Neural Networks with Transfer Learning for Computer Vision-Based Data-Driven Pavement Distress Detection". *Construction and Building Materials, 157*, 322-330. doi:https://doi.org/10.1016/j.conbuildmat.2017.09.110

Ibragimov, E. et al. (2020). "Automated Pavement Distress Detection Using Region Based Convolutional Neural Networks". *International Journal of Pavement Engineering*, 1-12. doi:https://doi.org/10.1080/10298436.2020.1833204

Li, S., & Zhao, X. (2019). "Image-Based Concrete Crack Detection Using Convolutional Neural Network and Exhaustive Search Technique". *Advances in Civil Engineering, 2019*. doi:https://doi.org/10.1155/2019/6520620

Lindell, M. K., & Prater, C. S. (2003). "Assessing Community Impacts of Natural Disasters". *Natural Hazards Review, 4*(4), 176-185. doi:10.1061/(ASCE) 1527-6988 (2003) 4:4 (176).

Morton, M., & Levy, J. L. (2011). "Challenges in Disaster Data Collection During Recent Disasters". *Prehospital and disaster medicine, 26*(3), 196-201. doi:10.1017/S1049023X11006339.

Nie, M., & Wang, K. (2018). "*Pavement distress detection based on transfer learning"*. Paper presented at the 2018 5th International Conference on Systems and Informatics (ICSAI), Nanjing, China.

Restas, A. (2015). "Drone Applications for Supporting Disaster Management". *World Journal of Engineering and Technology, 3*(03), 316. doi: 10.4236/wjet.2015.33C047.

Wang, W.et al. (2018). "*Road damage detection and classification with Faster R-CNN"*. Paper presented at the 2018 IEEE International Conference on Big Data (Big Data), Seattle, WA, USA.

Wang, X., & Hu, Z. (2017). "*Grid-based pavement crack analysis using deep learning"*. Paper presented at the 2017 4th International Conference on Transportation Information and Safety (ICTIS), Banff, AB, Canada.

Weinmann, T. L., Lewis, A. E., & Tayabji, S. (2004). "*Pavement sensors used at accelerated pavement test facilities"*. Paper presented at the Proceedings of the Second International Conference on Accelerated Pavement Testing, Minneapolis, MN, USA.

Xie, D., Zhang, L., & Bai, L. (2017). "Deep Learning in Visual Computing and Signal Processing". *Applied Computational Intelligence and Soft Computing, 2017*. doi:https://doi.org/10.1155/2017/1320780

Zakeri, H., Nejad, F. M., & Fahimifar, A. (2016). "Rahbin: A Quadcopter Unmanned Aerial Vehicle Based on a Systematic Image Processing Approach Toward an Automated Asphalt Pavement Inspection". *Automation in Construction, 72*, 211-235. doi:https://doi.org/10.1016/j.autcon.2016.09.002

Cite as: Chawla V., Massarra C., Sadek H., Sadeq M. & Zhu Z., "Pavement Automated Condition Assessment Model Using Unmanned Aerial Vehicle and Convolutional Neural Network", *The 2nd International Conference on Civil Infrastructure and Construction (CIC 2023)*, Doha, Qatar, 5-8 February 2023, DOI: https://doi.org/10.29117/cic.2023.0015

Strategies for Improving Construction Safety Performance in Developing Context

Wesam Beitelmal
Civil & Environmental Engineering Department, College of Engineering, Dhofar University, Salalah, Oman
wbeitelmal@du.edu.om

Wael M. Alruqi
Department of Civil Engineering, Jouf University, Skaka, Saudi Arabia
waelalruqi@ju.edu.sa

Mohamed Zoubi
Civil Engineering Department, Misurata University, Misurata, Libya
mohamed.zoubi@eng.misuratau.edu.ly

Abstract

Inexperience and lack of awareness of workplace appropriate actions are the common reasons behind accidents and injuries. Researchers and industry practitioners in developed countries identified more than 12 strategies that might lead to preventing worksite injuries. However, these strategies are specific to the developed context. Developing countries still fail to identify safety strategies that might align with their safety policies and procedures. This paper aims to take the first step towards identifying the best safety strategies in the developing context. Thus, the main research question is how can companies start to implement safety strategies with consideration of their context? This study applied a mixed method to meet the objectives of the study. The Delphi method was used to obtain the needed data. The descriptive analysis shows that four important strategies are identified out of the 12 strategies: Upper Management Support, Safety and Health Committees, Record Keeping and Accident Analysis, and Job Hazard Analyses. The findings of this paper can be used by managers to make defendable decisions to start implementing safety strategies in their organizations. Also, they will illuminate the developing countries' safety culture perspective and the implementation processes.

Keywords: Construction safety; Developing context; Libya; Delphi method

1 Introduction

In the field of construction, workers are exposed to accidents and get injured. Such a problem can be avoided by implementing safety management through identified strategies. As an example, construction industry in the US employs approximately 25% of the industrial workforce but has generally accounted for the highest rate of all industrial workers in the fatalities rate (NIOSH, 2018). This is twice in cost compared to all industries (Waehrer et al., 2007). Due to the lack of contribution from previous studies in the field of safety in construction, this study aims to contribute to safety in the construction industry in a developing context specifically. This research introduced the topic to Libyan practitioners as one of the developing countries to open the door for newly filed of research to be investigated. Researchers and industry practitioners in developed countries identified more than 12 strategies that might lead to preventing worksite injuries. This study aims to explore the possibility of implementing these strategies and techniques in the work zone with local practitioners. The main research question for this research is: "*What are the important safety management strategies that*

construction companies should start implementing with consideration to their local context?"

2 Literature Review

This section focuses on reviewing the accidents in the construction industry historically; then the identified safety strategies by the developed countries' experts were presented.

2.1 Accidents in Construction Industry

It is appropriate to consider construction work as inherently dangerous if no proactive steps are taken to improve the work conditions and to ensure that the work is undertaken in a safe manner. Looking back at history helps us to realize that the incidence of injuries and fatalities has decreased by more than 60% in the past three decades (OSHA, 2001). Over the years, since 1997, the Ocuppational Safety and Health Adminstration (OSHA) has changed rules and obligations to support workers' safety (Arbury et al., 2022). The incidence recordable rates have dropped as shown in Figure 1. Other sources such as (US Bureau of Labour Statistics, 2017) confirmed those results. Some researchers such as Hallowell and Gambatese (2009) believe that these improvements are the result of the increased adoption of highly effective safety strategies.

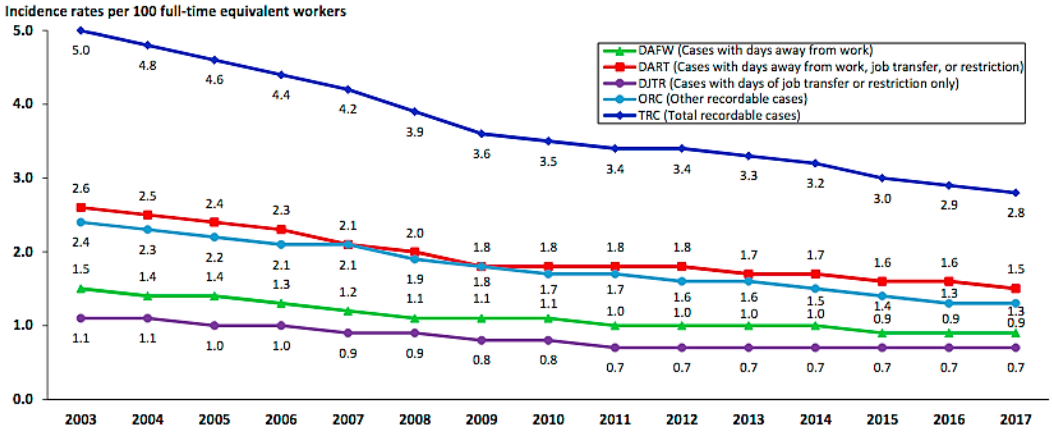


Fig. 1: Rate of Total Recordable Injuries and Illnesses (U.S. Bureau of Labor Statistics, 2018)

Developing countries still fail to identify safety strategies that might align with their safety policies and procedures. In general, accident prevention and its cost are accepted as the responsibility of management. However, not all construction firms commit the same amount of effort or funds to accident prevention. The differences may stem partially from differences in the perception of the degree of influence that management can have on reducing worker injuries (Beus et al., 2015). They may also be consequences of different perceptions of the actual costs related to worker injuries. If the true costs of injuries were well defined, management would be in a better position to make informed decisions concerning safety, rather than addressing safety solely from an altruistic point of view. Companies spent, on average, for managing safety and minimizing accident rates from less than 1 % to 10% of project costs (Dorji & Hadikusumo, 2006).

2.2 Identified Safety Strategies in Construction Industry

Based on the conducted studies about construction safety in developed countries, there were 12 highly effective administrative safety innovations identified (Esmaeili and Hallowell 2012). In this study, we will depend on these findings to introduce safety strategies to local practitioners as shown in Table 1:

Table 1: The Proposed Safety Strategies and Techniques

No.	Strategy name	Description
1	Upper management support	In most companies, it is important to ensure the support of upper management to successfully implement any strategic changes. In this strategy, the employer must warn all the employees/workers before starting work about various risks that they may face at the worksite. They need to know the ways of how to protect themselves based on the provided training. All the needed instructions should be in a noticeable and visible place (Hallowell & Gambatese, 2009).
2	Job hazard analyses	Injuries usually occur as a result of working in unsafe physical environments or unsafe practices or both. Knowing and recognizing an unsafe physical condition could directly reduce the probability of injury (Wang et al., 2021). Nevertheless, full dependence could never be placed on a checklist that is used for all kinds and sizes of projects. Therefore, training workers to help them distinguish or identify unsafe physical conditions and follow appropriate and safe work techniques helps to achieve good safety performance.
3	Safety and health orientation; training	According to Kinn et al. (2000), training should be an essential element/factor of every safety program; therefore, it is important that the areas in which training is necessary are classified. All employees need to be trained in hazard communication to make every worker completely knowledgeable about all substances that are expected to be on site. Even the most skillful workers and experienced foremen should become familiar with what is called the job-site plan, the project management personnel, company strategies and rules, and a range of other topics that may be related to an unknown project.
4	Frequent worksite inspections	This strategy is important to identify all circumstances that can efficiently and successfully be corrected. The inspection tour should cover the whole construction work, with specific consideration given to subcontractors' work. This strategy will deliver the same message to all of the workers and subcontractors regarding the importance of the safety (Muto et al., 1997).
5	Emergency response planning	There should be plans for dealing with and managing the emergency situations such as floods, fires, power outages, windstorms, etc. This could be done by recording and reporting all injuries and illnesses and related investigations. It is widely known that the requirements of the safety program may differ because it depends on the nature of the project (Brown & Dunn, 2007).
6	Record keeping and accident analysis	This strategy involves documenting and reporting the specifics of all accident information such as time, location, worksite condition, and cause. The analysis should point out the weakness in the company's safety program or the poor implementation of a program element (Ahmed et al., 2019).
7	Project-specific training and pre-job safety meetings	Hinze (1997) states that safety meetings include a discussion between a supervisor and all workers on a construction site. These safety meetings might be conducted formally and informally. In addition, safety sessions may be carried out for many levels of supervision (Arquillos et al., 2015).
8	Safety and health committees	The objective of this strategy is to have a different angle to support the management in their effort to recognize safety improvement. The safety committee is established including some workers. Thus, the members of the committee bring different viewpoints to the group (Milgate et al., 2002).
9	Substance abuse programs	Requirements that might be carried out by the owner contain the testing (planned and unplanned) of every worker. The goal of this strategy is to demonstrate that when an employee fails a test then it is seen to be common for the company to mandate rehabilitation or help (Hersch et al., 2002).
10	Safety manager on-site	A knowledgeable person at the job site, chosen by the contractor is usually designed to serve the safety representative, who will be responsible for implementing the safety program. The safety manager or the representative should have adequate authority to improve the work performance, and conditions to minimize hazards and/or dangers. The safety manager or representative must be qualified, and knowledgeable to recognize and identify safety and health hazards (Levitt & Samelson, 1993).

11	Subcontractor selection and management	This involves covering all aspects of on-site construction, operations, and activities related to a particular contract. Many owners now ask contractors to submit what is called project-specific safety programs including subcontractors' selection. It is the commonly required approval before starting construction. Thus, the owner will not accept to process/progress payments if the project safety is not approved (Aksorn & Hadikusumo, 2008).
12	Employee involvement and evaluation	It is essential to create a means of evaluating safety performance. That will make it possible to evaluate, assess and even measure the impact of a specific change that the company may aim to achieve. This is an indication that for evaluating and assessing safety performance and employee involvement, there should be what is called a reliable measure (Williams, 2008).

3 Methodology

This study applied a mixed method to meet the objectives of the study. The Delphi method was used to obtain the needed data.

3.1 Research Setting

The current study presents the research that was conducted in Libya's Misurata city. Both public and private companies and organizations were involved as follows: The Company of Free Zone Misurata; Libyan Iron and Steel Company-the construction department; The Company of Highways and Bridges; The Organization of Development of Administrative Buildings; The General Construction Company; The Office of Maintenance of Misurata International Airport.

3.2 Questionnaire Design

The questionnaire was the main source for collecting research data. To ensure the understanding of the questionnaire's questions and to have reliable answers and feedback, the original questionnaire was written in Arabic. It consisted of three main parts. In the first one, the participants were asked 12 descriptive questions related to personal experience in construction. Also, the previous involvement of the participants in accidents related to construction work. The second part focused on exploring the proposed safety strategies in participants' agencies and organizations. This was assessed using five Likert-scaled ratings from "not applied," to "completely applied." Before asking the participants for their assessments, short descriptive of the proposed safety strategies were presented to them to ensure all have the same understanding of the strategies, thus reliable inputs were obtained. The third part was designed to gain qualitative data about the participants' recommendations about the proposed strategies. The question was-"Which of the strategies does he/she recommend to a company aiming to enhance its safety management performance? After finalizing the questionnaire design, the researchers piloted the questionnaire with professors, and students to ensure the clarity of the questions from the participants' perspectives. Moreover, according to the busy schedule of the potential participants, the length of the questionnaire was checked to ensure its reasonability. The important feedback of this step was the suggestion to add definitions to the proposed strategies which were added in the final design of the questionnaire.

3.3 Data Collection

The questionnaires were distributed to all the targeted companies and organizations following snowballing techniques, which are recommended to be used if there is no database for the potential participants' information such as names, contact numbers, and emails. According to Oppenheim (2001), the researchers could ask a few appropriate individuals to distribute the questionnaire to who might also fit within the targeted sampling in terms of field of experience and topic of the study. The

data collection process lasted for about a month from December 12th, 2017 to January 10th, 2018. A total of forty-four questionnaires were distributed; however, the response rate was about 84% (i.e. thirty-seven were received). All the participants volunteered to participate in the study and no constraint was applied. In addition, they were informed about their anonymity and were given the right to withdraw from the process at any time.

3.4 Analysis Techniques

The researchers conducted a descriptive analysis based on the collected data to present the participants' historical experience in safety-related work. Also, the individual's feedback about which of the proposed safety strategies was implemented in his/her company. The second step of analysis includes using Analytical Hierarchy Process (AHP) technique to obtain the collective ranking of the strategies' importance. The data was collected in three rounds using the Delphi method through emails. Six participants were involved in the whole process of AHP which according to Krueger and Casey (2009) is enough for studies, and aims to reach a consensus among practitioners. The independent participants who were selected according to predefined guidelines from the 37 participants in the first step, were asked to participate in two or more rounds of structured surveys (Hallowell & Gambatese, 2010). Adapting Wind & Saaty (1980) scale, the authors of the current study used the scales, definitions, and explanations as shown in Table 2. A pairwise comparison was carried out between the most important safety strategies. The needed calculations to check the validity of the inputs were conducted and confirmed.

Table 2: Rating Scale Used in AHP (Saaty & Vargas, 1991)

Intensity of importance	Definition	Explanation
1	Equal importance	Two strategies contribute equally to the objective.
3	Somewhat more important	Experience and judgment slightly favor one over the other.
5	Much more important	Experience and judgment strongly favor one over the other.
7	Very much more important	Experience and judgment very strongly favor one over the other. Its importance is demonstrated in practice.
9	Absolutely more important	The evidence favoring one over the other is of the highest possible validity.

4 Results and Discussion

This section will include the results from the questionnaire under two categories: (1) Descriptive Result; and (2) Analytical Hierarchy Process (AHP) outcomes Descriptive Analysis. The range of current jobs includes general managers, project managers, managers of departments, and workers' supervisors. The participants' roles allowed most of them to witness construction accidents and injuries. The types of injuries and the associated treatments are shown in Table 3.

Table 3: Participants' Construction Safety Experience

Involvement in field accidents	Yes	27
	No	10
Types of injuries and treatments	Fatality	11.0%
	Disability	7.5%
	Hospital	48.0%
	On-site	33.5%

Those participants were asked in the questionnaire about the applied safety strategies in their current companies and/or organizations. The five Likert-Scale ranged from “not applied,” “weakly applied,” “acceptable application,” “well applied,” and “complete application.” Most of the participants indicated that at best the application of the strategies was between the “not applied” and the “weakly applied” categories. Then, the participants suggested the best safety strategies for their companies. Based on the questionnaire design, the participants were allowed to suggest up to two strategies (Table 4). The selected six strategies were selected for the next step of analysis using AHP for comparison and ranking.

Table 4: The Suggested Strategies Based on Participants’ Opinions

#	Proposed Safety Strategies	Suggestion 1	Suggestion 2
1	Upper management support	22	11
2	Job hazard analyses	2	8
3	Safety and health orientation and training	6	7
4	Frequent worksite inspections	0	0
5	Emergency response planning	0	0
6	Record keeping and accident analysis	2	3
7	Project-specific training and safety meetings	5	2
8	Safety and health committees	0	6
9	Substance abuse programs	0	0
10	Safety manager on-site	0	0
11	Subcontractor selection and management	0	0
12	Employee involvement and evaluation	0	0
Total		37	37

4.1 Analytical Hierarchy Process (AHP) technique

In the questionnaire, the authors asked the participants to provide their contact information if they agree to be involved in the second phase of the study. Six participants agreed and were invited to the AHP technique. To obtain the pairwise comparison between the six suggested strategies, the authors applied Delphi methods targeting two rounds to reach a consensus among the participants. The authors sent the six participants a matrix that includes the six strategies asking for their pairwise comparison using the scale in Table 1. In the first round, no consensus was achieved among the participants. Therefore, the authors decided to go for another round. The second round started by redistributing the matrix to each one of the participants. In the matrix, the previous participants’ inputs and the mode of the group assessment were provided. The participants were asked to review their assessments, they can keep or change them if needed, and provide the final decision. Table 5 shows the mode pairwise assessment for the participants after the second round.

Table 5: The Mode Assessment of the Participants

	Upper management support	Job hazard analyses	Safety and health orientation and training	Record keeping and accident analysis	Project-specific training and safety meetings	Safety and health committees
Upper management support	1	1	5	5	3	1/3

Job hazard analyses	1	1	5	1/3	3	1/5
Safety and health orientation and training	1/5	1/5	1	7	1	1/5
Record keeping and accident analysis	1/5	3	1/7	1	7	5
Project-specific training and safety meetings	1/3	1/3	1	1/7	1	3
Safety and health committees	3	5	5	1/5	1/3	1

To ensure that the obtained judgments (results) are not based on random inputs, the Consistency Ratio (CR) was calculated to measure how consistent the judgments have been relative to large samples of purely random judgments. According to Wind & Saaty (1980), if the CR is more than or equal to 0.9 then the judgments were random and the AHP assessments should be re-applied. Based on Table 5, the CR was found to be 0.86. Even though the CR value was close to 0.9, the authors accepted it and calculated the weights of each strategy. Based on these weights, the rank of the safety strategies is as follows: Upper Management Support (0.266); Safety and Health Committees (0.203); Record Keeping and Accident Analysis (0.187); Job Hazard Analyses (0.155); Safety and Health Orientation and Training (0.096); Project-Specific Training and Safety Meetings (0.093).

5 Discussion and Conclusion

This study investigated the safety strategies and their application in the construction field with consideration to the developing context. Questionnaires were distributed among practitioners in Libya as a case study. Their characteristics show that their experiences were relative to the research. The AHP technique facilitated determining the rank among the safety strategies. It is rare in developing countries to have a high number of knowledgeable practitioners. The results indicated that upper management support ranked as highly safety strategy. Recent studies showed that the support and involvement of upper management in all safety aspects stood as a leading indicator for preventing injuries in worksites in the developed context (Alruqi & Hallowell, 2019). The findings of this paper can be used by managers to make defendable decisions to start implementing safety strategies in their organizations. Also, they will illuminate the developing countries' safety culture perspective and the implementation processes. Based on the findings future research paths were opened such as investigating the repeatability of the finding in a wide range of developing countries focusing on MENA and Gulf regions.

References

Ahmed, A., A. F. M. Sadullah & A. S. Yahya. (2019). "Errors in Accident Data, its Types, Causes and Methods of Rectification-Analysis of the Literature." *Accid. Anal. Prev.*, Road Safety Data Considerations, 130: 3–21. https://doi.org/10.1016/j.aap.2017.07.018.

Aksorn, T. & B. H. W. Hadikusumo. (2008). "Critical Success Factors Influencing Safety Program Performance in Thai Construction Projects." *Saf. Sci., Construction Safety*, *46*(4): 709–727. https://doi.org/10.1016/j.ssci.2007.06.006.

Alruqi, W. M. & M. R. Hallowell. (2019). "Critical Success Factors for Construction Safety: Review and Meta-Analysis of Safety Leading Indicators." *J. Constr. Eng. Manag.*, *145*(3): 04019005.

https://doi.org/10.1061/(ASCE)CO.1943-7862.0001626.

Arbury, S. et al. (2022). "OSHA Workplace Violence Enforcement." *J. Occup. Environ. Med.*, *64* (4): e211–e216. https://doi.org/10.1097/JOM.0000000000002482.

Beus, J. M., L. Y. Dhanani & M. A. McCord. (2015). "A Meta-Analysis of Personality and Workplace Safety: Addressing Unanswered Questions." *J. Appl. Psychol.*, *100*: 481–498. US: American Psychological Association. https://doi.org/10.1037/a0037916.

Brown, D. F. & W. E. Dunn. (2007). "Application of a Quantitative Risk Assessment Method to Emergency Response Planning." *Comput. Oper. Res.*, Hazardous Materials Transportation, *34*(5): 1243–1265. https://doi.org/10.1016/j.cor.2005.06.001.

Dorji, K. & B. H. W. Hadikusumo. (2006). "Safety Management Practices in the Bhutanese Construction Industry."

Esmaeili, B. & M. R. Hallowell. (2012). "Diffusion of Safety Innovations in the Construction Industry." *J. Constr. Eng. Manag.*, *138*(8): 955–963. https://doi.org/10.1061/(ASCE)CO.1943-7862.0000499.

Hallowell, M. R. & J. A. Gambatese. (2009). "Construction Safety Risk Mitigation." *J. Constr. Eng. Manag.*, *135*(12): 1316–1323. American Society of Civil Engineers. https://doi.org/10.1061/(ASCE)CO.1943-7862.0000107.

Hallowell, M. R. & J. A. Gambatese. (2010). "Qualitative Research: Application of the Delphi Method to CEM Research." *J. Constr. Eng. Manag.*, *136*(1): 99–107. https://doi.org/10.1061/(ASCE)CO.1943-7862.0000137.

Hersch, R. K., T. L. McPherson, and R. F. Cook. (2002). "Substance Use in the Construction Industry: A Comparison of Assessment Methods." *Subst. Use Misuse*, *37*(11): 1331–1358. Taylor & Francis. https://doi.org/10.1081/JA-120014081.

Hinze, J. (1997). *Construction Safety*. Prentice-Hall.

Kinn, S. et al. (2000). "Evaluation of Safety Orientation and Training Programs for Reducing Injuries in the Plumbing and Pipefitting Industry." *J. Occup. Environ. Med.*, *42*(12): 1142–1147. Lippincott Williams & Wilkins.

Krueger, R. A. & M. A. Casey. (2009). *Focus Groups A Practical Guide for Applied Research*. United State of America: SAGE Publications.

Levitt, R. E. & N. M. Samelson. (1993). *Construction Safety Management*. John Wiley & Sons.

Arquillos et al. (2015). "Effectiveness of Construction Safety Programme Elements." *Enhancing Synerg. Collab. Environ.*, Lecture Notes in Management and Industrial Engineering, P. Cortés, E. Maeso-González, & A. Escudero-Santana, eds., 285–289. Cham: Springer International Publishing.

Milgate, N., E. Innes & K. O'Loughlin. (2002). "Examining the Effectiveness Of Health And Safety Committees And Representatives: A review." *Work*, *19*(3): 281–290. IOS Press.

Muto, T. et al. (1997). "Methods to persuade higher management to invest in health promotion programmes in the workplace." *Occup. Med.*, *47*(4): 210–216. https://doi.org/10.1093/occmed/47.4.210.

NIOSH. (2018). "Construction Statistics | NIOSH |CDC." Accessed December 22, 2022. https://www.cdc.gov/niosh/construction/statistics.html.

Oppenheim, A. N. (2001). *Questionnaire Design, Interviewing, and Attitude Measurement*. London ; New York : New York: Pinter Publishers ; Distributed exclusively in the USA and Canada by St. Martin's Press.

OSHA. (2001). "OSHA's 30th Anniversary | Occupational Safety and Health Administration." Accessed December 22, 2022. https://www.osha.gov/aboutosha/30-years.

Saaty, T. & L. Vargas. (1991). *Prediction, Projection and Forecasting-Applications of the Analytic Hierarchy Process in Economics, Finance, Politics, Games and Sports*.

US Bureau of Labor Statistics. (2018). "2018 Home : US Bureau of Labor Statistics." Accessed December 22, 2022. https://www.bls.gov/opub/mlr/2018/.

US Bureau of Labour Statistics. (2017). "Total Nonfatal Work Injury and Illness Rates, Private Industry : U.S. Bureau of Labor Statistics." *US Bur. Labour Stat.* Accessed December 14, 2022. https://www.bls.gov/charts/injuries-and-illnesses/total-nonfatal-work-injuries-and-illnesses-by-year.htm.

Waehrer, G. M. et al. (2007). "Costs of Occupational Injuries in Construction in the United States." *Accid. Anal. Prev.*, *39*(6): 1258–1266. https://doi.org/10.1016/j.aap.2007.03.012.

Wang, B. et al. (2021). "Workplace Safety and Risk Analysis Using Additive Heterogeneous Hybridized Computational Model." *Aggress. Violent Behav.*, 101558. https://doi.org/10.1016/j.avb.2021.101558.

Williams, J. H. (2008). "Employee Engagement Improving Participation In Safety." *Prof. Saf.*, *53*(12).

Wind, Y. & T. L. Saaty. (1980). "Marketing Applications of the Analytic Hierarchy Process." *Manag. Sci.*, *26* (7): 641–658. https://doi.org/10.1287/mnsc.26.7.641.

Cite as: Beitelmal W., Alruqi W. & Zoubi M., "Strategies for Improving Safety Performance in Developing Context", *The 2nd International Conference on Civil Infrastructure and Construction (CIC 2023)*, Doha, Qatar, 5-8 February 2023, DOI: https://doi.org/10.29117/cic.2023.0016

TBM Challenges on Musaimeer outfall tunnel

Saad Zayed Al-Marri
Public Works Authority, Doha, Qatar
smarri2@ashghal.gov.qa

Gary Peach
Mott MacDonald, Doha, Qatar
gary.peach@mottmac.com

Hernan Vigil Fernandez
HBK-PORR JV, Doha, Qatar
hernan.vigil@auccqatar.com

Abstract

Musaimeer outfall tunnel is the longest outfall tunnel in the Middle East. The tunnel was excavated by Earth Pressure Balance (EPB), Tunnel Boring Machine (TBM) and encountered three distinct rock masses namely Rus Formation, Midra-Shale, and Simsima Limestone along with water inflows at high pressure, complex mixed ground, and weaker ground strata prone to cavities with the presence of vertical and lateral fractures connected to the seabed.

These conditions resulted in the TBM operating in very dry conditions where the addition of soil conditioners and water sprayed in the excavations chamber and cutter head were required to avoid clogging situations and create a pasty excavation material, which impacted TBM operation. The opposite scenario occurred when the TBM encountered very wet conditions while passing through weathered Simsima Limestone fully connected hydrostatically with the seabed. Such situations directly impacted the productions rates, quantities of consumables, extra cost on the tunnel enabling activities and finally, the need of both atmospheric and hyperbaric interventions into the cutter head up to 3.5 bar to replace cutting tools. Long tunnels with only one access shaft pose many programme problems for logistics, combine these with the requirement to drive directly out under the seabed for 10.2 km, and the programme issues become even more challenging. To meet and eventually improve on the planned completion date required a complex and extensive management of all tunnel logistics activities required to support consistent tunnelling for a two-year period. This technical paper will discuss the management issues and solutions implemented to meet the challenges of the outfall tunnel construction.

Keywords: TBM; Sub- Sea tunnel; Hydrostatic pressure, Non-intrusive radar system (BEAM), TBM parameters

1 Introduction

The outfall tunnel extends from the pump station, 10.2 km offshore and connects via a riser shaft to a diffuser field. This allows the safe and environmentally compliant discharging of storm and ground water flows into the Arabian Gulf. The discharge from the structure to the sea is via 84 duckbill valves located at the equal spacing along the 6-arm structure (Public Works Authority, 2017). The project location is shown in Figure 1.



Fig. 1: Project Location

2 Geological and Geotechnical Conditions

Referring to boreholes information and additional geophysical investigation the TBM excavated through three general geological formations: Rus Formation (RF), Midra Shale (MS), and Simsima Limestone (SL). As the TBM passes from one to another the excavation face will include both strata. Water pressure both Low (LP) and high (HP) was expected and encountered, hence, the TBM excavated through 7 mining zones, as follows. The three geological formations are shown in Figure 2.

- Rus Formation (RF) – full face.
- Rus Formation with Midra Shale (MS).
- Midra Shale – full face.
- Midra Shale with Simsima Limestone (SL)
- Simsima Limestone – full face (Low Pressure (LP) and High Pressure (HP)).
- Simsima Limestone with Midra Shale.
- Simsima Limestone – full face (Low Pressure (LP) and High Pressure (HP)).

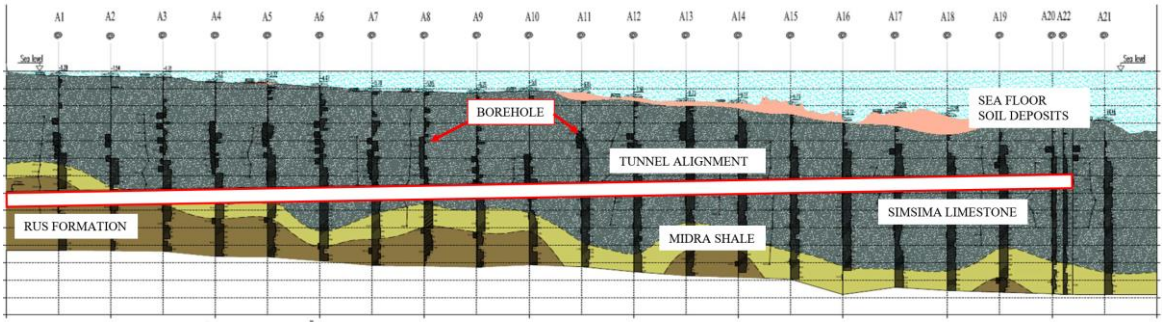


Fig. 2: Outfall Tunnel Geotechnical Section

From a hydrological point of view, the most crucial aspect is the aquifers at the Simsimal Limestone-Midra Shale interface and the interface between Midra Shale-Rus Formation, where the transmissivity was very high in both locations.

3 Tunnel Boring Machined (Tbm) Selection

The TBM was designed, Specification for tunnelling (2010), and manufactured by CREG/Wirth. The TBM selected to excavate the outfall tunnel was an EPB (Earth Pressure Balance) designed as per Qatar Construction Standards (2014) to support a maximum face working pressure of 4.5 bar (full

hydrostatic). EPB configuration has a cutter head, excavation chamber, main bearing or drive, screw conveyor, front, middle and tail shields, personnel locks, thrust system, articulation, erector, and special brushes as part of the tail shield seal system. In addition, there are 18 gantries, 160 m long accommodating all electromechanical parts, additive tanks, and rescue chambers. The TBM was designed to erect a concrete tunnel ring of six segments with a linear length of 1.35 m, the internal diameter being 3.7 m (Maidl, 2014).

The TBM Technical description (2018), was designed and equipped with:

- Optimized cutting tools combination for hard rock and soft rock.
- Operate in open mode or closed mode.
- Materials and equipment to support a maximum face working pressure of 4.5 bar.
- Eliminate the risk of uncontrolled water inflow into the tunnel during construction.
- The screw conveyor had two sets of gates for emergency purpose in high pressure.
- Long screw conveyor to dissipate the maximum pressure of 4.5 bar.
- Extra wire brush seals to withstand high pressure.
- Removable probe drilling machine.
- Real time probing system using BEAM (The Bore-tunnelling Electrical Ahead Monitoring).

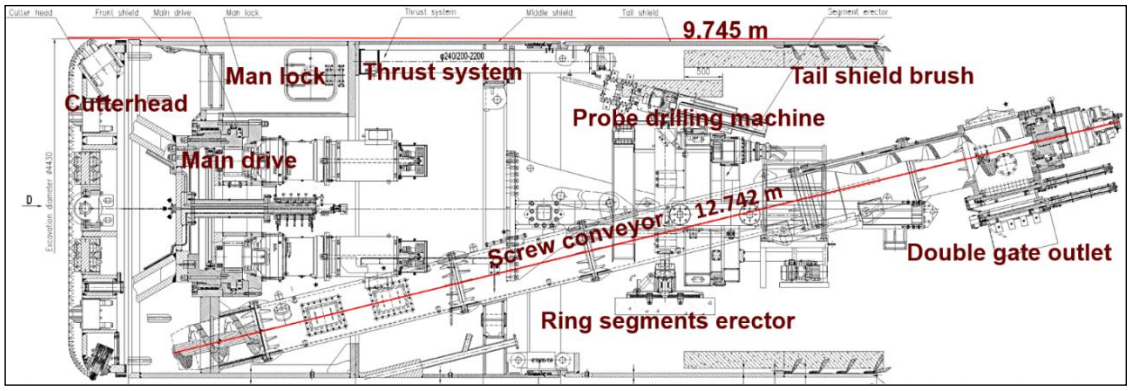


Fig. 3: TBM main components

4 Access Shaft Arrangements

4.1 Introduction

The project configuration included a drop shaft from the pump station, which connected to the outfall tunnel. This allows the treated surface and stormwater to transfer from the pump station to the outfall tunnel.

4.2 Drop Shaft

The Drop shaft was considered as a possible access shaft for the TBM works but at only 12 m in diameter is too restricted and this shaft would not be able to be completed until after TBM works had finished. This would put severe pressure on the overall completion date of the project. It was decided to not use the drop shaft for TBM access.

4.3 Logistic shaft

It was decided that a temporary logistics shaft has the most effective structure to construct the outfall tunnel. It was located directly behind the drop shaft (48 m deep) and along the same alignment is the

outfall tunnel. This structure consisted of a 26 m diameter shotcrete lined shaft and an extension tunnel of 26 m, capable of installing three separate rail tracks side by side. The logistic shaft and extension tunnel arrangement is shown in Figure 4 along with the two types of rail transport systems].

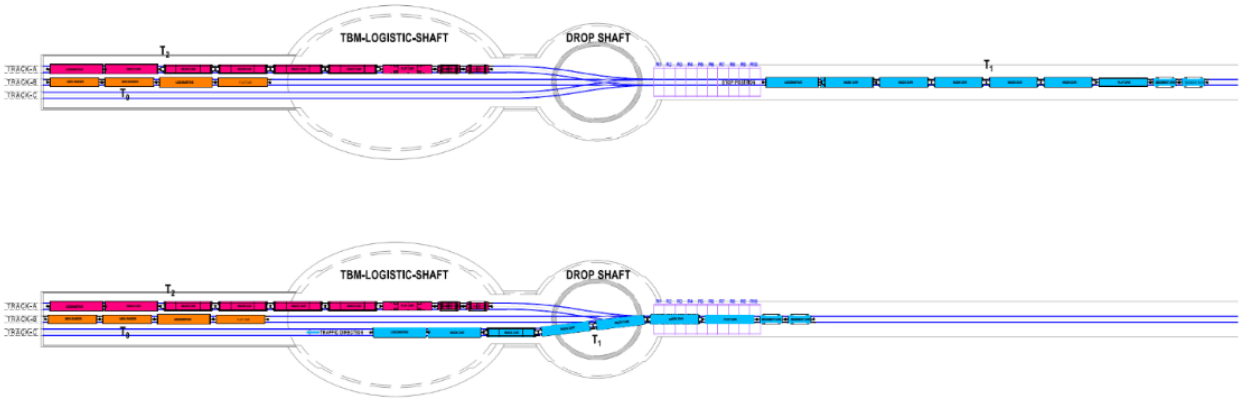


Fig. 4: Logistic & Drop shafts and Outfall tunnel arrangements.

5 Tunnel Logistics Options

5.1 Introduction

As the tunnel construction progresses the locomotive journey times increase until, at some point, they result in the TBM having to stop and wait for the locomotive bringing the next tunnel segmental ring, empty material skips and additional supplies back to it before it can start excavating again. To avoid this, one or more California (rail) crossings can be introduced in long tunnels to keep the tunnelling continuous. This allows more than one locomotive to operate on the railway line at once, and allows locomotives to wait closer to the TBM, ready to supply it from a shorter distance. Figure 5 illustrates the simple arrangement with one California crossing.

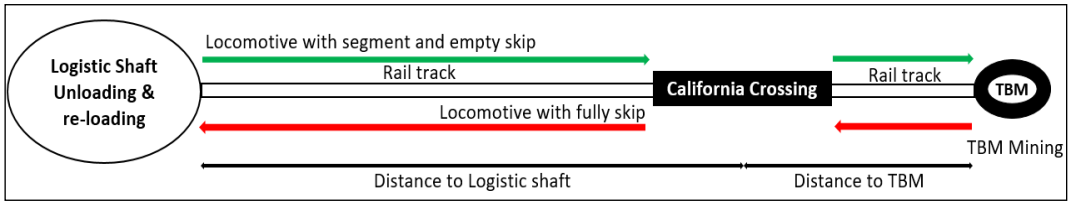


Fig. 5: Train traffic plan with California crossing

5.2 Single and Multiple Crossings considerations

During the planning stages analysis must be made as to the expected delay time which would be incurred supplying the TBM as the tunnel length increases daily. A California crossing is a complex structure which must take into consideration many variables and as such will take many months to fabricate. The variables to be considered in the design of a California crossing for the outfall tunnel are:

- Safety of TBM personnel.
- Working shifts number and duration per day.
- Number of working days per week.
- Length of combined material/segment and personnel trains (normal conditions).

- Additional excavated material skips for adverse conditions.
- Ease of installation.
- Ease of relocating within the tunnel 2 days per relocation.
- Impact of TBM services within the tunnel.
- Minimal impact on ventilation system.
- Efficient access and exit of the structure for the various rolling stock.

With the above design complete, the next stage was to simulate how the California crossing(s) would affect the tunneling production and to decide on how many would be required for the 10.2 km tunnel length. During this simulation the following would be estimated, and various ranges considered:

- Accelerate from logistic shaft.
- Top speed expected of the rail.
- Deaccelerated on approach to California crossing.
- Access onto California crossing.
- Traversing the Californian crossing.
- Exit California crossing.
- Accelerate from California crossing.
- Top speed expected of rail.
- Deaccelerated on approach to TBM/additional California crossing.
- Time to travel within the TBM Gantries.

During the tunnel construction, decision was taken to implement one California crossing.

6 Soil Conditioning

The primary necessity of soil conditioning is to obtain a suitable mixture of excavated material to build up and maintain the necessary pressure in the bulkhead to support the pressure of the soil and the water at the tunnel face, improvement of advance rates, reduction in the wear of cutting tools and cutter head torque.

The ground conditioning is carried out during the excavation at the tunnel face, in front of the cutter head, to avoid the clogging of the cutter head (cutting tools) with openings in the screw conveyor and excavation chamber. The TBM was provided with 4 injection lines for conditioning direct into the front of the cutter head, 3 lines to the chamber and screw conveyor, and the water spray injection lines to the excavation chambers. These lines were designed for different soil conditioners requiring foam, polymers, and bentonite in exceptional cases. During the design stages, the estimation of soil conditioners consumption assumed for the excavation of 1 ring (20 m^3) was 12 to 15 liters of concentrated liquid of foam, depending on the manufacturer, and 1,000 to 2,000 liters of water per tunnel ring.

7 TBM in Very Dry Conditions

During the initial stage and the learning curve of the TBM operation, the TBM was passing through the Rus Formation, the regular operation, the consumption of soil conditioners, the consistency of the paste, the quantity of excavated material per ring was as per expectations. However, after passing ring Number 450, the TBM entered mixed face conditions of Rus Formation and Midra Shale with higher clay content, which resulted in a reduced advance rate.

Once the TBM entered fully in Midra Shale occurring between tunnel ring 550 and 1150 the ground conditions were extremely dry, requiring extra addition of soils conditioning materials such as foam and water spray in the cutter head and excavation chamber to control the TBM parameters such as torque, thrust and reach and maximize possible advance rates in the difficult ground conditions.

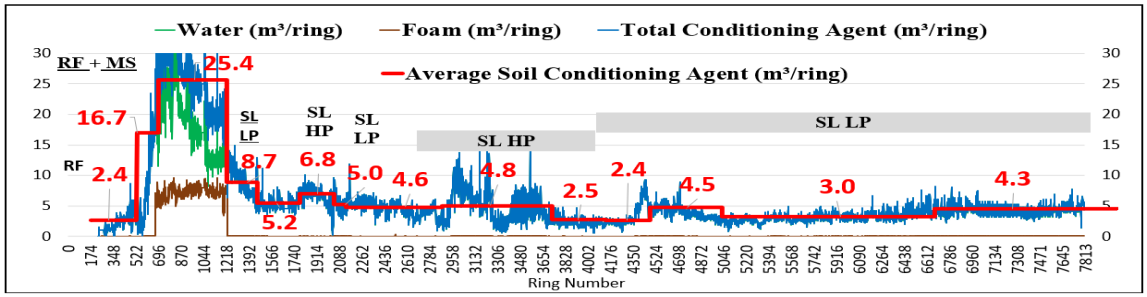


Fig. 6: Average Consumption of Soil Conditioning Agent at Each Geological Formation and Conditions

Figure 6 above shows the volume of soil conditioners (foam and water) added increased from 2. 4 m³/ring up to 25.5 m³ per tunnel ring. Therefore, the addition of soil conditioners, the swelling factor greatly increased the quantity of excavated material per tunnel ring from 4 to 8 skips per tunnel ring and occasionally 9 skips per tunnel ring as shown in Figure 7. This resulted in an increase of supply trains by 2 and sometimes 3 trains to excavate a ring instead of 1 as planned. To help mitigate the impact of increasing the number of trains, the installation of the California crossing was brought forward to tunnel ring 550. Figure 7 illustrates the number of skips required to remove the excavated material for one tunnel ring against ground condition types over the length of the tunnel. Figure 7 also indicated the net boring time take to excavate one tunnel ring, which increased with increasing quantity of excavated material.

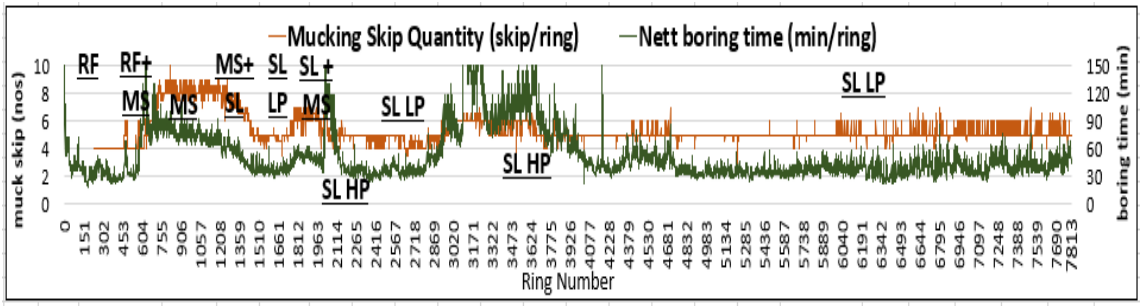


Fig. 7: Quantity of Muck Materials against the Boring Time

8 TBM in Very High Water Pressures

Opposite to the previous scenario occurred when the TBM encountered 2 areas of high-water pressure conditions while excavating through the weathered Simsima Limestone Formation fully connected hydrostatically to the seabed.

The first area was from tunnel ring 2,000 to 2,130 and the second area was from tunnel ring 2,830 to 4,100 where the TBM passed through a fault area (Figure 2), the EPB pressure instantly reached 3.5 bar.

After the necessary assessment of the geological conditions, adjustment on the main drive seal of the TBM to work in close mode, safety toolbox talk with the operatives, specifics drive instruction

parameter sheet was issued to the TBM operator on how to excavate through these areas.

From a soil-conditioning point of view, polymers were added in the excavation chamber and screw conveyor to control the effect of high-water inflow. Unfortunately, the results were not satisfactory enough in this situation considering the size of the excavation chamber.

To evaluate the differences of excavation with or without addition of polymer, two options were observed. The first was adding polymers and pushing the TBM slow enough to have time to condition the soil in the chamber and get it pasty enough, but the TBM's speed was slow, around 4 to 6 mm per minute. The second was without adding polymer, getting the muck without pasty consistency, to reach the advanced speed of 12 to 15 mm/min.

After analyzing the data and evaluating the advantages, disadvantages, and risk of the second option mentioned above, it was decided to continue advance without polymers and conditioning only with foam for lubrication purposes only to reach the maximum safe advance rate speed in relation to the conditions.

The logistics, as expected, was affected due to the excavated material quantity being higher than the theoretical. In this case, five skips per tunnel ring becomes the usual. For that, all the trains (3 units) were modified to be able to accommodate five skips. Regarding the California crossing, only one unit was installed and relocated based on not more than 20 hours idle time per week.

9 Cutter Head Interventions

A total of 7 cutter head interventions in atmospheric conditions were performed while excavating Midra shale, replacing 17 cutter discs. Two interventions in hyperbaric conditions, BS 6164 (2011) The life of cutter discs was expected to be around 70 tunnel rings per cutter, the actual cutter disc life per geological formation type is shown in Figure 8. The average being 77 tunnel rings per cutter.

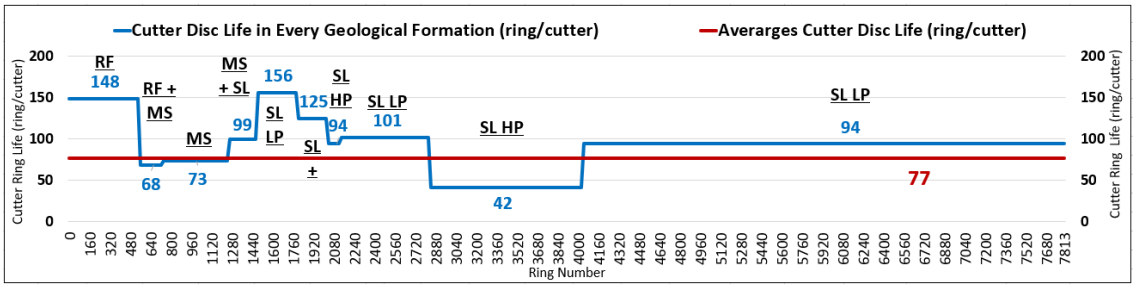


Fig. 8: Cutter Disc Life in Every Geological Formation and Condition



Clogging Clogging Disintegrated cutter

Fig. 9: Status of the Opening during Cutter head Intervention (clogging issues)

Some of the cutter head interventions were required to clean the clogged openings, as shown in Figure 9, which affects the speed of the TBM advance.

In terms of cutting tools consumption, the wearing was higher than expected due to hyperbaric conditions, in these cases, the lifetime decreased to 42 tunnel rings per cutter.

10 TBM Average Progress

Figure 10 shows the average progress along the different geological formations being 7.6 tunnel rings per day and 8.7 tunnel rings per day while the TBM was working in high water pressure conditions.

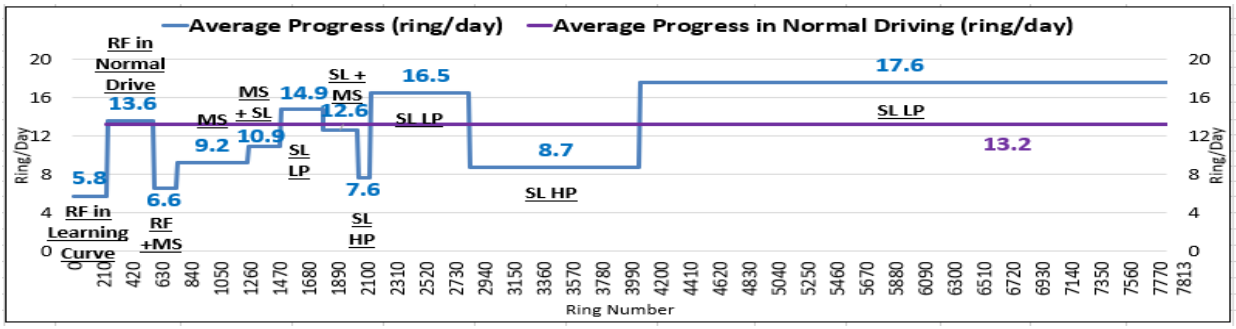


Fig. 10: TBM Average Progress

While the TBM was excavating in hyperbaric conditions, unusual wearing was observed in the screw conveyor gates as consequence of poor soil conditioning and high pressures in the excavation chamber, along the screw conveyor and rubber conveyor belt requiring early replacement.

11 Conclusions

The TBM completed the drive 58 days ahead of programme despite the difficulties, passing through geological formations in extreme ground water conditions. The lowest performance of the TBM occurred in these two extreme conditions. This is because the consumption of the consumables like soil conditions and greases were up to 4 times higher than average values along the tunnel.

The constant monitoring of the TBM parameters helps the crew to adjust them and obtain the best possible performance, minimizing lost time. The logistics' flexibility helped during the adverse scenarios during TBM drive, allowing modifying the train and using only one California crossing, which greatly reduced lost time.

The wearing of cutting tools was high but somehow expected when the TBM is mining in hyperbaric conditions. The lack of high-water pressure nozzles in the bulkhead might help in case of clogging issues, a lesson learned for following similar projects. Poor soil conditioning during high water pressure conditions resulted in some mechanical issues in terms of excessive wearing of the screw conveyor gates and the rubber conveyor belt.

References

British Standards Institution. (2011). BS 6164:2011 Code of Practice for Health and Safety in Tunneling in the Construction Industry, BSI Standards Publication, London.www.bsigroup.com.

Maidl, B. (2014). Manual for Construction of Tunnels and Galleries, Verlag: Glueckauf, Essen, ISBN 3-7739-0512-2.

Public Works Authority. (2017) Contract Documents for Design, Build, Operate and Maintenance of Musaimeer Pimping Station and Outfall, Project ID: IA 14/15 C 015 G, Contract Number: C2017/109.www.ashghal.gov.qa

Qatar Construction Specifications (2014). (QCS-2014).

Specification for tunneling. (2010). Third edition, The British Tunneling Society, and Institution of Civil Engineers.

TBM Technical Description. (2017) C2017_109-RPT-TU-000.

Cite as: Peach G., Fernandez H.V. & Al-Marri S.Z., "TBM Challenges on Musaimeer outfall tunnel", *The 2nd International Conference on Civil Infrastructure and Construction (CIC 2023)*, Doha, Qatar, 5-8 February 2023, DOI: https://doi.org/10.29117/cic.2023.0017

Performance of an Infrastructure Project Following the Deployment of a Customized Lean Strategy

Ramez Alchamaa
Dorsch Gruppe–Middle East, Doha, Qatar
ramez.alchamaa@dorsch.com

Hisham M. S. Abushaqra
Public Works Authority (Ashghal), Roads Projects Department, Doha, Qatar
habushaqra@ashghal.gov.qa

Abstract

This paper highlights the benefits of adopting and implementing a tailored lean construction strategy with its dynamic action plans during the construction phase of one of Qatar's recently completed infrastructure projects. The study includes using various enhancement measures and criteria combined with best practices by different project teams from all involved parties. The paper also proves the influence of producing a systematic work process during the project life cycle on overcoming challenges and barriers, in which the critical elements of accomplishment, improvements, and the conditions of satisfaction are adequately outlined and recorded. Through this paper, the lead author claims to achieve one primary goal, which is to name the most crucial barriers that affect the deployment of the Lean Construction concept within the construction industry based on data collected from four infrastructure projects, including the evaluated one in this paper. The required data was collected and collated through questionnaire surveys conducted on 57 professionals following many interactive workshops held by the lead author about the importance of Lean Construction implementation in construction projects. Concurrently, data analysis outcomes were used in the PDCA cycle of continuous improvement. The findings emphasize the importance of leadership engagement in lean deployment processes, and training sessions/workshops, besides rewarding the project team members as a pillar towards an ideal productivity level with the practical usage of resources and delivering the utmost value to the client.

Keywords: Continuous improvement; Lean Construction (LC); Enhanced Contract (EC); Enhancement Check Sheet (ECS) Score; Conditions of Satisfaction (CoS)

1 Introduction

Modern construction projects face frequent burdens related to shorter durations and uncertainty throughout their life cycle (Koskela et al., 2002). The crucial challenge in these current projects lies in the miscoordination of activities and tasks among the project's different teams as the traditional approach for delivery of projects is typically utilized. Given that the implementation of the Lean Construction (LC) principles and tools becomes a recognized approach worldwide to help reduce the uncertainty of activities scheduled in the preliminary plan (initial) schedule at high-level details. The problem seems obvious when new activities or unforeseen changes appear at a particular week of their execution on-site. Then, going ahead in the execution of such activities without properly eliminating the associated constraints might lead to an unreliable workflow that can hinder the overall project progress. In this regard, and as a considerable step forward, the Public Works

Authority (ASHGHAL) has lately adopted the Lean Construction (LC) principles by introducing the Enhanced Contracts in the Construction of infrastructure projects for the first time in the State of Qatar. Adopting this advanced approach in project management has become a strategic intent to enhance communication with stakeholders and residents, safety measure, and the overall appearance of the workplace. As a result, this would speed up the delivery time of projects and improve overcoming challenges the project may face promptly by recognizing and prioritizing them early.

Likewise, by implementing the (LC) principles appropriately, each stage of the construction project is planned for and controlled closely. In addition, holding regular Collaborative Planning sessions in the Project Performance Centre (i.e., The Big Room) would involve as many stakeholders as possible. Using various facilitation techniques to encourage consensus and cooperation is an efficient tool for monitoring the project's performance in all aspects. Furthermore, this implementation provides a more accurate prediction about the work completion schedule considering any emergent constraints and changes in priorities. The project works are also divided into zones and sub-zones for completion according to a zonal delivery plan that intends to minimize the impact of construction works on the residents of the target area or zone (disruption management).

This paper describes a thorough record of the main events of a sensible lean journey for one of the recently completed roads and infrastructure projects. The paper also outlines and evaluates the adopted enhancement measures by the project team, best practices during the life cycle of the cited infrastructure construction project, and the benefits realized through the following sections.

Finally, it is worth noting that the studied project in this paper is governed by the Public Works Authority (ASHGHAL), through the Enhanced Contract (EC) for infrastructure construction projects.

2 Project Overview

The designated project in this paper is a major project of roads and infrastructure construction in residential areas, namely Project A. The project consists of three zones– Zone 0, Zone 1, and Zone 2, with a total area of 117 hectare that covers over 119 residential plots; the scope of work is summarized as follows:

- The construction of drainage networks, including foul sewer, surface water, and groundwater lowering networks. Besides a treated sewerage effluent system (TSE) and portable water network with an approximate length of 33.5 km.
- The construction of a road network with an approximate length of 7.5 km and about 1,112 parking bays. The construction of pedestrian walkways and cycleways within the road corridors with an approximate length of 14.97 km and landscaping a length of 30.36 km.
- The construction of electrical and telecommunications networks.
- The installation of streetlights, traffic signals, and Intelligent Transportation Systems (ITS).

3 Overcoming Challenges and Emergent Barriers

The chronological chart in Figure 1 illustrates a summary of the project's schedule performance from the starting date of Project A in July 2019 till the end of December 2021. A couple of months later, following the start date, particularly in October 2019, the project started suffering from a gradual increment of the reported percentage of variance (delays) as per the original baseline schedule. The

peak point of the reported delays (i.e., a cumulative variance of 37%) occurred in June 2020 due to different events including, but not limited to, COVID-19, where the project has been forced to adapt significant challenges and formulate tailored solutions to mitigate the delays and other impacts caused by COVID-19. In July 2020, the project's leadership, from the Supervision Consultant to the Contractor, built an effective collaborative environment.

In the first place, the formed collaborative environment has targeted overall cultural change and the spread of the collaborative set mindset among team members in the project. The established environment has encouraged the interactive transfer of knowledge in a structured way inside the organization. All voices are heard, and contributions are valued within a safe, open dialogue space focused on asking questions and providing input on various subjects and issues. Furthermore, a recovery plan to minimize the excessive delays was prepared collaboratively between different teams, from the Supervision Consultant to the Contractor, in July 2020. It resulted in the production and implementation of a new revision of the Activity Program as a practical tool for monitoring the performance against planned activities with actual daily rates. It also allocated resources for each activity to ensure a predictable and reliable workflow of on-site construction activities.

Remarkably, the weekly performance of the project started to improve dramatically, with a considerable decrement in delays in the schedule as of August 2020 onwards. The delays began to decrease to an acceptable magnitude of ≤ 5% in February 2021 following the active implementation of the Lean Construction philosophy and tools in the project with the operative engagement of the leadership and teams from different disciplines.

It is worth mentioning that recorded delay in schedule has decreased significantly around the magnitude of ≤ 1% as of June 2021 and maintained to be around this percentage till the end of the year 2021, as demonstrated in Figure 1. This productivity improvement is attributed to the effective collaborative pull production planning and other lean implementation activities with the broad participation of different teams from both the Supervision Consultant and the Contractor associated with an operative implementation of the approved enhancement and lean strategy for the project as of May 2021.

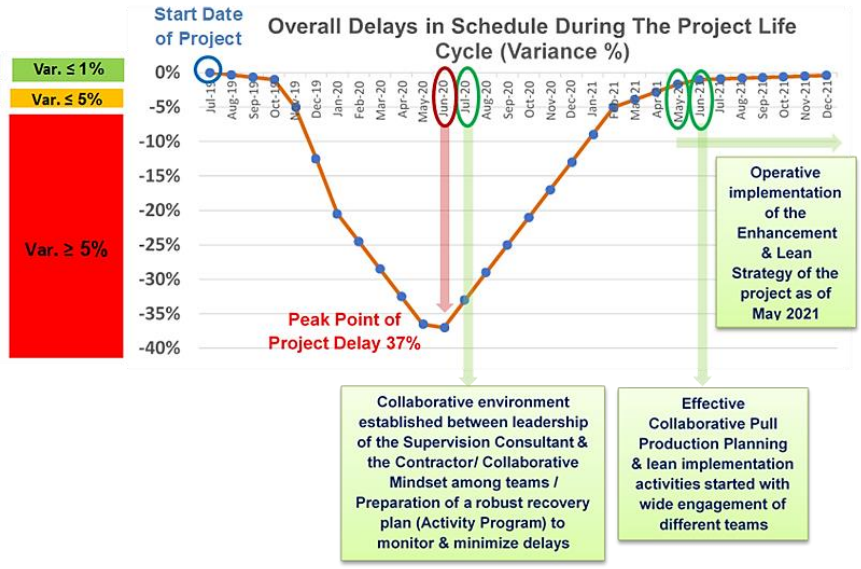
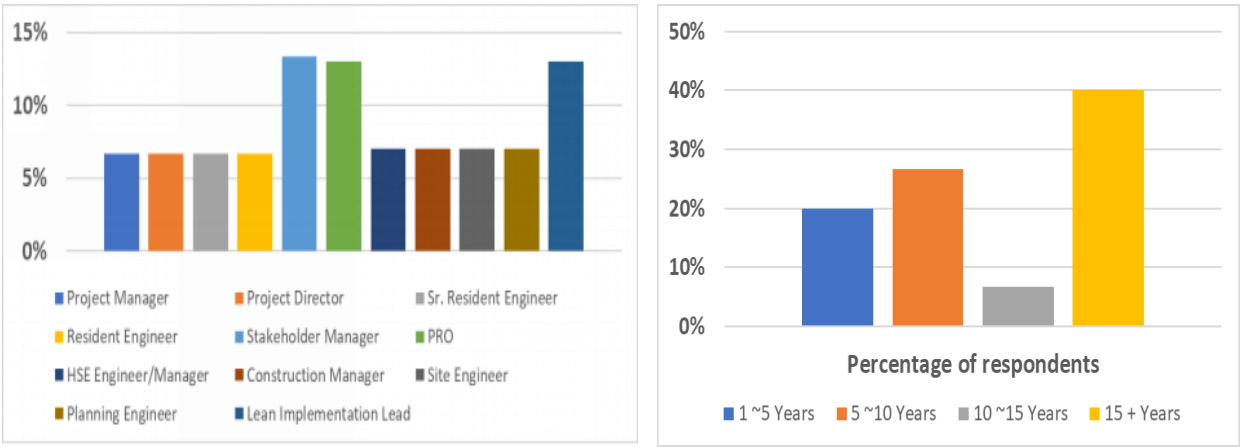


Fig. 1: Major Events in Project Performance

Additionally, the analysis of the chronological chart formed the keystone to conducting a deep-rooted survey to understand the barriers to LC implementation. For this purpose, the lead author has undertaken a series of structured questionnaire surveys to highlight these broadly experienced barriers and challenges in most of the ongoing construction projects to support a successful LC implementation. The cited questionnaire surveys were conducted on a sample of 57 professionals from four infrastructure construction projects, namely Project A, B, C, and D, as primary respondents following several interactive workshops held by the lead author about the importance of Lean Construction principles and implementation in construction projects. As a sample validation, Figure 2 demonstrates the survey respondents' position and total years of experience. According to the



corporation type, the survey respondents represent two parties: The General Contractor (53%) and the Supervision Consultant as representative of the Client (47%).

Fig. 2: Position and Total Years of Experience of Survey Respondents

Based on the gathered information, the lead author performed a descriptive exploratory analysis of the data to extract the most critical and influential barriers, as illustrated in Figure 3. As a result, the significant obstacles defined in this study are the lack of knowledge and understanding of LC due to insufficient training, which is the most effective barrier (45%), followed by the lack of knowledge about the expected benefits of Lean Construction implementation to the construction projects (27%). On the other hand, lack of leadership engagement and collaborative teamwork is a slightly less effective barrier (20%), followed by cultural barriers and attitude to work besides resistance to change by management (8%).

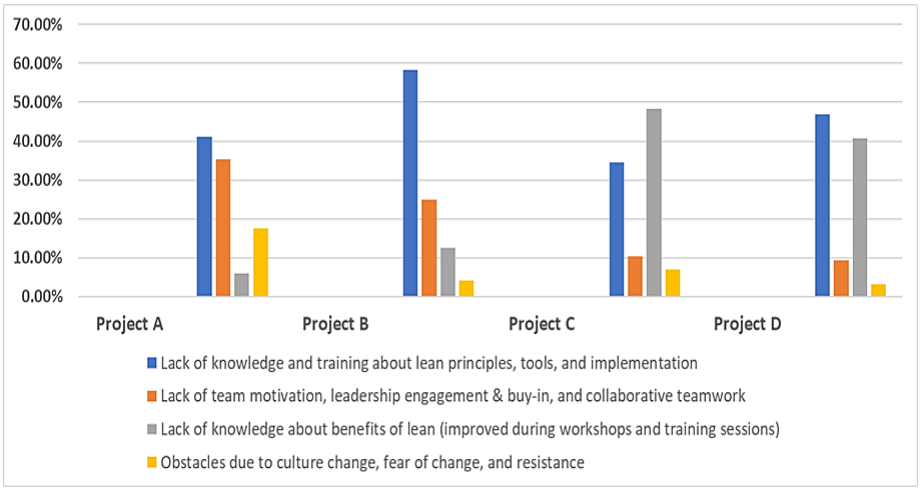


Fig. 3: Summary of the Most Influential Barriers to Lean Construction Implementation

The identified barriers are used for producing a customized enhancement and lean strategy for Project A that aligns with ASHGHAL's pre-set enhancement strategy that targets the enhanced infrastructure projects of 2021. Also, the practical implementation of the LC principles and tools has resulted in improving productivity by eliminating different types of reported wastes of available resources, time, and effort in addition to the repeated observations, minimizing the non-added value activities, and generating the maximum possible amount of value to the client and end-users. The upcoming sections of this paper present all these particulars. The efficient implementation of the approved robust enhancement strategy for Project A during the 2nd Quarter of 2021 has drawn the roadmap to achieve the target productivity, enhanced quality & safety performance, public satisfaction, schedule performance, and early delivery of various project's key stages, and authority satisfaction in alignment with ASHGHAL's pre-set enhancement strategy targets and predefined six categories and criteria for the enhancement process in Enhanced Contract projects (i.e., 1) Project delivery. 2) Site organization and management. 3) Planning and control. 4) HSEQ & KPIs. 5) Public relations and stakeholder management, and 6) Lean construction implementation. These six categories are the major components of the Enhancement Check Sheet (ECS). Hence, the ECS is the monthly evaluation and scoring system with over 100 criteria.

4 The Status of Enhancement & Lean Implementation Before and During the First Quarter of 2021 for Project A

Figure 4 illustrates the status of the Enhancement Check Sheet (ECS) Scores at the end of 2020 and early 2021 before preparing and implementing the Enhancement & Lean Strategy for the Project as of May 2021.

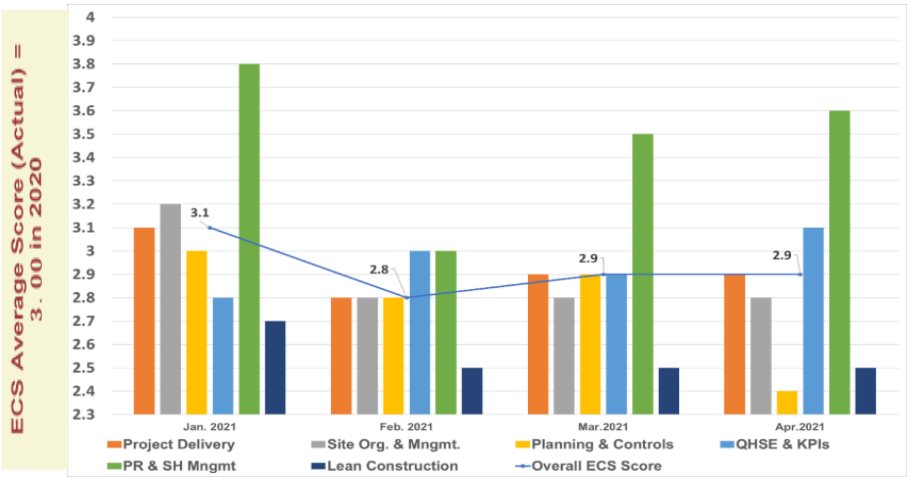


Fig. 4: The Scores of Major Enhancement Categories Before the Implementation of the Enhancement & Lean Strategy For 2021

5 Development of Operative Action Plans for Project A, Based on the Pre-Set Enhancement and Lean Strategy Targets by Ashghal

The continuous improvement (Kaizen) of the ECS categories following the approval and implementation of the enhancement & Lean Strategy for 2021 is demonstrated clearly in Figure 5.

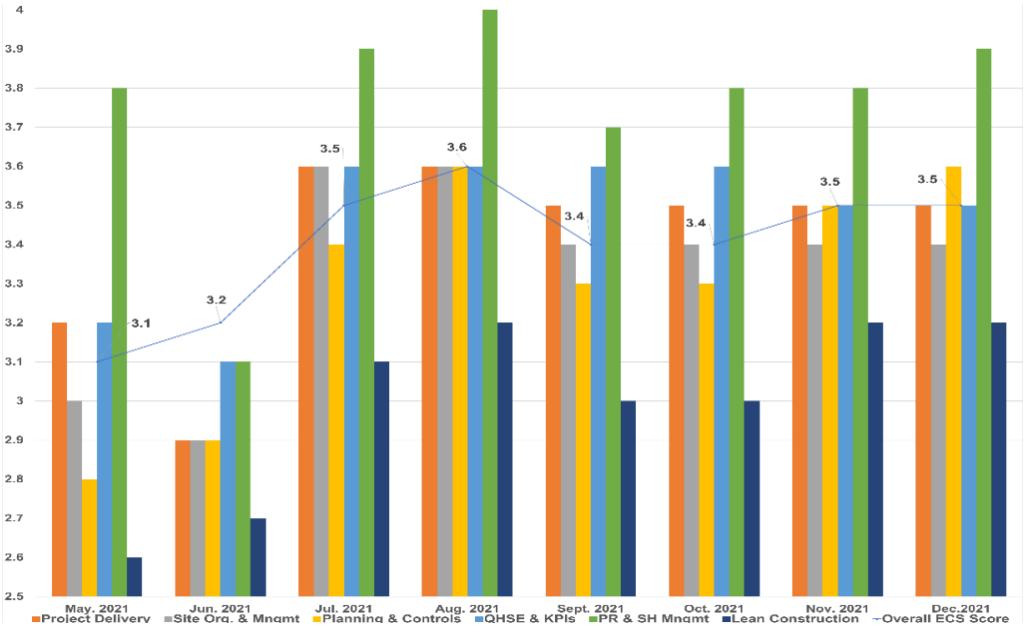


Fig. 5: The Continuous Improvement (Kaizen) of the ECS Categories Following the Implementation of the Approved Enhancement & Lean Strategy for 2021

Table.1 highlights the continuous improvement in the achievement rate of the strategic objectives against the strategic target task as commitments over Q2, Q3, and Q4 of the year 2021.

Table 1: The Enhancement Strategy Performance against the Target Strategic Tasks

(A) Target Strategic Tasks	**Q2 2021**		**Q3 2021**			**Q4 2021**		
	May 21	June 21	July 21	August 21	Sept. 21	Oct. 21	Nov. 21	Dec. 21
	29		40			44		
(B) Achieved strategic objectives	24		37			41		
Achievement rate (B/A) % per quarters during 2021	**89%**		**92%**			**93%**		

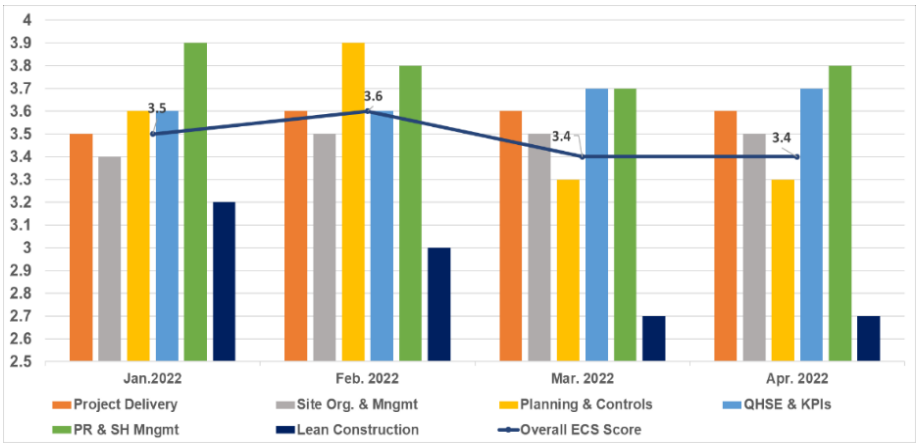


Fig. 6: Status of the ECS Categories During 2022 (January 2022 to April 2022)

Figure 6 displays the status of the ECS categories during the first four months of 2022 until the end of April 2022, when the Project entered the handover and closure phase as the completed tasks are being transferred to the client. The approved enhancement & Lean Strategy for 2021 for Project A

has been completed collaboratively, engaging all team members' inputs and commitments to achieve the targeted strategic tasks from the discipline's representatives in May 2021.

6 The Conditions of Satisfaction for the Ecs Categories During 2021

Table 2 summarizes the ECS categories and their respective conditions of satisfaction (CoS).

Table 2: ECS Categories and Their Respective Conditions of Satisfaction (CoS)

ECS Categories	Conditions of Satisfaction (CoS)
1. Project Delivery	Conduction of regular Collaborative Handing Over sessions with all assigned vital actions.
2 . Site Organization & Management	Site organization, elevated workplace, and proactive resolution of forecasted issues/ bottlenecks collaboratively.
3. Planning & Controls	Use of the actual productivity rate to develop the planning process.
4. HSEQ & KPIs	As a pre-set condition, the observations related to quality, health, safety, and welfare will be reduced by 70% at the end of Q4-2021.
5. Public Relations & Stakeholder Management	Standardize look & feel and achieve ZERO complaints status from the public at the end of Q4-2021 with a reduction in PR complaints by 50% from the previous year.
6. Lean Construction Implementation	The early completion dates of Key Stages due to the successful embedding of lean tools in all Key Stages & challenging pulling sessions of activities.

7 The Adopted PDCA Cycle for Continuous Improvement of ECS Categories and Regular Lean Implementation Activities

Figure 7, Figure 8, and Figure 9 illustrate the improvement of the ECS categories and the regular Lean Implementation Activities (e.g., Gemba walks as stated afterwards) using the PDCA Cycle. All crafted satisfaction conditions and their criteria were met as per the targeted objectives in the Project enhancement strategy for each quarter in 2021. As it is known, conducting the Gemba walk is a great event to allow managers and leaders from the Supervising Consultant and the Contractor to jointly observe the actual work process, engage with other teams and disciplines to gain knowledge about the work process, and explore opportunities for continuous improvement. Figure 7 illustrates the continuous improvement in the number of reported observations from the monthly Gemba walks as of February 2021. The recorded number of observations has decreased dramatically to be limited to 2 observations per month during the 4th quarter of 2021, with a significant improvement in the number of closed observations within ten days from the observations' day. This improvement relates to the satisfactory conditions of the entire ECS categories (see Table 2).

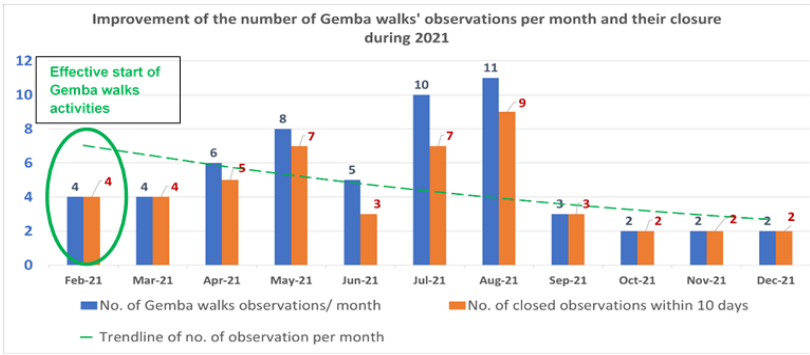


Fig. 7: Continuous Improvement in the Gemba Walks' Observations and their Closure

Likewise, Figure 8 presents the continuous improvement in the number of Public Relation Complaints (PRC) and the overall status of disruption management for Project A following the effective implementation of the enhancement strategy for 2021. Figure 8 reveals that the total number of PRC during 2021 is eight complaints, three of them were reported by the PR team from May 2021 till the end of 2021 (i.e., ZERO complaints status was achieved during Q3 and Q4 of 2021).

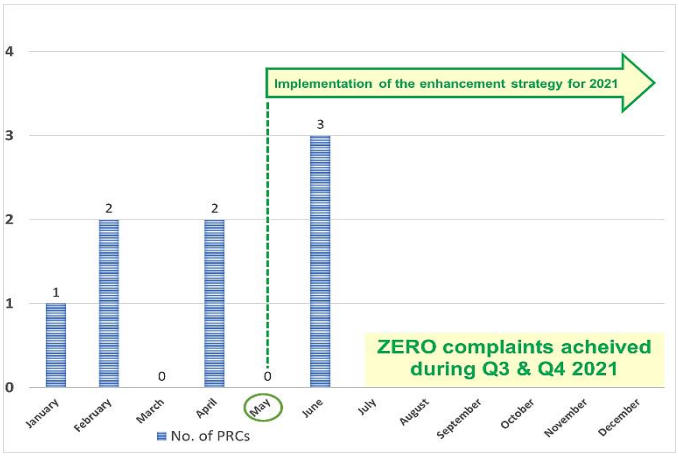


Fig. 8: Continuous Improvement in The Number of PR Complaints During 2021

This recorded status reflects an effective collaboration between various teams in implementing the enhancement strategy that meets the respective CoS for the PR & stakeholder management category (see Table 2). As for the site safety observations, they decreased dramatically during 2021, as illustrated in Figure 9, in which 99 observations were recorded by the respective HSE team early in Jan. 2021.

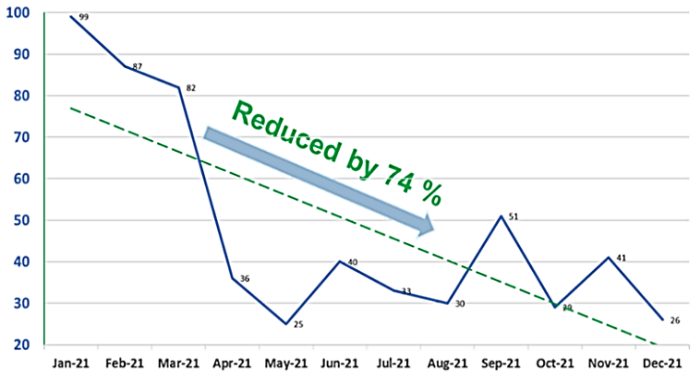


Fig. 9: Continuous Improvement of the Number of Safety Observations During 2021

These observations were eliminated significantly over 2021 quarters to record only 26 observations by the end of 2021 to indicate the outstanding engagement of all teams from various disciplines in the process. A considerable reduction of 74% of the observations is reported during the 4th quarter of 2021; this meets the respective CoS stated in Table 2 for the HSEQ & KPIs category.

8 Leadership Engagement in Lean Deployment, Training Sessions, Workshops, and Recognition (as a Pillar & Key Critical Factor of Continuous Improvement)

Systematic learning and knowledge transfer are proven to have a valuable role in the continuous improvement of this project as they focused on the following perceptions: 1) Empower teams' members with the support of leadership and encourage their collaborations and inputs to the project's

enhancement. Moreover, recognizing and awarding the team members as champions for their outstanding performance every month is proven to be a perfect asset to improve the project's enhancement process. 2) The collected feedback from questionnaire surveys is used to improve the process, have new commitments, and concentrate the teams' efforts on specific areas of improvement as required. 3) Use the monthly assessment of the ECS scores to adjust the strategic tasks that are part of the enhancement strategy of Project A.

9 Conclusion & Recommendations

This paper offered an inside view of a successful lean journey for a designated infrastructure project in the State of Qatar, including a description of the project status and emergent impediments at the initial stage of a selected project under the EC. The study in this paper displays that the leadership and teams' non-adoption of the lean culture is influenced by barriers that are mostly related to people, organizational processes, and other operational aspects. The analysis of these barriers was used to form a solid base for a productive preparation and deployment of a customized LC strategy and its target strategic tasks, remarking that addressing the organizational culture factors in construction was necessary for a successful implementation of practices (Cheung, Wong, & Wu, 2011). The outcome of this study emphasizes the importance of setting good Conditions of Satisfaction and strategic objectives to support LC adoption. In addition, the applied performance evaluation system on LC implementation outcomes of this study utilized the monthly evaluation and scoring system of the (ECS) that has already been stipulated by the Client (ASHGHAL) at an early stage of the construction. The ECS formed a handy tool for closely monitoring the implementation, the success factors, and the crafted CoS for the project. This performance evaluation system proved to help drive change and assess the quarterly performance of the customized action plans. The plans are updated as needed to ensure they are well linked to the CoS and achievable within the pre-determined timeframe for each condition. The cited system also accounts for implementation barriers that should be considered together with the lean-specific factors and CoS (Bassioni, Price, & Hassan, 2005). Lastly, the outcomes of this study can contribute to the further development of effective evaluation systems for future infrastructure projects.

References

Bassioni, H. A., Price, A. D. F., & Hassan, T. M. (2005). Building a Conceptual Framework for Measuring Business Performance in Construction: An Empirical Evaluation. *Construction Management and Economics, 23*(5), 495–507. DOI: 10.1080/0144619042000301401

Cheung, S. O., Wong, P. S. P., & Wu, A. W. Y. (2011). Towards an Organizational Culture Framework in Construction. *International Journal of Project Management, 29*(1), 33-44. DOI: http://dx.doi.org/10.1016/j.ijproman.2010.01.014

Koskela, L. & Howell, G. (2002). The Theory of Project Management: Explanation to Novel Methods, In Proc. 17th Ann. Conf. of the Int'l Group for Lean Construction, Gramado, Brazil, August 6-10.

Cite as: Alchamaa R. & Abushaqra H.M.S., "Performance of an Infrastructure Project Following the Deployment of a Customized Lean Strategy", *The 2nd International Conference on Civil Infrastructure and Construction (CIC 2023)*, Doha, Qatar, 5-8 February 2023, DOI: https://doi.org/10.29117/cic.2023.0018

Digitalization and usage of QR-code System in Documents Management

Loai Abdrabou- Adnan
IRIS Construction, Doha, Qatar
loai.a.abdrabou@gmail.com

Abstract

Multiple official documents from various departments have contributed to the rising number of printed pages in construction projects. The dominant explanation for this trend is that printed pages have a direct relationship with the progression of the project as the number of quality assurance, quality control documents, health and safety documents, technical documents, lean and enhancement documents, and store documents get increased with the project timeline. The research data was obtained from one of the infrastructure projects in the north of Qatar between 2020 and 2023 and in line with multiple academic references as listed in the last section of the paper (Ågren, 2014). Contrary to what has often been assumed, the rise in printed pages due to mentioned documents contributes to impacting the earth's environment badly, affecting global warming, cutting additional trees from green lands, reducing project KPIs, increasing overall project budget cost, and generating material waste. Lean enhancement engineers proposed replacing all the above-mentioned documents to be used in the digital format.

Keywords: Digitalization; Waste; Environmental; Sustainability; Quality

1 Introduction

The construction industry is a continuous cycle of producing printed pages due to the obligations of various departments that require physical documents to be in place. Therefore, a case study has been established by the lean enhancement team at an infrastructure project in the north of Qatar. The aim of this case study is to identify the root causes, required actions, and sustainable solutions to prevent such issues from occurring. The case study's need comes to reduce the impact on the environment and greenhouse gases, cut overhead costs, easy accessibility, and save efforts.

2 Methodology of the Proposal

The methodology of using the digital method of the QR-code system can be applied by following simple steps using smartphones. Firstly, collaboration meetings with all focal departments involved in the project, and secondly, identification of the documents in demand for daily usage at project printers. Thirdly, the root cause analysis shall be performed by each department using the Fish-Bone analysis technique and the 5 Whys method. Fourthly, discussion and brainstorming sessions of the pluses and deltas using the case study. Leading to establishing an agreed process to be followed by the concerned parties of the project. Nevertheless, maintaining and checking the proposal to evaluate the outcomes and adoption by the project teams.

3 Benefits of the Proposal

The expected positive outcomes from using the proposed innovative solution are enormous in multiple sectors. For example, it can reduce the impact on forests; cut energy use and climate change emissions and reduce other pollution forms. Also, reducing the demand for paper will also help lessen the social impacts and human rights abuses linked to paper production making it environmentally

friendly (Bikas et al., 2016). Moreover, lessen the cost required and cut overhead costs for the project. It is important to highlight that the scanned file can be either replaced, updated, or deleted which strongly agrees with the concept of saving time as with one click, a document will be updated and can be accessed globally by every personnel.

4 Methods and Tools to Measure Proposal Success

Multiple highlighted tools can be used to examine the case study's success such as measuring compliance by the team from GEC and the contractor. Also, measuring the outcome on both parties using IT department statistics. The number of printed pages has significantly decreased after the QR-code system implementing (Barlow et al, 2003). Nevertheless, financial results can be measured from the number of requested paper boxes from suppliers' quotations. Finally, before and after quantity tables were used in the lean case study to use the power of visual management aids in examining the success of the case study.

5 Environmental, Quality, Sustainability Standards

Using the QR-code digital system, compliance with multiple major environmental, quality and sustainability standards will be fulfilled for current as well as future projects. For example, ISO-9001 is customer-focused and places an emphasis on continuous improvement and top management processes that extended throughout the organization (Atkin, 2014), also, complying with ISO-14001 principles by saving printed pages, energy, costs, and efforts for the staff members. Moreover, confirming with ISO-50001 standards as an Energy Management System (EMS) is dedicated to improving energy usage and efficiency. This includes reducing an organization's energy footprint by reducing greenhouse gas emissions as well as energy costs. Finally, in line with ISO-20121 by sustaining energy savings and reducing the environmental footprint (Barlow, 2000).

6 Equations and Data Sheets

The enhancement team has gathered data about the number of printed pages in both contractor and consultant offices as shown below in Table 1.

Table 1: Data Collection

Printer location	**Day 1**	**Day 2**	**Day 3**	**Day 4**	**Day 5**	**Day 6**	**Day 7**	**Day 8**	**Day 9**
Contractor printer "Pages"	1600	1550	1400	2000	2200	2100	1900	1700	1450
GEC offices "Pages"	400	350	250	500	550	600	320	160	330

Although a collaboration awareness session on the importance of keeping the environment safe and minimizing the usage of printed pages was held, the number is yet to be increased as shown in Figure 1.



Fig. 1: Unused printed pages

$$Y = x\,A \qquad (1)$$

Where:

- Y: The overhead cost from printed pages $= QR\,\frac{21{,}840}{year}$.
- x: The unit price of 1 pack of white paper around QR 14.
- A: The daily average number of printed pages multiplied by the working days/year 780,000 pages.

$$Z = \frac{B}{w} \qquad (2)$$

Where:

- Z: The number of trees cut per year = 98 $Trees/year$.
- w: One tree makes over 8,000 pieces of paper (Fratzl, 2018).
- A: The daily average number of printed pages multiplied by the working days 780,000 pages.

$$O = \frac{Z}{p} * 100\% \qquad (3)$$

Where:

- O: Hectare of forest being demolished per year for the process of paper production = 9.8%.
- p: The number of trees planted per hectare will vary from 1,000 to 2,500 trees, depending on the species and the type of planting (Gurav, 2003).
- Z: The number of trees cut per year = 98 $\frac{Trees}{year}$.

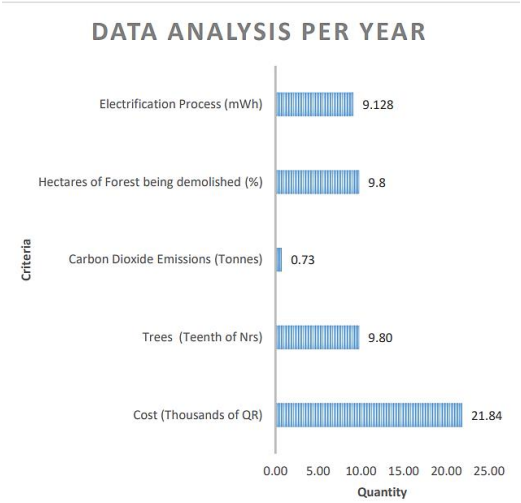


Fig. 2: Savings Per Year (ASTM, 2012)

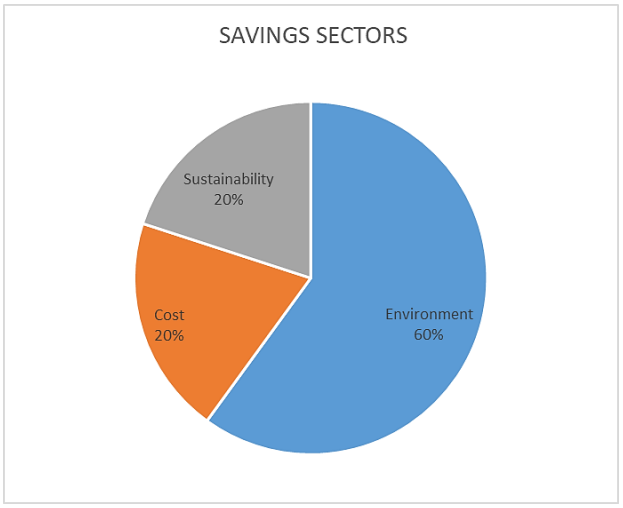


Fig. 3: Savings Per Sector

7 Proposal Usage Road Map

Case study implementation can be illustrated below in Figure 4. At the infrastructure project in the north of Qatar, 4 different departments are using the digital format of documents such as safety, quality, stakeholder, and lean departments. Firstly, each department will have to upload the document as a normal unofficial, transmittal, or submittal. Then, the file needs to be uploaded to specific software that can generate the QR code for each document. In this process, the generator may choose to have a lock or not to increase the safety and secure the information shared with others as some documents may be sensitive and cannot be shared with everyone. Finally, the document control centre starts by submitting the official document in the client portal for the consultant to be printed and reviewed. In this process either the consultant approves and uploads the document in the authority platform, or it is rejected and revised by the contractor for resubmission.

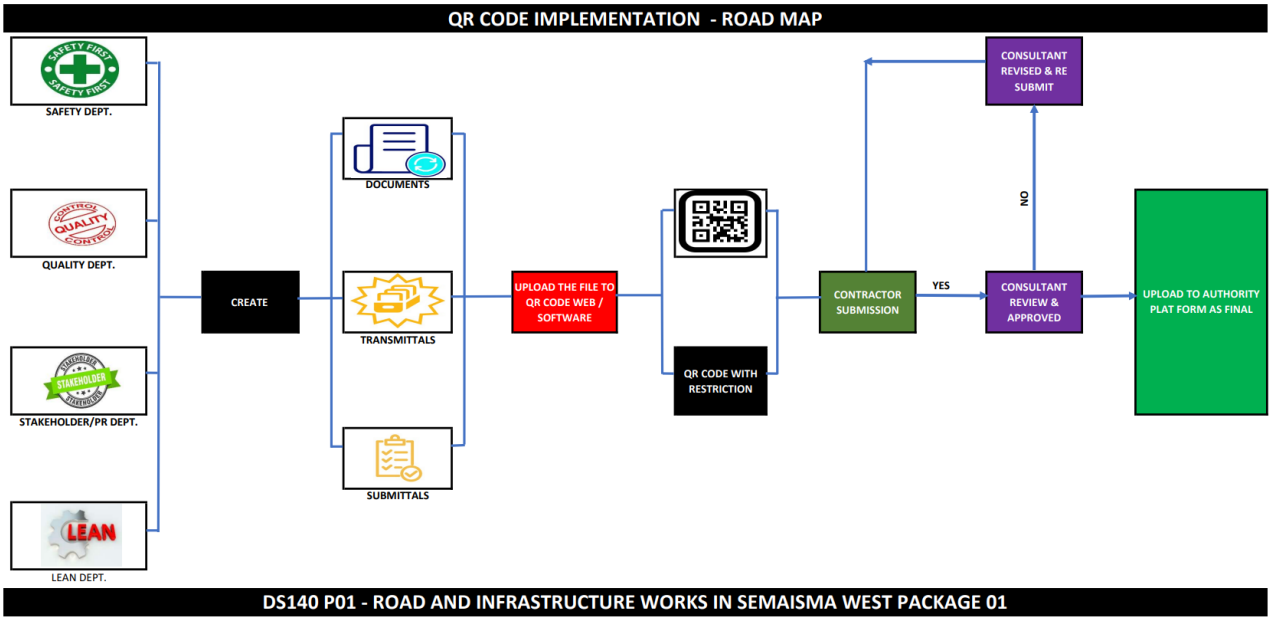


Fig. 4: QR-Code System Implementation Road Map

8 Conclusion

Enhancement engineers believe in the environment as the future of growth countries and in PWA's vision, "Qatar deserves the best." The case study has been submitted officially to ASHGHAL for their review and comments to specify the limitations of work in current projects and the future for upcoming projects if needed. Nevertheless, the contractor is using the digital study and started the implementation process internally among project staff to minimize the daily usage of paper. Finally, the proposal and implementation are under study in the phase of the data collection process in order to cover all aspects of the proposal in terms of the positive and negative points by the contractor, the supervision consultant, and the client. It is important to highlight that it is being used to enhance reducing overhead budget costs and saving efficient energy, feasible method and user-friendly, easy to use and convenient, more accessible by others, and confirming future needs. (Ballard & Howell, 2003).

References

ASTM International (2012). ASTM Standard Terminology for Additive Manufacturing Technologies, ASTM Committee F42 on Additive Manufacturing Technologies ASTM Committee F42 on Additive Manufacturing Technologies Subcommittee F4291 on Terminology.

Atkin, B. (2014). Industrialized building Construct. *Manag. Econ.*, pp. 1-6.

Fratzl, P. (2018). Wood made Denser and Stronger.

Ballard, G. & Howell, G. (2003). Lean Project Management Build. *Res. Inf.*, pp. 119-133.

Barlow, J. (2000). Innovation and Learning in Complex Offshore Construction Projects. *Res. Pol.*, pp. 973-989.

Barlow, J. et al. (2003). Choice and Delivery in Housebuilding: Lessons from Japan for UK House Builders. *Build. Res. Inf.*, pp. 134-145.

Bikas, H., Stavropoulos, P., & Chryssolouris, G. (2016). Additive Manufacturing Methods and Modelling Approaches: A Critical Review. *Int. J. Adv. Manuf. Technol.*, pp. 389-405.

Gurav, S. P. et al. (2003). Mechanical Properties of Paper-Pulp Packaging. *Composites Science and Technology*, *63*(9), 1325-1334.

M'hamdi, A. I. et al. (2017). Life cycle Assessment of Paper Production from Treated Wood. *Energy Procedia*, *128*, 461-468.

Cite as: Abdrabou L., "Digitalization and usage of QR-code System in Documents Management", *The 2nd International Conference on Civil Infrastructure and Construction (CIC 2023)*, Doha, Qatar, 5-8 February 2023, DOI: https://doi.org/10.29117/cic.2023.0019

Study on Business Value of Building Information Modelling – Applied in Developing Countries

Amr W. Sadek
King Abdul Aziz University, Civil and Environmental Engineering Department,
Jeddah, Saudi Arabia
asadek@kau.edu.sa

Abstract

This research investigates the business value of implementing building information modelling (BIM) in developing countries. The study of BIM in this research is conducted with a focus on its return on investment (ROI) in the construction sector. There is an imperative need for such new systematic studies to contribute to the growing knowledge of the practicing communities. After studying the extensive body of literature, it was determined that there were numerous surveys and/or workshops that addressed the same topic from various angles. This led to the research methodology used in the current paper. Such existing research analysed respondents' responses to arrive at some conclusions. Based on this, the author chose to analyse these prior studies and not necessarily create an independent questionnaire that would ultimately add more questions than it would solve. The study's key conclusion is that no quantitative formula for ROI can be used, and the only option to address this issue is to rely on qualitative research that claim adopting BIM has a high potential to provide both direct and indirect income. Due to disputed underlying assumptions, every attempt to estimate the ROI of BIM discovered in the literature cannot be generalised.

Keywords: Business Value; Building Information Modelling; Construction

1 Introduction

Over the past two decades, a growing number of construction projects have used building information modelling (BIM). Although there is not a single definition for BIM, it can be described as a process used to develop and handle digital information about a construction project throughout the project lifetime (NBS, 2019). Another description of BIM is a method that involves the development and administration of illustrations of the physical and functional attributes of places and is supported by a variety of tools, technologies, and contracts (Wikipedia, 2021).

It is reasonable to wonder why concerns regarding the adoption's return on investment (ROI) have not been raised to the same extent as with other tools, such as AutoCAD, which completely and quickly transitioned the building industry from conventional to computerized drawing, in 2D but with attributes. Among other things, vendor lists and material take-off have both utilised these properties. However, despite the fact that BIM was launched as a breakthrough technology that goes back to the 1990s, there are still concerns or scepticism about its total commercial worth, and out of the vast body of literature, not a single research paper or report has been able to address this problem.

If we take into account the fact that the majority of research focus on industrialised nations, the scenario and statistics in developing nations, where BIM adoption or awareness are still issues, look very different. Lack of support from the government and, more directly connected to this current study, risk regarding the business value of BIM adoption are among the elements that are frequently

deemed to be having a negative impact on the proliferation of BIM in developing nations.

The BIM by providing a description of individual features of the building is considered as one of the major outcomes (NBS, 2019). Building a BIM in the digital space allows for interaction with the structure to optimise actions, increasing the asset's whole life value.

There have been plenty of listed benefits of using BIM in construction throughout the project's end-to-end cycle (Qian 2012, Stowe et al., 2015). It represents the future solution that can be capable of comprehensively enhancing the productivity of different players in the construction industry in addition to enabling a more effective delivery process of buildings and structures (Qian, 2012). Whereas the value proposition and economical gains of BIM adoption are still under scrutiny (Jupp, 2013), especially by the classical stakeholders, there is perception of it as luxury, hype and not necessarily an enabling technology. The research by (Won & Lee, 2016) looked into this very question in an attempt to provide some criteria of when BIM is needed and suggested some indicators of the added value of implementing BIM.

A gap in the open literature has been identified to stem from the aforementioned concluding remarks from different reports. The proposed research puts more emphasis on how to evaluate ROI of BIM adoption in construction projects by associating available methods (Kouch, Illikainen, & Perälä, 2018; Kulaksiz, 2019; Salih, 2012). The standard definition of ROI used in this research is that provided in (Wikipedia. 2021); it is defined to be the quantitative relation between the net income and the amount of invested resources. It is worth highlighting that the ROI can be used to evaluate the potential profitability of a certain investment, but at the same time it may not provide a means of quantitative measurement of such investment (Feibel, 2003). As mentioned in (Schachner, 1973), return on investment (ROI) allows both financial managers and financial analysts to have a quick look at the ability of an investment to generate profit now or in the future. It compares the expected benefit obtained via the investment with the cost of the investment (Autodesk, 2007).

This research focuses on BIM adoption in developing countries in order to shed some light on the consequence of a country's economic status on implementing BIM. Despite the available data's scarcity, some prior research can still be relevant (Sahil, 2016; Durdyev et al., 2021); Masood, Kharal, & Nasir, 2014).

2 Research Objectives

This research aims at studying the ROI aspect of the business value associated with adopting BIM in the developing countries. The prior research summarized in the introduction section highlights the imperative need to investigate and comprehend the factors of ROI of BIM adoption, which represents the most significant advancement in the digital transformation of the construction industry since the breakthrough done by AutoCAD, which took place in the form of comprehensive and swift switch from manual conventional drawing to digital 2D drawing with attributes to enable material identification and vendor lists. Three decades ago, BIM was introduced as an innovative technology, however, there's no systematic study in the vast literature that addresses the concerns or doubts regarding its overall business value. This is further compounded by the fact that most studies focus on case studies in the big economies only, while the indicators are significantly different in developing countries that are facing challenges with the paradigm shift to digital systems in construction, not to mention the adoption of digital transformation enablers (e.g. BIM in the construction industry). The research addresses the main findings of the literature. It also investigates the possible adoption of unified measurement tools in different countries as well as companies or

organizations that implement BIM.

3 Methodology

The research methodology for the current study was established after examining the extensive body of literature (Sadek, 2022) and discovering that there are many questionnaires and/or workshops that address the same subject in various ways. Such existing research investigated respondents' responses to arrive at some conclusions that were then shown either visually or statistically. Based on this, the author chose to analyse these prior studies rather than create a separate questionnaire that would ultimately add more questions than it would solve.

4 Literature Review

This section reviews the prior literature relevant to this current research. The author believes that although important, other methods of literature reviews, such as bibliometric, scientometric, or latent semantic analysis, which are frequently utilised in cases of large volumes of literature, are ineffective for the current study's objectives. Therefore, in the following, an analysis of the critical literature content is conducted.

4.1 The BIM Definition

The current definitions of BIM in the open literature stem from the understanding of the author that are influenced by their range and scope of experience. There is a general misconception across the construction industry community that BIM is nothing but a software package or an add-on tool. However, the definition of BIM is portrayed as using 3D data in handling building data during its end-to-end lifecycle, with the right BIM tools to enhance building design and construction productivity. The BIM comprises different aspects and outputs that are produced from the process. This includes, but is not limited to, geographic information, spatial relationships, building geometry, quantities, and properties of building systems and components.

Aside from that, BIM also facilitates information transfer through digital presentations and provides a solid foundation for decision-making throughout the course of a project (Abanda & Joseph, 2014). Every researcher defines BIM from his or her own point of view; there isn't a single definition of BIM as can be found in the body of existing literature. Due to the definer's experience or purpose, the definition of BIM has been developed from different perspectives (Amin & Abanda, 2019; Mena et al., 2009).

5 BIM Measurement Tools

In this section, the research question on unified measurement tools to be applied is addressed based on (Succar, 2010). The research in (Succar, 2010) classified organizations with respect to their strategy of BIM implementation. The Yellow Organisation adopted an approach to invest heavily to adopt software packages that are object based in their nature. The management gave its marketing team the go-ahead to insert BIM labels onto the website of the Yellow corporate and begin acquainting potential customers with their new potential capabilities as well as the commercial potential of the new technologies and tools. The Blue Organization put a lot of time and effort into researching, creating, and then progressively putting into place a comprehensive BIM strategy, customised training programmes, modelling standards, and workflow processes. In order to communicate with, educate, and teach workers about BIM technologies and processes, both internal and external assistance was sought. After taking the helm in this implementation effort from the beginning, the management team was able to inspire and involve every employee in the creation of

BIM products and procedures. They did ongoing internal evaluations to make sure that BIM productivity was steady enough and that they could consistently and predictably generate high-quality models and drawings.

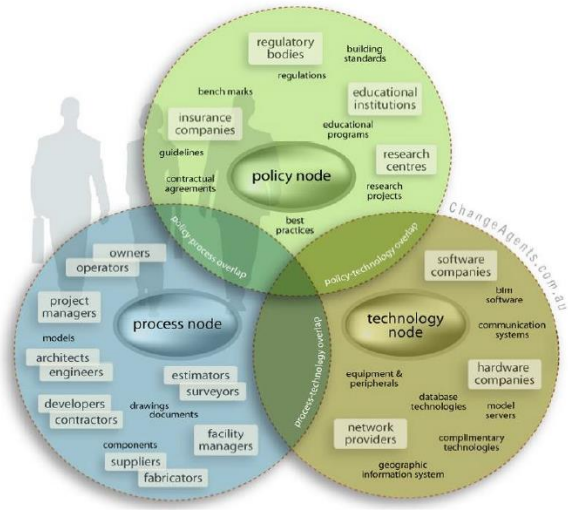


Fig. 1: The Interacting Elements of BIM Activity (Succar, 2010)

They enabled the marketing team to insert BIM visuals onto the website of the Blue Corporate website and begin alerting potential customers about their new capabilities since they were certain that BIM is the most effective approach to deliver services. Thus, the idea of capability differs greatly from that of maturity. A 'maturity model' puts together the main performance improvement levels, which need to be achieved by a certain entity (organization or a project team). The maturity models reported by COBIT, ISACA and CMMI, are some examples of several maturity models reported in the literature that respond to the first quest.

Previous research studied the BIM benefits. As this study relates to the return on investment of BIM, the research related to BIM implementation cost analysis is the focus of this article. The authors of (Azhar, 2008) conducted a study on the Atlanta Hilton Aquarium project and detailed the time and cost savings of BIM implementation. An estimated cost saving has been assigned for each resolved cost conflict.

Research in Holness (2006) has stated that the potential savings resulting from the use of BIM in the sector of construction are expected to range from 15% to 40% of total construction costs. In addition, the author states that for industrial projects that are deemed large scale projects with budgets of $75 to $150 million, the cost of BIM implementation ranges between 0.25% and 0.5% with respect to the total construction costs. The percentage of BIM costs to the total cost of construction is anticipated to change as the type and size of the project changes.

The available studies reported in the literature have concentrated on either the budgetary benefits or the speculation investigation of BIM in a single development company and its particular applications and project deliverables, which may not be scalable to other applications in the construction industry. This is expected since these investigations are limited to the company in question within its particular conditions and circumstances.

6 Adopting Bim: The Business Value

It was decided to review the extensive existing literature and finalize its findings, rather than conduct a new study that would repeat the same approach and compound the general problem of conflicting

conclusions and comments. Basically, the existing research evaluating the business value of BIM adoption in the construction industry can be divided into two groups. The first group of the existing literature, attempted to assess the ROI of implementing BIM by conducting a relevant questionnaire with carefully worded questions targeting a set of homogenous companies or organizations practicing AEC. After receiving the questionnaire completed by the respondents, an analysis including statistical evaluation is carried out and the results are listed. A sample article is (Enshassi, A., & AlKilani, 2018). Although there is wide variation in outcomes related to the foreseen ROI of implementation of BIM in the construction sector, it is more realistic to adopt such outcomes.

The second group, with a much smaller count of contributors than the first, followed an analytical methodology and developed an analytical model of his ROI, including the direct and/or indirect benefits and costs of adopting BIM. A number of assumptions have to be made to quantify his ROI of BIM implementation. The aforementioned assumptions may not be unanimously accepted. The sample release is (Giel & Issa, 2013).

7 Developing Countries

Developing countries that still struggle with BIM adoption presents another complication. The lack of data leads to undesirable interdependence on conditions and conclusions drawn from cases of implementation in the developed countries. Data were collected through the conducted focus group interviews. The analysed data were interpreted into a theoretical context representing the synthesis of various BIM activities using a grounded theory approach. The resulting work plan was then compared to the traditional phases of the Egyptian project life cycle to identify the strengths and weaknesses of each method.

7.1 BIM Awareness and Implementation in Africa

A fast growth of the Architecture, Engineering and Construction (AEC) industry in Africa is foreseen in the next few years. This will position the African continent as a major player worldwide in such industry. To highlight the size of major AEC projects conducted in the regions of Eastern, Southern, Central, Western and Northern Africa, the Deloitte report (Deloitte, 2022) listed the values of such key projects with a total of around $187bn, $125bn, $26bn, $82bn and $148bn, respectively. Such a challenge is compounded by the slow rate of digital solutions adoption in the AEC industry.

The adoption rate of BIM in Africa is lower compared to the developed countries. According to the research in (Abubakar et al., 2014) the level of BIM awareness in the above-mentioned five African regions ranged between 30% (Zambia) and 100% (Cameroon). The level of BIM awareness in Egypt (as indicated by the contributions to literature) exceeds 90% which is relatively high. Nigeria has contributed a high number of publications and awareness. However, the subjective sampling approach adopted in these surveys makes such results less indicative of the real situation. Nevertheless, they effectively depict their relative level of awareness. In the case of some leading countries (Egypt, South Africa and Nigeria), the high number of BIM publications indicates an advanced level of awareness but does not necessarily indicate an associated high level of implementation in AEC projects.

The BIM research is still at an early stage in the African continent. In general, the studies across Africa have shown that the implementation of BIM in Africa is facing the challenges of the barriers related to people/process interactions (e.g. lack of awareness, training, demand, and government support) followed by those related to economic and technological factors.

Therefore, increasing the awareness is mandatory as well as changing the mindset of the stakeholders in the AEC industry to start appreciating the benefits of BIM. The governments in Africa seem to have no clear mandates or policies towards such a paradigm shift, which necessitates adopting a bottom-up approach.

The cost of software and personnel training has been repeatedly reported especially by small and medium enterprises (SMEs) in different parts of Africa as a major challenge that hinders the spread of use of BIM in the AEC industry. This is merely attributed to the limited resources available for such SMEs to invest in such a risky transition to BIM. Finally, challenges related to lack of BIM standards, and inadequate infrastructure have adversely affected the development of BIM implementation in the AEC sector in Africa. Developing detailed action plans in the African context are necessary to target the resolution of the aforementioned challenges in order to support diffusing the BIM technology.

7.2 BIM Adoption in the Egyptian context

The feedback from practitioners in sales, design and construction in Egypt have been used to explore the benefits and challenges of BIM integration. In this case, BIM was developed based on Egyptian architectural practices. Focus group discussions revealed topics necessary for a successful implementation of BIM that included training on design coordination, as well as redefining the current detail levels, in addition to the necessity of governmental BIM mandating policies. A limitation, however, was the difficulty in reaching out to staff with extensive facility management experience.

Despite BIM's wide adoption in the industrial and developed countries since the onset of this century (Jung & Lee, 2016), the regions of Africa and the Middle East have been lagging and still struggling to actively catch up with other regions in such aspects. Although the number of BIM adopted projects has been going on (Gerges 2017, Jung & Lee 2016), more systematic and systemic efforts are still needed in order to perform such paradigm shift in the region. The creation of obligatory regulations with the aid of using governments' groups to sell the endorsement of BIM is an essential aspect that have motivated the adoption of BIM in international locations just like the UK (Abanda & Tah, 2014 and Cheng, 2015). However, Egypt's construction sector does not have enough expertise on the implementation of BIM, urging for the need to offer additional information and data to the industry (Elyamany, 2016). This is compounded by the circumstance in Egypt where the government is not promoting the use of BIM in addition to the lack of BIM published documents and standards (Elyamany, 2016). Elyamany (2016) and Gerges (2017) reported results of a survey on the BIM status in the Middle East. The survey showed that only 20% of AEC companies are either currently or have been using BIM or in the course of the BIM implementation process. On the other hand, the same survey depicted indicators of increased BIM awareness among the individuals of the workforce and end-users. This was evident from the high percentage (60%) of respondents who indicated that they possess between three and nine years of experience through which they have conducted a minimum number of projects adopting BIM. It is important to highlight that the findings from BIM research in the GCC countries and Egypt can be interchangeably applied. This is attributed to the resemblance of such regions' construction practices (Salama et al., 2006).

8 Conclusions

A quantitative formula for ROI of BIM implementation cannot be applied, and the only way to address that aspect is relying on qualitative studies. Such studies indicate a well-established potential

for BIM adoption to generate different forms of revenue. All the attempts reported so far throughout the open literature to quantify BIM ROI could not be generalized due to the controversial assumptions involved. A full list of literature is available in (Sadek, 2022) and reader is referred to such reference for extended bibliography to support all statements made herein. This reference is salient as it is a doctoral dissertation by the author. It contains around 400 references, only a fraction is cited in the present paper for simplicity and clarity.

References

Abanda, F. H. & Joseph H. M. Tah (2014). Free and open source Building Information Modelling for developing countries, ICT for Africa 2014, 1-4 October.

Abubakar, M.et al. (2014). Contractors' Perception of the Factors Affecting Building Information Modelling (BIM) Adoption in the Nigerian Construction Industry Computing in Civil and Building Engineering.

Amin, K. F. & Fonbeyin H. A. (2019). Building Information Modelling Plan of Work for Managing Construction Projects in Egypt, J. Construction in Developing Countries, 24: 23-61.

Aranda et al. (2009). 'Building Information Modelling Demystified: Does it Make Business Sense to Adopt BIM? *Int. J. Of Managing Projects in Business*, 2: 419-34.

Azhar, S., Hein, M. & Sketo, B. (2008). Building Information Modelling: Benefits, Risks and Challenges.

Cheng, J. C. P. & Lu, Q. (2015). A Review of the Efforts and Roles of the Public Sector for BIM Adoption Worldwide. *Journal of Information Technology in Construction*, 20: 442-78.

Deloitte Report, 2022, http://www2.deloitte.com.

DMG - Dar Al-Mimar Group, 2011, President's Report.

Durdyev et al. (2021). BIM Adoption in the Cambodian Construction Industry: Key Drivers and Barriers. *ISPRS Int. J. of Geo-Information*, 10: 215.

Elyamany, A. H. (2016). Current Practices of Building Information Modelling in Egypt, *Int. J. of Eng. Mgt. and Economics*, 6: 59.

Enshassi, Adnan, Abu Hamra A., & Suhair AlKilani. Studying the Benefits of BIM in Architecture, Engineering and Construction Industry in the Gaza Strip, *Jordan J. of Civil Eng*., 2018.

Feibel. 2003. Oxford University Press.

Gerges, M. et al. (2017). An Investigation into the Implementation of Building Information Modelling in the Middle East, *J. of Information Technology in Construction*, 22: 1-15.

Giel, Brittany K., & Raja R. A. Issa. (2013). Return on Investment Analysis of Using Building Information Modelling in Construction. *J. of Computing in Civil Engineering*, 27: 511-21.

Holness, G.V.R. (2006). BIM: Future Direction of the Design and Construction Industry. *J. of IT in Construction*, 48: 38-44.

Jung, W. & Ghang L. (2016). Slim BIM Charts for Rapidly Visualizing and Quantifying Levels of BIM Adoption and Implementation. *J. of Computing in Civil Eng.*, 30.

Jupp, J. (2013). Building Information Modelling Investment-Understanding Value, Return and Models of Assessment. Proceedings. In 38th AUBEA Int. Conference 1-10.

Kouch, A. M., Kimmo Illikainen, & Seppo Perälä. (2018). Key Factors of an Initial BIM Implementation Framework for Small and Medium-sized Enterprises (SMEs). In Proceedings of the International Symposium on Automation and Robotics in Construction (IAARC). Int. Association for Automation and Robotics in Construction (IAARC).

Masood, R., M. K. N. Kharal, & A. R. Nasir. (2014). Is BIM Adoption Advantageous for Construction Industry of Pakistan? *Procedia Engineering*, 77: 229-38.

The National-Bureau-of-Standards (NBS). 2019.

Qian, A.Y. (2012). Benefits and ROI of BIM for Multi-Disciplinary Project Management.

Sadek, A.W. (2022). ROI of BIM Adoption in Construction Industry in Developing Countries, DBA thesis, European International University.

Sahil, A. (2016). Adoption of BIM in Developing Countries: Degree Of Master Thesis, Colorado State University.

Salama, M. (2006). Investigating the Criteria for Contractors' Selection and Bid Evaluation in Egypt, Proceedings, and Engineering Business.

Salih, S. 2012. The Impact of BIM/VDC on ROI: Developing a Financial Model for Savings and ROI Calculation of Construction Projects.

Schachner, L. (1973). Return on investment-its Values, Determination and Uses. *The CPA Journal*, 43.

Stowe, K. et al. (2015). Capturing the Return on Investment of All-In Building Information Modelling: Structured Approach', Practice Periodical on Structural Design and Construction, 20.

Succar, Bilal. (2010). Building Information Modelling Maturity Matrix. In Handbook of Res. on Building Information Modelling & Construction Informatics, 65-103. IGI Global.

Kulaksiz T. (2019). Analysis of Factors Influencing ROI for BIM Implementation.

Wikipedia. 2021. BIM in Wikipedia.

Won, Jongsung, & Ghang Lee. (2016). How to Tell if a BIM Project is Successful: A Goal-Driven Approach. Automation in Construction, 69: 34-43.

Cite as: Sadek A., "Study on Business Value of Building Information Modelling – Applied in Developing Countries", *The 2nd International Conference on Civil Infrastructure and Construction (CIC 2023)*, Doha, Qatar, 5-8 February 2023, DOI: https://doi.org/10.29117/cic.2023.0020

Implementing the Last Planner System in a Design Project

Dawlat Elmosalmi
Engineering Consultants Group, Doha, Qatar
dawlatmossalamy@hotmail.com

Abstract

Through the past few years, the last planner system (LPS) as one of the main important methods of lean implementation in the (AECO) industry proved to improve efficiency, performance, reliability, planning and coordination. LPS can be implemented in design projects as well as in construction projects. This research reports the implementation process of the LPS as a basis for continuous improvement in the design stage. The first part is about Lean Concept definition, values and wastes; challenges faced, and Lean implementation. Second part is focusing on the last planner system, its definition and method of implementation. Third part is a case study of how LPS is implemented in managing a design project in a design consultancy firm, how to lead the lean enterprise, and how to deal with change resistance within the team.

Keywords: Lean; Last Planner System; Lean Design; Consultants; Collaborative Planning; Project Management

1 Introduction

The Architecture, Engineering, Construction and Operation (AECO) industry is always impacted by variations, which affect efficiency, profitability and quality. Lean practice is implemented in design and construction projects to eliminate wastes, add value and improve work processes. Last Planner System as a planning tool is one of the highly recommended collaborative planning processes. This paper aims to define clearly the concept of Last Planner System and how it can be implemented in a design project to achieve best results.

2 Lean Thinking

Lean is keeping everything in its most valuable form addressing efficiency, adding value and eliminating wastes while considering continuous improvement (Womack & Jones, 2005).
Lean Definition

Lean is adding value to the process and the elimination of waste from the production cycle leading to better quality, higher efficiency, lower costs, shorter time schedule and higher profits. Lean is about delivering the right things (including information) to the right place in the right amount, at the right time and under the right conditions. Value is what the customer needs at the end of the process. While waste can be defined as any step or action which takes place in the process but does not add value. (Badurdeen, 2007; Arleroth & Kristensson, 2011; Elmosalmi, 2014).

2.1 Lean Thinking Principles

The Lean thinking main principle is about respect for people since the human factor is the most important factor in any process, work or organization. People can make anything succeed or fail. When people feel respected, appreciated, trusted and supported, their performance changes and they

become more efficient. The Lean tenets after Respect for People are: (1) Identify Customer Value, which is understanding the client needs and what he/she is willing to pay for. (2) Generation of Value; adding value to the process considering the end user or client's main value, (3) Removal of Waste; which is removing any unnecessary activity from the process; (4) Optimize the Whole; which means that Lean is about the big picture not just the small parts or small activities. Success can be achieved when all project elements are working for the sake of success of the one big whole. (5) Focus on Process & Flow of Materials, Information, etc. to achieve smooth workflow without any constraints or obstacles. (6) Continuous Improvement (Kaizen) which is focusing on engaging employees/stakeholders in improving work processes in parallel with their ongoing tasks through a Plan-Do-Check-Act (PDCA) cycle. It also seeks to standardize processes and eliminate waste (Forbes & Ahmed, 2011; Elmosalmi 2014).

2.2 Wastes Classification

Wastes are classified into eight categories; (1) Overproduction waste is producing or delivering more than what is needed resulting in excess stocks and inventory. (2) Waiting time waste is people waiting for work or work waiting for people or equipment waiting for a production process to be completed or resources to arrive. (3) Transport waste is moving equipment or materials unnecessarily without any added value. (4) Motion waste is the movement of people unnecessarily due to poor layout of working area (ergonomic issues). (5) Stocks waste is the material or information stored at office, site or yard, excess work in progress (processing work), unused tools and data (often held as an acceptable buffer but should not be excessive). (6) Defects (errors) waste is the rework or output that does not reach the required quality standard. (7) Over processing waste is the added steps which are not adding value to the process like unnecessary reporting, non-value-added activities, unnecessary reviews. (8) Unused employee creativity waste is the poor utilizing of resources and not working on developing human skills in the fields. One of the most popular methods to eliminate waste is the 6S which are sort, set in order, shine, standardize and sustain. Sort is by separating the items into two groups: using and not using. Set in order is categorizing the items in the group of "using". Shine is keeping the area clean and everything in its location. Standardize is to apply the standards to the work area. Sustain is maintaining the gain (Bottirov, 2011).

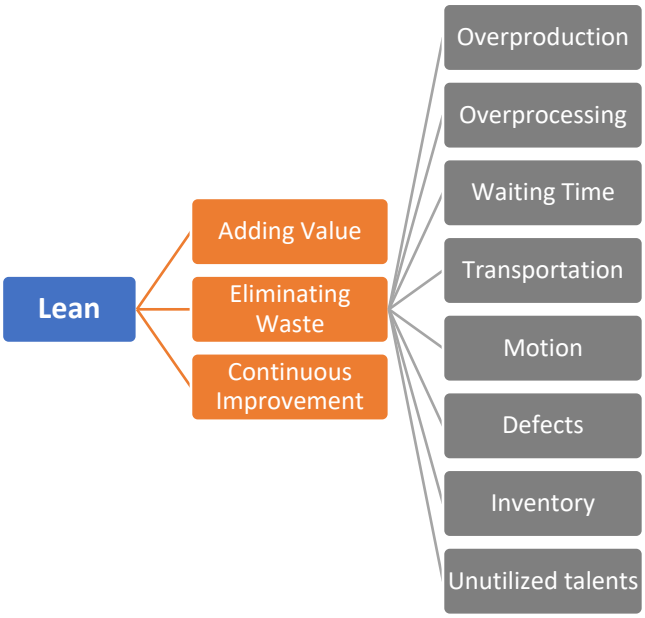


Fig. 1: Lean and Wastes Classification

3 Last Planner System (LPS)

LPS is the collaborative, commitment-based planning system and production control system that follows lean principles based upon reliable not just predictable plans. It is a collaborative planning process that involves everyone including Last Planners in a pull planning process. LPS follows Just-in-Time (JIT) delivery, Value Stream Mapping (VSM) and Pull Planning.

The Last Planner system involves (1) Lean Workstructuring; which includes the planning schedules and (2) Production Control; which includes the variance analysis and the percent of plan completed (PPC).

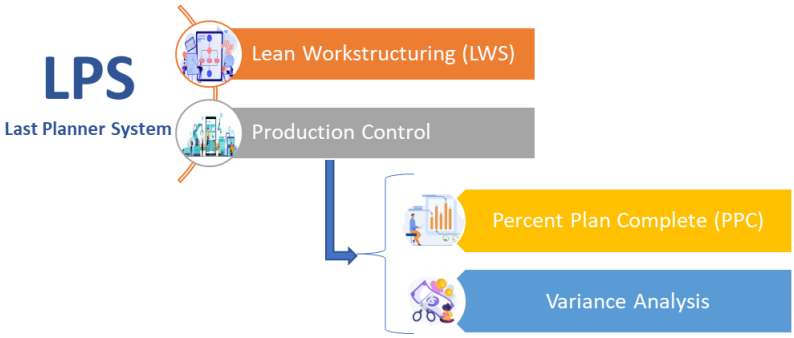


Fig. 2: Last Planner System

3.1 Principles of LPS

LPS is based on the following principles; (1) Plan in greater detail as you get closer to doing the work, (2) Produce plans collaboratively with those who will do the work, (3) Reveal and remove constraints on planned tasks as a team, (4) Make and secure reliable promises, (5) Measure promises kept (planning capabilities, PPC) in order to improve by learning from variance (work flow disruptions), (6) Continuously improve as a team, (7) Remove waste and adjust performance based on what has been learned as a means to optimize work flows. Operations based on Lean thinking and practice also continually strive to achieve flow, in which material and information move through the value stream without stopping. When flow is not possible between process steps, each step in a value stream should "pull" precisely what it currently needs from the previous step in the value stream and that's how waste is eliminated completely.

3.2 LPS Schedules

The schedules of LPS start at a very high level of information as in the Master Schedule which contains the main milestones. The second LPS level is the Phase schedule at which more details are being put into the master schedule and phases start to appear more clearly. Master and Phase schedules are about the work that should be done and not yet analyzed.

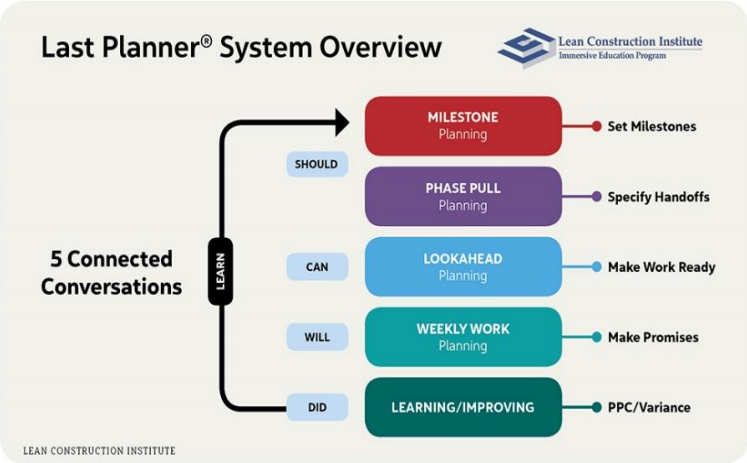


Fig. 3: Levels of Last Planner System

The third level of LPS is the Make Ready Planning/Look Ahead Planning; also, named 6 weeks look ahead plan. In this level, work is being planned on a six to eight weeks timeline with gives and gets for each trade to find out what every trade exactly needs to give or submit their part of the work. It is always observed that the first two weeks include more details and tasks than that of later weeks since everyone is planning in greater detail as they get closer to doing the work. The make ready plan is about the work which can be done by the team as per the collaborative planning session at which they are involved. The fourth level is the weekly work plan which is about what exactly will be done during this week with day to day tasks. This is where promises change into actions.

The fifth level is the Learning/Improving or also called daily huddles which is the day to day follow up through a daily 10-15 minutes meeting to hear from the team what has been finished, what will be done today and what are their notes for improvement.

LPS is based on visual management where all communication and data sharing is through visual management using data lists, bar charts, network schedules, graphic schedules, linear schedules, and sticky notes to define the gives and gets.

4 Case Study

4.1 About the Project

The project is a large-scale mixed-use development located at Doha. The project features 4 (Four) Administration Buildings associated with other additional facilities designed to provide support for both administrative and recreational activities.

4.2 Project Challenges

- Fast Track/Crashed Time Schedule.
- Working remotely during the COVID-19 Pandemic.
- Lack of information of existing utilities.
- Modifications to end-user requirements and additional requirements in space program.
- Resources utilization.
- Lack of Lean knowledge on the part of some team members.
- Teams culture (change resistant).

4.3 LPS Implementation Plan

ECG implementation plan for LPS internally in design phase was based on: (1) Kick off meeting. (2) The project management team create the master time schedule from the project proposal agreed with the client (main milestones of client submissions, meetings, workshops, etc). (3) The project management team create the phase schedule based on the phases or project stages agreed with client. (4) The project management team send a schedule template for all disciplines to fill their requirements from other trades and dates. (5) The disciplines send their requirements with dates to PM team. (6) PM team prepare the Look Ahead Plan (6-8 weeks Plan) from: The master schedule and phase schedule agreed with the client, PM estimated internal dates for DC Submission, Internal, coordination meetings, data exchange with BOQ and specifications teams, BOQ and specifications submission dates, etc., all disciplines requirements as received with planned dates. (7) On Sunday, PM team send the weekly work plan for Week 1 (Week 1 Plan) to all disciplines to be implemented. (8) Daily follow up should be implemented (daily huddles) by the PM team to ensure that the weekly work plan is running smoothly so that any new issues can be solved as quickly as possible and do not affect the work flow. (9) On Thursday of the same week, the PM team update the status of the weekly work plan and make the below changes: The finished tasks or work activities to be marked in green, the unfinished/delayed tasks to be marked in red, any issues which need response or feedback from the client to be marked with purple, The red tasks to be moved and added to Week 2 plan in red to remain a priority. (10) PM team to send week 2 plan to all disciplines highlighting that the red tasks are the ones delayed from week 1 and should take the highest priority. (11) Daily Follow up (Daily Huddles). (12) As part of continuous improvement, the first created detailed Look Ahead Plan to be standardized for the future same type of projects. (13) Measuring percentage of work completed (PPC) regularly. (14) Variance Analysis Charts checks are carried out every week to ensure compliance with main master schedule and control project budget. (15) A mitigation plan to mitigate the variance is carried out as a part of continuous improvement. (16) LPS implementation process is documented to ensure continuous improvement and lessons learnt to be shared with all other projects teams. (17) Wastes analysis reports were carried out to reduce over processing waste.

4.4 LPS Impact on the Project

It was found out that implementing Lean and LPS in the design phase is inherently important for better coordination, collaboration, quality and higher profits. The project was finished with less design cost than the planned budget (77% of the planned budget) achieving extra profit 33% of the project budget in spite of all the challenges that the team faced from the beginning of the project.

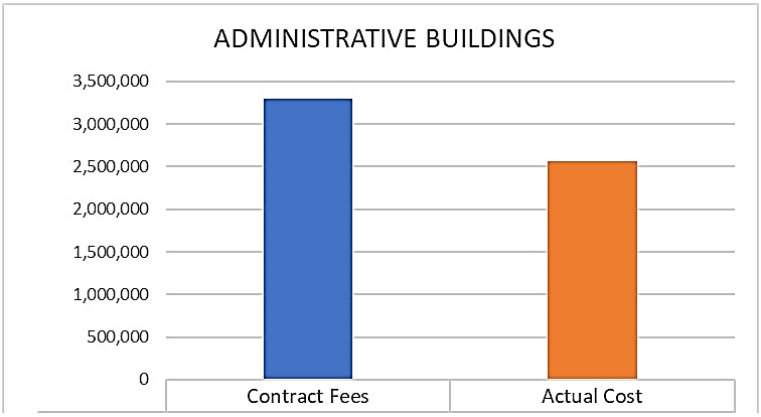


Fig. 5: Project budget vs. Actual Cost

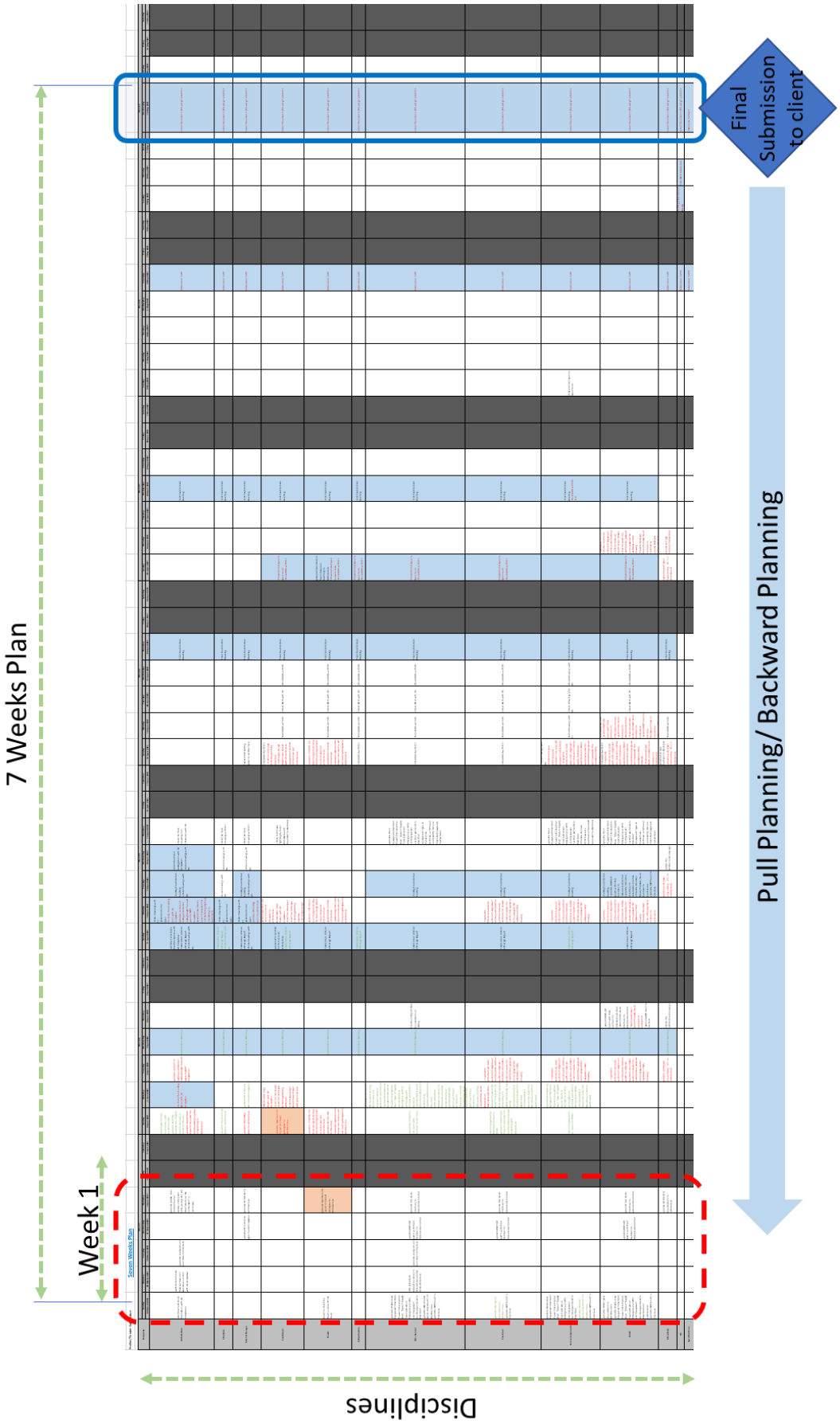


Fig. 6: From Make Ready Planning to Weekly Planning on a Spreadsheet

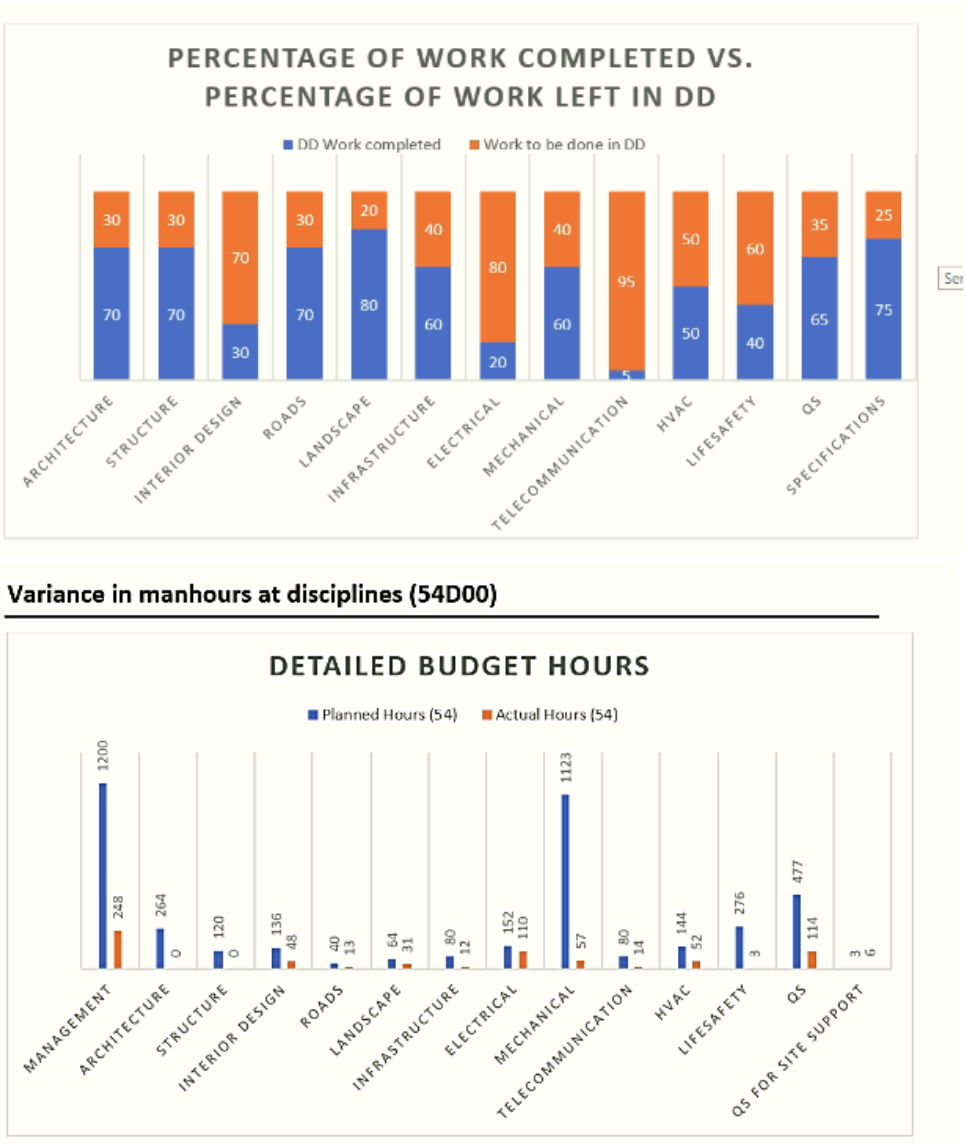


Fig. 7: PPC and Variance Analysis in the Case Study Project

5 Conclusion

Benefits of applying LPS on the project (1) Enhanced workflow reliability and predictability by improving coordination. (2) More detailed and reliable time schedule. (3) Get all team members committed and feel responsible from the first beginning of the project. (4) Get the planning and management team as close as possible to the production team. (5) Better commitment to time schedule. (6) Transparency. (7) More smooth workflow. (8) Less wastes. (9) Identifying and resolving issues and constraints as early as they appear and accordingly avoiding much rework. (10) Focusing on root causes of variance. (11) Standardizing the plans for future projects with the same type and circumstances. (12) Achieving the three project goals of higher quality, less cost and less time; leading to: (13) Client Satisfaction.

References

AGC Lean Construction Education Program.

Arleroth, J. & Kristensson, H. A. (2011). Waste in Lean Construction (M.Sc., Thesis, Department of Technology Management and Economics). Chalmers University of Technology, Gothenburg, Sweden.

Ballard, G. (2002). Managing Work Flow on Design Projects: A Case Study. Engineering, Construction, and Architectural Management.

Bottirov, O. (2011). Lean Construction in Construction Company (Phd, Viauc University, Department of Construction Management). Denmark.

Elmosalmi, D. (2014). Building Information Modeling (BIM) Technology Implementation in Lean Architecture through Managing Human Resource (M.Sc., Thesis, Department of Architecture). Ain Shams University, Egypt.

Forbes, Lincoln H. & Ahmed, Syed M. (2011). Modern Construction: Lean Project Delivery and Integrated Practices. CRC press, Taylor and Francis Group, LLC.

Womack, James P. & Daniel T. Jones (1996). Lean Thinking: Banish Waste and Create Wealth in Your Corporation. New York: Simon and Schuter.

——. (2005). Lean Solutions: How Companies and Customers Can Create Value and Wealth Together. Simon and Schuster, New York, NY.

Cite as: Elmosalmi D., "Implementing the Last Planner System in a Design Project", *The 2nd International Conference on Civil Infrastructure and Construction (CIC 2023)*, Doha, Qatar, 5-8 February 2023, DOI: https://doi.org/10.29117/cic.2023.0021

Investigation and Comparative Study between Research Methods used in the Five Categories of BIM-Based Built Environment Sustainability Studies

Hanane Bouhmoud
FSTM – Hassan II University of Casablanca, Mohammedia, Morocco;
ICEA – University of Padua (Università degli Studi di Padova, UNIPD), Padua, Italy
hb.bim.phd@gmail.com

Dalila Loudyi
FSTM – Hassan II University of Casablanca, Mohammedia, Morocco
dalila.loudyi@fstm.ac.ma

Andrea Giordano
ICEA – University of Padua (Università degli Studi di Padova, UNIPD), Padua, Italy
andrea.giordano@unipd.it

Salman Azhar
McWhole Building Science School – Auburn University, Auburn AL, USA
sza0001@auburn.edu

Mounia Farah
Hassania School of Public Works, Casablanca, Morocco
farah.mounia@gmail.com

Abstract

Using Building Information Modelling (BIM) helped enhance the environmental performances of building and civil infrastructure projects throughout their life cycle. However, the construction industry continues to be one of the most impactful industries on the environment, hence the imminent need for further research in this area. The choice of the right Research Method and Design (RMD) was always important to ensure relevant results for the Five Categories (Cs) of BIM-based Built Environment Sustainability (BIMBES) studies: BIM-based studies discussing either sustainability in general 'C1'; carbon emissions 'C2'; construction and demolition wastes 'C3'; water supply or use 'C4'; or energy 'C5', but the availability of a wide array of research methods and the absence of a clear mapping of the best methods to be used for each category remain significant challenges. The purpose of this study is to thoughtfully investigate the RMDs used for BIMBES studies. Thus, based on scoping review of 458 relevant papers, the study showed that BIMBES topics are contemporary and C1 and C5 are the most discussed. Similarly, the paper disclosed the evolution of BIMBES studies including categories' overlap, identified and mapped the RMDs used for BIMBES studies and highlighted 9 mixed research designs, 1 paradigm, 12 research instruments, and 4 data analysis approaches. This research paper could be the starting point for any study related to the BIMBES as it allows scholars to have a clear and well understanding of the used and useful RMDs to be adopted according to the topic they are exploring.

Keywords: BIM; Sustainability; Mixed method; Qualitative method; Quantitative method

1 Introduction

The Construction Industry (CI) is one of the most impactful industries on the environment (Bouhmoud *et al.*, 2022a). Scholars and practitioners joined forces to help reduce this impact towards green buildings by developing structured guidelines and/or standards such as LEED, BEAM+, and BREEAM (Awadh, 2017); providing innovative conceptual methods such as Lean Construction (Mellado & Lou, 2020) and Life Cycle Assessment (LCA) (Jalaei *et al.*, 2019); and implementing green construction alternatives such as recycling

(Guerra *et al.*, 2020), prefabrication (Liu *et al.*, 2019), and renewal resources (Chudikova *et al.*, 2019). Krygiel & Nies (2008) underlined that adopting green buildings could averagely save 30% of energy consumption, 35% of Carbon Emissions (CEs), 30–50% of potable water use, and 50–97% of Construction and Demolition Wastes (CDW).

1.1 Environmental Impact of the CI and Related BIM benefits

The CI environmental impact is a significant concern all over the world. Indeed, Bouhmoud et al. (Bouhmoud *et al.*, 2022a) emphasized that, globally, construction work and buildings are responsible for 39% of CEs, 40% of raw materials' consumption, 30% of energy-related CEs, and 20-50% of wastes deposited in landfills. This critical impact is basically due to operational, technological, and managerial issues related to currently used practices in the CI. Yet, these can significantly be lessened using the innovative technology of Building Information Modelling (BIM) including issues related to the fragmented nature of the CI (Haruna *et al.*, 2021), the poor coordination and communication, and the tasks synchronization between different construction disciplines (architecture, structure, topographical surveys…) within the same project (Bouhmoud & Loudyi, 2021).

BIM has a great potential to reduce construction impacts on the environment in the different phases of a building lifecycle as it enables the incorporation of multi-disciplinary data into one 3D model, then simulates and analyses different sustainability parameters during the same design process to find the most optimized eco-friendly scenario (Bouhmoud & Loudyi, 2021). Jen and Vernatha (Tu and Vernatha, 2016) conceptualized a BIM-based energy management support system to monitor and track the real-time energy performance of different zones in a building and optimize energy consumption. Similarly, adopting a BIM-based approach to lifecycle data management, helped the Shanghai Center, the tallest building in China, to achieve a material waste rate of 4% instead of 10% that is considered the common rate in China (Bouhmoud & Loudyi, 2021).

BIM provides the opportunity to considerably reduce time, cost and effort required to manage building information and life cycle assessment (LCA) data and remarkably accelerates the establishment of the LCA model (Bouhmoud & Loudyi, 2021). This technology helps to quantify, anticipate and optimize materials' production and transportation, onsite construction workflow, building operational consumption (equipment use, lighting, heating, ventilation and air conditioning), and demolition process and wastes; and considerably reduces the CEs at all buildings' stages (Bouhmoud *et al.*, 2022b).

1.2 Research Methods and Designs

Scholars (Creswell & Clark, 2017; Ellis & Levy, 2009; Rahi, 2017) distinguish between method types and development instruments. Method types are differentiated into quantitative, qualitative, and mixed according to the nature of the research questions. Mainly, quantitative methodologies are applied to research questions about causality, generalizability, or magnitude of effects whereas qualitative methodologies are used to investigate research questions aiming to develop a theory, explore why or how a phenomenon occurs, or describe the nature of individuals' experience (Fetters *et al.*, 2013). Mixed methods research studies combine the strengths of both quantitative and qualitative methods (Creswell & Clark, 2017) and provide an inventive approach to examine contemporary and/or complex research topics in the Architecture, Engineering and Construction (AEC) fields including the use of BIM for Buildings and Infrastructure (B&I) Environmental Sustainability (ES).

In the meantime, method development instruments, called also approaches (Ellis & Levy, 2009) or strategies (Rahi, 2017), refer to the adopted process to collect and interpret data with clear objectives. The choice of the method instrument depends on the stage of studying the addressed problem: exploration, description, evaluation, development, validation or applied exploitation (Ellis & Levy, 2009). The method instrument could be quantitative, qualitative or mixed. Interviews and focus groups are mostly qualitative whereas case studies and pre-test/post-test are commonly quantitative. However, some instruments could be either quantitative or qualitative according to the data analysis approach such as Literature Review (LR) which could be quantitative

such as scientometric LR or qualitative such as narrative or systematic ones.

Both quantitative and qualitative research methods follow three key steps: data collection, data analysis, and results. Though, mixed methods consist of the following three steps: (1) collect and analyse both qualitative and quantitative data separately, (2) integrate the findings either concurrently or sequentially by comparing, correlating, contrasting, validating, and/or interrelating both data types, and then (3) get the results by interpreting the findings to address the research question (Creswell & Clark, 2017).

1.3 Research Objectives

Considering both BIM considerable ecological potential and the current environmental harm caused by the CI, it is necessary to endorse research and development to permit more BIM-based studies enabling efficient solutions toward greener B&Is with less environmental impact in their different life cycle stages. In this vein, this study aims to provide both scholars and practitioners with the key tools and data needed to develop further studies helping to create innovative approaches, strategies, or technological tools serving this purpose. Hence, based on an exploratory mixed method design (Section 2), the study aim is achieved through the following research objectives:

i. to present the different categories of B&Is environmental sustainability (§2.1),
ii. to explore the publication evolution of topic-related studies (§3),
iii. to investigate the used method-development instruments in each defined studies' category (§4),
iv. and to examine the used method types and designs (§5).

2 Methodology

To meet the study objectives, the authors adopted a two-phase exploratory mixed method design where the qualitative results of the first phase were used as fundamentals to develop both quantitative (metrics) and qualitative results of the second phase.

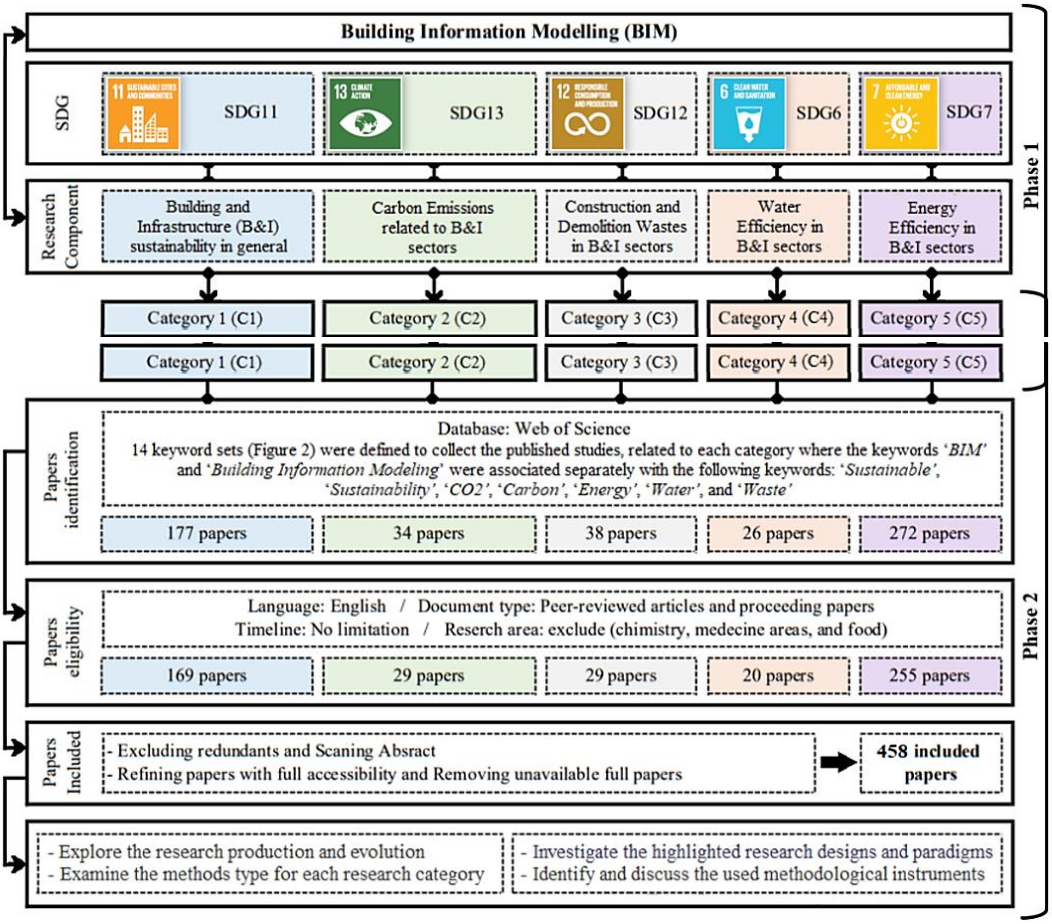


Fig. 1: Methodology flow – (a) Phase 1: preparatory study / (b) Phase 2: scoping review

2.1 Phase 1: Preparatory Study

The first phase consisted of a qualitative preparatory study to define the environmental aspects related to B&I in the CI that should be considered for the investigation. For this purpose, the authors reviewed the global main environmental strategies adopted by most countries, namely the Sustainable Development Goals (SDG) defined by the United Nations Development Programme (UNPD) (United Nations Development Programme (UNPD), n.d.) and reports of Conferences of the Parties (COP) administrated by the United Nations of Climate Change (UNCC) (n.d.). The investigation showed that the SDGs are strongly interconnected but five SDGs are considered closely connected to the ES in the CI:

- SDG6 "Clean Water and Sanitation" intends to endorse actions helping '*ensure availability and sustainable management of water and sanitation for all*.' For the CI, B&Is are responsible for 16% of the global water consumption (Ou *et al.*, 2017).
- SDG7 "Affordable and Clean Energy" focuses on '*ensuring access to affordable, reliable, sustainable and modern energy for all.*' Most undertaken actions, to reduce the environmental impact, concern substituting fossil energy with renewable ones and decreasing their consumption (UNCC, n.d.). Yet, the CI is responsible for 45% of global energy consumption (Ou *et al.*, 2017).
- SDG11 "Sustainable Cities and Communities" consists of actions to '*make cities and human settlements inclusive, safe, resilient and sustainable.*' The CI concerns the urban dimension as well where community management, green area versus built area, disasters risk management, and transportation/connectivity management represent big part of the AEC studies and projects. Several standards have been released to manage the sustainability of these aspects including environmental ones (Awadh, 2017).
- SDG12 "Responsible Consumption and Production" consists of '*Ensuring sustainable consumption and production patterns*' where '*achieve the environmentally sound management of chemicals and all wastes throughout their life cycle*' and '*substantially reduce waste generation through prevention, reduction, recycling and reuse*' are two of the main fixed targets. Construction work and buildings consume 40% of global raw materials and produce 20-50% of wastes deposited in landfills (Bouhmoud *et al.*, 2022a).
- SDG13 "Climate Actions" supports actions to '*take urgent action to combat climate change and its impacts.*' While, the total CEs per year is one of the most considered indicators for this purpose, construction materials and building operations are responsible for 28% and 11% of the global CEs, respectively (Bouhmoud *et al.*, 2022a).

As shown in Fig. 1, the study of the BIM-based Built Environment Sustainability (BIMBES) involves five categories of studies: C1, C2, C3, C4 and C5 that refer to BIM-based studies related to B&I sustainability in general, B&I CEs, CDWs, water and energy components, respectively.

2.2 Phase 2: Scoping Review – Metrics and Thematic Analysis

Considering the pre-defined category in phase 1, 14 keyword sets (Fig. 1) were defined to collect the published studies, related to each category where the keywords '*BIM'* and '*Building Information Modelling*' were associated separately with the following keywords: '*Sustainable'*, '*Sustainability'*, '*CO2'*, '*Carbon'*, '*Energy'*, '*Water'*, and '*Waste'*. The papers were collected from the largest scientific databases Web of Science. The paper-identification step led to the collection of 547 indexed papers, which were shortlisted to 458 included papers after applying eligibility criteria, excluding redundant, and refined available and accessible papers. The last three objectives of this study were investigated by using scoping LR as a method development instrument (Fig. 1).

3 Research Evolution in Bim-Based Built Environment Sustainability

The BIMBES research production experiences an upward trend with a significant disparity between the 5 studies categories. Energy and general sustainability represent the most discussed CI environmental aspects as

they represented 55.7% and 36.9% of the included papers respectively (Fig. 2). Similarly, since 2013, the energy and general sustainability-related research using BIM had the highest production rates, with 23.4 and 15.8 papers per year respectively, compared to other categories whose production rates did not exceed 2.8 papers per year. CDW-related research was the first to consider BIM use in 2005, followed by energy-related research in 2007 whereas water-related research started evoking BIM only in 2013 (Fig. 2).

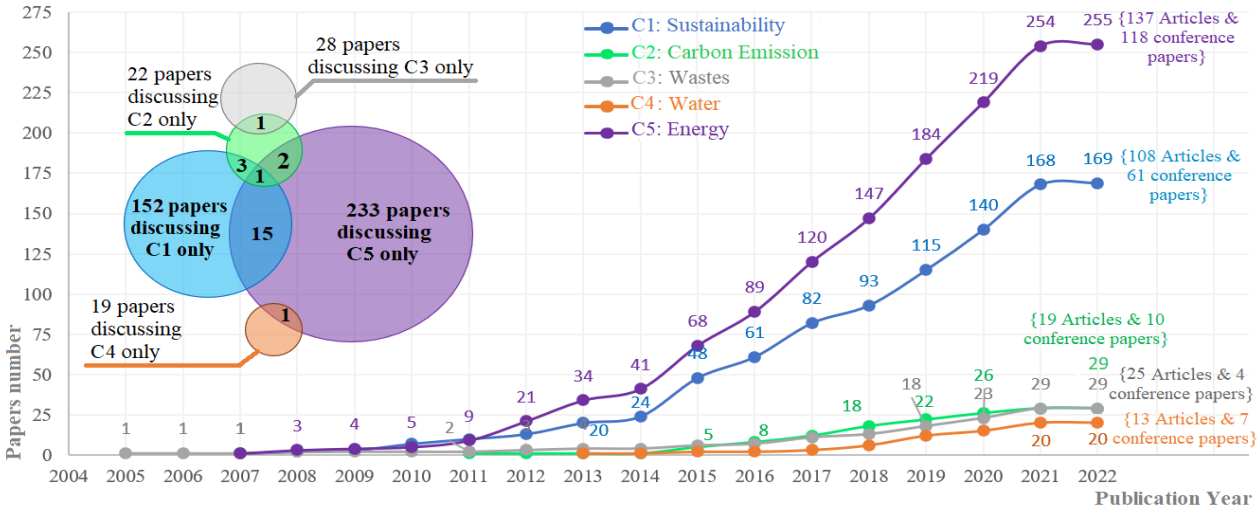


Fig. 2: Evolution of Research Production in BIM-Based Built Environment Sustainability: Dispatching by Research Category and Overlaps

4 Research Method Types and Research Designs and Paradigms

In the BIMBES research, scholars mainly use either quantitative or mixed methods which are adopted in 43.7% and 34.7% of the published studies, respectively (Fig. 3). However, the distribution of the used method types is dissimilar for each study category. Quantitative methods are mostly adopted for BIM-based research addressing water and energy efficiencies (C4 and C5), as they represent more than half the used methods with 55.6% and 53%, respectively, whereas they correspond to only one-third for the other ES aspects in BIMBES research (Fig. 3). On the other hand, qualitative methods are less considered for BIM-based studies addressing CEs (C2), CDW (C3), and energy efficiency (C5) as this type represented for these three categories less than one-fifth (21.4%) which corresponds to the rate of qualitative methods used for BIMBES research in total. However, qualitative methods are significantly adopted in BIM-based research tackling either B&I sustainability in general or water efficiency where it was considered for 30.1% and 27.8% of the related research respectively (Fig. 3).

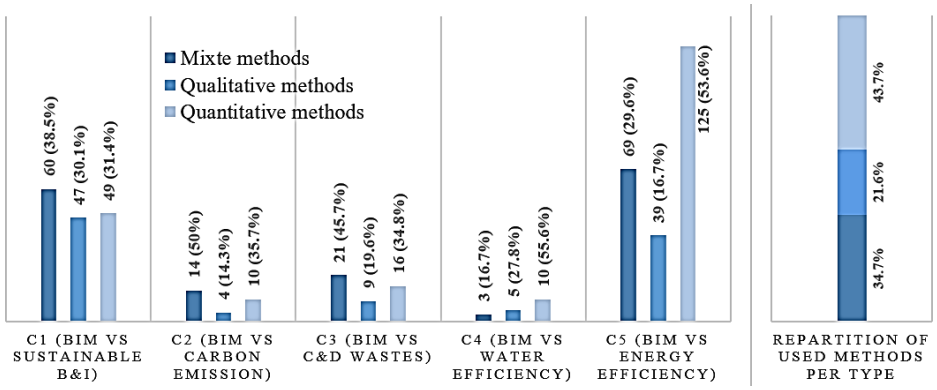


Fig. 3: Breakdown of the used Research Methods by Type and Per Research Category

The mixed method is the dominant method type in research associating BIM with CEs (C2), CDW (C3) and/or B&I sustainability in general (C1) with respective shares of 50%, 45.7% and 38.5%, whereas it

represents 29.6% for C5 studies and only 16.7% for C3 research (Fig. 3). Nine mixed research designs were explicitly highlighted in the reviewed work: Development Strategy Formulation and Evaluation Methodology (DSFEM) (Kim *et al.*, 2015), Design Science Research Methodology (DSRM) (Kang *et al.*, 2022), Sensitivity Analysis Method (Li *et al.*, 2020), Triangulation Design (Afaifia *et al.*, 2021), Axiomatic Design (GhaffarianHoseini *et al.*, 2019), Integrated Design (Schlueter & Geyer, 2018), Exploratory Design (Akinade *et al.*, 2016), Collaborative Science Research Design (CSRD) (Michaud *et al.*, 2021), Multi-Objective Optimization Approach (MOOA) (Abbasi & Noorzai, 2021). Among the four research paradigms (Rahi, 2017), one was explicitly mentioned: Constructivist (Akinade *et al.*, 2016).

5 Research Method Development Instruments and Data Analysis

The review study revealed that BIMBES research mostly utilizes literature review, modelling and case study instruments (Fig. 4). Scholars employed the LR instrument to either collect data to be used as input to develop the research delivery or to explore or describe research problems, the modelling instrument to develop a new framework, approach, or algorithm or upgrade existing ones to handle pre-defined research questions and the case study instrument to either evaluate a research problem or validate/refute research outcomes mainly the modelled elements or the findings of a previous study. As a result, most papers are studying research problems at mature stages namely evaluation, development, validation, or applied exploitation stages (§1.2).

The LR instrument, including all forms, is highly used in BIM-based research related to CEs (C2) and CDW (C3); with 66% and 97% of the related papers, respectively; and moderately used in studies addressing B&I general sustainability (C1), water and energy efficiencies (C4 and C5) with 42%, 40% and 31% of the related papers, respectively (Fig. 4). Scholars in topic-related research use five forms of the LR: Systematic, Scientometric, Scoping, Narrative, and General LR, which were used completely in C1 and C5 of BIMBES research and partially in the other categories. Systematic is the most used form followed by scientometric ones (Fig. 5).



Fig. 4: Used Research Instruments for Each of the Five Topic-Related Research Categories

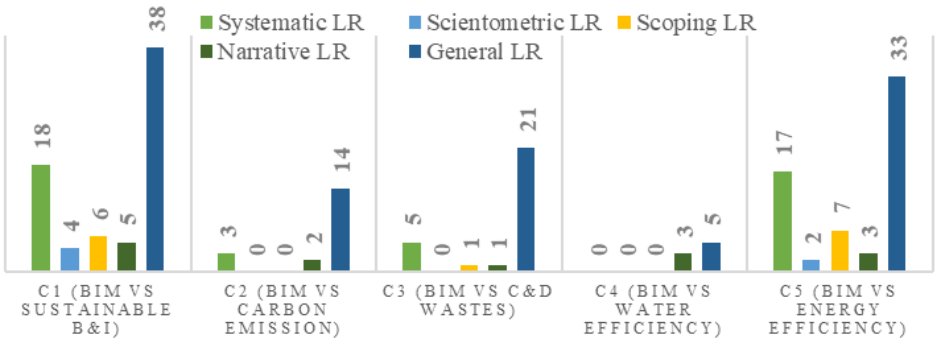


Fig. 5: The LR Breakdown into the Five Used LR Forms for Each Topic-Related Research Category

The modeling and case study instruments are commonly applied among CDW, CEs, and water efficiency studies using BIM (C3, C2, and C4) with respective percentages of 79%, 55%, and 50% for modeling and 62%, 52%, and 40% for case study. Likewise, the simulation instrument is frequently adopted for energy efficiency topics (C5), moderately used for B&I general sustainability (C1) and CEs (C2) topics, and lightly applied for CDW (C3) and water efficiency (C4) (Fig. 4).

In total, twelve method instruments are employed in BIMBES research: Ethnography, Survey, Interview, Focus Group, Modelling, Case study, Archival data, Document scan, Pre-test | Post-test, Simulation, Experiment, and Literature review. In the same vein, four data analysis approaches were emphasized: regression analysis (Afaifia *et al.*, 2021), statistical analysis (Schlueter & Geyer, 2018), Tukey's method (Alshibani & Alshamrani, 2017) , and hierarchical cluster analysis (Afaifia *et al.*, 2021).

6 Conclusion

The review study revealed that, referring to the SDGs, BIM could be used to enhance the B&Is ES by acting on five environmental aspects: B&I sustainability in general (C1), CEs (C2), CDW (C3), water efficiency (C4) and energy efficiency (C5). The topics within the BIMBES research are contemporary as the first paper was published in 2005 in C3 category followed by a 1st paper in C5 category in 2007 whereas C4 category was the last category to involve the BIM use with a 1st paper in 2013. Moreover, the study showed that C5 and C1 are the most discussed ES categories and have the highest production rates, with 23.4 and 15.8 papers per year respectively, whereas the remaining categories are still very limited.

The scoping review showed that most presented BIMBES research address mature stages of research problems study; namely evaluation, development, validation, or applied exploitation stages; and primarily apply quantitative and mixed methods with 43.7% and 34.7%, respectively. In the same vein, the study demonstrated that the LR, Modelling and Case study are topping the used development instruments for BIMBES research especially C3 category, with 62 to 97% of the used methods, followed by C2, with 52 to 66% of the used methods, and then C4, with 40 to 50% of the used methods. In terms of research methods metrics, this paper disclosed that the BIMBES research employs twelve method-development instruments: Ethnography, Survey, Interview, Focus Group, Modelling, Case Study, Archival Data, Document Scan, Pre-test | Post-test, Simulation, Experiment, and Literature Review. Similarly, four data analysis approaches were emphasized: Tukey's Method, Hierarchical Cluster Analysis, Regression Analysis and Statistical Analysis; and nine mixed research designs were explicitly highlighted in the reviewed work: DSFEM, DSRM, Sensitivity Analysis Method, Triangulation Design, Axiomatic Design, Integrated Design, Exploratory Design, CSRD, MOOA. Among the four research paradigms, one was explicitly mentioned: Constructivist.

By presenting a thoughtful investigation of the BIMBES research production and used research methods and designs for each category of the B&Is ES, this study endorses research and development to permit more studies using the considerable BIM abilities to enable efficient solutions toward greener B&Is in

different life cycle stages. Hence, this study would provide both scholars and practitioners with the key tools and data needed to develop and create innovative approaches. Although, this study is still limited since it used one scientific database which enabled omitting several published studies in the BIMBES research. In the meantime, this paper represents a first study discussing this topic hence further studies are needed to confirm this study findings and cover more scientific databases.

References

Abbasi, S. & Noorzai, E. (2021). "The BIM-Based Multi-optimization Approach in Order to Determine the Trade-off between Embodied and Operation Energy Focused on Renewable Energy Use", *Journal Of Cleaner Production*, Vol. 281, doi: 10.1016/j.jclepro.2020.125359.

Afaifia, M. et al. (2021). "An Energy Consumption Model for the Algerian Residential Building's Stock, Based on a Triangular Approach: Geographic Information System (GIS), regression analysis and hierarchical cluster analysis", *SUSTAINABLE CITIES AND SOCIETY*, Vol. 74, doi: 10.1016/j.scs.2021.103191.

Akinade et al. (2016). "Evaluation Criteria for Construction Waste Management Tools: Towards a Holistic BIM Framework", *International Journal of Sustainable Building Technology and Urban Development*, Vol. 7 No. 1, pp. 3–21, doi: 10.1080/2093761X.2016.1152203.

Alshibani, A. & Alshamrani, O. (2017). "ANN/BIM-based Model for Predicting the Energy Cost of Residential Buildings in Saudi Arabia", *Journal of Taibah University for Science*, Vol. 11 No. 6, pp. 1317–1329, doi: 10.1016/j.jtusci.2017.06.003.

Awadh, O. (2017), "Sustainability and Green Building Rating Systems: LEED, BREEAM, GSAS and Estidama critical analysis", *Journal of Building Engineering*, Vol. 11, pp. 25–29, doi: 10.1016/j.jobe.2017.03.010.

Bouhmoud, H. & Loudyi, D. (2021). "Building Information Modeling (BIM) Framework, Potential and Challenges", *International Journal of Information Science and Technology*, Vol. 5 No. 3, pp. 24–35, doi: 10.57675/IMIST.PRSM/ijist-v5i3.173.

Bouhmoud, H., Loudyi, D. & Azhar, S. (2022a). "Building Information Modelling (BIM) for Lifecycle Carbon Emission: Scientometric and Scoping Literature Reviews", *Smart and Sustainable Built Environment*, Vol. ahead-of-print No. ahead-of-print, doi: 10.1108/SASBE-05-2022-0086.

Bouhmoud, H., Loudyi, D. & Azhar, S. (2022b). "Evaluation of Building's Life Cycle Carbon Emissions Based on BIM and LCA: A Case Study of Affordable Housing in Morocco", presented at the CITC-12. The Twelfth International Conference on Construction in the 21st Century, Amman, Jordan, pp. 378–386.

Chudikova, B., Faltejsek, M., & IOP. (2019). "Advantages of Using Virtual Reality and Building Information Modelling When Assessing Suitability of Various Heat Sources, Including Renewable Energy Sources", Vol. 542, presented at the 2018 The 6th International Conference on Mechanical Engineering, Materials Science and Civil Engineering, doi: 10.1088/1757-899X/542/1/012022.

Creswell, J.W. & Clark, V.L.P. (2017). "Chapter 4: Choosing a Mixed Methods Design", *Designing and Conducting Mixed Methods Research*, 3rd ed., SAGE Publications, Inc., pp. 58–88.

Ellis, T. & Levy, Y. (2009). "Towards a Guide for Novice Researchers on Research Methodology: Review and Proposed Methods", *Issues in Informing Science and Information Technology*, Vol. 6, pp. 323–337, doi: 10.28945/1062.

Fetters, M.D., Curry, L.A. & Creswell, J.W. (2013). "Achieving Integration in Mixed Methods Designs—Principles and Practices", *Health Services Research*, Vol. 48 No. 6 Pt 2, pp. 2134–2156, doi: 10.1111/1475-6773.12117.

Ghaffarian Hoseini et al. (2019). "ND BIM-integrated Knowledge-Based Building Management: Inspecting Post-Construction Energy Efficiency", *Automation in Construction*, Vol. 97, pp. 13–28, doi: 10.1016/j.autcon.2018.10.003.

Guerra, B.C., Leite, F. & Faust, K.M. (2020). "4D-BIM to Enhance Construction Waste Reuse and Recycle Planning: Case Studies on Concrete and Drywall Waste Streams", *Waste Management*, Vol. 116, pp. 79–90, doi: 10.1016/j.wasman.2020.07.035.

Haruna, A., Shafiq, N. & Montasir, O. (2021). "Building Information Modelling Application for Developing Sustainable

Building (Multi Criteria Decision Making Approach)", *Ain Shams Engineering Journal*, Vol. 12 No. 1, pp. 293–302, doi: 10.1016/j.asej.2020.06.006.

Jalaei, F., Zoghi, M. & Khoshand, A. (2019), "Life Cycle Environmental Impact Assessment to Manage and Optimize Construction Waste Using Building Information Modelling (BIM)", *International Journal Of Construction Management*, Vol. 21 No. 8, pp. 784–801, doi: 10.1080/15623599.2019.1583850.

Kang, K. et al. (2022). "Building Demolition Waste Management Through Smart BIM: A Case Study in Hong Kong", *Waste Management*, Vol. 143, pp. 69–83, doi: 10.1016/j.wasman.2022.02.027.

Kim, J. et al. (2015). "BIM-based Decision-Support Method For Master Planning of Sustainable Large-Scale Developments", *Automation in Construction*, Vol. 58, pp. 95–108, doi: 10.1016/j.autcon.2015.07.003.

Krygiel, E. & Nies, B. (2008). *Green BIM : Successful Sustainable Design with Building Information Modeling*, Wiley Pub.

Li, H. et al. (2020). "Exploring and Verifying BIM-Based Energy Simulation for Building Operations", *Engineering Construction and Architectural Management*, Vol. 27 No. 8, pp. 1679–1702, doi: 10.1108/ECAM-06-2019-0314.

Liu, H. et al. (2019). "Towards Sustainable Construction: BIM-Enabled Design and Planning of Roof Sheathing Installation for Prefabricated Buildings", *Journal of Cleaner Production*, Vol. 235, pp. 1189–1201, doi: 10.1016/j.jclepro.2019.07.055.

Mellado, F. & Lou, E. (2020), "Building Information Modelling, Lean and Sustainability: An Integration Framework to Promote Performance Improvements in the Construction Industry", *Sustainable Cities and Society*, Vol. 61, doi: 10.1016/j.scs.2020.102355.

Michaud, M. et al. (2021). "A Taxonomy of Sources of Waste in BIM Information Flows", *Buildings*, Vol. 11 No. 7, doi: 10.3390/buildings11070291.

Ou, X., Li, Q. and Li, D. (2017). "Low-Carbon Architectural Design and Data Analysis Based on BIM", in Fei, M et al. (Eds.), *Advanced Computational Methods in Life System Modeling and Simulation, Lsms 2017, Pt I*, Vol. 761, Springer-Verlag Berlin, Berlin, pp. 390–399, doi: 10.1007/978-981-10-6370-1_39.

Rahi, S. (2017), "Research Design and Methods: A Systematic Review of Research Paradigms, Sampling Issues and Instruments Development", *International Journal of Economics & Management Sciences*, Vol. 6, doi: 10.4172/2162-6359.1000403.

Schlueter, A. & Geyer, P. (2018). "Linking BIM and Design of Experiments to Balance Architectural and Technical Design Factors for Energy Performance", *Automation in Construction*, Vol. 86, pp. 33–43, doi: 10.1016/j.autcon.2017.10.021.

Tu, K. J. & Vernatha, D. (2016). "Application of Building Information Modeling in Energy Management of Individual Departments Occupying University Facilities", *International Journal of Architectural and Environmental Engineering*, Vol. 10 No. 2, pp. 225–231, doi: doi.org/10.5281/zenodo.1112113.

United Nations Development Programme (UNPD). (n.d.). "The 17 Goals | Sustainable Development", available at: https://sdgs.un.org/fr/goals (accessed 18 December 2022).

United Nations of Climate Change (UNCC). (n.d.). "UNsFCCC: Session at COP | Documents, decisions and resources", available at: https://unfccc.int/ (accessed 18 December 2022).

Cite as: Bouhmoud H., Loudyi D., Giordano A., Azhar S. & Farah M., "Investigation and Comparative Study between Research Methods used in the Five Categories of BIM-Based Built Environment Sustainability Studies", *The 2nd International Conference on Civil Infrastructure and Construction (CIC 2023)*, Doha, Qatar, 5-8 February 2023, DOI: https://doi.org/10.29117/cic.2023.0022

Enhancement of Workers' Occupational Health, Safety and Welfare in Ashghal Projects

Naji Mohammed Al-Faridi
Quality & Safety Department (Safety Section), Public Works Authority (Ashghal), Doha, Qatar
nalfaridi@ashghal.gov.qa

Yasser Berzan
Quality & Safety Department (Safety Section), Public Works Authority (Ashghal), Doha, Qatar
ymberzan@ashghal.gov.qa

Hamad Saed R Kh Al-Hajri
Quality & Safety Department (Safety Section), Public Works Authority (Ashghal), Doha, Qatar
alkhayareen2@ashghal.gov.qa

Abstract

One of Ashghal's core values and top priority is the occupational health and safety of customers, employees and contractors. Ashghal prioritizes and is concerned about developing the welfare of workers on the site and in the camp. Ashghal develops welfare specifications for the projects to protect workers and be sure the specifications align with international and national requirements. The specification covers the facilities within the site, such as: number of toilets, handwashing basins, rest area/mess hall, shelter, drinking water, first aid room, transportation, clinic, etc. Ashghal develops an implementation and monitoring system to be sure welfare specifications are provided to all workers, referring to welfare specifications as contractual requirements, then linking workers' welfare as one of the monthly KPIs for the project, implementing it by the contractor, and monitoring it by the consultant. Ashghal is also working on developing specifications and requirements for workers' welfare, for example, developing and updating the specifications and requirements for their welfare on Ashghal construction sites, which will be issued soon as the "ACS."

Keywords: Ashghal - Public Works Authority of Qatar; OHS - Occupational Health and Safety; KPI - Key performance indicators; QCS - Qatar Construction Specifications; ACS - Ashghal Construction Specifications; SCH - Supreme Council of Health; HACCP - Hazard Analysis Critical Control Point; NCC - National Command Centre; MoPH – Ministry of Public Health; HMC – Hamad Medical Corporation

1 Introduction

Welfare facilities are an important requirement of any workplace, and they should be of high quality to make sure your workforce is healthy and productive. These facilities enable workers to work in a safe, hygienic, comfortable environment and help them do their work in an efficient and comfortable manner.

Providing the necessary welfare facilities will positively affect your employees' ability to work to their best capabilities, as there will be no room for time wastage. Having the necessary welfare facilities also gives employees a sense of appreciation and satisfaction, which will, in turn, lead to higher productivity. It is a human right to have access to this facility, and if it is not provided or is in poor condition, this increases worker stress and leads to accidents. Therefore, welfare facilities need

to be close to the workplace or within the worksite.

On the other hand, poor welfare facilities can result in several negative outcomes. Poorly maintained facilities, for example, can increase disease among workers, and limited access to rest areas can have a negative impact on morale, productivity, and individual health.

2 Current Status and Initiatives to Update

In Ashghal, the occupational health and safety of customers, employees, and contractors is one of the top priorities, and because workers are the main element in all Ashghal projects and programs, it is a priority to develop workers' welfare on the site.

Ashghal set out and developed standards to reinforce its commitment to improving the quality of workers' welfare across all projects and programs and be sure the specifications aligned with international and national requirements, for example, the number of toilets, hand washing basins, rest areas/mess halls, shelters, drinking water, first aid rooms, transportations, clinics, etc. It also linked some requirements with the total number of workers in the project, which covers the facilities within the site such as the number of toilets.

Based on these requirements, the Public Works Authority has issued Update No. 3 for the Evaluation Plan for Workers Accommodation and Welfare Standards, which includes important updates in the workers' welfare requirements on the workers' accommodation and site as well as setting out minimum mandatory requirements with respect to workers to ensure that their welfare is always maintained.

This update will also be included in the Ashghal Construction Specification ("ACS"), which will be released and published shortly and will cover all Ashghal requirements, including welfare facilities on the jobsite.

These two documents clearly define the workers' welfare requirements, which must be provided within the worksite area. Examples for this important update are:

3 Toilet and Washing Facilities

In the previous edition of QCS 2014, the requirements were "suitable and which allowed the contractors to provide facilities below the required standards, that affected the health and safety of workers and spread diseases among them. Also, it affects the level of worker productivity at work sites. but in those two new documents, it defines the total number of toilets that must be provided on the worksite according to the total number of workers within the same worksite area (1 WC and 1 urinal per 25 workers) and that they should be located within a 3-minute walk of the worksite area.

4 Drinking Water Facilities

One of the important updates in this part is the monthly third-party test for water quality. This reduces diseases resulting from the poor quality of drinking water tankers, which are strictly checked for cleanliness and condition to ensure the safe transportation of drinking water at the worksite, and forces contractors to provide thermos water flasks (with employee name tags or ID details) for all workers to carry potable water with them while working. This will raise the psychological state of the workers by making them realize that they are among the priorities of the higher management.

5 Food Handling and Storage

Public Works Authority is also concerned about the workers' food; therefore, Ashghal requires the

contractors to comply with SCH guidelines and ISO-22000/HACCP for foods that will be stored, transported to the worksite, and served to workers by licensed staff according to MoPH requirements.

Even in the food storage on the worksite, Ashghal asked that food be stored off the floors, preferably in refrigerators and on proper shelves, and to avoid bringing food in plastic bags.

6 Working in Summer Season

One of the significant updates to the worker's welfare requirements concerns the summer season. Qatar is one of the countries with high summer temperatures. Working in hot conditions may pose special hazards to safety and health.

Temperature, humidity, and radiant heat (such as from the sun) are the most effective factors in determining the amount of heat stress, as are some workers' medical histories, such as high blood pressure or heart conditions. Heat stress can lead to several problems, including heat exhaustion, heat stroke, cramps, fainting, and heat rash.

The previous requirements for working during the summer season required all activity to cease between 11:30 a.m. and 3:00 p.m. from June 15 to August 31, but the new update extends the time and dates to June 1 through September 15 and the time from 10:00 a.m. to 3:30 p.m.

7 Worker Rest Area Facilities

This is one of the welfare requirements, which Ashghal also insists to provide with the highest standards of health and safety requirements, with a specification of "suitable and sufficient" for these facilities. It should be safe and easy to access, as well as well-ventilated and equipped with enough tables and chairs (with backrests).

Also, it should include adequate washing facilities that must be clean and in orderly condition, with a team for periodic cleaning. It must include a suitable hall for practicing religious rites.

8 COVID-19 Restrictions

During the COVID-19 pandemic, Ashghal required contractors to follow actions and procedures issued by the MoPH and NCC in Qatar that helped prevent the spread of the pandemic, such as wearing a facemask, keeping a safe distance between workers on the jobsite, getting vaccinated, and so on. This is an example of Ashghal's concern for the safety and health of workers at its sites and its commitment to providing a good welfare facility.

9 Chronic Diseases Screening & Medical Requirements

Ashghal has also taken care of the healthcare of workers at worksites by obligating contractors to conduct periodic check-ups for chronic disease screening for all workers to ensure their health and fitness to perform the tasks assigned to them successfully.

As a result, any worker identified with one of these chronic diseases within Ashghal projects must be referred to HMC for further evaluation and additional medical care, and an individualized treatment plan must be provided for each worker identified with one of these chronic diseases.

In addition to providing medical requirements at work sites according to the requirements of the Ministry of Health, ensuring contractors' commitment and implementation, and imposing fines in case of non-compliance is also done.

10 Transportation Requirements

Transportation from and to the worksite is an important welfare measure, and Ashghal requires contractors to use fully air-conditioned buses, especially during the summer when temperatures and humidity levels are high. The buses' windows must be almost completely tinted.

In addition to providing flashlights and reflective stickers at the back of the bus, as well as determining the busload and the number of passengers allowed to be on the bus is also important.

11 Conclusion

Lack of appropriate welfare facilities can pose a significant threat to the health and safety of workers. If welfare facilities are not suitable and sufficient, it can result in physical and psychological illness and it can cause low morale and low productivity if employees feel that the employer is not bothered about their welfare. Therefore, the work environment should be safe and healthy for workers on worksites.

The health and safety of workers and customers is one of Ashghal's top priorities. In Ashghal's strategy, OHS objectives are effectively applied to projects and implemented to departments to ensure on-time delivery without deviation from OHS requirements and to improve OHS performance across projects, departments, and asset affairs.

Improvement in OHS welfare performance is an on-going process, and Ashghal wants to show all its support to customers and contractors, from inspection, feedback, and findings, then update the regulations and requirements for improvements.

References

Ashghal Evaluation Plan for Workers Accommodation and Welfare Standards, Rev.03, pp. 28, 60, 68, 77 & 82.

International Labor Organization (ILO) Welfare Facilities Recommendation No. 102.

Qatar Construction Standards – Current Revision - QCS 2014, Section 1, Parts 10.6, 10.9 & 10.9.5.

Cite as: Al-Faridi N. & Berzan Y.M., "Enhancement of Workers' Occupational Health, Safety and Welfare in Ashghal", *The 2nd International Conference on Civil Infrastructure and Construction (CIC 2023)*, Doha, Qatar, 5-8 February 2023, DOI: https://doi.org/10.29117/cic.2023.0023

A Side-by-Side Comparison of Shaft Excavation locally in Qatar

John Brown
Parsons International Limited, Qatar
john.brown@parsons.com

Sunit Saurabh
Parsons International Limited, Qatar
sunit.saurabh@parsons.com

Ahmed Akslakhi
Public Works Authority (Ashghal), Qatar
aalslakhi@ashghal.gov.qa

Eisa Al-Mohannadi
Public Works Authority (Ashghal), Qatar
ealmohannadi@ashghal.gov.qa

Abstract

The city of Doha has grown and expanded rapidly in the last 20 years, but this growth has strained the city's infrastructure, including its aging sewerage system and treatment facilities. The Public Works Authority (Ashghal) has therefore launched several strategic schemes which involve shallow and deep sewer tunnels and a new sewage treatment works (STW) to serve Doha's growing population in the years to come. One such schemes is the C853/1 Wakrah-Wukair Drainage Network Branches (WWDNB), which includes more than 15 km of bored pipes between 400mm and 2.4m inner pipeline diameter, with more than 60 shafts ranging in depths from 10m to 47m. The geology in the Wukair area is made up of several distinct strata, typically ranging in material strength between 10 and 48MPa, and it is the range of strengths that decides the method of shaft excavation. This paper will provide a production comparison between two types of excavation methods adopted for the same depth shafts and geological conditions. In the first method, the Contractor adopted the more traditional method using an excavator with appropriate attachments to break the ground, where this progressed in a cyclical manner until the shaft base was reached. The second method incorporated a piling rig to drill a specific pattern of holes within the shaft envelope, which enabled a faster excavation cycle and allowed for time and cost savings as well as improved safety. This paper will assess both methods, why both were utilised, and the lessons learnt.

Keywords: Wakrah-Wukair; Shaft excavation; Piling rig; Comparison

1 Introduction

Wakrah-Wukair Drainage Network Branches project shafts have 2 main purposes, to act as a launch and/or a reception shaft for the micro-tunnel/pipe-jacking tunnel boring machines and also in their final state as an access point for monitoring and maintaining the sewage network.

The design process for the excavation of these shafts considers these purposes and incorporates the regional geology, available equipment, skills, safety, schedule and costs.

The shafts at WWDNB have been categorized as 2 types:

1. Local network, which is approximately 8m-30m in depth; these are primarily in local residential areas.
2. Main network shafts; these are 30m-48m in depth and are generally located closer to the final processing area, such as a sewage treatment plant.

2 Geology and Design Considerations

Several peer-reviewed geotechnical studies are available on the geology of the Wakrah-Wukair region of Qatar. This paper only provides a basic summary of the typical stratigraphic units encountered in the project area according to the Geotechnical Interpretative Report (2021) of the project, see Table 1 below.

Table 1: Project Geological Strata overview

Geological Strata	**Unit thickness (m)**	**Material Strength (Avg. Uniaxial Compressive Strength of intact rock in MPa)**	**Brief description**
Made ground & residual soils	0-2	-	Asphalt and gravel, poorly graded
Simsima Limestone	22-28	40	Limestone to dolomite weathered
Midra shale	5-7	15	Calcareous siltstone interbedded with limestone/dolomite
Rus Formation (Drilling didn't reach the bottom of this layer)	19-20	10	Limestone to Dolomite

To summarise the typical groundwater conditions that need to be considered, two main aquifers with a depth up to 50m, the first aquifer is located within the saturated zone of the Simsima Limestone and the second aquifer is in the Rus Formation located below the Midra shale. Both aquifers are hydraulically interconnected, meaning a dewatering design needed to be established during shaft construction to manage the high level of seepage, also possible karstic conditions needed to be considered.

2.1 Design Considerations

To establish the level of ground support required and to confirm the design, detailed ground investigation including borehole drillings, laboratory & in-situ tests along with the geophysical surveys such as the Multichannel Analysis of Surface Waves (MASW) and Electrical Resistivity Tomography (ERT) techniques were carried out for this project. MASW and ERT are the non-destructive site characterization techniques used for evaluating the stiffness of the ground for geotechnical engineering purposes. Details of correlation and matching between the results of surface geophysical methods, with available drilling boreholes or other subsurface data of the area, and the anomalies if any were highlighted and interpreted.

Later during the execution stage, an observational approach was adopted where the rock face mapping was performed by the geotechnical team for every 3m of unsupported depth reports in accordance with EN-ISO 14689-1 & 2 and BS-5930:1999 + A2:2010. Based on the mapping report, Q-value (NGI, 2015) was evaluated to interpret rock mass support category. For both shaft excavation methodologies, rock support was applied based on the Q value range recommended in the temporary works design for shaft excavation and support. Basis temporary lining type consists of a certain thickness of shotcrete with or without steel mesh along with additional measures if required.

The purpose of this analysis is extremely vital in terms of decision-making whether what approach is required to ascertain the choice of equipment and method of excavation based on the hardness of the

rock, which in-turn helps speculate the production rate of excavation. For analysis purpose of this research, we will be studying Shaft SH 8/3 and SH 8/1, which are both excavated with different methodologies, one with traditional method and the other with the aid of a piling rig. The geotechnical investigation and face mapping reports show that both the shafts are in the strata of calcareous, stable limestones with Q value ranges up to 4. This concludes the fact that we are required to deploy Jackhammer/Pile-rig excavators to break into the ground for reaching formation level.

3 Methodology

An analytical approach has been adopted to compare both methods of excavation, where two shaft SH 8/3 and SH 8/1 were selected for correlating the site parameters.

3.1 Methodology 1 – Shaft Excavation by Excavators only Shaft 8/3

Shaft SH 8/3 is a 47m deep shaft excavated in 11m diameter. Excavations have been done with different sized excavators depending on the depth. First 6 meters of excavation has been done with a standard boom wheeled excavator and breaker. Beyond this depth and down to 14 meters of depth, excavation proceeded with long boom and long reach tracked chain excavators and breaker, see Figure 1.

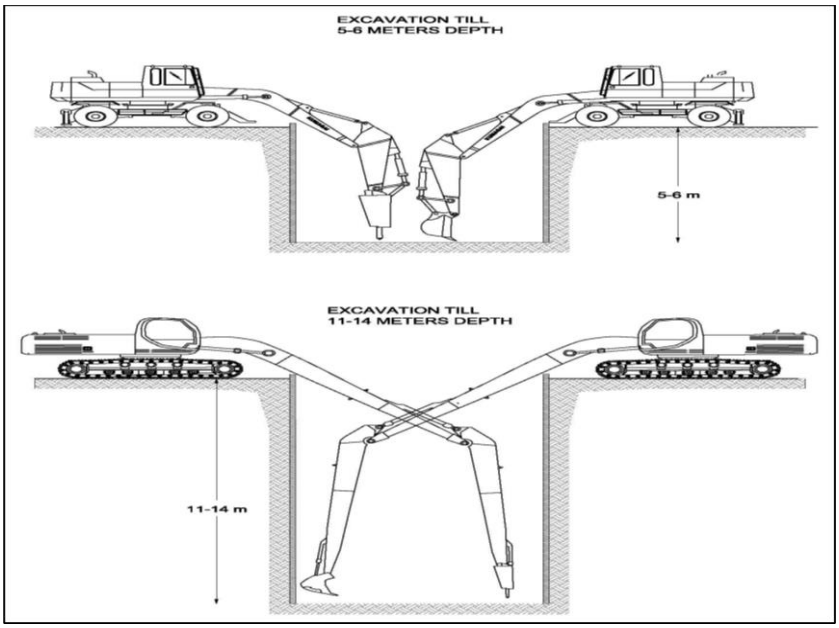


Fig. 1: Method 1 Initial Excavation of Shaft with Excavator and Breaker Attachments

Deeper than this and up to maximum depth of 50 meters, excavation then proceeded with mini/ compact excavators (6-8 tons) which were lowered into the shaft while the excavated material was loaded into soil skips lowered and lifted by a mobile crane.

3.2 Methodology 2 – Excavation by a Combination of Excavators and a Piling Rig Shaft 8/1

Excavations for shaft 8/1 was carried out using the BAUER BG-11 H piling rig see Figure 2. The contractor used 2 piling rigs from Bauer: BG-28 (larger) and BG-11 H (smaller). The BAUER BG-11 H rig is able to drill down to maximum depth of 28 m, whereas the bigger rig BAUER BG-28 is able to reach the maximum depth of shafts on WWDNB Project.

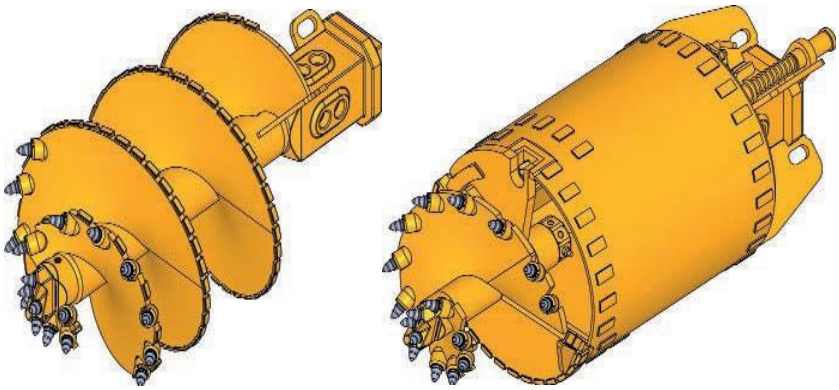
The BAUER BG-11 H piling rig first drilled uncased bores within the shaft perimeter spaced (outside diameter to outside diameter) 50 cm in a grid configuration see Figure 3, then in each marked out bore location, drilled down to final depth of the shaft. The piling rig partly removed the ground spoil from the bore, leaving as much spoil inside the bore, yet not so much to maintain the balance of torque

power of the rig. Upon finishing the bore, the spoil that was brought out of the excavated hole was pushed back into the hole. This method was repeated for each bore.



Fig. 2a: Photograph of BAUER BG-11 Piling Rig in Action

The Progressive Auger BAUER SBF-P2 and Rock drilling bucket BAUER KBF-P (with progressive bottom gate) were used as cutting tools. SBF-P2 and KBF-P are recommended in uncased bores or for the bigger diameters. Mainly it suited for strong rock (50-100MPa).



SBF-P2 **KBF-P**

Fig. 2 b: Photograph of BAUER SBF-P2 & KBF-P

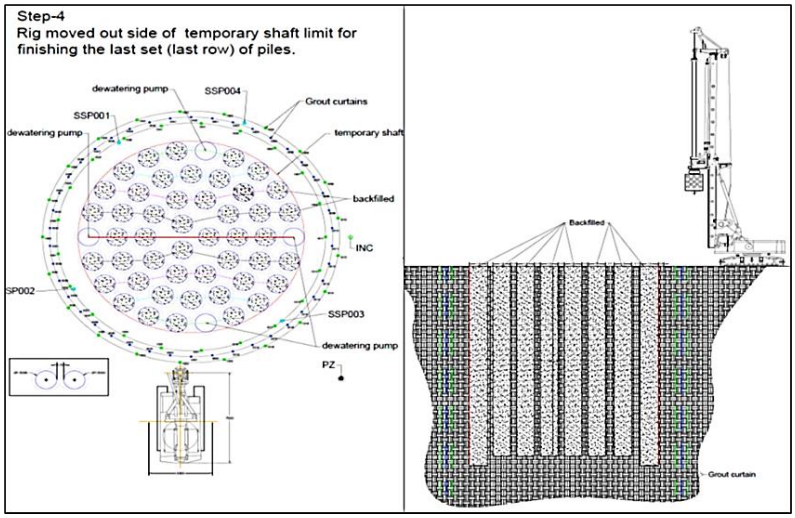


Fig. 3: Piling Rig Excavation Layout Plan and Section

When all the holes within the perimeter of the shaft have been drilled, the next stage is similar to method 1, using an excavator with a bucket to remove the broken spoil see Figure 4, making the excavation process significantly quicker as the material within the shaft has now been significantly broken up, the same methods of using shotcrete as shaft support was still used.

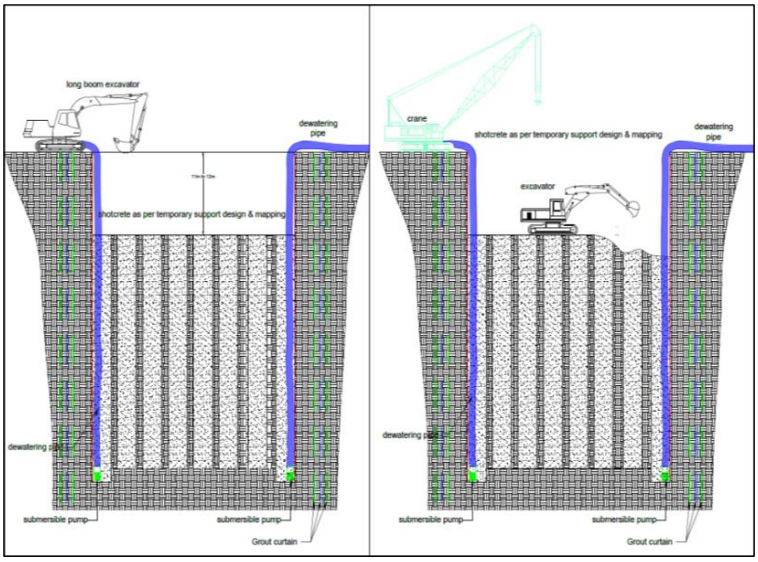


Fig. 4: Excavation of Shaft after Piling Rig has Drilled the Holes

4 Comparison of Both Shaft Excavation Methodologies

Table 2 shows a side-by-side comparison using Method 1 and Method 2 to excavate the shafts; these results are typical across the project.

Table 2: Side-by-side comparison of both methods

Detail/Type	**Excavation by Excavator Only Method 01**	**Excavation Aided by Piling Rig Method 02**
	SH 8/3	SH 8/1
Shaft Excavation Diameter	11m	11m
Shaft Depth	47m	47
Total volume to be excavated in (m^3)	~4470 m^3	~4470 m^3
Start of excavation (actual)	13th Mar 2022	14th Sep 2022
End of excavation (actual)	19th Oct 2022	21st Dec 2022
Total no. of days from start till end	220 days	98 Days
Total lifts for Shafts Lining	12 Lifts (every 4m of depth = 47/4)	12 Lifts (every 4m of depth = 47/4)
Total number of days for each Lift lining	02 days	02 days
Total number of days for full depth for lining work	24±5 (12x2)	24±5 (12x2)
Total days actual excavation	**196 days (220-24)**	**74 Days (98-24)**
Production rate (total volume/total day actual excavation) m^3/day	~23 m^3/day (4467 m^3/190 days)	~60 m^3/day (4470 m^3/74 days)
Limitations	Not suitable with areas of existing utilities thus requires extensive existing utility survey	1. More breakdown since machines working with impact/jackhammers 2. Changing jackhammer to bucket and bucket to jackhammer in the excavators cause extra time slippage

Equipment type used	1. Excavator 30T or 20T (Tire or Chain) 2. Excavator long mast Arm 18m 3. Crane 100T or 150T	1. Piling rig 2. Excavator 30T or 20T (tire or chain) 3. Excavator long mast Arm 18m 4. Crane 100T or 150T

5 Conclusion and Lessons Learned

Data shown in above Table 2 clearly indicates the following results:

1. Productivity rate in method 02 is recorded nearly ~ 2.6 times greater than that of the conventional method.
2. If the groundwater and geological conditions are similar, it is recommended to adopt method 2 for faster progress of the construction.
3. Probability of breakdowns of machines/equipment in method 01 is more since it required consistent effort of jack-hammer excavators for rock breaking, causing repetitive wear and tear.
4. Quality process using both methodologies was observed the same.
5. Although the risk/hazards are increased in method 2 due to deployment of additional resources, this is still recommended to adopt it, considering the higher productivity rate.
6. Since the productivity is substantially increased in method 2, that saved the considerable duration of the construction and therefore it leads to a cost effective solution.

6 Acknowledgements

The authors are grateful to the Public Works Authority, Qatar (ASHGHAL) for giving the opportunity to publish this paper. Token of thanks to the management of Parsons International Ltd. for the necessary support and guidance and as well as the contractor's management for inputs during the paperwork.

References

British Standards Institution. (2013) *Eurocode 7: Geotechnnical Design - Part 1: General rules.* BS EN 1997-1:2004+A1: 2013.

Geotechnical Interpretative Report (2021). Doc. no. C853/1-QTC-GEO-RPT-00008 Rev.2, Wakrah and Wukair Drainage Network Branches –C853/1.

Norwegian Geotechnical Institute. (2015) *Using the Q-system: Rock Mass Classification and Support Design.* s.l.: NGI, 2015.

Cite as: Brown J., Saurabh S., Alslakhi A. & Al-Mohannadi E., "A Side-by-Side Comparison of Shaft Excavation locally in Qatar", *The 2nd International Conference on Civil Infrastructure and Construction (CIC 2023)*, Doha, Qatar, 5-8 February 2023, DOI: https://doi.org/10.29117/cic.2023.0024

Flow of Activities: Utilizing Parade of Trade to Develop Visual Management Tool Tailored for Infrastructure Projects

Yehia Zakaria Abdelkader Ibrahim
Dorsch Qatar, Doha, Qatar
yehia.ibrahim@Dorsch.com

Saoud Ali Al-Tamimi
Public Works Authority (Ashghal), Doha, Qatar
stamimi@ashghal.gov.qa

Abstract

Parade of Trade (PoT) is a game used in Lean Construction to demonstrate the impact of variability on a production system and to promote the value of constraint management in an environment of dependent events. Infrastructure projects usually have a sequence of construction works to an extend matching with the PoT model. Different trades and activities distributed over a large-scale area combined with its arising particular issues, creates a challenging efficiency paradox. Therefore, there is a need to adapt a new tool that identifies pace maker of the production flow, shows the interactions between different construction stages and trades, and explains the impact of trade progress on one another. The PoT idea used to develop new Visual Management (VM) tool, tailored to bridge the gap in the current model of infrastructure construction management traditional tools, supports the effectiveness of resources utilization and optimizes the project as a whole. Starting from maximizing client's values and passing through selection methodology; this paper records the journey of developing and utilizing sustainable VM tool; tailored for infrastructure construction projects. It supports decision-making regarding resources allocation; adapting construction batch size; assist in determining takt time and takt zones. Furthermore, it opens the way for further studies from Lean researchers and practitioners to develop new Lean Construction tools tailored to serve infrastructure construction projects.

Keywords: Lean Construction; Infrastructure; Ashghal Enhanced Projects; Parade of Trades; Visual Management

1 Introduction

Although, Lean Construction tools, started and developed in building projects are utilized in infrastructure projects, insufficient attention has been paid for developing new tools particularly tailored for infrastructure projects. Infrastructure projects have a particular characteristics that differentiate it from building projects: it covers larger horizontal area, more affected by weather conditions, as it has no envelope to control the weather within the project's limit; has more interfaces with and impact on the public community. The previously mentioned characteristics denote that special cause variations would more affect infrastructure projects than building projects. Accordingly, there is an essential need to develop particular tools, tailored for infrastructure projects, focusing on minimizing the impact of special cause variations and maximizing owner's values.

Visual Management (VM) is a strategy for information management strongly related to one of the

core concepts of Lean production, which is increasing the process transparency and enhance shared understanding. In addition, the Parade of Trades (PoT) simulation game introduces concepts of sequential dependence and process variability in order to illustrate the detrimental impact such variability has on a system's performance (Tommelein, 2020). Deep utilities in infrastructure projects have a sequence of construction activities matching with the PoT model.

Public Work Authority (Ashghal), introduced Lean in construction programme as a part of their enhanced projects' contract form, intended to minimize project disruption and maximize residences satisfaction. This paper presents practical endeavour of developing a new VM tool; based on the Parade of Trade simulation idea, tailored for a programme of infrastructure projects worth approximately 1.7 billion QAR in the State of Qatar.

2 Pot as a Powerfull Learning Tool

The use of games in engineering teaching is common practice in classes with lecturers all over the world (Biotto, et al. 2021). PoT has been an iconic simulation game in teaching Lean main principals for three decades. The purpose of this game is to demonstrate the impact variability and dependence have in a construction environment where multiple trades follow each other in a linear sequence and work output by one trade is handed off to the next trade (Choo & Tommelein, 1999). Greg Howell used the Parade of Trades Game at the 6th Annual Conference of the International Group for Lean Construction. The Lean Construction Institute has been using it at many of their workshops, and the Associated General Contractors of America (AGC) have it as a part of their lean construction education program. As described by Bolivar A. Senior, (2011), it is a powerful learning tool showing the effects of dependency and variability in consecutive trades operating in a construction project. Therefore, PoT simulation game became a fundamental element of enhanced project's Lean Construction training. The game is physically played at the projects by both: Contractor and Supervision Consultant construction management teams; in order to elevate shared understanding, increase relatedness between project team members and focus on enhancing the project as a whole. The game highlighted the effectiveness of batch planning and clarified the efficiency paradox as explained by (Modig & Ahlstrom, 2021). Three rounds played simulating: the impact of variations on construction flow, the impact of bottle nicks even with providing additional resources, and the enhancement of construction flow by working in small batches.

3 Development of the New VM Tool

From early on, visual management VM has been a fundamental pillar of the Toyota Production System (TPS) and subsequently in Lean applications (Koskela et al., 2018). Mental operations, such as communication and decision-making are strictly seen waste in production; they are not adding value to the customer. Through VM, communication and decision-making can be accelerated. On the other hand, the higher reliability of VM translates into lower variability. Thus, VM has emerged as an intrinsic part of lean production as it is compatible with its first principles (Koskela et al., 2018). In Ashghal enhanced contract form, VM is included as one of four elements of Lean Construction Implementation Programme. Thereafter, the idea evolved for developing a new tool particularly tailored for the infrastructure construction activities. The focus of the new tool was to: maximize client values, support construction management decisions and enhance the project delivery as a whole.

3.1 Maximizing Client Values

The Associated General Contractors of America (AGC, 2013), describe Lean Construction as a set of ideas, practiced by individuals in the construction industry, based on the holistic pursuit of continuous improvements aimed at minimizing costs and maximizing value to client, (Forbes & Ahmed, 2020). Accordingly, maximizing clients' value was the starting point towards developing a new tool.

Two of the main values addressed in Ashghal enhanced contract are: residents' satisfaction, and disruption management. Open trenches for prolonged time affects both values. Open trenches accompanied as well with: HSE hazardous, operational costs, and impact on site look and feel. The foregoing justified why open trenches are a major concern for Ashghal. Subsequently, minimizing the length and the duration of open trenches is one of Ashghal's main targets.

3.2 Selection of Activities to be Presented

Deep utilities in infrastructure projects have a sequence of construction works typical to the PoT simulation model. In addition, deep utilities present an average of 53% of the project's total construction duration as shown in Table 1. An improvement in deep utilities construction duration certainly will contribute the most to the improvement of the project's overall duration.

Table 1: Deep Utilities Duration Relative to Project's Overall Duration

Project	A	B	C	D	E	F
Total Duration (months)	39	28	36	28	40	36
Deep Utilities Duration (months)	22	14	18	14	22	20
Deep Utilities Relative Duration to Project's Construction Duration (%)	56.4	50	50	50	55	55.5

Accordingly, deep utilities related activities were selected for the application of the new VM tool. However, with each activity measured in a different unit, there is a need to develop a new measuring unit to link between different activities and be the base for data presentation.

3.3 The Need for a New Measuring Unit

A contractor typically measures the progress of different construction activities by different units; pipe laying (by linear meter), excavation (by cubic meter), backfilling (by ton) or based on specific layer thickness by (square meter), and surrounding material (by tons). The typical progress reporting methods of plan vs actual quantities, will not explain the interaction between different activities nor correlate between different units. The typical highlighted progress on a layout drawing needs considerable mental operations and time to correlate between–location, activities, corresponding quantities for different utilities and will not show the before and after conditions. Accordingly, there was a need for a reference-measuring unit that correlates between different activities and can be visually presented in a simple and clear way.

Hereafter the "Linear Meter of Trench" became a new measuring unit for deep utilities activity progress. Regardless of trench's; depth, width, number or size of pipes; progress reported in linear meter of trench, e.g., two parallel pipes laid in the same trench for one meter reported as one linear meter of trench pipe laying; similarly, backfilling of three different utilities in the same trench

reported as one linear meter of trench backfilling. Complete accepted work only considered to report progress. Accordingly, a new VM graph was developed and standardized for progress reporting.

4 Results and Discussion

A new graph, Flow of Activities (FoA), developed based on the new measuring unit as shown in Figure 1, which represent a matured status of the project after utilizing the FoA graph.

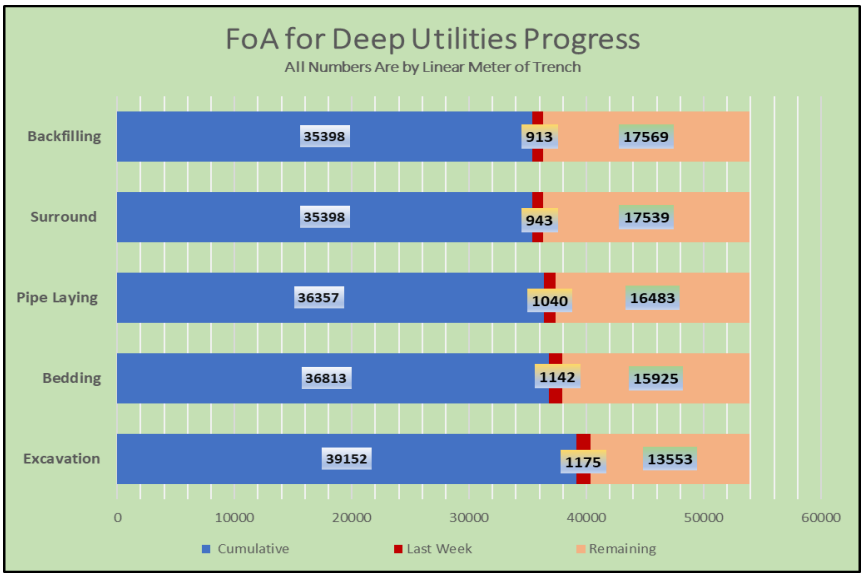


Fig. 1: FoA for the Deep Utilities' Activities

The FoA presented deep utilities; Foul Sewer (FS), Ground Water (GW), and Surface Water (SW) activities as physically constructed; from bottom to top; plotted over a scale refenced to the new measuring unit: linear meter of trench. It presented for each activity: cumulative length completed, last week length completed, and remaining length till the end of project. Major activities visualised for the project; interaction and dependence are clear in one page. It showed the progress of each activity relative to its predecessor and successor activity. It gave guidance for: which activity has an open front work, which activity is blocked, which activity is proceeding faster than the others, which activity needs more resources or even less resources to slow down and direct its resources to another activity.

When the FoA started to be used, a clear gap identified between excavation and subsequent activities; rate of progress of each trade was found different from the others; some activities found with no open front work, as predecessor and successor activities have almost the same completed quantity. Furthermore, through the first few weeks, pipe laying activity was identified to be the pace maker of the progress. Pipe laying and connection's production rate controlled the ability to achieve more progress with other activities. Hereafter, GEMBA Walk took place to identify probable gaps in pipe laying and connection process, followed by Value Stream Mapping (VSM) for pipe laying and connection, to find better methods for increasing productivity. Furthermore, it was noticed that; while resources increased and excavation work became more efficient; there were no considerable improvements in final product delivery (trench backfilling). Hence, efficiency paradox became clear. All the foregoing gave the project management quick reference for effective decisions making related to: resource allocation and material utilization. In addition, open trench status is clearly displayed with numbers, which is a client's main value.

The FoA included project's visual KPIs: A ladder shape in the graph, is an indicator of open front work for all activities; having on the graph approximately the same thickness of the weekly progress, is an indicator of effective utilization of resources and smooth flow of work; increase in the thickness of weekly progress, is an indicator for productivity improvement; In addition; the difference between completed excavation and backfilling quantities present the project open trench status, and the volume of Work In Progress (WIP); both are client's main concerns.

One of the added values of the FoA is the determination of the work batch size. Working in small batches is a key factor to speedy delivery and reduction of WIP. The determination of the batch size has been a challenge, as it has no theoretical method of determination. However, with the new graph the batch size can be determined by interpreting the weekly progress (by linear meter of trench) to a particular quantity of work for each separate activity and allocate the required resources accordingly. Furthermore, batch size will be a reference for short-term planning and further improvement. For over a year the project's Percent Plan Completed (PPC), for the first project started to implement FoA, which was between 85% to 95%.

The utilization of the FoA extended to cover road works and micro-tunnelling work as well. Furthermore, it could be used to support takt planning in determining the preliminary takt time and takt zones for infrastructure projects.

5 Conclusion

This paper provides an example of developing new VM tool for infrastructure projects. It illustrates practical method for determining construction batch size. It can be used further to identify the preliminary takt time and takt zones for takt planning purposes in infrastructure projects. VM provide better shared understanding and guidance for decision making, more than the traditional methods. There is still considerable room of enhancement for lean construction implementation that requires more studies from researchers and practitioners to develop innovative Lean tools to serve the particular conditions of infrastructure projects.

Acknowledgement

The implementation of the FoA was supported by Eng. Asghar Kamal, Dorsch Qatar, and Eng. Jamaluddin Hakouz, QBEC. The idea of adding the weekly progress to the graph is introduced by Eng. Hamad Salem Almejaba, Ashghal Project Manager. The support is gratefully acknowledged.

References

Biotto et al. (2021). "Virtual Parade Game for Lean Teaching and Learning in Students from Brazil and Chile", 29th Annual Conference of the International Group for Lean Construction (IGLC 2021), Lima, pp. 340-349.

Choo, Hyun & Tommelein, Iris (1999). "Parade of Trades: A Game for Understanding Variability and Dependence", Construction Engineering and Management Program, Civil and Environmental Engineering Department, University of California, Berkeley, Technical Report 99-1, pp. 1-4.

Forbes, Lincoln & Ahmed, Syed (2020). *Lean Project Delivery and Integrated Practices in Modern Construction*, (pp. 25-50), Routledge, New York.

Koskela, Lauri, Tezel, Algan., & Tzortzopoulos, Patrecia (2018). "Why Visual Management?", 26th Annual Conference of the International Group of Lean Construction (IGLC 26), Chennai, pp. 250- 260.

Modig, Niklas, & Åhlström, Par. (2021). "This is Lean: Resolving the Efficiency Paradox", Chapter 3&4, Rheologica, Stockholm.

Senior, Bolivar (2011). "Enhancing the Construction Parade of Trades Game", 47th ASC Annual International Conference, Omaha.

Tommelein, Iris (2020). "Takting the Parade of Trades: Use of Capacity Buffers to Gain Work Flow Reliability". 28th Annual Conference of the International Group for Lean Construction (IGLC-28), Berkeley, pp 421-432.

Ward, Steven, & McElwee, Andrew, (2007). "Application of the Principle of Batch Size Reduction in Construction", 15th Annual Conference of the International Group for Lean Construction (IGLC-15), Michigan, pp. 15-17.

Cite as: Ibrahim Y., Al-Tamimi S.A., "Flow of Activities: Utilizing Parade of Trade to Develop Visual Management Tool Tailored for Infrastructure Projects", *The 2nd International Conference on Civil Infrastructure and Construction (CIC 2023)*, Doha, Qatar, 5-8 February 2023, DOI: https://doi.org/10.29117/cic.2023.0025

Enhancing Micro-Tunnelling Activity in Infrastructure Construction Adopting Hybrid Lean Approaches: A Case Study

Asghar Kamal
Dorsch Gruppe, Doha, Qatar
asghar_civil@yahoo.com

Saoud Ali Al-Tamimi
Public Works Authority (Ashghal), Doha, Qatar
stamimi@ashghal.gov.qa

Jamal Hakouz
QBEC, Doha, Qatar
j.hakouz@outlook.com

Maryam Shalabi
Al Tawfeeq & Partners, Doha, Qatar
maryamshalabi@outlook.com

Ayman Naser
Engineering Management Program, College of Engineering, Qatar University, Doha, Qatar
an1401569@qu.edu.qa

Abstract

Micro-tunnelling Shaft Excavation (MTSE) is a major part in the development of infrastructure networks in Public Works Authority (ASHGHAL) projects in the State of Qatar. Despite the importance of this activity there has been minimal improvement to the existing methodology. Traditional methods are producing large amount of operational waste such as extra manhours, over-excavation and excess of backfilling materials used. Using collaborative pull planning, a system involving key stakeholders and last planners have been developed to streamline the micro-tunnelling activity. Using a panoply of lean tools, data collection and analysis, MTSE was monitored and evaluated through the Plan, DO, Check and Act (PDCA) cycle that led to around 60% of time saving. The paper summarises the process improvement using collaborative pull planning and applying PDCA with project stakeholders' engagement.

Keywords: Lean Construction; Collaborative Pull Planning; Last Planner System; Micro-Tunnelling; PDCA

1 Introduction

Micro-tunnelling (MT) techniques became necessary as the demand for utility service lines with minimal surface disruption increased. MT is "a trenchless construction method for installing pipelines with all of the following features: remote-controlled from a control panel on the ground surface, laser-guided, pipe sections jacked simultaneously as soil is excavated, with continuous support at the face of the excavation" (Moharrami et al., 2021). MT is a term used to describe remotely controlled pipe jacking operations.

Construction planning for MT projects is a complex process, leading activity and it is considered usually in the critical path for an infrastructure project. Therefore, delay in the construction of MT will lead to delay in project delivery (Moharrami et al., 2021). Despite the importance of this activity, the employed methodology has undergone minimal improvement. Traditional methods generate a

substantial amount of operational waste, such as additional labour hours, over-excavation, and excess backfilling materials (Jain et al., 2022). As a framework for directing future research to improve MT operations, Jain et al. (2022) interpreted the impact factors that are affecting the productivity of MT. Then, they argued that empirical and practical studies to improve the conventional MT method are lacking in the existing literature. Therefore, this paper is developed to answer the research questions, "How can the traditional processes of existing methodologies be enhanced?" and "What tools can be used to enhance these endeavours?"

ASHGHAL has recently introduced the enhanced infrastructure project framework to maximize customer's value and minimize non-value activities (Aslam et al., 2020). Lean Construction is a set of ideas that are practiced by individuals in the infrastructure construction industry (Habibi et al., 2022). These ideas are based on the holistic pursuit of continuous improvements (Malinova et al., 2022) that are aimed at minimising costs and maximising value to clients in all dimensions of the built and natural environment, including planning, design, construction, activation, operations, maintenance, salvaging, and recycling. Lean Construction is also known as "just-in-time" construction (Gunduz & Naser, 2017).

The purpose of this research is to customise a set of improvement tools based on a case study in order to improve the MT process.

2 Methodology

The authors followed the case study methodology in developing this research paper, case studies are suitable for studying phenomena in their real-life contexts where researchers have not previously studied (Naji et al., 2022). ASHGHAL introduced Lean Construction to enhance infrastructure projects performance and delivery. Accordingly, to fulfil the enhanced contract requirements, multiple stages of improvement has been performed. This paper was developed to study the enhanced MT activity as a case study in construction of infrastructure and deep utility.

2.1 First Stage of Improvement – Collaborative Target Planning

A kick-off meeting was held at the beginning of the project with all of the key parties involved in MT activities. The purpose of the meeting was to review the overall scope of the project and to prepare the required data for the subsequent session, which will utilize Collaborative Target Planning (CTP), Pull Planning, Last Planner System (LPS), and Make Ready Plan:

- Collaborative Target Planning (CTP): A workshop held at least six weeks prior to the commencement of the planned works and involving representatives from all key parties (client, consultant, designer, contractor, and subcontractors) with the objective of establishing and update a 12 weeks schedule.
- Pull Planning: A collaborative approach to project scheduling that reverses the sequencing process. This entails gathering team members in order to identify and isolate important project milestones. The team then works backwards to add all required details and specifications.
- Last Planner System: is project production system that encourages the development of a predictable workflow between various parties in order to produce reliable results.
- Make Ready Planning: Ensures the planned work can occur by removing constraints in advance. These constraints are defined using an acronym of DRAMPPSS (i.e., Design, Resource, Access, Materials, Plant, Permits, Safety, and Shared Understanding).

As explained earlier, MT is a leading activity and it is considered as a critical path for the project. A

collaborative session was conducted between all the concerned parties: contractor key personnel, construction team, consultant, client, dewatering subcontractor, MT subcontractor and geotechnical subcontractor. The first step during the session was identifying the milestones from the original monitoring program baseline schedule. During the session, an effective pull planning took place. Moreover, during the session the team focussed on the productivity for equipment and the manpower, the handoffs between the activities, the flow of the work and identifying any constraints. Moreover, DRAMPPSS were discussed and recorded as a commitment with a dedicated individual responsible for the each identified constraint including completion dates and linked with the corresponding activity in the CTP. The practice of all above steps supports the Last Planner System (LPS) exercise.

2.2 Second Stage of Improvement - Direct Work Observation from GEMBA Walk

As part of monthly GEMBA audit, the process of demobilisation and mobilisation of the Micro tunnelling jack setup was observed and considerable waste was noticed, therefore a direct work observation has been performed to verify and enhance the duration of time and productivity for machines and manpower that were discussed in the CTP. Performing the Direct Work Observation is essential in any enhanced project as it provides a clear indication of the Value Adding (VA) activities and Non-Value Adding (NVA) activities and a clear vision on how to improve the process (Gunduz & Naser, 2019):

- GEMBA: is a Japanese term meaning “the real place.” It is a practice of physically walking to the site construction location where value is generated to discover opportunities for improvement in a Lean Construction process.
- Value adding (VA): activities that transform the production or delivery of something that generate value to the customer or next activity; it needs to be maximized.
- Non-Value Adding (NVA): activities that are sheer waste but essential to perform VA activities; it needs to be minimized.
- Waste (W): Anything that consumes time, resources, or space without adding value to the customer’s given goods or services; it needs to be eliminated.
- Direct Work Observation: collecting VA, NVA, and W, which are then analyzed and studied to determine how to improve the process.

The paper examines MT network including around 8.5 km of utilities network and 90 connection shafts. During the site visit and data analysis with the last-planners, it was observed that demobilisation and mobilisation of the tunnel boring machine and its jacking setup is a non-added value activity that should be minimised in order to maximise added value in the micro tunnelling process.

The MT contractor has agreed to increase the number of jacking setups so that each tunnelling machine will operate with two jacking setups. This helped to maximise the utilisation of the tunnelling machine (one to be used with the machine and the other one to be ready for usage once first drive is completed). This will allow overlap in the procedure, allowing for more efficient use of tunnel-boring machines.

2.3 Third Stage of Improvement - Process Continuous Improvement using PDCA

The shaft excavation phase is the first and most critical step in the MT process. Any delay in the excavation plan will have a significant influence on all subsequent activities, the critical path would

be derailed eventually. Utilising continuous improvement approach, the traditional excavation method has been run through two PDCA cycles, each having its own impact and improvement as it will be demonstrated later:

- Continuous Improvement: is an ongoing effort to improve products, services, or processes. These efforts can seek "incremental" improvement over time or a "breakthrough" improvement all at once.
- PDCA cycle: (Plan, Do, Check, Act) is an improvement cycle based on the scientific method of proposing a change in a process, implementing the change, measuring the results, and taking appropriate action.

Traditional Excavation Method

The traditional and basic method to excavate a shaft, requires a regular jackhammer excavator of 20 tons, and a ramp system as an access to excavate reaching a depth more than 5 meters, as it can be seen in Figure 1. This method was used at the initial period of the project to expedite shaft excavation date but was generating a great number of operational wastes that can easily be avoided.

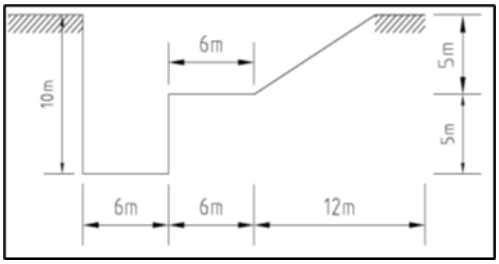


Fig. 1: Traditional Ramp shaft dimensions

First PDCA Cycle: Shaft excavation using Long Boom

The first PDCA cycle preformed to the shaft excavation process. After a thorough process analysis and discussion, the construction team decided to eliminate the use of ramps as it showed it can be improved with the replacement of regular jackhammers of 20 tons by long-boom jackhammers. The discussion revealed that the depth of 10 meters can be reached without the need of using a ramp as shown in Figure 2.

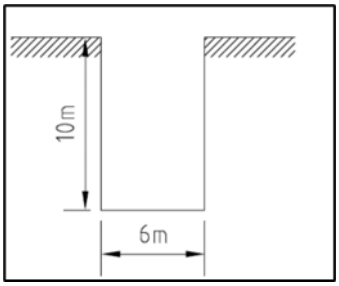


Fig. 2: Improved Shaft Dimensions

Second PDCA: Shaft Excavation using Long Boom Drum Cutter

Following the success of the first PDCA cycle and its implementation on site, a second PDCA cycle was performed. This cycle was supported by data analysis from direct work observations. Facts illustrated that the trimming process took a considerable amount of time. Therefore, the use of a drum cutter was proposed as it has better accuracy and shaft edges quality. The jackhammer tip was

changed from pin head to a drum cutter head and which resulted in major improvements in the process that will be explained later.

3 Outcomes' Analysis

It is evident that performing three stages of improvement concurrently on the MT activity have yielded in beneficial results.

First Enhancement: Collaborative Target Planning

As result of implementing the first stage Collaborative Target Plan (Figure 3), a change into the final plan from the baseline was done, and numerous decisions were made based on the outcomes of the session. Table 1 displays the contrasts between the two planning methods:

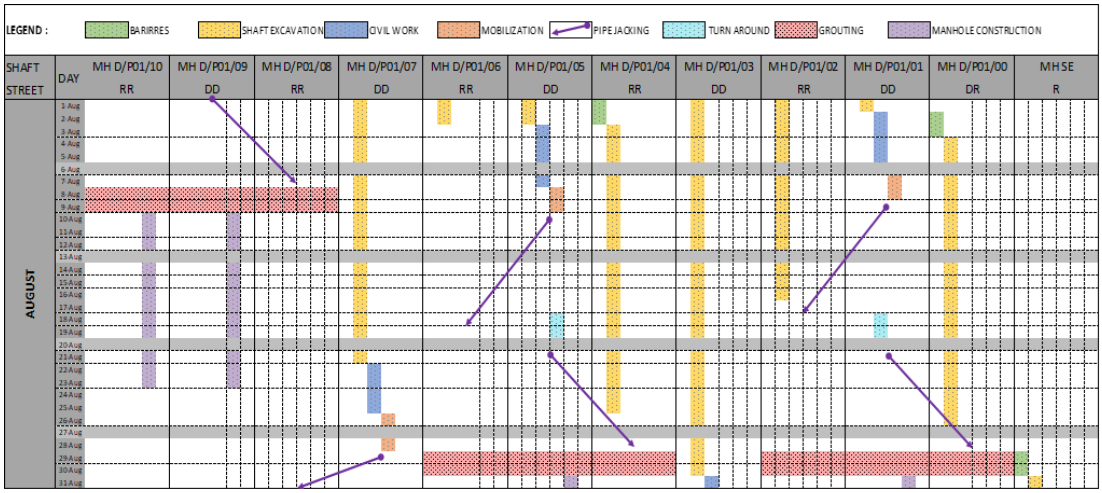


Fig. 3: Final Product of Collaborative Target Planning

Table 1: Comparison between the Baseline Schedule (original Plan) and Pull planning schedule

	Pull Planning Schedule	**Baseline Schedule**
Starting date	18th May 2021 (3 months ahead of Baseline schedule)	1st August 2021 (Project's Original Starting Date)
Slurry Lagoon	Size, Capacity and Possible locations were identified and shared	No common understanding of slurry lagoon details.
Storage Area	Storage Area required for Subcontractors identified	No allocated area
Pre-requisites	Materials, Resources, manpower, permits required were identified before commencement of work. Allowing more time to resolve the requirements	No record of requirements were recorded ahead of time
TBM Machine Numbers	1 TBM machine (Less resources and equipment required to operate at the same time)	3 TBM machine
Dewatering system	Schedule for the system route, sequence, pumps required during the upcoming MT activities	No clear indication on the requirements to operate the system
Dewatering capacity	Municipality have been contacted ahead of time to increase the number of Deep wells from 1 no. to 2.5 nos. Based on the site requirements and geotechnical report	Shortage in capacity would have occurred as only one Deep Well was dedicated to the project
Shaft Excavation sequence	Sequence has been modified to give priority and a head start for shafts that are above the water table	No criteria to decide sequence of the shaft

Second Enhancement: Direct Work Observation from GEMBA Audit

Applying this tool to the MT would potentially save about 120 days of mobilization and demobilization (Figure 4), in addition enabling the team to capture and rectify any issue before shifting the MT boring machine to the next shaft. Further, it allows early detection and resolution of issues faced when setting up the jacking system.

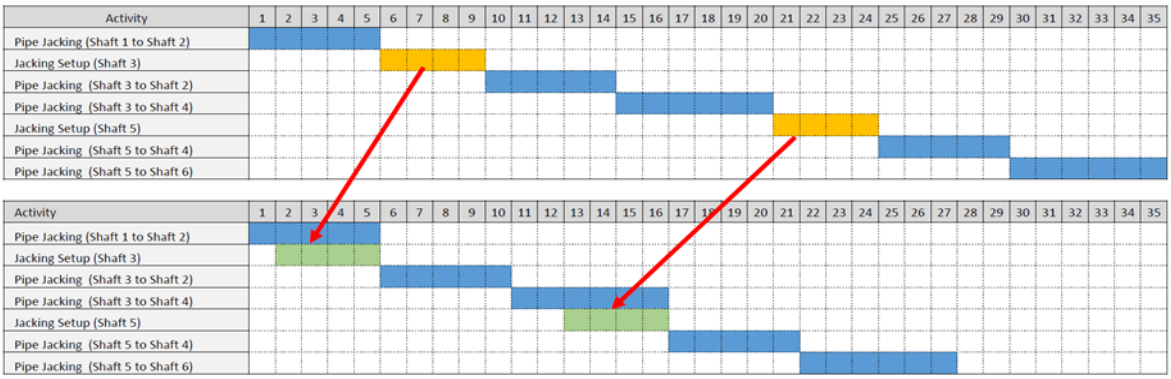


Fig. 4: Optimisation of NVA (Yellow) in MTSE to be Performed Concurrently with Other Tasks

Third Enhancement: Process Continuous Improvement using PDCA cycle

As indicated in Tables 2 and 3, the quantity of excavation material decreased by 63%, excavation time decreased by 33%, shaft working space decreased by 44%, and around 60% of trimming time saved.

Using the final approach with Long-Boom Drum cutters, Table 4 summarizes the considerable reduction in manhours needed to dig the shaft while the size remained unchanged. As trimming is eliminated, shaft excavation duration is optimised by 27%.

Table 2: Size and Time required to Excavate and Trim the Shafts Using the Traditional Method

Traditional Method: Excavation Ramp		
Type of Shaft	Shaft Excavation volume	Ramp Excavation Volume
Jacking	6x6x10= 360 m3	(12x6x5)/2=180m3
Receiving	6x6x10= 360 m3	(12x6x5)/2=180m3
Total Volume Excavated	1080 m3	
Excavation Time needed	120 Manhours	
Trimming Time needed	120 Manhours	
Total Hours needed	240 Manhours	

Table 3: Size and Time required to Excavate and Trim the Shafts using the Long-Boom method

First PDCA cycle: Long-Boom Jackhammers		
Type of Shaft	Shaft Excavation Volume	Ramp Excavation Volume
Jacking	6x4x10= 240 m3	N/A
Receiving	4x4x10= 160 m3	N/A
Total Volume Excavated	400 m3	
Excavation Time needed	112 Manhours	
Trimming Time needed	48 Manhours	
Total Hours needed	160 Manhours	

Table 4: Size and Time required to Excavate and Trim the Shafts using the Long-Boom Drum cutter

2nd PDCA Cycle: Long Boom Drum cutter		
Type of Shaft	Shaft Excavation Volume	Ramp Excavation Volume
Jacking	6x4x10= 240 m3	N/A
Receiving	4x4x10= 160 m3	N/A
Total Volume Excavated	400 m3	
Excavation Time needed	64 Manhours	
Trimming Time needed	N/A	
Total Hours needed	64 Manhours	

MTSE Enhancement benefits

Benefits of this process improvements can be summarized in a quantitative and qualitative comparison, as shown in Table 5. Figures 5 and 6 illustrate the considerable optimisations realized.

Table 5: Qualitative and Quantitative Benefits

Quantitative	Qualitative
Foam Concrete required dropped by 56%	Eliminate Ramp
Shaft excavation area reduced by 44%	Less impact on other nearby trades as ramps are eliminated.
Excavation manhours required decreased to 27% of original time.	Less concrete barriers and edge protection is required to protect the shaft.
Trimming time reduced to 0%	Better utilization of manpower and equipment.
	Minimize disruption by reducing time required to backfill the shaft.
	Increase public satisfaction
	Noise Reduction

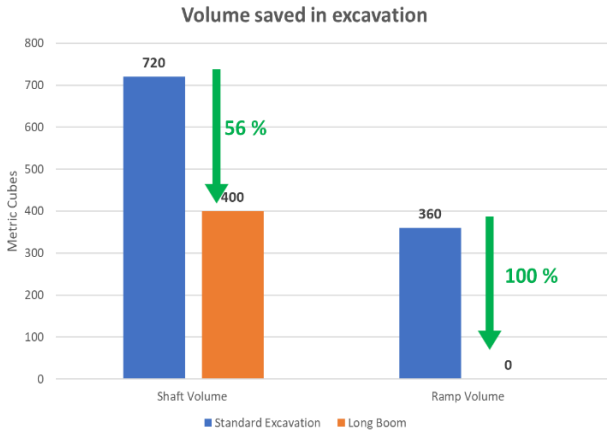


Fig. 5: Reduction in Excavation Volume

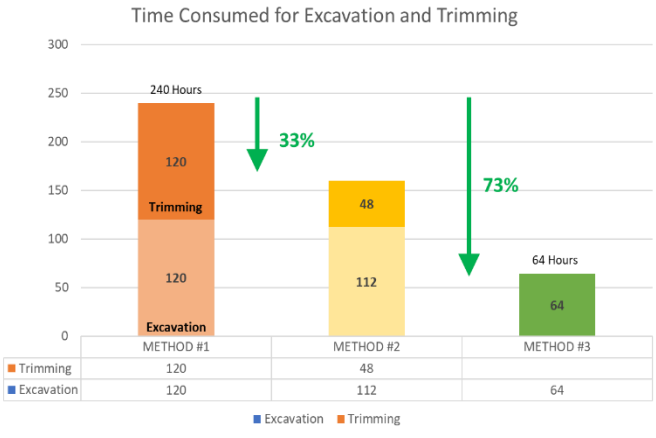


Fig. 6: Reduction in Excavation Time

4 Conclusion

Implementation of Lean tools in the construction industry has vital achievement to enhance the project delivery, mainly, in the construction of the infrastructure. This article demonstrates how the project has undergone three concurrent stages of improvement, with all stages interconnected to

achieve the goal of delivering the final product with less waste and greater value.

CTP addresses the conventional planning approach failures in a lack of cooperation, communication, and transparency. All participants in the collaborative session agreed on the order in which the tasks were to be performed, the required mission for each individual present, the start and end dates, and the required manpower, equipment, and Tunnel Boring Machine (TBM) numbers, which strengthen accountability on the promises taken. In addition, DRAMPPSS identification supported mapping critical prerequisites and deliver accountability for fulfilment.

In addition, the GEMBA has resulted in the implementation of direct work observation, which is an effective method for monitoring an activity and identifying gaps directly. The improvement made to the MT jack setup is a practical example on the GEMBA importance to optimise processes and generate savings.

References

Aslam, M., Gao, Z., & Smith, G., (2020). "Framework for selection of Lean Construction tools based on Lean objectives and functionalities". *International Journal of Construction Management*, 1-12.

Gunduz, M. & Fahmi Naser, A., (2017). "Cost based Value Stream Mapping as a sustainable construction tool for underground pipeline construction projects". *Sustainability*, *9*(12), 2184.

Gunduz, M. & Naser, A., (2019). "Value stream mapping as a lean tool for construction projects". *International Journal of Structural and Civil Engineering Research*, *8*(1), 69-74.

Habibi et al. (2022). "A Conceptual Framework for Implementing Lean Construction in Infrastructure Recovery Projects". *Buildings*, *12*(3), 272.

Jain, M., Reja, V. K. & Varghese, K., (2022). "Exploring the critical factors affecting the productivity of microtunneling pipe installation.

Malinova, M., Gross, S. & Mendling, J., (2022). A study into the contingencies of process improvement methods. *Information Systems*, *104*, 101880.

Moharrami et al. (2021), "A hybrid simulation approach for microtunneling construction planning," *Construction Innovation*, vol. 21 No. 3, pp. 363-378.

Naji, K. K., Gunduz, M., & Naser, A. F., (2022). "Construction change order management project support system utilizing Delphi method". *Journal of Civil Engineering and Management*, *28*(7), 564-589.

List of Acronyms

ASHGHAL	: Public Works Authority
CTP	: Collaborative Target Planning
DRAMPPSS	: Design, Resources, Access, Materials, Plants, Permits, Safety, Shared Understanding
GEMBA	: Japanese term meaning "the real place."
Km	: kilo-meters
LPS	: Last Planner System
MT	: Micro-tunnelling
MTSE	: Micro-tunnelling Shaft Excavation

NVA : Non-Value Adding

PDCA : Plan, Do, Check and Act

TBM : Tunnel Boring Machine

VA : Value adding

W : Waste

Cite as: Kamal A., Hakouz J., Zakaria Y., Shalabi M., Naser A. & Al-Tamimi S.A., "Enhancing Micro-Tunnelling Activity in Infrastructure Construction Adopting Hybrid Lean Approaches: A Case Study", *The 2nd International Conference on Civil Infrastructure and Construction (CIC 2023)*, Doha, Qatar, 5-8 February 2023, DOI: https://doi.org/10.29117/cic.2023.0026

Assessment of Workflow Reliability in Two Infrastructure Projects Considering Efficient Adoption of Lean Leadership Culture and Engagement

Zied Dahmani
AECOM, Doha, Qatar
zdahmani@ashghal.gov.qa

Saoud Ali Al-Tamimi
Public Works Authority (Ashghal), Doha, Qatar
stamimi@ashghal.gov.qa

Ramez Alchamaa
Dorsch Gruppe – Middle East, Doha, Qatar
ramez.alchamaa@dorsch.com

Abstract

An organization leadership culture is the corner stone of success or failure. This paper focuses on Lean Leadership as an emergent concept introduced to many organizations where leaders are role models, empower their teams and make them accountable. In construction projects, culture is usually the combination of behaviours, attitudes, and communication inherited from previous experiences. A culture change is not welcomed unless mandated by the leadership and practiced daily. Where many factors are similar, two projects had different outcomes. A root cause analysis, on two infrastructure projects with the Public Works Authority ASHGHAL in the State of Qatar, reveals that project culture is the driving factor on a successful delivery on time and budget, and complying to quality, health and safety, and environment standards, with a public satisfaction focus. Client pre-set strategic objectives are achieved through a collaborative effort of project team where accountability is the bonding agent between promises and accomplishments. This paper summarizes a lean leadership culture adoption where it established a psychological safe working environment that delivers project to client expectations.

Keywords: Workflow reliability; Lean Leadership; Accountability; Empowerment; Daily huddles

1 Introduction

Construction industry has been characterized by a top-down management structure, similar to a military organization structure where instructions just need to be followed. Then, accountability is not shared, and those who perform the work are responsible just in front of their superiors on how they performed their missions, without being involved in any assessment or actions of improvement (Demirkesen et al., 2019).

The difference between these two structures is in the amount of information received, where in construction accurate data is scarce and incomplete. As Simon Sinek stated in his book “Start with why”: “The point is, we make assumptions. We make assumptions about the world around us based on sometimes incomplete or false information.” This is the norm in construction projects, even if few exceptions exist. To be an exception, special behaviour and organization culture should be adopted and practiced at all levels in a standard manner (Ebbs et al., 2018).

In two infrastructure projects (project A & project B), with similar scope of work (roads and infrastructure in residential areas) and the same external factors (client management, consultant,

stakeholders) outcomes had been widely different, and on several occasions, responses had been totally opposite. Adopting a different working culture (Walter et al., 2020) had been a key difference as witnessed by both projects' stakeholders.

2 Context

In a disrupted ecosystem impacted by COVID-19 pandemic, most of infrastructure projects had suffered a disrupted supply chain, decreasing productivity, poor predictability, and a lack of proper communication between project team members.

Leaders arise in complicated situations to draw a vision and inspire others with a set of attitudes and practices characterized by consistency and efficiency (Manion, 2011). Organization's "Noise" (Kahneman et al., 2016) is intensified in a disruptive environment. Project Manager (PM) should act like a Maestro to clear this "Noise".

A Maestro's skill is to be a good listener at first hand and have the ability to inspire his musical groups to show the best of their talents. Similarly, a PM needs to have a good listening capability to understand and have better view and visibility of how the project is running (Howell & Macomber, 2006). Plus, PM should help his project team member to excel and improve their performance capability through transparency, delegation, and accountability.

PMs of project A & project B had different approaches to drive their teams for the completion stages, with significant different performances, attitudes, and work culture. Data, analysis, and observations supported the Lean Leadership management aspects.

3 Data and Facts

Basic project metrics used to evaluate project performance have been collected from Jun-2019 until Jul-2022. Analysis shows the following:

3.1 Progress:

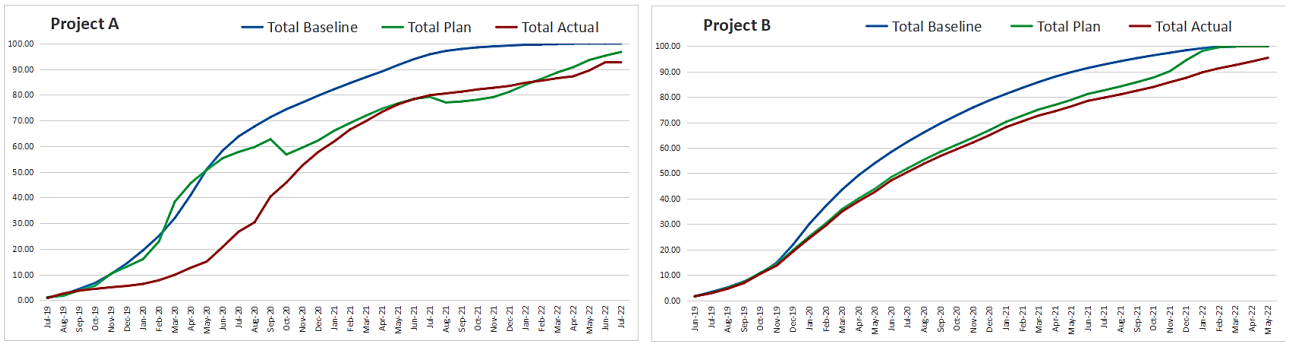


Fig. 1: Progress Curve for Project A & Project B

Project A progress shows a cumulative variance reaching -34.6 on Jun-2020. This led to the appointment of a new Contractor's PM to develop a recovery plan. The recovery took 12 months to catch-up with the Plan. Despite Plan instability due to scope change, project performance remained stable and project completion had been on-time. While project B showed a stable progress almost matching the Plan, the project could not stand ahead and did not deliver on-time.

3.2 Public Satisfaction

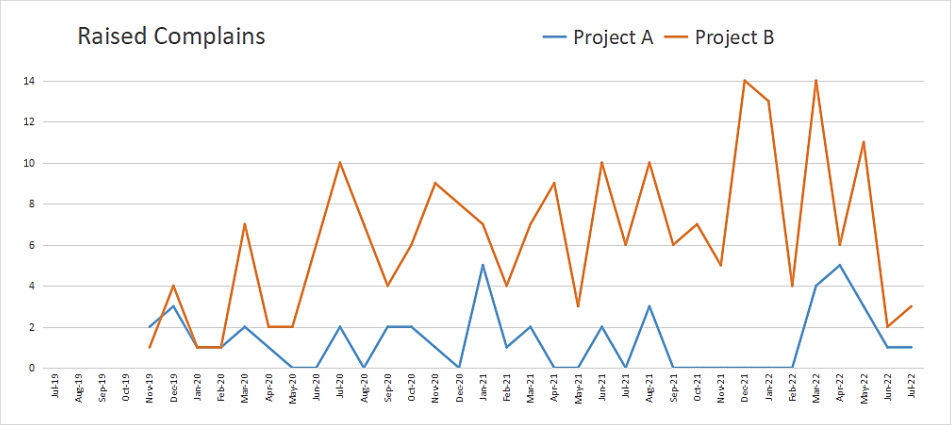


Fig. 2: Raised Complaints per month for Project A & Project B

A key client value is proper coordination with project stakeholders, and especially residents within project zones. Dedicated Public Relations officers are appointed to improve communication and ease any special requests. This section is measured by complaints raised to the client hotline. Figure 2 shows constant complaints track for project B with a monthly average of 5.4 complaint/month, while project A had a monthly average of 1.3 complaint/month and during several months of zero complaints record reaching six consecutive months.

3.3 Quality Management

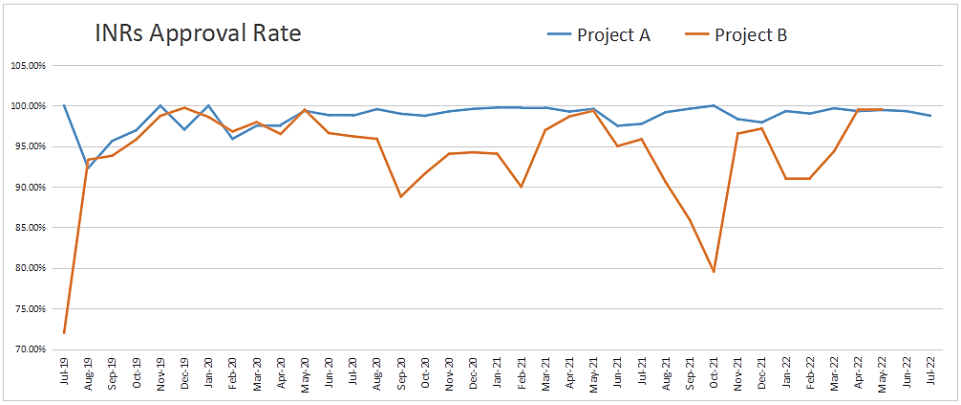


Fig. 3: Monthly Inspection Requests approval rate for Project A & Project B

Inspection Requests (INRs) approval rate is considered as one of the leading project KPI. It reflects the proper planning of inspections with work progress beside the quality compliance. Project A progress recovery from Jun-2020 has been characterized by a stable work inspection and approvals with an average INRs approval rate 99.3% over the 12 months recovery period. Despite its stable progress, project B inspection and approval have been unstable during most of the project life. Figure 3 illustrates this instability in inspection approvals in comparison to the stable performance of project A. Moreover, Figure 4 summarizes the INRs approval ranges, usually a quality assessment approach, where it demonstrates further the instable performance in the presence of a “wider” range of “INR approval probability” in comparison to the narrow range of project A. This stable quality performance helps to strengthen reliability between project shareholders: Client, Consultant, and Contractor. Project A efforts in having a stable quality record was rewarding as it won the client “Quality best practice award” in its first edition.

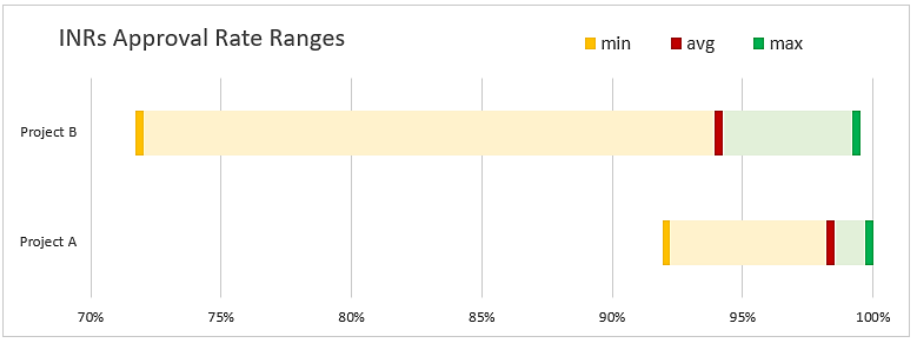


Fig. 4: Inspection Requests Approval rate ranges for Project A & Project B

Another fact that impacted the handover stage in Project B was the high approval proportion of Code B. Figure 5 visualizes the INRs statistics, where in Project B, the Code B INRs yellow area (45%) almost equals the Code A INRs green area (49%). In contrast, project A Code A INRs green area is dominant (80%) and it supported a smooth handover process for completed work.

The revision of Code B INRs to receive Code A approval is a time-consuming process that has a hidden commercial risk of final payment delays, usually not properly identified or assessed. Plus, Code B approval can be avoided with a proper planning of work and coordination of inspections. The time and efforts spent to transfer INRs from code B to code A can be saved easily with a better organization and accountability.

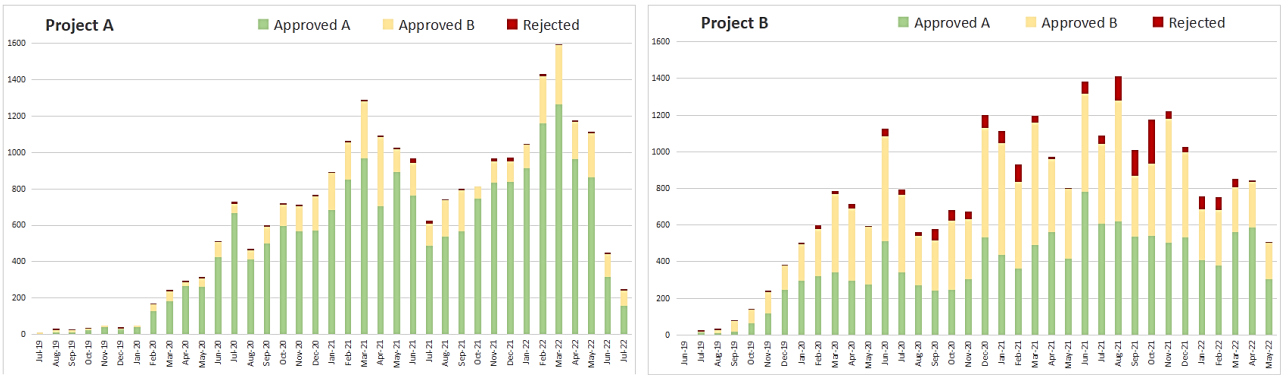


Fig. 5: Monthly Inspection Requests stats for Project A & Project B

Besides, Figures 1 & 5 indicate that submitted INRs had been in line with the Project A on-site progress, on the contrary to Project B where INRs approvals had been delayed in several cases to later stages, which increased rejection rate or Code B approvals, and subsequently impacted the handover process.

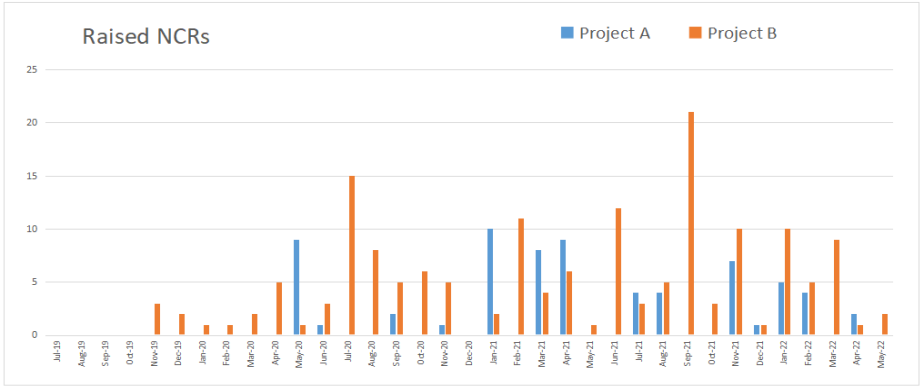


Fig. 6: NCR Issued per month for Project A & Project B

Another index of proper quality compliance is the Non-Conformance Reports records. Figure 6 proves that Project A has a significant different approach towards quality as only 67 NCRs are issued to the 163 NCRs in project B. Details show that NCR close-out was smoother and direct in project A, while project B suffered to reach an agreement with client and consultant rooted in the low reliability level, as stated before.

3.4 Variations and Changes

Typical contractors focus on the cost analysis dashboards during the assessment of project performance. In this aspect, again, both projects had different tactics: Project A focused on delivering value for the client that will support building a relationship of trust, and Project B used each and every argument to challenge client and claim inconsistent cases.

Table 1 summarizes that while both projects had similar percentages of overall change orders amounts (descope in both cases), the overall percentages of approved Extension of Time (EoT) was extensively disproportionate (more than the double). It reiterates the consistency in Project A performance especially a relationship of trust with client versus a devious attitude with the client of Project B management.

Table 1: Variations and Changes stats for Project A & Project B

	Project A	Project B
Change orders amounts (% in reference to original project cost)	-13.38	-13.26
EoT (% in reference to original project duration)	27.62	61.33

4 Root Cause Analysis

Project A success in progress recovery and on-time delivery resulted in receiving client appreciation. Despite its traditional stable progress records, Project B suffered the typical project issues: late delivery, poor quality records, rework phase, delayed handover, and cost overrun.

Project A achievement requires an investigation to uncover the foundations for such success. Most of the common stakeholders to project A and project B acknowledge the contractors' culture as the main difference factors, especially PM's leadership approaches to handle the projects. For this reason, authors used Simon Sinek's Golden Circle questions as an approach to investigate the root causes, as described in Table 2: **What** the project team did? **How** they did it? **Why** they did it?

Table 2: Lean Construction performance root cause analysis for Project A & Project B

	Project A	**Project B**
What	1) Daily huddles for 30 minutes at the end of shift with the participation of all project team, facilitated by PM, and attended by supervision consultant staff. 2) Weekly follow-up on prerequisite for the 3 months look ahead plan, ensuring all requirements are achieved on-time. 3) Critical issues are attended on-site by engineers and managers and resolved on the spot. 4) Site engineers have the authority to take decisions on resources distribution, and weekly and daily targets, assessing all risks incurred.	1) Daily huddles happen occasionally without all project team attendance. 2) Despite having a good planning approach, site engineers were not empowered to take decisions without PM's approval on simple tasks. 3) Site visits had been attended individually to have an update for "just in case" purpose. Joint site visits happened twice during project life. 4) All issues are escalated to PM to get resolved.

	Project A	Project B
How	1) All project team members had the freedom to express their opinions and thoughts, take decisions when necessary and be responsible for the outcomes. 2) PM have direct and open communication with all project team and shares all information and updates. On several occasions PM consults site engineers prior taking any decisions. 3) Work culture had been founded on harmony and transparency without any top-down barriers. 4) Productivity improvement is a weekly discussion point to share lessons learnt and try/use new methodologies.	1) Site engineers take a defensive approach on productivity topics and a "push back" response for issues/risks. 2) PM had an authoritarian approach that resulted in slow progress during his absence. 3) Work culture is the standard of "silos" despite several attempts to improve horizontal communication and coordination. 4) Labour productivity is not a concern as no data is available to discuss. During commercial assessment, manpower reduction is an immediate solution without productivity evaluation.
Why	1) To deliver the project and mitigate the -34.6% variance, project team stated that adaptability, especially during COVID19, need empowerment and accountability by all project team members. 2) As stated by PM "disruption requires strong adaptability, and there is no other option than having a strong team culture and accountability."	3) Lack of work culture. 4) Lack of leadership's long-term visibility. 5) Traditional ad-hoc remedy mindset to issues and concerns.

5 Key Success Factors

Project B shows that a classic authoritarian project management system can no longer respond to external and internal constraints and remain manageable. Project A records reflect the flexibility generated through leadership engagement and project members empowerment. Establishing the Lean activities routine manifested the development of "Tuckman Ladder Model" five stages within the project (Kumar et al., 2014).

The comparison between the two projects lead to three key success factors that made the difference. Table 3 describes the key success factors identified:

Table 3: Lean Construction key success factors for Project A

Success Factors	How?
Strong Team Communication	1) Ensure daily huddles are attended by all project team and led by PM for 15-20 min as a recap of: what is achieved? any missed targets? Why it is was missed? How to mitigate? What is the target for tomorrow? Is it achievable? Any support needed? 2) Visualization using proper charts and layout in a big room or visual performance centre is essential for an effective daily huddle.
Empowering the team	1) Delegation of decision making at operational level with an acceptable tolerance; setting clear and measurable commitments; establish an accountability culture through engagement in planning and execution (Tillmann et al., 2012). 2) Create a psychologically safe working environment, where project members speak freely without concerns to be punished or humiliated. It is the foundation for the team to trust each other and set-up a mindset of reliability in making and keeping promises.
Continuous Improvement	1) Challenging the status-quo: it is an attitude that needs space and time to be harnessed. 2) Adopting Standard Lean Construction practices such as GEMBA walks, 5S, etc to collect, analyse and assess data for the purpose of finding what can be improved? Then how?

A project team relationship is key contributing factor of failure or success of the project (Fauchier et al., 2013). Vertical relationships pattern is designed by the PM and defines the leadership model to be exemplified by the PM himself (Howell et al., 2004). Lean Leadership is a new and powerful approach to steer a project toward success in a disruptive ecosystem.

6 Conclusion

Project A and Project B exemplify a case of traditional management culture and another of adaptive management culture. Records from both projects reflect how success is being established during and upon delivery of the project.

Fayol "command and control" model build on central authority of planning and administration is no longer the right approach to manage a disruptive ecosystem. Lean Leadership model based on being a role model, establishing a team culture, coaching and mentorship, and motivating others to improve and excel is the new norm of successful project delivery. Lean Leadership training (Shang, 2014) is the vehicle for bringing PMs to this contemporary need. PMI incorporates Lean Management concepts in the PMBOK seventh edition, especially on new performance domains in project management, namely, Domain I: People, Domain II: Process, and Domain III: Business Environment. To be able to practice those newly introduced concepts, PMs should have a set of Lean Leadership skills learnt and practiced on daily basis as a standard working attitude. Lean Leadership is a component of an organization transformation that requires a "Lean Strategy" to standardise and sustain the development and practice of the new norm requirement.

References

Demirkesen et al. (2019). 'Identifying Barriers in Lean Implementation in the Construction Industry' In:, Proc. 27th Annual Conference of the International Group for Lean Construction (IGLC). Dublin, Ireland, 3-5 Jul 2019. pp 157-168.

Ebbs, P. J., Pasquire, C. L. & Daniel, E. I. (2018). 'The Last Planner® System Path Clearing Approach in Action: A Case Study' In: 26th Annual Conference of the International Group for Lean Construction. Chennai, India, 18-20 Jul 2018. pp 724-733.

Fauchier, D. & Alves, T. C. L. (2013), 'Last Planner® System is the Gateway to Lean Behaviors.' In: Formoso, C. T. & Tzortzopoulos, P., 21th Annual Conference of the International Group for Lean Construction. Fortaleza, Brazil, 31-2 Aug 2013. pp 559-568.

Howell et al. (2004). 'Leadership and Project Management: Time for a Shift from Fayol to Flores.' In: Bertelsen, S. & Formoso, C. T., 12th Annual Conference of the International Group for Lean Construction. Helsingør, Denmark, 3-5 Aug 2004.

Howell, G. & Macomber, H. (2006). 'What Should Project Management Be Based On?' In:, 14th Annual Conference of the International Group for Lean Construction. Santiago, Chile, 1-. pp 41-50.

Kahneman et al. (2016). Noise: How to Overcome the High, Hidden Cost of Inconsistent Decision Making, Harvard Business Review October 2016 issue (pp.36–43).

Kumar S, Deshmukh V & Adhish VS. (2014) Building and Leading Teams. *Indian J Community Med., 39*(4): 208-13. doi: 10.4103/0970-0218.143020. PMID: 25364143; PMCID: PMC4215500.

Manion Jo. (2011), From Management to Leadership: Strategies for Transforming Health, pp.40, Josey-Bass, San Francisco, CA.

Shang, G. (2014). 'Toyota Way Lean Leadership: Some Preliminary Findings From the Chinese Construction Industry.' In: Kalsaas, B. T., Koskela, L. & Saurin, T. A., 22nd Annual Conference of the International Group for Lean

Construction. Oslo, Norway, 25-27 Jun 2014. pp 1145-1156.

Sinek Simon (2009). Start with Why, ch. 1 pp. 11, and ch. 3 pp. 41-56, Portfolio, Penguin Group, London WC2R ORL, England.

Tillmann, P. et al. (2012). 'A Case Study on Benefits Realisation and its Contributions for Achieving Project Outcomes.' In: Tommelein, I. D. & Pasquire, C. L., 20th Annual Conference of the International Group for Lean Construction. San Diego, California, USA, 18-20 Jul 2012.

Walter, R et al. (2020). 'A Requirement Model for Lean Leadership in Construction Projects.' In: Proc. 28th Annual Conference of the International Group for Lean Construction (IGLC). Berkeley, California, USA, 6-10 Jul 2020. pp 145-156.

Cite as: Dahmani Z., Alchamaa R. & Al-Tamimi S.A., "Assessment of Workflow Reliability in Two Infrastructure Projects Considering Efficient Adoption of Lean Leadership Culture and Engagement", *The 2nd International Conference on Civil Infrastructure and Construction (CIC 2023)*, Doha, Qatar, 5-8 February 2023, DOI: https://doi.org/10.29117/cic.2023.0027

Implementation of Building Information Modelling (BIM) on Public Infrastructure and Building Projects in Qatar

Robert Grys
Public Works Authority (Ashghal), Doha, Qatar
rgrys@ashghal.gov.qa

Abstract

Building Information Modelling (BIM) is a term that has been referenced around the world by many practitioners and researchers. This modern methodology for project delivery improves the quality, time, and cost of any type of asset. BIM is not just applicable for buildings, it is equally applicable to utilities, infrastructure, and civil engineering projects. The Public Works Authority of Qatar recognizes the importance and the imperative of collaborative BIM to enhance design, construction, operation and maintenance of its building and infrastructure assets. The authority commits to the implementation of BIM and mandates its use on all public infrastructure and building projects over the complete lifecycle. This paper illustrates the implementation roadmap and strategy, in accordance with the Corporate Strategy and Qatar National Vision 2030, to adopt modern methodologies for design and construction delivery across the country. Anticipated benefits in each project stage will be highlighted, as well as the selection of standardized BIM uses within the authority and its supply chain. The authority has developed and published the *Ashghal BIM Standards* (ABIMS), which comprise of various specifications, templates, and guides. Those standards build on the existing code of practice for the collaborative production of architectural, engineering and construction information (ISO-19650: 2018). Finally, the historic establishment of a corporate BIM policy is fundamental for an enterprise and industry-wide adoption, building the governance on a unique concept – the four components of BIM Implementation – namely foundation, organisation, operation, and technology.

Keywords: Digital Transformation; BIM; Building Information Modelling; Information Technology; BIM Implementation

1 Introduction

More than USD $200bn was budgeted for the investment in the massive development of new roads, stadiums, facilities, and other major projects in the State of Qatar in the period between 2011- 2022. Most of this budget is dedicated to the transport sector that is required to support FIFA World Cup Qatar 2022 and Qatar National Vision (QNV) 2030 to meet the rapid infrastructure and economic growth (Ministry of Municipality, 2016). The QNV 2030 aims at transforming Qatar into an advanced country, capable of sustaining its own development and providing for a high standard of living for all its people for generations to come (General Secretariat For Development Planning, 2008). Qatar's National Vision defines the long-term goals for the country and provides a framework in which national strategies and implementation plans can be developed, such as the Corporate Strategy 2018-2022 of the Public Works Authority 'Ashghal'. This strategy aimed at "continuously enhancing customer satisfaction through leading project and asset management services and solutions" (Public Works Authority, 2018) and has set the foundation for the implementation of Building Information Modelling (BIM) within Ashghal for public infrastructure and building projects in the State of Qatar.

Before initiation of the 'Implementation of BIM programme' the subject has not been entirely new to Ashghal, since several design and construction projects have been tendered and delivered with 'some' BIM requirements. In 2017, the Public Works Authority piloted the implementation of lean construction principles within a few projects in Qatar to improve project performance and predictability of delivery. Following realization of tangible benefits through the pilot application, Ashghal made it contractual to implement Lean in future projects (Al-Buenain et al., 2020).

One of the major challenges can be observed in the way projects are managed by different departments within Ashghal, where each is responsible to tender, deliver or even maintain specific assets, like roads, drainage networks, or buildings. This occasionally has led to variations in project BIM requirements and non-uniform contractual scope within projects in different departments. The implementation of BIM in project contracts was not mandatory, since no new or existing company policy has demanded it. In addition, the lack of relevant standards within the authority and local industry has led to misinterpretations and different understanding of delivery requirements. It has been a logical consequence that a unified and company-wide digital transformation initiative, including revision of policies and processes, development of standards and templates, shall be the only way forward.

The purpose of this paper is to highlight and summarize key efforts in the BIM implementation journey of Ashghal. It shall elaborate how to structure the implementation of BIM within an authority with a variety of infrastructure and buildings projects. Further it illustrates a realistic timeline for an implementation considering existing inhouse staff and supply chain capabilities. The paper starts with a review on literature and methodology, before results of the Ashghal BIM implementation programme will be discussed. Finally, the paper will give a conclusion and recommendations.

2 Methods

Benefits of BIM as a methodology for project delivery to improve efficiency and quality of work were proven by numerous case studies and implementations on company and national level. The complex-scale project "Lusail Plaza" in Qatar has demonstrated how BIM integration in the coordination process can decrease clashes and improve progress of work during the construction phase (Abotaleb et al., 2020). Benefits can be expected in each project stage for a variety of stakeholders, including the owner, the designer, contractor and facility manager. Especially, benefits for the authority as the owner and operator have been aimed at, such as design benefits, increased building quality, improved collaboration, improved commissioning and handover of facility information, and integration with asset operation and maintenance systems (Eastman et al., 2011).

A majority of construction companies report a positive return on invest (ROI) on their BIM programs and that contractors in all markets are planning to expand their BIM programs over the next years (McGraw Hill Construction, 2014). A report on the business value of BIM for infrastructure revealed that BIM users at a high level of implementation (on at least half of their projects) grew from 20% in 2015 to 52% in 2017. Between 2017 and 2019, the growth in BIM implementation is most dramatic among those deploying BIM on nearly all (75% or more) of their projects, with the percentage almost doubling from 17% to 32% (Dodge Data & Analytics, 2017).

The higher management in Ashghal has not questioned if BIM can generate benefits for future design and construction projects, but has proclaimed a top-down implementation of BIM programme and tasked the project team to develop a respective scope and roadmap, tailored to the nature of Ashghal's business. The team investigated the "state of the art" and maturity of BIM adoption internationally,

where reports display the significant adoption of BIM by Governments throughout the world (McAuley, 2017). A focus has been set on Hongkong and Singapore as a case study, which are not only comparable to the size of Qatar but also have taken a pragmatic approach in mandating BIM, including adequate technical specifications and education programmes.

The *Roadmap for Digital Design and Construction* from the Federal Ministry of Transport and Digital Infrastructure in Germany aims on a gradual introduction of BIM, in which the first phase constitutes the preparatory phase and a second phase which starts with systematic scaling up the application of BIM in a larger number of pilot projects, before the broad implementation will begin in a third phase (Federal Ministry of Transport and Digital Infrastructure, 2015). This has ultimately inspired the Ashghal BIM implementation roadmap, which will be elaborated in the next chapter.

3 Results

3.1 Objectives

At the programme kick-off, the team has defined main corporative objectives for the BIM implementation to highlight areas for improvement and emphasize on a project lifecycle approach:

- Deliver intelligent 3D models for building and infrastructure projects to be used throughout the lifecycle of the programme.
- Facilitate collaboration, design proofing, and constructability reviews.
- Ensure a coordinated design by clash avoidance to reduce errors in the field.
- Streamline planning, progress reporting, and cost control.
- Improve commercial and contract management.
- Enhance visualization for communication and decision making.
- Support operation & maintenance with handover of reliable and accurate asset data.
- Take leadership in national BIM implementation.

3.2 Implementation Roadmap

Taking leadership in the national BIM implementation has been imperative to the senior management, since the Public Works Authority of Qatar is in a prominent position to lead innovation initiatives and drive a country-wide adoption of construction technologies, especially when it comes to improvements of industry standards and policies. The *Ashghal BIM Implementation Roadmap* (**Fig. 1**) illustrates a staged implementation strategy, consisting of three stages from the year 2018 to 2022.

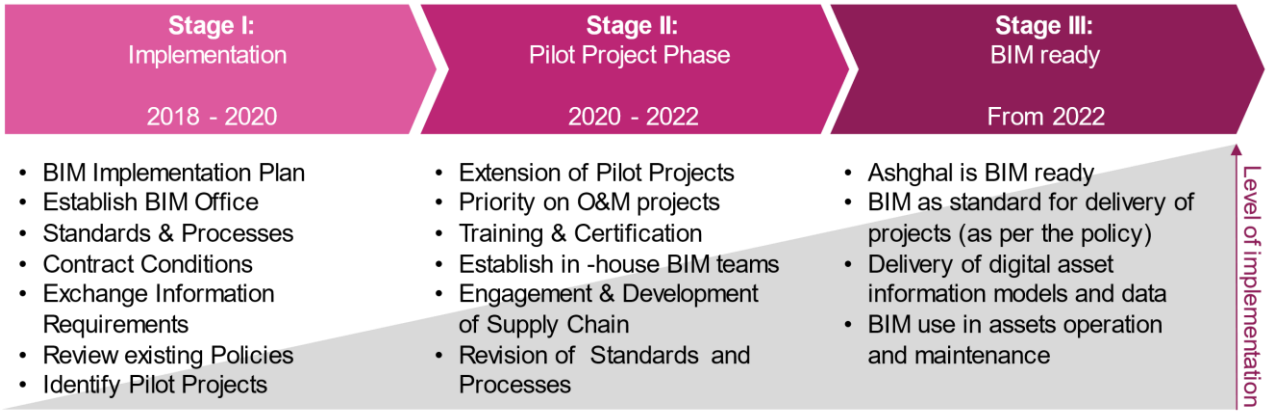


Fig. 1: Ashghal BIM Implementation Roadmap

The first stage ‘Implementation’ describes the foundational development of documents, from the overall implementation plan to other paperwork like policies, standards, and templates. It also included the organisational setup and implementation of one core team to lead and govern the subject within the company and coordinate between departments and other internal or external stakeholders. The second 2-year stage ‘Pilot Project Phase’ allowed the practical use of documentation on pilot projects, where the focus was set on the asset handover and technical procedures to integrate data from As-Built information models into operation & maintenance, in particular geospatial information system (GIS) and enterprise asset management system (EAMS).

The application of new standards on pilot projects also allowed to engage with the supply chain to gather valuable feedback for a revision of standards and processes. A training and certification programme has been rolled out to develop existing staff capabilities and establish in-house teams in concerned departments. The third stage from 2022 onwards marks the readiness of the authority, where BIM is mandatory for the delivery of design and construction projects as per company policy with the ultimate objective to use asset information models and data for the operation & maintenance.

BIM is not just about publishing a mandate or procuring software licenses, hence the definition of the implementation scope required an analysis of all relevant aspects including the inclusion of new roles like the *Information (or BIM) Manager* where challenges have to be identified along the project lifecycle and categorized (Grys & Westhorpe, 2011). The Ashghal implementation team has applied this unique concept to structure the implementation and governance into the *Four Components of BIM* (**Fig. 2**), namely *Foundation*, *Organisation*, *Operation*, and *Technology*.

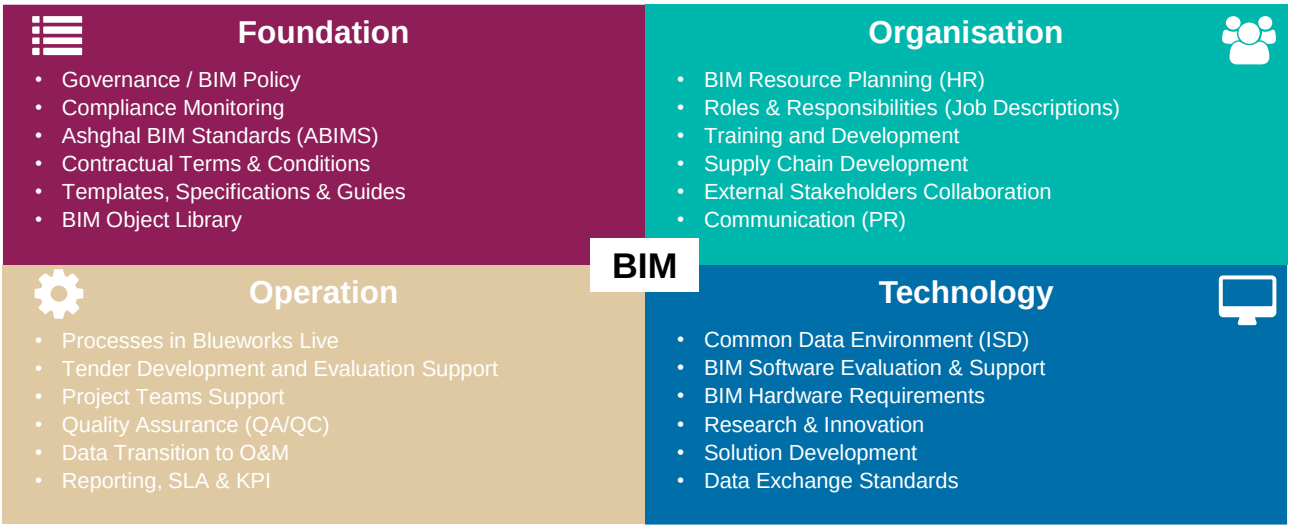


Fig. 2: Four Components of BIM

3.3 Foundation

The core of the *‘Foundation’* component is the corporate BIM policy, in which Ashghal commits to implement key aspects like to ensure delivery of *Asset Information Models* (AIM), produce in-house design works using model-based workflows and processes, implement a *Common Data Environment* (CDE), and train employees to achieve necessary BIM software capabilities. The Policy is applicable to all roads, highways, drainage, and buildings tenders and projects across the design, construction, and operation & maintenance phases, unless they are specifically exempted by Ashghal (Public Works Authority, 2022). The policy also defines guidelines, roles, and responsibilities of concerned departments, structured into the four components of BIM.

The team has developed and published the *Ashghal BIM Standards* (ABIMS), which comprise of various specifications, templates and guides. Those standards build on the existing code of practice for the organization and digitization of information about buildings and civil engineering works, including Building Information Modelling, namely *Part 1: Concepts and principles* (ISO, 2018a), *Part 2: Delivery phase of the assets* (ISO, 2018b), *Part 3: Operational phase of the assets* (ISO, 2020a), *Part 4: Information exchange* (ISO, 2022), *Part 5: Security-minded approach to information management* (ISO, 2020b).

Qatar Railways Company has cooperated with Ashghal before initiation of the programme and provided support including the full documentation of *Qatar Rail BIM Guidelines* (QRBG) as input for Ashghal standards development. The goal of the QRBG implementation is to secure consistent information delivery of the projects contracted under the Qatar Rail BIM programme. This is achieved by providing contractors with clear guidance and delivery requirements in the form of BIM guidelines (Qatar Railways Company, 2017). Another supporting documentation has been provided by the *Qatar-BIM Project* (Dawood, 2014) directed by Prof. Nashwan Dawood (School of Science and Engineering, Teesside University) and funded by the *Qatar National Research Fund* (QNRF). The publications and objective reports of this project have given recommendations for the development of standards and requirements in Qatar. Hafeez et al. (2016) aimed to develop a set of principles and recommendations for the employers information requirements (EIR), which are applicable to Qatar's construction sector.

Finally, to support in-house design, a library with an initial amount of 250 BIM objects has been developed in coordination with the Designs Department. The objects have been modelled to an agreed level of development for drainage (93 objects), roads (57), and buildings (100).

3.4 Organisation

The '*Organisation'* component is focusing on the people, internal staff as well as external supply chain. The implementation programme has been executed by a core team of specialists, managed by a corporate BIM Lead, and supported by an external consultant. The assignment of focal points and BIM champions in each department ensured the internal support and coordination within the organisation. A crucial factor for success has been the setup of a decentralized BIM organisation with one governance team on top and a Lead in each department, which is responsible to grow the internal team as per department needs based on project workload and requirements. This structure allows an allocation of expertise and knowledge at the place where BIM is happening, instead of centralising all staff in one place and risk that BIM is executed in a silo.

For the standardisation of internal BIM positions, the team has developed job descriptions with required competencies, key responsibilities, and qualification criteria. The *BIM Specialist* is in a senior role and is managing and overlooking BIM delivery for Ashghal projects within the department. The *BIM Coordinator* assists the *BIM Specialist* in coordination and execution of BIM projects, while the *BIM Technician* has the primary function to support in the production and management of information models and creation of accurate design drawings or other model derivatives, as well as quality assurance.

To ensure internal knowledge transfer, a comprehensive learning and development programme has been rolled out. A total of 17 training modules have been developed (refer to Fig. **3**), which were divided into seven (7) management and ten (10) software trainings.

BIM Management Training

Code	Module Name
M1	BIM Implementation and Fundamentals
M2	BIM Strategy, Procurement, and Governance
M3	BIM QA & QC
M4	BIM for Management
B1	BIM for Design
B2	BIM for Construction
B3	BIM for Operation and Maintenance

BIM Software Training

Code	Module Name
S1	Software Training: Design Authoring (Architecture)
S2	Software Training: Design Authoring (Structure)
S3	Software Training: Design Authoring (MEP)
S4	Software Training: Design Authoring (Infrastructure)
S5	Software Training: Construction Scheduling 4D
S6	Software Training: Measurement & Cost Management 5D
S7	Software Training: Design Review
S8	Software Training: Design Coordination
S9	Software Training: Model Viewing
S10	Software Training: Rendering & Visualisation

Fig. 3: Ashghal BIM Learning & Development Modules

The management modules cover topics like BIM fundamentals, procurement, quality assurance and include sessions for practical application during design, construction, and operation & maintenance. The software modules cover hands-on trainings in selected software applications, including design authoring and review, design coordination, construction scheduling and measurement. Due to the global pandemic in the years 2021-2022 the training programme has been rolled out in a mix of classroom and online training sessions.

3.5 Operation

The *'Operation'* component refers to the operational setup of the authority to perform BIM, specifically the integration into internal business processes and establishment of communication procedures and reporting methods. The majority of practical BIM execution on projects is being delivered by Ashghal's supply chain, such as design consultants, supervision consultants, and contractors. However, a significant amount of activities is assigned internally, such as design authoring, design review and approvals, model compliance checks, clash detection, quantity surveying, document & data management, etc.

The BIM governance function within Ashghal is assigned to the Engineering Information Systems Section within the Engineering Services Department, the 'home' of BIM, CAD & GIS. This core team has established a number of internal services to support BIM activities, including digital request forms, procedures and a service level agreement. In addition, the team has identified around 35 touch points in the existing business processes across departments and made required amendments to enable BIM-based project delivery, such as 'Develop Tender Documents,' 'Develop in-house Design & Design Development,' 'Manage Projects Handover, and 'Manage Design Review.'

A concept and procedure for project monitoring and reporting has been established, which includes project dashboards for status tracking during tender and delivery stages. An essential element is the continuous coordination with focal points and specialists of internal departments, supported by a communication website for any BIM matters, such as access to standards, templates, contacts, dashboards, and training documentation.

The practical application of information models for specific purposes is often referred by the industry as 'Model Uses' (Succar, 2019) or 'BIM Uses' (Pennsylvania State University, 2019). BIM Uses are intended or expected project deliverables and can be defined as a method of applying Building Information Modelling during an asset lifecycle to achieve one or more specific objectives.

Pennsylvania State University (2019) initially lists 25 BIM Uses, and Succar (2019) expands a Model Uses Table to 52 general uses with hundreds of potential synonyms. The Ashghal team decided to initially focus on ten (10) main BIM Uses (refer to Fig. **4**), to standardise general requirements on projects and encourage the concept of practicality and simplicity.

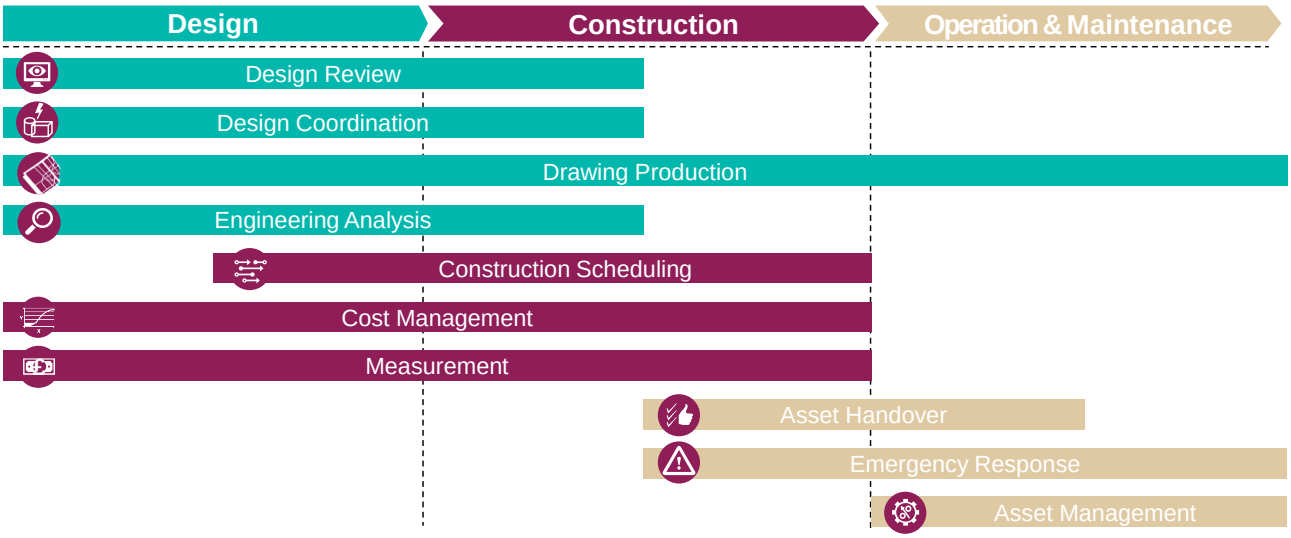


Fig. 4: Main Ashghal BIM Uses

According to the corporate BIM policy, all projects shall employ those selected BIM Uses, as applicable for the project stage and detailed in the project requirements and BIM standards, but not limited to (1) Design Review, (2) Design Coordination, (3) Drawing Production, (4) Measurement, (5) Construction Scheduling, (6) Cost Management, (7) Engineering Analysis, (8) Asset Handover, (9) Emergency Response, (10) Asset Management.

3.6 Technology

The *'Technology'* component involves all required IT-related topics to enable a smooth transition to BIM-based project delivery, such as computer hardware, software applications, data exchange, and cloud collaboration technologies. Personal computers for approximately 2000 Ashghal employees have to be regulary maintained, upgraded and exchanged. The team has identified required hardware specifications for desktop and laptop computers. A 'Standard' and 'Performance' configuration has been defined for each, which resulted in four different specifications. The 'Standard' has been assigned to users mainly working in regular office applications, having low interaction with 3D models (e.g. viewing only) and drafting in CAD applications. Power users primarily authoring 3D models and running clash detection or other engineering analysis applications have been assigned for the 'Performance' configuration.

The selection and procurement of software licenses followed an analysis of market leading solutions for certain BIM activities and consideration of existing internal staff skills and capabilities. The intention was to define a corporate software standard for main activities, such as buildings design authoring, roads and drainage design authoring, clash detection, design review, structural analysis, planning & scheduling, quantification, cost management, and visualisation. To enable smooth collaboration with the supply chain and enable compatibility of data submissions, selected software applications and file formats have been incorporated in the *Ashghal BIM Standards*.

Another strategic decision has been made with the introduction of cloud-based BIM technologies, which allows architects and engineers to easily access 3D information models and coordinate from

virtually anywhere. Storing information models in the cloud means project members can upload and access the latest version of their models, and work from one single source of truth. Design issues and clashes on a construction project can be detected quicker since actual data is used by the entire team. Further, cloud technology has been implemented for project visualisations and reviews of data submission by Ashghal's supply chain, which required an integration with existing project management systems.

4 Conclusion & Recommendation

This paper highlighted key elements of Ashghal's BIM implementation programme to emphasize that BIM impacts various business areas and is not just about technology alone. The focus has not been set on the question if BIM should be implemented for public projects in Qatar, but rather how the implementation scope shall be structured and what roadmap is suitable considering staff and supply chain capabilities. A staged implementation roadmap with an embedded phase for pilot projects can be recommended to any organisation where internal capabilities are middle to low.

Essential for a successful implementation and commitment from all staff is the foundation component with a corporate policy and standards. The methodology of using the four components of BIM can be transferred to any organisation in the construction sector. A top-down approach with a committed support by the higher management is fundamental for a structured and sustainable implementation programme.

Finally, it can be expected that the Public Works Authority will continue to improve BIM project delivery on public projects and take leadership in the national BIM implementation to contribute towards a country-wide adoption and development of national BIM standards for the entire Qatar construction sector.

References

Abotaleb M. M., Saab E., & AbdelZaher M. (2020). Integrating Building Information Management (BIM) in Civil Infrastructure Coordination: Application at Lusail Plaza. *International Conference on Civil Infrastructure and Construction (CIC 2020).* Doha, Qatar, 2-5 February 2020. DOI: https://doi.org/10.29117/cic.2020.0032

Al-Buenain A., Al-Muhanadi S. & Falamarzi M., (2020). The New Construction Approach Adapted by Ashghal for the Public Projects in Qatar. *International Conference on Civil Infrastructure and Construction (CIC 2020).* Doha, Qatar, 2-5 February 2020, DOI: https://doi.org/10.29117/cic.2020.0027

Dawood, N. (2014). *Development of a Whole Life Cycle Information Flow Approach enabled by BIM Modeling Protocols and Technologies for Qatar Construction Industry.* QNRF. https://www.qatar-bimproject.org

Dodge Data & Analytics (2017). *The Business Value of BIM for Infrastructure 2017*. Stephen A. Jones, Research & Analytics, Bedford MA, United States.

Eastman et al. (2011). *BIM handbook: A guide to building information modeling for owners, managers, designers, engineers and contractors*. John Wiley & Sons.

Federal Ministry of Transport and Digital Infrastructure (2015). *Road Map for Digital Design and Construction, Introduction of modern, IT-based processes and technologies for the design, construction, and operation of assets in the built environment*. December 2015. Berlin, Germany.

General Secretariat for Development Planning (2008). *Qatar National Vision 2030*. https://www.gco.gov.qa/en/about-qatar/national-vision2030.

Grys, R. & Westhorpe, M. (2011). 'The BIM Manager', *BIM Journal, Volume 3 – 2011-2012, Issue 33,* pp. 63–67. https://www.linkedin.com/pulse/bim-manager-20-robert-grys/

Hafeez et al. (2016). 'Principles and recommendations for client information requirements for BIM enabled construction projects in Qatar', *International Journal of Product Lifecycle Management*, vol. 9, No. 3, pp.198–218.

ISO (2018a). *Organization and digitization of information about buildings and civil engineering works, including building information modelling (BIM) – Information management using building information modelling – Part 1: Concepts and principles* (ISO 19650-1: 2018).

ISO (2018b). *Organization and digitization of information about buildings and civil engineering works, including building information modelling (BIM) – Information management using building information modelling – Part 2: Delivery phase of the assets* (ISO 19650-2: 2018).

ISO (2020a). *Organization and digitization of information about buildings and civil engineering works, including building information modelling (BIM) – Information management using building information modelling – Part 3: Operational phase of the assets* (ISO 19650-3: 2020).

ISO (2022). *Organization and digitization of information about buildings and civil engineering works, including building information modelling (BIM) – Information management using building information modelling – Part 4: Information exchange* (ISO 19650-4: 2022).

ISO (2020b). *Organization and digitization of information about buildings and civil engineering works, including building information modelling (BIM) – Information management using building information modelling – Part 5: Security-minded approach to information management* (ISO-19650-5: 2020).

McAuley, B., Hore, A., & West, R. (2017). BICP global BIM study-Lessons for Ireland's BIM programme. *Dublin Institute of Technology: Dublin, Ireland.*

McGraw Hill Construction (2014). *The Business Value of BIM for Construction in Global Markets.* Harvey M. Bernstein, McGraw Hill Construction, Bedford MA, United States.

Ministry of Municipality (2016). *Qatar National Development Framework*. https://www.mme.gov.qa/QatarMasterPlan /English /QNDF.aspx?panel=qndf

Pennsylvania State University (2019). *BIM Project Execution Planning Guide v2.2*. https://psu.pb.unizin.org /bimprojectexecutionplanningv2x2/

Public Works Authority (2018). *Ashghal Corporate Strategy 2018-2022: Vision, Mission, Values – Our Strategic Themes*. Doha, Qatar. https://www.ashghal.gov.qa/en/AboutUS/Pages/Mission.aspx

Public Works Authority (2022). *Building Information Modelling Policy v1.0*. Doha, Qatar.

Qatar Railways Company (2017). *Qatar Rail BIM Guidelines (QRBG)*. Doha, Qatar.

Succar, B. (2019). *211in Model Uses Table (1.26)*, Zenodo. DOI: https://doi.org/10.5281/zenodo.3563403

Cite as: Grys R., "Implementation of Building Information Modelling (BIM) on Public Infrastructure and Building Projects in Qatar", *The 2nd International Conference on Civil Infrastructure and Construction (CIC 2023)*, Doha, Qatar, 5-8 February 2023, DOI: https://doi.org/10.29117/cic.2023.0028

Using Value-Stream Mapping to Enhance the Production Performance in Infrastructure Construction Projects in Qatar: A Case Study

Ayman Naser
Engineering Management Program, College of Engineering, Qatar University, Doha, Qatar
an1401569@qu.edu.qa

Juhaina Essa Al-Sulaiti
Public Works Authority (Ashghal), Doha, Qatar
jalsulaiti@ashghal.gov.qa

Zied Dahmani
AECOM, Doha, Qatar
zdahmani@ashghal.gov.qa

Abstract

Current research on sustainable construction has primarily concentrated on the design and operation phases of projects. However, the enhancement of execution and production phases of infrastructure construction projects have received little attention. In this paper, Value Stream Mapping (VSM) is used, as a Lean production tool, to evaluate production operational waste during the project construction phase. VSM considers the development of process maps that support project managers in diagnosing the current state of production in order to propose future improvements. VSM addresses the underlying causes of issues, as opposed to the symptoms addressed by traditional tools. This paper presents a case study of the application of VSM in the construction of infrastructure projects to improve the manhole and high-density polyethylene pipe connection process. This study's primary contribution is to provide a comprehensive account of the application of VSM in the infrastructure construction industry, confirming its ability to identify the sources of production waste, quantify them, suggest reduction strategies, and develop a TAKT planning. The case study's result demonstrates an effective approach to enhance the performance of construction projects targeting to optimize the resources used and reduce costs, improve quality standards, mitigate the associated wastes and enhance the TAKT time concept in construction of deep utilities in infrastructure construction project.

Keywords: Lean Construction; Value Stream Mapping; Sustainable Construction Management; Enhanced Infrastructure Projects – Qatar; Project Planning and Design

1 Introduction

In order to streamline operations, Rother & Shook (1999) developed a Lean methodology known as Value Stream Mapping (VSM). Information and material flow in a value stream are typically analysed to determine which activities add value and which do not. It has been shown to be effective in decreasing lead time and inventory (Gunduz & Naser, 2019) and it is a core of visual management process (Gunduz & Naser, 2017).

Sustainable practices and efficiency goals are gaining traction in the construction industry. Part of contractual enhancements in infrastructure projects in the State of Qatar, Lean Construction was introduced to support project delivery and minimise programme disruption. Many businesses have employed Value Stream Mapping as a Lean technique to remain competitive in a rising global market.

Value Stream Mapping is intended to remove any production process operations that do not contribute value. Essentially, it is a novel term derived from Toyota's material and information flow diagrams that was created to assist Toyota's suppliers in learning the Toyota Production System. Value Stream Mapping's core idea has been used internationally in services, manufacturing, healthcare, and construction (Gunduz & Naser, 2017). Despite attempts to study sustainable practices in construction and infrastructure development, the construction ecosystem disruption challenges remain a barrier. VSM practice in infrastructure projects is limited that cannot reflect the extent of its impact on identifying and resolving typical operational losses, specifically manhours. Moreover, abstract concepts like "waste," "value," "process," "conversion," and "flow" of processes common to Lean manufacturing can be difficult for construction engineering and management practitioners to grasp and adopt. Therefore, it is crucial for construction professional skills to incorporate practical experience into the curriculum (Ramalingam, 2018). Without a thorough and accurate introduction to VSM, practitioners risk misapplying the method in practice. Therefore, the purpose of this study is to establish a VSM layout that will illustrate to construction practitioners' circumstances where waste is ingrained and must be eliminated. It provides a solid foundation and efficient methodology for construction professionals to develop an effective plan to boost productivity and maximise resource utilisation.

2 VSM in Construction Industry

The value stream mapping process may be divided into six main steps as follows: 1) Identify the process that requires improvement; 2) Establish a map of the process's current state; 3) Select a suitable metric for improvement; 4) Establish a map of the process's future state; 5) Define improvement methods to transfer from the current state to the future state in a manner that achieves the appropriate metric; and 6) Proceed making improvements (Espinoza et al., 2021). Ioannou and Yang (2016) demonstrated that on-site practitioners may use VSM to observe the daily flow of work in order to evaluate the impact of workflow adjustments. VSM may aid in the detection of possible bottlenecks in the building process, hence contributing to the reduction of waste in the construction industry (Kanai & Fontanini, 2020).

3 Identifying Takt Time in Construction Industry

The time that is allotted for the provision of a certain process is called the TAKT time, and it is determined by the demand placed by customers. According to Liker's (2004) research, "it is the heart pulse of one-piece flow." The advantages that are brought to the project by the use of TAKT time include a reduction in variability, a reduction in the total length of the project, and a reduction in the cost of the project (Gunduz & Naser, 2017). In manufacturing, when the consumer demand can be readily determined via the market, the TAKT time may be defined with relative ease. When it comes to determining the demand rate in the construction industry, there are several open questions that arise. One approach is to determine how much time is available to do the task and verify it so that it can be used as the basis for demand; another is to investigate whether or not it is possible to increase the capacity of the trade that moves the most slowly (Frandson et al., 2013). The part of the process that moves the least quickly functions as a bottleneck for the rest of it, which slows it down. It is now the responsibility of the system as a whole to strive towards increasing the pace of output in order to make it match the TAKT time in terms of its speed (Gunduz & Naser, 2019). Here in this paper, the authors utilize Frandson et al. (2013) approach to calculate the TAKT time.

4 Research Methodology

To demonstrate how theory can be applied in the real world, a case study was chosen as the research

method because it is appropriate for answering "why" and "how" questions, as well as when the researcher has little or no control over the events, or when the general circumstances of the phenomenon to be studied are contemporary, in a context of real situation (Gunduz & Naser, 2019). The selected case study was suitable since it concentrated on a project that was substantially behind schedule. Therefore, it gave a chance for VSM flow line visualization-based planning to recommend options after presenting their prospective benefits. In an effort to make things as simple and controllable as possible, the scope of this inquiry was restricted to a subset of the project's underlying structure. The construct validity was addressed by triangulating data from numerous sources, including direct observation, interviews, and documents. External validity is connected to analytical generalisations, in which the researcher attempts to generalise a specific set of data to a broader theory.

4.1 Data Collection

The construction of deep utilities (underground pipeline) is one of the infrastructure construction industry sectors that produce a huge amount of operational waste. As the deep utilities usually form part of project' critical path, any intermediate delays could lead to a direct impact on the project completion date. For this study, construction process of the manhole and high-density polyethylene pipe connection in infrastructure project was selected as a case due to the repetitive nature of this activity and easiness to visualize it. While the required resources to achieve the planned activities were provided, and no prerequisite (DRAMPPSS: Design, Resources, Access, Materials, Permits, Plants, Safety, Share-understanding) were missing; the Percentage Plan Completed (PPC) for construction of Road "A" was 54%. An initial analysis shows a slow progress during the backfilling of utilities trench. GEMBA walk was conducted by construction team to look at work-in-process, understand the current state and identify the obstacles. Outcomes of the walk highlight that the manhole connection process is the bottleneck activity of the backfilling of construction of road "A".

VSM is a powerful tool used to provide a macro level view of sequence of activities that are rarely fully understood. This view supports tactical improvements to remove obstacles to the flow and increase customer value. After data collection, the current state of VSM was developed (mapping of process, material, and information flows), the current metrics were recorded (i.e. value-added (VA), non-value added (NVA), Lead time (LT), manpower, batch size, and Takt time) as shown in Figure 1.

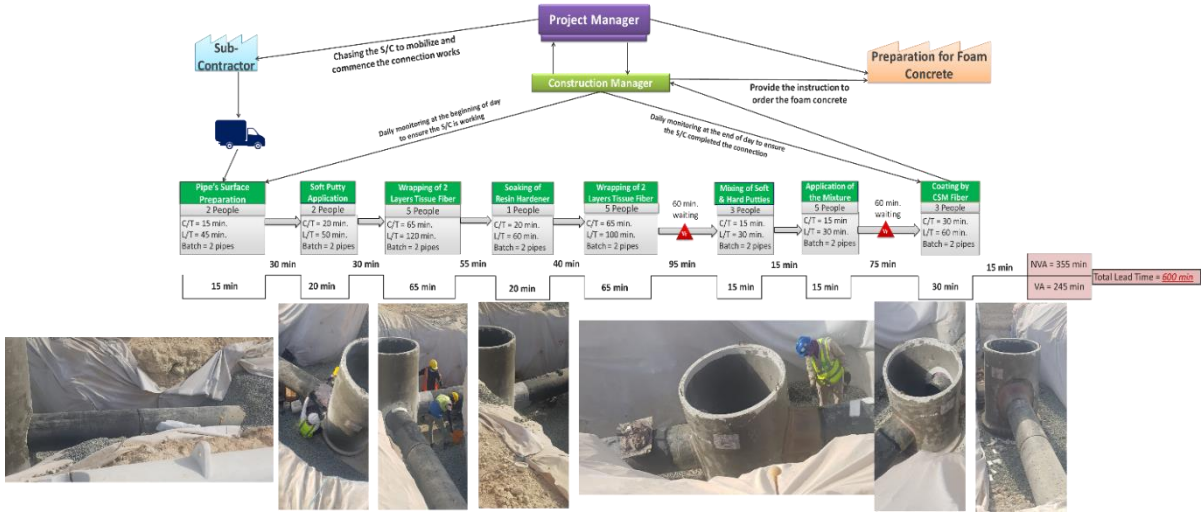


Fig. 1: Current State of Manhole's Connection Process

4.2 Future State of VSM

Moving from current state to future state, the following countermeasures were proposed to enhance the

process of the manhole connection. Table 1 provides a tracking template for the VS transformation plan:

- Implementing standard work for referral process using an approved method statement.
- Assigning a competent Forman.
- Increasing the batch size of 4 pipes per day by utilizing and monitoring a manpower properly to increase VA and reduce NVA.
- Introducing a supermarket after completing the installation of 4 pipes to perform Barcol hardness test to control and improve the quality of HDPE pipe connection with manhole.

Table 1: Value Stream Transformation Plan

Value Stream Transformation Plan															
Value Stream		Manhole's Connection with HDPE pipe			**Scheduled Review Dates**										
Executive Sponsor		Project Team			Weekly									21-Feb-2022	
Value Stream Champion		A.N.			Weekly									28-Feb-2022	
Value Stream Mapping Facilitator		A.N.			Weekly									7-Mar-2022	
Date Created		4/2/2022			Weekly									14-Mar-2022	
Kaizen Burst No.	**Measurable Target**	**Proposed Countermeasure**	**Exec. Method***	**Owner**	**Planned Timeline for Execution**										**Status**
					1	**2**	**3**	**4**	**5**	**6**	**7**	**8**	**9**	**10**	**11**	**12**	
1	Batch Size shall be targeted of 4 pipes per day	Implementing standard work for referral process using an approved method statement	KE	Project Manager													**100%**
2	Monitoring the work activity and installation closely	Provide VSM Training	JDI	Project Manager													**100%**
3	Targeting of batch size of 4 pipes per day	Reducing manpower, utilizing manpower properly, increase VA, and reduce NVA	KE	Project Manager													**75%**
4	Targeting of batch size of 4 pipes per day. The activity "mixing" is re-arranged in parallel with another activity.	Utilizing manpower properly, increase VA, and reduce NVA	KE	Project Manager													**75%**
5	Targeting of batch size of 4 pipes per day	Reducing manpower, utilizing manpower properly, increase VA, and reduce NVA	KE	Project Manager													**75%**
6	Targeting of batch size of 4 pipes per day	Reducing manpower, utilizing manpower properly, increase VA, and reduce NVA	KE	Project Manager													**75%**
7	Targeting of batch size of 4 pipes per day	Reducing manpower, utilizing manpower properly, increase VA, and reduce NVA	KE	Project Manager													**75%**
8	Targeting of batch size of 4 pipes per day	Reducing manpower, utilizing manpower properly, increase VA, and reduce NVA	KE	Project Manager													**75%**

9	Targeting of batch size of 4 pipes per day	Reducing manpower, utilizing manpower properly, increase VA, and reduce NVA	KE	Project Manager		**75%**
10	Supermarket is introduced after completing the installation of 4 pipes to perform Barcol hardness test	Improving the quality of Manhole's connection with HDPE pipes	KE	Project Manager		**100%**
11	Targeting of batch size of 4 pipes per day	Reducing manpower, utilizing manpower properly, increase VA, and reduce NVA	KE	Project Manager		**75%**

Agreement		
Executive Sponsor	**Value Stream Champion**	**Value Stream Mapping Facilitator**
Signature:	Signature:	Signature:
Date:	Date:	Date:

* Execution Method = JDI (Just-do-it), KE (Kaizen Event), or Proj (Project).

After identifying and eliminating operational wastes, the future state was developed with a clear picture of how the process should look. Implementing was utilized as a blueprint to standardize and sustain the process of developing a future state of VSM to maintain a continuous flow as indicated in Figure 2.

To prevent delays, TAKT time was introduced to the procedure. With little buffers, the activities were made as repetitious as feasible. Without interruption, the same crew will go from zone to zone doing identical activities. This will save resources and increase efficiency. The process included two steps, with the first stage's resources and therefore production rate remaining unchanged. Activities have been synchronised in accordance with pace to ensure that all activities are effective from the moment they begin until the time they conclude. The second stage was modified in accordance with TAKT time. The summary metrics and advantages of VSM are shown in Table 2.

Table 2: Value Stream Transformation

Value Stream Mapping Summary Metrics				
Executive Sponsor	Project Team	**Event Name**	Manhole Connection with pipes	
Value Stream Champion	A.N.	**Event Start Date**	04/02/22	
Facilitator	XXX	**Coordinator**	XXX	
Activity	**Processing Time (Hours)**	**Lead Time (Hours)**	**%C&A**	**Takt Time**
Current State				
Pipe's Surface Preparation	15	45	85.0%	300 min
Soft Putty Application	20	50	75.0%	
Wrapping of 2 Layers Fiber Tissues	65	120	95.0%	
Soaking of Resin Hardener	20	60	75.0%	
Wrapping of 2 Layers Fiber Tissues	65	100	75.0%	
Mixing of Soft & Hard Putties	15	30	75.0%	
Application of the Mixture	15	30	75.0%	
Coating by CSM Fiber	30	60	75.0%	
Future State				
Pipe's Surface Preparation	30	35	90.0%	109 min
Soft Putty Application	30	40	85.0%	
Wrapping of 2 Layers Fiber Tissues	80	90	95.0%	
Soaking of Resin Hardener	30	50	95.0%	
Wrapping of 2 Layers Fiber Tissues	80	90	95.0%	

Mixing of Soft & Hard Putties	30	30	95.0%	
Application of the Mixture	20	30	95.0%	
Coating by CSM Fiber	45	50	95.0%	
VSM Metrics	**C. S.**	**F. S.**		
VA	245	345		
LT	600	435		
NVA	355	90		
% VA	40.83%	79.31%		
Manpower	8	5		
Batch Size	2 pipes	4 pipes		

Takt planning can be developed based and after the implementation of VSM to maintain a continuous flow by using TAKT time. Dividing workstations by zones, each zone includes all locations that have same production rate for a certain task generated from VSM.

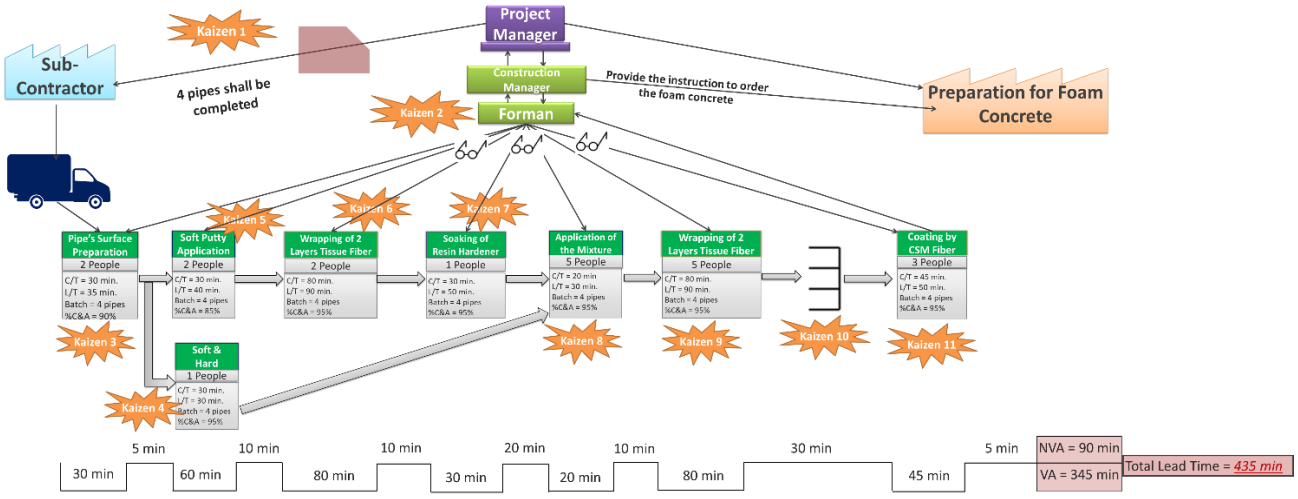


Fig. 2: Future State of Manhole's Connection Process

5 Discussion of Results

The objectives of this research have been accomplished mainly through demonstrating of:

- VSM is a Vital Visual Management and Lean tool to visualize materials and information flow in the process of the manhole and high-density polyethylene pipe connection process in infrastructure project.
- The potential of VSM to enhance the performance of construction projects targeting by reducing the construction Lead time by 27.5%, increase the VA by 30%, reduce the manpower by 37.5 %, reduce the NVA by 74%, and increase the batch size by 50%.
- Optimize the resources use through TAKT time to level the resources for each work trade and TAKT zone.
- Enhance the quality of each process's output and handoff between two trades, meaning that they do their work without having to correct it.
- Mitigate the associated wastes in construction of deep utilities in infrastructure construction project.
- Develop a TAKT planning through splitting the zones to ensure a proper resources utilization. In this paper, the construction area is splitted into 6 optimized TAKT's zone to ensure a proper resource optimization.

6 Conclusion

The optimization of both time and resources within the construction industry is becoming an increasingly important factor for the industry's success, and as a consequence, new planning and scheduling methodologies are being suggested for implementation. The purpose of this study was to provide a methodical approach to using VSM and TAKT time planning that is based on the idea of location-based management. A local initiative of modest to high scale served as the basis for the case study example. Because so many of the construction jobs included in this case study were similar to one another, it was the ideal choice for this article. Alternatively, the applicability of this technique could be restricted for more complicated building projects that include a large number of non-repetitive jobs. When tasks were first represented using the prevalent mode of operation, it was discovered that there were significant time wastages in the form of extra time buffers.

In addition to this, it was discovered that the number of resource allocation was not balanced. Following that, two measures were taken in order to attain production according to TAKT time: (1) the introduction of phased production rather than "as soon as feasible" while maintaining resources constantly. (2) The process of aligning the production rates of the various tasks and arranging them to be equivalent to the TAKT time that is being applied.

According to the findings, the total length of the connection process after the aforementioned adjustments has decreased in accordance with the existing conventional working style. This results in a reduction of the project duration. In addition to this, the future state implemented VSM and TAKT time-based schedule resulted in the optimization of a resource. The findings of the case study indicate that working to the TAKT time assists in the establishment of a continuous flow, which results in less waste, a shorter duration, and thus, lower costs.

This paper has offered a methodical approach to the determination and application of VSM and TAKT time to the various stages of the infrastructure project planning process. It has also been determined that using TAKT time as a pacing mechanism for productivity results in less waste. In the future, research might be done to expand on this subject by evaluating the approach and digitization of application and using VSM in large-scale projects.

Authors find that VSM can be combined with other process mapping tools such as SIPOC to harness the flow of activities and information within construction activities. This will provide further cases to be studied.

References

Espinoza, L. R., Herrera, R. F. and Brioso, X. (2021). "Use of Value Stream Mapping in a Case Study in Basement Construction." *Proc. 29th Annual Conference of the International Group for Lean Construction (IGLC29), Alarcon, L.F. and González, V.A. (eds.)*, Lima, Peru, pp. 995–1004

Frandson, A., Berghede, K. & Tommelein, I. (2013). "Takt Time Planning for Construction of Exterior Cladding." Proceedings, 21st annual conference of the International Group for Lean Construction, Fortaleza, Brazil.

Gunduz, M., & Fahmi Naser, A. (2017). "Cost based Value Stream Mapping as a sustainable construction tool for undergraound pipeline construction projects". *Sustainability*, *9*(12), 2184.

Gunduz, M., & Fahmi Naser, A. (2019). "Value stream mapping as a lean tool for construction projects." *International Journal of Structural and Civil Engineering Research, 8*(1), 69-74.

Ioannou, P. G., & Yang, I. (2016). "Repetitive Scheduling Method: Requirements, Modeling, and Implementation." *Journal of Construction Engineering and Management, 142*(5), 1–13.

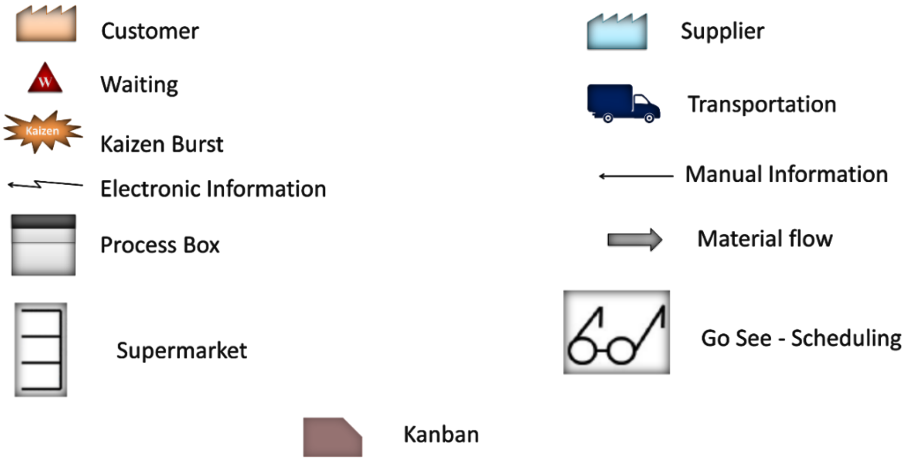
Kanai, J. & Fontanini, P. S. P. (2020). "Value Stream Map and Visilean® for Prefabricated Concrete Panels Management". *Proceedings of the 28th Annual Conference of the International Group for Lean Construction (IGLC).* Berkeley, California, USA, 6-10 Jul 2020, 673-684.

Liker, J. (2004). "The Toyota Way," McGraw-Hill, New York.

Ramalingam, S. (2018). "Mapping of BIM Process for Teaching Lean". *Proceedings of the 26th Annual Conference of the International. Group for Lean Construction (IGLC)*, González, V.A. (ed.), Chennai, India, 1291– 1301.

Rother, M., & Shook, J. (1999). "Value Stream Mapping". *Lean Enterprise Institute, Cambridge*.

Appendix A: Symbols Used in VSM



Cite as: Naser A., Kamal A., Al-Tamimi S.A. & Dahmani Z., "Using Value-Stream Mapping to Enhance the Production Performance in Infrastructure Construction Projects in Qatar: A Case Study", *The 2nd International Conference on Civil Infrastructure and Construction (CIC 2023)*, Doha, Qatar, 5-8 February 2023, DOI: https://doi.org/10.29117/cic.2023.0029

Marketing Strategies for Smart Buildings

Ahmed Mahfouz
College of Engineering, Qatar University, Doha, Qatar
ahmed.mahfouz@qu.edu.qa

Ahmad Mohammad Ahmad
College of Engineering, Qatar University, Doha, Qatar
am.ahmad@qu.edu.qa

Shimaa Basheir Abdelkarim
College of Engineering, Qatar University, Doha, Qatar
shimaa666@hotmail.com

Nada Hammam
College of Engineering, Qatar University, Doha, Qatar
nh1802279@qu.edu.qa

Maryam AlMulla
College of Engineering, Qatar University, Doha, Qatar
ma1702207@qu.edu.qa

Yongcheol Lee
Louisiana State University Louisiana, United States
yclee@lsu.edu

Khalid Naji
College of Engineering, Qatar University, Doha, Qatar
knaji@qu.edu.qa

Abstract

Globally, there is a growing proportion of the need to optimize monitoring and facility management of new and existing built facilities. Smart buildings provide waste reduction to the environment, flexibility to facility users, and optimization opportunities to the owner. Several research projects explore the monitoring, management, and maintenance of smart buildings towards efficient facility management (FM). However, there is a lack of defined, effective, efficient, and successful marketing schemes for smart buildings. Furthermore, smart buildings utilize the different technological possibilities and advancements in the smart building business and impact relevant stakeholders such as clients, facility managers, and users. Therefore, the study aims to develop a marketing strategy for smart buildings. The study adopts an integrative approach as the underpinning theory. The study's methodology adopts a robust analysis of different market strategies for various building types in the construction industry. In addition, lessons are deducted from the building typologies, such as sustainable buildings, tall and green buildings. The proposed marketing strategy requires four defined phases: segmentation, targeting, positioning and differentiations. The marketing directions focus on activities, actors, and tools through a comprehensive, detailed, and interpretative literature review. The proposed adaptable market strategy integrates client and facility users, focusing on the main drivers for marketing smart buildings. Therefore, the study is significant for facility managers, developers, and facility users.

Keywords: Smart buildings; Marketing; Strategy; Sustainability; Users

1 Introduction

There is need for reducing waste and adopting sustainable features by the three pillars of sustainability—economic, environmental, and social in the construction industry. The impact of buildings on energy consumption and carbon emissions is enormous. It is believed that intelligent buildings play a key role in enhancing the energy performance of buildings and cities (Doukari, 2022). In 2002, the Continental Automated Buildings Association (CABA) described a "smart building" as a building and its infrastructure that provide inhabitants with an efficient, adaptable, safe, and comfortable environment by integrating technology systems, controls, and communications (Karimi, 2021). The International Facility Management Association (IFMA), for instance, defines facility management as "the discipline of managing a company's activities and responsibilities within its working environment." It involves developing a business facilities strategy, making long-term projections, real estate, space inventory, projects (through design, construction, and restoration), building service and maintenance plans, and taking inventory of furniture and equipment (Milala, 2022). In smart building environments, facility management performance is elevated beyond normal buildings to include BMS platform operations. With its graphical representation of parameters, the BMS system is an effective tool for facility managers to gain an overview of the building's current operating values and the function of the individual systems while also allowing the parameters to be modified in response to changing needs (Paek, 2018). However, smart buildings have lacked substantial marketing strategies that can clarify the benefits of their use to all beneficiaries, including stakeholders, users, and facility managers.

2 Methodology

According to Synder (2019), the integrative theory described in Table 1 defines the integrative approach to managing mature or emergent topics. The objective of an integrative review approach is to provide an overview of the knowledge base, critically examine and maybe re-conceptualize it, and develop the theoretical basis of the topic as it matures. For newly emerging issues, the objective is to develop first or preliminary conceptualizations and theoretical models as opposed to reviewing older models. This form of review frequently necessitates a more innovative approach to data collection. Furthermore, the objective is typically not to cover all articles written on the issue but rather to mix viewpoints and insights from many fields of research traditions.

Table 1: Approaches to Literature Reviews Adapted from (Synder, 2019)

Approach	Integrative
Typical purpose	Critique and synthesize
Research questions	Narrow or broad
Search strategy	Usually not systematic
Sample characteristics	Research articles, books, and other published texts
Analysis and evaluation	Qualitative
Examples of contribution	Taxonomy or classification

This study aims to develop a smart buildings marketing strategy framework, using the methodology in Figure 1, within the construction industry, in which the strategy will outline the significance of marketing smart buildings and will outline the involvement of different parties, including the end user, the client, the government, etc. The study outlined the existing marketing strategies and available qualitative data collected within the current literature review, analysing the data and developing a marketing strategy framework. The framework was developed through a focus group that highlighted the existing marketing strategies related to smart buildings and adapted a qualitative approach to develop the outcome of the framework.

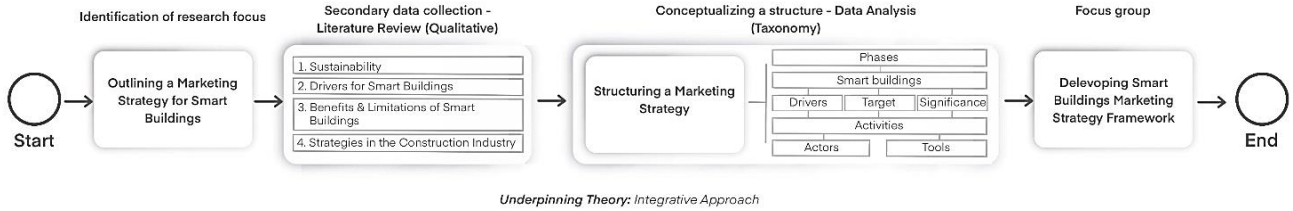


Fig. 1: Marketing Smart Buildings Framework Methodology

3 Literature Review and Analysis

In accordance with the commonly accepted concept of sustainability, meeting the needs of the public should not compromise the ability of future generations to do the same. The principles of sustainability include not just environmental but also social and economic factors. When the Earth's environmental systems remain stable, and their natural resources are used at a rate at which they can renew, environmental integrity is preserved (Froufe et al., 2020). Globally, the economic pillar works to preserve the economic autonomy that allows access to the financial and other resources required to meet the needs of the public, ensuring that economic systems remain intact and everyone has access to activities. The social pillar often refers to public policies that support social concerns. These social issues affect our well-being, including healthcare, education, housing, employment, etc. Sustainability is a shared ideal across several individuals and organizations, as seen by their policies, daily operations, and conduct. The concept of "smart buildings" has gained prominence in recent years. The evolution of the smart product market and the energy management service sector has propelled the global expansion of smart home technology. Several studies have documented the numerous benefits of smart home/building systems, such as better thermal comfort and safety, lower energy costs, and greater flexibility. There are many drivers for smart buildings, as described (Froufe et al., 2020) in Figure 2. These are categorised to the owner, user and environment.

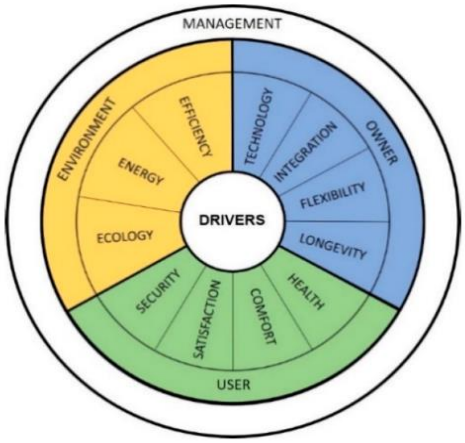


Fig. 2: Smart Building Drivers grouped by Category (Froufe, et al., 2020)

When it comes to environmental monitoring, sensor-actuator networks, embedded systems, and distributed software engineering are converging in exciting ways, as seen by the rise of "smart" buildings and cities. Therefore, it is crucial that smart buildings be included into the smart city ecosystem. New technologies are driving the growth of smart buildings because they enable smarter resources and processes, which in turn improve the building's efficiency, adaptability, interactivity,

and sustainability. A few certifications have been tailored to certify whether the building is smart or not, as shown in Table 2. The key target audience is decision-makers, interested in or supporting the certification process or conveying their knowledge to the market (Habash, 2022). Developers, builders, architects, government representatives, real estate businesses, and foreign companies engaged in market development are examples. The end users who want to buy or rent-smart buildings should be guaranteed that the decision-makers and developers certify the buildings and adopt the smart building certification requirements once they are applied.

Table 2: Smart Buildings Certifications (non-exhaustive list)

Certification	Focus	Country	Reference
SmartScore-WiredScored	Design & Operations	US, UK, Singapore	https://wiredscore.com/certify-a-building/smartscore/
Smart Building Collective	Design	Netherlands	https://smartbuildingcollective.com/
SPIRE™ Qualification Program	Assessment	US, Canada, Australia, Belgium	https://spiresmartbuildings.ul.com/
SpaceWell	Operations	Belgium	https://spacewell.com/
TIA-Telecommunication Industry Association	Assessment	US	https://tiaonline.org/
Kriea - Korea Research Institute of Eco-Environment Architecture	Design	South Korea	https://www.kriea.re.kr/eng_index.php

The energy consumption of a building may be drastically reduced by using data collected from a building's smart features to predict and adapt to the needs of its inhabitants. The automation of routine duties and the resulting reduction in operating costs are two major advantages for building owners. They have the ability to detect leaks such as ones arising out of fire, water, and gas. In the event of a breakdown or a deterioration in performance, smart buildings' built-in diagnostic systems will send a warning to the building's residents. Embedded expert systems may contain information regarding any home or industrial domain. In all smart construction decisions, the health of the occupants takes precedence; temperature, light intensity, air conditioning factors, etc., reflect this by providing a safe and comfortable environment, intelligent buildings can enhance the quality of life for the elderly and disabled who live alone (Habash, 2022).

Smart buildings boost the owner's market competitiveness and return on investment and boost ROI and competitiveness, making them more desirable. Even when construction process improvements may reduce costs, it is important to note that the cost-benefit ratio must be evaluated throughout the building's lifespan. Smart buildings cost more because of their technology, but the same technology improves energy efficiency, reduces water use, and optimizes infrastructure maintenance to save on lifecycle costs (Yang et al., 2021). Interoperability across processes, products, and people, adaptability to new environments and setups, and longevity thanks to regular technological upgrades, maintenance, and the incorporation of new features are all enhanced by system integration. These points strengthen the case for smart buildings in general, and certified smart buildings will soon become the norm. Smart buildings that have earned the Value Certification will be more reliable than those that have not. As a result, the hope for growth in the future is the primary factor luring investors. The price difference is admittedly due to the higher quality certified buildings and the guarantee of sustainable investment value. This expectation is strongly aligned with the overall trend of moving

towards sustainability (Angelidou, 2014).

Several elements, including return on investment, financial risk, pre-integration, and initial planning influence the construction industry's entry into the smart building market. The budget and investment of a project always determine its success. The bank loans typically finance such large projects, and risk is a significant deciding element. Slow and non-agile businesses, such as those in the construction industry, cannot afford to provide value to the end user without a return on investment or a reduction in cost risk (Kim et al., 2022). Due to the high risk of building projects, it is difficult to convince construction companies to include more stakeholders and vendors in a project with a limited budget. Integration is crucial for both stakeholders and builders. Retrofitting is expensive and does not necessarily offer value to individual users, particularly when the end user becomes unclear after the product's completion (could be a tenant, owner, renter, etc.). Stakeholders are enthusiastic about contributing their funds to the pre-planning and planning phases of a smart building. Laws and regulations govern the initial phases of a building project. By involving small stakeholders in the planning process, it is possible to save money instead of incurring fixed costs (Ma, 2016).

Table 3: Marketing Strategies for different types of buildings

S. No.	Description	Focus Area	Reference
Client Dimension			
1	Targeting the owners into marketing green development of buildings and developing the business aspects of different successful cases	*Sustainable Buildings*	Yudelson (2007)
2	Discussing the policies in japan to promote more sustainable development of buildings and facilities in order to encourage the industry of sustainable buildings.		Sunikka-Blank (2011)
3	The development of sustainable buildings history in the middle east and Africa and how their growth is a profitable business enterprise		Sayigh, A. (2013)
4	The connection of strong integration of sustainability and health with intelligence is needed in the future to market smart buildings to owners	*Intelligent buildings*	Habash, R. (2022)
User Dimension			
1	Comparison of the benefits when renting or selling sustainable/green properties owned by stakeholders	*Sustainable Buildings*	Kozlovská et al. (2014)
2	Using the summary index of the top sustainable buildings in the world to promote users to invest in sustainable properties		Sayigh, A. (2013)
3	Segmentation, targeting, positioning, and differentiation	*Green Building*	Popescu et al. (2015)

Various marketing strategies have been developed targeting different types of buildings, sustainable, intelligent, and green buildings as shown in Table 3. Yudelson (2007) developed a marketing strategy that targets smart buildings and discusses different cases that have shown success in construction. Popescu et al. (2015) developed a scheme, when approached to market green buildings, it showed major success, in which a 4-phase marketing scheme was developed accordingly.

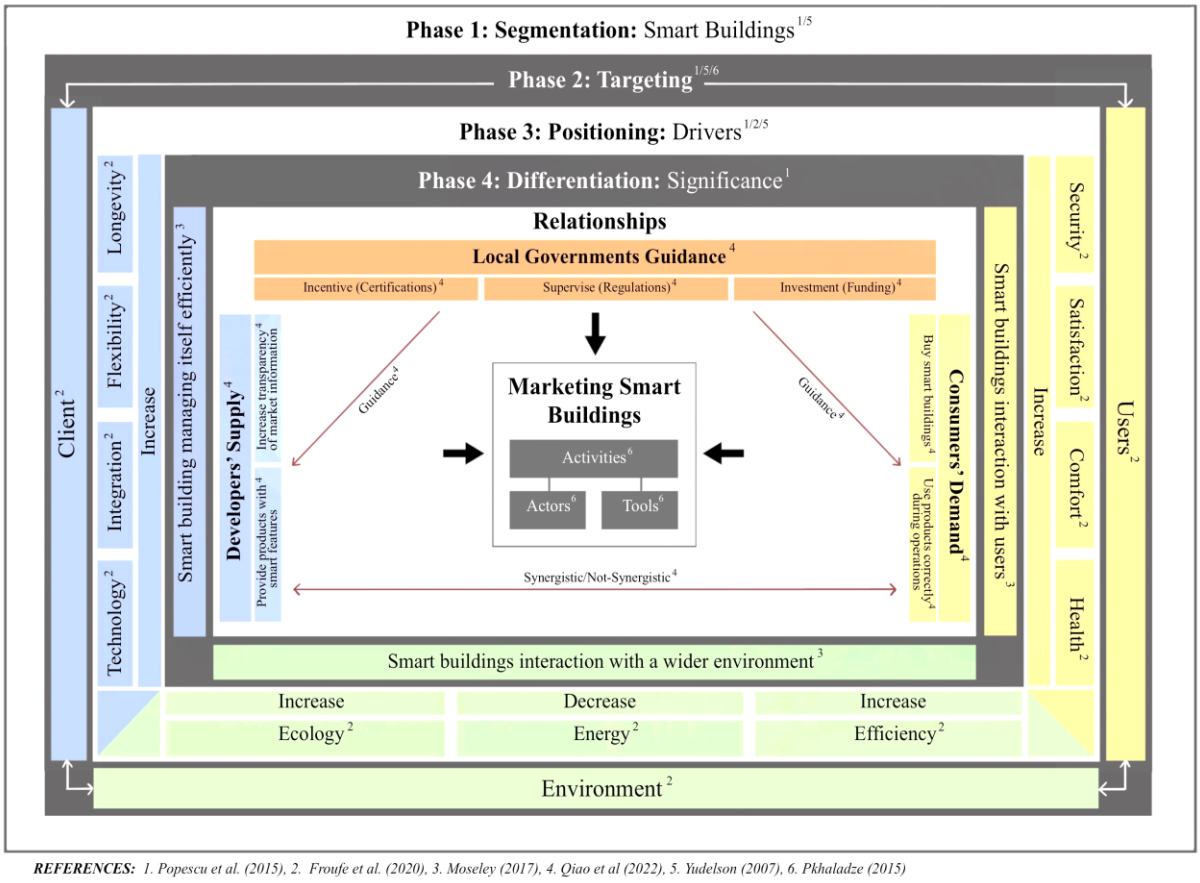
Table 4: Benefits and Limitations of Smart Buildings

S.No.	Description	Sustainability Pillar	Reference
Benefits			
1	Increasing entertainment and comfort	Economical	Kim et al. (2022)
2	Increasing energy-saving schemes that cut out costs for the owner		Yang et al. (2021)
3	Increasing economic benefit for the user as well as the owner		Yang et al. (2020)
4	Increasing utilization of other technologies integration		Yang et al. (2021)
5	Increasing equipment's monitoring activities		Rameshwar (2020)
6	Increasing healthcare services	Social	Kim et al. (2022)
7	Increasing users comfort		Yang et al. (2020)
8	Improving the users' quality of life		Yang et al. (2020)
9	Reducing energy waste	Environmental	Karimi et al. (2021)
Limitations			
1	Increased project cost at initial installation	Economical	Angelidou (2014)
2	Increased complications during adoption and implementation		Yang et al. (2021)
3	Increased cyber security risks	Social	Kim et al. (2022)
4	The unfamiliarity of the user with the user interface		Karimi et al. (2021)

Smart buildings have limitations that are considered a back draw in both the development and marketing processes they accompany. Table 4 identifies the benefits and limitations of smart buildings within the current market. Angelidou (2014) hints that, although smart buildings increase the economic benefits for the client as an owner and the end user, the initial installation cost of a smart building is significantly high, which makes the investment in a smart building questionable to the extent of not considering it, depending on the owner's budget, as most owners are more interested in the initial construction cost, rather than looking at the long term benefits of investing in a smart building. Kim et al. (2022) mention that a major limitation within smart buildings is the increased cyber security risks when is developed, as a smart building would be completely dependent in majority on the internet connection, there are more chances that an external attack, would occur and target the data acquired within the smart building database, whether from the owner or the end users.

4 Focus Group

Blackstone (2014) described a focus group as scheduled and aimed to generate group involvement and "get perceptions on a designated area of interest in a nonthreatening setting." A group of 3 to 5 is optimal. Groups larger than that, particularly when discussing contentious issues, can soon become unmanageable. Some advocate a group size of between 6 and 10 members for focus group research (Morgan, 1997). A group of six participants participated. These include four architects (4) and two engineers (2) focused on developing the framework for marketing smart buildings. The participants had an average of five years of experience. The participants attended three sessions that lasted from 45 minutes to one hour. The study adopted a qualitative approach. The focus group questions included highlighting and deducting relevant themes for the smart buildings with a significance on the smart building drivers and relationships between user and developer. The group focused on the existing marketing schemes for other types of buildings, including green and sustainable buildings, while adapting the qualitative approach to develop the framework. The framework was developed to link the accompanied parties within the process, the government, the client, and the user.



REFERENCES: *1. Popescu et al. (2015), 2. Froufe et al. (2020), 3. Moseley (2017), 4. Qiao et al (2022), 5. Yudelson (2007), 6. Pkhaladze (2015)*

Fig. 3: Marketing Smart Buildings Strategy Framework

The developed framework in Figure 3 approaches marketing smart buildings in four different phases that will lead to the essential target, Segmentation, Targeting, Positioning, and Differentiation (Popescu et al., 2015). *Phase 1* starts by segmenting the smart buildings from other types of buildings to be called out. *Phase 2* would target the audience, the user, the client, and the environment, which are the key targets in this framework. *Phase 3* is then adapting the drivers, in which the marketing strategy for smart buildings is needed. *Phase 4* incites the significance of smart buildings as per Table 3. The marketing strategies developed by Yudelson (2007) linking the client, the user, the developer, and the government institutions; a relationship link is created between them, developing a closed loop that guides the user and client by the government.

5 Discussion

The incentive to certify a smart building by the government, supervise the process, and invest in the development of smart buildings, as described by Yudelson (2007) is the motive to market smart buildings to owners, developers, and end users. The government will guide the construction industry concerning the user and the client. In contrast, the synergistic information exchange between the client and the user will adhere to better development of smart buildings.

Whether the user is renting or buying, they will be able to see the value of investing in a smart building thanks to the marketing strategy that emphasizes their safety, satisfaction, comfort, and health. In addition to making an investment in the technology, the user must also operate and utilize it in accordance with the developer's guidelines and applicable government requirements. The marketing plan for a smart building would explain the technology employed in its construction and the extent to which the owner may exercise discretion in overseeing the building's operations. The longevity of

the technology used is a long-term investment that would show value within the project's lifespan. Integrating the technology into the building to develop a better understanding of the investment choice taken by the owner. The developer must supply genuine, smart products with features that will best serve the client and user and match the cost invested in the project. Transparency is a key factor for the developer to follow while being guided by the government by acquiring the required certification. The environment as a target would be driven by the decrease in energy waste, the increase in ecological enhancements, and the increased efficiency of using all natural resources such as water and energy. The smart building marketing strategy framework guides the involved parties to understand the process scheme, starting from identifying the segment of the construction industry as smart building and developing the scheme to understanding the role and requirements of user, developers and government to satisfying needs and demands. The marketing tools require the participation of relevant actors and end-user demands to meet defined targets.

6 Conclusion and Recommendation

Smart buildings lack a clear marketing strategy that drives them into the market and recognizes them from other types of buildings. Smart buildings are a part of smart cities, which are being adapted worldwide and aim to be the future of all cities, as adapting smart integration is the leading innovation of the day. Hence, directing investors, governments, users, developers, etc., to adapt and develop the adaptation of smart buildings within smart cities is the way to advancement. Therefore, the study targeted the development of a marketing strategy for smart buildings in the construction industry. The framework targets the government as the guiding authority, the owner and user as parties of investment, the developers as the integrators of smart buildings, and the environment as the medium of effective resource and concern. Future research can further validate the developed framework with developers, clients and users to respond to further limitations of smart buildings.

7 Limitations

The study develops a conceptual framework model that aligns with the construction industry's marketing strategy adopted by different building categories. However, the framework focuses on smart buildings. Furthermore, the strategy proposes that the government encourage certification to enable the users to receive effective and efficient buildings. Conversely, there are limited certification institutions worldwide. Moreover, the framework was only validated with the focus group members.

Acknowledgement

This publication was made possible by the NPRP grant (NPRP 12S-0304-190230) from the Qatar National Research Fund (a member of Qatar Foundation) and Qatar University, College of Engineering (CENG) with project number QUCP-CENG-2020-1. The statements made herein are solely the responsibility of the author(s);

References

Angelidou, M. (2014). Smart city policies: A spatial approach. Cities, 41. DOI: https://doi.org/10.1016/j.cities.2014.06.007

Blackstone, A. (2014). Principles of sociological inquiry: Qualitative and Quantitative Methods (Vol. 1). Saylor Foundation.

Doukari et al. (2022). An Interoperable Approach for Modelling and Managing Smart Building Data - CESI Smart Building Demonstrator. Buildings.12.362.10.3390/buildings12030362.

Froufe, M. et al. (2020). Smart Buildings: Systems and Drivers. Buildings 2020, 10, 153. pp. 1-20. DOI: 10.3390/buildings10090153

Habash, R. (2022). Sustainability and Health in Intelligent Buildings. Woodhead Publishing Limited.

Karimi et al. (2021). Smart Built Environment Including Smart Home, Smart Building and Smart City: Definitions and Applied Technologies. DOI:10.5772/intechopen.95104.

Kim et al. (2022). Design and Implementation of Smart Buildings: A Review of Current Research Trend. *Energies*, *15*(12), 4278. DOI: https://doi.org/10.3390/en15124278

Kozlovská, Švajlenka, & Struková. (2014). Arguments for Marketing Benefits of Sustainable Buildings. Nehnuteľnosti a Bývanie.

Ma, Zheng & Badi, Adrian & Jørgensen, Bo. (2016). Market Opportunities and Barriers for Smart Buildings. DOI: 10.1109/IGESC.2016.7790078.

Milala, Sani & Ariffin, Khadijah & Kasim, Rozilah. (2022). Facilities Management Business Opportunities. International *Journal of Sustainable Construction Engineering and Technology*. 13. DOI: 10.30880/ijscet.2022.13.02.023.

Moseley, P. (2017). EU Support for Innovation and Market Uptake in Smart Buildings under the Horizon 2020 Framework Programme. Buildings, 2017, 7, 105. pp. 1-24. DOI: 10.3390/buildings7040105

Pašek, J. & Sojková, V. (2018). Facility management of smart buildings. International Review of Applied Sciences and Engineering. 9. 181-187. DOI: 10.1556/1848.2018.9.2.15.

Pkhaladze (2015). Green Building Marketing Action Plan. Enhancing Capacity for Low Emission Development Strategies (EC-LEDS) Clean Energy Program. USAID, Georgia

Popescu, M., Oaneca-Negescu, M. & Predescu, A. (2015). Green Marketing Strategies in Real Estate in Romania. Theoretical and Applied Economics. Volume 22 (2015), Special Issue, pp. 99-108.

Qiao, W., Dong, P. & Ju, Y. (2022). Synergistic Development of Green Building Market under Government Guidance: A Case Study of Tianjin, China. *Journal of Cleaner Production*, *340*(2022) 130540. pp. 1-16. DOI: https://doi.org/10.1016/j.jclepro.2022.130540

Sayigh, A. (2013). Sustainability, Energy and Architecture. In Case Studies in Realizing Green Buildings. Academic Press.

Snyder, H. (2019). Literature Review as A Research Methodology: An Overview and Guidelines. *Journal of Business Research 104*(2019). pp. 333-339. DOI: https://doi.org/10.1016/j.jbusres.2019.07.039

Sunikka-Blank, Minna & Iwafune, Yumiko. (2011). Sustainable Building in Japan – Observations on a Market Transformation Policy. Environmental Policy and Governance. 21. 351-363. DOI:10.1002/eet.580.

Yang, Ang & Han, Mingzhe & Zeng, Qingcheng & Sun, Yuhui. (2021). Adopting Building Information Modeling (BIM) for the Development of Smart Buildings: A Review of Enabling Applications and Challenges. Advances in Civil Engineering. 2021. 1-26. DOI: 10.1155/2021/8811476.

Yudelson, J. (2007). Marketing Green Building Services - 1st Edition. pp. 1-312. London. ISBN: 9780080942315. DOI: https://doi.org/10.4324/9780080942315

Cite as: Mahfouz A., Ahmad A.M., Abdelkarim S., Hammam N.N., Almulla M.A., Lee Y. & Naji K., "Marketing Strategies for Smart Buildings", *The 2nd International Conference on Civil Infrastructure and Construction (CIC 2023)*, Doha, Qatar, 5-8 February 2023, DOI: https://doi.org/10.29117/cic.2023.0030

The Impact of COVID-19 on Contracts and Claims for Infrastructure Projects

Mona Adam
Sudan University of Science and Technology, Khartoum, Sudan
monaadam2004@yahoo.com

Amani Mohammed
Redes Company, Khartoum, Sudan
amanimohamed5449@gmail.com

Abstract

Infrastructure projects have greatly affected the economy of countries, as they have contributed to supporting all economic sectors by providing them with many executive and operational projects. Despite the important role of infrastructure projects in Khartoum State, they are exposed to problems at various stages due to the Covid-19, which led to the failure to complete these stages. This study aimed to identify the extent of the impact of the Covid-19 on infrastructure projects in the Khartoum state and its relationship to claims and construction contracts in terms of costs, time and risks, and who bears and how to distribute the burden of additional costs and losses resulting from this pandemic, and how to contain and overcome the crisis and how to avoid the emergence of conflicts. The survey's descriptive approach was adopted by designing a questionnaire and distributing it to the affected sample. The questionnaire was collected and analyzed using the statistical analysis program and Excel. The results showed revenue losses for the public and private sector by 63.1%, and the Covid-19 also affected infrastructure projects in financial terms by 55%, and the prices of construction materials and direct and indirect costs by 50%, and the cash flow of projects by 49.2%. Based on these results, proposed solutions have been developed to improve the current situation, by standardizing the project cost in dollars to avoid exchange rate hesitation and following FIDIC contracts and formulating it to redress the damage in all sectors, which helps in improving the performance of projects in Khartoum state, which is trying to pass this unprecedented period.

Keywords: Contracts; Claims; Disputes; Costs; Time; Covid-19 and risks

1 Introduction

The construction industry is one of the important industries in the economies of any country, as the building and construction sector is defined as the sum of activities related to the planning, design and implementation of construction projects for various social and economic sectors in the country of all kinds, as well as private sector buildings and infrastructure such as roads, bridges, tunnels, ferries, sewage networks and all similar facilities. Infrastructure has significantly affected the economy of countries, as it has contributed to supporting all economic sectors by providing them with many executive and operational projects, which have contributed to supporting individual and industrial production and increasing the provision of employment opportunities for individuals. It also saved from public domestic spending, especially after it was able to establish roads that helped transportation to move correctly and at high speed, and it also

worked on the construction of railways, which linked many cities, saving transportation expenses, and encouraging the role of investment projects in the advancement of society.

The outbreak of the new Covid-19 has affected many sectors and industries in the world, including the construction industry, as many engineering companies have been forced to reduce their operations, and follow new practices in order to deal with the decline in demand for real estate, as well as the presence of new safety standards, and the increase in the number of employees working from home. Construction projects are likely to move at a slower pace than usual during the Covid-19, due to challenges and new practices across the supply chain, and suppliers may face challenges represented by re-lockdown, reducing operations. On the other hand, engineering companies will continue to adhere to practices imposed by the pandemic, such as social distancing, sterilization, and other changes that companies in various industries have been forced to adhere to.

The impact of Covid-19 included basic elements of construction projects, including environmental. We hope this paper provides an overview of the processes for managing the completion time and managing the time of the session, which includes: Identification of activities, sequence of activities, estimation of activity responses, estimation of periods timeline for activity, set the schedule of, monitor the schedule in addition to risk, as it has a negative impact on at least one of the project's goals, such as scheduling, cost, quality and occupational safety.

2 Data Collection Methods

The descriptive analytical method was used, due to its suitability for this type of study. The data was collected through secondary and primary sources. Secondary sources have included many previous studies in this area, as well as numerous references, reports, scientific papers and some related websites on the Internet. As for the primary data, it was obtained through the design of a questionnaire distributed to a random sample of consulting offices and construction companies.

3 Questionnaire Design

The questionnaire was designed to identify the most important problems facing contracting companies, institutions and consulting companies from the impact of the Covid-19 on infrastructure projects in Khartoum State, where the questionnaire consists of two parts:

Part I: General information, academic qualification, nature of work, type of work, years of experience and average projects implemented annually.

Part II: Questions about the impact of the Covid-19 on infrastructure project claims and contracts in Khartoum State from the design stage to the final delivery of the project and how to resolve disputes resulting from contracts and claims in terms of costs, time and risks.

After receiving the questionnaire forms after filling them out, the statistical analysis of the results of the questionnaire was carried out, where the statistical program for social sciences was approved.

4 Study Population and Sample Selection

The research sample is a subset of the study population and represents the basic characteristics of the community, so it is selected in an appropriate way to obtain accurate results on the subject of the study and thus circulate it to the study community as a whole, the researcher saw that the research sample within a group of consultants and contractors in various fields of construction and the study community is represented in the registered membership in the council of organizing houses of expertise for consulting services and the council for the regulation of engineering contractors, and the sample was randomly selected scientifically so that it represents the study community in a Correct way.

5 Data Analysis

To achieve the objectives of the study and verify its hypotheses, the following statistical methods were used:

Graphs, frequency distribution of answers, percentages, Cronbach's alpha coefficient to calculate the stability coefficient, arithmetic mean, standard deviation and median, relative importance coefficient, chi-square test to indicate differences between answers. To obtain as accurate results as possible, the statistical program SPSS was used and the Excel program was used to implement the graphs required in the study.

6 Analysis and Discussion f Results

- **Academic Qualification:** 11 Diploma, 73 Bachelor, 32 Master and 6 Doctorate.
- **Nature of work:** 49 Owner, 44 Contractor and 29 Consultant.
- **Type of Work:** 116 Public Sector and 6 Private Sector.
- **Years of work experience:** 24 Less than 5 years, 35 between 5-10 years, 31 between 11-15 years, 20 between 16-20 years and 12 more than 20 years.
- **Average Number of Projects Implemented Annually:** 43 Less than 5, 41 from 5-10, 10 from 11-15, 11 from 16-20 and 17 more than 20.

The First Axis: The Impact of Covid-19 in Terms of Contracts

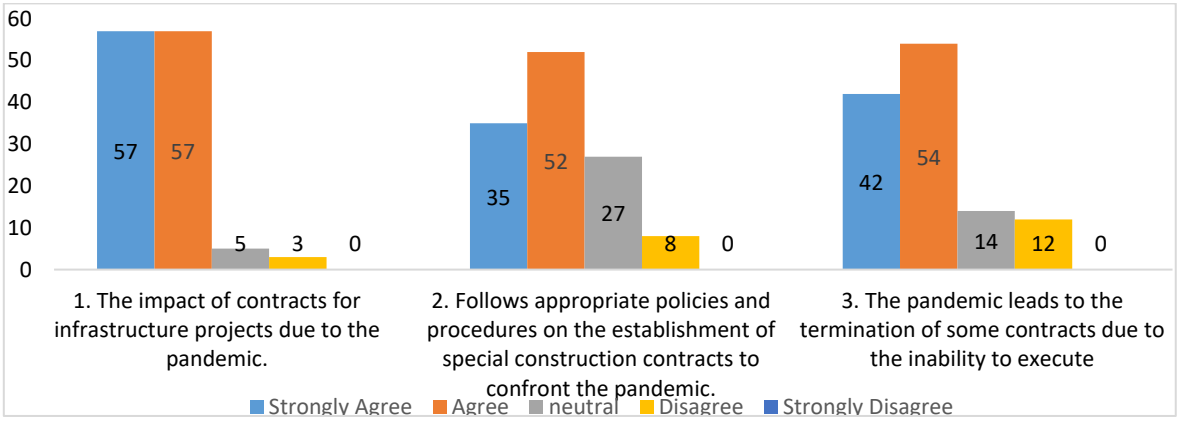


Fig. 1: Shows the Frequency Distribution of the Responses of the Study Members to the Statements of the First Axis

The Second Axis: The Impact of the Covid-19 in Terms of Conflicts

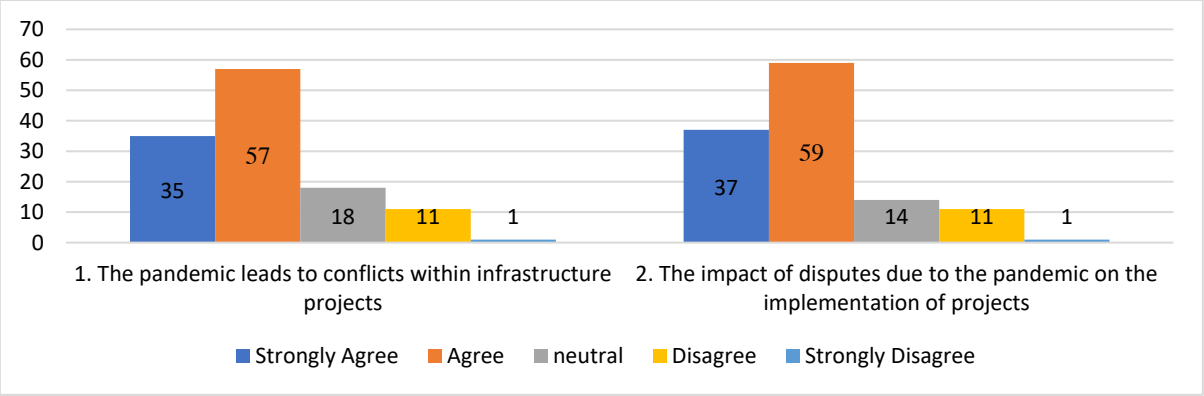


Fig. 2: Shows the Frequency Distribution of the Responses of the Study Members to the Statements of the Second Axis

The Third Axis: The Impact of the Covid-19 in Terms of Costs and Claims

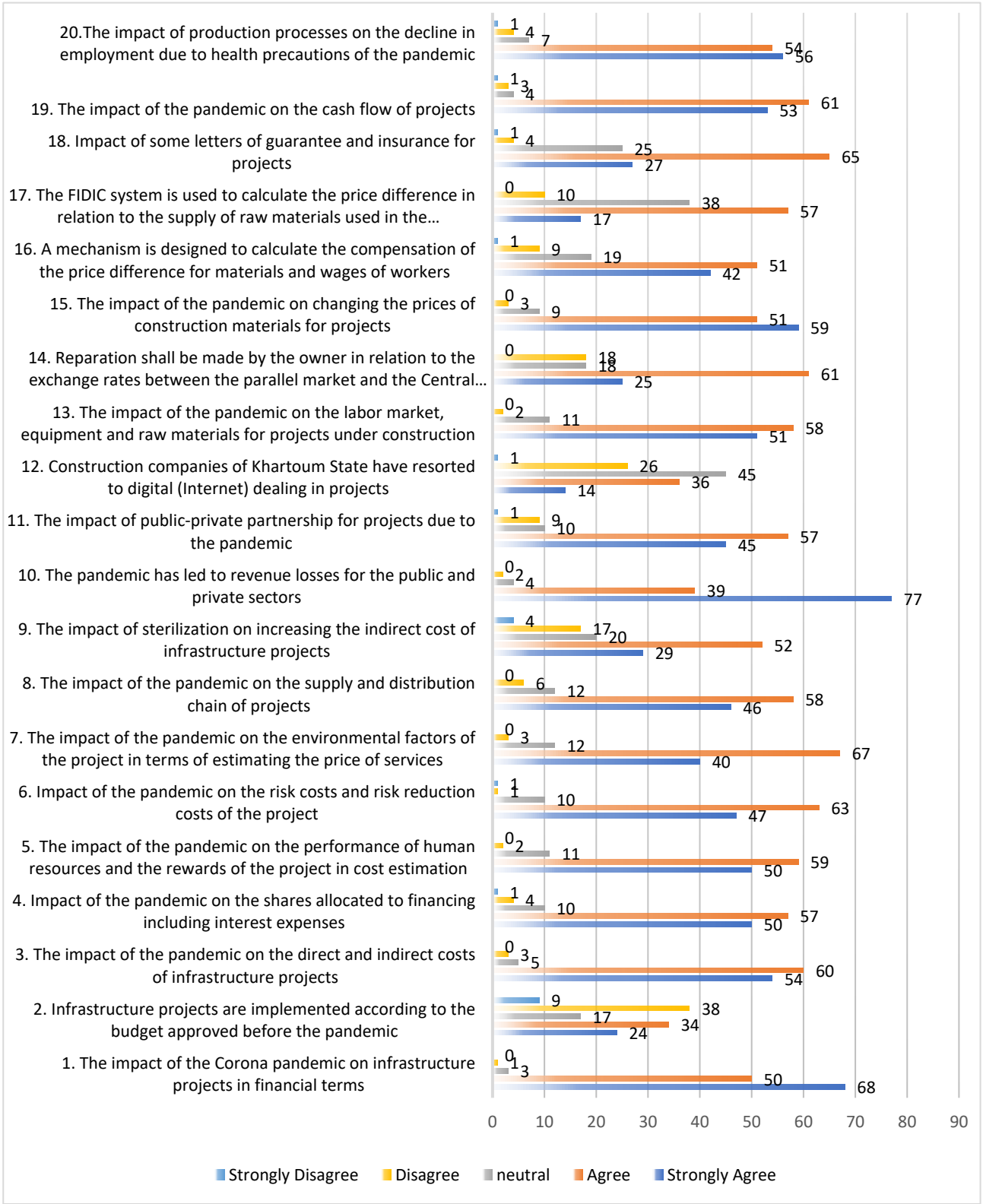


Fig. 3: Shows the Frequency Distribution of the Responses of the Study Members to the Statements of the Third Axis

The Fourth Axis: The impact of the Corona Pandemic in terms of Time

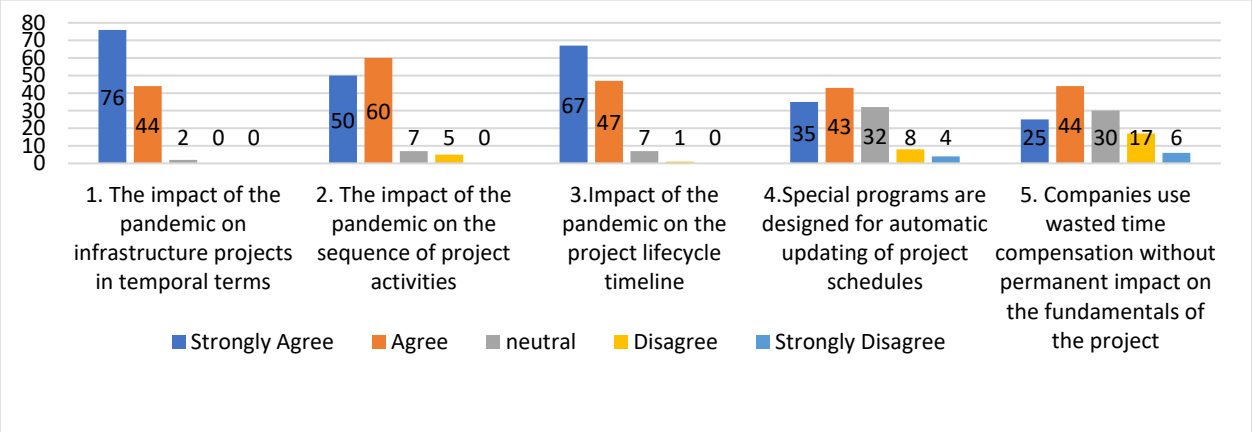


Fig. 4: Shows the Frequency Distribution of the Responses of the Study Members to the Statements of the Fourth Axis

Fifth Theme: The Impact of the Covid-19 in terms of Risks

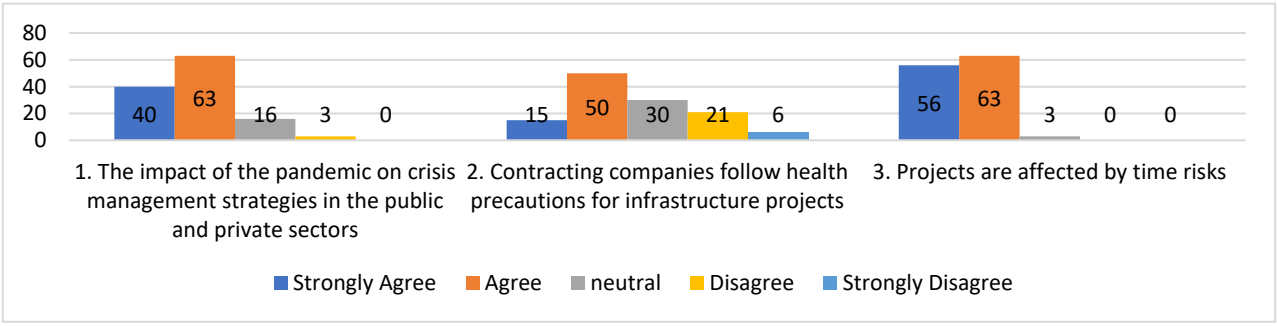


Fig. 5: Shows the Relative Distribution of the Responses of the Study Members to the Statements of the Fifth Axis

- **Hypothesis testing**

The first hypothesis (there is an impact of the Covid-19 on infrastructure project contracts and claims in terms of costs, time, risks and their direct and indirect effects) The chi-square test was used to indicate the differences between the answers to each of the questionnaire statements, the following table summarizes the test results for these statements.

Table 1: Results of the Initial Hypothesis Test

Axis	Ferry	Arithmetic mean	Standard deviation	Phrase measurement		Kai's moral value
				Weight	Grade	
The impact of the Covid-19 in terms of costs and claims	The impact of the Covid-19 on infrastructure projects financially	4.52	.592	5	Strongly agree	.000
	Infrastructure projects are implemented according to the budget approved before the Covid-19	3.21	1.281	3	neutral	.000
	The impact of the Covid-19 on the direct and indirect costs of infrastructure projects	4.35	.679	4	Ok	.000

	The impact of the Covid-19 on the shares allocated for financing, including interest expenses	4.24	.803	4	Ok	.000
	The impact of the Covid-19 on the performance of human resources and rewards for the project in estimating the cost	4.29	.698	4	Ok	.000
	The impact of the Covid-19 on risk costs and risk reduction costs for the project	4.26	.714	4	Ok	.000
	The impact of the Covid-19 on the environmental factors of the project in terms of estimating the price of services	4.18	.704	4	Ok	.000
	The impact of the Covid-19 on the supply and distribution chain of projects	4.18	.803	4	Ok	.000
	The effect of sterilization on increasing the indirect cost of infrastructure projects	3.70	1.082	4	Ok	.000
	The Covid-19 led to revenue losses for the public and private sectors	4.57	.643	5	Strongly agree	.000
	The impact of public-private partnership for projects due to the Covid-19	4.11	.902	4	Ok	.000
	Construction companies in Khartoum State resorted to digital dealing (Internet) in projects	3.30	.959	3	neutral	.000
	The impact of the Covid-19 on the labor market, equipment and raw materials for projects under construction	4.30	.701	4	Ok	.000
	The damage is reparated by the owner for the exchange rates between the parallel market and the Central Bank of Sudan in the supply of imported raw materials and foreign labor	3.76	.945	4	Ok	.000
	The impact of the Covid-19 on changing the prices of construction materials for projects	4.36	.728	4	Ok	.000
	A mechanism is designed to calculate the price difference compensation for materials and workers' wages	4.02	.936	4	Ok	.000
	FIDIC system is used to calculate the price difference for the supply of raw materials used in the implementation of projects	3.66	.819	4	Ok	.000
	The impact of some letters of guarantee and insurance for projects	3.93	.794	4	Ok	.000
	The impact of the pandemic on the cash flow of projects	4.33	.732	4	Ok	.000
	The impact of production processes on the decline in employment due to the health precautions of the pandemic	4.31	.793	4	Ok	.000
	Total	4.07	0.376	4	Ok	.000

The impact of the Corona pandemic in terms of time	The impact of the pandemic on infrastructure projects in terms of time	4.61	.523	5	Strongly agree	.000
	The impact of the pandemic on the sequence of project activities	4.27	.750	4	Ok	.000
	The impact of the pandemic on the project lifecycle timeline	4.48	.646	5	Strongly agree	.000
	Special programs are designed for automatic updating of project schedules	3.80	1.036	4	Ok	.000
	Companies use lost time compensation without a lasting impact on the fundamental factors of the project	3.80	1.115	4	Ok	.000
	Total	4.14	0.536	4	Ok	.000
The impact of the Corona pandemic in terms of contracts	Impact of Infrastructure Project Contracts Due to the Pandemic	4.38	.684	4	Ok	.000
	Follows appropriate policies and procedures on the establishment of special construction contracts to confront the pandemic	3.93	.879	4	Ok	.000
	The pandemic leads to the termination of some contracts due to lack of implementation	4.03	.927	4	Ok	.000
	Total	4.11	0.622	4	Ok	.000
The impact of the Corona pandemic in terms of conflicts	The pandemic leads to conflicts within infrastructure projects	3.93	.934	4	Ok	.000
	The impact of disputes due to the pandemic on the implementation of projects	3.98	.927	4	Ok	.000
	Total	3.95	0.873	4	Ok	.000
The impact of the Corona pandemic in terms of risks	The impact of the pandemic on crisis management strategies in the public and private sectors	4.15	.735	4	Ok	.000
	Contracting companies follow health precautions for infrastructure projects	3.39	1.064	4	Ok	.000
	Projects are affected by time risks	4.43	.545	4	Ok	.000
	Total	3.99	0.550	4	Ok	.000
Total all Ferries		4.06	0.445	4	Ok	.000

From the results in the Table 1, we notice that the arithmetic means of all hypothesis statements range between (3.95-4.14), the standard deviation of these phrases ranges between (0.873-0.376) and this indicates the homogeneity of the respondents' answers towards the phrases (whenever the standard deviation is small, this indicates the homogeneity of the answers of the study members). (There is an impact of the Corona pandemic on the contracts and claims of infrastructure projects in terms of costs, time, risks and their direct and indirect effects), and the table above indicates that the value of the Kai-squared probability to indicate the differences between the answers of the study members were (0.000) and this value is less than the level of significant (0.05), and this indicates that there are statistically significant differences between the answers and in favor of the approvers, meaning that there is an impact of the Covid-19 on contracts and claims of infrastructure projects in terms of costs, time, risks and their direct and indirect effects.

The second hypothesis (there are treatments for conflict resolution in infrastructure projects according to the existing variables and the effects of the Covid-19 on them).

Table 2: Second Hypothesis Test Results

Ferry	Arithmetic mean	Standard deviation	Phrase measurement		Level of significance
			Weight	Grade	
Reparation is made by the owner in relation to the exchange rates between the parallel market and the Central Bank of Sudan in the supply of imported raw materials and foreign labor	3.76	0.945	4	Ok	.000
A mechanism is designed to calculate the price difference compensation for materials and workers' wages	4.02	0.936	4	Ok	.000
FIDIC system is used to calculate the price difference for the supply of raw materials used in the implementation of projects	3.66	0.819	4	Ok	.000
Companies use lost time compensation without lasting impact on the fundamental factors of the project	3.53	1.115	4	Ok	.000
Follows appropriate policies and procedures on the establishment of special construction contracts to confront the pandemic	3.93	0.879	4	Ok	.000
Total	3.78	0.608	4	Ok	.000

From the results in Table 2, we note that the arithmetic means of all hypothesis statements range between (3.53-4.02), while the standard deviation of these statements ranges between (0.819-1.115) and this indicates the homogeneity of the respondents' answers towards the statements (whenever the standard deviation is small, this indicates the homogeneity of the answers of the study members). (There are treatments for conflict resolution in infrastructure projects according to the variables currently present and the effects of the pandemic on them), we note that the value of the Kai-square probability to indicate the differences between the answers of the study members was (0.000) and this value is less than the level of significance (0.05) and this indicates that there are differences statistically significant between the answers and in favor of the approvers, that is, there are treatments for conflict resolution in infrastructure projects according to the variables currently present and the effects of the Covid-19 on them.

7 Conclusion

The study presented in this paper showed the reality of the impact of the Covid-19 on the contracts and claims of infrastructure projects in Khartoum State and the obstacles facing local and foreign construction companies to confront the Covid-19 in terms of costs, time, risks and how to resolve disputes, the results of the survey and analysis of the results of the questionnaire showed the order of problems in terms of importance. The order of problems will be from the most important to the least important.

- As for costs and claims, the Covid-19 led to revenue losses of 77% for the public and private sectors, and affected infrastructure projects financially by 68%. Covid-19 also affected the changing prices of construction materials by 59.0% and 54.0% on direct and indirect costs and also affected the cash flow of projects by 53.0%.

- In terms of **time** impact, Covid-19 affected infrastructure projects by 76.0%. Covid-19 affected the project lifecycle timeline by 67.0%, and by 50.0% on the sequence of activities of the project.
- Conflicts affected the implementation of some projects by 59.0%; Covid-19 lead to conflicts within infrastructure projects by 57.0% for infrastructure projects.
- As for the risks of the Covid-19 affecting crisis management strategies in the public and private sectors by 63.0%, construction companies follow health precautions by 50.0% for infrastructure projects.

Recommendations

- It is necessary for institutions and companies operating in the construction industry to unify the cost of the project in dollars to avoid exchange rate hesitation.
- Follow the FDIC formula to compensate for damage in all sectors, design a special contract formula to combat the epidemic and similar force majeure, adopt FIDC contracts instead of standard contracts followed, make epidemic safety measures for construction projects**,** resort construction companies to deal digitally in projects.

References

Al-Mhdawi et al. (2022). Capturing the impact of COVID-19 on construction projects in developing countries: A case study of Iraq. *Journal of Management in Engineering, 38*(1).

Rehman**,** M.S.U., Shafiq, M.T. & Afzal, M. (2021). Impact of COVID-19 on project performance in the UAE construction industry. *Journal of Engineering, Design and Technology*.

Biswas et al. (2021). The impact of COVID-19 in the construction sector and its remedial measures. In: *Journal of Physics: Conference Series*, Vol. 1797, No. 1, p. 012054. IOP Publishing.

Biz Vibe (2020). How has the Coronavirus affected the global construction industry?, available at https://www.argaam.com

Omar Amoudi, Al-Obaid, Ali & Hamadeh, Mona. (2015). Identifying and Allocating Risks in Construction Projects from the Owner's Perspective in Syria. *Journal of King Abdulaziz University: Engineering Sciences*, 26.

Umar, T. (2022). The impact of COVID-19 on the GCC construction industry. *International Journal of Service Science, Management, Engineering, and Technology (IJSSMET), 13*(2), pp.1-17.

Cite as: Adam M. & Mohammed A., "The Impact of COVID-19 on Contracts and Claims for Infrastructure Projects", *The 2nd International Conference on Civil Infrastructure and Construction (CIC 2023)*, Doha, Qatar, 5-8 February 2023, DOI: https://doi.org/10.29117/cic.2023.0031

An Integrated Workflow for Transforming Infrastructure Projects Data into the Metaverse

Mohammed Amer Younus Al-Shaheen
GIS Senior Engineer, Public Works Authority (Ashghal), Doha, Qatar
malshaheen@ashghal.gov.qa

Raj Mukta Sundaram
GIS Engineering Expert, Public Works Authority (Ashghal), Doha, Qatar
rmukta@ashghal.gov.qa

Thirunavukkarsu Ramalingam
GIS Senior Engineer, Public Works Authority (Ashghal), Doha, Qatar
tramalingam@ashghal.gov.qa

Abstract

The infrastructure construction industry is typically characterized by large-scale, complex technologies, long completion times, and challenging collaborations. The provisioning of digital representations in 3D by combining physical properties with geospatial data would assist in addressing some of these challenging issues. These technologies would also provide a fundamental basis for the creation of Metaverse to support sustainable, innovative infrastructure design and construction. Hitherto most studies were focused primarily on integration techniques rather than providing comprehensive workflow for exploiting projects data to support engineers. This study aims to help engineers and decision makers better understand the opportunities and implications of the virtual 3D environment or Metaverse by examining the key emerging trends driving and enabling the development of data workflows for a selected infrastructure project. To build possible levels of workflow, the methodology involved incorporating 3D geometric data acquired from Building Information Models (BIM) and processed with geospatial location. The optimum data workflow and associated advantages for the construction industry have been determined. This paper also describes the concept and workflow approach, including specific data structures, data conversion, and a prototype solution. The results demonstrate the feasibility of the concept's robustness and both in terms of technical implementation and adoption for expediting business processes.

Keywords: Geographical Information System (GIS); Sustainability; Building Information Modelling (BIM); Metaverse; 3D

1 Introduction

The importance of collaboration in the construction industry has led to the development of its information and communication technologies in recent years. In the last few years, digital technology has gained a lot of intangible ground in many parts of the world. This is because COVID-19 sparked a flood of strategies for making workplaces and markets more resilient (Allam et al., 2022). Collaboration between parties and processes, assisted by digital technologies, is frequently cited as a crucial requirement for the effective completion of infrastructure projects.

In spite of the fact that the definition of the Metaverse remains unclear, everyone agrees that users will be immersed in virtual worlds–sometimes in VR, sometimes not, which implies that spatial data

will be crucial to the experience (Collins, 2022). As a word, Metaverse also comes up with a meaning like “Metaverse” by combining the words “meta” meaning “after, beyond” in Greek and “universe” meaning “universe” in English (Teknosa, 2022). There is no complete implementation of the Metaverse, however certain platforms incorporate Metaverse-like components. Video games offer the closest experience to the Metaverse at this time (Türk, 2022).

1.1 Virtual Reality (VR)

Due to technical advancements, digital technologies such as VR has acquired prominence and popularity in recent years (Shen et al., 2022). The term virtual reality (VR) refers to an experience that resembles or is completely different from reality based on the combination of hardware and software. It enables people to interact within a computer-generated simulated environment (Lo & Tsai, 2022). VR head-mounted displays (HMDs) provide the most immersive VR experiences to date due to their sophisticated technical capabilities, including high-quality image rendering and a variety of accessories that allow freedom of movement within the virtual environment (Parong et al., 2020).

Today, HMD-based Virtual reality (VR) produces virtual settings that can influence how users think, conduct, and feel in ways that no other technology can (Hershfield et al., 2011; Neguţ et al., 2016; Spence et al., 2017). By delivering functions such as immersive vision, hearing, feeling, and experiencing, virtual reality (VR) technology can build a region that resembles the actual world (Mandal, 2013; Zhou & Deng, 2009).

1.2 BIM and GIS

Increasingly sophisticated systems are being created for buildings, cities, and infrastructure (Najeh et al., 2019). Building Information Modelling (BIM) and Geographical Information System (GIS) are two inter-disciplinary scientific fields that use computers to integrate and visualize diverse project data and provide an objective source of project information to aid project managers in making project-related decisions (Wei et al., 2021).

As a result, a number of studies have examined new approaches and technologies to address these issues in the construction industry, such as Building Information Modelling (BIM) and Geographic Information Systems (GIS) (Celeste et al., 2022). The Building Information Model (BIM) is used to share and transmit all types of building information throughout the entire project planning, construction, operation, and maintenance life cycle (Xu, 2021). BIM can streamline the construction process for all MEP utilities, civil, architectural, and landscaping works by adopting a new process across the various phases of the design and construction process (Abotaleb et al., 2020).

In addition to the 3D model and the 3D Geographic Information System (GIS), there are also many opportunities for growth in many other areas. Examples include urban planning and management, planning and design, local government construction, housing industry development, land management, and environmental evaluation (Xu, 2021).

GIS technology enables access to infrastructures in the actual world based on their coordinates. Therefore, it can model infrastructures based on the actual locations of their components (Carneiro et al., 2018). Implementation of GIS reduced costs and improved the timeliness and accuracy of project and program planning for large transportation infrastructure developments (Ford et al., 2012; Wei et al., 2021).

Interoperability of data between BIM and GIS technologies is a formidable obstacle. Existing solutions emphasize integrating BIM and GIS based on their respective schemas (Zhao et al., 2019).

Yet, BIM and GIS derive from distinct sources with varied levels of detail, it is possible that certain data will never be correctly transferred (Karan & Irizarry, 2015). Compared to BIM, GIS is more advanced and well-developed, and it is mostly used to analyse spatial linkages and patterns (Wang et al., 2016).

To properly manage infrastructure projects, the data must be accurately represented geometrically and semantically. BIM has limitations on these types of projects in several respects, including precision in finding objects over large regions, information about the surrounding area, and spatial analytics. Considering the vast quantity of spatial data utilized in infrastructure project planning, GIS can be quite useful for managing the project's surroundings(Zhao et al., 2019). As BIM can give extensive project information, the integration of BIM and GIS is becoming a prominent topic under these circumstances.

Despite some attempts to integrate BIM and GIS systems, BIM and GIS are two very different systems, as they have different standards, data types, and levels of detail. As part of this study, BIM data was processed using a GIS application, which minimized information loss and linked the model interactively with the retrieval of domain data (architecture, structure, and mechanical engineering).

To this end, the integration of BIM and GIS can help to create a broader perspective in the assets management and its training by incorporating, via GIS, all the additional spatial information that falls within the territory and relates to infrastructures, subservices, and all the existing surroundings. The combination of BIM data and spatial data pertaining to the context in which the 360 VR is placed, enables spatial analysis and observation with scenarios to be performed on a large number of projects and assets. All of this makes intervention planning more informed and hence more effective and robust.

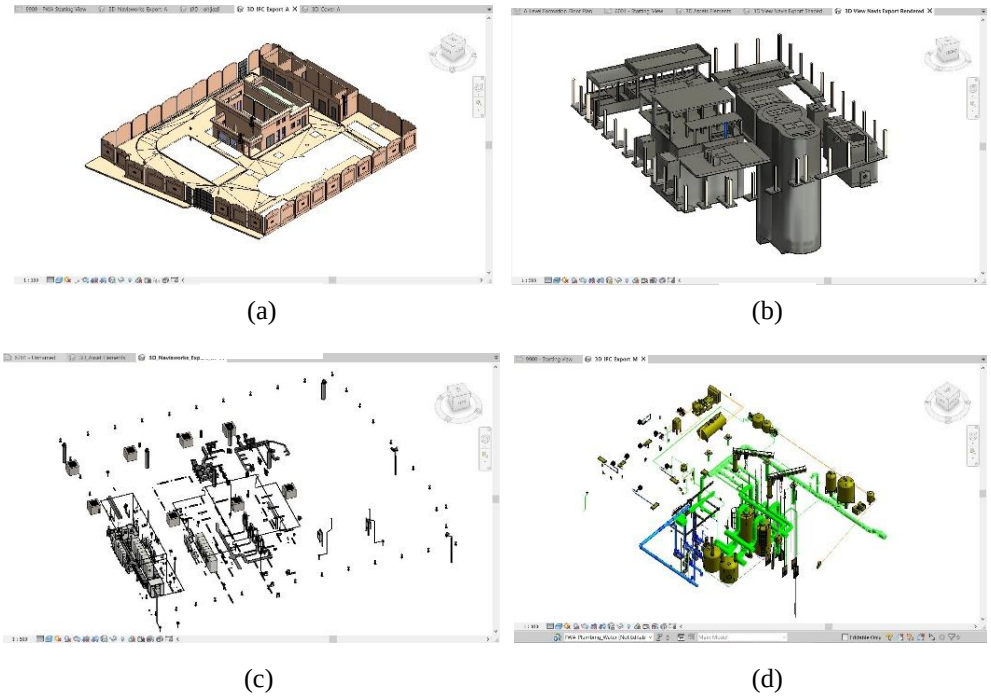
2 Methods and Workflow

As a case study, this paper focuses solely on infrastructure works. The selected project is Pumping Station Project PS16 North/PS16. The project is one of the projects submitted in BIM format by the contractor. A goal of this paper is to specify, formulate, and develop a workflow utilizing BIM and GIS technologies that will aid engineers in the entire data process and conversion, from start to finish, so that it becomes an essential workflow to resolve all issues that may arise along the way to produce web-based 360 VR experiences.

The value of reaching this goal is to develop a comprehensive procedure for using BIM to its maximum 3D modelling details that merge different 3D modelling disciplines to visualize and identify all the engineering domains (architectural, structural, mechanical, and electrical) during the data processing phase and extends to the 360 VR phase to assist in visualization and resolve any issues that may arise, formulating a coordination platform that could not have been conceived without this workflow and technology. The methodology for this paper is a case study done by exploring the data of a pumping station project, project code: PS16 North/PS16, of the infrastructure projects at the Public Works Authority (PWA/ASHGHAL). The first step was to collect the BIM files from the contractor. Four files collected which are as follows:

1. Architectural Model.
2. Structural Model.
3. Mechanical Model.
4. Electrical Model.

The federated project model was shared as well in Autodesk Navisworks format, due to the limitations highlighted in several literature including the software application in exporting the information of the model (Grosso et al., 2017; Shaw et al., 2007; Wetzel & Thabet, 2018).



(a) (b)

(c) (d)

Fig. 1 BIM Model Files: (a) Architecture Model (b) Structural Model (c) Mechanical Model (D) Electrical Model

This study uses BIM and GIS as the foundation for a collaborative process environment. Modelling indoor spaces is the strength of BIM, whereas outdoor mapping spaces are the strength of GIS (Amirebrahimi et al., 2015). This study is divided into three stages: First Stage: Processing the model into 3D GIS, Second Stage: Export geometries (Discipline based) and import into ESRI CityEngine, Third Stage: Publishing 360 VR Experience, Figure 2.

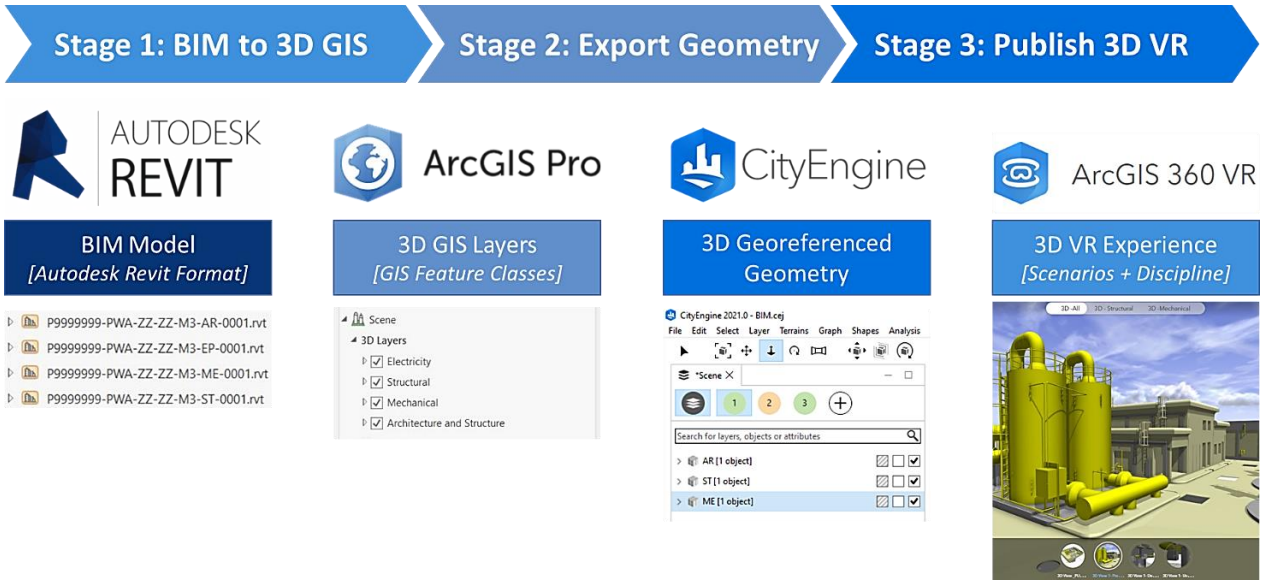


Fig. 2: The Study Workflow

3 Results and Processed Data

Due to the final outcomes of the data being rendered via ESRI 360 VR Experience, it is critical to use the native format, Revit, as a data source. As a 3D-based VR application, ESRI 360 VR Experience uses only 3D models. (Ioannis Pispidikis & Athanasiou, 2020). Starting with the. rvt format and reading by ArcGIS Pro application of these files. Subsequently, the Revit files will be investigated and extract the data needed for each discipline. The second step and in order to avoid the complexity a selected feature layer is reflected in ArcGIS Pro.

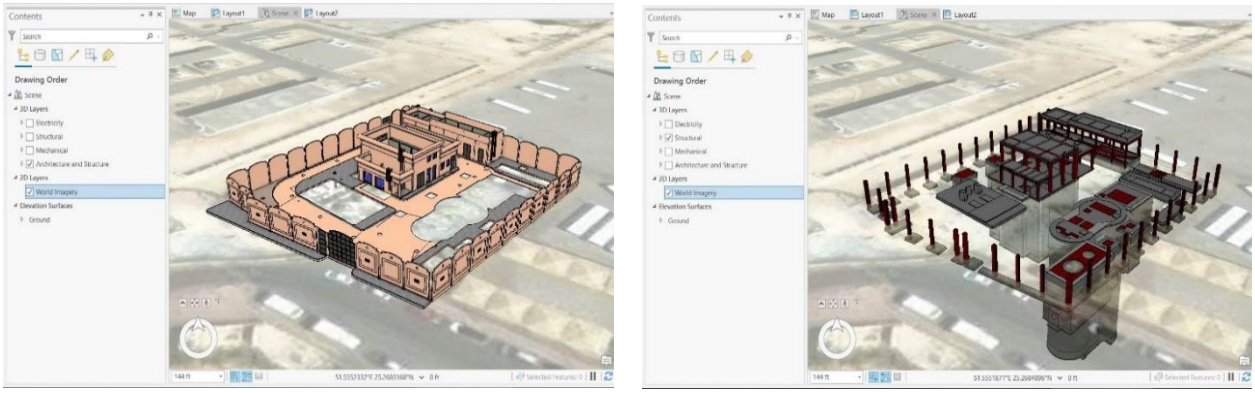
The import of BIM data into 3D GIS was accomplished through a simple workflow that integrated several steps at first stage. ArcGIS Pro 2.8 and a higher version can read natively the Autodesk Revit format. Only selected layers for the purpose of demo have been transferred and imported into .gdb file via ArcGIS Pro and viewed in a local scene tab. This method enabled the REVIT 3D virtual model to be transferred into the 3D GIS completely and without loss of data. Next, the model is georeferenced and navigable within the context of the urban environment in which it is placed as illustrated in Figure 3.



(a) (b)

Fig. 3: Pumping Station Project PS16 North/PS16: (a) Processed 3D GIS Data (b) Processed Top View Data

3D GIS data is arranged according to engineering disciplines as part of the processing of 3D GIS data. As a result, three sets of feature layers have been created to facilitate visual filtering of the 3D GIS data elements as shown in Figure 4.



(a) (b)

Fig. 4: Pumping Station Project PS16 North/PS16: (a) 3D GIS Architecture Model (b) 3D GIS Structure Model

At stage two, all required layers and data was exported to ESRI CityEngine. Since the aim is to maintain geometrical data for the model and avoid loss of the project information, all 3D GIS layers were converted and exported to fbx format and results rendered in Figure 5.

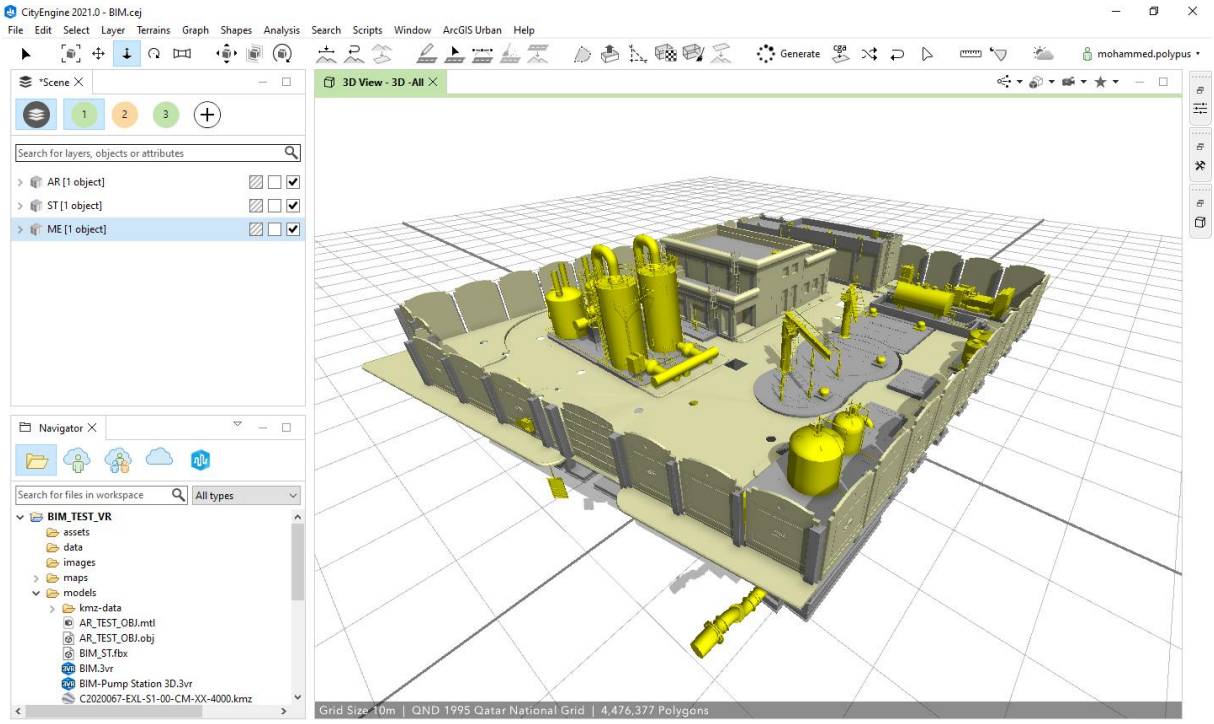


Fig. 5: Pumping Station Project PS16 North/PS16 - 3D Render in ESRI City Engine

The CityEngine Modelling application from ESRI allows users to create accurate 3D models of urban environments that can be used for simulations. This software is primarily known for its ability to create 3D content using rule-based modelling to generate detailed 3D objects from 2D data. In addition, rules can use attributes stored in GIS data, such as building heights and information specific to cadastral systems (Ribeiro et al., 2014).

After successfully importing the model in CityEngine and based on the methods followed, scenarios are created for the purpose of VR experience. These scenarios are created to render the capability of filtering the geometry based on the engineering discipline. As for the last stage of processing the 3D georeferenced model to VR experience, scenarios should be created. As a result of the exporter, CityEngine scenarios or layer compositions are converted into 360 VR Experience scenarios; turning CityEngine camera bookmarks into 360 VR Experience viewpoints (ESRI, 2022) , Figure 6.

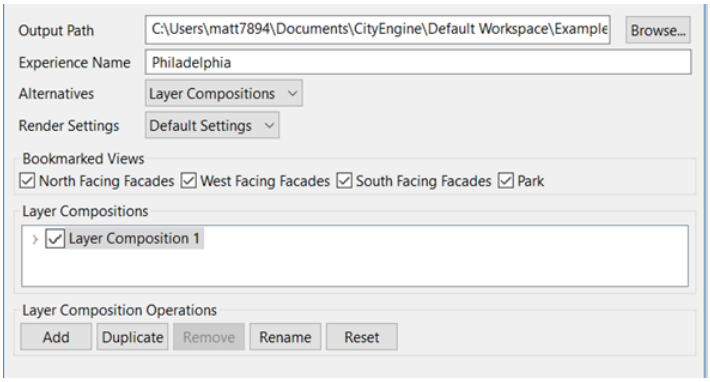


Fig. 5: 360 VR Experience Export Window

Despite the fact that CityEngine can export generated content to ArcGIS Online, it is not a web client or contains any web-enabled functionality (Ribeiro et al., 2014). At its core, the CityEngine 360 VR Experience exporter is an automated method of taking a series of viewport snapshots based on camera bookmarks. This collection of snapshots is combined into panoramic images (one for each bookmark). After uploading the exported 360 VR Experience, the experience may be consumed either locally or through the cloud (ESRI, 2022). The output format is .3vr file which can be uploaded to ESRI cloud account and viewed in the ArcGIS 360 VR environment. Figure 7 illustrates the results examined using Oculus (Quest 2) VR headset after publishing the results.



Fig. 6: 360 VR Experience Public on ArcGIS Online Cloud

With the 360 Virtual Reality Model built into the project, participants will be able to see it in three dimensions, which will help them understand the details and surroundings of the project better. Also, a 3D visualization makes it easier for users to talk to each other and share information, which reduces the chance of mistakes and misunderstandings.

4 Conclusion

Combining GIS (Geographic Information System) with BIM (Building Information Modeling) to create a spatial database that describes the built environment could be effective in supporting more informed and effective decision-making in the design scenarios and infrastructure asset management (Cecchini, 2019). Organizations can benefit from the affordances of immersive VR to provide richer and personalized user experiences. The implementation of VR capturing the lifecycle of the infrastructure projects at the Public Works Authority 'Ashghal' will have multi-faceted benefits. As compared to traditional collaboration platforms, immersive VR would provide richer and more effective collaboration platforms. A combination of VR's affordances makes it distinguishable from other collaboration technologies in its ability to foster a sense of community among engineers (Dincelli & Yayla, 2022; Nunamaker, 1997; Kane, 2017).

Additionally, studies have demonstrated that VR training is superior to traditional training methods. By focusing on the create-ability aspect of VR training, organizations can increase employee efficiency at the workplace (Dincelli & Yayla, 2022). The Public Works Authority 'Ashghal' will

have a greater opportunity to implement the VR in assets management and operation training particularly for complex infrastructure facilities and projects.

Thus, Ashghal can tailor the training material for each trainee to create more personalized learning experiences in a simulated environment. Next, this technology provides many opportunities for the Public Works Authority to reduce operational costs, such as the ability to create, embody, and interact with it (Stone et al., 2021). Also, it will be possible to provide safer and more accessible services by focusing on the create-ability, navigation, and sense-ability affordances (Dincelli & Yayla, 2022).

Even though VR offers businesses a lot of great opportunities, it also has a number of problems that could make it harder for businesses to use it and keep using it. One of the greatest obstacles is the availability of VR content that organizations can utilize for their purposes (Mattila et al., 2020). In other words, the data and source of the data is essential to create a meaningful content to be consumed as VR contents. The delivery of high performance and visual fidelity has been a challenge for virtual reality since its founding. For the successful adoption of immersive VR, potent computers and seamless connections to other peripherals are essential. In fact, low-quality graphics was one of the primary reasons why early VR technologies were not widely adopted. Infrastructure should be considered as key item to provide the robust VR adaptation.

Due to the vast number of design criteria and their complex interrelation, which are unique across businesses and industries, successful VR applications would create a sustainable competitive advantage and value for the Ashghal over the coming years. The study emphasizes the simplicity of contemporary technologies to produce data and contents for VR consumption comprising of complex infrastructure project details. Ashghal is embarking on gaining and exploiting the advantages by considering these as strategic opportunities in order to increase operational efficiency, improve corporate social responsibility, create new markets, and, overall, increase operational efficiency with this emerging technology.

References

Abotaleb, M. M., Saab, E. & AbdelZaher, M. (2020). Integrating Building Information Management (BIM) in Civil Infrastructure Coordination: Application at LUSAIL Plaza.

Allam, Z. et al. (2022). The Metaverse as a virtual form of smart cities: Opportunities and challenges for environmental, economic, and social sustainability in urban futures. *Smart Cities*, *5*(3), 771-801.

Amirebrahimi, S. et al. (2015). A data model for integrating GIS and BIM for assessment and 3D visualisation of flood damage to building. *Locate*, *15*(2015), 10-12.

Carneiro, J. et al. (2018). BIM, GIS, IoT, and AR/VR integration for smart maintenance and management of road networks: a review. 2018 IEEE international smart cities conference (ISC2),

Cecchini, C. (2019). From data to 3D digital archive: a GIS-BIM spatial database for the historical centre of Pavia (Italy). *J. Inf. Technol. Constr.*, *24*, 459-471.

Celeste, G. et al. (2022). Innovating the construction life cycle through BIM/GIS integration: a review. *Sustainability*, *14*(2), 766.

Collins, M. (2022). *The geospatial industry's key place in the metaverse*. Geo Week News. Retrieved December 21, 2022 from https://www.geoweeknews.com/news/the-geospatial-industry-s-key-place-in-the-metaverse

Del Grosso et al. (2017). Infrastructure management integrating SHM and BIM procedures. Conf. Smart Monit. Assess. Rehabil. Civ. Struct.,

Dincelli, E. & Yayla, A. (2022). Immersive virtual reality in the age of the Metaverse: A hybrid-narrative review based

on the technology affordance perspective. *The Journal of Strategic Information Systems*, *31*(2), 101717.

ESRI. (2022). *Export 360 VR Experiences from CityEngine*. ESRI. Retrieved Jaunary 1, 2023 from https://doc.arcgis.com/en/cityengine/latest/help/help-export-360vr.htm

Ford, M. et al. (2012). Benefits of geographic information systems in managing a major transportation program: evaluation and lessons learned. *Transportation research record*, *2291*(1), 1-7.

Hershfield et al. (2011). Increasing saving behavior through age-progressed renderings of the future self. *Journal of marketing research*, *48*(SPL), S23-S37.

Ioannis Pispidikis, K. D., Eftychia Kalogianni, Katerina, & Athanasiou, A. L. A. E. D. (2020, 10–14 May 2020). 3D Modelling and Virtual Reality for the Management of Public Buildings. Smart surveyors for land and water management, Amsterdam, the Netherlands.

Jay F Nunamaker, J. (1997). Future research in group support systems: needs, some questions and possible directions. *International Journal of Human-Computer Studies*, *47*(3), 357-385.

Kane, G. C. (2017). The evolutionary implications of social media for organizational knowledge management. *Information and organization*, *27*(1), 37-46.

Karan, E. P. & Irizarry, J. (2015). Extending BIM interoperability to preconstruction operations using geospatial analyses and semantic web services. *Automation in Construction*, *53*, 1-12.

Lo, S. C. & Tsai, H. H. (2022). Design of 3D Virtual Reality in the Metaverse for Environmental Conservation Education Based on Cognitive Theory. *Sensors*, *22*(21), 8329.

Mandal, S. (2013). Brief introduction of virtual reality & its challenges. *International Journal of Scientific & Engineering Research*, *4*(4), 304-309.

Mattila, O. et al. (2020). Restoration in a virtual reality forest environment. *Computers in human behavior*, *107*, 106295.

Najeh, H. et al. (2019). Diagnosis in buildings: New trends illustrated by an application. 2019 International Conference on Control, Automation and Diagnosis (ICCAD),

Neguț, A. et al. (2016). Task difficulty of virtual reality-based assessment tools compared to classical paper-and-pencil or computerized measures: A meta-analytic approach. *Computers in human behavior*, *54*, 414-424.

Parong, J. et al. (2020). The mediating role of presence differs across types of spatial learning in immersive technologies. *Computers in human behavior*, *107*, 106290.

Ribeiro, A., de Almeida, J. P. & Ellul, C. (2014). Exploring CityEngine as a visualisation tool for 3D cadastre. 3D Cadastres 2014-4th International FIG 3D Cadastre Workshop,

Shaw, N., Bouchlaghem, D. & Kerr, D. (2007). Strategic Review of the Production of a 4d Construction Sequencing Model–The Lessons Learnt.

Shen, S. et al. (2022). Exploring the factors influencing the adoption and usage of Augmented Reality and Virtual Reality applications in tourism education within the context of COVID-19 pandemic. *Journal of hospitality, leisure, sport & tourism education*, *30*, 100373.

Spence, C. et al. (2017). Digitizing the chemical senses: Possibilities & pitfalls. *International Journal of Human-Computer Studies*, *107*, 62-74.

Stone, N. J. et al. (2021). Virtual reality for hazard mitigation and community resilience: An interdisciplinary collaboration with community engagement to enhance risk awareness. *AIS Transactions on Human-Computer Interaction*, *13*(2), 130-144.

Teknosa. (2022). *Metaverse Nedir? - Teknosa Blog*. Teknosa Blog. https://blog.teknosa.com/populer-konular/metaverse-nedir

Türk, T. (2022). The Concept of Metaverse, Its Future and Its Relationship with Spatial Information. *Advanced Geomatics*, *2*(1), 17-22.

Wang, J. F., Zhang, T. L., & Fu, B. J. (2016). A measure of spatial stratified heterogeneity. *Ecological Indicators*, *67*, 250-256.

Wei, J. et al. (2021). BIM and GIS applications in bridge projects: A critical review. *Applied Sciences*, *11*(13), 6207.

Wetzel, E. M. & Thabet, W. (2018). A case study towards transferring relevant safety information for facilities maintenance using BIM.

Xu, S. (2021). Three-Dimensional Visualization Algorithm Simulation of Construction Management Based on GIS and VR Technology. *Complexity*, *2021*.

Zhao, L., Liu, Z. & Mbachu, J. (2019). Highway alignment optimization: an integrated BIM and GIS approach. *ISPRS International Journal of Geo-Information*, *8*(4), 172.

Zhou, N. N. & Deng, Y. L. (2009). Virtual reality: A state-of-the-art survey. *International Journal of Automation and Computing*, *6*(4), 319-325.

Cite as: Al-Shaheen M., Sundaram R.M. & Ramalingam T., "An Integrated Workflow for Transforming Infrastructure Projects Data into The Metaverse", *The 2nd International Conference on Civil Infrastructure and Construction (CIC 2023)*, Doha, Qatar, 5-8 February 2023, DOI: https://doi.org/10.29117/cic.2023.0032

Use of Immersive Augmented Reality Technology in Public Works: Myth or Reality? – A Case Study on Implementation Challenges

Balamohan Narayanasamy
Public Works Authority (Ashghal), Doha, Qatar.
nmohan@ashghal.gov.qa

Suresh Manicakam
Public Works Authority (Ashghal), Doha, Qatar.
smanickam@ashghal.gov.qa

Abstract

The State of Qatar witnessed an unprecedented transformation during the past three decades in various sectors, more specifically in public infrastructure. The rapid transformation coupled with urbanization has increased the density of public infrastructure assets both at the surface and sub-surface. Ashghal, the Public Works Authority (PWA) contributes to achieving the goals of Qatar National Vision 2030 (QNV) by leading the transformation of Qatar's public infrastructure delivery and improving operational efficiency. Augmented Reality (AR) Technology that interfaces digital information with the real-world environment both spatially and temporally engenders tangible impact in the area of construction planning, operations, and maintenance of public works and assets. AR Initiative is identified as part of the Geospatial Strategic Master Plan for PWA. AR Technology has proven successful in various industries like entertainment, health, manufacturing, etc., however, it has serious limitations and lacks adopting changes in large-scale implementation in the context of public works. In this paper, the intent, technology selection, and implementation roadmap are discussed through a case study. This case study presents various use cases considered in the public works domain including the use of AR with Geospatial and BIM Technology. This paper further discusses the strategy for deployment, best use, limitation, and factors to be considered for full-scale deployment. This paper summarizes the study outcomes of the current effort undertaken by PWA in deploying AR solutions and discusses the feasibility of AR solutions in public work is a myth or reality.

Keywords: Augmented Reality; Innovation; Public works; Geospatial Transformation; 3D Visualization

1 Introduction

Since the beginning of this century, the use of digital technology has evolved with multipurpose uses, and become an essential component of everyday digital life. The way users consume business services on handheld devices is gaining importance nowadays. As the new industrial revolution takes up a cognitive form, the use of innovative technologies increased its footprint beyond the private & industrial sectors. We live in the generation of Big Data. With the availability of valuable and variety of data, the velocity at which the data availability, decisions, and actions remain still confined in two-dimensional maps and drawings. This creates a major gap between availability and the best use of data. Emerging technologies such as BIM, IoT, and Virtual Reality (VR) gained importance to use of multi-dimensional information for the decision-making process. Augmented Reality (AR), one of the emerging technologies, promises to minimize the gap and maximize the utilization of enriched information.

In the space of civil engineering, the use of AR is increased during the last five years and the percentage of its application is around 10% in underground and about 45 in construction (Xu & Moreu, 2021). Typically, excavation damages to underground infrastructure cause huge financial losses in public sector organizations (Hansen et.al, 2021). In most cases, this is contributed by human errors with a lack of situational awareness of the underground assets. This indicates considering AR to improve upon traditional paper-based or 2D information-based inspection, planning, or maintenance procedures. Public Works Authority 'Ashghal' (PWA) the infrastructure implementation organization delivers the majority of the projects in the civil engineering domain.

In this paper, we summarize and share our industry experience in the implementation of AR initiatives in PWA, covering the business context and strategy. The key aim of this paper is to enable the reader, to understand the potential application areas of AR in the public works domain as well as implementation challenges and limitations.

2 Anatomy of Augmented Reality

Augmented Reality (AR) Technology superimposes computer-generated data on top of a user's perception of the real world in real time. AR falls closer to the real-life context by supplementing the real world with virtual computer-generated objects that appear to coexist in the same space as the real-world (Juan et.al, 2018). Two diverse types of AR are identified, (i) Location-based AR, the application relies on the spatial position and orientation of the device to select and display location-relevant information, (ii) Image-based AR, and the applications use an image recognition algorithm to trigger the display of relevant content over a recognized physical pattern (Vogt et.al, 2013). The application of AR technology is determined by the two available categories, Marker and Markerless (covers location-based, superimposition, projection, and outlining) abased. Understanding the specifics of these categories is crucial before the selection of AR products to be employed for use.

3 Business Context

Ashghal, the Public Works Authority (PWA) contributes to achieving the goals of Qatar National Vision 2030 & delivery mandates for hosting the FIFA World cup 2022 by leading the transformation of Qatar's road & drainage infrastructure and public buildings to develop the nation into one of the most advanced and smart countries in the world. The objectives in the pillars of sustainable development and high-quality urban lifestyle of QNMP-Qatar National Development Framework 2032 of QNMP highly influence the increase in the urban space and utility densities. The rapid transformation by taking advantage of the enormous opportunities of smart technology in developing more sustainable asset management. The "Smart Qatar" initiative also known as TASMU is one of the key components of QNV 2030. The TASMU emphasizes harnessing the power of innovative technology in the delivery of public infrastructure and improving operational efficiency.

Augmented Reality (AR) Technology interfaces digital information with real-world environments both spatially and temporally. It is considered as one that engenders tangible impact in the areas of operation and maintenance of public works assets. AR Initiative is part of smart city initiatives, identified as part of the Geospatial Strategic Master Plan for PWA. This plan provides a clear road map for geospatial business with PWA for the next five years to meet the strategic objective to achieve operational excellence in geospatial services.

3.1 Business Challenges and Needs

To understand the business case of this initiative, understanding the organization and its core

functions is almost important. Being a construction and asset management organization of critical capital assets, Ashghal depends on Geospatial Information (GIS) for carrying out its various key activities like design, project monitoring, asset operations, and maintenance. Ashghal is the owner of GIS data specifically for roads & highways, and sewers, and the TSE Network and its facilities. The spatial information of the core data acts as the source for key functions and departments' requirements during design, project management, project handover, and asset management. This information is used for various enterprise business applications like EAMS, CRMS, QPRO, QDRS, TDP, etc.

The key constraint in the State of Qatar for the development of road and utility infrastructure is the availability of right of way and it is limited. Thus, the utilities like foul sewer, TSE, ducts for telecommunication, electricity, water network, etc. are placed under the narrow corridor. Any maintenance or inspection activities that would be planned impact the free flow of traffic (Hamidy, 2020). The built environment and high-density underground utilities provide complex challenges to the field crew in locating the service assets. To understand the spatial placement of the underground assets, the density change was analyzed using geospatial information over the past decade and Figure 1 illustrates a qualitative assessment of utility density change in Doha and Al Khor. More than a 25% increase has been witnessed only from sewer density without consideration of other utility assets like electricity, water, telecom, ITS, and metro network assets, etc.

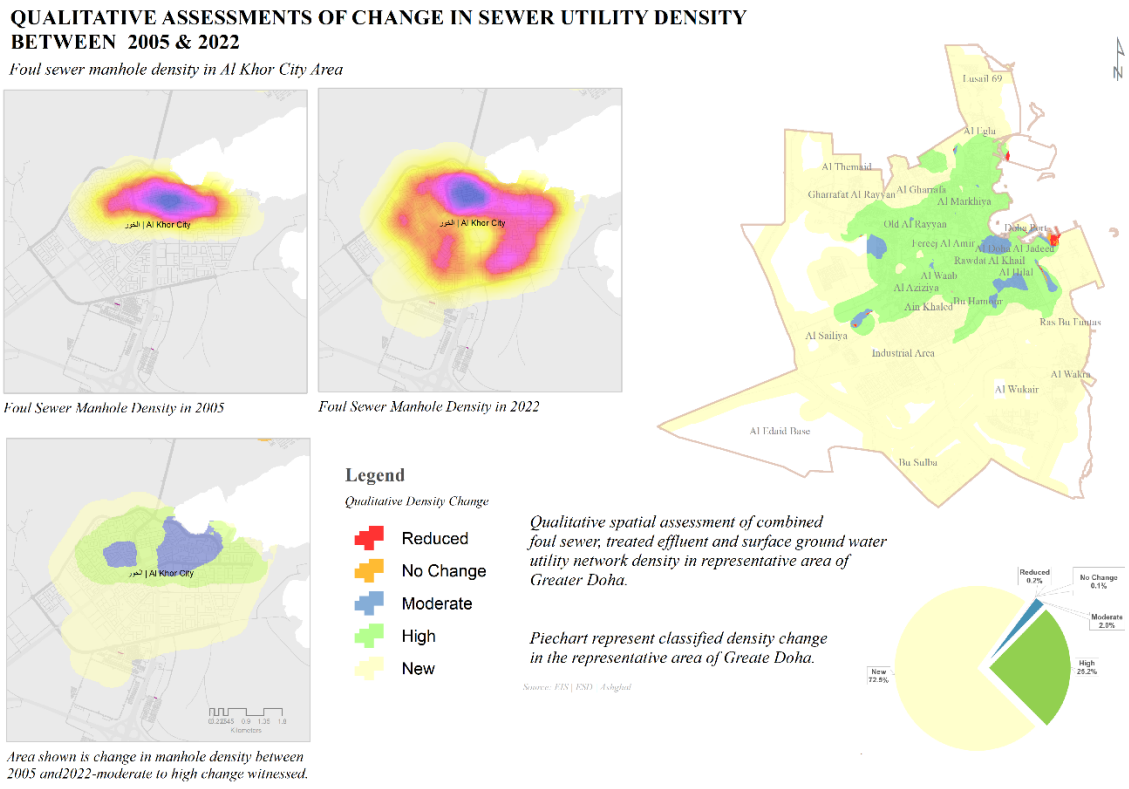


Fig. 1: Change in Utility Network Density in Doha and Al Khor Areas

Implementing AR technology would help the PWA field crew in visualizing/identifying any underground/hidden assets. AR implementation is expected to overcome the challenges and optimize any maintenance /inspection activities and design validation. Building Information Modeling (BIM) is being implemented in Ashghal more specifically in design phase of the work. As BIM is playing a critical role in virtual reality space, it creates a vacuum in the design validation in correlation with the real world. This leads to possible design changes based on the field condition during the construction stage. To support the above argument, one of the studies in PWA observed that the root cause for

variation orders and prolongation cost was contributed by the design changes, design clashes, delayed decisions, and unforeseen site conditions. The need for this initiative is expected to realize the following value proportion: (i) reduce the damage of PWA's assets and 3rd party underground assets and reduce claims (ii) improve the safety of the organizational personnel by eliminating accidentally hitting hazards and sub-surface infrastructure during the work activities and (iii) quick turnaround decisions, (iv) early error detection and design changes.

4 Methodology

A structured approach is being followed from the selection of the product to full-fledged implementation. This approach aims to use public investment to be more efficient and effective by finding out what works and what doesn't, at the earliest. The approach focuses on agility in implementation to identify challenges and hasten learning. There are two key factors considered to ensure the technology is compatible with the work environment, acceptable to the end users, has business value, and potential to have continuous enhancement. Figure 2 illustrates the context of the methodology adopted for this initiative. It is a modified approach suggested by Bas Leurs & Kelly Duggan (2018).

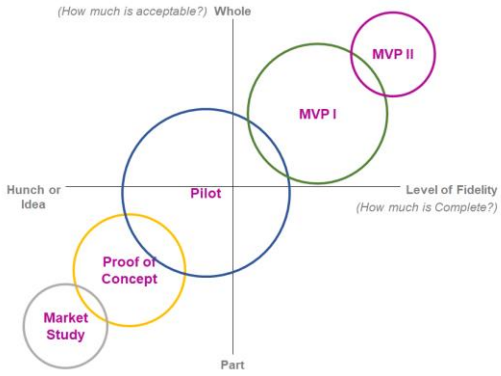


Fig. 2: AR Implementation Roadmap based on MVP Approach

A market study is to explore various commercially available AR products that are used in public works business space. We engaged with the product vendors to understand the capabilities of the product and their roadmap for the next five years. Based on the information available the simplified Technology Acceptance Model (TAM) is used to identify the most preferable product. As this model collects information from five dimensions, it is considered an appropriate framework for product selection. It has perceived usefulness, perceived ease of use, perceived enjoyment, and attitude towards its use (Cabero et.al, 2022).

Proof of Concept (POC) was followed to get real-life confirmation of the product and technology focus. The POC was conducted with three user groups including asset management, engineering information, and positional survey with limited users and dataset. The outcome of the POC helped to fine-tune the drafting of requirements specifications for the next phase and product procurement. Following the POC, the pilot phase is planned and targeted with a full license product of all functionalities, to a wider user base and datasets. This phase is business focused, to place the product in real-life business life cycle activities like inspection, validation, data collection, etc., A longer span pilot period of up to six months to one year is planned, this is typical to collect data from seamless user experience, varying working, and climate and environment, and to realize the product roadmap release from the vendors. Procurement of limited licenses with additional lidar scanner add-ons has been initiated.

The full-fledged implementation is planned with the Most Viable Product (MVP). The MVP shall provide the core functionality that will continuously adapt to create value in the business operation. The MVP will be rolled out to extended business users including partners and contractors. The implementation landscape will continuously increase and incrementally roll out enhanced versions of the project as MVP II/III etc.

5 Case Study Discussions

As PWA is transforming from a project delivery organization to an asset management organization, the case study is specifically designed and addressed to asset management business cases. To support the study, users from the GIS, Asset Management, and Positional Survey engaged to evaluate the technical aspects and position accuracy of the product. The POC case study is handled in two categorical cases (i) Business Cases and (ii) Usability Cases.

5.1 Business Cases

The case study used four distinct business cases for field assessment as part of the proof of concept (POC). The *situational awareness* case is to visualize sewer network assets in the real world in three-dimensional space from the handheld device. This task is to have awareness of the underground asset where the visibility of the asset is obstructed by a physical object (like a building, roadside structure) or inaccessible. The business case of *asset association* is to visualize associated assets to show proximity details of the assets like distance to the asset and refurbishment. The *Reality Viewing case* is to overlay geotagged images with real scenes. The case uses photographs taken from past maintenance work, typically captured before the backfill of utility maintenance work of trenches. The task of selecting an asset on the AR tool and being able to view the specific asset information is performed through an *asset information* case. The task is expected to be able to update some of the key attribute information from the field. Figure 3 shows screenshots captured during the POC exercises.

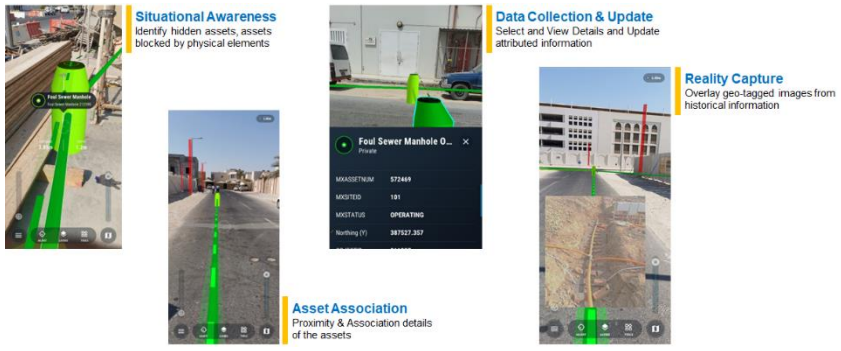


Fig. 3: Illustration of the AR Tool screenshot from POC Testing of various use cases

In the Pilot Phase, PWA intends to incorporate the following business cases:

i. AR indicates a remarkable opportunity as a functional extension of the BIM model during the design and construction phase of the infrastructure development life cycle. The case study scenario is to visualize the BIM model through AR handheld devices from the field and identity clashes with the built environment for design validation.

ii. Reality capturing, a 3D scanning of assets or works with lidar-enabled mobile devices empower the review of historical works with more accuracy. The case will be used along with work order data on the associated assets or work. This case will be validated to see the practicality of capturing the lidar data as part of the maintenance workflow.

iii. Using BIM and Reality Capturing to validate construction site inspection for audit and quality checks.

iv. Display work orders and associated assets with location information for data updates from the field.

v. Back-office collaboration - able to annotate and provide feedback on the design element remote inspections, review of remote site condition review if there is a conflict with existing assets to optimize response time.

vi. Image recognition case is to retrieve asset-specific documentation like manual, SOPs, and maintenance history by recognizing the asset captured from the device.

5.2 Usability Case

The product was evaluated for its useability in terms of ease of use, usefulness, reliability, and performance. The useability case is very important to achieve technical acceptance of the product and to have an attitude towards using the technology by the end user. Figure 4 below shows ten cases that were evaluated during the POC and its outcome. The size of the bubble represents ease of use for the selected product.

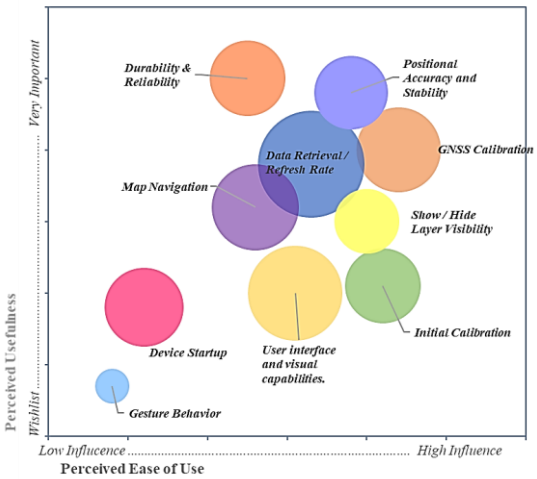


Fig. 4: Usability Cases and User Perception from POC

5.3 Characteristics of the data and devices

Table 1 below lists eight key data set used for the case study for POC. The nature and profile of the data used for the POC has been discussed with the business users to ensure it has representative data. The dataset was extracted from the geospatial information published as ESRI feature services in WGS84 format.

Table 1: Spatial dataset used for POC

No.	Spatial Layer	Characteristics
1	Foul sewer manhole	The point feature represents the location of the manhole used in the foul sewer network. The feature contains z value and invert-level information.
2	Foul sewer network	The data represents the utility network information of the foul sewer. It contains depth information, condition, and pipe material.
3	House connection manhole	This is a point feature and has similar characteristics to a foul sewer manhole. This asset is usually located inside a property boundary and accessibility is a big concern for the field crew.

No.	Spatial Layer	Characteristics
4	House connection network	The dataset connects the land property with the main foul sewer and has similar characteristics to the foul sewers.
5	Work Order	Work order location is mostly represented in point, in some cases, it is also reported as a polygon when there is a road cutting. Able to view historical details where the images are captured.
6	Traffic Signal Pole	Signal Pole was constructed at the road intersection and represented a point feature with height specifications.
7	Street Light Pole	Above ground and represented as a point with the height of the pole. The asset used as a reference for the calibration point for AR Device
8	Images	Images captured before backfilling of underground asset construction/maintenance to use for reality viewing functionalities. These are geotagged images captured from mobile devices.
9	Base Map Layers	A map service contains satellite imagery, road networks, landmarks, etc.,

There were 8 different mobile devices with different form factors & operating systems employed for the POC exercise viz., iPAD, iPhone, Samsung Tablets & Phones, Huawei P30 Pro and Trimble R10 GNSS with Bluetooth® and connectivity.

5.4 Case Study Findings

The study concludes with the lesson learned from the POC exercise with the following findings:

i. The technology demonstrated the best use in situational awareness scenarios (like viewing underground or hidden assets in 3D and augmented with the real scene) for the field crew.

ii. To have a truly augmented rendering of the depth of information highly depends on the way data is modeled in the database. In the case of unavailability of 3rd dimension information, the product is considered a default depth/height value as configured in the tool.

iii. Able to identify proximity for nearby/hidden assets is displayed with distance measures. This is very handy for the field crew for tracing the hidden/inaccessible assets.

iv. Able to query the assets and limit the query output through systems configuration. The utilization of the product shall be further explored for asset data updates or reporting of asset defects during the pilot phase.

v. Losing the positional accuracy as we move. The device location calibration is not reliable and sustained with mobile device internal GPS. However, with the use of external GPS Trimble R10 GNSS, the reliability is considerably improved and consistent. With the use of internal GPS and walking along the dotted line provided in the solution, calibration is required for every 25-30m. For external GNSS it sustains for more than 50m. It is observed that about 1-3cm accuracy was achieved with external GPS using Trimble R10 GNSS and the reliability of calibration is auto-calibrated with GNSS.

vi. On extreme summer temperatures, it is observed that the AR device is heated up quickly and in turn drains the battery.

6 Myth or Reality

The key barrier to harnessing any innovative technology is the myth around it. The top five myths about AR technology based on user perception are discussed in Table 2.

Table 2: AR – A Myth or Reality Facts

No.	Myth	Reality
1	Many users consider AR and VR the same, thus, they dissuade AR initiatives.	Though both technologies are related, with respect to the user experience AR is completely different. VR is an entirely desktop digital experience. VR information can be considered as one of the inputs for AR Technology and a good example is the use of BIM data in AR. AR combines with reality.
2	Too early to use AR Technology in public works areas and impractical to use.	The use of AR in public infrastructure works and civil engineering areas increase over the last five years. In addition to the use cases specified above, there are many use cases like HSE training in treatment plants, that can demand AR.
3	It is presumed that the implementation is more expensive, and deployment is too hard for data and the environment.	With the capability of consumer-level mobile devices and the availability of AR platforms on clouds, it becomes very much reachable on a subscription-based model. With respect to data, the latest AR platform consumes GIS and BIM data seamlessly as services. Thus, harnessing the technology even small organizations are more affordable provided the use cases are demanding.
4	Field calibration of this tool is difficult and time-consuming.	Though the reliability of the device calibration to a certain extent is true, it can be overcome by features like on-the-go calibration.
5	Due to various AR advertisements and exposure to the technology, the user believes that AR required additional expensive gadgets like glasses that are mandatory in order to use the technology.	For public works field activities, consumer-level mobile devices like smartphones, and tablets can provide an ease-of-use experience. In reality, the need for AR glasses, HoloLens depends on the use case. The use of a headset is optional, and the key purpose is to make the hands-free and comfortable for users while operating multiple field devices or tasks.

7 Conclusion

This paper considered a proof-of-concept case study, using AR for effective use of situational awareness, reality capture, and asset association for asset management personnel. The study indicates that the proposed AR technology has good potential for inspection and maintenance in the asset management life cycle. Selection of the right AR product eliminates any myth, and the use of TAM establishes user acceptance of the right fit product selection. The authors emphasize that the data needed shall have the right balance with respect to adding value to the business and sustaining its utilization. The implementation of AR technology would enable and encourage PWA to improve the characteristics and value of data to meet further technological needs. Beyond the cognitive limitations, AR technology is a reality and provides opportunities to become even more relevant when organizations incorporate it as an integral part of day-to-day asset management and public works operational areas to improve user experience and process efficiency.

References

Cabero-Almenara, Julio, Llorente-Cejudo, Carmen & Martinez-Roig, Rosabel. (2022).The use of mixed, Augmented and Virtual Reality in History of Art Teaching: A Case Study. Applied System Innovation. 5, 44.

Cheng et al. (2018) Construction of Interactive Teaching System for Course of Mechanical Drawing Based on Mobile Augmented Reality Technology, *IJETL 13* (02). Austria.

Fleck et al. (2021). Augmented Reality for Subsurface Utility Engineering, Revisited, *IEEE Transactions on Visualization and Computer Graphics*, 27(11).

Frederic, P .A. Vogt & Shingles, L. J. (2013). Augmented Reality in Astrophysics, Astrophysics and Space Science.

Hamidy M. M. (2020). Utility Impact Assessment of Road Projects in the State of Qatar, *International Conference on Civil Infrastructure and Construction. (CIC 2020)*, Doha, Qatar, 2-5, February 2020, doi: https:/doi.org/10.29117/cic.2020.0015.

Klaus, Schwab. (2016). The Fourth Industrial Revolution, World Economic Forum, Switzerland.

Leurs, Bas & Duggan, Kelly. (2018). Proof of Concept, Prototype, pilot, MVP – what's in a name? Four methods for testing and developing solutions, https://nesta.org.uk.

Ministry of Municipality and Environment. (2016). Qatar National Master Plan- Qatar National Development Framework 2032 (QNDF).

Xu, Jiaqi & Moreu, Fernando. (2021). A Review of Augmented Reality Application in Civil Infrastructure during the 4th industrial revolution, Frontier in Built Environment, 2 June 2021, DOI: 10.3389/fbuil.2021.640732

Cite as: Narayanasamy B. & Manickam S., "Use of Immersive Augmented Reality Technology in Public Works: Myth or Reality? – A Case Study on Implementation Challenges", *The 2nd International Conference on Civil Infrastructure and Construction (CIC 2023)*, Doha, Qatar, 5-8 February 2023, DOI: https://doi.org/10.29117/cic.2023.0033

GIS-Based Solutions for Monitoring and Controlling COVID-19 in ASHGHAL Construction Projects: Improving Construction Sector Resilience

Mohammed Amer Younus Al-Shaheen
GIS Senior Engineer, Public Works Authority (Ashghal), Doha, Qatar
malshaheen@ashghal.gov.qa

Amna Mohammed Al-Sayed
Planning Engineer – 2, Public Works Authority (Ashghal), Doha, Qatar
aalsayed@ashghal.gov.qa

Ahmad Yacoub Hasan
GIS Technical Expert, Public Works Authority (Ashghal), Doha, Qatar
ahasan@ashghal.gov.qa

Abstract

Early in 2020, doctors around the globe identified the virus responsible for Coronavirus disease 2019 (COVID-19). Rapidly spreading, the virus reached every continent. As part of its efforts to prepare for the FIFA World Cup in 2022 and Qatar National Vision 2030, the Public Works Authority (Ashghal), the State of Qatar, is on a fast-track mission to implement major infrastructure projects to revamp roads and sewer networks. Managing the human workforce on construction project sites becomes a significant challenge considering the pandemic. Large infrastructure projects are always characterized by many workers interacting in proximity at the work site. Immediately at the pandemic's beginning, management was instructed to leverage technology to empower decision-makers with COVID-19 monitoring tools across all the infrastructure construction projects. Thus, the Engineering Services Department created an ArcGIS Dashboard for engineers, contractors, and higher management to track the construction projects' COVID-19 status. Maps and data are combined in ArcGIS Dashboards to highlight significant patterns and measures. This paper explores the workflow established with direct communication and a submission system from the contractors and project managers to help collect and monitor critical health parameters of workers to prevent the propagation of COVID-19 infection. The study concluded that implementing a GIS safety dashboard for workers can help reduce the risk of project shutdowns due to novel Coronaviruses and provide an effective tool for organizations to improve occupational health and safety standards at worksites.

Keywords: Workforce; Occupational Health; Safety; Construction; COVID-19; Dashboard

1 Introduction

The worldwide impact of Coronavirus on the construction industry has led to a poor economic structure; countries are experiencing difficulties in developing their infrastructure (Majumder & Biswas, 2021). COVID-19 is the largest health and safety threat to the global construction industry. The COVID-19 crisis has decreased site productivity, increased regulatory costs, hindered project completion, and increased construction workers' risk and infection exposure (Olanrewaju et al., 2021). An outbreak of the novel Coronavirus disease of 2019 (COVID-19) poses a significant public health concern of international concern. This outbreak has serious economic and social implications ((WHO), 2022). The COVID-19 epidemic directly threatens the achievement of the above health

goals and affects their realization in terms of economic and social development.

A sufficient understanding of COVID-19's transmission characteristics has not been developed in light of global environmental changes ((CDC), 2022). In addition, the acceleration of global urbanization, the concentration of the population, the frequency and complexity of interactions, and the lack of medical protection in developing countries all contribute to the difficulty of preventing and controlling COVID-19 (Zhou et al., 2020).

COVID-19 has a wide-ranging, complicated, and sophisticated effect on the construction industry, just as it does on other major parts of the economy. Over 80% of construction workers on sites use hazardous materials and components, work in harsh weather conditions, carry or convey heavy materials and components, have poor health and safety practices, work in unhygienic conditions, and are exposed to harsh weather conditions (Olanrewaju et al., 2021).

In state of Qatar the Public Works Authority 'Ashghal' is responsible for majority of the infrastructure related to roads and drainage. Ashghal was established in 2004 to be responsible for the planning, design, procurement, construction, delivery, and asset management of all infrastructure projects and public buildings in Qatar ((ASHGHAL), 2022).

Following the announcement of awarding the FIFA 2022 World Cup hosting rights to the State of Qatar on December 02, 2010, the State was estimated to spend significantly on hundreds of new construction projects and the pressure started to build up for infrastructure projects. As of 2015, the construction sector contributed 10% to Qatar's gross domestic product (Al-Nuaimi, 2019). Then, on both the construction sites/offices and in the accommodation facilities, Ashghal took a series of measures to prevent the spread of Coronavirus disease (COVID-19); also policies and guidelines were reviewed and updated frequently as the pandemic evolved ((ASHGHAL), 2020).

Combined with large-scale population flow and other factors, the strong infectivity, long incubation period, and uncertain detection of COVID-19 made it imperative to provide scientific and technological support to prevent and control the spread of the epidemic. Ashghal aims to reduce the impact and spread of the COVID-19, hence, the pursue for monitoring tools was inevitable.

2 Role of Location Intelligence

At the 2020 Esri User Conference, the Center for Systems Science and Engineering (CSSE) at Johns Hopkins University won the Making a Difference Award for creating the Johns Hopkins COVID-19 Dashboard. The iconic dashboard visualization created by Ensheng Dong, a doctoral student at Johns Hopkins University, is used around the globe to assess the spread of the Coronavirus disease 2019 (COVID-19) pandemic (Milner, 2020).

This dashboard is intended to provide researchers, public health authorities, and the general public with an easy-to-use tool for tracking outbreaks. By providing data based on the date of report rather than the date of event, the dashboard functions as a snapshot of the cumulative data reported as of the date of report (Dong et al., 2022).

The use of location intelligence has changed the process of fighting Coronavirus (COVID-19). An organization's ability to respond to crises, maintain continuity of operations, and support the process of reopening can be significantly enhanced through the use of maps and geographical information systems (GIS). There are variety of utilizations of the GIS and its technology at early adoption of the spatial solutions; these are captured as part of the published studies which are summarized in Table 1.

Table 1: Summary of Studies Grouped by the Geospatial Solutions Theme

(Franch-Pardo et al., 2020)

Spatial Subject	Number of studies
Spatial Temporal Analysis	23
Health and Social Geography	17
Environmental Variables	15
Data Mining	11
Web-based Mapping	5

A wide range of GIS tools are being used to control the pandemic, particularly in relation to spatiotemporal analysis and web-based mapping (Fatima et al., 2021; Franch-Pardo et al., 2020). COVID-19 prevention and control were enhanced through the use of GIS data for decision-making, measure formulation, and effectiveness assessment. As a technology, GIS provides a complete solution for preparing data, building platforms, creating models, and producing maps. In a number of recent studies, spatial solutions provided by GIS has been found to have much potential for preventing and controlling COVID-19, with the most significant aspects being enhanced prevention measurements and the evaluation of controls (Karabegovic et al., 2021; Sarwar et al., 2020).

Different Web-based GIS services have been launched by governments, public health agencies, and academic institutions. ArcGIS is a commercial technology developed by Esri that is well-known and widely used throughout the world. All ArcGIS dashboard implementations have the same user interface, which makes them easy to identify. Despite the modular interface, each dashboard can be assembled in a different manner, although most organizations use either the same or a very similar interface.

The purpose of this study is to explore the implementation of geographical and geospatial analysis in Ashghal. A key objective of the study is to highlight current geospatial analytical methods that can be used to collect, process, analyze, and visualize COVID-19 cases in infrastructure construction projects.

3 Methods

Since the start of the pandemic, the Public Works Authority ‘Ashghal’ has continued to take all necessary precautions to protect the health and safety of its employees and stakeholders and ensure the continuity and on-time delivery of its projects. As information is of utmost importance today, particularly in times of post-pandemic crisis, it is imperative that Ashghal Infrastructure Projects share data promptly and confidentially.

Before implementing this transformation, all information related to COVID-19 was collected manually for each site in each project, then it was transferred to Excel sheets by email to be reviewed and finally checked to proceed through a certain analysis and reporting cycle. GIS technology allows for rapid construction of an information system for a relevant subject, especially in terms of database management, spatial analysis tools, and mapping (Zhou et al., 2020). An instrumental aspect of large-scale epidemic prevention and control is the use of data to support decisions and actions, particularly in the case of Asghal infrastructure projects.

Ashghal has unfurled a robust health and wellness initiative. As soon as the pandemic hit us, a core committee comprising of Projects Affairs Health Advisor, Information Technology Team Engineers, Engineering services GIS experts, Planning and Quality experts, and Safety Experts worked together

to create an online Covid reporting dashboard. Through ArcGIS Dashboards, users are able to convey information by using intuitive and interactive data visualizations that present location-based analytics. Data dashboards provide a visual representation of geographic information and data that can be used for monitoring events, making decisions, communicating with others, and identifying trends. A dashboard is a display that consists of multiple visualizations grouped together on a single screen. With them, you can obtain a comprehensive view of your data as well as key insights for making quick decisions based on the data.

3.1 Ashghal COVID-19 Dashboard

As part of various initiatives implemented by the Authority, Ashghal has created a unique GIS-based live COVID-19 Dashboard that helps Ashghal generate daily COVID reports that include the number of positive cases, number of suspected cases, and the number of recovered cases across Ashghal's projects and offices. One of the biggest challenges during the pandemic has been the flow of information and the sharing of knowledge and how the information will contribute to the organization's ability to contain the outbreak. As part of Ashghal's effort to make information sharing spontaneous, live, and practical, it launched a live COVID Dashboard, an online platform accessible from anywhere within the organization, allowing members of the organization to view information regarding the number of COVID cases. With the latest Geographical Information Systems for location intelligence, Ashghal could map all its work sites and thousands of employees across Qatar in real time to reflect where the cases were distributed, how many were positive, and how many were suspect.

Engineering services experts and engineers undertook an exercise to determine the cost saved and number of hours spent before using the manual entry and analysis and after implementing the online automation Table 2. The amount of time spent on online applications is small in comparison to the amount of time spent on manual applications. More than 219,000 QAR as total cost savings from reporting and tracking COVID-19 cases in Ashghal's Affairs and departments and with more than 168 contractors as sources of information, Table 2.

Table 2: Cost Saved Monthly in Using the Online Application

Affairs & Departments	Activity	Monthly Man-Hours Spent Before	Monthly Cost Saved QR (NOW)
Asset Affairs including **60** Contractors	Data Entry	180*	27,000
	COVID Tracking	300	45,000
Project Affairs Including **108** Contractors	Data Entry	324	48,600
	COVID Tracking	540	81,000
GSD Including All Towers	Data Entry	44	6,600
PQD	Data Entry	66	9,900
President Office	Data Entry	11	1,650
Total		**1,465**	**219,750**

**An average hourly rate of 150 /hour.*

Engineering services experts at Ashghal explore a two stages method to enhance the production of data for the COVID-19 Dashboard. Stage One: Enhance the workflow of data, Second Stage: Create and reflecting the information in meaningful manner including maps and ensure the sharing in the organization.

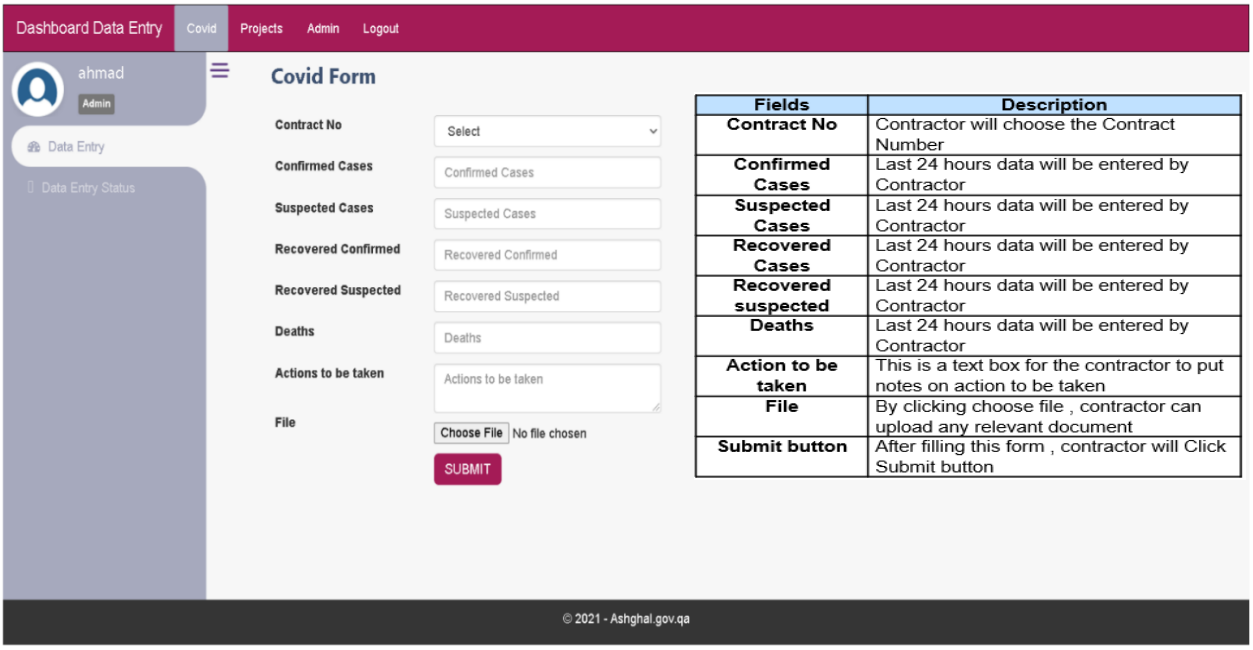
3.1.1 Stage One: COVID-19 Reporting – Workflow

The Dashboard provides the mechanism to enter COVID cases data through secured data entry form to restricted, responsible persons for each project and Ashghal office spaces. The contractor shall enter COVID related data on daily basis (if no cases to be reported, the contractor shall enter 0 as a value). Cut of time is 5 PM daily, however the system is open for reporting till midnight. The system will be sending notifications to PMs in case the contractor didn't enter any data before 5 PM daily.



Fig. 1: COVID-19 Reporting – Workflow

Any case reported before 5 PM shall be closed by the consultant and project manager on the same day, otherwise a notification will be sent to the defined focal point in Ashghal and any case reported after 5 PM will be considered the next day, Figure 1. The development of the workflow was essential to control and streamline the data from all contractors and engineers work on projects. As first step the contractor is required to fill the COVID-19 form online on a daily basis as illustrated in Figure 2.



Fields	Description
Contract No	Contractor will choose the Contract Number
Confirmed Cases	Last 24 hours data will be entered by Contractor
Suspected Cases	Last 24 hours data will be entered by Contractor
Recovered Cases	Last 24 hours data will be entered by Contractor
Recovered suspected	Last 24 hours data will be entered by Contractor
Deaths	Last 24 hours data will be entered by Contractor
Action to be taken	This is a text box for the contractor to put notes on action to be taken
File	By clicking choose file , contractor can upload any relevant document
Submit button	After filling this form , contractor will Click Submit button

Fig. 2: Data Entry COVID Form UI

As per the suggested workflow, and once the contractor submits the daily entry COVID-19 form, the Consultant must approve the data to be processed, Figure 3.

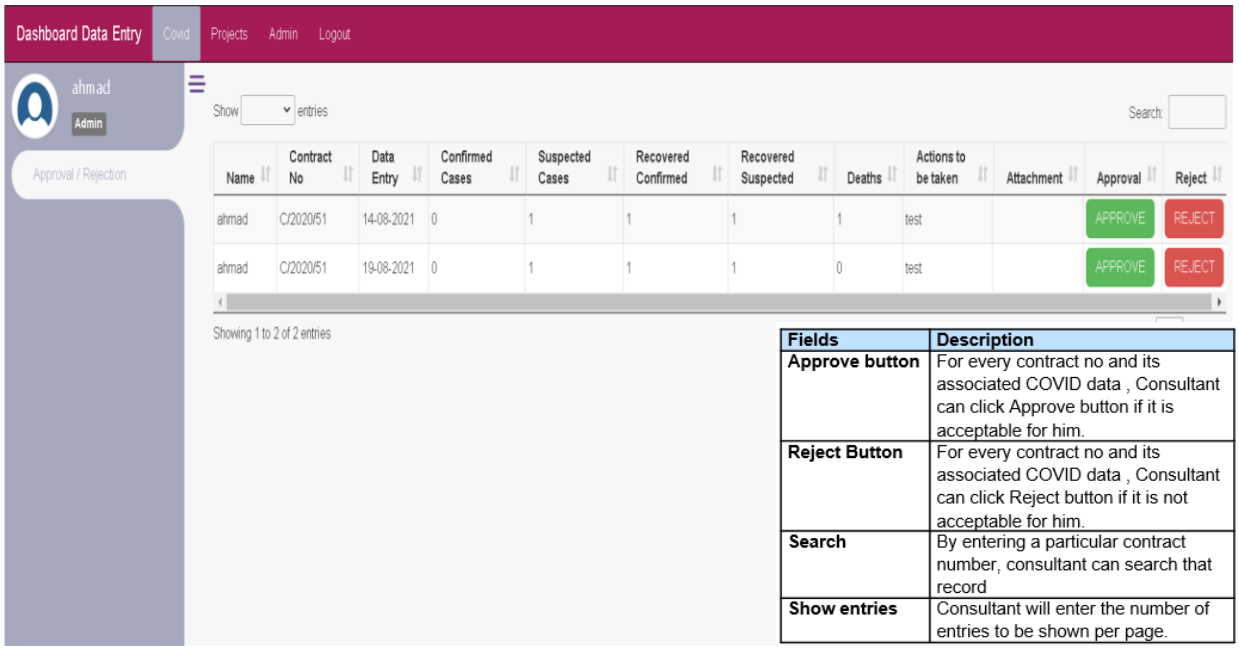


Fig. 3: COVID Form – Approval by the Consultant

A data approval must be obtained from Ashghal PM after the consultant has approved the daily COVID form as shown in Figure 4.

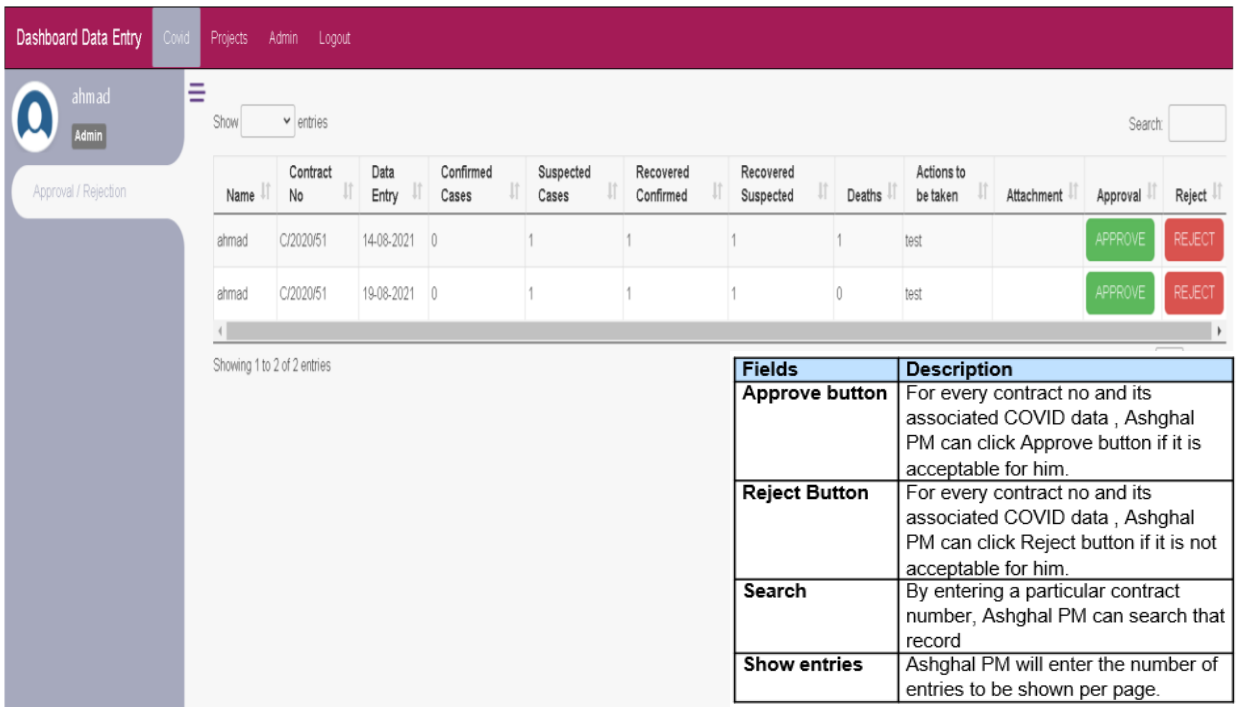


Fig. 4: COVID Form – Approval by Ashghal PM

As final step, user chooses reports option from the menu to generate reports for all reported cases and customized the outputs, Figure 5.

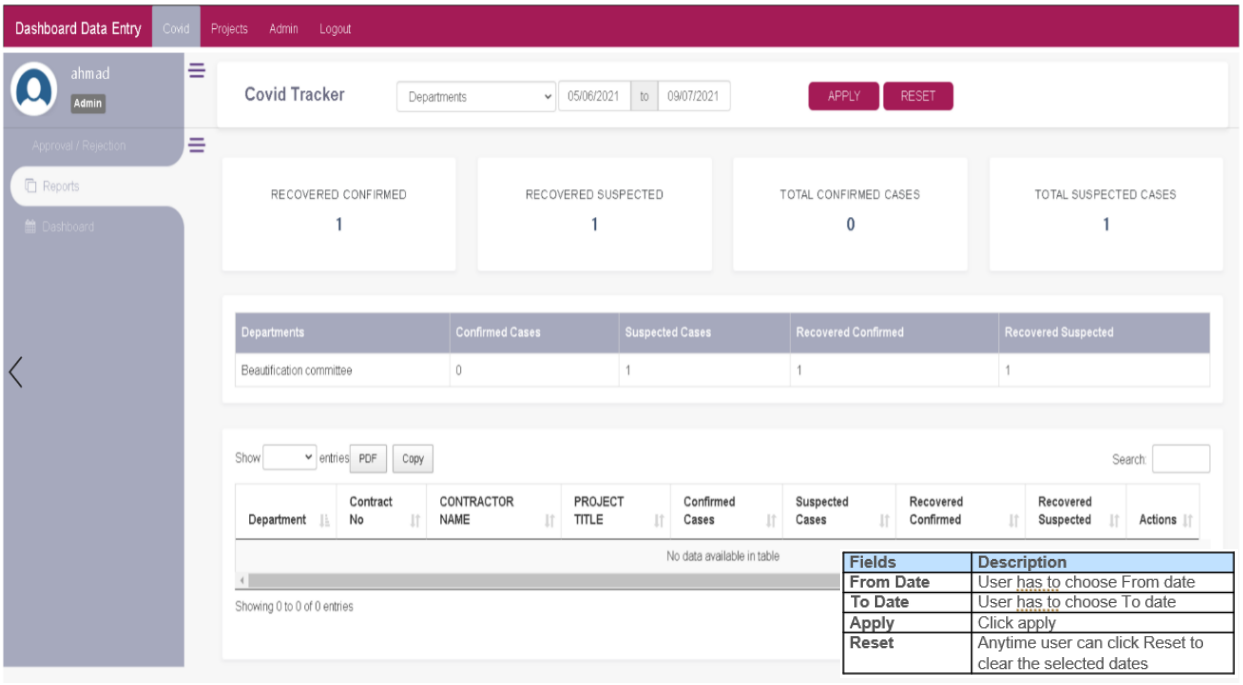


Fig. 5: COVID - Report Generation

Once the report is displayed, the users can generate the report in various formats including PDF and MS Word.

3.1.2 Stage Two: COVID-19 Map Dashboard – Visualization

The Dashboard provides a visual data representation with maps reflecting all approved collected data from stage one. The COVID-19 data is analysed in real-time and presented through meaningful graphs to understand the patterns of cases. The data is also presented on the GIS Map to display the impact on Ashghal's construction or maintenance projects across Qatar. The map depicts the risk factor as – high, medium, or low in red, blue and green colour, Figure 6.

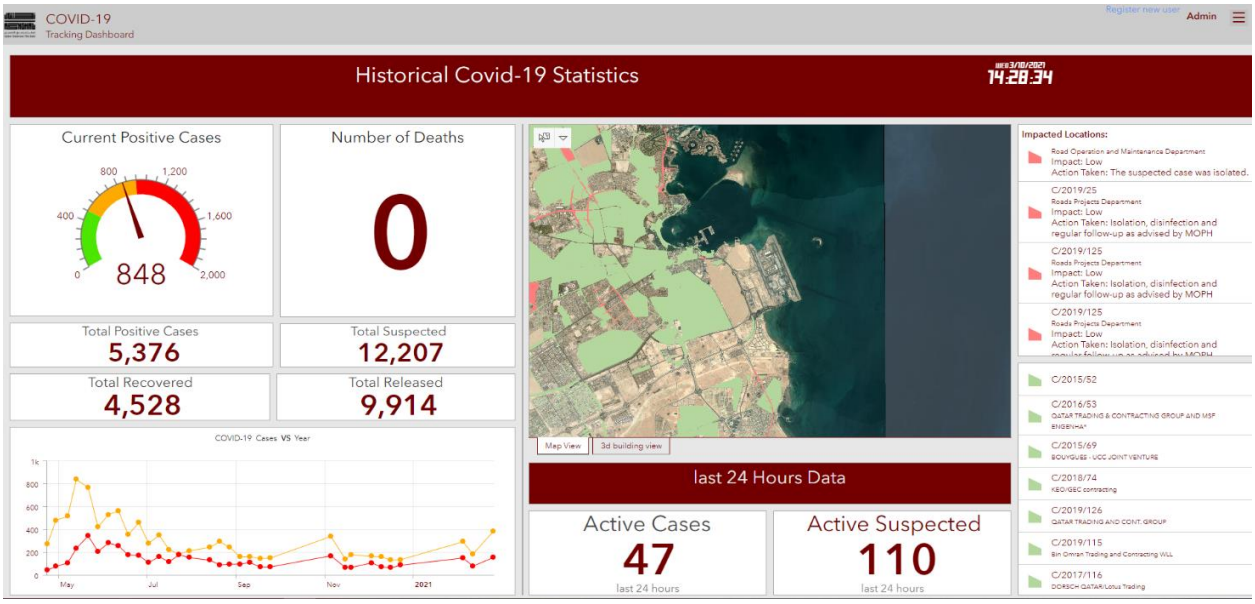


Fig. 6: Automated Online Dashboard – with Key Indicators and Summary of Cases

As part of additional enhancements, the Live Data Entry of COVID cases with visibility of site, which can be seen in mobile or laptops to take instant decisions, Figure 7.

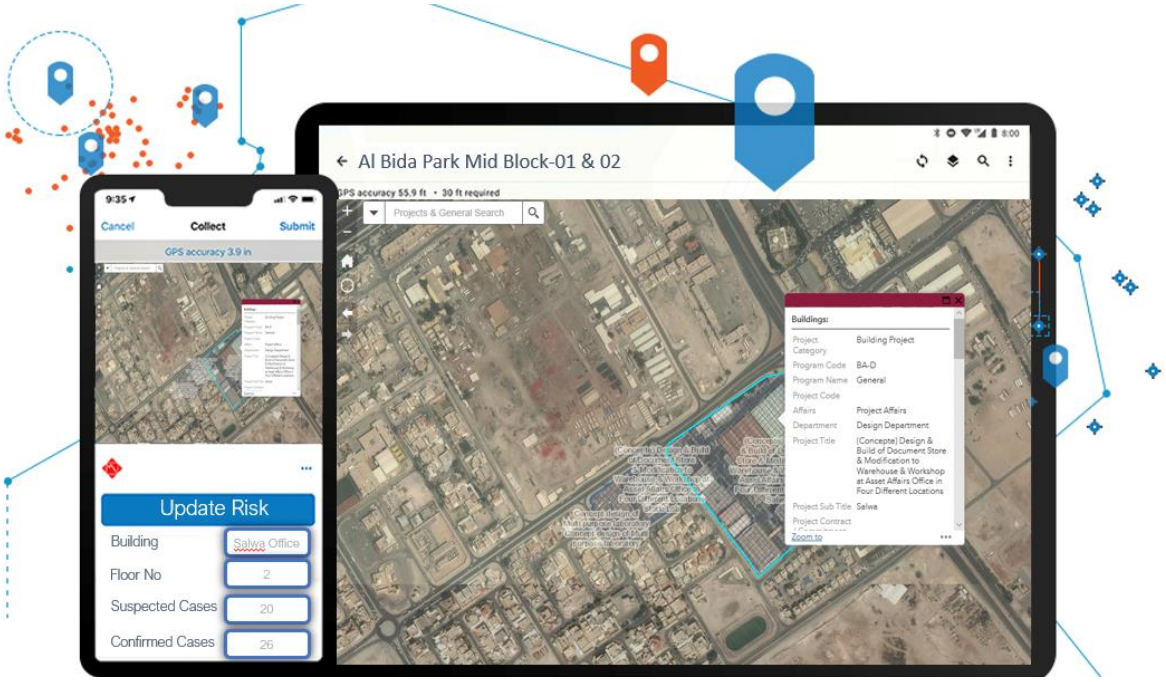


Fig. 7: COVID - Mobile Data Entry for Risk Updates

In the monitoring process, interactive maps and control panels are used between participants to communicate quickly about the current situation and to anticipate its development. In addition to displaying key indicators and providing critical information summaries, interactive dashboards, such as those shown in Figure 6, are remarkable tools. Ultimately, the GIS dashboard is to support the exchange of epidemiological and other data between internal departments, relevant agencies, and the public during the pandemic crisis.

The dashboard reported all positive and suspected cases in the last 24 hours. In addition, cumulative number (total number) of positive cases/suspected cases were reported. The recovered cases were also reported. Thus, GIS based software is an online dashboard that enabled the users to see the map of Qatar and identify the location where the positive and suspected cases were located.

4 Discussion and Conclusion

This system includes interfaces that facilitate the implementation of geospatial processes to meet the requirements of each research area, which vary from one to another. This way, an expert in their field can use GIS functionality, geo-information, and related processes in one web environment.

The spatial solution achieved the objective set by Ashghal team by providing 1) Early identification of positive cases through PCR Test result, 2) Identifying potential contacts as per Ministry of Public Health, Qatar Guidelines, 3) To report this information to doctors/nurses/ HSE managers and project directors confidentially and quickly to avoid spread, 4) To use the information to ensure immediate isolation and treatment of COVID positive workers and suspected cases, 5) To control and reduce COVID spread into workers accommodations and projects sites, 6) To use this online COVID dashboard to develop statistics and analyse trends to see projects reporting increasing number of cases and projects reporting decline in number of cases.

The identification and isolation of suspected COVID positive cases in the earliest possible time period. These two vital pieces of information were captured by the online dashboard. The medical team of doctors and nurses and managers were able to track all COVID cases and order effective isolation, testing, rehabilitation and monitor recovery of these cases on a daily basis.

As Ashghal works in bringing to life multi-billion-dollar infrastructure projects, the most important factor in this journey is the health and wellbeing of the human capital involved. This project enabled Ashghal to block only infected zones where non infected zones were able to continue with adhering to other constrains and the policy. The transformation enabled Ashghal to monitor the health of its employees on daily basis comparing to monthly basis before this project.

This transformation reduces the cost of monitoring and reporting by a monthly sum of 219,750 QAR equal to US $60.000. The online health and wellness dashboard helped us to save costs, save lives and provide timely and effective medical management of COVID cases.

The live COVID dashboard gives an immediate real-time update on the number of COVID cases in any Ashghal project and the link of the dashboard to the GIS system so the end user can see all projects, zoom in on any project, and detect the number of active and suspected cases. Historical data (from last year), including cumulative overall total in all projects, are also available. According to the statistics, Ashghal appears to be taking all necessary preventative measures to control the pandemic. Ashghal has always adapted innovative technology and human skills to work together to produce effective results. Despite enormous challenges, Ashghal continues to provide the best services for Qatar and its communities with passion, care, and promise. The Government of Qatar has implemented improvement measures that will set the benchmark for regional performance in the areas of Health, Safety, and Welfare. As part of this objective, Ashghal is continuously designing, building, operating, and managing infrastructure with the highest priority being given to the health, safety, and welfare of its employees, contractors, and customers.

References

Al-Nuaimi, B., & Al-Ghamdi. (2019). Environmental and Economic Life Cycle Analysis of Primary Construction Materials Sourcing Under Geopolitical Uncertainties: A Case Study of Qatar. *In Sustainability*, *11*(21). https://doi.org/https://doi.org/10.3390/su11216000

(ASHGHAL), T. P. W. A. (2020, 07 September 2020). *Roads and Subdivision Projects on Track while Maintaining Precautionary Measures*. ASHGHAL. Retrieved December 31, 2022 from https://www.ashghal.gov.qa/en/MediaHub/News/Pages/Roads-and-Subdivision-Projects-on-Track-while-Maintaining-Precautionary-Measures.aspx#.Y7BjZXbMKUk

(ASHGHAL), T. P. W. A. (2022). *The Public Works Authority 'Ashghal' - An Overview*. ASHGHAL. Retrieved December 31, 2022 from https://www.ashghal.gov.qa/en/AboutUS/Pages/default.aspx

(CDC), C. f. D. C. a. P. (2022). *Clinical Questions about COVID-19: Questions and Answers*. https://www.cdc.gov/coronavirus/2019-ncov/hcp/faq.html/

Dong, E., Ratcliff, J., Goyea, T. D., Katz, A., Lau, R., Ng, T. K., Garcia, B., Bolt, E., Prata, S., & Zhang, D. (2022). The Johns Hopkins University Center for Systems Science and Engineering COVID-19 Dashboard: data collection process, challenges faced, and lessons learned. *The Lancet Infectious Diseases*.

Fatima, M., O'Keefe, K. J., Wei, W., Arshad, S., & Gruebner, O. (2021). Geospatial Analysis of COVID-19: A Scoping Review. *Int J Environ Res Public Health*, *18*(5). https://doi.org/10.3390/ijerph18052336

Franch-Pardo, I., Napoletano, B. M., Rosete-Verges, F., & Billa, L. (2020). Spatial analysis and GIS in the study of COVID-19. A review. *Science of The Total Environment*, *739*, 140033. https://doi.org/https://doi.org/10.1016/j.scitotenv.2020.140033

Karabegovic, A., Ponjavic, M., & Hukic, M. (2021). Epidemic Location Intelligence System as Response to the COVID-19 Outbreak in Bosnia and Herzegovina. *Applied System Innovation*, *4*(4), 79.

Milner, G. (2020). Creating the Dashboard for the Pandemic. *ArcUser: The Magazine for Esri Software Users*, *23*(3), 56-59. https://www.esri.com/content/dam/esrisites/en-us/newsroom/arcuser/arcuser-summer-2020.pdf

Olanrewaju, A., AbdulAziz, A., Preece, C. N., & Shobowale, K. (2021). Evaluation of measures to prevent the spread of COVID-19 on the construction sites. *Cleaner engineering and technology*, *5*, 100277.

Sarwar, S., Waheed, R., Sarwar, S., & Khan, A. (2020). COVID-19 challenges to Pakistan: Is GIS analysis useful to draw solutions? *Sci Total Environ*, *730*, 139089. https://doi.org/10.1016/j.scitotenv.2020.139089

(WHO), W. H. O. (2022). *Coronavirus disease (COVID-19) Weekly Epidemiological Updates and Monthly Operational Updates*. https://www.who.int/emergencies/diseases/novel-coronavirus-2019/situation-reports/

Zhou, C., Su, F., Pei, T., Zhang, A., Du, Y., Luo, B., Cao, Z., Wang, J., Yuan, W., & Zhu, Y. (2020). COVID-19: challenges to GIS with big data. *Geography and sustainability*, *1*(1), 77-87.

Cite as: Al-Shaheen M., Al-Sayed A.M., & Hasan A.Y., "GIS-Based Solutions for Monitoring and Controlling COVID-19 in ASHGHAL Construction Projects: Improving Construction Sector Resilience", *The 2nd International Conference on Civil Infrastructure and Construction (CIC 2023)*, Doha, Qatar, 5-8 February 2023, DOI: https://doi.org/10.29117/cic.2023.0034

Challenges and Perspectives on Resilient Collaboration for Building Information Modelling (BIM) Education in the GCC Context

Raya Atour
Department of Architecture and Urban Planning, College of Engineering, Qatar University, Doha, Qatar
ra2010351@qu.edu.qa

Ahmad Mohammad Ahmad
Department of Architecture and Urban Planning, College of Engineering, Qatar University, Doha, Qatar
am.ahmad@qu.edu.qa

Abstract

Building Information Modelling (BIM) is revolutionizing the construction industry and education through digitization. The construction industry expects higher institutions to create graduate students that are BIM-aware and enabled through the understanding of BIM. There are four pillars of BIM, which are people, process, policy, and technology. Less focus is given to the people dimension, as BIM is perceived as 90% technology and 10% sociology, while in reality, it is 90% sociology and 10% technology. This study would embed its focus on people, which are students in the context of the educational implementation, and on female students in the GCC region. This paper aims to identify the complexity of collaboration in BIM education for female students in the GCC region, as many educational institutions create specific atmospheres for female students aligned with the local customs of the region. The investigation focuses on identifying the challenges in BIM collaboration in education in this specific context through a multifaceted theoretical investigation with a comprehensive literature review. The findings of this paper include identifying the multivariate factors involved in the collaboration of BIM education. The recommendations involve the inclusion of resilient strategies to integrate the long-lost 'soft' attributes of people in technology in the realm of optimization and efficiency. This study would be a significant milestone in the region and a promising approach to utilizing local and indigenous tools, approaches, and contexts to meet educational excellence.

Keywords: Building Information Modelling (BIM); Higher education; Collaboration; Female students; GCC region

1 Introduction

BIM is a digital technology that may aid the construction industry in maximizing its efficiency and profitability across the whole project lifecycle by facilitating communication and coordination between project teams (Yusoff, Brahim, & Mat Yusoff, 2021). Building Information Modelling (BIM) is transforming the Architecture, Engineering, and Construction (AEC) industry and education through digitization. The construction industry expects higher institutions to train graduate students that are BIM-aware and enabled through the understanding of BIM. BIM is one of the most important technologies in the worldwide AEC industry's shift towards digitalization to boost project efficiency (Maharika et al., 2020).

BIM consists of four pillars, which are people, process, policy, and technology. Less focus is given to the people dimension, as BIM is perceived as 90% technology and 10% sociology, while in reality,

it is 90% sociology and 10% technology (Ahmad, Aliyu, & Mohammed, 2020). In spite of substantial research and development efforts in academic and professional BIM literature, there is a lack of study on BIM collaboration management (CM), particularly for BIM model production (Yusoff et al., 2021). BIM is not a stand-alone technology, but rather a technology-enabled collaborative process (Ahmad et al., 2020; Munir & Jeffrey, 2013; Saka & Chan, 2019). Most literature focuses on the technical elements of BIM use while disregarding its social and cultural applicability (Reychav, Maskil Leitan, & McHaney, 2017).

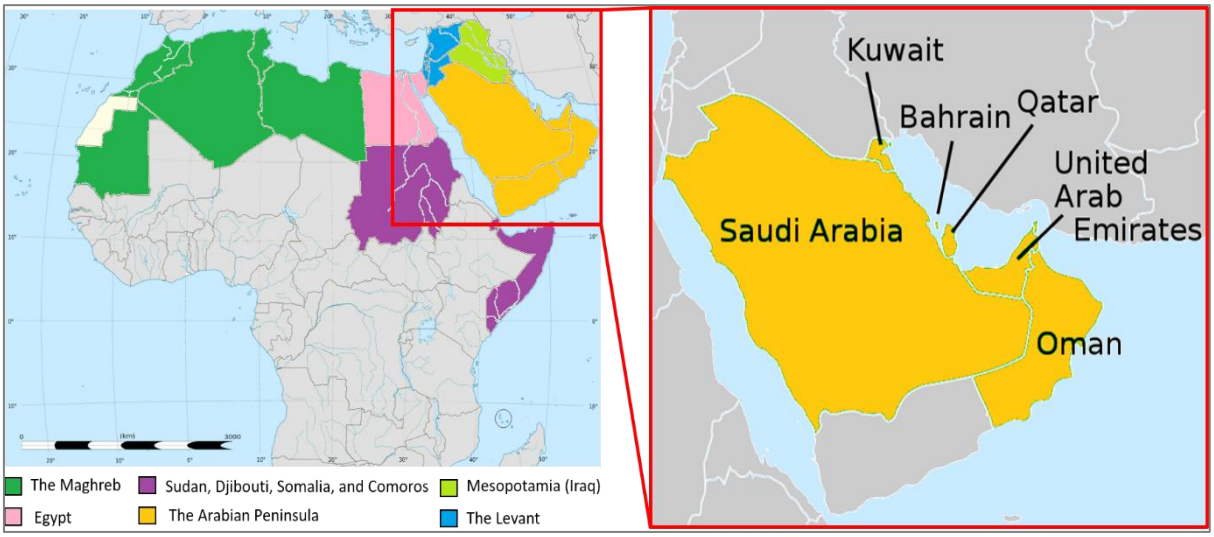


Fig. 1: Location of Research Study Scope. Source: Authors after World Map

This paper aims to explore the limitations observed in BIM-based Education in the GCC context and the limitations' impact on BIM-based collaboration. To do this, understanding the nature of BIM and its components was essential in order to know the angle and point of view this research is taking, and while the data and literature obtained in this study are not limited to addressing the GCC context, the incorporation of various sources was important as this topic is continuously expanding and has a multifaceted nature. Additionally, this study gives the results of a thorough review of the implementation of BIM education from 2019 onwards as well as reviewing literature before 2019. It provides a summary of BIM's current teaching techniques and highlighted collaboration problems. This document also serves as a resource and introductory guide for universities and educational institutions in the GCC areas that are new to BIM education or in the process of introducing it. Knowing that the Arab world and the MENA region consists of multiple cultures ranging in different geographical locations, as shown in Figure 1. The scope of this research will focus on the Arab Peninsula, the GCC region in specific as it constitutes of similar cultural context, aiding this research's target.

2 Methodology

Finding answers to the research questions was done by literature review. Many studies used the bibliometric analysis method (Ali, Alhajlah, & Kassem, 2022; Jin, Guo, Adamu, Kangwa, & Chohan, 2021; Küçük-Avci, Topal, & stanbullu, 2022; Saka & Chan, 2019). A detailed map of a certain study area can be provided through a manual review of literature (Ali et al., 2022). Particular attention must be paid to the requirements of the local industry (Boton, Forgues, & Halin, 2018), which can be done by observing the local context, theorise the context into logical patterns that are able to be understood universally, and creatively find solutions that are responsive to the specific case of the context. The methodology used for

this study can be seen in Figure 2 below.

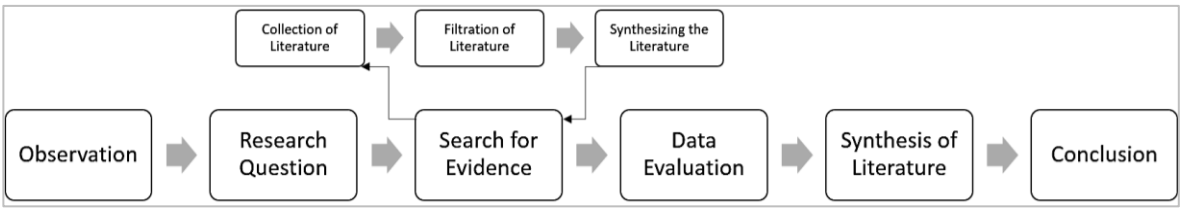


Fig. 2: Study Methodology. Source: Authors, adopted from *(Abdulazeez Abdulmumin, B. K. Bolo, Y. G. Musa Haddary, & Chindo, 2021)*

Many scientometric and bibliometric literature reviews position and analyse the scientific data into clear distinctions in a quantitative manner. However, not many critical reviews were done. The level of detail of this study is quite broad as it is a first step as a pilot study that describes the current situation regarding BIM collaboration within the specific context of GCC as a case study. The filtration process used to collect and include the literature used for this study can be seen in Figure 3 below.

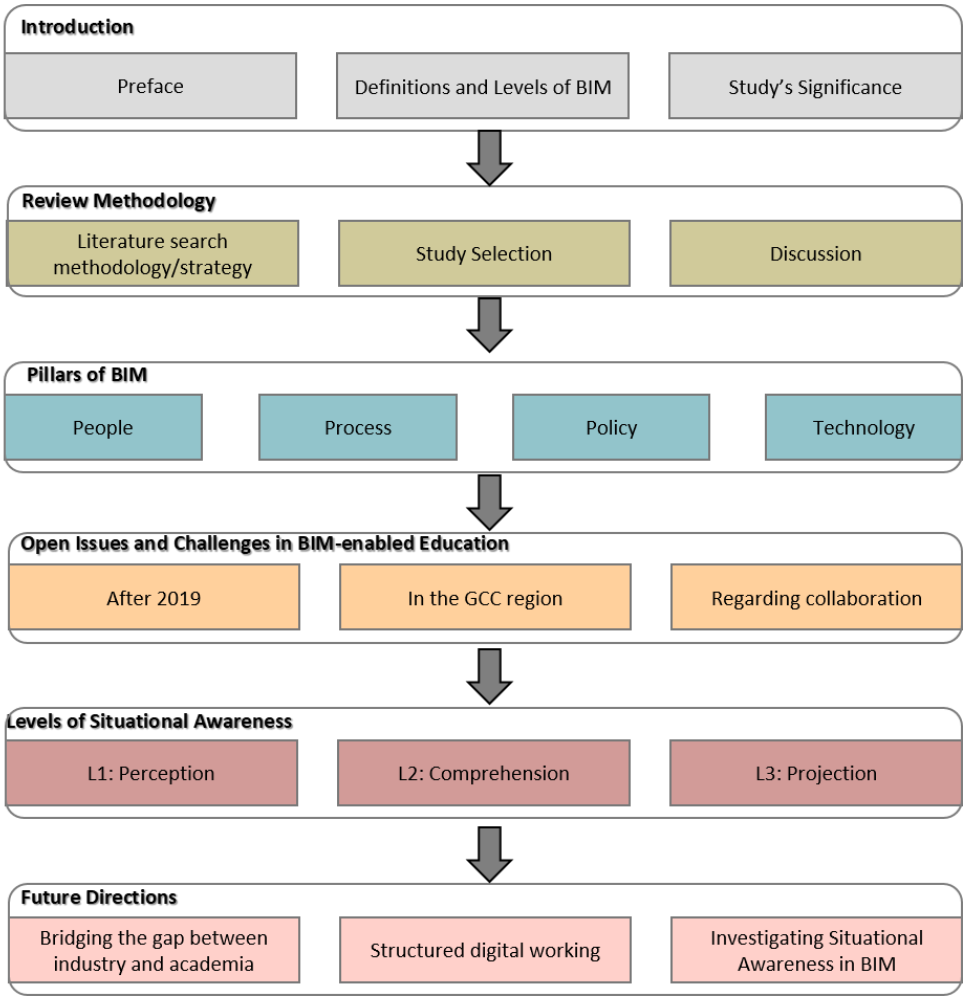


Fig. 3: Literature Review Scope: BIM-Collaboration Dimensions. Source: Authors

The methodology was initially adopted from (Jin et al., 2021). This research began with a comprehensive literature evaluation of the current situation of Building Information Modelling (BIM) in the education sector. The literature search was not confined to undergraduate level education, but

included all activities linked to teaching and learning. However it was limited to specific disciplines such as Architecture, Construction, and Engineering. The scope of the analysis was intended to include the following topics: collaboration and integration.

3 Literature Review and Analysis

According to a study done by (Ali et al., 2022), greater attention was paid to documents that included cooperation and collaboration in 2020, whereas in 2017, 2019, and 2021, increased emphasis was placed on risk, integration, and uncertainty. The result of that systematic literature review found that there are only 88 publications out of 650 that were directly associated with collaboration in building information modelling. Still, there has been a definite upward trend in their number over the last several years owing to the topic's significance, especially in 2019 with a trend of 20 published studies, 2021 with 19 studies, and 2020 with 17 published studies (Ali et al., 2022).

There are different levels of BIM, ranging from Level 1 to Level 4. This study will be generic and will not focus on certain levels specifically. According to (Ali et al., 2022), collaboration in the development of BIM models presents many crucial practical concerns, such as inadequate management systems for collaborative work, difficulty in successfully handling BIM model conceptualization issues and revisions, difficulty communicating and detecting pertinent alterations with connected BIM engineers, inefficiency in controlling BIM model generation self-inspections and findings, and an inability to properly regulate BIM model build versions throughout a process where the BIM model must be regularly altered and updated.

Collaboration and standardization are the pillars of BIM procedures in industry (Besné et al., 2021). Where BIM installations and BIM collaborative work are enabled by a number of standards increasingly used by public agencies (Besné et al., 2021). It is important to investigate whether the GCC context has what makes it unique from international contexts, specifically in education and BIM-enabled education. As challenges facing BIM in education could be universal in most cases, but also context-specific whenever the socio-cultural dimension comes into play.

Educators need to develop effective learning environments when using new technology such as Building Information Modelling (BIM), as it can be argued that in BIM-based collaboration, peer pressure promotes student learning (Zhao, 2021).

According to (Bishop & Verleger, 2013; Boton et al., 2018) with the crisis in education, the combination of two linked movements is transforming engineering education:

- "*The technological movement (to overcome related information flow and the physical barriers).*
- *The ideological movement (to remove the man-made and artificial barriers).*"

The competitive spirit between Gulf nations and even between various states within a country is a significant obstacle. This rivalry restricts cross-border or inter-institutional research collaboration (Badry & Willoughby, 2016). Additionally, colonial education and ethnology were instruments of power that served to define identities in order to sustain dominance relationships (2010). In this context, finding solutions relevant to the context of GCC would be a way to decolonize knowledge and learning approaches.

The worldwide Covid-19 epidemic has brought about enormous disruptions in higher education, especially the built environment (BE) industry (Jin et al., 2021). The Coronavirus produced a sense

of urgency and a matter of survival, which expedited the speed of research and invention and facilitated cooperation (Adnan et al., 2022). Uncertainty over the nature and limits of current collaboration models was associated with collaboration-related issues (2020).

Building on the previously mentioned pillars of BIM, which are People, Process, Policy, and Technology (Ahmad et al., 2020)**,** (Abdulazeez Abdulmumin et al., 2021; Boton et al., 2018) introduced a categorization of BIM education to be based on the following pillars:

- Technologies, Organisations' Infrastructure and Curriculum, as in data management as a technical pillar.
- Organization and Integration, as in team collaboration as a procedural pillar.
- Policies and Implementation, as in risk management for regulatory topics.

Using these pillars as a cornerstone in categorizing the phenomena and issues observed and related to this study's scope would contribute to linking multidisciplinary and interdisciplinary concepts into the research problem and therefore become a theoretical model in which recommendations would be provided.

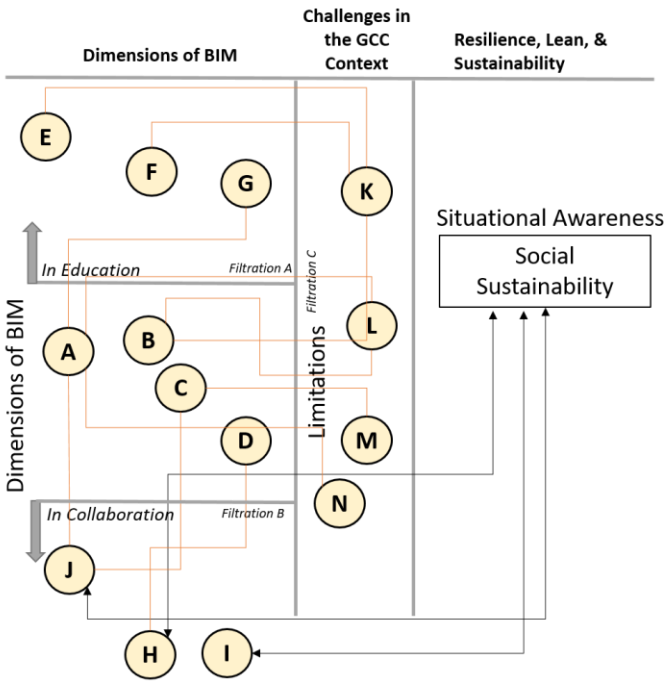
4 Discussion

4.1 Situational Awareness

Some scholarly references refer to BIM as a 'disruptive' approach (Boton et al., 2018) as it resulted in significant modifications to the design, management, and execution of construction projects. Diverse manifestations of identity are associated with sociocultural sustainability (Reychav et al., 2017; Wu, Fan, & Chen, 2015).

What has been noted for the literature review is that successful implementation of BIM collaboration was found to be most dependent on social aspects in an organization, which shows that the need for a perspective that includes social sciences is evident when incorporating technology within an organization. Based on the input of a workshop titled *When Social Science Meets Lean and BIM*, the fragmentation in the BIM implementation could be a challenge for social scientists to explore. The context of the current situation shows that there are specific challenges in the GCC region, especially for female students, where predefined gender roles continue to dominate the culture in which educated women function (Levers & Brock, 2007). Another challenge is that in the Arab nations, distance and open education are little established (A. Badran, Baydoun, & Hillman, 2018).

There many aspects and dimensions of BIM, such as Technology, Time (stage of the project), People, Document Management Collaboration (Shafiq, Matthews, & Lockley, 2013), and many more. Categorized aspects of BIM can be seen in Figure 4 and Table 1 below, which shows the relations between different aspects of BIM and its potential contribution to the concept of social sustainability and Situational Awareness (Adamu, Emmitt, & Soetanto, 2015) as a potential solution to this research problems, where the term 'Situational Awareness' is in fact a concept that has a developed a theoretical model provided by (Endsley, 1995) and could serve as a theoretical guideline in mapping and categorizing issues observed in this study's specific context. For this, the figure below serves as a map in categorizing each aspect related to the research problem and understanding how it connects and relates to finding a solution towards social sustainability and resilience in BIM-education collaboration within the GCC context.



Label	Aspects of BIM	Source
A	Process	(Ahmad, Aliyu, & Mohammed, 2020)
B	Policy	
C	People	
D	Technology	
E	Curriculum	(Abdulmumin, Bolo, Haddary, & Chindo, 2021)
F	Integration	
G	Implementation	
H	Cloud Computing	(Adamu, Emmitt, & Soetanto, 2015)
I	Optimisation of group efforts and Task Delegation	
J	Real-time visual Consensus and consent	
K	Culturally-specified roles for certain Educational Programs	(Levers & Brock, 2007)
L	Limited interdisciplinary collaboration between colleges	(Jabbour, Yamout, Giacaman, Khawaja, & Nuwayhid, 2012)
M	Limited skills and expertise	(Abdalla, 2016)
N	Gap Between Industry and Academia	(Abdalla, 2016)

Fig. 4: Left: The application of BIM elements in Education and Collaboration towards Social Sustainability within the GCC Context. Right: General Dimensions of BIM in Education – Collaboration. Source: Authors.

4.2 Paradigm Shift

There is a need for a shift in working processes across the industry. This applies to educational institutions. The construction industry expects higher institutions to graduate students that are BIM-aware and enabled through the understanding of BIM. Four distinct forms of architectural education were formed by the prior historical approaches to architecture: academic, craft, technological, and sociological (Salama, 2022).

When departments are structured along disciplinary lines, interdisciplinary cooperation and involvement may be challenging, particularly in teaching (Jabbour, Yamout, Giacaman, Khawaja, & Nuwayhid, 2012). Successful implementations have been dependent on social factors such as teamwork and the corporate environment, demonstrating a strong need and potential for a social science approach in this setting. Such as situational awareness as it was a recommendation of a previous study (Adamu et al., 2015).

4.3 Appreciative Inquiry

Appreciative inquiry has the power to decolonize the curriculum's content and the manner in which knowledge is generated and reproduced (Salama, 2022). Finding solutions to the current context of the GCC can be quite challenging yet vital for sustainable development measures. This proposal and recommendation includes multi-school collaboration within the GCC while keeping their cultural values as a form of cultural resilience and social sustainability. In this sense, investigating the model of Situational Awareness and its contribution to delivering a sense of collaboration, in the context of BIM-enabled education in the GCC context could be a promising approach to utilizing local and indigenous tools, approaches, and contexts to meet educational excellence.

Table 1: BIM Collaboration issues in the Educational Context in GCC and the Hypothesis Presented on its Relevance and Impact on the Model of Situational Awareness. Source: Authors

Label	References	Education Limitation in GCC	BIM Collaboration context	Relevance to the model of Situational Awareness (Largely Affected, Mildly Affected, Not Affected) [Hypothesis; to be tested in further research]
K	(Levers & Brock, 2007)	Culturally-specified roles for certain Educational Programs	BIM as a model that depends on interdisciplinary work in the engineering field, may be affected by the fact and reality that some educational programs are specified for female students whereas some are for male students	Perception: Largely Affected Comprehension: Largely Affected Projection: Largely Affected
L	(Jabbour et al., 2012)	Limited interdisciplinary collaboration between colleges	Apart from previously-mentioned barriers, students of a certain department need continuous contact in order to collaborate on a BIM-enable education level	Perception: Mildly Affected Comprehension: Largely Affected Projection: Largely Affected
M	(Abdalla, 2016)	Limited skills and expertise	BIM as a method that adapts emerging technologies, need enough time and expertise in multiple regions in the world, including the GCC	Perception: Largely Affected Comprehension: Largely Affected Projection: Largely Affected
N	(Abdalla, 2016)	Gap between Industry and Academia	According to a survey done in the UAE regarding BIM collaboration (Abdalla, 2016), 61.5% of respondents in the AEC academia agreed that a gap exists and therefore affects BIM collaboration	Perception: Mildly Affected Comprehension: Largely Affected Projection: Largely Affected

4.4 Interdisciplinary Approaches

Learning theories about the phenomena can be quite contrasting when getting an in-depth understanding of the phenomena's behaviour (Salama, 2022). BIM as an interdisciplinary object-oriented three-dimensional model (Boton et al., 2018), can include many risk factors, as multidisciplinary team works include "*communication barriers, accessibility and availability of resources, group size, and accountability*" (A. e. Badran, Baydoun, & Hillman, 2022).

The most popular teaching approach in the BIM educational framework in the publications between 2010 to 2017 is the one that considers a cross-disciplinary and multidisciplinary module, it was a topic of many publications in this research field, covering 54% of research topics about BIM educational framework and teaching approaches (S. K, Osman, Razak, & Shazwan, 2019), which stresses the need to include a social sciences perspective within investigating BIM challenges, especially when people are involved through collaboration. The concept of Situational Awareness as a solution to the research problem could be further analysed through more in-depth research in the future.

5 Conclusion and Recommendations

Future research advancement would need to perform a study that addresses specifically the Gulf environment using expert opinions and survey studies, including a quantitative research

methodology, where more analysis of the case study would be done via collecting quantitative data to investigate the inquiry of whether post-Covid scenario has an influence on the need to work digitally, facilitating BIM implementation and collaboration. Additionally, it is vital to find ways to bridge the gap between industry and academia, which would facilitate collaboration on many levels, as well as promote interdisciplinary and multidisciplinary approaches in learning, teaching, research, and overall knowledge production that gives space to structured digital working to ensure collaboration starts from a bottom-up approach, sprouting from the depth of the rich context it is in.

References

Abdalla, S. 2016. “The Architecture, Engineering and Construction (AEC) paradigm shift: BIM trend in the UAE.”

Abdulmumin et al. (2021). "BIM education ontology."

Abi-Mershed, O. (2010). Trajectories of education in the Arab world: legacies and challenges

Adamu, Z., Emmitt, S. & Soetanto, R. (2015). "Social BIM: Co-creation with shared situational awareness." *Journal of Information Technology in Construction, 20*, 230-252.

Adnan, B. et al. (2022). "Higher Education in the Arab World: New Priorities in the Post COVID-19 Era".

Ahmad, A., Aliyu, A. & Mohammed, N. (2020). "Understanding People Dimension towards BIM Culture Change in Consultancies". Solid State Technology, Vol. 63, 1911-1918.

Ali, K. N., Alhajlah, H. H. & Kassem, M. A. (2022). "Collaboration and Risk in Building Information Modelling (BIM): A Systematic Literature Review." 12(5), 571-594.

Badran, A., Baydoun, E. & Hillman, J. (2018). "Universities in Arab Countries: An Urgent Need for Change: Underpinning the Transition to a Peaceful and Prosperous Future."

Badran, A. E., Baydoun, E. E. & Hillman, J. R. E. (2022). "Higher Education in the Arab World: Research and Development."

Badry, F. & Willoughby, J. (2016). "Higher education revolutions in the Gulf: globalization and institutional viability".

Besné, A. et al. (2021). "A Systematic Review of Current Strategies and Methods for BIM Implementation in the Academic Field." *Applied Sciences, 11*(12), 5530.

Bishop, J. L. & Verleger, M. (2013). "The flipped classroom: A survey of the research." ASEE Annual Conference and Exposition, Conference Proceedings.

Boton, C., Forgues, D. & Halin, G. (2018). "A framework for building information modeling implementation in engineering education." *45*(10), 866-877.

Endsley, M. R. (1995). "Toward a Theory of Situation Awareness in Dynamic Systems." Human Factors, 37, 32-64.

Jabbour, S. et al. (2012). Public Health in the Arab World: Cambridge University Press.

Jin, R. et al. (2021). "A critical analysis of collaborative and disruptive digital-driven built environment education."

Küçük-Avci, i., Topal, M., & stanbullu, A. h. (2022). "The Effects of the Covid-19 Pandemic on Distance Education in Higher Education: A Bibliometric Analysis Study." *24*(2), 457-488.

Kirdar, S. (2020) Education in the Arab world.

Levers, L. Z. & Brock, C. (2007). Aspects of education in the Middle East and North Africa.

Maharika, I. F. et al. (2020). "Building Information Modelling (BIM) Adoption Model for Architectural Education." *20*(3), 22-42.

Munir, M. & Jeffrey, H. (2013). "Building information modelling (BIM): a summary of some UK experiences as guide to adoption in Nigeria."

Reychav, I., Maskil Leitan, R. & McHaney, R. (2017). "Sociocultural sustainability in green building information

modeling." *Clean Technologies and Environmental Policy, 19*(9), 2245-2254. doi:10.1007/s10098-017-1409-y

Suhaida, S. K, et al. (2019). "Evaluation of BIM Education for Quantity Surveying: A Review of Teaching Approaches.", 546-557.

Saka, A. B. & Chan, D. W. M. (2019). "A Scientometric Review and Metasynthesis of Building Information Modelling (BIM) Research in Africa." *Buildings, 9*(4), 85.

Salama, A. (2022). Decolonizing Architectural Knowledge: Situating Middle Eastern Pedagogies in a Globalizing World. In (pp. 221-232).

Shafiq, M., Matthews, J. & Lockley, S. (2013). "A study of BIM collaboration requirements and available features in existing model collaboration systems." Electronic Journal of Information Technology in Construction (ITcon), 18, 148-161.

Wu, S., Fan, P. & Chen, J. (2015). "Incorporating Culture Into Sustainable Development: A Cultural Sustainability Index Framework for Green Buildings." Sustainable Development, 24.

Yusoff, S. N. S., Brahim, J., & Mat Yusoff, Z. (2021). "Incorporation of Building Information Modelling (BIM) in Malaysian Higher Education Institutions: A Review."

Zhao, D. (2021). "Peer Pressure in BIM-Based Collaboration Improves Student Learning." *Journal of Civil Engineering Education," 147*(2), 04020019.

Cite as: Atour R. & Ahmad A.M.,"Challenges and Perspectives on Resilient Collaboration for Building Information Modelling (BIM) Education in the GCC Context", *The 2nd International Conference on Civil Infrastructure and Construction (CIC 2023)*, Doha, Qatar, 5-8 February 2023, DOI: https://doi.org/10.29117/cic.2023.0035

Assessment of Contractor's Extension of Time Claim (Eot)

Neveen Asaad Saleh Ahmed
Project Controls Manager, WS ATKINS, Doha, Qatar
asaadneveen@gmail.com

Abstract

Project Management tools and techniques are simply the process of coordinating the contractor's resources to achieve the Employer's Target. Each project has its own level of project management tailored to the project unique case. In project initiation stage, various inputs drive the main project key assumptions relevant to Project Scope, Duration, Cost and Stakeholders. Those same assumptions could impose a reason for the contractor not to meet project completion date and to be titled as causes of delay or Delay Events. Some of you might understand that since the topic is Time Extension Claim, so we focus on project timeline, this is correct, and within this, we will explain why the "Project Programme of Work (Baseline)" where assigned resources, cost, quantities, and sequence of work will drive Project Progress need to be agreed. Regardless the debate of whither or whither-not, the Baseline is a contractual document, and it requires approval or not, this paper assumes that; the contractor has signed the contract, secured approved programme, and managed to follow all contract clauses to submit a proper extension of time claim. Hence, he/she is concerned about the Contract Administrator action upon receiving this claim, methods of delay analysis, and determination report contents.

Keywords: Delay Events; Time Extension Claim; Project Programme of Work (Baseline); Methods of Analysis; Determination

1 Introduction

The relation between the Contractor and the Employer is defined through the signed contract that defines all contractor's obligations regarding scope, time cost quality, risk, deliverables...etc. However, the Employer in most cases assigns the administration of the contract to the Engineer/ Supervision consultant or even to the Project Management consultant.

Both the contractual parties have the right to raise claims at any time of the contract, and it is the responsibility of the contract administrator to assess those claims and provide fair recommendation or determination to the Employer. Types of claims and reasoning can be detailed under a separate topic. But for this topic, we will focus on construction Extension of Time Claim raised by the contractor (claimant) for the Contract Administrator determination, Hence, we will adopt the Contract Administrator (C.A) view and proceed step by step in assessing the submitted claim. In this paper the author puts his 20 years of experience in the field in addition to his readings and reviews, the author here is intended to use simple words to simplify the industry expressions.

2 Objective of an Extension of Time Claim

The contractor submits extension of time claim to demonstrate that on the balance of the probability, the claimant is entitled to a compensation and to prove and substantiate the amount of such

compensation. In simple words, contractor in this claim is explaining why he is unable to comply with the contract completion date for all the work or section of work. Contractor also shows that this failure is out of his control. If this done successfully, then the completion date of the work/section of work will be revised, which will relief the contractor from any delay penalties and could be compensated for the added cost attributed to these delays.

3 What is Included in Contractor Submission?

For a claim submission to be successful and ready for the Contract Administrator assessment, the contractor should fully understand the claim process as stated in the contract, maintain the time bar for his submission, fully understand the risk owner, and full understanding of each contract party's obligation under the conditions of the contract.

The Contract Administrator must be able to assess the claim, the contractor should prove contractual entitlement and provide enough exhibitions for each claim event. Contractor also needs to demonstrate that he has exerted all efforts to avoid/ reduce the impact of the delay. A successful EoT submission should include the following:

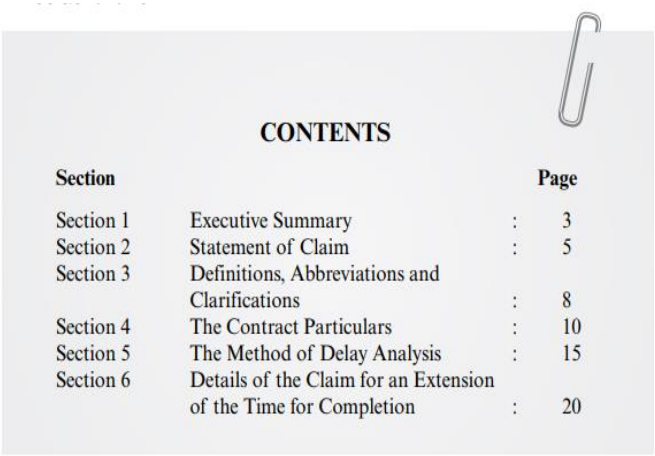
1. Full Narrative report.
2. Latest Approved Project Baseline: utilising agreed software.
3. Cause-and-effect matrix.
4. Delay Analysis: utilising agreed software.
5. Full set of substantiations related to each event.

An Explanation of each of the above will be listed below along with a hint of how the contract administrator will use every exhibit to produce the Claim Assessment Report.

3.1 Narrative Report

A successful narrative is measured as if it is red by a third party, it provides all the necessary information to understand the project. Narrative Report introduction should include brief of the project scope, list of contract documents arranged by priority, a project map or render photo is a good addition to the introduction. Baseline approval status and approval date should be part of the introduction, in next section of the report, the contractor lists the delay events and summarise the impact of each event and the overall impact. In this section contractor is encouraged to mention the duration, the revised date, and the cost he is claiming. Following section; the contractor is to include the contractual entitlement under the contract conditions, referring to each clause of the contract that could support his claim. Before last, comes the delay events section, for each delay event, contractor need to detail the cause, effect, circumstances and chronology of each delay event. The last section is the technical and delay analysis; contractor to explain the chosen delay analyse methodology and the reason of selecting this method. Finally, contractor is to conclude his claim with a table indicating the claimed duration, revised date and the related cost if applicable.

Figure 1 is a sample of the Report Content of the narrative report – Construction Claims & Responses Effective Writing & Presentation edition.



CONTENTS

Section			Page
Section 1	Executive Summary	:	3
Section 2	Statement of Claim	:	5
Section 3	Definitions, Abbreviations and Clarifications	:	8
Section 4	The Contract Particulars	:	10
Section 5	The Method of Delay Analysis	:	15
Section 6	Details of the Claim for an Extension of the Time for Completion	:	20

Fig. 1: Report Content

3.2 Latest Approved Project Baseline and Progress Update

Contractor upon signing the contract is requested to develop a fully detailed cost loaded work schedule which will demonstrate all the activities need to be executed to deliver the project deliverables. It presents the activities arranged in logical sequence and linked in proper relationships (FS, SS & FF), it also demonstrates the resources, the durations, and the quantities required for the contractor to submit the programme for the Engineer/Supervision consultant review. Once accepted/agreed, it is saved as The Project Baseline and should not be changed unless instructed. Contractor, on agreed periodic interval reports the updates of the programme which is known as progress update, it presents the actual status of work at site, those updates are to be compared against the planned baseline. In case of critical delay, the updated programme will forecast a finish date of activities/work/section of work that is shifted from the signed agreement- this indicates that contractor is unable to deliver project as committed-contractor then need to do analysis of the updated programme to figure out the cause of the delay. Most common method is analysis of the critical path.

3.3 Cause-and-effect Matrix

This is the main output of the Updated Programme Analysis. The contractor in this matrix lists the delay events, defines the root cause, the start and finish date and the impact of each event. This matrix is important for the Contract Administrator for better understanding of the Delay Event, and he uses it to develop the Delay Event Register Summary, where he will summarise the contractor submission and his final determination in one spreadsheet.

Cause & Effect analysis - EOT assessment

Contractor Calim #xx cut off date dd/mm/yy

DE	Title	Description	Cause	Effect	Start of Delay Event	Finish of Delay Event	Delay Event Status	Selected Host	Host Finish Date	Impact Finish Date	Status of the effect resulting from the Delay Event (*)	Delta Δ
[illegible]	DE09 - Changes in the Pipe Fittings @ Road Bridges due to PWW Requirements	Additional requirements to use flexible connectors for the PWN, TSE & FSN networks: thru bridges	Long lead item (DI Fittings), which takes average 18 weeks to be delivered	- PWN: complete the pressure testing & handover - TSE: complete the pressure testing & handover - Foul Sewer: complete the pressure testing, pumping station commissioning & handover	22-Dec-21	13-Oct-22	Closed	Approved revised program baseline	30-Sep-22	19-Dec-22	Closed	80.00
[illegible]	DE12 - Delay in the Landscape Signage for the LP	Ambiguity of the names on the landscape signage LP	Engineering missing data, Technical queries Drawing approvals	- Manufacturing of the signages - Erection of the Landscape signages	06-Aug-20	23-Nov-22	Closed	Approved revised program baseline	30-Sep-22	15-Jul-23	Active	288.00
13	DE13 - Promenade Granite wall -	Repeating the Mock-up approval process many	- Changing the approved pattern multiple times	- Granite Installation for the promenade wall								

Fig. 2: Cause and Effect Matrix

3.4 Delay Analysis

Contractor is to submit the Delay Analysis as per the agreed software and a PDF copy. It is preferable for the contractor to run the assessment for each Delay Event separately, however this depends on the utilised method such as window analysis when events occurred in same period are all combined in same window slice. In case the contractor is claiming for multiple delay events, global analysis should be strongly avoided. Contract Administrators do check the submission to ensure the contractor has used each of the following correctly:

1. **Delay Analysis Methodology:** C.A to check if the utilised methodology is the most suitable for analysing this Delay Event and the method is applied correctly. C.A if he finds the method is unsuitable, he may run his assessment utilising different a method, however, this change must be explained in the assessment report.
2. **Updated Programme:** Contractor in his selected analysis method, might need to refer to a specific updated programme's date, then the C.A needs to ensure this is the correct programme update for this event. C.A might use different data date, and to report this within his report.
3. **The Delay Event is Effective:** D.E is impacting a critical path activity, so it would delay the completion date of the work/section of the work.
4. **Delay Fragnet and Sub-fragnet:** Should be logically linked with the dependent activities, proper relationship, duration, resources, and quantities assigned are factual or as per the baseline. Again C.A has the right to do changes on all those items if necessary.

3.5 Full Set of Substantiations

"*The Three Most important aspects to successful claim are Good Records, Good Records and Good Record*"- Roger Knowles.

I can say no more! Many potential good claims were returned by the C.A. for the lack of substantiations. Consultant/supervision Consultant might have records to help, however it is the contractor's responsibility to keep and submit detailed records. Contract Administrator refers to those record to be able to understand and run proper assessment of the claim

4 Methods of Delay Analysis

"*Many extensions of time claim flounder on the method of delay analysis that should be used to demonstrate the effect of delays. The contractor often wishes to perform one method of delay analysis and the engineer considers that another method is more appropriate. Such disagreements will only serve to prolong the resolution of a claim*" - Andy Hewitt.

Choosing the correct Delay Analysis methodology is critical for demonstrating the impacted duration. Some contracts impose the methodology to avoid the conflict between the claimant and the C.A, however this might be unfair for the contractor as the selection of method of analysis depends on availability of records, nature of event, and the submission date.

The following table illustrates some of the most common methods of Delay Analysis–basically modelled methods either additive or subtractive modelling- and minimum requirement to be able to utilise. Please note that the BL is for Approved Baseline, UBL is Updated Programme and the IMP is Impacted Programme.

Table 1: Methods of Delay Analysis

Method of Analysis	Delay Impact Determined	Requirements	Implantation Steps
Impacted as Planned (IAP) (Fig. 3)	Prospective	• Requires approved BL • When the event starts in early stage of the project or before the first update of the approved baseline	• Add the fragnet to the approved BL. Schedule the program • The resultant deliverable dates are the revised dates
Time Impact Analysis (TIA) (Fig. 4)	Prospective	• Approved BL • Nearest update just before the D.E starts UBL (record the completion date UBL completion Date)	• Add the fragnet to the UBL, link logical - this program is now called IMP. Schedule the IMP • Record the resultant deliverable date: IMP completion date • Impacted duration= UBL completion date- IMP Completion date = X days • Revised Completion date = BL date + X days
Collapsed as Built	Retrospective	As Built program logically linked	• Extract the delay event of the program and run • The resulted date is the date that contractor could have finished the project on if the event did not occurr
Time Slice Analysis with Time Impact Analysis (Fig. 5)	Retrospective	• Approved BL • Periodic update of the program • Identification of Critical and near critical path • Time Slice Window of selected Updated Program – all windows to be equal time frame	• Record the BL completion date • Utilize the Window Start Date program to add the fragnet (IMP) • Utilize the Window finish Date program as the UBL • Compare the longest Path from IMP and UBL and the completion dates • (IMP completion date Later than (UBL) = duration is Employer Delay

4.1 Impacted as Planned

- Most straightforward way.
- Ignores actual progress on site.
- Depends on logical links, duration as demonstrated in the approved programme.
- Unless contractor has float, or other dependency linked to the critical path, the impact is straight forward and predictable.

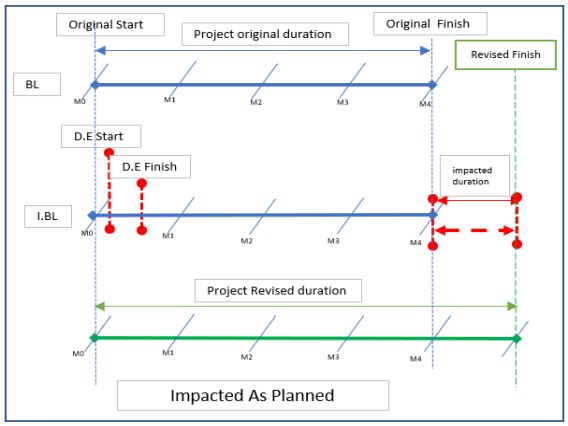


Fig. 3: Impacted as Planned

4.2 Time Impact Analysis

- Uses the nearest programme update just before the event occurs to clearly understand the project progress and the change in the critical path from the baseline.
- Better to use one delay event (including sub-events) at the time, but also can include same period near event.
- Critical path analysis is mandatory.

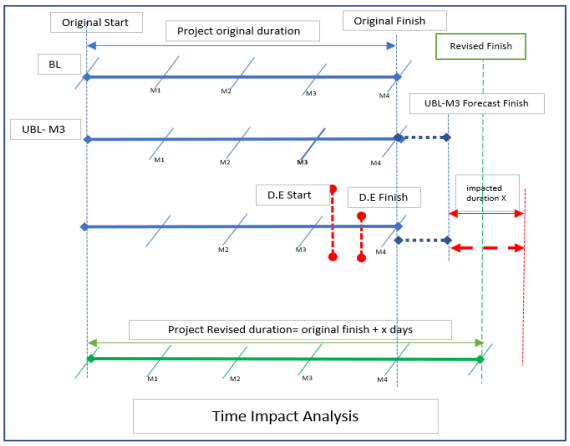


Fig. 4: Time Impact Analysis

4.3 Time Slice Analysis with Time Impact Analysis

- Most accurate method to define the entitlement and the concurrency.
- This method is basically implementation of TIA but on selected slice of time of the claim duration.
- Time and effort consuming method for both claimant and C.A.
- Considers both longest path and completion date changes.

Window No	Input Programme	Input Programme DD	Progress Cut off	Window Duration	Base Prog Finish	Impacted Finish (Step 1)	Updated Finish (Step 2)	Entitled Duration	Entitlement up to
1									
2									
3									
4									
5									
6									

Fig. 5: Time Slice Analysis with Time Impact Analysis

5 Time Entitlement Calculation

Depends on the Delay Event scenarios. Example given below:

Scenario 1: Possession of site/suspension of work: contractor is directly entitled for the time he was disrupted to proceed with work.

Scenario 2: Employer delay event occurs during the contractual duration Fig. (6).

Scenario 3: Employer delay event occurs beyond the contract completion date and before issuance of completion certificate Fig. (7).

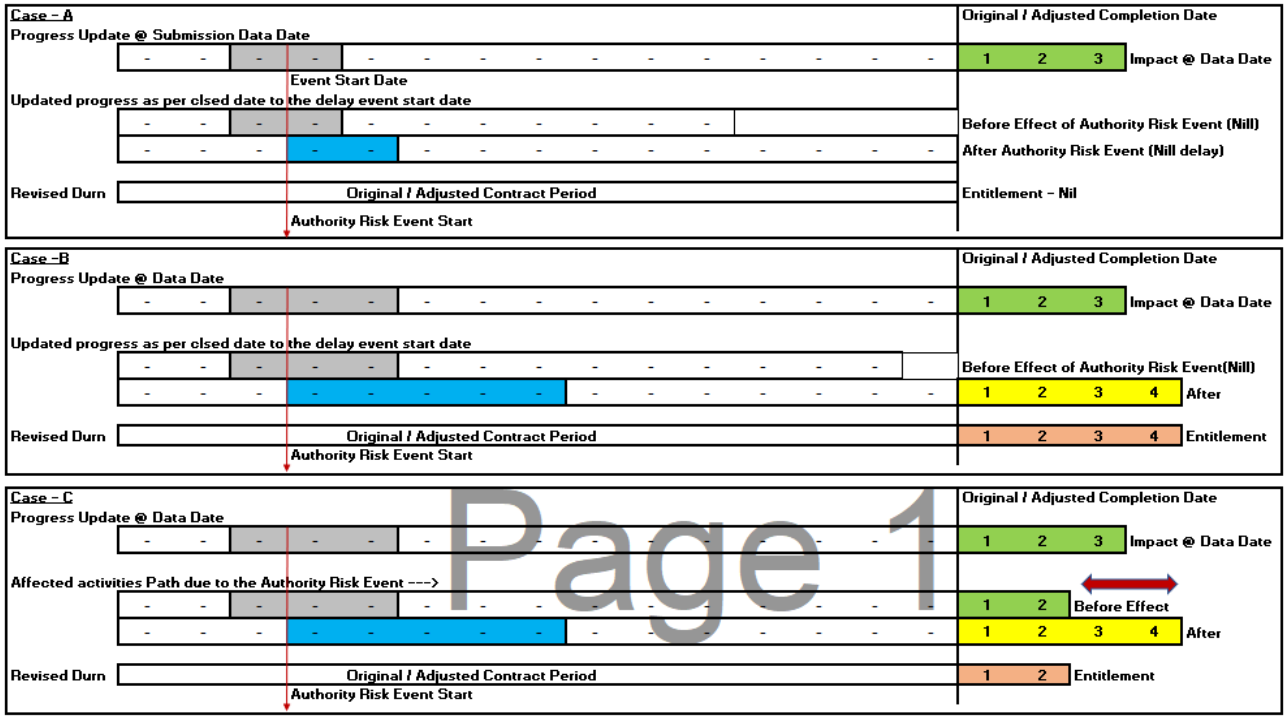


Fig. 6: Scenario 2 -Delay Event occurs during the contractual period

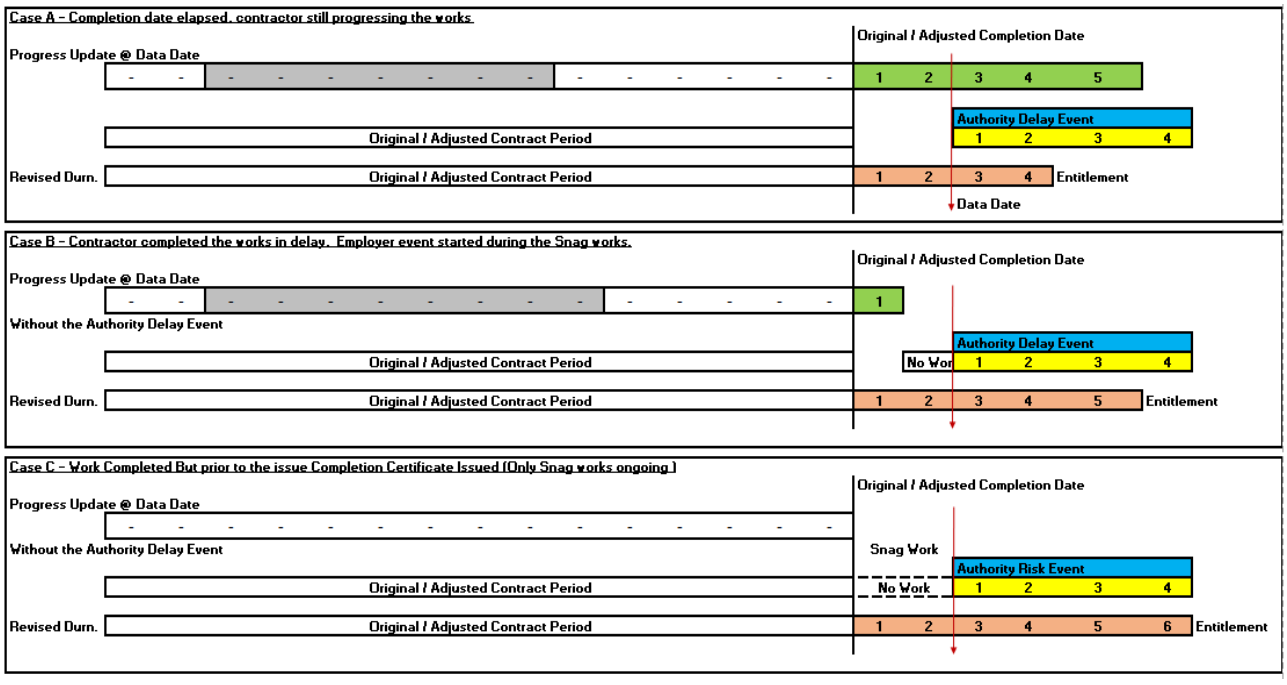


Fig. 7: Scenario 3 -Delay Event occurs beyond the Contractual Period

Presenting the data in the report:

Table 2: Determination Table

Delay Event	**Impacted Period**	**Impacted duration**
D.E #03	10 Feb 2021 to 10 March 2021	28 days
D.E #07 (suspension of work in zone 2)	29 Jan 2021 to 15 Feb 2021	17 days
D.E #012	25 Feb 2021 to 3rd April 2021	36 days
Excusable delays	29 Jan 2021 to 3 April 2021	64 days
Original contract duration date	254 days	
Revised contract duration	254 days + 64 days = 318 days	
Revised contract completion date	Commencement date + revised duration	

6 Concurrent Delay Events

Under the signed contract conditions, when 2 or more effective Delay Events have occurred in the same period of which one is caused by the employer and one caused by the contractor, where both are impacting the completion of deliverables. In this case the contractor is entitled for time compensation only and not for cost compensation.

Table 3: Concurrency Table

	D.E Description	**D.E Start**	**D.E Finish**	**Duration**
Contractor D. E	Delay in S.D Submittals	01 Jan 2020	10 Feb 2020	41 days
Employer D. E	DC2 Approval	28 Dec 2019	15 Feb 2020	48 Days
Compensation duration				**7 days**

7 Determination

Concluding section in the claim determination report that includes all the above details. A final table to demonstrate the revised deliverable dates and the attributed compensation cost if applicable.

Table 4: Determination Table

Description		**Date / Duration**
1	Commencement	Date as per signed Contract
2	Project Duration	1037 Calendar Days
3	Project Completion (Original Contract)	Date as per signed Contract
4	Revised Project Completion (EOT-1 award)	If applicable

8 Conclusion

Claim assessment basically depends on the contractor submission, mainly records and the delay analysis methodology. Contract Administrator determination is only a first step contract modification. Both contractor and employer have the right to accept/disagree the determination, in this case the signed contract should recommend the next step once disagreement is raised.

References

AACE International Recommended Practice NO. 29R-03- FORENSIC SCHEDULE ANALYSIS – TCM Framework: 6.4-Forensic Performance Assessment

FIDIC; Conditions of Contract for Plant & Design and Build (2017). 2nd Edition; International Federation of Consulting Engineers.

Gibson, R. (2008). 1st Edition Construction Delays Extensions of Time and Prolongation claims; Routledge Tylor & Francis Group. USA.

Hewitt, A. (2016). 2nd Edition. Construction Claims & Responses Effective Writing & Presentation, Wiley Blackwell, UK.

Khlousy, M. M. & Kandil, H. M. (2018). 1st Edition. Claims in Construction & FIDIC Contracts- Arab arbitration Centre-Egypt.

Knowles, R. (2012). 3rd Edition. 200 Contractual Problems and their solutions. Wiley Blackwell, UK.

Society of Construction Law Delay and Disruption Protocol (2017). 2nd addition. Society of Construction Law-UK.

Cite as: Ahmed N.A.S., "Assessment of Contractor's Extension of Time Claim (Eot)", *The 2nd International Conference on Civil Infrastructure and Construction (CIC 2023)*, Doha, Qatar, 5-8 February 2023, DOI: https://doi.org/10.29117/cic.2023.0036

Choosing by Advantages (CBA) Used as a Qualitative Assessment Methodology in Lean Construction

Zied Dahmani
AECOM, Doha, Qatar
zdahmani@ashghal.gov.qa

Juhaina Essa Al-Sulaiti
Public Works Authority (Ashghal), Doha, Qatar
jalsulaiti@ashghal.gov.qa

Ayman Naser
Dorsch Gruppe – Middle East, Doha, Qatar
an1401569@qu.edu.qa

Abstract

Decision making is part of the daily duties of researchers, engineers, and consultants, and taking the right decisions requires quantitative assessment which usually needs data and analysis. In construction industry, data collection or detailed analysis are practically complicated that cannot drive the right results. This fact leads to the common use of qualitative assessment where the numbers are not available, and the evaluation involves various criteria from diverse perspectives. As a Lean tool, Choosing by Advantage (CBA) is used predominately in the Design process. This paper's characteristics and contributions to the existing body of knowledge presents the CBA practice as a qualitative assessment tool in construction phases in the Lean Construction implementation in infrastructure projects, proposing equations through the technique which determines exactly how to assess the percentage advantage for each factor for qualitative factors with different grades or different ranks. The flexibility of CBA as a multicriteria decision-analysis (MCDA) model helped overcome the differences between criteria, categories, and value-based analysis. This paper describes the experience of selecting the option that considers advantages from various criteria in an extensive assessment.

Keywords: Choosing by Advantage (CBA); Multi-criteria decision-analysis (MCDA); Qualitative assessment; Public Works Authority

1 Introduction

The construction industry is very resource-intensive, and it is not uncommon for decisions to be made with inadequate information (Pryshlakivsky & Searcy, 2021). When it comes to the day-to-day operations of project management, poor decision-making may cause unnecessary expenditures and tension. Decisions may be made more intricately due to stakeholder participation and contemporary sustainability challenges (Zhuang et al., 2019). Lack of understanding of multi-criteria decision making is another barrier to good decision-making in the construction business (Belay et al., 2022). The challenges associated with making decisions needs a methodical approach. In addition, getting everyone on the same page requires a well-thought-out decision-making structure. Therefore, Lean Construction (LC) implementation is usually introduced as a new framework for project management to support decision-making for planning and project delivery (Gunduz & Naser, 2019). The typical project management assessment methodologies are based on quantitative data comparisons. In most cases, this data is incomplete and inconsistent between different disciplines such as Health and Safety

(H&S), Quality, Progress, Environment and Sustainability (E&S), and Public Relations (PR). This requires configuration of a multicriteria evaluation matrix, then alignment to a clear and consistent assessment tool. The assessment tool should summarize performance in reference to contractual requirements which are qualitative in nature (Agyekum-Mensah et al., 2020). In addition to other approaches to multicriteria decision-making, the CBA technique was used here. Using cost-benefit analysis (CBA), you may objectively evaluate how several options stack up against one another. The CBA framework relies on a small number of facts and criteria that have been established in advance in order to eliminate or greatly minimise the role of subjectivity in decision-making (Paredes & Herrera, 2020). Therefore, this study set out to provide a solid multi-criteria decision-making framework for analysing the critical factors contributing to the success of using CBA as a qualitative evaluation tool in the construction business. The findings of this research provide important additions to the existing body of knowledge and methods used to make decisions in the construction sector.

2 Literature Review

In the fields of Architecture, Engineering, and Construction (AEC), choices are often taken with just a cursory comprehension of the complexities of the issues at hand and after doing only the barest of analyses. When managers of a project are unable to make good judgements, the process of managing the project and operating it becomes fraught with conflict and waste. The complexity of decision-making is increased by factors such as the expanding involvement of project stakeholders and growing concerns over the social and environmental repercussions of a project (Li et al., 2016). Despite the fact that practitioners are looking for improved decision-making tools, there is a dearth of relevant literature, which makes it difficult for them to choose the most appropriate approach for every given situation (Danesh et al., 2018). In this context, a strategy of decision-making that is both methodical and scientific and that considers several factors is required in order to successfully navigate the problems connected with decision-making. In addition to this, it fosters openness and provides a common justification for advocating in favour of a more sustainable option (Danesh et al., 2018).

CBA has several examples of use in the construction literature. Parrish and Tommelein (2009), for instance, investigated the feasibility of using CBA to decide on a rebar design for a beam-column junction. In combination with set-based design, CBA enabled the engineer to systematically explore a wide range of options for satisfying both mandatory and desirable design requirements. Arroyo et al. (2014) examined the usage of Weighting Rating and Calculating (WRC) and Choosing by Advantages (CBA) in the selection of a structural system for a Palo Alto, California campus residential project. The case study revealed that both approaches led to the same conclusion, but their underlying assumptions were distinct. CBA contributed more to transparency than WRC. Karakhan et al. (2016) provided a case study on the use of CBA to a building project in order to make safety design choices for a facility's permanent elements. The findings suggested that CBA is a good decision-making technique that may be used by project teams to make early-stage safety judgements. Using the analytic hierarchy technique (AHP), Diabagate et al. (2015) provided a method for identifying the best offer for a tender (AHP). AHP has several restrictions. The first is that the phenomena of rank reversal must be taken into account in AHP procedures, which implies that when any choice alternative is added or withdrawn from the problem, the rank of decision alternatives changes. The subjectivity of the modelling process is seen as a second restriction of AHP (Arroyo et al., 2015).

Since it evaluates just the value-added benefits of a number of options, CBA is a reliable method for making decisions based on several factors. For the USDA Forest Service, Jim Suhr came up with the concept in 1999 (Suhr 1999). The CBA relies on mutually agreed-upon standards and relevant

information to make choices, making the process more objective and less prone to bias. This strategy entails focusing on the positive aspects of a situation instead than dwelling on its flaws, and grounding decisions in relevant facts and quantitative data to reduce the likelihood of prejudice and irrational thinking (Suhr, 1999). Although various multi-criteria decision-making methodologies, including linear optimization and weighting-rating calculation (WRC) and Analytical Hierarchy Process, were available for use in the research, the CBA method offers specific benefits over other frameworks (AHP). Collaboration, transparency of trade-offs across components, distinguishing the alternatives, maintaining consistency, and assessing the subjectivity of the alternative are all areas in which CBA has been shown to excel in previous research (Arroyo et al., 2015; Arroyo et al., 2016).

3 Point of Departure

As a part of contractual enhancements in infrastructure projects in the State of Qatar, Lean Construction was introduced to support project delivery and minimise programme disruption. While Lean Construction is not a typical discipline that performs beyond H&S, Quality, E&S and PR, integrating the overall lean performance needs to be aligned with other disciplines to reflect compliance and identify areas for improvement.

Besides, any discipline compliance can elude the added value behind the integration of Lean concepts at programme wide. Lean practitioners should "measure contractual compliance" to validate the Lean performance of each project (Nguyen & Akhavian, 2019).

Moreover, conventional project portfolio evaluation is often "progress oriented," which may lead to misguided strategy fulfilment and, in some circumstances, muddled reflections. Therefore, CBA was developed to evaluate the benefits of the alternatives, and decision-makers may readily pick the option that would provide the highest value for their project.

In a variety of ways, current research differs from all the related literature in different aspects. Choosing by Advantages is proposed as a straightforward method for choosing criteria in the present research. The suggested method provides contractors with equations that precisely specify how to calculate the percentage advantage for each qualitative factors with different grades/ranks basis.

4 Assessment Matrix

Construction projects' portfolios are managed through standardised performance dashboards, either combined per discipline or per project, highlighting several metrics to summarize performance in a report like format. Basic metrics, such as progress percentages, total manhours without Loss Time Injury (LTI), and work inspections approval rate, are quantitative measurement systems of single performance aspect. Usually, those metrics indicate a "status" and help take corrective actions when necessary. While this quantitative assessment can summarize staggered performances, it cannot reflect neither a holistic project performance nor the project compliance with contractual requirements.

Performance dashboards can be helpful for the "top performers' projects" to emphasize on their achievements, but they are helpless to depict the "low performers' projects" especially regarding contractual requirements. This dashboard's evaluation is part of a decision-making process for commercial approvals that needs a stringent outlook while the quantitative metrics can be confusing.

Such deficiencies require an extensive assessment involving all project's disciplines and considering multiple factors. This assessment is defined in the multicriteria decision-analysis (MCDA). MCDA approach is to have a set of criteria linked to specific requirements than develop a multi-dimensional model to integrate those criteria (Abraham et al., 2013). MCDA requires a configuration of decision criteria divided

into components for evaluation and interrelated for an overall insight (Seppälä et al., 2002).

The transition from typical construction project portfolio dashboards to a holistic assessment matrix using MCDA approach was explored to support group assessment and decision-making.

5 CBA Mathematical Model

For qualitative characteristics with n grades including, for example, excellent, very good, and good. Assign 100% to the attribute with the highest rating and 0% to the attribute with the lowest grade. Apply Eq. (1a – c) to any intermediate property. Therefore, if there is just one intermediate level, $A_{b=1}$ = 1 (A is: the order of the intermediate level) and C = 50%. Additionally, if there are two intermediate grades, the first will be allocated $A_{b=1}$ = 1 and C = 60%, while the second will be assigned $A_{b=2}$ = 0.5. Then, ${C_1}^*$equals 60% and, ${C_2}^*$ equals 30%. This means that the multiplier ($A_{b=1}$) for the first intermediate is 1 regardless of the number of intermediates, the multiplier ($A_{b=2}$) for the second intermediary is 0.5, the multiplier ($A_{b=3}$) for the third intermediate is 0.25, and so on.

Where C^* is the percentage of advantage in case of qualitative factors with n grades.

For $n \leq 3$, $use\ A_1 = 1$, and for $n > 3\ use\ A_b = \left[\frac{1}{2}\right]^{b-1}$, where $b = 2, \dots, n-2$ (1a)

$$C\ \% = 100\ [\tfrac{(n-1)}{(n+1)}] \quad (1b)$$

$$C^*\% = A_b \text{ x } C\ \% \quad (1c)$$

Then, to obtain importance advantage for each criterion at each factor, multiply the importance index (I-index) by the percentage of advantage for each criterion. For qualitative criteria with n grades, use equation (2).

$$Importance\ Advantage = (qualitative\ factors\ with\ n\ grades) = I\ index\ \text{X}\ C^* \quad (2)$$

6 CBA Implementation

While MCDA approach has a panoply of technical methodologies, CBA was chosen to structure the assessment for several reasons: it is a "mechanism" developed over 20 years that promotes decision-making at first hand (Suhr, 1999), and performance evaluation; it integrates different aspects with different measurement scales; it is flexible and can be customised to specific needs.

CBA has been practiced as a Lean Construction methodology mainly for design phase and pre-construction evaluations, focusing on advantages of alternatives and independent criteria integration.

Qualitative assessment enables not just performance comparison, but it fosters a deeper understanding of the problem from the people's perspective (Ivankova & Creswell, 2009). CBA's flexibility supports the qualitative assessment using a customised scale to reflect either contractual compliance or any other performance. This scale is developed from an inherited scoring scale of quality performance, covering INRs, NCRs, and other metrics, as indicated in Table 1.

Table 1: Scoring Scale

Score	Criteria
1	Not Acceptable
2	Needs improvement
3	Acceptable
4	Above Expectations

CBA practice had been performed on a three phases plan (Figure 1): Individual CBA, Combined CBA then Group CBA.



Fig. 1: CBA Phases

6.1 Phase One: Individual CBA

This phase aims to facilitate transition from quantitative metrics to MCDA approach and getting familiar to the new scoring scale. Each discipline lead develops qualitative criteria inspired by contractual requirement, with a focus on advantages. Then, each advantage was defined the acceptable performance either in numbers, when possible, or in an objective description. Once projects portfolio assessment is completed, an individual review should be conducted to level criteria scoring between projects. The criteria can be revisited to maximise the advantage consideration and address disbenefits if required.

6.2 Phase Two: Combined CBA

Once all discipline leads develop their criteria and the "Acceptable" performance, a joint discussion is facilitated to present the advantages considered in reference to the contract or strategic values. Then, alignment between similar criteria is performed to have a focused criteria list. In practice, 30%-40% of criteria will be combined or incorporated in other criteria especially when there are quantitative performance references. The discussion led not only to develop an assessment criteria system, but it improved understanding interfaces between disciplines and what is considered "important" for each aspect. This could not happen with traditional quantitative assessment systems or even several of MCDA methodologies.

6.3 Phase Three: Group CBA

With a clear list of assessment criteria, inspired by contractual requirements and integrated between different disciplines, a group review session involving all disciplines and management to confirm the validity of each criterion and ensure the list covers all project portfolio aspects and scope. Checks are done for practicality of assessment and accuracy of scores to reflect a holistic and fair project performance status.

7 Outcomes

This approach led to developing a robust multi-criteria tool to evaluate more than 40 infrastructure projects portfolio, then extended to include more than 160 projects with different scope of work that requires customization of a new list of criteria extracted from the first edition.

The new structured assessment system helped mitigate an existing bias usually driven by projects ahead of schedule while they have a low performance in other aspects. This biases free assessment is appreciated by different discipline leads as it helps them address non-compliance in a combined perspective.

Following a successful practice over 6 months, the scoring scale has been edited to reflect the contractual aspect of the assessment Table 2.

Table 2: Revised Scoring Scale

Score	Criteria
1	Not at required level
2	Partially in place or no proactive approach
3	Meets minimum standard; room for improvement
4	Proactively managed and exceeds requirements

The CBA mechanism practiced for a portfolio of projects in construction phase helped managers understand better the performance of supply chain, different sections, and different contractors.

While the scoring scale is a value-based assessment system, it is considered as qualitative rather than quantitative, as it is linked to a contractual requirement compliance description. However, the researcher utilized equations Eq. (1a – c) to evaluate the importance of advantages for implementation of Lean construction and related portfolio in construction projects.

8 Conclusion

Traditional selection models neglected the provided equations to quantify the percentage benefits for quantitative and qualitative parameters. This technique's main strength is approach, which quantifies important advantages using known significance indices for variables and equations for computing percentage advantages for quantitative and qualitative components, minimising subjectivity. The key addition to knowledge is a selection approach that calculates the percentage benefit of each factor of quantitative variables, qualitative elements with grades or rankings, and qualitative factors with yes/no foundation. The author believes this method will help industry practitioners pick the best option. Grouping the most relevant criteria that contribute to existing knowledge and offering the instruments (equations) to quantify each factor's percentage advantage for both quantitative and qualitative aspects achieves this.

CBA gives decision makers independence, unlike other existing methods. Due to intuitive component weights and scoring scales, ranking methods are more subjective. This study's innovative CBA approach compensates for extensive training. This is due to extracting many equations to express the percentage benefits for qualitative elements with n grades basis. The research will assist construction professionals by utilizing the CBA framework in understanding the relevance of multicriteria decision-making in construction project management. As construction is a highly opinionated sector, construction practitioners must recognise the necessity of making smart judgements. Due to the fact that CBA is predicated on value–adding benefits, it will facilitate effective decision-making. The collaborative aspects of CBA improve communication between team members and enhance understanding of interfaces. Managers found that CBA is essential for future strategy development as it can include different categories ranging from values to specifications. CBA consistency helped deliver a bias free qualitative assessment tool that supported decision-making with fairness. With the emergence of sustainability norms, CBA is a useful mechanism to consider sustainable advantages and environment friendly benefits while assessing options in any disciplines as future studies.

Acknowledgements

The authors wish to thank Paul Ebbs who initiated the CBA process for individual performance evaluation.

References

Abraham, K., Lepech, M., & Haymaker, J. (2013, July). Selection and application of choosing by advantages on a corporate campus project. In *Proceedings of 21st annual conference of International Group for Lean Construction (IGLC), Fortaleza, Brazil* (pp. 349-358).

Agyekum-Mensah, G., Reid, A. & Temitope, T. A. (2020). "Methodological pluralism: investigation into construction engineering and management research methods". *Journal of construction engineering and management, 146*(3), 04020006.

Arroyo, P., Tommelein, I. D. & Ballard, G. (2015). “Comparing AHP and CBA as decision methods to resolve the choosing problem in detailed design.” *Journal of construction engineering and management* 141, no. 1: 04014063.

Arroyo et al. (2016). “Collaborating in decision making of sustainable building design: An experimental study comparing CBA and WRC methods.” *Energy and Buildings* 128: 132-142.

Belay et al. (2022). “AHP based multi criteria decision analysis of success factors to enhance decision making in infrastructure construction projects.” *Cogent Engineering 9*, no. 1: 2043996.

Danesh, D., Michael J. R. & Abbasi, A. (2018). “Multi-criteria decision-making methods for project portfolio management: a literature review.” *International Journal of Management and Decision Making 17*, no. 1: 75-94.

Gunduz, M. & Naser, A. (2019). “Value stream mapping as a lean tool for construction projects”. *International Journal of Structural and Civil Engineering Research, 8*(1), 69-74.

Ivankova, N. V. & Creswell, J. W. (2009). “Mixed methods. Qualitative research in applied linguistics: A practical introduction”, 23, 135-161.

Li, T. H., Thomas Ng, S., & Skitmore, M. (2016). Modeling multi-stakeholder multi-objective decisions during public participation in major infrastructure and construction projects: A decision rule approach. *Journal of Construction Engineering and Management, 142*(3), 04015087.

Nguyen, P. & Akhavian, R. (2019). “Synergistic effect of integrated project delivery, lean construction, and building information modelling on project performance measures: a quantitative and qualitative analysis”. *Advances in Civil Engineering*.

Paredes, G. & Herrera, R. F. (2020). "Teaching multi-criteria decision making based on sustainability factors applied to road projects." *Sustainability* 12, no. 21: 8930.

Pryshlakivsky, J. & Searcy, C. (2021). "Life Cycle Assessment as a decision-making tool: Practitioner and managerial considerations." *Journal of Cleaner Production* 309: 127344.

Seppälä, J., Basson, L. & Norris, G. A. (2001). “Decision Analysis Frameworks for Life-Cycle Impact Assessment”. *Journal of Industrial Ecology, 5*(4), 45-68.

Suhr, J. (1999). ‘The choosing by advantages decision making system”. Greenwood Publishing Group.

Zhuang et al. (2019). "The role of stakeholders and their participation network in decision-making of urban renewal in China: The case of Chongqing." *Cities* 92: 47-58.

Cite as: Dahmani Z., Al-Sulaiti J.E. & Naser A., “Choosing by Advantages (CBA) Used as a Qualitative Assessment Methodology in Lean Construction”, *The 2nd International Conference on Civil Infrastructure and Construction (CIC 2023)*, Doha, Qatar, 5-8 February 2023, DOI: https://doi.org/10.29117/cic.2023.0037

The Implementation of Enterprise Resource Planning Systems for Roads and Infrastructure Construction Companies in Developing Countries

Marie-Belle Fawzi Boutros
BiBuilt, Hazmieh, Lebanon
marie-belle.boutros@bibuilt.com

Dima Jawad
Ontario Tech University, Oshawa, Canada
dima.jawad@ontariotechu.ca

Sophia Ghanimeh
Environmental Research Center, Qatar University, Doha, Qatar
s.ghanimeh@qu.edu.qa

Abstract

Construction Enterprise Resource Planning (CERP) systems started to infiltrate the construction world after ERPs became crucial in modern enterprises. In simple terms, CERP integrate and keep track of the various processes within construction companies. As a minimum, these possess include management of general contractors, subcontractors, financial work, accounting, payroll, logistics, workflow processes ... data related to different processes are stored within one unique database. Despite this intuitive objective, developing and standardizing CERP systems to fit the needs of all construction companies is not a straightforward course. This research focuses on the development of a framework that integrates the minimum required modules to be included within a CERP, specifically for road and infrastructure construction companies. This objective is achieved based on literature review on CERP despite its shortage, in-depth interviews with construction professionals requiring CERP, and the results of a structured questionnaire filled by CERP users and developers. The developed framework identifies the procurement module linked to the on-site deliveries as the first stone that should be developed and implemented. Then, budgeting and work progress modules must be added. After that, timesheet and equipment follow-up modules need to be implemented. Limitations encountered highlighted the main considerations to be considered in future work such as the cost, the company's size, development and implementation period, and type of work.

Keywords: CERP; ERP systems; ERP modules; ERP framework

1 Introduction

The origins of Enterprise Resource Planning (ERP) systems go back to the mid-20th century when the industrial sector used the Material Requirements Planning (MRP) system to plan and help in the decision-making of the production process. ERP systems included different integrated modules to help to manage and integrate the full business process. An important feature of the modules is that the data entered in one module is automatically routed to the other modules. So, all data are immediately updated and available to all functional areas (Stevens, 2018). The advantage of an ERP system is its capacity to provide financing, manufacturing, supply chain management, purchasing, selling, and planning in one single system (CFI Education Inc, 2021). These systems succeeded in the industry. Statistics show that the ERP software market around the world is more than $25 billion with a growth rate of 10% to 20% per year (Roul, 2021).

One major sector of the industry is construction where the challenges and complexities are unique. The execution of any construction engineering project passes by several stages. The larger the scale of the project is, the more complicated and interrelated the processes become, and the more critical management is required. Completing the scope construction projects on time and within budget remains the foremost challenge all over the world, specifically in developing countries. Lack of proper planning, collaboration, execution, and monitoring are identified as main reasons for not achieving these targets. Hence, the incorporation of the ERP systems within the construction field is increasingly recognized as the solution to these challenges with the main objective of avoiding failure of project completion in terms of quality, cost, and time. Findings show that Construction Enterprise Resource Planning (CERP) systems are a must but at the same time their proper implementation is very crucial. Several companies tried to implement CERP systems, however; varying success rates resulted after the implementation of CERP. The absence of standardized work in the construction field as well as the large cost of CERP can lead to improper implementation strategy of CERP. Moreover, the pandemic worldwide increased the need to prioritize the implementation of a system that reduces the contact between the engineers and decreases the papers transmittals while encouraging real-time follow-up remotely.

2 Objective and Methods

CERP system might include all the following modules: budgeting, cost control, procurement management, work progress management, revenues, inventory management, site operation, estimating and tendering, subcontractor management, asset management, document control, planning and scheduling, logistics, etc. Which modules to implement in your CERP depends on several strategic aspects: How can the CERP improve the business performance? How long will the CERP implementation project take? How will the CERP affect current business processes? What is the CERP total cost and what are the hidden costs of the CERP ownership (Stevens, 2018)? Other operational aspects include the size of the company, the number of employees, the type of construction, the operational need of the modules, the legislation in the country, the education and technical level of the users, and most importantly, the phases of implementation and deployment.

While being in the transition phase from an old system to a newer ERP, deep-rooted practices will remain an obstacle for most of the users until they get used to and accept the change. Hence, implementing the system in different phases is very critical while the choice of the correct modules to be implemented in each phase is also another predicament. During transitioning, the efficiency of the work that is being achieved cannot decrease, the mistakes should be minimized, the construction will continue, and the loss of data is not accepted. Thus, following a good strategy in the deployment of the correct modules at the correct time is a matter to be well-studied and investigated.

The objective of this paper is to present a developed framework for elaborating on the minimum required modules for road and infrastructure construction companies that can be adopted to reach a successful CERP transition and implementation.

The framework is established based on the results of three approaches: a review of the existing literature and existing CERP systems, structured questionnaire, and in-depth interviews with potential CERP clients. The questionnaire respondents and the interviewees are practitioners working and using CERP systems or professionals that participated in developing the system. Moreover, technical observation by the author is conducted through being part of a CERP development team and implementation team.

3 Background and Literature Review

In the last century, in their effort to organize and optimize their work, manufacturing industries based their production on systems known as the Material Requirement Planning (MRP). It was built to organize the storage and allocation of production materials. Then, this system was expanded to include the allocation of production equipment and labor, which represents the manufacturing process. This evolvement turned the system to be called Manufacturing Resource Planning or *MRP*II. As MRP II evolved, the addition of several modules such as purchasing, financials, human resources, and other front-office applications improved the management of different operations and led to the creation of Enterprise Resource Planning (ERP) systems (Jingsheng Shi & Halpin, 2003). The ERP systems provide a platform for different departments in an industry to share data and communicate through a fast process. Additionally, the information is stored under a common database (Vlachopoulou & Manthou, 2006). The main idea of ERP systems is to create a standard and synchronized base of information to improve the efficiency of the company (Chung, Skibniewski, Lucas Jr. & Kwak, 2008). Similarly, construction industries are searching for several solutions to improve their scheduling and planning and reduce their cost. Jingsheng Shi & Halpin (2003) and Nitithamyong & Skibniewski (2004) agreed that in opposition to the standard system within typical industries, construction firms are so diverse and differ in strategies applied. The main specificities in construction is recognized in the literature as varying durations, required resources, as well as the lack of the necessary technical staff and technical knowledge (Windapo, 2013). Moreover, remaining a strong competitor in the market demands continuity, technological innovations and sustainable solutions (Al Marri, 2014), along with the proper management of resources (Sutar, Kashid & Deshmukh, 2016) and integration of operation flows using information technology (Estébanez, Trigo & Belfo, 2016).

Several large ERP vendors can be named such as SAP, Oracle, PeopleSoft, JD Edwards, Microsoft Dynamics, Infor ERP, etc. However, these packages were mainly designed for manufacturing industries, hence; they were not able to succeed within the construction field (Tatari, Castro-Lacouture & Skibniewski, 2008). Furthermore, Shi and Halpin (2003) acknowledge that construction companies require specific functions: scheduling, planning, procurement, project-oriented, open, expandable, remotely accessible, etc. As a result, some ERP suppliers' companies developed construction ERP systems (Tatari, Castro-Lacouture & Skibniewski, 2008).

Hewavitharana and Perera (2019) established a logical framework that combines the organizational processes and ERP processes for construction companies, after studying the gap between construction and ERP procedures. The largest gap belongs to inventory management while the lowest belongs to sub-contractors' management. The major reasons leading to the largest gap are the variety of item codes, the incorrect process of purchasing procedures, unplanned payment methods, and the absence of a re-order level.

One of the most important features to take into consideration is to customize the ERP system, however; higher cost and longer time might be required to reach the implementation stage of the system (Mirian & Osvaldo, 2012). Furthermore, higher success rates are seen when the implementation of ERP modules is deployed in sequences not as a full bulk at a time (Hallikainen, Kivijärvi & Tuominen, 2009). Thus, Hadidi et al. (2016) suggested a decision model for ERP modules implementation in Saudi Arabia that helps in choosing the best sequence for ERP modules in construction firms. The results show that the highest CERP benefits are decision-making criteria and then improved efficiency, better information quality, cost reduction, improved flexibility, and user

satisfaction, respectively. The top three modules to be implemented at the first stage are ordered as follows: inventory control and logistics, procurement, project finance, and accounting. In addition to the results concluded by the literature stating the gaps among different modules (Hewavitharana & Perera, 2019) and the importance of implanting the ERP system in different stages (Hadidi, Assaf & Alkhiami, 2016), it is stated by the latter that the first three modules to be implemented in construction companies are inventory management, procurement, and accounting modules.

4 Results

4.1 Questionnaire's results

A structure questionnaire was created online using google forms and distributed to professionals working either as ERP users, developed, implementer, or manager. The first part of the questionnaire collected general information about the respondent and the company. The questionnaire was answered by 50 respondents where 29 out of them have used ERP systems during their career. The outcome identifying whether the ERP system utilized is customized or not is respectively 75.9% and 3.4%, while 20.7% of the respondents don't know. The departments where the respondents have worked are transportation and infrastructure engineering – contracting, cost control and planning, accounting, project control, operations, IT, estimation, and procurement department. The respondents' years of experience varied between 2 and 17 years and most of them are civil engineers. Currently 97% of the respondents are working. The average age is 29 years old and the different regions where the respondents have worked are Saudi Arabia, Egypt, Sultanate of Oman, UAE, Lebanon, Jordan, Nigeria, Congo, Ivory Coast, Europe, and Africa.

The second part of the questionnaire inquired about the CERP modules that the users have used along with the earliest year they have worked on the module. The highest percentage belongs to work progress module (96.55%) while the lowest to the tendering module (51.72%). The earliest module utilized was the procurement module in year 2005, followed by planning and scheduling, and document control modules in 2006 and 2007, respectively (**Table 1).** The user activity varied among different modules, however; the modules that are used the most, are based on the questionnaire results, respectively, work progress module (96.55 %), budgeting, site operations, and inventory management modules (82.76%), procurement and document control modules (75.86%), accounting module (68.97%), planning and scheduling module (58.62%), and tendering module (51.72%).

Table 1: Usage of Each Module

Module	%	Earliest Year
Work Progress	96.55	2008
Budgeting	82.76	2008
Inventory Management	82.76	2010
Site operations	82.76	2008
Procurement	75.86	2005
Document Control	75.86	2007
Accounting	68.97	2010
Planning and scheduling	58.62	2006
Tendering	51.72	2010

4.2 Summary of the Main Results from the in-Depth Interviews

Six in-depth interviews were conducted with construction professionals who are considering the adoption of CERP. The discussions tackled their experience, opinion, and goals from using the CERP. These interviewees were construction companies' owners/managers who are working in developing countries in specific Lebanon, Egypt, Morocco, Ivory Coast, Togo and Benin. The construction companies range between small to large and some specialized in buildings while others were involved in roads and infrastructure projects. Also, among these companies, two companies had limited implementation of CERP. Based on the discussions, first-time adopters are mainly interested in procurement and on-site deliveries. Timesheets and workforce monitoring comes next, inventory/stock management as well as equipment tracking, and logistics are identified as next modules by companies that have a limited CERP in place. Linking to budgeting and cost control/accounting was acknowledged by all interviewees with varying opinions on when to be implemented. The transitioning from established processes and systems—especially accounting—to a new system surfaced as the main concern. All interviewees agreed on the need for real-time data collection and tracking ultimately.

5 CERP Proposed Framework

After synthesizing the information collected from the three approaches while taking into consideration the differences among construction company's types, a framework suggesting the minimum required module adapted for roads and infrastructure engineering companies is presented below along with the order of integration of these systems. Figure 1 presented the suggested framework divided in three phases. The first phase includes the module for procurement and on-site deliveries. The second phase includes budgeting module and work progress module and the third phase includes the workforce timesheet module and equipment module.

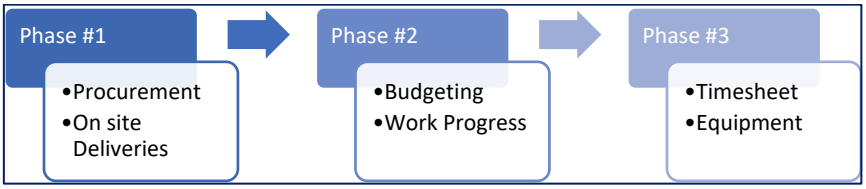


Fig. 1: Suggested Framework

5.1 Procurement and on-site Delivery Modules

One of the major activities in managing projects is procuring of resources. To this end, project managers send their requests of resources to the procurement department where a request for quotation and purchase orders are processed. The procurement manager searches for the required material to be purchased for all the company's projects while aiming to get the best offer and reach the most cost-effective and appropriate product. The more this task is properly handled, the more the project becomes cost-effective and profitable. The job does not end at the level of the orders, however; the procurement management team must ensure that the deliveries are achieved on time and within the specifications listed. The procurement department should be aware of the deadlines and lead times and ensure that the purchases will not delay any work. In the construction field, most of the time, the purchase orders are done from the offices while the deliveries are on-site. Two-way communication must be achieved within the two teams (on-site and procurement department) to make sure that the order has reached the site with the requested quantities and quality.

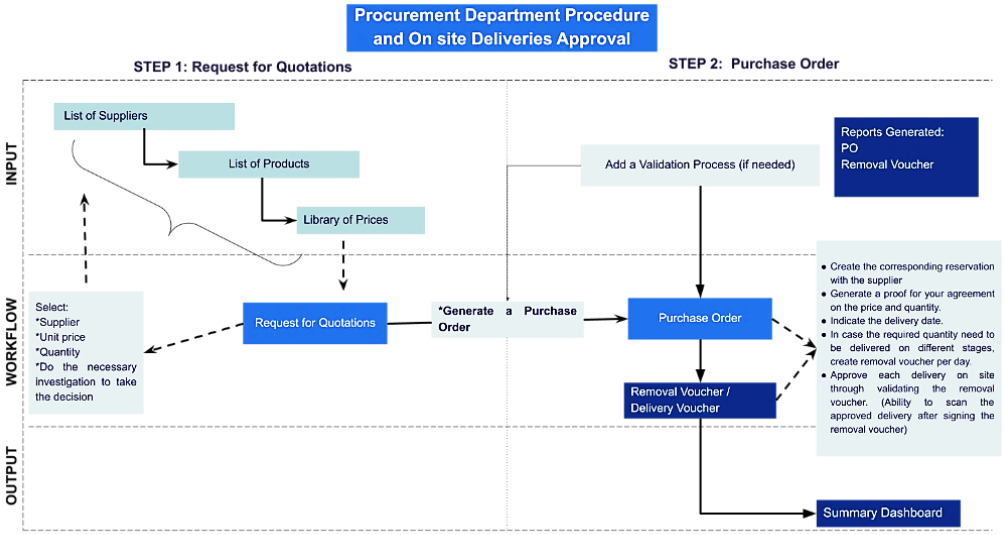


Fig. 2: Procurement and Delivery Module

Three main pillars contribute to this process:

1. The project's planning and required material.
2. The history of similar material previously purchased.
3. The on-site deliveries.

Figure 2 illustrates the suggested module for procurement procedures and on-site deliveries different where required input, workflow, and output are divided into two steps: request for quotations and purchase order processing.

5.2 Budgeting and Work Progress Modules

Comparing the projected and actual progress is very critical to measure some key performance indicators such as schedule performance indicator and cost performance indicator. A suitable budget makes it feasible to get a good cost estimation of the project. Also, a list of priority results for each project leads to better decision-making and more effective project management. Collecting regular data from the site helps measure the progress more accurately and allows the project manager to detect whether the project is behind schedule or not.

Figure 3 and **Figure 4** show respectively a plan for the budget and work progress modules.

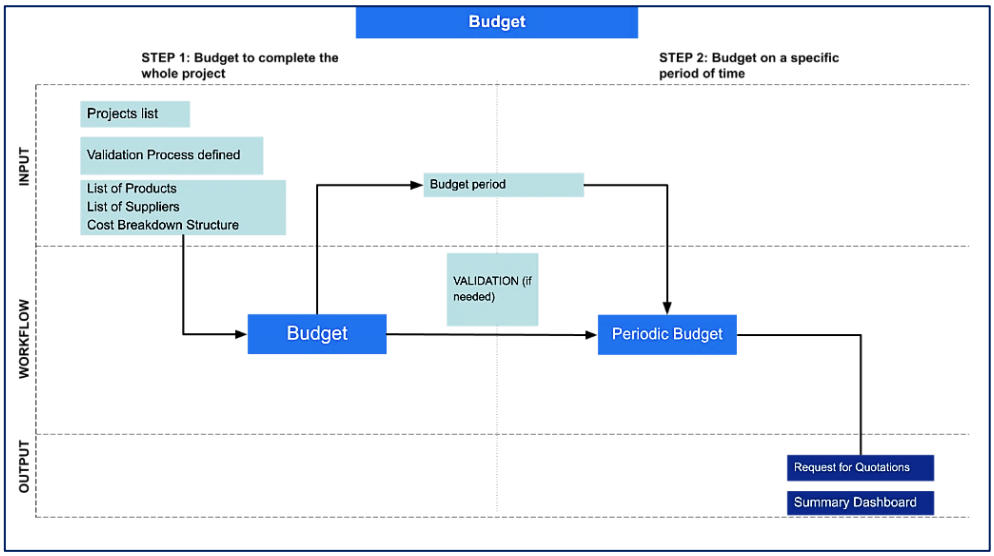


Fig. 3: Budget Module

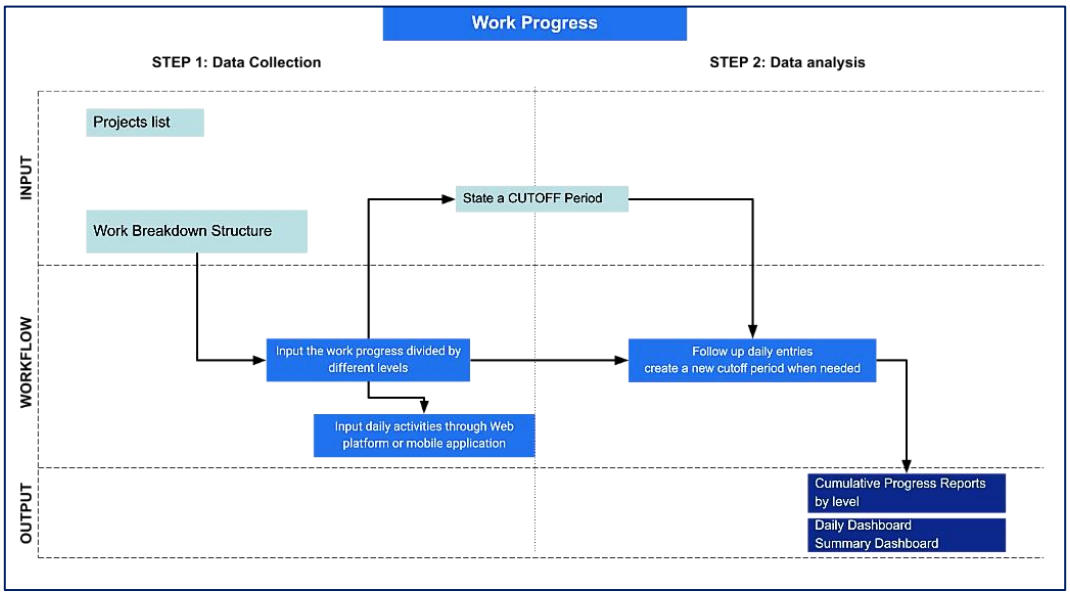


Fig. 4: Work Progress Module

5.3 Site Operations: Workforce Time sheet and Equipment Tracking Modules

Recording the workforce on-site on large-scale projects need to be well monitored to minimize any extra costs due to personnel mismanagement. It also helps track the lack of personnel in specific areas. Most importantly this work will be achieved in real-time. Moreover, due to improper equipment assignment among several projects, an operation on-site might be delayed or stopped due to a lack of equipment. Hence, it is very important to track all the equipment and make sure this equipment will reach the site on time. Also, collecting the working hours or working kilometres for each piece of equipment is needed to ensure project-based and activity-based costing. Figure 5 and Figure 6 present Workforce Timesheet modules and equipment tracking modules, respectively.

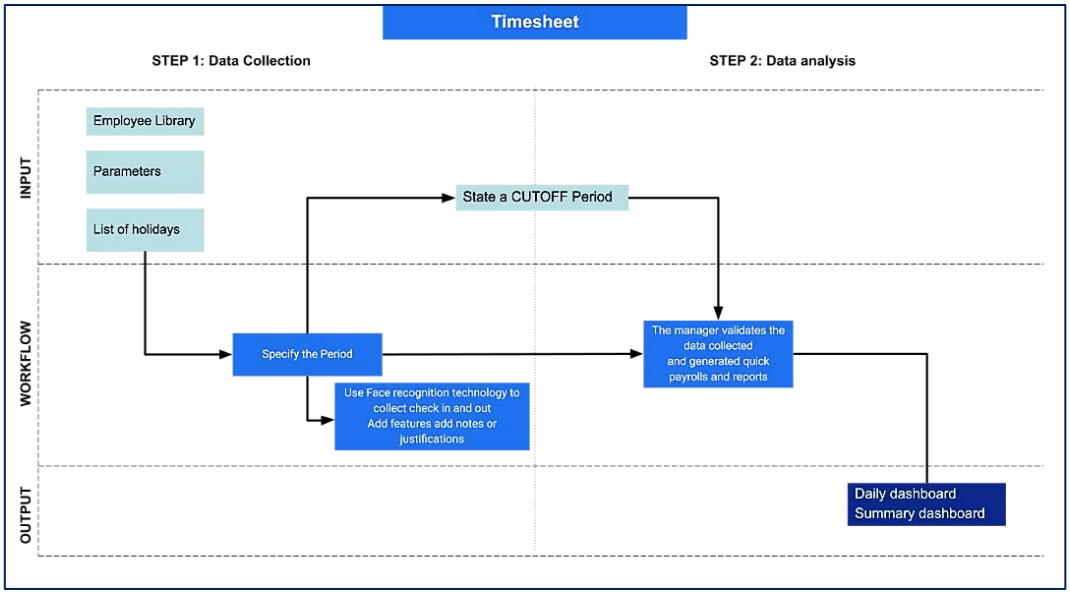


Fig. 5: Timesheet Module

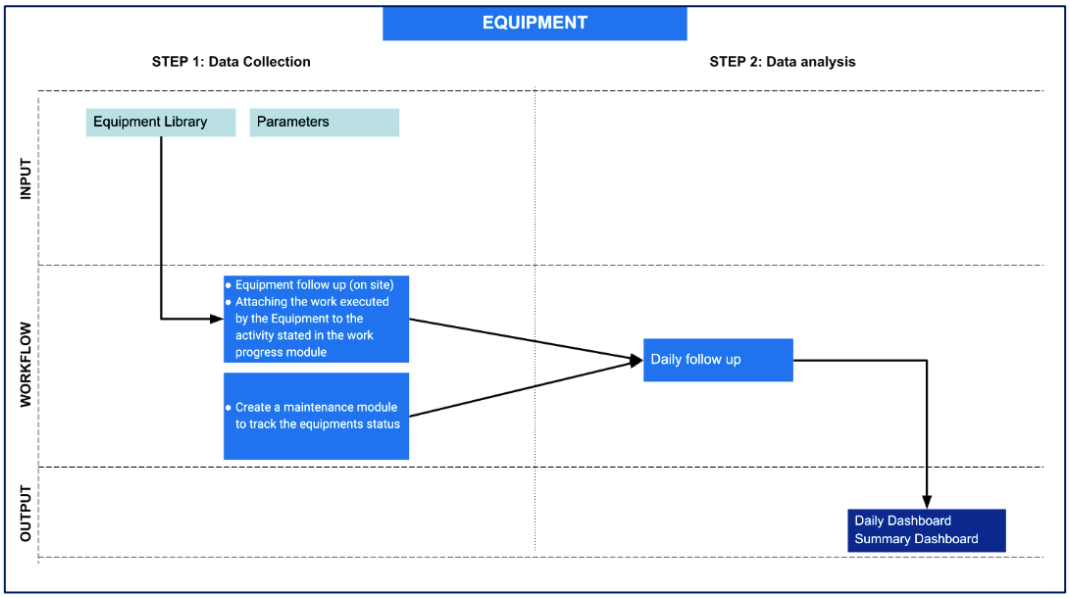


Fig. 6: Equipment Tracking Module

6 Conclusions

To conclude, this research is imperative for the modern management of construction companies successfully where this remains a challenge particularly in developing countries. Moreover, optimizing the resource allocation, cost, and time are the key elements of a good strategy design, but having the necessary tools to manage these resources across different departments and functions will guide any project to success. Hence, the role of CERP systems arises and the need for specific phased modules to be implemented will be in demand. Choosing the best framework to adopt and to prepare your company for the obstacles that might be faced will facilitate the integration of these systems. The outcome of this research presents a framework composed of three main phases including the following modules: procurement, delivery, budget, work progress, timesheet, and equipment. These results are observed from in-depth interviews with experts in the field, a survey distributed among users, and technical observations. However, further consideration might be taken in terms of cost, implementation time, size of the company, and the type of work achieved by the company.

References

Al Marri, K. (2014). ERP implementation in the project-based organisations of the construction industry. *The Business Management Review*.

CFI Education Inc. (2021). *www.corporatefinanceinstitute.com*. Retrieved from Corporate Finance Institute: https://corporatefinanceinstitute.com/resources/knowledge/other/material-requirements-planning-mrp/

Chen, J. (2001). Planning for ERP systems: Analysis and future trend. *Business Process and Management Journal*.

Chung, B. et al. (2008). Analyzing enterprise resource planning system implementation success factors in the engineering–construction industry. *Journal of Computing in Civil Engineering*.

Dilakshan, R., Disaratna, V. & Silva, K. (2018). *Tendency of Sri Lankan Construction Organizations in Adoptuing Entreprise Resource Planning Systems.*

Estébanez, R., Trigo, A. & Belfo, F. (2016). ERP systems adoption evolution in Iberian companies during the global financial and economic crisis and recession (2007–2014). *In Proceedings of the 2016 International Conference on Information Management*.

Hadidi, l., Assaf , S. & Alkhiami, A. (2016). A systematic approach for erp implementation in the construction industry. *Journal of civil engineering and management.*

Hallikainen, P., Kivijärvi, H. & Tuominen, M. (2009). Supporting the module sequencing decision in the ERP implementa¬tion process – an application of the ANP method. *International Journal of Production Economics*.

Hewavitharana , F. & Perera, A. (2019). Gap Analysis between ERP procedures and Construction procedures. *MATEC Web of Confrences.*

Hill. (1999). *A bona fide fit?* Manufacturing Systems.

Jingsheng Shi, J. & Halpin, D. (2003). Enterprise Resource Planning for Construction Business Management.

Luo, W. & Strong, D. (2004). A framework for evaluating ERP implementation choices. *Institute of Electrical and Electronics Engineers*.

Mirian, P. & Osvaldo, H. (2012). Prioritization of enterprise resource planning system criteria:Focusing on construction industry. *Production economics*.

Roul, R. (2021, January 22). *www.learn.g2.com*. Retrieved from Lear: https://learn.g2.com/erp-statistics#general-erp.

Stevens. (2018). *Operation Research.* Mcgraw Hill.

Sutar, A., Kashid, S. & Deshmukh, V. (2016). Management information system in construction project using MSP. *International Research Journal of Multidisciplinary Studies*.

Tatari, O., Castro-Lacouture, D. & Skibniewski, M. (2008). Performance evaluation of construction enterprise resource planning systems. *Journal of Management of Engineering*.

Vlachopoulou, M. & Manthou, V. (2006). Enterprise resource planning (ERP) in a construction company. *International Journal of Business Information Systems*.

Windapo, A. (2013). *Fundamentals of Construction Management.* Delhi.

Cite as: Jawad D., Boutros M.B. & Ghanimeh S., "The Implementation of Enterprise Resource Planning Systems for Roads and Infrastructure Construction Companies in Developing Countries", *The 2nd International Conference on Civil Infrastructure and Construction (CIC 2023)*, Doha, Qatar, 5-8 February 2023, DOI: https://doi.org/10.29117/cic.2023.0038

An Exploration into Delay-Influencing Factors on Healthcare Construction Projects: The Case of Saudi Arabia

Bader Almutairi
M.Sc. Student, Civil Engineering Dept., King Saud Univ., Riyadh, Saudi Arabia
438105191@student.ksu.edu.sa

Abdulrahman Bin Mahmoud
Assistant Professor, Civil Engineering Dept., King Saud Univ., Riyadh, Saudi Arabia
abinmahmoud@ksu.edu.sa

Abstract

The construction project's delay is one of the biggest challenges that concern practitioners in the construction industry. The success or failure of construction projects is usually measured by the building team's achievement of the project's goals and objectives (ex., time and cost). The Kingdom of Saudi Arabia (KSA), one of the largest construction industries in the MENA region, is experiencing significant delays in some construction industry projects for different reasons. The major causes of delays in project completion in the construction sector in the KSA and how sensitive it is to healthcare projects specifically differ from one project to another. Thus, there is an urgent need to identify construction project-specific causes of delay in the healthcare sector. The research is based on a quantitative approach using the systematic review methodology, where 100 delayed projects in Saudi Arabia were sampled from the healthcare sector, and the causes of delays were captured and recorded. Various factors contributed significantly to the projects' delays, such as change orders, high expenditure, and poor budgetary estimates. This study's results will help project managers reduce the risks of project delays by identifying the influencing factors and their local context, monitoring them, and finding the proper way to mitigate or element their impacts, if possible.

Keywords: Project delay; Healthcare construction project; Influencing factors; Saudi Arabia

1 Introduction

Delays in construction projects often occur, but the magnitude, scope, and overall impacts on project completion may be an essential consideration. For example, major construction projects often undergo long planning and approval phases that should eliminate any barriers that may hinder project progress. Construction delays in the healthcare sector in Saudi Arabia can be caused by various factors, including lack of funding, clear project plans, and difficulties obtaining necessary permits and approvals. Additionally, the complexity and scale of healthcare construction projects can make them particularly susceptible to delays. It's also possible that the COVID-19 pandemic has played a role in delaying construction projects in Saudi Arabia. To mitigate these delays, project managers must have clear project plans, adequate funding, and good communication with all stakeholders, including government officials and community members. Additionally, it may be helpful to bring experienced construction management teams with a track record of completing similar projects.

2 Literature Review

Zidane & Andersen (2018) established that the major factors accounting for delays in construction projects include change orders during construction, design issues, and internal bureaucracy, among others. Design issues may be associated with unclear technical obstacles, while internal bureaucracy affects the approval of financial procedures. According to Keane et al. (2010), change orders by the owner during construction occur due to a lack of coordination between the owner and reviewing team. Several other factors also cause change orders during construction, and their cumulative effects impact construction projects' cost, time, and quality. The impacts on project quality and organizational reputation may not necessarily occur, but the existing literature on the subject needs to consider the possibility of the same. Further surveys also show that the variations brought by the change orders increase the overall project cost while causing delays in construction schedules because of the additional work required. Assaf & Al-Hejji (2006) also identified change orders as the most common cause of delays in construction projects. It is the most critical contributor to time overruns in major construction projects, alongside delays in deliveries by external vendors and more extended review periods for the project materials. Failure to estimate the project's cost may account for delays in progress payments, while unclear technical obstacles occur due to planning and scheduling issues. Change orders generally occur due to common causes between the two parties, the owner and the contractor. According to Waty and Sulistio (2021), change orders are often associated with a mismatch between the designs and field conditions, delays by the contractors, and field security considerations. Natural factors, underground conditions, changes of authority, and working techniques may also account for this challenge.

Other factors accounting for delays in construction projects include cost planning inefficiencies associated with the failure to determine the project's cost (Maqsoom et al., 2019). It is regarded as a financial management challenge that affects even the major construction firms. Failure to estimate the project's cost accounts for most cases of cost overrun in large construction projects (Flyvbjerg et al., 2018). Cost overrun is a product of underestimation and mostly occurs several years after the commencement of the project. Outrun costs are often higher than the actual estimates due to changes in scope and complexities in the project, among other issues. Further investigations indicate that inaccurate cost estimates often occur because of incomplete information and errors in establishing the scope and complexity of the project. For example, Lesniak and Zima (2018) support these findings indicating that effective cost estimation is crucial for the sustainable development of the project schedule.

In addition, Unclear technical obstacles before the project's start occur due to failure to customize the standards and processes to the construction environment. This challenge may accrue because of the need to customize construction equipment to the construction site alongside other factors that may affect daily operations. Changes in the operating procedures may also have a similar impact by distorting the standard execution processes. Sambasivan and Soon (2007) established that delays in construction projects occur due to improper planning by the contractor, site management issues, material shortages, challenges in paying for completed work, mistakes during the construction stage, and time and cost overruns. Material shortages occur due to the failure of external vendors to make timely deliveries. At the same time, challenges in fulfilling financial obligations are a subset of the long time taken to approve financial decisions. Bad contractor experience also arose as a significant hindrance that is partly to blame for awarding contracts to the lowest bidders. Lastly, equipment availability challenges and failure to account for unclear technical obstacles significantly affect many construction projects.

The Kingdom of Saudi Arabia (KSA) is a rapidly developing country with numerous construction projects to attain its strategic developmental milestones (Alenazi et al., 2022). However, recent observations into the management of Saudi's healthcare construction projects indicate that the sector is experiencing significant delays. It is a sensitive issue, given that it occurs in the healthcare sector and significantly impacts project costs and completion times. Its impacts are significant in countries such as KSA, characterized by a fast-growing population that increases demand for expansive infrastructure projects. In addition, delays generally negatively affect the construction industry's reputation. Therefore, it is necessary to investigate the factors accounting for delays in KSA construction projects. Finally, this study focuses on the influencing factors causing these delays in the KSA.

3 Methodology

The study is a quantitative research using the systematic review methodology to assess the nature of the challenges affecting healthcare construction projects in KSA, focusing on establishing and evaluating the factors causing delays in healthcare construction projects. There are numerous ongoing healthcare construction projects in KSA. A total of 100 projects that are behind schedule within the last ten years were considered from the healthcare construction sector, and the most critical delay causes were collected and analyzed. These projects include the construction of medical cities, hospitals, medical rehabilitation, long-term care facilities, and the restructuring of primary care centers. The study utilizes insights from the literature review to establish the critical factors to this effect and how they play out in the progress of the overall construction project. The project reports detailing the progress of the ongoing construction projects that were obtained from the KSA Ministry of Health's Construction Projects Database. The project reports were analyzed to identify the critical factors contributing to project delays. The impact of each factor on the overall construction projects' progress was then tabulated in the results section.

Methodology Steps:

1. Collect projects that are behind schedule in the Ministry of Health database.
2. Investigate the most critical factors of delay.
3. Analyze the influencing factors, their impacts, and their frequency.

4 Results

Results indicate that several owners' and contractor-related factors account for the delays in construction projects. These factors, as identified from the healthcare construction projects' reports in Saudi Arabia, include change orders during construction, high expenditure, failure to estimate the project's cost, and unclear technical obstacles before starting the project. Other factors include long waiting times for the approval of financial procedures, failure by external vendors to make timely deliveries, and awarding contracts to the lowest bidder. Findings from the literature reviews show that a considerable proportion of these factors arise from design issues and elements of internal bureaucracy. Lack of coordination between the teams participating in the project also contributes to the most incidences of change orders. Cumulative impacts of these factors are experienced through time and cost overruns that accrue from the delays and implementation of design changes. The results also indicate that the project cost estimation challenges often contribute to delays in payment processing, and project planning and scheduling issues contribute to the technical challenges encountered during construction. Additionally, the outrun costs mainly resulted from cost overruns, incomplete information that made it difficult to estimate the project's cost, and erroneous projections.

The common factors influencing delays in KSA's healthcare construction projects are summarized in Table 1.

Table 1: The KSA's Healthcare Construction Projects Delays Common Factors and their Impacts

Factor	Impact
Change orders during construction	Time Overrun
High spending compared to the actual work completed	Time Overrun
Fail to estimate the project's cost	Time Overrun & Cost overrun
Unclear technical obstacles	Time Overrun & Cost overrun
Approval of financial procedures takes time	Time overrun
External vendors don't deliver on time	Time overrun
Contract awarded to the lowest bidder	Time overrun

The influencing factors causing delays, the responsible project party category, reasons for occurrence, and frequency are shown in Table 2. They are ranked from the highest to the lowest frequency.

Table 2: Factors Causing Delays in KSA's Healthcare Projects

Factor	Category	Main Reason\s	Frequency
Change orders by the owner during construction	Owner	Coordination challenges between the owner and the reviewing team	450
High spending compared to the actual work completed	Owner	Cost planning inefficiencies	321
Fail to estimate the project's cost	Owner	Incomplete information and failure to establish the scope of the project	209
Unclear technical obstacles before the start of the project	Contractor	Design issues & equipment availability challenges.	121
Approval of financial procedures takes time	Owner	Internal Bureaucracy	118
External vendors don't deliver on time	Materials Suppliers	Material shortages	92
Contract awarded to the lowest bidder	Owner	Inadequate contractor experience	54

5 Discussion

Healthcare construction projects in KSA are huge undertakings encompassing the development of complex structures. The complexity of these structures implies that their associated costs and time requirements are extensively huge. Given the need to adhere to strict timelines and tight construction budgets, major interventions must be deployed to minimize delays that may affect the project's progress. Unfortunately, despite the extensive design, approval, and implementation procedures, healthcare construction projects in KSA still need to be completed on time. The study utilized data from the database on Healthcare Construction projects in Saudi Arabia to establish the most probable

causes of delays. Outcomes from the exploration indicate that the delays accrue due to failures from the owners and contractors. The most common factors include change orders, failures in estimating the overall project cost, high expenditure, long waiting times for financial approvals, awarding contracts to the lowest bidder, unclear technical obstacles, and failure to make timely deliveries. These factors, alongside the reasons for their occurrence, are summarized in Table 2. According to the table, the owner accounts for 5 out of the 7 factors. The contractor only bears the blame for technical issues and procurement challenges. As highlighted in the literature survey, the most critical outcomes of these delay-causing factors are cost and time overruns. Therefore, the owner contributes a considerable portion of the delay influencing factors while the contractor plays a minor role.

In addition, exploring the occurrence frequency of these influencing factors in healthcare construction projects reveals insightful information regarding where efforts should be invested to minimize the impact of the delay. The utilized data of Healthcare Construction projects in Saudi Arabia shows that the change orders by the owner during construction were the most frequent factor that affected 450 healthcare projects, followed by high spending compared to the actual work completed and failure to estimate the project's cost which took place at 321 and 209 healthcare projects, respectively. Other influencing factors, such as the unclear technical obstacles before the start of the project, late approval of financial procedures, and delivery delay from external vendors, have occurred in 121, 118, and 92 healthcare projects, respectively. Lastly, the contracts awarded to the lowest bidder have a lower frequency of occurrence, which occurred in only 54 healthcare projects.

Future efforts should be dedicated to investigating the impact magnitude of these influencing factors to better project management and control. Additionally, the integrative design approach has a high potential for reducing the healthcare project delay through alignment and better stakeholders' communication, which will enhance the control and reduction of delay influencing factors.

6 Conclusion

The study has indicated that despite the sensitivity of healthcare construction projects, they still experience delays due to various factors. Owner-related factors include change orders during construction, high expenditure, cost estimation failures, long waiting times for approval of financial procedures, and awarding contracts to the lowest bidder. Failure by external vendors to deliver materials on time arises from the materials segment, while the contractor is to blame for technical obstacles. Consequently, these factors culminate in time and cost overruns as the major negative impacts. A major limitation faced by the investigator is the lack of accurate information or data. Data collection in the construction sector can be challenging due to the dynamic nature of construction projects and the lack of standardized data collection practices. This can lead to inaccuracies in the data and limit the conclusions drawn from the study. Moreover, the data about the construction project's performance may have a bias due to the involvement and influence of stakeholders, such as the project developers, contractors, and government officials.

References

Alenazi, E., Adamu, Z. & Al-Otaibi, A. (2022). Exploring the Nature and Impact of Client-Related Delays on Contemporary Saudi Construction Projects. *Buildings*, *12*(7), p.880. https://doi.org/10.3390/buildings12070880.

Flyvbjerg, B. et al. (2018). Five things you should know about cost overrun. *Transportation Research Part A: Policy and Practice*, *118*, 174–190. https://doi.org/10.1016/j.tra.2018.07.013

Keane, P., Sertyesilisik, B. & Ross, A. D. (2010). Variations and change orders on Construction Projects. *Journal of*

Legal Affairs and Dispute Resolution in Engineering and Construction, *2*(2), 89–96. https://doi.org/10.1061/(asce)la.1943-4170.0000016

Leśniak, A. & Zima, K. (2018). Cost calculation of construction projects including sustainability factors using the case based reasoning (CBR) method. *Sustainability*, *10*(5), 1608. https://doi.org/10.3390/su10051608

Maqsoom, A. et al. (2019). Influencing factors indicating time delay in construction projects: Impact of firm size and experience. *International Journal of Construction Management*, *21*(12), 1251–1262. https://doi.org/10.1080/15623599.2019.1613206

Sambasivan, M. & Soon, Y. W. (2007). Causes and effects of delays in Malaysian Construction Industry. *International Journal of Project Management*, *25*(5), 517–526. https://doi.org/10.1016/j.ijproman.2006.11.007

Zidane, Y. J. T. & Andersen, B. (2018). The top 10 universal delay factors in construction projects. *International Journal of Managing Projects in Business*, *11*(3), 650–672. https://doi.org/10.1108/ijmpb-05-2017-0052.

Cite as: Almutairi B. & Bin Mahmoud A., "An Exploration into Delay-Influencing Factors on Healthcare Construction Projects: The Case of Saudi Arabia", *The 2nd International Conference on Civil Infrastructure and Construction (CIC 2023)*, Doha, Qatar, 5-8 February 2023, DOI: https://doi.org/10.29117/cic.2023.0039

Investigating the Potential for Standardization of Glass Reinforced Polymer (GRP) Shutter Molds Designs in Bridge Projects in the UAE

Mhd Amer Alzaim
American University of Sharjah, Sharjah, United Arab Emirates
b00026779@alumni.aus.edu

Mariam Al Ali
American University of Sharjah, Sharjah, United Arab Emirates
g00093066@aus.edu

Ghassan Abu-Lebdeh
American University of Sharjah, Sharjah, United Arab Emirates
gabulebdeh@aus.edu

Abstract

This paper addresses the potential for design standardization of bridge construction moulds as a means to minimize waste and cost. Specifically, the paper looks at the potential for standardizing the design of bridge Glass Reinforced Polymer (GRP) shutter moulds that typically vary in size and design based on project-specific requirements. Environmental and economic sustainability aspects are addressed using a two-tiered approach views of construction experts were solicited, and production-to-demolition and disposing costs of a sample of completed projects estimated. There appears to be a consensus that there are significant benefits from standardizing the design of the modes including material waste reduction, cost savings, shorter procurement processes and possibly the reuse of shutter moulds. Given the size of the construction sector and its contribution to material and energy consumption and harmful emissions, and non-hazardous waste, the potential savings are significant.

Keywords: GRP; Shutter moulds; Bridge construction; Sustainability; Pier

1 Introduction

Globally, the construction industry is a major contributor to improving the quality of life in society, however, it still produces 45% to 65% of waste that is disposed in landfills, 35% of global CO_2 emissions, and nearly 30% of all greenhouse gas emissions, which further confirms the need for construction companies and government entities to focus on the implementation of effective strategies and policies to reduce the environmental impacts, as per (Li. *et al*., 2002). It is evident that the construction industry is experiencing challenges such as low level of automation in design and construction, and the scarcity of natural resources as well as the constant need for new "sustainable" construction methods. Accordingly, there is a need to address such challenges by looking at current practices and exploring the possibilities of enhancing performance in the industry, particularly for bridge projects where the reduction of costs and CO_2 emission, and energy savings would contribute immensely to improving the sustainability aspects. Therefore, according to (Qu *et al*., 2020) the future is seen to be moving in the direction of standardization of component production and manufacturing, equipment mechanization and automation and reducing complexity of structural elements assembly.

When looking at the design of bridges, specifically piers, they are designed primarily as a strong support system for the bridge superstructure, but they can also be aesthetically pleasing to the eye of the viewer. Therefore, sizes and shapes can vary in order to meet the demands of clients, which poses a challenge to designers where they have to be innovative and always come up with new designs thus increasing the potential for environmental impacts due to the increased number of bridge pier moulds used in every new project. To build a bridge, there are several types of moulds that can be used, such as column, beam moulds, wall, slab, staircase and customised moulds. Bridge piers are usually comprised of columns and heads, or a pier cap, which are customized in dimensions and shape based on the design requirements.

Qu *et al*. (2018) stated that in recent years, the design and construction of bridges have experienced advancements and innovations, which contributed time and cost savings, as well as simplifying the construction process e.g., Tandon (2019) mentioned that the use of pre-casting has accelerated the delivery of bridge projects by achieving several milestones, including reduction of environmental pollution to enhance the sustainability of a project, minimizing disturbance to traffic during construction with aesthetic quality of construction to support the social pillar of sustainability, in addition to accelerating construction and choice of durable structural components that boost the economic benefits through cost-reduction. As a result, the standardization of pre-casting moulds inside the casting facility is a major factor which determines the cost and speed of bridge construction projects.

As mentioned by Fitzgerald *et al*. (2021), Fibber reinforced plastics or polymers (FRP) are commonly used in the construction industry. They are made of composites that include either carbon, glass or aramid as the major fibre, and mixed with other elements like silica sand or limestone at a specific temperature. Usually, the glass fibre is named after the main element that is added. Accordingly, there is Carbon Fibre Reinforced Polymer (CFRP), Glass Fibre Reinforced Polymer (GFRP or GRP) and Aramid Fibre Reinforced Polymer (AFRP). Sundaram (2009) mentioned that the use of GRP material in bridge piers has been dominant over the traditional material like steel, aluminium and concrete, mainly due to its favourable traits like its ability to be designed in various shapes, as well as its long-life expectancy, corrosion resistance and uniform appearance. However, there are associated impacts of using GRP, such as the high emissions due to the complex production stages. However, according to Li *et al*., (2022) it still has lower CO_2 emissions compared to steel.

Although an experimental study of recycling GRP into concrete composite has shown that GRP waste can be used as a partial replacement for fine aggregate and an admixture in cement concrete, it still requires further investigation to evaluate durability and other compliance tests, which does not provide a feasible solution for the effective management of GRP waste, according to (Osmani & Pappu, 2010).Therefore, the reduction of construction waste should be considered, as it will be a more efficient approach compared to using treatment options that are costly and energy-demanding. A study in Wuhan, China conducted by Li. *et al*. (2022) revealed that construction managers with higher levels of education are willing to reduce construction waste as they understand the associated benefits, but fail to do so due to the tight project schedules, insufficient budgets, and the design changes factor which affects the waste reduction process, thus confirming the need for policies and regulations to regulate the use of GRP material and manage the associated waste.

The literature shows lack of studies in the UAE about the generation of waste and potential environmental and economic costs associated with bridge projects. Also, there is absence of information from the bridge construction industry about the effects of using different designs for bridge pier moulds and the willingness to consider standardization of designs to minimize waste generation. Given the importance of addressing waste associated with the construction industry, and given the fact that bridges are a main structural element of the infrastructure in any country, the aim of this work is to evaluate the sustainability aspects of bridge projects through the assessment of the environmental and economic impacts of construction moulds in bridge projects.This will be achieved by investigating whether there is waste associated with the GRP shutter moulds used in the construction of bridge projects, evaluating the environmental and economic impacts of the GRP materials during the manufacturing stage and exploring the perception of industry experts towards standardization of GRP shutter moulds design and the associated possible benefits.

2 Methodology

The research follows a pragmatic philosophy, with an abductive approach and a non-experimental strategy for exploratory purpose. Mixed-methods are used to address the qualitative and quantitative data obtained through interviews and a case study, respectively. The descriptive (qualitative) section includes literature review and interviews with subject matter experts (SMEs) in the field of bridge design and construction within the UAE, while the quantitative section is carried out by compiling a case study of different bridge projects that have been carried out within the UAE in the last 10 years. The interviews follow a non-probability snowballing sampling strategy to reach saturation, where: (i) Sampling population included: SMEs in construction projects in UAE; (ii) Study population: SMEs in bridge projects in UAE; (iii) Target: Minimum of 10 experts; and

(iv) Sampling frame: Mobile and email communication.

2.1 Data Collection

The case study section focused on twelve (12) real bridge projects constructed in 3 emirates (Dubai, Sharjah & Ajman), and consisted of data regarding quantities, sizes (dimensions), weights (in kilograms), and the cost (in Dirham) of the different shutter moulds that were used to construct the bridges (focusing on GRP moulds for heads and columns). Data was gathered to investigate the environmental effect of GRP moulds by calculating the emitted CO_2 gas, the Embodied Energy (EE) needed to produce the GRP moulds, the economic cost of the moulds manufacturing according to the costs obtained from the vendors that carried out the bridge projects, and the demolition cost (including loading, transport, and municipality waste management fees).The duration was specified to target the last 10 years, due to the ease of obtaining relevant documents, and the increased supply of bridge projects in recent years to ease the traffic jam issues resulting from the increased vehicle movements.

Subject Matter Experts (SMEs) were also approached for the participation in interviews. The sample collection followed non-probability convenient sampling approach to reach saturation by targeting project, technical and construction managers, in addition to project or structural engineers and technical consultants, with a specific criterion of having previous experience bridge construction projects and having technical experience of no less than five (5) years. Sampling limitations included time constraints and the specificity of the topic of interest being design and construction of bridge projects. This resulted in obtaining ten (10) SME participants, which satisfied the saturation limit for qualitative non-probability sampling.

The components of the interview were divided into two sections. The first, section included a declaration of consent to participate in the questionnaire, while the second part consisted of sixteen (16) questions related to different aspects of bridge design and construction, including Yes/No questions and descriptive aspect like reasons, factors or possible benefits. Due to difficulty in reaching the participants on site and given their commitments, they agreed to participate in a written format by answering the questions via email correspondence, while providing their personal contact information for further correspondence, if needed.

2.2 Data Analysis

When a product is produced, it requires a certain amount of energy during the manufacturing process, and that energy demand is a necessity throughout all the stages of production. According to Hanania *et al.* (n. d.), this includes raw material extraction, transportation, manufacture, assembly, installation, disassembly, and demolition of that product, which provides an idea of how sustainable this product is by showing how much energy is consumed through the entire life-cycle, which allows for lowering the impact on the environment by choosing products that have lower embodied energy. Simply said, simple materials like wood have lower embodied energy compared to highly processed material or complicated manufacturing processes, and the same applies for materials sourced closer to the homeland compared to those imported and transported from thousands of miles away. Moreover, the embodied energy of any object can be calculated by knowing what type of material is present within the object, the quantity (weight) of that material. Embodied Energy is then measured using "energy per unit mass" scale, such as mega joules per kilogram, according to Hendricks (2014). When it comes to GRP material, it is estimated to have an embodied energy rate of 100 Mega Joule (MJ) per kg of GRP and releases about 8.1 kg of CO_2 per kg of GRP, as stated by (Hammond *et al.*, 2011).

The quantitative portion (case study) had undergone statistical analysis to calculate the parameters indicated in Table 1, including total weight of all GRP moulds used in the bridge projects, the Embedded Energy (EE) consumed during mould manufacturing, Total Emitted CO_2 during manufacturing, and the total cost of manufacturing in AED (as shown in Table 3).Calculations were performed as follows:

$$Weight\ of\ GRP\ Mould\ (kg) \times factor\ (8.10) = X\ kg.\frac{CO2}{kg} of\ GRP\ (CO2\ Emissions) \quad (1)$$

$$Weight\ of\ GRP\ Mould\ (kg) \times factor\ (100) = X\ \frac{MJ}{kg}\ of\ GRP\ (Embodied\ Energy\ of\ EE) \quad (2)$$

$$Weight\ of\ GRP\ Mould\ (kg) \times factor\ (0.4) = X\ Dirhams\ \ (Cost\ of\ Demlition) \quad (3)$$

The data from the qualitative portion of the research (interviews) was analysed using Microsoft Excel to extract the answers of the participants and perform descriptive analysis using graphical representation and calculation of frequencies and percentages of the answers.

3 Results and Discussion

3.1 Bridge Projects Case Study

Based on the data collected (Table 1) the average number of mould designs per bridge project was found to be two (2) with some of the projects using up to three (3) different designs of moulds per bridge, and a quantity of seven (7) moulds (including replicates of the same design to facilitate project delivery). Data also suggested that none of the projects shared the same pier designs, evident by the different dimensions and shapes provided in the project sketches, thus moulds from one project could not be reused in another project. In addition, the collected data (Table 1) showed that

the combined weight of pier shutter moulds from the 12 projects was around 121 tons of GRP (assuming an average of 2 moulds per project multiplied by the average cost of a single mould), with an average of 4.8 tons for a single GRP Pier Shutter Mould and an average of 9.9 tons per project. Moreover, based on the current market, the average cost of a single pier shutter mould was found to be around AED 96,707 and about AED 193,413 for two mould per project, all of which had an average of 39,228 kg of CO_2 during manufacturing of a single GRP mould, and an average of 96,707 Mega joule (MJ) of energy consumed per kg of GRP produced for a single GRP mould.

Table 1: Sum and Average Statistics of 12 Bridge Projects Executed Between the Years 2014-2020 across Different Emirates in the UAE

GRP Shutter Mould Aspect	Weight (kg)	Embodied Energy (MJ per kg of GRP)	CO_2 Emissions (kg of CO_2 per kg of GRP)	Manufacturing Cost (AED)	Demolition Cost (AED) *
Sum	121,075	12,107,500	980,708	2,417,665	48,430
Average per mould	4,843	484,300	39,228	96,707	1,937
Average per project (2 moulds)	9,868	968,600	78,457	193,413	3,874
Note: Values calculated based on 25 GRP moulds used in 12 projects. *: Cost of demolition includes loading, transport, and municipality waste management fees.					

Through examining the case study of the bridge projects, the following points were noticed: (i) there was no standardization of design amongst the dimensions of the piers heads and pier columns shutter moulds, owing to the fact that the dimensions were not uniform (each project had a different design, resulting in new shutter moulds to be built); (ii) some projects required only one shutter mould for the pier head or pier column, which was reasonable, and showed that either there was uniformity in the design, which did not require having more than one type of shutter mould, or that the size of the bridge itself was not very large; and (iii) several projects required multiple types (designs) for the pier head, and also multiple quantities (units) of the same pier head, which was probably due to the size of the bridge and the different shapes incorporated into the design, therefore requiring multiple design. Table 2 below demonstrates such a case:

Table 2: Example of a Single Bridge Project Showing the Potential of Savings in Embodied Energy, CO_2emission and Economic Savings in Case of Standardization of Pier Head Design

Description	Qty of moulds	Weight (Kg)	Embodied Energy (MJ/kg)	CO_2 (Kg.CO_2)	Manufacturing Cost (AED)	Demolition Cost (AED)
Current Scenario (No Standardization):						
Total:	7	24,250	2,425,000	196,425	477,945	9,700
Proposed Scenario (Standardization):						
Total:	3	10,749	1,074,999	87,075	212,235	4,300
Amount of Saving:	**4**	**13,501**	**1,350,001**	**109,350**	**265,710**	**5,400**
Percentage of Savings:	**57%**	**56%**	**56%**	**56%**	**56%**	**56%**

The above estimates of potential savings were based on one project that had seven (7) types of moulds, which were standardized to 3. It is possible to generalize such figures on other bridge projects, however, the potential savings when applying such standardizations on a portfolio level vs.

project level is substantially increased. When the dimensions of bridge elements are standardized across the country, shutter moulds could be reused not only in a specific project, but also across different projects within the country, where mould costs will diminish and contractors would allow for only maintenance cost of those moulds, at which point the potential savings will way surpass those estimated in Table 2. The same was witnessed in precast of houses in UAE, were developers standardized design and created different prototypes to accelerate construction duration and reduce precast mould costs, were in many projects the mould cost becomes almost null when reused to build walls and slabs of hundreds of villas within individual projects.

3.2 Subject Matter Experts (SMEs) Interview

To determine if standardizing the designs of moulds reduces the negative effects on the environment, structured interviews were conducted with ten (10) industry subject matter experts (SMEs) from nine (9) construction companies in the UAE to explore current perspectives as engineering professionals towards designing & constructing bridge projects. Among these experts, the majority held at least 10 years of experience in the bridge construction industry, and included a variety of professionals, such as managers, engineers and a consultant, with 80% of them having previously worked on 1-10 bridge projects.

As shown in Table 3, eighty percent of participants said that typically, there were around two (2) to five (5) types/sizes of bridge piers in one project. Most respondents confirmed that the project or pier design is the main reason for using more than one type of mould in a single project, while the rest stated a variety of reasons like “site restrictions”, “project duration”, “number and size of bearing” and “carriageway width and proposed structure” just to name a few. Majority of the respondents also said that pier moulds contribute to a maximum of ten percent (10%) of project cost. There are several factors that determine the number of moulds required for a project. The respondents said that project duration, shutter mould and project cost, project construction method/work strategy plan, and number/type of piers are the main factors that determine the number of moulds required for a project.

Also, the respondents agreed that GRP is the most commonly used material in making shutters for bridge piers and when asked if they reuse the shutter materials for new projects, only thirty percent (30%) said yes while sixty percent (60%) said they don’t reuse these materials and most responded that the change in pier and architectural designs are the main reasons. Meanwhile, the majority of the respondents that did not reuse materials for new projects could not determine nor had usage for these materials, which more likely becomes waste materials, and when asked what they do with these materials after a project is completed, majority said they dispose of it at waste management point with demolition.

Additionally, experts have been asked if the design of piers can be standardized to maximize the use of shutters between various projects, and the majority of the respondents affirmed that the standardization of design in bridge piers in which they have mentioned that reuse of shutter moulds, material waste reduction, cost savings, and shorter procurement process are among the main benefits of design standardization. The respondents were also asked on their opinion on the single project use of pier shuttering moulds and its contribution to waste and pollution. Majority of the respondents agreed that using the moulds for a single project only contribute to additional waste and pollution. Majority of the respondents also stated that the decrease on project cost and duration as the main benefits of reusing the shutter moulds in future projects.

Table 3: Frequency and Percentage of Participants Responses to Technical Questions in the Interview

No.	Aspect	Frequency*	Percentage	No.	Aspect	Frequency*	Percentage
1	**Number of piers and types ***			**2**	**Cost of moulds in a project**		
	One type / different sizes	3	30%		1-10%	7	70%
	2-5 type / size	8	80%		>10%	1	10%
	>5 types / sizes	1	10%		>1%	2	20%
3	**Reasons for having more than one mould type***			**4**	**Material used in moulds***		
	Project or pier design	3	30%		GRP	8	80%
	Pier type specifications	1	10%		Steel	3	30%
	Number and size of bearing	1	10%		Wood	3	30%
	Orientation of super structure	1	10%		Composite of wood & steel	1	10%
	Carriageway width & structure	1	10%	**6**	**Agreement to reuse moulds**		
	Available space	1	10%		Yes	3	30%
	Site restriction	1	10%				
	Design calculation of bearings	1	10%		No	6	60%
	Project duration	1	10%				
	Bridge width & span length	1	10%		N/A	1	10%
7	**Factors determining number of moulds per project***			**8**	**Reasons for not reusing moulds**		
	Project Duration	3	30%		Different sizes & changes in pier or architectural design	6	76%
	Shutter mould / project cost	4	40%		Pier aging upon multiple usage	1	13%
	Number of piers	2	20%		Use of standard sizes only	1	10%
	Number of type of piers	2	20%		Need for repair / adjustments	1	10%
	Size of piers	1	10%	**9**	**Agreement on reusing moulds as shutters**		
	Manpower	1	10%		Yes	5	50%
	Project Construction Method / Work Strategy Plan	3	30%		No	2	20%
	Storage	1	10%		N/A	3	30%
	Probability of reusing shutter moulds	1	10%	**10**	**Purpose for not reusing moulds as shutters**		
	Effective use of moulds (productivity)	1	10%		Sale as second-hand material	1	10%
	Environment	1	10%		Shutter moulds	1	10%
	Authorities	1	10%		No Usage	2	20%
	Material used in mould	1	10%		N/A	5	50%
11	**Agreement on mould standardization in future**			**12**	**Benefits of moulds standardization***		
	Yes	8	80%		Reuse as shutter moulds / Material waste reduction	7	70%
					Shorter procurement process	1	10%
	N/A	2	20%		N/A	2	20%
					Cost savings	2	20%

13	**Actual Material Treatment upon project completion**			**14**	**Effect of one-time mould usage***		
	Stored with cleaning and maintenance	2	20%		Waste, pollution, harmful chemicals, environmental consequences	9	90%
	Disposal at waste management point with demolition	3	30%		Longer project duration	1	10%
	Sale as second-hand material	1	10%		Additional storage area	1	10%
	Recycled for use	1	10%		Mobilization cost	1	10%
	Re fabrication of non-reusable shutters for new projects	1	10%		Waste of resources and no effective utilization	2	20%
	N/A	2	20%		No effect	1	10%
15	**Benefits of reusing moulds***						
	Decrease project cost / shutter cost					9	90%
	Decrease project duration / shutter delivery time and fabrication / Time utilization for future projects (increase productivity)					10	100%
	Decrease waste					1	10%
	No effect					1	10%

* Frequency is calculated as one OR more than one answer per participant per question (Some participants mentioned more than one answer in selected aspects).

N/A: No Answer.

4 Conclusion

Based on the bridge drawings that were used for this study, most bridge piers did not vary aesthetically across different projects, and the design of these bridges had little to no differences, which is why the standardization of design for bridge pier moulds is a possibility that can be applied in future bridge projects in the UAE. This will not only help reduce the project cost and duration, which is beneficial for the clients, but also decreases the CO_2 emissions and waste pollution that greatly affects our environment. The contribution of this work, the first exploratory study of such a topic performed within UAE would benefit researchers as baseline to establish further research in the area of bridge construction waste.It is worth mentioning that there are some limitations associated with this research, such as that the evaluation of sustainability islimited to bridge piers only, as bridge decks and other elements are not included in the data set and scope within this research. Also, the aassessment is limited to bridges in Dubai and Northern Emirates only, with potential of expansion and inclusion of more bridge projects in different locations in future research.

Further research could be conducted on a comparative analysis of perceptions of stakeholders (i.e., designers, contractors, engineers) towards reducing and recycling bridge construction waste, and the possibility of using Structural Equation Modelling (SEM) and employing a detailed quantitative survey based on the results of this exploratory study to further understand the current perspectives of professional. Case study analysis could be performed to compare various construction and demolition waste management methods employed for the disposal or treatment of bridge projects waste. The economic and environmental effects in terms of the emitted CO_2 as a result of the treatment method, the required energy to treat the waste (and possible savings if reusing was an option), and the cost savings could be further explored. Such savings can be used for new bridge projects to improve the infrastructure of the country. Also, further studies should be conducted with focus on other elements and disciplines of bridge construction, and look for areas where there could be improvement in the processes and systems, and to find more element of bridge construction that

can be standardized in terms of design, all in attempt to reduce cost and duration of bridge construction, which can lead to more bridge and other infrastructure projects having positive economic and environmental impacts in a city or nation.

References

Fitzgerald, Amy et al. (2021). "A Life Cycle Engineering Perspective on Biocomposites as a Solution for a Sustainable Recovery." *Sustainability*, *13*(3).

Hammond, G. et al. (2011, January). *"The Inventory of Carbon and Energy (ICE)" in Embodied Carbon A BSRIA Guide.* University of Bath. https://greenbuildingencyclopaedia.uk/wp-content/uploads/2014/07/Full-BSRIA-ICE-guide.pdf.

Hanania, J., Stenhouse, K., & Doney, J. (n.d.) "Embodied Energy", University of Calgary. https://energyeducation.ca/encyclopedia/Embodied_energy .

Hendricks, C. (2014). *"Green Term Defined: Embodied Energy" in Gains Group Blog*. Gains Group Architects. https://thegainesgroup.com/embodied-energy/ .

Li, Jintao et al. (2022). "Triggering Factors of Construction Waste Reduction Behavior: Evidence from Contractors in Wuhan, China." *Journal of Cleaner Production*, 337, pp. 130396.

Li, Xuemei et al. (2022). "A Systematic Review of Waste Materials in Cement-Based Composites for Construction Applications." *Journal of Building Engineering*, 45, pp. 103447.

Osmani, Mohamed & Pappu, Asokan. (2010). "Utilisation of Glass Reinforced Plastic Waste in Concrete and Cement Composites.", *2nd International Conference on Sustainable Construction Materials and Technologies*, Università Politecnica delle Marche, Ancona, Italy, pp. 1127-1137.

Qi, Tiedong et al. (2020). "Research on Control of Precast Alignment of Short-line Method Precast Segmental Concrete Bridges Based on the Theory of Four-point Distance." *IOP Conference Series: Earth and Environmental Science*, 510.

Qu, Hongya et al. (2018). "Investigation and Verification on Seismic Behavior of Precast Concrete Frame Piers Used in Real Bridge Structures: Experimental and Numerical Study." *Engineering Structures*, 154: 1-9.

Sundaram, S. (2009). "GRP Builds a Future in the Gulf Region", *Reinforced Plastics*, 53, 40-43.

Tandon, Mahesh C. (2019). "Precast Concrete Construction Technologies for Metro Projects in India."

Cite as: Alzaim M.A., Alali M. & Abu-Lebdeh G., "Investigating the Potential for Standardization of Glass Reinforced Polymer (GRP) Shutter Molds Designs in Bridge Projects in the UAE", *The 2nd International Conference on Civil Infrastructure and Construction (CIC 2023)*, Doha, Qatar, 5-8 February 2023, DOI: https://doi.org/10.29117/cic.2023.0040

Digital Transformation Readiness in Infrastructure Project

Nada Wadi
Al Jaber and partners W.L.L, Doha, Qatar
nada.mohd.qa@gmail.com

Juhaina Essa Al-Sulaiti
Public Works Authority (Ashghal), Doha, Qatar
jalsulaiti@ashghal.gov.qa

Zied Dahmani
AECOM, Doha, Qatar
zdahmani@ashghal.gov.qa

Abstract

Digital technologies have brought a new performance momentum in all industries and businesses wherever it has been fully adopted from manufacturing to healthcare and to climate change monitoring. In construction, the digital transformation has been limited to design phases while missing the operations part. It becomes crucial for the world's largest ecosystem to accelerate this digitalization at full scale. In infrastructure projects, digitalization is introduced to the operational level as a ready-made tool that lacks flexibility. This paper describes the barriers to the digital transition in construction operations, combined with the emerging impact of the COVID-19 pandemic from planning and progress monitoring aspects. Adoption of lean construction implementation in infrastructure projects in the State of Qatar, requires adoption for digital tools for data collection, verification, and analysis. This process is continuously improved at the project level to deliver a digital tool that is tailored to the infrastructure projects. This paper describes the initial steps for digital transformation in infrastructure projects in-line with a digital maturity growth.

Keywords: Digital Transformation; Lean Construction; Planning and progress monitoring; Infrastructure project

1 Introduction

Digitization has been facilitated by the fourth industrial revolution Betti *et al*. (2020), which is allowing the use of Internet of Things (IOTs) and automation, and it also supports reduction in the environmental impact (Hasan *et al*., 2018). Eventually, digital change is affecting construction industry, and many new technologies are being developed by experts and implemented on pilot projects. These include Building Information Modelling (BIM), big data, cloud storage, multidimensional design [4D and 5D], automated prefabrication, robotics, 3D printing, artificial intelligence, and intelligent buildings (Sykes, 2018). Nevertheless, the construction sector is still considered as one of the least digitally advanced industries in terms of its adoption and usage of digital solutions and digital workforce engagement (Ribeirinho *et al*., 2020). One of the barriers to implementing automation in the construction industry is the different interpretations of the term construction automation (Chen *et al*., 2018). It tends to be a challenging issue due to the different levels of automation and digitalization during the various project phases. The application of the

digital solutions is a driver of change that helps increase efficiency in most aspects of the construction industry, especially design, construction, and operation phases (Aghimien *et al*., 2018).

Despite its importance, construction phase is least incorporated in digital solutions. Combined with a lean construction practice, developing a platform, which integrates the different modules in the construction phase environment, would be beneficial to manage sites through data collection, and analysis that will affect not only progress monitoring or planning, but also safety, quality, sustainability, and handover. This article will present a combination of lean thinking and digital transformation in infrastructure projects.

2 Lean Construction and Infrastructure Projects

The primary success criterion for any construction project is the completion of the project without cost and time overruns. As traditional project management approach is ineffective in resolving such issues, which may have a root in the organizational processes and historical pattern, a lean construction management is being slowly adopted as a new management technique. The adoption in several countries show enhancement in the project performance and increased likelihood of a project's success. According to Chung & Mutis (2020), lean construction concept processes or measures help minimize non-value adding activities and make sure that the value-adding activities are extensively controlled to increase productivity. Thus, the major intention of lean construction as a concept is to decrease wastage whilst increasing the value of the outputs. This can be done by using the right principles, resources, and measures to deliver things right the first time (Dehdasht *et al*., 2020). Several lean techniques are adopted in infrastructure projects such as continuous improvements, visual management, and collaboration between team members. Contrary to the traditional system, lean ensure reliable workflow and eliminate variation at an early stage of the project.

2.1 Challenges Facing Lean Implementation in Infrastructure Projects

In 2019, Public Work Authority (ASHGHAL) introduced the lean construction philosophy in infrastructure projects in Qatar. Since then, lean concepts, methods, tools, and thinking were implemented with different degrees of maturity and practice. However, some challenges related to understanding, adoption and exercise have emerged among them about the data collection, analysis, and visualization. Traditional methods of data life cycle are still being used by contractors, consultants, and clients. Those methods, such as storing the data on-premises in a local file server are an overburden to users and systems. Lean practice data analysis requires a smoother and more advanced approach on this particular side.

Besides, one of the main practices in lean is the daily huddle, where all engineers and team members gather in the visual performance centre to provide their progress updates, and reasons for non-conformance and assess the next day's plan. COVID-19 enforced a strict work regulation for health and safety. It resulted in stopping the physical gathering for daily huddles that hampered an essential part of lean not just for progress monitoring but also for production loss identification.

Moreover, complexity, ambiguity, and fragmented supply chain in infrastructure projects combined with uncertainty are typical challenges in construction, which requires a digitised lean intervention.

2.2 Digitised Lean Implementation

The imprecise performance of lean implementation within the contractors is rooted in a lack of bespoke requirements of processes and tools to be followed which limits standardization. The

existing lean implementation is not agile enough and requires optimization to have smoother process of data collection, reporting, interpretation, and visualization. Further, unpredictable plans and unreliable commitments, along with inadequate process, impact the lean practice assessment.

A study by Porter & Heppelmann (2015) stated that digitalization is expected to play an increasingly important role in the management and design of global chain supply primarily to companies vigorously involved in value-adding activities, including those involved in production of logistics systems.

The COVID-19 pandemic established an opportunity to consider digital transformation as the strategy to respond to the evolving disruptive environment and reinforce lean implementation through technology.

3 Digitization in Infrastructure

Digitization effect in progress monitoring specifically in infrastructure projects is not widely researched yet and few empirical evidence is found in the literature.

Before adopting digital solutions, contractors must understand the capabilities of each technology and the type of tasks that can be performed. It requires one to assess the strengths and limitations of each solution. The digital solution should process the data and deliver it to end users using personalized and reliable interactive dashboards.

Digital transformation can provide better collaboration, more control of the value chain, and enable more data-driven decision-making. It will make data more accessible and lower the risk of data loss and manipulation. From a lean perspective, the non-value-added communications will be eliminated.

3.1 Pilot Process Assessment Methodology

This study assesses the difficulties the project's current condition is encountering and how the proposed digital solution will effect the project's future state. DMAIC (Define, Measure, Analyse, Improve, and Control) which is the data-driven development method (Kurnia & Hardi, 2021) is used to study the digital change at an organizational level. Each stage of the process has a specific function to play in achieving the best results. This process was created as follows:

1. **Define:** by identifying the challenges facing data collection, reporting, and retrieving.
2. **Measure:** the time needed for data collection, reporting, and interpretation using the conventional method and compare it with the time spent with a simulated version of digitization.
3. **Analyse:** conduct a pilot study and evaluate the opportunities and challenges presented, and the factors that influence implementation.
4. **Improve:** suggest alternatives and recommendations within the experienced module.
5. **Control:** develop a process on how to emphasize certain process and sustain it.

3.2 Pilot Process Workflow

Figure 1 illustrates the process used in infrastructure projects to develop the weekly performance dashboard for monitoring and managing progress.

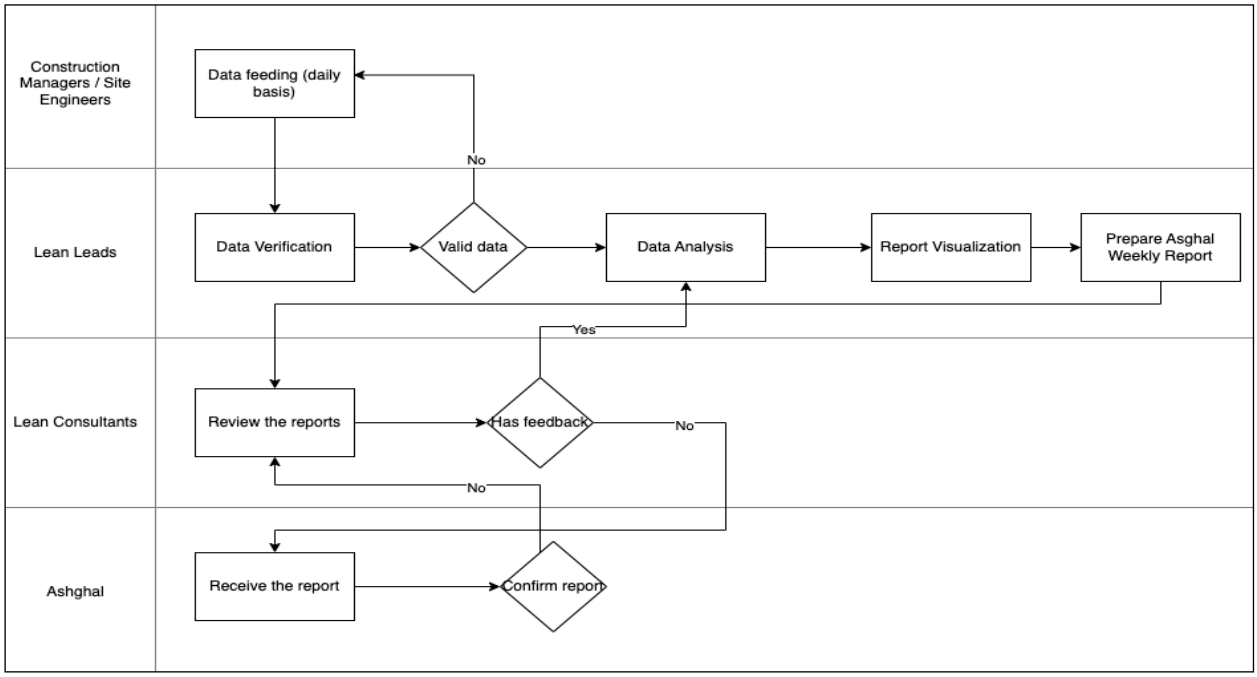


Fig. 1: Process Workflow

The workflow under research aim to enhance the data collection and analysis approach, increase its efficacy and accuracy, and optimize anion-value steps identified.

3.3 Pilot Process Simulation

A simulation pilot is conducted in one infrastructure project to evaluate the effects of digital transformation on productivity by examining the time savings for data collection, organization, documentation, interpretation, and analysis. An alpha version digital solution is developed to shift the daily huddle inputs into a comprehensive sheet with a user-friendly tab. The input process followed the same daily huddle steps for actual quantity update.

Table 1 summarizes a comparison of the findings during the simulation between conventional and pilot processes workflows.

Table 1 : Comparison between Conventional and Pilot Process Workflows

Variable	Conventional workflow	Pilot workflow
Data collection	Almost 2 days were needed for the engineers to provide their planned schedule data in addition to follow-up and reminder time.	Engineers will have the ability to modify progress data to some extent according to restricted rules and time limits emphasized by the system, which enables a more efficient and faster way.
Data reporting	It took the lean leads about 3 hours to review and revise the progress data for additional verification	The demand for repetitive entry of engineer's data will be reduced since the engineer will enter the data himself
Daily update	Updates took almost 30 min along with the daily huddle discussion	Manual update will no longer be needed since engineers update the actual on digital forms and just attend daily huddles
Data visualization	It took more than an hour to create or update the charts needed for progress dashboards	Once the data is entered, an automated visualization chart will be created
Data	Analysing various chart types and the causes	Automatic comparison and insights will be

Analysis	of shortfalls took almost two hours	generated along with the business intelligence tools
Data retrieval	Finding the required update, dashboard or PPC values took at least an hour going through the server	Any insights or data can be retrieved instantaneously with a single click using an interactive platform
Data Accuracy	Data accuracy was about 80 percent	Data accuracy reached 98 percent
Expansion analysis	Limited storage capacity and processing speed are set with no ability to improve	Storage is flexible and the processing time is dynamic and highly optimized

A fundamental change is observed in the progress reporting, monitoring and control mechanism.

Digitization of a basic and simple process showcased the tremendous savings not only in engineers' productivity, but also on the manager decision making approach as more accurate and reliable data is available.

3.4 Digitization Barriers

Resistance toward change, lack of top management commitment, lack of awareness and understanding about the significance and advantages of digitization, and limited financial tolerances are often seen as the barriers to digitization, similar to what is initially experienced in lean implementation. The inherent barrier to any transformation is typically rooted in human and organizational culture.

4 Future of Digitization in Infrastructure Project

Infrastructure projects need to initiate the shift towards a more digitised execution and management approach than being enforced to adapt to new sustainability requirement trends which are digital oriented. Digital transformation impacts productivity, data safety and decision-making approach as well.

A thorough assessment of the organization's culture and technological readiness must be emphasized to ensure the efficient adoption of digital solutions.

Virtual performance centres may be the new norm in construction projects management, that will shape the future of the industry and change the way of working as well as, it will shift the contractors and business owners toward data-driven decision-making.

Further, adopting artificial intelligence (AI) and machine learning to provide a predictive analysis and insights on future status based on current trends, will provide valuable insights for contractors and construction professionals to make better data-driven decisions.

Conclusion

Although technology has been used in the construction industry at different level of maturity, its application to the infrastructure sector is still unclear. Infrastructure projects have used lean construction to overcome the industry obstacles. However, the implementation of the lean concept had significant gaps, which were caused by the uses of traditional methods and lack of standardized process during implementation. This article tested the suggested digital solution pilot's possible effects on infrastructure projects, and the results showed definite advantages. Integrating digital solution in lean construction and other infrastructure modules for progress monitoring and control will reduce waste and increase efficiency of project delivery. However, there will be several obstacles confronting changes. Additionally, the future of digitalization points to a promising future in infrastructure and building, where AI will be essential for reliable insights from forecasted trends and predictions. If Lean implementation is backed up with digitization process, it creates an

infrastructure projects ecosystem with more consolidated, integrated, and standardized processes.

References

Aghimien et al. (2018). Digitalisation in Construction Industry: Construction Professionals' Perspective. In *Proceedings of the Fourth Australasia and South-East Asia Structural Engineering and Construction Conference, Brisbane, Australia*, pp. 3-5.

Betti, Francisco, Enno de Boer, & Yves Giraud. (2020). The Fourth Industrial Revolution and Manufacturing's Great Reset. *McKinsey Global Institute*.

Chen, Qian, Borja García de Soto, & Bryan T. Adey. (2018). Construction Automation: Research Areas, Industry Concerns and Suggestions for Advancement. *Automation in Construction* 94: 22-38.

Chung, Allan, & Ivan Mutis. (2020). Quality Assurance and Quality Control of High-Rise Enclosure Design Using Lean Principles. *Practice Periodical on Structural Design and Construction, 25*(1): 05019008.

Dehdasht, Gholamreza, et al. (2020). A Hybrid Approach Using Entropy and TOPSIS to Select Key Drivers for a Successful and Sustainable Lean Construction Implementation. *PloS one* 15, no. 2: e0228746.

Hasan et al. (2018). Factors Affecting Construction Productivity: A 30 Year Systematic Review. *Engineering, Construction and Architectural Management, 25*(7): 916-937.

Kurnia, Hibarkah & Humiras Hardi. (2021). A Systematic Literature Review of Lean Six Sigma in Various Industries. *Journal of Engineering and Management in Industrial System, 9*(2): 19-30.

Porter, Michael & JamesHeppelmann. (2015). How Smart, Connected Products are Transforming Companies. *Harvard business review, 93*(10): 96-114.

Ribeirinho, M. J. et al. (2020). The Next Normal in Construction McKinsey & Company.

Sykes, C. (2018). Smarter Construction, Stronger Economy, inclusive Society: The European Construction Industry Manifesto for Digitalisation.

Cite as: Wadi N. & Anabtawi M., "Digital Transformation Readiness in Infrastructure Project", *The 2nd International Conference on Civil Infrastructure and Construction (CIC 2023)*, Doha, Qatar, 5-8 February 2023, DOI: https://doi.org/10.29117/cic.2023.0041

Leading Technologies Adoption in Construction Safety Management

Yash Kumar Mittal
Malaviya National Institute of Technology Jaipur, Jaipur, India
yash.arch@mnit.ac.in

Pooja Tripathi
Malaviya National Institute of Technology Jaipur, Jaipur, India
2021rar9008@mnit.ac.in

Abstract

Existing research reveals that by adopting leading technologies in the construction industry, worker's safety could be maximized. Presently, the application of technologies to promote safety in the construction sector is limited. The data for accident cases on the construction sites are very limited. Many tools and techniques have been created to increase worker safety on construction sites by designing and implementing good safety plans. A bibliometric and scientometric approach was used to identify the most prominent technologies in construction safety management. The data was retrieved from WOS database, and the analysis of the study is based on using VOS viewer to visualize the domain-specific knowledge. This study helps in the identification of emerging digital technologies such as Building Information Modelling (BIM), IT applications, Augmented Reality (AR) and Virtual Reality (VR), its application, and barriers in adoption during safety management. This study also highlights critical factors that promote technology adoption in construction safety management. This research also traces the current trends, future directions and supports crucial knowledge on safety technology to construction researchers and practitioners.

Keywords: Construction industry; Technology adoption; Digital technologies; Safety Management

1 Introduction

The construction industry constitutes one of the most hazardous sectors around the world. The incident rates which measure the frequency of illness and injuries, in the construction sector are much higher than in any other industry (Jin *et al.*, 2019). Despite strict health and safety rules, there has been a noticeable increase in the incidence of building accidents. The most frequent causes of injuries and fatalities on construction sites include defective equipment, hazardous workplaces, and unsafe working conditions(Haupt, Akinlolu & Raliile, 2019). Safety planning is more difficult in an unstructured construction environment. Loss of life is the most severe effect of poor safety planning and implementation (Zhang *et al.*, 2013). Traditional safety planning is labour-intensive, time-consuming, and highly ineffective because it frequently relies on manual observations(Guo, Yu & Skitmore, 2017). In light of these, numerous technologies and interventions have been developed to reduce worker accidents and injuries and improve safety on construction sites. Modern technologies help clarify the work process and its applications in the virtual world. As a result of the expanding use of digital technologies in the building industry, researchers have been using BIM (Building Information Modelling), AR (Augmented reality), VR (Virtual reality), IOT (Internet of things), ICT (Information and Communication technologies) to improve safety management, planning and site monitoring in

the recent years (Hu & Zhang, 2011; Skibniewski, 2014; Guo, Yu & Skitmore, 2017; Park, Kim & Cho, 2017).

This review-based study used the science mapping approach by examining journal publications that have been published in the field of construction safety. The goals of this study are to (1) use science mapping to analyse the related journals, keywords, scholars, and articles in the field of construction safety; (2) analyse work on leading technology adoption in construction safety; (3) discuss the shortcomings and applications of the technologies in the construction safety domain and suggest directions for future research in sub-themes within the domain of construction safety.

2 Research Methodology

A bibliometric and scientometric approach was adopted to address the study's objective. The approach consists of a bibliometric analysis followed by scientometric analysis of the literature available on the concerned subject.

2.1 Biblio Metric Analysis

The bibliometric analysis is done using the Web of Science (WOS) database to examine research trends relevant to the use of technology in construction safety management. The search term is entered in the "Advanced search" field: “Construction Site”, “Safety Management”, and “Technology” are all represented by the acronyms “TO”. Without using filters, 292 papers in the years 2010 and 2022 are found. Filters are utilised in order to obtain more pertinent and concentrated literature results published in English. Review papers and articles are reviewed before being eligible for examination. The final list excludes documents containing meeting abstracts, conference proceedings, and editorial content. After applying all the filters, 236 papers related to the use of technology for safety management in the construction industry are found.

2.2 ScientoMetric Analysis

The scientifically retrieved data is mapped using scientometric analysis to identify themes and dynamic data properties, allowing the processing of a wide range of data. Current technology adoption patterns in the construction industry, gaps, key sources, organizations, and authors are studied using VOS viewer. This study performs a scientometric analysis using “mappings based on text data”. The most frequent terms in the title and abstract are then discovered using a “Co-Item Analysis”.

3 Results

3.1 Density of Publications

The yearly publishing history from 2002 to 2023 is depicted in Figure 2. It also demonstrates the yearly publications about the use of technology in construction safety management growing exponentially. The cumulative publications and exponential growth in publishing pattern are also shown and presented in the Figure 2. The graph shows that the number of articles on “Technology adoption in construction safety management” is rising. There has been a noticeable increase in number of publications between 2019 and 2022. Additionally, the deployment of technology is seen as being widely accepted, and there are ample evidences of studies and publications that highlight the need of using technology to manage construction safety.

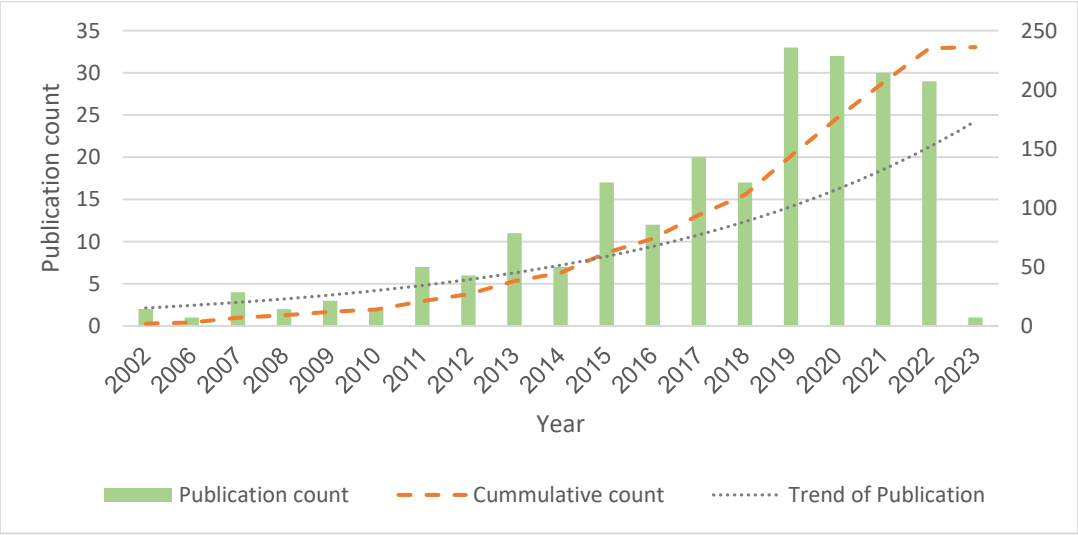


Fig. 1: Trend of Annual Publication

3.2 Most Occurring Keywords

Keyword identification in VOS Viewer is facilitated by choosing the data type and mapping the phrase "Co-Item" based on bibliographic data. The title and abstract fields are explored for words, and full counting is adopted as the counting mode. Out of 299 terms, 39 met the cut-off when the minimum number of occurrences of a term was set at 3. Figure 2 highlights the mapping of the most occurring keywords in the construction safety domain.

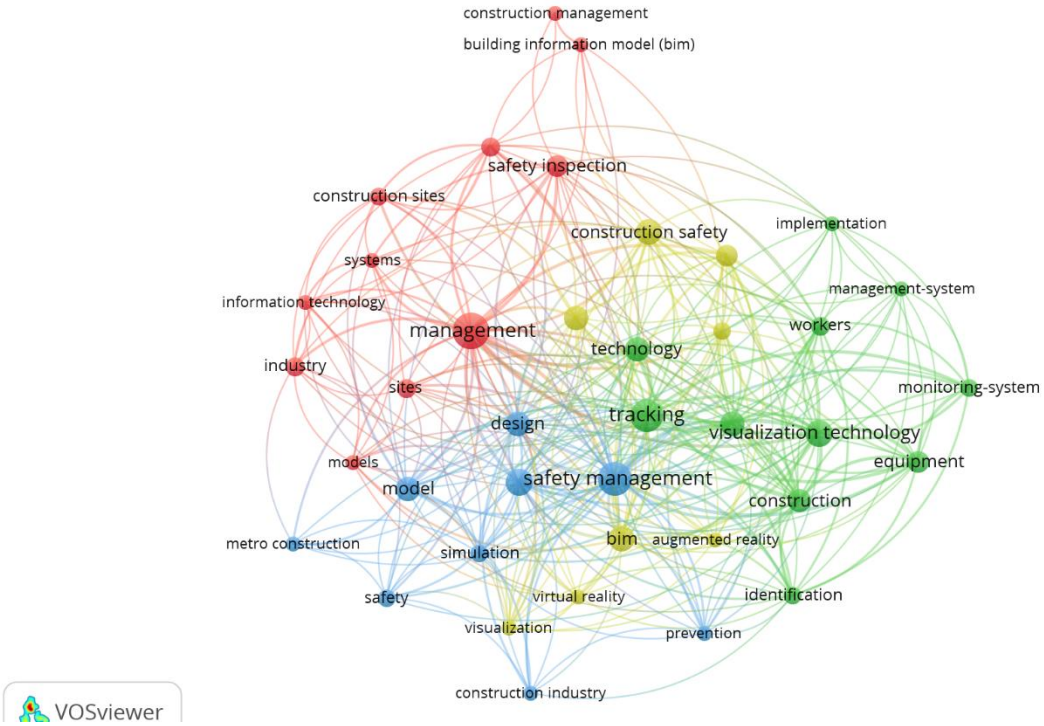


Fig. 2: Most Occurring Keywords

From the VOS viewer analysis, it is identified that Tracking (14), BIM (9), Visualization Technology (10), Augmented Reality (3), Virtual Reality (3), and Information Technology (3) are some mostly occurred keywords related to the construction safety domain. Four different clusters were generated from VOS viewer where blue colour indicates safety management with modelling

and simulations, green colour highlights monitoring of work process and hazards with the help of visualization technology, red colour shows safety management with inspection and information management system, while yellow colour shows different technology adoption in hazards prevention and mitigation.

3.3 Top Journal in Construction Safety Management

Figure 3 displays the top publications where technology adoption in the construction sector is addressed, with "Automation in Construction" receiving the most citations (1077). A table of published documents, citations, overall link strength, and scopus quartile is created based on the relevant journals.

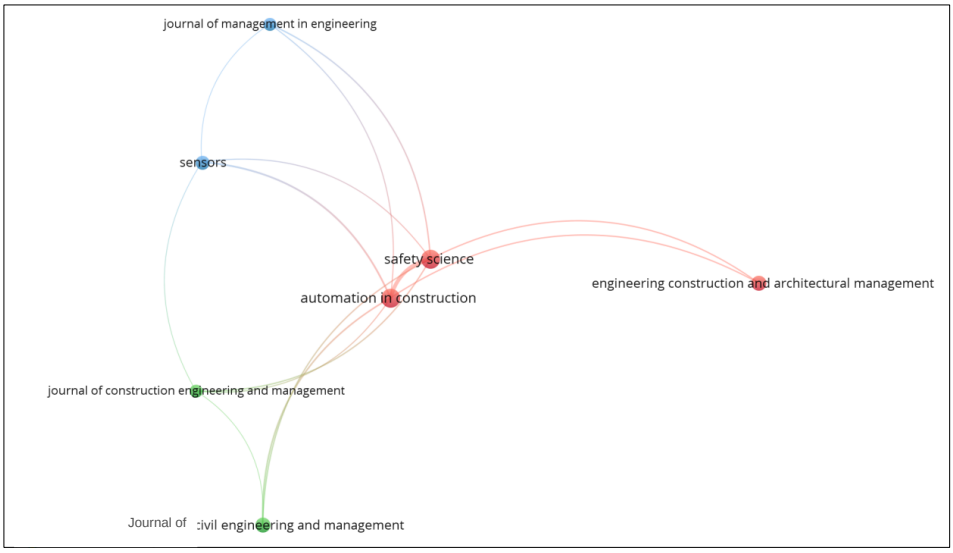


Fig. 3: Most Influential Journal in Construction Safety Management Domain

Table 1 shows that the most of the documents belong to the first and second quartile, indicating that they are the most acknowledged and frequently cited papers in the field of technology adoption in construction safety management. The Total Link Strength (TLS), which is automatically provided by VOS viewer upon mapping the research activity of chosen regions, was used to demonstrate the strength of international research collaboration. The degree of international research collaboration is inversely correlated with the TLS, with a higher TLS value indicating more collaboration (Sweileh, 2020).

Table 1 : Mapping of Journals as per Citation

S. No.	Source	Document	Citation	Total link strength	Quartile
1	Automation in Construction	13	1077	40	Q-1
2	Safety science	12	534	38	Q-1
3	Sensors	3	137	9	Q-2
4	Journal of construction engineering and management	2	137	7	Q-1
5	Engineering construction and architecture management	4	101	6	Q-2
6	Journal of management in engineering	2	18	6	Q-1
7	Journal of civil engineering and management	4	102	8	Q-2

4 Discussion: Digital Technologies and Trends in the Construction Safety Management

Big data, technological innovation, and construction have recently enhanced worker safety on construction sites. The usage of technology continues to receive attention as new technologies are

being developed. Various technologies have been designed to help contractors attain safety on their construction projects. BIM, VR, AR, drones, sensing and warning systems have been highlighted in numerous studies as useful for accident prevention and safe project delivery (Shen & Marks, 2016; Fan *et al.*, 2021; Tian *et al.*, 2021). The following sections provide a detailed examination of these technologies.

4.1 Building Information Modelling (BIM)

A cutting-edge technology in the development of the construction industry, building information modelling (BIM) combines various types of construction information into a 3D digital model. It can be used in all project lifecycle phases, including planning, design, construction, operation, and maintenance (Cheung, Lin & Lin, 2018). The current focus of construction site management systems is primarily on how to apply artificial neural networks, expert systems, and other numerical methods to improve the on-site management of uncertainty or optimize problems of space utilization (Hu & Zhang, 2011).

BIM technology can be used for 'facility maintenance', 'accident investigations', 'worker safety training', 'design for safety', and 'safety planning'. Visual evaluation of construction sites and the detection of potential dangers are made possible by BIM. The creation of safety training movies for site employees to help them better grasp the conditions on the jobsite is made possible by using BIM in construction activities (Akinlolu & Haupt, 2021). Innovative technologies were suggested to pair with BIM to improve its resolution and keep track of construction schedules (Tian *et al.*, 2021).

4.2 Virtual Reality (VR)

VR is an artificial, computer-generated experience of a real-life situation or environment (Haupt, Akinlolu & Raliile, 2019). In the construction demonstrates new ways of working using immersive displays to see, review, and alter virtual projects for all stages of the development cycle when integrated with BIM. Several authors have examined the benefits of using VR for construction safety instruction. VR enables the realistic simulation of many types of construction machinery for learning its operation and instructing employees about operational safety (Serrano, La Rivera & Valero, 2021). The user can enter a simulated construction site with the associated activities using immersive VR technologies. They can help a more efficient evaluation of the building plans, schedules and identify or assess relevant risks by improving real-scale spatial perception (Getuli *et al.*, 2020). VR is one powerful visualization tool used to advance state-of-the-art safety management practices (Park & Kim, 2013).

4.3 Augmented Reality (AR)

In contrast to VR, which simulates real-world situations with computer-generated visuals, augmented reality employs technology to improve reality (Zhao, 2017).It has been identified that the communication between the project team became difficult for safety manager while doing manual inspection with the help of site photos and checklists. By enhancing essential activities with digital content, AR technology can expand the scope of human recognition and reasoning (Park & Kim, 2013). Numerous researchers have investigated AR, creating systems and prototypes to assess its potential to enhance safety levels in construction. The System for Augmented Virtual Environmental Safety (SAVES) is one such system that was introduced to solve the shortcomings of the pre-existing training materials. Incorporating educational and performance-based tasks improves safety training (Shafiq & Afzal, 2020).

4.4 Internet of Things (IOT)

The Internet of Things (IOT) is described as the "interconnection of sensing and actuating devices offering the capacity to share information across platforms through a unified framework, generating a common operating picture for allowing creative applications" (Tang *et al.*, 2019). In collaboration with data transmission tools like Wi-Fi, Bluetooth, and 5G, IOT-related technologies like radio frequency identification (RFID), Unnamed Aerial Vehicles (UAVs), sensors, and laser scanners can be used to create seamless connectivity between physical devices on the construction site (Wang *et al.*, 2022). Researchers have used BIM and O technology to design a construction safety management system of deep foundation pits, as safety is related to accurate location tracking and real-time on-site monitoring (Fan *et al.*, 2021). IOT not only supports the BIM technology that provides safety incident warnings but also facilitates using various sensors to monitor hazardous factors at construction sites. In order to better achieve the integrated functional advantage of IOT technologies and correctly address potential safety hazards, various construction safety systems based on identifying and responding to dangers have been developed (Wang *et al.*, 2022). Figure 3 shows the interaction of the relevant covered technologies.

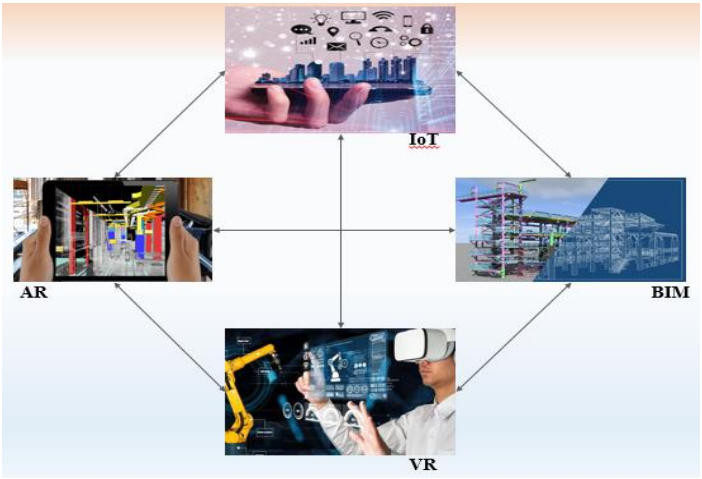


Fig. 4: Interaction of Digital technologies

A review of identified literature justifies that interaction of these technologies is an important decision-making tool. From site monitoring to virtual site planning, all critical decisions can be made possible with the help of technology implementation. Table 2 includes the summary of the existing literature review.

Table 2: Summary of Literature Review

S. No.	Technologies Integration	Application of Technology	Reference	Year
1	BIM and IOT	To improve construction and operational efficiencies by incorporating real time data streams	Tang et al. 2019	2019
2	BIM and VR	Safety training protocol based on BIM- enabled VR activity simulations	Getuli et al. 2020	2020
3	4D BIM	4D BIM tool for construction planning efficiency	Martins et al. 2020	2020
4	AR	Safety training module by AR technologies	Shafiq & Afzal 2020	2020
5	4D BIM	4D BIM simulation to prevent severe injuries and fatalities on building sites caused by spatial-temporal situations	Manzoor et al. 2021	2021

6	BIM and IoT	To improving the safety management efficiency of deep foundation pit construction sites	Fan et al. 2021	2021
7	4D BIM and VR	Effectiveness of (4-D) BIM and VR in simulating job-site safety instructions for a multilingual construction crew at a project	Afzal & Shafiq 2021	2021

5 Barriers in Adopting Digital Technologies

Digital technologies have a huge potential to enhance the efficacy of construction projects during design, construction, and maintenance phases. Despite this, several factors are limiting the advancement of technology adoption in the construction safety management. It was analyzed from numerous studies that there are various barriers in adopting technology for construction safety management purposes (Nnaji & Karakhan, 2020; Yap *et al.*, 2022):

- Costly investment associated with new technology.
- Workers training limitations.
- Lack or no government regulations for the implementation.
- Lack of legislations.
- Lack of decision support tools.
- Incompatibility of technology with current practices and current construction operations.
- Lack of professional knowledge.
- Technology performance concerns.

6 Conclusion

This study has offered a thorough review of earlier works on using technology in construction safety management. The use of different types of technology in construction safety issues, such as site safety education with training, safety communication and site monitoring and control, has been the subject of numerous research studies. A significant increase in innovation has occurred recently across several industries, creating numerous prospects for enhancing operational flexibility, efficiency, and safety. Many researchers have highlighted that the latest technology has more potential to address the issues of construction safety management. Latest technologies like BIM, AR, VR and IOT have significantly improved safety management on construction sites. In contrast to other businesses, the construction sector is slow in adopting technological improvements. Costly investments, lack of skilled staff and undefined government regulations are some significant barriers to adopting digital technologies. The study is limited to assessment of the safety management scenario in relation to technology implementation at various levels whereas occupational safety behaviors are not covered in the study. The study's findings would guide the construction stakeholders in formulating certain legislative recommendations that might significantly affect the adoption of digital technologies for construction safety management. The future scope of work includes practical implications of integrating technologies with the real-time construction process for managing safety.

References

Akinlolu, M. & Haupt, T. C. (2021). 'Effectiveness of BIM-based Visualization Technologies for Construction Site Health and Safety Management: A Meta-synthesis Approach', *IOP Conference Series: Materials Science and Engineering*, *1107*(1), p. 012176. doi: 10.1088/1757-899x/1107/1/012176.

Cheung, W. F., Lin, T. H. & Lin, Y. C. (2018) 'A Real-time Construction Safety Monitoring System for Hazardous Gas Integrating Wireless Sensor Network and Building Information Modeling Technologies', *Sensors (Switzerland)*, *18*(2). doi: 10.3390/s18020436.

Fan, W. *et al.* (2021). 'Safety Management System Prototype/Framework of Deep Foundation Pit Based on BIM and IoT', *Advances in Civil Engineering*, 2021. doi: 10.1155/2021/5539796.

Getuli, V. *et al.* (2020). 'BIM-based immersive Virtual Reality for construction workspace planning: A safety-oriented approach', *Automation in Construction*, *114*(February), p. 103160. doi: 10.1016/j.autcon.2020.103160.

Guo, H., Yu, Y. & Skitmore, M. (2017). 'Visualization Technology-based Construction Safety Management: A Review', *Automation in Construction*, *73*, pp. 135–144. doi: 10.1016/j.autcon.2016.10.004.

Haupt, T. C., Akinlolu, M. & Raliile, M. T. (2019). 'Emerging Technologies in Construction Safety and Health Management Management', in *International Conference on Innovation, Technology, Enterprise and Entrepreneurship*, pp. 413–420.

Hu, Z. & Zhang, J. (2011). 'BIM and 4D-based Integrated Solution of Analysis and Management for Conflicts and Structural Safety Problems During Construction: 2. Development and Site Trials', *Automation in Construction*, *20*(2), pp. 155–166. doi: 10.1016/j.autcon.2010.09.013.

Jin, R. *et al.* (2019). 'A Science Mapping Approach-based Review of Construction Safety Research', *Safety Science*, 113 (November 2018), pp. 285–297. doi: 10.1016/j.ssci.2018.12.006.

Mora-Serrano, J., Muñoz-La Rivera, F. & Valero, I. (2021). 'Factors for the Automation of the Creation of Virtual Reality Experiences to Raise Awareness of Occupational Hazards on Construction Sites', *Electronics (Switzerland)*, *10*(11). doi: 10.3390/electronics10111355.

Nnaji, C. & Karakhan, A. A. (2020). 'Technologies for Safety and Health Management in Construction: Current Use, Implementation Benefits and Limitations, and Adoption Barriers', *Journal of Building Engineering*, 29, p. 101212. doi: 10.1016/j.jobe.2020.101212.

Park, C. S. & Kim, H. J. (2013). 'A Framework for Construction Safety Management and Visualization System', *Automation in Construction*, 33, pp. 95–103. doi: 10.1016/j.autcon.2012.09.012.

Park, J., Kim, K. and Cho, Y. K. (2017) 'Framework of Automated Construction-Safety Monitoring Using Cloud-Enabled BIM and BLE Mobile Tracking Sensors', *Journal of Construction Engineering and Management*, 143(2), pp. 1–12. doi: 10.1061/(asce)co.1943-7862.0001223.

Shafiq, M. T. & Afzal, M. (2020) 'Potential of Virtual Design Construction Technologies to Improve Job-site Safety in Gulf Corporation Council', *Sustainability (Switzerland)*, *12*(9). doi: 10.3390/su12093826.

Shen, X. & Marks, E. (2016) 'Near-Miss Information Visualization Tool in BIM for Construction Safety', *Journal of Construction Engineering and Management*, *142*(4), p. 04015100. doi: 10.1061/(asce)co.1943-7862.0001100.

Skibniewski, M. J. (2014) 'Information Technology Applications in Construction Safety Assurance', *Journal of Civil Engineering and Management*, *20*(6), pp. 778–794. doi: 10.3846/13923730.2014.987693.

Sweileh, W. M. (2020). 'Bibliometric Analysis of Peer-Reviewed Literature on Climate Change and Human Health with an Emphasis on Infectious Diseases', *Globalization and Health*, *16*(1), pp. 1–17. doi: 10.1186/s12992-020-00576-1.

Tang, S. *et al.* (2019) 'A Review of Building Information Modeling (Bim) and the Internet of Things (Iot) Devices Integration: Present Status and Future Trends', *Automation in Construction*, 101(January), pp. 127–139. doi: 10.1016/j.autcon.2019.01.020.

Tian, J. *et al.* (2021). 'Crane Lifting Optimization and Construction Monitoring in Steel Bridge Construction Project Based on BIM and UAV', *Advances in Civil Engineering*, 2021. doi: 10.1155/2021/5512229.

Wang, X. *et al.* (2022). 'Development of an Internet-of-Things-Based Technology System for Construction Safety Hazard Prevention', *Journal of Management in Engineering*, *38*(3), pp. 1–16. doi: 10.1061/(asce)me.1943-5479.0001035.

Yap, J. *et al.* (2022). 'Barriers to the Adoption of New Safety Technologies in Construction: A Developing Country Context', *Journal of Civil Engineering and Management*, *28*(2), pp. 120–133.

Zhang, S. *et al.* (2013). 'Building Information Modeling (BIM) and Safety: Automatic Safety Checking of Construction Models and Schedules', *Automation in Construction*, 29, pp. 183–195. doi: 10.1016/j.autcon.2012.05.006.

Zhao, X. (2017). 'A Scientometric Review of Global Bim Research: Analysis and Visualization', *Automation in Construction*, 80 (February), pp. 37–47. doi: 10.1016/j.autcon.2017.04.002.

Cite as: Mittal Y.K.Y. & Tripathi P., "Leading Technologies Adoption in Construction Safety Management", *The 2nd International Conference on Civil Infrastructure and Construction (CIC 2023)*, Doha, Qatar, 5-8 February 2023, DOI: https://doi.org/10.29117/cic.2023.0042

Blockchain Technology Adoption in the State of Qatar: Qualitative Risk Analysis

Awad Alomari
AECOM, Roads Department, Public Works Authority (Ashghal) & PhD student at College of Engineering, Qatar Unversity, Doha, Qatar
aomari@ashghal.gov.qa

Noora Fetais
Department of Computer Science and Engineering, College of Engineering, Qatar University, Doha, Qatar
n.almarri@qu.edu.qa

Abstract

Businesses may gain from implementing Blockchain-based technology in terms of profitability, productivity, and efficiency, which may cause them to re-evaluate their current business strategies. However, because the technology is still evolving and there needs to be more study on the effects of the various Blockchain networks (such as public, private, and consortium), their significance in developing new business models needs more consideration. In this article, we identified the potential risks/opportunities associated with Blockchain adoption in the state of Qatar through the standard technique of Qualitative Risk Analysis suggested by the Project Management Institution (PMI) using a standard (5 x 5) probability impact diagram (PID) with seven areas of impact namely Cost/Budget, Schedule, Quality, Customer Satisfaction, Business Continuity or Service Disruption, Governance & Compliance, and Environment. We found that circa 84% (i.e. 10 risks) of the most significant risks are related to the organisational and environmental risks, while only 16% (2 risks) are related to the technology itself. Our research highlights the benefits of Blockchain advancements to decision-makers for strategic planning.

Keywords: Blockchain Adoption; Blockchain barriers; Qualitative Risk Analysis

1 Introduction

Blockchain technology, which has recently emerged, has been praised as the next revolution that will change the structure and scope of organizations and the way economic transactions are carried out . However, beyond the primary technological focus of the majority of current work, adopting - Blockchain technologies necessitates taking a wide variety of issues into account(Janssen et al., 2020a).

Qatar is one of the countries that show intent on blockchain adoption. The Regulatory Communications Authority announced the “Qatar National Blockchain Blueprint” (QNBB) in April 2022. Moreover, the QNBB was created by the Communications Regulatory Authority (CRA) in collaboration with Hamad Bin Khalifa University and Qatar University (QU). It made its debut as a national consultation document that the CRA released. QU has gone above and beyond by announcing its venture into the Metaverse, a system firmly rooted in Blockchain technology(AIBC, 2022).

In Blockchain, Each transactionmay be confirmed by the entire network, which can be either public, private, or a consortium, and is based on advanced cryptography and mathematics(Schlecht et al., 2021a); it’s a distributed ledger in which all participants share ownership over transaction data rather

than just one(Schlecht et al., 2021a).

In the following sections, we will critically review four previous studies that addressed the problem of blockchain adoption and identify the potential risks/opportunities related to adoption in the State of Qatar.

2 Literature Review

Blockchain is an electronic distributed ledger that holds a list of constantly expanding data verified by every/or assigned network nodes. It includes a history of the network's transactions and a complete list of all of them. Because blockchain is decentralised, there is no longer a requirement for a third party, and all network nodes can see the records. As a result, building a transparent blockchain takes much more work than building centralised ledgers. To maintain security and privacy with these ledgers, you must work hard and include third parties. This idea was presented on a white paper that launched the first crypto currency, bitcoin, and focused on a decentralised cash flow mechanism (Nakamoto, 2008). Its remarkable characteristics of blockchain to have stimulated the creation of more than 1600 crypto currencies (Arooj et al., 2022).

Since then, this subject has instigated researchers to explore the potential of this technology. The recent available literature on the adoption of blockchain technology placed a strong emphasis on its technical aspects [5, 6], while organizational adoption requires a much more comprehensive perspective (Janssen et al., 2020b). Thus, they offered a theoretical paradigm for Blockchain technology adoption that would capture the intricate interactions between institutional, market, and technological issues. Hence, to determine the critical elements around blockchain technology, the writers first researched the literature on existing organisations and technology adoption. This analysis uncovered various factors that organizations needs to consider and expressed concerns about how to manage best to adopt this disruptive technology. These factors were divided based on the institutional framework proposed by (Koppenjan & Groenewegen, 2005) into the institutional, market, and technological aspects. However, the said article has a limitation related to the study period (2015-2018), where significant development in blockchain technology has taken place in last three years.

Qatar is one of the countries that show intent on blockchain adoption. Where the Regulatory Communications Authority has announced the “Qatar National Blockchain Blueprint” (QNBB) by April, 2022. The QNBB was created by the Communications Regulatory Authority (CRA) in collaboration with Hamad Bin Khalifa University and Qatar University (QU), and it made its debut as a national consultation document that the CRA released A. QU has gone above and beyond by announcing its own venture into the Metaverse, a system firmly rooted in Blockchain technology(AIBC, 2022).

The generalisation of much-published research on this topic needs to be revised. Hence, we set by this study, the building block for the decision makers/executives in the State of Qatar related to the adoption of this technology by answering the following questions:

Q1: What are the risks/opportunities associated with Blockchain adoption?

Q2: How can we prioritise those identified risks/opportunities?

Moreover, we proposed the agenda for future research studies.

3 Research Methodology

The Qualitative Risk Analysis (QRA) technique, as per PMI best practices in risk management, as adopted. Risk Management is an integral part of Enterprise Portfolio Management. The purpose of

Risk Management is to enable organisations to succeed in delivering business objectives by adopting a systematic approach to the identification, assessment and management of uncertain events, which may impact the business value.

The Qualitative Risk Analysis (QRA) technique allows risks to be ranked using a single-point estimate for Probability and Impact. This technique will enable the organisation's pre-determined scoring scheme and will also allow organizations in the early stages of strategic planning to rank and prioritise their risks/priorities.

3.1 Risk Identification

In this study, we have identified the risks related to blockchain adoption through a structured literature review of the reported risks/barriers and opportunities to blockchain adoption, where we concluded that the study carried out by (Kouhizadeh et al., 2021)had addressed the most published risks related to blockchain adoption in addition to other few risks identified on Table 1 below:

Table 1: Identified Risks/Opportunities Related to Blockchain Adoption as Cited from the Literature

Risk ID	Risk Type	Risk Title	Reference	Description	Risk Category
O01	Opportunity	high traceability	(Biswas & Gupta, 2019a; Munim et al., 2022)	The lack of traceability limits consumers' capacity to judge the quality of the products they buy and prevents them from tracking their purchases throughout the entire delivery process. Hence, customers' trust is positively proportional to the degree of traceability.	Technological
R01	Risk	Security challenge	(Biswas & Gupta, 2019a; Sayogo et al., 2015; W. Wang et al., 2019; Yli-Huumo et al., 2016)	There are worries that data and information may be vulnerable to security issues like hacking, the spread of false information, and access to sensitive data.	Technological
R02	Risk	Access to technology		For the adoption of blockchain, the internet and IT infrastructure are crucial resources. Sometimes an organization's IT infrastructure is inadequate or technological access is impractical.	Technological
R03	Risk	The negative perception oftechnology		People could primarily connect cryptocurrencies like Bitcoin and blockchain technology. These advances could be seen as malicious behavior. Organizations may therefore be reluctant to use blockchain technology in general.	Technological
R04	Risk	Immutability challenge of blockchain technology	(Biswas & Gupta, 2019b)	According to the idea of immutability, records cannot be removed from ledgers. However, the history of an incorrect record that was added to the blockchain will always be there if it can be updated with new information.	Technological
R05	Risk	Immaturity of technology	(Biswas & Gupta, 2019b)	One technological problem resulting from blockchain's infancy is the difficulty scaling the technology. Blockchain technology would struggle to handle a high volume of transactions. Additionally, storing blocks that are getting larger is a concern because it runs into massive real-world data (the "bloat" problem in Bitcoin).	Technological
R06	Risk	Garbage-in_Garbage-Out related	(Powell et al., 2022)	Blockchain applications in food supply chains do not solve conventional IoT data quality issues. Data on a blockchain may be immutable garbage.	Technological

Risk ID	Risk Type	Risk Title	Reference	Description	Risk Category
		to data integrity			
O02	Opportunity	Increase in information security	(Munim et al., 2022)	Proof of work and proof of stake are examples of blockchain consensus protocols which are widely used.	Technological
R07	Risk	Lack of Tools for Blockchain Technology Implementation	(Munim et al., 2022)	Due to the lack of hardware and software tools within an organization to use the technology along with the maintenance, it could be expensive to invest in the companies.	Technological
R08	Risk	Increase in prices	(Biswas & Gupta, 2019a)	Additional implementation costs, in addition to environmental costs and training costs	Orgnizational
R09	Risk	Lack of Expertise about Technology	(Munim et al., 2022)	lack of skills to use the technology and a thorough understanding of itis largely stopping the growth of an organization.	Organizational
R010	Risk	Financial constraints	(Biswas & Gupta, 2019a; A. Hughes et al., 2019; Sayogo et al., 2015)	Due to supply chain information collecting and system conversion; organizations incur costs. Adopting sustainable techniques can also be expensive. The financial resources available to organizations to use this technology are limited.	Organizational
R011	Risk	Lack of management commitment and support	(Mangla et al., 2017; Y. Wang et al., 2019)	Some managers do not utilize disruptive technology and supply chain management (SCM) procedures to support sustainable practices over the long term.	Organizational
R012	Risk	Lack of new organizational policies for using blockchain technology	(Mendling et al., 2018; Y. Wang et al., 2019)	A successful implementation of blockchain technology by organizations can be achieved if new policies have been established (for example, where and how to use the technology	Organizational
R013	Risk	Lack of knowledge and expertise	(Angelis & Ribeiro da Silva, 2019; Kamble et al., 2021a; Sayogo et al., 2015)	Lack of technical know-how and understanding of sustainable supply networks and blockchain technology.	Organizational
R014	Risk	Difficulty in changing organizational culture	(Mangla et al., 2017; Mendling et al., 2018)	The adoption of blockchain technology alters or affects the culture of the firm. Organizational culture includes norms for workplace behavior and an appropriate code of conduct.	Organizational
R015	Risk	Hesitation to convert to new systems	(Angelis & Ribeiro da Silva, 2019; Govindan et al., 2014; Schlecht et al., 2021b)	Legacy systems would need to be modified or replaced in order to adopt new systems. Organizations and companies may object and hesitate torespond to this change.	Organizational
R016	Risk	Lack of tools for	(Andoni et al., 2019;	Lack of standards, proper procedures, tools, and criteria for using blockchain technology and	Organizational

Risk ID	Risk Type	Risk Title	Reference	Description	Risk Category
		blockchain technology implementation in sustainable supply chains	Govindan et al., 2014; Mangla et al., 2017; Morkunas et al., 2019)	assessing organizational sustainability performance.	
R017	Risk	high energy consumption	(Biswas & Gupta, 2019b)	Blockchain consumes a considerable amount of energy, aggravating the problem of global warming. In fact, despite the fact that blockchain engineers are constantly looking for greener solutions, the status of the technology now makes blockchain unsustainable.	Environmental
R018	Risk	Lack of customers' awareness and tendency about sustainability and blockchain technology	(Chkanikova & Mont, 2015; L. Hughes et al., 2019; Mangla et al., 2017)	Lack of customer understanding of supply chain sustainability techniques using blockchain technology	Environmental context (Supply chain view)
R019	Risk	Problems in collaboration, communication and coordination in the supply chain	(Chen et al., 2022; Janssen et al., 2020b; Kamble et al., 2021b; Kshetri, 2018; Y. Wang et al., 2019)	Lack of cooperation, coordination, and communication among supply chain participants who have various and occasionally incompatible operational motives, aims, and priorities; additional barriers to cooperation	Environmental context (Supply chain view)
R020	Risk	Challenge of information disclosure policy between partners in the supply chain	(L. Hughes et al., 2019; Y. Wang et al., 2019)	Participants in a supply chain may have varied privacy requirements and rules regarding the information and data utilized in blockchain technology and sustainable supply networks. Data's economic worth, confidentiality, and privacy may need to be revised to avoid problematic issues.	Environmental context (Supply chain view)
R021	Risk	Challenges in integrating sustainable practices and blockchain technology through SCM	(Govindan et al., 2014; Luthra et al., 2016; Morkunas et al., 2019)	Combining traditional supply chain procedures with sustainability strategies and blockchain is complex. Additionally, the development of technology, materials, and processes is required to enable sustainable practices. In order to connect to the internet of things or collect data from it for blockchain technology and sustainability, for instance, facilities and machinery need to be updated.	Environmental context (Supply chain view)
R022	Risk	Cultural differences of supply chain partners	(Mengelkamp et al., 2018; Y. Wang et al., 2019)	Different organizational or geographic cultures of supply chain participants could obstruct the adoption of blockchain technology.	Environmental context (Supply chain view)
R023	Risk	Lack of governmental policies	(Biswas & Gupta, 2019b; Govindan	Governments might be reluctant to direct blockchain technology adoption and sustainable supply chain practices	Environmental Context (External view)

Risk ID	Risk Type	Risk Title	Reference	Description	Risk Category
			et al., 2014; L. Hughes et al., 2019; Mangla et al., 2017; Y. Wang et al., 2019)		
R024	Risk	Market competition and uncertainty	(Biswas & Gupta, 2019b; Mangla et al., 2017; Y. Wang et al., 2019)	It takes time to implement blockchain technology and sustainable practices. It may have an impact on the organization's ability to compete in the market and provide competitive risks. Examples of uncertainty include client behavior, market expectations for sustainable products, and upcoming sales.	Environmental Context (External view)
R025	Risk	Lack of external stakeholders' involvement	(Biswas & Gupta, 2019b; Y. Wang et al., 2019)	The failure of relevant NGOs and communities to embrace blockchain technology and sustainable practices, as well as their competing goals.	Environmental Context (External view)
R026	Risk	Lack of industry involvement in blockchain adoption and ethical and safe practices	(L. Hughes et al., 2019; Luthra et al., 2016)	Lack of industry leadership in sustainability, blockchain technology, and safe and ethical procedures.	Environmental Context (External view)
R027	Risk	Lack of rewards and incentives	(Luthra et al., 2016; Y. Wang et al., 2019)	Lack of reward mechanisms, a problem in promoting sustainable practices and blockchain technology, or a lack of incentives from authorities and professional bodies to encourage these policies.	Environmental Context (External view)

3.2 Risk Assessment

Standard (5 X 5) Probability Impact Diagram (PID) was used, and the impact was assessed against seven potential areas of impact, namely Cost / Budget, Schedule, Quality, Customer Satisfaction, Business Continuity or Service Disruption, Governance & Compliance, and Environment. Then we adopted the Delphi technique for scoring the identified risks by collecting responses from the subject matter experts in the industry (SMEs); we received 5 responses out of 10 sent invitations as per the list below in Table 2:

Table 2: List of Respondents (SMEs).

No	Organization	Role	Yrs of Experience
1	Public Works Authority	Information Systems Department (ISD) Manager	-
2	Public Works Authority	ISD - Enterprise Architect	20
3	KEO International Consultants. Qatar	Risk Manager	23
4	AECOM – Qatar	Risk Manager	23
5	Parsons International - Qatar	Risk Manager	16

4 Results and Discussion

Normality was assumed in the received responses. Hence, the combined risk register was calculated by considering the average of the received responses. Then the risk and opportunities heat map was created as shown on figures 1 and 2 below:

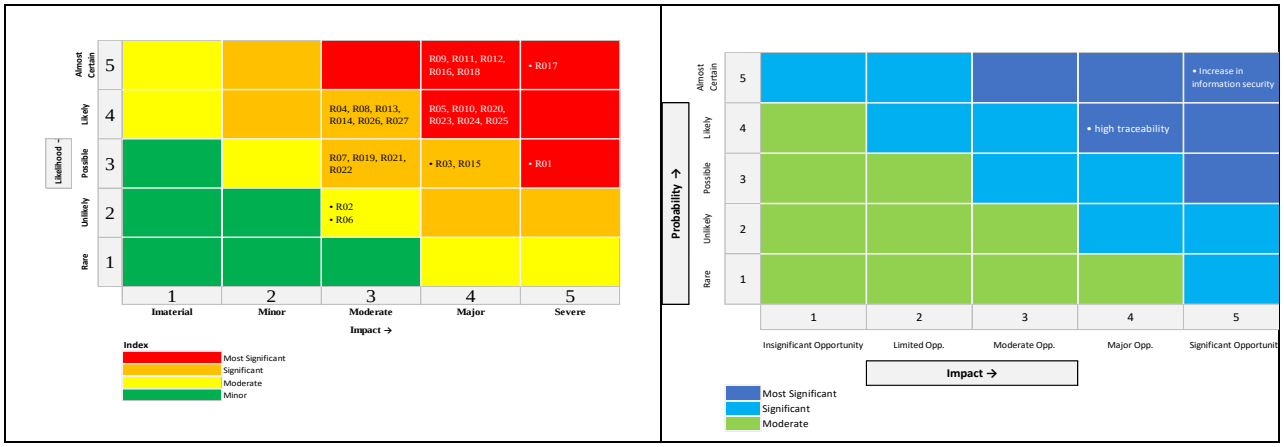


Fig.1: Combined Risks & Opportunities Heat Map

The first question in this study sought to determine the risks, while the second one was to determine the priority of those risks; by reviewing the heat maps mentioned above for risks and opportunities, it is evident that the following risks are the most significant risks related to blockchain adoption:

We found that circa 84% (i.e., 10 risks) of the most significant risks are related to organisational and environmental risks, while only 16% (2 risks) are related to the technology itself. Even the security challenges (Risk ID R01) were suggested by the IT SMEs (i.e. ISD Manager and ISD-Corporate Architect) to consider it as an opportunity with the following note:

"*Blockchain is built on security by design. This can be re-written as an opportunity*" *..ISD-Manager*

5 Conclusion and Future Work

Blockchain is a distributed electronic ledger in which every transaction is recorded publicly and is accessible to all users of the network or nodes. After Satoshi, originally, introduced the idea of a blockchain in 2008, scientists worldwide began to take notice. This new field of study has opened up new avenues for examination, leading to new research fields and resolving of problems in the current blockchain network.

The main purpose of this study was to identify the risks and opportunities associated with the adoption of blockchain in the State of Qatar and prioritize them. Both questions where answered through carrying out a systematic qualitative risk analysis using standard practices of risk management issued by Projects Management Institute (PMI) and the Delphi technique used in data collection from the industry SME. Although the current study is based on a small sample of participants, our findings suggests that the organisational and environmental risks are the most significant risks influencing the effective adoption of this technology in the state of Qatar. These findings will help managers and decision-makers in Qatar through the strategic planning for the adoption of Blockchain. Moreover, it adds to the body of knowledge by distinguishing the local differences associated with this part of the world.

However, this study has limitations related to the size of the sample and the diversity of the sample. Hence, it is recommended to run the study in a more diversified population to include SMEs from different sectors, mainly, Financial sector, Health care, and supply chain sector.

Refernces

AIBC. (2022). *Qatar's National Blockchain strategy*.

Andoni, M., Robu, V., Flynn, D., Abram, S., Geach, D., Jenkins, D., McCallum, P., & Peacock, A. (2019). Blockchain technology in the energy sector: A systematic review of challenges and opportunities. *Renewable and Sustainable Energy Reviews*, *100*, 143–174. https://doi.org/10.1016/j.rser.2018.10.014

Angelis, J., & Ribeiro da Silva, E. (2019). Blockchain adoption: A value driver perspective. *Business Horizons*, *62*(3), 307–314. https://doi.org/10.1016/j.bushor.2018.12.001

Arooj, A., Farooq, M. S., & Umer, T. (2022). Unfolding the blockchain era: Timeline, evolution, types and real-world applications. *Journal of Network and Computer Applications*, *207*, 103511. https://doi.org/10.1016/j.jnca.2022.103511

Biswas, B., & Gupta, R. (2019a). Analysis of barriers to implement blockchain in industry and service sectors. *Computers and Industrial Engineering*, *136*, 225–241. https://doi.org/10.1016/j.cie.2019.07.005

___. (2019b). Analysis of barriers to implement blockchain in industry and service sectors. *Computers and Industrial Engineering*, *136*, 225–241. https://doi.org/10.1016/j.cie.2019.07.005

Chen, R. R., Chen, K., & Ou, C. X. J. (2022). Facilitating interorganizational trust in strategic alliances by leveraging blockchain-based systems: Case studies of two eastern banks. *International Journal of Information Management*. https://doi.org/10.1016/j.ijinfomgt.2022.102521

Chkanikova, O., & Mont, O. (2015). Corporate supply chain responsibility: Drivers and barriers for sustainable food retailing. *Corporate Social Responsibility and Environmental Management*, *22*(2), 65–82. https://doi.org/10.1002/CSR.1316

Govindan, K., Kaliyan, M., Kannan, D., & Haq, A. N. (2014). Barriers analysis for green supply chain management implementation in Indian industries using analytic hierarchy process. *International Journal of Production Economics*, *147*(PART B), 555–568. https://doi.org/10.1016/j.ijpe.2013.08.018

Hughes, A., Park, A., Kietzmann, J., & Archer-Brown, C. (2019). Beyond Bitcoin: What blockchain and distributed ledger technologies mean for firms. *Business Horizons*, *62*(3), 273–281. https://doi.org/10.1016/j.bushor.2019.01.002

Hughes, L., Dwivedi, Y. K., Misra, S. K., Rana, N. P., Raghavan, V., & Akella, V. (2019). Blockchain research, practice and policy: Applications, benefits, limitations, emerging research themes and research agenda. *International Journal of Information Management*, *49*, 114–129. https://doi.org/10.1016/j.ijinfomgt.2019.02.005

Janssen, M., Weerakkody, V., Ismagilova, E., Sivarajah, U., & Irani, Z. (2020a). A framework for analysing blockchain technology adoption: Integrating institutional, market and technical factors. *International Journal of Information Management*, *50*, 302–309. https://doi.org/10.1016/j.ijinfomgt.2019.08.012

___. (2020b). A framework for analysing blockchain technology adoption: Integrating institutional, market and technical factors. *International Journal of Information Management*, *50*, 302–309. https://doi.org/10.1016/j.ijinfomgt.2019.08.012

Kamble, S. S., Gunasekaran, A., Kumar, V., Belhadi, A., & Foropon, C. (2021a). A machine learning based approach for predicting blockchain adoption in supply Chain. *Technological Forecasting and Social Change*, *163*. https://doi.org/10.1016/j.techfore.2020.120465

___. (2021b). A machine learning based approach for predicting blockchain adoption in supply Chain. *Technological Forecasting and Social Change*, *163*. https://doi.org/10.1016/j.techfore.2020.120465

Kouhizadeh, M., Saberi, S., & Sarkis, J. (2021). Blockchain technology and the sustainable supply chain: Theoretically exploring adoption barriers. *International Journal of Production Economics*, *231*. https://doi.org/10.1016/j.ijpe.2020.107831

Kshetri, N. (2018). 1 Blockchain's roles in meeting key supply chain management objectives. *International Journal of Information Management*, *39*, 80–89. https://doi.org/10.1016/j.ijinfomgt.2017.12.005

Luthra, S., Mangla, S. K., Xu, L., & Diabat, A. (2016). Using AHP to evaluate barriers in adopting sustainable consumption and production initiatives in a supply chain. *International Journal of Production Economics*, *181*, 342–349. https://doi.org/10.1016/j.ijpe.2016.04.001

Mangla, S. K., Govindan, K., & Luthra, S. (2017). Prioritizing the barriers to achieve sustainable consumption and production trends in supply chains using fuzzy Analytical Hierarchy Process. *Journal of Cleaner Production*, *151*, 509–525. https://doi.org/10.1016/j.jclepro.2017.02.099

Mendling, J., Weber, I., van der Aalst, W., Brocke, J. vom, Cabanillas, C., Daniel, F., Debois, S., di Ciccio, C., Dumas, M., Dustdar, S., Gal, A., García-Bañuelos, L., Governatori, G., Hull, R., la Rosa, M., Leopold, H., Leymann, F., Recker, J., Reichert, M., … Zhu, L. (2018). Blockchains for business process management - Challenges and opportunities. *ACM Transactions on Management Information Systems*, *9*(1). https://doi.org/10.1145/3183367

Mengelkamp, E., Notheisen, B., Beer, C., Dauer, D., & Weinhardt, C. (2018). A blockchain-based smart grid: towards sustainable local energy markets. *Computer Science - Research and Development*, *33*(1–2), 207–214. https://doi.org/10.1007/S00450-017-0360-9

Morkunas, V. J., Paschen, J., & Boon, E. (2019). How blockchain technologies impact your business model. *Business Horizons*, *62*(3), 295–306. https://doi.org/10.1016/j.bushor.2019.01.009

Munim, Z. H., Balasubramaniyan, S., Kouhizadeh, M., & Ullah Ibne Hossain, N. (2022). Assessing blockchain technology adoption in the Norwegian oil and gas industry using Bayesian Best Worst Method. *Journal of Industrial Information Integration*, *28*. https://doi.org/10.1016/j.jii.2022.100346

Powell, W., Foth, M., Cao, S., & Natanelov, V. (2022). Garbage in garbage out: The precarious link between IoT and blockchain in food supply chains. *Journal of Industrial Information Integration*, *25*. https://doi.org/10.1016/j.jii.2021.100261

Sayogo, D. S., Zhang, J., Luna-Reyes, L., Jarman, H., Tayi, G., Andersen, D. L., Pardo, T. A., & Andersen, D. F. (2015). Challenges and requirements for developing data architecture supporting integration of sustainable supply chains. *Information Technology and Management*, *16*(1), 5–18. https://doi.org/10.1007/s10799-014-0203-3

Schlecht, L., Schneider, S., & Buchwald, A. (2021a). The prospective value creation potential of Blockchain in business models: A delphi study. *Technological Forecasting and Social Change*, *166*. https://doi.org/10.1016/j.techfore.2021.120601

___. (2021b). The prospective value creation potential of Blockchain in business models: A delphi study. *Technological Forecasting and Social Change*, *166*. https://doi.org/10.1016/j.techfore.2021.120601

Wang, W., Zhang, J., Sun, M. te, & Ku, W. S. (2019). A scalable spatial skyline evaluation system utilizing parallel independent region groups. *VLDB Journal*, *28*(1). https://doi.org/10.1007/s00778-018-0519-4

Wang, Y., Singgih, M., Wang, J., & Rit, M. (2019). Making sense of blockchain technology: How will it transform supply chains? *International Journal of Production Economics*, *211*, 221–236. https://doi.org/10.1016/j.ijpe.2019.02.002

Yli-Huumo, J., Ko, D., Choi, S., Park, S., & Smolander, K. (2016). Where is current research on Blockchain technology? - A systematic review. *PLoS ONE*, *11*(10). https://doi.org/10.1371/JOURNAL.PONE.0163477

Cite as: Alomari A. & Fetais N., "Blockchain Technology Adoption in the State of Qatar: Qualitative Risk Analysis", *The 2nd International Conference on Civil Infrastructure and Construction (CIC 2023)*, Doha, Qatar, 5-8 February 2023, DOI: https://doi.org/10.29117/cic.2023.0043

Investigating the Barriers Involved in the Sustainable Implementation of LC and BIM Approaches in Qatar's Construction Industry

Faheem Memon
Heriot – Watt University Scotland, UK
faheemquest@hotmail.com

Abstract

The construction industry has never been as open to welcoming new ideas and strategies from other industries as it is now. Excessive waste in the three pillars of the construction industry, time, cost, and quality, led to adopting certain concepts tried and proven to work successfully in other sectors. Lean is one of such ideas that made its way to the construction industry after years of success in the manufacturing sector. Building Information Modelling (BIM), on the other hand, has been around for quite a while in the construction industry. Imagine how amazing it would be for the construction professionals and designers to live in what is yet to be constructed. BIM made it possible to foresee the future of the project. The question is not how successful these two strategies are, as this has already been proven through numerous studies, but how sustainable would that project be if both Lean and BIM are used concurrently. Qatar construction industry has embraced Lean and BIM concepts and Sustainability measures on its own, owing to a multitude of external and internal factors. Through a mixed-method approach of research strategy, an in-depth review of the literature helped explore the synergies between Lean Construction, BIM and Sustainability. However, the survey questionnaire and interviews led to identifying the two main barriers to implying Lean and BIM in Qatar's construction industry, "Culture and Attitude" and "Commitment & Support from Top Management". The survey results also indicated the interaction of Lean, BIM and Sustainability at different project stages and helped identify misunderstandings about Sustainability among the industry professionals. The proposed performance measurement strategy also received an overwhelming response.

Keywords: Sustainability; BIM; Lean Construction; Barriers; Construction

1 Aim

The aim of this research is to look into the effects of LC and BIM in achieving Sustainability objectives on infrastructure projects in the state of Qatar.

1.1 Objectives

- To investigate the barriers involved in the implementation of LC and BIM in achieving sustainable project delivery.
- To analyse the synergies between LC, BIM and Sustainability.
- To propose the framework for performance measurement of Sustainability with the support of tools like Lean and BIM.

2 Literature Review

2.1 Sustainability and the Emerging Technologies

The construction industry has started realising to change the way of thinking. In the Netherlands, for instance, one cannot build anything unless 20% of the demolished building is utilised in the new building (ICE, 2020).

Large construction companies have started investing in R&D (Research & Development) to come up with innovative technologies to achieve sustainability goals. BIM & LC are two of those technologies that have emerged so quickly (Memon, 2022).

2.2 BIM & LC for Sustainable Design and Construction

2.2.1 Synergies between Lean Principles and BIM to achieve Sustainability Goals

No much work is carried out to report the synergies amid Lean principles and BIM to achieve sustainability objectives on the projects. Moakher & Pimplikar (2012) suggest that the application of BIM in an integrated and collaborative work environment helps achieve sustainability goals like energy efficiency, reduction in operational costs, reduction in water consumption, and improvement in building air quality.

Clash detection is an effective tool that BIM provides, which directly contributes to the Lean goals of waste reduction at an early stage of design. BIM also offers a collaborative tool of 4D planning, which is considered an effective tool in LC. Cost management and Carbon footprint management carried out through auxiliary information system provided by BIM may reduce the waste produced by the environmental issues by early design iterations (Bhargav, *et al*., 2013).

Based on the literature analysis and evidence from various researchers, Rafael et al. (2010) in their matrix of interactions identified fifty-six interactions amid Lean and BIM.

Although, Lean and BIM, both with all their benefits, contribute to sustainable construction individually, however, blend of both is the need of the time (Ritu, *et al*., 2017).

2.2.2 Barriers Involved in the Application of Lean and BIM Practices in Qatar

Eastman *et al*. (2011) classified four challenges that the construction industry is facing to implement BIM standards. These challenges include Collaborative teamwork, legislations, Information communication and Operational issues.

Apart from the challenges as mentioned above, the main barriers to the implementation of the BIM by (Atif, *et al*., 2015) and (NBS, 2018) are availability of skilled staff, availability of training, no client demand.

Other barriers identified by (Saad, 2011) through an extensive study conducted in the UK and with the recommendation to test these barriers globally in different countries are, lack of commitment to change and continuous improvement (Saad, 2011), fragmentation and subcontracting (Saad, 2011), procurement and contracts type (Saad, 2011), culture and attitude (Saad, 2011), adherence to traditional management concepts due to time and commercial pressure (Saad, 2011), financial issues (Bashir, *et al*., 2010) cited in (Saad, 2011), lack of top management commitment and support (Bashir, *et al*., 2010) cited in (Saad, 2011), design/construction dichotomy (M, *et al*., 1998) cited in (Saad, 2011), lack of awareness (Memon, 2022), lack of customer-focused and process-based performance measurement systems (Saad, 2011)

2.2.3 Sustainable Development in Qatar

Sustainability has been considered as a pivotal element of QNV 2030 in terms of Qatar's future development, considering the "needs of the present without compromising the ability of future generations to meet their own needs" (Brundtland, 1987).

Qatar's response to the UN's Sustainability Development Goals (SDGs) is overwhelming. The

formation of the CSD is a significant step of Qatar towards the achievement of SDGs. CSD is currently working on five major areas; food and water security, natural resources governance, renewable energy, waste management, algal technology program (CSD, 2020).

As mentioned in section 2.8, the sustainability rating system GSAS in Qatar only deals with building construction. However, some project-tailored international rating systems like CEEQUAL (International), Green Roads, Envision TM and INVEST are jointly used on Qatar's major infrastructure projects as per QHDM.

3 Analysis of Results & Discussion

The outline and the approaches adopted for this research are illustrated below. Figure below shows the outline of the different steps adopted.

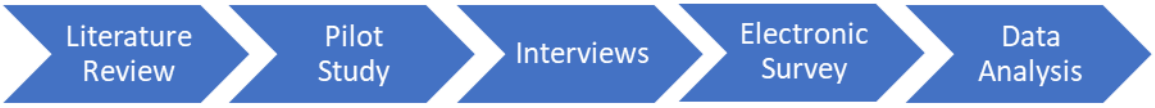


Table 1: Data Collection Source, Type and Nature of the Data and Approaches to Collecting the Data with the Scale of the Sample

Mixed-Method Approach for the research					
	Data Collection	**Nature**	**Data Type**	**Data Collection Approach**	**SampleTarget**
1	In-depth Literature Review	N/A	Secondary	N/A	N/A
2	Pilot Study of Survey Questionnaire	Structured	Primary	Qualitative	10
3	Survey Questionnaire (Google Forms)	Structured	Primary	Quantitative and Qualitative	150
4	Interviews through phone call	Semi-Structured	Primary	Qualitative	3

3.1 Survey Questionnaire

In survey questionnaire to study and analyze the objectives of the paper, the participation constituted of 60% of the post graduate & 8% of PhD scholars with 27% at the managerial level from large scale companies of both private and public sector. Pertaining to a question related to Sustainability, around 67% of the participants agreed that the design on the infrastructure projects follows the international Sustainability standards as mentioned in QHDM (Qatar Highway & Design Manual) which is alarming.

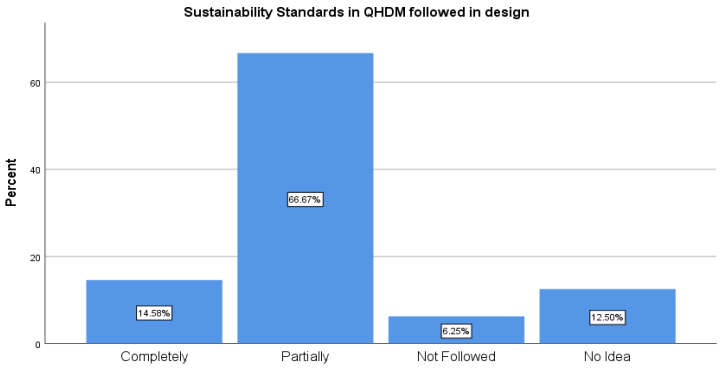


Fig. 1: Sustainability Standards in QHDM followed in Design

Considering, Qatar's construction industry, the Author, shortlisted some barriers for the survey questionnaire to test their impact on sustainable project delivery. Friedman's non-parametric test of ranking was conducted to check these barriers based on the participant's response. The test indicates that the top barrier with the highest mean rank is "Culture and Attitude." "Lack of Top Management Commitment & Support" is second in the ranking. "Lack of Commitment to Change", "Financial Issues", "Lack of Customer Focused and Process-Based Performance Measurement System" and "Adherence to the Traditional Management Concepts Due to Time and Commercial Pressure" can be considered of the same rank due to their mean rank values almost the same.

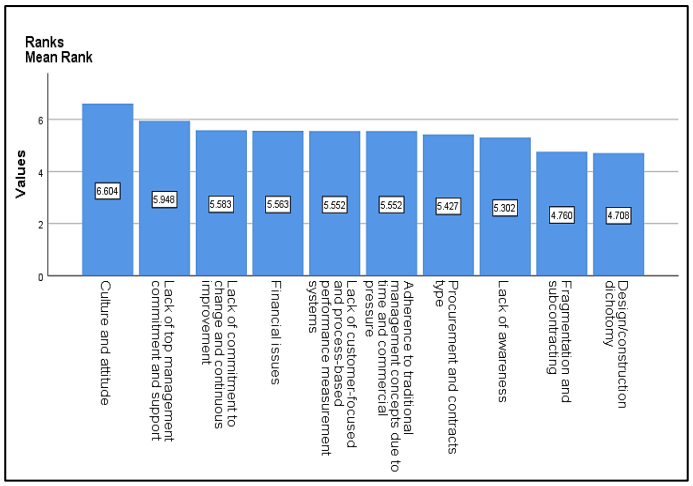


Fig. 2: Ranking of Barriers based on Survey responses through Friedman's non-parametric test of ranking

Descriptive Statistics

	N	Mean	Std. Deviation	Minimum	Maximum
Lack of commitment to change and continuous improvement	48	3.54	1.383	1	5
Fragmentation and subcontracting	48	3.29	1.202	1	5
Procurement and contracts type	48	3.44	1.319	1	5
Culture and attitude	48	3.77	1.403	1	5
Adherence to traditional management concepts due to time and commercial pressure	48	3.56	1.382	1	5
Financial issues	48	3.50	1.353	1	5
Lack of top management commitment and support	48	3.62	1.378	1	5
Design/construction dichotomy	48	3.25	1.158	1	5
Lack of awareness	48	3.44	1.382	1	5
Lack of customer-focused and process-based performance measurement systems	48	3.52	1.353	1	5

Fig. 3: SPSS - Friedman's non-parametric test of ranking

SPSS software was used to analyze the results of the study questionnaire. Approaches used for the analysis of each question are given in the table below:

Table 2: Data Analysis Approaches

Data Analysis Approaches			
Q. No.	**Data Type**	**Statistics Type**	**Approach**
1	N/A	N/A	N/A
2-3	Nominal	Descriptive	Frequency Distribution
4	Ordinal	Descriptive	Frequency Distribution
5-8	Nominal	Descriptive	Frequency Distribution
9	Ordinal	Exploratory	Frequency Distribution
10-12	Nominal	Descriptive	Frequency Distribution
13	Ordinal	Inferential	One Sample t-Test
14	Nominal	Exploratory	Frequency Distribution
15	Ordinal	Descriptive	Frequency Distribution
16-18	Nominal	Descriptive	Frequency Distribution
19	Ordinal	Descriptive	Mean & Mode
20	Ordinal	Inferential	Friedman's non-parametric test of ranking
21	Nominal	Descriptive	Frequency Distribution
22	Ordinal	Descriptive	Central Tendency (Mean, Median, Mode)
23	Nominal	Descriptive	Frequency Distribution
25-26	Ordinal	Descriptive	Frequency Distribution / Mean

Another objective of the study was to analyze the synergies between Lean, BIM and their impact on Sustainability. The literature review shows the different studies where the synergies between these Three aspects have been discussed. However, the participants were asked if the implementation of BIM and Lean construction (LC) help in achieving the following;

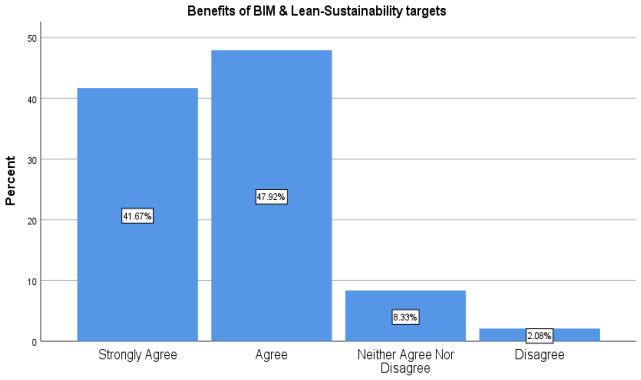


Fig. 4: Benefits of BIM & lean - Sustainability Targets

Sustainability targets, Increased Profit, Increased certainty of cost and schedule, Reduced risks, Competitiveness, Reduction in waste, Improvement in Health & Safety objectives, Improvement in Quality, Reduction in project or process completion time. Around 42% of the participants strongly agreed & 48% agreed that implementation of Lean and BIM combined help in achieving the above targets, which strongly indicates that there are synergies between Lean, BIM and Sustainability.

The author proposed the framework for performance measurement of Sustainability with the support of tools like Lean and BIM in the study and the participants were asked if they agree to a "Compatible re-alignment of the business process" is required for the performance measurement of BIM and Lean practices in line with sustainability objectives on infrastructure projects. Around 48% of the participants strongly agreed and 42% agreed to the proposal. Refer to the contents of the proposal modified by the author to suit the infrastructure projects;

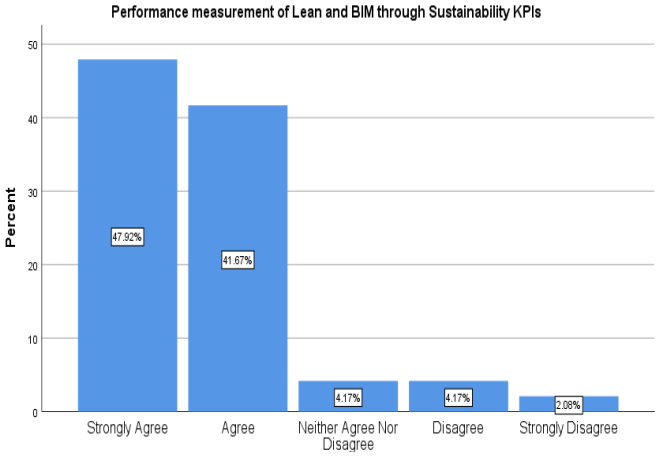


Fig. 5: Performance Measurement of Lean and BIM Through Sustainability KPIs

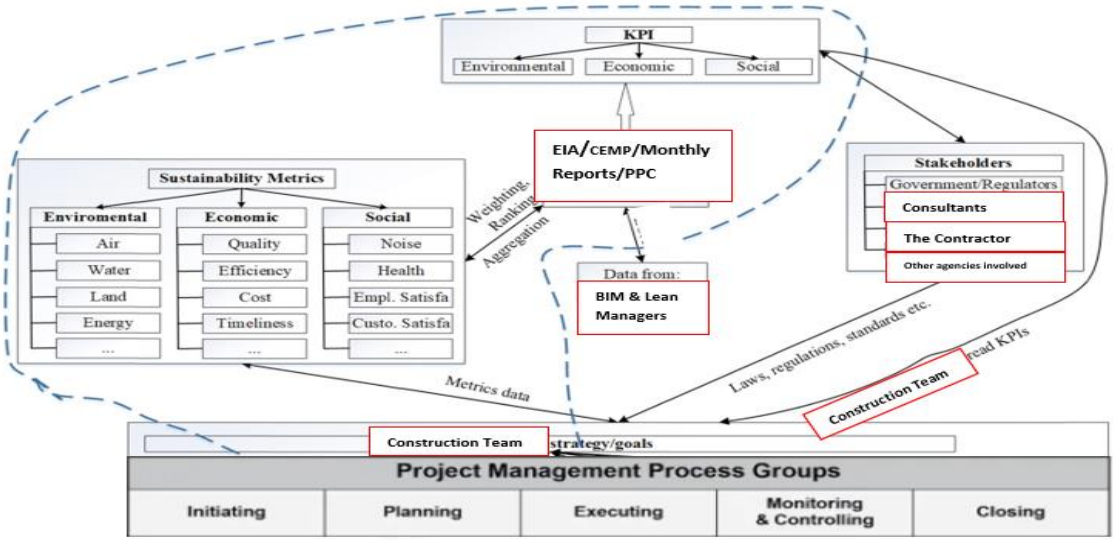


Fig. 6: Ardian, et al. (2018)'s conceptual framework for measuring sustainability performance of Supply Chains Modified by the Author to suit infrastructure projects

4 Conclusion and Recommendations

4.1 Impact of LC and BIM on Sustainable Project Delivery

The main objectives of the study were thoroughly investigated by conducting a thorough review of the literature previously available. However, the available literature is not enough to provide a concrete basis for the combined use of BIM with LC on infrastructure projects to achieve Sustainability objectives. The literature review, survey questionnaire and interviews somehow answered the questions of whether or not LC and BIM have an impact on Sustainability and are there any synergies between these three terminologies or not. A correlation between LC and Sustainability "LC = waste elimination = sustainability" as explained by Claire & BRE (2013, p. 10) is a partial answer to the questions. Nevertheless, a thorough review of various other studies and the survey helped in concluding and updating this synergy with a modified version of it, **"LC+BIM = waste elimination = sustainability."**

4.2 Barriers to the Implementation of LC and BIM for Sustainable Project delivery

Adapting the new innovative solutions to replace the old systems eventually end up with new challenges and barriers. The primary data collected through a survey questionnaire and the interviews helped in understanding the viewpoint of the industry regarding the objectives of this research. One of the objectives of this research was to point out the barriers involved in implementing LC and BIM to achieve Sustainability objectives. The survey results show that "Culture and Attitude" and "Lack of Top Management Commitment & Support" are the top barriers identified, indicating that Qatar's construction industry requires a strategic transformation from traditional project management techniques to new solutions like IPD.

4.3 Performance Measurement

The survey results revealed participants' strong agreement on the proposed modified performance measurement procedure by receiving Lean and BIM practitioners' feedback into the Sustainability KPIs and generating new streamlined KPIs. Figure 5 refers (Ardian, *et al*., 2018)'s conceptual framework for measuring sustainability performance of Supply Chains Modified by the Author to suit infrastructure projects. As mentioned in the previous section, the survey participants welcomed this new proposal by the Author and encouraged to have a system of performance measurement in the current KPI system.

4.4 Other Findings and Recommendations

A very strong opinion came about the need of producing a new rating system along with the legislation system separate for infrastructure projects, which may also consider the impacts of Lean and BIM on project Sustainability objectives. International Sustainability standards mentioned in QHDM are partially followed in design, indicating that the organizations need to be serious towards Sustainability. There is a lack of awareness about LC, BIM and Sustainability among the industry professionals. Specifically, there is a perception that Sustainability is all about the environment and recycling. Aspects of Sustainability from a Social and Economic perspective need to be highlighted or investigated. Further investigation on the case study basis is recommended for investigating the impact of LC and BIM on Sustainability. The questionnaire was distributed equally to Lean, BIM,

Sustainability practitioners and the rest of the industry. Yet, the results show a disproportion of the data gathered as not 100% of the people responded from each category.

More interviews from the industry professionals are recommended to be conducted for any studies in future.

4.5 Limitations of the Research

The Author could have conducted a further secondary analysis, but it was not possible due to the time limit. Further secondary analysis of this subject is highly recommended for future studies. Interviews were conducted from a limited sample due to the limited time frame. The limit of words did not allow the Author to dig down the literature review and conduct further secondary analysis.

References

Alex, O., (2018). Biodiversity and the Built Environment: Implications for the Sustainable Development Goals (SDGs). Resources, *Conservation & Recycling, 141*(February 2019), pp. 1-7.

Bashir et al. (2010). Barriers towards the Sustainable Implementation of Lean Construction. UK: s.n.

Bhargav, D. et al. (2013). Implementing Lean in construction : Lean Construction and BIM C725. London: CIRIA.

Brundtland, G. H. (1987). Our Common Future—Call for Action. *Environmental Conservation, 14*(4), pp. 291-294.

Claire, C. & Bre, C. (2013). Implementing Lean in Construction: Lean and the Sustainability-CIRIA, C726. London: CIRIA.

CSD (2020). Center for Sustainable Development Qatar. [Online] Available at: http://www.qu.edu.qa/research/sustainable-development-center/projects [Accessed 19 November 2020].

Eastman, Paul, T., Rafael, S. & Kathleen, L. (2008). BIM Handbook-A Guide to Building Information Modeling for Owners, Managers, Designers, Engineers, and Contractors. 2nd ed. SI: John Wiley & Sons.

Esam, E. (2018). The Adverse Impact of Non-Engineered Energy Efficiency Standards, Benchmarks and Designs on Buildings' Energy Consumption. Doha, Qatar Green Building.

ICE (2020). UN75-Sustainable Engineering In Action–Institution of Civil Engineers. UK: Pureprint Limited.

Kilani, H., Assaad, S. & Othman, L. (2007). Al-Hima: A way of life. Beirut: IUCN; SPNL.

Koskela, L. et al. (2002). The foundations of Lean Construction.

Atif et al. (2015). BIM Adoption in Qatar: Capturing High Level Requirements for Lifecycle Information Flow. [Online] at: https://www.researchgate.net/publication/282856004_BIM_ADOPTION_IN_QATAR_CAPTURING_HIGH_LEVEL_REQUIREMENTS_FOR_LIFECYCLE_INFORMATION_FLOW [Accessed 20 September 2020].

M, S. T., Seymour, D. & Clark, L. (1998). Obstacles to Implementing Total Quality Management in the Uk Construction Industry. UK: s.n.

Naoum (2007). Dissertation Research and Writing for Construction Students. 2nd ed. OXFORD: Elsevier Ltd.

NBS (2018). Building Information Modelling (BIM): Reports from NBS, National Buildings Specification. [Online] Available at: https://www.thenbs.com/knowledge/the-national-bim-report-2018 [Accessed 06 December 2020].

Rafael, S. et al. (2010). The Interaction of Lean and Building Information Modeling in Construction. *Journal of Construction Engineering and Management, 136*(9), pp. 968-980.

Ritu, A., Anil, S. & Mohammed, A. (2017). Driving Lean and green project outcomes using BIM: A qualitative

comparative analysis. *International Journal of Sustainable Built Environment*, 6, pp. 69–80.

Saad, S. (2011). A Strategy for Overcoming Barriers to the Successful Implementation of Lean Construction in the UK. at: https://www.researchgate.net/publication/275583500_A_Strategy_for_Overcoming_Barriers_to_the_Successful_Implementation_of_Lean_Construction_in_the_UK [Accessed December 2020].

Cite as: Memon F., "Investigating the Barriers Involved in the Sustainable Implementation of LC and BIM Approaches in Qatar's Construction Industry", *The 2nd International Conference on Civil Infrastructure and Construction (CIC 2023)*, Doha, Qatar, 5-8 February 2023, DOI: https://doi.org/10.29117/cic.2023.0044

Medical Facility Management under BIM Paradigm for Hospital Operations Performance in China During COVID-19

Georgios Kapogiannis
Oryx Universal College, Doha, Qatar;
Ningbo (China) Institute of Supply Chain Innovation – Member of MIT Global SCALE Network
georgios.k@oryx.edu.qa

Tianlun Yang
Ningbo (China) Institute of Supply Chain Innovation;
Member of MIT Global SCALE Network, Ningbo, China
tianlun.yang@nisci.edu.cn

Jiequn Guo
Ningbo (China) Institute of Supply Chain Innovation;
Member of MIT Global SCALE Network, Ningbo, China
guojq@nisci.edu.cn

Michael Gerges
University of Wolverhampton, Wolverhampton, United Kingdom
Michael.Gerges@wlv.ac.uk

Abstract

Hospitals operation is becoming a major focusing points on China as there is a huge market because of aging population. The management of healthcare institute is crucial as it contains operational activities that can be harmful to public health such as medical waste as well as medical equipment that has to be maintained timely. In particular with the pandemic COVID-19 situation, the maintenance of the medical equipment is the foundation to ensure the healthcare service can operate functionally. Hence, this research is focusing on how medical facilities are being managed in Chinese healthcare institute as well as to understand whether and how BIM can impact healthcare facility management. A mixed methodology was used to interview facility managers in the province of East China region during COVID-19 period. The result of this research shows that by adopting BIM, the quality and efficiencies of facility management for key hazard assets in hospitals can be improved in principle because of the large amount of asset data and hospitals' information.

Keywords: BIM; Healthcare Management; Operation Management; Facility Management, Integration

1 Introduction

Poor facility management in healthcare institute will cause multiple problems, for example, delay in diagnosis and treatment, which will end up with medical malpractice. Modern healthcare institutes contain large amount of medical facilities, which demand efficient management to ensure the normal operation of healthcare services. Traditional way of managing these facilities has limitations because these facilities require information coordination and data visualization to assist management team to make sufficient decisions. BIM is playing important role not only in design and construction, but also in facilities and assets management stages (Eastman, 2011). ISO-19650 specified in 2018 has defined Assets Information Requirement (AIR) and Assets Information Model (AIM) to regulate how BIM can be implemented to maintain building operation. BIM have board capacities in facility management, e.g., comprehensive visualized management (Wanigarathna et al., 2019) and can improve the productivity in AEC industries (He, Wang & Ying, 2011). With the situation of pandemic COVID-19, the hospital management in China is becoming more strict, all

medical facilities operation are required to follow rigorous rules for public safety purposes.

There needs to be an efficient solution to manage medical facilities, therefore, adopting BIM paradigm for facility management in healthcare institute can potentially increase its operation performance. It has been studied the impact from BIM to facility operation, which shows the earlier intervention of BIM, the more impact it can have to the later facility management (Deutsch, 2011) Implementation of BIM can significantly increase the resource allocation (Elbeltagi, 2014), hence, BIM has potentials to fill the gap in healthcare facilities management. This researchers explored all kinds of medical facilities in healthcare institute, like what their contribution to the hospital operation is, and what things people need to be aware of during its management. Then, the research concludes how BIM intervention can contribute to these operations from information management aspects.

2 BIM and Facility Management in Healthcare

2.1 Medical Facility Classification

Modern healthcare institute in China consists of all set of medical equipment, ranging from emergency to outpatient and inpatient. China has large population, which will cause large number of people seeking medical diagnosis and treatment daily. How to efficiently operate the hospital with modern medical facility is always a concerning issue, despite the fact that many solutions are implemented, there is still space for improvement. There comes a demand as to how these facilities need to be managed under modern techniques. Research shows different facilities need to be listed based on their priority and accessibility (Shehata & Rodrigues, 2018). Also, the facility information needs to be well-organized and managed to ensure the normal operation (Holzer, 2016).

With the above situation and criteria, this research goes into classification of medical facilities, and how the medical facilities can be categorized into fixed assets and portable assets (Table 1). Certain large medical devices have high radiation; therefore, need special insulated space to place them. Small size medical equipment is usually together with the out-patients office in order to have prompt action. A case study in Sutter Medical Centre Castro Valley in the United States proves the added value of BIM and Integrated Product Delivery (IPD) to better patients' experience, hence shorter stay at the hospital (Khemlani, 2009).

Table 1: Classification of Medical Facilities

Fixed Assets	
Medical Treatment Properties	To take the action as medical treatment and medical examination
Non-Medical Treatment Properties	To assist the operation of healthcare service.
Portable Assets	
Emergency Medical Facilities	To take along with ambulance the action of first aid
Non-Emergency Medical Facilities	To assist the medical service both inside hospital and outside hospital.

Another important aspect that we need to be aware of during the healthcare facility management is the medical waste because of the potential hazards. According to the review of relevant medical regulations, medical equipment can be categorized into hazardous and non-hazardous (Table 2). These hazard facilities will potentially cause contamination in both physical and chemical way, which requires strict regulations during the operation to ensure the public safety. The operation of healthcare facilities require data to be properly recorded and archived. Therefore, the intervention of BIM in healthcare can impact information coordination during the asset management.

Table 2: Potential Hazard of Medical Facilities

Potential Hazards	
Physical Hazards	This contains the radiation, noise, light pollution.
Medical Wastes hazards	This contains the medical residues which have a potential to contaminate the surrounding environment.
No potential Hazard	
Heavy Equipment	Large size facilities, which are not easy to remove, and must be installed in one place.
Light Equipment	Portable device, can be carried anywhere both inside and outside the hospitals.

Ensuring efficient patient diagnosis, treatment, and public safety requires good management of healthcare facilities; however, current researches do not contain any relevant study into healthcare justifying additional reasons of BIM integration besides, capital expenditures and operational expenditures. Henceforth, the intervention of BIM paradigm that could organize and visualize this information in a structural way could enable facilities managers to understand holistically the deployment and the properties of the key hazards as part of the facility operations.

2.2 BIM and Medical Facilities Operation

The management of different medical facilities need to consider their difficulties to operate. Due the potential risks, the operation of healthcare facilities requires certain skills, which needs different levels of training. Efficient management of medical facilities provides good treatment qualities, thus will save the life of patient, however the poor facility management will lead to poor treatment due to delay in diagnosis and decision making, and will potentially terminate the life of patient, especially in the emergency situation such as car accident and heart attack. Precedent research has demonstrated that adopting BIM in healthcare system can enhance the information operation coordination, thus can benefit the decision-making progress (Zuo, 2018). The facilities in healthcare institutes require sufficient information coordination to ensure the efficient maintenance, and a previous study shows the use of BIM model can contribute to avoid resource waste and to avoid maintenance mistake (Dixit et al., 2019). Figure 1 shows within BIM paradigm, information coordination in medical facility management can be impacted by data visualization and accessibility, which can impact the hospital operation performance.

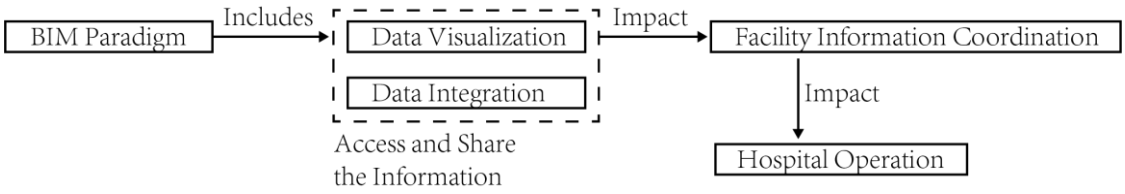


Fig. 1: BIM Impact on Facility Management

The management of medical facility is an important aspect in hospital operation. Implementation of BIM can enhance facility management performance and those relevant detailed methods have been well researched by many scholars (Shehata & Rodrigues, 2018). Precedent researches have shown that BIM enables optimization and faster operation process in facilities management (Fu, 2018). The relation between BIM and facilities management and offered valuable solutions has also been studied to show its feasibility (Hilal, Maqsood & Abdekhodaee, 2019). The outcome of adopting different measurement to investigate facility management have been explored by previous studies, which provides the valuable assessment solutions (Bröchner, 2017). Adopt BIM is a tendency in

Architecture Engineering Construction Operation (AECO) market regardless of time span (Reng, 2018). Talking from these perspectives and considerations, healthcare institute requires efficient resource allocation and management methods to ensure good medical treatment qualities. Regardless BIM having great advantages in managing data and information, its role and impact on healthcare facility management needs to be further investigated.

2.3 Management of Medical Facilities with BIM

In modern Chinese hospitals, national and local standards have regulated how medical equipment in hospitals needs to be operated. Precedent researches have been taken into consideration as to how information system can help the management of hospital, which shows the importance of clear and systematic asset information (Cui et al., 2016). Many high-tech medical equipment in Chinese healthcare institutes are imported, hence, it is quite important to know the daily operation and maintenance. With the intervention of BIM and many state-of-art technologies, e.g., Internet of Things (IoT), Near Field Communication (NFC), and Radio Frequency Identification (RFID), many facilities are becoming easier to manage. Some researchers have explored numerous technologies in AECO industries and have verified their impacts during the practical implementations (Wei et al., 2019) BIM paradigm highlights that these technologies need to be implemented by using appropriate methods and process (ISO, 2018a). In addition, improvement of the energy performance of facility management in Chinese public-funded healthcare institutes through integrating BIM has been validated by precedent researches (Wang et al., 2016).

The management of medical facilities need to comply with relevant criteria, and well-coordinated information that can improve the facility operation performance. Medical facilities are healthcare assets, due to their complexities and large numbers, they demand the intervention of information management in modern hospitals. BIM has strong capability in managing building asset information because the operational performance of building assets relies on the action taken by facilities management team (Fraser, Gunawan, & Goh, 2013). The powerful information integration capability from BIM can help medical team to have better coordination to make efficient decisions. Application of BIM will enable management of the building asset information from life-cycle perspective (Andersen & Findsen, 2019). Adopting BIM can reduce certain risks and avoid fatal error because it has strong visualization capabilities to increase the management performance (Cheng, 2017). Hence, modern Chinese hospitals can improve medical operation from the increased building asset management.

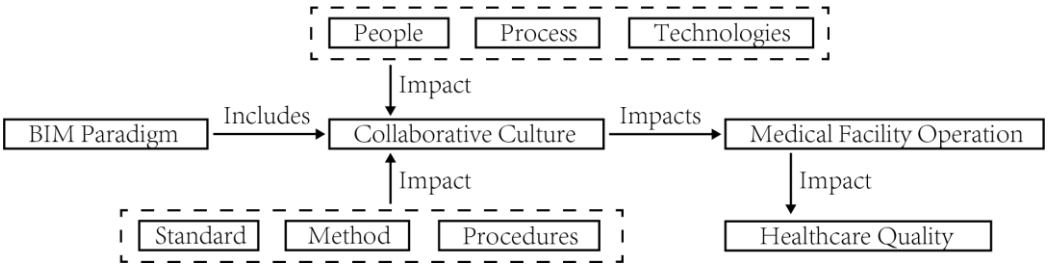


Fig. 2: BIM Impact on Healthcare

Furthermore, the development of a collaboration culture allows better integration of the overall management performance (Kapogiannis, Fernando & Alkhard, 2021). Figure 2 shows the impact from collaborative culture to facility management in healthcare institutes, the collaborative culture is not only impacted by people, process, and technologies, but also by standard method and

procedures. Hence, under BIM paradigm, it is widely accepted for its strength in collaborative management, and its role on information coordination has been well-recognized, therefore, precedent researches are considering BIM as a system that helps to clarify the process and development in AECO industry (Gholizadeh, Esmaeili & Goodrum, 2018), then its role is to support efficiency on hospital building operation and to prevent operational difficulties (Sijtsema, Gluch & Sezer, 2019).Therefore, the discussion of secondary data shows if facilities management in healthcare institutes fully adopt BIM in their medical equipment operation, it should enable a range of benefits that might impact patient experience and an efficient way to manage their resources. Section 3 of this paper has discussed the analysis of primary data to measure the feasibility of taking features of BIM into hospital management.

3 Potential Application of BIM in Healthcare in China

3.1 Research Methodology

The research uses mixed method approach. In total researchers received samples from 9 facility managers from 9 different hospitals in the East China region, therefore, the research is limited in lack of generalization. However, considering COVID -19 phase where the region was in lockdown and had limited access, the research is being considered as a preliminary and feasibility study. From this perspective, structured interviews took place followed by surveys, which were used to learn the opinion of facility managers in relation to the current status of asset management systems in Chinese hospitals, which reviews the potential of BIM integration in China retrospectively.

3.2 Qualitative Data Analysis-Understanding Facilities Managers Perception on BIM Integration

Considering a brief introduction on BIM and its benefits, for the first question in relation why BIM might help facilities management in Chinese hospitals, the word counts from the interview data shows that “Hospital”, “Use”, and “Design” have top frequencies (0.90%, 0.89%, and 0.87%). However, on the question of which factors should be used prior BIM integration, data shows “Think (28 times)” and “Reason (20 times)” have top frequencies. That means that it is mandatory to explore how BIM could be better utilized to understand the reasoning behind (business case) justifying the investment. As part of the reasoning the interviewees highlighted the importance of “Design (57 times)” and “Management (46 times).” These two words reflect BIM having potential in design stage within the hospital operation stages.

According to interview data, healthcare management is categorized into four parts: Finance, Treatment, Logistic, and Procurement. For the healthcare information, it goes into: Patient, Medicine, and Facilities. These functions and information are equally important to make healthcare institute running properly. The interview data shows in current Chinese hospital, there is already an information management solution being implemented, which uses a software named Tute, and its role is to manage the medical and patient information. The potential advantage of BIM is to improve the information coordination in healthcare management because BIM has great advantages in facilities management that can improve medical treatment performance. This happens because of technology inclusion. The major concern of an interviewee toward BIM implementation in healthcare management is focusing on whether this can increase the information coordination compared with current technical solutions.

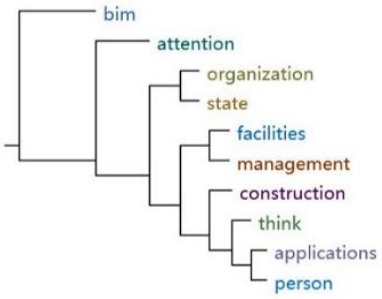


Fig. 3: Macro Perspective

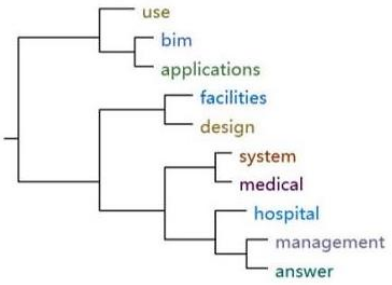


Fig. 4: Medium Perspective

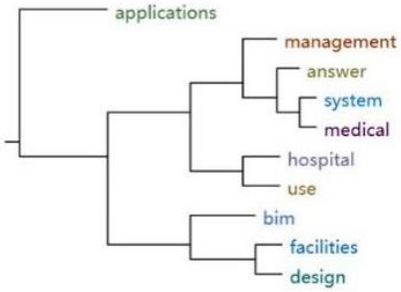


Fig. 5: Micro Perspective

To further explore the interrelations, this research uses NVivo to make clustering analysis from macro to micro perspective (Figure 3 to Figure 5).The macro perspective is focusing on the overall impacts from BIM. Figure 3 shows the role of BIM has the leading position to the entire hospital operation. The entire procedure is driven by people, process and technology under BIM criteria. The medium perspective is focusing on the impact from BIM to medical treatment. Figure 4 shows the role of BIM is assisting facilities management to make the healthcare services, which acts as tools to manage all the relevant information. Figure 5 shows the role of BIM in micro perspective. In this scenario, BIM is guiding the design of healthcare facilities, which is impacting the overall healthcare operation and management.

From the above data analysis, it can be concluded that the implementation of BIM in Chinese hospitals is: a) Acting as a leading power, to provide process and assign tasks to the entire project. b) Acting as tool to solve certain issues, driven by demand. c) Acting a solution to address certain group of problems and manage a range of tasks.

3.3 Quantitative Data Analysis-Potential BIM Integrated System Intervention

To measure whether BIM is a possible solution to improve healthcare services, a quantitative survey has been taken to analyze people's attitude towards the way healthcare facility management needs to be in the future. For understanding whether information management is required in a hospital, data shows despite the fact that there are 75% of people having certain degree of expectation towards the future healthcare management, still 50% of people have no idea what kind of system needs to be adopted. There are 37.5% people who think integrated system will be adopted in hospitals in the future and 12.5% people think other system will be adopted. The interview also goes into the satisfaction of current healthcare management. The data shows that 75% of people are satisfied with current management solutions.

There are certain barriers to promoting BIM in healthcare service, according to the statistics, there are over 60% of people who think adopting BIM will increase costs. Also, the understanding of BIM is another concern, the result shows that 50% of people have never heard about BIM, while only 12.5% of people understand BIM very well. The rest 37.5% of people have just briefly heard about BIM. Moreover, the interview goes to investigate how people think that BIM can be integrated with medical facilities management, results show that 50% of people think BIM will never be integrated with healthcare facilities and 12.5% of people provide no answer, there are 37.5% of people who think BIM has great potential to make intervention.

With the quantitative data analysis from the primary interview and questionnaire data, it can be

concluded that: a) Integrated information system is needed for healthcare service development. b) BIM needs to minimize its costs during the implementation. c) The advantages of BIM need to be better promoted and educated.

4 Conclusion, Limitations, and Future Research

This research has clarified that it is possible to integrate BIM into healthcare facilities/asset management based on primary and secondary data analysis. The collaborative culture from BIM paradigm can impact information coordination in medical facility management, thus to further impact on medical treatment quality and the enhance hospital operation performance. Considering the fast growth of designing integrated solution for the AECO sector, then hospital buildings have to integrate BIM paradigm in a way to solve critical problems such as equipment operation and waste disposal, so that the treatment quality and public responsibility can be assured. According to the findings from primary data, the demand from information to hospital management is listed in Table 3, thus, there is a high demand to use the strength of BIM to access and visualize healthcare data, which particularly can fill the gap in facility information and treatment management.

Table 3: Demand from Information to Hospital Management

	Finance Management	Logistic Management	Treatment Management	Procurement Management
Patient Information			Yes	
Medicine Information			Yes	
Facility Information	Yes	Yes	Yes	Yes

The research identifies the demand of hospital operation from the outstanding, and the findings shows different medical facilities need to be accommodated with diagnosis and treatment to ensure patients can mitigate the suffering. The research also identifies the potential hazard generated by medical facility operation need to be properly managed to respond to public liability. The research highlights the strength of BIM, compares its advantages from AECO disciplines regarding building operation management, reiterates its potential role in healthcare facility management. The findings show the facility information is highly linked with treatment management as facility rely on finance, logistic, treatment, and procurement, while treatments rely on patient, medicine, and facility information. (Figure 6) shows under BIM paradigm, it can have impact on developing an improved integrated system to increase the coordination of above information, thus, the performance of hospital management can be enhanced.

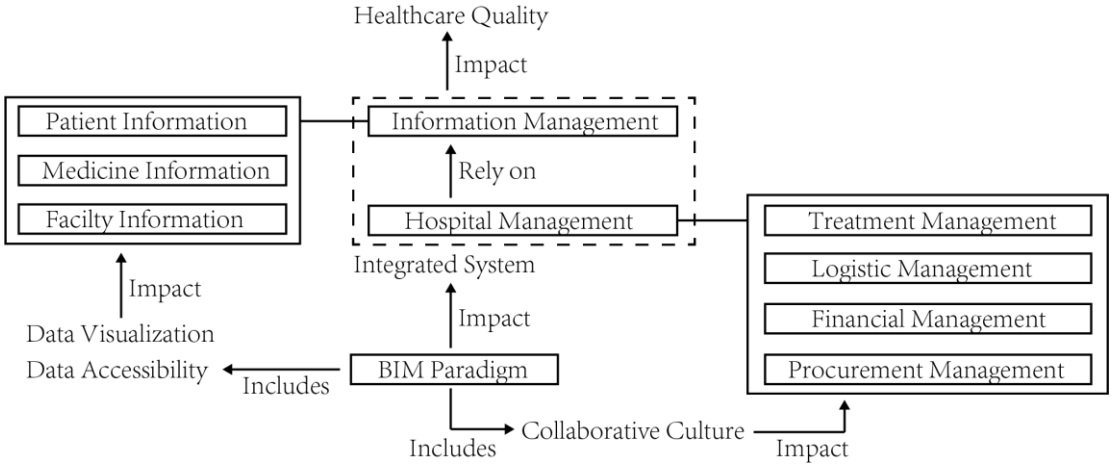


Fig. 6: Research Findings

However, the findings from this research is limited in sample quantity and diversity, therefore, it does not comprehensively cover all the situations in the country. Due to the medical resources not being evenly distributed, some areas still operated in a very traditional way, which is lack of digitization to manage healthcare services. Thus, how BIM can impact these area's hospitals is still waiting to be investigated. Furthermore, the research is standing from AECO asset information perspective, which has limited focus on how medical services are operated, hence, it may cause some bias regarding whether BIM can contribute to medical information management. This research is a preliminary study to measure the feasibility of using BIM in hospital management. The future research will go deep into medical diagnosis and treatment in healthcare institutes, to take in-depth exploration with medical professionals to examine how those characteristics in BIM can impact on healthcare service.

References

Andersen, M. T. & Findsen, A. L. (2019). Exploring the Benefits of Structured Information with the Use of Virtual Design and Construction Principles in a BIM Life-Cycle Approach. *Architectural Engineering & Design Management, 15*(2), 83-100.

Bröchner, J. (2017). Measuring the Productivity of Facilities Management. *Journal of Facilities Management, 15*(3), 285-301. https://doi.org/10.1108/JFM-04-2016-0013

Cheng et al. (2017). BIM Integrated Smart Monitoring Technique for Building Fire Prevention and Disaster Relief. *Automation in Construction, 84,* 14-30.

Cui et al. (2016). Effects of the Performance Management Information System in Improving Performance: An Empirical Study in Shanghai Ninth People's Hospital. *Springerplus, 5*(1). https://doi.org/10.1186/s40064-016-3436-2

Deutsch, R. (2011). *BIM and Integrated Design: Strategies for Architectural Practice.* Hoboken.

Dixit et al. (2019). Integration of Facility Management and Building Information Modeling (BIM). *Facilities, 37*(7/8), 455-483.429p.

Eastman, C. M. (2011). *Bim Handbook: A Guide to Building Information Modeling for Owners, Managers, Designers, Engineers and Contractors* (2nd ed.). Hoboken.

Elbeltagi et al. (2014). BIM-Based Cost Estimation/ Monitoring for Building Construction. *Emad Elbeltagi Int. Journal of Engineering Research and Applications, 4*(7), 56-66.

Fraser, K., Gunawan, J. & Goh, M. (2013). Facility Management Teams. *Journal of Facilities Management, 11*(3), 253-265. https://doi.org/10.1108/JFM-04-2012-0023

Fu, Y. J. (2018). Application Research of BIM Technology in Building Facilities Management Pay Eternal Construction. *Building Technology Development-Construction Technology, 45*(19), 28-29.

Gholizadeh, P., Esmaeili, B. & Goodrum, P. (2018). Diffusion of Building Information Modeling Functions in the Construction Industry. *Management in Engineering, 34*(2).

He, G., Wang, Y., & Ying, Y. (2011). *BIM Generalization.* China Architecture Industrial Press

Hilal, M., Maqsood, T., & Abdekhodaee, A. (2019). A Scientometric Analysis of BIM Studies in Facilities Management. *International Journal of Building Pathology and Adaptation, 37*(2), 122-139. https://doi.org/10.1108/IJBPA-04-2018-0035

Holzer, D. (2016). *The BIM manager's Handbook: Guidance for Professionals in Architecture, Engineering, and Construction*. Wiley

ISO. (2018). *BS EN ISO 19650-1: Organization and Digitization of Information About Buildings and Civil Engineering Works, Including Building Information Modelling - Information Management Using Building Information*

Modelling: Concepts and principles. International Organization for Standardization.

Kapogiannis, G., Fernando, T. & Alkhard, A.M. (2021), "*Impact of Proactive Behaviour Antecedents on Construction Project Managers' Performance*", Construction Innovation, vol. 21 No. 4, pp. 708-722. https://doi.org/10.1108/CI-02-2020-0029

Khemlani, L. (2009). A Sutter Medical Center Castro Valley: Case Study of an IPD Project. Accessed on August 2022 [available https://www.aecbytes.com/feature/2009/Sutter_IPDCaseStudy.html].

Reng, Y. (2018). Discussion on Application of BIM Technology in Medical Construction Engineering. *Engineering Technology and Application*, 64-65.

Shehata, M., & Rodrigues, F. (2018). *Project Management and BIM for Sustainable Modern Cities.* Egypt the Official International Congress of the Soil-Structure Interaction Group.

Sijtsema et al. (2019). Professional Development of the BIM Actor Role. *Automation in Construction, 97*, 44-51. https://doi.org/10.1016/j.autcon.2018.10.024

Wei et al. (2019). Analysis of Current Status and Prospects of BIM Technology Application. *Residential and Real Estate, 1*, 180.

Wang et al. (2016). Building Energy Efficiency for Public Hospitals and Healthcare Facilities in China: Barriers and Drivers. *Energy, 103*, 588-597. https://doi.org/10.1016/j.energy.2016.03.039

Wanigarathna et al. (2019). Building Information Modelling to Support Maintenance Management of Healthcare-Built Assets. *Facilities, 37*(7/8), 415-434.

Zuo, F. (2018). Research on Overall Process Control Technology for Hospital Building Construction Based on BIM. *Digital Construction, 40*(10), 1827-1830.

Cite as: Kapogiannis G., Yang T., Guo J. & Gerges M., "Medical Facility Management under BIM Paradigm for Hospital Operations Performance in China During COVID-19", *The 2nd International Conference on Civil Infrastructure and Construction (CIC 2023)*, Doha, Qatar, 5-8 February 2023, DOI: https://doi.org/10.29117/cic.2023.0045

Advancement in Construction Management

Ravish Kumar
Assistant Professor, Department of Architecture & Planning, NIT Patna, Bihar, India
ravish@nitp.ac.in

Arpita Srivastava
M. Arch. 3rdSem., Department of Architecture & Planning, NIT Patna, Bihar, India
arpitas.pg21.ar@nitp.ac.in

Manoj Kumar Rajak
Bureau of Indian standard, -New Delhi, India
manoj@bis.gov.in

Fulena Rajak
Professor, Department of Architecture & Planning, NIT Patna,Bihar, India
fulenarajak@nitp.ac.in

Bijay Kumar Das
Associate Professor, Department of Architecture & Planning, NIT Patna, Bihar, India
bijay@nitp.ac.in

Abstract

Building construction and infrastructure development have been a component of major civilizations throughout their history. Great examples, of architecture include the Great Pyramid, the Great Wall of China, and many more ancient constructions of historical significance. The fundamental component for the completion of these buildings is design, planning, execution, and closure. Planning of project execution is the most critical aspect, to have the ability to accomplish the required project execution in the allotted time and on framed expenses. Certainly, some outstanding quality and construction management procedures were implemented in the past, and someone was present to supervise the resources and time schedule. In today's construction project management, many mathematical tools and techniques such as bar charts, CPM, PERT and so on are employed for project planning. To manage the multi-tasking and complicated building environment, other standalone computer software and web-based packages are also in use. This paper aims to investigate advancements in construction management when dealing with extremely complicated building procedures in a complex environment. The methodology applied is to study and cite the literature of various preferred software management tools in the construction industry with the sequential order of the year, purpose, uses and process of the particular software. The results obtained are the analytical study of the software tools used in the construction industry.

Keywords: Construction Management; Computer Software; Web-based Construction Management

1 Introduction

Numerous researchers have identified construction industry characteristics that are distinct from those of other industries, e.g., ‘field oriented’ (Paulson, 1985), ‘extremely conservative (Rosenberg, 1982), ‘too many small firms’ (Cassimatis, 1969), ‘fragmented’ (Barrie & Paulson, 1978), and ‘technologically stagnant’ (Business Roundtable, 1982b). But a closer look at construction technology shows that these are only some of the ways in which the different qualities of built products and the limitations of construction technology lead to different results. A key part of

making the construction industry more technologically competitive is for people to learn more about the important features of built stuffs and how these features affect construction technology and its capability to improve. The Construction Industry includes services for building, changing, re-building, and fixing up different kinds of structures. For success of every project time and cost are very important parameters. The purpose of project management is to finish the project in the time allotted and within the budget that was planned. The total cost of a project goes up when it takes longer to finish. A Guide to the Project Management Body of Knowledge (PMBOK Guide) – Sixth Edition (Project Management Institute, 2017) explains that traditional view of project success is that scope, time, and cost are all met.

To enhance the performance of the construction activities, digital skills are important. The project environment is extremely complicated, and it is inconceivable that decisions could be made without software tools. The software tools enable the application of concepts and the visualisation of issues and solutions. Some of the mathematical tools for construction management include CPM (Critical Path Method), PERT (Program Evaluation Review Technique), Bar chart, Pie-charts etc. The software tools include Primavera, Microsoft Project etc. Some web-based packages, WPMS (Web-based Project Management System) like PM-ASPs (Project Management System-Application Service Provider) are also there. This paper explains the traditional and advanced construction project management tools and software in addition to web-based packages to investigate recent developments in construction management.

2 Bar Chart, CPM & PERT

A wide range of strategies required to be created in response to the practical problems of project execution are focused on establishing the project work, organization, as well as generating complete plans and budgets for inspection and managing execution throughout the project duration (Nicholas,1990).The different approaches make an important significant addition to communication by providing graphical representations, reports, observations, and assistance for review meetings (Nicholas,1990).

Bar charts or Gantt charts, due to their popularity of the advantages of dividing big projects into smaller tasks, mask a significant role in the development of Construction project management. Henry Gantt created his charts known as Bar chart in the 1910, and they followed employment in significant projects during World War I and the building of the Hoover Dam, which therefore facilitated the widespread usage. Therefore, his name started to appear on the charts (Seymour & Hussein, 2014). Bar charts are a straightforward depiction of the project schedule. They are not for displaying the priority relationships between activities.

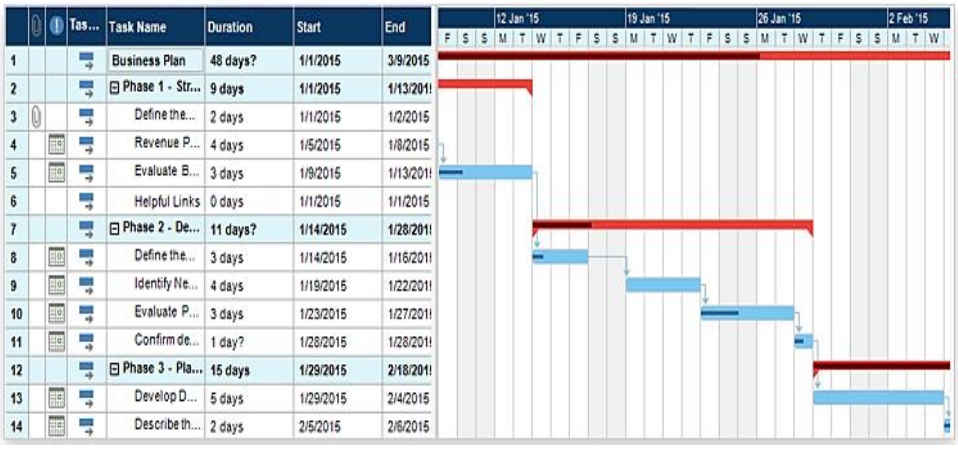


Fig. 1: Gantt Chart Outlines the Tasks that must be Completed and their Respective due dates (The Schedule) (Gantt.com, 2023)

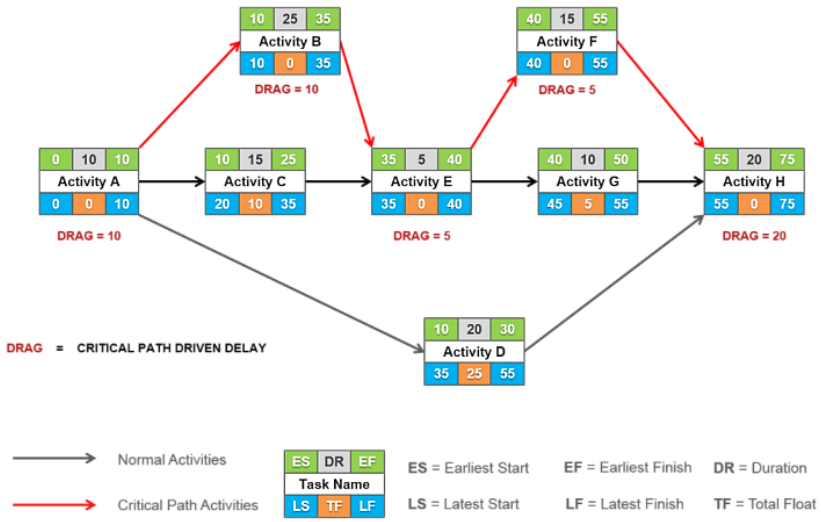


Fig. 2: Node Network Diagram for CPM Technique (Shuttleworth, 2017)

(Snyder, James, & Kline, 1987) Claim that the advent of CPM/PERT in 1958 marked the successful starting of the contemporary project management period (KWAK, 2003).It's fair to say that CPM/PERT has received special attention in the growth and, in some ways, the commencement of modern project management. Despite some overlap, CPM/PERT was developed in parallel to the chemical industry and the navy, two very different industries. The Polaris project, the first SLBMs with nuclear warheads, was spearheaded by the American Navy in 1958. One of today's most widely utilised methods was developed by the U.S. Navy, according to legend, Program Evaluation Review Technique (PERT), through the Polaris project. PERT worked effectively to represent the many scheduling possibilities of the project because of the significant complexity and unpredictability involved with project scheduling. Nearly at the same time as PERT, the Critical Path Method (CPM) was created. The upshot of a significant building project acted upon by the E.I. du Pont de Nemours Company was the creation. A sizeable chemical factory was to be constructed as part of the project. The necessity for the business to make an accurate cost and time estimate for the project resulted in the creation of the CPM. They initially called the approach they devised Project Planning & Scheduling (PPS), but it was eventually transformed into the well-known CPM method. (Seymour & Hussein, 2014).Project network techniques like PERT, CPM utilise network strategies to schedule work and provide an examination of the scheduling effects that activities have on one another, as well as the identification of critical and float activities, are basis for estimation of cost, allotment and administration of resources, and analysis of risk. The project organisation is interwoven with the work structure of project, allowing for the responsibility distribution to project participants. As according, to this viewpoint, the notion that the traditional method procedure for implementation advances, management and planning are practised on a regular basis is "static & closed" (Davidson, 1991) can be countered.

3 Software Packages

In order to accomplish various project management responsibilities, software support is required (Shtub, Jonathan & Globerson, 2005).Project management software programmes such as Microsoft Project, Primavera, and others are frequently used by professionals. According to some surveys [by (Liberatore & Johnson, 2003; Liberatore, Johnson, & Smith, 2001)], these tools are mostly used for critical route planning, with little usage of more advanced approaches such as time-cost trade-off analysis, simulation, and probabilistic analysis.

3.1 Microsoft Project

Microsoft Project (www.microsoft.com/project/) released its first version for the DOS operating system in 1984. The major purpose of application in design was to make it easy to use. Since its introduction, project managers have preferred MS Project as a tool (Hilo, Rashid, & Ismail, 1985-1989; Travica et al., 2007; Galloway, 2006), although it has never surpassed any other PM product. This is particularly evident in the construction sector, where it was never fully compliant with the sector's specific practises and processes. The most often used programme is Microsoft Project, which is mostly used for planning. Despite the fact that EVA (Earned Value Analysis) tools are accessible in this programme, they have largely been utilised in practise gathering and presenting data in several ways. These variables might be the source of the restriction: management, or they may find them too hard to utilise. Furthermore, getting these tools may be deemed impossible given the project budget or too expensive considering the anticipated advantages (Hazır, 2014).

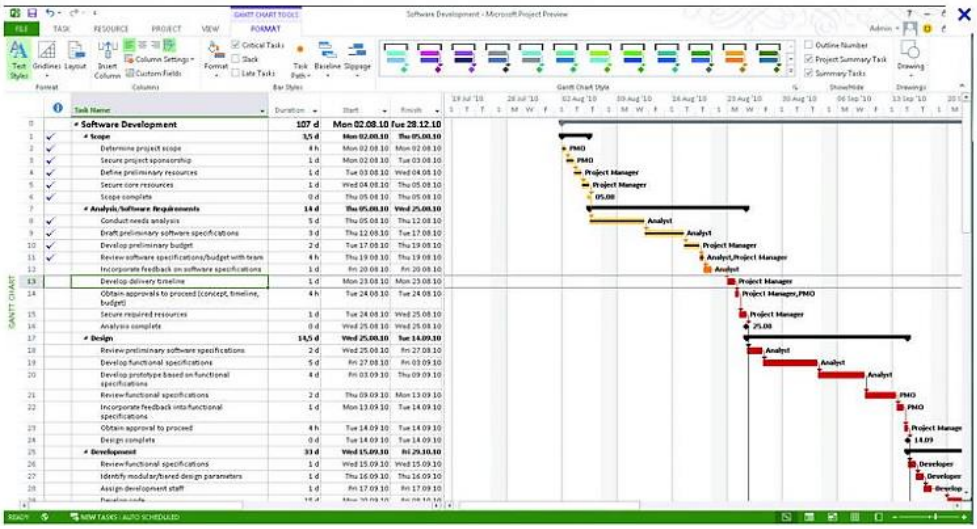


Fig. 3: Demonstration Project on Microsoft Project (Abramova, Pires, & Bernardino, 2016)

3.2 Primavera

The Primavera Systems (http://www.oracle.com) has been creating its PMS (Project Management System) package for the construction industry since 1983, and it is now a top supplier of Project Portfolio Management (PPM) solutions for the sector (Galloway, 2006). Estimation, activity sequencing, resource allocation, and timing are all part of the Primavera software scheduling process. The purpose of construction scheduling is to complete projects on schedule and to allocate resources efficiently. Primavera scheduling provides effective control (Kumar & Krishnamoorthi, 2015). Chopra & Dewangan (2014) indicated that, if used appropriately, the Activity ID and Activity Description—two of the underutilised components—can significantly improve the schedule's quality. The planning team has a responsibility to carefully choose the Activity ID structure in advance to ensure that schedule preparation proceeds without any problems. Scheduling involves the following steps: Creating EPS (Enterprise Project Structure). The initial stage in developing an optimum timeline for a project is to compile all of the project's data. Some of the steps illustrated below may be completed with the Primavera P6 programme creating the whole structure of the firm, including its branches, that is carrying out the project with Primavera P6. This may be referred to as Enterprise project structure (EPS). A project is a development approach that consists of a number of separate activities and supporting materials. The project is overseen by the different sections of EPS (Enterprise Project Structure). Given planned start and end dates, this is

possible. The project assigns a global, resource, or project calendar (Mahure & Ranit, 2018). Following the Primavera P6 methodology and analysis for the project planning and scheduling processes, drawings in the company's collections: Some methods and analysis for the Primavera P6 doing Project Planning and Scheduling, Drawing Collections from the Company stages are provided. The following approaches are used for project tracking and application administration. It contains detailed information about the quantities, the generation of OBS (Organisational Breakdown Structure) for the project, the generation of EPS for the project, the creation of a new project, the generation of a calendar for the project, the generation of a WBS (Work Breakdown Structure) for the project, the creation and characterization of project activities, definition of project function and resources, assignment of resources to activities, resource analysis and levelling of the project, and establishment of a new baseline for the project (Zerin & Joy, 2020).

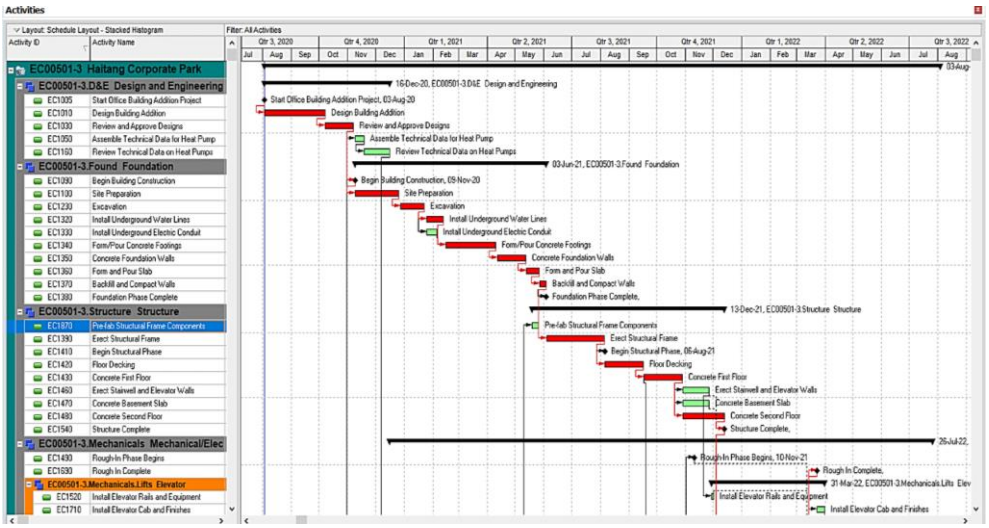


Fig. 4: Demonstration of a Project on primavera (The Standard for Planning and Scheduling, 2022)

3.3 MS Excel

Excel was developed to take use of Windows Vista, the eagerly anticipated next iteration of Windows (see www.microsoft.com/windowsvista). Microsoft's product interfaces are continuously refined and improved in order to expand the capabilities of knowledge workers, according to the company's developers. Because each office application contains so many features and options, Microsoft developers felt obligated to make the products easier to use and provide users with less obvious options. Microsoft Office 2007 has the latest edition of SharePoint Technologies, which consists of two distinct components: MOSS (for a Measure of Software Similarity) and Office. Documents are created and checked into MOSS using Office's built-in "check-in" procedure. As a result, version numbering, revision tracking, and strict collaboration rules are in place. Simple publication, retrieval of published materials, tracking, and other aspects of collaboration activities are available in Office 2007 programmes such as Word and Excel. The extra capabilities in Excel 2007 (together with those kept from earlier versions) are ideal for project managers, providing a one-stop shop where you may not only write (or link to) project documents, but plan and add the schedule, charts, and other components also. Excel defies conventional spreadsheet definitions. As the project progresses, the following Excel features can be implemented: generating custom forms, creation of a database, using Visual Basic for Applications (VBA), create macros and module programming, and design statistical and mathematical formulas that may be utilised to calculate and present project data (Heldman & Heldman, 2007).

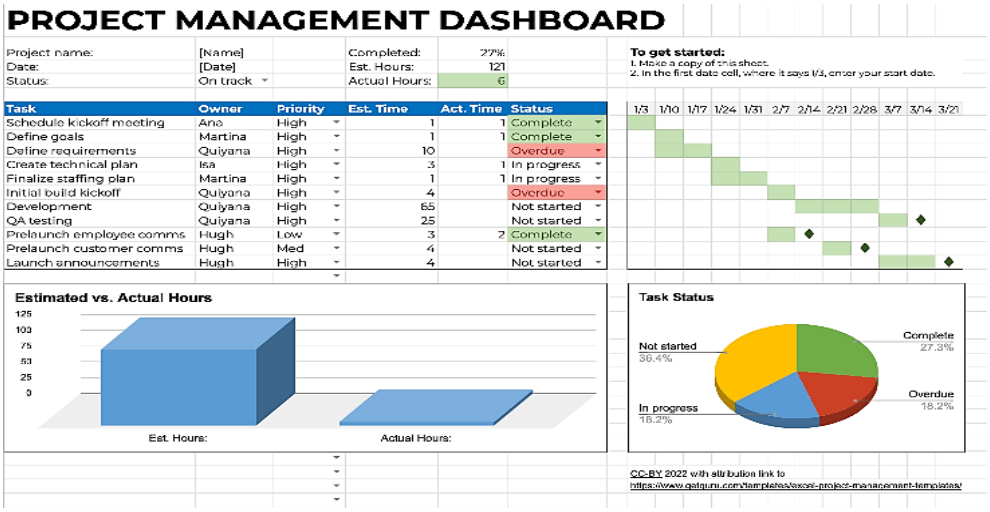


Fig. 5: Demonstration of Project on MS Excel (9 Free Project Management Excel Templates & Examples, 2023)

4 Web-Based Packages

Through savvy servers and browsers, the Web can also get around incompatibilities in data formats. The same system may therefore be shared over the Web by independent project members utilising various hardware platforms (Rojas & Songer, 1999). The benefits of Web technologies in the construction industry may be roughly grouped into three categories, as stated in (Skibniewski & Abduh, Web-based project management for construction: search for utility assessment tools, 2000): the facilitation of relevant information services, participant communication, and computers for engineering and management. In recent years, the concept of managing construction projects via the Internet and similar technology has become increasingly popular among practitioners. The purpose of Web-based Project Management System (WPMS) is to document construction project and management. WPMS is an electronic project management system and a personal network which uses Internet protocols to convey information (Brien, 2000).

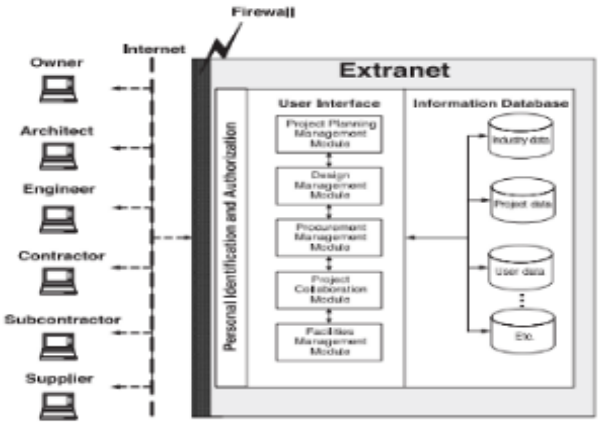


Fig. 6: Functional scheme of WPMS (Skibniewski & Nitithamyong, Web-based construction project management systems: practical advantages and disadvantages, 2004).

Only the project team has access to the system, which may be spread across many organisations. It essentially provides a centralised, widely accepted, and reliable way to distribute and store project information. All kinds of variations like geographic and border-related are completely eliminated by keeping project data within the server and sharing it via a regular web browser operating as a gateway. Project, design, management, and finance information are the four fundamental kinds of

construction project details that are often carried out through WPMS, as noted by Mead (Mead, 1997). In addition to information about the project, it also includes design information, management information, financial information, including cash flow, and information created by the project's accounting team. Information for design covers any data produced by the design team, such as CAD drawings. When project information shifts, the server's database may be quickly updated with the new information. Project members of the team may approach the updated data at any time from faraway places by inputting a digital user ID and password, overcoming the issues with linear communication systems (Thorpe & Mead, 2001).

4.1 Project Management System-Application Service Provider (PM-ASP)

"Project Management System-Application Service Provider (PM-ASP)," is gaining popularity because it requires less technical, building and managing resources, both financial and human resources (Thorpe & Mead, 2001).Due to the fact that PM-ASP is contracted out to an ASP, it does not require internal design and maintenance, has a cheap initial investment and administrative expenditures, and is easy to stay on top of cutting-edge technology. As a result, it is a workable option for a small A/E/C company that lacks the funds to support a complex networking infrastructure or an internal IT group. Although PM-ASP is a subject that is becoming more and more important and is still quite fresh and its optimum usage patterns and expansions have not yet undergone comprehensive examination by both practitioners and researchers in the field of building. Existing business models of PM-ASPs include Project Collaboration Network (PCN), Project Information Portal (PIP), Project Procurement Exchange (PPE) etc. The known visage of PM-ASPs include document management, process of workflow of project, directory of project, revision control and central logs, advancement in searching, conferencing, online related discussion, scheduling and calendar, project camera, converting a file, services related to printing, customized website, access while being offline, outside the system messaging, wireless integration, project information archiving, service related to information, service related to finance, E-bidding , procurement. Some other features which affects PM-ASPs include cost advantage, outsourcing advantage, clash among various IT professionals, Competition of ASPs etc. (Skibniewski & Nitithamyong, Web-based construction project management systems: practical advantages and disadvantages, 2004).

5 Conclusion

The Bar Charts / Gantt Charts, PERT/CPM network, are some of the tools and techniques used in conventional project management to implement. They are governed by the project team's network and organisational structure as well as the method used to disassemble the project into its constituent elements. On the other hand, software like Primavera, Microsoft Project adopts a strategy that views project activity from a high level. It is often depicted as a continuous flow of work units assigned to the project to carry out its duties. In short software, also expands the capabilities of construction project managers, architects having basic knowledge. Lastly, in WPMS, project data is saved on the server, and a regular Web browser is utilised as a medium to interchange the required data, removing geographic and hardware platform disparities. This paper's focus was on identifying the traditional and advanced construction management tools (including web-based packages) in an effort to comprehend the restrictions that emerge from building technology and to examine efforts made to get beyond those limitations. The building industry's driving drivers of development were mostly left out of this narrative. Therefore, there is a huge possibility for additional research when it comes to comprehending the dynamics of the

construction technology related constraints they bring about. The paper also aims to dispel the myth that software management tools are too complicated and time-consuming to learn, despite the fact that they are simple, time-saving, resourceful, and tend to increase one's proficiency. This myth is held by construction managers and other people in the building industry.

References

9 Free Project Management Excel Templates & Examples. (2023). Retrieved from Guru Technologies, Inc: https://www.getguru.com/templates/excel-project-management-templates.

Abramova, V., Pires, F. & Bernardino, J. (2016). Open Source and Proprietary Project Management Tools for SMEs. *Journal of Information Systems Engineering & Management*. Retrieved from Ten Six Consulting, LLC: https://tensix.com/displaying-the-task-path-in-microsoft-project/

Barrie, D., & Paulson, B. (1978). *Professional Construction Management.* New York: McGraw-Hill.

Brien, W. (2000). Implementing issues in project web sites: A practitioner's viewpoint. *Journal of Management in Engineering, vol. 16(3), ASCE, New York, USA,*, 34 – 39.

Business Roundtable (1982b). *Technological progress in the construction industry. A Report of the Construction Industry Cost Efectiveness Project, Report B-2.*

Cassimatis, P. (1969). *Economics of the Construction Industry.* New York: The National Conference Board, Inc.

Chopra, S. & Dewangan, A. (2014). Developing an Efficient Schedule in Primavera P6: Significance of Activity ID & Descriptions. *International Journal of Innovative Research in Science, Engineering and Technology (An ISO 3297: 2007 Certified Organization) Vol. 3, Issue 7*.

Davidson, F. P. & J. H. (1991). Large-Scale Projects-Management Trends for Major Projects. *Cost Engineering 33*, 15-23.

Galloway, P. (2006). Survey of the construction industry relative to the use of CPM scheduling for construction projects. *Journal of Construction Engineering and Management, 132*.

Gantt.com. (2023). Retrieved from What is a Gantt Chart?: https://www.gantt.com/

Hazır, Ö. (2014). A review of analytical models, approaches and decision support tools in project monitoring and control. *International Journal of Project Management 33(2015)*, 808–815.

Heldman, K. & Heldman, W. (2007). *Excel for Project Managers.* Indianapolis, Indiana: Wiley Publishing, Inc., Indianapolis, Indiana.

Kumar , E. & Krishnamoorthi , S. (2015). In their study they focused on the scheduling using MSP and earns value analysis for an apartment building. *IOSR Journal of Mechanical and Civil Engineering (IOSR-JMCE)*, 01-06.

Kwak, Y. (2003). Brief History Of Project Management. *The Story of Managing Projects by Carayannis, Kwak, and Anbari*.

Liberatore, M.J. & Pollack-Johnson, B. (May 2003). Factors Influencing the Usage and Selection of Project Management Software. *IEEE Trans. Eng. Manag. 50*, 164–174.

Liberatore, M.J., Pollack-Johnson, B. & Smith, C.A. (2001). Project management in construction: software use and research directions. *J. Constr. Eng. Manag. 127*, 101-107.

M. Nicholas, J. (1990). *Managing Business and Engineering Projects: Concepts and Implementation.* United States: Englewood Cliffs, NJ: Prentice-Hall.

Mahure, A. & Ranit, A. (2018). Project Management using Primavera P6. *International Journal of Engineering Research & Technology (IJERT),Vol. 7 Issue 04*.

Marsh, E. (1975). The Harmonogram of Karol Adamiecki. *The Academy of Management Journal Vol. 18, No. 2*, 358–364.

Mead, S. (1997). Project-specific intranets for construction teams,. *Project Management Journal, vol. 28(3), Project Management Institute, Pennsylvania, USA*, 44 – 51.

Patricia D Galloway. (2005). CPM Scheduling and How the Industry Views Its Use. *nAACE International Transactions*.

Paulson, Jr., B. (1985). Automation and robotics for construction. *Journal of Construction Engineering and Management,ASCE, 111*.

Project Management Institute. (2017). *PMBOK Guide 6th Edition.*

Rojas, E., & Songer, A. (1999). Web-centric systems: a new paradigm for collaboration engineering. *Journal of Management in Engineering, vol. 15 (1), ASCE, New York, USA*, 39 – 45.

Rosenberg, N. (1982). *Inside the Black Box, Technology and Economics.* Cambridge: Cambridge University Press.

Seymour, T. & Hussein, S. (2014). The History Of Project Management. *International Journal of Management & Information Systems –Third Fourth Volume 18, Number 4*, 233-311.

Shtub, A., Jonathan F., B. & Globerson, S. (2005). *Project Management: Processes, Methodologies, and Economics (2nd Edition) 2nd Edition.* Pearson,Prentice Hall.

Shuttleworth, M. (2017). *Project Risk Manager*. Retrieved from Project Schedule Planning: PERT vs. CPM: https://www.project-risk-manager.com/blog/pert-vs-cpm/

Skibniewski, M. & Abduh, M. (2000). Web-based project management for construction: search for utility assessment tools. *Proceedings of INCITE 2000, Hong Kong Polytechnic University*.

Skibniewski, M. & Nitithamyong, P. (2004). Web-based construction project management systems: practical advantages and disadvantages. *Proceedings of 4th International Conference on Construction Project Management*.

Snyder, J. R. & Kline. (1987). "Modern Project Management: How Did We Get Here – Where Do We Go?". *Project Management Journal*.

The Standard for Planning and Scheduling. (2022). Retrieved from ORACLE: https://www.oracle.com/in/industries/construction-engineering/primavera-p6/

Thorpe, T. & Mead, S. (2001). Project-specific web sites: friend or foe? *Journal of Construction Engineering and Management, vol. 127*(5), ASCE, NewYork, USA, 2001, 406 – 413.

Travica, B., et al. (2007). E-Commerce in Serbia: Where Roads Cross Ellectrons Will Flow. *Journal of Global Information Technology Management 10(2)*, 34-56.

W. Hilo, Rashid, K. & Ismail, A. (1985-1989). The Use of Project Management Software in Construction Industry. *Journal of Applied Sciences, 9 10(2009)*.

Zerin, F. & C. Joy, A. (2020). Construction Management Using Primavera. *International Journal of Science and Research (IJSR),Volume 9 Issue 6*.

Cite as: Kumar R., Srivastava A. Rajak M.K., Rajak F., & Das B.K., "Advancement in Construction Management", *The 2nd International Conference on Civil Infrastructure and Construction (CIC 2023)*, Doha, Qatar, 5-8 February 2023, DOI: https://doi.org/10.29117/cic.2023.0046

Offsite Construction in the UK: Economic and Environmental Benefits

Mohammad Maleki Sadabad
School of Science, Engineering & Environment, University of Salford, Manchester, UK
m.n.malekisadabad1@salford.ac.uk

Abstract

In contrast to traditional piece meal onsite construction, offsite construction comprises the planning, designing, production, transporting, and assembly of building elements for speedy site assembly to a higher degree of completion. Offsite building utilises a wide range of materials, scales, and systems, as well as modern manufacturing and fabrication techniques and computer software. Offsite construction is utilised to create componentised, panelised, and modular elements that support structural, enclosure, service, and interior partition systems. Integrating these systems with the supply chain through research, design, testing, and prototyping is an off-site optimisation technique. Due of economic, health and safety, and environmental factors, major UK contractors have adopted offsite construction over the past decade. Large projects are requiring major contractors like Mace, Laing O' Rourke, and Balfour Beatty to invest in off-site manufacturing. Offsite construction is defined in detail in this paper, along with how it can help construction projects to succeed economically and environmentally. The impact of offsite construction was examined in this research using a narrative review of the existing literature, and the findings demonstrate that there are numerous advantages both economically and environmentally. Offsite construction is more environmentally friendly because it requires less energy and large machinery uses on site. Since it is simpler to anticipate the amount of material required and buy in bulk, the organisation may reduce waste and the number of vehicles required to transport the finished product to the site. Cost savings always result from transferring site processes to a production workshop setting. The cost of labour in mechanical and electrical installation is one of the highest costs in construction industry, therefore, as prefabricated solutions have been fully or partially completed before they arrive on-site, labour can be reduced with offsite construction.

Keywords: Offsite construction; Sustainability; Cost efficiency

1 Introduction

Construction is a relatively diversified industry that involves tasks such as building infrastructure and facilities, manufacturing and supplying goods, as well as maintaining, operating, and disposing. It also includes activities like mining, quarrying, and forestry. The UK's annual construction activities exceed £110 billion and accounts for around 6.5% of GDP. The public sector produces about 25% of construction activity, whilst the private sector produces 75% of the industry output (Reporting to HM Treasury and Cabinet Office Government Construction, 2016).

Offsite construction is the process of completing components or elements of a construction project at a site other than the one where they will be installed permanently. Planning, design, production, and assembly are frequently included in these processes in specially designed offsite facilities, then the finished product is delivered to the project location for final assembly processes. The UK's

housing shortage has forced a reconsideration of the country's building strategy. The Lyons Review (Lyons, 2014) and Off-site Housing Review Miles & Whitehouse (2013) of the Construction Industry Council both recommend utilising offsite construction technology to help improve the availability of affordable housing. In comparison to other developed countries, the UK is relatively cautious when it comes to home building innovation, despite the potential of offsite construction potential (Nadim & Goulding, 2010).

Offsite technique has been acknowledged as a key enabler of the industry's productivity in numerous government assessments into construction productivity and housing supply, including Barker 2004 and Farmer 2016. This is due to its many advantages. Meanwhile, the industry, which is renowned for its innovation bias and risk aversion, has been resistant to change (Sinesilassie *et al*., 2017). The UK government's 2018 construction sector deal (HMG, 2018), which was released in response to its industrial strategy from a year earlier, outlined an ambition to change the industry by linking the construction, manufacturing, digital, and energy sectors (HMG, 2017). The plan aims to create new procedures and standards, including modular components for offsite building manufacturing that is being advanced through a variety of investments in a programme called "transforming construction" (through Innovate UK).

This paper has identified the benefits and pitfalls of offsite construction for the UK construction industry's social, economic, and environmental goals. Through the critical review of existing literature, this research has demonstrated that offsite building can be a better way to address the housing shortfall in the UK while having several advantages for the economy and environment.

2 Literature

Offsite construction is not anything new and it can be traced back to the Middle Ages when carpenters would often assemble the frames of buildings in the yards to ensure that all elements fitted together. The frames were then marked and dismantled to be transported to sight and reassembled this system was known as quick frame in the 19th century. This technique developed into the familiar timber balloon and platform framing. In the 1830s john manning a London carpenter and builder pioneered the manning cottage a timber house that was standardised and designed to be transported overseas and assembled by unskilled workers, then during the Crimean war in the 1850s British engineer Isambard kingdom Brunel designed the Renkioi hospital. The timber frame structure was manufactured in the UK flat packed shipped and assembled on site by unskilled workers in under six months (Deluxe Modular, 2019).

A consultation by the house of lords in 2018 revealed that there is a real confusion in terms of terminology or terms such as modular, off-site, pre-fabrication, modern methods of construction volumetric and panelised all being used. Modern method of construction (MMC) includes older approaches that aim to optimise the construction process to obtain better products in less time. This can mean for example any building method that improves efficiency quality or environmental performance, in this way MMC include but are not limited to off-site construction instead off-site construction is a way to achieve MMC, off-site on the other hand is a construction method that adds substantial value to a product via the manufacture and pre-assembly of components, elements or modules in a factory before installation in the final location, so off-site is all about transferring some of the building works to a factory. There are four main categories of off-site construction: sub-assemblies and components, panelised systems, volumetric systems and hybrid systems. These can be in any material steel concrete timber or indeed a hybrid material (publications.parliament.uk, 2018).



Fig. 1: Offsite Construction

In order to increase the overall value of a project, off-site construction typically incorporates sizable amounts of production in a factory setting. Prefabrication, manufacturing, modularization, standardisation, pre-assembly of components and modules are some of the several components that this technique encompasses (Constructing Excellence, 2015).

Offsite construction has several advantages in the housing industry, including the ability to produce higher quality in less timing and at a lower cost, as well as potential to better control expenses. Additionally, efficiency is increased, waste is decreased, the impact of bad weather is decreased, labour and material requirements are decreased, and the total environmental impacts are decreased with less inconvenience to locals (Building Societies Association, 2017).

The focus on the specific offsite construction techniques is not usually prominent, even though much has been written on the possible advantages that offsite construction and the associated procedures offer however, many authors and practitioners, including Goh & Goh (2019), suggest that using prefabricated components rather than on-site fabrication will result in higher-quality products. This is because of improved monitoring and the corresponding quality assurance standard in a production setting (Smith, 2011). Prefabrication, according to Blismas & Wakefield (2009), improved accuracy, quality, and component life while lowering whole-life costs and faults. This is accomplished by using highly specialised equipment under controlled circumstances and quality assurance in a regulated industrial environment.

3 Research Method

This research required several constructs to understand offsite construction method and its economic and environmental benefits in construction. In publications like peer-reviewed studies, construction manuals and reports, as well as rules and regulations, many of these constructs were discovered. These publications mostly concentrated on the benefits of applying offsite construction techniques in the construction sector. The accuracy of this study claim cannot be based on one, well-defined hypothesis. In practice, there were other realities to be understood, both from offsite construction as a developing innovative tool and other sustainable measures applied in the building sector. Due to the exploratory and interpretive nature of this topic, the analysis of data was essentially guided by an inductive theory building approach performed through a narrative literature review, from which the collection and examination of data informed the compilation of this research discussion and findings (Gray, 2013).

In continuing education, narrative literature reviews are frequently used to impart the most recent information about a particular subject or theme (Creswell, 2013; Denzin & Lincoln, 2005). This narrative review was conducted to present new and developing theories on the application of offsite construction methods in the building industry. The narrative review employed in this context,

however, was not carried out to describe the methodology that would allow data reproduction across the publications examined or to respond to specific quantitative research questions. In order to provide a realistic understanding of offsite construction's contribution during construction phases, the evaluation enabled the investigation of innovative strategies employed to enhance sustainability in the construction sector. The purpose of this project was to re-examine and critically analyse the existing data on off-site construction's potential to enhance both the economic and environmental aspects of the UK construction industry. The literature review carried out for this study established the link between the increased environmental and financial measures brought about by the employment of offsite construction techniques in the construction industry.

4 Research Results

The result from the analysis of existing literature shows that there is a strong relationship between implementing offsite construction techniques and the economic and environmental impact in construction industry.

The UK is facing a housing crisis, and only half of the 300,000 homes required to meet demand are being created each year. The potential of offsite construction for residential housing has been highlighted as a modern method of construction (MMC) that harnesses digital techniques, such as building Information Modelling (BIM), have been supported as answers to the industry difficulties which could be up to $22 billion in annual savings in Europe and the US (Cast Consultancy, 2019).

According to research released in, 2019 by the consulting firm McKinsey & Company, compared to traditional construction methods, offsite construction reduces the time required to provide housing, improves building quality, decreases waste, and requires fewer trades on-site (Mckinsey, 2019). Due to manufacturing precision, offsite construction can also result in greater insulation efficiency, which reduces home energy needs and improves occupant comfort. Offsite construction also contributes to the sustainable growth of urban areas by enhancing waste management, minimising onsite activity, and minimising interruptions to local communities.

The UK National Audit Office (NAO) states that offsite construction has financial gains result from quicker construction and less on-site work.

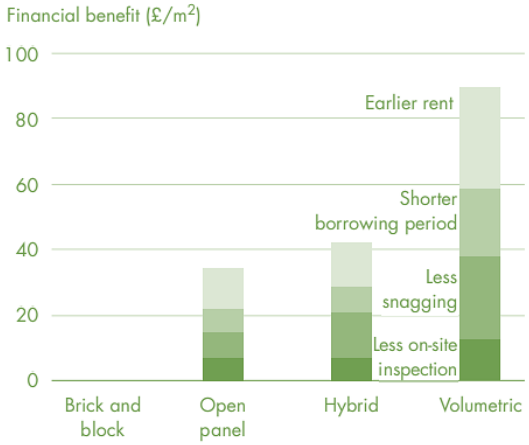


Fig. 2: Offsite Economic Benefits

In addition to the financial advantages of off-site construction, MMC simplifies the process to reuse and recycle materials at the end of a building’s existence by implementing design for deconstruction methodologies. This might be an effective technique to manage construction and demolition waste

in an integrated way that promotes circular construction (Ghaffar, Burman & Braimah, 2020).

Offsite construction has been recognised as one of the most innovative methods for improving quality, efficiency, and environmental performance in the housing construction industry. Results of studies back up these claims, including one from Hong Kong that demonstrates a 52% reduction in waste generation across all building types when adopting offsite construction techniques (Jaillon, Poon & Chiang, 2009). Similar results were discovered in a comprehensive review of high-rise residential projects in the UK, where MMC resulted to an average cost reduction of 30% while reducing waste by 70% and overall construction time by 50% (Lawson, Ogden & Bergin, 2012).

By moving onsite operations to the facility, material waste can be cut by up to 90%. Additionally, because fewer deliveries are needed during the construction phase, the energy consumed to move traffic around the site can be decreased by up to 70%. Nevertheless, it may be argued that their most important result is the 20% reduction in building lifespan energy consumption. Significant improvements are made possible by better insulation and a more tightly sealed building shell. Off-site techniques can, therefore, provide significant environmental advantages over time considering that in the UK, building life-cycle energy use is regarded as an important concern (Miles & Whitehouse, 2013).

Apart from reduction of solid waste, offsite construction generates less green house. Construction equipment can't help but release a variety of pollutants into the atmosphere. Although, air pollution cannot be eliminated, it can at least be reduced. Greenhouse gases like carbon dioxide are a more global issue that is already having a substantial impact on the global climate; however, offsite construction would reduce greenhouse gas emissions by 17% to 30% compared to on-site building (Barrat & Wiedmann, 2007).

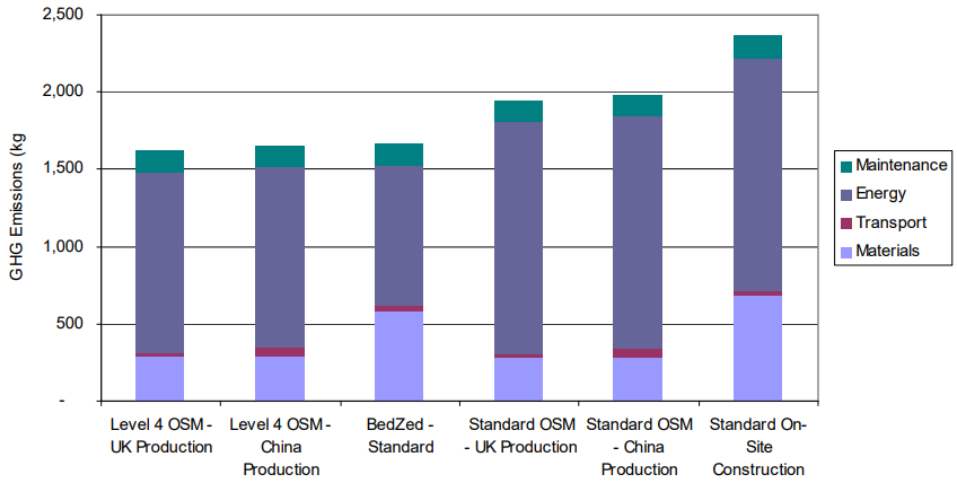


Fig. 3: Greenhouse Gas Comparison between Onsite and Offsite

The benefits of off-site construction are well backed by research, but we must also consider the barriers to off-site construction adoption, including cost, standardisation, skill needs, customer and industry perception, and others.

5 Conclusion

According to a literature analysis, adopting offsite construction methods in the construction sector has several advantages, including those related to social, environmental, and economic factors. Offsite construction improved health and safety as well as working conditions since conventional

construction is a risky activity and that many tasks involve taking risks, operatives are still required to work at heights, in all weather conditions, outdoors, near heavy machinery and at other risks that are not present in other industries, even though site safety has greatly improved over the past 20 years. Offsite construction has various advantages for the environment, including reducing road traffic movement which offer substantial improvements regarding environmental pollution and traffic disruption over the conventional approach. Another benefit of offsite construction is reduced energy use on site and in operation. The usage of energy on site is decreased by offsite construction, which is associated to a variety of activities such transportation, section staff accommodation and services, Lighting, and Equipment. Since the finished buildings typically meet higher standards, off-site construction methods have the potential to use less energy overall. Final environmental benefit is reduced material wastes due to controlled production environment during the construction phase as well as reusing of the some building elements after decommissioning. Offsite construction has several benefits when it comes to economic and financial considerations, but the most visible and commonly mentioned benefit is speed of construction. The time needed to build and commission an offsite building is often cut in half or by 60% compared to conventional methods, which is widely regarded to be a significant improvement. The building developer has a significant financial benefit from speedy construction in the form of lower financing costs and a quick return.

In summary, Offsite construction has a wide variety of sustainability advantages, some of which are also highly advantageous financially. The faster pace of construction results in a shorter construction schedule, which lowers financing costs and has positive effects on the environment which are the biggest financial benefits. Furthermore, early completion and the resulting early sale or rental income offer major cash-flow advantages. Although various studies demonstrate the advantages of offsite construction, a comprehensive analysis of the market and sector barriers to offsite construction is still required.

References

Barrett, J. & Wiedmann, T. (2007). *A Comparative Carbon Footprint Analysis of On-Site Construction and an Off-Site Manufactured House*. [Online] Available at: http://www.carbonconstruct.com/pdf/comparative_carbon_footprint_analysis.pdf.

Blismas, N. & Wakefield, R. (2009). Drivers, constraints and the future of offsite manufacture in Australia. *Construction Innovation*, *9*(1), pp.72–83. doi:10.1108/14714170910931552.

Construction Excellence. Offsite Production. 2015. Available online: http://constructingexcellence.org.uk/wpcontent/uploads/2015/03/preassembly.pdf

Creswell, J. W. (2013). *Qualitative inquiry & research design: Choosing among five approaches*. 3rd ed. Los Angeles: Sage Publications.

Denzin, N. & Lincoln, Y. (2003). Introduction: The Discipline and Practice of Qualitative Research. *N. Denzin & Y. Lincoln (Eds.). The Landscape of Qualitative Research. Theories and Issues*, 1-45.

Ghaffar, S.H., Burman, M. & Braimah, N. (2020). Pathways to circular construction: An integrated management of construction and demolition waste for resource recovery. *Journal of Cleaner Production*, 244, p.118710. doi:10.1016/j.jclepro.2019.118710.

Goh, M. & Goh, Y. M. (2019). Lean production theory-based simulation of modular construction processes. *Automation in Construction*, 101, pp. 227–244. doi:10.1016/j.autcon.2018.12.017.

Gray, D.E. (2021). *Doing research in the real world*. Washington, D.C.: SAGE Publications Ltd.

Jaillon, L., Poon, C. S. & Chiang, Y. H. (2009). Quantifying the waste reduction potential of using prefabrication in building construction in Hong Kong. *Waste Management*, *29*(1), pp.309–320. doi:10.1016/j.wasman.2008.02.015.

HM Government. (2017). Industrial strategy: Building a Britain fit for the future. *Government White Paper*.

HM Government. (2018). Industrial strategy: Construction sector deal. *HM Government: UK*.

Lawson, R.M., Ogden, R.G. & Bergin, R. (2012). Application of Modular Construction in High-Rise Buildings. *Journal of Architectural Engineering*, *18*(2), pp.148–154. doi:10.1061/(asce)ae.1943-5568.0000057.

Laying the foundations for MMC Expanding the role of Modern Methods of Construction One potential solution to the UK housing crisis. (2016). [online] Available at: https://www.bsa.org.uk/BSA/files/0e/0e05f081-6bb4-4ea2-a87d-aab6c1f5b4c4.pdf.

Lyons, M. (2014). *Mobilising the nation to build the homes our children need*. London: Labour Party.

Miles, J. & Whitehouse, N. (2013). Offsite housing review. *Department of Business, Innovation & Skills and the Construction Industry Council, London*

Modern Methods of Construction. (2019). [online] Available at: https://www.cast-consultancy.com/wp-content/uploads/2019/03/MMC-I-Pad-base_GOVUK-FINAL_SECURE.pdf.

Modular, D. (2019). *A Brief History of Modular Construction*. [Online] Medium. Available at: https://medium.com/deluxe-modular-news-updates/a-brief-history-of-modular-construction-b0177163ec7a.

Nadim, W. & Goulding, J. S. (2010). Offsite production in the UK: the way forward? A UK construction industry perspective. *Construction innovation*.

Publications.parliament.uk. (2018). *House of Lords - Off-site manufacture for construction: Building for change - Science and Tecnology Select Committee*. [Online] Available at: https://publications.parliament.uk/pa/ld201719/ldselect/ldsctech/169/16902.htm.

Reporting to HM Treasury and Cabinet Office Government Construction. (2016). [online] Available at: https://assets.publishing.service.gov.uk/government/uploads/system/uploads/attachment_data/file/510354/Government_Construction_Strategy_2016-20.pdf.

Sinesilassie, E. G., Tabish, S. Z. S. & Jha, K. N. (2017). Critical factors affecting schedule performance: A case of Ethiopian public construction projects–engineers' perspective. *Engineering, Construction and Architectural Management*.

Smith, R. E. (2011). *Prefab architecture: A guide for architects and construction professionals*. [Online] Hoboken, N.J.: John Wiley & Sons. Available at: https://www.wiley.com/en-us/Prefab+Architecture%3A+A+Guide+to+Modular+Design+and+Construction-p-9780470275610.

www.mckinsey.com. (2019). *Modular construction: From projects to products | McKinsey*. [Online] Available at: https://www.mckinsey.com/business-functions/operations/our-insights/modular-construction-from-projects-to-products.

Cite as: Sadabad M.M., "Offsite Construction in the UK: Economic and Environmental Benefits", *The 2nd International Conference on Civil Infrastructure and Construction (CIC 2023)*, Doha, Qatar, 5-8 February 2023, DOI: https://doi.org/10.29117/cic.2023.0047

Mitigating Legal Risks in Construction Project Contracts: The Importance and the Applicability of Force Majeure Clauses

Dana Ahmad Al Marri
Public Works Authority, Doha, Qatar
d.ahmed.almarri@gmail.com

Abstract

Contracts in the construction industry are structured in a manner that splits the risks between different contracting parties; hence risk allocations within the contract affect the price and operation. As most Construction Contracts are long-term contracts, therefore, it is essential to consider having provisions to mitigate foreseeable and unforeseeable risks which may reduce the positive economic prospects and gains, if not, properly evaluated, managed and considered under the contract. For those reasons and many others, the *Force Majeure* (FM) or the act of God clauses are included in almost all construction project contracts.

This paper will provide an analysis of the FM clause in the Public Works Authority (PWA) General Conditions of Contracts (GCOC) for 2018 in terms of the meaning of FM, a list of examples, and the consequences of invoking the FM clause and others. Moreover, the FM clause in PWA GCOC 2018 will be compared with other drafts of the FM clause in other forms of contracts that are used internationally, such as the International Federation of Consulting Engineers General Conditions of (FIDIC) Red Book, 1999 and 2017, and others. This comparison was conducted by taking into consideration scholarly opinions and existing literature on the topic. Finally, the paper addresses the gaps in the existing PWA GCOC FM clause and the applicability of the FM clause in cases such as COVID-19 and then recommends some amendments that could be considered in future contracts.

Keywords: Force Majeure; Contraction; Contracts; General Conditions; FIDIC; COVID-19 Pandemic

1 Introduction

Every construction project is unique and has special requirements to fit its purpose, hence project challenges and risks are also unique and sometimes unforeseen. For those reasons and many others, contracts in this industry are structured in a manner that splits the risks between different contracting parties; hence risk allocations within the construction contracts affect the price and operation.

As most construction contracts are middle to long-term contracts, therefore, it is essential to consider having provisions to mitigate the risks that are foreseeable or not foreseeable. If not properly evaluated and managed, these risks may reduce the positive economic prospects and gains, as poor management of projects risk and uncertainties lead to project failure (Arcadis, 2019). Over the past few years, severe disruption to supply chains due to COVID and others, some activities on projects are impossible to deliver on time, raising all sorts of contractual challenges and therefore, putting all parties in a critical stage during project delivery. For those reasons and many others, the FM or the act of God clauses are provided for in almost all construction contracts.

This paper aims to analyze the gaps in existing GCOC in PWAFM clause that makes it challenging to deal with the situation of health disasters such as COVID-19 or similar unforeseen risks where

performance is not prevented but rather became more expensive and difficult, by comparing it with other forms of contract that are used internationally. Lately, it has become essential to review the FM clauses in construction contracts as we live in a dynamic world with a lot of changes and risks that are new and unforeseen. Moreover, the actual language of the FM clause will be crucial for determining contracting parties' rights and responsibilities in such cases, courts will interpret the FM clause very narrowly.

The paper will start with a literature review and then analyze the existing FM clause in GCOC 2018 in PWA and compare it with the FM clause in other forms of contract. Then, the article provides recommendations that address the gaps in the clause to be considered in future contracts. For this purpose, the paper is divided into four sections as follows, (1) Literature Review, (2) Analysis and Discussion, (3) Recommendation, and (4) Conclusion.

2 Literature Review

This section will provide an overview of the scholarly opinion of FM clauses in construction contracts. At first, this will be for FIDIC, and afterward it will be followed by other forms of Contracts. In addition, an overview of model clause proposed by scholars is also included.

2.1 FIDIC Red Book FM Clause

The FM clause 19 in FIDIC Red Book, 1999 have defined the conditions that have to be satisfied for an event to be considered as a *Force Majeure* event; those conditions are (1) the event has to be beyond the party's control, (2) the party could not have provided against the event before going into contract, (3) the event could not be avoided or overcome, and (4) the event is not attributable to either party. Moreover, the (19.1) sub-clause has listed some examples of *Force Majeure* events.

However, under FIDIC 2017, the term "Exceptional Event" instead of "*Force Majeure*" has been used, and the same four conditions are to be met and are stated under clause (18). Sub clause (18.2) emphasizes on the notice requirement to trigger an exceptional event clause by the affected party. Sub clause (18.3) discusses the duty to mitigate delay and sub clauses (18.4), (18.5) & (18.6) address the consequences of exceptional event occurrence, such as notice to terminate and conditions of release from performance under the law.

In, both FIDIC Red Book 1999 & 2017, the list of events that would constitute *Force Majeure*/exceptional events is not limited to the stated events provided under sub-clauses (19.1) and (18.1) respectively, where the epidemic was not listed. However, the word "epidemic" appears in clause (8.5) of FIDIC 2017, which states that the contractor shall be entitled to a time extension, if unexpected shortages in the supply of personnel or materials result from epidemics or governmental actions (Hansen, 2020).

2.2 FM Clause in other Forms of Contracts

A comparative study, for contract administration guidelines to deal with the FM clauses and other provisions, has been conducted to compare the standard bidding documents for procurement of works (SBDW) used in World Bank (WB) Contracts and FIDIC conditions of contract for construction issued in 1987 and 1999. According to (Fawzy *et al*., 2012) both forms of general conditions of construction have dealt with the consequences of the FM and the difference between *Force Majeure* and employer's risks, differently. It has been found that for the definition of FM event, both contracts are merely identical, except that for the SBDW in WB Contracts, a statement was added with the examples listed to be considered as FM events. The statement was "sabotage by persons other than

the Contractor's Personnel," and this sentence is relevant to stating the difference between *Force Majeure* and risks that are attributed to one party. Moreover, when looking at the consequences of FM event, FIDIC entitled the contractor to payment and extension of time if the contractor suffered cost and delay in fulfilling his obligation under the contract as a result of such an event subject to raising a notice. In this regard, the WB Contract differs from FIDIC in that and the WB Contract specified the payment of the such cost to be "including the costs of rectifying or replacing the Works and Goods damaged or destructed by *Force Majeure*, to the extent they are not indemnified through the insurance policy referred to in Sub-Clause (18.2) [Insurance for Works and Contractor's Equipment]" which entails that the risk of such events has been transferred to the insurer (Fawzy *et al*., 2012).

2.3 Proposal of Different Drafts of FM Clause

Due to the limitation of the existing drafts of the *Force Majeure* scholars, Shafik *et al*., (2016) have proposed an FM clause applicable to contracts governed by civil or common law. When looking into the definition of FM the author found that some contracts provide specific definitions and others refer to a specific law for the needed definition. For those Shafik (2016) suggests that the drafter of such clause should take care when referring to the definition to the governing law to avoid doubts caused by vague formulations. Moreover, it was suggested the clause to list events should be considered FM and those events can be classified into basic groups such as natural, political, incidental, and accidental events. In addition, the clause entails the necessary procedure to invoke *Force Majeure* which includes notice to FM and submission of evidence of the event. With regard to the consequences of the FM event the proposed clause by scholars (Shafik *et al*., 2016) first emphasizes the non performing party's duty to overcome and mitigate the event effects as much as possible. Then, the clause details the consequences of FM such as suspension, an extension of time, or termination.

2.4 FM Clause and Civil Codes

It is essential to highlight that the decision regarding an event as FM is determined in addition to the contract by the governing law of the contract. A study Ezeldin (2018) has addressed the application of FIDIC 1999 contracts under the Egyptian Civil Code (ECC). The ECC Article 373 sets two conditions for an event to be considered as *Force Majeure*, therefore, relieving the party affected from performance. Those conditions are (1) fulfilling the obligation becomes impossible because of an alien reason; (2) the debtor (the affected party) shall have no control over the alien reason.

In Qatar, article 188 of the Qatar Civil Code, the *Force Majeure* concept is recognized as is described in case of the impossibility of performance then the contract would be automatically terminated. Article 171 considers cases whereby the performance is possible but cause losses to the party performing it and court will consider decreasing the losses to a reasonable limit. Moreover, article 172 emphasis that in any cases the execution of the contract must be in accordance to the contract provisions that was agreed of between the contracting parties.

3 Analysis and Discussion

This section will present an overview of the *Force Majeure* Clause in Public Works Authority General Conditions of Contract. Then, a discussion as to what extent this clause is similar to and different from the *Force Majeure* Clause in other contracts used internationally. Finally, a discussion to what extent this clause could be used for claiming Relief of Cost and Relief of Delay as a result of COVID-19.

3.1 Overview of PWA GCOC 2018 FM Clause in Light of FIDIC FM Clause

In Public Works Authority (PWA), there are many forms of general conditions of contracts (GCOC) to suit different types of projects that PWA entered with contractors, consultants, suppliers, and many others. This section provides an overview of the FM clause that is used in multiple forms of contracts such as building and engineering and design and build contracts which are the most used GCOC.

3.1.1 Meaning of *Force Majeure* Event

In GCOC, Clause (14) covers the FM Sub-Clause (14.1) and describes the meaning of FM event, stating that it is an 'exceptional event or circumstance which prevents a party from performing its obligations under the Contract'. Then the Sub-Clause continues to provide the conditions by which the event will be regarded as *Force Majeure*, those conditions are as followed:

a) which is beyond the control of the affected party; and

b) which the affected party, despite all reasonable efforts, could not have provided against before entering into the contract; and

c) which could not have been prevented, overcome or remedied in whole or in part by the exercise by the affected party of reasonable skill, care and diligence to a standard as would be exercised by a party in the same position as the party affected but excluding such event that could be prevented but for either party's breach of its obligations under the contract.'

Furthermore, Clause (14.1.2) provides a list of events that would be regarded as FM Events and includes war, hostilities, rebellion, terrorism, revolution, riot, commotion, disorder, natural catastrophes, loss or damage to goods arising during transportation, and many others. The Clause starts by stating that 'A *Force Majeure* Event shall include any of the following events or circumstances' before providing examples that limit the events that would be regarded as FM events to those listed in the Clause.

Similar to FIDIC 1999, the GCOC in PWA highlighted that the event shall be unforeseen, unavoidable, and uncontrollable and that the event is caused by other than Contractor's Personnel.

3.1.2 Notice of *Force Majeure* Event

Sub-Clause (14.2) emphasizes the requirement of triggering an FM clause to 'give notice to the other Party and the Engineer of the event or circumstances constituting the Force Majeure event and shall specify the obligations, the performance of which is or will be prevented.' The notice shall be given within five working days. Moreover, sub-clause (14.2.4) required the affected party to provide the Engineer with periodic reports on the status of the Force Majeure Event and the efforts to avoid or mitigate the impact. FIDIC has notice of requirement as well.

3.1.3 Notice of Cessation of *Force Majeure* Event

Sub-Clause (14.3) highlights that the affected party shall give notice within 5 days to the Engineer on the cessation of the FM event or its effect and the resumption of performance and obligations under the contract.

3.1.4 No Relief from Payment Obligations

In all circumstances, the occurrence of a *Force Majeure* event shall not relieve any party from payment as described under Sub-Clause (14.4).

3.1.5 Duty to Mitigate

All parties shall work on minimizing any disruption or delay in the performances as a result of FM event and resume full performance of its obligations as soon as practicable as per Sub-Clause (14.5).

3.1.6 Consequences of *Force Majeure* Event

In the occurrence of FM event as described in Sub-Clause (14.1), 'Sub-clause (19.1) [Contractor's Claims] and Sub-clause (14.2) [Notice of *Force Majeure* Event]'the contractor shall be entitled to bring a claim for (a) Relief for Delay, (b) Relief for Cost resulted from measures taken by the contractor as a result of FM event, and (c) Relief for Cost resulted from an instruction by the engineer to undertake remedial measures.

However, the Relief for Cost resulting from measures taken by the contractor as a result of the FM event under Sub-Clause(14.6.1) (b) is subject to 'the Contractor having notified the Engineer of the measures being undertaken within twenty-four (24) hours after initiation of those measures and complying with any instructions of the engineer following such notice'.

3.1.7 Sub-Contractor *Force Majeure* Event

Sub-Clause (14.7.1) highlight that in cases of '*Force Majeure* Event on terms additional to or broader than those specified in Sub-clause (14.1) [Meaning of *Force Majeure* Event]' such events shall not excuse the contractor's non-performance or entitle it to any relief under Clause (14). Sub-Clause (14.7.1) indirectly emphasized the importance of limiting the meaning of FM events to those specified under Sub-Clause (14.1) and that PWA will not take the risk of FM events beyond the signed contract with the contractor of sub-contractors.

3.1.8 Optional Termination, Payment, and Release

Sub-Clause (14.8) highlights that in cases of work prevented because of *Force Majeure* event for more than 63 continuous days or multiple periods of more than 100 days in a year, then either party may give the other party a notice to terminate the contract and the termination shall take effect seven days after the notice. Moreover, Sub-Clause (14.8.2) specifies the requirement related to the submission of final accounts by the contractor within 28 days after the termination and that the authority will only be required to pay the contractor the cost set out in the sub-clause.

3.2 Comparison between GCOC 2018 and FIDIC Red Book FM Clause

Similarities:

- Both clauses have similar conditions that are considered pre-requisite for an event to be regarded as an FM event, except that FIDIC 1999, has added a fourth condition that is not substantially attributed to the other party.
- Both clauses do not specify epidemic and pandemic as an example of an event that could be regarded as an FM event.
- Both highlight that FM event shall not suspend any payment performance under Sub-Clause (19.2) and (14.4) of FIDIC 1999 and GCOC, respectively.
- Sub-Contractor FM Event under GCOC Sub-Clause (14.7) is identical to the one provided under FIDIC 1999 Sub-Clause (19.5).

Differences:

- FIDIC 1999 under Sub-Clause (19.2) required the FM event to be an event that prevented the affected party from performing ‘any’ of its obligations, whereas under GCOC the word ‘any’ was not part of the FM definition, which emphasized that the standard of triggering FM, under GCOC is stricter.
- Unlike the GCOC, which provides a specific list of examples of an event that would be regarded as FM event, FIDIC 1999 started the list of examples by using the phrase 'may include, but not limited to', which indicates that it is a non-exhaustive list. However, the cost entitlement resulting from the FM event under FIDIC 1999 Sub-Clause (19.4) is limited to the list of events provided under Sub-Clause (19.1).

3.3 Applicability of GCOC FM Clause in Case of a Pandemic

On 12 Mar 20, the World Health Organization declared COVID-19 a global Pandemic; this declaration was followed by international travel restrictions and lockdown measures taken by countries to stop the spread of the virus. Those measures have invaded the world and significantly affected contracts and agreements between individuals, companies, and countries. Therefore, there is a significant effect on dealings between the parties and, consequently, on the laws adjudicating cases arising from COVID-19. Whether COVID-19 is considered an FM event or not, it does affect the performance of obligations under many construction contracts fully or partially.

To some extent, construction projects have been isolated from the immediate consequences of the lockdown and COVID-19. Although the laws and circulars that had been issued have effected all day-to-day work and the whole supply chain, exemptions were specifically made to the construction sites in order to be able to meet the deadlines, especially considering the vital delivery of projects that were critical for the host of the world biggest event that is the FIFA 2022 world cup.

To determine whether COVID-19 is an FM event, one needs to scrutinize the contract and the underlying facts that led the affected party to the required relief of obligation. That is because the existence of the COVID-19 event does not automatically mean that the parties are being delayed and the work costs more than planned. The wording of the FM clause and the evidence around the event is crucial when deciding whether an event amount should be considered FM. Therefore, careful thought must be given as to whether a FM event has arisen in exploring the wording of the clause. For instance, according to FIDIC 1999 Clause (19.2) eventual circumstance of an event must have prevented the party from performing an obligation to be rendered as *Force Majeure*. Moreover, deciding whether an event amount to an FM event or not is, in fact, a question of whether the obligation is still capable of being performed as opposed to it becoming more costly and time-consuming to be performed as per the definition of FM under GCOC Sub Clause (19.1) and (19.2).

It is important to highlight that Clause 14.1.2 in GCOC starts by stating that ‘A *Force Majeure* event shall include any of the following events or circumstances’ before providing the list of examples. The use of ‘shall include’ can be interpreted in a manner that limits the use of the FM Clause to the listed example only, and the listed examples do not include Epidemic and Pandemic which could mean the consequences of COVID-19 cannot be claimed under FM Clause in GCOC used in PWA.

4 Recommendation

The effectiveness of using a *Force Majeure* provision depends heavily on how it is drafted (Hansen, 2020). For this reason, this section will provide some insights or propose multiple insights and some amendments which could be adopted to encounter events such as the Pandemic.

4.1 The Difficulty in Performance.

The application of the impossibility test to the specific event shall be addressed amongst all the conditions outlined in FM Clause. COVID-19 is more likely to be classified as a disruption as it does not necessarily prevent performance but makes it more difficult and costly. Moreover, it is important to consider that the event has affected the performance temporarily for a specific period which does not last forever, even though it was unforeseeable when this would happen.

The limitation in the existing GCOC is relevant because it considers events that not only prevent performance but also make the performance difficult or cost more than it should be.

4.2 Options Available for New Drafts

There is not a single FM clause that applies to all circumstances and agreements. Still, when it comes to formulating a *Force Majeure* Clause, the parties have a choice between two options: (1) an explicit list of occurrences with a cross-reference to a term that defines *Force Majeure* should be included in an FM Clause, or (2) in addition to the already existing *Force Majeure* occurrences, the parties might want to think about including a standalone Pandemic provision Zin *et al*., (2021). Regardless of the choice parties decided to adopt, it is essential to draft provisions related to the risk of an unforeseen event, such as the Pandemic, that may not necessarily lead to the impossibility of performance but rather a frustration of the contract to leave no room for ambiguity.

4.3 Procedural Provisions Do Matter

The failure of contracting parties to understand and comply with contractual obligations has emerged as the leading cause of construction disputes. According to Arcadis (2017) the Middle East construction contractor continues to fail to comply with the notice and procedural provisions in the contract; therefore, claim quality is not up to date to ensure an early and fair resolution. Consequently, the FM Clause needs to include provisions that specify the procedure that the party has to follow in any event that amounts to FM. Moreover, it is important for the FM Clause to be holistic and address all aspects of FM events from occurrence to closure. Most importantly, the relief of delay and cost in case of FM event occurrence must be specified and detailed.

4.4 Relief of Time and Relief of Cost

It is very important for FM clause to address the type of relief available, either cost or time or both cost and time, for the affected party as a result of the occurrence of FM event. This is mainly to consider the different nature of FM events as some entitle the affected party only relief of time only and not relief of costs.

4.5 Beyond the FM Clause

In cases where the FM does not cover events like the Pandemic, using other provisions in the contract to request Relief of Delay and Cost resulting from an FM event can be an alternative. Therefore, it will be a wise decision from both parties to reconsider the other provisions to cover the effect of the

event on obligations. For instance, under FIDIC 1999, if COVID-19 consequences were not considered under Clause (19) [*Force Majeure*] it could be considered under other provisions such as Clause (8.4) [Extension of Time, (d) Epidemic or governmental actions] as COVID could be considered as Epidemic and all the lockdown and its consequences could be considered as governmental actions. Moreover, Clause (13.7) [Change of Law] as, governments put restrictions on the movement of people, materials, and many other things and put it in the form of laws, regulations, and circulars. In addition, Clause (13.8) [Changes of Costs], Clause (19.7) [Impossibility], or others could also be adopted for the same, notwithstanding those other theories of impracticality or frustration that might relieve a party from obligations under the contract.

5 Conclusion

We live in a world that has many universal risks which are unforeseen and unavoidable. If construction contracts are silent on such risks, this will create vagueness. To avoid protracted and expensive disputes to resolve the issues on their projects, contracting parties must concentrate on their ability to successfully navigate through turbulent times as the construction industry in the region continues to grow throughout 2022 (Arcadis, 2022). Tighter programs, more complex projects, price inflation, and the supply chain crisis are just a few factors that will undoubtedly make this the case.To address such challenges with certainty contracting parties should consider adopting any of the earlier recommendations that cover situations like the Pandemic. Therefore, it is recommended to have provisions covering risks similar to FM events but not necessarily preventing the performance outcome that would result from the performance of the obligation being much more expensive and the completion of the obligation being delayed. For that, it will be wise to rethink the GCOC to consider future issues and to make those anticipated unforeseen risks well thought of in the contract in terms of their scope, procedural matter relevant to the risk, and the consequences because of the risk occurrence.

Doing so will clear the vagueness if, such risk aurally occurs, and for that, this paper proposes rethinking the risk allocation and management in PWA GCOC to account for the future. Keeping in mind that, according to Arcadis (2022), as a result of COVID the number of disputes in the market will rise in 2022 as business owners and contractors re-engage coming out of COVID. Finally, it should be noted that neither the conclusions nor the assertions made in this paper are meant to be interpreted as legal advice. Instead, it provides an initial proposal to be taken further and rethink in the future.

References

Arcadis. (2022). *Global construction disputes 2019: The higher stakes, the bigger the risk*, pp. 1-28.

——. (2019). *Global construction disputes 2019: The higher stakes, the bigger the risk*, pp. 1-32.

——. (2017). *Global construction disputes 2017: The higher stakes, the bigger the risk*, pp. 1-29.

Ezeldin, A. Samer & Amr Abu Helw. (2018). "Proposed force majeure clause for construction contracts under civil and common laws." *Journal of legal affairs and dispute resolution in engineering and construction* 10.3, 04518005.

Fawzy, Salwa A. & Islam H. El Adaway (2012). "Contract administration guidelines for managing conflicts, claims, and disputes under World Bank–funded projects." *Journal of Legal Affairs and Dispute Resolution in Engineering and Construction*, 4.4, 101-110.

FIDIC (Fèdèration Internationale des Ingènieurs-Conseils), (1999). "Conditions of contract for construction." 1st Ed., Geneva.

FIDIC (Fèdèration Internationale des Ingènieurs-Conseils), (2017). "Conditions of contract for construction." 1st Ed., Geneva.

Hansen, S. (2020). "Does the COVID-19 outbreak constitute a force majeure event? A pandemic impact on construction contracts", *Journal of the civil engineering forum*, Vol. 6, No. 1, pp. 201-214.

Shafik, Noha, et al. (2016). "Application of FIDIC contracts under the Egyptian civil code." *Journal of Legal Affairs and Dispute Resolution in Engineering and Construction*, 8.3, 04516004.

PWA (2018). Building and Engineering (traditional) General Conditions of Contract, *Public Works Authority*, Doha, 1-86.

Zin, S. M. et al. (2021). "A proposed pandemic clause for force majeure events under construction contracts in Malaysia", *Environment-Behaviour Proceedings Journal*, *6*(16), 33-37.

Cite as: Al Marri D.A. & Al Kaabi N., "Mitigating Legal Risks in Construction Project Contracts: The Importance and the Applicability of Force Majeure Clauses", *The 2nd International Conference on Civil Infrastructure and Construction (CIC 2023)*, Doha, Qatar, 5-8 February 2023, DOI: https://doi.org/10.29117/cic.2023.0048

Why Construction Projects are delayed in PWA: Problems and Solutions

Dana Ahmad Al Marri
Public Works Authority, Doha, Qatar
d.ahmed.almarri@gmail.com

Noof Mohamed Al Kaabi
Public Works Authority, Doha, Qatar
nalkaabi@ashghal.gov.qa

Abstract

Construction is, by its nature, complex and uncertain. Changes and variations are inherently part of many construction projects, which require serious efforts to overcome. Project delay is a construction problem resulting in contractual claims, increased project cost, and decreased end-user satisfaction. This study investigates the root causes of project delay in Public Works Authority construction projects and gathers different perceptions on the causes of delay to propose a solution matrix that mitigate the effect of those delays and prevents its reoccurrence in future projects. A sample of over two-handed projects in 2021 have been granted an extension of time to its original completion date have been studied to identify and analyse the root causes of project delay and the risk relevant to the project delivery being prolonged. For these reasons, a categorization of delay has been adopted, and every cause of delay has been coded. The method adopted to identify the top root causes of project delay was the Pareto Analysis (Pareto analysis is premised on the idea that 80% of problems can be traced to 20% of the causes). The result of the study was the development of a holistic solution matrix to address the root causes of delay. The solution consists of two parts, (1) identify the relevant corrective, immediate and preventive actions, and (2) develop a responsibility matrix for the implementation of those solutions to ensure its governance.

Keywords: Construction projects; Delay; Cost; Problem Solution Matrix; Public Works Authority

1 Introduction

Delay in the project delivery led to additional cost associated with in direct cost (prolongation cost), additional consultant fees, disruption / Loss of Profit and the most critical impact related to the customer satisfaction. The objective of this study is to (1) identify major root cause of projects delays and to (2) propose the required actions to resolve the issue of project delays. To focus on delay causes related to the risk and responsibility of PWA result in Contractor's entitlement to bring forth claims for relief associated to the time for completion and/or additional costs.

The study was planned to be conducted in two phases as follows:

1. Phase (1) in 2022 focused on delay related to the authority (Public Works Authority) and other government agencies or end users
2. Phase (2) in 2023 cover the other causes of delay attributed to Contractor or other causes.

The reasons of limiting the scope on phase (1) to the Authority delay causes was because first it represents the controllable and internal causes compared to the other causes, and second it is the causes which leads to awarding extension of time completion to the projects.

2 Methodology

This section will present the steps taken to identify the issue of project delay and propose the necessary action to resolve it.

2.1 Classifying the Cause of Delays

The first step to identify the majors root causes to delay the projects by categorising the reasons of the delay using delay code. For that scholar exercises have been adopted such as the one presented by Lo *et al.*, (2006) which was further adjusted to fix the context in PWA. This exercise results shows the delay category presented in Fig. 1 below.

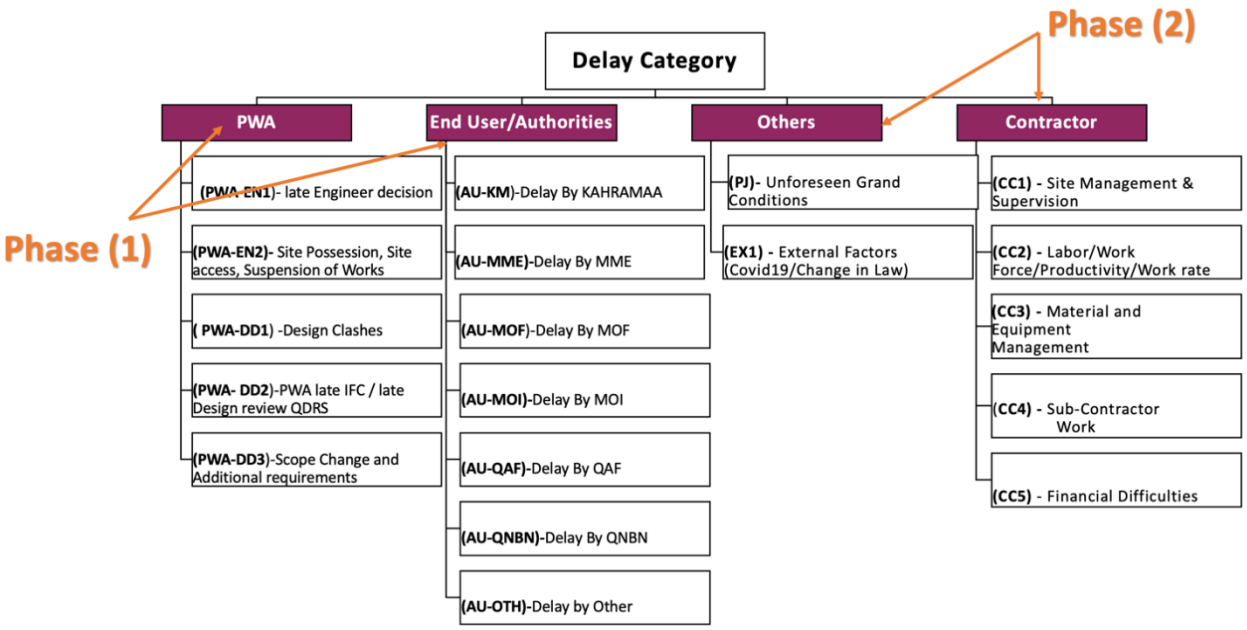


Fig. 1: Causes of Delay Categorization

It is important for delay category in PWA to have a common language used by all parties within the organization and in describing a particular delay. The delay category was discussed and agreed on during workshops which were conducted with project delivery departments.

2.2 Study the Existing Status

We will not be able to address a problem without the accurate diagnosis by analysing the available data which was the second step taken in this study. The diagnosis starts from determining the current situation based on data related to extensions of time (EOT) which was awarded to the construction contracts. The EOT issued by the competent department in PWA to construction projects in 2021 were approximately 200 No's, those EOT were analysed according to the agreed delay category. There are multiple reasons for project delays, 15 reasons, and it is, not possible, at a first stage to identify all of them. For that we used Perto chart to identify the fundamental reasons, which represent 20% of the reasons and have an impact of 80% on the problem as presented in the below chart.

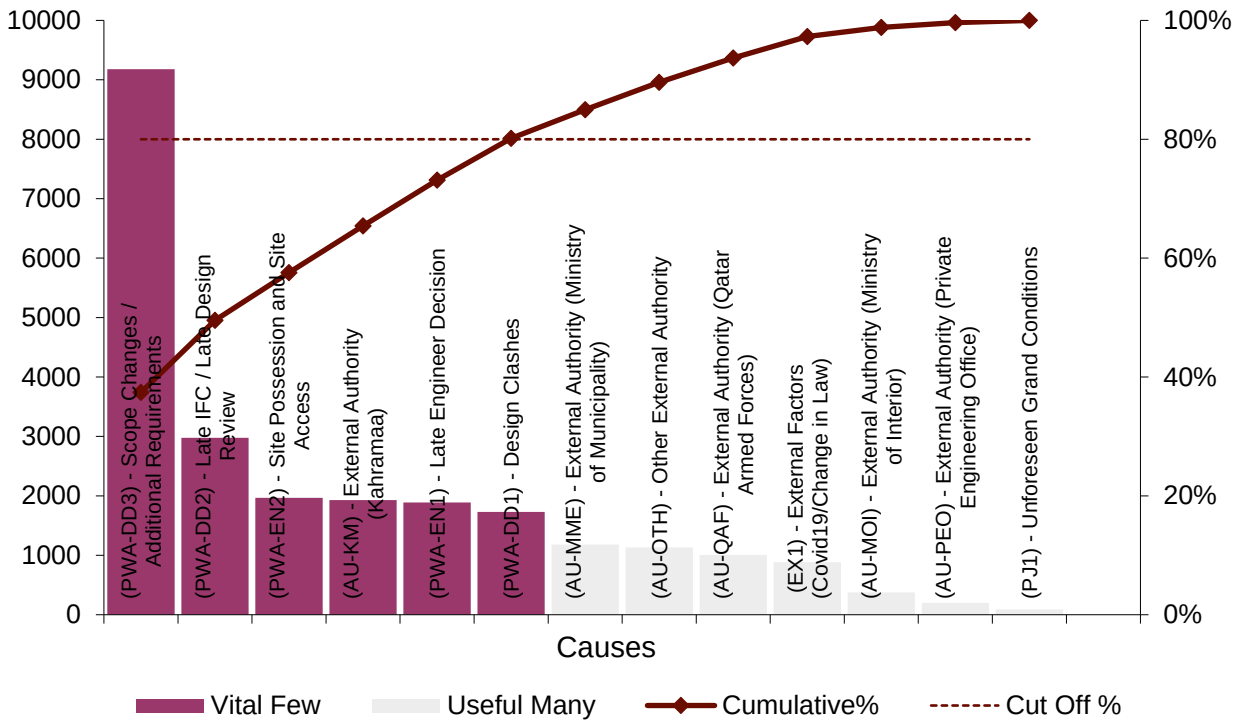


Fig. 2: Root Causes Pareto Analysis

The result shows that 6 delay reasons contribute to 80% of the problem, those delay causes are as follows:

1. (PWA-DD3) - Scope Changes / Additional Requirements
2. (PWA-DD2) - Late IFC / Late Design Review
3. (PWA-EN2) - Site Possession and Site Access
4. (AU-KM) - External Authority (Kahramaa)
5. (PWA-EN1) - Late Engineer Decision
6. (PWA-DD1) - Design Clashes

Changes in the scope of the project include, its requirements, and additional works amounting to approximately 40%, but are not limited to change in drainage strategy, adding additional network, change in construction method, switch from temporary to permanent roads and many others. The sound top cause is last issuance of issue for construction drawings and securing the relevant road opening permits.

2.3 Holistic Actions

As presented in Fig. 3 the action required to resolve the delay causes are split into three different forms of action, (1) preventive actions to eliminate the cause of the future potential delay, (2) immediate action to make the right and correct interventions that take place immediately to respond to the delay while occurring, and (3) corrective actions to prevent the reoccurrence of the delay in the future.



Fig. 3: Type of Action / Intervention

2.4 Development of Responsibility Matrix

There could not be one entity on the responsibility of projects delays, in PWA all affairs, departments, personnel take own responsibility to address the issue. For that as represented in Fig. 4 a responsibility matrix was developed for all the proposed actions. The responsibility matrix divides into five different roles for different entities towards implementing a specific action, those roles are (1) accountable, (2) responsible, (3) support, (4) consulted, and (5) informed. The importance of developing the responsibility matrix lies on the fact that they needed governance for the actions to be carried continuously to address the problem.



Fig. 4: Responsibility Matrix

2.5 Solution Implementation

Several workshops were conducted with different parties within the organization to come up with the actions required. Actions are visiting monthly for follow up and to make the necessary amendments if required.

3 Challenges

The main challenge which faces this study can be summarized as following:

1. Some proposed solutions are already on existing system such as the enterprise risk management and project charted application for which we must study what the existing system provides and not what the gaps are within that existing system. This does not address the issue on hand.

2. The development of the responsibility matrix was a bit challenging because it requires the management consent on taking some responsibilities and accountability toward the proposed actions.

4 Future Thoughts

Expand the scope of the study to phase (2) in 2023, and take into consideration literature in the matter that addresses the issue especially in terms of expectation of delay occurrence and avoidance.

5 Conclusion

Thank all of our colleagues for the support and collaborative work that was conducted for the purpose of this study and we are looking forward to much more collaboration in the future.

References

Lo et al. (2016). "Construction delays in Hong Kong civil engineering projects," *Journal of construction engineering and management*, 132.6, 636-649.

Cite as: Al Marri D.A. & Al Kaabi N., "Why Construction Projects are Delayed in PWA: Problems and Solutions", *The 2nd International Conference on Civil Infrastructure and Construction (CIC 2023)*, Doha, Qatar, 5-8 February 2023, DOI: https://doi.org/10.29117/cic.2023.0049

Theme 2:

Advances in Infrastructure Sustainability, Renovation, and Monitoring

Modeling Short-Term Deflection of Reinforced Concrete Slabs using the Layered Approach

Abeer A. Fageer
Department of Civil Engineering, Faculty of Engineering, University of KhartoumKhartoum, Sudan
abeerfageer97@gmail.com

Shahd K.Abdelgadir
Department of Civil Engineering, Faculty of Engineering, University of KhartoumKhartoum, Sudan
shahdkabdelgadir17@gmail.com

Anfal A. Abdelgadir
Department of Civil Engineering, Faculty of Engineering, University of KhartoumKhartoum, Sudan
Anfal.ali98.5@gmail.com

Amina M. Elbagir
Department of Civil Engineering, Faculty of Engineering, University of KhartoumKhartoum, Sudan
Aminaelbagir9@gmail.com

Mohammed A.Kabosh
Department of Civil Engineering, Faculty of Engineering, University of KhartoumKhartoum, Sudan
mohammedkabosh@hotmail.com

Amged O. Abdelatif
Department of Civil Engineering, Faculty of Engineering, University of KhartoumKhartoum, Sudan
Amged.Abdelatif@uofk.edu

Abstract

This paper examines the short-term deflection of reinforced concrete slabs taking the tension-stiffening phenomenon into account. The main goal of this study is to develop a model that predicts the deflection of one-way slabs made of reinforced concrete. The model takes into account concrete contribution in carrying tension between cracks thoroughly considering the stress-strain relationship material model. The model has been developed using MATLAB Program incorporating a numerical technique known as the layered approach. The developed layered approach model was validated using experimental deflection results reported in a previous study. Based on the experimental validation, the model showed its tendency in predicting the real-case deflection of one-way concrete reinforced slabs. It was concluded that different types of tension stiffening models can be added to the program to model deflection and crack propagation.

Keywords: Short-term deflection; Tension stiffening; Modeling; Stress-strain relationship

1 Introduction

Cracking of Reinforced Concrete (RC) member takes place when the tensile stress acting on the flexural mebmer exceeds the tensile strength of the extreme fiber. The diversity in the rigidity of the member throughout its length due to cracking creates difficulty in the estimation of deflection. In a cracked member, the uncracked area has the most rigidity, while it is the smallest in the cracked area (Gilbert & Warner, 1978). However, at intermediate regions between adjacent cracks, due to the bond action, concrete surrounding reinforcement keeps part of its tensile force, which effectively stiffens the member's reaction and decreases deflection. This effect is recognized as tension-stiffening (Gribniak, 2009). If the effect is ignored, Calculated Deflection may be significantly overestimated.

Cracking and tension stiffening (Lam et al., 2010) factors have the greatest impact on the numerical outcomes of concrete members under short-term loading. Numerical techniques are an effective way to examine the performance related to the design and optimization of deflection. They can comprise all conceivable material effects that give reinforced concrete's behavior its complicated nature. Numerical solutions are usually used in finding a solution for structural behavior governed by pre-defined material models. Commonly, a material model consists of equations that illustrate the relation between the stress and strain for a specific material. Material models are classified into different groups and in each group, a detailed principle is governing the stress-strain relation. In each material model, certain parameters are defined, which represent the specification of the characteristics of a specific material. Those parameters could be obtained by performing a nonlinear analysis to experimental results, where curve fittings and statistical methods are used to identify the parameter's values. For example, material models such as stress-strain relationships are implemented to obtain the values of curvature for further analysis of deflection (Sokolov, 2010).

The stress-strain model permits the tensile stresses to be produced using a tensile stress block, in the concrete in the spaces between adjacent fractures. It is commonly more applicable for any variety of shapes in members whether or not subject to axial loads and being bent uniaxially or biaxially. Tensile stress blocks can be efficient when performing full-range analysis under both service & ultimate conditions. The exact tensile stresses' magnitude in a cracked concrete member is incredibly challenging to assess. Therefore, current tensile stress blocks have been produced by suggesting a certain tensile stress block with unspecified parameters. Theoretical moment-curvature or load-deflection curves derived from the experiment are used to obtain the value of these parameters by curve fitting. Tensile stress blocks with linear ascending and descending branches are expressed in terms of $\alpha_1 \; and \; \alpha_2$ and these parameters have a different range of values according to a different type of load, tension reinforcement ratio, applied moment, and effective depth to total depth ratio (Lam *et al.*, 2010).

Recently, numerical techniques have been widely used to simulate structural complexity in real-case scenarios. Main equations are frequently simple and fail to reflect the material's complex multi-factor nature; therefore, don't assure higher statistical precision of deflection for flexural RC members (Sokolov, 2010). One of the numerical techniques that is well-known in calculating the deflection of RC members is the layered approach (Gribniak et al., 2012). A Layer model can be conveniently used for calculating stresses and internal forces at every cross-section along the length of the RC member. For steel reinforcement, stresses can be predicted from the longitudinal strains utilizing its experimental stress-strain curves. Since the applied moment is known, the problem could be solved considering the equilibrium equations for both axial force Eq (1), and bending moment Eq (2).

$$A_o \varepsilon_o - A_1 \psi_0 = 0 \qquad (1)$$

$$A_1 \varepsilon_o - A_2 \psi_0 = M \qquad (2)$$

$$A_o = \sum_{i=1}^{m} R_{ci} b h_i + E_s A_s + E_s A_s \qquad (3)$$

Where, ε_o the strain at the top fiber (reference point), ψ is the curvature, M is the applied moment at the section, and:

$$A_1 = \sum_{i=1}^{m} R_{ci} b h_i \, y_i + E_s A_s d + E_s A_s' d' \qquad (4)$$

$$A_2 = \sum_{i=1}^{m} R_{ci} b h_i \, {y_i}^2 + E_s A_s d^2 + E_s A_s' d'^2 \qquad (5)$$

m is the number of concrete layers in each section.

R_{ci} is the material stiffness for each concrete layer.

b is the width of the cross-section.

A_s is the cross-section area of the steel reinforcement in tension.

$A_s'$is the cross-section area of the steel reinforcement in compression.

E_s is the elasticity modulus of steel.

d is the depth of reinforcement in tension.

d' is the depth of reinforcement in compression.

y_i is the coordinate of the layer measured downwards from the reference point (top fiber).

h_i is the thickness of the layer.

2 Method of Analysis

The slab was split into several equal sections throughout its entire length. Then, the moment was calculated for each segment. The procedure of calculating short-term deflection using the Stress-Strain relationship layered approach starts by finding the average cracked curvature using the stress-strain material model. However, initially, the values of the curvature and strain (of the top fiber) were assumed to proceed with further calculations. Afterward, the model will substitute those initial values in equations (1) and (2). Unless the two expressions on the left-hand side and the right-hand side of eq (1) & (2) are equaled, MATLAB's solver will assume new initial values of strain and curvature iteratively. The conditions for the averaged crack section used in the MATLAB model script are given below (Carreira DJ & Chu, 1986; Torres et al., 2004).

$$\varepsilon_i \leq \varepsilon_{ct}\ , \qquad \mathrm{R_{ci}} = \mathrm{E_C} \qquad (6)$$

$$\varepsilon_{ct} \leq \varepsilon_i \leq \alpha_2 \varepsilon_{ct}, \quad \mathrm{R_{ci}} = \mathrm{E_t} \qquad (7)$$

$$\alpha_2 \varepsilon_{ct} < \varepsilon_i, \qquad \mathrm{R_{ci}} = 0 \qquad (8)$$

$$\varepsilon_{ct} = \frac{f_{ctm}}{E_c} \qquad (9)$$

$$\varepsilon_i = \varepsilon_o - \psi y_i \qquad (10)$$

$$E_t = \frac{\frac{\alpha_1 f_{ctm}(\alpha_2 \varepsilon_{ct} - \varepsilon_i)}{(\alpha_2 \varepsilon_{ct} - \varepsilon_{ct})}}{\varepsilon_i} \qquad (11)$$

ε_i is the strain at the top fiber (reference point).

ε_{ct} is the mean value of the strain of concrete.

ε_i is the strain at the midpoint of each layer.

R_{ci} is the material stiffness for each concrete layer.

E_t is the secant deformation modulus in the descending branch.

α_1,α_2 are dimensionless coefficients considered in this study, the values of α_1 and α_2 are 0.5 and 10, respectively, according to Damjanic & Owen (Lam *et al.*, 2010).

f_{ctm} is the mean concrete tensile strength.

Using the curvature values obtained from the above equations, the deflection values were calculated using the following Equations (9-11) (Eurocode 2, 2008).

$$\theta_i = \theta_{i-1} + 0.5\frac{l}{n}\left(\psi_{m(i)} + \psi_{m(i-1)}\right) \quad (12)$$

$$\delta_i = \delta_{i-1} + \frac{l}{2}\left(\frac{\theta_{(i)}+\theta_{(i-1)}}{n}\right) \quad (13)$$

$$\delta_{corrected(i)} = \delta_b \frac{x_i}{l} - \delta_i \quad (14)$$

Where θ_i, is the cumulative slope for each section, δ_i is the cumulative deflection for each section, and δ_b is the cumulative deflection at the right support.

3 Validation of the Model

To validate the numerical MATLAB model, its results were compared against experimental results which were previously reported in (Abdelatif & Wahab, 2016). In the previous experimental study, the slab was simply supported and tested under a point load positioned at the mid of the beam. In order to conduct an accurate validation of the model, the same dimensions and slab material properties were identical to those reported in the experimental study. The slab material properties and dimensions are shown in Table 1.

Table 1: The Properties of the Slab

Parameter	Value
Length of the slab, L (mm)	2000
Width of the slab, b (mm)	550
Concrete Elastic Modulus, E_c (Gpa)	32.8366
Steel Elastic Modulus, E_s (Gpa)	200
Area of Steel Reinforcement, A_s (mm^2)	1146
Characteristic Cylinder Strength, f_{ck} (Mpa)	30
Mean Characteristic Tensile Strength, f_{ctm}(Mpa)	2.89
Max Pointed load, P (kN)	14.715
Thickness of slab, h (mm)	80

Furthermore, Load-mid span deflection curve obtained from the model was compared to the experimental one as shown in Figure 1. It can clearly be seen that the developed model has a good match with the outcomes of the experiment. Therefore, such models can be used widely to study different flexural members.

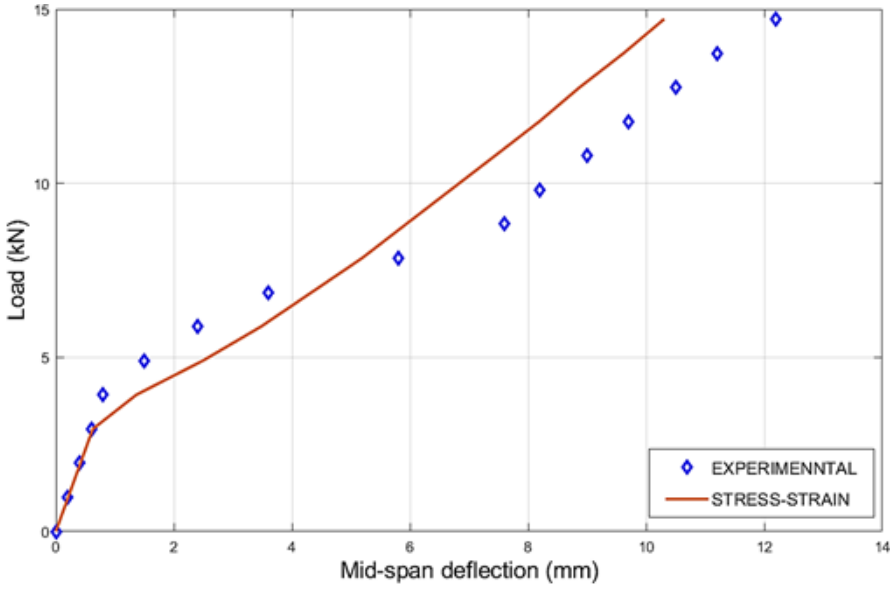


Fig. 1: Load-Deflection for a slab subjected to point load

3.1 Simulation of Strain Contour

In order to visualize the strain results on a concrete surface at different load steps before and after cracking, 2D contours were generated from the results using MATLAB as shown in Figure 2(a). In this example, only in 6 loading steps, as in the experiment, the contours are generated, however it could be generated for uncountable loading steps. As reported in the literature Abdelatif and Wahab (2016), concrete starts cracking when the tensile strain exceeds 0.01 % (i.e 0.0001). Accordingly, this limit is reached at the second loading step where the mid-span load is 3.924 kN in this case. This will directly interpret why the load-deflection curve goes in non-linear behavior after this step. These strains kept increasing as the load increased.

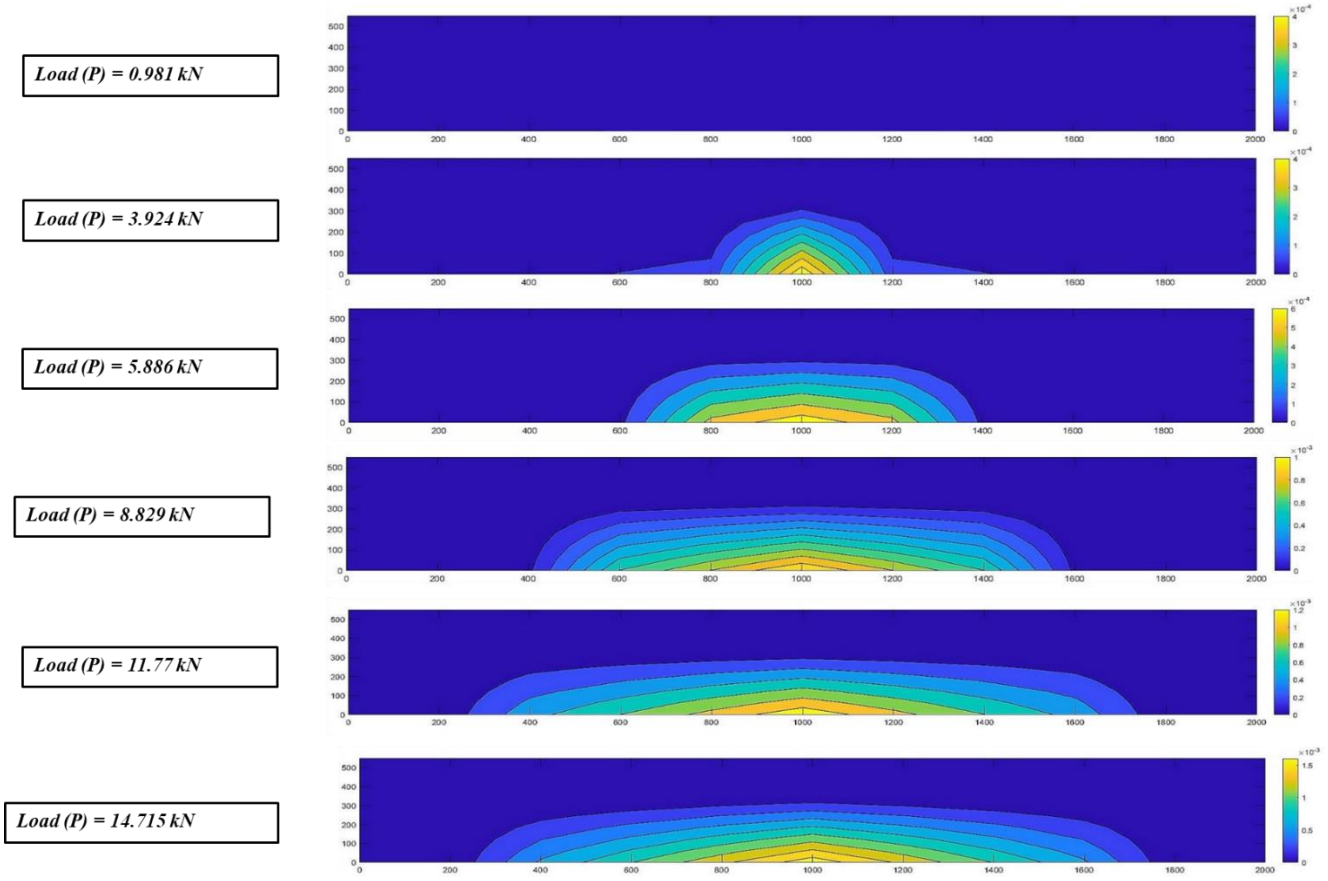


Fig. 2: Simulation of Strain Contour of One-Way Slab

4 Conclusion & Recommendations

In the study, a numerical model is developed to estimate the one-way slabs reinforced concrete's short-term deflection using the layered approach based on the average stress-strain material model. The model has been developed and created from the material model and layered method's fundamental equations using the MATLAB program to solve those equations iteratively. By comparing the developed model deflection results to the experimental deflection results for the same slab, good agreement was observed. One of the advantages of the developed model is that different tension stiffening models can be incorporated to estimate deflection and crack propagation. For future work, such models can be extended to study different reinforced concrete structural members under flexure considering different loading systems and different material models. In connection, the obtained results from this model can be compared to other simulation models that adopt different numerical techniques such as Finite Element Modelling.

References

Abdelatif, A. & Wahab, A. (2016). 'Flexural Strengthening of One-Way Slabs Using Concrete Overlay', *Journal of the Audio Engineering Society*, *62*(May), pp. 17–21.

Carreira, D. J., & Chu (1986). 'The moment–curvature relationship of reinforced concrete members.', *ACI Journal*, *83*(2), pp. 191–198.

Eurocode 2 : Design of concrete structures (2008). London: British Standards Institution.

Gribniak, V. (2009) *Vilnius Gediminas Technical University Shrinkage Influence on Tension-Stiffening of Concrete Structures*, https://doi.org/10.1016/j.proeng.2011.07.180.

Lam, J. Y. K., Ng, P. L. & Kwan, A. K. H. (2010) 'Tension stiffening in concrete beams. Part 2: Member analysis', *Proceedings of the Institution of Civil Engineers: Structures and Buildings*, *163*(1), pp. 29–39. doi: 10.1680/stbu.2009.163.1.29.

Gilbert, R. I., & Warner, R. F. (1978) 'Tension Stiffening in Reinforced Concrete Slabs', *Journal of the Structural Division*, *104*, pp. 1885–1900, https://doi.org/10.1080/13287982.2008.11464997.

Sokolov, A. (2010) '*Tension stiffening model for reinforced concrete beams*',PhD Thesis, Vilnius Gediminas TechnicalUniversity,Vilniaus,Lithuania.

Torres, L., López-Almansa, F. & Bozzo, L. M. (2004). 'Tension-Stiffening Model for Cracked Flexural Concrete Members', *Journal of Structural Engineering*, *130*(8), pp. 1242–1251. doi: 10.1061/(asce)0733-9445(2004)130:8(1242).

Gribniak, V. (2012). 'Improving efficiency of inverse constitutive analysis of reinforced concrete flexural members', *Scientific Research and Essays*, *7*(8). doi: 10.5897/sre11.1752.

Cite as: Fageer A., Khalid S., Abdelgadir A., Elbagir A., Kabosh M. & Abdelatif A., "Modeling Short-Term Deflection of Reinforced Concrete Slabs Using the Layered Approach", *The 2nd International Conference on Civil Infrastructure and Construction (CIC 2023)*, Doha, Qatar, 5-8 February 2023, DOI: https://doi.org/10.29117/cic.2023.0050

Early Thermal Cracking Control of Concrete Structures in Qatar

Firas Alkadour
Public Works Authority (Ashghal), Doha, Qatar
falkadour@ashghal.gov.qa

Christina Anagnostaki
Public Works Authority (Ashghal), Doha, Qatar
canagnostaki@ashghal.gov.qa

Theodoros Tzaveas
Public Works Authority (Ashghal), Doha, Qatar
ttzaveas@ashghal.gov.qa

Anil Kumar Oruganti
Public Works Authority (Ashghal), Doha, Qatar
aoruganti@ashghal.gov.qa

Ali Kara
Public Works Authority (Ashghal), Doha, Qatar
akara@ashghal.gov.qa

Abstract

Thermal cracks can occur in concrete elements at early stages during the hardening process. Also, the impact of thermal contraction and drying and autogenous shrinkage, may lead to excessive tensile strains and as a result cracks will occur. Consequently, an increase in reinforcements may be required to satisfy Early Thermal Cracking (ETC). ETC remains a major concern for concrete structures, especially for structures with high demand of water tightness. Considering the significance of water leaking in underground structures and the rising of the groundwater table in Qatar in the recent years, the Public Works Authority (ASHGHAL) has set the criteria to control early thermal cracks for Highway and Drainage Structures. This paper aims to present a comparison between the Early Thermal Cracking (ETC) codes and guidelines aiming towards providing sustainable and efficient design. This study compares the design method and parameters considered in BD 28/87, CIRIA C660 and CIRIA C766 currently used in Qatar for ETC calculations such as crack width permissible limit, minimum area of reinforcements, temperature change at early age, long term ambient temperature, autogenous shrinkage, drying shrinkage and restraint conditions. In addition, ETC calculations are carried out for a tunnel reinforced concrete box section with wall and top slab thicknesses ranging from 300mm to 1000mm. The least required area of reinforcements ($A_{s,req}$) for wall subject to edge restraint was by CIRIA C766 and for top slab subject to end restraint was by BD 28/87.

Keywords: Early Thermal Cracking; Underground Concrete Structures; CIRIA C766; CIRIA C660; BD 28/87

1 Introduction

After casting, concrete is subjected to volumetric changes at early age and in the long-term leading to cracks when subjected to restraint. The volumetric changes are caused by imposed deformations from temperature caused by heat of hydration due to concrete cooling from its peak temperature and ambient temperature contraction due to concrete cooling to lowest ambient temperature. Further, volumetric

changes result from shrinkage due to drying shrinkage where concrete shrinks while drying and autogenous shrinkage where the concrete shrinks due to chemical hydration (Gilbert & Ranzi, 2010).

In Qatar, Public Work Authority (PWA)'s design criteria for highway structures follows Ashghal Interim Advice Note No. 009, Revision No. A2 (Ashghal, 2016) which states that checking for early thermal cracking is to be carried out by either BD 28/87 (Highway Agency, 1989) or CIRIA Report C660 (Bamforth, 2007). Further, design criteria for drainage structures such as water retaining structures follows PWA Standard Drawing # SD 8-4-106_Rev.03 (Ashghal, 2019), which requires structures to be designed following BS EN 1992-1-1 (BSI, 2004) and BS EN 1992-3 (BSI, 2006). In NA to BS EN 1992-3 (BSI, 2009), reference to CIRIA C660 (Bamforth, 2007) is specified for complementary guidance on ETC. Moreover, CIRIA C660 was superseded by CIRIA C766 (Bamforth, 2018) where several parameters were modified.

This paper aims to present salient points of our study with a comparison between the Early Thermal Cracking (ETC) codes and guidelines aiming towards providing sustainable and efficient design. This study will compare the design method and parameters considered in BD 28/87, CIRIA C660 and CIRIA C766 currently used in Qatar for ETC calculations such as crack width permissible limit, minimum area of reinforcements, temperature change at early age, long term ambient temperature, autogenous shrinkage, drying shrinkage and restraint conditions. In addition, example of a tunnel under a constant water table is considered to quantify the required reinforcements for ETC of typical concrete elements subject to similar configurations and restrain conditions.

2 Early Thermal Cracking Guidelines

2.1 Key differences between ETC guidelines

The approach followed by the guidelines, as listed below, is generally similar but there are key differences impacting the calculated required reinforcements to meet the allowable crack width limit.

- BD 28/87 (Highway Agency, 1989) generally follows the method of BS 8007 (BSI, 1987) and CIRIA C660 (Bamforth, 2007) & C766 (Bamforth, 2018) follow BS EN 1992-3 (BSI, 2006).
- Concrete effective area is calculated differently impacting the required minimum area of reinforcement and calculated steel ratio considered in crack width calculations.
- Concrete cover is included in crack width calculations with CIRIA C660 (Bamforth, 2007) & C766 (Bamforth, 2018). In contrast, BD 28/87 Highway Agency (1989) only states to place the reinforcement as close to the surface in compliance with cover requirements without including the influence of cover on crack width.
- In CIRIA C660 (Bamforth, 2007) & C766 (Bamforth, 2018), expressions for crack width calculations (i.e. crack-inducing strain) varies depending on the nature of the restraint (i.e. continuous edge restraint, end restraint or internal restraint) unlike BD 28/87 (Highway Agency, 1989).
- Autogenous shrinkage is included in CIRIA C660 (Bamforth, 2007) & C766 (Bamforth, 2018).

2.2 Key Differences between CIRIA C660 and CIRIA C766

The approach followed by the guidelines, as described below, is generally similar but there are key differences impacting the calculated required reinforcements to meet the allowable crack width limit:

- Minimum area of reinforcements ($A_{s,min}$):

  $A_{s,min}$ required in CIRIA C766 compared to C660 is significantly reduced by considering $f_{ct,r} = 0.7\ f_{ctm}$ instead of f_{ctm} and introducing the k_{Redge} coefficient, where f_{ctm} is the concrete's mean value of tensile strength, $f_{ct,r}$ is the concrete's low characteristic tensile strength and k_{Redge} is a coefficient accounting for transferring part of the load to the restraining element (edge) when crack happens.

- The crack-inducing strain (ε_{cr}):

  In crack-inducing strain calculations, CIRIA C766 recommends using $f_{ct,r} = 0.7\ f_{ctm}$ instead of f_{ctm} used in CIRIA C660 as the value of concrete tensile strength.

- Coefficient for bond properties of reinforcements (k_1):

  CIRIA C660 recommended to increase k_1 value proposed in BS EN 1992-1-1 from 0.8 to 1.14 by implementing a reduction factor of 0.7 to cover cases with poor bond, unless the lower value is verified by experience. CIRIA C766 stated that poor bond applies to elements with thickness larger than 300 mm and also have concrete cover ≤ 50 mm.

- Concrete cover (C):

  CIRIA C660 considers using nominal cover (C_{nom}) in compliance with BS EN 1992-1-1 by adding an allowance for deviation (ΔC_{dev}) of 10 mm to the minimum cover (C_{min}). However, in CIRIA C766, C_{min} is recommended to be used.

- External Edge Restraint (R):

  Restraint factor is adjusted in CIRIA C766 to consider the restraint at the location of the maximum crack width and not at the joint and accordingly reducing the restraint value.

2.3 Minimum Area of Reinforcements ($A_{s,min}$)

$A_{s,min}$ is required to control crack width by limiting the steel stress to its yield strength due to the stress transfer to steel after cracking. For $A_{s,min}$ calculation, refer to equations 2, 3.12 and 3.20 provided in BD 28/87, CIRIA C660 and CIRIA C766, respectively.

2.4 Crack Width (CW)

Area of reinforcements required to meet allowable crack width limit ($A_{s,cw}$) is determined in accordance with equations 3, 3.15 and 3.23 provided in BD 28/87, CIRIA C660 and CIRIA C766, respectively.

2.5 Other Factors Affecting ETC

2.5.1 Temperature drop from hydration peak to mean ambient (T1).

The main variables affecting T1 are summarized under Table 1. In BD 28/87, tabulated T1 values are provided depending on the defined cement content, formwork type and casting season. In addition, for sections with thickness larger than 500 mm, T1 is increased by 10 ^{o}C. On the other hand, in CIRIA C660 and C766, T1 values maybe determined from excel spreadsheets developed by CIRIA taking into consideration many influencing variables such as binder content, binder type, concrete placing temperature, temperature ambient conditions, section thickness, formwork and insulation, etc.

Estimated T1 values considering the variables as defined under Table 1 were plotted in Figure 1 and Figure 2. Figure 1 shows a comparison between the guidelines under consideration for binder type CEM 1 considering different temperature values for Qatar (QA) and United Kingdom (UK). Unlike BD 28/87, the spreadsheet calculator provided by CIRIA considers the placing and ambient temperatures as variables and therefore can be adjusted to accommodate Qatar's hot climate. This can be observed in Figure 1 where higher T1 values resulted from CIRIA when placing temperature and ambient temperature were adjusted to suit Qatar's hot climate.

Figure 2 shows estimated T1 calculated in accordance with CIRIA guidelines for different binder types and taking into consideration Qatar's higher temperatures. It can be observed that T1 values obtained for binder Type CEM1 and Fly Ash are exactly similar. However, the key difference is the overestimated T1 values obtained from C660 for concrete with ground granulated blast-furnace slag (GGBS) binder type which were recalibrated in C766 based on feedback from users.

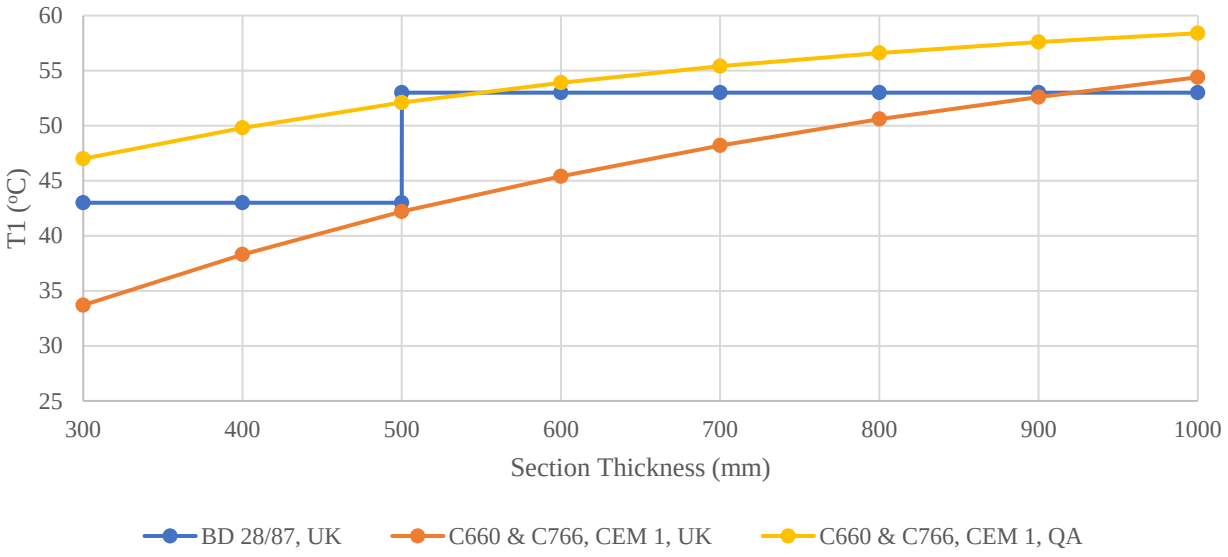


Fig. 1: T1 Values for CEM 1 Binder Type in Qatar (QA) and United Kingdom (UK)

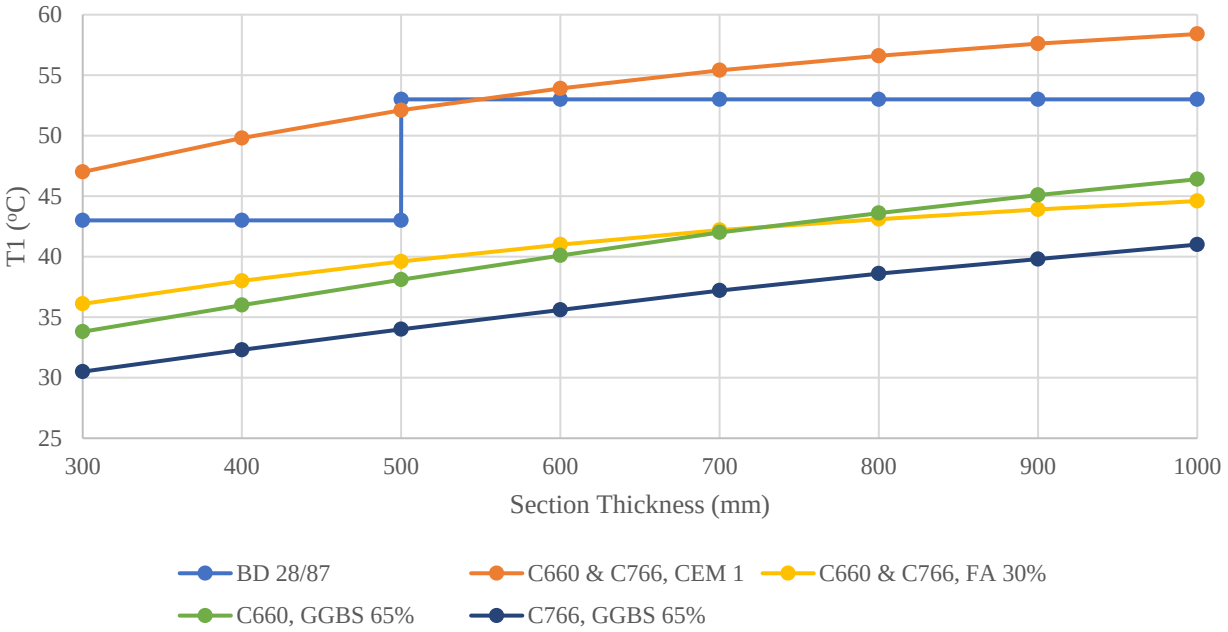


Fig. 2: T1 Values for Different Binder Types in Qatar (QA)

Table 1: Variables Impacting T1

Variable			Standards			Assumed Values	Reference to Local Conditions Applicable to Qatar
			BD 28/87	CIRIA C660	CIRIA C766		
Concrete Mix Details	Binder Content		✓	✓	✓	400 kg/m^3	Maximum cementitious content without special consideration as per QCS 2014, Section 05, Part 06, Cl. 6.3.1(2) (Technical Regulation, 2014)
	Binder Type	CEM 1	✓	✓	✓	CEM 1, 100%	-
		Fly Ash	×	✓	✓	Fly Ash, 30%	% of cementitious material is based on ranges specified under QCS 2014, Section 05, Part 06, Table 6.6 (Technical Regulation, 2014)
		GGBS	×	✓	✓	GGBS, 65%	
	Wet Density		×	✓	✓	2400 kg/m^3	-
	Specific Heat		×	✓	✓	1 kJ/kg^{o}C	-
	Thermal Conductivity		×	✓	✓	2 W/m^{o}C	Applicable to Aggregate from Gabbro type with siliceous sand as per CIRIA C766, Cl. 4.5 (Bamforth, 2018).
Temperature Input	Casting Season		✓	×	×	Summer	-
	Placing Temperature		×	✓	✓	32 ^{o}C (QR)	Maximum fresh concrete temperature as per QCS 2014, Section 05, Part 06, Cl. 6.3.1(4) (Technical Regulation, 2014)
						20 ^{o}C (UK)	
	Ambient Temp.	Min.	×	✓	✓	5 ^{o}C (QR)	Qatar (QA) values are as per QCS 2014, Section 01, Part 01, Cl. 1.5.2(4) (Technical Regulation, 2014). UK values are as per CIRIA 766, Cl. 4.2.2 (Bamforth, 2018).
						10 ^{o}C (UK)	
		Mean	×	✓	✓	27.5 ^{o}C (QR)	
						15 ^{o}C (UK)	
		Max.	×	✓	✓	50 ^{o}C (QR)	
						20 ^{o}C (UK)	
		Constant or variable	×	×	✓	Variable	-
	Placing Time		×	✓	✓	10 hours	Assumed placing time for maximum impact
Section and formwork details	Section Thickness		✓	✓	✓	300 mm to 1000 mm	-
	Formwork/ Insulation Type		✓	✓	✓	18mm plywood	-
	Wind Speed		×	✓	✓	0 m/s	Wind speed assumed for underground structure
	Formwork Removal time		×	✓	✓	48 hours	Minimum period prior to stripping of formwork is 24 hours for walls as per QCS 2014, Section 05, Part 09, Table 9.1 (Technical Regulation, 2014)

3 Practical Example in Qatar

Area of reinforcements (A_s) required to satisfy early thermal cracking requirements is calculated in accordance with BD 28/87, CIRIA C660 and CIRIA C766. The calculation is carried out for a below ground tunnel structure subject to high water table and stringent requirements for watertightness. The tunnel consists of reinforced concrete box section with an in-situ concrete top slab, integral with side walls on reinforced concrete base slab. ETC required area of reinforcements is determined for top slab and walls of varying thicknesses ranging from 300 mm to 1000 mm.

3.1 Qatar's Parameters

Parameters impacting ETC which are applicable to Qatar are summarised in Table 2.

Table 2: Qatar's Design Parameters

Parameter		Value	Unit	Reference
Concrete Grade		**C40**	Cubic Strength	IAN009_Rev.A2, Design Criteria # 13 (Ashghal, 2016)
Binder Type		Fly Ash 30	%	QCS 2014, Section 05, Part 06, Table 6.6 (Technical Regulation, 2014)
Actual Cover (C_{actual})	Base slab Bottom Face	**100**	mm	IAN009_Rev.A2, Design Criteria # 17 (Ashghal, 2016)
	Earth Face	**75**	mm	
	Internal Face	**50**	mm	
Minimum Cover (C_{min})		**35**	mm	BS EN 1992-1-1, Section 4.4.1.2, $C_{min,dur}$ for Structural Class S6 and Exposure Class XC3 (BSI, 2004)
Nominal Cover (C_{nom})		**45**	mm	BS EN 1992-1-1, Section 4.4.1.3 Δc_{dev} = 10mm (BSI, 2004)
Reinforcement Grade		**500**	MPa	IAN009_Rev.A2, Design Criteria # 14 (Ashghal, 2016)
Temperature Drop - T1		**See Section 2.5.1**		
Temperature Drop After Early Age- T2		**0**	ºC	BD 28/87, Cl. 5.9 (Highways Agency, 1989) CIRIA C660 and CIRIA C766, Cl. 4.3
Coefficient of Thermal Expansion		**12 x 10^{-6}**	/ ºC	IAN009_Rev.A2, Design Criteria # 6 (Ashghal, 2016)
Ambient Relative Humidity		**70**	%	IAN009_Rev.A2, Design Criteria # 6 (Ashghal, 2016)
End of Curing		**7**	Days	QCS 2014, Section 05, Part 10, Cl. 10.2 (Technical Regulation, 2016)
Design Life		**120**	Years	IAN009_Rev.A2, Design Criteria # 3 (Ashghal, 2016)
Allowable Crack width		**0.2**	mm	IAN009_Rev.A2, Design Criteria # 11 (Ashghal, 2016)

3.2 ETC for Walls

The nature of the restraint considered for walls cast onto base is external edge restraint. Restraint factors considered are provided in Table 3.

Table 3: External Edge Restraint Factors

Standard	Restraint Factor			Reference
	Restraint (R)	**Early Age Restraint (R1)**	**Long Term Restraint (R2 & R3)**	
BD 28/87	0.6	-	-	BD 28/87, Table 2
CIRIA C660	-	0.59	0.5	CIRIA Annex A, Restraint Calculator (R1, An/Ao = 1 & En /Eo = 0.7) (R2 and R3, An/Ao = 1 & En /Eo = 1.0)
CIRIA C766	-	0.45	0.38	

3.3 ETC for Top Slab

The nature of the restraint considered for top slab cast between rigid walls is external end restraint. CIRIA C660 and C766, recognize that cracks resulting from end restraint would be larger than those resulting from edge restraint. In end restraint, the restrained strain only impacts crack occurrence and the number of cracks and not the crack width. Crack width is dependent on the concrete strength and reinforcement ratio. On the other hand, following BD 28/87, ETC calculations for top slab are considered similar to walls subject to external edge restraint but with a restraint factor of 0.5.

3.4 Results and Discussion

Required area of reinforcements ($A_{s,req} = \max[A_{s,min}, A_{s,cw}]$) for ETC calculated as per Sections 2.3 and 2.4 are presented in Figure 3 for walls and Figure 4 for top slab with thicknesses varying from 300 mm to 1000 mm.

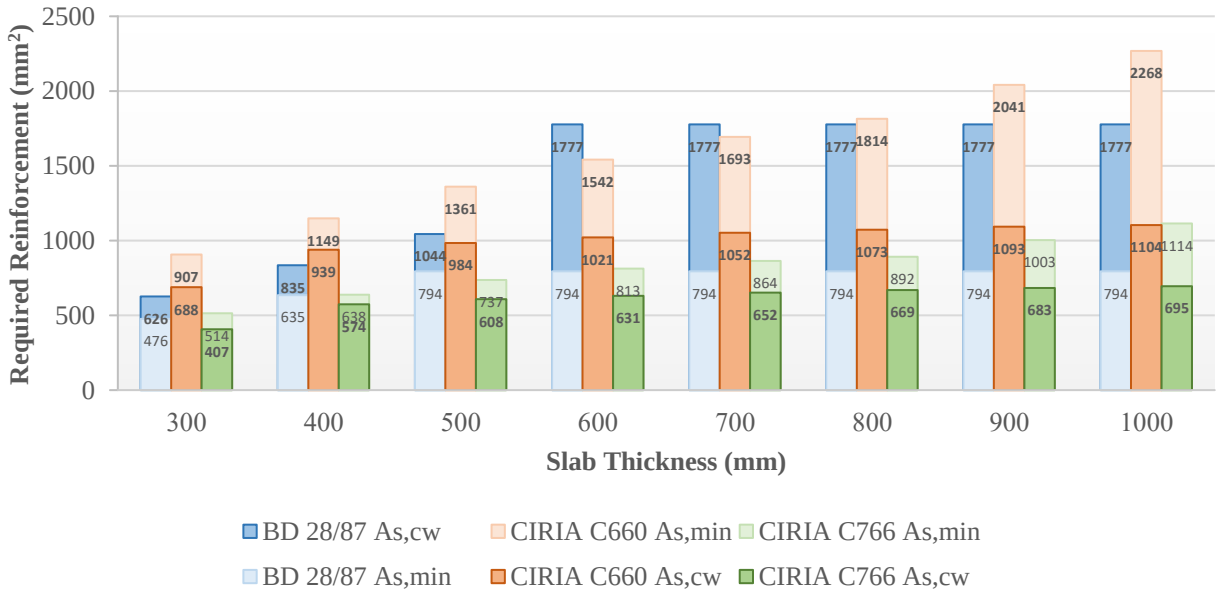


Fig. 3: Edge Restraint Required Area of Reinforcement (As,req)

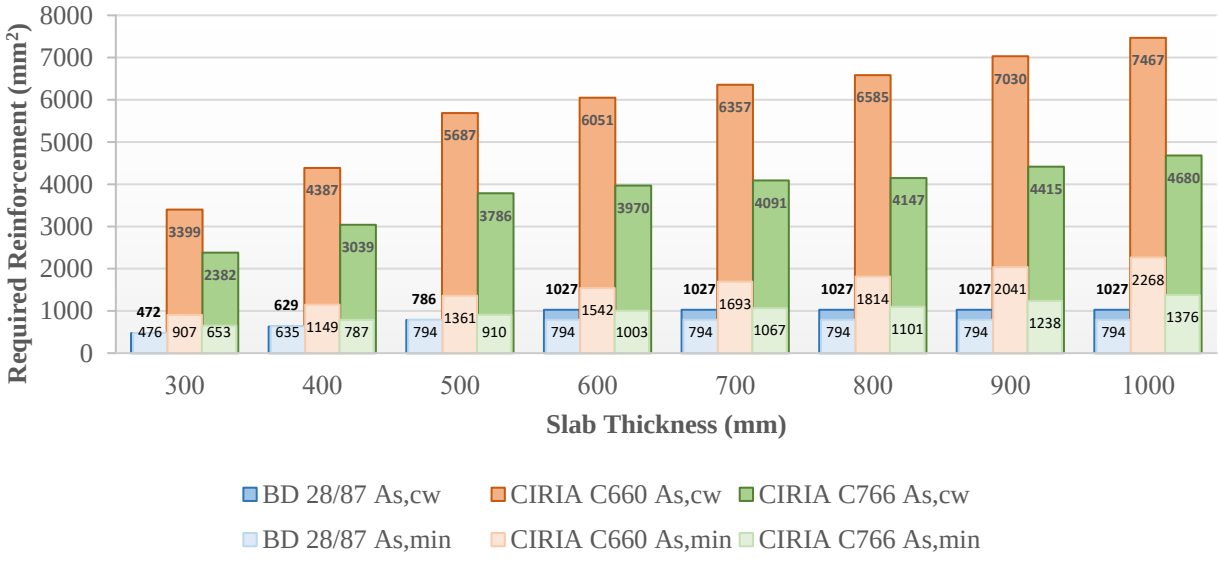


Fig. 4: End Restraint Required Area of Reinforcement (As,req)

The below can be observed from Figure 3 and Figure 4.

- There is a significant decrease in the required area of reinforcements in the latest CIRIA C766 in comparison with CIRIA C660 due the changes listed under Section 2.2. This decrease ranges from 43 to 51% for edge restraint and 30 to 37% for end restraint.
- $A_{s,min}$ requirements in CIRIA guidelines are generally more stringent than BD 28/87 especially for members with thickness larger than 500 mm as the effective area of concrete is considered as half the thickness but limited to 250 mm maximum in BD 28/87. $A_{s,min}$ required by CIRIA C766 is higher than BD 28/87 by a factor of 1.40 and 1.73 for 1000 mm thickness subject to edge restraint and end restraint, respectively.
- External Edge restraint (walls): $A_{s,min}$ is higher than $A_{s,cw}$ following CIRIA C660 and C766 and the opposite applies to BD 28/87 where $A_{s,cw}$ is controlling. Also, following CIRIA C766 requires the least reinforcements with reduction in required area of reinforcement of 18% to 54% compared with BD 28/87 and 43% to 51% compared with CIRIA C660.
- External End restraint (top slab): Higher crack width is anticipated in cracks developed due to end restraint which is not captured in BD 28/87. $A_{s,cw}$ is noted to be more than 3.4 times $A_{s,min}$ for CIRIA guidelines. Accordingly, the required area of reinforcement following BD 28/87 is significantly lower than CIRIA guidelines. However, it is recognized in the latest CIRIA C766, that in many situations where end restraint exists, the magnitude of the restraint might not be sufficient for cracking to develop. Thus, risk of cracking shall be calculated prior to unnecessarily increase in the reinforcements.

4 Conclusion

This paper provides a brief overview of Early Thermal Cracking (ETC) codes and guidelines used in Qatar, which are BD 28/87, CIRIA C660 and CIRIA C766. BD 28/87 has several limitations such as not accounting for the impact of concrete cover and Qatar's hot climate in crack width calculations. On the other hand, the updated CIRIA C766 guideline provides sustainable design in comparison with CIRIA C660 mainly due to adjustments in calculating minimum area of reinforcements and crack-inducing strain. ETC calculations were carried out for walls and top slabs of a tunnel reinforced concrete box section. For walls subject to edge restraint, CIRIA C766 requires the least reinforcements with reduction in required area of reinforcement of 18 to 54% compared with BD 28/87 and 43 to 51% compared with CIRIA C660. For top slab subject to end restraint, although $A_{s,req}$ by CIRIA C766 is 30 to 37% less than CIRIA C660, it is significantly higher than BD 28/87 as the higher crack width anticipated in members subject to end restraint is not captured by BD 28/87.

References

Ashghal (2019). PWA Standard Drawing, SD 8-4-106 Rev 3 Structural Notes, Ashghal.

Ashghal. (2016). IAN No. 009: Design Criteria for Highway Structures, Revision No. A2, Ashghal.

Bamforth. P. B. (2018). CIRIA C766, Control of cracking caused by restrained deformation in concrete, UK.

Bamforth. P. B. (2007). CIRIA C660, Early-age thermal crack control in concrete. London, UK.

BSI. (2009). NA to BS EN1992-1-1:2004 UK National Annex to Eurocode 2: Design of concrete structures - Part 1-1: General rules and rules for buildings, BSI.

BSI. (2006). BS EN1992-3:2006, Eurocode 2 Design of concrete structures - Part 3: Liquid retaining and containment

structures, BSI.

BSI. (2004). BS EN1992-1-1:2004 Eurocode 2 Design of concrete structures - Part 1-1: General rules and rules for buildings, BSI.

BSI. (1987). BS 8007:1987, Code of practice for design of concrete structures for retaining aqueous liquids, BSI.

Gilbert, R. I. & Ranzi, G. (2010). Time-dependent behaviour of concrete structures, CRC Press.

Highways Agency. (1989). Early thermal cracking of concrete, design manual for roads and bridges, Vol. 1 Highways structures: Approval procedures and general design, Section 3: General design, HA BD 28/87, Incorporating Amendment No. 1, HMSO.

Technical Regulation QS 27/2014 (2014). Qatar Construction Specification 2014 (QCS 2014).

Cite as: Alkadour F., Anagnostaki C., Tzaveas T., Oruganti A.K. & Kara A., "Early Thermal Cracking Control in Concrete Structures in Qatar", *The 2nd International Conference on Civil Infrastructure and Construction (CIC 2023)*, Doha, Qatar, 5-8 February 2023, DOI: https://doi.org/10.29117/cic.2023.0051

Box Jacking Method Implementation in Rock for Mesaimeer Pedestrian Underpass Structure in Qatar

Firas Alkadour
Public Works Authority (Ashghal), Doha, Qatar
falkadour@ashghal.gov.qa

Anbalagan Chelliah
Public Works Authority (Ashghal), Doha, Qatar
anchelliah@ashghal.gov.qa

Theodoros Tzaveas
Public Works Authority (Ashghal), Doha, Qatar
ttzaveas@ashghal.gov.qa

Ali Kara
Public Works Authority (Ashghal), Doha, Qatar
akara@ashghal.gov.qa

Abstract

Mesaimeer pedestrian underpass is proposed under the live traffic of Sabah Al Ahmad Road, Doha, Qatar which consists of a four dual lane carriageway, in addition to diverge lanes, service road lanes and right turn lanes by box jacking/pushing method for a total distance of 80.6 m. Due to the necessity of maintaining undisturbed traffic and to avoid disruption of the existing utilities crossing over the underpass alignment, the use of conventional Cut and Cover method is not feasible. Accordingly, trenchless construction method by box jacking/pushing is to be implemented in weathered limestone rock overlaid by fill soil. The method of construction of box jacking includes constructing shaft as launching pit for jacking operation, aligning the precast concrete box into position, excavating the soil/rock at the face of the precast concrete box, then pushing the box into the excavated length, and repeating the process. This paper includes overview of the project and its challenges intending to bring greater familiarity with the box jacking process in rock formation. The design and anticipated construction challenges are discussed from both structural and geotechnical perspectives. The challenges faced include box segment protection details, waterproofing details, construction and expansion joint details, high jacking loads due to rock formation, excavation advancement rate, necessity of grouting at box over-head and impact on existing utilities. Both structural and geotechnical analysis/design are assessed by numerical finite element modelling (FEM). Further, instrumentation and monitoring measures are planned to monitor various utilities and assess the impact during construction.

Keywords: Box Jacking in rock; Underpass construction; Trenchless construction; Structure in Qatar

1 Introduction

Mesaimeer pedestrian underpass is proposed under the live traffic of Sabah Al Ahmad Road, Doha, Qatar which consists of a four dual lane carriageway, in addition to diverge lanes, service road lanes and right turn lane. The underpass is located perpendicular to Sabah Al Ahmad Road and adjacent to Al Ghariya Street, to facilitate and provide safe connections for the pedestrian movement between two urban areas, Al Waab and Fereej Al Soudan as shown in Figure 1.

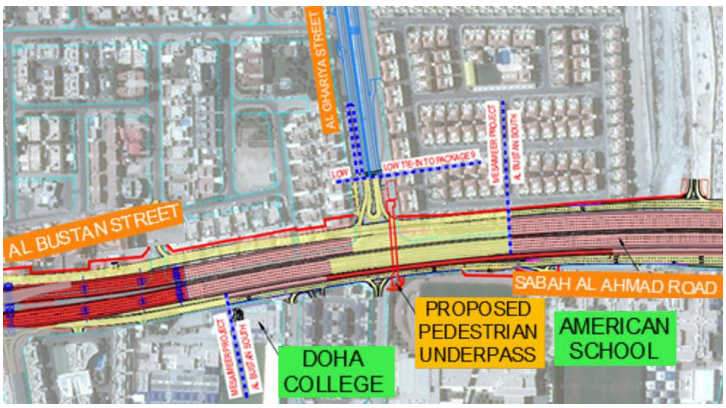


Fig. 1: Project Location

Due to the necessity of maintaining undisturbed traffic and avoid disruption of the existing utilities crossing over the underpass alignment, the use of conventional Cut and Cover method is not feasible. Accordingly, trenchless construction method by box jacking/pushing is to be implemented in weathered limestone rock overlaid by fill soil. Considering the geological conditions in Qatar, construction methodology implemented worldwide needs to be modified. Generally, box is pushed into ground and simultaneously excavation takes place. However, due to the rock formation, excavation must be done ahead of box pushing, which makes it a unique case. Further, the groundwater table is above the underpass top slab level, which would require waterproofing measures and water-tight joints at construction and expansion joints. Konstantis and Massinas (2020) discussed the challenges faced during construction of Doha Metro, Gold Link project by the box jacking method. However, construction sequence presented was not detailed. In addition, the authors did not discuss the waterproofing protection measures and joint details, and the ground improvement works were not presented.

This paper includes overview of the project and its challenges intending to bring greater familiarity with the box jacking process in rock formation. The proposed construction sequence is described and the design and anticipated construction challenges are discussed from both structural and geotechnical perspectives. Structural challenges include box segment protection details, waterproofing details, construction and expansion joint details, high jacking load due to rock formation and detailed design of jacked concrete segments. On the other hand, geotechnical challenges include excavation advancement rate, necessity of grouting at box over-head and impact on existing utilities.

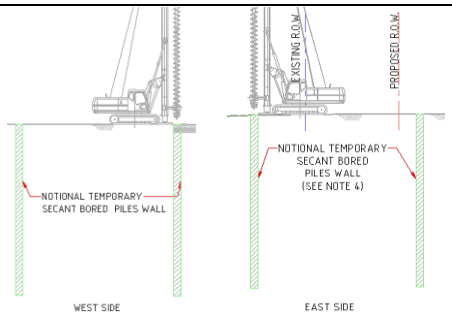
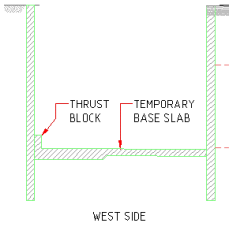
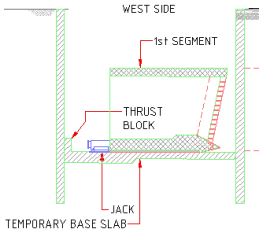
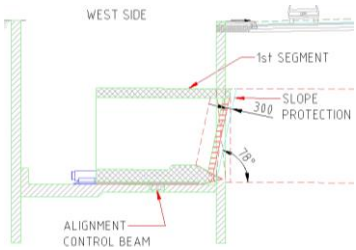
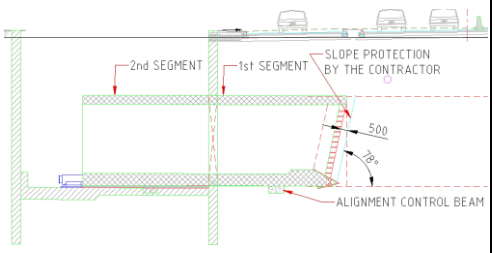
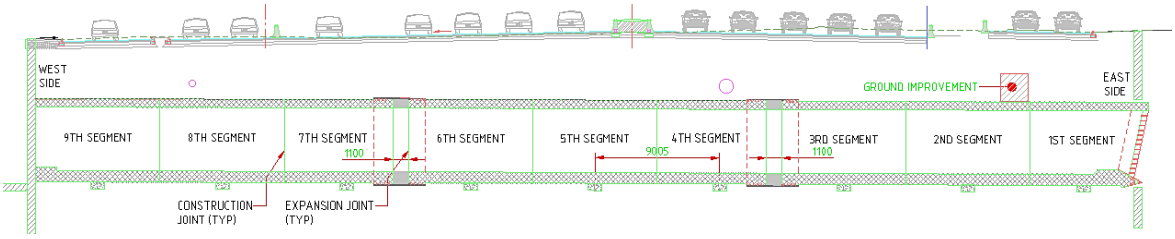
2 General Arrangement

The section of the underpass is a single cell box section with clear width and height of 6.20 m and 4.60 m, respectively. The overall length of the jacked underpass is 80.6 m with variable fill height above the box segments ranging from 4.3 m to 5.0 m. At both ends of the underpass, the pedestrian movement is facilitated with stairs and lifts. The underpass comprises of nine segments, each with length of 9.0 m. The joint types between the segments are either construction joints or expansion joints. The thicknesses of top slab, walls and base slab are 600 mm, 800 mm and 800 mm, respectively. The segments will be cast in excavated pits, which will later be jacked into their final position.

3 Proposed Construction Sequence

The general construction sequence for the jacked tunnel will be as presented in Table 1.

Table 1: Construction Sequence

Stages	Steps	Figures
1	a) Setting up and install temporary piles. b) Perform ground improvement to strengthen the fill material within the utility trench. c) Install ground and structure monitoring geotechnical instruments and take base readings.	
2	a) Excavate the access shafts on both sides of tunnel. b) Drilling of pilot hole horizontally below tunnel crown level to confirm the geological profile (soil/rock) to be encountered at tunnel face and perform laboratory tests to determine the ground properties. c) Install horizontal inclinometer and take the base reading. d) Cast smooth concrete slab and cast thrust block for pipe jacking.	
3	a) Cast in situ the first box segment within the access shaft. b) Install jacks and prepare for box jacking.	
4	a) Break in the tunnel portal. b) Excavate maximum of 300 mm and jack the first box segment immediately. The contractor shall verify the tunnel portal stability and provide any strengthening measures as required. c) Perform geological mapping of the full tunnel face. d) Monitor the installed instruments during the excavation and box jacking. The contractor shall immediately report the monitoring results to the engineer prior to future excavation.	
5	a) Excavate ahead of the first jacked box segment to maximum of 500 mm and jack the first box further. b) Jack the first box segment up to the last 1m, to allow the construction of the second box segment with the relevant construction joint with advancement rate of 500 mm maximum. c) Continue geological mapping after each excavation round, monitor the ground and structure instruments during the excavation and jacking and review the monitoring results. d) Adjust the excavation advancement rate based on the monitoring results to maximum rate of 1000 mm.	
6	a) Continue jacking the box sections one by one. b) Cast alignment control beams as necessary along the box jacking alignment. c) Cast the gaps at intermediate jacking location. d) After box pushing is completed, voids will be filled with grout using preinstalled grout holes at segments.	

4 Structural Challenges

4.1 Box Segment Protection Shield

At the front face of the first segment, a protection shield is provided to protect the reinforced concrete from any damages that might occur during excavation such as falling rocks as shown in Figure 2. The steel sheets which are fixed to the concrete by threaded bars can be easily removed to allow for installation of shear dowels at the Expansion Joint between first segment and east cast in situ shaft.

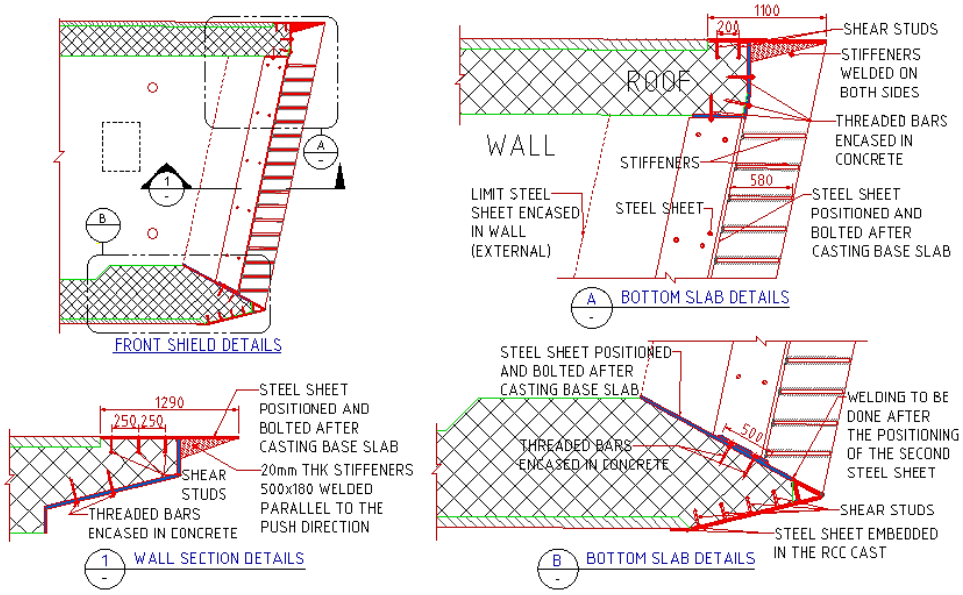


Fig. 2: Protection Shield details

4.2 Waterproofing Details

Ashghal specification for waterproofing of cut and cover tunnel and underpass highway structures which are designed to exclude groundwater are specified under Interim Advice Note No. 004 (IAN 004), Rev. A1 (Ashghal, 2013). The external faces of concrete shall be protected by waterproofing membrane. However, the waterproofing member is subject to damage during box jacking. Therefore, surrounding concrete protection of 100 mm thickness with steel mesh is proposed all around the box section to protect the waterproofing from any damage during construction and jacking as shown in Figure 3.

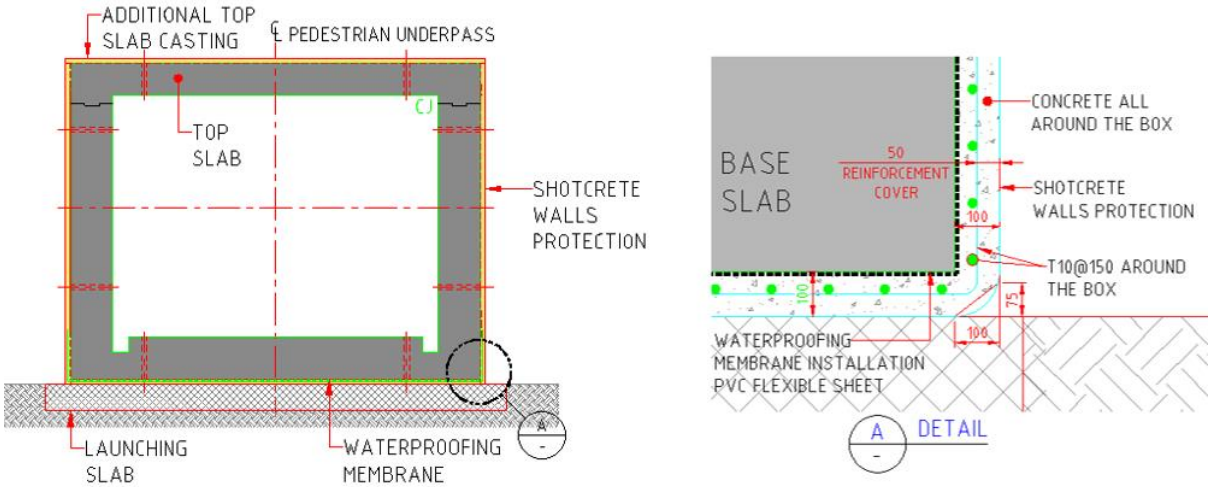


Fig. 3: Waterproofing Membrane Protection

4.3 Construction and Expansion Joint Details

As per Public Works Authority (PWA), IAN 004, Rev.A1 (Ashghal, 2013), waterstops shall be provided at both internal and external locations of the concrete structure.

4.3.1 Construction Joints

Following the construction sequence described under Section 3, segments are to be jacked to last 1m (i.e., projection of 1m from the tunnel portal) to allow the construction of the following box segment. Construction joint details are shown in Figure 4.

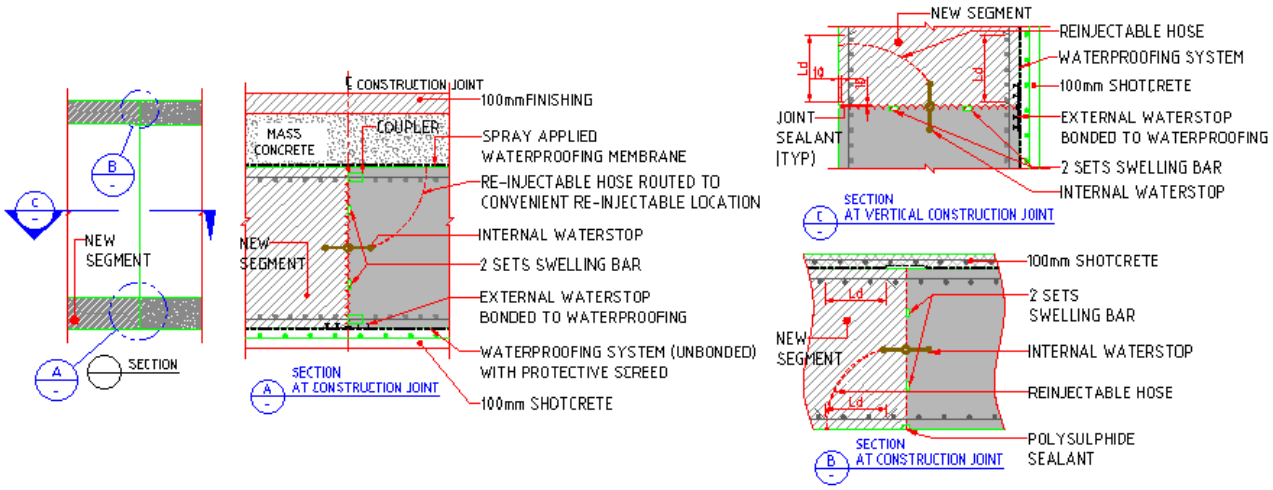


Fig. 4: Construction Joint Details

4.3.2 Expansion Joints

Two intermediate jacks are provided prior to box segments 3 and 6 to allow pushing of segments 1 to 3, 4 to 6 and 7 to 9 individually. Further details on box jacking arrangement are provided under Section 4.4. After completing jacking operation and removing the intermediate jacks, the gap is filled by stich concrete with Krystol Internal Membrane (KIM) Crystalline admixtures. Stainless steel plates are anchored into the segments by shear studs to prevent any misalignment in the segments by restraining them. Expansion joint detail at base slab is shown in Figure 5.

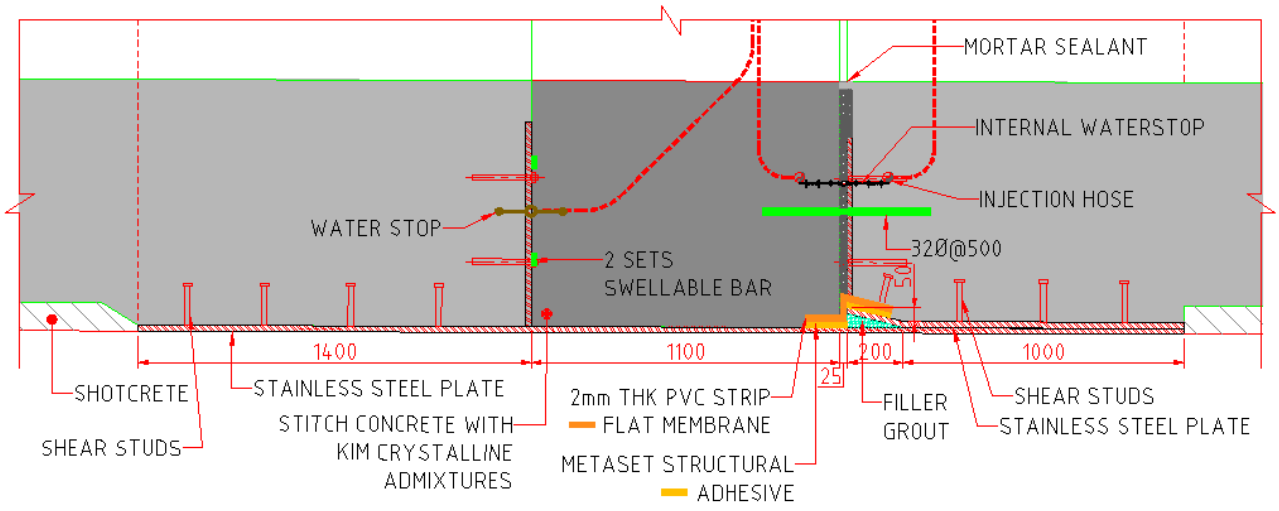


Fig. 5: Expansion Joint Detail at Base Slab

4.4 Box Jacking Loads and Arrangement

Based on the box-jacking specialist's experience in Qatar, the friction coefficient of 0.5 was appropriate for the estimation of jacking forces. This was considered in Doha, Metro, Gold Line Project (Konstantis & Massinas, 2020). However, friction coefficient of 0.8 is considered in this project for estimating the required jacking forces. Considering the higher friction coefficient at design stage will capture the worst-case scenario during box pushing and minimize the risk of segments being jammed during the pushing operations. The contractor shall validate the assumed value by measuring the actual coefficient of static friction between the concrete and the ground during construction. Furthermore, jacking force calculations are conservatively done considering the frictional resistance of the ground applied at the total perimeter of the box segment (i.e., roof, walls, and base slab).

Moreover, intermediate jacking locations are provided after every three segments (i.e., prior to box segments 3 and 6) leading to maximum jacking length of 21.0 m. Thus, the size of jacks is optimized and the impact of the jacks on the permanent structure is minimized. Based on the above considerations, the estimated required jacking force is 7,072 tons and this force shall be provided by seventeen jacks of 500 tons capacity each. Box jacking arrangement is shown in Figure 6.

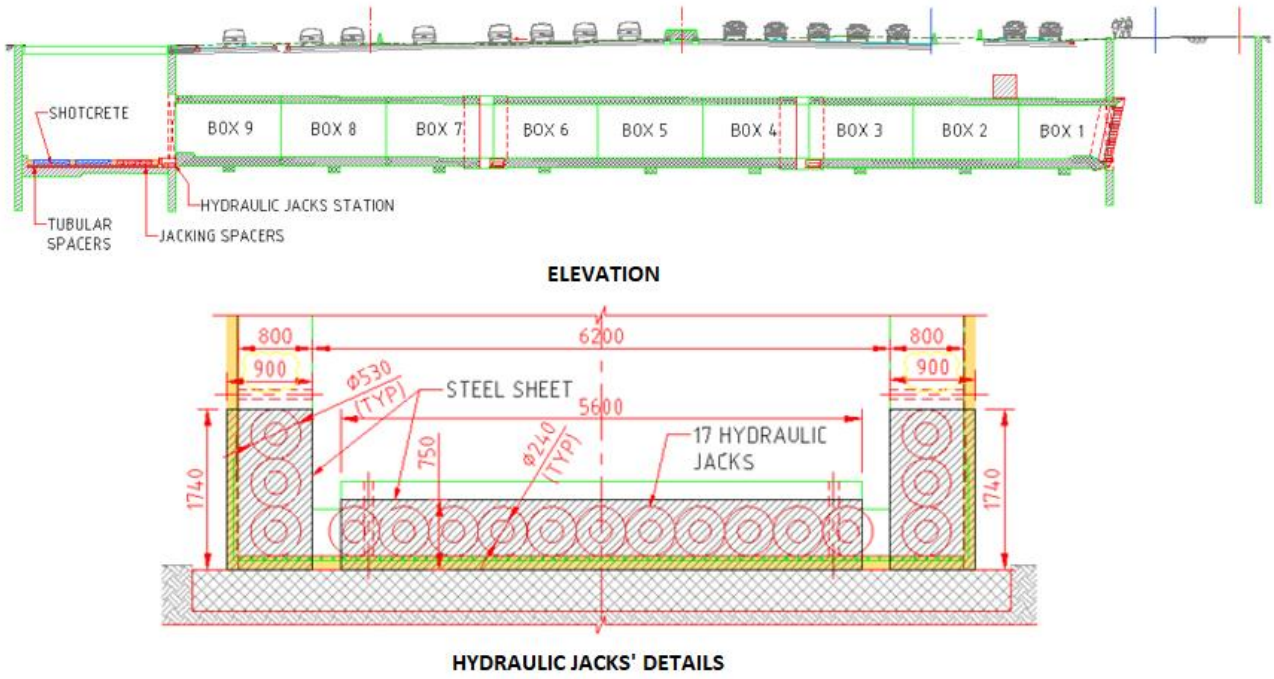


Fig. 6: Box Jacking Arrangement

4.5 Detailed Design of Jacked box RC Segments

The design criteria for highway structures are specified under Ashghal Interim Advice Note No. 009, Revision No. A2 (Ashghal, 2016) which requires the design to be carried out as per BS-5400-4 (BSI, 1990) and BD 31-01 (Highway Agency, 2001).

The global analysis of the structure was performed by finite element model (FEM) using CSiBridge software and the design was carried to cover both construction and permanent conditions. Top slab, walls, and foundations for box segments were modelled as frame elements in 2D model. Further, to capture the jacking force effect, the underpass was modelled as shell elements in 3D model. The earth pressure coefficients were based on the backfill properties specified in the Geotechnical Interpretative Report (GIR). The design considered upper and lower bound approach for the geotechnical

parameters to cover all critical cases listed below:

- Case of no lateral ground loads due to over excavation.
- Case of full lateral loads considering the highest anticipated at rest coefficient (ko) value of 0.7 as per the GIR.
- Case of full lateral loads due to grouting. (ko) of 1.0 is conservatively considered.
- Case of no vertical overburden due to over-excavation.

In addition, the design forces resulting from the soil-structure analysis performed using finite element analysis software (PLAXIS 3D) were also taken into consideration in the structural design. The reinforced concrete sections were designed for the most stringent forces.

5 Geotechnical Challenges

5.1 Ground and Groundwater Conditions

The subsurface condition at this site consists of a made ground/fill layer to a maximum depth of 3.5 m to 4.50 m below the existing ground level, followed by weathered Simsima Limestone (WSL) extending to depths varying between 4.0 m to 7.4 m below existing ground level. The weathering condition of WSL improved with depth as moderately to slightly weathered Simsima limestone. The Simsima/Dukhan Limestone is underlain by the Midra Shale formation extending to a maximum depth of 19.7 m to 22.9 m below ground.

At some sections of the underpass, due to existing utilities (like the Treated Sewage Effluent pipeline), filled up soils encountered at varying depths. A geophysical investigation performed along the underpass alignment showed potential variations in the compactness of overburden soil and the strength of the WSL formation.

The groundwater level was encountered at a level between 5.16 m and 5.64 m Qatar National Height Datum (QNHD) where the structural slab level of the underpass's top slab varies between 4.858 m to 5.030 m QNHD.

5.2 Geotechnical Analysis

The geotechnical analysis was performed by the Design Consultant using Plaxis 3D Finite Element Analysis. In the analysis, the overburdened fill soil depth was taken as 4.7 m followed by 4.0 m thick weathered limestone formation. As per this consideration, a 0.50 m thick WSL formation will exist on top of the underpass concrete box. In the analysis, it is considered that WSL formation will have minimum Cohesion of 50 kPa and Friction angle of 30 degrees.

A systematic excavation with advancement rate of 0.30 m to maximum of 1.0 m was considered. A face angle of 78 degrees was also considered at every advancement of the cutter during excavation. It is assumed that tunnel excavation will be carried out in dry conditions after lowering the groundwater level by dewatering. With the above assumptions, the analysis was carried out and the resultant forces and displacement were estimated.

5.3 Variation in WSL formation

Currently, it is assumed that a minimum of 0.50 m thick WSL formation will exist on top of the tunnel concrete box and this formation will have minimum cohesion of 50 kPa and angle of internal friction of 30 degrees. As geotechnical boreholes were drilled only on the road edges and geophysical

investigation along the underpass alignment showed varying velocity in the WSL formation, any variations will seriously impact the ground improvement cost and overall construction duration. Hence, before construction, it was recommended to perform horizontal drilling of borehole along the underpass alignment at the tunnel crown level and assess WSL formation existence and strength of the formation by performing relevant field and laboratory testing. Based on the findings, the excavation with or without improvement shall be finalized.

5.4 Impact on Existing Utilities and Road Pavement

Above the proposed pedestrian underpass box crown level, many existing pipelines are present at varying depths. The current analysis proved that the deflections are within the allowable limits of new construction limits. However, as these pipelines have already experienced the surcharge loading and some settlements might have already occurred, it was recommended to carry out deflection and condition assessment survey of the pipe by performing CCTV survey or other approved method before commencing and after finishing the tunnel excavation work. Further, instrumentation and monitoring were recommended during and after construction works to assess and decide on ground improvement requirement. It was also emphasized to coordinate with respective owners of these utility assets and get their approval before commencing these works. Localised ground improvement at the existing utility locations might be required to avoid any further settlement of these utilities.

5.5 Ground Improvement

Ground improvement was recommended at existing deep utilities' locations constructed by cut and cover method and at locations where WSL formation is weak at the underpass crown level. Upon exploring multiple ground improvement options, most conservative approach is to grout the entire length of the ground formation at the underpass crown level (like umbrella pattern). However, due to the high cost, an optimal approach was explored, and it was decided to identify the weak zones and perform ground improvement only at these locations. Horizontal borehole at underpass crown level before excavation was recommended to assess the ground improvement requirement. The location, extent and type of ground improvement will be finalized based on pilot horizontal borehole study at underpass crown level. The improved ground shall have minimum uniaxial compressive strength (UCS) of 500 kPa. It is expected that drilling and grouting execution in steps of 2.0 m to 3.0 m length in front of the segment opening is done to maintain 0.50 m height of grouting zone. The successful Tenderer/Contractor will design and execute the ground improvement works.

6 Conclusion

Mesaimeer pedestrian underpass is proposed under live traffic by box jacking method in rock. First, the proposed construction sequence was presented. In addition, details for tanking membrane, construction joint and expansion joint were provided for watertight structure considering the high groundwater table. Further, jacking force was calculated assuming a higher friction coefficient of 0.8 and frictional resistance of the ground applied to the total perimeter of the box segment. Moreover, structural analysis was carried out by FEM models using CSiBridge software covering both construction and permanent conditions and considering upper and lower bound approach for the geotechnical parameters. Furthermore, the geotechnical analysis was carried out assuming the presence of a WSL formation having a minimum thickness of 0.50 m with a cohesion of 50 kPa and an angle of internal friction of 30 degrees along the entire alignment of the underpass. Given the potential variations in ground formation, suitable mitigation measures such as ground improvement works were recommended in the event of weak formation at the underpass crown level.

References

Ashghal. (2013). Interim Advice Note No. 004: Design Criteria for Highway Structures, Revision No. A2, Ashghal.

Ashghal. (2016). Interim Advice Note No. 009: Specification for Waterproofing for Cut and Cover Tunnel and Underpass Highway Structures, Revision No. A1, Ashghal.

BSI. (1990). BS 5400-4:1990, Code of practice for design of concrete bridges, BSI.

Highways Agency. (2001). The Design of Buried Concrete Box and Portal Frame Structures, Design manual for roads and bridges, Vol. 2 Highways structure Design, Section 2: Special Structures, BD 31/01, HMSO.

Konstantis, S. & Massinas, S. (2020). Box Jacking/Pushing Method for Tunnel Construction in Rock: Doha Metro, Gold Line Project, International Conference on Civil Infrastructure and Construction.

Cite as: Alkadour F., Chelliah A., Kara A. & Tzaveas T.,"Box Jacking Method Implementation in Rock for Mesaimeer Pedestrian Underpass Structure in Qatar", *The 2nd International Conference on Civil Infrastructure and Construction (CIC 2023)*, Doha, Qatar, 5-8 February 2023, DOI: https://doi.org/10.29117/cic.2023.0052

Production of Self-healing Concrete using Gum Arabic for Immobilizing of Bacterial Spores on Sand

Amged O. Abdelatif
Department of Civil Engineering, Faculty of Engineering, University of Khartoum, Khartoum, Sudan
Amged.Abdelatif@uofk.edu

Ahmed A. Ibrahim
Department of Civil Engineering, Faculty of Engineering, University of Khartoum, Khartoum, Sudan
Ahmedalmansor156@gmail.com

Khadija E. Elamin
Microbial Culture Collection Unit (MCCU), Faculty of Science, University of Khartoum, Khartoum, Sudan
k2a.4e44@gmail.com

Adil A. El Hussein
Microbial Culture Collection Unit (MCCU), Faculty of Science, University of Khartoum, Khartoum, Sudan
adilelhussein@uofk.edu

Marmar A. El Siddig
Microbial Culture Collection Unit (MCCU), Faculty of Science, University of Khartoum, Khartoum, Sudan
marmarelsiddig@uofk.edu

Abstract

This paper studies the feasibility of producing self-healing concrete by immobilization of bacteria on the sand. In this study, the Gum Arabic (Acacia Senegal) was used to immobilize bacterial spores and its nutrient (Calcium lactate) on sand surface as a novel technique. Due to its availability and environment-friendly character, Bacillus subtilis bacteria have been selected and prepared. To achieve the aim of this study, three concrete mixes were made with 10%, 5%, and 2.5% of gum-capsulated sand with bacteria. The ability of self-healing of cracks was monitored using stereomicroscope and digital image camera. The experiments have shown that the proposed technique is efficient in healing of cracks without impairing the prisms' strength for mixes with 2.5% and 5% of gum-capsulated sand with bacteria. The results give a proof-of-concept to use Gum Arabic as an adhesion to immoblize the bacteria and its nutrient on sand to produce self-healing concrete.

Keywords: Self-healing concrete; Cracks; Gum Arabic; Immobilization; Bacteria; Capsulation

1 Introduction

Self-healing concrete is defined as the ability of concrerte to repair its cracks and recovery of the water-tightness throught bacterial consumption of calcium-based nutrient in concrete (Han et al., 2014; Pacheco-Torgal et al., 2017). It mimicks the healing of body wounds by production of a healing material without any manual intervention and relying only on the bacterial ones (De Belie et al., 2018). The most used type of bacteria and nutrient (i.e. healing agents) in the literature are "*Bacillus*" and Calcium Lactate ($CaC_6H_{10}O_6$), repectively (Khaliq & Ehsan, 2016). The self-healing of concrete activated once the cracks' mouths open and the water/mosture find its way through the surface cracks. Then bacteria starts to consume the nutrient and oxygen producing calcium carbonates ($CaCO_3$) that healed cracks ib concrete, Figure 1.

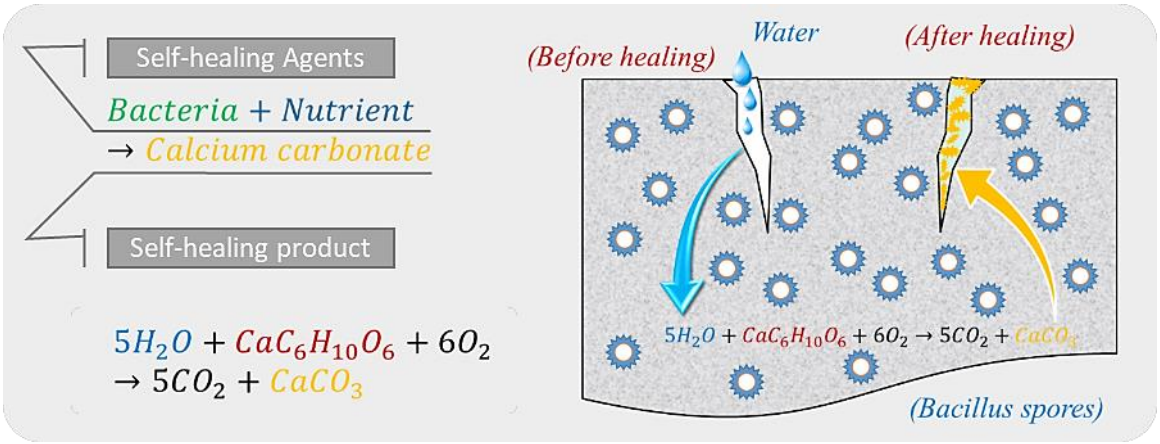


Fig. 1: Mechanism of Self-Healing Concrete

In general the production of self-healing concrete follows two techniques: direct method and immobilization/encapsulation method. In the direct method both bacteria and nutrient are mixed directly with the concrete. The main disadvantages of this method is that: 1) There is an early conversion of calcium source (Afiq et al., 2018); 2) Subjection of bacteria to mechanical stresses during concrete mixing; 3) Subjection of bacteria to chemical reactions of cement and the heat of hydration; and 4) Reaching the nutreitent by the bacteria is not granted (Alves et al., 2019; Jr et al., 2020). In the later method, many techniques and carriers are used to capsulate/immoblize bacteria and nutrient during the mixing and protect it from the harsh environment before releasing at the onset of the cracks (Talaiekhozan et al., 2014). Many carries and capsules are used in previous studies such as: light weight aggregate and graphite nano platelets (Khaliq & Ehsan, 2016); iron oxide and bentonite particles (Shaheen et al., 2019); diatomaceous earth (Wang et al., 2012); expanded clay particle (Jonkers, 2021); geo-polymer (Jadhav et al., 2018); and microcapsules (Al-Tabbaa et al., 2019). Use of organic and clay/earth based materials to concretize for immobilizing the bacteria can lead to ufavourable effects on properties of the produced concrete (Jonkers, 2021).

This research aims to experimentally prove the concept of immobilization of bacteria and its nutrient on sand using Gum Arabic as an adhesive material to produce self-healing concrete. It is known that sand (as a crrier) is one of the main concrete constituent materials. On the other hand, the literature shows that Gum Arabic is used as concrete admixture that works in both retardation of the setting time and reduction of mixing water (Satti & Ahmed, 2018). Therefore, both carrier and immoblizer are expected to show minimal or no adverse effects on concrete strength.

2 Materials and Methods

The main aim of the experimental work is to examine the self-healing ability of the proposed concrete mixture. In the self-healing concrete mix, the Hashab Gum Arabic *Acacia Senegal gum* (as adhesive material) is utilize as immoblizer of bacteria together with calcium-based nutrient, on sand. In this study Bacillus subtilis spores and Calcium Lactate are used as bacteria and nutrient, respectively.

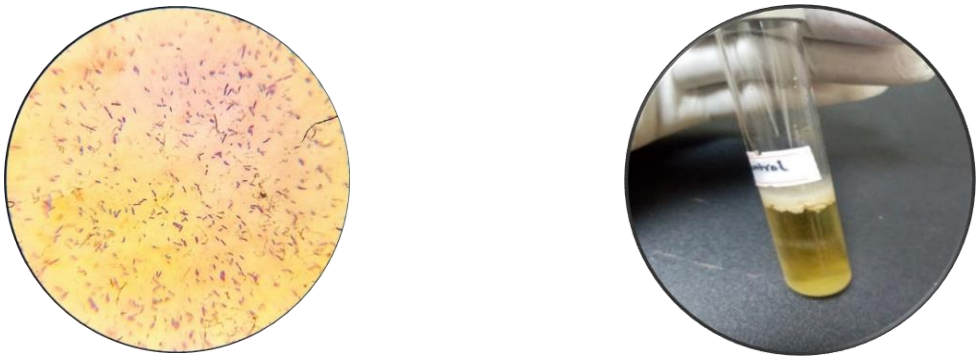
The following steps were taken to achieve the aim of the experiments:

1) Prepration of bacteria.
2) Immobilization of bacteria.

3) Preparation of the self-helaing concrete mixes.
4) Pre-cracking of the prisms.
5) Monitoring self-healing over the time.

2.1 Prepration of Bacteria

In this study, the *Bacillus subtilis* was isolated and provided as spores. The type of bacteria was identified and confirmed (**Fig. 2**a). To test its ability to produce calcium carbonat, *B. subtilis* spores were dissolved in peptone water supplemented with calcium lactate. Three days later, the $CaCO_3$ precipitated as shown in **Fig. 2**b. The X-ray diffraction (XRD) phase analysis showed that the calcium carbonate precipitation crystalline polymorphs structure is calcite (Abdelatif et al., 2022).



(a) (b)

Fig. 2: (a) Growth of rod-shaped Gram-positive Bacillus on Nutrient Agar medium; (b) Precipitation of Calcium Carbonate

2.2 Immobilization of Bacteria

Simply, dried Bacillus Subtilis bacterial spores, Hashab Gum Arabic, Calcium Lactate, and sand were thoroughly mixed. Then, tap water was added gradually with continious mixing until spore-coated sand pellets (gum-camsulated sand) were formed and then left to dry, Figure 3.



Fig. 3: Immoblization of Bacillus Subtilis and Calcium Lactate on sand using Gum Arabic

2.3 Prepration of Self-healing Mixes

Four mixes were used with capsulated sands of percentages of 0% (the control mix), 2.5%, 5%, and 10%. Three prisms of each mix were prepared with the dimension of $40\ mm \times 4\ 0mm \times 160\ mm$. The test matrix is shown in **Table 1**.

Table 1: Test Matrix

Mix	No. of prisms	Cement (g)	Water (g)	Sand (g)	Gum-capsulated Sand			
					Coated Sand (%)	Gum Arabic (g)	Calcium Lactate (g)	Bacterial Spores (g)
A (Reference)	3	450	250	1640	0.0	0.0	0.0	0.0
B				1584	2.50	5.60	5.60	3.30
C				1528	5.00	11.25	11.25	6.75
D				1512	10.00	22.5	22.50	13.50

2.4 Pre-cracking of Mortar Prisms

After 7 days of curing, the prisms were cracked using 3-point bending test under controlled loading rate. It is worth mentioning that the prisms are lightly reinforced to ease cracking of the prisms without complete splitting. The test setup and reinforcement of the prisms are shown in **Fig. 4**.

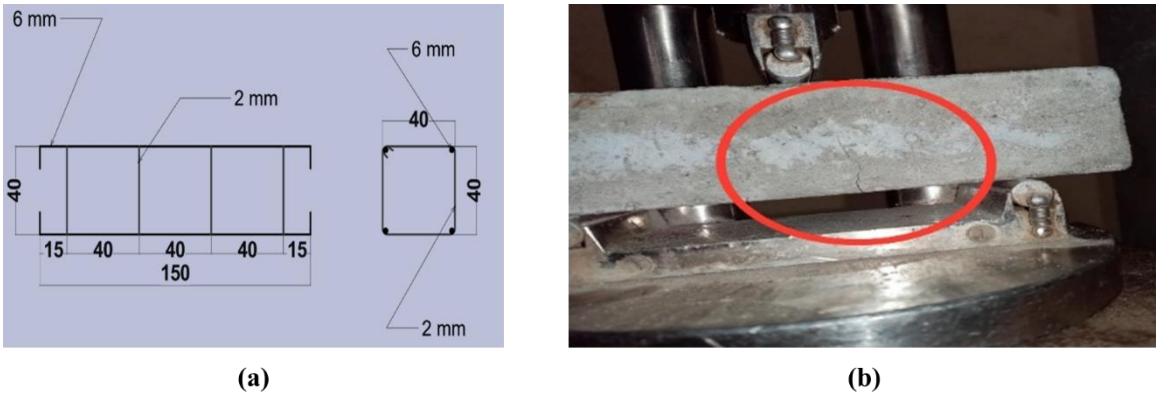


Fig. 4: Pre-cracking of Mortar Prism

2.5 Monitoring of Self-healing of Prism Cracking

Then, self-healing ability was monitored through the perception of the Calcite on the cracks. The healing and perception of Calcite were regularly monitored using stereomicroscopy and digital image photo.

3 Results and Discussions

Both the influence of gum-capsulated sand on the prism strength and self-healing-ability of the different mixes are discussed in this section.

3.1 Influence of Gum-Capsulated Sand on the Strength of the Mortar Prisms

As shown in **Fig. 5**, the strength of 2.5% and 5% of capsulated sand on mixes results in just 8% and 10%, respectively in comparison to the reference mix. In Mix D where 10% of capsulated sand is used, the strength is reduced by 36% in comparison to the reference prism's cracking load. This result is satisfactory (and far better for Mix A and Mix B) in comparison to 40 % reduction in mixes where expanded clay is used (Jonkers, 2011).

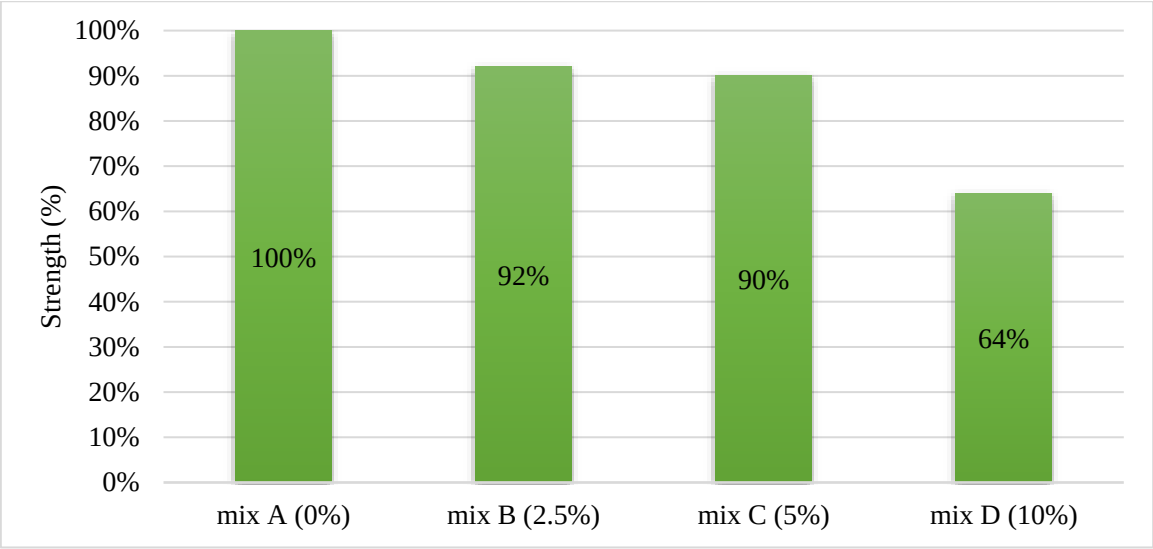


Fig. 5: Strength of Different Prisms in Comparison to the Cracking Load of the Reference Mix

3.2 Self-healing Ability of the Proposed Technique

Only the results of Mix C (5%) are presented in this paper, the rest of the results can be found elsewhere (Abdelatif et al., 2022). In Mix C, the progess of cracks healing was photographed in 3 days, 7 days and 14 days (Figure 6). The 25x stereomicroscope image clearly shows full healing of the crack by the bacterial product of Calite after 14 days.

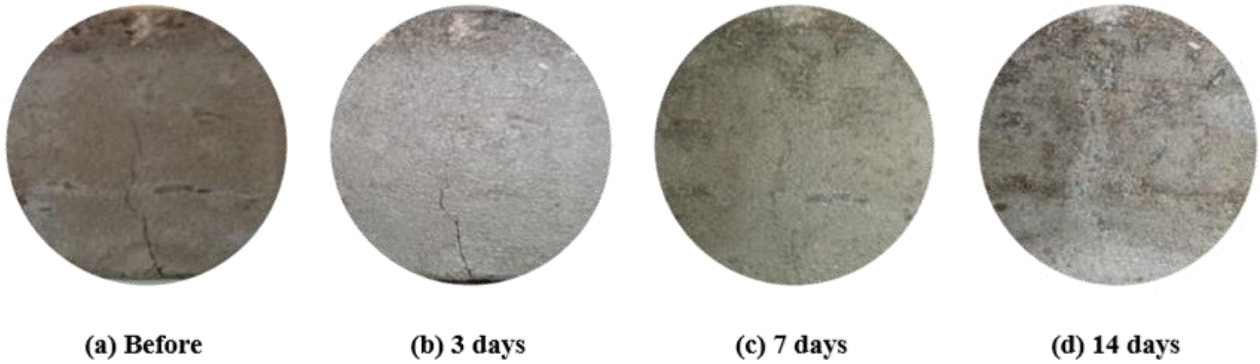


Figure 6: Self healing of a Crack Mix C over the Time

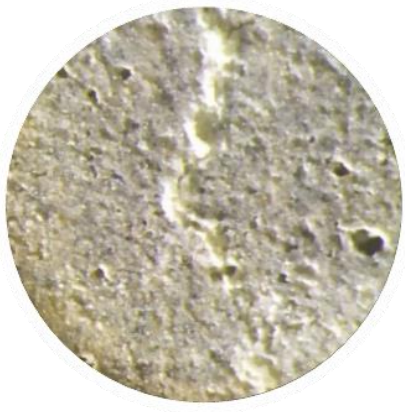


Fig. 7: 25x Stereomicroscope Image Showing the Formation of Calcite on a Crack

4 Conclusion

This study gives a proof-of-concept to use this novel, simple, and sustainable immobilization technique of bacteria for self-healing concrete. The Bacillus Subtilis (bacteria) was immobilized on sand (carrier) and capsulated with its Calcium Lactate (nutrient) by using Hashab Gum Arabic (adhesion) in the production of self-healing concrete. Three different percentages of capsulated sand was used to proof and examine the self-healing-abilty of the proposed technique. The results show the novelty of the proposed technique and how it is easy and simple to apply for self-healing of cracks without impairing the strength.

References

Abdelatif, A.O. et al. (2022). Production of Self-Healing Concrete by Bacillus Subtilis Spores Immobilized on Sand Using Gum Arabic as an Adhesion Material: Proof of Concept. J. Mater. Civ. Eng. 34, 4022310.

Afiq, M. et al, (2018). Development and Performance of Bacterial Self-healing Concrete - A Review Development and Performance of Bacterial Self-healing Concrete.

Al-Tabbaa et al. (2019). First UK field application and performance of microcapsule-based self-healing concrete. *Constr. Build. Mater*. 208, 669–685.

Alves et al. (2019). Characterization of Bioconcrete and the Properties for Self-Healing. Proceedings 38, 4.

De Belie, N. et al. (2018). A review of self‐healing concrete for damage management of structures. Adv. Mater. Interfaces 5, 1800074.

Han, B., Yu, X. & Ou, J. (2014). Self-sensing concrete in smart structures. Butterworth-Heinemann.

Jadhav, U. U. (2018). Viability of bacterial spores and crack healing in bacteria-containing geopolymer. *Constr. Build. Mater. 169*, 716–723.

Jonkers, H. M., 2011. Bacteria-based self-healing concrete 56, 1–12.

Jonkers, H. M., 2021. Bacteria-based self-healing concrete. In-Genium 56, 1–12.

Jr, A. A. G., Daly, M. K. M., Ongpeng, J. M. C. (2020). Applied sciences Bio-Influenced Self-Healing Mechanism in Concrete and Its Testing : A Review.

Khaliq, W. & Ehsan, M.B. (2016). Crack healing in concrete using various bio influenced self-healing techniques 102, 349–357.

Pacheco-Torgal, F. et al. (2017). *Eco-efficient repair and rehabilitation of concrete infrastructures*. Woodhead Publishing.

Satti, S. A. A. & Ahmed, Y. H. (2018). Use of Gum Arabic (Acacia Seyal) as Concrete Admixture. In: Conference Proceedings Civil Engineering 2018. pp. 198–202.

Shaheen, N. (2019). Synthesis and characterization of bio-immobilized nano / micro inert and reactive additives for feasibility investigation in self-healing concrete. *Constr. Build. Mater. 226*, 492–506.

Talaiekhozan, A. (2014). A Review of Self-healing Concrete Research Development 2, 1–11.

Wang, J. Y., De Belie, N. & Verstraete, W. (2012). Diatomaceous earth as a protective vehicle for bacteria applied for self-healing concrete. J. Ind. Microbiol. Biotechnol. 39, 567–577.

Cite as: Abdelatif A.O., Ibrahim A.A., Elamin K.E., El Hussein A.A. & El Siddig M.A., "Production of Self-healing Concrete using Gum Arabic for Immobilizing of Bacterial Spores on Sand", *The 2nd International Conference on Civil Infrastructure and Construction (CIC 2023)*, Doha, Qatar, 5-8 February 2023, DOI: https://doi.org/10.29117/cic.2023.0053

Top-Down Construction Method: A Case Study For Underpass Structure in Qatar

Ali Kara
Public Works Authority (Ashghal), Doha, Qatar
akara@ashghal.gov.qa

Anbalagan Chelliah
Public Works Authority (Ashghal), Doha, Qatar
anchelliah@ashghal.gov.qa

Theodoros Tzaveas
Public Works Authority (Ashghal), Doha, Qatar
ttzaveas@ashghal.gov.qa

Abstract

The Cut and Cover construction method has been applied to build several underpass structures within the expressway programme of the Highway Projects Department, Public Works Authority, Qatar. Booming in the construction industry contributes to increasing existing traffic in Qatar. This subsequently failed existing road junctions and required updating the road network parallel to the traffic studied. Underpasses and bridges were planned across many locations in Qatar to increase the level of service at road junctions, enhance the traffic capacity, reduce traffic congestion, and improve the free flow of traffic. This paper discusses the design and construction challenges of the underpass structure constructed by top-down construction method located on D ring Road in Doha, Qatar. The top-down construction method has been suggested by the construction contractor as an alternative to the conventional cut-and-cover construction method to minimize the traffic disruption and meet updated temporary traffic management (TTMs) due to underpass construction works, restore traffic at the junction on top of the underpass prior to the completion of construction works and overall optimize the construction duration. A numerical modelling research was carried out to study the change in arrangements. The site-specific challenges, such as modification in the structural arrangement of the underpass, change in ground conditions, lateral displacement of pile walls and dewatering challenges, are discussed in this paper.

Keywords: Top-Down construction; Underpass construction; Construction method; Deep excavation; Structure in Qatar

1 Introduction

The top-down construction method is preferred for constructing substructures in urban areas where tieback installation is not feasible in the deep excavation and when the aboveground area, such as roads above the substructure, is to be utilized during the construction. This approach allows simultaneous underground and aboveground structure construction.

In a conventional cut-and-cover method, after the construction of the diaphragm wall, excavation proceeds for a certain depth and an anchoring system (one or more layers) are installed to support the diaphragm walls and the excavation proceeds, followed by construction of the underground structure. This process takes more time, and the whole area can only be utilized once the structure is completed. In roadway underground structures, this approach causes much inconvenience to the public as the

road cannot be utilized, and traffic must be diverted for a longer duration. Lengthy occupation of road sites with noise disturbances and disruption to access is a prime disadvantage of the cut-and-cover method in busy urban areas (Puller, 2003). This paper presents a case study of an underpass constructed by top-down methodology on D-Ring Road, Doha, Qatar. In this case study, the design approach followed for the top-down construction, the construction sequence adopted, the challenges encountered, advantages and limitations of this approach are discussed.

The D-Ring Road in Doha connects many crowded areas such as Freej Hilal, Al Nuaija, Old Airport and Doha Expressway. D-Ring Road improvements were planned to avoid traffic congestion and reduce travel time. As part of this project, a 420m long underpass with 3 lanes in each direction, with a capacity of 12,000 vehicles per hour, was proposed to provide uninterrupted traffic movement. Underpass construction was planned as a combination of conventional cut-and-cover and top-down construction approach in the design stage. However, during construction, the construction contractor preferred to execute the construction implementing fully the top-down construction approach to minimize traffic disruption and optimize the construction duration (Hossein et al., 2018).

2 Literature Review

Puller (2003) stated that peripheral sheeting/walling, ground and groundwater conditions, geographical location, skills, and preferences of local contractors influence the substructure construction method (cut-and-cover or top-down). The top-down construction will likely minimize wall movements, soil deformation, and settlements. When the excavation depth increases, excavation becomes more complex, leading to top-down techniques which allow simultaneous substructure and superstructure construction.

Whittle et al. (1993) demonstrated the importance of finite-element analysis for top-down modelling construction for reliable and consistent predictions of soil deformations, nevertheless, emphasizes the need for adequate characterization of engineering properties for the entire soil profile.

Marchant et al. (1994) stated that the top-down construction approach was driven by economics from the main contractors' point of view. Moreover, adopting the top-down method can have a far-reaching impact on the design, and implications are also site-specific, per consultants' point of view. It emphasized the significance of involving the contractor at an early stage to enhance the efficiency of the design and construction process.

The top-down approach is well suited for most situations of the urban construction environment. However, it demands rigorous quality adherence, thorough planning, managerial expertise, and a detailed understanding of construction sequences for inclusion in the design and analyses (Basarkar et al. 2010).

Wong et al. (2019) studied the effectiveness of the top-down construction method in Malaysia. They concluded that adopting the top-down construction approach is most suitable and efficient in urban areas and busy traffic locations. The study highlighted the necessity of highly experienced contractors and special machinery for executing top-down construction. Further, the study identified that confined working environments and machine idling are limitations of this approach.

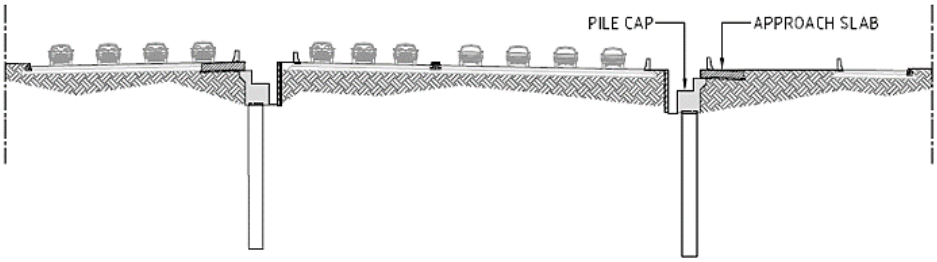
3 Top-down Construction

3.1 Construction Methodology

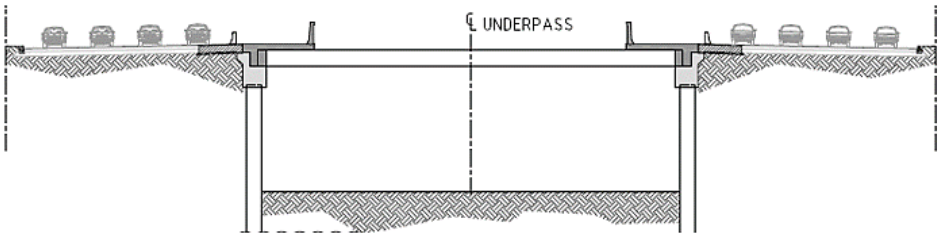
A top-down approach is instrumental in construction of the underpass. Piles and the top deck slab are first constructed to allow traffic at the ground level, then excavation to the bottom, where the underpass foundation slab and side walls are constructed.

At the site, the following construction sequence was followed, as shown in Figure 1.

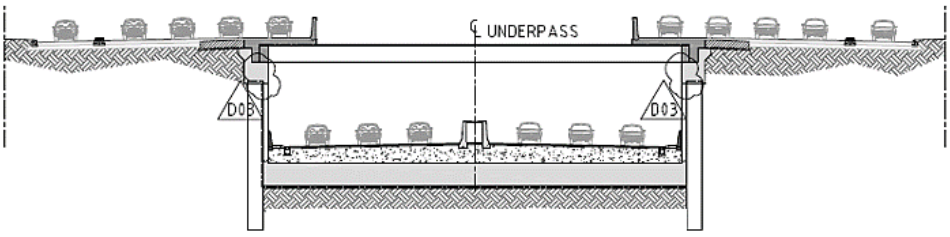
- Construction of Contiguous/Tangent-pile Walls and then pile cap construction on both sides. Construction of temporary piles in the middle for the deep sections.
- Construction of approach slab.
- Erection of concrete girders (post-tensioning) and casting of deck slab.
- Proceeding the excavation (with dewatering) to the foundation level in stages using temporary struts supports. Access for the removal of soil was provided.
- Construction of base slab, shotcrete on the pile walls, pouring mass concrete as a counterweight against uplift.
- Construction of underpass box wall.



Stage-1: ***Construction*** **of Pile Walls & Pile Cap**
Stage-2: Construction of Approach Slab



Stage-3: Placing precast girder, casting deck slab and barriers
Stage-4: Dewatering and Excavation up to the foundation level



Stage-5: Construction of Foundation, shotcrete and walls
Stage-6: Construction of mass concrete, wearing course
Stage-7: Open the underpass to traffic

Fig. 1: Construction Stages

Some of the site construction photos showing various stages of construction are shown below in Figure 2.



Boring of Piles



Constuction of Approach Slab



Deck slab reinforcement fixing



Excavation below Deck Slab



Excavation work



Application of Shotcrete at inner face of piles



Formwork installation for wall



Casting Central wall in between temporary piles

Fig. 2: Site Construction Photographs

3.2 Design Approach

The pile wall-ground interaction analysis was carried out using the finite element program Plaxis 2D and forces, displacement, and pile-wall stiffness were assessed. The contractor's geotechnical consultant performed the analysis following each section's Construction Industry Research and Information Association (CIRIA) C760 Guidance on Embedded Retaining Wall Design (Gaba et al.,

2017) of the underpass. In the analysis, each construction stage excavation condition, groundwater level, excavation support system, and loadings were modelled, and the analysis was carried out accordingly. The pile-wall flexural inertia for short-term (temporary condition) and long-term (permanent case) conditions of 0.7EoI and 0.50EoI (where E is the modulus, and I is the moment of inertia) were used. The resultant forces were used in the structural design.

4 Ground and Groundwater Conditions

4.1 Ground Conditions

The subsurface at the proposed underpass location consists of residual soil cover up to about 0.45m to 3.0m below the ground level, comprising *SILTY SAND* with occasional limestone fragments, followed by moderately weak *SIMSIMA LIMESTONE* up to about 10.0 -12.0m depth. *MIDRA SHALE* was encountered below Simsima limestone with a thickness varying from 1.4m to 4.4m which is underlain by a weak to moderately strong *RUS formation* up to the maximum drilled depth of 30m below the ground level. No cavities were found.

4.2 Groundwater Conditions

The groundwater level measured in the piezometers varied between 3.75m and 6.50m below the existing ground level, i.e., between Elevation +3.28m and +7.11m Qatar Highway National Datum (QNHD). The ground surface elevation at the project varied between elevation +13.0m and +15.0m QNHD.

5 Design and Construction Challenges

5.1 Change in Ground conditions

After completing the detailed design and before the underpass construction, wet utility pipeline construction was carried out by another contractor as part of a different project. Due to this, on one side of the underpass close to the pile-wall location, the existing natural formation was excavated and backfilled with soil fill material to about 8.0-10.0m depth (Table 1).

Table 1: Change in Subsoil Conditions

Subsoil Conditions	
During Detailed Design	**After Detailed Design (Before Construction)**
0.0-3.0/4.0m Residual Soil 3.0/4.0-20m and below Rock Formation	0.0-8.0/10.0m Backfilled soils in medium-dense condition 8.0/10.0m – 20.0m and below the Rock Formation

Initially, the pile wall was designed considering frictional resistance from rock formation encountered at about 3.0m below existing ground level. However, as rock formation was excavated and backfilled with soil, the pile wall was redesigned for the latest ground formation, and pile-wall length was increased at these locations.

As the piles must resist the lateral earth pressures and vertical loading, any reduction in pile capacity might have endangered the entire top-down construction approach. The additional ground investigation helped identify the fill areas. Accordingly, the piles at this alignment of the underpass were redesigned by sufficiently extending into the rock formation below the base slab level.

5.2 Modification in Structural Arrangement

Two rows of temporary piles were necessary to be constructed for the deep sections to allow casting the final intermediate wall. Then temporary piles were removed at a level below the base slab. After

the installation of side piles and excavation of soils for the construction of the underpass, it was observed that at deeper sections of the underpass where the box structure was proposed, and the exposed tangent piles at some locations exceeded the pile wall alignment tolerances. Revised wall thicknesses were structurally assessed to ensure the safety of construction. This issue has forced the contractor to make some minor modifications to the final structural configurations of the underpass. The final structural arrangement of the underpass structure is shown below in Figure 3.

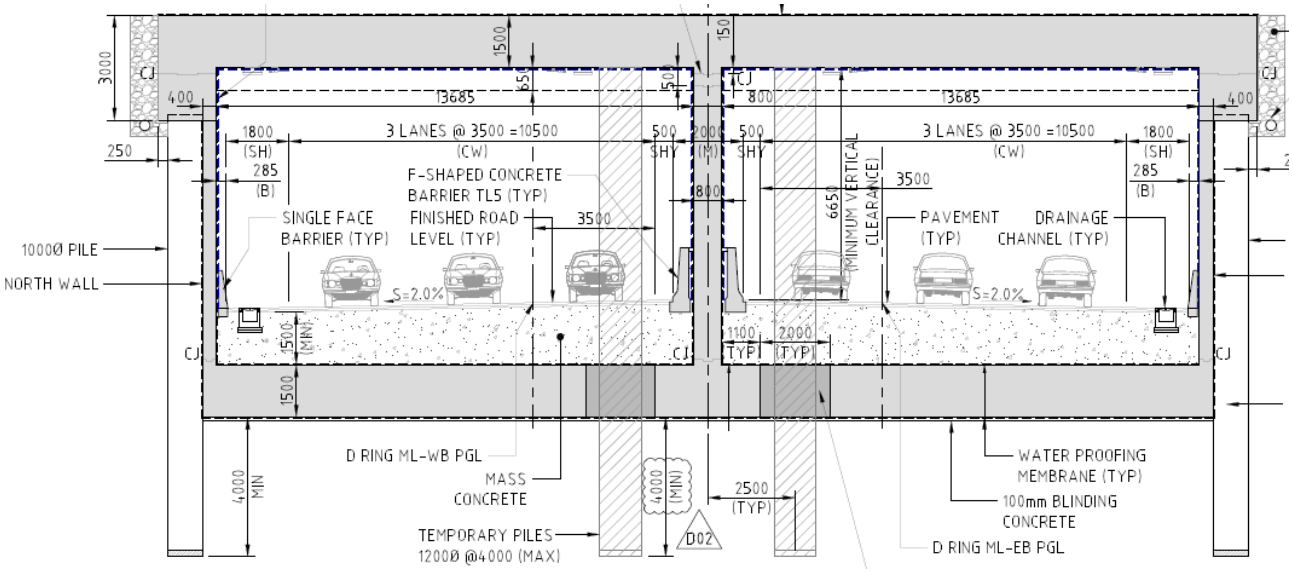


Fig. 3: Final Arrangement of Underpass Structure

5.3 Dewatering

The WellPoint Dewatering Method was adopted at the project site to lower the groundwater during excavation and underpass construction. The dewatering groundwater level was maintained at 1.0m below the excavation level. The existing WellPoint system could not achieve the required dewatering at deeper underpass sections. Hence, additional French drains 1.0m wide and 1.0m thick on both sides of the pile walls and 0.60m x 0.60m in the middle of the underpass at the base level were installed along the underpass alignment, as shown in Figure 4 below.

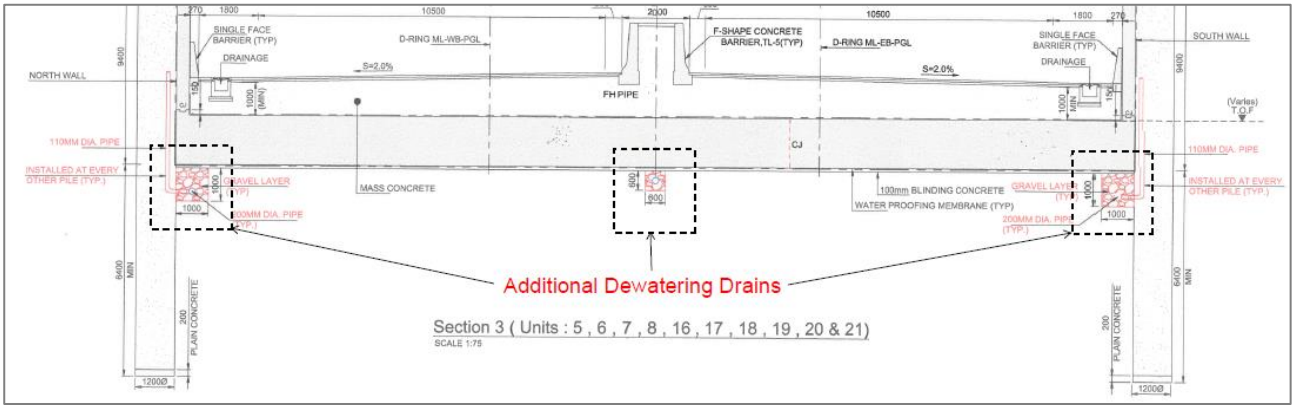


Fig. 4: Additional Dewatering Drains

As the new drain system requires an additional 1m, the pile wall design was checked by performing soil-structure interaction analysis using Plaxis 2D for the additional excavation. Initially, the detailed design of the pile wall design was performed considering additional excavation of 0.50m depth considering possible over-excavation meeting CIRIA C760 Standard (Gaba et al., 2017)

requirements. Hence, the net increase in excavation depth was about 0.50m only, and the increase in forces in the pile walls due to this additional excavation is marginal. As dewatering was under progress for some construction activities, the final deflection of walls for the static water level condition is not available.

6 Discussion and Conclusion

The Top-down Construction Method was very useful for temporary traffic management in this project with less traffic disruption. Compared to the conventional Cut & Cover Approach Method, this approach reduced construction duration, and the contractor could complete the construction works on time. Further, this case study reiterates the importance of precise location and structure-specific geotechnical investigation for the design of various structural elements of the underpass. Post geotechnical investigation, nearby below-ground construction activities that could alter the ground conditions must be reported to the designer. The design of deep pile-wall sections shall allow sufficient tolerances considering possible deviations in the verticality of piles, and underpass box structure geometry shall be designed accordingly. Implementing this method in locations with high water table, increases the complexity of the construction and complicates configurations to ensure that specifications for waterproofing details are met.

7 Acknowledgements

UCC Infraroad Limak JV company W.L.L is the construction Contractor, PARSONS International is the Design Consultant, and the Supervision Consultant of this project is WSP International, Qatar, acting also as Independent Checker for the detailed design. ACTS, Qatar, acted as a geotechnical consultant for the contractor and was responsible for the geotechnical design for the Top-down Construction Shoring System. The opinions expressed in this paper are those of the authors and do not necessarily reflect those of the organizations mentioned above and Public Works Authority.

References

Basarkar S. S. et al. (2010). 'Emerging Trend in Deep Basement Construction: Top-Down Technique', *IOSR Journal of Mechanical and Civil Engineering (IOSR-JMCE)*, ISSN: 2278-1684, PP: 01-11.

Gaba, A. et al. (2017). 'CIRIA C760 Guidance on Embedded Retaining Wall Design', CIRIA, London.

Gui, Y. et al. (2020). Study on deformation law of deep foundation pit with the top-down method and its influence on adjacent subway tunnel. *Advances in Civil Engineering*.

Hossein, Z. S & Mirmohamadi S. & Mostafa (2018). 'Top-Down Construction Method: A Case Study of Commercial Building', 11th International Congress on Civil Engineering May 2018, University of Tehran, Iran.

Marchant, S., Wren, G. & Lamb, R. (1994). 'Top-down construction and its implications', Proceedings of the Institution of Civil Engineers - *Geotechnical Engineering,107*(2), pp. 123-124.

Puller, M. (2003). *Deep excavations – a practical manual* (2nd Edition), Thomas Telford Ltd., London.

Whittle, A. J., Hashash, Y. M., & Whitman, R. V. (1994). 'Analysis of deep excavation in Boston'. *Journal of Geotechnical Engineering, 120*(10), 1911-1912.

Wong, J. Y. et al. (2019). 'Effectiveness of top-down construction method in Malaysia'. *International Journal of Innovative Technology and Exploring Engineering, 8*(6), 386-392.

Cite as: Kara A., Chelliah A. & Tzaveas T., "Top-Down Construction Method: A Case Study For Underpass Structure in Qatar", *The 2nd International Conference on Civil Infrastructure and Construction (CIC 2023)*, Doha, Qatar, 5-8 February 2023, DOI: https://doi.org/10.29117/cic.2023.0054

Experimental Investigation on the Flexural Capacity of Reinforced Concrete Beams with Treated Wastewater and Recycled Concrete Aggregates

Abdelrahman Abushanab
Department of Civil and Architectural Engineering, Qatar University, Doha, Qatar
aa1104287@qu.edu.qa

Wael Alnahhal
Department of Civil and Architectural Engineering, Qatar University, Doha, Qatar
wael.alnahhal@qu.edu.qa

Abstract

Eco-friendly concrete is the most recommended sustainable option to reduce the excessive diminution of concrete natural resources and the high generation of greenhouse gas emissions. Therefore, the present study explores the feasibility of employing treated wastewater (TWW), recycled concrete aggregates (RCA), and fly ash (FA) in concrete mixes. A total of 4 reinforced concrete (RC) beams were investigated under 4-point bending setup with three parameters investigated; namely, mixing water (fresh water and TWW), coarse aggregates (gabbro and RCA), and cementitious binders (cement and FA). The experimental results revealed that the beams' ductility was decreased by 9% and 16% with TWW and RCA, respectively. Moreover, the flexural performance of the TWW-RC beams was decreased by 14%, whereas RCA-RC beams showed comparable flexural strength to its counterpart with natural aggregates. In addition, the utilization of FA at a 20% replacement ratio enhanced the flexural strength by 5% to 7%.

Keywords: Treated wastewater; Eco-friendly; Recycled concrete aggregates; Flexural capacity; Ductility

1 Introduction

Concrete is the workhorse material in the construction industry in the 21st century. Nonetheless, the worldwide production of concrete has significantly increased over recent years due to population boom and urbanization (Abushanab & Alnahhal, 2021). The global concrete manufacturing rate has currently reached 10 billion tons per year, with an expectation to explosively increase by 80% by 2050 (Abushanab et al., 2021). The growing volume of concrete is raising concern about carbon emissions and overwhelming employment of concrete natural ingredients. Previous studies have reported that the utilization of fresh water (FW), natural aggregates, and ordinary Portland cement (OPC) for concrete applications is 2, 48.3, and 4.1 billion tons per year, respectively (Abushanab et al., 2021; Abushanab & Alnahhal, 2022b). Moreover, 10% of the worldwide CO_2 emissions are due to the concrete industry (Abushanab & Alnahhal, 2022b). In response, recyclable concrete ingredients should be adopted for concrete elements.

In a bid to save the environment and concrete natural resources, researchers have recently proposed the employment of treated wastewater (TWW), recycled concrete aggregates (RCA), and fly ash (FA) in reinforced concrete (RC) structures (Abushanab et al., 2021; Abushanab & Alnahhal, 2022b; Abushanab & Alnahhal, 2022c). Several studies have investigated the impact of utilizing TWW on

plain concrete properties (Meena & Luhar, 2019; Abushanab et al., 2021; Arooj et al., 2021; Abushanab & Alnahhal, 2022a). Abushanab & Alnahhal (2021) reported that the mechanical properties of TWW concrete decreased by 5% to 12% compared to that made with FW. Furthermore, the authors demonstrated that the chloride permeability was decreased by 40% at a TWW replacement ratio of 100%. Asadollahfardi et al. (2016) obtained similar results. Moreover, the employment of RCA in concrete applications has been reviewed by several researchers (Behera et al., 2014; Abushanab et al., 2021; Abushanab & Alnahhal, 2022b). It has been shown that concrete with 100% RCA experienced a 30% drop in compressive strength and a 13% increase in chloride permeability (Behera et al., 2014; Abushanab & Alnahhal, 2022b). Due to the inferior properties of TWW and RCA concrete, researchers have recently incorporated FA in concrete to improve the characteristics of RCA concrete (Abushanab & Alnahhal, 2021; Abushanab & Alnahhal, 2022b). Abushanab & Alnahhal (2022b) reported that partially replacing OPC with FA in TWW and RCA concrete has improved concrete chloride permeability by 50%. Furthermore, the influence of RCA and FA has been demonstrated for RC applications (Choi & Yun, 2013; Seara-Paz et al., 2018). Choi and Yun (2013) showed that RC beams with RCA had a 20% drop in the flexural strength. In addition, Seara-Paz et al. (2018) recorded narrower flexural cracks in RCA-RC beams compared to those made with natural aggregates.

Even though the characteristics of plain concrete with TWW, RCA, and FA have been tested, a gap remains in their combined effect on the flexural capacity of RC beams. Accordingly, this study investigated the impact of TWW, RCA, and FA on the flexural performance of RC beams.

2 Experimental Program

2.1 Mixing Water

The study at hand investigates two types of mixing water: FW and TWW. The TWW used was obtained from a local wastewater treatment plant. The chemical composition and concentration of FW and TWW are listed in Table 1.

Table 1: Chemical Properties of FW and TWW

Component	FW (mg/l)	TWW (mg/l)
Sulfate (SO_4^{-2})	6	6
Zinc (Zn^{+2})	0.0046	0.11
Phosphate (PO_4)	<0.03	9.19
Chloride (Cl^-)	14.1	511
Total dissolved solids	93	1690
Total suspended solids	2	3

2.2 Aggregates

In this study, coarse natural gabbro aggregates and RCA were considered. The particle size distribution of both types of aggregates was between 4.75 and 20 mm, as shown in Fig. 1. Furthermore, washed sand with a particle size of 0.075 to 4.75 mm was employed in the mixes as fine aggregates. The properties of fine aggregates, GA, and RCA are presented in Table 2.

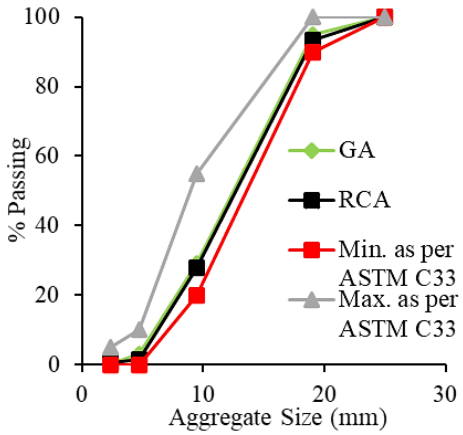


Fig. 1: Particle Size Distribution of GA and RCA

Table 2: Properties of Sand, GA, and RCA

Property	Sand	GA	RCA
Los Angeles Abrasion (%)	—	8.9	17.6
Water Absorption (%)	0.6	0.72	3.51
Specific Gravity	2.63	2.91	2.55

2.3 Cementitious Binders

Two types of cementitious binders were considered in this study: OPC and FA. The OPC considered had a particle size distribution of 10 to 90 μm and specific gravity of 3.15. The FA used was of type F with a particle size distribution and specific gravity of 3 to 55 μm and 2.15, respectively.

2.4 Steel Reinforcement

Deformed steel bars with diameters of 8, 10, and 12 mm were used to reinforce the RC beams. The characteristics of the bars are shown in Table 3.

Table 3: Characteristics of Steel Reinforcement

Property	Bar Diameter (mm)		
	8	10	12
Yield Strain	0.0268	0.00267	0.00266
Yield Strength (MPa)	512	515	525

2.5 Concrete Mixtures

In this study, a total of four concrete mixtures were fabricated. The parameters considered were the type of concrete mixing water (FW and TWW), coarse aggregates (GA and RCA), and cementitious binders (OPC and FA). Both TWW and RCA were employed at a 100% replacement ratio, whereas FA was tested at replacement ratios of 0% and 20%. The volume replacement method was used for RCA, whereas the weight replacement method was considered for both TWW and FA. Concrete mix ingredients are presented in Table 4. Regarding the notation used for the concrete mixes, the first digit belongs to the mixing water type (F for FW and T for TWW). The second digit corresponds to the coarse aggregate type (G for GA and R for RCA). The third digit belongs to the cementitious binders (C for 100% cement and F for a mixture of 20% FA and 80% cement).

Table 4: Concrete Mix Ingredients

Mix	Mix Proportion (kg/m^3)						
	FW	TWW	OPC	FA	GA	RCA	Sand
F-G-C	156	0	349	0	1075	0	708
T-G-C	0	156	349	0	1075	0	708
T-R-C	0	156	349	0	0	942	708
T-R-F	0	156	279	69	0	942	708

2.6 Concrete Compressive Strength Test

The compressive strength of concrete was tested at 28 days using 3 cylinders of 100×200 mm for each mix as per ASTM C39/C39M-20 (ASTM C39/C39M-20, 2020).

2.7 Concrete Flexural Tensile Strength Test

The flexural tensile strength of concrete was tested at 28 days using 3 prisms of 100×100×500 mm for each mix as per ASTM C78/C78M-18 (ASTM C78/C78M-18, 2018).

2.8 Flexural Capacity Test of RC Beams

Four RC beams measuring 180 mm width, 250 mm height, and 2000 mm length were constructed and tested up to failure under a four-point flexural bending setup to evaluate the effect of concrete mixes on the flexural capacity of RC beams. The beam's designations followed the same designations of the concrete mixes. To measure the beams' displacement, two linear variable displacement transducers (LVDT) were added at each midspan. The tests were performed using a displacement rate of 1 mm/min. The details of the test setup and instrumentations are shown in Fig. 2.

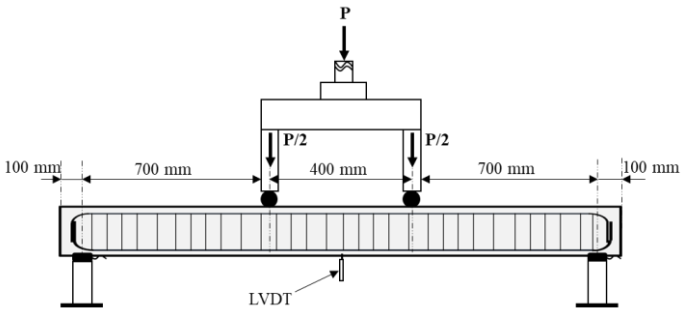


Fig. 2: Details of Test Setup and Instrumentations

3 Results and Discussion

3.1 Concrete Compressive Strength

Table 5 lists the compressive strength results. It can be revealed that mix T-G-C had a 6% lower compressive strength than mix F-G-C, attributable to the high amounts of phosphate and zinc in TWW, which alerted the hydration of OPC. In addition, the results show that mix T-R-C recorded 10% lower compressive strength than mix T-G-C due to the residual mortar on RCA, which affected the interface between aggregates and matrix and consequently generated more internal cracks. Moreover, mix T-R-F, which incorporated 20% FA, reported a drop of 16% in the compressive strength compared to T-R-C. This could be attributed to the decreased OPC hydration products due to the reduced OPC content, which consequently reduced the binding between aggregates and matrix. These observations agree with Sunayana & Barai (2019) and Alnahhal et al. (2023).

Table 5: Concrete Mechanical Properties

Specimen ID	Compressive Strength (MPa)	Flexural Tensile Strength (MPa)
F-G-C	57.03	3.77
T-G-C	53.50	3.29
T-R-C	48.04	3.43
T-R-F	40.54	2.96

3.2 Concrete Flexural Tensile Strength

The flexural tensile strength results are depicted in Table 5. It could be noticed that the use of TWW in mix T-G-C decreased the flexural strength by 13% compared to mix F-G-O, ascribable to the high pollutants of TWW. Furthermore, mix T-R-C achieved comparable flexural strength to mix T-G-C, indicating that RCA had no effect on the flexural strength of concrete. On the other hand, mix T-R-F reported 14% lower flexural strength than mix T-R-C due to the decreased OPC products. Abushanab & Alnahhal (2022b) also reported similar observations.

3.3 Flexural Strength of the Beams

Fig. 3 illustrates the load-deflection curves of the beams. In addition, Table 6 presents a summary of the ultimate load capacity and ductility index of the beams. It can be seen from the results that beam T-G-C had a drop of 14% and 9% in the ultimate flexural capacity and ductility index, respectively, compared to beam F-G-C. Furthermore, the deflection of beam T-G-C at service was 17% higher than that of beam F-G-C. The drop in the flexural properties of beam T-G-C is attributed to the chemical contaminants of TWW, which decreased the OPC hydration products and thus decreased the binding capacity between reinforcement and surrounding concrete. It can also be seen that beam T-R-C showed comparable flexural strength to its counterpart with natural aggregates. However, the beam recorded 9%, 6%, and 16% lower failure load, deflection, and ductility than beam T-G-C, respectively, compared to beams with natural aggregates. This might be attributed to the cracks and voids developed at the interface between aggregates and concrete matrix, which increased the brittleness of the beams. On the other hand, the flexural strength of beam T-R-F was increased by 7% and 5% compared beams TG-0 and TR-0, respectively. In addition, beam T-R-F reported marginally higher ductility than beam T-R-C. The improvement achieved with the 20% FA is ascribed to the calcium-silicate hydrates (C-S-H) gel, which densified the matrix and enhanced the bond strength between concrete and reinforcement. The obtained results are in line with Yoo et al. (2015).

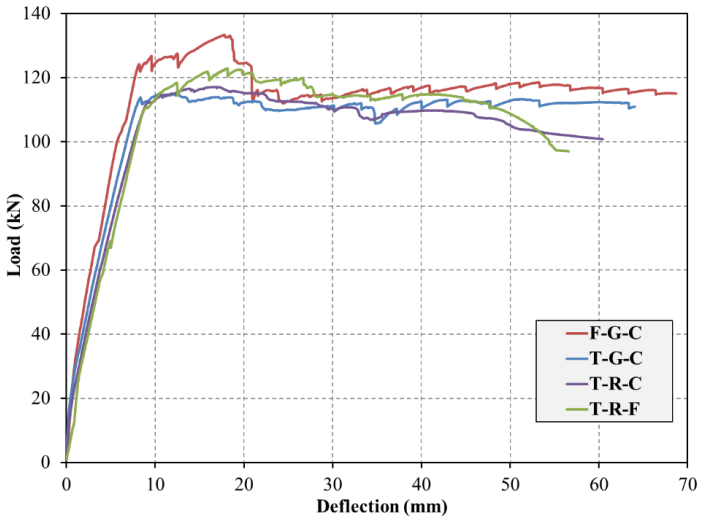


Fig. 3: Load-deflection curves of the beams

Table 6: Beam test results

Beam ID	Ultimate Strength (kN)	Ductility Index
F-G-C	133.35	8.32
T-G-C	115.12	7.60
T-R-C	117.09	6.39
T-R-F	122.90	6.43

4 Conclusion

In this study, the effect of TWW, RCA, and FA was investigated on the mechanical properties of concrete and flexural strength of RC beams. A total of four concrete mixtures were manufactured. The parameters considered were the type of concrete mixing water (FW and TWW), coarse aggregates (GA and RCA), and cementitious binders (OPC and FA). Based on the obtained results, the following conclusions are drawn:

1. TWW has a slight effect on the compressive strength of concrete. Nonetheless, RCA and FA showed a reduction of 10% and 16% in the compressive strength, respectively.
2. The use of TWW decreased the flexural strength and ductility of the beams by 14% and 9%, respectively.
3. RCA-RC beams had 9% and 16% lower failure load and ductility compared to beams with natural aggregates.
4. Incorporating FA with RC beams improved the flexural strength by 5% to 7%.

Acknowledgment

This publication was made possible by GSRA grant GSRA6-1-0509-19022 from the Qatar National Research Fund (QNRF, a member of Qatar Foundation). Also, the financial support from Qatar University through grant no. QUST-1-CENG-2021-20 is acknowledged. The findings achieved herein are solely the responsibility of the authors.

References

Abushanab, A. & Alnahhal, W. (2021). "Combined Effects of Treated Domestic Wastewater, Fly Ash, and Calcium Nitrite Toward Concrete Sustainability", *Journal of Building Engineering, 44,* 103240. https://doi.org/10.1016/j.jobe.2021.103240.

___. (2022a). "Characteristics of Concrete Made with Treated Domestic Wastewater", Proceedings of 2021 4th International Conference on Civil Engineering and Architecture, Thomas Kang and Youngjin Lee, Springer, Singapore, 231–35. https://doi.org/10.1007/978-981-16-6932-3_20.

___. (2022b). "Performance of Sustainable Concrete Incorporating Treated Domestic Wastewater, RCA, and Fly Ash", *Construction and Building Materials, 329,* 127118. https://doi.org/10.1016/j.conbuildmat.2022.127118.

___. (2022c). "Flexural Behavior of Reinforced Concrete Beams Prepared with Treated Wastewater, Recycled Concrete Aggregates, and Fly Ash", *Structures, 45,* 2067–79. https://doi.org/10.1016/j.istruc.2022.10.029.

Abushanab et al. (2021). "Mechanical and Durability Properties of Ultra-High Performance Steel FRC Made with Discarded Materials", *Journal of Building Engineering, 44,* 103264. https://doi.org/10.1016/j.jobe.2021.103264.

Alnahhal et al. (2023). "Mechanical characteristics of ultra-high performance steel FRC made with recycled concrete

aggregates", Proceedings of the 11th International Advances in Applied Physics And Materials Science Congress & Exhibition, 040009. https://doi.org/10.1063/5.0143845

Arooj et al. (2021). "A Sustainable Approach to Reuse of Treated Domestic Wastewater in Construction Incorporating Admixtures", *Journal of Building Engineering*, *33*. 101616. https://doi.org/10.1016/j.jobe.2020.101616.

Asadollahfardi, G. et al. (2016). "Use of Treated Domestic Wastewater before Chlorination to Produce and Cure Concrete", *Construction and Building Materials 105*, 253–61. https://doi.org/10.1016/j.conbuildmat.2015.12.039.

ASTM C78/C78M-18, (2018). Standard Test Method for Flexural Strength of Concrete (Using Simple Beam with Third-Point Loading). https://doi.org/10.1520/C0078_C0078M-18.

ASTM C39/C39M-20, (2020). Standard Test Method for Compressive Strength of Cylindrical Concrete Specimens. https://doi.org/10.1520/C0039_C0039M-20.

Behera, et al. (2014). "Recycled aggregate from C&D waste & its use in concrete – A breakthrough towards sustainability in construction sector: A review", *Construction and Building Materials, 68*, 501–16. https://doi.org/10.1016/j.conbuildmat.2014.07.003.

Choi, W. C. & Yun, H. D. (2013). "Long-Term Deflection and Flexural Behavior of Reinforced Concrete Beams with Recycled Aggregate", *Materials & Design, 51*, 742–50. https://doi.org/10.1016/j.matdes.2013.04.044.

Meena, K. & Luhar, S. (2019). "Effect of Wastewater on Properties of Concrete", *Journal of Building Engineering, 21*, 106–12. https://doi.org/10.1016/j.jobe.2018.10.003.

Seara-Paz et al. (2018). "Flexural Performance of Reinforced Concrete Beams Made with Recycled Concrete Coarse Aggregate", *Engineering Structures, 156*, 32–45. https://doi.org/10.1016/j.engstruct.2017.11.015.

Sunayana, S. & Barai, S. V. (2019). "Performance of Fly Ash Incorporated Recycled Aggregates Concrete Column under Axial Compression: Experimental and Numerical Study", *Engineering Structures, 196*, 109258. https://doi.org/10.1016/j.engstruct.2019.05.099.

Yoo, S. W., Ryu, G. S. & Choo, J. F. (2015). "Evaluation of the Effects of High-Volume Fly Ash on the Flexural Behavior of Reinforced Concrete Beams", *Construction and Building Materials, 93*, 1132–44. https://doi.org/10.1016/j.conbuildmat.2015.05.021.

Cite as: Abushanab A. & Alnahhal W., "Experimental Investigation on the Flexural Capacity of Reinforced Concrete Beams with Treated Wastewater and Recycled Concrete Aggregates", *The 2nd International Conference on Civil Infrastructure and Construction (CIC 2023)*, Doha, Qatar, 5-8 February 2023, DOI: https://doi.org/10.29117/cic.2023.0055

Widening of an Existing Bridge to Accommodate Two Traffic Lanes – Al Bustan South Project in Qatar

Theodoros Tzaveas
Public Works Authority (Ashghal), Doha, Qatar
ttzaveas@ashghal.gov.qa

Christina Anagnostaki
Public Works Authority (Ashghal), Doha, Qatar
canagnostaki@ashghal.gov.qa

Yoji Matsuo
Parsons International Limited, Doha, Qatar
Yoji.Matsuo@parsons.com

Georgios Sergakis
Parsons International Limited, Doha, Qatar
Georgios.Sergakis@parsons.com

Abstract

Driven by Qatar National Vision 2030 and catering to the 2022 FIFA World Cup, Qatar is undertaking an extraordinary and ambitious programme of infrastructure development to deliver a world-class new and upgraded road infrastructure network. Projects designed to improve highway capacity, connectivity, and safety through the urban and rural parts of Qatar and to meet current and future demands of population and economic growth.

In this paper, the authors discuss some of the most critical and challenging considerations in putting a planning and design process on a path to deliver successfully a bridge deck-widening project, implementing a collaborative approach. The case study of upgrading an existing ramp bridge will be presented, where the one lane deck was converted to two lanes to accommodate the heavy traffic flow. The fast-track construction schedule necessitated the widening from one side by 1.15m, while the extended slab was supported on a steel strut connected monolithically on the concrete box girder web (bottom) and extended part (top) through shear dowels. To meet the tight construction schedule and the local market material constraints, built-up sections were utilized with variable configurations along the length of the bridge. Further, several epoxy resin products were studied and utilized for the drilled bars on the extension part and the drilled dowels of the web. The replacement of the existing bearings was necessitated due to the additional weight of the extension.

Keywords: Deck widening; Steel-concrete composite; Bridge assessment

1 Introduction

The requirement of accommodating a second lane in the 350m long Ramp Bridge was aimed to improve the traffic flow that was observed during the operation of the structure as a single lane bridge. Several options were studied (See Figs. 1 & 2) to conclude on the preferred option, which would meet the fast-track schedule set by the client, and at the same time adhere to the site constraints, the required road geometry on the bridge, approaches and the local market availability of material resources.

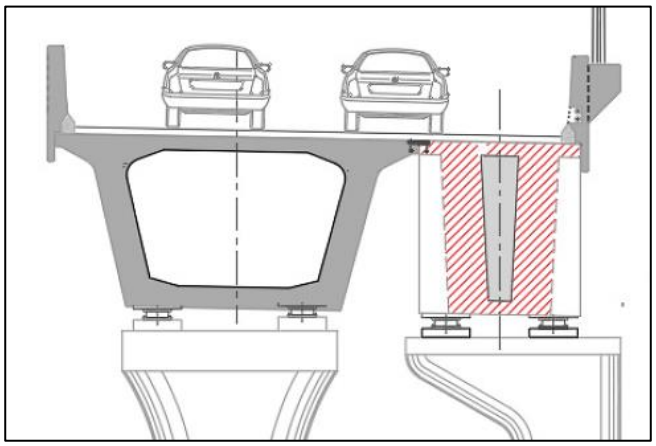


Fig. 1: Option of Adding a New Bridge Deck

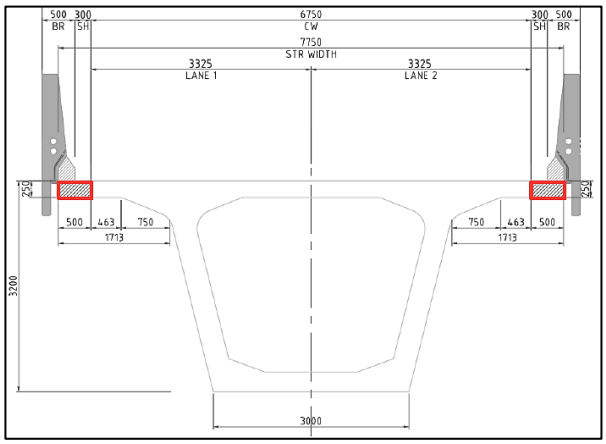


Fig. 2: Option of Extending Both Sides of the Deck (dimensions in mm)

In the preferred one-sided widening option (See Fig. 3), the addition of one lane on the bridge increased the cross-section width from 6.75m to 7.90m. The proposed 1.15m deck widening consisted of cast-in-place reinforced concrete deck slab supported on steel strut. The newly casted concrete of the extension was monolithically connected with the existing deck slab through additional rebar that was drilled and bonded to the deck slab using suitable epoxy resin. During the design, the number of rebars to be installed, the embedded length, and safe distance from the existing tendons were taken into consideration, to ensure the construction feasibility and safety. A key consideration was to keep the number of post-installed bars to a minimum and reduce the invasive operations on the existing deck flange. The steel strut was originally designed as the hot rolled section, but during construction stage the section was altered to built-up section to compensate for the local market constraints in obtaining the standard sections. The built-up section proposed by the contractor was not identical to the hot rolled section, as a result the design was checked once more utilizing the actual section to be installed.

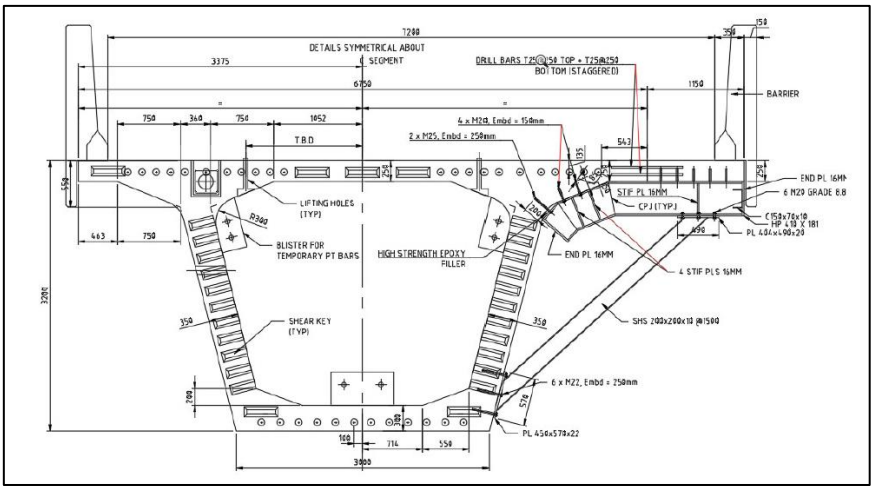


Fig. 3: Bridge Deck Cross-section (dimensions in mm)

2 Design Approach

The design was separated in two main stages and those were the positive assessments of the existing bridge to carry the additional loads (Stage 1) and the design of the new components for the widening of the existing bridge deck to accommodate the extra traffic lane (Stage 2).

The activities listed below were conducted for the preparation of the preferred option. Those were the following for each one of the above-mentioned stages:

2.1 Stage 1 (Existing Bridge)

- Check the structural safety of the existing Ramp Bridge (substructure & superstructure) for the widened deck slab.
- Provide the updated bearing schedule due to the increased permanent loads. These loads necessitated the bridge bearing replacement, an activity that was conducted by jacking of the existing deck (See Fig. 4) and replacing the bearings with larger capacity bearings.



Fig. 4: Caption of Bearing Replacement

2.2 Stage 2 (New Components)

- Design of the steel strut installed at a maximum spacing of 1.5m.
- Conduct all the necessary checks on both connection points of the strut.
- Design of the steel corbel at the abutment diaphragms. Due to the different geometry of the abutment diaphragm compared to the typical section (solid rectangular beam), a different detail was developed for this location, which proposed three rectangular hollow sections (RHS) closely spaced, supported to the side of the diaphragm segment. The RHS were developed in a horizontal plane, as opposed to the typical section strut, which was inclined.
- Provide the details of the extended expansion joints.
- Design of the new approach slab with the 1.15m projection corresponding to the deck extension.
- Provide the necessary construction steps/sequence of works.

The structural elements as listed below and form part of Stage 1 as it is mentioned above, were identified as affected by the deck widening and checked to confirm that no retrofit is necessary due to the increased dead, live and seismic loading:

- Foundations.

- Columns.
- Abutment.
- Bridge deck (Service Stress, Flexure, Shear & Torsion, and Transverse checks were performed).

3 Advantages of the Selected Option

The option of implementing the extension on one side of the bridge (i.e., eccentric) and supporting the newly casted extension with a steel bracket and strut was selected due to the below advantages:

- Minimization of the negative moment on the overhang.
- No local effects on the web of the existing bridge (i.e., strut supported on the height of the bottom slab haunch).
- The steel beam functioned as a shoring for widened deck construction (i.e., sacrificial formwork supported on this beam) thus the reduction of time for temporary works.
- One-sided widening minimized the traffic and utilities diversions. It also required the removal of the existing precast barrier and drilling of the deck slab on one side only. This reduced the construction duration.

4 Risk Mitigation Approach

The strut anchor bolts and steel reinforcement were detailed aiming to reduce the risks during the construction. Below are the locations that the anchor bolts and steel reinforcement were designed with particular attention to reduce the risk of adverse impact on the existing structure and ensure constructability.

4.1 Bracket Anchorage to the Bridge Deck Haunch (Soffit)

The anchor bolts embedded depth was designed to ensure a minimum of 55mm clearance to the post tensioning tendons (See Figs. 5 & 6). Further, the number of rows of the anchor bolts was reduced from 3 to 2, to avoid the embedment of a row of anchor bolts in the curved part of the bridge box girder deck. This increased the number of bolts in the 1st & 2nd rows as shown in the snapshots below.

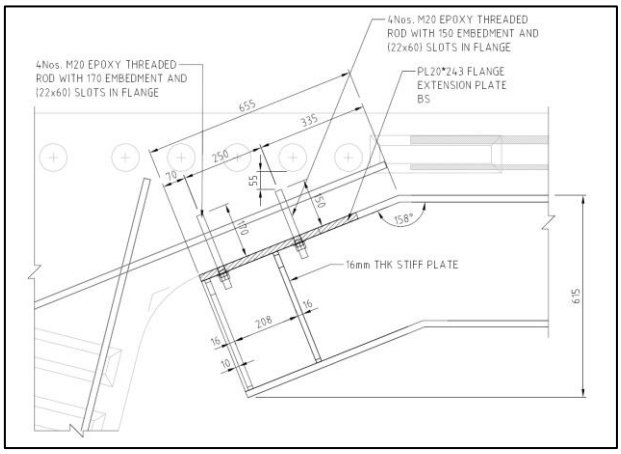


Fig. 5: Bracket (Section) (dimensions in mm)

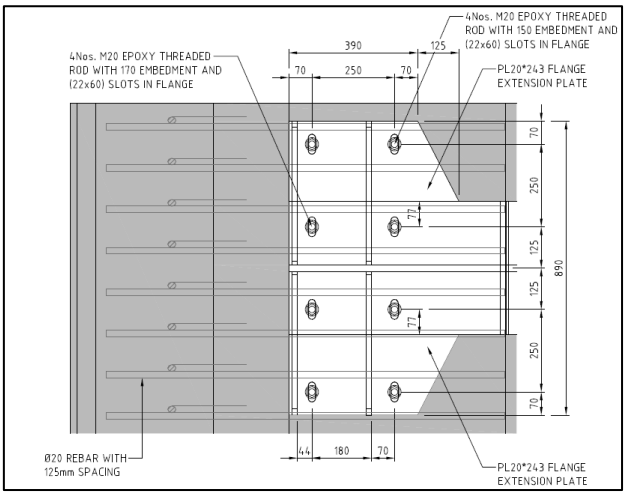


Fig. 6: Bracket (Plan view) (dimensions in mm)

4.2 Anchor Bolts providing the Connection of Strut Support and the New Extended Deck

The number of anchor bolts was increased and distributed on the bracket top flange to decrease the embedment depth to 150mm. This allowed the development of the anchor bolts within the 250mm deck slab extension to avoid crossing of the anchor bolt heads with the top mat of slab reinforcements for ease of construction (See Figs. 7 & 8).

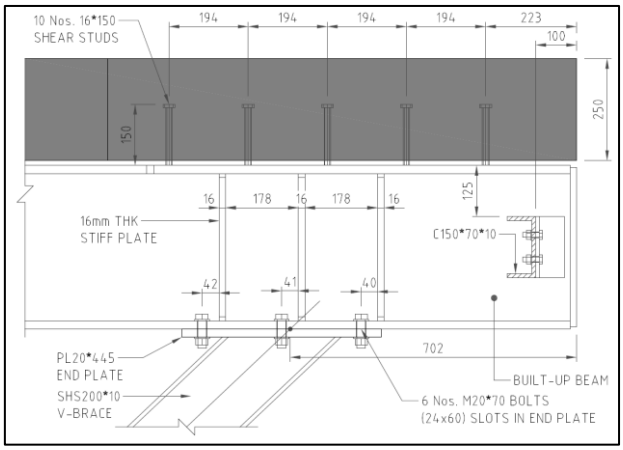


Fig. 7: Strut & Bracket (Section) (dimensions in mm)

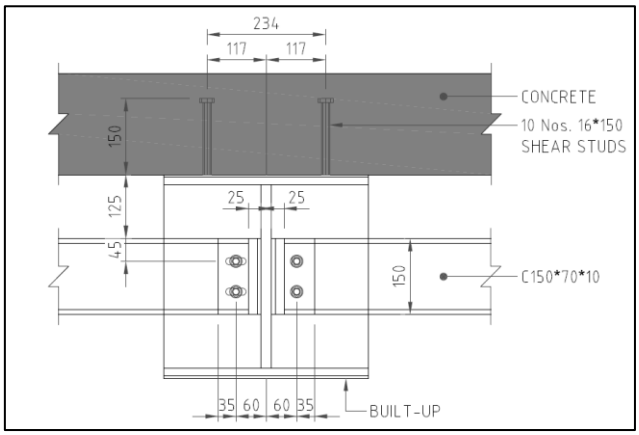


Fig. 8: Struct & Bracket (Section) (dimensions in mm)

4.3 Anchor Bolts of the Strut Bottom Connection with the Box Girder Bottom Slab Haunch

The number of anchor bolts increased to 6 and the embedment depth was optimized to reduce the risk of clashing with the bottom slab post-tensioning ducts. Further, the location was selected to ensure suitability to carry the straining actions transferred from the strut support. The design considered small deviations due to the uneven surface of the concrete, allowing grouting up to 15mm thickness (See Figs. 9 & 10).

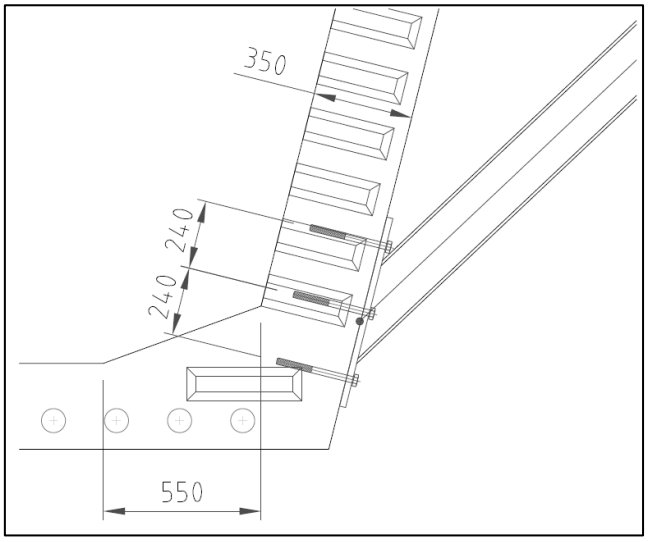


Fig. 9: Strut-Girder connection (Section) (dimensions in mm)

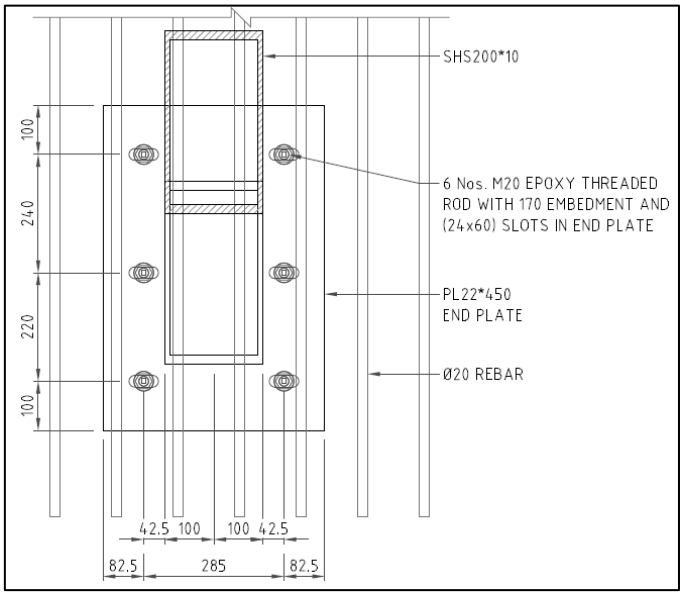


Fig. 10: Strut-Girder connection (Plate details) (dimensions in mm)

4.4 Drilling and Bonding of the Steel Reinforcement on the Existing Deck Slab to Accommodate the Extension

The steel reinforcement diameter and spacing were selected based on the required embedment depth, minimizing the number of drilling locations along the 250mm thick slab, while keeping a safe distance from the top slab post-tensioning ducts (See Fig.11).

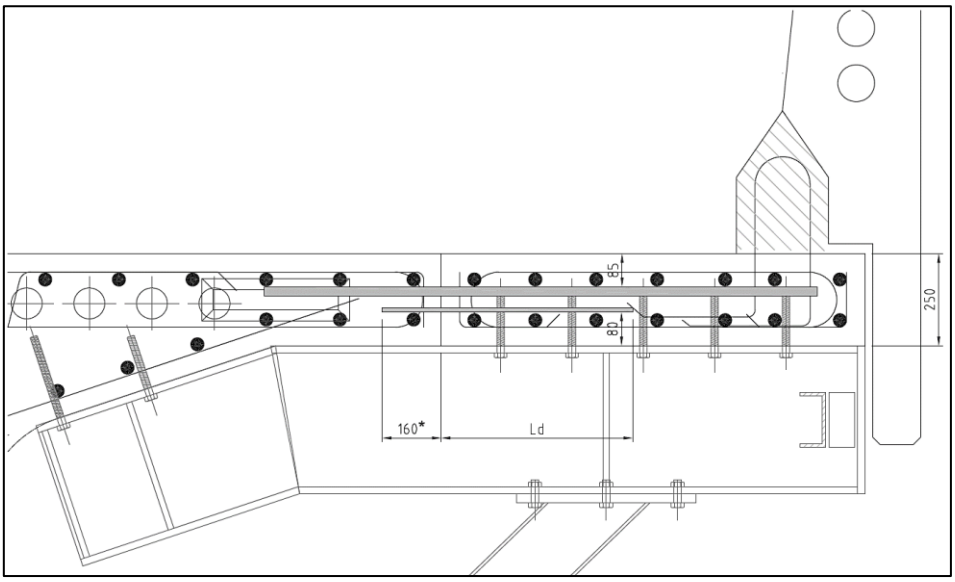


Fig. 11: Caption of Embedded Reinforcement (dimensions in mm)

5 Conclusion

The Ramp Bridge 8 of the Al Bustan South Project required the extension of the existing bridge deck by 1.15m to allow the placement of a second traffic lane. The design of this extension aimed to create a robust solution that would be constructed in a fast-track schedule with tight deadlines for delivery while considering the site constraints and market material availability.

The challenges that were encountered in the proposed one side deck widening were mainly the installation of the steel strut in the existing post-tensioned concrete deck, considering that the anchorage of the steel strut in both top and bottom plates, would have to be done in such a way to avoid any potential damage to the existing post-tensioning tendons. Further challenge was the jacking up of the bridge deck for the replacement of the spherical bearings, that would carry the increased loads due to the deck extension. The design proposal, the contractor's execution plan and the continuous engagement of all project stakeholders (Client/Contractor/Designer), were factors that enabled to overcome the above challenges and provide a robust structural design, speedy construction, with an aesthetically unintrusive configuration. Fig.12 shows the completed bridge deck.



Fig. 12: The Completed Deck Extension (site photo)

References

Ashghal. (2016). Interim Advice Note 009 – Design Criteria for Highway Structures, Revision A2, Ashghal.

Ashghal. (2016). Interim Advice Note 006 – Specification of Bridge Bearings, Revision A1, Ashghal.

BSI. (1990). BS 5400-4:1990, Code of practice for design of concrete bridges, BSI.

BSI. (2006). BS 5400-2:2006, Steel, concrete, and composite bridges. Specification for loads, BSI.

Cite as: Sergakis G., Matsuo Y., Anagnostaki C. & Tzaveas T., "Widening of an Existing Bridge to Accommodate Two Traffic Lanes – Al Bustan South Project in Qatar", *The 2nd International Conference on Civil Infrastructure and Construction (CIC 2023)*, Doha, Qatar, 5-8 February 2023, DOI: https://doi.org/10.29117/cic.2023.0056

Influence of Adding Demolition Wastes on the Mechanical Properties of Concrete in Sultanate of Oman

Said Almaawali
University of Nizwa, Nizwa, Oman
salmaawali@unizwa.edu.om

Samiya Alhamrashdi
University of Nizwa, Nizwa, Oman
23661994@uofn.edu.om

AmeeraAlsiyabi
University of Nizwa, Nizwa, Oman
09454731@uofn.edu.om

Abstract

Nowadays the global trend in construction industry is to reduce the cost, saving energy and preserving the environment. Using other industries' waste material as a construction material is one of several methods followed to meet these trends. Management of solid waste is considered as one of the most significant environmental issues not only in a country like Oman, but globally as well. Around 1.7 million tons of solid waste is yearly generated in Oman. More than 120 million tons of constriction demolition waste is yearly generated over the world. Besides, 10-30 % of solid wastes produced from construction field (concrete wastes and aggregate) in Oman is just dumped in the landfill area without any further use. In this paper, the influence of replacing the demolition waste with coarse aggregate on the mechanical properties of concrete was studied in terms of compressive, flexural, and tensile strengths, and workability. The concrete properties were evaluated by replacing of 20, 30 and 40% of coarse aggregates with demolition waste in the mix proportion of C-35 concrete and the experiment's results were compared with each other as well as with the conventional one, based on two different periods of 7 and 28 days. The results were satisfactory so it could be concluded that replacing of up to 40% of coarse aggregates with construction and demolition waste is still safe and not causing dramatic reduction in the concrete strength.

Keywords: Oman; Concrete; Recycling; Construction waste; Demolition

1 Introduction

Nowadays in the developed countries, the demolition waste from construction has become a real problem and major portion of the solid waste. In addition, there is a need for several methods that either reduce the use of natural resources, reuse them, or recycle them to other materials that can be used for the same purpose or another purpose due to the continuous consuming of natural resources on the planet. Besides, there are more than 120 million tons of construction demolition waste, which is yearly generated over the world (Elchalakani, 2012; Akter & Samah, 2018). However, 10-30 % of Oman solid wastes produced from construction field (concrete wastes and aggregate) is dumped in the recognized landfill area without any further use. Besides, management of solid waste is considered as one of the most significant environmental issues not only in Oman, but globally as well. Around 1.7 billion tons of solid waste is yearly generated in Oman, which is expected to reach 2.2 billion tons

by 2025 due to the increase in Oman's population (Ithraa, 2016). Moreover, construction industry consumes huge amounts of material, water, and energy, but unfortunately, all of these resources are non-renewable natural resources such as water and rocks. In addition, the process of producing aggregate is consuming a huge amount of diesel to generate the crusher and the screen as well as the gas emission due to that (Al-Manthari, 2018). Therefore, it becomes extremely necessary to find a useful method to recycle the demolition waste (Annual sustainability report, 2020).

In this research, the influence of replacing the demolition waste with coarse aggregate on the mechanical properties of concrete will be studied in terms of compressive, flexural, and tensile strengths, and workability will be discussed.



Fig. 1: Examples of Demolition Waste from Al-Masnaah- Al Batanah Region – Oman

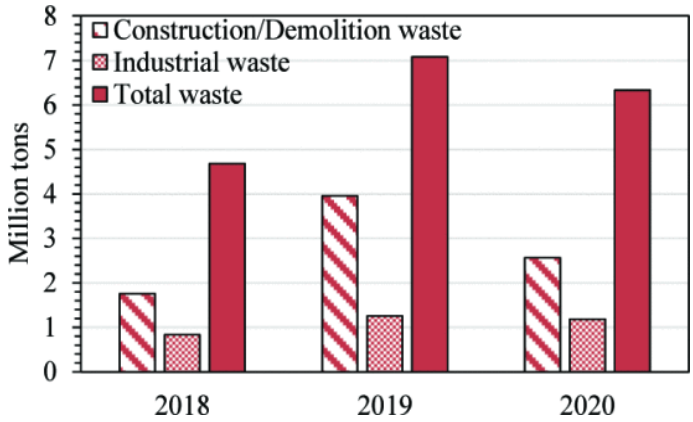


Fig. 2: Industrial and Construction Waste in Oman according to be'ah

2. Methodology

In order to complete this research and achieve its objectives, the experiments of compressive, flexural, and tensile strengths, and workability tests were performed on the concrete grade C-35 with replacement percentages of 0, 20, 30 and 40% and specimens ages are 7 and 28 days. Potable water, fine aggregate with 4.75mm particle size, 20mm crushed coarse aggregate, grade 53 ordinary Portland cement and demolition waste were crushed and sieved to obtain 20mm particles size, which are the materials used in this research. Later on, the findings were compared with the results of previous literature.

Table 1: Mix Proportions

W/C Ratio	Concrete Constituents (kg)			
	Cement	Fine Aggregate	Coarse Aggregate	Demolition Waste
0.51	411.8	698.7	889.4	0
0.51	411.8	698.7	711.52	177.88
0.51	411.8	698.7	622.88	266.82
0.51	411.8	698.7	533.64	355.76

3 Results and Discussion

The experiments had been done to find the differences between the normal concrete and replacing demolition waste as coarse aggregates or it can be called Recycled Aggregate Concrete (RAC). The demolition waste was taken from Al-Masnaah and Barka- North of Al Batinah Region – Oman. However, four experiments done are compressive strength, splitting tensile strength and flexural strength, as well as the workability (slump cone) test. The results are matching with the findings of other researches such as (Ramadevi & Chitra, 2017; Wahih, El-Karmoty, Ebid & Okba, 2013).

3.1 Compressive Strength

Test cubes were prepared for different concrete mixes with 0, 20, 30 and 40% replacement of coarse aggregates with recycled aggregates taken from demolition waste. Then universal compressive strength test was applied to the concrete cubes after 7 and 28 days. The results are shown in Table 2 and 3 and Figure 3. There is a slight decrease between normal concrete and 20% of the replacement ratio of demolition waste and there is more decreasing in 30% and 40% of replacement ratio of concrete waste. The reduction percentage after 7 days of curing was 2% between normal concrete and the 20% RAC. The normal concrete was 30 MPa and for 20% RAC was 29.4 MPa. In addition, the 30% of RAC was 24.2 MPa after 7 days of curing, and 22.9 MPa for 40% of RAC.

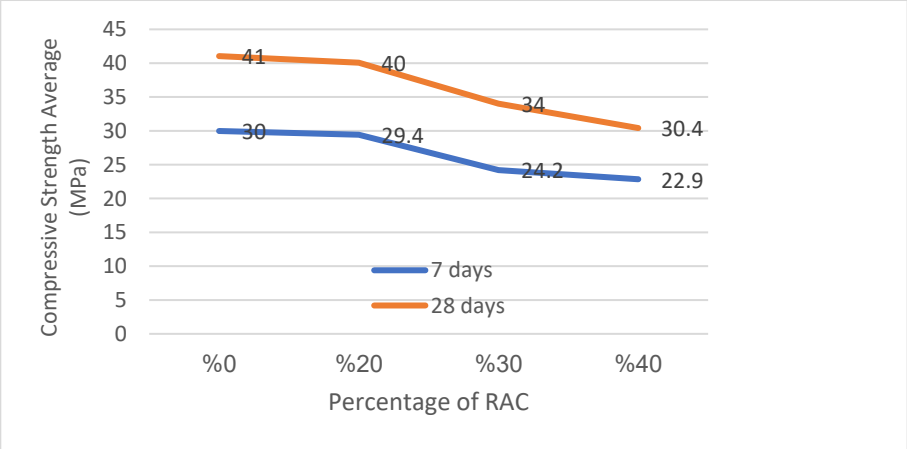


Fig. 3: Compressive Strength Results for 7 & 28 days

Table 2: Compressive Strength Results

% Demolition Waste	Testing age	Maximum Load (KN)	Compressive Strength (MPa)	Average Compressive Strength (MPa)
0%	7 Days	590.1	29.4	30
		576.7	28.8	
		583.6	30.7	

% Demolition Waste	Testing age	Maximum Load (KN)	Compressive Strength (MPa)	Average Compressive Strength (MPa)
	28 Days	689.8	39.1	41.0
		909.7	41.5	
		916.5	42.6	
20%	7 Days	680	30.2	29.4
		672.4	29.9	
		634.1	28.2	
	28 Days	900.5	40.2	38.4
		815.9	36.3	
		871.4	38.7	
30%	7 days	422	18.8	24.2
		605.2	26.9	
		606.9	27	
	28 days	773.9	34.4	34.0
		781.6	34.7	
		741.3	32.9	
40%	7 Days	517.6	23	22.8
		509.9	22.6	
		512.4	22.8	
	28 days	714.5	31.7	30.4
		662.5	29.4	
		689.5	30	

Moreover, the results after 28 days were 41.0 MPa for normal concrete, 38.3 MPa for 20% of RAC, 34.0 MPa for 30% and for 40% was 30.4 MPa. Therefore, it can be said that the results were nearly to achieve the goal of the compressive strength, which is C35, and the best percentage was20 %, which was 38.4 MPa, for 30% it was 34.03, which is close to 35 MPa. The 40% percentage of replacement ratio of demolition waste was 30.4 MPa, which is not bad and can be used for C30 concrete and lower. The quality of the concrete decreased when the percentage of the demolition waste replacement increased and by this experiment the differences of the compressive strength results for all percentages were shown, that there is a minor difference between normal concrete and other percentages of replacement ratio of demolition waste. The results show that demolition waste can be used as coarse aggregate in the concrete, especially for lower grades of concrete.

3.2 Splitting Tensile Strength

Concrete cylinders were cast also to test the tensile strength of concrete. The splitting tensile test had been done and as it is shown in Tables 4, 5 and Figure 3; that the normal concrete has 14.6 MPa splitting tensile strength after curing 28 days and according to BS 81I0; the concrete tensile strength has good reasonable value as well as the 20% of Recycled Aggregate Concrete, which was 14.3 MPa. Moreover, the results of 30% and 40% were 14.0 MPa and 13.5 MPa, respectively. It can be said that there is a minor decrease between the normal concrete and the other percentages of recycled aggregate concrete.

Table 3: Splitting Tensile Results

Percentage of RAC	Testing Age (Days)	Maximum Loads (KN)	Splitting Tensile (MPa)	Splitting Tensile Average (MPa)
0%	28	249.7	14.1	14.6
		251.9	14.8	
		254	14.8	

Percentage of RAC	Testing Age (Days)	Maximum Loads (KN)	Splitting Tensile (MPa)	Splitting Tensile Average (MPa)
20%	28	250	14.1	14.3
		270.7	15.3	
		234.5	13.5	
30%	28	232.6	13.2	14.0
		264.2	15	
		248.6	14.0	
40%	28	237.5	13.4	13.5
		240.5	13.6	
		238.4	13.5	

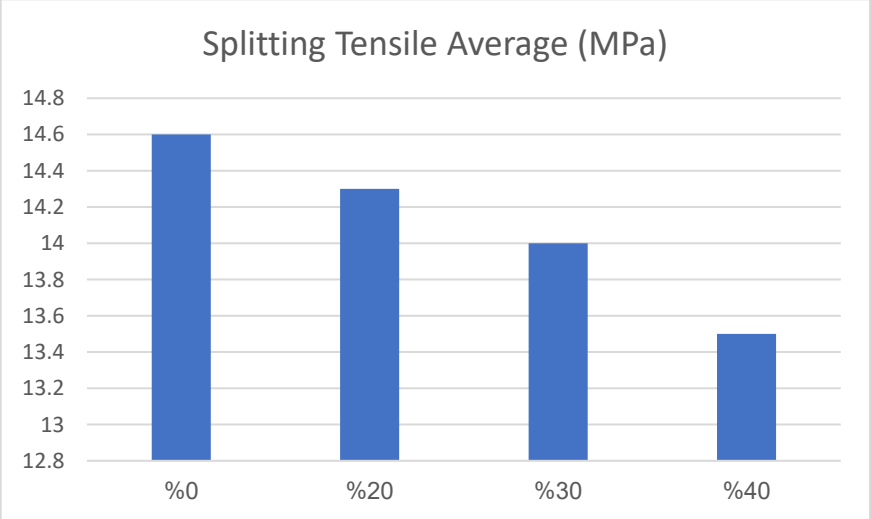


Fig. 4: Splitting Tensile Results for 28 days

3.3 Flexural Strength

In order to determine the flexural strength, 12 prisms, three from each percentage had been cast and cured for 28 days. As it is shown in Tables 6, 7 and Figure 5; the normal concrete has 15.7 MPa of the flexural strength and the 20% of recycled aggregate concrete was 14.4 MPa of the flexural strength. Where for 30% and 40% of recycled aggregate concrete it had a minor difference with normal concrete, the 30% of recycled aggregate concrete has 13.8 MPa of the flexural strength. Figure 5 is clearly showing the drop of the strength of the concrete when the percentage of the recycled aggregate concrete increases. The experiment's results show that the best percentage is 20%, which has 14.4 MPa, that is nearly same to the normal concrete quality, and it can be said that the results were nearly to achieve the goal of the strength. Generally, the results show that demolition waste can be used as coarse aggregates in the concrete especially for grades lower than C30.

Table 4: Compressive Strength Results

% of RAC	Testing Age (Days)	Maximum Loads (KN)	Splitting Tensile Average (MPa)
0%	**28**	15.76	15.7
		15.89	
		15.53	
20%	**28**	15.57	14.4
		13.03	
		14.73	

% of RAC	Testing Age (Days)	Maximum Loads (KN)	Splitting Tensile Average (MPa)
30%	**28**	14.30	13.8
		13.33	
		13.86	
40%	**28**	13.92	13.3
		13.03	
		12.89	

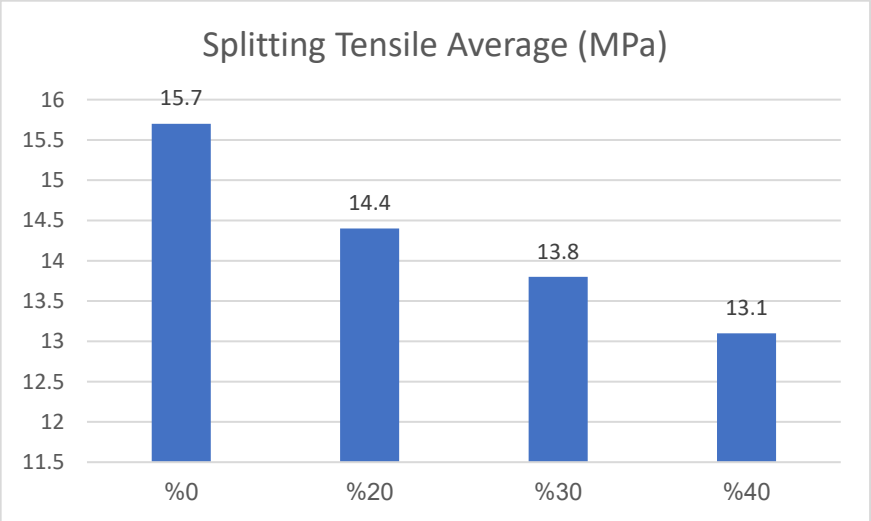


Fig. 5: Flexural Strength Results

4 Conclusion

The aim of this paper was to find a cheap and environmentally friendly concrete by using Recycled Aggregate from demolition waste. In this paper the mechanical properties of the concrete had been discussed such as compressive strength, flexural strength and splitting tensile strength. These experiments were done to check the differences between normal concrete, after replacing Recycled Aggregate Concrete. The demolition waste was taken from Be'ah plant-Barka – Oman.

In compressive strength test, there was a slight decrease between normal concrete and 20% of replacement ratio of demolition waste, which has been used as coarse aggregates and there is a decrease in 30% and 40% of replacement ratio of concrete waste. The quality of the concrete decreased when the percentage of the demolition waste replacement increased and by this experiment, the differences of the compressive strength results for all percentages were shown, that there is a minor difference between normal concrete and other percentages of RAC. The splitting tensile test had been also done and the results were shown that the normal concrete has 14.6 MPa of the splitting tensile strength after curing 28 days and according to BS 8110 the concrete strength has a reasonable quality as well as the 20% of Recycled Aggregate Concrete has 14.3 MPa, which is nearly same. Moreover, the results of 30% and 40% were 14.0 MPa and 13.5 MPa of the splitting tensile strength after curing 28 days. The quality of the concrete decreased when the percentage of the demolition waste replacement increased and by this experiment the differences of the strength results show that the best percentage is 20% which is has 14.3 MPa, which is nearly same to the normal concrete quality.

To test the flexural strength, the prisms had been casted and cured 28 days. The flexural strength of the normal concrete has 15.7 MPa and for the 20% of recycled aggregate concrete was 14.4 MPa, which is nearly same to normal concrete. Moreover, the 30% and 40% of recycled aggregate concrete had a minor difference with normal concrete. The 30% of recycled aggregate concrete has 13.8 MPa of the flexural strength. The results show that demolition waste can be used as coarse aggregates in the concrete. The workability of the concrete was tested using slump test. The result was 50 mm for normal concrete. The workability of the concrete with demolition waste was less than the workability of normal concrete. The result of first percentage which is 20% of recycled aggregate concrete was 42 mm which is less than normal concrete by 8 mm. The concrete which has 30% of recycled aggregate concrete was found 37 mm. There is a dropping in the workability of the concrete between the normal concrete and the re-cycled aggregate concrete. Generally, it can be concluded that 20% of coarse aggregates can be replaced in confidence with demolished grounded waste for C30 and C35 concretes. 30% and 40% can be used also for concrete of grades less than C30. For higher percentages of coarse aggregate replacement or higher grades of concrete, it should be tested before deciding to use such replacements.

References

Akhtar, A. & Sarmah, K. (2018). Construction and demolition waste generation and properties of recycled aggregate concrete: A global perspective. *Journal of Cleaner Production Volume 186,* 10 June 2018, pp. 262-281.

Annual sustainability report 2020. (2020). Available at: https://www.beah.om/Other/be-ah-ASR-2020.

Elchalakani, M. (2012) Sustainable Concrete made of Construction and Demolition Waste Using Recycled Wastewater in the UAE, *Journal of Advanced Concrete Technology 10*(1), 110.

Ithraa. (2016). Briefings from Oman Waste Management. Available at: https://issuu.com/ithraaoman/docs/ithraa_briefings_waste_eng_aw

Ramadevi, K. & Chitra, R. (2017). Concrete Using Recycled Aggregates. *International Journal of Civil Engineering and Technology 8*(9), 413-419.

Wagih, A. M. et al. (2013). Recycled Construction and Demolition Concrete Waste as Aggregate for Structural Concrete, *Housing & Building National Research Canter 9*(1), 193 – 200.

Cite as: Almaawali S., Alhamrashdi S. & Alsiyabi A., "Influence of Adding Demolition Wastes on the Mechanical Properties of Concrete in Sultanate of Oman", *The 2nd International Conference on Civil Infrastructure and Construction (CIC 2023)*, Doha, Qatar, 5-8 February 2023, DOI: https://doi.org/10.29117/cic.2023.0057

RSM Analysis for Optimum Content of Graphene Nanoplatelets for 3D-Printed Clay Strength

Mohamed Mohsen
Department of Civil & Architectural Engineering, Qatar University;
Tajarub Research & Development, Doha, Qatar
200202128@qu.edu.qa,

Malak Al-Diseet
Tajarub Research & Development, Doha, Qatar
malak.aldiseet@tajarub.org

Mervat Abu Rumman
Tajarub Research & Development, Doha, Qatar
mervat.ruman@tajarub.org

Ramzi Taha
Engineering Program, Schreiner University, Texas, USA
ramzitaha@gmail.com

Khalid Naji
Department of Civil & Architectural Engineering, Qatar University, Doha, Qatar
knaji@qu.edu.qa

Abstract

This study applies Response Surface Methodologies (RSM) methods to maximize 3D-Printed clay mechanical properties. Mixes containing different Graphene Nanoplatelets (GNPs) contents were printed and tested in compression and flexure. The Central Composite Design method was used by coding the mixes fabrication method, i.e. moulding and printing, and GNPs content as variables. The analysis showed that the mixes containing low GNPs content of 0.1 wt.% attained higher compressive and flexural strengths than those containing a higher content of 0.2 and 0.3 wt.%. The results also highlighted that GNPs' efficiency was better observed in the printed samples other than the moulded ones, indicating that the printing process contributed to a better and uniform dispersion of GNPs in the clay matrix. RSM analysis confirmed that the maximum flexural strength response could be obtained using a GNPs content of 0.1 wt.%. Furthermore, the desirability analysis showed that a maximum predicted flexural and compressive strength improvements of 21% and 36 % compared to the control mixes could be obtained, respectively. In summary, this study proposed the importance of using Nanofilaments in 3D printing activities to achieve the desired elements' mechanical properties.

Keywords: 3D-printed clay; Graphene Nanoplatelets; Mechanical strength; RSM

1 Introduction

Three-dimensional printing (3DP), also known as rapid prototyping, is an additive manufacturing (AM) technique in which a variety of structures and complicated geometries are fabricated using computer-generated model data (Ngo et al., 2018). The printing process comprises printing a material layer-by-layer on top of each other. Over the years, this technology gained wide attention and tremendous development in different industrial sectors such as construction, medicine, and biomechanical. Despite the numerous advantages of 3DP, e.g. design freedom, time efficiency, labour

safety, and environmental hazard reduction, imparting this technology to the construction industry is still relatively limited and very slow. However, the limited selection of printable materials is the key challenge. Currently, conventional ceramics engineering, involving clay and concrete sectors, is the largest materials industry in the world in terms of materials produced (Revelo & Colorado, 2018).

Clay is one of the oldest human-made materials, still widely utilized in construction and infrastructure today (Moropoulou et al., 2005). Building with clay has many features in the 21st century since it has superior thermal mass characteristics to any other material, acting as a buffer to exterior temperature fluctuations by delaying the release of immersed solar energy, resulting in a stable interior (Rael & San, 2017). Furthermore, it is easily available, affordable, fire-resistant and arguably the most earth-friendly material. These advantages are the main reasons the ceramic industry is of great interest to additive manufacturing technologies that use clay as raw materials. Although several additive processing techniques for ceramic components have been studied, research on ceramic and clay 3D printing for construction applications is still in its early stages (Wolf et al., 2018). To date, few studies in this area dealt with the performance of 3D-printed clays under different conditions and printing parameters, while research on the impact of various additives such as Nanomaterials was absent (Manikandan et al., 2020; Sangiorgio et al., 2022). A major challenge hindering the expansion of the cementitious materials 3D-printing industry is the reduced mechanical properties due to the layering process.

Nano-inclusions such as Graphene Nanoplatelets (GNPs) have gained interest in building technologies due to their exceptional properties at the nanoscale (Balaguru & Chong, 2006; Shen et al., 2013). Past work in this field showed that small additions of GNPs could effectively enhance cementitious composites' rheological, mechanical, and microstructural characteristics (Wang et al., 2016; Baomin & Shuang, 2019; Tao et al., 2019). However, using this technology to advance the production of 3D-printed clay elements is still missing. This research used the RSM methods to study the optimum GNPs content needed to maximize 3D-printed clay compressive and flexural strengths.

2 Research Methodology

Three different GNPs-to-clay dosages of 0.1, 0.2 and 0.3 wt.% were employed to evaluate the moulded and printed clay mechanical properties. Study samples were divided into two main groups: printed and moulded, with and without Nano-inclusions. Table 1 shows the tested batches. The experimental methodology consisted of samples preparation, first. Then, sample testing for flexure and compression. After that, test results were analysed using RSM techniques and reported accordingly.

Table 1: Test Batches

Test Group	Production Technique	Batch #	Batch Code	GNPs/clay Wt.%
Moulded Group	Moulding	1	MC	0.0
		2	M-0.1%GNPs	0.1
		3	M-0.2%GNPs	0.2
		4	M-0.3%GNPs	0.3
Printed Group	3D printing	5	PC	0.0
		6	P-0.1%GNPS	0.1
		7	P-0.2%GNPS	0.2
		8	P-0.3%GNPS	0.3

2.1 Materials and Equipment

The clay used was a high-quality Italian clay paste with a solid appearance. The GNPs used were industrial-grade 4 COOH Graphene Nanoplatelets of 4 nm thickness and 700 m^2/g surface area. The equipment included a clay 3D printer, an ultrasonic wave mixer, an electric ceramic kiln, a strength testing machine, and a scanning electron microscope (SEM).

2.2 Experimental Procedure and Testing

First, an aqueous solution of GNPs and water was prepared using an ultrasonic wave mixer for 30 minutes at a power of 400W to achieve a good dispersion of GNPs inside the clay matrix. The hard clay was cut into small pieces, and the aqueous solution was added gradually. After that, the clay was kneaded manually until a homogeneous paste free of cracks and not sticking to the hand was obtained; hence, the clay was ready to print. The same type of clay was used for all batches with a fixed water-to-clay ratio of 0.05. Printing of clay samples was performed using a Delta WASP 2040 3D printer along with an LDM WASP Extruder having a nozzle 3 mm in diameter. The printed specimens were sketched using the computer-aided design software Onshape, and a 3D printing slicing software simplifying 3D was utilized to generate g-code print paths. The compression and flexure sample configuration and the layered printing are presented in Figures 1a and 1b, respectively. After preparing the clay mixture, it was directly loaded into the 3D-printing system storage container. Then, a pressure of 6 bar was used on the storage container piston and kept constant during printing. Figure 2a shows the 3D-printing process for a cube sample. The best results were obtained using a printing speed of 90 mm/s and 300% flow. The same mix of proportions of each printed batch was used to make the same size moulded specimens using steel moulds. Finally, high-temperature heating was employed to turn raw clay into ceramic inside an electric ceramic kiln, as illustrated in Figure 2b. After the burning process, flexural and compressive strength tests were performed according to ASTM C348 and ASTM C109 standards.

(a) (b)

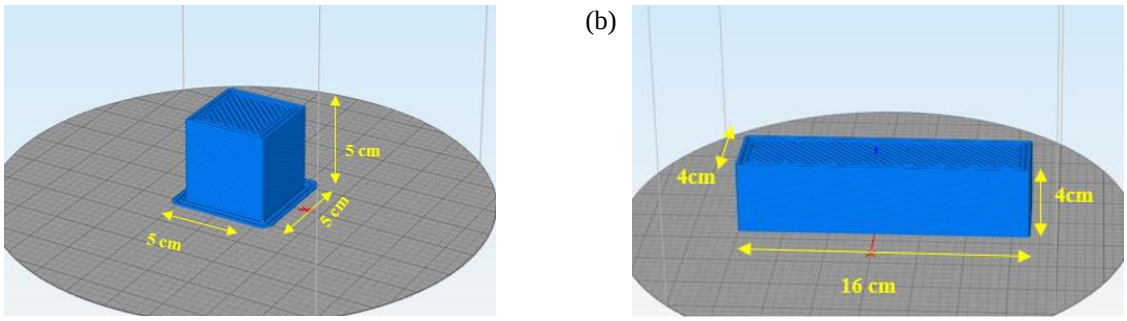


Fig. 1: (a) Details of ready-to-print 3D models of a) cube for compressive strength and b) prism for flexural strength

(a) (b)

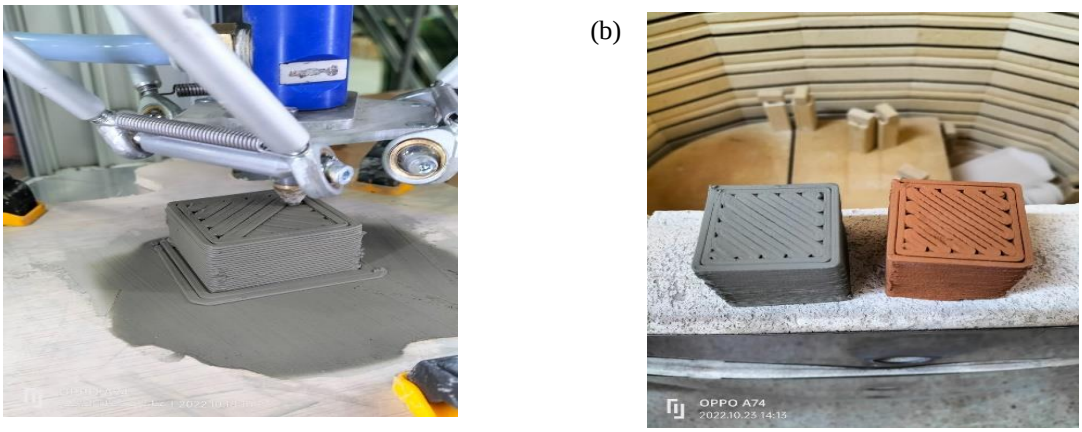


Fig. 2: (a) 3D-printing process, and (b) burnt vs unburnt sample

2.3 Response Surface Methods (RSM) Techniques

Response Surface Methodologies (RSM) techniques were used to study the effect of the fabrication method and GNPs weight fraction variables on the 3D-printed clay flexural and compressive strength factors' response. The following procedure was used to conduct this analysis:

1) Production type and Nanofilaments' weight fractions variables are coded (Table 2).
2) Second-order equations were employed to predict the flexural and the compressive strength functions as:

$$FS = b_0 + b_1x_1 + b_2x_2 + b_{11}x_1^2 + b_{22}x^2 + b_{12}x_1x_2$$

$$CS = a_0 + a_1x_1 + a_2x_2 + a_{11}x_1^2 + a_{22}x^2 + a_{12}x_1x_2$$

Where, FS is flexural strength, (MPa), CS is compressive strength, (MPa), $x1$ is samples production technique, $x2$ is GNPs' weight fraction, (%), and $a0$, $a1$, $a2$, $a11$, $a22$, $a12$, $b0$, $b1$, $b2$, $b11$, $b22$, and $b12$ are the response surface coefficients.

3) The prediction models and coefficients were measured.
4) The contour lines and desirability functions were plotted by optimizing the desirability function.

Table 2: Coding of production technique and GNPs weight fraction variables for RSM analysis.

Batch Code	Production Technique	Coding Production Technique	GNPs/clay Wt.%	Coding GNPs/clay Wt.%
MC	Moulding	-1	0.0	-1
M-0.1%GNPs	Moulding	-1	0.1	-0.333
M-0.2%GNPs	Moulding	-1	0.2	0.333
M-0.3%GNPs	Moulding	-1	0.3	1
PC	3D-printing	1	0.0	-1
P-0.1%GNPS	3D-printing	1	0.1	-0.333
P-0.2%GNPS	3D-printing	1	0.2	0.333
P-0.3%GNPS	3D-printing	1	0.3	1

3 Results & Discussion

3.1 Flexural and Compressive Strength

Figures 1a and 1b show the flexural and compressive strength results of all tested batches. Among all batches, the moulded mix containing 0.1 wt.% GNPs achieved the highest flexural strength of 18 MPa with an enhancement of about 7.5% compared to the moulded plain control mix. This finding indicates the role of proper Nanofilaments' dispersion on the strength enhancement of clay. The mix containing lower GNPs' content of 0.1 wt.% would probably have better dispersion quality than those containing higher GNPs' content of 0.2 and 0.3 wt.%. On the other hand, GNPs' efficiency was better observed in the printed samples using both low and high concentrations, as the printing process may contribute to a better and uniform dispersion of GNPs in the clay matrix. Compressive strength results revealed that both fabrication methods resulted in approximately equivalent compressive strength regardless of the weight fraction used. The maximum compressive strength improvement of about 42-48 % was obtained using a GNPs' weight fraction of 0.1%. The bridging and pore-filling impact of GNPs at low concentrations maybe responsible for this improvement pattern.

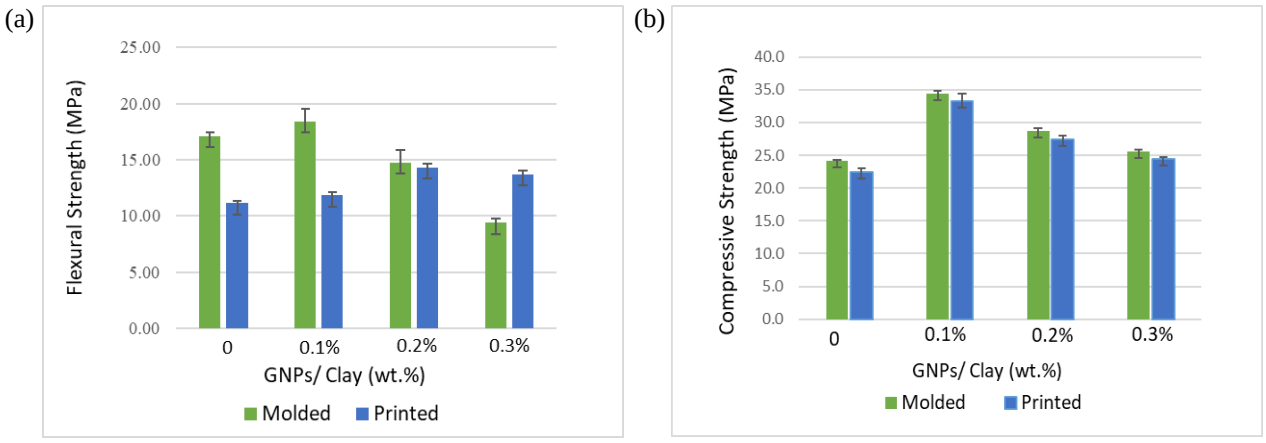


Fig. 3: (a) Flexural strength test results, and (b) Compressive strength test results

3.2 RSM Analysis

Figure 4 shows flexural and compressive strength factors' surface response against the production type and GNPs' weight fraction variables. The figure also shows the quadratic prediction formulas obtained using the RSM analysis techniques. The flexural strength response (Figure 4a) shows peaks at the negative coding boundaries indicating the highest flexural strength response at the moulded production type with 0.1 wt.% GNPs content. Alternatively, the compressive strength model (Figure 4b) shows the peaks at the mid boundaries indicating the success of both 0.1 and 0.2 wt.% GNPs at attain maximum compressive strengths peaks regardless of the production type. Figure 5a shows the production type and GNPs' weight fraction variables combined contour profiles versus the flexural and compressive strength. The coloured areas shown include all strengths falling below the plain clay flexural and compressive strengths. This analysis illustrates the significance of having a GNPs' weight fraction not exceeding 0.2625 wt.% (corresponds to a code of 0.75 on the chart) in case an improvement in both flexural and compressive strengths of printed clay is required.

Figure 5b shows the maximized Desirability Strength Function's behaviour of both production type and GNPs' weight fraction variables. The results showed that maximum flexural and compressive strength behaviours of printed elements could occur at a GNPs' weight fraction of 0.1125 wt.% (corresponds to a code of -0.25 on the chart). The maximum predicted flexural and compressive strengths are 13.45 and 30.70 MPa, respectively. Compared to the plain clay batch, these values represent 21% and 36% improvement in flexural and compressive strengths, respectively.

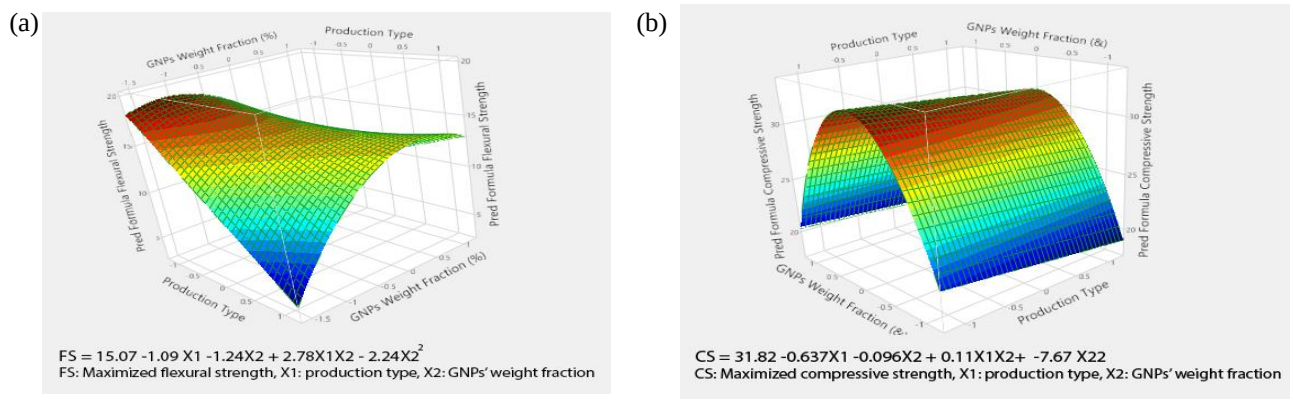


Fig. 4: RSM plots production type and GNPs' weight fraction (a) flexural strength and (b) compressive strength

(a) (b)

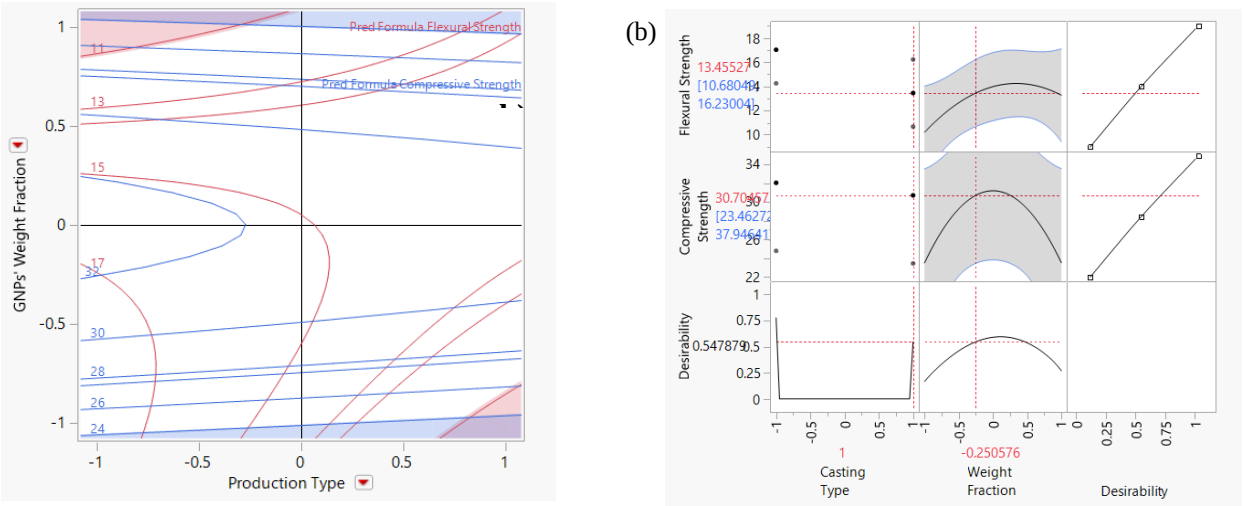


Fig. 5: (a) Production type and GNPs' weight fraction variables contour profiles and (b) maximized desirability functions

4 Conclusions

In this research, the RSM methods were used to investigate the impact of adding different GNPs' concentrations on the mechanical properties of 3D-printed clay. Mixes containing several Nanoparticles weight fractions were tested for flexure and compression, and the results were then analysed. Considering the study's findings, the following conclusions have been drawn:

i. The results showed that adding an appropriate dosage of GNPs to conventional clay could significantly improve the mechanical properties, thus increasing its suitability for construction printing applications without effecting the structural components' capacity, such as clay walls.

ii. Among all mixes, the one fabricated by traditional moulding with 0.1% GNPs had the highest flexural strength, while the mix containing 0.2% GNPs achieved the highest flexural strength between the printed mix, with an increment of about 7.5% and 21.1%, respectively, compared to the plain mix of each series.

iii. The compressive strength results showed a similar trend for the clay samples fabricated by both methods under the different dosages of GNPs.

iv. RSM techniques proposed empirical formulas to determine the compressive and flexural strengths of GNPs-modified 3-D printed clay.

v. RSM analysis showed that the maximum flexural and compressive strength response for 3D-printed clay was obtained at low dosages of GNPs (0.1 wt.%).

Acknowledgements

We gratefully acknowledge the generous assistance and valuable information provided by TecWorks-Jordan on the additive manufacturing of clay. In addition, we express our sincere appreciation and gratitude to the Department of Quality Control at Cementra Jordan Factory for their aid in testing samples.

References

Balaguru, P. & Chong, K. (2006). Nanotechnology and concrete: research opportunities. Proceedings of the ACI Session on Nanotechnology of Concrete: Recent Developments and Future Perspectives, 15-28.

Baomin, W. & Shuang, D. (2019). Effect and mechanism of graphene Nanoplatelets on hydration reaction, mechanical properties, and microstructure of cement composites. *Construction and Building Materials, 228*, 116720.

Manikandan, K. et al. (2020). Effects of nozzle geometries on 3D printing of clay constructs: Quantifying contour deviation and mechanical properties. *Procedia Manufacturing, 48*, 678-683.

Moropoulou, A., Bakolas, A. & Anagnostopoulou, S. (2005). Composite materials in ancient structures. *Cement and concrete composites 27*(2), 295-300.

Ngo, T. D. et al. (2018). Additive manufacturing (3D printing): A review of materials, methods, applications and challenges. *Composites Part B: Engineering, 143*, 172-196.

Rael, R. & San Fratello, V. (2017). Clay bodies: Crafting the future with 3D printing. *Architectural Design 87*(6), 92-97.

Revelo, C. F. & Colorado, H. A. (2018). 3D printing of kaolinite clay ceramics using the Direct Ink Writing (DIW) technique. *Ceramics International 44*(5), 5673-5682.

Sangiorgio, V. et al. (2022). The New Boundaries of 3D-Printed Clay Bricks Design: Printability of Complex Internal Geometries. *Sustainability 14*(2), 598.

Shen, M. Y. et al. (2013). Mechanical properties and tensile fatigue of graphene nanoplatelets reinforced polymer nanocomposites. *Journal of Nanomaterials*, 2013.

Tao, J. et al. (2019). Graphene Nanoplatelets as an effective additive to tune the microstructures and piezoresistive properties of cement-based composites. *Construction and Building Materials, 209*, 665-678.

Wang, B., Jiang, R. & Wu, Z. (2016). Investigation of the mechanical properties and microstructure of graphene nanoplatelet-cement composite. *Nanomaterials 6*(11), 200.

Wolf, A., Rosendahl, P. L. & Knaack, U. (2022). Additive manufacturing of clay and ceramic building components. *Automation in Construction, 133*, 103956.

Cite as: Mohsen M., Al-Diseet M., Abu Rumman M., Taha R. & Naji K., "RSM Analysis for Optimum Content of Graphene Nanoplatelets for 3D-Printed Clay Strength", *The 2nd International Conference on Civil Infrastructure and Construction (CIC 2023)*, Doha, Qatar, 5-8 February 2023, DOI: https://doi.org/10.29117/cic.2023.0058

A Static and Free Vibration Analysis of Porous Functionally Graded Beams

Lazreg Hadji
Department of Civil Engineering, University of Tiaret, Tiaret, Algeria
lazreg.hadji@univ-tiaret.dz

Vagelis Plevris
Department of Civil and Architectural Engineering, Qatar University, Doha, Qatar
vplevris@qu.edu.qa

Royal Madan
Department of Mechanical Engineering, G H Raisoni Institute of Engineering and Technology, Nagpur, India
royalmadan6293@gmail.com

Abstract

In this work, the static and free vibration analysis of functionally graded (FG) porous beams is investigated using a new higher-order shear deformation model (HSD). The porosity that develops naturally during the fabrication of a material is arbitrary in nature. Therefore, in the present study, a variation is considered taking into account three distribution patterns, namely (i) even distribution, (ii) uneven distribution, and (iii) the logarithmic-uneven pattern. Furthermore, the impact of several micromechanical models on the bending and free vibration behavior of the beams was investigated. Different micromechanical models were used to examine the mechanical properties of functionally graded beams, the properties of which change continuously throughout the thickness following a power law. Using the HSD model, the equations of motion are obtained using Hamilton's principle. To obtain displacements, stresses, and frequencies, the Navier type solution method was employed, and the numerical results were compared to those published in the literature. The impact of porosity and volume fraction index, different micromechanical models, mode numbers, and geometry on the bending and natural frequencies of imperfect FG beams were investigated.

Keywords: FG beam; Bending; Free vibration; Functionally graded materials; Porosity

1 Introduction

Functionally graded materials (FGMs) are special materials whose properties change along the length/thickness because of a change in the composition of two materials' porosity, and microstructure (Avcar, 2019; Hadji & Avcar, 2021; Sankar, 2001). A functionally graded material has varied thermo-mechanical properties and as a result, the yield strength of FGMs will vary. The effect of porosity on the limit speed analysis of a rotating disk was studied using variational principles under different loads, such as rotation and thermal (Madan & Bhowmick, 2021). The detailed dynamic analysis of a beam can pose significant computational challenges (Plevris & Tsiatas, 2018). In this work, the dynamic analysis was performed using finite element analysis, shear deformation theory, and modified shear deformation theory (Benaberrahmane et al., 2021; Larbi et al., 2013; Nguyen et al., 2017; Şimşek, 2010; Thai & Vo, 2012). The present study investigates the effect of porosity and volume fraction index, different micromechanical models, and geometry on the bending and natural frequencies of imperfect functionally graded (FG) beams. The power law variation of composition was considered to grade the beam in the transverse direction. Different material models were used to model the effective material properties of the FG beam. Hamilton's principle was used

in combination with Navier's method. The natural frequency of FG beams was calculated for different grading indices for both the longitudinal and the thickness directions. The analysis of imperfections in FGM beams reveals a logarithmic uneven distribution compared to other imperfection types studied. An even porosity distribution must be avoided and accordingly the proper manufacturing process has to be selected.

2 Effective Properties of FGMS

Fig. **1** shows the different models that are used to estimate the material properties effectively. The different models used are Voigt, Reuss, Tamura, local representative volume element (LRVE), and Mori-Tanaka model. Voigt and Reuss assume perfect bonding between fibers, so when the reinforcement is of particulate type and not long fibers, then Voigt and Reuss do not give good results. In such cases, the Tamura model (an empirical model) can be used. In this model, the term q is the stress-strain transfer ratio that can be calculated experimentally and numerically. A detailed description of all these models for different material properties and their estimates for different material combinations can be found in (Madan & Bhowmick, 2022).

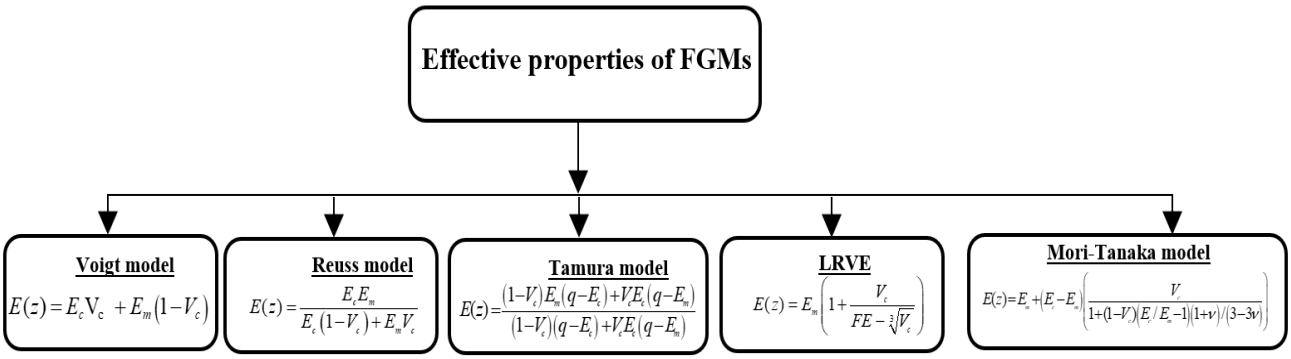
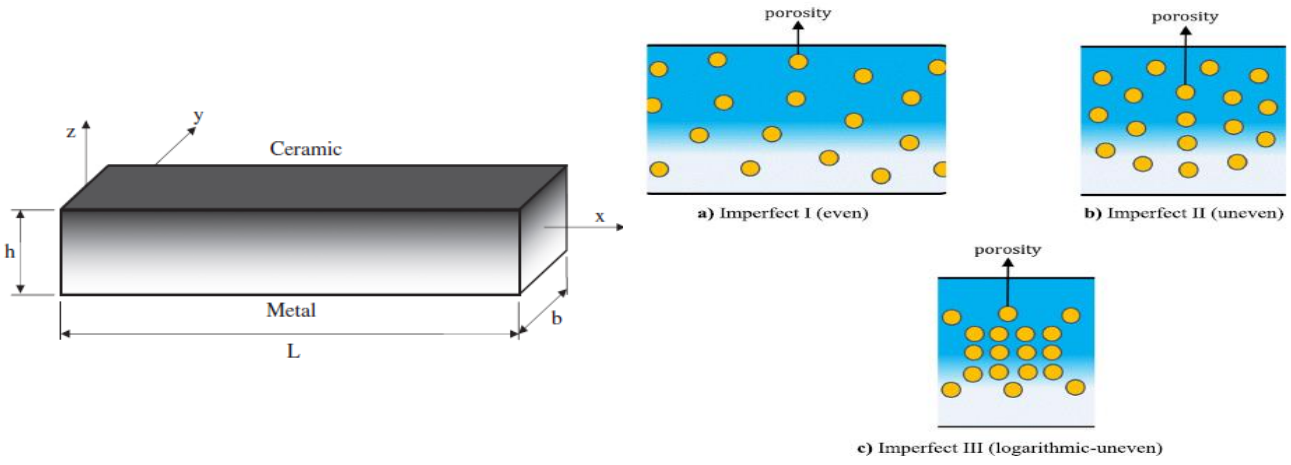


Fig. 1: Different material modeling methods

3 Preliminary Concepts and Definitions

We consider an FG beam of length L and cross section $b \times h$, as shown in Fig. **2**(a). The gradation of the beam is changing along the thickness direction.



(a) (b)

Fig. 2: (a) Geometry and coordinate system of an FG beam, (b) Porosity models

A beam is made of FGMs of which the volume fraction variation of ceramic and metal are denoted as $V_c(z)$ and $V_m(z)$, respectively, and are given by the formulas:

$$V_c(z)=\left(\frac{z}{h}+\frac{1}{2}\right)^p \tag{1}$$

$$V_m(z)=1-V_c(z) \tag{2}$$

Where, p is the volume fraction index that defines how the combination of metal and ceramic is distributed, with $0 \le p \le \infty$. For $p=0$, the beam is purely made of ceramic, whereas for $p=\infty$, it is purely metal.

3.1 Porosity-dependent Functionally Graded Materials

The characteristic of materials of FG porous beams can be written as

$$P(z)=(P_c-P_m)\left(\frac{z}{h}+\frac{1}{2}\right)^p+P_m-P_{por} \tag{3}$$

In this study, three types of porosity are considered; the first of them presents an even distribution (called hereafter Imperfect I), whereas the other ones are characterized by an uneven distribution (Imperfect II and III hereafter), along the beam thickness direction, as shown in Fig. **2**(b). The various expressions of the porosity distribution are presented in detail in Table 1.

Table 1: Porosity Distribution Types

Imperfect I	**Imperfect II**	**Imperfect III**
$P_{por}=\frac{\alpha}{2}(P_c+P_m)$ (4)	$P_{por}=\frac{\alpha}{2}\left(1-\frac{2\lvert z\rvert}{h}\right)(P_c+P_m)$ (5)	$P_{por}=\log\left(1+\frac{\alpha}{2}\right)\left(1-\frac{2\lvert z\rvert}{h}\right)(P_c+P_m)$ (6)
$\begin{bmatrix}E(z)\\ \beta(z)\\ \rho(z)\end{bmatrix}=\begin{bmatrix}E_{cm}\\ \beta_{cm}\\ \rho_{cm}\end{bmatrix}\left(\frac{z}{h}+\frac{1}{2}\right)^p+\begin{bmatrix}E_m\\ \beta_m\\ \rho_m\end{bmatrix}-\frac{\alpha}{2}\begin{bmatrix}E_c+E_m\\ \beta_c+\beta_m\\ \rho_c+\rho_m\end{bmatrix}$ (7)	$\begin{bmatrix}E(z)\\ \beta(z)\\ \rho(z)\end{bmatrix}=\begin{bmatrix}E_{cm}\\ \beta_{cm}\\ \rho_{cm}\end{bmatrix}\left(\frac{z}{h}+\frac{1}{2}\right)^p+\begin{bmatrix}E_m\\ \beta_m\\ \rho_m\end{bmatrix}-\frac{\alpha}{2}\left(1-2\frac{\lvert z\rvert}{h}\right)\begin{bmatrix}E_c+E_m\\ \beta_c+\beta_m\\ \rho_c+\rho_m\end{bmatrix}$ (8)	$\begin{bmatrix}E(z)\\ \beta(z)\\ \rho(z)\end{bmatrix}=\begin{bmatrix}E_{cm}\\ \beta_{cm}\\ \rho_{cm}\end{bmatrix}\left(\frac{z}{h}+\frac{1}{2}\right)^p+\begin{bmatrix}E_m\\ \beta_m\\ \rho_m\end{bmatrix}-\log\left(1+\frac{\alpha}{2}\right)\begin{bmatrix}E_c+E_m\\ \beta_c+\beta_m\\ \rho_c+\rho_m\end{bmatrix}$ (9)

For the various porosity distribution models, the material parameters of FG porous beam, such as the elastic modulus *E*, the thermal expansion coefficient β, and mass density ρ, were then calculated by employing the rule of mixture.

3.2 Equations of Motion

The Hamilton's principle was employed, for which the strain energy (*U*) and kinetic energy (*K*) relations are shown in Fig. **3**. A detailed solution algorithm is not included here, to maintain the brevity of the manuscript. For details on the solution algorithm, the interested reader is referred to the work of (Avcar, 2019).

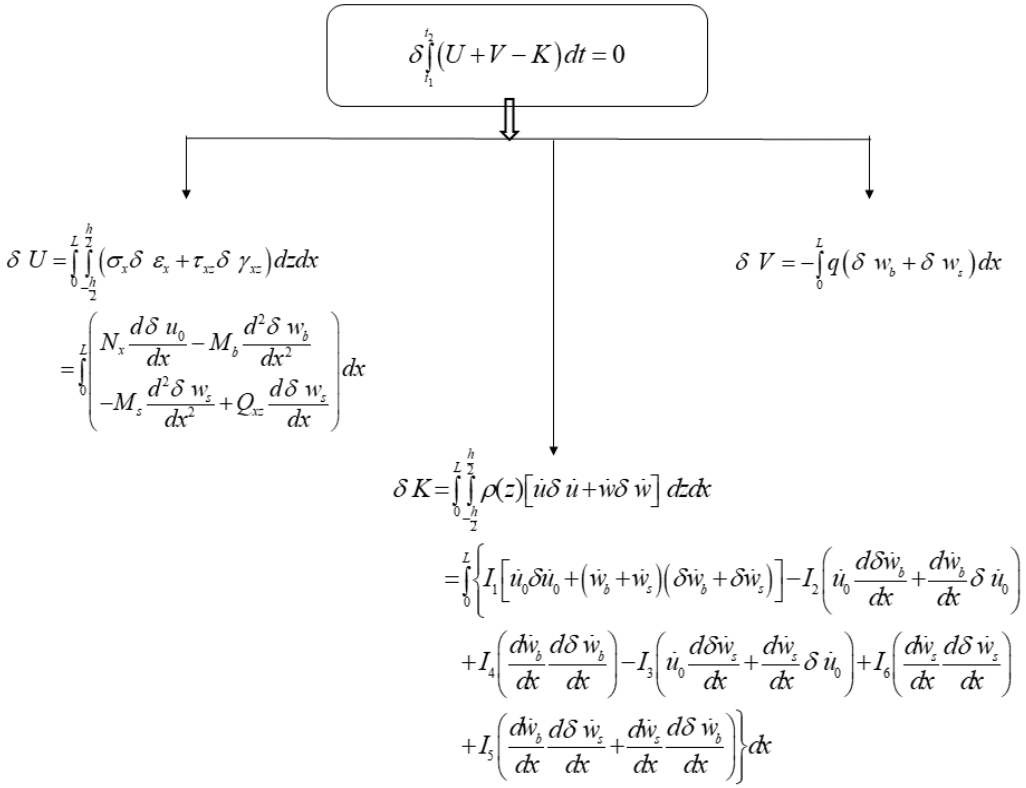


Fig. 3: Solution Methodology

4 Results and Discussion

The validation study of the bending and free vibration responses of simply supported porous FG beams was performed with comparison to published results. To perform the analytical calculations of this work we used the Maple software. The beam material selected has the following characteristics:

- Ceramic (P_c : Alumina, Al_2O_3): $E_c = 380$ GPa; $\nu = 0.3$; $\rho_c = 3960$ kg/m^3.
- Metal (P_m : Aluminium, Al): $E_m = 70$ GPa; $\nu = 0.3$; $\rho_m = 2702$ kg/m^3.

For convenience, the following dimensionless forms are used:

$$\bar{w} = 100\frac{E_m h^3}{q_0 L^4} w\left(\frac{L}{2}\right) \qquad (10)$$

$$\bar{\sigma}_x = \frac{h}{q_0 L}\sigma_x\left(\frac{L}{2},\frac{h}{2}\right) \qquad (11)$$

$$\bar{\tau}_{xz} = \frac{h}{q_0 L}\tau_{xz}(0,0) \qquad (12)$$

$$\bar{\omega} = \frac{\omega L^2}{h}\sqrt{\frac{\rho_m}{E_m}} \qquad (13)$$

Table 2 presents the deflection results corresponding to uniform and sinusoid loads for different *L/h* and *p*. The deflection increases with increasing *p* and decreases with increasing *L/h*. For the sinusoidal loading case, the deflection is found to be lower compared to the one of the uniform load cases. Table 3 demonstrates the results of displacement and stresses induced in an FG beam for various theories. The displacements are less for uniform load than the ones for sinusoidal load. Except for the classical beam theory, all other theories give similar results.

Table 2: Non-dimensional deflection of functionally graded (P-FGM) beams (Voigt model)

L / *h*	*p*	Theory	Uniform load	Sinusoidal load
5	0	(Sayyad & Ghugal, 2018)	3.1635	2.5004
		Present study	**3.1654**	**2.5019**
	1	(Sayyad & Ghugal, 2018)	6.2563	4.9432
		Present study	**6.2594**	**4.9457**
	2	(Sayyad & Ghugal, 2018)	8.0666	6.3745
		Present study	**8.0677**	**6.3754**
	5	(Sayyad & Ghugal, 2018)	9.8414	7.7830
		Present study	**9.8281**	**7.7723**
	10	(Sayyad & Ghugal, 2018)	10.940	8.6547
		Present study	**10.9381**	**8.6530**
10	0	(Sayyad & Ghugal, 2018)	2.9496	2.3271
		Present study	**2.9501**	**2.3275**
	1	(Sayyad & Ghugal, 2018)	5.8951	4.6506
		Present study	**5.8959**	**4.6512**
	2	(Sayyad & Ghugal, 2018)	7.5671	5.9698
		Present study	**7.5673**	**5.9699**
	5	(Sayyad & Ghugal, 2018)	9.0238	7.1207
		Present study	**9.0204**	**7.1179**
	10	(Sayyad & Ghugal, 2018)	9.9411	7.8452
		Present study	**9.9403**	**7.8446**

Table 3: Non-dimensional displacements and stresses of P-FGM beams (Voigt model, $L = 5h$)

p	Theory	Model	Uniform load			Sinusoidal load		
			$\overline{w}$	$\overline{\sigma}_x$	$\overline{\tau}_{xz}$	$\overline{w}$	$\overline{\sigma}_x$	$\overline{\tau}_{xz}$
0	**Present**	**RBT**	**3.1654**	**3.8019**	**0.7329**	**2.5020**	**3.0916**	**0.4769**
	(Sayyad & Ghugal, 2018)	ESDBT	3.1635	3.8084	0.7764	2.5004	3.0979	0.5072
	(Reddy, 1984)	HSDBT	3.1654	3.8028	0.7305	2.5020	3.0916	0.4769
	(Timoshenko, 1921)	FSDBT	3.1657	3.7501	0.4922	2.5023	3.0396	0.3183
	(Euler, 1744)	CBT	2.8783	3.7501	–	2.2693	3.0396	–
1	**Present**	**RBT**	**6.2594**	**5.8835**	**0.7329**	**4.9458**	**4.7856**	**0.4769**
	(Sayyad & Ghugal, 2018)	ESDBT	6.2563	5.8957	0.8288	4.9432	4.7964	0.5430
	(Reddy, 1984)	HSDBT	6.2594	5.8850	0.8031	4.9458	4.7856	0.5243
	(Timoshenko, 1921)	FSDBT	6.1790	5.7960	0.8313	4.8807	4.6979	0.3183
	(Euler, 1744)	CBT	5.7746	5.7960	–	4.5528	4.6979	–
2	**Present**	**RBT**	**8.0677**	**6.8824**	**0.6704**	**6.3754**	**5.6004**	**0.4368**
	(Sayyad & Ghugal, 2018)	ESDBT	8.0666	6.8971	0.8485	6.3745	5.6149	0.5553
	(Reddy, 1984)	HSDBT	8.0677	6.8842	0.8446	6.3754	5.6004	0.5521
	(Timoshenko, 1921)	FSDBT	7.9253	6.7678	1.0791	6.2601	5.4856	0.2709
	(Euler, 1744)	CBT	7.4003	6.7678	–	5.8346	5.4856	–
5	**Present**	**RBT**	**9.8281**	**8.1104**	**0.5904**	**7.7723**	**6.6057**	**0.3856**
	(Sayyad & Ghugal, 2018)	ESDBT	9.8414	8.1331	0.7654	7.7830	6.6281	0.5024
	(Reddy, 1984)	HSDBT	9.8281	8.1127	0.8114	7.7723	6.6057	0.5314
	(Timoshenko, 1921)	FSDBT	9.4987	7.9430	1.5373	7.5056	6.4382	0.2085
	(Euler, 1744)	CBT	8.7508	7.9430	–	6.8994	6.4382	–
10	**Present**	**RBT**	**10.9381**	**9.7119**	**0.6465**	**8.6530**	**7.9080**	**0.4224**
	(Sayyad & Ghugal, 2018)	ESDBT	10.940	9.7345	0.6947	8.6547	7.9300	0.4560
	(Reddy, 1984)	HSDBT	10.938	9.7141	0.6448	8.6530	7.9080	0.4224
	(Timoshenko, 1921)	FSDBT	10.534	9.5231	1.9050	8.3259	7.7189	1.2320
	(Euler, 1744)	CBT	9.6072	9.5231	–	7.5746	7.7189	–

Table 4 presents the non-dimensional natural frequency of P-FGM beams of various theories for varying *p*. It can be seen that the present methodology shows good agreement with results from the published literature. The natural frequency decreases as *p* increases.

Table 4: Non-dimensional flexural natural frequencies ($\overline{\omega}$) of simply supported P-FGM beams (Voigt model)

L/*h*	Mode	Theory	Model	Power law index (p)					
				0 (ceramic)	**1**	**2**	**5**	**10**	**∞ (Metal)**
5	1	**Present**	**RBT**	**5.15274**	**3.99042**	**3.62643**	**3.40120**	**3.28160**	**2.67732**
		(Sayyad & Ghugal, 2018)	ESDBT	5.15423	3.99140	3.62671	3.40000	3.28135	2.67810
		(Reddy, 1984)	HSDBT	5.15274	3.99042	3.62643	3.40120	3.28160	2.67732
		(Şimşek, 2010)	FSDBT	5.15247	3.99023	3.63438	3.43119	3.31343	2.67718
		(Şimşek, 2010)	HSDBT	5.15274	3.99042	3.62643	3.40120	3.28160	2.67732
		(Thai & Vo, 2012)	HSDBT	5.15275	3.99042	3.62644	3.40120	3.28160	2.67732
		(Vo et al., 2014)	FSDBT	5.15260	3.97108	3.60495	3.40253	3.29625	2.67725
		(Vo et al., 2014)	HSDBT	5.15275	3.97160	3.59791	3.37429	3.26534	2.67732
		(Timoshenko, 1921)	FSDBT	5.15247	3.99023	3.63438	3.43119	3.31343	2.67718
		(Euler, 1744)	CBT	5.39530	4.14840	3.77930	3.59490	3.49210	2.80336
20	1	**Present**	**RBT**	**5.46032**	**4.20505**	**3.83613**	**3.64849**	**3.53898**	**2.83714**
		(Sayyad & Ghugal, 2018)	ESDBT	5.46043	4.20513	3.83614	3.64830	3.53895	2.83720
		(Reddy, 1984)	HSDBT	5.46030	4.20503	3.83611	3.64850	3.53896	2.83716
		(Şimşek, 2010)	FSDBT	5.46032	4.20505	3.83676	3.65088	3.54156	2.83713
		(Şimşek, 2010)	HSDBT	5.46030	4.20503	3.83611	3.64850	3.53896	2.83716
		(Thai & Vo, 2012)	HSDBT	5.46032	4.20505	3.83613	3.64849	3.53899	2.83714
		(Vo et al., 2014)	FSDBT	5.46033	4.20387	3.83491	3.64903	3.54045	2.83714
		(Vo et al., 2014)	HSDBT	5.46032	4.20387	3.83428	3.64663	3.53787	2.83714
		(Timoshenko, 1921)	FSDBT	5.46032	4.20505	3.83676	3.65088	3.54156	2.83713
		(Euler, 1744)	CBT	5.47770	4.21630	3.84720	3.66280	3.55470	2.84618

Table 5 presents the displacement and stress results at different loads, namely under uniform and sinusoidal, for different material models. The difference in the results is because each case estimates the properties using different material models. The displacement is minimum for the Voigt and maximum for the Reuss model because these models are the ideal models and are best applicable for long fibers in which the bonding is perfect. Naturally, the results of the other models such as LRVE, Tamura, and Mori-Tanaka fall inside these upper and lower bands formed by the Reuss and Voigt models. The rule of mixture could not predict the properties of particle composite effectively, but it can be applied for lower ratios of material combinations. Its applicability can be extended in modeling the porosity effects, as well. The magnitude of results is found to be lower for the sinusoidal load and higher for the uniform load.

Table 5: Non-dimensional displacements and stresses of P-FGM beams (p=2 and L = 5h)

		Uniform load			Sinusoidal load		
Theory (Model)		$\overline{w}$	$\overline{\sigma}_x$	$\overline{\tau}_{xz}$	$\overline{w}$	$\overline{\sigma}_x$	$\overline{\tau}_{xz}$
Present	Voigt (Voigt, 1889)	8.0677	6.8824	6.3754	2.4047	5.6004	0.4368

	Reuss (Reuss, 1929)	10.1403	8.9372	8.0184	2.8647	7.2756	0.4231
	LRVE (Gasik, 1998)	9.3292	7.8585	7.3756	2.7326	6.3981	0.4104
	Tamura (Nakamura et al., 2000) (q=0) (q=100)	10.1403 9.2981	8.9372 7.9333	8.0184 7.3504	2.8647 2.7089	7.2756 6.4583	0.4231 0.4184
	Mori-Tanaka (Tanaka et al., 1993)	9.8633	8.5824	7.7989	2.8166	6.9869	0.4206

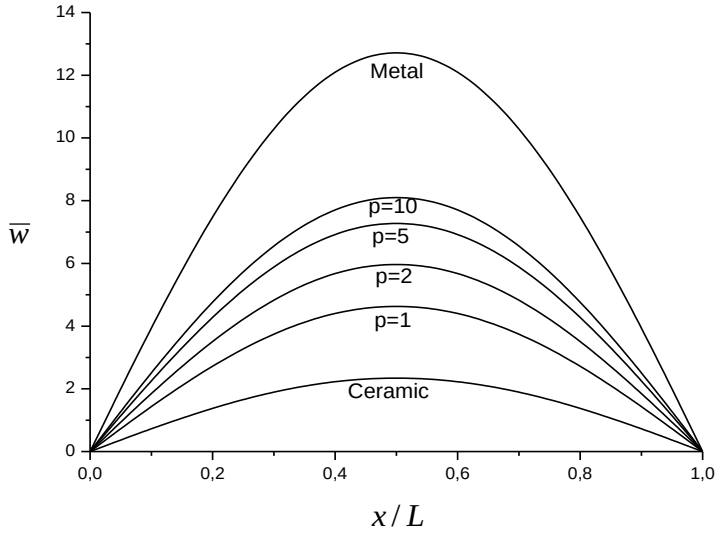


Fig. 4: The variation of the transverse displacement $\overline{w}$ for L/h

Fig. **4** shows the variation of displacement along x/L. The displacement is maximum for the pure metal case ($p=\infty$), and it decreases with decreasing p and reaches its minimum for the pure ceramic case ($p=0$) because ceramics have higher modulus of elasticity compared to metal.

Finally, Table 6 presents the natural frequency results for the cases $L/h=5$ and $L/h=20$. The frequency is maximum when there is no porosity present and decreases as the porosity fraction increases. Three different types of porosity variations were considered, namely the even case (Imperfect-1), the uneven case (Imperfect-2), and the logarithmic-uneven (Imperfect-3). The analysis shows that the Imperfect-1 case has the lowest frequency; the maximum is achieved for Imperfect-3, while Imperfect-2 gives intermediate results. The results of Imperfect-2 and Imperfect-3 yield quite similar results. As the natural frequencies obtained for Imperfect-2 and Imperfect-3 are similar, a fabrication process that leads to uneven porosity distribution can be selected.

Table 6: Variation of frequency parameters $\overline{\omega}$ of perfect and imperfect FG beam ($p=2$)

	Perfect	**Imperfect I (even)**		**Imperfect II (uneven)**		**Imperfect III (Logarithmic-uneven)**	
L/h	$a=0$	$a=0.1$	$a=0.2$	$a=0.1$	$a=0.2$	$a=0.1$	$a=0.2$
5	3.6264	3.4418	3.1489	3.6069	3.5785	3.6075	3.5816
20	3.8361	3.6335	3.3123	3.8226	3.8004	3.8230	3.8029

5 Conclusion

The conclusion of the research work can be summarized in the following points:

1. If the distribution of porosity in the beam is of imperfect type-1 (even) then the natural frequency would be minimum. The natural frequency is maximum for the case of imperfect type-3 (logarithmic-uneven). Therefore, a manufacturing technique would be intended to get a porosity development of logarithmic type and not evenly distributed. As expected, the natural frequency decreases with the introduction of porosity because of the degradation of material properties.
2. The dimensionless transverse displacement is minimum for ceramic and maximum for metal and intermediate in the case of FGMs, so a beam which is ceramic rich (p=0) yields lower displacements compared to a beam which is metal-rich (p=10) in composition.
3. The Voigt model gives the lowest displacement and the Reuss model gives the maximum. The Tamura model and Reuss gave identical results. The results of the present method show good agreement with the ones of the other theories published in the literature.

References

Avcar, M. (2019). "Free vibration of imperfect sigmoid and power law functionally graded beams." *Steel and Composite Structures*, *30*(6), 603-615. DOI: https://doi.org/10.12989/scs.2019.30.6.603.

Benaberrahmane, I. et al. (2021). "Investigating of free vibration behavior of bidirectional FG beams resting on variable elastic foundation." *Geomechanics and Engineering*, *25*(5), 383–394. DOI: https://doi.org/10.12989/gae.2021.25.5.383.

Euler, L. (1744). *Methodus inveniendi lineas curvas maximi minimive proprietate gaudentes, sive solutio problematis isoperimetrici lattissimo sensu accepti*, apud Marcum-Michaelem Bousquet & Socios, Lausannae & Genevae.

Gasik, M. M. (1998). "Micromechanical modelling of functionally graded materials." *Computational Materials Science*, *13*(1), 42-55. DOI: https://doi.org/10.1016/S0927-0256(98)00044-5.

Hadji, L. & Avcar, M. (2021). "Free Vibration Analysis of FG Porous Sandwich Plates under Various Boundary Conditions ".*Journal of Applied and Computational Mechanics*, *7*(2), 505-519. DOI: https://doi.org/10.22055/jacm.2020.35328.2628.

Larbi, L. O. et al. (2013). "An Efficient Shear Deformation Beam Theory Based on Neutral Surface Position for Bending and Free Vibration of Functionally Graded Beams#." *Mechanics Based Design of Structures and Machines*, *41*(4), 421-433. DOI: https://doi.org/10.1080/15397734.2013.763713.

Madan, R. & Bhowmick, S. (2021). "A numerical solution to thermo-mechanical behavior of temperature dependent rotating functionally graded annulus disks." *Aircraft Engineering and Aerospace Technology*, *93*(4), 733-744. DOI: https://doi.org/10.1108/AEAT-01-2021-0012.

___. (2022). "Modeling of functionally graded materials to estimate effective thermo-mechanical properties." *World Journal of Engineering*, *19*(3), 291-301. DOI: https://doi.org/10.1108/WJE-09-2020-0445.

Nakamura, T., Wang, T. & Sampath, S. (2000). "Determination of properties of graded materials by inverse analysis and instrumented indentation." *Acta Materialia*, *48*(17), 4293-4306. DOI: https://doi.org/10.1016/S1359-6454(00)00217-2.

Nguyen, D. K. et al. (2017). "Vibration of bi-dimensional functionally graded Timoshenko beams excited by a moving load." *Acta Mechanica*, *228*(1), 141-155. DOI: https://doi.org/10.1007/s00707-016-1705-3.

Plevris, V. & Tsiatas, G. (2018). "Computational Structural Engineering: Past Achievements and Future Challenges." *Frontiers in Built Environment*, *4*(21), 1-5. DOI: https://doi.org/10.3389/fbuil.2018.00021.

Reddy, J. N. (1984). "A Simple Higher-Order Theory for Laminated Composite Plates." *Journal of Applied Mechanics*, *51*(4), 745-752. DOI: https://doi.org/10.1115/1.3167719.

Reuss, A. (1929). "Berechnung der Fließgrenze von Mischkristallen auf Grund der Plastizitätsbedingung für Einkristalle." *ZAMM - Journal of Applied Mathematics and Mechanics / Zeitschrift für Angewandte Mathematik und Mechanik*, *9*(1), 49-58. DOI: https://doi.org/10.1002/zamm.19290090104.

Sankar, B. V. (2001). "An elasticity solution for functionally graded beams." *Composites Science and Technology*, *61*(5), 689-696. DOI: https://doi.org/10.1016/S0266-3538(01)00007-0.

Sayyad, A. S. & Ghugal, Y. M. (2018). "An inverse hyperbolic theory for FG beams resting on Winkler-Pasternak elastic foundation." *Advances in aircraft and spacecraft science*, *5*(6), 671-689. DOI: https://doi.org/10.12989/aas.2018.5.6.671.

Şimşek, M. (2010). "Fundamental frequency analysis of functionally graded beams by using different higher-order beam theories." *Nuclear Engineering and Design*, *240*(4), 697-705. DOI: https://doi.org/10.1016/j.nucengdes.2009.12.013.

Tanaka, K. et al. (1993). "An improved solution to thermoelastic material design in functionally gradient materials: Scheme to reduce thermal stresses." *Comput. Methods Appl. Mech. Engrg.*, *109*(3), 377-389. DOI: https://doi.org/10.1016/0045-7825(93)90088-F.

Thai, H. T. & Vo, T. P. (2012). "Bending and free vibration of functionally graded beams using various higher-order shear deformation beam theories." *International Journal of Mechanical Sciences*, *62*(1), 57-66. DOI: https://doi.org/10.1016/j.ijmecsci.2012.05.014.

Timoshenko, S. P. (1921). "LXVI. On the correction for shear of the differential equation for transverse vibrations of prismatic bars." *The London, Edinburgh, and Dublin Philosophical Magazine and Journal of Science*, *41*(245), 744-746. DOI: https://doi.org/10.1080/14786442108636264.

Vo, T. P., Thai, H.-T., Nguyen, T.-K., Maheri, A., and Lee, J. (2014). "Finite element model for vibration and buckling of functionally graded sandwich beams based on a refined shear deformation theory." *Eng. Struct.*, *64*, 12-22. DOI: https://doi.org/10.1016/j.engstruct.2014.01.029.

Voigt, W. (1889). "Ueber die Beziehung zwischen den beiden Elasticitätsconstanten isotroper Körper." *Annalen der Physik*, *274*(12), 573-587. DOI: https://doi.org/10.1002/andp.18892741206.

Cite as: Hadji L., Plevris V. & Madan R., "Static and Free Vibration Analysis of Functionally Graded Beams with Porosities", *The 2nd International Conference on Civil Infrastructure and Construction (CIC 2023)*, Doha, Qatar, 5-8 February 2023, DOI: https://doi.org/10.29117/cic.2023.0059

The Effect of Atrium on the Thermal Comfort in Buildings in Hot Arid Zones

Hamida Bencheikh
Architecture, Civil Engineering and Architecture, Amar Telidji University, Laghouat, Algeria
h.bencheikh@lagh-univ.dz

Boussebsi Khalida
Architecture, Civil Engineering and Architecture, Amar Telidji University, Laghouat, Algeria
ismakatya@yahoo.fr

Abstract

The atrium is an open interior space that may be linked to the external environment; it is becoming more and more popular and a key element in the architectural design of many buildings, due to its attractive and symbolic aesthetic characteristics for the public. It is a filter against unwanted external environmental phenomena such as rain, snow and wind. A well-designed atrium can contribute towards having a significant effect on the indoor environment, affecting the comfort of the occupants. However, in certain hot and arid regions such as the city of Laghouat in the south of Algeria characterized by a scalding and dry summer, and cold winter, these fully enclosed atrium spaces with their untouched typological and architectural diversity, and due to lack of a good renewal of the indoor air, can cause considerable thermal discomfort to the occupants of space, and thermal stratification inside, especially in summer. The present work studies the impact of the atrium configuration on the inside thermal environment, for summers and winter periods, and to provide a sufficient air renewal within the atrium to ensure good air quality. As a result, a rectangular, fully enclosed, unventilated central atrium building was examined with its adjacent spaces, by a series of field measurements to study two geometric factors that have a considerable impact on the interior thermal comfort, the height width ratio (SAR Index) and the glazed coverage ratio. The impact of SAR index and glazed area ratio on thermal comfort and stratification of the air in summer and winter period were also examined.

Keywords: Atrium configuration; Thermal comfort; Air stratification; SAR index; Hot and arid climate

1 Introduction

The basic requirement for a building is to provide shelter from the environment and the weather. Although buildings are not just structures, they house occupants who must be comfortable and healthy in the intended environment. The architectural solutions adopted in modern buildings were the integration of the atrium, especially in regions with a temperate climate; this architectural form is generally defined as a large open glazed space in a multi-tiered building. Large glassed surfaces can lead to excessive solar heat gain in summer, heat loss in winter, and air stratification, especially in summer, which can affect the building user's comfort and energy performance. Many recent studies that deal with the role of atrium geometry in energy consumption were done by a group of researchers (Wang, Huang, Zhang, Xu, & Yuen, 2017; Shafqat, 2012; Moosavi, Mahyuddin, Ghafar, & Ismail, 2014; Pichatwatana & Wang, 2013). The studies aim to investigate how the geometry of the atrium affects the indoor thermal, lighting and natural ventilation. The present work studies the impact of

atrium configuration on the internal thermal environment, for summers and winter periods by field measurements of the indoor temperature distributions, in order to study two geometric factors, which have a considerable impact on the interior thermal comfort namely: the height/width ratio (SAR Index) and the glazed coverage ratio.

2 Presentation of the Study Case

In order to better concretize the expected objective of this research, a building with an atrium, was taken as a case study in our investigation, the studied building located in the western part of Laghouat city with an average altitude of 750 meters, latitude 33°46'N and longitude 2°56'E; it has a hot dry climate. Figure 1 presents the annual minimum-maximum temperature and Figure 2 presents the mean monthly insolation hours recorded from 2006-2015.

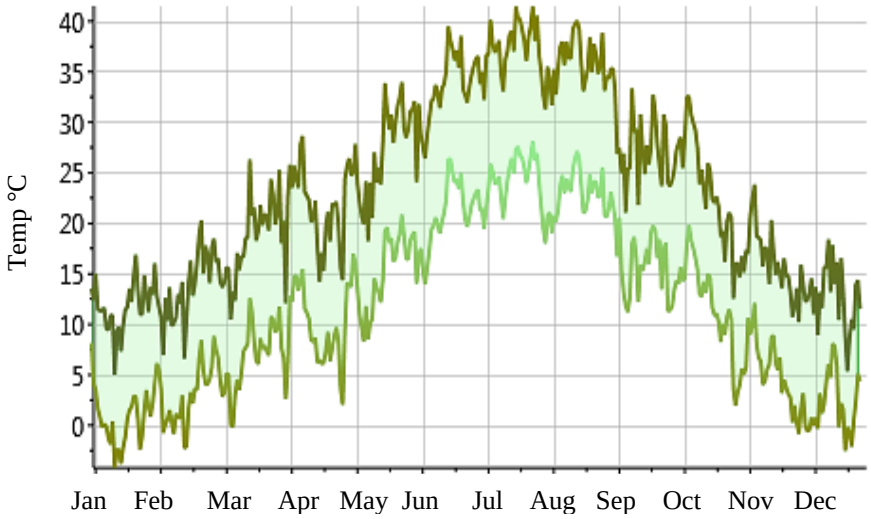


Fig. 1: Annual min and max temperature

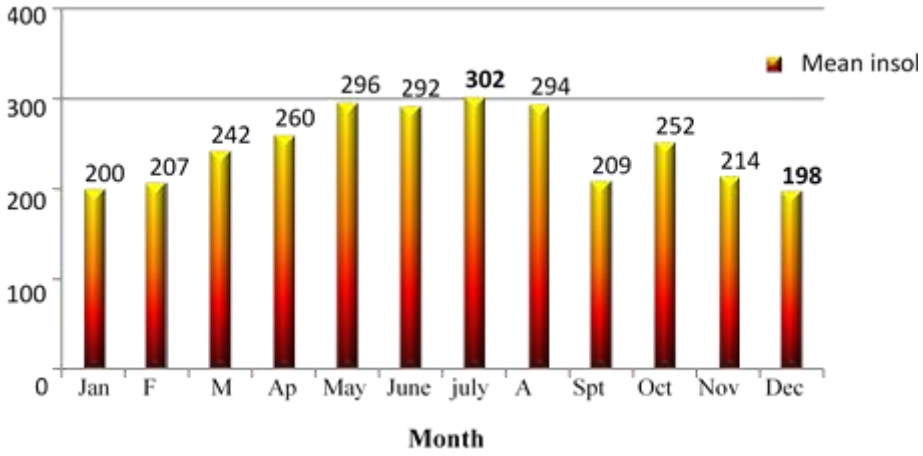


Fig. 2: Mean monthly insolation hours (2006-2015)

The studied building has two interior patios and a central atrium preceded by an entrance hall. The atrium represents a multifunctional, unifying, important gathering space, and can be used even as an exhibition and display space. It is rectangular in shape, naturally lit only from above by a huge canopy inclined at 10° to the south, covers the atrium roof without any solar protection, or openings. Rising along the levels of the building, this atrium is surrounded by corridors serving the adjacent spaces (classrooms), which are designed to receive natural light from the atrium through non-opening glazed transoms in their adjacent walls. The atrium space has an area of 141.96 m^2 and a volume of 1868.19

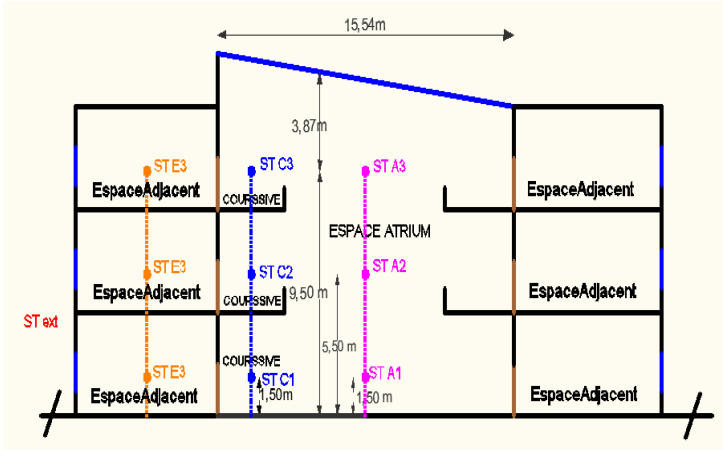
m^3; see Figure 3 shows plan Vue, the atrium and the atrium glazed cover.



Fig. 3: View of atrium space

3 Results and Discussions

The first measurement campaign was carried out during the winter period, February for four days separately (the 12, 13, 19, and 26), in weekend days in order to eliminate the heating, and the users heat gain, which help in estimating the level of the passive heating by atrium. The second measurement campaign was carried out during the summer period in July for a duration of 4 successive days (10, 11, 12, and 13), knowing that the building was also not occupied. The measurements were taken at 13 points, 12 distributed vertically over the three levels of the building and the 13th point was outside the building; see Figure 4, the measurements were limited to the period of occupation by users, from 8.00 a.m. to 5.00 p.m. at a height of 1.50m.



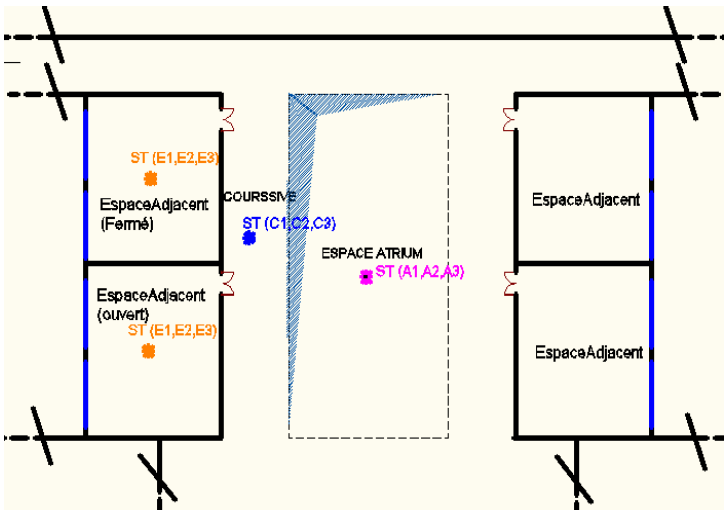


Fig. 4: Measurements points

3.1 Summer Period

The day of 11th July was a hot summer day, sunny with clear skies, characterized by an average wind speed of 2.5m/s, and an average temperature equal to 33°C, with a maximum of 41°C and a minimum temperature of 30°C. As previously mentioned, this measurement campaign was carried out in the raw internal conditions of the building (without internal gains) in order to better experience the almost raw thermal behaviour of the atrium.

Indoor air temperatures in the atrium space, in global reading and the results given by the graphs in Figure 5 show that the profiles of the air temperatures measured inside the atrium take the same shape with the outside air temperatures. Similarly, we can see a gradual evolution of the interior temperatures for the first hours of the morning (sunrise) to reach its maximum during the afternoon time slot, and falling slightly for the last hours of the afternoon (towards sunset), obviously this variation in temperature corresponds to the degree of intensity of the solar radiation received by the atrium glass roof. We can thus see that the temperature always exceeds those recorded in the various points of the measurements in the atrium, by recording a heat peak equal to 42.1°C at 3:00 p.m. for the outdoor temperature measured on-site. Similarly, a peak of 33.6°C is recorded at the same time in the ground floor with the lowest thermal zone, while the other peaks (1st and 2nd floor) are recorded after one hour, respectively, 34.8°C and 37°C. This phase shift is strongly influenced by the thermal capacity of the building envelope. A temperature difference of 4°C at 4:00 p.m., between the lower and the upper level confirms that the upper zone which is exposed to the higher solar intensity gets the higher air temperature, and that in the total absence of natural ventilation, in the roof, the warm air will not be able to escape to the outside and will remain trapped in the upper part creating this amplification. According to Figure 5, which illustrates the indoor temperatures measured in the atrium in relation to the thermal comfort zone calculated for the month of July by the Humphrey formula, hence, according to (Humphreys & Fergus, 2002), temperature of 28.4°C is higher than the limits of the comfort zone particularly for the 2nd floor during all the hours of occupation. On the other hand, the air temperatures on the ground floor are located within the limits of the comfort zone, only for the 8:00 to 12:00 a.m. time slot, in a temperature range of 26.6°C and 30.4°C, and for the first floor in a range of 29.9°C and 30.4°C from 8:00 to 9:00 a.m. It expresses a situation of discomfort generally felt inside the atrium.

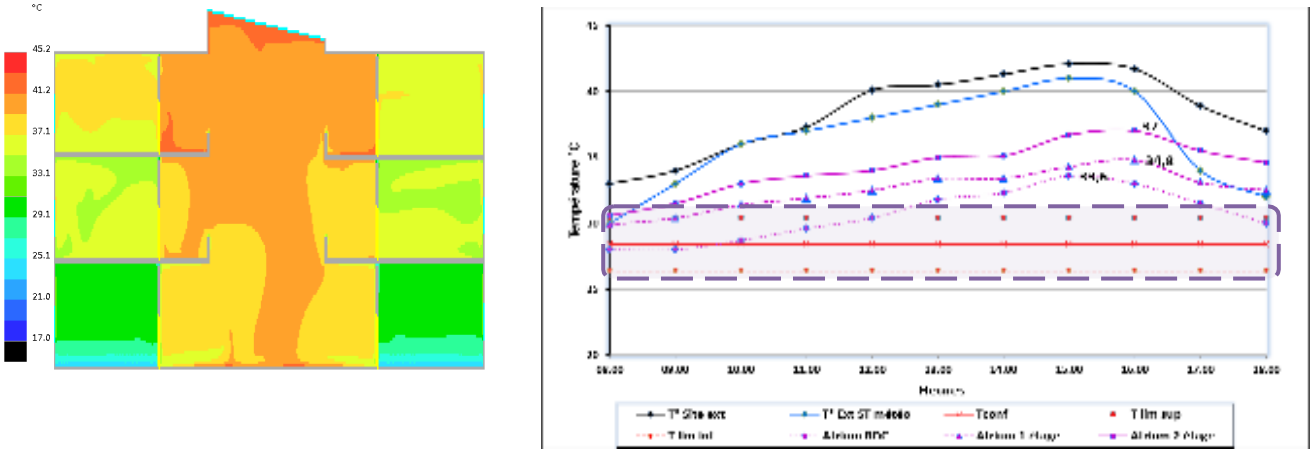


Fig. 5: Summer: The indoor temperatures compared to the adaptive thermal comfort

Analysis of thermal stratification in the middle of the atrium, the graphs shown in Figure 6 present the vertical thermal profiles of the air temperatures recorded in the middle of the atrium for the different hours of the day corresponding to the different intensities of solar radiation during the building occupancy schedule. From the profiles in Figure 6, we can see that there are three types of profiles in accordance with the profiles cited by Heller:

1. Non-linear profile for the first hours of the morning, where the temperature decreases slightly at the upper level. The low intensity of solar radiation and the low temperature levels during the morning are the factors responsible for the cooling of the area under the glass roof.

2. Non-linear profile, increasing in the upper level for the afternoon hours, especially at 3:00 p.m. This is the frequent case of a stratification produced at a high level inside the atrium, where the heat sources are distributed only in the upper part (Miray Gemi, 2006). This is strongly influenced by the high intensity of solar radiation.

3. Profile of a linear increase, from 1:00 p.m. to 2:00 p.m., when the sun is at its zenith, and at the last hours of occupation (4:00, 5:00 and 6:00 p.m.). This is the typical case in atriums where the heat sources are uniformly distributed in the space and its surfaces (Gemi, 2006).

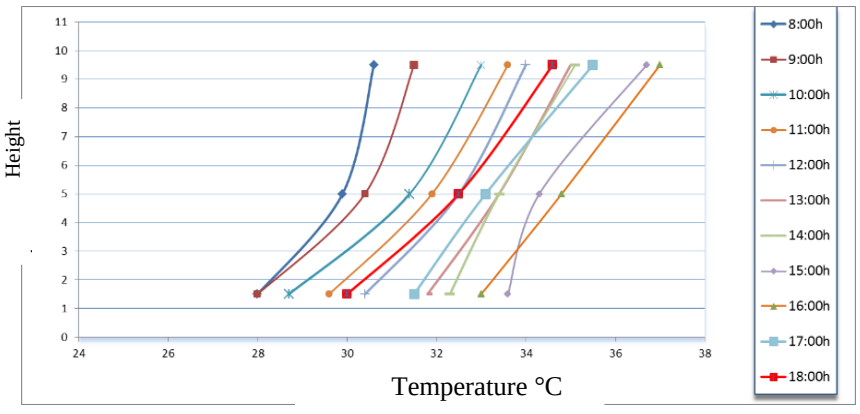


Fig. 6: The vertical thermal profiles of air temperatures recorded in center of the atrium for different hours of the day

3.2 Winter Period

A second measurement campaign was carried out in winter period, in order to complete the atrium thermal behaviour evaluation. A representative day was taken for the analysis; this day takes a drop

in air temperature of an average of 12°C, and a wind speed of 5 m/s. A partly cloudy sky during the morning hours before noon and from the afternoon onwards the scenario changes and the sky becomes clear and uncluttered.

From the curves in Figure 7, the temperatures measured at the different points in different levels of the atrium maintain the same profile and follow the same pattern as the outside air temperatures, with very small differences between them. It can also be seen that the temperatures recorded indoors are generally higher than those outside, revealing the strong influence of the weather conditions outside in terms of sky coverage, so that the highest values are recorded during the afternoon time slot, which coincides with the clearing of the sky after being cloudy, recording almost equal peaks on the ground, first and second floors, i.e. 15.8°C, 16.1°C and 16.5°C at 5:00 p.m., respectively. This rise in temperature is close to the lower limit of the comfort temperature "15.7°C," only in the afternoon hours from 02:00 to 04:00 p.m., and finally in the comfort zone during the peak heat hour (05:00 p.m.), recording temperatures equal to: 15.8°C, 16.10°C and 16.5°C on the ground floor, first floor and top floor, respectively. Therefore, we can say that the comfort situation during the winter period is strongly influenced by the state of the sky and the solar radiation.

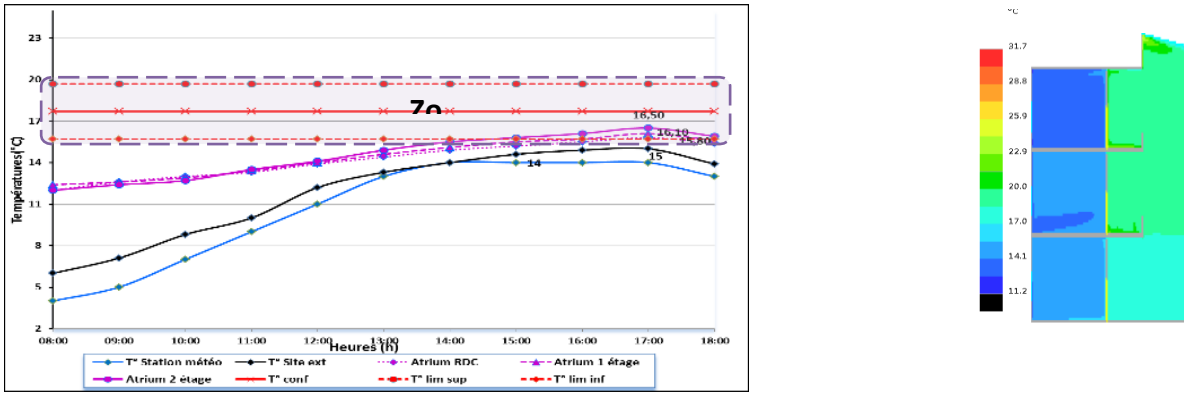


Fig. 7: Winter: The temperatures measured at different points on the different level

Analysis of thermal stratification in the middle of the atrium, from the vertical thermal gradient profiles that show the vertical interior temperature distributions in the atrium (Figure 8), here the space is weakly stratified, with moderate temperature gradients. Although there are profiles that conform to the three types of Heller profiles.

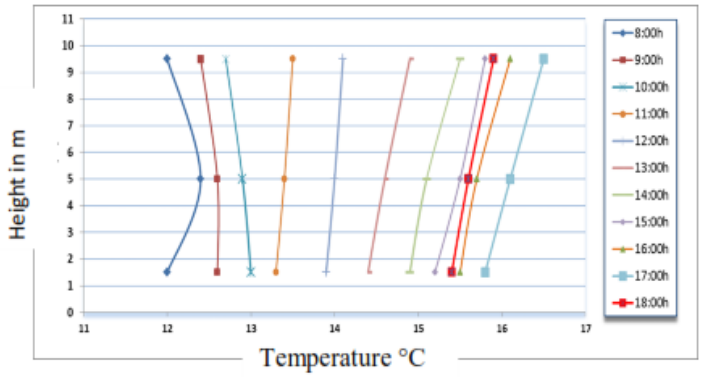


Fig. 8: The vertical thermal profiles of air temperatures recorded in center of the atrium for different hours of the day

4 Conclusion

The analysis of the results obtained from the investigation shows that the measured temperatures in

the atrium type in question remained outside the comfort zone for the summer period in the presence of a well-illustrated stratification. As it has considerably influenced the corridors surrounding it. On the other hand, the temperatures in the adjacent spaces showed a more or less destabilizing influence due to many of the factors already mentioned, the most influential ones in our case being: the exchange of ventilation between the atrium and the adjacent space, the wall glazing separating the atrium from its adjacent space and its opening, which did not exist in our case, as well as the presence of the adjacent walls exposed to the external conditions.

For the thermal behavior of the atrium and its adjacent spaces, we were able to observe that in winter, the atrium in question can be heated passively by freely admitting solar rays to the interior through the glazed cover, while depending on the external climatic conditions (mainly cloudiness of the sky), and on surface area of the atrium in relation to the total surface of the building. Nevertheless, the indoor temperature of the adjacent spaces will be influenced by several parameters, mainly by the direct gains absorbed through the external walls (opening or closing of external windows, spaces located on the top floor), the type of the atrium itself, such as the characteristics of the adjacent wall of the atrium, its glazed surface and its degree of opening. Therefore, we can say that the atrium can be considered as a passive strategy in winter, achieving relative comfort, but its influence on the adjacent spaces will remain conditioned by several parameters mentioned above.

References

Humphreys, M. A. & Fergus, N. (2002). The validity of ISO-PMV for predicting comfort votes in every-day thermal. *Energy and Buildings, 34*(6), 667-684. doi:https://doi.org/10.1016/S0378-7788(02)00018-X

Gemi, A. M. (2006). *Environment control and building technology an estimation approach for thermal performance of atrium buildings through a case study'.* Istnabul: technical university institute of science and technology.

Moosavi, L. et al. (2014). Thermal performance of atria: An overview of natural ventilation effective designs. *Renewable and Sustainable Energy Reviews, 34*, 654-670.

Pichatwatana, K. & Wang, F. (2013). Modelling Analysis of Thermal Performance of Internal Shading Devices for a Commercial Atrium Building in Tropical Climates. *3rd International Conference on Ecological, Environmental and Biological Sciences (ICEEBS).* Singapore.

Shafqat, H. (2012). *Nnumerical investigations of the indoor thermal environment in atria and of the buoyancy- driven ventilation in a simple atrium building.* Ontario: Queen's University (Canada) ProQuest Dissertations Publishing.

Wang, L. et al. (2017). Role of atrium geometry in building energy consumption: the case of a fully air-conditioned enclosed atrium in Cold Climates, China. *Energy and buildings, 151*(15), 228-241. doi:https://doi.org/10.1016/j.enbuild.2017.06.064

Cite as: Hamida B. & Khalida B., "The Effect of Atrium on the Thermal Comfort in Buildings in Hot Arid Zones", *The 2nd International Conference on Civil Infrastructure and Construction (CIC 2023)*, Doha, Qatar, 5-8 February 2023, DOI: https://doi.org/10.29117/cic.2023.0060

Theoretical Simulation of Thermal Deformations in Concrete Beams Reinforced with Two Overlapped FRP Bars in Cold Regions

Ali Zaidi
Professor, Structure Rehabilitation and Materials Laboratory (SREML), University of Laghouat,Laghouat, Algeria;
Associate Professor, Department of Civil and Building Engineering, University of Sherbrooke, Sherbrooke, QC., Canada
a.zaidi@lagh-univ.dz

Hizia Bellakehal
Structure Rehabilitation and Materials Laboratory (SREML), University of Laghouat, Laghouat, Algeria
h.bellakehal@lagh-univ.dz

Radhouane Masmoudi
Department of Civil and Building Engineering, University of Sherbrooke,Sherbrooke, QC., Canada
Radhouane.Masmoudi@USherbrooke.ca

Oumelkhir Terbagou
Structure Rehabilitation and Materials Laboratory (SREML), University of Laghouat, Laghouat, Algeria
rimassrimass1995@gmail.com

Naima Nia
Structure Rehabilitation and Materials Laboratory (SREML), University of Laghouat, Laghouat, Algeria
sreml@lagh-univ.dz

Abstract

The thermal incompatibility in transverse direction between concrete and fiber reinforced polymer (FRP) bars may cause tensile circumferential cracks within concrete under low temperatures, and consequently, the failure of concrete cover. This paper presents a theoretical study to investigate the transverse thermal deformation of concrete beams reinforced with two overlapped FRP bars in cold regions where the climate temperature may drop to -40°C. Numerical and analytical models are developed to predict the transverse thermal strains at the FRP bar/concrete interface of the concrete cover zone and the bars interaction zone and also at the external surface of concrete cover for overlapped glass FRP (GFRP) bars reinforced concrete beams under low temperature variations, having a ratio of concrete cover thickness to FRP bar diameter varied from 1.0 to 3.2. Comparisons between the results predicted from non-linear finite element model and those obtained from the analytical model in terms of transverse thermal strains are presented.

Keywords: Low temperatures; Overlapped GFRP bars; Transverse deformations; Concrete cover; Cracking thermal loadings

1 Introduction

Various deteriorated reinforced concrete constructions (bridges and parking) due to the corrosion of steel bars need repairs. However, the repair cost of deficient structures can be estimated to billions of dollars. Numerous studies were carried out to substitute the steel by an anticorrosive material such as fibers reinforced polymer (FRP). This composite material is characterized by high immunity to corrosion, lightweight, high tensile strength, and long service life (ACI, 2015). Nonetheless, the transverse thermal expansion of FRP bars is higher than that of concrete. This difference in thermal expansion may cause circumferential tensile cracks in concrete at low temperatures if the confining action of concrete is not sufficient (Zaidi & Masmoudi, 2012). Many

researches on thermal behavior of FRP reinforced concrete elements were investigated taking into account many parameters such as temperature variation, type and diameter of FRP bar, concrete cover thickness, shape of the cross section, and spacing between bars. However, the overlapped FRP bars effect on the thermal behavior of reinforced concrete beams submitted to low temperatures was not investigated in the previous studies (Zaidi & Masmoudi, 2012; Rahman et al., 1995; Masmoudi et al. 2005; Bellakehal et al., 2018). For this reason, a nonlinear numerical investigation using finite element ADINA software is performed to study the thermal behavior of concrete beams reinforced with two vertical overlapped glass FRP (GFRP) bars under low temperature variation of up to -60 °C. This study permits to predict transverse thermal strains at the interface of FRP bar/concrete and at the interface of the two FRP bars/concrete and at the external surface of concrete covervarying the ratio of concrete cover thickness to FRP bar diameter for overlapped FRP bars-reinforced concrete beams under low temperatures. Comparisons between transverse thermal strains predicted from the numerical model and those obtained from the analytical model are presented.

2 Nonlinear Numerical Model

A nonlinear numerical model has been established using ADINA software to investigate the prismatic concrete beams reinforced with two overlapped glass FRP (GFRP) bars under low temperature variations of up to -60°C, varying the ratio of concrete cover thickness to FRP bar diameter (c/d_b) from 1 to 3.2. The cross-section of beams had dimensions (b_oxh) of 76×100; 100×125 and 100 mm ×150 mm. Five GFRP bars diameters (d_b) have been used 9.5; 12.7; 15.9; 19.1 and 25.4 mm. The concrete cover thickness (c) considered was equal to 20; 25; 30 and 35 mm. Details of GFRP bars-reinforced concrete beams are illustrated in Figure 1. The GFRP bars used had a linear elastic behavior; however, the concrete had a nonlinear behavior. Both materials were supposed to have a perfect bond at the interface level. GFRP bars properties and concrete are described in Table 1 and 2, respectively.

The coefficient of thermal expansion (CTE) of concrete measured using experimental tests was equal to $11.6\text{x}10^{-6}$/°C. The average tensile strength (f_{ct}) and compressive strength (f'_c) have been determined according to ASTM standard tests (ASTM, 2002a, 2002b). The Poisson's ratio of concrete (ν_c) has been considered equal to 0.17. The concrete elasticity modulus (E_c) has been evaluated according to CAN/CSA-S806-02 guidelines. The longitudinal CTE of GFRP bars obtained by experimental tests was found to be equal to $\alpha_l = 8\text{x}10^{-6}$/°C while the transverse CTE was found to be equal to $\alpha_t = 33\text{x}10^{-6}$/°C. The elasticity modulus (E_t) and Poisson's ratio (ν_{tt}) of GFRP bars in the transverse direction were determined theoretically using the rule of mixture and were found equal to 7.1 GPa and 0.38, respectively. The cross-section of overlapped GFRP bars-reinforced concrete beam was modeled by means of two dimensional plane stress elements because of the constant of the axial deformations. The study has been carried out only for the half of the cross-section of concrete beams since the cross-section is symmetric respect to z-z axis. The temperature variation (ΔT) applied statically on the concrete and the overlapped GFRP bars, was decreased from 0 to -60°C with an increment of -5°C. The meshing of the concrete and the overlapped GFRP bars was established using triangular elements with six nodes, as shown in Figure 1(c). Moreover, the GFRP bars and the concrete materials share the same nodes at the interface.

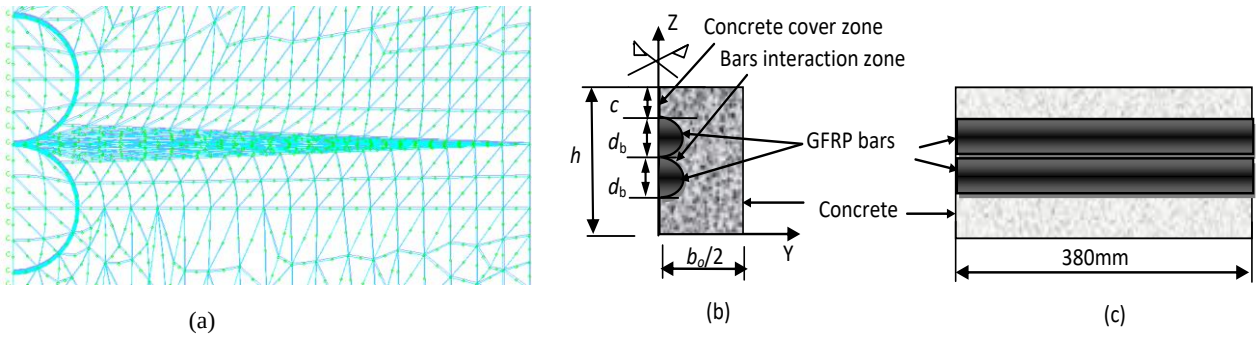


Fig. 1: Detail of reinforced concrete beam: (a) Meshing of the both GFRP bars and concrete through the width $b_o/2$, (b) The half of the modelled cross-section of beam,(c) Concrete beam reinforced with two overlapped GFRP bars

Table 1: Mechanical properties of glass FRP (GFRP) bars

Bar diameter d_b, mm	**Ultimate tensile strength f_{fu},MPa**	**Longitudinal modulus of elasticity E_l,GPa**	**Longitudinal Poisson's ratio, ν_{lt}**	**Ultimate tensile Deformation (%)**
9.5	627 ± 22	42 ± 1	0.28 ± 0.02	1.8 ± 0,2
12.7	617 ± 16	42 ± 1	0.28 ± 0.02	1.5 ± 0,2
15.9	535 ± 9	42 ± 1	0.28 ± 0.02	1.4 ± 0,2
19.1	600 ± 15	40 ± 1	0.28 ± 0.02	1.5 ± 0,2
25.4	N/a	N/a	0.28 ± 0.02	N/a

Table 2: Mechanical and physical properties of concrete

Compressive strength f'_{c28}, MPa	**Tensile strength f_{ct28}, MPa**	**Modulus of elasticity E_c, GPa**	**Coefficient of thermal expansion, α_c (x10^{-6}/°C)**
40 ± 3	4.1 ± 0.1	28 ± 2	11.6 ± 2.1

3 Linear Analytical Model

Based on research works carried out by Bellakehal et al. (2018) on concrete beam reinforced with two overlapped GFRP bars under high temperature, the following analytical model is developed for overlapped two FRP bars embedded in prismatic concrete element under low temperatures. The radial tensile stresses $\sigma_{\rho 1}$ due to the radial pressure P_1 exerted by FRP bar1 and $\sigma_{\rho 2}$ due to the radial pressure P_2 exerted by FRP bar2, in a concrete element situated at a distance ρ measured from the each FRP bar center, as shown in Figure 2, are given as follows:

$$\sigma_{\rho 1}(\rho) = \frac{P_1}{r_1^2 - 1}\left(1 - \frac{b_1^2}{\rho^2}\right) \tag{1}$$

$$\sigma_{\rho 2}(\rho) = \frac{P_2}{r_2^2 - 1}\left(1 - \frac{b_2^2}{\rho^2}\right) \tag{2}$$

Where, $r_1 = \frac{2c_1 + d_b}{d_b}$; $r_2 = \frac{2c_2 + d_b}{d_b}$; $b_1 = c_1 + a$; $b_2 = c_2 + a$; $a = d_b / 2$; c_1 and c_2 are the concrete cover thickness of the first and the second FRP bars, respectively. The radial pressures P_1 and P_2 exerted by the first and the second FRP bars, respectively, are given by the following expressions:

$$P_1 = \frac{(\alpha_t - \alpha_c)\Delta T}{\frac{1}{E_c}\left(\frac{r_1^2+1}{r_1^2-1}+\nu_c\right)+\frac{1}{E_t}(1-\nu_{tt})} \quad (3)$$

$$P_2 = \frac{(\alpha_t - \alpha_c)\Delta T}{\frac{1}{E_c}\left(\frac{r_2^2+1}{r_2^2-1}+\nu_c\right)+\frac{1}{E_t}(1-\nu_{tt})} \quad (4)$$

Where, E_c is the modulus of elasticity of concrete; ν_c is Poisson's ratio of concrete; α_c is the coefficient of thermal expansion of concrete; E_t is the modulus of elasticity of the FRP bar in the transverse direction; ν_{tt} is Poisson's ratio of the FRP bar in the transverse direction and α_t is the transverse coefficient of thermal expansion of FRP bar.

For FRP bar1 (Figure 2), the maximum radial tensile stress due to the radial pressure P_1 at the interface of FRP bar1/concrete in the concrete cover zone is obtained from Eq.(1) for $\rho = a$:

$$\sigma_{\rho 1max} = -P_1 \quad (5)$$

For FRP bar2 (Figure 2), the maximum radial tensile stress is:

$$\sigma_{\rho 2max} = -P_2 \quad (6)$$

In the bars interaction zone, the radial tensile stress due to radial pressures P_1 and P_2 exerted by the first and the second FRP bars, respectively, in concrete element situated at a distance ρ from the each bar center (Figure 2), is given as follows:

$$\vec{\sigma}_\rho(\rho) = \vec{\sigma}_{\rho 1}(\rho) + \vec{\sigma}_{\rho 2}(\rho) \Leftrightarrow \sigma^2(\rho) = \sigma^2{}_{\rho 1} + \sigma^2{}_{\rho 2} + 2\sigma_{\rho 1}\sigma_{\rho 2}\cos(2\alpha) \quad (7)$$

From Eq. (1) and (2) in Eq. (7), the radial tensile stress becomes:

$$\sigma_\rho{}^2(\rho) = \left[\frac{P_1}{r_1^2-1}\left(1-\frac{b_1^2}{\rho^2}\right)\right]^2 + \left[\frac{P_2}{r_2^2-1}\left(1-\frac{b_2^2}{(\rho)^2}\right)\right]^2 + \frac{2P_1P_2}{(r_1^2-1)(r_2^2-1)}\left(1-\frac{b_1^2}{\rho^2}\right)\left(1-\frac{b_2^2}{(\rho)^2}\right)\cos(2\alpha) \quad (8)$$

The maximum radial tensile stress due to radial pressures P_1 and P_2 of the first and the second bars, respectively, in the bars interaction zone, where $\rho = a$ and $\alpha = 0°$, is given by:

$$\sigma_{\rho max}(a) = \sigma_{\rho 1}(a) + \sigma_{\rho 2}(a) = -(P_1 + P_2) \quad (9)$$

The first circumferential cracks appear in concrete cover zone, at the interface of FRP bar1/concrete ($\rho = a$), when the maximum radial tensile stress $\sigma_{\rho 1max}$ reaches the concrete tensile strength f_{ct} ($\sigma_{\rho 1max} = -P_1 = f_{ct}$). Thus, the thermal load producing the first cracks, at the FRP bar1/concrete interface, obtained from Eq. (3) and (5) for $\sigma_{\rho 1max} = f_{ct}$, is given by:

$$\Delta T_{cr1} = \frac{f_{ct}}{(\alpha_t - \alpha_c)}\left[\frac{1}{E_c} + \frac{r_1^2-1}{r_1^2+1}\left(\frac{\nu_c}{E_c}+\frac{1-\nu_{tt}}{E_t}\right)\right] \quad (10)$$

While, the thermal load producing the first crack, in the concrete of bars interaction zone taking account of the two overlapped bars effect, is obtained from Eq. (9), (4) and (3) when $\sigma_{\rho max} = f_{ct}$, as follows:

$$\Delta T_{cr} = \frac{-f_{ct}}{(\alpha_t - \alpha_c)} \left[\frac{1}{\frac{1}{E_c}\left(\frac{r_1^2+1}{r_1^2-1}+\nu_c\right)+\frac{1}{E_t}(1-\nu_{tt})} + \frac{1}{\frac{1}{E_c}\left(\frac{r_2^2+1}{r_2^2-1}+\nu_c\right)+\frac{1}{E_t}(1-\nu_{tt})} \right]^{-1} \quad (11)$$

The transverse strain ε_{ct1} in the concrete cover zone, at FRP bar1/concrete interface ($\rho = a$), due to the radial pressure P_1 and the temperature variation ΔT, is given by:

$$\varepsilon_{ct1} = \frac{P_1}{E_c}\left(\frac{r_1^2+1}{r_1^2-1}+\nu_c\right)+\alpha_c \Delta T \quad (12)$$

Nevertheless, the transverse thermal strain ε_{ct} due to the radial pressures P_1 and P_2 exerted by the first and the second FRP bars (bar1 and2), respectively, at the interface of the two bars/concrete ($\rho = a$), and also the temperature variation ΔT, is given by:

$$\varepsilon_{ct} = \varepsilon_{ct1}(a) + \varepsilon_{ct2}(a) = \frac{P_1}{E_c}\left(\frac{r_1^2+1}{r_1^2-1}+\nu_c\right)+\frac{P_2}{E_c}\left(\frac{r_2^2+1}{r_2^2-1}+\nu_c\right)+\alpha_c \Delta T \quad (13)$$

The transverse thermal strain ε_{ct1} in concrete, at the external surface of concrete cover zone ($\rho = b_1$), due to the radial pressure P_1 and the temperature variation ΔT, is given by:

$$\varepsilon_{ct1} = \frac{2P_1}{E_c(r_1^2-1)}+\alpha_c \Delta T \quad (14)$$

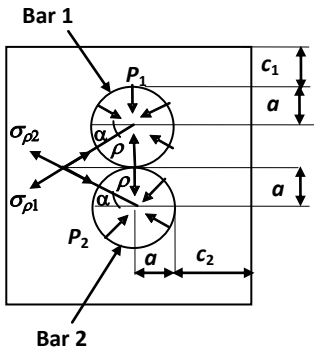


Fig. 2: Analytical model of overlapped FRP bars in concrete under low temperatures.

4 Comparison Between Numerical and Analytical Results

Figures 3 to 8 show comparisons between analytical and numerical curves in terms of transverse thermal strains of concrete at the interface of FRP bar/concrete of the concrete cover zone and at the interface of the two FRP bars/concrete of the bars interaction zone as well as at the external surface of the concrete cover of typical concrete beams reinforced with two overlapped GFRP bars varying c/d_b ratio from1 to 3.2. It is observed that the transverse thermal strain curve at the bar/concrete interface of the concrete cover zone is linear for temperature variations, in algebraic value, ΔT>-30 °C (Figures 3 and 4). However, for ΔT<-30 °C, in algebraic value, the strain curve becomes parabolic due to the formation of cracks in the concrete surrounding GFRP bars as shown in Figure 9(b). The same remarks can be noted for the thermal transverse strains at the interface of FRP bars/concrete of bars interaction zone except that the change of the slope of strain curves is done in

general at ΔT = -10 °C approximately as shown in Figures 5, 6 and 9(a). Furthermore, the transverse thermal strain at the interface of the two GFRP bars/concrete of the bars interaction zone is generally higher, particularly before the failure of the concrete cover compared to that predicted at the interface of FRP bar/concrete of the concrete cover zone. In addition, it is observed that transverse thermal strain curves at the external surface of concrete cover are linear for beams having ratios $c/d_b \geq 2$ (Figure 7), because cracks did not reach the external surface of concrete cover of these beams. However, for ratios $c/d_b < 2$ (Figure 8), the transverse thermal strain curves are linear up to the temperature variation ΔT_{sp}, producing the failure of concrete cover, from which the thermal strain curves become parabolic because of cracks, which reached the external surface of concrete cover as shown in Figure 9(c). In addition, transverse strain curves predicted from the non-linear numerical model are in good agreement with those obtained from the linear analytical model until thermal loads ΔT around -30 °C, -10 °C, -30 °C measured, respectively, at the interface of FRP bar/concrete of the concrete cover zone, at the interface of the two FRP bars/concrete of the bars interaction zone, and at the external surface of the concrete cover. Beyond these thermal load values, transverse thermal strains predicted from the numerical model are higher than those evaluated by the linear analytical model because of cracks developed within concrete, which are not considered in the analytical model.

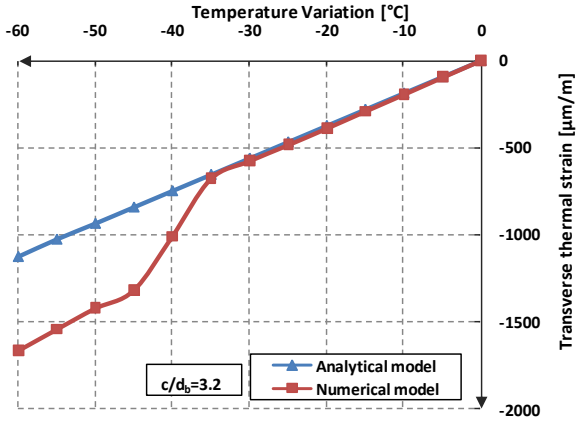


Fig. 3: Transverse thermal strain at FRP bar/concrete interface of concrete cover zone of beam having c/d_b = 3.2 - Comparison between analytical and numerical results

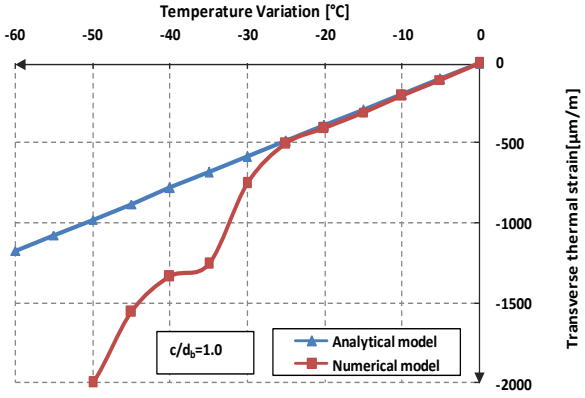


Fig. 4: Transverse thermal strain at FRP bar/concrete interface of concrete cover zone of beam having c/d_b= 1.0 - Comparison between analytical and numerical results

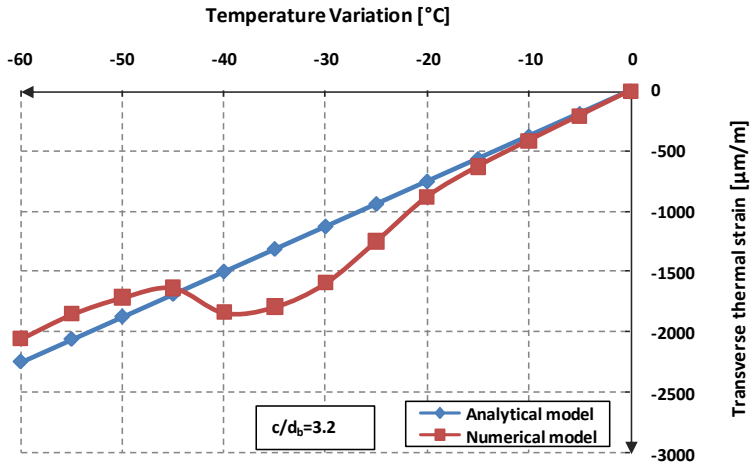


Fig. 5: Transverse thermal strain at two FRP bars/concrete interface of bars interaction zone of beam having c/d_b = 3.2 - Comparison between analytical and numerical results

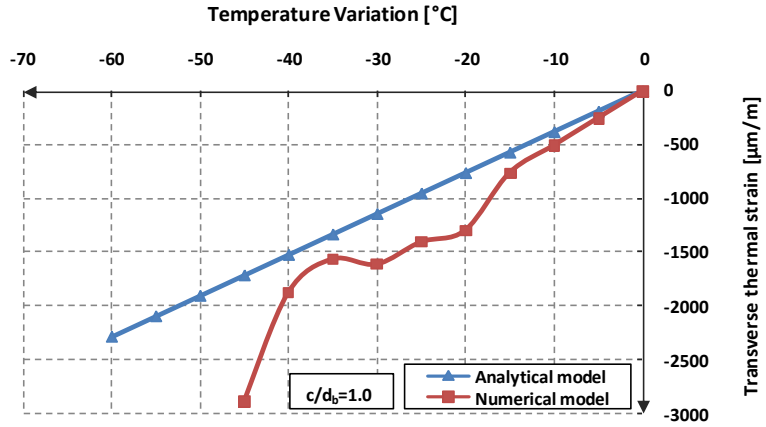


Fig. 6: Transverse thermal strain at two FRP bars/concrete interface of bars interaction zone of beam having c/d_b = 1.0 - Comparison between analytical and numerical results

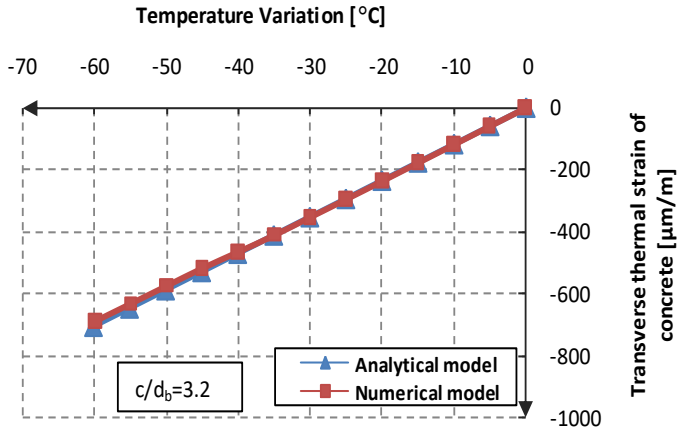


Fig. 7: Transverse thermal strain of concrete at external surface of concrete cover zone of beam having c/d_b = 3.2 - Comparison between analytical and numerical results

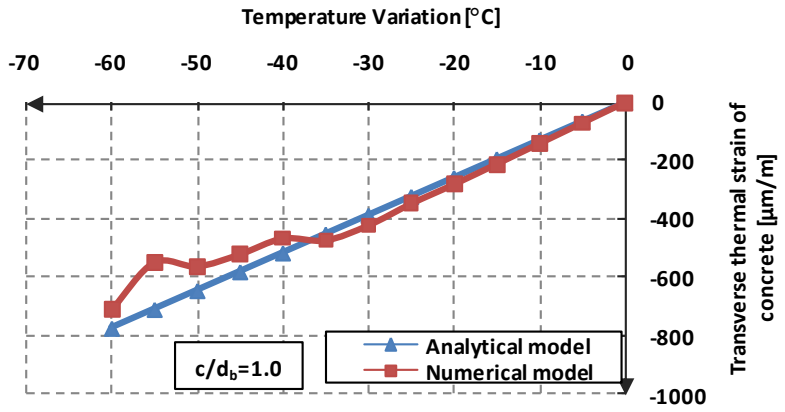
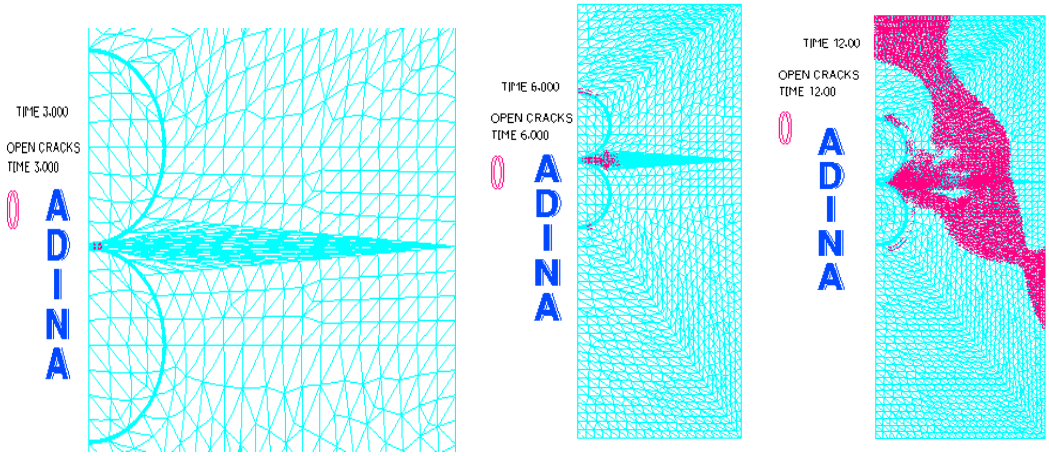


Fig. 8: Transverse thermal strain of concrete at external surface of concrete cover zone of beam having c/d_b = 1.0 - Comparison between analytical and numerical results



(a)At ΔT_{cr}=-10°C. (b)At ΔT_{cr}=-25°C. (c)At ΔT_{sp}=-60°C

Fig. 9: Cracks development in concrete at FRP bar/concrete interface for concrete cover zone and bars interaction zone (Beam having c/d_b = 1): (a) First cracks at bars interaction zone; (b) First cracks at concrete cover zone; (c) Failure of concrete cover

5 Conclusion

Analytical and numerical analysis of low temperature effects on thermal deformations of two glass FRP bars embedded in a prismatic concrete beam, allow to draw the following conclusions:

- From the linear analytical model, GFRP bar diameter and concrete cover thickness variations do not have a great influence on transverse thermal strain which depend mainly on the temperature variation.
- Numerical and analytical results in terms of transverse thermal strains at the FRP bar/concrete interface of concrete cover zone and at the interface of two FRP bars/concrete of bars interaction zone of prismatic beams, are almost similar for ΔT >-30 °C and ΔT >-10 °C, respectively. However, for $\Delta T \leq$ -30°C and $\Delta T \leq$-10 °C, the numerical strains are higher because of circumferential cracks developed in concrete, which are not taken into account in the analytical model.

References

American Concrete Institute. (2015). Guide for the Design and Construction of Concrete with FRP Bars, ACI 440.1R-15, Farmington Hills, Mich.

American Society for Testing and Materials. (2002a). Standard test method for splitting tensile strength of cylindrical concrete specimens, In: annual book of ASTM standards, *ASTM C 496-96, USA, 04*(2): 281–4.

American Society for Testing and Materials. (2002b). Standard test method for compressive strength of cylindrical concrete specimens, In: Annual book of ASTM standards, *ASTM C 39/C 39M-01, USA, 4*(2): 21–5.

Bellakehal, H. et al. (2018). Theoretical Analysis of Thermal Behavior of Overlapped GFRP Bars Embedded in Reinforced Concrete Beams. *Arabian Journal for Science and Engineering, Springer, 43*(10): 5255–5263. https://doi.org/10.1007/s13369-018-3086-5.

Canadian Standards Association. (2002). Design and construction of building components with fiber–reinforced polymers, CAN/CSA-S806-02, Toronto, Ontario, Canada.

Masmoudi, R., Zaidi, A.& Gérard, P. (2005). Transverse thermal expansion of FRP bars embedded in concrete, *Journal of composites for construction, 9*(5): 377-387. https://doi.org/10.1061/(ASCE)1090-0268(2005)9:5(377)

Rahman, H.A., Kingsley, C. Y. & Taylor, D.A. (1995). Thermal stress in FRP reinforced concrete, Proceedings of Annual Conference of the Canadian Society for Civil Engineering, Ottawa, Canada, 605-614.

Zaidi, A. & Masmoudi, R. (2012). Numerical Analysis of Thermal Behavior of Concrete Cover around FRP-Bars in Cold Region, *Arabian Journal for Science and Engineering, Springer, 37*(2): 489-504. https://doi.org/10.1007/s13369-012-0173-x.

Cite as: Zaidi A., Bellakehal H., Masmoudi R., Terbagou O. & Nia N., "Theoretical Simulation of Thermal Deformations in Concrete Beams Reinforced with Two Overlapped FRP Bars in Cold Regions", *The 2nd International Conference on Civil Infrastructure and Construction (CIC 2023)*, Doha, Qatar, 5-8 February 2023, DOI: https://doi.org/10.29117/cic.2023.0061

ABAQUS Modelling and Experimental Tests Comparison for Certain Classes of Composite Isolated Joints

Bashir Saleh
Libyan Academy, Tripoli, Libya
bashir.saleh@academy.edu.ly

Abstract

Depending on the type of configuration and connector arrangement, beam-to-column end-plate joints can be rigid, semi-rigid, or pinned. Fully restrained joints are required for rigid frames in which it is anticipated that the frame joints will have adequate rigidity to maintain the angles between intersecting parts in the service condition, ensuring full moment transfer. In contrast, partially restrained joints in semi-continuous frames are distinguished by relative rotations between crossing members, allowing the bending force to be transferred only partially. The concept of utilizing partially restricted, unstiffened joints in construction has gained traction since it looks to be more feasible and inexpensive. Bending transfer in partially constrained joints allows semi-continuous frames to withstand actions. Semi-continuous frames can survive actions due to bending transfer in partially restricted joints. At the same time, a certain degree of rotation is permitted, which improves the overall ductility of these structures. Using thinner end plates than those used in practical applications is one of the most effective ways to affect the ductility of end-plate beam-to-column joints. It was confirmed in a previous experimental study that the composite joints, where the thickness of the end plates is equivalent to about 60% of the diameter of the bolt used in composite joints, were taken into account in subsequent tests, and these studies can be confirmed using ABAQUS and Ls-Dyna modelling. All of these concerns are addressed, and recommendations for numerical modelling methodologies are made in order to ultimately analyse the reaction of the symmetric extended end plate joints with 8-bolts under hogging and sagging bending moments.

Keywords: Joint; Robustness; Finite elements; ABAQUS; LS-DYNA

1 Introduction

The bonding interaction between the concrete and steel elements composing the insulated joint makes nonlinear analysis of composite structures up to the point of failure somewhat difficult due to the complexity of the physical processes that precede the structural failure process under increasing procedures. The reason is a combination of different shear bolt behaviours in steel beams, concrete, and steel columns; the presence of any lateral metal surface; stress redistribution between concrete and rebar after cracking; slippage between steel sections and reinforced concrete slabs; and a variety of other conceivable local effects. This occurs in a structure made of diverse materials such as steel and concrete, and it is all connected to the distinct and complicated behaviours, the influence of overall ductility, and the behavior of the elements, which produces the collapse stress. This research gives a comprehensive investigation into the modelling of composite beam-to-column symmetric extended end plate connections with eight bolts. The class of joints evaluated is based on their steel equivalents, which the authors tested in previous investigations (Gizejowski & Barcewicz 2008). Because the design of these joints varies so greatly, developing a generic mathematical model for

predicting joint reaction is unfeasible. Instead, beam-to-column joint tests were performed to find the connection that describes how the moment is conveyed via the joint components. The optimal joint model for this study contains its practical behavior, which is often a modest number of parameters generated from experimental test data. As a result, a dependable rotational moment response for semi-rigid composite joints is required in order to calibrate the analytical formula for the spring rotational momentary characteristic utilized in engineering practice for analysis and design. In order to correctly replicate the different configurations of tested composite joints, the FE analysis performed herein gives advantage to the ABAQUS and Ls-Dyna codes (Hallquist, 2007, 2008). The composite concrete joints, according to the authors Barcewicz W. (2016), have the same composition and patterning as bare steel spans from an end plate spanning from beam to column. The major distinction is that composite joints consist of a poured concrete slab on a steel surface made of rolled sheets, as well as steel shear wire connectors to produce a composite, continuous action between the reinforced concrete slab, beams, and steel-rolling section. The modelling technique was carried out to advanced standards and correctly mimics the laboratory experiment; in particular, the position of the rebar buried inside the concrete slab and the modelling of the concrete itself differ from earlier studies. An essential topic to address when discussing structural robustness and design requirements for circumstances of extraordinary action is a structure's capacity to redistribute pressures internally and so limit the progression of damage. The development of so-called alternate loading routes is primarily accomplished by joint ductility, that is, by ensuring that the joints have adequate rotational capacity.

A structure's resilience is typically examined in analysis by analysing the potential removal of the main structural element(s) and determining if local impact can be absorbed by the decaying structural system. This necessitates research into joint responses to flaccid flexion with axial ligation. In an earlier study of isolated joints (flush and asymmetric extended end-plate), it was discovered that we needed to test the symmetric extended end-plate joint to be more resistant in the presence of positive and negative bending moments, as well as when the joints were subjected to member collapse (column loss scenario). Current advanced modelling approaches are then applied to joints as part of a complicated procedure that arises in the case of progressive collapse and is confirmed through comparisons with experimental test findings. Through energy-based static and nonlinear dynamic studies, the contribution seeks to expand knowledge in the relevant field of study and provide the groundwork for a global evaluation of structural susceptibility to disproportionate collapse. All of the specifics of modelling and simulation of the structural components involved in joint fitting, as well as the method of analysis employed in the software in this research, are the same as those used in earlier finite element analyses (Saleh, 2013). The flanges, web, and stiffener, for example, are 8-node, doubly curved thin shell elements, whereas the concrete deck slab plates of the steel girder are represented by thick shell components. The ABAQUS code's "rebar" layer option was used to represent reinforcement. To account for the geometric and materially nonlinear behavior of continuous steel composite structures, a 3D FE model was developed.

2 Symmetrical Model Development

The finite element model under consideration in this work is an extension of one presented by (Saleh, 2015). The previously utilized finite element joint model Saleh (2020) is transformed into a new model with the following precise requirements: The concrete slab reinforcement is represented by truss components and is situated in the same location as in the tested specimens. The finite element model utilized in this work is an extension of the model used to represent isolated extended end plate joints with 4-6 bolts Saleh (2022), and it has also been employed in earlier investigations of a basic

package of isolated joints. The reinforced concrete slab of the composite joint is modelled using various layers of brick finite elements structured so that the slab mesh nodes of certain layers correspond with the top of the shear studs and are in line with the reinforcement. This allows you to simulate the real stud length as well, the matching end nodes of the connected shell components of the beam flange and brick elements of a slab of reinforced concrete. There are two types of numerical analysis considered: static general and explicit dynamic. The influence of finite element mesh size, type, and time step is carefully determined. In the case of steel specimens, both methodologies produce equivalent findings; however, numerical time-explicit analysis is less precise in reproducing the experimental behavior of composite steel-concrete frame specimens. The concrete slab reinforcement is represented by truss components and is situated in the same location as in the tested specimens. The composite reinforced concrete slab is represented by multiple layers of brick-based finite elements organized so that the slab mesh nodes of certain layers correspond with the tops of shear studs and are in line with the reinforcement. This enables the modelling of the actual stud length as well as the matching end nodes of the linked shell components of the beam flange and brick elements of a reinforced concrete slab. The profiled sheeting effect is featured, and the concrete ribs are represented by brick finite elements in the shape of cubes and tetrahedrons, with a homogenous 8-nodal solid element C3D8. Sheeting is represented by thin shell pieces. Bolts are modelled using 3D beam elements of type B31 that allow for transverse shear strain. A circular cross-section between the end plate and the shaft flange represents the bolt section profile; a tiny and particular sliding contact interface is utilized.

3 Test Scenarios

These studies were carried out as part of a prior research effort at the Warsaw University of Technology, in which laboratory experiments were devised to explore the behavior of compound joints subjected to severe stresses Barcewicz (2016). As a follower interested in a scientific study on composite connections (steel and concrete) and their design under service and exceptional loads, I have attended this experimental test since its start. The specimens' beam elements were built of IPE 300, while the columns were composed of HEB 200. Steel grade S235JR was used for all steel elements (beams, columns, and end plates). M20 bolt connections of class 10.9 were used, and the Cofraplus 60 composite flooring was used to cast the concrete slab on the dip-profiled sheeting. The sheeting's ribs were positioned in a transverse orientation to the supporting beams. End plate types are utilized in symmetric extended end plate connections with eight bolts. End plates with a diameter of about 60% of the bolt size used in the endplate-to-column-flange connection were utilized, (Barcewicz, 2008).The sheeting and the headed studs (SD 19 by 100 mm) that were friction welded to the top flange of the beam contributed to the composite action. C25/30 was the concrete class (B30) used, and the main slab reinforcing bars were composed of BSt500S steel. All tests were carried out with the static loads rising monotonically until failure. Two independent jacks were used at 1540 mm from the column face to supply the equal weights to each cantilever point. The symmetrical structure was used to control specimen behavior as well as the impact of defects that might lead to column collapse. Figure 1 depicts the experimental test in general, as well as the lobe structure, whereas Figure 2 shows the experiment's modelling and simulation. The test methods and static loads applied to the joint were designed to model the negative and positive moments of a column loss, and the relationship between the quantity of bending moments on the joint, rotation, and deformation was estimated using Eurocodes EN 1-8 component approach.

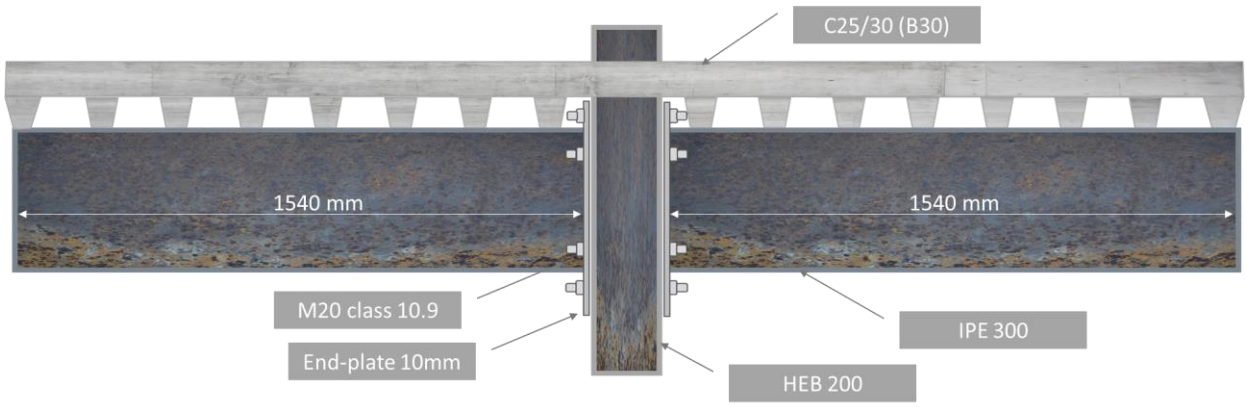


Fig. 1: Composite symmetric extended end plate joint eight Bolts test (Barcewicz, 2016)

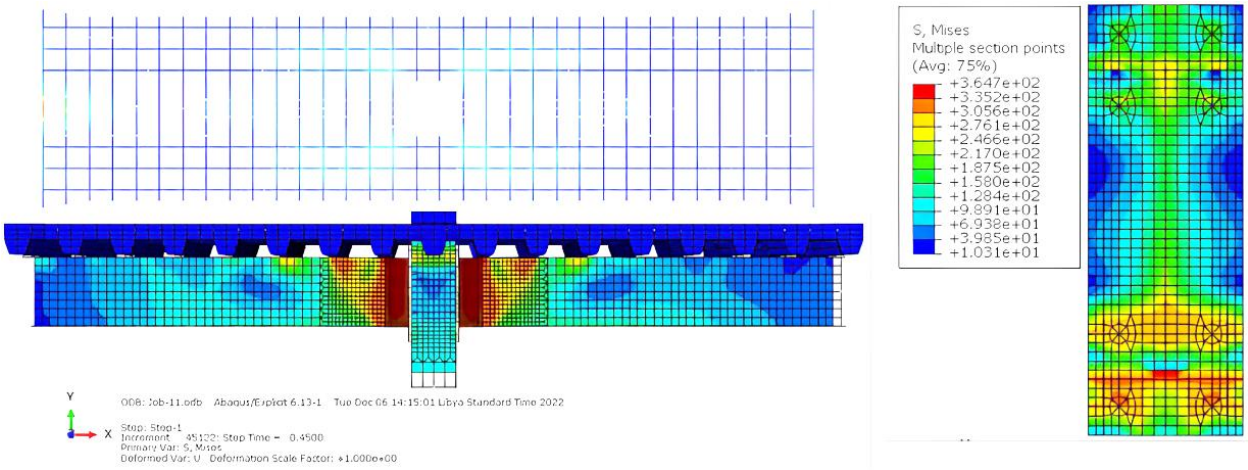


Fig. 2: Displays the stresses in the joint and the overall model using ABAQUS FE modeling

4 FEM Modeling Validation

Since the loading was supplied gradually in the experiment to remove dynamic effects, numerical models reproduce the same time-load characteristic. The chosen FEA modelling technique is validated by comparing the local and global behaviour of the experimentally verified joint and the conformity of force versus displacement relationships is the first indicator of its acceptability. In general, the global behaviour of the investigated composite specimens may be divided into two separate circumstances. Figure 3 illustrates the comparison of joint deformation experimentally and numerically, as well as the percent of agreement between them. For the joints subjected to hogging bending, a significant local deformation takes place at the bottom of the steel plate, both above and below the tensioned beam top flange. The same distortion occurs in the opposite direction in the joint subjected to a sagging bending force. Based on these figures, one might deduce that the symmetrically extended end-plate joints exhibit behaviour that is more ductile. This is owing to the accurate modelling technique utilized, which resulted in consistent and dependable results when compared to the results of the processes experimental test, as well as the appropriate selection of the rebar's diameter and plate thickness. Bolts exhibit no significant elongation in any circumstances, including those subjected to the greatest tensile pressures.

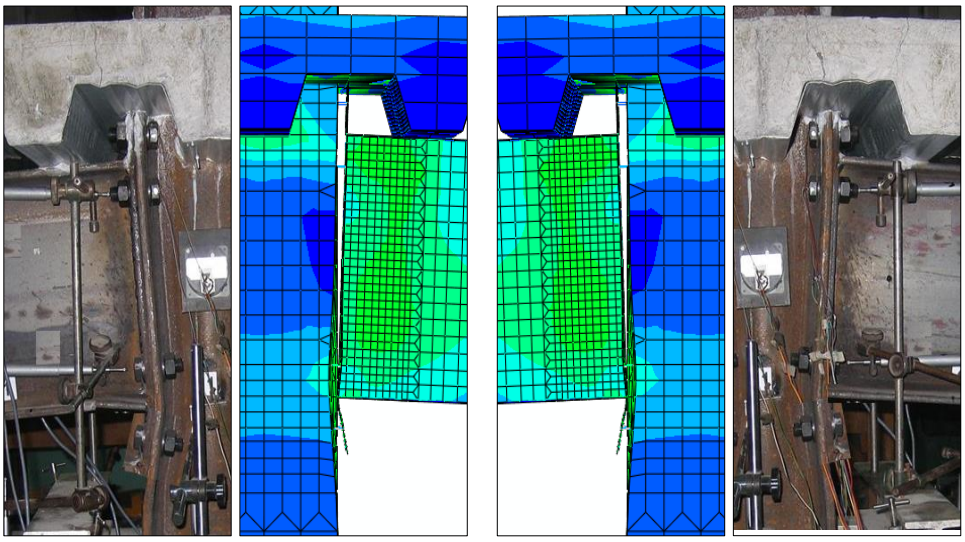


Fig. 3: Joint deformation comparison between experimental testing and FEA modelling

Load-displacement curves and M-ø joint characteristics are provided for the symmetric extended end-plate with 8 bolts specimen. The highest value of the applied load and the ultimate moment derived from the tests and FE models are almost identical (the discrepancy between the ultimate moments does not exceed 9%). The only difference is that the M- ø curve obtains these final values at a different angle of joint rotation, whereas the load-displacement curve obtains them at a different displacement. The highest agreement between the FEM findings and the test data is shown in the elastic range up to about 94% of the final moment, and the impact of the reduction in joint stiffness on the moment value is also clearly visible (see Figure 4 A and B). For the symmetric extended end plate with 8 bolts specimen, load-displacement curves and M- ø joint parameters are shown. The maximum applied load and the ultimate moment determined from the tests and FE models are almost equal (the difference between the ultimate moments is less than 9%). The M- curve obtains these final values at a different perspective of joint rotation, but the load-displacement curve acquires them at a different movement. The best agreement between the FEM results and the test data is demonstrated in the elastic range up to about 94% of the final moment, and the influence of joint stiffness decrease on the moment value is also clearly evident (see Figure 4 A and B).

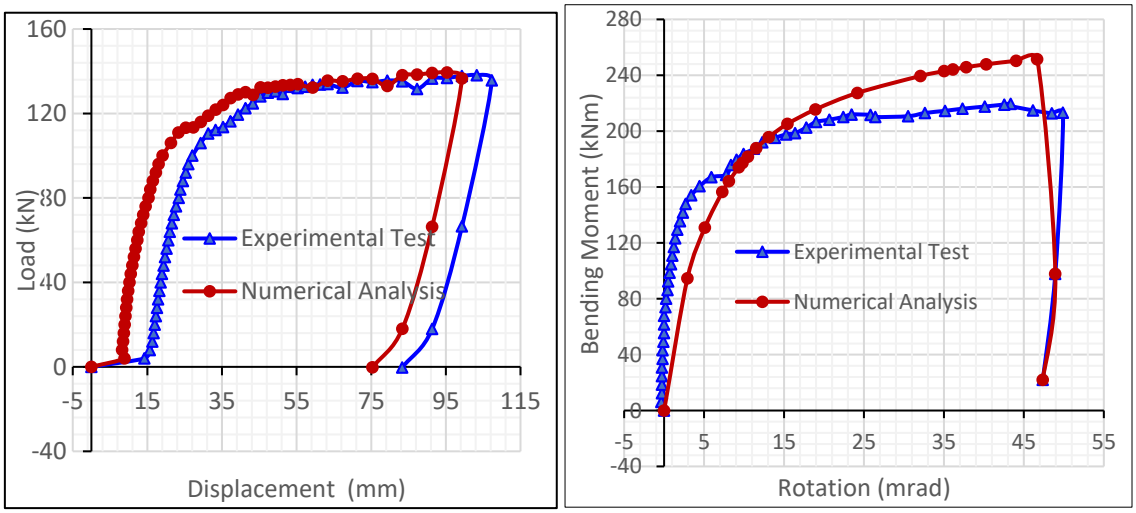


Fig. 4: (A) Force – Displacement relationship (B) Moment – Rotation Relationship of composite joint in experimental testing and FE modeling

5 Conclusion

The strengthening of a concrete slab is reproduced using truss components in the same place as in the tested cases. A composite joint's reinforced concrete slab is modelled using numerous layers of brick finite elements structured so that the slab mesh nodes of certain layers correspond with the tops of shear studs and are in line with the reinforcement. This allows for the modelling of the actual stud length as well as the matching end nodes of the linked shell components of the beam flange and brick elements of the reinforced concrete slab, so this updated numerical model of joint activity has greater accuracy than the previous one and was thus used for the representation of the physical frame evaluated to replicate global behavior for future study. Resistance to progressive collapse scenarios is the most important feature of structural resilience. Both testing and FEA modelling for resilient structural systems should demonstrate that the structure could bear the given load in the case of a worsening static scheme because of local damage modelling. The findings show that structural systems with thin, symmetrically extended end plates are resilient and robust. The numerical model also provides some additional useful information that is difficult to notice during testing, such as the distribution of tension and frictional forces induced by the bolt pre-tension and the moment at the joint, as well as the principal stress flow in the connections. This information is used to build mechanical simulations that comply with the Eurocode component approach to joint design. More emphasis should be placed on discovering creative joint constructional aspects in terms of their ductile behavior, specifically the position of bolts and welding scenarios that minimize the effect of ductility deterioration in the heat-affected zones (HAZs) of beam-to-column joints.

Knowledge of isolated joint stiffness, strength, and ductility in typical conditions and static loads must be increased to incorporate the effect of deformation rate on joint behavior in severe scenarios of local damage.

References

Eurocode 4: EN 1994-1-1: Design of composite steel and concrete structures, Part 1-1: General rules and rules for buildings. CEN, Brussels.

Gizejowski, M., et al. (2012). Evaluation of a unified moment-rotation characteristic of steel and steel-concrete composite joints, SEMC, The Fifth International Conference on Structural Engineering, Mechanics and Computation, Cape Town, South Africa.

___. (2013). Composite steel-concrete joints for efficient applications in modern building structures, *Botswana Journal of Technology*.

Gizejowski, M., Salah W. & Barcewicz W. (2008). Finite element modeling of the behaviour of steel end-plate beam-to-column joints, Archives of Civil Engineering.

Hallquist, J. O. (2007, 2016) LS-DYNA: Keyword User's Manual, Version 970, Livermore Software Technology Corporation: Livermore, California.

Saleh, B. (2013). Modelling of Beam-to-Column Joint of Steel-Concrete Composite Frames Subjected to Standard and Extreme Load Combinations. PhD thesis, WUT.

——. (2015). Moment-Rotation Characteristic of Joints of Steel-Concrete Composite Frame under Exceptional Events, IABSE Nara, pp. 504-505.

——. (2016). Experimental investigation for the steel-concrete composite joints subjected to in exceptional load, 6th Conference of Building Materials and Construction, Ghryan, Libya.

——. (2020). Numerical Study of Four Bolts End-Plate Joint Behaviour for Robustness Assessment. International Conference on Civil Infrastructure and Construction, Doha, Qatar.

——. (2022). Numerical analysis to evaluate the effective asymmetric expanded steel plate with semi-rigid joint. The Ninth National Conference on Building Materials and Structural Engineering, Tripoli University-Libya.

Cite as: Saleh B., "ABAQUS Modelling and Experimental Tests Comparison For Certain Classes of Composite Isolated Joints", *The 2nd International Conference on Civil Infrastructure and Construction (CIC 2023)*, Doha, Qatar, 5-8 February 2023, DOI: https://doi.org/10.29117/cic.2023.0062

Recycled Polypropylene Fibres for Reinforcing Cement Mortar under Arid Conditions

Khadra Bendjillali
Laboratory of Structures Rehabilitation and Materials, Faculty of Civil Engineering and Architecture, University Amar Telidji, Laghouat, Algeria
k.bendjillali@lagh-univ.dz

Mohamed Chemrouk
Laboratory of Buildings in the Environment, Faculty of Civil Engineering, University of Sciences and Technology Houari Boumediene, Algiers, Algeria
mchemrouk@yahoo.fr

Abstract

Concreting in arid environment is a delicate operation, due to many problems, such as the premature evaporation of mixing water, which affects the material consistency and the shrinkage cracking which threatens its durability. The present experimental work is conducted to investigate the physical and the mechanical behaviour of cement mortar reinforced by recycled polypropylene fibres under arid conditions, at 45 °C and 30% RH. The used polypropylene fibres are recycled from a domestic plastic waste. The tests realized in this investigation include the workability, the total shrinkage, the flexure and the compression tests. Through this investigation, the beneficial effect of recycled polypropylene fibres as reinforcement of cement mortar is well demonstrated, particularly under arid environmental conditions. The obtained results showed a substantial increase in the flow time of about 53% in mortar reinforced by 1% of recycled polypropylene fibres (1RPFM). It is also shown that under arid conditions, the presence of 1% of recycled polypropylene fibres in cement mortar leads to a considerable decrease in total shrinkage of about 46% and an increase in the flexural and compressive strength of about 24% and 26%, respectively, compared to control mortar (CM) at the age of 194 days. Overall, the used recycled polypropylene fibres have presented a high capacity to improve the different properties of cement mortar and make it a suitable composite for concreting in arid environment.

Keywords: Cement mortar; Recycled polypropylene fibres; Arid conditions; Shrinkage; Mechanical strength

1 Introduction

Algeria is the largest country in Africa; it comprises 2.4 million square kilometres of land, more than 80% of which is occupied by the Sahara Desert. The Sahara is covered by immense areas of sand dunes and it is characterised by hot and dry climate, especially during summer, with high temperature (50 °C), low humidity, frequent and violent winds and intense solar radiations. The properties of concrete and mortars are significantly affected by these climatic conditions. Construction materials are subjected to high risk of evaporation of their mixing water, which can affect even constitution water, if their exposure to arid climate is long. In hot and dry climate, the evaporation is about 10 times, than in hot and humid climate (Almusallam, 2001). The premature loss of water causing by this accelerate evaporation increases the cracking risk in cement materials and reduces their mechanical strength at later ages and also their durability performances. To improve the materials

quality and prevent their cracking, when exposed to arid and hot climate, several standards, as ACI 308R-16 and studies (Al-Amoudi et al., 2007; Khan & Abbas, 2017; Khan et al., 2021) recommend the application of an immediate curing technique. The incorporation of fibres in the mass of cement materials is considered by many authors (Zhang & Zhao, 2012; Cifuentes et al., 2013) as a good solution to reduce cracking risk and increase their ductility. Today, polypropylene fibres are among the most used fibres in concrete, because they have many qualities, such as their low price, their low density, their high chemical resistance, their non-water absorption and as reported by (Bin et al., 2020), their high ability to improve the fire resistance of concrete. The recycling of fibres coming from waste for the fabrication of some construction materials has become an important ecologic challenge as well as a major technological advantage (Bendjillali et al., 2013; Sengul, 2016; Pešić et al., 2016; Borg et al., 2016; Mohammad Hosseini & Tahir, 2018; Mohajerani et al., 2019; Adnan & Dawood, 2020; Faraj et al., 2020; Jain et al., 2021; Mohammed & Mohammed, 2021).

In the present paper, an experimental work is made on the re-use of recycled polypropylene fibres, as fibrous reinforcement, in cement mortar exposed to arid conditions (T = 45 °C and 30% RH). The used fibres are obtaining from a plastic waste of polypropylene resulting from the fabrication of domestic sweeps, which ends up in landfills. The valorisation of this waste in construction materials can improve their performances and participate in the protection of the environment. The work consists to measure the workability, the flexure and the compression strength and the total shrinkage of cement mortars reinforced by these recycled fibres.

2 Materials and Tests

For the preparation of tested mortar, Portland cement (CEM II/A 42.5), crushed limestone sand (0/2 mm), potable water, recycled polypropylene fibres, a superplasticizer (SIKA VISCOCRETE TEMPO12) are used. The sand characteristics are shown in Table 1. The fibres having the properties given in Table 2 are recycled from a domestic plastic waste (Figure 1).

Mortar mixtures are prepared according to the Standards EN196-1 (2005), with a water/cement and a sand/cement ratio of 0.55 and 3, respectively. The amount of the admixture, which is the same in all mortars is about 2.88%. The fibres are added in the last of mixing operation with weight contents of 0.5 and 1%. Three mortar mixes are tested, control mortar fabricated without fibres, noted CM, mortar prepared with 0.5% of recycled polypropylene fibres, noted 0.5RPFM and mortar prepared with 1% of recycled polypropylene fibres, noted 1RPFM. For each mixes, prismatic samples 40x40x160 mm are prepared and immersed in water for 14 days, immediately after their demoulding and then conserved under arid conditions, at 45 °C and 30% RH until testing day. Due to their very small size, compared to real structural elements that are already protected by the formwork, mortar samples if not protected will be exposed to a rapid evaporation of mixing water, immediately after their demoulding (24 hours) that can touch even the water required for cement hydration. Therefore, this initial curing of samples in water is an essential procedure that must be applied before exposure to arid conditions to prevent the premature water evaporation and allow the achievement of a sufficient strength for resisting to the various environmental conditions. The workability of the mixtures is estimated by the measure of the flow-time, according to the Standards P 18-452. Strength tests are conducted at different ages, 14, 21, 28, 42, 70, 105, 134 and 194 days. The strengths reached after 14 days in water conservation are considered as reference values. The total shrinkage is measured during 190 days of age of mortars.

Table 1: Characteristics of crushed limestone sand

Specific density	Fineness modulus	Sand equivalent	Methylene blue value	Water absorption
2.52 g/cm^3	1.80	63%	0.13 ml/g	4.50%

Table 2: Properties of recycled polypropylene fibres

Specific density	Diameter	Length	Water absorption	Elasticity modulus	Tensile strength
0.99 g/cm^3	0.38 – 0.51 mm	20 ± 2 mm	Nil	4 - 5 GPa	230 MPa



Fig.1: Recycled polypropylene fibres

3 Results and Discussions

3.1 Flowability

The flow-time of cement mortar has a significant effect on the facility of their production and also on their performances. It is well noted that mortars with recycled polypropylene fibres need more flow-time than control mortar (Figure 2). The increase of the flow-time will be interpreted in construction site by implementation difficulties of the material that requires additional finishing work. In composite materials, the cement paste may be trapped by fibres, giving the impression that the material is less workable. The negative effect of fibres on materials flowability is mentioned in many experimental works (Silva et al., 2013; Al-Hadithi & Hilal, 2016; Belferrag et al., 2016; Zeyad, 2019). This effect is less important with polypropylene fibres, by comparison to others (Dreux & Festa, 2002).

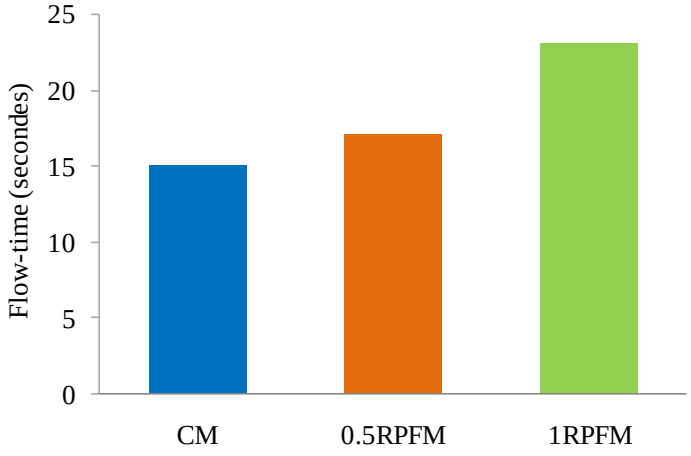


Fig.2: Variation of flow-time in cement mortars

3.2 Flexure Behaviour

Until 194 days of aging, the flexure strength of all mortars is the highest, compared to reference strength values (Figure 3). It is well observed that there is a quick strength evolution during the first 28 days of aging (14 days in water following by 14 days in arid conservation), where the evolution ratio reaches 116, 86 and 101% in mortars CM, 0.5RPFM and 1RPFM, respectively, compared to reference values. Kriker et al. (2008) have already concluded that the conservation of fibre concrete in hot-dry environment positively affects its performances at early age. A flexure strength reduction is detected beyond the age of 28 days; at 194 days, this reduction reaches 46% in CM, 37% in 0.5RPFM and 38% in 1RPFM, by comparison to maximum strengths obtained at 28 days. The decrease of flexure strength of mortars is probably due to the conservation conditions (T = 45 °C, 30% HR) that negatively affect the hydrated cement quality produced at early ages which in turn, weakens their long-term mechanical strength. These results are in agreement with others' studies (Park & Noguchi, 2017; Tang et al., 2017) who reported that the hot temperature favours early strength evolution but decreases the long-term strength. It is well known that the effect of hot temperature on the mechanical behaviour of cement materials becomes more influential with the low humidity. With the use of more recycled polypropylene fibres, the flexure strength becomes more important. By comparison, to control mortar, the flexure strength at the age of 194 days is increased by 19% and 24% in 0.5RPFM and 1RPFM, respectively. In this regard, it is very important to note that the recycled polypropylene fibres used in this investigation have a great ability to reduce the strength fall of cement mortars conserved in arid environment, which encourages their use for reinforcing concrete in arid climates. As other types of fibres, the used recycled fibres have improved the ductility of mortars by absorbing more energy, during flexure tests. These findings were mentioned in many literature studies (Oliveira et al., 2011; Yin et al., 2015; Caggiano et al., 2016).

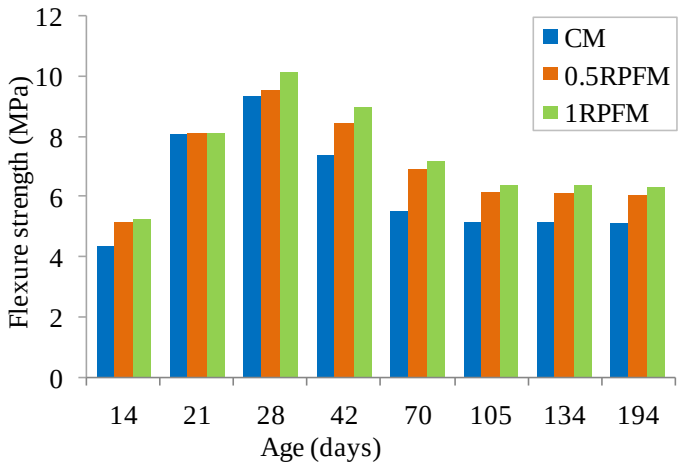


Fig.3: Variation of flexure strength of cement mortars

3.3 Compressive Behaviour

As with flexure behaviour, the compressive strengths of mortars in any age are higher than reference values (Figure 4). After a conservation of one week under arid conditions, a compressive strength increase of about 76, 63 and 49% is reached in CM, 0.5RPFM and 1RPFM, respectively, compared to reference values. These important percentages reflect the good effect of the temperature (T = 45 °C) associated with a low humidity (30% HR) to accelerate the evolution of the compressive strength by the activation of hydration reaction, during early time. The conservation conditions continue to affect positively, the compressive behaviour of mortars reinforced by recycled polypropylene fibres

until 42 days of aging (14 days in water and 28 in arid conditions) and then a decline of about 20% in 0.5RPFM and 15% in 1RPFM in the compressive strength will take place at 194 days of aging. Gallucci et al. (2013) justify the low final strengths of materials exposed to a temperature of 60 °C by the coarser and the porous microstructure of the cement paste, resulting from the increase of the C-S-H apparent density. After a conservation of 180 days (194 days of age) under arid conditions, the compressive strength increase reaches 39% in CM, 47% in 0.5RPFM and 45% in 1RPFM, by comparison to reference mortars. Recycled polypropylene fibres have improved also the compressive behaviour of cement mortars conserved under arid conditions; where an increase of the compressive strength of about 14% and 28% is detected at 28 days aging, in 0.5RPFM and 1RPFM, respectively, by comparison to CM. At the age of 194 days, the compressive strength increases from 15% in 0.5RPFM to 26% in 1RPFM, by comparison to CM. According to some previous studies (Santos et al., 2005; Ramezanianpour et al., 2013; Alaskar et al., 2021), the use of polypropylene fibres as reinforcement in cement composites, reduces their compressive strength. Bentur & Mindess (2007) justify the compressive reduction by the difficulties to achieve a full compaction, which encourages the creation of porosity in the material, particularly by using high amount of fibres. The positive effect of the recycled polypropylene fibres is not limited only to mechanical strength of mortars, but also to their post-cracking, when the high capacity of these fibres to bridge cracks and to prevent their opening is well observed during all crush concrete tests.

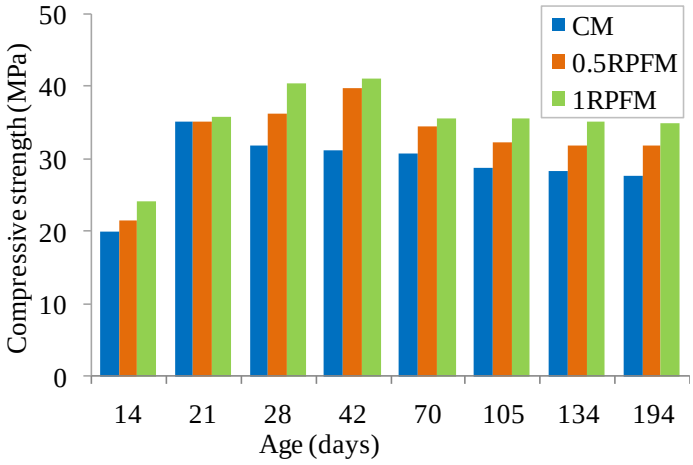


Fig.4: Variation of compressive strength of cement mortars

3.4 Total Shrinkage

The total shrinkage in all tested materials is in continuous evolution with the time, as seen in Figure 5. It is well observed that the shrinkage evolution is more important at early age, due to the effect of the conservation conditions (45 °C and 30% HR) on the evaporation of mixing water. The heat generated by the hydration reaction of cement during the first time of the preparation of mortars is also other parameter accelerating the water evaporation, which increases the risk of shrinkage. Several studies (Tolêdo Filho et al., 2005; Bouziadi et al., 2016), confirmed that the curing conditions do not affect only the initial rate of shrinkage, but also its magnitude. A stabilization of the values of shrinkage is observed at 78 days in CM and at 108 days in 0.5RPFM and 1RPFM. Furthermore, the presence of recycled polypropylene fibres in cement mortar considerably reduces the evolution and the amount of the shrinkage; in 1RPFM, the shrinkage is reduced by 74%, 56% and 46% at 1, 28 and 190 days of aging respectively, compared to CM. In other study (Branch et al., 2002), the reduction of the shrinkage reached up to 85% compared to ordinary concrete. It is remarked through these results that the used fibres act as a barrier against any shrinking movement in cement mortar. The

efficiency of recycled polypropylene fibres to reduce the total shrinkage can also be due to their good dispersion into the mortar mass. Jafarifar et al., (2014) confirmed that in fibre reinforced concrete, the evolution of free shrinkage is more uniform than in unreinforced concrete. Nevertheless, some authors (Mesbah & Buyle-Bodin, 1999) see that the ability of fibres to reduce cracking width is more than their ability to reduce free shrinkage value in mortars. Other researchers (Ma et al., 2004) have confirmed that polypropylene fibres decrease the number of larger cracks in cement mortar, but they increase the finer ones.

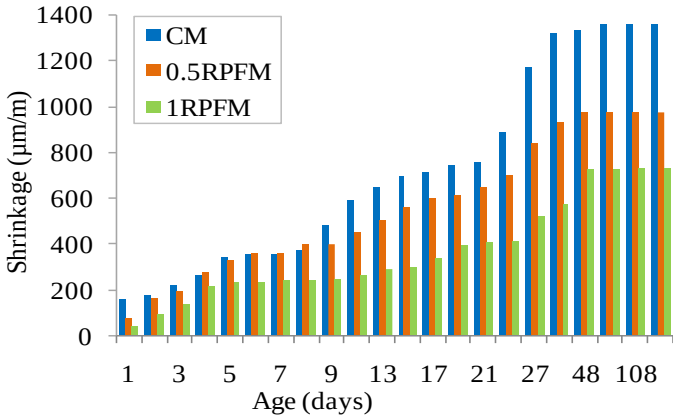


Fig.5: Variation of total shrinkage in cement mortars

4 Conclusion

From the present study, the following conclusions can be drawn:

- As many other types of fibres, the recycled polypropylene fibres have an adverse effect on the mortar consistency, particularly under arid conditions.
- The arid conditions which are characterised by low humidity and high temperature improve the early age mechanical strength of cement mortars, while their effect on the long-term strength is negative. At 28 days aging, the increase percentage of the flexure strength is about 116%, 86% and 101% in CM, 0.5RPFM and 1RPFM, respectively, compared to reference values; for the compressive strength, it reaches 76%, 63% and 49%, respectively. At the age of 194 days, the percentage decreases to 18% in CM and 0.5RPFM and 20% in 1RPFM for the flexure strength and to 39%, 47% and 45%, respectively, for the compressive strength.
- The recycled polypropylene fibres improve both the flexure and the compressive strength of mortars under arid conditions; in the mortar 1RPFM, the improvement is about 24% and 26% for the flexure and the compressive strength respectively, compared to CM, at the age of 194 days.
- The mortars conserved under arid condition rapidly develop more shrinkage with high values.
- The presence of recycled polypropylene fibres into the mass of mortars conserved under arid conditions shows down the evolution of their shrinkage and reduces its final values, when the reduction exceeds 46% in 1RPFM, by comparison to CM.
- The recycled polypropylene fibres improve the failure mode of tested mortars, by bridging cracks.

References

ACI Committee 308R-16. (2016). Guide to External Curing of Concrete, American Concrete Institute.

Adnan, H. M, & Dawood, A, O, (2020). "Strength behavior of reinforced concrete beam using re-cycle of PET wastes as synthetic fibers", *Case Studies in Construction Materials, 13*, e00367. https://doi.org/10.1016/j.cscm.2020.e00367.

Al-Amoudi, O. S. B, Maslehuddin, M., Shameem, M., & Ibrahim, M. (2007). "Shrinkage of plain and silica fume cement concrete under hot weather", *Cement & Concrete Composites, 29*(9), 690-699. https://doi.org/10.1016/j.cemconcomp.2007.05.006.

Alaskar, A, Alabduljabbar, H., Mohamed, A. M., Alrshoudi, F., & Alyousef, R. (2021). "Abrasion and skid resistance of concrete containing waste polypropylene fibers and palm oil fuel ash as pavement material", *Construction & Building Materials, 282*, 122681. https://doi.org/10.1016/j.conbuildmat.2021.122681.

Al-Hadithi, A. I., & Hilal, N. N. (2016). "The possibility of enhancing some properties of self-compacting concrete by adding waste plastic fibers", *Journal of Building Engineering, 8*, 20-28. https://doi.org/10.1016/j.jobe.2016.06.011.

Almusallam, A. A. (2001). "Effect of environmental conditions on the properties of fresh and hardened concrete", *Cement & Concrete Composites, 23*(4-5), 353-361. https://doi.org/10.1016/S0958-9465(01)00007-5.

Belferrag, A., Kriker, A., Abboudi, S., & Tié Bi, S. (2016). "Effect of granulometric correction of dune sand and pneumatic waste metal fibers on shrinkage of concrete in arid climates", *Journal of Cleaner Production, 112*(4), 3048-3056. https://doi.org/10.1016/j.jclepro.2015.11.007.

Bendjillali, K., Chemrouk, M., Goual, M. S., & Boulekbache, B. (2013). "Behaviour of polypropylene fibre mortars conserved in different environments", *European Journal of Environmental & Civil Engineering, 17*(8), 687-699. http://dx.doi.org/10.1080/19648189.2013.812685.

Bentur, A., Mindess, S., (2007). Fibre Reinforced Cementitious Composites, 2nd ed, Pub Taylors & Francis.

Bin, C., Ansheng, W., & Feng, F. (2020). "Bond behavior of PP fiber-reinforced cinder concrete after fire exposure", *Computers & Concrete, 26*(2), 115-125. https://doi.org/10.12989/cac.2020.26.2.115.

Borg, R. P., Baldacchino, O., & Ferrara, L. (2016). "Early age performance and mechanical characteristics of recycled PET fibre reinforced concrete", *Construction & Building Materials, 108*, 29-47. https://doi.org/10.1016/j.conbuildmat.2016.01.029.

Bouziadi, F., Boulekbache, B., & Hamrat, M. (2016). "The effects of fibres on the shrinkage of high-strength concrete under various curing temperatures", *Construction & Building Materials, 114*, 40-48. https://doi.org/10.1016/j.conbuildmat.2016.03.164.

Branch, J, Rawling, A., Hannant, D. J., & Mulheron, M. (2002). "The effect of fibres on the plastic shrinkage cracking of high strength concrete", *Materials & Structures, 35*(3), 189-194. https://doi.org/10.1007/BF02533588.

Caggiano, A., Gambarelli, S., Martinelli, E., Nisticò, N., & Pepe, M. (2016). "Experimental characterization of the post-cracking response in hybrid steel/polypropylene fiber-reinforced concrete", *Construction & Building Materials, 125*, 1035-1043. https://doi.org/10.1016/j.conbuildmat.2016.08.068.

Cifuentes, H., García, F., Maeso, O., & Medina, F. (2013). "Influence of the properties of polypropylene fibres on the fracture behaviour of low-, normal-and high-strength FRC", *Construction & Building Materials, 45*, 130-137. https://doi.org/10.1016/j.conbuildmat.2013.03.098.

Dreux, G, & Festa, J. (2002). Nouveau guide du béton et de ses constituants, 8th ed, Eyrolles.

Gallucci, E., Zhang, X., & Scrivener, K. L. (2013). "Effect of temperature on the microstructure of calcium silicate hydrate (C-S-H)", *Cement & Concrete Research, 53*, 185-195. https://doi.org/10.1016/j.cemconres.2013.06.008.

García Santos, A., Rincón, J. M., Romero, M., & Talero, R. (2005). "Characterization of a polypropylene fibered cement composite using ESEM, FESEM and mechanical testing", *Construction & Building Materials, 19*(5), 396-403. https://doi.org/10.1016/j.conbuildmat.2004.07.023.

Faraj, R. H., Hama Ali, H. F., Sherwani, A. F. H., Hassan, B. R., & Karim, H. (2020). "Use of recycled plastic in self-compacting concrete: A comprehensive review on fresh and mechanical properties", *Journal of Building Engineering, 30*, 101283. https://doi.org/10.1016/j.jobe.2020.101283.

Jafarifar, N., Pilakoutas, K., & Bennett, T. (2014). "Moisture transport and drying shrinkage properties of steel-fibre-reinforced-concrete", *Construction & Building Materials, 73*, 41-50. https://doi.org/10.1016/j.conbuildmat.2014.09.039.

Jain, A., Sharma, N., Choudhary, R., Gupta, R., & Choudhary, S. (2021). "Utilization of non-metalized plastic bag fibers along with fly ash in concrete", *Construction & Building Materials, 291*, 123329. https://doi.org/10.1016/j.conbuildmat.2021.123329.

Khan, M. I., & Abbas, Y. M. (2017). "Curing optimization for strength and durability of silica fume and fuel ash concretes under hot weather conditions", *Construction & Building Materials, 157*, 1093-1105. https://doi.org/10.1016/j.conbuildmat.2017.09.173.

Khan, M. U., Nasir, M., Al-Amoudi, O. S. B., & Maslehuddin, M. (2021). "Influence of in-situ casting temperature and curing regime on the properties of blended cement concretes under hot climatic conditions", *Construction & Building Materials, 272*, 121865. https://doi.org/10.1016/j.conbuildmat.2020.121865.

Kriker, A. et al. (2008). "Durability of date palm fibers and their use as reinforcement in hot dry climates", *Cement & Concrete Composites, 30*(7), 639-648. https://doi.org/10.1016/j.cemconcomp.2007.11.006.

Mesbah, H. A., & Buyle-Bodin, F., (1999). "Efficiency of polypropylene and metallic fibres on control of shrinkage and cracking of recycled aggregate mortars", *Construction & Building Materials, 13*(8), 439-447. https://doi.org/10.1016/S0950-0618(99)00047-1.

Mohajerani, A., Hui, S. Q., Mirzababaei, M., Arulrajah, A., Horpibulsuk, S., Abdul Kadir, A., Rahman, M. T., & Maghool, F. (2019). "Amazing types, properties, and applications of fibres in construction materials", *Materials, 12*, 2513. https://doi.org/10.3390/ma12162513.

Mohammadhosseini, H, & Tahir, M. M. (2018). "Durability performance of concrete incorporating waste metalized plastic fibres and palm oil fuel ash", *Construction & Building Materials, 180*, 92-102. https://doi.org/10.1016/j.conbuildmat.2018.05.282.

Mohammed, A. A., & Mohammed, I. I. (2021). "Effect of fiber parameters on the strength properties of concrete reinforced with pet waste fibers", *Iranian Journal of Science & Technology, Transactions of Civil Engineering, 45*, 1493-1509. https://doi.org/10.1007/s40996-021-00663-2.

Park, K., & Noguchi, T. (2017). "Effects of mixing and curing temperature on the strength development and pore structure of fly ash blended mass concrete", *Advances in Materials Science & Engineering*, 2017, Article ID 3452493. https://doi.org/10.1155/2017/3452493.

Pereira de Oliveira, L. A., & Castro-Gomes, J. P. (2011). "Physical and mechanical behaviour of recycled PET fibre reinforced mortar, *Construction & Building Materials, 25*(4), 1712-1717. https://doi.org/10.1016/j.conbuildmat.2010.11.044.

Pešić, N., Živanović, S., Garcia, R., & Papastergiou, P. (2016). "Mechanical properties of concrete reinforced with recycled HDPE plastic fibres", *Construction & Building Materials, 115*, 362-370. https://doi.org/10.1016/j.conbuildmat.2016.04.050.

Ramezanianpour, A. A., Esmaeili, M., Ghahari, S. A., & Najafi, M. H. (2013). "Laboratory study on the effect of polypropylene fiber on durability, and physical and mechanical characteristic of concrete for application in sleepers", *Construction & Building Materials, 44*, 411-418. https://doi.org/10.1016/j.conbuildmat.2013.02.076.

Sengul, O. (2016). "Mechanical behavior of concretes containing waste steel fibers recovered from scrap tires", *Construction & Building Materials, 122*, 649-658. https://doi.org/10.1016/j.conbuildmat.2016.06.113.

Silva, E. R., Coelho, J. F. J., & Bordado, J. C. (2013). "Strength improvement of mortar composites reinforced with newly hybrid-blended fibres: Influence of fibres geometry and morphology", *Construction & Building Materials, 40*, 473-480. https://doi.org/10.1016/j.conbuildmat.2012.11.017.

Standards EN 196-1. (2005). Methods of testing cement - Part 1: Determination of strength. European Committee for Standardization, Brussels.

Tang, Y., Su, H., Huang, S., Qu, C., & Yang, J. (2017). "Effect of curing temperature on the durability of concrete under highly geothermal environment", *Advances in Materials Science & Engineering*, 2017, Article ID 7587853. https://doi.org/10.1155/2017/7587853.

Tolêdo Filho, R. D., Ghavami, K., Sanjuán, M. A., & England, G. L. (2005). "Free, restrained and drying shrinkage of cement mortar composites reinforced with vegetable fibres", *Cement & Concrete Composites, 27*(5), 537-546. https://doi.org/10.1016/j.cemconcomp.2004.09.005.

Yin, S., Tuladhar, R., Shi, F., Combe, M., Collister, T., & Sivakugan, N. (2015). "Use of macro plastic fibres in concrete: A review", *Construction & Building Materials, 93*, 180-188. https://doi.org/10.1016/j.conbuildmat.2015.05.105.

Zeyad, A. M. (2019). "Effect of curing methods in hot weather on the properties of high-strength concretes", *Journal of King Saud University-Engineering Sciences, 31*(3), 218-223. https://doi.org/10.1016/j.jksues.2017.04.004.

Zhang, S., & Zhao, B. (2012). "Influence of polypropylene fibre on the mechanical performance and durability of concrete materials", *European Journal of Environmental & Civil Engineering, 16*(10), 1269-1277. https://doi.org/10.1080/19648189.2012.709681.

Cite as: Bendjillali K. & Chemrouk M., "Recycled Polypropylene Fibres for Reinforcing Cement Mortar under Arid Conditions", *The 2nd International Conference on Civil Infrastructure and Construction (CIC 2023)*, Doha, Qatar, 5-8 February 2023, DOI: https://doi.org/10.29117/cic.2023.0063

Corrected Rock Fracture Parameters Applied to Qatari Rock Masses

Hrvoje Vučemilović
Faculty of Civil Engineering and Architecture, University of Osijek, Osijek, Croatia
hvucemilovic@gfos.hr

Abstract

This paper is the continuation of the author's previous publications and an attempt to shed light on some of the presented propositions, therein. In his previous work, the author introduced a novel parameter for borehole rock mass evaluation, the FI_C, (Fracture Index Corrected) and applied it to Qatari rock masses along with RQD_C (Rock Quality Designation Corrected). This was the first case of such wide scale application of these borehole evaluation parameters. A short history is given on alternative proposals by several authors for improvements and amendments of *RQD* (Rock Quality Designation) since its proposal in 1963, with their authors' commentaries. Scale considerations are presented for both parameters, which are an essential consideration factor for any borehole parameter. The paper is concluded with remarks on assumed advantages and limitations of the two parameters and their future research and usage prospects. The paper is concluded with statements that Qatari rock masses are of unique type, which has not been sufficiently researched or classified by the leading world scientists in this field.

Keywords: Qatar; Rock masses; Rock mechanics; Corrected Rock Quality Designation; Corrected Fracture Index

1 Introduction

In this paper, the author has utilized the same data set which was used by Vučemilović et al. (2021), which consisted of exploration data from 201 boreholes spread over the southern regions and suburbs of the city of Doha. An analysis of relationship between *RQD* and λ (fracture frequency equivalent to *FI* – Fracture Index, or *FF* – fracture frequency) parameters shows how Qatari rock masses cannot be compared with a database of worldwide rock masses e.g. from (Russo & Hormazabal, 2019).

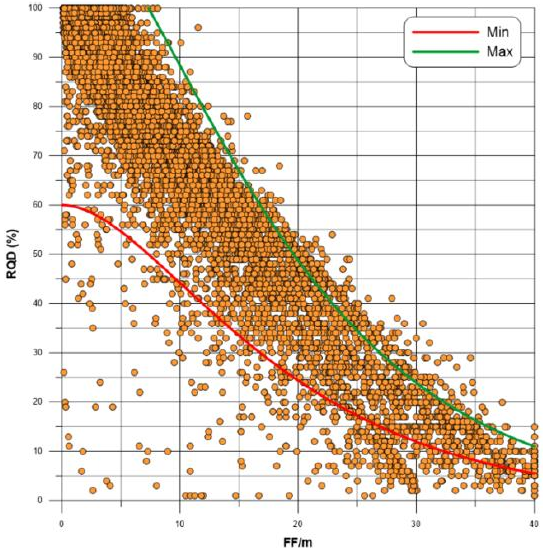


Fig. 1: Relation between *RQD* and mean fracture frequency λ (*FF* – Fracture Frequency) according to Russo & Hormazabal (2019)

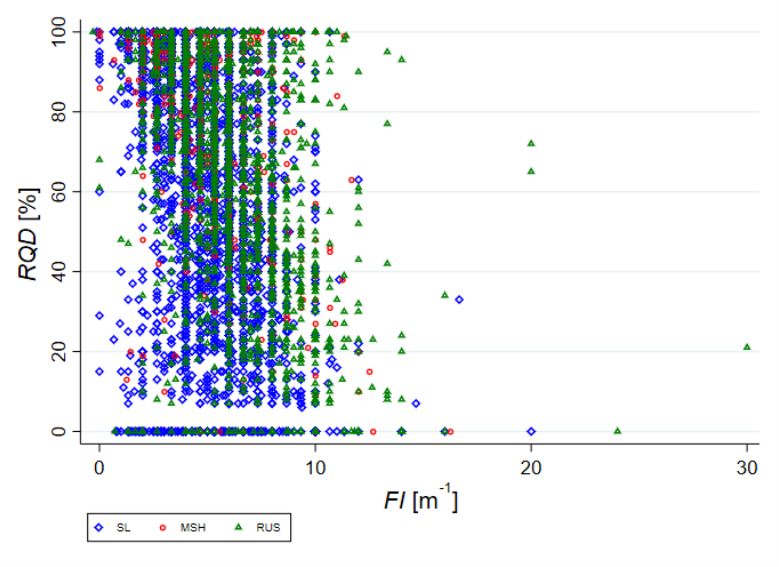


Fig. 2: Relation between *RQD* and frequency λ (*FI*) for Qatari rock masses

The theoretical relationship between *RQD* and λ is loosely linear and has been established by Priest and Hudson (1976) as one where *RQD* tends to decrease with the increase of λ in a more or less a narrow band diagonally. This was confirmed by Russo and Hormazabal (2019) who have collected over 30,000 data points from varied rock mases (Figure 1). This is not the case, however, for elaborated Qatari rock masses, which display a different trend in Figure 2, where the dependence is also in a (wider) band but vertically down across entire span of *RQD* values. The graph is differentiated for SL (Simsima limestone), MSH (Midra shale) and RUS (Rus formation) geological members. It can be observed that RUS member assumes minimal *RQD* values to a lesser extent than SL member, which is likely owed to the fact that SL layer Weathered Simsima is the most fractured of all layers from all three geological members. Data points for MSH member do not allow any similar conclusions.

Section 2 provides definitions in connection with *RQD*, λ (*FF*, *FI*), RQD_C and FI_C parameters relevant to this paper. Section 3 gives a review from the existing literature of some proposals on alternative parameters, improvements, and amendments of *RQD*, as it was originally proposed by Deere (1963) and Deere and Deere (1988), and includes their authors' commentaries on the prospects of their usage. At the end of this section, the most suitable parameter for Qatari rock masses is discussed and chosen. In section 4, scale considerations for both parameters are discussed in detail with conclusions on the applicability of scanning length adjustments of subject parameters for Qatari rock masses, given the maximum core box length utilized in Qatar. The conclusions section, similarly, discusses the author's stance on the advantages and limitations of the new parameters and presumed prospects for their further research and usage, and ends with a general commentary on uniqueness of Qatari rock masses in wider terms.

2 Definitions

RQD is a rock evaluation parameter introduced by Deere (1963) as a parameter of estimation using exploratory boreholes. It is defined as sum of all solid core pieces, which are at least 10 cm long in a core run, divided by the total length of the core run. The equation by Hudson and Harrison (2000) addresses the theoretical relationship between the theoretical *RQD* (*RQD**), fracture frequency λ, and length of the threshold *t*, which is assumed to have an arbitrary value.

$$RQD^* = 100(t\lambda + 1)e^{-t\lambda} \quad (1)$$

Fracture frequency λ is number of discontinuities in a core run divided by its total length, that is, number of discontinuities per meter of core run.

Li et al. (2009) have proposed a corrected *RQD* parameter, or RQD_C, which is expressed by a formula:

$$RQD_C = \frac{p_r}{N^a} \quad (2)$$

Where p_r is percentage of core recovery, or *SCR* (Solid Core Recovery), and *N* is the number of unbroken core pieces in a core run and *a* is the exponent of a power law function.

Author's proposed corrected *FI* parameter (FI_C) can be defined as (Vučemilović et al. 2021):

$$FI_C = \frac{100(N-1)}{p_r L} \quad (3)$$

where p_r is the percentage of recovery, or *SCR* (0–100), *N* is the number of cores in a core run, and *L* is the length of a core run.

3 Some Alternative Borehole Fracturing Parameter Proposals

Azimian (2015) has proposed an improved *RQD* parameter (*RQDI*), which takes into account joint angles and orientations from the *WJD* (Weighted Joint Density) method developed by Haftani et al. (2015) but also considers fractured zones, crushed zones, and void zones (referred to as vuggy or karstic zones). The proposal is presented with the formula

$$RQD_I = 100 - \left[100 \frac{f_i + CW + Fr + Cr + K}{L_t} \right] \quad (4)$$

Where, f_i is the value from Haftani et al. (2015), *CW* is the length of the void, or *K* washed core segment, *Fr* is the length of the fragmented core segment (with spacing of 15 – 50 mm), *Cr* is the length of the crushed core segment (with spacing < 15 mm). L_t is total core run length.

Araghi et al. (2006) proposed the modified *RQD* parameter, *MRQD*. This parameter is obtained by subtracting the weak zone parameter *WZ* from the value 100.

$$MRQD = 100 - WZ \quad (5)$$

$$WZ = \frac{1.5nd + CW + Fr + Cr + VZ + C}{L_t} \quad (6)$$

Where, *nd* is the number of discontinuities, *CW* is washed core portion length, *Fr* is fragmented core portion length, *Cr* is crushed core portion length, *VZ* is vuggy core portion length, *C* is void core portion length, and L_t is total core run length. The method is very similar to the one introduced by Azimian (2015) but it does not include the joint orientation parameter f_i.

Ahmed (2013) proposed a modified *RQD*, which is similar to that of RQD_C, designated as *RQDm*. He suggested that the logging session includes the core pieces lesser than 10 cm and lesser than 5 cm, along with those larger than 10 cm.

$$RQDm = \frac{\sum pu}{N^f} \quad (7)$$

$$\sum pu = pu1 + pu2 + pu3 \quad (8)$$

$$f = f1 \times f2 \times f3 \quad (9)$$

Where, $f1 = 1.003 pu1$, $f2 = 1.001 pu2$ and $f3 = 0.99005 pu3$

and where,

$pu1$ - percentage of core pieces less than 5 cm

$pu2$ - percentage of core pieces 5 – 10 cm

$pu3$ - percentage of core pieces > 10 cm

N – number of cores

f – exponent of the power function

The next question raised is; which *RQD* modification is best suited for the rock masses at hand? The author has concluded that the most suitable parameter for estimation of the subject rock masses is the *RQD* corrected, RQD_C, which was proposed by Li et al. (2009).

1. The parameter is simple and does not have a very detailed decomposition of types, length wise, of core run segments;
2. Its starting point is p_r, percentage of recovery, or *SCR*, as opposed to the maximum value of 100 (as proposed for *RQDI* and *MRQD*), which is considered a bias;
3. Unlike *RQDm*, the RQD_C does not have a fixated exponent value, which proves to be very useful since it lends adjustability.

4 Scale Considerations for Rqd_c And Fi_c

If we consider the data at hand from the Qatari rock masses, we must note the following:

1. RQD_C and FI_C values were calculated, for great majority of data, with 1.5 m scanning interval.
2. It would be of interest to develop theoretical dependencies of RQD_C vs FI_C, such as for 1.0 metre scanning intervals.
3. Similarly, it would be of interest to present theoretical dependence of RQD_C vs FI_C for different lengths of scanning interval and how this dependence changes for different values of *SCR* parameter.

Figure 3 shows theoretical FI_C versus RQD_C for different values of solid core recovery (*SCR*, or p_r). All curves display a logarithmic relationship. The larger the *SCR*, the lower is the maximum reached FI_C value. The lesser *SCR*, the steeper is the increase of FI_C over smaller RQD_C spans, and this span gradually shifts toward ever lower RQD_C values.

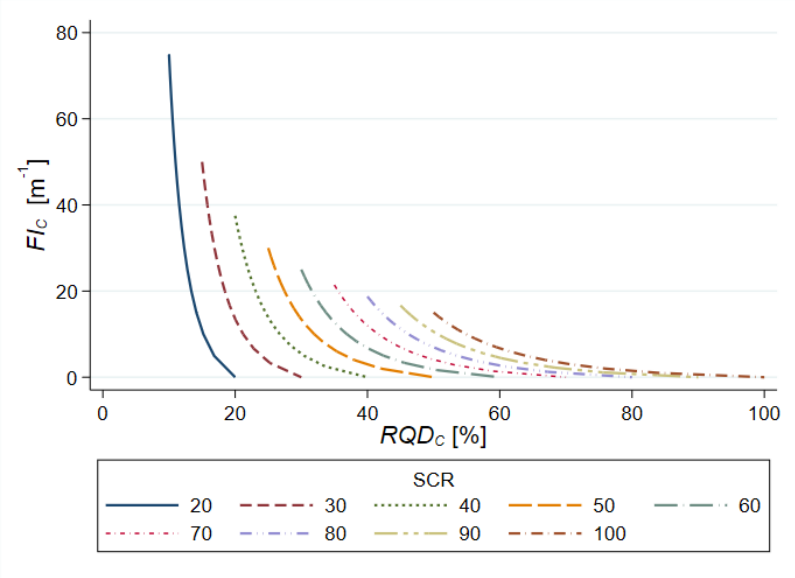


Fig. 3: Theoretical variation of FI_C versus RQD_C, for different values of *SCR* and exponent *a* value (of RQD_C) of 0.25, and scanning interval of 1.0 m

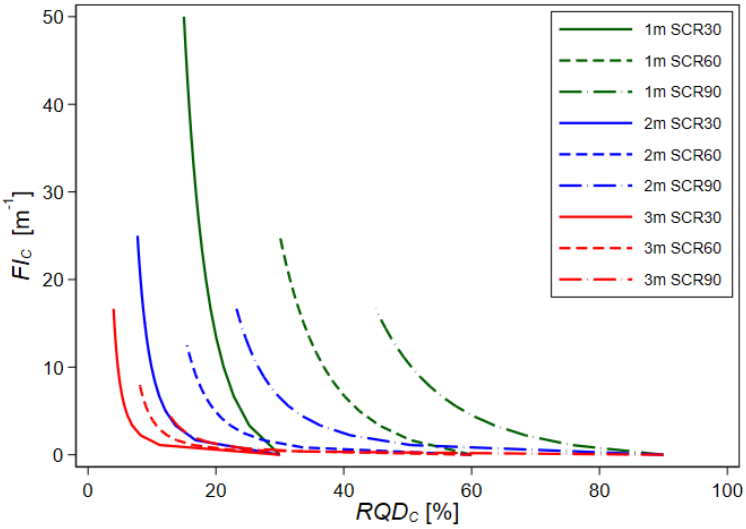


Fig. 4: Theoretical variation of FI_C versus RQD_C, for different scanning intervals and values of *SCR* for exponent *a* value (of RQD_C) of 0.25

In Figure 4, the theoretical dependence of RQD_C vs FI_C is shown for three different scanning interval lengths including 1.0 m, 2.0 m, 3.0 m, and *SCR* values of 30, 60, and 90. We can see overall reduction of FI_C and RQD_C in magnitude and span with increased scanning interval, but within the same scanning interval, FI_C is decreasing and RQD_C is increasing with the increase of *SCR*. The latter is an identical tendency as in Figure 3.

The graphs in Figures 5 and 6 display the values of RQD_C and FI_C versus scanning intervals, which were given to obtain the borehole core box data. The predominant interval is 1.5 m although it may not be readily visible from the graphs due to the point density. Table 1 shows the percentages of three most frequent scanning interval lengths, over the entire data sets for RQD_C and FI_C.

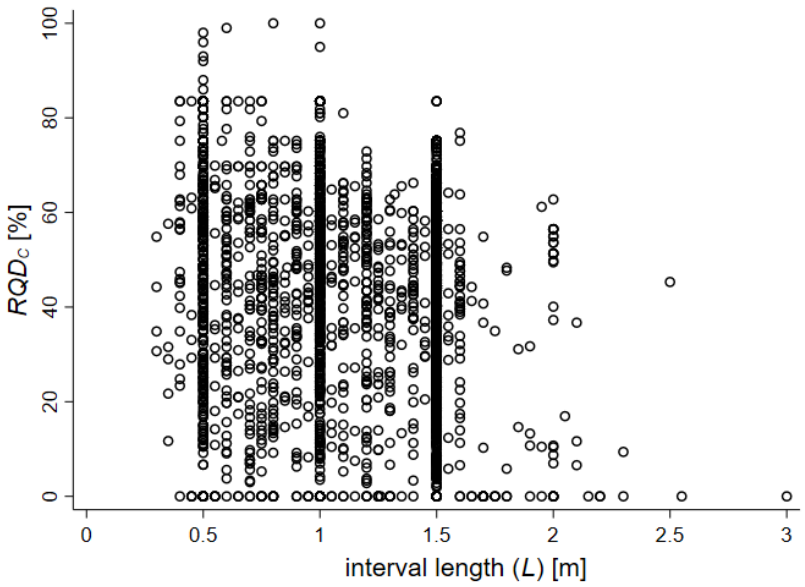


Fig. 5: RQD_C values against scanning interval lengths

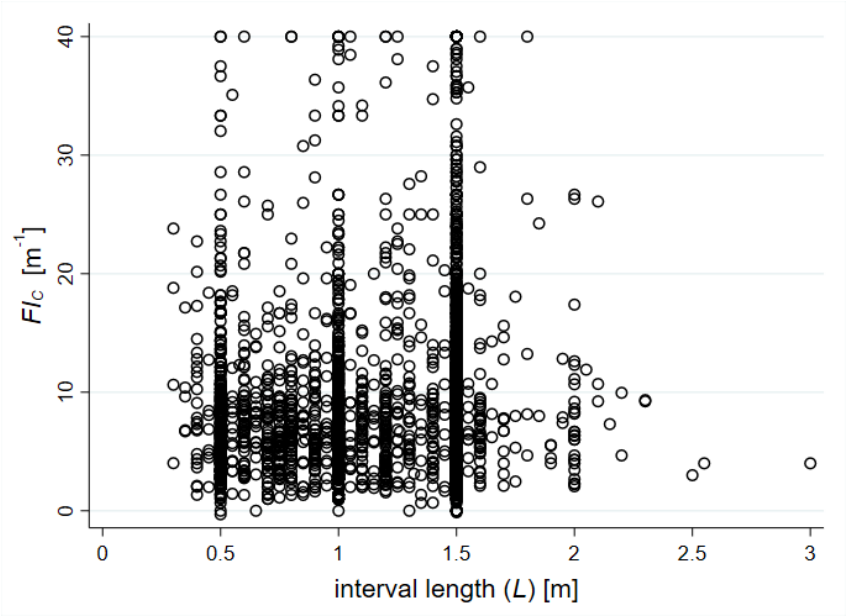


Fig. 6: FI_C values against scanning interval lengths

Table 1: Proportions of different scanning intervals for RQD_C and FI_C

	***L* = 0.5 m**	***L* = 1.0 m**	***L* = 1.5 m**	***L* = other**
***RQD*C & *FI*C**				
n	359	627	3314	1363
percentage	6.3 %	11.0 %	58.5 %	24.0 %

5 Conclusions

RQD is the most frequently used ubiquitous rock evaluation parameter, but obviously it does not work on all rock masses, e.g. on jointed shales as testified by Barton (2021 – personal correspondence). In

this paper, a short review is presented on some propositions from the available literature on alternatives to standard *RQD* by previous authors, along with commentaries from authors which argue against the wide spread usage of their parameters. Author has used these previous proposals to come up with the comparative conclusion on which parameter could be suited for Qatari rock masses. A new corrected parameter was selected and investigated, the RQD_C together with author's proposed corrected fracturing index (FI_C). The RQD_C parameter applied to Qatari rock masses displays, as opposed to *RQD*, statistical soundness and accordingly possesses the potential for practical usage and further research. The advantage of using the corrected parameters is their greater sensitivity for detection of fractures (RQD_C and FI_C) and loose core portions (FI_C). Possible limitations of the FI_C parameter are that it can only be used for slightly and moderately weathered rock masses, otherwise it might not be useful for detecting weathered spots within fresher rock masses. Scale considerations were also taken into account for both parameters towards the end of this paper and, as expected, both parameters reduce with scale increase. However, these considerations are warranted only in locations, countries or areas which use core box lengths above 1.5 m, which is maximum length used in Qatar. Minor adjustments at smaller scanning lengths are considered not impactful. Conclusively, Qatari rock masses are a separate "stock" of rock masses not falling under any group of rock masses researched so far by the world's-leading scientists in the field, and as such they possess features worthy of a wider systematic research effort.

References

Ahmed, T. M. F (2013). Modified Value of Rock Quality Designation Index RQD in Rock Formation. International Conference on Case Histories in Geotechnical Engineering. 1. https://scholarsmine.mst.edu/icchge/7icchge/session05/1

Araghi, M. S., Samani, F. B. & Goudarzi, M. T. (2006). A proposal for the modification of RQD (MRQD), ISRM International Symposium 2006, 4th Asian Rock Mechanics Symposium, Rock mechanics in underground construction, 8-10 November Singapore, Leung CF and Zhou YX (eds) © 2006 by World Scientific Publishing Co. Pte. Ltd, ISBN 981-270-437-X.

Azimian, A. (2015). A New Method for Improving the RQD Determination of Rock Core in Borehole. Rock Mechanics and Rock Engineering. Springer-Verlag Wien 2015. 10.1007/s00603-015-0789-8.

Deere, D. U. (1963). Technical description of rock cores for engineering purposes. *Rock mechanics and engineering geology 1*(1): 18. Vienna: Springer.

Deere, D. U. & Deere, D. W. (1988). The Rock Quality Designation (RQD) Index in Practice. In: Rock Classification Systems for Engineering Purposes, Kirkaldie, L. (Ed.). American Society for Testing and Materials, Philadelphia, ISBN: 0-8031-0988-1, pp: 91-101.

Haftani, M. et al. (2015). Practical Investigations on Use of Weighted Joint Density to Decrease the Limitations of RQD Measurements. Rock Mechanics and Rock Engineering, June 2015. 10.1007/s00603-015-0788-9.

Hudson, J. A. & Harrison, J. P. (2000). *Engineering Rock Mechanics*. Amsterdam: Pergamon.

Li, L., Ouellet, S. & Aubertin M. (2009). An improved definition of rock quality designation, RQDc. ROCKENG09: Proceedings of the 3rd CANUS Rock Mechanics Symposium, Toronto, May 2009 (Ed: M.Diederichs and G.Grasselli).

Priest, S. & Hudson, J. (1976). Discontinuity Spacings in Rock. *Int. J. Rock Mech. & Min. Sci & Geomechanics Abstracts, 13*(5), 1976, pp. 135-148.

Russo, A. & Hormazabal, E. (2019). Correlations between various rock mass classification systems including Laubscher (MRMR), Barton (Q) and Hoek and Marinos (GSI) systems. Geotechnical Engineering in the XXI century1: lessons and future challenges, NP Lopez-Acosta et al. (Eds), © the Authors and IOS Press, CC BY-NC 4.0, https://doi.org/10.3233/STALI90347

Vučemilović, H., Mulabdić, M. & Miščević, P. (2021). Corrected Rock Fracture Parameters and Other Empirical Considerations for the Rock Mechanics of Rock Masses of Doha, Qatar. *Geotech Geol Eng*, *39*, 2823–2847 (2021). https://doi.org/10.1007/s10706-020-01658-y

Cite as: Vučemilović H., "Corrected Rock Fracture Parameters Applied to Qatari Rock Masses ", *The 2nd International Conference on Civil Infrastructure and Construction (CIC 2023)*, Doha, Qatar, 5-8 February 2023, DOI: https://doi.org/10.29117/cic.2023.0064

Significance of GOs, GNPs and CNTs' Nanomaterials on the Mechanical Properties of Cement

Malak Al Diseet
Tajarub Research & Development, Doha, Qatar
malak.aldiseet@tajarub.org

Mervat Abu Rumman
Tajarub Research & Development, Doha, Qatar
mervat.ruman@tajarub.org

Mu'tasim Abdel-Jaber
Al-Ahliyya Amman University, Amman, Jordan
m.abdeljaber@ammanu.edu.jo

Ramzi Taha
Engineering Program, Schreiner University, Texas, USA
ramzitaha@gmail.com

Mohamed Al Ansari
Department of Civil & Architectural Engineering, Qatar University, Doha, Qatar
m.alansari@qu.edu.qa

Ala AbuTaqa
Department of Civil Engineering, Aqaba University of Technology, Aqaba, Jordan
Aabutaqa@aut.edu.jo

Mohamed Mohsen
Department of Civil & Architectural Engineering, Qatar University;
Tajarub Research & Development, Doha, Qatar
200202128@qu.edu.qa, mohamed.mohsen@tajarub.org

Abstract

This study reports the statistical significance of using Graphene Oxides (GOs), Graphene Nanoplatelets (GNPs) and Carbon Nanotubes (CNTs) on the mechanical properties of cement paste. Samples containing several nanoparticles' weight fractions were prepared and tested for flexure and compression. The testing results were then statistically analysed using the t-statistical method to investigate the significance of using Nanomaterials on the properties of cement paste. The results highlighted the significance of using GOs and CNTs on the flexural strength of cement paste. Mixes containing 0.04% GOs, 0.08% GOs and 0.12% CNTs could enhance the flexural strength by at least 45% compared to the plain control mix. On the other hand, test results showed the significance of using 0.04% GNPs, 0.08% CNTs and 0.12 % GOs in increasing the compressive strength of cement paste by at least 10% compared to the plain control mix. Microstructural analysis using Scanning Electron Microscope (SEM) showed that proper Nanofilaments dispersion in most batches. Furthermore, the analysis highlighted the nanoparticles' impediment within the cement hydration products.

Keywords: Graphene Oxides; Cementitious Nanoparticles; Nano concrete; t-statistical analysis

1 Introduction

In recent years, Nano-inclusions have been given great interest for their use in building materials due to their exceptional thermo-physical, electrical, chemical, and mechanical properties at the Nanoscale (Balaguru & Chong, 2006). In the construction field, Carbon Nanotubes (CNTs), Graphene

Nanoplatelets (GNPs), and Graphene Oxide (GO) are the most promising Nanofillers used to develop concrete, cement mortar, and cement paste with high mechanical performance and smart characteristics. This is due to their unique properties, as each of CNTs, GNPs, and GO possess excellent mechanical properties, high tensile strength, and Young's modulus (Liu et al., 2012; Salvetat et al., 1999; Shen et al., 2013), as well as thermal and electrical conductivity. However, they all differ in structure. CNTs are 1D tubes of carbon with nanoscale diameters and a large aspect ratio (length-to-diameter ratio) (Iijima, 1991). While GNPs are made from a series of parallel 2D graphene sheets of approximately 0.7-100 Nano-meters variation in thickness (Suárez & Prolongo, 2020). On the other hand, GOs is a 2D Nanosheet of highly oxidized carbon atoms decorated with oxygen-containing functional groups on its edges and basal plane (Wang et al., 2010). A literature survey has indicated that incorporating a small dosage of CNTs, GNPs, or GO effectively improves the cement matrix's mechanical properties (Baomin & Shuang, 2019; Mohsen et al., 2017; Yang et al., 2017). No study has reported the best Nanomaterial to achieve the highest cement paste's mechanical properties. This study investigates the significance of using CNTs, GNPs and GOs on the flexural and compressive strength of cement paste.

2 Research Methodology

In this study, three types of Nanoparticles, CNTs, GNPs, and GOs, were added to the cement paste using three weight fractions of 0.04%, 0.08%, and 0.12% Nanofiller-to-cement weight. Table 1 provides a summary of the experimental design including the test groups, prepared batches, types of Nano-inclusions and weight fractions. The testing methodology consisted of preparing and testing hardened samples for flexure and compression after 90 days of curing. Then analysing the results statistically using the t-test method to report the significance of every group combination. Finally, the microstructure of the fractured samples was inspected using a scanning electron microscope (SEM).

Table 1: Test Batches

Test Group	Batch #	Batch Name	Nano-cement Wt.%
Control	1	Plain	-
CNTs	2	0.04 CNT	0.04
	3	0.08 CNT	0.08
	4	0.12 CNT	0.12
GOs	5	0.04 GO	0.04
	6	0.08 GO	0.08
	7	0.12 GO	0.12
GNPs	8	0.04 GNP	0.04
	9	0.08 GNP	0.08
	10	0.12 GNP	0.12

2.1 Materials and Equipment

The cement used was Pozzolana Portland Cement (PPC), complying with EN 197-1:2011. The CNTs used were multi-walled carbon nanotubes of 10-20 nm diameter and 30 μm. The GOs used was a few-layer graphene oxide produced by a modified hummer's method with a layers' thickness of 1 nm. The GNPs used were COOH-functionalized Graphene Nanoplatelets consisting of several sheets of graphene that are chemically exfoliated from natural graphene. Finally, the surfactant used in the dispersion process was a polycarboxylic ether-based superplasticizer. The equipment used included a laboratory mixer, an ultrasonic

wave mixer, a strength testing machine and a scanning electron microscope (SEM).

2.2 Mixing and Testing

The mixing process started by performing the Nanofilaments' dispersion in an aqueous solution using an ultrasonic wave mixer for 30 min at a power of 400 W. The cement was added to the solution, and samples were poured, demoulded after 1 day, and cured for 90 days. After curing, flexural and compressive strength tests were performed according to ASTM C348 and ASTM C109.

2.3 Microstructural Analysis

Microstructure analysis was done using SEM to understand the dispersion and compatibility of the added nanoparticles within the cement hydration products. The procedure was performed using fractured samples that were dried and coated with conductive palladium.

2.4 t-Statistical Analysis

t-statistical tests were used to evaluate the significance of using Nanoparticles compared with the plain cement paste batch. The test determines if a difference in the means of two groups happens due to a random possibility. The following conditions were taken into consideration:

- A two-tailed significance level of 0.05 was considered.
- The null hypothesis is correct when the average strength values of the Nanocomposite mix and the control are equal.
- The null hypothesis is rejected if the t-statistic (τ_{st}) is equal to or larger than the critical t-test value (τ_{cr}).
- When the null hypothesis is rejected, the strength value of the composite mix and the control are considered not equivalent, indicating that the incorporated Nanoparticles improve the strength significantly.
- The degree of freedom (D_f) was determined as:

$$D_f = [(S_1^2/ y_1) + (S_2^2/ y_2)]^2/ [[(S_1^2/ y_1)^2 / (y_1-1)] + [(S_2^2/y_2)^2/ (y_2-1)]] \quad (1)$$

  Where, S_1, S_2 are the standard deviations of samples; 1, 2 and y_1, y_2 are the size of samples 1, 2.

- The standard error (SE) could be computed by the following equation:

$$SD = \sqrt{\left(\left(\frac{S_1{}^2}{y_1} + \frac{S_2{}^2}{y2}\right)\right)} \quad (2)$$

- The T-statistics value (τ_{st}) is determined by:

$$\tau_{st} = |(\boldsymbol{\mu}_1 - \boldsymbol{\mu}_2) / SE| \quad (3)$$

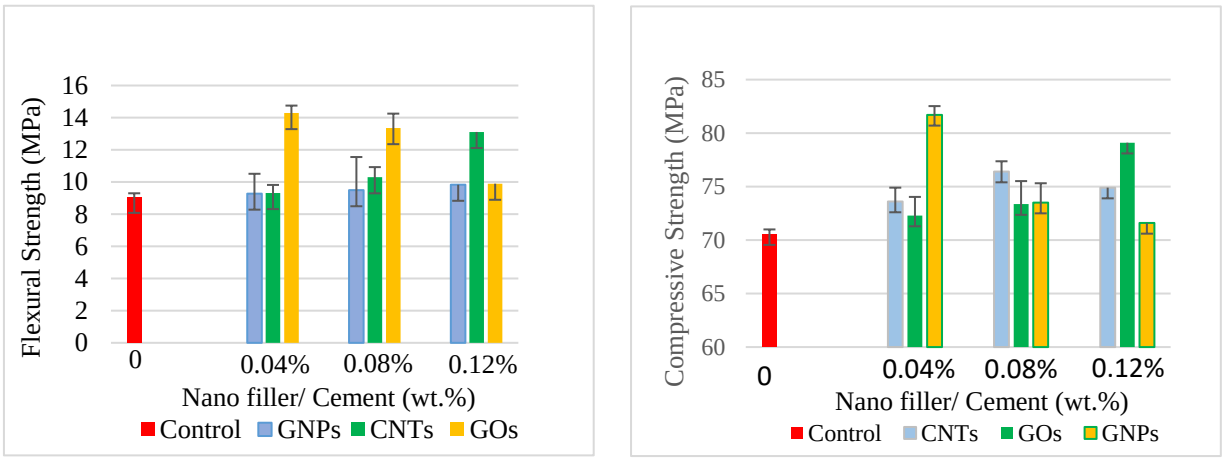
  where$\boldsymbol{\mu}_1$ = average value of sample 1, and $\boldsymbol{\mu}_2$ = average value of sample 2.

3 Results and Discussion

3.1 Flexural and Compressive Strength

Figures 1a and 1b show the flexural and compressive strength results of all batches. Among all batches, the mix containing 0.04 wt.% GOs attained the maximum flexural strength of about 58% compared to the plain cement paste mix. In addition, the mix having 0.08 wt.% GOs had an enhancement of about 48%

compared to the control cement paste mix. For CNTs, the mix containing 0.12% CNTs could attain a flexural strength increase of about 45% compared to the control mix. Unlike GOs and CNTs, GNPs did not show outstanding flexural strength increments regardless of the weight fraction used. All GNPs cementitious composites improvements were in the range of 2-8%. Compressive strength results showed that composites with 0.04 wt.% GNPs attained the highest strength improvement of about 16% compared to the plain cement batch. For CNTs, the results showed that the maximum compressive strength improvement of about 10% could be obtained using a CNTs' weight fraction of 0.08wt.%. For GOs composites, compressive strength results showed that the batch containing 0.12% GOs achieved the greatest improvement of about 12% compared to the control mix.

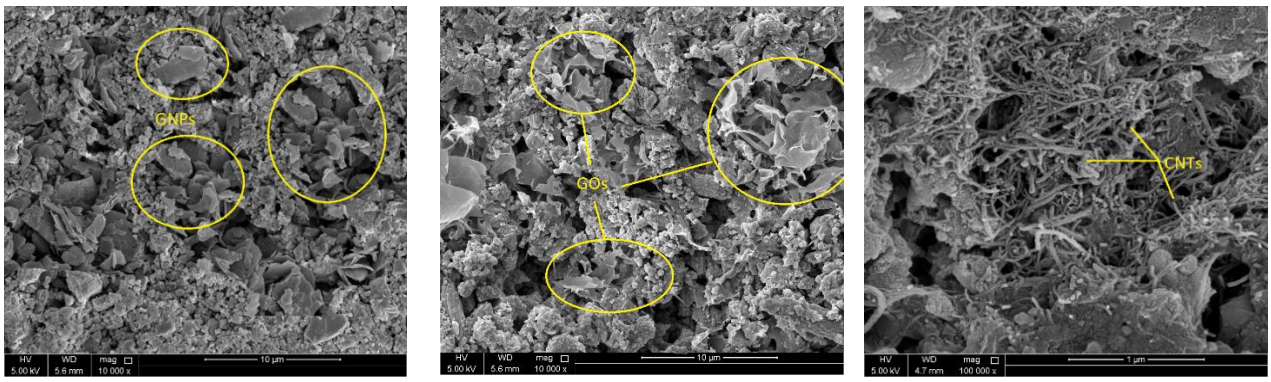


(a) (b)

Fig. 1: (a) Flexural Strength Test Results, and (b) Compressive Strength Test Results

3.2 Microstructural Analysis

SEM images showed that the Nanoparticles were impeded within the cement hydration products. Microstructural investigations of the fractured surfaces did not show clumps or agglomerations, indicating the success of the implemented dispersion procedures. GNPs (Figure 2a) appeared very similar in shape and size to the Calcium hydroxide (CH) hydration products. Similarly, GOs with larger surface areas and a more ductile appearance were impeded into the hydration products showing dense pore structure (Figure 2b). Unlike GNPs and GOs, CNTs were easily located due to their 1 D shape (Figure 2c). CNTs appeared to be dispersed well in all implemented weight fractions representing a proof sheet filing the Nanoscale voids.



(a) (b) (c)

Fig. 2: SEM image of mix containing (a) 0.12wt. % GNPs, (b) 0.12wt. % GOs, and (c) 0.12 wt. % CNTs

3.3 t-Statistical Analysis

t-statistical analysis of the flexural and compressive test results is presented in Tables 2 and 3, respectively. The results showed a significant enhancement in the batches containing 0.12 CNTs, 0.04 GOs and 0.08 GOs. When analyzed statistically, most remaining batches showed no significant enhancement in their flexural strength compared to the control mix. For compressive strength improvements, the statistical analysis showed that significant enhancements occurred in the batches containing 0.08 and 0.12 wt.% CNTs. Also, significant compressive strength enhancements were seen in the batches containing 0.12 GOs and 0.04 GNPs. These findings indicate the significance of adding Nanoparticles to increase both the flexural and compressive strength of cement paste.

Table 2: Flexural Strength Results t-Test

Mix	Degree of Freedom (DF)	Standard Error (SD)	T-Statistic Value (Tst)	Critical T-test Value	Remarks
0.04 CNTs	1	0.264	0.9	12.71	A
0.08 CNTs	2	0.305	3.99	4.303	A
0.12 CNTs	2	0.376	10.73	4.303	R
0.04 GOs	3	0.399	13.04	3.182	R
0.08 GOs	3	0.285	14.98	3.182	R
0.12 GOs	2	0.528	1.54	4.303	A
0.04 GNPs	2	0.684	0.29	4.303	A
0.08 GNPs	2	0.097	4.23	4.303	A
0.12 GNPs	1	0.097	7.69	12.71	A

* A: Accept Null Hypothesis, No Significant Enhancement

** R: Reject Null Hypothesis, Significant Enhancement

Table 3: Compressive Strength Results t-Test

Mix	Degree of Freedom (DF)	Standard Error (SD)	T-Statistic Value (Tst)	Critical T-test Value	Remarks
0.04 CNTs	2	1.213	2.52	2.571	A
0.08 CNTs	2	0.794	7.42	4.303	R
0.12 CNTs	3	0.615	7.12	3.182	R
0.04 GOs	3	0.502	3.47	3.182	A
0.08 GOs	2	1.04	2.7	2.571	A
0.12 GOs	2	1.269	6.72	4.303	R
0.04 GNPs	2	1.546	7.19	4.303	R
0.08 GNPs	2	1.083	2.7	4.303	A
0.12 GNPs	2	0.257	4.24	4.303	A

* A: Accept Null Hypothesis, No Significant Enhancement

** R: Reject Null Hypothesis, Significant Enhancement

4 Conclusions

This study investigates the significance of adding various concentrations of CNTs, GNPs, and GOs on the mechanical properties of cement paste. Mixes containing several Nanoparticles weight fractions were tested for flexure and compression and the results were statistically analysed. SEM images were also captured to visualize the reinforcing mechanism of the Nanoparticles. The following conclusions have been drawn:

i. CNTs, GNPs, and GO exhibited varying behaviors in terms of compressive and flexural strengths; however, all dosages demonstrated an improvement in mechanical properties over the control mix at 90 days.

ii. Among all mixes, the one prepared with 0.04% GNPs achieved the highest compressive strength, while the mix containing 0.04% GO achieved the highest flexural strength, with an increment of about 16% and 58%, respectively, compared to the plain cement paste mix.

iii. t-statistical analysis confirmed the significance of using 0.12 CNTs, 0.04 GOs and 0.08 GOs in increasing the flexural strength of cement paste.

iv. On the other hand, the statistical analysis showed the significance of using 0.12 GOs and 0.04 GNPs in increasing the compressive strength of cement paste.

v. Microstructural analysis using SEM highlighted the impediment of the Nanoparticles within the cement hydration products with proper dispersion all over the matrix.

Acknowledgements

We express our sincere appreciation and gratitude to the Department of Civil Engineering at Al-Ahliyya Amman University and the Department of Quality Control at Cementra Jordan Factory. The statements made herein are solely the responsibility of the author[s].

References

Balaguru, P. & Chong, K. (2006). Nanotechnology and concrete: research opportunities. Proceedings of the ACI Session on Nanotechnology of Concrete: Recent Developments and Future Perspectives, 15-28.

Baomin, W. & Shuang, D. (2019). Effect and mechanism of graphene nanoplatelets on hydration reaction, mechanical properties, and microstructure of cement composites. *Construction and Building Materials, 228,* 116720. https://doi.org/10.1016/j.conbuildmat.2019.116720

Iijima, S. (1991). Helical microtubules of graphitic carbon. *Nature, 354*(6348), 56-58.

Jiménez-Suárez, A. & Prolongo, S. G. (2020). Graphene nanoplatelets. *Applied Sciences, 10,* 1753. https://doi.org/10.3390/app10051753

Liu, L. et al. (2012). Mechanical properties of graphene oxides. *Nanoscale, 4*(19), 5910-5916. https://doi.org/10.1039/C2NR31164J

Mohsen, M. O. et al. (2017). Optimum carbon nanotubes' content for improving flexural and compressive strength of cement paste. *Construction and Building Materials, 150,* 395-403. https://doi.org/10.1016/j.conbuildmat.2017.06.020

Salvetat, J. P. et al. (1999). Mechanical properties of carbon nanotubes. *Applied Physics A, 69*(3), 255-260. https://doi.org/10.1007/s003390050999.

Shen, M. Y. et al. (2013). Mechanical properties and tensile fatigue of graphene nanoplatelets reinforced polymer nanocomposites. *Journal of Nanomaterials*. https://doi.org/10.1155/2013/565401.

Wang, Y. et al. (2010). The chemistry of graphene oxide. *Chem Soc Rev*, *39*, 228-240. http://doi.org/10.1039/B917103G.

Yang, H. et al. (2017). Experimental study of the effects of graphene oxide on microstructure and properties of cement paste composite. *Composites Part A: Applied Science and Manufacturing*, *102*, 263-272. https://doi.org/10.1016/j.compositesa.2017.07.022.

Cite as: Al-Diseet M., Abu Rumman M., Taha R., Al Ansari M., Abutaqa A., Mohamed Mohsen M. & Abdel-Jaber M., "Significance of GOs, GNPs and CNTs' Nanomaterials on the Mechanical Properties of Cement ", *The 2nd International Conference on Civil Infrastructure and Construction (CIC 2023)*, Doha, Qatar, 5-8 February 2023, DOI: https://doi.org/10.29117/cic.2023.0065

A Comparison between Natural Pozzolana and Fly Ash Replacements on the Mechanical Properties of Concrete

Mervat O. Aburumman
Tajarub Research & Development, Doha, Qatar
mervat.ruman@tajarub.org

Malak M. Al-diseet
Tajarub Research & Development, Doha, Qatar
malak.aldiseet@tajarub.org

Mohamed O. Mohsen
Department of Civil and Architectural Engineering, Qatar University;
Tajarub Research & Development, Doha, Qatar
200202128@student.qu.edu.qa, mohamed.mohsen@tajarub.org

Mu'tasim Abdel-Jaber
Al-Ahliyya Amman University, Amman, Jordan
m.abdeljaber@ammanu.edu.jo

Khalid Kamal A A Naji
Department of Civil &Architectural Engineering, Qatar University, Doha, Qatar
knaji@qu.edu.qa

Ala Abu Taqa
Department of Civil Engineering, Munib and Angela Masri Faculty of Engineering,
Aqaba University of Technology, Aqaba, Jordan
aabutaqa@aut.edu.jo

Abstract

This study investigates the effect of Natural Pozzolana (NP) and Fly Ash (FA) substitutes on concrete's mechanical and microstructural properties. Mixes containing 10 – 50 % cement substitute ratios were prepared and tested for flexure and compressive strength after 28 days of curing. Then, qualitative microstructural analysis was performed using Scanning Electron Microscope (SEM). In terms of compressive strength, the mixes containing only 10 % replacement ratios of both NP and FA showed an improvement of 10 % compared to the plain control mix. On the other hand, all mixes containing FA could attain at least a 25 % development in their flexural strength compared to the control mix. The microstructural analysis illustrated that adding FA and NP enhances cement hydration by improving the formation of dense hydration products such as calcium silicate hydrate (C-S-H) and calcium hydroxide (C-H), which are mainly responsible for the performance of the improved mechanical properties of concrete.

Keywords: Natural Pozzolana; Cement Replacements; Strength; Fly Ash; Microstructural Analysis

1 Introduction

Supplemental Cementitious Materials (SCMs), known as pozzolanic materials, are commonly used as fillers in concrete to partially replace cement. SCMs have become popular due to growing sustainability concerns in the construction industry, the need to produce more durable and sustainable concrete, and long-term resistance to harmful chemical reactions (Uzal et al., 2010). Fly ash (FA) is the most widely utilized type of SCM, which has proven itself as the industry standard for producing high-quality and durable concrete due to its low cost and widespread availability (Golewski et al.,

2018; Zabihi-Samani et al., 2018). Since the late 1980s, many studies have been conducted on the properties of concrete impregnated with FA, and many innovative outcomes have been reached. For example, different studies indicate that mechanical performances are generally better at 20-40 % replacement of cement (De Matos et al., 2019; Mehta, 2004; Atiş, 2002). Still, these levels can reach 60 % or higher (Yu et al., 2017; Huang et al., 2013). In addition, no significant reduction in concrete strength was observed at an early age, but more excellent strength gain properties appeared in the long term. It should be noted that the test results for samples treated for a short period could have been very different if the treatment period was longer (Golewski et al., 2018; Toutanji et al., 2004). Also, FA contents can significantly affect the rheological properties of concrete (Khodair et al., 2017; Bentz et al., 2013). In other words, using FA in concrete can produce an environmentally safe green material for civil engineering with structural, financial and environmental advantages.

However, finding practical natural substitutes that perform similarly to FA to improve mechanical and rheological concrete properties is essential because upcoming environmental and safety laws threaten its availability and quality. Therefore, there has been a great trend recently to use Natural Pozzolana (NP) as a natural material resulting from volcanoes with variable mineral, chemical and reactivity properties (Hossain et al., 2021; Shukla et al., 2020; Camacho et al., 2002; Ghrici et al., 2007). In addition to its abundance in different geographical locations, it is an economically viable option as a supplementary cementitious material in concrete production (Khan & Alhozaimy, 2011). Consequently, researchers recently turned to conduct experimental studies to determine the NP effect on concrete. For example, most studies found that using NP to replace approximately 20-30 % of Portland cement improved mechanical performance, particularly compressive strength, reduced chloride ion permeability by 66 %, and self-shrinkage by 40% (Ababneh & Matalkah, 2018; Hijazin et al., 2012). Also, replacing the cement by 50 % improved the concrete's resistance to alkali-silica reactions and sulfate attacks (Turanli et al., 2005). This study aims to compare concrete impregnated with FA and NP in mechanical and microstructure properties with cement replacement ratios ranging from 10 to 50 % in 10 mixes and compare them with a reference mix. The effect of these pozzolanic materials on concrete compressive and flexural strength was evaluated at 28-day. After that, a scanning electron microscope (SEM) was used to analyze the microstructure of the examined samples. Based on the strength results at 28-day, future tests will be directed towards improving and modifying these pozzolanic materials' physical properties and compositions to obtain specific and acceptable cement replacement ratios in concrete composites that give better results in the early ages and long term.

2 Experimental Program

2.1 Materials and Equipment

Cement (CEM II / B-P 42.5 N) conforming to EN 197-1: 2011, coarse aggregate (dolomite limestone) and fine aggregate (sand) used comply with ASTM C-33, in addition to natural pozzolana (ManaseerCrete) complied with ASTM C-618 class N, also, fly ash (class F), which complied with (ASTM C-618). Table 1 presents NP and FA composition and physical properties. A Polycarboxylate-ether superplasticizer (Master Glenium 51) was used in the concrete mixes preparation. The technical properties of Master Glenium 51 are shown in Table 2. A strength testing machine supplied by Controls Inc. was used for compression and flexural strength testing. Humboldt supplied a concrete mixer with an 85 L capacity. Finally, a scanning electron microscope (SEM), supplied by FEI Inc., was used for the microstructural analysis of the samples.

Table 1: Composition and Physical Properties of FA and NA

Characteristics	Sum (SiO_2,Al_2O_3, Fe_2O_3), Min%	Sulfur trioxide, Max%	Moisture Content Max%	Loss on ignition, Max%	Fineness% retained on 45 micron-sieving, Max%
Fly ash (Class F)	70	5	3	6	34
Natural pozzolana	70.5-75.5	0.2-0.8	0.4-1.2	0.8-1.2	1.7-3.3

Table 2: Technical Properties of Superplasticizer Master Glenium 51

Technical properties	
Appearance	Brown liquid
Specific gravity	1.10 ± 0.03 g/cm³
pH value	6.0 ± 1
Chloride content (%)	≤ 0.10 by mass

2.2 Concrete Mixing and Testing

The mixing of samples in this study was carried out in the proportions summarized in Table 3. To ensure that the components formed a homogeneous mix, the mixing period lasted 30 minutes. After the concrete mixing process was completed, five 100-mm cubes and five 150 mm x 150 mm x 550 mm prisms were poured from each mix in accordance with ASTM C39 and ASTM, C78, respectively. They were removed from the molds after 24 hours and cured for 28-day in a curing tank at a constant temperature of 25 °C and 90 % relative humidity. ASTM C39 and ASTM C78 were followed to conduct the compressive and flexural strength tests on the prepared samples using the strength testing machine.

Table 3: Mixtures' Compositions

Component	Batch No. / Quantity										
	# 1	**# 2**	**# 3**	**# 4**	**# 5**	**# 6**	**# 7**	**# 8**	**# 9**	**#10**	**# 11**
Cement (kg)	20	18	16	14	12	10	18	16	14	12	10
Fly Ash (kg)	-	2	4	6	8	10	-	-	-	-	-
Natural Pozzolana (kg)	-	-	-	-	-	-	2	4	6	8	10
Coarse Aggregate (kg)	50										
Fine Aggregate (kg)	46										
Water (kg)	10										
Superplasticizer (g)	200										

2.3 Microstructural Analysis Using Scanning Electron Microscopy (SEM)

Microstructure analysis of the fractured samples was performed at the Qatar University Central Laboratories Unit to understand better the influence of FA and NP on the strength properties. The microscope FEI-Nova Nano SEM Model was used to scan and take high-resolution images at various imaging scales.

3 Results and Discussion

3.1 Compressive and Flexural Strengths

Figures 1 and 2 present the average compressive and flexural strength results of the batches listed in Table 3. The standard deviations were also determined for each batch. The results showed different behavior of each material on compressive and flexural strength. There was a strength increase for the

batches prepared with 10 and 20 % FA by 8.9 and 0.3 %, respectively, compared to the control batch. After that, there was a significant decrease in strength for batches prepared using 30, 40 and 50 % FA. Whereas NP achieved an increase of 5.6 % in compressive strength when replacing 10 % of cement and a decrease in strength at the rest of the replacement ratios, compared to the control batch, as shown in Figure 1.

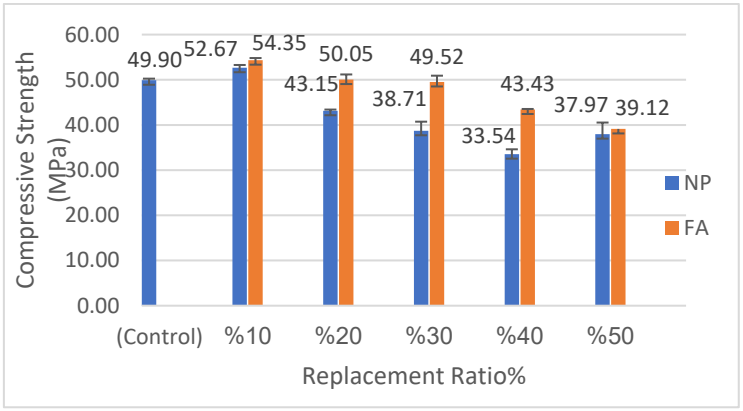


Fig. 1: Compressive Strength at 28-day

Flexural strength results were different from the above. There was an increase in strength in all batches impregnated with FA. The batches containing 10, 20, 30, 40 and 50 % of FA achieved 30.1, 26.8 %, 29.7 %, 25.1 % and 15.6 % respective increases in flexural strength compared to the control batch. In addition, in batches containing 10 % and 20 % of NP, the increase in the ratio was 35.6 % and 18.7%, respectively. This improvement in concrete strength can be attributed to the interaction between these materials and calcium hydroxide that results in the formation of re-crystallized calcium carbonate in the concrete matrix, which causes a decrease in the porosity and the transition zone in concrete.

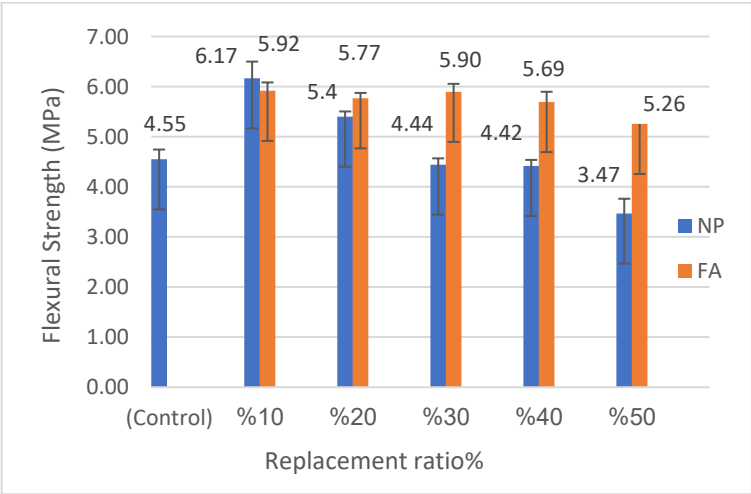


Fig. 2: Flexural Strength at 28-day

3.2 Microstructural Analysis

Figures 3 and 4 present the microstructure and morphology of randomly selected concrete mixes containing FA and NP at images of a 5, 10 and 50 µm scale. The samples were analysed after 28 days to ensure that the pozzolanic reaction with the cement stabilized and to be able to make comparisons between them.

Figure 3 shows the smooth and fine surface of FA particles, which improves the concrete surface

roughness and stimulates the pozzolanic reaction. The figure also shows calcium silicate hydrate (C-S-H) covering of the FA elements, that is probably caused by the pozzolanic reaction of the FA and calcium hydroxide ($Ca(OH)_2$). It is noticeable from Figure 4 that the NP-containing sample contains fewer calcium hydroxide crystals and the concrete matrix is more porous. Samples may tend to crack early; Therefore, lower mechanical strength properties were obtained.

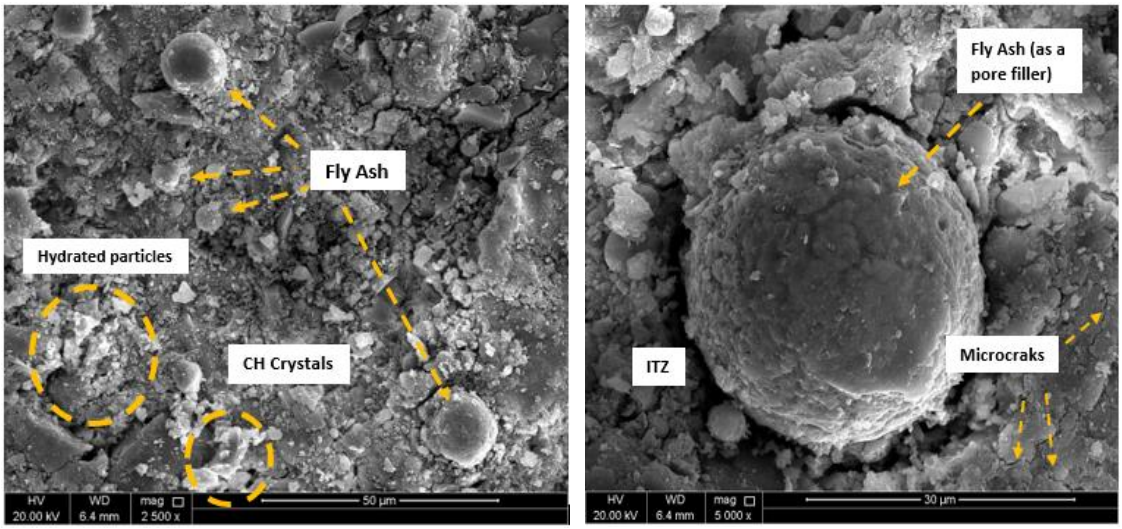


Fig. 3: SEM Micrographs of Concrete Matrix Impregnated with FA

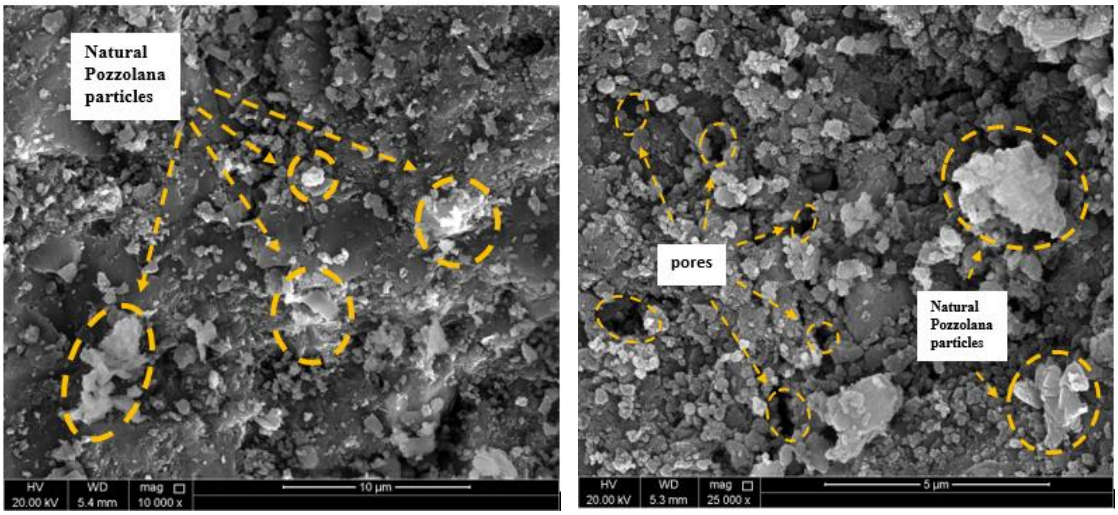


Fig. 4: SEM Micrographs of Concrete Matrix Impregnated with NP

4 Conclusions and Recommendations

The main experimental results drawn from this research are:

- Concrete impregnated with FA achieved better strength results than those containing NP.
- Incorporating FA material in concrete has good effects on mechanical properties. The batches prepared with 10 %, 20 %, 30 %, 40 % and 50% of FA increased flexural strength by 30.1 %, 26.8 %, 29.7 %, 25.1 % and 15.6%, respectively, compared to the control batch. Also, compressive strength enhancement by 8.9 % when replacing 10 % cement with FA.
- Replacing 10 % of cement with NP in concrete led to an improvement of compressive and flexural strength by 5.6 % and 35.6 %, respectively, compared to the control batch.

- Adding FA and NP promotes the cement hydration process by improving the formation of dense C-S-H and C-H crystals, primarily responsible for concrete's improved mechanical properties performance.
- Future tests should be directed towards improving and modifying the compositional and physical properties of FA and NP materials to obtain an acceptable cement replacement ratio that can improve concrete's mechanical properties, permeability and microstructure.

Acknowledgments

We express our sincere appreciation and gratitude to the Departments of Civil and Architectural Engineering at Qatar University and the Faculty of Engineering at Al-Ahliyya Amman University.

References

Ababneh, A. & Matalkah, F. (2018). Potential use of Jordanian volcanic tuffs as supplementary cementitious materials. *Case studies in construction materials*, *8*, 193-202. https://creativecommons.org/licenses/by-nc-nd/4.0/

Atiş, C. D. (2002). Heat evolution of high-volume fly ash concrete. *Cement and Concrete Research, 32*(5), 751-756.

Bentz, D. P., Ferraris, C. F. & Snyder, K. A. (2013). Best practices guide for high-volume fly ash concretes: Assuring properties and performance. https://doi.org/10.1016/S0008-8846(01)00755-4

De Matos, P. R., Foiato, M. & Prudêncio Jr, L. R. (2019). Ecological, fresh state and long-term mechanical properties of high-volume fly ash high-performance self-compacting concrete. I, 282-293. https://doi.org/10.1016/j.conbuildmat.2019.01.074

Espinoza-Hijazin, G., Paul, Á. & Lopez, M. (2012). Concrete containing natural pozzolans: new challenges for internal curing. *Journal of Materials in Civil Engineering, 24*(8), 981-988. http://dx.doi.org/10.1061/(ASCE)MT.1943-5533.0000421

Golewski, G. L. (2018). Green concrete composite incorporating fly ash with high strength and fracture toughness, *J. Clean. Prod. 172*, 218–226. https://doi.org/10.1016/j.jclepro.2017.10.065

Ghrici, M., Kenai, S. & Said-Mansour, M. (2007). Mechanical properties and durability of mortar and concrete containing natural pozzolana and limestone blended cements. *Cement and Concrete Composites, 29*(7), 542-549. https://doi.org/10.1016/j.cemconcomp.2007.04.009

Golewski, G. L. (2018). Evaluation of morphology and size of cracks of the Interfacial Transition Zone (ITZ) in concrete containing fly ash (FA). *Journal of hazardous materials*, *357*, 298-304. https://doi.org/10.1016/j.jhazmat.2018.06.016

Hossain, M. U. et al. (2021). Sustainable natural pozzolana concrete–A comparative study on its environmental performance against concretes with other industrial by-products. *Construction and Building Materials, 270*, 121429. https://doi.org/10.1016/j.conbuildmat.2020.121429

Khan, M. I. & Alhozaimy, A. M. (2011). Properties of natural pozzolan and its potential utilization in environmental friendly concrete. *Canadian Journal of Civil Engineering, 38*(1), 71-78. https://doi.org/10.1139/L10-112

Khodair, Y. & Bommareddy, B. (2017). Self-consolidating concrete using recycled concrete aggregate and a high volume of fly ash, and slag. *Construction and Building Materials, 153*, 307-316. https://doi.org/10.1016/j.conbuildmat.2017.07.063

Mehta, P. K. (2004, May). High-performance, high-volume fly ash concrete for sustainable development. In Proceedings of the international workshop on sustainable development and concrete technology (pp. 3-14). Ames, IA, USA: Iowa State University.

Rodrıguez-Camacho, R. E. & Uribe-Afif, R. (2002). Importance of using the natural pozzolans on concrete durability. *Cement and Concrete Research, 32*(12), 1851-1858. https://doi.org/10.1016/S0008-8846(01)00714-1

Shukla, A. et al. (2020, April). Natural Pozzolans a Comparative Study: A Review. In IOP Conference Series: Materials Science and Engineering (Vol. 804, No. 1, p. 012040). IOP Publishing. https://doi.org/10.1088/1757-899X/804/1/012040

Toutanji, H. et al. (2004). Effect of supplementary cementitious materials on the compressive strength and durability of short-term cured concrete. *Cement and concrete research, 34*(2), 311-319. https://doi.org/10.1016/j.cemconres.2003.08.017

Turanli, L, Uzal, B. & Bektas, F. (2005). Effect of large amounts of natural pozzolan addition on properties of blended cements. *Cement and concrete research, 35*(6), 1106-1111. https://doi.org/10.1016/j.cemconres.2004.07.022

Uzal, B. et al. (2010). Pozzolanic activity of clinoptilolite: A comparative study with silica fume, fly ash and a non-zeolitic natural pozzolan. *Cement and Concrete Research, 40*(3), 398-404. https://doi.org/10.1016/j.cemconres.2009.10.016

Yu, J. et al. (2017). Mechanical properties of green structural concrete with ultrahigh-volume fly ash. *Construction and Building Materials, 147*, 510-518. https://doi.org/10.1016/j.conbuildmat.2017.04.188

Zabihi-Samani, M., Mokhtari, S. P. & Raji, F. (2018). Effects of Fly Ash on Mechanical Properties of Concrete. *Journal of Applied Engineering Sciences*, *8*(2). https://doi.org/10.2478/jaes-2018-0016

Cite as: Abu Rumman M., Al-Diseet M., Abdel-Jaber M., Abutaqa A., Naji K. & Mohsen M., "A Comparison between Natural Pozzolana and Fly Ash Replacements on the Mechanical Properties of Concrete", *The 2nd International Conference on Civil Infrastructure and Construction (CIC 2023)*, Doha, Qatar, 5-8 February 2023, DOI: https://doi.org/10.29117/cic.2023.0066

Analysis of Factors Affecting the Performance of Dynamic Compaction Technique: A Study of Coastal Area of Eastern Province in Saudi Arabia

Ahmad Salah
Civil & Construction Engineering Department, College of Engineering, Imam Abdulrahman Bin Faisal University, Dammam, Saudi Arabia
aaasalah@iau.edu.sa

Mahmoud Sodangi
Civil & Construction Engineering Department, College of Engineering, Imam Abdulrahman Bin Faisal University, Dammam, Saudi Arabia
misodangi@iau.edu.sa

Eyad Sameer Derdas
Civil & Construction Engineering Department, College of Engineering, Imam Abdulrahman Bin Faisal University, Dammam, Saudi Arabia
eyad.dardas@hotmail.com

Jawad Nadhem Al Nasser
Civil & Construction Engineering Department, College of Engineering, Imam Abdulrahman Bin Faisal University, Dammam, Saudi Arabia
jksa1432@gmail.com

Ayad Abdulrahman Alshehri
Civil & Construction Engineering Department, College of Engineering, Imam Abdulrahman Bin Faisal University, Dammam, Saudi Arabia
2170002633@iau.edu.sa

Abstract

Coastal areas of the Eastern Province of Saudi Arabia have soil with low bearing capacity due to saturation with water, high contents of salt and inclusion of organic materials. The dynamic compaction (DC) technique, which is the most prevalent method for soil improvement in the area has not been effective in terms of cost, safety, and serviceability of the buildings. Thus, this paper aims to identify and assess the factors that prevent the efficient soil improvement performance using dynamic compaction technique. The desktop search and expert-based survey were used for data collection while the Analytic Hierarchy Process (AHP) was employed to analyze and prioritize the factors. The results indicate "difficulty in using the DC technique within 30m from buildings and 15m from underground services" as the most crucial factor. Above all, the practical and managerial implications implied in this paper are targeting a more efficient DC technique for soil improvement particularly in coastal areas of the Eastern Province of Saudi Arabia with expansive spread of Sabkha soil. Thus, the findings are expected to provide support to policy and decision makers in overcoming the performance shortfalls of DC technique.

Keywords: Analytic Hierarchy Process; Buildings; Dynamic compaction; Soil improvement; Sustainable construction

1 Introduction

The Vision 2030 of the Kingdom of Saudi Arabia driven by the National Transformation Plan has been the backbone of remarkable socio-economic transformation being witnessed in the Kingdom (Kumar & Albashrawi, 2022; Alshihri et al., 2022). The transformation plan pushes the agenda of transforming Saudi

Arabia into a major economic powerhouse and lays the groundwork for the country's shifts towards post hydrocarbon era (Sodangi, 2022; Balabel & Alwetaishi, 2021). In line with this, the construction sector being an integral component of this transformation plan, is projected to deliver by the year 2030, over 500,000 residential buildings, about 6,000,000 m² of new office space, and over 4,000,000 m² of retail space (Vision, 2030, 2022). Thus, to set the ball rolling, various giga projects like the futuristic NEOM city and other infrastructure projects worth over $1 trillion have been duly initiated across all regions in the Kingdom since the inception of the transformation plan in 2016 (Vision 2030, 2022). This inarguably positions the country as one of the biggest global construction sites.

For many decades now, building construction in the coastal areas of the Eastern Province of Saudi Arabia and the Arabian Gulf region in general have been tremendously plagued by the presence of low bearing capacity soils that are highly saturated with water and have high salt content and organic materials (Kazmi & Sodangi, 2021). Not that alone, incessant changes in groundwater table, extensive spread of problematic Sabkha soil, and ineffective earthwork techniques lead to high cost and time overruns during the construction stage while end-users of the buildings are exposed to the dangers of building failure and settlement, which are hurriedly remedied by inefficient, costly, and time-consuming repairs (Kazmi & Sodangi, 2021).

The study area for this paper is Dammam; a coastal city located in the Eastern Province of Saudi Arabia, which encompasses a total land area of 800 km² and a population of about 1.3 million (Almulhim & Aina, 2022). The city being Saudi Arabia's nerve centre for oil businesses and capital of the Eastern Province has been witnessing massive expansion in the construction of residential buildings, basic social and industrial infrastructure due to exponential economic and population growths (AlQahtani et al., 2022). Accordingly, the areas very close to the coastal line being the most preferred by clients and end-users have over the years become a beehive of new construction projects (AlQahtany & Abubakar, 2020). Nonetheless, the massive increase in the number of construction projects in these areas could be equally attributed to the continuous drive in achieving the objectives of the Kingdom's ambitious Vision 2030.

Many residential and industrial areas along the coastal line of Dammam city are affected by the wide spread of Sabkha soil, which is problematic to new construction projects as well as existing buildings in the areas due to its high water and salt contents, loose density, and high compressibility that necessitate ground improvement (Kazmi & Sodangi, 2021). While there are various soil improvement techniques that are utilized for ground improvement in these areas, remarkably, the dynamic compaction (DC) technique has been the most prevalent over the years. However, this technique has been noted to be grossly ineffective in terms of costs savings, safety, and serviceability of the buildings (Alimohammadi et al., 2022). Thus, this study will seek to determine and assess the factors that prevent the efficient soil improvement performance using dynamic compaction technique as evidence from the literature (Alimohammadi et al., 2022; Majik & Savoikar, 2022; Yao et al., 2022; Abdel-Rahman, 2021; Ghorbani et al., 2020; Li et al., 2020; Wu et al. 2020; Zhou et al., 2020; suggests that previous attempts have been made to empirically identify these factors, however, the studies have been mainly based on fragmented perspectives. Above all, the outcomes of the study are expected to provide support to policy and decision makers in overcoming the performance shortfalls of this soil improvement technique.

2 Literature Review

The built environment consists of different structures constructed on various types of soils. While some of these soils are non-problematic and appropriate for building construction in their natural

form, other soils are considered problematic as they require significant improvement to be appropriate for construction purposes and withstand the loads imposed on them. For instance, prior to the construction phase, problematic soil like Sabkha requires special treatment due to its high water and salt contents, low shear strength, low bearing capacity, and loose density to prevent causing damages that impair the structural integrity of buildings constructed on it.

Although several soil improvement techniques are utilized in building construction in the coastal areas of Dammam (Figure 1), the dynamic compaction (DC) approach is notably the most widely used over the past few decades (Alnaim et al., 2022). This is not surprising because of the technique's economic advantage, which makes the total costs involved relatively low as material addition or soil replacement are not required and simple equipment are used during the compaction, which shortens the duration. Not that alone, the DC technique is prominent among construction practitioners in the area considering its ability to enhance strength and bearing capacity of the soil while lowering the hydraulic conductivity of the soil.



Fig. 1: Soil Improvement Techniques

However, DC technique has some major shortfalls despite its notable advantages over other soil improvement techniques. For instance, there are many cases where building users, after few years of occupancy, are subjected to untold hardships associated with costly repairs due to serious damages that threaten safety of the buildings and its users (Alimohammadi et al., 2022).

Table 1: Review of factors preventing the efficient soil improvement performance of dynamic compaction technique

Factors	References
• Damage to surrounding structures due to vibrations	Yao et al. (2022); Abdel-Rahman (2021); Ghorbani et al. (2020); Wu et al. (2020)
• Serious danger when applied cohesive soils	Alimohammadi et al. (2022); Majik & Savoikar (2022); Wu et al. (2020)
• Inappropriate for expansive, organic, or clayey soil with low hydraulics conductivity	Li et al. (2020); Ghorbani et al. (2020); Zhou et al. (2020)
• Not suitable for construction sites that are underlain by landfills & soil layer that suffered from large settlements	Alimohammadi et al. (2022); Abdel-Rahman (2021); Ghorbani et al. (2020)
• Difficult to use within 30m from buildings & 15m from underground services.	Yao et al. (2022)
• Unsuitable when water depth is less than 1.5m	Yao et al. (2022); Ghorbani et al. (2020); Li et al. (2020)
• Inappropriate for soft cohesive soils located in the upper part of the compaction	Abdel-Rahman (2021); Zhou et al. (2020); Wu et al. (2020)

On the other hand, the Scopus database was used during the literature search to extract available journal articles that are peer-reviewed and empirically associated with the factors that prevent the efficient soil improvement performance of the dynamic compaction technique (Table 1). Essentially, the rationale for using peer-reviewed articles was to ensure that only authentic studies were retrieved, and the Scopus database provides a much quicker indexing process that improves the prospects of gathering available articles that are closely related to the present study being reported in this paper. While there are several existing studies on examining the disadvantages and challenges associated with the DC technique for improving the ground condition for construction purposes, the studies have been generally on buildings and structures constructed in non-coastal areas. Thus, the outcomes are primarily peculiar and may not be relevant and applicable for improving the efficiency of DC technique in coastal areas like Dammam city due to the peculiarity of the Sabkha soil spread in the area. Considering the poor attributes of the problematic Sabkha soil present in Dammam city, it became pertinent to investigate the factors that affect the efficiency of the DC technique for improving ground condition for construction purposes.

3 Methods

In this section, the techniques that were used to attain the goal of this paper are presented. Most importantly, the desktop search was utilized to review the relevant literatures and to identify factors that prevent the efficient soil improvement performance of DC technique. Subsequently, the authors deemed it is necessary to further consolidate the desktop search findings by improving the authenticity and wider applicability of the findings through an expert-based evaluation survey while Analytic Hierarchy Process (AHP) would be employed to analyze and prioritize the factors.

3.1 Expert-based Evaluation of the Adoption Factors

The expert-based survey was meticulously designed to focus on geotechnical engineers that are actively involved in soil improvement for construction projects in coastal areas of Dammam City.

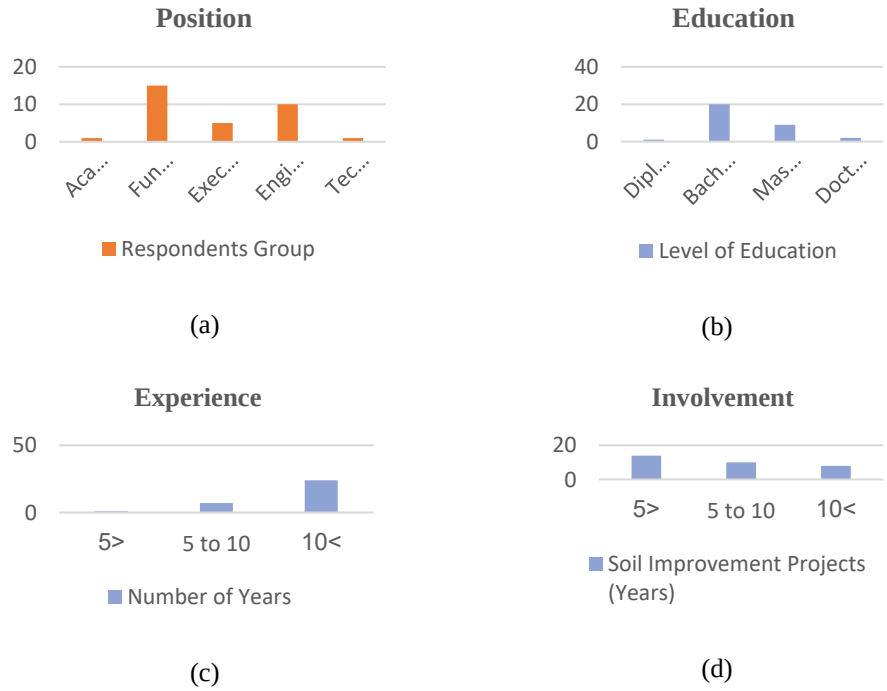


Fig. 2: Demographics and the characteristics of respondents

The list of the experts was generated using judgmental sampling to ascertain that only geotechnical practitioners that fit the requirements were invited to participate in the survey (Makoye et al., 2022). Remarkably, out of the entire 50 questionnaires that were administered, 32 complete responses were received, which are adequate for a study of this nature (Sodangi & Kazmi 2021).

3.2 The Analytical Hierarchy Process (AHP)

Essentially, the AHP was utilized in this study as one of the decision-making techniques to establish the importance weights of alternatives, which would be converted into a structural ranking order. The rationale for the selection of this technique is the ease with which it can be used to form a hierarchal structure of a given set of criteria. While utilizing experts' judgments ensures achieving an ideal solution; reaching out to the experts helps to mitigate the risk of using this technique.

The pairwise was generated using the collected data from 32 respondents which evaluates the factors on a scale from 1-5, where 1 = Very Low and 5 = Very High. The experts were requested to rate the effects of each factor on the performance of DC as a soil improvement technique in the coastal areas of the Eastern province of Saudi Arabia. To start with, the experts examined the importance and general impact of each factor obtained from the review of the relevant literatures and merged similar factors together. Subsequently, other factors that were mainly unique to soil improvement using DC technique in Dammam city which were not obtained from the desktop search were included by the experts. A list of six factors was generated as shown in Table 3 below:

Table 3: List of Factors

Factor Code	Description
F1	Inhibits vegetation growth
F2	Destabilizes the surrounding infrastructure due to strong vibration
F3	Disturbs surface & sub-surface flow of water
F4	Inappropriate where water depth is less than 1.5m.
F5	Difficult to use within 30m from buildings and 15m from underground services
F6	Unsuitable where soft cohesive soils are located in the upper part of the compaction

Furthermore, the pairwise generation was performed automatically by converting the raw data into AHP scale and then generating pairwise comparisons accordingly. Based on the procedure of pairwise comparison in AHP as described by Saaty and Sagir (2009), the comparisons are based on a scale from 1-9. Thus, the raw data needs to be converted from scale 1-5 into scale 1-9. The conversion process utilizes a systematic conversion equation (Eq. 1) that can be used to interchange between the two scales as shown in Table 4.

The conversion of raw data to 1-9 scales transforms the evaluations of participants into the scale recommended by Saaty (1970). However, the implementation of AHP requires the generation of pairwise comparison to evaluate the weights for each factor (i) from each decision maker (k). Equation 2 allows the generation of pairwise comparison between two factors (i.e., i and j) using their respective 1-9 scales given by decision maker (k).

$$X_{ik} = 2 \times Y_{ik} - 1 \qquad (1)$$

where,

X_{ij} represent the values in scale 1 to 9.

Y_{ij} represent the values in scale 1 to 9.

i represents the factor.

k represents the decision maker.

Table 4: Results of the conversion between the two scales

Y_{ij}	1	2	3	4	5
X_{ij}	1	3	5	7	9

$$P_{ijk} = \begin{cases} \frac{X_{ik}}{X_{jk}}, if\ mod\left(\max\left(X_{ik}, X_{jk}\right), \min\left(X_{ik}, X_{jk}\right)\right) = 0 \\ 2^{m}, if\ mod\left(\max\left(X_{ik}, X_{jk}\right), \min\left(X_{ik}, X_{jk}\right)\right) \neq 0;\ where, m = \begin{cases} -1, & X_{ik} < X_{jk} \\ 0, & X_{ik} = X_{jk} \\ 1, & X_{ik} > X_{jk} \end{cases} \end{cases} \quad (2)$$

After generating the pair wise comparisons, the following AHP procedure is used to calculate the weight score of the evaluation from each decision maker using the equations (3)-(5):

1. Calculate the sum of each column

$$\sum_{j=1}^{j=n} X_{ijk} \quad (3)$$

2. Calculate the normalized values by dividing each value by the sum of its respective column

$$r_{ijk} = \frac{X_{ijk}}{\sum_{j=1}^{j=n} X_{ijk}} \quad (4)$$

3. Calculate weight of each factor by averaging the normalized values of pairwise comparison

$$W_{ik} = \frac{\sum_{i=1}^{i=n} r_{ijk}}{n} \quad (5)$$

The AHP calculation procedure is repeated to calculate the weights provided by all respondents. Eq. (6) is used to calculate the total weight of each factor and to rank all factors in descending order

$$Wi = \frac{\sum_{k=1}^{k=m} W_{ik}}{m} \quad (6)$$

4 Results

The AHP results obtained are presented and discussed in this section. The AHP results include the importance weights and ranks of the factors that prevent the efficient soil improvement performance of dynamic compaction technique. Using the AHP, the six factors were prioritized based on their importance weights as shown in Table 5. The results indicate that the difficulty of using DC where buildings are within a radius of 30 m and underground services are on a depth of 15 m or less (Factor # 5), which represents the main challenges for practitioners. Also, it indicates that the existence of soft cohesive soils on the upper part of compaction (Factor 6) has a considerable effect on the implementation of DC techniques. On the other hand, the disturbs of flow of water (Factor # 3) represents the factor that has the least effects on the implementation of DC technique in improving

the soil. Also, the possibility of destabilizing the surrounding infrastructure due to the strong vibration (Factor # 2) has relatively low impact on the implementation of DC techniques. Nevertheless, the inhabitation of vegetation growth (Factor #1) and appropriateness when water table is in a depth of 1.5m or less (Factor #4) has average impact on the implementation of DC technique. Finally, the results highlight the importance and criticality of each factor on implementing the DC technique for soil improvement in under-developed coastal areas where cohesive/organic materials are existing on the upper part of the soil.

While the objective of this study has been accomplished, it is essential to underline the limitations of this paper. The study adopted a judgmental sample, which may seem small. However, a specialized study of this nature requires authentic responses from participants who are experts in the subject. Not that alone, examining a much larger sample size would be complicated and could result in findings that are ambiguous, unreliable, and invalid. Thus, the opinions and judgment of the experts involved in this study were considered reliable and authentic owing to their sheer proficiency in the practice of soil improvement for construction purposes, which in turn adds validity to the findings of the paper. Notwithstanding the aforementioned limitations, the factors evaluated and prioritized in this study symbolize the judgments of experts in ground improvement for construction projects in Saudi Arabia. However, there is a need for future research works to ensure that the findings reported in this paper are empirically validated.

Table 5: Weighting and Ranking Results

	Weights of Factors					
DM#	W1	W2	W3	W4	W5	W6
DM1	0.221	0.221	0.074	0.044	0.221	0.221
DM2	0.23	0.23	0.046	0.033	0.23	0.23
DM3	0.028	0.25	0.083	0.139	0.25	0.25
…	…	…	…	…	…	…
DM31	0.342	0.038	0.049	0.114	0.342	0.114
DM32	0.359	0.04	0.051	0.12	0.359	0.072
Weights	**0.168**	**0.136**	**0.119**	**0.141**	**0.231**	**0.205**
Rank	**3**	**5**	**6**	**4**	**1**	**2**

5 Conclusion

This paper determined and assessed the factors that prevent the efficient soil improvement performance using dynamic compaction technique in the coastal areas of the Eastern Province of Saudi Arabia. The expert-based survey was deployed to strengthen the factors identified in the literature review while the AHP was used for analysis and prioritization of the factors. The results indicate that the most crucial factors are “difficulty in using the DC technique within 30m from buildings and 15m from underground services” and the DC technique is unsuitable where soft cohesive soils are located in the upper part of the compaction. The outcomes of this paper provide thorough understanding of the factors affecting the efficiency of soil improvement performance using dynamic compaction technique. The outcomes can be applied to overcome the effects of these factors as well as to promote efficiency of the DC soil improvement technique. Above all, the practical and managerial implications implied in this paper are targeting more efficient DC technique for soil improvement particularly in coastal areas of the Eastern Province of Saudi Arabia with expansive spread of Sabkha soil. Thus, the findings are expected to be utilized to provide support to policy and

decision makers in overcoming the performance shortfalls of DC technique. Although the findings of this paper are largely based on problems related to building construction in coastal areas of the Eastern Province of Saudi Arabia, the outcomes could as well be appropriate and valid to other residential areas along the coastal line of other countries in the Middle East.

References

Abdel-Rahman, M. M. (2021). "Review of Soil Improvement Techniques". In: Shehata, H., Badr, M. (eds) Advancements in Geotechnical Engineering. Sustainable Civil Infrastructures. Springer, Cham. https://doi.org/10.1007/978-3-030-62908-3_14

Alimohammadi, H., Amirmojahedi, M. & Tahat, J. N. (2022). "A Case History of Application of Deep Compaction Method with Comparison to Different Ground Improvement Techniques". *Transportation Infrastructure Geotechnology*. https://doi.org/10.1007/s40515-022-00229-3

Almulhim, A.I. & Aina, Y.A. (2022). "Understanding Household Water-Use Behavior and Consumption Patterns during COVID-19 Lockdown in Saudi Arabia". *Water, 14*, 314. https://doi.org/10.3390/w14030314

Alnaim, A. et al. (2022). "A Systematic Framework for Evaluating the Effectiveness of Dynamic Compaction (DC) Technology for Soil Improvement Projects Using Cone Penetration Test Data". *Applied Sciences*, 12, 9686. https://doi.org/10.3390/app12199686

AlQahtany, A. M. et al. (2022). "Land Reclamation in a Coastal Metropolis of Saudi Arabia: Environmental Sustainability Implications". *Water, 14*, 2546. https://doi.org/10.3390/w14162546

AlQahtany, A.M. & Abubakar, I. R. (2020). "Public perception and attitudes to disaster risks in a coastal metropolis of Saudi Arabia". *International Journal of Disaster Risk Reduction, 44*, 101422.

Alshihri, S., Al-Gahtani, K. & Almohsen, A. (2022). "Risk Factors That Lead to Time and Cost Overruns of Building Projects in Saudi Arabia". *Buildings, 12*, 902. https://doi.org/10.3390/buildings12070902

Balabel, A. & Alwetaishi, M. (2021). "Towards Sustainable Residential Buildings in Saudi Arabia According to the Conceptual Framework of Mostadam Rating System and Vision 2030". *Sustainability, 13*, 793. https://doi.org/10.3390/su13020793

Ghorbani, J., Nazem, M. & Carter, J. P. (2020). "Dynamic compaction of clays: Numerical study based on the mechanics of unsaturated soils." *International Journal of Geomechanics, 20*(10), 04020195. https://doi.org/10.1061/(ASCE)GM.1943-5622.0001840

Kazmi, Z.A. & Sodangi, M. (2021). "Integrated Analysis of the Geotechnical Factors Impeding Sustainable Building Construction-The Case of the Eastern Province of Saudi Arabia." *Sustainability, 13*, 6531. https://doi.org/10.3390/su13126531

Kumar, V. & Albashrawi, S. (2022). "Quality Infrastructure of Saudi Arabia and Its Importance for Vision 2030." *MAPAN 37*, 97–106 (2022). https://doi.org/10.1007/s12647-021-00523-4

Li, X. et al. (2020). "New Method to Evaluate Strengthen Efficiency by Dynamic Compaction." *International Journal of Geomechanics, 20*(4), p.04020024. https://doi.org/10.1061/(ASCE)GM.1943-5622.0001586

Majik, R. K. & Savoikar, P. P. (2022). "Ground modification techniques for deep soft soils sites in Goa region." *Lecture Notes Civil Engineering, 152*, 409 - 421. https://doi.org/10.1007/978-981-16-1831-4_38

Makoye, M., Mlinga, R. S. & Ndanshau, M. O. A. (2022). "Impact of macroeconomic factors on performance of construction industry in Tanzania." *International Journal of Construction Management*. https://doi.org/10.1080/15623599.2022.2084259

Saaty, T. L. & Sagir, M. (2009). "Extending the measurement of tangibles to intangibles." *International Journal of Information Technology & Decision Making (IJITDM), 8*(01), pages 7-27. https://doi.org/10.1142/S0219622009003247

Sodangi, M. (2022). "Towards attaining efficient joint ventures in international construction: the case of Saudi Arabia".

Engineering, *Construction and Architectural Management*, Vol. ahead-of-print No. ahead-of-print. https://doi.org/10.1108/ECAM-07-2021-0647

Vision 2030, (2022). "The Progress & Achievements of Saudi Arabia. *Vision 2030 Kingdom of Saudi Arabia*." Available at: https://www.vision2030.gov.sa/ (Accessed: November 18, 2022).

Wu, S. et al. (2020). "Dynamic compaction of a thick soil-stone fill: Dynamic response and strengthening mechanisms." *Soil Dynamics and Earthquake Engineering, 129*, 105944. https://doi.org/10.1016/j.soildyn.2019.105944

Yao, Z. et al. (2022). "Effect of dynamic compaction by multi-point tamping on the densification of sandy soil". *Computers and Geotechnics, 151*, p.104949. https://doi.org/10.1016/j.compgeo.2022.104949

Zhou, C. et al. (2020). "Evaluation of dynamic compaction to improve saturated foundation based on the fluid-solid coupled method with soil cap model". *Computers and Geotechnics, 125*, 103686. https://doi.org/10.1016/j.compgeo.2020.103686

Cite as: Salah A., Sodangi M., Dardas E., Alnasser J. & Alshehri A., "Analysis of factors affecting the performance of Dynamic Compaction technique: A study of coastal area of Eastern province in Saudi Arabia", *The 2nd International Conference on Civil Infrastructure and Construction (CIC 2023)*, Doha, Qatar, 5-8 February 2023, DOI: https://doi.org/10.29117/cic.2023.0067

Comparison of Geotechnical Investigation Results with Encountered Ground Conditions during Subsea Tunnelling in Qatar

Saad Zayed Al-Marri
Project Coordinator of Musaimeer Pumping Station and Outfall Project,
Public Works Authority, Doha, Qatar
smarri2@ashghal.gov.qa

Gary Peach
Project Manager, Mott MacDonald, Doha, Qatar
gary.peach@mottmac.com

Furqan Hameed
Senior Geotechnical Engineer, MM Pakistan, Lahore Pakistan
furqan.hameed@mottmac.com

Abstract

Starting in 2018, Musaimeer Pumping Station and Outfall Project (MPSO) was constructed to manage ground and storm water received from 270 km^2 area of southern Doha, Qatar. The project consists of a pumping station, subsea tunnel, (constructed through Rus formation, Midra shale and Simsima limestone), riser shaft and diffuser bed structure. An Earth Pressure Balance (EPB) Tunnel Boring Machine (TBM) was used for subsea tunnelling where ground water inflows, mixed ground condition with the presence of vertical and lateral fractures connected to the seabed were encountered during tunnelling activity. This paper analyses the reliability of geotechnical investigation results and interpretations by comparison with encountered conditions. This will be beneficial to design a reliable geotechnical investigation programme for future projects of similar scope in the state of Qatar. Results and interpretations from drilled bore holes and geophysical survey provided an overall picture of underground conditions along the tunnel alignment, which identified the critical tunnelling areas for cutter head intervention and maintenance. These results were then compared with the built geotechnical conditions accessed by collecting data through the onboard TBM monitoring equipment, collecting rock mass samples, and performing geological face mappings during tunnelling activity. Comparison of pre-tendered investigation results with the built geotechnical conditions concluded that investigation results and encountered rock mass conditions were in line with each other. Geotechnical investigation programme followed for this project and interpretation as a result, made the tunnelling under sea to be carried out in more careful and low risk manner.

Keywords: TBM Tunnelling; Subsea tunnelling; Geotechnical investigation; Encountered ground conditions; Qatar

1 Introduction

Musaimeer pumping station and outfall project was constructed south of Hammad International Airport, Doha. The project is designed to manage surface and rainwater received from the drainage networks from 270 km^2 of urban areas in southern Doha. It consists of pumping station with pumping capacity of 19.7m^3 per second and 10.2 km long subsea outfall tunnel. The project outline is shown in Figure 1.

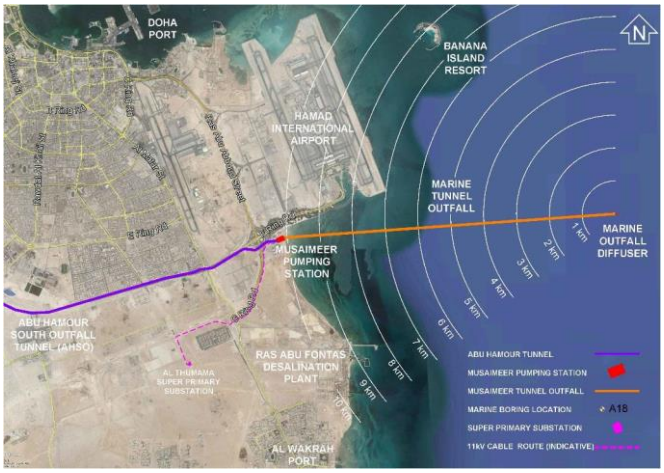


Fig. 1: Project Location

The objective of this paper is to compare the results of geotechnical investigations conducted for the project with encountered geotechnical conditions during the construction of outfall tunnel. Geotechnical information was collected by drilling bore holes and geophysical surveys. Foreseen ground information was used to predict ground condition along the alignment of tunnel. Observations during tunnel excavation operations were made by collecting rock mass samples, measuring fluctuations in water pressure, performing rock mass classification.

2 Geotechnical Investigation Results

As part of pre-tendered geotechnical investigations, borehole drilling (A1 to A22) and geophysical surveys, including Seismic reflection, Seismic refraction, were performed to access the in-situ ground conditions. Figure 2 shows the tunnel alignment, bore holes and geological formations.

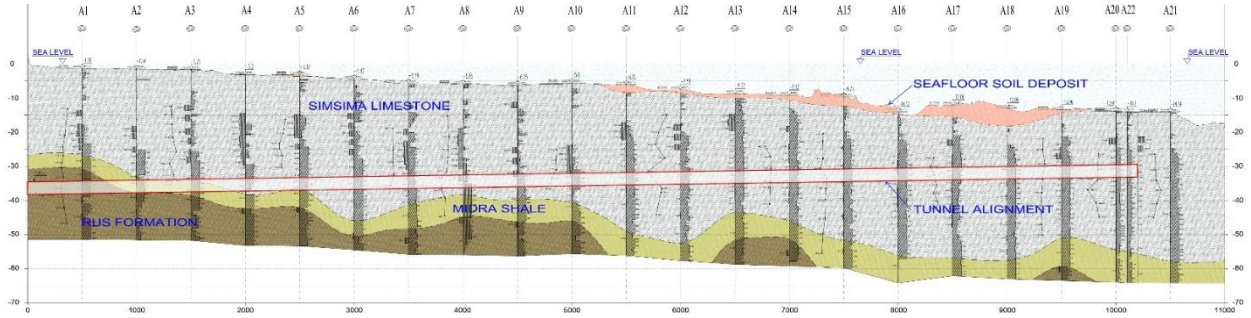


Fig. 2: Lithological Cross Correlation from drilled boreholes

2.1 Core Drilling Results

Core drilling was carried out along the tunnel alignment by 22 marine boreholes, 50 m in depth and 500 m apart from each other along the tunnel alignment. The rock stratigraphic units encountered were identified as made ground, unconsolidated soil, Simsima limestone, Midra Shale and Rus formation.

The characteristics of these geological units were poor bedding structures oriented in horizontal to sub-horizontal as cross-correlated from all the boreholes findings. There was no evidence of active faulting across the lithological units. Jointing systems indicated the predominant development of horizontal to sub-horizontal joint sets in the project area. The characteristics of stratigraphic units of the project are described as follows.

2.1.1 Made Ground

Made ground was encountered as unconsolidated sediment with shells from the marine borings, at a thickness varying from 0.45 to 5.20 m.

2.1.2 Simsima Limestone

The Simsima limestone was encountered as an underlying stratigraphic unit of made ground or unconsolidated superficial deposits. Typical geological characteristics observed from the Simsima limestone was the occurrence of poorly developed bedding structure with horizontal to sub horizontal dipping angle and generally increased in thickness towards the east. The thickness of this rock unit varies from 20.7 m to 44.0 m. Simsima limestone is predominantly dolomitic in composition and illustrates considerable variations in rock quality as indicated by Rock Quality Designation (RQD) values in association with weathering degree also illustrated by frequency of solution features with increasing depth. The uppermost section of the rock is distinctly weathered and fractured and is poor to very poor in quality compared to the deeper parts which are less weathered and more competent.

2.1.3 Midra Shale

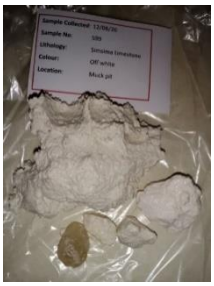
Midra shale was encountered in all boreholes at variable thicknesses ranging from 4.0 m to 8.6 m, yellowish brown to greenish in colour. Weak to medium strong mudstone, interbedded with layers of pinkish grey coloured, moderately strong, slightly to moderately weathered limestone. This rock stratigraphic unit is moderately to highly weathered with intense yellowish-brown iron oxide staining in parts. Midra shale is overlain by Simsima limestone and underlain by Rus formation.

2.1.4 Rus Formation

This is the oldest rock stratigraphic unit encountered boreholes, underlying the Midra shale in the project area. Rus formation is composed of beige, tan, grey, yellowish-brown coloured, medium strong to strong, slightly to moderately weathered, moderately fractured dolomitic limestone interbedded with less prominent, pale grey to brown/greenish brown coloured, weak to medium strong, moderately weathered, moderately fractured calcitic layers. This rock unit contains gypsum inclusions and veins, with the presence of solution cavities and vugs having occasional silty sand infills. The unit shows horizontal to sub-horizontal fractures with spacing close to wide. The joint surfaces are generally undulating and rough.

2.2 Encountered Rock Mass Sampling and Results

During tunnel excavation, rock mass samples were collected, at the chainages where investigation boreholes were drilled. Rock mass properties, RQD, weathering, hardness, from samples were observed and compared with the results of investigation. Reports were produced for sample collected from borehole locations whenever TBM crossed that location. Figure 3 shows the type of samples taken at these locations



(a): Simsima limestone



(b): Midra Shale



(c): Rus Formation

Fig. 3: Samples collected during TBM Tunnelling (Representative)

From the findings of the sampling reports, rock mass condition, its physical properties were found to be same as observed during investigation stage except at two locations where mixed rock mass was found. This validates the reliability of methods, procedures used during borehole drilling. As built geological plan and section was prepared in the form of geological sheet. Each geological sheet was composed of 260 m of tunnel alignment. Table 1 contains the pretender geological data along with details of the encountered ground conditions. The table shows in the remark's column that the "Lithological conditions confirmed" is the predominate finding.

Table 1: Lithology found in investigation vs encountered lithology

Bore hole No.	Borehole depth (m)	Sea Floor Elevation (m)	Lithology encountered at Tunnel elevation	Start Date of excavation through borehole location	End date excavation across borehole location	Ground conditions encountered during TBM Tunnelling	Remarks
A1	50	-1.39	Rus	03.4.2019	4.4.2019	Rus	Lithological conditions confirmed
A2	50	-1.54	Rus	22.5.2019	23.5.2019	Mixed Ground	Rus formation and Midra shale mixed
A3	50	-1.71	Midra Shale	13.7.2019	14.7.2019	Clay-Midrashale	Lithological conditions confirmed
A4	50	-3.20	Midra Shale	25.8.2019	26.8.2019	Clay- Midra shale	Lithological conditions confirmed
A5	50	-3.32	Simsima	27.9.2019	29.9.2019	Mixed ground	Midra Shale and Simsima limestone mixed
A6	50	-4.47	Simsima	7.11.2019	9.11.2019	Simsima	Lithological conditions confirmed
A7	50	-5.79	Simsima	2.12.2019	3.12.2019	Simsima	Lithological conditions confirmed
A8	50	-5.95	Simsima	3.1.2020	3.1.2020	Simsima	Lithological conditions confirmed
A9	50	-6.25	Simsima	26.3.2020	26.3.2020	Simsima	Lithological conditions confirmed
A10	50	-5.60	Simsima	4.4.2020	4.4.2020	Simsima	Lithological conditions confirmed
A11	50	-6.15	Simsima	9.6.2020	9.6.2020	Simsima	Lithological conditions confirmed
A12	50	-7.58	Simsima	7.7.2020	7.7.2020	Simsima	Lithological conditions confirmed
A13	50	-8.73	Simsima	2.8.2020	2.8.2020	Simsima	Lithological conditions confirmed
A14	50	-9.17	Simsima	26.8.2020	27.8.2020	Simsima	Lithological conditions confirmed

Bore hole No.	Borehole depth (m)	Sea Floor Elevation (m)	Lithology encountered at Tunnel elevation	Start Date of excavation through borehole location	End date excavation across borehole location	Ground conditions encountered during TBM Tunnelling	Remarks
A15	50	-9.73	Simsima	17.9.2020	18.9.2020	Simsima	Lithological conditions confirmed
A16	50	-14.12	Simsima	11.10.2020	11.10.2020	Simsima	Lithological conditions confirmed
A17	50	-12.60	Simsima	03.11.2020	03.11.2020	Simsima	Lithological conditions confirmed
A18	50	-12.98	Simsima	30.11.2020	30.11.2020	Simsima	Lithological conditions confirmed
A19	50	-13.46	Simsima	27.12.2020	27.12.2020	Simsima	Lithological conditions confirmed
A20	50	-13.91	Simsima	24.01.2021	24.01.2021	Simsima	Lithological conditions confirmed
A21	50	-14.14	TBM did not pass through this location as this borehole was located away from end of TBM tunnel				
A22	50	-14.10	This borehole was located near BH-A20 and investigated lithological conditions were confirmed as TBM passed through this location				

2.3 Geophysical surveys

Seismic refraction and reflection surveys were performed as part of pre-tendered investigations. Electric resistivity tomography (ERT) survey was performed as post-tendered investigation.

2.3.1 Seismic Refraction Survey (Pre-Tender)

Generally, four to five different seismic mediums (SM) were determined. SM-1 (Weak Limestone) started first 5m-10m from the sea floor and velocity range Vp=1600-2250m/s, SM-2 (Weak to medium strong Limestone) between 10m-20m, Vp= 2250-3400 m/s, SM-3 (Medium Strong to Strong Lime Stone) between 20m to 30 m and Vp= 4100-4900 m/s, SM-4 (Strong to very strong Limestone) between 30m-50m, Vp=4100-4900 m/s. Values of Vp=4900-5400 m/s were also recorded which were considered as compact material. Figure 4 shows a typical Seismic velocity section.

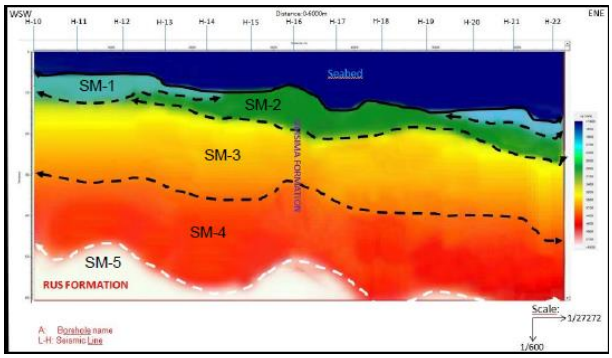


Fig. 4: Seismic velocity section

2.3.2 Seismic Reflection Survey (Pre-Tender)

Seismic reflection data was well matched with seismic refraction and core drilling results. Three seismic mediums M1, M2, M3 were observed. Figure 5 sows a typical seismic reflection survey result.

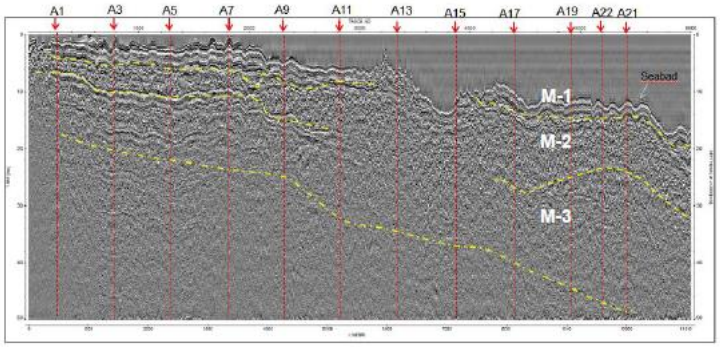


Fig. 5: Cross section of seismic reflection

Seismic refraction and reflection sections are in harmony with each other. Depth and thickness of layer for seismic reflection cross section were calculated based on thickness of layer obtained from seismic refraction for time to depth conversion. Seismic interpretations were made by the developed cross sections. The thickness of the layers was correlated with drilling logs. The yellow lines in Figures 5 & 6 represent the layers from reflection anomalies.

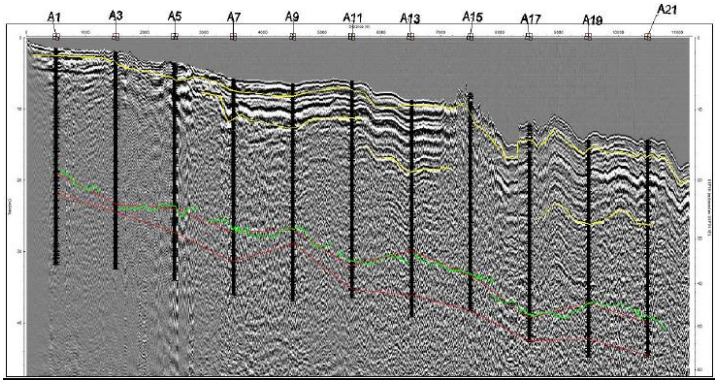


Fig. 6: Seismic reflection cross section and boreholes

Generally, two units were determined, Sismsima limestone and Rus formation. In addition, from time to time at different depths, thin Midra shale, mudstone layers were detected in bands. Interpretation of pre and post tender investigations result in the identification of 20 anomalies of note classified as F1 to F20.

2.3.3 Electric Resistivity Tomography

Electric resistivity tomography (ERT) was performed at post tendered stage along the entire tunnel alignment. Several conductive anomalies and resistive anomalies were detected during the first 2km of the survey. The final phase of study confirmed that those anomalies were probably connected to fractures or fracturing systems. Distances along the tunnel alignment start at zero at the pump station and increase to 10.2km at the end of the outfall tunnel

The resistive anomalies are associated to possible different nature and geological risks, however only the one between chainage 6.7 and 6.9 km at depth greater than 50.0 m, could be associated to a possible karstic risk (cavity). However, the tunnel alignment was above that anomaly. The area

between 5.2 to 7.4 km was affected by a significant increasing degree of fracturing and was considered as potential high permeability zone.

The area between 7.6 to 8 km was also considered an anomalous area. The evidence of a drop of resistivity values of more than 10 ohm-m along the tunnel alignment, was a warning of increasing permeability, and possible hydrostatic connection to the seabed. Figure 8 shows ERT for the entire tunnel alignment.

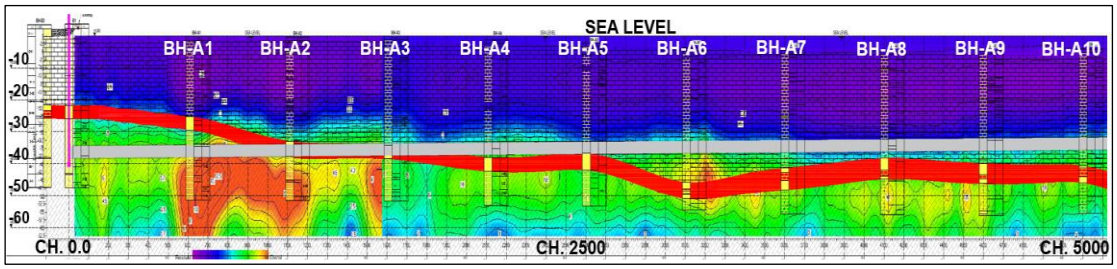


Fig. 8: ERT line from 0 to 10.2 km

3 Foreseen Geotechnical Conditions along the Tunnel

Pre-tender and post tender geotechnical information were combined according to the tunnel chainage to classify potential ground condition and were classified as favourable, moderately favourable, unfavourable and a reference chart was developed by combining geotechnical investigation data and ground classification. That chart was used to plan for TBM cutter head maintenance operations, the principal aim was to avoid unfavourable ground conditions for cutter head intervention, since that scenario would greatly increase the complexity and safety of the operations.

3.1 Bored Tunnelling Electric Ahead Meter Results

The TBM was equipped with Bored Tunnelling Electric Ahead Meter (BEAM) system, which is a non-intrusive electrically induced polarization system able to predict ground conditions up to 12 m ahead. Information is displayed in a matrix which combines resistivity and percentage frequency effect (PFE).

The interpretation of the matrix, which is shown in Figure 9, is based on the columns and rows; factors on the columns refer to the karst interpretation (P1:P4) while factors on the rows (R3:R1) refer to the possibility of water inflow.

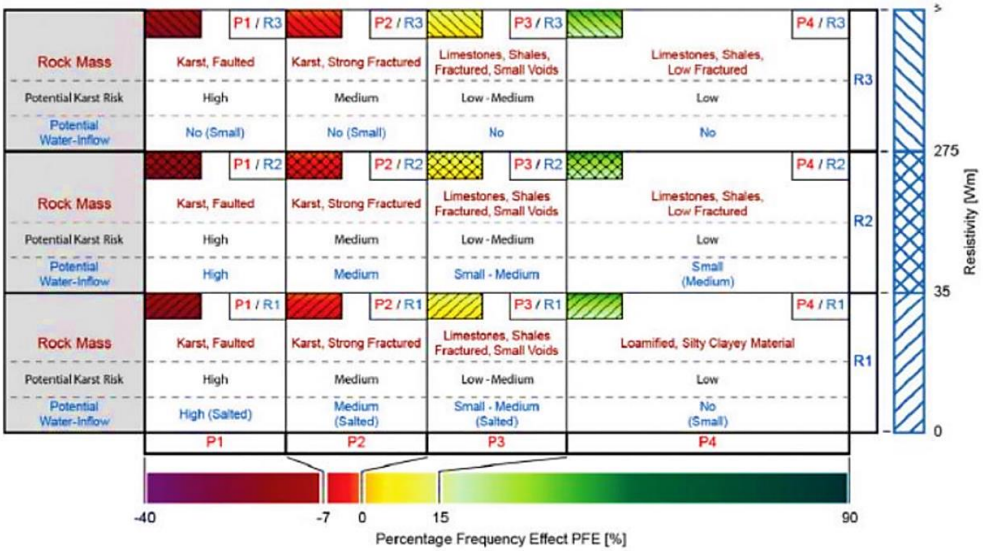
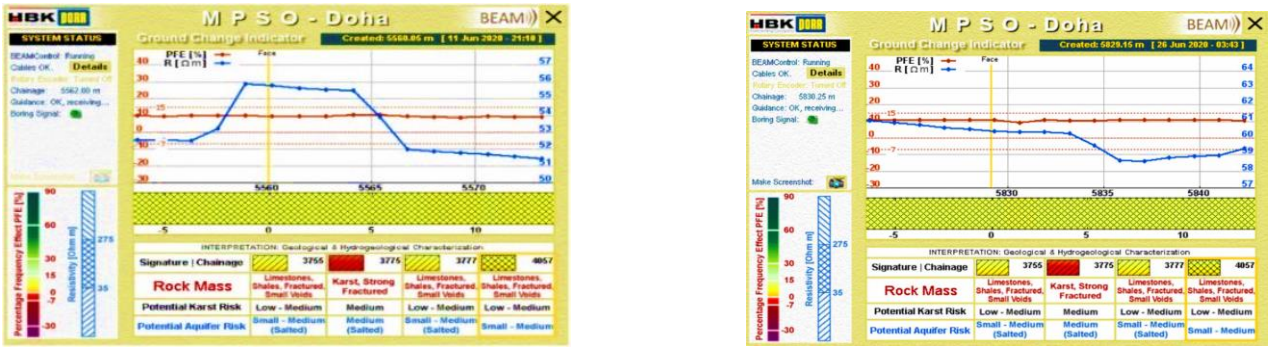


Fig. 9: BEAM Interpretation Matrix

3.2 Examples of Bored Tunnelling Electric Ahead Meter Results

In Figure 10 the bored tunnelling electric ahead meter (BEAM) display indicates the results of crossing two anomaly zones identified by the post tender geotechnical surveys.



(a): Fault zone F10 **(b):** Fault zone F13

Fig. 10: BEAM Display at Fault zone F10 – F13

It is important to note that there are limitations on the precision accuracy of the system. The system is not able to identify whether the TBM is passing through Rus formation, Midra Shale or Simsima limestone; it can only identify intrinsic properties of rock mass. It is not possible to measure the exact amount of water inflow and location. The system can provide an estimation of the possibility that water inflow or aquifers might be encountered.

3.3 Comparison of Foreseen Rock Mass Condition with Bored Tunnelling Electric Ahead Meter Data

With reference to foreseen ground conditions, it was predicted that the TBM will pass through 20 zones classified as F1 to F20. During tunnelling, the BEAM system also predicted those anomalies 10 to 15 m before encountering them. Table 2 shows the anomalies predicted during investigation stage and those picked by BEAM system during tunnel excavation.

Table 2: Foreseen geotechnical condition Vs actual and BEAM

No.	Fault Zone	Predicted Location	Actual Chainage		Picked up by BEAM		Remark
		Chainage	From	To	Yes	No	
1	F1	500	528	608	✓		Increase the pressure (2.6 bar)
2	F2	900	-	-		✓	In the Midra Shale, the fractured condition did not affect the EPB and TBM operation, the fracture looked like not connected to the seabed.
3	F3	1150	-	-		✓	
4	F4	1300	-	-		✓	
5	F5	1750	-	-		✓	
6	F6	1900	-	-		✓	
7	F7	2600	2638	2756	✓		High groundwater pressure (3.5 bar)
8	F8	3700	3678	-	✓		High groundwater pressure (3.5 bar) for 1569 m
9	F9	5200	-	5247	✓		
10	F10	5500	5437	5600	✓		Increase the pressure (2.4-3.4 bar)
11	F11	5800	5808	5884	✓		Fluctuated pressure (2.4-3.2 bar)
12	F12	6100	6079	6170	✓		Fluctuated pressure (2.4-2.8 bar)
13	F13	6350	-	-		✓	Not increase the pressure
14	F14	7000	6620	6820	✓		Fluctuated pressure (2.2-2.7 bar)
15	F15	7100	-	-		✓	Not increase the pressure

No.	Fault Zone	Predicted Location	Actual Chainage		Picked up by BEAM		Remark
		Chainage	From	To	Yes	No	
16	F16	7300	-	-		✓	Not increase the pressure
17	F17	8250	7820	8260	✓		Fluctuated pressure (2.2-2.7 bar)
18	F18	8450	-	-		✓	Not increase the pressure
19	F19	9550	9550	9650	✓		Low pressure, muck material increase
20	F20	9750	9650	9760	✓		Low pressure, muck material increase

4 Conclusion and Lesson Learned

- Geotechnical investigations, performed at pre-tender stage provided enough necessary information about rock mass along tunnel alignment.
- Plan for advance of tunnel proved to be a good tool for deciding intervention location.
- Although BEAM is giving good results about the presence of water ahead of tunnel, however it cannot predict the quantity of water and rock mass type through which TBM passes
- Around 60% of the rock mass condition is accurately encountered, as marked before start of mining operation through a different investigation.
- Observation and record of excavated material provides a good check no rock mass condition.
- Face mapping during cutter head intervention provides a good overview of rock mass condition, which was encountered during mining.
- Monthly updates of geotechnical properties of rock mass provides an opportunity to actively keep on observing the built geotechnical condition in comparison with pre-tendered observations.

References

Karagkounis, N. et al. (2016). Geology and geotechnical evaluation of Doha rock formations. *ICE Geotechnical Research UK*, 3(3). pp 120-121. https://doi.org/10.1680/jgere.16.00010

Sadiq, A.M. & Nasir, S.J. (2022). "Middle Pleistocene Karst Evolution in the state of Qatar, Arabian Gulf. *Journal of cave and Karst studies*, pp. 137-139.

Poulos, H.G. (2018). A review of geological and geotechnical features of some Middle Eastern countries – Innovative Infrastructure solutions, Springer, pp. 6-8.

Cite as: Al-Marri S.Z., Peach G. & Hameed F., "Comparison of Geotechnical Investigation Results with Encountered Ground Conditions during Subsea Tunneling in Qatar", *The 2nd International Conference on Civil Infrastructure and Construction (CIC 2023)*, Doha, Qatar, 5-8 February 2023, DOI: https://doi.org/10.29117/cic.2023.0068

A Review on the Performance of Bored Pile Foundations through Instrumented Pile Load Tests in Qatar

Muhammad Humza
Parsons International Limited, Doha, Qatar
muhammad.humza@parsons.com

Mannan Ali
Parsons International Limited, Doha, Qatar
mannan.ali@parsons.com

Majid Naeem
NSCC International, Abu Dhabi, UAE
majid.naeem@nsccme.com

Abstract

The level of infrastructure development Qatar has accomplished over the past 10 years has not been reached by any other country and this pace is expected to continue to achieve Qatar's 2030 Vision. High-rise buildings and bridges are mostly constructed on pile foundations which play an important role in overall cost of the project, but there is limited published literature available on the performance of pile foundations in Qatar. In this article, the performance of fully instrumented pile foundations embedded in rock formations of Qatar is reviewed, and discussion on observed behaviour is presented. This paper also uncovers the conservatism in pile design adopted by the piling industry. A total of more than 65 pile load test results were compiled to perform this study. Good practices are suggested that can be considered by the authorities and consultants in specifying a preliminary pile load test in order to reap its full potential. In projects, where the unit skin friction was validated through performance of pile load tests and later on pile design was optimized, 11% to 50% savings in piling cost was achieved contributing to sustainable projects.

Keywords: Preliminary pile load test; Pile performance monitoring; Rock skin friction; Qatar geology; Design optimization.

1 Introduction

Qatar has experienced rapid development of infrastructure and construction of high-rise buildings and bridges over the last 10 years. High-rise buildings and bridges are mostly constructed on pile foundations which contribute significantly to the overall cost of the project. Qatar is currently ranked as 19th tallest city in the world and second in the Middle East by numbers of completed buildings higher than 150m. Over 77 high-rise buildings (of heights over 100m) and several bridges have been built and many buildings are still under construction or are in the planning stages. This indicates the piling industry in Qatar has gathered a vast amount of information in recent years.

However, limited published literature is available on the performance of pile foundations, particularly in Qatar. The aim of this paper is to share interpretation of compiled instrumented pile load tests with the industry to help colleagues understand the behaviour of bored pile foundations embedded in rock formations of Qatar.

1.1 Available Database

Pile load test records and reports were gathered from some piling projects completed in Qatar. Details of these projects are not disclosed in order to ensure the confidentiality of data used to prepare this article. The compiled data comprised 65 pile load test results including 28 preliminary pile load tests, which were conducted using load cells. Among the available pile load test results, only those tests were considered for this study that fulfilled the criteria below:

- Preliminary and working pile load tests performed using bidirectional load cells.
- The pile load test reports are available including pile details, coordinates, strain, and measured skin friction values.
- Site-specific geotechnical factual reports with boreholes are available at or adjacent to the test pile location.

1.2 Bi-Directional Static Load Test (BDSLT)

Detailed description and operating principles of BDSLT are outside of the scope of this study. BDSLT is faster to perform, incurs less cost, reduces construction time and provides direct measurements of the load distribution and pile movement response. Through BDSLT, much higher test loads can be applied than with conventional pile load tests. The cost saving from using BDSLT ranges between 1/3 and 2/3 of conventional top load tests and increases further with any increase in applied load (Schmertmann et al., 1997).

A bi-directional cell is composed of a hydraulic piston assembly welded through steel plates on either side of this sacrificial cell assembly through steel reinforcement. When hydraulic pressure is applied, the piston or hydraulic cell extends, and the load is transferred to the pile. The pile side (or skin) and pile bottom take the load and generate resistance from the ground surrounding the pile and at the pile toe. The load cell applies the load both upward and downward in equal parts. The upper part of the test pile provides resistance to the upward load through the skin friction. The lower part of the pile (below the cell assembly) provides resistance to the downward load through either end bearing alone (if the cell is installed at the pile's toe) or through combined resistance provided by skin friction and end bearing (if the load cell is installed above the toe of the test pile). Telltale rods cased inside a pipe are attached to the top and bottom of hydraulic cell to measure the upward and downward movements against the reference frame at the surface. The movements are measured using displacement transducers.

2 Geological Conditions

At depths relative to civil engineering, the main geological formations, in stratigraphic succession, consist of upper Dammam formation (Simsima Limestone member), Lower Dammam formation (Dukhan Limestone and Midra Shale member) and Rus Formation. The geological formations are comprised of limestone, shale, siltstone, claystone, marl and gypsum. The Simsima Limestone member is present over 80% of the land surface of Qatar. In general, pile foundations have been formed in Simsima Limestone member with average thickness of 20m. **Fig. 1** illustrates variation of UCS[1] encountered in all the project sites with elevation. Simsima Limestone varies from weak to strong, while Rus Formation is generally extremely weak to moderately strong.

[1] Unconfined compressive strength

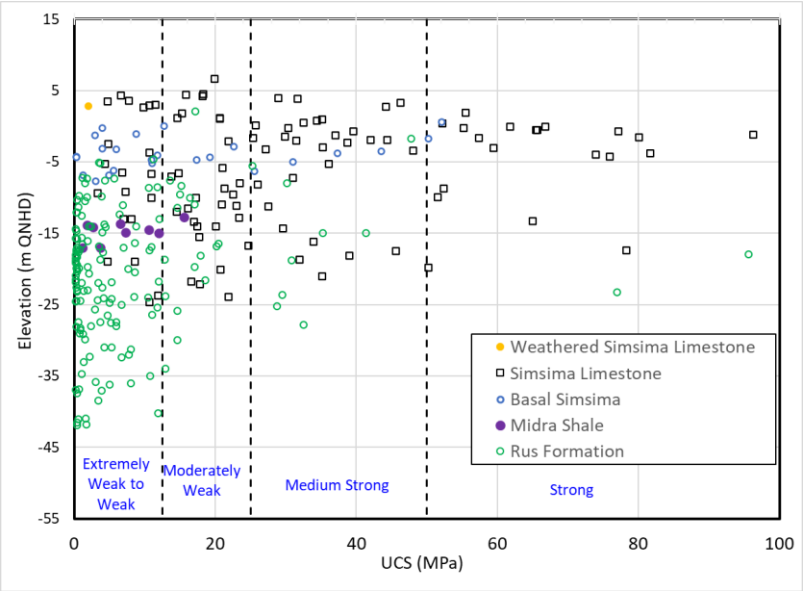


Fig. 1: Plot of UCS vs. elevation for the database

3 Empirical Correlations for Pile Design

The empirical correlations based on which piles are designed in Qatar relate the ultimate unit skin friction of pile with unconfined compressive strength (UCS) of rock considering correction factors for the rock discontinuities. In practice, the ultimate skin friction is estimated by relations provided by (Horvath et al., 1983) and (Williams and Pells, 1981).

$$f_s = 0.3 \times (UCS)^{0.5} \quad (1) \quad \text{Horvath et. al (1983)}$$

$$f_s = \alpha\beta \times UCS \quad (2) \quad \text{Williams and Pells (1981)}$$

$$f_s = 0.40 \times (UCS)^{0.5} \quad (3) \quad \text{Zhang (1998)}$$

$$f_s = 0.375 \times (UCS)^{0.515} \quad (4) \quad \text{Rosenberg \& Journeaux (1976)}$$

Where,

f_s = Ultimate unit skin friction

UCS = Rock Unconfined Compressive Strength

α = Reduction factor with respect to UCS

β = Reduction factor with respect to rock discontinuities

4 Load Transfer Behaviour along the Trial Pile

Vibrating wire strain gauges are installed typically at predefined levels along the length of the trial piles to measure the strains. Load transfer (P) at each strain gauge level is calculated using the following equation. Subsequently, the mobilised skin friction is derived using the known pile stiffness. The computed skin friction at each level of strain gauge was obtained from the pile load test report.

$$P = \Delta_{SG} \times AE_p \quad (5)$$

Where,

Δ_{SG} = Change in Strain Gauge reading

AE_p= Pile Axial Stiffness

It is well-known that the elasticity of concrete material does not remain constant over the range of stressing history during loading and unloading cycles but exhibits a strain-softening behaviour with increasing stress level. However, for this study, the pile stiffness used (AE) is based on the correlation of static elastic modulus (Ec) and cube compressive strength of the concrete (fc), as Ec = 4700 x $\sqrt{}$ fc. The load carried by the pile is estimated by the difference between the loads calculated at any two levels of strain gauges. Consequently, the average unit skin friction is calculated between any two strain gauge levels by the change in calculated load divided by the circumferential area of pile between the two strain gauge levels.

Fig. **2** illustrates the load transfer behaviour along the test pile calculated from data collected by strain gauges installed along the length of the trial piles. The distance of each strain gauge above (d1) and below (d2) the cell level is normalized by pile length segment above (L1) and below (L2) the jack level. At every strain gauge, computed skin friction is available in the test report. It is obvious from the review of PTPs report data that the maximum load is transferred to the pile at the load cell level, thus, strain measurements close to the location of the load cell assembly provide the highest values of unit skin friction, irrespective of the ground conditions and the strength of rock. The values of measured skin friction gradually decrease as the distance to the load cell increases, as shown in Fig. **2**, and it is also observed that the transferred load to pile is reduced to about 90 to 97% at the level of strain gauges placed at 3/4th distance of pile length above and below the jack level.

This means that skin friction values measured in the zone of the load cell may represent the expected design values since within this zone the load being applied by the cell begins to be transferred to surrounding rock. Consequently, rock in this zone carries a major part of the test load that mobilizes the maximum skin friction of rock. Hence, the remaining test load may not be sufficient to mobilize the rock's maximum skin friction along the entire length of test pile. Therefore, in the authors' opinion, geotechnical failure in rock formations of Qatar may only be reached, locally, at the load cell location.

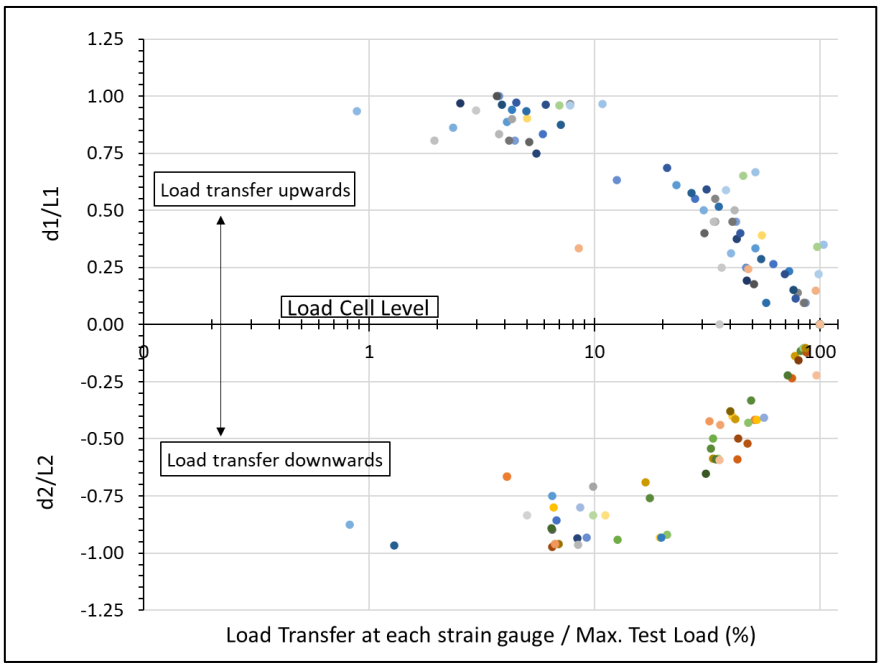


Fig. 2: Load distribution along the normalized PTPs length

5 Mobilized Skin Friction during Trial Pile Testing

Pile foundations in Qatar are usually designed in a way such that the geotechnical resistance is considered to be provided only by the skin friction and end-bearing is ignored. Hence, correct estimation of the unit skin friction becomes essential to get a cost-effective pile foundation system. **Fig. 3** presents ultimate skin friction values estimated by the empirical correlations commonly used in practice. This figure also shows mobilized skin friction achieved during the preliminary (trial) pile load tests. The unit skin friction measured within the load cell zone of the 27 selected PTP[2]s (as shown in **Fig. 2**) are the highest values measured during the tests. The rock UCS and RQD[3] values were taken from the boreholes drilled in the close vicinity of the each PTPs location.

The skin friction values near the cell assembly placed within the extremely weak to weak rock (as classified in accordance with BS EN ISO 14689) are considered to be fully mobilized exceeding the ultimate skin friction designed using empirical relationships. The approaches by Horvath et al (1983) and Williams and Pells (1981) may underestimate the ultimate skin friction that can be mobilized within extremely weak to weak rock (rock mass with UCS < 12.5 MPa[4]). However, empirical relation reported by Rosenberg & Journeaux (1976), originally developed for weathered and soft rocks, appears to be more suitable for pile design in extremely weak to weak rocks of Qatar.

On the other hand, the skin friction has not fully mobilized within the moderately weak to medium strong rock (UCS > 12.5 MPa). By looking at the pile deformations against the applied loads on PTPs, it implies that the skin friction is yet to reach its ultimate value. The data shows a clear and consistent trend of mobilized skin frictions for the rocks below and higher than the weak category.

The author suggests that the test load should be increased/designed such that the pile shall be loaded until pile failure or until the jack capacity is reached to determine the ultimate skin friction and capacity of pile in Qatar. However, in projects where the unit skin friction was validated through performance of pile load tests and skin friction was found not fully mobilized, pile design was optimized and 11% to 50% savings in piling cost was achieved contributing to accomplishment of sustainable projects as reported by Cherian (2021) and for a project where the authors were involved.

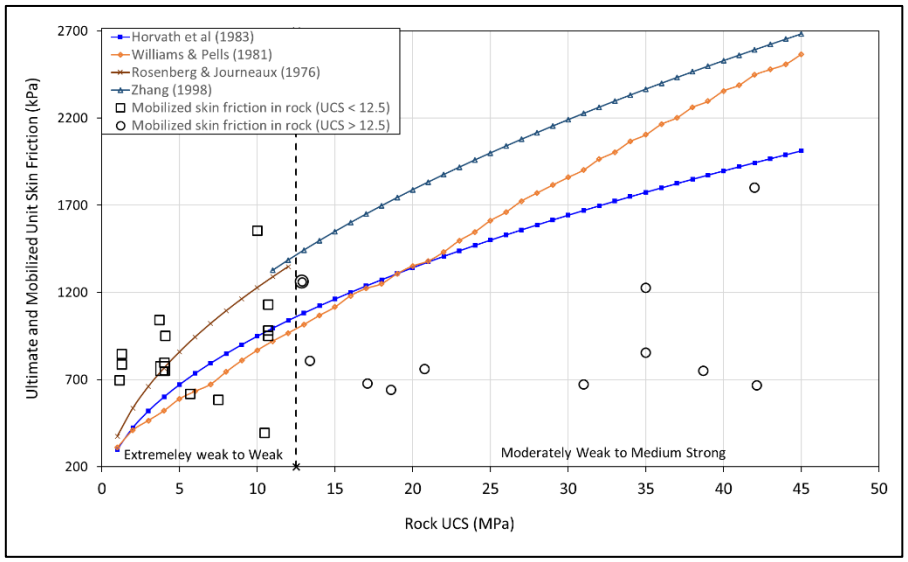


Fig. 3: Mobilized Skin Friction vs. Ultimate Skin Friction estimated by correlations.

[2] Preliminary Test Piles.
[3] Rock Quality Degeneration.
[4] MegaPascal.

6 Geotechnical Failure of Pile

In Qatar, almost all the pile load test reports conclude the results with a confirmation statement that "the test pile met the design requirements with regard to the design capacity, allowable settlement and hence concluded that the test result is acceptable", with no differentiation made for the failure criteria related to ultimate or working pile test whatsoever.

Geotechnical failure of a pile should be defined in terms of ultimate and serviceability limit states and these limit states should be considered when conducting load tests on trial piles and on working piles and failure criteria should be specified by the designer for each pile load test.

6.1 Ultimate Limit Failure Criteria for load tests

The target for the ultimate load testing on preliminary test pile (PTP) is to achieve the Ultimate Limit State (ULS) criterion. Table 1 provides the ULS criteria for the ultimate load test on trial piles (PTP) specified in the literature and codes.

Table 1: ULS failure criteria for bored piles in compression

Pile Type	**Failure Criteria**		
	Settlement	Residual settlement	Creep rate of head settlement
Preliminary Trial Pile	Settlement of the pile base diameter exceeds 10% of the pile diameter Or total axial movement exceeds 15 % of the pile diameter.	The residual settlement upon unloading from the ultimate load is 2.5% of the diameter or the load at which the pile head settlement = 0.15 + 0.1xDia (inches)	The load at which a sudden increase in the slope of the settlement-time curve occurs (plunging failure) – unlikely to occur in rock formations of Qatar
Reference	BS EN 1997-1, QCS 2014, ASTM D1143	DIN4026, Davisson (1972)	Bell and Robinson (2012)

Geotechnical failure for PTPs (using bidirectional load cells) may also be defined in terms of continued pile movement when the full elongation of cell stroke (typically around 200mm) occurs. The published guidelines and rule of thumbs for the pile failure criteria relate to the overall pile performance during a load test on preliminary pile (PTP) and working pile.

For this study, the authors have considered geotechnical failure as 10% of pile diameter. Fig. **4** shows measured settlement values (normalized by pile diameter) of 27 numbers of trial piles tested up to 300% of design verification load (DVL). It is evident from this figure that the majority of the piles have settled less than 2% of pile diameter with a couple of piles up to 4% mark except three tests (carried out for one particular project) where the maximum settlement of about 7% of diameter was achieved, indicating that none of the test piles reached the ultimate failure state.

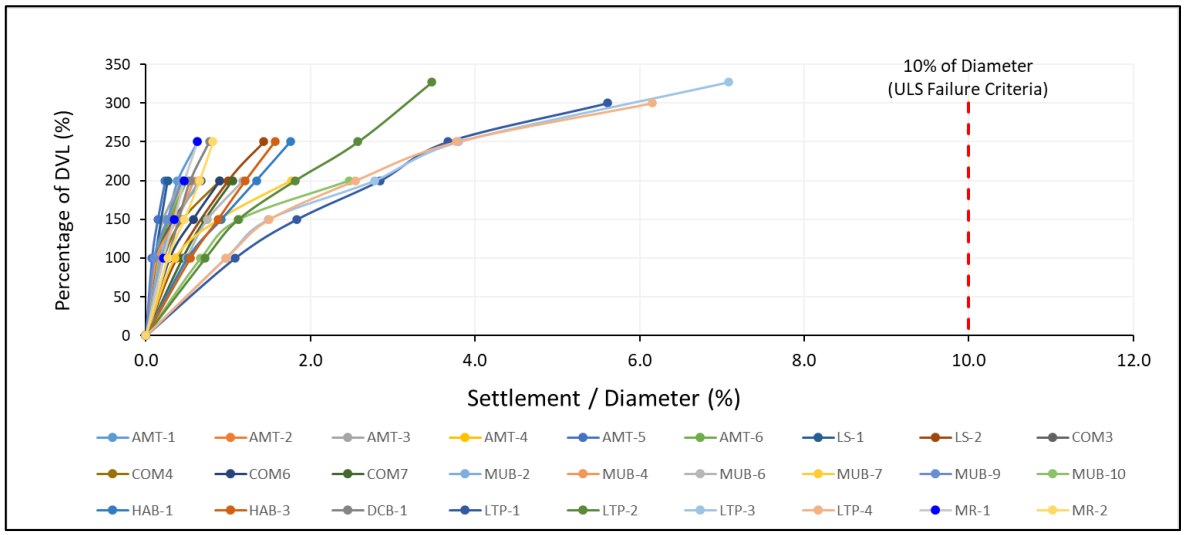


Fig. 4: Settlement of trial piles

Preliminary pile load tests are performed on trial piles, installed for test purposes only, before the design is finalised. As such, the pile design can only be optimized if skin friction has fully been mobilized. In case of a large diameter pile, it is often impracticable to perform a load test on a full-size trial pile such that the maximum skin friction could be mobilized, therefore, trial piles with smaller diameter may be considered for preliminary load tests in accordance with EN1997 and QCS 2014, provided that:

- the ratio of the trial pile diameter/working pile diameter is not less than 0.5
- the trial pile having smaller diameter is constructed using the same method as foundation working piles

6.2 Serviceability Limit Failure Criteria for load tests

Table 2 presents the suggested failure criteria to be considered for pile load tests on working piles. It is expected that the maximum accepted settlement suggested here does not exceed the tolerable movement limits of the structure. In any case, it is the responsibility of the engineer to state the performance specification in terms of maximum allowable pile settlement during load test at the design verification load (DVL).

Table 2: SLS failure criteria for bored piles in compression

Pile Type	Failure Criteria		
	Test Load	Max. Settlement	Residual Settlement
Working Pile	100% DVL	Exceeds 10 mm + elastic shortening; or 1% of Diameter; or Exceeds 7mm (second cycle)	The residual settlement upon the final release of the load exceeds 5mm
	150% DVL	14 mm + elastic shortening	
The maximum settlement values may be increased by 2.2% for every metre length of pile beyond 30 metres			
References: Federation of Piling Specialists (UK), Civil Design Criteria (Singapore)			

Bi-directional load tests on working piles are performed to measure the pile settlement against the design load. The settlements of a total of 44 numbers of preliminary and working piles at 100% and 150% of DVL are shown in **Fig. 5**. It is to be noted that the settlements presented in the figure are combinations of elastic shortening and pile vertical movements as given in the pile test reports. The details on adding elastic shortening to the pile vertical movements from the field tests are described by Loadtest (2002). It is clear that none of the piles has exceeded the serviceability limit state and even the combined settlement of pile at service load remains less then 10mm. The settlement criteria at 150% of DVL could not be verified due to unavailability of appropriate data to compute elastic shortening.

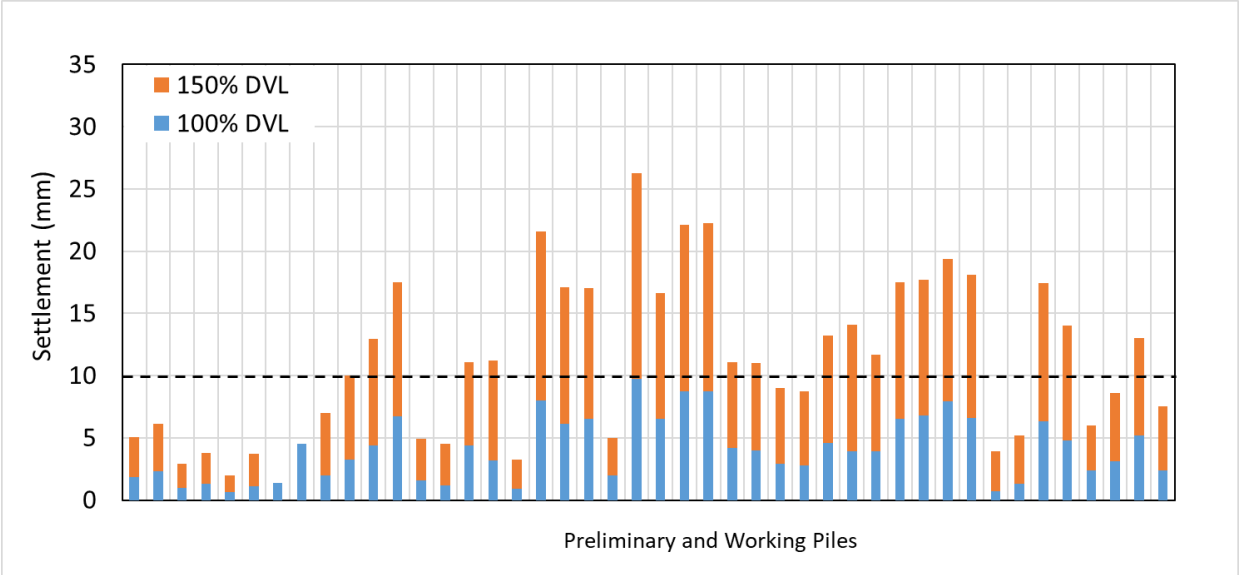


Fig. 5: Settlement of 44 test piles at 100% and 150% of DVL

7 Conclusions and Recommendations

This paper presents a review on the performance of pile foundations based on the typical geological conditions found in Qatar, aiming to provide an insight to engineers for optimizing the design of preliminary test piles. The following good practices are suggested for consideration by the authorities and consultants in specifying a preliminary pile load test in order to reap its full potential:

- The preliminary pile load test should be conducted on a trial pile with the aim of achieving ultimate failure criteria, and this shall not be considered as a means of verifying the proof or design load with some margin of safety. The ultimate bearing capacity of the piles may not be established if a pile load test ceases at a settlement less than 10% of the pile diameter. The results of trial pile test with ultimate failure will help in selecting more Optimized pile dimensions for the project, hence achieving savings in the overall project cost.
- If it is not practicable to perform preliminary pile load tests on a large-diameter pile with heavier loads, trial piles with smaller diameters may be constructed provided that the diameter of the trial pile is not less than 0.5 times the diameter of the working pile, and the trial pile with smaller diameter is constructed using the same method used for the foundation piles.
- For trial test pile designed as friction only pile, a “soft toe” or a compressible material of known thickness should be placed below the pile toe before construction and testing. This will ensure the loads are transferred to the shaft sides during the testing without any load being transferred

to the pile toe. The trial pile should be instrumented in such a way that the measurements could be used to derive the skin and end-bearing resistance separately.

References

Bell, A. & Robinson, C. (2012). Single piles. In ICE Manual of Geotechnical Engineering (Burland J, Chapman T, Skinner H and Brown M (eds)), ICE Publishing, London, UK, vol. II, pp. 803–821.

Cherian, A. (2021). "Geotechnical Evaluation of Multi-Layered Simsima Limestone using Bi-Directional Static Load Test." *Journal Geological Society of India,* Vol.97, 670-674.

Davisson, M. T. (1972). "High-capacity piles" in *Proc. Lecture Series on Innovations in Foundation Construction*, ASCE, Illinois Section, Chicago.

Federation of Piling Specialists. (2006). "Handbook on Pile Load Testing," FPS, Forum Court, 83 Copers Cope Road, Beckenham, Kent, BR3 1NR.

Horvath R.G, Kenney, T.C. & Kozicki, P. (1983). Methods of improving the performance of drilled piers in weak rock. *Canadian Geotechnical Journal, 20*(4): 758–772.

Loadtest. (2002). "Report on drilled shaft test, Osterberg method at US82 over Mississippi River", Washington County, Missouri, Project LT-8800-1, 61.

Qatar Construction Specification (2014). Ministry of Municipality and Environment, Qatar.

Rosenberg, P. & Journeaux, N. L. (1976). "Friction and end-bearing tests on bedrock for high-capacity socket design." *Canadian Geotechnical Journal, 13*(3): 324–333.

Schmertmann, J. H. & Hayes, J. A. (1997). "The Osterberg Cell and Bored Pile Testing – A Symbiosis," *The Third International Geotechnical Engineering Conference*, Cairo, Egypt.

Williams, A. F. & Pells, P. J. N. (1981), "Side resistance rock sockets in sandstone, mudstone, and shale", McMahon, Burgess and Yeates, Sydney, Australia.

Zhang, L. (1998). "Analysis and Design of Axially Loaded Drilled Shafts Socketed into Rock," Thesis, Massachusetts Institute of Technology, Cambridge, Massachusetts.

Cite as: Humza M., Ali M. & Naeem M., "A Review on the Performance of Bored Pile Foundations through Instrumented Pile Load Tests in Qatar", *The 2nd International Conference on Civil Infrastructure and Construction (CIC 2023)*, Doha, Qatar, 5-8 February 2023, DOI: https://doi.org/10.29117/cic.2023.0069

Tunnel Surveying Works: A Technical Challenge of 10 km-long tunnel under the Arabian Gulf-Qatar

Gary Peach
Mott MacDonald, Doha, Qatar
gary.peach@mottmac.com

Saad Zayed Al-Marri
Public Works Authority (Ashghal), Doha, Qatar
smarri2@ashghal.gov.qa

Hernan Vigil Fernandez
HBK-PORR JV, Doha, Qatar
hernan.vigil@auccqatar.com

Simbarashe Kazingizi
Noack Engineers GmbH & Co.KG, Passau, Germany
simbarashe.kazingizi@noack-engineering.com

Pavel Chumakou
Noack Engineers GmbH & Co.KG, Passau, Germany
Pavel.Chumakou@noack-engineering.com

Abstract

The Musaimeer Pump Station & Outfall Tunnel project (MPSO) was constructed as one of the longest Outfall tunnels in the World with a total length of 10.189m and at the same time being the longest undersea tunnel in the Middle East. MPSO will manage ground- and storm-water from the Southern Doha District and dispose of this water via a diffuser bed connected to the outfall tunnel. Difficulties faced during the project execution were firstly, the tunnel network itself. It was necessary to maintain precision and reliability of the 10km network, in a tunnel of smaller than 5m in diameter, starting from a 26m diameter drop shaft. Secondly, the breakthrough was into a 3m diameter vertically positioned riser shaft encased in a 5m x 5m concrete block which was positioned and constructed offshore by utilizing different network of 10km Global Positioning System Real-Time Kinematic (GPS RTK) readings. The key problem was confirming that both survey networks used were homogenous as the marine tolerances in comparison to the tunnel tolerances were very different. Thirdly, the actual Tunnel Boring Machine (TBM) connection was under the sea. The TBM excavated through a concrete filled shaft 0.6m beneath the riser shaft invert, then excavated 35m to create working space for civil works. The tunnel's crown was then cut using a 3m diameter opening to connect into the bottom of the riser shaft. This study serves to describe the Survey technical issues faced in the construction and coordination of underground tunneling and interfacing with offshore works.

Keywords: Tunnel; Surveying works; Network; Onshore; Offshore; Tolerance; Gyroscope

1 Introduction

1.1 General Information

Construction of outfall tunnels is often an effective and sustainable solution to improve the quality of life in the coastal areas. Also, the cities are interested in building longer tunnels as they allow to

spread the wastewater further away from the coast. At the same time the longer the tunnel – the bigger is the potential survey error. So, the importance of the topic lies in the solution of the survey problem for a long underwater tunnel.

The basis for this research was some previous publications done by our surveyor colleagues. Robert Benecke and Uwe Kalz from DMT (Benecke & Kanz, 2006), leading company in producing of gyroscopic survey equipment, published their work 'Ensuring tunnel navigation by cost-effective gyroscope control measurements'. Their paper clarifies by practical examples, how the problem of positioning errors in tunnel surveying can be solved cost-effectively with high-accuracy gyroscopic measurements.

Another valuable research was done by Andrew Hung Shing Lee. It is also a case study research which among others describes the 'double zigzag' traversing method used at 3.2 km TBM Tunnel of Lok Ma Chau Spur Line, Hong Kong and 7.5 km railway project constructed for Kowloon Canton Railway Corporation, Hong Kong (Lee, 2007).

The article by 'Implementation of gyroscope measurements in underground mines' (Szafarczyk & Skaba, 2019) is a case study research describing the implementation of gyroscopic measurements with gyrotheodolite Sokkia GYRO X1 II into the survey procedures in the coal-mining industry. The work deals with the parameters of the network and describes improvements achieved with the use of gyroscopic measurements.

1.2 Methodology

The research is also a case study based on the survey works done by Noack Engineering GmbH for the Musaimeer Pumping Station and Outfall Tunnel. This is qualitative research describing methods used to achieve required construction tolerance of the breakthrough. Stage-by-stage descriptions of different levels of our network are provided. The chosen approach for the tunnel network was developed internally and includes multiple network observations to a high accuracy prism installed every 50m and combined with the tunnel brackets installed every 200m, allowing to create one of the most stable network structures. In addition, an important part of the network was the gyroscopic survey.

All described activities were based on the Method Statement prepared prior to the start of the mining and approved by the client.

The data was processed and analysed using specialized survey software Microsurvey Star*net.

1.3 Technical Information

The Musaimeer Pumping Station and Outfall tunnel is a 10km long undersea tunnel. By the time of its construction, it was reported to be the 7th longest underwater tunnel in the World and the longest outfall tunnel in the Middle East. Being one of the major infrastructural projects of Qatar to be completed before the FIFA 2022 World Cup, it will have huge impact on the city's development in the future decades. The project aims to discharge the surface and stormwater, thus decreasing the surface water level and reducing pumping costs in construction projects around the country. It will also preserve the foundations of buildings and reduce land subsidence due to rain.

The client of the project was Ashghal, construction was awarded to the joint venture (JV) of Hamad Bin Khalid Contracting Company and PORR Qatar Construction Company (HBK-PORR). The tunnelling survey works were completed by Noack Engineering, Germany. The offshore works by installation of Polyvinyl Chloride (PVC) pipe were performed by MIC Construct (MIC). The mining

started on February 3, 2019 and was completed on February 3, 2021, exactly 2 years later. The maximum daily mining speed was achieved on November 28, 2019 – 33.8m (26 rings).

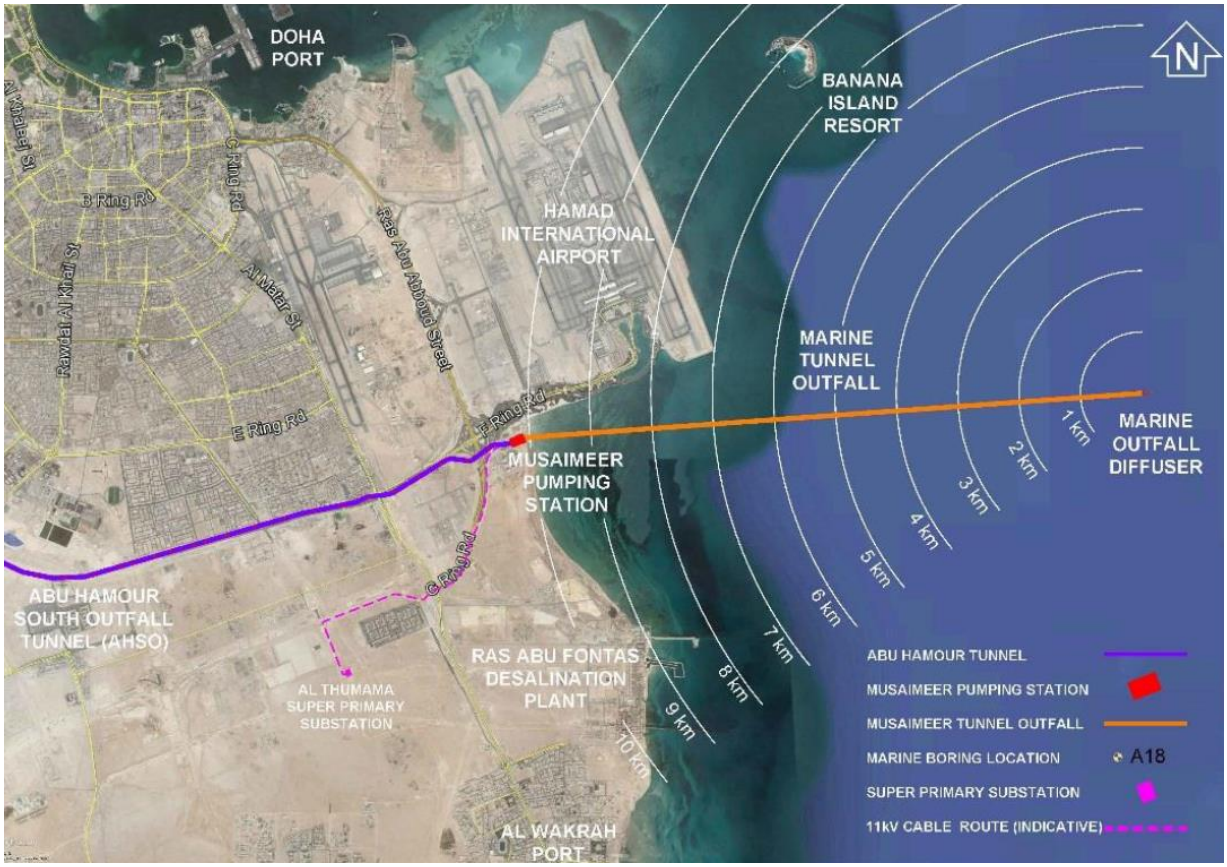


Fig. 1: Tunnel Alignment

Figure 1 shows the project alignment. The tunnel starts from a 37m deep shaft on the shore and follows a 10km alignment under the seabed. The horizontal alignment of the tunnel was a straight line connecting the launching shaft and the receiving riser shaft. The vertical alignment was also a straight line with a permanent inclination of +0.05% (50 mm/m). The vertical alignment increased from -36m to -31m below sea level. Which was approximately 15m below the seabed level. Mining was completed by a TBM. The tunnel has a diameter of 3.7m, with each ring at a length of 1.3m. The launching shaft had a 26m diameter and was 40m Deep with the receiving PVC pipe with a 3m diameter and encased in a 5m block of concrete.

1.4 Challenges

The survey works were faced with a few challenges:

1. Breakthrough to a riser shaft constructed offshore by another subcontractor –MIC. Therefore, it was extremely important to provide uniformity of survey networks between the two parties.
2. Accurate transference of the survey network from the surface to the base of the launching shaft and subsequently the TBM guidance system.
3. The length of the tunnel. The tunnel is 10km long without exit to the surface (no shafts, wells, openings etc.). This is combined with a small diameter of 3.7m. In addition, the tunnel started from a 40m deep shaft with a 26m diameter, which drastically reduced the accuracy of the launching bearing.

4. Differences in atmospheric conditions inside the tunnel, especially for the first 1,300m were very humid. Obviously, sudden changes of temperature and humidity caused air refraction and additional distortion to the measurement's accuracy.
5. Tough conditions of the mining required full time presence of survey team on the TBM. The inner space of the TBM was very congested. The survey window in which the navigation system was located was unfortunately located on the walkway; this meant the instrument had to be always manned to protect it from outside interference.

2 Main Surface Network

The network originated from 4 survey control pillars installed on the site by utilising Global Navigation Satellite System (GNSS) measurements. The points were located by utilising GNSS Static measurements which were processed against Qatar Network for Continuously Operating Reference Stations (QCORS) reference points.

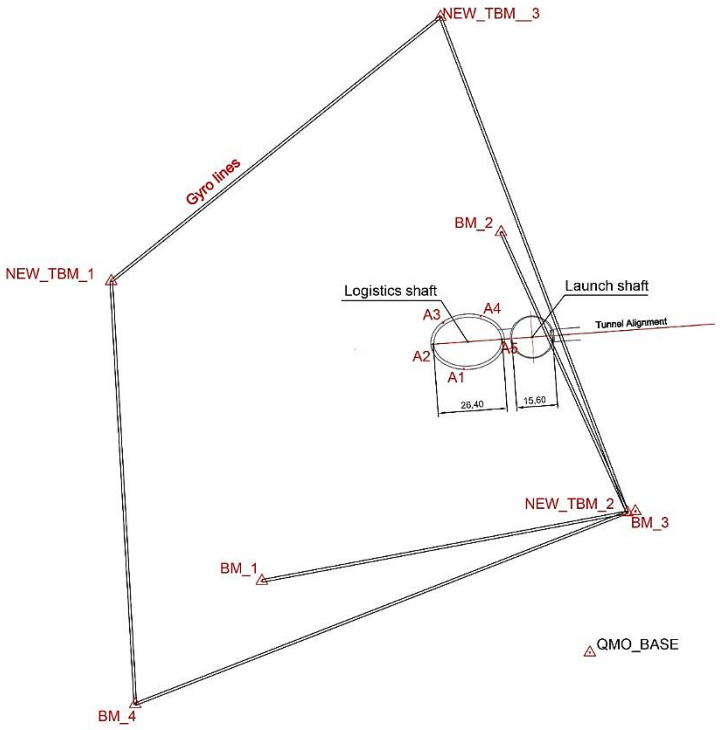


Fig. 2: Control points of the First and Second levels

These benchmarks where then also precisely levelled and coordinated from a minimum of Order 1 Qatar National Datum (QND) issued points to ensure they tied in with the QND network. In total these 4 points were located strategically on the edges of the site to maximise sighting distance and angle geometry. Figure 2 shows the location of site controls.

At the same time, MIC was responsible for the offshore works namely, PVC pipe installation (Riser shaft). MIC installed their first-order network base – point QMO_Base on the roof of HBK-PORR workshop at MPSO Site office. Government control point GD17 was used as main control point to calibrate the base station QMO_Base. A GNSS antenna receiver was set up on a tripod and tribrach plumbed above the control points; and GPS RTK measurements were recorded for at least 20 minutes (1200 epochs). After being established, QMO_Base broadcast the signal, ±10 kilometre offshore, to

the barge area. Noack Engineers Survey team did some verification of this point in Horizontal and Vertical positions to make sure that both parties work with a matching and consistent network.

3 Second Level Network

3.1 Site Network

The network derivative from the Main Surface Network was developed on site. As some of the primary pillars were obstructed on later stages – the survey team had to create derivative points NEW_TBM1, NEW_TBM2, NEW_TBM3. In addition to the pillars, in the Second level network 5 control points were created on the edge of the Launching shaft (A1 – A5) which has the largest diameter. The points on the edge of the shaft were 3D mini prism which could be observed both from the surface and the shaft. These points became the basis for the shaft network.

The points BM1, BM2, BM3, BM4 as well as NEW_TBM1, NEW_TBM2, NEW_TBM3 were built as pillars with the forced centering plate. They were designed this way to be used for the gyroscopic campaigns. In this case pillars were the best solution. They were located in protected areas on site (e.g. corners of the site) so that they could survive the duration of the project. It proved much easier and more precise to execute gyroscopic measurements on pillars rather than ground points.

3.2 Barge Network

MIC completed the works on installation of the PVC pipe, 10 km away from the seashore. The construction works were carried out from an anchored self-elevating platform (barge).

On specific locations of the barge, the survey team bolted tribrachs where a GNSS antennas were installed, and measurements conducted. Once coordinated with GPS coordinates on the QND grid system circular prisms were placed on the tribrachs. These points were measured with GPS in reference to the site office base point QMO Base. A total of 3 control points were installed on the barge. Each of them was observed in fast-static mode with a minimum period of 5 min. This exercise was conducted 4 times to verify the concordance of the observations. The barge points BM0, BM2, BM3 were used to install the PVC pipe according project coordinate system. Figure 3 shows the location of these points.

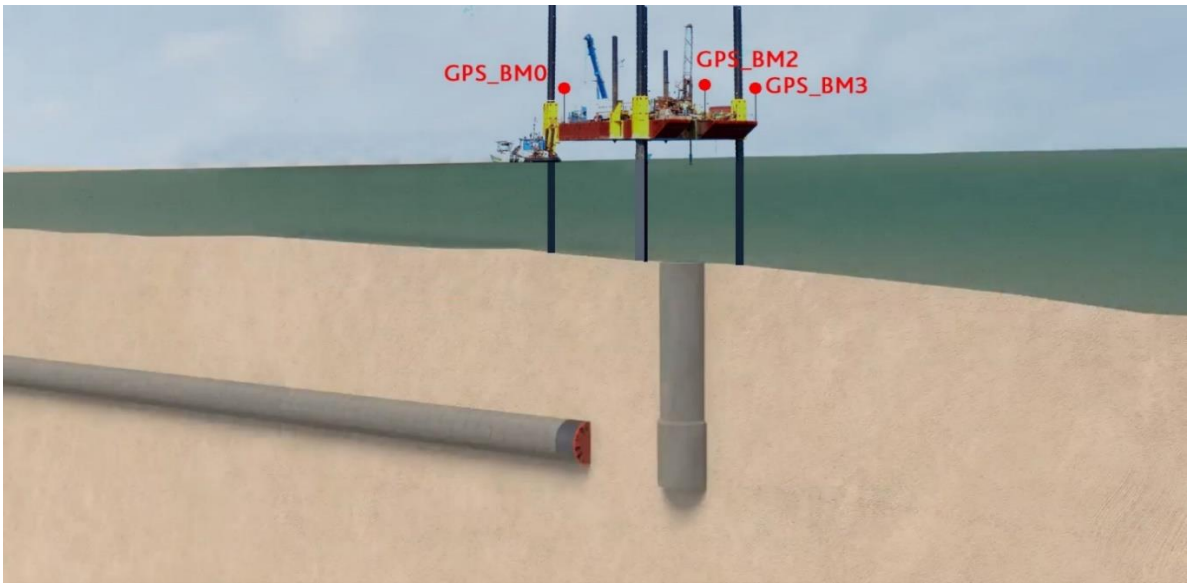


Fig. 3: PVC pipe installation from the Barge

Due to the different approaches of network creation, there were challenges to be overcome to ensure an accurate breakthrough. The surface points at the shaft area were measured by Noack Engineering for 4 hours on static GPS measurements. However, MIC used GPS RTK measurement which inherently had a 20 mm 3DCQ (3D Quality) and this would have increased over the 10km. This gave 70 mm displacement of the PVC pipe. Hence, course correction was applied to the TBM at breakthrough to align to this. Also, the MIC team were working on a scale factor of 1 whereas the project scale was 0.99999 meaning at 10km there was already a 100 mm error in distance. This factor was also taken into consideration by the Noack team.

4 Third Level Network – Shaft Network

The aim of the 3rd Level network was to bring the coordinates from the Site network down to the tunnel portal. Inside the shaft there are installed four arrays of 3D prism. From top to bottom there were there 3 levels of targets. Each level consists of 5 targets. As mentioned before, the prisms on the top edge were the part of the 2nd Level network – they were linked with observations to the pillars. Also, they were observed from the bottom of the shaft. As many measurements as possible are recorded to tighten the network. Figure 4 shows the location of shaft controls.

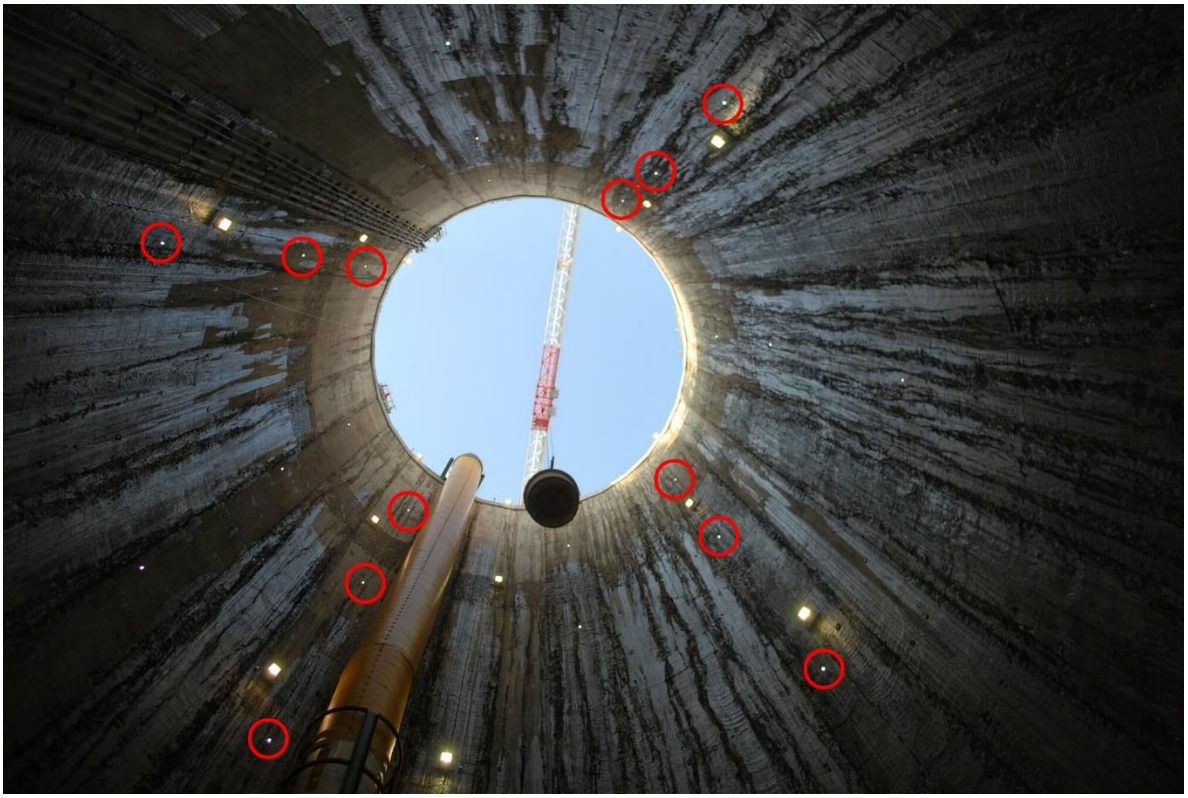


Fig. 4: Location of Shaft network controls (masked with red circles)

5 Fourth Level – Tunnel Network

Tunnel network was derivative from the shaft network. It was used for the TBM navigation and on-going wriggle as built in the rings. This network consisted of 3D prisms installed and anchored to the constructed segment via a brass spigot. These spigots were installed in pairs every 30 rings (about 48 meters) (e.g. on ring 840 left side, ring 845 right side, ring 870 left side, ring 875 right side). All tunnel control points were installed and observed with 11R5-W Leica Prism Adaptors with circular prism. The length offset from base of adaptor to prism centre is 100 mm. Figure 5 illustrates the sample of the tunnel control point.

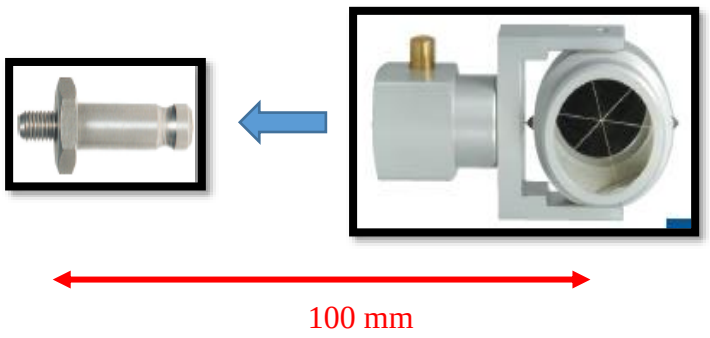


Fig. 5: Tunnel Control Point

The gyroscope brackets were installed every 126 rings (about 200 m) from each other. All network measurements were completed using a robotic 1-inch total station. From each station the surveyor observed as many targets as possible. As the result a dense, multi-shot network was formed. All the traverse works were repeated 3 times. Height values were controlled by precise levelling carried out by a digital level. The scheme of tunnel network is shown on Figure 7.

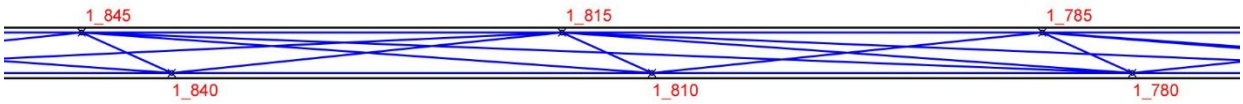


Fig. 6: Scheme of tunnel network

Concerning the fact that this network was created from transferring coordinates from the surface via a deep narrow shaft, it was expected that there would be a gyroscopic shift applied after the first gyroscope measurement as the initial launch bearing would be affected by the depth and narrow network transferred from the surface. Gyroscope measurements in the humidity and climate of Qatar meant all measurements had to be done in cooled shelters and also at night to mitigate the effects of the heat and humidity. The baselines had to be shorter to eliminate distortion due to the high humidity and temperature.

The gyroscopic measurements were done with the GYROMAT 3000 instrument by DMT, Germany. Initially the measurements were planned to be executed once the TBM would reach 500 m, and then subsequently every 1000-1500m. However, COVID-19 pandemic changed this schedule dramatically. The first campaign was taken at 779m, the second at 2210m, as planned. But the third campaign had to be postponed as no engineers from Germany could travel to Qatar during the lockdown. Due to such restrictions the third campaign (at 8138m) and the fourth campaign (at 9295m) were carried out by the Noack survey team, controlled via online internet connection by engineers from DMT offices in Germany.

In gyroscopic calculation the surface network baselines between pillars NEW_TBM_1, NEW_TBM_2, NEW_TBM_3 and BM_1, BM_2, and BM_4 were used.

6 Discussion and Conclusion

This is the case study, and it has limitations inherently peculiar to the MPSO project based on its specification, location and design. This being said, the issues, achievements and methodology used are not 100% representative of all industry practices and methods.

To sum up:

The accuracies utilized for the offshore work were determined by the 10km baseline achieved the Real-Time kinematic GNSS measurements, this in addition to the marine construction tolerances provided a large discrepancy in comparison to the strict tunnel drive tolerances. The depth and acute diameter of the launch shaft proved difficult to transfer accurate levels & Coordinates to the base. The 3.7m diameter of the tunnel and the 26m diameter of the shaft increased the initial error prior to launch as the horizontal angles measured in the launch adit were very acute with this alongside the short sighting distance meant the error factor was increased.

Temperature and humidity affected greatly our instrumentation from corrosion and reduction in accuracy on our network measurements and on the guidance system. Surveyors had to overcome harsh atmospheric conditions at the TBM, and these conditions were difficult for the navigation equipment. The total stations often required repairing – this is why there were 2 total stations on site – operational and spare.

All these major challenges were solved: A consistent surface network was built on the shore and offshore using the GNSS method, in order to make sure that the tunnel is constructed. This case study shows importance of coordination between two interface companies, Transfer the surface network to the shaft, then build an accurate tunnel network for the whole length of 10 km, Proper organization of the works helped to avoid delays in construction and minimize delays. A crucial part of the solution was introduction of 4 gyroscopic campaigns which were carried out during the Covid-19 travel restrictions, which was yet another challenge to the project.

Finally on February 3, 2021 the TBM has reached its final destination, passing through the concrete block of the shaft. Later the tunnel crown was opened and the final breakthrough result, considering all tolerances was 0.200m. Efforts and deep cooperation of the tunnel construction team and survey team made this landmark project true.

References

Benecke, N. & Kalz, U. (2006). Ensuring tunnel navigation by cost-effective gyroscope control measurements. Tunnelling and Underground Space Technology - TUNN UNDERGR SPACE TECHNOL. 21. 253-253. 10.1016/j.tust.2005.12.115.

Kazingizi Simbarashe. (2018) 'Method Statement for TBM Tunnel Survey', Musaimeer Pumping Station Outfall, Document reference number: C2017_109-MST-QM-0051.

Lee, Andrew Hung Shing. (13-17 May 2007) 'Engineering Survey System for TBM (Tunnel Boring Machine) Tunnel Construction Strategic Integration of Surveying Services', FIG Working Week 2007, Hong Kong SAR, China.

Specification for Tunnelling, Third Edition (2010), The British Tunnelling Society and The Institution of Civil Engineers, Thomas Telford Limited.

Szafarczyk, A., Skaba, A. & Sokalla, K. (2019). Implementation of gyroscope measurements in underground mines; focus on the mine of ruch (unit) „Borynia" in the Jastrzębie Coal Company. *Geoinformatica Polonica. 18*. 113-120. 10.4467/21995923GP.19.009.11576.

Thomas, R. K., Elwyn, H. K. & Bickel, J. O. (2012). '*Tunnel Engineering Handbook*', Springer Science & Business Media, Dec *6*, 2012 - Technology & Engineering.

Cite as: Peach G., Al-Marri S.Z., Fernandez H.V., Kazingizi S. & Chumakou P., "Tunnel Surveying Works. A challenge of 10 km long tunnel under the Arabian Gulf - Qatar", *The 2nd International Conference on Civil Infrastructure and Construction (CIC 2023)*, Doha, Qatar, 5-8 February 2023, DOI: https://doi.org/10.29117/cic.2023.0070

Numerical Study on the Pull-out Behavior of Steel Fibers in Cement-Based Composites

Ammar Babiker
School of Civil Engineering, College of Engineering, Sudan University of Science and Technology
Khartoum, Sudan
ammar.babiker@sustech.edu

Ebtihaj Abu-Elgasim
School of Civil Engineering, College of Engineering, Sudan University of Science and Technology,
Khartoum, Sudan
ebtihaj.gasim@sustech.edu

Abstract

The interaction between steel fiber and surrounding cement-based matrix and concrete materials is crucial in the behavior of Steel Fiber-Reinforced Concrete (SFRC). This interaction is generally measured through a single fiber Pull-out test. Considerable research has been conducted in this field. However, efforts have been largely directed to the analytical and experimental methods, whereas very limited research has been performed using the finite element method. Having an authentic numerical model, numerical parametric studies together with experiments can serve as an essential tool to enhance the understating of bond behavior. Therefore, this study attempts to numerically investigate the behavior of fiber bonds in SFRC composites. The bond behavior was investigated using different approaches of modeling bonds in the LS-Dyna explicit software. The validation of the finite element model was performed with the comparison of computed and experimental pull-out force obtained from the literature. It is shown that the validation is possible for all investigated approaches and the computation results showed a strong agreement between pull-out force and relative displacement with experimental results of previous studies. Finally, the validated model is employed as a powerful tool to simulate the bond behavior of a single steel fiber embedded in a cement-based matrix.

Keywords: Pull-out; Bond behaviour; Fiber-reinforced composite; Steel fiber; Cement-based; Finite element

1 Introduction

In fiber-reinforced composites, the fiber and its surrounding matrix are rendered tight together through the so-called bond interaction. Understanding this interfacial behavior is essential for interpreting the global behavior of these materials. To investigate the bond behavior of the steel fiber and its adjacent cement base, numerous studies examined fiber pull-out tests using different testing configurations and different materials, for instance, see Friedrich & Wang (2016); Gray & Johnston (1984); Li et al. (1991); Morrison et al. (1988); Pinchin & Tabor (1978); Stang & Shah (1986). Though it is a big challenge to derive and extract the properties of steel fiber-reinforced composites from single fiber pull-out tests, the results obtained from these tests can provide an excellent idea of how to identify the mechanical properties of SFRC materials (Hughes & Fattuhi, 2012; Maage, 1977). Previous investigations performed by Naaman et al. (1992) and Banthia & Trottier (1995) reported that fiber to its adjacent matrix interfacial bond quality is always evaluated using the single fiber pull-

out test configuration, in which fiber slip is addressed as a function in the fiber applied load خطأ! لم يتم العثور على مصدر المرجع. illustrates a typical pull load-slip behavior for straight, rounded and hooked-end steel fibers.

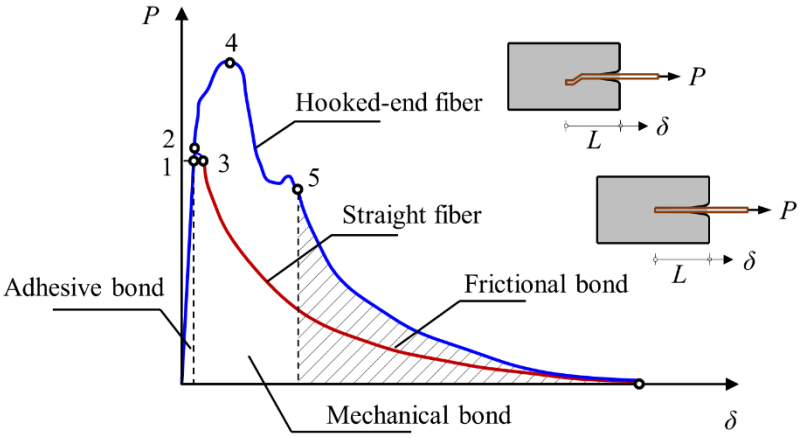


Fig. 1: Schematic representation of pull-out load-slip behavior, adapted from Kooiman (2000)

2 Methods of Modeling Bonds in Fiber-Reinforced Composite

Bond interaction between the reinforcing steel and surrounding matrix provides an essential process for SFRC composites. Embedding steel bars into the concrete matrix or cement-based materials should be implemented in such a manner that the cement-based matrix resists the compressive stresses acting in the structural elements. In contrast, steel reinforcement resists tensile stresses. Bond action of the matrix and embedded steel bars is generally acquired by three different mechanisms: chemical adhesion, mechanical friction, and mechanical interlocking. The function of each depends highly on the composition of the particular structural member. Many techniques are nowadays available in LS-Dyna commercial finite element software to model bond, de-bond, and sliding mechanisms between the reinforcing bar and the surrounding matrix, for instance, shared nodes, constraint nodes, and one-dimensional contact algorithms. If needed, the constraint method can be operated with a pre-defined bond-slip relationship. These methods are described in the following:

2.1 Merged Common Nodes

The merged common nodes are widely known as shared nodes. In this technique, the so-called perfect bond between the continuum Lagrangian and the embedded beam or truss elements can be realized by merging the common nodes of the two parts. This process enables the nodes of the continuum Lagrangian to share the same locations as those of the beam or truss elements (LSTC, 2018; Schwer, 2014). خطأ! لم يتم العثور على مصدر المرجع. shows a representation of the concept of shared nodes.

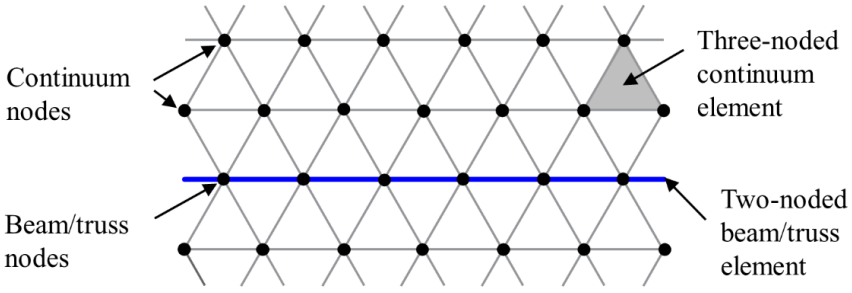


Fig. 2: Concept of the shared or merged nodes

2.2 Constraint Methods

Unlike the previous method, here in a method, the keyword *CONSTRAINED_BEAM IN_SOLID (CBIS) can be utilized to achieve the perfect bond by embedding the beam or truss elements into the Lagrangian elements with full kinematic compatibility. The CBIS option was developed and implemented in LS-Dyna code to avoid certain limitations of the previous keyword *CONSTRAINED LAGRANGE_IN_SOLID keyword (CLIS). In this option, the beam or truss elements are constrained to move over with the Lagrangian continuum. In the CBIS, no coincidence nodes of solid elements and beam elements are required, therefore; each part can be discretized independently, and the movement of the two discretizations is constrained automatically (Bermejo et al, 2014; LSTC, 2018; L. Schwer, 2014). A schematic representation of the constraint nodes method is presented in خطأ! لم يتم العثور على مصدر المرجع.

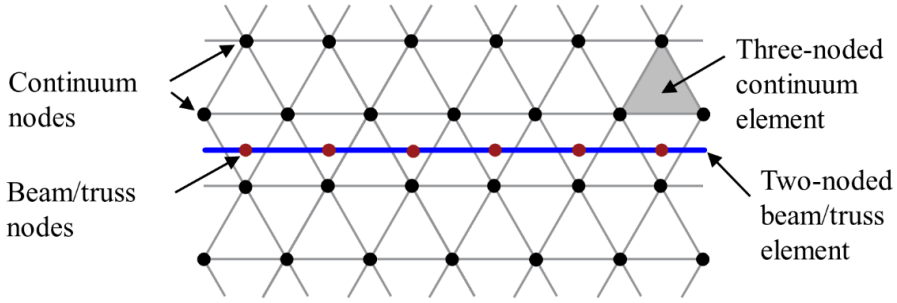


Fig. 3: Concept of the constraint nodes

2.3 One Dimensional Contact Algorithmic

The bond behavior of the reinforcing steel and the surrounding concrete and cement-based matrix can also be modeled using the so-called 1D (one-dimensional) contact law implemented in LS-Dyna explicit finite element software. This contact algorithm can be defined using LS-Dyna keyword *CONTACT_1D using the following expression.

$$u_{max} = SMAX\, e^{-EXP \cdot D} \tag{1}$$

where D defines the damage parameter, which is the sum of the absolute values of the plastic displacement increments $D_{n+1} = D_n + \Delta_u$, u_{max} represents the maximum permissible slip-strain, EXP is the damage curve exponent, and $SMAX$ the maximum shear strain.

By taking into consideration accumulative damage, the interfacial bond between the reinforcing bar and the surrounding concrete matrix is decomposed in a two-phase model. In the elastic range, the bond strength is linearly proportional to the relative slip S. After reaching the maximum bond strength τ_{msx}, the bond shear will decay exponentially in the plastic zone.

$$\tau = \begin{cases} GBS, & S \le SMAX \\ \tau_{max} e^{(-EXP \cdot D)}, & S > SMAX \end{cases} \tag{2}$$

3 Experimental Setup

In FRC structural members, bond failure is most often achieved due to fiber Pull-out and splitting. خطأ! لم يتم العثور على مصدر المرجع. presents a test setup of the single fiber Pull-out test set-up. It is a servo hydraulic apparatus. An experimental investigation of Shannag et al. (1997) will be adopted in this

work to validate the reliability, convergence, and accuracy of the finite element models and their chosen contact algorithms. For more details, see (Shannag, 1997).

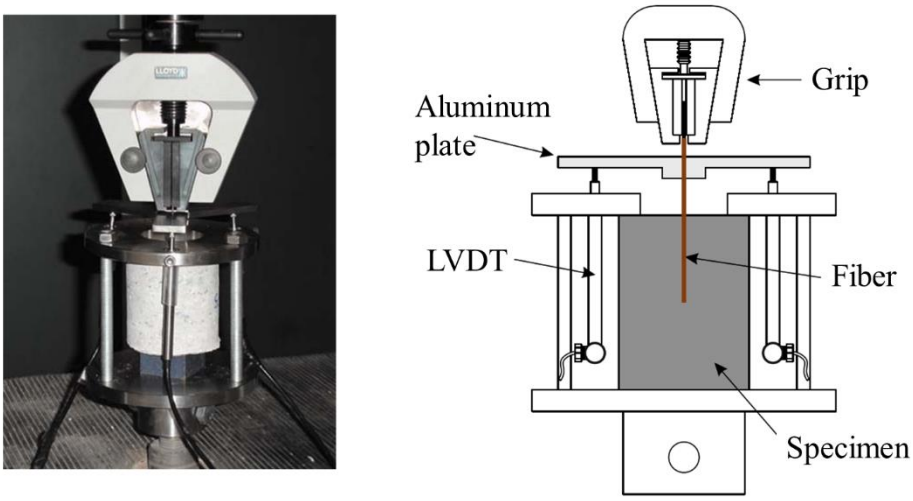


Fig. 4: Single fiber pull-out test setup, according to Shannag et al. (1997)

4 Finite Element Simulations

In this research, three different finite element models were developed to investigate the behavior of the single fiber pull-out test in a cement-based composite. Each model has a different contact algorithm that defines the interfacial contact between the cement-based matrix and steel fiber. Their properties and modeling aspects are presented in the following section:

4.1 Geometry and Discretization

A three-dimensional numerical model of the single fiber pull-out test was developed, including the cylindrical cement-based matrix and the embedded straight and rounded steel fiber. The bonded segment of the fiber is set to 12 mm, which is located in the middle of the cement-based cylindrical specimen and has a diameter of 16 mm and a length of 32 mm, see خطأ! لم يتم العثور على مصدر المرجع.

Each numerical model has 1,248 eight-noded hexahedron Lagrangian elements for the cement-based matrix and 5 two-noded beam elements for the fiber. To keep the model simple and minimize the computational time, the Hughes-Liu formulation was adopted for the steel fiber, whereas one point integrated solid formulation was used in the simulation for the cement-based matrix. The mesh size chosen for both parts, cement-based matrix and steel fiber, was 4 mm. The overall number of the elements and nodes used for any part in each model is listed in **Table 1**. The static displacement loadings were applied at the top endpoint of the steel fiber using LS-Dyna keyword *PRESCRIBED_MOTION_NODE, see خطأ! لم يتم العثور على مصدر المرجع. The cylindrical specimen was constrained against any movement in the x, y, and z directions at the top surface nodes. In this study, the time-step scale factor is set to a default value of 0.9, which is the most significant value to ensure minimum computational time and result accuracy.

Table 1: Elements and nodes in each simulation

Phase	Number of elements	Number of nodes
Matrix	1,248	1,521
Steel fiber	5	6

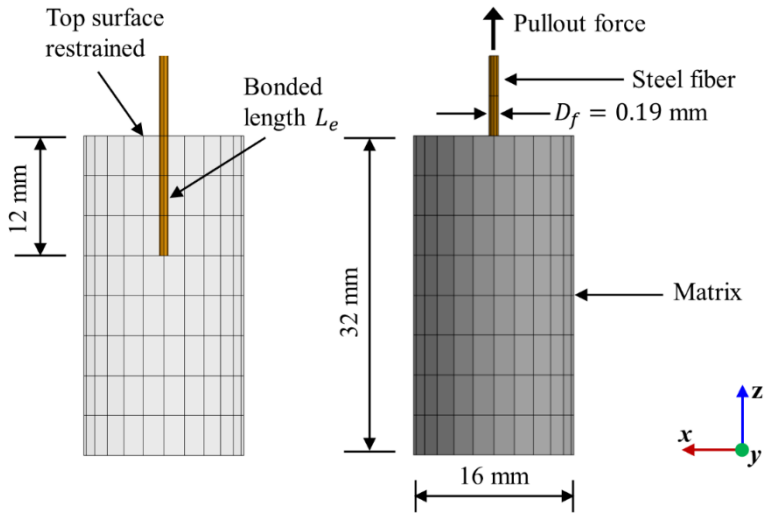


Fig. 5: Finite element discretization of single fiber Pull-out test

4.2 Conistitutive Material Model

For any phase of the finite element model, an adequate material formulation needs to be defined. In this work, the mechanical material parameters of Shannag et al. (1997) were adopted. This allows the verification of the simulated results with the experimental ones. Within previous studies, a large number of constitutive material formulations in the LS-Dyna finite element were investigated and analyzed by many researchers to their capabilities of modeling such types of bond problems (Babiker et al., 2022; Fang & Zhang, 2013).

LS-Dyna finite element code provides a large number of material models that can be applied for concrete and cement-based materials, including the Continous Surface Cap Model (*MAT_159), Schwer and Murray Cap Model (*MAT_145), Winfrith Concrete (*MAT_084), Karagozian and Case (*MAT_072R3) and many others. In this work, Schwer & Murray Cap Model (SMCM) was adopted due to its better capabilities of simulating such problems. The SMCM is a three-invariant extension of the Geological Cap formulation. This material involves visco-plasticity to account for the strain-rate effect and also utilizes damage mechanics to include strain softening and modulus degradation in both tension and compression. More details about this formulation and parameters adjacent can be found in (Schwer (1994; Schwer & Murray, 2002).

The steel fiber is assumed to behave as elastic ideal plastic without hardening. The material model Piecewise Linear Plasticity (*MAT_024) was employed to define the material parameters of the steel fiber. The rate effect is irrelevant in the research, therefore; it was ignored. **Table 2** gives the material parameters defined in each model according to the experimental data.

Table 2: Material parameters

Parameter	**Matrix**	**Fiber**
Unit weight [kg/m^3]	2400	7850
Compressive strength [G[1]Pa]	0.040	-
Tensile strength [GPa]	0.0035	2.99
Modulus of elasticity [GPa]	25	200
Poisson's ratio [-]	0.2	0.3

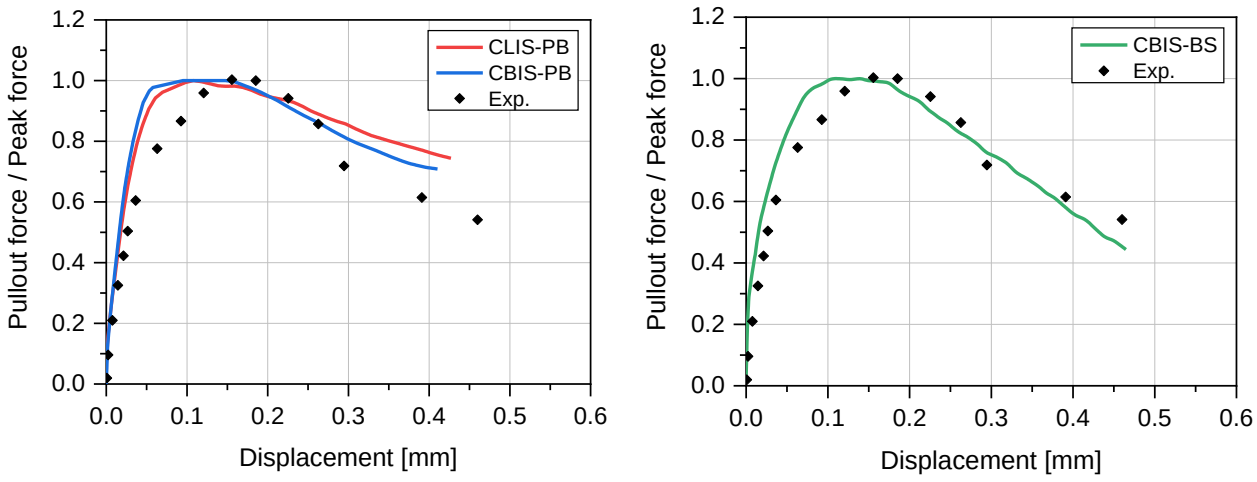
[1] GigaPascal

4.3 Contact Algorithm

As discussed in Section 2, numerous methods are available in the LS-Dyna finite element to simulate the interfacial behavior of the steel fiber and the cement-based matrix. In this research, three different methods were investigated. In the first step, the perfect bond was achieved with constrained nodes using *CONSTRAINED_BEAM_IN_SOLID. In the second step, the perfect bond was modeled with constrained nodes using *CONSTRAINED_LAGRANGE_IN_SOLID. Finally, the constrained method was used again, but this time with a pre-defined bond-slip curve. This method was utilized using the *DEFINE_FUNCTION keyword. The pre-defined bond-slip curve was written in Fortran syntax and then implemented into the LS-Dyna finite element code. The three investigated methods will be identified later as CBIS-PB, CLIS-PB, and CBIS-BS, respectively.

5 Finite Element Results

The computed pull-out force versus relative displacement curves are illustrated in **Fig. 6**, along with the experimental data.



(**a**) perfect bond (**b**) bond-slip

Fig. 6: Pull-out-displacement curve in comparison to the simulation results

According to **Fig. 6**(a), it can be observed that there is a good correspondence between the predictions of the simulated perfect bond methods and the experimental results. Accordingly, both the constraint nodes and shared nodes methods in LS-Dyna are considered to be acceptable approaches for handling the perfect bond between the embedded fiber and the adjacent cement-based matrix. The pull-out versus displacement relationship computed using a pre-defined bond slip, seen in **Fig. 6**(b), also largely corresponds to experimental results, especially when it comes to the strain-softening behavior.

Based on the obtained result of this work, it can be concluded that the CBIS and CLIS techniques of LS-Dyna finite element code can well capture the bond interaction between the cement-based matrix and the embedded steel fiber; therefore, they are recommended for modeling such problems and also can be used in comprehensive parametric studies on different aspects such as fiber diameter, fiber embedded length, fiber shape, material formulation, bond law, loading rate, and many others.

Furthermore, **Fig. 7** gives the propagation of the effective plastic strain on the cement-based matrix during the analysis. It should be mentioned that the damage patterns in **Fig. 7** are the result of the PB-CBIS method.

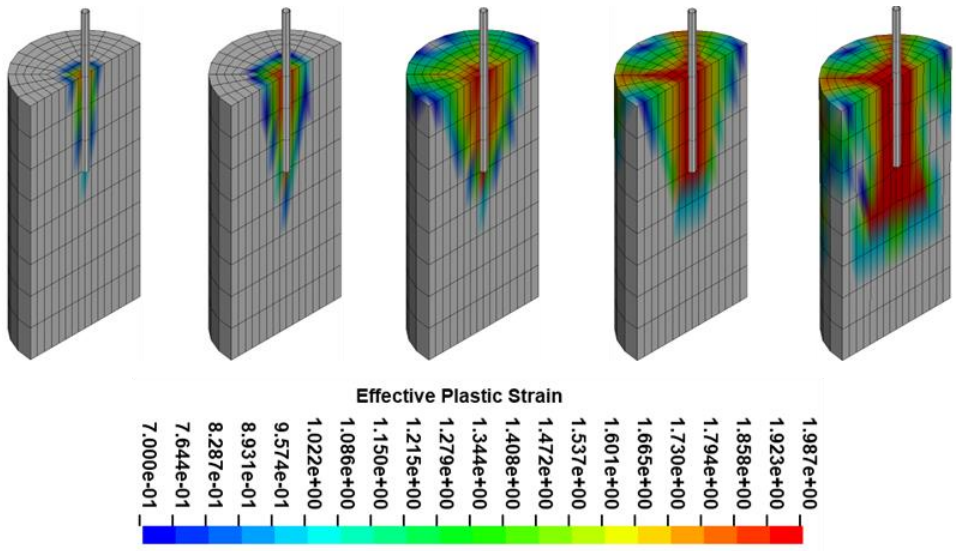


Fig. 7: Damage states at the center cut plane for the CBIS-PB configuration

6 Conclusions

The presented paper gave a brief description of finite element investigation on the pull-out behavior of steel fiber in a cement-based composite. Three different methods of bond modeling in LS-Dyna finite element commercial software were examined. The developed finite element models were validated against the experimental result with good agreement. Based on the simulated results of this work, the following conclusions may be derived.

It is demonstrated that the merged and constrained nodes methods of LS-Dyna finite element code can well capture the pull-out behavior of steel fiber in a cement-based matrix. A future study has to investigate the capabilities of the 1D (one dimensional) algorithm of LS-Dyna, and the influence of mesh density and many other influential parameters to derive further benefit from these models and also to identify any exciting limitations they may have.

References

Babiker, A., Dean, A., Abu-Elgasim, E. & Abdel-Magid, T. (2022). Numerical modeling of steel fiber reinforced concrete spallation exposed to medium loading rate. *Global Journal of Engineering and Technology Advances*, *12*(2), 001–014. https://doi.org/10.30574/gjeta.2022.12.2.0130

Banthia, N. & Trottier, J. F. (1995). Concrete reinforced with deformed steel fibers part II: toughness characterization. *ACI Materials Journal*, *92*(2), 146–154. https://doi.org/10.14359/9765

Bermejo, M., Santos, A. & Goicolea, J. M. (2014). A methodology to calibrate structural finite element models for reinforced concrete structures subject to blast loads. *Proceedings of the IX International Conference on Structural Dynamics, EURODYN2014, July*, 3497–3502. http://oa.upm.es/36297/

Fang, Q. & Zhang, J. (2013). Three-dimensional modelling of steel fiber reinforced concrete material under intense dynamic loading. *Construction and Building Materials*, *44*, 118–132.

Friedrich, L. F. & Wang, C. (2016). Continuous modeling technique of fiber Pull-out from a cement matrix with different interface mechanical properties using finite element program. *Latin American Journal of Solids and Structures*, *13*(10), 1937–1953.

Gray, R. J. & Johnston, C. D. (1984). The Effect of Matrix Composition on Fiber/Matrix Interfacial Bond Shear Strength

in Fiber-Reinforced Mortar. *Cement and Concrete Research*, *14*(2), 285–296.

Hughes, B. P. & Fattuhi, N. I. (2012). Fibre bond strengths in cement and concrete. *Magazine of Concrete Research*, *27*(92), 161–166. https://doi.org/10.1680/macr.1975.27.92.161

Kooiman, A. G. (2000). Modelling Steel Fibre Reinforced Concrete for Structural Design. In *PhD thesis*. PhD thesis, Delft University of Technology.

Li, Z., Mobasher, B. & Shah, S. P. (1991). Characterization of Interfacial Properties in Fiber ‐ Reinforced Cementitious Composites. *Journal of the American Ceramic Society*, *74*(9), 2156–2164. https://doi.org/10.1111/j.1151-2916.1991.tb08276.x

LSTC. (2018). *Keyword User ' S Manual Volume 1: Vol. I*.

Maage, M. (1977). Interaction between steel fibers and cement based matrixes. *Matériaux et Constructions*, *10*(5), 297–301. https://doi.org/10.1007/BF02478831

Morrison, J. K., Shah, S. P. & Jenq, Y. (1988). Analysis of Fiber Debonding and Pull-out in Composites. *Journal of Engineering Mechanics*, *114*(2), 277–294. https://doi.org/10.1061/(ASCE)0733-9399(1988)114:2(277)

Naaman, A. E. et al. (1992). Fiber Pull-out and bond slip. I: Analytical study. *ASCE Journal of Structural Engineering*, *117*(9), 2769–2790.

Pinchin, D. J. & Tabor, D. (1978). Interfacial phenomena in steel fiber reinforced cement II: Pull-out behavior of steel wires. *Cement and Concrete Research*, *8*, 15–24.

Schwer, L. (2014). *Modeling rebar: the forgotten sister in reinforced concrete modeling*. http://sce.umkc.edu/blast-prediction-contest/

Schwer, L. E. (1994). Viscoplastic augmentation of the smooth cap model. *Nuclear Engineering and Design*, *150*(2–3), 215–223. https://doi.org/10.1016/0029-5493(94)90138-4

Schwer, L. E. & Murray, Y. D. (1994). A three ‐ invariant smooth cap model with mixed hardening. *International Journal for Numerical and Analytical Methods in Geomechanics*, *18*(10), 657–688. https://doi.org/10.1002/nag.1610181002

Schwer, L. E. & Murray, Y. D. (2002). Continuous surface cap model for geomaterial modeling: A new LS-DYNA material type. *7th International LSDYNA Users Conference*, *2*, 35–50.

Shannag, M. J., Brincker, R. & Hansen, W. (1997). Pull-out behavior of steel fibers from cement-based composites. *Cement and Concrete Research*, *27*(6), 925–936. https://doi.org/10.1016/S0008-8846(97)00061-6

Shi, Y., Li, Z. X. & Hao, H. (2009). Bond slip modelling and its effect on numerical analysis of blast-induced responses of RC columns. *Structural Engineering and Mechanics*, *32*(2), 251–267. https://doi.org/10.12989/sem.2009.32.2.251

Stang, H. & Shah, S. P. (1986). Failure of fibre-reinforced composites by pull-out fracture. *Journal of Materials Science*, *21*(3), 953–957. https://doi.org/10.1007/BF01117378

Cite as: Babiker A. & Abu-Elgasim E., "Numerical Study on the Pullout Behavior of Steel Fibers in Cement-Based Composites", *The 2nd International Conference on Civil Infrastructure and Construction (CIC 2023)*, Doha, Qatar, 5-8 February 2023, DOI: https://doi.org/10.29117/cic.2023.0071

Development and Implementation of Ashghal Guidelines for the Evaluation and Repair of Sinkholes

Jamal Essa M Al-Ansari
Roads Operation & Maintenance Department, Public Works Authority (Ashghal), Doha, Qatar
alansari@ashghal.gov.qa

Khaled E Hassan
Stantec UK Limited, Qatar Branch, Doha, Qatar
khassan@ashghal.gov.qa

Kempaiah Kantha Kumar
Roads Operation & Maintenance Department, Public Works Authority (Ashghal), Doha, Qatar
kkumar@ashghal.gov.qa

Khaled N Helali
Stantec UK Limited, Qatar Branch, Doha, Qatar
khilali@ashghal.gov.qa

Abstract

Sinkholes are a common and recurring problem with potential safety risks to road users and authorities. A sinkhole is a void in the ground caused by natural and/or manmade activities, and mainly associated with carbonate rocks and underground water movement. It occurs suddenly and manifests as a hole in the ground, with the potential to cause significant problems of road closure and interruption to road users and construction activities. With the vast infrastructure, development over the last two decades and the majority of soil formation of Qatar exposes limestone and dolomites, the number of reported sinkholes has increased dramatically. This paper presents the development and implementation of new guidelines for the evaluation and repair of sinkholes for the Roads Operation and Maintenance Department (ROMD) at the Public Works Authority (Ashghal). It reviews the methodology adopted for the classification of sinkholes, application of Ground Penetrating Radar (GPR) technique for the early detection of subsurface voids and sinkholes before they become major problems. It also covers the approach adopted by ROMD and its Framework Partners for the repair of sinkholes. A case study is presented on the implementation of the new guidelines for the effective evaluation and repair of sinkholes, with performance monitoring in service. Successful implementation of the new guidelines contributes to enhanced management of road network in Qatar by maximizing asset performance and minimizing accidents and service disruption.

Keywords: Carbonate rock; Grout; Foamed concrete; Sinkhole geometry; Repair strategy

1 Introduction

With the rapid development of Qatar's infrastructure, there is an increasing concern about subsurface voids and sinkholes that pose health and safety hazards to road users and operators. Geologically, Qatar lies on a bed of sedimentary rock mostly made up of tertiary limestone and dolomite with interbedded clay, shale, gypsum and marl (Cavelier et al., 1970). These dominantly carbonate strata are highly variable, with strong bands interbedded with much weaker materials and dissolution cavities infilled with uncemented material. The strata have been subject to extensive dissolution and

formation of cavities and sinkholes due to underground water movement (Leblanc, 2008). Sub-surface voids/sinkholes result from the simultaneous or sequential activity of subsurface dissolution and downward movement of the overlying material by internal erosion and/or gravity.

Sinkholes appear suddenly as a hole in the ground or pavement, even though they occur over a long time of bedrock erosion. Natural sinkholes are generally formed over thousands of years, whereas manmade activities can greatly accelerate their occurrence. For example, construction activities tend to increase overburden loads or lowering groundwater level, causing existing voids at deeper depths to collapse. In addition, breakage of water and sewer pipelines results in washing out the fine particles of soil and void formation (Iqbal, 2019). Many shallow depressions of 9736 are reported in Qatar over the last three decades, with the average intensity of 1 per km^2 (Sadiq & Nasir, 2002).

This paper summarises the guidelines developed by the Roads Operation and Maintenance Department (ROMD) at the Public Works Authority (Ashghal) for the evaluation and repair of sinkholes (Ashghal, 2020). The guidelines provide a quick and simple way for the classification of sinkholes, based on underground investigation using ground-penetrating radar (GPR), and effective procedures for repair, considering conventional construction materials and equipment currently in use in Qatar. A case study on the evaluation and repair of a sinkhole is presented along with performance monitoring approximately 20 months in service.

2 Detecting and Evaluation of Sub-Surface Voids/Sinkholes

Various techniques have been used for the detection of ground subsidence including GPR, electrical resistivity tomography, acoustic sensing, ultrasonic sensing, and seismic sensing. The GPR is a subsurface imaging method that provides high-resolution information to a depth of up to 30 m. Low frequency waves are generally used for deep ground investigation whereas high frequency waves are used for near surface. Ashghal is utilising a piece of advanced GPR equipment with a step frequency between 10 MHz and 10 GHz that enables high resolution scans up to four metres beneath the road surface. Fig. 1 shows the Ashghal GPR equipment, which operates by sending electromagnetic radar waves into the pavement structure to detect changes in subsurface properties.



Fig. 1: 3D-GPR equipment utilised by Ashghal for Sinkhole investigations

3 Sinkhole Repair Methodology

The methodology for sinkhole repair is dependent on appropriate evaluation of sinkhole causes and dimensions that need to be considered before repair. Fig. 2 illustrates the methodology of sinkhole evaluation and repair. The most important factors in the evaluation process are the causes of sinkhole and geometrical dimensions. The location of a sinkhole adjacent to a highway structure or building may influence the repair method to be followed.

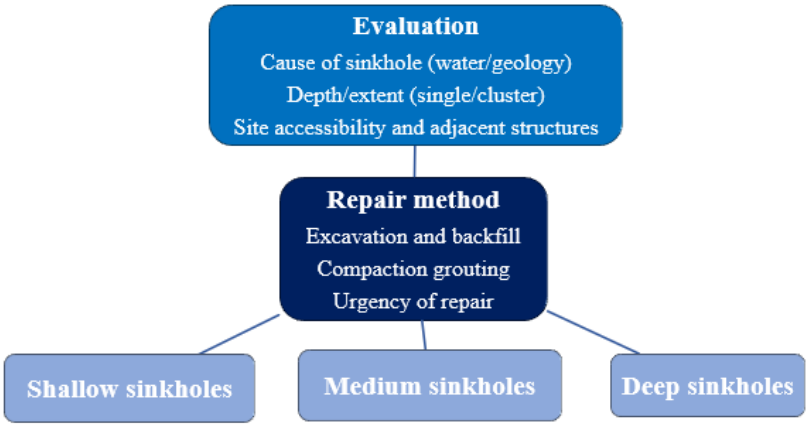


Fig. 2: Sinkhole Repair Methodology

4 Evaluation of Sub-Surfcae Voids/Sinkholes

4.1 Causes of Sinkholes

Water is the main triggering mechanism for sinkhole formation and development. Natural sinkholes are generally formed due to extensive dissolution of carbonate rocks due to changes in water/sea level and rainfalls. Manmade sinkholes are mainly associated with construction activities such as deep excavation of soil, dewatering, improper compaction, or breakage of pipelines. Increased construction activities and water movement result in increased soil erosion and weakening of the pavement structure. When the overburden loads exceed the load-bearing capacity of the foundation, the upper pavement surface eventually falls through and collapses as shown in Fig. 1. If water is found in a sinkhole, the source shall be identified. Water leaks caused by broken utility pipes should be immediately reported to the appropriate authority, who will undertake the remedial measures to stop the leak or discharge before repairing the sinkhole and reinstating the pavement layers.

4.2 Depth of Sinkhole

Sinkholes are generally circular in plan with a funnel shape, where the wide end opens at the surface and the narrow end is at the bottom. The depth of a sinkhole refers to the depth from the pavement surface (Finished Road Level, FRL) to the bottom of the sinkhole, as shown in Fig. 3. For repair purposes, sinkholes are classified into shallow, medium and deep as given below:

- Shallow sinkholes – up to 1.5m depth from the Finished Road Level (FRL)
- Medium sinkholes – greater than 1.5m and less than 5m depth from the FRL
- Deep sinkholes – greater than 5m depth from the FRL

Shallow and medium sinkholes are generally reached at their bases using regular excavation equipment, whereas deep sinkholes require drilling to reach their bases. In addition to the evaluation of a sinkhole depth, the length and width as shown in Fig. 3 are also required for appropriate repair.

Sinkholes can vary in size and depth and could be isolated or connected to other voids to form a cluster of sinkholes. The presence of a sinkhole throat indicates connected voids or cavities, which need to be sealed before repair, as discussed later in this paper. Evaluating the size and extent of sinkholes are essential for selecting the appropriate repair method.

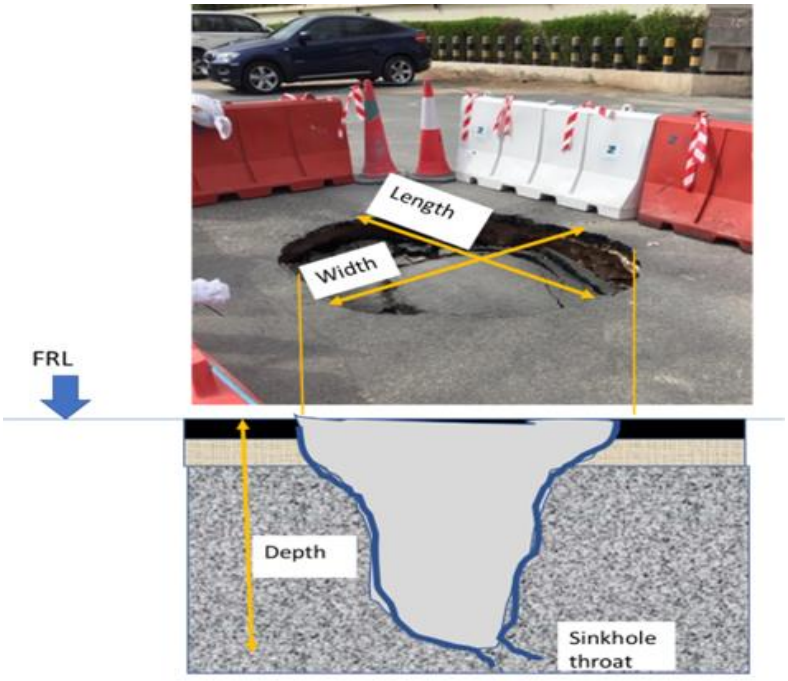


Fig. 3: Measurement of sinkhole dimensions

4.3 Adjacent Structures

The position of existing infrastructure in relation to the sinkhole location shall be identified together with any damaged of subsurface utility services. The foundation of a building or a structure could be greatly affected by the adjacent sinkhole. Utility pipelines and ducts that cannot be shut down or rerouted need to be considered during the repair process.

5 Repair Methods

Two techniques are considered in the Ashghal guidelines (Ashghal, 2020) for the repair of sinkholes to include excavation and backfill and compaction grouting. The excavation and backfill method is used for the repair of shallow- and medium-depth sinkholes, whereas the compaction grouting is used for the repair of deep sinkholes. The repair work needs to be carried out in coordination with the relevant authorities to ensure nearby utilities of water, sewer, telephone lines or cables are identified to prevent interference and damage during repair.

5.1 Excavation and Backfill

The method is used for shallow and medium depth sinkholes, and includes excavation, backfill and reinstatement of pavement layers as illustrated in Fig. 4. Excavation shall be carried out in a manner that removes loose and erodible materials and avoids undue damage to existing pavement and utilities. The surface dimensions of excavation should be at least 1.0 m away from the surface dimensions of the sinkhole until a firm excavated material is found. The excavation walls should be vertical, even and free from fractured materials.

In case of a sinkhole throat is detected during excavation, it should be plugged with rocks, stones, or concrete blocks of at least 1.5 times the maximum width of the throat. All service utilities under the road shall be surrounded in accordance with the service provider's standards and specified in the Code of Practice and Specification for Road Openings in the Highway (Ashghal, 2014).

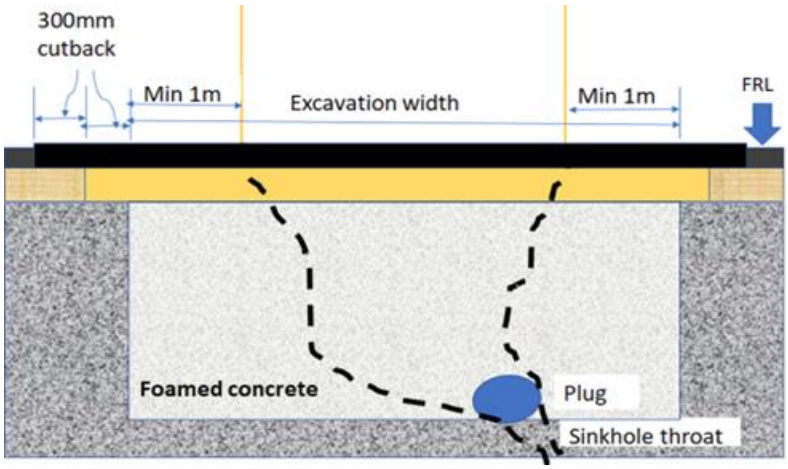


Fig. 4: Schematic diagram of the excavation and backfill repair method

A flowable fill of Foamed Concrete (C5) shall be used as the backfill material for the entire layer. The Foamed Concrete shall be flowable and self-levelling that complies with the requirements of the Qatar Construction Specification of Section 8: Part 2 (QCS, 2014). It may be placed by chutes, conveyors, or pumps in layers of up to 1.0 m single lift depth and should not be tamped or compacted on site. The placed concrete should be left to cure for at least 8 hours to attain adequate strength before reinstating the pavement layers. Reinstatement of the pavement layers shall be made to match existing pavement construction and in accordance with the Code of Practice and Specification for Road Openings in the Highway (Ashghal, 2014).

5.2 Compaction Grouting

Compaction grouting is generally considered for the repair of deep sinkholes that are adjacent to structures, with difficulties of excavating and accessing the bottom of sinkholes. It involves the injection of a low-slump mortar under a specific pressure, down a pre-drilled borehole, to fill voids or to densify subsurface soil. The thick mortar grout forms a series of bulbs in the soil and increases its density as shown in Fig. 5.

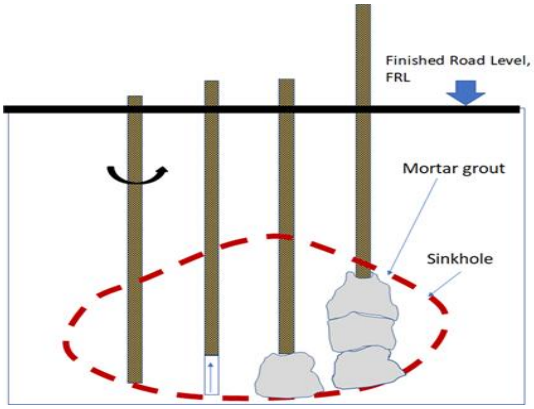


Fig. 5: Schematic diagram of the staged compaction grouting for deep sinkholes

Deep sinkholes cause depression and settlement of the pavement surface and are generally detected using underground investigation. Compaction grouting repair is usually planned as a series of primary and secondary boreholes. The primary points are drilled first and grouted followed by the secondary points, which are usually located midway between the primary points. Before drilling and grouting, the levels of the pavement surface and structures around the working area shall be recorded. The injection pressure shall be limited to a maximum of 5 bar, and vertical movement of the pavement surface and surrounding structures shall be limited to a maximum of 2.0 mm.

The grout mixture shall be of stiff consistency, slump of 50±10 mm as per BS EN 12350-2 (BSI, 2019), and 28-day compressive strength between 10-15 MPa. Compaction grouting shall start with primary holes, in increments of 400-900 mm, under continuous pressure by the bottom-up injection method as shown in Fig. 5. Monitoring during grouting is essential for the grout consistency, injection rate, injection pressure and injected volume. The grouting data shall be used for the determination of grout quantity and compared with the pre-assessed sinkhole dimensions. A reliable relation should be obtained only if sufficient sinkhole and soil information are available. Controlling the grout consistency and injection method enables accurate verification of quantities injected during grouting. In addition to the grout volume verification, it is recommended to carry out underground investigation before and after grouting to clarify the percentage of voids filling.

6 Case Study

Implementation of the Ashghal guidelines for the evaluation and repair of sinkholes commenced in late 2020, with more than 50 sites investigated over the last two years. Investigations revealed only shallow and medium sinkholes, caused mainly due to leakage of water or sewers, and none of the investigated sites revealed deep sinkholes. A case study is presented on the evaluation and repair of a sinkhole, which was reported at a residential area. A GPR investigation was performed, and the analysis indicated inconsistent layers of up to 0.75m below the pavement surface, i.e., a shallow-depth sinkhole. The GPR investigation also indicated a wider length and width of the sinkhole than what the hole appeared at the surface. Fig. 6 shows the reported sinkhole in March 2021 with the surface hole detected near a manhole cover, together with the GPR report of the depth and extent of sinkhole.

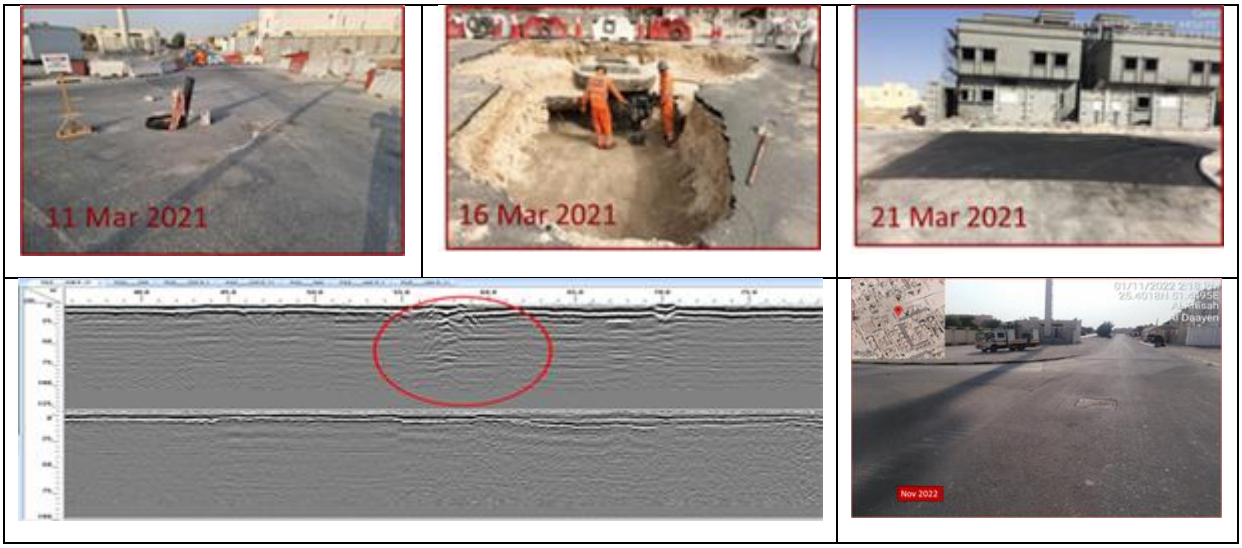


Fig. 6: Different stages of sinkhole evaluation and repair – Case Study 1

Excavation was conducted to remove all weak soil and erodible materials until a firm soil surface was reached. The bottom layer of the excavation was compacted to ensure a dense foundation support. A layer of Foamed Concrete (C5) was poured into the excavation hole and left to harden overnight before reinstating the pavement layers. The site was opened to traffic 24 hours after completion of repair and monitored periodically to assess performance under traffic and environmental loadings. No signs of depression or defects were observed up to the last monitoring date of November 2022, 20 months after repair. The pavement layers were intact with no evidence of surface or subsurface defects. ROMD worked with their Framework Partners on implementing the new guidelines for the evaluation and repair of sinkholes, and several sites are selected for performance monitoring. Excellent performance has been achieved to date from the monitoring sites, which is encouraging for wider implementation. Efficient detection and repair of sinkholes contributes to enhanced road safety and more efficient operations and maintenance of the road network in Qatar.

7 Conclusion

This paper presents the new guidelines developed at Ashghal for the evaluation and repair of sinkholes. Investigating the causes and assessing the dimensions of sinkholes are essential for appropriate repair. Underground investigation is recommended to assess the extent of sinkhole dimension below the pavement surface. The Ashghal guidelines classify sinkholes, based on depth from surface, into shallow, medium, and deep. Excavation and backfill repair is used for shallow and medium sinkholes, whereas deep sinkholes are repaired by compaction grouting.

The Ashghal guidelines for the evaluation and repair of sinkholes have been implemented in late 2020 at various locations. Performance monitoring after repair indicated excellent performance with no observed defects at pavement surface or subsurface. A case study is presented on the successful implementation of Ashghal guidelines for the repair of a shallow sinkhole with excellent performance for up to 20 months in service. Further monitoring is planned for the continuous improvement and enhancement of the safety and efficiency of the road network in Qatar.

The implementation of the new guidelines has been limited to shallow and medium-depth sinkholes, as no deep sinkholes have been identified by Ashghal over the last 2 years. Consideration shall be taken when implementing the repair procedures for deep sinkholes as no performance data is available to date.

References

Ashghal. (2014). Amendment to the Code of Practice and Specification for Road Opening in Highway. Roads Operation and Maintenance Department (ROMD) at the Public Work Authority (Ashghal), Doha, Qatar.

Ashghal. (2020). Sinkhole Repair Guidelines. Roads Operation and Maintenance Department (ROMD) at the Public Work Authority (Ashghal), Doha, Qatar.

BS EN 12350-2. (2019). Testing fresh concrete Slump test. British Standards Institution, London, UK.

Cavelier, C., Sallatt, A. & Heuze, Y. (1970). Geological Description of the Qatar Peninsula (explanation of the 1/100,000 geological maps of Qatar). Bureau de recherches geologiques et minieres, Department of Petroleum Affairs, Government of Qatar. https://pascal-francis.inist.fr/vibad/index.php?action=getRecordDetail&idt=GEODEBRGM71110099

Iqbal, M. A. (2019). Decades of Engineering Experiences with Sinkholes. 8th International Conference on Case Histories in Geotechnical Engineering, Philadelphia, Pennsylvania. Published by the American Society of Civil Engineers. ISBN: 9780784482117, pp. 65-78. DOI:/10.1061/9780784482117.006.

Leblanc, J. (2008). A Fossil Hunting Guide to the Tertiary Formations of Qatar. DOI:10.13140/RG.2.1.3850.0966.

QCS. (2014). Qatar Construction Specification. Ministry of Municipality, Doha, Qatar. https://www.mme.gov.qa/cui/view.dox?id=1441&contentID=3815&siteID=2.

Sadiq A. M. & Nasir S. J. (2002). Middle Pleistocene Karst Evolution in the State of Qatar, Arabian Gulf. *Journal of Cave & Karst Studies*, Vol. 64, No. 2, pp132-139.

Cite as: Al-Ansari J., Hassan K., Kumar K. & Helali K., "Ashghal Guidelines for the Evaluation and Repair of Sinkholes", *The 2nd International Conference on Civil Infrastructure and Construction (CIC 2023)*, Doha, Qatar, 5-8 February 2023, DOI: https://doi.org/10.29117/cic.2023.0072

Characterisation of Sewage Sludge and Municipal Solid Waste for Use as Cementitious Materials

Mohammed Bin Saif Al-Kuwari
Ministry of Environment & Climate Change, Doha, Qatar
msakuwari@mm.gov.qa

Khaled E. Hassan
Infrastructure Research & Development IRD at the Qatar Science & Technology Park (QSTP), Doha, Qatar
khassan@irdme.net

Abstract

Volumes of accumulated solid waste materials of sewage sludge (SS) and municipal solid waste (MSW) in Qatar continue to increase annually with a potentially negative impact on the environment. This paper presents an innovative technology for the production of green cement and advanced construction products from SS and MSW. Chemical composition analyses of the solid waste materials indicated the presence of main oxides available in Portland cement, but at lower contents. The three solid waste materials were incinerated and ground to produce consistent powder materials of similar sizes to Portland cement. The physical and chemical characteristics of the solid waste materials were investigated and compared to that of Portland cement. Paste and mortar mixtures were prepared by replacing 25, 50, and 75% of Portland cement with the different solid waste materials. Solid waste materials were found to influence the fresh properties of concrete, mainly water demand and setting time. Increasing the content of solid waste materials resulted in reduced compressive strength at all tested ages. SS gave the best performance within the solid waste materials investigated. Recommendations are made on the effective use of solid waste materials in various construction applications.

Keywords: Cementitious materials; Compressive strength; Fresh properties; Green construction; Solid waste

1 Introduction

The rapidly developing infrastructure in Qatar, for the 2022 and beyond, consumes large quantities of resources and impacts on the environment. Considering the shortage of quality construction materials in Qatar and waste generation from massive infrastructure projects, there is a need to develop advanced and environment-friendly construction materials to support the government strategy of sustainable development.

Portland cement (PC) production is an energy-intensive process through the heating of limestone and clay together in kilns at elevated temperatures of 1100-1700°C, with each tonne of PC producing a similar amount of CO_2. Cement remains a globally important product with approximately 4.4 billion tonnes produced in 2021, compared to 1.39 billion tonnes in 1995 (Statista, 2022), indicating the growth rate of cement production. Its environmental impact worldwide cannot be ignored, especially with the current technological race against time to reduce greenhouse gas (GHG) emissions, in particular CO_2 emission as the main cause of global warming.

Large quantities of municipal solid waste (MSW) and domestic sewage sludge (SS) are produced

every year in Qatar, as seen in Table 1 (PSA, 2019). The production of both MSW and SS increases every year due to population growth, leading to environmental challenges related to the treatment of wastes.

Table 1: Annual production of MSW and SS in Qatar (PSA, 2019)

Year	2013	2014	2015	2016	2017	2018
Population (M)	2,004	2,216	2,438	2,617	2,725	2,760
Domestic solid waste (000s tonnes)	930	1,048	1,096	1,155	1,184	1,313
Sewage sludge (000s tonnes)	27	32	40	42	42	38

MSW is incinerated in an Energy-from-Waste plant in the Domestic Solid Waste Management Centre (DSWMC), under the management of the Ministry of Municipality. The incinerated MSW produces fly ash (FA) and incineration bottom ash (IBA) of approximately 50,000 tonnes per year with the majority of it being IBA. The production of SS biosolids is relatively lower at 45,000 tonnes per annum, and is managed by the Public Works Authority (Ashghal). Current practice in Ashghal is to transfer the SS to the Doha North Sewage Treatment Works (DNSTW), which is equipped with facilities for thermal drying to reduce the volume of SS. The dried SS is produced in pellets, 2-5mm in size, with reduced moisture content of less than 10%. The majority of incinerated MSW and SS waste is sent to landfills with potential impact on the environment.

Landfilling of organic waste without appropriate treatment can pollute the surrounding air, soil, and groundwater environments. When organic landfilled wastes decompose, they create methane gas (CH_4), which is very explosive and flammable. Another significant landfilling concern is leachate management, where heavy metals can become mixed with and contaminate surface water, groundwater and soils. Inappropriate waste disposal can also attract pests and rodents that carry infectious diseases, causing severe environmental health consequences due to pollution and spread of diseases. Dried waste materials, especially fine particles, may be resuspended by wind thereby spread disease and may also increase the risk of fire and explosion (Cai & Zhang, 2013).

This paper presents a methodology for the utilisation of solid waste materials, originating from other sources than construction, for use as cementitious materials in construction applications. Incinerated MSW and SS are used to replace PC in the production of non-structural concrete products, with the double environmental benefits of reducing waste in landfills and carbon emissions from cement production. The work presented is part of a research project funded by the Qatar National Research Fund (QNRF NPRP 12S – 0306 – 1902417) on the "Development of a Novel Technology for Producing Green Cement and Advanced Construction Materials from Solid Waste". The project is delivered by the Ministry of Environment and Climate Change together with Infrastructure Research & Development (IRD) at the Qatar Science & Technology Park (QSTP) and in collaboration with the Public Works Authority (Ashghal) and stakeholders from the construction industry.

2 Characterisation of Solid Waste Materials

The solid waste materials considered in this investigation are incinerated MSW of fly ash (MSW-FA), incinerated MSW of bottom ash (MSW-IBA), and incinerated sewage sludge ash (SSA). The MSW materials were sourced from the DSWMC, Ministry of Municipality, whereas the SSA material was supplied by Ashghal (DSWMC). The MSW ashes are already incinerated during production at 800-900°C for a duration of 45 minutes. The SS waste material was incinerated in a furnace at the

same temperature range of 800-900°C for 2 to 3 hours. The increased incineration time is considered for SSA to minimise the organic content of the material. Fig. 1 shows the incinerated waste materials of MSW-FA, MSW-IBA, and SSA before grinding.



MSW-FA MSW-IBA Incinerated SSA

Fig. 1: Incinerated waste materials used in the investigation (prior to grinding)

The MSW-FA material is collected as a residue of the flue gas, and therefore supplied in a powder form as shown in Fig. 1. The MSW-IBA and SSA waste materials were ground into powder of similar particle size to PC to enhance reactivity as cement substitutes. Grinding was carried out in a dry process using a ball-mill to produce powder, passing 120µm (microns), with homogeneous and consistent appearance.

2.1 Properties of Solid Waste Materials

The grading curves of the solid waste materials together with the grading curve of PC are shown in Fig. 2. The waste materials showed coarser grading than PC, with finer grading of the MSW-FA in comparison to SSA and MSW-IBA. Powder materials passing 75 µm play the greatest part of cement hydration, and the results in Fig. 2 show that more than 90% of the PC particles are passing 75 µm, whereas between 65% and 76% for the solid waste materials.

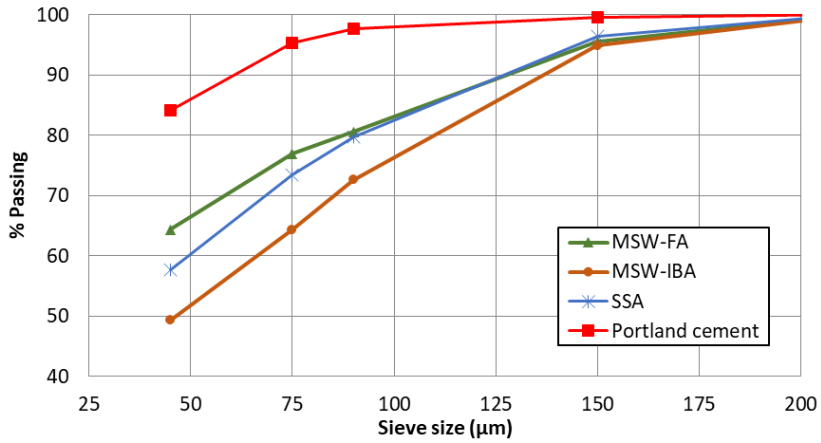


Fig. 2: Grading of waste materials and Portland cement

Table 2 summarises the physical properties of the waste materials and PC powders. PC has the highest specific gravity, followed by the SSA, MSW-IBA and MSW-FA. The Blaine Fineness method was used for the determination of the fineness of powder materials, as per BS EN 196-6 (BSI, 2018).

Despite the finer grading of PC, it gave the lowest surface area of 3130 cm^2/g. The MSW-FA, collected as dust from the hot flue gas, exhibited the highest surface area of 7220 cm^2/g. The difference between the grading and surface area results may be attributed to the surface texture and particle shape of the waste materials. The pH results indicate that all materials are alkalis, with PC exhibiting the highest alkalinity of 12.3 and the lowest of 9.8 for the MSW-IBA.

Table 2: Properties of waste materials and Portland cement

Property	MSW-FA	MSW-IBA	SSA	PC
SG	2.61	2.66	2.99	3.17
Blaine (cm^2/g)	7220	4670	4950	3130
pH	12.3	9.8	11.4	13.0
Chloride (%)	12.59	0.58	0.12	0.09
SO_3 (%)	7.0	0.7	0.9	3.3
LOI[1] (%)	18.0	12.9	2.8	1.6

BS EN 197-1 (BSI, 2011) limits the chloride content of cementitious materials to a maximum of 0.1%. The results in Table 2 show that only PC complies with the chloride requirement, whereas the SSA gave a marginally higher value of 0.12%. MSW-FA exhibited the highest chloride content of 12.59%. BS EN 197-1 also limits the sulfate content (SO_3) to a maximum level of 3.5% and the loss on ignition (LOI) to a maximum of 5.0% by weight of the total binder content. The results in Table 2 show that all the waste materials contain less than 3.5% of SO_3, except the MSW-FA which contains a high sulfate content of 7.0%. Only PC and SSA satisfied the BS EN 197-1 requirement of <5.0% LOI.

The properties of solid waste materials indicate lack of compliance to BS EN 197-1 as cementitious materials, especially for the MSW-FA and MSW-IBA. Despite the chloride and LOI contents, the solid waste materials were investigated further for potential use as cementitious materials in non-structural concrete products. Only SSA has the potential for use in structural concrete applications.

2.2 Chemical Composition

The chemical composition of the solid waste materials is investigated using X-ray fluorescence (XRF) and the results are presented in Table 3. The chemical composition of PC is generally expressed as oxides with main elements of calcium, silica, alumina and iron oxides. PC contains almost 80% of CaO and SiO_2, with less of aluminium oxide (AI_2O_3) and iron oxide (Fe_2O_3). The ratio by mass (CaO) / (SiO_2) shall be not less than 2.0, and the content of magnesium oxide (MgO) shall not exceed 5.0 % by mass (BS EN 197-1, 2011).

Table 3: Chemical composition of waste materials and Portland cement

Binder	SiO_2	Al_2O_3	Fe_2O_3	CaO	MgO	SO_3	Na_2O	K_2O	P_2O_5	LOI
MSW-FA	11.24	4.25	1.17	39.16	2.40	5.94	4.97	4.00	1.39	15.01
MSW-IBA	33.84	7.02	10.39	25.60	2.51	0.72	2.26	0.83	2.52	13.32
SSA	20.17	5.70	8.11	28.85	8.87	0.76	1.05	1.78	13.58	2.75
PC	20.49	4.43	3.13	61.78	3.63	3.27	0.21	0.95	0.11	1.58

The main oxide components of the incinerated waste materials are those of CaO, SiO_2, Al_2O_3, Fe_2O_3, similar to that of PC. The SSA is mainly composed of CaO, SiO_2, P_2O5, MgO, and Fe_2O_3, making

[1] Loss on Ignition.

88% of the total oxides. The SSA is low in calcium (CaO) compared to PC, but contains adequate amounts of silica and alumina that could possess pozzolanic reaction. SSA has a high phosphorus content, 13.6 % of P_2O_5, which is not available in other waste materials and PC. MSW-FA has a relatively higher content of CaO and less SiO_2, compared to IBA and SSA. MSW-FA also has the highest content of alkalis (Na_2O and K_2O) and sulfur trioxide (SO_3) compared to IBA and SSA, which are detrimental to the properties of concrete and may limit its use in concrete.

3 Paste And Mortar Mixtures and Properties

The waste materials were used to replace PC at different proportions of 25%, 50%, and 75% by weight of binders and their effects on the fresh and hardened properties of concrete were investigated. Paste specimens were used for investigating the consistency and setting time properties, as per BS EN 196-3 (BSI, 2016). Mortar specimens were prepared in the weight proportions of 1 part of cementitious material: 3 parts of sand: 1 half part of water (water to cement ratio of 0.5), and used for the determination of compressive strength at 2, 7, and 28 days. A summary of the mixtures and test results is given in Table 4.

Table 4: Properties of mixtures prepared with solid waste materials

Mix	Consistency (%)	Setting time (min)		Compressive strength (MPa)			Strength factor ($k=fck_x / fck_{PC}$)
		Initial	Final	2d	7d	28d	
100% PC	26.5	135	210	22.9	36.6	44.8	1
25% FA	27.0	45	75	11.7	20.0	30.4	0.68
50% FA	28.5	30	75	0.0	8.5	17.5	0.39
75% FA	31.0	15	45	0.0	0.0	5.3	0.12
25% IBA	25.0	150	210	13.2	20.6	23.4	0.52
50% IBA	26.0	195	225	3.9	11.3	11.6	0.26
75% IBA	27.5	225	315	0.0	0.0	3.7	0.08
25% SSA	25.0	180	255	21.6	30.6	37.1	0.83
50% SSA	26.0	285	355	11.8	18.2	24.9	0.56
75% SSA	26.5	375	625	0.0	5.3	7.6	0.17

The control mixture was made with 100% PC and labelled (100% PC) in Table 3. Mixtures made with solid waste materials were labelled based on the type of waste materials and percentage of cement replacement. For example, mixture labelled as (25% FA) is made by replacing 25% of PC with MSA-FA, (50% IBA) means replacing 50% of PC with MSW-IBA, and (75% SSA) for replacing 75% of PC with SSA.



Fig. 3: Casting of the fresh mortar prisms

The mortar ingredient materials were mixed mechanically using an electrical mixer for 3 minutes and cast into prism moulds of the dimensions of 40x40x160mm, as shown in Fig. 3. The fresh mortars, inside their moulds, were covered with wet hessian and polyethylene sheets for 24 hours and demoulded on the following day. Curing of the mortars mixtures was made in a water tank maintained at 20±2°C until testing.

3.1 Paste Results

The paste specimens are tested for consistency and setting time and the results are given in Table 3. The consistency test determines the amount of water required for the complete hydration of cement particles. The consistency of PC is 26.5% and the use of solid waste materials resulted is similar or higher consistency values. Increasing the FA content from 25% to 75% increased the consistency to 27% to 31%, respectively. FA had the highest particles surface area, almost double of PC, and would require more water to achieve the standard consistency. The IBA and SSA mixture had marginal effects on the standard consistency, compared to PC.

The setting time results are also given in Table 3. The initial and final setting times of the 100% PC are 135 and 210 minutes, respectively. The use of MSW-FA significantly reduced the setting time compared to PC, with high replacement level results in faster setting. The lowest initial setting of 15 minutes and final setting of 45 minutes are achieved for the 75% FA mixture. In contrast, the use of MSW-IBA and SSA delayed the setting time. Increasing SSA replacement level resulted in a delay in both initial and final setting times. Replacing 75% of PC with SSA increased the initial and final setting times to 375 and 625 minutes, respectively, almost triple the values obtained for the control 100% PC. Similar findings on the retarding effect of SSA have been reported by previous studies due to the presence of phosphorus oxide (Cyr, 2007; Piasta & Lukawska, 2016). The delay in setting times may be an advantage in hot regions for use in specific applications.

3.2 Mortar Results

Compressive strength testing was conducted at the ages of 2, 7, and 28 days on the different mortar mixtures, and the results are given in Table 3 and also presented in Fig. 4. Table 3 also provides the 28-day strength reduction factor (k) defined as the ratio of compressive strength of the mixture made with different proportions of waste materials in relation to the compressive strength of the 100% PC mortar. The PC mortar attained compressive strength values of 22.9 MPa at 2 days (≥20 MPa) and 44.8 MPa at 28 days (≥42.5 MPa), and therefore classified as a Strength Class 42.5 R according to BS EN 197-1. The use of waste materials, as cement replacement, resulted in lower compressive strength, and the strength reduction is proportional to the replacement level.

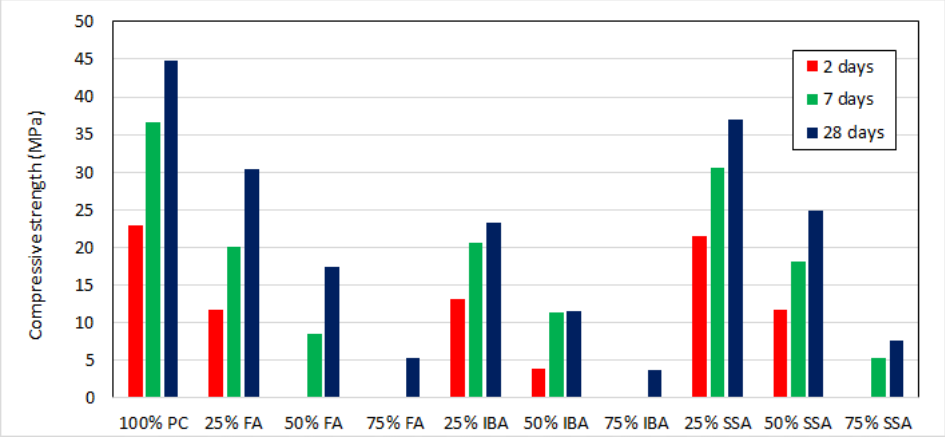


Fig. 4: Compressive strength of the mortar mixtures

Replacing 25%, 50% and 75% of PC with FA reduced the 28-day compressive strength to 30.4, 17.5, and 5.3 MPa, respectively. A strength reduction of 32%, 61%, and 88%, respectively. In fact, the 75% FA mixture did not attain any measurable strength at 2 and 7 days, and only achieved 5.3 MPa at 28 days. Similar trend to the FA was observed for the IBA mortars, but with lower compressive strength values at all tested ages. The 28-days compressive strength of the 25% IBA was 23.4 MPa, a reduction of 48% compared to the 100% PC. The 50% IBA and 75% IBA mixtures gave 28-day strength values of 11.7 and 3.7 MPA, reduction of 74% and 92%, respectively. Similar to the FA mixture, the 75% IBA mortar did not achieve any measurable strength at the ages of 2 and 7 days, and only reached 3.7 MPa at 28 days.

The best compressive strength results among the investigated waste materials are found in the 25% SSA. The inclusion of SSA reduced the compressive strength but at a lower magnitude than the FA and IBA materials. The 25%, 50%, and 75% SSA mortar mixtures exhibited 28-day strength values of 37.1, 30.6, and 21.6 MPa, a loss of 17 %, 32 %, and 52 % compared to 100% PC, respectively. In other words, the SSA mixtures attained 48% to 83% of the 28-day compressive strength of 100% PC at the different replacement levels of 25 to 75%., compared to 12 to 68% for the FA and 8 to 52% for the IBA.

The use of waste materials in construction has the double environmental benefits of reducing waste sent to landfills as well as the carbon emission associated with the production of PC. The new development of "Green Cement" is towards the achievement of a substantial reduction in CO_2 emission while transforming waste from landfills to useful construction products. SSA was found to be the most viable material that resulted in moderate reduction in strength properties, and better performance compared to the other two solid waste materials. Its physical and chemical properties suggest that SSA could be blended with other cementitious materials to satisfy most of the requirements of a cementitious binder for structural and non-structural concrete applications. SSA retardation of the setting time may be an advantage in hot countries, especially in applications that require longer setting time. Replacing 50 to 75% of PC with SSA will produce concrete with 28-day strength of 7 to 25 MPa, which could be widely used in non-structural concrete applications as green products with less impact on the environment. Further work is planned to use different activation techniques of SSA to enable its utilisation in a range of construction application.

4 Conclusion

Three solid waste materials of municipal solid waste (MSW) of fly ash (FA) and incineration bottom ash (IBA) and sewage sludge ash (SSA) were considered in this investigation for use as cement replacement materials. The solid waste materials contain similar oxide components to PC but failed to comply with BS EN 197-1, especially for the MSW-FA and MSW-IBA in terms of salt and LOI contents. Only SSA possessed any potential for use in structural concrete applications.

The solid waste materials were used to replace PC at different levels of 25, 50, and 75%, by weight of binder, for the development of paste and mortar mixtures. FA increased the water demand of the paste whereas the IBA and SSA had marginal effect on consistency. FA also accelerated the initial and final setting whereas SSA and IBA delayed the setting time. The retarding effect was more pronounced for the SSA with its high content of phosphorus oxide. The use of solid waste materials reduced the compressive strength of mortars, and the reduction was proportional to the replacement level. Within the investigated solid waste materials, SSA exhibited the best performance in terms of water demand and compressive strength when compared to MSW-FA and MSW-IBA materials. Non-

structural concrete products of 7 to 25 MPa could be achieved by replacing 50 to 75% of Portland cement with SSA.

The work conducted in this investigation is limited to small patches received from two recycling plants in Qatar for the processing of domestic municipal and sewer waste materials. Variations of the processed waste materials may affect the derived conclusions. Further work is currently being undertaken for assessing the variability of waste materials produced at different ages and also investigating the use of different techniques for the activation of solid waste materials to develop innovative concrete products.

Acknowledgement

The work presented in this paper is part of a research project funded by the Qatar National Research Fund (NPRP 12S – 0306 – 1902417) on the "Development of a Novel Technology for Producing Green Cement and Advanced Construction Materials from Solid Waste". The authors are grateful to QNRF for funding this project.

References

BS EN 196-3. (2016). Methods of testing cement. Determination of setting times and soundness. British Standards Institution, London, UK.

BS EN 196-6. (2018). Methods of testing cement - Determination of fineness. British Standard Institution, London, UK.

BS EN 197-1. (2011). Cement Composition, specifications and conformity criteria for common cements. British Standard Institution, London, UK.

Cai, L. & Zhang, T. (2013). Detecting human bacterial pathogens in wastewater treatment plants by a high-throughput shotgun sequencing technique. *Environmental Science and Technology*, *47*(10), pp.433-41. https://doi.org/10.1021/es400275r.

Cyr, M., Coutand, M. & Clastres, P. (2007). Technological and environmental behavior of sewage sludge ash (SSA) in cement-based materials. *Cement and Concrete Research*, *37*(8), pp1278-1289. https://doi.org/10.1016/j.cemconres.2007.04.003.

Piasta, W. & Lukawska, M. (2016). The Effect of Sewage Sludge Ash on Properties of Cement Composites. *Procedia Engineering*, *161*, pp1018–1024. https://doi.org/10.1016/j.proeng.2016.08.842.

PSA. (2019). Environmental statistics. Planning and Statistics Authority (PSA). Doha, Qatar. https://www.psa.gov.qa/en/statistics/Statistical%20Releases/Environmental/EnvironmentalStatistics/Environment_11_2018_AE.pdf.

Statista. (2022). https://www.statista.com/statistics/1087115/global-cement-production-volume/. Reviewed online on 17th October 2022.

Cite as: Al-Kuwari M.S. & Hassan K., "Characterisation of Sewage sludge and municipal solid waste for Use as Cementitious Materials", *The 2nd International Conference on Civil Infrastructure and Construction (CIC 2023)*, Doha, Qatar, 5-8 February 2023, DOI: https://doi.org/10.29117/cic.2023.0073

Parametric Optimization of RC Beams Strengthened with FRCM Using FE Modelling and Response Surface Methodology

Qusai Aborahmeh
Department of Civil and Architectural Engineering, Qatar University, Doha, Qatar
qa1901097@qu.edu.qa

Mohamed Rabie
Department of Civil and Architectural Engineering, Qatar University, Doha, Qatar
m.rabie@qu.edu.qa

Usama Ebead
Department of Civil and Architectural Engineering, Qatar University, Doha, Qatar
uebead@qu.edu.qa

Abstract

This study focuses on the numerical and statistical analyses to predict the mid-span moment capacity of RC beams strengthened with fabric reinforcement cementitious mortar (FRCM) laminate. A finite element model (FEM) has been built to simulate twelve RC beams strengthened with two types of FRCM, namely Polyparaphenylene benzobisoxazole (PBO) FRCM and Carbon (C) FRCM. The FE models were verified based on experimental work available in the literature. The finite element models have shown a good agreement with experimental results in terms of maximum load-carrying capacity, load-deflection curves, and concrete strain values. The numerical simulation was followed by a parametric study on 42 models using face centred response surface methodology (RSM). Combining FEM and RSM, a novel mathematical model has been proposed to predict the mid-span moment capacity of the RC beams strengthened with FRCM. The results of the proposed model have shown optimal predictability with R^2 equal to 90.34%. In addition, the proposed model agreed with the ACI design procedures and the existing literature.

Keywords: FEM; Nonlinear modelling; FRCM; Strengthening; Response surface method

1 Introduction

Textile reinforced mortar, also known as fabric reinforced cementitious matrix (FRCM), is a material that consists of fabric grids made of fibers such as carbon, glass, and PBO Polyparaphenylene benzobisoxazole (PBO) embedded in mortar (Awani et al., 2017). These fabric grids are mounted on a concrete surface and their grid geometry allows the penetration of mortar, creating an interlocking between the matrix and the host surface. The use of FRCM in strengthening reinforced concrete (RC) structures has many advantages, including higher durability and greater bond efficiency (Al-Lami et al, 2020; Ebead & Wakjira, 2018; Elghazy et al., 2018; Wakjira & Ebead, 2019; Wei et al., 2022; Younis et al., 2017). There is a significant amount of literature on the experimental use of FRCM in various structural applications, such as flexural strengthening, shear strengthening, and durability, and these studies have shown improvements in ultimate load-carrying capacity and durability (Aljazaeri & Myers, 2017; Azam & Soudki, 2014; Babaeidarabad et al., 2014; Ebead et al., 2017; El-Sherif et al., 2020; Elghazy et al., 2018; Kadhim et al., 2022; Pino et al., 2016; Wakjira & Ebead, 2018).

However, there has been less research on numerical studies of FRCM, and the numerical models that

have been developed have primarily been used to verify experimental data. This is in contrast to traditional finite element (FE) models, which are often used to predict the behavior of a system before it is built or tested. In this context, the authors of the paper are proposing the use of response surface methodology (RSM) to update the FE model of an FRCM-strengthened RC beam and improve its predictive accuracy. RSM is a statistical approach that can be used to model the relationships between multiple input variables and an output variable, and it can be used to optimize the performance of a system by identifying the optimal values of the input variables.

The proposed RSM-based FE model is then validated using experimental data and compared to a traditional FE model. The results show that the proposed RSM-based FE model has improved predictive accuracy and can be used to accurately predict the behavior of FRCM-strengthened RC beams. This means that the model can be used to design FRCM-strengthened RC beams without the need for physical testing, potentially saving time and resources. Overall, the use of RSM to update the FE model of FRCM-strengthened RC beams represents an important step forward in the use of numerical modeling to predict the behavior of these structures. A graphical representation of the process followed in the presented study is shown in Figure 1.

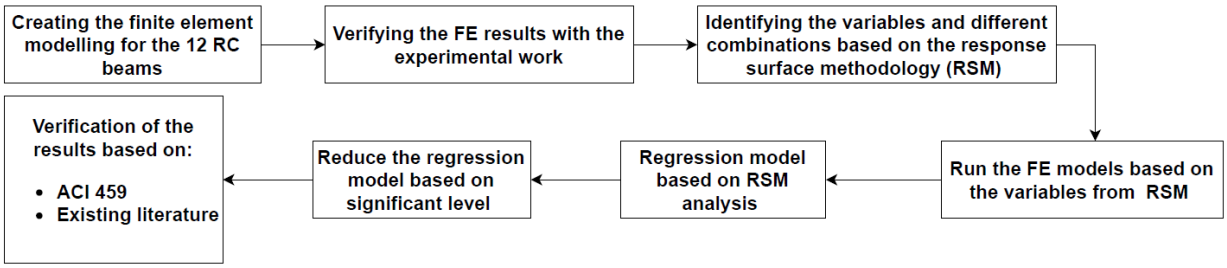


Fig. 1: Flow chart of the proposed methodology

2 Summary of the Prevous Experimental Study done by (Ebead et al., 2017)

2.1 Experimental Dataset

A total of twelve RC beams were strengthened in flexural form using two types of FRCM (PBO-FRCM and C-FRCM) based on a previous study (Ebead et al., 2017). The experimental dataset of the RC beams was chosen according to the following criteria: (a) experiment-based tensile constitutive relations for (PBO-FRCM and C-FRCM) were used allowing for an accurate FE model; (b) The beam details such as reinforcement, and material properties, surface preparation for the strengthening and dimensions were accurately known; and (c) concrete strains, load-deflection curves, and failure modes were clearly presented.

In the experimental work, the RC beams were tested under four points pending load. All beams had a rectangular cross-section of 150 mm × 260 mm and a length of 2500 mm with a clear span of 2000 mm. Reinforcement consisted of two steel bottom and top bars. The bottom bar size was varied between 12 mm and 16 mm to consider the reinforcement ratio as a study parameter, namely ρ_s(D12) =0.72% and ρ_s(D16) =1.27%. 8-mm diameter stirrups spaced at 100 mm were used, the schematic drawing for the RC beam is shown in Figure 2.

2.2 FE analysis

A total of twelve 3D models were built using the finite element software ABAQUS 6.14 (Smith, 2009).A 30 mm mesh size has been used after doing a mesh sensitivity study. The reference beams

in the experimental work were simulated as a benchmark for the FE models as illustrated in Figure 3, followed by adjusting the FE models based on parameters investigated in the experimental work. To increase the reliability of the FE model a mesh sensitivity study was conducted and therefore a mesh size of 30 mm was selected and applied for all the simulated beams.

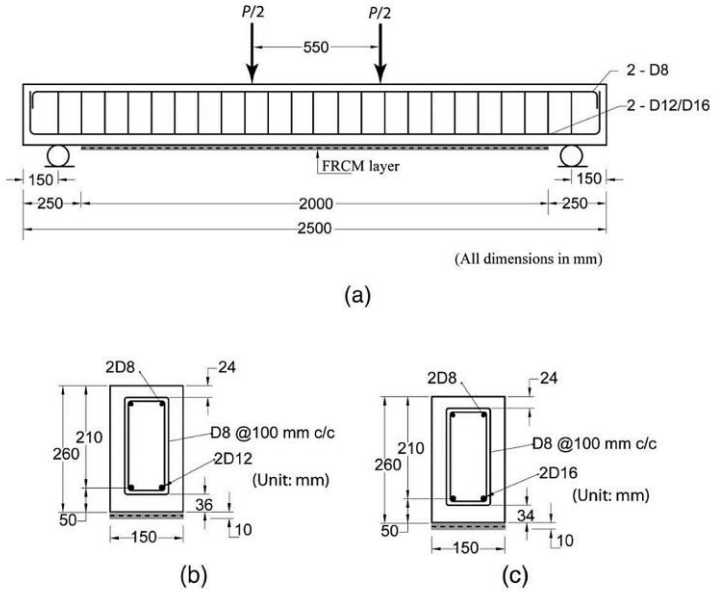


Fig. 2: Experimental beam details (Ebead et al., 2017).

2.3 Material Models

The concrete damage plasticity (CDP) model has been used for concrete while an elastic perfectly plastic model has been used for the steel rebar and the FRCM shell.

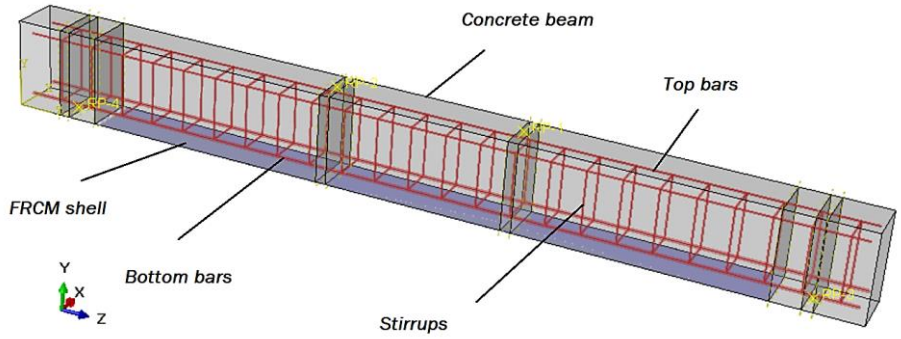


Fig. 3: Numerical beam 3D view

2.4 Boundary conditions and interactions

The overall assembly of the applied boundary conditions is shown in Figure 4. Constraints were applied to the reference points (RP) that have been assigned to the indicated regions and constrained with tie constrains. For RP4 and RP3, only transitional restrain in the y-direction has been assigned to provide the roller restrain effect used in experiment. The out-of-plane movement was restrained by locking the z-transition along the end faces. The load has been applied to points RP1 and RP2 as incremental displacement in the negative y-direction.

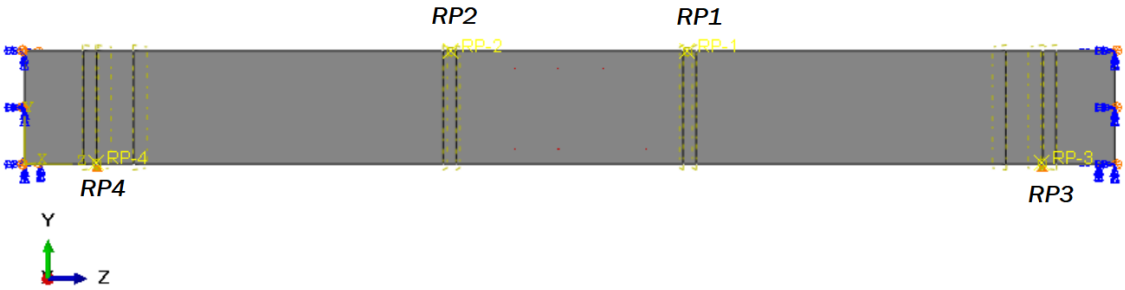


Fig. 4: Boundary conditions applied to the numerical model

3 Methodology

3.1 RSM analysis

Response surface methodology (RSM) analysis has been used to develop a mathematical equation that can be used to predict the mid-span moment capacity.

A face-cantered design (FCD) approach is adopted here. The selected parameter and levels of each are shown in Table 1.

Table 1: Variables level for RSM analysis

Variables	Description	Low	Mid	High
R (%)	1000ρ	7.18	9.94	12.7
Fc (MPa)	$\frac{F_c'}{10}$	3	4.85	6.7
Kf (MPa)	$10 \times K_f$	2.3	7.8	13.3
D (mm)	$\frac{d}{100}$	26	31	36
L (mm)	$\frac{L}{100}$	22	26	30

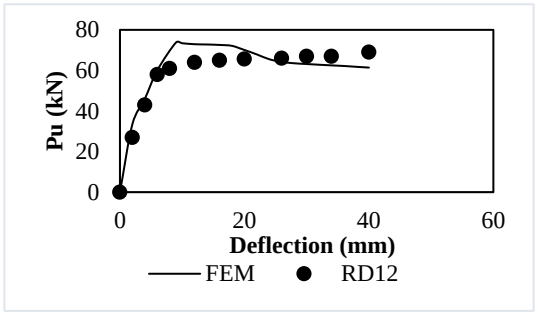
3.2 FE analysis

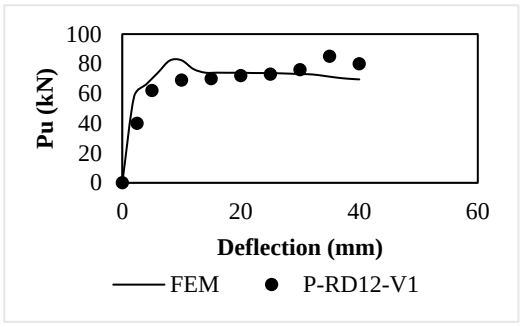
A total of twelve 3D models were built using the finite element software ABAQUS 6.14 (Smith, 2009). A 30mm mesh size has been used after doing a mesh sensitivity study. The reference beams in the experimental work were simulated as a benchmark for the FE models as illustrated in Figure 3, followed by adjusting the FE models based on parameters investigated in the experimental work. To increase the reliability of the FE model a mesh sensitivity study was conducted and therefore a mesh size of 30 mm was selected and applied to all the simulated beams.

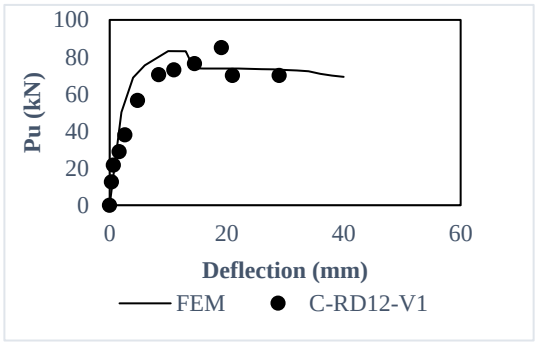
4 Results and Discussion

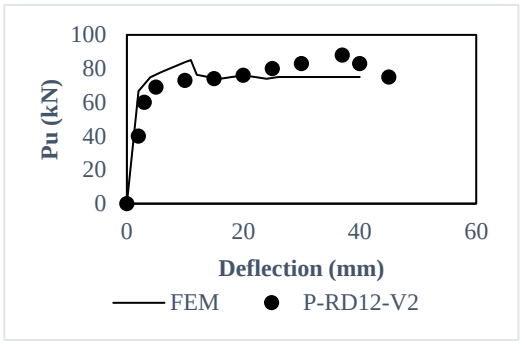
4.1 Load-deflection responses

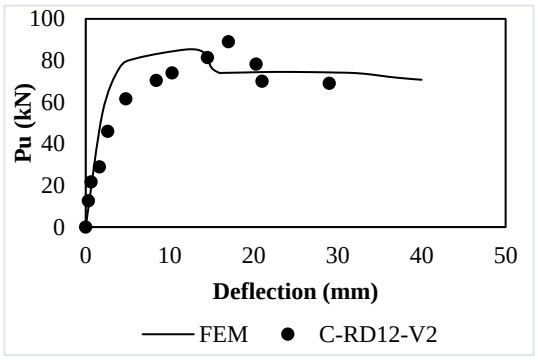
The comparison of the load-deflection curves of the experimental and the FE analysis is shown in Figure 5. It can be observed the well-predicted load-deflection curves and maximum load capacity resulted from the FE analysis in all FE models.

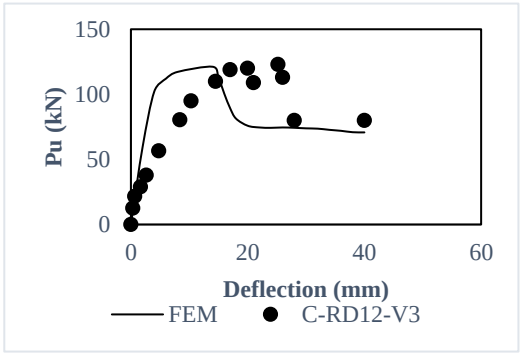


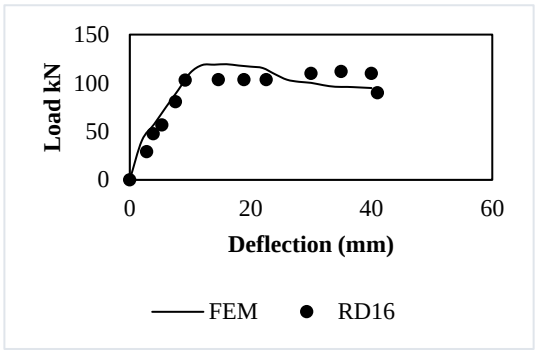


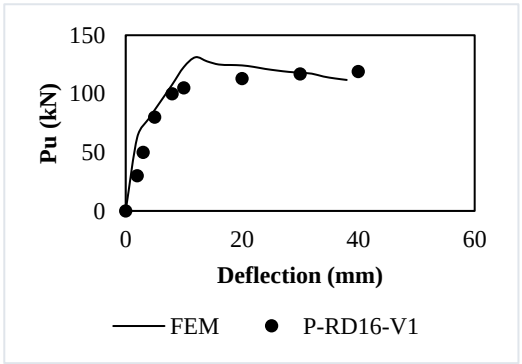


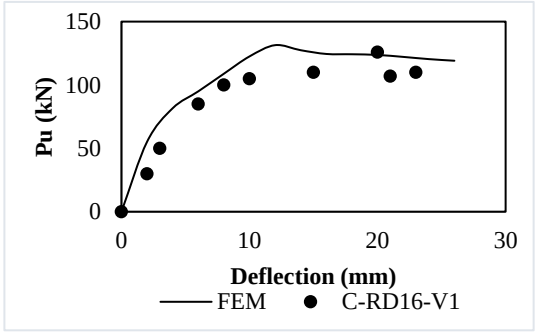












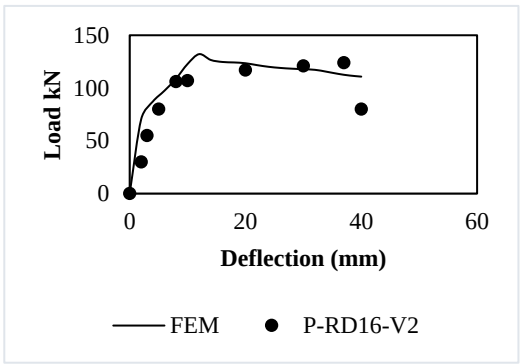


Fig. 5: Maximum load capacity curves for 10 numerical beams

4.2 RSM results

A total of 42 numerical models have been built to conduct the required statistical combinations and runs. A response surface regression in Eq. (1) has been generated with a significant level of 0.05.

$$Mu = 106.4 - 11.64R - 20.71Fc - 7.05K_f - 2.62D - 0.64L + 0.541R \times D + 0.453Fc \times K_f + 0.69Fc \times D + 0.275K_f \times L \quad (1)$$

It can be observed that there are no second-order effects in the study parameters. However, four interactions between R, D, F_c', K_f and L have a significant effect.

4.3 RSM model verification

The generated equation has been compared with the results obtained in several experimental works from literature as shown in Table 2.

Table 2: RSM comparison with experimental work

Reference work	Considered sample	Mu - Experiment (kN-m)	Mu-predicted (kN-m)	Absolute varince (kN-m)	Percentage (%) variance
(Hashemi & Al-Mahaidi, 2010)	MSF	46.3	45	1.3	3%
(Ombres, 2011)	S1-T1-P1-1	39.2	36.6	2.6	7%
(Haustein et al., 2012)	sample 2	79	55	24	30%
(Babaeidarabad et al., 2014)	L-4	24.2	37	12.8	53%
(Jung et al., 2015)	B2	33.1	39	5.9	18%
(Akbari Hadad et al., 2020)	FB-6k-4P	50.8	49	1.8	4%

Furthermore, a comparison with the moment value obtained from following ACI code procedures has been generated and plotted against the results obtained from the RSM equation and the FE models as shown in Figure 7.

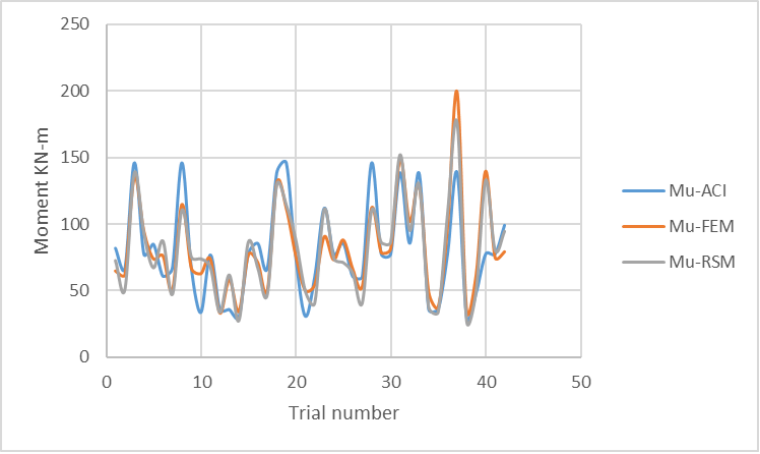


Fig. 7: Moment results comparison

Both comparisons showed a good agreement with the results obtained from the FE procedures and the RSM. However, the moment values from ACI design codes are overestimated (safer) in the cases where the maximum moment is above 100 kN-m. This can be attributed to the assumption of full bond between concrete and FRCM layers by the ACI equations that ignores the debonding and slippage of FRCM.

5 Conclusions

In this study, numerical and statistical analyses of 12 RC concrete beams strengthened with different types and layers of FRCM laminate has been carried out. The non-linear finite element simulations used concrete damage plasticity constitutive model for concrete. The study parameters included FRCM stiffness, number of laminates, reinforcement ratio, beam depth and clear span. The following conclusions can be drawn:

1. The proposed equation to predict the mid-span moment of RC beams strengthened with FRCM is of high accuracy and has been validated using available experimental data in the literature and using code provisions and guidelines.
2. The response surface methodology along with the finite element modeling can be used to optimize parameters and conduct virtual experimentation with high accuracy.
3. The proposed equation has best accuracy for the cases where the loading scheme and test setup matches the one in this study. However, further investigation is needed to generalize the equation for other cases.

References

Akbari, H., H., Erickson, B. & Nanni, A. (2020). Flexural analysis and design of FRCM-strengthened RC beams. *Construction and Building Materials*, *244*, 118371. https://doi.org/10.1016/j.conbuildmat.2020.118371

Al-Lami, K., D'Antino, T. & Colombi, P. (2020). Durability of fabric-reinforced cementitious matrix (FRCM) composites: A review. In *Applied Sciences (Switzerland)* (Vol. 10, Issue 5). https://doi.org/10.3390/app10051714

Aljazaeri, Z. R. & Myers, J. J. (2017). Strengthening of Reinforced-Concrete Beams in Shear with a Fabric-Reinforced Cementitious Matrix. *Journal of Composites for Construction*, *21*(5), 04017041. https://doi.org/10.1061/(asce)cc.1943-5614.0000822

Awani, O., El-Maaddawy, T. & Ismail, N. (2017). Fabric-reinforced cementitious matrix: A promising strengthening technique for concrete structures. *Construction and Building Materials*, *132*, 94–111. https://doi.org/10.1016/j.conbuildmat.2016.11.125

Azam, R. & Soudki, K. (2014). FRCM Strengthening of Shear-Critical RC Beams. *Journal of Composites for Construction*, *18*(5), 04014012. https://doi.org/10.1061/(asce)cc.1943-5614.0000464

Babaeidarabad, S., Loreto, G. & Nanni, A. (2014). Flexural Strengthening of RC Beams with an Externally Bonded Fabric-Reinforced Cementitious Matrix. *Journal of Composites for Construction*, *18*(5), 04014009. https://doi.org/10.1061/(asce)cc.1943-5614.0000473

Ebead, et al. (2017). Effectiveness of Fabric-Reinforced Cementitious Matrix in Strengthening Reinforced Concrete Beams. *Journal of Composites for Construction*, *21*(2), 1–14. https://doi.org/10.1061/(ASCE)CC.1943-5614.0000741

Ebead, U. & Wakjira, T. G. (2018). FRCM/stirrups interaction in RC beams strengthened in shear using NSE-FRCM. *IOP Conference Series: Materials Science and Engineering*, *431*(11), 112001. https://doi.org/10.1088/1757-899X/431/11/112001

El-Sherif, H. E., Wakjira, T. G. & Ebead, U. (2020). Flexural strengthening of reinforced concrete beams using hybrid

near-surface embedded/externally bonded fabric-reinforced cementitious matrix. *Construction and Building Materials*, *238*, 117748. https://doi.org/10.1016/j.conbuildmat.2019.117748

Elghazy, et al. (2018). Corrosion-Damaged RC Beams Repaired with Fabric-Reinforced Cementitious Matrix. *Journal of Composites for Construction*, *22*(5), 04018039. https://doi.org/10.1061/(asce)cc.1943-5614.0000873

Hashemi, S. & Al-Mahaidi, R. (2010). Investigation of Bond Strength and Flexural Behaviour of Frp-Strengthened Reinforced Concrete Beams Using Cement-Based Adhesives. *Australian Journal of Structural Engineering*, *11*(2), 129–139. https://doi.org/10.1080/13287982.2010.11465061

Haustein, et al. (2012). Atmospheric dust modeling from meso to global scales with the online NMMB/BSC-Dust model - Part 2: Experimental campaigns in Northern Africa. *Atmospheric Chemistry and Physics*, *12*(6). https://doi.org/10.5194/acp-12-2933-2012

Jung, et al. (2015). Prediction of Flexural Capacity of RC Beams Strengthened in Flexure with FRP Fabric and Cementitious Matrix. *International Journal of Polymer Science*. https://doi.org/10.1155/2015/868541

Kadhim, et al. (2022). Analysis and design of two-way slabs strengthened in flexure with FRCM. *Engineering Structures*, *256*, 113983. https://doi.org/10.1016/J.ENGSTRUCT.2022.113983

Ombres, L. (2011). Flexural analysis of reinforced concrete beams strengthened with a cement-based high-strength composite material. *Composite Structures*, *94*(1), 143–155. https://doi.org/10.1016/j.compstruct.2011.07.008

Pino, et al. (2016). Performance of FRCM strengthened RC beams subject to fatigue. *Sustainable Construction Materials and Technologies*, *2016-Augus*(10). https://doi.org/10.1061/(asce)be.1943-5592.0001107

Smith, M. (2009). *ABAQUS/Standard User's Manual, Version 6.9*. Dassault Systèmes Simulia Corp.

Wakjira, T. G. & Ebead, U. (2018). Hybrid NSE/EB technique for shear strengthening of reinforced concrete beams using FRCM: Experimental study. *Construction and Building Materials*, *164*, 164–177. https://doi.org/10.1016/j.conbuildmat.2017.12.224

——. (2019). Internal transverse reinforcement configuration effect of EB/NSE-FRCM shear strengthening of RC deep beams. *Composites Part B: Engineering*, *166*, 758–772. https://doi.org/https://doi.org/10.1016/j.compositesb.2019.03.004

Wei, L. et al. (2022). Performance of FRCM composites and FRCM-strengthened RC beams subjected to anodic polarization and cyclic loading. *Engineering Structures*, *250*, 113475. https://doi.org/10.1016/J.ENGSTRUCT.2021.113475

Younis, A., Ebead, U. & Shrestha, K. C. (2017). Different FRCM systems for shear-strengthening of reinforced concrete beams. *Construction and Building Materials*, *153*, 514–526. https://doi.org/10.1016/j.conbuildmat.2017.07.132

Cite as: Aborahmeh Q., Rabie M. & Ebead U., "Parametric Optimization of RC Beams Strengthened with FRCM Using Finite Element Modelling and Response Surface Methodology", *The 2nd International Conference on Civil Infrastructure and Construction (CIC 2023)*, Doha, Qatar, 5-8 February 2023, DOI: https://doi.org/10.29117/cic.2023.0074

Modeling Asphalt Pavement Frictional Properties using Different Machine Learning Algorithms

Mohammad Ali Khasawneh
Civil Engineering, Prince Mohammad Bin Fahd University, Al Azeziya, Eastern Province, Kingdom of Saudi Arabia
mkhasawneh@pmu.edu.sa

Mohammad Ahmad Alsheyab
Civil, Construction and Environmental Engineering, Iowa State University, Ames, Iowa, USA
alsheyab@iastate.edu

Haneen Issa Al Akhrass
Civil Engineering, Jordan University of Science and Technology, Irbid, Jordan
hialakhrass18@eng.just.edu.jo

Abstract

The objective of this work is to use some machine learning algorithms and test its efficiency in developing models to predict Locked Wheel Skid Trailer (LWST) values from Dynamic Friction Tester (DFT) and Circular Texture Meter (CTM) measurements conducted on asphalt pavement surfaces. For this prediction, three models were developed using DFT measurements at different speeds starting from 20km/h (12.5 mph) up to 64 km/h (40 mph) and then same DFT measurements as combination with Mean Profile Depth (MPD) and the last model used the International Friction Index (IFI) parameters (F60 and SP). The machine learning techniques includes two supervised learning algorithms: the Multi-Layer Perceptron (MLP) type of Artificial Neural Networks (ANN) and M5P tree model. In addition to one lazy algorithm called the K Nearest Neighbor (KNN) or Instance-Based Learner (IBL). The results showed that MLP models are the best in terms of the correlation coefficient that resulted in 81% prediction power using DFT parameters. Additionally, it was shown that the result of tree models was close to ANN but with much simpler regression. However, KNN models were recommended for LWST prediction of similar data characteristics and it is expected that this algorithm will be more efficient as the training data set becomes larger.

Keywords: Friction; Texture; International Friction Index (IFI); Machine Learning Algorithms

1 Introduction

Pavement skid resistance is defined as the impeding force generated by the interaction between a tire and a pavement under a non-rotating wheel (ASTM 867-02, 2015). Since skidding occurs when the frictional demand exceeds the available friction force at the interface between a tire and pavement, it is important to measure the ability of a pavement to resist the skidding of a tire on a motor vehicle.

Lack of sufficient surface friction is one of the factors contributing to crashes on roads. The tire-pavement interaction has been a vital field of study due to the volume and severity of motor vehicle accidents on roads as in Hofko et al. (2019). Theoretically, the surface frictional force developed between a pavement and a tire is composed of two components: adhesion and hysteresis. Adhesion is only significant on dry surfaces at low vehicle speed and hysteresis has a considerable

significance at high vehicle speed on wet surfaces (Khasawneh & Alsheyab, 2020).

Multiple methods and procedures have been developed to evaluate the tire-pavement interaction and surface textures. There are two major devices used for the measurement of pavement surface friction in the laboratory, namely; British Pendulum Tester (BPT) as outlined in (ASTM E 303-93, 2002) and Dynamic Friction (DF) tester as specified in (ASTM E 1911-98, 2002). Both are highly portable, easy to handle and can be used in the field.

There are four basic types of full-scale friction-measuring devices. These are side-force, locked wheel, fixed-slip, and variable-slip devices. Unlike the portable devices, these devices can measure friction at or close to highway speeds, see (Henry, 2000).

To our knowledge, no available devices can measure pavement micro-texture directly. However, they can be measured indirectly at low-speed levels using laboratory friction devices, such as the British Pendulum Tester at 10km/h and the Dynamic Friction Tester at 20 km/h as demonstrated in (Khasawneh, 2008). However, three common methods are utilized for measuring pavement macro-texture: profilometers (ASTM E 1845-15, 2015), volumetric (ASTM E 965-96, 2001) and outflow (ASTM E 2380, 2005).

Statistical interpretation and Machine Learning (ML) techniques are vital in pavement surface evaluation nowadays. Multiple technicians collect and interpret the information for pavement friction could result in contradicting viewpoints and subjectivity, see (Marcelino et al., 2021). In addition, the cost of the equipment used for pavement surface evaluation is another important factor to be considered; this was addressed by (Hall et al., 2009). In essence, many researchers globally are utilizing these tools since they can make predictions and generalizations in real time and save effort and money for many industries. Accordingly, ML-based approaches, including Support Vector Machine (SVM), artificial neural network (ANN) and classification and regression tree (CART) are widely used in pavement surface condition and damage detection applications and this can be shown in several studies such as Majidifard et al., (2020); (Karballaeezadeh et al. 2020); and (Yang, 2017). A thorough study conducted by Majidifard and co-workers showed a full procedure to evaluate the Pavement Condition index (PCI) from images using Deep Learning (DL) and ML techniques. Karballaeezadeh and co-workers introduced another use of AI-based methods in the year 2020. In this study, the authors were able to generate models to predict PCI based on the Falling Weight Deflector (FWD) deflection results. The methods used are the single multi-layer perceptron (MLP) and radial basis function (RBF) neural networks as well as their hybrids. Both studies proved that using computer-based approaches can be significantly advantageous for pavement surface evaluation. Bashar and Torres-Machi (2021) utilized Artificial Neural Networks (ANN), Random Forest (RF) and Support Vector Machine (SVM) algorithms to predict International Roughness Index (IRI) and the study resulted in good prediction models for estimating IRI from images. In addition, researchers were able to use computer-based models in the friction aspect of pavement engineering. Yang (2017) utilized the Convolutional Neural Networks (CNN) to build a friction prediction model having the pavement surface spectrogram as an input and the friction number as an output. The model predicted the friction values with 90.63% testing accuracy. Zhan et al. (2020) utilized the Deep Residual Networks (ResNets) for the prediction of pavement friction and the resulted accuracy for the model was 91.95%.

Furthermore, Cummings (2010) presented a strong relationship between Locked Wheel Skid Trailer (LWST) and IRI values. Quiros et al. (2018) satisfactorily compared the network-level friction measurements obtained with the Sideway-force Coefficient Routine Investigation Machine (SCRIM)

with measurements made with the traditional LWST. Praticò & Vaiana (2015) investigated the correlation between Mean Profile Depth (MPD) and Mean Texture Depth (MTD) and it was shown that there is no linear relationship between the two. However, significant regression models were generated for estimation purposes. Kouchaki et al. (2018) investigated the correlation between Dynamic Friction Tester (DFT), Grip Tester, and Circular Texture Meter (CTM) and found a good correlation between DFT results at high- and low- speed levels. The study also showed a greater correlation between MPD and the friction values at high speed. However, the type of surface also plays in important role in the significance of the models. Yu et al. (2020) investigated the relationship between DFT and BPN or MPD and found that at speeds of 20 km/h, correlation with BPN was significant and as speed increases, the correlation becomes stronger with MPD.

As can be seen from literature, the computer-based models are vastly used for pavement functional and surface performance prediction, and hence, this article mainly aims at generating different ML models to predict LWST values from DFT and CTM measurements. The data was taken from actual measurements made in different counties within the state of Ohio. Different techniques of ML were employed and significant models were developed.

2 Methodology

After data collection, three different Machine Learning (ML) techniques were used to predict the LWST values from DFT and CTM measurements. Three models have been produced for each ML technique; the first model using DFT results at seven (7) different speeds and the second one using the IFI parameters (F60 and Sp) and the final one using DFT and CTM parameters.

The ML techniques are Multi-Layer Perceptron (MLP), which is a type of Artificial Neural Networks (ANN), the Decision Tree model (M5P), and a lazy learning algorithm called K-Nearest Neighbor (KNN) or Instance Based Clustering Learner (IBK). Waikato Environment for Knowledge Analysis (Weka version 3.8.5) software was used to conduct the above-mentioned models. Weka is known as powerful tool in data analysis due to its portability and comprising a huge collection of data modeling techniques, together with graphical user interfaces for easy access to these functions (Kulkarni & Kulkarni, 2016).

Multi-Layer Perceptron (MLP) is a feed-forward network used as a supervised learning algorithm without any brief assumption about the distribution and pattern in the data. It consists of at least three layers namely input layer, hidden layer, and the output layer. Each layer consists of several neurons or nodes that are fully connected to the next layer by weights (Gardner & Dorling, 1998). A weighted sum of the normalized parameters is the input to each node in the hidden layer. The hidden layer modified this sum by a certain activation function and transferred it to the output layer. In this study, sigmoid activation function was used to handle the nonlinearity in the data and due to its relatively easy computations and efficiency (Gardner & Dorling, 1998). The output layer signal is then a function of the weighted sum signals from the previous hidden layer signals that can be calculated using Eq. 1 below.

$$Y' = \sum_{i=1}^{n} (\omega_i * \mathrm{sig}(\alpha)_i) + \vartheta. \quad (1)$$

Y': The predicted normalized value.
n: Number of nodes in the hidden layer.
ω_i: Node weight.
$\mathrm{sig}(\alpha)_i$: Sigmoid value for the weighted sum of the inputs to the hidden layer.
ϑ: The output bias.

The MLP learns through the training data and assigns the weight for each connection in the model. The predicted value calculated using the previous equation and the weight is then adjusted based on the error term between the actual and predicted values and using one of the back-propagation training algorithms to find the weights with minimum error term (Hornik et al., 1989).

All decision tree models are also non-parametric supervised learning algorithms that use the training data to build a decision rule to predict the target variable in both classification and prediction issues. M5 tree model follows the classical process for building decision trees and was first developed by Quinlan (1992) then modified by Wang and Witten (1997) to handle missing values and attribute with fixed possible values. According to Shmueli et al. (2006), the tree is built by two steps: recursive partitioning and pruning. The recursive partitioning step starts by splitting the data into two branches according to the strongest variables and by trying different values (threshold) for that variable to get the one with the least sum of squared errors (SSE) from the mean. Then, the second strongest variable is used to split each branch into smaller branches, and the process is repeated until no further development achieved or one of the stopping criteria is met. Each split point becomes a node on the tree and is represented by a single or multiple linear regression (MLR) called tree model or by a numeric value and called tree regression.

The second step (pruning step) is an alternative for the stopping criteria to reduce the overfitting problem. After building a full tree where each leaf contains one or a few data points, it is pruned back by removing the nodes that do not improve the quality of the predictive model. In this step, the utility of each node on the tree is tested to generate a successively smaller tree. The best tree is the one with minimum sum of squared errors or minimum cost complexity. The resulting model will represent the non-linearity in the data by a piece-wise linear function with smoothing function to fill the gaps that formed at leaf nodes. In this study M5P tree model was used.

K Nearest Neighbor (KNN), or what is known in Weka as Instance-Based Learner (IBL), is a lazy learning algorithm. In the Lazy method, unlike other Machine Learning (ML) methods such as ANN and decision trees, no generalization or action is made on the data until a call to the system is done (Webb, 2016). It also means that this method generates a prediction for the test instance when it enters the system rather than building a model. KNN methods generate a prediction based on an average of a K number of instances of the nearest neighbor in the system data set (training data). The number of instances (K) is defined by the user or using the cross-validation option. The user chooses an integer value between 1 and the number of instances in the training data set. It is not recommended to use K as a large number to avoid giving a prediction equal to the mean of the training dataset for all the testing data points. Cross-validation defines the optimal K number between one and the number defined by the user based on mean absolute error or mean squared error.

Then, the nearest neighbor instances are chosen based on some search algorithms that calculate the distances between the test point and each value in the database. Different distance functions are available, including; Euclidean, Manhattan, Minkowsky for regression, and Hamming distance for classification. Euclidean is the simplest and most used function for regression purposes based on a mathematical calculation of the distance (length of segment) between the neighbor points using the Pythagorean Theorem. The main disadvantages of KNN are the high sensitivity to noise, outliers, and irrelevant data points. Another point is that a large training database and memory are needed to increase the accuracy of the results. In turn, this makes the process slower and less efficient. Weka 3.8.5 was used to conduct the KNN modeling due to its ability to provide different alternatives to overcome some of these problems and get the best results.

3 Results and Discussion

Before starting the modeling process, all the data were normalized to a value between [-1, 1] using the attribute normalize filter in the pre-processing analysis tools, so each attribute can have the same attention in the model. Outliers were also detected and removed to improve the prediction model without any significant change or improvement for the model or the error term. Then, data was split into two subsets; training for model building and validation for testing the performance of the models based on unseen data. Finally, three different models were generalized using each ML technique. The first model using DFT results at seven (7) different speeds and the second one using the IFI parameters (F60 and Sp) and the final one using the DFT and CTM parameters.

For MLP, one hidden layer was used as recommended and proved to be sufficient for any prediction problem by Goodfellow et al. (2016) and number of nodes were determined using the process suggested by (Shahin et al., 2002). The process based on starting with a small number of hidden layers and increasing it until there was no further improvement in the model. The model improvement was represented by the Mean Absolute Error (MAE) term and correlation coefficient. The results of optimization process are shown in Fig. 1. The process started with zero nodes in the hidden layer up to 20 nodes. Zero nodes means that the relation is expected to be linear between LWST and the predictors. The results using zero nodes in terms of R^2 was almost equal to results using MLR that presented in Khasawneh (2015) and this result was improved significantly using more nodes. It can be noticed that the optimum number of nodes were different for the three models and using DFT10 up to DFT64 as predictors for LWST provided the minimum MAE.

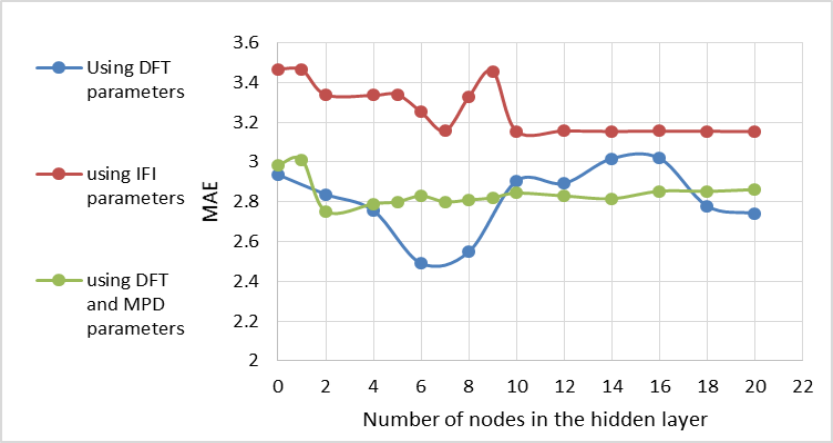


Fig. 1: Results of optimization process

For weight adjustment during the model building, small learning rate of 0.01 and a momentum of 0.1 were used, which is not uncommon in past research since the dataset and number of parameters are considered small,. Large training time (epochs) of 500,000 was assigned but with an early stopping criterion. The model building and weight adjustments stop when the error increases in the ValidationSetSize data and exceeds the validation threshold. In other words, if the error term in the training data increases for several consequence epochs (validation threshold), then the modeling stops. The weights before the last increase in error term are shown on the final model. Table 1 summarizes the final structure, training time, Root Mean Square Error (RMSE) and coefficient of determination (R^2) for the three generalized models in this study for both training and validation sets.

Table 1: Summary of the MLP results

Model	Structure	Training time (sec.)	RMSE	R^2 training	R^2 validation
DFT model	7-6-1	85.2	3.26	81.38	79.01
IFI model	2-7-1	12.9	4.16	69.60	82.64
DFT and MPD model	8-2-1	2.2	3.57	77.67	75.69

The first model is the best model, which explains 81% of the variance in the data with minimum RMSE. However, the third model gives also a close coefficient of determination with much smaller training time and simpler model with only two nodes in the hidden layer. The second model was with the least predictive power and even less than MLR models; see (Khasawneh, 2021).

Tree model was built based on 85% of data points. The remaining 15% were used as a validation set. For the first and third models, the data was represented by four (4) different linear regressions (rules) whereas one linear rule represents the data in the second model. In this case, where there is no split point in the data that can minimize the SSE from the mean, the final model of M5P is one linear rule that is very similar to the regular MLR. Table 2 summarizes the three final models.

Table 2: Summary of M5P models

Model	Linear rules	R^2 training	R^2 validation
DFT Model	$LWST_{rule1}$=0.035 DFT_{10}+0.642DFT_{64}+5.496	75.69	70.49
	$LWST_{rule2}$=0.129 DFT_0-0.322 DFT_{10}-1.269DFT_{64}+99.820		
	$LWST_{rule3}$=0.354 DFT_{10}-0.319DFT_{20}+0.435DFT_{40}+0.264DFT_{50} +0.316DFT_{64}+23.761		
	$LWST_{rule4}$=0.349 DFT_{30}+19.813		
IFI Model	$LWST_{rule1}$=0.05 Sp+0.851F_{60}+12.426	63.73	61.20
DFT and MPD Model	$LWST_{rule1}$=11.508 MPD+0.090DFT_{10}-0.247DFT_{10}+0.178DFT_{20} +0.114DFT_{50}+0.451DFT_{64}+27.8	77.19	84.64
	$LWST_{rule2}$=1.569 MPD-0.017$DFT1_0$-0.126 DFT_{10}+0.090 DFT_{20} +0.114 DFT_{50}+0.296 DFT_{64}+31.678		
	$LWST_{rule3}$=4.389 MPD+0.051DFT_0-0.441 DFT_{10}+0.566 DFT_{50} +0.462 DFT_{64}+23.860		
	$LWST_{rule4}$=1.010 MPD+ 0.349 DFT_{30}+ 0.232 DFT_{64}+20.020		

The best model for LWST prediction using M5P tree was the third model with R^2 of 77.19% and 84.64% for both training and validation sets, respectively. It was also found that DFT64 is a very important variable affecting the LWST and was included in most LWST rules. However, the second model still provided the least explanation and prediction of LWST data. Figure 2 shows the split point and ranges for each linear rule for the DFT and MPD Model.

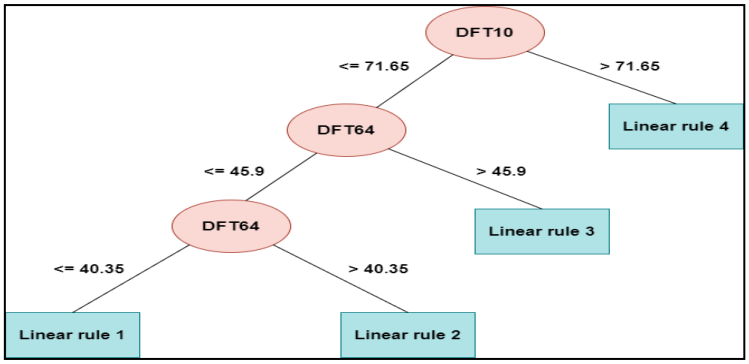


Fig. 2: Best M5P model tree

For the K Nearest Neighbor (KNN), the maximum number of nearest neighbor was set to 10 to avoid prediction values equal or near to the mean and cross-validation option was used to choose the best number of instances to be averaged. In addition, weighted average by one over the distance was used to give the closest case or point the highest weight during the prediction process. Using 85% of data set to train the KNN, the result of KNN modeling process was prediction values for each data point that were represented graphically in Figure 3 (a-b) for both training and validation datasets.

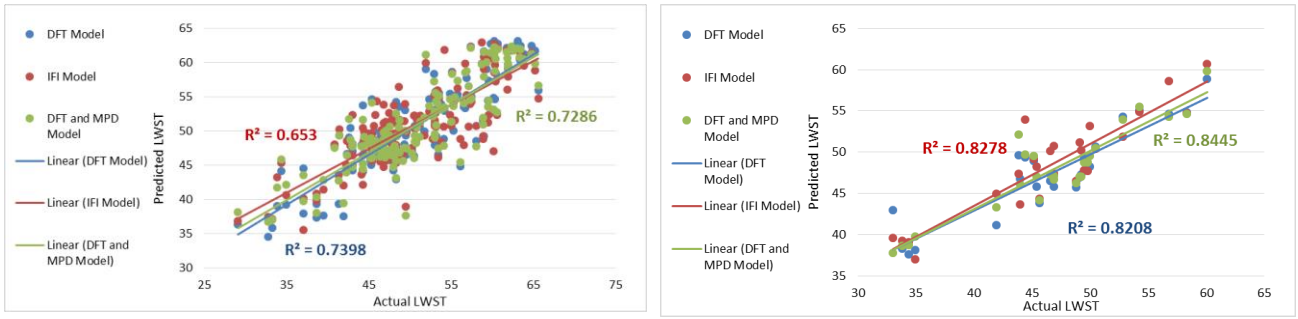
4 Conclusions

Using machine-learning techniques has a significant effect on the power of LWST prediction. Yet increasing the data points in the training set will continuously enhance the models. The best model in LWST prediction was the MLP model. The first model that used DFT parameters give the highest explanation for the variance in the data followed by DFT and MPD model. Including the MPD parameter in MLP model along with DFT parameters unexpectedly reduce the prediction power in term of R^2 from 81% to 78% but with less than 3% of training time of the first model.

However, if we are looking for simplicity, the M5P model could give good results, especially by using both DFT and MPD parameters that resulted with R^2 of 77%. Whereas, KNN model that gives the least coefficient of determination can be repeatedly improved by increasing the training data and would give the best results in case the tested points have similar characteristics to the data in training set.

For validation purposes, the results were very close using all models which can be explained by the fact that the validation dataset was chosen as a representative sample that follows almost the same distribution of the LWST data in the training set; so for each point there would be several nearest values in each model.

Finally, it can be concluded that MLP was the best technique in this study with maximum R^2 of 81% using DFT parameters to predict LWST values and that IFI parameters were not good enough to get a satisfied predictions.



(a) **(b)**

Fig. 3: (a) Graphical display of KNN results based on training data, (b) Graphical display of KNN results based on validation data

References

Alsheyab, M. A. & Khasawneh, M. A. (2022). "Quantifying the effect of modified mixture volumetrics and compaction effort on skid resistance of asphalt pavements," *Int. J. Pavement Eng.*, vol. 23, no. 5, pp. 1552–1560. doi: 10.1080/10298436.2020.1810688.

ASTM 867-02. (2015) "Standard Terminology Relating to Vehicle- Pavement Systems," doi:

https://doi.org/10.1520/e0867-02.

ASTM E 2380. (2005). “Standard Test Method for Measuring Pavement Texture Drainage Using an Outflow,” Am. Soc. Test. Mater., vol. i, pp. 2–5. https://doi.org/10.1520/e2380_e2380m-15.

ASTM E 303-93. (2002). “Standard Test Method for Measuring Surface Frictional Properties Using the British Pendulum Tester”. doi: 10.1520/E0303-93R13.2.

ASTM E 965-96. (2001). “Standard Test Method for Measuring Pavement Macrotexture Depth Using a Volumetric Technique”. https://doi.org/10.1520/e0965-15.

ASTM E1845-15. (2015). “Standard Practice For Calculating Pavement Macrotexture Mean Profile Depth”. https://doi.org/10.1520/e1845-09.

ASTM E1911-98. (2002). “Standard Test Method for Measuring Paved Surface Frictional Properties Using the Dynamic Friction Tester”. https://doi.org/10.1520/e1911-09ae01.

Bashar, M. Z. & Torres-Machi, C. (2021). “Performance of machine learning algorithms in predicting the pavement international roughness index,” *Transp. Res. Rec.* https://doi.org/10.1177/0361198120986171.

Cummings, P. (2010). “Modeling the Locked-Wheel Skid Tester to Determine the Effect of Pavement Roughness on the International Friction Index,” University of South Florida.

Gardner, M. W. & Dorling, S. R. (1998). “Artificial neural networks (the multilayer perceptron) - a review of applications in the atmospheric sciences,” *Atmos. Environ.*, vol. 32, no. 14–15, pp. 2627–2636, doi: 10.1016/S1352-2310(97)00447-0.

Goodfellow, I., Bengio, Y. & Courville, A. (2016). *Deep Learning (Adaptive Computation and Machine Learning series)* Illustrated Edition, Illustrate. The MIT Press.

Hall et al. (2009). “Guide for Pavement Friction”. doi: 10.17226/23038.

Henry, J. J. (2000). “Evaluation of Pavement Friction Characteristics. NCHRP Synthesis of Highway Practice,” *Transp. Res. Board*, vol. 291. https://doi.org/10.5703/1288284314663.

Hofko et al. (2019). “A laboratory procedure for predicting skid and polishing resistance of road surfaces,” *Int. J. Pavement Eng.*, vol. 20, no. 4, pp. 439–447. doi: 10.1080/10298436.2017.1309191.

Hornik, K., Stinchcombe, M. & White, H. (1989). “Multilayer feedforward networks are universal approximators,” Neural Networks, vol. 2, no. 5, pp. 359–366. doi: 10.1016/0893-6080(89)90020-8.

Karballaeezadeh et al. (2020). “Intelligent road inspection with advanced machine learning; Hybrid prediction models for smart mobility and transportation maintenance systems,” *Energies*, vol. 13, no. 7. doi: 10.3390/en13071718.

Khasawneh, M. A. (2008). “The development and verification of a new accelerated polishing machine,” University of Akron.

___. (2015). “The prediction of LWST Values from DFT and CTM measurements using linear and nonlinear regression analyses,” *Jordan J. Civ. Eng.*, vol. 9, no. 4, pp. 487–498. doi: 10.14525/jjce.9.4.3121.

Khasawneh, M. A. & Alsheyab, M. A. (2020). “Effect of nominal maximum aggregate size and aggregate gradation on the surface frictional properties of hot mix asphalt mixtures,” *Constr. Build. Mater.*, vol. 244, p. 118355. doi: 10.1016/j.conbuildmat.2020.118355.

Kouchaki et al. (2018). “Field Investigation of Relationship between Pavement Surface Texture and Friction,” *Transp. Res. Rec.*, vol. 2672, no. 40, pp. 395–407. doi: 10.1177/0361198118777384.

Kulkarni, E. G. & Kulkarni, R. B. (2016). “WEKA Powerful Tool in Data Mining General Terms,” *Int. J. Comput. Appl.*, 2016.

Majidifard, H., Adu-Gyamfi, Y. & Buttlar, W. G. (2020). “Deep machine learning approach to develop a new asphalt pavement condition index,” *Constr. Build. Mater.*, vol. 247. doi: 10.1016/j.conbuildmat.2020.118513.

Marcelino et al. (2021). “Machine learning approach for pavement performance prediction,” *Int. J. Pavement Eng.*, vol. 22, no. 3, pp. 341–354. doi: 10.1080/10298436.2019.1609673.

Praticò, F. G. & Vaiana, R. (2015). "A study on the relationship between mean texture depth and mean profile depth of asphalt pavements," *Constr. Build. Mater.*, vol. 101, pp. 72–79. doi: 10.1016/j.conbuildmat.2015.10.021.

Quinlan, J. R. (1992). "Learning with continuous classes," *Aust. Jt. Conf. Artif. Intell.*, vol. 92, pp. 343–348.

Quiros, et al. (2018). "Interconversion of Locked-Wheel and Continuous Friction Measurement Equipment (CFME) Friction Measurements," *Transp. Res. Rec.*, vol. 2672, no. 40, pp. 452–462. doi: 10.1177/0361198118797455.

Shahin, M. A., Maier, H. R. & Jaksa, M. B. (…). "Predicting Settlement of Shallow Foundations using Neural Networks," *J. Geotech. Geoenvironmental Eng.*, vol. 128, no. 9, pp. 785–793.

Shmueli, G., Patel, N. R. & Bruce, P. C. (2006). Data mining for business intelligence: concepts, techniques, and applications in Microsoft Office Excel with xlminer, 1st edition. John Wiley & Sons.

Wang, Y. & Witten, I. H. (1997). "Inducing Model Trees for Continuous Classes," *Eur. Conf. Mach. Learn.*, pp. 1–10.

Webb, G. I. (2016). "Lazy Learning," in Encyclopedia of Machine Learning and Data Mining, pp. 2016–2017.

Yang, G. (2017). "Exploring Pavement Texture and Surface Skid Resistance Using Soft Computing Techniques," Oklahoma State University.

Yu et al. (2020). "Dynamic friction coefficient between tire and compacted asphalt mixtures using tire-pavement dynamic friction analyzer," *Constr. Build. Mater*, vol. 258, doi: 10.1016/j.conbuildmat.2020.119492.

Zhan et al. (2020). "Friction-ResNets: Deep Residual Network Architecture for Pavement Skid Resistance Evaluation," *J. Transp. Eng. Part B Pavements*, vol. 146, no. 3, p. 04020027. doi: 10.1061/jpeodx.0000187.

Cite as: Khasawneh M.A., Alsheyab M.A. & Al Akhrass H.I., "Modelling Asphalt Pavement Frictional Properties using Different Machine Learning Algorithms", *The 2nd International Conference on Civil Infrastructure and Construction (CIC 2023)*, Doha, Qatar, 5-8 February 2023, DOI: https://doi.org/10.29117/cic.2023.0075

Modeling Thermal Conductivity, Thermal Diffusivity and Specific Heat of Asphalt Concrete Using Beta Regression and Mixture Volumetrics

Mohammad Ali Khasawneh
Civil Engineering, Prince Mohammad Bin Fahd University, Al Azeziya, Eastern Province, Kingdom of Saudi Arabia
mkhasawneh@pmu.edu.sa

Mohammad Ahmad Alsheyab
Civil, Construction and Environmental Engineering, Iowa State University, Ames, Iowa, USA
alsheyab@iastate.edu

Abstract

The main objective of this paper is to develop predictive models using Beta regression for laboratory-prepared hot mix asphalt (HMA) specimens' thermal properties, including thermal conductivity (TC), thermal diffusivity (TD) and specific heat (SH). Thirty such specimens were prepared while varying the mixture's nominal maximum aggregate sizes (NMAS) and gradation coarseness. The widely used Transient Plane Source (TPS) method was employed to determine the thermal properties of the asphalt concrete. Only one type of asphalt binder was used for preparing all specimens. The air void volume (V_a) and the effective binder volume (V_{be}) were calculated for each mixture. To this end, the multiple linear regressions and the non-linear beta regressions were employed. Laboratory work resulted in hundred and fifty (150) data points. Three nominal maximum aggregate sizes, two gradation coarseness levels, five replicates and five different locations of measurements to ensure accuracy and repeatability in the obtained results. In conclusion, using V_a and V_{be} as predictors provided reliable predictive models for the thermal properties of different asphalt mixtures. The distribution of V_a and V_{be} was identified, and synthetic data was created to evaluate the accuracy of the models. Apart from R^2 values, beta regression was more reliable to predict thermal properties of asphalt mixtures than multiple linear regression.

Keywords: Beta regression; Multiple linear regression; Superpave; Thermal conductivity; Thermal diffusivity; Specific heat; Air void volume; Effective binder volume

1 Introduction

Since temperature has a significant impact on how well pavements perform, it follows that different pavement temperatures cause varying structural reactions, and hence various distresses. In order to understand how the asphalt binder responds under specific conditions, it is essential to be aware of the various qualities of asphalt concrete. In addition, asphalt concrete's thermal qualities primarily define its characteristics for heat storage and heat transport (Tritt, 2005) and (Geng & Heitzman, 2016). Thermal conductivity (TC), thermal diffusivity (TD), and specific heat (SH) are three basic terms used to describe heat transmission. Thermal conductivity, in its simplistic term, is the quantity of heat transmission through a material per unit surface area and per unit temperature difference. Specific heat is a constant that relies on the type of material used to transfer heat and it implies the heat required to raise the temperature of the unit mass for a known substance in order to cause an increase of one unit in temperature. Lastly, thermal diffusivity measures rate of temperature spread through a material. High diffusivity means that heat is transferring rapidly as in (Shi, 2014) and (Cengel & Heat, 2003).

Various techniques are available to assess thermal parameters of different engineering materials. Axial flow, hot-wire, guarded heat flow meters, guarded hot plate and transient plane sources are some examples (TA Instruments, 2012). The transient plane source (TPS) approach, however, is the most popular technique for evaluating thermal characteristics because of its reliable design, and its ability to detect thermal conductivity, diffusivity, and specific heat in a timely manner (Warzoha & Fleischer, 2014).

Thermal properties of asphalt concrete have been investigated by many researchers with emphasis on the influencing variables that affect the thermal behavior of asphalt mixtures. This is demonstrated in studies conducted by Mrawira and Luca (2006); Kim et al. (2003); Côté & Konrad (2005); Çanakci et al. (2007); Hall & Allinson (2009); (Pan et al., 2017); (Hassn et al., 2016); (Bai et al., 2015); (Tang et al., 2014); and (Wang et al., 2016).

To substantiate the findings of previous studies, this study aims at utilizing analytical modeling techniques for the prediction of thermal properties of asphaltic materials. In this study, the TPS method was employed to investigate the thermal characteristics of Superpave laboratory-compacted hot mix asphalt (HMA) specimens. The study included both experimental and analytical parts focused on the effect of HMA volumetrics in governing the thermal properties of asphalt mixtures. Since aggregate plays a key role in regulating the engineering properties of asphaltic materials, changing the aggregate gradation of the asphalt mixture is the primary issue under examination in this work, see Elliott et al. (1991); Garcia et al. (2020); Cai et al. (2022); and (Khasawneh & Alsheyab, 2020). As a result, the gradation was controlled by altering the nominal maximum aggregate size (NMAS) and aggregate gradation (i.e., fine gradation or coarse gradation). The air void volume (V_a) and the effective binder volume (V_{be}) were used as predictors since these two variables are significantly influenced by the gradation and the asphalt binder type (Asphalt Institute SuperPave Fundamentals Reference Manual).

Two approaches of statistical modeling were used: multiple linear regression (MLR) and nonlinear beta regression (NLBR). The models can be used to forecast these thermal properties; in some cases, they may aid specialists in the asphalt industry in forecasting the thermal performance of asphalt mixtures with less resources by limiting the need for comprehensive testing in the lab and highlighting the need for additional research in the future that considers other design variables.

2 Methodology

Thirty HMA specimens with three different NMAS values of 19.0 mm, 12.5 mm and 9.5 mm and two types of aggregate gradation: fine aggregate gradation (FG) and coarse aggregate gradation (CG) were arranged. The Superpave fundamentals documented by the Asphalt Institute Reference Manual, and used by Alsheyab and Khasawneh (2022), outlines the mix design procedure in accordance with Superpave specifications. The asphalt binder utilized in this investigation has a 60/70 penetration grade (PG) and is produced in Jordan. The crushed limestone used in the aggregate component of the prepared mixtures was purchased from Khaled Al-Rijob quarries in the Jordanian city of Irbid. Table 1 shows information related to aggregate fractions and volumetric measures including voids in the total mixture (VTM), V_a and V_{be}. All mixtures were regulated at VTM of 4%.

The transient plane source (TPS) method follows the procedure described in Mirzanamadi *et al* (2018). It is widely used method and easy to operate. It is not considered a time consuming method and can get the job done in a timely manner. Therefore, TPS was selected to meet the objectives of this study. The

experimental setup is shown in Figure 1. The experimental setup of the device comes in two forms; the typical form, which is a two-sided experimental sample setup in which the sensor is sandwiched between two pieces of the material. The second setup is the single-sided, which is used under different circumstances that are beyond the scope of the present study. Both setups are equally effective and regularly used.

Table 1: Mixtures' properties

Mixture	Aggregate Skelton				HMA Volumetrics		
	Coarse Aggregate Proportion,%	Fine Aggregate Proportion,%	Dust Proportion,%	VTM,%	V_a avg,%	V_{be} avg,%	No of specimens
AC-9.5 (F)	31	64	5	4.2	77.552	246.421	5
AC-9.5 (C)	38	58	4	4	80.040	251.724	5
AC-12.5 (F)	44	52	4	4	80.693	219.305	5
AC-12.5 (C)	50	47	3	4.1	82.882	217.260	5
AC-19 (F)	50	44	6	3.9	83.951	218.84	5
AC-19 (C)	63	34	3	3.8	84.302	214.61	5



Fig. 1: The laboratory arrangement of Hot-Disk 2200 used in this study

3 Results and Discussion

The correlation coefficient (R) and p-value matrix were investigated for the interpretation of the variables eventually used for developing the proposed predictive models. RStudio 2022.02.3+492 software was utilized to analyze the data. Table 2 shows the descriptive statistics (including measures of central value and measures of scatterness in the distribution) for the data collected.

Table 2: Descriptive statistics of the thermal data

Variable	Minimum	25th Percentile	Median	Mean	75th percentile	Maximum	Standard Deviation	Remarks
V_a, cc	77.36	80.66	82.83	82.10	83.95	84.50	2.19	Predictor
V_{be}, cc	193.9	205.4	217.3	218.4	219.3	251.7	18.72	Predictor
TC,W/(m.K)	0.8419	1.2220	1.4850	1.5140	1.7953	0.0286	0.384	Response
TD, mm^2/s	51.76	85.81	103.30	105.22	123.47	181.30	25.43	Response
SH, $(M.J)/(m^3.K)$	0.007	0.0111	0.0134	0.0154	0.0176	0.03613	0.0064	Response

Table 3 shows correlations and p-values for V_a, V_{be}, TC, TD, and SH and it can be seen in the table that both V_a and V_{be} had a significant effect on the thermal properties values; negative relationship against Va and positive relationship against V_{be}. V_a had higher correlation for TD and SH, but lower than V_{be} for TC.

Table 3: Correlation and P-value matrix

		V_a	**V_{be}**	**TC**	**TD**	**SH**
	Correlation, R	p-value				
V_a			≤0.001	≤0.001	≤0.001	≤0.001
V_{be}		- 0.462		≤0.001	≤0.001	≤0.001
TC		- 0.807	0.819		≤0.001	≤0.001
TD		- 0.836	0.784	0.716		≤0.001
SH		- 0.852	0.774	0.849	0.788	

The main purpose of the study is to generate predictive models that describe the behavior of asphalt concrete thermal enactment to assist in better understanding the behavior of this thermoplastic mixture. For comparison purposes, two regression techniques were carried out; multiple linear regression (MLR) and nonlinear Beta regression (NLBR). The inputs were the air void volume (V_a) and the effective binder volume (V_{be}), and the outputs were thermal capacity metrics. All these regression techniques were performed using RStudio 2022.02.3+492. It is important to note that including both variables in any model will always enhance the prediction. Table 4 shows the generated MLR models. The TC, TD and SH models had R^2 values of 0.700, 710, and 796, respectively. It is also important to mention that the multicollinearity was not encountered for the generated MLR models.

Table 4: Multiple Linear Regression Results

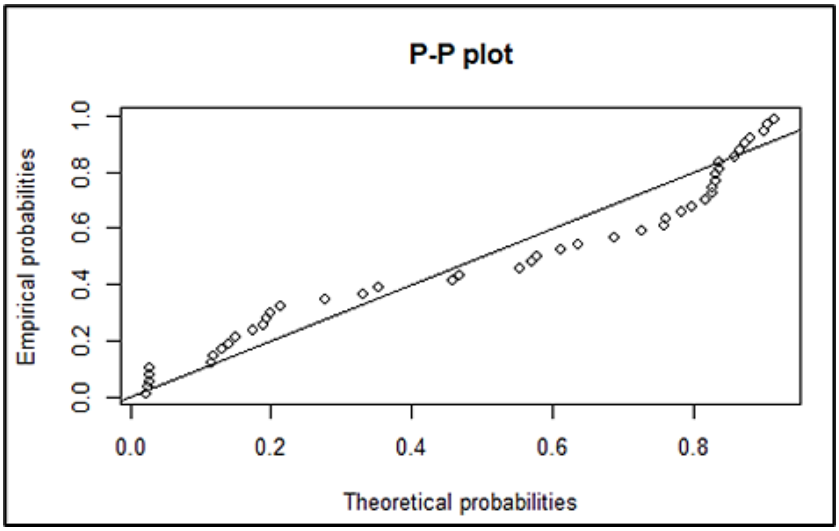
Notation	**Linear Regression**		
	Independent Variable	**Model**	**R^2**
ML	$V_a + V_{be}$	TC = 4.152 - 0.0665 V_a + 0.0122 V_{be}	0.730
		TD = 493.60 - 6.20 V_a + 0.516 V_{be}	0.732
		SH = 0.135 - 0.00176 V_a + 0.0001 V_{be}	0.746

When dealing with datasets that have a wide range of uncertainty, beta distribution is a useful choice. Unlike linear regression, Beta regression analysis assumes flexible shapes depending on the nature of the datasets and, therefore, provide reliable estimations. It is evident that Beta distributions are efficient in "rate" estimation (Ferrari & Cribari-Neto, 2004)) as it will provide better prediction when compared to linear regression (Cetin et al., 2019). Similarly, Table 5 shows the generated NLBR models and it is clearly shown that R^2 values for the Beta regression are comparable with R^2 values in MLR models, where R^2 values were 0.700, 0.710, 0.796 for TC, TD and SH, respectively.

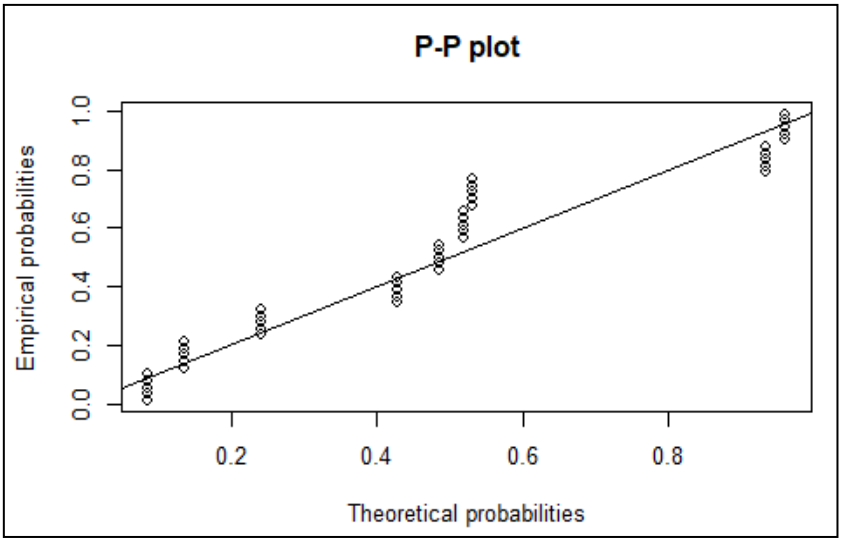
Table 5: Results of Beta regression modelling

Notation	**Multiple Linear Regression**		
	Independent Variable	**Model**	**R^2**
NLB	$V_a + V_{be}$	$TC = \frac{100}{1+e^{-(-2.0966 - 0.047\ Va + 0.075\ Vbe)}}$	0.700
		$TD = \frac{1000}{1+e^{-(1.998 - 0.066\ Va + 0.0052\ Vbe)}}$	0.710
		$SH = \frac{1}{1+e^{-(0.1352 - 0.00175\ Va + 0.000102\ Vbe)}}$	0.796

RStudio 2022.02.3+492 was used to identify the best distributions that fit the inputs V_a, and V_{be}. An approximation can be made to find the most suitable distribution for each input based on the data fitting line sloped at 45° in the P-P plot generated in RStudio 2022.02.3+492. It was found that Weibull distribution was the best fit for V_a and Gamma distribution was found to be the best fitting machine for V_{be}. The P-P plots for each input are shown in Figure 2. Table 6 shows the shape and the scale parameters for each distribution associated to each input (predictor). Table 7 shows descriptive statistics of the synthetical data for the predictors. It is important to note that when comparing the descriptive statistics of the synthetical data in Table 7 to the descriptive statistics of actual data, minimal differences were observed indicating that the simulation is quite accurate to the actual data. Once the distribution was identified representative data set points of 1000 scenarios were plugged into the models and responses (outputs) were monitored.



(a) V_a P-P Plot



(b) V_{be} P-P Plot

Fig. 2: Predictors P-P Plots: **(a)** V_a and **(b)** V_{be}

Table 6: Predictors variables distribution parameters

Predictor Variable	Distribution	Parameters	
		Shape	Scale
V_a	Weibull	53	83
V_{be}	Gamma	143.1	0.66

Table 7 shows the descriptive statistics of the three thermal properties estimated by multiplying inputs into the developed models (MLR and NLBR). By comparing synthetical data in Table 7 to the actual data, it can be observed that NLBR models were the more accurate in estimating thermal properties values. The MLR models were good in predicting the values near the mean for all thermal properties. However, the standard deviations of the resulted data from NLBR models are closer to the actual standard deviation implying that NLBR models provide better estimates than MLR models. That is, MLR models tend to overfit the output and therefore the prediction becomes less reliable when new data is introduced to the developed models.

Table 7: Descriptive statistics of the response variables

Model	Variable	Minimum	25th Percentile	Median	Mean	75th percentile	Maximum	Standard Deviation
N/A	*Actual*							
	TC,W/(m.K)	0.8419	1.2220	1.4850	1.5140	1.7953	2.441	0.384
	TD, mm^2/s	51.76	85.81	103.30	105.22	123.47	181.30	25.43
	SH, $(M.J)/(m^3.K)$	0.005	0.0111	0.0134	0.0154	0.0176	0.0361	0.0064
	Synthetical							
MLR	TC,W/(m.K)	0.852	1.206	1.350	1.375	1.527	2.550	0.246
	TD, mm^2/s	61.26	85.25	95.32	96.85	106.63	162.74	15.97
	SH, $(M.J)/(m^3.K)$	0.006	0.0107	0.0129	0.0134	0.0154	0.0313	0.0038
NLBR	TC,W/(m.K)	0.638	1.186	1.366	1.373	1.557	2.40	0.277
	TD, mm^2/s	50.98	84.92	96.61	97.07	108.82	160.36	17.27
	SH, $(M.J)/(m^3.K)$	0.002	0.0104	0.0134	0.0135	0.0163	0.0317	0.0044

4 Conclusion

The findings of this study about thermal properties of asphalt mixtures using multivariate regression techniques are succinctly summarized below:

1. V_a and asphalt mixtures thermal properties had inverse significant relationship. On the other hand, V_{be} and thermal properties had positive significant relationship.
2. Multiple linear regression models provided higher R^2 values than nonlinear Beta regression models.
3. After the synthetical simulation was conducted Beta regression models were more accurate to predict the actual data.
4. After the synthetical simulation was conducted the standard deviations of beta regression models' outputs were closer to the actual standard deviations.

5. Multiple linear regression models overfitted the actual results which made them less accurate than nonlinear Beta regression models.
6. Although non-linear beta regression models showed better prediction, multiple linear regression models can still be reliably used for estimation.

References

Alsheyab, M., A. & Khasawneh, M., A., (2022). Quantifying the effect of modified mixture volumetrics and compaction effort on skid resistance of asphalt pavements. *International Journal of Pavement Engineering, 23*(5), pp.1552-1560, doi.org/10.1080/10298436.2020.1810688

Asphalt Institute Superpave Fundamentals Reference Manual. (1999). NHI Course #131053: Federal Highway Administration, US Department of Transportation.

Bai, et al. (2015). Thermal properties of asphalt mixtures modified with conductive fillers. *Journal of Nanomaterials*, 2015, doi.org/10.1155/2015/926809

Cai, et al. (2022). Gradation of limestone-aggregate-based porous asphalt concrete under dynamic crushing test: Composition, fragmentation and stability. *Construction and Building Materials, 323*, p.126532, doi.org/10.1016/j.conbuildmat.2022.126532

Çanakci, et al. (2007). Thermal conductivity of limestone from Gaziantep (Turkey). *Building and environment, 42*(4), pp.1777-1782, doi.org/10.1016/j.buildenv.2006.01.011

Cengel, Y. (2003). Heat Transfer: A practical approach. Second Edition.

Cetin, B., Ashlock, J. & Jeong, H. D. (2019). Development of Granular Roads Asset Management System. Final Report, Iowa State University, Institute for Transportation. Sponsored by Iowa Highway Research Board (IHRB Project TR-729) Iowa Department of Transportation (Intrans Project 17-615).

Côté, J. & Konrad, J. M. (2005). Thermal conductivity of base-course materials. *Canadian Geotechnical Journal, 42*(1), pp.61-78, doi.org/10.1139/t04-081

Elliott, et al. (1991). Effect of aggregate gradation variation on asphalt concrete mix properties. Transportation Research Record, (1317).

Ferrari, S. & Cribari-Neto, F. (2004). Beta regression for modeling rates and proportions. *Journal of applied statistics, 31*(7), pp.799-815, doi.org/10.1080/0266476042000214501

Garcia, et al. (2020). Effect of aggregate gradation on performance of asphalt concrete mixtures. *Journal of materials in civil engineering, 32*(5), p.04020102.

Geng, A. P. & Heitzman, M. (2016). Measuring the thermal properties of pavement materials. In Fourth Geo-China International Conference Shandong University Shandong Department of Transportation University of Oklahoma Chinese National Science Foundation American Society of Civil Engineers.

Hall, M. & Allinson, D. (2009). Assessing the effects of soil grading on the moisture content-dependent thermal conductivity of stabilised rammed earth materials. *Applied Thermal Engineering, 29*(4), pp.740-747, doi.org/10.1016/j.applthermaleng.2008.03.051

Hassn, et al. (2016). Effect of air voids content on thermal properties of asphalt mixtures. *Construction and Building Materials, 115*, pp.327-335, doi.org/10.1016/j.conbuildmat.2016.03.106

TA Instruments (2012). Principal Methods of Thermal Conductivity Measurement. TA Instruments, pp.1-5.

Khasawneh, M., A. & Alsheyab, M., A. (2020). Effect of nominal maximum aggregate size and aggregate gradation on the surface frictional properties of hot mix asphalt mixtures. *Construction and Building Materials, 244*, p.118355, doi.org/10.1016/j.conbuildmat.2020.118355

Kim, et al. (2003). An experimental study on thermal conductivity of concrete. *Cement and concrete research, 33*(3), pp.363-371.

Mirzanamadi, R., Johansson, P. & Grammatikos, S. A. (2018). Thermal properties of asphalt concrete: A numerical and experimental study. *Construction and Building Materials, 158,* pp.774-785, doi.org/10.1016/j.conbuildmat.2017.10.068

Mrawira, D., M. & Luca, J. (2006). Effect of aggregate type, gradation, and compaction level on thermal properties of hot-mix asphalts. *Canadian Journal of Civil Engineering, 33*(11), pp.1410-1417, doi.org/10.1139/l06-076

Pan, P. et al. (2017). Effect of material composition and environmental condition on thermal characteristics of conductive asphalt concrete. *Materials, 10*(3), p.218, doi.org/10.3390/ma10030218

Shi, X. (2014). Controlling thermal properties of asphalt concrete and its multifunctional applications (Doctoral dissertation).

Tang, N. et al. (2014). Effect mechanism of mixing on improving conductivity of asphalt solar collector. *International Journal of Heat and Mass Transfer, 75*, pp.650-655, doi.org/10.1016/j.ijheatmasstransfer.2014.04.014

Tritt, T., M. (2005). *Thermal conductivity: theory, properties, and applications*. Springer Science & Business Media.

Wang, et al. (2016). Electrical and mechanical properties of asphalt concrete containing conductive fibers and fillers. *Construction and Building Materials, 122*, pp.184-190, doi.org/10.1016/j.conbuildmat.2016.06.063

Warzoha, R. J. & Fleischer, A. S. (2014). Determining the thermal conductivity of liquids using the transient hot disk method. Part II: Establishing an accurate and repeatable experimental methodology. *International Journal of Heat and Mass Transfer, 71*, pp.790-807, doi.org/10.1016/j.ijheatmasstransfer.2013.10.062

Cite as: Khasawneh M.A. & Alsheyab M.A., "Modeling Thermal Conductivity, Thermal Diffusivity and Specific Heat of Asphalt Concrete Using Beta Regression and Mixture Volumetrics", *The 2nd International Conference on Civil Infrastructure and Construction (CIC 2023)*, Doha, Qatar, 5-8 February 2023, DOI: https://doi.org/10.29117/cic.2023.0076

Planning and Implementing of Effective Enabling Works for a Successful TBM Tunnelling Project

Saad Zayed Al-Marri
Public Works Authority, Doha, Qatar
smarri2@ashghal.gov.qa

Gary Peach
Mott MacDonald, Doha, Qatar
gary.peach@mottmac.com

Hernan Vigil Fernandez
HBK-PORR JV, Doha, Qatar
hernan.vigil@auccqatar.com

Abstract

The outfall tunnel, which forms part of the Musaimer Pump Station and Outfall project (MPSO), is a 10.2 km long subsea tunnel that extends from the south coast of Doha, starting onshore, and continues under the Arabian Gulf to end in a connection with a diffuser field via riser shaft. The excavation of the outfall tunnel using a Tunnel Boring Machine (TBM) with a 4.42 m diameter and 180 m long backup, starts from a 40 m deep shaft and has an inclination of 0.05% upward to the riser shaft. The tunnel is constructed by precast concrete elements of 3.7 m internal diameter passing through different geological formations typical in the State of Qatar. Although planning a TBM tunnel involves a significant amount of engineering knowledge and experience, what is equally challenging is the enabling works which are required to be designed and constructed before the TBM even arrives at the site. On this project, these works which were substantial within themselves commenced 16 months before the TBM arrived on site. This paper will discuss the planning and execution of these outstanding underground enabling works, the logistic shaft required to facilitate the assembly and launch of the TBM at the initial stage of tunnelling and also how to arrange the sequence and space in terms of TBM logistics supply requirements to allow simultaneous construction of key permanent structures, namely the drop shaft structure which resulted in 6 months saving on the overall completion on this section of the works.

Keywords: TBM; Sub-sea tunnel; Enabling works; Logistics tunnel; Logistics shaft; Drop shaft

1 Introduction

The construction of the outfall tunnel using a TBM was complex in terms of enabling works, which required detailed planning, execution, and a clash avoidance analysis with other temporary or permanent works within the project boundaries to reach the successful conclusion to the project.

The complex enabling work starts on the surface where all the required facilities to run the TBM must be strategically deployed, in general terms those facilities are related to the logistics to receipt of the container where the TBM is delivered in major and/or minor parts, areas to store TBM parts and preassemble them. Other facilities are related to the storing of temporary materials, e.g., high and low voltage cables, water pipes in the tunnel, ventilation ducts, rails and rails preassembly facilities, power plant generation, silos for cement, bentonite, additives, and precast segments. In addition, the road layout and traffic management must be perfectly designed to allocate the heavy traffic while transporting all the consumables required including the precast rings to the site and then removal from site of the excavated material for disposal.

There is another type of enabling works with less visual impact, but it is one of the most critical from the TBM operatives' point of view. This is the access to the tunnel portal via shaft not only the lowering and assembly the TBM but also to provide the rail sidings via tunnel to park and operate the rolling stocks which supply the TBM on an hourly basis, i.e., transportation of personnel in and out of the tunnel, removal of excavated soil, transportation of the precast rings, grout and general consumables needed to operate the TBM on a regular basis.

The project rolling stock and railway requirements were determined as 3 trains, which in turn determined the length of the logistic tunnel to have space enough to park the trains and facilitated the operation of loading and unloading at the bottom of the shafts.

Finally, the location and quality of the welfare to serve the TBM operations had to be designed to ensure safe day-to-day operation with the project boundaries along with the workshop area, which provide services to the TBM.

2 Underground Enabling Works

The connection between the outfall tunnel and the pumping station is through a drop shaft. Water is pumped out from the wet well into an outfall chamber before being discharged via the drop shaft into the outfall tunnel. The drop shaft will be used to support TBM launching and during the construction phase to provide the logistics and access to the TBM and outfall tunnel.

The drop shaft is a 10 m internal diameter circular shaft, and approx. 11.4 m above ground level and extend to about 43 m below ground with a total height of approx. 54.4 m. The diameter size of the drop shaft is not big enough to be used as TBM logistics shaft and for that, the initial plan was to enlarge it to allow the assembly of the TBM, its regular operation including logistic operations and access during the construction of the outfall tunnel.

Once the Qatari Public Works Authority (Ashghal) awarded the MPSO project to the joint venture Hamad Bin Khalid Contracting Company and Porr Qatar Construction (HBK-PORR) at the end of 2017, the idea was to use a launching shaft with rectangular pit shape and size of (31 x 20 on the surface and 25 x 14 at the bottom) and 43 m deep. The bottom of the launching shaft provides access to the logistics tunnel and TBM launcher chamber and was planned to be excavated to allocate the 3 tracks and rail switches required to operate the rolling stock which serves the logistics to operate the TBM and the required chamber to launch the TBM. Figures 1 and 2 show the top and longitudinal profiles of the logistics tunnel, drop shaft and TBM launching chamber. This was first proposal considered.

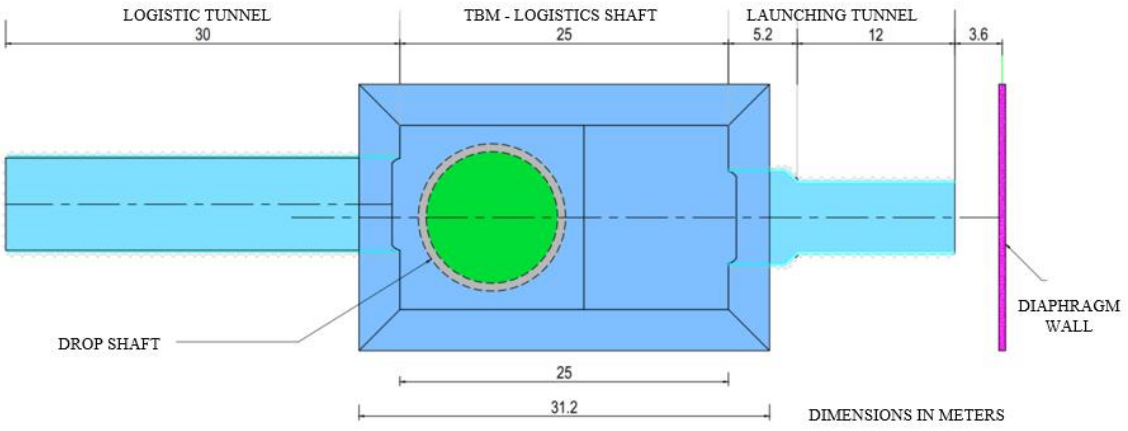


Fig. 1: Top view of Launching Shaft and tunnel, Logistics tunnel initial stage plan

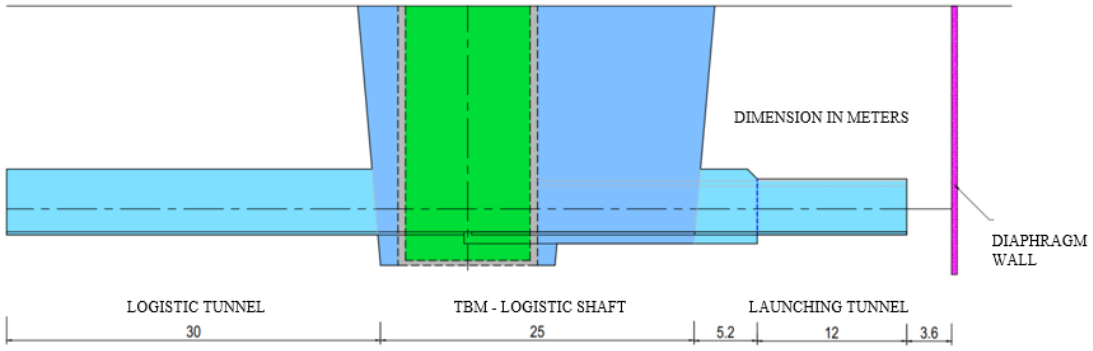


Fig. 2: Longitudinal profile of Launching Shaft and tunnel, Logistics tunnel initial stage plan

The second option evaluated at the initial stage was one oval-shaped launching shaft. Instead of a rectangular pit, the aim is to reduce the excavation and support quantities simultaneously improving the stability of the shaft due to the oval shape.

The options of a launching shaft and the drop shaft all in one excavation once the TBM finishes the excavation of the outfall tunnel seems to be the optimum solution. However, on further analysis and risk evaluation and considering the constraints and particularities of the outfall tunnel i.e., only one TBM to excavate the outfall tunnel, a long subsea tunnel with more than 10 km and only one access and egress. This represented a severe risk increment for unexpected delays. If any delay happens during construction of the outfall tunnel, it directly impacts the construction of the drop shaft and the connection of the outfall chamber and subsequent installation of utilities and land scape activities on the surface, jeopardizing the overall completion date of the project.

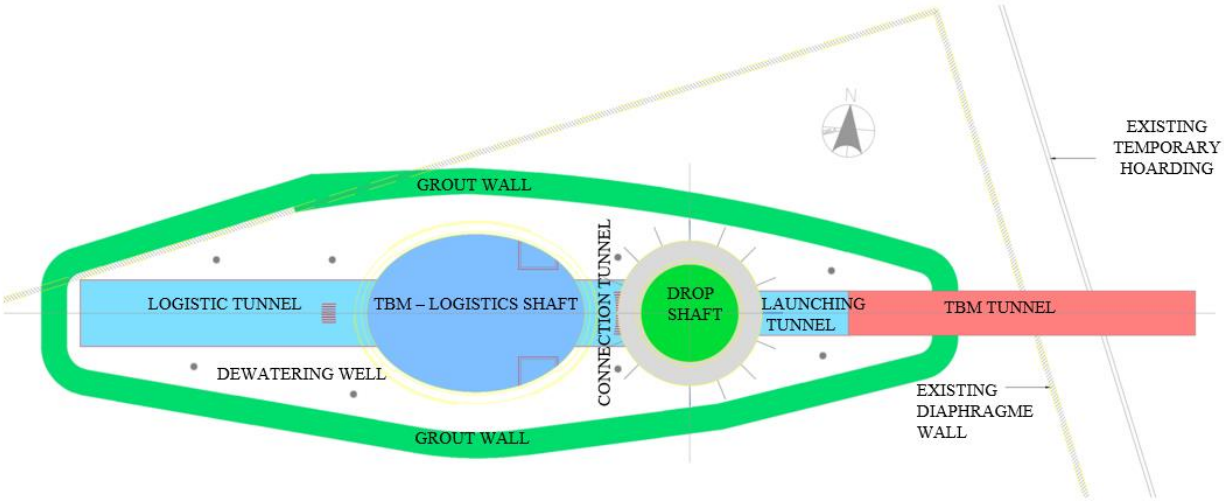


Fig. 3: Top view final concept of Launching and drop Shaft, Logistics and Connection Tunnel and Launching tunnel

The solution adopted to reduce and mitigate the risk described was to split the drop shaft from the logistics shaft, as indicated in Figure 3. There would now be 2 independent shafts which require larger efforts and resources but adding a tremendous value in term of advantages to project scheduling and providing improved TBM logistics facilities at both the bottom and the surface locations.

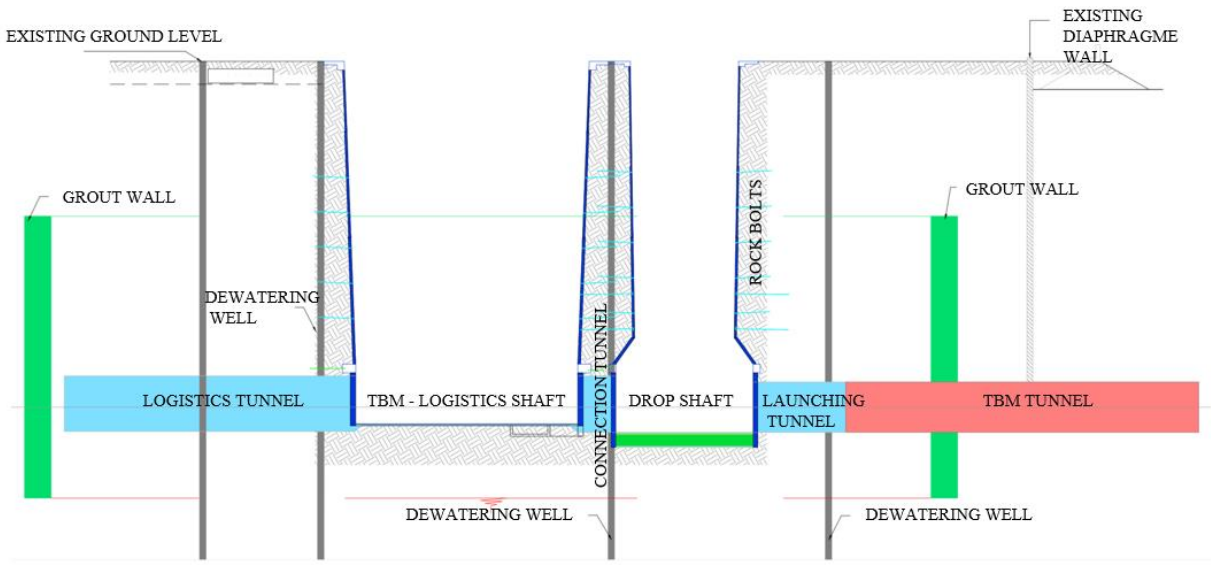


Fig. 4: Longitudinal profile of the final arrangement of drop and logistics shafts, connection and launching tunnels

2.1 Logistics Shaft and Drop Shaft (concept)

The decision to excavate independent shafts simultaneously aims to reduce the pressure on the project completion date. Delays during the construction of the outfall tunnel still allows the construction of the permanent works of the drop shaft, its connection with the outfall chamber and the surrounding landscape and rock armour among others to go ahead. This method also foresees the possibility of back-filling of the logistics shaft with low strength mass concrete in the case of any time constraints.

Figures 3 and 4 show the location of the Drop shaft, Logistics shaft and a short connection tunnel.

The Sequential Excavation and Support (SES) method was selected to excavate both shafts and support using Sprayed Concrete Lining (SCL) with wet shotcrete, wire mesh and rock bolts as primary lining support. The logistics shaft presents particular consequence of the oval shape that is the construction of concrete reinforced stiffening rings to improve the stability of the shaft. The drop shaft has the provision of the key at the bottom, not only to allocate the base slab and to control the buoyancy, but also to allow the simultaneous construction of the final concrete lining support and provide the required openings to allow the passage of the TBM logistics trains.

2.2 Logistics Shaft and Drop Shaft (Grouting and dewatering works)

The TBM project area is enclosed within a cut-off wall of an average depth of -34.3 m Qatar-National Height Data (QNHD). This cut off wall has been constructed on a pretender project phase. Thus, up to a certain excavation level (approximately 18m, below ground level), no water or very small water ingress was expected. When the excavation depth reaches a maximum depth of -40 m QHND, dewatering is required to lower and maintain the water table below formation excavation level. Dewatering is performed through 8 deep wells, with installed submersible pumps which convey the ground water to surface sedimentation tanks before discharging to the sea

In addition to dewatering, to mitigate the risk of water ingress, extensive rock grouting was carried out around the drop and logistics shaft and the TBM launching chamber tunnel. Figure 5 shows the location of the bore holes to create a second cut of wall (with primary and secondary bore holes for water tightness) around the shafts and tunnels. Tertiary bore holes within the excavation area of the shaft and tunnel acted as a grout plug on the bottom to prevent the ingress of water from the invert of

the excavations and reduce the settlements which are expected to be in the range of 5 to 10 mm, refer to Figure 6. In total 76 primary, 75 secondary and 62 tertiary boreholes were drilled reaching 10,468 meters of boreholes and 1,421,754 litres of grout was injected into the strata to seal the excavation. The grout mix design was based on Ordinary Portland Cement (OPC), bentonite, and stabilizer with water and cement ratio from 1.2 to 1.8 depending on the site conditions.

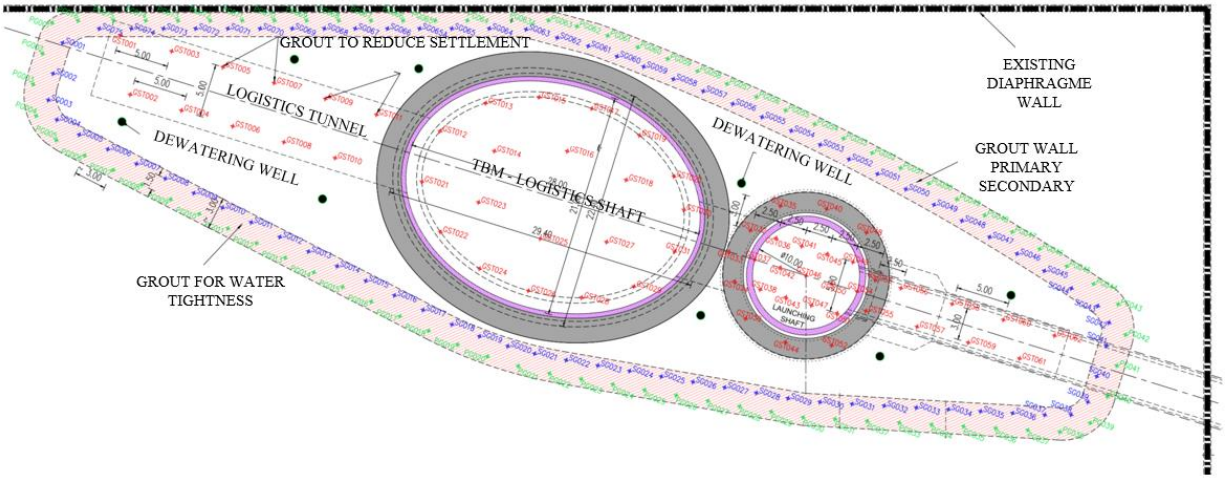


Fig. 5: Rock-grouting primary, secondary and tertiary

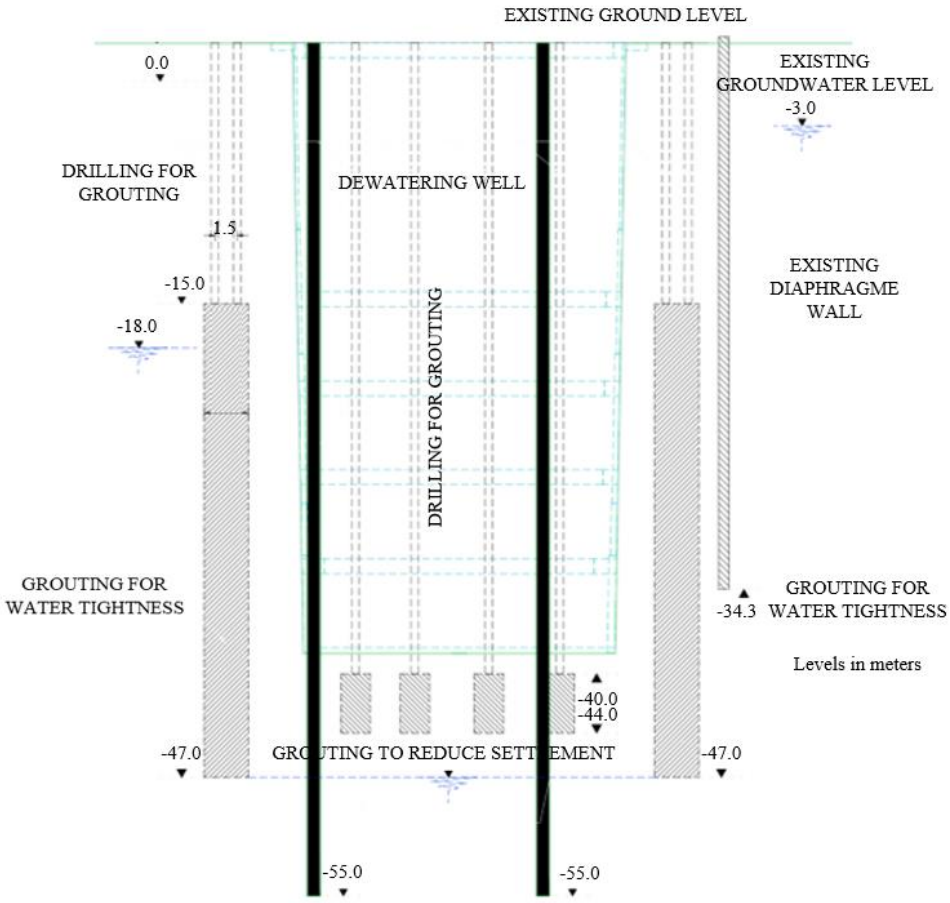


Fig. 6: Arrangement of grouting bore holes and grouting length

2.3 Logistics Shaft and Drop Shaft (excavation works)

The excavation works and application of the primary support consisting in SCL for the logistics and drop shaft was designed and implemented simultaneously. The excavation is carried out by using conventional excavators (with more than one excavator working in the shaft at the time as shown in Figure 7), a drum cutter and hydraulic hammer. The primary support was sprayed wet shotcrete reinforced with wire mesh (double layer) and installation of rock bolts.

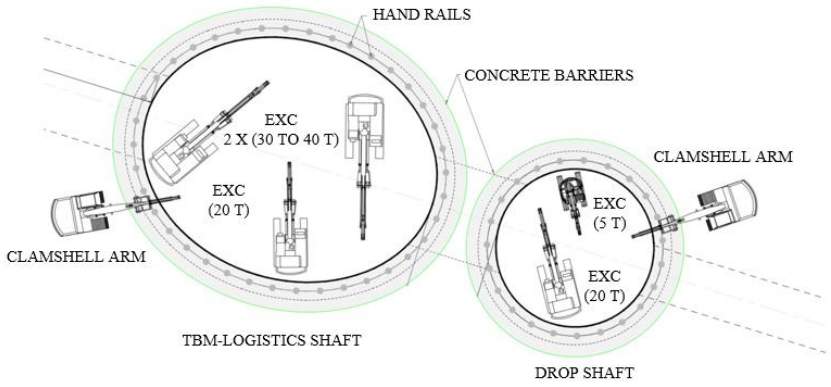
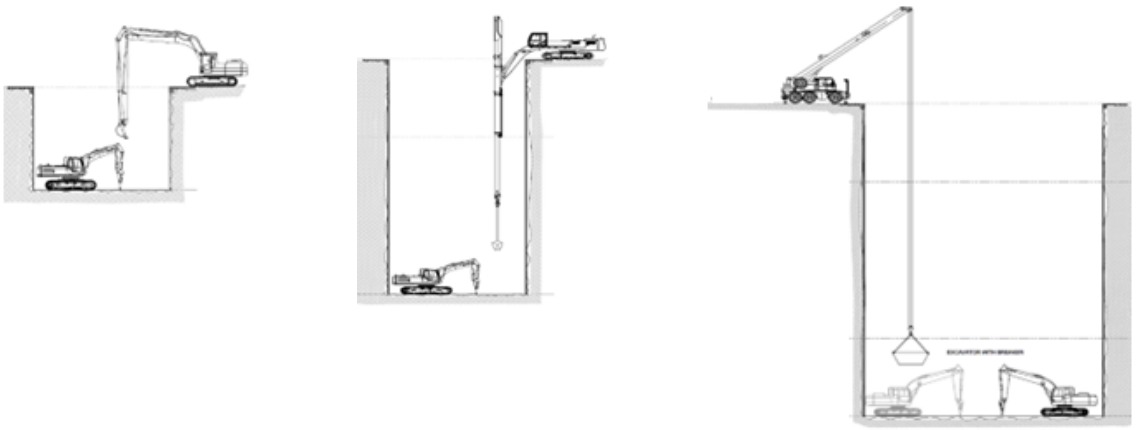


Fig. 7: Logistics and Drop Shaft Excavation Plan

The adjustment of every cycle length (between 2 and 3 m) along with the type of support to be applied was determined on site by the geotechnical engineer by related face mapping results. Excavation was planned to be carried out in three different phases, each phase having its own method of works. Figure 8 illustrates the 3 separate phases of excavation for the logistics and drop shaft works:



Phase 1: from GL to -8 m **Phase 1: from -8 to -30 m** **Phase 3: from -30 m to -43 m**

Fig. 8: Logistics and drop shaft excavation stages

As a preventive measure, water in isolated locations penetrated inside the shaft because of the rock porosity and where rock-grouting method could not seal all the gaps in hard rocks, weep holes were installed to drain the water and to reduce the water pressure over the shotcrete.

The water will be collected at the specially excavated water sump at the bottom of the excavation (one sump at each step of excavation), from the sump the water will be vertically pumped up by the means of the submersible pump into a water sedimentation tank. Figure 9 shows the general surface site layout of the logistics and drop shaft.



Fig. 9: Photo of the logistics and drop shafts during TBM operations

2.4 Logistics and Connection Tunnels. Launching Chamber Tunnel (excavation works)

The configuration of logistic and drop shafts required an internal connection tunnel, the rolling stocks require this access to operate, load, off load, park the trains underground. The launching technique of the TBM required a special launching chamber/tunnel. The New Austrian Tunnelling Method (NATM) was the method selected to excavate the required tunnels, therefore there are 3 NATM tunnel section executed on the MPSO project:

- The NATM connection tunnel section between the 2 shafts of 4.30 m in length.
- The NATM logistics tunnel extending 30 m to the land side
- The NATM launching tunnel extending to the seaside (launching tunnel) of 10 m length.

The first NATM activity was the connection tunnel between drop and logistic shaft to connect the two shafts and provide full access to the equipment and labour on formation level. The next NATM activity is the logistics and launching tunnel excavation which started together.

NATM tunnel construction sequence includes several steps, which are repeated in the same order until full completion of each excavation cycle is achieved. Once the excavation cycle is fully supported in line to the design and the relevant drawings, then the following cycle can commence following the same sequence. For this design the following steps shall be followed to comply with NATM design requirements:

Survey works; excavation; soil disposal; scaling; survey check of the excavation line and correction if and where required; geological mapping and classification of the rock mass. Recommendation of the supporting class in line to the applied rock mass classification and Detail Design criteria.

Continue with safe application of shotcrete (3 cm to 5 cm); installation of wire mesh; application of full structural thickness of shotcrete; drilling, installation and grouting of rock bolts and installation of monitoring targets on the shotcrete lining.

The Figure 10 summarized the NATM tunnel sections required for each NATM tunnel.

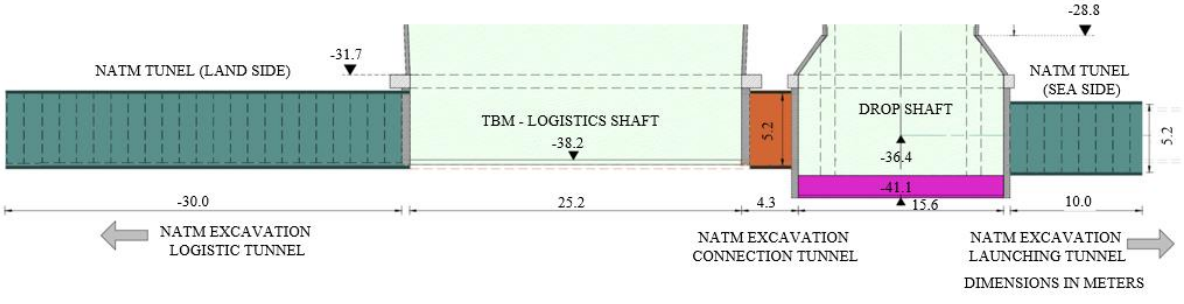


Fig. 10: Longitudinal profile logistics tunnel, connection tunnel and TBM launching tunnel all of them excavated in NATM along with logistics shaft and drop shaft

Figure 11 shows the view looking into the outfall tunnel through both logistics and drop shaft and from the back of the TBM launching chamber/tunnel.

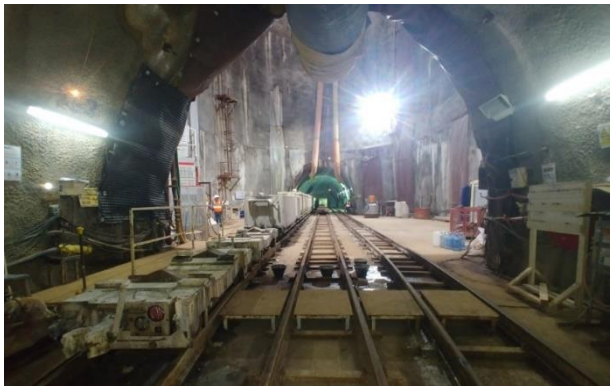


Fig. 11: View from base of drop shaft with the setup of rolling stocks tracks and logistics shaft and tunnel

3 Conclusion

The construction of the drop shaft and its connection to the outfall chamber was accomplished before the TBM achieved the tunnel completion; this was a key decision that helped to shave off 6 months from the project duration.

There were no significant TBM idle times due to logistics issues either on the surface or under the ground.

The construction of other permanent structures was not impacted due to clashing with the TBM enabling works, which confirms the importance of good planning and clash analysis at the early stage of the project.

Starting the required enabling works 16 months ahead of arrival of the TBM mitigated the risks associated with the underground enabling works.

The highlights of the facts in terms of planning, plan and implementation of enabling works related to the TBM discussed have no limitations unless contractually what is stated is something different and every contractor should follow a similar strategy to increase the possibilities of a successful TBM project.

References

Construction Management Plan C2017_109-PLN-CO-0003.

Design criteria report for Drop Shaft C2017_109-RPT-PD-ST-DS-0001.

Public Works Authority. (2017). Contract Documents for Design, Build, Operate and Maintain of Musaimeer Pumping Station and Outfall, Project ID: IA 14/15 C 015 G, Contract Number: C2017/109.www.ashghal.gov.qa

Qatar Construction Specifications 2014. (QCS-2014).

Specification for tunneling, Third edition, The British Tunnelling Society, and Institution of Civil Engineers, 2010

The British Standards Institution (2011). BS 6164:2011 Code of practice for health and safety in tunnelling in the construction industry, BSI Standards Publication, London.www.bsigroup.com.

Cite as: Al-Marri S.Z., Peach G., Fernandez H.V., "Planning and Implementing of Effective Enabling Works for a Successful TBM Tunnelling Project ", *The 2nd International Conference on Civil Infrastructure and Construction (CIC 2023)*, Doha, Qatar, 5-8 February 2023, DOI: https://doi.org/10.29117/cic.2023.0077

Ashghal Quality Assurance & Quality Control system – QSD Role in Monitoring & Reporting the Quality Performance in Ashghal Projects

Aisha Abdulaziz A. M. Al-Ibrahim
Ashghal, Doha, Qatar
aalibrahim@ashghal.gov.qa

Aisha Abdulla N. J. Al-Thani
Ashghal, Doha, Qatar
salthani4@ashghal.gov.qa

Effrosyni Plexousaki
Ashghal, Doha, Qatar
eplexousaki2@ashghal.gov.qa

Mounera Ismail R M Al-Ansari
Ashghal, Doha, Qatar
malansari2@ashghal.gov.qa

Abstract

Ashghal has established a robust system of quality control and quality assurance for all projects constructed by Ashghal. Ashghal Departments are supervising a sophisticated system of quality control and quality assurance processes and procedures, implemented by the Consultants, Contractors, and Key Supply Chain Partners of Ashghal projects (e.g., Sub-Contractors, Key Suppliers, and Independent Laboratories). This paper illustrates how Ashghal Quality & Safety Department (QSD) monitors and reports the quality performance in Ashghal constructed projects to ensure continuous improvement and adherence to Ashghal quality strategy, policy mission, and targets. QSD is operating as Third Party, reporting directly to Ashghal President, and is monitoring and reporting the compliance of the industry to the quality requirements defined in Qatar Construction Specifications (QCS, 2014), Contracts, Professional Services Agreements, ISO 9001:2015 Standard and specific Ashghal requirements. Effective root cause analysis carried out by the auditing team has led to value-adding activities. QSD has established specific Key Performance Indicators (KPIs) for the management of non-conformities and corrective actions, to improve the performance and minimize the deviations and failures of compliance. QSD is conducting focused and system audits at Ashghal projects and the supply chain and is liaising with departments and individual projects as necessary, to agree on Lessons Learned and Actions to improve the quality of works. These activities include the establishment of consistent criteria of the qualifications and experience of the quality staff of Ashghal departments and Consultants' teams. QSD is making quarterly presentations to the Ashghal President regarding the performance of the Departments (including Contractors' and Consultants' performance) and of the Ashghal Project Managers. The established criteria and evaluation related to the quality are dynamic and reviewed/updated periodically to ensure the improvement of the Quality Performance of Ashghal Projects.

Keywords: PWA; QA/QC; NCR KPIs; Quality requirements

1 Introduction

Ashghal (Public Works Authority in Qatar) is responsible for the design and construction of the Qatari infrastructure and other large-scale projects (Buildings for education, health, etc.). Ashghal is also responsible for the asset management of many of the constructed projects (mainly Roads, Drainage & Sewage Networks) (Emiri Decree, 2014a) The effective delivery of the projects, at the required quality, in conformity with contractual, legal, and technical requirements and specifications, is ensured through a sophisticated quality system, with interrelated processes and procedures, across and within Ashghal Departments.

The minimum quality requirements are defined in Qatar Construction Specifications (QCS), latest edition of 2014. These minimum requirements are expected to be met by all Ashghal projects and the level of compliance is to be verified and reported by QSD.

Ashghal is currently developing its own specifications, Ashghal Construction Specifications (ACS), to incorporate the latest technical and managerial developments, procedures, and best international practices.

Ashghal is supervising and verifying the quality of its projects through direct supervision (in-house projects) but mainly with the assistance of Consultants who operate under the capacity of the Engineer Representative and mobilize experienced quality staff at each project. The day-to-day quality monitoring of projects is performed by Ashghal QSD staff and the quality control staff of the Consultants.

Quality & Safety Department (QSD) in Ashghal is reporting directly to the Ashghal President and is conducting third party audits to verify the compliance to quality, safety, and environmental requirements. The Quality Section of QSD is responsible of monitoring and reporting of the quality performance and levels of compliance to quality requirements to the Ashghal President (Emiri Decree, 2014b).

2 Ashghal Requirements for Quality

The quality requirements expected to be fulfilled in Ashghal projects are defined in QCS (2014) (minimum requirements, applicable for all projects), in the contracts of the Construction Contractors and the Professional Service Agreements (PSA) of the Consultants.

ASHGHAL departments are also issuing circulars on quality control, either with technical content (for example, sampling and testing of materials and works by independent laboratories) or with managerial content (for example, handing-over procedures, management of non-conformities, etc).

2.1 Quality Requirements in Construction Contractor Contracts

Construction Contractors must comply with specific requirements for quality assurance and quality control defined in their contracts. To achieve this, they prepare, obtain approval, and implement a quality management system that includes Project Quality Plan, quality & operational procedures, Inspection & Test Plans, Method Statements, etc. QSD is verifying the implementation periodically through focused audits.

2.2 Quality Requirements in Professional Services Agreements of Consultants

Ashghal has established specific requirements regarding the duties and the responsibilities of the

awarded Consultants in the PSAs, and compliance is verified periodically by QSD through focused audits.

2.3 Quality Requirements in QCS (2014)

QCS (2014) requirements for quality are detailed in several sections and include prescriptive sub-sections and templates to promote understanding and facilitating the implementation.

Section 2 of QCS (2014) details the quality requirements all Ashghal Construction Contractors shall comply with.

Section 1, Part 23 of QCS (2014) defines the role and responsibilities all Ashghal Design & Supervision Consultants shall comply with.

All other QCS (2014) Sections include specific technical requirements directly related with the quality, such as material properties, workmanship and testing of finished works. (Qatar Construction Specifications, 2014)

3 Pwa (Ashghal Qatar) Quality & Safety Department Role in Quality

The role of the Quality & Safety Department (QSD) of Ashghal, by Emiri Decree, is to ensure quality of all Ashghal projects. To deliver on our mandate, we have developed and are continuously improving and implementing a robust auditing programme, with system and focused audits, most of them unannounced, with defined audit scope and mechanisms to record findings, managing non-conformities and identifying areas for improvement.

QSD reports directly to HE the Ashghal President, and as a supporting department of Ashghal, we operate as a third party to ensure the compliance with quality requirements in Ashghal. QSD started issuing Non-Conformity Reports (NCRs) in January 2020 instead of simply submitting audits reports to the Ashghal departments, after receiving authorization and instruction from the Ashghal President. This new approach has proven very fruitful and valuable; noticeable improvements can be identified in the quality performance of all departments since 2020.

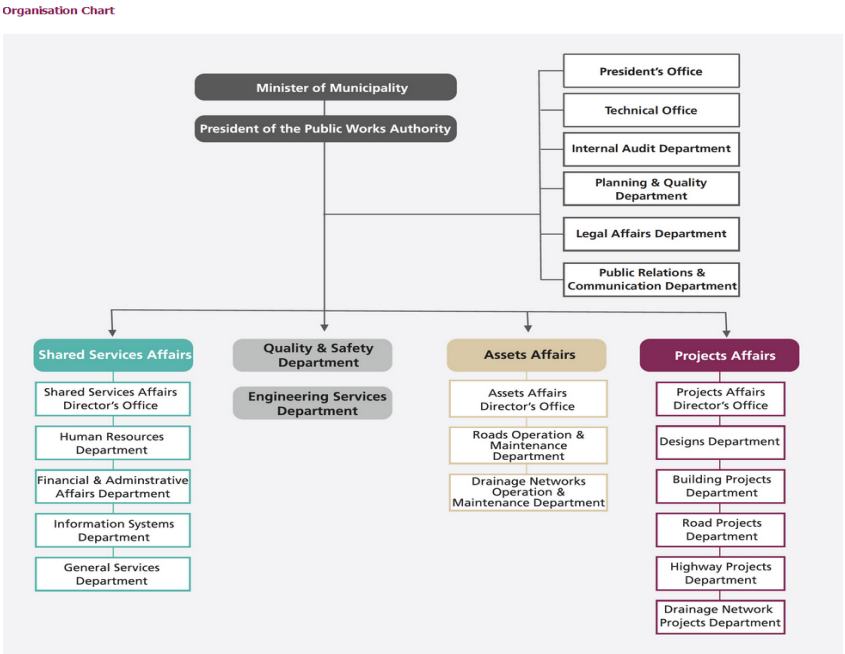


Fig. 1: Ashghal Organization Structure

QSD organization structure comprises four sections with direct interaction with Ashghal and Industry Key supply Chain Partners: Quality, Safety, Environment and Laboratory Sections. The Quality Section team is the team responsible for the monitoring and reporting of the quality performance of Ashghal projects. (Public Work Authority, 2023)

4 QSD Quality Section Auditing on Ashghal Projects

4.1 Summary of Quality Section Audit Process

QSD Quality Section is operating as a Third Party that conducts audits based on a monthly/annual audit plan. There are three different types of audits QSD auditors focus on e.g. (Construction practice, Material management and Quality Management System (QMS)), The monthly audit plan presents the planned audits for active projects in every month of the year and the audits which have been conducted by the auditors of QSD. Annual audit plan gives a brief look on the number of audits conducted for each project through the year.

QSD conducts the audits mainly unannounced and includes in the audit scope the activities of the Key Supply Chain Partners (KSCP) in each project: Consultant, Construction Contractor & main Sub-Contractors (for example Road-Works Sub-Contractor, Independent Site Laboratory) and critical suppliers (for example Asphalt Plants & Qatar Primary Material Company).

QSD Quality Section has scheduled and conducted 1,254 focused and system audits in Ashghal projects until now, since January 2020. The target was to audit all projects under construction, with minimum scope on the quality management systems, the management of materials, the sampling and testing of materials & finished works and the applied construction practices.

4.2 QSD Quality Section Personnel

All Quality Section employees hold various degrees in Engineering (for example Civil, Chemical, Industrial and Systems) alongside other employees with various levels of knowledge and expertise, many of them with more than twenty years' international experience in large-scale infrastructure projects. This multicultural and multi-generation environment allows the staff to be immersed in a work environment that is unique, challenging and always evolving.

Every Quality Auditor processes IRCA Lead Auditor ISO 9001: 2015 certificate and receives specific, on-the-job training in quality management of construction projects by the Quality Experts of the department. In addition, the employees attend internal and external training courses on project management and asset management to attain a higher level of experience in project management and ensure effective and efficient auditing.

4.3 Audit findings – Management of Non-Conformities – Continuous Improvement

Most of the identified non-conformities are related to construction practices, management of materials (including sampling and testing) and completeness & suitability of quality procedures and methodologies applied in the projects by both the Consultants and Contractors' teams. It has become evident over the last three years, that quality awareness among team members of the Consultants and Contractors, not only the assigned quality staff, could be significantly improved.

The main challenges identified during the follow-up on the issued NCRs and the implementation of the action plans was the lack of full understanding of the root cause analysis of the non-

conformities. QSD has established a mandatory classification of the root causes as per the 6-M method and provides expert opinion and support to the audited teams to ensure the differences between Correction & Corrective Action are understood, and the evidence of the implementation of those actions are identifiable, traceable, and legitimate.

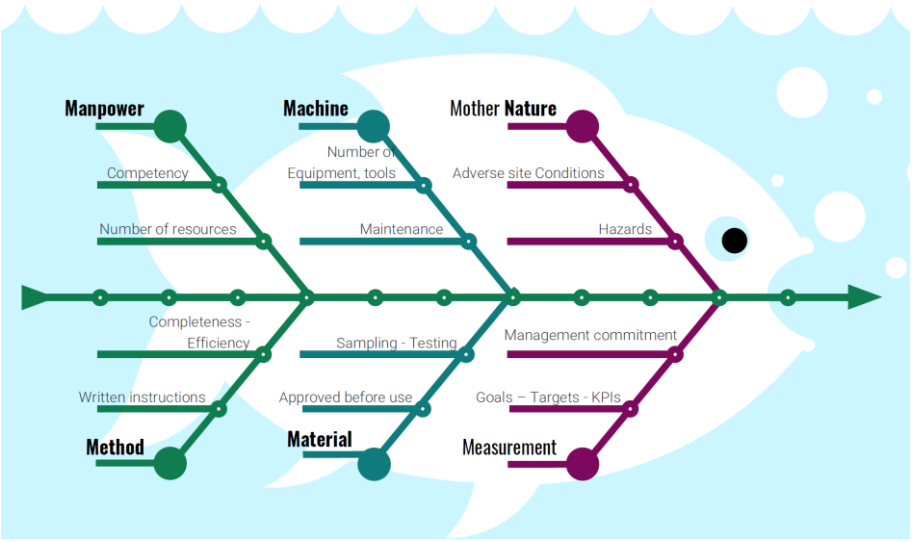


Fig. 2: Root Cause Analysis as per 6-M methodology (Fishbone – Ishikawa diagram)

The whole process resulted in the improvement of the applied corrective actions and the reduction in recurrence of non-conformities. The challenge is continuous and QSD has established more challenging targets through specific KPIs presented in the following section.

5 Key Performance Indicators (KPI) For Quality

5.1 KPIs for Management of Non-Conformities at Projects

KPIs can be developed to increase the functional value of a project by managing its development against a value determined by the owner (Gongbo et al., 2011). To enhance the quality performance, standardize the management methodology and ensure consistency across departments and within project teams, QSD has established specific KPIs for the project NCRs (issued by all involved parties) that are implemented since 2021. Those KPIs will be reviewed and revised accordingly in 2023.

6 Quarterly Performance Evaluation

6.1 QSD Evaluation of Quality Performance for the Ashghal President and Top Management

QSD prepares and conducts quarterly presentations to the Ashghal President regarding the performance of Ashghal projects in quality (including Contractors and Consultants' performance) and of the Ashghal Project Managers. The established criteria and evaluation related to the quality are dynamic, and reviewed/updated periodically, to ensure continuous improvement and adherence to Ashghal Quality Strategy, Quality Policy, Mission, Purpose, and Targets.

The QSD Manager presents quarterly evaluation reports of quality performance of projects to the Ashghal President and top management. QSD Quality Section has developed, established, maintains, and continuously improves the evaluation process. The assigned team analyses the data

of QSD Quality Section Database and presents the results of the analysis with recommendations and actions for improvement.

Objective approach and evidence-based decision making is effectively applied in every performance evaluation process. The Departments follow up each presentation with specific action plans. Critical areas that have been improved to date are:

- Standardization of full-time quality staff requirements in consultants' teams and in each department.
- Monthly Quality Working Committee for Project Affairs Departments.
- Minimization of Stop of Activities incidents.
- Customized software for the management of Non-Conformities.
- Mandatory Quality Walks at projects with the participation of each project top management.
- Quality Awareness Sessions for all project staff, not only for quality staff.
- Quality Awards.
- Penalization system to minimize the recurrence of non-conformities.

6.2 Evaluation of PWA Project Managers

Ashghal top management is materializing the international understanding that quality stops from the top and in achieving so all Ashghal Project Managers are evaluated by QSD Quality Section for performance in quality, as per the Ashghal President instruction, from October 2020. The evaluation criteria are dynamic and are reviewed periodically for suitability and effectiveness.

QSD is currently applying the revision 1 of the evaluation criteria and is intends to conduct a second review of the criteria in July 2023.

The revision 1 applied criteria are:

- Accepted Responses to issued NCRs
- Available system to monitor and report the recurrence of non-conformities as per established criteria.
- Consultant's full-time quality staff at the project.
- Number of Stop of Activities Incidents

The observed improvement in quality of Ashghal projects in the past twelve months can also be attributed to the improvement of awareness and understanding of the quality requirements among Project Managers, after the quarterly evaluations of QSD and the shared feedback with the departments.

7 Promoting Quality Awareness in Ashghal Projects

Ashghal President initiated the top-down approach to the quality performance of the whole organization because of the QSD quarterly presentations and evaluation of the PWA Project Managers. The demonstration of the management commitment has been materialized through customized training sessions delivered by QSD to Ashghal staff and to project staff at the sites.

7.1 Training PWA Project Managers

QSD delivered customized high-level quality training sessions in quality to all Ashghal Project Managers in the years 2021 and 2022. QSD prepared the content and Ashghal Human Resources Department awarded a consultant in year 2022 to provide quality-training sessions to all Ashghal Project Managers.

New quality sessions are under preparation by QSD for the year 2023, with more technical, contractual, and construction-oriented quality management content.

7.2 Training Consultants & Contractors in Quality Control

Ashghal has awarded internationally recognized consultant in the projects, with proven previous experience in similar projects in Qatar and in the world. Nevertheless, the full compliance with quality requirements has proven to be a challenge, despite the experience records and robust tender submissions of technical proposals by the Consultants. QSD identified gaps between the assumed experience of the consultants' staff and their actual performance in the projects. The COVID-19 restrictions on travel imposed more challenges on the mobilization of the best-in-their-fields Quality Managers & Quality Engineers in their fields.

QSD stepped-in and provided customized, in many cases project-oriented, quality trainings to the Consultants' staff, starting in September 2020.

Ashghal has been implementing the nationalist approach to empowering and utilising local Contractors in the projects. Most local contractors had no previous experience in Ashghal quality requirements and, despite (QCS) 2014 establishing the minimum quality requirements in construction, had not been implementing (QCS) 2014, especially the Section 2, in their previous projects. QSD provided awareness sessions to the contractors' quality staff in 2021 & 2022. More training sessions are scheduled for 2023, that will also include the contractors' top management.

7.3 QSD Cooperation with Project Affairs (PA) Departments to Improve Quality

Ashghal Project Affairs incorporates the delivery teams and departments who procure, award and construct the Ashghal projects. QSD has established close cooperation with Project Management Office (PMO) to promote quality awareness and communicate the quality KPIs and objectives to all departments.

PWA Departments have dedicated core quality teams that work closely with QSD to improve quality performance. Monthly meetings have been established and Lessons Learned have been shared among departments and projects.

8 QSD Tools for Quality Management

8.1 QA/QC Questionnaires

All active Ashghal projects submit monthly to QSD, through a specific electronic platform, the project QA/QC questionnaire that includes information on used materials, conducted sampling and testing, mobilized independent laboratories, project progress, submissions and approvals of drawings, NCR status, etc. QSD uses the questionnaire database for managing each project's risk aspect and effectively planning the QSD audits and site assessments. (QSD, 2020).

8.2 Ashghal List of Approved Tests & Laboratories

Ashghal projects and awarded construction contractors can mobilize in their projects only private laboratories approved by QSD to conduct only the tests included in the Ashghal List of Tests & Laboratories. QSD Quality Section administers this list through specific software and publishes the list periodically on Ashghal website for industry information and use. QSD Laboratory Section receives the industry applications for laboratories and tests to be included in the list and conducts the relevant document review, site assessments, and verifications to grand the approval.

8.3 Ashghal Laboratory Data Tracking System - LDTS

Quality Section collects, analyzes, and periodically reports the compliance status of the sampling and testing activities at Ashghal projects through a specific software: the Ashghal Laboratory Data Tracking System. All mobilized laboratories must upload the relevant testing data monthly, and all Ashghal Departments and Consultants have view-only access to the system (The President's Office, 2020)

8.4 Ashghal Quality Tracker System – AQTS

Quality Section has developed specific software for the evaluation and reporting of the level of quality compliance of each project, each Construction Contractor, and even each Department. The system is named Ashghal Quality Tracker System (AQTS), and QSD is currently cooperating with the Information Systems Department to incorporate it into the whole Ashghal Programme Management System (APMS). AQTS provides general and detailed quality control reporting on the incorporated materials, applied construction practices, the workmanship of finished works, and used quality management systems.

9 Conclusion

The Quality Section of QSD Ashghal has established a sophisticated quality assurance and quality control system to monitor and report the compliance of all active Ashghal projects by means of technology, highly-experienced expatriate staff training and mentoring Qatari staff, applying best international practices, and maintaining an eye for lessons learned and opportunities for improvement that is shared with Ashghal Departments.

Ashghal top management has provided QSD with authorization, encouragement, and resources to develop and implement a robust quality assurance and quality control system, and expects QSD and especially the Quality Section, to be vigilant and fully immersed in site activities, the progress of works and the level of quality of KSCPs.

Absolute quality and 100% compliance are the ultimate targets in all Ashghal departments and QSD Quality Section is actively and continuously striving to reach this target.

References

Emiri Decree. (2014-a). Emiri Resolution No. (34) of 2014 Organising the Public Works Authority.

___. (2014-b). Emiri Resolution No. (34) of 2014 Organising the Public Works Authority.

Gongbo, et al. (2011) Identification of Key Performance Indicators for Measuring the Performance of Value Management Studies in Construction, *Journal of Construction Engineering and Management*, Vol. 137, No. 9.

Public Works Authority. (2023). “Organisation Chart”. www.ashghal.gov.qa

Qatar Construction Specifications – QCS. (2014). Published by Ministry of Municipality and Environment.

Quality and Safety Department. (2020). Data Entry in the Electronic Quality Program. 2020/0001697/7

The President’s Office. (2020). Mandatory Guidelines for the Quality Control of Publics Works Authority Projects. Circular No. 38.

Cite as: Al-Ibrahim A.A.A.M., Al-Thani A.A.N.J., Plexousaki E. & Al-Ansari M.I.R.M., “Ashghal Quality Assurance & Quality Control system – QSD Role in Monitoring & Reporting the Quality Performance in Ashghal Projects”, *The 2nd International Conference on Civil Infrastructure and Construction (CIC 2023)*, Doha, Qatar, 5-8 February 2023, DOI: https://doi.org/10.29117/cic.2023.0078

Utilisation of Waste Plastics Admix with Laterite Soil for Production of Road Pavement Interlocking Blocks

Yamusa Bello Yamusa
Department of Civil Engineering, School of Engineering Technology, Nuhu Bamalli Polytechnic, Zaria, Kaduna State, Nigeria
yamusabello@yahoo.com

Mubarak L. Liman
Department of Science Laboratory Technology, School of Applied Sciences, Nuhu Bamalli Polytechnic Zaria, Kaduna State, Nigeria
mubarak.liman@gmail.com

Bilkisu Danjuma
Department of Civil Engineering, School of Engineering Technology, Nuhu Bamalli Polytechnic, Zaria, Kaduna State, Nigeria
danjumabilkisu15@gmail.com

Abubakar Sani
Department of Civil Engineering, School of Engineering Technology, Nuhu Bamalli Polytechnic, Zaria, Kaduna State, Nigeria
abubakarsani832@gmail.com

Yusuf Walliyullah
Department of Science Laboratory Technology, School of Applied Sciences, Nuhu Bamalli Polytechnic Zaria, Kaduna State, Nigeria
yuswaliy@gmail.com
a)

Abstract

Plastic wastes are non-biodegradable and hence pile up in refuse dumps and streets constituting an eyesore and menace to the environment. Some of them end up in drainages and waterways where they block water passages resulting in flooding. This is in addition to the fatalities they cause to livestock and marine life that ingest them unknowingly. Globally, plastic waste proliferation has been recognized among the biggest environmental challenges mitigating the achievement of the United Nations Sustainable Development Goals (SDG). This research intends to transform the unwanted plastic wastes by mixing with laterite soil to produce road-paving interlocking blocks. Laterite soil was mixed with plastic waste at various proportions by respective weight denoted as P1 (60:40%), P2 (70:30%), and P3 (80:20%) to determine their usability as road paving material. Maximum compressive strength of 9.68, 10.40, and 6.88 N/mm^2 were achieved for P1, P2, and P3 respectively, implying the P2 mix has the best strength. The paving interlocking blocks made from plastic-laterite composite registered a relatively high performance and met the minimum compressive strength required by the Nigerian Building and Road Research Institute for interlocking paving blocks deployed for non-traffic use.

Keywords: Plastic waste; Laterite soil; Interlock paver block; Compressive strength; Waste management

1 Introduction

Nigeria is estimated to have a population of over 180 million people with an average daily per capita waste generation rate of 0.65kg per day (Orhorhoro & Oghoghorie, 2019). This amounts to 42 million

tonnes of waste generated annually in Nigeria (Ike et al., 2018). The total global production of plastics recently is estimated at 8,300 million metric tons and Nigeria estimated plastics generation is about 25 million tons (Olanrewaju & Oyebade, 2019). Globally, plastic waste constitutes more than 60% of the total global municipal solid waste (MSW) of which was recovered and 78% disposed of. Therefore, converting these plastic wastes to useful products such as interlocks for road construction will go a long way in solving the plastic waste menace.

This research looks at the possibility of mixing this quantum of plastic waste with laterite soil. Laterite is a soil found in wet and hot tropical areas of the world that are rich in iron and aluminum (Ahmad et al., 2018). Due to the high content of iron oxide, laterite soils are reddish in color and are formed from the intense weathering of their parent rock. Persistent weathering, known as laterisation, results in a wide variability in their physical and chemical properties (Gidigasu, 2012). Laterite soil is the most common and abundant soil in Nigeria. Using this soil would help save a lot on cost of production of plastic-laterite paver blocks.

Soil reinforcement is undertaken for various ground improvement schemes in geotechnical engineering applications, encompassing backfill for earth-retaining structures, repair of slopes, landfill liners and covers, soil stabilization, and sub-grades for footings and pavements (Schlosser & Delage, 1988; Stanciu et al; Vaníček & Kazda, 2000). Technically, the soil has intrinsically high compressive strength but low tensile strength that is just restricted by the capability of the soil to resist applied shear stresses. Ground improvement is targeted to overcome the inability of the soil to capture any tensile loads and shear stresses which might result in deformation. Using tensile reinforcement improves the reliability and stability of geotechnical structures (Chebet & Kalumba, 2014). Plastics will be used as the tensile element in this regard.

Globally, the construction industry depends greatly on typical materials like sand, cement, and gravel which remain the major cause of natural materials' depletion (Sojobi, 2016). Local materials that are abundant and cheaper than conventional materials should be an alternative in construction (Yamusa, 2018). Utilization of abundant local materials to reduce construction costs to achieve sustainable development is paramount, especially in developing countries (Sojobi, 2016; Yamusa et al., 2016, 2017). Thus, laterite soil commonly available is investigated in composition with plastic waste to produce efficient, economic, and durable interlock blocks.

Paving blocks made from polyethylene/laterite composite could register higher performance relative to conventional concrete. They will lower the chances of surface rutting development, and eliminate spalling and weathering while minimizing susceptibility to cracking. If made and put into use, these blocks will not only reduce construction costs, especially those for repairs but also assist in environmental conservation. In this regard, it can be adjudged an innovative and remarkably feasible human project. Roads and walkways will be cheaply constructed, and with the increased durability, accessibility will be improved, and economic growth bolstered. In conclusion, this research could achieve its objectives and if applied, can help improve the quality of human life and mitigate the future of plastic waste.

2 Materials and Methods

2.1 Plastic Waste and Laterite Soil

The recyclable plastic waste (RPW) that was used in manufacturing the paving blocks was bought from collection points within the municipality gotten from refuse dumps, waterways, and landfill sites, and then sorted and classified. These RPW were cleaned and air dried, and then taken to the

laboratory for experimentation.

Laterite soil was bought from the available burrow pits within the catchment area (Zaria city) of this research. The soil was powdered using a mechanical grinder and then sieved through a 5mm aperture to eliminate oversize gravel. The RPW and laterite soil are shown in Figure 1.



Fig. 1: Plastic Waste Bags and Laterite Soil

2.2 Physicochemical Tests on Waste Polyethylene Bags

Samples of waste Polyethylene bags were collected from recycling refuse dumps in the Sabon Gari area of Zaria, Nigeria, and transported as bales to the workshop at Nuhu Bamalli Polytechnic. They were sorted and classified; where only Transparent High Density Polyethylene (T-HDPE) were selected for use in this experiment.

The clean samples of waste T-HDPE obtained were freeze-dried overnight in a laboratory freezer at -12°C to improve their crystallinity to allow for easy pulverization. They were subsequently ground in a pulverizer for 30 mins. until they become finely divided particles of less than ≤2mm diameter. Physicochemical assays including melting point, crystallinity, density, solubility, and index were determined using standard methods according to AOAC (1990). Determination of thermal physicochemical properties and degree of crystallinity: The enthalpies of fusion and degree of crystallinity were determined. The specific gravity and density were determined by the displacement method according to standards as described in (ASTM, 2008).

2.3 Physicochemical Tests on Laterite Soil

The laterite soil samples undergo the following physical property tests adopting the British Standard (BSI, 1990): Specific gravity test, particle size distribution test, Atterberg limit test, and compaction test. The sample was classified using the plasticity chart of the British Standard Classification System (BSI, 1999).

2.4 Mix Ratio of Waste Plastic and Laterite Soil

Creating a ratio mix for melting/solubilisation of the various classified waste plastics stream based on their known physicochemical characteristics. The mix proportions of laterite and plastic waste materials were obtained by weight. The following mix ratios were investigated:

b) 60% laterite and 40% plastic contents by weight denoted as P1.

c) 70% laterite and 30% plastic contents by weight denoted as P2.

d) 80% laterite and 20% plastic contents by weight denoted as P3.

The waste plastic was put inside a lagged portable improvised plastic melting and mixing machine (mixer-densifier) at a temperature of about 180ºC and laterite was thereafter introduced and mixed. The densifier machine was fabricated through mechanical modification of a typical concrete mixer machine in such a way that a heating chamber was introduced with a heat-lagging covering to minimize heat loss. This machine automatically mixes the composite samples in a closely monitored and adjusted temperature to minimize the effect of thermal oxidation and its effect on molecular mass, ensuring preservation of physicochemical characteristics as well as the efficiency of the system. Three samples were taken after curing for the strength characteristic test. The test complies with (ASTM, 2014) for RPW.

2.5 Physicochemical Characteristics of Plastic-Laterite Interlock Bricks

Evaluation of the physicochemical characteristics of the produced materials and quality assessment checks in comparison with conventional concrete materials. In order to determine the load capacity of polyethylene and laterite composite, and to evaluate the effect of compressive strength, Compressive Test was carried out using a universal compressive machine tester (Model: Yes-3000; S/N: 110310) and Flexural strength was determined using universal flexural machine tester (Model: SEIDNER 3000; S/N: 5993).

a) Compressive Strength Test: To determine the loading capacity of polyethylene and laterite soil on the compressive strength of mixed polyethylene, the compressive strength test was carried out using a universal compressive machine tester. The test complies with BSI (2009b) for control paving blocks. Three samples per each mix were tested and average strength was determined by averaging the three results.

b) Flexural Strength Test: Unlike the compressive strength test, the flexural strength test is to be carried out according to the BSI (2009a) standard on the composite samples that gave the highest compressive strength.

3 Results and Discussion

3.1 Physicochemical Properties of Waste Polyethylene Bags Sample

The physical test shown in Table 1 on the polyethylene shows varying properties with respect to thermal behaviors. The T-HDPE has a melting point of 148°C. The enthalpy of fusion and percentage crystallinity were 98.6J/g and 33.6% respectively. Crystallinity of the samples is an important physical parameter in this project since the melt flow; hardness and brittleness of the bricks to be produced depend on it.

Table 1: Physical Properties of Waste Polyethylene Bag Samples

Sample Description	Initial Melt. Temp/ Melting Point (°C)	Final Melting Temp (°C)	Enthalpy of Fusion (J/g)	Crystallinity (%)	Density (g/cm^3)
T-HDPE	148.00	163.10	98.60	33.64	0.954

3.2 Physical Properties of Laterite Soil

Results of the laboratory tests carried out to determine the physical properties of laterite soil samples are shown in Table 2. According to the British Standard (BS) classification, the soil sample is classified as a silty clay of medium plasticity (ML).

Table 2: Physical Properties of Laterite Soil

Property	Value
Specific gravity	2.70
% Fineness	10
% Sand	70
% Gravel	20
OMC, %	16
MDD, Mg/m^3	1.6
Liquid limit, %	47
Plastic limit, %	31
Plasticity Index, %	16
Linear Shrinkage, %	5
BS Classification	ML
Colour	Brown

3.3 Compressive Strength Test on Plastic-Laterite Blocks

Figure 2 shows the compressive strength at different mix ratios, where P1, P2 and P3 have 9.68 N/mm^2, 10.40 N/mm^2 and 6.88 N/mm^2 respectively. It was observed that the weight of the interlocking blocks increases with increase in the laterite content and decreases with increase in the plastic content. The blocks from the P2 mix ratio have the highest compressive strength, with an average of 10.4 N/mm^2. From the results obtained, these show that plastic-laterite interlocking paver blocks can be used in non-vehicular traffic areas such as public parks, building premises, footpaths, and landscaping because the compressive strength is adequate for the smooth service of users (Agyeman et al., 2019; Olofinnade et al., 2021). This also conforms with the minimum compressive strength of 3.45 N/mm^2 by Nigerian Building and Road Research Institute (NBRRI, 2006).

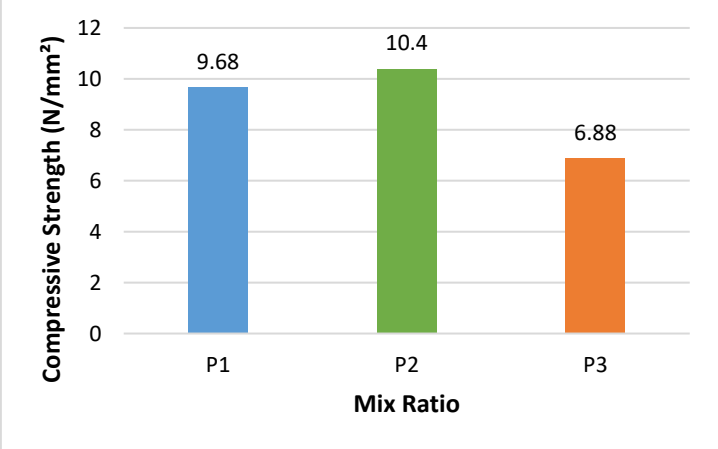


Fig. 2: Compressive Strength of Interlock at Different Mix Ratios

3.4 Flexural Strength Test on Plastic-Laterite Blocks

Figure 3 shows the flexural strength at different mix ratios, where P1, P2, and P3 have 7.14 N/mm^2,

5.10 N/mm^{2,} and 3.94 N/mm^2 respectively. It was observed that the weight of the interlock increases with an increase in the laterite content and decreases with increased plastic content. The interlocks from the 60:40 mix ratio have the highest flexural strength, with an average of 7.14 N/mm^2.

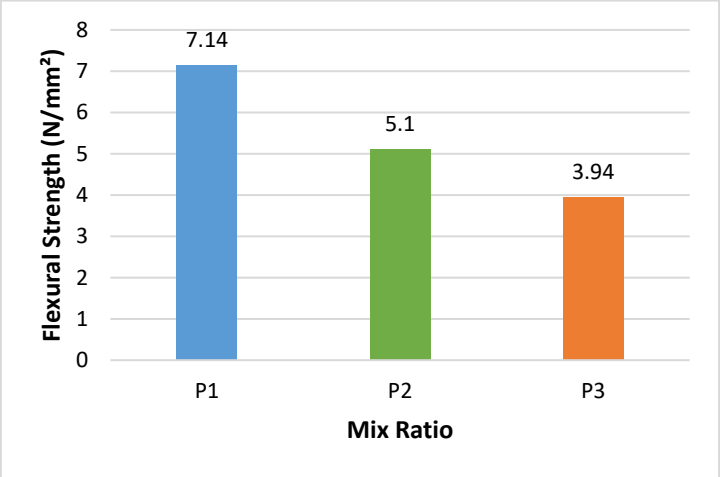


Fig. 3: Flexural Strength at different mix Ratios

The relationship between compressive strength and flexural strength of paving blocks is shown in Figure 4. It was observed that the flexural strength increased with an increase in compressive strength. A preceding study conducted by Djamaluddin *et al* (2020) likewise established that the flexural strength is directly proportional with the compressive strength.

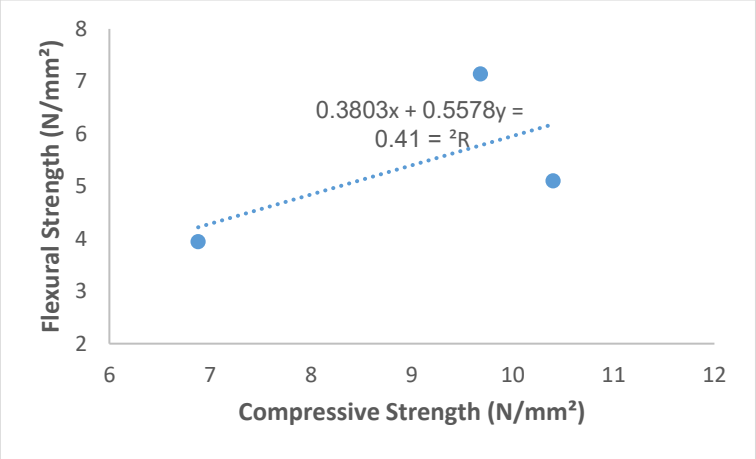


Fig. 4: Relationship between Flexural and Compressive Strength

3.5 Finished Product of Interlock blocks

Based on the analysed results, the plastic-laterite interlocking blocks were produced with the optimum mix ratio of 70-30. Figure 5 shows the finished product laid at the production workshop. Colorants were added to give different looks in order to enhance the aesthetic view where needed.



Fig. 5: Densifier Machine and Various Colors of Plastic-Laterite Interlock Bricks

4 Conclusion

This research efficiently demonstrates how to transform recyclable waste plastics into suitable paving construction materials i.e. interlocking blocks which can tremendously reduce environmental pollution. The results showed that the P2 ratio has the maximum compressive strength even though P1 and P3 also satisfy the requirement of the Nigerian Building and Road Research Institute (NBRRI) to be used for non-vehicular traffic pavements. Nonetheless, more tests such as water absorption and acid resistance need to be conducted in addition to compressive strength and flexural strength tests. In conclusion, the research brought about selection of best mix-ratio and production procedures leading to qualitative interlock products that are three times stronger than conventional concrete interlocking bricks that requires a minimum compressive strength of 3.45N/mm^2 by NBRRI. This can serve as a waste management approach that would decrease the problem of waste plastics in the society. Rather than the waste plastics going into landfills or incinerators they can be used as construction materials. Although this study shows that plastic waste can be curbed by utilizing it as a construction material, it was observed that its cost of production was high. This was due to the high consumption of liquefied petroleum gas (LPG). So, an alternative to LPG should be used to reduce cost.

Acknowledgment

This research work was supported by the National Research Fund (NRF) Grant of the Nigerian Tertiary Education Trust Fund (TETFund) Grant No: TETF/DR&D-CE/NRF-2020.

References

Agyeman, S., et al. (2019). Exploiting recycled plastic waste as an alternative binder for paving blocks production. *Case Studies in Construction Materials*, 11, e00246. doi.org/10.1016/j.cscm.2019.e00246.

Ahmad, et al. (2018). Effects of soil recompaction on permeability. *Science World Journal, 13*(3), 6-9.

AOAC. (1990). Official methods of analysis of the AOAC. Standard methods of the Association of Official Analytical Chemists, Maryland, USA.

ASTM. (2008). Standard test methods for density and specific gravity (relative density) of plastics by displacement. Committee d-20 on plastics: ASTM international. doi: 10.1520/ D0792-20.

ASTM. (2014). D638-14, 2014 standard test method for tensile properties of plastics. ASTM International, West Conshohocken, PA. doi**:** 10.1520/D0638-14.

BSI. (1990). Methods of testing soil for civil engineering purposes (BS1377: Part 1-9). British Standards Institute, London.

BSI. (1999). Code of practice for site investigations (BS 5930). British Standards Institute, London.

BSI. (2009a). Testing hardened concrete. Flexural strength of test specimens 12390-5 (2009). British Standards Institution, London.

BSI. (2009b). Testing hardened concrete; compressive strength of test specimens, part 3: BS EN 12390-3: 2009. British Standards Institute.

Chebet, F. & Kalumba, D. (2014). Laboratory investigation on re-using polyethylene (plastic) bag waste material for soil reinforcement in geotechnical engineering. *Civil Engineering and Urban Planning: An International Journal (CIVEJ), 1*(1), 67-82.

Djamaluddin, A. R., et al. (2020). Evaluation of sustainable concrete paving blocks incorporating processed waste tea ash. *Case Studies in Construction Materials*, 12, e00325. doi.org/10.1016/j.cscm.2019.e00325.

Gidigasu, M. (2012). Laterite soil engineering: Pedogenesis and engineering principles (Vol. 9): Elsevier.

Ike, C., *et al.* (2018). Solid waste management in Nigeria: Problems, prospects, and policies. *The Journal of Solid Waste Technology and Management, 44*(2), 163-172. doi:10.5276/JSWTM.2018.163.

NBRRI. (2006). Nigerian building and road research institute. *Newsletter, 1*, 15-17.

Olanrewaju, O. & Oyebade, A. (2019). Environmental menace of plastic waste in Nigeria: Challenges, policies and technological efforts. World Environmental Conservation Conference 2019.

Olofinnade, O., et al. (2021). Solid waste management in developing countries: Reusing of steel slag aggregate in eco-friendly interlocking concrete paving blocks production. *Case Studies in Construction Materials, 14*, e00532. doi.org/10.1016/j.cscm.2021. e00532.

Orhorhoro, E. & Oghoghorie, O. (2019). Review on solid waste generation and management in sub-Saharan Africa: A case study of Nigeria. *Journal of Applied Sciences and Environmental Management, 23*(9), 1729-1737. doi: 10.4314/jasem.v23i9.19.

Schlosser, F. & Delage, P. (1988). Reinforced soil retaining structures and polymeric materials. *The application of polymeric reinforcement in soil retaining structures* (pp. 3-65): Springer. doi: 10.1007/978-94-009-1405-6_1.

Sojobi, A., O. (2016). Evaluation of the performance of eco-friendly lightweight interlocking concrete paving units incorporating sawdust wastes and laterite. *Cogent Engineering, 3*(1), 1255168. doi.org/10.1080/23311916.2016.1255168.

Stanciu, et al. (2019). Evolution of the design methods for reinforced soil works. Paper presented at the 15th Computational Civil Engineering CCE2019, Iasi, Romania.

Vaníček, I. & Kazda, I. (2000). Application and design of earth structures from the reinforced soils. *Acta Polytechnica, 40*(2).

Yamusa, Y. B. (2018). Effects of gradation on engineering properties of compacted laterite soil liner. PhD Thesis, School of Civil Engineering, Faculty of Engineering, Universiti Teknologi Malaysia.

Yamusa, et al. (2016). Effects of gradation on hydraulic conductivity properties of compacted laterite soil liner: A review. *International Journal of Scientific & Engineering Research, 7*(6), 1088-1091.

Yamusa, et al. (2017). Sustainable design of compacted laterite soil liner. Paper presented at the Global Civil Engineering Conference. DOI:10.1007/978-981-10-8016-6_84.

Cite as: Yamusa Y.B., Liman M.L, Danjuma B., ani A. & Walliyullah Y., "Utilisation of Waste Plastics Admix with Laterite Soil for Production of Road Pavement Interlock Blocks", *The 2nd International Conference on Civil Infrastructure and Construction (CIC 2023)*, Doha, Qatar, 5-8 February 2023, DOI: https://doi.org/10.29117/cic.2023.0079

Utilization of Recycled Materials in Infrastructure Projects: Ashghal Approach

Osman Elhussein
Quality & Safety Department (CML - Laboratories Section), Public Works Authority (Ashghal)
Doha, Qatar
osmane@ashghal.gov.qa

Aljazi Al-Mansoori
Quality & Safety Department (CML - Laboratories Section), Public Works Authority (Ashghal)
Doha, Qatar
aalmansoori2@ashghal.gov.qa

Abstract

As a result of numerous infrastructure projects which have taken place in Qatar in the last decade, there has been an unprecedented increase in demand for construction materials. In addition, the huge program of infrastructure development has led to production of massive quantities of construction waste. Consequently, the Public Works Authority of Qatar (Ashghal) launched an initiative to use recycled materials in projects in line with Qatar National Vision 2030 and Qatar National Development Strategy 2018 – 2022. A roadmap was developed in 2018 considering the available resources and experiences. Recyclable materials which can be used in Ashghal projects were identified. Excavation waste, demolition waste, Reclaimed Asphalt Pavement (RAP), Wadi Aggregate, Crumb Rubber and Steel Slag were selected for reuse. Controlled logistic areas to store, manage and process recyclable materials were established. Moreover, guidelines and prequalification procedures were developed for both materials sources and recycled materials producers. Testing programs were carried out on these materials to identify their basic characteristics. Laboratory trials and field trials were carried out at selected projects. Field trials were monitored and assessed using the local construction specifications QCS 2014. Based on lab and field trials, customized specifications were developed for the utilization of the selected recyclable materials in Ashghal projects. These specifications establish the baseline for construction using the selected recycled materials and determine the criteria and methods needed for quality control. Furthermore, Key Performance Indicators (KPIs), were established for Ashghal project departments to monitor their performance in relation to recycling. Ashghal's phenomenal performance in utilization of recycled materials in the last three years is presented.

Keywords: Ashghal; Recycling; Construction; Materials; Specifications

1 Introduction

Environmental development, which includes environmental protection, is one of the pillars of Qatar National Vision (QNV) 2030. Qatar shall protect its environment through balancing the needs of economic growth and social development with the conditions for environmental protection (QNV, 2008). Consequently, Qatar National Development Strategy (NDS), developed to achieve the QNV 2030. NDS-2 (2018-2022), encouraged recycling of construction waste to make use of them as construction materials, which reduces the cost of imported materials and preserves the environment. A target was set to increase the proportion of recycled materials in projects to 20% of the total materials used by 2022 through implementing specific programs and projects (QNDS, 2018) as shown in Table 1.

Table 1: NDS-2 Intermediate Outcome 1, Target, Projects, and Implementing Agencies

Intermediate outcomes	Targets	Programmes/Projects	Implementing Agencies	Supporting agencies
Intermeditae Outcome 1: An infrastructe created by economic and sustainable materials	1.1 Increase the proportion of recycled materials in projects to 20% of the total materials used by 2022	Develop a manual on the exploitation of local materials and waste, including methods of sorting and labelling, and identifying areas of optimum exploitation after the necessary specialized studies have been conducted.	MME	Ashghal Qatar General Organization for standards and metrology QU
		Develop legislation and building specifications to encourage the recycling of waste that include methods of dealing with waste, binding ratios, incentives, and penalties		
		Established a material research center	Ashghal	MME

The unprecedented programs of urbanization and establishment of infrastructure in the State of Qatar have led to generation of massive amounts of construction waste. Construction waste accounts for more than 75% of all solid waste generated in Qatar and most of this waste is landfilled in the desert contaminating an increasingly large area of land (Reid et al., 2016). Reuse of this waste requires establishment of a robust waste management plan, which includes a set of regulations and legislations that cover waste collection, sorting, recycling and disposal (Hahladakis et al., 2020). Alternative eco-friendly materials shall be utilized in projects to replace natural and imported materials. Some recycled materials such as steel slag may outperform natural aggregates in some characteristics such as skid resistance and fatigue life (Ziauddin et al., 2002). In addition, Reuse of recycled materials such as reclaimed asphalt pavement (RAP) has economic and environmental benefits as it reduces the rate of depletion of non-renewable resources such as aggregate and asphalt binders (MS-2, 2014). Moreover, properly managed stockpile of RAP may have more consistent gradation than virgin aggregates (West, 2015). Ashghal recycling initiative has ultimately led to encouraging the use of crumb rubber modified bitumen in lieu of polymer modified bitumen especially in local road projects, which are overseen by Road Projects Department of Ashghal (Ezio et al., 2020).

As stated in the roadmap, project departments of Ashghal were instructed to identify recyclable waste materials in their projects and thereafter retain and store it avoiding cross mixing and contamination of different types of materials. Such materials shall be transferred to Ashghal Central Storage Area, which is located at Rawdat Rashid as shown in Figure 1 (Ashghal Recycling Manual, 2021).

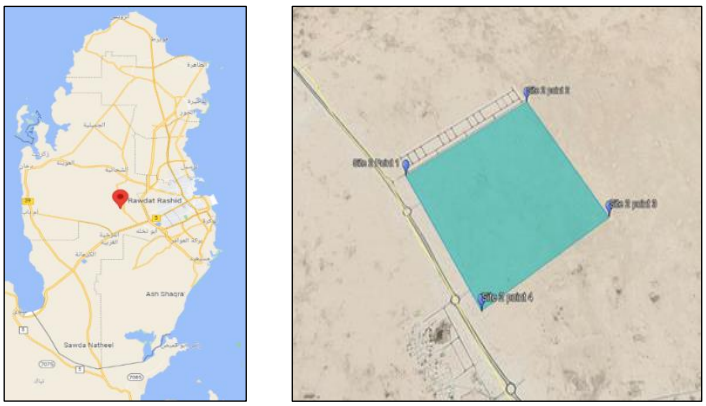


Fig. 1: Ashghal Central Storage Area for Recyclable Materials in Rawdat Rashid

2 Testing Programs

After launching Ashghal Initiative to use Recycled Materials in Projects on 5 November 2017 (Ashghal, 2017), which followed by Ashghal Recycling Roadmap on 9 May 2018 (Ashghal, 2018), the following materials were identified as the recyclable materials that can be used in Ashghal projects:

1. Excavation waste.
2. Demolition waste.
3. Reclaimed asphalt pavement (RAP).
4. Wadi aggregate.
5. Crumb rubber.
6. Steel slag.

These materials were selected based on the availability of considerable amounts and the ease of processing and recycling. Materials characterization program was carried out on recycled materials, which were collected from different sources. Based on the characteristics and compliance with the relevant specifications of Qatar Construction Specifications (QCS, 2014), the adequate utilization of each material was identified.

2.1 Demolition Waste, Excavation Waste and Wadi Aggregate

Total of 8 different blends were studied for fill and road subgrade materials and 5 blends for subbase materials. For fill and subgrade materials, the blend was considered successful based on compliance with fill and subgrade materials specifications, which are stated in Section 6, Part 3 of (QCS, 2014) as shown in Table 2. The successful blend consisted of Wadi Aggregate, which is a by-product of sand washing industry, Demolition Waste and Excavation Waste.

Table 2: Test Results of Fill and Subgrade Materials

Parameter	Test Standard	Result	QCS (2014) Specifications	
			Min.	Max.
Materials Passing 75.0mm	ASTM D6913	-	100	-
Materials Passing 0.075mm	ASTM D1140	7.0	-	30.0
Liquid Limit, %	ASTM D4318	Non-Plastic	-	30
Plastic Limit, %			-	-
Plasticity Index			-	10
Soaked CBR value, %	ASTM D1883	182	15	-
Swell, %		0.06	-	2.0

For road subbase materials, the successful blend following QCS (2014), Section 6, Part 4, consisted of 0-5mm, 5-10mm, 10-20mm and 4-50mm Demolition Wastes. Test results compared to (QCS, 2014) specifications are shown in Table 3. Subgrade, fill and subbase materials constituents are illustrated in Figure 2.

Table 3: Test Results of Subbase Materials

Parameter	Test Standard	Result	QCS (2014) Specifications	
			Min.	Max.
Materials Passing 50.0 mm	ASTM C136, ASTM C117	100.0	100	100
Materials Passing 37.5 mm		99.1	90	100

Materials Passing 19.0 mm		81.2	70	90
Materials Passing 9.5 mm		46.9	45	75
Materials Passing 4.75 mm		35.3	30	60
Materials Passing 0.600 mm		12.4	10	30
Materials Passing 0.075 mm		4.1	0	12
MDD, Mg/m^3	ASTM D1557	2.16	2.05	-
Soaked CBR value, %	ASTM D1883 BS 1377-4: 1990	250	70	-
Swell, %		0.04	-	1.0
Liquid Limit, %	ASTM D4318	Non-Plastic	-	25
Plastic Limit, %			-	-
Plasticity Index			-	6



Fig. 2: (a) Subgrade/Fill Materials Blend **(b)** Subbase Materials Blend

2.2 Reclaimed Asphalt Pavement (RAP) Materials

Major emphasis has been put on Reclaimed Asphalt Pavement (RAP) derived from milling of bituminous courses. This is due to the abundancy of this material in the fast-growing Qatari infrastructure network and the need to replace the imported bituminous courses constituents such as the aggregate and bitumen with less costly materials. A field trial was carried out to assess the feasibility of producing and laying hot asphalt mix containing 15% RAP. Test results of a sample collected from the field trial is shown in Table 4.

Table 4: Results of Asphalt Mix Containing 15% RAP Compared with QCS Specifications

Parameter	Result	Target JMF[1]	QCS Limits
Bulk specific gravity, G_{mb}	2.542	-	-
Bulk density (kg/m^3)	2534	-	-
Maximum Theoretical Density, G_{mm}	2.718	2.738	-
Air voids (%)	6.5	6.6	4.5 - 8.0
Stability (kN)	18.40	13.2	≥ 9.5
Flow (mm)	2.75	2.6	2 - 4
Quotient (kN/mm^2)	6.69	5.1	≥ 4.75
Air voids @ 400 blows (%)	4.8	4.0 / 5.1	≥ 3.4

[1] Job Mix Formula

Based on the evaluation of the field trial and the results obtained from laboratory testing, it was concluded that the production and laying of asphalt mix containing 15% RAP is compatible with the Contractor's plant layout and field equipment. The produced asphalt mix met QCS requirements and the desired level of compaction in the field consistently. Paving operations of the asphalt mix with 15% RAP are shown in Figure 3.



Fig. 3: Paving Operations of Asphalt Mix with 15% RAP

2.3 Crumb Rubber

Crumb rubber is the product of reducing scrap tyres into uniform grains after removing the reinforcing materials such as steel and fibre along with any other type of contaminants. Plant trials showed that asphalt mixes containing crumb rubber modified bitumen (CRMB) can comply with QCS, Section 6, Part 5 requirements. Test results of two plant trials are shown in Table 5.

Table 5: Results of Asphalt Mixes containing CRMB produced from Plant Trials

Parameter	Plant Trial 1	Plant Trial 2	QCS Limits
Optimum binder content, OBC (%)	4.1	4.1	3.4 – 4.4
Air voids, V_a (%)	7.2	6.5	5.0 – 8.0
Voids in mineral aggregate, VMA (%)	15.6	15.4	≥ 14.0
Voids in filled with asphalt, VFA (%)	54	58	50 – 75
Stability (kN)	13.5	18.5	≥ 13.0
Flow (mm)	2.5	2.5	2 - 4
Quotient (kN/mm^2)	5.40	7.40	≥ 5.25
Air voids @ 400 blows (%)	4.4	4.5	≥ 4.0
Retained stability (%)	94	90	≥ 75
Tensile strength ratio, TSR (%)	81	84	-
Filler to bitumen ratio	0.95	0.76	0.75 – 1.35
Rut depth from HWT test (mm)	4.7	7.2	-

2.4 Steel Slag

Ashghal, in collaboration with Qatar Steel Company and TRL, constructed trial sections in Qatar Steel premises in the Mesaieed Industrial Area. Two sections were constructed with asphalt courses containing 20% and 40% steel slag aggregate. Loose samples from the hot mixes were collected and tested. Test results compared with QCS requirements are shown in Table 6. After monitoring the trial sections and testing of the extracted samples, the study concluded that steel slag can be used as coarse

aggregate (5-20 mm) to replace gabbro in asphalt base mixes; however, the Ministry of Environment has limited the use to a maximum of 20% in asphalt base courses and in non-structural ancillary concrete such as soakaways, manholes and cable covers (Hassan et al., 2017). Paving operations of asphalt mix with 20% steel slag are shown in Figure 4.

Table 6: Results of Asphalt Mix containing 20% and 40% steel slag aggregate

Parameter	20 % Slag	40% Slag	QCS Limits
Air voids, V_a (%)	8.2	7.0	4.0 – 8.0
Voids in mineral aggregate, VMA (%)	16.3	15.2	≥ 13.0
Voids in filled with asphalt, VFA (%)	49.6	53.8	50 – 70
Stability (kN)	16.6	18.1	≥ 9.5
Flow (mm)	2.9	2.6	2 – 4
Quotient (kN/mm^2)	5.7	7.0	≥ 4.75
Air voids @ 400 blows (%)	4.7	4.1	≥ 3.2



Fig. 4: Paving Operations of Asphalt Mix with 20% steel slag

3 Developing Specifications and Guidelines

After launching Ashghal Recycling Initiative, lack of materials specifications, manufacturers' and suppliers' prequalification procedures were identified as challenges for implementation. After selecting the potential recyclable materials, which can be used in Ashghal projects, it was required to prepare guidelines related to permissible uses of materials, materials handling in processing plants, materials control in projects, technical specifications, quality control measures and supplier's prequalification. Hence, recycling specifications and guidelines were developed by Quality and Safety Department taking into consideration the conducted laboratory and field trials, Ashghal technical requirements, joint research projects, the best regional and international practices and Qatar Construction Specifications. Hence, the following technical documents were issued for implementation:

1. Roadmap for Implementation of Ashghal Initiative of Recycling in Construction Projects.
2. Ashghal Recycling Manual.
3. Reclaimed Asphalt Pavement (RAP) Management Guidelines.
4. Recycled Materials for Road Works. Public Works Authority (Ashghal) Issue, (QCS, 2018), Section 6, Part 9.
5. Factory Production Control of Bituminous Mixtures – Part A: Technical Guidance.

6. Pre-qualification Guidelines for Crumb Rubber and Crumb Rubber Modified Binder Producers.
7. Guidelines for Mix Design and Quality Control of Asphalt Mixes with Crumb Rubber Modified Binders.

4 Ashghal Performance in Recycling

For corporate performance monitoring in relation to recycling, Quality and Safety Department (QSD) established KPIs for different recycled materials to ensure Ashghal will achieve the maximum value and cost savings. The established KPIs and targets are shown in Table 7. As requested by Ashghal top management during the 2019 Full Year Performance Review, Quality and Safety Department conducted a review on the applied recycling processes to provide challenging targets for recycling KPIs. Consequently, the established KPIs, which were segregated for each material type, were provided for implementation and reporting by project departments starting from 2020. Segregation of KPIs allowed an enhanced monitoring of recycling performance for each recyclable material in Ashghal projects.

Table 7: Key Performance Indicators per Recycled Materials type

No.	KPIs for Recycling	Target (%)	Overall Average (%)
1	Percentage of RAP in asphalt	1	20
2	Percentage of recycled materials in Subbase and Road Base layers	20	
3	Percentage of recycled materials in Fill and Subgrade materials	20	
4	Percentage of Crumb Rubber in asphalt	0.1	
5	Percentage of recycled aggregate in masonry blocks, kerb and paving blocks	1	
6	Percentage of recycled aggregate in non-structural concrete	1	
7	Percentage of recycled aggregate for cable and pipe bedding & surround	1	

Ashghal performance in recycling is monitored every quarter. Data received from project departments is collected and reviewed by Quality and Safety Department and then reported to Ashghal top management. Quantities of recycled materials used in Ashghal projects are reported in line with the performance indicators. During 2021, 41,553 tons of RAP were used in hot asphalt mixes out of 1,798,651 tons placed in Ashghal projects. 914,701 tons of recycled unbound road base materials were used out of total 1,915,643 tons total materials used. In addition, 13,556,350 tons of subgrade and fill materials were reused out of total 16,485,304 tons. 1,190 tons of crumb rubber was utilized to modify bitumen replacing the imported polymers. 38,407 tons of recycled aggregate were used in concrete blocks out of 3,345,146 tons used. For non-structural concrete, 44,892 tons of recycled aggregate were utilized in concrete mixes out of total 2,118,697 tons of aggregate used. Nevertheless, 605,405 tons of recycled bedding and surrounds materials were utilized for pipe and cable bedding out of total 3,079,833 tons of materials used in projects. Hence, during the last year, Ashghal was able to use 15,202,498 tons of recycled materials out of 28,743,274 tons total materials, which were identified as recyclable materials. Hence, about 52.9% of the total materials consumed in projects,

was successfully recycled and reused. Summary of year 2021 recycling performance is shown in Figure 5.

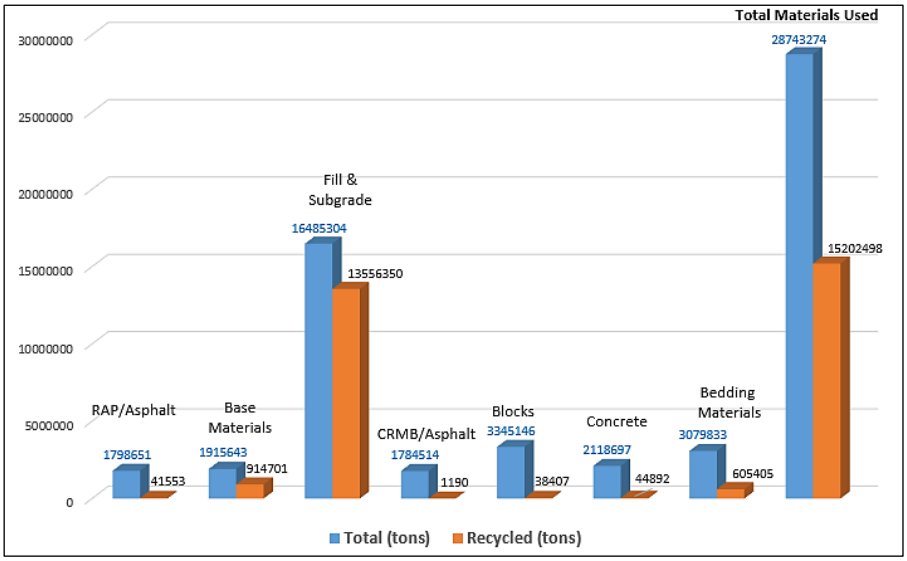


Fig. 5: Ashghal Recycling performance during 2021

Recently, the target of the percentage of materials to be recycled in Ashghal projects was suggested to be increased from 20% to 30% of the total consumed materials. Implementation of the new target is expected to start within 2023.

5 Conclusion

Based on the illustrated approach, which was followed by Ashghal to use recycling materials in projects, the following can be concluded:

1. Implementation of recycling plan in public works projects is facilitated and supported by the country strategy and vision.
2. Lack of local specifications, regulations and legislations that cover waste handling, recycling and reuse pose major challenges for the utilization of recycled materials in projects.
3. Developing specifications was facilitated through conducting lab experiments, performance testing schemes and field trials.
4. Based on Ashghal experience, up to 15% RAP can be added to hot mix asphalt with no need to modify the standard job mix formula and without addition of rejuvenators.
5. A well-designed blend of 15% Wadi aggregate, 30% recycled demolition waste and 55% recycled excavation waste was found to comply with QCS (2014) requirements for subgrade and fill materials. This blend can fully replace the natural burrowed materials.
6. Natural road subbase materials can fully be replaced by a graded recycled demolition waste blend as it was found to comply with (QCS, 2014) requirements.
7. Public Works Authority (Ashghal) of Qatar has successfully achieved 52.9% recycling rate in 2021 by recycling and reusing of 15,202,498 tons out of 28,743,274 tons of the recyclable materials consumed in infrastructure projects.

References

Ashghal. (2017). Ashghal Initiative of using Recycled Materials in Ashghal Projects (Circular No. (131)). Doha, Qatar, 05/11/2017.

Ashghal. (2018). Roadmap for Implementation of Ashghal Initiative of Recycling in Construction Projects (Circular No. (69)). Doha, Qatar, 09/05/2018.

Ashghal Recycling Manual. (2021), Ashghal Center for Research and Development, Public Works Authority. 1st Edition.

Ezio, et al. (2020). Use of Crumb Rubber Modified Binders and Asphalt Mixtures in Public Works Authority Road Projects - State of Qatar, *International Conference on Civil Infrastructure and Construction (CIC 2020), February 2-5, 2020*, Doha, Qatar.

Hahladakis, J. N., Purnel,l P. & Aljabri, S. J. (2020). Assessing the Role and Use of Recycled Aggregates in the Sustainable Management of Construction and Demolition Waste via a Mini-Review and a Case Study, Waste Management Research, Vol. 38, Issue 4.

Hassan, et al. (2017). Optimising Steel Slag in Construction (July 2017), TRL Report.

MS-2, Manual Series No. 2, Asphalt Mix Design Methods (2014), 7th Edition, Asphalt Institute.

Qatar National Development Strategy 2018-2022, Ministry of Development Planning and Statistics (2018), Gulf Publishing and Printing Company, Doha.

Qatar National Vision 2030, General Secretariat for Development Planning (2008), Doha.

Reid, J., M., Hassan, K., E. & Al-Kuwari, M., S. (2016). Improving the Management of Construction Waste in Qatar (2016), Proceedings of the Institution of Civil Engineers - Waste and Resource Management, Vol. 169 - Issue 4.

West, R. (2015). Best Practices for RAP and RAS Management, Quality Improvement Series 129. Lanham: National Asphalt Pavement Association (NAPA), Federal Highway Administration, United States.

Ziauddin, et al. (2002). Review of steel slag utilization in Saudi Arabia, Dec. 2002, The 6th Saudi Engineering Conference, KFUPM, Dhahran, Saudi Arabia.

Cite as: Elhussien O. & Al-Mansoori A., "Utilization of Recycled Materials in Infrastructure Projects: Ashghal Approach", *The 2nd International Conference on Civil Infrastructure and Construction (CIC 2023)*, Doha, Qatar, 5-8 February 2023, DOI: https://doi.org/10.29117/cic.2023.0080

Launching a 148m-Long Tunnel Boring Machine from a 15m-Inner Diameter Shaft

Volkan Salepciler
Parsons International Ltd.,Doha, Qatar
volkan.salepciler@parsons.com

John Brown
Parsons International Ltd.,Doha, Qatar
john.brown@parsons.com

Jacek Bogdan Stypulkowski
Public Works Authority (Ashghal),Doha, Qatar
jstypulkowski@ashghal.gov.qa

Sheikh Abdulrahman Al-Thani
Public Works Authority (Ashghal),Doha, Qatar
aalthani@ashghal.gov.qa

Abstract

The city of Doha has grown and expanded rapidly in the last 20 years, but this growth has strained the country's infrastructure, including its aging sewerage system and treatment facilities. ASHGHAL has therefore launched several schemes which involve shallow and deep sewer tunnels and new treatment works to serve Doha's growing population in the years to come. Wakrah and Wukair Drainage Tunnel (WWDT) project scope includes 13.3 km long of bored and lined tunnel using 2 no's 5.85m Diameter Earth Pressure Balance (EPB) TBMs, 8 Shafts, adits with provisions for future connections, ancillary hydraulic structures and Odour Control Facility. Based on WWDT project restrictions the Contractor was required to launch a 148m long Tunnel Boring Machine (TBM) inside a 15m Diameter shaft at a depth of 59.4m. This paper describes how the WWDT project contractor overcame these constraints and successfully launched both TBMs. The TBM launch and commissioning were a contract milestone. The methodology used involved partially mining a stub adit/logistics tunnels using a Sequential Excavation Method (SEM) to accommodate several TBM sections at the bottom of the shaft at the same time several of the TBM gantries were operational on the surface umbilically connected to the cutterhead. This paper will also provide a brief overview of 2 types of TBM launches used recently in Qatar for comparison.

Keywords: WWDT; EPB-TBM; TBM Launch; Shaft; SEM

1 Introduction

The Wakra–Wukair Foul Sewage Conveyance System (WWFSCS) & Treated Sewage Effluent (TSE) Return System Projects consists of three sub-projects (Figure 1) whose scopes are elaborated below:

Wakra-Wukair Drainage Network Branches Project - WWDNB

This drainage network is for collecting sewage from commercial & residential areas in Wakra & Wukair and Industrial area. The length of this project is 16 km, and it is being executed using micro tunnelling methods to install concrete pipes with internal diameters ranging from 400mm to 2400mm.

Wakra Wukair Drainage Tunnel Project – WWDT

Wakra Wukair Drainage Tunnel (Figure 2) will collect the sewage from WWDNB and transfer it to a future sewage treatment plant (STP). Details are mentioned below at WWDT scope of Work Section.

Wakra Wukair Treated Sewage Effluent Project – WWTSE

Wakra Wukair Treated Sewage Effluent (WWTSE) project is for transporting treated sewage effluent (TSE) from the STP through lines placed in trenched excavations using conventional open-cut excavation method. Length of line is 29 km, with diameters varying from 600 to 1400mm.

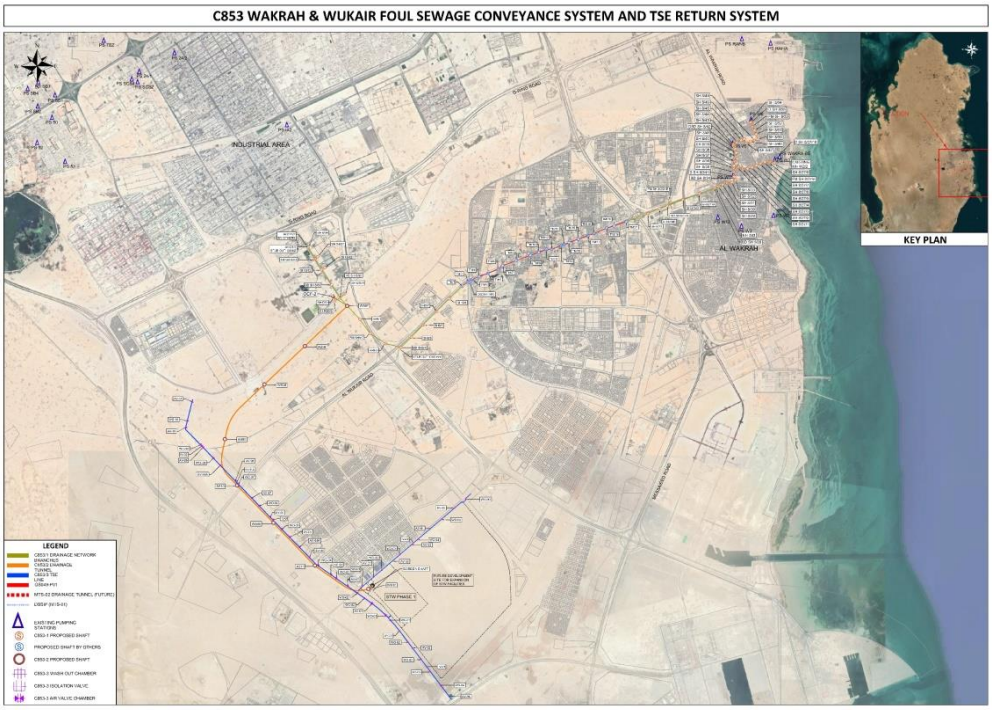


Fig. 1: General layout of WWDNB, WWDT & WWTSE

In summary, the WWFSCS will collect and transfer sewage flows from the existing and future sewerage networks of Wakra & Wukair to the upcoming Sewage Treatment Plant (STP). From the STP, treated sewage will be transferred to different locations for irrigation and other purposes.

2 Project Overview - WWDT Scope of Works

The Project comprises the design, construction, testing, commissioning, and handing over of the Drainage Tunnel. The Drainage Tunnel (DT) is approximately 13.3-km long with four temporary work shafts for TBM launch and/or reception – WS07, WS08, WS09 and WS10 and four additional temporary shafts for the construction of permanent access shafts in between the TBM work shafts – AS08, AS09, AS10 and AS11 which shall all be converted to permanent access shafts.

The DT final inner diameter shall be 4.5m. The lining concept consists of primary lining which is 300mm thick segmental concrete, (C50/60) and a Secondary Corrosion Protection Lining (CPL) of 250mm thick concrete (C35/45) with a 2.5mm thick HDPE protective membrane.

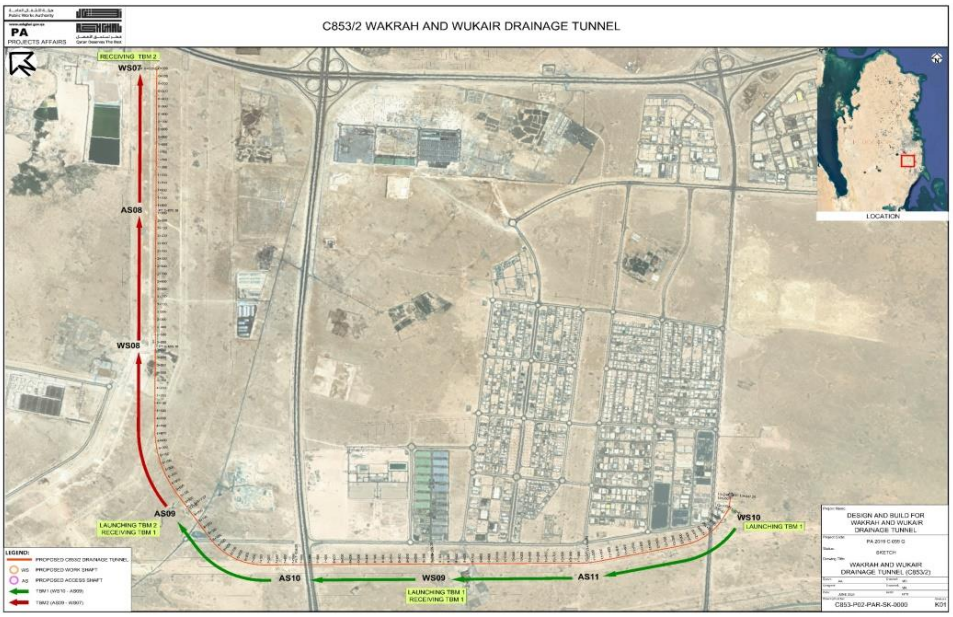


Fig. 2: WWDT Tunnel overall plan

3 TBM Introduction

EPB-TBMs were utilized for tunnelling of the WWDT. The overall length of each TBM, including 11 backup gantries is 148m which includes TBM shield parts (Cutter head, front, middle and tail shield) of 11.1m in length. The TBM tunnel is permanently supported by precast fiber reinforced concrete segmental lining rings erected within the TBM tail skin. The annulus between the excavated face and the segment extrados is filled with grout.

Tunnel backup gantries were designed for the supply of supporting systems for TBM mining works. In WWDT each TBM consists of 11 backup gantries and the supporting details are provided below (Table 1).

Table 1: Technical details of TBM Gantries-WWDT

Gantry-1	Operator cabinet, Foam generator and control cabinet
Gantry-2	Grouting system and Quick unloading device
Gantry-3	Foam solution tank, foam tank, transfer pump, polymer tank and Hydraulic pump station
Gantry-4	Grease system, grease barrel transfer hoist
Gantry-5	water tank and frequency Converter cabinet
Gantry-6	Bentonite tank, Transformer, HV switch cabinet and metal detector device
Gantry-7	Wastewater tank, cooling water tank (internal circulating water tank), Generator and air compressor
Gantry-8	Chiller unit and Emergency refugee chamber
Gantry-9	Emergency refugee chamber
Gantry-10	Pipe extension hoist, pipe storage area and crew room
Gantry-11	Working area, office room and emergency generator

4. TBM Launch

TBM launch consists of a set of procedures that need to be implemented prior to start-up of the TBM for full production. The launch includes pre-assembly, lowering down the shaft and the site assembly process both at the surface and at the bottom of the shaft. This procedure is intended to

lead to the initial drive followed by full production run of the TBM.

The mechanized excavation of the tunnel follows a standard sequence forming the overall production process. While boring, the EPB TBM moves forward by pushing on the segmental lining while at the same time, backfilling the annular gap behind the segments (clearance in between the excavation outline and the outer ring surface) with grout. Friction and bond between the constructed tunnel and surrounding rock provides resistance to the thrust forces.

The main procedure for the TBM launch in the absence of segmental lining is that a special thrust frame must be installed to provide counterforce. After the cutting of the ground (mining) has started the annular gap is created which needs grouting. Special bulkheads were needed to provide confinement and prevent grout leakage into the shafts before its setting.

This paper illustrates two different TBM launch processes which have already been used in Qatar.

4.1 Musaimeer Pumping Station and Outfall Tunnel (MPSO)

Musaimeer Pumping station and outfall tunnel (MPSO), consists of a 4.43m diameter, subsea tunnel, 10.1 km in length connected via a riser shaft to a seabed diffuser field. For tunnelling purposes, an EPB TBM of 170m length (approx.) was used which included 18 back up gantries and TBM shield with a cutter head.

A construction of the tunnel was required to facilitate launch from a shaft within a relatively small construction site, while a pump station structure was being constructed simultaneously. In order to facilitate assembly of the TBM below ground, a temporary logistics shaft was constructed together with mechanically excavated sprayed-concrete lined tunnels. The size of the shaft and length of the temporary shaft was minimized to limit time and costs but had to be balanced with practical requirements for TBM assembly and tunnel construction logistics.

TBM lowering and launching preparation commenced with excavation of launch (drop) shaft which later was converted to permanent drop shaft whose diameter is 15.6m. The shaft excavation was followed by excavation of logistic shaft whose diameter was 25.2m and a SEM logistic tunnel 31.5m long along the tunnel alignment. Later both shafts were connected with a SEM connecting tunnel of 4.3m length as shown in the below Figure 3.

The launching adit was constructed for the initial position of TBM cutterhead so that the screw conveyor and other cutterhead parts could be lowered down the drop shaft for assembly. Lowering of TBM commenced with TBM shields and was followed by the backup gantries. Gantry #1 to #7 were lowered into the logistic shaft and pushed up to cutter head and was followed by lowering of gantries #8 to #11in logistic shaft. The TBM was then powered up and tunnelling started. As the TBM moved forward the remaining gantries (gantry #12 to #18) were added. Muck removal required a special arrangement to allow muck skips to be moved to a second rail line so they could exit the backup system and go to the logistic shaft to be lifted out and emptied.

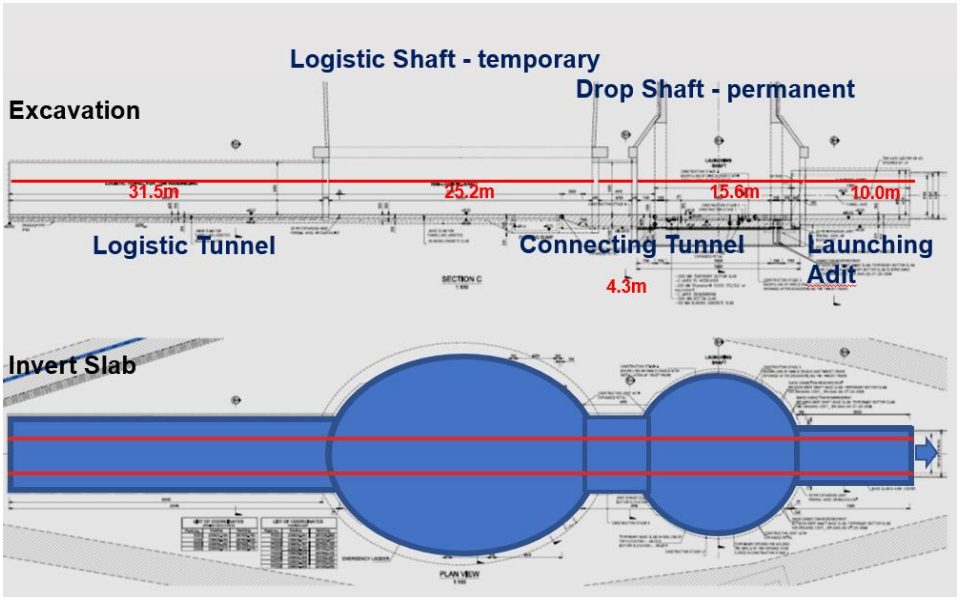


Fig. 3: Cross section and Plan view of Logistic shaft and SEM logistics tunnel

However, logistic shaft and tunnel were temporary and built solely for the purpose of TBM launch and as tunnelling completed both structures were backfilled. The 10m long Launch adit was constructed from the launch shaft towards the tunnel alignment and later became a part of the permanent tunnelling structure. The TBM lowering and launching layout is shown below (Figure 4).

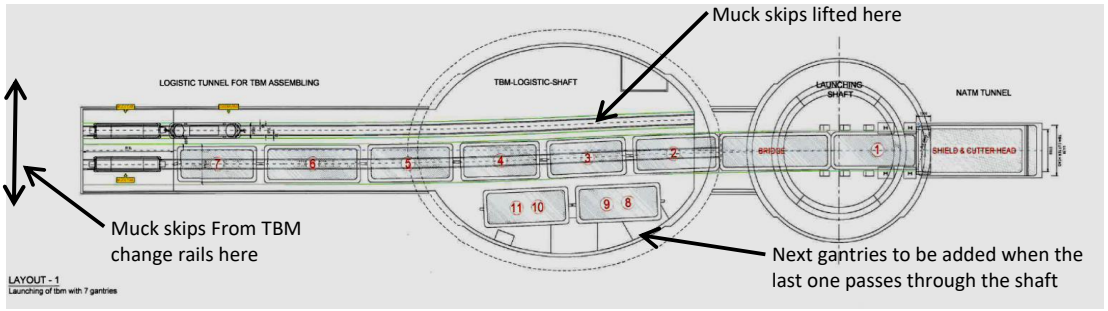


Fig. 4: Plan view of Logistic shaft and SEM logistic tunnel

Due to the existing space constraints in MPSO the method followed for the TBM launch was not as convenient as an optimal launch where full length of TBM including all back-up gantries could be locate into launching area.

4.2 Wakra Wukair Drainage Tunnel Project - WWDT

4.2.1 Shaft and SEM - Tunnels for Lowering and Launching of TBM

One launching shaft was constructed for the purpose of lowering and launching each of the WWDT EPB TBM's, namely shaft WS10 and shaft AS09, whose diameters are 17m and 15m and depths are 52.29m and 61.6m respectively. Both will be later converted to permanent access shafts.

Similar to MPSO Project launch, adits and logistics tunnels were constructed using SEM method for the TBM launch, due to space constraints and only single shaft was constructed at each site. The launch adit tunnels are approx. 15 m long and facilitate shield cradle while the logistic tunnels facilitate the TBM gantries during initial drive. The tunnel logistic layout respectively with 25m long as shown in Figure 5 below.

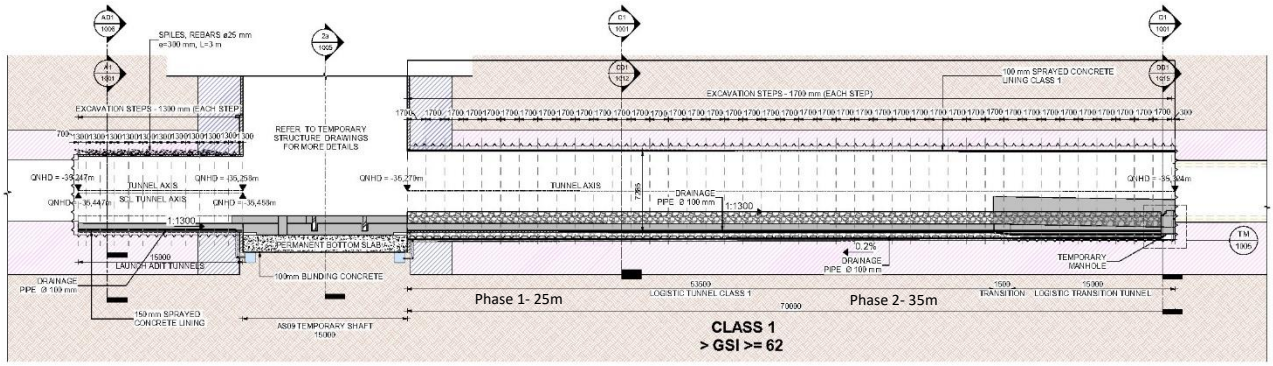


Fig. 5: Cross sectional view of launch adit & logistic tunnels

4.2.2 TBM Pre-assembly Works/Preparatory Works on Surface for Lowering

Due to the limited space at the bottom of the shaft, temporary concrete slabs were constructed at the surface. Before lowering down the shaft the preassembling of TBM parts was done at ground surface level as follows:

- Pre-assembly of Drive motor, Reducers to Main drive, Middle shield's front and rear parts.
- Preparation of Tail Skin.

4.2.3 Preparatory Works Required at Shaft Bottom Prior to TBM Lowering and Assembling:

- Completion of TBM launch adit and logistic tunnel SEM Works.
- Construction of temporary slab with TBM cradle along with the welding pit.
- In order to reach the first contractual milestone only 25m long logistic tunnel was constructed in shaft WS10.

4.2.4 Lowering and Assembly Works Inside the Shaft

Due to space constraint at shaft, the sequence of lowering and assembling works of TBM used three phase Umbilical Launch Method. The sequence of TBM Shield parts lowering and back up gantries lowering was optimized as per the space availability and site conditions. Lowering, assembling and umbilical launch in WS10 is explained below.

5 Lowering, Assembling and Umbilical Launch of TBM Parts in Ws-10 Shaft

5.1 Phase 1: TBM Shield and Backup Lowering & Assembly consisted of:

Phase 1 consisted of lowering and assembling of TBM shield in the shaft and sliding into launch adit, along with lowering and assembling of gantry #3 and gantry #2 in the logistic tunnel. Gantry #3 was lowered initially followed by gantry #2 due to TBM manufacturing setup. Installation of parts from bridge and gantry #1 was done at shaft bottom.

Lowering and assembly of thrust frame was completed at this stage and connections were made between gantry #2, #3 (refer to Table 1) from logistic tunnel and parts at shaft bottom to the TBM shield through umbilical pipes & cables (Figure 6 and Figure 7). All other TBM backup gantries were located at the surface level using extended power cables and hydraulic pipes running down the shaft to the TBM in order to launch (Figure 8).

TBM launch with umbilical advanced until 90m was completed (only main machine/shield).

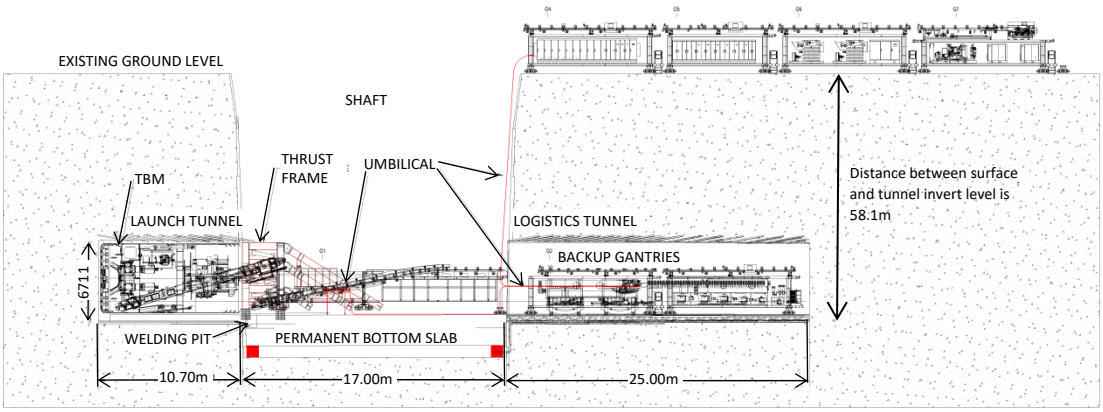


Fig. 6: TBM Umbilical launch Illustrative sketch



Fig. 7: TBM Umbilical site setup

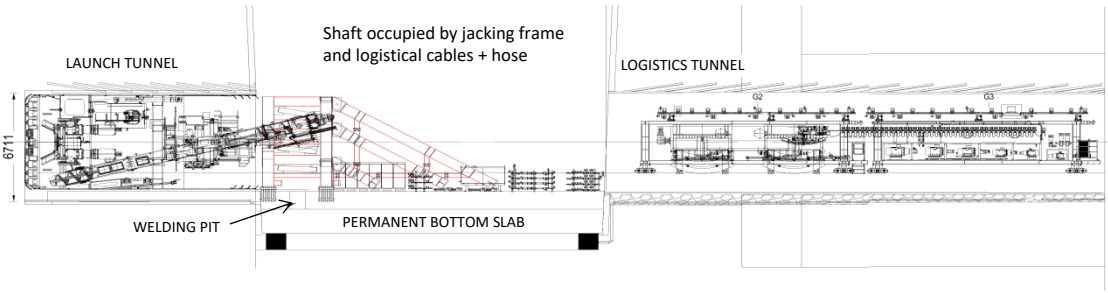


Fig. 8: TBM Pre-assembling works through shaft

5.2 Phase 2: Transfer and Connection of Backup Gantries #1 to #7, to the Shield Consisted of:

After completion of 90m of tunnelling (Figure 9), mining stopped and all the umbilical connections were disconnected and thrust frame removed from shaft, since installed rings were sufficient to resist thrust force.

Gantry #1 and bridge gantry were lowered from the surface and all the removed components for initial drive were reinstalled and pulled towards main machine and also gantry #2 and gantry #3 from logistic tunnel.

All the backup gantries from #4 to #7 were lowered and pulled towards the TBM shield and connections done for next 80 m of tunnel advance. However, gantries 8 to 11 having rescue chamber and cable extensions were not connected to the main TBM, which were not essential for initial drive.

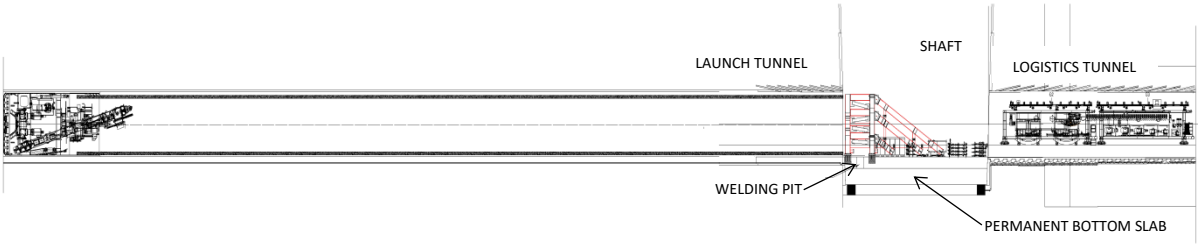


Fig. 9: TBM mining through umbilical system

Before phase 3, balance 45m of logistic tunnel was excavated via SEM and temporary concrete fill was done in the tunnel invert for locomotive logistic usage.

5.3 Phase 3: Lowering and Assembly of Remaining Backup Gantries #8 to #11 Consisted of:

In Phase 3, lowering and connections were made for gantry #8 to gantry #11 to the TBM and backfilling of tunnel entrance invert was performed for installation of rail switch. After completion of Phase 3 works, TBM Main Drive was started.

The main reason why this method as described above was implemented was to achieve the first contractual milestone of the WWDT Project. The length of the launching audit & logistic tunnel which have been constructed by SEM method and sequence of the umbilical launch had been decided accordingly. The TBM has been launched on time and the first milestone has been achieved successfully.

A simplified process of lowering and launch of TBM was followed in Shaft AS09 since entire tunnel excavation of 70m could be completed and no contractual milestone defined for the second TBM launch.

6 Conclusions

Two different TBM launching methods have been presented in which the optimal option of launching a full-length TBM at the required tunnel level was not practicable. Since the available space was limited on both presented methodologies the assembly and launch were accomplished by innovative engineering. One using an additional logistics shaft and tunnels, and one utilizing a single shaft with short launch tunnels and staged installation of TBM sections as the tunnel progressed, using an umbilical system.

The challenge was to fit as many TBM gantry sections in as short a space as possible at tunnel level, and to use lengths of cable and pressurized hydraulic hoses as an umbilical to connect to the rest of the TBM gantries at the shaft bottom, or at ground level. Due to the confined space and limited access a lot of re-work was inevitable in removal and reinstallation of gantry parts as the TBM progressed into the tunnel and up to the limits of the umbilical.

The presented methods demonstrate that even in constrained spaces, if an umbilical launch method can be used, it is possible to successfully launch a 148m long TBM in a 15m diameter shaft on time and, in the case of the WWDT project, achieve the first project milestone.

Acknowledgements

The writers acknowledge PWA (client) and PHM-JV (PORR-HBK-MIDMAC) for all the construction and design efforts and Parsons International Ltd. for actively supervising the project.

References

HBK-Porr-JV. (2018). Method of Statement of TBM Launching, C2017_109-MST-QM-0038 at MPSO Project.

PHM-JV/ (2022). Method of Statement of TBM Launching, C853/2-PHM-GEN-TUN-MST-9 at WW Drainage Tunnel Project.

Public Works Authority. (2020). Contract Document for Wakrah and Wukair Drainage Tunnel C853/2, Contract Number: C2020-127

Qatar Construction Specifications. (2014). (QCS-2014).

Cite as: Brown J., Salepciler V., Stypulkowski J. & Al-Thani A., "Launching a 148m-Long Tunnel Boring Machine from a 15m-Inner Diameter Shaft", *The 2nd International Conference on Civil Infrastructure and Construction (CIC 2023)*, Doha, Qatar, 5-8 February 2023, DOI: https://doi.org/10.29117/cic.2023.0081

Backfilling Manhole Surround Using Recycled Concrete Waste Material

John Brown
Parsons International Ltd., Doha, Qatar
john.brown@parsons.com

Suvish Valsan
Parsons International Ltd., Doha, Qatar
suvish.valsan@parsons.com

Nand K Vashisht
Parsons International Ltd., Doha, Qatar
nand.vashisht@parsons.com

Anna Olliver
Public Works Authority (Ashghal), Doha, Qatar
aolliver@ashghal.gov.qa

Eisa Abdulla S A Al Mohannadi
Public Works Authority (Ashghal), Doha, Qatar
ealmohannadi@ashghal.gov.qa

Abstract

The massive development in the State of Qatar to fulfil the Qatar National 2030 Vision requires efforts to direct the construction sector towards reducing economic, social and environmental impacts through the application of more sustainable construction techniques. The Public Works Authority, Qatar (Ashghal) has acknowledged that using available domestic sources to produce quality aggregate by recycling pavements, construction and demolition waste, and industry by-products is beneficial when natural sources are getting depleted. One of the projects exploring the possibility of utilizing the recycled concrete waste as surround backfill material is Contract C853/1 named the Wakrah-Wukair Drainage Network Branches (WWDNB). This is an ongoing mega drainage project associated with the construction of 67 number of shafts and approximately 17 km of sewer pipes at a maximum depth of 48m below ground level. The proposed material would be replacing the conventionally used materials such as graded limestone, gabbro aggregate and foamed concrete. This paper assesses the feasibility of utilizing recycled concrete aggregate (RCA) for backfilling of permanent shafts whilst satisfying the requirements of the Qatar Construction Specifications (QCS). A number of laboratory tests were therefore conducted, and the proposed material was found to be of acceptable quality. Additionally, mock-up tests are scheduled to confirm the field attributes before implementation on site for shafts in non-traffic areas. Using RCA as shaft backfill is more beneficial from a sustainability perspective as it will decrease the carbon footprint by 70% when compared with using traditional backfill materials. The goal of the study is to introduce an industry-wide application which is both sustainable and economical.

Keywords: Recycled concrete; RCA; Sustainability; Backfilling; Compaction; Construction

1 Introduction

The Wakrah and Wukair Drainage Network Branches (WWDNB) (Contract C853/1) is an ongoing

mega drainage project associated with the construction of 67 number of shafts and approximately 17km of sewer pipes at a maximum depth of 48m below ground level. The Public Works Authority (Ashghal) is the designated engineer who is represented by the Engineer's Representative, Parsons International Limited (PIL). PIL provides construction supervision services in the form of site management and engineering review of all designs completed by the Contractor's team. The three-year design-build construction contract was awarded in November 2020 to the Qatar Trading and Contracting Group (QTCG).

The geological strata of the WWDNB project area are comprised of rock formations such as Simsima Limestone, Midra Shale and Rus formation (QTCG, 2022a). The construction includes the excavation of temporary shafts and the installation of drainage pipeline and permanent manholes. Shafts will serve the purpose of launching and retrieval of a Micro Tunnel Boring Machine (MTBM) used for pipe jacking operations. After the completion of pipe jacking and permanent manhole construction, the temporary shafts are backfilled with a selected material which is durable and resistant to settlement (Figure 1).



Fig. 1: Temporary shafts on the WWDNB project used for micro tunneling and manhole installation (left side) and ongoing conventional backfilling works (right side)

The traditional backfilling method in Qatar is to dispose of the excavated material and backfill the shafts using suitable granular fill material. As the suitable material is not naturally available in Qatar, it has to be imported which makes it an unsustainable construction practice. The Qatar National Development Strategy 2018-2022 (NDS-2) acknowledged the existing recycling activities in the construction industry and set a target to increase recycling levels (Hassan et al., 2022). Ashghal has acknowledged that and issued Ashghal Recycling Manual in 2021 to encourage reusing and recycling construction waste in new construction projects.

The project has taken several steps to find innovative approaches and sustainable solutions to be adopted during construction and proposing RCA as a backfill material for deep shaft can be considered as one of them. This initiative can lead similar construction projects in the direction to try out-of-the-box solutions rather than following a conventional approach. Utilising Recycled Concrete Aggregate (RCA) to backfill shafts is an attractive option for Ashghal as it is more sustainable and also more cost-effective. RCA is the resultant of construction and demolition waste which contains relatively clean concrete aggregates which can be crushed and graded into different sizes as required.

The RCA (Figure 2) analysed in this study has been supplied by Qatar Primary Material Company (QPMC), an agency processing and supplying aggregates and other construction materials in the State of Qatar. This paper presents an assessment of the locally available material and pursues various studies conducted on this subject to understand if the material's properties are fit-for-use.



Fig. 2: RCA material stockpile and sampling at QPMC

2 Properties of the Proposed Material

2.1 Gradation

The requirements for backfilling material as per QCS (2014), Section 08 [Drainage Works], Part 02 [Earthworks], Sub-clause 2.3.4 [Backfilling Excavation] specify the use of a suitable selected fill material with no specific requirements related to the material gradation, except that "the uniformity coefficient should be more than 10 and the maximum stone size shall be 75mm with less than 15% of material passing through 0.063mm sieve". The material gradation adopted for the study complies with QCS (2014), Section 08, Part 02, Table 2.2 [Gradation Requirements for Pipe Bedding, Rigid Pipes], which specifies gradation for pipes above a Nominal Diameter (DN) 800 mm. The QCS requirements against the laboratory test results for the RCA are presented in Table-1. The bedding material gradation provides a high load-bearing capacity and a stable base below the pipes. Thus, using such a graded material for backfilling lowers the risk of settlements and creep (QTCG, 2022b).

Table 1: Gradation requirements as per QCS and RCA test results (QTCG, 2022b)

Sieve Size (mm)	Acceptance Limits (% by Mass Passing)	RCA Test Value (% by Mass Passing)
25	100	99.5
20	90-100	94
14	50-80	68
10	40-70	54
5	25-60	40
2.36	10-40	24
0.5	0-15	8

It has been demonstrated that systematic processing of the material through crushing and screening can achieve the required gradation for the purpose of application. The sieve analysis results of RCA sample have fulfilled the gradation criteria as per the desired property requirements.

The RCA is not expected to exhibit any alarming settlement, since as presented above, the material is well graded which will reduce the void ratio of the compacted material.

2.2 Physical and Chemical properties

The proposed RCA material has been tested to assess the physical and chemical properties listed in Table-2 against the requirements of QCS (2014), Section 08 [Drainage Works], Part 02 [Earthworks] and applicable requirements of Section 05 [Concrete], Part 02 [Aggregate] and Section 06 [Roadworks] Part 03 [Earthworks] along with proposed target engineering properties by the contractor's designer.

Table 2: Required properties of the RCA material and test results (QTCG, 2022b)

Property	Requirement Reference	QCS Reqd. value	Targeted value	Test Result
Organic content	QCS (2014), Section 08, Part 02, clause 2.3.4 3(f)	2% max	Free of organic impurities	No impurities
Clay Lumps and Friable Particles	QCS (2014), Section 05, Part 02, Table 2.1	2% max	Free of content	0.16%
Minimum Index Density	For reference only	None	1.8 g/cm^3	1.840 g/cm^3
Maximum Index Density	For reference only	None	2.0 g/cm^3	2.045 g/cm^3
Shell content	QCS (2014), Section 05, Part 02, Table 2.1	3% max	None	Nil
Resistance to fragmentation: Los Angeles abrasion	QCS (2014), Section 05, Part 02, Table 2.1	30% max	None	14 %
Flakiness Index	QCS (2014), Section 05, Part 02, Table 2.1	35% max	None	4%
Water Absorption	QCS (2014), Section 05, Part 02, Table 2.1	2% max	None	4.36% & 5.92 % when retested
Soaked Compacted California Bearing Ratio at 95%	QCS (2014), Section 08, Part 02, clause 2.3.4 3(g) QCS 2014, Section 06, Part 03, Table 3.1	15% min	15% min	55%
Maximum Dry Density (MDD) and Optimum Moisture Content (OMC)	For reference only	None	None	2.14 g/cm^3 at 7.1% OMC
Swelling	QCS (2014), Section 06, Part 03, Table 3.1	2% max	2% max	0.28%
Angle of Internal Friction	For reference only	None	30˚ min	32˚
Cohesion	For reference only	None	None	2.5kN/m^2
Aggregate 10% fines value (Dry Condition),	QCS (2010), Section 05, Part 02, Table 2.1	150kN min for 20mm and 100kN min for 10mm	125kN min for graded RCA[1]	130kN
Aggregate 10% fines value (Soaked Condition)	For reference only	None	For wet/dry TFV ratio	99kN
Aggregate 10% fines value - Ratio (Wet/Dry)	(Stålheim, 2014)	None	75 min	76.2
Fines content (Material passing #200 sieve[2])	QCS (2014), Section 08, Part 02, clause 2.3.4 3(b)	15% max	10% max	0.6%
Plasticity Index	QCS (2014), Section 08, Part 02, clause 2.3.4 3(c)	6% max	6% max	Non-plastic

Notes:

[1] Average of the required values in QCS 2010 taken.

[2] 0.075mm sieve was used while QCS states 0.063mm, however, since the fines content is very low, therefore this is acceptable.

The test results in Table-2 have been studied in order to assess the suitability of the material, and the following has been concluded:

Organic content, Clay Lumps and Friable Particles: RCA is expected to be free of organic impurities, clay lumps and friable particles unlike naturally excavated material. The proportionate settlement by permitting 2% of organic content, clay lumps and friable particles is eliminated by

using an impurity-free material. The tested samples are observed to practically be impurity free with a negligible 0.16% content of clay lumps and friable particles.

Minimum and Maximum Index Density: Although the limits of index density test are not defined, the minimum and maximum index density tests were conducted to get relative results in order to compare the material with the properties of the existing ground and conventional backfill materials. The test results which range between 1.840 g/cm^3 and 2.045 g/cm^3 can be compared against the density of the in-situ rock mass (approx. 2200 kg/m^3 for Simsima limestone) and general backfill material (2000 to 2100 kg/m^3).

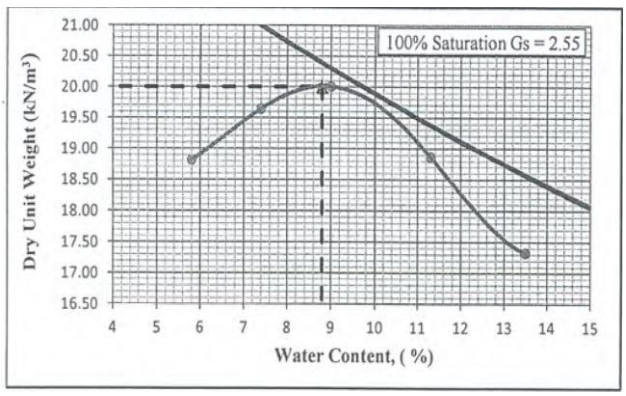
Shell content: Although the inclusion of shell content has no impact on the proposed application, the tests were conducted to ensure no external contamination. The tests indicated no presence of shell content in the RCA material.

Resistance to fragmentation/Los Angeles (LA) abrasion: The result of the LA test, which in this case is 14% and within the stipulated maximum 30%, satisfies the criteria for resistance to fragmentation or abrasion.

Flakiness Index: The test provides an indication of the level of achievable compaction, as flaky material tends to break down and lose strength during compaction which may cause further settlement. The flakiness index of the RCA material is only 4%, which is far below the max 35% limit.

Water Absorption: Crushed concrete typically has a higher water absorption since the crushed mortar has higher absorption than natural aggregates (Aminur et al., 2014), and this can be observed from the performed tests (4.36% and 5.92% when retested). Despite the relatively porous nature of the RCA as reflected by the absorption results, the RCA is typically relatively strong with good resistance to weathering and aggressive environment (Hassan et al., 2022). Furthermore, the water absorption property is usually specified and necessary for aggregates intended for use in bound layers, such as structural concrete or asphalt. Therefore, since the RCA exhibited higher strength (LA abrasion) and resistance to weathering (soundness) complying with QCS 2014, the recorded higher water absorption values are not considered detrimental for the backfilling application and will have no impact on the bearing capacity and/or performance of the unbound/backfill layers.

Maximum Dry Density (MDD) and Optimum Moisture Content (OMC): The MDD value is measured for the RCA backfill material to determine the optimum moisture content required for the material to attain maximum compaction. The MDD value of 2.14g/cm^3 at 7.1% OMC obtained during testing as per Figure 3.



Uncorrected:	
Optimum water Content, (%)	**8.8**
Maximum Dry Density, (g/cm³)	**2.04**
Maximum Dry Unit Weight, (kN/m3)	**20.01**
Corrected:	
Optimum water Content, (%)	**7.1**
Maximum Dry Density, (g/cm3)	**2.14**
Maximum Dry Unit Weight, (kN/m3)	**20.96**

Fig. 3: Compaction curve and RCA test results for MDD and OMC

Soaked Compacted California Bearing Ratio (**CBR) and Swell Potential:** The obtained results for the soaked compacted CBR (55%) and swell potential (0.28%) at 95% MDD were found to be within the required limits of min 15% CBR and max 2% swell, which indicates that there is a low probability of settlement due to volume change.

Angle of Internal Friction: Although there are no specific shear and deformation parameter requirements for backfill materials, the strength of the RCA material was tested by carrying out a direct shear test as a potential comparison against similarly graded natural aggregate. An angle of 32° was obtained with a cohesion value of 2.5kN/m^2, where the angle of friction is greater than the stipulated minimum 30°.

Aggregate 10% fines value (TFV): Test conducted on the RCA provided a value of 130kN in dry condition which is more than the desired 125kN min. Tests were also carried out in soaked conditions to drive a soaked/dry TFV ratio, with an obtained value of 76.2. Considering the results of the soaked/dry TFV ratio, a value of min. 75 indicates a better-quality material in terms of durability (Stålheim, 2014). The TFV test is planned to be repeated post-compaction on site to reassure the results are within the required limits.

Fines content: A result of 0.6% using the 0.075mm (Sieve No. 200) separating sieve indicates very low fines, which suggests a low potential for settlement.

Plasticity Index (PI): Although the requirement allows max 6%, the RCA is found to be free from any clay content and similar materials.

3 Planned Mock-Up and Field Tests

Following the laboratory tests and evaluation of results, and to confirm how the RCA would behave in practice after compaction, a mock-up with pre-construction field testing as per Table 3 is planned to be performed in a shallow excavation replicating the actual site conditions.

The method of backfilling is proposed to be conducted as follows: The RCA will be evenly spread in layers not exceeding 300mm in height and compacted to achieve a minimum of 95% compaction of the standard MDD. It is expected that larger layer thicknesses are required due to the coarser grain composition of the RCA when compared to traditional backfill. During the compaction trial, the target will be to establish the maximum possible loose layer thickness at the achieved target compaction level. The achieved compaction will then be checked for verification on site through Nuclear Dry Density (NDD) testing. Further samples will be collected from the compacted layer and tested for gradation properties to ensure that any increase in the percentage of fines (Sieve No. 200) does not exceed 10% post compaction. This will be compared to the gradation results for uncompacted material, a sample which will be taken prior to compaction.

Additionally, settlement monitoring will be conducted to study the long-term behaviour of the backfill to properly assess the behaviour of the reinstated ground. Since cyclic load-bearing capabilities due to vehicle traffic need to be considered for the application in traffic areas, shafts backfilled with RCA will initially only be approved for use in non-traffic areas.

Upon successful mock-up results, testing in accordance with Table 4 will be performed for quality control (QC) purposes as well as settlement monitoring.

Table 3: Recommended pre-construction tests during the mock-up

Stage	Tests	Frequency
Before compaction	Gradation Proctor – MDD Abrasion Ten Per cent Fines	Once
During compaction	Compaction level (nuclear gauge)	Each layer (95 %)
After compaction	Gradation Ten Per cent Fines	Once (selected layer that has reached 95 %)

Table 4: Recommended tests during site execution for QC purposes

Stage	Tests	Frequency
Before compaction	Gradation Proctor – MDD Abrasion Ten Per cent Fines	Once
During compaction	Compaction level (nuclear gauge)	Each layer (95 %)

4 Sustainability Benefits

Utilising concrete waste material is an excellent example of how to implement and follow the 'Reduce, Reuse and Recycle' philosophy. It will also reduce the usage of equipment & accessories, manpower and overall cost of a project.

The NDS-2 has estimated construction waste to constitute approximately 80% of the solid waste generation across Qatar, with estimated stockpiles of 80 to 100 million tonnes (Mt) accumulated in landfill sites (Hassan et al., 2022). The weighted average carbon footprint for various recycled materials is 3.0 kg CO_2e/t, compared to that of local limestone, which is 8.2 kg CO_2e/t and imported material that is 10.3 kg CO_2e/t (Hassan et al., 2022).

On this project, the usage of waste concrete is estimated to replace approximately 83,000 tons of quarried rock aggregate. Therefore, an approximate estimation indicates that a 60-70% reduction of the total carbon footprint can be achieved when the conventional backfill materials such as limestone, gabbro or foamed concrete are replaced by RCA.

It is also worth mentioning that significant cost savings can be achieved by adopting RCA for the proposed application which is a motivating factor from a project perspective. An approximate estimation of the cost of RCA is expected to be half that of limestone or gabbro aggregate and one-third of the foamed concrete. Once regularised, further cost reductions could be achieved from mass producing RCA with the added advantage of environmental benefits.

Furthermore, using a recycled material for construction will also raise the project's score on contractually mandated participation in the Civil Engineering Environmental Quality Assessment & Award Scheme (CEEQUAL).

5 Discussion

Assessment of the laboratory test results indicated a positive sign to proceed further to use this

material as backfill, however, the planned mock-up tests and long-term settlement monitoring are still required to properly assess the behaviour of the reinstated ground.

The authors would also like to highlight some viewpoints and recommendations for further research and studies to be conducted for the following:

- While in contact with water, RCA material may precipitate calcium carbonate contained in the leachate from the crushed concrete, also known as tufa, which is formed through a series of chemical reactions. To control tufa precipitation, washing the RCA is required by some agencies to remove the dust, which typically contains free lime and calcium hydroxide (Ellen et al., 2001).
- The recycled concrete may react with groundwater which may result in a change of material properties. This is subject to further studies by others.

6 Conclusions

Based on the performed suitability testing on the recycled concrete aggregate, the tested material is found to be of acceptable quality and is adequately satisfying the minimum requirements specified under QCS for suitable backfill. Additional tests were also carried out to analyse the durability and strength of the aggregate under dry and soaked conditions.

RCA is not expected to exhibit alarming settlement, since the material is well graded which will reduce the void ratio of the compacted material. Also, the material has low crushing and abrasiveness potential, high soaked CBR values and a satisfactory TFV value, which reduces the risk of disintegration. Furthermore, the post compaction settlement behaviour of the RCA aggregates will be evaluated during the mock-up testing. If the requirement will be achievable in the field for compaction criteria of minimum 95% of the laboratory established MDD value, the material would be proven to have no adverse impacts in performance when compared to the conventional backfill material produced from excavated rock.

Since the long-term behaviour of the material is yet to be evaluated in terms of settlement, as cyclic load-bearing capabilities are still unknown, shafts backfilled with RCA on the project will initially only be approved for use in non-traffic areas.

Using RCA as shaft backfill is more beneficial from a sustainability perspective as it will decrease the carbon footprint by 70% when compared with using traditional backfill materials such as limestone, gabbro or foamed concrete.

Acknowledgements

The authors are grateful to the Public Works Authority, Qatar (ASHGHAL) and for giving the opportunity to publish this paper. Our token of thanks to the management of Parsons International Ltd. for the necessary support and guidance and as well as the Contractor’s management for inputs during the paperwork.

References

Ellen, et al. (2001). Use of Recycled Asphalt Pavement and Crushed Concrete as Backfill for Mechanically Stabilized Earth Retaining Walls, Research Report Number 0-4177-1, Center for Transportation Research, The University of Texas at Austin, pp 55

Hassan, K., Reid, M. & Al-Kuwari, M. S. (2022). Implementation of Recycled Aggregate in Construction, QNRF

NPRP NO: 7 – 795 – 2 – 296, pp 2, 5, 149.

Rahman, et al. (2014). Suitability of recycled construction and demolition aggregates as alternative pipe backfilling materials, *Journal of Cleaner Production 66*, 75-84, pp 78. https://doi.org/10.1016/j.jclepro.2013.11.005

Elhussien, et al. (2021). Ashghal Recycling Manual.

Qatar Construction Specification. (QCS) 2014.

QTCG. (2022a). Geotechnical Interpretative Report, Doc. no. C853/1-QTCG-GEN-GEO-RPT-00008 Rev.2. Public Works Authority. Doha: 236 p

QTCG. (2022b). Technical Note for Designer's Recommendation on the Use of Crushed Concrete Recycled Aggregate for Backfilling, Doc. no. C853/1-QTCG-GEN-DES-TNE-00008 Rev.2. Public Works Authority. Doha: 50 p

Stålheim, J. (2014). Comparative study of established test methods for aggregate strength and durability of Archean rocks from Botswana, Published digitally at the Department of Earth Sciences, Uppsala University, pp 11, 12.

Aqil, et al. (2005). Strength and deformation characteristics of Recycled Concrete Aggregate as a Backfilling Material. Vol. 45, Issue 5, pp 53-72. https://doi.org/10.3208/sandf.45.5_53

Cite as: Brown J., Valsan S., Vashisht N.K., Olliver A. & Al-Mohannadi E.A.S.A., "Backfilling Shaft Surround Using Recycled Concrete Waste Material", *The 2nd International Conference on Civil Infrastructure and Construction (CIC 2023)*, Doha, Qatar, 5-8 February 2023, DOI: https://doi.org/10.29117/cic.2023.0082

Impact of the Fiber Distribution Characteristics on the Uniaxial Behaviour of Fiber-Reinforced Composites- An Experimental Study

C.B. Kameswara Rao
Department of Civil Engineering, NIT Warangal, Warangal, India
raocbk@nitw.ac.in

S.R.R. Teja Prathipati
Department of Civil Engineering, V.R.Siddhartha Engineering College, Vijayawada, India
teja@vrsiddhartha.ac.in

Hanuma Kasagani
Department of Civil Engineering, V.R.Siddhartha Engineering College, Vijayawada, India
hanumakasagani@vrsiddhartha.ac.in

Abstract

The demand for development of fiber-reinforced composites has enhanced as the practise of integrating fibres into concrete has become prevalent over the past few decades.. The intersection zone where the fiber crossing the fracture surface and fiber distribution characteristics in the composite plays an important role in predicting the overall performance of the Fiber Reinforced Composite (FRC). To ascertain the orientation and distribution of the fibres in various FRC's, a variety of experimental methods have been proposed in the literature. This study aimed to assess the impact of fibre orientation and fibre distribution characteristics on the fresh and hardened properties of Hybrid FRC's and Hybrid Graded FRC's containing glass and steel fibres. It can be concluded that the methods adopted in this study for calculating the fiber distribution and orientation characteristics were reliable and the proposed equations were successful in predicting the uniaxial behaviour of FRC. Positive synergy was observed in the Hybrid Graded FRC specimens, which was attributed to the superior fibre distribution characteristics displayed by hybrid grading of fibres, which was rationalised by the fact that modifying the fibre distribution characteristics would affect the FRC's behaviour.

Keywords: Fiber-reinforced composite; Fiber distribution characteristics; Graded fibers; Hybrid graded fibers; Uniaxial behaviour

1 Introduction

Fibers have long been employed in cement-based products to enhance material performance. The best-known attribute of fiber-reinforced composites is a significant increase in tensile strength and toughness (Prashanth et al.,1994; Zollo,1997). Other advantages of employing fibres include higher shear strength, resilience to dynamic stresses, and reduced shrinkage cracking (Ngo et al., 1994). Many types of fibres have been used to reinforce building materials, including concrete. Fiber Reinforced Concrete (FRC) typically uses either steel or glass fibres as reinforcement. High Strength Concrete (HSC) has been shown to be successful at higher stress levels (Singh et al., 2018) because of its increased strength and dense microstructure. HSC has very poor tensile strength and a brittle failure mode. Because of this, using fibres in HSC reinforcement projects increases mechanical characteristics and post-peak performance behaviour.

Most modern fiber-reinforced High Strength Concretes (FR-HSC) are made with a single fibre type that has a finite effectiveness called Mono Fiber-reinforced High Strength concretes (MFR-HSC). It was determined that the inclusion of mono fibres did not significantly enhance the composite as a whole (Kasagani et al., 2021). The Reinforcement of Hybrid Fibers to high strength concrete (HyFR-HSC), is extremely flexible and can be used in a variety of applications because of its ability to increase mechanical qualities and prevent multi-level cracking (Koniki et al., 2021). Positive synergy may be due to mixing fibres of varying lengths, diameters, and Young's moduli (Prathipati et al., 2020; Prathipati et al., 2021).

Different lengths of fibers incorporated into the composite will be beneficial in bridging of micro-cracks by short length fibers and long length fibers will address macro cracking and the composite formed by using both the fibers is called Graded Fiber Reinforced Concrete (GrFR-HSC) (Teja et al., 2021). Concrete's workability and mechanical qualities will be enhanced by using fibres of varying lengths instead of a single strand length (Doyon-Barbant et al., 2018). Therefore, Hybrid Graded Fiber-Reinforced High Strength Concrete (HyGrFR-HSC) refers to the practise of incorporating multiple types of graded fibres into a single batch of concrete in order to increase the mechanical properties of the concrete by making use of the modulus and geometry of the fibres in the blend (Koniki et al., 2021).

The FR-HSC's behaviours are significantly affected by fibre distribution features such the fibre orientation factor and fibre dispersion factor. The distribution of the fibres within the material affects their ability to serve as reinforcement (Doyon-Barbant et al., 2018). Poorly-distributed fibres in some areas offer little to no reinforcement, which causes flaws in the composite material. Uniformly scattered fibres reduce the maximum size of such faults, maximising reinforcing efficiency. Fiber dispersion characteristics influence FRC fresh state qualities and vice versa. Given that mechanical performance is significantly correlated with fresh state attributes & fibre dispersion characteristics, all of which must be controlled for optimal mechanical performance, increasing the number of fibres may improve mechanical qualities, however because fibres are not always aligned in the direction of stress, the effectiveness is questionable. Better would be the homogeneous distribution of fibers, which could enhance FRC performance in a structure at reduced cost. In addition to strength, ductility will also be addressed. The mechanical properties of the composite are improved by the fibres' uniform orientation and distribution (Prathipati et al., 2021a; Prathipati et al., 2021b). Therefore, in order to acquire the high-performance FRC, it is crucial to study the effects of fibre distribution characteristics on the mechanical properties of various FR- HSC's. This suggests that a proper analysis of the FR-HSC's mechanical performance necessitates an examination of fibre dispersion characteristics. Therefore, a reliable testing strategy was required to identify the characteristics of fibre distribution in the FRC mixtures, enabling a more appropriate relationship to be established between fibre distribution features and material behaviour.

X-ray transmission photography, electrical resistivity measurement, and image analysis approach are just a few of the experimental methods that can be used to evaluate the fibre dispersion properties in composites (Yang et al., 2018). The fibre distribution features of all the FRC specimens in this study were assessed using digital image analysis methodology, as suggested by Lee et al., (2003). The necessary specimen cross-section was removed and a picture of it was captured for use in the image analysis. By feeding the collected image into the software, the features of the fibre dispersion may be assessed. Although numerous researchers made use of image analysis, there were discrepancies in their interpretation of fibre dispersion features. In addition,

there was a lack of information in the literature between the correlation of mechanical performance and fibre distribution characteristics for different types of FR-HSC's. Hence in this manuscript an investigation was attempted to figure out how different fibre distributions affect the functionality of MFR-HSC, HyFR-HSC and HyGrFR-HSC mixes. Fiber density, dispersion and orientation in the composite are computed by conducting image analysis.

2 Investigational Study

2.1 Materials

The materials used were of the following specific gravities: 3.13 for OPC 53 grade, 2.68 for fine aggregate (Zone-II River sand), and 2.78 for coarse aggregate (crushed granite, 10 mm nominal size). The combination of Silica Fume and Class F Fly Ash as two different SCMs were incorporated. The study employs potable water, Conplast SP430 as a superplasticizer, crimped steel fibres, and AR glass fibres. Fiber characteristics are summarised in Table 1.

Table 1: Fibers properties

Mixes	Steel (mm)		Diameter (mm)	Aspect Ratio		Elastic Modulus (GPa)	Tensile Stength (MPa)
Crimped Steel Fiber	25	50	0.5	50	100	200	1400
Alkali-Resistant Glass Fiber	6	12	0.0135	444	888	73	1168

2.2 Mix Proportions and Designations

The control mix of M70 grade concrete was made in accordance with Indian Standards (IS 10262, 2019). Water-binder ratio of 0.31 and mix proportion of 1:1.05:1.52 were determined from the trail mixes and used in this investigation. Steel fiber: lengths (25 mm & 50 mm), dosage (0.5%, 0.75%,1% & 1.25%) and Glass fiber: lengths (6 mm & 12 mm); dosage (0.1%, 0.2%,0.3% & 0.4%) are also included as independent variables. 1 Control Mix CM, 16 MFR-HSC Mixes were formed, 4 HyFR-HSC Mixes and 1 HyGrFR-HSC Mixes were formed in the study, and their respective mix denotations are given in Table 2 and Table 3.

Table 2: MFR-HSC Mix designations

Mix	Designation	Volume Fraction (%)	Steel Fiber		Glass Fiber	
			25 mm	50 mm	6 mm	12 mm
MFR-HSC	CM	0	-	-	-	-
	M1	0.5	100%			
	M2	0.75	100%			
	M3	1	100%			
	M4	1.25	100%			
	M5	0.5		100%		
	M6	0.75		100%		
	M7	1		100%		
	M8	1.25		100%		
	M9	0.1			100%	
	M10	0.2			100%	
	M11	0.3			100%	
	M12	0.4			100%	
	M13	0.1				100%
	M14	0.2				100%
	M15	0.3				100%
	M16	0.4				100%

Table 3: HyFR-HSC & HyGrFR-HSC Mix designations

Mix	Designation	Volume Fraction (%)	Steel Fiber		Glass Fiber	
			25 mm	50 mm	6 mm	12 mm
HyFR-HSC	Hy1	1.65	100%	-	100%	-
	Hy2	1.65	-	100%	100%	-
	Hy3	1.65	100%	-	-	100%
	Hy4	1.65	-	100%	-	100%
HyGrFR-HSC	HyGr	1.65	50%	50%	50%	50%

2.3 Mixing and Testing Methodology

A pan mixer with a 100 kg capacity was used to mix the concrete. Both aggregates were introduced to the mixer separately at the first stage of mixing, where they were combined for one minute. In the second step, the mixer received different additions of fly ash, cement, glass fibres, and steel fibres for an additional minute. The final step involved thoroughly mixing water and superplasticizer for an additional two minutes to create a uniform mixture. Concrete is poured into moulds, which are then compacted on the vibrating table. The specimens were demolded and allowed to cure for 28 days after casting for 24 hours.For evaluating the compressive strength of all the mixes, steel cube moulds of 100 mm were chosen. According to IS: 516-1959 , compressive strength of all mixes was evaluated in the current investigation using a 1000 kN servo-controlled test system. For the uniaxial tensile test, we employed a dog bone specimen measuring 150 mm in length and 80 mm by 40 mm in cross section. Displacement (at a rate of 0.2 mm/s) was controlled using a servo-hydraulic testing frame. After tensile testing, the damaged samples were chopped with a concrete cutter until the crack was nearly invisible by maintaining the cross-sectional size after cutting at 80 mm by 40 mm. Each failure plane specimen was polished and smoothed using a grinding machine before being photographed using an optical microscope. Micrographs are processed in Image J, with the RGB image converted to greyscale and the scale calibrated. A thresholding method is used to transform a grayscale image into a binary one, and the fibres were discovered in the binary image. There will be an analysis of the fibre distribution parameters, including fibre count, major axis length, and minor axis length. It was not until much later that the fibre dispersion properties were established.

3 Experimental Outcomes

3.1 Compressive Strength

Below, Figure 1 represents the compressive strength of all the different mixtures. There is a shift in the compressive strength of concrete produced using MFR-HSC mixes whenever there is an increase in either the fibre length or the fibre volume. There was an improvement in compressive strength values for MFR-HSC mixes when the volume of glass fibre was increased from 0.1 percent to 0.3 percent and when the volume of steel fibre was increased from 0.2 percent to 1 percent. With an increase in glass fibre length from 6 mm to 20 mm and steel fibre length from 25 mm to 50 mm, compressive strength values decreased regardless of fibre content. When compared the compressive strength values of HyFR-HSC and HyGrFR-HSC mixes from the figure 2, it can be observed that hybridizing fibers at higher volume fraction has resulted in the decrimental effect and which can be compensated by hybridizing graded fibers.

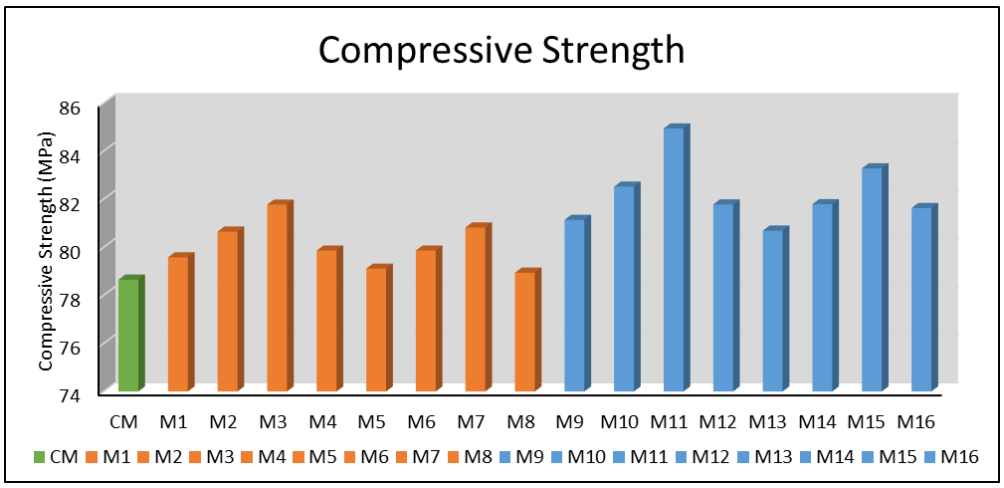


Fig. 1: Compressive Strength of MFR-HSC mixes

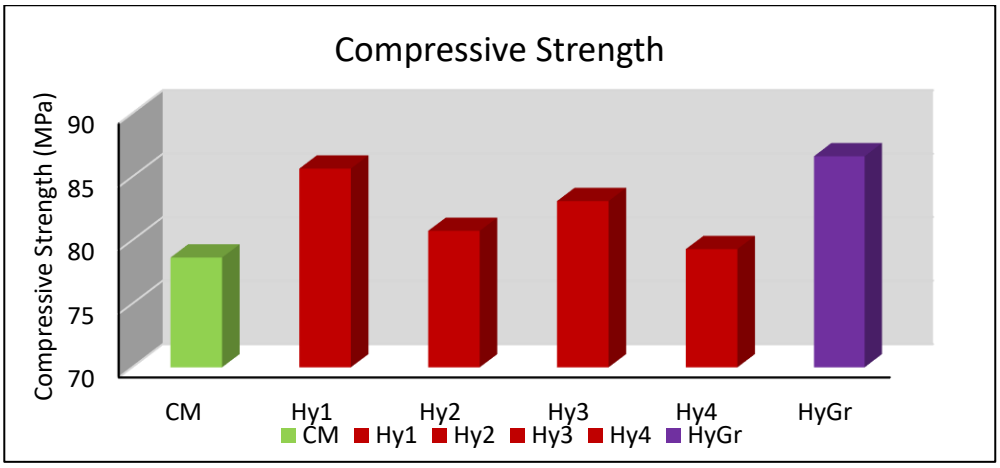


Fig. 2: Compressive Strength of HyFR-HSC and HyGrFR-HSC mixes

3.2 Tensile Strength

In the Figure 3 below, we can see that the hybridization of graded fibres has increased the direct tensile strength of the HyGrFR-HSC mixes in comparison with HyFR-HSC mixes and this can be validated by evaluating the fiber dispersion characteristics of the HyFR-HSC and HyGrFR-HSC mixes and presented in the next section.

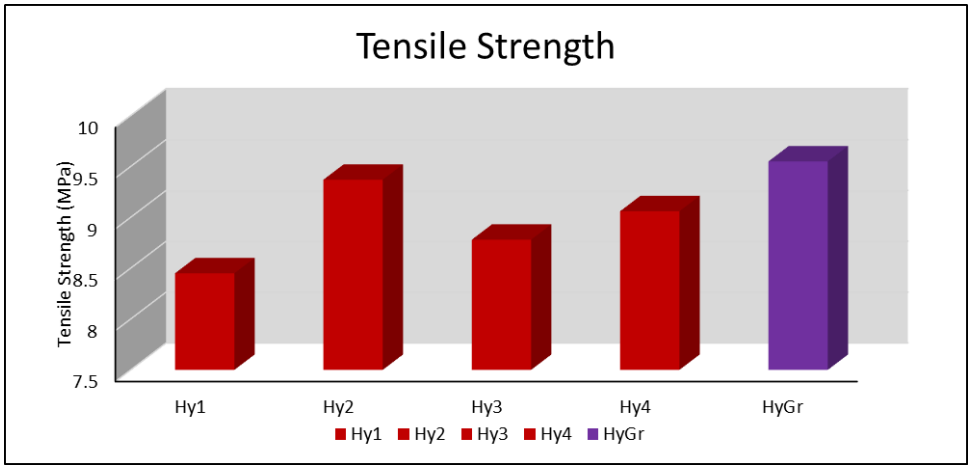


Fig. 3: Tensile Strength of HyFR-HSC and HyGrFR-HSC mixes

3.3 Fiber Dispersion Characteristics

By determining the distribution coefficient (η_d), also known as the fibre dispersion coefficient, as determined by Lee et al., (2009) and given in Eq (1), the orientation coefficient (η_θ) was calculated by superimposing an image of a fibre on a broken plane and dividing the minor axis length by the main axis length of the fibre. The Eq (2) was used to calculate the η_θ. Fiber length affects the Fiber Length Coefficient (η_l). Equations (3) and (4) yield η_l under the assumption of a uniform interfacial shear stress transfer. (Chiang, 1994).

$$\eta_d = exp\left[\sqrt{\frac{\Sigma(x_i - 1)^2}{n}}\right] \quad (1)$$

$$\eta_\theta = \frac{1}{n}\sum_{i=1}^{n}\frac{bi}{ai} \quad (2)$$

$$\text{For } L_f < Lc \ \eta_l = L_f / 2L_c \quad (3)$$

$$\text{For } L_f \geq L_c \ \eta_l = 1-(L_c / 2L_f) \quad (4)$$

n : total number of fibers at the image's grid location.

x_i : *i*th square's fibre count.

ai & bi : major & minor axis of the fiber's elliptical imprint on the cutting plane.

L_f & L_c : fiber length and fiber critical transfer length.

The values of η_d, η_Θ and η_l for HyFR-HSC and HyGrFR-HSC mixes were computed and are presented in Table 4 below.

Table 4: Fiber distribution, fiber orientation and fiber length coefficients of HyFr-HSC&HyGrFR-HSC mixes

Mix (1)	Mix Designation (2)	η_d (3)	η_θ (4)	η_l (5)
HyFR-HSC	Hy1	0.421	0.470	0.449
	Hy2	0.466	0.544	0.466
	Hy3	0.401	0.536	0.509
	Hy4	0.372	0.548	0.526
HyGrFR-HSC	HyGr	0.479	0.529	0.488

4 Analytical Modeling

The law of mixtures can be used to measure the tensile strength of a composite (σ_{ct}). Fiber contribution to composite strength is determined by fibre orientation and distribution. As a result, the tensile capabilities of composites are primarily influenced by the dispersion, orientation, and quantity of fibres in the cracking area, as well as fibre dispersion parameters. The frequently used Rule of Mixtures equation was modified by Kasagani, et al., (2019), which introduced the fibre dispersion coefficient (d) to account for fibre dispersion in the fracture plane, is used to forecast tensile strength and is given in below equation

$$\sigma_{ct} = \eta_d \ \eta_\theta \ \eta_l \ V_f \ \sigma_{fu} + V_m \ \sigma_{mt} \quad (5)$$

The experimental peak tensile stress values for all the mixes are given in column 4 of Table 5. The tensile strength of fibre reinforced composite for HyFR-HSC, and HyGrFR-HSC mixes for M70 grade is calculated using equation (5), and the results are shown in column 3 of Table 5. Table 5, column 5, shows the comparison between calculated and experimental composite strengths. From Figure 4 which

represents the plot of Analytical vs Experimental Composite Tensile Strength of HyFR-HSC & HyGrFR-HSC mixes, it is clear that the values for composite strength obtained from Equation 5 are remarkably similar to the experimental values. Further analysis of Table 5 reveals that HyGrFR-HSC specimens outperformed HyFR-HSC specimens in terms of positive synergy. This is due to the superior fibre distribution characteristics displayed by hybrid fibre grading, which is supported by the idea that changing the fibre distribution characteristics will affect FRC behaviour.

Table 5: Experimental and Theoretical Tensile strength of HyFr-HSC&HyGrFR-HSC mixes

Mix (1)	**Mix Designation (2)**	**$\sigma_{ct} = \eta_d \eta_\theta \eta_l V_f \sigma_{fu} + V_m \sigma_{mt}$ (3)**	**Experimental Peak Stress (4)**	**Ratio of Theoretical stress to Experimental stress (5)**
HyFRC	Hy1	8.14	8.45	0.96
	Hy2	8.94	9.37	0.95
	Hy3	8.71	8.78	0.99
	Hy4	8.65	9.06	0.95
HyGrFRC	HyGr	9.39	9.55	0.98

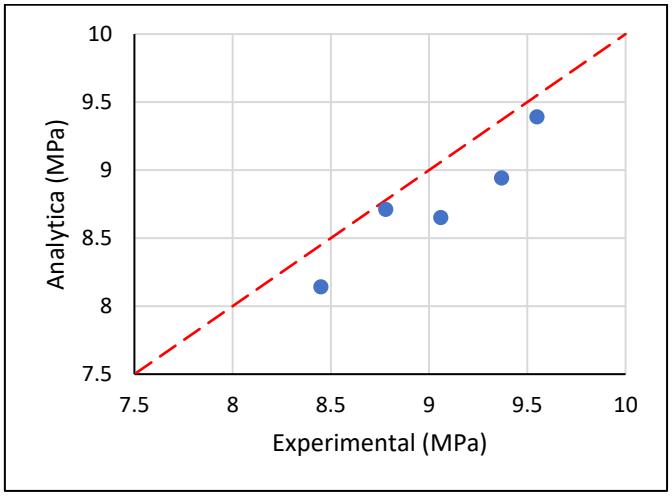


Fig. 4: Analytical vs Experimental Composite Tensile Strength of HyFR-HSC & HyGrFR-HSC

5 Conclusion

The following are some of the important conclusions drawn from this study:

- Irrespective of fiber length in MFR-HSC mixes glass fiber with 0.3% fiber volume and steel fiber with 1% fiber volume have exhibited higher compressive strength.
- When compared to HyFR-HSC mixes, the peak stresses under both compression and tension improved for HyGrFR-HSC mixes.
- HyGrFR-HSC mixes have shown higher values of fiber dispersion coefficient (η_d), fiber orientation coefficient (η_θ) and fiber length coefficient (η_l) when compared to HyFR-HSC mixes at the same fiber volume fraction and thereby indicating better fiber distribution and fiber pullout strength in HyGrFR-HSC mixes.
- It has been found that the composite's strength in uniaxial tension is affected by the fibre dispersion, fibre orientation, and fibre embedded length. In this investigation, the tensile strength of the composite was estimated using an equation that takes into account the aforementioned properties, and the predicted values are more in line with the experimental values.

The mechanical properties and fibre dispersion characteristics of Hybrid Graded FRC incorporating steel and glass fibres were only studied in this study; therefore, in the future, the impact of using fibers of varying geometries on the properties of HyGrFRC will be studied.

References

Chiang, C. R. (1994). A statistical theory of the tensile strength of short-fiber-reinforced composites. *Composites science and technology*, *50*(4), 479-482. https://doi.org/10.1016/0266-3538(94)90056-6

Doyon-Barbant, J. & Charron, J. P. (2018). Impact of fibre orientation on tensile, bending and shear behaviors of a steel fibre reinforced concrete. *Materials and Structures*, *51*(6), 1-16. https://doi.org/10.1617/s11527-018-1282-0

Kasagani, H. & Rao, C. B. K. (2019). Effect of short glass fibre on dilated concrete in compression and tension. *Proceedings of the Institution of Civil Engineers-Structures and Buildings*, *172*(3), 214-225. https://doi.org/10.1680/jstbu.17.00017

Kasagani, et al. (2021). Influence of graded glass fibres on strain hardening and strain softening behaviour of CGGF under uniaxial stress. *Magazine of Concrete Research*, *73*(13), 674-700. https://doi.org/10.1680/jmacr.19.00303

Koniki, et al. (2021). Mechanical behavior of triple-blended hybrid fiber-reinforced concrete: an experimental and numerical study. *Innovative Infrastructure Solutions*, *6*(3), 1-14. https://doi.org/10.1007/s41062-021-00526-9

Lee, et al. (2003). Measurement and numerical simulation of three ‐ dimensional fiber orientation states in injection ‐ molded short ‐ fiber ‐ reinforced plastics. *Journal of applied polymer science*, *88*(2), 500-509. https://doi.org/10.1002/app.11757

Ngo, et al. (2017). Shear resistance of ultra-high-performance fiber-reinforced concrete. *Construction and Building Materials*, *151*, 246-257. http://dx.doi.org/10.1016/j.conbuildmat.2017.06.079

Prathipati, et al. (2021a). A study on the fiber distribution characteristics of hybrid fiber reinforced high strength concrete with steel and glass fibers. *Materials Today: Proceedings*, *43*, 962-969. https://doi.org/10.1016/j.matpr.2020.07.341

Prathipati, et al. (2021b). Assessment of fiber distribution characteristics in the hybrid fiber reinforced concrete–An experimental study. *Materials Today: Proceedings*, *38*, 2541-2548. https://doi.org/10.1016/j.matpr.2020.07.556

Prashanth, et al. (2017). Fiber reinforced composites-a review. *J. Mater. Sci. Eng*, *6*(03), 2-6. https://doi.org/10.4172/2169-0022.1000341

Singh, B., Arora, V. V. & Patel, V. (2018). Study on stress strain characteristics of high strength concrete. *Indian Concrete Journal*, *92*(6), 37-43.

Prathipati, S. R. R. & Rao, C. B. K. (2021). A study on the uniaxial compressive behaviour of graded fiber reinforced concrete using glass fiber/steel fiber. *Innovative Infrastructure Solutions*, *6*(2), 1-14. https://doi.org/10.1007/s41062-020-00438-0

Prathipati, S. R. R., Rao, C. B. K. & Murthy, N. R. (2020). Mechanical behavior of hybrid fiber reinforced high strength concrete with graded fibers. *International Journal of Engineering*, *33*(8), 1465-1471. https://doi.org/10.5829/ije.2020.33.08b.04

Yang, Y. (2002). Methods study on dispersion of fibers in CFRC. *Cement and Concrete Research*, *32*(5), 747-750. https://doi.org/10.1016/S0008-8846(01)00759-1

Zollo, R. F. (1997). Fiber-reinforced concrete: an overview after 30 years of development. *Cement and concrete composites*, *19*(2), 107-122. https://doi.org/10.1016/S0958-9465(96)00046-7

Cite as: Rao C.B.K., Prathipati S.R.R.T. & Kasagani H., "Impact of the Fiber Distribution Characteristics on the Uniaxial Behaviour of Fiber-Reinforced Composites- An Experimental Study", *The 2nd International Conference on Civil Infrastructure and Construction (CIC 2023)*, Doha, Qatar, 5-8 February 2023, DOI: https://doi.org/10.29117/cic.2023.0083

Influence of Pier Stiffness on Track-Bridge Interaction

Ali Mubarack C. K.
Indian Institute of Technology Roorkee, Roorkee,Uttarakhand, India
ak@ce.iitr.ac.in

Akhil Upadhyay
Indian Institute of Technology Roorkee, Roorkee,Uttarakhand, India
akhilfce@iitr.ac.in

Abstract

The bridge is a common engineering structure over which a rail track is often laid. With the introduction of continuous welded rail (CWR), major rail tracks have shifted worldwide from jointed rail to continuous welded rail. CWR eliminates fish plates and overcomes many of the drawbacks of the jointed rail, resulting in a long, smooth track with no joints. Track-bridge interaction (TBI) is important when a continuous welded rail is provided over a bridge structure. Since numerous parameters influence the phenomenon, a numerical model has been developed in SAP2000. Longitudinal pier/abutment stiffness is an important structural property of bridge substructure, and its magnitude changes significantly from one bridge to another. Due to the coupling between CWR track and the bridge, the bridge pier stiffness affects the rail stress developed in addition to pre-existing stress. Pier stiffness has been identified as an important parameter affecting the track-bridge interaction phenomenon as its value changes with the site conditions. The developed numerical model has been utilized to study the influence of pier stiffness on support reaction and additional rail stress in CWR subjected to thermal loading. Both the support reaction and rail stress have been found to be considerably influenced by pier stiffness. Additional rail stress in CWR is a source of concern because the track is a long, slender member that can buckle if excessive compressive stress develops in the track.

Keywords: Track-bridge interaction; Continuous Welded Rail; Pier stiffness; Additional Rail Stress; Horizontal Support Reaction

1. Introduction

Rail tracks are an essential engineering structure generally supported on an embankment and very often by a bridge structure. Continuous welded rail (CWR) is progressively replacing conventional jointed rail because of its inherent advantages over the latter. A seamless track system without intermittent joints is the main benefit of deploying CWR. The other benefits of CWR over a jointed rail track include better ride quality, lower noise pollution, decreased track maintenance requirements, and better track structural longevity (IRICEN, 1996). Also, the elimination of fishplate joints considerably reduces the dynamic effects of the vehicle load on the track, especially when the vehicle wheel passes from one rail segment to another over the joint (Cai, et al., 2007). The special expansion joints (SEJs), which are undesirable on a high-speed track, are eliminated by CWR over the bridge (Sanchez et al., 2021). However, the track-bridge system provided by CWR needs special attention as additional rail stress and support reactions are developed due to the interaction between the two inter-coupled systems.

The interaction between track and bridge systems arises due to the inter-coupling between the two structures through the support medium of the track and various fastening elements. Forces are developed at the track-bridge interface due to various load effects. For steel bridges, temperature variation significantly contributes to the track-bridge interaction (TBI) effects. Several studies have highlighted the influence of TBI in the presence of thermal loading (Fryba, 1985; Mubarack & Upadhyay, 2021; Yun et al., 2019). The development of high rail stress is not desirable, especially in the transition zone to the bridge (Strauss et al., 2015). To calculate the final reaction at the support, these additional horizontal support reactions must be added to the conventional support forces (UIC, 2001). Ballasted tracks are advantageous in both the dynamic and economic aspects of the bridge design (Quesada et al., 2021). The accurate estimation of rail stresses, displacements, and support reactions is essential during the design stage of the bridge. UIC Leaflet has been the pioneer in developing a codal provision in Europe based on earlier research on track-bridge interaction phenomena (UIC, 2001). The UIC code outlines criteria and methodology for conducting track-bridge interaction studies, and it provides rail stress and displacement limits to define track failure criteria. In addition, to account for the non-linear nature of the ballast, the code allows the bi-linear approximation of the track stiffness in the longitudinal direction.

Dutoit identified the role of pier stiffness as an important parameter for high-speed rail bridge design criteria (Dutoit, 2009). A detailed investigation of the influence of pier stiffness on the development of track stress and rail displacement is missing in the present literature. This paper will investigate the influence of pier stiffness on support reaction and additional rail stresses for a single-span simply supported steel bridge subjected to thermal loading. The well-maintained ballasted track is considered for the present study.

2. **Track-bridge Interaction**

As the CWR track is directly exposed to the environment, and the rail is a slender metallic structure with low thermal inertia, the track absorbs and emits heat rapidly and undergoes large temperature variations on a day-to-day basis. Any change in track temperature with respect to neutral temperature (the temperature at which the track develops no thermal stress) induces thermal strains in the track, and the track will tend to move longitudinally. Figure 1 shows the development of track forces due to the restrainment of these thermal movements. In Figure 1, F is the track force, the parameter α is the coefficient of thermal expansion for steel, ΔT_R is the rail temperature change relative to laying temperature, E is Young's modulus (steel), and A is the cross-sectional area of two rails combined. In Figure 1, the track movements occur in the end zone or the expansion zone in CWR, where the thermal strain is gradually relieved. However, the immovable central zone of CWR develops the full track force.

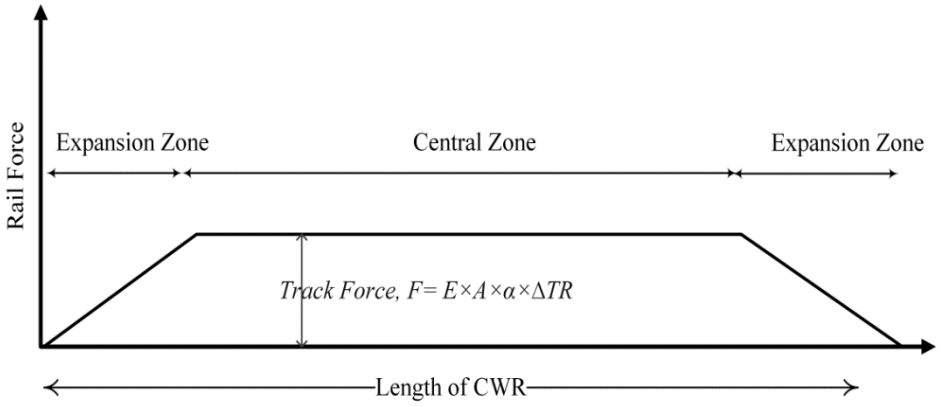


Fig. 1: Variation of longitudinal rail force in CWR

When the CWR track is allowed to pass over a bridge, the track is made to rest on a surface that is subjected to movement, and additional rail stresses are induced in CWR due to the coupling between them (Kumar & Upadhyay, 2012). The above phenomenon is called track-bridge interaction. In the case of a ballasted track, track and bridge are coupled through rail, sleeper ballast, and fastening. In the case of a ballast-less track or a slab track, the rail, fastenings, and concrete slab are supported directly on the bridge superstructure. The TBI phenomenon causes the creation of additional rail stress as well as additional horizontal support reactions at the bridge support. The interaction between the track and bridge is caused by temperature changes, horizontal braking and acceleration, traffic-induced bridge deck end rotations, and deformations and settlements due to creep and shrinkage. For steel bridges, temperature changes are a major source of TBI effects. This paper considers the temperature loading effects for a single span simply supported steel bridge.

3. Numerical Modelling of TBI

As numerous parameters affect the TBI phenomenon, the evaluation of various forces and stresses are computationally intensive. For the purpose of this study, the authors' previously developed and validated numerical model for the track bridge interaction has been used (Mubarack & Upadhyay, 2021). The numerical model was developed in SAP2000 (Computers and Structures Inc., 2016). Figure 2 shows the model for the track bridge system for a single span bridge, where CWR passes over a bridge that is located in the central zone of CWR track. The single span bridge has been modeled with fixed support at one end and movable/roller support at the other. The special expansion joint (SEJ) is not provided. Rail and deck elements were modeled with linear elastic beam elements.

In Figure 2, K_s, the resistance of the deck to horizontal displacement represents the longitudinal stiffness provided to the bridge deck by the bridge substructure. The support stiffness (K_s) was incorporated in the present model through linear spring elements in SAP2000. K considers the combined stiffness of the pier, bearing, base, foundation, and the subgrade on which the foundation rests. The stiffness of the movable bearing is ignored. The rail is modeled by combining two UIC rail sections. The bridge deck is modeled with linear beam elements. Only the effect of the uniform temperature load on the bridge deck has been considered.

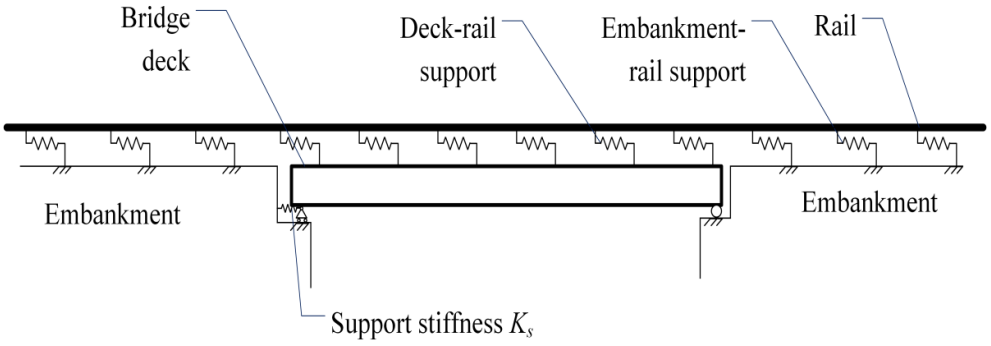


Fig. 2: Model for track-bridge interaction

Track stiffness is an important parameter that affects the phenomenon. Ballast behavior is essentially non-linear in nature. Figure 3 shows the track stiffness in the longitudinal direction for a well-maintained ballast under frozen and normal conditions. The deck-rail support and embankment rail support are modeled with two-noded connection elements called link elements, which simulates ballast stiffnesses. In the present model, well-maintained ballast under normal condition is

considered. For investigating the influence of thermal loading, track is considered vertically unloaded with vehicle traffic. The longitudinal track stiffness has been incorporated by employing nonlinear link elements in SAP2000.

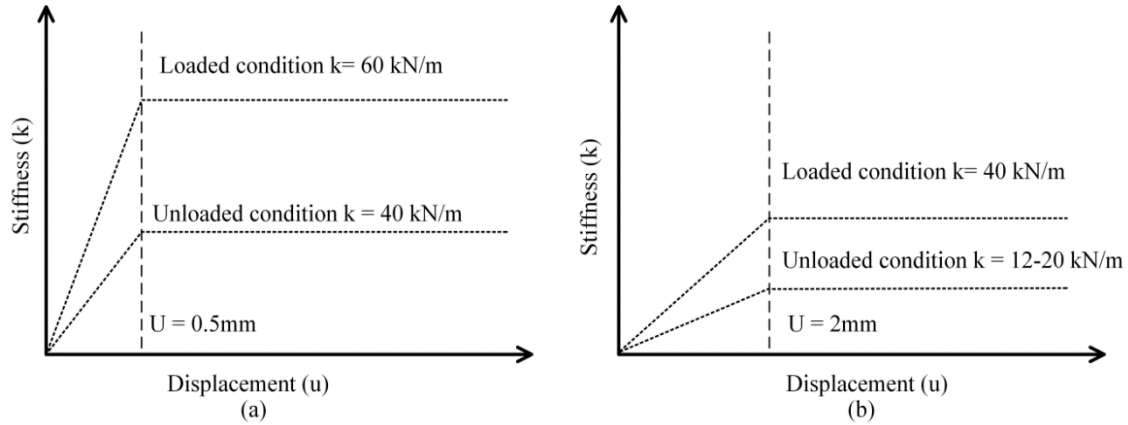


Fig. 3: Longitudinal track stiffness **(a)** frozen ballast **(b)** normal ballast

4. **Numerical Studies**

The model described in the previous section has been used to find the effects of the stiffness variation of the bridge deck support. A normal ballasted track having horizontal ballast stiffness 20 kN/m of the track with a yield displacement of 2mm is considered. The horizontal support stiffness variation of 0 kN.mm to 1000 kN.mm has been considered to investigate the influence of pier stiffness on additional rail stresses in CWR and the corresponding pier reactions. The length of the bridge deck considered is 75m. The UIC 60 rail section is used, and the combined cross-sectional area of the two rails is 1,540 mm^2. The bridge deck has the following specifications: Young's modulus, E=2.1x10^5 N/mm^2, coefficient of thermal expansion α = 1.0 x 10^{-05} °C^{-1}, cross-section area = 0.71 m^2, moment of inertia I = 3.84 m^4. The temperature increment applied to the bridge deck is 35 °C. The application of thermal loading caused the development of additional rail stress at the fixed and moveable ends of the bridge, as well as the support reaction.

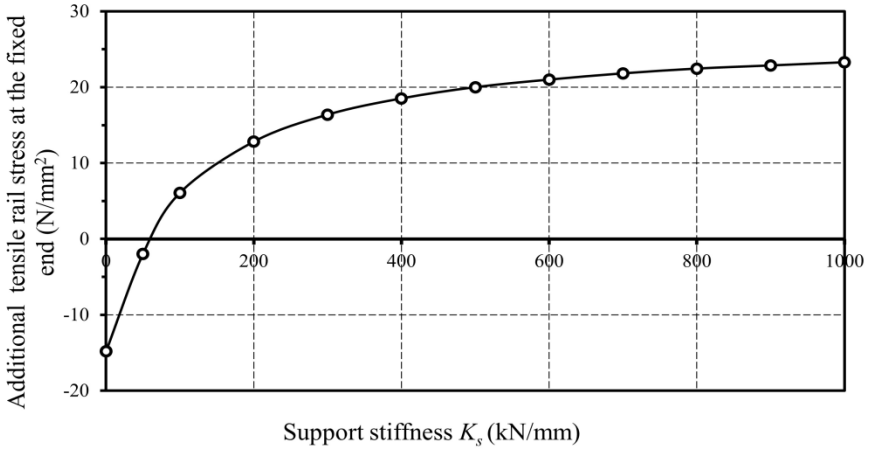


Fig. 4: Variation of additional rail stress at the fixed end with support stiffness

Figure 4 shows the variation of additional rail stress at the fixed end of the bridge corresponding to different support stiffness values. Initially, the track develops a stress equal to -14.8MPa (compressive) under zero-support stiffness, which is a floating-deck condition (represents an

extremely flexible support condition). The nature of the track stress at the fixed end was reversed by slightly increasing the support stiffness. From Figure 4, higher support stiffness results in larger tensile stress at the fixed-elastic end, but the increase in rail stress tends to decrease.

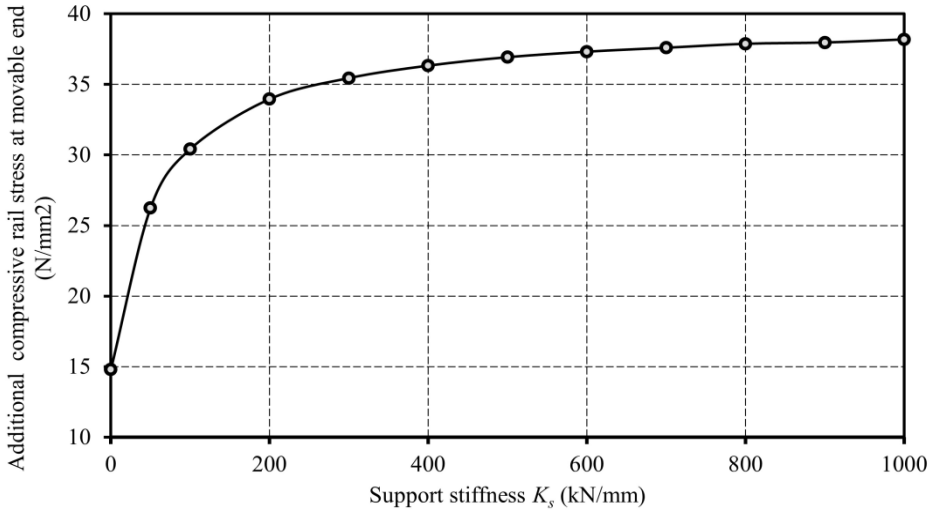


Fig. 5: Variation of additional rail stress at the movable end with support stiffness

Figure 5 shows the additional compressive rail stress variation at the movable end corresponding to various support stiffness values. Initially, for K_s =0, compressive rail stress at the movable end = 14.8 N/mm^2, matching the value at the fixed end. For all stiffness instances, CWR at the movable end of the bridge develops compressive stress. A higher support stiffness increases additional compressive stress at the movable end. Figure 6 shows the variation of rail stress along the track length as viewed in the present model.

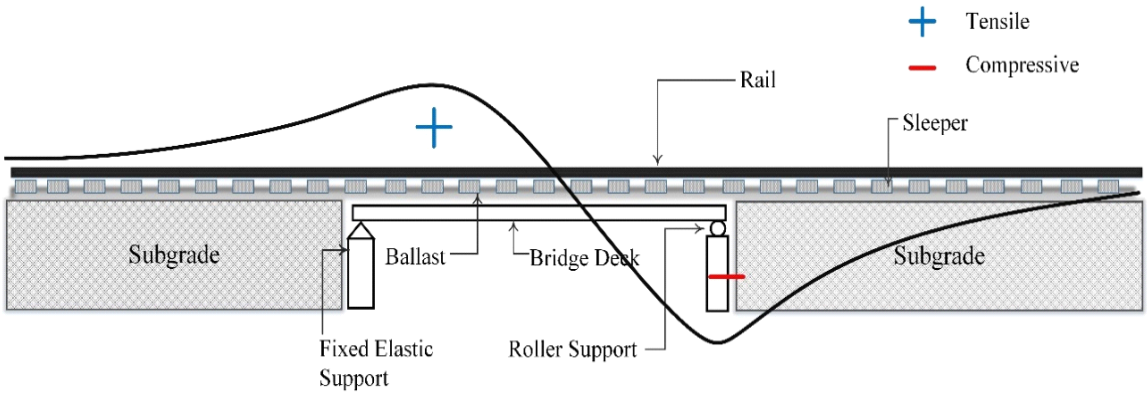


Fig. 6: Variation of additional rail stress along the length of CWR due to TBI as realized in the present model

Figure 7 shows the variation of horizontal bridge support reactions at the fixed end with support stiffness. The bridge support reaction is increasing considerably with an increase in support stiffness. A higher support stiffness increases the support reaction. However, at higher support stiffness, due to the nonlinear nature of the phenomenon, the increase in support reaction tends to decrease. From Figure 7, a significant amount of force is observed to be developed by the bridge pier even at a moderate value of pier stiffness. This reaction is in addition to the reaction due to existing loads. The development of such large horizontal forces is not desirable for long, slender piers due to the possibility of developing high overturning moments in the pier foundation, which highlights the importance of the present study.

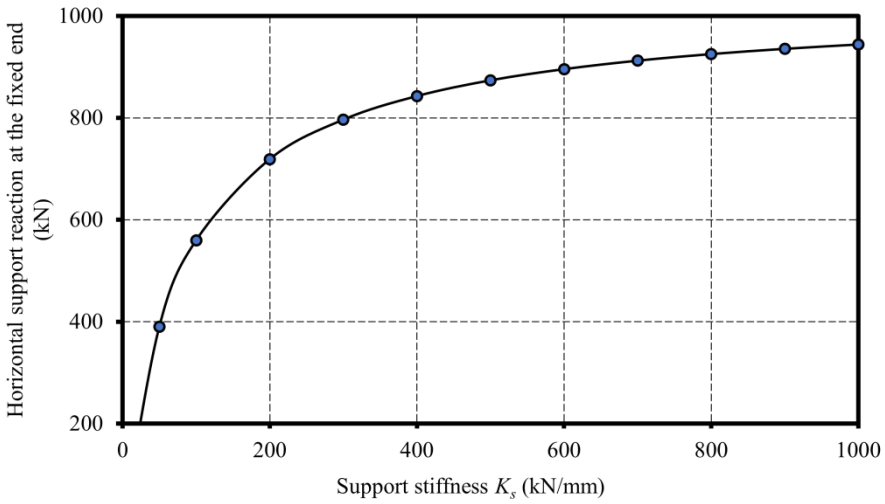


Fig. 7: Variation of horizontal support reactions at the fixed end with the change in support stiffness

5. Conclusion

CWR is gaining popularity over jointed rail because of its inherent advantages. However, the designer should have a good understanding of the TBI-related issues for the safe and efficient design of the track-bridge system. This paper studied the effect of pier stiffness on the TBI phenomenon considering thermal loading for single-span simply-supported bridges. The simplified numerical model, which handles the non-linearity associated with the ballast, has been utilized to find additional rail axial stresses and support reactions. In the present study, it has been observed that in a steel bridge with simply-supported decks, due to thermal loading, stiff piers develop more rail stress and support reaction because of the continuity of the CWR track passing over it. With an increase in support stiffness, both the maximum compressive and tensile rail stresses increase; however, the increase in both stresses tends to decline with higher support stiffness. At lower support stiffness, changes in interaction effects were more sensitive. Measuring rail stress at the fixed and movable ends of the bridge as well as estimating support responses are essential during the bridge design stage. The present study contributes to the knowledge of the behavior of CWR over bridges, especially under thermal loading. The designer may assess the final bridge forces considering the effect of other load cases on the interaction and the local stiffness variations of the ballast.

References

Cai, et al. (2007). Dynamic stress analysis of rail joint with height difference defect using finite element method. *Engineering Failure Analysis, 14*(8), 1488–1499. https://doi.org/https://doi.org/10.1016/j.engfailanal.2007.01.007

Computers and Structures Inc. (2016). CSI Analysis Reference Manual for SAP2000, ETABS, SAFE and CSIBridge. Computers and Structures Inc. http://docs.csiamerica.com/manuals/ etabs/Analysis Reference.pdf

Dutoit, D. (2009). New evolutions for high-speed rail line bridge design criteria and corresponding design procedures. Track-Bridge Interaction on High Speed Railways, 1–6.

Fryba, L. (1985). Thermal Interaction of Long Welded Rails with Railway Bridges. Rail International, 16, 5–24.

IRICEN. (1996). Long Welded Rails (Vol. 1, Issue 2). Indian Railways Institute of Civil Engineering.

Kumar, R. & Upadhyay, A. (2012). Effect of temperature gradient on track-bridge interaction. *Interaction and Multi-scale Mechanics, 63*(1), 1–12. https://doi.org/10.12989/imm. 2012.5.1.001

Mubarack, C. K. A. & Upadhyay, A. (2021). Stability of continuous welded rail on steel bridge subjected to thermal

loading. Structures, 34, 4524–4531. https://doi.org/https://doi.org/ 10.1016/j.istruc.2021.10.050

Quesada, et al. (2021). Ballasted track interaction effects in railway bridges with simply-supported spans composed by adjacent twin single-track decks. *Engineering Structures, 247*, 113062. https://doi.org/10.1016/j.engstruct.2021.113062

Sanchez, et al. (2021). Rail expansion devices and maximum dilation length in railway bridges. An experimental study. *Engineering Structures, 229*(May 2020). https://doi.org/10.1016/j.engstruct.2020.111605

Strauss, et al. (2015). Monitoring-based performance assessment of rail-bridge interaction based on structural reliability. *Structural Concrete, 16*(3), 342–355. https://doi.org/10.1002/suco.201500019

UIC (International Union of Railways). (2001). UIC 774-3R Track/bridge Interaction Recommendations for calculations (UIC 774-3R; 2nd ed.). International Union of Railways.

Yun, et al. (2019). Quantification of ballasted track-bridge interaction behavior due to the temperature variation through field measurements. NDT and E International, 103, 84–97. https://doi.org/10.1016/j.ndteint.2019.01.009

Cite as: Mubarack A. & Upadhyay A., "Influence of Pier Stiffness on Track-Bridge Interaction", *The 2nd International Conference on Civil Infrastructure and Construction (CIC 2023)*, Doha, Qatar, 5-8 February 2023, DOI: https://doi.org/10.29117/cic.2023.0084

The Use of Demolished Concrete Lumps (DCL) in Rectangular CFSTs Under Flexure

Salem Khalaf
Graduate Research Assistant, American University of Sharjah, Department of Civil Engineering, Sharjah, UAE
b00074986@alumni.aus.edu

Farid Abed
Professor, American University of Sharjah, Department of Civil Engineering, Sharjah, UAE
fabed@aus.edu

Abstract

This paper investigates the flexural performance of rectangular concrete-filled steel tube (CFST) beams that are partially incorporated with demolished concrete lumps (DCLs). In total, three CFST beams were prepared and tested under flexure through a four-point bending setup. These three specimens are selected from a bigger ongoing research project that considers further parameters. The three beams varied in the presence of DCLs within the CFST section and the maximum particle size of the DCLS. The DCLs were mixed with mortar and were isolated at the center of the CFST section and surrounded by normal concrete. The flexural behavior of the CFST beams was analyzed and discussed through the use of moment versus displacement, moment versus strain, and deflected shape graphs. The test results showed that the CFST beams with partially incorporated DCLs had similar flexural behavior to the normal CFST beam. The displacement at ultimate capacity was reported to be lower for the beams with incorporated DCLs, especially the beam with the higher DCL maximum particle size. However, the displacement at yield was found to be lower for the specimen that was fully cast with normal concrete. Finally, it was observed that the failure mode was the same for all three beams.

Keywords: Recycled concrete; DCL; CFST; Flexure; Beam

1 Introduction

Concrete-filled steel tubes (CFSTs) have been used over the past decade due to their superior mechanical properties. The steel tube provides confinement for the concrete infill and enhances its strength and ductility, while the concrete infill delays the local buckling of the steel tube (Roeder et al., 2010 and Han, 2004). CFSTs are mainly used as column members where the confinement is significantly utilized (Abdalla et al., 2013; Elyoussef et al., 2019; Abed et al., 2013). However, many studies have been conducted that investigated the flexural performance of CFST members under bending which can be found in the literature (Abed et al., 2018a; Abed et al., 2018b,; Abed et al., 2015; Wang et al., 2014; Hou et al., 2016).

Research interest in using recycled and waste materials in CFSTs has increased in the past decade. These recycled and waste materials include recycled aggregates, supplementary cementitious materials, and demolished concrete lumps (DCLs). For instance, (Abed et al., 2021) investigated the flexural response of rectangular and circular CFSTs with different recycled aggregates' replacement ratios up to 100%. The results showed insignificant changes in the flexural behavior or the moment capacities with different replacement ratios. In addition, it was reported that the increase in the

concrete strength from 30 to 50 MPa led to a minor increase in the ultimate capacity, whereas the yielding moment was approximately the same. Another study, (Wu et al., 2018) investigated the effect of using DCLs on the axial behavior of CFST columns. The DCLs were poured into a mold with fresh concrete to create precast segments. These precast segments were then isolated at the center of the section and surrounded with normal concrete. It was reported that the precast segment's area had a negligible effect on the axial capacity of the CFST specimen.

As of now, one study was published (Khalaf et al., 2022) which investigated the flexural performance of circular CFST specimens with partially incorporated DCLs. This study was done by the authors of this paper, in which a very similar specimen preparation and testing procedure were followed. The DCLs were isolated at the center of the section and were surrounded by normal concrete. Test results revealed that the incorporation of DCLs had a negligible effect on the flexural performance of circular CFST beams. This paper aims to study the effect of DCLs on the flexural performance of rectangular CFSTs, and assess the feasibility of using DCLs in a unique arrangement without compromising any of the flexural properties. The main parameters of this study are the presence of DCLs, and the maximum DCLs particle size.

2 Experimental Program

2.1 Specimen Preparation

The experimental program investigated the flexural performance of three rectangular CFST beams. All beams had the same steel-tube section dimensions (200x100 mm), thickness (4 mm), and length (1.5 m). One of the three beams served as the control specimen, denoted R-Control-F, in which it was fully cast with normal concrete, while the other two beams incorporated DCLs with two different maximum particle sizes (19 and 25 mm). For the two beams that incorporated DCLs, they were isolated at the center of the section. The isolation process included installing 100x50 mm rectangular foams at the center of the section with the use of spacers, followed by pouring the normal concrete surrounding the foams. The foams were then removed using liquid thinner that dissolves the foam easily without harming the concrete. Finally, DCLs were poured together with mortar in the DCL's region. The section details of all three beams can be shown in Figure 1. The process of isolation of the DCLs at the center of the section was done for two main reasons: to avoid bond loss between the steel and the DCLs due to the excessive shrinkage expected, and minimize the flexural contribution of the DCLs as the stresses and the corresponding strains at the DCL's region is lower than the rest of the section. The DCL's region within the section remained constant between the two beams that incorporated DCLs. The test matrix for all three beams in this study is summarized in Table 1. It is important to note that this paper is a part of a bigger project which includes more specimens and parameters considered.

Table 1: Test matrix

Beam Label	Tube Height X base (mm)	Tube Thickness (mm)	DCL's particle size range (mm)	DCL's region dimensions (mm)
R-Control-F	200 X 100	4	N/A	N/A
R-100x50-D19	200 X 100	4	12.5-19	100 X 50
R-100x50-D25	200 X 100	4	19-25	100 X 50

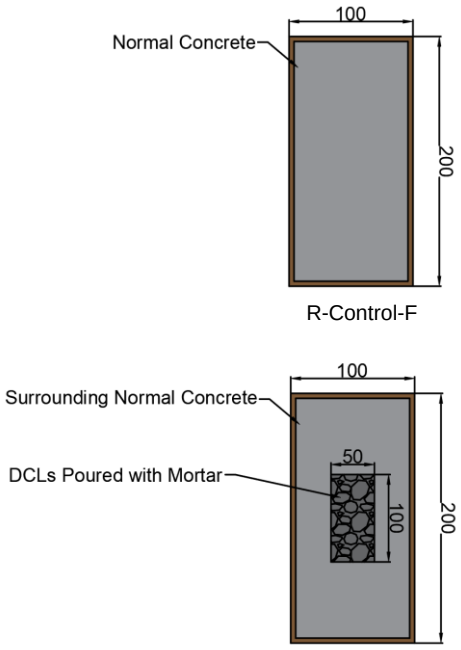


Fig. 1: Section details of CFST beam specimens, dimensions in mm

2.2 Material Properties

All CFST beams were filled from the same concrete batch. Three cylinders and three cubes were cast to obtain the compressive strength of the concrete after 28 days of curing. The compressive strength values were 28 and 36 MPa for the cylinders and cubes, respectively. Similarly, three cylinders and three cubes were cast with mortar and DCLs for each maximum particle size. The results showed that the two different DCLs sizes gave very close compressive strength values, which were 16 and 20 MPa for the cylinders and cubes, respectively. In addition, two steel coupons were shaped and fabricated from the original steel tubes according to the ASTM specifications to obtain the tensile properties. The average yield and ultimate strength reported were 230 and 274 MPa respectively.

2.3 Four-Point Bending Setup

All beams were tested under flexure using the four-point bending setup utilizing the universal testing machine (UTM), as shown in the schematic test setup in Figure 2. The beams had a clear span of 1350 mm and a pure moment region of 450 mm. Three strain gauges were installed at the top, center, and bottom of the section at the midspan to record the longitudinal strain values. In addition, three LVDTs were used to record the deflection at midspan and at a distance of 250 mm from the supports. One rigid plate was used as a spreader that was placed on top of two plates located at a distance of 450 mm from the supports. The load cell from the UTM was applied at a rate of 2 mm/min.

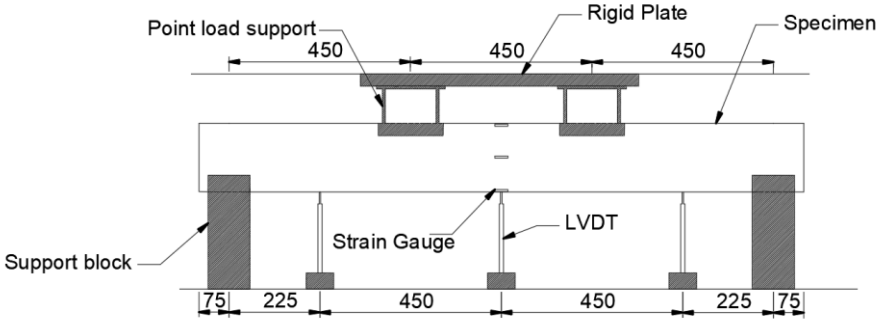


Fig. 2: Schematic test setup, dimensions in mm

3 Results and Discussion

The flexural performance of all three beams is evaluated through the use of moment versus midspan deflection, moment versus microstrain, and the deflected shape curves. In addition, the failure modes of the steel and the concrete infill for all beams are also discussed. Figure 3 shows the moment versus midspan deflection for all three beams. It is observed that the overall flexural response of all three beams is very similar. The initial stiffness of all three beams is approximately the same, and the transition from the elastic to the plastic stage is also comparable between the specimens. Furthermore, all three beams failed in a ductile manner as indicated by the deflections recorded after yielding. The flexural results of the specimens can be found in Table 2. The yielding moment (My) was recorded at a bottom microstrain equal to the yielding strain of the steel obtained from the coupon test. As for the ultimate moment (Mu), it was recorded at a bottom microstrain of 0.01, which is a value recommended by many researchers as the results are very comparable to design codes. It is observed that the yielding and ultimate moment values are close, where the maximum percentage difference is around 2% and 0.5%, respectively, which was between beams R-100x50-D25 and R-Control-F. As for specimen R-100x50-D19, the yielding and ultimate moment values were very similar to R-Control-F.

Table 2: Test results

Specimen Label	Yield Moment, My (kN.m)	Deflection at My (mm)	Ultimate Moment, Mu (kN.m)	Deflection at Mu (mm)
R-Control-F	53.2	6.44	65.2	19.26
R-100x50-D19	53.1	7.01	65	18.78
R-100x50-D25	54.3	7.8	64.9	16.39

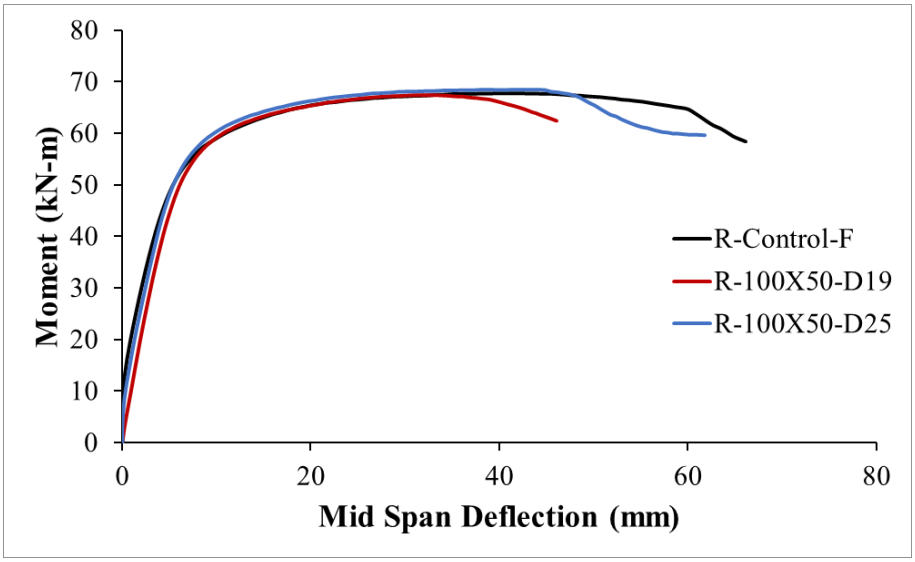


Fig. 3: Moment versus midspan deflection curves

The moment versus microstrain curves of the three beams can be shown in Figure 4. Similar to the moment versus deflection curves, the flexural behavior of the three beams was very similar. It is observed that for the bottom strain (positive x-axis), the moment values for the specimen R-100x50-D25 become slightly higher than the other two specimens. This behavior is also noticed for the top strain (negative x-axis). Figure 5 shows the deflected shape of the beams at the yielding and ultimate

stages. It is observed that the deflection at yield for R-Control-F was the lowest, whereas beam R-100x50-D25 had the highest deflection with a percentage increase of 20%, indicating that its stiffness was the lowest out of the three beams. However, the pattern flips for the ultimate deflections, where beam R-100x50-D25 had the lowest deflection, while R-Control-F had the highest deflection, where the percentage increase was around 17.5%. When comparing the beams with DCLs, the deflection at yield of specimen R-100x50-D25 was around 11% higher than specimen R-100x50-D19, whereas the deflection at ultimate of specimen R-100x50-D19 was 14% higher than specimen R-100x50-D25.

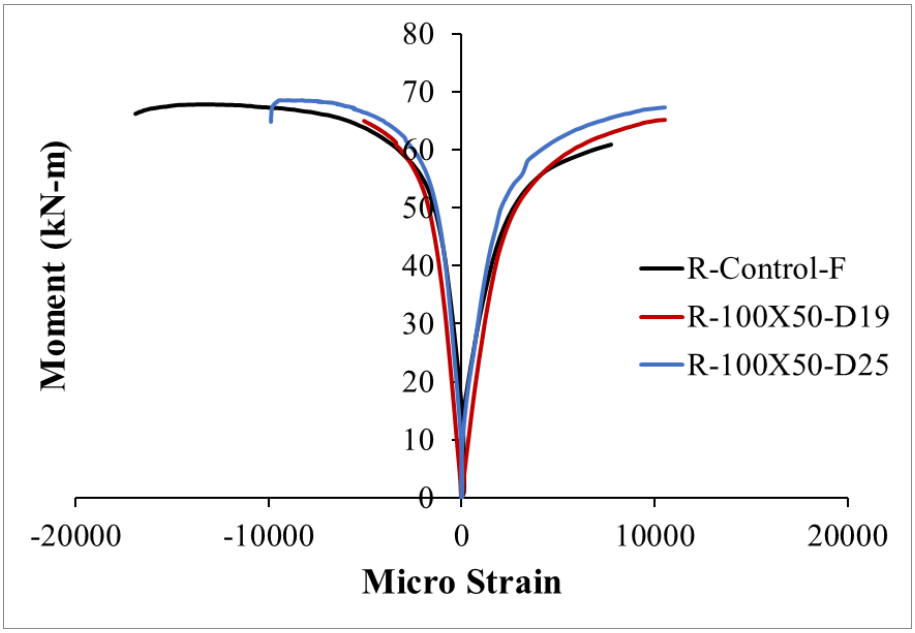


Fig. 4: Moment versus microstrain curves

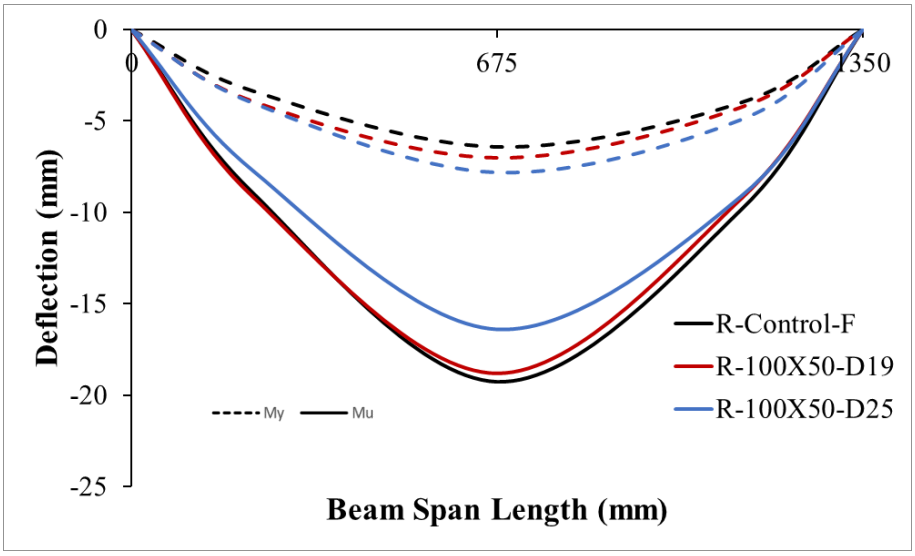


Fig. 5: Deflected shapes

Figure 6 shows the CFST failure modes of the steel and concrete, which was the same for all three beams. It was observed that an outward local buckling occurred in the compression zone of the steel between the two point loads. As for the concrete, it was observed that crushing occurred in the compression zone, and tensile cracks formed in the tension zone of the section.



Fig. 6: Failure mode of steel and concrete

4 Conclusion

This paper investigated the flexural performance of rectangular CFST columns with partially incorporated DCLs. The following conclusions can be drawn from this study:

- In general, the overall flexural response of all three beams was very similar, and they all failed in a ductile manner.
- The maximum percentage difference recorded between the specimens was 2% and 0.5% for the yielding and ultimate moment values, respectively.
- The highest and lowest deflection at yielding were reported by beams R-100x50-D25 and R-Control-F. However, the deflection at ultimate gave opposing results, where beam R-100x50-D25 had the lowest deflection, and beam R-Control-F had the highest deflection.
- All three beams had the same failure mode. The steel in the compression zone exhibited outward local buckling, while the concrete was crushed in the compression zone, and tensile cracks were formed in the tension zone.
- This study is limited to the used DCL maximum particle sizes, which were 19 and 25 mm. Further research on the effect of larger DCL sizes is recommended.

References

Abdalla, S., Abed, F. & AlHamaydeh, M. (2013). Behavior of cfsts and ccfsts under quasi-static axial compression. *Journal of Constructional Steel Research, 90*, 235–244. https://doi.org/10.1016/j.jcsr.2013.08.007

Abed, F. H., Abdelmageed, Y. I. & Kerim, I. A. (2018). Flexural response of concrete-filled seamless steel tubes. *Journal of Constructional Steel Research, 149*, 53–63. https://doi.org/10.1016/j.jcsr.2018.06.030

Abed, F. & Abdelmageed, Y. (2018). Finite element simulations of the flexural response of cfsts. 2018 Advances in Science and Engineering Technology International Conferences (ASET). https://doi.org/10.1109/icaset.2018.8376766

Abed, F., Abdelmageed, Y. & Alhoubi, Y. (2021). Effect of different cross-sections and concrete types on the flexural behavior of cfsts. *Composite Structures, 276*, 114570. https://doi.org/10.1016/j.compstruct.2021.114570

Abed, F., AlHamaydeh, M. & Abdalla, S. (2013). Experimental and numerical investigations of the compressive behavior of concrete filled steel tubes (cfsts). *Journal of Constructional Steel Research, 80*, 429–439. https://doi.org/10.1016/j.jcsr.2012.10.005

Abed, F., Najib, M. & Ilgun, A. (2015). "Flexural behavior of concrete filled seamless steel tube (CFST) beams." In the 10th International Conference on Composite Science and Technology (ICCST/10), Lisbon, Portugal.

Elyoussef, M., Elgriw, M. & Abed, F. (2019). Fe parametric study of the compressive behavior of cfsts. 2019 8th International Conference on Modeling Simulation and Applied Optimization (ICMSAO). https://doi.org/10.1109/icmsao.2019.8880323

Han, L., H. (2004). Flexural behaviour of concrete-filled steel tubes. *Journal of Constructional Steel Research, 60*(2), 313–337. https://doi.org/10.1016/j.jcsr.2003.08.009

Hou, et al. (2016). Flexural behavior of circular concrete filled steel tubes (CFST) under sustained load and chloride corrosion. *Thin-Walled Structures, 107*, 182–196. https://doi.org/10.1016/j.tws.2016.02.020

Khalaf, et al. (2022). Flexural response of CFST beams with incorporated dcls. 2022 Advances in Science and Engineering Technology International Conferences (ASET). https://doi.org/10.1109/aset53988.2022.9734909

Roeder, C., Lehman, D. & Bishop, E. (2010). "Strength and Stiffness of Circular Concrete-Filled Tubes". *Journal of Structural Engineering, 136*(12). https://doi.org/10.1061/(ASCE)ST.1943-541X.0000263

Wang, et al. (2014). Flexural performance of rectangular CFST members. *Thin-Walled Structures, 79*, 154–165. https://doi.org/10.1016/j.tws.2014.02.015

Wu, et al. (2018). Axial loading tests of thin-walled circular steel tubes infilled with cast-in-place concrete and precast segments containing dcls. *Thin-Walled Structures, 127*, 275–289. https://doi.org/10.1016/j.tws.2018.02.008

Cite as: Khalaf S. & Abed F., "The Use of Demolished Concrete Lumps (DCL) in Rectangular CFSTs Under Flexure ", *The 2nd International Conference on Civil Infrastructure and Construction (CIC 2023)*, Doha, Qatar, 5-8 February 2023, DOI: https://doi.org/10.29117/cic.2023.0085

Marine Dredging Sediments Valorization in Self-Compacting Concretes

Walid Maherzi
University Lille, IMT Lille Douai, University Artois, JUNIA, UL, Laboratory of Civil Engineering and Geo-Environment,
Lille, France
walid.maherzi@imt-nord-europe.fr

Mahfoud Benzerzour
University Lille, IMT Lille Douai, University Artois, JUNIA, Laboratory of Civil Engineering and Geo-Environment,
Lille, France
mahfoud.benzerzour@imt-nord-europe.fr

Nor-Edine Abriak
University Lille, IMT Lille Douai, University Artois, JUNIA, Laboratory of Civil Engineering and Geo-Environment,
Lille, France
nor-edine.abriak@imt-nord-europe.fr

Ahmed Senouci
Department of Construction Management, College of Technology Building,
Texas, United States
asenouci@Central.UH.EDU

Abstract

Rock and eroded soil are transported by wind, tide, and human action (development works), and deposited as sediment in ports, estuaries, and rivers. The sediment accumulation at the bottom of ports disrupts maritime activities and disturbs the physicochemical balance of water bodies. As a result, dredging is necessary to reduce sediment deposits and restore the natural environment for proper port functioning. At the national level, the maintenance of the 6,500-kilometer French coastline would require the extraction of about fifty million cubic meters of marine sediment every year. These dredged sediments have been used in civil engineering applications for about ten years, in order to reduce their economic and environmental impact. The proposed study addresses the potential use of sediments to produce accropode blocks for maritime public works applications. It consists in developing concrete mixtures using dredged marine sediment treated to protect against erosion. A study of material characterization, optimization of the composition of the concrete formulation, as well as a determination of the mechanical, physical and durability properties of the concrete were necessary to validate the technical feasibility of this new solution. Around 700 small accropode blocks were then prepared to better analyze the structure stability against swell effects. The obtained results show that the sediments could not produce Self Compacting Concrete (SCC). However, sediment treatment with 6% by weight of cement has enabled the production of SCC. It is worth noting that the use of superplasticizer was essential to ensure concrete workability. Increasing the cement percentage has also improved the composite workability. Finally, a concrete compressive strength greater than 40 MPa has been achieved when using 300 kg/m^3 of treated sediments.

Keywords: Circular economy; Dredged sediments; Workability; Concrete; Valorization

1. Introduction

Materials that are produced as a result of rock and soil erosion are transported by climatic actions (wind, tides) and human actions (development works) and deposited as sediment in ports, estuaries,

and rivers. Sediment accumulation at the bottom of ports disrupts maritime activities and disturbs the physicochemical balance of water bodies. As a result, dredging is a necessary to reduce sediment deposits to restore the natural environment for proper port functioning. At the national level, the maintenance of the 6,500 kilometers of French coastline would require the extraction of about 50 million m^3 of marine sediments every year.

Even though considered as waste, these sediments have been used in civil engineering applications for several years. They have been used in road construction (Miraoui et al., 2012), brick manufacture (Achour et al., 2019), mortar and concrete production (Benzerzour et al., 2018), and cement production (Amar et al., 2018). Use of dredged sediments as a substitute for traditional aggregates could provide a number of advantages: improved management of dredged sediments, efficiency/ease of access to resources at site of use, and prevention of harm caused by the resource as it is used in its original environment.

This study explores the potential use of these sediments in the manufacture of accropode blocks for the protection of the coastline against the effects of swells (Figure 1). It consists of developing concrete mixes using marine dredged sediments that required sediment treatment, material characterization, concrete composition and formulation, and determination of concrete mechanical, physical, and durability properties. Around 700 small accropode blocks were then prepared to better analyze the structure stability against swell effects. The obtained results show that the raw sediments could not produce Self Compacting Concrete (SCC). However, sediment treated with 6% by dry weight of cement has enabled the production of SCC. It is worth noting that the use of superplasticizer was essential to ensure concrete workability. Increasing the cement percentage has also improved the composite workability. Finally, a concrete compressive strength larger than 40 MPa has been achieved when using 300 kg/m^3 of sediment.

2. Experimental Program

2.1. Materials

The cement used for this study is ordinary Portland cement CEM I 52.5R. Limestone fillers were used to improve the workability of self-compacting concrete by improving particle size distribution and to increaseconcrete strength of concrete especially at a young age. The limestone fillers were supplied by the Aucais factory (Urville – 14). They came in the form of an odorless powder with a light ochre color.

Three types of aggregates were used, namely 0/4 mm sand, 2/6 mm gravel, and 6/10 mm gravel. The particle size distribution is given in Figure 1 and the different characteristics of the aggregates used are given in Table 1 and Figure 1. The aggregates were dried in an oven at 105 ° C to a constant mass. Two concrete additives were used in the concrete mixtures. The first one was a superplasticizer, which was used to improve the fluidity of the mixture and act on the de-flocculation of the cement grains but also of all the fines present in the concrete. The second one was a hardening accelerator, which was added to reduce the setting time of cement due to sediments, and also to increase concrete early age strength.

Table 1: Aggregate physical properties

Physical Properties	Standard	S 0/4 mm	G 2/6 mm	G 6/10 mm
Actual density (kg/m^3)	NF EN 1097-6	2620	2571	2596
Bulk density (kg/m^3)	NF EN 1097-6	1469	1343	1357
Compacted bulk density (kg/m^3)	LCP method	1790	1473	1476

Bulk compactness	NF EN 1097-3	0.561	0.522	0.523
Compactness measured by shaking table	LCP method	0.683	0.573	0.569
Sand equivalent	NF EN 933-8	82.1	-	-
Water absorption coefficient (%)	NF EN 1097-6	0.40	1.22	0.70

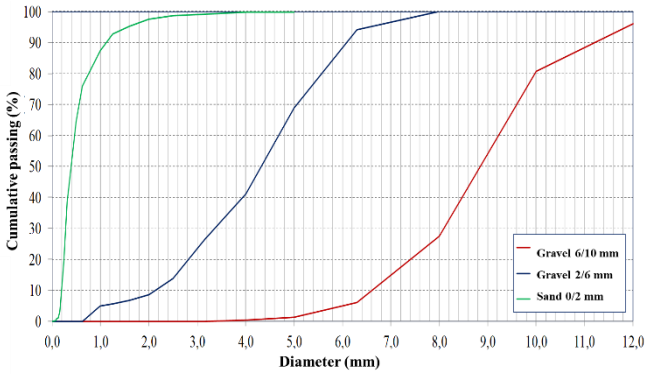


Fig. 1: Aggregate particle size distribution

The sediments were wet and stored in 100 L buckets. Table 2 summarizes the sediment density, organic matter content, particle size distribution and Atterberg limits..خطأ! لم يتم العثور على مصدر المرجع

Table 2: Dredged sediment physical properties

Physical properties		Values
Density (kg/m^3)		2545
Organic matter content (%)		7.02
Particle size distribution	D_{10} (µm)	5.4
	D_{50} (µm)	51.4
	D_{90} (µm)	235.3
	Average size (µm)	94.1
Atterberg limits	Liquidity limit w_L (%)	86.8
	Plasticity limit w_P (%)	40.4
	Plasticity index I_p	46.4

2.2. Dredged sediment treatment

To obtain a self-compacting concrete, the dredged sediments were treated with cement to reduce their shortcomings such as high water absorption, cohesion, and organic matter content as well as large specific surface area. The dredged sediments were treated as follows:

- Dried to a constant mass.
- Crushed to a fine powder.
- Dry-mixed using CEM cement I 52.5 R. 6% is the cement rate used for sediment treatment.
- Added water very slowly in the mixer while rotating. The amount of added water should be 25 to 28% of the dredged sediment mass. Water is added as slowly as possible, even by spraying, to obtain a porous and powdery mix.
- Dried the mix in an oven at 40°C to speed up drying.

The treated sediments included 74.1% of dredged sediment, 4.4% of cement, and 21.5% of water: 21.5%. These values make it possible to calculate the amount of treated sediment to be added to concrete using the amount of raw sediment.

2.3. Concrete preparation and specimen casting

100-liter concrete batches were prepared. The fresh properties were tested immediately after six minutes of mixing. After that, the molds were filled and vibrated for 5 minutes. All the molds were covered with plastic sheets and stored for 24 hours in the laboratory prior to demoulding. Then, they were cured at 20^0C and relative humidity (RH) of 80–95% until testing.

3. Testing Program

3.1. Fresh properties

The slump was measured using Abram's cone after each concrete batch according to EN 12350-8. Fresh mix percent entrapped air was measured using an 8L pressure gauge meter according to EN 12350-7 standard. The density was determined by measuring the mass and volume of the vibrated molds according to the NF EN 12350-6 and NF EN 12350-10.

3.2. Mechanical properties

Concrete compressive strengths were measured according to EN 12390-3. On the other hand, dry bulk densities were computed according to NF P18-459. Both tests were performed on hardened 100x200mm concrete cylinders.

3.3. Durability properties

The Water Accessible Porosity (WAP) of hardened concrete specimens was measured using vacuum saturation and hydrostatic balance according to NF P18-459 standard after curing periods of 28 and 90 days. For each concrete mix, two 100x200mm concrete cylinders were removed the 20-mm upper and lower portions and then sliced in three identical portions. The saturated surface dry state (SSD) of the specimens was obtained using vacuum saturation. Initially, the specimens were placed in a vacuum chamber with silica gel to decrease the contact angle of the water and dry pores in the specimens. The water was introduced in the chamber after 4 hours to immerse the specimens and the vacuum was kept on for an additional 44 hours. The WAP was obtained from the mass of SSD specimens measured in air and in water, and that of oven dried at 105 C specimens.

3.4. Formulation and Implementation of Cementitious Composite with and without Dredged Sediments

- **Control Concrete Mix Designs (without sediments)**

Table Three control concrete mixes were designed (BT1, BT2 and BT3). The aggregate quantities for the control concretes were computed based on the granular stacking (MEG) method. A mix design with maximum compactness was retained for the control concretes, namely, 45% of sand, 18% of gravel#1, and 37% of gravel#2. Table 3 summaries the control concrete mix designs. Table 4 summarizes the concrete properties in the fresh and hardened states.

Table 3: Control concrete design mixes (without sediment)

Mixtures	**BT1**	**BT2**	**BT3**
Cement (kg/m^3)	338	361	368
Limestone filler	113	120	123
Equivalent binder	365	391	399
Efficient water	152	162	147
Gravel 2/6 mm	329	319	325
Gravel 6/10 mm	675	655	668
Sand 0/4 mm	821	797	812

Superplasticizer concrete additive (kg/m^3)	5.4	5.8	5.9
Setting accelerator concrete additive (kg/m^3)	7.8	8.3	8.5
Effective E/C ratio	0.45	0.45	0.40

Table 4 shows that BT3 concrete exhibited increased performance. Thus, BT3 was chosen as the reference for the composition of sediment concrete with and without treatment.

Table 4: Control concrete mechanical properties

State	**Physical properties**		**BT1**	**BT2**	**BT3**
Fresh condition	Air content (%)		3.8	3.3	3.5
	Abrams cone spread (cm)		71.0	70.0	67.5
	Waiting time 50cm spreading (s)		5.5	6.5	5.0
	Box L	Ratio H_1/H_2	0.91	0.90	0.90
		Time T_1 (s)	5.1	1.5	1.5
		Time T_2 (s)	6.9	2.5	4.8
	Fresh density (kg/m^3)		2387	2409	2397
Hardened state	Compressive strength at 28 days (MPa)		53.8	59.6	74.3
	28-day tensile strength (MPa)		4.7	4.9	5.3
	Dry bulk density (kg/m^3)		2282	2307	2292
	Porosity accessible to water (%)		12.4	11.9	11,5
	Static Elastic Modulus (GPa)		41.0	41.9	43.4
	Dynamic Elastic Modulus (GPa)		44.3	44.2	44.8
	Total Shrinkage at 90 days (μm/m)		288	298	288
	Total mass loss after 90 days of drying (%)		0.95	0.85	0.63

- **Dredged Sediment Based Concrete Mix Designs**

Several wastes were tested to achieve the performance of a self-compacting concrete having a 28-day compressive strength greater than 40 MPa. Two design approaches were implemented. The sand was substituted with dredged sediment in the first approach. On the other hand, limestone filler was totally replaced with the dredged sediments.

First approach: 30% by weight of the sand was replaced by dredged sediments. Table 5 summarizes the mix design of sediment-based concrete batches, which were named BS (Sediment Concrete).

Table 5: First approach concrete design mixes

Parameters	**BS1***
Cement (kg/m^3)	368
Limestone filler (kg/m^3)	123
Equivalent binder (kg/m^3)	399
Effective water (kg/m^3)	222
Gravel 2/6 mm (kg/m^3)	325
Gravel 6/10 mm (kg/m^3)	668
Sand 0/4 mm (kg/m^3)	568
Superplasticizer concrete additive (kg/m^3)	14.7
Setting accelerator concrete additive (kg/m^3)	8.5
Sediment noise (kg/m^3)	244
Effective E/C ratio	0.65

* BS1: concrete with 30% sediment.

The workability of BS1 concrete did not have self-compacting properties even with E/C ratio = 0.65 and 4.0% of the superplasticizer. For these reasons, BS1 concrete was excluded from this study.

Second approach: The grain size of the sediment particles is almost equivalent to limestone filler. Therefore, limestone fillers were substituted by dry raw sediment (a substitution of 100% mass). The superplasticizer additive concrete was used instead of setting accelerator concrete additive for a better performance in the de-flocculation of cementitious particles. Tables 6 and 7 summarize the composition and the properties of the second approach concrete design mixes, respectively.

Table 6: Concrete formulation according to Approach 2

Composition (kg/m^3)	**BS2**
Cement	368
Equivalent binder	368
Efficient water	209
Gravel 2/6 mm	325
Gravel 6/10 mm	668
Sand 0/2 mm	812
Superplasticizer concrete additive	11.3
Setting accelerator concrete additive	8.5
Raw sediments	123
Effective E/C ratio	0.58

Table 7: Concrete characteristic where sediment replaces limestone filler

BS2	
Characteristics	Value
Occluded air content (%)	6.5
Abrams cone subsidence (cm)	9.3
Fresh density (kg/m^3)	2234
Compressive strength at 28 days (MPa)	39.2
28-day tensile strength (MPa)	3.5
Shrinkage at 90 days (µm/m)	616
Total mass loss after 90 days of drying (%)	1.24

In the two approaches, the cement treatment was necessary for achieving self-compacting workability.

- **Cement-treated sediment-based concrete mix**

In this part of the study, the concrete mix included a partial replacement by mass (5, 10, 15 and 20%) of fine and coarse aggregates with treated sediments. The amount of binder was increased by 20% to improve the workability of concrete mix. Table 8 summarizes the treated sediment-based concrete mixes. On the other hand, Table 9 summarizes the main characteristics of these concrete mixes.

Table 8: Concretes mixes with treated sediments partially replacing aggregates

Composition	**BS3 –** 5.0%		**BS4 –** 10.0%		**BS5 –** 15.0%		**BS6 –** 20.0%	
	F.I	F.F.	F.I	F.F.	F.I	F.F.	F.I	F.F.
Cement (kg/m^3)	407	373	447	381	540	423	590	441
Limestone filler (kg/m^3)	136	124	149	127	180	141	197	147
Equivalent binder (kg/m^3)	441	404	484	413	585	549	639	478
Effective water (kg/m^3)	186	170	246	210	297	233	325	242
Gravel 2/6 mm (kg/m^3)	309	283	292	249	276	216	260	194
Gravel 6/10 mm (kg/m^3)	634	581	601	512	576	451	534	399
Sand 0/4 mm (kg/m^3)	771	706	730	623	689	541	649	485
Superplasticizer 1(kg/m^3)	6.5	6.0	7.2	6.1	8.6	6.8	9.4	7.1
Superplasticizer 2 (kg/m^3)	8.1	7.5	8.9	7.6	10.8	8.5	11.8	8.8
Raw sediment (treated) (kg/m^3)	90	83	180	154	271	212	361	270

Raw sediment/aggregates (%)	5.0	10.0	15.0	20.0
Treated sediment/BT3 aggregates (%)	6.8	13.5	20.3	27.0
Effective W/C ratio	0.46	0.55	0.55	0.55

Table 9: Characteristics of concrete mixes with treated sediments partially replacing aggregates

State	Characteristics		**BT3 –** 0.0%	**BS3 –** 5.0%	**BS4 –** 10.0%	**BS5 –** 15.0%	**BS6 –** 20.0%
Fresh condition	Occluded air content (%)		3.5	3.6	3.0	3.2	4.2
	Abrams cone spread (cm)		67.5	81	68	71	65
	Time for 50cm spreading (s)		5.5	0.88	1.98	1.53	2.09
	Box L	Ratio H_1/H_2	0.90	0.91	0.87	0.91	0.91
		Time T_1	1.5	0.8	1.1	0.8	1.1
		Time T_2	4.8	1.9	2.0	1.9	2.0
	Fresh density (kg/m^3)		2397	2324	2261	2222	2182
Hardened State – Physics and Mechanics	Compressive strength at 28 days (MPa)		74.3	59.7	50.5	45.9	44.6
	28-day tensile strength (MPa)		5.30	4.09	3.78	3.59	3.40
	Dry bulk density (kg/m^3)		2292	2222	2147	2088	2052
	Porosity accessible to water (%)		11.5	14.6	16.6	19.3	20.3
	Static Elastic Modulus (GPa)		43.4	36.3	30.3	26.7	22.6
	Dynamic Elastic Modulus (GPa)		44.8	39.7	35.3	31.7	30.4
	Shrinkage at 90 days (μm/m)		288	468	656	834	966
	Total mass loss drying (%)		0.64	1.01	1.34	1.74	1.74

We can conclude that treated sediment-based concretes meet the specifications initially planned. The compressive strength of all these concretes is greater than 40 MPa and the spreading of these concretes is greater than 60 cm. The flow time at t_{50} and the filling ratio H1/H2 are also satisfactory. The BS3, BS4, BS5 and BS6 concretes meet the requirements of self-compacting concretes.

4. Conclusion

The study addressed the potential use of dredged sediments to produce accropode blocks for maritime public works applications. Concrete mixes were developed using dredged sediments that required treatment, material characterization, concrete composition and formulation, and determination of concrete mechanical, physical, and durability properties.

The study has the following conclusions:

- The dredged sediment is not favorable for obtaining a self-compacting concrete,
- The treatment of sediments with cement at 6% by weight achieves a self-compacting concrete,
- To ensure the workability of concrete, the use of concrete additive, such as superplasticizer, is essential,
- Increasing the quantities of cement in concrete mix improves the workability of the composite,
- Using 300 kg/m^3 of sediment allows the concrete to reach a compressive strength greater than 40 MPa.

The obtained results of this study show the feasibility of using sediments in the formulations of self-compacting concretes (SCC). Nevertheless, this study should be complemented by an estimate of the economic impact as well as a life-cycle analysis in order to develop on an industrial scale this new sector for the recovery of dredging sediments.

References

Emmanuel, et al. (2015). Valorization of sediments in self-consolidating concrete: mix-design and microstructure. *Construction and Building Materials*. Vol. 81, pp.1–10. doi: https://doi.org/10.1016/j.conbuildmat.2015.01.080.

Junakova, N., Jozef, J. & Magdalena, B. (2015). Reservoir sediment as a secondary raw material in concrete production. *Clean Technologies and Environmental Policy*, Vol. 17, pp.1161-1169. doi: https://doi.org/10.1007/s10098-015-0943-8.

Mahfoud et al. (2018). Formulation of mortars based on thermally treated sediments. *Journal of Material Cycles and Waste Management*, Vol. 20, pp. 592-603. doi: https://doi.org/10.1007/s10163-017-0626-0.

Mohamed, M., Rachid, Z. & Nor-Edine, A. (2012). Road material basis in dredged sediment and basic oxygen furnace steel slag. *Construction and Building Materials*, Vol. 30, pp. 309-319. doi: https://doi.org/10.1016/j.conbuildmat.2011.11.032.

Raouf, et al. (2019). Durability study of concrete incorporating dredged sediments, *Case Studies in Construction Materials*, vol. 11, pp 841–847. DOI: https://doi.org/10.1016/j.cscm.2019.e00244.

Zhao, et al. (2018). Use of uncontaminated marine sediments in mortar and concrete by partial substitution of cement. *Cement and Concrete Composites*, Vol. 93, pp. 155-162. doi: https://doi.org/10.1016/j.cemconcomp.2018.07.010.

Cite as: Maherzi W., Benzerzour M., Senouci A. & Abriak N., "Marine Dredging Sediments Valorization in Self-Compacting Concretes", *The 2nd International Conference on Civil Infrastructure and Construction (CIC 2023)*, Doha, Qatar, 5-8 February 2023, DOI: https://doi.org/10.29117/cic.2023.0086

Self-compacting Backfills using Fly Ash and Dredged Marine Sediments for Public Work Applications

Walid Maherzi
University Lille, IMT Lille Douai, University Artois, JUNIA, Laboratory of Civil Engineering and Geo-Environment, Lille, France
walid.maherzi@imt-nord-europe.fr

Mahfoud Benzerzour
University Lille, IMT Lille Douai, University Artois, Laboratory of Civil Engineering and Geo-Environment, Lille, France
mahfoud.benzerzour@imt-nord-europe.fr

Nor-Edine Abriak
University Lille, IMT Lille Douai, University Artois, Laboratory of Civil Engineering and Geo-Environment, Lille, France
nor-edine.abriak@imt-nord-europe.fr

Ahmed Senouci
Department of Construction Management, College of Technology Building, Texas, United States
asenouci@Central.UH.EDU

Abstract

Sediment accumulation at the bottom of ports disrupts maritime activities and disturbs the physicochemical balance of water bodies. In France, the maintenance of the 6500-kilometer long coastline would require the extraction of about 50 million m^3 of marine sediments every year. For several years, these sediments were considered waste. However, they are increasingly being acknowledged as a resource in need of management. Several research studies were conducted to find valorization ways that satisfy technical and regulatory requirements. These sediments present interesting heterogeneous physicochemical, mineralogical, and geotechnical characteristics. However, they may contain contamination, which could limit their uses. This paper deals with the possibility of producing self-compacting backfills using dredged marine sediments, fly-ash, and hydraulic binders for public work applications. The impact of dredged sediments on the composition of self-compacting backfills was studied. Moreover, the impact of fly ash and binder type and percentage on the backfill behavior and mechanical properties was discussed.

Keywords: Sediment; Valorization; Sustainable materials; Backfill; Waste management

1. Introduction

The accumulation of sediments in ports for several years causes capacity- and efficiency losses, which emphasize the importance of sediment dredging management in the world. For example, the European countries generate sediment-dredged volumes of 100 and 200 million cubic meters per year (Maherzi et al., 2018). Placing dredged sediments in landfills, which is expensive, is only practiced when there are no other solutions (Maherzi et al., 2018). However, dredged sediments can be considered as alternative resources rather than waste (Brahim et al., 2022). With the current limited availability of high-quality aggregates, using dredged sediments as a construction material can optimize their future management (Maherzi et al., 2018).

The suitability of using dredged sediments in lightweight aggregate production has been reported in the literature due to their perpetual availability, homogeneity, and mineralogical and chemical composition (Liu et al., 2018; Ennahal et al., 2021). Dredged sediments have also been used in brick production (Brahim et al., 2022; Slimanou et al., 2019). The replacement of 15% of quartz sand with sediments has resulted in a 63% increase in compressive strength and a 10% decrease in porosity (Ouédraogo et al., 2021). The compressive strength of bricks passed the very strict grade requirements of the American Society for Testing and Materials (ASTM) requirements when 50% of their natural making clay was replaced by dredged sediments (Wang et al., 2018). Ouédraogo et al. (2021) have studied replacing up to 19% of sand with dredged sediments in construction. Benzerzour et al. (2018) have studied mortar compressive strength and weight loss for cement partial substitution of dredged sediments at 5%, 10%, 15% and 20% by mass. The results showed that a 15% substitution of cement by dredged sediments was most suitable for mortars (Benzerzour et al., 2018).

This paper studies the suitability of self-compacting backfill materials using dredged marine sediments, fly-ash, and hydraulic binders for heavy construction applications. The impact of self-compacting backfill composition including type and percentage of fly ash and binder on its physical and mechanical properties is discussed.

Self-compacting backfills are usually injected with pressure to fill cracks, cavities, or ground interstices to improve the mechanical performance and hydraulic characteristics of the soil. In general, backfill stability decreases when its fluidity increases due to water content.

2. Materials and Methods

2.1. Materials

The physicochemical, geotechnical, and mineralogical characteristics of backfill materials are described as follows.

- **Sediments:** The dredged marine sediments were collected from Dunkirk port (France). Table 1 summarizes the sediment physicochemical properties.

Table 1: Sediment physicochemical characteristics

Average water content w (%)	22.35
Average organic content (%)	9.10
Plasticity index PI (%)	13.00
Blue methylene value (g/100g)	2.99
Density of solid grains (t/m^3)	2.44
Grains < 2µm	3.00
2µm < Grains < 63µm	72.00
63µm < Grains	25.00

- **Fly ash:** fly ash, which was taken from Eurovia Harnes site, was composed mainly of silica (SiO_2) and alumina (Al_2O_3). Other elements such as iron oxide (Fe_2O_3/FeO_4) and lime are also present to a lesser extent.
- **Fiber:** Polypropylene fibers are ideal additives in cementitious mixes to reduce plastic withdrawal and cracking and to improve surface properties. The mechanical properties of the fibers that had an average size of 12mm, are shown in Table 2.

Table 2: Polypropylene fibre characteristics

Characteristics	**Values**
Elastic modulus	3500 – 3900 N/mm^2
Extensibility	320 – 400 N/mm^2
Melting point	160 – 170 °C
Electrical conductivity	0

- **Hydraulic binders:** Three hydraulic binders were used: Cement CEM I 52.5 N, cement CEMI 52.5 PM-ES and Road hydraulic binder RolacPI LH.
  - **ROLAC® PI:** It is a hydraulic binder containing clinker to speed up trafficability after the completion of fills and platforms. The binder ROLAC PI LH consists of more than 60% of lime and 20% of silica dioxide (SiO_2).
  - **Cement CEM I 52.5 N:** This cement is comprised between 95% and 100% of clinker, up to 5% of secondary components, and a small quantity of calcium sulphate to ensure product regularity. The initial setting time, measured at a temperature of 20°C, is greater than 40 min. The density is of about 3.12 g/cm^3, and the compressive strengths, determined based on NF EN 196-1, shows that the compressive strength at 28 days is 62 MPa.
  - **Cement CEM I 52.5 PM-ES:** this cement type is used for concrete products and backfills that would be exposed to aggressive environment, such as maritime environment, zones of marling and water with high sulphate contents, freezing and thawing, and acid medium. The cement produces high-strength concrete after 28 curing days with limited sulphide content.

2.2. Methodology

Several adopted mix designs were optimized for backfill applications, such as trench backfill materials, by improving strength and handling easiness. The essential criteria to satisfy backfill applications are listed below:

- Specimen spread out due to own weight must lie between 350 mm and 500 mm.
- Bearing Capacity Index (IBI) must reach a value of at least 10 within 24 hours to speed up the return to circulation.
- 28-day unconfined compressive strength (UCS) values must lie between 0.5 MPa and 1MPa to ensure material easy handling.
- Slump values must reach at least 15 cm for better drain coating.
- Adequate compressive strength after immersion for better material behavior with water.

Ten mix designs were used to evaluate the impacts of hydraulic binder types and contents on backfill application criteria. The mixes contained 30 % of sediment and 70% of fly ash and cement, respectively. The reference mixture (control) did not contain dredged sediments.

Furthermore, three mix designs containing different type of cement and dredged sediments were tested using a water to cement ratio of 1:2 (W/C=0.5). The dredged sediment percentage was obtained by studying the interaction between sediment and cement.

3. Results and Discussion

3.1. Mechanical study

3.1.1. Sediment and Cement Mix Behavior

Figure 1 shows the variation of the mix mechanical strength with the Sediment / Cement (S/C) ratio. Increasing the (S/C) ratio has adversely affected the mix mechanical properties. Indeed, increasing the (S/C) ratio from 0.2 to 0.8 has decreased the mix mechanical strength by about 67 %, which may be due to the sediment chemical disruptive elements on cement setting such as sulphates and chlorides.

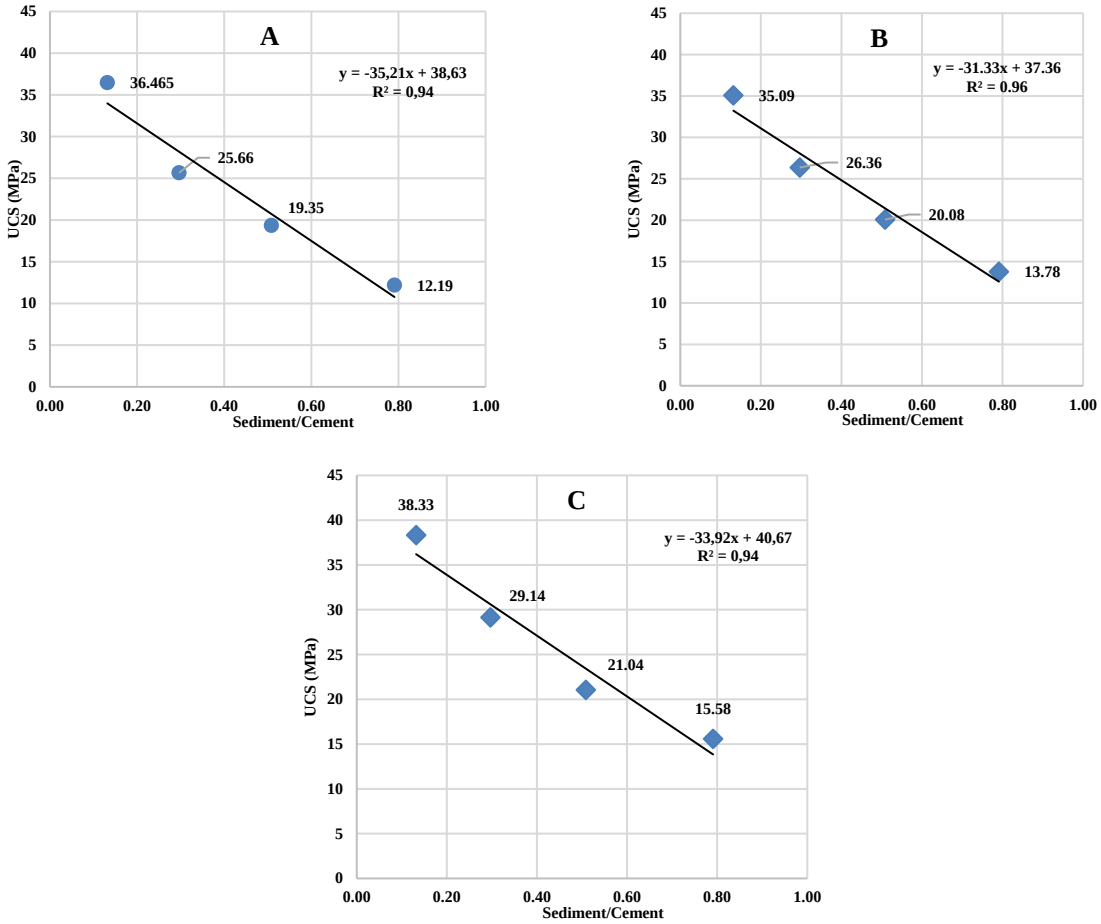


Fig. 1: Mix mechanical strength versus S/C ratios (A: Cement CEM I 52.5 N, B: Cement ROLAC PI LH, C: Cement CEM I 52.5 PM ES)

3.1.2. Abrams Cone Slump

The test, which is defined by standard NF P 18-451, determines four consistency levels according to the slump 10 minutes after pouring. The results presented in Table 3 show that the binder ROLACPI LH gives the best fluidities compared to the other two cements. This can be explained by its low water demand because it is composed of more than 40% blast furnace slag. The formulations were classified according the consistency results.

Table 3: Slump test results

Rate of cement (%)	ROLACPI LH (cm)	CEM I PM (cm)	CEM I N (cm)
6	20.5	18.0	20.0
8	22.0	20.0	24.0
10	24.0	19.5	19.0

3.1.3. Bearing capacity index

The Bearing Capacity Index (IBI) is determined using the following equation:

$$IBI=p/ps\ .100\% \quad (1)$$

Where p = measured pressure for binders [N/mm^2] and ps = pressure to achieve equal penetration on standard crushed stone [N/mm^2]

Table 4 summarizes the IBI results for the various mixes after 24 and 72 hours. All tested mixes satisfied the fluidity criterion. These results can be attributed to the compactness on granular media composed of 30% sediment and 70% fly ash (Ennahal et al., 2021).

Table 4: Bearing index results for different mixtures

	ROLACPI LH		CEM I 52.5 PM		CEM I 52.5 N	
Rate of cement (%)	CBR (24h)	CBR (72h)	CBR (24h)	CBR (72h)	CBR (24h)	CBR (72h)
6	26.98	35.58	15.15	32.45	22.76	29.96
8	54.14	64.64	18.30	39.85	22.90	32.30
10	56.50	65.70	23.00	41.81	34.96	44.94

3.1.4. Unconfined Compression Strength

The unconfined compressive strength values (UCS) represent the average of measures taken from three samples. The standard deviation of measurements varied between 0.01 and 0.10 MPa. The compression strength results for the tested samples are shown in Figure 2. They show that increasing cement substitution rates increased the compressive strengths of the tested mixes. It is worth noting that the mixes prepared with cement Rolac PI showed the best mechanical performance compared with those prepared with the cements CEM I 52.5PM and CEM I 52.5 N. This can be explained by the fact that cements containing blast furnace slags are more resistant to chemical elements contained in sediments such as heavy metals, chlorides, sulfates, etc. (Maherzi et al., 2018).

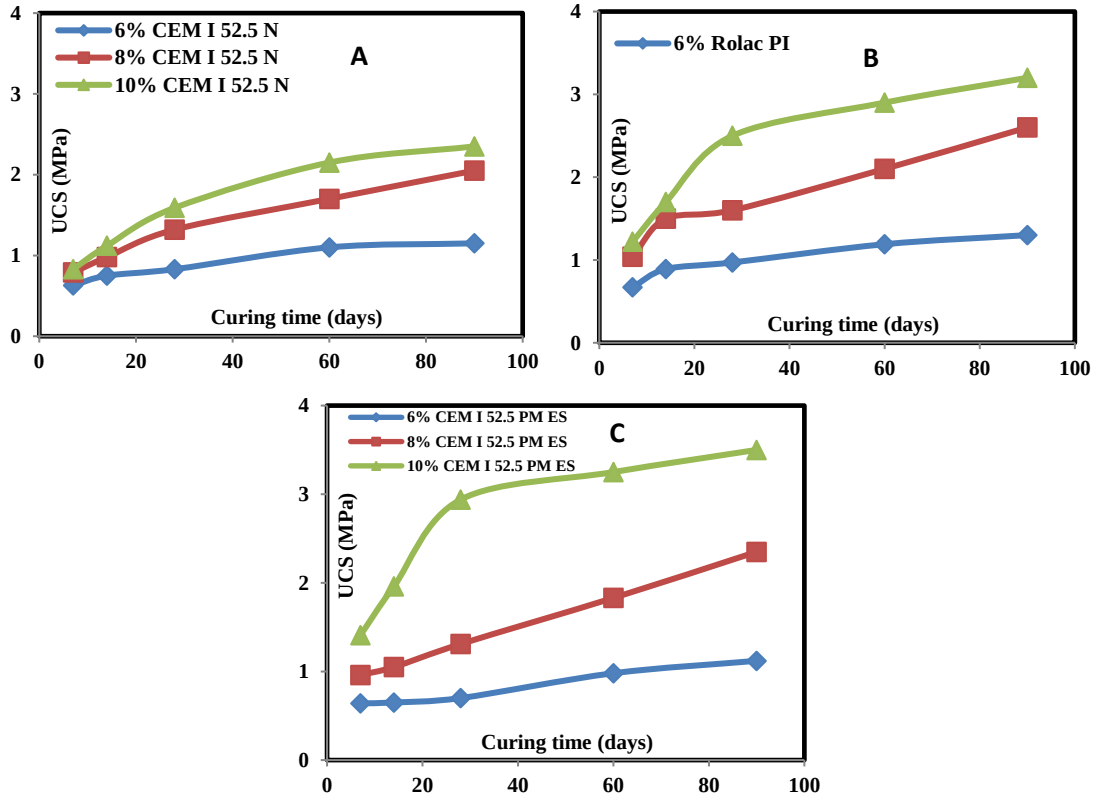


Fig. 2: Compressive strength of various prepared mixes (A: Cement CEM I 52.5 N, B: Cement ROLAC PI LH, C:

Cement CEM I 52.5 PM ES)

3.2. Environmental study

The environmental study was carried out on backfill blocks using the cement ROLAC PI. The blocs were permanently watered and their runoff water was recovered (Figure 3). The runoff water samples, which were recovered after 7, 28, and 60 days, were environmentally analyzed.

Table 5 summarizes the environmental analysis results obtained on the recovered water samples. The environmental analysis results show that the concentration of the leachate environmental elements remain low and did not change drastically with time. Moreover, there were no major changes in the concentrations of the detected elements. Indeed, the use of hydraulic binders prevented the contaminants from the hydration-formed products, which helped mix stability in the short and medium terms.

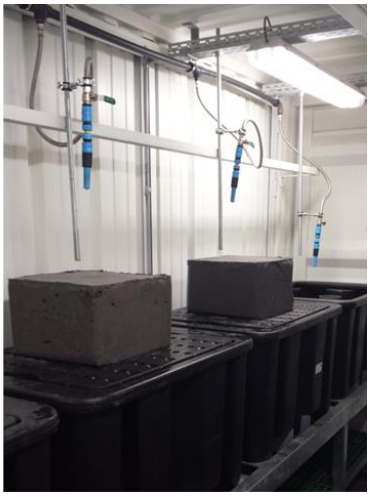


Fig. 3: Grout block leaching test

Table 5: Environmental analysis results

		With sediment			**Without sediment**			**Thresholds of inert waste**	
Analysis	**Unit**	**7**	**28**	**60**	**7**	**28**	**60**		
PAH	µg/l	<1	<1	<1	<1	<1	<1	-	µg/l
PCB	µg/l	<0,07	<0,07	<0,07	<0,07	<0,07	<0,07	-	µg/l
COT	mg/l	3,2	2,8	3,4	3,0	3,0	3,5	-	µg/l
Heavy metals									
Arsenic	µg/l	<5	<5	<5	<5	<5	<5	10	µg/l
Cadmium	µg/l	<0,20	<0,20	<0,20	<0,20	<0,20	<0,20	5	µg/l
Chrome	µg/l	5,9	3,7	2,9	<1	<1	<1	50	µg/l
Copper	µg/l	8,6	<2,0	7,1	5,9	4,6	4,9	50	µg/l
Mercury	µg/l	<0,05	<0,05	<0,05	<0,05	<0,05	<0,05	2000	µg/l
Lead	µg/l	<2,0	<2,0	<2,0	<2,0	<2,0	<2,0	50	µg/l
Nickel	µg/l	<3	<3	<3	<3	<3	<3	20	µg/l
Zinc	µg/l	29	21	10	17	13	11	5000	µg/l

4. Conclusion

The accumulation of sediments at the bottom of ports disrupts maritime activities and disrupts the physicochemical balance of water bodies. For several years, these sediments were considered waste. However, several research studies have been carried out to find ways of valorization that meet

technical and regulatory requirements. The research presented in this article examines the suitability of self-compacting embankments using dredged marine sediments, fly ash and hydraulic binders for heavy construction applications. The impact of dredged sediments on the composition of self-compacting embankments has been studied. In addition, the impact of the type and percentage of fly ash and binder on the backfilling behavior and mechanical properties was discussed. According to the results presented above, the following conclusions can be addressed:

1. According to the consistency standard of cementitious materials, the set of self-compacting grouts are qualified as fluid (slump>160mm).
2. The values of the bearing index are greater than 15 after 24 hours of hardening, and greater than 30 after 72 hours of hardening.
3. ROLAC cement comprised of 40% blast furnace slag, has the highest IBI values compared to other cements.
4. After 28 days of normal cure, the self-compacting backfills using ROLAC PI cement had compressive strength values comprising between 0.97 MPa and 2.5 MPa.
5. The results of accelerated environmental monitoring of the tested formulations show the safety of these new materials.

Based on the obtained test results, self-compacting embankments seem to be a promising means of recovery of dredged sediments that meet technical and regulatory requirements.

References

Benzerzour, et al. (2018). Formulation of mortars based on thermally treated sediments. *Journal of Material Cycles and Waste Management, 20*(1), pp.592-603. DOI: https://doi.org/10.1007/s10163-017-0626-0

Brahim, et al. (2022). Valorization of Dredged Sediments in Manufacturing Compressed Earth Blocks Stabilized by Alkali-Activated Fly Ash Binder. *Buildings, 12*(4), pp. 419. doi: https://doi.org/10.3390/buildings12040419

Ennahal, et al. (2021). Performance of lightweight aggregates comprised of sediments and thermoplastic waste. *Waste and Biomass Valorization, 12*(1), pp. 515-530. doi: https://doi.org/10.1007/s12649-020-00970-1

Lei, et al. (2018). Recycling dredged sediment into fill materials, partition blocks, and paving blocks: Technical and economic assessment. *Journal of Cleaner Production, Vol. 199*, pp. 69-76. doi: https://doi.org/10.1016/j.jclepro.2018.07.165

Liu, et al. (2018). Effects of sintering temperature on the characteristics of lightweight aggregate made from sewage sludge and river sediment. *Journal of Alloys and Compounds, 748*, pp. 522-527. doi: https://doi.org/10.1016/j.jallcom.2018.03.216

Maherzi, et al. (2018). Beneficial reuse of Brest-Harbor (France)-dredged sediment as alternative material in road building: laboratory investigations. *Environmental technology, 39*(5), pp. 566-580. doi: https://doi.org/10.1080/09593330.2017.1308440

Ouédraogo, et al. (2021). Environmental assessment, mechanical behavior, and chemical properties of self-compacting mortars (SCMs) with harbor dredged sediments to be used in construction. *Environmental Science and Pollution Research, 28*(39), pp. 55003-55013. doi: https://doi.org/10.1007/s11356-020-12279-6

Slimanou, et al. (2020). Harbor-Dredged Sediment as raw material in fired clay brick production: Characterization and properties. *Journal of Building Engineering, Vol. 28*, pp.101085. doi: https://doi.org/10.1016/j.jobe.2019.101085

Cite as: Maherzi W, Benzerzour M., Abriak N. & Senouci A., "Self-compacting Backfills using Fly Ash and Dredged Marine Sediments for Public Work Applications", *The 2nd International Conference on Civil Infrastructure and Construction (CIC 2023)*, Doha, Qatar, 5-8 February 2023, DOI: https://doi.org/10.29117/cic.2023.0087

Sustainability Driven Strategy for Achieving Sustainable Infrastructure: Musaimeer Pumping Station and Outfall Project

Dila Ersenkal
Technical Principal, Environment & Sustainability Lead, Mott MacDonald, Doha, Qatar
dila.ersenkal@mottmac.com

Gary Peach
Project Manager, Mott MacDonald, Doha, Qatar
gary.peach@mottmac.com

Biliana Paskova
QA/QC Manager, HBK-PORR JV, Doha, Qatar
b.karamukova@auccqatar.com

Abstract

The increasing emphasis on global sustainability issues such as climate change, loss of biodiversity, deforestation, and water scarcity has provided a strong mandate for the construction industry to incorporate sustainable practices, more efficient processes and innovative technologies to deliver sustainable project outcomes. Implementing sustainability rating and assessment schemes throughout the lifecycle of projects has been instrumental in achieving high levels of environmental and social performance. This paper presents a case study; the Musaimeer Pumping Station and Outfall (MPSO) project, a strategic asset for Qatar, and discusses the sustainability strategy adopted for achieving the 'Very Good' level Civil Engineering Environmental Quality and Assessment Award Scheme (CEEQUAL) certification for the project. The paper sets out how the project's registration with CEEQUAL International resulted in achievement of sustainability best practice in design and construction phases. Specific achievements with regards to the key CEEQUAL topic areas including project strategy, project management, people and communities, land use and landscape, historic environment, ecology and biodiversity, water environment, physical resources use and management (such as energy, water, materials), and transport are also highlighted in this paper. The paper also provides the importance of the adopted strategy in translating the overarching Qatar National Vision 2030 and alignment with the United Nations (UN) Sustainable Development Goals (SDGs). The challenges faced throughout the project lifecyle and the benefits achieved by undertaking a CEEQUAL assessment for this project are also discussed in this paper.

Keywords: Sustainability; Infrastructure; CEEQUAL; SDGs

1 Introduction

Musaimeer pumping station and outfall (MPSO) project is designed to manage surface and rainwater received from the drainage networks from 270 km² of urban areas in southern Doha, which has witnessed rapid urbanization and has experienced heavy rains over the recent years. To address the urbanization challenges and to alleviate the flooding in the catchment area, MPSO project has been designed. The project includes a pumping station with a capacity of 19.7 m^3/s, a 10.2 km long, 3.7 m internal diameter under seabed outfall tunnel, an offshore riser shaft and 84 port diffuser field. MPSO project organization comprises of Ashghal, Qatar's Public Works Authority (PWA), Project Management Consultant (PMC), Mott MacDonald and HBK-PORR, the main Contractor.

2 PROJECT ACHIEVEMENTS

2.1 Strategy

The key objective of the MPSO project was to build a sustainable asset, achieving a minimum 'Good' rating level with Civil Engineering Environmental Quality and Assessment Award Scheme (CEEQUAL), and delivering social, environmental and economic benefits. To achieve this objective, the MPSO project adopted a sustainability-driven strategy, registering the project with CEEQUAL and implementing a wide range of practices that led to sustainability outcomes. The project has focused on the following practices throughout the project lifecycle:

- Assessing the impact of climate-change and consideration of future projections
- Minimizing the carbon footprint of the project
- Minimizing the impact on the environment and the communities
- Utilizing innovative technologies to enhance resource consumption
- Achieving financial savings and commercial benefits.

2.2 People and Communities

The southern and western areas of Doha have been experiencing a rapid urbanization in recent years. As a consequence, the need to increase the drainage capacity to accommodate additional storm-water runoff and construction activities has become critical. The MPSO project is built to increase the drainage capacity within Doha to accommodate storm-water runoff, addressing potential flooding risks, and enhancing the communities' living quality and to minimize the potential adverse impacts of flooding on the residents and communities of Doha, as well as minimizing negative impacts on the environment, particularly the marine ecosystems. The site selection for the MPSO project was carried out strategically to ensure that the location of the pumping station was remote from the residential communities eliminating the potential environmental impacts. Furthermore, a rigorous site-wide environmental monitoring programme has been implemented throughout the construction phase to mitigate the potential environmental and social impacts.

2.3 Land Use and Landscape

The following 'land use and landscape' measures were implemented by the MPSO project:

- A comprehensive Environmental Impact Assessment (EIA) was carried out.
- 22 design alternatives were assessed for disposing of storm and ground water to ensure the optimal solution was chosen in terms of engineering viability, cost effectiveness, operational efficiency, environmental impact and climate-resilience.
- A 10. 2km-long outfall tunnel was constructed 15m below the seabed by Tunnel Boring Machine (TBM) to avoid seabed disturbance of seabed.
- Geotechnical studies have been carried out to assess the potential geotechnical hazards and risks; associated mitigation measures were established and implemented.
- Comprehensive Hazard and Operability Study / Control Hazard Operability Study (HAZOP/CHAZOP) were undertaken to assess the severity and the likelihood of flooding hazards and the adverse impacts on the equipment, materials, buildings, and other assets. Associated mitigation measures were established and implemented.
- The pumping station was designed for flood resilience; integrating measures to address potential flooding risks from a 1-in-50-year storm event.

2.4 Historic Environment

The status of the historic environment of the project site was assessed during the Environmental Impact Assessment (EIA) process to determine the presence of any features that are of archaeological, historical and cultural nature and value, which may be adversely affected by the project activities. As on outcome of the rigorous engagement and consultation held with the local authorities, and the baseline studies carried out, the project site was determined to be of no archaeological, cultural, or historical nature and value.

2.5 Ecology and Biodiversity

The following 'ecology and biodiversity' measures were implemented by the MPSO project:

- Sensitive receptors around the MPSO project and their proximity to the site location were identified and considered for design options.
- Out of all 22 design options, the project selected an outfall chamber with the least potential to have an impact on the environment and the communities.
- The outfall chamber was extended from 7 km to 10. 2 km, to increase the distance from the sensitive receptors.
- Instead of an outfall pipeline with dredged trench on the seabed, the project considered the construction of an outfall chamber below the seabed, to minimize the potential adverse impacts on the marine ecology.
- A detailed Biodiversity and Ecology Management Plan was developed and implemented.
- A comprehensive environmental management and monitoring program (that included air quality, noise, water quality, marine water quality management and monitoring) was implemented for monitoring and management of identified ecological features on and around the project footprint.
- Acacia trees located nearby the site were preserved.
- Birds' and honeybees' colony observed on site were protected.

2.6 The Water Environment

The following measures were implemented by the MPSO project for the protection and enhancement of the 'water environment':

2.6.1 Storm Water and Ground Water during Operation

As per the design requirements, the MPSO pumping station is equipped with mechanical process equipment such as bar screens, grab rake mechanism, grit collection system & grit classifier, and oil & grease removal system to achieve high level primary treatment to remove debris, grit, oil & grease. This allows the collected storm water runoff to be discharged into the marine environment after going through primary treatment.

2.6.2 Marine Water

During the operation of the MPSO project, the storm and groundwater from Abu Hamour tunnel will be discharged 10.2 km offshore via the outfall chamber. To ensure that the marine environmental conditions are not affected by the discharge of this water, it was key to understand the existing seawater quality baseline data throughout the design & build phase, evaluating the trends and to compare with the operational data. To gather this information, a comprehensive seawater quality program was established. The program included establishing online, oceanographic buoys that

allowed for continual monitoring of seawater quality on an hourly basis, and monthly seawater sampling by a third-party accredited laboratory. The results of the monitoring program have been shared with the respective authorities throughout the project lifecycle.

2.6.3 Water from Tunneling Works

The water generated from the tunnelling works – the TBM water, as well as the dewatering water from the shafts was treated by a water treatment plant (WTP) that was established on site. A specific environmental permit was obtained from the Ministry of Environment and Climate Change (MOECC) for the operation of the WTP. To meet the general and specific conditions set forth within this permit; a comprehensive monitoring program (including daily, weekly, and monthly sampling & analysis) was established to mitigate the potential environmental impacts associated with the tunneling activities.

2.6.4 Dewatering

A specific environmental permit for dewatering was obtained from the Ministry of Environment and Climate Change (MOECC) and Kahramaa, for the dewatering activities carried out around the construction site. To meet the general and specific conditions set forth within this permit; a comprehensive monitoring program (including daily, weekly, and monthly sampling & analysis) was established to mitigate the potential environmental impacts associated with the dewatering activities.

2.7 Physical Resources – Use and Management

2.7.1 Energy

The following ‘energy’ measures were implemented by the MPSO project:

- The outfall tunnel is a gravity-based tunnel with no pumping energy midway.
- The operational power demand is met via the 11kV power connection reducing the need for on-site diesel generators.
- Energy star equipment and energy-efficient light fixtures have been used.
- Using daylight resulted in reduced energy consumption.
- Materials were selected considering the energy conservation measures.
- Variable Frequency Drives (VFDs) were utilized to reduce the energy consumption and line losses.
- The cast in-situ roof was replaced with prefabricated elements reducing the CO_2 emissions and eliminating the need for 190 tons of form work and scaffolding.
- The adopted energy conservation measures helped the project to reduce the overall carbon footprint of the project.

2.7.2 Water

The following ‘water’ measures were implemented by the MPSO project:

- The water fixtures that comply with international codes and standards for efficient plumbing were selected.
- Treated TBM and dewatered water was reused for dust suppression and cleaning activities at the project site.
- Daily, weekly, and monthly monitoring and reporting of accumulative water consumption data was carried out throughout the project lifecycle.

2.7.3 Materials

The project used prefabricated construction elements to deliver substantial savings and efficiencies. The following 'materials' measures were implemented by the MPSO project:

- Principles for Design for Manufacture and Assembly (DfMA) were followed.
- Material resource efficiency measures were established and integrated into the design and construction.
- Pre-cast tunnel segments were used for the 10.2 km tunnel.
- Geometrical optimization and enhancement of the shafts resulted in generation of reduced quantity of excavated materials and reduced concrete consumption.
- Use of 4D BIM model eliminated over-procurement and helped reduce waste and rework.
- Concrete & steel with pre- and post-consumer recycled contents were procured.
- Responsibly-sourced wood & timber products with Forest Stewardship Council (FSC) and Program for the Endorsement of Forest Certification (PEFC) certificates were utilized for both temporary & permanent works.
- 49% of total material used was procured from local and regional businesses.
- Low Volatile Organic Compound (VOC)/bio-degradable coatings were used as applicable.

2.7.4 Waste

The following 'waste' measures were established by the MPSO project:

- A comprehensive Waste Management Plan (WMP) and associated waste hierarchy procedures were implemented.
- 100% of the excavated materials generated by the tunneling works are reused for a regional coastal reclamation project.
- 100% of the dredged materials generated by the dredging works were reused in the backfilling works.
- A 'Pledge for a Plastic-free Future' was established for the project, eliminating the single use plastics (SUPs) at project office and site.
- High recycling rates were achieved for paper, cardboard, steel, wood, and plastics; by establishing well-managed, individual waste segregation, storage, and disposal areas for each waste stream.
- Comprehensive training and awareness sessions were delivered, responsible waste management and resource conservation related project bulletins were prepared and shared with project staff.

2.7.5 Transport

The following 'transport' measures were implemented by the MPSO project:

- Proactive logistics and transportation planning was implemented.
- Sustainable transportation awareness programs were delivered, resulting in 30% of staff utilizing carpooling instead of individual vehicles.
- Traffic flow design was followed during all project site works.
- Designated traffic paths and schedules were allocated for construction vehicles.
- Materials delivery measures were established.
- Rigorous monitoring and management of site access road were implemented.

3 Summary of Project Challenges

There were various challenges faced throughout the project lifecycle, which also impacted the smooth delivery of the sustainability strategy of the project.

The site allocated for the MPSO project was very tight, requiring detailed scheduling and organization of construction activities. The lack of storage space within the project site for excavated materials from tunneling works was the key obstacle that the project team had to resolve. Then there were the environmental challenges, specifically the marine environmental impacts associated with the dredging, drilling, and other offshore works.

Another challenge was the construction of the outfall tunnel below the seabed under high water pressure conditions. There was only one access/exit point with potential hazards, requiring continual monitoring and control of every single operation inside the tunnel.

Last but not least, the site activities did not pause or stop during the COVID-19 pandemic. Rigorous measures to meet the Qatar Ministry of Public Health (MoPH) requirements were implemented to mitigate the adverse effects of the pandemic.

4 Summary of Benefits Achieved

Below is a summary of the immediate economic benefits achieved by the project:

- The project is designed to withstand climate change effects up to the year 2060 and to minimize the environmental impact during operation.
- An in-depth assessment of the potential flooding hazards was carried out.
- The final design incorporated measures to address potential flood risks from a one-in-50-years storm event.
- 100% of the excavated materials are fully reused for a regional coastal reclamation project.
- 100% of dredged materials were fully utilized during the backfilling works.
- Pre-cast tunnel segments were used for the 10.2 km tunnel.
- Pre-cast beams and slabs were used for the roof structure saving steel formwork.
- A gravity system with low-maintenance requirements has been utilized for the outfall.
- Environmentally friendly materials were considered and selected for the project.
- A local segment factory was used to supply the tunnel segments.
- Local manpower and local companies were considered and engaged with for various project activities such as marine works, oceanographic buoy supply and maintenance services.

5 Conclusion

Registering the project with globally recognized and third party audited CEEQUAL International enabled the MPSO project to incorporate sustainability considerations into the key project components and milestones. Sustainability, effective resource allocation, a sustainable, innovative and durable design, the use of local goods and service providers and meeting future capacity needs were prioritized for the MPSO project. Despite all the challenges faced throughout the project lifecycle, the project received environmental awards including the Ashghal Green Award in 2020 and the CEEQUAL '**Very Good**' in 2022, the highest rating ever in Qatar. Adopting a sustainability-driven strategy helped the project not only achieve CEEQUAL '**Very Good**' rating (that is higher than the contractually required 'Good' level), but also further receive industry excellence awards from ICE Qatar and MEED. The project also yielded value far beyond its immediate benefits contributing

directly to the United Nations (UN) Sustainable Development Goals (SDGs); particularly UN SDG 9, SDG 11, SDG 12, SDG 13, SDG 14, and SDG 17.

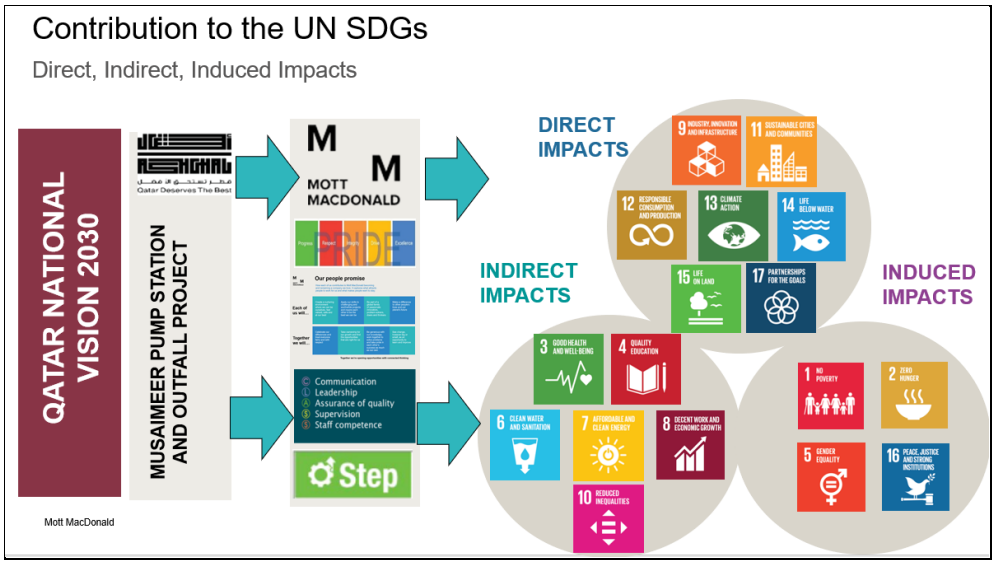


Fig. 1: Alignment of the MPSO project with the UN SDGs

The alignment of the MPSO project with the UN SDGs is shown in Fig. 1 and also summarized below:

- MPSO project contributes directly to the **UN SDG 9** through building a resilient, sustainable infrastructure, focusing on efficient resource consumption and adopting innovative technologies, minimizing the potential adverse environmental impacts.
- The main objective of the MPSO project is to increase the drainage capacity within Doha to accommodate storm-water runoff, and to minimize the potential adverse impacts of flooding to the residents and communities of Doha, as well as minimizing the negative impacts on the environment, and particularly the marine ecosystems, contributing directly to the **UN SDG 11**.
- The innovative and sustainable practices adopted for the project, local supply of materials and selection of local/regional companies have resulted in achieving economic benefits, directly contributing to the **UN SDG 12**, and leading to positive outcomes for the national economy as well.
- Utilization of advanced Building Information Modeling (BIM) for the design of prefabricated roof slabs has also enabled the MPSO project contribute directly to the **UN SDG 12**.
- MPSO project contributes directly to the **UN SDG 13** by implementing mitigation measures to minimize the CO_2 emissions as much as possible. Selected examples include considering more sustainable solutions during design; use of new, innovative technologies with reduced emissions during construction; and enhanced office settings to reduce the project overall carbon footprint.
- To ensure that the marine and coastal ecosystems are protected during the construction of the 10.2 km outfall chamber below the seabed, and the potential significant adverse impacts are avoided, a comprehensive seawater quality monitoring is undertaken for the project, contributing directly to the **UN SDG 14**.
- MPSO project contributes directly to the **UN SDG 15** by protecting the natural habitats, preventing the loss of biodiversity, and protecting the threatened species.

- MPSO project promoted collaboration and partnerships to create opportunities for delivering a sustainable, socially inclusive asset for the country, while raising awareness on sustainability, and capacity building for future generations, contributing to the **UN SDG 17**.

References

CEEQUAL Version 5.2 Assessment Manual for Projects: Qatar International Edition. (2015).

Sustainable Development Goals. (2020). United Nations Department of Global Communications

Cite as: Ersenkal D., Peach G. & Paskova B., "Sustainability Driven Strategy for Achieving Sustainable Infrastructure: Musaimeer Pumping Station and Outfall Project", *The 2nd International Conference on Civil Infrastructure and Construction (CIC 2023)*, Doha, Qatar, 5-8 February 2023, DOI: https://doi.org/10.29117/cic.2023.0088

A Markovian-Genetic Algorithm Model for Predicting Pavement Deterioration

Ala Sati
College of Engineering, University of Sharjah, Sharjah, United Arab Emirates
u20200159@sharjah.ac.ae

Saleh Abu Dabous
College of Engineering, University of Sharjah, Sharjah, United Arab Emirates
sabudabous@sharjah.ac.ae

Hissam Tawfik
College of Engineering, University of Sharjah, Sharjah, United Arab Emirates
htawfik@sharjah.ac.ae

Abstract

Pavement structures are constantly deteriorating due to many distresses, for instance cracks and rutting that are initiated and expanded. Deterioration models of pavement structures is an important component of pavement management systems (PMS). The deterioration of pavements has been extensively modeled using Markov chains. This paper aims at formulating a more efficient deterioration model to predict the condition of pavement sections. It is proposed to accomplish this by developing a Markovian deterioration model coupled with a meta-heuristic search optimization method, namely genetic algorithms (GA). An essential component of the Markov chain model is the transition probability matrix. In the proposed model, a standard percentage prediction method was used to calculate the transition probabilities. This is then calibrated by integrating the GA method with the Markov chain. The model is based on the historical international roughness index (IRI) data retrieved from the long-term pavement performance (LTPP) database. To test the validity of the method, a real-life case study is used and the performance of the developed model was assessed using both validation and testing data. For predicting pavement conditions, this study concluded that calibrating calculated transition probabilities using meta-heuristic optimization results in better performance than developing the transition probabilities using classical methods. The Markovian-GA model developed in the present study can be used to predict the future condition of pavement facilities in order to assist engineers in planning the optimum maintenance and rehabilitation (M&R) actions.

Keywords: Pavement condition; Infrastructure deterioration; PMS; LTPP; Genetic algorithm

1 Introduction

Civil infrastructure such as roads, bridges, airports, telephones, water networks, etc. are essential to society. Due to the importance of these facilities, infrastructure agencies are responsible for monitoring them to ensure that they remain in good condition to help the economy. Generally, there are many types of transportation infrastructure, including roads, streets, bridges, and parking lots. It is essential for researchers to pay attention to these since their deterioration can lead to serious consequences. Pavement structures that provide the surface of roads, streets, and bridges on which vehicles are especially essential due to their impact on vehicle serviceability and safety. Structural and surface characteristics both influence pavement performance in meeting design criteria throughout its service life.

Pavement deterioration refers to the worsening of pavement or the drop of pavement conditions.

The deterioration of the pavement state continues until the pavement fails and reaches the point where it can no longer serve its function. Deterioration has stochastic nature, and because sometimes a sudden necessity for immediate maintenance and rehabilitation (M&R) actions are needed, pavement management systems (PMS) have become an important part of the decision-making process. As an example, Abaza et al. (2004) integrated PMS with the Markovian model. The designed system becomes an effective decision-making tool that assists the engineers in planning and scheduling the M&R for pavement sections. The primary responsibilities of any PMS is to increase the effectiveness of the pavement decision-making process, broaden the decision-making scope, provide feedback on the decisions made, and maintain a consistent decision-making process at all organizational levels (Hudson et al., 1979). PMS can be used at local, country, state, and federal levels (Beckley, 2016) as illustrated in Golabi et al. (1982), which developed a PMS for the state of Arizona and Picado-Santos et al. (2004) that created a PMS for managing Lisbon pavements. Particularly, pavement management studies confirmed that PMS has proven to be an extremely useful tool in managing large state and metropolitan paving networks (Wolters et al., 2011). However, measuring and predicting the pavement performance is a critical part of any PMS.

In recent years, researchers have shown considerable interest in studying the mechanisms underlying infrastructure deterioration and developing models to forecast the state of various forms of infrastructure, both of which are crucial tasks. In order to make successful, advantageous M&R decisions, an accurate deterioration prediction method is necessary (Ahmed et al., 2020). In deterioration research, there is a great variety in using different data types and different methods to predict the condition of infrastructure facilities, as well as in each research, every developed model is based on a unique set of data. Models of deterioration are categorized into three categories.

The first category is deterministic models, which are the models formulated by a mathematical or statistical equation. The second category is stochastic models, which rely on random variables which create uncertainty in the model. The last category is Artificial Intelligence Models, which are a type of model based on computer techniques that require human intelligence to be developed. In general, all the deterioration models, regardless of the method used in its development, describe how the facility will perform over time. Deterioration models have been extensively simulated using Markov chains (Yosri et al., 2021). For instance, Ranjith et al. (2013) developed a Markovian model to predict the future condition of a timber bridge. Moreover, Li et al. (2014) proposed a Markov chain to generate a deterioration model for urban bridges in Shanghai. For pavement, (Kobayashi et al., 2010; Surendrakumar et al., 2013; and Anyala et al., 2014) implemented the Markov chain method to predict the deterioration of pavement in different places. Among all the discussed Markovian deterioration models, the transition probabilities were the essential part of the Markov chain method.

In this study, the Markov chain approach was proposed to develop the pavement deterioration model. Transition probabilities were developed using a simple percentage prediction method and then calibrated using an optimization method in order to enhance the accuracy of the model prediction. To verify the accuracy of the suggested technique, the produced model's performance was compared to results from previous research.

2 Materials and Methods

2.1 Data Extraction

In this study, historical pavement roughness data was utilized in developing the models. The data

was retrieved from the Long-Term Pavement Performance (LTPP) database. LTPP is the largest pavement study ever conducted for the pavement sections of the United States (US) and Canada (Sati et al., 2020). This study was focused on pavement sections that had not been maintained or rehabilitated, which were 431 sections. The sections with the missing international roughness index (IRI) data were removed. The remaining sections used in this study were 362 sections. The characteristics of the pavement sections, which are the Age, Roadway Functional Class, Climatic Region, Freezing Index, Precipitation, Temperature, AADT, and AADTT were extracted, also from the LTPP database, to categorize the pavement sections.

2.2 Research Methodology

In this study, the methodology framework adopted, presented in Figure 1, consists of many stages. Many steps were executed in each stage. In the first stage, one stage has been performed, which is the collection and preparation of the roughness data. In the second stage, the collected data was converted into condition states utilizing the Federal Highway Administration (FHWA) ranges presented in Table 1. The data was categorized using cluster analysis. K-means cluster analysis is the most popular clustering method. In this method, the sum of the squared error (SSE), calculated by (1), between a cluster's empirical mean and the point within the cluster is minimized.

$$SSE = \sum_{k=1}^{K} \sum_{i=1}^{n} \|x_i - \mu_k\|^2 \quad (1)$$

Where n represents the number of observations within the cluster, K is the cluster number, x_i is the center of the observation, and μ_k is the cluster center.

The elbow method, which is a graphical method where the graph represents the relationship between the number of clusters and the sum of squared error, was proposed to find the optimum number of clusters. In the last stage, which is the core of this study, the model was first developed, then validated, and lastly tested. The following subsections will explain each in detail.

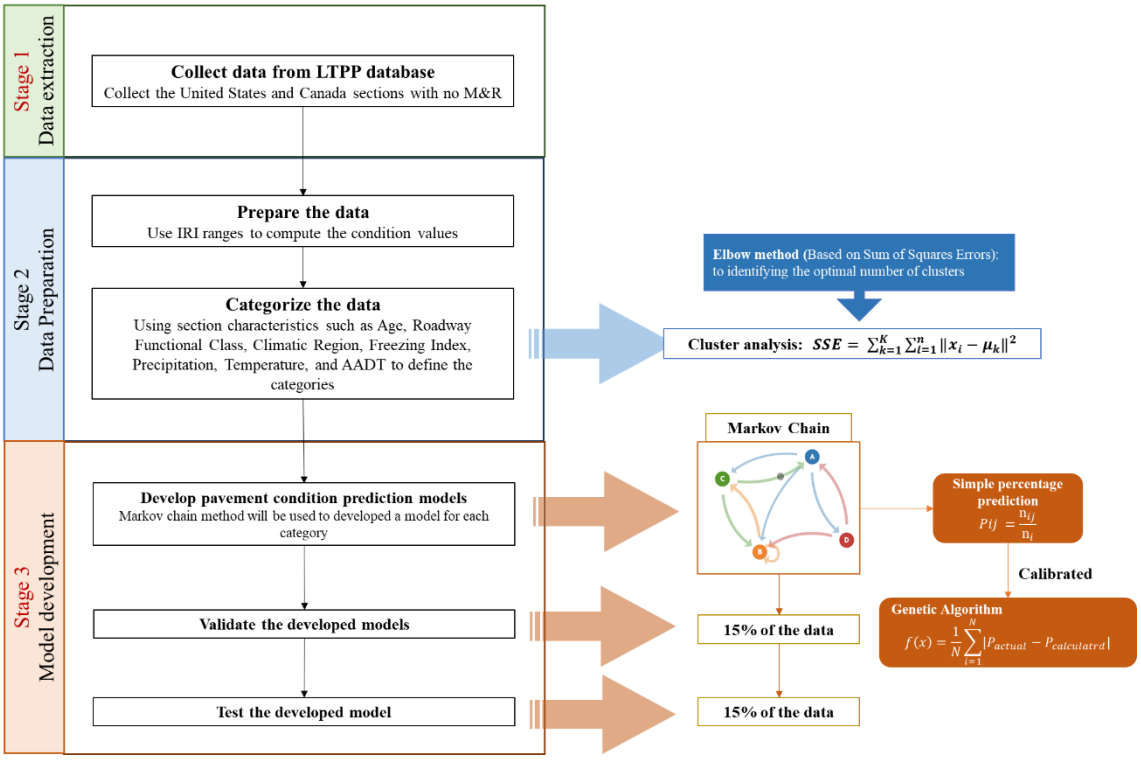


Fig. 1: Research methodology

Table 1: FHWA ranges

State	Category	IRI (m/km)	
		Roadway Functional Class	
		Interstate	Other
1	Very good	< 0.95	< 0.95
2	Good	0.95 – 1.49	0.95 – 1.49
3	Fair	1.50 – 1.89	1.50 – 2.69
4	Mediocre	1.90 – 2.69	2.70 – 3.48
5	Poor	2.69 <	3.48 <

2.3 Proposed Methods

2.3.1 Markov Chain

The Markov chain approach explains the sequence of potential events using a discrete number of events. The aim of the Markovian process is to base predictions purely on the current situation while ignoring the entire history. In a scientific sense, the probability of an event depends entirely on the current situation, regardless of the previous state. The following equation illustrates this process of independence, which is known as the Markov property:

$$P(X\,j) = P(X\,t+1 = i\,t+1 | X\,t = i\,t, X\,t-1 = i\,t-1, \ldots, X\,1 = i\,1, X\,0 = i\,0)) = P(X\,t+1 = i\,t+1 | X\,t = i\,t) \quad (2)$$

Where $P(X_j)$, represents the probability of a future condition, t is the current state, while j is the state in the future. The odds of transitioning from state i to state j are known as the transition probabilities and are represented by P_{ij}. The transition probability matrix (n×n), or P, is depicted in (3) and contains all possible outcomes. The number of condition states is n, as well.

$$P = \begin{bmatrix} P_{11} & P_{12} & \cdots & P_{1j} \\ P_{21} & P_{22} & \cdots & P_{2j} \\ \vdots & \vdots & \cdots & \vdots \\ P_{i1} & P_{i2} & \cdots & P_{ij} \end{bmatrix} \quad (3)$$

Using the Markovian process, the time step should be selected first. Then, the future condition vector (P_t) will be predicted by the multiplication of the transition probability matrix and the initial condition vector (P_0). This multiplication is raised to the power represented by the time step, as shown in (4). Lastly, the expected future condition will be calculated using (5).

$$P_j = P_0 \times P^t \quad (4)$$

$$Ev = \sum_{j=1}^{5} j \times P_j \quad (5)$$

In the simple percentage prediction method, the condition data was used to calculate the transitioning probability from state i to state j in terms of the simple mean. This probability is donated by P_{ij} and determined using the following equation.

$$Pij = \frac{n_{ij}}{n_i} \quad (6)$$

Where n_{ij} represents the transitions' number from state i to state j, and n_i represents the total number of elements in state i.

2.3.2 Genetic Algorithm Optimization

The most popular meta-heuristic optimization algorithm utilized recently due to its diversity of applications is the genetic algorithm (GA) (Vasuki, 2020). It computes successive generations of

solutions based on a set of initial solutions and hypotheses.

The first step in GA is the random creation of the initial population of the solution. The next step is to evaluate each chromosome in the population using the objective function. Then, GA operations will be utilized to create new chromosomes. The new chromosomes will be evaluated as well. The old population will be replaced with new ones. Then, these procedures will be repeated until a near-optimal solution is found. GA has three important operations, reproduction, crossover, and mutation. In addition, there are other operations that can be added to the algorithm based on the need, such as Elitism.

1. Reproduction: is a GA operation that first arranges the chromosomes according to their objective function values, then selects the members from the current population randomly and copies them to the next population. The most commonly used method for selection is the roulette wheel.
2. Crossover: is an operator that crosses over the genes of randomly selected parents to produce a new offspring. It may be one point, two points, or multipoint.
3. Mutation: is a GA operator that is implemented to ensure diversity in the population. In this operation, one or more genes in the parent chromosome string are altered to produce totally new offspring.
4. Elitism: is an operation that can be added before the main GA operations to ensure the survival of the best solutions. This operation copies the elite solutions to the next generation without any changes. If the predefined number of iterations has been reached, an elitist chromosome does not change significantly from one iteration to the next, or when an absolute number of generations is reached, the production of the new generation will cease.

In this study, GA was chosen because of its capability to search for a population of solutions on a global scale instead of a single-based search solution. In this study, GA was used as a calibration process of the transition probabilities generated by the percentage prediction method.

2.3.3 Genetic Algorithm-Based Markovian model

In this case, GA was used to minimize the mean absolute error (MAE) between the transition probabilities based on historical data, which are actual, and the estimated transition probabilities, as shown in (7).

$$Min\ MAE = \frac{1}{N}\sum_{i=1}^{N}|P_{actual} - P_{calculated}| \quad (7)$$

Where N is the number of probabilities in the raw, and P_x is the transition probability. Since the problem is using data for the sections with no M&R, the transition probabilities that were optimized are:

$$P = \begin{bmatrix} P_{11} & P_{12} & P_{13} & P_{14} & P_{15} \\ 0 & P_{22} & P_{23} & P_{24} & P_{25} \\ 0 & 0 & P_{33} & P_{34} & P_{35} \\ 0 & 0 & 0 & P_{44} & P_{45} \\ 0 & 0 & 0 & 0 & P_{55} \end{bmatrix}$$

These probabilities are subject to many constraints. The first one is the summation of each row, which is equal to one.

- $\sum_{j=1}^{5} P_{ij} = 1$, i= 1,2,3,4, & 5

The second one is the probability of staying in the same condition rather than transitioning to the

next condition for one time step that is always higher. Following is the mathematical formulation of this constraint:

- $P_{11} > P_{12}$, $P_{12} > P_{13}, P_{13} > P_{14}, P_{14} > P_{15}$
- $P_{22} > P_{23}, P_{23} > P_{24}, P_{24} > P_{25}$
- $P_{33} > P_{34}, P_{34} > P_{35}$
- $P_{44} > P_{45}$

The last constraint is that the probabilities are always between zero and one. Rarely can they be exactly zero or one.

- $0 \leq P_{ij} \leq 1$

Based on the nature of the problem in this study, each row is optimized separately since the row's probabilities are related to each other, while the probabilities of different rows are not related. MATLAB software was used to implement the GA calculations. Before the main GA operation, 0.05 of the population was counted as elite solutions. In addition, the rate of the crossover was 0.8, which means that 80% of the population was crossed over. Moreover, the default mutation option in MATLAB, which is mutation Gaussian, was used. In this option, each entry of the parent vector is given a random number according to a Gaussian distribution.

3 Results and Discussions

3.1 Cluster analysis

After performing K-means cluster analysis and in order to identify the number of clusters, the Elbow method was applied. The results were based on the sum of squared errors (SSE). Table 2 represents the SSE results that vary with the clusters' number. By graphically representing the results (Figure 2) the cluster's optimum number is equal to three. In addition, the number of sections in each cluster and the division of the data in each cluster are represented in Figure 3.

Table 2: SSE Results

No of clusters	SSE
2	2,305.33
3	1,731.75
4	1,658.42
5	1,466.28
6	1,200.77
7	1,181.78
8	1,119.79
9	994.86
10	949.14

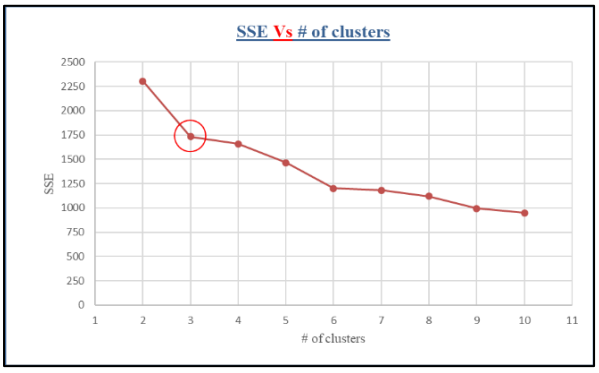


Fig. 2: SSE vs. the number of clusters

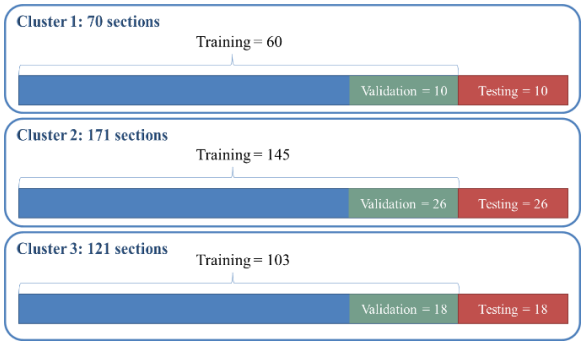


Fig. 3: Data division for each cluster

3.2 Markov Chain Transition Probabilities

The following matrices represent the results of calculating the transition probabilities using the traditional method, percentage prediction, then calibrating these probabilities using a Genetic algorithm.

Cluster 1

$$\begin{bmatrix} 0.9577 & 0.0276 & 0.0110 & 0.0047 & 0.0000 \\ 0 & 0.9411 & 0.0493 & 0.0104 & 0.0001 \\ 0 & 0 & 0.9508 & 0.0467 & 0.0025 \\ 0 & 0 & 0 & 0.9902 & 0.0098 \\ 0 & 0 & 0 & 0 & 1 \end{bmatrix}$$

Cluster2

$$\begin{bmatrix} 0.8705 & 0.0787 & 0.0364 & 0.0147 & 0.0007 \\ 0 & 0.9521 & 0.0332 & 0.0137 & 0.0010 \\ 0 & 0 & 0.9762 & 0.0206 & 0.0038 \\ 0 & 0 & 0 & 0.9730 & 0.0270 \\ 0 & 0 & 0 & 0 & 1 \end{bmatrix}$$

Cluster 3

$$\begin{bmatrix} 0.9367 & 0.0363 & 0.0182 & 0.0089 & 0.0002 \\ 0 & 0.9596 & 0.0325 & 0.0078 & 0.0002 \\ 0 & 0 & 0.9875 & 0.0110 & 0.0016 \\ 0 & 0 & 0 & 0.9167 & 0.0833 \\ 0 & 0 & 0 & 0 & 1 \end{bmatrix}$$

3.3 Performance Results

Table 3 represents the root mean squared error (RMSE), coefficient of determination (R^2), and mean absolute percentage error (MAPE) results for both validation and testing data. In addition, the performance of different studies was collected and presented in Table 4 to compare it with the performance of the proposed model in this study.

Table 3: RMSE results

	Validation		Testing		
Cluster No.	**RMSE**	**MAPE**	**RMSE**	**MAPE**	**R^2**
1	0.447	0.070	0.316	0.025	0.8334
2	0.277	0.051	0.555	0.115	0.7505
3	0.408	0.065	0.236	0.014	0.8622

Table 4: The models' performance in different studies

The study	**Method**	**RMSE**	**R^2**
Yang et al. (2006)	ANN	0.379	-
	Markov chain	0.346	-
Attoh-Okine et al. (2009)	MARS	-	0.76
Bianchini & Bandini, P. (2010)	Multiple linear regression	0.2272 - 0.3790	0.8022 - 0.9196

In summary, after developing the models, the performance of each one was calculated. Focusing on the testing results, the RMSE was found to be 0.316, 0.555, and 0.236 for cluster 1, cluster 2, and cluster 3, respectively. Moreover, the MAPE values are 0,025 for the first cluster, 0,115 for the second one, and 0,014 for the third cluster. The R^2 ranges between 0.07505 and 0.08622. The results of this study were compared with previous studies that used different methods (Table 4); the results demonstrated that the developed models have acceptable performance. In addition, it is clear from the results that the model of Cluster 3 has the highest performance while Cluster 2 has the lowest performance. To summarize, this study found that the Markov chain performed very well in predicting pavement conditions when calibrating the transition probabilities using GA.

4 Conclusion

This study was performed to enhance the accuracy of the Markov chain deterioration model for pavement sections. Data on pavement roughness was collected from the LTPP database. IRI values were converted into condition states using the ranges specified by FHWA. In order to classify the data into categories, pavement characteristics such as age, roadway functional class, climatic region, freezing index, precipitation, temperature, AADT, and AADTT were used. K-means cluster analysis was integrated with the elbow method to define the number of clusters. According to the results, three clusters were found to be the optimum partitioning. Each cluster's models were developed using the Markov chain method. A simple percentage prediction approach was presented to determine the transition probabilities, which are an essential part of the Markov chain.

Then, the developed transition probabilities were calibrated using genetic algorithms. The data in each cluster was divided into training, validation, and testing sets. The validation and testing data were used to test the model's performance by utilizing RMSE, MAPE, and R^2. The ranges of RMSE, MAPE, and R^2 were 0.236 – 0.555, 0.014 – 0.115, and 0.7505 – 0.8622, respectively. The developed models in this research were compared to other models utilized in previous studies and were found to outperform previous models. This research concluded that the Markov chain models have better accuracy in predicting pavement conditions rather than other models. Furthermore, using the genetic algorithm to calibrate the transition probabilities improves the model's accuracy.

This study was limited to sections with no maintenance and rehabilitation. For future work, other statistical methods such as Poisson distribution can be used to calculate the transition probabilities and then calibrated using a genetic algorithm or other optimization methods. Additionally, data from other infrastructure systems can be used to implement the proposed model to ensure its applicability.

References

Abaza, K. A., Ashur, S. A. & Al-Khatib, I. A. (2004). "Integrated pavement management system with a Markovian prediction model". *Journal of Transportation Engineering*, *130*(1), 24-33. https://doi.org/10.1061/(ASCE)0733-947X(2004)130:1(24)

Ahmed, R., Zayed, T. & Nasiri, F. (2020). "A hybrid genetic algorithm-based fuzzy Markovian model for the deterioration modeling of healthcare facilities". *Algorithms*, *13*(9), 210. https://doi.org/10.3390/a13090210

Anyala, M., Odoki, J. B., & Baker, C. J. (2014). "Hierarchical asphalt pavement deterioration model for climate impact studies". *International Journal of Pavement Engineering*, *15*(3), 251-266. https://doi.org/10.1080/10298436.2012.687105

Attoh-Okine, N. O., Cooger, K., & Mensah, S. (2009). "Multivariate adaptive regression (MARS) and hinged hyperplanes (HHP) for doweled pavement performance modeling". *Construction and Building Materials*, *23*(9), 3020-3023. https://doi.org/10.1016/j.conbuildmat.2009.04.010

Beckley M. E. (2016), "Pavement Deterioration Modeling Using Historical Roughness Data," *Arizona State University*.

Bianchini, A. & Bandini, P. (2010). "Prediction of pavement performance through neuro‐fuzzy reasoning". *Computer‐Aided Civil and Infrastructure Engineering*, *25*(1), 39-54. https://doi.org/10.1111/j.1467-8667.2009.00615.x

Golabi, K., Kulkarni, R. B. & Way, G. B. (1982). "A statewide pavement management system." *Interfaces*, *12*(6), 5-21. https://doi.org/10.1287/inte.12.6.5

Hudson, W. R., Haas, R. & Pedigo, R. D. (1979). Pavement management system development. *NCHRP report*.

Kobayashi, K., Do, M. & Han, D. (2010). "Estimation of Markovian transition probabilities for pavement deterioration forecasting". *KSCE Journal of Civil Engineering*, *14*(3), 343-351. https://doi.org/10.1007/s12205-010-0343-x

Li, L., Sun, L. & Ning, G. (2014). "Deterioration prediction of urban bridges on network level using Markov-chain model". *Mathematical Problems in Engineering*. https://doi.org/10.1155/2014/728107

Santos, et al. (2004). "Pavement management system for Lisbon". In *Proceedings of the Institution of Civil Engineers - Municipal Engineer*, 157(3), 157-165. Thomas Telford Ltd. https://doi.org/10.1680/muen.2004.157.3.157

Ranjith, et al. (2013). "Deterioration prediction of timber bridge elements using the Markov chain." *Journal of Performance of Constructed Facilities*, *27*(3), 319-325. https://doi.org/10.1061/(ASCE)CF.1943-5509.0000311

Sati, A. S., Dabous, S. A. & Zeiada, W. (2020). "Pavement deterioration model using Markov chain and international roughness index". In IOP Conference Series: *Materials Science and Engineering*, *812*(1), 012012). IOP Publishing. DOI: 10.1088/1757-899X/812/1/012012

Surendrakumar, K., Prashant, N. & Mayuresh, P. (2013). "Application of Markovian probabilistic process to develop a decision-support system for pavement maintenance management". *International Journal of Scientific & Technology Research*, *2*(8), 295-303.

Vasuki, A. (2020). *Nature-inspired optimization algorithms*. CRC Press.

Wolters, et al. (2011). "Implementing Pavement Management Systems for Local Agencies: Implementation Guide" (No. ICT-11-094-1).

Yang, et al. (2006). "Modeling crack deterioration of flexible pavements: Comparison of recurrent Markov chains and artificial neural networks". *Transportation Research Record*, *1974*(1), 18-25.

Yosri, et al. (2021). "Genetic algorithm-Markovian model for predictive bridge asset management". *Journal of Bridge Engineering*, *26*(8), 04021052. https://doi.org/10.1061/(ASCE)BE.1943-5592.0001752

Cite as: Sati A., Abu Dabous S. & Tawfik H., "A Markovian-Genetic Algorithm Model for Predicting Pavement Deterioration", *The 2nd International Conference on Civil Infrastructure and Construction (CIC 2023)*, Doha, Qatar, 5-8 February 2023, DOI: https://doi.org/10.29117/cic.2023.0089

Potential Implementation of Warm Mix Asphalt (WMA) in Pavement Construction in the State of Qatar

Mohammad Hasan Anshasi
AECOM/Public Works Authority, Doha, Qatar
mohammad.anshasi@aecom.com

Charles N. Nunoo
AECOM/Public Works Authority, Doha, Qatar
charles.nunoo@aecom.com

Abstract

Warm-mix asphalt (WMA) technology has been used in many countries around the world, in lieu of Hot Mixed Asphalt (HMA), due to its ability to allow significant reduction in the temperatures at which asphalt mixes are produced and placed, leading to performance that is comparable to HMA. The resultant is a reduction in the viscosity of the asphalt due to the incorporation of WMA technologies, which facilitates the coating of aggregates at lower temperatures (as much as 30°C less temperature) that translates to a reduction in energy consumption and greenhouse gas emissions, which in turn supports sustainable development. WMA technology has been successfully implemented in several countries across the globe, especially in Europe and USA, aiming at saving energy, reducing emissions throughout the production, and paving process, without compromising the in-service performance. This paper discusses how the long-term benefits and sustainability advantages of WMA technology can be harnessed to augment the Qatar roadmap and aspiration towards achieving 25% reduction in greenhouse gases (GHG) by 2030 and achieving Net Zero by 2050.

Keywords: Warm Mix Asphalt (WMA); Sustainability; Emission; Lower energy consumption; Lower emissions; Safer work conditions

1 Introduction

Hot Mix Asphalt Mixes (HMA) are the only asphalt mixes specified in the Qatar Construction Specification (QCS, 2014), and currently used for all the asphalt pavement layers construction in road projects in Qatar. Notwithstanding that, these mixes have demonstrated an acceptable level of short and long-term performance, in most cases; the process of production, placement and compaction of HMA is associated with high levels of greenhouse gas (GHG) emissions. This emanates from the substantial amount of energy or fuel consumption during the asphalt production and construction process, considering the high aggregate heating and plant mixing temperatures for the HMA which can reach up to 171°C for mixes produced with modified stiff binders. Shacat J. et al. (2022) estimated that CO_2 emission equivalency associated with the production of 421.9 million tons of asphalt mixes during 2019 in the USA was 21.7 MMT CO_2e with emission cradle-to-gate intensity of 51.4 Kg CO_2e per ton of asphalt mix.

One of the major challenges experienced in pavement construction using HMA is how to maintain adequate mix temperature during breakdown and intermediate compaction to achieve the required density and in place air voids for stiff HMA with polymer-modified binder (PMB) or Crumb Rubber Modified Binder (CRMB). Moreover, overheating of this binder during storage and mixing of the

HMA may result in premature aging and affect the binder properties and the overall pavement in-service performance.

Several alternative technologies have been considered to mitigate this negative environmental impact and high levels of GHG emission including the following, as indicated in (EAPA, 2014):

- Cold mixes produced using unheated aggregate and bitumen emulsion or foamed bitumen.
- Half-warm asphalt: produced between approximately 70°C and roughly 100°C.
- Warm mix asphalt: produced and mixed at temperatures roughly between 100°C and 150°C.

WMA technology was developed in the late 1990s and is considered an acceptable alternative to the HMA for its ability to allow the reduction of asphalt mixing and compaction temperature by as much as 20°C to 40 °C, leading to lower energy/fuel consumption, lower GHG emission, and in turn create and enable safer work conditions by reducing human exposure to fuel emissions, fumes, and odors, while achieving the required asphalt MAT density at lower compaction temperature.

This is even more critical when paving during cold weather with long haul distances when paving and compacting asphalt mixes with stiff modified binders such as CRMB or PMB. Details of these benefits are discussed in Section 3 of this paper. Warm Mix Asphalt mixes have been implemented successfully internationally for years, including in Europe, United States, and South Africa. Table 1 below, based on European Asphalt Pavement Association (EAPA) document, indicates considerable quantities of WMA have been produced during the period from 2013 to 2020 in these countries. The estimated total quantity of WMA produced in Europe alone during this period is approximately 56 million tons.

Table 1: WMA production period from 2013 to 2020 (Millions of Tons) (EAPA, 2020)

Country/Continent	2013	2014	2015	2016	2017	2018	2019	2020
Europe	3.401	7.33	6.833	7.014	7.241	7.099	8.961	8.678
USA*	69	103	109	106	133	143	150	169
Ontario Canada		0.75	0.9	0.75	No data	No data	No data	No data
South Africa	0.15	0.15	0.2	0.2	No data	No data	No data	No data

* The figures for USA include both WMA and HMA

2 WMA Asphalt Technologies

The production of WMA does not require a major modification of the conventional asphalt plant infrastructure and equipment. However, several proprietary techniques in the form of materials additives have been developed and incorporated into the asphalt mixing process, including foamed bitumen, chemicals, and organic additives, as shown in the following sections. These additives facilitate proper mixing and coating of the aggregates, as well as improve workability and the ultimate compaction of the asphalt mixes.

2.1 Organic Additives

Organic additives are mainly composed of wax or fatty acids amides which helps to reduce the viscosity of the binder. The type of wax must be carefully selected so that the melting point of the wax is higher than expected in-service temperatures (otherwise permanent deformation of the asphalt layer may occur). The following are examples of organic additives used in the industry:

- **Sasobit** is a form of Fischer-Tropsch synthetic which can be added to the mix by blending with the binder in a binder tank in the form of flakes in a molten state or by pneumatically blowing it into the plant mixing drum through a modified feed line in the form of prills. The

mixing dosage of Sasobit is between 1% and 2.5% and can help reduce plant-mixing temperatures between 20°C and 30˚C (D'Angelo J, et. al, 2008).

- **Asphaltan-B** is a refined Montan wax. These materials can be either blended in the bitumen tank at 2.5% of the binder weight or added to the mix in the plant pugmill and can help decrease the production temperature between 20°C and 30 ˚C (D'Angelo, et. al, 2008).

2.2 Chemical Additives

Chemical Additives are mainly considered to improve workability, compatibility and aggregate coating of the mix at a lower mixing temperature, Evotherm™ DAT is an example of the chemical additives, which is delivered in a dispersed emulsion form. The manufacturer recommends the addition of Evotherm DAT at 0.25 to 0.75 % by weight of asphalt cement. Evotherm can be pumped to the plant with a minimum mixing temperature of 104°C and compaction temperature of minimum 66°C. (Aschenbrener, et. al, 2011) and (D'Angelo, et al., 2008).

2.3 Foaming Techniques

The main concept of the foaming technique is to introduce a small and controlled amount of water to the bitumen, which increases the bitumen volume and reduces viscosity and temperature. Additionally, expansion of bitumen will allow proper coating of aggregates at lower mixing temperatures. The foaming is done by adding water directly through injecting nozzles such as WAM-FOAM technique or through foaming agent/additive such as Synthetic Zeolite:

- **Synthetic Zeolites** "are framework silicates with large empty spaces in their structures that allow the presence of large cations, such as sodium and calcium. They also allow the presence of large cation groups (positive ions), such as water molecules. Zeolites contain approximately 20% of water, the material is added to the mixture by 0.3% of the weight and releases small amount of water when exposed to heat, creating a controlled foaming effect, which slightly increases binder volume and reduces viscosity. Examples of Synthetic Zeolite are Alpha-min and Advera, which have been reported to reduce the production temperatures by up to 30°C. (D'Angelo J, et. al, 2008).
- **WAM-FOAM®** is a process and not an additive; initially developed by Shell in cooperation with Kolo Veidekke in Norway in the late 1990s (D'Angelo, et. al, 2008). The process includes blending of two grades of binder, one nominally soft binder (viscosity grade 1500 Centistoke at 60°C) and hard binder (about PG58/64-22).

3 Benefits of WMA

3.1 Energy savings and Reduction in Emissions of Greenhouse Gases

One of the crucial benefits of implementing WMA is its positive impact on the environment, reduction in GHG emissions, achieving sustainability advantages, fuel/energy savings, and is considered a step-in alignment with the Qatar roadmap towards achieving the target of 25% reduction in GHG by 2030 and reaching to Net Zero by 2050. Several technical references indicated considerable reduction in asphalt production-and compaction-temperatures of between 20°C and 30°C, fuel savings of between 20% and 35%. Reduction of plant gases, including carbon dioxide emissions, between 15% and 60% have been achieved by implementing WMA as follows:

1. D'Angelo J, et al. (2008) indicated that fuel savings with WMA typically range from 20% to 35%. Additionally, they indicated significant reduction in plant stack gas emissions reported

in several European countries. For example reduction in Carbon dioxide CO_2 (15%-40%), sulfur dioxide SO_2 (18%-35) and carbon monoxide CO (10%-30%). The table below lists the reduction in plant stack emissions in different countries.

Table 2: Reduction in Plant Gas Emissions (D'Angelo J, et al., 2008)

Emission	Norway	Italy	Netherlands	France
CO_2	31.5	30-40	15-30	23
SO_2	NA	35	NA	18
CO	28.5	10 to 30	NA	NA

2. Milad, et al. (2022) summarized the reduction in gas emissions using different warm mix additives, processes and techniques based on the review of several references. For example, the highest reduction in carbon dioxide CO_2 was between 17.35% and 60% when using chemical additive (Evotherm) and a reduction of 63% in carbon monoxide CO. Table 3 below summarizes the reduction in gas emission percentages using different warm mix techniques and additives as indicated:

Table 3: Reduction in gas emissions using different WMA additives (Milad, et al., 2022)

Additive/process	CO_2	CO	SO_2	NO_x	VOC
Evotherm (Chemical additive)	17.35%- 60%	19.51-63%	75.2%	20-72.6%	-
Synthetic Zeolites (Foaming)	15.8%	18.4%	9.67%	16.5%	-
WAM-FOAM	31.4	28.5	-	61.5	-
Alpha-min		62.0	83.3	30.8	62.8
Sasobit	-	63.2	83.3	21.2	51.3

3. NCHRP report 779 (2014) summarizes the fuel consumption and stack gas emission measurements for 5 projects in the USA comparing HMA and WMA mixes. The results show an average reduction in the mix, a temperature of 27° C and fuel saving of 22%. It also shows reduction of carbon dioxide (CO_2) emissions because of lower fuel usage.
4. In NAPA report SP106, Shacat, et al. (2022) suggested the fuel saving to be 1,000 Btu/°F/ton of the asphalt mix.

3.2 Approximate Potential Energy Saving and Gases Emission Reduction in Qatar

The amount of energy savings and reduction in GHG emissions depend on several factors including the kind of fuel (natural gas or diesel) used, aggregate types, moisture content (wet aggregates required more heating), production rate, technique used, binder type and weather condition, and should be measured and calculated based on the overall Life Cycle Inventory.

Therefore, further field trials and investigations need to be performed to evaluate the energy fuel saving and reduction in GHG emissions in Qatar in Warm Mix asphalt over Hot Mix asphalt.

However, a very rough estimate of the CO_2e emission reduction forecast and energy saving can be proposed based on several assumptions including the following:

- The approximate forecast total asphalt quantity for PWA Road Projects Department (RPD) for the period from 2023 to 2026 is approximately 7,500,000 tons.
- Considering using WMA in the asphalt base course layers for only 20 % of the total forecast quantity.

- Assuming the same CO_2e equivalent emission intensity of 51.4 Kg CO_2e/ton for material production and transportation estimated based on NAPA SIP-106 report, and based on several technical references, it can be assumed that the average reduction in CO_2e is approximately 25% when using WMA.
- Assume 20^oC (68 ^{o} F) reduction in production temperature and energy saving estimated based on the formula suggested in NAPA SIP 106, i.e. 1,000 Btu/°F/ton. This varies depending on several factors such aggregates' moisture and bitumen type, technique used, plant operations and fuel type.

Based on the above assumptions (1-3), the reduction in CO_2e emission can be estimated to be approximately 19,300 metric tons, which is equivalent to approximately 1390 passengers' vehicles, on the consideration that a typical passenger vehicle emits about 4.6 metric tons of carbon dioxide per year as per the US Environmental Protection Agency (EPA). Additionally, based on assumptions 1 and 4 above, the energy saving can be estimated to be approximately 102,000 MMBtu.

3.3 Safer Working Condition

Maintaining safe working conditions and eliminating work-related hazards and injury/illness is a major goal for all entities involved in the pavement construction. The implementation of WMA can help in achieving this target considering the following:

- The lower mixing- and paving- temperatures minimize fume and odor emissions and create cooler working conditions for the asphalt workers. per EAPA, the release of fumes is reduced by around 50% for every 12°C reduction in temperature. (EAPA, 2014).
- Reduction in the exposure of laborers to higher temperatures and fumes that cause burns, irritation, and associated with potential long-term illnesses such as cancer.
- More comfortable work conditions, which will have positive impact on the productivity.

3.4 Plant Mixing and Paving Operations Benefits

Using WMA techniques has multiple benefits on mixing and paving operations; however, these techniques and mix designs should be carefully controlled, implemented and tested to achieve the required quality and performance of the pavement layer equivalent to HMA. Below is a list of major benefits as indicated by D'Angelo J, et al. (2008) and (EAPA, 2014).

- Reduction in viscosity to ensure coating at lower mixing temperature, reduce compaction effort and compact the mix at lower temperatures.
- Decrease in binder aging.
- Increase the haul distance while maintaining the mix workability.
- Reduction in thermal segregation, improved fatigue performance.
- Ability to increase the RAP percentage and use of CRMB to improve sustainability.
- Place thicker lifts and open to traffic in a short period.

4 WMA Materials Selections, Production, Construction and Perforamance Evaluation

The mix design of the WMA can follow the same known procedures of HMA. However the Superpave mix design and volumetric analysis per AASHTO R 35 (2022) is recommended to be used as a mix design procedure. The objective of the WMA is to produce sustainable and environmentally

friendly mixes by reducing the mixing temperature and binder viscosity at the same time while achieving strength, durability, and performance similar to of the HMA. To achieve this, major steps need to be considered and further investigated including materials selection, WMA mix design process, production, construction, and performance evaluation.

4.1 WMA Materials Selection

Table 4 summarizes some of the WMA materials selection requirements and findings on WMA based on several references including NCHRP 691(2011), NCHRP 779 (2014) and (AASHTO R 35, 2022):

Table 4: WMA Materials Selection Requirements and Findings

Steps	Requirements and Findings
Mix Design	• The recommended mix design method is Superpave based on AASHTO R35.
Binder Grade Selection	• The same binder grade for HMA can be used; the performance grade binder selection is based on AASHTO M 323 considering environment and traffic loading. • Reduced mixing temperature may produce less aged binder which may result in rutting; however, in many cases stiffer high-temperature binder grade may be needed for satisfactory rutting performance (NCHRP 691, 2011).
Aggregates Properties and Gradation	• No major changes from HMA.
Reclaimed Asphalt Pavement (RAP)	• The RAP and new binders can mix at the lower temperatures used in WMA provided the mixture remains at elevated temperatures for a sufficient time. To ensure good mixing of RAP and new binders, the planned field compaction temperature for WMA exceeds the high-temperature grade of the RAP binder (NCHRP 691, 2011). • Small percentage of RAP to WMA can greatly help in drying the virgin aggregate. • RAP may improve rutting resistance of WMA mixes. • The performance of WMA mixes containing RAP is affected by the degree of mixing between the RAP binder and the new binder and the WMA technology used.
Anti-strip agent	• Essential to improve WMA moisture sensitivity.

4.2 WMA Production and Construction

Table 5 summarizes some of the materials production, construction steps requirements and recommendations based on several references including (NCHRP 691, 2011), (NCHRP 779, 2014) and (AASHTO R 35, 2022).

Table 5: Summary of some of the materials production, construction steps requirements

Steps	Requirements and Recommendation
Mixing Temperature	20-30°C lower than Hot Mix Asphalt (HMA). The minimum mixing temperature will depend on WMA additive technique, binder grade, level of aggregates coating, moisture condition of the aggregates and performance of the mix (moisture sensitivity and rutting).
Aggregates Moisture Content	Moisture content of aggregates in the stockpiles should be minimized.
Binder Absorption	Based on NCHRP 691 (2011) volumetric properties of WMA mixes with binder absorption $\leq$ 1% is the same as HMA. On average binder absorption for WMA is less by 0.11% than corresponding HMA, however the reduction depends on the WMA additive or technique and aggregates moisture.
Aggregates Coating	• Testing done as per AASHTO TP195. • Mixing time should be verified to ensure proper coating at low mixing temperature. • $\geq$95% of the coarse aggregates should be fully coated (AASHTO R035).
Plant Equipment and Operations	Ensure proper plant maintenance for example the following: • Dryer and lifters maintained and burner proper tuning. • Keeping baghouse temperatures high enough above due point to prevent condensation.

	• Mitigate air leak. • Inspect the fines return lines more frequently to ensure that no build-up occurs due to moisture. • Control and reduce aggregates stockpiles moisture to reduce energy required for drying.
Mix Workability/COmpatibility	• Compaction temperature could not evaluated based on binder viscosity. • The recommended compaction can be determined as specified in AASHTO R 35, which specified based on the gyration ratio of 1.25, which is the ratio between the number of gyrations to reach the density (92%) at planned compaction temperature and the number of gyrations to reach the 92% density at planned compaction temperature minus 30ºC. • AASHTO R35 recommends that the planned field compaction temperature for WMA should exceed the high temperature grade of the RAP binder when using RAP.
WMA Construction equipment and operations	Similar to HMA except WMA has a lower compaction temperature and less compaction effort. Additionally, the following should be considered: • High pre-computation by paver screed (i.e. tampers and vibrators) • Perform a test section to establish the compaction procedure and rolling pattern for each mix type

4.3 WMA Performance Evaluation

Table 6 summarizes some of the performance tests, significance, requirements, criteria and related findings of using different materials and methods on the performance of the WMA based on several references including (NCHRP 691, 2011, (NCHRP 779, 2014) , (AASHTO R 35) and (NCHRP 843, 2017):

Table 6: Performance Evaluation Requirements, Criteria and Findings Summary

Performance Evaluation	Requirements and Criteria	Major Technical Findings
Mix Moisture Sensitivity	Major criteria to evaluate the Warm Asphalt mix durability and resistance to moisture damage. Stipulated in AASHTO R 35 and tested in accordance with AASHTO T283. The minimum recommended tensile strength ratio is 0.80	**NCHRP report 691 (Project 9-43A)** Anti-strip agent may be required to improve the moisture sensitivity. WMA technologies with anti-strip additives improved the tensile strength ratio (TSR) of some of the mixtures. The tensile strength ratio remained the same or improved in 67 per cent of the mixtures.
Mix Rutting Susceptibility	Evaluate WMA mix's ability to resist permanent deformation and rutting **NCHRP report 691 (Project 9-43A):** Rutting resistance is evaluated using Flow number test in AASHTO TP 79. **NCHRP report 843 (Project 9-43A)-**In the report, the rutting is evaluated using the Hamburg Wheel Tracking Test (HWTT) per AASHTO T324 and stipulated different scenarios for the rutting ranking based on rutting resistance index (RRI) and rut depth: Good: Rut depth 2.54 mm at 20000 cycles, RRI=18000, Average: Rut depth 12.5 mm at 20000 cycles, RRI=10,000 and Poor: Rut depth 12.5mm at 10,000 cycles, RRI=5000.	**NCHRP report 843 (Project 9-43A)** The report indicated equal or better Rutting Resistance for HMA and WMA mixes (using Evotherm, Sasobit and foaming) for one of the projects. **NCHRP report 779 (Project 9-47A)** The report indicated that the rut depth for WMA sections were slightly higher than of the HMA mainly for the traffic exceeding 3.5 million ESALs. Also, WMA mixes produced using foaming technique showed better rutting performance than with additives.
Fatigue Performance	Not a major concern for WMA mixes and may improve by implementing Warm Mix asphalt except for some organic additives.	**NCHRP report 843 (Project 9-49)** The reports show that HMA and WMA pavement exhibited comparable wheel path longitudinal cracking. The three WMA techniques discussed

		have similar resistance to wheel-path longitudinal cracking in relatively short service periods. However, in the longer term, the effect of aging on organic WMA technology is more prominent. The chemical and foaming WMA pavements appear to have better resistance to longitudinal cracking than the organic WMA pavements in the long term.

4.4 Proposed Potential Implementation Plan of WMA in Qatar

Notwithstanding the significant experience in implementing different types and techniques of the WMA worldwide, the experience of WMA in Qatar and GCC is still very limited. Previous studies on WMA and a trial done using WMA technology on a temporary traffic diversion on one expressway project in Qatar during 2014 produced no documented data to evaluate the short-and long-term performance of the WMA pavement section.

Further steps are required before the WMA can be fully incorporated in Qatar road projects which will consider also local materials and climatic conditions. These steps can be summarized as follows:

a. Perform several presentations and training to stakeholders involved in the pavement industry in Qatar, explaining the technology, implementation techniques, requirements, and overall benefits of WMA.

b. Compile information on the materials locally available.

c. Compile data on plants and industry-readiness to adopt WMA.

d. Conduct multiple trials to evaluate the performance of the WMA compared to HMA using several local binder grades and types (Neat, PMB and CRMB), using RAP, using different mixing plant fuel types and different mix types. The evaluation will cover materials selection, mix design process, materials production, construction practices, carbon emissions measurement (i.e., using gas meter reading from plant stacks), fuel consumption, cost per ton, performance testing (e.g. Moisture and Rutting Susceptibility).

e. The trials may be performed incorporating different WMA techniques; organic additives blended with the binder can be considered as a starting point.

f. Develop or update the current specifications and guidelines based on the international standards and local materials properties to cover WMA Technologies.

g. Perform a life-cycle cost analysis of WMA taking into consideration the commercial impact of its implementation considering fuel saving and cost of additives.

5 Conclusion and Recommendations

The benefits of using WMA are well-documented worldwide with the major driver for its implementation in Qatar being the reduction of paving costs, improvement of asphalt compaction, allowing asphalt mix to be hauled longer distances, and improvement of the working conditions by reducing exposure to fuel emissions, fumes, and odors. The following summarizes the salient points and recommendations of the papers:

1. WMA is an acceptable alternative to the HMA since it cuts down asphalt mixing-and compaction- temperatures by 20°C to 30°C and enables fuel savings, lower gas emissions, and a safer working environment.

2. In general, WMA can achieve comparable performance to HMA, in terms of aging and fatigue cracking. However, rutting performance is limited to a lower traffic load, and anti-strip may be required to improve moisture sensitivity when modified binders are used for the asphalt mix.
3. Customized WMA specifications need to be developed for Qatar's local conditions after successful implementation and monitoring of pilot projects.
4. The WMA mix design, materials selections, production and construction methods should be developed and incorporated into the next revision of the QCS.
5. Local materials, recycled asphalt pavement (RAP) and Crumb Rubber Modified Binders (CRMB) should be considered in the implementation of WMA in Qatar, to enhance pavement performance in addition to the sustainability and environmental benefits.

References

AASHTO R35. (2022). "Special Mixture Design Considerations and Methods for Warm Mix Asphalt (WMA)"

Aschenbrener, T. & West, R. (2011). "NCAT Report 11-02 Three-Year Evaluation of the Colorado Department of Transportation's Warm-Mix Asphalt Experimental Feature on I-70 in Silverthorne, Colorado Final Report"

D'Angelo, et al. (2008). "Warm-Mix Asphalt: European Practice", *FDHW, FHWA-PL-08-007*.

European Asphalt Pavement Association. (2020). "*Asphalt in Figures*".

European, Asphalt Pavement Association. (2014). "*The Use of Warm Mix Asphalt*".

Milad, et al. (2022). "A Comparative Review of Hot and Warm Mix Asphalt Technologies from Environmental and Economic Perspectives: Towards a Sustainable Asphalt Pavement", *Journal of Environmental Research and Public Health 2022*, 19, 14863. https://doi.org/10.3390/ ijerph192214863

NCHRP Report 619 (Project 9-43A). (2011). "*Mix Design Practices for Warm Mix Asphalt.*"

NCHRP Report 779 (Project 9-47A). (2014). "*Field Performance of Warm Mix Asphalt.*"

NCHRP Report 843 (Project 949). (2017). "*Long-term Field Performance of Warm Mix Asphalt Technologies.*"

Shacat, et al. (2022). "GHG Emissions Inventory for Asphalt Mix Production in the United States. Current Industry Practices and Opportunities to Reduce Future Emissions", *NAPA*, SIP 106.

Cite as: Anshasi M. & Nunoo C., "Potential Implementation of Warm Mix Asphalt (WMA) in Pavement Construction in The State of Qatar", *The 2nd International Conference on Civil Infrastructure and Construction (CIC 2023)*, Doha, Qatar, 5-8 February 2023, DOI: https://doi.org/10.29117/cic.2023.0090

Potential Utilization of Alternative Construction Materials in Qatar, in lieu of Conventional Washed Sand

Subrahmanyam Pilaka Venkata
AECOM/ Public Works Authority (Ashghal), Roads Projects Department, Doha, Qatar.
svenkata@ashghal.gov.qa / pvsubbu23@gmail.com

Ahmed Ghanim Abdulsalam Abunahia
Public Works Authority (Ashghal), Roads Projects Department, Doha, Qatar
anahia@ashghal.gov.qa

Aisha Zayed M. A. AlKhayareen
Public Works Authority (Ashghal), Roads Projects Department, Doha, Qatar
aalkhayareen@ashghal.gov.qa

Noora Ibrahim Q. S. Al-Ansari
Public Works Authority (Ashghal), Roads Projects Department, Doha, Qatar
nalansari@ashghal.gov.qa

Abstract

Natural sand that has been washed is an essential material used in infrastructure development and construction projects of all sizes. Due to the depletion of natural sand sources in Qatar, there has arisen a need to develop alternate materials to replace it. Substitutes such as wadi gravel, marine sand and manufactured sand, including crushed imported limestone, recycled sand and crushed gabbro have been considered and explored. Consequently, a proposal to encourage local washed sand producers to incorporate varying proportions of these alternate materials into the various material demands was considered by the Public Works Department, depending on the application in either structural and/or precast members. This paper primarily focuses on providing an overview of some of the available alternate materials to washed sand that could be utilized without affecting the physical, mechanical, or strength properties of concrete, precast, and other construction materials that use washed sand, while at the same time providing a long-lasting, durable and economically beneficial alternative material to the national economy.

Keywords: Alternative materials; Recycled aggregates; Wadi gravel; Washed sand; Imported limestone; Marine sand; Strength aspects; Economically beneficial

1 Introduction

Sand is the world's second most consumed raw material after water and an essential ingredient in the construction industry. In the future, industrialization, population growth, and urbanization are all likely to fuel explosive growth in sand demand. The global use of sand and gravel has been discovered to be ten times that of cement. This means that the world consumes 50 billion tonnes of sand and gravel per year just for construction. (United Nations, 2022)

Qatar's waste generation output is expected to rise in the near future due to the country's growing population, and increase in construction related to the World Cup 2022 projects, and a general increase in industrial output. More than 2.5 million tonnes of municipal solid waste are produced annually in Qatar, or around 2.5 kg per person per day. Qatar's waste generation problem is not just limited to municipal solid waste; the construction sector is also a major contributor. Currently, Qatar

generates 8.0 million tonnes per year of construction waste, and this number is predicted to remain above 6.0 million tonnes per year through 2030 (Qatar Development Bank, 2017).

Domestic demand for sand in Qatar, like in many other countries, is increasing, raising the possibility that the country's reserves will be consistently reduced. As a result, there is a risk that washed sand will soon be a scarce commodity. This can be mitigated by systematically implementing certain alternative materials through sustainability policies and regulations. This paper provides an overview of identified alternative materials to washed sand that do not affect the physical, mechanical, or strength aspects of concrete, precast, and all other construction elements that use washed sand, while also being long-lasting, durable, and economically beneficial to the national economy.

This paper will cover the following alternative construction materials, with a particular emphasis on alternatives to washed sand.

1. Recycled aggregates.
2. Wadi gravel.
3. Marine sand.
4. Imported crushed limestone sand.
5. Imported crushed gabbro sand.
6. Imported processed washed sand.

2 Alternative Materials

2.1 Recycled Aggregates

The Building Projects Department of the Public Works Authority (PWA) completed a pilot project using recycled aggregates in the State of Qatar for a holding tank, part of the Quarantine Veterinary & Laboratory Project at Hamad Seaport through Envi-Beton Company & Qatar Primary Materials Company (QPMC). The results were more than satisfactory, exceeding the Qatar Construction Specifications (QCS, 2014) requirement. Durability tests were conducted at the request of Ashghal's Quality and Safety Department (QSD), and the results exceeded the requirements of all applicable specifications.

The main issues with recycled aggregates include high values of acid soluble sulfate and chloride, sand equivalent, water absorption and fractions falling grading limits. The solutions include new system of recycling processes and modification of impact crushers and the use of new technology. The conclusion is that using recycled aggregates with no extra natural aggregates or sand will undoubtedly benefit the industry. Increased usage of recycled aggregate will reduce waste accumulation in landfills while decreasing demand for natural aggregates.

2.2 Wadi Gravel

Despite being a potential supply of fine and coarse aggregate, substantial processing was necessary to remove gypsum and make the aggregates appropriate for use in concrete to avoid internal sulfate attack. However, the savings in transportation costs and greenhouse gas emissions from not importing gabbro or other aggregates from distant sources more than compensate for this disadvantage. "Wadi gravel — a new concrete aggregate in Qatar: Part 1 — investigation, processing, and trials," a paper published by Khalid et al. (2020), demonstrated the successful processing of local Wadi gravel from Mekaines using Qatar's existing advanced washing and crushing facilities to produce QCS 2014-compliant aggregate for use as a coarse aggregate in concrete. The research also indicated several promising things to consider when using crushed wadi gravel sand as an alternative through numerous

trials, test results, and petrographic analysis. However, it emphasizes the challenges in processing crushed wadi gravel sand to remove gypsum that has adhered to it. The studies give some recommendations for the quantities of wadi gravel that are required to replace traditional washed sand in concrete.

Based on the current state of washed sand in Qatar and the above-mentioned study, Qatar Sand Treatment Plant (QSTP) conducted some trials with various wadi gravel crushed sand approved proportions, with the following results and conclusions:

Table 1: Trial results for wadi gravel crushed sand

0-5mm Natural wadi crushed sand 100%				
	Mix design	**Qty %**	**Compressive Strength, N/mm^2**	**Average N/mm^2**
Trial#1	Cement-OPC	17.3		**31N/mm^2**
	0-5 Natural wadi crushed sand	33.0	22.6	
	Water	7.2	33.8	
	Admixture	0.09		
	5-10mm Gabbro Aggregate	12.4		
	10-20mm Gabbro Aggregate	30.0	35.8	
0-5mm Natural wadi crushed sand 70%+ 0-5mm Washed sand 30%				
	Mix design	**Qty %**	**Compressive Strength, N/mm^2**	**Average N/mm2**
Trial#2	Cement-OPC	17.1		**47N/mm^2**
	0-5mm Natural wadi crushed sand	22.8	46.1	
	0-5mm Washed sand	9.7		
	Water	8.5	49.1	
	Admixture	0.09		
	5-10mm Gabbro Aggregate	12.2		
	10-20mm Gabbro Aggregate	29.6	44.9	
0-5mm Natural wadi crushed sand 50%+ 0-5mm Washed sand 50%				
	Mix design	**Qty %**	**Compressive Strength, N/mm^2**	**Average N/mm^2**
Trial#3	Cement-OPC	17.1		**52N/mm^2**
	0-5mm Natural wadi crushed sand	16.2	52.0	
	0-5mm Washed sand	16.2		
	Water	8.5	50.8	
	Admixture	0.09		
	5-10mm Gabbro Aggregate	12.2		
	10-20mm Gabbro Aggregate	29.6	52.5	

1. Trial#1-Strength is good but the surface finish is unsatisfactory.
2. Trial#2-Strength is high and the surface finish is satisfactory.
3. Trial#3-Strength is too high and the surface finish is satisfactory.

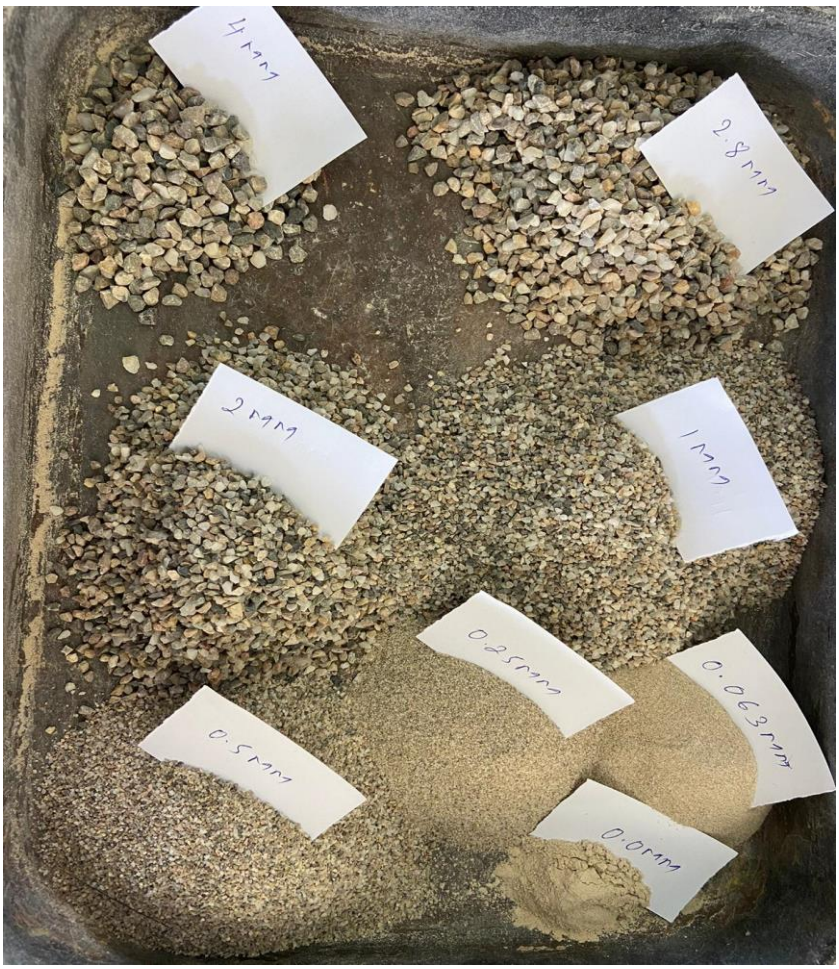


Fig. 1: Wadi gravel crushed aggregates of various sizes

If we propose to use the locally available wadi gravel as fine aggregate, local washed sand producers are prepared to invest and bring in specialized and cutting-edge technological equipment to crush, screen, process, and remove undesirable gypsum-bound deposits sticking to gravel.

2.3 Marine Sand

Due to the high chloride content of marine sand, more processing, washing, and cleaning are required to meet applicable specifications. Given the current situation, marine sand can be considered one of the viable alternatives to washed sand. Another study was conducted and published by Al Kuwari and Khaled (2015), for the Ministry of Environment, Science, and Technology Park. Advantages and disadvantages of marine sand are detailed below:

Advantages of Marine Sand

1. Marine sand particles are rounded or cubical.
2. The grading of sea sand is finer than that of river sand.
3. It contains no silt or organic materials.
4. It is readily available, but requires cleaning.
5. Material grading and consistency are uniform.
6. Reasonable cost of mining.
7. Countries with access to the sea such as Qatar can make extensive use of this natural resource.

Disadvantages of Marine Sand

1. Corrosion of reinforcements.
2. Cost and time for processing sea sand.
3. Production may require larger capital investment.
4. The mining of marine sand has an environmental impact, which can be mitigated.
5. May contain seashell.
6. Higher chloride content.

Table 2: Test results of marine sand

e	TEST REQUIREMENT	QCS 2014 S.5, P.2 PERMISSIBLE LIMITS	WASHED SEA SAND
1	Clay Lumps and Friable Particles (%)	2 % max	2%
2	Oven Dried (mg/m^3)		2.22 (mg/m ^{3})
3	S.S.D (mg/m ^{3})		2.38 (mg/m ^{3})
4	Apparent (mg/m ^{3})	2.0 min	2.66 (mg/m ^{3})
5	Water Absorption (%)	2.3 max	2%
6	Sand Equivalent Value (%)	60% min	90%
7	Shell Content (%)	3 % max	2%
8	Acid-soluble Chlorides (%)	0.06 % max	0.04%
9	Acid-soluble Sulphate^2 (%)	0.40 % max	0.35%
10	Material Fine Than 0.063 mm (%)	3 % max	2%
11	Bulk Density Un-Compacted (mg/m ^{3})		1.05 (mg/m ^{3})
12	Bulk Density Compacted (mg/m^3)		1.17 (mg/m ^{3})
13	Sand Color		Grey

2.4 Imported Crushed Limestone Sand

The UAE and Oman Musandam (Oman) limestone is considered among the best quality in the world. This imported limestone is widely used in ready-mix concrete plants and the manufacture of cement precast products. M/s Readymix Qatar is already using imported limestone from Musandam (Oman) for the “Nakhilat Ship Repair Yard Project” in Ras Laffan in Qatar. Test results comply with (QCS, 2014).

2.5 Imported Crushed Gabbro Sand

Gabbro is a coarse-grained, dark-colored, intrusive igneous rock. It is usually black or dark green in color and is made up mostly of the minerals plagioclase and augite. Gabbro, due to its durability and strength, has a wide range of applications in the building industry. It is brought into Qatar from the UAE and Oman. Before being utilized as fine aggregates in concrete, crushed gabbro must be treated to eliminate filler. In the face mix of the paving blocks, processed crushed gabbro was used. Cost, on the other hand, is a major issue determining the use of crushed gabbro sand, necessitating serious consideration of other materials such as wadi gravel.

2.6 Imported Processed Washed Sand

The Public Works Authority's Road Project Department (RPD) explored the possibility of importing washed sand from the region (Iran, Kingdom of Saudi Arabia KSA, etc.) via a few ready mix plants and precast manufacturers, but doing so would require approval from multiple government agencies and would most likely be expensive from Iran, but the option is open from Al Hofuf, KSA.

3. Conclusion

This paper proposes that using alternative materials (recycled aggregates and Wadi gravel) will provide Qatar with numerous advantages, including enhancing environmental protection, productive use of otherwise waste materials, reducing natural aggregate imports, cost savings, new business opportunities, and a reduction in greenhouse gas emissions. Simultaneously, alternatives such as sand imports from Al Hofuf, KSA, and the usage of marine sand (while mitigating environmental issues) should be explored for future demands.

Producers of washed sand should be permitted to utilize different proportions of available materials, including washed sand, imported limestone, crushed wadi gravel sand, and crushed gabbro sand, particularly for precast elements and non-structural concrete subject to QCS compliance.

All government bodies, including all PWA departments, QSD, the Central Laboratory, and universities, should hold discussions on the above proposals and develop application-focused specifications, particularly for structural, non-structural, precast, and marine structures. Depending on the importance of the structural members, different alternative options should be made available to ready mix and precast producers, while also taking critical requirements compliance, such as durability, into consideration.

Acknowledgements

The authors would like to thank the Manager of Road Projects Department, (RPD) PWA, Eng. Saoud Ali A. A. Al-Tamimi, Dr. Osman Elhussain Mohamed Idris, Quality and Safety Department (QSD), Dr. Charles Nunoo (RPD) and Qatar Primary Materials Company (QPMC). The acknowledgement also goes to the Building Projects Department (BPD), Design Department (DD), Qatar Sand Treatment Plant (QSTP) for their valuable contributions and ongoing support from proposals to conducting trials for various alternatives such as wadi gravel, recycled aggregates, and crushed gabbro sand for various pilot projects.

References

Al-Kuwari, M.S. & Hassan, K. (2015). "Concrete Sand Sustainability Report (In Arabic), prepared for Ministry of Environment.

Hassan, K. et al. (2019) "Wadi Gravel- a new concrete aggregate in Qatar: Part1-investigation processing and trials" *Quarterly Journal of Engineering Geology and Hydrology* (QJEGH)

Qatar National Research Fund, QNRF NPRP NO: 7 – 795 – 2 – 296 2022 – Implementation of recycled aggregates in construction. QDB-2017, Material Recovery Products in Qatar (qdb.qa),

United Nations Environment Programme. (2022). Our use of sand brings us "up against the wall". https://www.unep.org/news-and-stories/press-release/our-use-sand-brings-us-against-wall-says-unep-report

Cite as: Venkata S.P., Alkhayareen A.Z.M.A., Al Ansari N.I.Q.S. & Abunahia A.G.A., "Potential Utilization of Alternative Construction Materials in Qatar, in lieu of Conventional Washed Sand)", *The 2nd International Conference on Civil Infrastructure and Construction (CIC 2023)*, Doha, Qatar, 5-8 February 2023, DOI: https://doi.org/10.29117/cic.2023.0091

Experimental Validation of Repair Methods for Earthquake-Damaged Bridges Incorporating Pipe-Socket Precast Pier System

Kathryn Hogarth
Idaho State University, Pocatello, Idaho, United States
hogakat2@isu.edu

Arya Ebrahimpour
Idaho State University, Pocatello, Idaho, United States
ebraarya@isu.edu

Mustafa Mashal
Idaho State University, Pocatello, Idaho, United States
mashmust@isu.edu

Abstract

This project focuses on the retrofitting of concrete bridge piers. In the first phase of the project, a half-scale bridge bent was designed and experimentally tested in the Idaho State University (ISU) Structural Lab (SLAB) under earthquake-style loading. The bents modeled a pier connection developed by ISU and Idaho Transportation Department (ITD) (pipe-socket connection). The bridge bent was tested until failure and the results were processed and compared to one another. After testing the bent specimens ISU and ITD have come back to work on another project to retrofit the half-scale bridge piers and experimentally test and quantify the design. Many post-earthquake repair methods have been suggested by ISU and ITD to repair the pier's stiffness, strength, and ductility after a design-level event. This paper focuses on ultra-high-performance concrete (UHPC) jacketing as the retrofit method. Methods to retrofit concrete-filled steel tubes (CFSTs) have only been used in analytical studies and have not been experimentally tested. In order to combat this issue of lack of experimental data, ISU is testing four piers with a UHPC jacket retrofit. The objective of this research is to experimentally validate the proposed UHPC retrofit for the pipe connection.

Keywords: Seismic retrofit; Bridge piers; UHPC; CFST; Jacket

1 Introduction

The first phase of this project was to test the pipe connection of an Accelerated Bridge Construction (ABC) bridge bent and compare the results to a typical cast-in-place (CIP) bridge bent. A diagram showing the design of the pipe connection can be seen in Figure 1. The pipe connection is advantageous because it incorporates ABC, it has ample installation tolerance, it has improved onsite safety, and it allows deformation during smaller movements.

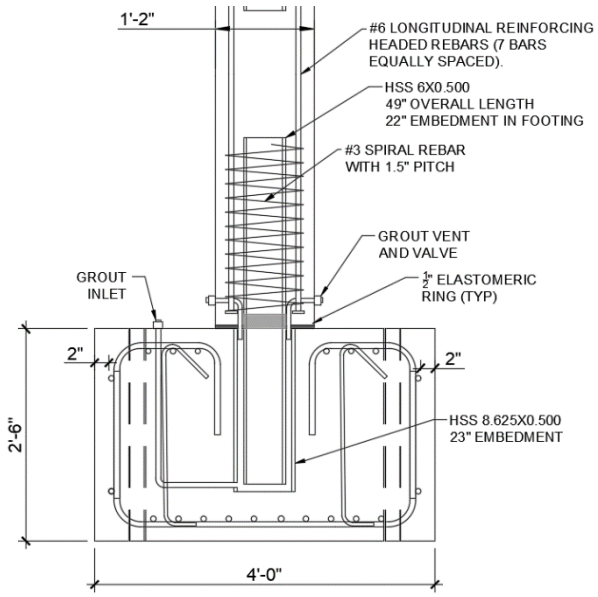


Fig. 1: Pipe-Socket Connection for Column-to-Footing Connection

In the first phase of the project, both bents were tested under quasi-static loading using a hydraulic actuator. The results from comparing the half-scale bridge bents show that the precast bent had more ductility and energy dissipation compared to the CIP bent. Figure 2 shows the numerical results in the form of the hysteresis loops.

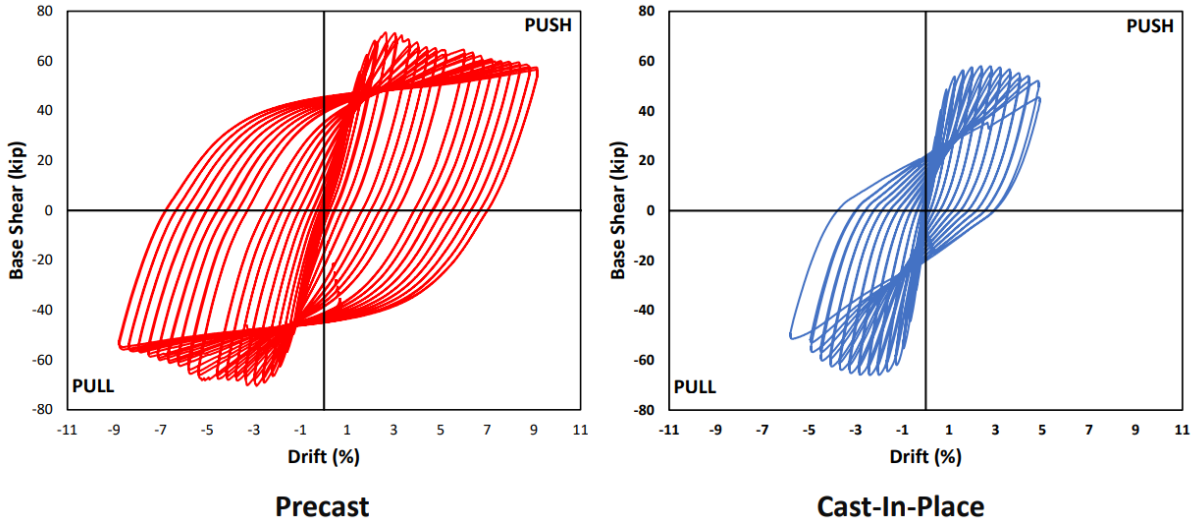


Fig. 2: Hysteresis Graphs of Half-scale Bridge Bents (1 kip = 1.45 kN)

After the specimens were tested, they were dissembled and stored at ISU. As shown in Figure 2, the precast bent with the pipe connection outperformed the CIP bent. Now ISU and ITD are presented with an opportunity and interesting research question: What is the best method for retrofitting of bridge piers with a pipe connection after an earthquake event?

The objective of this research is to experimentally validate some of the proposed retrofitting options for the pipe connection. The final design for the retrofit needs to be effective in restoring stiffness, strength, and displacement ductility of the pier by 70-80%. The design must also be practical, fast, cost-effective, and durable.

2 Literature Review

To find a sufficient repair method for the pipe-socket connection, a literature review of retrofitting

methods for bridge piers was conducted. Through the review the following methods were investigated: steel jacketing (Bemstead et al., 2019), concrete jacketing (Krish et al., 2018), fiber-reinforced polymers (FRP), and external yielding elements (Wang et al., 2017). From the literature review it was obvious that a UHPC jacket would be the most ideal retrofit method for the project.

2.1 Steel Jacketing Literature Review

Many research projects have been conducted to investigate steel jacketing to seismically retrofit bridge piers. The concept is to confine the original concrete pier with a steel jacket through bolting or welding. The gap between the jacket and the damaged concrete is then filled with grout. Steel jackets can be the partial or full height of the pier. Steel jacketing significantly increases the pier stiffness due to an increase in the size of the cross-section of the pier (Chail et al., 1991). While steel jacketing is effective in restoring seismic performance; it is considered very costly and labor-intensive (Raza et al., 2019).

2.2 FRP Literature Review

FRP is advantageous compared to traditional jacketing methods (concrete and steel jacketing) because installation of FRP is less labor-intensive, installation is easy and relatively quick, and minimizes changes to the cross-sectional geometry of the bridge piers. The biggest disadvantage to FRP is de-bonding. In a study performed by Kotynia et al. (2008) on the strengthening of reinforced concrete beams using FRP, failure occurred in all specimens due to premature de-bonding of the FRP from the concrete surface which led to a lower strength utilization ratio (i.e. the ratio of strain in FRP at failure to its ultimate strain). Another disadvantage of FRP is that it is expensive and does not perform as well as in high temperatures or wet environments (Raza et al., 2019). The most common type of FRP used in seismic retrofitting is carbon fiber reinforced polymers (CFRP). Many studies have been conducted on the use of CFRP as a seismic retrofit technique. In an experimental study, it was found that CFRP can increase lateral load capacity by 7% in bridge piers, (Faustino & Chastre, 2016).

2.3 UHPC Jacketing Literature Review

UHPC is a concrete material that is composed of steel fibers, silica fume, fly ash, Portland cement, fine aggregates, admixtures and water. UHPC typically has a compressive strength of 18 to 35 ksi (124-228 MPa). A comparison of UHPC to normal-strength concrete (NSC) and high-strength concrete (HSC) can be seen in Table 1. The comparison in Table 1 shows that UHPC has many beneficial qualities over typical concretes.

Table 1: Comparison of properties of UHPC with NSC and HSC (Ahlborn et al., 2011)

Property	NSC	HSC	UHPC
Compressive Strength	3,000-6,000 psi (20.7-41.3 MPa)	6,000-14,000 psi (41.3-96.5 MPa)	18,000-33,000 psi (124.11-227.5 MPa)
Tensile Strength	400-500 psi (2.75-3.45 MPa)	-	1,000-3,500 psi (6.89-24.13 MPa)
Elastic Modulus	2,000-6,000 ksi (13.8-41.4 GPa)	4,500-8,000 ksi (31.02-55.16 GPa)	8,000-9,000 ksi (55.16-62.05 GPa)
Poisson's Ratio	0.11-0.21	-	0.19-0.24
Porosity	20-25%	10-15%	2-6%
Chloride Penetration	>2000	500-2000	<100
Water-Cement Ratio	0.40-0.70	0.24-0.35	0.14-0.27

UHPC has been a popular repair method recently in Canada. Many retrofit projects in Canada are using UHPC jacketing methods. For example, Mission Bridge was recently seismically retrofitted in Abbotsford, British Columbia (Figure 3). Mission Bridge is a 1,126-meter bridge that crosses the Fraser River. One of the nineteen V-shaped concrete piers was retrofitted with UHPC jackets for two of the existing concrete columns. The jackets incorporated UHPC with a mild steel reinforcing cage. The retrofit was the final step in a series of seismic upgrades performed over several years, to ensure the integrity of this vital link in a high seismic zone. The project was completed in June 2014 (Doiron, 2016).



Fig. 3: Mission Bridge Seismic Retrofit Project Abbotsford, British Columbia, Canada, Doiron (2016)

3 Concept for Retrofit

After some preliminary literature review and discussion with ITD, the basis of retrofitting the precast pier is to utilize a UHPC jacket in the plastic hinge zone of the pier. The concept can be seen in Figure 4.

Preliminary calculations have been done for the design of the UHPC jacket using SAP2000. The precast column section with the UHPC jacket can be seen in the cross-section (Figure 5). Note that it has been decided to test using twelve no. 6 rebar dowels to push the plastic hinge above the jacket/pipe region and provide sufficient shear and flexural resistance at the column-to-footing interface for the first specimen. The first specimen will also include circular stirrups (no. 3 at a 1.5 in. spacing) for better confinement.

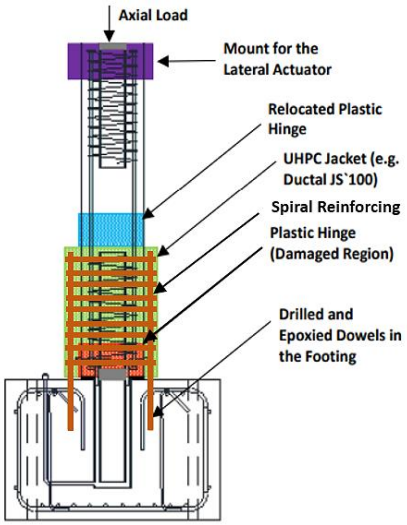


Fig. 4: Concept for UHPC Jacket (Green Section)

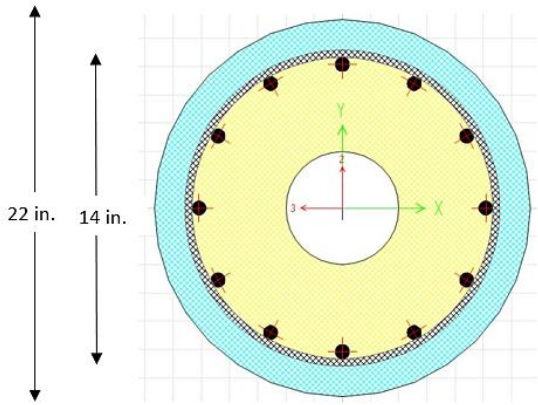


Fig. 5: Precast 1 Design

Note that since the pipe in this specimen is fractured, the moment capacity contribution from the pipe is conservatively taken to be negligible. Also note that for this specimen all of the cover concrete

spalled, therefore the entire section, excluding the pipe, is taken to be UHPC. The jacket is designed to sit at a 4 in. (10.16 cm) thickness out from the original column diameter (14 in. or 35.56 cm), with an overall diameter of 22 in (55.88 cm).

4 Experimental Program

The experimental program follows the flowchart in Figure 6. Preliminary testing is done to quantify UHPC and NSC bond strength, tensile strength, and compressive strength. The UHPC used in the experimental program is JS1000 provided by Ductal.

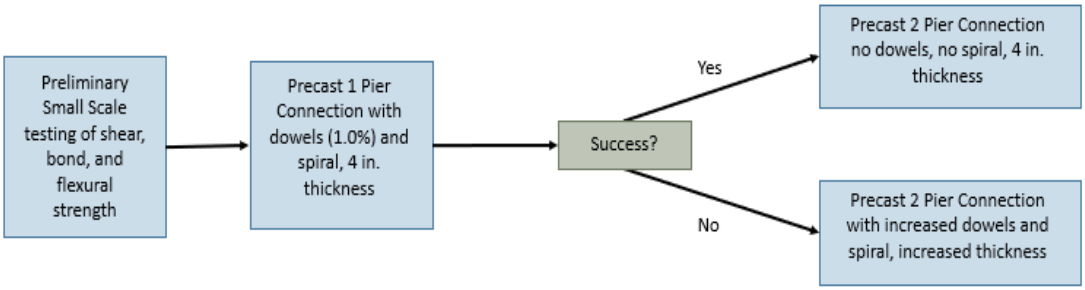


Fig. 6: Experimental program

5 Construction of Precast 1 and Testing

The design for the jacket of Precast 1 was accepted by ITD and construction began by ISU in July of 2022. The first step is to roughen the surface for the pour, as well as drill the concrete to allow for the tension dowels to be epoxied in (Figure 7-a). The next step is to assemble the cage (Figure 7-b). Lastly, the form is assembled and the UHPC is poured (Figure 7-c). Note that the jacket is poured while the pier is under a 30-kip (133kN) axial load to simulate the structure of a bridge.

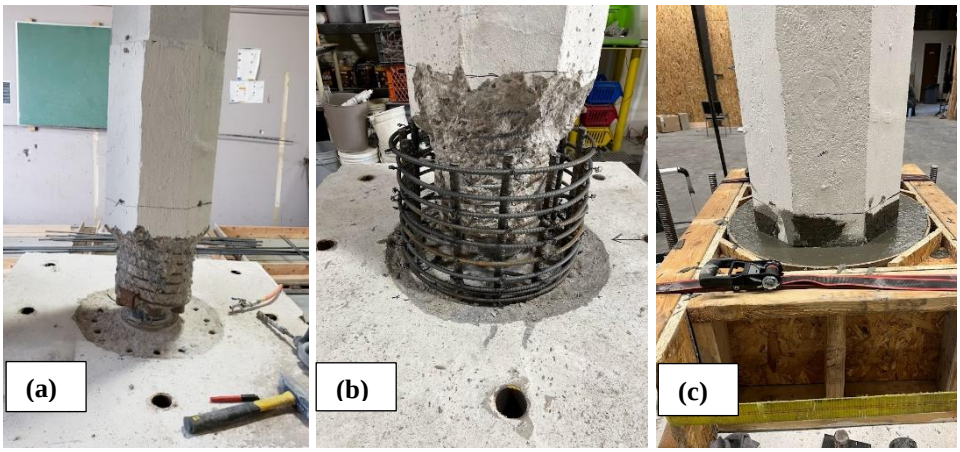


Fig. 7: Construction of Precast 1

After the pier is poured and cured, Precast 1 is instrumented and moved into the lab to get ready for testing. The test setup can be seen in Figure 8. The test is accomplished by programming the hydraulic actuator to run a loading protocol similar to the bent loading protocol, which has been scaled down for one pier. The loading protocol is a quasi-static cyclic loading protocol. During testing, the pier is monitored for cracks and spalling. Photos, videos, and documentation were taken as necessary.

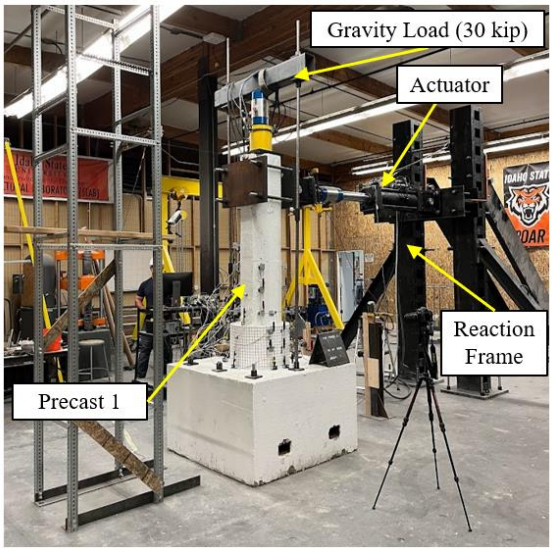


Fig. 8: Test set-up

6 Results for Precast 1

The results for Precast 1 can be seen in Figure 9. The jacket performed as expected and was successful in pushing the plastic hinge up the face of the column. The jacket saw no uplift from the footing and no separation from the column.

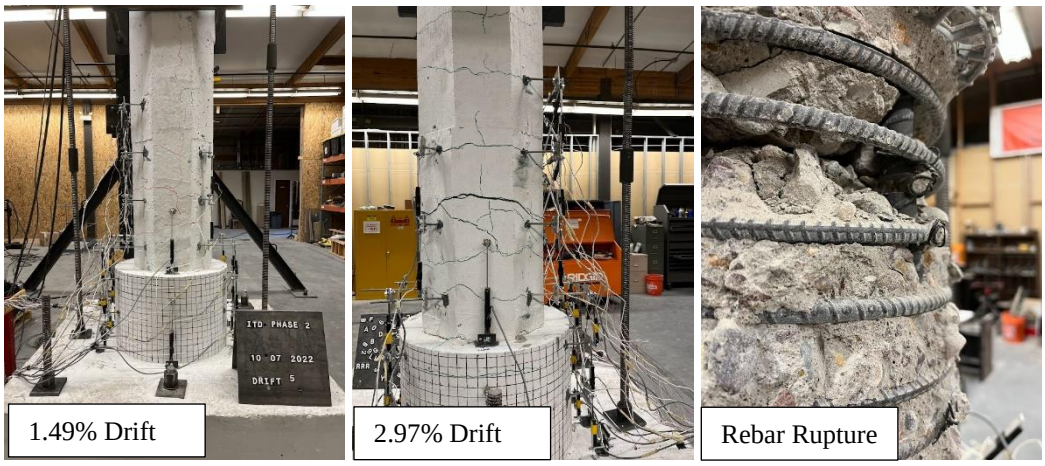


Fig. 9: Photos from Precast 1 Testing

The hysteresis of Precast 1 can be seen in Figure 10. The ultimate force for Precast 1 is 30.76 kip (137 kN) at 2.6% drift. Data from Precast 1 is still being analyzed and processed and will be presented in the future.

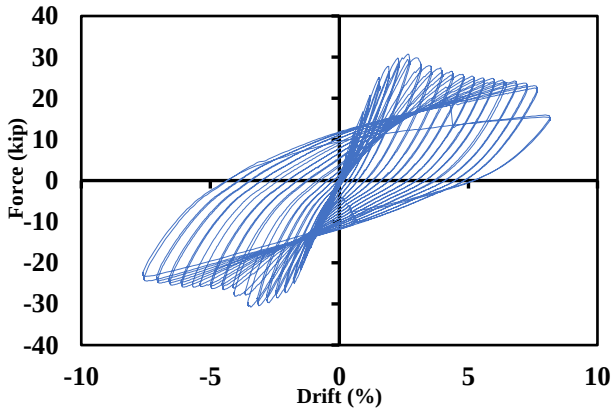


Fig. 10: Precast 1 Force vs Displacement (1 kip = 1.45 kN)

7 Construction of Precast 2 and Testing

After the success of Precast 1, Precast 2 was constructed. The design for Precast 2 was a 4 in. jacket with no steel reinforcing. The construction process follows the same steps as that of Precast 1, except for the concrete drilling. After Precast 2 is constructed, it was tested in the same manner as Precast 1. The testing used the same test setup and instrumentation. The same loading protocol was used for Precast 2. During testing documentation, photos, and videos were taken as necessary.

8 Results for Precast 2

The results for Precast 2 can be seen in Figure 11. The jacket succeeded in pushing the plastic hinge up the face of the column. Due to no tension dowels being used, the jacket and footing interface separated, creating rocking during testing. Despite the rocking, the column was still able to deform above the jacket. Due to the rocking, testing of Precast 2 ran longer by 4 cycles. The force vs drift hysteresis for Precast 2 can be seen in Figure 12. The rapid decline around at 6.64% drift is due to the rebar rupture.

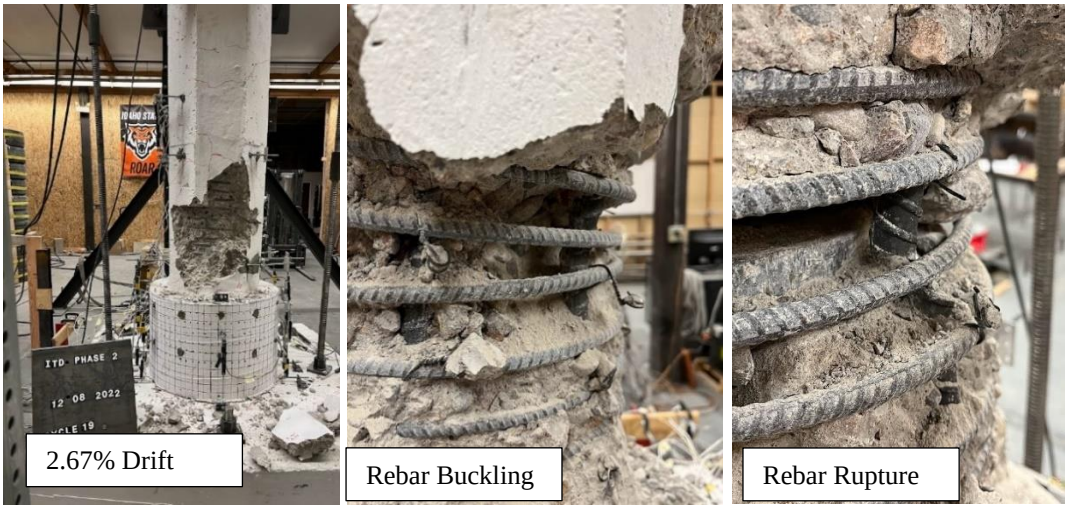


Fig. 11: Photos from Precast 2 Testing

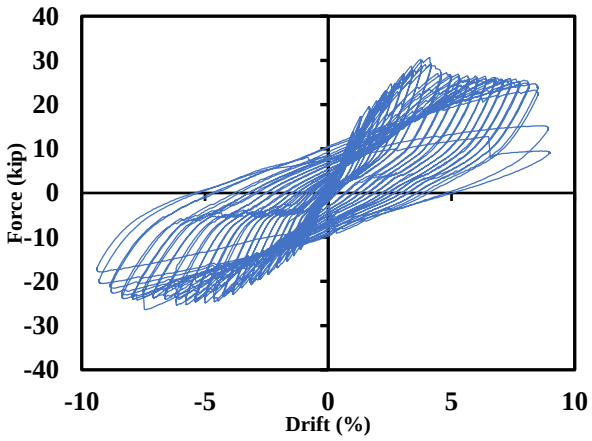


Fig. 12: Force vs Drift for Precast 2 (1 kip = 1.45 kN)

9 Conclusion

This project covers seismic retrofit of pipe-socket connected piers. The project investigated the suitability of UHPC jacketing methods. For Precast 1, a 4” UHPC jacket is used with light caging. Precast 2 incorporated a 4” UHPC jacket with no caging. Both methods for retrofit were successful. Precast 1 pushed the plastic hinge up the column face with no separation from the footing. Precast 2

succeeded in pushing the plastic hinge up the face of the column with separation from the footing and partial failure due to rocking. Precast 2 has just been tested in the ISU SLAB in December of 2022. More results are to become available as they are processed for comparison with the original pier and the two retrofit options. From observation, it is clear that the UHPC jacket method is a suitable method to retrofit the pipe-socket connection.

References

Ahlborn, et al. (2011). "Characterization of Strength and Durability of Ultra-High-Performance Concrete under Variable Curing Conditions", *Transportation Research Record*, *2251*(1), 68–75. DOI: 10.3141/2251-07

Bumstead, J., Korat, J. & Stephens M. T. (2019). "Repair Strategies for Earthquake-Damaged CFST Bridge Columns", *ASCE Structures Congress*, DOI: 10.1061/9780784482230.016

Chail, Y. H., Priestley, M. J. N. & Seible, F. (1991). "Seismic Retrofit of Circular Bridge Columns for Enhanced Performance", *ACI Structural Journal*, *88*(5), 572-584. DOI: 10.14359/2759

Doiron, G. (2016). "Pier Repair/Retrofit Using UHPC – Examples of Completed Projects in North America", *International Interactive Symposium on Ultra-High Performance Concrete*, *1*(1). DOI: 10.21838/uhpc.2016.99

Faustino, P. & Chastre, C. (2016). "Damage Effect on Concrete Columns Confined with Carbon Composites", *ACI Structural Journal*, *113*(5), 951-962. DOI: 10.14359/51687916

Kotynia, et al. (2008). "Flexural Strengthening of RC Beams with Externally Bonded CFRP Systems: Test Results and 3D Nonlinear FE Analysis", *Journal of Composites for Construction*, *12*(2), 190-201. DOI: 10.1061/(ASCE)1090-0268(2008)12:2(190)

Krish, et al. (2018). "Rapid Repair of Reinforced Concrete Bridge Columns via Plastic Hinge Relocation Utilizing Conventional Materials", *Alaska Department of Transportation & Public Facilities*, URL: http://www.dot.alaska.gov/stwddes/research/search_lib.shtml

Raza, et al. (2019). "Strengthening and Repair of Reinforced Concrete Columns by Jacketing: State-of-the-Art Review", *Sustainability*, *11*(11), 3208. DOI: 10.3390/su11113208

Wang, Z. et al. (2018). "Seismic Behavior of Precast Segmental UHPC Bridge Columns with Replacable External Cover Plates and Internal Dissipaters", *Engineering Structures*, *177*(1), 540-555. DOI: 10.1016/j.engstruct.2018.10.012.

Cite as: Hogarth K., Ebrahimpour A. & Mashal M., "Experimental Validation of Repair Methods for Earthquake-Damaged Bridges Incorporating Pipe-Socket Precast Pier System", *The 2nd International Conference on Civil Infrastructure and Construction (CIC 2023)*, Doha, Qatar, 5-8 February 2023, DOI: https://doi.org/10.29117/cic.2023.0092

Efficacy in developing a Sustainable, Resilient, and Interdependent Infrastructure System in the Gulf Region

Mohamed G. Mohamed
PhD student, University of Washington, Seattle, USA
mcmgs@uw.edu

Muiruri Kevin
PhD student, University of Washington, Seattle, USA
kevinmb@uw.edu

Abstract

The world is becoming increasingly interconnected, and the exchange of information, knowledge, and services assists in developing and managing many aspects of the built environment. Sustainable, resilient, and interdependent development of infrastructure emphasizes relationships among systems with benefits of creating one system-of-systems that includes enhancing the delivery of primary services, increasing systems efficiency in performing more than one function, exchanging benefits between systems, sharing information among systems, reducing carbon emission, eliminating waste, enhancing the operation of all systems, and reducing the cost of developing, managing, operating, and maintaining them. Infrastructure development in the Gulf region presents many challenges, such as excessive use of scarce natural resources, limited areas of development, and high cost of development, operation, and maintenance in each system. This study addresses the importance of developing a sustainable, resilient, and interdependent infrastructure system that can work with the natural processes and flows and respond to challenges specific to the Gulf Region. Its findings will guide decision-makers in the appropriate choices and the economic, environmental, and social opportunities in developing an integrated and efficient one-system network. Relationships between infrastructure systems, such as simple, colocation, or geographical relationship, and an integrated relationship in the Gulf region will be compared with other relevant international projects. Data from project-specific literature and case studies were used to carry out this study.

Keywords: Infrastructure system; Sustainable; Resilient; Interdependent; Gulf region

1. Introduction

Infrastructure systems, such as telecommunications, electric power systems, movement of natural gas and oil, transport, and water treatment and supply, are essential for the continuous and reliable functioning of economic and social systems, as they supply the main services that support economical production, safety, security, and a high quality of life. Infrastructure systems are developed, operated, and maintained to meet service requirements, resist deterioration such as fatigue, cracking, and corrosion, and withstand hazards such as floods, earthquakes, and winds. Many factors must be considered during infrastructure development, such as strength, rigidity, serviceability, and maintainability, in addition to sustainability, resilience, and interdependence of infrastructure (Grafius et al., 2020).

Sustainable infrastructure is based on development that meets the needs of the present without compromising the future. It must respond to environmental protection concerns, reduce

consumption of scarce and non-renewable natural resources, and adapt to climate change, economic development, and social equity. Sustainable development must have a friendly impact on the environment during the design, construction, rehabilitation, and maintenance stages. This should involve all project elements, including structural systems, construction materials, and maintenance plans. Infrastructure resilience is the ability of the developed systems to absorb or mitigate the impact of damage or hazard and to restore normal operation as soon as possible with minimum cost. Infrastructure interdependency is a two-way relationship between two or more systems in which the serviceability of any one system can influence other systems; operate depending on each other; and be developed to be part of or follow the natural systems (Chester et al., 2019).

This paper emphasizes and discusses the importance of developing sustainable, resilient, and interdependent infrastructure systems in the Gulf Region and the benefit of developing a practical and reliable level of relationship among the systems towards an integrated system that makes all systems work as one system.

2. Sustainable, Resilient and Interdependent Infrastructure Systems

2.1 Sustainable Infrastructure System

Sustainable development is development that addresses the requirements of the present without adversely affecting the needs of future generations. Sustainability is accepted as an important performance measure that should be included in the design, construction, operation, and maintenance of infrastructure systems (Hinge et al., 2020). Sustainable infrastructure can be achieved through three main execution measures, economic measures that meet the operation and maintenance requirement throughout the life cycle at minimal cost, environmental measures that utilize suitable materials and construction with the least influence on the environment during the construction, operation, repair, and dismantling, and social measures related to security, safety, and social equity. Infrastructure systems' construction, operation, and maintenance require large amounts of resources such as land, water, materials, and energy, which pollute the environment, including water contamination, sound, and greenhouse gas emissions.

Scarce natural resources and the environment must be protected by the proposed high-level workable design and rehabilitation strategies that reduce the impact on the natural environment, such as flora, fauna, soil, water, and air. The socioeconomic development of communities must be considered during the infrastructure development, including health, security, safety, equity, reliability, functionality, accessibility, operability, serviceability, maintainability, and costs (Lounis & McAllister, 2016).

2.2 Resilient Infrastructure System

Infrastructure resilience is the ability of substantial networks to withstand hazards, reduce interruption of functionality, and minimize recovery periods and costs. Various hazards and deterioration act and periods, such as reduction in capacity, corrosion, and fatigue (Kong et al., 2019). The resilience of an infrastructure system depends on many factors, such as the system’s function within the community. Important services of the infrastructure systems that serve the community, such as power, transportation, and communication systems, are required to be at a high-performance level of continuous operation, minimum damage, fewer hazard events, and quick recovery to normal operations.

The consequences of damage to any system affect the system’s operativity and functionality to meet

the required objectives (Ouyang & Wang, 2015). The recovery period is subject to the infrastructure system's condition during the hazard period, the degree of deterioration, and the required maintenance and repair. Resilience development examines economic, social, and community influences, functionality, and performance during recovery. Design solutions enhance structural designs to reduce loss of functionality and damage during hazard events and shorten recovery periods (Lounis & McAllister, 2016).

2.3 Interdependent Infrastructure System

Infrastructure interdependency is the approach in which one or more systems need the services of one or more systems to operate or in which the service of one or more systems is influenced by the service of other systems (Hasan & Foliente, 2015). Interdependent infrastructure can be defined as networks in which the circumstances of one or more networks affect another (Grafius et al., 2020). According to Rinaldi et al. (2001), there are four different types of interdependent relationships among infrastructure systems according to the nature of resources of each system. These include:

- Physical/geographic relationship: the systems are connected by sharing the same material or proximity, such as in colocation in corridors and tunnels.
- Cyber relationship: systems are related to each other by transferring information or data between systems.
- Logical relationship: in which systems are connected according to developing, managing, operating, and financing resources.
- Integral relationships: the relationship in which one system can use the output or advantages of another system or systems.

3. Development of Sustainable, Resilient and Interdependent Infrastructural System

The goal of developing resilient and interdependent infrastructure systems is to promote interdisciplinary studies and research that propose innovative approaches and creative solutions for designing and operating infrastructure, to enhance the realization of the design for interdependent infrastructure networks and procedures, to generate awareness and expertise for innovation in interdependent infrastructure which enhances the networks and their serviceability and operability in term of security, safety, efficiency, and effectiveness (Wang et al., 2011). The mentioned goals guide many defined objectives in the development, including creating advanced knowledge approaches and creative solutions to enhance resilience, achievement, and operation in interdependent infrastructure, building conceptual frameworks to analyze the adapting behavior of the interdependent system during the natural and/or climatic change and its impact on the serviceability, maintainability, and repairability, developing a workable strategy that links the opportunities in interdependent infrastructure such a cyber, logical, physical, economic, environmental, social, and integral relationship, and understanding the barriers to interdependent infrastructure development that hinder the upgrade of systems such as the legal, political, psychological, and socioeconomic barriers (Hasan & Foliente, 2015). According to Brown (2014), the concept of the future infrastructure network is the design of a multipurpose, interconnected, multifunctional, resilient, and sustainable system in a closed loop that exchanges characteristics with the natural ecosystem and benefit from each other. The steps in developing sustainable, resilient, and interdependent infrastructure of existing and new systems are shown in Figure (1).

The benefits from the emphasis on the relationships within the infrastructure systems include enhancing the delivery of the main services; increasing system efficiency in performing more than one function and/or exchanging benefits between them; sharing information among systems; reducing carbon emission; eliminating waste; enhancing the sustainability and resilience of the overall system, and reducing the cost of development, management, and maintenance (Brown, 2014).

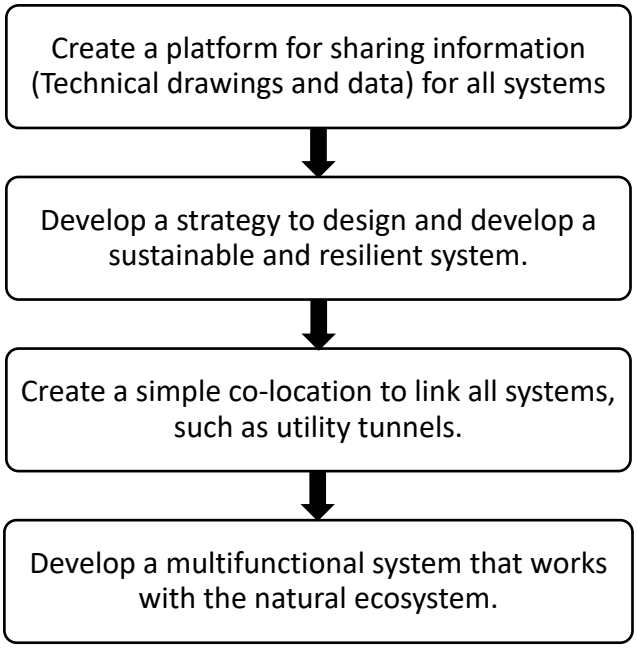


Fig. 1: Steps for developing Sustainable, Resilient and Interdependent Infrastructure

In the platform, different data models and workflow processes can be utilized in the development, management, operation, and maintenance of the infrastructure systems, such as Building Information Modeling (BIM), Digital Twins (DTs), and Emerging Technologies (EMs), (Callcut et al., 2021).

4. Case Studies

The following group of case studies on sustainable, resilient, and interdependent infrastructure development can be used to understand the different approaches for linking the systems and the benefits gained from each development. Table (1) shows the relationship and Locations of each case study.

4.1 Case Study 1: Underground Utility Tunnel in Shanghai, China

This is a new sustainable underground structural system developed in 2015 in Shanghai, China, to house more than one network of the utility system to enhance the development, renovation, adaptation, maintenance, and repair of the systems without any obstructions to the urban area and to improve the quality of urbanization. In contrast, the standard procedure of building the utility systems separately under the roads or in congested shallow-level corridors can lead to recurrent road cutting for maintenance, causing leakage, damage, or rupture to other systems. These can cause damage to the surrounding environment as well as noise, safety, and security problems (Yang & Peng, 2016).

4.2 Case Study 2: Photovoltaics Noise Barriers

Photovoltaic noise barriers are a combination of noise barrier systems and photovoltaic systems

used to reduce traffic noise while at the same time producing renewable energy. It includes a grid-connected solar panel array located along railways or highways and mounted to produce electricity for the grids and deflect noise away from a densely populated area. It can be utilized in a limited area in crowded locations, supply the area with electricity, reduce energy transmission costs, enhance energy efficiency, reduce carbon dioxide (CO_2) emissions, and minimize traffic noise. Examples of large photovoltaic noise barriers are those located along the A90 highway near Ouderkerk, Amsterdam, the Netherlands, and another along a viaduct near Zurich, Switzerland (Vallati et al., 2015).

4.3 Case Study 3: The Stormwater Management and Road Tunnel in Kuala Lumpur, Malaysia

The Stormwater Management and Road Tunnel (SMART) project, completed in 2007, was developed to serve two main purposes required by the city, to solve the problem of traffic congestion and to manage stormwater flooding. The tunnel is about 9.7 km in length with two sections, used according to the seasons; during the light rain season, no water is rerouted into the tunnel, and the traffic moves as normal during moderate rainfall; the lower section of the tunnel acts as storage for the water and the upper section used for traffic; during heavy rain, no traffic is allowed in either section, and the tunnel is used completely for water storage. this occurs about twice a year (Grafius et al., 2020). This innovative colocation project emphasizes the relationships between the two systems and works with nature to manage flooding, which cannot be avoided. The project solves two significant urban problems, saving costs and using fewer resources (Kim-Soon et al., 2016).

4.4 Case Study 4: Infrastructure Ecology in Stockholm, Sweden

This is an interactive and cooperative exchange project between the energy and materials flows of the locality. It uses a transformative approach based on an integrated and nearly closed system in which energy and resources flow and cycle from one utility to another. The heat from the Combined Heat and Power plant (CHP) and the sewerage treatment facility is retrieved to supply district heating. Biogas drawn out from the sewage plant is processed as fuel for local vehicles and domestic cooking stoves, and a portion of the sewage facility returns sludge for agricultural use. Mixed combustible household waste and forestry waste are appropriated for combustion in the CHP plant, and household commercial organic waste returns as fertilizer for agriculture or landscape use. Solar panel arrays supply local and distributed energy and domestic hot water systems (Brown, 2014).

4.5 Case Study 5: Combined Power and Distillation Plant in the Gulf Region

In the Gulf region, electrical power and freshwater supplies are developed at the same time. Thermal distillation of seawater needs large amounts of steam as an energy source. However, the latest technologies require only low-pressure and grade steam. Thermal distillation can be multi-stage flash (MSF) form and/or multiple-effect distillation (MED) units. The water and steam plants are firmly interconnected. The integrated cycle plant gives low-pressure steam to the desalination plant's MSF units and goes back through the condensate recovery process. A distillate from the desalination plant is supplied to the combined cycle plant, which utilizes it for cooling towers and steam cycle (Maadhah & Wojcik, 1981). Some examples of combined power and flash distillation plants are the Marafiq integrated water and power plant in Jubail, Kingdom of Saudi Arabia, and the Ras Laffan power and water plant located in Ras Laffan industrial city, Qatar (Rahman & Zidih, 2018).

4.6 Case Study 6: Water Treatment Plants in the Gulf Region

Wastewater treatment plants in the Gulf region use a combination of physical, chemical, and biological processes to treat sewage water from household, industrial and commercial use. Specialized equipment and technical chemical feed stations sanitize the water effectively. Wastewater treated at a sewage treatment plant can supply nutrient-rich water for irrigation, agricultural, industrial, and municipal purposes. Wastewater treatment also offers economic value by contributing to conserving the country's very scarce freshwater resources. The environmental benefits include reducing the pollution of water resources and sensitive receiving bodies and controlling saline water intrusion through groundwater recharge (Ouda, 2015).

4.7 Case Study 7: Doha Metro Project

This is one of the most recent and significant infrastructure projects in Qatar; phase one was completed in 2020, which includes three main metro lines (the red line from Al Wakra to Lusail, the green line from Al Mansoura to Al Riffa, the gold line from Ras Bu Abboud to Al Azizyah), and 37 passenger stations. The stations were developed on three levels: the first level includes the entrance and creative hard and soft landscape features; the second level is the station hall which includes the ticket office, restrooms, retail shops, restaurants, and other facilities; the third level is the platform for accessing the metro. The metro station is an innovative example of colocation that enhances connectivity between different modes of transportation, reduces environmental impact, enhances sustainability, and creates multifunctional activities. The metro is electrically powered, which can reduce air pollution and energy consumption and enhance economic development (Amerio, 2020).

Table1: Interdependent Relationship and Locations of the Case Studies

No.	Case Study	Location	Interdependent Relationship
1	Underground Utility Tunnel	Shanghai, China	Geographical
2	Photovoltaic Noise Barriers	Amsterdam, Netherlands, and Zurich, Switzerland	Geographical
3	The Stormwater Management and Road Tunnel	Kuala Lumpur, Malaysia	Geographical
4	Infrastructure Ecology	Stockholm, Sweden	Cyber and Integral
5	Combined Power and Distillation Plant	Gulf region (Qatar, Saudi, and UAE)	Cyber and Integral
6	Water Treatment Plants	Gulf region (Qatar, Saudi, and UAE)	Cyber and Integral
7	Doha Metro Project	Doha, Qatar	Geographical and logical

5. Conclusion

Historically, infrastructure networks such as energy, telecommunication, and transportation were developed, managed, operated, and maintained separately. With the development and expansion of urban areas in the cities in the Arabian Gulf Region, the development of additional new systems such as district chilled water systems and district heating water systems, the logical need to link systems with each other, and the requirement for more efficient and reliable services, there is an urgent need to develop a more sustainable, resilient, and interdependent system that enhances the

delivery of major services, raises the efficiency of the system in operating many functions, interchanging benefits, sharing information between systems, reducing carbon emission, minimizing waste, improving the sustainability and resilience of the overall system, and minimizing costs. This kind of development can start with creating a platform to share information such as technical drawings and data, developing a strategy for designing and managing the networks as one system, developing a collocation program to link all systems in an underground utility tunnel, and later creating a multifunctional network that is linked with natural ecosystem if possible. In this regard, the infrastructure systems must be multipurpose, interconnected, and synergistic, contribute fewer carbon emissions, be resilient and adaptable to predicted changes in nature and the climate, work with natural processes, improve social contexts and serve local communities.

References

Amerio, M. (2020). Doha Metro Project: 3TI Lesson Learned, *Transportation Research Procedia*, *45*, 866-873. DOI: 10.1016/j.trpro.2020.02.082.

Brown, H. (2014) Next Generation Infrastructure: Principles for Post-industrial Public Works, 1-39, *Island Press*, Washington.

Callcut, et al. (2021). Digital Twins in Civil Infrastructure Systems, *Sustainability*, *13*, https://doi.org/10.3390/su132011549

Chester, M., Markolf, S. & Allenby, B. (2019) Infrastructure and the Environment in the Anthropocene, *Journal of Industrial Ecology*, (23) 1006-1015. DOI: 10.1111/jiec.12848.

Grafius, D., Varga, L. & Jude, S. (2020). Infrastructure Interdependencies: Opportunities from Complexity. *Journal of Infrastructure Systems*. *26*(4), 1-11. DOI:10.1061/(ASCE)IS.1943-555X.0000575.

Hasan, S. & Foliente, G., (2015). Modeling infrastructure system interdependencies and socioeconomic impacts of failure in extreme events: emerging R&D challenges. *Natural Hazards*, *78*, 2143-2168. https://doi.org/ 10.1007/s11069-015-1814-7.

Hinge, G., Surampalli, R. & Goyal, M., (2020). Sustainable Infrastructure. *Sustainability*, ResearchGate, 295-311. DOI: 10.1002/9781119434016.ch14.

Kim-Soon, et al. (2016). Relationship between Stormwater Management and Road Tunnel Maintenance Works, Flooding and Traffic Flow. *Advanced Science*," *22*(7), 1845-1848. DOI: 10.1166/asl.2016.7047.

Kong, J., Simonovic, S. & Chao, Z. (2019). Resilience Assessment of Interdependent Infrastructure Systems: A Case Study Based on Different Response Strategies. *Sustainability 11*(23), http://doi.org/10.3390/su11236552.

Lounis, Z. & McAllister, T., (2016). Risk-based Decision Making for Sustainable and Resilient Infrastructure Systems. *Structural Engineering*. *142*(9), https://doi.org/10.1061/(ASCE)ST.1943-541X.0001545#sthash.3xdbK88L.dpuf

Maadhah, A. & Wojcik, C., (1981). Performance study of water desalination methods in Saudi Arabia, *Desalination*, *39*, 205-217, https://doi.org/10.1016/S0011-9164(00)86125-1

Ouda, O. (2015). Treated Wastewater Use in Saudi Arabia: Challenges and Initiatives, *International Journal of Water Resources Development*, *32*(5), 799-809. https://doi.org/10.1089/079000627.2015.1116435.

Ouyang, M. & Wang, Zh., (2015). Resilience assessment of interdependent infrastructure systems: With a focus on joint restoration modeling and analysis. *Reliability Engineering and System Safety*, *141*, 74-82, https://doi.org/10.1016/j.ress.2015.03.011

Rahman, H. & Zaidi, S., (2018) Desalination in Qatar: Present Status and Future Prospects. *Civil Engineering Research Journal*, *6*(5), 133-139, DOI: 10.19080/CERJ.2018.06.555700

Rinaldi, S., Peerenboom, J. & Kelly T., (2021) "Identifying, understanding, and analyzing critical infrastructure interdependencies" *IEEE Control System Management*, *21*(6), 11-25. https://doi.org/10.1109/37.969131.

Vallati, et al. (2015) Photovoltaic Noise Barrier: Acoustic and Energetic Study. *Energy Procedia*, *82*, 716-723. DOI: 10.1016/j.egypro.2015.11.797.

Wang, et al. (2011). Review of interdependent infrastructure systems vulnerability analysis. *IEEE 2*(11) 446-451. DOI: 10.1109/ICICIP.2011.6008284.

Yang, C. & Peng, F. L. (2016) Discussion on the Development of Underground Utility Tunnel in China, *Procedia Engineering*. *165*, 540-548. DOI:10.1016/i.proeng.2016.11.698.

Cite as: Mohamed M.G. & Kevin M., "Efficacy in developing a Sustainable, Resilient, and Interdependent Infrastructure System in the Gulf Region.", *The 2nd International Conference on Civil Infrastructure and Construction (CIC 2023)*, Doha, Qatar, 5-8 February 2023, DOI: https://doi.org/10.29117/cic.2023.0093

Digital Twins in AEC Infrastructure and Building Management Systems

Mohammad Oditallah
Swinburne University of Technology/Department of Civil & Construction Engineering, Melbourne, Australia
moditallah@swin.edu.au

Md Morshed Alam
Swinburne University of Technology/Department of Civil & Construction Engineering, Melbourne, Australia
mmalam@swin.edu.au

Palaneeswaran Ekambaram
Swinburne University of Technology/Department of Civil & Construction Engineering, Melbourne, Australia
pekambaram@swin.edu.au

Abstract

The current practice of Architecture, Engineering, and Construction (AEC) management systems relies on time-consuming, manual methods for data collection, analyzing, and decision-making. This affects the productivity of the industry in all phases: design, construction, operation, and maintenance of their assets. Adoption of innovative technologies is the key solution for the AEC industry to overcome the challenges they face and follow other reinvented industries. Although recent advancements have been proposed for more productive data acquisition and decision support by leveraging digital tools, Building Information Modeling (BIM), Internet of Things (IoT), and Artificial Intelligence (AI), the fragmented approach of adoption and the absence of a connected workflow is a barrier. Digital Twin (DT) is a digital presentation of a physical entity that replicates the status and behavior of its physical counterpart. It can help to improve overall system effectiveness and reliable data-informed decisions. However, the concept of DT and its key features is still not well-understood in the AEC industry. Therefore, this paper aims to review and investigate the twinning requirements and characteristics of DT and discuss its structure and potential solutions in terms of AEC infrastructure and buildings assets operations and maintenance systems. The DT concept, main characteristics, and critical considerations for the AEC sector are highlighted and classification for DT levels is introduced and discussed.

Keywords: AEC; Digital twin; Smart infrastructure and building systems; Intelligent operation management; Predictive maintenance

1. Introduction

Annual construction industry contribution was estimated as 13% of the world gross domestic product (GDP) (Barbosa et al., 2017), and is expected to reach $14 trillion by 2030 (Perspectives & Economics, 2015). In 2018, this sector contributed to 10% of the Australian economy with around $110 billion and employed more than 1 million people. Despite the significance of its contribution, the growth of its global labor productivity has averaged only 1% per year over the past twenty years, which is extremely low compared with 2.8% and 3.6% growth rates for the total world economy and manufacturing sector, respectively. International programs were established to identify key objectives for the development of this industry. It was found that it needs to achieve more integrated processes with new information and production technologies, aiming to enable the construction industry to follow the manufacturing sector (Milford, 2009).

The construction industry has started to adopt Building Information Modeling (BIM) and digital tools in the current industrial revolution. However, the implementation of technologies is still in its infancy, as the industry is characterized by slow adoption of new technologies partly due to the fragmented nature of the industry, segmentation, and resistance to change (Beetz, et al., 2020). These factors influenced the adoption of cutting-edge technologies, such as Digital Twin (DT) for integrated digital systems. (Callcut et al., 2021) observed that the adoption of DT in AEC industry tends to be fragmented and dispersed. Consequently, the industry continues to rely on traditional tools and techniques in collecting, analyzing and driving the decision process. This resulted in the absence of a centric dataset and the lack of smart capabilities and systems efficiencies across all phases of a construction project.

Moreover, since the start of the current industrial revolution, advancements in technology have enhanced productivity in various industries. This digital transformation includes data sensors, machines, big data modeling, cloud computing, and Information Technology (IT) systems, which led to the use of predictive approaches and improved decision-making, improved data exchange, and applications by leveraging Artificial intelligence (AI) algorithms and smart techniques. Currently, there is a focus on introducing Digital Twins (DT) for enabled data-driven decisions and more integrated applications in various industries (van Dinter et al., 2022). DT is a digital representation of a physical product that mimics real-world behavior by leveraging data from the physical element, process, or system to its virtual counterpart. The virtual models are supported by simulation tools, cloud-based connections, sensors and databases that are introduced to enable remote management and interaction with physical assets (Tao & Zhang, 2017).

The understanding of DT in the AEC industry is currently fragmented (Callcut et al., 2021). The adoption of DTs is still in its evolutionary stage due to inconsistencies in definitions and characterizations (Jones et al., 2020). This lack of knowledge will affect the overall digitization of the industry as the transition movement aimed to integrate subsystems that can work as part of one inter-connected system to improve productivity and performance.

Moreover, intelligent systems comprise digital subsystems that communicate through a digital data; therefore, the currently developed subsystems will remain fragmented and lack an integrated systematic workflow unless the integration frameworks and capabilities of these systems have been well understood in the AEC assets context. There is also a lack of prototypes and studies, and possible solutions that digital twins may provide (Jones et al., 2020; Broo & Schooling, 2021). Therefore, this work aims to investigate the current state of the DT concept and adoption in the AEC industry and provide insight into future research and a developmental requirement to implement true DT in this sector and maximize the benefits.

2. Digital Twin: Definition and Characteristics

DTs' core characteristics were identified as follows; life-cycle phases data of the asset, synchronization rate of data, types of connections between spaces (bi-directional or one-way flow), and sensor data. In addition, advanced analytical techniques were developed for enabling twinning capabilities such as predicting, forecasting, alerts, or fault detection through data-driven models and physics-based simulations.

In terms of connections, the core definition established by Grieves focuses on the linkage nature between two spaces being bidirectional and having multiple virtual spaces for a single real one (Grieves, 2014). However, the latter proposed data flow types were based on the level of automation between the physical and the virtual parts of an asset (Kritzinger et al., 2018), where three types of DTs are classified

as a digital model, digital shadow, and digital twin. The twin is when data transfer is bi-directional, digital shadow has one-way data transfer and the digital model is where no automatic transfer of data exists. Figure 1 shows the three types mentioned.

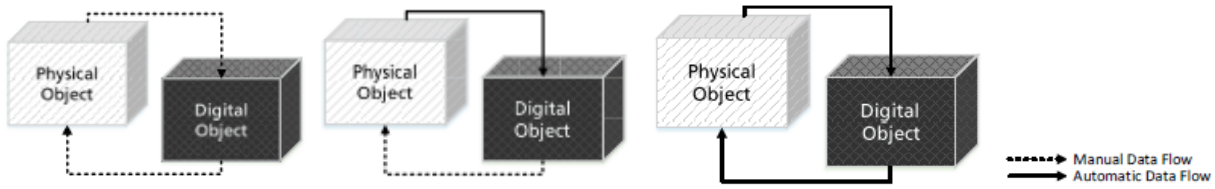


Fig. 1: (a) Digital model, **(b)** Digital shadow, and **(c)** Digital twin, based on data flow type (Kritzinger et al., 2018)

In terms of lifecycle inclusion in DT, (Söderberg et al., 2017) considered the life cycle of manufacturing phases as a core point in their definitions. (Zhang et al., 2017) added product life cycle and simulation of integrated data and defined the prediction component to be the main part of DT. Others included mechanical analysis, advanced analytical algorithms, and simulation models (Dassisti et al., 2017; Tao, et al., 2019). (Schleich et al., 2017) considered the need for a two-way connection between a physical and virtual entity, whereas (Trauer's et al., 2020) definition focuses on the need to exchange data information involving sensors, data, and models.

(Semeraro et al., 2021) described the DT in terms of a system capable of synchronizing data, modeling the behavior of the physical space, and communicating services by the virtual space, with the ability to simulate the product life cycle. Visualization and simulation, along with continuous data updates are features also found to be a main part of the DT. As stated in ISO (2019), ongoing updates in the virtual part reflect the changes in the physical counterpart to represent status. (Defraeye et al., 2021) included all the essential elements, geometrical components, and properties of the material; they also included continuously updated sensor data and realistic simulation for the relevant processes throughout the product lifecycle. The core features of DT found in literature definitions and descriptions are summarized in Figure 2 below.

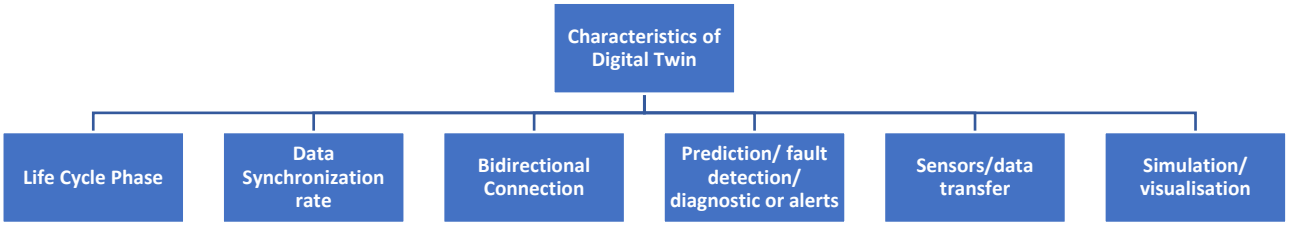


Fig. 2: Characteristics of Digital twin

DT can be developed for any real-world asset, for example, buildings and civil infrastructure assets (Bado, 2022). It can be developed at the unit level, system level, and system-of-systems level. At the system level, the DT can be developed for the process (Bao et al., 2019). DT in the manufacturing process aimed to improve resource allocation, process controls and production plans to validate the production process before or during it. Therefore, process twinning can be possible in AEC processes, such as the use of a DT for construction methods, processes, and operations for monitoring and control.

In terms of the synchronization rate for DT, most definitions stated the need for real-time data transfer. However, continuous data transfer might not be necessary in some cases or not possible either in the construction sector. The frequency of data transfer and updating the DT model status depends on the frequency of the decision-making cycle or when a significant change in the physical asset occurs, i.e. periodic asset inspection data. (Callcut et al., 2021) compared the need for real-time data in two different scenarios and reported that data rates could be varied based on need. For example, twinning traffic on roads networks for navigation maps use, as digital maps collect traffic data from the location data of users' GPS in real-time, along with local traffic information (rules, directions, priorities etc.) and automatically learn from historical and live traffic data to provide directions, optimize driving routes, and predict arrival time along with dynamic visualizing. Note that, the decisions during this operation including driving speed, traveling time, selecting routes, and optimizing options are performed continuously for the user and system.

On the other hand, the solid, or static physical assets such as structural assets might not need to have bidirectional connections, as in this case, the feedback from virtual to physical can be physical action orders such as scheduling maintenance or manual responses. (Stark & Damerau. 2019) noted that plans or reactions based on virtual feedback and decision-making can affect physical space and change its status. It can be considered as a feedback flow of data transferred indirectly by the users or decision-makers and divided into virtual flow to a decision maker and the decision to the physical part, where the decision-maker can be a user, operator, asset owner, etc. According to that, the digital shadow structure can be presented in a more realistic flow as shown in Figure 3.

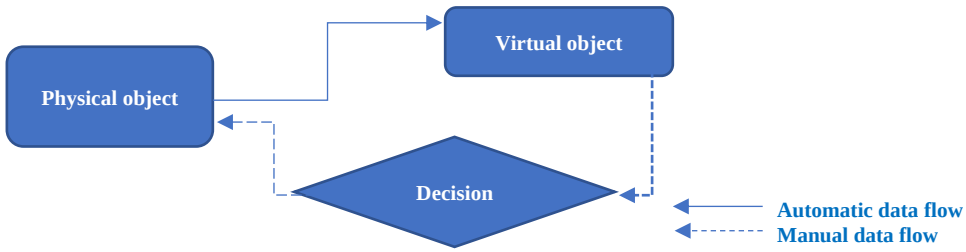


Fig. 3: Digital shadow data flow structure

The life cycle of the product is a necessity included in most definitions of DT (Schroeder et al., 2016; Söderberg et al., 2017; Zhang et al., 2017), and it was the main core of the DT concept introduced by (Grieves, 2014). Asset life cycle models and data serve as crucial sources of information regarding the various life phases of physical assets. These models aim to facilitate effective communication of operational activities and responses related to the assets, thereby enabling better decision-making processes (Zhanget al., 2019). The data related to asset life cycle phases encompass essential information for each stage of the asset, including planning, design, construction, operation, and maintenance. Integrating all relevant asset data in a holistic model providing a comprehensive view of the purpose and function of the DT utilization. (Defraeye et al., 2021) emphasized that the comprehensive model should incorporate all essential elements, including geometrical components and material properties.

DT features such as monitoring, diagnosing, and predicting the state and behavior of the twinned entity, indicated the prediction capability, and fault detection for observing a discrepancy and abnormality in the behavior and performance of a system (Amruthnath & Gupta, 2018), by using rules, analytical models, and machine learning, such as use failure data for predicting machine failure. The simulation is

also an essential part, as it can generate failure to be used in predicting defects (Aivaliotis et al., 2019). Simulation can be implemented for predictive modeling, visualization components (Gunal, 2019), and optimizing future operations (van der Horn & Mahadevan, 2021). As a result, a digital twin for AEC use can be defined as a virtual copy (graphical and non-graphical information) of a certain asset, process, or system of connected assets that comprise the purpose-related lifecycle data, reasonable data exchange and synchronization, analytical and simulation models, and intelligent techniques, to model real-world conditions and responses of the physical entity.

3. Current State of Digital Twin in AEC

In the construction industry, the potential reported applications of DT include supporting decision-making in energy management, procurement, the feasibility of a project, and sustainability (Opoku et al., 2021), as well as improving future actions and extending the lifetime of the built infrastructure and improving sustainability. Many different works leveraged an integration of BIM models in the AEC industry with external data sources and processes such as cloud computing, scanning sensors and IoT. Integrations purposed for the design phase, operation and maintenance, construction progress and quality processes. In terms of the design phase, (Jiang et al., 2021) discussed the mechanism of the fatigue management system using Digital Twins and noted that fatigue data including historical fatigue after the bridge retirement, can be supported by the integration of information for the more insightful design and management of new bridges. For road pavement design, digital twin included structured geometric and attribute data of a constructed road using secondary raw materials (SRMs), including real-time material characteristics using sensors to support data centralization and graphical presentation of road performance indicators (Meža et al., 2021).

For the maintenance phase, DT was used to predict the highway tunnel pavement performance where sensors were used for asset performance, data collection along with other life cycle-related data (maintenance records, traffic flow, etc.), in addition to advanced analytical modeling; multisource spatial-temporal data and dynamic visualization, which allowed for enhanced maintenance method (Yu et al., 2020). Visualization of anomalies to assess the conditions of assets is a major step in decision-making and maintenance planning such as defects, cracks, etc. For that purpose, an interactive system to display pavement cracks in 3D visualization was developed (Cao et al., 2022), where cracks detection and segmentation were implemented via 3D edge detection and deep learning algorithms, and data was collected using a camera and laser scanning sensors.

At a system level, (Dan et al., 2022) developed a DT system for a group of bridges, where traffic load is measured by a camera sensor, machine vision, Weigh-In-Motion (WIM) System, and cloud-based finite element models integrated to analyze mechanical responses for real-time fatigue analysis and monitoring. Another work presented the progressive settlement based on road traffic, using LIDAR (Light Detection and Ranging) sensor data, UAV-based camera sensors for traffic counting, and environmental air quality sensors, where scanned assets were converted into standard CAD packages (Steyn & Broekman, 2021). In terms of health monitoring, BIM and GIS integration process was used for a cable-stayed bridge in Africa, the structure as-built was modeled using a point cloud, and geographic information of the external environment represented and visualized as 3D GIS objects for flatness and distortion monitoring. In that work, an IoT network was used to stream data such as temperature, tilt, and deformation (Sofia et al., 2020).

Few works used a bi-directional flow of data in their systems, aiming at activating alerts in the physical space and issuing action orders. For instance, advanced monitoring and control for underground garage

environment management using BIM and Wireless Sensor Networks (WSN) to capture environment conditions presented visually for an effective monitoring system with abnormality data detection and alerts execution (Lin & Cheung, 2020). As a conceptual framework for web-based building management, (Deng et al., 2021) discussed a framework, in which the authors described BIM integrated with simulations, IoT, and AI for real-time indoor environment and occupant's comfort with predictions and responding controls automatically. (Valinejadshoubi et al., 2021) used BIM model, IoT, database system integrated via Dynamo (Visual Programming Environment), and cloud-based services to enable cloud-based monitoring systems to detect the thermal comfort levels of office occupants based on predefined targeted thresholds for monitoring alerts.

Building energy-related works were found to be the most studied area, because of the need for an intelligent platform for real-time management. (Peng et al., 2020) developed a hospital building operations system by integrating BIM models, multisource data, and algorithms to monitor and identify abnormal consumption patterns to enable effective administrative management with automated feedback from the digital platform to the real space. (Rafsanjani & Ghahramani, 2020) proposed a system using IoT sensors to evaluate the behavior of energy consumption by individuals. They were able to identify and classify occupants' consumption trends for energy savings reaction.

In road construction, a recent study developed a framework for an intelligent real-time roller compaction system to assess the quality and manage road layers compaction process (Han et al., 2022), where IoT is adopted to connect physical and virtual space for actual operations in road construction, and the quality of the process assessed and visualized. As a smart city planning use, DT for green spaces and skylines planning was developed by (White et al., 2021). The authors aimed at creating a publicly open digital twin that enabled data feedback exchange from users to interact on planned changes. A summary of DT applications in AEC is presented in Table 1.

Table 1: Digital Twin Applications in AEC

Author	Description	Bidirectional	Synchronization (real time)	Sensors	Visualization/Simulation	Prediction, fault detection
(Rafsanjani & Ghahramani, 2020)	Energy consumption		x	x		x
(White et al., 2021)	DT for smart city		x	x	x	
(Lin and Cheung, 2020)	Underground Garage	x	x	x	x	x
(Lu, et al., 2020)	Energy demand			x		x
(Peng, et al., 2020)	Hospital building operations	x	x	x	x	x
(Meža et al., 2021)	Pavement secondary material		x	x	x	
(Yu et al., 2020)	Highway Tunnel Pavement			x	x	x
(Xie et al., 2020)	Anomaly detection		x	x	x	x
(Steyn & Broekman, 2021)	Settlement of bridge			x	x	
(Dan et al., 2022)	Bridge fatigue monitoring		x	x	x	x
(Sofia et al., 2020)	Monitor health of the bridge		x	x	x	
(Shim et al., 2019)	Pre-stressed concrete bridge			x	x	x
(Deng et al., 2021)	Building management	x	x	x	x	x
(Cao, 2022)	Cracks visualizing system			x	x	x
(Han et al., 2022)	Intelligent compaction system		x	x	x	x
(Valinejadshoubi et al., 2021)	Thermal monitoring		x	x	x	x

4. Discussion

To identify the status of DT applications in AEC, a classification of the main DT features and relevant AEC studies was conducted. In addition, understanding DT applications and capabilities from different sectors were used to interpret the AEC-related works into levels of twinning. Identified levels can be discussed as follows, the first level is where BIM is integrated with IoT and visualized live data for monitoring, predefined triggers, alerts etc. The second level incorporates integration with artificial intelligence (AI) techniques, analytical models, or computational models for predictions and simulation to support the decision-making process. The predictive feature is a key feature at this level that can enable predicting defects or the future status of the asset.

The third level shall include more advanced integration and involves the prediction of the state of the asset combined with automated decision guidance, process, or optimized actions. These actions can be descriptive plans based on predefined policies and informative embedded data, or actual actions for real-time control as a feedback capability to manage the operations of the asset. However, control actions can only be adopted when this automation is possible in the physical part i.e., mechanical, electrical process or computerized object, as this can be implemented through a bi-directional connection between two spaces for the developed DT.

Most of the studies' prototypes are based on local BIM platforms, using visual programming in most cases, a few (Valinejadshoubi, et al., 2021; White, Zink, et al., 2021) have shared the developed prototype to cloud-based access. However, recently, cloud services such as Amazon and Google Cloud developed cloud-supported tools for analyzing and visualizing data with the integration possibilities of AI and IoT. Nevertheless, cloud-based frameworks can expand to a more collaborative involvement of stakeholders in the management platform for better decisions and monitoring.

Monitoring the interior environment, operation, and maintenance management was also found as the key focus of AEC DT adoption (Lu et al., 2020; Rafsanjani & Ghahramani, 2020). On the other hand, applications for bridge health monitoring are found common in infrastructure assets applications (Shim et al., 2019; Sofia et al., 2020; Dan, Ying et al., 2022). However, most of these studies were classified in levels 1 & 2, which helped in supporting decision making in an efficient and real-time manner in some cases. Other proposed frameworks involved predictive ability using analytical modeling, or artificial intelligence algorithms to predict status or health measures, (Yu et al., 2020; Deng et al., 2021).

These works are considered a promising start toward a higher level of twinning, as they can perform predictive monitoring for the future state, which might lead to enhanced maintenance planning and actions by optimizing the traditional maintenance approach. DTs have more capabilities to be leveraged in this industry. DTs (level 3) utilizations are needed for automation in actions, optimization, and guidance for maintenance operations. Many utilization methods found effective in optimizing maintenance, such as integrating knowledge-based systems using ANN (Li, Yin et al., 2022), and Reinforcement learning (RL) in optimizing maintenance (Yao et al., 2020). This will overcome the current challenges of corrective and preventative approaches used in building and infrastructure assets.

5. Conclusion

This paper investigated the DT concept, definition, and characteristics as implemented in other advanced sectors and provided a fundamental understanding of the characteristics of the required

Digital Twin for the AEC industry. DT characteristics and types are identified and discussed along with critical features applicable to AEC. The current literature works were reviewed and evaluated. Three levels of DT based on enabled capabilities were introduced and described in this study. The results can help to develop a true Digital Twin in terms of automated building operation and predictive infrastructure maintenance in AEC, by integrating IoT, advanced modeling and simulation methods, predictions, decision support systems and automation. This study has limitations that could be addressed by future research. First, the study focused on conceptual aspects of DT implementation in AEC with limited focus on technical aspects. Second, only the most relevant publications in DT lifecycle phases were considered in this review.

References

Aivaliotis, P., Georgoulias, K. & Chryssolouris, G. (2019). The use of Digital Twin for predictive maintenance in manufacturing. *International Journal of Computer Integrated Manufacturing 32*(11): 1067-1080.

Amruthnath, N. & Gupta, T. (2018). A research study on unsupervised machine learning algorithms for early fault detection in predictive maintenance . 2018 5th *International Conference on Industrial Engineering and Applications* (ICIEA).DOI: 10.1109/IEA.2018.8387124.

Bado, et al. (2022). Digital Twin for Civil Engineering Systems: An Exploratory Review for Distributed Sensing Updating. *Sensors*, *22*(9), 3168.

Bao, et al. (2019). The modelling and operations for the digital twin in the context of manufacturing. *Enterprise Information Systems 13*(4): 534-556.

Barbosa, F., Woetzel, J. & Mischke, J. (2017). Reinventing construction: A route of higher productivity , *McKinsey Global Institute*.

Beetz, et al. (2020). BuildingSMART. [Online] Available at: https://www.buildingsmart.org/wp-content/uploads/2020/05/Enabling-Digital-Twins-Positioning-Paper-Final.pdf [Accessed 10 12 2022].

Broo, D. G. & Schooling, J. (2021). Digital twins in infrastructure: definitions, current practices, challenges and strategies. *International Journal of Construction Management*: 1-10.

Callcut, et al. (2021). Digital twins in civil infrastructure systems. *Sustainability 13*(20): 11549.

Cao, T., Wang, Y. & Liu, S. (2022). Pavement Crack Detection Based on 3D Edge Representation and Data Communication With Digital Twins. *IEEE Transactions on Intelligent Transportation Systems*: 1-10.DOI: 10.1109/tits.2022.3194013.

Dan, D., Ying, Y. & Ge, L. (2022). Digital Twin System of Bridges Group Based on Machine Vision Fusion Monitoring of Bridge Traffic Load. *IEEE Transactions on Intelligent Transportation Systems 23*(11): 22190-22205.DOI: 10.1109/TITS.2021.3130025.

Dassisti, et al. (2017). Hybrid production-system control-architecture for smart manufacturing . *OTM Confederated International Conferences On the Move to Meaningful Internet Systems* , Springer.

Defraeye, et al. (2021). Digital twins are coming: Will we need them in supply chains of fresh horticultural produce? *Trends in Food Science & Technology 109*: 245-258.

Deng, M., Menassa, C. & Kamat, V. (2021). From BIM to digital twins: A systematic review of the evolution of intelligent building representations in the AEC-FM industry. *Journal of Information Technology in Construction 26*: 58-83.DOI: 10.36680/j.itcon.2021.005.

Grieves, (2014). Digital twin: manufacturing excellence through virtual factory replication. *White paper 1*(2014): 1-7.

Gunal, M. M. (2019). Simulation and the fourth industrial revolution. Simulation for Industry 4.0 , *Springer*: 1-17.

Han, et al. (2022). A BIM-IoT and intelligent compaction integrated framework for advanced road compaction quality monitoring and management. *Computers and Electrical Engineering 100:* 107981.DOI:

https://doi.org/10.1016/j.compeleceng.2022.107981.

ISO (International Organization for Standardization) (2019) ISO23241:2021: Automation systems and integration–digital twin framework for manufacturing – Part 1:Ooverview and general principles. *ISO*, Geneva, Switzerland. See https://www.iso.org/standard/75066.html (accessed 23/10/2022).

Jiang, et al. (2021). An architecture of lifecycle fatigue management of steel bridges driven by Digital Twin. *Structural Monitoring and Maintenance 8*(2): 187-201.

Jones, et al. (2020). Characterising the Digital Twin: A systematic literature review. *CIRP Journal of Manufacturing Science and Technology 29*: 36-52.DOI: https://doi.org/10.1016/j.cirpj.2020.02.002.

Kritzinger, et al. (2018). Digital Twin in manufacturing: A categorical literature review and classification. *IFAC* - PapersOnLine *51*(11): 1016-1022.DOI: https://doi.org/10.1016/j.ifacol.2018.08.474.

Li, et al. (2022). Automated decision making in highway pavement preventive maintenance based on deep learning. *Automation in Construction 135*: 104111.DOI: 10.1016/j.autcon.2021.104111.

Lin, Y. C. & Cheung, W. F. (2020). Developing WSN/BIM-Based Environmental Monitoring Management System for Parking Garages in Smart Cities. *Journal of Management in Engineering 36*(3): 04020012.DOI: 10.1061/(ASCE)ME.1943-5479.0000760.

Lu, et al. (2020). Digital twin-enabled anomaly detection for built asset monitoring in operation and maintenance. *Automation in Construction 118*: 103277.DOI: https://doi.org/10.1016/j.autcon.2020.103277.

Meža, et al. (2021). Digital Twins and Road Construction Using Secondary Raw Materials. *Journal of Advanced Transportation* 2021: 1-12.DOI: 10.1155/2021/8833058.

Milford, R. (2009). Construction industry development in developing countries; lessons and opportunities. 3rd *International Conference on Concrete & Development.*

Opoku, et al. (2021). Digital twin application in the construction industry: A literature review. *Journal of Building Engineering 40*: 102726.

Peng, et al. (2020). Digital Twin Hospital Buildings: An Exemplary Case Study through Continuous Lifecycle Integration. *Advances in Civil Engineering* 2020: 8846667.DOI: 10.1155/2020/8846667.

Perspectives, G. C. & Economics, O. (2015). Global construction 2030: a global forecast for the construction industry to 2030. *Global Construction Perspectives and Oxford Economics*: London, UK.

Rafsanjani, H. N. & Ghahramani, A. (2020). Towards utilizing internet of things (IoT) devices for understanding individual occupants' energy usage of personal and shared appliances in office buildings. *Journal of Building Engineering 27*: 100948.DOI: https://doi.org/10.1016/j.jobe.2019.100948.

Schleich, et al. (2017). Shaping the digital twin for design and production engineering. *CIRP Annals 66*(1): 141-144.

Schroeder, et al. (2016). Digital twin data modeling with automationml and a communication methodology for data exchange. *IFAC* - PapersOnLine 49(30): 12-17.

Semeraro, et al. (2021). Digital twin paradigm: A systematic literature review. *Computers in Industry 130*: 103469.DOI: https://doi.org/10.1016/j.compind.2021.103469.

Shim, et al. (2019). Development of a bridge maintenance system for prestressed concrete bridges using 3D digital twin model. *Structure and Infrastructure Engineering 15*(10): 1319-1332.DOI: 10.1080/15732479.2019.1620789.

Söderberg, et al. (2017). Toward a Digital Twin for real-time geometry assurance in individualized production. *CIRP Annals 66*(1): 137-140.

Sofia, H., Anas, E. & Faïz, O. (2020). Mobile Mapping, Machine Learning and Digital Twin for Road Infrastructure Monitoring and Maintenance: Case Study of Mohammed VI Bridge in Morocco . 2020 *IEEE International Conference of Moroccan Geomatics* (Morgeo).DOI: 10.1109/Morgeo49228.2020.9121882.

Stark, R. & Damerau, T. (2019). Digital Twin. *CIRP Encyclopedia of Production Engineering* . S. Chatti and T. Tolio. Berlin, Heidelberg, Springer Berlin Heidelberg: 1-8.

Steyn, W. J. & Broekman, A. (2021). Process for the Development of a Digital Twin of a Local Road – A Case Study, *Springer International Publishing*: 11-22.

Tao, et al. (2019). Digital twin-driven product design framework. *International Journal of Production Research 57*(12): 3935-3953.

Tao, F. & Zhang, M. (2017). Digital Twin Shop-Floor: A New Shop-Floor Paradigm Towards Smart Manufacturing. *IEEE Access* 5: 20418-20427.DOI: 10.1109/ACCESS.2017.2756069.

Trauer, et al. (2020). What is a digital twin?–definitions and insights from an industrial case study in technical product development . *Proceedings of the Design Society*: DESIGN Conference, Cambridge University Press.

Valinejadshoubi, et al. (2021). Development of an IoT and BIM-based automated alert system for thermal comfort monitoring in buildings. *Sustainable Cities and Society 66*: 102602.DOI: https://doi.org/10.1016/j.scs.2020.102602.

van Dinter, R., Tekinerdogan, B. & Catal, C. (2022). Predictive maintenance using digital twins: A systematic literature review. *Information and Software Technology 151*: 107008.DOI: https://doi.org/10.1016/j.infsof.2022.107008.

VanDerHorn, E. & Mahadevan, S. (2021). Digital Twin: Generalization, characterization and implementation. *Decision Support Systems 145*: 113524.DOI: https://doi.org/10.1016/j.dss.2021.113524.

White, et al. (2021). A digital twin smart city for citizen feedback. *Cities 110*: 103064.DOI: https://doi.org/10.1016/j.cities.2020.103064.

Xie, et al. (2020). Digital Twin Enabled Asset Anomaly Detection for Building Facility Management. *IFAC* - PapersOnLine *53*(3): 380-385.DOI: https://doi.org/10.1016/j.ifacol.2020.11.061.

Yu, et al. (2020). Prediction of Highway Tunnel Pavement Performance Based on Digital Twin and Multiple Time Series Stacking. *Advances in Civil Engineering* 2020: 8824135.DOI: 10.1155/2020/8824135.

Zhang, et al. (2017). A digital twin-based approach for designing and multi-objective optimization of hollow glass production line. *EEE Access* 5: 26901-26911.

___. (2019). Modeling and simulation in intelligent manufacturing. *Computers in Industry 112*: 103123.

Cite as: Oditallah M., Alam M.M. & Ekambaram P., "Digital Twins in AEC Infrastructure and Building Management Systems", *The 2nd International Conference on Civil Infrastructure and Construction (CIC 2023)*, Doha, Qatar, 5-8 February 2023, DOI: https://doi.org/10.29117/cic.2023.0094

Sustainable Alternatives for Concrete by adding Different Types of Natural and Industrial Waste Materials

Rana Ezzdine Lakys
Australian University of Kuwait/College of Engineering, West Mishref, Kuwait
r.lakys@au.edu.kw

Mohammad Hany Yassin
Australian University of Kuwait/College of Engineering, West Mishref, Kuwait
m.yassub@au.edu.kw

Adel Jumaah
Australian University of Kuwait/College of Engineering, West Mishref, Kuwait
jumaah@auedukw.onmicrosoft.com

Abstract

The construction industry accounts for a high percentage of global energy-related CO_2 emissions (37 % in 2021 based on data from United Nations Environmental Program - UNEP) leading to an increasing need for solutions to aggressively reduce the energy demand in the built-up environment. Previous research showed that adding natural fibers such as Palm Tree Fronds (PTF) enhances the thermal behavior of concrete but may have negative effect on its mechanical properties as it may dramatically reduce its compressive strength and hence its durability. The work conducted previously by the authors confirms the research findings for different grades of concrete. Therefore, the possibility of adding another type of waste to compensate the compressive strength of concrete was explored. This additional material was chosen based on environmental consideration and the solution of adding Ceramic Waste Powder (CWP) was adopted. According to literature review, adding CWP may enhance not only the mechanical resistance of concrete but also its workability and its resistance to segregation. In this aim, different groups of mixes are performed to obtain the optimal mix for a high strength sustainable concrete: Control mix, CWP mix where CWP was added to replace 33% of the cement mass, and (CWP+PTF) mix where CWP (33% of the cement mass) and PTF (0%, 0.5% and 1% of sand volume) were added to the mix. The results of the compressive strength at early age (1 day) showed that the best results were obtained for the (CWP + PTF) mix with 0.5 % of added PTF.

Keywords: Sustainability; Concrete Mix; Palm Tree Waste; Ceramic Waste Powder; Compressive strength

1 Introduction

Concrete is the most used material in the modern built environment. The annual production of concrete is continuously increasing resulting in consuming large amounts of component materials. It is estimated that concrete production consumes around 15 billion tons of aggregates and 4.2 billion tons of cement per year according to (Langer et al., 2004).

One the greatest environmental drawbacks of concrete production is its large CO_2 footprint. On average, around 700-900 g of CO_2 is released per each kg of cement (Marincovic et al., 2010; Muller et al., 2014). Despite continued efforts to move towards renewable energy sources in the cement production process, CO_2 emissions cannot be reduced due to the unpreventable release of CO_2 during

the calcination reaction in addition to the emissions resulting from transportation. Globally, the construction industry is responsible for more than 34% of energy demand and around 37% of CO_2 emissions in 2021 according to the *2022 Global Status Report for Buildings and Construction* published by the United Nations Environment Program (UNEP, 2022).

Nowadays, the topic of developing sustainable construction materials to reduce both financial and environmental load resulting from construction-related activities has become a priority for researchers. The work presented in this paper falls within this context. It aims to search for the optimal concrete mix including two types of waste: a natural (organic) waste material, the Palm Tree Fronds (PTF) fibers, and an industrial waste material, the Ceramic Waste Powder (CWP) to optimize the thermal resistance of concrete reducing the energy consumption of the built environment without compromising its mechanical properties, the compressive strength in particular. Therefore, different mixes with different percentages of added wastes are investigated in this study.

2 Background

In recent years, the research on developing sustainable concrete to address the issue of global climate change has gained increasing interest all around the world. The main focus of this research is on:

1- The reduction of cement in concrete to reduce the financial and environmental cost generated by the cement production process by partially substituting the cement with alternative natural or industrial binding materials. In most of the related research, the cement substitute assured an equivalent or even higher mechanical performance of the concrete due to its pozzolanic properties such as rice husk ash (Zareei et al., 2017), waste paper ash (Kejela, 2022), waste brick powder (Mansoor et al., 2022), silica fume (Khalid et al., 2019; Imam et al., 2018), waste glass powder (Yassen et al., 2018), fly ash (Khalid et al., 2019), ground granulated blast furnace slag (Khalid et al., 2019), ceramic waste (Raval, 2013), demolition waste (Srivastava et al., 2013), glass waste (Yaseen et al., 2018) and others.

2- Adding or partially replacing concrete natural components such as fine and coarse aggregates with natural or industrial materials. In conventional concrete, around 70% of the concrete volume consists of natural aggregates. Replacing part of these natural components helps in saving natural materials for future generations and participates in enhancing concrete properties such as the workability, the density, the thermal resistance, the flexural strength, etc. The aggregates' substitutes may consist of organic materials such as natural fibers derived from coconut shell (Gunasekaran, 2013; Kumbhar, 2018) (Sujatha & Deepa, 2020), coir, palm, kenaf, jute, sisal, banana, pine, sugarcane and bamboo (Ahamed et al., 2020) or industrial waste such as construction and demolition waste materials (Jagan, 2017) (Singh & Sancheti, 2019), waste plastic (Sharma et al., 2021), waste tyre rubber (Rohini et al. 2016), waste ceramic tiles (Sekar, 2017), recycled aggregates (Marinkovic et al., 2020) and others. Using these various natural and industrial wastes contribute not only in saving the natural sources but also in reducing the waste to be dumped and thus reducing groundwater pollution.

The use of palm tree fronds (PTF) in construction has been applied for long time especially in hot dry climate region. The concept of introducing fibers to the concrete mix was found beneficial to compensate for the weak tensile resistance of concrete, thus reinforcing fibers in concrete can minimize or eliminate the formation of shrinkage cracks (Al-Kutti, 2017; Machaka et al., 2014). In addition to its mechanical effects on the performance of concrete, previous studies showed that PTF fibers improve the overall thermal resistance of the material when added to the mix (Benmansour et

al., 2014; Yassin et al., 2020). A previous study conducted by the authors investigated the effect of adding ground PTF (as replacement for sand) on the mechanical behavior of concrete (Ezzdine Lakys, 2021). The study concluded that ground PTF should be added in very low percentages (1% of sand replacement) to avoid excessive reduction in compressive strength.

Nowadays, an extremely large number of ceramic tiles is produced annually to meet the increasing need in construction as a result of the fast-growing populations. Large volumes of production inevitably result in large volumes of waste; the ceramic tiles waste resulting from construction works are estimated at 30% of total ceramic production, according to (Torkittiku & Chaipanich, 2010). This waste is generally dumped on the ground leading to environmental damage. On the other hand, adding ceramic waste powder (CWP) to concrete as a partial cement substitute was investigated by Irassar et al. (2014) and Mohit & Sharifi (2019) and many others, and it was found that the CWP enhances the hydration reaction due to its cementitious properties and reduces the alkali-silica reaction expansion resulting in a higher strength of concrete.

In this study, PTF fiber was chosen due to its ability to enhance the thermal resistance of concrete while CWP was chosen for its pozzolanic properties to increase the strength of concrete.

3 Experimental Plan

The experimental plan consisted of preparing the two type of wastes, the PTF and the CWP, in the first phase. The second phase included the concrete mix preparation: mix design for all mixes, concrete mixing and samples casting and curing. Three cylinders of 100 mm diameter and 200 mm length were cast for each mix. The final phase consisted of testing the concrete samples.

3.1 Materials Preparation

The PTF is chemically treated, then ground as explained in a previous work (Lakys, 2022). **Fig. 2** shows the particle size distribution for the ground PTF fibers, 85% of the fibers range between 0.5mm and 2 mm while 35% fall below 0.15 mm.

The CWP was obtained by crushing waste ceramic tiles in an aggregate crushing machine then by reducing the coarse particles into fine particles by placing them in a Los Angeles Abrasion for minimum 30 minutes. As a final step, the ground particles were sieved by a No. 200 sieve to obtain the powder shown in **Fig. 1**.



Fig. 1: Ceramic waste powder and PTF fibers

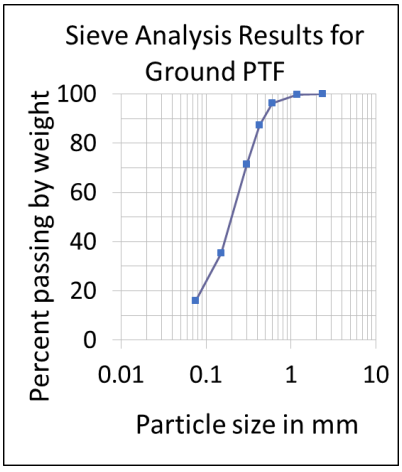


Fig. 2: PTF Sieve analysis

3.2 Mix Design

The concrete mix should be designed to ensure at the same time a great workability/fluidity of the concrete and a high resistance to segregation, which can be very challenging given that these two properties are contradictory. In a typical concrete, when the workability increases, the resistance to segregation decreases. The key factors for a successful mix design for a high strength concrete with great workability are high cementitious/fine powder dosage (450-600 kg/m3), limited aggregate content (ratio of coarse aggregate volume to total mixture volume limited to 45-48 %), low water-powder ratio (ratio of water to cementitious material limited to 0.28-0.45 %) and use of superplasticizer. Our mix design was performed based on these factors to obtain M60 grade concrete.

Five groups of mixtures (families) are cast to investigate the addition of PTF in different percentages as replacement for sand and the partial replacement of cement by ceramic powder. The families are defined as follows:

1. S0-P0: is the control mix designed with 0 % CWP and 0 % PTF;
2. S33-P0: is the mix designed with 33 % CWP and 0 % PTF;
3. S33-P0.5: is the mix designed with 33 % CWP and 0.5 % PTF;
4. S33-P1: is the mix designed with 33 % CWP and 1 % PTF;
5. S0-P1: is the mix designed with 0 % CWP and 1 PTF.

Table 1: Mix Design for all families (mixes)

Mix	Cement [kg]	CWP [kg]	Water [ℓ]	Aggregate (12.5 mm) [kg]	Aggregate (9.5mm) [kg]	Sand [kg]	PTF [kg]	Admixture [ℓ]
S0-P0	450	0	150	598	598	625	0	6.5
S33-P0	300	150				625	0	
S33-P0.5						622	1.92	
S33-P1						619	3.85	
S0-P1	450	0				616	5.76	

4 Results

The results, shown in the following sections, aim to evaluate the effect of adding the wastes with various percentages on fresh concrete, in terms of workability, and on concrete cured for one day (hardened concrete) in terms of compressive strength.

4.1 Fresh Concrete

The slump test (ASTM C143-78, 2017) was performed for all mixes. The control mix S0-P0 slumped by 50 mm (low to medium workability) while all other mixes showed a collapse slump resulting in a high workability concrete (**Fig. 3** and **Fig. 4**). Therefore, the traditional slump test was considered inappropriate for these mixes and the inverted slump test (ASTM C192–19, 2020) was performed instead. The mixes including ceramic waste powder and PTF gave similar results, the concrete flowed during 20 to 25 seconds to spread into a circle of a diameter varying from 420 mm to 500 mm. These mixes did not achieve the self-consolidating concrete condition but were very close.



Fig. 3: Slump test for S0-P0



Fig. 4: Collapse slump for S33-P0.5

4.2 Hardened Concrete

The concrete samples were cured for one day according to ASTM C192–20, 2020 and demolded and tested for compression according to ASTM C39–21, 2021. The compression test set-up is presented in Figure 5. The results of the compressive strength are given in **Table 2**. It is observed that when considered separately the effect of PTF (Mix S0-P1) and the effect of CWP (Mix S33-P0), the compressive strength decreased for both, while an increase in strength was detected for the combined effect of PTF and CWP (Mix S33-P0.5), a percentage of 1% of sand replacement by PTF resulted in reducing the concrete strength.

Replacing 33% of the weight of cement with CWP reduced the compressive strength of the concrete by 23%, similar result was found by Shaikh-ul-Karim (2020) where a reduction of 26,7% was observed due to 30% replacement of cement by CWP after 3 days of curing. Shaikh-ul-Karim (2020) found that there is no significant reduction of the strength when adding CWP as cement substitute with a limit of 20%. The results of our study show that the control mix (0% CWP and 0% PTF) and the mix S33-P0.5 (33% CWP and 0.5% PTF) have almost similar strength, around 16 MPa at Day 1. Replacing 0.5% of sand volume by PTF increased the strength of concrete after one day of curing by around 27% compared to its strength when no PTF is added (S33-P0) while replacing 1% of sand volume by PTF decreased it by around 30%.



Fig. 5: Compression test set-up

Table 2: Compression test results for all samples

Mix	Compression test results (MPa)			Average (MPa)	Standard Deviation (MPa)
S0-P0	16.60	12.67	19.01	16.09	3.20
S33-P0.5	14.4	16.25	16.42	15.69	1.12
S0-P1	11.78	10.47	16.26	12.84	3.04
S33-P0	12.47	12.2	12.47	12.38	0.16
S33-P1	11.14	10.3	11.84	11.09	0.77

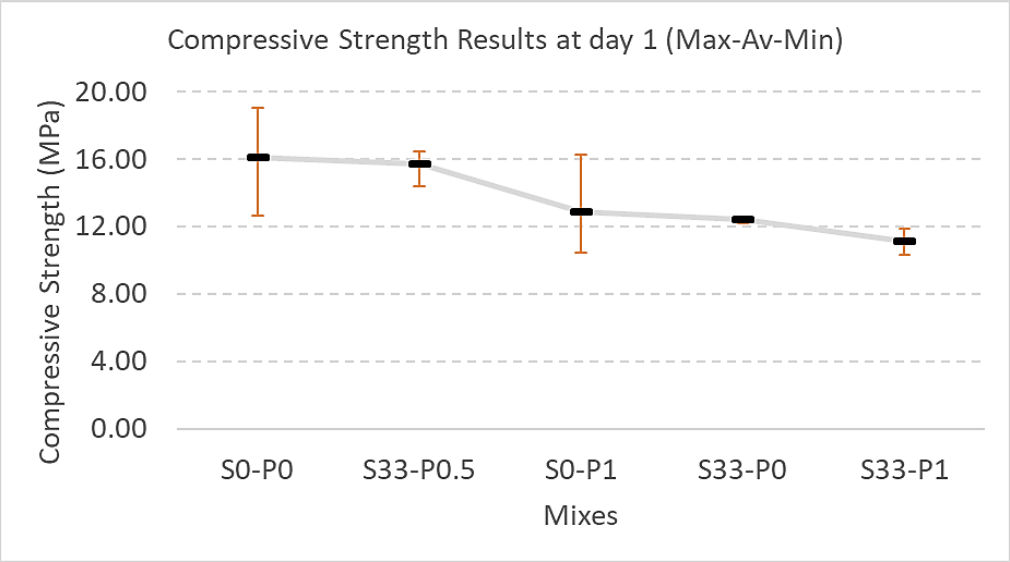


Fig. 6: Compression test results showing maximum-average-minimum values for each mix

5 Conclusion

In this study, the results of adding two types of wastes to concrete are investigated: CWP as cement substitute and PTF as sand substitute. To achieve this aim, various mixes were designed and cast. The workability of the fresh concrete was explored and three samples from each mix were tested after one day of curing to investigate the effect of the added wastes on the compressive strength of concrete. The results showed that the workability of concrete was greatly enhanced when adding the two wastes. The compression test results showed that adding one type of waste reduced the strength of concrete while no significant strength reduction was found when adding both (CWP at 33% of cement replacement and PTF at 0.5% of sand replacement). This combination was considered to be the optimal mix in terms of compressive strength when compared to others mixes. The results are promising particularly when considering that CWP may lead to higher strength after a longer curing period (more than 28 days) due to pozzolanic reactions (Mohit & Sharifi, 2019).

The results of this study represent a great significance in terms of sustainable construction since it emphasizes on the re-use of ceramic tile waste as CWP in a relatively high proportion as cement replacement (33%) with no significant reduction of compressive strength of concrete particularly when considering that the cement production accounts for 5 to 8% of global greenhouse gas emission according to (El-Dieb & Kanaan, 2018). On the other hand, incorporating the PTF in the concrete mix, even in small percentages, enhances the thermal resistance of the concrete according to a

previous study conducted by the authors (Yassin, 2020) resulting in reducing the energy consumption of the construction. Further studies are needed to investigate the effect of adding these two wastes with various percentages on the concrete (flexural strength, water absorption, density, absorptivity, durability, etc.) for both short and long terms.

Acknowledgments

The authors acknowledge the financial support of the Kuwait Foundation for the Advancement of Sciences (KFAS) for funding this project via Grant# PN20-35EV-02.

The authors also acknowledge the contribution of the students Dana Alshatti, Fajer Alfailakawi, Fahad Hasieh, Issa Alsamad and Talal Alhamad to the experimental tests reported in this paper.

References

Ahamed, M., Ravichandran, P. & Krishnaraja, A. R. (2021). Natural Fibers in Concrete – A Review. IOP Conference Series: *Materials Science and Engineering*, *1055*(1): 012038. DOI: 10.1088/1757-899X/1055/1/012038.

Al-Kutti, W., Islam, A. B. M. & Nasir, Muhammad. (2017). Potential use of date palm ash in cement-based materials. *Journal of King Saud University - Engineering Sciences*, *31*(1). DOI: 10.1016/j.jksues.2017.01.004.

ASTM C 39/C39 M-21. (2021). Standard test method for compressive strength of cylindrical concrete specimens. *American Society for Testing and Materials*, West Conshohocken, PA

ASTM C143-78 (2017). Standard Test Method for Slump of Portland Cement Concrete, *04*(02). ASTM International, West Conshohocken, PA.

ASTM C 1611/C 1611 M-09b. (2009). Standard test method for slump flow of self-consolidating concrete. *American Society for Testing and Materials*, *04*(02). ASTM International, West Conshohocken, PA.

ASTM C192/C192M–19. (2020). Standard practice for making and curing concrete test specimens in the laboratory. *American Society for Testing and Materials*, *04*(02). ASTM International, West Conshohocken, PA.

Babita, et al. (2019).Review Paper on Partial Replacement of Cement and Aggregates with Various Industrial Waste Material and Its Effect on Concrete Properties. 10.1007/978-981-13-7017-5_13.

Benmansour, et al. (2014). Thermal and mechanical performance of natural mortar reinforced with date palm fibers for use as insulating materials in building. *Energy and Buildings*. *81*. 98–104. DOI: 10.1016/j.enbuild.2014.05.032.

El-Dieb, A. & Kanaan, D. (2018). Ceramic waste powder an alternative cement replacement – Characterization and evaluation. *Sustainable Materials and Technologies*. *17*. e00063. ISSN 2214-9937.

Ezzdine Lakys, R., Yassin, M. H. & Merouani, Z. (2022). Preliminary Study on the Effect of Adding Palm Tree Fronds to Concrete. 7th International Conference on Civil Structural and Transportation Engineering. Niagara Falls, Canada. June 05-07, 2022. Paper No. 189. DOI: 10.11159/iccset22.189.

Gunasekaran, K., Annadurai, R. & Kumar, P. (2013). A study on some durability properties of coconut shell aggregate concrete. *Materials and Structures*. *48*. 1253-1264. DOI: 10.1617/s11527-013-0230-2.

Hiremath, M. N., Sanjay, S. J. & Poornima, D. (2017), Replacement of Coarse Aggregate by Demolished Brick Waste in Concrete, (IJSTE) - *International Journal of Science Technology & Engineering*, Vol. *4*(2), 31-36.

Imam, A., Kumar, V. & Srivastava, V. (2018). Review study towards effect of Silica Fume on the fresh and hardened properties of concrete. *Advances in Concrete Construction*, *6*(2). 145-157. DOI: 10.12989/acc.2018.6.2.145.

Irassar, et al. (2014). Utilization of ceramic wastes as pozzolanic materials. *Technical Proceedings of the 2014 NSTI Nanotechnology Conference and Expo*, NSTI-Nanotech 2014. 3. 230-233.

Jagan, V. M. R. (2017). Study on Replacement Level of Concrete Waste as Fine Aggregate in Concrete. *International Journal for Research in Applied Science and Engineering Technology*. V *5*(2). DOI: 241-246. 10.22214/ijraset.2017.2038.

Kejela, B. (2020). Waste Paper Ash as Partial Replacement of Cement in Concrete. *American Journal of Construction and Building Materials*. Vol. 4. 8-13.

Khalid, et al. (2019). Comparison of different waste materials used as cement replacement in concrete. *IOP Conference Series: Earth and Environmental Science*, *357*(1). DOI: 10.1088/1755-1315/357/1/012010.

Kumbhar, V. (2018). Comparative Analysis of Coconut Shell Concrete to Traditional Concrete. *International Journal of Research Technology in Engineering & Management*, *2*(6), 107-113.

Machaka, et al.. (2014). The Effect of Using Fan Palm Natural Fibers on the Mechanical Properties and Durability of Concrete. *International Journal of Materials Science and Engineering*, *2*(2). 76-80. DOI: 10.12720/ijmse.2.2.76-80.

Mansoor, S. S., Hama, S. & Hamadallah, D. (2022). Effectiveness of replacing cement partially with waste brick powder in mortar. *Journal of King Saud University - Engineering Sciences*. DOI:10.1016/j.jksues.2022.01.004

Marinkovic, S. et al. (2010). Comparative environmental assessment of natural and recycled aggregate concrete,*Waste Management*., Vol. 30, pp. 2255–2264.

Mohit, M. & Sharifi, Y. (2019). Ceramic Waste Powder as Alternative Mortar-Based Cementitious Materials. *ACI Materials Journal*. *116*. DOI: 10.14359/51716819.

Müller, H., Haist, M. & Vogel, M.. (2014). Assessment of the sustainability potential ofconcrete and concrete structures considering theirenvironmental impact, performance and lifetime. *Construction and Building Materials*, vol. 67, pp. 321–337.

Raval, A., Patel, I. & Pitroda, J. (2013). Ceramic Waste: Effective Replacement of Cement for Establishing Sustainable. *IJETT*, *4*(6). 2324-2329.

Rohini, I., Arularasi, V. & Muthu, A. C. (2016). Investigation based on partial replacement of coarse aggregate with waste tire rubber in concrete. *International Journal of Latest Research in Engineering and Technology*, *2*(8), 100-109.

Shaik-ul-Karim, S.M., Ahmed, S. & Saifullah, I. (2020). Performance of Mortar Incorporating Ceramic Waste Powder as Partial Replacement of Cement. *5th International Conference on Civil Engineering for Sustainable Development* (ICCESD 2020). Khulna, Bangladesh

Sekar, M. (2017). Partial Replacement of Coarse Aggregate by Waste Ceramic Tile in Concrete. *International Journal for Research in Applied Science and Engineering Technology*, *5*(3). 472-479. DOI: 10.22214/ijraset.2017.3086.

Sharma, et al. (2021). Recycled Plastic as Coarse Aggregate for Structural Concrete. UKIERI Concrete Congress – *Concrete Research Driving Profit and Sustainability*. Jalandhar, India. 1070-1074

Singh, S. & Sancheti, G. (2019). Replacement of Aggregate by C&D Waste. *International Research Journal of Engineering and Technology*, *06*(03), 2293-2300.

Sujatha, A. & Balakrishnan, D. (2020). Properties of Coconut Shell Aggregate Concrete: A Review. 10.1007/978-981-15-5644-9_60.

Srivastava, V., Monish, M. &, Agarwal V. C. & Mehta, P. K., (2013). Demolition Waste as Cement Replacement in Concrete. *Journal of Environmental Nanotechnology*, *2*(3), 16-19, DOI: 10.13074/jent 2013.09.132026

Torkittiku, P. & Chaipanich, A. (2010). Utilization of ceramic waste as fine aggregate within Portland cement and fly ash concretes. *Cement & Concrete Composites*, *32*(6), 440-449.

United Nations Environment Programme. (2022). 2022 Global Status Report for Buildings and Construction: Towards a Zero-emission, Efficient and Resilient Buildings and Construction Sector. Nairobi.

Yaseen, M., Hama, S. & Mahmoud, A. (2018). Reusing of Glass Wastes as Powder as Partial of Cement in Production of Concrete. *11th International Conference Development In E-Systems Engineering* 2018, pp. 330-334. DOI: 10.1109/DeSE.2018.00065.

Yassin, et al. (2020). Optimizing the Thermal Resistance of Concrete Using the Palm Tree Fronds Fibers. *The International Conference on Civil Infrastructure and Construction (CIC 2020)*, Doha, Qatar, 452-461. DOI: 10.29117/cic.2020.0057.

Zareei, et al. (2017). Rice husk ash as a partial replacement of cement in high strength concrete containing micro silica: Evaluating durability and mechanical properties. *Case Studies in Construction Materials*. *7*. 73-81. DOI: 10.1016/j.cscm.2017.05.001.

Cite as: Lakys R.E., Yassin M.H. & Jumaah A., "Sustainable Alternatives for Concrete by adding Different Types of Natural and Industrial Waste Materials", *The 2nd International Conference on Civil Infrastructure and Construction (CIC 2023)*, Doha, Qatar, 5-8 February 2023, DOI: https://doi.org/10.29117/cic.2023.0095

Exploration of Carbonate Aggregates in Road Construction using Ultrasonic and Artificial Intelligence Approaches

Mohamed Abdelhedi
Research Laboratory GEOMODEL (LR16ES17), Department of Earth Sciences, Faculty of Sciences, University of Sfax, Sfax, Tunisia
mohamed.abdelhedi.etud@fss.usf.tn

Rateb Jabbar
KINDI Center for Computing Research, College of Engineering, Qatar University, Doha, Qatar
rateb.jabbar@qu.edu.qa

Chedly Abbes
Research Laboratory GEOMODEL (LR16ES17), Department of Earth Sciences, Faculty of Sciences, University of Sfax, Sfax, Tunisia
chedlyabbes8@gmail.com

Abstract

The COVID-19 pandemic has significantly impacted the construction sector, which is highly sensitive to economic cycles. In order to boost value and efficiency in this sector, the use of innovative exploration technologies such as ultrasonic and Artificial Intelligence techniques in building material research is becoming increasingly crucial. In this study, we developed two models for predicting the Los Angeles (LA) and Micro Deval (MDE) coefficients, the two important geo-technical tests used to determine the quality of carbonate rock aggregates. These coefficients describe the resistance of aggregates to fragmentation and abrasion. The ultrasound velocity, porosity, and density of the rocks were determined and used as inputs to develop prediction models using multiple regressions and an artificial neural network. These models may be used to assess the quality of rock aggregates at the exploration stage without the need for tedious laboratory analysis.

Keywords: Ultrasonic pulse velocity; Los Angeles (LA) coefficient; Micro Deval (MDE) coefficient; Carbonates; Rock aggregates; Artificial Intelligence

1 Introduction

Over the past decade, there has been a significant increase in the development of new methods for subsurface geological exploration, particularly in the exploration of sources of building materials (Pell et al., 2021). The increasing global economic crises have amplified the need for new exploration methods such as the ultrasonic method and the application of artificial intelligence in the exploration of geo-resources, including building materials, particularly for developing countries. The construction of smart cities, such as the over 300 projects in China and the more than 100 planned in India, require a significant amount of building materials, particularly for road construction. Transportation is a fundamental function of a smart city (Toh et al., 2020). Additionally, the population of the world's urban areas is increasing by 200,000 people per day, seeking affordable housing as well as social, transportation, and utility infrastructure. This has led to an increasing demand for sustainable construction materials globally (Marangu et al., 2017).

The traditional methods for construction materials prospecting seem inadequate compared to the significant international demand for these materials. These techniques are labor-intensive, costly,

and time-consuming. Therefore, finding more practical, faster, and less expensive prospecting techniques is of great interest (Abdelhedi & Abbes, 2021). While the ultrasonic method has not yet been well-developed for geomaterial applications, it is a very attractive tool. In recent years, several authors have applied this method in the exploration of carbonate rocks (Abdelhedi et al., 2017), in gold mine exploration (De Souza et al., 2022), and in mortar quality control (Abdelhedi et al, 2018).

Artificial intelligence (AI) is a set of computational algorithms used for clustering, predicting, and classifying tasks (Ebid, 2020). Because AI has superhuman abilities, it has revolutionized all spheres of technology and science (Jabbar, Jabbar & Kamoun, 2022; Moulahi et al., 2022). AI is becoming more ubiquitous across several areas, including healthcare (Elleuch *et al.*, 2021), agriculture (Ayadi et al., 2020), sustainability (Jabbar et al., 2021; Abulibdeh, Zaidan & Jabbar, 2022; Zaidan et al., 2022) and transportation (Jabbar et al., 2018; Ben Said & Erradi, 2022).

In the field of geology, AI technology has attracted significant academic and industrial attention in recent years. AI has been applied in geoscience for the determination of reservoir rock properties, drilling optimization, and enhanced production facilities (Solanki et al., 2022). Furthermore, these techniques have been used in carbonate rock exploration for the prediction of rocks and mortar UCS (Uniaxial Compressive Strength) values (Abdelhedi et al., 2020). Additionally, AI has been applied in mining and geological engineering, including rock mechanics, mining method selection, mining equipment, drilling-blasting, slope stability, and environmental issues (Bui, Bui & Nguyen, 2021).

This study applied AI and ultrasonic methods to establish predictive models linking porosity, density, and ultrasonic velocity to Los Angeles (LA) and Micro Deval (MDE) coefficients, with the aim of increasing the exploration of high-quality carbonate aggregates used in road construction.

The remainder of this paper is organized as follows. Section 2 presents the methods and materials used in this study. Section 3 discusses the computational results obtained from experiments. Finally, in Section 4, conclusions are presented.

2 Methods and Materials

Seven samples were collected from carbonate formations and crushed into aggregates with particle sizes ranging from 10mm to 14 mm.

2.1 Ultrasonic Velocity

The ultrasonic method involves exciting the structure of the material using a vibratory source, such as a piezoelectric transducer, which converts electrical energy into mechanical energy and vice versa. The use of transducers allows control over the shape and duration of the pulse, providing a repetitive and energetic source. The measurements were carried out with direct contact, requiring the use of a coupling material between the transducer and the sample to reduce the loss of the signal (Abdelhedi et al., 2018).

2.2 Artificial Neural Network ANN

An artificial neural network (ANNs) is a type of AI algorithm used to solve complex non-linear problems. ANNs are modeled after the structure of the human brain and are composed of interconnected nodes, or "neurons," that process and transmit information. ANNs have been applied as a method of artificial intelligence in a variety of fields, including geo-materials applications.

In this study, we used an artificial neural network (ANN) with three layers: an input layer, an output layer, and a hidden layer. The input layer is composed of three neurons, each representing a

different variable (ultrasonic pulse velocity, density, and effective porosity) that is used as input data for the ANN. The output layer is formed by a single output neuron, which produces the predicted value of the LA or MDE coefficient based on the input data. The hidden layer is a single layer that processes the input data and generates an intermediate output that is used by the output layer to produce the final result.

The back-propagation neural network (BP-NN) (Wengang et al., 2019) used in this study is a learning algorithm used to train the ANN. The BP-NN uses a technique called "back-propagation" to adjust the weights of the connections between the neurons in the ANN based on the difference between the predicted output and the actual output. The BP-NN adjusts the weights during a number of iterations, called “epochs,” and uses a learning function called Levenberg-Marquardt (TRAINLM) (Kipli et al., 2012) to determine the rate at which the weights are adjusted. By iteratively adjusting the weights in this way, the BP-NN is able to "learn" from the input data and improve the accuracy of its predictions over time.

2.3 Los Angeles Coefficient

The resistance to fragmentation of aggregates is an important characteristic that can affect the performance of materials in various applications, such as road construction. To determine this property, the Los Angeles (LA) coefficient is commonly used. The LA coefficient is measured according to standards P18-572 (1990) (Amrani et al., 2019) using a test that involves subjecting the material to standard ball shocks in a Los Angeles machine. The mass of the ball load used in the test varies based on the granular class of the material. The resistance to fragmentation is calculated as:

$$LA = 100\frac{m}{M} \qquad (1)$$

Where M is the mass of the material being tested and m is the mass of the particles smaller than 1.6 mm produced during the test.

2.4 Micro-Deval Coefficient

The abrasion resistance of aggregates is an important property that can impact their performance in various applications. To determine this characteristic, the micro-deval coefficient is commonly used. This test, described in standards P18-573 (1990), measures the wear resistance of rocks under both dry and wet conditions. The test involves subjecting the material to reciprocal friction in a rotating cylinder under controlled conditions, using abrasive filler for tests on gravel between 10 and 14 mm. The micro-deval coefficient (MDE) in the presence of water is calculated as

$$MDE = 100\frac{m}{M} \qquad (2)$$

Where M is the mass of the material being tested and m is the mass of the particles smaller than 1.6 mm produced during the test. The wear resistance of the material is expressed by the quantity of these particles

3 Results and Discussion

Artificial neural networks (ANNs) have been shown to be effective models for predicting complex rock properties in multiple studies (Kahraman et al., 2010; Madhubabu et al., 2016). Therefore, ANNs were used to create two models that linked the physical parameters to the mechanical parameters of carbonate rock aggregates, allowing for the estimation of their resistance to fragmentation and abrasion. Ultrasound velocity, porosity, and density were first determined and analyzed, and then used to create predictive models using Excel and ANN. The datasets were used for training, validation, and

verification of the prediction efficiency of the models. The input parameters for the models were ultrasonic velocity, porosity, and density, while the outputs were either the MDE or LA coefficient. The MDE and LA coefficient values predicted by the models created using multiple regression are plotted against the measured values in Figures 1 and 2, respectively.

We note that these two relationships exhibited significant correlations ($R^2 > 0.8$). However, the first correlation shows a negative estimated value of MDE, which is not acceptable.

The models produced by the artificial neural network give two correlations between the predicted MDE and LA coefficient values and the measured values (figures 3 and 4 respectively). The plotted data for the output parameters for both models was close to Line 1, indicating a favorable prediction. Models generated by ANN analysis were more accurate than models generated by multiple regressions. Figure 1 shows that the multiple regression model produced a false estimation of MDE (a negative value), demonstrating the ANN model's superiority.

Abdelhedi et al. (2020) conducted a similar study in which they used ANNs to predict uniaxial compressive strength (UCS) in carbonate rocks. Tariq et al. (2017) used ultrasonic pulse velocity and density to develop an ANN model with a correlation coefficient of $R^2 = 0.84$ to predict UCS values in carbonate rocks.

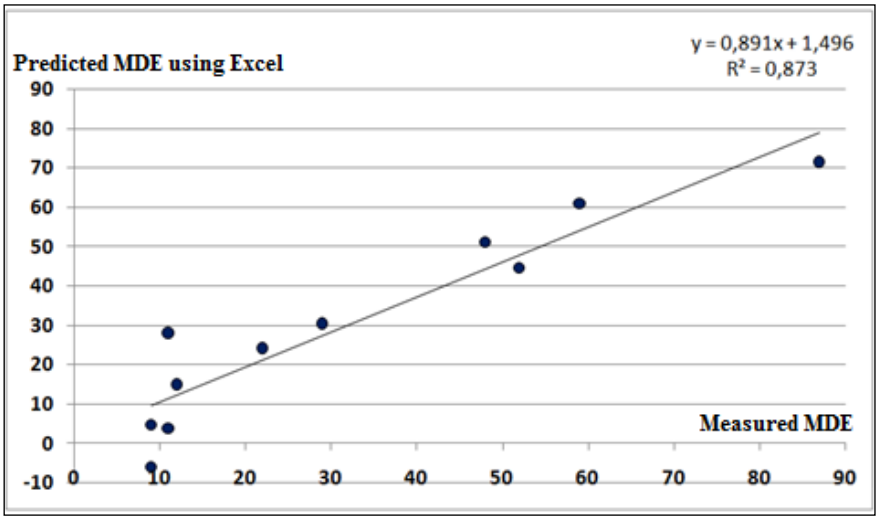


Fig. 1: Correlation between MDE values estimated by multiple regression and measured MDE

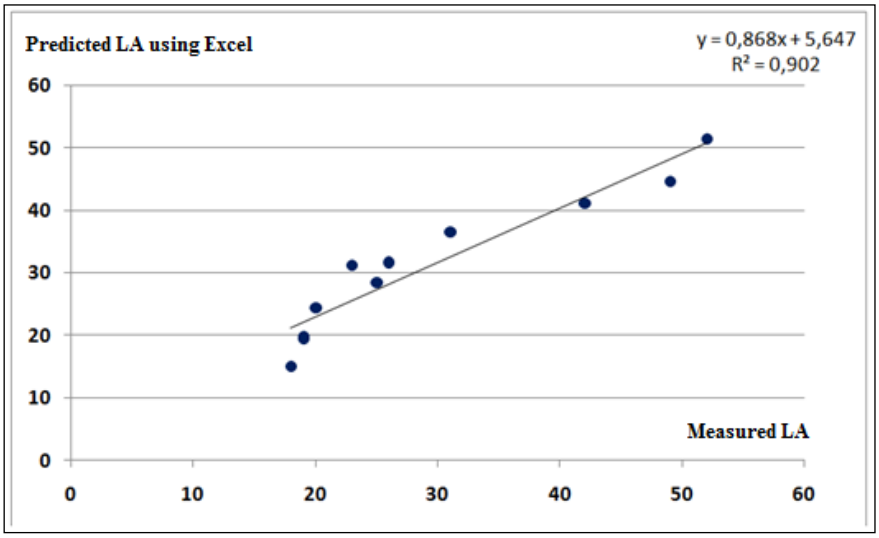


Fig. 2: Correlation between LA values estimated by multiple regression and measured LA

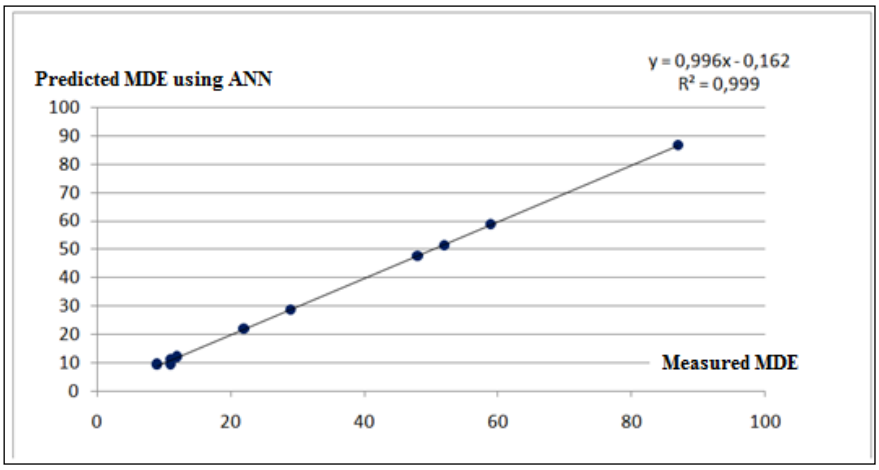


Fig. 3: Correlation between MDE values estimated by ANN and measured MDE

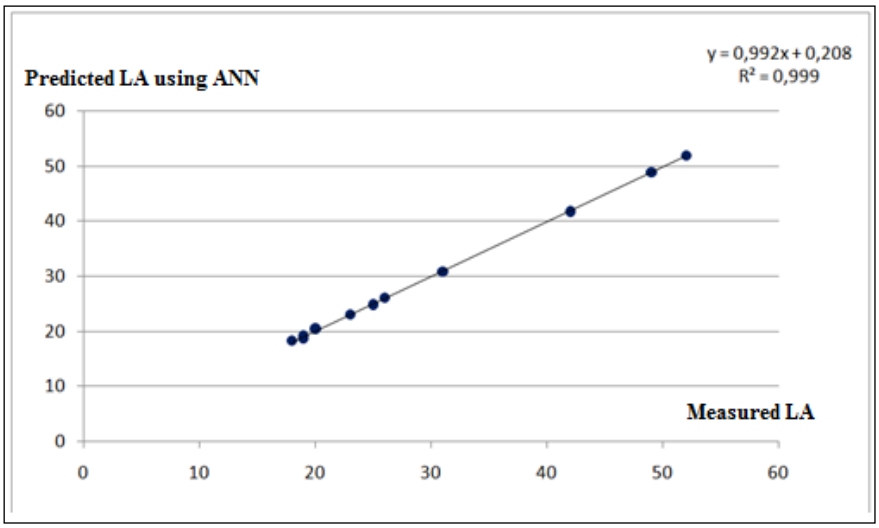


Fig. 4: Correlation between LA values estimated by ANN and measured LA

4 Conclusion

The performance of construction materials, such as aggregates, can significantly affect the strength and durability of structures. In order to evaluate the suitability of different aggregates for different applications, it is important to measure their physical and mechanical properties. Two important properties that are commonly tested for aggregates are their resistance to fragmentation and abrasion. These properties can be evaluated using the Los Angeles (LA) and micro-deval (MDE) tests, respectively.

In this study, a number of carbonate rock aggregates were subjected to the LA and MDE tests in order to determine their resistance to fragmentation and abrasion. Multiple correlation methods were then used to develop predictive models linking the physical parameters of porosity, density, and ultrasonic velocity to the LA and MDE coefficients. These models can be used to predict the resistance to fragmentation and abrasion in the exploration of new mining sites of aggregates based on their physical properties.

The LA and MDE coefficients are particularly important for aggregates used in the construction of roads and hydraulic concretes. By using this technique, it is possible to easily assess the potential of new aggregate geo-resources for use in these applications.

Despite some limitations, such as the small sample size, this research is an important step towards improving our understanding of the behavior of aggregates and their suitability for use in construction.

References

Abdelhedi, et al. (2017). “Ultrasonic velocity as a tool for mechanical and physical parameters prediction within carbonate rocks”, *Geomechanics and Engineering*, *13*(3), 371-384. DOI: https://doi.org/10.12989/gae.2017.13.3.371

Abdelhedi, M., Mnif, T., & Abbes, C. (2018). “Ultrasonic velocity as a tool for physical and mechanical parameters prediction within geo-materials: Application on cement mortar”, *Russian Journal of Nondestructive Testing*, *54*(5), 345-355. DOI: https://doi.org/10.1134/S1061830918050091

Abdelhedi, M., Jabbar, R., Mnif, T., & Abbes, C., (2020). “Prediction of uniaxial compressive strength of carbonate rocks and cement mortar using artificial neural network and multiple linear regressions”, *Acta Geodynamica et Geromaterialia*, *17*(3), 367-378. DOI: 10.13168/AGG.2020.0027

Abdelhedi, M. & Abbes, C., (2021). “Study of physical and mechanical properties of carbonate rocks and their applications on georesources exploration in Tunisia”. *Carbonates and Evaporites*, *36*(2), 1-13. https://doi.org/10.1007/s13146-021-00688-8

Abulibdeh, A., Zaidan, E. & Jabbar, R. (2022). “The impact of COVID-19 pandemic on electricity consumption and electricity demand forecasting accuracy: Empirical evidence from the state of Qatar”, *Energy Strategy Reviews*, *44*, p. 100980. https://doi.org/10.1016/j.esr.2022.100980

Amrani, et al. (2019). “Valorization of phosphate mine waste rocks as materials for road construction”, *Minerals*, *9*(4), 237. https://doi.org/10.3390/min9040237

Ayadi, et al. (2020). “Dairy cow rumination detection: A deep learning approach”, In *International Workshop on Distributed Computing for Emerging Smart Networks*, 123-139. Springer, Cham. DOI: https://doi.org/10.1007/978-3-030-65810-6_7

Bui, X. N., Bui, H. B. & Nguyen, H. (2021). “A Review of Artificial Intelligence Applications in Mining and Geological Engineering”, *Proceedings of the International Conference on Innovations for Sustainable and Responsible Mining*, *109*, pp. 109–142. DOI: https://doi.org/10.1007/978-3-030-60839-2_7

De Souza, et al. (2022). “Laboratory measurements of ultrasonic wave velocities and anisotropy across a gold-hosting structure: A case study of the Thunderbox Gold Mine, Western Australia”, Ore Geology Reviews, *146*, 104928. https://doi.org/10.1016/j.oregeorev.2022.104928

Ebid, A. M. (2020). “35 Years of (AI) in Geotechnical Engineering: State of the Art”, *Geotechnical and Geological Engineering*, 2, *39*(2), pp. 637–690. DOI: https://doi.org/10.1007/s10706-020-01536-7

Elleuch, et al. (2021). “Real-time prediction of COVID-19 patients health situations using Artificial Neural Networks and Fuzzy Interval Mathematical modeling”, *Applied Soft Computing*, *110*, p. 107643. https://doi.org/10.1016/j.asoc.2021.107643

Jabbar, et al. (2021). “Reshaping Smart Energy Transition: An analysis of human-building interactions in Qatar Using Machine Learning Techniques”, arXiv preprint arXiv:2111.08333. https://doi.org/10.48550/arXiv.2111.08333

Jabbar, et al. (2018). "Applied Internet of Things IoT: Car monitoring system for Modeling of Road Safety and Traffic System in the State of Qatar", *Qatar Foundation Annual Research Conference Proceedings*, Volume 2018 Issue 3. Vol. 2018. No. 3. Hamad bin Khalifa University Press (HBKU Press). https://doi.org/10.5339/qfarc.2018.ICTPP1072

Jabbar, R., Jabbar, R. & Kamoun, S. (2022). “Recent progress in generative adversarial networks applied to inversely designing inorganic materials: A brief review." Computational Materials Science, 213. 11612. https://doi.org/10.1016/j.commatsci.2022.111612

Kahraman, et al. (2010). “The usability of Cerchar abrasivity index for the prediction of UCS and E of Misis Fault

Breccia: regression and artificial neural networks analysis". *Expert Systems with Applications*, *37*(12), 8750-8756. https://doi.org/10.1016/j.eswa.2010.06.039

Kipli, et al. (2012). "Performance of Levenberg-Marquardt backpropagation for full reference hybrid image quality metrics", *Proceedings of International Conference of Muti-Conference of Engineers and Computer Scientists* (IMECS'12) (pp. 704-707).

Madhubabu, et al. (2016). "Prediction of compressive strength and elastic modulus of carbonate rocks", *Measurement*, 88:202-213. https://doi.org/10.1016/j.measurement.2016.03.050

Marangu, J. M., Latif, E & Maddalena, R., (2021). "Evaluation of the reactivity of selected rice husk ash-calcined clay mixtures for sustainable cement production." Edited by R. Maddalena and M. Wright-Syed: 81.

Moulahi, et al. (2022). "Privacy-preserving federated learning cyber-threat detection for intelligent transport systems with blockchain-based security". *Expert Systems*, e13103. https://doi.org/10.1111/exsy.13103

Pell, et al. (2021). "Towards sustainable extraction of technology materials through integrated approaches", *Nature Reviews Earth & Environment*, 2(10), 665-679. https://doi.org/10.1038/s43017-021-00211-6

Ben Said, A. & Erradi, A. (2022) "Spatiotemporal Tensor Completion for Improved Urban Traffic Imputation", *IEEE Transactions on Intelligent Transportation Systems*, *23*(7), pp. 6836–6849. DOI: 10.1109/TITS.2021.3062999

Solanki, et al. (2022). "Artificial intelligence: New age of transformation in petroleum upstream", *Petroleum Research*, *7*(1), pp. 106–114. https://doi.org/10.1016/j.ptlrs.2021.07.002

Standard P18-572 (1990) Aggregates. Micro-deval attribution test. *Association française de normalisation, Bureau de Normalisation Sols et Routes*. Géotechnique-normes. Décembre 1990, Paris, France.

Standard P18-573. (1990). Aggregates. Los Angeles test–granulate. Los Angeles pruefung. *Association française de normalisation, Bureau de Normalisation Sols et Routes*. Géotechnique-normes. Décembre 1990, Paris, France.

Tariq, et al. (2017). "A new technique to develop rock strength correlation using artificial intelligence tools", *SPE Middle East Oil and Gas Show and Conference*, 18-21, March, Manama, Bahrain. https://doi.org/10.2118/186062-MS

Toh, et al. (2020). "Advances in smart roads for future smart cities", *Proceedings of the Royal Society* A, *476*(2233), 20190439. https://doi.org/10.1098/rspa.2019.0439

Wengang, et al. (2020). "Back-propagation neural network modeling on the load–settlement response of single piles." *Handbook of probabilistic models*. Butterworth-Heinemann, 2020. 467-487. https://doi.org/10.1016/B978-0-12-816514-0.00019-9

Zaidan, et al. (2022). "Motivation, preference, socioeconomic, and building features: New paradigm of analyzing electricity consumption in residential buildings", *Building and Environment*, 109177. https://doi.org/10.1016/j.buildenv.2022.109177

Cite as: Abdelhedi M., Jabbar R. & Abbes C., "Exploration of Carbonate Aggregates in Road Construction using Ultrasonic and Artificial Intelligence Approaches", *The 2nd International Conference on Civil Infrastructure and Construction (CIC 2023)*, Doha, Qatar, 5-8 February 2023, DOI: https://doi.org/10.29117/cic.2023.0096

Identification of Karstic Features with Extensive Geophysical Investigation for Underground Infrastructure - South of Wakrah Pumping Station and Outfall (SWPSO) Project

Ali Akbar
Stantec UK Limited, Doha, Qatar
ali.akbar@stantec.com

Fathelrahman Dafalla
Stantec UK Limited, Doha, Qatar
fathelrahman.dafalla@stantec.com

Ilayaraja Kumba Krishnamurthi
Public Works Authority (Ashghal), Doha, Qatar
ikrishnamurthi@ashghal.gov.qa

Andres E. Pinto Candia
Stantec UK Limited, Doha, Qatar
andres.pinto@stantec.com

Abstract

There has been a significant increase in the number of underground infrastructure projects built in a short period because of Qatar's goal of effective mass transit and robust urban drainage infrastructure, as well as the country's recent fast urbanization and harsh weather events. The Doha Metro, the Inner Doha Re-sewerage Implementation Strategy (IDRIS), and most recently the Doha South Terminal Pumping Station (DSTPS) and the Musaimeer Pumping Station and Outfall (MPSO) projects faced difficulties in identifying and quantifying the Karstic features and the remedial approach for underground works to ensure the completion of the projects on schedule and within budget due to the unknown ground conditions. One of the most important risks for underground construction in Qatar is the presence of karst environments, which are concentrated mainly within the limestone, dolomite, gypsum, and anhydrite horizons of the Eocene strata. The proper assessment of Karstic features requires an appropriate selection of geophysical methods and a high level of skills and expertise to interpret the data. To do so, a comprehensive geophysical survey campaign was deployed at the early stages of the project's execution to identify the Karstic features of concern associated with subsurface conditions at shallow and deeper depths up to 80 meters below ground level. This paper presents an example of a recently developed geophysical investigation program for the pre-tender design of the South of Wakrah Pumping Station and Outfall project. The project team carried out a comprehensive geophysical study to identify the Karstic features of concern along the tunnel alignments, shaft locations, and at the pump station area. Most of the identified Karstic features are categorized as low risk, but there was a high-risk anomaly (cavern) identified, and the extent of this cavern was verified with well-known geophysical methods like Multichannel Analysis of Surface Waves (MASW), seismic refraction, and 3D crosshole seismic tomography.

Keywords: Karstification; Caverns; Cavities; Geophysical methods; 3D model

1 Introduction

In most civil engineering works, it is critically important to characterize the mechanical behavior of

geotechnical materials under various types of loading. This characterization has normally been expressed in terms of elastic moduli, of which shear modulus is most important because it is directly related to the stiffness of the subsurface material. In general, there are two methods to characterize the mechanical behavior of geotechnical sites under various types of loading. One is the deflection-response method which measures stress-strain behavior of the sites caused by static or dynamic load. The major drawbacks of this method are that the overall stiffness is measured and, therefore, it is not possible to measure the stiffness at different depths, and the method can be destructive to the sites. The other method of characterization is the wave-propagation method which estimates the shear moduli at different depths by measuring seismic velocities with different methods. These methods offer the most direct and non-destructive approach to determining stiffness at different depths of geotechnical sites. Advantages of mapping the bedrock surface with the shear wave velocity field calculated from surface waves include the insensitivity of geophysical methods to velocity inversions, ease of generating and propagating surface wave energy in comparison to body wave energy, and sensitivity to lateral changes in velocity.

2 Geological Setting

The Tertiary to Quaternary periods account for all of Qatar peninsula's formations. The Simsima Limestone, middle Eocene, makes up most Qatar's territory. The Midra Shales member of the Lower Dammam Formation, middle Eocene, lies beneath the Simsima Limestone, which is a component of the Upper Dammam Formation. The Rus Formation, lower Eocene, is beneath the Midra Shales. A thin layer of loose to medium-dense silty, gravelly sand covers the solid geology.

3 Geophysical Investigations

Combination of multi-channel analysis of surface waves (MASW), seismic refraction seismic crosshole tomography and geophysical borehole logging methods were utilized to achieve the objective of the geophysical study in order to investigate the underground cavities and/or weak zones to a depth of 60-80 meters below ground level (BGL); the methods provide an accurate and consistent technique for estimating near-surface shear wave and P wave velocities, respectively.

3.1 Multichannel Analysis of Surface Waves (MASW) and Seismic Refraction Tomography

The surveys were performed as fixed static spreads and the collected data was processed for both MASW and refraction. The geophones were planted into soil and because of the direct receiver coupling, the signal-to-noise (SN) ratio of acquired data was higher than surveys made by the land streamer. To determine phase velocities at low frequencies precisely, Park et al. (1999a) pointed out that it is essential for the MASW method to use as long a receiver array as possible. However, a longer receiver array might decrease the lateral resolution of the survey, because the conventional MASW method provides a velocity model averaged over the total length of the array. A smaller array is better for increasing lateral resolution. Improved lateral resolution offsets the accuracy of phase velocity. CMP cross-correlation analysis will be used to overcome this trade-off.

Two different geophone arrays were used over parallel lines separated by 5-10 meters to provide the necessary depth of investigation and resolution. For high resolution and shallow depth of investigations (less than 25 meters), a geophone array consisting of at least 48 geophones spaced at 2.5 meters (120 meters receiver spread length) was used. For deeper investigation (greater than 25 meters) with moderate resolution, a geophone array consisting of 48 geophones spaced at 5 meters (240 meters receiver spread length) was used.



(a) **(b)**

Fig. 1: (a) and **(b)** view of XLR8-1450

A crawler-mounted accelerated weight drop (XLR8-1450) was used to create seismic energy for both shallow and deep investigations (Figure 1a) and (Fig 1 b).

For deep works, an array consisting of 96 active geophones with 5 meters spacing was used to investigate until 80-meters with moderate resolution. For shallow works, an array consisting of 96 active geophones with 2.5 meters spacing was used to investigate up to 25 meters with high resolution.

A mixed geophone array configuration (the first -near to AWD- 24 geophones with 0.5-meters and the last 24 geophones 1-meter spacing) land streamer was used to have a shallower resolvable depth while maintaining at least 15-meters depth of investigation.

3.2 Seismic Crosshole Tomography

Seismic crosshole tomography surveys were conducted by lowering the seismic source in one of the four boreholes and the string of geophones in another borehole. The seismic source used was a Geotomographie BIS-SH-DS electro-mechanical probe capable of producing both P waves and horizontally polarized S-waves. During the tests, the source probe was lowered into each of the test boreholes at a depth interval of two meters and locked into position by inflating the packer so that it is tightly clamped to the borehole wall. The receiver system consisted of a string of ten 30Hz-geophone stations with a station interval of one meter. Each individual station contained three geophones arranged in a tri-axial orthogonal manner and a digitizer for the analogue- to-digital conversion (24 bit). Crosshole tomography program; both P-wave and S-wave crosshole seismic tomography were carried out between borehole pairs at 11 shafts location across the project area. Crosshole tomography was performed from top to bottom of borehole, with boreholes depth ranging from 45 to 70-meters, which were drilled at 10-14 meters BH spacing.

3.3 Geophysical Borehole Logging

3.3.1 P-S Logging

The main purpose of this test is to acquire shear wave velocities (V_s) and compressional wave velocities (V_p) as a function of depth of engineering and environmental concern, which in turn, can be used with density to derive the dynamic soil parameters. P-S logging offers very high resolution (typically one meter) to resolve thin layers that can have a dramatic effect on surface response. The

shear wave velocities (V_s) and compressional wave velocities (V_p) were calculated at one-meter depth intervals. The dynamic ground parameters obtained by considering the seismic velocities from the PS log measurement were calculated for each testing location. PS logging tests were carried out in thirty-five (35) exploratory boreholes in the project site. After completion of drilling, the P-S logging was performed in uncased-well conditions.

Data measurements were performed at 1-meter interval by drawing the probe from bottom to top in the water-saturated section of the open hole. To acquire data, the probe was stopped at the required depth and the source was fired under surface command. The resultant signals were created from the measuring software as two horizontal and one vertical shot to allow measuring P and S wave velocities. The graphical representation of the P and S wave velocities is presented in the below section.

3.3.2 Acoustic & Optic Televiewer (ATV & OPTV) Logging

The HRAT (high resolution acoustic televiewer) logging was carried out in 10 exploratory boreholes and optic televiewer logging was carried out in 25 exploratory boreholes in compliance with ASTM-D-5753-05 *Standard Guide for planning and conducting borehole geophysical logging*. ATV & OTV logging were applied in designated open holes before any other in situ testing was conducted after completing drilling, ATV or OTV probe was lowered to the bottom of the open hole (filled with clean water) to scan the features of the borehole wall as it travelled up to the ground. Each borehole location was left to rest in order to stabilize the groundwater condition since it does not offer travel time measurements and is unsuitable for boreholes containing mud or cloudy fluids. Measurement was taken in both directions, from top to bottom and from bottom to top. The final measurement was taken while pulling up to get a better-quality image, and to prevent vibration of the probe. When the probe was taken down, the amplitude settings were adjusted to find the optimum setting and additionally the vibration of the probe was less when pulling up. HiRAT software was used during measurements. The levels, depths, and speed of the probe down the hole were monitored using a computer unit during data acquisition.

4 Correlation of Geophysical Results with Borehole Data

Comparison of the geophysical results with rock core information allowed calibration of the geophysical data interpretation. The top-made ground, significant notable fractures/voids, and drilling conditions for each boring were compared to the velocity signature for each MASW profile. A good correlation was assigned if two or more of the previously stated conditions could be correlated to the modeled velocity profile. For example, if the boring log indicated the overburden was relatively weak rock existed at 10 meters below ground level and the corresponding S-wave velocity profile identified low velocity at this depth, and then a good correlation existed. Conversely, if the boring log did not indicate conditions that correlated to the modeled velocity value, a poor correlation was assigned. The interpreted 2-D section shear-wave velocity correlates very well with subsurface materials encountered in the geotechnical boreholes. Examples of correlation between geophysical results and geotechnical boreholes are presented in Figure 2. Based on the above observed anomalies, verification diagraphy boreholes were recommended to be drilled to verify the nature of the anomalies in geophysical profiles.

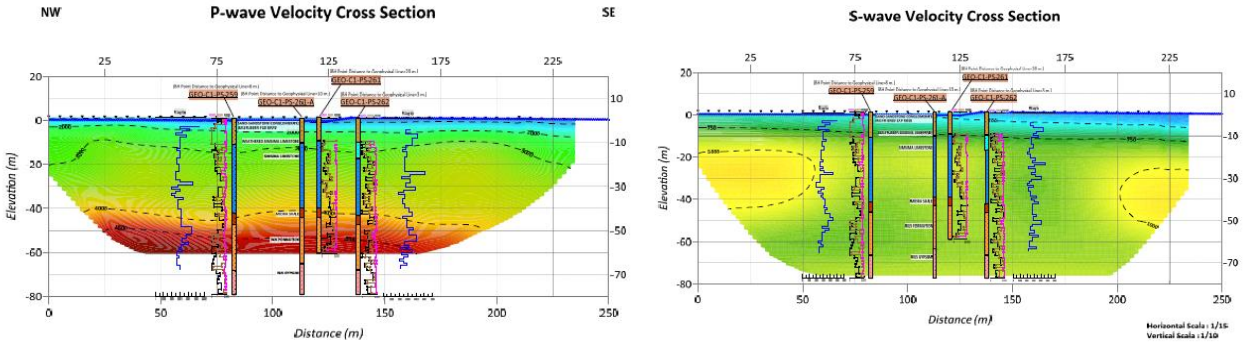


Fig. 2: Comparison of the MASW & Refraction data with the borehole controls

Fortunately, low V_s values in the first 5 meters (less than 1000 m/s correspond to the soft unconsolidated topsoil) followed by a V_s increase (as also observed in the PS-logging data). The blue line in-between the two boreholes illustrates the base of the Simsima Limestone and the base of the Midra Shale and the orange line indicates the transition from the Rus Formation to the Rus Gypsum formation. Apart from the change from unconsolidated soil to Simsima Limestone, only minor variations in V_s are visible in the MASW result.

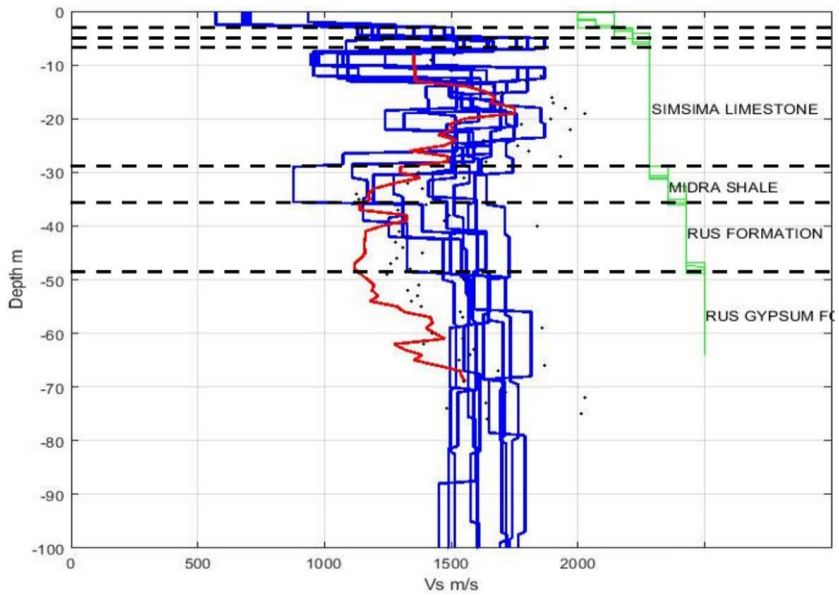


Fig. 3: Plot showing the average of all PS-logging values and the geological interpretation (The black dashed lines map the geological transitions onto the geophysical profiles

Crosshole tomograms showed high shear wave velocities except at one critical shaft location. At this location, a zone of medium velocity (the moderately weathered/fractured zone with $750<V_s<1000$ m/s) was observed (Figure 3). This zone started at the surface and continued till final depth (60 meters). A cavern was discovered during drilling which starts around 55-60 meters under this shaft location. It is believed that this weak zone is the result of settling of the zones above the cavern roof. It was observed that, the P and S-wave velocity models seem to agree well with the trends in the borehole log values.

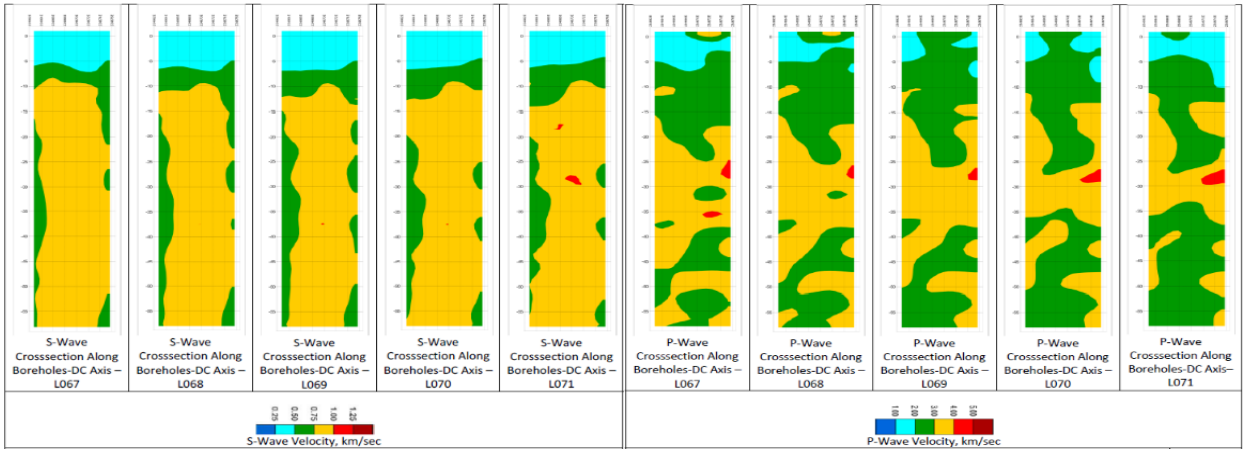


Fig. 4: 2D presentation of Results of Seismic Crosshole Tomography

Based on the correlation of all geophysical results presented in Figure 4 and Figure 5, it is observed that the P and S-wave velocity models, OTV and OTV and Crosshole results seem to agree well with the trends in the core borehole (RQD, TCR and SCR) and diagraphy log values.

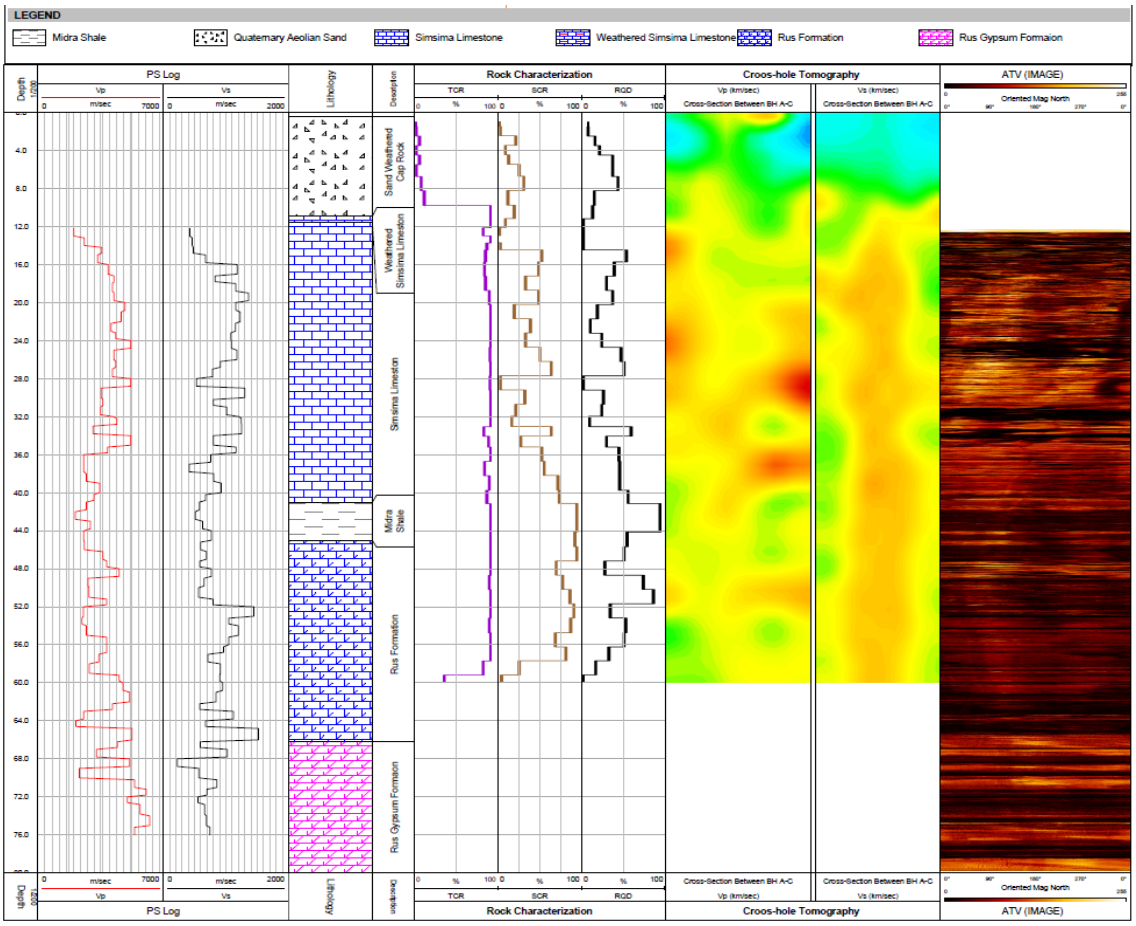


Fig. 5: Correlation of Geophysical methods results with the borehole control

5 Results and Discussion

5.1 MASW and Seismic Refraction

The MASW and refraction survey was completed as a "screening tool" to provide subsurface information that would ultimately be used to determine the above-mentioned geotechnical areas of

concern. The shear wave and P wave velocity surveys provided a two-dimensional image of the subsurface along the proposed tunnel and shaft locations at specific traverse line locations. The shear wave velocity results indicated that the study area of the project site exhibited distinct velocity conditions and contrasts. Low-velocity areas within the MASW profiles were consistent with unconsolidated surficial materials and deep highly fractured/weathered bedrock with a high percentage of *attapulgite* clay, while higher velocity materials were consistent with harder materials. Within this type of geologic setting, unconsolidated materials are attributed to soft, weak (less competent) rock. The shear wave and P wave velocity profiles across the project area is characterized by several geologically significant changes in material properties. Unique signatures of low, medium, and high shear wave velocity values across the site at different depths have been recorded on the processed shear wave velocity sections. Summary of Geological Strata Shear Wave Velocity Values for all MASW profiles is presented in Table 1 and 3D models P and S wave at one of the critical locations are presented in Figure 6 below.

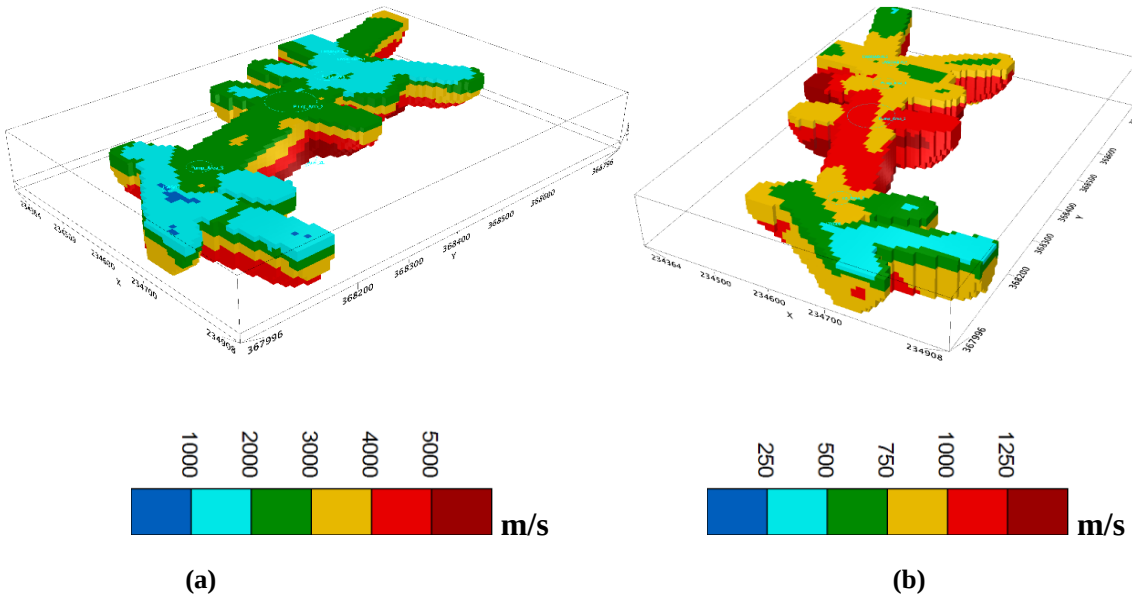
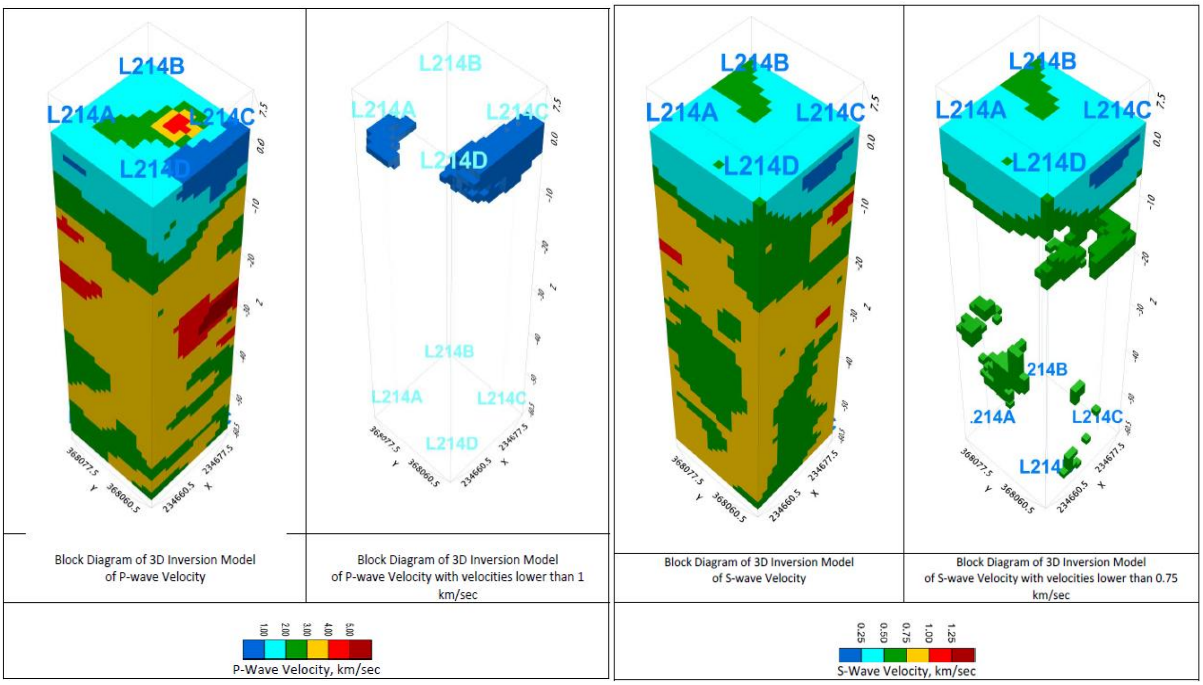


Fig. 6: P and S wave 3D Velocity model of one of the critical locations of the project

5.2 Seismic Crosshole Tomography

After inversion of the travel time data, 3D models were prepared after which level maps and vertical cross-sections were produced. And the resulting velocity tomograms were then compared with the available borehole log data (RQD, SCR, TCR, Lithology, ATV and PS-log) of the nearby boreholes. At the critical shaft location, there was a zone of medium velocity (the moderately weathered/fractured zone with $750<V_S<1000$ m/s). This zone started at surface and continued till final depth (60m). A cavern was discovered during drilling which starts 55-60 m under this shaft location. It is believed that this weak zone is the result of settling of the zones above the cavern roof. It is observed that the P and S-wave velocity model seems to agree well with the trends in the borehole log values. The results of crosshole tomography are presented as 3D in Figure 7 below.



(a) **(b)**

Fig. 7: The inverted V_p and V_s 3D models at one of the critical shaft locations

6 Conclusions

Comparison with conventional geophysical methods (PS-logging, seismic Refraction, MASW and seismic Crosshole Tomography), shows the result describes the vertical geological sequences along the site well and allows for a 2D and 3D interpretation of lithology and geotechnical parameters derived from V_s. Based on the review of the geotechnical boring logs, shear wave and P wave velocity results, the following conclusions can be drawn from the present survey:

- 2D Sections for shear wave (V_s) and P wave (V_p) from MASW Refraction and Crosshole tomography data versus Depth (m) were presented.
- Poison's Ratio, Shear Modulus, Young 's Modulus and Bulk Modulus values were calculated from (V_s) and (V_p) data and 2D sections for these engineering parameters versus depth (m) were also calculated and presented.
- The geotechnical boreholes were proposed and considered to correlate and calibrate the obtained results within the site to verify the nature of the identified anomalies in MASW profiles.
- To know the extent of the cavern, additional diagraphy boreholes were drilled and OPTV was performed to map the roof of the cavern at various levels at each borehole location.

References

Curtis et al. (2006). Seismic interferometry – turning noise to signal, *The Leading Edge* 2006, 25:9, 1082-1092.

Milsom, J. & Erikson, A. (2011). *Field Geophysics*. John Wiley & Sons, Inc., New York, USA.

O'Connell, D. & Turner J (2011). Interferometric Multichannel Analysis of Surface Waves (IMASW), *Bulletin of the Seismological Society of America*, Vol. 101, No. 5, pp. 2122-2141, October 2011, Doi: 10.1785/0120100230

Orndoff, et al. (2018). Linking Geology and Geotechnical Engineering in Karst: *The Qatar Geologic Mapping Project.*

Pánek, T., Margielewski, R. (2000). *An Introduction to Applied and Environmental Geophysics*, John Wiley & Sons, Inc., New York USA.

QCS Technical Committee and Associated Subcommittees. (2014). Qatar Construction Specifications Revision IV (QCS 2014), Doha, Qatar.

Sadiq, A. & Nasir, S. (2002). Middle Pleistocene Karst Evolution in the State of Qatar, Arabian Gulf. *Journal of Cave and Karst Studies*. *64*(2):132-139.

Scotney., Harwood M., Sanderson D. (2012). A multi-disciplined approach to mapping the Pre-Triassic land surface near Bradgate Park, Charnwood Forest, Leicestershire, UK. *Journal of the Yorkshire Geological Society*.

Bourbié, T., Coussy, O. & Zinszner, B. (1987). *Typical Rock Velocities Acoustics of Porous Media*. Houston TX, *Gulf Publishing Co*.

Yilmaz, Ö. (2001). Seismic data analysis: Processing, inversion, and interpretation of seismic data. *Society of Exploration Geophysicists*.

Cite as: Akbar A., Dafalla F., Krishnamurthi I.K. & Pinto A., "Identification of Karstic Features with Extensive Geophysical Investigation for Underground Infrastructure - South of Wakrah Pumping Station and Outfall (SWPSO) Project", *The 2nd International Conference on Civil Infrastructure and Construction (CIC 2023)*, Doha, Qatar, 5-8 February 2023, DOI: https://doi.org/10.29117/cic.2023.0097

Robust Geotechnical Hazard Identification and Assessment for Major Underground Projects in Qatar. Case Study: South of Wakrah Pumping Station and Outfall (SWPSO) Project

Mohamed Khalil
Stantec UK Ltd. (Qatar Branch), Doha, Qatar
Mohamed.Khalil@stantec.com

Fathelrahman Dafalla
Stantec UK Ltd. (Qatar Branch), Doha, Qatar
Fathelrahman.Dafalla@stantec.com

Andres Pinto
Stantec UK Ltd. (Qatar Branch), Doha, Qatar
Andres.Pinto@stantec.com

Atif Galal Ahmed
Public Works Authority (Ashghal), Doha, Qatar
agahmed@ashghal.gov.qa

Abstract

The recent global development in geotechnical and geophysical investigation methodologies has continued to improve the possibility of early identification of critical geohazards and mitigation of risks associated with construction of large underground projects. This is not only limited to highlighting the potential risks, but also minimizing the cost and time for construction by avoiding or mitigating unexpected risks. A case study is presented by a recent unprecedented tunneling project in the State of Qatar featuring a 4.5-8.5 meters diameter, 55 kilometers in length, with various deep shafts, pumping station, and outfall in the Al-Wakrah city. Following an extensive desk study from available geotechnical and geophysical data in the vicinity of the project area and from previous practical experience from similar projects, a thorough geotechnical and geophysical investigation campaign was planned and executed. The result of the comprehensive ground investigation gave a clear picture of expected geohazards and prospective mitigation measures to be taken during the construction of the works. The paper presents a description of the main identified geohazards, including the presence of chert bands, karstic areas, massive caverns, high permeability areas, and high aggressiveness ground conditions along with its implications and mitigation measures, to be taken into account in the next stages of the project. A similar approach can be adopted for future infrastructure projects to support the geotechnical risk assessment and to minimize the impact of construction activities on the environment.

Keywords: Geotechnical hazards; Geohazard; Risk assessment; Deep excavations; Underground project

1 Introduction

In the State of Qatar, the recent, fast urban development around the capital city, Doha and its commercial and residential areas, Al-Wakrah city and Al-Khor city (all three collectively named Greater Doha), has led to an increase in the population and, consequently, an increase in the demand for all life needs, which has necessitated fast planning and construction of adequate and efficient infrastructure such as roads, drainage systems, water distribution networks, and all other

related facilities. This rapid development in residential and commercial buildings without the presence of suitable infrastructure services has resulted in the rise of groundwater table and led to the creation of isolated water bodies (commonly called perched water) exacerbated by the presence of sabkha soils (which always facilitate the creation of perched water).

Historical events of recent storm rains that caused complications and even flooding in key areas were recorded and various levels of damage to the existing infrastructure was observed. In fact, a recent study carried out by Public Works Authority (Ashghal) in Greater Doha to monitor the existing groundwater conditions illustrated the continuous rise in groundwater and surface water tables. Thus, a strategic plan to find solution to these undesirable occurrences was considered as part of the local development strategy in line with the Qatar National Vision 2030.

Even though the extensive experience gained during the execution of significant infrastructure projects in Qatar, like the Inner Doha Re-sewerage Implementation Strategy (IDRIS), the Doha South Terminal Pumping Station (DSTPS), and the Musaimeer Pumping Station and Outfall (MPSO) (Ashghal and Stantec, 2019), has improved current understanding of the expected hazards, the role of geotechnical, hydrogeological, geophysical, and geo-environmental conditions in the proper project risk assessment continues to be one of the major challenges during the engineering design and construction stages.

Therefore, to support the geotechnical risk assessment and reduce the negative effects of construction activities for upcoming infrastructure projects, a more objective and consistent assessment of hazards is proposed using the information obtained during the respective ground investigation campaign (Ashghal & ZETAS, 2022). This information consists of geotechnical, hydrogeological, geophysical, and geo-environmental assessments employing lessons learned from a recently completed ground investigation program for the South of Wakrah Pumping Station and Outfall (SWPSO) project.

2 Project Background

2.1 General

The South of Wakrah Pumping Station and Outfall (SWPSO) project is a key capital project in the State of Qatar, whose major goal is to provide a long-term optimum strategic drainage system for stormwater and groundwater in the catchment area of Al-Wakrah city and South of Wakrah area. This is one of the most severely affected areas by the water rise and flooding during storm events. The project is currently in the tender design stage with Public Works Authority (Ashghal) at an estimated value (Capex) of $2 billion USD. The SWPSO project is divided into three biddable contracts, as presented in Fig. 1, and comprises the following main components:

1. Catchment area of 475 square kilometers approximately.
2. Onshore micro tunnels and tunnels:
    - Total length – 46 kilometers approximately.
    - Internal diameter ranges 1.0 – 8.0 meters approximately.
    - Depth ranges 15 – 50 meters approximately.
3. Onshore access and tunnel boring machine (TBM) launching/receiving shafts:
    - Internal diameter ranges 8.0 – 20.0 meters approximately.
    - Depth ranges 15 – 50 meters approximately.
4. Onshore pumping station shaft and screen shafts:
    - Internal Diameter ranges 40 – 80 meters approximately.
    - Depth ranges 45 – 55 meters approximately.

5. Emergency flooding area/lagoon (EFA) next to the Pumping Station.
6. Marine outfall tunnel:
    - Total length – pending authority's decision.
    - Internal diameter – 8.5 meters approximately.
7. Cross-catchment connection tunnel options:
    - Total Length – 9 kilometers maximum.
    - Internal diameter ranges 3.0 – 4.5 meters approximately.
    - Depth ranges 20 – 40 meters approximately.

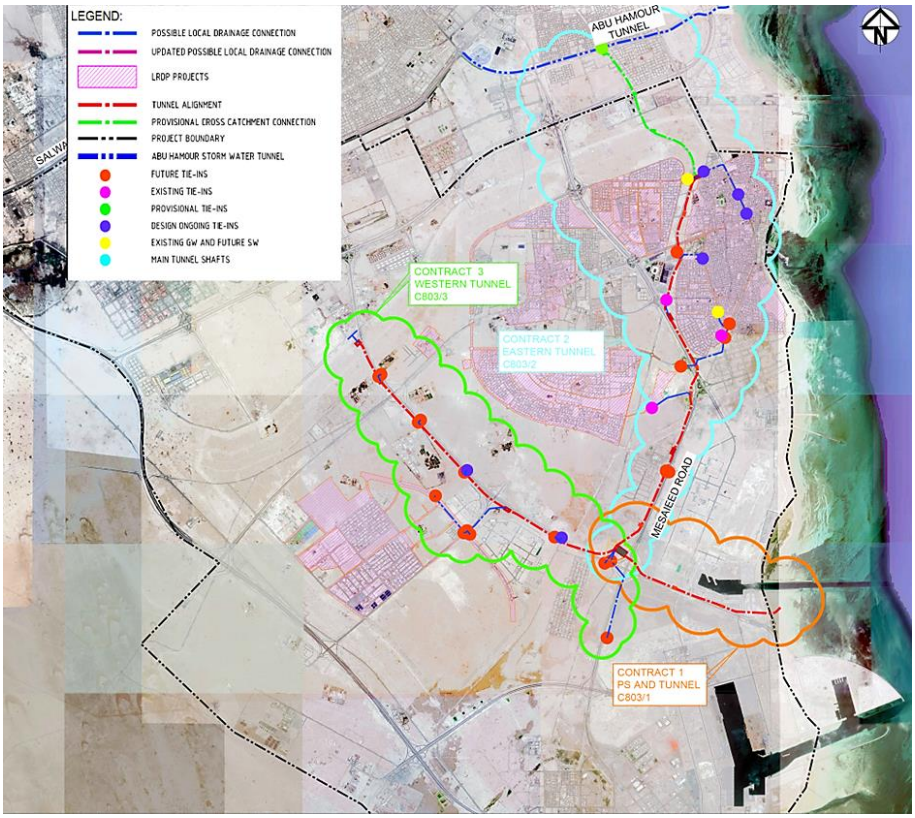


Fig. 1: SWPSO Project Plan Showing Pumping Station Area with EFA (Middle Junction) and Tunnel Alignment for Contract 1 (Orange), Contract 2 (Blue), and Contract 3 (Green)

2.2 Ground Investigation

The construction of deep underground works with changing ground and geological conditions, excessive groundwater inflow, presence of potential cavities and karstic features, aggressive chemical conditions, and the existence of chert bands and other hard strata as identified from previous major infrastructure projects in Qatar constitute the majority of the SWPSO project's potential geohazards.

As such, a comprehensive subsurface investigation program was planned and conducted to delineate the soil, rock, and groundwater conditions in the project area. The program consisted mainly of land-based geotechnical exploratory borehole drilling along the tunnel alignments and pumping station area followed by field testing efforts conducted in the boreholes and laboratory testing works conducted on extracted rock core and groundwater samples. The ensuing onshore site characterization and geotechnical interpretation are based on an integrated approach that combines the site-specific data collected from exploratory borings, field, and laboratory testing in combination with subsurface geometry imaged by the onshore geophysical survey works.

The purpose of this geotechnical exploration program was basically to reveal the site data obtained by exploratory core drilling, in-situ, and laboratory testing, geophysical and hydrogeological surveys in the perspective of physical, dynamic, and chemical properties of encountered soil and rock units towards geotechnical assessment of subsurface conditions in project area. This exploration program was undertaken to provide information necessary for the assessment of ground and groundwater conditions, and in turn the identification and assessment of potential geohazards, at the underground tunnels, launching/receiving shafts open excavations, and the pumping station site.

3 Geotechnical Hazard Identification & Assessment

3.1 Purpose

The main goal of the proposed methodology is to provide a more objective and consistent assessment of geohazards along SWPSO project tunnel alignment using the factual information obtained during the respective ground investigation campaign. The proposed methodology enables both qualitative and quantitative risk assessment, risk mitigation, and contingency planning by prospective future bidders for SWPSO project. The following main criteria are to be considered in the geohazard assessment based on applicable construction-related risks as identified from previous similar projects in Qatar all with consideration to the existing ground environment in the project area:

1) Groundwater Inflows/Permeabilities at tunnel footprint and open excavations.
2) Karstification/Cavities/Geophysical Anomalies at tunnel footprint and open excavations.
3) Chert/Hard strata (UCS over 50 MPa) at tunnel footprints and open excavations.
4) Ground conditions for open excavation (extent of soil cover and weak rock).
5) Ground/groundwater chemical aggressiveness at tunnel footprint and open excavations.

3.2 Proposed Methodology

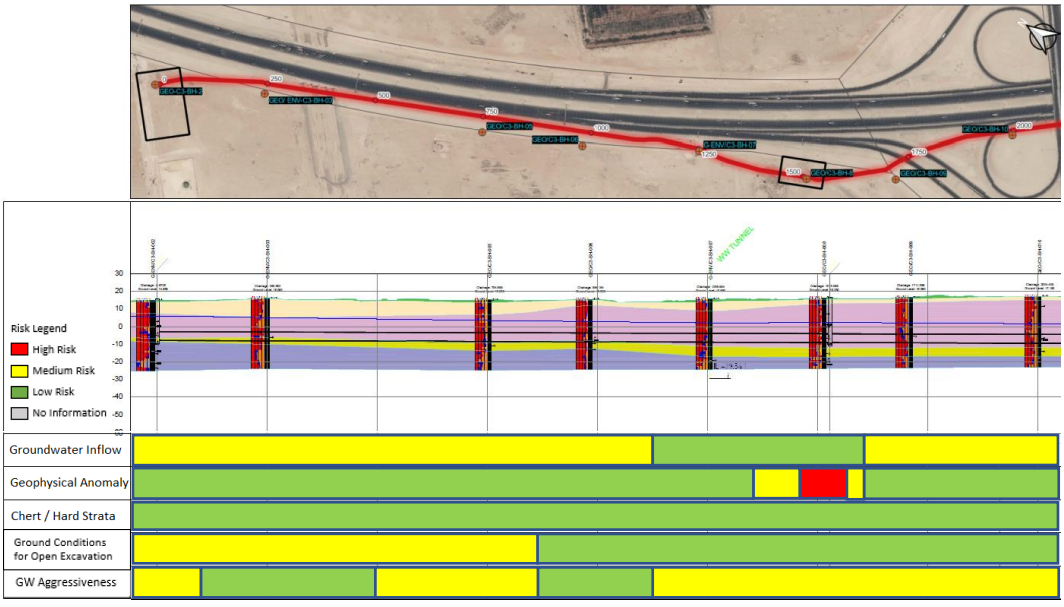


Fig. 2: Hazard Identification and Assessment Sample Schematic

A sample hazard identification and assessment for the first two kilometers (CH 0 – CH 2000) for Contract 3 (C3) project tunnel alignment is shown above in Fig. 2. The five (5) specific construction-related geohazards are presented along the tunnel alignment longitudinal profile with a color scale for an easy visual identification of the geohazards. In assessing and eventually deciding

on the corresponding occurrence probability (color) of each geohazard, an objective, and systematic approach was adopted to ensure consistent assessment that inherently takes into consideration the varying encountered conditions along the tunnel alignment profile. The geohazard-pertaining calculation is explained in detail below.

3.2.1 Hazard #1: Groundwater Inflows/Permeabilities

Experience shows that the primary hazard to be immediately identified from the ground investigation campaign for this type of underground project in Qatar is the potential high groundwater inflows during open excavations or tunnel boring machine (TBM) advancement due to:

1) Existing high rock mass hydraulic conductivities/permeabilities.
2) Excavation through Simsima limestone/Midra shale or Midra shale/Rus formation interfaces.
3) Presence of interconnected karstic features and associated preferential groundwater flow paths.

The impact of an unexpected high groundwater inflow is the potential flooding of deep excavations and tunnels, which will in turn cause delays and additional design and construction costs, making this a considerable risk that needs to be identified and prepared for before starting construction. To address each of the above three (3) reasons for potential high groundwater inflows, the following three (3) criteria are considered along the tunnel footprint (1.5 diameter above and 1.5 diameter below the tunnel centerline):

1) Lowest rock quality designation value (*RQD*%), as determined from exploratory boreholes.
2) Coefficient of hydraulic conductivity, *k* (m/s), as determined from Falling head or Packer tests.
3) Number of geological formations crossed (e.g., Simsima limestone, Midra Shale, RUS formation).

Both the RQD and k-value criteria are assigned specific contributions (weights) to the overall hazard score based on their relevance and how they compare against the respective practical maximum values. An additional hazard score is added whenever more than one formation is crossed along the tunnel footprint during TBM advancement or during open excavation. A sample calculation is shown in Table 1 below, with the hazard criteria and hazard scores for the first two kilometers (CH 0 – CH 2000) for Contract 3 (C3) project tunnel alignment, as shown above in Fig. 2.

Table: 1 Groundwater Inflow Hazard Assessment Calculation

Groundwater Inflow Hazard Assessment		**Max RQD = 100%**		**Max k-value = 1x10^{-5}**				
Tunnel Footprint (1.5D Above & Below)	BH-02	BH-03	BH-05	BH-06	BH-07	BH-08	BH-09	BH-10
Lowest RQD (%)	20	15	60	50	30	60	25	0
Permeability (m/s)	5.4 x 10^{-7}	5.4 x 10^{-7}	5.4 x 10^{-7}	1.7 x 10^{-6}	2.4 x 10^{-6}	3.0 x 10^{-6}	3.2 x 10^{-6}	3.4 x 10^{-6}
Formations Crossed	2	2	2	2	1	1	1	1
Lowest RQD (%)	16%	17%	8%	10%	14%	8%	15%	20%
Permeability (m/s)	4%	4%	4%	13%	19%	24%	26%	27%
Formations Crossed	40%	40%	40%	40%	0%	0%	0%	0%
Hazard Score (Out of 100%)	60%	61%	52%	63%	33%	32%	41%	47%
Hazard Criteria	0-33% Low	33-66% Medium	66-100% High		Weights: RQD → 20% k-value → 80% Crossing more than one formation → +40%			

3.2.2 Hazard #2: Geophysical Anomalies/Cavities

Experience also shows that one of the critical hazards to be identified from the ground investigation for this depth, especially for the encountered ground conditions, is the presence of karstic features, cavities, caverns, or sinkholes, all of which constitute geophysical anomalies, specifically when clashing with vicinity of open excavations or tunnels footprint.

As evident from multiple previous similar underground projects, the fractured sedimentary rock mass of Qatar exhibits karstic features due to progressive dissolution of soluble carbonate sequences, such as limestone, dolomite, and gypsum, which may or may not be filled with groundwater. The impact of an unexpected geophysical anomaly is the potential relocation of open excavation shafts or shifting of tunnel level and the additional time and cost for adjusting the design, construction, and remedial works, marking this as another considerable risk that needs to be identified and accounted for.

To identify the possibility of having a geophysical anomaly, the following three (3) criteria are proposed to be considered along the tunnel footprint (2 diameters above and 2 diameters below the tunnel centerline):

1) Shear wave velocity, V_s (m/s), from geophysical survey (e.g., MASW, Seismic refraction).
2) Shear wave velocity, V_s (m/s), from P-S logging at exploratory boreholes locations.
3) Penetration drilling rate (m/h) from diagraphy drilling method.

Both shear wave velocities (*Vs*) are indicative of the stiffness of the scanned rock mass and, thus, are direct indicators of open/filled cavities or vugs. Both are relatively assigned the same contribution (weight) to the overall hazard score based on how they compare against a practical range of Vs values that were selected based on actual observations from previous projects.

Although seldom occurring, geophysical anomalies can be readily identified through normal and diagraphy borehole rotary drilling operations through an abnormal freefall of drilling rods or a considerably low total core recovery (TCR %) at which the drilled area shall also be marked as high possibility of having a geophysical anomaly. Hazard level may be exceptionally chosen based on other evidence or project location (e.g., near the shore). A sample calculation is shown in Table 2 below, with the hazard criteria and hazard scores for the first two kilometers (CH 0 – CH 2000) for Contract 3 (C3) project tunnel alignment.

Table 2: Karstification/Cavities/Geophysical Anomalies Hazard Assessment Calculation

Karstification/Cavities/Geophysical Anomalies Hazard Assessment									
Tunnel Footprint (2D Above & 2D Below Centerline)	BH-01	BH-02	BH-03	BH-05	BH-06	BH-07	BH-08	BH-09	BH-10
Vs from Geophysical Survey (m/s)	Low Risk	Low Risk	Low Risk	Low Risk	Low Risk	Low Risk	Low Risk	Low Risk	Low Risk
Diagraphy Drilling Rate	Low Risk	Low Risk	Low Risk	Low Risk	Low Risk	Low Risk	High Risk	Low Risk	Low Risk
Hazard Level									
	Hazard Determination: Vs > 1250 m/s → Low Risk 750 m/s < Vs < 1250 m/s → Medium Risk Vs < 750 m/s → High Risk					Diagraphy Drilling Rate: Low Risk: < 200 m/h Medium Risk: 200-500 m/h High Risk: > 500 m/h			

3.2.3 Hazard #3: Chert / Hard Strata

Experience also shows another crucial hazard to be identified from the ground investigation campaign for this deep underground project: the presence of chert bands within the Simsima limestone formation. These are high-strength sedimentary rock with unconfined compressive strength (UCS) values of 120-250 MPa, which can cause damage to excavation and drilling equipment.

Previous similar underground projects reported multiple occurrences of chert bands at varying depths during the excavation and construction and were mainly documented as follows:

- Chertified zones in Simsima limestone that were typically found at 6 to 10 meters depths and,
- RUS chert veinlets that were mostly at 35 to 50 meters depths, but much thinner.

The presence of unusually strong rock bands or hard strata can impose detrimental time and cost impacts due to low excavation production rates and potential damage to the cutting tools of the excavators and the TBM's discs and cutter heads during tunnel drilling operations. Therefore, this hazard constitutes a considerable risk that needs to be properly identified and planned against.

To identify all locations with problematic hard strata, the following two (2) criteria are proposed for consideration along the tunnel footprint (1.5 diameter above and 1.5 diameter below the tunnel centerline) and open excavation/shaft footprint (up to tunnel depth):

1) Presence of chert bands of any thickness or form as determined from exploratory borehole logs.
2) Hard Rock Strata of UCS values greater than 50 MPa as determined from laboratory testing.

Both the above parameters are direct indicators of the hardness and excavatability of the rock mass. The presence of chert bands is assigned a higher contribution (weight) to the overall hazard score since they are considerably stronger than any of encountered rock formations.

The UCS value of 50 MPa is statistically nominated as the upper bound value ($\mu + 2\sigma$) based on findings and distribution of UCS testing results from previous similar projects, and thus, any UCS value exceeding 50 MPa is deemed an outlier. Other than that, the hazard score may be exceptionally chosen based on other evidence that supports the need for stronger excavation or tunneling equipment. A sample calculation is shown in Table 3 below, with the hazard criteria and hazard scores for the first two kilometers (CH 0 – CH 2000) for Contract 3 (C3) project tunnel alignment.

Table 3: Chert or Hard Strata Hazard Assessment Calculation

Chert or Hard Strata (UCS >= 50 MPa) Hazard Assessment								
Borehole Location	BH-02	BH-03	BH-05	BH-06	BH-07	BH-08	BH-09	BH-10
Tunnel Footprint (1.5D Above & Below)	None	None	None	None	None	None	None	None
Shaft Footprint (Up to Tunnel Depth)	None	None	None	None	None	None	None	None
Hazard Score	Low	Low	Low	Low	Low	Low	Low	Low
Hazard Criteria	Low	Medium	High	Hazard Determination: If Either has Chert → High If Either has Hard Strata → Medium If Both are None → Low				

3.2.4 Hazard #4: Ground Conditions for Open Excavation

It is foreseen that at the open excavation locations, the overburden soils shall be retained by an engineered slope and that the excavation in the rock strata shall be near-vertical to vertical open cut excavation that is either unsupported or supported using shotcrete, combination of shotcrete and rock bolting, secant pile walls, or diaphragm walls depending on the overall geotechnical designs for temporary and permanent works. Thus, an additional important hazard that must be identified from the ground investigation campaign for this underground project is the presence of weak ground conditions that can affect ground stability of deep excavations, wherever they may be (not necessarily at open excavation locations only). Indeed, varying thicknesses of weak ground conditions (soil and weak rock) were encountered along the project tunnel alignments, with the thicknesses characteristically increasing toward the shoreline.

The impact of a considerable extent of loose quaternary deposits (QD) and/or highly-weathered Simsima limestone rock (WSL) will detrimentally affect the overall stability of deep unsupported open cut excavations and may cause large displacements that might affect assets in the vicinity of the excavation, all of which can cause additional time and cost impact for the design and construction of a proper excavation lateral ground support (shoring) system to guarantee the stability of the excavation and construction of additional remedial works.

To identify locations with problematic weak zones, the following two (2) criteria are proposed to be considered along the tunnel alignment, most confidently at the exploratory borehole locations:

1) Extent of Soil / Quaternary Deposits (QD) formation in meters (m).

2) Extent of Highly Weathered Simsima Limestone (WSL) formation in meters (m).

Summation of above two formation thicknesses is indicative of risky weak zones for the vertical excavation of unsupported shafts since the loose QD layer will not sustain itself vertically and the WSL layer is highly susceptible to progressive degradation due to air exposure and weathering.

The hazard criteria values are conservatively selected based on safe uptime of an unsupported excavation depth in zones with similar weak ground conditions as evident from previous excavations in Qatar, with more attention paid to the depth of QD layer to not exceed a limiting value of 5 meters. A sample of the calculation is shown in Table 4 below, with the hazard criteria and hazard scores for the first two kilometers (CH 0 – CH 2000) for Contract 3 (C3) project tunnel alignment.

Table 4: Ground Conditions for Open Excavation Hazard Assessment Calculation

Ground Conditions for Open Excavation Hazard Assessment								
Borehole Location	BH-02	BH-03	BH-05	BH-06	BH-07	BH-08	BH-09	BH-10
Soil / QD Depth	1	0	1	0.5	1	0.5	0.5	0
WSL Depth	4	7	4	2	3	1.5	1.5	1.5
Hazard Score	5	7	5	2.5	4	2	2	1.5
Hazard Criteria	Good (0-5 m) Low	Medium (5-10 m) Medium	Poor (< 10 m) High					

3.2.5 Hazard #5: Ground/Groundwater Chemical Aggressiveness

For the design of deep tunnels and shafts, the expected exposure conditions, driving deterioration mechanisms (chloride-induced corrosion, sulfate attack, and/or abrasion), and the measures taken

against them are considered the principal factors which may influence the long-term durability of the concrete structures. In terms of groundwater exposure conditions, the most important parameters are the availability of oxygen and moisture, temperature, surface levels of chlorides, sulfates, and pH levels.

Following the above brief narrative, the last, but not least, hazard that must be identified from the ground investigation campaign for this underground project is the existence of aggressive ground and/or groundwater conditions affecting the durability of the permanent concrete structures. Historically, the majority of the recorded ground and groundwater chemical compositions in Qatar ground environment are indicative of an aggressive/corrosive environment to reinforced concrete members and structures. The considerable amounts of sulfates and chlorides in the encountered groundwater are expected to be particularly corrosive to steel reinforcement.

The impact of unaddressed high concentrations of sulfates and chlorides in the ground and groundwater can cause chemical and physical attacks on concrete structures, leading to surface deterioration, corrosion, and loss of reinforcement cover, causing the durability and service lives of permanent structures to be immediately damaged and reduced, eventually leading to additional time and cost impact for operations and maintenance works and increasing the life-cycle cost of the project.

To identify all locations with potential high ground/groundwater aggressiveness, the following main two (2) chemical contents were proposed to be measured along the tunnel alignment, as readily available from laboratory-tested groundwater samples from exploratory borehole locations:

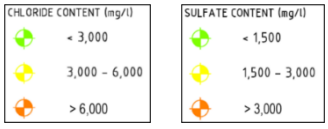
1) Chloride (Cl) Groundwater Chemical Content (mg/L).

2) Sulfate (SO_4) Groundwater Chemical Content (mg/L).

Experience shows that the above two chemical contents are the most relevant factors in the durability of concrete structures in Qatar's ground conditions, as evident from concrete durability assessments from previous similar underground projects and as referred to immensely in Qatar Construction Specifications (QCS Technical Committee and Associated Subcommittees, 2014). The hazard criteria values are conservatively selected based on ranges of groundwater chemical composition and recommendation of durable concrete properties as stated in *QCS 2014, Section 05: Concrete.* A sample of the calculation is shown in Table 5 below, with the hazard criteria and hazard scores for the first two kilometers (CH 0 – CH 2000) for Contract 3 (C3) project tunnel alignment.

Table 5: Groundwater Chemical Aggressiveness Hazard Assessment Calculation

Groundwater Aggressiveness Hazard Assessment								
Borehole Location	BH-02	BH-03	BH-05	BH-06	BH-07	BH-08	BH-09	BH-10
Chloride (Cl)	Low	Low	Low	Low	Low	Medium	Low	Medium
Sulphate (SO_4)	Medium	Low	Medium	Low	Medium	Low	Medium	Low
Hazard Score	Medium	Low	Medium	Low	Medium	Medium	Medium	Medium
Hazard Criteria	Low	Medium	High	Hazard Determination: Both Low → Low Both Medium → Medium Both High → High If (1) Medium → Medium If (1) High → High				



4 Conclusion

The main purpose of this paper is to document the assumptions, methodology, and lessons learned from the proposed geotechnical hazard identification and assessment exercise carried out for South of Wakrah Pumping Station and Outfall (SWPSO) project.

The main goal of the proposed methodology is to provide a more objective and consistent assessment of geohazards along deep underground projects using the information obtained during the respective ground investigation campaign. The proposed methodology enables both qualitative and quantitative risk assessment, risk mitigation, and contingency planning by prospective future bidders for deep underground infrastructure projects in the State of Qatar.

The five (5) main construction-related geohazards pertaining to Qatar were explained in detail throughout the course of the paper and the assessment of geohazards was presented along the tunnel alignment longitudinal profile of a case study project with a color scale for a rapid and simple understanding of the geohazards and their probability of occurrence.

References

Public Works Authority (Ashghal) and Stantec. (2019). Geotechnical Desk Study Report South of Wakrah Tunnels, Pumping Station and Outfall Project, Doha, Qatar.

Public Works Authority (Ashghal) and ZETAS, (2022). Geotechnical Interpretative Reports for Contracts 1, 2 and 3, South of Wakrah Tunnels, Pumping Station and Outfall Project, Doha, Qatar.

QCS Technical Committee and Associated Subcommittees. (2014). Qatar Construction Specifications Revision IV (QCS 2014), Doha, Qatar.

Cite as: Khalil M., Dafalla F., Pinto A. & Ahmed A.G., "Robust Geotechnical Hazard Identification and Assessment for Major Underground Projects in Qatar. Case Study: South of Wakrah Pumping Station and Outfall (SWPSO) Project", *The 2nd International Conference on Civil Infrastructure and Construction (CIC 2023)*, Doha, Qatar, 5-8 February 2023, DOI: https://doi.org/10.29117/cic.2023.0098

Influence of Fine Dune Sand on Modulus of Elasticity of Eco-Self-Compacting-Concrete

Makani Abdelkadir
EMIA ex. LFGM (Laboratory of Eco-Materials: Innovations & Applications), Department of Civil Engineering & Hydraulic, TAHRI Mohamed University, Algeria
makkaniabdelkadir@univ-bechar.dz

Tafraoui Ahmed
EMIA ex. LFGM (Laboratory of Eco-Materials: Innovations & Applications), Department of Civil Engineering & Hydraulic, TAHRI Mohamed University, Algeria
ahmedtafraoui@yahoo.fr

Zaoiai Said
EMIA ex. LFGM (Laboratory of Eco-Materials: Innovations & Applications), Department of Civil Engineering & Hydraulic, TAHRI Mohamed University, Algeria
zawi.said@yahoo.com

Benmerioul Farid
EMIA ex. LFGM (Laboratory of Eco-Materials: Innovations & Applications), Department of Civil Engineering & Hydraulic, TAHRI Mohamed University, Algeria
benmerioulfarid@gmail.com

Abstract

The aim of this research was to study the effect of fine dune sand on the mechanical performance of Eco-Self-Compacting Concrete (SCC). For that, the fine dune sand of the Western erg (Taghit – Algeria) was being like mineral addition to formulate the SCC, and a comparison was carried out on their effect on the properties of SCC. Our study also showed that the substitution of fine dune sand (DS) by cement in the composition of the SCC, contributes to a slight variation of workability in the fresh state parameters still remaining in the field of SCC required by the AFGC recommendations. The experimental results show that the compressive strengths and modulus of elasticity of SCC improved by substituting of 20% cement by DS.

Keywords: Eco-Self-Compacting concrete; Fine Dune sand; Formulation; Mechanical performance

1. Introduction

The Self-Compacting Concretes (SCC) are very fluid concretes whose implementation without vibration has several advantages at divers levels which interest more and more industries (Neville, 2004: Bethmont et al., 2009). The stability and perfect homogeneity of SCC are ensured by the use of the superplasticizer and the incorporation of the mineral additions in their compositions (Benmerioul et al., 2017, Ayed et al., 2020). In the eighties and nineties, the studies relating to the high performance concretes showed the harmful role of the excess water in concretes. The reduction of this quantity of water, by the use of deflocculants and by the correction of granular stacking via ultrafine, has led to the strength and durability gains that are now known (Okamura & Ouchi, 1999, Bouhamou et al., 2008).

As part of the development, dune sand is now incorporated in the new concrete (Tafraoui, 2012). The negative impact of dune sand on the performance of concrete was due to poor grading and fineness (Ali et al., 2021; Ahmad et al., 2022). Fine aggregate (amount and type) is a primary component of concrete; it significantly affects fluidity, strength and dry shrinkage of concrete.

Increases in dune sand concentration lowered workability (slump) of concrete to 30% (Dawood & Jaber, 2022), The concrete made with a fine dune sand with ratio of 10% showed the highest mechanical performance (Rennani et al., 2020; Lee et al., 2022).

The present work aims to understand the influence of fine dune sand on the mechanical performance of the SCC based on local mineral addition.

2. Materials Used

2.1 Cement and Mineral Additions

The cement used is a Portland cement [NF EN 1971]. Fine dune sand is a crushed dune sand to 80 µm from Taghit, Bechar - Algeria (Figure 1). The granularity, uniformity, chemical purity and nature of the dune sand make it a unique resource.



Fig. 1: Location of dune sand of Tgahit (Bechar -Algeria)

Table 1 presents the physical and mechanical characteristics of Portland cement and dune sand.

Table 1: Physical and mechanical properties of Portland cement and fine dune sand

Properties	Unity	Portland Cement	Fine Dune Sand
Absolute density	kg/m^3	3050	2800
Finesse	cm^2/g	3200	3000
Weight of Unit	kg/m^3	1120	1300
Mechanical strength at 2 days	MPa	24	-
Mechanical strength at 28 days	MPa	50	-

The results of chemical analysis in Table 2 show that the quartz (SiO_2) level in the six fraction of dune sands was found to be greater than 80 %, which means that these sands are of a siliceous nature.

Table 2: Chemical properties of dune sand (Tafraoui, 2012)

Fraction (mm)	0-0.04	0.04-0.10	0.10-0.12	0.12-0.16	0.16-0.20	0.20-0.25
%SiO_2	81.60	92.40	95.20	96.30	97.30	97.20
%Al_2O_3	3.80	2.10	1.40	1.00	0.83	0.80
%Fe_2O_3	2.20	1.00	0.60	0.30	0.24	0.20
%CaO	3.90	0.90	0.30	0.30	0.10	0.10
%MgO	0.60	0.20	0.02	0.50	0.40	0.05
%SO_3	0.20	0.20	0.20	0.20	0.20	0.10
%K_2O	1.10	0.60	0.33	0.10	0.04	0.02

Fraction (mm)	0-0.04	0.04-0.10	0.10-0.12	0.12-0.16	0.16-0.20	0.20-0.25
%Na_2O	0.50	0.20	0.10	0.10	0.10	0.20
%P_2O_5	0.10	0.02	0.01	0.01	0.01	0.00
%TiO_2	0.90	0.60	0.30	0.10	0.05	0.05
%MnO	0.04	0.03	0.02	0.01	0.02	0.01
%Cr_2O_3	0.01	0.01	0.01	0.01	0.01	0.01

The shape of dune sand particle is round form according to Figure 2.

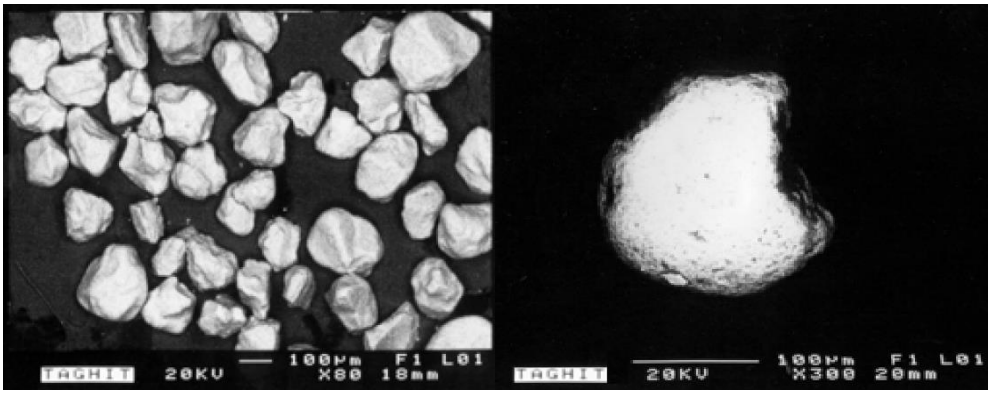


Fig. 2: SEM photographs of dune sand (Tafraoui, 2012)

2.2 Aggregates

The influence of aggregates is very strong on mechanical performance of concrete. All classes used (0/3), (3/8), (8/15) come from the quarry (Bechar).

The distribution curves of all aggregates are presented in Figure 3.

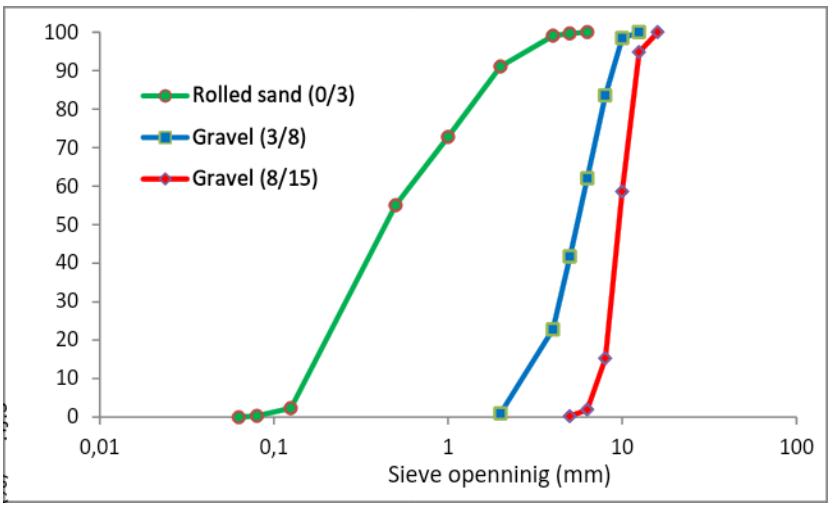


Fig. 3: Sifting of the materials used

The physical characteristics of aggregates used are presented in Table 3.

Table 3: Physical properties of aggregates

Parameters	Unity	Rolled sand	Gravel	Gravel
d/D	-	**0/3**	**3/8**	**8/15**
Equivalent of Sand	%	74	—	—
Modulus of fineness	-	2.1	—	—
Volumetric mass-Absolute	kg/m^3	2604	2630	2666
Volumetric mass-Apparent	kg/m^3	1761	1606	1444

2.3 Mixing Water and Superplasticizer

Mixing water was used from the tap of the laboratory at Bechar University. This water is treated for drinking Standard [NF EN 1008].

The admixture used is superplasticizer SIKAPLAST 5045 according to [NF EN 934 -2].

2.4 Composition of SCC

The final composition of the SCC is given in Table 4. Five concretes are thus obtained with varying percentage of fine dune sand, SCC%DS (0, 5, 10, 15 and 20%).

Table 4: Formulations of Self-Compacting-Concrete (kg/m^3)

	SCC%DS				
Addition	**0%**	**5%**	**10%**	**15%**	**20%**
Cement	520	494	468	442	416
W/C	0.5				
Aggregate 0/3	903				
Aggregate 3/8	151				
Aggregate 8/15	578				
Admixture	6.8				

3. Experimental Methods

3.1 Fresh properties test

The principal properties of SCC in the fresh state (fluidity, static and dynamic stability) are presented in Table 5.

Table 5: Values of principal properties of SCC in the fresh State according to AFGC norm

	Slump Flow test	**L – box test**	**Test of Stability in sieve (%)**
Limit values	600 - 750 mm	≥ 0.8	≤ 15 %
			

2.2 Mechanical Performance Test

The compressive strength was measured by hydraulic press (Figure 4-a) with a loading rate of 0.5 MPa/s. The European standard NF EN 12390-5 has been complied.

The elasticity modulus of concrete is a necessary parameter in structural design for the determination of the strain distributions and deformations, especially when the design of the structure is based on elasticity of materials. This property is conventionally measured using

standardized tests based on specimens of concrete subjected to uniaxial compressive loading. The elasticity modulus test was performed according to recommendations RILEM CPC8 1972 (Figure 4-b). The modulus of elasticity is measured with an extensometric system with two induction sensors.



(a) Compressive strength test **(b)** Elasticity Modulus test

Fig. 4: Mechanical performance test

4. Experimental Results and Interpretations

4.1 Fresh properties of SCC

According to the results presented in Table 6, it was found that all self-compacting concretes comply with the self-acceleration criteria recommended for recommendations AFGC (2008).

Table 6: Fresh state of concrete

	SCC 0%DS	**SCC 5%DS**	**SCC 10%DS**	**SCC 15%DS**	**SCC 20%DS**
T50 (s)	2.00	2.65	3.00	3.24	3.24
Slump flow (mm)	720	660	650	700	670
L-box test	0.89	0.83	0.88	0.89	0.88
Stability in sieve (%)	10.4	6.8	6.1	11.6	14.1

From the experimental results, all concretes have an acceptable fluidity according to AFGC norm (Slump-flow 650-720 mm). T50 time of the respective mixes recorded to reach 500 mm spread circle was observed to increase gradually from 2.00 sec (SCC 0%DS) to 2.24 sec (SCC20% DS). All the concretes have a good mobility of fresh SCC (L-box 0.83-0.89). These concretes present a good stability (Stability in sieve 6.1-14.1%: do not present segregation).

4.2 Compressive Strength and Modulus of Elasticity

The mechanical strength and modulus of elasticity are essential characteristics for the material concrete and the fundamentals parameters of our study. The mechanical performance (the evolution of compressive strength and modulus of elasticity) for the various compositions of concrete are presented graphically in Figure 5.

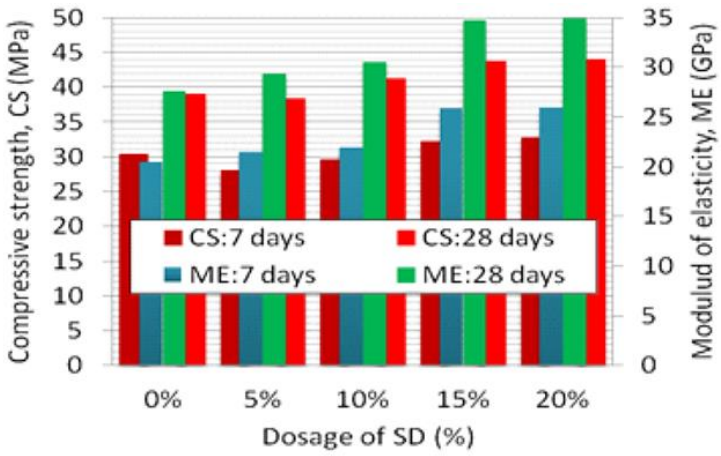


Fig. 5: Compressive strength and modulus of elasticity of SCC

It can be noted from Figure 5 that the increase in the dosage of SD has resulted in an increase in compressive strength and modulus of elasticity for 7 and 28 days. This confirms the positive influence of the fine dune sand on the mechanical performance of concrete. This is due to the physical properties of better bonding, as addition of dune sand approved the compressive strength due to the denser cementitious matrix and better bonding in transition zone (Rennani et al., 2020).

5. Conclusion

Our study focused on the use of fine dune sand as partial replacement of cement in the composition of Eco-self-compacting concrete (SCC). The fresh properties, compressive strength and modulus elasticity of SCC were presented. In general, the following conclusions were made:

- Through this research, we have demonstrated that it is possible to manufacture SCC of different composition parameters, having good rheological and mechanical characteristics.
- The use of fine dune sand in the composition of SCC by varying the dosage (0, 5, 10, 15 and 20%) of fine dune sand contributes to a slight variation of the fresh workability parameters while still remaining in the SCC range required by the AFGC recommendations for these concretes.
- The mechanical behavior of the SCC (compressive strength and modulus of elasticity) is proportional with the dosage of fine dune sand.
- The experimental results show that dune sand has the attitude to be used in SCC. The best substitute dosage for experimental study has been found to be between 15 and 20 %.
- Detailed investigations on durability performance should be explored.

Acknowledgements

The authors wish to thank the Directorate General for Scientific Research and Technological Development (D.G.R.S.D.T., Algeria) for financial support of this work. Thanks to professors and students members of EMIA ex LFGM (Laboratory of Eco-Materials: Innovations & Applications).

References

AFGC, Association française de génie civil, recommandations for SCC applications, 2008.

Ahmad, et al. (2022) “Concrete Made with Dune Sand: Overview of Fresh, Mechanical and Durability Properties”.

Materials, *15*, 6152. https://doi.org/10.3390/ma15176152

Ayed, K., Kerdal, D. E. & Leklou, N. (2020) "Durability of self-compacting concretes made with the natural pozzolan and siliceous fines", *Journal of Materials and Engineering Structures*, *7*(2), 227–240

Benmerioul. et al. (2017) "Valorization of the crushed dune sand in the formulation of self-compacting-concrete" *Procedia Engineering*, *171*, 672–678. https://doi.org/10.1016/j.proeng.2017.01.408

Bethmont, et al. (2009) "Contribution of granular interactions to self-compacting concrete stability: Development of a new device". *Cement and Concrete Research Volume 39*, Issue 1, 30-35. https://doi.org/10.1016/j.cemconres.2008.10.007

Bouhamou, et al. (2008) "Influence des paramètres de composition sur le comportement du béton autoplaçant à l'état frais". *Afrique Science*, *4*(1), 1– 20. DOI: 10.4314/afsci. v4i1.61626

Dawood, A. O. & Jaber, A. M. (2022) "Effect of Dune Sand as Sand Replacement on the Mechanical Properties of the Hybrid Fiber Reinforced Concrete". *Civil and Environmental Engineering*, *18*, 111–136. DOI: https://doi.org/10.2478/cee-2022-0012

Lee, et al. (2022) "Effect of Dune Sand on Drying Shrinkage Cracking of Fly Ash Concrete". *Applied Sciences*., 12(3). https://doi.org/10.3390/app12063128

Moulay, A., A. Abdeldjalil, M. & Khelafi, H. (2021) "An experimental study on the optimal compositions of ordinary concrete based on corrected dune sand—Case of granular range of 25 mm". *Case Studies in Construction Materials*, Volume 1, https://doi.org/10.1016/j.cscm.2021.e00521

Neville, A. (2004). "The confused world of sulfate attack on concrete". *Cem. Concr. Res.*, *34*, 1275-1296. https://doi.org/10.1016/j.cemconres.2004.04.004

Okamura, H. & Ouchi, M. (1999) "Self-compacting concrete Development present use and future", *First International RILEM symposium* on self-compacting concrete. *Rilem Publication*, vol. 3-14.

Rennani, et al. (2020) "Mechanical properties of high-performance concrete made incorporating dune sand as fine aggregate",. *Rev. Rom. Ing. Civ*, *11*, 37–46.

Tafraoui, A. (2012) "Valorisation du sable de l'erg occidental (Algérie): Application aux nouveaux bétons". *Editions Universitaire Européennes*.

Cite as: Abdelkadir M., Ahmed T., Said Z. & Farid B., "Influence of Fine Dune Sand on the Modulus of Elasticity of Eco-Self-Compacting-Concrete", *The 2nd International Conference on Civil Infrastructure and Construction (CIC 2023)*, Doha, Qatar, 5-8 February 2023, DOI: https://doi.org/10.29117/cic.2023.0099

Upgrading Existing Infrastructure – The Case Study of Industrial IC Bridge

Theodoros Tzaveas
Public Works Authority, Doha, Qatar
ttzaveas@ashghal.gov.qa

Christina Anagnostaki
Public Works Authority, Doha, Qatar
canagnostaki@ashghal.gov.qa

Yoji Matsuo
Parsons International, Limited, Qatar
yoji.matsuo@parsons.com

Georgios Sergakis
Parsons International, Limited, Qatar
georgios.sergakis@parsons.com

Abstract

Doha, the capital of Qatar, has been facing phenomenal growth of vehicular traffic owing to rapid development which has resulted in traffic congestion causing significant rise in travelling time in some areas. To mitigate these problems, upgrading existing intersections and consequently retrofitting the contained structures along significant corridors is a strategy implemented by the Public Works Authority in some cases. A case study presented herewith, is a project awarded as a *Design & Build* Contract by the PWA to upgrade the infrastructure at the junction of a major corridor (Junction 101 – Industrial Interchange). This paper covers the tender stage and the final design solutions, outlining the simulation models, assessment of the existing structures, the design analysis and the construction methodology adopted to address the operation and maintenance conditions as well as the project specific requirements and constraints.

Keywords: Steel-concrete composite; Condition assessment; Retrofitting; Bridge expansion joints

1 Introduction

The Industrial Interchange is located at the junction 101 of the Salwa Road and Furousiya Street. Salwa Road is categorized as an expressway and the Furousiya Street as a major artery before upgrading and shall be categorized as an expressway in the future. The junction is a 4-level grade-separated junction (Figure 1) with Furousiya Street at -1 level, existing roundabout bridges at-grade (level 0), Salwa Road bridges at +1 level, and left turn directional ramp at +2 level.

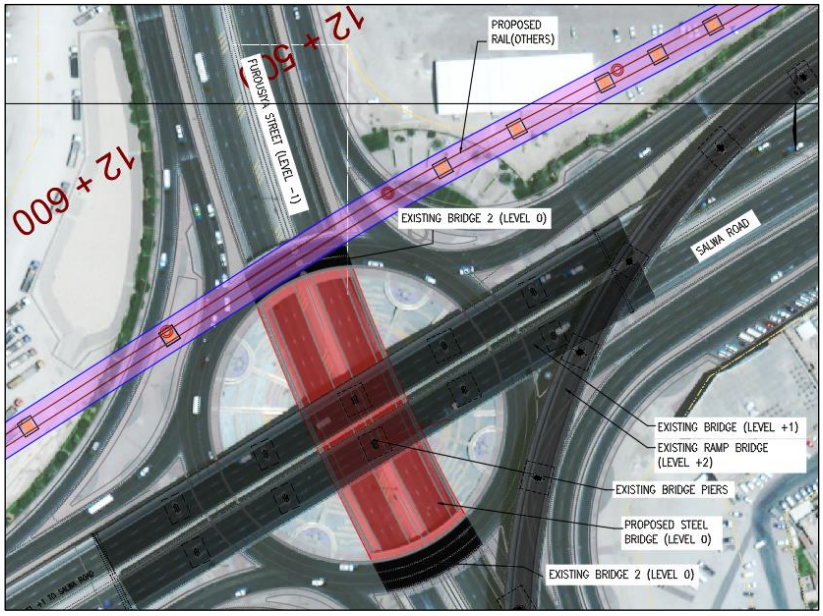


Fig: 1: Layout of Junction 101 with the existing and proposed bridges

The scope of the project was to upgrade the at-grade (level 0) portion of the intersection to improve the traffic performance and to accommodate the future demand. The reference design in the tender stage (Figures 2 & 3) proposed/dictated the construction of a single span bridge with steel-concrete composite decking over the Furousiya Street extending between the two existing roundabout bridges, converting the current signalized roundabout to a signalized junction.

2 Tender Stage

At the pre-design/tender stage the design approach considered a single-span steel-concrete composite bridge, with 37.80m width and 104.48m length approximately, supported on the existing retaining walls with the necessary retrofitting (Figure 2), to carry safely the additional loads due to the new configurations and accommodate the installation of the new bridge bearings. The bridge was initially designed as a steel- concrete composite bridge with steel tub girders spaced in a nominal distance and concrete slab on top. The monolithic/composite connection of the two structural elements was achieved with shear studs projecting at the tub girder top flanges. The two existing piers of the Salwa ramp bridges (level +1), maintain their structural independence through openings in the newly proposed deck.

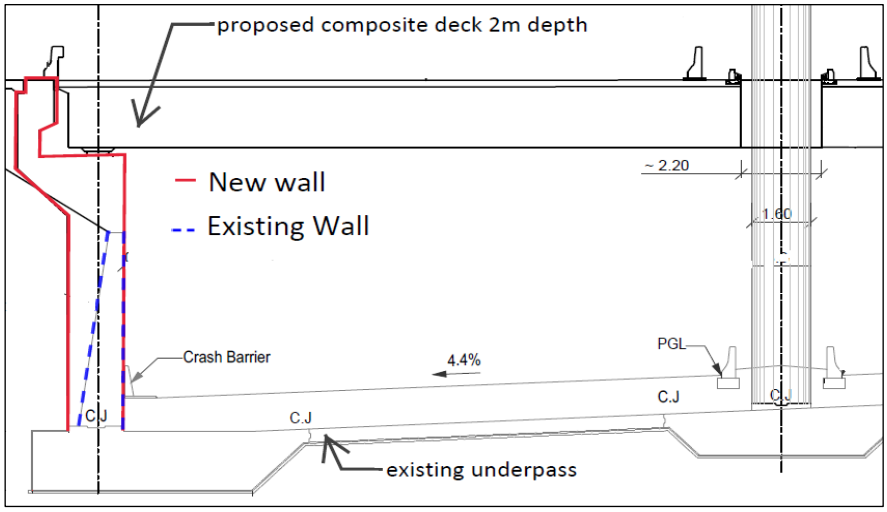


Fig. 2: Reference Design Typical Section

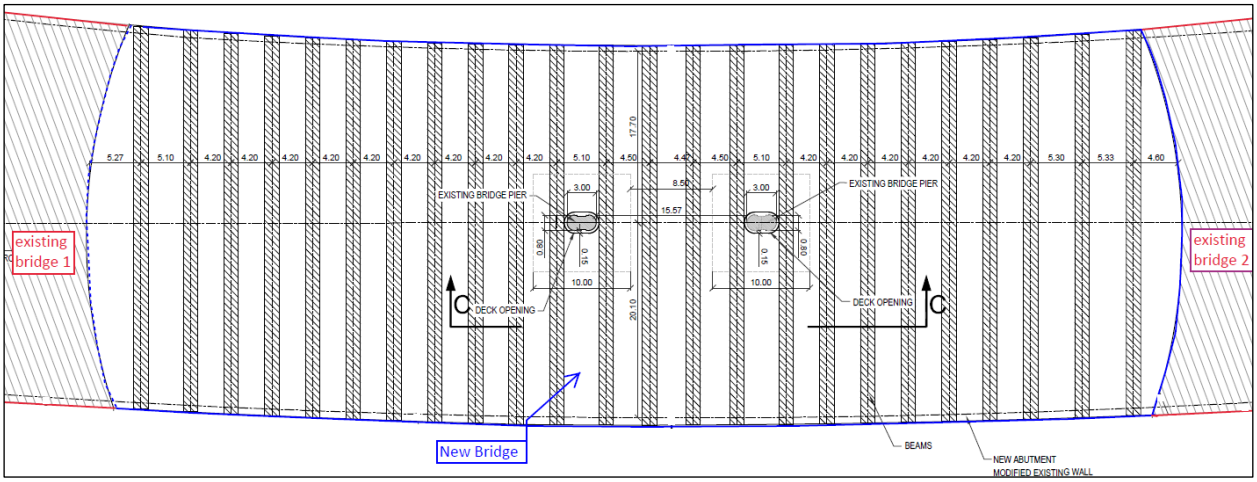


Fig. 3: Reference Design Layout

Due to the challenging site conditions, a number of constraints had to be considered in the preliminary design stage which included the following:

- **Vertical Clearance**: As the newly installed deck is bound by the existing underpass at -1 Level and the existing Salwa Road Bridge deck at +1 Level, the design was constrained by the fixed total height to provide vertical clearances below and above the proposed deck. To provide acceptable vertical clearances, the new deck depth had to be optimized.
- **High Groundwater Table**: Due to the consideration for high groundwater table present at the site, particular attention was given to ensure the watertightness of the existing underpass structure by avoiding penetration of the bottom slab.
- **Existing Salwa Bridges Piers**: Piers for the existing Salwa Bridges are present behind the proposed abutments and founded at a higher level than the existing underpass. The design was required to mitigate against the risk of undermining the piers' foundations and complications of installing temporary shoring to support the piers during construction.
- **Unknown Existing Structure Capacity**: There is an inherent risk in relying on the capacity of the existing structure. The design considered minimizing additional load transfer to the existing underpass.

Several design options were considered which included the modification in the following structural features:

- **Number of spans**: A single-span structure would eliminate the need for placement of the median support; however, this will require an increased deck depth, which would make the vertical clearances unacceptable.
- **Abutment types**: Modification of the existing underpass retaining walls to support the new deck as envisaged in the tender design would require major retrofit of the walls and enlargement of the existing footings, including complicated shoring to support the existing Salwa Bridge piers during the construction. Installing a piled abutment behind the existing underpass walls would mitigate this risk.

After consideration of the above factors, the design option as presented in the following sections was selected.

3 Design Stage

3.1 General Description

The optimal solution finally adopted in the design was a two-span composite bridge with a median support integrated with the existing base slab and new abutments at both sides with piles placed behind the existing retaining walls (Figure 4). The challenge of this solution is the construction of the foundation of the median piers, without overstressing the existing 400mm base slab and maintaining the integrity of the slab and the underlying waterproofing membrane, considering the high-water table in the area. Further, the proposed solution of the independent piled abutments eliminated any need for temporary shoring walls that would be necessary to support the existing Salwa Piers located behind the existing underpass walls.

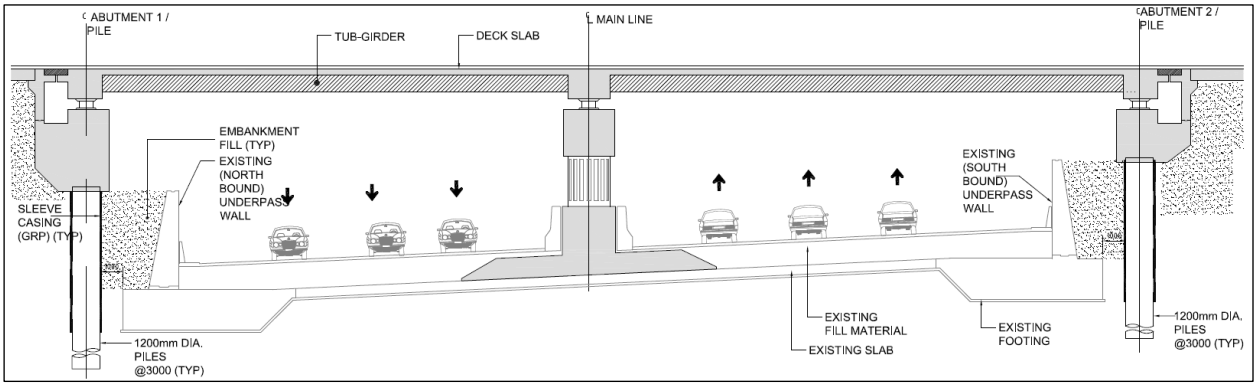


Fig. 4: Final/Adopted Bridge Section

3.2 Advantages

The preference of this option was based on many advantages in regards to the feasibility and constructability of the bridge, as well as its minimal impact to adjacent structures in a compressed construction schedule as presented below:

- Achieved maximum vertical clearance below the deck (min 5.7m).
- Achieved maximum vertical clearance between the proposed deck FRL and Salwa Bridge deck soffit.
- Deck depth is reduced to 1.0m in total.
- The durability requirement of 120 years is satisfied.
- The bridge is supported on new abutments and piers.
- No loads transferred on the existing retaining walls and therefore avoided extensive and complicated retrofit works.
- Applied stresses on existing slab within allowable code limits.
- No major temporary shoring system is required.
- Excavation and backfilling activities are significantly reduced.
- Eliminated the requirement of extensive de-watering activities that would be necessary if the underpass wall would be converted to a bridge abutment.

3.3 Existing Structures Assessment

A condition assessment of the existing structures has been conducted at the early stages of the design in order to understand the properties of materials incorporate any strengthening actions and determine the feasibility of the proposed solution. All the tests/measurements/site inspections/verifications of as-built

configurations required by the codes have been conducted and the results were analyzed and provided in assessment reports. The results have shown that the existing trough structure and the roundabout bridges are in a good condition and no strengthening was deemed necessary. In addition, the base slab of the underpass and the foundation of the Salwa Bridge piers could accommodate the additional loads due to the construction of the median support.

3.4 Structural Type & Design Approach

The superstructure for the Industrial Interchange Bridge extends between the two existing roundabout bridges with an overall length of 107m approximately (Figure 5). The 1.0m composite deck depth consists of 0.25m of cast-in-place concrete slab and of 0.75m steel girder with a typical spacing of approximately 3.0m (Figure 6). The steel tub girders are connected at the abutments and median supports through concrete diaphragms. The connection of those elements is monolithic and is achieved through shear studs (Figure 6).

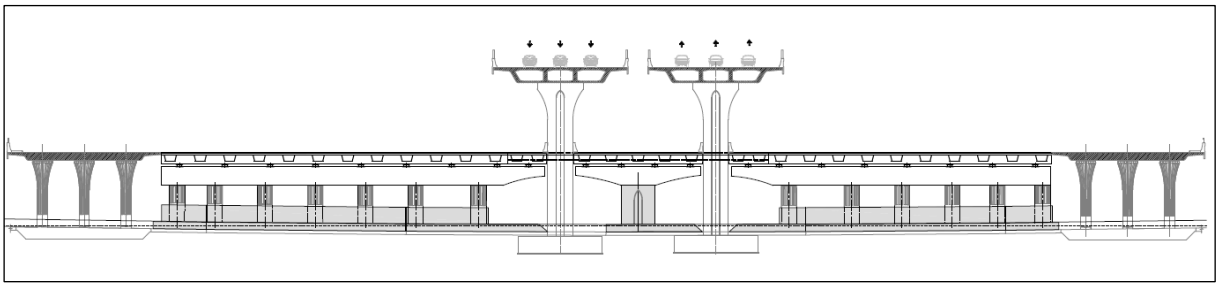


Fig. 5: Longitudinal Section

The bridge deck rests on spherical bearings at all supports. The articulation over the middle support consists of free sliding bearings in order not to transfer additional moments at the bottom of the median piers. In accordance with the new road layout, the traffic direction is not always perpendicular to the expansion joint axis between the parts on the bridge (Figure 7). For this reason, flexible plug joints were chosen to connect the parts of the bridge to allow the movement in both directions and accommodate the altering super-elevation throughout the 107m deck width (Figure 7).

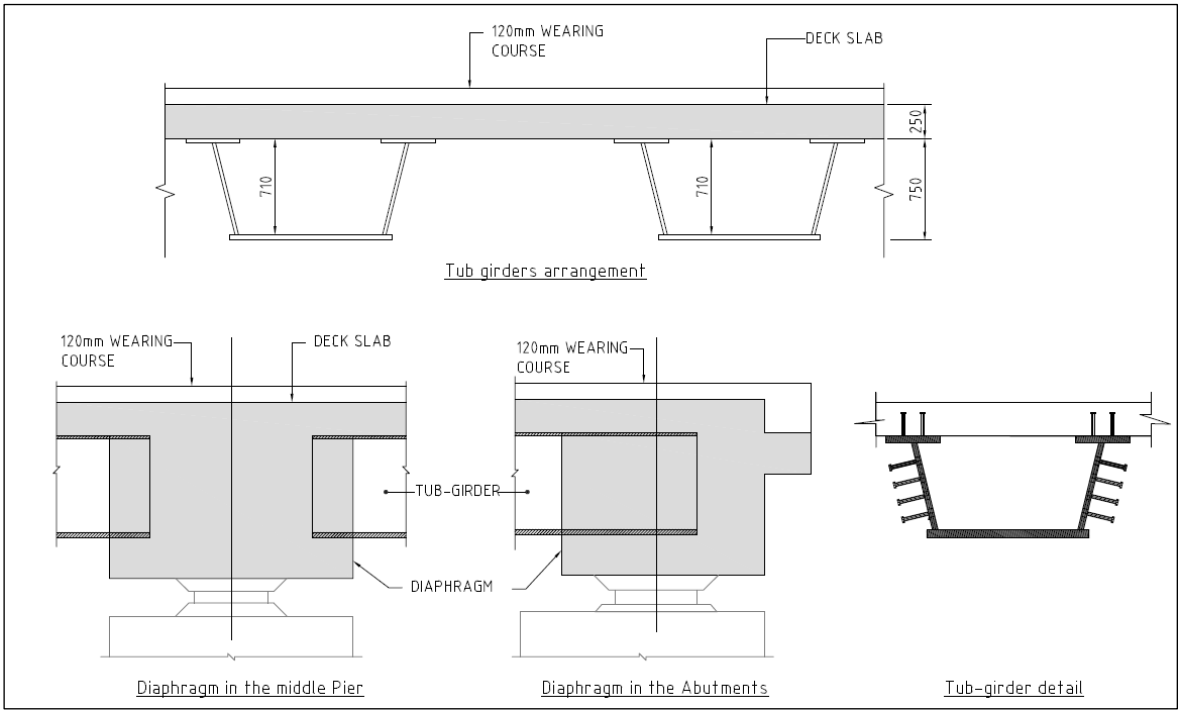


Fig. 6: Typical deck details

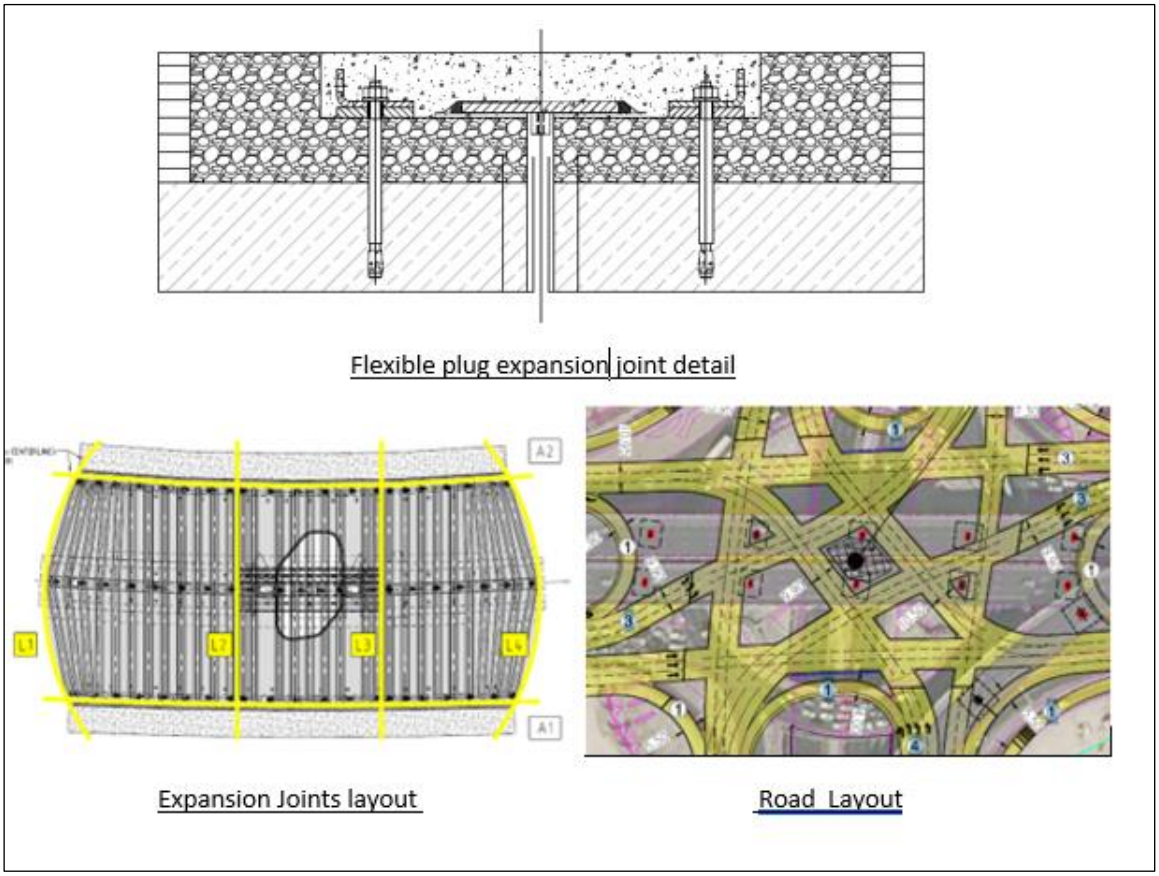


Fig. 7: Flexible plug expansion joints details and layout

The abutments are designed as piled supports with pile cap. The piles are sleeved for the top 5.5m to avoid transferring loads on the existing retaining Underpass walls. The median pier is designed with pad strip footings of 11,000 to 12,000 mm width and 850mm to 900mm thickness, integrated with the 400mm existing base slab with shear studs (Figure 8) in order to accommodate the additional loads transferred from the pier. By implementing these substructure types the risk of damaging the existing Underpass walls is avoided and the amount of temporary works is minimized.

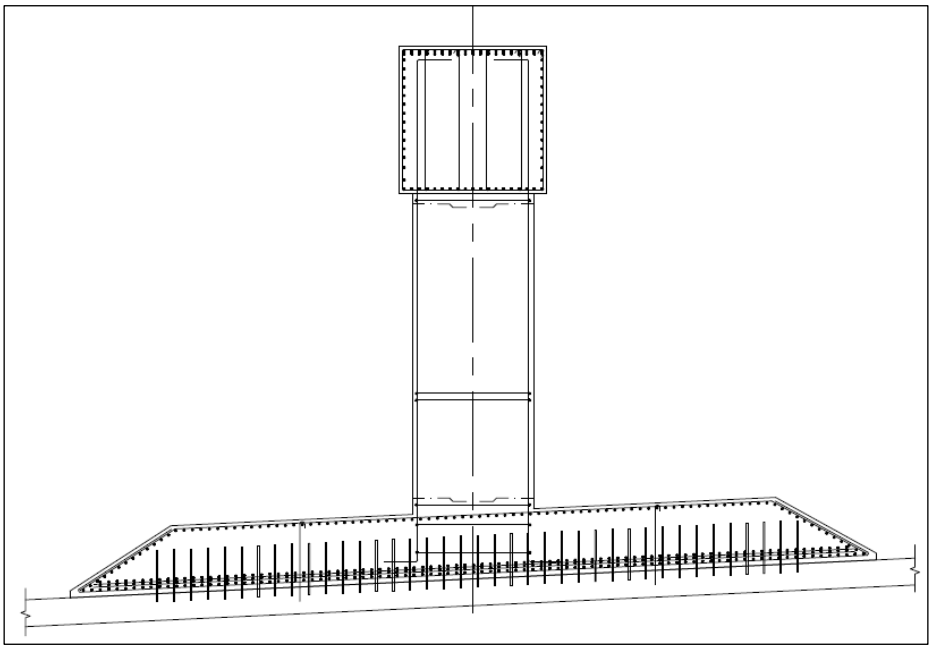


Fig. 8: Median Pier integrated footing

4 Conclusion

The case study presented in this paper, highlights the challenges faced to develop and implement a retrofitting solution to address multiple requirements such as a compressed construction time-frame, constraints in the vertical clearances below and above the new bridge deck due to the presence of the existing structures, as well as efforts to preserve the existing structures without strengthening (Furousiya Underpass/ Roundabout Bridges/ Salwa Road Ramp Bridges).

Further, the need for temporary shoring walls and the extensive dewatering were both eliminated by using piled abutments.

The use of prefabricated steel girders decreased the weight of the bridge deck superstructure, allowed a significant portion of works to be completed off-site, minimized the impact to the existing underpass slab and at the same time it provided an ease of handling in the site space that is limited due to the presence of diverted traffic.

The design proposal that was developed was an integrated and robust solution to accommodate all the site constraints and allow the construction of this complex interchange to be conducted in a safe (for the existing structures) and timely (considering the demanding construction schedule) manner.

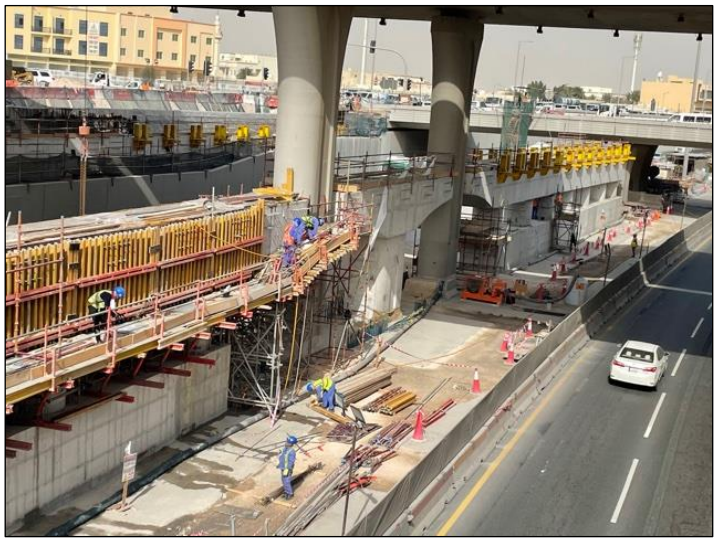


Fig. 9: – Median Piers during construction

References

Ashghal. (2016). Interim Advice Note 009 – *Design Criteria for Highway Structures*, Revision A2, Ashghal.

Ashghal. (2016). Interim Advice Note 006 – *Specification of Bridge Bearings*, Revision A1, Ashghal.

Ashghal. (2016). Interim Advice Note 031 – *Expansion Joints of Highway Structures*, Revision A1, Ashghal.

BSI. (1990). BS 5400-4:1990, *Code of practice for design of concrete bridges*, BSI.

BSI. (2006). BS 5400-2:2006, *Steel, concrete, and composite bridges. Specification for loads*, BSI.

BSI. (2000). BS 5400-3:2000, *Steel, concrete, and composite bridges. Code of practice for design of steel bridges*, BSI.

Cite as: Anagnostaki C., Tzaveas T., Sergakis G. & Matsuo Y., "Upgrading Existing Infrastructures - The Case Study of Industrial IC Bridge", *The 2nd International Conference on Civil Infrastructure and Construction (CIC 2023)*, Doha, Qatar, 5-8 February 2023, DOI: https://doi.org/10.29117/cic.2023.0100

Data Interpretation Framework for Pile Thermal Integrity Testing

Qianchen Sun
Department of Engineering, University of Cambridge, Cambridge, UK
qs217@cam.ac.uk

Mohammed Elshafie
Department of Civil and Architectural Engineering, Qatar University, Doha, Qatar
melshafie@qu.edu.qa

Chris Barker
Ove Arup & Partners Limited, London, UK
chris.barker@arup.com

Anthony Fisher
Skanska Cementation International, London, UK
anthony.fisher@skanska.co.uk

Andrew Bell
Skanska Cementation International, London, UK
andrew.bell@skanska.co.uk

Abstract

Given the inherent nature of how deep cast in-situ concrete foundations (piles and diaphragm walls) are constructed, evaluating their integrity is difficult. Several well-established methods for testing integrity have been established, but each has its own advantages and disadvantages. In recent years, a new integrity test method called thermal integrity profiling (TIP) has been put into use in deep foundation construction. The primary characteristic utilised in this test is the early-age concrete release of heat during curing; abnormalities such as voids, necking, bulging, and/or soil intrusion inside the concrete body lead to local temperature fluctuations. During concrete curing, temperature sensors installed on the reinforcing cage collect precise temperature data along the entire pile, allowing empirical identification of these temperature variations. This paper proposes a staged data interpretation framework for pile integrity assessment, with the thermal integrity test serving as the initial step. The framework, which is adaptable to different concrete mixtures and pile designs, utilises the heat of hydration and the theory of heat transmission, as well as numerical modelling with the Finite Element (FE) method. It also adopts a staged procedure to assess the *as-built* quality; for a particular pile, more details are revealed about any anomalies being investigated (including location, size and shape) at each subsequent stage. The primary advantage of this staged process is that it enables practitioners to follow a risk-based approach and decide whether or not to pursue subsequent stages of construction depending on the results they get at the end of each stage. This provides practicing engineers with vital information about the quality of the pile immediately after pile building, so permitting immediate and less expensive repair and remedial work if required.

Keywords: Thermal Integrity Test; Pile Anomaly Detection; Structural Health Monitoring; Non-destructive Test

1 Introduction

Pile foundations transfer loads deep into the ground where it is stronger and stiffer. Hence, they are

commonly employed in construction practice to avoid the weaker soils closer to the surface. In developing pile systems, designers must evaluate how *as-built* construction works are compared to performance specifications. Understanding the integrity and quality of these piles is a significant challenge – not least because they are buried in the ground. In recent years, pile repair and the associated maintenance accounted for a significant part of the construction cost. In the United Kingdom, infrastructure repair and maintenance costs account for approximately £15 billion each year – 20% of the total construction costs (*Infrastructure UK*, 2010). It is therefore very important to assess the quality of the piles at/during their construction. However, as underground structures they have limited accessibility which makes it very difficult to inspect the structural quality (Matsumoto et al., 2004; Kister et al., 2007). Anomalies in piles or other deep members could lead to structural instability and/or other durability problems. Studies on about 10,000 bored piles, conducted in the United States and Germany, showed that more than 15% of pile test results had signs of minor defect signs and 5% of tested piles had major defects (DiMaggio & Hussein, 2004; Brown & Schindler, 2007). The discovery of these defects could result in large financial losses and could cause undue delays. It is therefore very important to identify the pile construction defects early on, particularly when heavy loads are involved.

In the last decade, a new integrity assessment test called thermal integrity profiling (TIP), has been employed by the piling industry. It monitors the temperature changes and thermal profiles of early age concrete throughout the casting and curing processes. The heat production and dissipation within the pile concrete body are influenced by the design mix of the concrete, the nature of the ground and the pile geometry. If defects are present inside the pile, they will cause local temperature fluctuations relative to the predicted heat produced during the curing process. The observed temperature information is utilised to deduce the *as-built* shaft shape, the position of the reinforcement cage and eventually the presence of defects. The current practice of data interpretation of this temperature-based integrity method is mostly based on empirical experience in the piling industry. The detection of anomalies by directly interrogating the temperature profiles can only provide suggestive results. Temperature signal changes are similar, and it is not easy to separate the potentially many causes behind these changes.

This paper presents a staged-based framework to interpret the temperature data obtained from the field thermal integrity test. The proposed data interpretation framework employs Finite Element (FE) numerical modelling to systematically study the pile *as-built* quality through one-dimensional and two-dimensional analyses. Following this staged investigation procedure, the integrity information, such as overall quality, defect location, defect size and severity, along the pile are identified and evaluated. The detailed staged data interpretation method is explained in detail in this paper and demonstrated through a field case study.

2 Staged Data Interpretation Framework

The thermal integrity method utilises the exothermic characteristic of the cement hydration process. The generated hydration heat increases the concrete temperature. Defects within piles, such as necking, inclusions or segregation, produce less heat and therefore lower the concrete temperatures; in contrast, bulges in the shaft lead to higher concrete temperature.

In order to numerically evaluate the pile integrity using monitoring temperature data, a staged data interpretation framework is proposed as illustrated in Figure 1. The first stage is to conduct the field thermal integrity test – this comprises collecting continuous temperature data from sensors installed

before casting along the entire length of the pile. Following that, a cement heat-of-hydration test (Calorimetry) should be conducted in order to provide input for the cement hydration model, which will be employed by the FE model in the later stages. Upon obtaining temperature data and ground information, the data interpretation process is then followed as follows: Stage 1, the "vertical scanning" stage, employs a 1D finite element model to perform a quick evaluation of all temperature data along the pile length. Through this scanning process, the maximum temperatures at the respective sensor locations are converted into pile effective radii, which are then used to generate a 3D pile shape for more intuitive identification of potentially defective regions. A more detailed explanation for the 1D finite element process and the pile effective radii are presented in (Sun et al., 2022).

Assuming that potentially defective regions are identified in Stage 1, the investigation moves to Stage 2, the "slicing" stage. Temperature development data is extracted from cross-sections within the defective regions and the defect investigation is performed using a 2D FE model. The information retrieved from Stage 1 is used for setting up (a) an initial defect configuration (assumed size and location) and (b) suitable search zones within the cross-sections. A series of 2D FE simulations for the heat-of-hydration are then conducted, taking into account the appropriate boundary conditions, with the temperature development data from the model then compared with the actual field data using an appropriate cost function (Δ). It is worth mentioning that more sensors (measuring points) within the cross-section provide better results.

At the end of each 2D simulation, based on the comparison with the field data, the assumed defect configuration (size and location) is optimised within the search zones through algorithms (such as differential evolution and/or particle swarm optimization) before a new 2D simulation is conducted. This is continued until the cost function is minimised to an appropriate value. The defects are assumed to be circular in shape; however, this is not the case in practice. Nonetheless, the proposed framework is not limited by this assumption as different shapes and different sizes could be assumed instead within the cross section seeking to minimise the cost function as much as possible. More detailed explanation for the 2D finite element analysis can be found in (Sun et al., 2020). The detailed procedure of the staged method will be demonstrated using a field case study in the following sections.

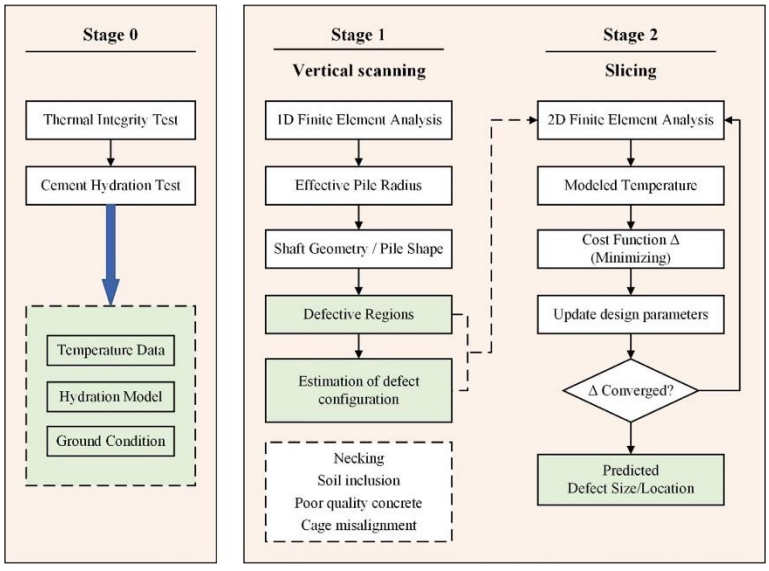


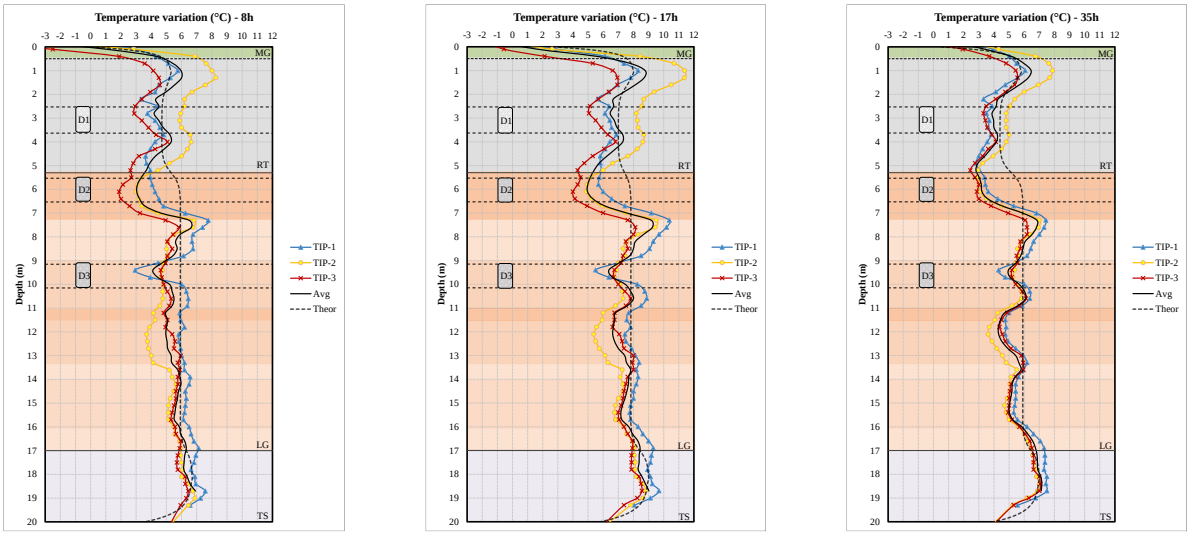
Fig. 1: Staged Data Interpretation Framework

3 Field Trial Pile Data Interpretation

3.1 Pile Instrumentation and Measured Temperature

This field case study investigated the monitoring of a continuous flight auger test pile designed to evaluate the capability of thermal integrity testing. The test pile had an exterior diameter of 900mm and a height? of 20m. Before casting concrete into the pile, temperature sensors were installed inside the reinforcing cage, which had a 750mm diameter. A total of three temperature sensing cables were installed at equal intervals; these are designated as TIP-1, TIP-2, and TIP-3 in the following text.

The measured longitudinal temperature fluctuation profiles are illustrated in Figure 2. The whole pile started to heat up between 4 and 8 hours after casting, with the exception of the top half meter, which was exposed to ambient air overnight. Seventeen hours after casting, the pile temperature peaked at between 8°C and 11°C. The temperature reduced at a fairly moderate rate after that such that 35 hours after casting, the average temperature was around 5°C for all three profiles.



(a) (b) (c)

Fig. 2: Temperature Profiles at **(a)** 8 hour **(b)** 17 hours **(c)** 35 hours

3.2 The Stage One Analysis

The first stage of the analysis involves using a 1D finite element model to quickly evaluate all temperature data along the length of the pile. This stage, also known as the vertical scanning stage, aims to assess overall pile quality and identify any defective zones for further analysis. The observed temperature at the sensor position is influenced by several parameters, such as shaft diameter, boundary conditions, and the presence of anomalies, which make it difficult to distinguish between individual elements. Therefore, changes in the temperature profile in each layer of soil are interpreted as changes in the effective pile radius, i.e., the radius of an intact pile that generates the same temperature readings at the sensor position. The effective pile radius is an important parameter for quality assurance, as it enables engineers to quickly determine whether extensive integrity studies are necessary. The effective pile radius can be linked to the effective pile cover thickness using the equation R_eff=r_cage+D_cover, where r_cage is the radius of the reinforcement cage.

All temperature profile variations are assumed to result from changes in the effective pile radius, which is estimated using one-dimensional finite element studies of heat transport in three radial directions corresponding to the three sensor sites inside the pile. The effective pile radius is

modified at various positions along the pile depth to achieve a satisfactory match between the observed temperature profile and that estimated by the FE analysis. This approach enables the prediction of the effective radius along the depth of the pile in three sensor radial directions. After analyzing all cross-sections, the pile's geometry can be calculated.

Figure 3 illustrates a theoretical relationship between cage radius, shaft radius, and temperature at 16 hours after concrete pouring. The relationship was obtained through numerical simulation of early age concrete hydration heat development. The theoretical temperature measurement changes linearly as the shaft radius moves around the designed value, with the intersection of the solid and dotted lines representing the theoretical temperature measurement. The temperature measurement at the cage position is particularly sensitive to the concrete cover thickness, which may serve as an excellent signal for evaluating the *as-built* pile shape. Normally, pile concrete cover thickness would vary between 25mm and 200mm, with or without defects, so the measured temperature should fall within the linear zone.

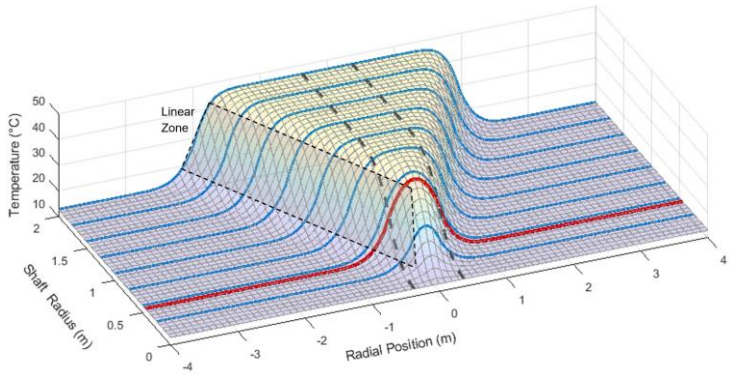


Fig. 3: Relationship between cage position, shaft size and temperature measurement at 16 hours

A strongly linear relationship is revealed through 1D FE analysis, which can be expressed in the following equation:

$$D_{cover} = \alpha_k * T_{max} - \beta_k \quad (1)$$

where D_{cover} represents the concrete cover thickness (cm) and T_{max} denotes the maximum temperature (℃) at the measurement point, α_k (cm/℃) and β_k (cm) are D-T parameters dependent on factors including sensor location and soil material. The values of these parameters were obtained through linear regression of the FE analysis data. In the primary body of soil (Lambeth Group), the values are α_k = 1.53 cm/℃ and β_k = 34.49 cm. Different soil layers would have different D-T parameter values. The obtained relationship allows the back-calculation of the cover thickness at three different sensor locations on the cross-sections along the pile depth. The effective pile radius can be subsequently obtained by adding the reinforcement cage radius.

Figure 4 demonstrates the 3D pile shape according to the calculated effective radius method. An expanded pile radius zone (larger than the average) is indicated in orange while the blue color indicates zones of pile radii that are smaller than average. The following could be seen from the figure:

- Two small deficient zones - between 2 to 4 m and 9 to 12m.
- One severely deficient zone - between 6 to 8 m.
- The pile radius ranges from 43 to 57 cm in the upper half while the lower half is consistently around 51 cm in radius.

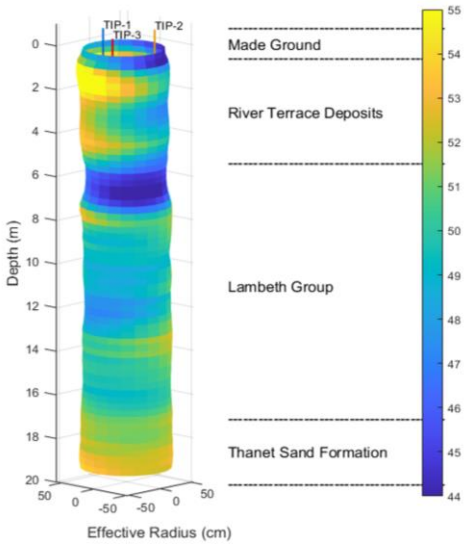


Fig. 4: Predicted pile 3D shape

3.3 The Stage Two Analysis

The 2D FE analysis in this stage aims to find the detailed defect location and size within each defective zone identified in the first stage. In this stage, known as the "slicing stage", the defective zones are cut into multiple cross-sections to evaluate the defects at two-dimensional level. Normally, if the *as-built* pile geometry is uniform and no defects are present, the temperature profile measured at depth for each one of the cables should be similar, the temperature development at three sensors within the same cross-section should be relatively similar. The temperature data at each cross-section can be a good indicator for pile integrity at the corresponding level. As shown in Figure 5, if a defect is located near sensor 1, the measurement temperature development should be lower than the expected values, owing to a loss of heat source. For those sensors away from defects, the reduction of temperature measurement should be insignificant, such as sensor 3 in the figure. Based on that, a search zone (using a grid) is then introduced around the expected defect location and a series of FE simulations are run in a systematic manner changing the radius of an assumed circular defect centered at each of the search grid points.

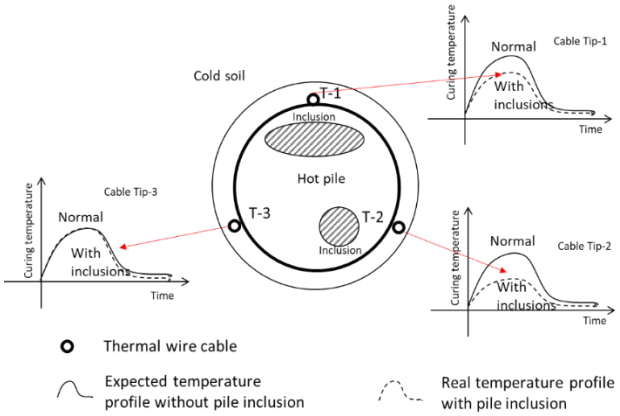


Fig. 5: Conceptual relationship between temperature development and pile integrity

A comprehensive assessment of anomalies is detailed below:

a. A numerical model is established for each cross-section at various depths within the pile depth, accounting for potential anomaly locations identified in the first stage analysis.

b. Temperature measurements from the three cables within each cross-section can provide an indication of the position of an assumed circular anomaly. For example, if a cable shows a larger temperature decrease compared to the other two at a certain depth, it suggests that the anomaly is inside the reinforcement cage and closer to that cable.

c. Based on the estimated defect locations, a starting "search origin" is determined for each cross-section. For instance, the origin is set at (0,0) for the section at 6m depth and at (0,19cm) for the section around 9m depth, as shown in Figure 6.

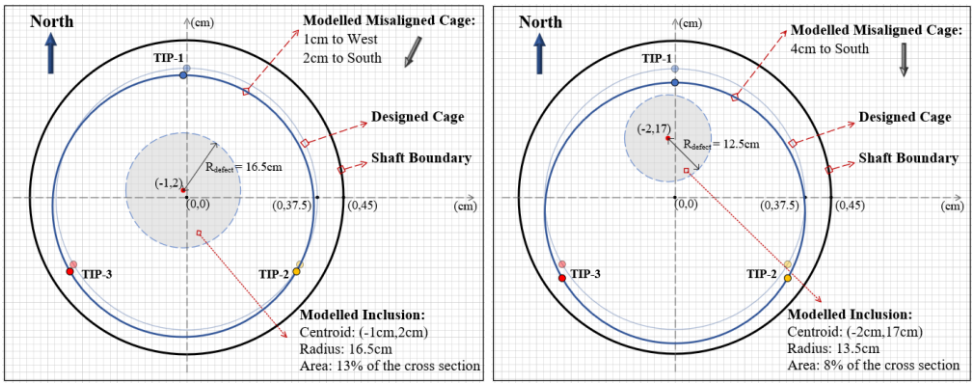
d. A search grid is established around the search origin for each cross-section. 2D FE simulations are then run in a systematic manner with a circular anomaly of varying radius centered at each point in the search grid zone.

e. After each simulation, the predicted temperatures at TIP-1, TIP-2, and TIP-3 are contrasted with the field measurements. The temperature difference, cumulatively, is minimized to obtain the cost function.

f. In order to consider reinforcement cage misalignment, a search zone is established within the numerical model for TIP-1, TIP-2, and TIP-3.

g. At a given cross-section, at the end of FE simulations the anomaly configuration that minimized the cost function consititutes the detected anomaly. The analysis takes cage misalignment into account.

The outcomes of the 2D FE defect forecasts at depths of 6.1m and 9.4m are depicted in Figure 6. At the 6.1m cross-section, a circular anomaly was detected with an assumed center at (-1cm, 2cm) and a radius of 16.5cm, accounting for 13% of the cross-sectional area. The cage eccentricity was found to be 1cm to the west and 2cm to the south. At the 9.4m cross-section, the FE simulation predicted an inclusion center at (-2cm, 17cm) with a size of 8% of the cross-section and a cage eccentricity of 4cm to the south. The stage 2 FE analysis provided an accurate prediction of the size and location of Inclusions 2 and 3. However, compared to the actual size of the engineered inclusions (9% cross-sectional area), the area for Inclusion 2 was slightly underestimated by 1%, while the FE analysis overestimated Inclusions 3 by 4%. Inclusion 1 was not detected in the FE studies, as it was simulated using four sandbags to mimic an externally attached concrete cover defect on the reinforcement cage. According to the on-site engineer, these sandbags were damaged during the reinforcing cage installation process. At this depth, sand spreads within the concrete body. As the volume of sand was negligible, totaling only 3% of the cross-sectional area of the pile, the concrete quality did not appear to have been considerably harmed.



(a) **(b)**

Fig. 6: Predicted Anomaly Configurations at **(a)** 6.1m, **(b)** 9.4m

In the work presented in this paper, the anomalies are assumed to be circular in shape; however, in practice, the flaws have different shapes and may consist of low-quality concrete. This does not restrict the methodology proposed above. Different shapes (of varying sizes) may be assumed in the studies, and more shapes (of varying sizes) could be gradually added inside the same cross-section to reduce the cost function and get the best possible outcome. In addition, a new technique of topology optimisation has been devised to discover faults in both 2D and 3D space. It can evaluate the quality of concrete in a precise manner and predict defects in any shape. The details can be found in the authors' future publications.

4 Conclusion

A relatively new and promising technique for assessing thermal integrity involves measuring temperature changes induced by hydration heat. In this paper, a framework for interpreting data from the test is proposed, and a case study of the test is presented using this new approach on a trial pile.

The stage one analysis uses a 1D finite element analysis to interpret the data while accounting for the parameters of the concrete mix and soil. The FE model establishes a linear relationship between maximum temperature and effective pile radius. The pile effective radii throughout the whole shaft could be determined using the linear relationship, and the expected *as-built* pile's 3D shape could then be recreated, making it possible to more effectively identify problem areas. After that, the stage two analysis, which used 2D finite element analysis, was able to accurately estimate the sizes and positions of the anomalies with less than 10% of the cross-sectional areas of the sections under consideration.

More information regarding the defects, such as their position, size, and shape, can be disclosed in each stage. This staged procedure enables practitioners to take a risk-based approach and choose whether or not to go on to the next stage based on the data they get at the conclusion of each stage. This innovative method may provide practicing engineers with vital test data about the quality of the pile immediately after pile building, so permitting immediate and less expensive repair and remedial work.

References

Brown, D. & Schindler, A. (2007). High performance concrete and drilled shaft construction. In *Contemporary Issues In Deep Foundations* (pp. 1-12).

DiMaggio, J. A. & Hussein, M. H. (2004, July). Current practices and future trends in deep foundations. American Society of Civil Engineers.

Infrastructure UK, H. T. and I. and P. A. Infrastructure cost review: technical report. (2010).

Kister, et al. (2007). Methodology and integrity monitoring of foundation concrete piles using Bragg grating optical fibre sensors. *Engineering Structures*, *29*(9), 2048-2055.

Matsumoto, et al. (2004). Monitoring of load distribution of the piles of a bridge during and after construction. *Soils and foundations*, *44*(4), 109-117.

Sun, et al. (2020). Thermal integrity testing of cast in situ piles: An alternative interpretation approach. *Structural Health Monitoring*, 1475921720960042.

___. (2022). Integrity monitoring of cast in-situ piles using thermal approach: A field case study. *Engineering Structures*, *272*, 114586.

Cite as: Sun Q., Elshafie M., Barker C., Fisher A., & Bell A., "Data Interpretation Framework for Pile Thermal Integrity Testing", *The 2nd International Conference on Civil Infrastructure and Construction (CIC 2023)*, Doha, Qatar, 5-8 February 2023, DOI: https://doi.org/10.29117/cic.2023.0101

Galvanized Steel as a Sustainable Material-Technology and Failure Analysis

Abdulwahab Ibrahim
University of Doha for Science and Technology, Doha, Qatar
Abdulwahab.ibrahim@udst.edu.qa

Scott MacIntyre
Atlantic Metallurgical Consulting, Dartmouth, Canada
scott.amcl@gmail.com

Abstract

The building industry is responsible for 40% of global CO2 emissions and 36% of global energy consumption. Therefore, it is not surprising that the industry is motivated to embrace more environment-friendly procedures and turning to more environment-friendly materials and manufacturing processes. Driven by ever-stricter environmental norms and regulations, as well as rising costs, galvanizing is considered as an affordable, again, an environment-friendly and 'green' corrosion protection method. In order to prevent corrosion and produce a tough, long-lasting surface, clean steel is coated with a layer of molten zinc during the hot-dip galvanizing process. It has the extra benefit of completely covering the steel, making it more durable than conventional coatings that just adhere chemically or mechanically. As a result, it is not only very efficient but also very environment-friendly. A single, one-time treatment will completely coat a product's interior and exterior, giving it a coating that can shield steel and keep it from needing maintenance for more than 70 years. In this paper, galvanizing will be introduced as an efficient, affordable, and environment-friendly anti-corrosion method. Technical issues related to the process are presented and challenges associated with galvanizing are addressed. The experimental part includes measuring the zinc coating layer using optical microscopy. Failure cases related to galvanized structures which include bridges, bolts, and fire affected monopole are discussed, root causes were analyzed, and recommendations are provided.

Keywords: Corrosion; Galvanized steel; Failure analysis; Sustainability

1 Introduction

Corrosion is a natural phenomenon and has a great impact on society. Its impact includes economic, security, energy, health, safety, and environment (Maeda, 1996; Krylova, 2001; Moodley, 2019; Romero et al., 2006). In 2002, the US federal highway Administration (FHWA) released its study on the direct cost associated with metallic corrosion, which was estimated at $276 billion that is approximately 3.1 of the nation's Gross Domestic Product (GDP) (Sharma et al., 2014). Corrosion and weathering resistance are key characteristics that affect the strength and longevity of building structures, especially those composed of metal. Corrosion can occur in buildings and structures with exposed metal and concrete (Sherrawi et al., 2018).

Climate change may have a significant impact on the damage risks of concrete infrastructure and, as a result their durability and sustainability. In many cases, the scale of the change in risk should not be overlooked. Wang et al. (2012) studied the impact of climate change on the corrosivity of concrete infrastructure in Australia using a mathematical simulation model. The authors concluded that some

measures, such as new materials and structures, can be adopted. Cover design, mixing, coating, and cathodic protection were recommended to protect the existing structures. The material of choice for all engineers, designers, architects, and fabricators is structural steel. Affordability, ductility, and tremendous strength make steel the perfect material for building and construction. A wide range of steel parts and structures used in infrastructure, construction, and other fields are all long-term protected by general galvanized steel.

Galvanizing is a process of coating steel structures with zinc in order to prevent corrosion. The most popular method is hot dip galvanizing (HDG) in which a steel part is soaked in a molten zinc bath. The galvanizing layer acts as a barrier that keeps corrosive substances like Cl^- ions from reaching the matrix steel. The build-up of zinc anti-corrosion products from this would increase the ability of the galvanizing layer for protection. Additionally, the galvanizing layer serves as a sacrificial anode, corroding zinc rather than steel more favourably (Carpio et al., 2010; Adetunji, 2010; Shibli, 2015). Using galvanized steel dramatically lengthens wind turbine service life while reducing costly maintenance and downtime caused by corrosion. Additionally, galvanizing has long been used to protect steel transmission towers, which serve as the backbone of many of the world's power grids.

HDG has limitations, such as a relatively insufficient level of protection to withstand the harsher environmental conditions (Maaß & Peißker, 2011; Maeda, 1996; Krylova, 2001; Moodley, 2019; Romero et al., 2006). McDonald studied the effect of using galvanized bars in concrete and how corrosion behaviour of the coated bars is different from other anti-corrosion protection. The author concluded that by adopting advanced methods in concrete marine structure, long design life can be achieved (McDonald, 2011). Joseph et al. (2021) investigated the corrosion resistance of galvanized steel roofing sheets in acidic and rainwater environments. They concluded that the corrosion rate was lower in the rainwater environment comparing to the acidic environment. Way et al. recommended different practices to ensure adequate durability of galvanized steel structures used as steel framing in residential buildings. Their recommendations include maintaining the building envelop, avoiding direct contact with moisture, and preventing any direct contact between the galvanized structure and any aggressive or moist material (Way et al., 2009).

In addition to other design aspects such as having concrete structure with adequate thickness to protect the rebar, HDG forms a coating that isolates the steel bars from the surrounding concrete (Sharma et al., 2014; Hegyi et al., 2015; Yeomans, 2018). Ortlon performed a comparative study on the corrosivity of reinforced concrete with unprotected steel and hot-dipped galvanized steel. The authors concluded that hot-dipped galvanized steel bars show better corrosion resistance when tested using four different concrete compositions (Ortlon & Tutikian, 2017).

The collapse of bridges has made corrosion-related infrastructure failures most obvious on a global scale. There has been a history of corroded bridge failures, frequently resulting in fatalities (Lee et al, 2013; Zhang et al, 2022; Deng et al, 2016). When considering the entire life cycle of a bridge, both weathering steel and HDGS with a coating thickness of at least 200 µm provide significant advantages over conventional coating techniques. Suzumura and Nakamura (2004) investigated the environmental factors that affect corrosion behaviour of galvanized steel wires used in bridges. They concluded that the corrosion is related to the wire position inside the tension cables. Similar to other researchers, the authors found that corrosivity of the steel wires increases with the increase of sodium chloride content and temperature. Morgado and Brito (2015) studied the failure causes of pre-stressed steel cables of a suspension bridge that collapsed during use. They concluded that the predominant failure cause was stress corrosion cracking (SCC).

2 Experimental Work and Analysis

2.1 Visual Examination

Failed components were initially examined visually in *as-received* condition. In some cases, failed parts were cleaned with acetone and ultrasound cleaner. Fracture surface initially examined either visually and/or using a stereo microscope.

2.2 Metallography and Microstructural Analysis

Samples cut from the failed components were prepared for metallographic investigation by hot mounting, grinding, polishing, and etching. The grinding step was performed using silicon carbide emery paper starting with 240, 320, 400, 600, and 1000 grit. Polishing was performed using alumina suspension solution with particle sizes of 9, 6, 3, and 1 μm. An optical microscope (OM) equipped with image analyzer software and magnification power up to 1000x was used for optical microscopy analysis.

2.3 Hardness and Microhardness testing

Rockwell hardness scale HRB and HRC were used for hardness measurements. In some cases, small samples, and microstructural features in the range of a micro scale were tested using Vickers (Hv) microhardness machine equipped with a 136° pyramidal diamond indenter and a load of 10 kg.

2.4 Chemical Analysis and Scanning Electron Microscopy (SEM)

Chemical analysis of sections cut from the failed components were analyzed using a Spectro test spectrometer equipped with ultraviolet spark probe under argon gas. SEM examination was conducted using Tescan field emission scanning electron microscope (FESEM) equipped with energy dispersive spectroscopy (EDS) analysis for microanalysis.

3 Failure Cases

3.1 Case 1 - Fire-damaged Monopole

In this failure case, galvanized steel samples removed from a fire-damaged monopole were analyzed for the extent of damage. The HRB hardness, as well as the expected ultimate tensile strength (UTS) and yield strength (YS) were calculated based on the Vickers hardness values. It is found that these values closely correspond to the values obtained from the mill certificate. The result of one of the samples is shown in Table 2. The galvanized layer thickness measurements were performed as shown in Figure 1. The thickness of the sample was in the range between 188μm and 277 μm with an average of 208 μm which was in the specification range.

Table 1: Mechanical properties of the monopole material

Property	ID Hardness	MID Hardness	OD Hardness	Average Hardness Hv10	Average Hardness HRB	Estimated UTS (MPa)	Estimated YS (MPa)
Values	222	219	225	222	97.1	721	576

The microstructure analysis of the samples revealed a typical pearlitic structure in a banding form. Some other samples show evidence of spheroidization of pearlite, and others show evidence of carbides dispersed to the grain boundaries. Alterations of the microstructure due to heat would be evident in loss of the elongated pearlite banding generated during rolling operations. At elevated temperatures, the pearlite begins to spheroidize, or decompose into iron carbide particles that diffuse

to the grain boundaries as shown in Figure 2. The strength of the steel is typically lower due to spheroidization, but ductility is typically increased. Spheroidization only becomes a problem when large amounts of carbides are deposited along the grain boundaries, resulting in embrittlement and potential cracking. This is a problem commonly seen in furnace heating tubes that are exposed to elevated temperatures for thousands of hours (Yang & Liu, 2016; Nasiri & Mirzadeh, 2019]. Hence, even the worst heat-affected samples showed adequate hardness values and strengths to remain in service, as the minimum strength required is 300 MPa is.

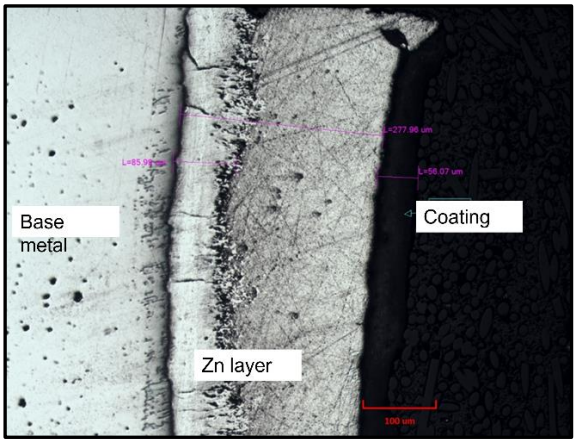


Fig. 1: Zinc layer thickness

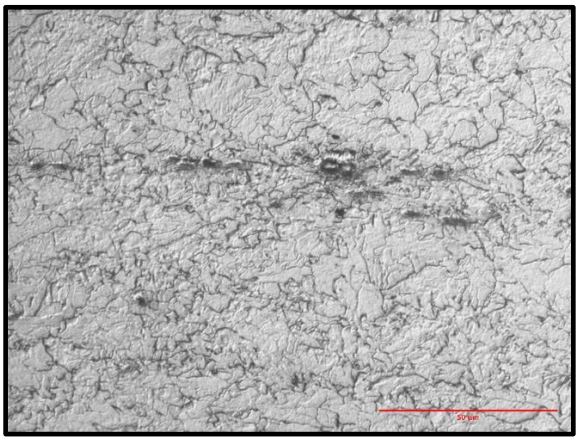


Fig. 2: Grain boundary carbide precipitates

3.2 Case 2-Corrosion Evaluation of Wrapping Wires of Mackay Bridge

This case involves corrosion evaluation of galvanized wrapping wires used to protect the tension wire cables in a Mackay bridge. Visual inspection shows clearly that the wrapping wires suffered corrosion. Figure 3 shows the sections, after cutting, with noticeable evidence of more corrosion at 6:00 o'clock than 12:00 o'clock positions. Figure 4 shows the galvanized cables and the wrapping wires used for protection as installed. The wrapping wires were zinc coated and painted orange. There are 61 cables inside the wrapping wires and wooden plates were placed inside the wrapping cables for separation. In addition to the wrapping wires, the cables show sign of corrosion, which is mostly associated with 6:00 o'clock position, evidence of localized corrosion was seen as shown in Figure 5 and Figure 6 respectively.

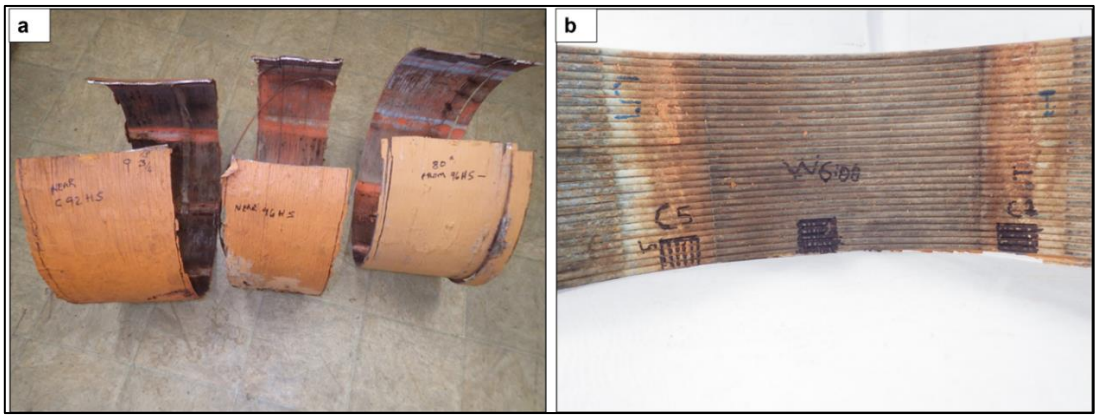


Fig. 3: Wrapping wires. **(a)** Sections cut; **(b)** wrapping wires show signs of corrosion

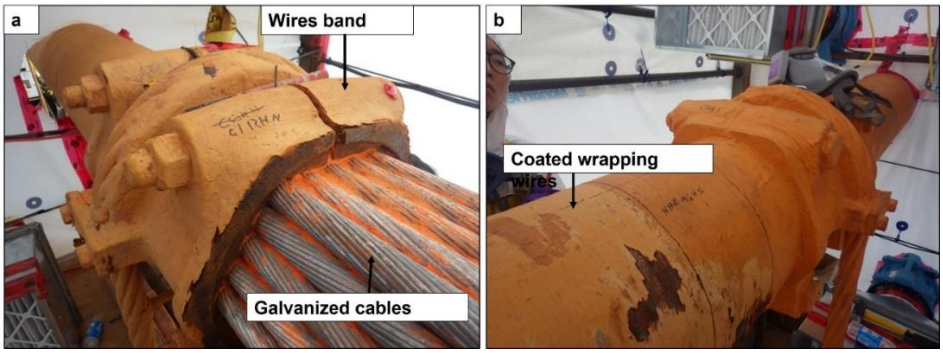


Fig. 4: Close up picture shows **(a)** exposed galvanized wires, **(b)** wrapping wires

The samples' locations were chosen to represent different positions such as 6:00, 4:00, and 12:00 o'clock. Each sample consists of 5 wires mounted together. Zinc layer thickness measurement was performed at the OD and ID on each wire. Five readings were taken at each side (OD & ID) which makes 50 measurements on each sample. The results show that the zinc layer thickness is higher on the outside (OD) than inside (OD). This is apparently due to the effect of paint on the outer side of the wrapping wires. Figure 7a shows optical micrograph of unaffected galvanized layer. However, some samples show complete deterioration of the galvanized layer and signs of pitting corrosion as shown in Figure 7b.

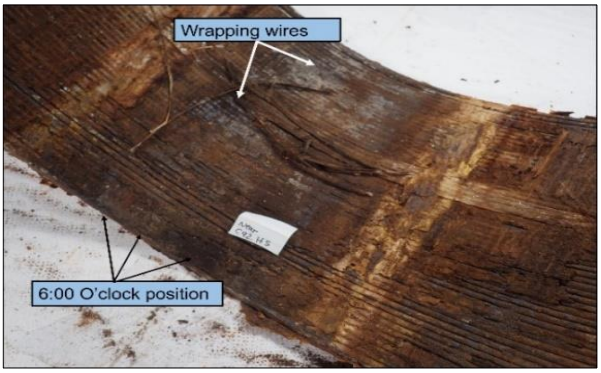


Fig. 5: Wires at 6:00 o'clock position

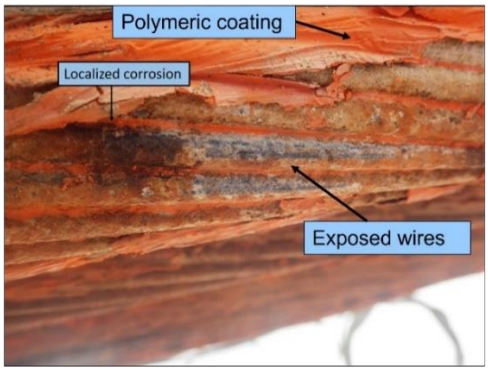


Fig. 6: Exposed wires show corrosion

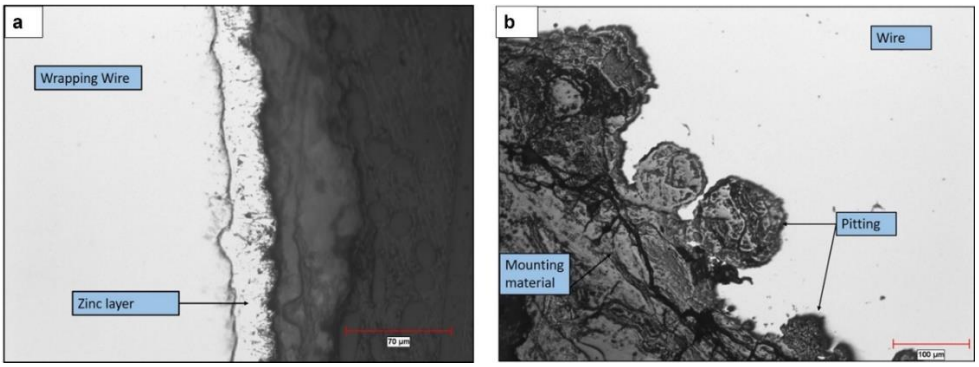


Fig. 7: Optical micrograph of, **(a)** zinc layer **(b)** corrosion pits formed on the wrapping wire

In general, bridge wires and cables are affected by atmosphere that contains acid rain, moisture, and dissolved gases. The exposure of the bridge wires to the de–icing salt and splash are considered as factors affecting corrosion. The main factor that contributes to corrosion of the wires is water entering the wrapping wires/cables and reacting with the cables. Water may enter the wires either as a liquid or as a vapour which may condense when the temperature drops. There was clear evidence that the wrapping wires did not provide enough protection to the cables and permitted water to penetrate. The

damage primarily starts due to the deterioration and depletion of the zinc coating layer which should prevent the wires from direct contact with the environment. The deterioration of the zinc layer is mainly due to contact with water which may contain dissolved carbon dioxide and sulfur dioxide. In conclusion, the wrapping wires will help to protect the cable wires as far as they can prevent water and humidity from getting into contact with the cable wires. Dehumidification is an option to minimize corrosion of the wrapping wires.

3.3 Case 3-High-strength galvanized bolt failure

This case represented galvanized bolts that fractured within very short time. The bolt in *as received* condition is shown in Figure 8. The bolt is classified as DG 10.9. Chemical composition analysis performed shows that the bolt is made from AISI 4140 alloy steel as shown in Table 2.

Table 2: Chemical analysis of the bolt material

Element (wt %)	C	Si	Mn	P	S	Cr	Mo	Ni	Cu	Fe
Failed bolt	0.401	0.271	0.733	0.012	<0.002	1.108	0.190	0.102	0.122	97.0

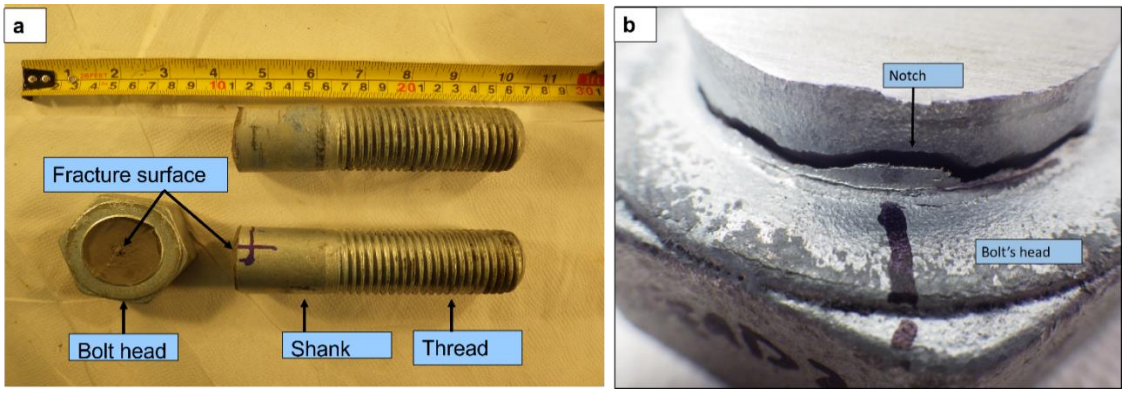


Fig. 8: Bolt as received **(a)** bolt parts, **(b)** fracture position and appearance

Microstructural analysis performed on the bolt material in its polished and etched condition did not show any abnormality in terms of inclusions, banded structure, or defects. The flow pattern observed from the macrographs suggest that bolts were manufactured by forging. Fracture surface examination shows a dis-coloured crescent-like zone that initiated at the edge of the bolt head and reached ~2 mm thickness in its center. To identify the nature of the crescent-like zone, the fracture surface examined under the SEM and EDS was used for the chemical analysis.

Figure 9 and Table 3 show the fracture surface and the EDS analysis, respectively. The result shows clearly that the crescent-like zone is rich in zinc (~50% by weight) and much thicker than the normal galvanized layer. This finding suggest that the crack happened during the galvanizing stage which consequentially allowed zinc to diffuse inside the crack. The crack eventually propagated and reached its critical length and the bolt failed. HDG cracks have been reported by many researchers (Elboujdaini et al., 2004; Elboujdaini et al., 1995; Carpio et al., 2010); one or more factors may contribute to HDG cracks. According to literature, local strain, hydrogen embrittlement, liquid metal embrittlement, etc. can act individually or together as a cause of cracking and failure (Mraz & Lesay, 2009).

It is reported that the cracking susceptibility during HDG increases with hardness and hence, a critical hardness threshold was proposed. Mraz proposed 34 HRC as a criterion for HDG cracking to start, the hardness measurement on the bolt material shows 39 HRC. This would suggest that the bolt

material is very susceptible to HDG cracking. Furthermore, ASTM F568M-02 standards does not recommend this type of steel (10.9) to hot dip galvanized due to its high strength and its high susceptibility for cracking during the galvanization process. In this case, other galvanizing options need to be considered such as thermal metal spry or painting.

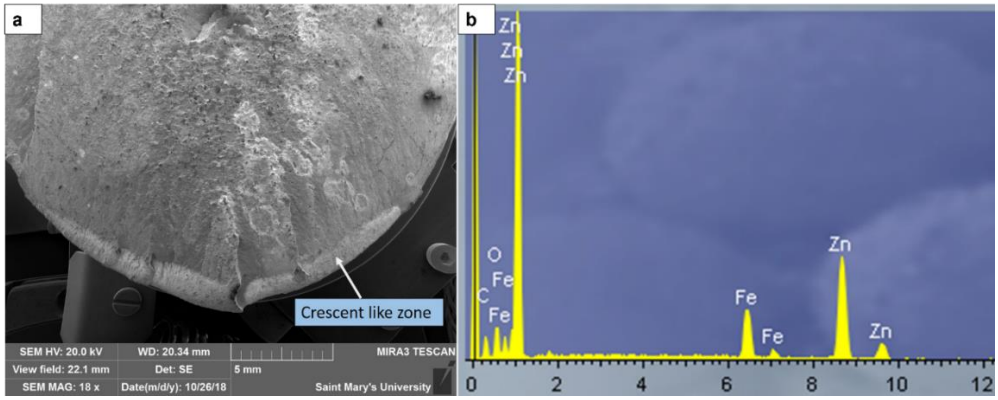


Fig. 9: SEM of the fracture surface, **(a)** Crescent-like zone **(b)** EDS shows presence of zinc

Table 3: EDS spectrum acquired from the crescent-like zone

Element	**O**	**Al**	**Cr**	**Mn**	**Fe**	**Zn**
Weight %	16.26	----	----	----	5.28	51.4

4 Conclusion

1 Galvanizing provides the most constant, effective, and affordable corrosion protection method for steel structures.

2 Galvanized steel can provide a sustainable solution for the construction industry as it needs less maintenance, last longer than other types of paints, and reduces time for maintenance.

3 Failure and root cause analysis provides information that can help to extend the life of infrastructure, reduce failure, and improve the sustainability.

References

Al-Sherrawi, et al. (2018). Corrosion as a Source of Destruction in Construction

Adetunji, O. R. (2010). Optimizing hot-dip galvanizing operations of steel sheets for better quality, *Journal of Natural Sciences Engineering and Technology*, *9*(2), 99-105

Carpio, et al. (2010). Stress corrosion cracking of structural steels immersed in hot-dip galvanizing baths, *Engineering Failure Analysis*, *17*(1), 19-27.

De Kayser Ortolan, V. & Tutikian, B. F. (2017). Comparative assessment of corrosion of concrete reinforced with unprotected steel and hot-dip galvanized steel, Revista de la Construcción. *Journal of Construction*, *16*(2), 238-248.

Deng, L., Wang, W. & Yu, Y. (2016). State-of-the-art review on the causes and mechanisms of bridge collapse, *Journal of Performance of Constructed Facilities*, *30*(2), 04015005.

Elboujdaini, M., Tyson, W.R., and Goodwin, F. (2004). Experiments on Delayed Failure during Galvanizing of Flame-Cut Structural Steels, 103-109.

Elboudjaini, M et al. (1995). "ZM-396: (Control of Cracking during Galvanised Structurals: Final Report Phase 2, 3 and 4b).

Moodley, K. (2019). (Advances in corrosion inhibition materials and technologies: A review. *Advanced Materials*

Letters, *10*(4), 231-247.

Hegyi, A., Păstrav, M., & Rus, M. (2015). Environmental And Economic Aspects Of Anticorrosion Protection By Hot-Dip Galvanized Method Rebars In Concrete, *Journal of Applied Engineering Sciences*, *18*(1).

Joseph, O. O., Dirisu, J. O., & Odedeji, A. E. (2021). Corrosion resistance of galvanized roofing sheets in acidic and rainwater environments, Heliyon, *7*(12), e08647.

Krylova, I. (2001). Painting by electrodeposition on the eve of the 21st century. *Progress in Organic Coatings*, *42*(3-4), 119-131.

Lee, et al. (2013). A study of US bridge failures: 1980-2012, Buffalo, NY: MCEER.

Maeda, S. (1996). Surface chemistry of galvanized steel sheets relevant to adhesion performance. *Progress in Organic Coatings*, *28*(4), 227-238.

Maaß, P. & Peißker, P. (Eds.). (2011). Handbook of hot-dip galvanization. John Wiley & Sons.

McDonald, D. B. (2011). Corrosion Protection for Concrete Structures in Marine Environments, In *Coastal Engineering Practice* (2011) (pp. 78-88).

Morgado, T. L. M. & e Brito, A. S. (2015). A failure analysis study of a prestressed steel cable of a suspension bridge, *Case Studies in Construction Materials*, *3*, 40-47.

Mraz, L. & Lesay, J. (2009). Problems with Reliability and Safety of Hot Dip Galvanized Steel structures, *Soldagem & inspecao* 14.2: 184-190.

Nasiri, Z. & Mirzadeh, H. (2019). Spheroidization heat treatment and inter-critical annealing of low carbon steel, *Journal of Mining and Metallurgy B*: Metallurgy, 55(3), 405-411.

Romero, et al. (2006). Behavior of Galvanized Steel in Tropical Marine Environments, *Materials Performance*, *45*(2), 24.

Sharma, R., Goodwin, F. E. & Dallin, G. W. (2014). Continuous Galvanized Rebar for Corrosion Control in RCC structures.

Shibli, S. M. A., Meena, B. N. & Remya, R. (2015). A review of recent approaches in the field of hot dip zinc galvanizing process, *Surface and Coatings Technology*, *262*, 210-215.

Suzumura, K. & Nakamura, S. I. (2004). Environmental factors affecting corrosion of galvanized steel wires, *Journal of Materials in Civil Engineering*, *16*(1), 1-7.

Wang, X., Stewart, M. G. & Nguyen, M. (2012). (Impact of climate change on corrosion and damage to concrete infrastructure in Australia), *Climatic Change*, *110*(3), 941-957.

Way, et al. (2009). Durability of Light Steel Framing in Residential Building.

Yeomans, S. R. (2018). Galvanized Steel Reinforcement: Recent Developments and New Opportunities, *Proceedings of 5th International Federation for Structural Concrete*, Melbourne, Australia.

Yang, C. C. & Liu, C. L. (2016). Optimization in Spheroidized Annealing of Two AISI 1022 Low Carbon Steels Used in Bolt Industry.

Zhang, et al. (2022). Causes and Statistical Characteristics of Bridge Failures: A Review, *Journal of Traffic and Transportation Engineering* (English Edition).

Cite as: Ibrahim A. & MacIntyre S., "Galvanized Steel as a Sustainable Material-Technology and Failure Analysis", *The 2nd International Conference on Civil Infrastructure and Construction (CIC 2023)*, Doha, Qatar, 5-8 February 2023, DOI: https://doi.org/10.29117/cic.2023.0102

Performance of Mild Steel and Corrosion-Resistant Steel Rebars in Chloride-Contaminated Concrete

Muazzam Ghous Sohail
Associate Professor, Department of Civil Engineering, Capital University of Science and Technology, Islamabad, Pakistan
Muazzam.sohail@cust.edu.pk

Nasser Al Nuaimi
AVP Research & Graduate Studies/ Associate Professor Department of Civil Engineering, Qatar University, Doha, Qatar
anasser@qu.edu.qa

Wael Alnahhal
Associate Professor, Department of Civil and Architecture Engineering, College of Engineering, Qatar University, Doha, Qatar

Ramazan Kahraman
Professor, Department of Chemical Engineering, College of Engineering, Qatar University, Doha, Qatar
ramazank@qu.edu.qa

Abstract

Reinforced concrete (RC) infrastructure in Arabian Peninsula is subjected to harsh climatic conditions of high temperatures, humidity, and airborne chlorides and there is a high concentration of salts in seawater and soils. These factors instigate corrosion of reinforcing steel in RC infrastructure at the early stages of the service life. To overcome the durability issues of RC infrastructures, corrosion-resistant reinforcing bars are employed. In this study, a comparison of microcell and macrocell corrosion of mild steel (MS) and two types of corrosion-resistant rebar namely the high chromium (HC) and stainless steel (SS) was established. Nine concrete block samples of $20 \times 10 \times 350$ mm were cast with top rows of reinforcements, the top row consists of MS, HC, or SS, and the bottom row contained only SS. Blocks were conditioned under 3.5% NaCl for 2 years and linear polarization resistance and macrocell currents were evaluated to compare the corrosion performance of mild and corrosion resistant steel rebars. It was observed that SS is the most corrosion-resistant steel rebar, where high chromium steel showed up to three times more corrosion resistance than mild steel under chloride attack.

Keywords: Corrosion of steel in concrete; High chromium steel; Stainless steel; Macrocell corrosion durability of reinforced concrete

1 Introduction

Chloride-induced corrosion is the major cause of concrete infrastructure deterioration. Corrosion causes spalling and cracking of concrete cover, which in turn reduces the serviceability of the structures. The repair cost to corrosion-damaged infrastructures is up to 3.5% of GDP in the US and up to 5% in the middle eastern region. Furthermore, the reduced service life of RC infrastructure has become a major burden on the economy (Al Hashem, 2011; Lim, 2012).

Concrete is inherently porous and allows several ionic species to diffuse or penetrate up to the steel surface. These ions, such as chlorides, CO2, and other gases cause the corrosion of steel. Even high-

performance concrete is prone to cracking (Sohail et al., 2018b, 2020b). That is why the rebars need to be corrosion-resistant under harsh climatic conditions (Ghous Sohail et al., 2022; Sohail et al., 2018a).

Stainless steel (SS) and high chromium (HC) steel are the two main candidates for this purpose. The SS has chromium contents of up to 18% while the HC has up to 9%. These additions reduce the corroding tendency of these two types of steel compared to mild steel. Mild steel has chromium from 0 to 1% max (Mohamed et al., 2013; Team, 2007; Sohail et al., 2019).

Several researchers have evaluated the corrosion performance of SS and HC in comparison to MS. The manufacturers of HC have suggested that its performance in resisting corrosion is similar to SS. However, other researchers have shown that its corrosion is up to 2-3 times higher than MS and several levels less than stainless steel (Cui & Krauss, 2008; Nachiappan & Cho, 2005; Sohail et al., 2020a, 2021). Fahim et al. (2019) tested in corrosion performance of MS, HC, 316 LN SS, 304 SS, and XM 28 SS in concrete pore solution, in cracked and uncracked concrete. The composition of steel rebar played a significant role in the chloride threshold values that initiate corrosion, the passive layer formation, and the corrosion rates. Sohail et al. (2020) observed that the corrosion resistance of HC is two times higher than MS under a chloride solution.

In this study, the corrosion performance of mild steel, high chromium steel and stainless was evaluated while under chloride attack. The acceleration was carried out in such a way that it matches the natural corrosion of steel in concrete. The southern exposure tests were applied on the concrete block samples, which comprised wetting and drying for two years under 3.5% NaCl solution. The geometry of block samples and reinforcement placement was also kept in such a way that it simulates the real condition in RC structures. The results of this study will help engineers and designers select the reinforcement type for the conditions encountered in the field. Especially in locations where corrosion due to chloride is a durability concern.

2 Experimental Detail

Three concrete block samples of $20 \times 10 \times 30$ cm were cast; the mold is shown in **Fig. 1**. Two reinforcement rows were fixed in the mold. The top was the bars to be studied while at the bottom for the reference to measure the macrocell corrosion were the stainless steels. Each bar was connected to an electric wire for electrochemical measurements. The length of each rebar was 30 cm and the diameter of 16 mm.



Fig. 1: Mold for block samples with a top row with either mild steel/high chromium/stainless steel, and a bottom row with stainless steel only

Concrete was cast using cement CEM I N42.5 from a local manufacturer. San was 0/4 mm, while aggregates were 4/10 mm. The water-to-cement ratio was 0.65 to keep the concrete flowable. The compressive strength at 28 days was 23 MPa.

The steel composition is given in **Table 1**. The MS, HC, and SS had chromium contents of 0.013, 9.54, and 18.180, respectively. This is the most significant variance in all the steel types. There are several other elements/constituents are there that are different in each steel type. The yield and tensile strengths of steel were respectively 561 and 664, 937 and 1158, and 609 and 738 for MS, HC, and SS, respectively.

Table 1: Chemical composition of studied steel types

Steel Type	1. Chemical Composition (%)													
	C	**Si**	**Mn**	**P**	**S**	**V**	**Nb**	**Cu**	**Ni**	**Cr**	**Mo**	**N**	**CE**	**Co**
MS	0.2	0.14	0.66	0.011	0.014	-	-	0.025	0.021	0.013	-	0.006	0.32	-
SS	0.020	0.290	-	0.0390	0.0240	-	-	0.520	8.010	18.180	0.340	-0.0830	-	0.180
HC	0.1	0.41	0.57	0.011	0.009	0.27	0.019	0.16	0.1	9.54	0.02	0.019	1.15	-

2.1 Conditioning of Block Samples

Samples were conditions under 3.5% NaCl solution. The wetting and drying cycle was applied for two weeks each. The corrosion state was monitored regularly during the testing by open circuit potentials (OPC). Once the OPC falls in a range for mild steel that the corrosion is 100% guaranteed, other electrochemical tests were performed.

2.2 Linear Polarization Resistance/Microcell Current Measurements

Linear polarization resistance (LPR) was applied after corrosion was initiated on each rebar in the block samples. Three electrodes set up were used to obtain the LPR/R_p values. Gamry® 3000 potentiostat was used to perform these experiments. The reference electrode (RE) was the saturated calomel electrode (SCE), while the counter electrode (CE) was titanium mesh. The mesh was placed at the top surface of the concrete block, which is near the top row of reinforcement. RE electrode was placed in the water in which block samples were immersed. A polarization of $\pm$ 20 from OCP was applied to rebars to perturb the system and currents were measured.

2.3 Macrocell current

The top rebars after corrosion were connected to the bottom bar to measure the macrocell corrosion current in each type of steel rebar. In this study, the results of only one rebar from the top row connected to a rebar at the bottom row are presented. That is the anode-to-cathode ratio is 1. This will compare the real-time corrosion behavior of steel rebars. Gamry® 3000 potentiostat was used for these experiments. The block samples were kept immersed under water till the top reinforcement row during the experiments. The macrocell between the top and bottom bar was measured until the current become stable.

3 Results and Discussion

3.1 Linear Polarization Resistance (LPR)

The typical results of LPR spectra are shown in Fig. **2**. It can be seen that the range of current range for SS was at least an order lower than the currents observed in the MS and HC. Principally the LPR curves should be straight lines as the polarization increase current should increase linearly around the OCP (Sohail, 2013). However, the LPR curves are slightly crooked at the cathodic polarization side, this is due to the experimental setup of titanium mesh which injects the current

that might get astray and results in a slightly nonlinear part in the curve. The Rp values were calculated on the straight/linear portion of the curve.

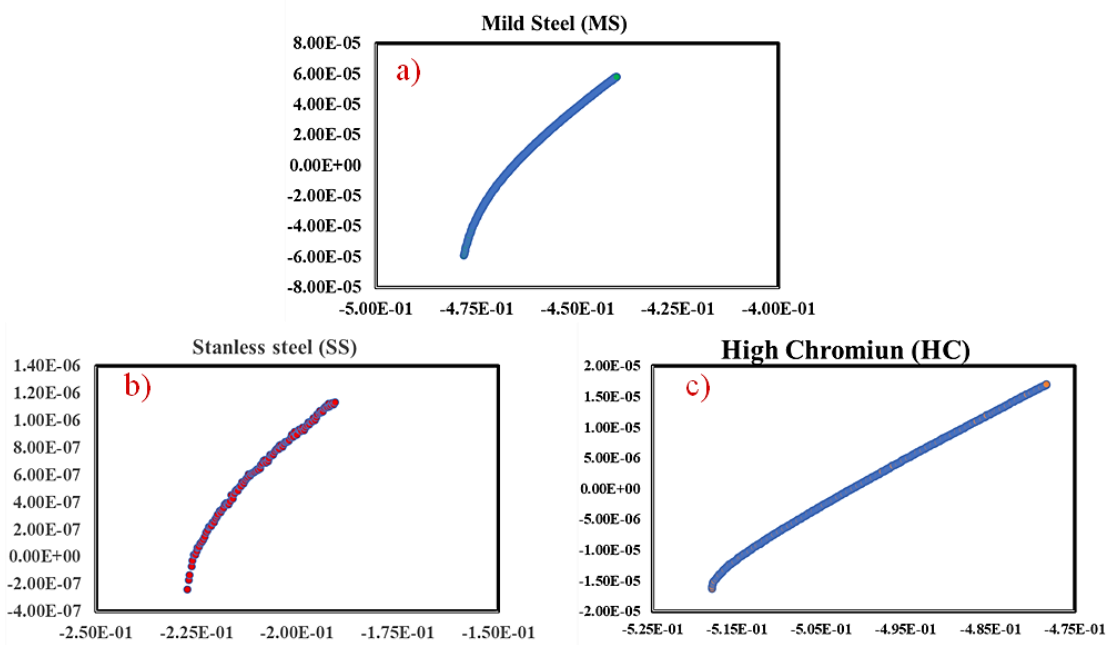


Fig. 2: Linear polarization resistance (LPR) curves. The slope of the LPR curve provides Rp values

The extracted polarization resistance, Rp, is shown in Fig. **3**, for three types of steel rebars. The values were 417, 1294, and 3414 Ohms from MS, HC, and SS, respectively. As the Rp value increases the resistance to corrosion is increased, and vice versa. The polarization resistance is more for SS compared to HC and MS. This is due to a higher amount of chromium in its composition. The HC showed three times higher resistance compared to MS. Sohail et al. (2020) demonstrated that HC has 2-3 times higher corrosion resistance compared to the MS. Which is similar to the results in this study.

Fig. **4** shows the microcell corrosion current extracted from the LPR/Rp values. The values are 62.47, 20.13, and 0.763 µA for MS, HC, and SS respectively. With these values, the corrosion rate is 0.01894, 0.006104, and 0.001143 mm/year respectively for MS, HC, and SS. This shows how fast the rebars will lose their cross-sectional area under active corrosion due to the chloride attack. Losing area will increase the corrosion products in concrete, hence increase the spalling, and cracking in the concrete cover.

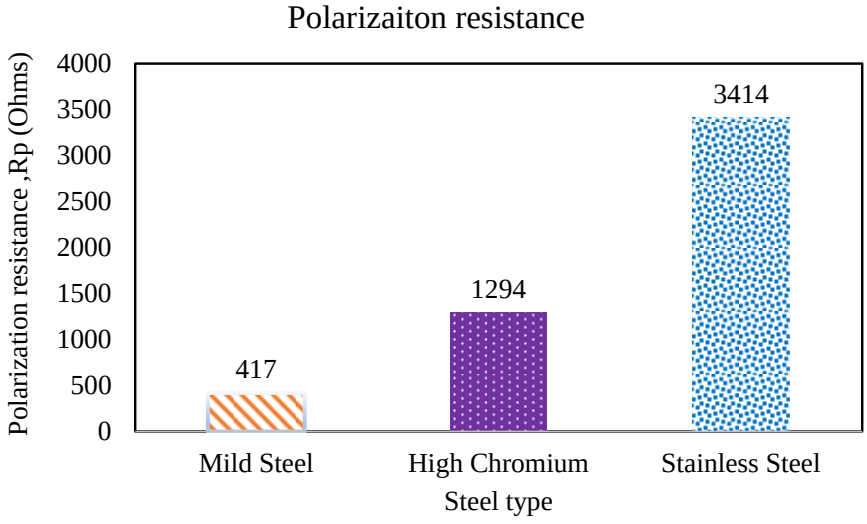


Fig. 3: Polarization resistance of mild steel, high chromium, and stainless steel in the active corrosion state under chloride attack

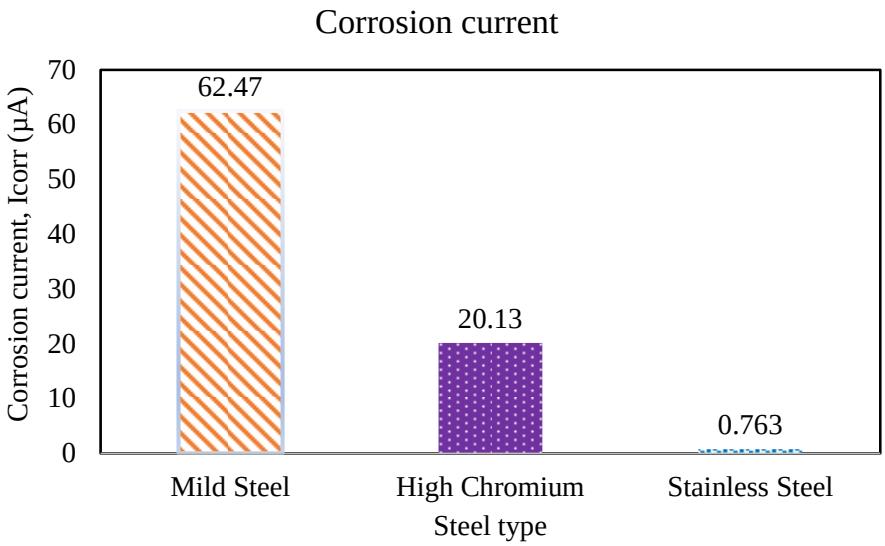


Fig. 4: Microcell corrosion current calculated based on the Rp values in mild steel, high chromium steel, and stainless steel

Fig. 5 presents the macrocell corrosion current in the MS, HC, and SS rebars in the block samples with an A/C ratio of 1. The top bar in the concrete block was connected to the bottom bar directly underneath the top bar. The current was measured until the values are stable between bars.

It is clear that SS performed much better than the other two bars. Its macrocell current was also in nano ampere (nA). Whereas, the macrocell current in the MS and HC was 60 µA and 10 µA, respectively. The macrocell current MS is 6 times higher compared to the HC. Macrocell corrosion causes higher loss in weight and cross-sectional area of steel rebars (Sohail et al., 2015). Hence, the macrocell is more damaging to reinforcement as compared to the microcell corrosion current.

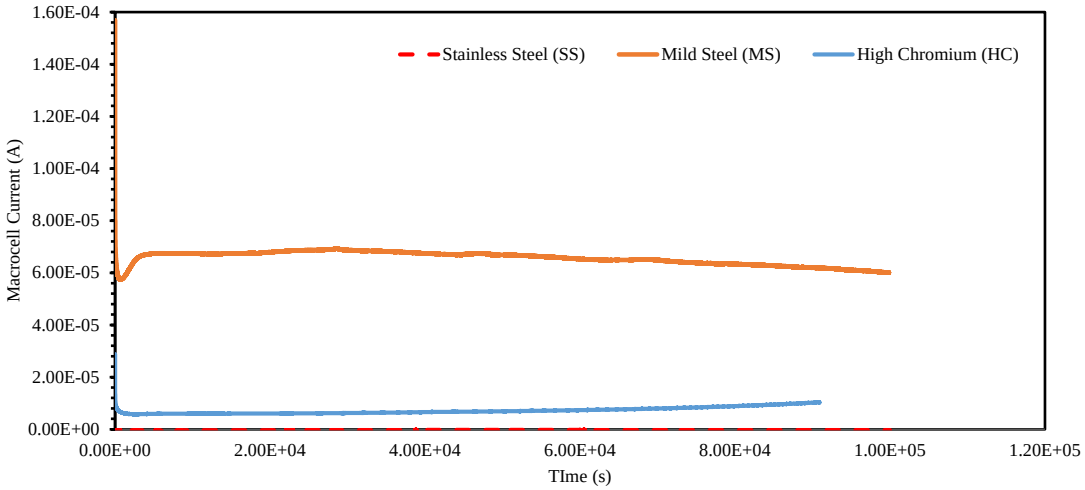


Fig. 5: Macrocell corrosion in block samples with an anode-to-cathode ratio of 1

4 Conclusion

Accelerated corrosion was induced using wetting and drying cycles in the concrete samples reinforced with either mild steel, high chromium steel, or stainless steel rebars. After two years of conditioning, the samples were electrochemically tested with linear polarization resistance, and macrocell current was measured.

Results show that the high chromium steel could be a viable solution as reinforcement where the

chloride environment is encountered and corrosion of mild steel is a concern. Stainless steel has performed better than mild and high chromium steel in harsh environments. However, the cost of stainless steel might hinder its use in normal construction. However, for important mega structures subjected to harsh environments, it could be employed to enhance durability.

References

Al Hashem, A. (2011). "Corrosion in Gulf Cooperation Councel (GCC) state: Statistics and figures." *The Corrosion UAE*, Abu Dhabi, UAE.

Cui, F. & Krauss, P. (2008). *Comparative Corrosion Testing and Analysis of MMFX 2 Rebars for Reinforced Concrete Applications*.

Fahim, et al. (2019). "Corrosion resistance of chromium-steel and stainless steel reinforcement in concrete." *Materials and Corrosion*, John Wiley & Sons, Ltd, *70*(2), 328–344.

Lim, H. L. (2012). "Assessing Level and Effectiveness of Corrosion Education in the UAE." *International Journal of Corrosion*, Hindawi, 2012, 1–10.

Mohamed, N., Boulfiza, M. & Evitts, R. (2013). "Corrosion of carbon steel and corrosion-resistant rebars in concrete structures under chloride ion attack." *Journal of Materials Engineering and Performance*, Springer US, *22*(3), 787–795.

Nachiappan, V. & Cho, E. H. (2005). "Corrosion of High Chromium and Conventional Steels Embedded in Concrete." *Journal of Performance of Constructed Facilities*, *19*(1), 56–61.

Sohail, M. G. (2013). "Corrosion of steel in concrete: development of an accelerated test by carbonation and galvanic coupling." PhD Thesis, Universite de Paul Sabatier, Universite de Toulouse III.

Sohail, et al. (2015). "Significance of macrocell corrosion of reinforcing steel in partially carbonated concrete: numerical and experimental investigation." *Materials and Structures*, *48*(1–2), 217–233.

___. (2019). Corrosion performance of mild steel and epoxy coated rebar in concrete under simulated harsh environment. International Journal of Building Pathology and Adaptation, 37(5), 657–678. https://doi.org/10.1108/IJBPA-12-2018-0099

___. (2018a). "Reinforced Concrete Degradation in the Harsh Climates of the Arabian Gulf: Field Study on 30-to-50-Year-Old Structures." *Journal of Performance of Constructed Facilities*, American Society of Civil Engineers (ASCE), *32*(5), 04018059 (1–12).

___. (2018b). "Advancements in Concrete Mix Designs: High-Performance and Ultrahigh-Performance Concretes from 1970 to 2016." *Journal of Materials in Civil Engineering*, *30*(3), 04017310.

___. (2020a). "Electrochemical behavior of mild and corrosion resistant concrete reinforcing steels." *Construction and Building Materials*, Elsevier Ltd, 232.

___. (2020b). "Durability characteristics of high and ultra-high performance concretes." *Journal of Building Engineering*, 101669.

___. (2021). "Electrochemical corrosion parameters for active and passive reinforcing steel in carbonated and sound concrete." *Materials and Corr osion*, John Wiley & Sons, Ltd, 1–18.

___. (2022). "Behavior of artificially corroded RC beams strengthened with CFRP and hybrid CFRP-GFRP laminates." *Engineering Structures*, Elsevier, *272*, 114827.

Team, P. E. (2007). "Purdue e-Pubs MMFX Microcomposite Steel (MMFX2)."

Cite as: Sohail M.G., Al Nuaimi N., Al-Nahhal W. & Kahraman R., "Performance of Mild Steel and Corrosion-Resistant Steel Rebars in Chloride-Contaminated Concrete", *The 2nd International Conference on Civil Infrastructure and Construction (CIC 2023)*, Doha, Qatar, 5-8 February 2023, DOI: https://doi.org/10.29117/cic.2023.0103

Bio-Based Self-Healing Concrete for Sustainable and Durable Concrete Infrastructure

MuazzamGhousSohail
Department of Civil Engineering, Capital University of Science and Technology,
Islamabad, Pakistan
Muazzam.sohail@cust.edu.pk

Nasser Al Nuaimi
VP Graduate Studies, Associate Professor Department of Civil Engineering,
Qatar University, Doha, Qatar
anasser@qu.edu.qa

Ramazan Kahraman
Professor, Department of Chemical Engineering, College of Engineering,
Qatar University, Doha, Qatar
ramazank@qu.edu.qa

Zulfa Al Disi
Postdoctoral Researcher, Department of Biological and Environmental Sciences,
College of Arts and Sciences, Qatar University, Doha, Qatar
zaldisi@qu.edu.qa

Nabil Zouari
Professor, Environmental Sciences Program, Department of Biological and Environmental Sciences,
College of Arts and Sciences, Qatar University, Doha, Qatar
Nabil.Zouari@qu.edu.qa

Bora Genturk
Associate Professor, Sonny Astani Department of Civil and Environmental Engineering,
University of Southern California, Los Angeles, California, USA
gencturk@usc.edu

Debora F. Rodrigues
Associate Professor, Department of Civil and Environmental Engineering, University of Houston,
Houston, Texas, USA
dfrigiro@central.uh.edu

Yucel Yildirim
Handar Engineering & Contracting WLL, Doha, Qatar
yyildirim@handar.com.tr

Abstract

In this study, bio-self-healing concrete was manufactured using a natural phenomenon called microbial-induced calcium carbonate precipitation (MICP). The *bacillus cereus* bacteria isolated from Qatari soil was used for this purpose. These bacteria have endured the harsh weather of high temperatures, humidity, and alkaline soil conditions. Hence, are a potential candidate for long-term self-healing in concrete structures that are subjected to the climate of the Middle Eastern region. The bacteria were encapsulated in sodium alginate beads then the beads were added to the cement-sand mortar. The nutrients for bacteria such as urea, calcium nitrate, yeast extract, and calcium chloride were mixed in mortar as dry constituents. After curing for 28 days, cracks were artificially induced in the prismatic samples, which were reinforced with steel rebars at the tensile side. Samples were placed in water to instigate self-healing. It was observed that the bacteria healed the cracks up to 0.70 mm. It is concluded that the used bacteria are viable in the alkaline concrete matrix and capable of producing calcium carbonate.

Keywords: Bio Self-Healing Concrete; MICP; *Bacillus Cereus;* Autonomous Crack Filling; Infrastructure Durability

1 Introduction

Reinforced concrete (RC) infrastructure in the Middle Eastern Region suffers cracking under the harsh climate of high temperature, humidity, and chloride environment. Cracks are generated in concrete under mechanical, as well as, environmental loading. These cracks allow the ingress of deleterious agents into concrete, which in turn cause the corrosion of reinforcing steel rebars. Once corrosion is initiated the durability of the RC structure is drastically reduced (Sohail et al., 2018, 2022a). Several remedies are available to enhance the lifespan of RC structures, namely strengthening with carbon fibers using repair mortar, or injecting the epoxy/slurry into the cracks (Sohail et al., 2021; Al Nuaimi et al., 2021 . However, these solutions do not protect against cracking and subsequent corrosion as the surface area of exposed concrete is so large that it is physically impossible to cover.

Autonomous self-healing using bacterial strains has emerged as a potential candidate to overcome the cracking issues of concrete under service (Tziviloglou et al., 2016; Van Tittelboom et al., 2010). The healing is done by the metabolism of bacteria who consume nutrients and produce calcium carbonates in the cracked portion. Calcium carbonate is inherently a binding material in itself and bonds with the cement matrix and hence concrete gets healed. This calcite precipitation is called microbial-induced calcium carbonate precipitation (MICP) (Wiktor & Jonkers, 2011; Wen et al., 2019; Sohail et al., 2022bb).

Several naturally occurring bacterial strains are capable of producing MICP under a suitable environment. Most commonly used are *Sporocarsinapastuerii* and most of the *bacillus genes*. The pathway for producing MICP is the urea decomposition by the urease enzymes produced by bacteria (De Belie & Wang, 2016; Tittelboom et al., 2016). The living cells produced enzymes through metabolism, which then work as a catalyst in the hydrolysis of urea into ammonia and carbonate, the pH of the surroundings is then increased. Ammonia (NH4+) and CO_3^{2-}(carbonic acid) are formed after upon further hydrolysis of urease. The bacterial walls are charged negatively, the form a bond with the cations of Ca^{2+}, and reach with CO3 ions and calcium carbonates (Anbu et al., 2016).

Among the MICP-forming bacteria, not all can produce calcites under a highly alkaline environment which is encountered in concrete. That is why they are needed to be encapsulated in the polymeric beads and then incorporated in to the concrete matrix. The beads used in literature are of different materials, sizes, and shapes. A few examples of encapsulating materials are ethylene oxide and propylene oxide (Wang et al., 2014b), silica sol-gel (Yang et al., 2011), lightweight clay particles (Tziviloglou et al., 2016), hydrogels (Wang et al., 2014a), engineered aggregates (EA) Pan et al., 2023), glass granules (Zhang et al., 2021), and expanded per lite (Alazhari et al., 2018). Sodium alginates, carrageenan, and chitosan are biopolymers that are used as carriers of healing agents.

In this study, a locally available *bacillus cereus* strain that was isolated locally from Qatari soil was studied for calcite precipitation in concrete. These strains have the advantages that they are weathered and evolved under a harsh climate of high temperature, humidity, salty environment, and high pH soils. Hence, it is expected that these strains will be viable in high-pH of concrete and could produce calcite precipitation in cracks. These strains were encapsulated in sodium alginate

beads. These strains are never been used in concrete, especially for application in the Middle Eastern Region. Bio self-healing concrete made *bacillus cereus* isolated from Qatari soils can arrest the degradation problem in structures subjected to Middle Eastern climates.

2 Experimental Detail

2.1 Bacterial Strains and Sodium Alginate Beads

The *bacillus cereus* bacteria were selected because already showed calcite precipitation in previous works where soil stabilization was performed with MICP. The *bacillus cereus* strains performed MICP at 40˚C in the field in previous works (Oualha et al., 2020; Bibi et al., 2018). These bacteria were preserved in 30% glycerol at –80° in the Qatari Mineral Precipitating Strains Bank. They were then revived as fresh living cells by striking them on a medium of Luria-Bertani (LB).

The growth media, Luria Bertani, and Urea Medium were used to grow the strains before adding in the beads. The LB was comprised of NaCl (5 g/l), tryptone (10 g/l), and yeast extract (5 g/l) whereas UM contained NaCl (5 g/l), Peptone (2 g/l), glucose (1 g/l), KH_2PO_4 (2 g/l), and of Urea (20 g/l). After that, the strains were recovered and inoculated in liquid media so that they could be placed in sodium alginates.

The beading procedure is presented in Fig.1. The sodium alginate of 1 % by weight was mixed in 1 litre of autoclaved water. A magnetic stirrer was placed in the bottle to mix the alginates homogeneously once the spores were formed in the urea media. The mixture of bacterial spores inside the media was added to the sodium alginates. They were stirred for 15 minutes. Then the mixture was introduced into a 2% calcium chloride solution, drip by drip, as shown in Fig.1a. Fig.1b shows the bead in the CaCl2 solution, and Fig.1c shows the dried bead.

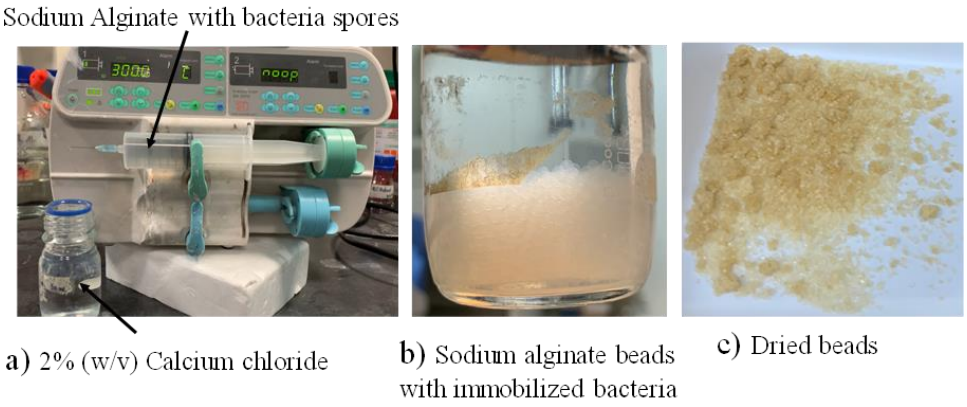


Fig.1: Procedure for encapsulation of bacteria in the sodium alginate beads, a) sodium alginate was dripped in to 2% calcium chloride solution, b) fresh beads, c) dried beads

Nutrients for the bacterial strains were mixed into the mortar. The nutrients such as urea, yeast and calcium nitrate were introduced as dry ingredients in the cement-sand mortar. Several researchers used the selected nutrients for bacteria. The selected amount was sufficient for bacteria to get food and grow.

2.2 Mortar for the Self-Healing Process

Table 1 shows the mortar mixture used in this study. A ratio of 1:2.5 of cement/sand was selected, whereas, water/cement ratio was 0.5. Three mixes were prepared, the control mix was cement, sand, and water. The second mix was comprised of urea, yeast, and calcium nitrate while keeping the other ingredient the same as the control mix. One mix was prepared by adding sodium alginate

beads containing *bacillus* species from local soil. The nutrients were mixed in a mortar in a dry state. The beads were dried before adding in mortar. The urea and yeast were 27 g and 4 g per cement weight, respectively, whereas, calcium nitrate was 33g by weight of cement.

Table 1: Concrete mix proportion for self-healing through bacterial strains

Number of mixes	Mortar Mix type	Cement in grams	Sand in grams	Water-cement ratio	SP (g)	Sodium Alginate Beads (g)	Urea in grams	Yeast Extract (g)	Calcium Nitrates (g)
1	Control mix	666	1665	333	10	-	-	-	-
2	Control + nutrients (CN)	666	1998	400	10	-	27	6	33
3	Control + nutrients + *B. cereus*	666	1665	333	10	16	27	6	33

2.3 Mortar Samples for Generating Cracks

The compressive strength was evaluated by casting and testing 50 x 50 x 50 mm cube samples following ASTM C109/C109M-02. (2002). Beads and Nutrients may affect the strength adversely, which is why compressive strength is essential to measure. To generate the cracks in the mortar matrix, prism samples of 40 x 40 x 160 mm were cast having steel rebar at the tensile side. The steel rebar was 4 mm in diameter and 15 mm in length. Bars were placed in their location with the help of fixing wires. Cube and prism samples were cured for 28 days by immersion in distilled water. Three cube samples were tested for each mix. Whereas prism samples were loaded using four-point bending using a manual hydraulic machine as shown in **Fig. 2**. The load was applied manually upto 5 MPa until the 3 to 5 cracks appeared in the mortar matrix. Formed cracks were between 50 to 1000 µm. Cracks appeared in the shear zone as no shear reinforcement was provided. All the prism samples were placed underwater for 3 days to increase the urease activities of the bacteria and observe if, there is, any mineral precipitation.

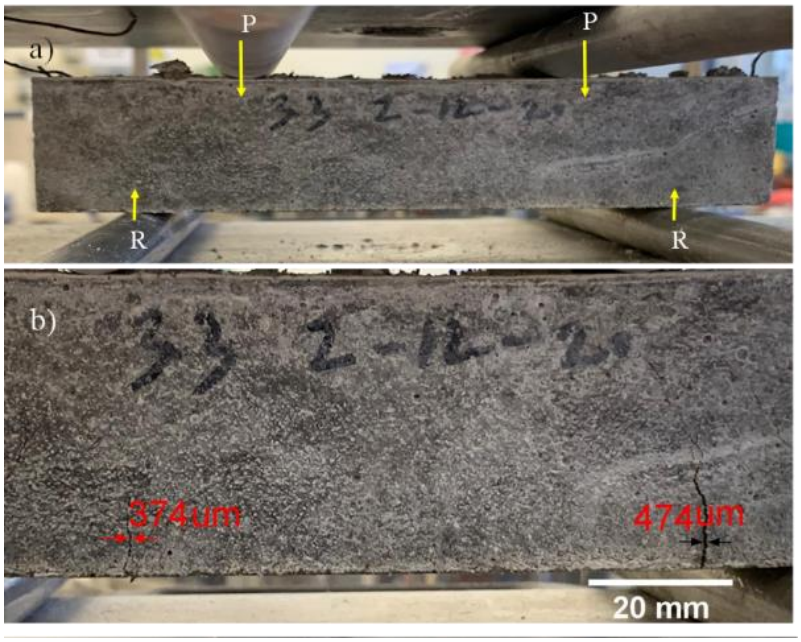


Fig. 2: a) prism samples under four-point loading for cracks formation. Crack generation in prism samples. b) Cracks up to 474 µm in the samples with *bacillus cereus*

2.4 SEM and XRD on the Cracked Surface

Broken samples from the cracked portion weres taken for SEM and XRD analysis. White precipitation was also analysed under XRD.

3 Results And Discussion

After the cracks were generated in the prisms, they were immersed under double distilled water this would instigate the transfer from spores to living cells of bacteria. The samples of mortar without beads (control), with only nutrients, and samples with only beads were also placed underwater after cracking. The samples having spores of *bacillus* are shown in **Fig. 3**.

Fig. 4 shows the sample of the beads containing bacillus cereus after immersion in water for 14 days. It can be observed that the formed cracks are filled with white precipitates of calcium carbonates. The cracks were filled where they passed through the beads. Cracks from 170 to 683 µm were filled with local strains.

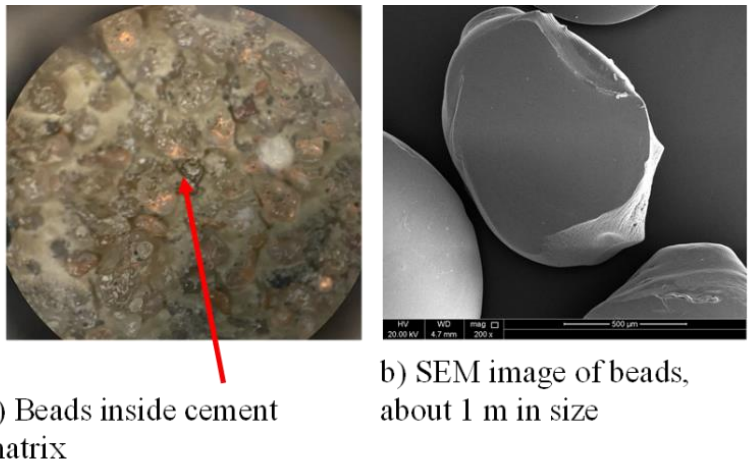


Fig. 3: a) Beads survival in mortar matrix under the microscope, b) SEM image of a bead before adding in mortar

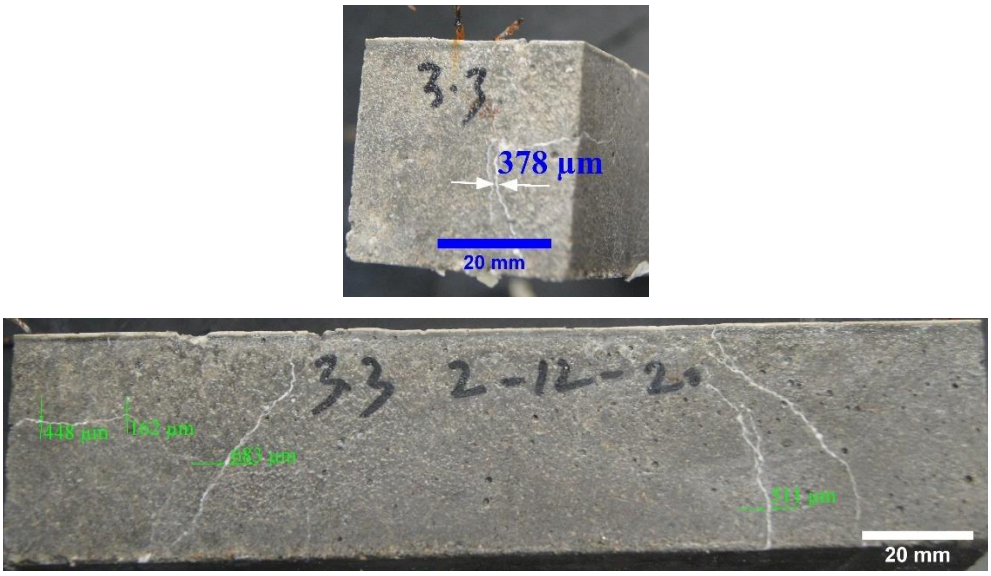


Fig. 4: The prism samples showing the self-healing of the cracks with local bacterial strains. The cracks of up to 680 microns were filled with calcium carbonates

Fig. 5 shows the SEM and EDX analysis of bacterial surroundings. It can be seen that bacteria were viable in the cement matrix. The presence of magnesium and phosphates in EDX analysis confirms the bacteria in concrete (**Fig. 5**b). **Fig. 5**c shows the hexagonal crystalline structure of calcium carbonates. **Fig. 5**d shows the EDX analysis of the white precipitates of calcium carbonates.

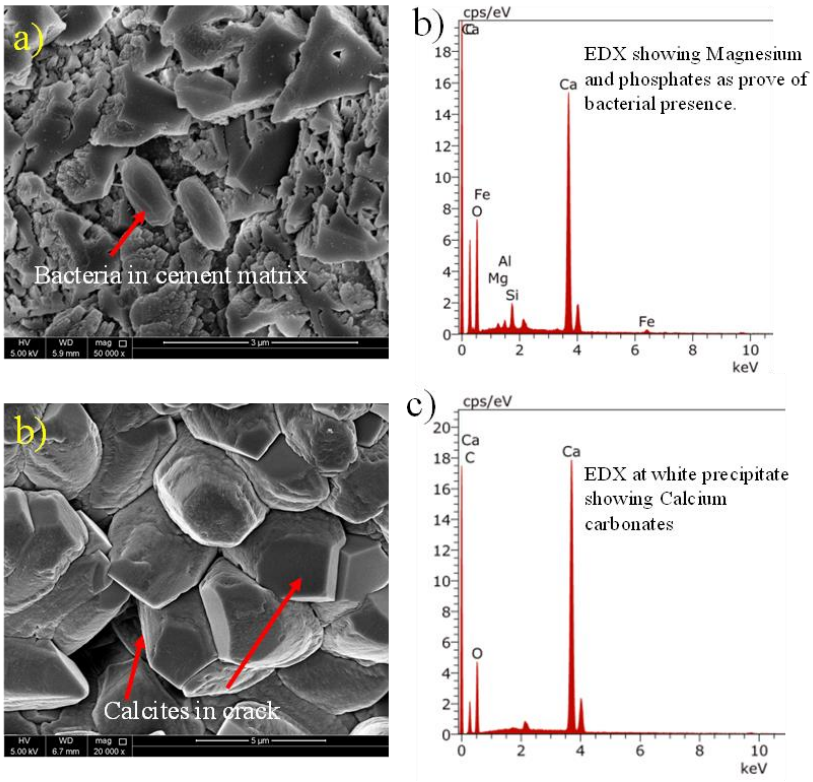


Fig. 5: a) SEM of bacterial survival in a cement matrix, b) EDX of bacterial surroundings, c) Calcium carbonate mineral (crystalline shape), d) EDX of calcium carbonate mineral

The XRD analysis of white precipitates filling the cracks was performed. Fig. **6** shows the XRD spectra of the material filling the cracks for *bacillus.* The materials were similar in mineralogy, that is, calcium carbonate.

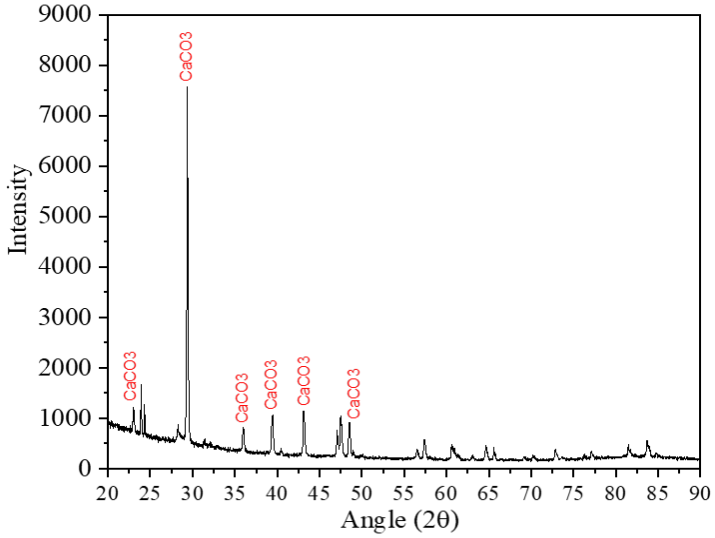


Fig. 6: XRD spectra of crack filling material in samples with local strains of bacillus cereus

4 Conclusion

The bio self-healing concrete is the need of the hour to arrest the degradation and enhance the infrastructure durability in the Middle Eastern Region. In this study, local bacterial strains of *bacillus cereus* were embedded in sodium alginate beads and then these beads were incorporated into the cement mortar. Then cracks were generated in the prism samples and placed in the water.

It was observed that locally isolated *bacillus cereus* from Qatari soil could survive in the cement matrix and also could perform healing of cracks. Crack from as small as 70 µm to 683 µm were healed with a white precipitate formed by bacteria in the cracks. Hence, the proposed bio-self-healing concrete could enhance the durability of RC structures subjected to harsh climatic conditions.

References

Alazhari, et al. (2018). "Application of Expanded Perlite Encapsulated Bacteria and Growth Media for Self-Healing Concrete." *Construction and Building Materials 160* (January): 610–19. https://doi.org/10.1016/J.CONBUILDMAT.2017.11.086.

Al Nuaimi et al. (2021). *Durability of Reinforced Concrete Beams Externally Strengthened with CFRP Laminates under Harsh Climatic Conditions.* Journal of Composites for Construction, 25*(2), 04021005. https://doi.org/10.1061/(ASCE)CC.1943-5614.0001113*

Anbu, et al. (2016). "Formations of Calcium Carbonate Minerals by Bacteria and Its Multiple Applications." *SpringerPlus 5:15* (1): 1–26. https://doi.org/10.1186/S40064-016-1869-2.

ASTM C109/C109M-02. (2002). "Standard Test Method for Compressive Strength of Hydraulic Cement Mortars." *Annual Book of ASTM Standards* 04: 1–6. https://doi.org/10.1520/C0109_C0109M-20B.

Belie, N. De & J. Wang. 2016. "Bacteria-Based Repair and Self-Healing of Concrete." *Journal of Sustainable Cement-Based Materials 5* (1–2): 35–56. https://doi.org/10.1080/21650373.2015.1077754.

Bibi, et al. (2018). "Isolation, Differentiation and Biodiversity of Ureolytic Bacteria of Qatari Soil and Their Potential in Microbially Induced Calcite Precipitation (MICP) for Soil Stabilization." *RSC Advances 8* (11): 5854–63. https://doi.org/10.1039/c7ra12758h.

Hawileh, et al. (2014). "Behavior of Reinforced Concrete Beams Strengthened with Externally Bonded Hybrid Fiber Reinforced Polymer Systems." *Materials & Design 53* (January): 972–82. https://doi.org/10.1016/J.MATDES.2013.07.087.

Oualha, et al. (2020). "Microbially Induced Calcite Precipitation in Calcareous Soils by Endogenous Bacillus Cereus, at High PH and Harsh Weather." *Journal of Environmental Management 257* (March): 109965. https://doi.org/10.1016/j.jenvman.2019.109965.

Pan, et al. (2023). "Numerical Simulation of the Fracture and Compression Response of Self-Healing Concrete Containing Engineered Aggregates." *Cement and Concrete Composites 136* (February): 104858. https://doi.org/10.1016/J.CEMCONCOMP.2022.104858.

Sohail, et al. (2018). "Reinforced Concrete Degradation in the Harsh Climates of the Arabian Gulf: Field Study on 30-to-50-Year-Old Structures." *Journal of Performance of Constructed Facilities 32*(5): 04018059 (1-12). https://doi.org/10.1061/(ASCE)CF.1943-5509.0001204.

___. (2021). "Durability of Plain Concrete Prism Strengthened with Galvanized Steel Mesh and CFRP Laminates under Harsh Environmental Conditions." *Construction and Building Materials 286* (June): 122904. https://doi.org/10.1016/j.conbuildmat.2021.122904.

___. (2022a). "Behavior of Artificially Corroded RC Beams Strengthened with CFRP and Hybrid CFRP-GFRP Laminates." *Engineering Structures 272* (December): 114827. https://doi.org/10.1016/J.ENGSTRUCT.2022.114827.

___. (2022b). “Bio Self-Healing Concrete Using MICP by an Indigenous Bacillus Cereus Strain Isolated from Qatari Soil.” *Construction and Building Materials 328* (April): 126943. https://doi.org/10.1016/J.CONBUILDMAT.2022.126943.

Tittelboom, et al. (2010). “Use of Bacteria to Repair Cracks in Concrete.” *Cement and Concrete Research 40*(1): 157–66. https://doi.org/10.1016/J.CEMCONRES.2009.08.025.

___. (2016). “Comparison of Different Approaches for Self-Healing Concrete in a Large-Scale Lab Test.” *Construction and Building Materials 107* (March): 125–37. https://doi.org/10.1016/j.conbuildmat.2015.12.186.

Tziviloglou, et al. (2016). “Bacteria-Based Self-Healing Concrete to Increase Liquid Tightness of Cracks.” *Construction and Building Materials 122* (September): 118–25. https://doi.org/10.1016/j.conbuildmat.2016.06.080.

Wang, et al. (2014a). “Application of Hydrogel Encapsulated Carbonate Precipitating Bacteria for Approaching a Realistic Self-Healing in Concrete.” *Construction and Building Materials 68* (October): 110–19. https://doi.org/10.1016/J.CONBUILDMAT.2014.06.018.

___. (2014b). “Application of Hydrogel Encapsulated Carbonate Precipitating Bacteria for Approaching a Realistic Self-Healing in Concrete.” *Construction and Building Materials 68* (October): 110–19. https://doi.org/10.1016/J.CONBUILDMAT.2014.06.018.

Wen, et al. (2019). “Impact of Bacteria and Urease Concentration on Precipitation Kinetics and Crystal Morphology of Calcium Carbonate.” *Acta Geotechnica*, January. https://doi.org/10.1007/s11440-019-00899-3.

Wiktor, V. & Jonkers, H. M. (2011). “Quantification of Crack-Healing in Novel Bacteria-Based Self-Healing Concrete.” *Cement and Concrete Composites* 33*(7)*: 763–70. https://doi.org/10.1016/J.CEMCONCOMP.2011.03.012.

Yang, et al. (2011). “A Self-Healing Cementitious Composite Using Oil Core/Silica Gel Shell Microcapsules.” *Cement and Concrete Composites 33*(4): 506–12. https://doi.org/10.1016/j.cemconcomp.2011.01.010.

Zhang, et al. (2021). “Crack Self-Healing in Bio-Green Concrete.” *Composites Part B: Engineering 227* (December): 109397. https://doi.org/10.1016/J.COMPOSITESB.2021.109397.

Cite as: Sohail M.G., Al Nuaimi N., Kahraman R., Aldisi Z., Zouari N., Gencturk B., Rodrigues D. & Yildirim Y., “Bio-Based Self-Healing Concrete for Sustainable and Durable Concrete Infrastructure”, *The 2nd International Conference on Civil Infrastructure and Construction (CIC 2023)*, Doha, Qatar, 5-8 February 2023, DOI: https://doi.org/10.29117/cic.2023.0104

Along-Wind Aerodynamic Forces on a Rectangular Plan Building in Vicinity of a Gently Sloped Two-Dimensional Hill

Abdul Haseeb Wani
Indian Institute of Technology Jammu, Jammu, India
abdulhaseeb.445@gmail.com

Rajendra Kumar Varma
Indian Institute of Technology Jammu, Jammu, India
rajendra.varma@iitjammu.ac.in

Ashok Kumar Ahuja
Indian Institute of Technology Jammu, Jammu, India
ahujashok@gmail.com

Abstract

Many engineering applications, such as wind energy distribution for optimum site selection for wind farms, pollutant dispersion, forest fire propagation and wind loads on structures in hilly terrains require a thorough understanding of the wind flow. The assessment of wind loads on buildings and structures located on exposed hill sites is a key application for understanding the effect of topography. This paper presents a wind tunnel investigation of along-wind aerodynamic forces on a rectangular plan building located near and on top of a gently sloped sinusoidal hill. The hill model has a slope equal to 15° and extends fully across the width of the wind tunnel in the direction perpendicular to the wind flow. A force measurement study is carried out on a rectangular plan rigid building model, which is placed near and on top of the hill at a total of 17 successive locations. Results measured include along-wind base shear forces and base moments. It is observed that the along-wind force gradually increases, as the building is moving closer towards the crest. The maximum along-wind base shear force for the building is reported just upstream of the crest. Increased along-wind base moment for the building up to a factor of 4.0 is observed at the crest. This paper is expected to be of great help to structural engineers for designing buildings in hilly terrains.

Keywords: Wind tunnel; Two-Dimensional hill; Rectangular building; Along-wind forces; Along-wind moments

1 Introduction

In order to evaluate the localized wind speed and direction at a location in a hilly terrain, a thorough understanding and knowledge of the atmospheric boundary layer modification caused by sudden changes in the local topography is required (Bowen & Lindley, 1977). The contemporary approach to the analysis of boundary layer flow over hills may be traced back to a series of theoretical studies published in early 1970's, the most notable of them being that of Jackson & Hunt (1975), where they provided an in-depth analytical answer for airflow over a gently sloped hill . Other fairly good numerical models for wind flow over hills include those of (Deaves, 1975, 1980). Among others, Britter et al., (1981) carried out wind tunnel investigation of air flow over a two-dimensional hill, and Pearse (1982) studied experimentally the wind flow over conical hills. Other studies on boundary layer flow over hills include the review papers by (Taylor et al., 1987; Finnigan, 1988).

Notable field studies on wind flow over hills include the work of (Mason, 1986; Salmon et al., 1988). Other wind tunnel studies include those of Gong & Ibbetson (1989), Ferreira et al., (1991, 1995); (Kim et al., 1997); (Carpenter & Locke, 1999); (Cao & Tamura, 2006); and (Li et al., 2017). Recent studies on flow over complex/hilly terrain include the work of Hyvärinen et al., (2018), Kozmar et al., (2018), Fang et al., (2019), and Kilpatrick et al., (2021). Most of the studies in the past reported mean wind flow and turbulence characteristics over the hill models of different geometries and slopes. A limited number of studies have been conducted from the perspective of structural loading which include the work of (Bitsuamlak et al., 2007) and (Cheynet et al., 2016). However, when it comes to evaluate wind effects on buildings or structures, which are located in hilly terrains, the literature available is scarce. Most of the structural designers follow the standard codes of practice for wind loads, which either underestimate or overestimate the wind loads for buildings located in vicinity of a topographic feature like a hill or an escarpment. This study is an attempt to evaluate the wind effects on a building located near and on top of a two-dimensional hill placed in a boundary layer wind tunnel.

The main objective of this paper is to evaluate the along-wind forces and base moments of the building model placed successively at a total of 17 locations between the upstream and downstream measuring points over the hill model and to compare them with that of a flat terrain. The work described in this paper should greatly assist in the prognosis of design wind loads, which are mostly calculated using standard codes of practice for wind loads of different countries.

2 Materials and Methods

2.1 Characteristics of Wind Flow

Experiments are carried out in an open-circuit boundary layer wind tunnel, which has cross-sectional dimensions as 2 m × 2 m and length of test section as 15 m. The wind tunnel has a contraction ratio of 9:1 at the entrance of the test section. To generate vortices and create a thick boundary layer, vortex generators and a barrier wall are fixed near the entrance of the test section (Fig. 1). The modelled atmospheric boundary layer is characterised by a power-law exponent of 0.2 for the incoming flow. The boundary layer thickness is approximately 900 mm measured from the wind tunnel floor. The approach flow (reference) mean wind velocity and turbulence intensity profiles are shown in Fig. 2.

2.2 Model Description

A two-dimensional symmetrical hill model is prepared using plywood. The hill model is sinusoidal in shape with H/L value equal to 0.54 (gently sloped/shallow hill) (Fig. 3). The geometrical shape of the hill is given by the equation used by Ferreira et al., (1995).

$$z = \frac{H}{2}\left(1 + sin\left(\pi \frac{x-L}{2L}\right)\right) \quad (1)$$

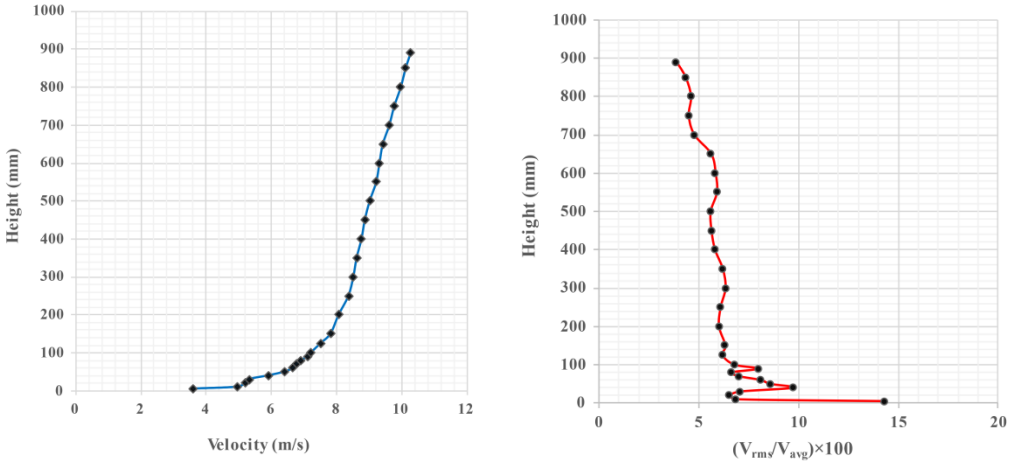
Where H is the hill height, L is the length measured in the direction of wind flow, for z = H/2.

The height of the hill is kept fixed at 300 mm. A geometric length scale of 1:100 is adopted throughout the study.

A force measurement study is carried out in which a rectangular plan shaped building model is made using plywood. The building model is rigid and hence static wind analysis is adequate to evaluate the wind loads. The building has plan dimensions of 200 mm × 100 mm and height equal to 300 mm (Fig. 4).



Fig. 1: Upstream Portion of the Test Section of the Wind Tunnel



(A) Mean Wind Velocity Profile (B) Turbulence Intensity Profile

Fig. 2: Wind flow characteristics without the presence of hill (flat terrain)

2.3 Measurement Technique

Mean wind velocity and turbulence intensity for the flat terrain are measured using Testo 480 instrument which has a probe with a 4-blade 16 mm diameter fan fixed on top of it. The Testo 480 instrument is connected to a computer for real time measurement of wind velocity. Force measurement study is carried out by using the 5-component Load cell Nissho LMC-5510-10 (LMC-5510-10 is the model no. and S.no. is 11554) which works at a frequency of 300 Hz. All the experiments are carried out at a mean free-stream wind velocity of 10.3 m/s measured at approximately 900 mm height above the wind tunnel floor. The measurements are made at several locations between 6H upstream and 10H downstream for the hill successively (Fig. 3 (b)). Testo easy climate software (v3.4) was used for real time measurement of wind velocity and dEX-2 data logger software was used for acquiring data from the load cell via, data acquisition system.

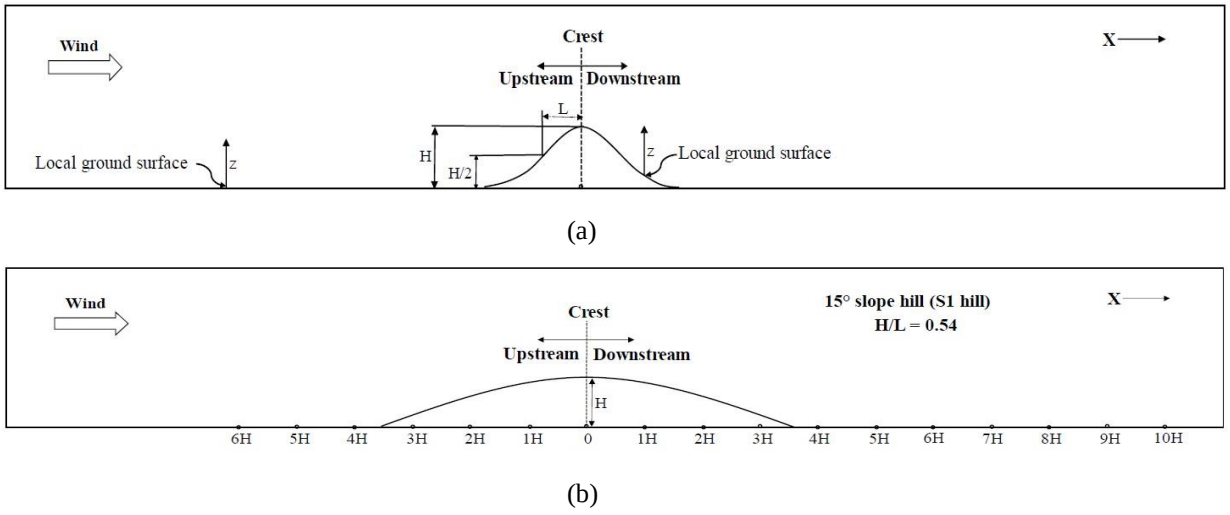


Fig. 3: Geometry of the hill models considered for the force measurement study; (a)-general notations of a hill, and (b)-hill model with slope equal to 15°

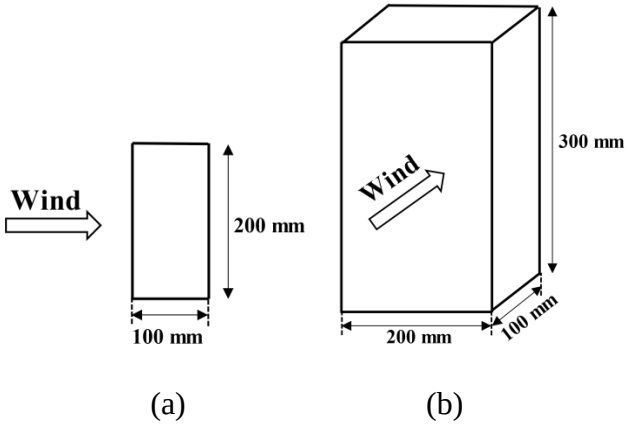


Fig. 4: Building model used in the force measurement study; (a)-plan, and (b)-isometric view

3 Experimental Results and Discussions

A force measurement study is carried out on the rectangular plan rigid building model having height equal to 300 mm. The building is placed at successive locations between 6H upstream and 10H downstream in presence of the hill (Fig. 5). The measurements from the five-component load cell include base shear (F_x) and corresponding moment (M_y) in the along-wind direction; base shear (F_y) and corresponding moment (M_x) in the across wind direction and the twisting moment at the base (M_z). The focus will be on results in the along-wind direction. Results are shown for F_x and M_y in Figs. 6 & 7. It is observed that there is increase in F_x as the building continues nearing to the crest and decrease in F_x as the building is placed on the downstream side of the hill. A similar trend is observed for the base moment (M_y). The along-wind force (F_x) is represented in a dimensionless form by a ratio 'F_R' defined as 'along-wind force on the building in presence of the hill at any location between 6H upstream and 10H downstream divided by the along-wind force on the building in an isolated condition (without the presence of hill). As the building location shifts from the farthest upstream location 6H towards the crest, a significant increase in the F_R value is seen. The highest value of F_R reported is 2.00 at 1H upstream. The value at the crest (1.97) is almost equal to the maximum value of 2.00. As the building location shifts from crest towards the downstream side, F_R keeps decreasing, the obvious reason being the flow deceleration occurring

beyond the crest till 3H downstream at a rapid rate. The lowest value of F_R reported is 0.91 at 3H downstream, which is just near the downstream foot of the hill. In the region extending from 4H downstream till 10H downstream, the F_R value is seen to be nearly constant and close to 1.00 which indicates that the along-wind force is close to that of the isolated case (flat terrain).



(a) (b) (c)

Fig. 5: Few photographs of the force measurement study done; (a)-building at an upstream location, (b)-building at crest, (c)-building at a downstream location

An insight into the numerical values of F_R is quite useful from a structural engineer's point of view. The increase in the value of F_R confined to the region extending from 3H upstream till 2H downstream affirms the need for consideration of increased wind loads for buildings in general, in these regions. At the time of writing this paper, the authors were aware of no other data to compare the results with.

Figure 7 shows the variation of base moment (M_y) ratio represented by M_R. M_R is defined, as the base moment on the building in presence of the hill at any location between 6H upstream and 10H downstream divided by the base moment on the building in an isolated condition (without the presence of hill). A similar insight into the values of M_R reveals that in the region extending from 3H upstream till 2H downstream, a drastic increase in the value of M_R is seen with the highest value being 3.96, occurring at the crest. This observation reaffirms the need of considering increased wind loads and thereby increased moment values at the design stage of the construction of buildings in hilly terrains having a similar feature described in this study.

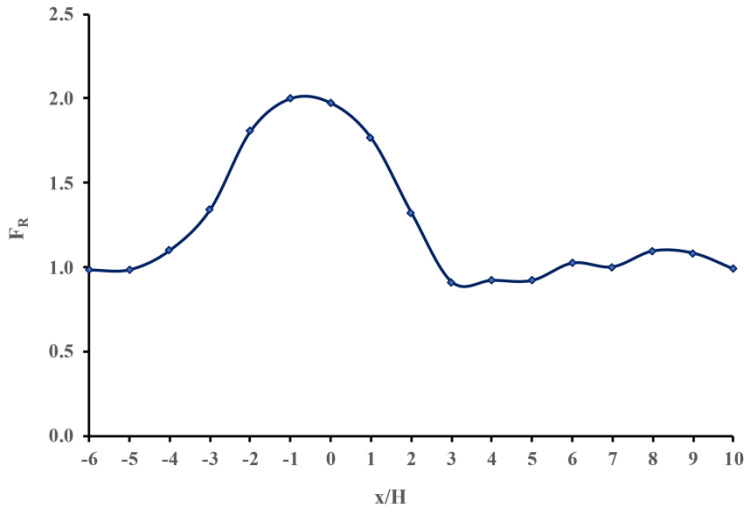


Fig. 6: Along-Wind Force Variation Represented by F_R

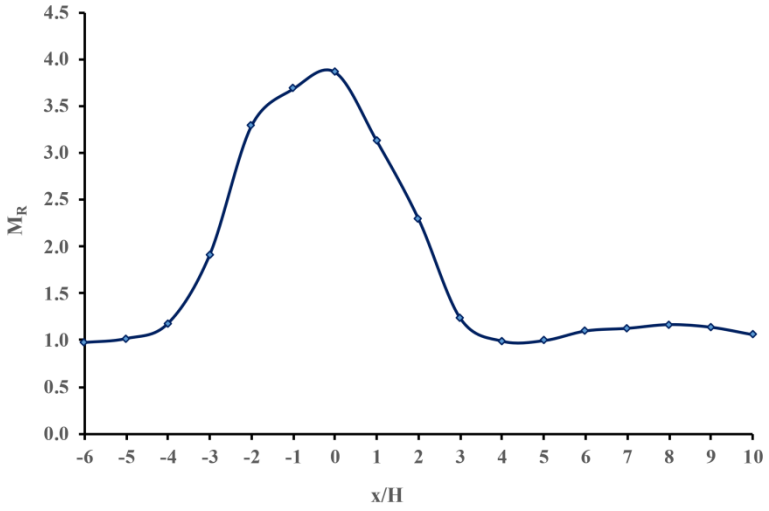


Fig. 7: Base moment variation represented by M_R

4 Conclusions

The present study investigated experimentally the wind effects on a rectangular plan building located near and on top of these hills. Following conclusions can be drawn from the study:

- The approach flow in presence of the hill does not change significantly until it reaches 4H upstream location.
- Due to the gentle slope of the hill, the flow in the upwind slope remains attached and no separation of flow takes place. It is also observed that the along-wind force gradually increases as the building is moving closer towards the crest owing to the significant acceleration of flow as it moves along the slope.
- The maximum along-wind base shear force (F_x) for the building in presence of the hill is observed to be exactly twice (at 1H upstream) the value of along-wind base shear force for the building without the presence of hill (isolated/flat terrain case).
- The highest value of M_R for the building is equal to 3.96 at the crest. This reaffirms the need to take increased base moments up-to a factor of 4.0 for the buildings at the design stage.
- The work presented in this paper should be of great assistance to structural engineers while designing buildings for wind loads in such hilly terrains.
- This paper presents the results for a two-dimensional hill with a gentle slope. Further studies can be carried out for hills with steep slopes.
- Only one row of hill is considered in the present study. Future scope of this work can include making the models of multiple hills and carrying out a similar study. Furthermore, the current study is based on a two-dimensional hill however, a study can be carried out on a three-dimensional hill.

References

Bitsuamlak, G. T., Bédard, C. & Stathopoulos, T. (2007). Modeling the Effect of Topography on Wind Flow Using a Combined Numerical–Neural Network Approach. *Journal of Computing in Civil Engineering 21*(6): 384–392.

DOI: 10.1061/(ASCE)0887-3801(2007)21:6(384).

Bowen, A. J. & Lindley, D. (1977). A wind-tunnel investigation of the wind speed and turbulence characteristics close to the ground over various escarpment shapes. *Boundary-Layer Meteorology 12*(3): 259–271. DOI: 10.1007/BF00121466.

Britter, R. E., Hunt, J. C. R. & Richards, K. J. (1981). Airflow over a two-dimensional hill: Studies of velocity speed-up, roughness effects and turbulence. *Quarterly Journal of the Royal Meteorological Society 107*(451): 91–110. DOI: 10.1002/qj.49710745106.

Cao, S. & Tamura, T. (2006). Experimental study on roughness effects on turbulent boundary layer flow over a two-dimensional steep hill. *Journal of Wind Engineering and Industrial Aerodynamics 94*(1): 1–19. DOI: 10.1016/j.jweia.2005.10.001.

Carpenter, P. & Locke, N. (1999). Investigation of wind speeds over multiple two-dimensional hills. *Journal of Wind Engineering and Industrial Aerodynamics* 83(1–3): 109–120. DOI: 10.1016/S0167-6105(99)00065-3.

Cheynet, E., Jakobsen, J. B. & Snæbjörnsson, J. (2016). Buffeting response of a suspension bridge in complex terrain. *Engineering Structures 128*: 474–487. DOI: 10.1016/j.engstruct.2016.09.060.

Deaves, D. M. (1975). Wind over hills: A numerical approach. *Journal of Wind Engineering and Industrial Aerodynamics* 1: 371–391. DOI: 10.1016/0167-6105(75)90031-8.

Deaves, D. M. (1980). Computations of wind flow over two-dimensional hills and embankments. *Journal of Wind Engineering and Industrial Aerodynamics 6*(1–2): 89–111. DOI: 10.1016/0167-6105(80)90024-0.

Fang, P., Zheng, D. & Li, et al. (2019). Numerical and experimental study of the aerodynamic characteristics around two-dimensional terrain with different slope angles. *Frontiers of Earth Science 13*(4): 705–720. DOI: 10.1007/s11707-019-0790-8.

Ferreira, A. D., Silva, M. C. G. & Viegas, et al. (1991). Wind tunnel simulation of the flow around two-dimensional hills. *Journal of Wind Engineering and Industrial Aerodynamics 38*(2–3): 109–122. DOI: 10.1016/0167-6105(91)90033-S.

Ferreira, A. D., Lopes, A. M. G. & Viegas, et al. (1995). Experimental and numerical simulation of flow around two-dimensional hills. *Journal of Wind Engineering and Industrial Aerodynamics* 54–55: 173–181. DOI: 10.1016/0167-6105(94)00040-K.

Finnigan, J. J. (1988). Airflow over Complex Terrain. In: Steffen WL and Denmead OT (eds) *Flow and Transport in the Natural Environment: Advances and Applications*. Berlin, Heidelberg: Springer Berlin Heidelberg, pp. 183–229. DOI: 10.1007/978-3-642-73845-6_13.

Gong, W. & Ibbetson, A. (1989). A wind tunnel study of turbulent flow over model hills. *Boundary-Layer Meteorology 49*(1–2): 113–148. DOI: 10.1007/BF00116408.

Hyvärinen, A., Lacagnina, G. & Segalini, A. (2018). A wind-tunnel study of the wake development behind wind turbines over sinusoidal hills: A wind-tunnel study of the wake development behind wind turbines over sinusoidal hills. *Wind Energy 21*(8): 605–617. DOI: 10.1002/we.2181.

Jackson, P. S. & Hunt, J. C. R. (1975). Turbulent wind flow over a low hill. *Quarterly Journal of the Royal Meteorological Society 101*(430): 929–955. DOI: 10.1002/qj.49710143015.

Kilpatrick, R. J., Hangan, H. & Siddiqui, et al. (2021). Turbulent flow characterization near the edge of a steep escarpment. *Journal of Wind Engineering and Industrial Aerodynamics 212*: 104605. DOI: 10.1016/j.jweia.2021.104605.

Kim, H. G., Lee, C. M., & Lim, et al. (1997) An experimental and numerical study on the flow over two-dimensional hills. *Journal of Wind Engineering and Industrial Aerodynamics 66*(1): 17–33. DOI: 10.1016/S0167-6105(97)00007-X.

Kozmar, H., Allori, D. & Bartoli G, et al. (2018) Wind characteristics in wind farms situated on a hilly terrain. *Journal of Wind Engineering and Industrial Aerodynamics 174*: 404–410. DOI: 10.1016/j.jweia.2018.01.008.

Li, Q., Maeda, T. & Kamada, et al. (2017). Experimental investigation of flow over two-dimensional multiple hill

models. *Science of The Total Environment 609*: 1075–1084. DOI: 10.1016/j.scitotenv.2017.07.259.

Mason, P. J. (1986). Flow over the summit of an isolated hill. *Boundary-Layer Meteorology 37*(4): 385–405. DOI: 10.1007/BF00117485.

Pearse, J. R. (1982). Wind flow over conical hills in a simulated atmospheric boundary layer. *Journal of Wind Engineering and Industrial Aerodynamics 10*(3): 303–313. DOI: 10.1016/0167-6105(82)90004-6.

Salmon, J. R., Teunissen, H. W. & Mickle, et al. (1988) The Kettles Hill Project: Field observations, wind-tunnel simulations and numerical model predictions for flow over a low hill. *Boundary-Layer Meteorology 43*(4): 309–343. DOI: 10.1007/BF00121711.

Taylor, P. A., Mason, P. J. & Bradley, E. F. (1987) Boundary-layer flow over low hills. *Boundary-Layer Meteorology 39*(1–2): 107–132. DOI: 10.1007/BF00121870.

Cite as: Wani A.H., Varma R.K. & Ahuja A.K., "Along-Wind Aerodynamic Forces on a Rectangular Plan Building in Vicinity of a Gently Sloped Two-Dimensional Hill", *The 2nd International Conference on Civil Infrastructure and Construction (CIC 2023)*, Doha, Qatar, 5-8 February 2023, DOI: https://doi.org/10.29117/cic.2023.0105

Effect of Chemicals on Compressive Strength of Plastic-Laterite Interlock Paving Blocks

Mubarak L. Liman
Department of Science Laboratory Technology, School of Applied Sciences, Nuhu Bamalli Polytechnic
Zaria, Kaduna State, Nigeria
mubarak.liman@gmail.com

Yamusa Bello Yamusa
Department of Civil Engineering, School of Engineering Technology, Nuhu Bamalli Polytechnic,
Zaria, Kaduna State, Nigeria
yamusabello@yahoo.com

BilkisuDanjuma
Department of Civil Engineering, School of Engineering Technology, Nuhu Bamalli Polytechnic,
Zaria, Kaduna State, Nigeria
danjumabilkisu15@gmail.com

Abubakar Sani
Department of Civil Engineering, School of Engineering Technology, Nuhu Bamalli Polytechnic,
Zaria, Kaduna State, Nigeria
abubakarsani832@gmail.com

Yusuf Walliyullah
Department of Science Laboratory Technology, School of Applied Sciences, Nuhu Bamalli Polytechnic
Zaria, Kaduna State, Nigeria
yuswaliy@gmail.com

Abstract

This research centres on the need to develop a simple but sustainable material for the utilization of the quantum of plastic wastes that litter our environment. The research uses waste plastics and laterite soil and converts them into construction materials (interlock blocks) with the help of the densifier, thereby reducing the plastic waste, which is a key contributor to environmental pollution. Literature has shown that concrete structure is prone to chemical actions; the durability of conventional concrete bricks gets affected by chemical effects. The chemicals may cause cracking of concrete, rutting, and deterioration of the structure. In the same vein, the plastic-laterite interlock bricks might not be free from such defects due to chemical action. Therefore, this research looks into the effects of different chemical curing conditions on the compressive strength of plastic-laterite paving blocks. Varying proportions of plastic wastes and laterite soil were mixed and processed into composite bricks and subjected to different chemical treatments; in acid, base, oil, and water for 3, 14, and 28 days relative to a concrete brick control. It was observed that samples cured in acid solution gave the lowest compressive strength, while those in base solution gave the highest. The paving interlock blocks made from polyethylene/laterite composite registered relative performance compared to concrete interlock bricks control. If made and put into use, these blocks will reduce construction costs, assist in environmental sustainability and improve circular economic growth. Therefore, using this innovative approach will bolster infrastructural projects and checkmate plastic pollution within our environment.

Keywords: Plastic waste; Laterite soil; Interlock bricks; Chemical effect; Compressive strength; Waste Management

1 Introduction

More production equals more waste; more waste creates environmental concerns of contamination. An economically viable solution to the waste problem should include the utilization of waste materials for new products, which could help in minimizing the heavy burden on the nation's landfills. The importance of recycling is huge because it saves natural resources, saves energy, reduces solid waste, reduces air, water, and land pollutants, and reduces greenhouse gases.

Waste polyethylene usage in road construction is trending. Some aggregates are water-loving (hydrophilic) such as concrete. Others like polyethylene and bitumen are water-hating (hydrophobic) in nature. Thus, polymers that are hydrophobic when added to asphalts mix make them repel the water and thereby increase the strength. Roads made of recyclable plastic wastes can bring about the reduction of these tons of waste in our environment by utilizing them as construction materials (Ansari et al., 2017).

Laterite soil is abundantly found in tropical parts of the world including Nigeria. Laterite soils are used for road sub bases or bases and other engineering applications (Yamusa et al., 2019). The viability of a project relies on the relative abundance of materials to be used which in turn helps in creating more economical construction (Yamusa et al., 2020), hence the justification of this research whereby laterite soil will be used as the major raw material.

In a report www.polygongroup.com (2022), natural freshwater has a neutral pH of 7. Alkaline has a pH above 7 while acidic is below 7. The main concrete binder i.e., Portland cement has a pH of 11 thus making it alkaline. Concrete deteriorates in an acidic solution by increasing its porosity, which makes it weak and lowers its strength. Therefore, the lower the pH the weaker concrete becomes. When cement in a concrete mixture reacts with the carbon dioxide in the air results in carbonation. Carbonation lowers concrete's pH, affecting its ability to hold the cementitious components within it together. When exposed to acidic environments, concrete dissolves into sand and rocks. The resulting pressure can cause the already weakened concrete around it to break and crack (www.polygongroup.com, 2022). In this study, the effects of chemical solutions i.e., acid, base, oil, and water were explored on the plastic-laterite paver blocks to analyze their significance on compressive strength.

2 Materials and Methods

2.1 Plastic Waste and Laterite Soil

The recyclable plastic waste (RPW) that was used in manufacturing the paving blocks was bought from collection points within the municipality gotten from refuse dumps, waterways, and landfill sites, and then sorted and classified. Thereafter, the RPWs were dry-cleaned and taken for experimentation in the laboratory.

Laterite soil was bought from the available borrow pits within the catchment area (Zaria city) of this research. The soil was powdered using a mechanical grinder and then sieved through a 5mm aperture to reduce oversize gravel. The RPW and laterite soil were as shown in Figure 1.



Fig. 1: Plastic waste bags and laterite soil

2.2 Physicochemical Tests on Waste Polyethylene Bags

The samples of waste Polyethylene bags were sorted at the Civil Engineering Workshop in Nuhu Bamalli Polytechnic and classified into three dominant categories viz.,

1) Transparent Low-Density Polyethylene (T-LDPE).
2) Transparent High-Density Polyethylene (T-HDPE).
3) Black Low-Density Polyethylene (B-LDPE).
4) Mixed Polyethylene comprising of 3 categories above (M-HLPE).

Thereafter, the determination of chemical composition/percentage purity, thermal physicochemical properties, degree of crystallinity, and specific gravity was carried out as described in (ASTM, 2008).

2.3 Physicochemical Tests on Laterite Soil

The laterite soil samples undergo the following physical property tests adopting the British Standard (BSI, 1990). Specific gravity, particle size distribution, atterberg limit (plasticity chart of British Standard Classification System) (BSI, 1999), linear shrinkage test, and compaction test.

2.4 Mix Ratio of Waste Plastic and Laterite Soil

Creating a ratio mix for melting/solubilization of the various classified waste plastics stream with laterite soil based on their known physicochemical characteristics; the mix proportions of laterite and plastic waste materials were obtained by weight. The following mix ratios were investigated:

a) 60% laterite and 40% plastic contents by weight denoted as P1.
b) 70% laterite and 30% plastic contents by weight denoted as P2.
c) 80% laterite and 20% plastic contents by weight denoted as P3.
d) Concrete control mixing ratio of 1:2:4 by weight denoted as P4.

2.5 Physicochemical Characteristics of Plastic-Laterite Interlock Bricks

Evaluation of the physicochemical characteristics of the produced interlocking bricks and quality assessment checks in comparison with conventional concrete materials; to determine the loading capacity of polyethylene and laterite composite, and to evaluate the effect of compressive strength, tests conducted include compressive strength, water absorption, and effects of chemicals on the produced paving interlocks.

a) Effects of Chemicals*:* This was carried out according to ASTM modified method. Respective samples were immersed in mild acid and mild base for 3, 14, and 28 days to test for the effect of the chemicals on the physicochemical characteristics of the products. Subsequently, the samples were washed and checked for any defect and were then subjected to compressive strength to determine their response as a result of the chemical effect.

***b) Compressive Strength Test*:** To determine the loading capacity on the strength of mixed polyethylene-laterite bricks, the compressive test was carried out using a universal compressive machine tester. The test complies with BSI (2009) for control paving blocks. Three samples per mix were tested and average strength was determined by averaging the three results.

3 Results and Discussion

3.1 Physicochemical Properties of Waste Polyethylene Bags Sample

The results from Table 1 show similar levels of purity among the samples, in particular, the T-LDP and T-HDPE have pure polyethylene at 98% while the B-LDPE and M-HLPE have polyethylene

purity percentages of about 92%. The lower percentages in the latter might be because B-LDPE is mostly used for multiple uses in grocery packing which might result in it harboring more impurities than other samples.

Table 1: Percentage purity of various samples of waste polyethylene bags

Sample Description	W1 (g)	W2 (g)	% Purity
T-LDPE	500	490	98.00
T-HDPE	500	492	98.40
B-LDPE	500	484	91.80
M-HLPE	500	481	92.20

While the physical test, shown in Table 2, on the various samples of polyethylene shows varying properties concerning thermal behaviors. The T-HDPE had a higher melting point (148°C) than the LDPE while the mixed sample M-HDPE has a melting point of 132°C. The enthalpy of fusion and percentage crystallinity (33%) is lowest in T-HDPE when compared to LDPE, which have a percentage crystallinity of 61% and 56% for T-LDPE and B-LDPE, respectively. Interestingly, the M-HLPE had an average percentage crystallinity of about 50%. The crystallinity of the samples is an important physical parameter in this project since the melt flow, hardness, and brittleness of the bricks to be produced are dependent on it. The M-HLPE was the sample of choice used for the study since polyethylene plastic wastes exist in mixed form and the novelty of the research lies in the ability of the process to utilize these mixed wastes with poor recyclable value.

Table 2: Physical properties of waste polyethylene bags samples

Sample Description	Initial Melt Temp/ Melting Point (°C)	Final Melt Temperature (°C)	Enthalpy of Fusion (J/g)	Crystallinity (%)
T-LDPE	112.50	126.70	180.40	61.34
T-HDPE	148.00	163.10	98.60	33.64
B-LDPE	114.20	125.50	165.80	56.46
M-HLPE	132.00	158.80	149.20	50.40

3.2 Physical Properties of Laterite Soil

Table 3 presents laboratory results on the physical properties of the laterite soil used in this study. According to the British Standard (BS) classification, the soil sample is classified as silty clay of medium plasticity (ML).

Table 3: Physical properties of laterite soil

Property	Value
Specific gravity	2.70
% Fines	10
% Sand	70
% Gravel	20
OMC, %	16
MDD, Mg/m^3	1.6
Liquid limit, %	47
Plastic limit, %	31
Plasticity Index, %	16
Linear Shrinkage, %	5
BS Classification	ML
Colour	Brown

3.3 Effect of Acid Curing on Compressive Strength

The effect of acid curing can be seen in Figure 2, where compressive strength increase with an increasing number of days, especially for concrete cured in acid for 28 days. The positive influence of test piece aging in aqueous media on their mechanical properties (compressive strength) was demonstrated. This result corresponds to Šiler et al., (2016) where a different effect of the pH environment on hydration was observed.

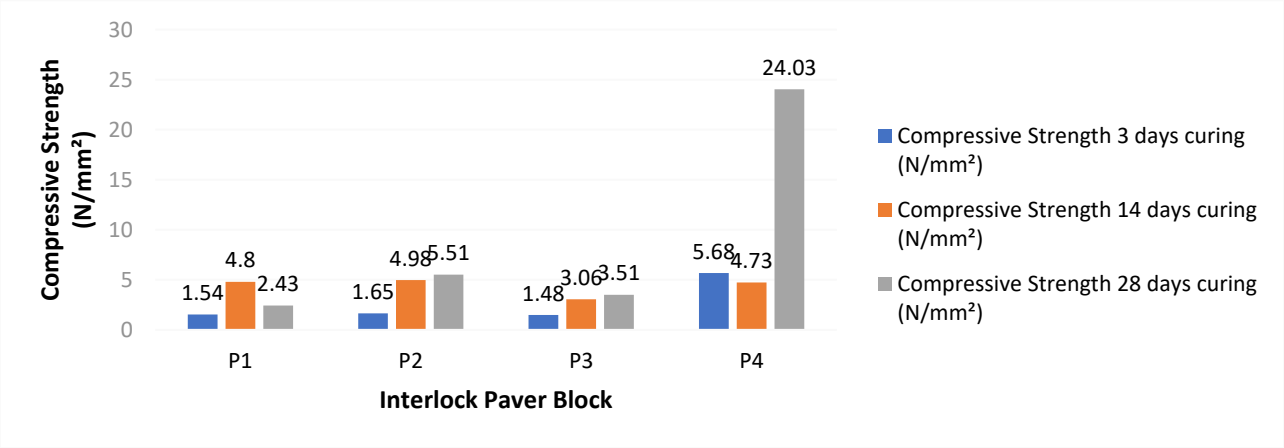


Fig. 2: Compressive strength of paver blocks after acid curing

3.4 Effect of Base Curing on Compressive Strength

The effect of acid curing can be seen in Figure 3. The compressive strength increased significantly for all mix ratios especially concrete cured with a base solution. These values indicate compressive strength performs better in an alkaline medium. Similar findings were also reported by Dutta et al., (2020) saying that the main reason behind the phenomena is that in alkaline media, both the formation of calcium carbonate and calcium silicate hydrate increases with time. These two elements of Portland cement are responsible for the hardening of cement composite. Thus, the compressive strength of concrete increases in the long run for all the tested series. In this study, the compressive strength at 14 days gives the peak values for P1 and P2, whereas, P3 and P4 show maximum compressive strength at 28 days. This depicts that plastic-laterite paver blocks P3 with a 20-80% mix ratio indicate similar properties with concrete because laterite soil has a concentration of iron and aluminum oxides (the sesqui oxides gibbsite and goethite), which act as cementing agents (Yamusa, 2018).

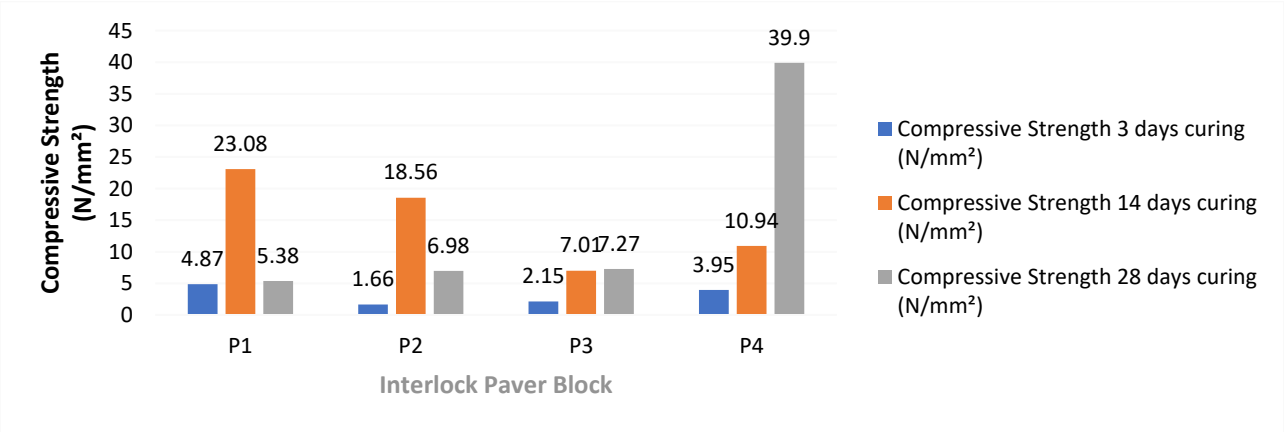


Fig. 3: Compressive strength of paver blocks after base curing

3.5 Effect of Oil Curing on Compressive Strength

The effect of engine oil curing can be seen in Figure 4. The compressive strength increased significantly for all mix ratios, especially for 14 days of curing. The reason may be attributed to what was observed by, Shafiq et al., (2018), that the chemical composition of used engine oil showed the presence SO_3 content which may be the reason for the plasticizing effect. In general, a small dosage of used engine oil caused a substantial reduction in the coefficient of oxygen permeability and porosity of all concrete mixes, which is an indicator of enhanced long-term durability.

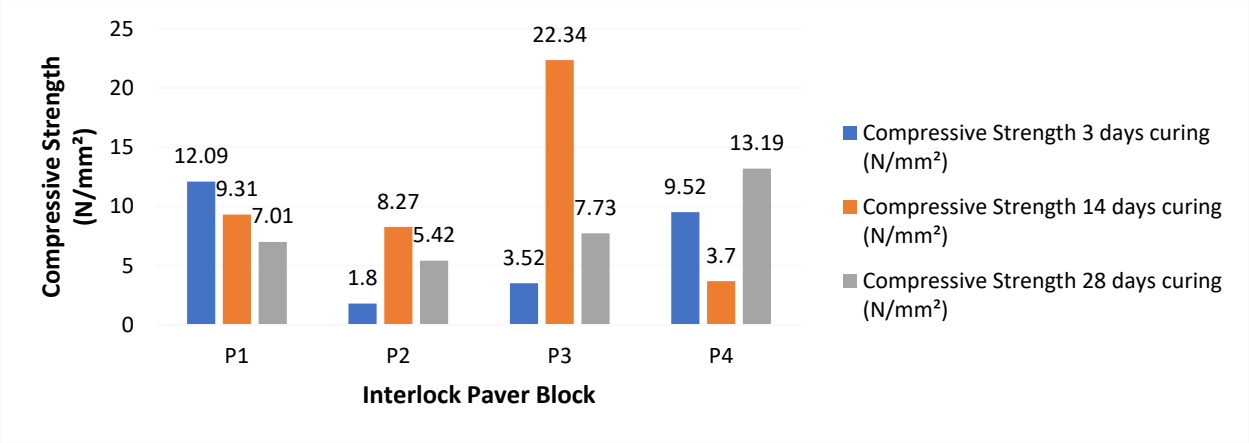


Fig. 4: Compressive strength of paver blocks using engine oil curing

3.6 Effect of Water Curing on Compressive Strength

Figure 5 displays the effect of water curing on compressive strength. The hydrophilic nature of the concrete block makes it absorb higher water in comparison with the hydrophobic nature of RPW blocks that absorbed less water as the results indicated. Similar results were reported by some researchers in the literature (Agyeman et al., 2019and Youssef et al., 2015).

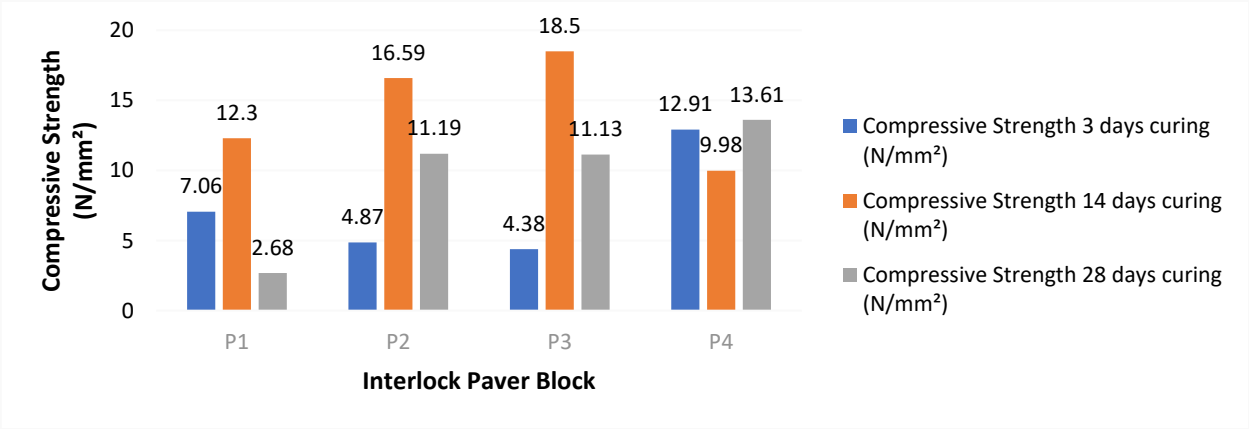


Fig. 5: Compressive strength of paver blocks after water curing

3.7 Evaluating the Effect of Chemicals on RPW Blocks for Pavement Construction Purposes

\Compressive strength is one of the significant physico- mechanical property parameters when evaluating the quality of paving blocks Agyeman et al., (2019). Figure 6 depicts the variance of compressive strengths across the various samples of paver blocks in different media. The most common solvent that pavements are exposed to is water and it can be seen that the compressive strength of all three plastic paver blocks (P1, P2, and P3) are relatively higher than that of concrete control (P4). This affirms that the plasticised paver bricks will serve well in presence of water. On the other hand, the acidic and oil environments significantly resulted in a decline in the compressive

strength of the paver blocks. Acids are known to be corrosive and can hydrolyse composites of laterites and cement while the effect of the oil might be attributed to its ability to percolate and create hydrophobic environments within the blocks which can affect the compressive strength. The effect of the base can be seen to have shown the best curing for compressive strength, particularly for the P1 and P2 samples. The decline for P3 and P4 might not be unrelated to the high content of laterite or sand in the two samples. Therefore the P1 mix is adjudged as the best mix-ratio for compressive strength that requires a minimum compressive strength of 3.45 MPa required by the Nigerian Building and Road Research Institute.

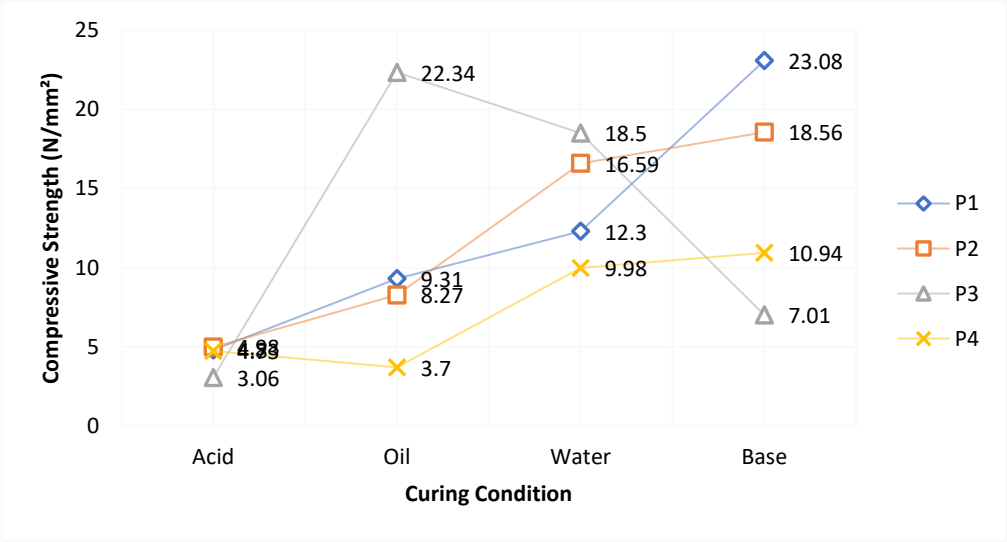


Fig. 6: Compressive strength of blocks under different curing conditions for 14 days

4 Conclusion

In conclusion, the research invented an auto-mechanical densifier machine that simplifies the plastic melting and mixing with laterite for efficient mass production of the interlocking bricks, which makes economic sense and promotes sustainability. The results indicated that the concrete paving blocks absorbed more water (hydrophilic) than the RPW paving blocks as they were gauged to be hydrophobic. The compressive strength increased significantly for all mix ratios after days of curing. Relatively, the effect of the base showed the best curing for compressive strength, particularly for the P1 and P2 samples.The research brought about the selection of the best mix-ratio and production procedures leading to qualitative interlock products that are similar or even stronger than conventional concrete interlocking bricks and which can withstand exposure to varying environmental solvents. However, more research and investigations are needed and are underway to ascertain the long-term resilience of the plastic-laterite paver bricks when exposed to real-life environmental conditions, which include routine exposure to chemicals as well as freezing or scorching temperature extremes.

Acknowledgment

This research work was supported by the National Research Fund (NRF) Grant of the Nigerian Tertiary Education Trust Fund (TETFund) Grant No: TETF/DR&D-CE/NRF-2020.

References

Agyeman, et al. (2019). Exploiting recycled plastic waste as an alternative binder for paving blocks production. Case *Studies in Construction Materials, 11*, e00246. doi.org/10.1016/j.cscm.2019.e00246.

Ansari, et al. (2017). Replace of asphalt with waste polythene in bitumen road. *International Journal of Advance Research, Ideas and Innovations in Technology, 3*(3), 602-608.

ASTM. (2008). Standard test methods for density and specific gravity (relative density) of plastics by displacement. Committee d-20 on plastics: ASTM international.DOI: 10.1520/ D0792-20.

ASTM. (2014). D638-14, 2014 standard test method for tensile properties of plastics. ASTM International, West Conshohocken, PA. DOI: 10.1520/D0638-14.

BSI. (1990). Methods of testing soil for civil engineering purposes (bs 1377:Part 1-9). British standards institute, london.

BSI. (1999). Code of practice for site investigations (bs 5930). British standards institute, london.

BSI. (2009). Testing hardened concrete; compressive strength of test specimens, part 3: Bs en 12390-3: 2009. British Standards Institute.

Dutta, et al. (2020). Effect of mixing water ph on concrete. Paper presented at the Proceedings of the 5th International Conference on Civil Engineering for Sustainable Development (ICCESD 2020), 7~9 February 2020, KUET, Khulna, Bangladesh (ISBN-978-984-34-8764-3).

Shafiq, et al. (2018). Effects of used engine oil on slump, compressive strength and oxygen permeability of normal and blended cement concrete. *Construction and Building materials, 187*, 178-184. doi.org/10.1016/j.conbuildmat.2018.07.195.

Šiler, et al.. (2016). The determination of the influence of ph value of curing conditions on portland cement hydration. *Procedia Engineering, 151*, 10-17. doi.org/10.1016/j.proeng.2016.07.393.

www.polygongroup.com. (2022). How humidity and ph affect concrete degradation.

Yamusa, Y. B. (2018). Effects of gradation on engineering properties of compacted laterite soil liner. PhD. Thesis, School of Civil Engineering, Faculty of Engineering, Universiti Teknologi Malaysia.

Yamusa, et al. (2019). A review on the fundamental engineering properties of compacted laterite soil at different gradations. *Journal of Advanced Research in Applied Sciences and Engineering Technology, 16*, 10-19.

___. (2020). Engineering characteristics of compacted laterite soil as hydraulic barrier in waste containment application. *Journal of Engineering Science and Technology, 15*(1), 508-523.

Youssef, et al. (2015). Evaluation of corn husk fibers reinforced recycled low density polyethylene composites. *Materials Chemistry and Physics, 152*, 26-33. doi.org/10.1016/j.matchemphys.2014.12.004.

Cite as: Liman M.L., Yamusa Y.B., Danjuma B., Sani A. & Walliyullah Y., "Effect of Chemicals on Compressive Strength of Plastic-Laterite interlock paving Blocks", *The 2nd International Conference on Civil Infrastructure and Construction (CIC 2023)*, Doha, Qatar, 5-8 February 2023, DOI: https://doi.org/10.29117/cic.2023.0106

Hardened Properties of Self-Compacting Concrete Incorporating Recycled Granite Waste as Fine Aggregate

Aboubakeur Boukhelkhal
Research Laboratory of Civil Engineering, University of Laghouat, Laghouat, Algeria
a.boukhelkhal@lagh-univ.dz

Abstract

The present paper investigates the hardened properties of self-compacting concrete by reusing granite waste to replace natural fin aggregates. The reuse of solid wastes as powder or aggregates allows us to produce sustainable concretes that have lower environmental impacts and reduced cost. In this work, granite waste was used as a partial replacement to natural river sand in self-compacting concrete (SCC). For this purpose, four mixtures were designed in which three contained a combination of river sand (RS) and recycled granite (RG) and one only included river sand (RS) as reference mix. Compressive strength, flexural strength, ultrasonic pulse velocity and water absorption were investigated for the hardened SCC at 28 days of hydration. The results showed that the introduction of RG has no effect on compressive strength of SCC. Adding 30% of RG increased flexural strength by 12%. According to ultrasonic pulse velocity results, the use of RG resulted in more compactness and homogeneous SCC. In addition, SCC including RG showed less water absorption.

Keywords: Self-compacting concrete; Recycled granite; Compressive strength; Flexural strength; Water absorption

1 Introduction

Self-compacting concrete (SCC) is an innovative concrete that can flow and fill all the form work without vibration or compaction. Concrete industry consumes large quantities of natural resources especially in the form of aggregates (60-70% by volume of concrete). In the same time, important amount of waste is generated and deposit in landfill, causing serious environmental problems. The use of waste in concrete industry as a partial substitution of cement and aggregates has become an attractive alternative from environmental and economical points of view Boucedra et al., (2020); Shaikh, (2016); Ouldkhaou et al., (2020), Boukhelkhal et al., (2017); Djelloul et al., (2018) and (Sadek et al., 2016). The performance of concretes may be affected by the homogeneities and the characteristics (shape, texture, specific gravity, water absorption) of recycled aggregates Chen et al., (2003); Cabral et al., (2010) and Oliveira et al., (2011),e.g., recycled aggregates have been showed to reduce the workability of concrete because of their high water absorption (Leite et al., 2013). It was reported that the use of coal bottom ash as replacement of sand has no negative effect on the durability and strength of concrete until a substitution level of 50% (Singh & Siddique, 2016). The incorporation of recycled glass was found to increase the slump flow of SCC (Ali & Al-Tersawy, 2012). However, mechanical properties decreased by increasing the recycled glass content.

Granite is a very hard magmatic rock consisting of silicates (quartz, feldspar and mica 75%), alumina (15%) and other metal oxides (10%) (Lemaître, 2012). Granite stone is characterized by its solidity, its impermeability and its variety in textures and colors. This noble stone is widely used for

manufacturing ornamental and decorative pieces. However, granite industry generates significant quantities of waste from sawing, shaping and lustration of granite block. This waste is generally rejected which can cause serious environmental problems. The incorporation of this waste into concrete as powder to partially replace cement, or as aggregate by substituting natural aggregates is an interesting solution that can contribute to reduce the environmental impact and the cost production of concretes. This paper examines the possible use of granite waste as recycled fine aggregates in order to produce sustainable self-compacting concrete. Recycled granite was incorporated as a partial replacement to river sand (10%, 20% and 30% by volume).

2 Materials And Methods

2.1 Materials

The cement used for the preparation of different mixtures is blended in cement (CEM II, 42.5). It has specific gravity and fineness of 3.09 g/cm^3 and 380 m²/kg, respectively, the chemical composition of cement is presented in Table 1.These properties meet the Algerian standard NA 442 as well as the European standard EN 197-1.

Table 1: Chemical composition of cement

Element (%)	**Cement**
SiO_2	18.21
CaO	62.54
MgO	2.23
Al_2O_3	3.62
Fe_2O_3	4.18
SO_3	1.85
K_2O	0.42
T_iO_2	0.21
Na_2O	0.07
P_2O_5	0.22
Loss ignition	1.72

As fine aggregate (FA), river sand characterized by granular class of 0/5, and a continuous particles size distribution was used. Recycled granite was used as a partial substitution of river sand (10, 20 and 30%). For coarse aggregate (CA), two classes 3/8 and 8/15 were used. The physical properties of aggregates are given in Table 2. Particles size distribution of fine and coarse aggregates is plotted in Figure 2. The median diameter of RS and RG is 0.51 and 0.8 mm, respectively. The proportion of fine particles is higher in RG (12%) as compared to RS (2%). The super plasticizer used is a polycarboxylates based High-Range Water Reducers (HRWR). It has a specific gravity and pH of 1.07g/cm^3 and 8, respectively. Locally available potable water was used for mixing SCC constituents.

Table 2: Physical properties of aggregates

Properties	**River sand**	**Recycled granite**	**C.A 8/15**	**C.A 3/8**
Absorption (%)	0.84	2.44	3.48	4.85
Density	2.62	2.72	2.58	
Fineness modulus	2.20	2.65	-	-

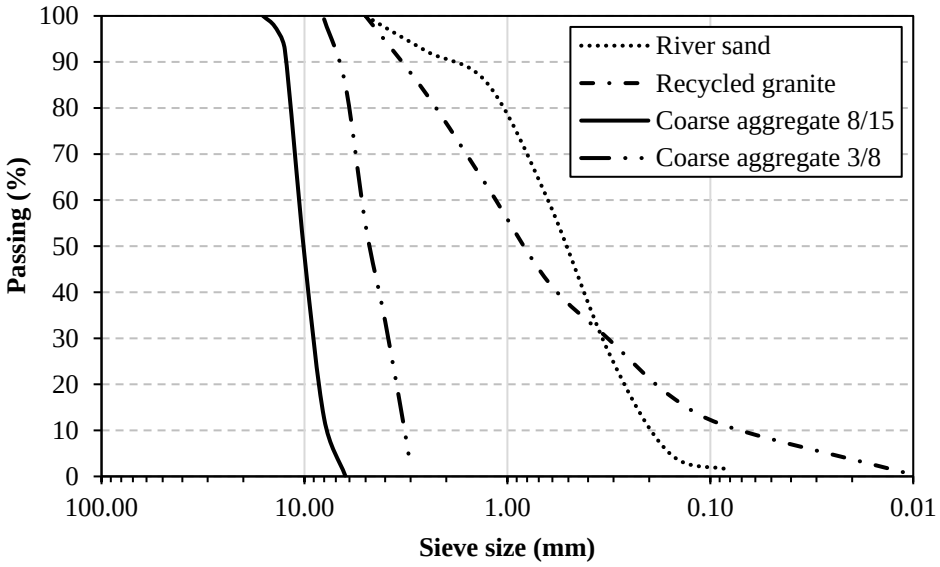


Fig. 1: Particles size distribution of used aggregates

2.2 Mix Proportion Design

To study the effect of RG on some hardened properties of SCC, four mixtures were prepared. The control mix includes only RS as a fine aggregate, whereas in the other mixtures, RS was partially substituted by RG at ratios of 10, 20 and 30%. In all SCC mixtures, the amount of binder, w/b ratio and dosage of SP were kept equal to 470 kg/m^3, 0.4 and 0.8-0.9%, respectively.

Table 3: Mix proportions of SCC

Mixture	w/c	River sand (kg)	Recycled granite (kg)	Cement (kg)	C.A 8/15 (kg)	C.A 3/8 (kg)	SP		Eau (kg)
							(%)	(kg)	
100RS	0,4	868.10	-	461.56	534.08	263.25	0.90	4.15	221.89
10RG		781.29	90.12						
20RG		694.49	180.23						
30RG		607.69	270.34				0.80	3.69	222.22

2.3 Testing Procedures

From each concrete mixture prismatic specimens 7×7×28 cm in sizes were cast. After casting, all specimens were covered with plastic sheets for 24 hours. After that, the specimens were unmolded and transferred to conservation in conditioned room at 20 ± 2 ºC and 100% relative humidity until the time of test. For each mix, three specimens were used to determine flexural strength and ultrasonic pulse velocity and six specimens to measure compressive strength at 28 days. These tests were conducted in accordance with European Standard (EN 196-1, 2002). Ultrasonic pulse velocity test was also carried out in agreement with American Standard (ASTM C597-16, 2016).

For water absorption by immersion test, three specimens of 70×70×280 mm in sizes from each mixture were cured in water for 28 days and dried after that at 105 ± 5 °C for 72 hours until, the specimens were weighed M_0 and immediately immersed in water at approximately 21 °C for not less than 48 hours before being weighed M_1 (ASTM C642-97, 1997). The coefficient of water absorption by immersion A_i is given by the following equation:

$$A_i = \left(\frac{M_1 - M_0}{M_0}\right) \times 100 \qquad (1)$$

Where

M_1: saturated mass (g); M_0: dried mass (g); A_i : coefficient of water absorption by immersion (%).

3 Results And Discussion

3.1 Compressive strength

The influence of recycled granite aggregates on 28-days compressive strength of SCC is shown in Figure 2. Compressive strength values are in the range of 38.03 and 40.20 MPa. As can be seen in this figure, the compressive strength is slightly decreased by increasing RG content. The mixtures contain 20% and 30% of RG developed a similar compressive strength as compared to reference mix (about 40 MPa) at 28 days. The reason behind this increment is the high percentage of fine particles in RG, which improved the compactness and therefore the resistance of SCC. In their work, Gupta & Vyes (2018) reported that the substitution of fine natural aggregate in cement mortar by waste granite powder improved the mechanical properties such as compressive strength. The use of crushed brick as a partial replacement of sand was found to decrease the compressive strength of concretes (Debieb & Kenai, 2008).

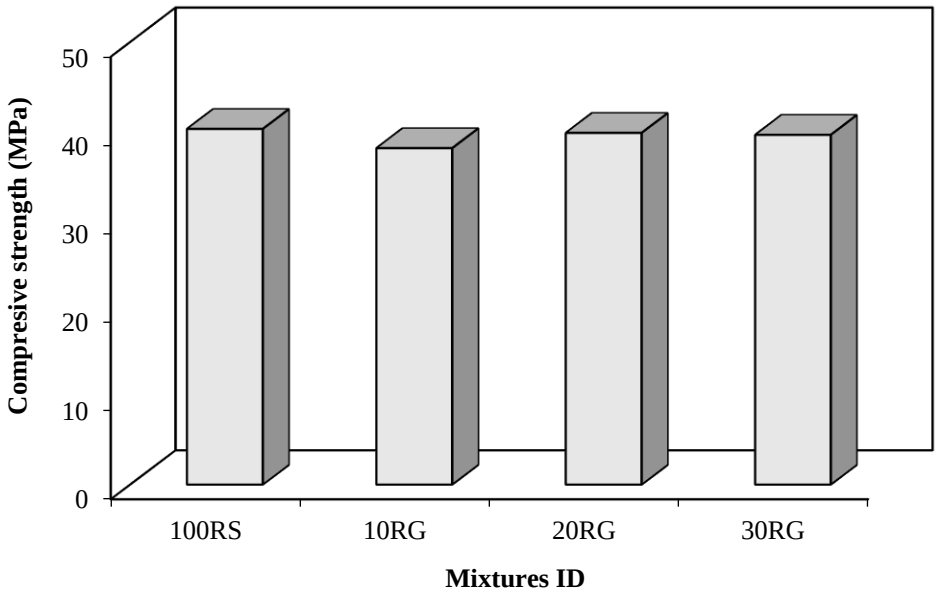


Fig. 2: Variation of 28 days-compressive strength vs RG content

3.2 Flexural strength

Figure 3 depicts the variation of flexural strength as a function of the amount of RG. The values of flexural strength are in the range of 4.36 – 5.64 MPa. The introduction of 10% and 20% of RG slightly decreased the flexural strength; however, a substitution level of 30% resulted in higher flexural strength in comparison to control mixture. This may be attributed to the irregularities in shape and texture for granite particles in comparison to river sand that is characterized by smooth and spherical particles.

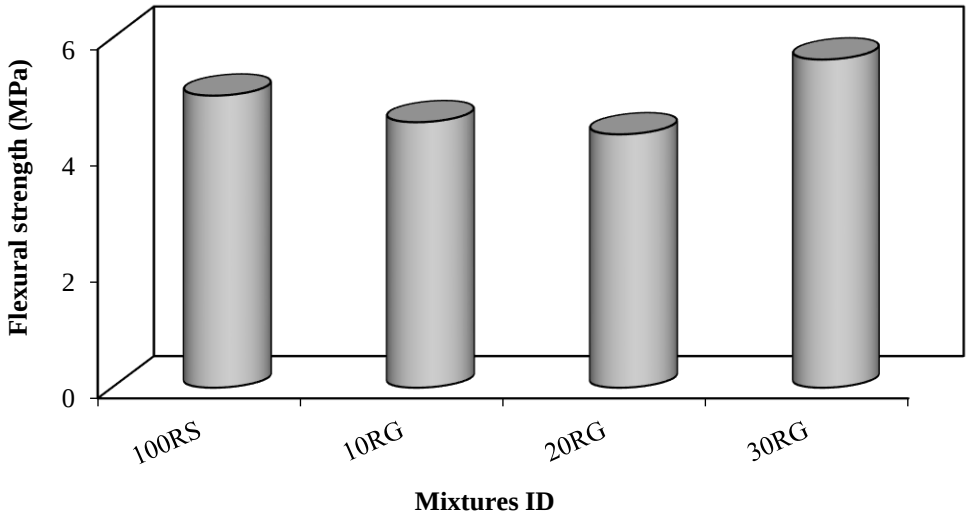


Fig. 3: Evolution of flexural strength of all SCC mixtures

3.3 Ultrasonic Pulse Velocity

The results of ultrasonic pulse velocity (UPV) test for various SCC mixtures are presented in Figure 4. UPV could be used to examine nondestructively the internal structure of concrete. The values of UPV are in the range of 4285–4405 m/s. The results revealed that UPV increased by increasing RG content. It was observed that 30RG mix has the highest value of UPV. The reason behind the increase in UPV could be due to the predominance of fine particles (<100 μm) in recycled granite in comparison to river sand as can be observed in figure 1.Whitehurst [29] classified the concretes according to their quality as following: excellent, good, moderate, bad and very bad for an UPV values above 4500 m/s, 3500 / 4500 m/s,3000 / 3500 m/s, 2000 / 3000 m/s, and lower or equal to 2000 m/s, respectively. This classification indicated that all the tested mixtures have a good quality.

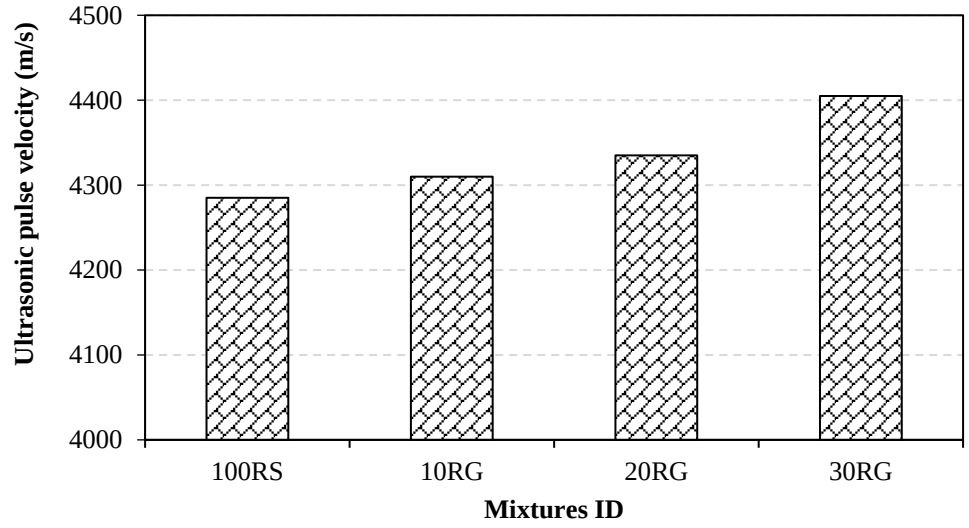


Fig. 4: Variation of ultrasonic pulse velocity of all mixtures

3.4 Water Absorption

The results of water absorption test are illustrated, in Figure 4. The values of water absorbed by immersion are in the range of 3.09 - 4.27 %. The results showed that water absorption decreased by increasing the amount of RG. Water absorption coefficient of mixtures with RG replacements of 10%, 20% and 30% is decreased by about 5%, 20% and 28% in comparison with control mixture,

respectively. This result may be attributed to the filling effect of recycled granite in which fine particles filled the voids and contributed to better packing of mixtures with RG.

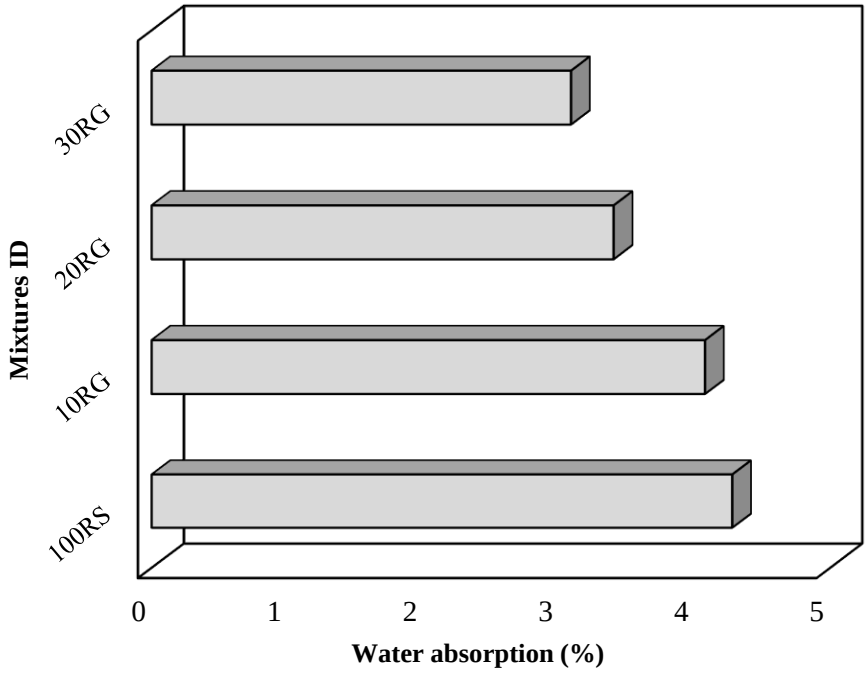


Fig. 5: Variation of water absorption of all mixtures

4 Conclusion

Based on the experimental results and evaluation of SCC with RG, the following conclusions can be drawn:

- All SCC mixtures have developed similar compressive strengths. SCC mixture included 30% RG exhibited the highest flexural strength.
- Mixtures containing recycled granite showed superiors ultrasonic pulse velocity values in comparison to control mix. This indicated the positive effect of RG in improving the density and homogeneities of SCC mixtures. Waster absorption of self-compacting concrete can be reduced by using recycled granite.
- Recycled granite waste may be successfully used as fine aggregate to produce green and low cost self-compacting concrete.

From the above conclusions, an optimum percentage of recycled granite of 30% can be recommended to manufacture sustainable self-compacting concrete.

References

ASTM C597-16. (2016). Standard Test Method for Pulse Velocity through Concrete, ASTM International, West Conshohocken, PA.

ASTM C 642-97. (1997). Standard test method for density, absorption, and voids in hardened concrete. American Society for Testing and Materials, USA.

Boucedra, A., Bederina, M. & Ghernouti, Y. (2020). Study of the acoustical and thermo-mechanical properties of dune and river sand concretes containing recycled plastic aggregates, *Construction and Building Materials*,

256.https://doi.org/10.1016/j.conbuildmat.2020.119447

Boukhelkhal, A. Azzouz, L. Benabed, B. & Belaid, A.S.E. (2017). Strength and durability of low-impact environmental self-compacting concrete incorporating waste marble powder. *Building Materials and Structures*, *4*, 31-41.https://doi.org/10.34118/jbms.v4i2.29

Cabral, A.E.B. Schalch, V. Dal Molin, D.C.C. & Ribeiro, J.L.D. (2010). Mechanical properties modeling of recycled aggregate concrete, *Construction and Building Materials*, *24*, 421–430. https://doi.org/10.1016/j.conbuildmat.2009.10.011

Chen, H-J. Yen, T. & Chen, K-H. (2003). Use of building rubbles as recycled aggregates, *Cement and Concrete Research, 33*, 125–132. https://doi.org/10.1016/S0008-8846(02)00938-9

Debieb, F. Kenai, S. (2008). The use of coarse and fine crushed bricks as aggregate in concrete, *Construction and building materials*, *22*(5), 886-893. https://doi.org/10.1016/j.conbuildmat.2006.12.013

De Oliveira, M.E.D. De Moraes Sales, R.J. De Oliveira, L.A.S. & Cabral, A.E.B. (2011). Generation and composition diagnosis of Fortaleza CDW, Engenharia Sanitaria e Ambiental, 16, 219–224. https://doi.org/10.1590/S1413-41522011000300003

Djelloul, O.K. Menadi, B. Wardeh, & G. Kenai, S. (2018). Performance of self-compacting concrete made with coarse and fine recycled concrete aggregates and ground granulated blast-furnace slag, *Advanced Concrete Construction*, *6*(2), 103-121. https://doi.org/10.12989/acc.2018.6.2.103

EN 196-1. (2002). Methods of testing cement-Part 1: Determination of strength.

Emam Ali, E. & Al-Tersawy S.H. (2012). Recycled glass as a partial replacement for fine aggregate in self-compacting concrete, *35*, 785–791. https://doi.org/10.1016/j.conbuildmat.2012.04.117

Gupta, L.K. & Vyas, A.K. (2018). Impact on mechanical properties of cement sand mortar containing waste granite powder, *Construction and Building Materials*, *191*, 155-164. https://doi.org/10.1016/j.conbuildmat.2018.09.203

Leite, M.B. Figueirêdo Filho, J.G.L. & Lima, P.R.L. (2013). Workability study of concretes made with recycled mortar aggregate, *Materials and Structures*, *46*, 1765–1778. https://doi.org/10.1617/s11527-012-0010-4

Lemaître, C. (2012). Mise en oeuvre et emploi des matériaux de construction. Editions Eyrolles, Paris.

Ouldkhaoua, Y. Benabed, B. Abousnina, R. & Kadri, E-H. (2020). Experimental study on the reuse of cathode ray tubes funnel glass as fine aggregate for developing an ecological self-compacting mortar incorporating metakaolin, *Building Engineering*, *20*: 1-11. https://doi.org/10.1016/j.jobe.2019.100951

Sadek, D.M., El-Attar, M.M. & Haitham, A.A. (2016). Reusing of marble and granite powders in self-compacting concrete for sustainable development, *Journal of Cleaner Production, 121*, 19-32. https://doi.org/10.1016/j.jclepro.2016.02.044

Singh, M. & Siddique, R. (2016). Effect of coal bottom ash as partial replacement of sand on workability and strength properties of concrete, *Journal of Cleaner Production, 112*(1), 620-630. https://doi.org/10.1016/j.jclepro.2015.08.001

Shaikh, F.U.A. (2016). Mechanical and durability properties of fly ash geopolymer concrete containing recycled coarse aggregates, *International Journal of Sustainable Built Environment, 5*, 277–287, https://doi.org/10.1016/j.ijsbe.2016.05.009.

Whitehurst, E.A. (1951). Soniscope tests concrete structures, *Journal of the ACI*, *47*, 433-444.

Cite as: Boukhelkhal A., "Hardened Properties of Self-Compacting Concrete Incorporating Recycled Granite Waste as Fine Aggregate", *The 2nd International Conference on Civil Infrastructure and Construction (CIC 2023)*, Doha, Qatar, 5-8 February 2023, DOI: https://doi.org/10.29117/cic.2023.0107

A Comparative Study on Punching Shear Strength Statistics for Ferrocement Slabs

Mohammed Ihtesham Hussain
University of Technology and Applied Sciences, Muscat, Oman
mohammed.ihtesham@hct.edu.om

Ahmed Majid Salim Al Aamri
University of Technology and Applied Sciences, Muscat, Oman
ahmed.alamri@hct.edu.om

Manjunath Shantharam Amalkar
University of Technology and Applied Sciences, Muscat, Oman
manjunath.amalkar@hct.edu.om

Chimdi Gadafa Benti
Adama Science and Technology University, Adama, Ethiopia
chimdi.gedfa@astu.edu.et

Abstract

Ferrocement is a modern material that is considered composite as it is made of cement mortar and tightly packed layers of wire mesh. Recent ferrocement applications include prefabricated rooftop elements, load-bearing panels, and bridge slabs. However, in various parts of the world, particularly the eastern hemisphere, numerous individuals and research groups have made significant efforts to study the engineering of ferrocement which includes tensile, compressive, impact, and fatigue strength, as well as, cracking behaviour. Despite this, the shear strength of ferrocement slabs has received scant consideration. However, since ferrocement is increasingly used in structural applications, transverse shear has become a determining design factor. This paper presents the behavior of ferrocement slabs when subjected to punching shear. Eleven square slabs with dimensions 916 mm were cast, and their thicknesses were adjusted along with the wire mesh and mortar strength. After 14 days of curing, these slabs were removed from the water tank, de-moulded, and tested. Prior to testing, the top surface of these slabs was bleached to reveal the crack pattern clearly. The slabs failed in punching instead of flexural failure and they demonstrated ductile behaviour. A comparison for the observed results for the strengths and behavior of the slabs was made.

Keywords: Ferrocement; Punching shear; Slabs; Comparison; Failure mode

1 Introduction

Ferrocement has been employed in a variety of applications during the last two decades, including strengthening and repairing existing reinforced concrete, steel, and concrete water tanks, sewers, and swimming pools, as well as seismic retrofitting masonry walls. Ferrocement coatings are relatively lightweight and, in the majority of cases, relatively simple to install. The reinforced material's homogenous distribution and high surface area to volume ratio result in a more effective fracture arrest mechanism, i.e., crack propagation is halted, resulting in the material's high tensile strength. The ultimate tensile resistance in Ferrocement is achieved by applying the reinforcement in the loading direction. Nevertheless, analysing and designing ferrocement members are quite complex and basically follows the principles of reinforced concrete elements specifically in flexure and shear. In comparison to studies on the flexural behaviour of ferrocement elements, very few

research publications exist on the shear behaviour of ferrocement elements. This could be because these elements have a very high span-to-depth ratio. Due to the scarcity of raw resources and the demand for low-level technical capabilities, ferrocement has a high potential for contraction in developing nations (ACI, 1997). Although ferrocement materials are typically thin and frail, they are equally robust and aesthetically pleasing and offer a diverse range of construction solutions, particularly for roofing and wall construction (Pushyamitra, 2011).

When ferrocement was used to examine the wear of concrete boxes, it resulted in a considerable improvement in stiffness, strength, and ductility (Abdullah & katsuki, 2002). Ferrocement is a coating that improves the shear strength of brickworks (Walker & Damu, 1997). Structural units formed of ferro cement planes can be used with confidence in a variety of applications such as low-cost housing plans, agriculture, and industrial use (Akhthar ET.AL, 1999). For the same steel stress, the fracture widths in ferrocement are orders of magnitude smaller than those in reinforced concrete, making it a superior material for water retention structures and suggested for the construction of water tanks (Balaguru ET.AL, 1997) and (Naaman, 1971). The failure modes and crack patterns of ferrocement box beams subjected to two-point stress tests show that the smaller the span to effective depth ratio, i.e., a/d1, the more pronounced the diagonal tension failure; if the ratio is greater than one, the beam tends to fail flexibly (Abdul Samad ET.AL, 1998). Another study looked at the location of diagonal cracks in rectangular reinforced concrete beams. The location of the crucial diagonal fracture as measured from the nearest support increases as the a/d ratio grows and, to a lesser extent, as 'fcu' decreases (Al-kubaisy & Nedwell, 1998). The ultimate moment and the behavior of ferrocement in flexure increase with increasing matrix grade and reinforcement volume fraction (Mansur & Paramasivam, 1986). Shear strength of ferrocement beams subjected to transverse shear with varied reinforcing volume percentages was found to be dependent on mortar, wire mesh strength, volume %, and shear span (Venkata & Basa, 1988). The punching shear capacities of the retrofitted test specimens were significantly higher than those of the bare specimens with apertures, and most structural code equations grossly underestimate the punching shear capacities of the test specimens (Durucan & Anil, 2015). There have been few studies into ferrocement members' behavior under punching shear (Tan, 1994; Al-Kubaisy & Jumaatco, 1999).

There is currently no code formula for the shear strength of ferro cement elements. There is a necessity to demonstrate that the shear strength equations supplied by existing norms of practice for reinforced concrete may also be applied to ferrocement. All samples of slabs A1, A2, A3, A4, and A5 were similar in dimensions except reinforcement, i.e., wire mesh and varying skeleton steel, volume fraction of reinforcement (vf). Slabs B1, B2, and B3 were developed to investigate the influence of slab thickness (h), using 20-, 25-, and 35-mm slab thicknesses. Slabs C1, C2, and C3 are composed of three identical slabs with varying compressive strengths of mortar (fcu). The load-deflection relationship is investigated, as well as the punching shear behaviour.

2 Materials and Methods

Cement, sand, water, superplasticizer, wire meshes, and skeletal steel were used in this experimental work. Throughout the experiment, ordinary Portland cement (OPC-43 grade) was employed. As a fine aggregate, well-graded locally accessible river sand down to 2.36 mm in size was used. Wire mesh is a significant component of ferrocement and is often composed of fine wires. As shown in Figure 1, the wire mesh is 1 mm in diameter and has 12.5 mm x 12.5 mm openings. The wire mesh has a yield strength of 390 N/mm^2 in tension.

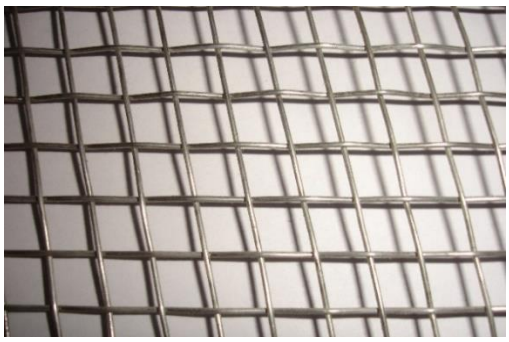


Fig. 1: Square wire mesh

Between the upper and lower layers of the wire mesh, skeletal steel bars 6 mm in diameter are symmetrically positioned in two orientations. Steel bars have yield strength of 430 N/mm2. The strength of the mortar was increased by changing the water-cement ratio and adding suitable admixtures to improve workability and speed-strength development. To aid in crack detection, the slabs' bottom and top faces were whitewashed. Table 1 contains information about the various specimens cast.

Table 1: Details of test specimens

Slab Notation	Investigated parameter	Thickness of slab h (mm)	No. of layers of wire mesh	No. of skeletal steel	Volume Fraction of Reinforcement V_f (%)	Mortar Strength (N/mm^2)
A1	V_f	30	2	10	1.45	40
A2		30	2	8	1.24	40
A3		30	1	8	1.03	40
A4		30	3	8	1.45	40
A5		30	2	-	0.42	40
B1	h	20	1	10	1.85	40
B2		25	2	9	1.85	40
B3		35	2	10	1.85	40
C1	f_{cu}	30	2	6	1.04	30
C2		30	2	6	1.04	20
C3		30	2	6	1.04	12

As seen in Figure 2, all specimens were exposed to a single concentrated force delivered through the centre of a rigid steel loading plate using a hydraulic jack.

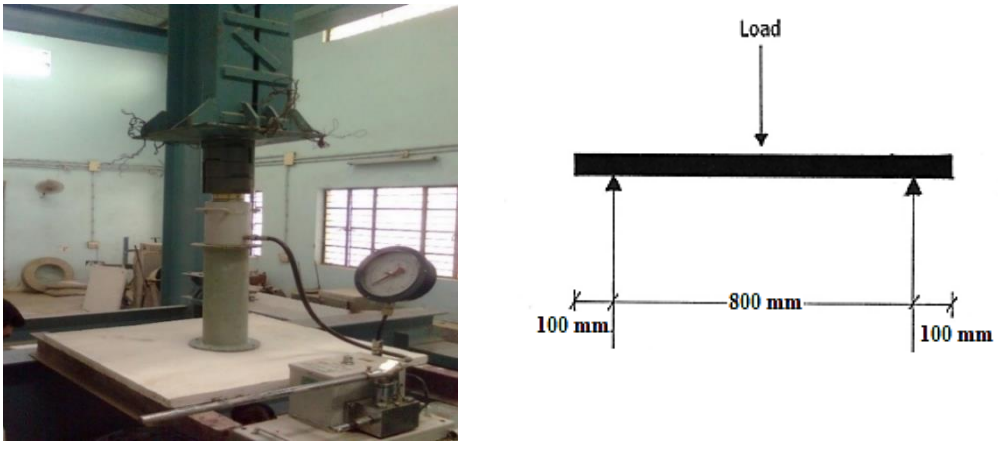


Fig. 2: Loading set up for the experimental work

By using the hydraulic jack, the load is gradually increased. The deflection under the load point was

determined using a dial gauge attachment (the least count is 0.01mm). The load was applied in about 2 kN increments. Following each load increase, the dial gauge reading was collected, and the area examined for the presence of cracks.

3 The Behavior of Slabs

In general, it was observed that, the load-deflection relationship is linear until the slab begins to crack. The first crack began at around 20%–35% of each slab's ultimate shear strength on the tension side of the slab beneath the loaded area and progressed radically across the slab to the sides.

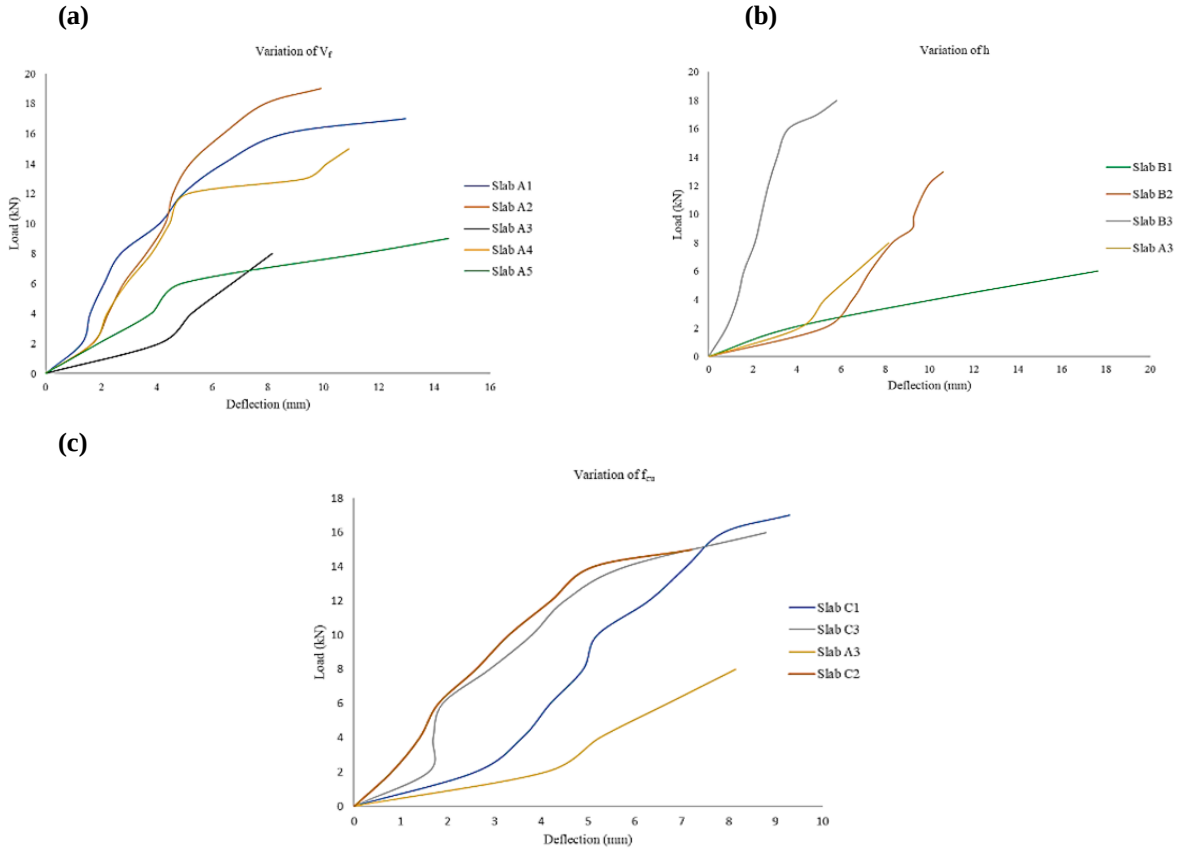


Fig. 3: Load-Deflection curves

(a) Variation of V_f **(b)** Variation of h **(c)** Variation of f_{cu}

When a slab cracks, its stiffness is reduced, and the load picks up once the fracture development has stabilized with insignificant slab deflection. As the ultimate load approaches, the stiffness of the curve is reduced further until it is almost horizontal. On the slab's top face, punching shear failure was evident, but on the slabs bottom face, just an outline of the truncated failure cone with a substantially larger diameter was created, along with the noticeable lifting of the slab's corners. When the ultimate load is attained, the load-carrying capacity suddenly decreases, and the slab fails in punching shear. Following the ultimate load, the load-bearing capacity is entirely determined by steel reinforcement and membrane action.

4 Failure Pattern in Slabs

Also in the slabs, radial cracks were observed on the bottom face, primarily between the loading point and the edges of the panel; on the upper surfaces, a circular punching effect of the loading area, as can be seen on the surface in Figure 4. It was mirrored on the bottom face with an enlarged picture, clearly indicating the truncated cone. Although this overall pattern of cracking is constant

across all slabs, depending on the test parameter, variances in the number and spacing of cracks, as well as the perimeter of the bottom failure cone, were noted. Around 40% to 50% of the ultimate load results in the formation of new cracks between the supports and at the loading site. Increased load exacerbated the cracks and brought them to the ultimate load point. Observation demonstrates that as the thickness (h) is raised, the bottom perimeter increases. Although the overall pattern of cracking is essentially comparable for the variations in f_{cu} and h.

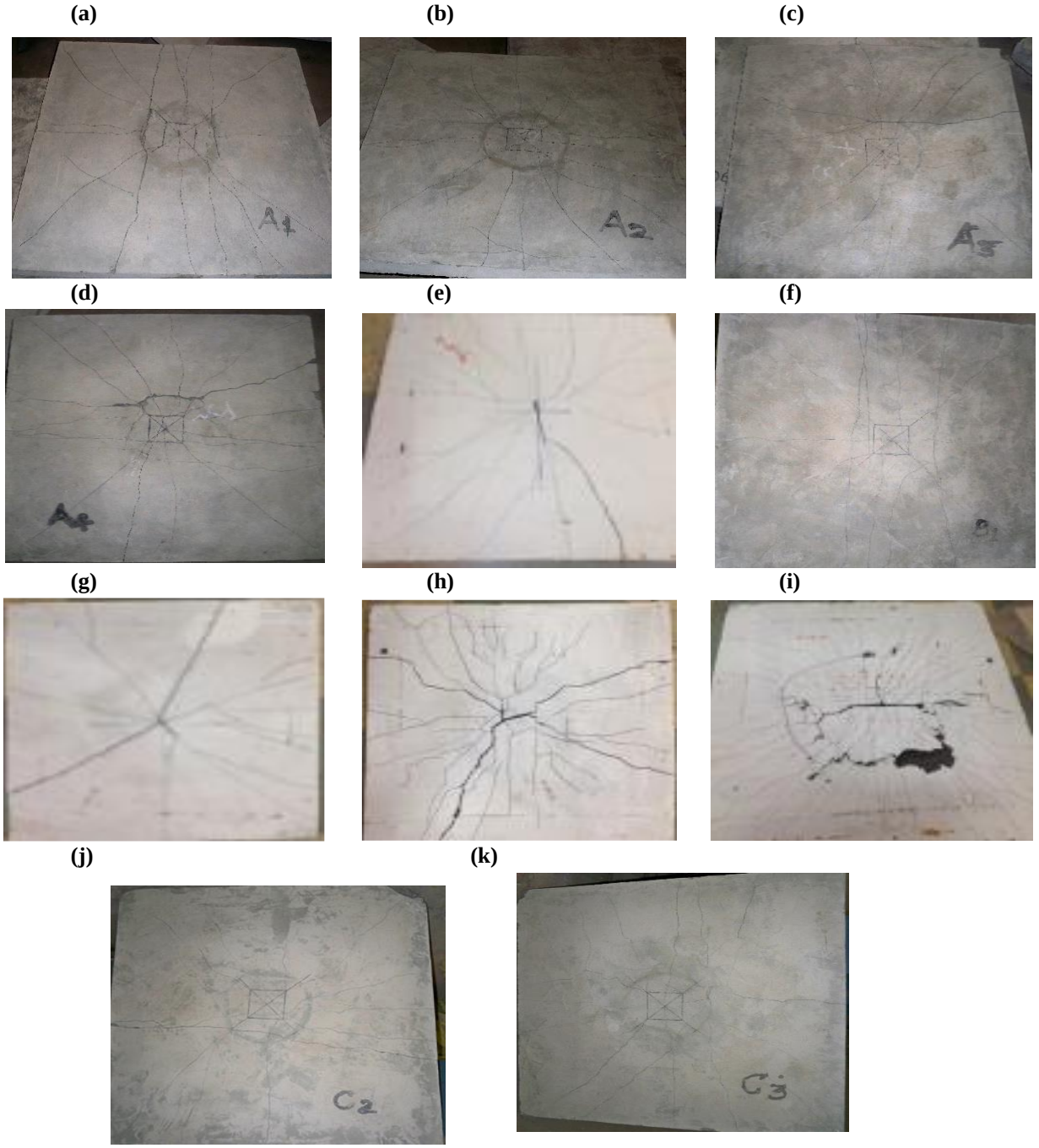


Fig.4: Cracked pattern and punching shear envelope for different slab

V_f has a major influence on the distribution of cracks. Increased reinforcement resulted in fewer larger fractures and more closely spaced cracks. Cracks were clustered near the loading point at exceptionally high V_f values, with the majority developing along the reinforcing grid lines. Most specimens tested failed in punching shear. Based on the experimental data, the critical perimeter on the slab's top surface typically occurred quite close to the plate's face. While the matrix bulged out

towards the bottom of the slab, this frequently resulted in a much larger perimeter than at the top. Additionally, the essential perimeter's size and form are consistent. This indicated that the shear plane generated was angled at an angle, resulting in the pyramidal or conical shape associated with the punching shear failure.

5 Conclusion

All the slabs were subjected to single concentrated load delivered using a hydraulic jack. It was observed that instead of flexure, the ferrocement slabs failed due to punching shear failure. On the top surface, the inclined shear plane typically originates near the periphery of the loaded area, with fewer cracks on the top surface than on the bottom. The load-deflection trend of the ferrocement slabs subjected to punching shear exhibits two peaks and demonstrated ductile behaviour. The first peak is caused by punching shear failure, whereas the second peak is caused by the development of tensile membrane action in response to high deformation. The second peak is often greater than the first in slabs with a high-volume proportion of reinforcement or a larger loaded area. In terms of stress, both cracking and punching shear strengths rise independently of V_f, f_{cu}, and h, but decrease as effective span increases. Punching shear strength has increased up to 1.04 percent of the volume percentage of reinforcement (V_f) and an additional increase in (V_f) resulted in a decrease in punching shear strength. Increases in slab thickness (h) resulted in an increase in punching shear strength while increased Mortar strength (f_{cu}) results in increased punching shear strength. The research parameters do not affect the number and extent of cracks that occur on the compression side. Ferrocement elements shear behaviour is almost identically to reinforced concrete elements.

References

Samad, et al. (1998). Fibrocement box beams subjected to pure bending and bending with shear. *Journal of Ferrocement, 28*.

Abdullah and Katsuki Takiguchi. (2002). “Strength and behavior of concrete confined by ferrocement boxes”. Journal of Ferrocement, 32.

ACI. (1997). State-of-the-Art report on ferrocement, ACI 549-R97. Manual of Concrete Practice. American Concrete Institute, Farmington Hills, Michigan.

Akhthar, S. et al. (1999). Experimental investigations on use of fly ash mortar in ferrocement panels.

Al-Kubaisy, M., & Jumaat, M. (1999). Punching Shear Strength of Ferrocement Slabs, *Journal of Ferrocement, 29*(2): 99-114.

Al-Kubaisy, M.A. & Nedwell, P.J. (1998). Location of Critical Diagonal Crack in Ferrocement Beams, *Journal of Ferrocement, 28*.

Balaguru, P. N., Naaman, A. E. & Shah, S.P. (1977). “Analysis and Behaviour of Ferrocement in Flexure, “proceedings, ASCE, V. 103, ST 10, oct.1977, pp.1937-1951.

Durucan, C. & Anil, Ö. (2015). Effect of opening size and location on the punching shear behavior of interior slab-column connections strengthened with CFRP strips. Eng Struct 2015. https://doi.org/10.1016/j.engstruct.2015.09.033

Mansur, M., A. & Paramasivam, P. (1986). Study of Sandwich Wall Panels, *Journal of Ferrocement 16*(3): 295-313.

Naaman, A. E., & Shah, S. P. (1971). “Tensile Tests of Ferrocement,” ACI Journal, Proceeding V. 68, No.9, Sept. 1971, pp. 693-698

Walker, P., J. & Damu, M. (1997). Shear reinforcement for Brickwork Beams using Ferrocement – Ferrocement Vol 27. no.1-Jan 1997 pp 33 – 45.

Pushyamitra, D. (2011). Use of ferrocement in construction industry. Proceedings of the National Conference on Ferrocement, FS-2011, Pune, India. 30-37.

Tan, K. H. & Paramasivam, P. (1994). Punching shear strength of steel fiber reinforced concrete slabs, *Journal of Material in Civil Engineering 6*: 240–253. https://doi.org/10.1061/(ASCE)0899-1561(1994)6:2(240)

Krishna, V. & Gouda, P .D. B. (1988). Some studies on the behaviour of ferrocement in shear. In Proceedings of the 3rd International Conference on Ferrocement: 99 – 105. Roorkee University of Roorkee.

Cite as: Hussain M.I., Al Aamri A.M.S., Amalkar M.S. & Benti C.G., "A Comparative Study on Punching Shear Strength Statistics for Ferrocement Slabs", *The 2nd International Conference on Civil Infrastructure and Construction (CIC 2023)*, Doha, Qatar, 5-8 February 2023, DOI: https://doi.org/10.29117/cic.2023.0108

Optimum Design of Plane Trusses Using Mathematical and Metaheuristic Algorithms on a Spreadsheet

Vagelis Plevris
Department of Civil and Architectural Engineering, Qatar University, Doha, Qatar
vplevris@qu.edu.qa

Ismail Hafez Mohammed Elias
Department of Civil and Architectural Engineering, Qatar University, Doha, Qatar
ie1707600@student.qu.edu.qa

Aristotelis E. Charalampakis
Department of Civil Engineering, University of West Attica, Athens, Greece
achar@uniwa.gr

Abstract

Mathematical optimization refers to the process of finding the values of variables that maximize or minimize a function. Structural optimization is the process of designing a structure in such a way as to minimize its weight or cost, while meeting a set of performance requirements, ensuring that it is robust, lightweight, and efficient. Two large categories of optimization algorithms are mathematical and metaheuristic algorithms. The ones of the first rely on mathematical principles, are deterministic and exact but may fail if the problem is too large or complex. The latter category, metaheuristics, represents algorithms that are used to find approximate solutions. They are high-level strategies that guide the search toward a good solution, rather than being a specific, deterministic algorithm. They are often used for problems where it is difficult or impractical to find the optimal solution using exact methods. Metaheuristics typically involve iteratively improving a solution through some type of search or exploration process. They make use of techniques from probability and statistics, such as randomization and stochastic optimization, to explore the search space and guide the search toward good solutions. Some examples include genetic algorithms, simulated annealing, differential evolution (DE), particle swarm optimization (PSO), and ant colony optimization. In this study, a mathematical optimizer and two metaheuristics (DE, PSO), are employed for the optimum structural design of plane truss structures aiming to minimize the weight of the structure under constraints on allowable displacements and stresses. A 10-bar plane truss is considered as the numerical example of the study. The constraints are checked by performing an analysis with matrix methods. All calculations are done on a spreadsheet. The results of the algorithms are compared to each other as well as to results from the literature in terms of convergence speed, number of function evaluations, and accuracy of the solution.

Keywords: Optimization; Metaheuristic; Differential Evolution; Particle Swarm Optimization; Spreadsheet

1 Introduction

A spreadsheet application is a computer program that allows users to create and edit spreadsheets. Spreadsheets are used to organize data and perform calculations with numerical information. They consist of rows and columns, with cells that can contain text, numbers, or formulas. Some popular spreadsheet applications include Microsoft® Excel® (hereafter, simply Excel), Google Sheets, Open

Office Calc., and Apple Numbers. Spreadsheets are commonly used for budgeting, financial analysis, and data management, but they also see significant applications in various engineering fields, such as structural engineering, (Christy, 2006), water engineering, (Pandit, 2015), geotechnical engineering, (Ozcep, 2010), among others. They can do basic calculations such as cost estimates, schedule and cost control, and markup estimation, as well as structural calculations of reactions, stresses, strains, deflections, and others. Many engineering firms rely on spreadsheets for complex engineering calculations of all kinds. Spreadsheets may not exhibit the full power and advanced capabilities that advanced coding with a computer language can offer, but they have the advantage that they are simple to use and easy to understand, without the need for the user to use coding to make simple or more complex calculations.

In this work, we employ Excel for the optimum design of plane truss structures. In particular, we use the Excel Solver, which is a built-in optimizer of Excel, and the xl Optimizer software[1] which is an external plug-in for Excel. The Solver has been successfully used for solving various kinds of structural analysis problems (Bhatti, 2005; Rady & Mahfouz, 2022; Shahnam, 2003).

2 Structural Optimization of Trusses

Structural optimization is the process of designing a structure (such as a bridge, building, or aircraft) in such a way as to minimize its weight or cost, while still meeting a set of performance requirements. It is a branch of engineering that involves the use of optimization techniques and principles of structural mechanics to design structures that are robust, lightweight, and efficient. Structural optimization typically involves three steps: (i) defining the design variables, constraints, and objective function; (ii) formulating the optimization problem; and (iii) solving the problem. The design variables are the parameters that can be varied in the design, such as the shape, size, and material of the structure. The constraints are the requirements that the structure must meet, such as strength, stability, and durability. The objective function is a measure of the performance of the structure, such as its weight or cost.

A truss is a structure that is composed of a set of slender, pin-jointed members that are used to span a distance and support loads. Trusses are commonly used in engineering and construction. They are usually made of steel or other metals and are used in a wide variety of applications, including bridges, buildings, towers, and other structures. In truss sizing optimization, the aim is usually to find the right sections of the structural members of a truss that would lead to minimum weight while satisfying the design constraints. Such a problem can be formulated mathematically as:

$$\begin{aligned} &\min_{x_i} \quad W(\boldsymbol{x}) = \sum_{i=1}^{N_e} L_i \cdot x_i \cdot \rho_i \\ &\text{Subject to} \\ &g_k(\boldsymbol{x}) \le 0, \quad k = \{1,\ldots,K\} \end{aligned} \tag{1}$$

Where $W(\boldsymbol{x})$ is the total structural weight (or mass), N_e is the number of elements, $\boldsymbol{x}$ is a vector with the cross-section areas x_i of each member, L_i is the length of each member, ρ_i is the material density of element i, and $g(\boldsymbol{x})$ are the behavioral constraints, K in total. Side constraints are also usually imposed on the lower and upper limits of the design variables, i.e. $lb_i \le x_i \le ub_i$, where lb_i and ub_i denote the lower and upper bounds of the i-th design variable, respectively.

[1] Xl Optimizer, Add-in version overview, accessed 5 January 2023, https://xloptimizer.com/overview

3 Optimization Algorithms

In this work, we have used the Excel Solver and the xl Optimizer plug-ins for our optimization needs. The Solver has been used for optimizing the truss structure using mathematical algorithms and in particular the **Generalized Reduced Gradient (GRG)** method. Various metaheuristic algorithms are available in the literature for dealing with constrained structural optimization problems (Lagaros et al., 2022). In xl Optimizer, we have used two of the offered metaheuristic algorithms, namely, **Differential Evolution (DE)** and **Particle Swarm Optimization (PSO)**.

3.1 Generalized Reduced Gradient: Single Point and Multi start

GRG is an algorithm for solving optimization problems with continuous variables and linear or nonlinear constraints. It is an iterative method that starts with an initial feasible point and then uses the gradient of the objective function to move toward the optimal solution. GRG works by constructing a quadratic approximation of the objective function at each iteration and then solving a series of quadratic programming sub problems to find the next iterate. The algorithm stops when the quadratic approximation is good enough, or when a specified termination criterion is met. One of the main advantages of the GRG method is that it can handle a wide range of optimization problems, including problems with linear constraints, nonlinear constraints, and mixed integer variables. It is also relatively efficient, especially for problems with a large number of variables. However, it can be sensitive to the initial point and may not always converge to the global optimum. It can also be computationally expensive for large problems with many constraints. GRG is the default algorithm used by Solver and it is offered in two variations: (i) “Single point” (default setting), where the algorithm is run once, and (ii) “Multi start” where GRG will run repeatedly, starting from different (automatically chosen) starting values for the decision variables. This process will usually find a better solution, at the expense of requiring more computing time.

3.2 Differential Evolution

Differential Evolution (DE) is a metaheuristic optimization algorithm that was introduced by (Storn & Price, 1995). It is a population-based algorithm used to find approximate solutions to optimization problems, particularly problems with a large number of variables. In DE, a population of candidate solutions is maintained, and each member of the population is represented by a set of variables or parameters. At each iteration, DE generates a new candidate solution by combining the variables of three existing solutions in a specific way. This new candidate solution is then evaluated, and if it is better than the worst of the three solutions that were used to generate it, it is added to the population. The key idea behind DE is that the combination of variables from different solutions can create new, potentially better solutions that would not have been found by simply exploring the search space randomly. DE uses several strategies to control the search process, such as scaling and crossover, which help to balance exploration and exploitation and avoid getting stuck in local minima. It is simple to implement and has been shown to be effective in many types of problems, particularly those with a large number of variables or complex, multimodal search spaces. DE comes in many variations Georgioudakis & Plevris (2020a); Georgioudakis & Plevris (2020b) and has been applied successfully to, many structural engineering optimization problems in the past (Georgioudakis & Plevris, 2018; Kao et al., 2020). In this work, we use the standard DE/Rand/1/bin scheme.

3.3 Particle Swarm Optimization

Particle Swarm Optimization (PSO) is a metaheuristic optimization algorithm that is inspired by the social behavior of birds. It was first introduced by Kennedy & Eberhart (1995) as a computational

method for optimizing continuous, nonlinear problems. In PSO, a set of "particles" are used to search for a good solution to a problem. Each particle represents a potential solution to the problem and is initialized with a randomly generated position and velocity. The position of each particle is updated at each iteration based on its previous position and velocity, as well as, the positions and velocities of the other particles in the swarm. The movement of the particles is guided by two types of information: the "personal best" position of each particle, which is the best position that the particle has achieved so far; and the "global best" position, which is the best position that has been achieved by any particle in the swarm. At each iteration, each particle adjusts its velocity and position based on these two sources of information, with the goal of moving toward better positions in the search space. PSO has several attractive properties, including simplicity, flexibility, and robustness. It is particularly well suited to problems with many variables, or problems that are multimodal or noisy. It has been applied to a wide range of optimization problems, including function optimization, clustering, and image processing. It has also very interesting applications in structural engineering (Charalampakis & Dimou, 2010; Plevris et al., 2011).

4 Numerical Example

The 2D truss that is investigated and optimized is presented in Fig. **1**. The Young's modulus *E*is equal to 10,000 ksi (68.95 GPa), the length *L* is 360 in (9.144 m), the load *P* is 100 kip (444.82 kN) and the material density ρ is 0.1 lb/in^3 (2767.99 kg/m^3). There are 10 truss members and each one represents a design variable; this results in 10 design variables for the optimization problem, corresponding to the section area for each member, in the interval [0.1, 35] (in^2) (0.64 to 225.81 cm^2). The constraints of the optimization problem are imposed on stresses and displacements. In particular, the maximum allowable stress is 25 ksi (172.37 MPa) for any member, in compression or tension, while the maximum allowable displacement is 2 in (5.08 cm), in any of the ±x and ±y directions. Buckling is not taken into account as a constraint in this problem. The optimization objective is the minimization of the total weight (or total mass) of the structure, under the imposed constraints. This example is a standard benchmark problem that has been studied thoroughly by several researchers in the literature (Plevris, 2009). All simulations and analyses are performed in Excel on a personal computer running Windows 11, equipped with an Intel Core i9-8950HK (2.90 GHz) and 64 GB Ram.

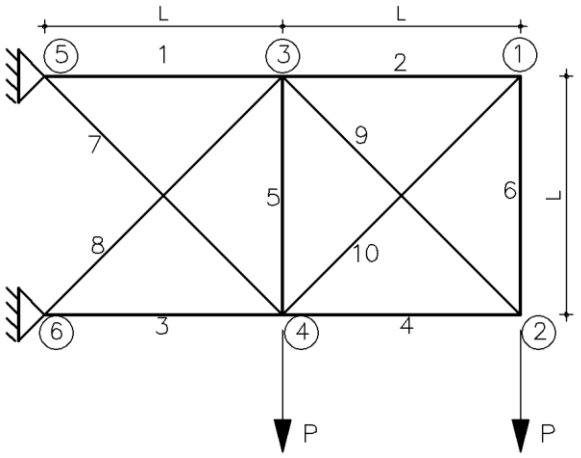


Fig. 1: The 10-Bar Plane Truss Model

4.1 Results from the Literature

Table 1 shows various results from the literature for the same problem. In this table, constraint violations are reported using a bold font. The best results that strictly do not violate any of the

constraints are the ones reported by (Plevris & Papadrakakis, 2011) and (Charalampakis & Tsiatas, 2019). Some authors report lower objective function values, but their designs violate some of the constraints, as shown in the table.

Table 1: Optimization results from the literature

	(Galante, 1992)	**(Haftka & Gürdal, 1992)**	**(El-Sayed & Jang, 1994)**	**(Memari & Fuladgar, 1994)**	**(Ghasemi et al., 1997)**	**(Perez & Behdinan, 2007)**	**(Plevris & Papadrakakis, 2011)**	**(Charalampakis & Tsiatas, 2019)**
A1 (in^2)	30.4400	30.5200	32.9700	30.5610	25.7300	33.5000	30.5218	30.5310
A2 (in^2)	0.1000	0.1000	0.1000	0.1000	0.1090	0.1000	0.1000	0.1000
A3 (in^2)	21.7900	23.2000	22.7990	27.9460	24.8500	22.7660	23.1999	23.1970
A4 (in^2)	14.2600	15.2200	14.1460	13.6190	16.3500	14.4170	15.2229	15.2280
A5 (in^2)	0.1000	0.1000	0.1000	0.1000	0.1060	0.1000	0.1000	0.1000
A6 (in^2)	0.4510	0.5510	0.7390	0.1000	0.1090	0.1000	0.5514	0.5500
A7 (in^2)	7.6280	7.4570	6.3810	7.9070	8.7000	7.5340	7.4572	7.4590
A8 (in^2)	21.6300	21.0400	20.9120	19.3450	21.4100	20.4670	21.0364	21.0450
A9 (in^2)	21.3600	21.5300	20.9780	19.2730	22.3000	20.3920	21.5285	21.5110
A10 (in^2)	0.1000	0.1000	0.1000	0.1000	0.1220	0.1000	0.1000	0.1000
Weight (lb)	4 999.22	5060.93	5013.39	4981.09	5095.64	5024.25	5060.85	5060.86
Max Stress (ksi)	**25.08667**	**25.00271**	**31.28849**	20.60011	18.52549	**25.01711**	24.99998	24.99991
Max Displ. (in)	**2.02798**	1.99996	**2.01307**	**2.06047**	**2.01368**	**2.03890**	2.00000^{-}	2.00000^{-}

4.2 Computational Tools: Excel Solver and Xl optimizer

In this work, we have used the built-in Solver of Excel and xl Optimizer software. In particular, we have used two variations of the GRG mathematical algorithm of the Solver, namely the Single point GRG and the Multi start GRG, and two metaheuristic algorithms of xl Optimizer, namely DE and PSO. It has to be noted that Solver also offers a third alternative, an Evolutionary Algorithm (a Genetic Algorithm, GA) (Goldberg, 1989), while xl Optimizer offers a variety of additional optimization algorithms, such as different variants of DE, Enhanced PSO (EPSO), GA, Simulated Annealing, Artificial Bee colony, and others. In addition, xl Optimizer can perform multi-objective optimization in which two or more objectives, usually conflicting with each other, are to be optimized simultaneously, an advanced topic with very interesting and useful engineering applications (Lagaros et al., 2005; Papadrakakis et al., 2002).

To use both tools, one first needs to set up the problem in an Excel spreadsheet. This typically involves defining the variables to be optimized and the constraints that must be satisfied. In our example, all these data are entered in Excel via their corresponding cells in a spreadsheet, i.e. the cell that contains the objective function, the cells that contain the variables, and the cells that contain the constraints. The truss analysis is done using matrix methods (the direct stiffness method) for plane trusses. For simplicity, no Macros or any other coding has been used for analysis or any other purposes. All the analysis is done using matrix operations in Excel, using standard Excel functions for matrix manipulation, such as “Mmult”, “Minverse” and “Transpose”, without the use of any coding. In most cases, we used the default settings of each optimization tool, unless otherwise stated.

Excel Solver is a tool for Microsoft Excel that allows one to find an optimal solution to a problem that has multiple variables and constraints. The Solver comes together with Excel, as part of its

basic installation, but it is deactivated by default and the user has to enable it through Excel options (Add-ins). Many different types of problems can be solved using Solver, including linear programming, nonlinear programming, and integer programming problems. It can also be used to solve problems involving complex formulas or large datasets.

Xl Optimizer is an advanced optimization toolbox that can be installed as an add-in to Excel. It implements a large variety of customizable, state-of-the-art metaheuristic algorithms in a single environment, featuring an intuitive user interface. The xl Optimizer add-in is installed in Excel's ribbon and does not require any external programs. It is ideal for very difficult (multi-parametric, non-differentiable, discontinuous, combinatorial, deceptive, etc.) and/or expensive optimization problems.

4.3 Optimization Results with Solver

Single Point Solution

First, we use the GRG Nonlinear optimizer, which is the default optimizer of Solver. The solver options used are the following default options: "*Max Time: Unlimited, Iterations: Unlimited, Precision: 0.000001, Use Automatic Scaling, Convergence: 0.0001, Population Size: 100, Random Seed: 0, Derivatives Forward, Require Bounds, Max Sub problems: Unlimited, Max Integer Sols: Unlimited, Integer Tolerance: 1%, Assume Non Negative*". In the single point solution, it is important to define a proper starting point, as the solution reached usually depends on the point initially set. In our case, we started the run with a "heavy" design, where design variables have been set to their upper limit, i.e., 35 in^2. We also tried other options, starting all design variables from the 25, 15, and 5 in^2points, but we did not notice any significant difference in the obtained results. The results of the Single point solution with the GRG Nonlinear optimizer are shown in Table 2. The minimum obtained is 5076.67 lb. The max displacement is reported as 2 in, with a very slight violation of this constraint. The solution time was very fast, 0.797 seconds, for 30 iterations of the algorithm.

Multi Start Solution

For the Multi start case, the default population size given by Solver is 100 but instead, we used the value of 10 as we noticed that there is no significant improvement in the objective function after the first runs, so a value of 100 would only cause delay. The starting point is again set with all design variables set at their highest value (35 in^2). Using Multi start, we obtain a better result (5060.84 lb), at the expense of spending more computing time (14.4 times more than the time needed for the Single Point Solution). In addition, there are slight violations of the constraints, as shown in Table 2.

4.4 Optimization Results with Xl optimizer

In xl Optimizer the termination criterion is set as "*OR (FE>=20000, TIME_MIN>10)*", which means that the maximum number of iterations is 20,000 for all methods used, and also the maximum time of calculations is 10 minutes. The latter criterion was never triggered as the criterion related to the maximum number of iterations was triggered before, for all cases. The default constraint function is "*1000*V+100*". In our case, we used a stricter constraint, "*1000*V+10000*", to make sure that the optimum design will be feasible (with no constraint violations) in the end.

Differential Evolution

The DE variant used is the default one offered by the program. It is the DE/Rand/1/bin scheme using the following default settings: "*Population code = '50', Population = 50, F = 0.5, Cr = 0.9, Asynchronous updating of solutions = No*". The results of DE are presented in Table 2. The

minimum obtained is 5060.87 lb with no violations of the constraints. The solution time was 69.098 seconds for 20,000 iterations of the algorithm.

Particle Swarm Optimization

The PSO variant used is the standard PSO with the following default program settings: "*Population code = '20', Population = 20, C1 = 2, C2 = 2, W0 = 0.8, Gamma = 0.4, Elitism = Yes.*" The results are presented in Table 2.The results of PSO are also presented in Table 2. The minimum obtained is 5080.57 lb with a very small violation of the displacement constraint. The solution time was 73.073 s for 20,000 iterations of the algorithm, which is the largest time required by any algorithm tested.

Fig. **2** shows the convergence histories for both DE and PSO metaheuristic algorithms. We see that PSO converges faster during the first runs, but then DE takes the lead after around 6000 iterations. The total number of iterations for each algorithm is 20,000 but this graph has been limited to the first 10,000 iterations for illustration purposes. After 10,000 iterations, DE had reached an objective value of 5062.67 (vs 5060.87 in the end), and PSO had already reached the same optimum as the one after 20,000 iterations (5080.57).

Table 2: Optimization results with all Optimization Algorithms

	Solver algorithms		**xlOptimizer algorithms**	
	Single point GRG	**Multistart GRG**	**DE**	**PSO**
A1 (in^2)	30.73067	30.52222	30.55354	32.28475
A2 (in^2)	0.10000	0.10000	0.10000	0.10000
A3 (in^2)	23.94943	23.20055	23.17546	23.54453
A4 (in^2)	14.72451	15.22289	15.24921	14.68662
A5 (in^2)	0.10000	0.10000	0.10000	0.10000
A6 (in^2)	0.10000	0.55103	0.55361	0.10000
A7 (in^2)	8.53892	7.45715	7.45930	8.52972
A8 (in^2)	20.95103	21.03627	21.02740	20.33665
A9 (in^2)	20.83663	21.52784	21.51037	20.75112
A10 (in^2)	0.10000	0.10000	0.10000	0.10000
Weight (lb)	5076.67	5060.84	5060.87	5080.57
Max Stress (ksi)	20.36570	**25.00002**	24.99954	20.43916
Max Displ. (in)	**2.00000**$^+$	**2.00001**	2.00000$^-$	**2.00000**$^+$
Solution time (s)	0.797	11.5	69.098	73.073

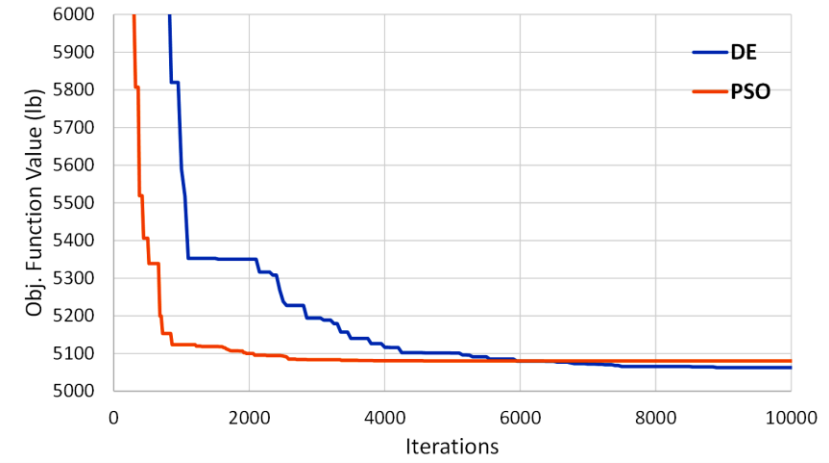


Fig. 2: The convergence histories for the DE and PSO algorithms

5 Conclusion

Spreadsheets have become very powerful and popular tools in the engineering community as they are easy to use, provide excellent results, and do not require any coding skills. Large engineering firms rely on spreadsheet calculations for the design of elements of various projects. Traditionally, the design was done with trial and error, where the engineer would try different sets of parameters before ending up with an acceptable good solution, while only expert programmers could have access to optimization algorithms. The addition of Solver and the availability of easy-to-use and powerful external tools such as xl Optimizer empowers the engineer who is now able to design elements optimally, without having to be an expert in optimization procedures or coding. The Solver is a robust and reliable tool, available in every Excel installation, offering two main optimization algorithms (a mathematical and an evolutionary one), while xl Optimizer goes far beyond, offering a host of metaheuristic optimization algorithms for a wide range of applications and the ability to deal with multi-objective problems. The addition of such tools gives tremendous power to Spreadsheet calculations. In this work, we showed that both Solver and xl Optimizer can be used to optimize 2D truss structures efficiently, using either mathematical or metaheuristic algorithms.

The next step in our research is applying the spreadsheet-based optimization techniques to larger scale problems Papadrakakis et al., (2001), 3D truss problems, frame problems, and multi-objective structural problems, while exploring additional metaheuristics, such as GA, EPSO, Simulated Annealing, Artificial Bee colony, and others.

Acknowledgement

The support of Qatar University is acknowledged, through the Student Grant entitled “Design Optimization of Truss Structures using Swarm Intelligence Methods” (QUST-2-CENG-2022-681).

References

Bhatti, M. A. (2005). "Structural Design Optimization using the MS Excel Solver and Computer Algebra Systems." in *Structures Congress*, 2005, 1-9. DOI: https://doi.org/10.1061/40753(171)83.

Charalampakis, A. E. & Dimou, C. K. (2010). "Identification of Bouc–Wen hysteretic systems using particle swarm optimization." *Computers & Structures*, *88*(21), 1197-1205. DOI: https://doi.org/10.1016/j.compstruc.2010.06.009.

Charalampakis, A. E. & Tsiatas, G. C. (2019). "Critical Evaluation of Metaheuristic Algorithms for Weight Minimization of Truss Structures." *Frontiers in Built Environment*, *5*. DOI: http://doi.org/10.3389/fbuil.2019.00113.

Christy, C. T. (2006). *Engineering with the spreadsheet: Structural engineering templates using excel*. DOI: http://doi.org/10.1061/9780784408278.

El-Sayed, M. E. M. & Jang, T. S. (1994). "Structural optimization using unconstrained nonlinear goal programming algorithm." *Comput. Struct.*, *52*(4), 723-727. DOI: https://doi.org/10.1016/0045-7949(94)90353-0.

Galante, M. (1992). "Structures optimization by a simple genetic algorithm." *Numerical Methods In Engineering And Applied Sciences*, Barcelona, Spain, 862-870.

Georgioudakis, M. & Plevris, V. (2018). "A Combined Modal Correlation Criterion for Structural Damage Identification with Noisy Modal Data." *Advances in Civil Engineering*, 2018(3183067), 20. DOI: https://doi.org/10.1155/2018/3183067.

___. (2020a). "A comparative study of differential evolution variants in constrained structural optimization." *Frontiers in Built Environment*, *6*(102), 1-14. DOI: https://doi.org/10.3389/fbuil.2020.00102.

___. (2020b). "On the Performance of Differential Evolution Variants in Constrained Structural Optimization." *Procedia Manufacturing*, *44*, 371-378. DOI: https://doi.org/10.1016/j.promfg.2020.02.281.

Ghasemi, M. R., Hinton, E. & Wood, R. D. (1997). "Optimization of trusses using genetic algorithms for discrete and continuous variables." *Eng. Computations*, *16*(3), 272-303. DOI: https://doi.org/10.1108/02644409910266403.

Goldberg, D. E. (1989). *Genetic algorithms in search, optimization and machine learning*, Addison-Wesley Longman Publishing Co., Boston, Massachusetts.

Haftka, R. T. & Gürdal, Z. (1992). *Elements of Structural Optimization*, Kluwer Academic Publishers.

Kao, C. Y., Hung, S. L. & Setiawan, B. (2020). "Two Strategies to Improve the Differential Evolution Algorithm for Optimizing Design of Truss Structures." *Advances in Civil Engineering*, 2020, 8741862. DOI: https://doi.org/10.1155/2020/8741862.

Kennedy, J. & Eberhart, R. (1995). "Particle swarm optimization." *IEEE International Conference on Neural Networks*, Piscataway, NJ, USA, 1942–1948.

Lagaros, N. D., Plevris, V. & Kallioras, N. A. (2022). "The Mosaic of Metaheuristic Algorithms in Structural Optimization." *Archives of Computational Methods in Engineering*. DOI: https://doi.org/10.1007/s11831-022-09773-0.

Lagaros, N. D., Plevris, V. & Papadrakakis, M. (2005). "Multi-objective Design Optimization Using Cascade Evolutionary Computations." *Comput. Methods Appl. Mech. Engrg.*, *194*(30-33), 3496-3515. DOI: https://doi.org/10.1016/j.cma.2004.12.029.

Memari, A. M. & Fuladgar, A. (1994). "Minimum Weight Design of Trusses by BEHSAZ Program." *Proceedings of 2nd International Conference on Computational Structures Technology*, Athens, Greece, August 30 - September 1.

Ozcep, F. (2010). "SoilEngineering: A Microsoft Excel® spreadsheet© program for geotechnical and geophysical analysis of soils." *Computers and Geosciences*, *36*(10), 1355-1361. DOI: https://doi.org/10.1016/j.cageo.2010.01.015.

Pandit, A. (2015). *Water engineering with the spreadsheet: A workbook for water resources calculations using excel*. DOI: https://doi.org/10.1061/9780784414040.

Papadrakakis, M., Lagaros, N. D. & Plevris, V. (2002). "Multi-objective Optimization of Skeletal Structures under Static and Seismic Loading Conditions." *Engrg. Optim.*, *34*(6), 645-669. DOI: http://dx.doi.org/10.1080/03052150215716.

Papadrakakis, M. et al. (2001). "Large Scale Structural Optimization: Computational Methods and Optimization Algorithms." *Archives of Computational Methods in Engineering*, *8*(3), 239-301. DOI: http://dx.doi.org/10.1007/BF02736645.

Perez, R. E. & Behdinan, K. (2007). "Particle Swarm Optimization in Structural Design." in *Swarm Intelligence: Focus on Ant and Particle Swarm Optimization*, F. T. S. Chan and M. K. Tiwari, eds., Itech Education and Publishing, Vienna, Austria, 373-394.

Plevris, V. (2009). "Innovative computational techniques for the optimum structural design considering uncertainties." National Technical University of Athens, Athens, Greece.

Plevris, V., Batavanis, A. & Papadrakakis, M. (2011). "Optimum design of steel structures with the Particle Swarm Optimization method based on EC3." *3rd International Conference on Computational Methods in Structural Dynamics and Earthquake Engineering (COMPDYN 2011)*, Corfu, Greece, 25-28 May 2011.

Plevris, V. & Papadrakakis, M. (2011). "A Hybrid Particle Swarm – Gradient Algorithm for Global Structural Optimization." *Comput.-Aided Civ. Infrastruct. Eng.*, *26*(1), 48-68. DOI: https://doi.org/10.1111/j.1467-8667.2010.00664.x.

Rady, M. & Mahfouz, S. Y. (2022). "Effects of Concrete Grades and Column Spacings on the Optimal Design of Reinforced Concrete Buildings." *Materials*, *15*(12), 4290. DOI: https://doi.org/10.3390/ma15124290.

Shahnam, N. (2003). "Utilization Of Excel In Solving Structural Analysis Problems." Nashville, Tennessee, 2003/06/22. DOI: https://doi.org/10.18260/1-2--12122.

Storn, R. & Price, K. (1995). "Differential Evolution - A Simple and Efficient Adaptive Scheme for Global Optimization Over Continuous Spaces." Berkeley, CA.

Cite as: Plevris V., Elias I.H.M. & Charalampakis A.E., "Optimum Design of Plane Trusses Using Mathematical and Metaheuristic Algorithms on a Spreadsheet", *The 2nd International Conference on Civil Infrastructure and Construction (CIC 2023)*, Doha, Qatar, 5-8 February 2023, DOI: https://doi.org/10.29117/cic.2023.0109

The Effect of Surface Treatment of Basalt FRP Bars on the Shear Capacity of Oneway High-Strength Concrete Slabs

Abathar Al-Hamrani
PhD candidate, Civil and Architectural Engineering, Qatar University, Doha, Qatar
aa1205725@qu.edu.qa

Wael Alnahhal
Associate Professor, Civil and Architectural Engineering, Qatar University, Doha, Qatar
wael.alnahhal@qu.edu.qa

Abstract

Corrosion is a common condition encountered by steel reinforcing bars which has a considerable negative impact on the structural integrity of concrete structures. Nowadays, applying anti-corrosive composite materials such as fiber-reinforced polymer (FRP) bars as reinforcing bars instead of steel bars is a major area of interest among researchers. The current study presents an investigation on the influence of surface treatment of the basalt (B) FRP reinforcing bars on the shear strength ofone-way high-strength concrete slabs. Two types of BFRP bars were tested, one with a sand-coated surface and the other with a ribbed surface.The testing results showed that the ribbed BFRP bars resulted in a slightly higher shear strength than the slab reinforced with sand-coated bars. The ultimate shear capacity in the ribbed bars reinforced slab was recorded as 95.65 kN, whereas it was recorded as 90.08 kN in the sand-coated bars reinforced slab. Moreover, in comparison to the slab with sand-coated bars, the first flexural crack was delayedin the slab with ribbed bars.Also, reinforcing the one-way slab with ribbed BFRP bars has shown higher stiffness represented by lower midspan deflection at all loading stages compared to the sand-coated bars. As a result, this has induced lower stresses on the ribbed bars, which caused lower midspan strain values in the ribbed bars than the sand-coated bars.

Keywords: Shear strength; Ribbed; Sand-coated; BFRP bars; One-way slab

1 Introduction

Despite the distinct mechanical characteristics of steel reinforcement, corrosion is still recognized as one of the main reasons that deteriorates and shortens the lifespan of many concrete structures worldwide such as parking garages and bridge decks (El-Sayed et al., 2005a). To tackle this problem, there is a growing body of literature investigating the structural performance of concrete structures that are reinforced with an anti-corrosive material known as fiber-reinforced polymers (FRP) Al-Hamrani & Alnahhal (2021); Al-Hamrani & Alnahhal (2022); (Balaguru et al., 2009); (El-Refai et al., 2022); (Zoghi, 2013). However, special care must be given to the concrete members designed with FRP bars due to the distinct difference in the mechanical properties between the FRP and the steel bars. The most critical difference is the low modulus of elasticity of the FRP bar compared to the steel bar, which leads to increased deflection and crack depth and width Abushanab et al., (2021); Attia et al., (2020); El-Sayed set al., (2005b); (El-Sayed et al., 2007); (Razaqpur et al., 2004). This in turn will reduce the depth of the uncracked compression zone and the aggregate interlock along the shear crack surface, which both are responsible for

reducing the ultimate shear capacity.

It is customary when conducting a study on the one-way slabs to consider the flexural behavior as done by several studies Attia et al., (2019); Benmokrane et al., (2005); Chang et al., (2012); (Michaluk et al., 1998); (Zheng et al., 2019). However, because of the brittle nature of both the FRP bars and concrete and the low elastic modulus of the FRP bars, it is also recommended to investigate the shear behavior of one-way slabs reinforced with FRP bars.

Recently, few studies have been published on the shear behavior of one-way slabs reinforced with FRP bars Abdul-Salam et al., (2013); (Abdul-Salam et al., 2016); (El-Sayed et al., 2005a). These studies have used the GFRP and the CFRP as the main reinforcing bars, while the BFRP bars are still not investigated. In addition,previous studies have concentrated on the effect of reinforcement ratio, concrete compressive strength, span-to-depth ratio, and depth of the slabs, but the effect of surface treatment of the bar on the shear behavior was not studied. Therefore, the present study was designed to determine the effect of the surface treatment of BFRP bars on the ultimate shear capacity of a one-way high-strength concrete slab. The effect of two surface treatments will be investigated herein, namely the ribbed and the sand-coated surfaces.

2 Materials

2.1 BFRP Bars

All the used BFRP bars were of 12 mm diameter with two different surface treatments. The first type of bars was manufactured with a sand-coated layer on the outer surface, while the second type of bars was manufactured with ribs on the outer surface as can be seen in Figure 1. The mechanical as provided by the manufacturer's data sheet were as follows: the ultimate tensile strength, the elastic modulus, and the ultimate strain values were 1177 MPa, 49.48GPa, and 2.55% for the sand-coated bars; whereas for the ribbed bars, these values were 1100 MPa, 50GPa, and 2.20%, respectively.



Fig. 1: The Used BFRP Bars

2.2 Concrete

In this study, a concrete mix with the proportions listed in Table 1 was prepared.To measure the concrete strength of each mix, three concrete cylinders of 200 mm height and ×100 mm diameter were cast, cured in water for 28 days, and tested according to ASTM C39. The obtained average compressive strength was 55.12 MPa.

Table 1: Concrete Mix Proportions

Concrete ingredients					
Cement (kg/m^3)	Water (kg/m^3)	Sand (kg/m^3)	Gabbro coarse aggregate, 10 mm (kg/m^3)	Gabbrocoarse aggregate, 20 mm (kg/m^3)	Superplasticizer (kg/m^3)
500	165	700	105	945	0.35

3 Test Set-Up

As shown in Figure 2, the testing set-up with the dimensions of the tested one-way slabs in mmis illustrated in Figure 2. The experimental work includes two one-way slabs with the following dimensions: 600 mm width × 150 mm height × 2550 mm length. The first slab was reinforced longitudinally with 8ϕ12mm sand-coated bars, while the second slab was longitudinally reinforced with 8ϕ12mm ribbed bars. The reinforcement ratio of the tested slabs was specified as 1.27%, which is equivalent to 3.62 times greater than the balanced reinforcement ratio. The slabs were loaded until failure with two symmetrical point loads located at the middle of the slab with a loading span of 1350 mm. The loading rate was specified to be 1 mm/min. At the midspan, two linear variable differential transformers (LVDTs) and two strain gauges were fixed to record the deflection of the slabs and the strain values in the longitudinal BFRP bars, respectively.

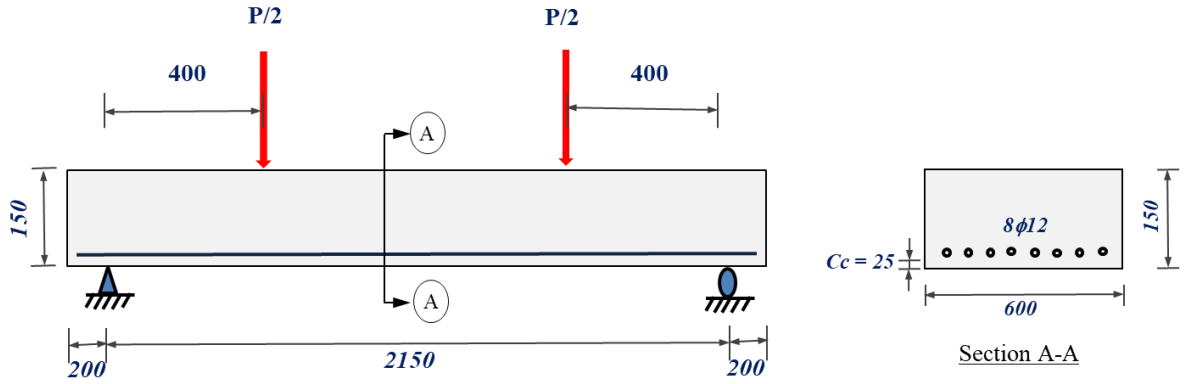


Fig. 2: Testing Set-Up. All Dimensions are in Mm

4 Testing Results

In this section, the obtained experimental results will be discussed in terms of the load versus midspan deflection and the load versus BFRP bar's strain behaviors that are shown in Figure 3 and Figure 4, respectively. Further details listed in Table 2 will be discussed, including the ultimate load and the corresponding midspan deflection, the BFRP bar's strain at the ultimate load, the onset of flexural crack, and the failure mode. Overall, when loaded, both slabs experienced a linear increase in the applied load with a small increment in the deflection as the slabs were utilizing their full moment of inertia before the onset of the first flexural crack as can be seen in Figure 3. At this stage, the stiffness of the ribbed bars reinforced slab was higher than the sand-coated bars reinforced slab. Moreover, as reported in Table 2, the load at the first flexural crack was recorded at 27.5 kN in the slab reinforced with ribbed bars, whereas it was recorded at 22.5 kN. Beyond this stage, the stiffness of both slabs was reduced progressively, then the loads continued to increase linearly with a higher increment in the midspan deflection. Similar to the pre-cracking stage, in the post-cracking stage, the slab reinforced with ribbed bars exhibited higher stiffness than that reinforced with sand-coated bars in all loading stages. To clarify this, the midspan deflection at 100 kNreached 10.34 mm in the former slab, however, a higher midspan deflection of 15.26 mm was reached in the latter slab. Similarly, the midspan deflection corresponding to the ultimate loading capacity was 27.86 mm in the slab with ribbed bars, while the midspan deflection was 35.52 mm in the slab with sand-coated bars. This could be due to the difference in the surface treatment of the used bars. According to Fahmy et al., (2021), the difference in the surface treatment can lead to different bonding characteristics. Therefore, they reported a significantly higher bond strength in the helically ribbed FRP barsthan in the sand-coated bars. This observation might also justify the higher

shear capacity of 95.65 kN that was attained by the slab reinforced with ribbed BFRP bars when compared to the shear capacity of 90.08 kN attained by the slab reinforced with sand-coated bars.

It is expected that the higher deflection in the slab will induce higher stresses in the bottom reinforcing bars. As a result, it can be observed in Figure 4 that the strain values in the ribbed BFRP bars were notably lower than the sand-coated ones in all loading stages after cracking load. For instance, the strain in the ribbed BFRP bars corresponding to the ultimate load was 0.0062, but the sand-coated bars demonstrated higher strain with a value of 0.0081 despite the failure of the latter at a lower loading level. As can be seen in Figure 5, both slabs have failed under diagonal tension failure.

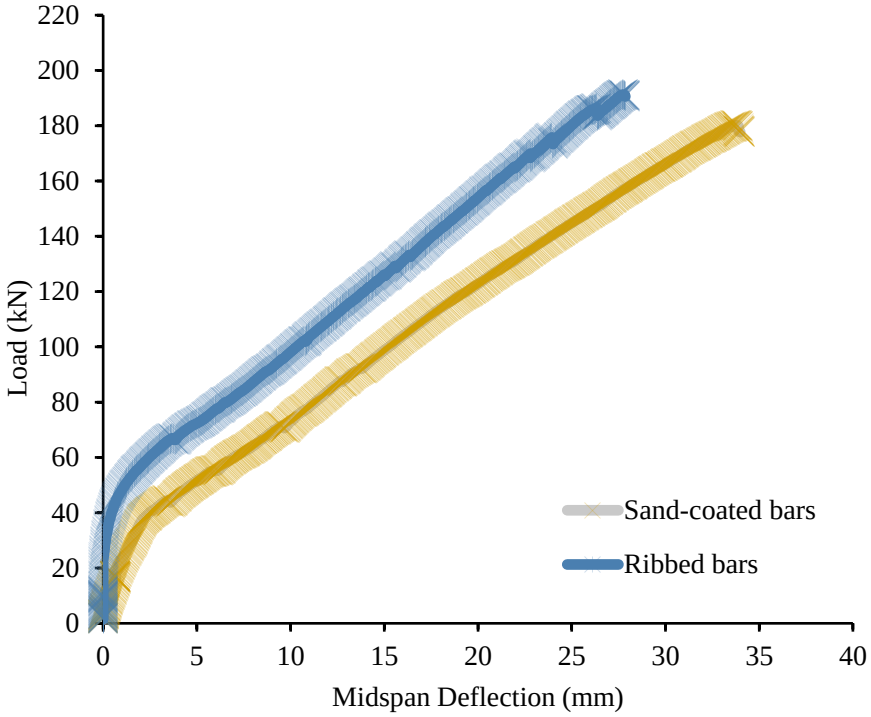


Fig. 3: Load vs Midspan Deflection relationship

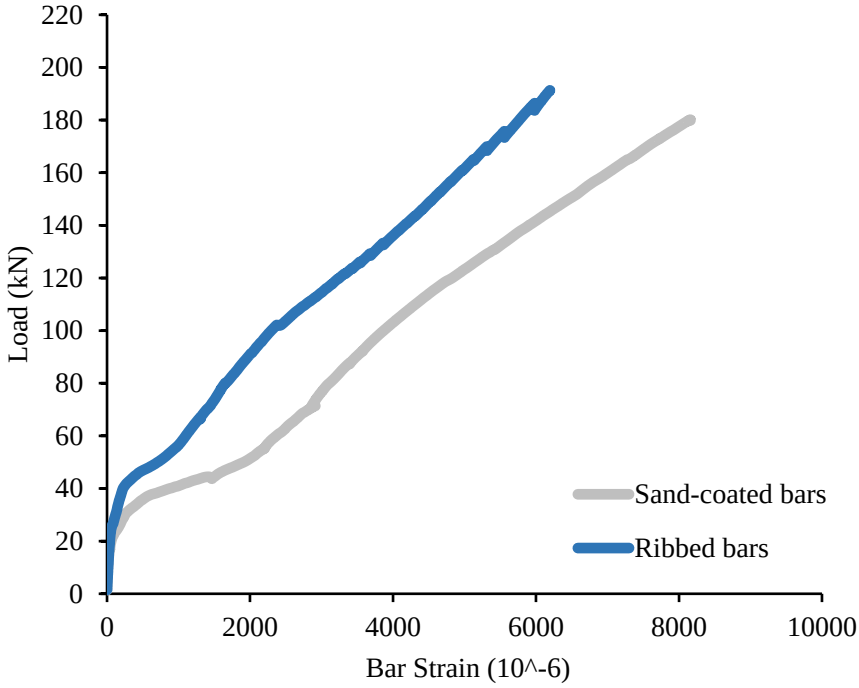


Fig. 4: Load Vs BFRP Bar Strain at Midspan

Table 2: Detailed Test Results

	Slab with sand-coated bars	Slab with ribbed bars
Ultimate load (P/2)	90.08 kN	95.65 kN
Midspan deflection at ultimate load	35.52 mm	27.86 mm
BFRP strain at ultimate load	0.0081	0.0062
Load at the first flexural crack	22.5 kN	27.5 kN
Failure mode	Diagonal tension	Diagonal tension



Slab with sand-coated bars



Slab with ribbed bars

Fig. 5: Failure Modes of the Tested Slabs

5 Conclusion

This study has assessed the effect of two surface treatments, namely ribbed and sand-coated surfaces on the shear behavior of one-way high-strength concrete slabs. The main outcomes obtained from the current study are as follows:

1. The slab reinforced with ribbed bars resulted in a higher stiffness and lower midspan deflection than the slab reinforced with sand-coated bars in all loading stages.
2. The load at the initial flexural crack in the concrete slab with ribbed bars was increased by 22.4% over the counterpart slab with sand-coated bars.
3. After cracking, the developed strain in the ribbed BFRP bars was notably lower than that in the sand-coated bars up to the ultimate stage.
4. Both slabs failed under shear, however, the shear capacity of the ribbed bars reinforced slab was higher than the sand-coated bars reinforced slab by 6%.

Acknowledgement

The authors show their gratitude to Qatar Foundation for their financial support through the GSRA grant no. GSRA6-1-0301-19005 and UREP grant no. UREP21-089-2-039 from the Qatar National Research Fund (QNRF, a member of Qatar Foundation).

References

Abdul-Salam, B., Farghaly, A. & Benmokrane, B. (2013). "Evaluation of Shear Behavior for One-Way Concrete Slabs Reinforced with Carbon-FRP Bars", CSCE General Conference, vol. 243, Montréal, Québec.DOI:10.13140/RG.2.1.3831.7609.

Abdul-Salam, B., Farghaly, A. & Benmokrane, B. (2016). "Mechanisms of shear resistance of one-way concrete slabs reinforced with FRP bars", *Construction and Building Materials*, vol. 127, pp. 959-970. DOI: 10.1016/j.conbuildmat.2016.10.015.

Abushanab, A., Alnahhal, W. & Farraj, M. (2021). "Structural performance and moment redistribution of basalt FRC continuous beams reinforced with basalt FRP bars", *Engineering Structures*, vol. 240, 112390. DOI: 10.1016/j.engstruct.2021.112390.

Al-Hamrani, A. & Alnahhal, W. (2021). "Shear behavior of basalt FRC beams reinforced with basalt FRP bars and glass FRP stirrups: Experimental and analytical investigations", *Engineering Structures*, vol. 242. DOI: 10.1016/j.engstruct.2021.112612.

Al-Hamrani, A. & Alnahhal, W. (2022). "The Influence of Reinforcement Ratio on the Shear Behaviour of Sand Coated Basalt FRP Bars Reinforced Beams", Lecture Notes in Civil Engineering, Ilki, Alper., Ispir, Medine., Inci, Pinar., vol. 198, Springer, Cham, pp. 972-979. DOI: 10.1007/978-3-030-88166-5_85.

Attia, K., El Refai, A. & Alnahhal, W. (2020). " Flexural Behavior of Basalt Fiber–Reinforced Concrete Slab Strips with BFRP Bars: Experimental Testing and Numerical Simulation", *Journal of Composites for Construction*, vol. 24, iss. 2. DOI: 10.1061/(asce)cc.1943-5614.0001002.

Attia, et al. (2019). "Flexural behavior of basalt fiber-reinforced concrete slab strips reinforced with BFRP and GFRP bars", *Composite Structures*, vol. 211, pp. 1-12. DOI: 10.1016/j.compstruct.2018.12.016.

Balaguru, P. N., Antonio, N. & Giancaspro, J. (2009). FRP composites for reinforced and prestressed concrete structures : a guide to fundamentals and design for repair and retrofit, 1, Taylor & Francis, Newyork.

Benmokrane et al. (2004). "Fibre reinforced polymer composite bars for the structural concrete slabs of a Public Works and Government Services Canada parking garage", *Canadian Journal of Civil Engineering*, vol. 31, iss. 5, pp. 732-748. DOI: 10.1139/L04-049.

Chang, K. & Seo, D. (2012). "Behavior of one-way concrete slabs reinforced with GFRP bars", *Journal of Asian Architecture and Building Engineering*, vol. 11, iss. 2, pp.351-358. DOI: 10.3130/jaabe.11.351.

Dhipanaravind, S. & Sivagamasundari, R. (2018). "Flexural Behaviour of Concrete Oneway Slabs Reinforced with Hybrid FRP Bars", *International Journal of Applied Engineering Research*, vol. 13, iss. 7, pp. 4807-4815.

El-Sayed, A., El-Salakawy, E. & Benmokrane, B. (2005a). "Shear Strength of One-Way Concrete Slabs Reinforced with Fiber-Reinforced Polymer Composite Bars", *Journal of Composites for Construction*, vol. 9, iss. 2, pp. 147-157. DOI: 10.1061/(ASCE)1090-0268(2005)9.

El-Sayed, A., El-Salakawy, E. & Benmokrane, B. (2005b). "Shear capacity of high-strength concrete beams reinforced with FRP bars", *ACI Structural Journal*, vol. 103, iss. 3, pp. 383-389. DOI: 10.14359/15316.

El-Sayed, A., El-Salakawy, E. & Benmokrane, B. (2007). "Shear Strength of FRP-Reinforced Concrete Beams without Transverse Reinforcement", *ACI Structural Journal*, vol. 104, iss. 1, pp. 113-114. DOI: 10.14359/15181.

El-Refai, et al. (2022). " Shear performance of basalt fiber-reinforced concrete beams reinforced with BFRP bars", *Composite Structures*, vol. 288. DOI: 10.1016/j.compstruct.2022.115443.

Fahmy, M., Ahmed, S. & Wu, Z. (2021). " Bar surface treatment effect on the bond-slip behavior and mechanism of basalt FRP bars embedded in concrete", *Construction and Building Materials*, vol. 289. DOI: 10.1016/j.conbuildmat.2021.122844.

Michaluk, et al. (1998). "Flexural behavior of one-way concrete slabs reinforced by fiber reinforced plastic reinforcements", *ACI Structural Journal*, vol. 95, iss. 3, pp. 353-365. DOI: 10.14359/552.

Zheng, et al. (2019). "Serviceability of one-way high-volume fly ash-self-compacting concrete slabs reinforced with basalt FRP bars", *Construction and Building Materials*, vol. 217, pp. 108-127. DOI: 10.1016/j.conbuildmat.2019.05.044.

Zoghi, M. (2014). *The International Handbook of FRP Composites in Civil Engineering*, 1, CRC Press, Newyork. DOI: 10.1201/b15806.

Cite as: Al-Hamrani A. & Alnahhal W., "The Effect of Surface Treatment of Basalt FRP Bars on the Shear Capacity of One way High-Strength Concrete Slabs", *The 2nd International Conference on Civil Infrastructure and Construction (CIC 2023)*, Doha, Qatar, 5-8 February 2023, DOI: https://doi.org/10.29117/cic.2023.0110

Bond Performance of Near-Surface Mounted BFRP Bars to Concrete

Omar Aljidda
Ph.D. Candidate, Department of Civil and Water Engineering, Laval University, Quebec City, Quebec, Canada
omar.aljidda.1@ulaval.ca

Ahmed El Refai
Professor, Department of Civil and Water Engineering, Laval University, Quebec City, Quebec, Canada
ahmed.elrefai@gci.ulaval.ca

Wael Alnahhal
Associate Professor, Department of Civil and Architectural Engineering, Qatar University, Doha, Qatar
wael.alnahhal@qu.edu.qa

Abstract

This paper presents the test results of a study on the bond performance of near-surface mounted (NSM) basalt fiber reinforced polymer (BFRP) bars to concrete. Twelve C-shape concrete specimens were tested under direct pull-out loading configuration. Test parameters included the bar surface configuration (deformed and sand coated), the types of epoxy adhesive (NSM Gel and Sikadur-30), and the bonded length (6, 12, and 24 times its diameter). The influence of various parameters on the overall bond performance of NSM-BFRP bars is analyzed and discussed. The obtained results confirmed the impact of the investigated parameters on the bond behavior of the tested specimens. It was found that the bond strength and failure mode varied considerably with the bar surface configuration and bonded length. Higher bond strength was obtained when the NSM Gel epoxy with high strength properties. The results also revealed that both the deformed and sand coated bars showed almost similar bond strengths. Moreover, the pull-out loads increased with the increase of the bonded length of the NSM bars.

Keywords: Near-surface mounted; pull-out; Basalt; Strengthening

1 Introduction

The Near Surface Mounted (NSM) strengthening technique is one of the most effective techniques in strengthening existing reinforced concrete (RC) structural elements. The technique necessitates the use of strips or bars embedded in grooves that were made into the concrete cover and then filled with an appropriate filling material to ensure their bond to the concrete. Fiber-reinforced polymer (FRP) strips or bars are frequently used as NSM reinforcement because of their superior tensile strength and resistance to corrosion (Gómez, Torres & Barris, 2020); Maljaee, Ghiassi, & Lourenço, 2018); Novidis & Pantazopoulou, 2008). Previous research demonstrated that NSM-FRP bars may offer great anchorage capacity, resulting in high resistance against debonding, and therefore, a high ratio of the tensile strength of the FRP bars can be utilized (Kalupahana et al., 2013; De Lorenzis & Teng, 2007; De Lorenzis & Nanni, 2001).

The structural efficiency of the NSM strengthening techniques depends on several parameters, such as the groove dimension in which the NSM reinforcements are embedded, the bar surface configuration, the bonded length, and the most importantly, the bond performance between bar-epoxy interface and the concrete-epoxy interface. The stress transmission and the interaction

processes occur via both interfaces: the cylindrical contact surface between the NSM-FRP bar and the epoxy and the boundary between the concrete substrate and epoxy. Perfect bond at both interfaces lets stress transfer between the NSM-FRP bars, the epoxy, and the concrete and guarantees a good composite behavior. In either case, the force transfer occurs at an earlier stage of loading via the chemical adhesion between the NSM bar and the epoxy, whereas friction and mechanical interlocking take place at higher load levels (Novidis & Pantazopoulou, 2008).

The majority of the earlier investigations have focused on the evaluating the bond behavior of NSM-FRP bars made of carbon (CFRP) or glass (GFRP) (Sharaky et al., 2013; De Lorenzis & Teng, 2007; Cruz & Barros, 2002). De Lorenzis et al. (2002) conducted direct pull-out tests on 36 concrete specimens reinforced with NSM-CFRP and GFRP bars with various groove-filling materials, bonded lengths, and groove sizes. The authors stated that specimens with epoxy resin failed at the epoxy-concrete interface rather than the bar-epoxy interface, whereas those bonded with cement mortars failed by splitting the mortar cover due to its low tensile strength as compared to epoxy. In addition, specimens with cement mortars showed 70% lower capacity than their epoxy-filled counterparts. Moreover, for a given groove size, the load-bearing capacity increased, and the bond strength decreased as the bonded length increased in all specimens. Soliman et al. (2011) investigated the effect of the bonded length, the FRP bar size, and the adhesive type on the bond performance of NSM-GFRP and CFRP bars. The results showed that the specimens with epoxy had a higher bond strength of about 40-56% than the corresponding specimens with cement adhesive. It was also stated that by increasing the bonded length, the load capacity of the specimen improved, in contrast to increasing the size of the groove, where a significant impact on the failure load was not recorded. Regarding the failure mode, concrete tension failure was the dominant failure mode. Lee et al. (2013) evaluated the bond behavior of NSM-CFRP and GFRP bars. The results verified the effect of the bar surface configuration on the bond behavior such that the use of spirally wound and sand coated bars showed the best performance, whereas CFRP bars displayed a higher bond strength than those of GFRP. Likewise, using epoxy adhesives with greater bond strength increased the bond strength of the tested pull-out specimens.

Recently, the BFRP bars have become known as promising substitutes for GFRP bars. However, despite many studies, noticeable lack of studies on using the BFRP bars in the NSM strengthening technique can be observed. This paper reports the experimental investigation in which pull-out tests were performed while investigating test parameters. The outcomes of this research were considered to be important before recommending the use of the BFRP bar in NSM strengthening technique application.

2 Experimental Program

2.1 Specimen Details

Twelve C-shaped concrete specimens were constructed and tested in the laboratory using a modified pull-out test, as illustrated in Figure 1. A square groove was made into the concrete pull-out specimen along its center using a special diamond saw to accommodate the NSM bars. The dimensions of the grooves were determined based on the diameter of the bars used (10 mm) and the minimum dimensions suggested by ACI 440.2R-17 (2017) provisions of $1.5d_b$. Prior to placing the NSM-BFRP bar into the groove, epoxy was first added to the groove until it reached the desired bonded length. The specimen's surface was leveled, and any extra epoxy was removed. All BFRP bars were anchored using long steel tubes and filled with cement grout in accordance with ASTM D7205M-21(2021) requirements. The pull-out specimens were then cured for 14 days in the

laboratory, which was kept at a constant temperature of 22°C.

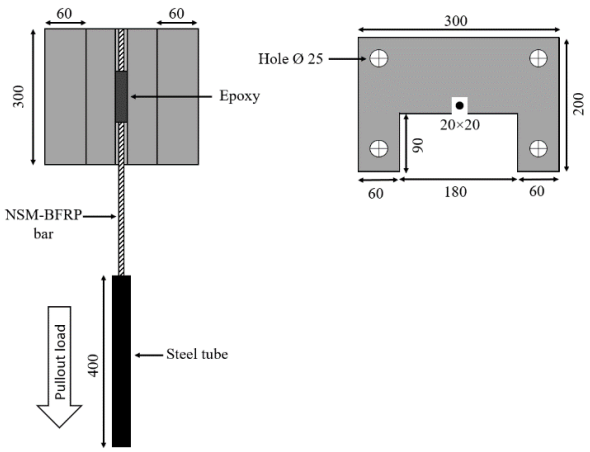


Fig. 1: Pull-out specimen (All dimensions are in *mm*)

2.2 Test Matrix

Various parameters were investigated in this study, including the bar surface texture (sand coated and deformed), the type of epoxy, and the bonded length ($6d_b$, $12d_b$, and $24d_b$), as summarized in Table 1. Each specimen is labeled in format A00-B. The first letter of the specimen's label, A, represents the bar surface configuration (SC for sand coated surface) and (D for deformed surface). The digits represent the bar's bonded length as a multiple of its diameter, while the letter B represents the type of epoxy (SD for Sikadure-30 epoxy) and (NG for NSM Gel). NSM-BFRP bars with a diameter of 10 mm embedded in a square groove of $2d_b$ are used in all specimens.

Table 1: Test Matrix

Specimen	Bar surface	Bonded length	Type of epoxy
D6-NG	Deformed	$6d_b$	NSM Gel
D6-SD	Deformed	$6d_b$	Sikadur-30
D12-NG	Deformed	$12d_b$	NSM Gel
D12-SD	Deformed	$12d_b$	Sikadur-30
D24-NG	Deformed	$24d_b$	NSM Gel
D24-SD	Deformed	$24d_b$	Sikadur-30
SC6-NG	Sand coated	$6d_b$	NSM Gel
SC6-SD	Sand coated	$6d_b$	Sikadur-30
SC12-NG	Sand coated	$12d_b$	NSM Gel
SC12-SD	Sand coated	$12d_b$	Sikadur-30
SD24-NG	Sand coated	$24d_b$	NSM Gel
SD24-SD	Sand coated	$24d_b$	Sikadur-30

2.3 Materials

All pull-out specimens were casted at the same time using ready-mix concrete with compressive strength at 28 days was 50 MPa. The mechanical properties of the sand coated and deformed BFRP bars were obtained from the manufacturer's datasheet, as summarized in Table 2. Two epoxies were used in the experimental study. The first type Sikadur-30 epoxy (SD), is a two-component epoxy, resins, and a special filler, designed for bonding structural reinforcement. The second type of epoxy NSM Gel (NG), is a high strength epoxy-based adhesive consisting of two parts resin and hardener. This epoxy is specially designed for NSM applications and may also be used for externally bonded

strengthening techniques. The epoxy properties are listed in Table 3.

Table 2: BFRP bars properties

Bar type	Bar surface	Tensile strength (MPa)	Ultimate strain%	Modulus of elasticity (GPa)
BFRP	Deformed	1200	2.31	52
BFRP	Sand coated	1278	2.22	57.5

Table 3: Epoxy properties

Epoxy type	Shear strength (MPa)	Modulus of elasticity (MPa)	Curing time
NSM Gel	27.2	1682	14 days
Sikadur-30	18	9600	7 days

2.4 Test setup

The pull-out tests were conducted using a Universal Testing Machine. A special steel frame setup, shown in Figure 2, was designed and fabricated to perform the tests. Each specimen was equipped with two LVDTs to measure the NSM bar's slippage at both loaded and free ends. The pull-out specimens were pulled with a displacement-controlled rate of 0.2 mm/min until failure. Outcomes from the LVDTs, the load cell, were collected using an automatic data acquisition system.

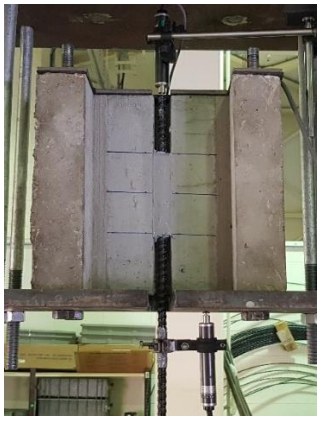


Fig. 2: Pull-out test setup

3 Experimental Results

The pull-out test results are listed in Table 4. The bond strength, τ_{max}, was calculated as per Equation (1) as follows:

$$\tau_{max} = \frac{P_{max}}{\pi d_b L_b} \quad (1)$$

Where P_{max} is the maximum pull-out force as obtained from the tests; d_b is the bar nominal diameter; L_b is the bonded length of the NSM bar.

Table 4: Pull-out test results

Specimens	P_{max} (kN)	τ_{max} (MPa)	$S_{max,\,le}$	$S_{max,\,fe}$	Failure mode
D6-NG	35.37	18.76	2.27	1.41	SEC
D6-SD	17.2	9.12	1.02	0.82	SEC
D12-NG	44.68	11.85	2.53	1.11	SEC
D12-SD	33.18	8.80	1.64	1.11	SEC
D24-NG	49.29	6.54	3.47	1.16	CS+ SEC

Specimens	P_{max} (kN)	τ_{max} (MPa)	$S_{max,\ le}$	$S_{max,\ fe}$	Failure mode
D24-SD	41.70	5.53	2.19	1.23	CS+ SEC
SC6-NG	33.42	17.73	2.24	1.08	P-SD
SC6-SD	31.66	16.80	2.01	0.82	P-SD
SC12-NG	44.26	11.74	4.09	1.64	P-SD
SC12-SD	33.47	8.88	1.77	0.76	P-SD
SC24-NG	49.86	6.61	3.31	1.40	CS+ P-SD
SC24-SD	49.14	6.52	3.31	1.12	CS+ P-SD

SEC= splitting of the epoxy cover; CS= concrete splitting; P-SD= NSM bar pull-out and surface delamination.

3.1 Failure Modes

- **Splitting of the epoxy cover**

This failure mode for all pull-out tested specimens with deformed bars surface with bonded lengths of $6d_b$ and $12d_b$, failure occurred by splitting of the epoxy cover companied by a varying degree of detachment of the concrete cover along the bar's bonded length were observed on most specimens, as shown in Figure 3(a).

- **NSM-bar pull-out and surface delamination**

This failure mode for all the specimens with sand coated bar surface texture with bonded lengths of $6d_b$ and $12d_b$. The bar's outer surface layer was entirely peeled off (delaminated) from the subsequent bar layers, as shown in Figure 3 (b).

- **Concrete splitting**

This failure mode characterized all pull-out tested specimens with a bonded length of $24d_b$. The crack started longitudinally at the loaded end and spread towards the free end along the center of the pull-out specimen, causing concrete splitting of the pull-out specimen, as shown in Figure 3 (c). It should be stated that this failure was brittle, with no earlier sign of cracking detected on the concrete surface.



(a) (b)

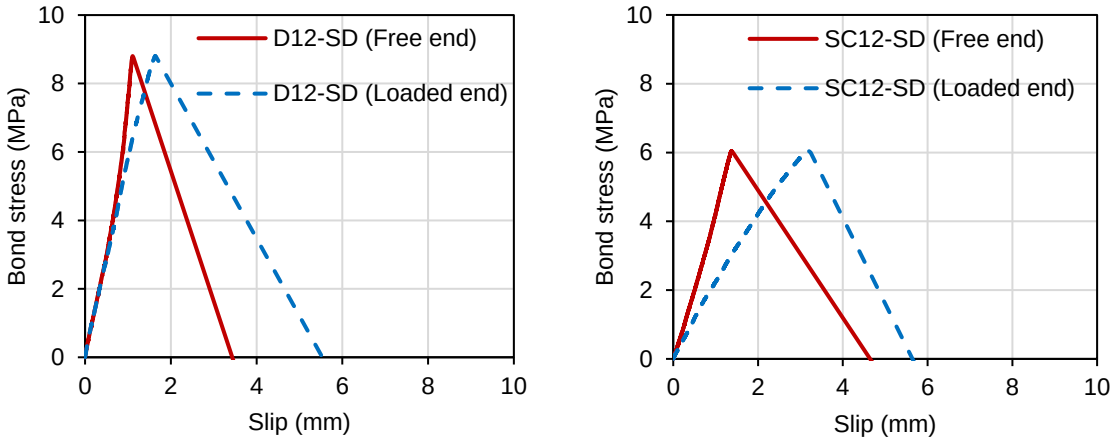


(c)

Fig. 3: Mode of Failure: (A) D12-NG; (B) SC12-NG; (C) D24-NG

3.2 Bond Stress-Slip Relationship

Figure 4 presents representative average bond stress versus free and loaded ends slip relationships for NSM-BFRP specimens with a bonded length of $12d_b$ with different bar surface configurations. Each bond stress-slip curves demonstrated a linear ascending branch up to maximum bond stress. At the beginning of loading, the pull-out load increased linearly with the slow increase of the relative slip up to 50-60% of the maximum bond stress, and there have been no cracks in either the concrete or epoxy. After reaching the maximum bond stress, explosive sounds were heard, showing signs of cracking in the concrete surrounding the groove and the epoxy cover. Additional increase in the pull-out load resulted in additional cracks that spread longitudinally in the epoxy towards the bar's free end, and further slippage between the bar and the epoxy was observed. Once achieving the maximum stress, the bond stress-slip curves exhibited an abrupt descending branch that was described by a considerable decrease in the bond stress accompanied by a significant increment in the NSM-bar slippage. This sudden loss of bond described the loud explosive noise when the pull-out specimens achieved their maximum load. This was attributed to the epoxy splitting in the case of deformed NSM-BFRP specimens and bar surface delamination for the specimens with sand coated NSM-BFRP bars.



(a) (b)

Fig. 4: Bond stress-slip curves: (A) D12-SD; (B) SC12-SD

3.3 Effect of Test Parameters

- **Effect of The Type of Epoxy**

Chemical adhesion is distinguished by a resistance to material separation. Therefore, the type of epoxy plays a significant role in ensuring a sufficient bond stress transfer from NSM bars to the concrete substrate. As plotted in Figure 5, the pull-out specimens with NG epoxy exhibited higher bond strength than the pull-out specimens with SD epoxy regardless of the bar surface configuration and bonded length due to high shear strength, as shown in Table 3. For example, the bond strength of specimens D12-NG and D12-SD were 11.9 and 8.9 MPa, respectively. A similar trend was observed for the specimens with different bonded lengths and the specimens with sand coated bar surface configuration, as illustrated in Figure 5.

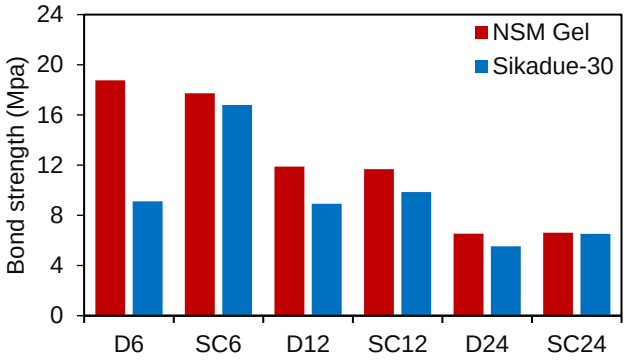


Fig. 5: Effect of the type of epoxy

- **Effect of the Bonded Length**

Relationships between the average bond strength and the bonded length are illustrated in Figure 6 for the specimens with different types of epoxy. In general, increasing the bonded length (L_b) leads to an increase in the maximum pull-out force (P_{max}). Contrarily, the average bond strength decreases due to the higher bonded area between the NSM bar and surrounding epoxy, as can be depicted from equation (1), and the non-uniform distribution of the bond stresses along the embedded portion of the bar, which increases with the increase of the bonded length, regardless of the type of the epoxy or bar surface texture. For example, the bond strengths of specimens with deformed BFRP bars decreased by 37% and 45% when their bonded lengths increased from $6d_b$ to $12d_b$ and $24d_b$, respectively. A similar trend was also observed by comparing the bond strength of the specimens with sand coated BFRP bars. The bond strengths decreased by 34% and 44% when their bonded length increased from $6d_b$ to $12d_b$ and $24d_b$, respectively.

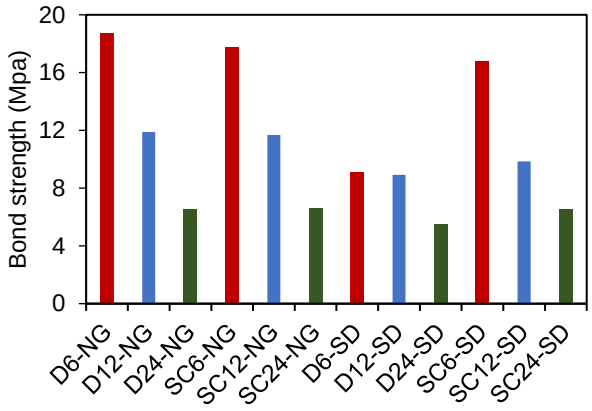


Fig. 6: Effect of the Bonded Length

- **Effect of the Bar Surface Configuration**

The bar surface configuration is critical to the bond behavior of NSM reinforcement because it directly affects the efficiency of the stress transfer from the NSM bar to the surrounding epoxy and concrete substrate through mechanical interlocking and frictional mechanisms (Wang & Cheng, 2021; Hassan & Rizkalla, 2004). As a result, several techniques, such as surface deformations or sand coating, or a combination of both, can be used to improve bond performance. The present experimental results showed that the bar surface configuration also governed the failure mode of the tested pull-out specimens. As shown in Table 4, all specimens with deformed BFRP bars failed due

to splitting their epoxy cover regardless of the epoxy type. The deformed surface configuration performed a significant role in improving the mechanical interlocking between the NSM-BFRP bar and the surrounding epoxy, which let the pull-out specimens develop their bond strengths. While the sand coated BFRP bars failed due to the delamination of the outer sand layer of the BFRP when the bar was pulled out. However, the epoxy surrounding the bar and the concrete remained undamaged along the bonded length indicated that the bond strength of the sand coated NSM-BFRP bar was developed mainly by friction and adhesion. However, the test results showed that the bar surface configuration had a minor impact on the bond strength of the pull-out tested specimens. This finding can be illustrated from the pull-out results shown in Figure 7.

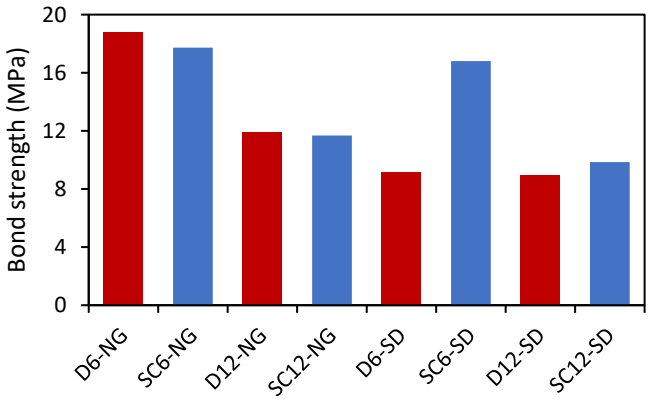


Fig. 7: Effect of the Bar Surface Configuration

4 Conclusion

This paper presented experimental investigations concerning the bond performance of BFRP bars when used for NSM application. From the experimental test results, the following conclusions are drawn:

1. The sand coated BFRP specimens with bond lengths of $6d_b$ and $12d_b$ failed due to NSM bar pull-out and surface delamination, while their deformed counterparts failed due to the splitting of the epoxy cover.
2. The concrete splitting was governor failure mode for the pull-out specimens with the bonded length of $24d_b$.
3. The epoxy's shear strength had a major impact on the bond behavior. The pull-out specimens with NSM Gel showed the best reliability producing the highest bond strength.
4. Increasing the bonded length caused a significant increase in the pull-out loads. However, the average bond strength decreased because of the non-uniform distribution of bond stress along the bonded length.
5. The sand coated and deformed NSM-BFRP bars exhibited almost similar bond strengths. The bar surface configuration had a slight impact on the bond strength of the tested specimens.

References

ACI 440.2R-17. (2017). *Guide for the Design and Construction of Externally Bonded FRP Systems for Strengthening Concrete Structures*.

ASTM D7205/D7205M-21. (2021). *Standard Test Method for Tensile Properties of Fiber Reinforced Polymer Matrix Composite Bars 1*. https://doi.org/10.1520/D7205_D7205M-21

Cruz, J. M. S. & Barros, J. A O. (2002). Bond Behavior of Carbon Laminate Strips into Concrete By Pull-out-Bending Tests. *"Bond in Concrete – from Research to Standards,"2002*, 8.

De Lorenzis, L. & Nanni, A. (2001). Characterization of FRP Rods as Near-Surface Mounted Reinforcement. *Journal of Composites for Construction*, *5*(2), 114–121. https://doi.org/10.1061/(asce)1090-0268(2001)5:2(114)

De Lorenzis, L., Rizzo, A. & La Tegola, A. (2002). A modified pull-out test for bond of near-surface mounted FRP rods in concrete. *Composites Part B: Engineering*, *33*(8), 589–603. https://doi.org/10.1016/S1359-8368(02)00052-5

De Lorenzis, L., & Teng, J. G. (2007). Near-surface mounted FRP reinforcement: An emerging technique for strengthening structures. *Composites Part B: Engineering*, *38*(2), 119–143. https://doi.org/10.1016/j.compositesb.2006.08.003

Gómez, J., Torres, L. & Barris, C. (2020). Characterization and simulation of the bond response of NSM FRP reinforcement in Concrete. *Materials*, *13*(7). https://doi.org/10.3390/MA13071770

Hassan, T. & Rizkalla, S. H. (2004). Bond Mechanism of Near Surface Mounted Fiber Reinforced Polymer Bars for Flexural Strengthening of Concrete Structures. *Repair and Strengthening of Concrete Structures*, *101*(6), 830–839. https://doi.org/10.1680/frasocs.16156.0003

Kalupahana, W. K. K. G., Ibell, T. J. & Darby, A. P. (2013). Bond characteristics of near surface mounted CFRP bars. *Construction and Building Materials*, *43*, 58–68. https://doi.org/10.1016/j.conbuildmat.2013.01.021

Lee, D., Cheng, L. & Yan-Gee Hui, J. (2013). Bond Characteristics of Various NSM FRP Reinforcements in Concrete. *Journal of Composites for Construction*, *17*(1), 117–129. https://doi.org/10.1061/(asce)cc.1943-5614.0000318

Maljaee, H., Ghiassi, B. & Lourenço, P. B. (2018). Bond behavior in NSM-strengthened masonry. *Engineering Structures*, *166*(April), 302–313. https://doi.org/10.1016/j.engstruct.2018.03.091

Novidis, D. G., & Pantazopoulou, S. J. (2008). Bond tests of short NSM-FRP and steel bar anchorages. *Journal of Composites for Construction*, *12*(3), 323–333. https://doi.org/10.1061/(ASCE)1090-0268(2008)12:3(323).

Sharaky, I. A. et al. (2013). Effect of different material and construction details on the bond behaviour of NSM FRP bars in concrete. *Construction and Building Materials*, *38*, 890–902. https://doi.org/10.1016/j.conbuildmat.2012.09.015

Soliman, S. M., El-Salakawy, E. & Benmokrane, B. (2011). Bond performance of near surface mounted FRP bars. *Journal of Composites for Construction*, *15*(1), 103–111. https://doi.org/1090-0268/2001/1-103-111/$25.00.

Wang, X. & Cheng, L. (2021). Bond characteristics and modeling of near-surface mounted CFRP in concrete. *Composite Structures*, *255*(August 2020). https://doi.org/10.1016/j.compstruct.2020.113011

Cite as: Aljidda O., El Refai A. & Alnahhal W., "Bond Performance of Near-Surface Mounted BFRP Bars to Concrete", *The 2nd International Conference on Civil Infrastructure and Construction (CIC 2023)*, Doha, Qatar, 5-8 February 2023, DOI: https://doi.org/10.29117/cic.2023.0111

Blockchain and its Potential in the Digitization of Land and Real Estate Property Records

Vagelis Plevris
Department of Civil and Architectural Engineering, Qatar University, Doha, Qatar
vplevris@qu.edu.qa

Hassan Abdallah
Department of Civil and Architectural Engineering, Qatar University, Doha, Qatar
ha2003260@qu.edu.qa

Azzam Alnatsheh
Department of Computer Science and Engineering, Qatar University, Doha, Qatar
aa1802605@qu.edu.qa

Abstract

A blockchain, is a decentralized digital ledger that is distributed across multiple computers, recording transactions in a way that cannot be altered without the consent of the network and the alteration of all subsequent blocks. In the context of land and real estate property records, a blockchain could be used to securely and transparently track the ownership and transfer of properties. Using a blockchain to digitize land and real estate records can have several benefits. For example, it can help reduce the risk of fraud, as all transactions are recorded on a secure and tamper-proof ledger. It can also make the process of transferring ownership more efficient, as it can automate many of the steps involved and reduce the need for intermediaries. Additionally, a blockchain can increase the transparency of the property market, as all records will be publicly available on the ledger. In this work, we examine the current situation and the related problems in registering land and real estate property records, especially in developing countries, and we state the challenges and opportunities of the application of blockchain technology in this field. We investigate whether blockchain has the potential to bring a positive change and play a significant role in the real estate market in the future and what are the prerequisites to achieve that.

Keywords: Blockchain; Distributed Ledger; Digitization; Real Estate; Property

1 Introduction

Blockchain is a digital ledger used to record transactions that are decentralized and distributed across a network of computers. It allows for the creation of a secure and transparent record of transactions without the need for a central authority or intermediary. Blockchain technology is still in its infancy, but it has the potential to greatly affect the Architecture, Engineering, and Construction (AEC) industry in the future, possibly even transforming it drastically for the better. Cheng et al. (2021)examined the present situation, investigating the challenges, benefits and future research opportunities of using blockchain in the AEC industry. Tezel et al., (2022) investigated the application of blockchain in the Built Environment field, with emphasis on cyber security, trust and transparency and the influence of the technology on them. Plevris (2022) presented a brief introduction to blockchain technology and its applications in fields related to civil engineering and construction. According to the study, although there are several early-stage challenges, the technology has the

potential to become a force of positive change in the AEC industry. Plevris et al. (2022) identified six key areas of the industry where blockchain can be successfully applied: (i) Building information modeling and Computer Aided Design; (ii) Contract management and smart contracts; (iii) Construction project management; (iv) Smart buildings and smart cities; (v) Construction supply chain management; and (vi) Property ownership, land titles, asset management and maintenance in real estate. The present study focuses on the sixth of the above key areas. It examines the potential of blockchain in the digitization of land and real estate property records and the improvement of the efficiency and transparency of the property ownership process. Finally, it discusses the relevant challenges in its implementation.

1.1 The Importance of Blockchain

The importance of blockchain and the increasing interest of the scientific community in it can be realized by looking at the scientific literature on the subject. By searching the Scopus database[1] with the keyword "*blockchain*" in the "*Article titled, Abstract and Keywords*" fields, one gets 39,623 document results. The query was made on January 11, 2023. Of these documents, 38,562 (accounting for 97.3% of the total) were published in 2018 or later, as there were only 1061 published articles on the topic between the years 1990-2018 (of them 817, i.e. 77%, in 2018). A similar trend can be observed when the search is limited to "Engineering". The relevant search gives 16,939 document results. Fig. **1** shows the results for every year, from 2013 up to 2022, for both cases.

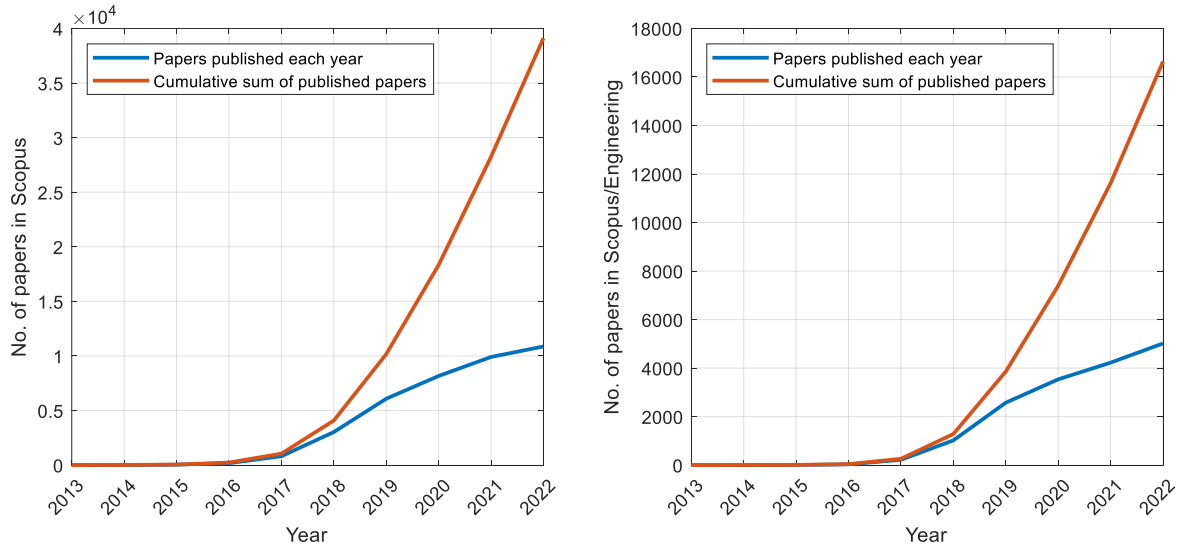


Fig. 1: Scopus Articles in "Blockchain" (Query Made on Jan. 11, 2023):
(a) All Fields, (b) Engineering Field

1.2 Literature Review

Latifi et al. (2019) investigated the applications of blockchain in real estate and how it can facilitate the industry. According to the authors, blockchain technology can sort out many of the classical issues that real estate is currently facing. By using the technology and by harnessing smart contracts, it is possible to provide liquidity to the markets, remove intermediaries and give satisfaction to all parties involved (tenants, owners, and investors). Saull et al. (2020) posed the question of whether digital technologies such as blockchain can speed up real estate transactions. The authors conducted group interviews to identify the parties involved and the individual steps of

[1] Scopus, www.scopus.com, accessed January 11, 2023.

transactions in real estate, concluding that wide collaborations in the industry are a prerequisite to help such technologies break through. The study of Kaczorowska (2019) investigated the possibilities and challenges of blockchain-based land registration. The author mentions the irreversibility of the transactions and the absence of an intermediary, highlighting the lack of independent verification and any external control, while also discussing the experience of specific countries in the implementation of the technology in land registration.

Many of the published works on the topic focus on applications in local markets or specific countries. Wouda & Opdenakker (2019) investigated applications of blockchain technology in commercial real estate transactions in the Netherlands, focusing on the development of a blockchain solution that can improve transactions related to office buildings. According to the authors, one of the major challenges is the difficulty in defining the property characteristics, due to the lack of data quality and structure. Veuger (2018) examined whether blockchain can change the game and the question of whether the entire value chain of the real estate market will embrace it in the future. The study is focused on the case of the Dutch real estate sector, but many of its findings have also a general value. The author states that the relationship between real estate and blockchain has yet to be proven in practice. In a follow-up work (Veuger 2020) it is stated that confidence in the blockchain is key for guiding that disruption. The work of Hoxha & Sadiku (2019) focuses on the case of Kosovo, studying the factors influencing the decision to adopt blockchain technology in real estate transactions in the country. According to the authors, sellers and buyers consider transparency and cost reduction as the most important factors in adopting blockchain in real estate transactions.

Ali *et al*., (2020)highlighted the limitations of traditional centralized land registry systems. Even if some of the related processes are nowadays digitized, problems remain, such as the lack of complete history of the land and no built-in mechanism for record tempering detection. They propose a transparent and trusted property registration system on a permissioned blockchain that addresses these problems. Konashevych (2020) focused on the constraints of blockchain use for real estate and property rights. According to the study, permissioned and private distributed ledger systems cannot be considered significant evolutionary steps forward in government systems. Such systems require a proper architecture of overlaid technologies to support changes in outdated and mistaken data, address issues of digital identity and privacy, legal compliance, and enforceability of smart contracts and scalability. Garcia-Teruel (2020) investigated the legal challenges and opportunities of blockchain technology applied in the real estate sector. According to the author, blockchain and the application of smart contracts can improve procedures, facilitate transactions and enhance interconnectivity. However, to not reduce the rights of the parties involved, the blockchain should have some special features, such as the possibility of being amended. Yadav and Kushwaha (2021) proposed a blockchain solution for the digitization of transactions in real estate that mitigates the possibility of falsifying documents and other fraudulent activities. The proposed system reduces overhead transmissions by around 50% by using a new consensus algorithm.

2 Distributed Ledger Technology

Distributed ledger technology (DLT) can be defined as a digital system that records the transactions of assets simultaneously, in multiple locations. It differs from traditional databases as it lacks a central data store or administrative function. Each node in a distributed ledger verifies and processes each item, creating a record and consensus on its authenticity. Distributed ledgers can be

used to store both static data, such as a registry, and dynamic data, such as financial transactions. Blockchain, a well-known application of DLT, is a decentralized, digital ledger that is used to record transactions across a network of computers. It grows constantly as new blocks with new recordings are added to it. Each block contains a link to the previous block and a timestamp, so the data in the blockchain cannot be altered retroactively without changing all the subsequent blocks and having the consensus of the network. This makes it a secure and transparent way to record transactions. The use of blockchain technology can revolutionize a wide range of industries, including supply chain management, finance, and more. There are several potential applications of blockchain technology in the construction and architecture industries, including asset tracking, i.e. tracking the ownership and transfer of immovable assets such as buildings and land.

2.1 Decentralized vs. Centralized Ledgers

A decentralized ledger is a record-keeping system that does not rely on a central authority but is rather maintained by a network of computers (nodes). In a decentralized ledger system, the nodes work together to validate and record transactions, and there is no single point of control or failure. This makes decentralized ledger systems highly resilient and resistant to tampering and censorship. On the other hand, a centralized ledger is a record-keeping system that is maintained by a central authority or organization. In a centralized ledger system, the central authority has complete control over the ledger and can decide which transactions are valid and which are not. This can make centralized ledger systems more vulnerable to tampering and censorship, as the central authority has the full power to alter or even delete transactions. Examples of such systems include traditional databases used by banks and government agencies. Both decentralized and centralized ledger systems have their advantages and disadvantages, and the appropriate choice of ledger system depends on the specific needs and goals of the application.

2.2 General Purpose Technologies

General Purpose Technologies (GPTs) are innovations that have a far-reaching and transformative impact on society and the economy. They can be implemented in many applications and sectors and have the potential to drive economic growth and productivity by enabling new products, services, and ways of operating. Some examples include the steam engine, electricity, and the internet. Such technologies have had a profound impact on society and have led to major economic and social changes, such as the industrial revolution and the information age. They are characterized by their ability to generate increasing returns and positive feedback loops, which can lead to rapid diffusion and adoption. On the other hand, they can also lead to disruption and creative destruction, as they can make existing products, services, and business models completely obsolete. GPTs often have high upfront costs and require significant investments in research and development, infrastructure, and human capital. However, they can also lead to significant long-term economic and social benefits, making them an important study area for policymakers, businesses, and researchers.

2.3 Blockchain as GPT

Blockchain has the clear potential to become a GPT due to its ability to enable new products, services, and ways of doing things across a wide range of applications and sectors. Some uses of blockchain include enabling transparent and secure supply chain management, facilitating the peer-to-peer exchange of assets, enabling the creation of smart contracts, and many more. It has the potential to transform industries by increasing efficiency, reducing the need for intermediaries, and increasing trust and transparency. However, it is still a new technology in its infancy, and its

adoption and impact will depend on many factors, including the development of supporting infrastructure and the creation of proper regulatory frameworks.

3 Technical Details

Blockchain relies on several novel technologies and advancements in mathematics and computer science, such as asymmetric cryptography, hash functions, Merkle trees, consensus mechanisms, and others. In the next section, we provide a very brief description of some of these. A more detailed description of these technologies can be found in (Plevris et al., 2022).

3.1 Asymmetric Cryptography

Asymmetric cryptography, or public key cryptography, is a method of encrypting and signing information that uses a pair of mathematically related keys: a public key and a private key. The public key can be distributed and shared freely while the private key must be always kept secret. This allows for the convenient and secure exchange of information between parties without the need for them to first establish a shared secret key. A common use of asymmetric cryptography is encrypting a message or document so that only a person with the private key can read it. Another one is digital signature, which is used to sign a document, guaranteeing the authenticity of the sender.

3.2 Cryptographic Hash Functions

A cryptographic hash function is a mathematical function or algorithm that takes an input ("message") and returns a fixed-size string of characters, often referred to as the "hash". One of the main properties of cryptographic hash functions is that they are highly sensitive to changes in the input. Although the same input will produce the same output always, even the slightest change to the input will result in a completely different output, which is known as the "avalanche effect". Another property is that it is computationally infeasible to generate the same hash output from two different input values ("collision resistance") or to determine the original input value from its hash value ("Preimage Resistance"). Some common uses of cryptographic hash functions include ensuring data integrity, generating digital signatures, and password storage.

3.3 Consensus Mechanisms

A consensus mechanism is a process used to ensure that all participants in a blockchain network agree on the state of the ledger. This is important because it ensures that all copies of the ledger are identical, which is essential for the integrity and security of the network. Proof of Work (PoW) is a popular mechanism used by some blockchain networks (including Bitcoin) to achieve distributed consensus. It involves network participants ("miners") competing to solve a computationally difficult problem and the first one to solve it is allowed to create the next block. The difficulty of the problem is adjusted so that it takes a certain average amount of time to solve, ensuring that the rate at which new blocks are created is kept constant. The main purpose of PoW is to prevent fraud and ensure the security of the network by making it expensive and time-consuming to produce fraudulent blocks. Since each block is linked to the previous one, tampering with a single block would require recalculating all subsequent blocks, which would require an enormous amount of computing power and time, making it practically infeasible to tamper with the blockchain without being detected. PoW has received criticism because of its high energy consumption and the potential for the centralization of mining power. Alternative approaches, such as Proof of Stake (PoS), have been proposed to address these issues. In PoS, the creator of a new block is chosen depending on their stake in the network, where "stake" refers to the amount of assets (such as

cryptocurrency) that a user holds. The higher the stake, the greater the chance a user will be chosen to create a new block and receive the block reward. A significant advantage of PoS is that it is much less energy intensive than PoW.

4 The Current Situation in Real Estate

4.1 Problems of the Traditional Real Estate Sector

The real estate industry is considered vital to the economy and plays a significant role in people's lives worldwide. The total value of the worldwide real estate market was calculated to be $3.7 trillion in 2021 and is projected to grow at a yearly rate of 5.2% between 2022 and 2030(Grand View Research Inc 2022).Investments in real estate typically provide better returns than the stock market while being less volatile and offering tax benefits. However, the industry has not undergone much change in recent years and is still reliant on outdated methods for transactions and record keeping, especially in developing countries. Problems such as limited participation, slow and costly verification procedures, and limited foreign investments, among others, plague the industry.Fig. **2** illustrates the current real estate ecosystem, the different parties involved, and the relevant interactions and transactions among them. This traditional system has several drawbacks and limitations:

- It involves many intermediaries that slow down transactions and increase the cost.
- It requires long and laborious due diligence and financial verification processes.
- Investing abroad is costly, difficult, and slow, due to the various requirements that need to be met, including obtaining international bank accounts, financing, accreditation, having a good credit score, and having access to fund managers, sponsors and even citizenship. Due to all these, the real estate business tends to be confined to specific geographic locations.
- Transactions are often made through wire transfers, which are costly and slow to verify.
- There is limited participation as the high cost of real estate investment makes it accessible only to the wealthy, although practically everybody is interested in housing.
- It does not support fractional ownership which would be convenient for very small investors with limited funds.
- The system suffers from low liquidity as traditionally, assets in real estate are hard to exchange or convert into cash due to their high value and the expenses associated with intermediaries, every time a deal is completed.

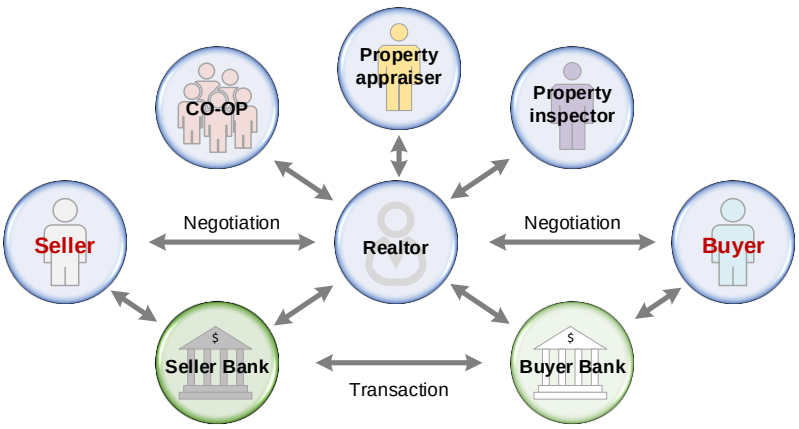


Fig. 2: An Illustration of the Traditional Real Estate Ecosystem

4.2 Solutions that Blockchain can Offer

The advent of blockchain technology can revolutionize the real estate industry by providing secure, tamper-proof digital records of ownership and transactions, stored in a decentralized way. Blockchain technology makes verification more efficient and eliminates the need for intermediaries, among other improvements.Below we discuss some of the benefits and solutions that blockchain technology can offer to the real estate industry, once it is embraced by it.

Decentralization: Decentralization in blockchain technology refers to the distribution of the system's components and decision-making authority among multiple actors, rather than being centralized in a single entity. In the context of real estate, this means that property ownership and transactions are recorded on a blockchain, rather than in a centralized database controlled by a single authority as is the conventional case today. In a decentralized blockchain system, there is not a single point of failure, and the information is shared among all the nodes, which makes it much harder to hack or tamper with the records. This reduces the cost of security and trust.

Immutability: The decentralized nature of blockchain allows for a more transparent and secure system. In the blockchain, the records that have been validated are irreversible. Thus, blockchain can ensure that the records are accurate, secure, and cannot be altered or deleted, providing a secure way to prove ownership, and simplifying transactions.

Intermediaries and Minimizing the Cost of Verification: In the traditional real estate ecosystem, the cost of verification can be quite high due to the need for various intermediaries, as illustrated in Fig. **2**, to verify ownership and transfer of properties and funds. By utilizing blockchain technology, the cost of verification can be greatly reduced. In a blockchain-based real estate system, each property and each individual will have a unique digital identity, which can be verified using digital signatures, this allows for a more efficient and secure verification process, as digital identities cannot be easily forged or tampered with. Overall, blockchain can greatly reduce the cost of verification in real estate by automating processes, increasing efficiency and security, and reducing the need for intermediaries.

Smart Contracts: Smart contracts are self-executing contracts, with the terms of an agreement being directly written into code. The code and the relevant agreements are stored and replicated on a blockchain network. Smart contracts allow for the automation of contract execution, which can streamline processes and reduce the risk of errors or disputes. Once the smart contract has been deployed to a blockchain network, it will automatically execute when certain conditions are met. Smart contracts can be used in a variety of applications, including supply chain management, real estate, and financial services. In real estate, they can be used to automate many processes, including the transfer of property ownership. This eliminates any need for intermediaries to manually verify and execute these transactions, reducing further the cost of verification.

Tokenization and Fractional Ownership: Blockchain technology allows for the full tokenization of real estate assets, making it possible for people with limited savings to participate in investments. Tokenization involves creating digital assets on the blockchain that represent ownership of a property. This process addresses issues of capital formation and liquidity, and it does not require intermediaries. Tokenization allows for the creation of a legal wrapper around the property, which makes it possible to securitize it and create an investment vehicle. It opens the door for more efficient foreign real estate investments and liquidity as anyone can purchase or sell small shares of the assets.

Providing a Universally Accessible Data Set: Throughout the entire life cycle of a building, it is important to track all information and data about it. Blockchain technology can provide a continuously updated record of everything about the asset, allowing for tracking and access to all necessary information and data. For example, any changes made to the building, such as repairs or renovations, can be recorded and tracked, and the entire record can be transferred to new owners when the property is sold. This way each property can have a universally accessible data set that includes information about past sales, repairs, and amenities, providing a digital history of actions and transactions. This will help stakeholders to prove ownership, increase transparency, and prevent fraud, which is important, especially in the case of countries where public authorities are not reliable.

Centralized systems may work well in developed countries where land records have been long certain and clear and there is trust. This is not the case in countries like India, where land records date back to the colonial era, and most land holdings have uncertain ownership. Putting these records on a blockchain could increase efficiency and reduce fraud Suganthe et al., (2021). Similarly, in various developing countries, property records are especially vulnerable to falsification and corruption and different parties can therefore claim varying degrees of authority over a specific piece of land. A decentralized approach can be used to increase the reliability of such systems (Khalid et al., 2022).

4.3 Challenges

Although blockchain can help revolutionize the real estate industry by making transactions faster, cheaper, and more secure, several challenges must be overcome before this can happen. Some of these challenges are summarized below.

Regulation: A major challenge that blockchain will face is related to governance and regulation. The technology is still relatively new, and there are no clear regulations in place for how it should be used in the real estate industry or in general. This can make it difficult for companies to know how to comply with laws and regulations. An adequate regulatory framework will provide market participants the stability they need to adopt the technology and fully engage with it, allowing blockchain innovation to flourish, but this may take time.

Interoperability: Different blockchain platforms have different technical standards, which can make it difficult for them to work together. This can be a problem for the real estate industry, where many different parties need to interact and share information, especially in a global market.

Data privacy: Blockchain technology is designed to be transparent and immutable, but this can be a problem when it comes to sensitive information like personal data. There needs to be a way to protect this data while still allowing for the benefits of blockchain.

Scalability: As the number of transactions on a blockchain network increases, the network can become slow and unwieldy. This can be a problem for the real estate industry, where large numbers of transactions need to be processed quickly.

Adoption: Finally, for blockchain technology to be successful in the real estate industry, it needs to be widely accepted and adopted. This means that all parties involved in a real estate transaction need to be willing to use the technology, which can be a difficult challenge to achieve.

5 Conclusion

The shift to a digital economy brings about new opportunities as financial and physical assets are given digital representations. By 2025, blockchains are expected to store around 10% of the world's

GDP, according to the World Economic Forum. Governments are working to adapt their laws and regulations to accommodate this change and take advantage of the new opportunities it presents. The impact of the blockchain technology on the economy and peoples' daily lives is uncertain, however, many experts believe blockchain could play a significant role across various industries in the future. This study examined the technical aspects and key concepts of blockchain and its application in the industry of real estate. While it is difficult to predict exactly how blockchain will impact the real estate industry in the long term, it certainly has the potential to bring a positive change and play a significant role in the future by increasing transparency, reducing errors and delays, and improving the overall efficiency of the industry. Nevertheless, there are also significant challenges that need to be tackled before this can become a reality, which can take time and effort.

Acknowledgement

The support of Qatar University is acknowledged, through the Student Grant entitled "Exploring the Potential of Blockchain Technology in Civil Engineering, Architecture and the Construction Industry" (QUST-2-CENG-2022-663).

References

Ali, T., Nadeem, A., Alzahrani, A. & Jan, S. (2020). "A Transparent and Trusted Property Registration System on Permissioned Blockchain." *2019 International Conference on Advances in the Emerging Computing Technologies (AECT)*10-10 Feb. 2020, 1-6. DOI: https://doi.org/10.1109/AECT47998.2020.9194222.

Cheng, et al. (2021). "When Blockchain Meets the AEC Industry: Present Status, Benefits, Challenges, and Future Research Opportunities." *Buildings*, *11*(8). DOI: https://doi.org/10.3390/buildings11080340.

Garcia-Teruel, R. M. (2020). "Legal challenges and opportunities of blockchain technology in the real estate sector." *Journal of Property, Planning and Environmental Law*, *12*(2), 129-145. DOI: https://doi.org/10.1108/JPPEL-07-2019-0039.

Grand View Research Inc. (2022). "Real Estate Market Size, Share & Trends Analysis Report By Property (Residential, Commercial, Industrial, Land), By Type (Sales, Rental, Lease), By Region, And Segment Forecasts, 2022 - 2030."

Hoxha, V. & Sadiku, S. (2019). "Study of factors influencing the decision to adopt the blockchain technology in real estate transactions in Kosovo." *Property Management*, *37*(5), 684-700. DOI: https://doi.org/10.1108/PM-01-2019-0002.

Kaczorowska, M. (2019). "Blockchain-based land registration: Possibilities and challenges." *Masaryk University Journal of Law and Technology*, *13*(2), 339-360. DOI: https://doi.org/10.5817/MUJLT2019-2-8.

Khalid, M. I. et al. (2022). "Blockchain-Based Land Registration System: A Conceptual Framework." *Applied Bionics and Biomechanics*, 2022, 3859629. DOI: 10.1155/2022/3859629.

Konashevych, O. (2020). "Constraints and benefits of the blockchain use for real estate and property rights." *Journal of Property, Planning and Environmental Law*, *12*(2), 109-127. DOI: https://doi.org/10.1108/JPPEL-12-2019-0061.

Latifi, S., Zhang, Y. & Cheng, L. C. (2019). "Blockchain-Based Real Estate Market: One Method for Applying Blockchain Technology in Commercial Real Estate Market." *2019 IEEE International Conference on Blockchain (Blockchain)*14-17 July 2019, 528-535. DOI: https://doi.org/10.1109/Blockchain.2019.00002.

Plevris, V. (2022). "A Brief Introduction to Blockchain Technology and its Applications in Civil Engineering and Construction." *1st International Conference on Advances in Civil & Environmental Engineering (1st ICACEE-2022)*, University of Engineering & Technology Taxila, Pakistan, 22-23 February 2022.

Plevris, V., Lagaros, N. D. & Zeytinci, A. (2022). "Blockchain in Civil Engineering, Architecture and Construction

Industry: State of the Art, Evolution, Challenges and Opportunities." *Frontiers in Built Environment*, 8. DOI: https://doi.org/10.3389/fbuil.2022.840303.

Saull, A., Baum, A. & Braesemann, F. (2020). "Can digital technologies speed up real estate transactions?" *Journal of Property Investment & Finance*, 38(4), 349-361. DOI: https://doi.org/10.1108/JPIF-09-2019-0131.

Suganthe, et al. (2021). "Blockchain enabled Digitization of Land Registration." *2021 International Conference on Computer Communication and Informatics (ICCCI)*27-29 Jan. 2021, 1-5. DOI: https://doi.org/10.1109/ICCCI50826.2021.9402469.

Tezel, et al. (2022). "Blockchain Opportunities and Issues in the Built Environment: Perspectives on Trust, Transparency and Cybersecurity." in *Industry 4.0 for the Built Environment: Methodologies, Technologies and Skills*, M. Bolpagni, R. Gavina, and D. Ribeiro, eds., Springer International Publishing, Cham, 569-588. DOI: https://doi.org/10.1007/978-3-030-82430-3_24.

Veuger, J. (2018). "Trust in a viable real estate economy with disruption and blockchain." *Facilities*, *36*(1/2), 103-120. DOI: https://doi.org/10.1108/F-11-2017-0106.

___. (2020). "Dutch blockchain, real estate and land registration." *Journal of Property, Planning and Environmental Law*, *12*(2), 93-108. DOI: https://doi.org/10.1108/JPPEL-11-2019-0053.

Wouda, H. P. & Opdenakker, R. (2019). "Blockchain technology in commercial real estate transactions." *Journal of Property Investment & Finance*, *37*(6), 570-579. DOI: https://doi.org/10.1108/JPIF-06-2019-0085.

Yadav, A. S. & Kushwaha, D. S. (2021). "Blockchain-based digitization of land record through trust value-based consensus algorithm." *Peer-to-Peer Networking and Applications*, *14*(6), 3540-3558. DOI: https://doi.org/10.1007/s12083-021-01207-1.

Cite as: Plevris V., Abdallah H. & Alnatsheh A., "Blockchain and its Potential in the Digitization of Land and Real Estate Property Records", *The 2nd International Conference on Civil Infrastructure and Construction (CIC 2023)*, Doha, Qatar, 5-8 February 2023, DOI: https://doi.org/10.29117/cic.2023.0112

Enhancing the Bond Durability of Basalt Fiber Reinforced Polymer Bars Using Basalt-Macro Fiber Reinforced Concrete

Alaa Taha
Department of Civil and Architectural Engineering, Qatar University, Doha, Qatar
at1301775@qu.edu.qa

Wael Alnahhal
Department of Civil and Architectural Engineering, Qatar University, Doha, Qatar
wael.alnahhal@qu.edu.qa

Nasser Alnuaimi
Department of Civil and Architectural Engineering, Qatar University, Doha, Qatar
anasser@qu.edu.qa

Abstract

This paper presents a study about the bond durability of basalt fiber reinforced polymers (BFRP) bars embedded in concrete incorporating basalt macro fibers (BMF) when conditioned in harsh saline environment at 60 °C. A total of 24 pullout specimens were tested to investigate the influence of concrete type (plain concrete and fiber reinforced concrete) and duration of conditioning (30, 60 and 90 days). The basalt-macro fiber reinforced concrete (FRC) incorporated BMF at 0.5% fiber volume fraction. The BFRP bars used had helically wrapped surface treatment. Moreover, the bond durability was assessed based on bond-slip behaviour, bond degradation, and service life predictions of bond strength retentions after 50 years of service life. The experimental results revealed that BFRP bars embedded in basalt macro FRC showed higher bond stiffness compared to those embedded in plain concrete. Additionally, BFRP bars embedded in basalt macro FRC showed slower bond degradation than their counterparts embedded in plain concrete. Finally, FRC increased the bond strength retentions of BFRP bars based on 50 years' service life predictions when compared to plain concrete.

Keywords: BFRP bars; Bond strength; Bond durability; Basalt-Macro FRC; Saline environment

1 Introduction

BFRP bars are becoming promising alternatives to the conventional glass fiber reinforced polymers (GFRP) bars because of their lower cost and similar mechanical properties (Attia et al., 2020; ElSafty et al., 2014). In general, basalt fibers possess larger failure strains and enhanced resistance to chemical attacks compared to carbon fibers and glass fibers respectively (Sim & Park, 2005)). Fiber reinforced polymer (FRP) bars may have different bonding mechanism compared to conventional steel reinforcements because of their anisotropic and linear elastic behaviours in addition to having wide variety of surface treatments. Numerous studies examined the bonding behaviour of FRP bars to concrete (El Refai et al., 2015; Yan & Lin, 2017).

Furthermore, exposing FRP reinforcements to high temperatures, environments of high humidity, chemical attacks, or any combination of these environments can cause strength reductions of FRP bars. These reductions can in turn result in negative alterations to the bonding behaviour of FRP reinforcements throughout their life use (El Refai et al., 2015). Few studies have been implemented on the durability of BFRP bars' bonding mechanism unlike the GFRP bars' bonding durability which have been examined thoroughly in the literature (D'Antino *et al.*, 2018; Yan & Lin, 2017). Hassan et

al., (2016) examined the effect of high alkaline environment at high temperature on the BFRP bars' bond durability. The variations in the BFRP bars' bond strength after 6 months of exposure were insignificant when compared to the specimens that were unconditioned. In the contrary, 25 % reduction in BFRP bars' ultimate bond stress was reported by (Altalmas et al.,(2015) when subjected to saline and alkaline conditions for a total of 90 days.

Besides, few research studies examined the influence of FRC on the FRP bars' bond durability. Majority of these investigations have been done on the conventional GFRP reinforcements. Commonly, using FRC mixes improved the FRP reinforcements' bond stress (Liu et al., (2017; Yan & Lin, 2017)). A research study about the influence of structural fibers on bond durability of GFRP reinforcements subjected to harsh seawater conditions was performed by Yan et al., (2017). The study indicated enhanced GFRP reinforcements' bond durability when FRC is used. Similarly Belarbi & Wang (2012) reported higher bond stress retentions of GFRP reinforcements embedded in FRC than plain concrete subjected to extreme temperatures, seawater conditions, as well as cycles of freeze and thaw.

Based on the aforementioned discussion and since the FRP bars' bond strength is what governs the structural capacity as well as the serviceability of FRP reinforced concrete structures, therefore the bond durability of FRP bars to concrete is critical in determining the durability performance of structures utilizing FRP reinforcements Davalos et al., (2008)). It is noteworthy to point out that the durability of BFRP bars' bond in FRC is lacking in the literature. Hence, this study provides experimental as well as analytical examinations on the BFRP bars bond performance and durability when surrounded by FRC while subjected to seawater conditions at high temperature for different conditioning durations.

2 Experimental Program

2.1 Preparation of Pull-Out Specimens

24 specimens for pullout testing were prepared to examine the influence of exposure duration and type of concrete on the BFRP bars' bond strength durability in seawater conditions. The tested specimens were divided into three groups. The 1st group denotes the unexposed specimens, and the remaining two groups correspond to the exposed counterparts. The labelling of the specimens was done in the subsequent order: concrete type, duration of conditioning, exposure temperature, and number of the specimen. For example, 0.5%BF-30-60-2 denotes the second identical pullout specimen of FRC with volume fraction at 0.5% conditioned for 30 days under 60 °C. The specimens of pullout testing were prepared in accordance with ASTM D7913 (2014) and a sample with its details is shown in Fig.1. Moreover, a total of 24 compressive strength cylinders were prepared according to ASTM C39 (2020) to track the compressive strength throughout the conditioning.

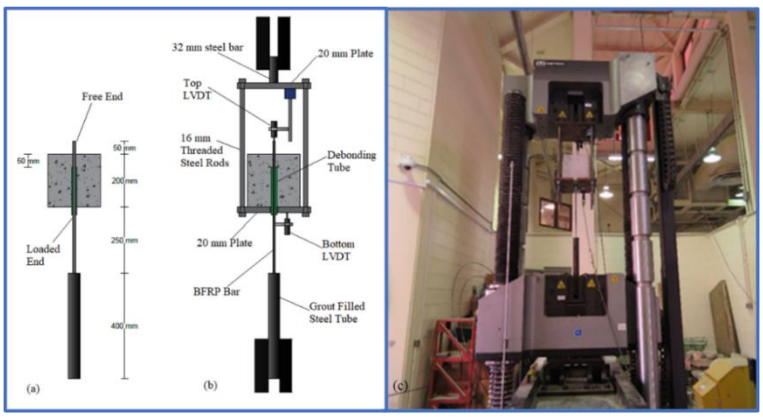


Fig. 1: (a) Details of Specimens for Pullout Test; (b) Details of Test Setup; (c) Test Setup Photo

2.2 Conditioning Environment

All the specimens were cured for 28 days. Control specimens were under lab conditions until the end of the conditioning, whereas other specimens were conditioned in saline environment at 3.9% NaCl concentration inside temperature-controlled tank to simulate the seawater of the gulf region. The temperature of the simulated seawater was chosen to be 60 °C to simulate accelerated conditions. Furthermore, the conditioning durations of this durability test were chosen to be 30, 60, and 90 days.

2.3 Materials

The BFRP bars and BMF used in the study are depicted in Fig. 2. Table 1 depicts the properties of the used BMFs as per the manufacturer's data sheet. Subsequently, Table 2 depicts the concrete mix design used, which was selected to achieve a 28 MPa target compressive strength. The bars used in this study were BFRP bars with surface treatment of helical wraps labelled as HWBFRP bars as depicted in Fig. 2(a). The nominal diameter of the used HWBFRP bars was 10mm. The polymeric resin used for manufacturing the HWBFRP bars was vinyl ester. The bars used had a modulus of elasticity of 44 GPa and a 1100 MPa of tensile strength with a density of 1900 kg/m^3.

Table 1: BMF Properties

Type	Diameter (mm)	Length (mm)	Aspect Ratio	Density (g/cm^3)	Tensile Strength (MPa)
BMF	0.72	43	59	2.1	900

Table 2: Concrete Mix Designs

Concrete Mix Type	Fiber Type	Water (kg/m^3)	Cement (kg/m^3)	Coarse Aggregate (kg/m^3)	Sand (kg/m^3)	Fiber Volume Fraction (%)	Superplasticizer (kg/m^3)
Plain concrete	-	204	350	1082	714	0	0
0.5%-BMF	BMF	204	350	1082	714	0.5	0.27



Fig. 2: (a) HWBFRP Bars; (b) BMF

2.4 Test Setup

To conduct the pullout test, a 1500 kN universal testing machine (UTM) was used. To measure the loaded and free end slippages, two linear variable displacement transducers (LVDTs) were used. The loading rate of the pullout specimens was 1.2 mm/min as per ASTM D7913 (2014). Fig.1(b) depicts the test setup details.

The following equation was used to obtain the average bond strength:

$$\tau = \frac{P}{\pi d_b L_d} \quad (1)$$

Where τ is the bond stress, d_b is the diameter of the bar, P is the ultimate load, and L_d is the embedded length of the bar inside the concrete.

3 Test Results and Discussion

3.1 Bond-Slip Response

Fig. 3 shows the response of the bond slip for control pullout specimens as well as conditioned specimens being immersed for 90 days. In general, the bond behaviour of pullout specimens consisted of an ascending branch till the point where the surrounding concrete starts to crack causing a reduction in the rate of increase in bond stress associated with increase in slippage. This continues until the ultimate stress is attained followed by descending branch where a gradual decay occurs in the bond stress caused by the wedging action of BFRP bar's indentation on the concrete surrounding it.

As can be inferred from Table 3, The usage of FRC increased the HWBFRP bars bond strength for control and conditioned specimens. This increase can be ascribed to the fibers crack effect of bridging throughout the induced cracks in the surrounding concrete because of the pullout loads. For unconditioned specimens the enhancement of adding 0.5%BF to concrete was insignificant, however it is worth to mention that the bond stiffness of HWBFP bars was significantly improved in FRC by achieving slightly higher bond strength at considerably lower slippage. Such behaviour will limit excessive cracking in reinforced concrete (RC) structures making basalt FRC and HWBFRP system highly recommended for serviceability limit state (SLS) design considerations of FRP RC structures. It is noteworthy to mention that the minimum bond stress obtained for control specimens was 13.1 MPa which is significantly higher than minimum requirement of ACI 440.6 M(2008).

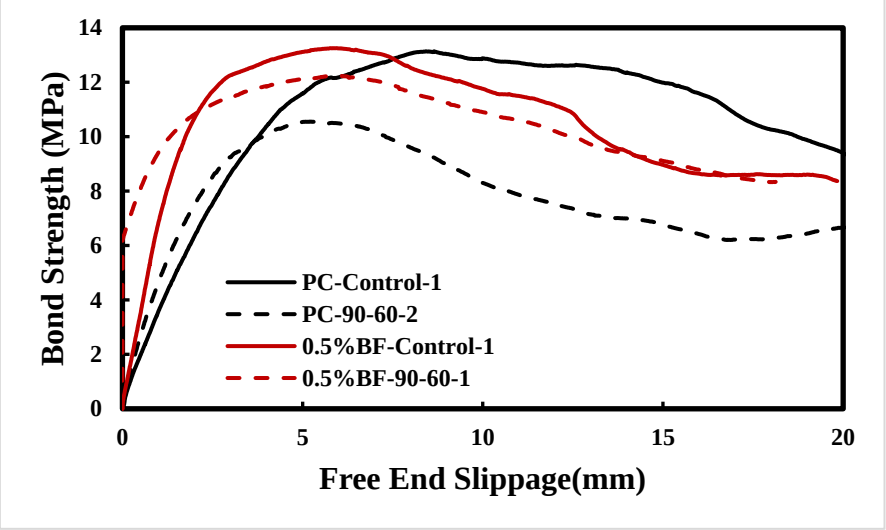


Fig. 3: BFRP Bars Bond-Slip Response

Table 3: Results of Bond Test

Specimen	$f'c$ (MPa)	τ_{max} (MPa)	τ^*_{max} (MPa)	δ_{FE} (mm)	Failure Mode	Retention (%)
Control Specimens at 23 °C						
PC-C-1	32.5	13.14	13.14	8.65	P	100
PC-C-2		11.78		6.21	P	
PC-C-3		14.49		6.44	P	
0.5%BF-C-1	30	13.25	13.27	5.84	P	100

0.5%BF-C-2		12.64		6.18	P	
0.5%BF-C-3		13.91		7.54	P	
Exposed Specimens at 60 °C for 30 days						
PC-30-60-1	29.3	12.14	13.4	6.59	P	102
PC-30-60-2		13.38		7.01	P	
PC-30-60-3		14.69		5.51	P	
0.5%BF-30-60-1	31.2	17.2	15.18	7.76	P	114
0.5%BF-30-60-2		12.32		4.45	P	
0.5%BF-30-60-3		16.02		5.77	P	
Exposed Specimens at 60 °C for 60 days						
PC-60-60-1	34.4	16.34	12.17	3.97	P/R	93
PC-60-60-2		11.65		7.07	P	
PC-60-60-3		8.52		5.49	P	
0.5%BF-60-60-1	33.1	12.28	14.72	9.07	P	111
0.5%BF-60-60-2		16.83		3.37	R	
0.5%BF-60-60-3		15.05		8.2	P	
Exposed Specimens at 60 °C for 90 days						
PC-90-60-1	35.6	11.6	11.77	8.68	P/R	90
PC-90-60-2		10.56		5.2	P	
PC-90-60-3		13.15		4.824	R	
0.5%BF-90-60-1	34.2	12.24	14.03	5.78	P	106
0.5%BF-90-60-2		14.05		4.5	P	
0.5%BF-90-60-3		15.81		4.87	R	

**f'c: The Compressive Strength of Concrete; $\tau_{max:}$ Ultimate Bond Stress; $\tau^*_{max:}$ Average Bond Stress; δ_{FE}: Free End Slippage; P: Pullout Failure; R: Rebar Fracture; P/R: Pullout Followed by Rebar Fracture.

3.2 Bond Degradation

Fig.4 shows the column chart of the average bond stress of all tested specimens. After 90 days of conditioning the decrease in the bond stress of plain concrete was 10 % compared to control specimens, whereas no reduction was noticed for conditioned FRC pullout specimens compared to their control counterparts. These results can be ascribed to the capability of BMF to limit the ingress of chlorides throughout the porous network of the concrete (Mohamed & Al-Hawat, 2016). After 30 days of exposure, all conditioned specimens tended to exhibit bond strength reduction with the increase of conditioning duration. Plain concrete pullout specimens vulnerable for 90 days experienced 12% reduction in comparison with their 30 days conditioned counterparts. On the other hand, 0.5%BF pullout specimens showed a decrease of 8% in comparison with the 30 days conditioned specimens. This degradation in the bond stress along with time can be ascribed to the presence of chloride environment and moisture at high temperature. The presence of chlorides can detrimentally affect the interfacial shear strength between the fibers and their surrounding matrix (Tam at al.(2019)). Furthermore, the differences in the coefficient of thermal expansion between concrete and the used bars can lead to different rates of expansions and contractions causing voids that can be filled with chlorides and thus accelerating the degradation of the bond performance between the bar and the concrete surrounding it (Belarbi & Wang, 2012).

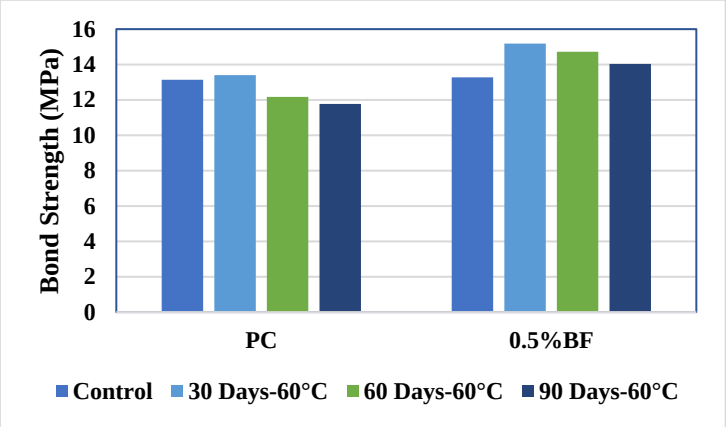


Fig. 4: Bond Degradation of HWBFRP Bars in Plain and FRC Concrete

3.3 Service Life Prediction

The methodology mentioned in the fib Bulletin 40 (2007) can be implemented to predict the bond stress retention after a specified service life. The bond stress of the used bars can be decreased by an environmental factor ,$\eta_{env,}$ mentioned in the following equations:

$$\eta_{env,b} = 1/[(100-R_{10})/100]^{n} \quad (2)$$

$$n = n_{mo} + n_T + n_{SL} \quad (3)$$

where R_{10} is the slope of the trend line of degradation fitted in double logarithmic scale. n_{mo},n_T and n_{SL} are parameters of humidity, temperature, and required service life respectively. Fig. 5(a) shows the double logarithmic fitting of the bond strength retention values of HWBFRP bars in plain concrete. Whereas, Fig. 5(b) shows the bond retention values of HWBFRP bars in FRC when fitting them in double logarithmic scale. Table 4 shows the obtained bond retention predications based on 50 years' service life. It can be inferred that after 50 years under service, the bond stress retentions of BFRP bars in plain concrete is in the range of 56 to 86% depending on moisture conditions whereas when embedded in 0.5%BF concrete, the retentions varied between 74 to 92%.

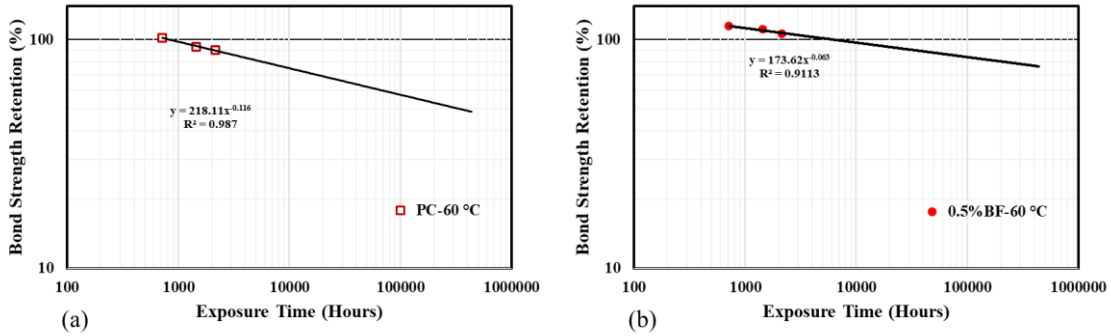


Fig. 4: Double Logarithmic Retention of HWBFRP Bars in (a) Plain Concrete; (b) FRC

Table 4: Bond Strength Service Life Predictions

					Plain Concrete		**Basalt FRC**	
n_{SL}	n_{mo}	MAT (°C)	n_T	n	$\eta_{env,b}$	$1/\eta_{env,b}$(%)	$\eta_{env,b}$	$1/\eta_{env,b}$(%)
2.7 (50 years of service life)	-1 (Dry)	<5	-0.5	1.2	1.16	86	1.08	92
		(5-15)	0	1.7	1.23	81	1.12	90
		(15-25)	0.5	2.2	1.31	76	1.15	87
		(25-35)	1	2.7	1.4	72	1.19	84

	0 (Moist)	<5	-0.5	2.2	1.31	76	1.15	87
		(5-15)	0	2.7	1.4	72	1.19	84
		(15-25)	0.5	3.2	1.48	67	1.23	81
		(25-35)	1	3.7	1.58	63	1.27	79
	1 (Moisture Saturated)	<5	-0.5	3.2	1.48	67	1.23	81
		(5-15)	0	3.7	1.58	63	1.27	79
		(15-25)	0.5	4.2	1.68	60	1.31	76
		(25-35)	1	4.7	1.79	56	1.36	74

4 Conclusion

In conclusion, this paper investigated the effect of concrete type and conditioning duration on the bond durability of HWBFRP bars under extreme seawater conditions. The following conclusions can be outlined:

- Basalt macro FRC significantly improved the bond stiffness of HWBFRP in comparison with plain concrete making the usage of basalt macro fibers recommended for SLS design considerations of FRP RC structures.
- The bond strength at 90 days of exposure for HWBFRP bars in basalt macro FRC was 19% higher than HWBFRP bars surrounded by plain concrete.
- The bond stress retentions throughout the conditioning of HWBFRP bars in plain concrete were 102, 93, and 90% at 30,60,and 90 days respectively, whereas the retentions of the bond stress for their counterparts embedded in basalt macro FRC were 114, 111, and 106% at 30,60,and 90 days respectively indicating slower degradation.
- Based on 50 years' predictions, the retentions of the bond stress for HWBFRP bars in plain concrete were in the range of 56 to 86% depending on moisture conditions, whereas when embedded in basalt macro FRC, the retentions varied between 74 to 92%.

Acknowledgement

This research was made possible through and through grant no. GSRA7-1-0419-20019 from Qatar National Research Fund (QNRF) and through Qatar University internal grant no. QUST-1-CENG-2020-17.

References

ACI Committee 440. (2008). "Specification for Carbon and Glass Fiber-Reinforced Polymer Bar Materials for Concrete Reinforcement," 6.

Altalmas, A., El Refai, A., & Abed, F. (2015). "Bond Degradation of Basalt Fiber-Reinforced Polymer (BFRP) Bars Exposed to Accelerated Aging Conditions." *Construction and Building Materials*, *81*, 162–71. doi:10.1016/j.conbuildmat.2015.02.036.

ASTM C39/C39M – 20 (2020). "Standard Test Method for Compressive Strength of Cylindrical Concrete Specimens." doi:10.1520/C0039.

ASTM D7913 / D7913M – 14 (2020) "Standard Test Method for Bond Strength of Fiber-Reinforced Polymer Matrix Composite Bars to Concrete by Pullout Testing."

Attia, K., El Refai, A., & Alnahhal, W. (2020). "Flexural Behavior of Basalt Fiber–Reinforced Concrete Slab Strips with BFRP Bars: Experimental Testing and Numerical Simulation." *Journal of Composites for Construction, 24*(2): 04020007. doi:10.1061/(ASCE)CC.1943-5614.0001002.

Belarbi, A. & Wang, H. (2012). "Bond Durability of FRP Bars Embedded in Fiber-Reinforced Concrete." *Journal of Composites for Construction*, *16*(4): 371–80. doi:10.1061/(ASCE)CC.1943-5614.0000270.

D'Antino, T., Pisani, M. A. & Poggi, C. (2018). "Effect of the Environment on the Performance of GFRP Reinforcing Bars." *Composites Part B: 141*, 123–36. doi:10.1016/j.compositesb.2017.12.037.

Davalos, J. F., Chen, Y. & Ray, I. (2008). "Effect of FRP Bar Degradation on Interface Bond with High Strength Concrete." *Cement and Concrete Composites*, *30*(8): 722–30. doi:10.1016/j.cemconcomp.2008.05.006.

ElSafty, A., Benmokrane, B., Rizkalla, S., Mohamed, H. & Hassan, M. (2014). "Degradation Assessment of Internal Continuous Fiber Reinforcement in Concrete Environment." University of North Florida, 270.

fib TG 9.3. (2007). Fib Bulletin 40: FRP Reinforcement in RC Structures. *Fib Bulletins No. 40*. fib. The International Federation for Structural Concrete. doi:10.35789/fib.BULL.0040.

Hassan, M., Benmokrane, B., ElSafty, A. & Fam, A. (2016). "Bond Durability of Basalt-Fiber-Reinforced-Polymer (BFRP) Bars Embedded in Concrete in Aggressive Environments." *Composites Part B*, *1*(6): 262–72. doi:10.1016/j.compositesb.2016.09.039.

Liu, H., Yang, J. & Wang, X. (2017). "Bond Behavior between BFRP Bar and Recycled Aggregate Concrete Reinforced with Basalt Fiber." *Construction and Building Materials*, *135*, 477–83. doi:10.1016/j.conbuildmat.2016.12.161.

Mohamed, O. A. & Al-Hawat, W. (2016). "Influence of Fly Ash and Basalt Fibers on Strength and Chloride Penetration Resistance of Self-Consolidating Concrete." In *Materials Science Forum*, *866*, 3–8. Trans Tech Publications Ltd.doi:10.4028/www.scientific.net/MSF.866.3.

El Refai, A., Abed, F. & Altalmas, A. (2015). "Bond Durability of Basalt Fiber-Reinforced Polymer Bars Embedded in Concrete under Direct Pullout Conditions." *Journal of Composites for Construction*, *19*(5): 1–11. doi:10.1061/(ASCE)CC.1943-5614.0000544.

El Refai, A., Ammar, M. A. & Masmoudi, R. (2015). "Bond Performance of Basalt Fiber-Reinforced Polymer Bars to Concrete." *Journal of Composites for Construction*, *19*(3): 1–12. doi:10.1061/(ASCE)CC.1943-5614.0000487.

Sim, J., Park, C. & Moon, D. Y. (2005). "Characteristics of Basalt Fiber as a Strengthening Material for Concrete Structures." *Composites Part B*, *36*(6–7): 504–12. doi:10.1016/j.compositesb.2005.02.002.

Tam, L., He, L. & Wu, C. (2019). "Molecular Dynamics Study on the Effect of Salt Environment on Interfacial Structure, Stress, and Adhesion of Carbon Fiber/Epoxy Interface." *Composite Interfaces 26* (5): 431–47. doi:10.1080/09276440.2018.1506901.

Yan, F. & Lin, Z. (2017). "Bond Durability Assessment and Long-Term Degradation Prediction for GFRP Bars to Fiber-Reinforced Concrete under Saline Solutions." *Composite Structures*, *161*, 393–406. doi:10.1016/j.compstruct.2016.11.055.

Cite as: Taha A., Alnahhal W. & Alnuami N., "Enhancing the Bond Durability of Basalt Fiber Reinforced Polymer Bars Using Basalt-Macro Fiber Reinforced Concrete", *The 2nd International Conference on Civil Infrastructure and Construction (CIC 2023)*, Doha, Qatar, 5-8 February 2023, DOI: https://doi.org/10.29117/cic.2023.0113

Synthesis of Calcium Nitrate Self-Healing Microcapsules Using Aerosol OT-Hexane Solution for Cementitious Materials

Ala Abu Taqa
Department of Civil Engineering, Munib and Angela Masri Faculty of Engineering,
Aqaba University of Technology, Aqaba-Jordan
aabutaqa@aut.edu.jo; aa1104819@student.qu.edu.qa

Ghassan Suleiman
Department of Civil Engineering, Munib and Angela Masri Faculty of Engineering,
Aqaba University of Technology, Aqaba-Jordan
GSuleiman@aut.edu.jo

Ahmed Senouci
Department of Construction Management, University of Houston, Houston, USA
asenouci@central.uh.edu

Mohamed O. Mohsen
Department of Civil and Architectural Engineering, Qatar University;
Tajarub Research & Development, Doha, Qatar
200202128@student.qu.edu.qa, Mohamed mohsen@tajarub.org

Abstract

Calcium nitrate synthesis of in urea-formaldehyde shell has recently been used to produce self-healing microcapsules for construction applications. The original synthesis was based on water-in-oil emulsion with sulfonic acid as fundamental ingredient of the oil (continuous) phase. It has been modified herein by changing the composition of the continuous (oil) phase by mixing anionic surfactant, Aerosol OT (AOT) with hexane to prepare the solution while keeping the aqueous phase unchanged. The submicron refined calcium nitrate microcapsules. In order to characterize the microcapsules encapsulated using the aforementioned, procedure, a Scanning Electron Microscopy (SEM) was utilized. The obtained microcapsules had satisfactory diameter and shell thickness. To assess the effect of the prepared microcapsules on the compressive and flexural strengths, mortar mixes containing 75% microcapsules (by weight of cement), as an introductory dosage, were made. It has been demonstrated that incorporating the self-healing microcapsules prepared using the procedure suggested in this study did not cause significant reductions in the mortar samples' strengths. Hence, the encapsulation methodology presented here may be utilized to investigate their self-healing efficiency in cementitious materials.

Keywords: Self-healing Microcapsules; Calcium Nitrate; Aerosol; Hexane; Cementitious materials; Compressive and flexural strengths

1 Introduction

Lately, microencapsulation has been extensively adopted to generate microcapsules that have been effectively used in various specialities such as pharmaceuticals, catalysts, electronics, etc. Arefin et al., (2020), Gao et al., (2021), Patil & Bendre (2022), Vintila et al., (2020). Moreover, self-healing microcapsules have been recently utilized to repair concrete structures Al-Ansari et al., (2017), Fayyad et al., (2016), Hassan et al., (2016), Huang & Ye (2011), Kaes et al., (2014), Milla et al., (2016), Mostavi et al., (2015), Podgornik & Šumiga (2008), Schlangen & Sangadji (2013), Van-

Tittelboom et al., (2011), (Van-Tittelboom & Belie, 2013), (Yang et al., 2011). When crack tips rupture microcapsule shells, the released healing agent forms the calcium-silicate hydrate gels (C-S-H) by reacting with a catalyst to fill the cracks and prohibit their propagation.

In construction applications, different healing agents, such as polyurethane and Sodium silicate, have been prosperously selected as healing agents, Maes et al., (2014), Pelletier et al., (2022), (Van Tittelboom et al., 2011). Due to the high costs of such agents, Hassan et al., (2016) attempted to encapsulate the calcium nitrate (as a low-cost material) into urea-formaldehyde shells, which exhibited satisfactory healing efficacy. However, incorporating these microcapsules into cementitious mixes caused compressive and flexural strengths reductions (Milla et al., 2016). Consequently, Hassan et al., (2016) proposed a modification to their original encapsulation procedure to mitigate strength reduction by using a low-Hydrophilic-Lipophilic (HLB) emulsifiers (such as Span 85 and Span 60) to replace the sulfonic acid catalyst, partially (Al-Ansari et al., (2017), Milla et al., (2016). The micro capsules caused a 40% reduction in the elastic modulus for mortar samples incorporating Span 85 (Al-Ansari et al., 2017). On the other hand, the microcapsules using Span 60 had less healing efficiencyin steel-fiber concrete mixes than the micro capsules synthesized using the original procedure (Milla et al., 2016).

Extensively in literature, various oil and water emulsions have been prepared using the anionic surfactant, Dioctyl Sodium Sulfosuccinate (Aerosol-OT, AOT) Aveyard et al., (1986), Hensel

et al., (2017), (Kalyanram et al., 2017), (La Mesa et al., 1992). The dominant advantage of AOT is that it does not need any other co-surfactant to effectively form aggregates in non-polar solvents. This makes AOT more appropriate for the preparation of water-in-oil emulsions than other surfactants (Kizling & Kronberg, 2001), (Leong & Candau, 1982). Accordingly, researchers had successfully used AOT in hexane solutions to synthesize different nano particles (Eastoe et al., (1991), Gupta & Gupta (2004), (Kizling & Kronberg, 2001), (Srivastava et al., 2011).

The paper presents a new modification to the encapsulation procedure of calcium nitrate as a self-healing agent that were proposed by Al-Ansari et al., (2017) and Hassan et al., (2016) to produce refined and smaller size microcapsules with no significant undesirable effects on the cementation's materials' mechanical properties. Such modification utilized the AOT to stabilize the continuous phase (hexane solution) while the aqueous phase components were kept unaltered. After that, the Scanning Electron Microscopy (SEM) was used to recognize the microcapsule's characteristics (shell thickness and diameter). Moreover, the effect of incorporating such microcapsules on the 7 day mortar compressive and flexural strengths was also assessed.

Based on the results, it has been recommended to direct future tests towards investigating the strengths of large concrete samples at different ages with incorporating different dosages of the prepared self-healing microcapsules.

2 Methodology and Design of Experiment

2.1 Preparing the Microcapsules

2.1.1 Synthesis

The procedure suggested by Hassan et al., (2016) for preparing the self-healing microcapsules forms the basis of this study. Calcium nitrate was utilized as the healing agent, encapsulated in a shell consists of urea and formaldehyde and polymerized in a water-in-oil emulsion. As per the original encapsulation procedure, the aqueous phase has been prepared by dissolving 10 grams of the calcium

nitrate, 0.5 grams of the resorcinol, 0.5 grams of the ammonium chloride, 12.67 grams of the formaldehyde and 5 grams of urea in filtered water. However, the components of the continuous phase were changed by mixing 5.8 grams of AOT with 180 grams of Hexane as an organic solvent.

2.1.2 Emulsification and Polymerization

40°C and 1500 RPM elevated temperature and shear rate, respectively, were used to stir the constituents of the continuous phase as suggested by (Hassan et al., 2016) and (Milla et al., 2016). Drops of the aqueous phase have been added to the continuous over 10 minutes. The emulsion was kept to react for 1.5 hours and then, it has been left to settle for few minutes. After settling, the hexane was poured and the produced microcapsules were spread on a wide pan for air drying.

2.2 Characterization by the Scanning Electron Microscopy

The characteristics of the microcapsules (i.e. diameter, shell thickness, shape…etc.), have been assessed by the scanning electron microscope (SEM) imaging technique. A tape with double sides tape was attached to a stubbed mount and the microcapsules were dispersed on top of such tape. Platinum was then used to cover the microcapsules for four minutes. Finally, a secondary electron mode of a 3 kV accelerating voltage was used to capture the images.

2.3 Testing of Mortar Samples

Three mortar mixes were made in this study. The first mix was considered as the control mix (normal mortar without microcapsules). The second and the third mixes incorporated a dosage of 0.75% (of cement weight) as the microcapsule's dosage, with the former being produced using the encapsulation procedure without AOT and the latter being produced using the proposed procedure in this study (with AOT). 740 grams of Portland cement CEM I Class 42.5 R were mixed with 2035 grams of natural sand and 359 grams of water. No microcapsules have been added to the control mix while 5.55 grams of microcapsules prepared using the original procedure have been incorporated to the second mix and same amount of the microcapsules prepared using the procedure proposed in this study have been added to the third mix.

From each mix, three standard mortar cubes (50mm x50 mm x50 mm) and three standard prisms (40 mm x 40 mm x 160 mm) were casted. The testing matrix is summarized in Table 1. After 24 hours, the casted samples were demolded and tested at 7 days for compressive and flexural strengths as per ASTM C109 and ASTM C348, respectively.

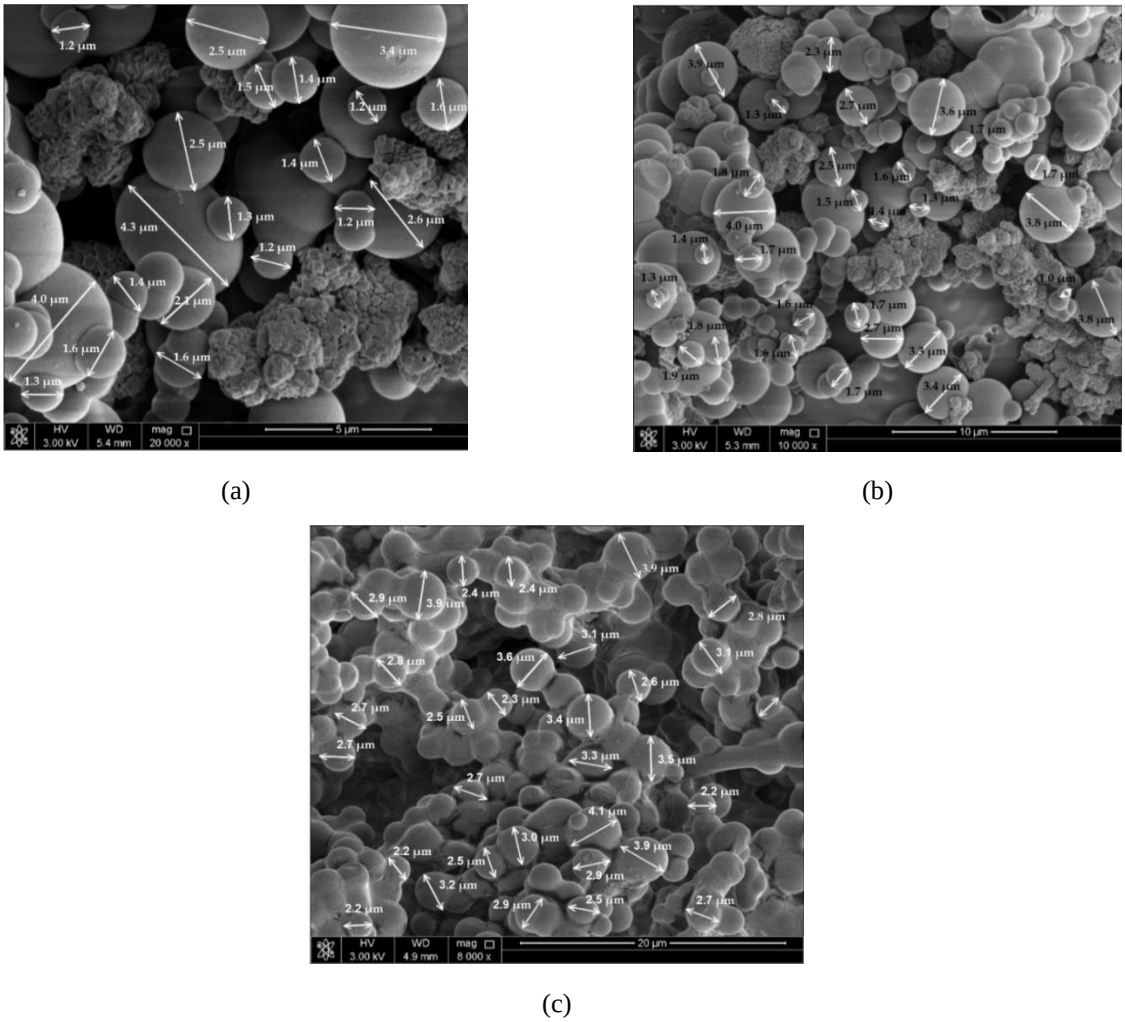
Table 1: Testing matrix of mortar samples

Mix No.	Batch ID.	MC dosage (% of the cement weight)	Samples for the compression testing	Samples for the flexural testing
Without MC (Control)	1	0.00	3	3
	2		3	3
With 0.75 MC (non-modified procedure, without AOT)	1	0.75	3	3
	2		3	3
With 0.75 MC (with AOT)	1	0.75	3	3
	2		3	3

3 Discussion Of The Results

3.1 Microcapsules' SEM Imaging

Figure 1 shows the prepared microcapsules' diameters at different imaging scales. A round more than 150 microcapsules were selected randomly from the images and the average diameter value of all of them was calculated. It has been found that the produced microcapsules had diameters in the range of 1µm to 5 µm and an approximated average diameter of 2.5 µm. Such values are smaller than the same of the microcapsules prepared using the procedures developed by (Al-Ansari et al., 2017) (70 µm) and (Hassan et al., 2016) (51 µm). A perfectly spherical and uniform shape of the produced microcapsules could be also noted in Figures1 (a-c).

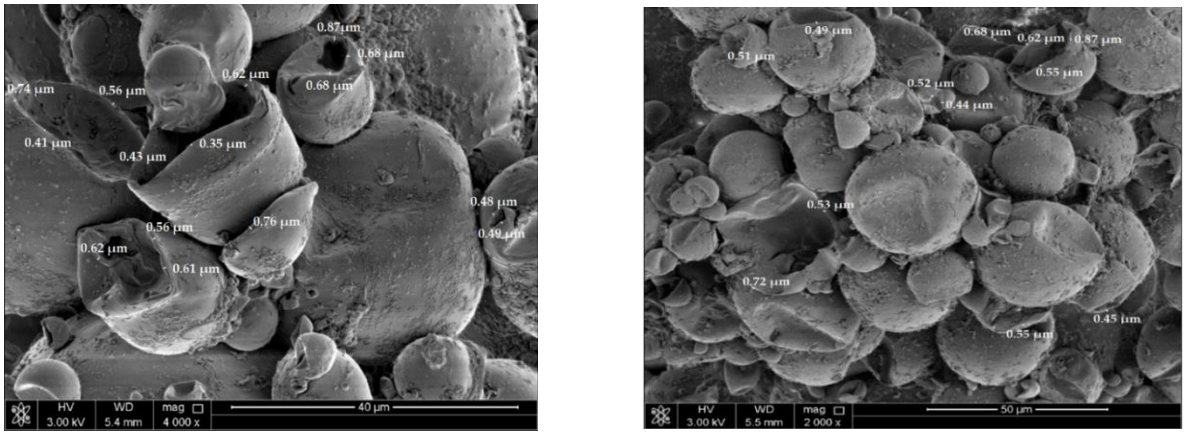


(a) (b)

(c)

Fig. 1: SEM images of the prepared microcapsules showing their diameters at different imaging scales (a) 5 µm (b) 10 µm (c) 20 µm

From Figure 2, the shell thicknesses of the prepared microcapsules could be approximated. As shown in Figures 2 (a) and (b), the shell thicknesses of randomly selected microcapsules were between 0.35 µm to 0.70 µm with an approximated average shell thickness of 0.60 µm. Such values are also smaller than the same which have been recorded by Al-Ansari et al., (2017) (0.80 µm) and (Hassan et al., 2016) (0.90 µm). This observation may support a conclusion that the efficiency of the self-healing of the AOT microcapsules be enhanced because the thinner shell thickness is easier to be ruptured by the crack tip when the cracks are initiated in cementitious elements.



(a) (b)

Fig. 2: SEM images of the prepared microcapsules of the prepared microcapsules showing their shell thicknesses at different imaging scales (a) 40 µm (b) 50 µm

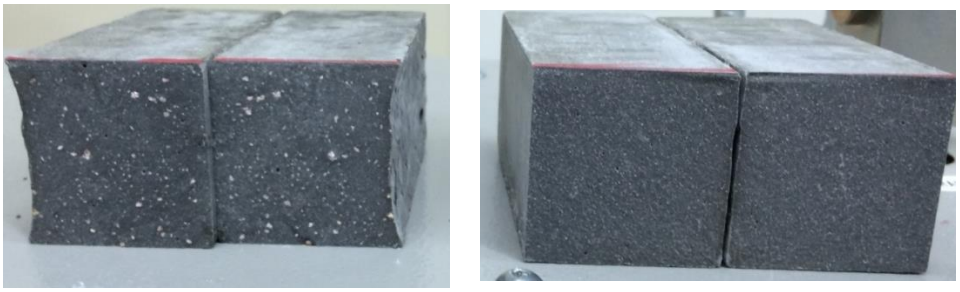
3.2 Testing the Compression & Flexural Strengths

As aforementioned, 6 mortar samples were tested for compression from each mix and same for the flexural strength. ASTM E178 standard was used to check the outlier observations and exclude them before computing the average values.

For the second and third mixes (containing microcapsules) and regardless the microcapsules preparation procedure, it has been found that the reductions in the compressive strength values (compared to the control mix that does not contain microcapsules) were very small and could be neglected (0.34% for the second mix and 0.27% for the third mix)

However, for the flexural strength, it could be found that the average reduction in the flexural strength values for the second mix (which contains microcapsules prepared with the non-modified procedure, without AOT) was about 15.3% which may be considered significant. On the contrary, the average reduction in the flexural strength's values was only 0.31% for the third mix (which contains microcapsules prepared with the modified procedure suggested in this study (with AOT)). Such results suggested that utilizing AOT for the polymerization of the self-healing microcapsules will decrease the undesirable effects on the cementitious mixes' strengths and mechanical properties.

After carrying out the flexural test on the mortar prisms, pictures of the fracture surfaces have been captured as shown in Figure 3. From the visual observation of such pictures, one may conclude that the distribution of the modified microcapsules (with AOT, Figure 3 (b)) was more uniform and the microcapsules sizes were smaller compared to the pictures of the samples containing microcapsules prepared with the non-modified procedure (without AOT, Figure 3 (a)). Such observation strengthens the results demonstrated previously in this study that using AOT for the synthesis of microcapsules results in refined microcapsules which may enhance the physical, chemical and mechanical properties of the cementitious mix.



(a) (b)

Fig. 4: Images of the Prisms' Fracture Surfaces after Flexural Strength Testing (a) Sample Incorporating microcapsules Prepared using the Non-Modified Procedure (without AOT) and (b) Sample Incorporating microcapsules prepared using the Modified Microcapsules (With AOT)

4 Conclusions

From this study, the following points could be concluded:

- The modified microcapsules prepared in this study (with AOT) had diameters in the range of 1.0 µm to 5.0 µm and an approximated average diameter of 2.5 µm. Such values are smaller than the same of the microcapsules prepared using the previous encapsulation procedures. Perfectly spherical and uniform shape microcapsules were obtained.
- The shell thicknesses of randomly selected microcapsules prepared using the procedure presented in this study (with AOT) were found to be in the range of 0.35 µm to 0.90 µm with an approximated average shell thickness of 0.60 µm. Such values are also smaller than the same of the microcapsules prepared using the previous encapsulation procedures. This observation may support a conclusion that the efficiency of the modified self-healing microcapsules (with AOT) may be enhanced because the thinner shell thickness is easier to be ruptured by the crack tip when the cracks are initiated in cementitious elements
- For the mix containing the modified self-healing microcapsules (with AOT), the average reductions in the compressive and flexural strengths of mortar mixes at 7 days were only 0.27% and 0.31%, respectively (which could be neglected). This observation demonstrates that using AOT for the synthesis of self-healing microcapsules can decrease the potential unfavourable effects on the cementitious mixes' mechanical properties in general and the flexural strength in particular.
- Using AOT for the synthesis of microcapsules results in refined microcapsules which may enhance the physical, chemical and mechanical properties of the cementitious mix.

References

Al-Ansari, et al. (2017). "Performance of modified self-healing concrete with calcium nitrate microencapsulation", *Construction and Building Materials, 149,* 525-534.

Arefin, et al. (2020). "An overview of microcapsule dosage form". *International Journal of Pharmaceutical Chemistry and Analysis , 7,* 155-160.

Aveyard, et al. (1986). "Interfacial tension minima in oil–water–surfactant systems. Behaviour of alkane–aqueous NaCl systems containing aerosol OT", *Journal of the Chemical Society, Faraday Transactions 1: Physical Chemistry in Condensed Phases, 82,* 125-142.

Eastoe, et al. (1991). "Structural studies of microemulsions stabilised by aerosol-OT", *Advances in Colloid and Interface*

Science, 36, 1-31.

___. (1992). "Variation of surfactant counterion and its effect on the structure and properties of Aerosol-OT-based water-in-oil microemulsions", *Journal of the Chemical Society, Faraday Transactions, 88*, 461-471.

Fayyad, E. M., Almaadeed, M. A. & Jones, A. (2016). "Preparation and characterization of urea–formaldehyde microcapsules filled with paraffin oil", *Polymer Bulletin, 73*, 631-646.

Gao, et al. (2021). "Structural regulation of poly(urea-formaldehyde) microcapsules containing lube base oil and their thermal properties", Progress in Organic Coatings, 150, 105990.

Gupta, M. and Gupta, A.K. (2004). "In vitro cytotoxicity studies of hydrogel pullulan nanoparticles prepared by AOT/N-hexane micellar system", *Journal of Pharmacy and Pharmaceutical Sciences, 7*, 38-46.

Hassan, et al. (2016). "Microencapsulation of Calcium Nitrate for Concrete Applications", Proceedings of the Transportation Research Record, 2016, 8-16.

Hensel, et al. (2017). "Molecular characterization of water and surfactant AOT at Nanoemulsion surfaces", Proceedings of the National Academy of Sciences, 114, 13351-13356.

Huang, H. & Ye, G. (2011). "Application of Sodium Silicate Solution as Self-Healing Agent in Cementitious Materials", Proceedings of the In Proceedings of International RILEM Conference on Advances in Construction Materials Through Science and Engineering, 2011, 530-536.

Kaes, M., Van-Tittelboom, K. & De-Belie, N. (2014). "The efficiency of self-healing cementitious materials by means of encapsulated polyurethane in chloride containing environments", *Construction and Building Materials, 71*, 528-537.

Kalyanram, P., Valenzuela, P. & Gupta, A.R. (2017). "Aerosol-Ot Stabilized Micro and Nano-Scale Emulsions for Pharmaceutical Formulations", *Organic & Medicinal Chemistry International Journal, 4*, 88-90.

Kizling, J. & Kronberg, B. (2001). "On the formation of concentrated stable w/o emulsions", *Advances in Colloid and Interface Science, 89-90*, 395-399.

La Mesa, et al. (1992). "Phase diagram and phase properties of the system water-hexane-Aerosol OT", *Langmuir, 8*, 2616-2622.

Leong, Y.S. & Candau, F. (1982). "Inverse microemulsion polymerization", *Journal of Physical Chemistry, 86*, 2269–2271.

Maes, M., Van Tittelboom, K. & De Belie, N. (2014). "The efficiency of self-healing cementitious materials by means of encapsulated polyurethane in chloride containing environments", *Construction and Building Materials, 71*, 528-537.

Milla, et al. (2016). "Evaluation of the Effect of Self-Healing Calcium Nitrate Microcapsules on Concrete Properties. In Proceedings of the Paper # 16-0422, submitted to the 95th Transportation Research Board Annual meeting, Washington, D.C, 2016.

___. (2019). "Measuring the crack-repair efficiency of steel fiber reinforced concrete beams with microencapsulated calcium nitrate", *Construction and Building Materials, 201*, 526-538.

Mostavi, et al. (2015). "Evaluation of Self-Healing Mechanisms in Concrete with Double-Walled Sodium Silicate Microcapsules", *Journal of Materials in Civil Engineering, 27*.

Patil, R. & Bendre, R. (2022). "Preparation, characterization and controlled release study of poly (urea–formaldehyde) microcapsules enclosing Pretilachlor herbicide", *Iranian Polymer Journal, 31*, 691-704.

Pelletier, et al. (2022). Self-healing concrete with a microencapsulated healing agent", Available online: http://energetics.chm.uri.edu/system/files/Self%20healing%20concrete%20-7-11.pdf, accessed March 2022.

Podgornik, B. B. & Šumiga, B. (2008). "Microencapsulation technology and its applications in building construction materials", *RMZ - Materials and Geoenvironment, 55*, 329-344.

Schlangen, E. & Sangadji, S. (2013). "Addressing Infrastructure Durability and Sustainability by Self-Healing Mechanisms - Recent Advances in Self-HealingConcrete and Asphalt", *Procedia Engineering, 54*, 39-57.

Srivastava, S., Sharma, S.K. & Sharma, R. K. (2011). "Synthesis of gold nanorods using concentrated aerosol OT in hexane and its application as catalyst for the reduction of eosin", *Colloids and Surfaces A: Physicochemical and Engineering Aspects*, *373*, 61-65.

Van-Tittelboom, K. & Belie, N. D. (2013). "Self-Healing in Cementitious Materials-a Review", *Materials*, *6*, 2182–2217.

Van-Tittelboom, et al. (2011). "Self-Healing Efficiency of Cementitious Materials Containing Tubular Capsules Filled with Healing Agent", *Cement and Concrete Composites*, *33*, 497–505.

Vintila, et al. (2020). "The Synthetization and Analysis of Dicyclopentadiene and Ethylidene-Norbornene Microcapsule Systems", 12, 1052.

Yang, et al. (2011). "A Self-Healing Cementitious Composite Using Oil Core/silica Gel Shell Microcapsules". *Cement and Concrete Composites*, *33*, 506-512.

Cite as: Abutaqa A., Suleiman G., Senouci A. & Mohsen M., "S Synthesis of Calcium Nitrate Self-Healing Microcapsules Using Aerosol OT-Hexane Solution for Cementitious Materials", *The 2nd International Conference on Civil Infrastructure and Construction (CIC 2023)*, Doha, Qatar, 5-8 February 2023, DOI: https://doi.org/10.29117/cic.2023.0114

Assessment of the Current Frequency Calculation Methods Used in the Determination of the Dynamic Modulus Value in Pavement Design and Analysis

Mohammed A. Alfarra
Qatar University, Doha, Qatar
ma2000372@student.qu.edu.qa

Mohammed Sadeq
Seero Engineering Consulting LLC, Doha, Qatar
mohammed.sadeq@seeroeng.com

Husam Sadek
Seero Engineering Consulting LLC, Doha, Qatar
husam.sadek@seeroeng.com

Abstract

The dynamic modulus |E*| is used in the Mechanistic-Empirical Pavement Design Guide (MEPDG) to express the viscoelasticity of asphalt material at a range of temperatures and loading frequencies. As a result, the current MEPDG method assumes that frequency is calculated as the opposite of vehicular loading pulse time. In addition, the loading pulse time can be calculated using the Odemark thickness equivalency method according to the MEPDG. On the other hand, the loading frequency as per Qatar Highway Design Manual (QHDM 2021) is estimated based on the average vehicle speed using Losa and Di Natale formula. However, studies found major inadequacies in the adopted method of MEPDG, which might affect the accuracy of the loading frequency and |E*| accordingly which leads to an impact on the pavement design and performance analysis. Hence, it was recommended that alternative frequency determination approaches like the Fast Fourier Transform (FFT) be used rather than traditional time-domain techniques. Therefore, this paper compares the results of the MEPDG and QHDM loading frequency procedure with the dominant frequencies (DF) obtained using the FFT. On the other hand, the loading time pulses are estimated using the Odemark approach and, compared to the ones simulated using 3D Move Analysis software that accurately considers the tire contact pressure, viscoelastic properties, & vehicle speed. It was found that the used frequency determination approach in the pavement design in Qatar, overestimates the frequency values by about 30% to 88%. Furthermore, the findings showed that the MEPDG method for determining loading time and frequency is not conservative.

Keywords: Asphalt; Dynamic Modulus; Loading Pulse; Fast Fourier Transform; Loading frequency

1 Introduction

The, fact that, Hot Mix Asphalt (HMA) is currently defined as viscoelastic material is one of the most significant benefits of the important improvements made by the MEPDG (Al-Qadi et al., 2008). As a result, the |E*| is used to express the viscoelastic behavior of the HMA, considering both the effects of temperature and the rate of loading, as shown in the belowsigmoidal equation (Pellinen et al., 2003).

$$log\,|E*| = \delta + \frac{\alpha}{1+e^{\beta+\gamma(\log f_r)}} \qquad (1)$$

where |E*| is the dynamic modulus (MPa); α is the vertical distance in logarithmic coordinates

between the |E*| master curve's lower and upper asymptotes.; δ is the |E*| master curve's lower asymptote in logarithmic coordinates; β, γ are the master curve's shape parameters; γ impacts the rate of change between the upper and lower asymptotes; β impacts the turning point's horizontal location, and f_r is a reduced frequency in Hz.The reduced frequency f_r is the frequency equivalent to the testing temperature in relation to the reference temperature. Furthermore, after determining the shift factor, Equation (2) can be used to determine the reduced frequency (Zhang et al., 2020).

$$f_r = f\times \alpha(T) \quad (2)$$

where f represents the loading frequency, T represents the temperature, and α(T) represents the temperature shift factoras explained below (Laukkanen et al., 2018):

$$\log(\alpha(T)) = a_1(T^2 - T^2_{ref}) + a_2(T - T_{ref}) \quad (3)$$

a_1, a_2 are fitting constants affected by material characteristics (Laukkanen et al., 2018).

During the mix design process, the |E*| of the HMA is captured in the frequency domain by using the Asphalt Mixture Performance Tester (AMPT) machine under a wide range of temperatures and frequencies applied to the samples, and it is used to establish the |E*| master curve. However, vehicular loading is applied on-site in the time domain (Harran, 2011). Therefore, several researchers have tested various time-to-frequency conversion methods to accurately measure the associated frequency from vehicle stress or strain pulse length. For example, MEPDG takes the method of calculating frequency to be the inverse of the time pulse (f=1/t). Where f is the frequency in Hz and t is the loading time in (s). The relationship between frequency and time in the dynamic modulus tests is currently a source of heated debate among researchers (Sullivan & Denneman, 2015). A recent study has examined the accuracy of the MEPDG's conversion equation(Dongre et al., 2006), and no supporting reference for that approach was found other than MEPDG. The approach (i.e., MEPDG) is fundamentally inaccurate because it cannot accurately simulate the pulse produced by vehicular loading, which has a complex frequency spectrum (Underwood & Kim, 2009).On the other hand, MEPDG uses equation (4) based on Odemark's thickness equivalency approach to calculate the effective length of the loading pulse at any depth within the pavement system (Al-Qadi et al., 2008).

$$t = \frac{L_{eff}}{17.6V_s} \quad (4)$$

Where t = time of loading (s); L_{eff} = effective length (in); and v_s = vehicle speed (mph).The Odemark method relies on the pavement structure being converted into a single subgrade layer system. Furthermore, the stress distribution for a given subgrade soil is assumed to be at 45°. The effective depth varies in the transformed section and is calculated as follows (Al-Qadi et al., 2008):

$$z_{eff} = \sum_{i=1}^{n-1} h_i \sqrt[3]{\frac{E_i}{E_{SG}}} + h_n \sqrt[3]{\frac{E_n}{E_{SG}}} \quad (5)$$

Where, Z_{eff} = effective depth, h_n = thickness of the layer of interest (layer n), E_{SG} = elasticity modulus of subgrade, and E_n= elasticity modulus of the layer of interest. However, many researchers found that the MEPDG method for frequency calculations is associated with a significant error, which affects the accuracy of the entire pavement design process (Katicha et al., 2008; Dongre et al., 2006). Therefore, Al-Qadi et al., (2008) compared the results ofusing the Odemark approachto the loading frequencies in the asphalt layer computed using the advanced Finite Element (FE) model. The results showed that the MEPDG method is not conservative and to

improve the MEPDG frequency, a correction factor was proposed by (Al-Qadi et al., 2008). Furthermore, Al-Qadi et al., (2008) used the (FFT) analysis to estimate the equivalent loading frequency based on the measured field loading time pulses to evaluate and quantify the MEPDG's time-frequency conversion process. The equivalent frequencies were assumed to be the weight center of the Fourier spectra. It was reported that the MEPDG frequency calculations method is associated with a frequency estimation error ranging from 40% to 140%, depending on the vehicle speed and pavement depth. Thus, (Al-Qadi et al., 2008)concluded that the inaccuracy in the MEPDG is due to using Odemark's hypothesis and the unrealistic time-frequency conversion approach. Another approach based on Losa and Di Natale equation (6) for frequency determination is adopted in pavement design and analysis in Qatar (Losa & Natale, 2012).

$$f_z = 0.043 \frac{V}{2a} e^{-2.65z+\beta(T)} \quad (6)$$

$$\beta(T) = 1.25x10^{-5}T^3 - 1.6x10^{-3}T^2 + 9.2x10^{-2}T \quad (7)$$

Where, f is the frequency in Hz, v= vehicle speed (m/s), a= radius of tire pressure (m), z= distance from the surface to the center of the asphalt layer (m), and T= average pavement temperature (^oC). However, this method is still not verified or compared by any reliable conversion method such as the FFT which wasrecommended by several studies to be used in the prediction of the frequency spectrum of vehicular loading (Al-Qadi et al., 2008). Therefore, this paper assesses the MEPDG loading frequency calculations and Losa & Di Natale approaches by comparing their results to the dominant frequency (DF) obtained by FFT. In addition, it provides a compersion between the current MEPDG loading time estimation method with the loading pulses generated by the 3D Move analysis software. The used softwareconsiders the viscoelastic material characterization for the pavement layers. The Loading time pules were extracted at different speeds and depths.

2 Methodology

2.1 Experimental Program

In this paper, two pavement sections with different asphalt mixtures were selected. Section 1 was produced with Pen 60–70 base bitumen and based on the Qatar Construction Specifications (QCS), which is following the Marshall procedure. While Polymer Modified Bitumen (PMB) with an SBS modifier was included in Section 2. The |E*| Master Curve parameters for the selected asphalt mixtures in this study can be seen below table.

Table 1: Parameters of the |E*| Master Curves (AMPT) at a Reference Temperature Of 21.1°C for the Selected Asphalt Mixtures

Mix	**δ**	**α**	**β**	**γ**	**a_1**	**a_2**
Pen 60–70 Based Mixture	-1.434	5.964	2.229	0.370	0.0010	−0.173
PMBBased Mixture	-1.388	5.912	2.041	0.316	0.0009	−0.170

Besides, to check the temperature influence on the estimation of the loading pulse and frequency, two seasons (spring & summer) were adopted as per Qatar's environmental conditions. During spring (i.e., low temperature)the average air temperatureof 23°C is considered and the average surface temperature of 25°C is assumed, while in summer (i.e., high temperature), the average air temperature is assumed to be 46°C while the average surface temperature was considered as 63°C. In addition, the average pavement temperatures at the center of the asphalt layers in each season were calculated based on BELLS2 model by Lukanen et al. (2000) which was also adopted in the

QHDM 2021 and considered in the analysis to count for the asphalt viscoelasticity properties. The estimated average pavement temperatures are presented in Table 2. Also, the module for each layer is assumed as per the typical results of the Falling Weight Deflectometer (FWD) test in Qatar.

Table 2 : Summary for the Assumed Modulus of Each Layer (Used in the Calculation of the L_{eff})

Season	Average Pavement Temp. °C	Layers	Assumed Module (MPa)	
			Section 1	Section 2
Spring	23.2	AC	8893	6923
		Subbase	1129	1072
		Subgrade	232	173
Summer	55.9	AC	2282	2171
		Subbase	575	562
		Subgrade	179	173

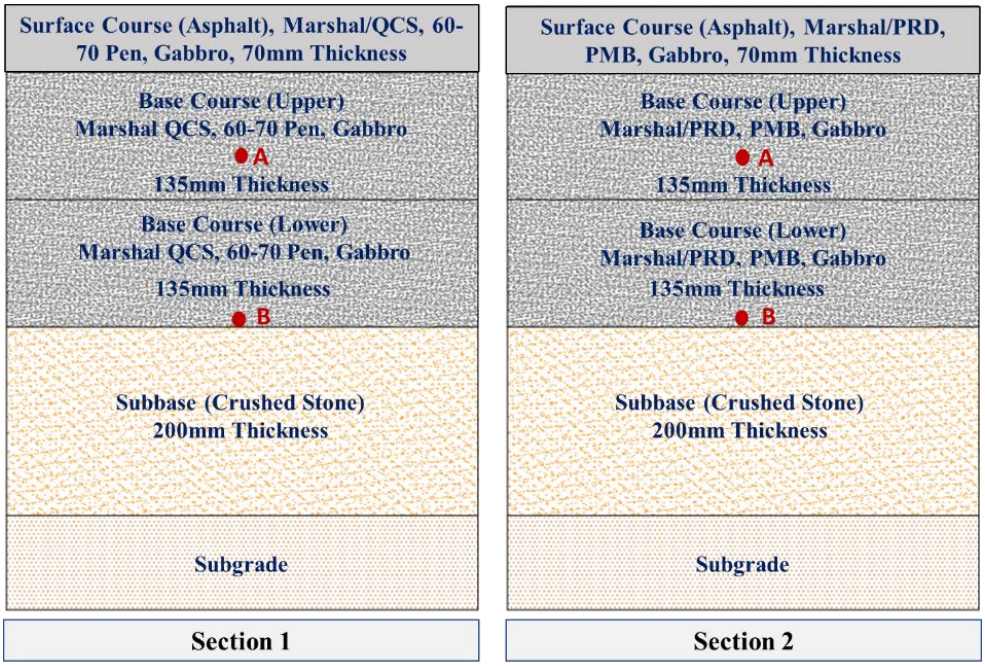


Fig. 1: Layers and Materials' properties of the two selected sections

2.2 Loading Time Pulse Generation

A single tire from a standard single-axle dual tire with a total axle weight of 80 kN was used to generate the vertical stress time pulse (σ_v) using 3D-Move Analysis software. The radius of the tire contact circular area (a_c) was determined by dividing the load on the tire by the inflation pressure (724 kPa). The (a_c) was found to equal 0.093 m. Three target speeds of 24, 40, and 72 km/hr were included in the study and applied in the 3D model at the two sections. Besides, the loading time pulses were captured at two different depths (point A = 170mm) and (point B = 340mm) as shown inFig. **1**. On the other hand, the bell-shaped equation (8) is used to represent the generated vertical compressive stress pulse for a moving vehicle.

$$y(t) = e^{-t^2/s^2} \qquad (8)$$

Where s= the standard deviation that controls the shape of the curve ($s=n_1v^{-n2}$). The standard

deviation (s) is a function of speed for the two variouslocations in the pavement structure, where v is the truck speed in km/hr. Also,n_1&n_2 are the controls factor that varies with the pavement depth (Loulizi et al., 2002).

2.3 Loading Frequency Determination

Four various scenarios were considered to determine the loading frequency from the Loading Time Pulse Duration (t) (see Table 3). The loading frequency determination methods adopted in the MEPDG and QHDM 2021, were compared to the dominant frequencies (DF) values of FFT that are calculated at the weight center of the resulting frequency spectrum to evaluate their accuracy.

Table 3 : Frequency calculation scenarios considered in this study

Scenario #	**Loading Time Duration**	**Loading Frequency Determination Method**
Scenario 1	3D Move Generated Pulse	$f = \frac{1}{t}$
Scenario 2	$t = \frac{L_{eff}}{17.6V_s}$	$f = \frac{1}{t}$
Scenario 3	Losa and Di Natale	$f_z = 0.043\frac{V}{2a}e^{-2.65z+\beta(T)}$
Scenario 4	3D Move Generated Pulse	DF - FFT

3 Results And Discussion

3.1 The Estimated Loading Pulse Time

Fig. **2** displays the vertical stress (σ_v) pulses for a vehicle speed of 40 km/hr, normalized to their peak values at 170mm in Section 1 through the spring and summer seasons. While the generated loading time pulses generated in Section 2 at the same speed in the two seasons were almost the same as the material characteristics have a minor impact on the generated loading pulses. With increasing the depth, the loading pulse width showed longer durations. However, the temperature affected slightly the length of the loading pulses on the two sections. This completely corresponds to the findings of (Loulizi et al., 2002) and (Al-Qadi et al., 2008) in their studies.

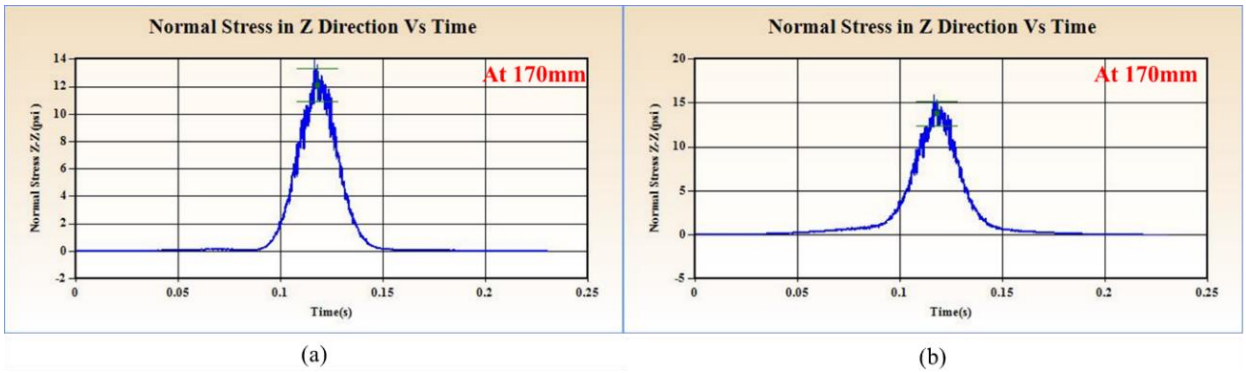


Fig. 2: Loading Time Pulse generated on Section 1 at 40 Km/Hr Speed
At Depth of 170mm (a) spring season (b) summer season

The normalized bell-shaped function has shown an accurate approximation of the produced loading pulse by 3D Move Analysisat different speeds and depths as shown in the below figures.

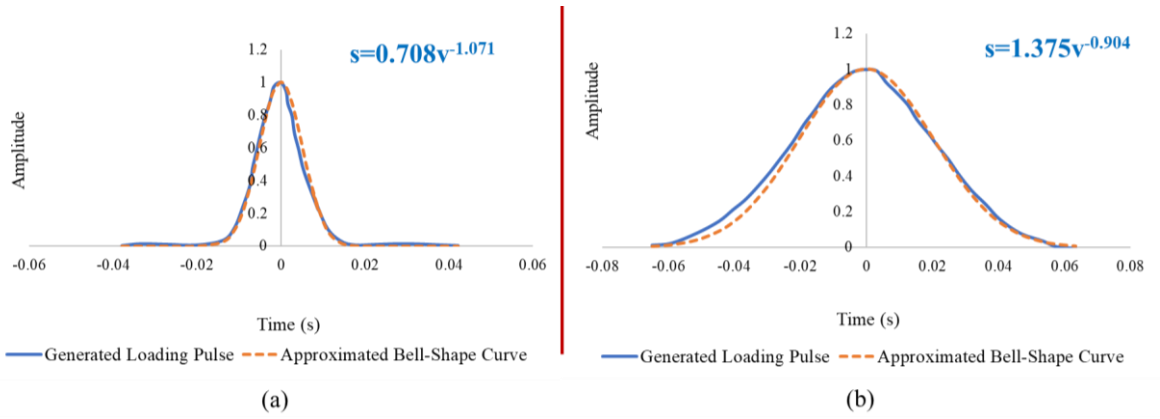


Fig. 3: Normalized Bell-shaped approximations of Loading Pulses for the 72 km/h test applied on section 1 in spring at (a) 170 mm (b) 340 mm

On the other hand, the same criteria and conditions considered in the 3D Move Analysis were used the calculate the vehicular loading time pulse (t) based on equation (4). A summary of the generated loading time pulses using 3D Move Analysis and Odemark approach at different operational conditions in Section 1 & Section 2 are presented in Table 5.

3.2 The Predicted Loading Frequency From Different Scenarios

The built-in FFT routine in Microsoft Excel® was used to perform the frequency analysis of vertical stress pulses in scenario 4 and to find the DF. The FFT analysis was done on a total of 2048 data points obtained at equal intervals. Furthermore, The DF values at the weight center of FFT Fourier spectra were compared against the other frequency calculation approaches. The corresponding normalized FFT wave of the σv pulse was generated at different depths as shown in Fig. **4**.At high depths, the area under the generated frequency spectrums tended to decrease. While,the frequency value significantly was not influenced by the temperature, especially at low speeds.

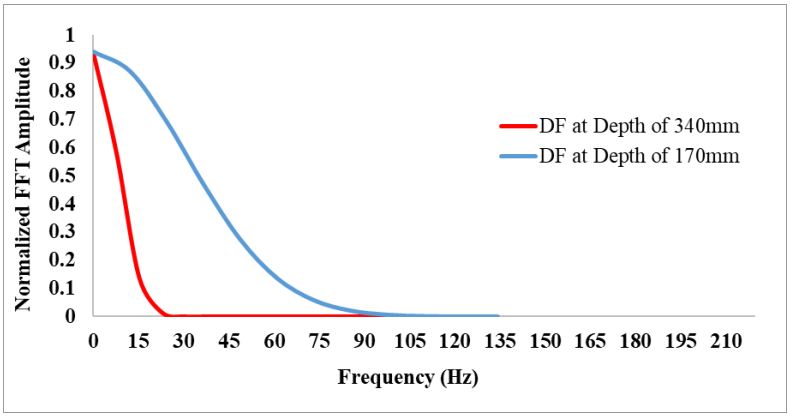


Fig. 4: The Frequency domain of loading pulse on section 1 at 72 km/hr during spring

Nearly similar frequency waves were obtained using FFT at the same conditions in Summer.Table 4 shows a summary of the calculated loading frequency using Losa and Di Natale and FFT methods. Results obtained using FFT agree with the findings of previous studies(Al-Qadi et al., 2008; Shafiee et al., 2015). The difference in frequency value becomes clearer as the speed increases, and it is influenced by the temperature. It's worth noting that in comparison to FFT results, the Losa & Di Natale equation used in the State of Qatar produced high-frequency values, particularly at higher speeds and temperatures.

Also, Table 5 relates the Fourier analysis results to the loading frequency obtained using the MEPDG and the Losa & Di Natale methods. Also, the calculated frequencies using FFT were generally lower than scenario 1 results, particularly at speeds of 40 km/hr and higher.

Table 4 : Summary of the calculated loading frequency using Losa and Di Natale and FFT methods

Sec.#	Depth mm	Speed km/hr	Loading Frequency (Hz) using Losa and Di Natale		Loading Frequency (Hz) using the DF-FFT	
			23.2 ºC	55.9 ºC	23.2 ºC	55.9 ºC
1	170	24	5.10	12.50	2.82	2.82
		40	8.49	20.83	4.41	4.34
		72	15.29	37.50	6.59	5.32
	340	24	4.07	9.98	2.25	2.26
		40	6.78	16.63	2.91	2.92
		72	12.20	29.93	3.35	3.66
2	170	24	5.10	12.50	3.57	2.64
		40	8.49	20.83	4.10	3.39
		72	15.29	37.50	6.00	5.01
	340	24	4.07	9.98	2.15	2.08
		40	6.78	16.63	3.05	2.91
		72	12.20	29.93	4.50	4.66

Table 5 : Percentage deviation from the DF -FFT based on the 3D Move Analysis loading pulses (%)

S#	Depth mm	Speed km/hr	Loading Pulse Duration (s) - Odemark approach		Loading Pulse Duration (s) - 3D Move Analysis		Scenario 1		Scenario 2		Scenario 3	
			23.2 ºC	55.9 ºC	23.2 ºC	55.9 ºC	23.2 ºC	55.9 ºC	23.2 ºC	55.9 ºC	23.2 ºC	55.9 ºC
1	170	24	0.200	0.147	0.308	0.308	13.1%	16.0%	43.6%	58.5%	44.7%	77.4%
		40	0.120	0.088	0.155	0.155	31.6%	33.2%	47.0%	61.6%	48.1%	79.2%
		72	0.067	0.049	0.080	0.080	47.3%	52.1%	56.0%	73.9%	56.9%	85.8%
	340	24	0.372	0.266	0.382	0.382	14.1%	13.9%	16.3%	39.9%	44.7%	77.4%
		40	0.223	0.160	0.225	0.225	34.6%	33.2%	35.1%	53.4%	57.1%	82.5%
		72	0.124	0.089	0.128	0.128	57.1%	55.1%	58.4%	67.5%	72.5%	87.8%
2	170	24	0.203	0.147	0.246	0.246	12.1%	14.1%	27.6%	61.3%	29.9%	78.9%
		40	0.122	0.088	0.162	0.162	33.6%	32.6%	50.2%	70.1%	51.7%	83.7%
		72	0.068	0.049	0.106	0.106	36.5%	39.4%	59.5%	75.5%	60.7%	86.6%
	340	24	0.377	0.265	0.381	0.381	18.0%	20.4%	19.0%	44.7%	47.2%	79.1%
		40	0.226	0.159	0.224	0.224	31.6%	34.1%	30.9%	53.7%	55.0%	82.5%
		72	0.126	0.088	0.128	0.128	42.4%	42.3%	43.4%	58.8%	63.1%	84.4%

From the previous table, it can be noticed that the loading pulses duration of the Odemark approach is less than the 3D Move Analysis generated loading pulses by (1% to 147%). In addition, using the Odemark approach might overestimate the loading frequency by an error of 0.10% to 59.5%, which will affect the estimation of the asphalt modulus. Moreover, the deviation of scenario 1 from

scenario 4 was ranging from 12.11% to 57.09%. This is in agreement with the findings of (Al-Qadi et al., 2008). In addition, the associated error with Scenario 3 (adopted in the state of Qatar) compared to the dominant loading frequencies obtained with FFT was ranging between about 29.88% to 87.77%, which means that it might overestimate the estimation of the loading frequency value and leads to an unreliable estimation of the HMA complex modulus.

4 Conclusion

This study was conducted to evaluate the accuracy of the MEPDG's time-frequency conversion process along with the Losa and Di Natale equation used in the state of Qatar. The 3D Move Analysis software was used to generate the loading pulses for two different sections and at various operational criteria., and the same conditions were used to determine the loading pulse using the Odemark methodapproach. On the other hand, the FFT analysis was performed to find the DF ofthe generated loading pulses using 3D Move Analysis. Four scenarios were developed for frequency determination based on the estimated loading pulse time. Accordingly, the following conclusions were drawn based on the selected sections, material properties, and the other study's conditions which are in line with pavement design criteria used in the state of Qatar:

1. Using Odemark's approach adopted in MEPDG for frequency calculation produces higher frequencies than those determined by using the 3D move analysis method, particularly at low speeds and high temperatures. This would result in higher complex moduli of the HMA.
2. The simple loading frequency estimation methods used in pavement design and analysis in the state of Qatar, based on this study, can overestimate the loading frequency depending on vehicle speed and measurement depth. The associated error with Losa and Di Natale method compared to the DF-FFT was ranging between 29.88% to 87.77%.
3. In addition, the Deviation of Scenario 1 from DF-FFT was ranging from 12.11% to 57.09%.

It is obvious that DF- FFT produces more accurate moduli and it is recommended to be used in the |E*| determination in the pavement design and analysis in Qatar. While the approach of considering DF at the weight centers of frequency waves needs to be further studied in the future.

References

Al-Qadi et al. (2008). "Accuracy of Current Complex Modulus Selection Procedure from Vehicular Load Pulse: NCHRP Project 1-37a Mechanistic-Empirical Pavement Design Guide." *Transportation Research Record*, no. 2087: 81–90. https://doi.org/10.3141/2087-09.

Al-Qadi, Imad L., Wei, X. & Elseifi, M. A. (2008). "Frequency Determination from Vehicular Loading Time Pulse to Predict Appropriate Complex Modulus in MEPDG." *Asphalt Paving Technology: Association of Asphalt Paving Technologists-Proceedings of the Technical Sessions* 77 (January 2008): 739–71.

Dongre, R., Myers, L. & D'angelo, J. (2006). "Conversion of Testing Frequency to Loading Time: Impact on Performance Predictions Obtained from the ME Pavement Design Guide." *Proceedings of the Transportation Research Board*.

Harran, G. (2011). "Improving the Determination of the Dynamic Modulus of Asphalt Concrete for Mechanistic-Empirical Pavement Design." *Ph.D. Thesis, University of Manitoba, Winnipeg, Manitoba, Canada*.

Katicha, et al. (2008). "Conversion of Testing Frequency to Loading Time Applied to the Mechanistic-Empirical Pavement Design Guide." *Transportation Research Record*, no. 2087: 99–108. https://doi.org/10.3141/2087-11.

Laukkanen, et al. (2018). "The Temperature Dependence of Relaxation Mechanisms in Amorphous Polymers and Other Glass-Forming Liquids." *Journal of Non-Crystalline Solids 483*(12): 10–17.

https://doi.org/10.1016/j.jnoncrysol.2017.12.029.

Losa, M., & Andrea, N. (2012). "Evaluation of Representative Loading Frequency for Linear Elastic Analysis of Asphalt Pavements." *Transportation Research Record*, no. 2305: 150–61. https://doi.org/10.3141/2305-16.

Loulizi, et al. (2002). "Measurement of Vertical Compressive Stress Pulse in Flexible Pavements: Representation for Dynamic Loading Tests." *Transportation Research Record 1816* (1): 125–36.

Lukanen, et al. (2000). "Temperature Predictions and Adjustment Factors for Asphalt Pavement." Turner-Fairbank Highway Research Center.

Pellinen, T. K., Matthew, W. W., & Bonaquist, R. F. (2003). "Asphalt Mix Master Curve Construction Using Sigmoidal Fitting Function with Non-Linear Least Squares Optimization," 83–101. https://doi.org/10.1061/40709(257)6.

Shafiee, et al. (2015). "Analysis of Loading Frequency in Flexible Pavement Using Fast Fourier Transform." *International Journal of Pavement Research and Technology 8*(6): 403–9. https://doi.org/10.6135/ijprt.org.tw/2015.8(6).403.

Sullivan, B., & Denneman, E. (2015). "Inter-Conversation of Australian Modulus Test Methods Inter-Conversation of Australian Modulus Test Methods." *16th AAPA International Flexible Pavements Conference*.

Underwood, B. S. & Kim, Y. R. (2009). "Determination of the Appropriate Representative Elastic Modulus for Asphalt Concrete." *International Journal of Pavement Engineering 10*(2): 77–86. https://doi.org/10.1080/10298430701827668.

Zhang, et al. (2020). "Predict the Phase Angle Master Curve and Study the Viscoelastic Properties of Warm Mix Crumb Rubber-Modified Asphalt Mixture." *Materials 13*(21): 1–26. https://doi.org/10.3390/ma13215051.

Cite as: Alfarra M., Sadeq M. & Sadek H., "Assessment of the Current Frequency Calculation Methods Used in the Determination of the Dynamic Modulus Value in Pavement Design and Analysis", *The 2nd International Conference on Civil Infrastructure and Construction (CIC 2023)*, Doha, Qatar, 5-8 February 2023, DOI: https://doi.org/10.29117/cic.2023.0115

Preliminary Study on the Use of Reclaimed Asphalt in Public Works Authority Road Projects in the State of Qatar

Ezio Santagata
Ashghal Chair, Qatar University, Department of Civil and Architectural Engineering, Doha, Qatar;
Full Professor, Politecnico di Torino, Department of Environment, Land and Infrastructure Engineering, Torino, Italy
ezio.santagata@qu.edu.qa; ezio.santagata@polito.it

Sadegh Yeganeh
PhD Candidate, Department of Environment, Land and Infrastructure Engineering, Politecnico di Torino, Torino, Italy
sadegh.yeganeh@polito.it

Haissam Sebaaly
Research Associate, Department of Engineering, Built Environment and Information Technology,
University of Pretoria, Pretoria, South Africa
haissam.sebaaly@tuks.co.za

Osman Elhussein
Senior Quality Engineer, Quality and Safety Department, Public Works Authority, Doha, Qatar
osmane@ashghal.gov.qa

Ali Mohammed Al Marri
Manager, Quality and Safety Department, Public Works Authority, Doha, Qatar
almarri@ashghal.gov.qa

Abstract

This paper describes the outcomes of a preliminary study focused on the evaluation of four full-scale pavement sections in which reclaimed asphalt (RAP) was used in partial substitution of virgin aggregates during the production of asphalt mixes. Considered mixes were produced with different RAP percentages and were thereafter laid on site for the formation of asphalt base course layers of pavements in local roads of the State of Qatar. For comparative purposes, two trials included asphalt mixes containing no RAP, and in one case use was made of a rejuvenating agent. Activities carried out for the monitoring of field trials included analysis of component materials, critical observation of production and laying operations, assessment of the most relevant characteristics of produced asphalt mixes, and evaluation of the degree of compaction achieved during construction. Experimental results were of crucial importance for the introduction of RAP-related paving technologies in the State of Qatar, providing a meaningful background to the preparation of the "Ashghal Recycling Manual" issued by Ashghal and of the draft updated version of Qatar Construction Specifications.

Keywords: Road pavements; Reclaimed asphalt; Field trials; Quality control

1 Introduction

Decades of research and field experience have shown that reclaimed asphalt (indicated as "RAP") obtained from the milling of distressed layers of flexible pavements can be used in partial substitution of virgin aggregates in asphalt mixes, thereby leading to the reduction of production costs and of the consumption of non-renewable resources (Copeland, 2011; Zaumanis & Mallick, 2015). It has also been proven that asphalt mixes containing RAP, when designed appropriately, can exhibit improved performance-related properties, especially with respect to their rutting resistance

at high temperatures and under severe loading (Widyatmoko, 2008; Pradyumna

et al., 2013). In such a context, rejuvenating agents may be needed to restore the original properties of the aged binder, allowing the use of significant percentages of RAP without jeopardizing field performance of resulting asphalt mixes (Im et al., 2014; Ali et al., 2016; Moghaddam & Baaj, 2016).

The above-mentioned potential benefits of employing RAP in asphalt mixes have been considered to be of premium relevance for pavements of the road network of the State of Qatar, managed by the Public Works Authority (Ashghal). Related implementation efforts commenced in 2018 with the launch of the so-called "Ashghal Recycling Initiative" in which a significant emphasis was placed on the use of RAP not only because of the availability of such a material in Qatar, but also due to the fact that asphalt mixes exclusively rely on the import of gabbro aggregates from foreign Countries.

Since versions of Qatar Construction Specifications (QCS) issued until 2014 allowed only the use of virgin aggregates, as part of the Recycling Initiative Ashghal planned a series of activities to gradually facilitate the local implementation and fine-tuning of RAP-related paving technologies. The collaboration of Contractors was sought, and with the support of competent Ashghal Departments field trials were constructed. These entailed the production and laying of base course (BC) asphalt mixes containing RAP in field trials that were limited to secondary or residential roads characterized by low volumes of traffic, with a negligible percentage of heavy trucks.

This paper describes the outcomes of a preliminary study focused on the evaluation of four full-scale pavement sections of the type described above.

2 Field Trials

A synthetic description of the four field trials included in the study is provided in Table 1. The BC mixes produced and laid in the first three trials were, as per QCS 2014 requirements, of the "B" type, with a nominal maximum aggregate size (NMAS) of 19 mm, while BC mixes considered in the fourth field trial were slightly coarser (of the "A" type indicated in QCS 2014), with a NMAS of 25 mm. Considered mixes were produced with different RAP percentages (comprised between 15% and 40%, with respect to the weight of total aggregates in the mix). For comparative purposes, two trials included asphalt mixes containing no RAP, and in one case use was made of a rejuvenating agent.

Identification codes of the mixes listed in Table 1 are given by the combination of trial number, Contractor code, mix type, RAP percentage and, whenever used, presence of rejuvenator. Paving sections of the first three trials were located in residential streets of Al Rayyan, while the fourth trial took place on the extension of an existing access road in the Municipality of Al Wakrah.

Table 1: Description of Field Trials

Trial	Contractor	Mix type	RAP (%)	Mix code
1	A	BC Class B	20	1A-B-20
2	A	BC Class B	40 40* 0	2A-B-40 2A-B-40R 2A-B-0
3	A	BC Class B	15	3A-B-15
4	B	BC Class A	15 0	4B-A-15 4B-A-0

* with rejuvenating agent

3 Job Mix Formulas and Preliminary Tests

Given the preliminary character of the trials, Job Mix Formulas (JMFs) of asphalt mixes containing RAP did not stem from specific mix design activities. Rather, Contractors referred to existing Conformity Certificates issued for asphalt mixes containing gabbro aggregates, designed according to the Marshall procedure. Thus, approved JMFs were adjusted to obtain the target binder content and size distribution of the aggregates of reference mixes. For mixes containing a limited quantity of RAP such an approach is standard practice in many Countries which already employ hot recycling of RAP on a routinely basis. Although use of higher RAP percentages was scheduled in the first two field trials, this simplified approach was maintained throughout the study.

In conformity with QCS (2014), bituminous binders employed for the production of asphalt mixes were all of the neat (unmodified) type and of 60/70 penetration grade. This generally corresponds to a PG64S-22 grade defined as per AASHTO M 332-14.

In most of the trials, asphalt mixes containing RAP were produced with no use of rejuvenating agents. However, in field trial #2 one of the mixes was produced with 40% RAP and 1.5% (by weight of RAP) of a commercial rejuvenator (Iterlene ACF 2000, supplied by Iterchimica, Italy). No preliminary study was carried out to verify to what extent such a dosage, which was suggested by the supplier, would affect the rheological and chemical characteristics of the aged bitumen contained in RAP. In such a context it should be mentioned that previous studies showed that the degree of field ageing of bitumen in Qatar is extremely high, thereby suggesting that the residual bitumen contained in RAP may be very close to the so-called “black rock” condition (Sirin et al., 2017).

In the case, of the first three trials, employed RAP was a 0-20 mm material available in a single fraction that did not derive from any granulation and/or separation process. On the contrary, in the case of the trial #4, available RAP was preliminarily processed with the consequent formation of three fractions (0-5 mm, 5-14 mm and 14-20 mm) that were thereafter recombined in pre-defined proportions to obtain a single fraction. Such an operation, which is in line with international best practice, was deemed necessary to better control the grading, composition and volumetrics of the final asphalt mix (Al-Qadi et al., 2012).

RAP was sampled during the planning phase of the first three field trials and on the day of production of trials #1 and #4. Samples were then subjected to analysis for the determination of particle size distribution before binder extraction (as per ASTM C136-14), binder content (as per ASTM D2172-17) and particle size distribution after binder extraction (as per ASTM D5444-15). Results of these tests are synthesized in Table 2 and in Figs. 1 and 2.

When considering the single-fraction RAP material employed in the first three trials, non-negligible differences were found, in terms of both bitumen content (Table 2) and particle size distribution (Fig. 1), between the results of analyses performed on samples taken in the planning and production phases. This was most likely due to the non-homogeneity of the stockpiled RAP, which was not subjected to any preparatory processing, with the possible presence of agglomerations and clusters. Such a hypothesis was confirmed by the size distributions of extracted aggregates (Fig. 2), that were found to be quite constant.

With respect to the results obtained on the reconstituted RAP employed in the fourth field trial, it was observed that extracted aggregates exhibited a particle size distribution which was similar to that of the aggregates contained in the single fraction used in the first three trials. Binder content

(equal to 3.4%) was intermediate between the previously obtained values and in line with the percentages normally adopted in base course and wearing course mixtures complying to QCS 2014.

Table 2: Binder Content of RAP

	Trials #1-3	**Trial #4**
Planning	3.7	-
Production	3.0	3.4

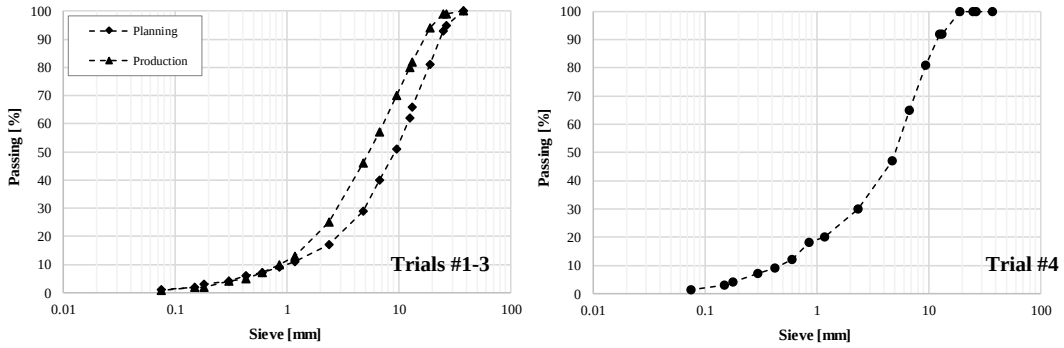


Fig. 1: Particle size distribution of RAP particles

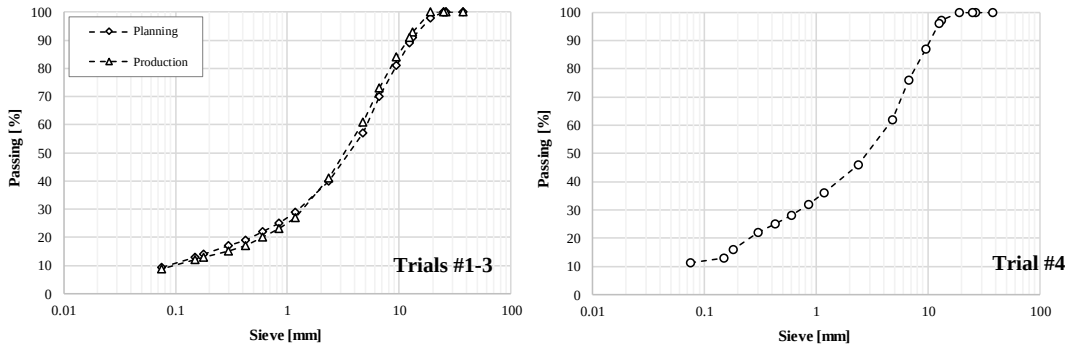


Fig. 2: Particle size distribution of aggregates extracted from RAP

4 Production and Laying

During production of the BC asphalt mixes, the RAP fraction was cold-fed directly to the pug mill. At the moment of mix discharge in hauling trucks, mix temperature was of the order of 170°C. Paving sites were prepared the day before the trials by applying a prime coat on the surface of the existing granular sub-bases. Asphalt mixes arrived on site with a temperature of approximately 155°C and in all cases environmental conditions at the time of laying were favourable, with air temperatures in the range of 20-30°C.Laying was carried out by employing two pavers operated in echelon in order to guarantee the formation of hot-on-hot longitudinal construction joints. Breakdown rolling was carried out by means of tandem steel rollers, while pneumatic tire rollers were used for completion of the densification process.

During the first three trials, due to the lack of RAP processing, agglomerates of fine RAP were visible in the asphalt mixes. Conversely, the appearance of the mix laid in trial #4, containing 15% of pre-processed RAP, was more homogeneous. The use of 40% RAP in trial #2 proved to be challenging from the viewpoint of laying. In particular, segregation phenomena were observed at

the paver's screed and it was observed that breakdown rolling needed to be carried out in an extremely timely manner to overcome the stiff response of the mixes under compaction.

5 Experimental Investigation

5.1 Characteristics of Asphalt Mixes

Test results obtained on loose samples of the asphalt mixes for the assessment of composition are synthesized in Tables 3 and 4 and in Fig. 3. Results of tests carried out on Marshall-compacted specimens are provided in Tables 5 and 6. Symbols adopted in the tables are: B for percent binder content, f/B for filler-bitumen ratio, v for void content, S for Marshall Stability, F for Marshall flow, S/F for Marshall quotient, S_{t1} for indirect tensile strength evaluated in dry conditions, S_{t2} for indirect tensile strength evaluated after conditioning in water, TSR for tensile strength ratio.

Composition of the mixes was assessed by referring to binder content (determined as per ASTM D2172-17) and to the particle size distribution of extracted aggregates (determined as per ASTM D5444-15). Corresponding results, synthesized in Fig. 3 and in Tables 3 and 4, highlighted non-negligible deviations from the JMFs and in some cases led to violations of QCS 2014 limits.

Use of lower RAP dosages (equal to 15% and 20% in trials #1, #3 and #4) led to a coarser grading of the fine fraction (passing the 4.75 mm sieve), whereas a finer grading in the entire range of particle sizes was found for the mixes containing 40% RAP (laid in trial #2). Such an outcome was explained by referring to the composition of RAP fractions, which did not replicate the combination of virgin fractions of the JMFs. Furthermore, it was postulated that when employing non-processed RAP, the presence of clusters led to an increase of the percentage of fines and filler in an unpredictable manner. As expected, particle size distribution of mixes containing no RAP was in line with JMFs.

Binder content of asphalt mixes significantly deviated from target, being in most cases lower, and higher only for the mixes laid in the second field trial. These results were presumably due to the variable contribution coming from RAP, especially in the case of the non-processed material employed in the first three trials. It should be also mentioned that the setting adjustments made by the Contractors during the production of mixes containing RAP had negative effects on the production of the reference mixes with no RAP, which were unfortunately characterized by binder over dosage (mix 2A-B-0) or under dosage (mix 4B-A-0).

Table 3: Binder content and Filler/Bitumen Ratio of asphalt mixes (BC Class B)

	1A-B-20	**2A-B-40**	**2A-B-40R**	**2A-B-0**	**3A-B-15**	**Target JMF**	**QCS limits**
B (%)	3.5	4.6	4.6	4.2	3.7	3.8	3.6 - 4.0
f/B	1.4	1.6	1.5	0.9	1.1	1.05	0.8 - 1.5

Table 4: Binder content and Filler/Bitumen Ratio of asphalt mixes (BC Class A)

	4B-A-15	**4B-A-0**	**Target JMF**	**QCS limits**
B (%)	3.1	3.4	3.6	3.3 - 3.9
f/B	1.2	0.9	1.19	0.8 - 1.5

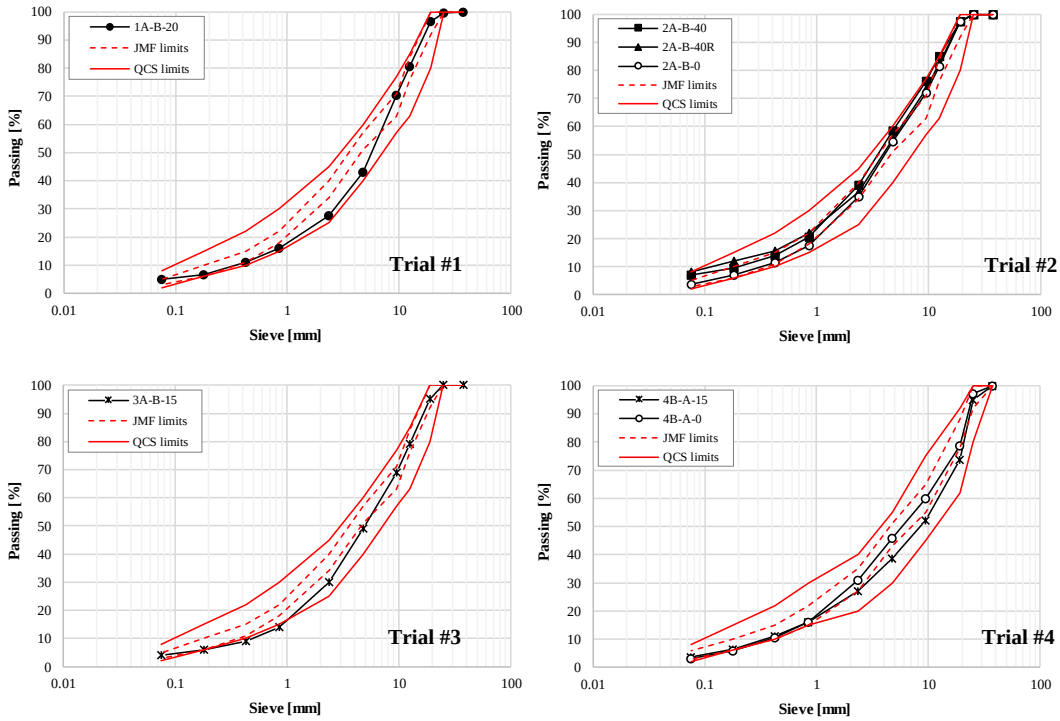


Fig. 3: Particle size distribution of aggregates extracted from asphalt mixes

Marshall-compacted specimens were prepared in the laboratory by following the procedure indicated in ASTM D6926-16 (75 blows per face). Specimens were thereafter characterized in terms of their volumetric properties and subjected to the Marshall stability test (as per ASTM D6927-15) as per (QCS, 2014). Further tests were performed to evaluate the tensile strength ratio (TSR) after water immersion (as per ASTM D4867-14). Although such a measurement was not mandatory in QCS 2014, it was considered to be a useful to assess asphalt mix durability. Finally, as required by QCS 2014, additional Marshall specimens were compacted with 400 blows per face in order to verify their void content (v_{400}) which in such extreme conditions can provide an indication of the resistance to bleeding. Results of the above-mentioned tests, synthesized in Tables 5 and 6, highlighted non-negligible deviations from the JMFs and in some cases led to violations of (QCS, 2014) limits.

In most cases the volumetrics of specimens compacted both with 75 and 400 blows per face deviated from target. In particular, very low void contents were found for the mixes with 40% RAP, possibly as a result of the very high content of bitumen, fines and filler. On the contrary, mixes containing lower RAP percentage (equal to 15-20%) with a coarse grading of the fine fraction, yielded void content values, which were higher than the target. As a result of the previously mentioned adjustments of production settings, mixes containing no RAP did not reach acceptable densification levels after standard compaction with 75 blows per face, with void content values that were above target both for the class B mix (2A-B-0) and for the class A mix (4B-A-0). Finally, use of the rejuvenating agent for the mix containing 40% RAP led to a void content reduction, thus suggesting that the employed additive may have softened the aged bitumen of the recycled fraction.

Assessment of the effects of RAP on the results of Marshall Stability tests was complicated by the variability of RAP composition and of added binder dosage. Nevertheless, use of 40% RAP was found to cause a significant increase of stability, while minor effects were recorded with respect to Marshall Flow. In the case of trial #4, the effect of RAP was highlighted more clearly, possibly as a result of the better control of RAP composition.

TSR results were mainly controlled by void contents, reaching values above 85% for highly compacted mixes (with 40% RAP), while lower values were achieved for the less compacted mix with 15% RAP (4B-A-15). In such a context, it should be mentioned that the threshold value normally referred to for acceptance purposes in standard technical specifications is equal to 80%.

Table 5: Results of tests carried out on Marshall Specimens (BC Class B)

	1A-B-20	**2A-B-40**	**2A-B-40R**	**2A-B-0**	**3A-B-15**	**Target JMF**	**QCS limits**
v (%)	7.5	3.3	2.5	7.0	6.5	6.6	4.5 - 8.0
S (kN)	16.3	21.5	33.8	19.4	18.4	13.2	≥ 9.5
F (mm)	2.5	2.7	2.3	2.2	2.7	2.6	2 - 4
S/F (kN/mm)	6.5	7.8	15.0	8.6	6.7	5.1	≥ 4.75
v_{400} (%)	5.9	2.1	1.5	4.8	4.8	5.1	≥ 3.4
S_{t1} (kPa)	-	1316	1017	-	-	-	-
S_{t2} (kPa)	-	1126	898	-	-	-	-
TSR (%)	-	86	88	-	-	-	-

Table 6: Results of tests carried out on Marshall Specimens (BC Class A)

	4B-A-15	**4B-A-0**	**Target JMF**	**QCS limits**
v (%)	7.6	9.0	6.8	4.0 - 8.0
S (kN)	17.4	14.8	14.4	≥ 9.5
F (mm)	2.4	2.5	2.7	2 - 4
S/F (kN/mm)	7.2	5.9	5.3	≥ 4.75
v_{400} (%)	5.6	6.1	5.0	≥ 3.2
S_{t1} (kPa)	1122	1159	-	-
S_{t2} (kPa)	808	793	-	-
TSR (%)	72	68	-	-

5.2 Field Compaction

The effectiveness of field compaction of asphalt mixes was evaluated by determining the void content of sets of 8 cores extracted from compacted layers and by thereafter calculating the degree of compaction with respect to corresponding Marshall specimens (see Tables 5 and 6). Average results obtained from the above-mentioned tests are given in Table 7, which also lists minimum and maximum values or measured void contents. Symbols adopted in the table are v for void content and %RD for percent relative density (referred to Marshall specimens). Cores were not available in the case of mix 4B-A-0, laid in trial #4 and containing no RAP.

As expected, average void content values of the laid asphalt mixes were consistent with those of the corresponding Marshall specimens, with QCS requirements that were not satisfied for three of the considered mixes. Although variability of test results was relatively high, it was observed to be lower for mixes containing 15% RAP and in particular, for the mix containing processed RAP, which during compaction operations was also observed to be the most homogeneous. Percent relative density was in all cases within the QCS acceptance range, thus indicating that regardless of the deviations from the JMFs, considered mixes could be efficiently compacted in the field.

Even though high in-place void content may be detrimental for long-term durability, given that the asphalt mixes were placed on roads characterized by low traffic levels and negligible percentage of heavy trucks, they were not removed and left to withstand the actions of vehicle loading.

Table 7: Volumetrics of cores extracted from compacted layers

	1A-B-20	2A-B-40	2A-B-40R	2A-B-0	3A-B-15	4B-A-15	QCS limits
v (%)	9.2	4.3	5.4	8.2	7.1	5.9	5.0 - 8.0
v_{min} (%)	7.4	2.8	3.3	7.0	5.5	4.8	-
v_{max} (%)	11.0	6.1	6.7	9.4	8.5	7.5	-
%RD (%)	98.2	99.0	97.0	98.7	99.4	101.8	97.0 - 101.8

6 Conclusions

Results obtained in the preliminary study described in this paper were of crucial importance for the introduction of RAP-related paving technologies in the State of Qatar, constituting a valuable reference for the preparation of the "Ashghal Recycling Manual" issued by Ashghal (Elhussein et al., 2021) and for the update of Qatar Construction Specifications (QCS, 2018).

Regardless of the fact that experimental results highlighted deviations from target JMFs and partial violation of requirements set in (QCS, 2014), it was proven that the production and laying of base course asphalt mixes containing RAP was feasible and compatible with the technical capabilities, plants and equipment of local Contractors. It was also confirmed that in order to fully exploit RAP as a valuable component of asphalt mixes, such a material needs to be subjected to preliminary processing, which consists in granulation followed by separation into size fractions, and to appropriate laboratory tests for the assessment of its composition.

Since it was envisioned that Engineers, Supervision Consultants and Contractors in Qatar would need some time to gradually gain confidence in the use of RAP, in the first phase of its widespread implementation it was decided, by setting proper constraints in (QCS, 2018), to limit its percentage to 15% in base course asphalt mixes laid exclusively on infrastructures characterized by low traffic volumes (up to 3 million Equivalent Single Axle Loads, ESALs) and on roads made for temporary use (for less than 20 years). However, plans were made to progressively increase (up to 30%) the maximum allowable RAP percentage in asphalt base courses and to extend the applicability of related technologies to the entire road network of the State of Qatar. Such a goal was made explicit in the "Ashghal Recycling Manual," where it was stated that for RAP contents comprised between 15% and 30% specific mix design studies, including additional performance-related tests, should be carried out for approval.

Further research activities related to the use of RAP in asphalt mixes are currently in development, focusing on the optimization of mix designs and on the assessment of performance-related properties. Additional activities are being planned for the monitoring of pilot and full-scale projects. It is envisioned that obtained results will lead to further refinements of specifications and guidelines, thereby contributing to the construction of more sustainable and durable road pavements in the State of Qatar.

Acknowledgements

Experimental activities documented in this paper were performed with the involvement of the laboratory of the Ashghal Center for Research & Development (ACRD) and of the Road Materials Laboratory of the Politecnico di Torino, Italy.

References

Al-Qadi, et al. (2012). *Impact of high RAP contents on structural and performance properties of asphalt mixtures*, Research Report FHWA-ICT-12-002, Illinois Center for Transportation, Urbana, IL, USA.

Ali, et al. (2016). "Investigation of the impacts of aging and RAP percentages on effectiveness of asphalt binder rejuvenators", *Construction and Building Materials*, 110, pp. 211-217.

Ashghal (2018). *Roadmap for implementation of Ashghal Initiative of recycling in construction projects*, Circular No (69), Doha, Qatar, 09/05/2018.

Copeland, A. (2011). *Reclaimed asphalt pavement in asphalt mixtures: State of the practice*, Report FHWA-HRT-11-021, Federal Highway Administration, Office of Research, Development, and Technology, McLean, VA, USA.

Ecker, A. (2001). "The application of Iatroscan-technique for analysis of bitumen", *Petroleum and Coal*, *1*(1), pp. 51-53.

Elhussein, et al. (2021). *Asghal Recycling Manual*, PWA-ACRD-1, Public Works Authority, Doha, Qatar.

Im, et al. (2014). "Impacts of rejuvenators on performance and engineering properties of asphalt mixtures containing recycled materials", *Construction and Building Materials*, *53*, pp. 596-603.

Leroy, G. (1989). "Bitumen analysis by thin layer chromatography (Iatroscan)", *Proceedings, 4th Eurobitume Congress*, 4-6 October 1989, Madrid, Spain, pp. 166-170.

Moghaddam, T.B. & Baaj, H. (2016). "The use of rejuvenating agents in production of recycled hot mix asphalt: a systematic review", *Construction and Building Materials*, *114*, pp. 805-816.

Nellensteyn, F.J. (1928). "Relation of the micelle to the medium in asphalt", *Journal of the Institute of Petroleum Technologists*, *14*, pp. 134-138.

Pradyumna, T.A., Mittal, A. & Jain, P.K. (2013). "Characterization of reclaimed asphalt pavement (RAP) for use in bituminous road construction", *Procedia - Social and Behavioral Sciences*, *104*, pp. 1149-1157.

Qatar Construction Specifications (QCS 2014) (2014). Ministry of Municipality and Environment, Doha, Qatar.

Qatar Construction Specifications (QCS 2018, draft) (2023). Ministry of Municipality and Environment, Doha, Qatar.

Santagata, E., Baglieri, O., Tsantilis, L. & Chiappinelli, G. (2015). "Fatigue and healing properties of nano-reinforced bituminous binders", *International Journal of Fatigue*, *80*, pp. 30-39.

Santagata, E. et al. (2020). "Test procedures for advanced characterization of bituminous binders employed for pavement construction in Public Works Authority road projects - State of Qatar", *Proceedings, International Conference on Civil Infrastructure and Construction*, 2-5 February, 2020, Doha, Qatar.

Sirin, et al. (2017). "Effect of ageing on asphalt binders in the State of Qatar: a case study", *Road Materials and Pavement Design*, *18*: sup4, pp. 165-184.

Widyatmoko, I. (2008). "Mechanistic-empirical mixture design for hot mix asphalt pavement recycling", *Construction and Building Materials*, *22*(2), pp. 77-87.

Zaumanis, M. & Mallick, R.B. (2015). "Review of very high-content reclaimed asphalt use in plant-produced pavements: state of the art", *International Journal of Pavement Engineering*, *16*(1), pp. 39-55.

Cite as: Santagata E., Yeganeh S., Sebaaly H., Elhussein O. & Al Marri A., "Preliminary Study on the Use of Reclaimed Asphalt in Public Works Authority Road Projects in the State of Qatar", *The 2nd International Conference on Civil Infrastructure and Construction (CIC 2023)*, Doha, Qatar, 5-8 February 2023, DOI: https://doi.org/10.29117/cic.2023.0116

Development of a Comprehensive Pavement Design System for Roads in Wind and Solar Farms

Ezio Santagata
Ashghal Chair, Qatar University, Department of Civil and Architectural Engineering, Doha, Qatar;
Full Professor, Politecnico di Torino, Department of Environment, Land and Infrastructure Engineering, Torino, Italy
ezio.santagata@qu.edu.qa; ezio.santagata@polito.it

Haissam Sebaaly
Research Associate, Department of Engineering, Built Environment and Information Technology,
University of Pretoria, Pretoria, South Africa
haissam.sebaaly@tuks.co.za

Vittorio Capozzi
Head of Civil Infrastructural Engineering, ENEL Green Power S.P.A., Rome, Italy
vittorio.capozzi@enel.com

Abstract

This paper briefly, illustrates the structure and contents of an ongoing research program aimed at developing a set of procedures and tools to be used for the design of pavements in renewable energy projects and mainly in wind and solar farms. Challenges related to this topic derive from the non-standard nature of several factors that affect the structural and functional performance of such pavements, with the consequent need of employing purposely defined prediction methods, design criteria and specifications. Further crucial aspects to be taken in account in the research program are related to the life cycle cost analysis of pavements, to be carried out in a multinational context by considering alternative scenarios according to an OPEX (operating expense) versus CAPEX (capital expenditure) philosophy. It is envisioned that results and deliverables of the project will contribute to the enhancement of the effectiveness of operations in wind and solar farms, optimizing investments and leading to the selection of more sustainable pavement solutions.

Keywords: Renewable energy; Wind and solar farms; Pavement design; Performance prediction; OPEX versus CAPEX; Experimental tests; Sustainability

1 Introduction

ENEL Green Power S.P.A. (hereafter indicated as “EGP”) is a Company of the Italian utility group ENEL S.P.A. that develops and manages power generated from renewable resources worldwide. It is currently in charge of more than 1,200 power plants located in five continents, with assets in operation or under construction in 21 Countries. The overall worldwide energy capacity of EGP plants, either in operation or under construction, is of the order of 56 GW, deriving from a mix of renewable resources, which include wind (yielding approximately 33% of total capacity), solar (21%), hydroelectric (45%), geothermal(1.4%) and biomass (0.1%).

In view of the impressive data indicated above, EGP can be considered one of the major private international players that are operating and investing resources in the global green energy transition, which will be crucial to react against ongoing climate change for a more sustainable future.

As part of its efforts to improve the effectiveness of its investments and operations, since its foundation EGP has been constantly supporting research activities both of the fundamental and

applied type in multiple areas of engineering and earth science. In such a context, in 2021 it secured appropriate resources for the development of a comprehensive pavement design system for roads in wind and solar farms. Following a competitive bid that involved the participation of several invited research institutions specialized in the area of pavement engineering, the research contract was awarded to the Politecnico di Torino, Italy. Activities were commenced in April 2022 and are expected to be completed by the end of 2023.

This paper briefly describes motivation, structure and contents of the abovementioned research program, with a synthetic illustration of specific challenges, inherent complexities, adopted approaches and expected deliverables.

2 Motivation

The need for a comprehensive research program focused on pavement design for wind and solar farms originated from the status of engineering operations managed by EGP worldwide, in which critical issues were identified. As described in the following, such issues are related both to the structural evaluation of pavement solutions and to the analysis of corresponding cost.

According to current practice, pavement design activities for each farm are carried out by Consultants designated by Contractors. Employed design procedures, such as the AASHTO 1993 method, are usually quite empirical and conservative, originally developed for standard roads and highways and lacking the possibility of taking in account the peculiar factors that characterize pavements to be constructed in wind and solar farms. These include non-standard and exceptionally high vehicle loadings, extreme climatic conditions, poor sub grade bearing capacity, and limited availability of high-quality materials. Further challenges that arise in the use of standard empirical methods stem from the need of implementing strengthening techniques, often unique to certain Countries, and of employing locally available recycled materials. Finally, complexity of design operations also derives from the need of differentiating pavement cross-section's as a function of the hierarchy and expected use of the different branches that compose the vast mobility network of a given farm. In such a context, it should be considered that these sites might have a remarkable land footprint, covering rural areas with an extension that for a reference energy capacity of 100 MW can be, depending upon the specific technology, of the order of 50-100 hectares for wind farms and of 150-250 hectares for solar farms. Corresponding infrastructures for internal mobility can form networks characterized by a significant extension, which in the worst-case scenario are constructed on uneven and steep terrain with potential ground instability.

While considering current practice followed by Consultants in design operations, it was also observed that unfortunately structural design evaluations are seldom combined with analyses related to construction or life cycle costs, thereby preventing the true optimization of investments. Such a limitation needs to be overcome in the research program by defining a sound assessment procedure that includes alternative scenarios according to an OPEX (operating expense) versus CAPEX (capital expenditure) philosophy. In turn, these should be translated in operative plans that may entail, depending upon the case, stage construction, planned maintenance and scheduled rehabilitation. The ultimate goal of part of the program is to create guidelines to be implemented at the multinational level, thereby ensuring the consistency of choices made worldwide by designers and decision-makers.

3 Structure and Contents

The research program is structured in multiple interconnected tasks, conceived to yield deliverables

that will be shared with Consultants, Contractors and EGP Technical Departments worldwide, with the added value of being reference milestones for future research activities. Further refinements of the scope and contents of each task may occur in the future phases of development as a function of achieved results.

3.1 Technical and Scientific Background

The technical and scientific background of the research program was defined in Task 01, already completed at the time of preparation of this paper, which consisted in a bibliographical study carried out by thoroughly analysing international literature. Task outcomes were synthesised in a report (Politecnico di Torino, 2022) that contained a general description of infrastructures and pavements, a synthesis of the most common pavement design procedures, a review of technical information on component materials and layers, and a discussion of financial and environmental aspects. Contents of this report constitute the reference baseline for many of the other tasks included in the project.

Given the scarcity of published documents focusing on pavements for wind and solar farms, literature analysis considered low-volume roads (LVRs) satisfying the mobility needs of local communities in rural areas, together with function-specific roads (FSRs) designed and constructed to serve the industry or to allow access to remote areas (such as mining haul roads, agricultural roads and forestry roads) Pretoria Department of Transport, (1990); Tannant & Regensburg, (2001); Thompson et al., (2019). In these contexts, it was recorded that studies and specifications generally refer either to “paved roads”, that entail the presence of flexible asphalt pavements and rigid concrete pavements, or to “unpaved roads”, which can be further divided into the categories of gravel roads, driving surface aggregate (DSA) roads and earth roads. Additionally, it was noted that unpaved roads can be either unsealed or, in particular cases, sealed (by means of bituminous or non-bituminous surface treatments). Typical distresses were identified for all pavement types, highlighting their origin and their implications on structural and functional performance (FHWA, 2003, 2015). Finally, pavement selection criteria were discussed, showing that they can be generally expressed by referring to average daily traffic (ADT) or annual average daily traffic (AADT) (Pasindu et al., 2020).

With respect to pavement design procedures, the literature review synthesized the principles and procedures more appropriate for pavement design of paved and unpaved roads. It was noted that while methods of the former group (such as AASHTO 1993 and those with a mechanistic framework) are well known to pavement engineers, those belonging to the latter group (such as those developed in Australia, Canada, Russia and South Africa) are more familiar to LVR and FSR specialists.

Technical information on basic and mechanical characteristics of materials were collected by focusing on aggregates used in unbound layers (including those derived from recycling), mechanically and chemically stabilized soils, and geo synthetics. Whenever relevant, mechanical modelling methods, selection criteria and design principles were also reviewed.

Finally, Task 01 addressed the themes of costs and environmental impact by introducing the basics of Life-Cycle Cost Analysis (LCCA) and Life Cycle Analysis (LCA). Preferred analysis approaches were highlighted, together with guidelines to be followed for interpretation of results.

3.2 Review of Current Practice

Review of current practice in the design of EGP projects was carried out in Task 02 of the research

program, close to completion at the time of submission of this paper in which available pavement-related design documents of EGP wind and solar farms, in operation or in construction throughout the world, were analysed in detail. The ultimate goals of such a review were to identify existing conceptual gaps and inconsistencies, and to perform a comparative evaluation of the various pavement cross-sections by employing a common approach for the assessment of expected design life and construction costs. Outcomes of these analyses were synthesized in a specific report (Politecnico di Torino, 2023a) that will be further integrated towards the end of the research program by making use of more advanced design concepts and more comprehensive financial evaluation methods in accordance with the work developed as part of Tasks 03 and 04.

It was observed that although design Consultants in most part make use of the AASHTO 1993 method, non-negligible inconsistencies exist with respect to the procedures followed, for both paved and unpaved roads, to compute (or assume) several input data. These are related to extraction of bearing capacity data from geological and geotechnical surveys (expressed in terms of CBR index and thereafter converted into resilient modulus), to the inclusion of seasonal effects that can account for changes of water content in the sub grade and unbound layers, to the assumption of meaningful layer coefficients for standard and non-standard materials, to the calculation of the number of Equivalent Single Axle Loadings (ESALs) in the design period, to the assignment of representative ESALs to different branches composing the network of transportation infrastructures (both temporary and permanent), and to the identification of acceptable serviceability at the end of the design life. Furthermore, it was confirmed that design Consultants seldom referred to stage construction or planned rehabilitation options, with a very limited attention to financial implication of their choices and with no formal value engineering assessment.

Based on the review outcomes synthesized above, in Task 02 comparative analyses were carried out, for a selected number of representative EGP projects, by applying the AASHTO 1993 procedure in a uniform and consistent way, thus amending previous design choices according to a common rationale. Special attention was reserved to design ESALs, that were expected to show a relationship with extension of farms, length of the infrastructure network and total energy capacity. Further calculations were made by hypothesizing alternative scenarios based on terminal serviceability changes and introduction of stage construction. Construction and life cycle costs were computed for all considered cases, thereby leading to the preliminary identification of preferred general design strategies. It was concluded that in the absence of strict guidelines on the use of the AASHTO 1993 procedure, the likelihood of significantly overdesigning or under designing pavements has been extremely high, with the consequent waste of financial resources due to excessive expenses for construction (in the case of overdesign) or for early maintenance and rehabilitation (in the case of under design). As a consequence, while still working on the development and implementation of improved pavement design methods, clear guidelines on the use of AASHTO 1993 will be shared by EGP with design Consultants and Contractors.

3.3 Development of Pavement Design Procedures

By taking in account the outcomes and conclusions of Task 02, specific pavement design procedures were purposely developed as part of Task 03, currently in its finalization stage (Politecnico di Torino, 2023b). These procedures present the distinctive character of including a sound mechanistic component based on the analysis of the results of specific experimental tests and environmental modelling activities, to be performed in the preliminary phases of site assessment, and to the evaluation of stresses and strains induced in pavement structures by vehicle loadings.

According to the philosophy adopted by the research team during their development, such procedures will yield results characterized by a higher reliability in comparison to empirical ones (such as AASHTO, 1993) but will also allow significant life cycle savings since the likelihood of overdesign or under design will be reduced.

The new procedures were developed for both paved and unpaved roads, although in the former case the main focus was on asphalt pavements since in wind and solar farms rigid structures are exclusively used in pads and platforms or to overcome high gradients of the road alignment in critical locations. Damage mechanisms and their relevance to pavements in wind and solar farms were highlighted for the most frequently occurring categories of distresses (cracking, distortion and disintegration for paved roads; surface defects and structural defects in the case of unpaved roads) (FHWA, 2003; Paterson, 1991). Corresponding design evaluations were introduced in the form of analytical (transfer) functions and specific calculation procedures AASHTO, (2008); Austroads, (2017); La Vern, (2016); NCHRP, (2002); SRSMT, (2001); (Yapp et al., 1991) that constituted the backbone of the proposed methods. Appropriate guidance was provided with respect to the assessment of traffic loadings in the design life and climatic conditions, and the steps to be followed for design verification (possibly to be carried out iteratively until reaching optimization) were clearly illustrated. Details of the procedures will be shared in the near future with the international technical and scientific community according to EGP policies.

3.4 Improved Use of Pavement Design Methods and User-Friendly Implementation

In order to make the best possible use of the pavement design procedures developed as part of Task 03, EGP requested to include in the research program specific tasks dedicated to the definition of guidelines for their improved use in adherence to the OPEX versus CAPEX philosophy (Task 04), to the creation of user-friendly software-based tools for their implementation into practice (Task 05), and to the formalization of a simple pavement design catalogue to be employed for budgeting purposes, in preliminary design, and in standard projects of limited importance (Task 06). Activities of these tasks are still in progress and related deliverables are expected to be finalized by the end of the second quarter of 2023.

3.5 Experimental Testing and Technical Specifications

As per the requirements set by EGP, it was planned that activities related to the development of pavement design procedures and tools (comprised in Tasks 03 to 06) would be supported by experimental investigations (Task 07) and by the review and update of existing EGP technical specifications (Task 08).These activities were commenced in the early stages of the program and will continue throughout its development until the end of 2023.

At the time of submission of this paper, activities of Task 07 have been exclusively carried out in the laboratory, mainly focusing on the physical and mechanical properties of sub grade soils and unbound and cement-treated materials for sub-bases and bases. Emphasis has been given to the assessment of the resilient modulus of granular materials by means of triaxial tests, exploring the full load spreading potential of these materials by operating on samples prepared with variable degrees of water saturation (representative of different climatic conditions and/or seasons) and of compaction level (representative of the variable effectiveness of construction operations). Relevant models are being fitted to experimental data to take in account their non-linearity in subsequent pavement design calculations. Samples currently being analysed were taken from two EGP farms (one wind and one solar project) and in two additional reference sites.

Review of technical specifications (EGP, 2021, 2022a, 2022b) is being performed in Task 08 by referring to international literature and past experience of the research team in similar projects. Furthermore, ongoing updates are taking in account the results achieved in the other tasks of the program (including Task 07) in order to ensure full consistency and completeness to the entire set of deliverables. Details of the contents of these improved specifications will be shared with the international technical and scientific community according to EGP policies.

4 Conclusions

At the time of submission of this paper, limited conclusions can be drawn from the work performed in the described research program since it is at less than 50% completion. Nevertheless, finalized and ongoing activities yielded interesting results that confirmed the relevance of addressed topics. Thus, it is envisioned that deliverables of the project will contribute to the enhancement of the effectiveness of operations in EGP wind and solar farms, optimizing investments and leading to the selection of more sustainable pavement solutions.

Further activities on the subject of pavements in wind and solar farms are being planned to validate the results coming from the ongoing research program. These will be part of a follow-up program that will include, but will not be limited to, full-scale validation of predicted pavement performance, implementation of emerging technologies in pavement construction operations, closed-loop recycling of materials in wind and solar farms, and development of tailored LCA models.

Acknowledgements

The team of the Politecnicodi Torino engaged in the research program is composed of prof. E. Santagata (Principal Investigator), prof. O. Baglieri, prof. G. Chiappinelli, prof. D. Dalmazzo, prof. P.P. Riviera, prof. L. Tsantilis, Dr. H. Sebaaly, Dr. S. Yeganeh, Eng. R. Rabezzana, and Eng. C. Sai Vangaveeti. The supporting team of ENEL Green Power S.p.A. is formed by Dr. Eng. V. Capozzi, Eng. F. Sannino, Eng. G. Favata, Dr. M. Sapigni, and Eng. A. Micchia. Experimental activities are being carried out in the Road Materials Laboratory of the Politecnico di Torino.

References

AASHTO. (1993). *Guide for Design of Pavement Structures*, American Association of State Highway and Transportation Officials, Washington, D.C., USA.

AASHTO. (2008). *Mechanistic Empirical Pavement Design Guide. A Manual of Practice*, American Association of State Highway and Transportation Officials, Washington, D.C., USA.

Austroads (2017). Guide to Pavement Technology Part 2: Pavement Structural Design, AGPT02-17, Austroads Ltd., Sydney, Australia.

EGP. (2021). *Technical Standard. Design Engineering Services for Wind Energy Installations*, GRE.EEC.S.73.XX.W.00000.00.064.01, ENEL Green Power S.p.A., Rome, Italy.

EGP. (2022a). *Technical Specification for Civil Works for Wind and Solar Farms*, GRE.EEC.S.25.XX.A.00000.00.218.02, ENEL Green Power S.p.A., Rome, Italy.

EGP. (2022b). *Technical Specification. Photovoltaic Power Plant. Engineering, Equipment Manufacturing, Civil and Electromechanical WOrks for the Execution Phase*, GRE.EEC.S.27.XX.A.00000.00.156.12, ENEL Green Power S.p.A., Rome, Italy.

FHWA (2003). *Distress Identification Manual for the Long-Term Pavement Performance Program*, FHWA-RD-03-031, Federal Highway Administration, McLean, VA, USA.

FHWA (2015). *Gravel Roads. Construction & Maintenance Guide*, Federal Highway Administration, McLean, VA, USA.

La Vern, M., Doré, G. & Bilodeau, J.P.(2016). "Mechanistic-Empirical Design of Unpaved Roads", *Proceedings, Conference of the Transportation Association of Canada, Innovations in Pavement Management, Engineering and Technologies*, Toronto, ON, Canada.

NCHRP (2002). *Contributions of Pavement Structural Layers to Rutting of Hot Mix Asphalt Pavements*, NCHRP 468, National Cooperative Highway Research Program, National Academy Press, Washington, D.C., USA.

Pasindu, H. R., Gamage D. E &, Bandara, J. M. S. J. (2020). "Framework for Selecting Pavement Type for Low Volume Roads", *Transportation Research Procedia*, 48, pp. 3924-3938.

Paterson, D. O. W. (1991). "Deterioration and Maintenance of Unpaved Roads: Models of Roughness and Material Loss", *Transportation Research Record, 1291*, pp. 143-156.

Politecnico di Torino. (2022). *Pavement Design for Roads and Platform in Renewable Energy Production. Sub-task 01 - Bibliographical study*, Final Report, ENEL Green Power S.p.A., Rome, Italy.

___. (2023a). *Pavement Design for Roads and Platform in Renewable Energy Production. Sub-task 02-Technical and Economic Analysis of Cross-Sections*, Draft Report, ENEL Green Power S.p.A., Rome, Italy.

___. (2023b). *Pavement Design for Roads and Platform in Renewable Energy Production. Sub-task 02 - Analysis of Pavement Damage*, Draft Report, ENEL Green Power S.p.A., Rome, Italy.

Pretoria Department of Transport. (1990). *The Structural Design, Construction and Maintenance of Unpaved Roads. Technical recommendation for pavements*, TRH 20, Pretoria, South Africa.

SRSMT (2001). *Design of Flexible Road Pavements*, ODN 218.046-01, Ministry of Transportation, Russia.

Tannant, D. D. & Regensburg, B. (2001). *Guidelines for Mine Haul Road Design*, University of British Columbia - Okanagan, Kelowna, B.C., Canada.

Thompson, R. J., Peroni, R. & Visser, A., (2019). *Mining Haul Roads*, CRC Press/Balkema, Leiden, The Netherlands.

Yapp, M. T. Y., Steward, J. & Whitcomb, W.G. (1991). "Existing Methods for the Structural Design of Aggregate Road Surfaces on Forest Roads", *Transportation Research Record*, 1291, pp. 41-57.

Cite as: Santagata E., Sebaaly H. & Capozzi V., "Development of a Comprehensive Pavement Design System for Roads in Wind and Solar Farms", *The 2nd International Conference on Civil Infrastructure and Construction (CIC 2023)*, Doha, Qatar, 5-8 February 2023, DOI: https://doi.org/10.29117/cic.2023.0117

Theme: 3

Sustainable Architecture and Urban Planning for Society Wellbeing

The Urban Morphology of Mshereib, the Heart of Downtown Doha

Rozan A. A. Amleh
College of Engineering, Qatar University, Doha, Qatar
ra2000540@qu.edu.qa

Mark David Major, Heba O. Tannous, Almaha M. Alyafei, Ghada H. Fetais, Mohammad A. Najjar, Reem Y. Awwaad
College of Engineering, Qatar University, Doha, Qatar
m.major@qu.edu.qa, heba.tannous@qu.edu.qa, as1204137@qu.edu.qa, gf1205513@qu.edu.qa, mn2101931@qu.edu.qa, ra084283@qu.edu.qa

Abstract

Doha experienced a remarkable transformation since oil and natural gas exportation began in the mid-twentieth century. Rapid urbanization and globalization ('process of interaction and integration among people, companies, and governments worldwide involving goods, services, data, technology, and capital') characterize this transformation. Doha expanded to accommodate significant population increases and lifestyle changes. The urban expansion was auto-centric and suburban, similar to post-war development in the United States and other western societies. Qatari citizens 'emptied' Old Doha as they moved to contemporary villas in new developments at the suburban periphery. In response, the Qatari government launched plans for Msheireb Downtown Doha. Its purpose is to attract Qataris back to Doha's historic center by providing a walkable, mixed-use urban environment promoting a new model of sustainable urbanism. The design and planning explicitly seek to become rooted in Qatari social identity while preserving cultural heritage and historic resources. Our paper investigates the urban form and function of Msheireb Downtown Doha to evaluate its success. It examines the urban morphology, including figure-ground and pedestrian sheds analysis from crucial locations and surveys of ground-level land uses, active/inactive frontages, and the pattern of building heights. The goal is to illustrate and understand the project's urban form and function logic. Based on this, we argue that Msheireb Downtown Doha does satisfy the inhabitants' desire for a downtown lifestyle. It offers a model for urban regeneration consistent with the Qatar National Vision 2030 for an advanced society, sustainable development, and a high standard of living for people.

Keywords: Development; Land use; Morphology; Regeneration; Urban studies

1 Introduction

Qatar, a country with a total land area of 11,571 km², occupies a small flat peninsula in the Persian/Arabian Gulf. It has a desert climate with very mild winters and hot summers. It has a post-war modernized economy that has witnessed unprecedented urban growth due to the discovery of oil and natural gas. Doha, initially an offset of the fishing village of Al Bidda, hosted the ruling families for the first migration in the 1800s due to tribal conflicts over land at Al Zubarah in northwest Qatar. With oil discovery from 1942-1947, the country transformed from patches of pearling and fishing villages along the coastline in the 18th century into an oil-producing country after the 1950s, focused on developing its capital city of Doha. As a result, the country encountered rapid urbanization and globalization like other Gulf Cooperation Council (GCC) cities. In addition, the rise of the oil and gas exporting industry led to a significant shift in lifestyle and economy in the late 20th and early 21st

centuries. Doha witnessed two primary waves of urbanization. The first included massive economic and population growth since the 1970s due to oil and gas revenues leading to dramatic urban development. The second wave of urbanization started in the 2000s, endorsed by the national governmental vision to diversify the economy and globalize the city by participating in international sporting events. Since then, urban sprawl and automobile dominance with minimal considerations for pedestrian design have come to represent significant urban challenges in Doha. As a result, ex-pat laborers and construction workers came to occupy the neglected neighborhoods in the old city center. Qatar's development has three main phases: traditional, transitional, and modernization:

1. **Traditional Phase–Pearling and Fishing Economy:** Early inhabitants shifted from the northwestern part of the country to Al Bidda and later its offshoot Doha and started developing a national government and policies that made Doha the capital and center of urbanization.
2. **Transitional Phase–Oil Discovery:** Resulting in the transformation of Qatar from 1942-1970, despite initial exploitation of resources halting due to World War 2.
3. **Modernization Phase–British withdrawal and Qatar's independence declaration in 1971:** Later, in 1972, the government contracted a foreign planning consultancy to start the construction of governmental buildings around the capital's seashore, which continues to this day.

Llewelyn Davies, a leading planner in the UK, proposed that the government buys back the central plot of Doha's traditional quarters and use it for high-density commercial and governmental buildings. As a result, significant urban regeneration efforts focused on the heart of Doha, including preserving Souq Waqif to maintain the city's architectural heritage and traditional urban fabric. Around 1977, William Pereira's firm was appointed to develop the reclaimed land of Al Dafna around the coastline of Doha Bay (today’s West Bay). The enhancement of the healthcare system resulting in life expectancy growth and population increases, and Qatari locals migrated to the suburbs. As a result, the city center became old and congested. Many migrants moved to Qatar as long-term residents or short-term construction workers to handle specific projects. Unfortunately, only Asian workers seemed to manage to live under those conditions in the abandoned city center. Today, according to the Planning and Statistics Authority, Qataris constituted only 10% of the population. In comparison, the expatriates and migrants compose 90%, which subsequently influenced planning strategies in the city to cater to varying cultures and backgrounds. Qatar's developmental framework shifted from focusing on the local and surrounding regions to the global context. As a result, city planning began purposely implementing elements to attract people to live and work in Qatar. This planning approach also helped position Qatar within the spectrum of the global economy. The strategic objective is to reverse the development pattern in Doha, which has tended towards isolated land use, dependence on car transportation, and energy-hungry structures. Mega-projects like Msheireb Downtown Doha (MDD) aim to change the direction of urban development by creating new social and civic hubs in the city where it is enjoyable to live, work, shop, visit and spend time. The project proposed creating compact, walkable, and well-connected neighborhoods with naturally cooled streets built at a human scale. Smart City technology and effective connectivity are the influential development aspects of this project. In addition, the plan embodies a diverse land-use mix that supports the national vision of economic diversification and real estate development.

MDD is the country’s first sustainable downtown regeneration project, developed by Msheireb Properties in 2010, a real estate developer owned by the Qatar Foundation, to revive the commercial district of Old Doha and bring new vitality to Doha's downtown by the highest standards in green building. Utilizing the latest innovative technologies supporting the old core areas while upgrading the surrounding land uses and street network. AECOM, with Allies and Morrison Architects,

designed the project in the center of Doha, adjacent to the historic site of Souq Waqif and the significant location of the Amiri Diwan, only minutes from the Hamad International Airport and midway between two critical routes into the city. It was opened for the public in 2019 after substantial completion (90%), yet stage 4 was delayed by the COVID-19 pandemic; however, it was recently completed in March 2022. Furthermore, it has a unique architectural language yet is inspired by traditional Qatari heritage and architecture based on its proportion, simplicity, space, light, layering, ornament, and response to climate while maintaining much of the traditional fabric pattern (**Figure 1**). The urban pattern of the area emerged from a process of restricted random aggregation of dwelling units over time, following simple rules catering to movement on foot and domesticated animals. There were later mid-twentieth-century interventions, primarily road width, to accommodate vehicles. MDD makes further accommodations with variations in the width of route sections for different modes of movement, including a local tram network (**Figure 2**). The MDD project aims to change the direction of urban development in Qatar by creating a livable neighborhood in response to the local climate. For these reasons, researchers selected MDD as a case study for three ongoing studies. The first examines the relationship between urban morphology and real estate economics. The second as one of several case studies in a comparative investigation of neighborhood structure in Doha. Lastly, a study examining the child-friendly provisions in the project's urban design. We limit this paper to reporting on aspects of the morphological survey work and analysis.

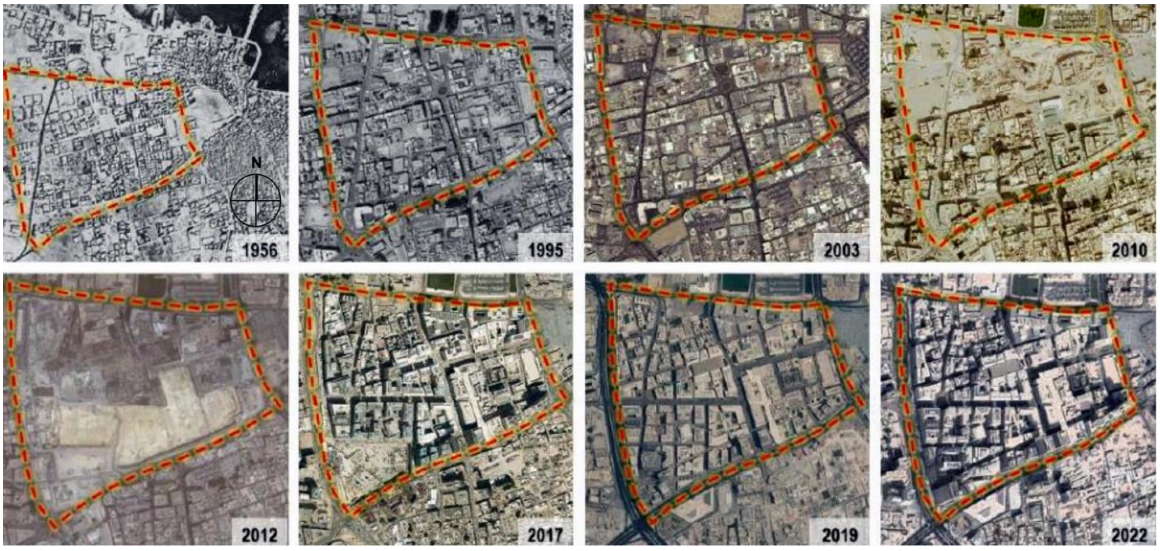


Fig. 1: Satellite views of the Msheireb area and subsequent redevelopment into Msheireb Downtown Doha from 1956-2022 (Source: Ministry of Municipality/Google Earth)



Fig. 2: Sketches of typical route section views in Msheireb Downtown Doha today including (left-to-right) the traditional pedestrian-only *sikka*, expanded pedestrian *sikka* routes to accommodate tramline and public plazas in *fereej* subareas, and primary routes accommodating all modes of movement including the tram and vehicles

2 Literature Review

In general, urban morphology refers to the study of urban form and its connected physical elements that structure and shape urban fabric, such as streets, buildings, and properties, considering the spatial logic of the space and the structured urban principles. It also includes the policymakers, governors, and regulatory processes involved in shaping and organizing cities. Urban morphology is a source of knowledge that highlights several aspects of life in cities. A comprehensive function of urban morphology recognizes the recurring spatial patterns in the structure, appearance, and transformation of the new and existing urban forms. As a resource of information on the historical urbanization process in Qatar and its contextual impact, researchers from Qatar University conducted morphological analyses for various projects in Doha. The projects are diverse in size, function, and date of creation. The purpose is to understand the design logic of the built environment and highlight the physical and functional parameters, such as ground-level land uses, pedestrian sheds, and active/inactive frontages, that might relate to the socio-economic factors influencing its urban morphology. Recent examples include an artificial island development, The Pearl-Qatar, and two souqs in Qatar, Souq Waqif and Souq al Wakra. The data about design and planning in each project's layout were collected based on on-site surveys, visualized concisely, and translated into quantitative numerical data in various forms. In early 2022, Qatar University researchers did the same for MDD to understand better the urban fabric and land use in the urban regeneration project.

Doha's recorded history includes the Al Thani tribe, the current ruling family that existed in the early settlement around 1847, which was called at that time Al Bidda. Like other Gulf cities, the early settlement started as a fishing village and later became a modern face in the Arab world and the Middle East after the discovery of oil. Moreover, the fishing village had a strategic location due to its proximity to the coastline as the central water resource, which helped facilitate trade purposes. As a result, early settlers of Al Bidda brought economic developments along the coastline, creating eight settlements representing two social classes at that time, original Qatari families and Persian immigrants. The mosque, port, and market represented the social hub for the two groups, except for their more isolated living spaces. Historically, Msheireb was the first ‘suburb’ of Doha and Souq Waqif and the original business district of old Doha, which is currently connected to the waterfront through Al Corniche Road. As population growth occurred over time, the inhabitants were strongly associated with the coastline. The area was accessible and connected to the central historical market, Souq Waqif, through old wadi routes, later called Wadi Msheireb or Al Kahraba Street. Al Kahraba Street recreated a commercial hub because it was the nation's first to have an electricity connection. Thus, it represented a meaningful street that was essential at that time. Later, the neighborhood of Msheireb was constructed using local materials. The design layout and logic of most buildings, transport networks, and vehicular movements are inspired by Islamic vernacular architecture. The continuous urban development of Doha as a commercial center led to the establishment of many vital neighborhoods, such as Al Asmakh and Al Najada, the areas surrounding MDD today.

3 Research Design

To explore the physical form and function of MDD and understand its design logic, the researchers utilized a mixed-method quantitative and qualitative approach with selective research tools during two stages. The first stage is a literature review as a resource for information about the historical urbanization process in Qatar and the transformation of the Msheireb area, which stands as a background study and links it directly to the current context to understand the influence of the local heritage in its contemporary design. Moreover, selective international readings in urban design and

planning served as a foundation for basic concepts such as urban morphology and morphological analysis, objectives, and approaches to deeply analyze and investigate the spatial urban fabric and the land use of MDD. The second stage represents a morphological analysis of the physical form and land use of MDD. The analysis was conducted to find the site's physical characteristics and began with collecting data about the building geometry, such as the size of the blocks, building heights, and route structure. The active and non-active frontages and ground-level land use help us to understand the probable impact on pedestrian behavior and movement. It also highlights the central issue in the urban fabric regarding shading and walking distances.

4 Data Analysis and Results

MDD has four quarters, created by 69 blocks, 22 are regular in shape, and 47 are irregular due to building footprints with an average area of 13,414 m^2. Therefore, while analyzing the built-up form, we calculated the average block size by dividing the total ground level area by the number of blocks resulting in 194.4m^2. The block sizes of residential buildings in MDD are diverse to support the three types of housing as specified by Msheireb Properties: townhouses, premium apartments, and prestige apartments. Many buildings utilize a courtyard typology, but increased building heights transform this into air wells, with the space only operating as a 'courtyard' at ground level. It is evident in the figure-ground of urban blocks and spaces in MDD today, as well as those of four restored courtyard houses adaptively reused as museums (**Figure 3**, left). One of the remarkable things about MDD is the pleasure of walking as it is a pedestrian-friendly environment with extensive shading via building form, massing, and relation to adjacent buildings with an extensive distribution of the underground parking points, cars, pedestrians, or mass-transit users, and residents. For pedestrians, the Wadi area is considered the primary target for this group. It is accessible from both gateways, and its *sikka* (narrow passageway) is dedicated to pedestrians. The southern part of Al-Kahraba Street is also walkable, while pedestrians need to spend more effort to arrive at the north part or use other modes of transportation. Biking could extend user reach to most of MDD's areas, especially with the bike rental service provided by Ooredoo at different spots. The tram service is more convenient for pedestrians because it has many stops in the neighborhood, mostly when the hot climatic conditions deter walking in the neighborhood. Using another mode of transportation involves more activities, renting in case of bikes or waiting on the tram, which hinders pedestrians' desire to walk. The spatial distribution of mosques in MDD allows the third group to walk everywhere. Like external groups, other transportation modes enable them to arrive at most destinations (**Figure 3**).



Fig. 3: (left) Figure-ground representation with space (white) and urban blocks (black) and (right) pedestrian sheds of 200 m from mosques in Msheireb Downtown Doha



Fig. 4: Survey of building heights based on the number of floors in Msheireb Downtown Doha in January-February 2022

The urban form of the townhouses reflects the courtyard style of traditional Qatari houses, while the apartment buildings reflect the modern living of contemporary Qatari architecture. The masterplan's buildings have been classed into three-character types according to scale and massing low, mid, and high-rise buildings. Low-rise buildings are up to four occupiable stories (including the ground level). These buildings have a domestic scale and typically do not incorporate ground-level colonnades. Mid-rise buildings are between five and ten occupiable stories (including ground) and comprise most facilities. These buildings usually have a clear base, middle and top. They often incorporate a street arcade at the bottom and set-back accommodation at the top. Tall buildings have over ten occupiable stories, typically found to the south of the site. They are comprised of a podium and tower element. The podium element rises to the defined top of street height. The tower element rises above this line and can reach the target building height (**Figure 4**).

In MDD, there are more than 100 buildings, each distinct yet all expressing a shared architectural language rooted in the local culture and climate. MDD comprises a diversity of uses, including residential, offices, retail, food and beverage, hospitality, cultural (museums), and other ancillary services, such as religious and civic buildings. Most residential buildings are in the northwestern part of Msheireb, moving from the low-rise townhouses to the high-rise premium and prestige apartments to the south. The residential land use in MDD concentrates near vital areas across the local scale of MDD. The housing types developed as townhouses harmonize with the surrounding built forms and heights. The size of townhouses is conveniently supported by neighborhood facilities such as a school, mosque, and green public spaces, all within walking distance. The residential land use extends downwards until Sahat Al Nakeel, the second prominent public space after the Barahat in MDD. The residential buildings near Sahat al Nakeel are developed as apartments serving a more comprehensive population sector.



Fig. 5: Survey of (left) ground-level land use and (right) active and inactive frontages in Msheireb Downtown Doha in January-February 2022

In contrast, the townhouses in the north are designed based on the *fereej* (neighborhood) concept and courtyard houses to attract Qatari nationals. There are medical facilities and a mosque near the apartment buildings to support the necessities of urban living. The townhouse cluster stands for the typical design of *fereej* with up to six townhouses, and the traditional urban courtyard form reinterpreted for modern living. The apartments in MDD range from compact business suites to homes for international residents and Qatari families. Each apartment has a formal and a family majlis, combined with a layout providing proper levels of privacy within the home. Community facilities such as pools, gyms, and majlis rooms also integrate into the common parts of the apartment buildings. They also have private outdoor space in various forms – roof terraces, balconies, and elevated courtyards. The three residential typologies aim at various end-users to provide critical density and mass in bringing activity to the area. A few buildings were preserved; including the five traditional buildings managed by Qatar Museums, Sheikh Suhaim Palace, and the original routes of Al-Kahraba and Abdallah bin Thani streets (**Figure 5**). It indicates the active and nonactive frontages along two types of routes. The active and inactive frontages are surveyed on the building's ground level only. Vacant shops with the provisions of active frontages (glazing) have a distinct color. Once operating, they are supposed to draw more attention from pedestrians. The nonactive frontages are limited to townhouses and civic buildings such as the tram depot. Building design does not leave any chance to activate the ground floor frontages. This matches the design intent for increased flexibility in ground floor uses. MDD's master development standards mandate that all ground floor levels have a 4-meter height to suit different uses and provide maximum flexibility in changing uses over time. This generous allocation of active frontages along the two sides of the routes significantly improves walkability, as users were motivated to walk more within the two routes. Active frontages allow people to mingle with others and interact with the goods displayed. This pattern is evident when comparing the already opened segments of *sikka* and streets with those still under construction (Phase 4) in early 2022. The people's movement decreases the more they move towards the west of Sikka or the south of the street. Therefore, plaza three will play a significant role in activating the connection between the two routes once more spaces around the plaza start to open.

5 Future Research

By 2030 around 60% of the world's population will reside in cities, and 70% of global children will live in cities by 2050 (Source: United Nations). Therefore, creating a healthy and sustainable

environment for children is a fundamental goal. However, according to UNICEF's Child-Friendly Cities Initiative (CFCI), Qatar does not host a child-friendly city or implement a CFCI design. Thus, creating MDD as a child-friendly city aims to bring children's needs into the urban planning agenda to contribute to Qatar's 2030 vision for more sustainable and inclusive communities. Since MDD succeeded in providing a sustainable and walkable neighborhood and family-oriented design for the residents and visitors, future research can explore the potential for the case of MDD as an example of a smart city to be a child-friendly neighborhood within the region. The research's primary objective will be to examine how MDD can be represented as a child-friendly city and highlight the guidelines to follow so the built environment can fill a gap in urban planning to complement the needs and views of the children in Qatar.

6 Conclusion

Qatar is a part of the Arabian Gulf's culture, economics, and society. Thus, residents of Qatar have sought a safe and stable life in various times and conditions, focused on making a living from the sea or land through grazing or desert life. However, the trajectory of social life changed after the discovery of oil and natural gas. Qatari society split into economic classes after being divided into multiple tribes for much of its history. With its distinctive vernacular architectural language and innovative green solutions, MDD is the country's first sustainable downtown regeneration project. The purpose behind this is to revive the commercial district of old Doha and bring new vitality to the downtown. The design is rooted in the Qatari heritage considering its proportion, simplicity, space, light, layering, ornament, and response to climate. On the environmental level, the MDD masterplan incorporates the *sikka* (narrow passageways) borrowed from Islamic architecture and *fereej* (neighborhoods) concepts to provide comfortable zones with natural cooling. The project also creates vehicle access with underground services and parking, facilitating contemporary urban life. Initially, the MDD aimed to reverse the development pattern in Doha, which has tended towards isolated land use, reliance on car transportation, and energy-hungry structures. Our study of the urban morphology of MDD suggests the project succeeds in creating a new social and civic hub in the city center where it is enjoyable to live, work, shop, visit and spend time.

Acknowledgments

The authors acknowledge Qatar University and the Office of Research Support (ORS) for the grant, which covered portions of the research in this paper (Grant ID: QUCG-CENG-22/23/472). The authors would like to acknowledge the contributions of MUPD graduate students for the fieldwork, namely Adheena K. Aliyar, Ahmed H. Keshk, Fatima R. Al-Esmail, Rakeen A. Razzak, Sreejaya Thankam, and Zolfa A. Mostafa for the research in this paper.

References

Al-Amadi, et al. (2022) "Form and Function in The Pearl-Qatar Artificial Island Development," *5th International Conference of Contemporary Affairs in Architecture and Urbanism (ICCAUA-2022) Conference Proceedings Book* (J.M.P. Madrigal, M. Nikoofam, Eds.), 11-13 May 2022, Alanya HEP University, Alanya, Turkey: Municipality of Alanya, 617-627, DOI: 10.38027/ICCAUA2022EN0100, E-ISBN: 978-605-71006-2-7, https://iccaua.com/PDFs/2022_Conference_fulL_book/SESSION_C_2022/ICCAUA2022EN0100_Alamadi_617-627.pdf.

Al-Buainain, F. A. A. A. (1999) *Urbanisation in Qatar: A Study of the Residential and Commercial Land Development in Doha City, 1970-1997*, Doctoral Dissertation, University of Salford, Salford.

Alattar, D., Nafi, S. & Boussaa, D. (2021). "The search for identity in a global world: The case of Doha in Qatar," *Journal of Urban Regeneration and Renewal*. *14*. 295-311.

Alraouf, A. (2016). "Dohaization: An Emerging Interface between Knowledge, Creativity, and Gulf Urbanity," *Gulf Cities as Interfaces* (Katodrytis, G., Syed, S., Eds.). KSA: Gulf Research Centre Cambridge; 47-69

Ibrahim, et al. (2020) "Investigating Land Use Dynamics in Emerging Cities: The Case of Downtown Neighborhood in Doha," *Journal of Urban Design*, *25*(3), 387-411. DOI: 10.1080/13574809.2019.1632179.

John, P. (2019) "Msheireb Downtown Doha 90% complete," *Gulf Times*, 31 March 2019. Accessed 2 April 2022 at https://www.gulf-times.com/story/627421/Msheireb-Downtown-Doha-almost-complete-open-for-public.

Khan, et al. (2021) "Tradition, Transformation, and Re-creation in Two Marketplaces: Souq Al Wakrah and Souq Waqif, Qatar," *Habitat International*, 116, 102438, ISSN 0197-3975, DOI: 10.1016/j.habitatint.2021.102438, https://www.sciencedirect.com/science/article/pii/S0197397521001272.

Łaszkiewicz, E., Nowakowska, A. & Adamus, J. (2022) "How Valuable is Architectural Heritage? Evaluating a Monument's Perceived Value with the Use of Spatial Order Concept," *SAGE Open*, 12(4). https://doi.org/10.1177/21582440221142720.

Major, M. D., Mirincheva, V. & Tannous, H. O. (2019) "Urban Transformations: From restricted random aggregation to designed cultural intent in Middle Eastern cities" (in Chinese and English), *China Journal of Urban Design*. Beijing: Tsinghua University Press, 5, 2019: 34-49, http://urbanism.com.cn/EN/abstract/abstract153502.shtml#1.

Nagy, S. (2008) "Dressing Up Downtown: Urban Development and Government Public Image in Qatar," *City and Society*, *1*(12), 125-147. DOI: 10.1525/city.2000.12.1.125

Oliveira, V. (2016). *Urban Morphology. An Introduction to the Study of the Physical Form of Cities*. Switzerland Springer International Publishing.

Pintos, P. (2021). Msheireb Downtown Doha Masterplan / Allies and Morrison + AECOM + Arup. *ArchDaily*. Accessed 2 April 2022 from: https://www.archdaily.com/966087/msheireb-downtown-doha-masterplan-allies-andmorrison-plus-aecom-plus-arup

Salama, A. M. & Wiedmann, F. (2013). *Demystifying Doha: On Architecture and Urbanism in an Emerging City*. Routledge, New York/London.

Salama, A.M. & Wiedmann, F. (2013) The Production of Urban Qualities in the Emerging City of Doha: Urban Space Diversity as a Case for Investigating the 'Lived Space'. *Archnet-IJAR: International Journal of Architectural Research*, *7*(2), 160-172. ISBN: 978-1-909864-08-5.

Wiedmann, F., Salama, A. M. & Thierstein, A. (2012) Urban Evolution of the City of Doha: An Investigation into the Impact of Economic Transformations on Urban Structures. *METU Journal of the Faculty of Architecture*, *29*(2), 35-61.

Cite as: Amleh R.A.A., Major M.D., Tannous H.O., Alyafei A.M., Fetais G.H., Mohammad A. Najjar M.A. & Awwaad R.Y., "The Urban Morphology of Mshereib, the Heart of Downtown Doha", *The 2nd International Conference on Civil Infrastructure and Construction (CIC 2023)*, Doha, Qatar, 5-8 February 2023, DOI: https://doi.org/10.29117/cic.2023.0118

Social Outcomes and Needs Study for Housing Development

Gozde Calim
Mott MacDonald, Dubai, UAE
gozde.calim@mottmac.com

Morgan Belsher
Mott MacDonald, Dubai, UAE
morgan.belsher@mottmac.com

Abstract

Mott MacDonald are providing advisory services for an accommodation project located in the Kingdom of Saudi Arabia (KSA). The project plan is to deliver more than 2000 housing and community facilities to teaching staff for a University in KSA. Currently subsidiaries are paid to faculty members who arrange accommodation with private proprietors. The current provision by private landlords offers limited choice with inconsistent availability of basic needs such as; security and safety, first point to healthcare, family' leisure activities, children's care, education needs, domestic cleaning and travel provision to campus, etc. The Project aims to provide high quality living conditions to education professionals via quality housing options, and to foster team and community spirit among the teaching staff. Mott MacDonald have prepared a Social Outcomes Study as this project has an opportunity to provide services to a range of end users from different ages, marital status and different backgrounds. Mott MacDonald understands that social objectives can be achieved fully by developing an equitable living environment. Believing that simple changes can make a big impact on individuals' lives, we help our clients to achieve accessible, safe and connected environments. We believe in the power of sustainable and equitable urban designs, in which people are at the core of activities. We have collected best practice approaches from across the globe and conducted surveys with end users to create a transparent process and choice of preferred living opportunities. More than 5 goals of the United Nations (UN) and Social Development Goals (SDG) are integrated within the project's social objectives. It is planned to have sustainable and nature protected solutions.

Keywords: Public Private Partnership ; Social Housing; Social Outcomes; United Nations Social Development Goals.

1 Introduction

As part of broader objectives of becoming an economic incubator for the region and significantly improving the level of educational provision for local, national, and international students, one of the prominent public universities in KSA plans to provide a housing development for educational staff within their campus (on a land of over area of 1,000,000.00 sqm). The current accommodation provided by private proprietors offers limited choice and a lack of basic services. Private housing options presents challenges such as–lack of large housing, security and safety, uncontrolled environment of living, unfavourable leisure and active daily life, and unfavourable travel conditions impacting the duration to campus, etc. Private housing for faculty members also makes allowances

(provided by the university) and budget spending dependent on the market thereby increasing the uncertainty.

Mott MacDonald have provided their technical advisory services for:

i) Needs assessment,

ii) Scope and Services structuring, and

iii) Social Outcomes Study.

2 Social Outcomes

Our unique way of exploring social outcomes helps us to ask right questions to deliver a project specific action plan to achieve accessible, inclusive and resilient living spaces.

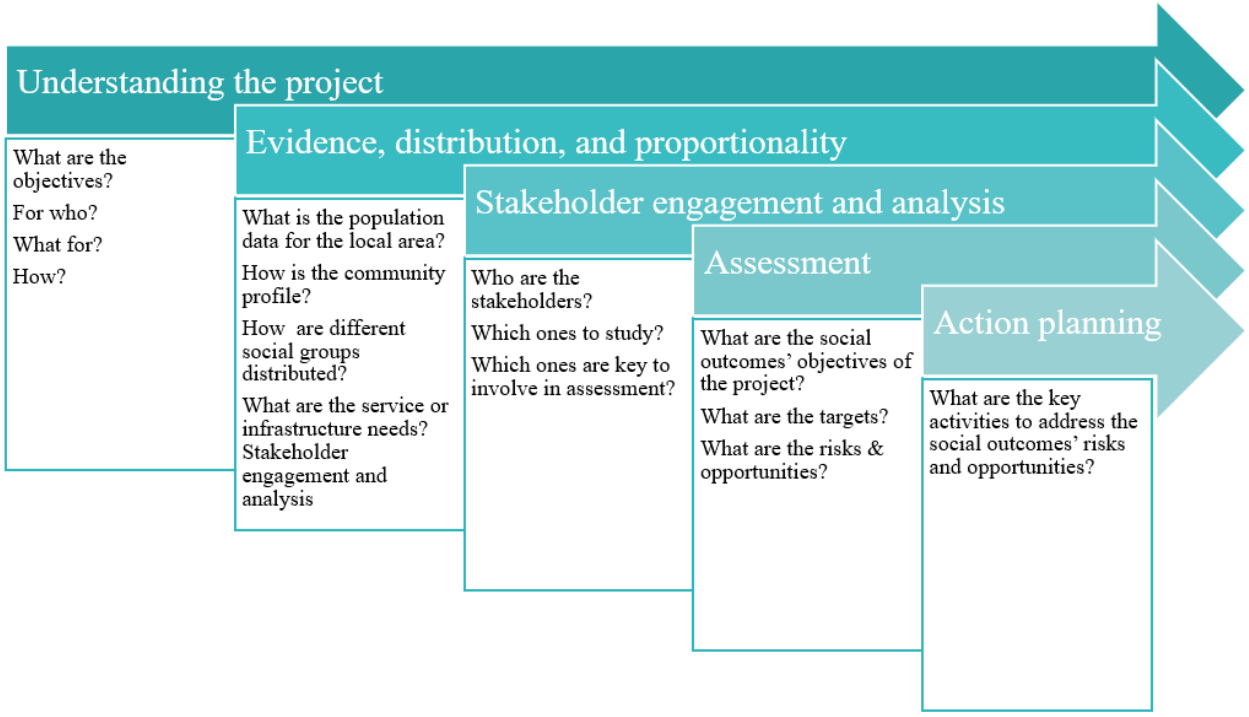


Fig. 1: Social Outcomes Study (Mott MacDonald, 2022)

3 Understanding the Project

We have first studied the alignment of the university's objectives against the over-arching objectives of KSA Vision 2030 (Kingdom of Saudi Arabia, Council of Economic and Development Affairs, 2016). By the nature of this development, it is important to capture the long-term vision of KSA during the project inception stage. Vision 2030 has been adopted as the roadmap for economic development in the Kingdom and is built around **three basic pillars, being a vibrant society, a thriving economy, and an ambitious nation. Vision 2030 plans to build these pillars via a number of Vision Realization Programs (VRPs, Kingdom of Saudi Arabia, Council of Economic and Development Affairs, 2017).**

Mott MacDonald have led discussions with key stakeholders to explore options to realise the Vision 2030 objectives and have provided guidance on the project's alignment. Key objectives and goals of the project are summarised in the table below:

Table 1: Vision 2030 – Vision realization programs, goals and action plan

Vision Realization Programs	Vision Goals	Project Objectives
Quality of life program	1. Improving the individual and families' quality of life by the environment to develop and support new liveable and lifestyle options. 2. Participation of citizens, residents, and visitors in cultural, entertainment, sports, tourism, and urban activities, and other activities that nurture their quality of life. 3. Diversifying economic activity, and consequently boost Saudi cities' ranking amongst the world's top liveable cities.	The Project is expected to improve the quality of life and secure high living standards for the faculty members. The role of the private sector investments in this Project ensures continuous development and sustainability of the faculty housing facility.
Housing Program	1. Housing solutions that enable families to own and benefit from suitable houses. 2. Improve housing conditions for current and future generations through the provision of suitable and guaranteed financing solutions. Supply of housing units at reasonable prices within record time.	The Project will stimulate supply in the housing sector for the new campus, specifically through effective partnerships with the private sector.
National Transformation Program	1. Governmental operational excellence, 2. Enabling the private sector, 3. Developing economic partnerships, and promoting social development, 4. Ensuring the sustainability of vital resources.	The Project is expected to significantly improve living standards & safety at faculty while ensuring the sustainability of vital resources and enabling the private sector investment.
Privatization Program	1. Enhance the role of the private sector in providing services and making government assets available. 2. Improving the quality of services provided and contribute to the reduction of costs. 3. Encouraging economic diversity and development and boosting competitiveness to face regional and international competition.	The Project is proposed to be developed under a private partnership approach, which incorporates a framework for defining public and private sector partnership to enhance the quality and efficiency of public services, and support contributions to economic development.

The housing project has strong and direct links with the National Vision and Objectives (VRPs, Kingdom of Saudi Arabia, Council of Economic and Development Affairs, 2017) as illustrated in the figures below:

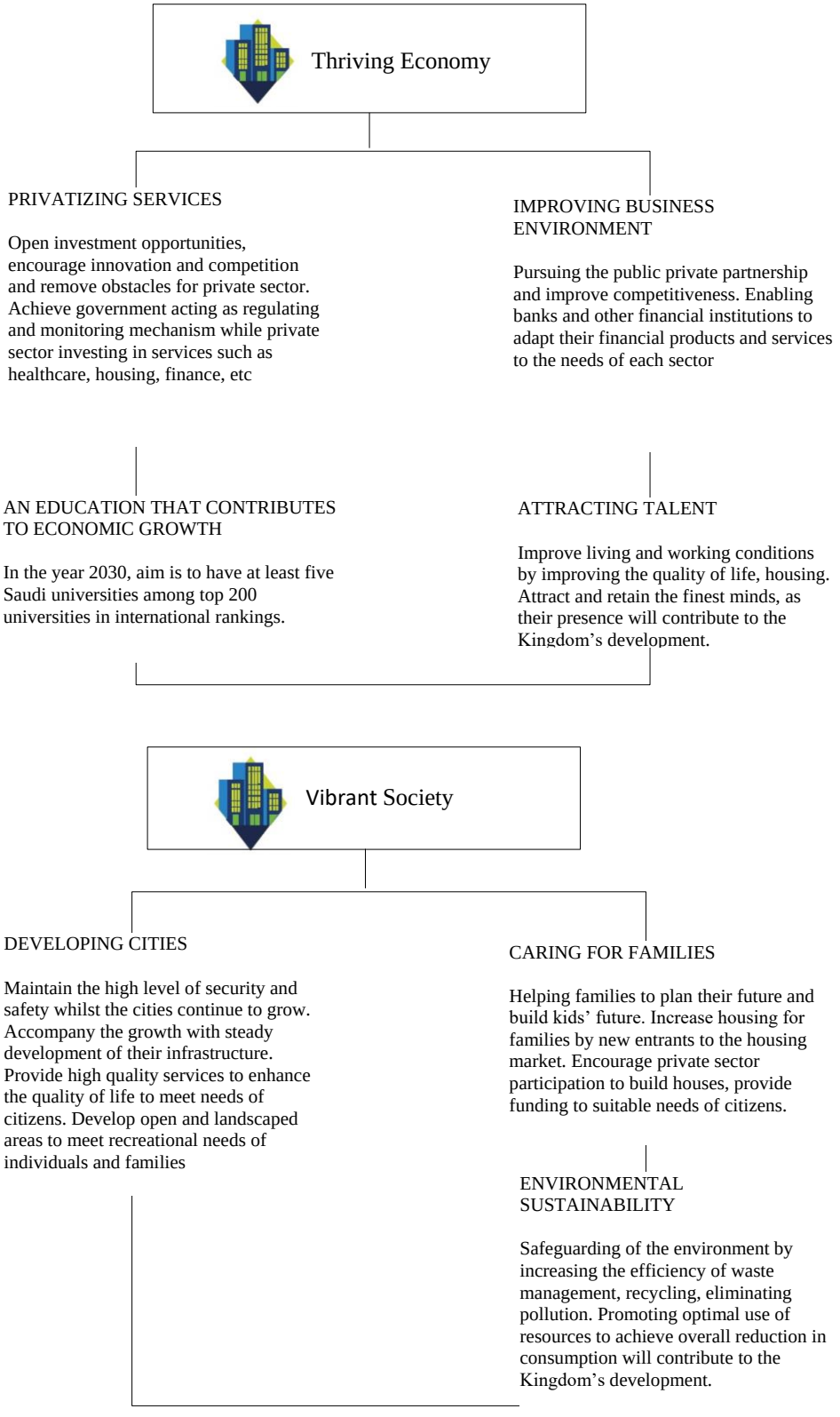


Fig. 2: National Vision and Objectives

After finalisation of the objectives alignment study, key social objectives for the project are as listed below:

- Affordable, safe, and quality housing options
  - Increasing level of innovation and efficiencies in design.
  - Security, privacy, and promoting the community's lifestyle.

- Full recovery of travel time and cost to campus.

➢ Stimulation of intellectual development

- Easy interaction with fellow peers in development.
- Attraction for strategic hiring.
- Fostering team and communal spirit among teaching staff.

➢ Establishment of guidelines in the university

- Structure for compatible and cooperative living.
- Adequate care and maintenance of the facilities as per the university's requirements and monitoring structure.

4 Evidence, Distrubution and Proportionality

The next step for the needs study was to identify the key features and components of the development. Firstly, we conducted desktop research to understand the total estimate relating to the number of occupants and their demographic to capture essential need requirements. The below graph summarises the overall estimated living, demographic and dedicated housing types.

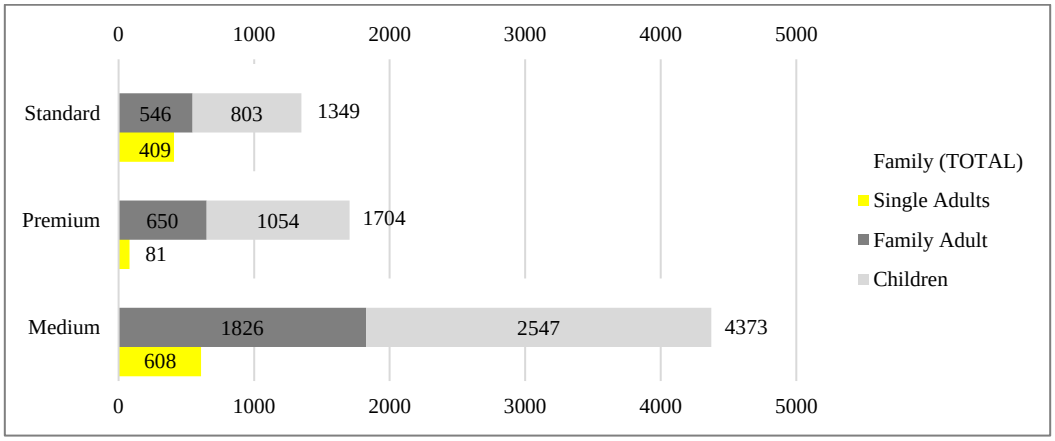


Fig. 3: Assessment of Overall Demographics vs Housing Type

Assumptions on demographics: We conducted studies to estimate the overall population within the housing project. To note, this will also support decision making on the selection of supporting facilities and sizes. Based on the statistics published by General Authority of Statistics (Population by Age Groups, and Gender mid-year 2020',GASTAT, 2020) the family population chosen conservatively suggests that the younger population (until 19 years of age) tends to take up a higher proportion of overall population.

The development will have approximately 2600 housing units (varies types) and residents of families and single adults.

5 Stakeholder Engagement and Analysis

At this stage, capturing the user's expectations (as key stakeholders) is highly important especially for such a long-term project. We have given higher attention to their needs as this development will be their livelihood, provided, they continue to be staffed at the university. One of the keys to enhance and improve the learning environment for a university is to attract the individuals who are among the best in their profession and offer them and their families a high-quality living environment.

User surveys conducted in the planning stage will improve the project's scope and its social viability.

We have developed key questions (total 25) to i) assess current living conditions and ii) identify their preferences. Some of the results are presented below:

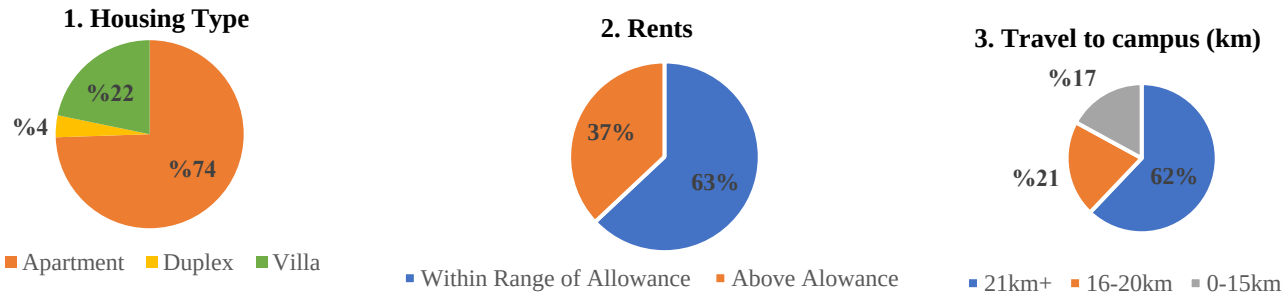


Fig. 4: i) Current living conditions (Users Survey – Source: Confidential)

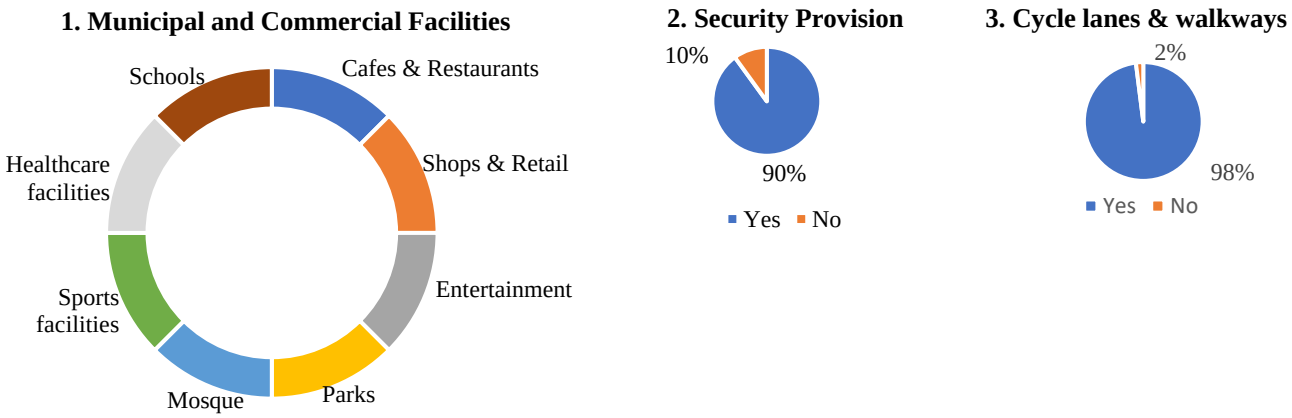


Fig. 5: ii) Future preferences (Users Survey – Source: Confidential)

6 Masterplan for the Project

We have then proceeded to define the key features of the development based on the i) global precedents, ii) stakeholder feedback and iii) user preference. The range of recommended housing options, based on preferences, professional degree in the university, and marital status is set out below:

Table 2: Recommended Housing Types

Housing Type	**Layout**	
	Size (m2)	**Features**
Premium	250 to 300	4 bedrooms, Live-in maid/laundry facilities, Large open areas of green space or Roof terraces.
Medium	200 to 250	3 to 4 bedrooms, Shared green amenity space, Live-in maid/laundry facilities.
Standard	100 to 150	2 to 3 bedrooms, Terrace balcony.

Furthermore, to enhance the day-to-day experience in the development; below services are also included:

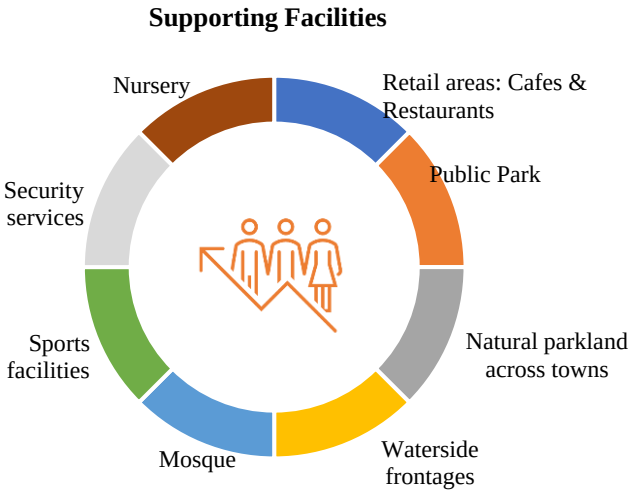


Fig. 6: Supporting facilities

7 Social Outcomes and Benefits Assessment

Lastly, we have explored the new social outcomes associated with the project, and further explored other potential activities and opportunities that can be added.

Sustainable Development Goals (SDGs) are an internationally recognised framework for delivering sustainable development for all countries, supported by the United Nations (UN). There are 17 SDGs, covering global challenges ranging from the elimination of poverty (SDG 1) and delivery of clean, safe drinking water (SDG 6) to sustainable economic growth (SDG 8) and taking action on climate change (SDG 13).



Fig. 3: Sustainable Development Goals (United Nations Department of Global Communications, 2020)

The United Nations Social Development Goals are used as a key reference for the study; therefore, we have listed **specific outcomes that can be aligned to the project**. These outcomes are then linked to the related SDGs.

Table 3: Project Social Framework and UN SDG Alignment

Outcomes	**UN SDGs**	**Success factors and opportunities for SDG alignment**
Accessibility, safety and security		Establishing non-motorized vehicles zones. Vehicular hierarchal network Pedestrian-friendly interface. Easy access to recreational spine. Connecting each building to nearby amenities and transit stops. Connections between major roads to enhance connectivity. Connectivity between housing urban spaces and recreational and services area.

Suitable living conditions	  	Open spaces spatial concept. Different housing types, forms and densities hence consideration of the human scale comfort vision. Smart living; an ecosystem of innovation; greener community; reduced operational costs. Plantation of trees to increase green cover, reduced GHG emissions by replacing conventional vehicles with electric vehicles & charging facilities.
Equitable living and social interaction	 	Roads designed to promote safe and secure mobility, having gender, age and disability responsive features; i.e., waiting rooms, lighting, pedestrian and disable friendly design elements. Inclusive access to community services and retails.
Connected places of work and opportunity		Generation of employment opportunities. FM staff to be accommodated in the housing areas; skills development. Employment creation, income generation, inclusive economic growth.
Partnership		Minimizing upfront costs through private partnership, value for money through controlled operation and maintenance of housing, high quality of services under the university's oversight. Stable payment mechanism hence better control on the budget.

8 Conclusion

Delivering social outcomes is about making a positive difference within the communities. Embedding social outcomes in projects involves **consciously thinking about users, communities and local people**. This needs to happen throughout the whole project, from inception and design stage, right through to construction, operation and decommissioning. Identifying the opportunities to deliver projects is the first step to enable positive outcomes. Focus and attention to identify opportunities from the outset, will considerably increase chances of success. When we first developed our action plan, we placed users and the local community at the heart of our due diligence process.

By spotting and developing social, environmental and economic opportunities, we believe the project can yield value far beyond its immediate benefits.

References

General Authority of Statistics. (2020). 'Population by Age Groups, and Gender mid-year 2020' (General Authority of Statistics, 2020. stats.gov.sa.

Ibrahim A., Musonda I. & Ibrahim K. (2018). Challenges of Student Housing Provision through Public Private Partnership, University of Johannesburg Institutional Repository.

Mott MacDonald Project Due Diligence – Confidential.

Provost Office. (2019). Eligibility and Allocation Guidelines for Administration of Restricted Faculty Housing Programs on UBC's Vancouver Campus, University of British Columbia.

Qatar University (2022). Policies and procedures of University Housing, Qatar University, http://www.qu.edu.qa/offices/housing_department/policies-and-procedures

Sustainable Development Goals. (2020). United Nations Department of Global Communications.

Vision Realization Programs (VRPs)' (2017). Kingdom of Saudi Arabia, Council of Economic and Development Affairs.

Vision 2030 (2026). Kingdom of Saudi Arabia, Council of Economic and Development Affairs.

Cite as: Calim G., & Belsher M., "Social Outcomes and Needs Study for Housing Development", *The 2nd International Conference on Civil Infrastructure and Construction (CIC 2023)*, Doha, Qatar, 5-8 February 2023, DOI: https://doi.org/10.29117/cic.2023.0119

Multimodal Transport For Smart Mobility in Emerging Cities: Case of Doha

Mahnoor Hasan
Department of Architecture and Urban Planning, College of Engineering, Qatar University, Doha, Qatar
mh1204286@qu.edu.qa

Fodil Fadli
Department of Architecture and Urban Planning, College of Engineering, Qatar University, Doha, Qatar
f.fadli@qu.edu.qa

Abstract

A mobility focused smart city ensures an urban place that is shaped with latest innovations accentuating the overall well-being of its citizens. One of the significant aspects for assessing the Smart Mobility in an emerging city is the assessment of its Multimodal Transport Network. Integrating diverse transportation modes into a single route for seamless mobility is necessary to revolutionize the cities into smart cities. Qatar is currently leading the pace of smart growth by investing profoundly in smart cities infrastructure and evolving mobility technologies. This paper explores: (i) the progress of the smart mobility development and initiatives in Qatar, (ii) the Multimodal transport system in one of its smart cities, Msheireb Downtown Doha (MDD) and (iii) how the Multimodal transport system could be influenced in the light of emerging transportation technologies like Autonomous Vehicles (AVs). The study investigates in-depth the transport network of the city and makes an exploratory analysis. The qualitative approach is used in doing secondary research and performing on-site observations. On-site observations for the smart mobility assessment involved assessing indicators like walkability, cycling, inter-modality and transportation hubs and the overall public transport system in MDD. It is concluded that there is still room for improvement when it comes to developing the intermodal network for the mobility enhancement and deployment of AVs. The outcome of the study is the investigation of the smart mobility initiatives adopted in Qatar, the assessment of multimodal transport pattern of MDD, and a bus route proposal in the era of AVs.

Keywords: Smart mobility; Multimodal Transport; Emerging technologies; Qatar

1 Introduction

This section emphasizes how crucial a robust Multimodal transportation system is for the development of smart mobility in a smart city. It also highlights how the Multimodal transport system is used for assessing the smart mobility. Smart mobility lays emphasis on transportation sector and logistics, with the smart usage of technology. It places a strong emphasis on reliable travel schedules, healthy communities, and user safety. Previous scientific studies confirm that intelligent transportation system (ITS) supports smart mobility (Papa et al., 2015). Despite the absence of a universal meaning for the term “Smart City,” several researchers define it as including the following areas: smart people, smart economy, smart environment, smart governance, smart transportation, and smart lifestyle (Giffinger et al., 2007; Stratigea & Panagiotopoulou, 2014).

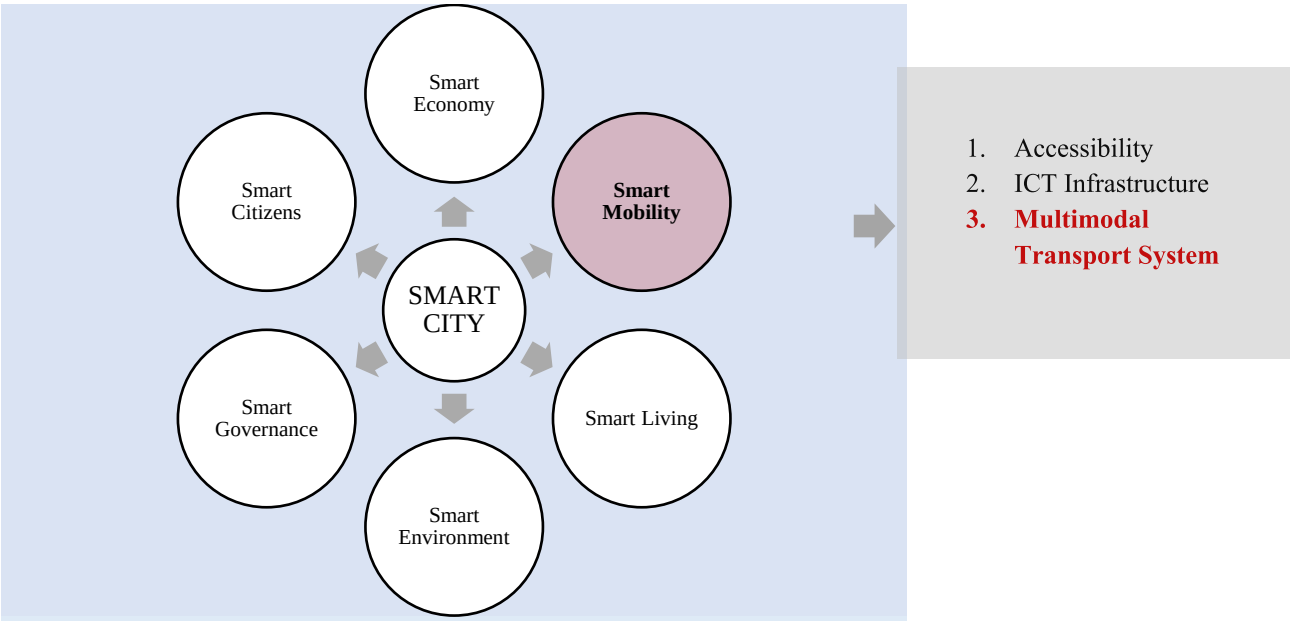


Fig. 1: Relationship between Smart city, Smart Mobility and Multimodal Transport System

Various researchers have made numerous efforts to define 'smart city' by combining diverse terms, representing the absence of a common definition (Chong et al., 2018; Schaffers et al., 2012; Zhuhadar et al., 2017). Smart Mobility, as one of the components of a smart city, is a crucial subject, impacting many facets of its residents' quality of life. According to Staffans & Horelli (2014), Smart Mobility refers to innovative and sustainable ICT-aided logistics, transport and communication systems with international and local accessibility. Multimodal transport often implies that one mode of transportation is employed as the primary way of travel while the other modes are used as egress or access routes (s). Interconnectivity, which allows for multimodal or inter-modal transit linking all of a city's resources, including its people, information, and commerce, is the crucial element of smart mobility or the transportation network of a city. Interconnections are the networks that link various transport network infrastructures (de Stasio et al., 2011).

Therefore, smart mobility is the way of connecting the Multimodal transport system used by commuters for day-to-day activities with the innovative use of technologies.

2 Multimodal Transport System as an Assessment Factor for Smart Mobility

Based on frameworks used in the past by various researchers for the assessment of smart mobility in a city, Table 1 has been created that summarizes the most important indicators used in the most recent researches for assessing smart mobility in a city. Most of the researchers agree that the deployment of multimodal transport system is considered as one of the most important assessment factors for smart mobility.

Table 1: List of most important Indicators for assessment of Smart Mobility conducted in the most recent researches

No.	Source and Year	Most Important Indicators	Cities Evaluated
1.	Biyik et al. (2021)	(i) Organizations (ii) Technology (iii) People	European Cities
2.	Munhoz et al. (2020)	(i) Accessibility (ii) Walkability (iii) Public policies	Brazilian cities

		(iv) Environmentally friendly policies (v) Urban mobility plans (vi) Maintenance (vii) Safety	
3.	Orlowski & Romanowska (2019)	(i) Technical infrastructure (ii) Information infrastructure (iii) Mobility methods (iv) Legislation	Poland
4.	Battarra et al. (2018)	(i) Accessibility (ii) Sustainability (ii) ICT	Italian Metropolitan cities
5.	Arce-Ruiz, Baucells, & Moreno Alonso (2016)	(i) Sustainable Urban Mobility Plans (SMUP) (ii) Payment integrated in Multimodal Transport system (iii) The use of ICT in traffic management (iv) Deployment of Multimodal Transport system	62 Spanish Cities

3 Methodology

Inductive approach is used as a research strategy in this research. It starts with observations and concludes that the intermodal network can be further enhanced in MDD for the deployment of AVs. Msheireb Downtown Doha (MDD) is used as the case study as the research strategy for investigating the real-life context of the transportation network. The study investigated in-depth the transport network of the city and makes an exploratory analysis. The qualitative approach was involved in doing secondary research and performing on-site observations. Analysis of the existing data was done through the theoretical and contextual background of smart mobility. On-site observations for the smart mobility assessment involved assessing indicators like walkability, cycling, inter-modality and transportation hubs and the overall public transport system in MDD. Site visits were made that investigated the site's settings. The observation approach was utilized to assess the urban design of the development. Plans were collected and maps were drawn based on relevant urban planning related indicators chosen from the most recent frameworks for smart mobility assessment.

4 Smart Mobility Initiatives Adopted in Qatar

Numerous mobility-related projects are being implemented in Qatar with the goal of influencing how people travel about the city. For instance, the Ministry of Information and Communications Technology is focusing on projects that assist sponsors in adopting smart technology and support the activities of various sectors (Sustainable Smart Cities: Improving Quality of Life, 2014). Qatar is a unique case study since it has undergone rapid urbanisation and through numerous stages of growth. It has noticed significant changes in its urban fabric recently, especially with respect to Msheireb Downtown Doha (MDD). Countless strategies have been commenced with the introduction of Qatar National Vision 2030, promoting it as an emerging regional and international service hub. The core of the country's National Vision 2030 is to have a technology-driven, diversified economy. Through it, the country intends to offer cutting-edge services to all stakeholders. Qatar has been striving to achieve the vision of smart cities, and its initiatives have propelled it to the position of a digital pioneer. Smart city designers set new standards for urban development, which will have an impact on forthcoming smart cities in the nation and beyond. MDD is the first downtown regeneration project of its kind in the world that makes use of connection and smart technology to improve the city's economics, way of life, and environment (Rider, 2021). With a comprehensive approach to creating settings where its residents, companies, and visitors can thrive, Qatar has demonstrated its dedication

to setting the standard for defining the future city. Qatar is dedicated towards making comprehensive public-private cooperation, investment in innovation centres, where co-creation will support the regional economy and future global initiatives as part of an integrated smart technology ecosystem (Rider, 2021).

As Msheireb Downtown Doha (MDD) is completed, Qatar is bringing its vision of smart cities to fruition. MDD is also the first to incorporate important dimensions of a smart city, including smart city technology, smart economy, smart environment, and interconnection.

By 2030, Qatar aims to be a developed society capable of maintaining its growth and providing a high standard of living to all of its residents. The National Vision of Qatar outlines the nation's long-term objectives and provides a framework for formulating implementation plans (Qatar National Vision 2030 booklet).

The Ministry of Transport and Communications (MOTC) is developing a smart transportation system as part of the Tasmu Smart Qatar Program. Using cutting-edge digital technology, Tasmu Smart Qatar seeks to transform Qatar into a world-class smart city in order to elevate living standards and increase the country's competitiveness on a global scale. The programme has a number of goals that range from sustainability to societal advantages. The program's main goal is to use technology and resources as effectively as possible for the benefit of society, the economy, and the environment. Their approach is both environment friendly and focused on providing a good service to the general people, and make use of electric buses, smart bus hubs, WiFi-enabled street lighting, and water taxis. The transportation industry seeks to promote mobility by providing a secure and safe transportation network. Through the integration of several transportation options, seamless mobility is intended to be created throughout Qatar's streets for a customised travel experience (Tasmu Smart Qatar).

5 Multimodal Transport System in Msheireb Downtown Doha (Mdd)

Utilizing two or more modes of transportation in one journey is known as multimodal transportation. The interconnection of various types of transportation is essential for transportation efficiency. It combines the benefits and makes up for the drawbacks of various modes of transportation. Increasing the usage of public transit while reducing reliance on cars as the primary form of transportation is one of the fundamental goals of multimodal transportation. Inter-modality in MDD, is reinforced very well by suitable infrastructure like designated bicycle pathways alongside streets, tram routes and pedestrian walkways.

Within 400 m of the metro station, public transport facilities like bus stations are accessible. The bicycle lanes and the pedestrian infrastructure are well integrated with the existing transit systems, connecting to the major metro line. There are two hubs with four and three modes of transport within the catchment area of 200m from the Metro Station. There are 4 modes of transportation namely tram, cycle, bus and metro line within the hub near to the Msheireb Metro station. The hub with three modes of transport namely; tram, bicycle, and bus lie towards the north west of Msheireb Downtown area. Inter modality is therefore considered strong because both the hubs with 3 and 4 modes of transport cover almost the entire area of MDD.

However, there is still room for improvement in the transport network of the Downtown. Inside MDD, there is no bus service available. The two bus stops existing on Al-Khail Street can be exploited to be part of a well-designed bus route. Part of the reason why there is no bus service inside MDD is that the Downtown is highly walkable and detached places have been already connected by 9 Tram stations all over the Downtown. Although the Msheireb Metro station is connected with the tram, it

necessitates commuters to walk certain number of meters to reach it. It has also been found that the cycling paths in most of the places are not ongoing and continuous. Moreover, the South-West area of the Downtown is devoid of any cycling tracks. Figure 2 demonstrates the Intermodal transportation network of Msheireb Downtown Doha (MDD).

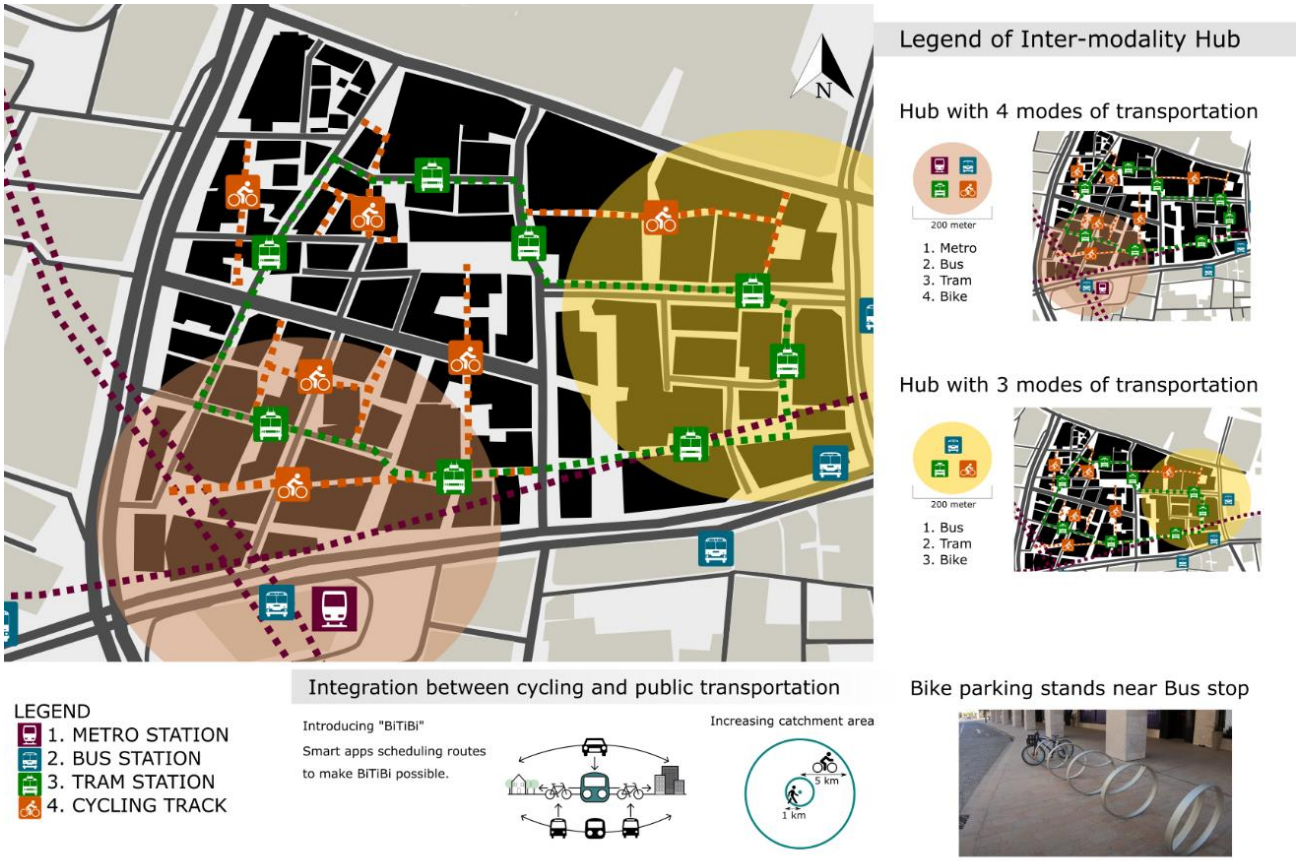


Fig. 2: Inter-modality and Transportation Hubs in Msheireb Downtown Doha

An incentive to support the bike-train-bike modal over vehicles and car-train hybrids is the BiTiBi (bike-train-bike) idea utilised in the European setting. The most significant guidelines in the BiTiBi approach are the establishment of adequate bike parking at metro stations and offer bikes, particularly for the last mile. In the case of MDD, this concept has been used with the provision of bike stands close to the metro station. This concept can be implemented at other metro stations in Qatar to ensure BiTiBi is applied.

6 Multimodal Network in the Light of Emerging Technologies like Autonomous Vehicles

According to (Bezai, Medjdoub, Al-Habaibeh, Chalal & Fadli (2021), infrastructure has a significant impact on the successful deployment of developing technologies like Autonomous Vehicles. Travelers must be able to reach a variety of transportation hubs, such as bus stops, railway stations, etc., in order to switch between AVs. Since AVs are expected to be the final mode of transportation utilised to get to the desired location in an urban setting, the mobility hubs must guarantee that there is an easy interchange of transportation modes. The mobility centres also need to have areas for bike stations and spacious walkways for both bikers and pedestrians. Re-designing the transit bus network is crucial for the effective implementation of AV technology. A traveller who plans his route from two points outside the city's downtown is compelled to take two buses—one to get him from his starting point to the downtown core and another from the downtown core to his destination—due to

the bus network configuration, which radiates from the central core into many metro areas.

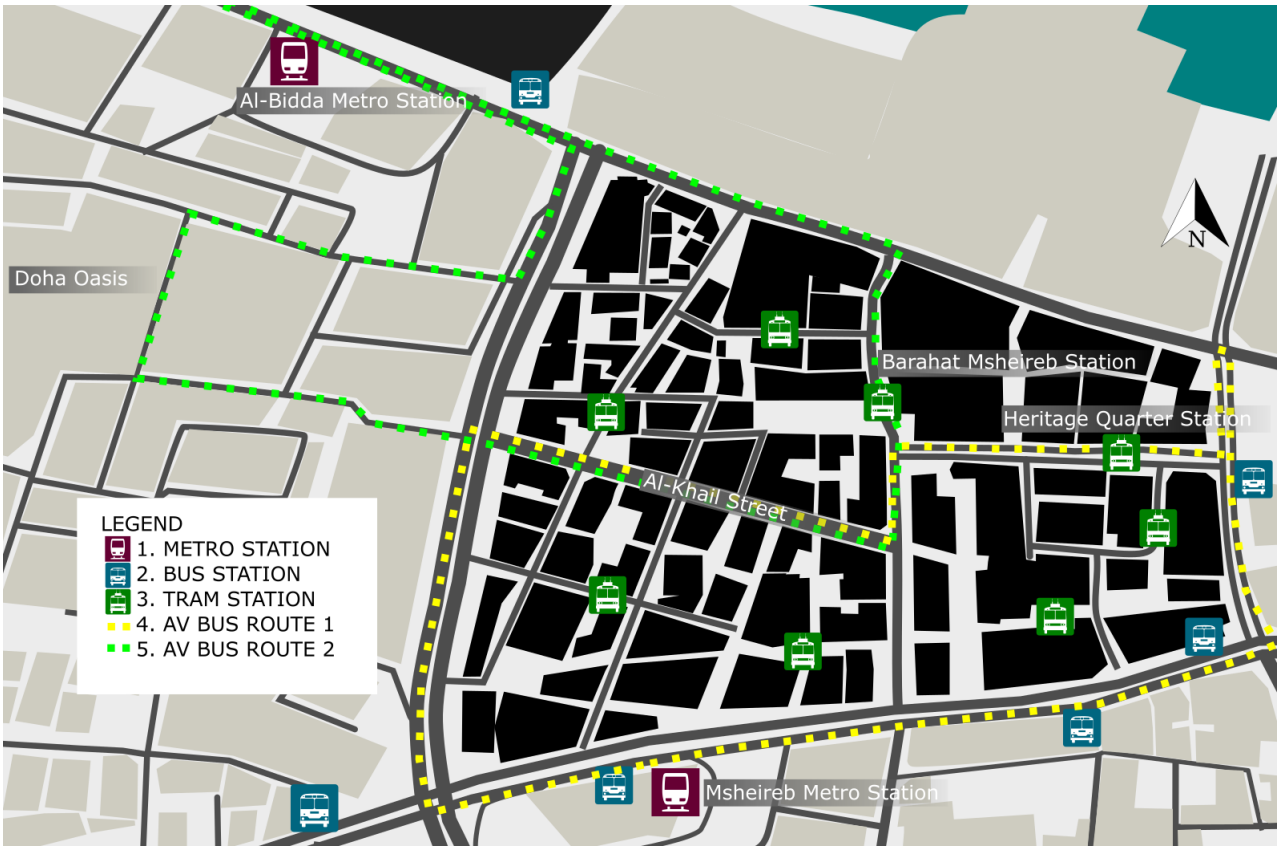


Fig. 3: AV bus route proposal

For the effective implementation of AVs on the streets of MDD, the following proposals are made with regard to the transport network. In close proximity to the MDD, are two Metro stations: (a) Msheireb Metro Station, which connects the red, green, and gold lines; (b) Al-Bidda Metro Station, which serves the red and green lines and which can be connected to the Tram stations by autonomous minibuses. Two routes could be created: one linking the Msheireb Metro Station with the Heritage Quarter Tram Station (for tourists visiting the Heritage Quarter) and Al Khail Street, a three-lane commercial street; the other linking the Al-Bidda Metro Station with the Barahat Msheireb Station and the Doha Oasis, a popular theme park for tourists (Figure 3). Both Metro stations already have bus stops that may be utilised by autonomous minibuses as well as regular buses. The minibus stop may be close to the Tram stations. It is possible to restructure both bus stops to make them more effective and smarter. Finally, instead of merely being located on the external main road, internal streets can also be used as locations for mini bus stops.

7 Conclusion

This paper investigated the smart mobility initiatives taking place in Qatar and the Multimodal transportation system in one of Qatar's smart cities, Msheireb Downtown Doha (MDD). It provided an insight into how the growth of smart mobility in Qatar, in light of cutting-edge transportation technology like autonomous cars, may affect the Multimodal transport system. There are several ways that this study might be developed in accordance with the idea of smart mobility. It gave an insight into how the multi-modal transport system could be influenced by the development of smart mobility in Qatar in the light of emerging transportation technologies like Autonomous vehicles. This study

can be advanced further in many ways in line with the smart mobility concept. Apart from assessing the Multimodal transport network, additional mobility indicators can be added for assessing the smart mobility from urban planning perspective allowing cities to adapt them in the most sustainable way. Using this paper as the base information, diverse ways can be recognised to integrate the globally available smart transportation technologies in the existing urban fabric of Qatar.

Acknowledgements

This paper was made possible by an Award [GSRA6-2-0514-19027] from Qatar National Research Fund (a member of Qatar Foundation). The contents herein are solely the responsibility of the author.

References

Arce-Ruiz, R., Baucells, N. & Moreno Alonso, C. (2016). *Smart Mobility in Smart Cities*.

Battarra, et al. (2018). Smart Mobility in Italian Metropolitan Cities: A comparative analysis through Indicators and actions. *Sustainable Cities and Society, 41*. doi: 10.1016/j.scs.2018.06.006.

Benevolo, C., Dameri, R. & D'Auria, B. (2016). Smart Mobility in Smart City. Action taxonomy, ICT intensity and public benefits. In (Vol. 11, pp. 13-28).

Bezai, et al. (2021). Future cities and autonomous vehicles: analysis of the barriers to full adoption. Energy and Built Environment, *2*(1), 65-81. doi:https://doi.org/10.1016/j.enbenv.2020.05.002.

Bıyık, et al. (2021). Smart Mobility Adoption: A Review of the Literature. *Journal of Open Innovation: Technology, Market, and Complexity, 7*, 146. doi:10.3390/joitmc7020146.

Chong, et al. (2018). Dynamic capabilities of a smart city: An innovative approach to discovering urban problems and solutions. Government Information Quarterly, 35. doi:10.1016/j.giq.2018.07.005.

de Stasio, C., Fiorello, D. & Maffii, S. (2011). Public transport accessibility through co-modality: Are interconnectivity indicators good enough? *Research in Transportation Business & Management, 2*, 48-56. doi:https://doi.org/10.1016/j.rtbm.2011.07.003.

Giffinger, et al. (2007). Smart cities - Ranking of European medium-sized cities.

Munhoz, et al. (2020). Smart Mobility: The Main Drivers for Increasing the Intelligence of Urban Mobility. *Sustainability, 12*, 10675. doi:10.3390/su122410675.

Orlowski, A. & Romanowska, P. (2019). Smart Cities Concept: Smart Mobility Indicator. *Cybernetics and Systems*. doi:10.1080/01969722.2019.1565120.

Papa, E. & Lauwers, D. (2015). Smart mobility: Opportunity or threat to innovate places and cities? , 543-550.

Qatar National Vision 2030. (n.d.). Retrieved December 06, 2021, from https://hukoomi.gov.qa/en/about-qatar/qatar-national-vision-2030#tab-3.

Rider, B. (2021, February 18). Qatar's Smart Cities of the Future [Web log post]. Retrieved from https://www.linkedin.com/pulse/qatars-smart-cities-future-beverly-rider.

Schaffers, H., Ratti, C. & Komninos, N. (2012). Special Issue on Smart Applications for Smart Cities - New Approaches to Innovation: Guest Editors' Introduction. *Journal of Theoretical and Applied Electronic Commerce Research, 7*, II-V. doi:10.4067/S0718-18762012000300005.

Staffans, A. & Horelli, L. (2014). Expanded Urban Planning as a Vehicle for Understanding and Shaping Smart, Liveable Cities. *The Journal of Community Informatics. 10*. 10.15353/joci.v10i3.3439.

Stratigea, A. & Panagiotopoulou, M. (2014). *Smart' Cities as a New Paradigm for Serving Urban Sustainability Objectives – A View in the Mediterranean Experience*.

Sustainable smart cities: Improving quality of life. (2014). Retrieved October 6, 2022, from https://motc.gov.qa/sites/default/files/sustainable_smart_cities_-_improving_quality_of_life.pdf.

Tasmu Smart Qatar, Retrieved from http://smart.gov.qa/en.

Zhuhadar, et al. (2017). The next wave of innovation—Review of smart cities intelligent operation systems. *Computers in Human Behavior, 66,* 273-281. doi:10.1016/j.chb.2016.09.030.

Cite as: Hasan M., Fadli F., "Multimodal Transport For Smart Mobility in Emerging Cities: Case of Doha ", *The 2nd International Conference on Civil Infrastructure and Construction (CIC 2023)*, Doha, Qatar, 5-8 February 2023, DOI: https://doi.org/10.29117/cic.2023.0120

A Bibliometric Study of Visual Quality Research in the Context of Urban Open Spaces

Mohammad Najjar
College of Engineering, Qatar University, Doha, Qatar
mn2101931@qu.edu.qa

Madhavi Indraganti
College of Engineering, Qatar University, Doha, Qatar
madhavi@qu.edu.qa

Goze Bayram
College of Engineering, Qatar University, Doha, Qatar
gbayram@qu.edu.qa

Abstract

Visual quality assessment has received much attention in research by forest management and landscape researchers after the mid-twentieth century with the advent of legal frameworks enacted to protect natural resources, including scenery. Since then, the field has gained momentum that is mostly attached to landscape change and assessing the environmental impact of changes. Urbanized areas, however, received less attention and just started to receive some exposure in the last two decades (concurrently with the emergence of new technologies of GIS and remote sensing). Developing a comprehensive understanding of the visual quality assessment research requires a reconnaissance survey of its history and the trends of its research growth. This study undertakes an analysis of visual quality assessment literature in the context of urban settings using bibliometric tools. The paper employs quantitative techniques to analyse 3,221 journal papers retrieved from the Web of Science using keywords co-occurrence, citation burst, and direct citation analyses with the help of VOSViewer, CiteSpace, and Gephi software. Here we show the discipline's status quo, trends, and patterns of development. They confirm the recency of urban-related research. Our study touches on the chronological emergence and decay of major visual quality notions. It also highlights the most central studies and the journals and research groups actively working in the field. Moreover, it points out research gaps related to urban spaces for future studies guidance.

Keywords: Visual quality assessment; Scenic beauty; Landscape visual quality; Urban aesthetics

1 Introduction

The assessment of scene visual quality goes back in history to the Greek philosophers, including Socrates and Plato. Yet the protection of the visual quality of natural landscapes and resources became mandated in the USA just five decades ago as per the National Environmental Policy Act in 1970. In other countries, guidelines for landscapers, like GLVIA in the UK, were established to regulate changes to landscapes so their impacts on visual quality and other ecological systems are mitigated. In many cases, the visual quality is assessed as part of Environmental Impact Assessments (EIA) that precede the permits of new projects. This legal and regulatory movement towards protecting natural landscape scenic beauty has initiated a parallel research movement on landscape visual quality

assessment methodologies and the impact of artificial changes. US Department of Agriculture (USDA), for instance, has funded several research projects and published dozens of works to create tools and methods that can be used to maintain and assess the visual quality of forests managed and administered under its scope. This momentum successfully shaped the formal approach based on the physical content of the landscape and descriptive sets of regulations and guidelines; such an approach is still dominant in landscape and forest management practice.

Bacon (1979) discussed using the Visual Management System (VMS) - a map-based geographical system for forest management- and identified a few physical characteristics of the natural landscape upon which visual quality assessment can be evaluated. The study provides a framework for identifying the landscape character and the respective allowable change. On the contrary, Daniel and Boster (1976) proposed the Scenic Beauty Evaluation (SBE) model based on human perception regardless of physical landscape characteristics. Kaplan (1979) discussed the use of perception-based surveys to identify the visual value of landscape characteristics. While these early studies and others were all published by USDA, they present distinct attempts to tackle landscape visual quality assessment. The first attempt is a map-based evaluation that neglects the public perception, while the second ignores the physical content of the scene. The third links the two ways of evaluation to avoid the dilemma of authority/public mismatch. These two ways of evaluation have initiated the primary lines of thought for following scholarly works. The other lines of thought were mainly branched from these two. Lothian (1991) conducted a chronological review of the two approaches and concluded with the triumph of the subjective approach, as it can be justified by statistical models. He argues that this approach is sincerely objective, as it is connected to communal human perception. In contrast, the objective approach is subjected to criteria determined by one or a few experts.

The objective (formal) approach has been widely considered in regulations and experts' practice because it provides clear and consistent criteria and guidelines for landscapers and practitioners to adhere to, such as those stipulated in GLVIA 3. On the other hand, the subjective approach has been widely investigated and improved in academia. This duality, with the different environmental and psychological layers, produced more sub-schools. Firstly, Daniel (2001) highlighted the potential growth of the field beyond the objective and subjective approaches supported by the new technologies of GIS and remote sensing. He proposed that a new approach will eventually combine the two schools to obtain an optimized correlation between the scene's physical characteristics and the users' psychological status with the help of the prevalent technology. Secondly, and from an environmental perspective, Gobster (1999) argued that the definition of forest aesthetics shouldn't be limited to scenic beauty but should go deeper into the site's physical and ecological characteristics. The study attempted to resolve the dilemma between landscape visual quality and ecological systems' sustainability through "ecological aesthetics". The protection of ecosystems and the ecological value in this approach are of prime importance in maintaining a specific visual quality. Thirdly, the perceptual approach was extended to a cognitive one, as evident in Kaplan's Attention Restorative Theory (ART) (1995), which positively correlates the restoration of users' attention with exposure to naturalness. The theory suggests that such exposure has a healing effect on users, translated to more productiveness in office spaces and schools. This approach was applauded by psychologists who took this theory further to propose more profound assessments of natural scenes and their contribution to enhancing mental health based on human perception, cognition, and experience, as suggested by (Celikors & Wells, 2022).

While this field emphasized forests, natural scenes, and rural settings for a while, given the conditions

of its emergence, recent studies started to discuss the visual quality of open spaces within the built environment. Luckily, these studies took advantage of using advanced methods and technologies like remote sensing, GIS, ML, and LiDAR, in addition to well-established statistical models like AHP and PCA, which helped correlate user preferences with the physical components for several applications. Yet, given the immaturity of visual quality assessments of urban open spaces, there is an urgent need to establish an urban-specific framework that considers using the most advanced tools. Urban areas are much more dynamic in terms of time, place, and vantage point than static homogenous natural scenery. Thus, high-resolution GIS data will facilitate more accurate assessments.

In this study, we investigate the status of this research field by analyzing literature extracted from Web of Science database. This study identifies the prominent directions through research clustering. It will detect the most influential studies and the primary keywords within each cluster. By doing so, this study acts as an entry point to the topic for new researchers as they will get familiar with the key terms, studies, authors, and journals. The significance of this study is also represented by several benefits, including identifying research groups and potentials for collaboration, and detecting theoretical research gaps in the field. The study will also shed light on the climax of the field's various paradigms represented by the phasing of their primary keywords. While classic paradigms could be considered non-active areas, researchers may find it worthy of activating some of their concepts if found valid for the current needs, or they may find it necessary to build up on a hot area with an urgent need. Thus, this study facilitates the alignment of new research works according to such patterns.

Therefore, this study aims to present the status quo of visual quality assessment in urban settings and the trends that have dominated visual quality since the 70s. The objectives of this research are:

- To study the clusters of visual quality assessment research and to map them.
- To identify central studies of the field and their interests, and
- To highlight active research outlets.

2 Methodology

This study uses science-mapping tools to form an understanding of the theoretical structure of the visual quality and scenic beauty field. These maps provide a high-level understanding of the field's trends (based on timelines) and clusters (based on research interests) and facilitate qualitative reviews of the body of knowledge. At the same time, generated trends and clusters draw implicit boundaries of the field's areas and explain the patterns connecting various studies by detecting mutual keywords and citations. By doing so, the most influential studies per cluster can be identified, in addition to the cluster's core concepts.

This study follows the methodology proposed by Darko et al. (2019) for their scientometric study on Green Buildings with few variations to suit the visual quality field and its specific conditions. While their study provided a step-by-step methodology that acts as a recipe for similar studies, they have also highlighted common shortcomings of previous scientometric studies, represented by excluding early studies through specifying a start date, the subjective deduction of research areas, and the lack of meaningful analysis of the extracted data resulting from confusing maps with plenty of overlaps between the clusters' nodes. Such cloudy maps hinder the interpretation of the field's areas and interests. Therefore, it is critical to specify options that mitigate anomalies within the maps, like

selecting author keywords (representing the author's interests) instead of generating them from the abstract (Abstract Keywords). This study considers one main variation to this methodology, given the smaller sample size and the sparse nature of the field. The study will use citation analysis instead of co-authorship, as it provides a better indicator of study influence based on citing and cited studies. Co-authorship analysis has specific use cases where researchers from different entities collaborate to produce a scholarly work. Therefore, it neglects studies by one author and provides very little about those co-authored by researchers from the same organization.

2.1 Data Collection

The first stage involves collecting bibliometric data from the two databases using "Visual Quality," "Scenic Beauty," and "Landscape Visual Quality" terms in combination with the "Urban" term. This combination is used to harvest the most relevant studies, as many use one or more of these terms. Web of Science databases was selected among others for multiple advantages; first, for strict indexing of journals which eliminates predatory journals and not credible publications. Secondly, it exports search results in a friendly format for most bibliometric tools with the ability to select only relevant data fields. The use of filters was necessary to avoid confusion with other fields. For instance, the Image Visual Quality topic, mainly tackled by computer engineering and computer sciences, shares similar keywords to landscape visual quality. The search was also limited to journal articles, as from one side, they represent the de facto form in the urban studies, and the process they go through, including the peer review, makes them the most reliable medium in research, and the most attractive way of publishing for quick yet reliable knowledge accumulation. On the other side, journal articles provide a consistent format for bibliometric data, enabling equal comparisons between scholarly works. Moreover, they facilitate the analysis for geographical distribution for two items; first, the research conducted, thus identifying research gaps in regions of different nature. Second, the interested academic bodies, their geographical distribution, and their level of interest. Such analysis will highlight the need for academic bodies in nonactive regions to initiate collaboration with others.

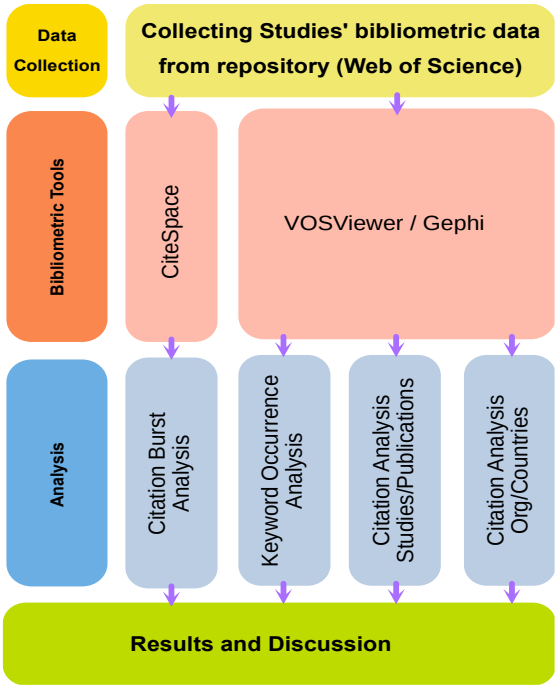


Fig. 1: Diagram of the proposed methodology (Source: Authors)

2.2 Process of Scientometric Analysis

The analysis considered for this study involves three distinct activities, as follows:

1. Keyword co-occurrence illustrates the most critical keywords in the field. It also groups them according to their co-occurrence in the same article. The proposed groups infer the different orientations of investigated studies. The main result of this analysis is the identification of the research clusters. Combined with the Centrality calculations, this analysis will also detect the most influential keywords within clusters. The analysis is mainly based on the incidence of two terms together. The weighted degree centrality metric is calculated based on the number and strength of links for each keyword with others. This metric allows for a more accurate ranking of the most important keywords.
2. Citation burst analysis traces the chronological emergence and decay of keywords in research. Using this technique, it reconstructs the prevalent patterns of the topic over its timespan and detects turning points of these patterns, which can be further linked with clusters mentioned earlier.
3. Study and journal citation analyses list the predominant academic journals with visual quality and scenic beauty as their primary journal aims. These journals are more likely to align the manuscripts they receive with their goals, and therefore, they form important resources for the visual quality body of knowledge.

2.3 Bibliometric Tools

The bibliometric analysis mentioned earlier can be conducted with the help of few tools; each with specific functions and configurations as follows:

1. VOSViewer for keyword co-occurrence and citation analyses. The main output of the tool is the network maps that express how far the nodes (keywords, authors, journals, countries) are central to the field or a cluster, based on links (lines) moving out to nodes of cited works or moving in from the citing ones. VOSViewer clustering for studies and keywords is based on their citation and co-occurrence. The software suggests several clusters according to a reasonable minimum number of nodes per cluster input.
2. Gephi for centrality calculations and network mapping. The tool uses maps exported by VOSViewer to conduct statistical calculations, including degree centrality and clustering coefficients.
3. CiteSpace for the citation burst analysis. While, VOSViewer provides the average publish year of each node in its overlay network maps, CiteSpace’s citation burst analysis generates more informative indicators for the calculated start year and end year for each keyword representing not only the time a keyword became popular in the field but also for how long, and when such keyword started to disappear and replaced by other terms for newer paradigms, interests, methods, and technologies.

3 Results and Discussion

The analysis discussed earlier reveals a few interesting results for the visual quality assessment field. One of the primary outcomes is the capabilities we have explored in the used methodology that could also be extended to other fields as needed. For visual quality analysis in specific, the following results were found.

3.1 Keyword Co-occurrence and Citation Burst Analyses

Keyword occurrence analysis has confirmed the history of the field paradigms discussed earlier. Using this, five clusters were thus generated with a few main keywords describing the interests of each cluster of the studies (Figure 2). The first considers the classical approach for assessing natural landscapes and the impact of changes proposed by landscapers. Checking their weighted centrality, the main keywords of this cluster are found to be scenic beauty, landscape change, landscape management, landscape planning, landscape perception, and forest management.

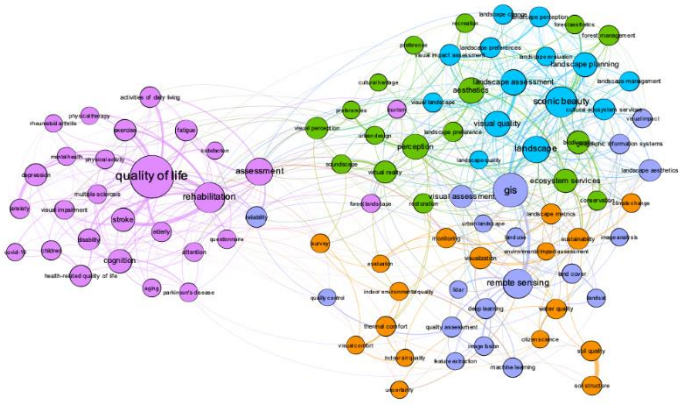


Fig: 2: Network map for Keyword Co-occurrence analysis

Table 1: Keyword Citation Burst Analysis

Keywords	Begin	End	77 - 2022
Recreation value	1993	1995	
Forest aesthetics	1994	2004	
Ecosystem management	1996	2004	
Scenic beauty	2004	2005	
Aesthetic assessment	2008	2009	
Forest management	2009	2011	
Visual assessment	2009	2010	
Visual impact	2011	2016	
Landscape planning	2011	2012	
Visual perception	2012	2014	
Principal component analysis	2012	2018	
Soil quality	2013	2014	
Visual impact assessment	2013	2016	
Cultural ecosystem service	2015	2019	
Landscape perception	2015	2018	
Landscape metrics	2016	2017	
Outdoor recreation	2017	2018	
Acoustic comfort	2017	2019	
Parkinson's disease	2017	2020	
Protected area	2018	2020	
Sustainable development	2018	2020	
Virtual reality	2018	2022	
Thermal comfort	2018	2022	
Public perception	2018	2020	
Ecosystem service	2019	2022	
Visual quality	2019	2020	
Rural area	2019	2022	
Machine learning	2020	2022	
Visual comfort	2020	2022	
Climate change	2020	2022	
Urban design	2020	2022	
Landscape management	2020	2022	
Landscape quality	2020	2022	
Landscape aesthetics	2020	2022	
Indoor air quality	2020	2022	

The research in these clusters is elaborated in the following sections. Compared with other keywords in burst analysis (Table 1), Scenic Beauty, Forest Management, and Forest Aesthetics represent this cluster's classical nature. Landscape terms, however, are prevalent in recent research. In other words, this cluster

represents professionals and authorities with landscaping and forest management backgrounds. It answers their needs for streamlined assessments of landscape decisions, obtaining or issuing the needed permits, and aligning efforts with the legal frameworks for natural resource preservation.

The second cluster represents studies that tackle visual quality assessment as one of the ecosystem services, side by side with the ecological and biodiversity assessments of the land. The cluster's keywords include Ecosystem Services, Biodiversity, Conservation, Restoration, Forest Management, and Aesthetics. The burst analysis failed to assess most of the cluster's keywords. However, it indicates an early presence of ecology-related keywords. The third cluster is associated with the psychological and medical applications of the field, as suggested by its keywords. Quality of Life is the most central term of the cluster, with keywords Cognition, Depression, Mental Health, Rehabilitation, and Attention supporting it. The attention restoration theory is present in this cluster's keywords in addition to medical terms like fatigue and Parkinson's disease. Although the study of psychological aspects began early in the field, the field recently witnessed intensive attention from medical studies. This cluster has extended the subjective approach for scenic beauty evaluations (evaluations built directly on user perception) to more psychological concepts such as Mental Health, Attention, Rehabilitation, and Experience.

The fourth cluster considers the use of relatively new technologies and tools in assessing the landscape visual quality, combining objective and subjective lines of thought as suggested by (Daniel, 2001). With GIS and Remote sensing being the most central in the cluster, other terms for technologies like LiDar, machine and deep learning, and Landsat shape the cluster interests. The preceding technologies used for objective assessments, like VMS, were limited to a few physical and topographical attributes. For instance, landscape character contained only three classes which, when combined with the other three sensitivity levels, can provide several scenarios and decisions made accordingly. The proposed assessments lacked numerical insights and were limited to very few choices for the level of human interventions (preservation, retention, and modification). Newer technologies like GIS, LiDAR, remote sensing, and spatial data management secure more numerical data, whether objective-based such as the site characteristics and components, or subjective-based, like user ranking and preference, allowing endless statistical applications like regression and PCA, and facilitating extensive integration with other modern technologies like deep learning, artificial and convolutional neural networks and virtual reality. Moreover, these technologies have been implemented in a wide range of geography-related sciences, including climatology, agriculture, regional and urban planning, and environmental studies.

The keywords of the fifth cluster indicate the proposed link between the sustainability of the built environment and the visual quality. Sustainability, climate change, soil and water quality, thermal comfort, and indoor environment quality shape the cluster's structure. The quality of views and daylight in buildings is an essential criterion in most green building rating systems. Although there is no direct relationship between most of the cluster's keywords and the visual quality, they generally represent qualities of adequate construction.

In summary, the five clusters are landscape and forest management, ecological, psychological and medical, technology-related, and sustainability-related. The clustering generated by VOSViwer does not suggest a stand-alone cluster for urban studies. Instead, nodes for urban subjects are fragmented between the last two clusters. The concentration of the field is still majorly limited by natural and rural scenery assessments. The same is noticed in studies discussed in the next part as well.

3.2 Citation Analysis – Studies and Journals

After conducting the weighted centrality analysis for the collected studies, it became obvious that most central articles (mostly cited) are quite old. Out of 26 articles with a weighted degree of centrality exceeding 15, only three were published in 2015 or after. Most of the 26 articles were published before 2010. Considering that, around 50% of the collected articles were published in 2017 or after; this indicator highlights the close-knit structure between new research works and traditional ones and the lack of breakthroughs in the field. This also indicates the need for a dedicated investigation of the most recent studies (in the last six years) to inform new research projects about the efforts done recently and to build upon them instead of starting anew or relying on old approaches, some of which became irreverent with the emergence of new methods, tools, and technologies.

The citation analysis for the studies shown in Figure 3 and Table 2, has resulted in 5 clusters in which the first has the highest share (52 out of 162 nodes) and includes the most central nodes. Studies in this cluster discuss the formal application of visual quality assessments to meet regulatory and legal requirements. The second cluster focuses on the influence of site ecology and user demography, and psychology on the landscape's visual quality. The third cluster is linked with assessing the scenic beauty at the forest level and the use of it as a tool for forest management. The fourth cluster of studies employs GIS and remote sensing tools in modeling land aesthetics. The use of GIS and spatial data management allows for large-scale implementation of scenic beauty metrics and facilitates shaping a more accurate understanding of the drivers influencing it in urban, rural, or natural settings. Finally, few studies in the fifth cluster discuss the change in agricultural lands for touristic purposes, especially for abandoned ones. In many European regions, the policies authorities considered for agricultural market liberalization and those related to ecological compensation caused the abandonment of agricultural lands at a massive scale. While this seems to be mainly pronounced in European countries, other pressures can be noticed in other regions where importing food is competitive to its production. The visual quality of abandoned agricultural lands received a great deal of research in this cluster.

In summary, the five clusters are professional-related, ecological/psychological, forest-level assessment, technological, and agricultural/touristic. Similar to keyword co-occurrence analysis, there is no specific concentration on the assessment of urban spaces' visual quality. Both analyses highlight the minimal interest in assessing urban public spaces compared with natural, agricultural, and rural ones. The dimensions discussed here are also psychological, medical, or technological. Urban spaces are fragmented under the hood of some of these dimensions, while most of the studies that discussed urban spaces are mostly recent.

Table 2: Studies clusters and central nodes (Source: Authors)

Study	Year	Cluster	Weighted Degree
Daniel	2001	1	42
Arriaza, et al.	2004	1	29
Dramstad, et al.	2006	1	26
Palmer & Hoffman	2001	1	25
Bulut & Yilmaz	2008	1	21
Yao, et al.	2012	1	21

Table 3: Journal clusters and central nodes (Source: Authors)

Journal	Cluster	Weighted Degree
Journal of environmental management	1	349
Forest science	1	190
Environmental monitoring and assessment	1	185
Ecological indicators	1	173
Landscape ecology	1	140
Soil & tillage research	1	124

Tveit	2009	1	20
Bulut & Yilmaz	2009	1	17
Zhao, et al.	2013	1	17
Wang & Zhao	2017	1	16
Meitner	2004	1	16
Hull & Stewart	1992	2	22
Gobster, et al.	2007	2	21
Daniel & Meitner	2001	2	19
Lindemann-Matthies, et al.	2010	2	19
Ode, et al.	2009	2	19
Svobodova, et al.	2012	2	17
Junge, et al.	2015	2	17
Brown & Daniel	1986	3	22
Ribe	2009	3	20
Schirpke, et al.	2016	4	17
Bishop & Hulse	1994	4	16
Hunziker & Kienast	1999	5	24
Schirpke, et al.	2013	5	20
de la Fuente de Val, et al.	2006	5	20
Schirpke, et al.	2019	5	16

Environment and behavior	1	113
Scandinavian journal of forest research	1	107
Soil use and management	1	81
Ecological engineering	1	78
Ecosystem services	1	57
Geoderma	1	54
Environmental management	1	51
Journal of forestry	1	51
Remote sensing	1	43
Sustainable cities and society	1	41
Applied geography	1	35
Renewable energy	1	31
Landscape and urban planning	2	1190
Urban forestry & urban greening	2	259
Journal of environmental psychology	2	217
Sustainability	2	216
Forests	2	209
Landscape research	2	164
Building and environment	2	102
Fresenius environmental bulletin	2	84
Journal of environmental engineering and landscape management	2	57
Water	2	54
International journal of environmental research and public health	2	48
Journal of the acoustical society of America	2	48
Applied acoustics	2	31

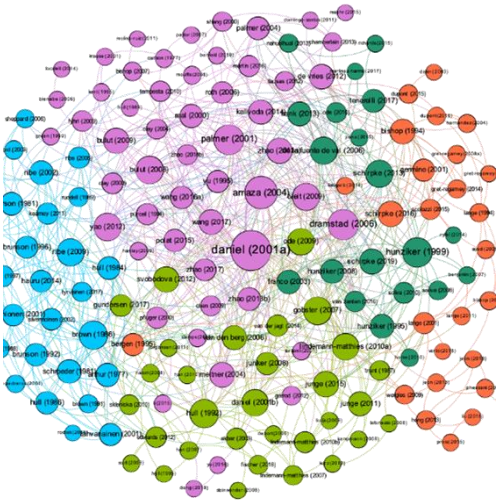


Fig 3: Network map for Studies Citation analysis

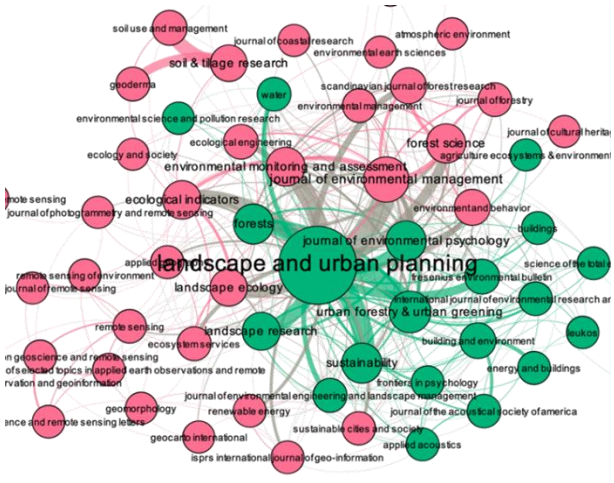


Fig. 4: Network map for Journal Citation analysis

Citation analysis for the journals shown in Figure 4 and Table 3, revealed the dominance of landscape and environmental studies in the field. Landscape and Urban planning journal is by far the most central journal when it comes to citation, followed by the Journal of environmental management and urban forestry and urban greening journal. Journal of environmental psychology came fourth, while most medical, remote sensing, artificial intelligence, and psychological journals had much lower centrality despite the rapid focus on the landscape visual impacts on human mental health and rehabilitation in the last few years and the new frontiers remote sensing and AI had brought to the topic. Similar to the studies' citation analysis, this can be connected with the reliance on old references, while recent studies have started to explore newer options for methods and technologies.

4 Conclusions

This study provided an overall understanding of the current status of visual quality assessment research using a dataset extracted from the Web of Science. The study has applied systematic bibliometric analyses on the extracted data and found a few patterns that govern the field's intellectual structure. Following are the conclusions:

1. The field has emphasized for long the assessment of rural and natural regions compared to urban areas. This emphasis is linked with the professional needs established by introducing new regulations for changes in the natural landscape.
2. The psychological dimension is evident in many studies and has been further extended to medical and demographical aspects. Together, they form a set of visual-quality applications.
3. The advent of new technologies has recently pushed the field in a new direction. Yet, these tools have endless capabilities to serve the topic, especially at the urban level, which comprises more dramatic views and more diversity in physical features.
4. Study citation analysis revealed the strong attachment of most studies to the earlier fundamental ones, despite the steep acceleration of published articles in the last few years. This invites us to review the recent efforts to shift this field to a new state that tackles the upcoming challenges, especially in the urban domain, similar to the shift witnessed in psychological and medical applications for the field.

Although Visual Quality research started early compared to other urban studies, it did not receive enough density until recently, particularly at the urban level. Therefore, the field needs more attempts to establish a set of methods and tools for public space assessment. This study has also presented a methodology for bibliometric analysis of the field that can be extended to others, or applied to the field's relationship with others, like computer sciences, medical or psychological studies. The study also met multiple challenges. Overlaps with other sciences using similar keywords for different applications were problematic and required deep filtration. For instance, image visual quality, intensely discussed by computer sciences, dominated the search results even though it has no direct relationship with landscape visual quality. Interpreting networks in the absence of a clear relationship between nodes, from another hand, is associated with some subjectivity. Some network maps include heterogeneous clusters with little cues to distinguish their common interests. Finally, using tools withdifferent algorithms caused some inconsistencies in the results. Citation burst analysis, for instance, generated the timelines of keywords different from those extracted by Keyword Co-occurrence analysis, which obstructed forming clear descriptions of the network.

References

Bacon, W. (1979). The Visual Management System of the Forest Service.. (pp. 660-665).

Bastian, M., Heymann, S. & Jacomy, M. (2009). Gephi: An Open Source Software for Exploring and Manipulating Networks. *Proceedings of the International AAAI Conference on Web and Social Media, 3*(1). doi:10.1609/icwsm.v3i1.13937

Celikors, E. & Wells, N. M. (2022). Are low-level visual features of scenes associated with perceived restorative qualities? *Journal of Environmental Psychology, 81*, 101800. doi:10.1016/j.jenvp.2022.101800

Daniel, T. C. (2001). Whither scenic beauty? Visual landscape quality assessment in the 21st century. *Landscape and Urban Planning, 54*(1-4). doi:10.1016/S0169-2046(01)00141-4

Daniel, T. C. & Boster, R. S. (1976). Measuring landscape esthetics: the scenic beauty estimation method. *USDA Forest Service Research Paper*.

Darko, et al. (2019, February). A scientometric analysis and visualization of global green building research. *Building and Environment, 149*, 501-511. doi:10.1016/j.buildenv.2018.12.059

Gobster, P. H. (1999). An Ecological Aesthetic for Forest Landscape Management. *Landscape Journal, 18*(1). doi:10.3368/lj.18.1.54

Hosseini, et al. (2018). Analysis of Citation Networks in Building Information Modeling Research. *Journal of Construction Engineering and Management, 144*(8). doi:10.1061/(asce)co.1943-7862.0001492

Kaplan, R. (1979). Visual Resources and the Public: An Empirical Approach. In *Proceedings of Our National Landscape Conference*. USDA Forest Service General Technical Report PSW-35. (pp. 209-2l6.)

Kaplan, S. (1995). The restorative benefits of nature: Toward an integrative framework. *Journal of Environmental Psychology, 15*(3). doi:10.1016/0272-4944(95)90001-2

Lothian, A. (1999). Landscape and the philosophy of aesthetics: Is landscape quality inherent in the landscape or in the eye of the beholder? *Landscape and Urban Planning, 44*(4). doi:10.1016/S0169-2046(99)00019-5

Ramos-Rodrígue, A. R., & Ruíz-Navarro, J. (2004). Changes in the intellectual structure of strategic management research: A bibliometric study of the Strategic Management Journal, 1980-2000. *Strategic Management Journal, 25*(10). doi:10.1002/smj.397

Santos, R., Costa, A. A. & Grilo, A. (2017, August). Bibliometric analysis and review of Building Information Modelling literature published between 2005 and 2015. *Automation in Construction, 80*, 118-136. doi:10.1016/j.autcon.2017.03.005

van Eck, N. J. & Waltman, L. (2010). Software survey: VOSviewer, a computer program for bibliometric mapping. *Scientometrics, 84*(2). doi:10.1007/s11192-009-0146-3

Cite as: Najjar M., Indraganti M. & Bayram G., "A Bibliometric Study of Visual Quality Research in the Context of Urban Open Spaces", *The 2nd International Conference on Civil Infrastructure and Construction (CIC 2023)*, Doha, Qatar, 5-8 February 2023, DOI: https://doi.org/10.29117/cic.2023.0121

Investigation of Indoor Thermal Perceptions and Comfort Temperature in Educational Spaces in Qatar

Madhavi Indraganti
Department of Architecture and Urban Planning, College of Engineering, Qatar University, Doha, Qatar
madhavi@qu.edu.qa

Abstract

We conducted thermal comfort field surveys in female educational spaces in Qatar in the autumn and winter of 2018 and 2020 – 21 and collected 324 datasets. They contained all the four environmental measurements and simultaneous thermal responses of female university students dressed in traditional Islamic clothing consisting of headgears and full-body cloaks (abayas) (mean clothing: 1.21 clo). Exacerbating the occupant discomfort, classrooms are overcooled/overheated in autumn/winter, respectively. About 89.9% respondents had no access to indoor temperature control and 43.5% had no access to any environmental controls. We evaluated the mean indoor comfort temperature as 22.9 (3.1) ˚C. In 64.2% cases, it did not conform to the comfort zone in international standards. We noted significant seasonal differences in indoor environments. Air speed was zero most of the time. Only 53.8% felt comfortable thermal sensations, and 66% accepted the environments, as against 80% in the international standards. The predicted mean vote (PMV) was significantly inaccurate up to three scale points and in 86.4% cases PMV mis-predicted by half a scale point or more. Therefore, framing the narrative around user-controlled air movement and indoor controls is necessary, so that indoor temperature can be effectively increased in autumn and lowered in winter.

Keywords: Adaptive comfort; Comfort temperature; Field study; Hot climates; Buildings

1 Introduction

Qatar is a gas rich country in the Arabian Gulf with highest per capita income and CO_2 emissions in the world (International Energy Agency (IEA), 2018); (The World Bank, 2019). Most public buildings are air-conditioned yearlong, often in disharmony with the outdoor conditions. Energy is heavily subsidized often served free to the government establishments. This often leads to energy wastage and excessive use of air-conditioning (AC). Recent studies in the Middle East have pointed out that the buildings are being over-cooled and heated much to the discomfort of the occupants (Elnaklah, et al., 2021) (Indraganti & Boussaa, 2018) (Alshaikh, et al., 2008). Qatar and the Gulf region are yet to have custom designed adaptive comfort standards (Global Sustainability Assessment System (GSAS), 2015). As a result, environmental engineers in the region propose prescriptions based on the predicted mean vote approach (PMV) (ISO, 2005). Internationally, many researchers demonstrated from field study results that the PMV greatly mis-predicted the actual sensation by as much as 60%, irrespective of the building type and mode of environmental control (Cheung, et al., 2019) (Humphreys & Nicol, 2002). Researchers pointed out that increasing the indoor set point in the Gulf region from 18˚C to 24 ˚C would potentially accrue 16 – 68% savings in Energy (Indraganti & Boussaa, 2018).There are no thermal comfort studies that reported the thermal comfort of occupants in the Middle Eastern classrooms. There are many studies on thermal comfort in naturally ventilated

classrooms and laboratories (Singh, et al., 2018), (Mishra & Ramgopal, 2015). Some reports also presented thermal comfort in air-conditioned university classrooms in Malaysia and Japan (Zaki, et al., 2017), Indonesia (Karyono, et al., 2015) and Ecuador (Guevara, et al., 2021). However, the climate, clothing, and cultural practices of people in the Middle East is quite different from these reports, which need to be studied for appropriate indoor environmental design. Therefore, this study has the following objectives: (a) to evaluate the thermal comfort temperature of the students in university learning spaces in autumn and winter seasons, (b) to compare the data with the related adaptive standards, and (c) to study the adaptative use of controls and limitations in using them.

2 Methodology

2.1 Survey Location and Buildings Surveyed

Qatar has hot humid desert climate (Bwh in Köppen climate classification). Doha (N25° 17', E51° 32') is its capital city and is 10 m above the mean sea level. The survey was conducted in autumn and winter seasons in Qatar University (QU), Doha, which is 2 km from the Gulf Shore. The surveys were conducted in three Women's college buildings named B1, B2 and B3 in two phases: November 8 – 30, 2018 (N= 165) and October 3, 2020 – February 15, 2021 (N = 159), avoiding the periods of examinations and vacations. The SARS-COV-19 pandemic after March 2020 affected the data collection. Overall, we invested 33 days in the surveys. The learning areas (Fig. **1**) in these buildings are randomly selected for field survey (Table 1).

Table 1: Details of the buildings surveyed

Building, N, age	Nature of Learning Space Surveyed	Survey Periods	Glazing/ Operable Windows/ Thermostats
B1, 276, 15 years	Lecture hall, computer classroom, architecture design studio, study hall	Nov 8, 2018 - Nov 30, 2018 (9 days), Oct 3, 2020 - Nov 10, 2020 (8 days), Jan 31, 2021- Feb 15, 2021 (7 days)	Fixed glazing; Operable windows in two ground floor studios; Wall mounted, but dysfunctional
B2, 18, 35 years	Lecture hall, computer classroom	Oct 6, 2020 - Oct 21, 2020 (6 days)	Fixed glazing: Wall mounted, but dysfunctional
B3, 30, 15 years	Lecture hall	Oct 24, 2020 - Oct 26, 2020 (3 days)	Fixed glazing: Wall mounted

2.2 Data Collection

This was a *right-now-right here* transverse survey. We collected occupant responses through a thermal and indoor environmental quality (IEQ) questionnaire survey through Google Forms and measured the indoor environment simultaneously as the subjects responded. The instrument tripod and the set-up used in the surveys are shown in Fig. **1** and Table 2. After setting up the instrument tripod close to a group of 5-10 subjects. We measured indoor air temperature (T_a), indoor globe temperature (T_g), and relative humidity (RH) in all the surveys. In addition, in 2020-21 we measured air velocity (V_a), CO_2 concentration also in all the surveys at a 5-minute interval. All the measurements are done with sensors at 1.1 m from the finished floor level. We obtained the outdoor daily mean temperature (T_o) from a meteorological website (Anon., 2021).

Table 2: Details of the dataloggers and sensors used in the surveys

Survey Period (sample size)	Description	Trade Name/ Manufacturer	Parameter Measured	Range	Accuracy
Nov 8, 2018 - 30 Nov 2018 (165)	Thermo-hygro data logger with probe thermometer with black painted table tennis ball	U12-013 (Temp/RH/2 Ext) with TMC1-HD/ Onset, Hobo, USA	Air temperature	0 to 50 °C	±0.35 °C (0° to 50°C)
			Humidity	5 to 90% RH	±2.5% (10 to 90%)
			Globe temperature	0 to 50 °C	±0.35 °C (0° to 50°C)
Oct 3, 2020 - Nov 10, 2020 (113)	Testo 400 IAQ and comfort kit with tripod Testo, Germany	IAQ probe with Bluetooth (0632 1551)	Air temperature	(- 60 to 155 °C)	±0.5 °C (0° to 50°C)
			Humidity	5 to 95% RH	±3% (10 to 35%) ±2% (35 to 65%) ±3% (65 to 90%)
Jan 31, 2021 - Feb 15, 2021 (46)			CO_2 Concentration	0-10,000 ppm	± 50 ppm (0 to 5,000 ppm)
		Globe thermometer Ø 150 mm (0602 0743)	Globe temperature	0 to +120 °C	Class 1. ±0.5 °C
		Omni directional turbulence probe, (0628 0152)	Air velocity	0 to +5 m/s	± 0.03 m/s (0 to 5 m/s)



Fig. 1: Instrument set-up and the surveys in progress in lecture halls, studios and computer classrooms

2.3 Thermal Questionnaire and Respondents

The participants in the survey are acclimatized students and teaching staff engaged with the surveyed space for over 15 minutes prior to the survey. Being a public university, the undergraduate campuses are gender-segregated and this research is conducted primarily in the women's campus. Therefore, we collected 96% data from females. The questionnaire survey included three age group options, viz., 18-30, 30-50 and above 50 years. The questionnaire was prepared in English and translated to Arabic, broadly following thermal satisfaction surveys of ASHRAE Standard-55 and other researchers (ASHRAE, 2020); (Huizenga, et al., 2006). We used ASHRAE 7-point scale for evaluating the thermal sensation (TSV). Satisfaction for various indoor environmental quality parameters were measured on 7-point scales based on the research of de Dear et al. (1997); Huizenga et al. (2006) and (Indraganti & Boussaa, 2018). The Internal Review Board (IRB) at QU approved them for ethical compliance (Permission number: QU IRB 1226-E/20). The questionnaire had three segments: (1) personal identifiers such as age group, building number, type of the surveyed space, and the period of engagement with the space prior to the survey, (2) questions on thermal comfort and environmental satisfaction and access to the environmental controls and (3) checklists for various pieces of garments, and list of activities. The surveyors made field notes about

the indoor environmental controls in use within the surveyed space, while the survey/measurement was going on. We collected a total of 324 valid responses overall.

3 Results and Discussion

3.1 Clothing Insulation, Metabolic Rates, Outdoor and Indoor Conditions

We estimated the clothing insulation (I_{cl}) values for Western and non-Western ensembles using standard checklists and earlier reports (ASHRAE, 2020); (ISO, 2005); (Indraganti, et al., 2015); (Havenith, et al., 2015) and (Al-ajmi, et al., 2008). Subjects in non-Western ensembles had significantly higher clothing insulation with a large effect size (mean of Western ensembles = 0.67 (0.11) clo, mean of non-Western ensembles = 1.21 (0.13) clo, t(322) = -24.41; p <0.001, eta squared = 0.65). It was noted that student subjects in the 18-30 years age group had higher I_{cl} values. In response to a direct question on satisfaction with their dress choice, 92% said they are satisfied with their choice of dress and 32.7% cited convenience was the reason behind their choice. Results show that 84.9% subjects were in non-Western clothing, which consisted of *abaya*, *hijab*, full length skirts, Punjabi scarves, *salwar-kameez* etc. This is much higher than 16% subjects in non-Western clothing as noted in an office building study in Qatar (Indraganti & Boussaa, 2018). We estimated the metabolic rates using the values in (ISO, 2005).

During the survey period the outdoor daily mean temperature varied from 19.3 – 34.3 °C while relative humidity also varied widely between 34 – 76% with 26.3 (3.5) °C and 63.3 (9.7)% as the mean values, respectively. High temperature coupled with moderate to high humidity causes perspiration and discomfort in September and October. Outdoor discomfort eases as the temperatures plummet in November to February while the humidity remains high, for Doha is a coastal place in the Arabian desert. Humphreys et al. (2016) suggested exponentially weighted running mean temperature as a superior predictor for indoor conditions. Therefore, we estimated the running mean temperature (T_{rm}) taking 0.8 for α indicating a half-life of 3.5 days. In this survey the range in running mean temperature was 19.6 – 34.4 °C while the mean was 27.4 (3.4) °C.

Table 3: Descriptive statistics of outdoor and indoor environmental variables

Season	N	Outdoor Daily Mean Temperature (°C)	Air Temperature (°C)	Globe Temperature (°C)	Mean Radiant Temperature (°C)	Operative Temperature (°C)	Air Velocity (m/s)	Relative Humidity (%)
Winter	48	19.6 (0.2)	24.3 (1.3)	24.3 (1.2)	24.3 (1.2)	24.3 (1.3)	0.01 (0.01)	48.5 (2)
Autumn	278	27.4 (2.3)	22.1 (1.1)	21.9 (1.5)	21.8 (1.5)	22 (1.3)	0 (0)	58 (6.6)
All	324	26.3 (3.5)	22.4 (1.4)	22.2 (1.7)	22.2 (1.7)	22.3 (1.5)	0 (0)	56.7 (7)

Comparatively, the indoor thermal conditions were less variable as the buildings were centrally air-conditioned throughout. We noted about 8 K variation in indoor air temperature through the survey period. However, independent t-test revealed significant seasonal differences in the means of all the indoor environmental parameters ($p < 0.05$). For example, there was a significant difference in To recorded in autumn (mean (standard deviation (s.d.)) = 21.9 (1.3) °C) and winter (mean (s.d.) = 24.3 (1.2) °C; t (322) = -11.771, $p < 0.001$ (two-tailed)). The magnitude of the differences (effect size) in the means (mean difference = 2.4 K 95% CI: -2.775 to -1.962) was very large (eta squared = 0.301) (Pallant, 2011). There were negligible inter-building differences in the thermal indices. All the four thermal indices viz. air, globe, mean radiant and operative temperatures correlated strongly with each

other ($p < 0.001$), and their mean values were also very similar (i.e., < 0.2 K difference). It means that any of these indices can be used in the analysis. Therefore, to compare the results with the literature and triangulation with the international standards we propose to use operative temperature (Zaki, et al., 2017), (ASHRAE, 2020), (European Committee for Standardization, 2019). Near still air conditions prevailed throughout the survey, with air velocity averaging at 0.0 m/s on all data. Of the 159 samples with V_a records, only in 27% cases, we had V_a >= 0.01 m/s. It indicates that there is much scope for increasing the air speeds.

3.2 Subjective Thermal Responses

Overall, the mean thermal sensation is found to be -0.29 (1.73), indicating subjects voting on the cooler side of the 7-point sensation scale (Fig. **2**). Importantly, only 23.5% and 48.8% subjects voted neutral and within the central three categories of the sensation scale, respectively.

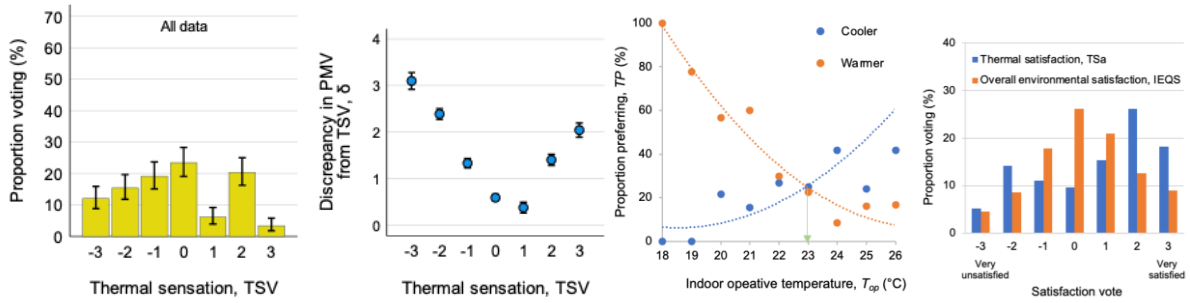


Fig. 2: Histogram of TSV; mean discrepancy in PMV from TSV (δ) varying with TSV; Proportion of subjects wanting cooler and warmer environments at various Top bins; Proportion voting on thermal satisfaction (TSa) and overall environmental satisfaction scales (IEQS); Error bars indicate 95% CI

Moreover, 46.6% and 27.5% subjects voted on the cooler side of sensation and on the cooler side of discomfort (TSV < -1), respectively, while 23.8% voted on the warmer side of discomfort (TSV > 1). This result clearly indicates that most subjects were feeling uncomfortable (mostly cold) sensations. Zaki et al. (2017) made a similar observation about air-conditioned classrooms in Malaysia and Japan. Mean thermal sensation vote varied significantly with season (autumn (mean (s.d.) = -0.55 (1.64)) and winter (mean (s.d.) = 1.26 (1.42); t (322) = -7.806, $p < 0.001$ (two-tailed)). The magnitude of differences in the mean was large (1.81) with large effect size (eta squared = 0.16). That most subjects felt uncomfortably warmer sensations in winter, colder sensations in autumn suggests that there was overheating in winter and overcooling in autumn. Thermal preference (TP) correlated very strongly with thermal sensation ($r = -0.729$, $p < 0.001$) and TP averaged at 0.11(0.76), indicating a preference for warmer environments on the whole (Table 4). Only 41% subjects preferred no change in their thermal conditions while as much as 34.2% subjects preferred warmer/cooler than the ambient conditions, even while voting neutral on TSV. We also noted similar significant seasonal variations in TP (mean difference = 0.56, $t(322) = 6.6$, $p < 0.001$, eta squared = 0.12), as was noted in TSV, implying overcooling/overheating in autumn/winter.

3.3 Evaluation of Predicted Mean Vote (PMV) and Predicted Percent Dissatisfied (PPD)

The mean PMV was 0.45 and PPD was 13.9%. In response to a direct question on thermal acceptability (TA), 33.6% subjects voted the environments unacceptable. It can be observed that PMV failed to accurately capture the actual thermal sensation in 86.4% cases, where |PMV – TSV| > 0.5. It can be noted in Fig. **2** that the discrepancy (δ) in PMV from TSV is significantly higher at all

scale points of TSV, by as much as 3 scale points towards the cold sensation. This finding is very important in the context of the Middle East where, PMV is used to evaluate the indoor environmental design. Hence, misprediction of such high proportions jeopardizes the accuracy of thermal comfort design, leading to intense discomfort to occupants. In response to a direct question on thermal satisfaction, 59.8% subjects considered the thermal environment satisfactory, while 42.7% subjects felt the same for the overall indoor environmental quality, even though the subjects felt the environments overcooled autumn and overheated in winter. The descriptive statistics of subjective thermal variables is presented in Table 4.

Table 4: Descriptive statistics (mean and standard deviation) of subjective thermal variables (Values in bold indicate significant seasonal difference at $p < 0.001$ with a large effect size)

Data (N)	TSV	PMV	TP	TA (%)	PPD (%)	TSa	IEQS
All (324)	-0.29 (1.73)	0.45 (0.46)	0.11 (0.76)	33.64 (47.3)	13.92 (9.52)	0.67 (1.88)	0.24 (1.55)
Autumn (278)	**-0.55 (1.64)**	**0.39 (0.45)**	**0.19 (0.76)**	34.5 (47.6)	**12.7 (8.65)**	0.62 (1.88)	0.23 (1.55)
Winter (46)	**1.26 (1.42)**	**0.8 (0.36)**	**-0.37 (0.48)**	28.3 (45.5)	**21.3 (11.17)**	1.02 (1.88)	0.33 (1.56)

3.4 Evaluation of Neutral Temperature by Linear Regression

Linear regression of indoor temperature with thermal sensation is regarded a simple method to estimate the neutral temperature. In this study we linearly regressed indoor operative temperature with measured TSV and PMV estimated from the indoor environmental and personal variables to evaluate the neutral temperature (Figure 3). We obtained 0.513 /K ($p < 0.001$) as the sensitivity of TSV which is the same as 0.51 /K reported from AC buildings of two large ASHRAE and European databases (Humphreys, et al., 2016). Our result is also comparable to 0.424 /K, the slope obtained in AC classrooms in Japan, but higher than 0.216 /K, the slope obtained in AC offices Qatar (Zaki, et al., 2017); (Indraganti & Boussaa, 2018). This returned a rate of change in sensation vote of 1.9 °C and neutral temperature of 22.9 °C, which matched closely with the preferred temperature of 23 °C obtained from thermal preference vote as shown in Fig. 2. This is about 1.9 K lower than the neutral temperature obtained in an office study in Doha (Indraganti & Boussaa, 2018). Further, we obtained 0.170 /K ($p < 0.001$) as the slope with PMV and corresponding a neutral temperature of 19.1 °C. It appears that the subjects in learning spaces in Qatar were more sensitive to ambient temperature changes, which the PMV index failed to capture.

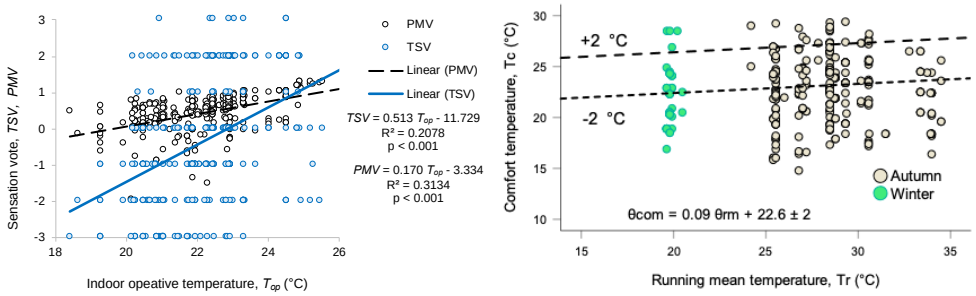


Fig. 3: (Left) Linear regression of indoor operative temperature with TSV and PMV, (right) Comfort data from the current study superimposed over the adaptive model suggested in the Chartered Institute of Building Services Engineers (CIBSE) Guide. Comfort temperature (Θ_{com}), daily outdoor running mean temperature (Θ_{rm})

3.5 Griffiths Method to Estimate the Comfort Temperature (T_c)

We used Griffith's method to estimate the comfort temperature (Griffiths, 1990). We tested the data with three Griffiths coefficients (α) 0.25, 0.33 and 0.5 as suggested in the literature (Rijal, et al., 2013); (Rijal, et al., 2017); (Humphreys, 2013). We noted that α at 0.5 returned the most reliable and consistent estimate of comfort temperature overall, when the data were split in two seasons. With smaller values of α, the variability in comfort temperature is much wider, often resulting in unreliable values of T_c. Therefore, we use 0.5 for α as Humphreys et al. (2016) suggested, similar to others (Zaki, et al., 2017); (Singh, et al., 2018).

The comfort temperature in winter is about 1.3 K lower than in autumn (23 °C) (95% CI). The mean comfort temperature overall was found to be 22.9 ± 3.1 °C. This value is identical with the (a) regression neutral temperature (22.9 °C), (b) comfort temperature of 23 °C, with the highest probability of expressing comfort (b) and comfort temperature 23 °C, obtained by intersecting the regression lines of thermal preference for warmer and cooler environments (Fig. **2**). Further, our result is slightly lower than the comfort temperature (24.0 ± 2.6 °C) reported through a yearlong study in offices in Qatar, where 64.1% of the respondents were men (Indraganti & Boussaa, 2018).

It is important to note that the current comfort temperature in classrooms in Qatar is 3-4 K less than the comfort temperatures in AC classrooms in Ecuador (25.4 – 26.4 °C) (Guevara, et al., 2021), Malaysia (25.2 °C) and Japan (26.2 °C) (Zaki, et al., 2017), where air speeds were effectively higher than Qatar. Increasing air movement in autumn allows higher indoor temperatures and reduces cold discomfort votes. Significantly, Taiwan (25.6 °C) (Hwang, et al., 2006), Indonesia (24.9 °C) (Karyono, et al., 2015) achieved higher comfort temperature by increasing air speed. Notably, cross-tabulation revealed that cold discomfort (TSV < = -2) increased thermal and IEQ dissatisfaction by 20%. Similarly overheating in winter when the subjects were dressed in warmer clothes also caused higher dissatisfaction. Overheating and overcooling were perhaps the two main reasons why thermal sensation satisfaction (TSa) was not even 50%, as against the 80% in standards (ASHRAE, 2020).

3.6 Evidence of Adaption and Lack of Adaptive Opportunities

Humphreys et al. (2016) define adaptive thermal comfort as "If a change occurs such as to produce discomfort, people react in ways which tend to restore their comfort." If adaptation is restrained, people express dissatisfaction. Fig. **4** (a) Fig. **4** (b) show the proportion of subjects voting dissatisfied on the 7-point equal interval thermal satisfaction scale (TSa) and the corresponding proportion of sensation of thermal drift felt in the environment. Results show that thermally dissatisfied subjects (30.6%) were most often feeling the environment cold (65%). While most of the spaces investigated had no operable windows (< 8%), only 11.1% occupants said that they have the ability to change the temperature in their room. Fig. **4** (c) shows the controls voted to have been adjusted around the time of the survey. It is important to note that most of the subjects were feeling handicapped with their ability to have access to temperature control (89.9%) and 43.5% subjects have not accessed any of the suggested controls. The following open-ended response on the thermal satisfaction and the feeling of thermal drift aptly summarizes the current overcooling situation and the ensuing discomfort to students in autumn: "la astadee'a tahamol alboruda ashar bala'eya wa alsabab shidat alboruda, لا أستطيع تحمل البرودة، أشعر بالإعياء والسبب شدة البرودة (I can't handle the cold. I feel tired/unconscious and the reason is the extreme cold)."

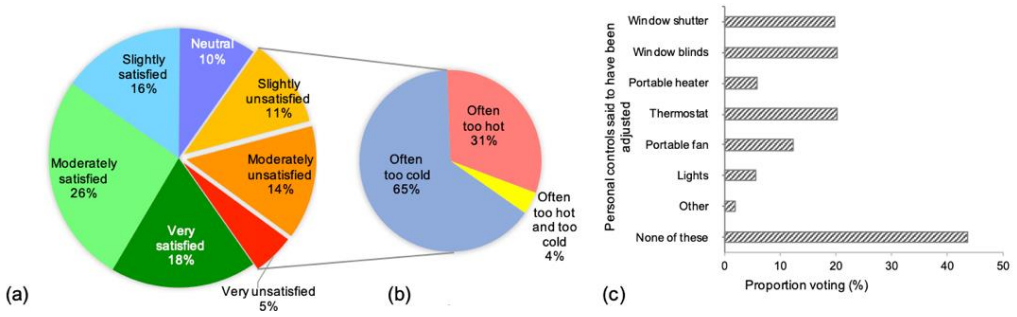


Fig. 4: (a) Proportion of voting thermal dissatisfaction (N: 324); **(b)** Proportion of sensation of thermal drift (N: 99); **(c)** Proportion of various controls said to have been adjusted

4 Conclusions

A thermal comfort and environmental quality evaluation (IEQ) survey was conducted in autumn and winter seasons in higher education learning environments in Qatar. Indoor temperatures were low compared to international surveys (mean T_{op} was 22.4 ˚C). Significant seasonal differences were noted in indoor and outdoor temperatures and we found overcooling in autumn and overheating in winter seasons with near still air conditions overall. This resulted in cooling/heating discomfort in these two seasons, respectively. As a result, maximum proportion voting comfortable was found to be only 53.8% as against the 80% suggested value in international standards. Thermal acceptability was only 66%. Fanger's PMV was inaccurate up to three sensation points. Moreover, in as much as 86.4% cases it mispredicted by half a scale point or more. Mean indoor comfort temperature was found to be 22.9 ˚C, which is about 3- 4 K lower than classrooms in Japan, Malaysia and Asia. The comfort data were juxtaposed with the international standards and 64.2% cases are outside the ± 2 K limits for the comfort zone suggested in the CIBSE Guide, the majority of which fell below the lower limit of the international standard. Most subjects (89.9%) said they have no access to control the indoor temperature. Overall, 30% felt thermal dissatisfaction and 65% of the dissatisfied felt the environments were often cold and 31% felt them too hot often. Less than 8% data were recorded with spaces with operable windows. Overall, 43.5% felt they have no access to any of the indoor environmental controls such as thermostats, windows and blinds.

These findings call for greater opportunities for personal control, increased air movement and corresponding elevation in indoor temperatures in autumn. It would not only improve user satisfaction but would also save energy. Further, it is necessary to frame the narrative around the use of operable controls in learning environments in Qatar, rather than simply overcooling/overheating them full throttle, exacerbating the occupant dissatisfaction.

Acknowledgments

We thank all the participants and the funding agencies: Qatar National Research Fund and Qatar University (Grant: UREP25-040-2-018 and Grant: QUST-2-CENG-2018-8).

References

Al-ajmi, et al. (2008). Thermal insulation and clothing area factors of typical Arabian Gulf clothing ensembles for males and females: Measurements using thermal manikins. *Applied Ergonomics*, p. 39 (2008) 407–414.

Alshaikh, A., Roaf, S. & Smith, R. (2008). *What is the relationship betwen humidity and comfort at high temperatures? In search of new ways of looking at the issue.* s.l., s.n.

Anon., (2021). *Weather Underground.* https://www.wunderground.com/weather/qa/doha [Accessed 23/6/2021].

ASHRAE. (2020). *ANSI/ ASHRAE Standard 55-2020 Thermal environmental conditions for human occupancy,* Atlanta: ASHRAE.

Cheung, et al. (2019). Analysis of the accuracy on PMV – PPD model using the ASHRAE Global Thermal Comfort Database II. *Building and Environment,* Volume 153, pp. 205-217.

CIBSE. (2015). *CIBSE Guide A: Environmental Design,* London: The Chartered Institution of Building Services Engineers .

de Dear, J. R., Brager, S. G. & Cooper, D. (1997). *Developing an Adaptive Model of Thermal Comfort and Preference (ASHRAE RP- 884),* Sydney, NSW 2109 Australia: Macquarie Research Ltd., Macquarie University, Sydney, NSW 2109 AUSTRALIA and Center for Environmental Desi.

Elnaklah, et al. (2021). Thermal comfort standards in the Middle East: Current and future challenges. May, p. 107899.

European Committee for Standardization, 2019. *EN 16798-1:2019 Energy performance of buildings - Ventilation for buildings - Part 1: Indoor environmental input parameters for design and assessment of energy performance of buildings addressing indoor air quality, thermal environment, lighting and acous,* Brussels: European Committee for Standardization.

Global Sustainability Assessment System (GSAS). (2015). *GSAS Building Typologies: Design Guidelines 2015 - v2.1,* Doha: Gulf Organization for Research and Development.

Griffiths, I. D. (1990). *Thermal Comfort in Buildings with Passive Solar Features: Field Studies ,* s.l.: s.n.

Guevara, G., Soriano, G. & Mino-Rodriguez, I. (2021). Thermal comfort in university classrooms: An experimental study in the tropics. *Building and Environment,* Volume 187, p. 107430.

Havenith, G. et al. (2015). A Database of Static Clothing Thermal Insulation and Vapor Permeability Values of Non-Western Ensembles for Use in ASHRAE Standard 55, ISO 7730, and ISO 9920. *ASHRAE Transactions, 121*(1), pp. 197-215.

Huizenga, C. et al. (2006). Air Quality and Thermal Comfort in Office Buildings: Results of a Large Indoor Environmental Quality Survey. *Proceedings of Healthy Buildings,* Volume III, pp. 393-397.

Humphreys, M. A. & Nicol, J. F. (2002). The validity of ISO-PMV for predicting comfort votes in every-day thermal environments. *Energy and Buildings ,* Volume 34, pp. 667-684.

Humphreys, M. A., Rijal. H. B. & Nicol. J. F. (2013). Updating the adaptive relation between climate and comfort indoors; new insights and an extended database. *Building and Environment,* Volume 63, pp. 40-55.

Humphreys, M., Nicol, F. & Roaf, S. (2016). *Adaptive thermal comfort, Foundations and Analysis.* Oxon: Routledge.

Hwang, R. L., Lin, T. P. & Kuo, N. J. (2006). Field experiments on thermal comfort in campus classrooms in Taiwan. *Energy and Buildings,* Volume 38, pp. 53–62.

Indraganti, M. & Boussaa, D. (2018). An adaptive relationship of thermal comfort for the Gulf Cooperation Council (GCC) Countries: The case of offices in Qatar. *Energy and Buildings,* Vol. 159, pp. 201–212.

Indraganti, M., Lee, J. & Zhang, H. A. E. A. (2015). Thermal adaptation and insulation opportunities provided by different drapes of Indian saris. *Architectural Science Review, 58*(1), pp. 87–92.

International Energy Agency (IEA). (2018). [Online] Available at: http://energyatlas.iea.org/#!/profile/WORLD/QAT

ISO. (2005). *ISO 7730:2005(E) Ergonomics of the thermal environment — Analytical determination and interpretation of thermal comfort using calculation of the PMV and PPD indices and local thermal comfort criteria ,* Switzerland: ISO.

Karyono, T. H., Heryanto, S. & Faridah, I. (2015). Air conditioning and the neutral temperature of the Indonesian university students. *Architectural Science Review, 58*(2), pp. 174-183.

Mishra, A. K. & Ramgopal, M. (2015). A thermal comfort field study of naturally ventilated classrooms in Kharagpur, India. *Building and Environment,* Vol. 92, pp. 396-406.

Pallant, J. (2011). *SPSS Survival manual: A step by step guide to data analysis using the SPSS program. 4th Edition.* Berkshire, England: Open University Press McGraw-Hill Education.

Rijal, H. B., Honjo, M., Kobayashi & T, N. (2013). Investigation of comfort temperature, adaptive model and the window-opening behaviour in Japanese houses. *Architectural Science Review,* Vol. 56, pp. 54-69.

Rijal, H. B., Humphreys, M. A. & Nicol, J. F. (2017). Towards an adaptive model for thermal comfort in Japanese offices. *Building Research & Information,* Issue Rethinking on Comfort, pp. 1-13.

Singh, et al. (2018). Status of thermal comfort in naturally ventilated classrooms during the summer season in the composite climate of India. *Building and Environment,* pp. 287-304.

The World Bank. (2019). *The World Bank.* https://data.worldbank.org/country/qatar?view=chart [Accessed 24/5/2021].

Zaki, et al. (2017). Adaptive thermal comfort in university classrooms in Malaysia and Japan. *Building and Environment,* Vol. 122, pp. 294-306.

Cite as: Indraganti M., "Investigation of Indoor Thermal Perceptions and Comfort Temperature in Educational Spaces in Qatar", *The 2nd International Conference on Civil Infrastructure and Construction (CIC 2023)*, Doha, Qatar, 5-8 February 2023, DOI: https://doi.org/10.29117/cic.2023.0122

The Use of Newly Developed Public Transportation System in Relation to People's Thermal Perception of Outdoor Climate

Deema Alattar
Department of Architecture and Urban Planning, College of Engineering, Qatar University, Doha, Qatar
da0801752@student.qu.edu.qa

Abstract

In the past decade, Doha the capital city of Qatar has witnessed a massive shift in various fields including economy, education, and sports sector. This flux caused rapid population growth, and as a result have led to an increase in the number of private cars in the city, leading to significant traffic congestion. The Transport Master Plan for Qatar (TMPQ) 2006-2026 included the introduction of a metro and rail system aiming to (1) solve the problem of traffic congestion, (2) meet the goals of Qatar National Vision (QNV) 2030, (3) and successfully sponsor the recently held FIFA World Cup 2022. Most of the people in Qatar have private cars, which they generally consider necessary for door-to-door trips. In addition, the existing public transportation system is mostly used by the lower class. Therefore, in order to develop a successful public transportation system, it is crucial to examine people's thermal perception of outdoor spaces, particularly in terms of microclimate, and people's adaptive actions in response to Qatar's hot humid climate. In this research paper, the thermal comfort issue was explored by considering both, subjective and objective parameters. The outcomes of the research reveal that people are largely able to adapt successfully to the heat through behavioural adaptation, which improves people's thermal tolerance to the outdoor climate in Qatar. However, the findings indicate that people's thermal comfort could be further enhanced through minor modifications to the outdoor environment including a high Height/Width ratio, provision of vegetation, and shading street furniture.

Keywords: Outdoor thermal comfort; Behavioural adaptation; Hot-arid climate; Public transportation

1 Introduction

The public transportation (PT) system is newly developed in Doha city, the capital of Qatar, where Doha Metro started operations in 2019 supported by an extensive network of infrastructure including buses, taxis, bicycles, and pedestrians. This system was designed as a solution to the issue of high traffic congestion, to meet the goals of Qatar National Vision 2030, and successfully host the world cup 2022 (Shaaban, 2012). However, people in Qatar are used to door-to-door trips with high reliance on private cars use. In addition, it is believed that Qatar's harsh weather conditions would be an impediment to the success of this system, where using PT requires walking and waiting outdoors.

Scholars highlighted that in order to achieve outdoor thermal comfort studying the microclimatic measurements solely is not sufficient as human behavioural adaption plays a fundamental role in the same. The physical microclimatic measurements reflect only 50% of actual sensation votes, and the remaining 50% is identified by human adaptation (Nikolopoulou, 2001; Nikolopoulou, 2006).

Therefore, it is crucial to study both the microclimatic measurements and human adaptation while the relationship between them is "complementary rather than contradictory." The term "adaptive approach" refers to the fact that people may take actions to enhance their thermal comfort level, by making use of more or less clothing or activity, as well as different ways of behaving within the built environment. (Nikolopoulou, 2003; Sugawara, 2008) have specified three measures of thermal adaptation: physical, physiological, and psychological.

Multiple microclimatic studies have focused on how the physical environment would have a positive impact on enhancing people's outdoor thermal comfort in hot climates (Krüger, 2010; Pearlmutter, 2006). This can be achieved if designers considered the following aspects of street design (including aspect ratio, urban geometry, solar orientation, street orientation, shade, and vegetation) (Ali-Toudert, 2006; Giridharan, 2008; Johansson, 2006; Park, 2012; Pearlmutter, 2007; Yang, 2011).

Although, the number of thermal comfort studies has increased in the last few years, still in Qatar the research work in this area is considered humble. Based on the Qatari standards, it is suggested to follow ASHRAE standard in order to achieve thermal comfort yet this is not validated to the local climate of Qatar. It is imperative to mention that, both Fanger's Thermal Comfort Model and ASHRAE standard were criticized by several researchers for being limited to uniform comfort conditions (Indraganti, 2010). To fill the gap in this area, an outdoor field study was conducted in both warm and cool seasons in 2017 in Qatar. The objectives of this paper are to understand: (a) people's thermal perception of the outdoor microclimate in Qatar, (b) people's adaptive actions, (c) the characteristics of the outdoor built environment, and how these aspects would affect the use of PT.

2 Research Method

According to the Köppen-Geiger climate classification, Qatar's climate is considered as the following:

The main climate is arid, the precipitation is desert, and the temperature is hot arid (Kottek, 2006). The mean air temperature across the year is between 14°C and 41°C. Qatar's climate is classified into three seasons: (a) the cool season enduring from December 6 to March 6, (b) the warm season enduring before and after the hot season from March 7 to May 10 and from September 27 to December 5, and (c) the hot season enduring from May 11 to September 26 (Climatemps, 2014; ColumbusTravelMedia., 2016; weatherspark, 2016).

The criteria for selecting the time and location of field measurements were based on fundamental issues. The climatic measurement was performed during the warm and cool seasons, where the hot season was excluded because most of the people travel outside the country at this time of the year. The data collection was scheduled from 8:00 until 18:00 hrs since this is the time most of the people use their cars/ or PT. The location of the field measurements was in Doha the capital of Qatar, in Al-Waab area. This location was chosen because both groups of the studied sample (current users and non-current users) can be studied in close proximity experiencing the same climatic conditions, and the selected metro station has similar characteristics to most metro stations in Doha (surrounded by residential and mixed-use land uses).

The methodology of this research paper consolidates both qualitative and quantitative methods. In order to study outdoor thermal comfort (Nicol, 2008) level III protocol of field studies took place focusing on the adaptive approach and using prediction and causality comparing two different groups of users (Groat, 2002), incorporating physical measurements (objective) and human behaviour (subjective) to grasp the outdoor thermal perception of people in Qatar's hot arid climate and its impact on the use of PT.

2.1 Climatic Variables

Climatic measurements were conducted during warm season (November 25, 2016 to December 2, 2016), and cool season (December 30, 2016 to January 6 and February 20-22, 2017) to investigate the climatic conditions. In order, to track the changes in the weather, the measurements were planned every two hours from 8:00 until 18:00 hrs. Microclimatic data was collected by measuring air temperature (Ta), relative humidity (RH), wind speed (W), and mean radiant temperature (MRT) using data loggers measured by the two devices shown in Figure 1(a). For all measurements, equipment was placed at a height of 1.1 m, corresponding to the centre of gravity for typical adults, appropriately in locations where people are expected to sit or walk (Mayer, 1987). To calculate the PET, the climatic data was used as input into the radiation and bioclimatic model RayMan. The PET is the main index for thermal comfort assessment, in contrast with the thermal sensation vote (TSV), which is an indicator of human thermal adaptation.



(a) **(b)**

Fig. 1: (a) EXTECH heat stress meter HT30 (Extech Instruments, 2016), and Kestrel 4200 pocket airflow tracker (Kestrel meters, 2016). (b) Site map shows Khalifa International Stadium, Aspire park, and Villagio Mall, locations of questionnaire responses where were collected

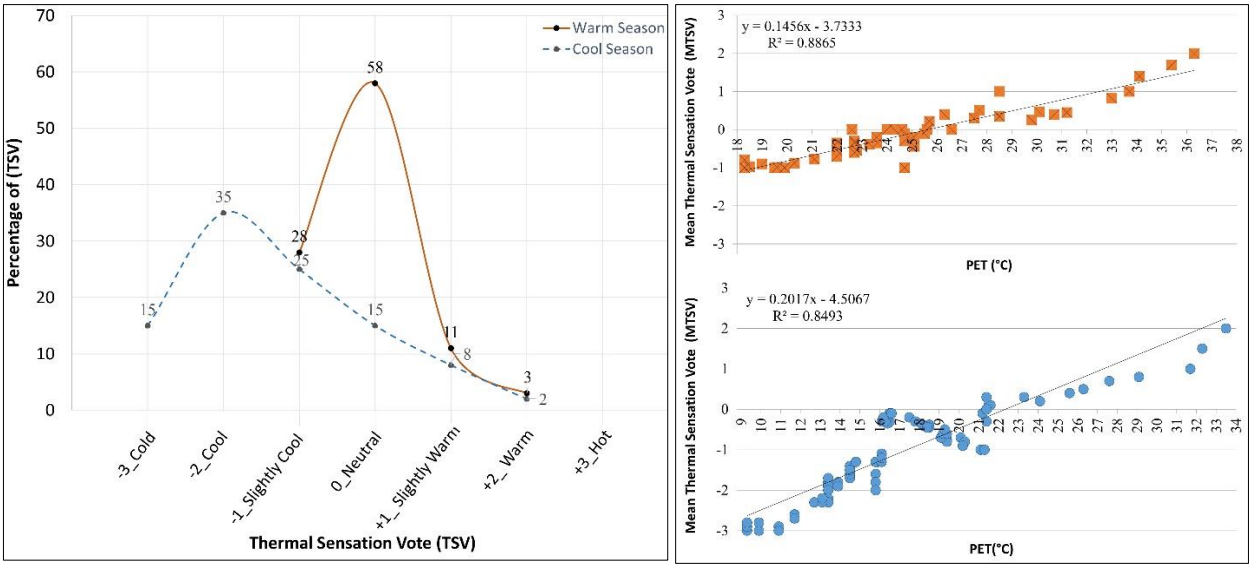
2.2 Questionnaire

Simultaneously with the climatic data measurements, the questionnaire was conducted, at the same time and in the same locations; since it was a right-now-right-here questionnaire, in order to be able to study the relationship between TSV and climatic measurements. The sample size was 200 participants; with two different groups, each constituted 100 responses (current users of PT and non-current users). The current user of PT was interviewed at bus stops and the non-current users were interviewed at Aspire Park (Figure 1(b)). In order to understand if there are any factors that affect the use of PT other than thermal comfort, it was mandatory to interview people in outdoor areas so they express their current thermal status. The sample was limited to citizens and residents who were living in Qatar for the past ten years to ensure that their thermal memory is linked to Qatar's climate. In the questionnaire, people were asked about their thermal status, thermal preference, and their use of PT in the meantime and in the future.

3 Results and Discussion

3.1 Subjective Thermal Responses

In contemplation of evaluating participants' thermal sensation votes (TSV), people from both groups were asked to express their thermal status in warm and cool seasons. Fanger's 7 points scale -3 (very cold) to +3 (very hot) was used to indicate the studied sample's thermal condition (Figure 2(a)). On one hand, in the warm season participants recorded the highest percentage of votes feeling neutral with 58%, and 97% of the votes fall within the three central categories (slightly cool= -1, neutral= 0, and slightly warm=1) on thermal sensation scale. Interestingly, this reflects that most of the people felt comfortable in the warm season. On the other hand, in the cool season the highest votes recorded 35% of feeling cool (-2 on the sensation scale). Unlike the warm season, in the cool season the majority of the votes were skewed to the left on the cooler side of the sensation scale constituting 75% of the votes.



(a) **(b)**

Fig. 2: (a) TSV percentage responses for each season. (b) Correlation between TSV and PET on right top side for warm season and right bottom side for the cool season

For the purpose of identitfying (1) people's thermal senstitivty (TSV) in realtion to Physiological Equivalent Temperature PET values, (2) people's thermal acceptable range, and (3) neutral temperature in both seasons; it was mandotry to perform a coorelation test. Using Excel's "Linear regression analysis," a test was performed. The Mean Thermal Sensation Votes (MTSV) were used as dependent variable, and the PET values served as independent variable, which is described in the following equations:

In the warm season:

$$y = 0.1456\ (PET) - 3.7333 \qquad R^2 = 0.8865 \qquad (1)$$

In the cool season:

$$y = 0.2017\ (PET) - 4.5067 \qquad R^2 = 0.8493 \qquad (2)$$

In the warm season, the value determined for the slope of the fitted line, namely 0.1456, indicates participants' overall thermal sensitivity to PET variables; this in turn indicates that a shift from one sensation category to the next corresponds to approximately 5 °C. The linear regression result indicates that 88.65% of the variation in participants' TSV is explained by the PET. In the cool season,

the corresponding linear regression value is 0.2017, and the results there indicate that 84.93% of the variation in participants' thermal sensation is similarly explained, with each category of TSV representing about a 6.8 °C shift as measured by the PET. This difference in results between seasons indicates that participants' thermal sensation tends to be more sensitive during the warm season than in the cool season.

(Markus, 1980) stated in order to determine the thermal acceptable range it should be indicated as +0.5 to -0.5 range on the thermal sensation vote scale. With the aim of identifying the thermal acceptable range for people in Qatar, the earlier linear regression equation was used. It concludes that, the thermal acceptable range in the warm season is 22.2 to 29.1 °C, and for the cool season is 19.8 to 24.8 °C. This indicates that people tend to tolarate higher temperatures in the warm season than in the cool season. The average acceptable thermal range overall for both seasons, excluding the hot season, is 21 to 26.9 °C PET.

In an effort to compute the neutral temperature (the temperature at which people vote zero on the sensation scale, expressing a feeling of neither too cool nor too warm), we utilize the previous equation– it has been found that, the neutral temperatures for the warm and cool seasons were 25.64 °C and 22.3 °C, respectively. This finding is similar to the previous one where people's neutral temperature tends to be higher in the warm season than in the cool season. This is can be referred to the expectation factor, where people expect that the temperature should be higher in the warm season. Hence, they adapt to higher temperatures in the warm season than in the cool season.

3.2 Behavioural Adaptation

3.2.1 Location in the Environment

(Yao, 2009) stated that human behaviour in a thermal environment is one part of human adaptation process. If a person feels thermally uncomfortable, he or she might make personal, environmental or cultural modifications, which are considered behavioural adaption actions (De Dear, 1998). In the questionnaire, participants were asked about the actions they would take if they felt too hot in an outdoor space, and reactions differing based on gender were noted, as shown in Figure 3. The first clear finding is that most participants of both genders said they would "move to the shade," with response frequencies of 32% for males and 40% for females. This indicates that protection from solar radiation is considered a key means for people to improve their thermal comfort. The second notable finding is that 29% of males would choose to reduce their amount of clothing to adapt to the surrounding environment, while only 5% of females said they would do so. This is presumably due to cultural issues, as women cannot easily reduce their clothing due to the local clothing norms (e.g., they cannot take off their veil).

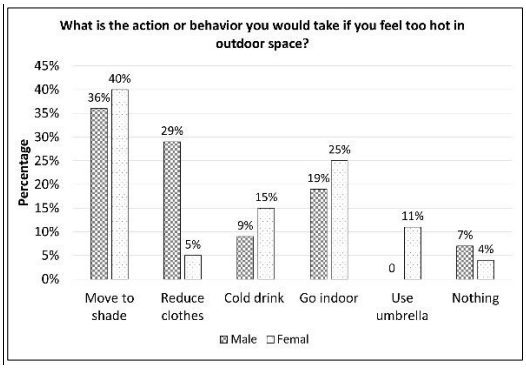


Fig. 3: People's behavior if they felt too hot in case of both genders–males and females

3.2.2 Level of Activity

One part of behavioural adaptation is level of activity, and this has a significant impact on the thermal comfort level of users (Clark, 1985). In order to gauge the influence that participants' level of activity would have on their thermal comfort, the relationship between these two factors was examined. Participants were asked how long they would enjoy walking or waiting (sitting or standing) during the warm or cool seasons. In this way, one can form a picture of how outdoor climate in the region contributes to people's activity level, which in turn is relevant in seeking to understand how people are likely to view the use of PT in Qatar (Figure 4). In the cool season, a slight majority (51%) of respondents said that the time they could comfortably wait for the next bus or metro car to arrive was 20 minutes, while 39% gave the same response during the warm season. This may be due to the impact of seasonal variation as well as people's expectations regarding thermal comfort; participants tended to express more willingness to wait outdoors during the cool season than during the warm season because of their different expectations about each season (Lin, 2009; Nikolopoulou, 2003).

The other tested activity was walking; participants were asked for how long they could enjoy walking in either of the seasons. This set of findings, shown in Figure 4, was consistent with the findings just discussed. Most participants opted for 15 or 20 minutes during both seasons, but during the cool season, people's willingness to walk for a longer period was greater than in the warm season. In the cool season, response rates of 38% and 53% were observed for the respective choices of 15 and 20 minutes as preferable walking times, while during the warm season, the corresponding respective response rates were 46% and 39%. Again, this can be explained by different seasonal expectations. However, comparing the waiting and walking time outcomes reveals that people tolerate staying in outdoor spaces for longer times when they are sitting or standing rather than walking. This shows how different activities have different influences on people's thermal conditions in outdoor spaces.

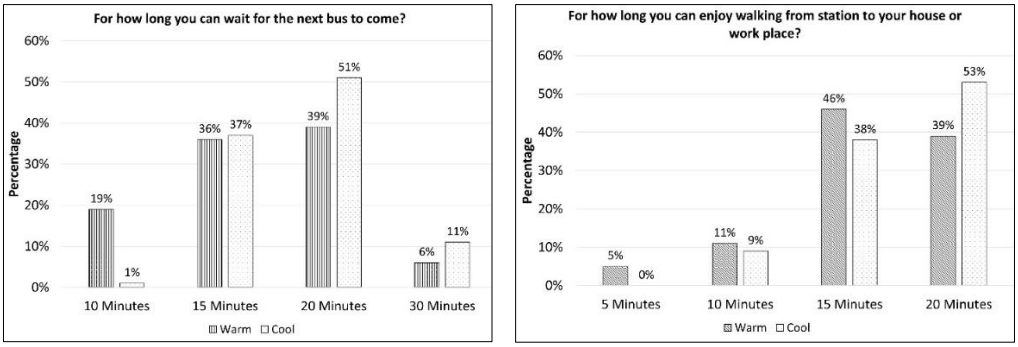


Fig. 4: People's responses regarding the waiting time in outdoors (left), and people's responses regarding their ability of walking duration outdoors (right)

3.3 Physical Built Environment and Better Outdoor Thermal Comfort

Values of PET varied between the warm and cool seasons, with values of 18.4 to 37.3 °C and 9.3 to 33.0 °C, respectively. It is noteworthy that the PET measures exceed the acceptable limit by almost 8 °C during both seasons. People's reactions when they feel uncomfortably hot were also studied; it was found that most respondents would choose to move to the shade in such a situation. This highlights the fact that an influential factor on people's thermal comfort is exposure to solar radiation. This has been found to be the case in a previous study of Qatar's Souq Waqif, where the difference in air temperatures between shaded and unshaded walkways can reach to 10 °C (Alattar, 2015). If shaded walkways are provided, the PET value can be reduced so that it falls into the acceptable range.

Shading in an outdoor area can be provided through a high H/W ratio, as well as by vegetation and other shading elements. In our case study, focusing on Villaggio Metro Station, we found the H/W ratio to be rather low, with a value of about 0.3, so that almost no shade is provided (Figure 5). Regarding vegetation, as yet no trees providing shade in the studied area have been planted. Shading devices have also not been provided. All of the above factors indicate a crucial need for vegetation and shading elements to enhance the microclimate and encourage more users to use the PT system currently being developed. The problems just discussed are evident not only around Al-Waab Street, but rather typical of the streets in Qatar more generally, even in areas with high-rise buildings like the West Bay area of Doha's Central Business District (CBD). Street orientations have generally not been taken into account, and as a result, the shade that these buildings could otherwise provide is essentially wasted, leaving the adjacent streets highly exposed to solar radiation.

A good solution to this problem is the creation of "vegetation islands" which can be used to form sheltered corridors. This concept of vegetation islands refers to the provision of shaded walkways at specifics distances, with these walkways shaded by trees. This can encourage people to spend more time in outdoor spaces and better enjoy walking there, as when people abandon one spot exposed to rain in favour of another which provides shelter.

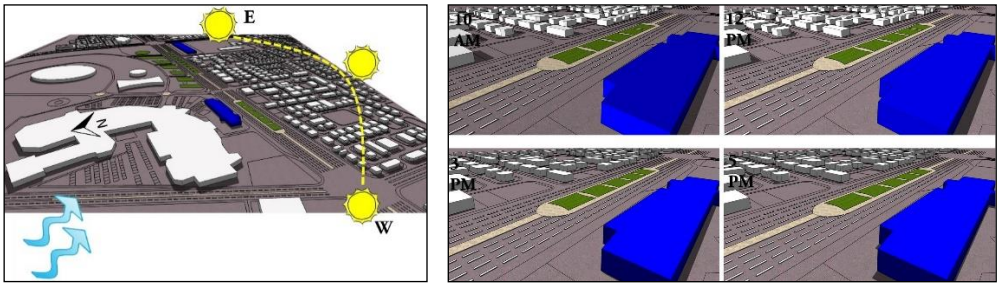


Fig. 5: To the (left), the street orientation of the studied site, to the (right), illustration to the shade and shadow created from the H/W in relation to different times of the day

4 Conclusion

A sample of 200 subjects were involved in outdoor thermal comfort study in Doha, hot arid climate of Qatar. The data collection was conducted during the warm and cool seasons using class III protocol for field study. The aim of this study was to understand if outdoor climatic conditions would be an obstacle to the use of newly developed Public Transportation System.

Following are the conclusions:

1. One of the objectives of this study was to understand people's thermal perception of the outdoor climate in Qatar. People expressed their thermal status using Fanger 7-point scale for both warm and cool seasons. It has been found that people's thermal acceptable range for the warm season is 22.2 to 29.1 °C, and for the cool season is 19.8 to 24.8 °C. This indicates that people tend to tolerate higher temperatures in the warm season than in the cool season. The average acceptable thermal range overall for both seasons, excluding the hot season, is 21 to 26.9 °C PET.
2. In addition, the neutral temperatures were identified for the warm and cool seasons 25.64 °C and 22.3 °C, respectively.
3. In order to understand the use of PT in relation to outdoor thermal comfort, people's behavioural adaption was studied. The first aspect was people's location in the environment, people were asked what action they would take if they felt too hot and most responses voted they would move

to the shade. This highlights that solar exposure is considered the most influential issue to achieve thermal comfort. The second aspect is the level of activity, in this case, people were asked about the duration of time they can enjoy waiting or walking in outdoors. Most of the respondents recorded longer waiting and walking times than required for the next bus to arrive or to reach the metro station. This emphasizes the fact that based on people's behavioural adaptation, the microclimatic conditions are not considered an impediment to the use of PT.

4. Interestingly, in accordance with our case study it has been found that the built environment is not well designed. The provision of shade is not considered in all aspects including H/W ratio, urban geometry, shading trees, shading elements, street orientation, and solar orientation.
5. The measured PET values for both warm and cool seasons exceed the thermal acceptable ranges with a value around 8 °C. This means that the PET should be decreased by 8 °C to promote a better outdoor microclimate. A previous study in Souq Waqif in Qatar found variation of 10 °C between shaded and unshaded walkways. This indicates if shade is provided in the studied area (in Doha's streets), the PET values will fall within the thermal comfort range.

Acknowledgment

I want to express my sincere appreciation to my supervisor Dr. Djamel Ouahrani, as this research paper is developed out of data collected during my master's thesis.

References

Alattar, D., Nafi, S. & Furlan, R. (2015). Built Form of the Souq Waqif in Doha and User's Social Engagement". *American Journal of Sociological Research, 5*(3), 73-88.

Ali-Toudert, F. & Mayer, H. (2006). Numerical study on the effects of aspect ratio and orientation of an urban street canyon on outdoor thermal comfort in hot and dry climate. *Building and environment, 41*(2), 94-108.

Clark, R. P. & Edholm, O. G. (1985). Man and his thermal environment, pages, Arnold, city.

Climatemps (2014). "Doha, Qatar Climate Graphs", Retrieved November 24 from http://www.qatar.climatemps.com/graph.php

ColumbusTravelMedia (2016). "Qatar Weather, climate and geography", Retrieved November 20 from http://www.worldtravelguide.net/qatar/weather-climate-geography

De Dear, et al. (1998). Developing an adaptive model of thermal comfort and preference/discussion, pages, ASHRAE transactions, city.

Extech Instruments (2016). "Extech Instruments Heat Stress WBGT Meter-HT30", Retrieved December 4 from http://www.homedepot.com/p/Extech-Instruments-Heat-Stress-WBGT-Meter

Giridharan, et al. (2008). Lowering the outdoor temperature in high-rise high-density residential developments of coastal Hong Kong: The vegetation influence. *Building and Environment, 43*(10), 1583-1595.

Groat, L. & Wang, D. (2002). Architectural research methods, pages, Wiley, city.

Indraganti, M. (2010). Behavioural adaptation and the use of environmental controls in summer for thermal comfort in apartments in India. *Energy and Buildings, 42*, 1019–1025.

Johansson, E. (2006). Influence of urban geometry on outdoor thermal comfort in a hot dry climate: a study in Fez, Morocco. *Building and environment, 41*(10), 1326-1338.

KestrelMeters.com (2016). "Kestrel 4200–Discontinued", Retrieved December 4 from https://kestrelmeters.com/products/kestrel-4200-pocket-air-flow-tracker

Kottek, et al. (2006). World Map of the Köppen-Geiger climate classification updated. *Meteorol. Z., 15*, 259-263.

Krüger, E., Pearlmutter, D. & Rasia, F. (2010). Evaluating the impact of canyon geometry and orientation on cooling loads in a high-mass building in a hot dry environment. *Applied energy*, *87*(6), 2068-2078.

Lin, T. P. (2009). Thermal perception, adaptation and attendance in a public square in hot and humid regions. *Building and environment*, *44*(10), 2017-2026.

Markus, T. A., Morris, E. N. & Reed, P. (1980). Buildings, climate and energy, pages, Pitman, city.

Mayer, H. & Höppe, P. (1987). Thermal comfort of man in different urban environments. T*heoretical and applied climatology*, *38*(1), 43-49.

Nicol, J. F. (2008). A handbook of adaptive thermal comfort towards a dynamic model, pages, University of Bath, city.

Nikolopoulou, M., Baker, N. & Steemers, K. (2001). Thermal comfort in outdoor urban spaces: understanding the human parameter. *Solar energy*, *70*(3), 227-235.

Nikolopoulou, M. & Lykoudis, S. (2006). Thermal comfort in outdoor urban spaces: analysis across different European countries. *Building and Environment 41*(11), 1455-1470.

Nikolopoulou, M., & Steemers, K. (2003). Thermal comfort and psychological adaptation as a guide for designing urban spaces. *Energy and Buildings*, *35*(1), 95-101.

Park, M.Et al. (2012). Effect of urban vegetation on outdoor thermal environment: field measurement at a scale model site. *Building and Environment*, *56*, 38-46.

Pearlmutter, D., Berliner, P. & Shaviv, E. (2006). Physical modeling of pedestrian energy exchange within the urban canopy. *Building and Environment*, *41*(6), 783-795.

Pearlmutter, D., Berliner, P. & Shaviv, E. (2007). Urban climatology in arid regions: current research in the Negev desert. I*nternational Journal of Climatology*, *27*(14), 1875-1886.

Shaaban, K. & Khalil, R. F. (2012). Proposed policies to support the new metro system in Qatar. *Procedia-Social and Behavioral Sciences*, *48*, 2315-2324.

Sugawara, et al. (2008). How much cool air does an urban green park produce?. Geogr Rep Tokyo Metrop Univ,), Geographical reports of Tokyo Metropolitan University, 43-89.

Weatherspark (2016). "Average Weather For Doha, Qatar", weather spark https://weatherspark.com/averages/32878/Doha-Ad-Dawhah-Qatar

Yang, F., Lau, S. S. & Qian, F. (2011). Urban design to lower summertime outdoor temperatures: An empirical study on high-rise housing in Shanghai. *Building and Environment*, *46*(3), 769-785.

Yao, R., Li, B. & Liu, J. (2009). A theoretical adaptive model of thermal comfort–Adaptive Predicted Mean Vote (aPMV). *Building and environment*, *44*(10), 2089-2096.

Cite as: Alattar D. & Indraganti M., "The Use of Newly Developed Public Transportation System in Relation to People's Thermal Perception of Outdoor Climate.", *The 2nd International Conference on Civil Infrastructure and Construction (CIC 2023)*, Doha, Qatar, 5-8 February 2023, DOI: https://doi.org/10.29117/cic.2023.0123

An Analytical Review of Attempts to Mitigate Visual Pollution in Urban Settings

Diala Al Midani
Department of Architecture and Urban Planning, College of Engineering, Qatar University, Doha, Qatar
da1805053@qu.edu.qa

Fodil Fadli
Department of Architecture and Urban Planning, College of Engineering, Qatar University, Doha, Qatar
f.fadli@qu.edu.qa

Abstract

Visual pollution is the main issue rising in urban settings these days. The residents of the built environment or the surrounding communities are negatively impacted by this sort of pollution. Visual pollution reduces quality of life and has an impact on the community's overall wellbeing. Urban planning developments in Qatar are progressively recognizing the issue of visual pollution in urban settings. Therefore, there are various efforts and actions that were adopted to minimize such an issue. This paper's primary aim is to formulate a set of suggestions to help in mitigating visual pollution impact. The aim will be achieved by focusing on producing an analytical review of methods to mitigate visual pollution impact in many countries generally and in the state of Qatar mainly, besides highlighting the country's laws, regulations, and act towards visual pollution. The methodology used was qualitative approach to review adopted methods and used solutions in mitigating visual pollution impact. The findings proposed a set of recommendations to help in reducing visual pollution impact and enhancing the attempts of mitigating visual pollution in urban settings. The paper concludes many practices used previously in various countries and mainly in the state of Qatar and identifies the most appropriate methods to control visual pollution and enhance the attempts of reducing its impact in urban settings.

Keywords: Visual pollution; Urban settings; Qualitative approach; The State of Qatar

1 Introduction

Humans have attempted to alter their environments repeatedly throughout history in an effort to fulfil their goals. Many concerns were raised because of changes in the environment and by the needs of the expanding population and industrial growth. Land, water, air, and noise pollution are the first things that come to mind when discussing environmental issues. However, visual pollution is not as significant as other sorts of pollution are; visual pollution is a type of pollution that has recently gained attention since it affects individuals psychologically and spiritually.

In an urban setting, it is difficult to find beauty in a single building; rather, beauty or visual chaos can be seen in relation to the whole urban context. Investigating visual pollution focuses on the unity as well as the disparities in urban design of the urban settings, such as architectural principles of the urban fabric, signage and advertisements, buildings' design, structural materials, and various existing physical objects, in order to investigate the visual quality and visual distortion in urban settings and the built environment.

According to Bodur and Kucur (1994), visual pollution is the act of bringing undesirable changes in

the environment that disrupt healthy people's visual acuity. Visual pollution can alternatively be characterized as the entirety of the erratic formations that are typically present in both natural and built settings, which are typically observed in an indirect manner and make a bad impression on people's thoughts (Oner & Konakli, 2009).

Oner & Konakli (2009) highlighted some of the visual pollution causes in cities, including poor judgement, legal shortcomings, a lack of oversight, usage that is incompatible with its intended purposes, lacking in culture and knowledge as well as insensitivity on the part of local government (Oner & Konakli, 2009). Both the city as a whole and the specifics, such as specific areas of buildings or urban spaces, reflect visual pollution.

Visual pollution is caused by environments that are monotonous, congested, lack greenery and distinctive character, as well as abandoned buildings with an unbalanced number of levels and poorly designed transportation networks. In addition, enormous billboards at the city's entrances and exits, garbage bins, direction signs, signboards, utility lines, cell phone towers, transformer structures, and air conditioning units affixed to building exteriors, and satellite dishes, all contribute to visual pollution.

Studies from both developed and developing nations have attempted to investigate the causes of the visual pollution problem, but all of these efforts have been limited by the complexity, subjectivity, researcher preferences, statistical measurement of the degree of visual pollution, and the visual pollution objects (Bankole, 2013; Nasar & Hong, 1999).

This paper's primary goal is to create a set of recommendations and principles to minimize the effect of visual pollution impact in urban settings. The goal will be accomplished through an analytical analysis review of internationally and locally used strategies for reducing the effects of visual pollution affect in urban settings by emphasising international and local laws, rules, and actions on mitigating visual pollution impact.

2 Methodology

The methodology in this study depends on qualitative approach to collect data about attempts and methods for mitigating visual pollution impact in urban settings through an analytical review of literature and relevant research papers. Firstly, it addresses the international attempts from different countries for reducing the impact of visual pollution based on reviewing their relevant laws, regulations, methods, and acts. Consequently, this study highlights local attempts for mitigating visual pollution impact in urban settings in the state of Qatar by reviewing governmental laws, authorities' actions and adopted solutions. The analytical review will be presented in detail as follows.

3 Analysis

3.1 International Attempts for Mitigating Visual Pollution

Since the city of Sao Paulo assigned the Clean City Law in September 2006, prohibiting the display of any outdoor advertising, such as billboards, transit, and that especially in front of shops. The city made a radical action in 2007 to remove all outdoor commercial signs.

The term "visual pollution" has gained popularity around the world, and scholars are studying it in relation to the excessive commercialization of public areas and urban settings (Baker, 2007; Koeck & Warnaby, 2014).

In the United States, they started to reduce the visual pollution since 1956 through the Highway Beautification Act, which restricts billboard placement on highways and roads (Nagle, 2009),

especially with regards to retail shops located near a highway that may have huge billboards, which creates visual problems and distractions. After the Beautification Act, another way for advertisers is gradually preventing the problem of visual pollution. For instance, signboards that direct drivers without deforming the urban settings are increasingly used and considered as the first step to mitigate visual pollution on highways in the United States (Maguire et al., 1997).

Moreover, there were many initiatives to make the public more aware of urban settings appearance and visual pollution, therefore, the Dunn Foundation organization was developed to design educational programs for students from grade 3 to grade 12. These programs highlight the impacts of visual pollution, and create awareness among students on how to enhance the appearance of their communities and enhance the visual environment (The Dunn Foundation, 2012). Another non-profit organization called Scenic America is seeking the reduction of visual mess and ensure scenic conservation.

One of their movements towards preventing the visual pollution was hiding the communication towers with artificial trees (Scenic America, 2013).



Fig. 1: Artificial tree to hide a communication tower.

3.2 Local Attempts for Mitigating Visual Pollution

In the State of Qatar, billboards were controlled since 1980 by a governmental law No (4). In 2012, Qatar set out a new Law No. (1) with additional requirements to control the advertisements/boards placement (Salt & Earley, 2012).

In order to display an advertisement board in Qatar, an approval from the municipality must be obtained. The applicant must submit the license application accompanied by a sketch of the advertisement content details. There are many requirements the advertisement must follow prior to the approval of the advertisement license, such as; a) the advertisement design must not be similar to directional sings, in terms of colour, size, or form, to avoid the distraction, b) the placement of advertisement must not harm the public facilities aesthetics or obstruct the pedestrians, c) if the advertisement is installed on a building it must not hinder the ventilation outlets or block the visibility.

In addition, the advertisement owner is responsible for maintaining the sign, if he didn't respond to the Municipality notification within seven days, the advertisement sign may be removed.

Moreover, the Advertising Law prevents placing an advertisement on historic buildings, religious sites, traffic signals and trees or plant containers (Law No. 1, Article 11).

In addition, Ashghal which is the Public Works Authority of Qatar, has launched the directional sign development strategy, that seeks to standardize and control the implementation of directional signs on roads and highways to make them easy to be read and reduce the confusion to drivers. The standardization will create an aesthetic characteristic and harmony on the roads in Qatar. Also, in some areas, where it's hard to place directional signs, some destinations are written on the asphalt road which reduce the signboards' visual impacts.

Regarding the communication towers and cellular mobile base station location, Qatar has assigned some requirements and regulations to control the visual impact of installed towers. The height and the appearance of the towers must meet the beautification principles of the Ministry of Municipality and Urban Planning. The installed communication towers must be designed, painted, and hidden with the respect to local pattern of streets, city skyline, building traditions, to reduce the contrast among these towers and the surroundings (Communication Regulatory Authority, 2014).

Moreover, Qatar attempts to minimize the visual pollution caused by various elements, in parallel to that the General Cleanliness Department, on behalf of the Ministry of Municipality and Environment (MME), has cleared the ports of Al Wakrah and Al Khor from abandoned motorboats and dhows that had become a problem. The Assistant Undersecretary for General Services Affairs at the Ministry of Municipality and Environment Safar al Shafi stated that abandoned boats "occupy a large space and produce visual pollution." He further added that in order to prevent removal and legal action, boat owners must follow the rules and maintain their boats.



Fig. 2: The abandoned dhows removal campaign by the Ministry of Municipality and Environment, Qatar



Fig. 3: The abandoned vehicles removal campaign by the Ministry of Municipality and Environment, Qatar

Since Qatar is witnessing rapid development and many construction projects, a systematic scheme to reduce the visual harm caused by construction work was needed. The Gulf Organization for Research and Development (GORD) developed GSAS (Global Sustainability Assessment System) to improve the overall quality of the construction projects (Al Midani & Fadli, 2020).

GSAS evaluates the aspects of the construction processes based on many categories such as the outdoor environment. The objective of assessing this category is to minimize the visual impacts during the construction phases. Negative visual impacts during the construction process could be formed by many factors, such as cranes, machines, trucks, site fencing, landscape alteration, etc.

GSAS proposed many mitigation measures to reduce the visual pollution resulting from any construction project. These measures must ensure the following: a) the fence material must respect the surrounding land use and act as a visual barrier, b) the piles must be covered with netting to minimize their visual impacts, c) any dirt or mud which has been spread onto the public streets by the construction vehicles must be cleaned and removed, d) reduce ground and vegetation disturbance that cause negative visual impacts in terms of contrast of texture, form, and colour, e) in order to give the suggested trees a chance to grow while construction work is being done, plant temporary tree nurseries earlier if it's possible, to mitigate visual pollution (GSAS Construction Management: Guidelines & Assessment, 2017).

4 Findings

Many cities thrive to have a beautiful urban image with well-known landmarks, advertisements, and other stimuli. However, many have accumulated so much that it has adversely changed the surrounding environment. Several cities make a concerted effort to precisely balance their aesthetics, although this effort often fails. A neighbourhood's atmosphere can be significantly disrupted by having too many structures and attractions.

The majority of cities and smaller towns have an excessive number of billboards. Even if it is pleasant to see advertisements, too many of them may worsen the town's surrounding visual. Cities should therefore restrict on how many advertisements are allowed while encouraging companies to advertise their goods online or through other means, like social media. As authorities consider upgrading the town centre, learning and educating the public and designers about visual pollution will enable the users to protect their cities from such issue and enable the architects change the future plans to incorporate more of the surrounding environment.

Based on the previous analysis, this study addresses a set of recommendations for reducing visual pollution to create techniques that lessen the detrimental effects of various visual pollution objects, such as:

1. When installing cellular mobile base stations, the architectural style of the nearby structures must be taken into consideration.
2. Instead of constructing new structures, consider about the possibilities of using existing structures as beacons, streetlight poles, mosque towers, etc. to hide transmitting equipment.
3. Regulate where directional signs are placed and make sure that their size, shape, and colour are all the same. To reduce the visual effects of signboards, write the destinations on the road's surface.
4. Control outdoor advertising and implement maintenance policy.

5. Choose the least obstructive locations for the new traffic management components, such as lights, radar, etc.
6. Implement a site fence with the right colour and material to minimize the unsightly effects of construction sites.
7. Remove any neglected items, including vehicles, bicycles, commercial signs, boats, etc., and impose a fine on the owners to stop them from occupying the space and ruining the view.

However, this paper identified that the most appropriate methods to control visual pollution and enhance the attempts of reducing its impact are to: a) assign governmental laws and implement strong acts that protect cities and towns from visual pollution, b) consider strong regulations and legislation for future development projects and take urgent action against violators.

5 Conclusion

Despite its severe effects on people's mental health and the quality of urban environments, visual pollution is a concern that urban areas often ignore. It is our responsibility to lessen environmental visual pollution and offer solutions. Controlling visual pollution remains difficult because of its complexity and subjectivity yet assessing it and enacting laws in urban contexts is a significant step towards reducing and preventing its effects. In keeping with the previous discussion, this paper highlights that visual pollution is an arising issue that affects the quality of urban environment and impact user's behaviour. Therefore, this issue started to gain attention from decision makers in several countries. Hence, this paper highlighted international and local efforts and acts in mitigating visual pollution impact in urban settings. Various approaches and techniques that had been used in different countries were addressed in this paper, besides a set of recommendations to boost and strengthen the efforts of mitigating visual pollution impact was provided.

References

Al Midani D. & Fadli F. (2020). An Analytical Review of Sustainable Green Buildings in Qatar: Implementations in the Architecture, Engineering and Construction (AEC) Sector. International Conference on Civil Infrastructure and Construction (CIC 2020), Doha, Qatar.

Baker, L. E. (2007). Public sites versus public sights: The Progressive response to outdoor advertising and the commercialization of public space. *American Quarterly 59*(4), 1187-1213.

Bankole, O. (2013). Urban Environmental Graphics: Impact, Problems and Visual Pollution of Signs and Billboards in Nigerian Cities. *International Journal of Education and Research, 1*(6), 1–12.

Bodur, S. & Kucur, R., (1994). On visual pollution. *Journal of Ecology Environment, 12*, 50–51.

Communications Regulatory Authority, Qatar. (2019). Construction Procedures and Standards of Cellular Mobile Base Stations and Towers Report.

Epidemiol. J. (2005). Multilevel analysis. Community Health.

GSAS Construction Management: Guidelines & Assessment, (2017). - Issue 3. Pp. 137-138.

Koeck, R. & Warnaby, G. (2014). Outdoor advertising in urban context: spatiality, temporality, and individuality. *Journal of Marketing Management*.

Maguire, M., Foote, R. & Vespe, F., (1997). Beauty as well as bread. American Planning Association. *Journal of the American Planning Association, 63*(3), 317-328.

Matramkot, S. (2018). The Peninsula Qatar newspaper.

___. (2019). The Peninsula Qatar newspaper.

Nagle, C. (2009). Cell phone towers as visual pollution. *Norte Dame Journal of Law, Ethics, and public policy*.

Nagle, et al. (2009). (The Idea of Pollution). Environments.

Nasar, J. L. & Hong, X. (1999). (Visual Preferences in Urban Signs capes. Environment and Behavior) *31*(5), 671–691.

Öner, S. & Konakl, N. (2009). (Applications Caused Visual Pollution in the City of Konya and Suggestions for Solutions), pp. 498-506.

Salt, D. & Earley, M., (2012). Qatar's New Advertising Law.

Shafi, S. M. (2015). Visual Pollution: Advertising, Signage and Environmental Quality. Design and the Built Environment. *European Scientific Journal*.

Visual pollution:' The Dun foundation (2012).

Washington, DC: Scenic America (2013).

Cite as: Al Midani D. & Fadli F., "An Analytical Review of Attempts to Mitigate Visual Pollution in Urban Settings", *The 2nd International Conference on Civil Infrastructure and Construction (CIC 2023)*, Doha, Qatar, 5-8 February 2023, DOI: https://doi.org/10.29117/cic.2023.0124

Environmental Sustainability Comparative Assessment of Low-Rise and High-Rise Neighbourhoods based on People's Lifestyle Preferences: The Case of Doha, Qatar

Shikha Patel
College of Engineering, Qatar University, Doha, Qatar
sp2009946@qu.edu.qa

Hatem Ibrahim
College of Engineering, Qatar University, Doha, Qatar
hatem_ibrahim@qu.edu.qa

Abstract

The urban form of Doha city has undergone numerous changes owing to rapid economic growth during the past few decades. The Qatar National Vision 2030 highlights Environmental Sustainability as one of the key sectors of Qatar's First National Development Strategy. Achieving Environmental Sustainability requires analysis from meso and micro scales. This study selected a high-rise neighbourhood (West Bay) and a low-rise neighbourhood (Onaiza) in Doha city to be analysed. The study objectives are to, a) investigate environmental factors based on two levels: meso and micro scales and, b) develop planning strategies to enhance Environmental Sustainability in both low-rise and high-rise neighbourhoods. The research tools include content analysis, observation study and open-ended interviews. The results revealed similarities in lifestyle preferences for meso parameters, walkability and waste segregation, and micro parameters, surroundings and green infrastructures. Backyard farming is preferred by the low-rise neighbourhood while high-rise neighbourhood residents choose more sustainable alternatives for mobility. The study emphasizes the importance of public awareness and participation in formulating urban policies due to the changing dynamics of the city's population.

Keywords: Environmental Sustainability; High-Rise and Low-Rise neighbourhood; Urban Planning; Meso and Micro environmental factors; Public participation

1 Introduction

The growing urban population and increased exhaustion of natural resources demand sustainable development to counter the environmental impacts. The sustainable development of cities requires planners to continuously engage and intervene at different scales - city, neighbourhood and household or macro, micro, and meso (Al-Thani et al., 2018). Qatar's National Vision 2030, established within Qatar National Master Plan, aims to recognize Qatar as a sustainable nation within the global community. Sustainable development is imperative for Qatar as about 60% of its GDP relies on a single resource, and the population relies on imported goods (The World Bank, 2021). While Doha was primarily characterised by low-rise mixed-use suburban neighbourhoods, several sustainable development initiatives have added high rises to Doha's urban form (Khalil & Shaaban, 2012).

Jacobs (1961) portrayed high-rise denser urban developments as the poster image for sustainability while associating low-rise sprawl with unsustainability. In support, Bakker (2020) compared Atlanta city (U.S.) to Barcelona (Spain) pointing out poor air quality, pollution, and congestion, in Atlanta city which is dominated by suburbs. In contradiction, Brown (2017), argued high-rise compact urban form as the ideal

generated by European and American urban theorists that was not applicable to the Middle East and Asian countries. Qatar's urban form is a mix of low-rise and high-rise urban forms; therefore, both must contribute to achieving the goal of being sustainable. Postulating that both arguments, that is, low-rise and high-rise can have the potential to be sustainable, the urban planning policies and action plans prioritise improving the quality of the built environment and hence, focus on the tangible elements of urban planning. The psychological aspects such as personal preference, motivation and attitudes are overseen resulting in an overestimation of the built environment's efficiency (Kim et al., 2014). It is, therefore, vital to investigate people's preferences at the meso and the micro-scales to intervene at the city scale.

2 Research Methods and Tools

This study employs the following research tools:

- **Literature Review and Content Analysis**: A related literature review develops an assessment framework for investigating meso and micro-scale parameters.
- **Observation Study:** Aimed to examine the neighbourhoods' physical features and the residents' activities. The neighbourhoods were observed between 15th October to 15th November 2022, one hour during the day and one hour during the evening on weekdays and weekends. The observations were not recorded in any specific hour ensuring non-repetition of activities and apprehending the necessary information needed to make inferences.
- **Questionnaire Survey**: Aimed to analyse residents' perception and behaviour toward environmental sustainability. A questionnaire survey form was drawn with "satisfied" and "unsatisfied" choices, the answer to which was investigated further with follow-up questions. A total of eighty interviews were conducted (forty residents of each neighbourhood) based on random sampling. The interviews were conducted in person that consisted of open-ended questions associated with the meso and micro-scale parameters of Environmental Sustainability.
- **Analytical Study**: A qualitative assessment of responses to address the differences in lifestyle preferences between the residents of a low-rise and a high-rise neighbourhood.

3 Literature Review

3.1 Background and Context

This study considers three parameters at meso and micro scales each. For the meso scale, that is the household scale, people's lifestyle preferences towards walkability, urban farming and waste management are investigated. While cities work and invest in developing sustainable public transportation, walkability is perceived as the core urban design parameter for Environmental Sustainability. People's preference for walking to work, leisure and daily activities depend on accessibility to places of interest, climate, pedestrian pathway infrastructure and an individual's desire to walk (Baobeid, et al., 2021). Given the positive environmental impact of urban farming, the lifestyle preference for urban farming depends on the climate, size of the house, availability of agricultural materials and willingness of an individual (Patel et al., 2021). To begin waste management at the city level requires waste segregation at the household scale, as a first step. People's preference to segregate waste depends on their awareness, the infrastructure for it and essentially the willingness to do it (Nwofe, 2013).

A study by Grenni et al. (2020) confirmed that a sense of place and location drive an individual in contributing to the environment. One of the factors that help people prefer walking over automobiles is proximity. Therefore, the surroundings, a neighbourhood offers to individuals are significant to

achieving Environmental Sustainability. Another important parameter is the choice of mobility. The choice between carpooling, public transportation and using an individual automobile depends on the destination, time of travel and an individual's preference (Kim et al., 2021). Last, introducing green infrastructures bridges the gap between environmental and economic sustainability. At the micro-scale, green infrastructure comprises instruments and mechanisms in the neighbourhood that run on solar or wind energy. The desire to invest in green infrastructures depends on awareness, availability of appropriate technology, affordability, and an individual's willingness (Khoshnava et al., 2020). While the factors influencing the various parameter are distinct, the common factor is people's preference and willingness to act. This study, therefore, aims to investigate people's preferences for a low-rise and a high-rise neighbourhood of Doha city to recommend and implement policies and regulations at meso and micro scales addressing environmental sustainability.

3.2 Environmental Sustainability Assessment Framework

The assessment framework for this study is categorized into two scales: meso and micro for a low-rise and a high-rise neighbourhood. The mesoscale parameters, walkability, urban farming and waste management and the micro-scale parameter, location, surroundings, mobility and green infrastructures are associated with indicators assessed by observation and survey studies. For meso parameters, the preference to walk is associated with pedestrian satisfaction which includes walking space, connectivity, and availability of pedestrian furniture such as benches, bus stops, and plants (Cambra, 2012). The challenges in the low-rise neighbourhood are connectivity and maintenance and walking space is a challenge in the high-rise neighbourhood. The indicators for urban farming are the availability of space, motivation and availability of materials and equipment (Swanepoel et al., 2018). The availability of land is an advantage for the low-rise and a challenge for the high-rise neighbourhood. The indicators for waste management selected are awareness, segregation and existing facilities (Ferdinan et al., 2022). Waste management challenges are similar for the low-rise and the high-rise neighbourhood in Doha, that is lack of awareness and facilities.

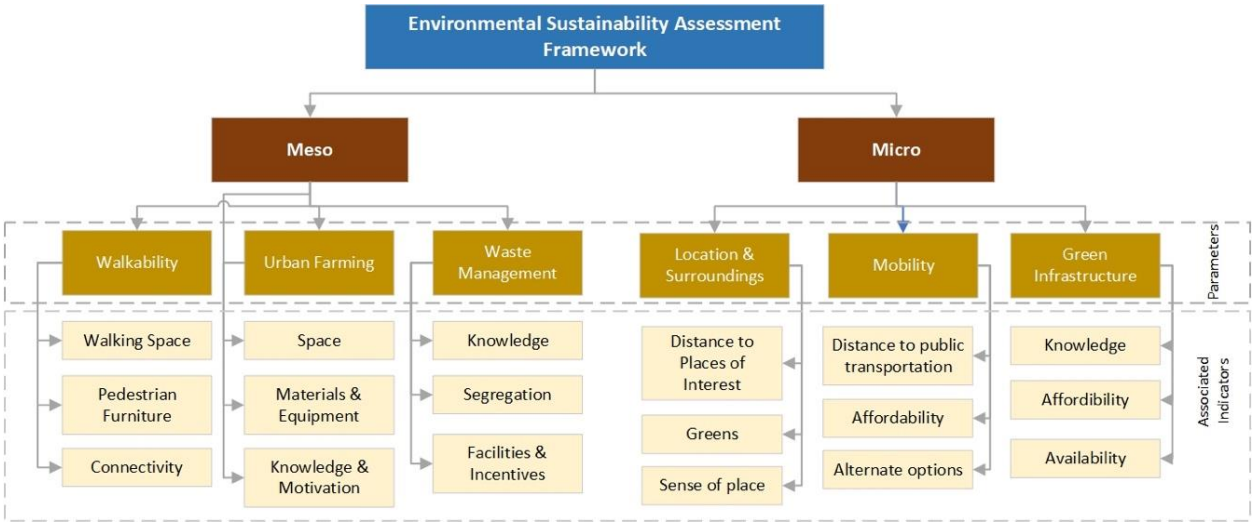


Fig. 1: Environmental sustainability assessment framework for Doha city (meso and micro-scale parameters)

The indicators for location, and surroundings, are distance to places of interest, availability of greens and sense of place. Distance to places of interest determines a person's preference for walkability, the availability of greens assures a pleasant living experience, and a sense of place determines a person's willingness to contribute to the environment. The indicators for preference for mobility are

distance to public transport, affordability, and other alternatives (Gillis et al., 2015). The indicators for choosing green infrastructure are knowledge, facilities, and availability (Pakzad & Osmond, 2015). Implementing green infrastructures is an important parameter aligning with Qatar's Sustainability Goals, Figure 1.

4 Case Studies: Low-Rise and High-Rise Neighbourhoods

Two adjacent neighborhoods, Onaiza comprising 80% of low-rise urban form and West Bay comprising 80% of high-rise urban form, are selected for the case study. Onaiza is situated in the northeastern part of Doha city and West Bay (the central business district) is situated on the northeastern coastline of Doha city, Figure 2.

4.1 Environmental Sustainability Assessment based on Observation Study of Onaiza and West Bay Neighbourhoods

The observation study investigates the physical characteristics of neighbourhoods and people's lifestyle preferences about the selected parameter.

Walkability: The observation of pedestrian pathways in Onaiza shows obtrusions in walking space such as a fallen tree, garbage spill and disconnected pedestrian pathway. The pedestrian pathways in Onaiza are observed to be unused due to poor connectivity and poor maintenance. A lack of street furniture, shading devices and landscaping are rectified as reasons for unused pedestrian pathways. In contradiction, the walking space in West Bay is interrupted by bikes, bicycles and construction materials. While the pedestrian pathways in West Bay are well-connected and maintained and harbour street furniture, the illegal car parking on pedestrian pathways makes walking unsafe, Figure 3 (A,B).

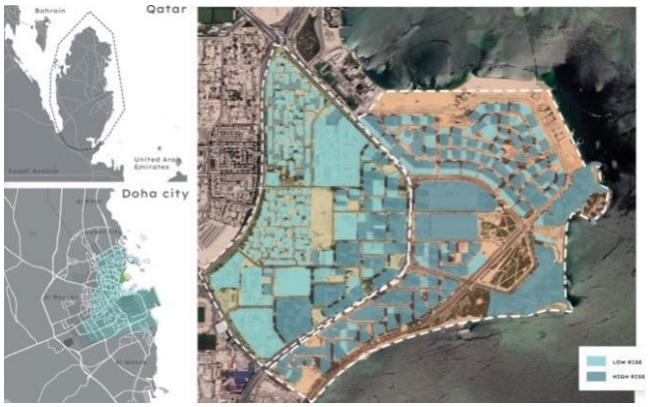


Fig. 2: The selected case studies: Onaiza (low-rise) and West Bay (high-rise) neighbourhoods

Urban Farming: Onaiza neighbourhood is characterised by single-family residences (villas) and multi-family residences (a group of small villas). Both types of residences show ample courtyard, backyard or front lawn space. West Bay neighbourhood is characterised by high-rise residential apartments, office buildings, hotels and mixed-use buildings. The plot space around the building footprints is occupied by parking and utilities, which leaves no space for urban farming. However, there seldom are buildings that bear space for landscaping around the plot, where urban farming is a possibility, Figure 3 (C, D).

Waste Management: For single-family and multi-family residences in Onaiza, solid waste is first collected in a common bin at the residence and then transferred to a community bin common between a group of residences and streets. No waste segregation or decomposing activities within the

compounds were observed. Following a similar organization in West Bay, the garbage chute collects solid waste from each floor of a high-rise building and is then transferred to a common bin. Waste is not segregated at any level in the process, Figures 3 (E, F).



Fig. 3: Observation study of meso scale parameters for Onaiza and West Bay

Location and Surroundings: There are about 14 restaurants/ coffee shops, 1 mall, 6 public parks, 5 grocery supermarkets and 4 pharmacies in West Bay. Most of the high-rise towers in West Bay have their private park and children's play area, which are well-used and enjoyed by the residents. In the case of Onaiza, which is approximately the same area as West Bay, there are 2 restaurants, 2 public parks, 1 grocery supermarket and 2 pharmacies. Imperatively, the streets, parks and public places are more crowded in West Bay compared to Onaiza.

Mobility: There are 12 bus stops and 2 metro stations (the West Bay metro station and the Doha Exhibition and Convention Center (DECC) metro station) added to well-connected and maintained pedestrian pathways that make public transportation accessible to West Bay residents. However, Onaiza has 10 bus stops and no metro stations, which makes it uncommon for residents to choose public transportation. However, the difference in choice of mobility from both neighbourhoods is also due to the ownership of homes. The probability of a homeowner in Onaiza investing in a private automobile is more than expats obliged to relocate after the contracted term.

Green Infrastructure: In early 2022, the "West Bay Beautification" retrofitting project was implemented that improved pedestrian connectivity and parks and installed energy-saving streetlights and other infrastructures. High-rise residential towers badge certificates that ensure energy efficiency leaving a minimum carbon footprint, Figure 4. In the case of Onaiza, no energy-saving equipment on the streets is observed. No green building certified badge was observed on individual homes.



Fig. 4: Observation study of micro scale parameters for Onaiza and West Bay

4.2 Environmental Sustainability Assessment based on Questionnaire Survey of Onaiza and West Bay Neighbourhoods

A follow-up question was asked for initial questions to investigate future aspirations, Figure 5.

Walkability: Only 30% of Onaiza residents are satisfied with available walking space while 80% of West Bay residents are satisfied with walking space and pedestrian pathway connectivity. West Bay residents (95%) are also satisfied with pedestrian furniture that makes the neighbourhood friendly to walkers. Less than 50% of Onaiza residents are satisfied with pedestrian connectivity and furniture. However, residents of both neighbourhoods (above 90%) are willing to change lifestyle preferences if proper facilities are given.

Urban farming: 80% of Onaiza residents are satisfied with the available space and have the knowledge to practice urban farming. However, the cost of materials and equipment is challenging as 75% of Onaiza residents are uncomfortable investing in urban farming. In the case of West Bay, only 5% of residents are satisfied with the available space and 95% of residents are uncomfortable investing in materials and equipment. Residents of both neighbourhoods (above 80%) are willing to practice and participate in urban farming when proper guidance and incentives are given.

Waste Management: Only 5% of Onaiza and West Bay residents segregate waste and are provided with the necessary facilities. Less than 50% of residents from both neighbourhoods possess knowledge of waste management. However, over 80% of Onaiza and West Bay residents are willing to improve waste management practices in homes with proper facilities, knowledge and incentives.

Location and Surroundings: Only 40% of Onaiza residents were satisfied with the distance to places of interest around the neighbourhood while the number increased to 85% in the case of West Bay. More than 80% of West Bay residents are satisfied with the green spaces around the neighbourhood and are willing to relocate for a better location. Only 30% of West Bay residents hold a sense of place, while in the case of Onaiza, more than 70% of residents hold a sense of place.

Mobility: Only 40% of Onaiza residents are satisfied with the distance of the nearest public transportation from their homes, while 85% of West Bay residents are satisfied with the distance to public transportation. While both the neighbourhood residents are satisfied with the cost of using public transportation, 85% of Onaiza residents and 55% of West Bay residents are satisfied with the alternatives of public transport that is walking, biking and carpooling. However, more than 90% of Onaiza and West Bay residents showed a willingness to use public transportation more often in future with improvements in the facilities.

Green infrastructure: The questions investigated residents' knowledge and awareness of the energy efficiency systems in the infrastructure around them. Only 35% of Onaiza residents and 60% of West Bay residents are knowledgeable about energy-efficient infrastructures in their neighbourhoods. Onaiza residents showed more enthusiasm (more than 90%) for investing in green infrastructures in the future as compared to West Bay residents. However, it is important to note that West Bay residents are more (95%) satisfied with the availability of green infrastructures in their neighbourhood as compared to Onaiza residents.

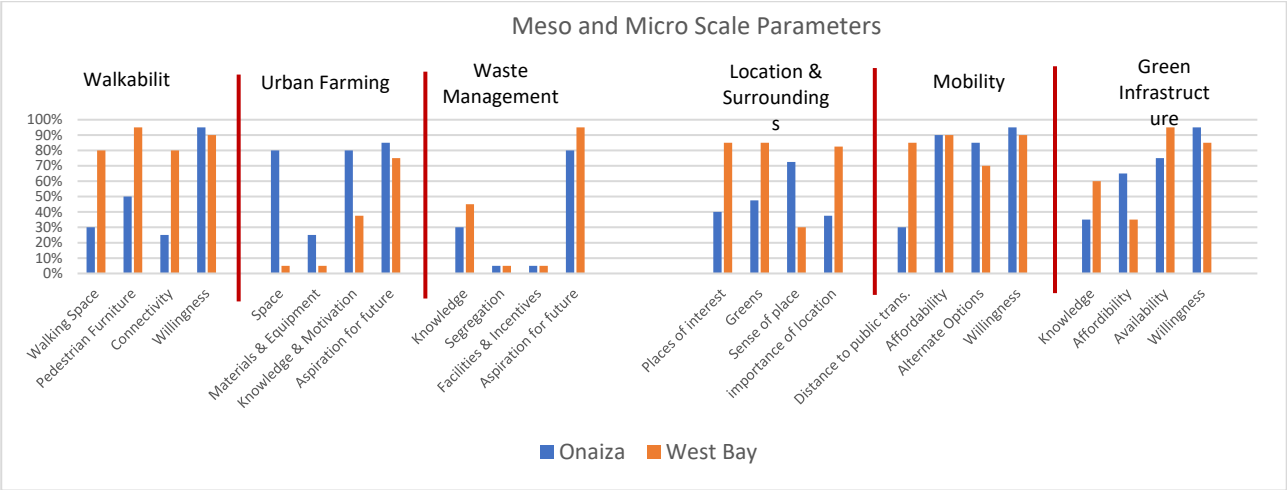


Fig. 5: Responses of residents' lifestyle preference to meso and micro-scale parameters

5 A Cumulative Analysis of Environmental Sustainability in Onaiza and West Bay Neighbourhoods

A qualitative assessment of environmental sustainability was performed through observation study and structured open-ended interviews, making a comparison between the lifestyle preferences of people residing in a low-rise neighbourhood (Onaiza) and a high-rise neighbourhood (West Bay) in Doha city.

5.1 Meso Scale Analysis

Walkability: The responses revealed that residents of Onaiza and West Bay rarely prefer to walk, even though the high-rise urban form of West Bay provides more opportunities for walking and using public transportation. This might be because of the general lifestyles of expatriates and the geographies they come from. Due to unfavourable weather conditions in Doha city, most expatriates take private vehicles as their preferred mode of transportation. While the lack of availability of places of interest is the reason for Onaiza residents, West Bay residents feel walking unsafe due to illegal parking. Onaiza residents unanimously agreed that pedestrian walkways in their surroundings are not well maintained and not well connected.

Urban Farming: West Bay and Onaiza residents are not involved in urban farming and lack knowledge of the concept. However, upon investigation, it was found that Onaiza residents are occasionally involved and interested in backyard/kitchen farming to grow certain spices and herbs. The lack of space is a major challenge for West Bay residents. All residents revealed a willingness to participate in community farming when proper knowledge and incentives are given.

Waste Management: Households in Onaiza and West Bay do not segregate waste and lack knowledge and awareness. The community bin at Onaiza and the garbage chute in the high-rise towers of West Bay are single units with no separation for different types of waste. This is the main reason people choose not to segregate waste at home as all the waste is eventually dumped into the same bin. Therefore, a regional-level policy is needed to promote waste management.

5.2 Micro Analysis

Location and Surroundings: West Bay residents have more opportunities and better facilities to walk to nearby places while Onaiza residents either carpooled or drove individually for leisure and shopping away from their neighbourhood. Onaiza residents preferred to go to far away parks rather

than neighbourhood parks, while West Bay residents chose to go to far away parks only during the weekends.

Mobility: West Bay residents more frequently use public transportation than Onaiza residents due to proximity and better connectivity. The feeder buses that commute between metro stations and bus stops in Onaiza have less frequency due to which Onaiza residents find it convenient to use private vehicles.

Green Infrastructures: While some of the Onaiza and West Bay residents are already using energy-efficient appliances, it is observed that residents do not prioritize user-friendliness, performance and convenience over energy efficiency when buying an appliance for their home. Onaiza residents showed more interest in investing in energy-efficient systems, which could be because of their ownership status. However, most of the residents were unaware if their neighbourhood has a green infrastructure or not, Table 1.

Table 1: Meso and Micro scale challenges for Onaiza (low-rise) and West Bay (high-rise) neighbourhoods

Scale	Parameters	Onaiza (Low-rise) Neighbourhood	West Bay (High-rise) Neighbourhood
Meso Scale	Walkability	Walking space, connectivity, quality of pedestrian pathways	Illegal parking
	Urban Farming	Cost of materials & equipment	Available space, facilities
	Waste Management	Lack of facilities & incentives	Lack of facilities & incentives
Micro Scale	Location & Surroundings	Proximity to places of interest and public parks	Too crowded
	Mobility	Proximity to metro stations, frequency of feeder buses	Connectivity
	Green Infrastructures	Lack of knowledge and availability	Lack of knowledge and availability

6 Conclusions and Recommendations

Beyond the anticipated FIFA 2022 World Cup, the Urban Planning Department of the Ministry of Municipality is expected to face several challenges. The oversupply of housing needs to be reappraised in response to the possible migration after the World Cup; rather than building new cities and neighbourhoods, planners must think of strategies to revive and retrofit old neighbourhoods. With a smaller population after the 2022 World Cup, amalgamated with continued sprawl, it will be a challenge to make the existing neighbourhoods environmentally sustainable. The following urban policies, strategies and interventions are recommended for low-rise and high-rise neighbourhoods to be environmentally sustainable, based on the findings of this study (Table 2).

Table 2: Proposed urban planning policies, strategies and interventions for meso and micro scale

Parameter	Proposed Urban Planning Policy	Proposed Strategies and Interventions
Walkability	Improving pedestrian walkway environment to enhance walkability at the neighbourhood scale in accordance with participatory approach.	• The street redesign should consider making it walkable by back-fitting connectivity. • Strict policies to maintain and monitor the quality of pedestrian pathways must be regulated. • Involve public participation to enhance small-scale pop-up infrastructures, parks and community spaces, promoting liveliness.

Parameter	Proposed Urban Planning Policy	Proposed Strategies and Interventions
Urban Farming	Promote urban farming to improve the environment and public health.	• Allot land for urban farming (a) within the plot area of low-rise development (b) within the common space in the plot area of high-rise developments (c) within public parks encouraging participation. • Strategies to incentivize urban farming must be regulated.
Waste Management	Spread awareness regarding low-cost strategies to manage domestic waste to support regional scale waste management	• Waste segregation at meso and micro scales must be mandatory and incentivized. • Composting green waste must be mandatory on-site and incentivized. • Technology for recycling 100% of the waste at regional level must be financed.
Location & Surroundings	Action plan to integrate urban development, green spaces and climate changes for improving public health	• Existing green spaces must be integrated with new green spaces to create approachable and health public space. • Promote mixed use neighbourhood. • Install mobile green elements through participatory approach.
Mobility	Action plans to improve efficiency of public transportation	• Focus on providing last mile connectivity to all neighbourhoods. • Create "only pedestrian" streets to increase the demand to use public transportation.
Green Infrastructure	Action plan to promote and finance energy efficient systems	• Spread awareness about energy-efficient systems that must be installed in homes and neighbourhoods. • Incentivize the usage of energy efficient appliances.

References

Al-Thani, et al. (2018). Smart Technology Impact on Neighborhood Form for a Sustainable Doha, *Sustainability, 10*(12). DOI: https://doi.org/10.3390/su10124764

Bakker, P. (2020). Can dense cities save the planet?, https://www.kone.com/en/news-and-insights/stories/can-dense-cities-save-the-planet.aspx. (Accessed: 18/5/2022).

Baobeid, A., Koc, M. & Al-Ghamdi, S. G. (2021). Walkability and Its Relationships with Health, Sustainability, and Livability: Elements of Physical Environment and Evaluation Frameworks. *Frontiers in Built Environment*, 7. DOI: https://doi.org/10.3389/fbuil.2021.721218

Brown, D. (2017). Challenging the conceptual boundaries of the compact city paradigm in sub-Saharan Africa, The Bartlett Development Planning Unit, pp. 2-6.

Cambra, P. J. (2012). Pedestrian Accessibility and Attractiveness Indicators for Walkability Assessment. *Technico Lisboa*.

Ferdinan, et al. (2022). "Household Waste Control Index towards Sustainable Waste Management: A Study in Bekasi City, Indonesia". *Sustainability, 14*. DOI: https://doi.org/10.3390/su142114403

Gillis, D., Semanjski, I. & Lauwers, D. (2015). "How to Monitor Sustainable Mobility in Cities? Literature Review in the Frame of Creating a Set of Sustainable Mobility Indicators". *Sustainability, 8*(1). DOI: https://doi.org/10.3390/su8010029

Grenni, S., Soini, K. & Horlings, L. G. (2020). The Inner Dimension of Sustainability Transformation: how a sense of place and values can support sustainable place-shaping. 15(1), pp. 411-422. DOI: https://doi.org/10.1007/s11625-019-00743-3

Jacobs, J. (1961). The Death and Life of Great American Cities. Random House Publisher, New York. ISBN: 978-0679741954

Khalil, R. & Shaaban, K. (2012). Rebuilding Old Downtown: The Case of Doha, Qatar, Real Corp 2012, Tahungsband, pp. 677 – 689. DOI: 10.13140/2.1.3296.1600

Khoshnava, et al. (2020). "Contribution of green infrastructure to the implementation of a green economy in the context of sustainable development". *Sustainable Development*, 28(1), pp. 320-342. DOI: https://doi.org/10.1002/sd.2017

Kim, S., Park, S. & Lee, J. S. (2014). Meso- or Micro-scale? Environmental Factors Influencing Pedestrian Satisfaction. *Transportation Research Part D: Transport and Environment*, pp. 10-20. DOI: https://doi.org/10.1016/j.trd.2014.05.005

Kim, et al. (2021). A comparative analysis of the users of private cars and public transportation for intermodal options under Mobility-as-a-Service in Seoul. *Travel Behavior and Society*, *24*, pp. 68-80. DOI: https://doi.org/10.1016/j.tbs.2021.03.001

Nwofe, P. (2013). "Waste Management and Environmental Sustainability: A Case Study of Selected Cities in Ebonyi State". *Journal of Environmental Sciences*, *7*(1), pp. 20-28. DOI: 10.5707/cjenvsci.2013.7.1.20.28

Pakzad, P. & Osmond, P. (2015). Developing a Sustainability Indicator Set for Measuring Green Infrastructure Solution. *Urban Planning and Architecture Design for Sustainable Development*, *216*, pp. 68-79. DOI: 10.13140/RG.2.1.2343.1121

Patel, S., Karanisa, T. & Khalek, M. A. (2021). Backyard Urban Agriculture in Qatar: Challenges and Recommendation. *Environmental Network Journal*, *1*(3), pp. 1-37. DOI: http://hdl.handle.net/10576/30946

Stedman, R. (1999). Sense of Place as an Indicator of Community Sustainability. *The Forestry Chronicle, 75*(5), pp. 765-770. DOI: https://doi.org/10.5558/tfc75765-5

Swanepoel, J. W., Van Niekerk, J. A. & Van Rooyen, C. J. (2018). An Analysis of the Indicators Affecting Urban Household Food Insecurity in the Informal Settlement Area of the Cape Town Metropole. *South African Journal of Agricultural Extension*, *46*(1), pp. 113-129. DOI: http://dx.doi.org/10.17159/2413-3221/2018/v46n1a467

The World Bank. (2021). Climate Change Knowledge Portal: Qatar. (Online). https://climateknowledgeportal.worldbank.org/country/qatar/climate-data-historical (Accessed 5/5/2022).

Cite as: Patel S. & Ibrahim H., "Environmental Sustainability Comparative Assessment of Low-Rise and High-Rise Neighbourhoods based on People's Lifestyle Preferences: The Case of Doha, Qatar", *The 2nd International Conference on Civil Infrastructure and Construction (CIC 2023)*, Doha, Qatar, 5-8 February 2023, DOI: https://doi.org/10.29117/cic.2023.0125

Transit-oriented Development from the View of Traditional City Model

Sara Nafi
Qatar University, Doha, Qatar
Sn1405549@qu.edu.qa

Djamel Ouahrani
Qatar University, Doha, Qatar
djamel@qu.edu.qa

Abstract

Several communities have adopted the transit-oriented development (TOD) model to improve the urban form of the city. Through the TOD model, citizens are enabled and encouraged to travel by public transit and live near it, resulting in a compact, walkable city. By emphasizing these principles, cities are able to create a sustainable urban environment that is beneficial to everyone. The purpose of this paper is to explore the relationship between transit-oriented development (TOD) and traditional city models and to promote the TOD model among Middle Eastern planners. Although Peter Calthorpe developed the TOD model in the early 1990s, the elements of TOD have existed in traditional cities for a long time. Literature has not explored the relationship between these two models; therefore, traditional cities and their development have been studied, such as Marrakech and Fes in Morocco. Marrakech and Fes are both examples of traditional cities in Morocco. The two cities have different features, such as *Marrakech's riads*, the old city walls, and the *souks* while Fes is known for its medina, the University of Al-Qarawiyyin, and its tanneries. This research, therefore, aimed to understand the correlation between traditional city models and TOD models by investigating: (a) the concept and diverse types of TOD models; (b) the relationship between TOD and traditional city models, and (c) the presence of TOD elements in traditional cities. This research provided insights into the opportunities and challenges of combining TOD models with traditional city models, in order to achieve more sustainable urban development.

Keywords: Transit-oriented development; Traditional city model; Connectivity; Public transportation

1 Introduction

Understanding our city's history is crucial to maintaining its identity and knowledge. Trade, commerce, and cultural exchange have always been taken place in cities over the centuries (Ali etal., 2021; Marthya, 2021). Streetcars were developed in the early 20th century by a single owner to serve suburban areas and increase real estate values (Carlton, 2009; Su, 2021). As a result, cities have developed around their transportation modes in the past. As these transit hubs grew into suburbs, urban development concentrated around them (Tamakloe, Hong, & Tak, 2021; Zhou, & Yang, 2021). The transit system was built early in the development of suburbs to serve city growth; therefore, it was known as "development-oriented transit". The suburban model eventually led to "transit-oriented development." (Ebrahimi, Rahimian, & Sahraei, 2013).

A Transit-oriented development (TOD) model is a well-established method for achieving compact and high-density development, using diverse land uses to promote open spaces, improving

accessibility and providing a variety of transportation options (Dong, 2021; Yildirim, & Arefi, 2021). The concept of TOD promotes sustainable development by reducing the use of cars and focusing on pedestrian-oriented development. Additionally, TOD serves as the centre of urban life where people can live, work, play, and socialize (Cervero, & Kockelman, 1997). As a result, long-distance driving becomes less necessary, greenhouse gas emissions from cars are reduced, and traffic congestion is lessened (Zhou, & Yang, 2021; Wey, & Hsu, 2014).

TOD have been used by a variety of city planners to promote the city's urban form in the past few years. In 1980, Peter Calthorpe, leader of the New Urbanist movement, recognized the TOD concept from a variety of perspectives (Hess, & Lombardi, 2004). As described by Calthorpe (1993), TOD typically consists of a mix of commercial, residential, office and public space located between 10-15 minutes (approximately 1 kilometre) from a public transportation stop (Su, 2021). Through TOD, cities become more compact and walkable, encouraging citizens to use public transportation and live near it (Dou et al., 2016). In TOD models, the city is developed around transit hubs, surrounded by markets, bazaars, and residential zones, returning to a traditional suburban and metropolitan centre (Ghasemi, Hamzenejad, & Meshkini, 2019; Mai, Zhan, & Chan, 2021).

To fill the gap in the literature regarding the relationship between traditional cities and TOD, this paper aims to make TOD more accessible to community members and planners in the Middle East. Even though TOD was developed by Peter Calthorpe in the early 1990s, TOD elements existed long before then. Therefore, this paper seeks to bridge the gap in knowledge by offering a better understanding of TOD principles, originating from traditional urban designs to planners and community members in the Middle East.

2 Methodology

Several reviews of recent literature related to transit-oriented development (TOD) were conducted to gain a deeper understanding of the concept. The overall data collection methods were based on an evaluation of literature from a variety of fields that emphasized TOD key factors and traditional city elements. To fill the gap between TOD and traditional city models, similarities and differences in their elements were identified. A meta-analysis was used to identify and analyze the various components of TOD and traditional city models, identifying relevant high-quality data sources and integrating findings to draw conclusions, allowing a broader and more systematic understanding of these two models. Through this analysis, it was possible to determine how various elements of TOD and traditional city models overlap and contrast, providing insights for future development. By utilizing a meta-analysis, it was possible to gain a deeper understanding of the differences and similarities between TOD and traditional city models, providing valuable insights for urban planners and decision-makers. This, in turn, could aid urban planners and decision-makers in formulating more effective urban and transport policies that incorporate the benefits of both TOD and traditional city models. Finally, it was possible to identify gaps in the existing literature, as well as opportunities for future research.

3 TOD Model

Several studies related to TOD at local, regional, and international levels were reviewed to gain greater insight into the concept. The TOD strategy has been widely recognized as an effective urban planning strategy in recent years. TOD promotes mixed land use, compact cities, walkability, and public transportation use and living (Mirmoghtadaee, & Abdi, 2021).

The concept of TOD has been discussed in numerous ways by urban and transport planners. However,

it is widely attributed to Peter Calthorpe, one of the leading figures of the New Urbanism movement. In 1993, Peter developed the TOD phrase, which was widely used in "The Next American Metropolis" book. TOD is defined by Calthorpe as "a mixed-use development in close proximity to a central public transportation stop, which is approximately 10-15 minutes' walk or cycle ride away (Su, et al., 2021). In TOD, pedestrian paths are integrated into mixed-use developments, which include residences, offices, public spaces and public transportation, encouraging citizens and employees to take public transportation, walk, cycle or drive" (Abdi, 2021) (see Figure 1).

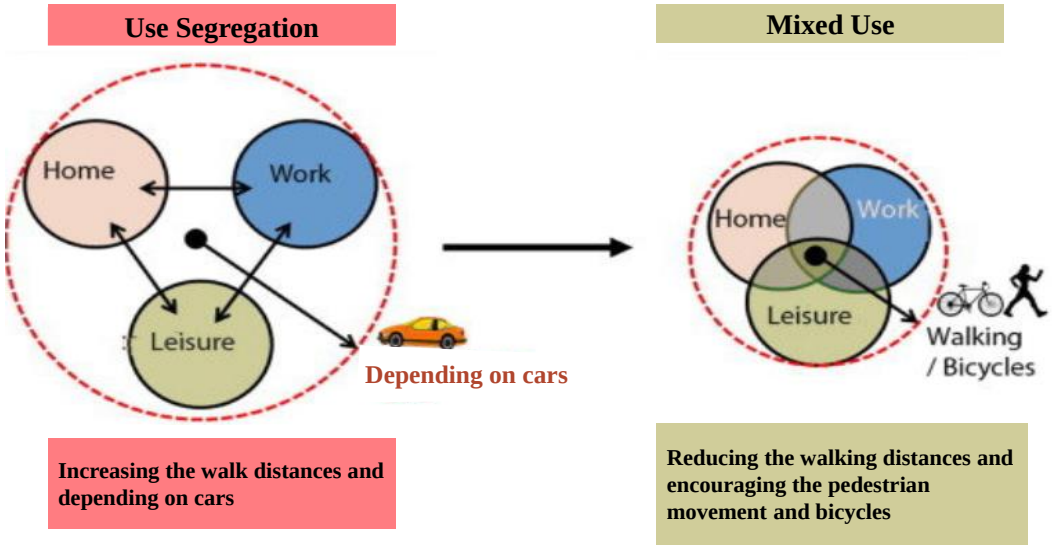


Fig. 1: Use segregation vs mixed use (Kamyar, & Spourezi, 2019)

3.1 **Distinct types of transit-oriented development**

The first type is single-node TOD (see Figure 2). This type is based on a single neighborhood centered on railway stations. It can be located in an urban or suburban area. Development is carried out in a circular pattern centered on a train station. There are a variety of radiuses ranging from 0.5 km (for pedestrian access) to 2-3 km (for bicycle access) (Zhang, 2022).

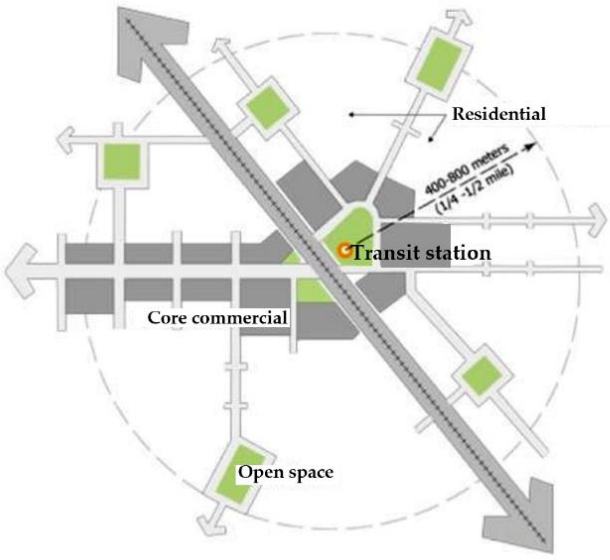


Fig. 2: Single-node TOD (Abdi, 2021)

The second type of TOD is multi-node TOD (see Figure 3). The purpose of this type is to create a regional network of nodes around railway stations, similar to single-node TOD. There are two types of nodes: circular and semicircular. TOD nodes are typically arranged in the form of "beads-in-a-string." TOD of this type aims to realign entire urban regions around rail transportation and away from automobiles (Abdi, 2021).

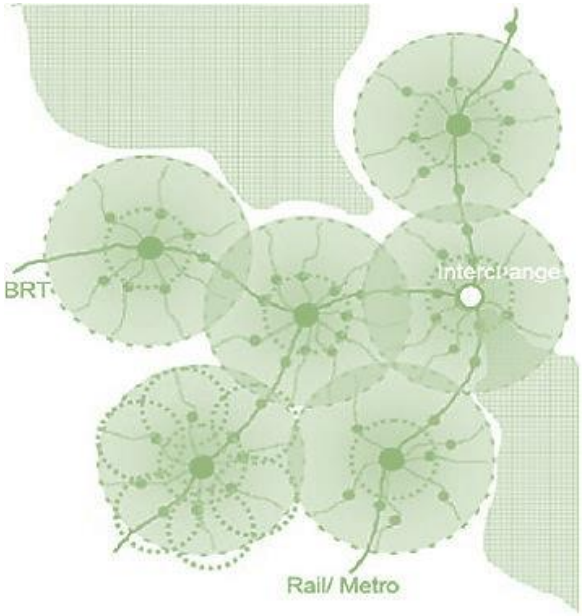


Fig. 3: Multi-node TOD (Kamyar, & Spourezi, 2019)

The third type of TOD is corridor TOD (see Figure 4). This type occurs in cities and is based around light rail or Bus Rapid Transit (BRT) stops. Due to the proximity of nodes along the transit line(s), the development pattern is linear or ribbon-like. TOD corridors can be used in existing urban areas as well as those that are being planned.

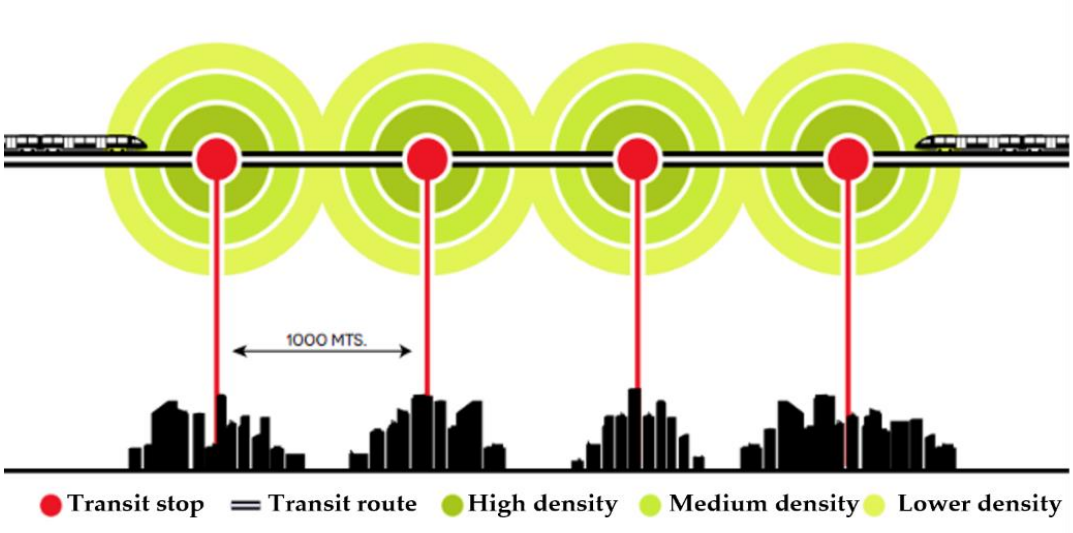


Fig. 4: Corridor TOD (Dabbour, 2021)

4 The Presence of TOD Features in Traditional Cities

4.1 The Traditional City Model

In 1969, the German geologist Dettman developed the traditional city model (Dabbour, 2021). City development was centered around the great mosque, with a bazaar, market, and residential areas surrounding it. The traditional city model emphasized the importance of the great mosque as the nucleus of the city, with all other activities deriving from it (see Figure 5).

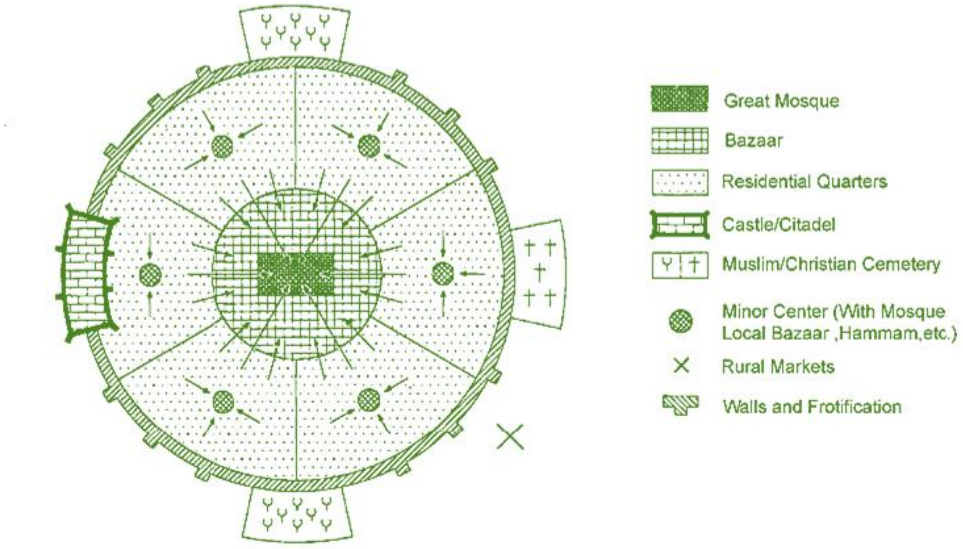


Fig. 5: Dettman Islamic City Model (Al-Harami, & Furlan, 2020)

A second German geographer, Ehlers, has developed a design for traditional cities. He identifies the characteristics of a traditional city as (a) Newly built streets that undo the ancient urban consistency of the bazaar area and disrupt the cohesion of the bazaar. (b) A new external area of the city that reflects the surrounding environment and has a patterned order (Calthorpe, 1993). Ehlers emphasizes that this new external area should be well integrated with the environment, providing a sense of continuity with the city's past. To ensure this continuity, Ehlers proposed that the design of this external area should incorporate elements of the surrounding environment, including the use of local materials and traditional patterns. As a result, Ehlers stressed the importance of creating a design that is both aesthetically pleasing and respectful of the city's cultural heritage (Al-Harami, & Furlan, 2020) (see Figure 6).

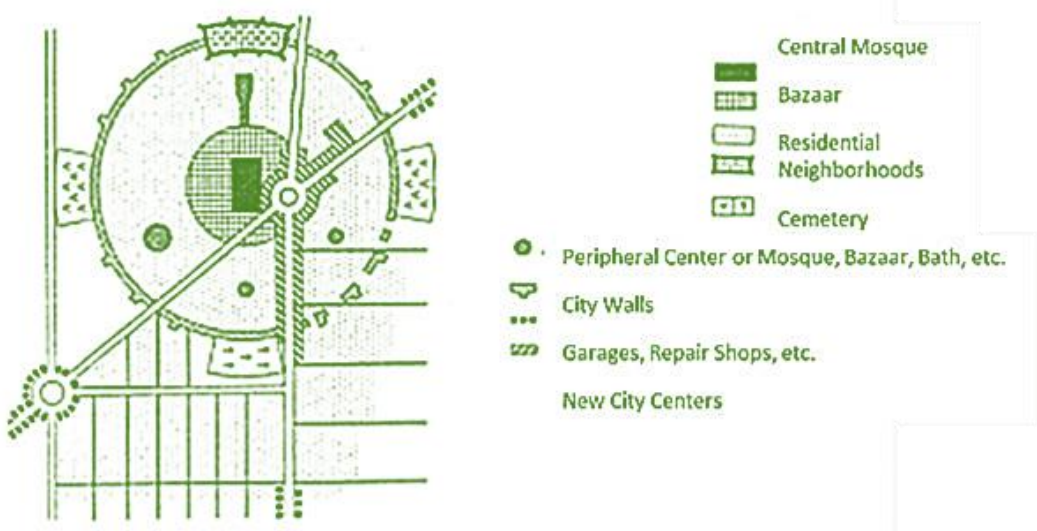


Fig. 6: Ehlers Traditional City Model (Al-Harami, & Furlan, 2020)

4.1.1 Connectivity and Compact City

The traditional city consists of residences, palaces, and public spaces such as mosques, hospitals, madrasas, and residential areas (Rogers, 2020). Most houses are internally oriented, segregated from the "outside" world by walls, or through hierarchically arranged streets. A street often runs from a major public road to a cul-de-sac and finally to a private parcel. There are very few connections between the various districts of the city. Returning to the major street is the only way to get from one sector to another (Caset, et al., 2020).

The image below shows Fes compact city, the cultural heart of Morocco. It is one of the oldest cities in the world. The area is one of the world's largest urban car-free areas and is listed as a UNESCO World Heritage Site. The city consists of two old Medina quarters, Fes el Bali and Fes el Jdid, and the modern Ville Nouvelle, built during the French colonial period (1912-1956) (Zhang, 2022). Fes is renowned for its traditional city layout, with its narrow alleyways, winding streets, and intricate architecture, which reflect its centuries-old history. These features, combined with the rich culture and vibrant atmosphere (see Figure 7 and 8).

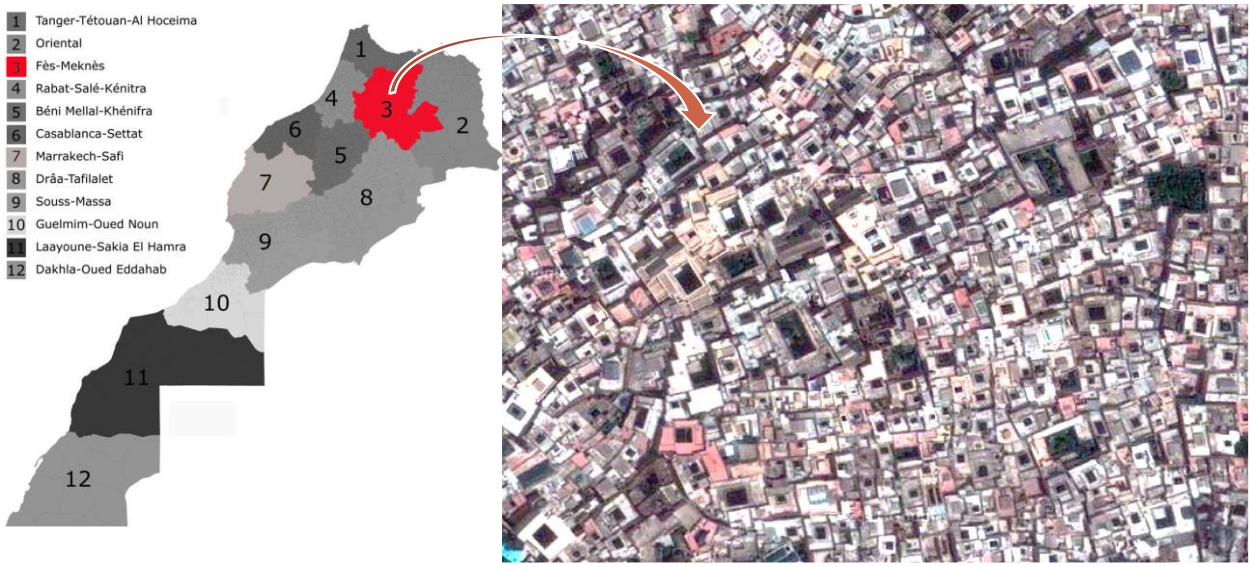


Fig. 7: Fes compact city, the cultural heart of Morocco



Fig. 8: Close interaction between the souq, mosque, alleyways, and surrounding residences (Zhang, 2022)

In the city of Fez, the area was divided according to professions, such as tanneries, copper craftsmen spice sellers. Chouara Tannery is one of the oldest tanneries in the entire city, in addition to being the largest. Located near the Saffarin Madrasa on the Oued Fes (also called the Oued Bou Khrareb), it is the oldest Medina quarter of the city (see Figure 9). Throughout the city's history, the tanning industry continued to operate in the same manner as it was in the early centuries. In modern day, the tanning industry is considered one of the main tourist attractions in the city (Zhang, 2022; Nafi, et al., 2021).



Fig. 9: Chouara Tannery in Fes (Nafi, et al., 2021)

4.1.2 Public Realm

Plazas, souks, parks, squares, and leisure areas are all examples of public realms that contribute to social cohesion. Low levels of pollution and a sense of safety contribute to a more comfortable living environment (Ehlers, & Floor, 1993). The public realm is an important component of a community's social life, contributing to community interaction, social cohesion, and a sense of belonging (Hakim, 2008). TOD includes public spaces in which people can determine their own cultural identities, participate in communities, and engage in social activities (Marthya, et al., 2021; Budiman, 2019).

Similarly, to TOD, the traditional city has a ''Barahat,'' an open area around the houses where traditional performances are held. There are several Barahat scattered throughout the old city neighbourhood. In addition to covering residents' needs, Barahat provides a comfortable, secure atmosphere for them (Rogers, 1998). A compact outdoor park, for example, was located near schools. There is also a public Majlis near mosques (Calthorpe, 1993).

In comparison to Fes, Marrakech in morocco was once one of the most significant trading centres for Atlas Mountain tribes, and it remains so today (Figure 10). The souks are located to the north, while the Koutoubia Mosque and Gardens are to the west. To the south lies the Kasbah area which is home to the Saadian Tombs, Bahia Palace, and El Badi Palace. Within the city, visitors can explore the spice markets at Souk el-Attarin, the blacksmith markets at Souk Haddadine, and the slipper markets at Souk Smata. The buildings have large open spaces and courtyards that enhance the sense of place. (Figure 10 & 11).

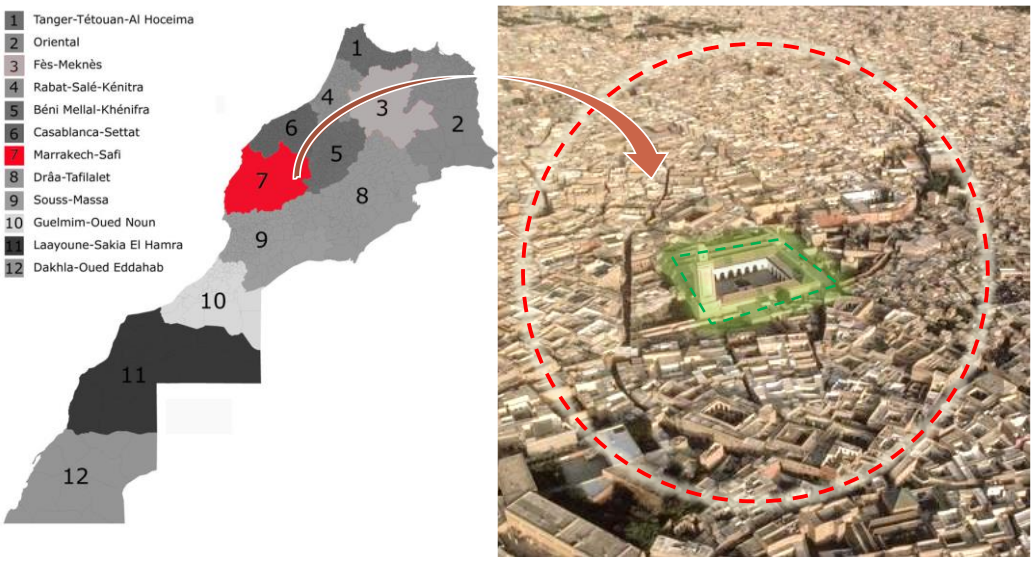


Fig. 10: Marrakech, Morocco



Fig. 11: Jemaa el Fna Square, Marrakech (Zhang, 2022)

4.1.3 Diversity and Density

Studies have shown that the TOD model promotes a mix of commercial, residential, recreational, and educational land uses, along with high pedestrian activity (29). A transit stop is usually surrounded by commercial buildings and public amenities, while the rest of the land is used for other purposes (Benzakour, 2020). The TOD approach also promotes compact development of moderate to high-density cities, allowing pedestrians to move easily within them (Yildirim, & Arefi, 2021; Al Saeed, & Furlan, 2019; Lamour, Morelli, & Marins, 2019; Mukhamedjanov, et al., 2021).

For the traditional city model, it promotes a compact development of a variety of land uses, including the bazaar (market), the madrasah (school), the mosque, the guesthouse, the hammam, the library, the cultural center, and residential buildings (Mirmoghtadaee, & Abdi, 2021). Typically, the central mosque is surrounded by a bazaar, a library, and schools. On the other hand, the traditional city model integrates these land uses with traditional spaces and maintains them (Calthorpe, 1993; Caset, et al., 2020).

5 Discussion

The concept of TOD and its different subtypes were examined. By comparing TOD with traditional city plans, as well as analyzing the similarities between their principles, it was demonstrated that

TOD elements are also found in traditional city plans. The results of this comparison provide insight into how TOD can be incorporated into traditional city plans to create more sustainable, efficient, and livable environments. This comparison, thus, suggests that TOD can be used to supplement traditional city plans, creating a more holistic approach to urban design and development.

The results show that TOD is a top-down, centrally planned process created by city planners, whereas the traditional city model is a bottom-up, collectively planned process determined by contextual conditions and society. Traditional cities created places for commerce and economic centers. However, the TOD model operates more as a commodity and a service to society to improve the quality of life. This has resulted in the TOD model becoming a popular approach to developing cities, offering a balance between economic and social needs, while also promoting a more sustainable and equitable urban environment.

Traditional cities were built on destination-based activities. Attractive destination to engage in activities and interactions. This is because traditional cities are designed from a human-centric perspective, where the focus is on providing places for people to gather and interact. In contrast, TOD is designed from a transportation-centric perspective, which focuses on providing efficient transportation to move people from one place to another. Therefore, even though TOD has its own distinct features, there are still elements of traditional city planning that are present.

Today, cities are increasingly organized around activities that are generated within the city itself, such as work, recreation, and entertainment. For instance, in many cities, the downtown area has become a hub of activity with people commuting there for work and entertainment, rather than just for shopping or business. A traditional city is a city that has developed organically over time, through the organic growth and expansion of its population. A TOD city is a city that has been designed and planned from the ground up to be a more efficient and sustainable place to live (see Figure 12).

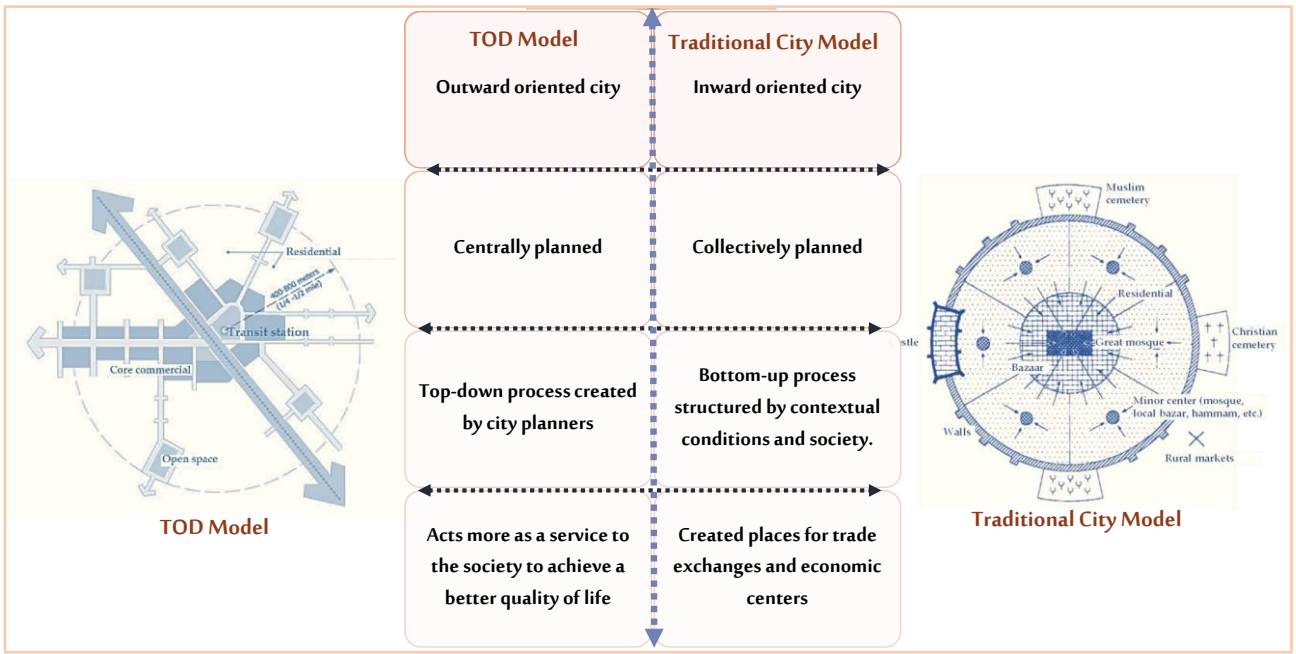


Fig. 12: Comparison between the traditional city and TOD model

6 Conclusion

Through high-quality transit, TOD promotes sprawl-free development and improves urban mobility. TOD enhances wealth building, improves opportunities for residents, and reduces air pollution by

promoting neighborhood diversity, walkability, and compact development near transit hubs. Although TOD is a more academically structured concept than traditional forms of city planning, the paper attempts to demonstrate that it is not a very new concept. By establishing a link between TOD and traditional city development, this paper aims to strengthen the concept of TOD in non-Western cities. This planning will not only preserve the traditional city but also enhance the newly urbanized areas as well. It is necessary to maintain traditional neighborhoods that contain elements of TOD while enhancing these elements to meet the needs of 21st-century residents. This paper argues that cities in non-Western countries can benefit from combining traditional city development with TOD. This will ensure that the traditional city is preserved and create new, modern spaces that can accommodate the needs of a modern society. The paper aims to establish a connection between these two concepts and show how they can be used together to create a sustainable urban environment.

Scholars, urban and transportation planners can benefit from the study for formulating TOD strategies in Middle Eastern cities while maintaining vernacular city structures and urban identity. For example, planners can use the findings of the study in order to design pedestrian-friendly streets that preserve the traditional urban fabric, as well as create dynamic public spaces for leisure and social activities. Furthermore, planners can use the results of the study to develop strategies that promote walkability and green infrastructure, while also preserving the unique character of Middle Eastern cities.

Finally, to achieve successful TOD planning that takes Middle Eastern culture, climate, and geography into account, efficient interaction and coordination between policymakers, planners, and stakeholder groups is essential. Long-term regional coordination would lead to more cohesive strategies and tools as well as stronger organizational links. Moreover, decision-makers and local planners will be better able to develop a consistent regional vision based on broader theories related to TOD. For TOD to be implemented successfully, the general population must be involved in decision-making processes. Therefore, it is essential to create a participatory approach to TOD planning, ensuring that the public is included in conversations concerning regional development.

Acknowledgements:

This study was created as part of my PhD thesis at Qatar University in Urban Planning. Thanks to Qatar University's assistance, the authors were able to conduct this type of research.

Funding:

This publication was made possible by an Award [GSRA7-1-0502-20030] from Qatar National Research Fund (a member of Qatar Foundation). The contents herein are solely the responsibility of the authors.

References

Abdi, M. H. (2021). What the newcomers to transit-oriented development are confronted with? Evidence from Iranian policy and planning. *Journal of Transport Geography*, *92*, 103005.

Alattar, D. A. & Furlan, R. (2017). Urban Regeneration in Qatar: A Comprehensive Planning Strategy for the Transport Oriented Development (TOD) of Al-Waab.

Al Saeed, M. & Furlan, R. (2019). Transit-oriented development in West Bay, Business District of Doha, State of Qatar: A strategy for enhancing liveability and sense of place. *Journal of Cultural Heritage Management and Sustainable Development*, *9*(3): 394-429.

Al-Harami, A. & Furlan, R. (2020). Qatar National Museum-Transit oriented development: The masterplan for the urban regeneration of a 'green TOD'. *Journal of Urban Management*, *9*(1): 115-136.

Ali, L., et al. (2021). Dynamics of Transit Oriented Development, Role of Greenhouse Gases and Urban Environment: A Study for Management and Policy. *Sustainability*, *13*(5).

Benzakour, S. (2020). "Guide Fez: Time Trip," https://bahaarofficial.com/en/blogs/infos/carnets-de-voyage-decouvrez-les-merveilles-du-maroc-avec-bahaar.

Budiman, H. (2019). Istanbul, The Development of Islamic City Thinking. *MATEC Web of Conferences, 280,* 02005.

Calthorpe, P. (1993). The Next American Metropolis: Ecology, Community, and the American Dream. New York: Princeton Architectural Press., ed. 10003. Vol. 1., Canada: Princeton Architectural Press. 175.

Carlton, I. (2009). Histories of transit-oriented development: Perspectives on the development of the TOD. Institute of Urban and Regional Development, University of California, Berkeley, *02*(2009).

Cervero, R. & K. Kockelman (1997). Travel demand and the 3Ds: Density, diversity, and design. *Transportation Research Part D: Transport and Environment*, *2*(3): 199-219.

Dabbour, L.M. (2021). Morphology of quarters in traditional Arab Islamic city: A case of the traditional city of Damascus. *Frontiers of Architectural Research, 10*(1): 50-65.

Dong, H. (2021). Evaluating the impacts of transit-oriented developments (TODs) on household transportation expenditures in California. *Journal of Transport Geography*, *90,* 102946.

Dou, et al. (2016). An empirical study on transit-oriented low-carbon urban land use planning: Exploratory Spatial Data Analysis (ESDA) on Shanghai, China. *Habitat International*, *53*, 379-389.

Ebrahimi, A., Rahimian, F. P. & Sahraei, M. (2013). Impacts of urban passages on formation of iranian bazaars: Case study of the historic bazaar of Tabriz. *International Journal of Architectural Research (IJAR), 61,* 61-75.

Ehlers, E. & Floor, W. (1993). Urban Change in Iran, *1920-1941*. *Iranian Studies*, *26*(3/4): 251-275.

Ghasemi, K., M. Hamzenejad & Meshkini, A. (2019). The livability of Iranian and Islamic cities considering the nature of traditional land uses in the city and the rules of their settlement. *Habitat International, 90,* 102006.

Hakim, B.S. (2008). Arabic-islamic cities: building and planning principles. Kegan Paul International Limited. 197.

Hess, D. & Lombardi, P. (2004). Policy Support for and Barriers to Transit-Oriented Development in the Inner City: Literature Review. *Journal of Transportation Research Board*.

Kamyar, M. & Spourezi, Z. J. (2019). Representing Iranian-Islamic Identity in Iranian Contemporary Cities Structure. *Journal of Contemporary Urban Affairs*, *3*(2): 55-62.

Lamour, Q., Morelli, A. M. & Marins, K. R. D. C. (2019). Improving walkability in a TOD context: Spatial strategies that enhance walking in the Belém neighbourhood, in São Paulo, Brazil. *Case Studies on Transport Policy*, *7*(2): 280-292.

Liang, et al. (2020). Planning for urban life: A new approach of sustainable land use plan based on transit-oriented development. *Evaluation and Program Planning*, *80*, 101811.

Mai, X., Zhan, C. & Chan, R. C. K. (2021). The nexus between (re)production of space and economic resilience: An analysis of Chinese cities. *Habitat International*, *109*, 102326.

McCarty, C. (2021). "Imperial Cities of Morocco", 2021 Feb. 18, 2021 [cited 2023 Feb. 11]; https://www.kimkim.com/c/imperial-cities-of-morocco-7-day-itinerary.

Marthya, K., et al. (2021). Place-Making of Transit Towns in Qatar: The Case of Qatar National Museum-Souq Waqif Corridor. *Designs*, *5*(1).

Mukhamedjanov, A., et al. (2021). Reshaping the concept of transit-oriented development in response to public space overheating near the transit nodes of Tokyo. *Cities*, *116*, 103240.

Nafi, S. (2021). Transit-Oriented Development in Doha: The Case of the Al Sadd Neighborhood and Hamad Hospital Metro Station. *Designs*, *5*(4): 61.

Su, S., et al. (2021). Unraveling the impact of TOD on housing rental prices and implications on spatial planning: A comparative analysis of five Chinese megacities. *Habitat International, 107,* 102309.

Tamakloe, R., Hong, J. & Tak, J. (2021). Determinants of transit-oriented development efficiency focusing on an integrated subway, bus and shared-bicycle system: Application of Simar-Wilson's two-stage approach. *Cities, 108,* 102988.

Tong, et al. (2018). Correlation between Transit-Oriented Development (TOD), Land Use Catchment Areas, and Local Environmental Transformation. *Sustainability*, *10*(12): 4622.

Wey, W. M. & J., Hsu (2014). New Urbanism and Smart Growth: Toward achieving a smart National Taipei University District. *Habitat International*, *42,* 164-174.

Yildirim, Y. & Arefi, M. (2021). How does mixed-use urbanization affect noise? Empirical research on transit-oriented developments (TODs). *Habitat International*, *107,* 102297.

Zhou, J. & Y. Yang. (2021). Transit-based accessibility and urban development: An exploratory study of Shenzhen based on big and/or open data. *Cities*, *110*, 102990.

Zhang, M. (2022). Chapter Eleven - Corridor transit oriented development: Concept, practice, and research needs, in Advances in Transport Policy and Planning, X.J. Cao, C. Ding, and J. Yang, Editors. *Academic Press*, 277-299.

Cite as: Nafi S. & Ouahrani D., "Transit-oriented Development from the View of Traditional City Model", *The 2nd International Conference on Civil Infrastructure and Construction (CIC 2023)*, Doha, Qatar, 5-8 February 2023, DOI: https://doi.org/10.29117/cic.2023.0126

Assessment of Aesthetic Control in Qatar's Urban Design

Nur Alah Abdelzayed Valdeolmillos
na1912807@student.qu.edu.qa

Almaha Ahmad E R Al-Malki
aa082370@qu.edu.qa

Shaligram Pokharel
shaligram@qu.edu.qa

Mohamed Arselene Ayari
arslana@qu.edu.qa
College of Engineering, Qatar University, Doha, Qatar

Abstract

Aesthetic control is concerned with the visual appearance of the built environment, specifically in the urban setting. The built environment aesthetics can directly influence place identity, property values and the business owners' financial status in the area. People's behavior in terms of choosing a place to live or do business is also affected by the locality's aesthetics. Qatar has invested heavily in the built environment over the last two decades, which has shed light on the importance of government adopted aesthetic control measures to preserve the identity of Qatar's built form. This paper reviews the current control measures and provides some directions to adopt in the building permit process in support of Qatar's National Master Plan 2032. The paper recommends a strategy to the Ministry of Municipality and Environment for a swift implementation of aesthetic/design control in Qatar until a fully integrated solution is adopted to align with the built environment as proposed in the Qatar National Master Plan 2032. Digital tools can foster designs that can restore the quality of compromised ecosystems. A partnership platform can be created between the building permit unit and pre-selected private design-oriented consultants. Lastly, this research initiative could be used by other countries subject to similar development dynamics as a precedent to further develop their own aesthetic control measures.

Keywords: Aesthetic controls; Design regulations; Design governance; Urban Planning; Qatar

1 Introduction

The appearance of the built environment can have a direct influence over different aspects of daily decisions such as property values and the financial status of the business owners in the area. It can unconsciously direct people's behavior by affecting the place they want to live in or the route they want to take to work (Gjerde & Vale, 2015). In addition, good design can promote well-being, decrease stress, increase cultural vitality and civic pride, and enhance the sense of place in their communities (Carmona M. , 2001). Places with high aesthetic qualities are also appealing due to increased economic values, the potential for business investment, and the attraction of high-caliber workers (Gjerde & Vale, 2015).

This research focuses on Qatar's situation in terms of aesthetic control and how the process can be evaluated and upgraded to achieve high-quality design outcomes. Aesthetic control is concerned with

the development's visual appearance in its urban setting (Hawkes, Scheer, & Preiser, 1994). It is used as a planning tool to control the aesthetics and the visual impact of a building to its context, focused mostly on the external appearance of a building. It is different from design review or design control, which is more focused on morphology, internal and external spatial design, and the study of other design features of the buildings. Lack of adequate handling of aesthetics in the built environment results in standardization and a monotonous environment or chaotic, unhealthy and unattractive urban spaces (Drew, 1965; Deng, 2009; Gjerde & Vale, 2015). Literature shows that there are best practices and available technologies on aesthetic control and design regulations, some of which can be implemented in Qatar's context.

The paper proposes a phased framework for aesthetic control to enhance the current building permit approval process and swiftly integrating design controls. Therefore, three research questions are addressed in this paper: i) What is the status of aesthetic control in Qatar's urban design? ii) What parameters should be considered in aesthetic control reviews? iii) What roles would emerging technology play to assist municipalities in implementing aesthetic control as per QNMP 2032 Vision?

2 Literature Review

2.1 Aesthetic Control

Aesthetic control is a determinant tool used by the government bodies to administer and control the design proposals and/or development projects with concerns to its urban context. These control measures are reviewed and implemented by an independent local government body either through informal and/or formalized processes (Hawkes, 1999; Scheer, Brenda, Preiser & Wolfgang, 1994).

The most prominent objective associated with aesthetic control is the image and character preservation for the urban environment, especially those deeply connected with heritage (Hawkes, 1999). Scheer and Preiser (1994) mention that the improvement in the quality of life in the urban environment, conservation of unique features around the built environment, creation of aesthetically and visually congruent environment are some of the objectives for aesthetic control. Deng (2009) mentions that an ideal control model should relate to the historical, cultural, social, political and economic status of every individual that lives within a given urban context (Deng, 2009). Nonetheless, external challenges facing urban developments such as the neighbourhood image, increase in urban density, environmental challenges, services and facilities; can affect the overall aesthetic control of the whole development (Arbab, Azizi & Zebardast, 2018).

Keira (2011) explains that the existing development approval process may only consider the immediate context concerning aesthetic control instead of the whole area or the entire city (Kiera, 2011). Mostly, there are areas where some regulations practices are adapted to control the appearance of each establishment. It should be noted that aesthetic control does not mean standardization of the buildings; it promotes spontaneity and the creativity of the architects and makes the built environment more visually cohesive. Carmona et al. (2001) indicate that the appreciation of the urban environment, as Gestalt psychologists suggested, comes from the recognition and grouping of patterns. Although, variation has great significance in designing visually appealing urban landscapes, six criteria have been identified by Cantacuzino (1994) to make for a greater harmonization of new buildings within existing contexts namely: siting, massing, scale, proportion, rhythm, and materials (Carmona M. , 2001).

In Qatar, currently, there are no statutory aesthetic control processes. The design is controlled via the building permit regulations and approval process in two stages: Design Control 1 (DC1) and Design

Control 2 (DC2). The DC1 stage approval process consists of the submission and review of architectural drawings, including the site plan with area statements, elevations, and sections (Doing Business 2020, Qatar). The building elevations are evaluated at DC2 stage through a 'no-'objection' approval methodology based on compliance with Qatari architecture style which takes place only if the building is intended for public use, and it is assessed by the Private Engineering Office (PEO) of the government mostly based on the building's facade features.

In recent years, the development of multiple megaprojects and cities within the city, for example, Msheireb, Lusail City, and The Pearl, have made project teams advance in regulating aesthetic control to meet their stakeholders' aspirations. However, the positivity of these efforts is still sporadic and not reflected in the majority of privately led projects, which in contrast give little attention to urban design or planning regulations (Qaddumi & Ahmadi, 2017). This contrast has been recently identified by the government launching in 2019 the Doha Central Development and Beautification Projects (The Peninsula Qatar, 2020a).

2.2 Design Regulations vs. Design Governance

From an urban design perspective, the process and product of development are primarily concerned with individual pieces of development that are often inconsistent and do not support the creation of places (Carmona, Marshall & Stevens, 2006). Zoning as a tool is often used to determine pre-approved architectural styles to maintain the character and property values (Staley & Claeys, 2005). The public sector's role in the form of control regulations on urban design is often emphasized even when it is strongly influenced by the sophistication of their capabilities. Staley's and Claeys's (2005) study discuss how such rigid system is based on the past and how a new framework needs to be developed that is more dynamic and innovation driven.

On the other hand, the notion of design governance can create a complex shared responsibility that positively influences the design outcomes. Design governance is a journey that supports continuous stewardship and change for adopting a good design process. A quality design process is crucial for the optimization of each of the other design quality forms– aesthetic, project, and place (Carmona, 2016). Doha's urban growth since the 1970s has followed a master plan through the urban planning department of the Ministry of Municipal Affairs and Agriculture (MMAA) that provided legal zoning plans, some of which have been detailed and adjusted to cater to the later fast urban growth due to the oil boom in Qatar (Adham, 2008).

The vision to transform Doha into a well-connected international hub required that the existing zoning plans be remodelled (Salama & Wiedmann, 2016) to reflect the new knowledge and needs for development and redevelopment of the areas. In this regard, the QNMP launched in 2011, introduced an extensive set of key development objectives, strategies, and regulations providing a strict framework as guidance to spatial and land-use decision-making for the development of Qatar until the year 2032. The master plan has been developed with a macro-urban context focus, and its most important current challenge is the possibility of its execution in particular development-constrained areas (Salama & Wiedmann, 2016). Special Zones are not regulated under the QNMP. Their planning and design guidelines have been produced by project teams to govern and guide these projects from inception to completion. A review of these documents for the development of Lusail, Msheireb, and Education City shows that they have used some common parameters for a coherent urban design. They have considered some for the regulation of aesthetic aspects such as design rationale, design quality, style, context & identity and aspect, along other aspects more related to urban planning like

building siting, building height and, orientation and form (Lusail City, 2015).

However, the developed policies of the master plan mainly target new developments whereas the addressing issues in the current fabric via tactics of retrofitting or upgrading is not clearly mentioned in the document apart from being described as opportunities under the "Enhancing Urban Form" section (Qaddumi & Ahmadi, 2017). Therefore, the master plan's transformative role for the urban governance in Qatar is highly dependent on the overall effectiveness, flexibility, and transparency of its comprehensive legal framework, becoming the new decision-making process for all major developments in the country.

3 Research Framework

خطأ! لم يتم العثور على مصدر المرجع. The research questions are set first based on the need for the research and the insight on aesthetic control is developed through the literature review. The review helps to define the parameters of aesthetic control and the extent it can be applied in building permit approval processes. The research focuses on two main topics: aesthetic control and design regulations. Data from literature is analysed through content analysis and additional data is gathered through semi-structured interviews with several industry professionals: consultants, and related staff at the Ministry of Municipality and Environment (MME), PEO, Arrus International, Arab Engineering Bureau, Building Permit Complex and Qatar Foundation. To demonstrate the aesthetic control process in Qatar, this research focuses on controls applied to "City within a City" projects as well as the controls applied by MME and the foreseen controls coming with the new QNMP implementation.

4 Data Analysis

This section of the research divulges in the aesthetic control imposed on private development versus that of public/government-related developments. Furtherly, this section explains the gaps in regulations and implementation of aesthetic control in Qatar's Urban Design.

4.1 Regulations of Private Development versus MME Regulations

The MME is the main government body that governs the practice of building approvals and other permits related to any construction project. The municipalities under the umbrella of MME are responsible for reviewing the design process and ensuring its implementation as per the approval.

The QNDF is concerned with municipal spatial development, zoning regulations, and urban centre plans. The zoning regulations control the land-use of the area and, accordingly, the built area ratio, building height, open spaces, and other aspects of urban design. It does not consider the aesthetical qualities of the building with its urban context; however, that soon might change when its Qatar Urban Design Compendium (QUDC) project is launched. The QUDC aims to put forward a set of policies that provide guidelines for the practice of urban design and it is meant to be used as a national planning tool to protect Qatar's physical development in the future. It will act as a guide to the rationale, values, and principles for Qatar's urban design, although there would still be a need to develop a clear set of rules to implement the guidelines envisaged in QUDC.

The zoning regulations as per the QNMP are administered through the Municipal Spatial Development Plans (MSDP) requiring assessment of buildings and provision of permits based on its location land-use requirement, which differs from one location to another and between the different municipalities. Areas in Qatar except for special zones like Lusail city, as mentioned earlier, have zoning regulations enforced

There are some basic regulations to follow for building facades such as window opening percentage,

glass/curtain wall material, and allowed colour tones on the facade. In governmental/public buildings, these aspects are reviewed by the PEO in the building permit application phase for compliance with traditional Qatari architecture style and in alignment with Building Permit Complex process. The PEO follows one of the most stringent processes about aesthetic requirements. A panel in the PEO reviews developments based on its style, colour of elevations, and proportions. **خطأ! المرجع الذاتي للإشارة المرجعية غير صحيح.** illustrates different roles and responsibilities for each stakeholder, depending on the project type. This comparison highlights the differences in how aesthetic control is administered throughout Qatar's built environment and the stakeholders involved in approving such a process.

Table 1: Difference of roles and responsibilities during building permit approval process

	Private Projects	**Public/Governmental Projects**	**Special Projects**
Client	Provide Requirements Personal Taste	Provide Requirements Provide Design Brief	Prepare Special Regulations Provide Requirements Provide Design Brief Thoroughly follow compliance through all design stages
Consultant	Check MME Regulations Produce Design Get Client Approval Apply for Building Permit	Check MME Regulations Follow PEO Design Requirements otherwise Provide strong justification Produce Design Get Client Approval Apply for Building Permit	Check any applicable MME Regulations Follow Client Regulations Produce Design Get Client Approval Apply for Building Permit
MME	Check Compliance with Regulations Approve Drawings	Check Compliance with Regulations Get PEO Approval on Elevations Approve Drawings	Check Compliance with Regulations if applicable or give exemptions as required. Get PEO Approval on Elevations Approve Drawings
PEO	No input	Review Elevations for compliance with Qatari traditional architectural style. Seek management approval for justified deviations.	Review elevations and seek management approval and exemption
Main decision-maker	Client	PEO	Client

In Table 2, a comparison between the high-level aesthetic control parameters implementation in projects under the QNMP or other zones is given. In most cases, land uses marked as special zones are designated for megaprojects where the design intent is clear from the beginning. For example, for Education City, the guidelines are categorized as mandatory, firm, flexible and optional. The degree for their enforcement is based on the needs and design requirements of the stakeholder. In the Lusail project or Msheireb, aesthetic control was considered early in the design phase. The implementation for other areas follows MME regulations that provide aesthetic control at the hands of the owner and the architect.

Table 2: Comparison matrix of aesthetic control parameters implemented currently between developments in regular zones versus special zones

	Regular zones	**Special projects (megaprojects)**		
		Education City	**Msheireb**	**Lusail City**
Design Rationale			X	X
Design Quality		X	X	X

	Regular zones	Special projects (megaprojects)		
		Education City	Msheireb	Lusail City
Style			X	X
Context & Identity			X	
Building siting	X	X	X	X
Building Height	X	X	X	X
Orientation & Form		X	X	X
Glass percentage	X			
Windows	X	X	X	X
Materials	X	X	X	X
Entrances	X	X	X	X

Aesthetic control of private residential or real estate developments may have been done in piecemeal concept as most regulations are concerned with the land use, buildings height, setbacks, openings, building colour, and built area. Thus, there might be a lack of creativity to promote a better aesthetic of the built environment. The design consultants consulted by some of the authors mentioned that such individual developments can be guided, advised, and improved. It is the role of the government bodies to educate and guide individuals and/or organizations.

4.2 Gaps in Regulations and Implementation of Aesthetic Control

With reference given to Table 2, it is apparent that there are disparities in aesthetic control regulations for developments that fall under regular zones, as the regulations are too general. MME regulations for these types of development focus on building height, building siting, location of entrances, and height of windows with some constraints related to sustainability aspects like the percentage of glazing. Apart from those, the designers and clients are free to incorporate their creativity without any limitation. Although the government buildings need to follow traditional Qatari architecture, there seem to be no guidelines on shaping the aesthetics in the development projects.

The interviews with urban design professionals in MME revealed that MME is shifting towards form-based codes, particularly in the West Bay and the prime urban centres. The Municipality Spatial Development Plans codes are currently used with some local municipality regulations, but these have been in-house efforts rather than a broad level adoption for the built environment.

There are three major actors in the aesthetic/design control of projects in Qatar: The Client, PEO, and MME. While MME is the authority entitled to direct the outcome of the built environment, it is noticed that it has minimal impact on the aesthetic/design control on private projects and thus on the generated urban context. In contrast, for the special projects, MME guidelines are superseded by the client requirements. In such cases, the design outcome is guided through workshops and discussions' involving all the project players. This aspect of design review through a multidisciplinary design panel has not been incorporated within MME procedures for building permit applications. With QUDC guidance under the MME, the urban context may be served better as it will provide instructions on design control implementation so that the design can be achieved to serve not only an individualistic purpose but also to make the urban context better.

Qatar is one of the pioneering countries to have an electronic system for building permits, launched by MME in 2014 to include all the transactions and procedures required for building, the platform

mostly works as a document management system to transfer the transactions to all parties involved in the process of issuing building permits (The Peninsula Qatar, 2020b). In contrast, the actual tasks required by different departments are still conducted traditionally, which makes it harder to track the information and decision-making streams in the aesthetic control process.

5 Discussion

A contemporary urban planning process demands human-cantered development, where future technologies are intertwined with traditional approaches. Innovative design, parametric planning, digital tools, experts and executive planners' experience allow the fostering of designs that can restore the quality of compromised ecosystems. A smart digital environment, supporting informative decisions and facilitating the exchange of information between stakeholders to design the built environment and public realm, is thus the key in developing cohesive aesthetic control regulations (Fink & Koenig, 2019).The challenge is that the different planning teams within MME and the planning and design industry use different technologies and software to run separate analyses and produce/review designs at the different scales of the city planning process. With this, the resulting data integration becomes almost impossible to achieve without the exhaustive time and resource deployment. This hampers a coordinated and informative decision on the outcome.

Some countries have already identified this gap and have put measures to support the integrated control process. For example, the Future of Planning Programme of the UK aims to transform its planning system into a data-driven and digitally enabled system. Developing a comprehensive vision with different stakeholders involved in the planning can help to establish the requirements and create a new planning technology platform. In the last Plan tech week, 2019, The Royal Town Planning Institute (RTPI) and Connected Places Catapult (CPC) launched a shared vision for the digital future of planning including a manifesto made up of 11 points as starting principles for mapping the road towards a digital planning system (Harris & Webb, 2019). These digital planning technologies can develop an aesthetic control system that is not biased and adaptive to each zoning regulations.

5.1 Steps to Cover the Gaps

A phase wise strategy proposed here can be adopted by MME to start a swift implementation of aesthetic/design control in Qatar until a fully integrated solution with the implementation of all QNMP, QNDF, and QUDC components using state-of-the-art technologies is achieved.

Phase1: As an immediate action, the upgrading of MME resources is recommended specifically to cater to the needs of private projects. A partnership platform can be created between the building permit unit and pre-selected private design-oriented consultants. The architectural drawings of building permit applications can be routed randomly to these consultants at the DC1 stage for review by design experienced architects targeting to identify the gaps in designs and their quality within their context and provide comments and guidance on their improvements. A pre-requisite to this step is to include in the building permit submittal for consultants a "Site Specific Appraisal," where the consultant studies the project context and highlights the needed design response. This review should be done with firm key performance indicators and in parallel with the building permit review process. In the site-specific appraisal, information to be evaluated can be like what is mentioned in Table 2, such as the context and identity of the site and design rationale.

For more significant real estate developments, it is recommended to have a similar partnership platform between MME and the "Special Projects" client teams, who have experience in guiding the design of large developments to create a multidisciplinary design review panel. It is recommended

that the consultants engage with the panel for guidance at early design stages to clarify design expectations for the specific project character and context. At this phase, making any changes to the current process for governmental projects is not recommended.

Phase 2: The second phase relies on the full implementation of the guidelines, regulations, and policies related to the QNDF and all its subcomponents supported by the planning regulation law. In this phase, MME is recommended to upgrade its human and technical resources concerning aesthetic/design control. This may come from phase 1 of the control process. In parallel, it is recommended to activate action areas where the outcome of the implemented regulations, the QUDC guidance and the localized form-based codes on intended urban design and aesthetic results can be visualized. At this phase, it is recommended that the design governance be managed entirely by MME through a governance network model, where collaborative and partnership arrangements between public, private and voluntary organizations are established (Adams & Tiesdell, 2012). The collaborative platforms created in Phase 1 can be strengthened through an integrated collaboration model. The awareness and adoption of these policies by the wider industry is also an important task that should be taken up by the MME. This could be achieved through educational campaigns, training sessions, incentives, and involvement through design competitions and awards.

5.2 Steps to be Adopted in the Future

The integration of digital technology into urban planning supports the development of smart cities for their efficient operations. Qatar is developing Lusail City as some of the world's first cities to be fully integrated with smart systems. Qatar aims to release the Qatar Smart City Framework in 2020 with guidelines and direction for the development of smart and sustainable cities (Oxford Business Group, 2020). The use of technology and data to its full potential can benefit the nation to become a more efficient place for services and socioeconomic development as mentioned in (Zhongwen, 2018; Catapult Future Cities, 2018). Although comprehensive planning is challenging to adopt in the absence of real data and plans (Qaddumi & Ahmadi, 2017), the use of technology and data analytics can support the development of data-driven solutions (Tomer, 2019) for urban planning. This strategy could include aesthetic control in relation to the urban context.

Several parameter-based modelling methods have been tested in recent years. These include the integration of BIM (Building Information Modeling), GIS (Geographic Information System), and CIM (City Information Modeling) to support form-based codes and to demonstrate that parts of the building permit process can be automated by the integration of BIM and geospatial data. Such an integration promotes analysis of the building design through quantitative, visual and qualitative criteria (Kim, Clayton, & Wei, 2011); (Olsson, Axelsson, Hooper, & Harrie, 2018) Olsson, Axelsson, Hooper & Harrie, 2018). Hence, the automation of design reviews would support municipalities to focus more on design governance through an integrative and informed decision-making process, and the implementation of a context conscious aesthetic/design control.

6 Conclusion and Recommendations

This research presented an investigative analysis of Qatar's current approval system regarding aesthetic control, how it is currently administered and how it can be improved. Although some design regulations need to be abided by, analysed evidence shows that the current system of building permit approvals has yet to implement any aesthetic control regulations. The ongoing special megaprojects in Qatar have their own aesthetic control regulations that are implemented to several degrees of success around the country and these, by comparison, could act as precedents to MME to put forth

their own regulations without limiting the creativity and aspirations of the end-users. In theory, the finding of this research highlights a clear gap between the current design regulations and implementation. Accordingly, the paper showcases steps that can be endorsed to overcome such gaps.

In answer to the three research questions posed in this paper and as can be summarized from all the literature reviewed and interviews conducted that there is still no urban planning legislation that is put in place for aesthetic control. The current focus is on the regulations based on zoning. Aesthetic control practices in Doha's urban design are limited to a site's physical attributes rather than the urban design aesthetic aspects of the built environment. It is found that the parameters integral to aesthetic control reviews are the design rationale, design quality, style, context and identity, building siting, height, orientation and form, glass percentage, windows, materials and entrance. MME can use these parameters and the megaprojects' expertise to implement a sound aesthetic control measure in the building permit process. It is also established that the use of technologies in assisting the implementation of aesthetic control and the aesthetic control review process for MME, provide a 'creative hub' for designers to focus on the scale of the urban context to achieve a better aesthetic control.

Research on aesthetic control can focus on land surroundings and physical form in neighbourhoods. This can help to build in localized form-based codes in aesthetic control. Additional studies can be on current aesthetic control applications in different buildings developed through different municipalities to find more common features of aesthetic control, differentiation needed and commonalities to be induced.

References

Adams, D., & Tiesdell, S. (2012). *Shaping places: Urban Planning, design and development*. New York: Routledge.

Adham, K. (2008). *Rediscovering the Island: Doha's urbanity from pearls to spectacle*. In Y. Elsheshtawy, The Evolving Arab City: Tradition, Modernity and Urban Development. London: Routledge.

Arbab, P., Azizi, M. & Zebardast, E. (2018). Place-Identity Formation in New Urban Developments of Tehran Metropolis. *Journal of Urban Planning and Development*, *144*(2), 05018010 (1-11).

Azzali, S. & Tomba, M. (2018). Urban Development and Planning Practice in Doha. Middle East Intitute.

Carmona, M. (2001). *Housing Design Quality, Through Policy, Guidance and Review*. London: Spon Press.

Carmona, M. (2016). Design governance: theorizing an urban design subfield. *Journal of Urban Design*, *21*(6), 705-730.

Carmona, M., Marshall, S. & Stevens, Q. (2006). Design Codes: their use and potentional. *Progress in Planning*, *65*(4), 209-289.

Catapult Future Cities. (2018). PLANTECH: A data-driven and digitally enabled planning. Retrieved April 29, 2020, from Future Cities: http://futurecities.catapult.org.uk/wp-content/uploads/2017/10/FoP-Plantech-lowres.pdf

Deng, Z. (2009). Design control in post-reform China: A case study of Shenzhen's commercial office development. *Urban Design International*, 118-136. doi:10.1057/udi.2009.13

Drew, K. (1965). Urban Aesthetics: theory and application of physical design control within the urban renewal program. Manhattan, Kansas, U.S.: Kansas State University.

Fink, T. & Koenig, R. (2019). *Digital Integrative Urban Planning. In Regenerative Design in Digital Practice: A Handbook for the Built Environment* (pp. 2017-214). Eurac Research.

Gjerde, M. & Vale, B. (2015). Aiming for a Better Public Realm: Gauging the Effectiveness of Design Control Methods in Wellington. Buildings, 69-84.

Griffin, M. (2019, June 13). AI gets to grips with designing cities so humans don't have to. Retrieved April 26, 2020, from Fanatical Futurist: https://www.fanaticalfuturist.com/2019/06/designing-communities-and-cities-using-ai-us-startup-secures-25m-in-investment/

Harris, J. & Webb, S. (2019, October 28). How the planning system can adopt new technologies to improve efficiency. Retrieved May 1, 2020, from pbc today: https://www.pbctoday.co.uk/news/planning-construction-news/digital-planning-manifesto/66046/

Hawkes, D. (1999). Aesthetic Control in Inner city area planning. University of Tasmania.

Kiera, A. (2011). The Local Identity and Design Code as Tool of Urban Conservation, a Core Component of Sustainable Urban Development - The Case of Fremantle, Western Australia. Retrieved from http://www.ct.ceci-br.org

Kim, J., Clayton, M. & Wei, Y. (2011). Parametric form-based codes: Incorportation of land-use regulations and object-oriented parametric modeling of BIM. Acadia 2011 Regional Conference, (pp. 217-223). Nebraska.

Lusail City. (2015). Planning & Design Guidelines: Qetaifan Islands. Doha.

Nasar, J. (1998). *The evaluative image of the city*. Sage Publications.

Olsson, et al. (2018). Automation of Building Permission by Integration of BIM and Geospatial Data. *ISPRS International Journal of Geo-Inofmration, 7*, 1-22.

Oxford Business Group (2020). The Report: Qatar 2020. Retrieved April 30, 2020, from Oxford Business Group: https://oxfordbusinessgroup.com/country/qatar

Pring, A. (2019, September 24). RTPI and Connected Places Catapult set out shared vision for digital planning. Retrieved April 23, 2020, from BIM+: http://www.bimplus.co.uk/news/rtpi-and-connected-places-catapult-set-out-shared-\

Qaddumi, D. & Ahmadi, A. (2017, April 28). Scaling down planning in Doha towards the neighborhood and its public realm. Special Issue on Shaping Qatar's Sustainable Built Environment-Part I.

Salama, A. & Wiedmann, F. (2016). Fragmentation and Continuity in Qatar's Urbanism: Towards a Hub Vision. 154 - 177. doi:10.1057/978-1-137-46639-6-6

Scheer, C., Brenda, Preiser & Wolfgang. (1994). *Design Review: Challenging urban aesthetic control*. Springer US. doi:10.1007/978-1-4615-2658-2

Schnabel, M., Zhang, Y. & Aydin, S. (2017). Using parametric modelling in form-based code deisgn for high-dense citites. *Procedia Engineering, 180*, pp. 1379-1387.

Staley, S. R. & Claeys, E. R. (2005). Is the Future of Development Regulation Based in the Past? toward a Market-Oriented, Innovation Friendly Framework. *Journal of Urban Planning and Development, 131*(4), 202-213.

The Peninsula Qatar. (2020a). Ashghal to commence beautification of six main areas between Corniche and A-Ring Road. Retrieved July 2020, from The Peninsula: https://thepeninsulaqatar.com/article/14/06/2020/Ashghal-to-commence-beautification-of-six-main-areas-between-Corniche-and-A-Ring-road

The Peninsula Qatar. (2020b). Ministry starts implementing amendments to building permit systems. Retrieved April 30, 2020, from The Peninsula: Ministry starts implementing amendments to building permit systems

Tomer, A. (2019). Artificial intelligence in America's digital city. A blueprint for the future of AI: 2018-2019. Retrieved April 27, 2020, from Brookings: https://www.brookings.edu/research/artificial-intelligence-in-americas-digital-city/

Zhongwen, H. (2018). Data Analytics in Urban Planning: New Tools for Old Problems. (B. Asia, Interviewer) https://www.brinknews.com/data-analytics-in-urban-planning-new-tools-for-old-problems/.

Cite as: Valdeolmillos N.A.A., Al-Malki A.A.E.R, Pokharel S. & Ayari M.A., "Assessment of Aesthetic Control in Qatar's Urban Design", *The 2nd International Conference on Civil Infrastructure and Construction (CIC 2023)*, Doha, Qatar, 5-8 February 2023, DOI: https://doi.org/10.29117/cic.2023.0127

Application of PERS to Evaluate Walkability in State of Qatar

Mohamed Elsayyad
Civil Engineering Department/ College of Engineering, Qatar University, Doha, Qatar
me1403383@qu.edu.qa

Deepti Muley
Qatar Transportation and Traffic Safety Center, Civil Engineering Department, College of Engineering, Qatar University, Doha, Qatar
deepti@qu.edu.qa

Abstract

Well-designed pedestrian facilities are essential to promote walking among residents. These facilities also act as safe space for use of cycling and other personal mobility vehicles. In 2018, Ministry of Transport developed a system to assess the pedestrian environment, called Pedestrian Environment Review System (PERS). The PERS system is intended to assess, in a consistent systematic way, the quality of the pedestrian environment. This paper applies the guidelines of this manual to assess the walkability in Doha City. A total of ten links and ten crossings were included in this study. On-street evaluation was completed for each selected element and relevant scores for each parameter was assigned. The links assessment demonstrated that, overall, there were some issues highlighted by the PERS Audit in the studied areas such as poor curb ramp design, placement of obstruction on the pavement, lack of tactile information, conflict between pedestrian and vehicles at side-entry intersections, unavailability of wayfinding materials, etc. The overall pedestrian environment in the wider area assessed was generally positive, adequately maintained and of an appropriate quality. The provision of poor-quality crossings was identified as a negative feature of the studied areas. The issues were related to the infrastructure itself. Recommendations are made based on findings to improve the walkability of pedestrian network in State of Qatar.

Keywords: PERS; Qatar; Walkability; Crossing; Road facilities

1 Introduction

Walking is an essential element of a conventional traffic system for communities. The walkability of road facilities captures the attention of transportation professionals in urban planning. Walking is widely recognised for its health promotion of individuals in terms of reducing chronic diseases and decreasing traffic congestions (Makhlouf et al., 2023). One of the key elements to stimulate the activity of walking is to provide walkable built environment. Specialists and scholars have studied the relationship between the walking environment and the prevalence of the walking activity in communities (LIANG et al., 2022). Several methods have been established to evaluate the walkability of street facilities such as Geographic Information System (GIS), surveys, deep learning, simulations and analysing data records (Li et al., 2023).

State of Qatar has introduced new system, known as Pedestrian Environment Review System (PERS), for assessing pedestrian facilities across the street network. This study was undertaken to determine the status of existing facilities by applying this new assessment system. This study describes detailed findings of the field audit conducted on ten links and ten crossings in Doha City. This audit was

undertaken as a part of the 2nd National Action Plan 2018–2022, Action No. 260: Analyzing local pedestrian behavior to update the guidelines of the design and control of pedestrian facilities. A link is defined as an infrastructure that connects two intersections. While crossings are the segments that allow pedestrian to pass/cross a road section. The audit allows for the identification and assessment of problems related to pedestrians in street facilities that lead to prioritizing resources allocation for rehabilitation efficiently and effectively. This audit was carried out in compliance with the Pedestrian Environment Review System developed by the Ministry of Transport and Communications guidelines (MOTC, 2018). The PERS Audit relies on a consistent systematic way to assess the quality of the pedestrian environment.

2 Methodology

PERS audit comprises of three main stages. First is the selection of study locations that is links and crossings. Second is the assessment based on predefined criterion. Finally, third stage is reporting the findings and presenting them for decision making and records.

2.1 Stage 1: Identification of Links and Crossings

The links and crossings were chosen in different zones/municipalities such as Al Markhiya, Al Gharaffa, Al Najma, etc. to assure the diversification of the locations with different built environments. The variation of suburb types was considered in which some locations were in residential, commercial, industrial, and diplomatic land uses. Moreover, these areas were free of roadworks to ensure a valid audit. The links that were selected for the assessment are summarised in Table 1 below. Furthermore, the identified crossings are shown in Figure 1.

Table 1: Links Name and Location

Link No.	Link Name	Location
1	Al Jassasiya St.	25.331308, 51.493410 to 25.331336, 51.485633
2	Bu Silla St.	25.345254, 51.446185 to 25.342906, 51.439620
3	Najma St.	25.239566, 51.547007 to 25.244890, 51.542866
4	Al Mansoura St.	25.270430, 51.543155 to 25.269530, 51.536206
5	Al Waab St.	25.255587, 51.440250 to 25.252200, 51.431266
6	Diplomatic St.	25.326298, 51.529497 to 25.330548, 51.529540
7	Marbella St.	25.367013, 51.549213 to 25.366615, 51.552624
8	Al Kahraba St.	25.288319, 51.525248 to 25.285469, 51.524755
9	Al Difaaf St.	25.282472, 51.502765 to 25.282427, 51.500949
10	Urwa bin Masoud St	25.305333, 51.485285 to 25.305328, 51.483689

ID	Legend	Intersection Name
1		Porto Arabia St. / Marbella St.
2		Diplomatic St. / Conference Centre St.
3		Al Mansoura St. / Al Khalidiya St.
4		Baaya I/C
5		Oqba Bin Nafie St. / Najma St.
6		Al Kahraba St. / Al Khail St.
7		Onaiza St. / Al Shabab St.
8		Najma I/C
9		Museum of Islamic Art I/C
10		Khalifa St. / Madinat Khalifa St



Fig. 1: Location Map of Crossings

2.2 Stage 2: On-street Evaluation

Once the abovementioned step has been completed, the on-street evaluation took place in late December 2020. For each review framework, manual entry of records through visual evaluation is reported in a review form on site. Each framework consists of several parameters where reviewer scores and comments on each parameter for each link and crossing. Each parameter is scored in a scale with a range from -3 to +3, where +3 represents the highest score and -3 represents the lowest. A parameter with a score of +3 reflects an excellent practice. Whereas 0 is an average score of the best and worst practices. While N is used when the parameter is considered irrelevant. The score reflects the level of service to the user ascribed by comments made to support each score and highlight key issues. The score is assigned based on the checklist factors identified for each parameter. The evaluation parameters for links and crossings are shown in Table 2.

Table 2: Links and Crossings Audit Parameters

Link Audit Parameters	Crossing Audit Parameters
Effective width	Crossing provision
Curb ramps / Dropped Kerbs	Deviation from desire line
Gradient	Performance
Obstructions	Crossing Capacity
Permeability	Delay
Legibility	Legibility
Lighting	Legibility for sensory impaired people
Tactile Information	Curb ramps / Dropped Kerbs
Colour contrast	Gradient
Personal security	Obstructions
Surface quality	Surface quality
User conflict	Maintenance
Quality of environment	-
Maintenance	-

A sample of assessment for link and crossing assessment form is included in Appendix A. The summary of link and crossing assessment for each site is provided in Appendix B.

3 Findings from Field Audit

3.1 Links

The effective width of the links, presence of obstructions, and road gradient are parameters used to rate the walkability of links. Most of the links had a sufficient effective width with obstructions in some cases, nevertheless. For example, lighting columns were installed in the middle of the sidewalk, which may cause issues for handicap users with wheelchairs. Some links perform very well in terms of effective width such as Al Kahraba St. in Msheireb Downtown Doha. Furthermore, most of the links scored 0 in gradient parameter since Qatar's land is almost flat. The presence of curb ramps at side-entries and intersections was considered in the evaluation for providing accessibility. Links are are classified into two categories, with curb ramps and without curb ramps. Links without curb ramps were also divided into two types, either complete absence of curb ramps or presence of speed humps instead of compensating the function of curb ramps while crossings in some cases. For links with curb ramps, some curb ramps were meeting the design requirements, while others did not meet the minimum requirements. Another accessibility parameter that was considered is the presence of tactile information for people suffering from visual impairment. All links lack tactile information except for

Al Kahraba St. in Msheireb Downtown Doha due to the recent development of these areas. Traffic volume/speed and pedestrian fences are factors used to rate the permeability parameter. Half of the links scores well in the permeability criteria due to the observed low traffic volume/speed without pedestrian barriers along the median. While other links perform poorly due to the parked vehicles along the links, wide links with high vehicle speeds, and/or high traffic volumes. User conflict is a parameter used to check if there is an adequate space provision for each road user. There is a conflict between pedestrians and vehicles at side-entry intersections and between pedestrians and cyclists on the sidewalk in most of the links, except for some parts of Al Waab, Najma, and Al Kahraba streets as there is a separation between different users eliminating conflicting movements. .

Legibility can be defined as the clearness of wayfinding instructions reflected by signage, information boards, markings, etc. It was found that some links suffer from poor legibility due to lack of information, improper placement of signs, and/or absence of landmarks. Whereas several links showed convenient wayfinding features that assist pedestrians/walkers in their journey. Additionally, two problems in some links presented with regards to lighting, poor old yellow lights and absence of lights on the sides of the roads. This may affect the visual contrast of the pedestrian during the journey. All these factors play a major role in the personal security of the pedestrian. Furthermore, several links had CCTV units and security guards as well as appearing aesthetically. All these factors contribute to the personal safety and security.

The built environment quality of walking facilities varied from one link to another in this study. Multiple locations exhibited issues such as surface defect and/or wet surface associated with dirty presence of garbage. Moreover, another major problem was found that some walking facilities were left without paving. It was apparent from the visual evaluation that inadequate maintenance was done to some links. On the other hand, some links appeared to have perfect surface and environment quality condition. Consequently, it is clear from the abovementioned discussion that there are roads of high quality, medium quality, and others of poor quality.

3.2 Crossings

The crossings evaluation followed similar procedure that was used for assessment of the links.. The crossing provision refers to the suitable planning of crossings facilities of the pedestrian. This depends on many factors including location, pedestrian volume, road type, traffic speed, and pedestrian type. Crossing provision, deviation from desire line, performance, and crossing capacity determines the functional performance level of the crossing facility in terms of walkability. Most crossings appeared with high quality, serving pedestrians' desire lines, along with having adequate capacity and width at peak hours. These crossings manifested good visibility for pedestrians. However, some flaws were visible in some crossings. For instance, absence of a crossing facility, absence of refuge island, inadequate waiting area were found in some locations. These defect may cause difficulties to the pedestrian while crossing as well as impacting the personal comfort of the individual. In terms of delay, most of the crossings allows adequate time for pedestrians to cross. Nevertheless, the waiting time at some crossings was relatively long unlike the waiting time at crossings at Msheireb and the Pearl areas. Additionally, it was observed that there is a pedestrian phase in Msheireb that allows pedestrians on the four sides of the roads to cross during the complete stop of vehicles due to the red light. In the Pearl, there was no delay since the red light immediately flashes after pressing the push button of crossing.

Crossing legibility evaluation was done based on different conditions from the legibility of links. Legibility parameter for crossings encompasses the clearance of crossing markings, illumination of

the crossing area. It was found that some crossings suffer from poor legibility due to the low quality of lightning or markings or absence of crossing markings. Whereas several crossings showed well-lit crossings and clear crossing markings. Only one crossing had very good legibility for sensory impaired users due to the available audible information and tactile warnings provided. Another parameter to check the accessibility of the pedestrians is presence of curb ramps for people suffering from movement impairment. Most crossings have well-designed curb ramps. Though, few crossings did not have curb ramps or have curb ramps that may cause difficulties for handicap users with wheelchair due to its size and/or gradient. The built environment quality of crossing facilities varied from one crossing to another in this study. The crossings appeared to have perfect surface and environment quality condition overall. However, it was noted during the audit that the surfacing of the crossings contains cracks and poor reinstatements in some places which could cause a potential trip hazards to pedestrians. Multiple locations exhibited issues such as high mast light poles and traffic signal poles reducing the effective width of the crossings and obstructing pedestrians' movement. Moreover, another major problem was found that some push buttons at crossing facilities were not working. This indicates that adequate maintenance was needed at some crossings.

4 Conclusion

A total of 20 locations, with 10 links and 10 crossings, were evaluated. The links assessment demonstrates that overall, there were some significant issues highlighted by the PERS audit in the studied areas such as poor curb ramp design, placement of obstructing objects on the pavement, lack of tactile information, clear conflict between pedestrian and vehicles at side-entry intersections, and unavailability of wayfinding materials. The overall pedestrian environment was generally positive, adequately maintained and of an appropriate quality. Poor-quality crossings were identified in multiple locations of the studied areas. Most of the issues were related to the infrastructure of the crossings. For example, lack of audible information, tactile information, count down signals, rotating cones, insufficient crossing time for elderly pedestrian, inconsistency of curb ramp design, placement of permanent obstructions on the refuge islands, and the deficiency of push buttons.

Based on the results of the PERS audit, the following recommendations can be made:

- Removal/relocation of obstructions that reduces pedestrian space.
- Improve existing curb ramps at side roads to be flushed and aligned.
- Installing correct new curb ramps and tactile paving.
- Provide wayfinding materials such as finger posts or maps.
- Placement of crossings at signal junctions.
- Installing new traffic signals with adequate facilities such as push button, audible information, countdown, and rotating cones to facilitate normal and sensory impaired pedestrians' movement.
- Increase the pedestrian phase to provide sufficient time for elderly and mobility impaired pedestrians to cross safely.
- Installing pedestrian signs at a suitable distance before the crossing points.

It should be noted that the PERS is an advanced system, expecting very high standards of walkability infrastructure. The newly developed suburbs have higher scores while older suburbs have lower scores. Hence, significant improvements are expected to achieve these standards for the entire network of Doha City.

Acknowledgments

Authors are thankful to National Traffic Safety Committee (NTSC), State of Qatar for providing support for this study.

References

Li, Y., Yabuki, N., & Fukuda, T. (2023). Integrating GIS, Deep Learning, and environmental sensors for multicriteria evaluation of Urban Street Walkability, *Landscape and Urban Planning*, *230*, 104603.

Liang, Z., Lo, H. K., & NG, K. F. (2022). Towards walkability enhancement: A systematic review and Future Directions, *SSRN Electronic Journal [Preprint]*.

Mohamed et al. (2023). Neighborhood Walkability and Cardiovascular Risk in the United States, *Current Problems in Cardiology*, *48*(3), 101533.

MOTC (2018). Pedestrian environment review system. Land Transport Planning Department, Ministry of Transport and Communications, State of Qatar.

Appendix A

3:30 9/7/2020

PERS [Software]

Link Assesment Form **Page 1 of 3**

Link Name: Al Jassasiya St.

Location: 25.381308, 51.493410 to 25.381336, 51.485633

Reviewers: M. E.

Parameter	Checklist Factors	Checklist +	Checklist +-	Checklist -	Score "-3 to +"	Comment Section	Comment Section
1.9 m 2.1 m Effective Width >5m	Width for pedestrian flow	✓			-1	• Some section are bigger than 5m	
	Wheelchair accessibility	✓					
	All sections acceptable width	✓					
	Separation from traffic	✓					
	Allowance for obstructions	✓					
	Pedestrian congestion			✓			
Dropped kerbs	Located on desire lines		✓		-3	Curb ramps are not provided but there are raised crossings at every side-entry intersection	
	Adequate capacity		✓				
	Level dropped/flush		✓				
	Gradient of drop		✓				
	Consistency		✓				
	Frequency of dropped kerbs		✓				
Gradient	Severity		✓		✓		
	Steps/ramps		✓				
	Rest points		✓				
	Undulations		✓				
	Appropriate handrails		✓				
	Presence of crossfalls		✓				
Obstrctions	Presence of obstructions	✓			0	lamp posts in middle of sidewalk	
	Location/alignment	✓					
	Overhead obstructions			✓			
	Tapering or transparent obstructions		✓				
	Tactile warnings			✓			
	Sight line reduction			✓			
Permeability	Frequency of crossing points			✓	+2		
	Parked cars/physical barriers			✓			
	Traffic flow			✓			
	Dropped kerbs			✓			
	Pedestrian barriers			✓			
	Sightlines	✓					
Legibility	Signage provision	✓			-1		
	Signage clarity	✓					
	Information boards			✓			
	Distances given on signs			✓			
	Sightlines	✓					
	Built form aids navigation			✓			

Link Assesment Form Page 2 of 3

Parameter	Checklist Factors	+	+-	-	Score "-3 to +	Comment Section	Comment Section
Lighting	Intensity/frequency	/			+3	but the light colour is yellow and it would be better if it is white	
	Definition/colour			/			
	Maintenance	/					
	Context suitability	/					
	After-Dark	/					
	Obstructions	/					
Tactile information	Evident		/		-3		
	Consistent/correct		/				
	Maintained		/				
	Appropriate Colour		/				
	Interruptions		/				
	Tapping Line		/				
Colour Contrast	Tonal contrast		/		/		
	Location		/				
	Assists navigation		/				
	Enhanced visibility of obstructions		/				
	Space identification		/				
	Made to specification		/				
Personal Security	Perceived/ sense of crime			/	+1		
	Activity on the street	/					
	Lighting	/					
	Police presence			/			
	CCTV			/			
	Visual appeal			/			
Surface Quality	Smoothness/trip hazards	/			0	one section only	has issues with Maintenance
	Surface friction	/					
	Slippery surfaces			/			
	UKPMS CVI hierarchy		/				
	Maintenance			/			
	Context suitability	/					
User Conflict	Conflicting movements			/	0	There is conflict at side-entry intersections and also with cyclists	
	User flows	/					
	Encroachment on pedestrian space	/					
	Segregation from cyclists		/				
	Bus queues an obstruction		/				
	Adequate space provision	/					
Quality of environment	Traffic/ noise			/	+2	no seating + no landscaping + low traffic volumes no noise	
	Aesthetics			/			
	Soft landscaping			/			
	Quality of materials	/					
	Quality of private frontages	/					
	Sense of place		/				

Link Assesment Form

Maintenance	Cleanliness		✓	+2		
	Drainage		✓			
	Evidence of neglect		✓			
	Seasonal foliage		✓			
	Graffiti		✓			
	Landscaping		✓			
	Durability of materials		✓			

Comments:

* There are some defect sections with poor Quality and others with poor ——— effective width
* Lighting columns are at the middle of the sidewalk at some sections
* there is a big vertical curve

Quick Wins (Maintence Recommendations)

	Enhanced street cleaning along the link	✓	A board and goods on footway enforcement to reduce obstructions
	Remove litter and gum stains from the link		Enforce parking restrictions on footways
	Remove graffiti from infrastructure along the link		Remove redundant signage poles / lighting columns
	Remove fly-tipped refuse from link		Clear foliage and overhanging branches on footways and paths
	Clean lights and mirrors in subway	**Dropped kerbs and tactile paving**	
	Clear blocked drains/gutters to reduce ponding		Improve existing dropped kerbs at side roads to be flush & aligned
	Repair/replace broken fencing along the link		Install new dropped kerbs that are flush and aligned
	Repair malfunctioning street/subway lighting		Improve existing tactile paving at side roads - correct colour and layout
Surface Quality		✓	Install new tactile paving at side roads - correct colour and layout
✓	Resurface footway along sections with		Install new corduroy tactile paving at steps
✓	Resurface footway along sections with trip hazards		
	Install bound resin in small tree pits		

9/7/2020

PERS [Software]

Crossing Assesment Form **Page 1 of 3**

Crossing Name: Al Kahraba St. / Al Khail St.

Location: 25.285469, 51.524755

Reviewers: M.E

Parameter	Checklist Factors	Checklist +	Checklist +-	Checklist -	Score "-3 to +3"	Comment Section	Comment Section
Crossing Provision	Type suitable for context	✓			+3		
	Suitable for pedestrian type	✓					
	Suitable for pedestrian volume	✓					
	Suitable for type of road	✓					
	Traffic speeds			✓			
	Traffic volumes			✓			
Deviation from the desire line	Deviations			✓	+2		
	Serve likely desire lines	✓					
	At grade/ by level change			✓			
	Pedestrian priority	✓					
	Distance minimisation	✓					
	Barriers causing deviation			✓			
Performance	Crossing operational	✓			+3	* the time is enough for normal and relatively fast pedestrians * the location, visibilty, and quality of crossing markings is good * traffic volume is low	
	Safety/protection of pedestrians	✓					
	Vehicle behaviour	✓					
	Traffic control measures			✓			
	Space ownership		✓				
	Obstruction to sight lines			✓			
2- Crossing Capacity	Minimum dimension standards met	✓			+3	*waiting area and refuge island are provided sufficiently	
	Peak hour performance		✓				
	Pedestrian flows coped with		✓				
	Waiting areas/ widths	✓					
	Refuge capacity	✓					
	Width for wheelchair users	✓					
Delay	Crossing stages			✓	+3	When the button is pressed, all the four traffic lights will become red	
	Effect of crossing type		✓				
	Traffic flow	✓					
	Pedestrian phase	✓					
	Waiting time			✓			
	Crossing time	✓					
Legibility	Surface Type continuity	✓			+2	* Clearly marked crossing. * surface quality is good * well lit	
	Obvious where to cross	✓					
	Driver stop line in place	✓					
	Delineation for pedestrians	✓					
	Positioning of infrastructure	✓					
	Lighting	✓					

9/7/2020

Crossing Assesment Form

Parameter	Checklist Factors	Checklist +	Checklist +–	Checklist –	Score "-3 to +3"	Comment Section	Comment Section
Legibility for sensory impaired people	Button position	✓			+3	*all Buttons are working * The only signal with audible information * there is tactile information.	
	Audible information	✓					
	Rotating cones			✓			
	Tactile Information provided/intact	✓					
	Appropriate Tactile information	✓					
	Colour contrast		✓				
Dropped kerbs	Suitable locations	✓			+3		
	Capacity	✓					
	Level dropped/flush	✓					
	Gradient of drop		✓				
	Provision	✓					
	Profile	✓					
Gradient	Crossing at grade		✓		/		
	Crossfall evident		✓				
	Impedience to access		✓				
	Camber		✓				
	Severity of gradient on approach		✓				
	Severity of gradient on exit		✓				
Obstrctions	Obstructions on approach			✓	+3	* bollards can be considered as obstruction	
	Obstructions on crossing			✓			
	Location/alignment	✓					
	Overhead obstructions			✓			
	Opaque/tapering obstructions			✓			
	Tactile warnings	✓					
	Sight line reduction			✓			
	Permanent obstructions			✓			
Surface quality	Smoothness/trip hazards			✓	+3	overall quality is perfect surface is smooth and consistent	
	Context suitability	✓					
	Consistency	✓					
	Quality of reinstatements		✓				
	Drainage		✓				
	Slippery surfaces			✓			
Maintenance	Cleanliness	✓			+3		
	State of repair		✓				
	Littering			✓			
	Evidence of neglect			✓			
	Impact of seasonal foliage			✓			
	Graffiti/stickers/ chewing gum			✓			
	Evidence of debris			✓			

Crossing Assesment Form	Page 3 of 3

Comments:

Quick Wins (Maintence Recommendations)

	Cleaning and Repairs
	Remove litter and gum stains from the crossing
	Remove graffiti from infrastructure at the crossing
	Clear foliage and overhanging branches at crossing
	Clear blocked drains/gutters to reduce ponding

	Signals
	Repair rotating cone on crossing signals
	Replace control button at crossing signals
	Repair 'wait' illumniation bulb in control box
	Re-align the green man to be visible to pedestrians
	Repaire broken bulbs in the green/red man signal head

	Surface Quality
	Highlight crossing area and markings
	Resurface crossing at sections with ponding
	Resurface crossing on carriageway with trip hazards
	Resurface crossing waiting areas with trip hazards

	Dropped kerbs and tactile paving
	Improve existing dropped kerbs so that they are flushed and aligned
	Install new dropped kerbs that are flush and aligned
	improve existing tactile paving so that it has correct colour and layout
	install new tactile paving with correct colour and layout

Appendix B

Table 3: Scores for Links and Crossings Audit Parameters for Selected Sites

Link Audit Parameters										
	Link 1	**Link 2**	**Link 3**	**Link 4**	**Link 5**	**Link 6**	**Link 7**	**Link 8**	**Link 9**	**Link 10**
Effective width	-1	+1	+3	-3	0	0	-3	+2	0	+2
Dropped Kerbs	-3	-3	+2	-1	-3	+3	-3	-1	-2	-3
Gradient	N	N	N	N	N	N	N	N	N	N
Obstructions	0	+1	+3	-2	-1	-3	0	+2	0	+2
Permeability	+2	+1	-3	-2	-2	+1	-2	+3	+1	+2
Legibility	-1	0	-1	0	-1	-3	0	+3	0	0
Lighting	+3	N	N	N	+2	N	N	N	N	N
Tactile Information	-3	-3	-3	-3	-3	-3	-3	+2	-3	-3
Colour contrast	N	N	N	N	N	N	N	N	N	N
Personal security	+1	+1	+1	-2	+2	+2	+2	+3	+1	-1
Surface quality	0	+2	+3	-1	-1	-1	+3	+3	0	-3
User conflict	0	0	+2	0	0	0	+1	0	+3	-3
Quality of environment	+2	0	+3	-3	-1	0	+3	+3	-1	-1
Maintenance	+2	+2	+3	-1	-3	-1	+3	N	+1	-3
Crossing Audit Parameters										
	Site 1	**Site 2**	**Site 3**	**Site 4**	**Site 5**	**Site 6**	**Site 7**	**Site 8**	**Site 9**	**Site 10**
Crossing provision	+3	+3	0	-1	-1	+3	+2	+3	+3	-3
Deviation from desire line	+3	+3	0	0	+2	+2	+3	+2	+2	+1
Performance	+3	+3	-1	0	+3	+3	+3	+3	+3	-3
Crossing Capacity	+1	-3	0	0	+2	+3	+3	+2	+2	-3
Delay	+3	+1	+2			+3	N	-1	-1	N
Legibility	+3	+2	0	0	+2	+2	+2	+2	+2	-3
Legibility for sensory impaired people	-3	-3	-3	-3	-3	+3	-3	-3	-3	-3
Curb ramps / Dropped Kerbs	+3	+3	-3	-1	+3	+3	+3	+2	+3	-3
Gradient	N	N	N	N	N	N	N	N	N	N
Obstructions	+3	+2	+2	0	+3	+3	+3	+1	+1	-3
Surface quality	+3	+2	+2	-1	+3	+3	+3	+2	+2	-2
Maintenance	+3	+3	-2	-1	+3	+3	+3	+1	+3	-2

Cite as: Elsayyad M.I. & Muley D., "Application of PERS to Evaluate Walkability in State of Qatar", *The 2nd International Conference on Civil Infrastructure and Construction (CIC 2023)*, Doha, Qatar, 5-8 February 2023, DOI: https://doi.org/10.29117/cic.2023.0128

Area-Specific Traffic Peak Hour Timing Using Traffic Signal Detectors: A Case Study of Qatar

Almodather Mohammed
Public Works Authority – Ashghal, Doha, Qatar
amohamed5@ashghal.gov.qa

Ali Al-Saudi
Public Works Authority – Ashghal, Doha, Qatar
aabdullah@ashghal.gov.qa

Mohammed Al-Marri
Public Works Authority – Ashghal, Doha, Qatar
malmarri6@ashghal.gov.qa

Abstract

This case study addresses peak hour traffic timing in Qatar after COVID-19 as traffic conditions returned to normal. Traffic data were provided for multiple areas, mainly around Doha City. Flow data were obtained from traffic signal detectors for 318 intersections. The peak periods in morning, mid-day, and evening were 06:30 am–08:30 am, 12:30 pm–2:30 pm, and 5:15 pm–7:15 pm, respectively. These findings align with the Ministry of Transport's state-wide study (Transportation Masterplan for Qatar, 2018). We found traffic in Qatar to differ on Thursday, Friday, and Saturday versus the rest of the week due to the weekend effect. Results offer useful insights for policymakers to reduce congestion and provide complex traffic solutions (e.g., understanding land use–specific peak hour timing, imposing zone-specific working hours). In addition, this case study highlights the potential to use existing infrastructure to expand traffic studies in Qatar at minimum cost.

Keywords: Traffic; Vehicles; Peak hour; Qatar; Congestion; SCAT

1 Introduction

Traffic congestion, which continues to increase, affects the economy and can disrupt cities' development (Downs & Downs, 2004). Qatar's road network is improving thanks to vast investment in new highways and roads. People's number of hours spent commuting in the area declined by 6% between 2018 and 2019 (QMIC, 2019). Although the COVID-19 pandemic decreased traffic congestion across most cities in 2020, this effect is diminishing. Yet congestion could assume a new pattern as it resumes (TomTom, 2022).

Gathering traffic data is crucial for accurately measuring congestion and understanding its patterns. Conventional temporarily installed traffic data collection methods, such as automatic pneumatic tube counts (ATCs), manual counts (MCs), and video-based turning movement counts (TMCs), are most common in practice (Leduc, 2008). Other traditional permanent methods like inductive loop detectors (ILDs) are also used, depending on the purpose of data collection. More technologically advanced methods of traffic data acquisition (e.g., based on cell phone tower data, GPS data, or Bluetooth data) are available as well; however, privacy and legal concerns have impeded their broader adoption. As state-wide data collection projects are typically initiated and overseen by government planning agencies, these concerns are given significant consideration (Losavio et al., 2018).

The Transportation Masterplan for Qatar (TMPQ) project, a state-wide data collection initiative, has been considered the most reliable source of traffic data in Qatar. The project was spearheaded by Qatar's Ministry of Transport. Data collection for this project took place between 2018 and 2019. The study was based on temporary conventional traffic data collection methods, namely ATCs, MCs, and TMCs (Ministry of Transport, 2020). In the current study, we aim to set the stage for in-depth research on traffic data collection using a conventional permanent method (i.e., ILDs) which already exists in Qatar and will require limited resources.

Our work makes two contributions in that we 1) reconfirm peak traffic periods in Qatar after the pandemic compared to TMPQ and 2) illustrate traffic patterns and peak hours in areas across the state. Results are intended to facilitate traffic studies among traffic engineers and to enable stakeholders to monitor traffic more efficiently using our data processing framework.

The remainder of this paper is organized as follows: Section 2 summarizes related work on traffic peak hour identification. Section 3 describes our traffic data collection procedure along with information about TMPQ. Section 4 presents our results, and Section 5 concludes.

2 Related Work

Traffic engineers have been interested in counting vehicles since urban congestion began rising (Goetz, 2019). Several widely accepted counting methods are available. TMCs are considered the most accurate vehicle-counting method, yet relevant literature is lacking (Zheng & Mike, 2012). Data processing is time-consuming and costly irrespective of whether this task is completed manually or via software. Therefore, ATCs have been deemed most feasible for long periods (i.e., more than a day; Puan et al., 2019).

Other traffic-counting technologies include the radio frequency identification system; license plate recognition systems; and ILDs, which are wires installed on the road pavement to detect vehicles (Oluwatobi et al., 2021). These approaches are unique in that they gather real-time data (vs. conventional TMCs and ATCs, which require post-processing). ILDs have an additional advantage over other methods because vehicle counting is not the sole purpose: ILDs are also used to optimize traffic signal timing under the Sydney Coordinated Adaptive Traffic System (SCAT) (NSW Government Department of Main Roads, n.d.).

ILDs are widely used in intelligent transport systems but not in traffic data collection. ILDs cannot measure a vehicle's speed and length, which are key factors when obtaining traffic data (Belenguer et al., 2019). Most traffic signals in Qatar have already installed and use ILDs via SCATS (SICE, 2020).

The largest data collection project in Qatar, carried out between 2018 and 2019, leveraged 500 ATC locations, 500 TMC locations, and 100 MC locations to evaluate traffic patterns across the country (Ministry of Transport, 2020). The study categorized traffic peaks into three blocks of a 3-hour period each: morning (6–9 am), mid-day (12–3 pm), and evening (5–8 pm). Peak traffic is thus apt to occur during these periods in any part of Qatar. ILDs can identify peak hours, and Qatar was equipped with this technology in 2018. However, ILDs have few data collection attributes, and their accuracy has yet to be determined in this state.

3 Methodology

In this case study, raw data from ILDs were obtained from 318 intersections connected to the road monitoring center system in Qatar's Roads Operation and Maintenance Department. Data were collected between October 14, 2022, and October 20, 2022, after which they were processed to

determine general traffic patterns. These patterns were then analyzed to identify area-specific peak hours.

3.1 Data Processing

Raw ILD data were processed via SCAT Traffic Reporter software based on data dumps in 5-min intervals. Sample data are presented in **Fig. 1**.

```
Friday 14 October 2022 00:05
Int 5632    1=0     2=6     3=4     4=0     5=6     6=2     7=3     8=119
 9=0    10=3    11=10   12=5    13=9    14=7    15=4    16=1
17=4    18=5    19=5    20=5    21=5    22=0    23=4    24=4
25=8    26=7    27=4    28=7
```

Fig. 1: Raw Data Snapshot for One Intersection (5-min Interval)

The number following "Int" is the intersection number. The detector number appears before "=", and the number after "=" denotes the vehicle count during the 5-min period.

A program was written in Anaconda Python to organize the raw data into hourly traffic data for each intersection (**Fig. 2**).

	A	B	C
1	time	intersection	sum
2	14-10-22 00:00	601	3771
3	14-10-22 00:00	2102	5267
4	14-10-22 00:00	2202	3754
5	14-10-22 00:00	2307	14079
6	14-10-22 00:00	3001	7993
7	14-10-22 00:00	3199	910
8	14-10-22 00:00	5107	24600
9	14-10-22 00:00	5108	1412

Fig. 2: Reorganized Detector Data

3.2 Understanding Data Patterns

Our data spanned a week in October (from Friday to Thursday) as shown in **Table 1**.

Table 1: Data and Day of Week

Date	Day	Type	Note
14-Oct-22	Friday	Weekend	Day off for all public/private sectors and schools
15-Oct-22	Saturday	Weekend	Day off for all public/some private sectors and schools
16-Oct-22	Sunday	Weekday	Workday for all
17-Oct-22	Monday	Weekday	Workday for all
18-Oct-22	Tuesday	Weekday	Workday for all
19-Oct-22	Wednesday	Weekday	Workday for all
20-Oct-22	Thursday	Weekend	Workday for all; some private sectors worked a half day

We assembled a daily profile for all intersections (**Fig. 4**) to further understand behavioral traffic patterns in Qatar over the focal week.

3.3 Area-specific Peak Hours

For the purposes of determining peak hours by area, we mapped the areas as arbitrary 2km squares covering all traffic signals with detectors. The 101 areas are depicted in **Fig. 3**. Distinctive patterns are discussed in Section 4.



Fig. 3: 2km × 2km Areas (N = 101) Covering All Signals with Detectors

4 Results

4.1 Daily Profile

Given the hourly traffic flow at each location throughout the week (as presented in Fig. **2**), we plotted a daily profile to clarify traffic patterns in Qatar (**Fig. 4**).

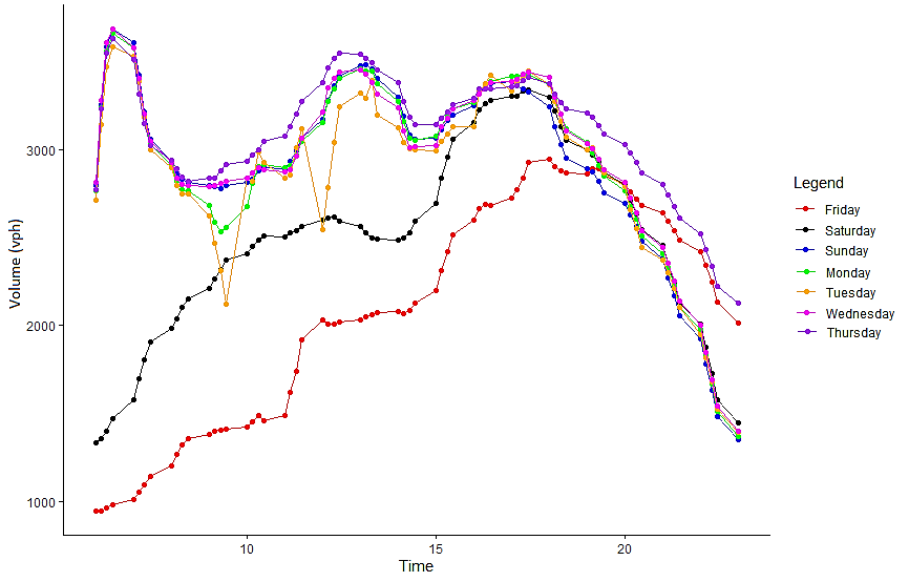


Fig. 4: Weekly Traffic Profile (October 14, 2022–October 20, 2022)

Traffic followed a typical pattern from Sunday to Thursday. The peak period was higher on Thursday evening, possibly due to leisure travel because most people in Qatar were not working the next day. This information is important when planning events for later in the day. We therefore treated Thursday as a distinctive pattern. Saturday's pattern resembled that of Friday: most people were not working, but the peak period was higher due to some work trips in the private sector.

Overall, traffic in Qatar assumed four patterns: 1) Sunday–Wednesday were typical workdays; 2) Thursday featured work in the morning and leisure in the evening; 3) All offices were closed on Friday; and 4) Saturday was a free day for some of the population. We focus on the weekday result (Pattern 1) in this section given that most traffic design is based on weekday volumes. Results for the other patterns are provided in the Appendix.



Fig. 5: Morning Result (Pattern 1)



Fig. 6: Evening Result (Pattern 1)

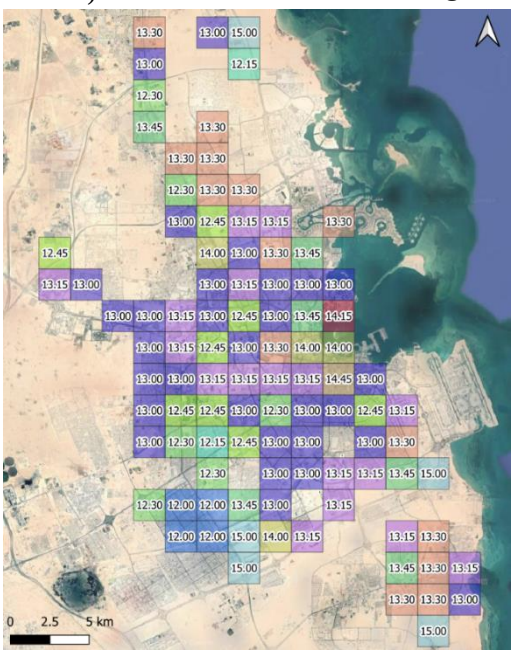


Fig. 7: Mid-day Result (Pattern 1)

The weekday results from Fig. **5** to Fig. **7** show that 6:45–7:45 was the most common peak hour in

the morning; 13:00–14:00 was the most common peak hour during mid-day. The most common evening peak hour was 17:45–18:45. The morning peak hour pattern was related to land use in the city: the further one is from Inner Doha, the earlier the peak hour tended to be, presumably due to vehicles traveling to offices in the area. An exception to this trend appeared in the Industrial Area, whose peak was later at 9:00. The mid-day and evening peak hour patterns were more complicated and merit further study along with land use.

4.2 Discussion

Although the accuracy of ILD results has not been studied in Qatar, peak hour periods confirm the TMPQ findings. In addition, the daily profile in this research aligns with that produced in TMPQ's Data Collection, Inventories and Survey Summary (Figure 4-2 in the original document). These consistencies are reassuring. However, studies which compare accuracy are still lacking.

This paper shed light on a possible use case of ILDs that may save costs and time. This research is intended to be a proof-of-concept of a framework to complete such a task rather than to serve as a reference for peak hours. One could argue that the accuracy (not volume) of peak hour timing can be used safely: even though ILD counters' accuracy may not be high, the error is eliminated because figures were consistent throughout the data collection period. A longer period of ILD data collection, to be verified with TMCs and ATCs, is needed for further verification.

5 Conclusion

Qatar has an advanced transportation infrastructure featuring more than 400 intersections with ILDs which are linked with one system and monitored constantly. This case study offers initial insight into capabilities of gathering ILD data. We examined traffic patterns over a week and identified distinctions. The peak hour for each area in Qatar aligns with research conducted in 2018. As such, traffic seems to have returned to normal since the COVID-19 pandemic. Practically, this case study can benefit traffic engineers who evaluate different areas in Qatar based on peak traffic during the morning, mid-day, and evening. We have also provided a framework for engineers to duplicate for mass traffic data collection in Qatar. Researchers can apply the developed framework to explore traffic patterns' relationships with land use. It will then be possible to modify peak hours based on transport demand management if needed to reduce traffic congestion. It is worth noting that a longer period study is required to take place and be verified against TMCs and ATCs to validate the accuracy of using ILDs for peak hour determination. Fortunately, introducing a longer period and more data points does not complicate this task or raise costs as with the on-site data collection method used in TMPQ.

References

A. Downs, Still Stuck in Traffic Coping with Peak-Hour Traffic Congestion. Washington, D.C.: Brookings Institution Press, 2004.

Belenguer, et al. (2019). "Advantages offered by the double magnetic loops versus the conventional single ones," *PLoS One,* Vol. 14, No., doi: 10.1371/journal.pone.0211626.

G. Leduc. (2008). "Road Traffic Data: Collection Methods and Applications," 2008. [Online]. Available: http://www.jrc.ec.europa.eu/

Losavio, et al. (2018). "The Internet of Things and the Smart City: Legal challenges with digital forensics, privacy, and security," *Security and Privacy,* Vol. 1, No. 3, p. e23, doi: 10.1002/spy2.23.

Ministry of Transport (2020). "Transportation Masterplan for Qatar - Data Collection, Inventories and Surveys," Doha,

2020.

NSW Government Department of Main Roads, “The New Generation SCATS 6.”

Oluwatobi, et al. (2021). “The design of a vehicle detector and counter system using inductive loop technology,” in *Procedia Computer Science*, Vol. 183, pp. 493–503. doi: 10.1016/j.procs.2021.02.089.

QMIC. “QMIC Launches the Qatar Traffic Report for 2019 Revealing Key Insights & Findings : QMIC : Innovative Solutions to Enable Smart Living,” *Qatar Traffic Report*, 2019. https://www.qmic.com/selections/qmic-launches-the-qatar-traffic-report-for-2019-revealing-key-insights-findings/ (accessed Oct. 15, 2022).

R. Goetz, “Transport challenges in rapidly growing cities: is there a magic bullet?,” *Transport Reviews*, Vol. 39, No. 6. Routledge, pp. 701–705, Nov. 02, 2019. doi: 10.1080/01441647.2019.1654201.

SICE. (2020). “Doha will prepare its ITS installations for the 2022 World Cup | SICE,” https://www.sice.com/en/news/doha-will-prepare-its-its-installations-for-the-2022-world-cup (accessed Dec. 11, 2022).

TomTom, “TomTom Traffic Index – Live congestion statistics and historical data,” *TomTom Traffic Index*, 2022. https://www.tomtom.com/traffic-index/ (accessed Oct. 15, 2022).

Zheng, P. & Mike, M. (2012). “An Investigation on the Manual Traffic Count Accuracy,” *Procedia Soc Behav Sci*, vol. 43, pp. 226–231, 2012, doi: 10.1016/j.sbspro.2012.04.095.

Appendix

Table 2: Peak Hour Results for All Patterns

Area	Pattern 1 (Sunday-Wednesday)			Pattern 2 (Thursday)			Pattern 3 (Friday)			Pattern 4 (Saturday)		
	AM	MD	PM	AM	MD	PM	AM	MD	PM	AM	MD	PM
1	6.30	13.30	17.30	6.30	12.45	17.45	9.00	15.00	17.45	9.00	15.00	17.30
2	7.45	13.00	20.00	7.45	14.00	20.00	7.00	15.00	18.30	9.00	15.00	17.00
3	7.30	15.00	17.00	7.45	12.15	17.30	7.30	15.00	19.00	9.00	15.00	17.00
4	6.30	12.15	19.45	6.30	12.00	17.00	-	-	-	9.00	13.00	19.45
5	6.15	13.00	17.30	6.15	12.45	17.45	8.00	15.00	17.45	9.00	15.00	16.15
6	6.30	12.30	17.45	6.30	12.15	17.45	8.45	15.00	17.45	9.00	15.00	17.45
7	6.30	13.30	17.00	6.30	12.15	17.15	9.00	15.00	19.15	9.00	13.30	17.00
8	6.45	13.45	17.00	6.45	14.00	17.45	8.45	15.00	18.00	9.00	15.00	17.15
9	6.30	13.30	17.45	6.45	12.15	17.45	9.00	15.00	19.45	9.00	15.00	17.45
10	6.45	13.30	17.00	6.45	12.45	18.00	9.00	15.00	20.00	9.00	14.30	18.30
11	7.00	13.30	17.00	6.45	13.30	17.00	8.45	15.00	19.30	9.00	15.00	17.00
12	6.45	13.30	17.00	6.45	13.45	17.00	9.00	15.00	18.15	9.00	15.00	17.00
13	9.00	12.30	17.45	9.00	14.00	18.45	9.00	15.00	17.00	9.00	13.45	17.45
14	6.45	13.00	17.45	6.30	12.45	18.00	9.00	15.00	20.00	9.00	15.00	17.45
15	6.45	12.45	17.45	6.45	12.30	17.45	9.00	15.00	18.00	9.00	15.00	17.30
16	7.00	13.15	17.00	6.45	13.45	17.00	8.30	15.00	19.15	9.00	15.00	17.00
17	6.45	13.15	17.00	6.45	13.15	17.15	8.15	15.00	18.00	9.00	15.00	17.00
18	8.15	13.30	17.45	8.30	14.00	18.15	9.00	15.00	19.45	9.00	15.00	17.45
19	7.00	13.45	17.30	6.45	14.00	19.45	9.00	15.00	18.00	9.00	15.00	17.30
20	7.00	13.30	17.00	6.45	12.30	17.00	9.00	15.00	18.00	9.00	15.00	17.15
21	7.00	13.00	17.00	6.45	13.45	17.00	8.45	15.00	18.00	9.00	15.00	17.00
22	6.30	14.00	17.00	6.30	12.45	17.00	9.00	14.00	19.15	9.00	15.00	18.00
23	6.45	12.45	17.00	7.15	15.00	17.45	7.30	14.45	18.00	9.00	15.00	18.15
24	6.45	13.15	17.30	9.00	13.15	18.30	9.00	14.45	20.00	8.30	15.00	17.30
25	6.30	13.00	17.30	6.30	13.45	18.00	8.30	14.30	19.15	9.00	15.00	17.45
26	6.45	13.00	17.00	7.00	13.15	17.00	9.00	15.00	18.00	9.00	12.45	17.45
27	6.45	13.15	17.45	6.45	12.45	17.45	8.45	15.00	18.00	9.00	12.45	18.00
28	6.45	13.00	17.45	6.45	13.00	19.15	8.45	15.00	18.15	9.00	15.00	17.30
29	7.00	13.00	17.30	6.45	12.30	17.45	8.45	15.00	19.45	9.00	12.30	17.45
30	7.30	13.00	17.00	8.00	13.00	17.00	8.45	15.00	18.00	9.00	14.30	17.00

Area	Pattern 1 (Sunday-Wednesday)			Pattern 2 (Thursday)			Pattern 3 (Friday)			Pattern 4 (Saturday)		
	AM	MD	PM	AM	MD	PM	AM	MD	PM	AM	MD	PM
31	7.30	14.15	17.00	7.30	14.15	17.00	9.00	15.00	19.30	9.00	15.00	17.00
32	7.15	13.45	17.00	7.15	13.45	17.00	9.00	14.00	19.15	9.00	15.00	17.30
33	6.45	13.00	18.00	6.45	12.45	17.45	9.00	12.00	19.30	9.00	12.15	17.45
34	6.45	12.45	18.00	7.00	12.45	18.00	9.00	12.00	17.45	9.00	12.00	18.15
35	6.45	13.00	17.15	6.45	13.15	15.15	8.30	12.00	17.45	8.30	15.00	17.15
36	6.45	13.15	17.00	6.45	13.30	17.45	8.45	15.00	18.00	9.00	15.00	17.45
37	6.30	13.00	17.45	6.30	12.45	18.45	9.00	13.45	18.00	9.00	12.15	18.30
38	6.30	13.00	17.45	6.30	12.30	17.45	9.00	15.00	19.30	9.00	15.00	18.00
39	6.30	13.00	17.45	6.45	12.45	17.45	9.00	15.00	18.00	9.00	15.00	17.45
40	6.30	13.15	19.15	6.30	13.00	17.45	9.00	15.00	18.00	9.00	15.00	17.45
41	6.45	12.45	17.45	6.45	12.45	17.45	9.00	12.00	18.00	9.00	15.00	17.45
42	6.45	13.00	17.30	6.45	13.15	18.00	9.00	12.00	18.00	9.00	15.00	17.30
43	6.45	13.30	17.30	7.00	13.30	17.30	8.45	13.30	19.30	9.00	15.00	17.30
44	7.00	14.00	17.00	7.00	14.00	17.30	9.00	13.45	19.30	9.00	15.00	17.30
45	7.15	14.00	17.45	7.00	14.45	17.45	9.00	15.00	19.00	9.00	15.00	17.30
46	-	-	-	-	-	-	-	-	-	-	-	-
47	6.45	13.00	17.30	6.30	14.45	17.15	6.00	12.00	18.45	9.00	12.30	17.30
48	7.15	14.45	17.00	7.15	15.00	17.45	9.00	15.00	18.30	9.00	15.00	18.00
49	7.00	13.15	17.15	7.00	13.15	19.00	9.00	15.00	19.30	9.00	12.30	18.00
50	7.15	13.15	17.30	7.00	13.30	17.30	9.00	13.30	19.45	9.00	12.30	17.30
51	6.45	13.15	17.15	6.45	12.45	17.00	9.00	15.00	17.45	9.00	15.00	17.45
52	6.45	13.15	17.45	6.30	12.45	17.45	9.00	15.00	17.45	9.00	15.00	17.45
53	6.45	13.00	17.30	6.30	12.45	17.45	9.00	15.00	17.45	9.00	15.00	17.45
54	6.30	13.00	17.15	6.15	13.15	17.00	9.00	12.00	17.45	9.00	15.00	17.00
55	6.30	13.00	17.45	6.30	12.45	17.45	9.00	15.00	17.45	9.00	15.00	17.45
56	6.30	12.45	17.45	6.30	12.45	17.45	9.00	15.00	18.00	9.00	15.00	17.30
57	6.45	12.45	17.45	6.45	12.45	18.00	9.00	15.00	17.45	9.00	15.00	17.45
58	6.45	13.00	17.30	6.45	13.30	17.30	8.45	15.00	18.00	9.00	12.45	17.00
59	6.45	12.30	17.45	6.45	12.30	17.45	9.00	12.30	17.45	9.00	12.15	17.45
60	7.00	13.00	17.15	6.45	12.45	18.00	9.00	12.15	18.45	9.00	12.30	17.45
61	7.15	13.00	17.45	7.30	12.45	17.30	9.00	15.00	18.00	9.00	12.30	17.45
62	7.15	12.45	18.00	7.15	12.30	17.15	9.00	12.00	18.00	9.00	12.30	18.00
63	7.00	13.15	17.30	6.45	12.45	17.45	8.30	13.00	20.00	9.00	12.15	17.30
64	6.45	13.30	17.15	6.45	13.15	17.00	9.00	12.30	18.00	9.00	12.15	17.45
65	6.45	13.00	17.45	6.45	12.45	18.15	9.00	12.30	17.45	9.00	12.45	17.45
66	6.15	13.00	19.15	6.15	13.15	18.45	6.00	12.00	20.00	8.00	12.30	20.00
67	6.45	13.00	17.45	6.45	13.00	17.45	6.00	12.00	19.30	8.00	12.15	17.45
68	6.45	12.45	17.45	6.45	12.45	17.45	9.00	12.00	18.00	9.00	12.00	17.45
69	6.30	12.15	18.00	6.30	12.30	19.15	9.00	12.00	19.45	9.00	12.15	17.45
70	6.30	12.30	17.00	6.30	12.45	17.30	9.00	15.00	18.00	9.00	15.00	17.45
71	6.30	13.00	17.15	6.45	12.45	17.45	9.00	15.00	18.00	9.00	12.30	18.00
72	-	-	-	-	-	-	-	-	-	-	-	-
73	-	-	-	-	-	-	-	-	-	-	-	-
74	6.30	12.30	17.45	6.45	12.45	18.30	9.00	12.00	18.00	9.00	12.00	18.00
75	6.30	13.00	17.45	6.30	12.45	19.30	9.00	12.00	18.00	9.00	12.30	18.00
76	6.30	13.00	17.45	6.30	13.00	18.00	8.45	12.00	17.45	8.30	12.45	17.00
77	6.30	13.15	17.45	6.30	12.45	17.45	9.00	14.45	19.00	8.30	15.00	17.45
78	6.45	13.15	17.45	6.45	12.30	18.15	9.00	12.00	18.15	9.00	12.15	18.00
79	6.45	13.45	17.15	6.45	13.15	17.45	6.00	12.30	19.30	9.00	12.00	17.45
80	7.45	15.00	17.00	7.45	13.00	17.00	6.00	13.00	17.45	9.00	12.45	17.00
81	6.15	13.15	17.00	6.30	13.15	19.45	8.45	12.30	17.30	8.15	12.00	18.00
82	6.30	13.00	17.30	6.30	12.30	17.00	9.00	12.00	17.45	9.00	15.00	17.45
83	6.30	13.45	17.00	6.30	13.45	17.45	9.00	12.00	17.45	9.00	15.00	17.00
84	9.00	12.00	17.00	9.00	12.00	17.00	8.45	15.00	17.45	9.00	12.00	17.00
85	9.00	12.00	17.00	9.00	12.00	17.00	9.00	15.00	17.15	9.00	12.00	17.00
86	8.00	12.30	17.00	9.00	12.30	17.00	9.00	15.00	17.15	8.00	15.00	17.00

Area	Pattern 1 (Sunday-Wednesday)			Pattern 2 (Thursday)			Pattern 3 (Friday)			Pattern 4 (Saturday)		
	AM	MD	PM	AM	MD	PM	AM	MD	PM	AM	MD	PM
87	9.00	12.00	17.00	9.00	15.00	17.00	9.00	15.00	17.30	9.00	12.00	17.00
88	7.15	12.00	17.00	6.45	12.15	17.15	9.00	15.00	17.45	9.00	15.00	17.00
89	7.45	15.00	17.00	9.00	15.00	17.30	9.00	15.00	18.00	9.00	15.00	17.15
90	7.15	14.00	17.00	7.30	13.45	17.45	8.45	15.00	17.00	7.45	12.00	17.00
91	6.30	13.15	17.00	6.30	13.30	17.45	9.00	12.00	17.45	8.30	15.00	17.00
92	6.45	13.15	17.45	6.45	13.00	17.45	9.00	12.00	18.15	7.45	12.45	17.45
93	6.30	13.30	17.45	6.45	12.45	18.00	9.00	12.00	18.00	8.45	12.15	17.45
94	6.30	13.15	17.45	6.30	12.30	19.15	9.00	12.00	19.30	9.00	12.30	18.30
95	6.30	13.30	17.45	6.30	13.45	18.00	9.00	15.00	18.00	8.45	15.00	17.45
96	6.45	13.45	17.45	6.45	13.15	18.15	8.45	12.00	18.30	9.00	15.00	18.15
97	9.00	15.00	17.00	8.45	14.45	17.00	9.00	15.00	18.00	8.15	12.00	17.00
98	6.30	13.30	17.45	6.30	13.30	17.00	9.00	12.00	17.45	8.15	15.00	17.45
99	6.30	13.30	17.45	6.30	12.30	17.45	9.00	12.00	17.45	9.00	12.15	18.00
100	6.30	13.00	17.45	6.30	12.30	19.15	8.45	12.00	18.00	9.00	15.00	17.00
101	6.15	15.00	17.00	6.15	15.00	17.00	6.15	15.00	18.00	6.15	15.00	17.15

Cite as: Mohamed A., Al-Saudi A., Al-Marri M. & Batran M., "Area-Specific Traffic Peak Hour Timing Using Traffic Signal Detectors: A Case Study of Qatar", *The 2nd International Conference on Civil Infrastructure and Construction (CIC 2023)*, Doha, Qatar, 5-8 February 2023, DOI: https://doi.org/10.29117/cic.2023.0129

Exploring Crowd Management and Evacuation Strategies using Microscopic Pedestrian Simulation: A Case Study of Souq Waqif

Shabna SayedMohammed
Qatar Transportation and Traffic Safety Center; Department of Civil and Architectural Engineering, Qatar University, Qatar
sk2000596@qu.edu.qa

Charitha Dias
Qatar Transportation and Traffic Safety Center; Department of Civil and Architectural Engineering, Qatar University, Qatar
cdias@qu.edu.qa

Wael Alhajyaseen
Qatar Transportation and Traffic Safety Center; Department of Civil and Architectural Engineering, Qatar University, Qatar
wyaseen@qu.edu.qa

Mohammed Yousef Alqaradawi
Qatar Transportation and Traffic Safety Center, Qatar University, Qatar
myq@qu.edu.qa

Abstract

Safe egress plans are critical for crowd evacuation at touristic attractions, particularly during special events, as visitors are often unaware of their options. Identification of bottlenecks in the walking spaces are vital for the development of safe and efficient crowd management and evacuation plans. This paper aims to explore crowd management and evacuation strategies for pedestrian egress flow in Souq Waqif, which is a famous touristic attraction in Doha, under varying crowd demand conditions. PTV Viswalk pedestrian simulation tool was used to evaluate crowd evacuation strategies and identify potential bottlenecks during the egress of crowds. Several guided and unguided evacuation scenarios were developed to understand the egress patterns to the allocated assembly areas inside the Souq. The crowd demands and densities were estimated using publicly available data. Eight major locations were identified as the bottleneck during the simulation. Simulation outcomes highlighted that the current evacuation plans and assembly locations are inadequate in providing safe evacuation routes. However, guided scenarios reduced evacuation times considerably when compared to unguided scenarios, particularly when the demand is high. A sensitivity analysis was also conducted to identify the effect of variations in walking behavior parameters in the simulation model. Variations in the walking behavior parameters changed the evacuation times considerably. Thus, proper calibration of walking behavior parameters considering local conditions could improve simulation accuracy. This study helps to identify probable bottlenecks and their characteristics that could help policymakers to assess the effectiveness of evacuation plans and crowd management strategies for crowd safety.

Keywords: Crowd management; Simulation; Pedestrian safety; Crowd evacuation; Historical sites

1 Introduction

Safe crowd egress, particularly during emergencies, is of utmost importance for the reduction of pedestrian injuries and fatalities. The causalities or fatalities might rise if evacuation times increase due to wrong exit selection caused by inadequate guidance or due to pushing and stampedes caused

by panic (Vilar et al., 2018; Zheng et al., 2009). Moreover, tourists are often unaware of safe egress routes and are thus highly vulnerable during emergencies (Sabashi et al., 2022). Proper signage including new innovative methods for wayfinding has been suggested by some researchers as effective means of escape during emergencies (Carattin & Brannigan, 2012). However, the evaluation and selection of suitable solutions and preventive measures for improving safety require consideration of numerous scenarios (Bakar et al., 2017). The number of scenarios to be tested and the cost related to testing such scenarios make crowd simulation tools to be the right decision-support tool that can be used to predict the behavior of the system (Chu et al., 2015). Thus, simulation tools can be used to model crowd evacuations under different conditions, particularly emergencies, to assist decision-makers to make the right solution. Moreover, simulation results can aid in the modification of the built environment to prevent emergencies (Sagun et al., 2011). This is crucial as experimental studies suggest that exiting pedestrians make exit choices based on the characteristics of the queue (speed and length) rather than route length or exit width (Bode et al., 2015).

A major challenge in using pedestrian evacuation simulation tools is the validation of such tools due to the complexity of acquiring data regarding social and psychological factors (Chen et al., 2021). Nevertheless, the Viswalk Crowd simulation tool based on Social Force Model has been found to simulate crowd escape under normal conditions with reasonable accuracy (Martén & Henningsson, 2014; Shi et al., 2021). However, the simulation of emergency conditions showed less frequency of the "faster is slower" effect, obstacle effect, and clogging effect when compared with the empirical data (Shi et al., 2021). Other studies suggest that the social force model and Viswalk simulation tool help illustrate pedestrian interactions, although a combination of more than one approach could provide better results (Jain et al., 2020; Zheng et al., 2009).

The present study focuses on the analysis of various scenarios for crowd evacuation at Souq Waqif which is a heritage site located in the Msheireb district of Doha and comprises an area of 164,000 m^2. Further, as shown in Figure 1, it is located in the vicinity of other famous tourist attractions. It is a labyrinth market founded 100 years ago for the trade of livestock goods (Furlan & Faggion, 2015; Khan et al., 2021). To preserve the architectural and historical identity of the Souq, it was reconstructed and restored in the years 2006 – 2008. It is now a blend of traditional Qatari architecture and modern functional spaces making it one of the top tourist attractions in Qatar. It is also anticipated that the Souq would be a prime destination for tourists visiting Qatar during future mega-events. Safety and efficiency of these crowd flows should be guaranteed, particularly during critical situations, i.e., potential evacuation situations and high-density situations. A simulation of crowd evacuation for a part of Souq Waqif was undertaken by Abdelaal et al (2020), who concluded that for higher crowd densities and emergencies, the route choice remains the same. Moreover, crowd densities as high as 6 p/m^2 were observed at junctions and gates (Abdelaal et al., 2020).

The present paper focuses on various scenarios for simulation designed based on the existing and forecasted demand on the pedestrian corridors of Souq Waqif to analyze the variation in evacuation times. The entire area designated as Souq was used for the simulation under normal conditions. A proposed solution based on providing effective guidance to pedestrians to the exit that will result in lesser evacuation time was simulated. In addition, the sensitivity of the simulated model to various walking behavior parameters was also studied.

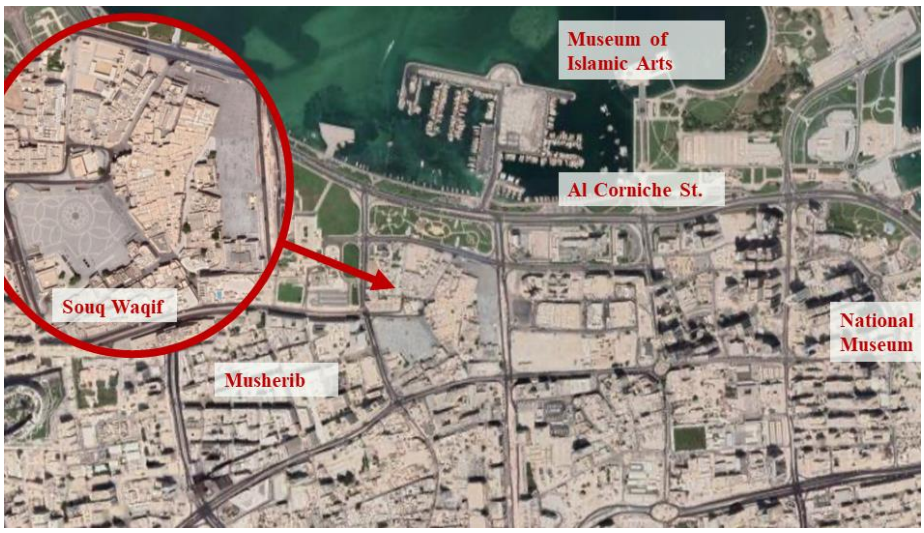


Fig.1: Souq Waqif area considered for the present study

2 Methodology

2.1 Data Collection

In this study, publicly available data, such as newspaper articles, Google Maps, and YouTube videos, were used to acquire the required data. The crowd demands were estimated for an event day scenario based on a press release ("2017 "زوار سوق واقف بالآلاف.. و12 الف زائر يوميا بسوق الوكرة,) that gives the total number of daily Souq visitors during the Eid period. This value was estimated at 60,000 visitors per day. To estimate the number of visitors per hour, data from google maps for different attractions in the Souq that shows the variations in demand was used. Projecting this data to the entire Souq gave the pedestrian demand (Figure 2). The demand reached 19800 pedestrians during the peak hour (9:00 pm -10 pm).

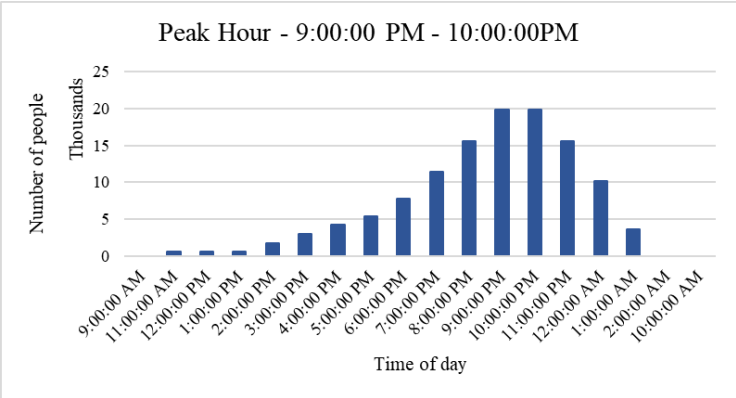


Fig. 2: Estimated pedestrian demand of Souq Waqif during an event

The crowd density was calculated based on video footage from (Rahman.YouTube., 2013) by counting the number of people within a known area. The footage highlights the main street in Souq Waqif as well as the square in front of the police station during the Eid period. The densities were estimated as 1.22 ± 0.07 p/m^2 and 1.59 ± 0.02 p/m^2 for the major walkway and junction in Souq Waqif. These pedestrian densities represented the level of service E – F based on Highway Capacity Manual criteria for walkways. The pedestrian demand for each corridor was determined based on the estimated densities so that the total demand remains at 19800 pedestrians per hour.

2.2 Scenario Design

A range of different scenarios was considered for the simulation as listed in Table 1. As per the Doha Metro Ridership forecast shown in Figure 3, it was predicted that there will be an increase of 50% in ridership by 2022 when compared with 2020 (Kovessy, 2015). Therefore, a similar projection for the number of pedestrians for the Mega Event scenario was assumed for the demand estimation of the number of pedestrians who will visit the Souq during future mega events that will be held in Qatar. An intermediate stage with an increase of 20% of the event day scenario was also considered. The normal day scenario was designed with half the demand of the event scenario.

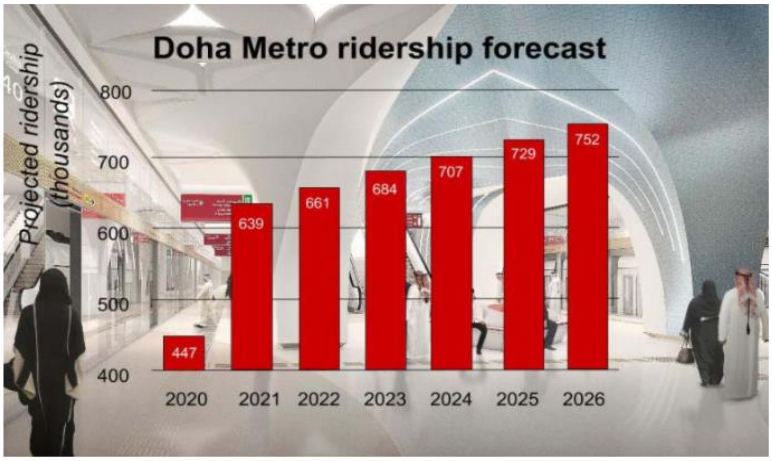


Fig.3: Doha Metro ridership forecast for 2020 to 2026

Table 1: Scenarios for simulation

Scenario	Conditions	Description	Number of Pedestrians in Peak Hour
NORMAL DAY	Guided Unguided	Friday/Saturday peak hour	9963
EVENT DAY	Guided Unguided	Spring Festival/National day peak hour	19800
EVENT DAY - FUTURE	Guided Unguided	20 % increase in event day demand during peak hour	23760
MEGA EVENT DAYS	Guided Unguided	50 % increase in event day demand during peak hour	29700

The destinations for the evacuation scenarios were determined based on the assembly areas as shown in Figure 4. The assembly areas marked are as per the designated assembly areas mentioned in the Souq Waqif evacuation plans displayed in the Souq corridors. For simulation, the pedestrians were assumed to evacuate to the designated assembly areas considering the shortest path for evacuation. Efficient guiding will improve the evacuation of pedestrians and also prevent anxiety, panic, and blind following of people during panic situations (Ma et al., 2017; Ma et al., 2016; Ren et al., 2021; Zhou et al., 2019). Therefore, in this study, the various demand scenarios for the unguided situation are compared with guided scenarios to evaluate their effectiveness.



Fig. 4: Simulated area of Souq Waqif showing the designated assembly areas

2.3 Simulation

The simulation of crowd evacuation for Souq Waqif has been carried out using PTV Viswalk, which is a microscopic simulation tool for pedestrian traffic (PTV, 2015). The Social Force Model developed by Helbing and Molnar is the basis of pedestrian behavior in Viswalk (Helbing & Molnar, 1995). This continuous model based on the concept of Newtonian Mechanics is capable of qualitatively reproducing many self–organizing phenomena. The global pedestrian walking behavior parameters can be assigned depending on the characteristics of the pedestrians being modeled. The default values represent a moderate conservative average value of an adult pedestrian (Alexandersson & Johansson, 2013). These parameters affect the route choice of pedestrians. They are based on the impact caused by other pedestrians and the relaxation time which determines the aggressiveness of the pedestrians. For the evaluation of various scenarios, the default walking parameter values have been used. Each pedestrian in Viswalk is assigned a destination and the pedestrian always chooses the quickest path to the assigned intermediate or final destination. The dynamic potential option can be utilized to model the pedestrian movement more realistically by making each pedestrian recalculate the path with the least travel time at each time step. The calculation for the dynamic potential option requires high computing capacity and has been thus utilized only for 75% of the routes in the present study.

2.4 Sensitivity Analysis

The social force model used in Viswalk suggests indirect forces that are psychological in nature exerted by the personal environment of the pedestrians and are a measure of the motivation of the pedestrians to perform a certain movement (PTV, 2015). This model is devised in such a way that (a) most of its parameters cannot be measured directly, (b) many characteristics of walking behavior are affected by a single parameter, and (c) more than one parameter determines a single walking behavior (Kretz et al., 2018). This makes calibration difficult. However, a sensitivity analysis was carried out by varying some of the Walking Behavior parameters of Viswalk. The parameters considered for the sensitivity analysis were Asocio mean and Bsocio mean where the parameter Asocio mean decides the strength of the force between pedestrians and the parameter Bsocio mean determines the range of the force between pedestrians in meters (PTV, 2015). Table 2 shows the default values as well as the values used for analysis. The values were increased and decreased by 50% for the analysis and were done for the evacuation of the event day scenario with 19800 pedestrians during the peak hour.

Table 2: Sensitivity analysis parameters and values

Walking Behavior Parameter	Value
ASOCIO MEAN	0.2
	0.4 (Default)
	0.6
BSOCIO MEAN	1.4
	2.8 (Default)
	5.6

3 Results

3.1 Analysis of Evacuation Scenarios

Evacuation scenarios as mentioned in Table 1 were simulated using Viswalk for the Souq Waqif. Figure 5 shows a comparison of the percentage of evacuation with time for varying demands for the unguided as well as guided scenarios. The time required to evacuate more than 98% of the crowd was compared for different scenarios. It can be visualized from Figure 5 that the guided evacuation provides faster evacuation for all the scenarios. Moreover, this tendency is very predominant for higher demand as seen in the Mega event days scenario. Table 3 shows the difference in evacuation time for each scenario. There is a reduction of 180 seconds for the Mega Event Days Scenario and a reduction of 130 seconds for the Event Day scenario while comparing the guided and unguided scenarios. Figures 6 and 7 show screenshots of guided and unguided evacuation scenarios at 300 seconds of simulation. It can be observed that the crowd densities are relatively lower in the guided scenario. It was noted that the route choices made for the unguided scenarios for the varying demand conditions were similar. This is in line with the findings of (Abdelaal, 2020). Moreover, eight locations were identified as potential bottlenecks for unguided scenarios. Some of these locations are wide corridors that are blocked due to the herding effect of the pedestrians. Similar bottleneck locations were identified in the guided scenario. However, the bottlenecks were cleared at a faster rate as some of the pedestrians used alternative routes to the guidance provided. Thus trained leaders as suggested by Zhou et al. (2019) could help redirect the evacuating pedestrian to routes that are insufficiently used.

Table 3: Comparison of evacuation time for different scenarios

Scenario	Conditions	Number of pedestrians/ hr (Demand)	Evacuation time for 98% evacuation (seconds)
Normal Day	Unguided	9963	300
	Guided	9963	280
Event Day	Unguided	19800	530
	Guided	19800	400
Event Day - Future	Unguided	23760	605
	Guided	23760	490
Mega Event Days	Unguided	29700	740
	Guided	29700	560

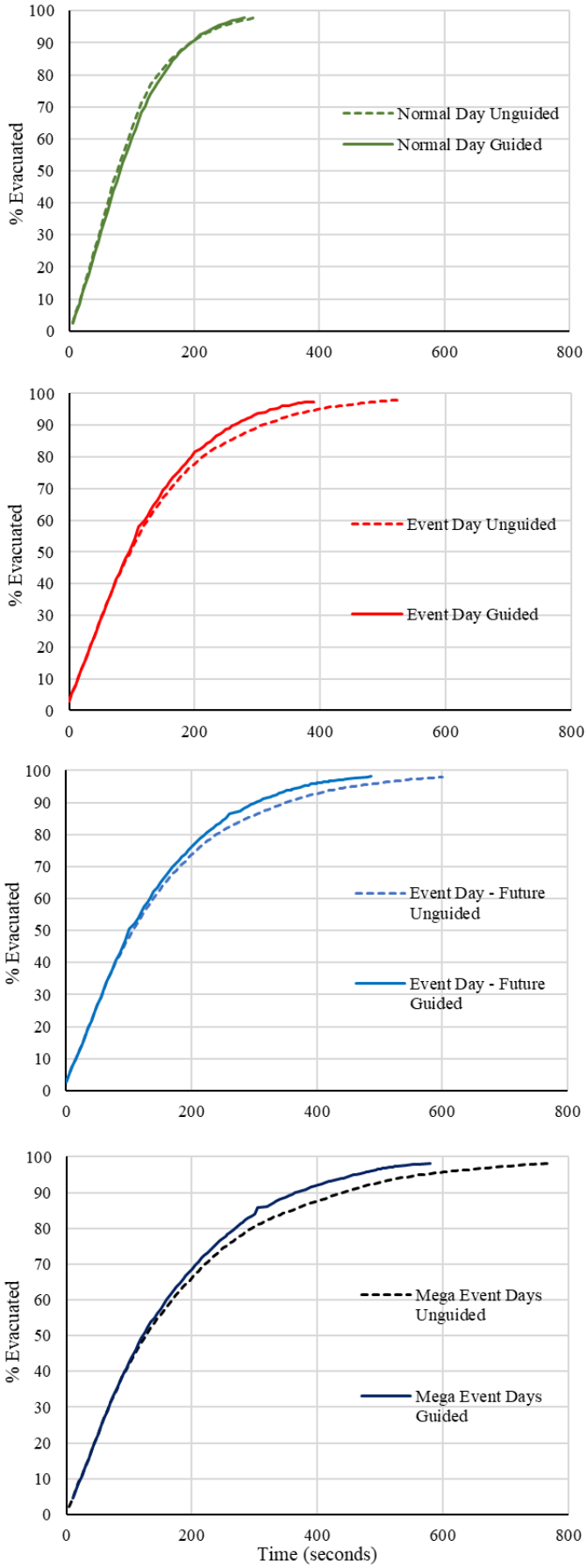


Fig. 5: Comparison of evacuation time for all scenarios

(a)

(b)

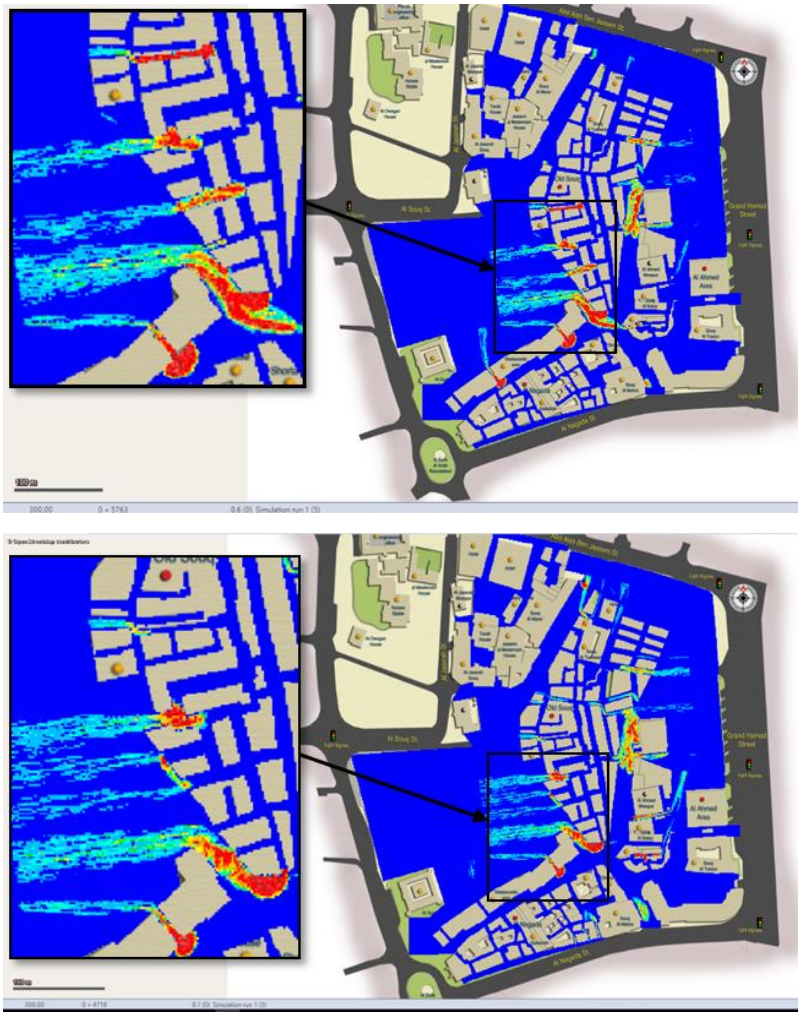


Fig. 6: Unguided scenario (a) and guided scenario (b) at 300 seconds of evacuation showed that the evacuation is proceeding with higher efficiency in the guided scenario

3.2 Sensitivity Analysis

The sensitivity analysis for the simulation of the event day scenario for the walking behavior parameters Asocio mean and Bsocio mean was performed to assess the effect on the evacuation performance. Figures 7 and 8 show the variation in the percentage evacuated at 400 seconds of simulation. Both the parameters show a decrease in the percentage evacuated as the parameter values are increased. However, the simulation model is more sensitive to the values of Asocio mean than Bsocio mean. This is extremely important as these parameters vary for different ethnicity. Further research is necessary for calibrating the parameters for the characteristics of people in Qatar.

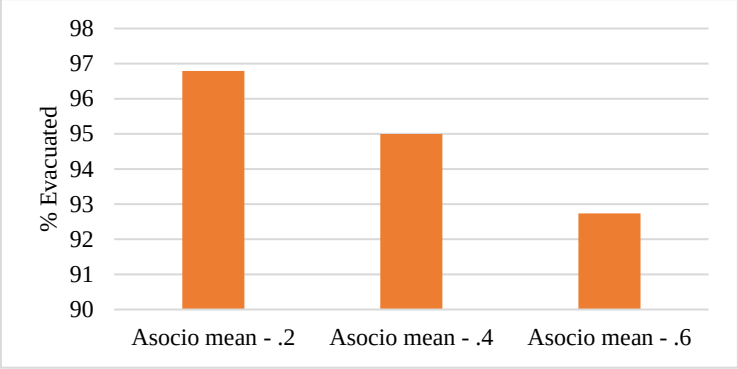


Fig. 7: Comparison of percentage evacuated at 400sec of evacuation time for different values of Asocio mean

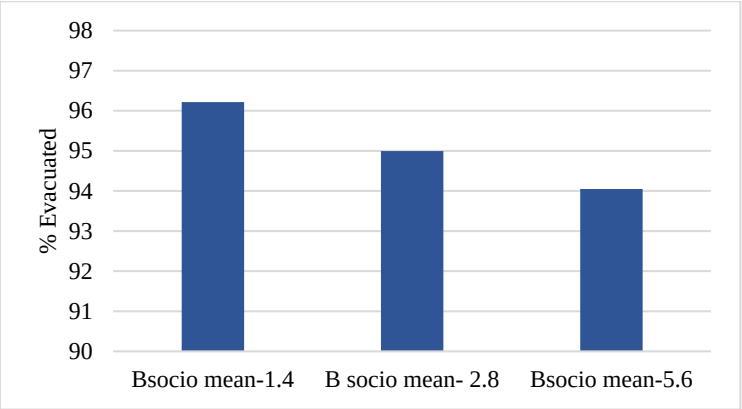


Fig. 8: Comparison of percentage evacuated at 400sec of evacuation time for different values of Bsocio mean

4 Conclusion

The crowd evacuation at Souq Waqif for different scenarios namely normal day, event day, future event day, and mega event days scenarios were simulated using PTV Viswalk crowd simulation software. The evacuation times for 98% of pedestrians evacuating for the various scenarios for guided and unguided conditions were compared. Eight potential bottleneck locations were identified from the simulation. It was found that the guided scenario substantially reduced the evacuation times and this was more predominant for higher pedestrian demand and density conditions. Thus an efficiently designed guiding system that comprises variable message signs or security staff to guide crowds, would help enhance efficiency in crowd flows and reduce injuries and fatalities in case of an emergency. Further, as understood from the sensitivity analysis both behavior parameters, i.e., Asocio mean and Bsocio mean show a decrease in the percentage evacuated as the parameter values are increased. These parameters could be significantly different for different ethnicities and are required to be calibrated using field data to improve the accuracy of the output of the model. Simulation models with actual empirical data as well as walking behavior parameters would provide more realistic results.

References

Abdelaal, A., Dias, C., Sarvi, M., Alhajyaseen, W., & Tarlochan, F. (2020). Crowd Dynamics, Management and Control at Tourist Attractions during Special Events: A Case Study at Souq Waqif Using Pedestride® Crowd Simulation Tool.

Alexandersson, S., & Johansson, E. (2013). *Pedestrians in microscopic traffic simulation. Comparison between software Viswalk and Legion for Aimsun*

Bakar, N. A. A., Majid, M. A., & Ismail, K. A. (2017). An overview of crowd evacuation simulation. *Advanced Science Letters, 23*(11), 11428-11431.

Bode, N. W., Kemloh Wagoum, A. U., & Codling, E. A. (2015). Information use by humans during dynamic route choice in virtual crowd evacuations. *Royal Society open science, 2*(1), 140410.

Carattin, E., & Brannigan, V. (2012). Controlled evacuation in historical and cultural structures: requirements, limitations and the potential for evacuation models. Proceedings of the 5th International Symposium on Human Behavior in Fire 2012,

Chen, J., Shi, T., & Li, N. (2021, 2021/10/01/). Pedestrian evacuation simulation in indoor emergency situations: Approaches, models and tools. *Safety Science, 142*, 105378. https://doi.org/https://doi.org/10.1016/j.ssci.2021.105378

Chu, M. L., Parigi, P., Law, K. H., & Latombe, J.-C. (2015, 2015/09/01). Simulating individual, group, and crowd behaviors in building egress. *SIMULATION, 91*(9), 825-845. https://doi.org/10.1177/0037549715605363

Furlan, R., & Faggion, L. (2015). The Souq Waqif Heritage Site in Doha: Spatial Form and Livability.

Helbing, D., & Molnar, P. (1995). Social force model for pedestrian dynamics. *Physical Review E, 51*(5), 4282.

Jain, H., Vanumu, L. D., & Ramachandra Rao, K. (2020, 2020//). Identifying a Suitable Pedestrian Simulation Software—

A Case Study on Emergency Evacuation of Classroom. Recent Advances in Traffic Engineering, Singapore.

Khan, A. H., Major, M. D., Tannous, H. O., & Paquet, T. (2021, 2021/10/01/). Tradition, Transformation, and Re-creation in Two Marketplaces: Souq Al Wakrah and Souq Waqif, Qatar. *Habitat International*, *116*, 102438. https://doi.org/https://doi.org/10.1016/j.habitatint.2021.102438

Kovessy, P. (2015, November 20). *Some 600,000 people a day expected to use Doha Metro by 2021*. https://www.dohanews.co/some-600000-people-a-day-expected-to-use-doha-metro-by-2021/

Kretz, T., Lohmiller, J., & Sukennik, P. (2018). Some indications on how to calibrate the social force model of pedestrian dynamics. *Transportation Research Record*, *2672*(20), 228-238.

Ma, Y., Lee, E. W. M., & Shi, M. (2017). Dual effects of guide-based guidance on pedestrian evacuation. *Physics Letters A*, *381*(22), 1837-1844.

Ma, Y., Yuen, R. K. K., & Lee, E. W. M. (2016). Effective leadership for crowd evacuation. *Physica A: Statistical Mechanics and its Applications*, *450*, 333-341.

Martén, J. B., & Henningsson, J. (2014). Verification and validation of Viswalk for building evacuation modelling. *Journal*, *5*, 135-144.

[Record #3439 is using a reference type undefined in this output style.]

Rahman.YouTube., K. (2013, November 3). *Souq waqif - Doha Qatar _1080 p-HD [Video]*

Ren, H., Yan, Y., & Gao, F. (2021). Variable guiding strategies in multi-exits evacuation: Pursuing balanced pedestrian densities. *Applied Mathematics and Computation*, *397*, 125965.

Sabashi, K., Ben-Moshe, B., Schmöcker, J. D., Hadas, Y., & Nakao, S. (2022, 2022/01/01/). Simulation of tourists' wayfinding during evacuation based on experiments in Kyoto. *Transportation research procedia*, *62*, 640-647. https://doi.org/https://doi.org/10.1016/j.trpro.2022.02.079

Sagun, A., Bouchlaghem, D., & Anumba, C. J. (2011, 2011/03/01/). Computer simulations vs. building guidance to enhance evacuation performance of buildings during emergency events. *Simulation Modelling Practice and Theory*, *19*(3), 1007-1019. https://doi.org/https://doi.org/10.1016/j.simpat.2010.12.001

Shi, X., Xue, S., Feliciani, C., Shiwakoti, N., Lin, J., Li, D., & Ye, Z. (2021, 2021/01/15/). Verifying the applicability of a pedestrian simulation model to reproduce the effect of exit design on egress flow under normal and emergency conditions. *Physica A: Statistical Mechanics and its Applications*, *562*, 125347. https://doi.org/https://doi.org/10.1016/j.physa.2020.125347

Vilar, E., Rebelo, F., & Noriega, P. (2018). Smart systems in emergency wayfinding: A literature review. International Conference of Design, User Experience, and Usability,

Zheng, X., Zhong, T., & Liu, M. (2009, 2009/03/01/). Modeling crowd evacuation of a building based on seven methodological approaches. *Building and Environment*, *44*(3), 437-445. https://doi.org/https://doi.org/10.1016/j.buildenv.2008.04.002

Zhou, M., Dong, H., Ioannou, P. A., Zhao, Y., & Wang, F.-Y. (2019). Guided crowd evacuation: approaches and challenges. *IEEE/CAA Journal of Automatica Sinica*, *6*(5), 1081-1094.

"زوار سوق واقف بالآلاف.. و12 الف زائر يوميا بسوق الوكرة". (2017, 4th February). *Al-Sharq Newspaper (2017)*. https://al-sharq.com/article/04/02/2017/زوار-سوق-واقف-بالآلاف-و12-الف-زائر-يوميا-بسوق-الوكرة

Cite as: Sayedmohammed S., Dias C., Alhajyaseen W. & Alqaradawi M., "Exploring Crowd Management and Evacuation Strategies using Microscopic Pedestrian Simulation: A Case Study of Souq Waqif", *The 2nd International Conference on Civil Infrastructure and Construction (CIC 2023)*, Doha, Qatar, 5-8 February 2023, DOI: https://doi.org/10.29117/cic.2023.0130

Adapting Smart Street Strategy for Post-Covid Built Environment

Ahmad Mohammed Ahmad
College of Engineering, Qatar University, Doha, Qatar
am.ahmad@qu.edu.qa

Shimaa Basheir Abdelkarim
College of Engineering, Qatar University, Doha, Qatar
shimaa666@hotmail.com

Nasir Mohammed
Department of Architecture, ABU Zaria, Kaduna State, Nigeria
nasirmakarfi@hotmail.com

Ahmed Mahfouz
College of Engineering, Qatar University, Doha, Qatar
ahmed.mahfouz@qu.edu.qa

Yongcheol Lee
Louisiana State University, Louisiana, United States
yclee@lsu.edu

Khalid Naji
knaji@qu.edu.qa
College of Engineering, Qatar University, Doha, Qatar

Abstract

The street networks occupy 25% of land use and are the veins of cities. By 2050, more than two-thirds of the world's population will live in urban areas. The urban street infrastructures and systems are expected to serve the public in performing mandatory and social activities on the streets. In addition, walkability and mobility within urban streets are linked with better public health demands. Therefore, there is a need for the public street to adopt smart features to provide better public health towards limiting the spread of covid.The study aims to develop a framework for smart street strategies to facilitate post covid built environment. The study adopts an integrative approach to deduct the smart street features through a robust literature review and workshops that influence post-Covid built environment within the urban design (Infrastructure) and information management. The study objective includes identifying the processes for adapting smart street strategies and healthcare concerns that can be leveraged to support public health in cities. As a result, the strategy can be adopted and applied by policymakers for implementation worldwide. The contributing features of the effort will focus on *tracking, controlling, and preventing analogy*. As a result, the framework will provide a baseline for neighborhoods, communities, and cities to develop and integrate novel strategies for managing public health to have an effective and efficient post-Covid pandemic built environment.

Keywords: Smart street; Post-Covid; Smart city; Pedestrians

1 Introduction

COVID-19 disproportionately impacted different countries worldwide, affected people's way of life, and had tremendous consequences on the world's economy. Gharipour and DeClercq (2021) stated that the

pandemic is a social, political and urban phenomena that should be considered to reduce its impact through public, practitioners and interdisciplinary collaboration. Therefore, there is a need to learn from the covid experiences to adapt to post-Covid built environment where measures including tracking, controlling and prevention strategies are adopted to manage future or seasonal pandemics. During epidemics, there is an acute relationship between shared urban public spaces and public health. The study focuses on a smart street intervention that requires urban infrastructure as its core. Furthermore, the streets are public spaces that link people from different communities in the urban fabric. However, the restriction on public movement can facilitate social distancing as one of the vital measures to manage Covid in the public realm. As a result, the streets will play a vital role in supporting the effort to limit the spread of the Covid-19 virus, contributing to making streets safer and healthier. The street is a public domain that allows interaction, communication and transportation of the public. Therefore, several urban interventions can facilitate the impact of pandemics on the street. In addition, urban infrastructure assists in reducing the impact of pandemics from previous knowledge of pandemics. However, the study proposes adopting smart street strategies with required urban infrastructure to mitigate and improve liveability in a post-pandemic built environment. The study adopted the integrative approach as the underpinning theory that supports the creation of new frameworks through a focus group study fostering creative thinking. The smart street framework was developed under five analogies, including infrastructure, smart features, data exchanged, contributions, and healthcare phases. The framework is significant as it provides the basis for interconnection between different devices to support tracking, controlling and prevention in a post-pandemic built environment. It can be adopted worldwide under the guidance of government institutions for implementation.

2 Literature Review

2.1 History of Pandemics

Pandemics spread to the public and caused loss of life and property. There have been several pandemics over the years. As a result, street management can be adopted to minimize the spread, which is not a panacea to the pandemic. Snowden (2019) described that several pandemics took place over the years; in 2008, the research found 335 human diseases between 1960-2004 originated from animals. He quoted virologist Brain Bird stating, “we live in an era now of chronic emergency” pandemic. As a result, the question is not whether but when it occurs and the prevalence of reoccurrence of a societal pandemic. After the Severe Acute Respiratory Syndrome (SARS) experience, the World Health Organisation (WHO) established a preparedness plan to establish country-based guidelines in 2005; they appointed a commission in 2018 that concluded in 2019 ‘*A World at Risk’* that the world and countries are unprepared for long-anticipated pandemics. In addition, funding and comprehensive planning are required to prepare for future pandemics.

2.2 Post-Covid Built Environment

Gillen et al. (2019) described the short and long-term challenges of the post-covid environment. Short-term consequences are becoming fewer, while long-term consequences are unpredictable. There are factors considered beyond the safety measures of social distancing, assigned seating and circulation roles. The post-Covid environment has some threads that include the design for flexibility and adaptability to future proof buildings or public spaces. There is a need to sustainably design spaces (existing and newly

built). Hughes and Armstrong (2021) stated that there is a need to rethink and reinvent the order in a post-pandemic environment. Kim and Kim (2022) described the WHO post-pandemic phases when the disease activity is at seasonal levels as described in Figure 1.

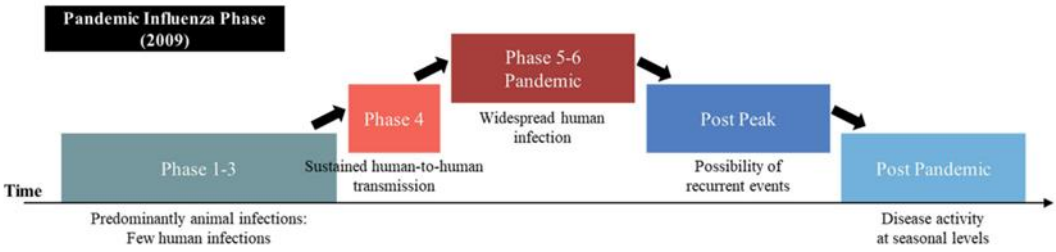


Fig. 1: The WHO (2009) Phases for the pandemic adapted by (Kim and Kim, 2022)

An integral part of the built environment is the street. The streets are destined for density. As the world must adapt and live with pandemics, well-designed and smart streets are needed. A street is a public place that allows the public to communicate, interact and move from one way to another. Street networks occupy 25% of land use and are the veins of cities (Gardner, 2011). By 2050, more than two-thirds of the world's population will live in urban areas (Ritchie & Roser, 2018). Cities are growth centres of population, consumption and waste generation.

The populations are expected to be serviced by the urban street infrastructures and systems. The public performs mandatory and social activities on the streets (Jung et al., 2009). Walkability and mobility within urban streets are linked with better health and transportation. However, restrictions and movement of people can facilitate social distancing as one of the vital measures to manage Covid in the public realm. The streets are public spaces that link people from different communities in the urban fabric. Therefore, there is a need to manage the spread of Covid smarter. As a result, the streets will play a vital role in supporting the effort to limit the spread of the Covid-19 virus, contributing to making streets safer and healthier. Shawket and El Khateeb (2020) and Lakshmi (2021) indicate the contributing factors for the Covid virus spread in the public realm through physical and air contact with contaminated solids. As a result, neighbourhoods, communities, and cities need to develop new and more innovative strategies for managing the spread to build a post-Covid pandemic-built environment (Klaus, 2020). Urban infrastructure defines the connection between cities and public health; and affects the number of people visiting healthcare services (Gharipour & DeClercq, 2021).

Post-Covid built environment can have an impact on the healthcare phases. Kim and Kim (2022) described the four Korean healthcare phases in Figure 2. The *Concern phases* indicate pre-outbreak while monitoring suspicious pandemic spread; the *Notice Phase* implies the first infection is reported with people in close contact affected and urban spread is initiated. *The Alert phase* describes a confirmed rapid increase in cases leading to an urban emergency. Finally, the *Serious Phase* indicates the rampant spread and disease response reaches its threshold levels. Sharifi et al. (2021) described three main contributions towards limiting the impact of the Covid-19 pandemic. These include tracking, controlling and preventing analogies. Furthermore, they indicated that smart solutions and technologies could facilitate the effort to manage pandemics in a post-Covid built environment.

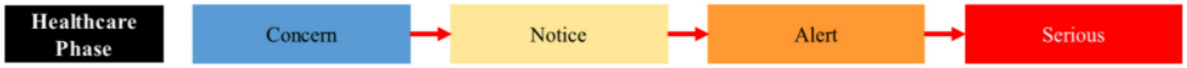


Fig. 2: Healthcare system phase with time series (Kim and Kim, 2022)

2.3 Urban Infrastructure

One of the contributing factors to the spreading of diseases is related to urban mobility. The travels occur within the streets, making them a valuable public realm that would enable mobility and virus spread. Urban infrastructural design and digital data management are vital for smart street interventions. Tešić et al. (2020) believe smart features can facilitate pandemic management. For example, sensors can be used at pedestrian zebra traffic lights to avoid contact with contaminated solids. The cycle lanes' intervention can be achieved by providing shade and using parked vehicles for cyclist safety in narrow streets. Well-designed cycle lanes can reduce the population on sidewalks and public transport use, supporting the challenges of overcrowding, as shown in Fig. 3. Furthermore, the lack of shading can result in pedestrians congesting shaded pathways. As shade is required during summer, which can be achieved through different shading strategies as described by Ahmad et al. (2021).

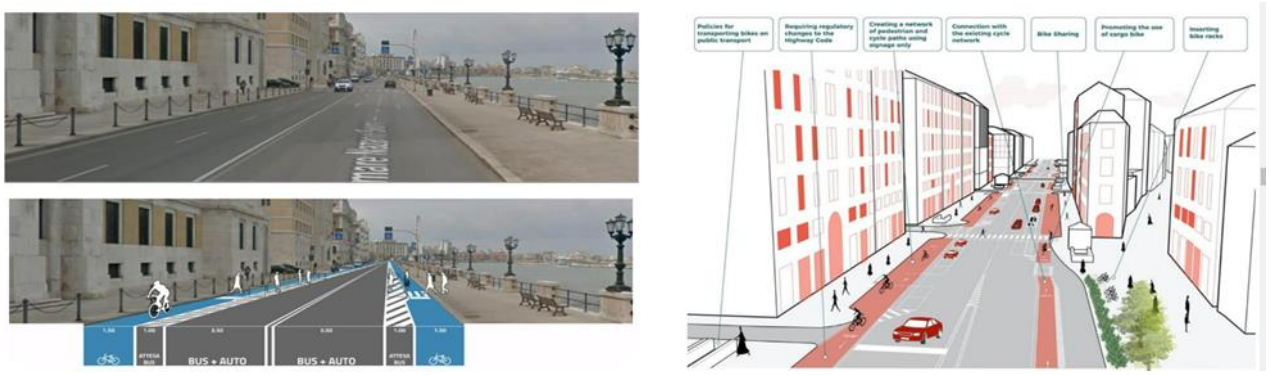


Fig. 3: Urban design (infrastructure) Al-Kindi and (Abbood, 2021)

2.4 Smart Street

Smart Street is defined as a fundamental building block for any smart city architecture. Smart streets have their basis in smart lighting systems (Pribyl & Pribyl, 2015); they include cyber-physical systems and services apart from space, traffic, waste management and environmental monitoring (Ahmed & Rani, 2018). The smart street concepts can be leveraged to support public health in the future. Figure 3highlights the focus on vehicles; however, there is a dire need for pedestrian focus.

Table 1: Principles and elements for the smart street

Principles for Smart Street		**Elements for Smart Street**	
Principles	**Description**	**Elements**	**Description**
People first	Priority-More walkable-pedestrian-cyclist-public transport-public services (goods and services) – Private vehicles	Connectivity corridor	To enable hardware and street furniture for connectivity within the smart street for a variety of direct and indirect socio-economic outcomes
Sense of place	Sense of place-local and cultural integration	Smart street information system	Urban information systems depend on national, regional and local agencies. Ability to collect data on fixed and moving things

From Input to impact	Measuring and communicating the impact of input (technological)	Traffic and transit management	The use of sensors and ability to manage different sections of the street at different times of the day
Connectivity counts	Free public wifi enables economic growth	Accessibility, security and safety	Lack of accessibility and protection of pedestrians
Available and accessible	To enable safe outdoor activities during times such as Covid	Smart street furniture	Items such as benches, transit stops, Covid kiosk to enable dialogue with the public. Lamps, waste management etc.
Flexible programmable public realm	Enable diverse commercial spaces to reduce clusters	Climate protection, environmental monitoring, weather mitigation	Measuring noise, air quality, climate, flood and water levels, weather monitoring and prediction, providing shelter, shade etc
Open not closed	Making government sector information openly available	Environmental sustainability	Reduced carbon emissions by simplifying public transport, bike riding and car-sharing
Evolution not revolution;	Minimize waste and maximize learning with limited budgets	Street activity	Ability to manage street activities through interactive technology.
Complex stakeholder environment	Adopting the bottom-up rather than a top-down focused solely on the achievement of local targets, not international		

Table **1** : Some principles and elements of the smart street. This study tends to deduct the relevant aspects that can be leveraged for public health only. It is noteworthy that the study will integrate smart street strategies to focus on public health.

3 Methodology

The study adopted qualitative data collection and analysis as described in Figure 4. Furthermore, it adopted the integrative research approach as the underpinning theory described in Table 2. Snyder (2019) stated that the integrative approach aims to assess, critique, and synthesize the literature to enable the development of new theoretical frameworks (Torraco, 2005). In addition, the approach allows focusing on newly emerging topics to create conceptual and theoretical models. The study aims to develop a novel and conceptual smart street strategy for a post-covid built environment. The data collection for the integrative approach analyses literature and main ideas in the context of their relationships. MacInnis (2011) stated that the process requires conceptual thinking.

Table 2: Integrative research features- adapted from Synder (2019)

No.	Approach	Integrative research
1	Typical purpose	Critique and synthesize
2	Research question	Narrow or Broad
3	Search strategy	Usually not systematic
4	Sample characteristics	Research articles, books,
5	Analysis and evaluation	Qualitative
6	Examples of contribution	Taxonomy or classification, theoretical model or framework

The literature review analysed smart features adopted in smart public spaces. Smart infrastructure provides the foundation for all the smart features related to a smart city, including smart health and improving city liveability. As a result, infrastructure is vital for the smart street adaptation into post-Covid built environment. The approach defined relevant analogies that include relevant infrastructure facilitating smart street features with their data exchange format and possible contributions towards the WHO healthcare phases. A focus group was further adopted. Morgan and Krueger, (1998) stated that they had between four to six participants, meanwhile, Krueger and Casey (2000) had between six to eight participants. Barbour (2018) stated that focus groups excel in providing a process outcome compared to a defined outcome. The approach's limitation is the unfolding of data in an unsequential manner. Six participants conducted the focus group; there were four architects and two engineers with an average of five years of experience.

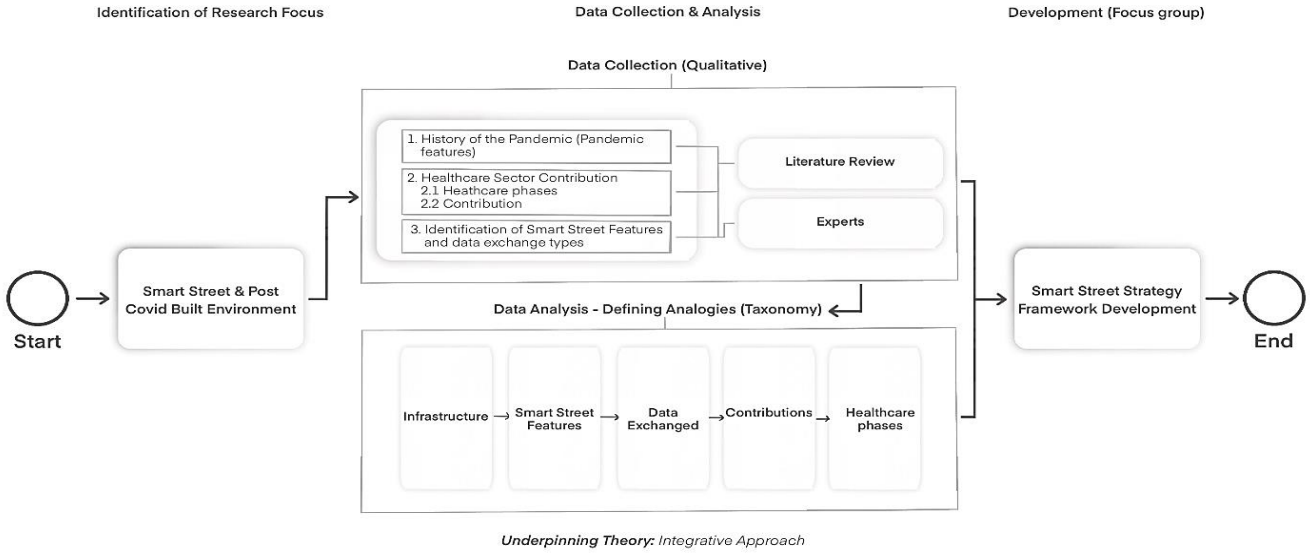


Fig. 4: Smart street framework methodology

The participants attended three sessions that lasted from 45 minutes to one hour. The study adopted a qualitative approach. The focus group questions included highlighting and deducting relevant themes for the smart street with a significance on pandemic tracking, monitoring and prevention. The participants deducted the findings from the literature review, and the framework was developed as a process linking relationships between different analogies.

4 Data Analysis and Discussion

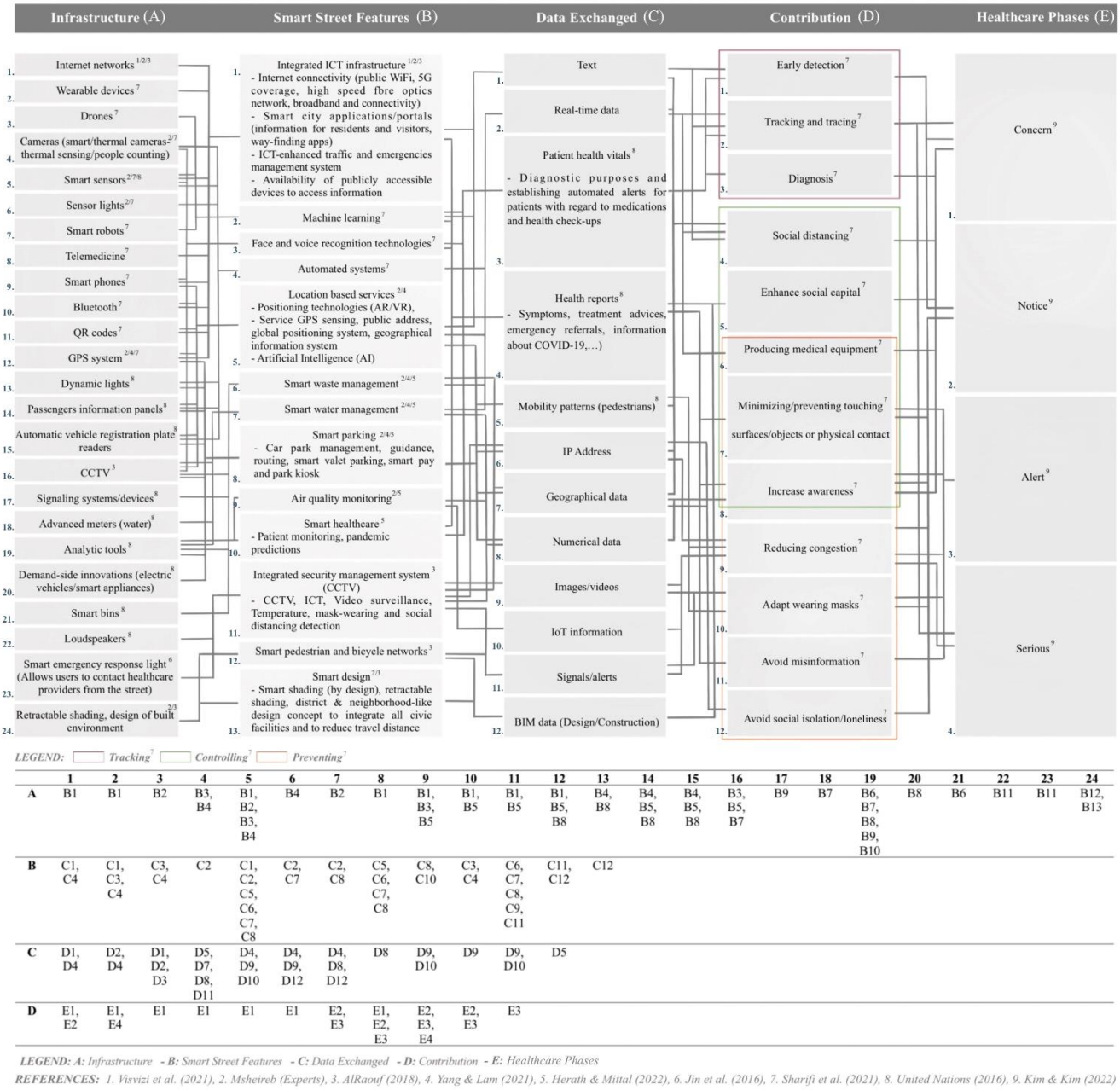
The study adopted an integrative research approach that facilitated deductions from secondary data leading to the development of the smart street framework. Smart infrastructure provides the core characteristic that underpins most of the smart components to connect and generate data, which may be used intelligently to ensure the optimal use of resources and improve the performance of the street. This section introduced some critical components of smart city infrastructure as described in Table 3.

Table 3: Smart digital layers, Adapted from United Nations (2016)

Smart Digit Layer	Description	Healthcare Contribution
Urban	They include physical and digital infrastructures. For example–smart buildings, mobility, and waste management systems.	Smart parking reduces congestion. Smart waste reducing physical contact
Sensors	They include smart devices that measure and monitor different parameters.	Smart sensors reduce physical contact and detect masking and social distancing.
Connectivity	They include data and information from the sensor level to storage and for further analysis	Smart data facilitate pandemic control identifying areas of concern for public
Data Analytics	They include the analysis of data collected by different smart infrastructure systems to help predict some events (such as traffic congestion)	Predictions can reduce congestion and prevent the spread of the virus
Automation	They include a digital enabling interface layer that enables automation and scalability for a large number of devices across multiple domains	To report/ update the public with timely data, the interface connected to several devices is vital to prevent the spread

The framework described in Figure 5 is developed based on analogies from the literature review. The focus group findings played a vital role towards developing the concepts and relationships between the different thematic analogies deducted from existing studies. The framework adopted five themes. These include Infrastructure, Data exchange, Smart features, Contributions and the Healthcare phases. The Infrastructure provides a platform for the smart function to take place. The Data exchanged format is vital to understand the nature of the information interoperable within an interface. The Smart features are non-exhaustive; there will be novel Smart features over time as technological advancement is imperative. The Contributions are towards healthcare management of covid. The Healthcare phases highlight relationship between healthcare contributions. For example, Smart camera can highlight the rise in public temperature, highlighting early detection and indicating concern as Healthcare phase.

The framework is the outcome of the focus group. It focuses on achieving the framework rather than the framework outcome. The study provides a platform for smart street features that facilitate the development of post-Covid built environment. Future research can highlight novel smart street features and adopt their contribution towards public health. For example, sensor on a zebra crossing to prevent the spread of the virus through physical contact. The practicality of the framework can be realised with government support and guidance due to the nature of the study, which centres on public spaces and public health. In addition, the framework can be adopted in the short term by retrofitting existing infrastructure. For example, CCTV cameras can be replaced with Smart cameras that allow temperature and masking detection to control and prevent the virus's spread. While on the long term, an established Central Command Centre is required to be developed to manage the interconnected Smart features effectively and efficiently.



	1	2	3	4	5	6	7	8	9	10	11	12	13	14	15	16	17	18	19	20	21	22	23	24
A	B1	B1	B2	B3, B4	B1, B2, B3, B4	B4	B2	B1	B1, B3, B5	B1, B5	B1, B5	B1, B5, B8	B4, B8	B4, B5, B8	B4, B5, B8	B3, B5, B7	B9	B7	B6, B7, B8, B9, B10	B8	B6	B11	B11	B12, B13
B	C1, C4	C1, C3, C4	C3, C4	C2	C1, C2, C5, C6, C7, C8	C2, C7	C2, C8	C5, C6, C7, C8	C8, C10	C3, C4	C6, C7, C8, C9, C11	C11, C12	C12											
C	D1, D4	D2, D4	D1, D2, D3	D5, D7, D8, D11	D4, D9, D10	D4, D9, D12	D4, D8, D12	D8	D9, D10	D9	D9, D10	D5												
D	E1, E2	E1, E4	E1	E1	E1	E1	E2, E3	E1, E2, E3	E2, E3, E4	E2, E3	E3													

LEGEND: A: Infrastructure - B: Smart Street Features - C: Data Exchanged - D: Contribution - E: Healthcare Phases

REFERENCES: 1. Visvizi et al. (2021), 2. Msheireb (Experts), 3. AlRaouf (2018), 4. Yang & Lam (2021), 5. Herath & Mittal (2022), 6. Jin et al. (2016), 7. Sharifi et al. (2021), 8. United Nations (2016), 9. Kim & Kim (2022)

Fig. 5: Smart Street Framework for post-Covid built environment. (Non-exhaustive list)

5 Conclusion and Recommendation

Most of the country's population will go more into the urban areas. As a result, the street network is taking up a large part of the urban land. Streets are a cornerstone to communication, interaction and transportation of the public. Smart streets are developed from the idea of smart lights that contribute towards developing more smart city features. Therefore, smart strategy initiatives are required to manage the communities and cities for resilient post-Covid built environments. The study aimed to develop a Smart street framework strategy towards the post-pandemic built environment. It is expected to be resilient towards Covid spread at seasonal levels by providing preventive and controlling inputs into the public streets. The integrative approach allows focusing on newly emerging areas of study to create

conceptual and theoretical models. Smart features from secondary data were analysed and deducted to develop the smart street framework; it targets smart city and public health researchers to contribute towards tracking, controlling and preventing the spread of Covid within the built environment. The smart street can be applied in densely populated areas in the short-term and to other streets in the long-term. Future research recommendation for the study suggests exploring the interoperability of the data exchanged between the muti-facet and disciplinary applications to enable efficient and effective information management of the spread in the communities and cities.

Limitation

The study highlights a conceptual framework that provides a basis for future Smart street strategies towards post-Covid built environment. However, the framework only provides an exhaustive list of all relevant Smart features identified from literature review sources. As a result, it is non-exhaustive. Furthermore, this study does not consider the cost implication of adopting the framework.

Acknowledgement

This publication was made possible by the NPRP grant (NPRP 12S-0304-190230) from the Qatar National Research Fund (a member of Qatar Foundation); and Qatar University, College of Engineering (CENG) with project number QUCP-CENG-2020-1. The statements made herein are solely the responsibility of the author(s).

References

Ahmad, A. M., Ahmad, A. M. & Aliyu, A. A. (2021). Strategy For Shading Walkable Spaces In The GCC Region, *Journal Of Urban Generation and Renewal, 14*(3), 312-328.

Ahmed, S. H. & Rani, S. (2018) A Hybrid Approach, Smart Street Use Case and Future Aspects for Internet of Things in Smart Cities," Future Generation Computer Systems, vol. 79, 2018, pp. 941–951.

AlRaouf, A. (2018). Lusail City Vision – Doha, Qatar. Proceeding of Mega Urban Projects Conference In Doha, Qatar. Retrieved from: https://www.researchgate.net/publication/322978187_Lusail_City_Vision_-_Doha_Qatar (Accessed on the 29th of May, 2022). DOI: 10.13140/RG.2.2.17117.51689

Barbour, R. (2018). Doing Focus Group. Sage Publishing. Los Angelos.

Gardner, C. (2011). Old Urbanist: We Are the 25%: Looking at Street Area Percentages and Surface Parking. Old Urbanist. Available from: https://oldurbanist.blogspot.com/2011/12/we-are-25-looking-at-street-area.html

Gharipour, M. & DeClercq, C. (2021). *Epidemic Urbanism: Contagious Diseases in Global Cities*. University of Chicago Press. US.

Herath, H.M.K.K.M.B & Mittal, M. (2022). Adoption of Artificial Intelligence In Smart Cities: A Comprehensive Review. *International Journal of Information Management Data Insights 2* (2022) 100076. https://doi.org/10.1016/j.jjimei.2022.100076

Hughes, R. & Armstrong, R. (2021). *The Art of Experiment: Post-pandemic Knowledge Practices for 21st Century Architecture and Design*. Routledge. US.

Jin, et al. (2016). Smart Street Lighting System: A platform for Innovative Smart City Applications and a New Frontier for

Cyber Security. *The Electricity Journal. 29*. Pp. 28-35

Jung, S., Lee, J. K. J. & Ha, J, (2009) A study on Analysis of User Behavior in Urban Central Street: On the Dongsung Street in Daegu. *Journal of the Regional Association of the Architectural Institute of Korea*, 2009,p. 300.

Al-Kindi, A. & Abbood, A. (2021). Urban Street Space after Covid-19: (Indicators of safe and healthy urban street space. *Turkish Journal of computer and Mathematics education.*

Kim, J. H. & Kim, J. Y. (2022). How Should the Structure of Smart Cities Change to Predict and Overcome a Pandemic? *Sustainability*, 14, 2981. https://doi.org/10.3390/su14052981

Klaus, I. (2020). Bloomberg CityLab. Retrieved from: The Post-Pandemic Urban Future is Already Here: https://www.bloomberg.com/news/articles/2020-04-06/how-will-the-pandemic-transform-urban-space.

Krueger, R. A. & Casey. M. A. (2000). *Focus Groups: A Practical Guide for Applied Research*. Sage Publishing. US.

Lakshmi, S. (2021) SARS- CoV-2 to Skin, finds study. News Medical Life Sciences. Available from: https://www.news-medical.net/news/20210429/Touching-contaminated-surfaces-can-transfer-SARS-CoV-2-to-skin-finds-study.aspx. Accessed on 15/05/2022.

Lynn, T., Rosati, P. & Fox, G., (2020) Smart Streets: Definition, Principles, and Infrastructural Elements. The Fourtheeth International Conference on Digital Society. Available from: https://www.researchgate.net/profile/Pierangelo-Rosati/publication/346205531_Smart_Streets_Definition_Principles_and_Infrastructural_Elements/links/5fbcd322a6fdcc6cc65ebe6b/Smart-Streets-Definition-Principles-and-Infrastructural-Elements.pdf

MacInnis, D. J. (2011). A framework for conceptual contributions in marketing. *Journal of Marketing*, 75, 136–154. https://doi.org/10.1509/jmkg.75.4.136.

Morgan, D. L. & Krueger., R. A. (1998). *Developing Questions for Focus Groups*. Sage Publishing. US.

Gillen, et al. (2021). *Rethink Design Guide: Architecture for a post-pandemic world*. Routledge, RIBA Publishing Press.

Pribyl, P. & Pribyl, O. (2015) Definition of a Smart Street as Smart City's Building Element," in 2015 Smart Cities Symposium Prague.IEEE,2015, pp. 1–6.

Ritchie, H. & Roser, M. (2018). "Urbanization". Published online at OurWorldInData.org. Retrieved from: 'https://ourworldindata.org/urbanization' [Online Resource]

Sharifi, A., Khavarian-Garmsir, A. R. & Kummitha, R. K. R. (2021). Contributions of Smart City Solutions and Technologies to Resilience against the COVID-19 Pandemic: A Literature Review. *Sustainability*, 13, 8018. pp. 1-29. DOI: https://doi.org/10.3390/su13148018

Shawket, I. M. & El khateeb, S. (2020). RedefiningUrban Public Space's Characters after COVID-19; Empirical Study on Egyptian Residential Spaces. 24th International Conference Information Visualisation (pp. 594-599).

Snowden, F. M. (2019). *Epidemics and Society: From the Black Death to the Present*. Yale University Press. United States.

Snyder, H. (2019). Literature Review: As A Research Methodology: An Overview and Guidelines. *Journal of Business Research 104* (2019). pp. 333-339. DOI: https://doi.org/10.1016/j.jbusres.2019.07.039

Tešić, D., Blagojević, D. & Lukić., A, (2020). Bringing "Smart" into Cities to Fight Pandemics – With the Reference to the Covid-19. *Tourism and Hotel Management*. Pp. 49–1/2020. DOI: 10.5937/ZbDght2001099T

Torraco, R. J. (2005). Writing integrative literature reviews: Guidelines and examples. Human Resource Development Review, 4, 356–367. https://doi.org/10.1177/1534484305278283

United Nations (2016). Smart Cities and Infrastructure. Report of the Secretary-General - Economic and Social Council. Commission on Science and Technology Development, Nineteenth Session, Geneva 9-1e May, Item 3(a) of the Provisional Agenda

Visvizi, A., Abdel-Razek, S., Wosiek, R. & Malik, R. (2021). Conceptualizing Walking and Walkability in the Smart City Through a Model Composite w2 Smart City Utility Index. Energies 2021, 14, 8193. pp. 1-20. DOI: https://doi.org/10.3390/en14238193

WHO Global Influenza Programme & World Health Organization. ((2009:Pandemic influenza preparedness and response . a WHO guidance document. World Health Organization. https://apps.who.int/iris/handle/10665/44123

Yang, W. & Lam, P. (2021). An Evaluation of ICT Benefits Enhancing Walkability In A Smart City. Landscape and Urban Planning 215, 104227.

Cite as: Ahmad A.M., Abdelkarim S., Mohammad N., Mahfouz A., Lee Y. & Naji K., "Adapting Smart Street Strategy for Post-Covid Built Environment", *The 2nd International Conference on Civil Infrastructure and Construction (CIC 2023)*, Doha, Qatar, 5-8 February 2023, DOI: https://doi.org/10.29117/cic.2023.0131

Nairobi MRTS Conceptualization: Transit-Oriented Development for Sustainable Transport

Bidhan Chandra Roy
RUPL, New Delhi, India
bcroy1944@gmail.com

Satyaki Bhattacharyya
Principal Track Engineer, DB Engineering & Consulting GmbH, Bengaluru, India
satyakib.backup@gmail.com

Abstract

Nairobi, famous for Nairobi National Park, the world's only game reserve found within a major city, started developing as a rail depot on the Uganda Railway. In 1963, Nairobi became the capital of the Republic of Kenya and showed phenomenal growth in terms of population ever since (from 11,500 in the year of 1906, to 3,138,369 by Year 2009, at growth rate of 4.1% a year). The city of Nairobi has experienced rapid urban sprawl. In 1970, average commuter distance was 0.8 km and increased to 25 km in 1998. Present commuter distance is over 40 km. The long commuter distances and heavy traffic congestion on the road has led to long travel time. At this rate, the difficulties commuting to the central business area is getting more and more complicated. The need of the hour is developing a world-class transport network, a combination of Road and Rail Based Mass Rapid Transit System (hereinafter mentioned as MRTS or MRT) technology. A comprehensive study was carried out in this direction to find out the feasibility of such MRTS in early 2000s. Based on the findings of the study, further study was conducted in 2013-2014 for developing the basis for a technical and financial harmonisation of measures. In 2019, the NMA Council gazetted 5 BRT and 7 Commuter Rail corridors vide Legal Notice No. 16 of 26th February 2019, which is outcome of all the efforts. This paper aims to put together the outcome of studies made so far.

Keywords: MRTS Planning; Nairobi MRTS

1 Introduction

The name Nairobi was derived from Enkare Nairobi, meaning "cool waters" in Maasai. In 1899, the Uganda Railway established a camp in what was then a swampy region that would become Nairobi. In 1905, the city served as the seat of government for both Kenya and the British East Africa Protectorate. The town was burnt down in the early 1900s and it had to be rebuilt, subsequent to spread of an infectious disease.

Nairobi's population reached above 15,000 in 1919, when it was officially recognised as a municipality with full corporate powers and a designated territory of 1.5 miles (3.9 Km). In 1950, Nairobi was officially recognised as a city, and its original 90 sq. km. expanded to include 690 sq. km. The colonial city's 1948 master plan called for a central business district (abbreviated as CBD) with easy access to the surrounding suburbs and industrial zone. Without any central planning, the town expanded along a gridiron layout of streets, and land use changed little in response to the prevailing racial dynamic (Africans, Asians and Europeans).

East of the main thoroughfare was where most African-American neighbourhoods were located. After

colonial limitations on Africans were lifted in 1963, migration into the city increased dramatically, catalysing rapid expansion. However, the city's public transportation infrastructure has not kept pace with its growth, leading to the chaos and stampedes that can be seen daily in the Central Business District.

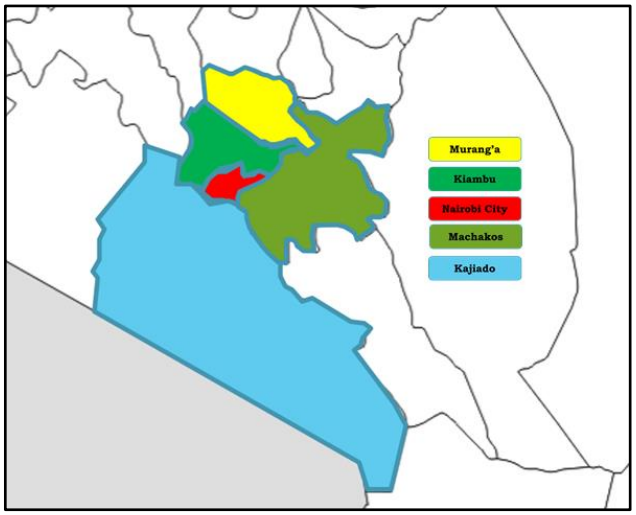


Fig. 1: Nairobi Metropolitan Area

Table 1: Population Distribution in NMR

COUNTY	Population (2019)	%	Area (KM^2)	%	Density (P/KM^2)
Nairobi	4,397,073	42.2%	694.9	2.1%	6,328
Kiambu	2,417,735	23.2%	2,449.2	7.5%	987
Kajiado	1,117,840	10.7%	21,292.7	65.1%	52
Machakos	1,421,932	13.7%	5,952.9	18.2%	239
Muranga	1,056,640	10.1%	2,325.8	7.1%	454
Totals	**10,411,220**	**100.0%**	**32,715.5**	**100.0%**	**318**

In 2009, 3.13 million people lived in Nairobi city, which covers 696 sq. km of the Nairobi Metropolitan Region (NMR); 47% of NMR residents. Nairobi's population density is 4509 people per sq.km. Compared to this, Kikuyu, Karuri, Thika, and Kangundo Town Councils had 1000–1500 people per sq.km; 400–600 people per sq.km live in Limuru, Kiambu, Ruiru, and Machakos Municipal Councils. The County Councils' population densities range from 18 in Kajiado to 437 in Kiambu.

Nairobi Metropolitan Region (NMR) begins at 2,300 m above sea level on the eastern side of the Rift Valley and progressively declines down to 1,400 m above mean sea level. The western and northern parts of NMR are hilly, whereas the eastern half has mild slopes. These districts' social-cultural zones are diversified, with urban areas having multi-ethnic groupings and rural areas having homogeneous ethnic groups like Kamba in eastern province, Kikuyu in central province, and Maasai in the Rift Valley.

2 Transportation Planning in Nairobi

2.1 History

In 1926, the Nairobi Municipal Council hired a town planning consultant team to reorganise the city (locate workers within walking distance to the CBD and industrial area). This was followed by a deal with a British transportation company (U.T.O.) to provide metropolitan public transportation services. This was the origin of the current bus services in Kenya. Prior to 1950, just 12 buses served predominantly Asian and European regions with good access roads to the town centre.

The CBD had ample open spaces before 1948. However, the master plan prevented spreading beyond Nairobi River in the North and the railway line in the South, and proposed a road system within the CBD with freedom of through traffic and easy exit for traffic into the city's suburbs and industrial area.

The 1970 Nairobi urban study group (N.U.S.G.) report, which led to the 1973 Nairobi Metropolitan expansion strategy, suggested decentralising industry to Dandora, Ruaraka, and Dagoretti in order to integrate work and housing zones. N.U.S.G. promoted exclusive bus ways, commuter rail transit, and staggered working hours, excluding the "Matatu" sector's role in public transport. Belgium Transurb consult group (1984) suggested three mass transit solutions for Nairobi-introduction of articulated

buses, light rail transit, and exclusive bus lanes.

2.2 Present Scenario

Because public transport is expensive and insufficient, most city journeys are made on foot. Nairobi's principal public transit is matatu and various private buses. Commuter train capacity is modest and limited to a few regions. Public transport cannot satisfy demand.

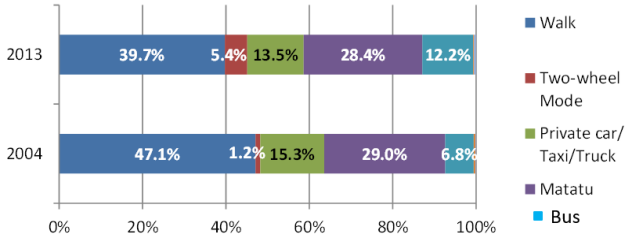


Fig. 2: Modal Split Changes



Fig. 3: Congestion in Central Business Area

Taxis are a well-liked means of transportation, not only among travellers but also among residents, and they are included in the category of intermediate public transport (IPT). Tuktuks are three-wheeled motor vehicles that can also function as an individual passenger transport (IPT). There are approximately 200 tuktuks that operate along the same lines as taxis but cater to shorter distances of travel. As part of the integrated public transport system, two-wheeled motor cycles known as boda bodas are used to transport passengers. Their primary route of operation is in the direction of and between the municipal towns. In the same vein, cycle taxis can also function as IPT in more remote locations.

Trains arrive and depart from Mombasa three times per week, making Nairobi reachable by rail. Only trains heading east to Mombasa are in operation. At the moment, Kenya Railway only runs one direction of intercity service per day from Nairobi Railway Station to each of (i) Embakasi Village (12.6 km), (ii) Kikuyu (31 km), (iii) Kahawa (24 km), and (iv) Ruiru (32 km). Normal speeds are around 12–20 kph. Despite being the more cost-effective public transportation option, most urban commuters avoid the commuter rail for a variety of reasons, including but not limited to: insufficient inter-modal transfer facilities; a lack of safety and comfort; and a lengthy distance between the station and their respective places of employment.

The bus system in Kenya is generally dependable, however it is insufficient. Nairobi serves as the hub of the country's bus system, and a number of bus companies offer services to and from the country's other major cities. Approximately 4% of all passenger trips in NMR are made on buses, which operate on approximately 67 routes and are projected to carry approximately 0.35 to 0.40 million passengers per day. The vast majority of buses compete with the Matatus for passengers on the same routes.

Commuters and tourists alike utilise Matatus (public minibuses) to get from the city centre to the outskirts of Nairobi. The smallest Matatus are the size of a van and seat capacity of 14, while the largest may hold up to 50 passengers. In the event of an accident, Matatus frequently have more passengers than seatbelts. Matatus are typically driven recklessly due to the lack of licence requirements, including passing on the sidewalk, exceeding the speed limit, and weaving in and out of traffic.

Transportation costs in the city are prohibitive for most residents due to high prices and low wages. The typical bus fare during rush hour is Ksh 50 in the central 0-10 km zone, and Ksh 100 in the 10-20 km zone. When compared to the minimum wage of Ksh 7, 334 (GOK, 2011) per month, which is roughly Ksh 200-300 per day, the expense of public transportation is quite high.

This necessitates the creation of a brand-new, cutting-edge mass transit system that is at once dependable, committed, and affordable. Consulting Engineering Services (India) Pvt. Ltd. conducted a feasibility study on the topic between 2009 and 2013 in order to find a workable solution for the ambitious Nirobi Mass Rapid Transit System. A second international consulting bid was issued to conduct a harmonisation study of the available alternatives and find the optimal way to improve traffic flow.

3 Outcome of Feasibility Study by CES & APEC (Ref 1)

3.1 Field Studies and Mode Selection Method

In order to determine the level of interest in travelling within the NMR, the research area was divided into 74 traffic analysis zones (TAZ). Simulation of the travel demand pattern between TAZs in NMR was carried out with the use of a four-stage urban transport-planning model. Based on the projections of the demand for transportation, it appears as though certain corridors in NMR may require the high capacity Metro Rail. On other lines, medium-capacity modes of transportation such as bus rapid transit systems (BRTS), light rail transit systems (LRT), and monorail will be sufficient. The level of demand, as shown by peak hour peak direction traffic (PHPDT), is the primary factor that determines which of these systems will be selected.

Corridors with a peak hour passenger demand threshold (PHPDT) of fewer than 5,000 passengers have not been evaluated for a new MRTS technology, and the same number of passengers can be fed by the present bus service. In areas with a PHPDT of more than 5,000 passengers, BRTS has been proposed as an alternative. Between these two options, the Bus Rapid Transit System (BRTS) is the one that has been deemed to be more suitable for Nairobi due to the fact that it would make the transition into a system with a higher capacity less cumbersome. There have been discussions about installing LRT in areas with a PHPDT of more than 12,000 passengers and installing Metro Rail in corridors with a PHPDT of more than 30,000 passengers (not envisaged in Scenario at present).

The following is a prediction of future travel demand on the specified MRTS corridors for the year 2030 based on low growth scenarios:

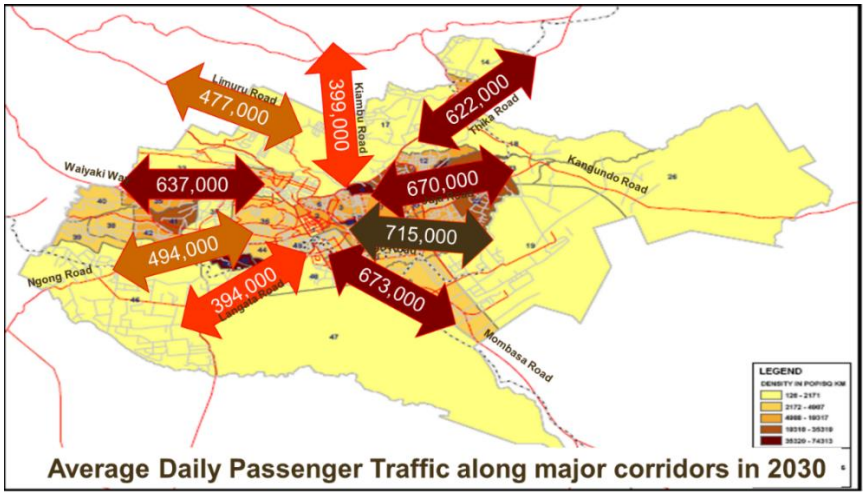


Figure 4: Travel Demand in the City of Nairobi

3.2 Study Outcome

A transit hub at NRS (Nairobi Railway Station) and connecting the entire city to this, with sufficient transit interchanges so that any commuter can bypass the Transit hub at NRS in case, would satisfy the movement demand of most commuters in the city, as most travel in Nairobi is directed toward NRS.



Fig. 5: Concept of Transit Hub

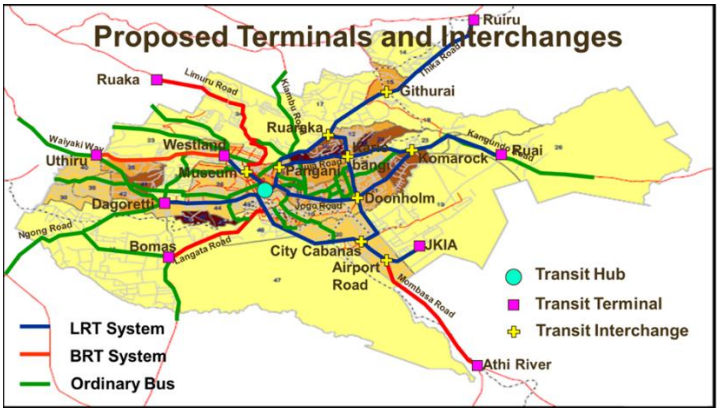


Fig. 6: Nairobi MRTS Corridors

The current Nairobi Railway Station and its adjacent yards might be repurposed into the Central Hub Terminal of the Nairobi Mass Rapid Transit System (MRTS), complete with sleek, environmentally friendly architecture. This terminal would be the starting point and final destination for all lines. This would make it simple to switch between different lines, shortening the time it takes to travel between different parts of the region/city.

In a perfect world, demand control strategies would complement the availability of public transportation options. Critical areas such as the Central Business District, proposed District Centres, Nodal Terminals, MRTS/BRTS proposed stations/stops, and corridors should be prepared for transit oriented development around rail stations, road terminals, and along the corridors/lines up to one km on either side, first for the construction stage of MRTS and then for the operation stage on a continuous basis.

3.3 Economic Viability

Economic viability study was done in all the corridors, and the project was found to be economically viable. The difference in the economic instances "without" and "with" the project is used to calculate the benefits of the project. The circumstance known as "without project" is referred to as the "base" case or the "do-nothing" case. In this scenario, the predicted development scenario is superimposed over the transport network that is already in place. The 'with project' case illustrates a potential future development scenario for the integrated multi-modal transport network following the successful completion of the MRTS project.

MRTS would reduce carbon emissions, travel time, and vehicle costs, in addition to reducing the amount of carbon emissions. The wage rate method was utilised in order to arrive at an estimation of the value of time (VOT) for passengers. The Consultants for PT consumers' Stated Preference Survey determined passengers' average monthly income. A carbon footprint software model was utilised to assess carbon emission decrease.

Table 2: Economic Viability Table

#	Corridor Name	Approx. Length kms	EIRR (%)	Technology Proposed
1	Thika Road	40.47	33.13	LRT/BRT
2	Juja Road	13.82	21.94	LRT
3	Jogoo Road	12.79	24.77	LRT

#	Corridor Name	Approx. Length kms	EIRR (%)	Technology Proposed
4	Ngong Road	20.30	24.44	LRT/BRT
5	Limuru Road	13.8	25.75	BRT
6	Mombasa Road	26.62	63.43	BRT
7	Outer Ring Road	12.93	25.10	LRT
8	Waiyaki Way	18.71	14.29	LRT
9	Langata Road	7.64	28.65	BRT

3.4 Financial Viability and Viability Gap Funding

Discounted cash flow (DCF) analysis estimates the Financial Internal Rate of Return (FIRR). Capital and operating costs were stated earlier. Each route's average daily ridership estimates revenue. This research assumes KSH 2.5 for BRTS and KSH 4 for LRTS per passenger-kilometre. The Phase 1 MRTS sections' Project FIRR and Equity FIRR were estimated. The Project FIRRs, or returns on total investment, were lower than the EIRRs, as is typical for such projects. With debt and equity financing and Viability Gap Funding (VGF), projects can be made feasible with Equity FIRRs of 18%.

Table 3: Project FIRR and VGF

Corridors	Name	Project FIRR (%)	VGF in Ml. Kshs
LRT-2(1)	Thika Corridor (NRS - Githurai)	4.33	37,713
LRT-3	Juja Corridor	7.61	36,669
LRT-4	Jogoo Corridor	7.70	29,864
LRT-6	Ngong Corridor	3.01	32,326
BRT-1	Limuru Road (NRS To Ruaka)	0.79	15,793
BRT-3	Mobassa (Athi River)	5.84	27,652
			1,80,017

It is envisaged that funding for the MRTS project will come from a public-private partnership (PPP), which will make use of the resources and core skills offered by the private sector. Building public and partner confidence will require a significant contribution from the government, which must take the lead in this endeavour.

Table 4: Recommended Sources for VGF

Sources	Amount (mn Ksh)	Percentage
Property development by Private Investors	9,000	5%
Soft Loan from Multilateral agencies	126,000	70%
Share of GoK (from Budgetary resources)	45,000	25%
Total	1,80,000	

3.5 Project Capital Cost

A period of approximately 15 years would be required for the implementation of the complete 170 kilometres of projected MRTS within Nairobi. The following is a summary of the estimated capital costs of all of the corridors at their pricing in 2010-2011:

Table 5: Project Capital Cost

Corridor	Financial Cost (mill Kshs)	Economic Cost (mill Kshs)
MRTS 1 : Waiyaki Way	54,864	45,770
MRTS 2 : Thika Road	108,115	89,361
MRTS 3 : Juja Road	63,207	52,414
MRTS 4 : Jogoo Road	43,183	35,938

Corridor	Financial Cost (mill Kshs)	Economic Cost (mill Kshs)
MRTS 5 : Outer Ring Road	42,021	34,953
MRTS 6 : Ngong Road	44,411	37,364
MRTS 7 : Limuru Road	17,357	15,100
MRTS 8 : Langata Road	9,120	7,934
MRTS 9 : Mombasa Road /Athi River	27,075	23,555

The cost estimate for the infrastructure was derived from the costs of similar works being performed as part of the ongoing Thika Road Improvement Project. The cost of BRT/LRT systems and rolling stock is determined based on the knowledge gained from previous projects of a similar nature that were carried out in India. We will assume that the cost of government land is zero. One percent of the total cost of the civil project is allocated to R&R and social impact.

3.6 Social and Environmental Viability

All MRTS corridors are planned on highways with right of way over 30 metres, enough for elevated LRT structures at the road centre. Construction, depots, and yards would require more land. Reduce project-affected persons. Transportation-related water quality factors need intensive monitoring. Some streams have 0.235mg/l of oil and grease, above the Water Quality Regulation's zero limit. Due to fewer public transport vehicles in major corridors, the high-capacity MRTS should reduce oil and grease in waterways. Sulphur, nitrogen, and carbon monoxide levels in Nairobi's ambient air are low. Carbon dioxide and particulate matter, the most common metrics, are low outside the city. These make the project socially and environmentally viable.

4 Implementation

Following the results of the feasibility study, additional research was conducted to lay the groundwork for a technical and financial harmonisation of measures aimed at improving the traffic situation and increasing the efficiency of the various transport networks in the Kenyan capital. This research included conducting a detailed traffic analysis and developing models, as well as formulating a concerted strategy for the implementation of an integrated transport solution (Ref: Harmonization of Public Transport done by H.P. Gauff Ingenieure GmbH consortium & inputs available in Nairobi Metropolitan Area Transport Authority Website https://namata.go.ke/mrts).

During this, a few corridors identified was merged together and mode converted to BRTS instead of providing a combination of BRT & LRT as proposed earlier, for the first phase. In later stage, some of the corridors are proposed for conversion to LRT.

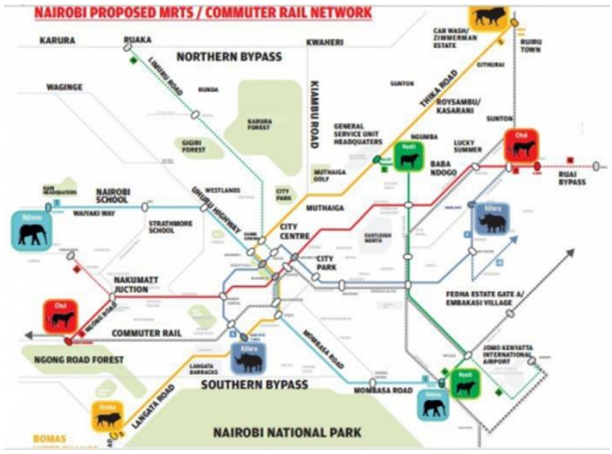


Fig. 7: Nairobi MRTS Schematic

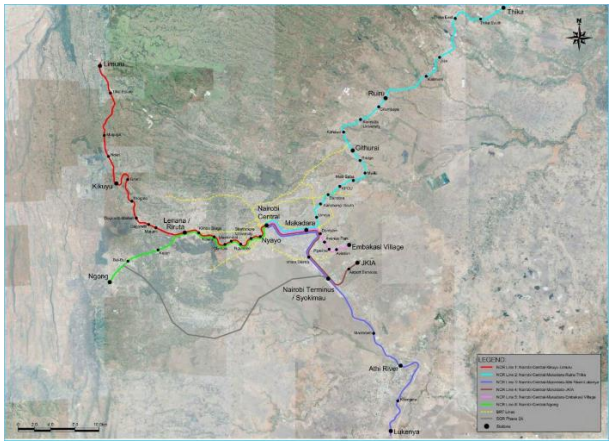


Fig. 8: Commuter Rail Master Plan

The proposed plan calls for a Bus Rapid Transit (BRT) system to be the primary mode of transportation in the first phase of the project, with five interconnecting lines named after Kenya's Big Five animals: Ndovu (elephant), Simba (lion), Chui (leopard), Kifaru (rhino), and Nyati (buffalo).

5 Conclusion

In order to meet the demand for transportation in the Nairobi Metropolitan Area, the MRTS Harmonisation Study of 2014 recommended the construction of Commuter Rail and five BRT lanes (NMA). Through the publication of Legal Notice No. 16 on February 26, 2019, the NMA Council officially designated the following 5 BRT lines and 7 Commuter Rail corridors for the year 2019:

One ticket gets a traveller from Kangemi to Imara Daima on Ndovu line. The Waiyaki Way and Mombasa Road line will contain drop-off and pick-up stations at ABC Place, Westlands, University Way, Kenyatta Avenue, Haile Selassie Avenue, Makaburini, Nyayo Stadium, and near General Motors. Some stations connect to other lines. This project is a proposed addition to the Expressway project that is currently being developed by KeNHA.

Simba Line will transport passengers from Bomas Interchange at the Bomas of Kenya to Ruiru town via the city. The 27-kilometer project follows Thika Superhighway from Ruiru to Kenyatta National Hospital through Nairobi CBD. The STECOL Corporation-SMEDI project began on August 4, 2020.

Chui Line passengers can take one bus from Njiru in Embakasi to Jamhuri Showground. Dandora, Kariabangi, and Gikomba market would be significant stops on the Ngong Road, Juja Road, and Komarock Road route. The MRTS will reach Ruai and Kawangware in Phase II. Detail Design of this corridor is being carried out at present.

Kifaru Line will connect Mama Lucy Hospital to T-Mall via the CBD in Nairobi's densely populated Eastlands. Donholm, City Stadium, Bee Centre, Nairobi Hospital, and Moi Avenue are prominent stops along Jogoo Road.

Nyati, the shortest of the five lines, will connect Balozi Estate near GSU headquarters to Imara Daima through Outering Road. Phase II extends the railway to Jomo Kenyatta International Airport (JKIA). This stretch is being developed under Korea Funding Plan.

In addition, the following Commuter Rail Lines are also given go-ahead for implementation:

a. Nairobi - Limuru Town
b. Nairobi - Ngong Town
c. Nairobi - Kenol, Murang'a
d. Nairobi - Kiambu Town
e. Nairobi - Ruai Town
f. Nairobi - Jomo Kenyatta International Airport
g. Nairobi – Konza

References

2009 Kenya Population and Housing Census: "Counting Our People for Implementation of Vision 2030" Volume XIV Population Projections.

King'ori Zacharia (2007). Nairobi Urban Transportation Challenges – Learning from Japan.

Report on Feasibility Study & Technical Assistance for Mass Rapid Transit System for the Nairobi Metropolitan Region

carried out by CES and APEC.

Report on MRTS Nairobi – Harmonization of Public Transport done by Group of H.P. Gauff Ingenieure GmbH & Co KG -JBG- ETC Transport Consultants GmbH - PB-Consult Planungs- und Betriebsberatungs-GmbH.

Study on Master Plan for Urban Transport in the Nairobi Metropolitan Area, 2006.

*For updated status of the project in Nairobi inputs taken from inputs available in Nairobi Metropolitan Area Transport Authority Website. https://namata.go.ke/mrts

Cite as: Roy B.C. & Bhattacharyya S., "Nairobi MRTS Conceptualization: Transit-Oriented Development for Sustainable Transport", *The 2nd International Conference on Civil Infrastructure and Construction (CIC 2023)*, Doha, Qatar, 5-8 February 2023, DOI: https://doi.org/10.29117/cic.2023.0132

An Adaptive Tabu Search OptimisationAlgorithm for Solving E-Scooters Battery Swapping Problem

Mahmoud Masoud[ab]
[a]Department of Information Systems & Operations Management, Business School,
King Fahd University of Petroleum and Minerals, Dhahran, Saudi Arabia
[b]Center for Smart Mobility and Logistics, King Fahd University of Petroleum & Minerals, Dhahran, Saudi Arabia
mahmoud.masoud@kfupm.edu.sa

Abstract

E-scooters have become a popular mode of transportation for first and last-mile excursions in recent years. Their usage as a short-distance public transit system is commonly regarded as an efficient solution to minimise carbon emissions while also being handy for individuals on the go. The need for charging, however, has become problematic as a result of the popularity of e-scooters because it effectively renders the scooter that is presently being charged inoperable. A relatively new method being used involves swapping batteries in e-scooters rather than transferring full scooters to be recharged, reducing out-of-service time to a few minutes rather than hours. To reduce trip distances and maximise fuel economy for battery swapping operators, a system for determining the most effective path to switch the e-scooters' batteries will be required. This paper aims to do this through the use of Tabu Search (TS) algorithm to determine the optimal number of battery swapping operators for an area and then to ascertain the most efficient routes for each operator. This method will then be compared to Simulated Annealing in order to determine which method is the most optimal for this scenario. The data used to evaluate this method was obtained from the 2019 Chicago pilot program . The results showed an adapted tabu search in the total distance travelled, leading to shorter charging trips comparing to simulated annealing.

Keywords: Micro-mobility; e-scooters; Freelancers; Tabu search; Assignment problem; Simulated Annealing

1 Introduction

With the rise in popularity of e-scooters, a new mode of transportation has emerged to finish the last-mile journey. This popular mode of transportation, however, faces its own set of challenges in order to improve and become more efficient. Some of these concerns include the necessity for e-scooters to be recharged, and their relatively hefty size, which can make it difficult for freelance chargers to carry multiples e-scooters home to recharge (Carey & Lienert, 2022). To address this, rechargeable batteries are rapidly becoming the standard. This implies that the people who charge these e-scooters may carry hundreds of batteries with their person at once and go on a path where they just need to replace the scooter's battery, saving time and effort. However, this procedure may be made more effective by optimising the route and cutting down on the distance the operators must drive, which will reduce the cost of fuel and the amount of time required (Masoud et al., 2019a; Almannaa et al., 2021a; Almannaa et al., 2021b). Using e-cargo bikes, which presently have a battery capacity of 20 and 40 batteries and have a range of around 30 kilometres, is one environmentally beneficial prospective option being investigated (Severengiz, et al., 2020). Reducing it as much as feasible might have a huge beneficial impact on the environment overall because the environmental footprint of recharging e-

scooters is rather large—it accounts for 43% of the entire environmental impact of an e-scooter.

This problem is blatantly similar to the capacitated vehicle routeing problem, which is a derivation of the travelling salesman problem (Eksioglu, Vural & Reisman, 2009). The main notion is that a travelling salesperson must go from site to location selling their wares; the salesman aims to limit the overall distance traversed because it will take less time. The capacitated vehicle routeing challenge entails adding a capacity to both the vehicle travelling around and the destinations the vehicles arrive at. This means that the trucks must not only decrease the total distance of their routes, but also deliver the appropriate capacity of commodities at each point (Clarke & Wright, 1964; Mingozzi, 2005).

This study proposes a modified tabu search to handle this problem, as well as a comparison to Simulated Annealing, both of which will be done using Google.

2. Methodology

The implementation of the separate methods for optimizing the routes for the capacitated vehicle routing problem described in this paper can be split into five major components:

1. Cleaning and extraction of data.
2. Run the data through the Google OR-Tools API with the different methods provided (Tabu Search (TS), Simulated Annealing (SA)).
3. Compare and analyse the results.

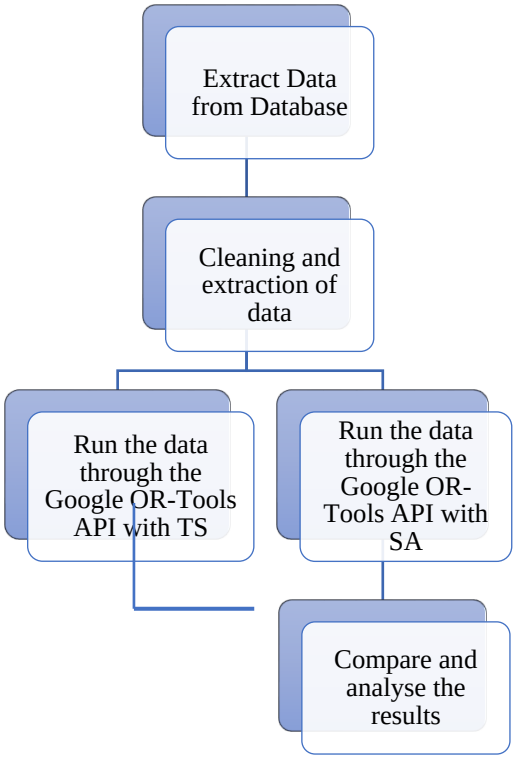


Fig. 1: Methodology Flowchart

1.1 Data Extraction

The E-Scooter Trips 2019 Chicago Pilot dataset (City of Chicago, 2020) is a large dataset that includes 710839 e-scooter trips with information on the trip's duration, location, and region. Only the e-position scooter's at the conclusion of the journey is necessary for our algorithm because that is likely the time when a scooter may need charging. The whole set of data will be cleaned by deleting any

rows that have NaN values in the necessary fields, such as the End Community Area Number, End Centroid Latitude, and End Centroid Longitude. The data is initially divided into its many sections in order to assess the efficacy of the various route optimisation techniques under a variety of circumstances. This will generate several sub datasets that may be assessed, such as a dataset in Table 1 which is relevant data columns used for implementation.

Table 1: Relevant Columns Used for Implementation

Column Name	Description
Trip ID	A unique code used for identifying each trip
End Time	Timestamp of when the trip ended, rounded to the nearest hour
End Community Area Number	A number identifying the Community Area where the trip ended
End Community Area Name	The Community Area name where the trip ended
End Centroid Latitude	The Latitude of the centre of the trip end census tract
End Centroid Longitude	The Longitude of the centre of the trip end census tract

The pseudo-code for the data extraction can be seen below:

1. **Load** data as $\text{Dataset}_{\text{all}}$
2. **Remove** unnecessary rows with NaNs as values for relevant columns in $Dataset_{all}$ as $Dataset_{cleaned}$ **For** 'i' = number of community areas:
    3.1 **Extract** all rows and columns of community area 'i' in 'End Community Area Number' from $Dataset_{cleaned}$ as $Dataset_{Area_i}$

    3.2 **Find** *timestamp* t_{max} in '*End Time'* from $Dataset_{Area_i}$ with maximum number of rows

    3.3 **Extract** all rows and columns of timestamp t_{max} in '*End Time*' from $Dataset_{Area_i}$ as $Dataset_{Area_i}$

    3.4 **Extract** '*End Centroid Latitude*' and '*End Centroid Longitude*' columns from $Dataset_{Area_i}$ as $Dataset_{Area_i}$

    3.5 **Convert** $\text{Dataset}_{\text{Area}_i}$ from 'End Centroid Latitude' and 'End Centroid Longitude' to '*X*' and '*Y*' (Gerdan & Deakin, 1999)
3. **Output** $Dataset_{AreaXY_i}$ as the datasets to be used for evaluation in each algorithm

2.2 Adaptive Tabu Search

Tabu search is a metaheuristic optimisation algorithm designed to locate effective solutions to problems that are challenging to resolve using conventional optimisation methods. The algorithm operates by incrementally enhancing a solution to a problem by making little adjustments to the existing solution, while avoiding making the same modification more than once. This is accomplished by keeping track of "tabu" moves, or modifications that are prohibited from being made again during the current search.

The initial solution to the problem is used as the basis for the tabu search method, which iteratively refines the answer. The algorithm finds the optimal option that is not forbidden at each stage after evaluating the alternatives that may be made to the present solution. The algorithm may make a tabu move, albeit with a lower probability, if no such move can be located. The algorithm keeps going until it meets a predetermined stopping criterion, such the maximum number of iterations or an acceptable level of solution quality (Masoud et al., 2019b).

Pseudo-code for the general formulation of the Tabu Search algorithm can be seen below:

1. **Initialize** solution (i.e. in this case a set of routes determined by using the First Solution Strategy: "PATH_CHEAPEST_ARC" from Google OR-Tools). PATH_CHEAPEST_ARC starts from a route "start" node and iteratively connects to the next node that is the shortest distance away from it until it returns to the "start" node.
2. **Initialise** the Tabu List to be empty
3. **While** the stopping condition has not been met (for e.g. 1000 iterations):
   3.1 **Generate** a set of potential routes by making small changes to the current route (e.g. using 2-opt which is swapping the order of the locations of two e-scooters on a route)
   3.2 **Evaluate** each potential route to determine distance travelled
   3.3 **Choose** the best route with the smallest distance travelled that is currently not on the Tabu List
   3.4 **Update** the Tabu List by adding the current route onto it
   3.5 **If** stopping condition has not been met return to 3a and loop.
4. **If** the stopping condition has been met, output the current set of routes as the optimal solution

2.3 Simulated Annealing

A heuristic optimisation approach called Simulated Annealing employs randomisation to determine a function's global minimum or maximum. It is based on the idea of metallurgy's annealing process, in which a material is heated and then gradually cooled to improve its hardness and minimise flaws. In simulated annealing, an algorithm employs random motions to explore various places in the search space where the problem's solution is represented as a point (Kirkpatrick, Gelatt Jr. & Vecchi, 1983).

The algorithm evaluates a new solution at each step and determines whether to accept it based on how well it compares to the existing solution. It is always accepted if the new answer is superior. If it is worse, it is occasionally accepted with a probability based on how much worse it is and a metric known as the temperature. The algorithm becomes increasingly selective and converges on the best answer when the temperature is continuously lowered over time. The temperature schedule, which controls how rapidly the temperature drops and how selective the algorithm gets over time, is crucial to the effectiveness of simulated annealing. The algorithm can locate the global minimum and avoid getting caught in local minima with the aid of a well-designed temperature schedule.

Pseudo-code for the general formulation of the Simulated Annealing algorithm can be seen below:

1. **Initialize** solution (i.e. in this case a set of routes determined by using the First Solution Strategy: "PATH_CHEAPEST_ARC" from Google OR-Tools). PATH_CHEAPEST_ARC starts from a route "start" node and iteratively connects to the next node that is the shortest distance away from it until it returns to the "start" node.
2. **Initialize** 'temperature' variable
3. **While** the stopping condition has not been met (for e.g. 1000 iterations) and the temperature is above a minimum threshold:
   3.1 **Generate** a set of potential routes by performing local search from the current route
      3.1.1 **Select** a random route from the set of routes
      3.1.2 **Select** a random e-scooter from the route
      3.1.3 **Generate** a set of possible new routes by removing the selected e-scooter from the selected route and inserting it into each of the other routes

3.1.4 **Evaluate** each of the new routes based on distance and load capacity

3.1.5 **Select** the new route with the smallest distance travelled that still satisfies the load constraint

3.2 **If** the new route is an improvement over the previous route, update the set of routes with the new route

3.3 **Else if** the new route is not an improvement, accept the new route based on a probability equal to $e^{-\frac{\Delta}{T}}$, where Δ is the difference in distance between routes, and T is the temperature

3.4 **Decrease** the temperature based on a pre-defined cooling schedule

3.5 **If** stopping condition has not been met return to 3a and loop.

4. **If** the stopping condition has been met, output the current set of routes as the optimal solution

3. Results

The the comparison of SA and TA techniques has been included in Table 2. The highlighted values show which algorithm performed the best and produced the smallest distance for each respective area. The algorithm with the largest number of highlighted values is Tabu Search compared to simulated annealing.

Table 2: Comparison of SA and TA Performance

Area	Load	No. of Locations	SA	TS
7	31	5	5147	5147
8	32	6	6882	6882
9	84	8	12143	11759
10	15	3	1326	1326
11	53	11	12226	10231
13	30	5	2185	2185
14	44	8	4796	4796
15	453	34	45873	45613
16	32	8	7462	7462
17	525	36	49702	49404
18	364	26	42005	40851
19	18	4	2175	2175
20	22	3	1786	1786
21	322	23	37904	37857
22	40	4	4160	4160
24	40	7	7563	7563
25	40	6	8053	8053
45	35	4	3746	3746
67	65	6	12119	12119
76	45	3	3910	3910
All	377	58	111503	99878

Table 1 demonstrates that TS is performing better than SA. The e-scooter chargers frequently cover shorter distances using TS than SA. The overall distance covered by chargers using TS for 20 locations was 99878 km, which is less than 10.5% of the total distance covered by chargers using the SA approach. From Figure 2, Tabu search as a best solution, will sometimes have routes that surround other routes but never have multiple operators arriving at the same destination.

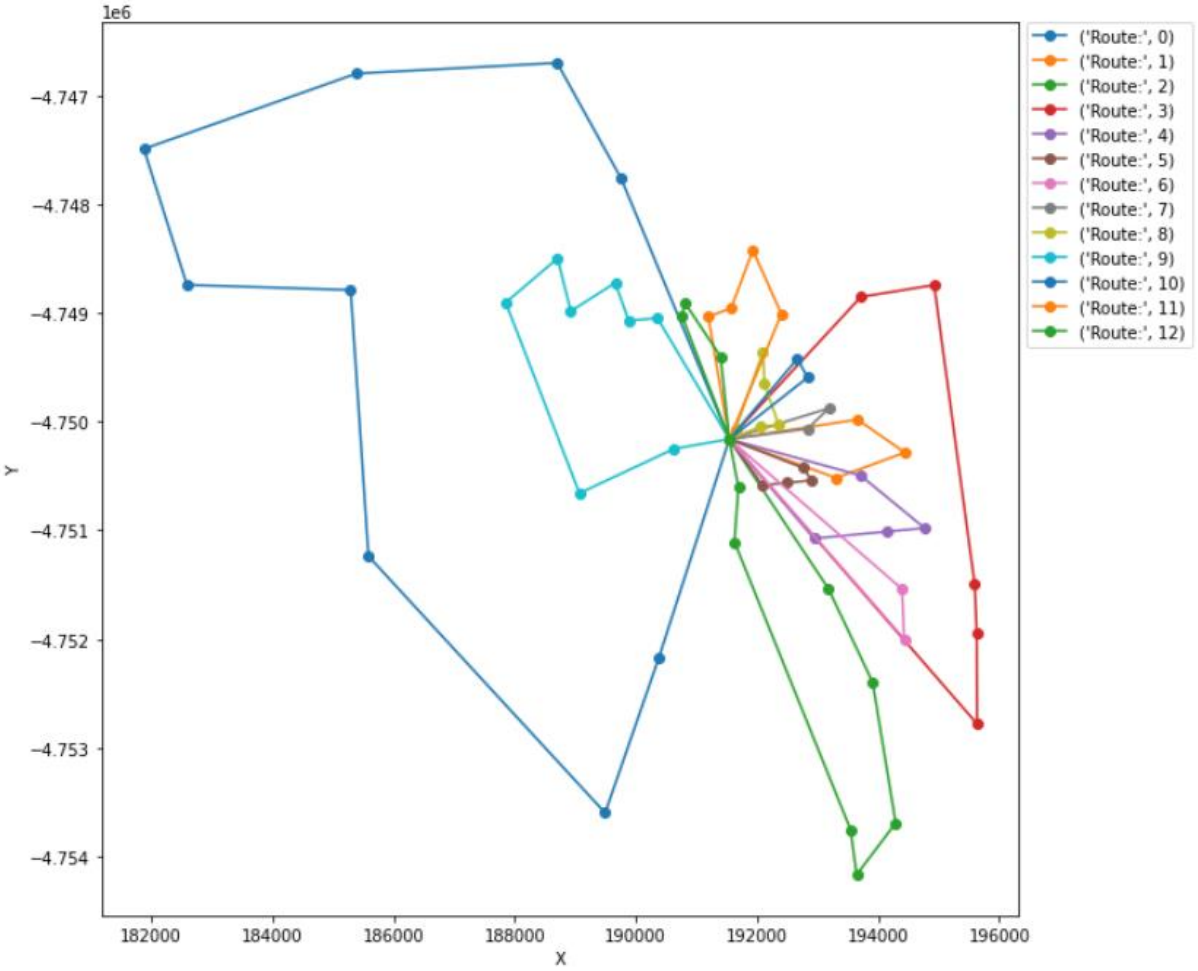


Fig. 2: Tabu Search for Chicago

4. Conclusion

E-scooters are frequently seen as an effective way to reduce carbon emissions while also being convenient for people on the go when used as a short-distance public transportation system. Instead of moving complete scooters to be recharged, e-scooters' batteries are swapped, decreasing out-of-service time to a few minutes rather than hours. A method for calculating the most effective way to exchange the batteries on e-scooters will be necessary to decrease travel lengths and maximise fuel economy for battery switching operators.

In this study, Simulated Annealing and Tabu Search were used to build, analyse, and compare a route optimisation method. The efficiency of the optimisation algorithms as a technique for optimising e-scooter battery charging routes was tested using an e-scooter trip dataset from the 2019 Chicago Pilot. The findings demonstrated that, in comparison to Simulated Annealing, which was somewhat inferior, Tabu Search was generally the best solution for many instances. The total distance travelled by chargers using the TS strategy for 20 sites was 99878 km, which was less than 10.5% of the total distance travelled by chargers using the SA approach.

References

Almannaa, et al. (2021a). A comparative analysis of e-scooter and e-bike usage patterns: Findings from the City of Austin, TX. *International Journal of Sustainable Trans-portation*, *15*(7), 571-579.

Almannaa, et al. (2021b). Perception anal-ysis of E-scooter riders and non-riders in Riyadh, Saudi Arabia: Survey outputs. *Sustainability*, *13*(2), 863.

Carey, N. & Lienert, P. (2022). “E-scooters fall head over wheels for battery swapping,” Reuters, p. 1, 25 March 2022.

City of Chicago, “E-Scooter Trips - 2019 Pilot,” 15 April 2020. [Online]. Available: https://data.cityofchicago.org/Transportation/E-Scooter-Trips-2019-Pilot/2kfw-zvte.

Clarke, G. & Wright, J. W. (1964). “Scheduling of Vehicles from a Central Depot to a Number of Delivery Points,” Operations Research, Vol. 12, no. 4, pp. 568-58.

Eksioglu, B., Vural, A. V. & Reisman, A. (2009). “The vehicle routing problem: A taxonomic review,” Computers and Industrial Engineering, vol. 57, no. 4, pp. 1472-1483.

Gerdan, G. P. & Deakin, R. E. (1999). “Transforming Cartesian coordinates X,Y,Z to Geographical coordinates φ, λ, h,” The Australian Surveyor, vol. 44, no. 1, pp. 55-63.

Kirkpatrick, S., Gelatt Jr., C. D. & Vecchi, M. P. (1983). “Optimization by Simulated Annealing,” Science, Vol. 220, No. 4598, pp. 671-680.

Masoud, et al. (2019a). Heuristic approaches to solve e-scooter assignment problem. IEEE Access, 7, 175093-175105.

___. (2019b). Optimal Assign-ment of e-scooter to Chargers. In 2019 IEEE Intelligent Transportation Systems Conference (ITSC) (pp. 4204-4209). IEEE.

Mingozzi, A. (2005). “The Multi-depot Periodic Vehicle Routing Problem,” in International Symposium on Abstraction, Reformulation, and Approximation, Berlin, 2005.

Severengiz, et al. (2020). “Life Cycle Assessment on the Mobility Service E-Scooter Sharing,” in IEEE European Technology and Engineering Managment Summit (E-TEMS), Dortmund, 2020.

Cite as: Masoud M., “An Adaptive Tabu Search OptimisationAlgorithm for Solving E-Scooters Battery Swapping Problem”, *The 2nd International Conference on Civil Infrastructure and Construction (CIC 2023)*, Doha, Qatar, 5-8 February 2023, DOI: https://doi.org/10.29117/cic.2023.0133

Multicriteria Approach in Developing Pedestrian Network Data for Sustainable Urban Mobility

Sagar Sonone
Public Works Authority, Ashghal, Doha, Qatar
ssonone@ashghal.gov.qa

Narayanasamy Balamohan
Public Works Authority, Ashghal, Doha, Qatar
nmohan@ashghal.gov.qa

Abstract

Building a reliable Infrastructure is a continuous activity, improving the accessibility to the known areas and connecting the origin to destinations with various modes of transportation. Having safe and secure pedestrian movement ensures sustainable urban mobility. Therefore, the study includes an approach for multi-criteria evaluation to reach from origin to destination. Factors strongly correlating that will affect the walkability were considered, including climatic conditions, type of network (crossings, pedestrian bridges, shared use, footpath), land use etc. which will affect the distance and time of the walkability. After capturing & tracing all the footpath locations in GIS for the most populated areas, the percentage of land use provides insights into typical pedestrian movements for a specific period of the day. Pedestrian movement is categorised into various levels and focused on locations of interest where huge volume travels a particular area at the same time & travel distance, which leads to analysing required infrastructure considering safety and convenience aspect such as availability of sufficient footpath width, availability of streetlights, locating a bus stops/ public transport etc. as an initial experiment using the above criteria for a known location such as a metro station was considered which will result in building more confidence on the factors and their integrity. The study will aid as a tool in designing and constructing infrastructure projects which will ensure the maintenance of seamless pedestrian connectivity & incorporate necessary assets within the project. Better connectivity will encourage people to walk further, safely & use public transportation facilities more often.

Keywords: Walkability; Pedestrians network; Sustainable infrastructure; GIS; Urban connectivity

1 Introduction

The pedestrian network is the fundamental unit of urban space and becomes the most crucial supply-side part of the transportation network. In addition, the pedestrian network provides last-mile connectivity for people, specifically for public transportation users. Recent studies show that the extent of availability of pedestrian networks and cycle tracks influences urban mobility. Pedestrian infrastructure is considered the primary means of access to public spaces and the most complex transport network as it joins all transport modes.

In this modern information age, the accessibility of maps for trip planning has become much easier compared to a decade ago. With the easy availability of online maps and mobile maps apps like Google Map®, HERE®, Wain®, etc., becoming day-to-day commodities, the use of maps for navigation and exposure to a suitable pedestrian network encourages people to walk and highly influence the travel behaviour of the population.

2 Qatar Context and Background

Doha, the capital of the State of Qatar, is transforming from a major city to a metropolis. Pedestrian linkages and networks are a critical element of a metropolis urban form. In addition, during the last two decades, public infrastructure, specifically the roads and highway infrastructure, have grown in multiple folds, and pedestrian and network is part of any road and highway design aspects. Figure 1 shows pedestrian space in local road design.

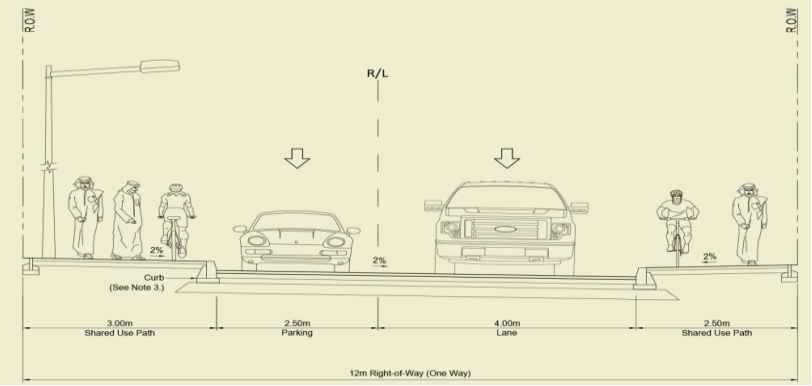


Fig. 1: Typical cross-section of the local road

As more than 90% of total pedestrian trips occur in the Doha Metropolitan Area (DMA), Qatar has prioritised pedestrian-friendly urban mobility. Thus a detailed study has been undertaken by MOTC to review Qatar's Pedestrian Environment as part of the Qatar Pedestrian Crossing Master Plan in 2017. The study employed PERS developed by TRL in the UK. Qatar 2050 Transportation Master Plan study identified about 263 km of dedicated off-road pedestrian footpaths: and 124 km of off-road cycle tracks with 53 km of shared-use pedestrian/ cyclist off-road routes.

Public Works Authority (Ashghal) is responsible for managing and maintaining the geographic information for road and highway infrastructure. Ashghal keeps the information both from an asset perspective and a network perspective. Ashghal maintains the schematic of road network data using a carriageway centreline representing the flow of traffic called a 'flowline.' Ashghal also developed a navigable network dataset derived from the flowline data set.

As the travel demand has a multi-purpose and inherently becomes a multi-model, the need for pedestrian network and cycle network track become highly warranted within the network perspective. A dedicated cycle lane has become part of the recent road and highway design. Currently, the dedicated cycle network covers about 930 km in Qatar, and Qatar gained a Guinness record for having the longest continuous cycle track of 32.89 km.

The pedestrian network information must be part of Ashghal's primary network dataset. As Qatar was hosting the FIFA World cup 2022 and expected more than two million visitors to visit during the event, the need for a pedestrian network of digital information was in high demand. The information facilitated visitors' smooth movement and prepared plans for safe and secure pedestrian walkways. To make the network more conducive for walking and to engage the FIFA fans to explore Qatar's Cultural Landmarks, various key areas were transformed entirely for pedestrian movement, and vehicle movement was restricted.

To develop a pedestrian network dataset in the shortest possible time, Ashghal has undertook a study to prioritise areas for capturing the geographic information of the pedestrian network. The key objective of the study is to (i) identify and prioritise the areas that needed a pedestrian network, (ii)

set an approach for constraints for links and crosses, (iii) define the classification of a pedestrian network, and (iv) build the network. This paper shares how Ashghal prepared the pedestrian network in a limited time and with a focused approach.

3 Methodology

A systematic 4-step methodology, as shown in Figure 2, was adopted to identify the priority areas for developing the pedestrian network dataset. The study used a multi-criteria analysis technique, which is robust and widely used in many fields in selection & prioritisation processes based on multiple influenced criteria. As spatial dimension has become one of the critical factors in evaluating options, integrating Geospatial Information System (GIS) with multi-criteria analysis was considered appropriate.



Fig. 2: Study Methodology

Step 1: Undertake a study and identify the factors influencing the development of the pedestrian network. Per the previous study conducted by MoTC, Pedestrian Environment Review System identified 14 factors for the quality of an environment for pedestrians. The proximity to Bus Stops, Metro Stations significantly impacts pedestrian movement (Khaled Shaaban et al., 2018). Land Use density, diversity & design are critical dimensions for the walkability index. The number of intersections facilitating the road crossing for pedestrians is considered one of the essential evaluation factors in assessing the pedestrian network (Pereira, 2022).

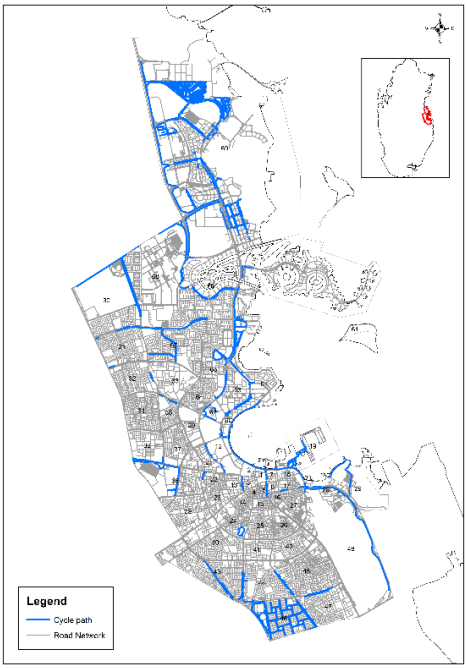


Fig. 3: Dedicated cycle tracks in urban zones

There is a high degree of preference for sharing pedestrians with available cycle track networks. It is also natural for a pedestrian to use the shared path that relies significantly on off-road routes for safety and security (Delaney, Hannah et al., 2016). Thus, while defining the criteria of zone selection, the cycle paths are not considered because the dedicated cycle lane in the urban zones contributes about 6% of the total road network, Figure 3.

Step 2: Previous studies provided various factors affecting pedestrian movement and the suitability of pedestrian networks. Though there are many factors identified, however by considering the following three factors for evaluating the quality of the pedestrian network in this study:

a. Accessibility - Proximity for Public Transport (Metro Stations & Bus Stops),

b. Land Use - Residential Areas, Offices/commercial, Point of Interest (PoI),

c. Street Connectivity – Intersections, Pedestrian structures.

The data required for this evaluation have been assessed, collected, and extracted. The following data in Table 1 represent criteria as the fundamental data unit for the assessment. The quality of the availability of the spatial data is assessed before its use to ensure the requirements can be quantifiable and spatial interpreted.

Table 1: Datasets and source

No.	Datasets	Source
1	Land use	CGIS / MME
2	Bus Stops	MoTC
3	Metro Stations	Q Rail
4	Road's data	Ashghal
5	Zones	CGIS / MME

Step 3: In this step, the conventional strategy is to determine the weightage and scoring for priority decisions in the multi-criteria approach. The strategy is a simple subjective scoring reliant on the judgments of subject matter experts. The key benefit of this approach is that it can be guided & performed quickly. The weightage and ranking scores for the criteria are valued and presented in Table 2.

Table 2: Weightage and scoring attributes

Weightage	Criteria	Sub-Criteria	Measure	Score
50%	Accessibility to Public Transportation	Proximity to Metro	< = 300 m	1
			> 300 m	0
		Proximity to Bus Stop	< = 200 m	1
			> 200 m	0
30%	Land use	Residential & PoI	> 20 %	1
			< 20 %	0
		Offices / Commercial	> 50 %	1
			< 20 %	0
20%	Street Connectivity	Intersections, Pedestrian Structures	> 200 (Number of intersections per sq. km)	1
			50-200 (Number of intersections per sq. km)	0.5
			< 50 (Number of intersections per sq. km)	0

Step 4: Performing prioritisation analysis using GIS as a tool. ESRI ArcGIS 10.8 as a GIS platform. Performing three spatial analyses and thematic maps supports all the outcomes.

4 Assessment

Building a pedestrian network database along an ~18000 km road network requires evaluating a critical assessment of the priority through a thorough analysis of influential factors and criteria and assessing with a multi-criteria analysis based on the factors of usage & importance of the network in the given area/street. Considering the proximity to public transportation using the buffer analysis and nearest neighbourhood analysis using the Thessian polygon technique to determine prevailing service areas for bus stops and to identify the areas influenced by the spatial spread of land use categories by conducting buffer analysis. The street connectivity factor was analysed using the spatial density technique on street intersections and pedestrian structures.

4.1 Assessing Proximity to Public Transport

The study includes assessing the proximity of metro stations using a 300m Euclidean buffer analysis. The land use with this 300m buffer was analysed, and calculating the percentage of each land use type within this buffer gives an estimate of land use diversity. The pairwise influence of Metro stations and land use criteria were analysed based on the set weightage and Score. Overlaying Zones on these metro stations are provided with high priority scoring considering the percentage overlay of the buffer within the zones. Figure 4 illustrates the buffer's proximity and the land use percentage.

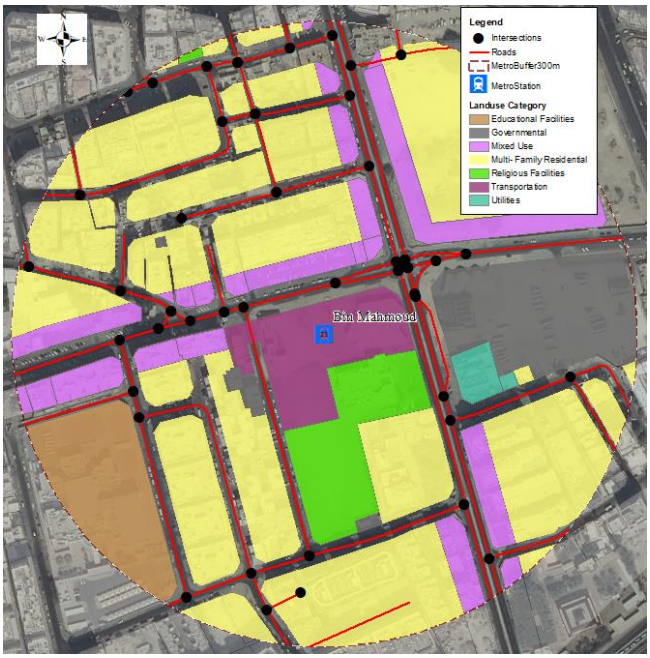


Fig. 4: Land Use within 300m of the proximity of the metro station

Generating Thiessen polygons using bus stop locations to address the proximity to public transportation for bus stops. The area of the polygon is the factor for the influence area of each bus stop. Smaller zones indicate closer proximity to bus stops and stronger influence for pedestrian users, deciding an appropriate area to signify the influence. It is assumed based on 15min walkable urban city concept. If a normal person walks 1.2km in 15 minutes, then any area less than 4.5 sqm would be highly influential. Considering Qatar's weather conditions during the peak summer, reducing the walking distance to 300m would cover approx. 0.3sqkm. Then all Thiessen polygon that meets this conditional is selected and merged to depict the map showing the influential area—considering the Zones with the maximum coverage of Thiessen polygons as thematically presented in Figure 5.

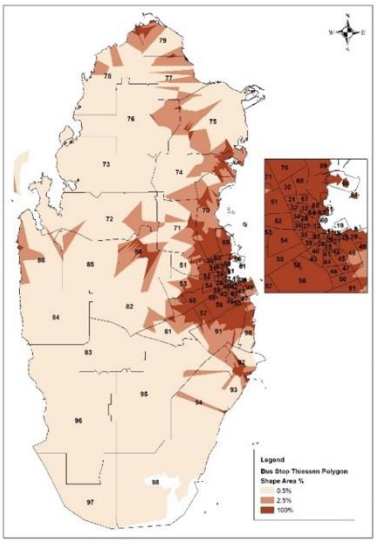


Fig. 5: Proximity of bus stop

4.2 Land Use: Assessing the Percentage of Land Use within Zones:

Land uses are differentiated into various categories. Reclassifying land use categories into four significant groups should simplify the analysis for this exercise as presented in Table 3. These groups will provide subjective weightage and scoring based on a judgmental valuation of pedestrian volume and movement for the zone.

Table 3: Land use categories collated into four significant groups

Residential	PoIs	Offices/Commercial	Other
• Multi- Family Residential • Single- Family residential	• Community and culture facilities • Educational Facilities • Health Facilities • Open Space Recreation (Indoor-Outdoor) • Religious Facilities • Tourism	• Governmental • Services/ Offices • Special Use • Commercial	• Agriculture and Green Areas • Heavy Impact industry • Logistics- Distribution-Warehouse • Low Impact industry • Medium Impact industry • Mixed Use • Sports Facilities • Transportation • Unknown/Undefined • Utilities • Vacant Land • Wholesale

4.3 Pedestrian Crossings

Pedestrian crossings on intersections & dedicated bridges serve as an effortless way to safely cross any significant junctions or roads. Typically, public movement around these areas is more than in other locations to cross any streets safely. Zones containing pedestrian bridges & a more significant number of intersections are likely to be used more by pedestrians. Pedestrian bridges & crossings positively correlate to the volume, and it becomes necessary to have enough space & need footpaths around it. Using a density range from 0.010 to 0.085 total of 53 zones are selected.

$$Zone\ Intersection\ Density = \frac{Number\ of\ intersections}{Total\ Zone\ Area\ (sq.km)}$$

Example: Zone 23- Bin Mahmoud total intersection is 396 for an area of 1161750 sq.m

Zone 23 intersection density = $\frac{396}{1161750}$ = 0.03408

5 Evaluating The Factors

Based on the assessment area, calculating the score for each criterion for each zone will help derive the final scoring of individual zones. Figure 6 illustrates the areas identified with the influential individual criteria.

Factor A = Accessibility Weightage x ∑ (metro proximity score, bus stop proximity score).

Factor B = Land Use weightage x Score for land use category.

Factor C = Street Connectivity weightage x Score for intersection density,

$$Total\ Score = Factor\ A + Factor\ B + Factor\ C$$

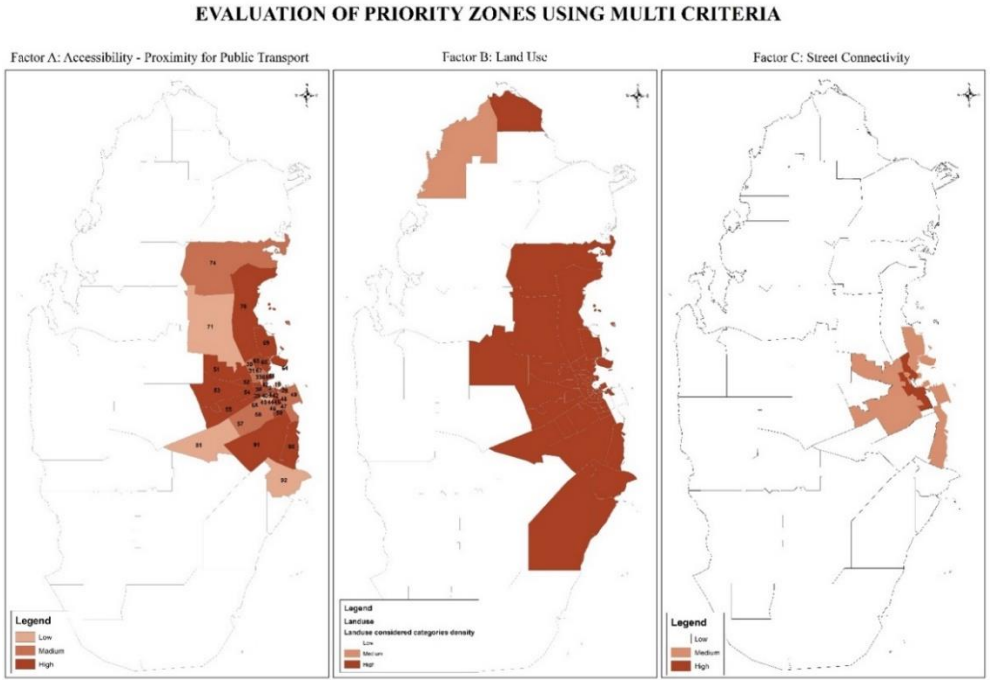


Fig. 6: Individual criteria evaluation

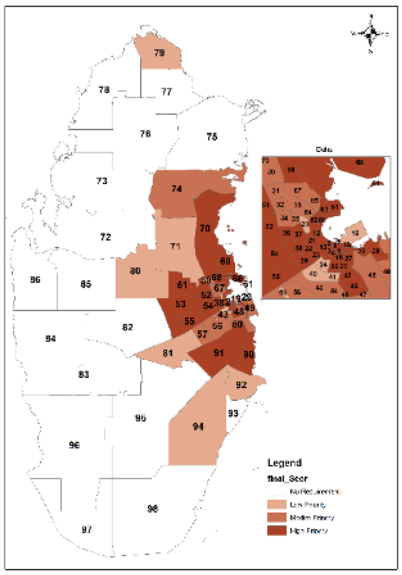


Fig. 7: Prioritised zone based on the combined normalised Score

The final scoring was evaluated based on the spatial addition of individual factor scores, normalised on the zone, and sorted based on the Score to prioritise the zones. Presenting the outcome of the assessment with priority zone is thematically in Figure 7. The combined scores are further normalised to classify the low, medium, and high-priority zones. The priorities of zones will assist in computing the lengths, further aiding in generating the prioritised pedestrian database, as presented in Table 4.

Table 4: Assessed priority zones and estimated length of pedestrian network data

No.	Priority Classification	Number of zones	Estimated Walkway Length(km)
1	High Priority	46	~ 8065
2	Medium Priority	25	~ 5280
3	Low Priority	3	~ 5071
4	No Requirement	17	-

6 Conclusion

The availability of pedestrian network information is necessary for the transportation network spatial dataset used for navigation and multi-model trip planning analysis. The main goal of this study is to support the data team in identifying and prioritising the zone where the pedestrian network data will be developed. This study considered three influential factors and applied multi-criteria analysis to determine the priority areas/zones. The assessment provides insights into the need for pedestrian network spatial information. Although the proposed method assigned the weight for all walkability elements based on subjective judgment, the above method can easily be modified by adding more or assigning different weights to different elements as needed. Combined values of evaluation scores of each criterion assist in identifying the priority areas for developing the pedestrian network dataset and implementing the necessary pedestrian safety infrastructure, maintaining the existing conditions of the assets, and promoting safe walking. This prioritisation and assessment of walkway length helped the data to estimate the resources required to develop the walkway database in a limited duration.

References

Delaney, et al. (2016), "Walking and cycling on shared-use paths: The user perspective", ICE Proceedings Municipal Engineer, http://dx.doi.org/10.1680/jmuen.16.00033.

MoTC (2021). Qatar Highway Design Manual, vol. 1, page 57, 130, Doha Qatar.

MoTC (2017a). Qatar Pedestrian Crossings Master Plan - Version 1.0, Doha, Qatar.

MoTC (2017b). Qatar Pedestrian Environment Review System - Version 1.0, Doha, Qatar.

Pereira, M. F., Santana, P. (2022) "Is walkability equitably distributed across socio-economic groups? – A spatial analysis for Lisbon metropolitan area," Vol. 106, *Journal of Transport Geography.*

Shaaban, et al. (2018). "A simple method to assess walkability around metro stations", Vol. 10, no 1, 19.

Yabuki, N. (2022), "Integrating GIS, deep learning, and environmental sensors for multi-criteria evaluation of urban street walkability". *Landscape and Urban Planning*.

Cite as: Sonone S. & Narayanasamy B., "Multicriteria Approach in Developing Pedestrian Network Data for Sustainable Urban Mobility", *The 2nd International Conference on Civil Infrastructure and Construction (CIC 2023)*, Doha, Qatar, 5-8 February 2023, DOI: https://doi.org/10.29117/cic.2023.0134

A Quantitative Evaluation of Urban Green Spaces in Rajshahi, Bangladesh

Md. Asaduzzaman
Department of Architecture, Faculty of Civil Engineering, Rajshahi University of Engineering & Technology, Rajshahi-6204, Bangladesh
md.asaduzzaman@arch.ruet.ac.bd

Nafis Sadat
Department of Architecture, Faculty of Civil Engineering, Rajshahi University of Engineering & Technology, Rajshahi-6204, Bangladesh
nafissadat123@gmail.com

Abstract

Being a developing country, Bangladesh has faced rapid growth in urbanization in the past few decades. This results in decreasing parks and other green spaces in urban areas. Rajshahi is one of the divisional districts in Bangladesh that is prone to rapid urbanization, though the urbanization rate of Rajshahi is less than the other megacities in Bangladesh. As a result, it is important to preserve the parks in Rajshahi before they are diminished. To assess the quantity and preserve the present urban green infrastructure in Rajshahi, it is necessary to identify and categorize them according to their regional characteristics. This paper aims at evaluating the urban green spaces in Rajshahi and finding out whether the existing urban green spaces are enough to meet the goal of a sustainable city. It is done by analyzing the regional characteristics of urban parks and green spaces located in Rajshahi, Bangladesh, based on GIS data and categorizing them according to their physical size to determine their catchment area. Statistical data and aerial images are processed and simulated through ArcGIS software and correlated with cadastral plans for accurate identification. Explanatory factors regarding UGS loss in a specific region are also investigated using socio-economic, cultural, and geographic in order to find out the reason for UGS change. The resultant data shows that only 6.14 m^2/capita urban open space is available for the urban inhabitants which are insufficient for achieving sustainability goals and should be preserved in order to enhance the liveability of the city.

Keywords: Sustainability; Parks; Urban greenery; Catchment area; Rajshahi

1 Introduction

Urban parks, at their core, directly affect the public health of the communities around them. They contribute to public health by reducing stress and enhancing the quality of life on a micro-scale. Despite being a vital urban element, the number of green spaces is decreasing rapidly. According to the World Wildlife Fund, green spaces cover almost 30% of the earth's surface which is decreasing at an alarming rate worldwide (Konijnendijk et al., 2013). Worldwide, the major cause of the diminishing of parks and green spaces is urbanization where around 55% of the world's population live (World Urbanization Prospects, 2018, 2018). Increased densification of urban areas results in an increase in built form thus a decrease in vegetation quantity.

In 1961, around 2.64 million people in Bangladesh lived in the urban areas which is 5.19% of the

population (Bangladesh Bureau of Statistics (BBS), n.d.). In the last few decades, Bangladesh has experienced an extremely high rate of urbanization exceedingly more than two to three times higher than that of the national population growth rate. This rapid urbanization requires more space for industries, commercial establishments, a housing facility for the increased population, and other grey areas of the urban areas.

This rapid urbanization has a negative impact on green spaces. In order to maintain ecological balance, a country should have 33% of greenery. According to FAO, the total forest area covers nearly seventeen percent of the total land area of Bangladesh and it decreasing day by day because of urbanization (Fisher et al., 1997). The overall scenario of Rajshahi is almost the same. Rapid urbanization in Rajshahi in the last few decades has resulted in a tremendous rate of increase in built form and a decrease in open spaces that include tree coverage. Only a few sets of public parks are left intact until now in the city corporation area in Rajshahi. "From 2001 to 2019, Rajshahi lost 12ha of tree cover, equivalent to a 2.9% decrease in tree cover since 2000, and 3.38kt of CO_2 emissions. In 2010, Rajshahi had 105ha of tree cover, extending over 0.043% of its land area. In 2012, it lost 140mha of tree cover" (*Rajshahi Deforestation Rates & Statistics | GFW*, n.d.). This loss in vegetation cover has occurred mainly in urban areas. Study shows that in 2029 and 2039, approximately 70% and 88% of Rajshahi will experience a temperature of more than 38 °C respectively as a result of urbanization, unplanned development, and drastic loss in vegetation cover (Kafy et al., 2020).

This reduction in vegetation cover has adverse effects. Rural and suburban regions generally have 2 to 4 degrees Celsius less land surface temperature than urban regions (Lai & Cheng, 2010). This phenomenon results from urbanization, climate change and rapid global warming (World Bank, 2016). Another study opined for the December-February period, the average maximum and minimum temperatures showed a decreasing and increasing trend of 0.1 0C and 1.60C respectively (Rahman & Lateh, 2017). On the contrary, "A city with substantial green spaces represents good planning and management, a healthy environment for its dwellers, vegetation and wildlife populations" (Adams, Leedy, 1986). The air remains comparatively cool by the urban green spaces it flows through. Thus, urban green spaces purify the air as the "lungs of the city" (*Open Space Protection Plan*, n.d.).

1.1 Study Area

Generally, urban open spaces serve the purpose of public assembly particularly e.g., open markets, parks, grand streets, plazas, playfields, etc. However, this research only focuses on the parks of Rajshahi Development Authority (RDA) authorized area in Rajshahi, Bangladesh, other than its streets and roads or plazas. These parks in Rajshahi have great impacts on human interaction through citizens' sensory involvement and their participation at both the community and district levels.

Public parks within the RDA-authorized area are taken under consideration for this particular research and their physical size and functional characteristics are analysed. According to their physical size, they will be categorized and their catchment area will be determined.

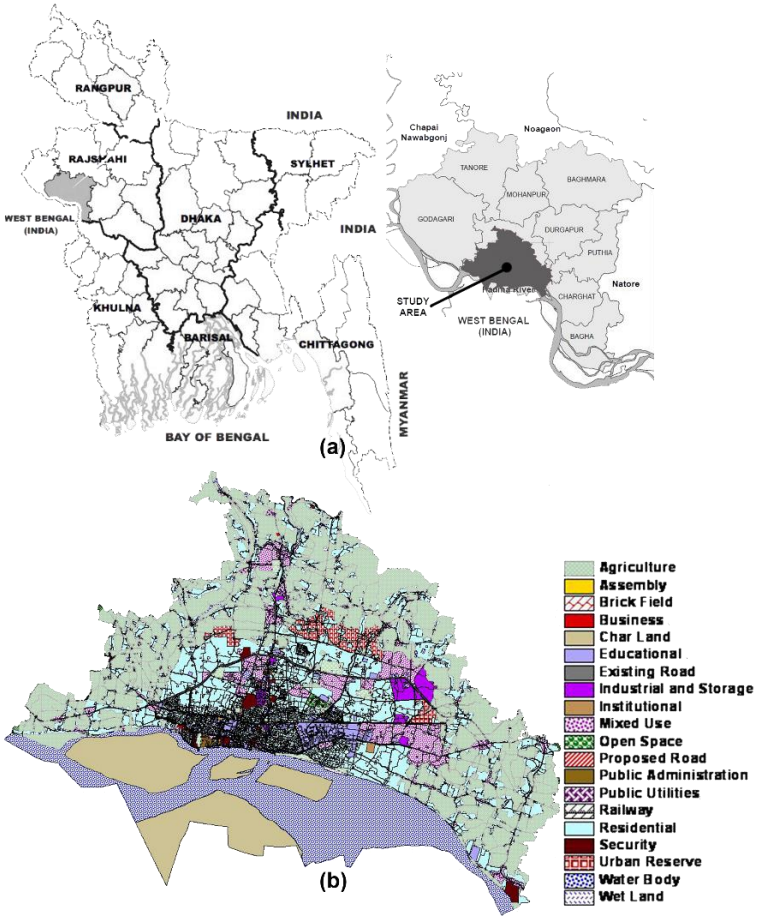


Fig. 1 :(a) Study Area Map, (b) Rajshahi Metropolitan Development Map

The land use map of Rajshahi Metropolitan Development plan shows that green spaces consist in only the suburban areas. These suburban areas contain all the agricultural lands where scarcity of parks can be seen within the dense CBD area. Again, Residential and Institutional zones constitute the most densely populated area of Rajshahi. Parks can be hardly seen in these areas.

2 Literature Review

Understanding the regional characteristics of urban green spaces is necessary prior to categorization. Preserving green spaces can improve the quality of urban life in terms of social and environmental aspects.

2.1 Urban Green Space Categorization

According to the standard, public parks and open spaces that work as community gathering spaces can be divided into seven different categories based on their physical size. This differs with the type of urban green space and the attractiveness and accessibility conditions.

Table 1: Green Space categorization (*Policy 7.18 Protecting Open Space and Addressing Deficiency | London City Hall*, n.d.)

Green Space categorization	**Size Guideline**	**Distance from Home**
Regional Parks Large areas, corridors, or networks of open space, the majority of which will be publicly accessible and provide a range of facilities and features offering recreational, ecological, landscape, cultural, or green infrastructure benefits. Offer a combination of facilities and features that are unique within London, are readily accessible by public transport, and are managed to meet best practice quality standards	400 hectares	3.2 to 8 kilometres

Green Space categorization	Size Guideline	Distance from Home
Metropolitan Parks Large areas of open space that provide a similar range of benefits to Regional Parks and offer a combination of facilities at a sub-regional level, are readily accessible by public transport and are managed to meet best practice quality standards	60 hectares	3.2 kilometres
District Parks Large areas of open space provide a landscape setting with a variety of natural features providing a wide range of activities, including outdoor sports facilities and playing fields, children's play for different age groups, and informal recreation pursuits.	20 hectares	1.2 kilometres
Local Parks and Open Spaces Providing for court games, children's play, sitting-out areas, and nature conservation areas.	2 hectares	400 meters
Small Open Spaces Gardens, sitting-out areas, children's play spaces, or other areas of a specialist nature, including nature conservation areas	Under 2 hectares	Less than 400 meters (300m)
Pocket Parks Small areas of open space that provide natural surfaces and shaded areas for informal play and passive recreation that sometimes have seating and play equipment.	Under 0.4	Less than 400 meters (200m)
Linear Open Spaces Open spaces and towpaths alongside the Thames, canals, and other waterways; paths, disused railways; nature conservation areas; and other routes that provide opportunities for informal recreation. Often characterized by features or attractive areas which are not fully accessible to the public but contribute to the enjoyment of the space.	Variable	Wherever feasible

2.2 Per Capita Urban Green Space (UGS)

UGS Per capita is determined by the ratio of total UGS covered area in square meters to the total urban population in the study area. The resultant value is expressed in m^2/capita unit (Russo & Cirella, 2018). Symbolically,

$$Per\ Capita\ UGS = \frac{Total\ UGS\ Area\ \ (TUGS)}{Total\ Population\ in\ the\ Study\ area\ (TP)} \qquad (1)$$

According to the WHO, a minimum of $9m^2$ of urban green space per capita is needed for healthy living (Russo & Cirella, 2018).

2.3 Urban Green Space Abundance (%UA)

Percentage of UGS abundance i.e., %UA is the rate of UGS area to the total study area where the areas are expressed in Km^2 unit (M'Ikiugu et al., 2012).

Symbolically,

$$\%UA = \frac{UGS\ Area(UA)}{Total\ Study\ Area\ (TA)} \times 100\% \qquad (2)$$

This percentage can be calculated for each UGS category as well which is then called Proportional UGS abundance (PUA). PUA is the percentage of total area (TA) comprised of a specific class of UGS (M'Ikiugu et al., 2012).

Symbolically,

$$PUA = \frac{Specific\ Class\ of\ UGS\ Area(SUA)}{Total\ Study\ Area\ (TA)} \times 100\% \quad (3)$$

Proportional UGS abundance (PUA) provides a basis for determining which category of UGS is deficient and needs expansion. Proportional diversity of UGS (PDU) is also used to evaluate the correlation among UGC categories. The proportional diversity of UGS (PDU) is the percentage area of UGS occupied by a specific class (M'Ikiugu et al., 2012).

Symbolically,

$$PDU = \frac{Specific\ Class\ of\ UGS\ Area(SUA)}{Total\ UGS\ Area\ (UA)} \times 100\% \quad (4)$$

3 Research Methodology

Statistical data from RDA and arial image with an average resolution of 5m is taken. To integrate the data into a spatial database, ArcGIS 10.8 software is used. The data were then correlated with cadastral plans for an accurate identification of the urban green categories.

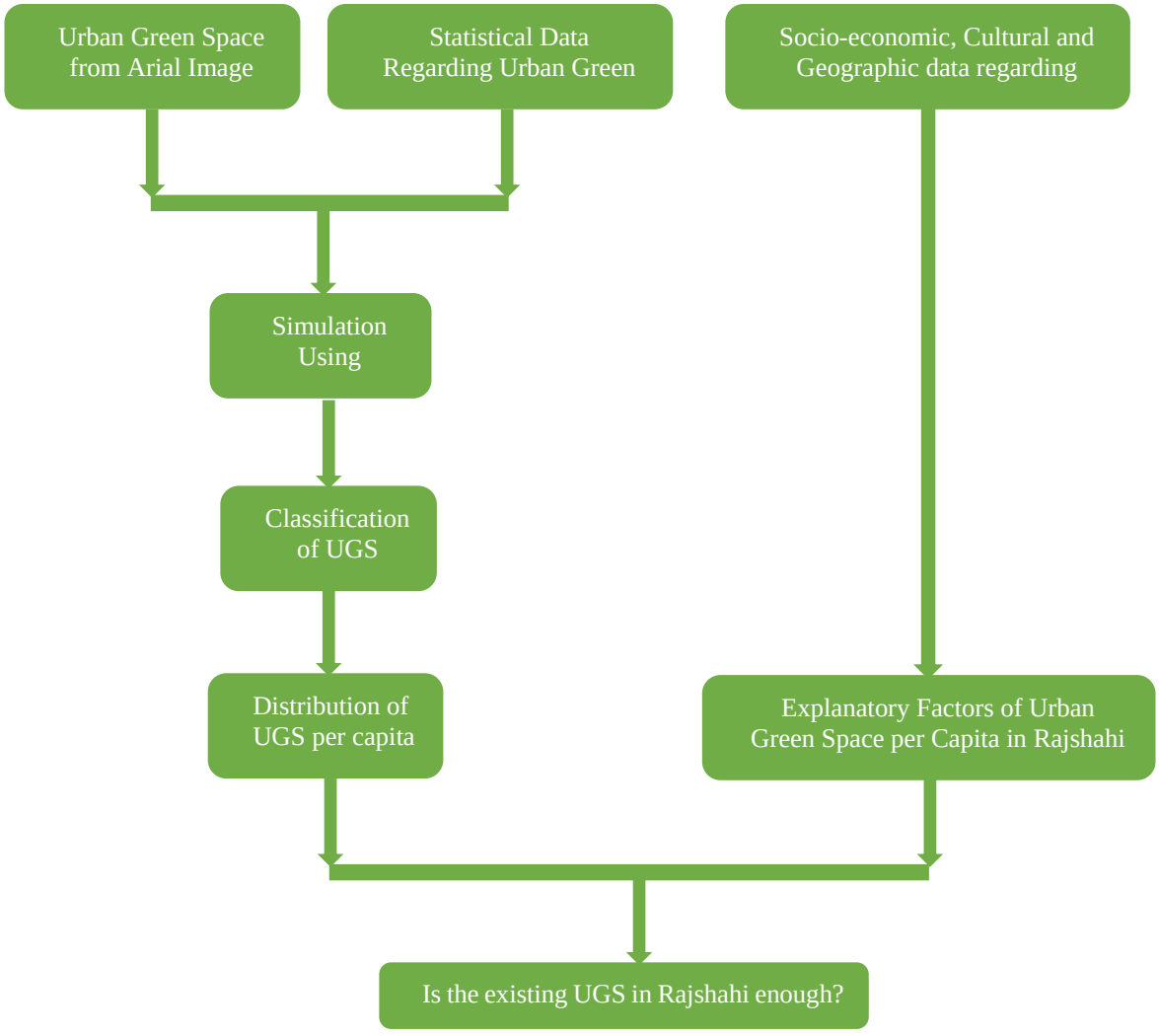


Fig. 2: Flow Diagram for Evaluating Urban Green Spaces in Rajshahi

3.1 Selecting Urban Green Spaces in Rajshahi

A set of regional characteristics of public open space is taken under consideration for selecting the suitable green spaces for this research. These regional characteristics include public accessibility, function, vegetation, etc. Green spaces which are not publicly accessible, such as private lawns, roof gardens etc. are not considered for this study.

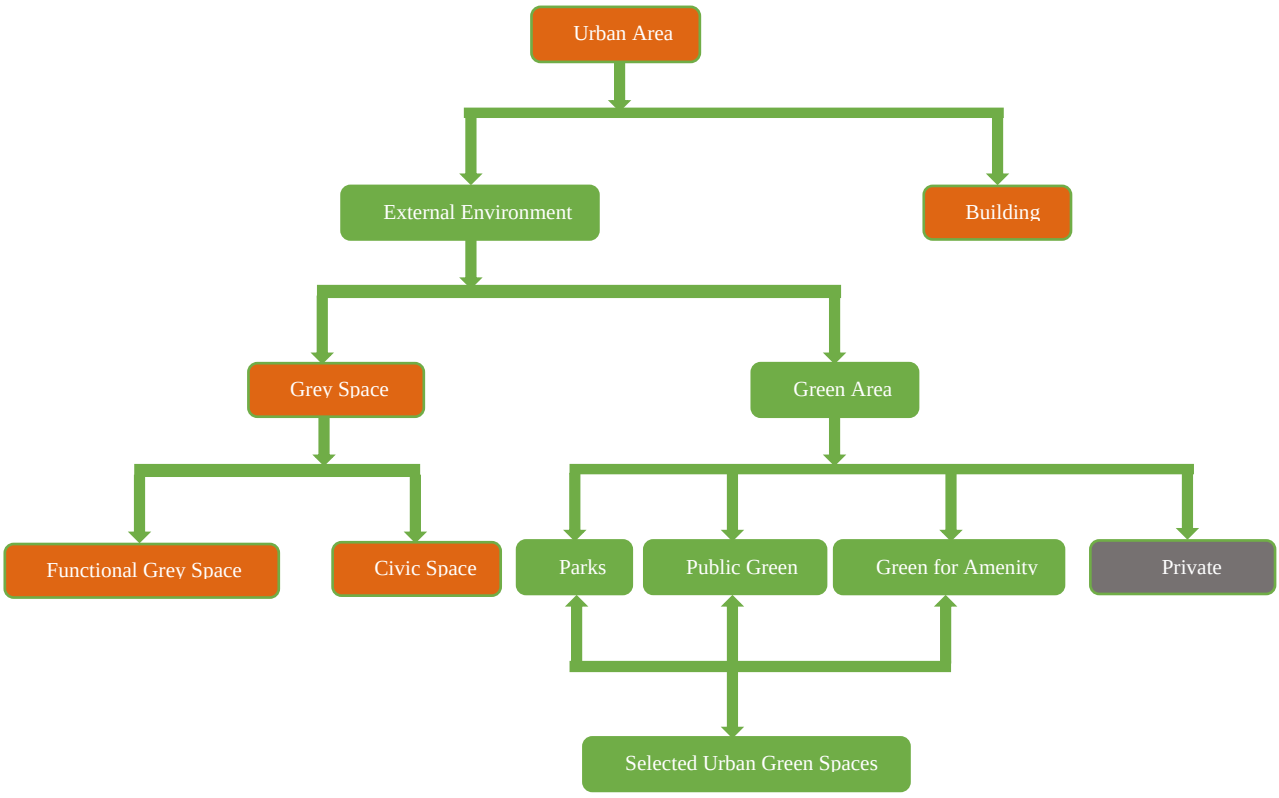


Fig. 3: Selection Criteria

3.2 Classification of Urban Green Spaces

A digitized land use map of the area authorized by the Rajshahi Development Authority (RDA) is considered as the base map in ArcGIS software. Urban open spaces that include public parks, gardens, playgrounds, and roadside linear parks are extracted from the attribute table content. These open spaces are then categorized according to their physical sizes. A universal urban open space categorization dataset prepared in the "London Plan" is used in categorizing the open spaces in Rajshahi (*Policy 7.18 Protecting Open Space and Addressing Deficiency | London City Hall*, n.d.). These urban open spaces are then extracted as separate shapefile layers according to their category.

3.3 Defining Catchment Area

After extracting the shapefiles of each category, they are linked in QGIS software for determining their catchment area. Each category of urban open space has a different catchment area. The universal urban open space categorization dataset prepared in the "London Plan" is also used herein determining the catchment area. QGIS buffer tool is used for determining the catchment area. Here the buffer area ranges from 200m to up to 1.2 km according to their category (*Policy 7.18 Protecting Open Space and Addressing Deficiency | London City Hall*, n.d.). This buffer area graphically shows the green catchment coverage in overall Rajshahi city and helps to determine the grey area where the green network is poor.

3.4 Analysing Urban Open Spaces

For Analysing and calculating the %UA, PUA, and PDU of the extracted open spaces from the digitized map, the 'Summary Statistics' tool is used in ArcGIS software. The summation of the area of each UGS category is calculated by the 'Summary Statistics' tool and then %UA, PUA, and PDU are calculated using equations (1), (2), and (3), respectively.

4 Result and Discussion

4.1 Mapping Urban Green Spaces according to Category

Analysing the GIS data, it is found that a total of 411 parks of four different categories are found within the site area. There are 53 district parks, 83 small open spaces, 270 pocket parks, and 5 linear parks present in the site area. No parks have met the criteria of being regional parks, metropolitan parks, or local parks.

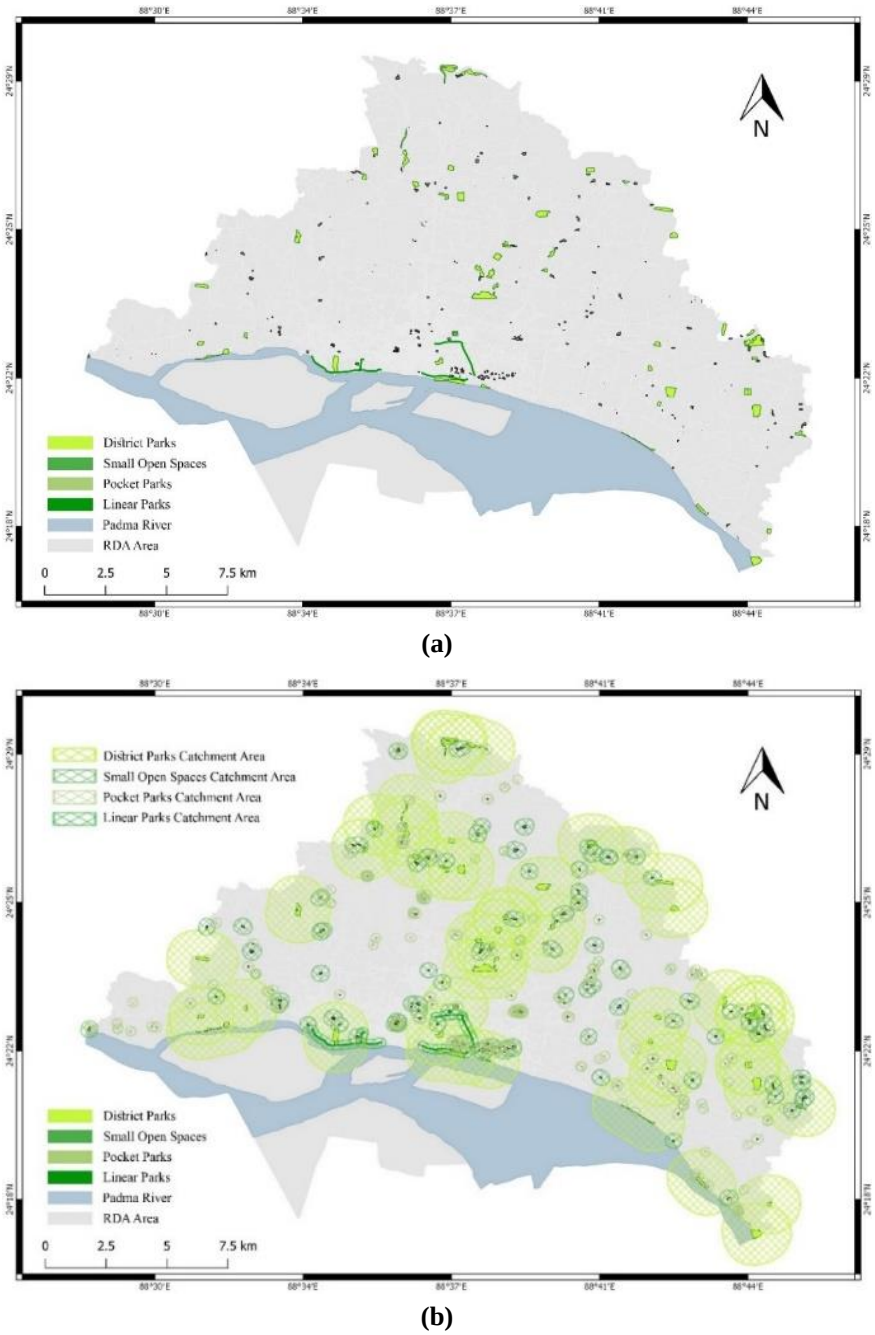


Fig. 8: (a) Urban Green spaces in Rajshahi, **(b)** Catchment Area of All Urban Green Spaces

Figure 8 shows the catchment area of each urban green spaces in Rajshahi. It shows that approximately 50% of the study area is deprived of the catchment area of any green spaces. Again, all the green spaces are in a clustered formation. It occurs due to clustered urban development characteristics of Rajshahi. The city centre is located at the bank of Padma River. This CBD area is covered with a large catchment area of a linear district park. Socio-demographic data shows that all the deprived neighbourhoods from the catchment area are commercially advanced compared to other zones. From the analysis of the catchment area of each urban park and open spaces available in Rajshahi, it is found that urban parks are situated in a clustered manner. Some locations have a considerable number of parks where the other parts of the city have no parks at all. Again, small open spaces and pocket parks cannot serve the city equally but accessibility is high here. The scarcity of linear parks shows the uninviting walking environment in the streets of Rajshahi.

4.2 Per Capita Urban Green Space (UGS) Calculation

Analysing the attribute tables of each urban park category, the area of District Parks, Small Open Spaces, Pocket Parks, and Linear Parks are found and their summation is calculated by using the 'Summary Statistics' tool in ArcGIS.

Table 2: Area of Each Park Category

Category	Area in Sqm Unit
District Parks	3319770
Small Open Spaces	753020
Pocket Parks	202080
Linear Parks	25200
Sum	**4300070**

From this data, UGS per capita in Rajshahi can be calculated using equation (1)

$$\text{Per Capita UGS} = \frac{4300070}{700133} = 6.14 \text{ m}^2/\text{capita}$$

Rajshahi has 6.14 m^2/Capita UGS where the mean ideal value is 9m^2/capita according to WHO. This result explains the deficiency of urban parks in Rajshahi City. This does not meet the minimum UGS per capita criteria. Hence, number of parks and other green spaces must be increased in order to enhance liveability.

4.3 Urban Green Space (UGS) Abundance (%UA) Calculation

The total area covered by urban parks in Rajshahi and the total study area are calculated from the attribute table. Data shows that the total area covered by urban parks in the study area is 4.30 km^2, and the total study area consists of 364.825 km^2. From this data, the percentage of urban green space abundance can be calculated using equation (2)

$$\%UA = \frac{4.30}{364.825} \times 100\% = 1.179\%$$

Proportional UGS abundance (PUA) is also calculated from the attribute table data. PUA is calculated using equation (3) for each category.

Table 3: PUA Calculation for Each Park Category

Category	$PUA = \frac{Specific\ Class\ of\ UGS\ Area(SUA)}{Total\ Study\ Area\ (TA)} \times 100\%$
District Parks	0.91%
Small Open Spaces	0.206%
Pocket Parks	0.06%
Linear Parks	0.007%

Proportional diversity of UGS (PDU) is also calculated with the data found from the attribute table using equation (4) to evaluate the correlation among UGC categories. This PDU data for each category helps to determine which category needs future expansion.

Table 4: PDU Calculation for Each Park Category

Category	$PDU = \frac{Specific\ Class\ of\ UGS\ Area(SUA)}{Total\ UGS\ Area\ (UA)} \times 100\%$
District Parks	77.20%
Small Open Spaces	17.51%
Pocket Parks	4.70%
Linear Parks	0.59%

5 Conclusion

The government of Bangladesh aims to make cities and human settlements inclusive, safe, resilient and sustainable and provide universal access to safe, inclusive and accessible, green and public spaces (Johnston, 2016). This study shows that only 6.14 m^2/capita urban green space is available for the inhabitants which are only 1.179% of the total study area. Proportional UGS abundance (PUA) and Proportional diversity of UGS (PDU) are also calculated for each open space type. These urban parks and open spaces safeguard the quality of precious life-giving resources that are very limited in quantity in the case of Rajshahi. Hence, preserving the open spaces in Rajshahi should be given top priority that ca be achieved through proper planning and collaboration of the governing bodies.

References

Adams, L.W. & Leedy, D. L. (Eds. . 1987. (1986). Integrating Man and Nature in the Metropolitan Environment. In *National Symposium on Urban Wildlife*.

Ahmed, et al. (2013). Simulating land cover changes and their impacts on land surface temperature in dhaka, bangladesh. *Remote Sensing*, *5*(11), 5969–5998. https://doi.org/10.3390/rs5115969

Bangladesh Bureau of Statistics (BBS). (n.d.). *Urbanisation cencus*. Retrieved July 27, 2020, from http://en.banglapedia.org/index.php?title=Urbanisation

Fisher, R. J., Srimongkontip, S. & Veer, C. (1997). The Asia-Pacific Forestry Sector Outlook Study is being undertaken under the auspices of the Asia-Pacific Forestry Commission . This report comes under Workplan Number C16 . *Forestry*, *December*. ftp://ftp.fao.org/docrep/fao/W7732E/W7732E00.pdf

Johnston, R. B. (2016). The 2030 Agenda for sustainable development. *Arsenic Research and Global Sustainability - Proceedings of the 6th International Congress on Arsenic in the Environment, AS 2016*, 12–14. https://doi.org/10.1201/b20466-7

Kafy, A. A., Sattar, G. & Mahmud-ul-islam, S. (2020). Reduction of Vegetation Cover in Rajshahi City Corporation of Bangladesh. *Rajshahi University Journal of Environmental Science*, *8*, 11–24.

Konijnendijk, et al. (2013). Benefits of Urban Parks - A systematic review. *International Federation of Parks and Recreation Administration, January*, 1–68.

Lai, L. W. & Cheng, W. L. (2010). Urban heat island and air pollution--an emerging role for hospital respiratory admissions in an urban area. *Journal of Environmental Health*, *72*(6), 32–35. https://pubmed.ncbi.nlm.nih.gov/20104832/

M'Ikiugu, M. M., Kinoshita, I. & Tashiro, Y. (2012). Urban Green Space Analysis and Identification of its Potential Expansion Areas. *Procedia - Social and Behavioral Sciences*, *35*, 449–458. https://doi.org/10.1016/j.sbspro.2012.02.110

Mst. Ilme, F. (2014). *A study on the role of the local level institutions in the development of rajshahi city*. Bangladesh University of Engineering and Technology.

Policy 7.18 Protecting open space and addressing deficiency | London City Hall. (n.d.). Retrieved September 6, 2020, from https://www.london.gov.uk/what-we-do/planning/london-plan/current-london-plan/london-plan-chapter-seven-londons-living-spac-20

Rahman, M. R. & Lateh, H. (2017). Climate change in Bangladesh: a spatio-temporal analysis and simulation of recent temperature and rainfall data using GIS and time series analysis model. *Theoretical and Applied Climatology*, *128*(1–2), 27–41. https://doi.org/10.1007/S00704-015-1688-3

Rajshahi Deforestation Rates & Statistics | GFW. (n.d.). Retrieved July 28, 2020, from https://rb.gy/rmgoes

Rajshahi Development Authority. (n.d.). *Rajshahi Metropolitan Development Map*. Retrieved July 27, 2021, from https://rdaraj.org.bd/wp-content/uploads/2010/12/MasterPlan-Jurisdiction-Map_big.jpg

Russo, A. & Cirella, G. T. (2018). Modern compact cities: How much greenery do we need? *International Journal of Environmental Research and Public Health*, *15*(10). https://doi.org/10.3390/ijerph15102180

Hossain, et al. (2020). Climate change impacts on farmland value in Bangladesh. *Ecological Indicators*, *112*, 106181. https://doi.org/10.1016/J.ECOLIND.2020.106181

Urban population growth (annual %) - Bangladesh | Data. (n.d.). Retrieved July 27, 2020, from https://data.worldbank.org/indicator/SP.URB.GROW?end=2019&locations=BD&start=2015

World Urbanization Prospects 2018. (2018). Department of Economics and Social Affairs; United Nations.

Cite as: Asaduzzaman M. & Sadat N., "A Quantitative Evaluation of Urban Green Spaces in Rajshahi, Bangladesh", *The 2nd International Conference on Civil Infrastructure and Construction (CIC 2023)*, Doha, Qatar, 5-8 February 2023, DOI: https://doi.org/10.29117/cic.2023.0135

Post-Covid-19 Ventilation Strategies for Shopping Malls in Hot Humid Climate

Wardah Fatimah Mohammad Yusoff
Department of Architecture and Built Environment; Centre for Engineering Education Research; Centre for Innovative Architecture and Built Environment, Faculty of Engineering and Built Environment,
Universiti Kebangsaan Malaysia, Malaysia
wardahyusoff@ukm.edu.my

Zinnirah Wellun
Department of Architecture and Built Environment, Faculty of Engineering and Built Environment,
Universiti Kebangsaan Malaysia, Malaysia
p102441@siswa.ukm.edu.my

Nur'Aina Farhana Norzelan
Department of Architecture and Built Environment, Faculty of Engineering and Built Environment,
Universiti Kebangsaan Malaysia, Malaysia
p114148@siswa.ukm.edu.my

Abstract

To date, many strategies have been executed to combat the COVID-19 disease, including the provision of good ventilation in buildings to reduce the spread of the virus. Open or semi-open space with good air exchange between indoor and outdoor provides better condition compared to enclosed space with mechanical ventilation. However, the design of public buildings, especially the shopping malls in hot and humid climate are mostly enclosed, with the high usage of air-conditioning systems. Due to the COVID-19 situation, it is found that the typical approach to shopping mall design needs to be revised and improved. Hence, this study is conducted with the intention to derive an initial idea regarding the new approach of a shopping mall that is able to be less dependent on the mechanical ventilation system. The method conducted for this preliminary study is a semi-structured interview with three respondents that possess experience of involving in shopping mall projects, namely the architect and mechanical engineer. The findings from the interview show that all respondents agreed that a new approach to ventilation systems should be implemented in shopping malls. They also emphasized that for shopping malls located in hot and humid climate, the usage of merely natural ventilation is impractical, especially in providing thermal comfort to the users. Hence, it is recommended to have hybrid ventilation, which combines mechanical and natural ventilation systems. This study is significant as it encourages other studies related to the new approach to shopping mall design, especially in the hot and humid climate.

Keywords: COVID-19; Shopping mall; Mechanical ventilation; Natural ventilation; Hot humid climate

1 Introduction

Severe acute respiratory syndrome Coronavirus 2 (SARS-CoV-2) is a virus that has caused Coronavirus disease (COVID-19). This disease has been spreading worldwide since 2019, and now it has become endemic, where this virus will always be in the community (Kumar & Morawska, 2019). To date, there are many studies indicate that this virus can be transmitted from one person to the other through the air inside a space (Srivastava et al., 2021). Urban morphology, population size, and building attributes also play roles in determining the spread of infectious diseases such as

COVID-19 (Tong et al., 2022). This has encouraged architects to explore new approach of design and planning in achieving a healthier environment. Among the consideration are providing natural light, good ventilation and green open areas (Waheeb & Hemeida 2022).

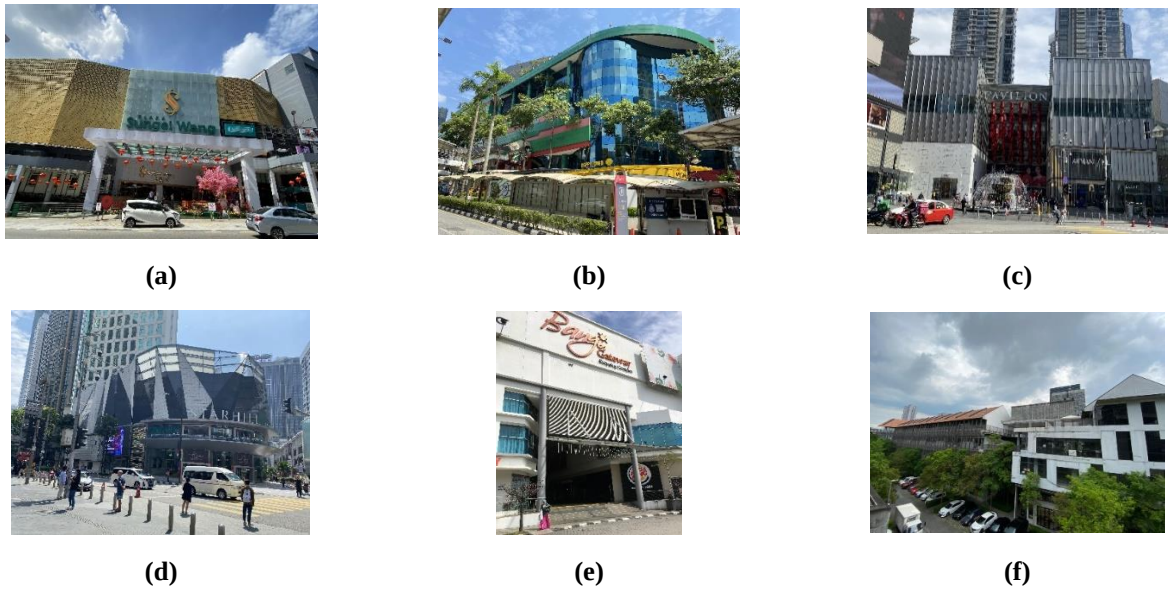
There are three main functions of ventilation, namely for health, thermal comfort and structure cooling. Good ventilation strategies in buildings are essential in ensuring ventilation functions are achieved optimally. The ventilation strategies can be categorized into two, which are the active and passive strategies. The active strategies include the utilization of mechanical tools to aid the airflow such as mechanical fans and air conditioning. Meanwhile, the airflow in the passive strategy is induced by the pressure or thermal differences. Several studies have insisted on the need to provide good airflow and air exchange between the indoor and outdoor in controlling the spread of COVID-19 disease. The study by Park et al. (2021) on the airborne transmission in school building indicated that under the condition of occupants, wearing masks, and the space is naturally cross ventilated with 15% window opening, the probability of infection would be less than 1%. Meanwhile, for a large office building, the usual ventilation system used is mechanical ventilation such as the heating, ventilation and air-conditioning (HVAC) system. Srivastava et al. (2021) suggested on the combination of local air cleaning with the HVAC system for the office building. The study investigated the usage of Ultraviolet-C (UV-C) disinfection device in cleaning the air that carried the SARS-CoV-2 virus. Besides school and office, a gymnasium is also a place that has high risk of spreading COVID19 disease due to the activities that involve high metabolism rates. Therefore, Wang et al. (2022) recommended the usage of a real-time metabolism-based ventilation control system at a gymnasium. The proposed system was able to decrease the infection probability of 4.3-6.3%, as well as encouraged energy savings of 13% compared to the fixed-fresh air ventilation system.

Shopping mall is a public building that also has many visitors. The current design of shopping malls is mainly influenced by the malls in the United State of America (Ibiyeye et al., 2015; Albuquerque et al., 2016; Akadiri et al., 2012). According to Federico (2008), this 'American Model' is a box lit with artificial light, and has the same thermal environment throughout the year, regardless of the changes in the surrounding environment and climate. Due to that approach of design, most shopping malls are fully ventilated with mechanical ventilation systems. The usage of such system had resulted in the enclosed approach of shopping mall design, which are unfavourable in controlling the COVID-19 disease. The virus particles spread quicker in enclosed space compared to open space. This is due to the natural ventilation factor in open space that aids to reduce the concentration of virus particles in the air (Kumar & Morawska, 2019). Chai et al. (2020) investigated the COVID-19 transmission in the shopping malls in Wenzhou, China. The findings indicated possible transmission among the visitors. With the current increase in the infectious diseases, especially via airborne transmission such as COVID-19, are the conventional ventilation systems applied in shopping malls appropriate? Hence, this study aims to investigate the appropriate ventilation strategies in shopping malls for post COVID-19 situation, particularly in the hot and humid climate of Malaysia. This is a preliminary study, which encourages more studies of post COVID-19 ventilation system in Malaysia's shopping malls.

2 Shopping Malls in Malaysia

In general, shopping malls in Malaysia can be divided into three phases which the first phase is from 1970 to 1989, the second phase is from 1990 to 1999 while the third phase starts from 2000 and above. The shopping malls during the first phase were developed along Sultan Street, Tunku Abdul Rahman Street, Petaling Street and Bukit Bintang Street in Kuala Lumpur (Zaki et al., 2012). Kuala

Lumpur is the capital city of Malaysia, and well known as the main business area in Malaysia. To date, the numbers of shopping malls are continuously increasing in Kuala Lumpur. During the early phases, namely the phases one and two, the shopping malls in Malaysia are designed with enclosed approach. The mechanical ventilation system commonly adopted is fully air-conditioning system such as centralized system. Due to the hot humid climate, where the air temperature is constantly high throughout the year, the heating system is not utilized in Malaysia. However, during the third phase, which is after the year 2000, the shopping malls in Malaysia have been designed with different approach. The open concept with greenery has started to be introduced. In addition, the semi-enclosed atrium which allows natural daylight and ventilation has also started to be applied in the shopping malls during the third phase. The new approach has also allowed other ventilation system to be applied such as the hybrid ventilation system, which combines the natural and mechanical ventilation. This new approach has actually been influenced by the green movement in Malaysia, which encourages sustainable design. For example, the development of Malaysia Green Building Index. The examples of shopping malls in Malaysia during the first phase are Sungei Wang Plaza (Figure 1a) and Sunway Putra Mall, while for the second phase, the examples are Lot 10 Shopping Centre (Figure 1b), Mid Valley Mega Mall, Pavillion (Figure 1c) and Starhill Gallery (Figure 1d). After the year 2000, shopping malls with different approaches are Publika Solaris Dutamas, Bangi Gateway (Figure 1e) and Tamarind Square (Figure 1f).



(a) **(b)** **(c)**

(d) **(e)** **(f)**

Fig. 1: The shopping malls constructed from the year 1970 to 2020, which are **(a)** Sungei wang Plaza, **(b)** Lot 10 Shopping Complex, **(c)** Pavilion, **(d)** Starhill Gallery, **(e)** Bangi Gateway, and **(f)** Tamarind Square

3 Methodology

The method used for this preliminary study is a semi-structured interview. The semi-structured interview technique was chosen as it provides more opportunity to explore the respondents' opinions, and still can be tailored within the intended topics. The interviews were conducted with respondents who had been involved in shopping mall projects, namely the architect and mechanical engineer. As aforementioned, this study is just a preliminary study. Therefore, there is a limited number of respondents involved in the interview, which are three only. More respondents with variety of backgrounds will be involved in future studies. The interviews were recorded and the analyses were executed using the Nvivo software. The coding system was used in the analyses. The thematic analyses were conducted to categorize the codes into specific themes.

The interview session was divided into two sections. The first section was conducted with the purpose to identify the respondents' backgrounds, while the second section focused on the discussion regarding the shopping mall designs and ventilation systems.

The interview questions were developed based on the themes or topics that were found in the literature review, as well as to achieve the aim of this study. However, the interviews were not restricted to the developed questions only, as the semi-structured interview method was employed. The additional topics raised by the respondents were also considered in analysing the results and findings.

4 Results and Discussion

Based on the interviews, there are 28 codes identified, and they have been grouped into several categories. The frequencies of the codes being discussed by the respondents are calculated. The thematic analyses of the codes and the interview questions have resulted in three main themes namely mechanical ventilation, hybrid ventilation, and space layout design. The results and discussion of the interviews are presented according to the themes. The frequencies of each code for each theme mentioned by the respondents are provided in table form for certain examples only. Meanwhile, for the other codes, the findings are explained and summarized in text. The first respondent who is an architect with 20 years of experience in building industry are represented by R1, the second respondent who is an architect who also possesses 20 years of experience is denoted as R2, while the third respondent who is a mechanical engineer who has 10 years of experience, and also owns a company that is specialized in the air-conditioning system, is indicated as R3.

4.1 Mechanical Ventilation

The aspects discussed in this theme can be classified into four namely the types of mechanical ventilation system, the factors that influence the selection of the system, the disadvantages of the system, and the appropriate location for the system. Based on the interview, all respondents agreed that the centralized system is the usual system used in shopping malls compared to the split unit and the combination of centralized and split unit. Meanwhile, for the factors of the system selection, all respondents agreed that thermal comfort is the main factor that influences the selection of the system. All respondents mentioned that the hot and humid climate of Malaysia has caused high demand for cooling. The air-conditioning system is the fastest and easiest method to achieve indoor thermal comfort. R1 also added that the enclosed design of the shopping malls has also made the air-conditioning system as the main choice. Besides thermal comfort, the other factors listed by the respondents are escapism, community awareness and client's request (Table 1).

R1 and R2 associated the provision of air conditioning with the escapism aspect, which had attracted the communities to visit the mall due to the cooler indoor environment compared to outdoor. R1 included community awareness as the factor that also causes high demand for air conditioning usage. The high dependence on the air-conditioning system in achieving thermal comfort, the lack of tolerance to the hot environment, as well as less awareness of the importance of energy savings have made air-conditioning the most favourable system in the community. Meanwhile, R1 and R2 also stated that the client's request also influences the selection of the ventilation system. R1 connected the client's request with the exclusivity justification. Large shopping malls which are occupied with leading brand tenants will obtain high profits. Therefore, their business models are able to cover the cost of expenses involving the ventilation system. Meanwhile, R2 added that the building concept intended by the client also influences the design of the shopping mall and the type of ventilation system used. For example, smaller shopping malls that have different target users and tenants have

applied hybrid ventilation systems compared to the large and exclusive shopping malls that prefer fully air-conditioning systems.

Table 1: Frequencies of each code mentioned by the respondents for the factors that influence the selection of the system

Code Category	Code	Frequencies mentioned by the respondents			Total
		R1	R2	R3	
Factors that influence the selection of the system	Thermal comfort (Hot humid climate)	4	5	6	15
	Escapism	1	3	0	4
	Community awareness	2	0	0	2
	Client's request	4	3	0	7

For the disadvantages of the system, the high cost involved by the mechanical ventilation system is mainly mentioned by all the respondents. Among many types of mechanical ventilation systems, air-conditioning involves great amount of costs such as installation costs, operating cost, and maintenance costs. Indoor air quality was the second most frequently mentioned by the respondents. R1 mentioned that area which involves activity such as cooking, is more appropriate to have air exchange between the indoor and outdoor. Meanwhile, R2 insisted that toilet should not be ventilated with mechanical ventilation, as good natural ventilation is essential to bring out the odour. Three factors that influence the air quality by mechanical ventilation system have been highlighted by all respondents. They are the maintenance of the system, the air filter quality and the polluted indoor air. Besides involving high cost and affecting indoor air quality, the other disadvantages mentioned by the respondents are the utilization of space and energy. R1 and R3 stated that the centralized air-conditioning which is normally used in shopping malls has involved many spaces to accommodate the system such as spaces for air handling unit, chiller, cooling tower and ducting. Meanwhile, for the energy usage, R2 and R3 insisted on the high-energy utilization by the air-conditioning system, which is more than 40% of the total building energy consumption.

For the location of the mechanical ventilation system, there are two aspects highlighted by the respondents namely the locations of zones that require mechanical ventilation system and zones that are unnecessarily ventilated by that system (Table 2). All respondents agreed that zone with high density of visitors such as retails area, can be ventilated with mechanical ventilation, while the areas such as toilets and service rooms are unnecessarily to be mechanically ventilated. However, for the service rooms that accommodate many electrical equipment, consideration can be given for the mechanical ventilation usage. The large volume area is also discouraged to be fully mechanically ventilated as it incurs high-energy load for cooling.

Table 2: Frequencies of each code mentioned by the respondents for the appropriate location of the system

Code Category	Code	Frequencies mentioned by the respondents			Total
		R1	R2	R3	
Appropriate location of the system	Location of zone	1	1	2	4
	Areas that are unnecessarily ventilated by mechanical ventilation	1	3	0	4

4.2 Hybrid Ventilation

The code category discussed in this theme can be classified into three namely the purpose of hybrid ventilation, the advantages and disadvantages of the system. The purpose of using hybrid ventilation highlighted by the respondents are the importance of air exchange, energy savings, as well as the requirements of Malaysia Uniform Building By-Law (UBBL) and Malaysia Green Building Index (GBI). The importance of air exchange is the most discussed by the respondents compared to the other code categories. All respondents agreed that air movement, which involves the air exchanges between the indoor and outdoor, is significant in the building. R1 mentioned on the necessity to provide openings to allow the cross-ventilation in the building. However, natural ventilation alone is insufficient to provide thermal comfort due to the low air velocity. Hence, R2 and R3 stated on the usage of mechanical fan to assist the natural ventilation. In term of energy savings, all respondents agreed that the hybrid ventilation system uses less energy compared to the fully mechanical ventilation system. Meanwhile, for the Malaysia UBBL requirement, it is already stated that certain areas have to be ventilated by natural ventilation such as the fire staircase, the habitable rooms and the toilets. The utilization of natural ventilation is also a point highlighted in the Malaysia GBI requirements. According to R1, natural ventilation is also important to get a high score in the evaluation of the GBI. Among the criteria included in the GBI evaluation scoring is energy efficiency. The Building Energy Index (BEI) is one of the components that is considered in energy efficiency scoring. By using natural ventilation, the BEI can be lowered significantly, which subsequently helps to increase the energy efficiency of the building.

The advantages of using hybrid ventilation mentioned by all respondents are the reduction of energy usage, the decrease of costs related to fully mechanical ventilation system, and the provision of good air exchange between indoor and outdoor. Good air exchange is essential in reducing the spreading of airborne diseases such as COVID-19. R1 had associated the benefits of good air exchange with the unnecessary of wearing masks, which helps to save the cost also. This subsequently has caused the visitors to prefer open areas compared to the enclosed or confined areas during the COVID-19 situation.

Meanwhile, different disadvantages had been highlighted by the respondents regarding the usage of natural ventilation. R1 mentioned the importance of understanding the surrounding condition and climate in the provision of natural ventilation. This is because, for natural ventilation, the outdoor air condition affects greatly the indoor air. The area with high levels of air pollution is inappropriate for natural ventilation application. Meanwhile, R2 indicated on the difficulty of controlling the indoor thermal condition with natural ventilation, compared to the usage of fully mechanical ventilation system such as air conditioning. This is because the outdoor air temperature and humidity influence the indoor air condition for natural ventilation. R3 mentioned the need for high cooling load to cool the indoor environment of huge space. The concern of cooling load was also raised by R2 who insisted that natural ventilation alone is insufficient to cool a building that has a large volume area such as a shopping mall. In addition, the high number of occupants at one time, the presence of many electrical equipment, as well as the enclosed building design with minimal number of openings, have also increased the demand for cooling load.

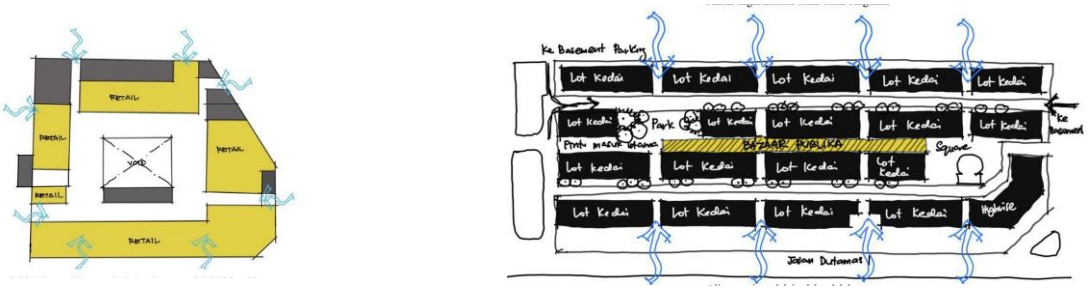
4.3 Building Layout Design

The design of shopping mall also plays a role in increasing the effectiveness of hybrid ventilation system in the building. All respondents agreed that among the effective design for hybrid ventilation

is the division into smaller or modular blocks compared to the large building block. In this way, the zoning of areas that utilize air-conditioning is only focused on smaller spaces compared to the large spaces that require greater energy consumption for cooling. In addition, air can also flow through the gaps between the building blocks, which allows for natural ventilation. R2 opined that a cluster layout of the blocks is more effective than a linear layout. This is because the cluster layout can reduce the cooling load in the space due to the smaller square footage (Figure 2).

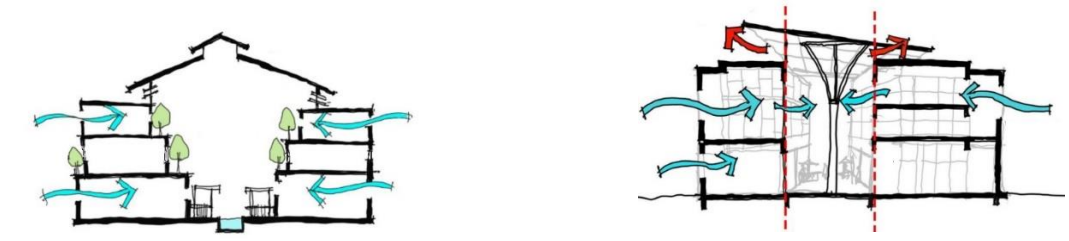
R1 and R2 also indicated that the layout design that includes courtyard and greenery is able to provide many open spaces that can be used by the public for socializing and relaxing. According to R1, shopping mall is a building typology which is normally large in size. Therefore, from a psychological point of view, it needs intermediate spaces for visitors to rest for a while. Hence, the inner courtyard is one of the good examples for this approach. This area is naturally ventilated. The presence of vegetation also helps to cool the surrounding environment (Figure 3).

As for the internal layout, R1 mentioned that the height and arrangement of the temporary wall partitions need to allow the air to flow through the gaps in between and above them. Besides that, the gaps are also essential to allow the penetration of daylighting, which subsequently reduce the dependence on the artificial lighting.



(a) **(b)**

Fig. 2: Example of shopping mall designs that consist of several blocks that are arranged in **(a)** cluster, and **(b)** linear layouts



(a) **(b)**

Fig. 3: Example of shopping mall designs that encompass **(a)** water features and greenery and **(b)** semi-open atrium that allows for natural ventilation

5 Conclusion

This study is a preliminary study on the appropriate approach of ventilation system at shopping malls located in hot and humid climate for post COVID-19 situation. Hence, the findings from this study provide the initial recommendations, which in the future have the potential to be expanded into guidelines via more intensive and extensive studies. The findings from the interview highlighted the disadvantages of the usual mechanical ventilation system applied at the shopping malls in the hot and humid climate, as well as the advantages and drawbacks of hybrid ventilation system. The findings can be concluded that there are many factors that influence the selection of the system. The main

factor is the provision of good thermal comfort for the users, as it can attract more people to the shopping malls. Nevertheless, the client's request also plays a role especially for the shopping malls that have their own target tenants and visitors. Hence, these two aspects, namely the user thermal comfort and the request of building owners need to be considered in the design. However, being in a hot and humid climate, where the cooling aspect is very essential, the challenge faced is the ability to control the indoor environment for thermal comfort, and at the same time able to achieve various savings such as the cost, energy and space.

Therefore, this study has recommended on the utilization of hybrid ventilation, which combines the mechanical and natural ventilation systems. By combining these two systems, many benefits can be derived such as the reduction in building space and energy usage, as well as the savings of cost for many aspects such as installation, maintenance and operation costs. All the considerations mentioned above are vital even though for post COVID-19 situation. Though the controlling of indoor thermal environment is more challenging with hybrid ventilation system compared to the fully mechanical system such as air conditioning, the hybrid system still provides more advantages in the post COVID-19 situation. The hybrid ventilation system is more appropriate as it is able to provide better indoor air quality due to the air exchange between the indoor and outdoor, which helps to reduce the spreading of airborne disease.

The study also summarizes that building layout design also plays significant role in the ventilation system used. To optimal the usage of hybrid ventilation system, the building layout should be designed to have several blocks, with the courtyard and greenery in between, compared to having just one large block. This is because, the approach allows for the zoning of ventilation system to be effectively implemented. Some areas are occupied with fully mechanical ventilation system, some areas are ventilated with hybrid ventilation, and some other areas are naturally ventilated. The presence of airflow and greenery in between of the blocks also helps to cool the surrounding environment. The building blocks that implement hybrid ventilation system should also be incorporated with many openings to allow for cross-ventilation. In a nutshell, the conventional shopping mall design that has one block with large volume area is irrelevant for the post COVID-19 situation, as the hybrid ventilation system is more appropriate compared to the fully mechanical ventilation system.

Acknowledgement

The authors would like to express appreciation to the Malaysian Ministry of Higher Education for the research grant FRGS/1/2019/TK10/UKM/02/4 - *Airflow characteristics and behaviour around openings with various types of shading elements*, which helps to fund this study.

References

Akadiri, P. O., Chinyio, E. A. & Olomolaiye, P. O. (2012). Design of a sustainable building: A conceptual framework for implementing sustainability in the building sector. *Buildings 2*(2): 126–152. doi:10.3390/buildings2020126

Albuquerque, D. & Carrilho da Graça, G. C. (2015). Use of building thermal and CFD simulation in the design of a large office building in Lisbon. Proceedings of BS2015:14th Conference of International Building Performance Simulation Association, Hyderabad, India.

Chai, et al. (2020). Indirect Virus Transmission in Cluster of COVID-19 Cases, Wenzhou, China. *Emerging Infectious Diseases*. *26*(6): 1343-1345.

Federico, M. (2008). 178: Sustainable Design for Retail Buildings. PLEA 2008 – 25th Conference on Passive and Low Energy Architecture. Retrieved on 10 November 2022.

Ibiyeye, et al. (2015). Mixed-Mode Ventilation In Malaysia's Shopping Malls: A Taxonomy Study. *International Journal on Sustainable Tropical Design Research and Practice*, *8* (Special Issue 2): 72-82.

Kumar, P. & Morawska, L. 2019. Could fighting airborne transmission be the next line of defence against COVID-19 spread? *City and Environment Interactions*, *4*:100033.

Park, et al. (2021). Natural ventilation strategy and related issues to prevent coronavirus disease 2019 (COVID-19) airborne transmission in a school building. *Science of the Total Environment, 789*: 147764.

Srivastava, et al. (2021). Effective ventilation and air disinfection system for reducing coronavirus disease 2019 (COVID-19) infection risk in office buildings. *Sustainable Cities and Society*, *75*: 103408.

Tong, H., Li, M. & Kang, J. (2022). Relationships between building attributes and COVID-19 infection in London. *Building and Environment*. *225*: 109581.

Waheeb, M. I. & Hemeida, F. A. (2022). Study of natural ventilation and daylight in a multi-storey residential building to address the problems of COVID-19. *Energy Reports*. *8*: 863:880.

Wang, J. et al. (2022). Metabolism-based ventilation monitoring and control method for COVID-19 risk mitigation in gymnasiums and alike places. *Sustainable Cities and Society*. *80*: 103719.

Zaki, A., Nor'Aini, Y. & Shardy, A. (2012). Exploring Malaysian Mall Manager's KSAOs. *Procedia-Social and Behavioral Sciences*, *62*:144-158.

Cite as: Yusoff W.F.M. Zinnirah Wellun Z., Norzelan N.F., "Post-COVID-19 Ventilation Strategies for Shopping Malls in Hot Humid Climate", *The 2nd International Conference on Civil Infrastructure and Construction (CIC 2023)*, Doha, Qatar, 5-8 February 2023, DOI: https://doi.org/10.29117/cic.2023.0136

Conceptual Framework for Planning Urban Roadside Vegetation to Enhance Air Quality for Roadside Users

Soujanya Mogra
Department of Architecture and Urban Planning, College of Engineering, Qatar University, Doha, Qatar
sm1513220@student.qu.edu.qa

Mohd Faris Khamidi
Department of Architecture and Urban Planning, College of Engineering, Qatar University, Doha, Qatar
mohd.khamidi@qu.edu.qa

Fodil Fadli
Department of Architecture and Urban Planning College of Engineering, Qatar University, Doha, Qatar
f.fadli@qu.edu.qa

Abstract

Vegetation is known for enhancing air quality. However, vegetation on urban roads can either increase or decrease exposure to air pollutants. The health of pedestrians and cyclists is particularly of great concern since they are exposed directly to air pollutants, unlike drivers. Dispersion of air pollutants is necessary for exposure reduction on urban roads. The local factors, including street geometry, meteorological conditions, and physical characteristics of vegetation, influence the dispersion of pollutants. There is a lack of framework for planning urban road vegetation to disperse air pollutants. This study summarizes the literature on the influence of local factors; analyses the interrelation between the local factors on the dispersion of air pollutants by trees and hedgerows. It provides a conceptual framework to provide clarity in planning urban roadside vegetation to enhance the air quality for roadside users.

Keywords: Urban roadside vegetation; Dispersion of air pollutants; Well-being of the roadside users; Conceptual Framework

1 Introduction

Urban vegetation is widely known for enhancing air quality. Ambient pollutants are reduced by vegetation through absorption and deposition, as well as dilution through dispersion (Garland, 2001). Vehicular traffic on urban roads is one of the main contributors to air pollutants in cities (World Health Organization, 2022). Accumulated air pollutants over a prolonged period in urban streets are detrimental to the health of road users. The health of roadside users, i.e., pedestrians and cyclists, are particularly at risk from traffic-borne air pollution since they are exposed directly to the pollutants, unlike drivers, who are partially protected. The ability of the street vegetation to disperse air pollutants plays a significant role in reducing roadside users' exposure to traffic-borne air pollutants.

Studies on the dispersion of air pollutants in street canyons have examined the influence of wind conditions (Baik & Kim, 1999; Huang et al., 2019); street geometrical characteristics (Hunter et al., 1992; Oke, 1988); variations in surface temperature (Xie et al., 2005; Xie et al., 2007). Studies have looked into the effect of vegetation on pollution dispersion in street canyons (Amorim et al., 2013;

Buccolieri et al., 2009; Gromke et al., 2016; Li et al., 2016). There are reviews on the deposition and the dispersion of air pollutants by street vegetation (Abhijith et al., 2017; Janhäll, 2015). In addition, Hewitt et al., (2020) discussed where and how certain vegetation forms improve air quality in different urban environments. Trees and hedgerows are common street elements. However, there is no clarity on planning trees and hedgerows in street canyons to reduce roadside users' exposure to air pollutants. Hence, a conceptual framework for planting trees and hedgerows to disperse air pollutants is worth developing. This study provides a conceptual framework for planning trees and hedgerows to enhance the dispersion of traffic-borne pollutants in street canyons.

2 Local Parameters

2.1 Street Geometry

Local urban spatial form and building regulations determine the geometrical characteristics of urban roads. 'Aspect ratio' is used to express the geometry of street canyons. 'Aspect ratio' is defined as the ratio of the building height (H) and the width of the street (W). Aspect ratios fall into one of three categories: shallow, which has aspect ratios less than 0.5; regular, which has aspect ratios between 0.5 and 2; and deep, which has aspect ratios greater than 2 (Abhijith et al., 2017; Vardoulakis et al., 2003). Street canyons are subcategorized into short, medium, and long based on the street canyon length (L) and street canyon height (H). The short canyon has $L/H \approx 3$; the medium canyon has $L/H \approx 5$; and the long street canyon has $L/H \approx 7$ (Vardoulakis et al., 2003).

When the wind direction is perpendicular to the street canyon, as shown in Figure 1, the airflow regime, i.e., the number of vortex formations and strength of the vortex, varies according to the street aspect ratio (Oke, 1988) and street canyon length (Hunter et al., 1992). In an isothermal condition, three types of airflow regimes are observed by Oke (1988), as shown in Figure 2. When $H/W < 0.33$, the vortex formed at the windward and leeward walls, has no interactions, as shown in Figure 2 (a), which is known as 'isolated roughness flow.' When $0.33 > H/W < 0.66$, the vortex near the windward and the leeward wall interfere, as shown in 2 (b), which is known as 'wake interference flow' When $H/W > 0.66$, a single complete vortex is formed as shown in 2 (c), which is known as 'skimming flow.' The transitions between airflow regimes occur at critical combinations of aspect ratio and length ratio (Hunter et al., 1992). Shallow and short-street canyons are better ventilated.

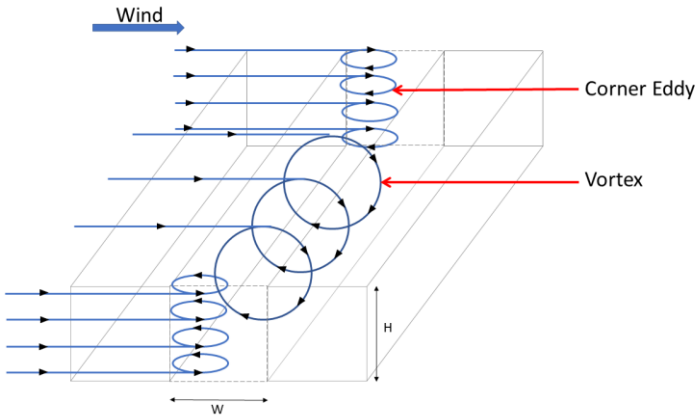


Fig. 1: Formation of vortex and eddies in a square street canyon (H/W=1)

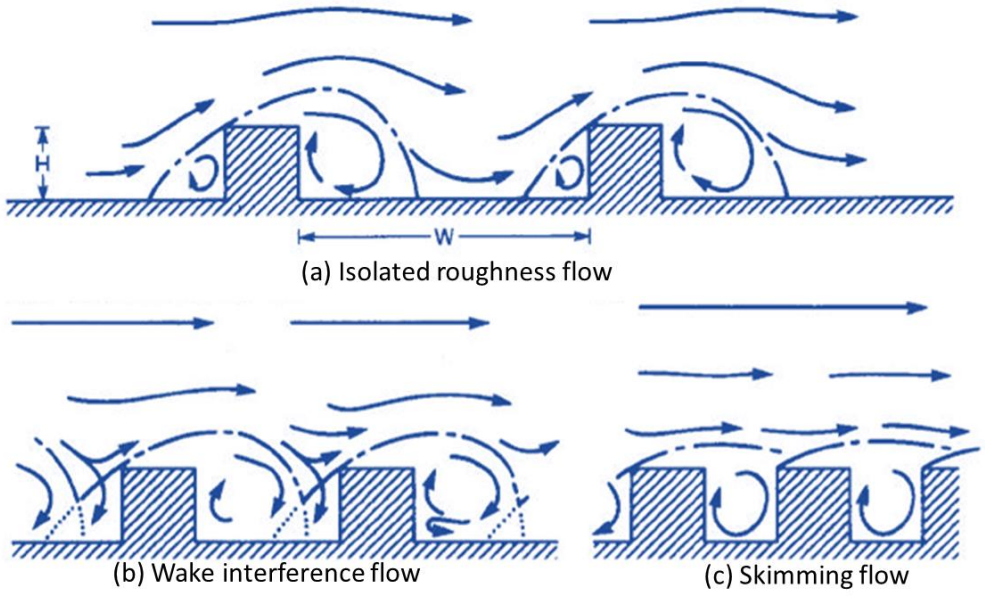


Fig. 2: Airflow regime in street canyons

Trees form a relatively complicated flow field, and the street aspect ratio does not influence the formation of vortices in the presence of trees (Wang et al., 2020). A study conducted by Buccolieri et al. (2009) showed that the effect of trees on the dispersion of pollutants decreases with an increase in aspect ratio, irrespective of the form and arrangement of trees. A study by Zhu et al. (2022) showed that a central greenbelt and a greenbelt on the leeward side of the street canyons are effective in pollutants' dispersion in street canyons having lower aspect ratios with aspect ratios less than 0.67.

2.2 Wind Direction

Typically, the wind directions perpendicular, parallel, and oblique to the street canyons are studied. When the wind is perpendicular to the street axis, the pollutants accumulate at the leeward bottom with a greater concentration at the canyon's centre. When the wind is oblique to the street axis, the pollutants build up at the leeward side of the downwind part of the canyon. When the wind is parallel to the street canyon, the pollutants accumulate in the downwind area (Vardoulakis et al., 2003; Yazid et al., 2014).

Studies show that trees perform better at dispersing pollutants when the wind is parallel to the street axis. For example, Amorim et al. (2013) in Portugal showed that when the wind direction was roughly 45°, CO concentration was increased by 12% in the street canyon with an aspect ratio of 0.33. When the wind is parallel, trees decreased CO concentration by 16% in the street canyon with an aspect ratio of 0.75. A study by Gromke & Ruck, (2012) showed that wall averaged pollutant concentration was higher in street canyon with avenues of trees compared to the tree-less street canyon. Wall averaged pollutant concentration in street canyon with avenues of trees was highest for oblique wind and lowest for parallel wind. Zhu et al. (2022) showed that a central greenbelt and a greenbelt on the leeward side of the street canyons are effective in reducing pollutants exposure of roadside users when the wind direction is almost perpendicular in street canyons with an aspect ratio less than 0.67.

A study by Gromke et al. (2016) showed that the presence of a central hedgerow in a street canyon of an aspect ratio of 0.5 reduced the area-averaged reduction of pollutant concentration by 46–61% at pedestrian head height level on the leeward side. Two sideways-arranged hedgerows reduced area-

averaged pollutant reduction on the leeward side between 18 and 39% at pedestrian head height. In the case of parallel wind direction, two sideways arrangements of hedgerows reduced the area-average pollutant concentration up to 60% at the head height of the pedestrians.

2.3 Wind Speed

Lower wind speeds weaken street ventilation by reducing vertical air mixing between the in-canyon volume air and the air above in the atmosphere. Higher wind speed enhances vertical air mixing by strengthening the vertices and has a significant role in pollutants' dispersion Zhang et al., (2015).

Niroobakhsh et al. (2021) revealed that an increase in ambient wind speed does not affect the number of vertices; however, it increases turbulence intensity and strength of the vertices. Nazridoust and Ahmadi (2006) observed the vanishing of the secondary vortex at the bottom upwind corner when the wind speed increased to 20 m/s from 1 m/s in a regular street canyon. Further, Baik and Kim (1999) observed the merging of the two secondary vertexes into a primary vortex at the canyon bottom in a deep street canyon when the wind speed increased from 1m/s to 4m/s. Additionally, the study found a threshold for the wind speed above which the number of vortices did not change.

Ries and Eichhorn (2001) observed an increase in volume averaged pollutant concentration when the speed was reduced to 5m/s from 6 m/s in a street canyon with an aspect ratio of 0.5 in the presence of trees. A study by Zhu et al. (2022) on Qianfoshan Road in Jinan, China, showed that a central greenbelt and a greenbelt on the leeward side of the street canyons are effective in pollutant exposure reduction in moderate to higher wind speeds. The study found an increase in exposure to PM2.5 when the wind speed was 2.45m/s and perpendicular to the street axis. When the wind speed increased from 2.45 to 4.7 m/s, 4.7 to 6.7 m/s, and 6.7 to 9.35 m/s, the residence time of PM2.5 decreased by 78%, 51%, and 40%, respectively.

A study by Li et al. (2016) showed that the optimum height of a hedgerow is 1.1 meters for the dispersion of pollutants in street canyons of an aspect ratio between 0.3 and 1.67. The study revealed that the dispersion of pollutants by hedgerows is not sensitive to wind speed when the wind is perpendicular to the street canyons.

2.4 Surface Temperature

According to the solar zenith angle and the weather during the day, buildings and street surfaces heat up. Studies by Xie et al. (2005) on a regular street canyon showed that when the leeward façade is heated, the airflow pattern remains the same as in the isothermal case. However, the vortex acquires greater strength due to upward advection flux along the leeward wall produced by buoyancy flux. Consequently, the pollutant concentration decreases when the windward wall is heated. On the other hand, when the windward façade is heated, the upward buoyancy flux produced opposes the downward advection flux and forms two contra-rotating vertexes. As a result, pollutant concentrations increase on the windward side. When the ground surface is heated, the buoyancy flux produces two counter-rotating vortices: one near the upper leeward wall and the other near the lower portion of the windward wall. With an increase in temperature, the clockwise vortex on the windward side expands, and the contraclockwise vortex on the leeward wall shrinks. As a result, pollutants accumulate on the windward side. However, overall, the pollutant concentration decreases in the street canyon when the ground is heated.

Di Sabatino et al. (2015) revealed that trees in the street canyon reduce the temperature at the bottom of the façade in a Mediterranean climate during the day. However, trees trapped heat closer to the

ground and released the heat at night time. As a result, night time air and façade temperatures were higher in street canyons with trees than in street canyons without trees. In addition, the tree crown hindered vertical air exchange and created thermal stratification, which caused reversal airflow. As a result, volume-averaged concentration in the bottom of the street canyon increased.

3 Intrerelation between the Meteorological Conditions, Street Geometry, and Dispersion of Pollutants by Street Vegetation

Dispersion of pollutants by street trees is lower at lower wind speeds (Ries & Eichhorn, 2001). Pollutant concentrations are higher when the wind directions are perpendicular and oblique to the street canyon axis (Zhang et al., 2015; Huang et al., 2019). The presence of trees in street canyons slows down the airflow velocity (Buccolieri et al., 2011; Wang et al., 2020). Trees perform better when the ambient wind direction is parallel to the street axis (Amorim et al., 2013; Gromke & Ruck, 2012). The dispersion of pollutants by street trees decreases with an increase in aspect ratios (Buccolieri et al., 2009). When the street canyon ratio is less than 0.67 with optimal tree spacing, the Central Greenbelt (trees and hedgerows) and leeward greenbelt have the potential to disperse pollutants even when wind direction is perpendicular to the street axis (Zhu et al., 2022). Variation in wind direction, i.e., perpendicular to parallel, has more influence than the variation in aspect ratio between 0.33 to 0.75 on the dispersion of pollutants (Amorim et al., 2013). Variations in wind speed considerably influence the dispersion of pollutants by street trees (Zhu et al., 2022). Dispersion of pollutants by street trees increased with an increase in wind speed; however, not at the same rate (Zhu et al., 2022). Diurnal temperature influences the dispersion of pollutants by street trees (Di Sabatino et al., 2015).

Central hedgerows reduce wall-averaged pollutants at pedestrian height for perpendicular wind directions in shallow street canyons (Gromke et al., 2016). A sideways arrangement of two hedgerows performs better in pollutants' dispersion when the wind is parallel to the street axis (Gromke et al., 2016). The effect of hedgerows on pollutant dispersion is less sensitive to changes in wind speed (Li et al., 2016).

There is no simple association between the meteorological conditions and the dispersion of pollutants by street vegetation. Therefore, planning urban road vegetation for the dispersion of pollutants necessitates local investigations. Field experiments can be resource intensive as well as time-consuming. Hence, Computational Fluid Dynamics (CFD) method is popular among researchers. Software such as Ansys Fluent (Buccolieri et al., 2009; Gromke et al., 2016), Open Foam (Jeanjean et al., 2016; Jeanjean et al., 2017), and ENVI-met (Vos et al., 2013; Wania et al., 2012) are used in the investigations.

4 Conceptual Framework for Planning Urban Road Vegetation for Dispersion of Air Pollutants

This study recommends the below parameters in the simulations:

1. Street geometrical characteristics: the typical length of an urban block, building height, and coverage according to the local regulation.
2. Street orientation: orientation of the local street patterns such as gridiron, radial, and circular according to the prevailing wind direction.
3. Meteorological conditions: the seasonal variations, hourly variations.
4. Vegetation: physical characteristics such as height, width, vertical coverage, and leaf area density (LAD).

5. Pollutants' Emission Rate: calculated using the Annual Average Daily Traffic (AADT)

   Figure 3 shows the theoretical framework for planning trees and hedgerows for pollutants' dispersion in urban streets.

Figure 3 shows the conceptual framework for planning trees and hedgerows for dispersion of pollutants by street vegetation.

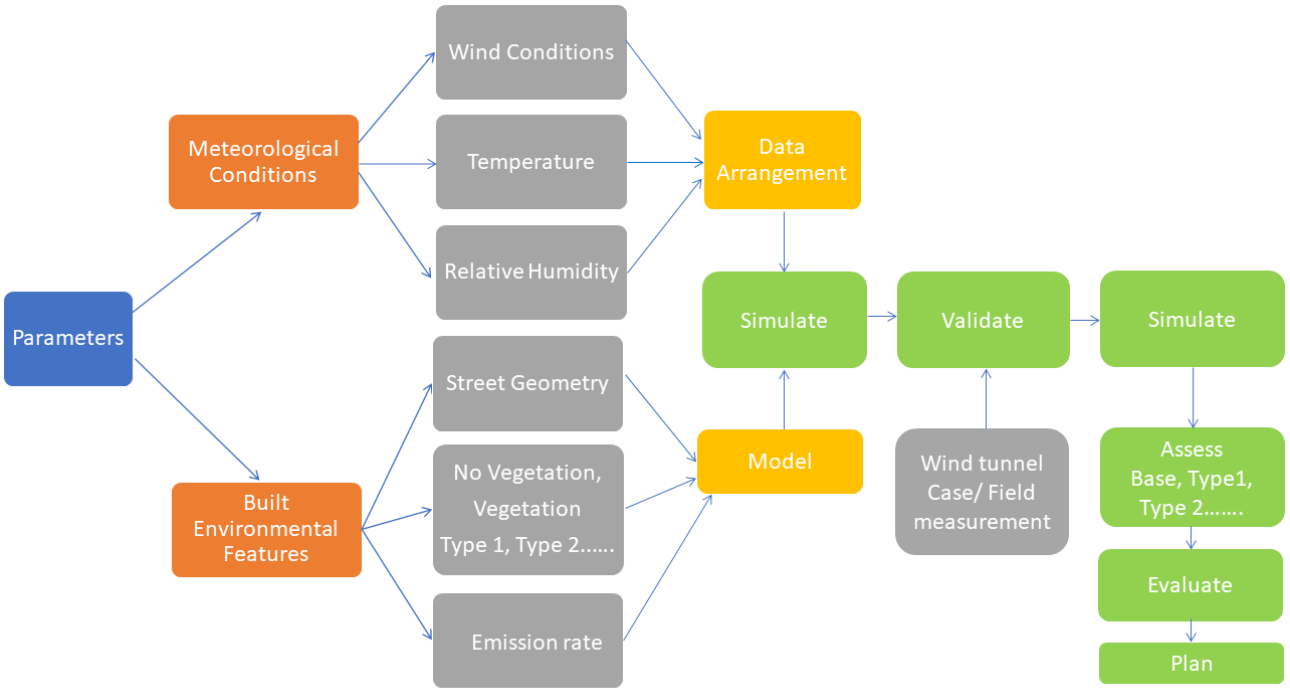


Fig. 3: Conceptual Framework for Planning Urban Road Vegetation for Pollutants' Dispersion

5 Conclusion

Street geometry plays a crucial role in street ventilation. Vertical air exchange is higher in shallow street canyons than in regular and deep street canyons. Vegetation has less effect than street geometrical characteristics on the dispersion of pollutants. Hence, vegetation is suitable for shallow street canyons.

Trees perform better in the dispersion of pollutants when the prevailing wind is parallel to the street axis. Hedgerows perform better than trees in pollutant exposure reduction when the wind is perpendicular to the axis in shallow and regular street canyons. At low wind speeds, street trees are less effective at dispersing pollutants. Dispersion of pollutants by hedgerows is less sensitive to wind speed when the wind is perpendicular to the street axis. Therefore, the physical form of vegetation plays a crucial role in the dispersion of pollutants.

Changes to any parameter, including the meteorological parameters, vegetation form, and street geometry, can considerably influence pollutant dispersion by street vegetation. Therefore, all the local parameters should be considered together in the simulations to plan urban road vegetation to reduce roadside users' exposure to pollutants.

References

Abhijith, et al. (2017). Air pollution abatement performances of green infrastructure in open road and built-up street canyon environments – A review. *Atmospheric Environment, 162*, 71-86. https://doi.org/https://doi.org/10.1016/j.atmosenv.2017.05.014

Amorim, et al. (2013). CFD modelling of the aerodynamic effect of trees on urban air pollution dispersion. *Science of the Total Environment, 461-462*, 541-551. https://doi.org/https://doi.org/10.1016/j.scitotenv.2013.05.031

Baik, J. J. & Kim, J. J. (1999). A Numerical Study of Flow and Pollutant Dispersion Characteristics in Urban Street Canyons. *Journal of Applied Meteorology, 38*, 1576-1589. https://doi.org/10.1175/1520-0450(1999)038<1576:ANSOFA>2.0.CO;2

Buccolieri, et al. (2009). Aerodynamic effects of trees on pollutant concentration in street canyons. *Science of the Total Environment, 407*(19), 5247-5256. https://doi.org/https://doi.org/10.1016/j.scitotenv.2009.06.016

Buccolieri, et al. (2011). Analysis of local scale treeâ€“atmosphere interaction on pollutant concentration in idealized street canyons and application to a real urban junction. *Atmospheric Environment, 45*(9), 1702-1713. https://doi.org/https://doi.org/10.1016/j.atmosenv.2010.12.058

Di Sabatino, et al. (2015). The effects of trees on micrometeorology in a real street canyon: consequences for local air quality. *International Journal of Environment and Pollution*, *58*(1/2), 100.

Garland, J. A. (2001). On the Size Dependence of Particle Deposition. *Water, Air and Soil Pollution: Focus*, *1*(5), 323-332. https://doi.org/10.1023/a:1013183911748

Gromke, C., Jamarkattel, N. & Ruck, B. (2016). Influence of roadside hedgerows on air quality in urban street canyons. *Atmospheric Environment, 139*, 75-86. https://doi.org/https://doi.org/10.1016/j.atmosenv.2016.05.014

Gromke, C. & Ruck, B. (2012). Pollutant Concentrations in Street Canyons of Different Aspect Ratio with Avenues of Trees for Various Wind Directions. *Boundary-Layer Meteorology*, *144*(1), 41-64. https://doi.org/10.1007/s10546-012-9703-z

Hewitt, C. N., Ashworth, K. & MacKenzie, A. R. (2020). Using green infrastructure to improve urban air quality (GI4AQ). *Ambio*, *49*(1), 62-73. https://doi.org/10.1007/s13280-019-01164-3

Huang, et al. (2019). Effects of Wind Direction on the Airflow and Pollutant Dispersion inside a Long Street Canyon. *Aerosol and Air Quality Research*, *19*. https://doi.org/10.4209/aaqr.2018.09.0344

Hunter, L. J., Johnson, G. T. & Watson, I. D. (1992). An investigation of three-dimensional characteristics of flow regimes within the urban canyon. *Atmospheric Environment. Part B. Urban Atmosphere*, *26*(4), 425-432. https://doi.org/https://doi.org/10.1016/0957-1272(92)90049-X

Janhäll, S. (2015). Review on urban vegetation and particle air pollution – Deposition and dispersion. *Atmospheric Environment, 105*, 130-137. https://doi.org/https://doi.org/10.1016/j.atmosenv.2015.01.052

Li, et al. (2016). The impacts of roadside vegetation barriers on the dispersion of gaseous traffic pollution in urban street canyons. *Urban Forestry & Urban Greening*, *17*, 80-91. https://doi.org/https://doi.org/10.1016/j.ufug.2016.03.006

Nazridoust, K. & Ahmadi, G. (2006). Airflow and pollutant transport in street canyons. *Journal of Wind Engineering and Industrial Aerodynamics*, *94*(6), 491-522. https://doi.org/https://doi.org/10.1016/j.jweia.2006.01.012

Niroobakhsh, A., Hassanzadeh, S. & Hoseinibalam, F. (2021). Flow and pollution concentration large-Eddy simulation and transition conditions for different street canyons and wind speeds: Environmental pollution reduction approach. *Urban Climate*, *35*, 100731. https://doi.org/https://doi.org/10.1016/j.uclim.2020.100731

Oke, T. R. (1988). Street design and urban canopy layer climate. *Energy and Buildings*, *11*(1), 103-113. https://doi.org/https://doi.org/10.1016/0378-7788(88)90026-6

Ries, K. & Eichhorn, J. (2001). *Simulation of effects of vegetation on the dispersion of pollutants in street canyons*. https://doi.org/10.1127/0941-2948/2001/0010-0229

Vardoulakis, et al. (2003). Modelling air quality in street canyons: a review. *Atmospheric Environment*, *37*(2), 155-182. https://doi.org/https://doi.org/10.1016/S1352-2310(02)00857-9

Vos, et al. (2013). Improving local air quality in cities: To tree or not to tree? *Environmental Pollution*, *144*(1), 41–64.

Vranckx, et al. (2015). Impact of trees on pollutant dispersion in street canyons: A numerical study of the annual average effects in Antwerp, Belgium. *Science of The Total Environment*, *532*, 474-483. https://doi.org/https://doi.org/10.1016/j.scitotenv.2015.06.032

Wang, et al. (2020). Effect of Street Canyon Shape and Tree Layout on Pollutant Diffusion under Real Tree Model. *Sustainability*, *12*(5).

Wania, et al. (2012). Analysing the influence of different street vegetation on traffic-induced particle dispersion using microscale simulations. *Journal of Environmental Management*, *94*(1), 91-101. https://doi.org/https://doi.org/10.1016/j.jenvman.2011.06.036

World Health Organization, W. (2022). *Ambient (outdoor) Air Pollution*. World Heath Organization. Retrieved 7 February 2023 from https://www.who.int/news-room/fact-sheets/detail/ambient-(outdoor)-air-quality-and-health

Xie, et al. (2005). Thermal effects on vehicle emission dispersion in an urban street canyon. *Transportation Research Part D: Transport and Environment*, *10*(3), 197-212. https://doi.org/https://doi.org/10.1016/j.trd.2005.01.002

Xie, et al. (2007). Impact of building facades and ground heating on wind flow and pollutant transport in street canyons. *Atmospheric Environment*, *41*(39), 9030-9049. https://doi.org/https://doi.org/10.1016/j.atmosenv.2007.08.027

Yazid, et al. (2014). A review on the flow structure and pollutant dispersion in urban street canyons for urban planning strategies. *Simulation*, *90*. https://doi.org/10.1177/0037549714528046

Zhang, et al. (2015). Influence of Meteorological Conditions on Pollutant Dispersion in Street Canyon. *Procedia Engineering*, *121*, 899-905. https://doi.org/https://doi.org/10.1016/j.proeng.2015.09.047

Zhu, et al. (2022). The influence of roadside green belts and street canyon aspect ratios on air pollution dispersion and personal exposure. *Urban Climate*, *44*, 101236. https://doi.org/https://doi.org/10.1016/j.uclim.2022.101236

Cite as: Mogra S. & Khamidi M.F., Fadli F., "Theoretical Framework for Planning Urban Roadside Vegetation to Enhance Air Quality for Roadside Users", *The 2nd International Conference on Civil Infrastructure and Construction (CIC 2023)*, Doha, Qatar, 5-8 February 2023, DOI: https://doi.org/10.29117/cic.2023.0137

The Challenges and Future Aspirations of Implementing Global Sustainability Assessment System (GSAS) in the Urban Facilities of Mega Sport Events [MSEs] in Qatar

Raya Atour
Department of Architecture and Urban Planning, College of Engineering, Qatar University, Doha, Qatar
ra2010351@qu.edu.qa

Fodil Fadli
Department of Architecture and Urban Planning, College of Engineering, Qatar University, Doha, Qatar
f.fadli@qu.edu.qa

Abstract

Sports facilities are built for a specific function and purpose. Once the demand for such purpose no longer exists, it is important to know how both the buildings and the city will adapt to the existence of such megastructures as to prevent turning them into *'white elephants'* in the city. This paper aims to study the environmental impact assessment tools and techniques used in promoting and implementing sustainability in mega sports projects in Qatar. The investigation focuses on assessing the cultural impact of the architectural design of sports facilities in Qatar using the global sustainability assessment system (GSAS) as a sustainability/EIA assessment tool. Most of the sports facilities in Qatar are GSAS-certified at the design and build (D&B) level and are ongoing their operational assessment. Data collection involves desktop and literature review of the current Qatar EIA methods. The findings of this paper include an objective overview of the global sustainability assessment system (GSAS) and its linkage to holistic sustainability. The recommendations involve the inclusion of mixed-methods analysis to integrate the long-lost concept of 'culture' in the realm of sustainability to prove that behind the modern exteriors of these newly-built structures lies a deep culture and a vernacular tradition. This study would be significant in the region and worldwide and a promising overview of utilizing local tools on an international level.

Keywords: GSAS; Sports facilities and stadiums; Mega Sport events; Sustainability; Environmental Impact Assessment

1 Introduction

Mega Sports Events (MSEs) is an international event which has many challenges, including how the city is planning to provide and build enough infrastructure that would take in this large load within a specific period of time. Infrastructure of the city used to host any major international event has many challenges, including designing effective quality and quantity of stadiums for the use of the games, in the case of the Mega Sports Events (MSEs). Achieving sustainable development is a key objective of any city's built environment that aims for excellence. In this regard, Global Sustainability Assessment System (GSAS) is the Middle East and North Africa's (MENA) first performance-based, independent green building certification system., which was designed and developed for evaluating and rating green buildings and infrastructure ((GORD), 2021). Such areas of research could help in filling the gap between practice and theory, by addressing local case studies and finding their position in the global context. Contemporary urban sustainability research frequently focuses on

environmental problems by investigating urban architecture as well as technology that is more efficient and decreases energy waste (Wiedmann, Salama, & Mirincheva, 2014). This paper presents a review of the Qatar EIA method and its cultural and economic value.

1.1 The Evolution and Development of Environmental Impact Assessment Tools

The progress in science and technology had great advantages to humanity, allowing various projects in building and infrastructure to provide people opportunities of liability. However, it began to have negative effects in terms of its environmental impact, as a result of compelling designers and planners to seek and think about alternatives. These adverse effects had made many organizations counter them by introducing laws to protect the environment, which emphasized the significance of Environmental Impact Assessment (EIA). The first country to prioritize EIA was the United States with the National Environmental Protection Act (NEPA) of 1969. However, a large number of countries followed, as was demonstrated in the table earlier.

Columbia was the first developing Latin American country to implement an EIA system in 1974. In Asia and the Pacific, Thailand and the Philippines have long-established EIA protocols, for example, EIA was mandatory in Sri Lanka. Whereas in Africa, the EIA process is continuously growing, despite the fact that several nations, including as Rwanda, Botswana, and Sudan, have some experience with EIA. The European Community mandated EIA in July 1985 (Ramachandra, 2012). And on the universal level, the integration of environmental considerations in development was pinpointed by The World Conservation Strategy in 1980; and in 1987, In accordance with World Bank policy, environmental problems must be addressed as part of a comprehensive economic agenda (Ramachandra, 2012). The general stages of EIA development have emerged in the following sequence, to be a decision-making method and tool around the world:

Table 1: Stages of EIA development

Stage	Development Description
Stage A	The major emphasis is on economic development. Decisions are made based on interest group lobbying and engineering feasibility. No formal accounting.
Stage B	The main concern is still economic development. Traditional cost-benefit analysis. Focus on efficiency criteria and engineering feasibility
Stage C	One of the goals is to promote economic growth. Innovative cost-benefit analysis. The utilization of numerous objectives and discount rates, as well as creative proxy pricing systems.
Stage D	The fundamental goal remains economic development. EIA is primarily concerned with describing the effects of proposals on biophysical processes.
Stage E	Economic development is not the sole objective. EIA with a greater emphasis on socio-cultural as well as bio-physical systems.

What can be observed from the stages above is that the main account of the EIA was the emphasis on economic development and engineering feasibility, followed by cost-benefit analysis. It was later followed by some focus on biophysical processes concerning the natural environment. It was only recently and in the latest stage of EIA development that the socio-cultural aspects of sustainability were taken into account, which shows an interesting transition worth investigating.

1.2 GSAS: Global Sustainability Assessment System

The Global Sustainability Assessment System (GSAS), which was previously called QSAS, is the first performance-based approach for assessing green buildings and infrastructures in the Middle East and North Africa (MENA) area ((GORD), 2021), and the development if its rating schemes is a ground-up approach that provides a smooth integration of the country's requirements with global sustainable goals (Fadli, Sobhey, Asadi, & Elsarrag, 2014). The assessment of the effect of new buildings on the environment and urban fabric is regarded to be the primary objective of QSAS/GSAS. Comparative improvement techniques advocated by QSAS may be the most applicable building design standard in the Gulf area, since it seeks to assess the different components of building design that may impact the natural and built environment (Ferwati, Saeed, Shafaghat, & Keyvanfar, 2019).

Sustainability and Environmental Impact Assessment Techniques have become a buzzword for some time in the industry and academia in architecture and engineering fields. Follow the GORD-GSAS framework developed by the Gulf Organization for Research & Development-GORD through its GSAS 2019 (v.4). The Benefits of the GSAS Approach are that they use a bottom-up approach and therefore allows for optimal integration of environmental measures and regional needs. Therefore it combines the greatest characteristics of the world's most renowned sustainability rating systems. In addition to being performance-based therefore relies on a method that is quantitative and results-oriented rather than feature-oriented. It is also flexible; where individual components can be applied to any project of any size without compromising the system's integrity.

1.3 Research Priorities

EIA's primary goal, as part of any organization's developmental decision-making, is to assist the methodical consideration of environmental concerns (Fadli et al., 2014). Sustainability and resilience are buzz words highly used in urban and environmental studies. However, this trend did not come from anywhere. This suggests and stresses its importance in the global context. The current research priorities in the context of place and time, are addressing the changes happening in that context and finding a way to better understand the most efficient techniques used to respond to them. The challenges are happening worldwide but are specific to a certain period, such as the challenges of Global Warming and the challenges which accompanied the Covid-19 pandemic. Other challenges are more specific and related to a certain place and time only, and are more temporary, such as international events including Qatar 2022 Mega Sports Events (MSEs). Focusing on research priorities could help us navigate the issues which are worth investigation, and also help in determining the most efficient research methods and methodologies to tackle the issues using the limitations of time and resources.

EA's practice can vary widely in quality and rigor. However, its theoretical foundation has grown in complexity and diversity (Mahmoudi, Sayahnia, Esmaeilzadeh, & Azadi, 2018). To address the challenges mentioned earlier, there must be an intellectual framework to follow. Such intellectual frameworks could sometimes manifest in certain architectural movements and buzz words, such as sustainability, adaptability, and resilience. Regarding the focus areas related to the techniques of environmental impact assessment, it includes main three aspects of sustainability, which are the environment, the society, and the economy. Therefore, the main focus of environmentally-friendly built areas is in relating these aspects in designing and evaluating the built environment includes studying energy efficiency and renewable energy, as well as the study of materials choice: building

materials and their relation and impact on building efficiency, sustainability, and resilience. Although the theoretical foundation of Environmental Assessment has become more broad and complex, but its implementation differs considerably in terms of quality and rigor (Mahmoudi et al., 2018). In this regard, Environmental Impact Assessment techniques could be considered from the most important laws and regulations which implement environmental regulations, laws, and other measures to grant environmental approvals in most countries that propose to establish spatial development projects (Alrikabi & Abbas Oudah, 2021).

1.4 The History and Chronological Growth of EIA

To understand the notion of measuring environmental effect more precisely, it is required to understand the concept of environmental impact (Alrikabi & Abbas Oudah, 2021). In dividing the years 1970 to 1999 to three phases. The table below summarizes the evolution and development of EIA in various countries, sorted ascendingly by year of initiation:

Table 2: The Historical Development of EIA Laws in Different Countries Worldwide

Country	Policy Name/ Description	Year	Phase I (1970-1979)	Phase II (1980-1989)	Phase III (1990-1999)
United States	US Environmental Policy	1969-1970	**x**		
USA (California)	California Environmental Quality Act (CEQA)	1971	**x**		
Australia	Environmental Protection (Impact of Proposals)	1974	**x**		
Philippines	Environment Policy	1975	**x**		
West Germany	Cabinet Resolution	1975	**x**		
France	Law on the Protection of Nature	1978	**x**		
Thailand	Environmental Quality	1978	**x**		
China	Environmental Protection Law	1979	**x**		
Canada	Federal Environmental Assessment and Review Process Guidelines Order	1984		**x**	
Japan	Environmental Agency Principles for Implementing EIA	1984		**x**	
India	Environment Protection	1986		**x**	
Sri Lanka	National Environmental	1986		**x**	
The Netherlands	EIA Policy	1986		**x**	
Western Australia	Environmental Protection	1986		**x**	
Malaysia	Environmental Quality (EIA) Order	1987		**x**	
New Zealand	Resource Management	1991			**x**
Vietnam	Environmental Protection Law	1994			**x**
Bangladesh	There was a declaration that all large development projects should undergo EIA. However, there is no specific EIA legislation.	1995			**x**

What could be observed from the table above is the tendency of each part of the world in implementing the laws of environmental impact assessment. The impression of this pattern suggests that the laws and policies regarding preserving the natural environment and its impact on human use of land first started in developed countries, mostly in the Western part of the world, in countries such as the USA and Western Germany (in 1975). Such policies were then shortly followed by Asian-Pacific countries due to high demand in land use and not efficient laws and policies to regulate them, therefore there was a high need

to solve problems related to pollution, urbanization, and population growth while maintaining the natural resources available. These laws were later officially implemented in other parts of the world such as the UK, New Zealand and Bangladesh. At the national level of EU member states, There have been a variety of policies and laws enacted to address and resolve the problem of land consumption, which are issues that are now being considered by the various EU member states. For instance, Germany, the Netherlands, and the United Kingdom place high importance on the environmental politics agenda and discuss methods and mechanisms to prevent the continued expansion of settlement and transit regions (Nuissl, Haase, Lanzendorf, & Wittmer, 2009).

2 Methodology

As Environmental Impact Assessment tools deal with a complex phenomenon that includes human beings and their behaviour, tackling problems could become a challenge since they are ever changing and continuously growing. Therefore, obtaining an objective approach could help researchers identify important issues and to navigate them through quantitative data feasible to be read and interpreted while limiting personal interpretation and intervention, thus creating a framework of analysis that is accurate and consistent. which is a commitment to the significance and practicability of monitoring scientific understanding of any phenomenon, whether it is social, cultural, or other disciplines; thus being able to tackle it into what could be comprehensible. To constantly improve this scientific objective approach, an understanding of the limitations of objective knowledge is essential, because it is continuously changing and growing, therefore prioritizing the need to differentiate credible information from more speculative knowledge claims (Hammersley, 2019).

Following the steps, details, and explanations related to the EIA process, the GORD GSAS training courses site visits, lectures-presentation and guest-lectures wrap-up sessions (DB+O), this study aims to cover the following stages in the EIA of a case study in Qatar:

Stage 1: Screening, Scoping Project Identification.

Stage 2: Impact Identification: Project Investigation.

Stage 3: Assessment: Project Assessment.

Stage 4: Mitigation: Project Analysis.

Stage 5: Mitigation Measures through Recommendation Guideline: Concluding an EIA Summary Which Would Include Mitigation and Development Recommendations in the studies project.

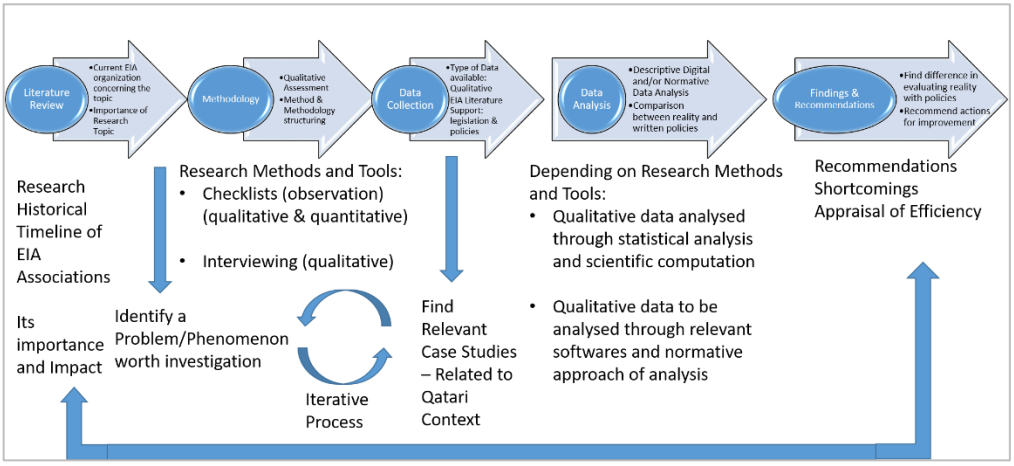


Fig. 1: Research Methodology and Approach

3 Literature Review

3.1 EIA Techniques in Qatar

To focus the research on the local context: the Case of Qatar, we must consider additional information about the geographical environment in which this portion of property is located (Nuissl et al., 2009). That is, to evaluate the "effect at the context level" of land-use transformation. Since it is insufficient to examine a single parcel of land experiencing land-use change, we must consider the whole landscape (Nuissl et al., 2009), rather we must look at it from different scales and dimensions. It is important to mention that complete sustainability in an urban environment is possible if the social, economic, and environmental factors are comprehended in connection to one another. (Wiedmann et al., 2014). Therefore Aside from ecological balance, the viability of urban environments depends greatly on economic expansion and social justice (Wiedmann et al., 2014). A significant challenge for urban governance nowadays is the mediation of multiple landowners' interests and newly constructed legal frameworks (Wiedmann et al., 2014). Building on this statement, analysing the current urban developments in Qatar could help us tackle which major issues are observed with regards to policies of EIA and how can they be solved in the governmental and private sector. More recent studies must be done to survey the urban developments in Doha, however, the picture below can give a glimpse of the priority of urban developments that were most important in 2014, which can be developed and compared to the current situation in 2021 for future studies.

The current focus on urban planning in Doha can be shifted towards everything related to Mega Sports Events (MSEs) in 2022; therefore developing studies concerning this special event could be of high importance. Which could be analysed from various aspects, including the socio-cultural disciplines, since it was started and showed earlier with the different stages encompassing the development of EIA with time, it is observed that previously, the development of sustainability tools did not include social issues and qualitative criteria, therefore future attention must be placed on this, and also backed up with recent studies who also recommend this transition (Fadli et al., 2014). In addition, recent studies show that the built heritage might be seen not just in terms of its individual disciplines pertaining to history and architecture, but also as a systemic, sustainable totality. This reasoning for cultural heritage protection through sustainable discourse views the built environment and space as a whole (Fadli & AlSaeed, 2019). Therefore, cultural values are not apart from environmental and energy-consumption reduction strategies and can go along hand-in-hand. To illustrate this, recent studies focus on the importance of implementing vernacular and local building and planning strategies to show that reusing and incorporating locally accessible building materials and bioclimatic design ideas drawn from existing vernacular buildings into contemporary residential building retrofitting projects can increase knowledge of energy-consumption reduction measures. (Ozarisoy & Altan, 2021).

3.2 Categories Explorations and Development

To state the purpose and rationale of this study, it is important to point that the GSAS Trust manual has the value that is given for Urban Connectivity and Cultural & Economic Value to be from the lowest values, as shown in the figure below. Such low weight for these categories can be concerning for architects who can argue on its significance and importance. Therefore, the purpose of this study is to find the reason for such low values and to find ways to increase their weight in the assessment, in case we find justifiable arguments.

Category	Sub-categories	
Cultural and Economic Value	Heritage and Cultural Identity	Support to National Economy



Fig. 2: GSAS Categories for Design and Build. The below on the right highlights the selected categories for this study

3.3 Cultural and Economic Value

The Cultural & Economic Value category focuses on cultural effects on the design of the built environment as well as contributions to the national economy ((GORD), 2021). In this regard, the architecture of the physical environment may aid in preserving the cultural identity and legacy of a community, where the design expression must be compatible with and interwoven into the existing cultural fabric. Furthermore, the utilization of local resources and skills helps the growth of the national economy ((GORD), 2021). The weight of Cultural and Economic Value has changed from 13% to 8% to 4% within few years. This huge drop in percentage is worth investigating, to know whether the tools of assessment are not functioning or whether cultural and economic value is not from the priority of the stakeholders involved. It is worth mentioning that there is increase in assessing intangible qualitative value in architecture and urban planning in the last few years, which signals an important paradigm shift into qualitative and mixed methods research. Additionally, the affirmation of the significance of intangible values of Cultural Heritage is one of the current goals of the World Heritage List (WHL) (reinforced by the adoption of the UNESCO Convention of 2003), as well as one of the goals of many governments that seek to foster a sense of national or local identity (Mezzino, 2017).

4 Findings

The findings of this case study analysis shows that improvement in assessing the qualitative-related categories might benefit from a mixed-method approach in data collection and analysis. And although this study does not provide the legislative background and way to achieve such outcomes, the recommendations rely on involvement of educational institutions in the process of evaluating and assessing buildings, as a way to include a bottom-up approach more effectively and engaging, especially for young and aspiring professionals.

4.1 Barriers to Sustainability Adaptation

The barriers to sustainability adaptation are many and interrelated. This study focuses on the technical and social factors as a wheel of change to the methodologies used from a technological and cultural point of view, by relying on research done in highly reputed institutions including Qatar University.

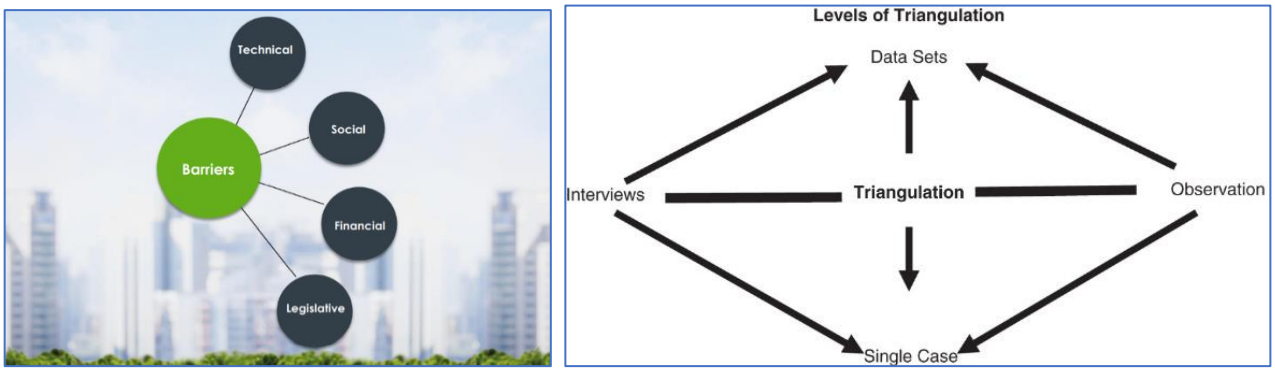


Fig. 3: (Left) EIA Barriers. (Right) Levels and Methods of Triangulation in Mixed-Methods Research

4.2 Conclusive Remarks on Argumentative Recommendations

On GSAS Design and Build (D&B) Toolkit and Calculators, which are considered the methodology in which data is collected and analysed, the results obtained through the case study assessment using the EIA model toolkit GSAS shows that mixed-methods research approach could help validate the data collected and provided more accurate conclusions, as part of the Triangulation Approach in social sciences studies, as shown in Figure 3. And although the EIA techniques confirms to scientific objectivity and quantitative results, this does not mean that qualitative data cannot be converted to quantitative measures. Therefore, providing perspectives for GSAS expansion and enhancement in terms of methodologies used rather than being feature-oriented, which would be an interesting project to be expanded in the future.

Therefore, in the category assessing Urban Connectivity, data collection and analysis could go beyond descriptive analysis, and behavioural mapping, space syntax could be suggested as a methodology, research, and analysis tool in understanding urban connectivity on a deeper and more profound level. In the category of Cultural and Economic Value, it would be worthwhile to include public participation and inclusion in evaluating heritage and cultural values, which can be achieved by collecting data through surveys, questionnaires, and interviews. A straightforward approach to achieve this is by introducing standard surveys templates with qualitative criteria about the heritage and cultural aspects. Revising methods and methodologies used in environmental impact assessment techniques on urban connectivity and cultural value: in the case of stadiums in Qatar would be an important topic to address in future research. Additionally, clearly drawing the distinct lines between what is objectivity and what is subjectivity in the current intellectual realm is of high importance, in order to restructure our perception of what is of objective value and what is of subjective. This attempt is of high value due to the increase number of post-modernist theories which erases the distinction between the two. Therefore, this is an attempt to balance the shifting paradigms and enhancing the academic tone to be rigorously scientific yet culturally sensitive and appropriate.

Acknowledgments

This manuscript was written and built on the work done in the course titled “Techniques of Environmental Impact Assessment MUPD657” taught by Dr. Fodil Fadli in the Master’s program of Urban Planning and Design in Fall 2021 at Qatar University. The authors would like to extend their acknowledgements to the Gulf Organization for Research and Development (GORD), especially Dr. Yousif Alhorr and Dr. Eiman Eliskandarani for their valuable help throughout the research and their generous contribution to the research topic on enhancing EIA in Qatar.

References

Alrikabi, N. K. & Abbas Oudah, A. (2021). Comparative study for Environmental Impact Assessment in Environmental Iraqi and Saudi legislation. *IOP Conference Series. Earth and Environmental Science, 754*(1). doi:http://dx.doi.org/10.1088/1755-1315/754/1/012018

Bhat, B., Bandh, S. & Shafi, S. (2020). *Environmental Management: Environmental Issues, Awareness and Abatement*.

Fadli, F. & AlSaeed, M. (2019). A Holistic Overview of Qatar's (Built) Cultural Heritage; Towards an Integrated Sustainable Conservation Strategy. *Sustainability, 11*(2277). doi:10.3390/su11082277

Fadli, et al. (2014). Environmental impact assessment of new district developments. *WIT Transactions on Ecology on The Built Environment, 142*. doi:10.2495/ARC140441

Ferwati, et al. (2019). Qatar Sustainability Assessment System (QSAS)-Neighborhood Development (ND) Assessment Model: Coupling green urban planning and green building design. *Journal of Building Engineering, 22*, 171–180.

Flick, U. (2018). The SAGE Handbook of Qualitative Data Collection. In. doi:http://dx.doi.org/10.4135/9781526416070.n34

GORD (2021). Website Description and Information. Retrieved from https://www.gord.qa/gsas-trust

Hammersley, M. (2019). From Positivism to Post-Positivism: Progress or Digression? *teoria polityki, 3*, 175–188. doi:10.4467/25440845TP.19.009.10292

Mahmoudi, et al. (2018). Integrating Resilience Assessment in Environmental Impact Assessment. *Integrated Environmental Assessment and Management, 14*(5), 567-570. doi:http://dx.doi.org/10.1002/ieam.4075

Mezzino, D. (2017). *Cultural Built Heritage's Tangible and Intangible Dimensions and Digitalization Challenges.* (Doctor of Philosophy). Carleton University, Ottawa, Ontario.

Nuissl, et al. (2009). Environmental impact assessment of urban land use transitions—A context-sensitive approach. *Land Use Policy, 26*(2), 414-424. doi:https://doi.org/10.1016/j.landusepol.2008.05.006

Ozarisoy, B. & Altan, H. (2021). Systematic literature review of bioclimatic design elements: Theories, methodologies and cases in the South-eastern Mediterranean climate. *Energy & Buildings*. doi:https://doi.org/10.1016/j.enbuild.2021.111281

Ramachandra, T. V. (2012). Principles of Environment Management. Retrieved from Indian Institute of Science: https://nptel.ac.in/courses/120/108/120108004/

Wiedmann, F., Salama, A. M. & Mirincheva, V. (2014). Sustainable urban qualities in the emerging city of Doha. *Journal of Urbanism*. doi:http://dx.doi.org/10.1080/17549175.2013.870088

Cite as: Atour R. & Fadli F., "The Challenges and Future Aspirations of Implementing Global Sustainability Assessment System (GSAS) in the Urban Facilities of Mega Sport Events [MSEs] in Qatar", *The 2nd International Conference on Civil Infrastructure and Construction (CIC 2023)*, Doha, Qatar, 5-8 February 2023, DOI: https://doi.org/10.29117/cic.2023.0138

Climate-cultural Conscious Design Approach to the Post-COVID-19 Built Environment

Mohd Shahrudin Abd Manan
Department of Architecture, Faculty of Design and Architecture, Universiti Putra Malaysia, Selangor, Malaysia
am_shahrudin@upm.edu.my

Nur Dalilah Dahlan
Department of Architecture, Faculty of Design and Architecture, Universiti Putra Malaysia, Selangor, Malaysia
nurdalilah@upm.edu.my

Abstract

The pandemic has accelerated the digital transformation, by enabling current work activities to be done online more efficiently. With the movement control restrictions being lifted, the conventional workspace is no longer stationary. The role of the built environment as a health determinant in the post-COVID-19 era should consider co-mitigation interventions for non-communicable and communicable diseases through physical activity campaigns. This study aims to provide a perspective on the influence of micro-climate-conscious design in various built environments in hot climate countries on physical activity behaviour. The challenges to the social context, the cultural aspects, and the environmental aspects of the cultural-climate design measures in existing built environments are synthesised from analytical themes made in line with the Preferred Reporting Items for Systematic Reviews and Meta-Analyses (PRISMA) standards. The implications for future research are discussed. The finding recognises the importance of spatial heterogeneity in the cultural-climate-conscious built environment design approach. This study provides insights for policymakers and employers to better understand the dynamic roles of built environment perceptions in the post-COVID-19 era in hot climate regions at different intervention levels.

Keywords: Post-Covid-19; Physical activity; Built environment; Multifaceted factors; Cultural-climate; Micro-climate conscious; Health awareness

1 Introduction

The COVID-19 pandemic has reshaped how we occupied our built environment, especially indoor spaces through rigorous climate-controlled application changes. The significance of healthy buildings via ventilation technology improvements and crowd control is vital to eradicate the transmission of the COVID-19 virus. Moreover, due to the movement control restrictions, residential, public and commercial buildings are operating to allow for a higher intake of fresh air and increased natural ventilation.

After a dramatic fall in the number of deaths following the global vaccine roll-out programme in 2021, many nations have welcome a new normal shift that provides hope to revive the economy and most importantly the people's spirit. As a determinant of health, the built environment in this post-COVID-19 era is anticipated to offer a more resilient quality that prioritises communicable disease mitigation interventions. However, the said interventions should not adopt the one-size-fits-all approach and addressed the climate and cultural uniqueness of a local context.

The pandemic has accelerated digital transformation, highlighting the fact that most of the activities

of the current world can be done online more efficiently than by manual operations. The possibility that the working space can expand beyond the office building has been proven through the practice of work-from-home culture enforced during the movement control restrictions. Operating in an increasingly volatile global environment requires conventional workplaces to build resilience and to re-design their operational activities making use of technological innovations. Due to the changing nature of technology, the physical activity behaviour of working adults may improve by expanding their workspace outside of the office building. Building for the post-COVID-19 era means more than just environmental effort, but also planning for co-mitigation interventions of non-communicable diseases (NCD) without compensating people's changing working culture.

Earlier reviews of physical activity suggest that it is the key to combating metabolic syndrome and can be based on complex interactions between individual, environmental and sociocultural factors (Dinu, Pagliai, Macchi & Sofi, 2019; Nunan, Mahtani, Roberts & Heneghan, 2013; Rawlings, 2019; Saunders, Green, Petticrew, Steinbach & Roberts, 2013). However, the unsafe built environment features, a lack of facilities providing healthy food and sensory pollution lead to the emergence of obesogenic environments in the cities. Reports have shown that sedentary office workers comprise the majority of obese individuals worldwide due to a lack of physical activity during work and non-work hours (Addo, Nyarko, Sackey, Akweongo & Sarfo, 2015; Cheng, 2016; Heinen & Darling, 2009; MalayMail, 2016; Nor, 2018).

In another alarming report, 73% of all recorded deaths were caused by NCDs that are evidenced to be preventable by changing one's physical activity behaviour (Economist, 2017; IPH, 2015). Moreover, obtaining a better understanding of obesogenic features of the built environment in hot climate regions by identifying distinct types of neighbourhoods may offer solutions to the growing physical inactivity in this region. That is why built environment design decision-makers need to be aware of the direct and indirect impacts their decisions have on longstanding health and societal welfare, given that they are primarily determined by environmental factors (Fitzpatrick, Shi, Willis, & Niemeier, 2018; Lee, Choi, Lee & Choi, 2019).

As a health determinant, the role of the built environment in the post-COVID-19 era should have equal considerations to reduce the spread of both communicable and non-communicable diseases. The promotion of physical activity both inside and outside of a building is seen as the most sustainable preventive strategy for both types of diseases following the global vaccine roll-out. It is more possible now especially in the hot climate regions thanks to our better understanding of epidemiology and the fourth industrial revolution. In response to that light, this paper aims to discuss through thematic synthesis (i) perspectives on climate-cultural conscious design approach shifts in built environments located in hot climate regions, and (ii) the available interventions designed to reduce the effects of obesogenic environments through physical activity.

2 Methodology

Our search includes four databases (Science Direct, PubMed, ProQuest and Google Scholar) and is made in line with the Preferred Reporting Items for Systematic Reviews and Meta-Analyses (PRISMA) standards. Keywords used are, 'post COVID-19', 'built environment', 'physical activity', 'NCD prevention', 'thermal transient condition perceptions', 'obesogenic environment', and 'walkability'. We include sources with samples consisting of working-age adults (18 to 60 years old) with minimal physical activity in their daily routine from both quantitative and qualitative studies. All included sources are published in peer-reviewed English journals.

Search activities were managed using Endnote X9 software. The thematic synthesis aims to determine to what extent interventions in the current tropical built environment address the factors that predominantly influence sedentary workers' participation in physical activity. By using NVivo 11, the data was organised into three stages, namely, line-by-line coding, descriptive themes coding, and analytical theme coding.

3 Results and Discussion

A total of 1374 titles and abstracts were identified following duplication removal. Subsequently, 1126 records were screened and deemed to be irrelevant to this search based on their article type, title, and abstract. A total of 248 full texts were screened implying 218 excluded records. The outcome of the previous screening was discussed to clarify the interpretation of inclusion criteria. The 30 included studies were further divided into 23 quantitative and seven qualitative or mixed-method studies. Only three records were found with the combined 'post-COVID-19' and 'built environment' keywords. However, all three were not peer-reviewed journal articles. The three themes synthesised are namely, micro-climate conscious design, obesogenic environment, and facilitating behavioural changes. The themes discuss the climate-culture consciousness in built environment design deemed suitable to deter NCD via physical activity. It is well documented that a healthy and active lifestyle helps to boost one's immune system.

3.1 Micro-climate-conscious design

People in hot climate countries preferred thermally cooler and dryer living, commuting and working environments, (Dahlan & Gital, 2016; Krüger et al., 2015; Le Gouais et al., 2020; Vidyarini & Maeda, 2019; Wan Omar et al., 2013). The use of air-conditioning systems has an effect on thermal sensation in the short term, which emphasises the relationship between micro-climatic conditions and the overall bodily thermal response. Behavioural changes such as an increase in perceived alertness and thermal satisfaction among office workers were observed following large indoor-outdoor air temperature differences (Cheung et al., 2017; Vidyarini & Maeda, 2019).

The design of indoor and outdoor spaces with interchangeable transient and stationary conditions elicit behavioural responses, as seen in inhabitants' choices in time spent, clothing insulation and type of activity. The provision of shade and protection from direct solar radiation is essential to promote participation in physical activity (Karuppannan & Sivam, 2013; McKay, 2015; Vidyarini & Maeda, 2019). Willingness to cycle and walk for daily trips is strongly influenced by the midday heat, the availability of trees or shaded pathways, and whether heavy sweating can be avoided or not (Hashim et al., 2017; Vidyarini & Maeda, 2019; Wan Omar et al., 2013). With considerable outdoor street designs, such as covered pathways, rain shelters and covered street furniture, inhabitants are prepared to participate in physical activity but only within a reasonable distance (Ahmed, 2003). In Bahrain, where the humidity level is lower than those in Malaysia, Singapore and India, engaging in walking during light rain is a pleasant experience (Silva & Akleh, 2018).

In Singapore, the use of an apartment void deck is preferred by residents over neighbourhood open spaces. This is because the former spaces are covered, equipped with facilities, thermally comfortable with cross ventilation, and well-lit, making them suitable for social activities and studying while being connected to main pedestrian pathways (Karuppannan & Sivam, 2013). Micro-climate-conscious designs are commonly complemented with comprehensive pedestrian networks located in mixed land-use development and within close distances of the inhabitants' homes and workplaces, making them ideal for walking and cycling (Adlakha et al., 2016; Dahlan & Kurmanbekova, 2019; Pinelo

Silva & Akleh, 2018 Hashim et al., 2017). Wider streets were interpreted as attractive, safe and inviting given that pedestrians were seen to stay longer in them and engage in more physical activity compared to narrower streets (Ahmed, 2003; Richards et al., 2020; Wijesundara & Wijekoon, 2017).

3.2 Obesogenic environment

The rise in obesity is associated with activities that have to do with the outdoors such as commuting for work and access to food stores, restaurants, sports facilities, health facilities and parks, all within the circulation buffer zone in the neighbourhood (Adlakha et al., 2016; Aizawa, 2019; Loo et al., 2017; Matozinhos et al., 2015; McKay, 2015; Yu et al., 2017). Nevertheless, the role of health and disease prevention even in low- and middle-income countries has a concordant relationship with physical activity despite built environment characteristics such as land slope, greenness, built-up and intersection density (Valson et al., 2019). Other authors (Arundhana, 2018; Dahly, 2013; Le Gouais et al., 2020; Matozinhos et al., 2015; Sarkar et al., 2018; Valson et al., 2019) have advised against a 'one-size-fits-all' method to mitigate the rising incidences of NCDs, thus calling for prioritisation of physical activity intervention based on local spatial heterogeneity.

The downstream interventions (i.e. reducing the use of air conditioning, wearing clothing appropriate for warm tropical weather, and controlling the air pollution level) mainly reflect people's likelihood of participating in physical activity when exposed to pro-environmental conditions while at home and work (Dahlan & Gital, 2016; Dahlan & Kurmanbekova, 2019; Tan et al., 2020). In terms of environmental quality, physical activity is associated with practices that comply with sustainable development goals (SDGs) through a reduction in traffic congestion and the level of air pollution (Rother, 2020; Wan Omar et al., 2013). Some authors second the notion that the walkable neighbourhood also contributes as a stress relief mechanism and extended exposure to features may reduce common health ailments such as hypertension (de Keijzer, 2019; Sarkar et al., 2018; Wan Omar et al., 2013).

3.3 Facilitating Behavioural Changes

Temporary urban characteristics defined by activities and structural and sensory interventions at shopping streets in Sri Lanka are strongly relevant to the human scale, walkability and mass, density and scale of the place, as documented by (Wijesundara & Wijekoon, 2017). Inhabitants of busy tropical cities such as Kuala Lumpur and Singapore also indicated that a variety of activities and facilities in public spaces is crucial for encouraging physical activity (Karuppannan & Sivam, 2013). The creation of mixed land-use developments and a continuous pedestrian network has promoted more utilitarian physical activity, albeit facilitating place-making processes, as reported in Bahrain (Pinelo Silva & Akleh, 2018), Malaysia (Hashim et al., 2017) and Singapore (Richards et al., 2020). The organization of street interventions fuels pedestrians' excitement and attempts to pursue pleasure and thus also serves as a stress release mechanism after a hard day's work (Alba & Williams, 2013). These issues are indicators of work-life balance, namely, adjustments to long working hours, ample leisure and personal care time, and a short commute time (Economist, 2017; OECD, 2011).

Reports on upstream interventions in many cities in both developed and developing countries, including Ghent, Hamburg, Helsinki, Madrid, Bogota, Brussels, Chengdu, Hyderabad, Salaya, Putrajaya, and Milan, urge the public to reduce their private car and motorcycle trip through policies set by the health ministry, transportation ministry and local governments. This can be done by engaging in any of the active travel modes (i.e., walking, cycling and public transportation) to increase health benefits, reduce traffic fatalities and air pollution exposure to provide a seamless and accessible

(i.e., affordable and universally designed) travel experience (Fraszczyk et al., 2019; Hashim et al., 2017; Thondoo et al., 2020). Despite resistance and a slow response from the public, the outbreak of COVID-19 has shown that an extreme reduction in motorization can become a reality (Thondoo et al., 2020).

4 The Implication

The authors acknowledge the influence of built environment variables such as travel time, safety (i.e., crime rate and traffic congestion), and health via environmental quality (i.e., air quality, heat stress and noise pollution) with the three types of physical activity behaviours commonly practised during daily city trips, namely, commuting to work, running errands and participating in leisure activities. Shortcomings or difficulties related to any of these variables have been reported to influence people to drive their motor vehicles. The workplace neighbourhood is a good example of a built environment that possesses all three built environment variables. The main attributes of workplace neighbourhoods, such as the ability to commute to work by walking and bicycling and the degree to which designated parking areas are available to workers, have been observed in planned cities, specifically Putrajaya in Malaysia (Hashim et al., 2017) and Singapore (Karuppannan & Sivam, 2013). Moreover, organic workplace-built environments can be seen in Chennai (Adlakha et al., 2016) and Kerala in India (Valson et al., 2019), mid to western regions of Indonesia (Arundhana, 2018), Cebu Province of the Philippines (Dahly, 2013) and Brazilian cities (Matozinhos et al., 2015).

The intervention reviewed in this theme mainly aims to understand the changes in people's response to dynamic environmental factors that can lead to healthy physical activity behaviour. Assessment of the reciprocal and dynamic relationships between people and places has been done using qualitative and quantitative methods, thus leading to a variety of physical activity intervention types suitable for each measured population. People's judgement and interpretations of the environment that lead to changes in physical activity patterns may take time. Currently, individual psycho-physical investigations show more objective and specific responses to micro-climatic and built environment characteristics. Moreover, an assessment of the individual's interpretation of his environment (i.e. workplace, home and neighbourhood) can be translated into spatial mapping to identify the effectiveness of physical activity design intervention at the street level. Both the interpretation and psycho-physical responses of the people should be considered for physical activity participation, thus warranting a built environment design that is responsive to the micro-climate and socioeconomic status of the population.

Sedentary office-working adults in the hot climate countries have shown similar health risk factors as their temperate-country counterparts. Uniform neutral operative temperatures in the workplace and a high-calorie diet contribute to low metabolism, thus leading to imbalances in energy expenditure. The authors emphasise that the spatial heterogeneity in high- and low-income communities causes a lack of localised influences on environmental determinants that are obesogenic and disparate in health information.

Consideration of providing flexible working hours by having intermittent break periods, coupled with a low-temperature difference between the indoors and outdoors will reduce workers' sedentary behaviour while indoors. There are many reviews on people's behaviour towards their built environment (Angkurawaranon, Jiraporncharoen, Chenthanakij, Doyle & Nitsch, 2014; Malambo, Kengne, De Villiers, Lambert & Puoane, 2016; Brian E Saelens & Handy, 2008; Tucker & Gilliland, 2007), but little has been said about changing work flexibility in hot-climate countries, where it can

be challenging to workers who are acclimatised to the air-conditioned indoor spaces of their workplace.

More creative and critical strategies in terms of self-reported status on health awareness and micro-environment adaptability data collections are needed to educate the public on the health benefits of physical activity. Mechanisms to promote physical activity behaviours should be designed based on downstream-level data gathered through a mixture of climate-cultural monitoring and ethnographic interviews. Discrepancies in the inhabitants' feedback between built environments in tropical and temperature are anticipated and should be adopted in future built environment health determinant policies.

The whole population intervention approach for physical activity in the tropical built environment can be summarised as shown in Figure 1. The two-way flows (i.e., up-mid and mid-down streams) show the occurrences of evidence-based information dissemination, which is commonly collected from the lower streams and used as a decision-making support for upstream-level intervention designs. However, appropriate methodologies are required through adaptation and refinement of the traditional research methods with a focus on the multifaceted factors discussed. The authors acknowledged the sentiment of local inhabitants in response to their microenvironment climate and physical conditions, and culture when deducing their behaviour towards physical activity. Emphasis on place-level prioritisation and individual adaptability to the environment suggests the importance of recognising spatial heterogeneity as physical activity triggers especially at the midstream and downstream levels.

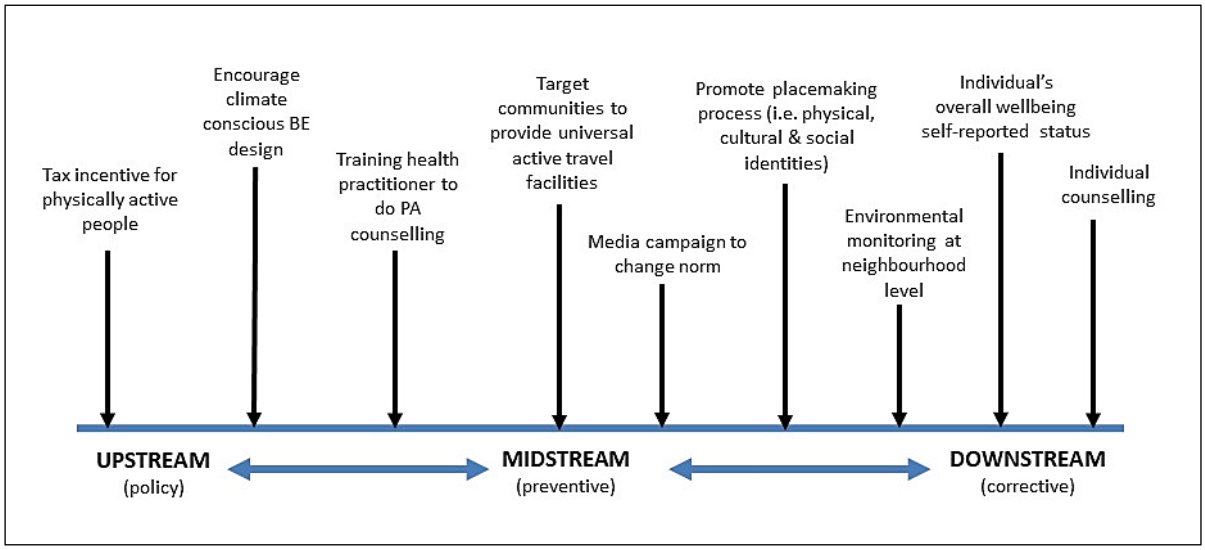


Fig. 1: Whole population physical activity intervention.
(BE: built environment; PA: physical activity)

5 Conclusion

This study aims to discuss the current literature regarding the participation in physical activities in response to their micro-climate conscious design, obesogenic environment and facilitating behavioural changes in the post-COVID-19 hot climate regions built environment. Like others, we noted that few evaluative studies that articulate environmental changes, particularly built environments act to promote physical activity or call for greater consideration for place-level prioritisation, which we found to be a more promising intervention strategy than its 'one-size-fits-all' counterpart. In addition, we deduced that 'place-level prioritisation' through multifaceted factors

encourages traits unique to the daily lives of the majority of people in hot climate built environments. Our findings suggest that downstream and midstream delivery levels of intervention will most likely empower the public to participate in physical activity in their daily lives.

References

Addo, et al. (2015). Prevalence of obesity and overweight and associated factors among financial institution workers in Accra Metropolis, Ghana: a cross sectional study. *BMC Research Notes, 8*, 599. doi:10.1186/s13104-015-1590-1

Adlakha, D., Hipp, J. A. & Brownson, R. C. (2016). Neighborhood-based differences in walkability, physical activity, and weight status in India. *Journal of Transport & Health, 3*(4), 485-499. doi:https://doi.org/10.1016/j.jth.2016.10.008

Ahmed, K. S. (2003). Comfort in urban spaces: defining the boundaries of outdoor thermal comfort for the tropical urban environments. *Energy and buildings, 35*, 103-110.

Aizawa, T. (2019). Urban developments and health: Evidence from the distributional analysis of biomarkers in China. *SSM - Population Health, 8*, 100397. doi:https://doi.org/10.1016/j.ssmph.2019.100397

Alba, J. W. & Williams, E. F. (2013). Pleasure principles: A review of research on hedonic consumption. *Journal of Consumer Psychology, 23*(1), 2-18. doi:https://doi.org/10.1016/j.jcps.2012.07.003

Andi Imam Arundhana, A. P. U., Muqni, A. D. & Thalavera, M. T. (2018). Regional differences in obesity prevalence and associated factors among Indonesian adults: Indonesia Basic Health Research 2007 and 2013. *Malaysian Journal of nutrition, 24*(2), 193-201.

Angkurawaranon, et al. (2014). Urbanization and non-communicable disease in Southeast Asia: a review of current evidence. *Public Health, 128*(10), 886-895. doi:https://doi.org/10.1016/j.puhe.2014.08.003

Cheng, N. (2016, 2 April 2016). Putrajaya Tops Obese List, Nation. *The Star*.

Cheung, et al. (2017). Longitudinal assessment of thermal and perceived air quality acceptability in relation to temperature, humidity, and CO2 exposure in Singapore. *Building and Environment, 115*, 80-90. doi:https://doi.org/10.1016/j.buildenv.2017.01.014

Dahlan, N. D. & Gital, Y. Y. (2016). Thermal sensations and comfort investigations in transient conditions in tropical office. *Applied Ergonomics, 54*, 169-176.

Dahlan, N. D. & Kurmanbekova, M. (2019). Impact of Built Environment on Thermal Perceptions among office Workers in Tropical Low Carbon City: A Physical Inactivity Awareness Assessment. *Alam Cipta, 8*(2), 57-73.

Dahly, et al. (2013). The spatial distribution of overweight and obesity among a birth cohort of young adult Filipinos (Cebu Philippines, 2005): an application of the Kulldorff spatial scan statistic. *Nutrition & Diabetes, 3*(7), 1-8. doi:10.1038/nutd.2013.21

de Keijzer, et al. (2019). Long-term exposure to greenspace and metabolic syndrome: A Whitehall II study. *Environmental Pollution, 255*, 113231. doi:https://doi.org/10.1016/j.envpol.2019.113231

Dinu, et al. (2019). Active commuting and multiple health outcomes: a systematic review and meta-analysis. *Sports Medicine, 49*(3), 437-452.

Economist, T. (2017). *Tackling obesity in ASEAN: Prevalence, impact, and guidance on interventions*. Retrieved from Asian Roundtable on Food Innovation for Improved Nutrition:

Fitzpatrick, et al. (2018). Obesity and place: Chronic disease in the 500 largest U.S. cities. *Obesity Research & Clinical Practice, 12*(5), 421-425. doi:https://doi.org/10.1016/j.orcp.2018.02.005

Fraszczyk, A., Weerawat, W. & Kirawanich, P. (2019). Commuters' Willingness to Shift to Metro: a Case Study of Salaya, Thailand. *Urban Rail Transit, 5*(4), 240-253. doi:10.1007/s40864-019-00113-3

Hashim, S. F., Hashim, H. & Shuib, K. B. (2017). Residents' Perspective on Cycling as an Option for Transportation in Putrajaya. *Planning Malaysia Journal 15*(2).

Heinen, L. & Darling, H. (2009). Addressing Obesity in the Workplace: The Role of Employers. *The Milbank Quarterly, 87*(1), 101-122. doi:10.1111/j.1468-0009.2009.00549.x

IPH. (2015). *National Health and Morbidity Survey 2015 (NHMS 2015).* (Vol. 2). Kuala Lumpur: Institute for Public Health.

Karuppannan, S. & Sivam, A. (2013). Comparative analysis of utilisation of open space at neighbourhood level in three Asian cities: Singapore, Delhi and Kuala Lumpur. *URBAN DESIGN International, 18*(2), 145-164. doi:10.1057/udi.2012.34

Krüger, E., Drach, P. & Bröde, P. (2015). Implications of air-conditioning use on thermal perception in open spaces: A field study in downtown Rio de Janeiro. *Building and Environment, 94*, 417-425. doi:https://doi.org/10.1016/j.buildenv.2015.07.024

Le Gouais, A., Govia, I. & Guell, C. (2020). Challenges for creating active living infrastructure in a middle-income country: a qualitative case study in Jamaica. *Cities & Health*, 1-12. doi:10.1080/23748834.2020.1767950

Lee, et al. (2019). P70 Association between built environment and cardiovascular diseases. In: BMJ Publishing Group Ltd.

Loo, et al. (2017). Association between neighbourhood walkability and metabolic risk factors influenced by physical activity: a cross-sectional study of adults in Toronto, Canada. *BMJ open, 7*(4), e013889.

Malambo, et al. (2016). Built Environment, Selected Risk Factors and Major Cardiovascular Disease Outcomes: A Systematic Review. *PloS one, 11*(11), e0166846. doi:10.1371/journal.pone.0166846

MalayMail. (2016, 3/2/2016). Nearly half Malaysia's population overweight or obese, Health Minister says. *Malay Mail*.

Matozinhos, et al. (2015). Neighbourhood environments and obesity among adults: a multilevel analysis of an urban Brazilian context. *Preventive medicine reports, 2*, 337-341.

McKay, et al. (2015). Associations between active travel and adiposity in rural India and Bangladesh: a cross-sectional study. *BMC Public Health, 15*, 1087. doi:10.1186/s12889-015-2411-0

Nor, et al. (2018). An update on obesity research pattern among adults in Malaysia: a scoping review. *BMC women's health, 18*(Suppl 1), 114-114. doi:10.1186/s12905-018-0590-4

Nunan, et al. (2013). Physical activity for the prevention and treatment of major chronic disease: an overview of systematic reviews. *Systematic reviews, 2*, 56-56. doi:10.1186/2046-4053-2-56

OECD. (2011). *How's Life?: Measuring well-being*. Retrieved from https://www.oecd-ilibrary.org/economics/how-s-life_9789264121164-en

Pinelo Silva, J. & Akleh, A. Z. (2018). Investigating the relationships between the built environment, the climate, walkability and physical activity in the Arabian Peninsula: The case of Bahrain. *Cogent Social Sciences, 4*(1), 1502907. doi:10.1080/23311886.2018.1502907

Rawlings, et al. (2019). Exploring adults' experiences of sedentary behaviour and participation in non-workplace interventions designed to reduce sedentary behaviour: a thematic synthesis of qualitative studies. *BMC Public Health, 19*(1), 1099. doi:10.1186/s12889-019-7365-1

Richards, et al. (2020). Demographic biases in engagement with nature in a tropical Asian city. *PloS one, 15*(4), e0231576. doi:10.1371/journal.pone.0231576

Rother, H. A. (2020). Controlling and preventing climate-sensitive noncommunicable diseases in urban sub-Saharan Africa. *Science of The Total Environment, 722*, 137772. doi:https://doi.org/10.1016/j.scitotenv.2020.137772

Saelens, B. E. & Handy, S. L. (2008). Built environment correlates of walking: a review. *Medicine and science in sports and exercise, 40*(7 Suppl), S550.

Sarkar, C., Webster, C. & Gallacher, J. (2018). Neighbourhood walkability and incidence of hypertension: Findings from the study of 429,334 UK Biobank participants. *International Journal of Hygiene and Environmental Health, 221*(3), 458-468. doi:https://doi.org/10.1016/j.ijheh.2018.01.009

Saunders, et al. (2013). What are the health benefits of active travel? A systematic review of trials and cohort studies.

PloS one, 8(8), e69912.

Tan, et al. (2020). Association between microenvironment air quality and cardiovascular health outcomes. *Science of The Total Environment, 716*, 137027. doi:https://doi.org/10.1016/j.scitotenv.2020.137027

Thondoo, et al. (2020). Participatory quantitative health impact assessment of urban transport planning: A case study from Eastern Africa. *Environment International, 144*, 106027. doi:https://doi.org/10.1016/j.envint.2020.106027

Tucker, P. & Gilliland, J. (2007). The effect of season and weather on physical activity: A systematic review. *Public Health, 121*(12), 909-922. doi:http://dx.doi.org/10.1016/j.puhe.2007.04.009

Valson, et al. (2019). Spatial Clusters of Diabetes and Physical Inactivity: Do Neighborhood Characteristics in High and Low Clusters Differ? *Asia Pacific Journal of Public Health, 31*(7), 612-621. doi:10.1177/1010539519879322

Vidyarini, E. & Maeda, T. (2019). Effects of Air Temperature Step Changes on Thermal Perception and Perceived Arousal in an Actual Environment under Hot-Humid Climate Conditions. *Journal of the Human-Environment System, 22*(1), 7-15. doi:10.1618/jhes.22.7

Wan Omar, W. R., Patterson, I. & Pegg, S. (2013). Using a Health Belief Model to investigate the walking behaviour of residents living in Kuala Lumpur, Malaysia. *Annals of Leisure Research, 16*(1), 16-38. doi:10.1080/11745398.2013.769422

Wijesundara, J. & Wijekoon, N. (2017). Transitory Urban Interventions for Effective Place making in Shopping Streets: Case of Pettah in Sri Lanka. *Cities People Places: An International Journal on Urban Environments, 2*(1), 10-25.

Yu, et al. (2017). Neighborhood walkability and hospital treatment costs: A first assessment. *Preventive Medicine, 99*, 134-139. doi:https://doi.org/10.1016/j.ypmed.2017.02.008

Cite as: Abd Manan M.S & Dahlan N.D., "Cultural-climate Conscious Design Approach to the Post Covid-19 Built Environment", *The 2nd International Conference on Civil Infrastructure and Construction (CIC 2023)*, Doha, Qatar, 5-8 February 2023, DOI: https://doi.org/10.29117/cic.2023.0139

Resilience Urban Planning from Climate Change Point of View: A Case Study for Qatar

Husam A. Samman
Ministry of Municipality, Doha, Qatar
hsamman@mm.gov.qa

Ruzanna Ahmed Zahir
Ministry of Municipality, Doha, Qatar
RAhmad@mm.gov.qa

Abstract

Qatar is a Middle Eastern country characterised by an arid climate. Key challenges in urban planning in general are uncertainties of the future, *especially when it comes to water resources and specifically storm water*. While textbook of urban planning concentrates the most on social and economic factors that promote prosperity for the communities, in many arid areas the concept of planning from a climate change and specially storm water might be looked at as the least important in the priority list of criteria required for a successful and practical urban planning. This situation poses a challenge to urban planners in general, especially with limited available standards and criteria of planning from a storm water and climate change perspectives. This paper intends to shed some light on the above-mentioned challenges of planning from storm water perspective and provide a more practical approach to urban planning from climate change perspective, and aims at providing the urban planning community with the basics of optimizing the challenge of rainfall and possible flooding in such an arid area like Qatar.

Keywords: Climate change; Storm water; Sea level rise; Urban planning; Qatar

1 Introduction

Changes to climate change in terms of changes to rainwater intensity and the sea level rise, and the consequences of poor planning of flood mitigation measures are not uncommon in the arid region of Middle East. For example, a devastating flood in Nov 2009 in Jeddah, Saudi Arabia caused deaths of over 100 people and major destruction of urban infrastructure (Al-Saud, 2010). Furthermore, the Gulf countries including Qatar, experienced unusual rainfall events in 1995 causing severe flash floods (Membery, 1997). Heavy rainfall and major flooding were also reported in 2015 across the Gulf regions including Qatar, Oman and Saudi Arabia (Al Saud, 2010; Al-Shaqsi, 2010; Subyani, 2011; Al-Rawas & Valeo, 2015). In the most recent years, multiple unexpected rainfall events have been encountered in the State of Qatar. And although the investment in Infrastructure in the State of Qatar is unexceptional in magnitude, it is still challenged by dealing with rainfall events that exceed expectations and thus pose some risks specially in the built environment.

The main challenges in urban planning in arid regions from a storm water point of view include lack of recorded available watercourses, rainfall, infrequent occurrence of floods and lack of defined storm water catchment (Xao Lin, 1999; Vivoni et al., 2006; Sen, 2008; Morin et al., 2009). The accurate identification of historical water courses and proper characterization of storm water catchment, in

addition to the set of available rainfall and flood data together with sea level - tidal station – data is an important first step for comprehensive watershed management.

A number of hydrological modelling approaches have been adopted to estimate design floods in arid regions (e.g., El-Hames & Richards, 1998; Jothityangkoon et al., 2001; Foody et al., 2004; Sevinç & Sen, 2007; Bracken et al., 2008). However, the calibration of rainfall runoff models in arid regions is problematic due to the lack of recorded rainfall and flood data, and simple empirical or semi-empirical models may perform equally well or even better than the complex modelling approaches (McIntyre et al., 2007). Numerous storm water and flood studies have been carried out in various parts of the world recently utilizing GIS based methods (e.g., Soussa et al., 2010; Metwaly et al., 2010; Fernandez & Lutz, 2010). These GIS based methods can also be applied to storm water management in the arid region of the Middle East.

This paper focuses on properly incorporating storm water into urban planning in Qatar. There have been limited holistic storm water studies in the Gulf region; in terms of storm water studies, there is no known significant rainwater study that linked its output with the urban planning community in Qatar until now. The Ministry of Municipality had carried out multiple studies related to rainfall and runoff, a national flood project, and an outfall assessment project in Qatar. The paper aims at providing the urban planning communities with some guidelines regarding better utilization of the outputs of the watershed and flood studies. In addition, introducing the major storm water watershed elements (including storm water catchments, major wadi lines, major natural depression areas), in addition to depth and risk of flood. Finally, it will also discuss the potential changes in rainfall intensity and possible location that might be affected by sea level rise from climate change point of view. Hence, provide a practical way to incorporate them into the urban planning, therefore providing a more climate change resilient planning for the built environment in general, coupled with added value planning from socioeconomic and environmental perspective to meet sustainability goals.

2 Study Area

The study area for this paper will focus on Qatar in general, (Figure 1) with an estimated area of 11,571 km^2, but will also include two pilot study areas with smaller size to better illustrate the objectives.

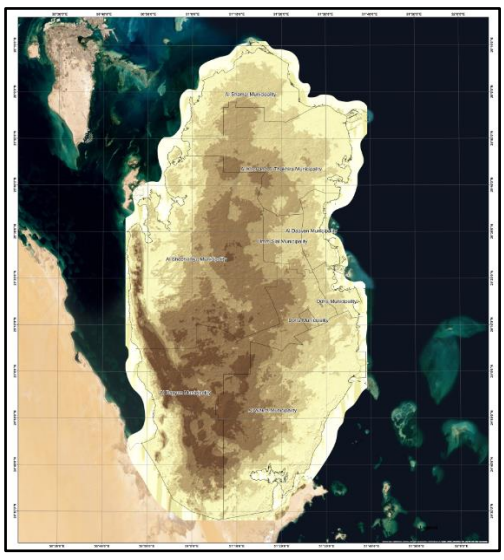


Fig. 1: Location map of Qatar

3 Data Collection and Assessment

Most of the data for this study were obtained from the Ministry of Municipality (MM), Qatar. An assessment was undertaken to identify any significant data gaps and to determine its implication on storm water modelling and mapping outcomes of this study. The objectives of data collection were to:

- Assess the level of detail and availability of existing topographic and bathymetric data to develop a Digital Elevation Model (DEM) of the study area.
- Collect and review available historical rainfall and flood data available, to calibrate and parametrize hydrologic model.
- Determine the availability and reliability of existing GIS information.

In relation to the most 2017-2018 current terrain data, the team has processed the DEM available to better fit the hydrological and watershed analysis. The study has also utilized the output of the Qatar flood study finalized by Ministry of Municipality together with available tidal station sea level rise analysis as part of a climate change analysis.

The rainfall runoff processes in arid regions are characterized by flat topography, poorly defined overland flow paths, poor vegetation and high transmission losses (Pilgrim et al., 2009).

The average annual rainfall in Qatar is 77.9 mm (Mamoon et. al 2016). The climate of Qatar is dominated by mild winters and very hot summers. Rainfall mainly occurs in the period from October to May, with significant inter-annual variability (Batanouny, 1981). Westerly disturbances are considered to be the main source of rainfall in Qatar.

4 Methodology

4.1 Overview of Methodology

The focus of this paper is to present the outputs of the watershed analysis and shed the lights on the importance of utilizing them in future urban planning efforts in general. The study will present the major water courses within the watershed under study, including main boundaries of catchment areas and the major Wadis within. In addition, it will present the natural depressed areas that would be potential storm water accumulation points, finally through incorporating the major areas of potential flood currently under future climate change scenarios, the paper will present the urban planning community with solid guidelines for better planning the future including the climate change scenario.

4.2 Model Setup

4.2.1 Preparing the Digital Terrain Model

The first step in carrying out an accurate watershed analysis is to prepare the topographical data, mainly the digital elevation model (DEM), by conducting a DTM analysis to produce the elevation topography model from LIDAR data set of 2017.

The available data was in point cloud format and further analysis is required to create the Digital Terrain Model (DTM). Accordingly, the team has carried out Post Data Processing phases by manipulating the LIDAR point cloud until creating seamless Digital Terrain Model (DTM) (Figure 2). An algorithm has been created to speed up the surfacing and interpolation analysis. The interpolated DTM is derived from the LIDAR point cloud in shapefile format and further involved mosaicking process which require approximately 13,152 tiles to create a seamless DTM for the whole Qatar. The team also generated two analyses from the DTM which are as follows (Figures 2 and 3).

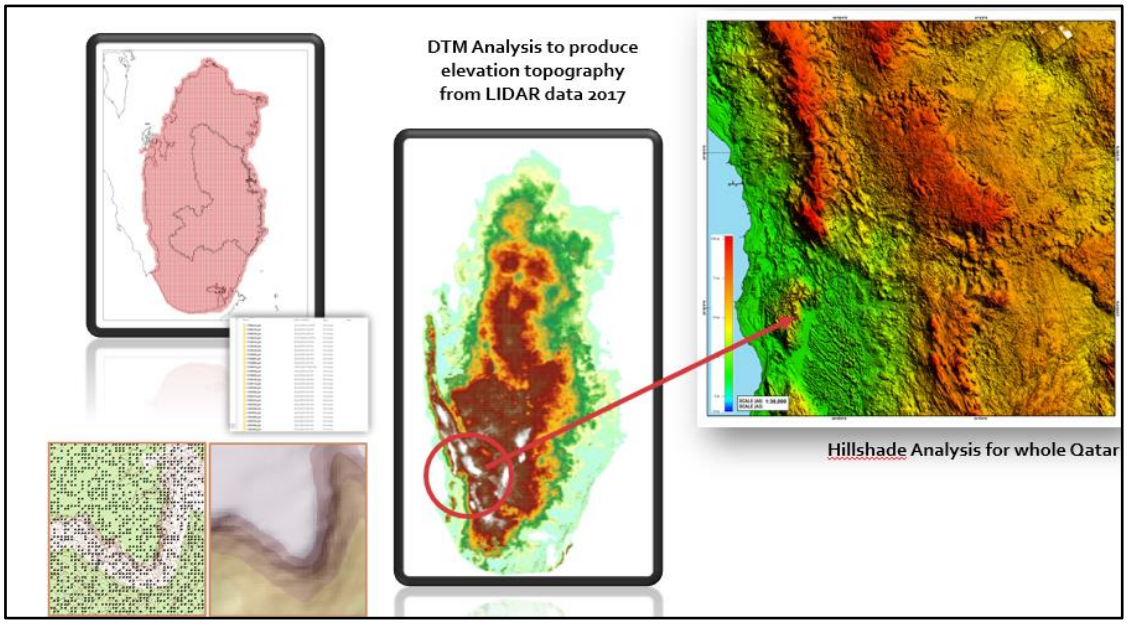


Fig. 2: Creating the digital Terrain model from Lidar Data set

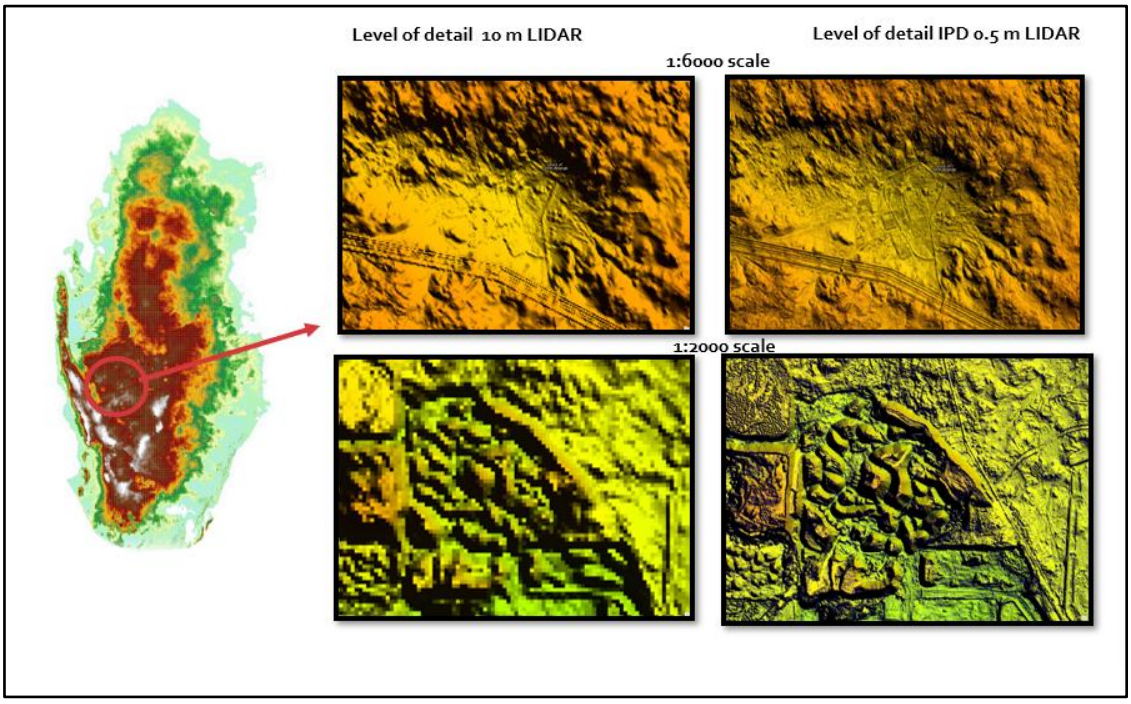


Fig. 3: Level of details after processing the elevation data

4.2.2 Conducting the Watershed Analysis

The second step in watershed analysis is to establish the main watershed and sub-catchments. Due to the flat nature of Qatar, the assessment considered various factors to design the hydrological level of the catchments to better suited the planning process. Figure 4 herein below provide more details on the steps taken.

Watershed area was delineated using the latest Digital Terrain Model that only consider the Qatar natural topographic and ground elevation. ArcGIS 10.7.1 and Global Mapper software were utilized to perform this watershed delineation. The hydrologic analysis tools were utilized for watershed delineation, flow accumulations and flow length. Figure 4 shows the workflow of how the watershed delineated.

The Sub-catchments were delineated using an automated ArcGIS tool (Arc Hydro). Sub-catchment slopes were calculated based on the study area DEM and the longest flow path lines generated using Arc Hydro. Catchment slopes ranged from 0.2% to 29.5% with an average slope of 3.02%, which is considered to be relatively flat. Manning's 'n' values for each sub-catchment were determined using an area weighted approach and ranged from 0.03 to 0.08. Fraction imperviousness for the sub-catchments ranged from 0.01 to 0.95 with 62% of sub-catchments being highly impervious with fraction impervious values in the order of 0.75 to 0.95 (a fraction value of 1.0 indicates 100% imperviousness).

A hydrologic model of the catchments was developed using XP-RAFTS software to estimate runoff hydrographs at the outlet of sub-catchments for a range of design storm events. Rain on grid hydraulic modelling was undertaken using the 2D hydraulic model developed, the rainfall runoff process was simulated through the application of design rainfall events directly across the detailed 2D hydraulic model domain. The 10% and 1% AEP design flood events were again assessed in the 'rain on grid' hydraulic model through the application of design rainfall intensities and temporal patterns as model boundary conditions. Rainfall loss and infiltration rates were initially set to a base case of zero to obtain conservative results. For the 1% AEP design event, a sensitivity analysis was undertaken on the rainfall loss and infiltration rates based on pre-set scenarios.

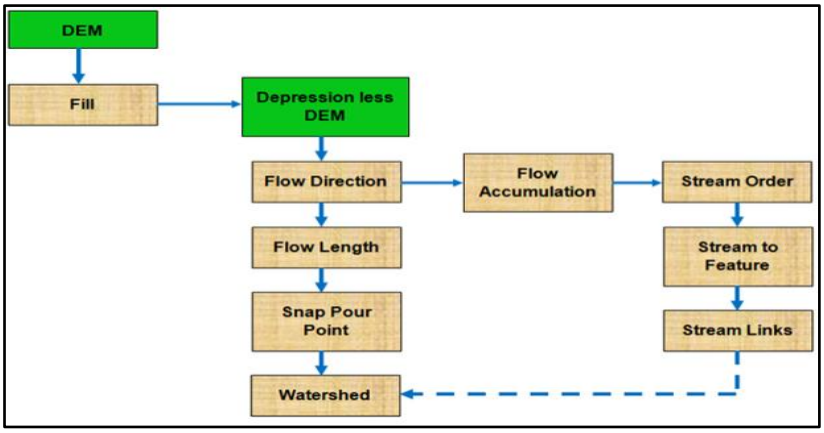


Fig. 4: Watershed Delineation Workflow

The Digital Elevation Model being utilized is a very high resolution elevation models which is possible to extract small wadis. In order to map the watershed area correctly, it is necessary to remove errors and artificial sinks in the Digital Elevation Model where pre-processing is required to allow water movement across the digital landscape. In addition, LIDAR data 2017 Ortho Image from CGIS with the resolution of 0.2m were used for visual assessment of the delineated watershed.

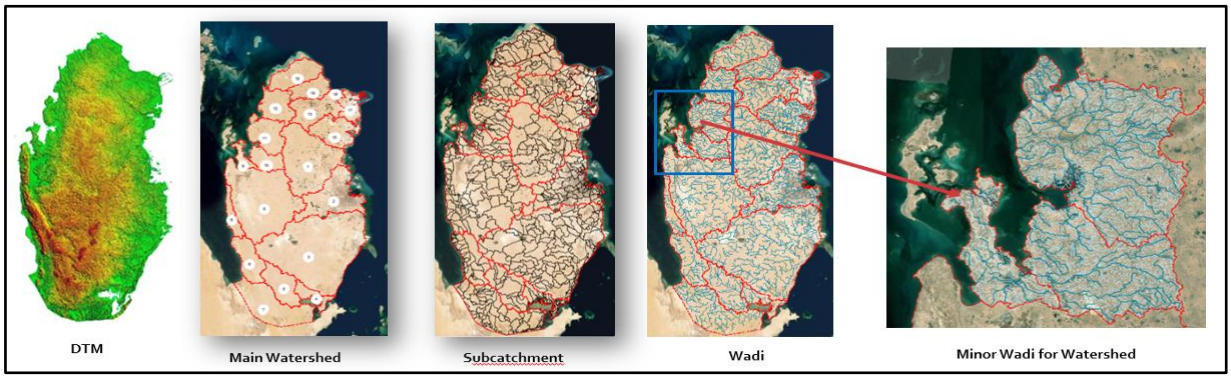


Fig. 5: Output of Watershed Analysis

4.2.3 Depression Area Using LIDAR

Depression area were identified from GIS analysis using an algorithm that extract sink information from the latest 2017 LIDAR data. These depressions may contribute to pinpoint the suitable location for natural wetland design as well as hydrologic connectivity to store the runoff water. Somehow the depth of the depression area requires elevation information or a contour data. Figure 6 shows the mechanism of nested depression that can be design as storm water storage areas.

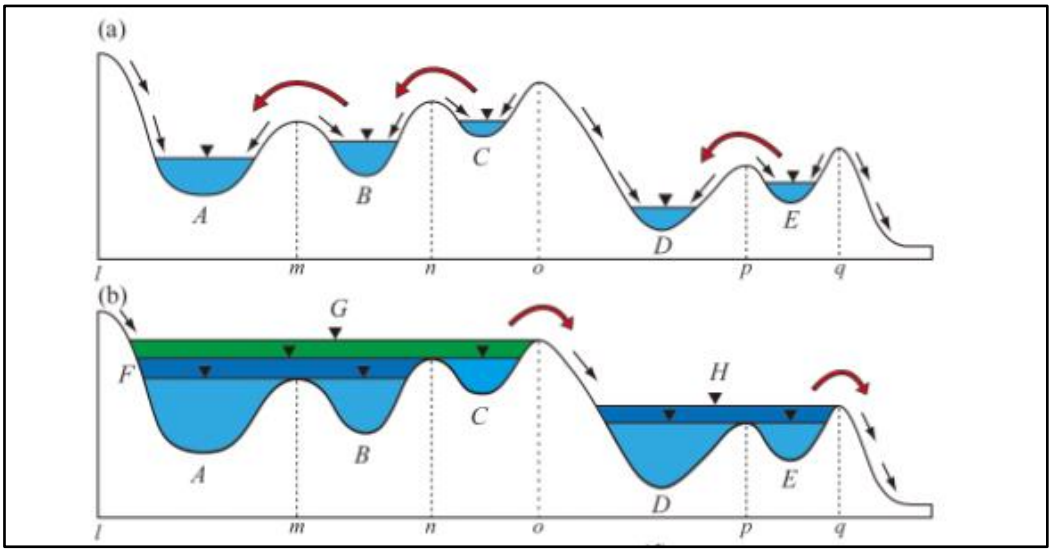


Fig. 6: Mechanism of Nested Depression area

4.2.4 Setting up the Hydrological Model - Rain on Grid Hydraulic Modelling Approach

A hydrologic model was established to estimate runoff hydrographs for a range of design storm events at key locations across the study area. Design event hydrographs were then applied as point source inflow boundary conditions in a two-dimensional (2D) TUFLOW GPU hydraulic model of the pilot catchment at specific inflow locations to simulate the two dimensional behaviour of flooding across the catchment study area. Key features of the model included a detailed DEM, a land use layer, building representation, walls/fences and cross drainage infrastructure.

The catchment model setup included the following features:

(a) The preparation of a detailed DEM using existing topographic and bathymetric data.

(b) The preparation of design rainfall dataset using existing guidelines and hydrologic parametrization/extrapolation techniques.

(c) The development of a detailed hydrologic model including representation of existing catchment area, slope, imperviousness, roughness and rainfall loss rates.

4.2.6 Climate Changes Scenario

In order to determine the potential impact of climate change on flood behaviour in each of the ten model sub-catchments, Year 2050 and 2100 future climate change scenarios were assessed for the 5 year and 100 year ARI design events using the future rainfall intensity and sea level conditions summarised in Table 1 below.

Table 1: Future Climate Change Scenarios

Scenario	Future Climate Era	Change in Rainfall Intensity (5year Ari)	Change in Rainfall Intensity (100 Year Ari)	Tide Conditions Relative to Qatar National Datum (Qnd95)	Sea Level Rise (M)	Storm Surge (M)	Resultant Sea Condition (M Qnd95)
1	2050	+10%	+10%	MHHW	+0.37	+0.5	MHHW +0.87
2	2100	+20%	+20%	MHHW	+0.98	+0.5	MHHW+1.48
3	2100	+30%	+30%	MHHW	+0.98	+0.5	MHHW+1.48
4	2100	+40%	+50%	MHHW	+0.98	+0.5	MHHW+1.48
5	2100	+60%	+60%	MHHW	+0.98	+0.5	MHHW+1.48

In relation to the derivation of the future climate scenarios, it is noted that:

- The rainfall intensity increases adopted for Scenarios 1 to 3 were determined to represent an approximately ‘median’ year 2050 and 2100 rainfall scenarios.
- The rainfall intensity increases adopted for Scenarios 4 and 5 are consistent with the future climate rainfall scaling factors of 1.4 (for 2 year to 10-year ARI design events) and 1.5 (for 100-year ARI design events) as recommended in the Qatar Rainfall Runoff project Technical Report. It is noted that these scaling factors represent a ‘conservative’ year 2100 rainfall scenario and will result in higher flood levels than Scenarios 1 to 3.
- Tidal levels vary along the coastline of Qatar. In accordance with Tidal Information (MM 2015), the Mean Higher High Water (MHHW) tidal levels and resultant future climate sea level conditions have been determined using the nearest tidal gauge location. The MHHW tidal levels adopted along the Qatar coast is provided in Table 2.
- The storm surge height of 0.5 m was adopted based on recommendations provided by an internationally recognized storm tide consultant as part of the Qatar Flood Study.

Table 2: Mean Higher High Water Tidal Levels (MHHW) Tide Levels

Flood Model Catchment Name	Nearest Tidal Gauge Location	Mhhw Tidal Level (M Qnd)
Al Khattiya	Dukhan	0.30
Al Nuaman	Ras Ushayriq	0.58
Al Ruwais	Al Ruwais	0.74
Al Thakira	Ras Laffan	0.64
Doha	Doha Port	0.69
Fuwairit	Ras Laffan	0.64
Mesaieed	Mesaieed Port	0.81
Ras Laffan	Ras Laffan	0.64
Rawdat	Doha Port	0.69
Sawda Natheel	Dukhan	0.30

4.2.6 Calibration/verification

Due to the lack of historical flood data in the pilot catchment, the pilot catchment flood model was not calibrated to historical flood events. However, following the heavy rainfall experienced in Qatar on the 25th of November 2015, and other heavy rainfall events in recent years including the latest this year 2022, it was decided that the event would be modelled and where possible model performance checked against available ground flood records.

Based on a review of modelled results against limited on ground flood records, the nature and pattern of flooding estimated by the flood model was found to be generally consistent with that experienced on ground. In the absence of detailed calibration data, this provided confidence in the flood model's ability to simulate the nature of flooding across the study area.

5 Case Study

To better illustrate the implementation of the watershed analysis and the assessment of a proposed development from a climate change perspective, the following case study in Al Ruwais area north of Qatar is presented. The main objective of this assessment is to identify areas prone to risk from possible surface drainage flooding and rise in sea level at the coastal area of al Ruwais.

Site Location and Topography

The area under assessment is located in Al Rwais in Al Shamal Municipality. In general, the average built area elevation is around **2m (QND)** especially for build area within the range of 30-350 m from the sea shoreline. However closer inspection of the elevation in the area suggests a dredge line elevated at around 4 m and form a natural separation line of expected storm water runoff. In addition to this there is some areas identified as naturally depressed areas where elevation drops to less than 10 cm, more details will be covered in depth in the following sections.

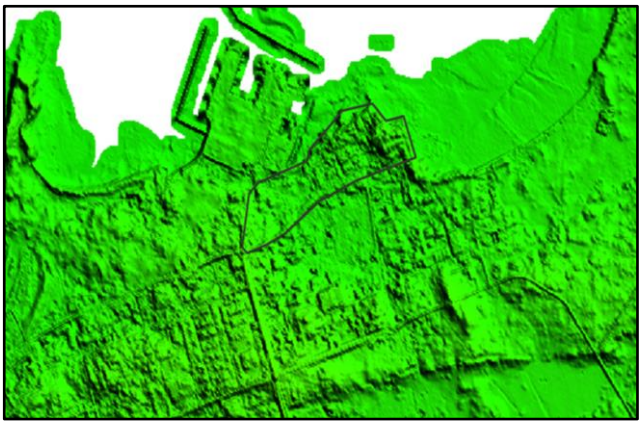


Fig. 7: Al Rwais Area – Digital Elevation Model

Watershed and Catchment Considerations

The line depicted in Green in **Figure 8: Watershed and Catchment Boundaries.** is the natural catchment separation line, with an elevation of around 4 m QND , accordingly the storm water runoff is expected to flow away from this line in both direction as depicted by arrows in black. The current surface drainage/runoff direction is expected to follow the main lines shown in light blue to the line shown in dark blue in **Figure 9: Natural Surface Runoff Direction to main Streams.**

In general the main storm water runoff stream flow direction shown in Dark Blue Figure 3 below indicates that the natural flow line is passing right through the developed area, thus it is expected that the northern part would experience some flooding issue during heavy rainfall events, especially if this natural flow line is blocked by development, accordingly it is highly recommended to take this into consideration during the design and development of the streets in the area, to consider the natural Stream flow line shown in dark blue in Figure 3 below. In addition, it is highly recommended to consider the minor stream flow lines during the development of the local roads and drainage projects in the area.

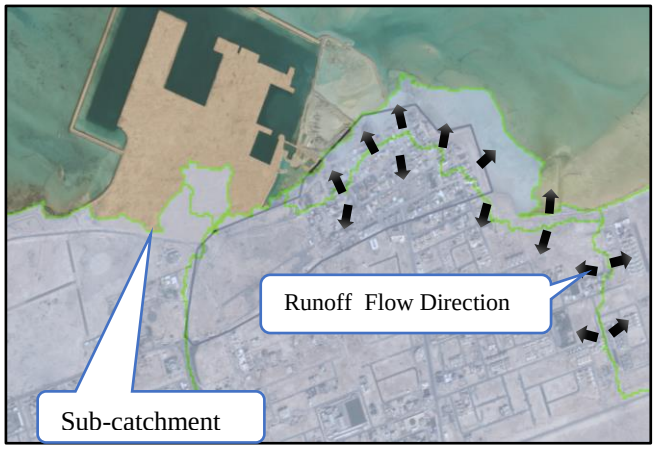


Fig. 8: Watershed and Catchments Boundaries

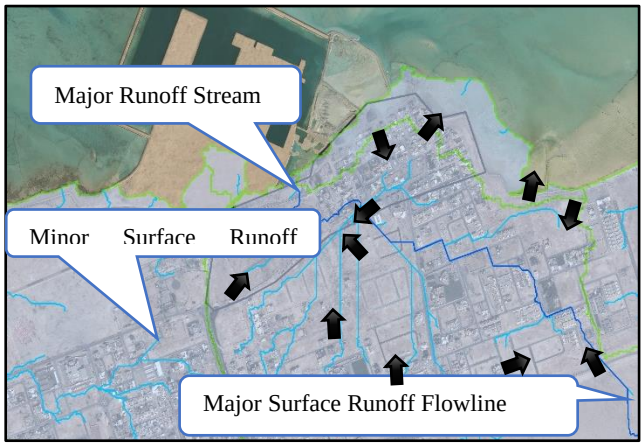


Fig. 9: Major and Minor Natural Surface Runoff Streams

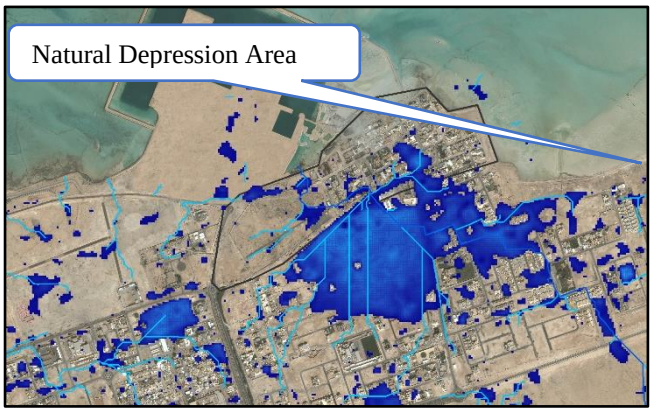


Fig. 10: Natural Depression areas within the Catchment

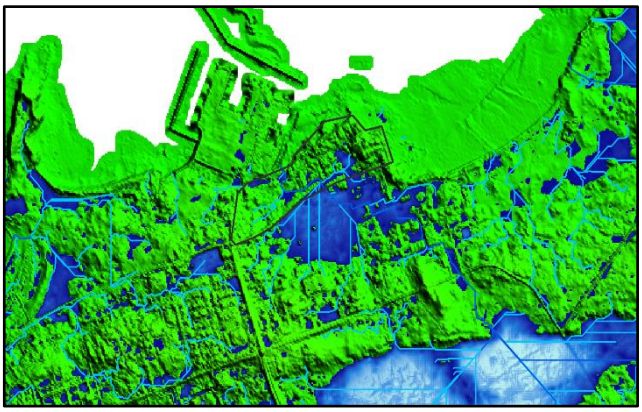


Fig. 11: Depression area and DTM integration

For better assessment IPD has considered a separate model run integrating the DTM together with flood model. **Figure 6** below shown the assessment based on DTM for reference, where the depressed areas shows depth in blue, the darker the blue the deeper the elevation.

Flood Assessment

To confirm the findings in the previous sections, a Flood Assessment is carried out based on the IPD Flood Model developed for the area tacking into consideration the 1 in 100 years event as a return period, to account for expected depth of runoff and associated hazards due to flooding if any. Figures 12 and 13 below confirm the fact that multiple inland areas are prone to flooding, especially in the naturally depressed areas.

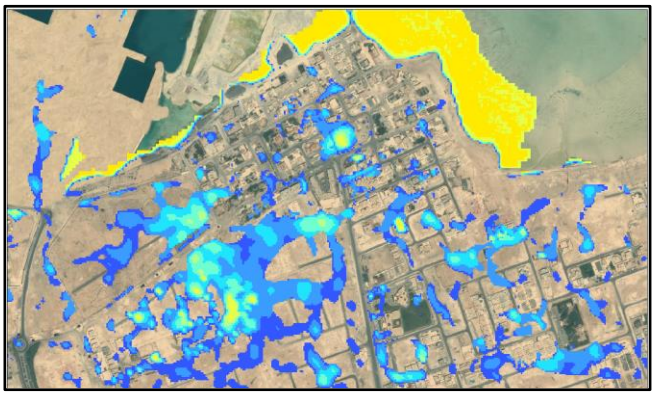


Fig. 12: Flood Depth for 1 in 100 Years – Base Model

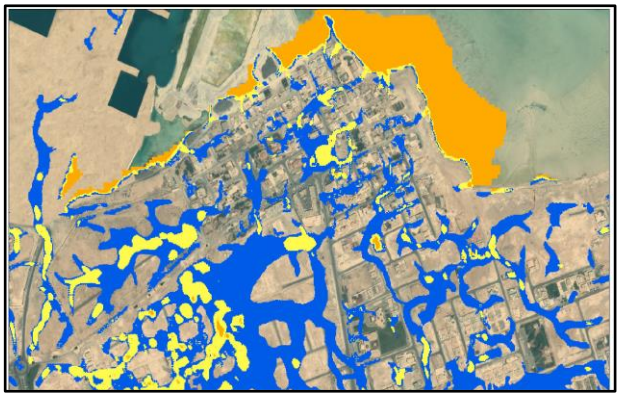


Fig. 13: Flood Risk for 1 in 100 Years – Base Model

Climate Change Scenario

In order to assess the area under extreme rainfall event based on Climate Change scenario, the team considered a Return period 1 in 100 years storm event with expected rise in rainfall intensity 20 % and Storm Surge of 0.5m. Based on the nearest Tide gage in the area (the Al Ruwais Tide gage) a Mean Higher High Water Tidal Levels is 0.74 m (relative to QND) and Considered Sea Level Rise of 0.98 m (QND)

Accordingly based on the above the expected final **Sea level is expected to be around 2.22 meter.**

Bases on this any development in the area that would be above the 2.22m mark would be considered safe from the effect of sea level rise. Based on best practices it is recommended that the final floor level to be 0.3m above the freeboard level from the flood levels expected in this area. Figure 14 and 15 below shows the result of the flood model run including sea level rise considering the above information related to climate change scenario.

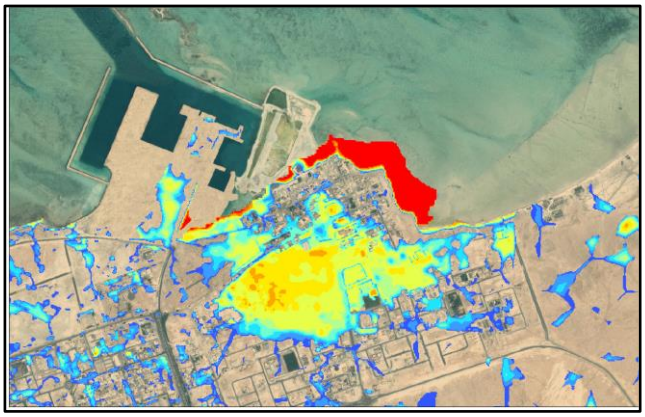


Fig. 14: Flood Depth 1 in 100 Years Climate/Ch Scenario

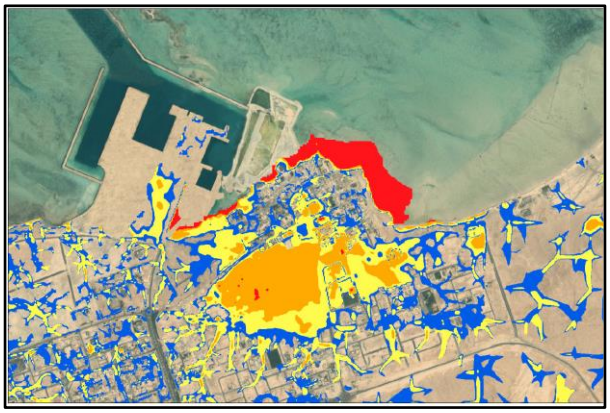


Fig. 15: Flood Risk 1 in 100 Climate Change Scenario

Findings:

- The assessment area is falling into two separate catchments within the Ruwais watershed area, where the elevation cut off point is found to be around 4m as shown Figure 9 in light green. Although might not be a continuous line, it is expected to form a high ground level, thus rainfall runoff would flow away from this line as shown in Figure 8 and 9, also same catchment boundary line would act as a natural protection against sea level rise in the future.
- Under current rainfall intensity and 1 in 100 years return period, specific locations in the area are expected to have flooding in the range of 0.30 to 0.75 cm as shown in Figure 12, and thus low to medium level of hazard risk as shown in Figure 13.
- Under climate change scenario however, with 20% increase in intensity and 0.5 m surge in storm, the same areas identified would experience more flooding in the range of 0.75 to 1.5 m as shown in Figure 14 herein above.
- The expected rise in sea level based on the climate change scenario is expected to be in the range of 0.98m. The adopted Mean Higher High Water Tidal Levels based on Al Ruwais Tidal gage is 0.74 m. Thus The Expected Sea level rise based on Climate Change conditions coupled with storm surge is found to be around 2.22m.
- The flood model run based on the criteria considered in the above mentioned climate change scenario indicate that the risk in specific areas would be medium to high as shown in Figure 15 herein above.

Recommendations:

Based on the findings summarized herein above, it is recommended to:

- Regulations for developing the area could be more flexible and tailored to take into considerations the findings above, to guarantee safety of development.
- The area east of Al Ruwais Port is not considered a high-risk area from a sea level increase point of view, even under climate change scenario for 100 years.
- The area discussed above might be considered under higher risk of flooding with expected change in rainfall intensity and thus flood protection measures need to be considered especially for the areas prone to high-risk hazard risk shown in Figure 15 hereinabove.
- It is recommended to regulate development within the high-risk area in such a way that would enforce implementing a 30 cm first floor level above the expected flood freeboard depth in the area, accordingly placing only development within the high-risk area on-hold to guarantee safer development until final regulations are developed for the area.

  Example: Property is located in high-risk area (orange), the expected flood depth is 1 m, and accordingly final first floor elevation shall be 1.3 at minimum.
- Development north of Street 840 could be considered safe to develop as it is not falling within the high-risk area, but it is recommended to consider a 2.22m +30 cm final first floor level to be safer considering a climate change scenario.

6 Conclusion

Urban Planning communities in close coordination with storm water engineers shall consider storm water and watershed elements at an early stage of the planning process, mainly to prevent development in major storm water streams/Wadis and naturally depressed areas. Land use and zoning regulations shall consider the major watercourses within the catchment areas, and more attention shall be granted to developing naturally depressed areas as parks and storm water collection infrastructure as possible to avoid flooding risks rather than randomly allocated land uses without respecting the natural runoff topography. Finally, assessment of future development from a climate change perspective shall take precedence during the early stages of urban planning new areas, especially areas close to coastal line.

References

Al-Rawas & Valeo. (2008). Issues with Flash Flood Modelling in the Capital Region of Sultanate of Oman. http://www.rcuwm.org.ir/En/Events/Documents/Workshops/Articles/8/3.pdf. Accessed on 01 July 2015.

Al-Shaqsi, S. (2010). "Care or Cry: Three years from Cyclone Gonu. What have we learnt?" *Oman Medical Journal 25*(3).

Al-Saud, M. (2010). Assessment of Flood Hazard of Jeddah Area 2009, Saudi Arabia, *Journal of Water Resources and Protection 2*, 839-847.

Batanouny, K.H. (1981). Ecology and flora of Qatar. Qatar University.

BMT Group Ltd. (2015). United States Department of Agriculture (USDA) soil type parameters as defined in the TUFLOW 2011-09 and 2012-05 Release Notes.

Bahat, et al. (2009). Rainfall–runoff modelling in a small hyper-arid catchment. *Journal of Hydrology, 373*(1–2), 204–217.

Borah, D. K. (2011), Hydrologic procedures of storm event watershed models: A comprehensive review and comparison,

Hydrol. Processes, 25, 3472–3489, doi:10.1002/hyp.8075.

Dang N, Babel M & Luong H. (2011) Evaluation of food risk parameters in the Day River flood diversion area, Red River delta, Vietnam. *Natural Hazards 56*:169–194.

Dawod, G.,Mirza M. & Al-Ghamdi, K. (2011). GIS-Based Spatial Mapping of Flash Flood Hazard in Makkah City, Saudi Arabia. *Journal of Geographic Information System, 3*, 225-231.

Fernandez D & Lutz, M. (2010). Urban flood hazard zoning in Tucumán Province, Argentina, using GIS and multicriteria decision analysis, *Engineering Geology*, 111: 90-98.

Farquharsen F.A.K., Meigh, J.R., Sutcliffe, J.V. (1992) Regional flood frequency analysis in arid and semi-arid areas. *Journal of Hydrology*, 138:487–501.

Foody, G.M., Ghoneim, E.M. & Arnell, N.W. (2004). Predicting locations sensitive to flash flooding in an arid environment. *Journal of Hydrology, 292* (1–4), 48–58.

Forkuo E. (2011) Flood hazardmapping using Aster image data with GIS. *International Journal of Geomatics and Geosciences 1*(4):932–950.

Haque, et al. (2015). Development of a regional flood frequency estimation model for Pilbara, Australia, 21st International Congress on Modelling and Simulation, 29 Nov to 4 Dec 2015, Gold Coast, Australia.

MME/GHD (2016). Flood Study for the State of Qatar – Pilot Catchment Flood Modelling Study Report and Flood Risk Maps. June 2016.

McIntyre, N., Al-Qurashi, A. & Wheater, H. (2007). Regression analysis of rainfall–runoff data from an arid catchment in Oman. *Hydrological Sciences Journal, 52*(6), 1103–1118.

Membery, D. (1997). "Unusually wet weather across Arabia", *Weather*, *52*(6): 166-174. DOI: 10.1002/j.1477-8696.1997.tb06303.x.

Morin, et al. (2009). Towards flash-flood prediction in the dry Dead Sea region utilizing radar rainfall information. *Advances in Water Resources, 32*, 1066–1076.

Mouri G, Kanae S & Oki T. (2011). Long-term changes in flood event patterns due to changes in hydrological distribution parameters in a rural–urban catchment, Shikoku, Japan. *Atmos Res*. doi:10.1016/j.atmosres.2011.02.002.

Parker D., Priest S. & McCarthy S. (2011) Surface water flood warnings requirements and potential in England and Wales. *Applied Geography*, 31:891–900.

Pilgrim, D., Chapman, T. & Doran A. (2009). Problems of Rainfall-Runoff Modelling in Arid and Semiarid Regions. *Hydrological Sciences Journal, 33*, 4, 379-400.

Rahman, et al. (2014). Australian Rainfall and Runoff Revision Projects, Project 5 Regional flood methods, Stage 3 Report, Engineers Australia, Water Engineering, 145.

Sen, Z. (2008). *Wadi Hydrology*, CRC Press, USA.

Sen, et al. (2013). Flash flood inundation map preparation for wadis in arid regions, *Arab Journal of Geoscience*, 6:3563-3572.

Cite as: Samman H. & Zahir R.A., "Resilience Urban Planning from Climate Change Point of View: A Case Study for Qatar", *The 2nd International Conference on Civil Infrastructure and Construction (CIC 2023)*, Doha, Qatar, 5-8 February 2023, DOI: https://doi.org/10.29117/cic.2023.0140

Megaprojects to Improve Public Transport from the User' Perspective

János Varga
Keleti Károly Faculty of Business and Management, Óbuda University, Budapest, Hungary
varga.janos@uni-obuda.hu

Ágnes Csiszárik-Kocsir
Keleti Károly Faculty of Business and Management, Óbuda University, Budapest, Hungary
kocsir.agnes@uni-obuda.hu

Abstract

Globalisation and our fast-paced world have opened up new horizons all over the world. Population growth, rising energy prices and their declining nature are creating problems for transport. Road congestion, drastic increases in journey times and rising travel costs have highlighted the importance of improving public transport. However, for public transport to be attractive, it is essential that the transport alternative itself is fast, comfortable and modern. In this paper, we examine two metro construction projects in cities with high populations from a project management perspective, with a particular focus on the main purpose of the project, its usability. In this study, we want to highlight the visible goals expressed by the end users and their reflection in the project. We want to focus on the different phases of project management that lead to the success of the project.

Keywords: Public transport; Sustainability; Project; Project management

1 Introduction

Sustainability has become a popular term today. If you search the internet for sustainability, you will get 2.2 billion results in 0.55 seconds. This shows that sustainability is a much sought-after and popular topic for many people, but it is not the only reason why we need to address it. Indeed, the planet has undergone a major transformation and the last decades have seen an unprecedented explosion in many ways. The world's GDP or the volume of world trade has risen at an unprecedented rate since 1960, as has been seen in the change in population numbers, among other things. In a very short space of time, we have witnessed large-scale increases that have shed new light on the finite capacities of our planet. We have finite resources and opportunities in the face of infinite growth, so it is only a matter of time before the two are finally separated. Sustainability has become not only a fashionable term, but also a concept that increasingly affects our lives. It indicates a major problem, behind which we can assume that something is not working very well and that major change is needed. Meanwhile, globalisation and increasingly intense change are placing new challenges on the shoulders of humanity.

The question rightly arises: in what ways can we sustainably maintain or improve our quality of life? Today, our lives are hampered by many problems. Rising energy prices, population growth and dwindling resources are all pushing us to look at sustainability in a new light. We also need to be clear that sustainability is no longer just about our consumption, but also about being sustainable in areas such as public transport, which is used by many people. In the case of public transport, too, the increasing number of passengers, the drastic rise in energy prices or the shortage of raw materials and commodities that are important for transport can cause problems on a daily basis. From this

perspective, sustainability must also be interpreted and even examined in relation to public transport, given that we are talking about a system that offers a significant proportion of humanity a choice of alternatives and services. However, while we are striving for sustainability in transport, we must not lose sight of the fact that we must at the same time be able to provide a service that is of the right quality, up-to-date and that offers maximum passenger satisfaction. We must provide a sustainable, economical, efficient and high-quality service, which is often not easy, but the challenges of the 21st century have made such demands on transport.

2 Literature Review

Sustainability is most often associated with consumption (Tseng et al, 2016), where it is often thought that all that is needed to have a sustainable world is to consume more consciously or less (Harjato et al, 2021; Wang et al, 2019). If we want to understand sustainability in this dimension for transport, we could say that sustainable transport means travelling less. Most definitions associate sustainability with the finite resources and potential of our planet, but again this implies a consumption-centred approach (Dolan, 2002; Pogutz & Micale, 2011).

However, sustainability cannot be linked to consumption alone, as the pursuit of sustainability has a well-defined purpose. Namely, to protect the condition and quality of our environment so that we can live in an environment that provides a suitable living space for all. Defining sustainability is still a challenge today, as many things can be sustainable. Sustainable systems, sustainable cities, sustainable budgets, sustainable tax systems, sustainable business environments, and so on. We also hear a lot about sustainable transport or transport systems. It is safe to say that sustainability has a slightly different meaning everywhere, as it means something different in economic, ecological or even transport terms (Morelli, 2011).

However, all definitions of sustainability have something in common. Wherever sustainability is pursued, it is always aimed at having a positive impact on the environment. We want to strive for sustainability in order to make a positive change and a positive impact on our environment. The definition of transport and sustainable transport, which is the subject of this study, is a perfect example of this. The OECD links sustainability and transport. It mentions that transport faces the same challenges of resource scarcity or increasing demand for services as other productive or service sectors. Moreover, public transport is often under an even greater burden, often having to provide a sustainable service to millions of people on a daily basis. Sustainable transport, according to the OECD, is transport that does not endanger public health and the ecosystem, but provides a service that meets transport needs at the right quality (OECD, 2022).

Sustainable transport is expected to use renewable resources at a slower rate than the time it would take to recycle them; and resources that cannot be renewed are used much more slowly than renewable resources. All this points to the need for sustainable transport in this sense to have a positive impact on people’s environment, but also to ensure an adequate level of service. The significant positive and negative impacts of transport systems on both the sustainability of cities and people’s lives have been demonstrated in several cases. In order to promote sustainability, a number of transport improvement projects are being launched, often with technical or financial constraints. This makes it difficult to implement such projects (Mahmoudi et al, 2021). Creating sustainable transport can be important not only at regional, state or city level. The European Union itself has set significant climate targets, one of the most important of which is the decarbonisation of the transport sector. The EU has pledged to reduce emissions to 0% by 2050 and achieve a form of climate neutrality. This requires a significant

reduction in greenhouse gas emissions, but still providing services and solutions that are affordable for citizens (EC, 2022).

Among these initiatives, we can assume a significant transformation, with a large number of investments and projects (Varga & Csiszárik-Kocsir, 2019; Dobos et al., 2022). Achieving zero emissions in the transport sector will require replacing, upgrading or adapting many of the technologies or devices that have been in place in the past. But transport cannot be left out of the continuous improvement and regular investment. Public transport is seen as a key element in building sustainable cities and should therefore be central to the sustainability of cities and regions (Miller et al, 2016). Sustainable transport is not just about the environmental quality of the means of transport themselves. It means at the same time environmentally sustainable transport, sustainable transport system and sustainability of transport processes (Cheba & Saniuk, 2016). A sustainable transport system should enable mobility for all inhabitants, but in a way that is safe and environmentally friendly. This is not an easy task, as the needs and demands of people from different income groups are different, and it is not always possible to provide this at the same level (Mohan & Tiwari, 2000). However, transport sustainability in this interpretation is also strongly linked to its impact on the immediate environment. The positive relationship between transport sustainability and quality of life has also been clearly confirmed (Steg & Gifford, 2005).

Sustainable transport also seeks to maintain a balance. This balance should not only be between transport and quality of life, but should also focus on environmental, economic and social aspects. Sustainable transport must therefore be able to provide environmental, economic and social benefits at the same time (Gilbert & Tanguay, 2000). The relationship between transport and the environment is very closely linked, and this includes the development of transport infrastructure or the modernisation of transport facilities in such a way that transport itself becomes more environmentally friendly and environmentally aware. Challenges in implementing sustainable transport programmes and projects include the complexity of transport problems in the urban environment, conflicts of interest or lack of adequate resources (Fernandez-Sanchez et al., 2020).

There is also a strong link between sustainable transport development and project management. While it has become essential to apply sustainability criteria to public transport, economic aspects cannot be ignored. Development projects often have significant cost and time requirements, in addition to the scarcity of other resources in the transport sector. In most cases, development takes the form of major projects or programmes, all with a single objective: to achieve a positive impact that safeguards environmental assets without depriving citizens of transport services. In this way, public transport projects try to achieve the desired impact by maximising resource constraints and, while at the same time being cost and time-constrained, by trying to produce an outcome that meets citizens' expectations while at the same time having a positive impact on their quality of life and the environment.

3 Material and Method

The megaprojects presented in this study are included in the top 50 projects list published by the Project Management Institute (PMI, 2021), an organisation that develops project management standards and selects each year the most inspiring and exemplary projects of the year to be used as a model for future similar initiatives. In this study, we would like to present two projects that aim to improve public transport, educate people about the use of cars and reduce the time and safety of transport. The modernisation of public transport will encourage more people to choose surface or

underground solutions rather than driving and generating congestion. The two projects presented are metro projects in cities with very high populations (Ryad and Mumbai). The two projects under study are analysed from a user perspective, so no filtering criteria were applied in the selection of the sample of respondents, i.e. educational qualifications, previous project management knowledge were not criteria, i.e. anyone could fill in the questionnaire as a basis for the evaluation. Respondents were asked to rate the selected projects on the basis of some factors related to the scope of the project. Respondents rated the factors on a scale of 1 to 4, with a score of 1 indicating a very weak factor and a score of 4 indicating a very strong factor. The characterisation of project scope is presented using a word cloud. 39.5% of the sampled respondents have a tertiary education; while 60.5% have a secondary education. 12.2% of respondents are Generation Y, 23.3% are Generation X and 64.5% are Generation Z. The survey was conducted in April and May 2022.

The two projects selected are both in countries where both GDP and population have grown enormously since the turn of the millennium. Population growth requires that country leaders think about improving public transport and implement them in the form of huge megaprojects; and GDP per capita clearly shows the room for manoeuvre of cities in terms of the technologies and constructions used, which explains the differences between the two developments.

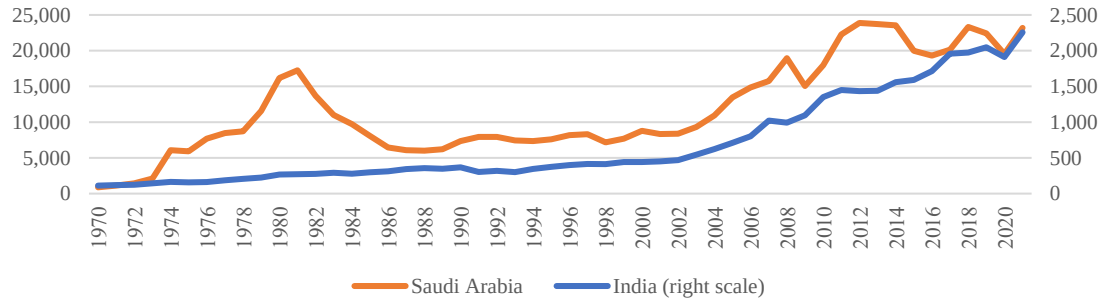


Fig. 1: GDP per capita in the countries hosting the examined megaprojects

4 Results

4.1 Evaluation of the Riyadh-Metro project

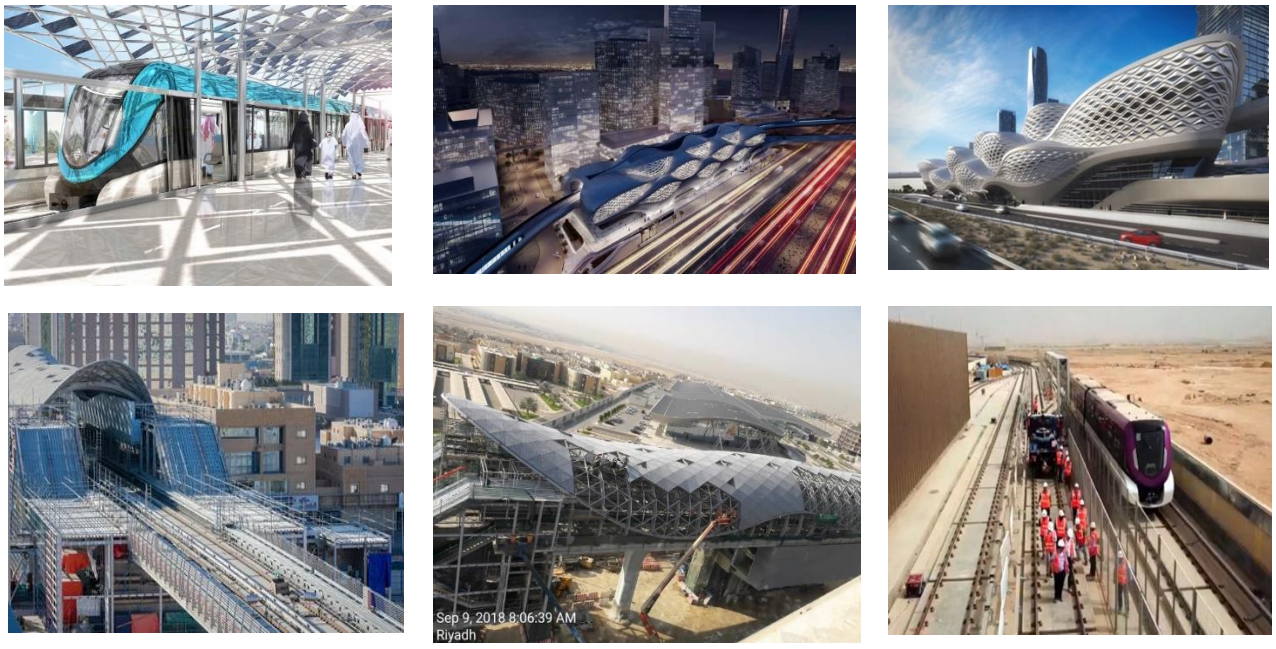


Fig. 2: Visual plans and process of metro construction

Saudi Arabia's largest city, Riyadh, previously had no culture of public transport use. With a population of 8.3 million expected by the end of the decade, the vast majority of people in the city will be travelling by car, causing huge environmental damage, congestion and air pollution, and degrading the quality of life of the people living there. The metro project to be unveiled consists of six autonomous lines totalling 176 km, making it the largest public transport project in the world. This is complemented by an extensive network of bus lines, which will cover a further 1150 km (PMI, 2021). The project had a budget of USD 23 billion and was planned to be completed in seven years. The project has a constant focus on a greener approach to a more sustainable future. The design has also taken care of cooling and shading the surrounding areas, using innovative solutions (irrigation channels, canopy, internal and external vegetation).

As a first step, we asked survey respondents to rate in one word the essence of the project scope, what they as users see and what the main message of the project is for them. From the responses received, we created a word cloud, shown in the figure below. Most of them identified "public transport" as the main element in the project scope. Here, respondents tended to name the main objective of the project. The next most frequent terms were "useful" and "metro", with 20-20 votes. In addition, the terms "environmental awareness" and "sustainability" were also mentioned, but many also mentioned the essence of the project. It can therefore be said that the outcome of the project itself played a decisive role in defining the scope.



Fig. 3: Scope of the Riyadh-Metro project

Respondents were then asked to rate one characteristic of project scope on a four-point scale. Here, the highest average scores were given for usefulness, public interest, usability and future focus. The four attributes were all rated above 3.5. In addition, a very high proportion considered the project to be environmentally friendly, sustainable, relevant and feasible, as indicated by average scores above 3.0. The project was considered least profit-oriented, as it received the lowest average rating. Similarly, cost-effectiveness was also rated low, with the uniqueness and uniqueness of the project ranking third from the bottom. The latter is not surprising as the public transport infrastructure is not particularly unique in itself, but the technology used, the architectural solutions and the solutions to protect the environment fall into this category. However, this is not something that the survey respondents have seen from the outside at this stage of the project.

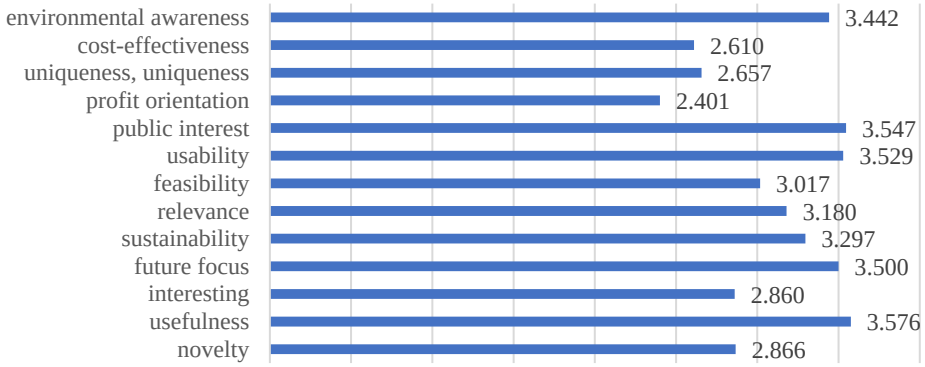


Fig. 4: Evaluation of the scope of the Riyadh-Metro project

4.2 Evaluation of the Mumbai-Metro project

Mumbai is one of the world's most populous cities. The city's rail system moves more than 7 million people commuting daily, which means that situations that endanger passengers are very common. Due to the large crowds, passengers often fall in front of trains or get injured in the crowd. This is why the city authorities decided to modernise the public transport network. The construction of metro line 3 was a huge challenge for the contractors. The first step was to create one of the longest tunnel systems in the world, 33.5 km of underground tunnels with 27 stations. This was a huge challenge, as the line ran through highly populated parts of the city, passing under many tall and listed buildings, and was complicated by overpasses, metro viaducts and railway lines. Getting the tunnel boring machine to the starting point was also a major challenge. During the construction, 8,000 workers and 17 drilling machines worked 24 hours a day to ensure that the plans could be kept on schedule. (PMI, 2021). However, an outbreak of the coronavirus made it very difficult to complete the work on time. Every time a worker fell ill, a team was quarantined, resulting in huge delays to the project. In addition, the works were scheduled during the monsoon season, which meant that flooding also posed a risk to the people working in the tunnel. This project was also specifically designed with the environment in mind. The basic mission of the project is also to reduce the city's carbon dioxide emissions, both by reducing the number of vehicles and by the forest development associated with the project.

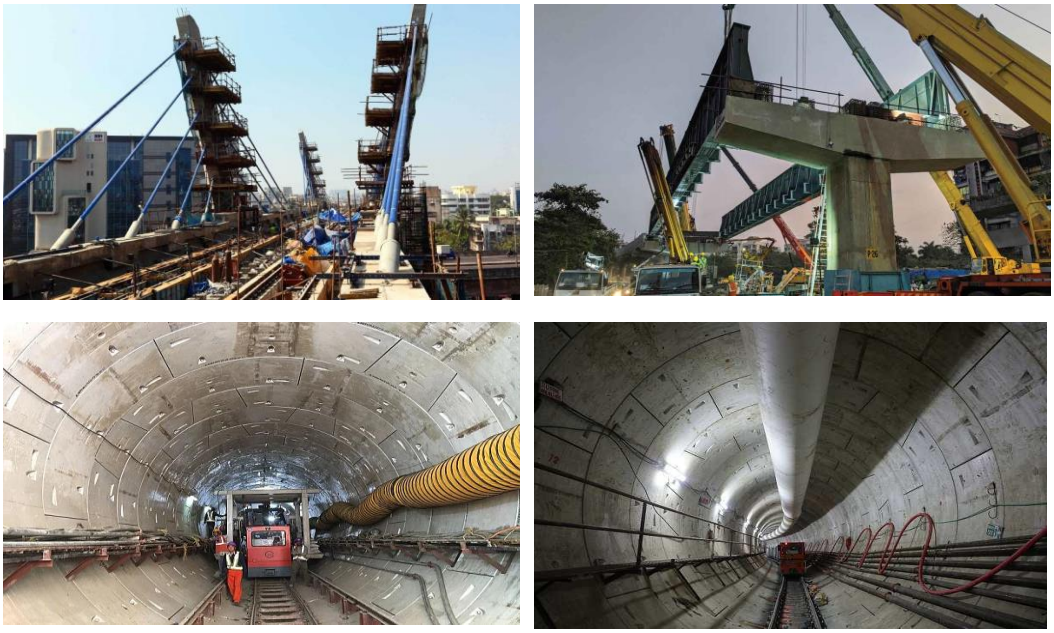


Fig. 5: The process of metro construction

The present project was also described by respondents mainly in terms of its visible objective. The most frequently mentioned scoping elements were the words “public transport” and “metro”. These were followed in terms of frequency of mention by ‘useful’, ‘appropriate’ and ‘important’. In several cases, the project scope was interpreted as infrastructure or development, but the words safe, challenge and public interest also appeared.



Fig. 6: Characterisation of the scope of the Mumbai-Metro project

When respondents were asked to characterise the project scope along the given characteristics, it was seen that it was rated as being of public interest, useful and usable with a much higher ratio compared to the previous project, as the average score for these three characteristics was above 3.6 in all cases. This was followed by a markedly lower average score (around 3.2) for relevance, future focus and feasibility. Respondents ranked the project scope as the least cost-efficient and innovative, with the uniqueness and uniqueness of the project ranking third.

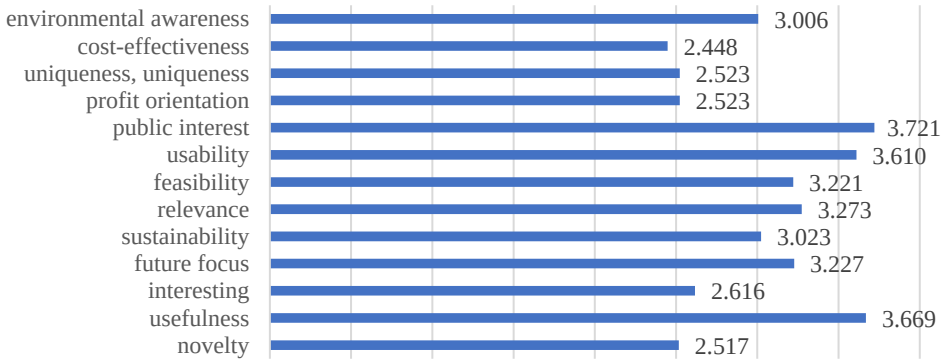


Fig. 7: Evaluation of the scope of the Mumbai-Metro project

5 Conclusion

If we evaluate the two projects as a whole, it can be said that the social utility of each of them is outstanding. Many cities, including Riyadh and Mumbai, have realised that while car transport is more convenient and practical in many cases than public transport, it still places a huge burden on cities and therefore the planet. Public transport offers an alternative to environmentally damaging car travel, by providing an efficient way to get large numbers of people where they need to go. By reducing air pollution, congestion and the negative impact on the environment. The evaluation of the projects shows that they were very positively received by the respondents, even though they may not be direct users. The message value of the projects was that they were perceived as being of most

public interest, useful and usable, as these three main characteristics dominated the top three places in the respondents' opinion. In terms of cost-effectiveness, however, respondents had doubts. Obviously this is not a coincidence, as a project to improve public transport is implemented with a huge budget, the benefits of which will only be felt after several years or even decades. Adequate quality public transport and education can certainly be a solution to the environmental problems of our time. The two projects presented in this case and their evaluation by users are certainly a message for future developments, which can help to determine the purpose and direction of similar projects.

Acknowledgement

The paper was prepared with the support of Széll Kálmán Public Finance Research Group of the University of Public Service.

References

Cheba, K. & Saniuk, S. (2016). Sustainable Urban Transport - The Concept of Measurement in the Field of City Logistics. *Transportation research Procedia, 16*, pp. 35-45. https://doi.org/10.1016/j.trpro.2016.11.005

Deakin, E. (2003). Sustainable Development and Sustainable Transportation: Strategies for Economic Prosperity, Environmental Quality and Equity. Working Paper 2001-03.

Dobos, et al. (2022). How Generation Z managers think about the agility in a world of digitalization. In: Szakál, Anikó (ed.) IEEE 20th Jubilee World Symposium on Applied Machine Intelligence and Informatics SAMI (2022): Proceedings, Poprad, Slovakia, pp. 207-212.

Dolan, P. (2002). The sustainability of sustainable consumption. *Journal of Macromarketing, 22*(2), pp. 170-181. DOI: 10.1177/0276146702238220

Fernandez-Sanchez, G., Terrón, J. A. & Fernandez-Heredia, Á. (2020). Evolution towards a Sustainable Public Transport in the City of Madrid. Sustainable Mobility April 22nd, 2020. DOI: 10.5772/intechopen.90102

Gilbert, R. & Tanguay, H. (2000). Sustainable transportation performance indicators project. Brief review of some relevant worldwide activity and development of an initial long list of indicators. The Centre for Sustainable Transportation, Toronto, Ontario, Canada

Harjoto, et al. (2021). Sustainable consumption and production, climate change and firm performance. *Journal of Impact and ESG Investing Winter 2021, 2*(2), pp. 8-34.

Mahmoudi, R., Shetab-Boushehri, S. N. & Emrouznejad, A. (2021). Sustainability in the evaluation of bus rapid transportation projects considering both managers and passengers perspectives: A triple-level efficiency evaluation approach, *International Journal of Sustainable Transportation, 16*(12).

Miller, et al. (2016). Public transportation and sustainability: A review. *KSCE Journal of Civil Engineering 20*(3):1076-1083 DOI: 10.1007/s12205-016-0705-0

Mohan, D. & Tiwari, G. (2000). Sustainable Transport Systems: Linkages between Environmental Issues, Public Transport, Non-Motorised Transport and Safety. Transportation Research and Injury Prevention Programme. Indian Institute of Technology

Morell, J. (2011). Environmental sustainability: a definition for environmental professionals. *Journal of Environmental sustainability, 1*(1), Article 2.

OECD Environmental Criteria for Sustainable Transport. https://www.oecd.org/env/greening-transport/environmentalcriteriaforsustainabletransport.htm

Project Management Institute (2021). Most Influential Projects: 2021 Edition. https://www.pmi.org/most-influential-projects-2021 (letöltve: 19/03/2022)

Pogutz, S & Micale, V. (2011). Sustainable consumption and production. *Society and Economy. 33*(1), pp. 29-50.

Steg, L. & Gifford, R. (2005). Sustainable transportation and quality of life. *Journal of Transport Geography, 13*, pp. 59-69

Tseng, et al. (2016). Sustainable consumption and production in emerging markets. *International Journal of Production Economics, 181*, Part B, pp. 257-261

Varga, J. & Csiszárik-Kocsir, Á. (2019). Redefining the Role of Project Leader for Achieving a Better Project Result. *PM World Journal, 8*(8). pp. 1-18.

Wang, et al. (2019). A literature review of sustainable consumption and production: A comparative analysis in developed and developing economies. *Journal of Cleaner Production*, *206*, pp. 741-754.

Cite as: Varga J. & Csiszárik-Kocsir A., "Megaprojects to Improve Public Transport from the User' Perspective", *The 2nd International Conference on Civil Infrastructure and Construction (CIC 2023)*, Doha, Qatar, 5-8 February 2023, DOI: https://doi.org/10.29117/cic.2023.0141

An Inclusive Transportation for Iraya-Mangyan IP in Accessing Social Infrastructure using Scalogram Analysis

Junekaycelle Aubrey Grace N. Carillo
Mapua University, Mandaluyong City, Philippines
jagncarillo@mymail.mapua.edu.ph

Frances Dale Danielle F. Dadiz
Mapua University, Bulacan, Philippines
fddfdadiz@mymail.mapua.edu.ph

Samantha Nicole T. Regala
Mapua University, Laguna, Philippines
sntregala@mymail.mapua.edu.ph

Geoffrey L. Cueto
Mapua University & MES Construction, Quezon City, Philippines
glcueto@mapua.edu.ph

Abstract

Indigenous people (IP) were the first residents who originally lived and hosted their represented nations or domains. Therefore, these natives were initially acknowledged as the first individuals, meaning they were included in the country's population and must be prioritized over the rest of the civilians, considering they were part of the country's history. However, despite being a small population, most of these individuals were poor and illiterate. In addition, they were unable to catch up with those normal citizens living in the modern world because of not being socially identified in institutional industry, being discriminated against due to their origins, and being deprived of social support like access to education, transportation, hospital, and other essential facilities. This research sought to study the quality-of-life Iraya-Mangyan IPs had and the present conditions in their inhabited area to determine how they lived their everyday lives and how they moved around their domain. By conducting this study, the proponents found no inclusive transportation and comprehensive social support infrastructure available and accessible for Iraya-Mangyan IP, and thus, the transportation system was insufficient and defective.

Keywords: Indigenous People (IP); Inclusive transportation, Social infrastructure, Scalogram Analysis

1. Introduction

Indigenous people (IP) were the first residents who originally lived and hosted their represented nations or domains. There were also distinct kinds of indigenous people worldwide or even within a country. Indigenous people (IP) or also known as natives, first populace, aboriginals were one of the minority population groups characterized by shared history with pre-colonial cultures, strong attachment to their heritage, beliefs, motherland, natural resources, linguistic, and other significant to them (United Nations, 2021). Therefore, these natives were first acknowledged as the first individuals, meaning they were part of the country's population and must be prioritized over the rest of the civilians, considering they were part of the history. However, despite being a small population, most of these individuals were poor and illiterate. According to the United Nations Development Programme (2010), even with some policies and

programs for indigenous people and their ancestral domains, they were still part of the country's poorest and most deprived individuals (United Nations Development Programme, 2010).

The most prominent Philippine indigenous groups were from the mountains of northern Luzon, called Igorot IPs. At the same time, the ethnic groups in southern Mindanao were also known as Lumad IPs (International Work Group for Indigenous Affairs, 2021). There were also smaller groups like the Mangyan IPs in the central islands, Magbukun Ayta IPs in Bataan, Kalanguya IPs of Nueva Vizcaya, Tongrayan IPs of Kalinga, and others. However, this research aimed to study the indigenous people from the central islands, which were the Mangyan IPs, particularly the Iraya-Mangyan IPs. Mangyan was the umbrella term for the eight tribes, which were Iraya, Alangan, Tadyawan, Tawbuid, Buhid, Hanunuo, Ratagnon, and Bangon. Each had its own separate language and traditions, yet, such features belonged to the Iraya-Mangyan, the richest cultural tribe among the Mangyans (Pomelo, 2020).

Researchers chose Mangyan IPs as they were less popular than other ethnic tribes, like Igorot IPs. Likewise, Iraya-Mangyan was the most prominent compared to the rest of the Mangyan tribes. Additionally, the research study would be conducted on Sitio Calomintao, Alacaak, in Santa Cruz, Occidental Mindoro, the motherland of the Mangyan tribes. The criteria for choosing the research location were based on where the enormous number of indigenous people lived and must be far from the urban areas.

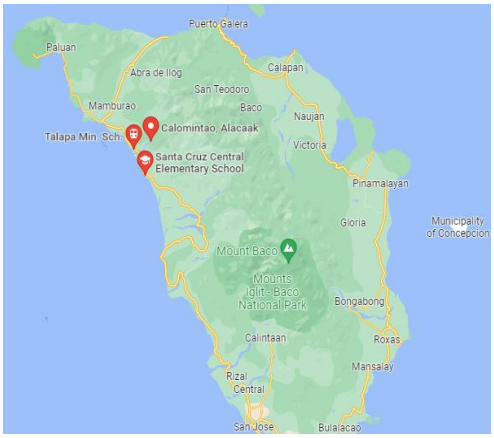


Fig. 1: Location Map of Mindoro, Philippines (Google Maps, 2023)

Indigenous people were left behind in the era of the modern world, which has rapid, advanced, and refined technologies and infrastructures. Other than their strong attachment to the land, they were born on and the nature around it, indigenous people struggle to adapt to non-indigenous people's modern way of life. This was because they were not socially identified in institutional industry, discriminated against due to their origins, and deprived of access to education, transportation, hospital, and other essential facilities. Indigenous people in the Philippines have always been subject to historical prejudice and marginalization from political circles and economic advantages (United Nations Development Programme, 2010).

Additionally, previous studies reveal the shortcomings of different governments in providing inclusive access to basic life processes and necessities for the Indigenous People. These are access to health care (Bjerregaard, Petersen & Larsen, 2018; Burnett, et al. 2020), protection of the environment (Camargo, Winchenbach, & Maguirre, 2022), preservation of culture and heritage (Muir, 2022), lack of representation in policymaking (De La Cruz, et al., 2020), and little to no access to innovative education systems (Li, Brar, & Roihan, 2021). A research study was also conducted in Africa that studied the experiences and cases of older people residing in its cities, as they are one of those

population groups often neglected in terms of transportation access and livelihood support (Wignall, et al., 2019). This meant that even older people were deprived of those social supports; what more, the indigenous people who also composed of elders.

The actual case was the Mangyan IPs, who have lived their entire lives in the mountains or at the foot of the hills, far from the nearest urban areas. This also meant they struggled to travel to urban areas and access transportation, health care, technology, etc., as they were surrounded only by nature, and there was little to no progress and encouragement from local governments. Furthermore, some remote areas like mountains or islands in the Philippines were not easily accessible as there was still little to no transportation infrastructure available in those places. That was why researchers sought to examine the chosen respondents' domains to help and provide them access to social infrastructures, which normal people living in the city always had and acquired.

The study's main objective was to develop the components and approaches to how inclusive transportation will help indigenous people. This aimed to propose a feasible and sustainable Inclusive Transportation for Iraya-Mangyan IP in Accessing Social Infrastructure using Scalogram Analysis. Specifically, this research intended to:

1. Assess the present condition and quality of life of the Iraya-Mangyan indigenous people in terms of:

    1.1 Education
    1.2 Employment and Livelihood
    1.3 Health
    1.4 Social Relations

2. Analyze the condition of the area inhabited by the Iraya-Mangyan indigenous people, particularly:

    2.1 Geographic features
    2.2 Accessibility
    2.3 Mobility
    2.4 Available Modes of Transportation
    2.5 Nearest Urban Area

3. Determine the requirements set by the governing bodies, as well as the practical and social significance of constructing a social support infrastructure and system for the Iraya-Mangyan indigenous people, particularly of:

    3.1 Mode of Transportation
    3.2 Type of Transportation Infrastructure

4. Assess the most feasible, suitable, and sustainable social support infrastructure and system to propose for the Iraya-Mangyan indigenous people, with respect to their demography

2. Methodology

The theoretical framework intended to produce a more precise depiction of the research study's scope in which guided data collection. The variables presented in this study are education, employment and livelihood, health, environment, and social relations.

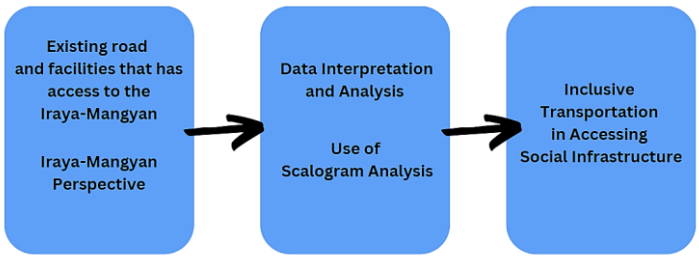


Fig. 2: Framework of the study

The research design refers to the overall strategy that one might choose to integrate the different components of the study coherently and logically. The researchers utilized qualitative method in analyzing the current condition of the target population by using a scale to know the factors that greatly affect their daily lives. On the other hand, the data collected from the scale analysis was treated quantitatively by computing the coefficient of likeability. This allowed the researchers first to describe the existing condition and correlate it to investigate how the difference of one variable affected the variation of the other. In this research, a survey was used because it involved respondents and questionnaires to provide answers to the problems related to the study, specifically on the following aspect:

1. Education – access to educational establishments, means of transportation going to school, and easiness in purchasing school materials.
2. Employment and Livelihood – access to infrastructures that generates employment or cater livelihood activities, having means of transportation going to workplace, and earning sustainable salary.
3. Health – access to health and medical establishments, having a way of transportation going to medical establishments, accessibility of the area for emergency vehicles to enter.
4. Social Relations – feeling of belongingness around people outside of their indigeneity, accessibility of the area for people outside their indigeneity to enter, having means of transportation to go to social activities outside their area.

This study used a convenience sampling technique, a non-probability sampling technique where subjects were selected because of their convenient accessibility and proximity to the researchers. Largely, convenience sampling included the individuals who were most accessible to the researchers. This was an easy and inexpensive way to gather initial data. Still, there was no way to tell if the sample was representative of the population, so it could not produce generalizable results. The sampling design was justified to be selected for this study as the population was not well defined, or there was no accurate data that showed the population of the Iraya-Mangyan people. As of 01 May 2020, the province of Occidental Mindoro had a total population of 525, 354 persons. Of this total, the household population comprised 99.3 percent or 521,444 persons. Based from this 2020 census of population, the 8.07% was the population of the municipality of Santa Cruz (Philippine Statistics Authority, 2022). The sampling size was based on the randomly selected population in the tribe of the Iraya-Mangyan Indigenous People. These sampling techniques focused on recruiting more potential participants that were difficult to locate.

The data gathered in this study would be analysed using the following statistical tools:

- **Simple Percentage** would be utilized to determine the respondents' demographic profile, including sex, age group, educational attainment, and income range. To compute the percentage, the following formula would be utilized:

$$P = F\ 100N$$ where: P = percentage

F = frequency

N = total number of respondents

- **Guttman Scale**, also known as the **Scalogram Analysis**, comprises components that can be sorted hierarchically. It reflects respondents' extreme "attitude," whether they are exceedingly favourable or unfavourable about the topic. The Guttman scale is beneficial because a single answer can predict responses to all items; therefore, it is deterministic. Guttman scale is

depicted by their items' "implicational" or "scalable" nature (Gothwal, et al., 2019).

Guttman Scale would be utilized to determine how likely it was to build a transportation system for the Iraya-Mangyan IP to connect them to the nearest urban area. The scale consisted of twenty questions that were arranged in ascending difficulty order. Participants would be asked to answer positively or negatively to each question. A positive reaction was assessed as a 0 (yes), while a negative response would be counted as a 1 (no). This should follow a Guttman scale because the reply could only potentially affirm the following question after confirming the preceding question (Gothwal, et al., 2019). This was comparable to the likelihood that respondents would agree or disagree with the construction of a road and bridge, given the current state of their daily lives, where the reader should only be able to decide on the next item if he/she had been able to answer the previous item. As a result, responses on a Guttman scale should be able to be separated into two categories, indicating whether a participant "passed" or "failed" an item. The proportion of participants who passed or failed a question was used to create an item hierarchy, which was created by categorizing items from most to least difficult (Gothwal, et al., 2019).

- The **Coefficient of Reproducibility (CR)** was used to validate the Guttman Scale, which measures scalability when instituting a hierarchy using the Guttman Scalogram technique (Jobling, & Snell, 1961). However, instead of calling it the way it was, the researchers used different terminology, **Coefficient of Likelihood (CL)**, which was more fitting to the objectives of the present study. Nevertheless, both coefficients' computation process does not differ much from each other. This value was calculated as one minus the total number of errors divided by the total number of responses. A CL score of higher than 0.90 was regarded as acceptable, indicating that the Guttman scale was both cumulative and unidimensional.

3. Results and Discussion

The compilation of the questionnaire, the results and analysis of the study's qualitative findings, and the results and analysis of the qualitative data were all covered in this chapter. With the help of scalogram analysis, this study sought to propose inclusive transportation for Iraya-Mangyan IP to access social infrastructure.

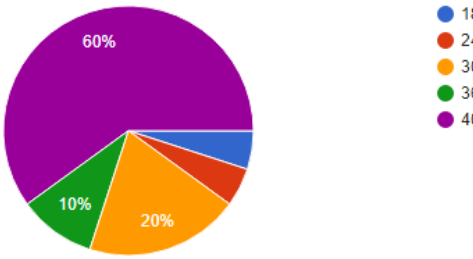


Fig. 3: The Demographic Profile of the Respondents

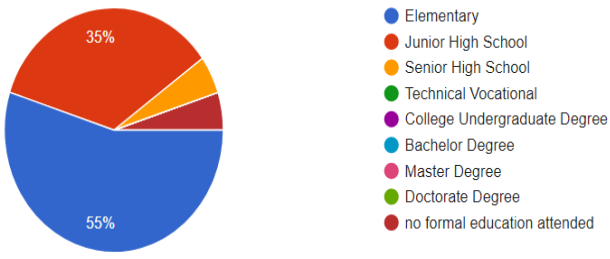


Fig. 4: The Demographic Profile of the Respondents

This figure 3 represented the frequency of the age brackets of Iraya-Mangyan IP. Based on the graph, the majority of the respondents were aged 40-60 years old, followed by 30-35 years old, 36-40 years old, 18-23 years old, and finally, 24-29 years old. Figure 4 shows the frequency of the educational attainment of the Iraya-Mangyan IP. According to the graph, 55% of the respondents finished elementary school, while 35% graduated from high school. A significantly small percentage of the respondents finished senior high school, which had an equal number as those who never attended any formal educational institution.

HEALTH						SOCIAL RELATIONS					
	Statement 3.1	Statement 3.2	Statement 3.3	Statement 3.4	Statement 3.5		Statement 4.1	Statement 4.2	Statement 4.3	Statement 4.4	Statement 4.5
SCORE	16	20	15	14	19	SCORE	6	7	20	7	0
%	0.8	1	0.75	0.7	0.95	%	0.3	0.35	1	0.35	0
RII	0.84					RII	0.4				

EDUCATION						EMPLOYMENT AND LIVELIHOOD					
	Statement 1.1	Statement 1.2	Statement 1.3	Statement 1.4	Statement 1.5		Statement 2.1	Statement 2.2	Statement 2.3	Statement 2.4	Statement 2.5
SCORE	17	19	19	12	18	SCORE	19	19	19	10	20
%	0.85	0.95	0.95	0.6	0.9	%	0.95	0.95	0.95	0.5	1
RII	0.85					RII	0.87				

Fig. 5: Assessment of the status of the Iraya-Mangyan IP using Scalogram Analysis

The figure above shows the scalogram analysis of the data gathered by the researchers from their survey interview for the Iraya-Mangyan IP. A mark of one (1) means that the respondent agreed with the given statement, while a grade of zero (0) 58 means that they disagreed with the statement. Each aspect (education, employment and livelihood, health, and social relations) had a separate tally to assess what was most needed by the respondents regarding each aspect.

The Coefficient of Likeability (CL) is a term derived from Coefficient of Reproducibility (CR), which is often used as a criterion of scalability when forming a scale by the Guttman Scalogram technique (Jobling, & Snell, 1961). The researchers used the same equation as Guttman defined CR.

Definition of Coefficient of Reproducibility

Guttman defines the coefficient of reproducibility to be

$$C_R = 1 - \frac{\text{total number of errors}}{\text{number of items} \times \text{number of persons}}$$

and is thus equal to the overall proportion of responses which can be correctly reproduced. (Jobling, & Snell, 1961).

CL measures the extent to which an observed set of response patterns agrees with that expected to form a perfect scale (CL = 1.0). In connection, a high value of CL indicates a close agreement, which is expected to be at least 0.70. Meanwhile, CL lower than 0.70 indicates that the response pattern is not close to a perfect scale. Table 1 shows the tabulated results of the CL computations done by the researchers.

Table 1: Coefficient and Likeability

	Education	Employment and Livelihood	Health	Social Relation
No. of errors	15	13	16	60
No. of items	5	5	5	5
Coefficient of Likeability	0.85	0.87	0.84	0.4

As observed in the table above, in terms of education, the response pattern of the respondents has a CL of 0.85, meaning that the answers of the sample will most likely be the same as the whole population. In connection, this also shows that there is a difficulty in accessing basic education for the Iraya-Mangyan IP. Moving on to the aspect of employment and livelihood, the computed CL is 0.87, which indicates another close agreement to a perfect scale. In this light, this also shows that there is a crisis in employment and livelihood for the Iraya-Mangyan IP. Meanwhile, the health aspect has a CL of 0.84, which shows that the response pattern of the respondents also has a close agreement to a perfect scale. Again, this indicates that there is a problem accessing basic health services for the Iraya-Mangyan IP. On the other hand, the CL for the social relation aspect is only 0.4, which is below the acceptable CL of 0.70. This indicates that the Iraya-Mangyan IP do not experience extreme injustice or discrimination from the people

outside their indigeneity.

Based on the actual setting of the Iraya-Mangyan IP first handedly witnessed by the researchers, there was little to no social support infrastructure around their area. From the Municipality of Sta. Cruz, at least thirty (30) minutes of a tricycle ride to go to the location of their tribe. The route to the Iraya-Mangyan IP area was not paved and only had one lane. Moreover, the roads were next to agricultural lands owned by the private sector. The area of the tribe was very secluded. Their way of living was not primitive, but when compared to the lifestyle of the people in the nearest urban area, one could observe a massive gap. For instance, the municipal hall of Santa Cruz was well architectured and was next to a stadium wherein sports and other huge events could be conducted.

Based on the data collected from the respondents, the social support infrastructure they all agreed they needed was a bridge that could be built to connect two points that went over the creek. According to the Iraya-Mangyan IP, if the water level rose, it would be impossible for them to go through it because the current would also be substantial. When an emergency happened, it was challenging to transport sick patients. Moreover, it would also greatly help the tricycle drivers who would pick up and/or drop off passengers to and/or from the tribe's location. On the other hand, the only mode of transportation that could pass through the narrow roads going to the Iraya-Mangyan Tribe was only tricycles. However, no tricycle lanes were designated to serve the people coming out and/or in their area. Based on the data gathered, these two particular projects were needed by the Iraya-Mangyan people, and they would benefit from a faster and safer trip when they needed to go to and from their tribe.

4. Conclusion

This research sought to study the quality-of-life Iraya-Mangyan IPs had and the present conditions in their inhabited area to determine how they lived their everyday lives and how they moved around their domain. This would also indicate if they had access to social infrastructure, whether a transportation system was available throughout their locations, or how far they could access transportation infrastructure in their area. In addition, knowing their difficulties in life would make this study feasible as it aimed to provide help and convenience for indigenous people around the country, especially in Iraya-Mangyan IP.

In conclusion, no inclusive transportation and comprehensive social support infrastructure were available and accessible for Iraya-Mangyan IP. The transportation system was not sufficient and was defective. According to them, they had requested the local government several times to build a bridge since there was a stream along their route. However, they have failed miserably since, up until now, no construction was happening. In addition, the road was bumpy and not sustainable. In addition, the healthcare system provided for them by the government was flawed since they had to wait for a week before they could get financial assistance. If this were the case, the critical patient would die by the end of the week. Moreover, the clinic provided for them in their domain was useless, as they would still not be treated since no health professionals and medical equipment were available. They would borrow money just for them to acquire medicine or medical services. Additionally, they hardly got any assistance for their farms, like even fertilizers, knowing they needed the aid since most of them only do farming.

The statements mentioned above would indicate that the government did still not prioritize indigenous people. This might be because they were just one of the minority groups and not profit-makers that could contribute drastically to the economy. That was why Iraya-Mangyan struggled so much to survive and endure all the hardships they had experienced. They might be starting to catch up to people in the modern world, but that would take a while and not that easy as they have limited

exposure, especially to education. However, with the help of the government and the other people around them, it would be possible and safe for them, especially the new generation of Iraya-Mangyan, to dream big and go out of their comfort zone. One aspect that would help them be exposed to the modern world is transportation. Once they have easy access to the urban areas and other social infrastructure, many opportunities might arise, like job opportunities. Their way of living would improve. They could also broaden their horizons and perspectives. In addition, once they could access higher education, they would be knowledgeable, which would help them elevate their lives. There would be a big chance that some of the Iraya-Mangyan could be successful in their chosen field or become one of the country's presidents. Moreover, they would now have the power and resources to help other minority groups and contribute to the country's success.

References

Bjerregaard, P., Petersen, I. K. D. & Larsen, C. (2018). Measuring social inequality in health amongst indigenous peoples in the Arctic. A comparison of different indicators of social disparity among the Inuit in Greenland.

Burnett, et al. (2020). Indigenous Peoples, settler colonialism, and access to health care in rural and northern Ontario.

Camargo, B., Winchenbach, A. & Maguirre, M. (2022). Restoring the dignity of indigenous people: Perspectives on tourism employment.

De La Cruz, et al. (2020). Indicators of well-being among indigenous peoples of the Colombian Amazon: Tensions between participation in public policy making and autonomy.

Google Maps. (2023). Sitio Calomintao, Alacaak, Santa Cruz, Occidental Mindoro, Philippines.

Gothwal, et al. (September 2009). Guttman Scale Analysis of the Distance Vision Scale. Invest. Ophthalmol. *Visual Science. 50*(9):4496-4501.

International Work Group for Indigenous Affairs. (2021). Indigenous peoples in Philippines.

Jobling, D., & Snell, E. J. (1961). The Use of the Coefficient of Reproducibility in Attitude Scaling. *The Incorporated Statistician, 11*(2), 110–118.

Li, J., Brar, A. & Roihan, N. (2021). The use of digital technology to enhance language and literacy skills for Indigenous people: A systematic literature review.

Muir, B. (2022). Consequences and implications of British Columbia's failed cumulative effects assessment and management framework for Indigenous peoples.

Philippine Statistics Authority. (2022). Household Population, Number of Households, and Average Household Size in Occidental Mindoro based from the 2020 Census of Population and Housing | Philippine Statistics Authority MIMAROPA.

Pomelo, G. (2020). A week with the Iraya, Mangyan of Puerto Galera and the Warriors of Light.

United Nations Development Programme. (2010). Fast Facts: Indigenous Peoples in the Philippines.

United Nations. (2021). UNPFII Twentieth Session: 19-30 April 2021 for Indigenous Peoples. United Nations.

Wignall, et al. (2019). 'We built this city': Mobilities, urban livelihoods and social infrastructure in the lives of elderly Ghanaians. *Geoforum*, 103, 75–84.

Yap, E. (2021). Why you should visit the culture-rich Mangyan in Mindoro. Smile Magazine.

Cite as: Regala S.N., Carillo J.A.G., Dadiz F.D.D. & Cueto G., "An Inclusive Transportation for Iraya-Mangyan IP in Accessing Social Infrastructure using Scalogram Analysis", *The 2nd International Conference on Civil Infrastructure and Construction (CIC 2023)*, Doha, Qatar, 5-8 February 2023, DOI: https://doi.org/10.29117/cic.2023.0142

Revisiting the Building Design Attributes and Indoor Radon: A Survey of 36 Homes in the Commonwealth of Kentucky

Osama E. Mansour
School of Engineering & Applied Sciences, Western Kentucky University,
Bowling Green KY, United States Of America
Oe.Mansour@Wku.Edu

Shahnaz Aly
School of Engineering & Applied Sciences, Western Kentucky University,
Bowling Green KY, United States Of America
Shahnaz.Aly@Wku.Edu

Peter Hall
School of Engineering & Applied Sciences, Western Kentucky University,
Bowling Green KY, United States Of America
Peter.Hall702@Topper.Wku.Edu

Abstract

Radon is an odorless radioactive gas that exists in the soil underneath buildings in areas that is rich in Radium and Uranium. It seeps from the soil and accumulates in the indoor environment. In 2009, radon gas has been classified by the International Agency for Research on Cancer as being carcinogenic to humans. According to the US Environmental Protection Agency (EPA), indoor radon is the second leading cause of lung cancer after smoking in the United States. EPA recommends homeowners mitigate their houses against radon if the indoor radon concentration exceeds 4 pCi/L. Building new healthy homes while developing affordable building renovation strategies is one of the key solutions to mitigate the impacts of such environmental hazards. This research explores the relationship between building design attributes and radon gas in areas prone to higher concentrations of indoor radon. 36 homes with different age, design features, and construction materials were tested in Bowling green Kentucky, an area classified as zone 1 by the Environmental Protection Agency (EPA). Zone 1 is defined by the EPA as an area where the predicted indoor radon average is greater than 4 pCi/L. The survey also collected data about the architectural design, construction materials, structure systems, HVAC systems, and building envelope design of each house that participated in the study. The purpose is to feedback to the construction industry with potential improvements to help with the current indoor radon mitigation efforts. The results open the doors for further research needed to enhance the current building design and construction methods in areas prone to a higher concentration of indoor radon.

Keywords: Indoor radon; Design attributes; Home; Kentucky

1 Introduction

Radon gas exists in the soil of areas rich in radioactive substances such as Radium and Uranium (Dieu Souffit et al., 2022; Missimer et al., 2019). It seeps from the soil to indoor environment and accumulates to higher levels during the winter months. One of the adverse health effects of indoor radon is being one of the primary causes of lung cancer for non-smokers (Cheng et al., 2021; Riudavets et al., 2022; Su et al., 2022; Vogeltanz-Holm & Schwartz, 2018). EPA set 4 pCi/L indoor radon concentration as a threshold for homeowners to mitigate their houses. The current study investigates various design attributes and potential impacts on indoor radon in Warren County, Kentucky. The average indoor radon in this area is higher than 4 pCi/L.

A previous geological research was done to study the fact that Bowling Green is a city built on Karst landscape is subjecting homes to environmental issues such as high indoor radon (Webster, 1990). The study found indoor radon concentration average of 25 pCi/L with 47% of the homes in the area above the 4.0 pci/L limit. The EPA reported in 2020 that the average indoor radon is 14.0 pci/L in Bowling Green Kentucky homes (EPA). However, the geological research did not include building design attributes regarding indoor radon in such areas.

2 Building Design Attributes

There are many design attributes that contribute to indoor radon. The attributes include building structure, foundation type, building envelope design, construction materials, heating and cooling systems, building location, and cost of construction. Homeowner's requirements or needs are the main driver to the building design attributes (Barros-Dios et al., 2007; Li & Hopke, 1991; Lu et al., 2019; Mansour, 2021; Stabile et al., 2016; Webster, 1990). However, homeowners are not fully aware of such important design attributes. According to the realtor association of US only 5-10% of home buyers are aware of indoor radon issue who ask to get the house tested before signing the contract (Momin et al., 2018). Homeowner's choice of home location is mostly based on their work location (Manaugh et al., 2010). Also, according to The National Association of Home Builders (NAHB) analysis of the Census Bureau's Survey of Construction (SOC), Custom homes accounted for only 17.6% of new single-family homes started in 2021. This indicates that most of home design attributes are not a result of feedback from the current homeowners or building users. For instance, homeowners might have a preference in the foundation type but most of the time they buy a house with certain type of foundation based on the availability in the area they want to live in. they don't choose the construction details, they just choose from what is available and already built by the contractors.

Homeowners find wood frame structure as a first and dominant choice when buying a house in the United States. They only have a few choices for building envelope style and materials, either exterior wood frame wall covered with vinyl siding, or covered with brick veneer. They also don't have various choices for heating and cooling systems. For example, in Bowling Green Kentucky with its humid subtropical climate, all new construction homes are mechanically ventilated with forced air HVAC system, A combination of a furnace for heating in winter and a heat pump for cooling in summer. The authors surveyed various factors that could attribute to the indoor radon concentration, however, only 4 attributes were examined in the current study; foundation type, ventilation type, building envelope materials, and availability of mitigation systems in the tested homes, Figure 1 shows the building design attributes considered in the current study.



Fig. 1: Building design attributes considered in the study

3 Method

Most of the research into indoor radon involves measurements of radon averages in the indoor environment using one of two ways (Yarmoshenko et al., 2016). Short-term testing using passive devices or active devices that usually take between 2 and 90 days. The passive devices include Alpha track detectors, charcoal canisters, or charcoal liquid scintillation detectors. After using passive devices for testing, they are usually sent to a laboratory for analysis. On the other hand, active devices require power to operate. Continuous monitors and Alpha trackers are commonly used for long-term testing (George, 2008). A long-term test gives a reading that is more likely to reflect the building's year-round average radon level than a short-term test (Barros et al., 2014). In the present study, active digital Alpha trackers were used to offer more precise readings for greater potential for generalization.

Professional digital radon monitors were used to identify the average indoor radon concentrations in thirty-six houses, each house was tested for at least 72 hours. Some houses were tested for longer term up to three months period because they were part of another experiment. Each monitor has a passive diffusion chamber and uses Alpha spectrometry to calculate the average indoor radon. Table 1 shows the sample characteristics such as age, mitigation status, foundation type, building envelope materials, ventilation type, and average indoor radon in pCi/L. Figure 2 shows the sample clustered based on building design attributes.

Table 1: Building characteristics aligned with the indoor radon averages

House number	Time it was built	Mitigation status (Mitigated/ non-mitigated)	Foundation type	Building Envelop materials	Naturally/ Mechanically Ventilated	Average indoor radon concentration pCi/L
1	1970	Mitigated	Crawlspace	Brick	Mechanically	5.3
2	1999	Mitigated	Crawlspace	Vinyl siding	Mechanically	5.1
3	1920	Mitigated	Slab	Brick	Mechanically	8.9
4	2006	Mitigated	Crawlspace	Brick	Mechanically	2.5
5	1924	Mitigated	Slab	Brick	Mechanically	6.4
6	1993	Mitigated	Crawlspace	Vinyl siding	Mechanically	5.4
7	2004	None	Crawlspace	Brick	Mechanically	4.1
8	1981	Mitigated	Basement	Brick	Mechanically	1.4
9	2005	None	Crawlspace	Brick	Mechanically	2.0
10	1951	None	Crawlspace	Vinyl siding	Mechanically	8.1
11	2021	None	Crawlspace	Vinyl siding	Mechanically	13.2
12	2017	None	Crawlspace	Vinyl siding	Mechanically	2.9
13	2010	Mitigated	Crawlspace	Brick	Mechanically	1.8
14	1974	Mitigated	Slab	Brick	Mechanically	8.4
15	2018	None	Crawlspace	Vinyl siding	Mechanically	5.9
16	2018	None	Crawlspace	Vinyl siding	Mechanically	7.6
17	2019	None	Crawlspace	Vinyl siding	Mechanically	9.2
18	2019	None	Slab	Vinyl siding	Mechanically	4.3
19	2019	None	Crawlspace	Vinyl siding	Mechanically	13.1
20	2020	None	Crawlspace	Vinyl siding	Mechanically	7.6
21	2020	None	Crawlspace	Vinyl siding	Naturally	0.7
22	2020	None	Crawlspace	Vinyl siding	Mechanically	5.5
23	2020	None	Crawlspace	Vinyl siding	Mechanically	8.9
24	1938	None	Basement	Vinyl siding	Mechanically	2.9
25	1950	None	Crawlspace	Brick	Mechanically	54.5
26	1950	None	Crawlspace	Stone	Mechanically	4.0

House number	Time it was built	Mitigation status (Mitigated/ non-mitigated)	Foundation type	Building Envelop materials	Naturally/ Mechanically Ventilated	Average indoor radon concentration pCi/L
27	1972	None	Crawlspace	Vinyl siding	Mechanically	13.8
28	1971	None	Crawlspace	Brick	Mechanically	26.0
29	1972	None	Crawlspace	Brick	Mechanically	21.8
30	1973	None	Crawlspace	Brick	Mechanically	25.8
31	1971	None	Crawlspace	Brick	Mechanically	25.3
32	1936	None	Basement	Stone	Mechanically	16.8
33	1936	None	Crawlspace	Brick	Mechanically	5.5
34	1978	None	Crawlspace	Brick	Mechanically	22.0
35	1992	None	Crawlspace	Brick	Mechanically	26.4
36	1993	None	Crawlspace	Vinyl siding	Mechanically	14.1

The radon data was analysed to find out whether is there a corelation between building age and indoor radon, to identify the mean and median of indoor radon in the 36 houses, the mean and median of indoor radon in each foundation type, the mean and median of each building envelope type, and compare these averages. The purpose is to explore a potential impact of such building design attributes on indoor radon concentration in Bowling Green KY an area classified as zone 1 by the EPA.

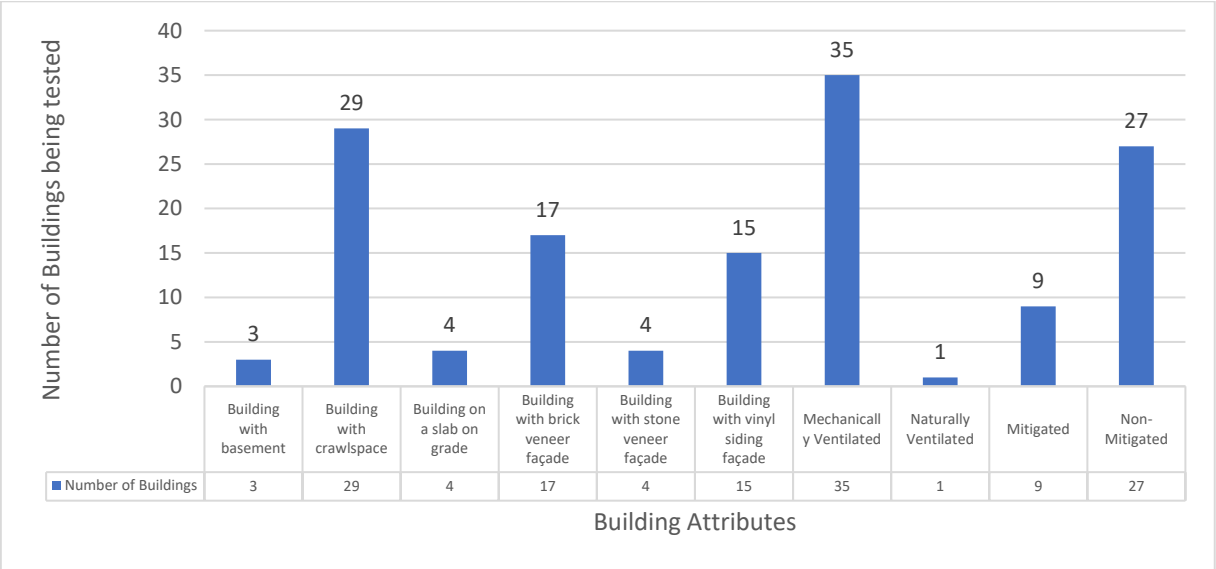


Fig. 2: Buildings included in the study clustered based on the design attributes

4 Results

The indoor radon readings range between 2 to 54.4 pCi/L in the 36 houses with average of 11.03 pCi/L and median 7.6 pCi/L. The indoor radon concentration average in the 36 houses exceeds the limit set by the EPA 4 pCi/L (the mitigation threshold set by the EPA). This result updates the work of Webster (Webster, 1990) that showed the average of indoor radon in 113 homes in Bowling Green Kentucky in 1990 to be 25 pCi/L. in the current study, only 3 (8.3%) of the 36 houses have indoor radon concentration less than 4pCi/L. 9 (25%) of the 36 houses have radon mitigation systems installed, however, it has been found that only 2 of the 9 mitigated houses have indoor radon concentration less than 4pCi/L.

Figure 3 shows the radon readings with the indoor air temperature, relative humidity, and atmospheric pressure in one of the houses. This house was tested for long term indoor radon. The readings were collected around the clock for five months, the average indoor radon concentration was found 14.1 pCi/L.

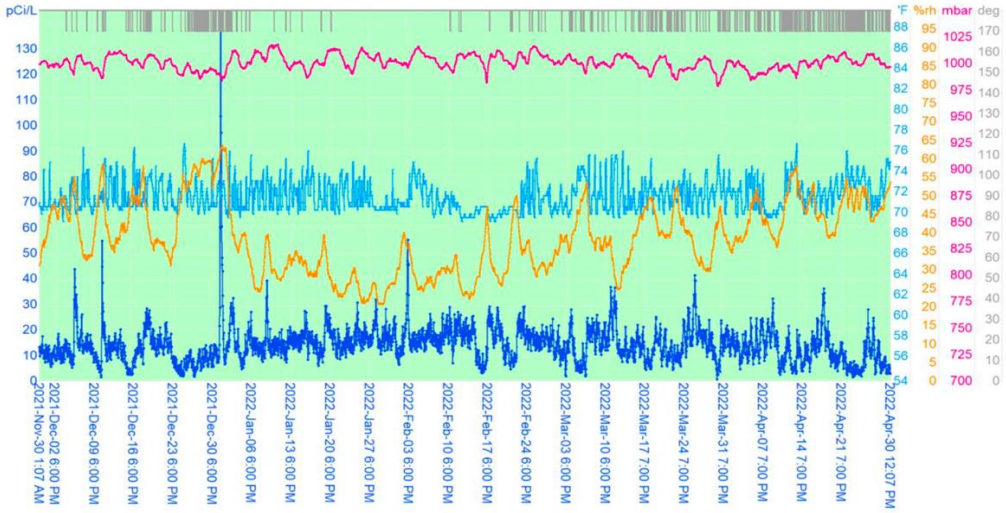


Fig. 3: Indoor radon readings pCi/L aligned with indoor air temperature, relative humidity, and atmospheric pressure in one of the houses included in the study

Figure 3 shows the relationship between the house age and the averages of indoor radon. The analysis shows that there is a weak or almost no correlation between building age and indoor radon averages in the 36 houses. The correlation coefficient is 0.2718. This result contradicts with the authors previous pilot study on mitigated houses in Bowling Green Kentucky (Mansour, 2021)

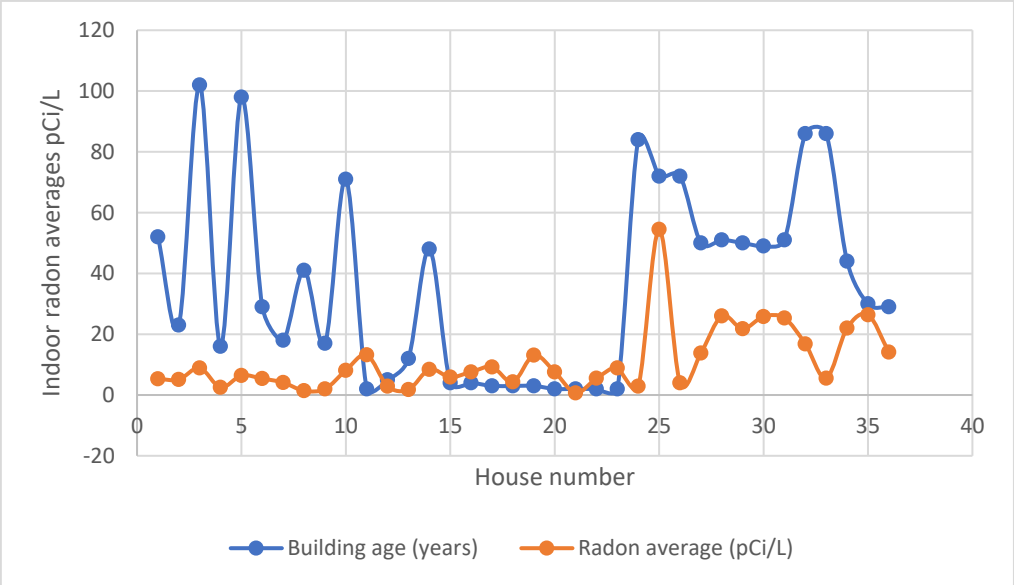


Fig. 4: The correlation between house age and radon averages in the 36 houses

Figure 5 shows the relationship between the mean and median of indoor radon in pCi/L of the 3 different types of foundation included in the study. The foundation type that was associated with the least indoor radon averages was slab-on-grade. The average indoor radon concentration in the houses built on concrete slabs is 7 pCi/L while the median value is 7.4 pCi/L. in the houses with basement the mean value is 7.03 pCi/L while the median value is 2.9 pCi/L. In the houses built on crawlspace, the mean value is 12 pCi/L while the median value is 7.6 pCi/L.

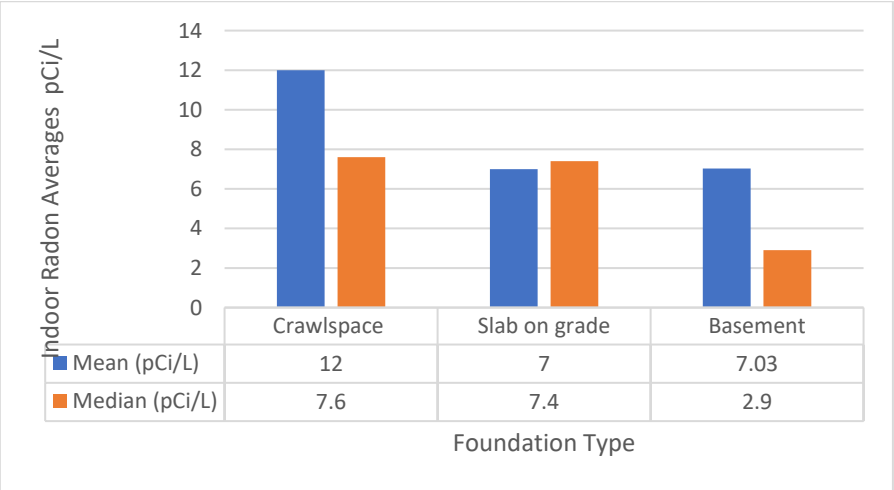


Fig. 5: The Mean and Median of indoor radon averages associated with the three different foundation types found in the 36 houses

Figure 6 shows the relationship between the mean and median of indoor radon in pCi/L of the 3 different types of building envelop materials included in the study. The building envelope type that was associated with the least indoor radon averages was wood frame covered with vinyl siding. The average indoor radon concentration in the houses with vinyl siding is 6.69 pCi/L while the median value is 5.9 pCi/L. In the houses with stone veneer, the mean value is 12,18 pCi/L while the median value is 13.95 pCi/L. In the houses with wood frame and brick veneer facads, the mean value is 14.59 pCi/L while the median value is 8.4 pCi/L.

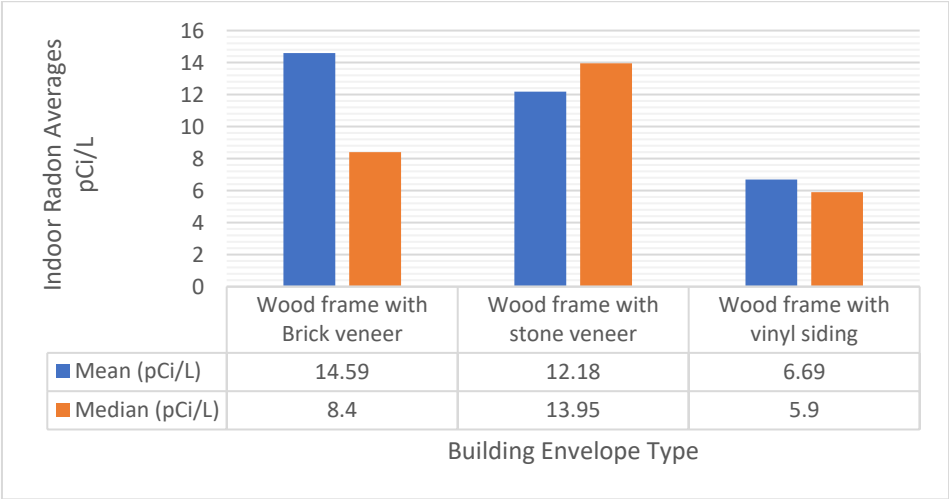


Fig. 6: The Mean and Median of indoor radon averages associated with the three different building envelope types found in the 36 houses

5 Conclusion

In the present study, 36 random homes were tested for indoor radon in Warren County, Kentucky. The average of indoor radon in this area is higher than 4 pCi/L. The objective is to investigate weather building design attributes impact or correlate with the indoor radon concentration average in these homes. This research builds on a previous study done in 1990 to investigate the impact of the Karst landscape on indoor radon in Bowling Green single family houses (Webster, 1990).

Digital radon monitors were used to measure the indoor radon concentration in each house. The indoor radon concentration was measured through monitoring the Alpha particles in the indoor environment around the clock. The test period ranges from short term testing for 72 hours in some

buildings to long term testing for 5 months in other buildings. The study focusses on building age, construction type, building materials, foundation type, and ventilation system type as building design attributes that could impact the concentration of indoor radon.

The measurements indicate that there is a weak or almost no correlation between the building age and indoor radon averages in the 36 houses. The indoor radon concentration ranges between 2 to 54.4 pCi/L in the 36 houses with average of 11.03 pCi/L and median 7.6 pCi/L. The radon average exceeds the limit set by EPA 4 pCi/L. only 13% of the sample had indoor radon concentration less than 4 pCi/L. Houses built on a slab on grade had indoor radon concentration lower than houses with crawlspace. Houses with facades covered with vinyl siding had indoor radon averages lower than houses with brick or sone veneer building envelope.

The results show a novel perspective for the relationship between building design attributes and indoor radon in areas classified as zone 1 by the EPA. It also, helps homeowners to better understand the importance of mitigating their homes against such environmental hazards. The authors suggest that radon mitigation should be regulated in areas classified as zone one by EPA. Further investigation in more houses is currently underway to generalize the conclusion of the current study.

References

Barros, N. G., Steck, D. J., & Field, R. W. (2014). A comparison of winter short-term and annual average radon measurements in basements of a radon-prone region and evaluation of further radon testing indicators. *Health physics*, *106*(5), 535.

Barros-Dios, J., Ruano-Ravina, A., Gastelu-Iturri, J., & Figueiras, A. J. E. R. (2007). Factors underlying residential radon concentration: results from Galicia, Spain. *103*(2), 185-190.

Cheng, E. S., Egger, S., Hughes, S., Weber, M., Steinberg, J., Rahman, B., Worth, H., Ruano-Ravina, A., Rawstorne, P., & Yu, X. Q. (2021). Systematic review and meta-analysis of residential radon and lung cancer in never-smokers. *European Respiratory Review*, *30*(159).

Dieu Souffit, G., Jacob Valdes, M., Bobbo Modibo, O., Flore, T. S. Y., Ateba Jean Félix, B., & Tokonami, S. (2022). Radon risk assessment and correlation study of indoor radon, radium-226, and radon in soil at the cobalt–nickel bearing area of Lomié, Eastern Cameroon. *Water, Air, & Soil Pollution*, *233*(6), 196.

George, A. C. (2008). World history of radon research and measurement from the early 1900's to today. AIP Conference Proceedings,

Li, C.-S., & Hopke, P. K. J. H. p. (1991). Efficacy of air cleaning systems in controlling indoor radon decay products. *61*(6), 785-797.

Lu, M., Chen, D., & Nicol, A. M. (2019). A study of radon concentration in homes in the Sea to Sky corridor and the North Shore of Vancouver British Columbia. *BCIT Environmental Public Health Journal*.

Manaugh, K., Miranda-Moreno, L. F., & El-Geneidy, A. M. (2010). The effect of neighbourhood characteristics, accessibility, home–work location, and demographics on commuting distances. *Transportation*, *37*(4), 627-646.

Mansour, O. E. (2021). *Re-examining the Efficacy of Radon Mitigation Systems in Single-Family Dwellings: A Pilot Study* ZEMCH 2021, Dubai, United Arab Emirates.

Missimer, T. M., Teaf, C., Maliva, R. G., Danley-Thomson, A., Covert, D., & Hegy, M. (2019). Natural radiation in the rocks, soils, and groundwater of Southern Florida with a discussion on potential health impacts. *International journal of environmental research and public health*, *16*(10), 1793.

Momin, B., McNaughton, C., Galanek, J. D., Neri, A., Gallaway, M. S., & Puckett, M. (2018). A qualitative study of Realtor knowledge, attitudes, and practices related to radon health effects: Implications for comprehensive cancer control. *Cancer Causes & Control*, *29*(12), 1249-1255.

Riudavets, M., Garcia de Herreros, M., Besse, B., & Mezquita, L. (2022). Radon and lung cancer: current trends and future perspectives. *Cancers*, *14*(13), 3142.

Stabile, L., Dell'Isola, M., Frattolillo, A., Massimo, A., & Russi, A. (2016). Effect of natural ventilation and manual airing on indoor air quality in naturally ventilated Italian classrooms. *Building and Environment*, *98*, 180-189.

Su, C., Pan, M., Liu, N., Zhang, Y., Kan, H., Zhao, Z., Deng, F., Zhao, B., Qian, H., & Zeng, X. (2022). Lung cancer as adverse health effect by indoor radon exposure in China from 2000 to 2020: A systematic review and meta-analysis. *Indoor Air*, *32*(11), e13154.

Vogeltanz-Holm, N., & Schwartz, G. G. (2018). Radon and lung cancer: What does the public really know? *Journal of environmental radioactivity*, *192*, 26-31.

Webster, J. W. (1990). Radon Contamination of Residences in a City Built Upon a Karst Landscape Bowling Green, Warren County, Kentucky.

Yarmoshenko, I., Vasilyev, A., Malinovsky, G., Bossew, P., Žunić, Z. S., Onischenko, A., & Zhukovsky, M. (2016). Variance of indoor radon concentration: Major influencing factors. *Science of The Total Environment*, *541*, 155-160. (Science of the Total Environment)

Cite as: Mansour O.E., Aly S. & Hall P., "Revisiting the Building Design Attributes and Indoor Radon: A Survey of 36 Homes in the Commonwealth of Kentucky", *The 2nd International Conference on Civil Infrastructure and Construction (CIC 2023)*, Doha, Qatar, 5-8 February 2023, DOI: https://doi.org/10.29117/cic.2023.0143

Effect of Double Decker Flyover Construction on Urban Fabric of Ashok Rajpath, Patna, India

Bijay Kumar Das
Associate Professor, Dept. of Architecture &Planning, NIT Patna, Patna, Bihar, India
bijay@nitp.ac.in

Arpita Srivastava
M. Arch, 3rd Sem., Dept. of Architecture &Planning, NIT Patna, Patna, Bihar
arpitas.pg21.ar@nitp.ac.in

Avi Kush
B. Tech, Civil Eng. (3rd Sem.), SMVDU, Katra, Jammu and Kashmir, India.
avikush@ymail.com

Abstract

Rapid urbanization and increase in number of vehicles has led to diminishing vehicular spaces on the street. This has led to construction of flyovers, which has dominated the streets. They reduce the "Sky-View" factor and has a put a serious threat to "Enclosure" widely used in Urban Design concepts. It has reduced the openness for the pedestrians and severely obstructed the views. This paper examines the effect of fly-over on the "Urban Fabric of an ancient street "Ashok Rajpath" of Patna, India.

Keywords: Sky-view factor; Urban fabric; Fly-over; Enclosure ratio; Street

1 Introduction

According to 2019, Pedestrians, bikers, and users of motorised two-wheelers account for more than 58% of all road mortality casualties in Patna (MoRTH, 2020). The three groups can be known for vulnerable to utilising road and are prone to accidental damage. When compared to no flyover, the existence of a flyover raises the relative risk by 15% (Goela, Jain & Tiwari, 2017).

Flyovers are major road structures that are generally erected on crossings to take away continuous influx, mainly in non-urban areas. To alleviate Karachi's transportation issues, the city government built approximately fifty flyovers at major city crossings. However, in most cases, thorough end long planning have been implemented, resulting in half fulfilment of the city's removal of traffic-allied problems (Zubair, 2019).

According to a recent survey in Bangalore, traffic congestion is the most pressing public problem, followed by poor road conditions "No 1 reason..., followed closely by poor traffic management and lack of proper (sic) infrastructure like flyovers" (TOI Survey, 2008) for the issue. Widening of road, grade-separated crossings (often known as flyovers), restricted access motorways, integrate lights, and traffic management strategies in urban areas were among the former set of improvements (Tiwari, 2002). Using flyovers can save a lot of time and energy by avoiding congestion and minimising negative environmental impacts like smog and traffic jams. Even though its primary function is to make roads safer, flyovers also improve the city's visual appeal. People using the flyover will have a bird's-eye view of the city below.

While there are certainly some drawbacks to using flyovers, these are mostly the result of poor construction of buildings, improper planning, etc.

2 Research Methodology

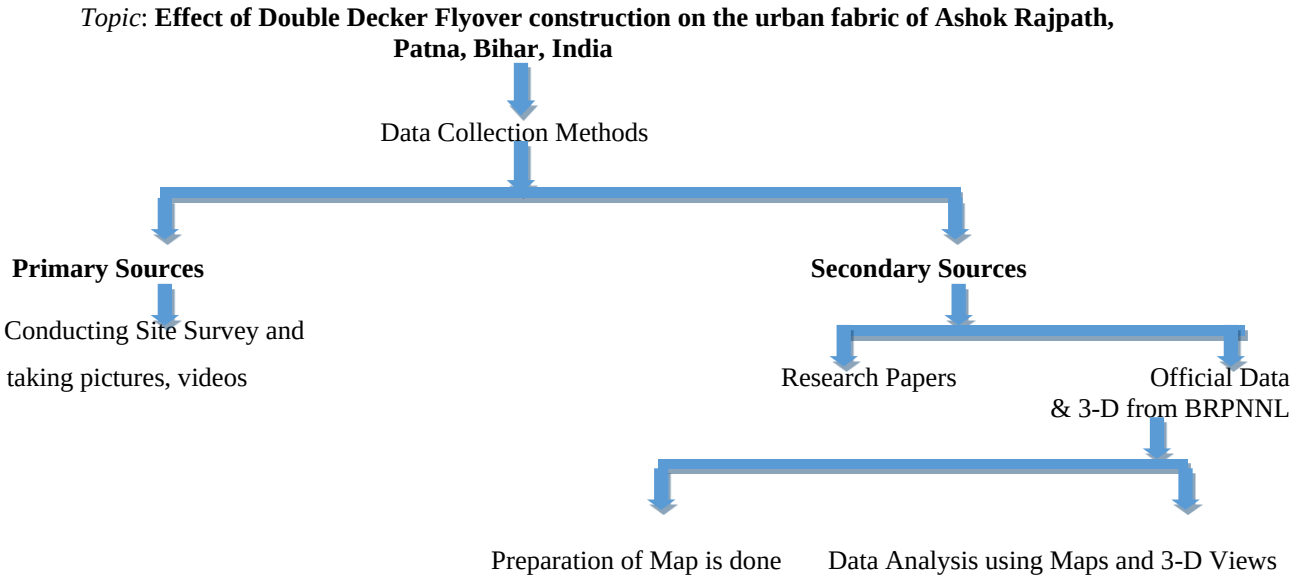


Fig. 1: Research Methodology Flowchart

3 Effect Of flyover on the Urban Fabric

Urban expansion and use of transport are intertwined because transportation networks assist create the urban layout while also promoting the city's economic, cultural, and social development. Similar to how a city's characteristics influence its architecture (Anwar, HONG & Afia Zubair, 2020).

The physiognomies of built-up places, also the characteristics of cities are related with urban fabric, which is different from urban density, land use, and transportation infrastructure. There are differences in the spatial distributions of urban density as a result of new constructions and redevelopments, and new facilities for transportation impacts accessibility and land use. Transport infrastructure is critical to the study of urban form because it separates and unites urban territory into well-defined city segments and allows humans to perform tasks that connect the social, economic, and environmental systems to population growth and urbanization increase.

In architectural sense, flyovers affect the view of street and façade of buildings thus affecting the urban fabric of area. The skyline of an area totally changes giving flyover a static object as a monumental scale and food carts, vehicles as dynamic objects as human scale.

4 Upcoming Flyover in Ashok Rajpath, Patna

On Ashok Rajpath, a 2.2 km-long double-decker flyover has to be built (TOI, 2021). The flyover runs from Kargil Chowk, which is near to Gandhi Maidan to Patna Science College. Rajya Pul Nirman Nigam Pvt. Ltd. Vehicles will be moved at three levels after this project is completed: Tier 2, tier 1and the add-grade level, which is the existing road. There will be no change in grade level. All four lanes of tier 1 and tier 2 will conclude at Patna Science College with three exits for the PMCH via its multi-level parking. The double-decker flyover would be connected to the Loknayak Ganga Path by the Krishna Ghat (Ganga Expressway) (Wikipedia, 2022).

Table 1: Details of Ashok Rajpath 2-Lane Double Decker Flyover

Name of Project	**Construction of Elevated Corridor from Kargil Chowk, Gandhi Maidan to Science College via PMCH, Ashok Raj Path, Patna, Bihar (2-Lane Double Decker)**				
District/Head	Patna				
Description of Project	(i) Type of Structure-RCC/PSC / Steel Composite, (ii) Length of elevated corridor-2.2 km, Length of Tier-1 is 1.5 km and Tier-2 is 2.2 km (iii) Carriage way-2 x 2-lane Double Decker (Tier-1 two lanes + Tier-2 two lane)				
Administrative Approval	Rs.422.00 Crore {RCD, Lt No.-5566 (S) dated-24.09.2020}				
Agreement Amount	Rs.324.0049 Crore (Agreement no.-16/2021-22).				
Date of Start	15.01.2022				
Schedule Date of Completion	14.01.2025				
Contractor	Gawar Construction Limited, DSS- 378, Sector: 16-17, Hisar 125 005 (Haryana)				
Physical Progress					Remarks
Foundation	Sub-Structure	Super-Structure	Approach	Expenditure (Rs. in Cr.)	Work in Progress
20%	15%	15%	-	5.40	

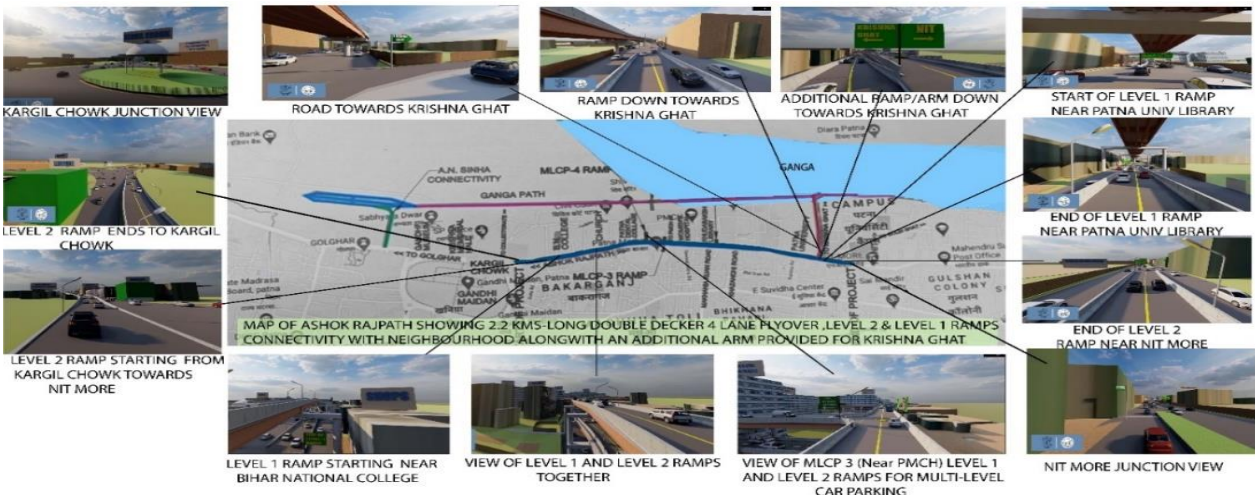


Fig. 2: Map of Double decker flyover on Ashok Rajpath alongwith detailed views

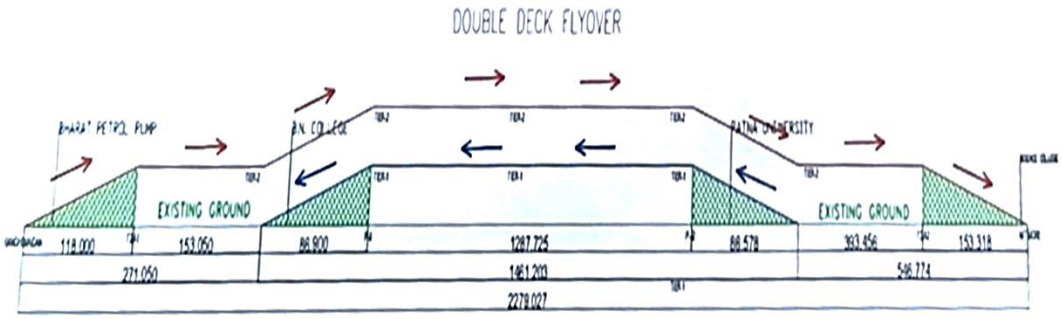


Fig. 3: Sectional Elevation of Double decker flyover on Ashok Rajpath

5 Sky-view Factor and Flyover

The sky view factor (SVF) is the ratio of a point's viewable sky area to the overall sky area. It establishes the link between the observable sky region and the surrounding covered areas, like built

structures, big trees etc. (Miao, et al., 2020). The SVF, as a key criterion in urban climate analysis and urban planning practices is used worldwide (Miao, et al., 2020).

The planning of structures and canyons in urban streets on both edges of a roadway is a critical issue influencing urban micro - climatic and air pollution (Ali-Toudert & Mayer, 2006). The ratio of building heights (H) to street canyon width (W), often known, as the aspect ratio, and the sky view factor (SVF), are two indices that can be used to identify the geometric properties of urban street surfaces.(Arnfield & John, 2003), (Unger, 2009). The aspect ratio illustrates the concentration of built structures in comparison to their heights (Unger, 2009). The SVF is a more favorable parameter than the aspect ratio since it better captures the complicated urban environment (G.T. & Watson, 1984). It denotes the ratio of sky to regions where buildings or plants are blocking it (Matzarakis & Algeciras, 2015), (An, et al., 2013), (Tzu-PingLin, Kang-TingTsai, Ruey-LungHwang & Andreas Matzarakis, August 2012), (SantosNouri, PedroCosta & Matzarakisb, December 2017). Oke (1981) proposed the concept of SVF to evaluate the impact of urban heat islands in urban settings (Oke, 1981; Watson & G., 1987). It is now utilized as a geometric notion to offer the fraction of the observable area of the sky inside the street canyons, which dimensionless values provide an explanation. (Oke, 1981; Xiaodong, et al., 2019). It is stated as a value between 0 and 1, with 0 signifying a completely closed region and 1 representing an open area (Oke, 2015; Scarano & Mancini, 2017). Increasing the elevation of structures along open spaces blocks the sky and reduces the SVF, whereas lowering the elevation increases the SVF (Bourbia & Boucheriba, 2010; Adeb Qaid, Hasanuddin Bin Lamit, Dilshan Remaz Ossen & Mohd Hisyam Rasidi, 2018). SVF influences the surface heat balance, micro-scale airflow, air pollution, and microclimate of the urban environment, to name a few (Venhari, Martin Tenpierik & Taleghani, 2019). It has been widely used in urban climate research, such as renewable energy utilization (Compagnon, 2004), outdoor thermal comfort and urban heat island studies (Unger, 2009; Liang Chen, et al., 2010; Hämmerle, Gál, Unger & Matzarakis,2009), Biometeorology of humans (F. Lindberg & C. S. B. Grimmond, 2010), (Andreas Matzarakis, Frank Rutz, & Helmut Mayer , 2007) and urban planning practices (F.Bourbia & F.Boucheriba, 2010), (Eliasson, 2000), (Ruihan Weia, Dexuan Song, Nyuk HienWong, & Miguel Martin, 2016).

Furthermore, the SVF is buildings which obstructs the sky around a street may significantly restrict how much sun radiation reaches canyons, therefore they should be included in an urban solar radiation model. (Ali-Toudert & Mayer, February 2006), (J.A.R., Tablada, & Matzarakis, 2003), (Corripio, 2003), (Christine Ketterer & Andreas Matzarakis, 2014), (Herrmann & Andreas, 2012), (T.Nguyen & Joshua, 2012), (Qaid A & Ossen D, 2003). It might be integrated in studies on enhancing the thermal setting in an urban region using remote sensing (Yang, Man, Massimo, & Janet, 2015).

Areas having lower SVF values cool more quickly at night and get warmer gradually within the day, owing to shadowing from buildings and trees (Loyde, Lucila, & Andreas, 2015), (Robert D. Brown & Terry J. Gillespie, 1990), (M.Scarano & J.A. Sobrino, 2015). As a result, deep roadway canyons with narrow widths and tall buildings may limit thermal exchange (M.Scarano & F.Mancini, 2017).

Urban climate change studies and urban planning have recently focused heavily on how thermal comfort levels vary across various urban SVF values, particularly in light of climate change and population growth. (Ruihan Weia, Dexuan Song, Nyuk HienWong, & Miguel Martin, 2016), (Kim & Yun, 2019), (Xiaojiang Li, Carlo Ratti, & Ian Seiferling, 2018), (Yun Kyu Yi & Hyoungsub Kim, 2017).

6 Enclosure and Flyover

The relationship between building height and floor area, as well as their relationship to the surrounding landscape, structures, and roadways. In addition, it includes the solar direction, site coverage, and building envelope. Dimension and mass affect the amenity of streets, spaces, and other buildings by creating a sense of openness or enclosure. Enclosure: height to distance ratio h/d = 1:1 (full enclosure) = 1:2 (minimal enclosure) = 1:3 (threshold of enclosure) = 1:4 (loss of enclosure).

Table 2: Explanation of different types of Enclosure Ratio

Enclosure Ratio	Explanation
1:1	Enclosure 1:1 is when one tends to see details of building more than façade.
1:2	Enclosure 1:2 is when the object perceived in relationship with surrounding.
1:3	Enclosure 1:3 is when all perceived together with details.
1:4	Enclosure 1:4 is when an object seen as an edge.
1:6	Enclosure 1:6 is when the backdrop of building more than its façade.

Enclosure can be seen on Ashok Rajpath on different locations through the following pictures.



Fig. 4: Loss of Enclosure (1:4) happens on Ashok Rajpath after coming of the flyover

7 Results & Discussion

This paper explains the effect on urban fabric of an area with the coming of double-decker flyover between Kargil Chowk and NIT More. Thus, by connecting it to Krishna Ghat will help keep traffic moving without interruptions. Hence, it will reduce the travelling time for two and four wheeler vehicles.

In addition, by coming of Double decker flyover, the skyline of the street will change, thus affecting buildings front facade and increase in their height. This will induce a total change in the street canyons, as perceived from the bird's eye view. Usually with the increase in the height of buildings around street canyons, the sunrays from the sky gets blocked, that leads to a reduction in the SVF.As sky is less visible and solar access is limited and this will affect the lives of people, animals and plants. The study of enclosure is also done along the Ashok Rajpath, as the coming of double decker flyover will thus affect the enclosure ratio, hence loss of enclosure will be seen at several points along the street.

Acknowledgements

I am grateful to Bihar Rajya Pul Nirman Nigam Ltd. (BRPNNL) who provided the resourceful data to work for this research paper.

References

Algeciras, J. , Tablada, J. & Matzarakis, A. (2003). Effect of asymmetrical street canyons on pedestrian thermal comfort in warm-humid climate of Cuba. *Theor. Appl. Climatol.*, 1 - 17.

Ali-Toudert, F. & Mayer, H. (February 2006). Numerical study on the effects of aspect ratio and orientation of an urban street canyon on outdoor thermal comfort in hot and dry climate. *Building and Environment,Volume 41, Issue 2*.

Arnfield, J. (2003). Two decades of urban climate research: A review of turbulence, exchanges of energy and water, and the urban heat island. *International Journal of Climatology,Volume 23, Issue 1*, 1-26.

An, et al. (2013). Three-dimensional point cloud based sky view factor analysis in complex urban settings. *RMets,International Journal of Climatology*.

Anwar, A., Hong, L. & Afia Zubair, R. (2020). Effect of Transport Infrastructure in changing the urban form of a historical city: A case study of Lahore. *ISOCARP 2020* (p. 11). Doha: ISOCARP.

Bourbia, F. & Boucheriba, F. (2010). Impact of street design on urban microclimate for semi arid climate (Constantine). *Renewable Energy, Volume 35, Issue 2*.

Chen, et al. (2010). Sky view factor analysis of street canyons and its implications for daytime intra-urban air temperature differentials in high-rise, high-density urban areas of Hong Kong: a GIS-based simulation approach. *RMetS International Journal of Climatology*.

Compagnon, R. (2004). Solar and daylight availability in the urban fabric. *Energy and Buildings,Volume 36, Issue 4*.

Corripio, J. G. (2003). Vectorial algebra algorithms for calculating terrain parameters from DEMs and solar radiation modelling in mountainous terrain. *International Journal of Geographical Information Science,Volume 17 - Issue 1*.

Eliasson, I. (2000). The use of climate knowledge in urban planning. *Landscape and Urban Planning,Volume 48,Issues 1–2*, 31-44.

Goela, R., Jain, P. & Tiwari, G. (2017). Correlates of fatality risk of vulnerable road users in Delhi. *Accident Analysis and Prevention*, 86-93.

Hämmerle, et al. (521–527). Comparison of models calculating the sky view factor used for urban climate investigations. *Theoretical and Applied Climatology volume 105*, 2011.

Harbich, L., Labaki, L. & Matzarakis, A. (2015). Effect of tree planting design and tree species on human thermal comfort in the tropics. *Landscape and Urban Planning,Volume 138*, 99-109.

Herrmann, J. & Matzarakis, A. (2012). Mean radiant temperature in idealised urban canyons—examples from Freiburg, Germany. *International Journal of Biometeorology,volume 56,* 199–203.

Ketterer, C. & Matzarakis, A. (2014). Human-biometeorological assessment of heat stress reduction by replanning measures in Stuttgart, Germany. *Landscape and Urban Planning,Volume 122, February 2014*, 78-88.

Kim, H. & Y. K. (2019). QuVue implementation for decisions related to high-rise residential building layouts. *Building and Environment,Volume 148*, 116-127.

Li, X., Ratti, C. & Seiferling, I. (2018). Quantifying the shade provision of street trees in urban landscape: A case study in Boston, USA, using Google Street View. *Landscape and Urban Planning,Volume 169*.

Lindberg, F. & Grimmond, C. S. B. (2010). Continuous sky view factor maps from high resolution urban digital elevation models. *Inter-Research Science Publisher, CR 42:177-183*.

Matzarakis, A. & Algeciras, J. R. (2015). Quantification of thermal bioclimate for the management of urban design in Mediterranean climate of Barcelona, Spain. *International Journal of Biometeorology,60, (2016),* 1261–1270.

Matzarakis, A., Rutz, F. & Mayer, H. (2007). Modelling radiation fluxes in simple and complex environments—application of the RayMan model. *International Journal of Biometeorology volume 51*, 323–334.

Miao, et al. (2020). Review of methods used to estimate the sky view factor in urban street canyons. *Building and Environment 168*, 1-8.

MoRTH. (2020, September 24). *Road Accidents in India – 2019.* Retrieved from Ministry of Road Transport & Highways

Transport Research Wing New Delhi,GOI: www.morth.nic.in

Nguyen, H. & J. M. (2012). Incorporating shading losses in solar photovoltaic potential assessment at the municipal scale. *Solar Energy,Volume 86, Issue 5*, 1245-1260.

Oke, T. (2015). Street design and urban canopy layer climate. *International Journal of Biometeorology volume 59*, 285–297 .

Oke, T. R. (1981). Canyon geometry and the nocturnal urban heat island: Comparison of scale model and field observations. *Journal of Climatology*.

PTI (2022). Patna Metro"s Ashok Rajpath alignment shifted to institutional area due to flyover project. *Financial Express*.

Qaid A & Ossen D. (2003). Effect of asymmetrical street aspect ratios on microclimates in hot, humid regions. *Int. J. Biometeorol.Volume 56,*, 1-56.

Qaid, et al. (2018). Effect of the position of the visible sky in determining the sky view factor on micrometeorological and human thermal comfort conditions in urban street canyons. *Theoretical and Applied Climatology volume 131*, 1083–1100.

Robert D. Brown & Terry J. Gillespie. (1990). Estimating Radiation received by a Person under Different Species of Shade Trees. *Arboriculture & Urban Forestry Online,Volume 16, Issue 6*.

SantosNouri, A., PedroCosta, João. & Matzarakisb, A. (2017). Examining default urban-aspect-ratios and sky-view-factors to identify priorities for thermal-sensitive public space design in hot-summer Mediterranean climates: The Lisbon case. *Building and Environment,Volume 126*, 442-456.

Scarano, M. & Mancini, F.. (2017). Assessing the relationship between sky view factor and land surface temperature to the spatial resolution. *International Journal of Remote Sensing Volume 38 Issue 23*.

Scarano, M. & Sobrino, J.A.. (2015). On the relationship between the sky view factor and the land surface temperature derived by Landsat-8 images in Bari, Italy. *International Journal of Remote Sensing Volume 36, 2015 - Issue 19-20: Fourth International Symposium on Recent Advances in Quantitative Remote Sensing*.

Steyn, D. , Hay, J. , Watson, I. & Johnson, G. (1984). The determination of view-factors in urban canyons. *Journal of Climate & Applied MeteorologyVolume 23, Issue 2*, 329 - 335.

Tiwari, G. (2002, April). Urban Transport Priorities: Meeting the Challenge of Socio-economic Diversity in Cities, a Case Study of Delhi, India. *Cities,Volume 19,Issue 2*, 95-103.

TOI. (2008). Poor Roads No 1 Cause of Congestion:TOI Survey, Bangalore. *TOI*, p. 1.

TOI. (2013). Bomb scare on Ashok Rajpath. *TOI*.

TOI. (2021). CM lays stones for Patna"s first double-decker flyover. *TOI*.

TOI. (2021). Double-decker flyover: CM Nitish Kumar likely to lay stone tomorrow. *Times of India,Patna*, p. 2.

TOI. (2022, September 5). Patna metro alignment slightly changed. *TOI*.

Tzu-PingLin, et al. (August 2012). Quantification of the effect of thermal indices and sky view factor on park attendance. *Landscape and Urban Planning,Volume 107, Issue 2*, 137-146.

Unger, J. (2009). Connection between urban heat island and sky view factor approximated by a software tool on a 3D urban database. *International Journal of Environment and Pollution,Volume 36, Issue 1-3*, 59-80.

Venhari, A. A., Tenpierik, M. & Taleghani, Mohammad. (2019). The role of sky view factor and urban street greenery in human thermal comfort and heat stress in a desert climate. *Journal of Arid Environments,Volume 166*.

Watson, I. D. & G. T. (1987). Graphical estimation of sky view-factors in urban environments. *Journal of Climatology*.

Weia, et al. (2016). Impact of Urban Morphology Parameters on Microclimate. *Procedia Engineering,Volume 169*, 142-149.

Wikipedia. (2022). *Wikipedia*. Retrieved from Wikipedia: https://en.wikipedia.org/wiki/Ashok_Rajpath.

Xiaodong He, et al. (2019). Influence of sky view factor on outdoor thermal environment and physiological equivalent temperature. *International Journal of Biometeorology, volume 59*, 285–297.

Yang, et al. (2015). Modeling the effective emissivity of the urban canopy using sky view factor. *ISPRS Journal of Photogrammetry and Remote Sensing,Volume 105*, 211-219.

Yi, Y. K. & Hyoungsub Kim. (2017). Universal Visible Sky Factor: A method for calculating the three-dimensional visible sky ratio. *Building and Environment*, 390-403.

Zubair, S. (2019). Impact of Flyovers on Traffic Situation of a Metropolitan City: A Case Study of Karachi-Pakistan. *26th World Road Congress.* Abu Dhabi, United Arab Emirates: National Academies,Transportation Research Board.

Cite as: Das B.K., Srivastava A. & Kush A., "Effect of Double Decker Flyover construction on Urban Fabric of Ashok Rajpath, Patna, India", *The 2nd International Conference on Civil Infrastructure and Construction (CIC 2023)*, Doha, Qatar, 5-8 February 2023, DOI: https://doi.org/10.29117/cic.2023.0144

Built Environment Attributes and Walking Patterns: A Case Study of Abu Dhabi Downtown

Jiin Baek
Department of Architecture, College of Engineering, Qatar University, Doha, Qatar
jiin.baek@qu.edu.qa

Abstract

Walkability is crucial in sustainable urban design. Our understanding on the walkability in cities in hot and arid climate needs to be improved due to shortage of our knowledge and previous studies about this. Thus, this study aimed to demonstrate the value of sustainable urban design in enhancing downtown Abu Dhabi residents' walking experience. Urban neighbourhoods' quality of walking environment and the scale of the downtown's super block in Abu Dhabi Main Island were measured. In addition, it is examined how its urban design influences walking behaviour by selecting two study sites based on land use diversity. To measure them, the current study investigated the (1) walkable distance in Abu Dhabi; (2) scale of pedestrian movement; and (3) potential purpose of walking patterns of pedestrians of urban infrastructure. Site observation and surveys were carried out for collecting data that supports people's perceptions linked to walking purpose, quality, frequency, and intensity. To analyse these data, the geographic information system was employed. With this study, walking distance for the utilitarian purpose service in Abu Dhabi block cover by 0.5 miles. There is the active movement regardless of the extreme weather conditions both weekday and weekend. This study data could potentially guide designers and policy-makers to create a healthier walking environment for Abu Dhabi residents as well as some cities in hot and arid climate.

Keywords: Walkability; Land use; Urban form; Pedestrian movement

1 Introduction

In a sustainable community, walkability is an important planning factor that can promote city scales and socioeconomic benefits (Speck, 2013; Claris & Scopelliti, 2016). Walkable neighbourhoods are crucial for sustainable communities as they encourage good health (Alfonzo, 2005), lead to economic improvement (Carmona et al., 2018), reduce CO_2 emission (Chapman et al., 2018), and bring about social development for the community instead of car-based urbanism. Talen (2013) revealed that a Google Scholar search for a "walkable neighbourhood" returned 500 entries, 96% of which had been published since 2000, demonstrating scholars' interest in walkable environments. Academic and practicing planners access the links between the built environment and physical activity as an influence for individual health (Cervero & Kockelman, 1997, 2000; Handy et al., 2002; Moudon et al., 2006). Several studies have presented examples of how to build transportation infrastructure, (e.g., direct proximity or transit-oriented development); support travel behaviours through urban forms (e.g., density, diversity, and design); and create positive walking experiences for individual pedestrians' safety and comfort (Neighborhoods, 1998). However, these factors of creating a sustainable community with walking behaviour are a debatable question in the United Arab Emirates (UAE); the National Bureau of Statistics of UAE recorded the summer temperature to be 38~42°C, and reached to 48°C in August, high air temperatures exceed the comfort zone range. The current

study aims to demonstrate the value of sustainable urban design in enhancing Abu Dhabi downtown residents' walking experience. To find out how the built environment influences pedestrian movement in a walkable neighborhood, we conduct empirical observation in two sites in different land-use characteristics of blocks. To measure the scale of pedestrian's movement framed on demographic composition, the number of pedestrians who passed by the street segment in the downtown superblock (approximately 200 m × 200 m) is counted. For walking, a random survey is administered to identify the preference of micro-scale of urban design elements (mainly land use store pattern) and preferred times for walking.

2 Literature Review (Factor of Walkability)

Walkability has received significant attention because of its role in sustainable development and its diverse benefits associated with public health, social life, sustainable environment, and the economy. As per Speck (2013), walkability is important for determining how a city is sustainable, healthy, and vibrant. Shimitz and Scully (2006) supported the idea that a pedestrian-friendly street design may help residents' biological health, contribute to positive lifestyle changes, and improve overall quality of life. Additionally, a pedestrian-friendly walkable environment enhances the street vitality (Gauvin et al., 2008). In post-modern urban planning, walkability is how safe and convenient on foot in their neighbourhood and it involved the many discourse and efforts how to define and measure walkability.

As outlined in Handy (2002) and Frank and Pivo (1994), the dimension of density can increase opportunities for walking or cycling rather than using a car through compact city development. With a similar logic, other dimensions of built environments, such as design and diversity, also affect people's travel mode choices. For example, Ewing and Cervero (2010) found a strong correlation between land use diversity and different frequencies of walking based on the type of amenity. Another built environment aspect, "connectivity and accessibility," is an essential criterion for enhancing walkability in terms of pedestrian comfort (Hillier and Hanson, 1989; Legeby, 2010). These two aforementioned elements help public transportation network planning and facilitate the desired and intended use of city development. Moreover, many scholars have measured connectivity, accessibility, and proximity with street configuration to analyse built environment characteristics (Legeby, 2010). Handy (2002) claimed that street connectivity, mixed use development, and good design improve the attractiveness of walking and bicycling despite physical and psychological barriers. Another aspect of walkability research focuses on the purpose of walking. Owen (2004) examined walking and walking environments in terms of aesthetic attributes, convenience of facilities, destination accessibility, and car perception, finding that "walking for exercise" differed from "walking to destination." Lee and Moudon (2006) individually observed micro-scale environment elements and proposed destination, distance, density, and route (3D+R) with objective measures. In their study, the number and accessibility of amenities had a solid relation to walking time (Cerin et al., 2007). Additionally, walkability increased when more grocery and retail shops, churches, and schools were in the neighbourhood, and when amenities were closely located, there was a positive relationship to the destinations within a 5-min walking distance (Southworth, 2005; Lee and Talen, 2014). Talen (2013), who is a new urbanist, emphasized a small, walkable block size with wide sidewalks and trees. Walkable neighbourhoods also sustain pedestrian-based services within walking distance, and social interaction and a sense of community contribute to a safe neighbourhood environment and increase the property value of the community. Walkable access to amenities creates a "pedestrian shed," where destinations are within a 5-min walking distance or a

radius measuring approximately 400 meters, considered to be the distance that people are willing to walk before opting to drive (Mehta, 2008).

2.1 Physical Built Environment and Characteristics of the Research Sites.

Since 1963, Abu Dhabi has been characterized by extensive growth as a modern city concept (Bani Hashim, 2015). During that period, the old core of the downtown expanded along the northern shoreline (Corniche), and the Airport Road became the main link to areas situated in the mainland. With the increase of oil prices, the city grew rapidly between 1972 and 1980. The urban form of the 1970s was characterized by arterial roads in a gridiron pattern, square blocks, and buildings within the superblocks. During this period, the inner part of the superblocks started to form, including secondary service roads that ran parallel to the arterial roads, passageways between buildings for pedestrian movement, etc. High-rise buildings were constructed at the perimeters of the superblocks, while mid- and low-rise buildings were built inside. Commercial and mixed buildings were 30-floors tall. From 1975 to 1979, 628 buildings were built in Abu Dhabi's mainland, which is a significant increase compared to the construction of 90 buildings during 1970–1974 (Bani Hashim, 2015).

This study focuses on the city's central downtown area built during the 1970s urban evolution (Figure 1). The superblock is situated in one of highest population density areas in the Abu Dhabi Main Island (average density = 156.5 ppl/acre). Designated as a visual climax of high-rise building composition in the early development stage (1970s–1980s), the buildings exhibit distinctive characteristics in terms of their height: high-rise at the rim of the superblock and low-, mid-, or high-rise in the middle. Numerous studies have investigated how density, land use, street connectivity, and perception affect walking patterns. Various methodologies were utilized to evaluate walkability quality for the examined areas. The ways of measuring walkability have been discussed from planning and transportation to the environment and health fields, with various theories on pedestrian movement (Frank and Pivo 1994; Handy et al. 2002; Newman 1996). To measure pedestrian movement objectively, researchers created audit tools and developed measurement methods, qualitative and quantitative (Lee and Talen, 2014).

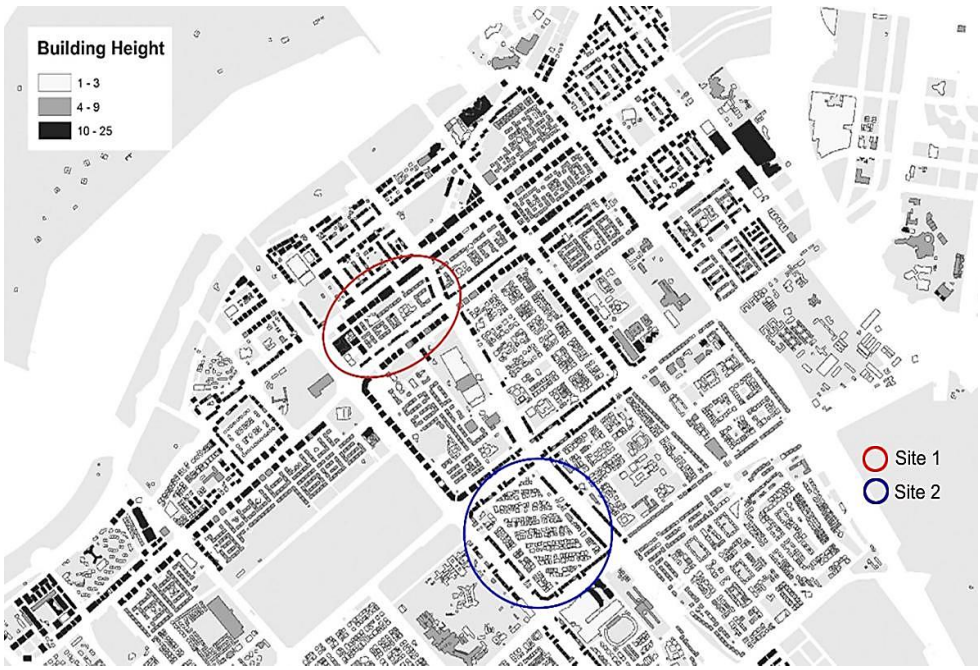


Fig. 1: Building density based on height. Case study area: Hamdan St. Block (Site 1; circled in red) and Al Falah St. Block (Site 2; circled in blue)



Fig. 2: Study Site 1 (left): High- and mid-rise typology; Study Site 2 (right): High-rise and low-rise typology

3 Materials and Methods

3.1 Physical Built Environment and Characteristics of the Research Sites

To analyse what extent the built environment and individual perception affect walkability in the region, two different land use feature were chosen. Both are located in Abu Dhabi's central district constructed during the 1970s along with the most significant streets in the city centre. The site design is based on principles of modern urbanism, especially the gridiron street pattern. An individual, single block is considered a super block (forming a square, some of which are more than 400 × 400 m), with secondary service roads running parallel to the arterial roads and pathways between the buildings for pedestrian movement. Assuming Abu Dhabi block size covers a walkable distance of about 0.25 mile (400 m), the current study measured the walkable distance for an individual block boundary. The methodology is designed to capture pedestrian natural movement in the research sites with survey analysis.

As we can see the table 3, the main difference between the two sites is their land uses and building densities. Site 1, Hamdan Street block (Sector E3-01), has an area of 0.2598 km^2 and comprises high-rise buildings[1] constructed along the perimeter of the superblock, with mid-rise buildings on the inner side. As both building types are used for commercial and residential purposes, the area contains low-rise retail stores and high-rise buildings for residential use. Further, Site 1 has a high percentage of diverse land use characteristics, such as various types and scales of retail businesses, offices, public institutional uses for school or mosque, and vertical residential buildings. Site 2, Al Falah Street block

[1] Low-rise buildings have 1–3 stories, mid-rise buildings have 4–9 stories, and high-rise buildings have 10 stories or more.

(Sector E18-01), has an area of 0.4175 km^2 comprising high-rise (commercial and residential) buildings along the perimeter of the block and low-rise residential villas or one- to two-story buildings in the inner block. Site 2 was primarily designed for residential use or single land use, with small-scale retail business at the boundary of the block. Additionally, Site 2's street layout of the superblock interior is rotated in the east–west direction instead of being parallel to the Corniche.

The analysis of walkable environment characteristics at each site was conducted by targeting residents and visitors in two different areas that had varied building densities. Considering the site characteristics in detail (Table 3) shows that they are alike in population with diverse housing components from single to multi-families: Site 1 has a population[2] of 38,880 and an area of 0.18 km^2 (215.55 ppl/acre), while Site 2 has a population of 44,987 and an area of 0.22km^2 (146.49 ppl/acre). Since Abu Dhabi was designed as a car-oriented city, pedestrian sidewalks on both blocks lacked consistency in terms of sidewalk width, design, street furniture, and trees. Site observation was conducted at the end of winter and spring, which is a suitable time for collecting pedestrian movement data in consideration of the culture and temperature of the region. Because of Arabic cultural customs, including *qayloulah* (afternoon nap), more active movement is observed on the streets after 4 p.m.

Site observation was conducted at both sites over a 2-week period, including weekdays and weekends, from January 2015 to early April 2015. Observations were carried out on sunny days with an average temperature of 32 °C between 4:30 p.m. and 7:00 p.m. This time of the day was chosen because it has the most active movement. To investigate how many people walked and moved around, a pedestrian audit was conducted at both sites. The method employed was a cross-section counting method[3] developed by Bauer, which counts pedestrian numbers at various time stamps. To achieve reliable observation data, counting points in each area were designated to 25 points from a block in Site 1 (high- and mid-rise with mainly retail shops) and 23 points from a block in Site 2, (high- and low-rise with mainly residential villas). For precise and rigorous observation, pedestrian movement and counting were observed at two levels: (1) the block perimeter and (2) selected intersections of the internal blocks. Entry points and the middle of each street segment were taken as additional counting points. As this study investigates how different urban forms or configurations indicate different walking patterns in each block as well as the natural pedestrian movement in Abu Dhabi's downtown area, observations were conducted at various points of urban characteristics at each site.

4 Results

4.1 Site Observation

Site 1, Hamdan Street, is a 4 km stretch in the heart of the capital city, known for its retail hubs, commercial buildings, and apartment complexes (a ground floor, mezzanine, plus 18 floors). With large new developments constructed in Abu Dhabi within the last decade, this area could be considered the old downtown. The Hamdan street area shows the most dynamic pedestrian movement and traffic congestion in Abu Dhabi.

The area is one of the oldest neighbourhoods with affordable shopping outlets, a series of hotels, and a vertical residential community close to the Corniche and Madinat Zayed. Retail businesses on the

[2] The population as mentioned in the GIS data from 2016 provided the number of floors through building footprints.

[3] Cross section counting method: The most basic measurement of a crowd is pedestrian counts at a cross section. A cross-sectional count is a pair of pedestrian numbers and time stamp indicating the number of people that crossed a particular virtual gate (henceforth called counting line) either since the last measurement or exactly at the indicated time stamp. This method enables obatining information on volume flow, flow rates, and (for suitable configuration and directional counts) occupation level/average pedestrian density

ground floor include jewellery shops, clothing shops, cafés, restaurants, food outlets, electronic stores**,** fruit markets, travel agencies, and vegetable markets. The Hamdan street area is a geographically significant location in the early development Abu Dhabi during the 1970s. There are many various ethnic groups,[4] mainly Arabs, Filipinos, Indians, and Pakistanis, in the area. A noticeable finding is streets can be used as a social gathering place for the same ethnic group of blue-collar workers every Friday. Site 2, Al Falah Street, is a family-friendly environment with many facilities at hand's length. The locals consider it the landmark of Emirati's residential area. In the block, there are many restaurants and an array of retails shops for residents, such as supermarkets, a school, a mosque, a medical centre, and a bank in the building complex surrounding the block. The perimeter comprises high-rise apartment complexes and a two-story villa inside the block. The street pattern of the internal block is uniquely faced to the north and south rather than parallel to the Corniche.

Although the two sites have different land uses, building heights, and density characteristics, they have similar streetscape features. Examining the micro-scale urban elements of Sites 1 and 2 revealed that the 2.5-m wide sidewalk is narrow and makes people feel uncomfortable while walking, especially during busy times. A parking ticket machine (Mawaqif pole) located in the middle of the pedestrian pathway restricts the flow of pedestrian movement. Overall, parking spaces and car traffic are prioritized over pedestrian movement. It is rare to find parks or benches for neighbourhood visitors. At some instances, people were observed sitting in informal areas, such as road curbs, building corners, or building entrances. The alleyways (Sikka) are unhygienic and unsafe places with no maintenance, although they have the potential benefit to create shade for pedestrians.

4.2 Pedestrian Counting (Scale of Pedestrian Movement)

To measure how many people moved around during the peak time (from 4:30 p.m. to 7 p.m.) at the two sites (weekdays and weekends during winter and spring), a pedestrian audit was conducted. An auditing point was designed based on the segment in the street, and the land use pattern was the average number of pedestrians within a 5-min interval at each observation point. Generally, Site 1 had a much higher number of pedestrians than Site 2, and in both regions, the number of pedestrians was higher on weekends than on weekdays (total average for Site 1: 1,800 people on weekends, 1,073 people on weekdays; Site 2: 322 people on weekends, 289 people on weekdays) (Figure 3). As the spider web diagram (Figure 4) shows, the two sites had comparable seasonal patterns of winter and spring but different patterns for weekdays and weekends. Figure 3 shows that Site 1 (mixed land use) had a more consistent pattern across weekends and weekdays than Site 2 (residential area) owing to particular land use features. Although Site 2 (Figure 3) showed s comparable pattern, movements that are more pedestrian were observed on weekdays in the area surrounding the Site 2 block owing to pedestrians passing by on their way to other blocks. With the diurnal pattern for Site 2, the weekday movement follows the shade direction of the perimeter's high-rise building depending on the time.

For Site 1 (mixed land use area), a high number of pedestrian movement in the perimeter corner (253 people on weekends), pedestrian crossing (119 people), and bus stops (206 people) was observed. Inside the block, inner street segment shows a high number of pedestrians in the inner segment from perimeter (188 people) and around the mosque (142 people). Specifically, a huge pedestrian movement was bordered in the Bangladeshi ethnics' social gathering area inside the small block

[4] According to the World Atlas data, the ethnic composition of the UAE in 2019 was as follows: 11.6% Emiratu South, 59.4% Asian (38.2% Indians, 9.5% Bangradeshis, 9.4% Pakistanis, and 2.3% others), 10.2% Egyptians, 6.1% Filipinos, and others 12.8%.

(comprising a seven-storied height); as its street is open, many people come and chat in the street (119 people). Some people sit on the curve with their group instead of using small pocket park inside of Site 1. Street can be social gathering space instead of movement.

For Site 2 (residential villa area), most of the natural movement was recorded near the retail stores, and many people were seen to pass through the internal long segment (segment of point 7, 17, 20) rather than the pedestrian pathway next to the road for going to other blocks. In Al Falah Street, a high number of pedestrian movement occurred around the bus stop (28 people on weekends), the perimeter of the block. Pedestrian movement was rarely observed inside the block surrounding the residential villa block. The inner segment between the villa shows the seldom movement (4–17 people), mosque entrance (19 people), and Indian ethnic restaurants (34 people).

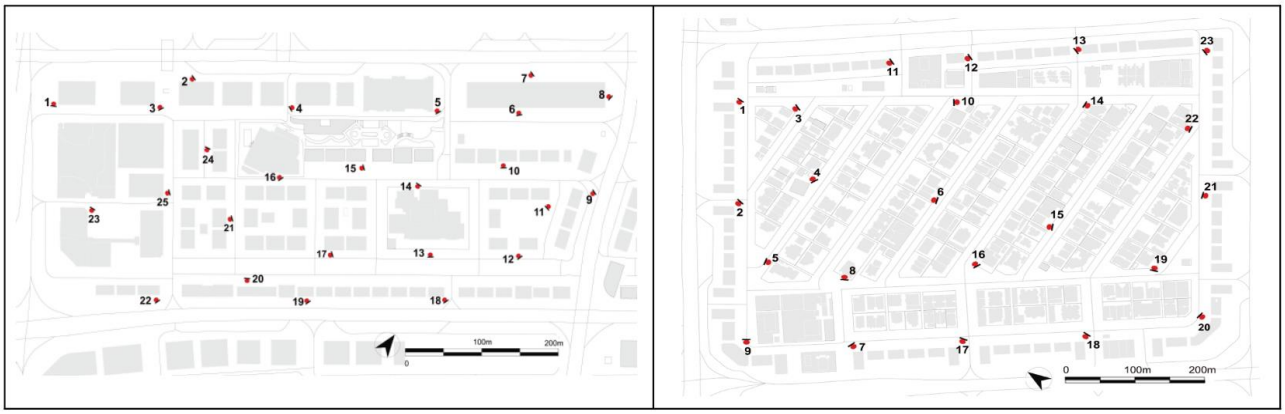


Fig. 3: Pedestrian counts points for Sites 1 and 2

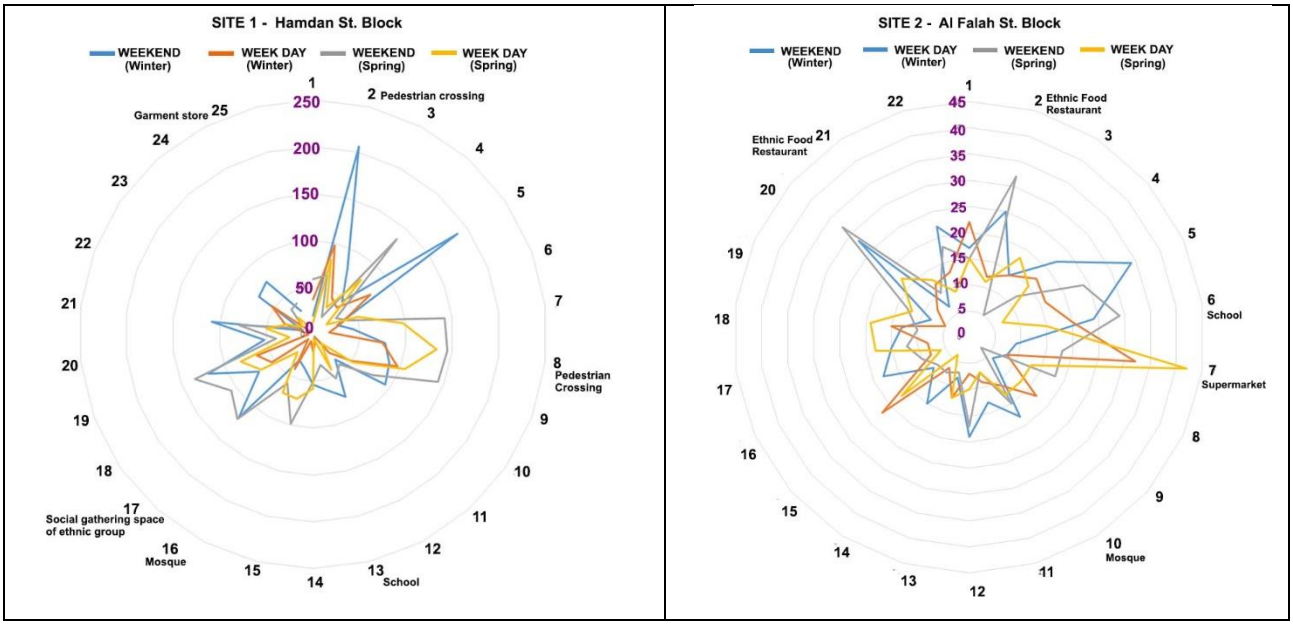


Fig. 4: Spider web diagram of Sites 1 and 2

5 Conclusion

The main finding of the current study can be given that walking behavior in both blocks in Abu Dhabi is strongly associated to a physical built environment. Subsequently, pedestrian perception of the city is found the positive aspect of walking environment in downtown block. The connectivity and accessibility, measured by the ratio between the number of intersections and straight lines in GIS, were sufficient for pedestrian movement. However, consistency of sidewalk pavement in microelement from design perspective is low, although the ratio of overall pavement in sidewalk is

high. The block size is too big to achieve an approachable physical metric for a neighborhood community as a small block size for frequent street access. This research also found the similar results that pedestrian movements in Abu Dhabi have relevance of land use and density to walkability. The design of land use and density are important factor to enhance the walkability in Abu Dhabi downtown. High-density areas with multi-land-use with small stores showed the highest pedestrian movement. Site 1 (Mixed land-use area) showed around four times higher pedestrian movement than site 2 (residential area). In a various ethnic group of pedestrians, Indian sub-continent ethnic has been observed at highest percentages in the block. The current study findings expand our understanding of hot arid region's walking environments and highlight the requirements for enhancing walking experiences. These observed results and analysis of the physical built environments show the potential of walkability to adapt to the other GCC countries and cities in hot arid climate conditions.

References

Alfonzo, M. A. (2005). To walk or not to walk? The hierarchy of walking needs. *Environment and behavior 37*(6):808-36.

Bill, H. & Hanson, J. (1989). The social logic of space: Cambridge university press.

Carmona, et al. (2018). Street appeal: The value of street improvements. *Progress in Planning* 126:1-51.

Cervero, R. & Kockelman, K. (1997). Travel demand and the 3Ds: Density, diversity, and design. *Transportation research part D: Transport and environment 2*(3):199-219.

Ewing, R. & Cervero, R. (2010). Travel and the built environment: A meta-analysis. *Journal of the American planning association 76*(3):265-94.

Frank, L.D., & Pivo, G. (1994). Impacts of mixed use and density on utilization of three modes of travel: single-occupant vehicle, transit, and walking. Transportation research record 1466:44-52.

Gauvin, et al. (2008). Association between neighborhood active living potential and walking. *American journal of epidemiology 167*(8):944-953.

Handy, et al. (2002). How the built environment affects physical activity: views from urban planning. *American journal of preventive medicine 23*(2):64-73.

Hashim, B. & Reem, A. (2015). Planning Abu Dhabi: From Arish Village to a Global, Sustainable Arab Capital City. Doctoral dissertation, UC Berkeley.

Lee, C. & Moudon, A. V. (2006). Correlates of walking for transportation or recreation purposes. *Journal of physical activity and health 3*(s1): S77-S98.

Lee, S., & Talen, E. (2014). Measuring walkability: A note on auditing methods. *Journal of Urban Design 19*(3):368-388.

Legeby, A. (2010). Urban segregation and urban form: From residential segregation to segregation in public space. Doctoral dissertation, KTH.

Mehta, V. (2008). Walkable streets: pedestrian behavior, perceptions and attitudes. *Journal of Urbanism 1*(3):217-245.

Moudon, et al. (2006). Operational definitions of walkable neighborhood: theoretical and empirical insights. *Journal of physical activity and health 3*(s1):S99-S117.

Handy. S. et al. (1998). The Effectiveness of Land Use Policies as a Strategy for Reducing Automobile Dependence: A Study of Austin Neighborhoods. Southwest Region University Transportation Center

Newman, O. (1997). Creating defensible space: Diane Publishing.

Owen, et al. (2004). Understanding environmental influences on walking: review and research agenda. *American journal of preventive medicine 27*(1):67-76.

Schmitz, A., & Scully, Jason. (2006). Creating walkable places: compact mixed-use solutions.

Southworth, M. (2005). Designing the walkable city. *Journal of urban planning and development 131*(4):246-57.

Speck, J. (2013). Walkable city: How downtown can save America, one-step at a time: Macmillan.

Susan, C. & Scopelliti, D. (2016). Cities Alive: Towards a walking world.

Talen, E., & Koschinsky, J. (2013). The walkable neighborhood: A literature review. *International journal of sustainable land use and urban planning 1*(1).

Cite as: Baek J., "Built Environment Attributes and Walking Patterns: A Case Study of Abu Dhabi Downtown", *The 2nd International Conference on Civil Infrastructure and Construction (CIC 2023)*, Doha, Qatar, 5-8 February 2023, DOI: https://doi.org/10.29117/cic.2023.0145

Ganga Riverfront Development at Patna, India: Urban Rejuvenation Project

Fulena Rajak
National Institute of Technology Patna, Patna, India
fulenarajak@nitp.ac.in

Bijay Kumar Das
National Institute of Technology Patna, Patna, India
bijay@nitp.ac.in

Sandeep Kumar
National Institute of Technology Patna, Patna, India
sandeep.ar@nitp.ac.in

Abstract

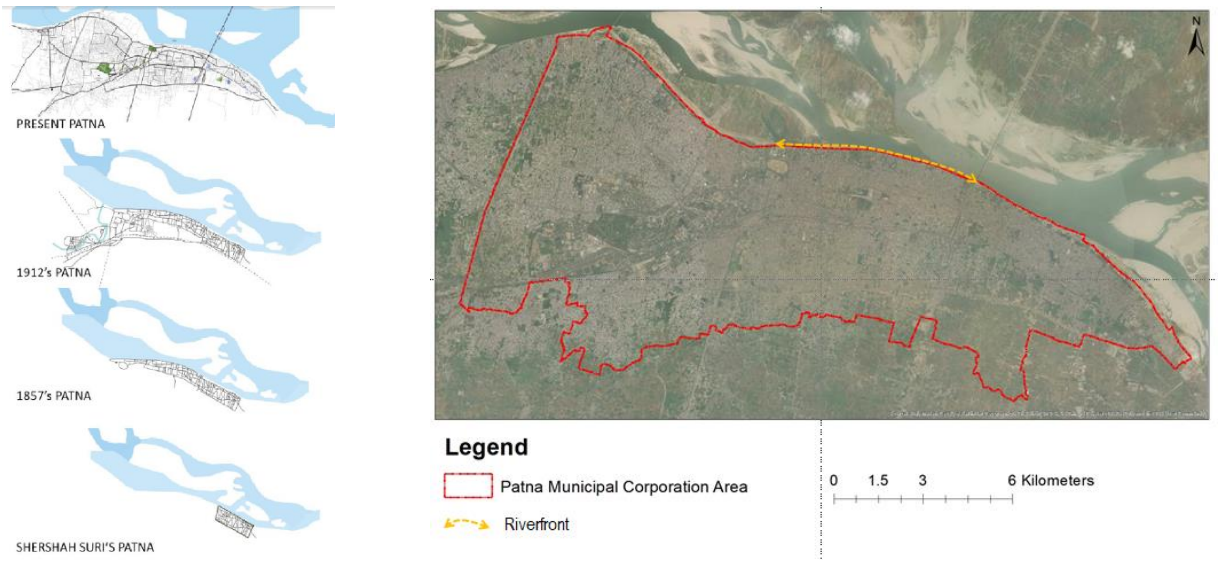
River front project at Patna, India along the river Ganga has rejuvenated the linear city of Patna, India. Patna is a historic city having lived for more than two thousand years. The city has grown linearly on the bank of Ganga. Like other cities of India, it faces the problem of pollution, congestion and lack of public open spaces and recreation spaces. After the completion of River front project, this city has a new life. Once neglected and treated as back yard of city, it has opened up for the residents and has added new avenues of urban open spaces. It has added the recreation space to the city and the happiness index of the city will certainly rise. This paper examines the positive aspects of River front development in the city and how the residents have reacted to it.

Keywords: Public Open Space; Recreational Open Space; River Front; Patna

1 Introduction

Open spaces play a very important role in city's landscape. They have physical, social, economic and environmental benefit. With increase in Urban Population and land use change, these spaces are very vulnerable. This change and pressure of increasing population density is more on the urban core areas. (Ghose, 2015). The growth of Patna is Linear from east to west. Then it grew towards a little of south and then towards west. As per the report and older map, the older city is the special area demarcated in the City's master plan. (Sharma, 2016) (See Figure 1). Patna being the historic City whose history goes back to 600 BC, the core area faces the space crunch for people recreational need. As per the study by Kumar recreational, there is lacuna of open spaces in the core city of Patna (Kumar, 2015).

The core city area lacked the recreational open space (Kumar, 2015). There was a need to fill this lacuna with the potential open space, which will cater the needs of the people. The Riverfront Ghats, which was earlier, isolated, were also unsafe. These potential recreational spaces was then connected and developed as riverfront. Total 6.6 km stretch has been connected alongside of the river, as Ganga river front development out of 21 km stretch touching the Ganga of Patna city. Which, tries to cater the recreational need of nearby residents of the old city area, and now this acts as an active public space.



(a) (b)

Fig. 1: Figure showing **(a)** Evolution of Patna city **(b)** Patna city map with Patna Municipal corporation boundary showing Ganga riverfront

2 River Front of Patna

The riverfront benefits a population of 1 million (Urban Development and Housing Department, 2010) in the special area zone as nearby Residents with accessible open space, Fisherman with more mooring capacity, and infrastructure for Low income communities such as new community hall electric crematorium for the city (Lall, 2021). The developed riverfront with promenade and Ghats comprise of many activities and acts as an active public space which caters the diverse activity, ranging from leisure seating, walking, jogging, skating, outdoor classroom, religious gathering, skits, etc. Apart from these formal activities, it also support informal economy such as local tea and snack seller, religious goods kiosks, which support the formal activity on the riverfront. Earlier before 2016, the riverfront was the neglected space and was acting as backyard of the city. The rejuvenation of Patna riverfront has contributed to the healthy and psychological well-being, of the residents. This also helps in increasing the happiness index of the city with activities like cultural, educational, environmental, health and psychological wellbeing.

The riverfront promotes the walkable city, creation of usable open space catering diverse activity and sensitivity toward local context as per the development vision (Lall, 2021). We will try to assess the vision with the current context and condition based on the observation.

2.1 Accessibility

Ganga river front is accessible from Ashok Rajpath catering diverse land uses. It starts with Collectorate Ghats and Anta Ghat on west and ends at Hanuman Ghat and Gosai Ghat in east. In terms of accessibility, it supports the concept of walkability as it connects the dense area of Patna through walking and non-motorised vehicle network. The major road in old city area is Ashok Rajpath, which is very congested and have very high vehicle commute time, with less pedestrian walking facility. The Ganga River front earlier being the backyard now is accessible and connected through out to provide commute through walking and justifies the walkable city vision for this old city area. It has several accessible puncture from different land use along the river (see Figure-2). However, a few places, it does not have universal accessibility, which gives a break to NMV and makes it difficult to differently abled to connect throughout the riverfront.



(a)



(b)



(c)

Fig. 2: Figure showing **(a)** Accessibility through the residential area towards riverfront **(b)** Connection from the Patna College (Institutional Land use) **(c)** Connection from Kali Temple

2.2 Usability and Activity of Ganga River Front

Open spaces provide many functions in urban context that benefits people's quality of life (Ghose, 2015). It provides physical, psychological, social, environmental, and economic benefit, for that should support diverse activity (Rukiye, 2014). Ganga Riverfront being a recreational open space caters a variety of activity throughout the day like, walking, cycling, jogging, group gathering, outdoor classroom, and caters informal kiosks. It supports the religious activity also; as river Ganga in the Hindu mythology is considered the goddess and rituals such as, Ganga Aarti happens once a week. The spaces also caters the activity for which it is not designed for such as classrooms or group reading at the steps of the Ghats especially near Institutional land use. Pictures showing different activity at Ganga river front is shown in Figure 3.

Physical and Social Activity



Liesure walking and seating



Cycling at Ganga river front



Group gathering at Ghat

Religious Activity



Praying near Ghat



Regional Chhath Festival



Ganga Aarti on Saturday evening

Educational Activity



Steps used as knowledge sharing space

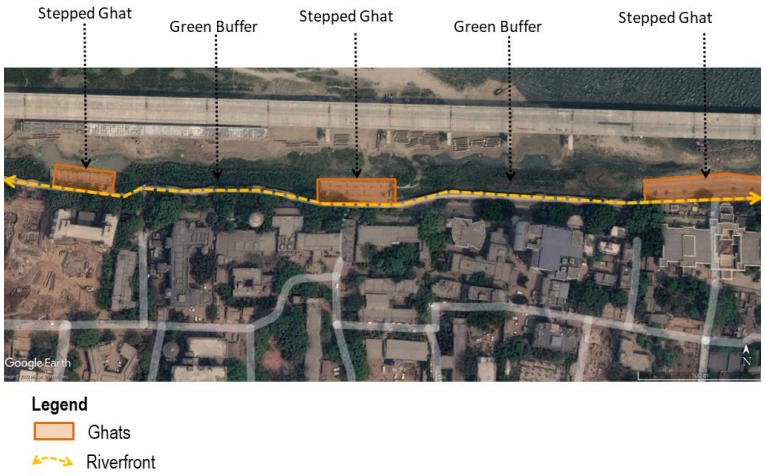


Group reading at Patna College Ghat

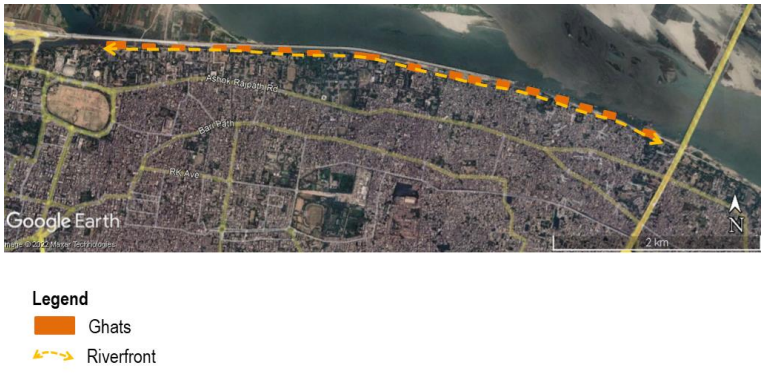
Fig. 3: Figure showing different activity at Ganga River front, Patna

2.3 Sensitivity towards Local Context

The spaces in Ganga River front have diverse spaces to accommodate the local context. The riverfront is mix of natural and constructed edges. Ghats provide connection with the nearby land use to the river, especially near religious and institutional areas. The green buffer in between Ghats acts as riparian buffer (See Figure-4). Riparian Buffer consists of macrophytes, native grasses, sedges, climbers, shrubs and trees (Dutta, 2011). It is the most significant component in ecology and environment as they help in conserving soil, habitat of that area and indirectly influencing fauna and aquatic ecosystem with grassland, wetland, for their habitat. The riverfront shows the combination of grey and green zones within the developed stretch. The local context of social connection as well as the environment connection can be seen in the Ganga riverfront development. However, the expressway proposed in front of the riverfront promenade can affect the riparian buffer of the stretch.



(a)



(b)

Fig. 4: Figure showing **(a)** Ghats and Buffer green spaces, **(b)** 6.6 km Ganga riverfront

3 Discussion

As per the observation analysis of accessibility and usability of the riverfront and contextual analysis through map, the riverfront stands as per the vision. However, it lacks in the universal accessibility as all the places have not been connected with ramps wherever the level difference area there. In usability, the spaces cater variety of activity and support flexible open space to cater different needs of people (see Figure 3). In terms of the context local land use and river connection has been stablished on the basis of accessibility, and usability. Environmentally the grey and green buffer combination has been provided to support riparian buffer (see Figure 4 (a)). The main findings of the study are that, the riverfront is making city more accessible and walkable and it is creating usable open space in the open space scarce core city area. It is also accommodating the green buffer zone, which helps in conserving the riparian zone, ecology and environment.

4 Conclusion

Patna lacks urban green open spaces especially in the core area (Kumar, 2015). The core area also faces congestion and traffic issue. Ganga riverfront tries to solve these two main issues and justifies the vision for the development i.e. walkable city, creation of usable open space catering diverse activity and sensitivity toward local context. The creation of public open space and green areas also support the Sustainable Development Goal 11, and 13 of United Nation. Patna has total 14.5 km stretch touching the river edge excluding the developed 6.6 km riverfront. The remaining area also can be connected to make it one of the spine to connect city, and make city walkable.

References

Dutta, R. B. D. (2011). Influence of riparian flora on the riverbank health of a Himalayan river before being regulated by a large dam in North East India. *Annals of Biological Research*, 268-280.

Ghose, A. A. (2015). An Assessment of Declining Urban Greens under Patna Municipal Corporation Based on Normalized Difference Vegetation Index. *Universal Journal of Environmental Research and Technology, 5*(5: 220-232), 220-232.

Kumar, S. (2015. Study & analysis of urban green spaces and an integrative approach to sustainable development in historic city Patna. *International Journal of Advanced Research, 3*(4), 66-75.

Nishant, Lall. (2021). UIA 2021 RIO: 27th World Congress of Architects, volume ii of iii.

Rukiye Duygu Çay, F. A. (2014). Benefits of Urban Green Spaces for Citizens: Ankara Case Study. *IV International Conference. "Ecology of Urban Areas" 2014.* Zrenjanin, Serbia.

Sharma, R. T. (2016). Safe and Inclusive Cities, Patna: City Profile, Poverty, Inequality and Violence in Urban India: Towards Inclusive Planning and Policies. New Delhi: Institute for Human Development.

Urban Development and Housing Department (2010). City Development Plan (2010-30) PATNA. Government of Bihar.

Cite as: Rajak F. & Das B.K., "Ganga Riverfront Development at Patna, India: Urban Rejuvenation Project", *The 2nd International Conference on Civil Infrastructure and Construction (CIC 2023)*, Doha, Qatar, 5-8 February 2023, DOI: https://doi.org/10.29117/cic.2023.0146

The Impact of Land Mix-use on Inhabitants' Social Wellbeing in the Qatari Neighbourhoods

Hameda Janahi
Assistant professor, College of Engineering, Qatar University, Doha, Qatar
hameda.janahi@qu.edu.qa

Abstract

Health and wellbeing have been key considerations in designing sustainable environments. However, most research on built environments and wellbeing has been conducted in Western communities, with very little research in the context of Middle Eastern countries. This study aims to fill the gap by investigating the impact of the residential built environment on social wellbeing in the cultural context of Doha, the capital of Qatar. The research studied six neighbourhoods in Doha. The investigation used subjective and objective methods such as interviews and spatial models (space syntax), complemented by questionnaires and an observation survey. The data were analysed separately; however, they are thematically discussed in this research. The findings of this research broadly support the work of other studies in this area, linking public spaces with the inhabitants' casual interactions. However, this research found that some uses have a higher impact than others. In Doha, mosques significantly influenced inhabitants' social interaction, especially men. The social relationships between neighbours were maintained in private spaces – *Majles*-. *Majles* had low integration with other spaces in the dwelling, which ensures household privacy. Based on the findings of this investigation, recommendations are made and guidelines developed for future residential developments in Qatar and the surrounding region to ensure the social wellbeing of communities.

Keywords: Wellbeing; Doha; Neighbourhood; Mix-use; Social

1 Introduction

Researchers have examined the use of space in residential environments under many different names, including land mix-use, community spaces, public spaces, and third spaces. Communal space is defined by the Ministry of Housing, Communities and Local Government (2021) as a public space in which most inhabitant movements take place. Communal space includes streets and squares designed as multi-purpose and multi-user. Small and Adler (2019) refer to communal spaces as 'fixed spaces' and define them as sites for unplanned social and direct interaction. Finlay et al. (2019) identify communal space as a 'third space' with a wide range of uses in which people can meet beyond home and work. Third spaces substantially impact social interaction, social support, social network, sense of community, and belonging (Finlay et al. 2019). The mixed uses include the local services, facilities, and functions available in the neighbourhood, supporting the daily lives of inhabitants (Földi, 2006; Ministry of Housing Communities and Local Government, 2021).

Wickes et al. (2019) categorised spatial-use typologies into four groups. These are shown in Table 1, along with the nature of the interactions that occur within the space and the types of interactions. Wickes et al. (2019) claim that collective community identity and social cohesion differ, as some inhabitants who use the space have no interest in its social role.

Table 1: Wickes et al. (2019) categorisation of communal spaces

Type of Land Use	Nature of Interaction	Type of Interaction	Example
Anchoring sites	Scheduled and routinised opportunities for copresence	Frequent interactions between a regular group of users	Schools, libraries, health clubs
Local exposure sites	Unscheduled	Frequent interaction which encourages acquaintanceship ties between regular users	Park
Scheduled conduits sites	Scheduled activities for different users	Unplanned interaction between the same users	Train stations, Cinemas
Extra-local exposure sites	Unscheduled and sporadic interaction	Sporadic interaction with diverse users	Shopping mall

Finlay et al. (2019) noted that communal spaces are associated with quality of life –QOL-, health, and wellbeing. The academic literature on the impact of communal space on social wellbeing examines 1) the characteristics of the neighbourhood's layout design, as well as its functions and the user's proximity to them (Montford, 2013; Wickes et al., 2019; Williams, 2006) and 2) the location, accessibility, and visibility of the communal space (Abu-Ghazzeh, 1999; Cooper, 2014; Francis et al., 2012; Karuppannan and Sivam, 2011; Williams, 2006). It is argued that street syntactic accessibility influences land-use mix, as some uses – such as retail – benefit from high levels of pedestrian movement (Ozbil et al., 2011), while short and direct routes encourage short-distance walking (Ozbil et al., 2011; Stevenson et al., 2016). Other researchers point out that integrating public gathering spaces into the street fabric enhances inhabitants' copresence at different times and for various purposes that facilitate constant street monitoring (Brown and Lombard, 2014; Ministry of Housing Communities and Local Government, 2021; Wickes et al., 2019). It is claimed that communal spaces are a critical motivator for frequent and spontaneous social interaction between inhabitants (Francis et al., 2012; Jackson, 2003; Mouratidis, 2018), which is found to subsequently increases place attachment (Zhu & Fu, 2017) and lead to social support (Finlay et al. 2019). It is argued that living in close proximity to a communal space results in denser social networks (Small & Adler 2019). Additionally, Francis et al. (2012) found that the social interaction that results from a mix of land use enhances community cohesion and, therefore, creates a stronger sense of safety. However, social cohesion may be negatively affected if the neighbourhood includes communal spaces that attract large numbers of strangers, as this can reduce local interaction between inhabitants (Wickes et al. 2019).

However, the spatial-use impact cannot be generalised, as Muzayanah et al. (2020) found no correlation between mixed-use density and social capital variables in Indonesian metropolitan cities. Historically, in Middle Eastern culture, the mosque has been a critical communal space (Mortada, 2003). The mosque has been used as a multi-purpose space that unifies and strengthens relationships and facilitates conflict resolution (Mortada, 2003). However, recent literature on land use has failed to emphasise the role of the mosque as a critical social space in the residential environmental context.

2 Methodology

There is a need for both qualitative and quantitative approaches based on the identified indicators in this research. Combining subjective and objective data in a mixed-methods study enhances the research results and allows for comprehensive analysis (Bonaiuto 2004; Hanson et al., 2005; Bonaiuto & Alves, 2012; Rezvani et al., 2013; Bakar et al., 2015; Creswell & Creswell, 2018). The methods

used in this study are listed in Table 4.5. The ethics committee at the Welsh School of Architecture approved all the methods and tools used in this study.

Case studies of low-density neighbourhoods were utilised to investigate the impact of different residential environments on the social wellbeing of residents in the cultural context of Doha. According to the proposed national masterplan for Doha city and the percentage of detached dwellings in Qatar, low-density neighbourhoods dominate the majority of city land. (Ministry of Development Planning and Statistics – Qatar, 2017). The case study selection ctiteria was based on the physical characteristics of the neighbourhood such as 1) ensure comparable travel distance to the city centre, 2)variety of residential layout design, 3) public facilities within walkable distance.

A basic socio-economic and physical analysis of the neighbourhoods was the starting point for the fieldwork. After this activity, each neighbourhood underwent a structured mapping of social behaviour. A questionnaire survey was then distributed to public space residents after the observation mapping was completed. Interviewing the residents was the final fieldwork activity.

As for the participants, the researcher introduced the research to local networks and then used snowball sampling to interact with other residents. Residents who have lived in the neighbourhood for at least five years were eligible to participate. The demographic characteristics of the selected participants were vetted to ensure the inclusion of a range of social groups, age groups (>16 years), genders, and work statuses.

Table 2: Indicators and methods of measuring social wellbeing and residential environment design

	Indicators	**Measure**	**Tool**
Social wellbeing	Social interaction	Frequency interaction Type of interaction	Interview
	Privacy	Personal privacy Family privacy	Interview Spatial analysis
Residential environment	Layout Spatial use	Connectivity Integration	Spatial analysis Space Syntax

3 Impact of Land Mix Use on Social Interaction

Public spaces within the neighbourhood were categorised as indoor or outdoor facilities. No significant correlation was found between the total number of public spaces within the neighbourhood and the interviewees' average number of social contacts (Table 3). Furthermore, some demographic and cultural characteristics (discussed below) were found to affect the relationship between public space use and social wellbeing.

Table 3: Comparison of the total number of mix-uses and average number of contacts

Case study	**Layout**	**Case study area (hectare)**	**Average number of social contacts (neighbour)**	**Total number of public buildings**
Thumama	Semi- gridded	42.3	21	10
Dahl Alhamam	Semi- gridded	18.5	14	13
Onaiza	Cul-de-sacs	31.0	13	13
Hazem Almarkhiya	Cul-de-sacs, Loops	30.3	20	5
Duhail	Loops	33.4	20	8
Khulaifat	Loops	13.8	17	28

3.1 Outdoor Spaces and Social Interaction

In general, satisfaction with outdoor spaces was found to correlate with more frequent gatherings between neighbours (Spearman correlation coefficient of 0.151, p-value 0.017) and create more opportunities for casual interaction (Spearman correlation coefficient of 0.130, p-value 0.042). The following subsections discuss sidewalks and public parks separately as outdoor spaces and their impact on social wellbeing.

Sidewalks

The impact of sidewalks was investigated using several data analysis methods. The correlation test found that, in general, satisfaction with the sidewalks in the neighbourhood had a significant positive relationship with various indicators of networking and social interaction (Table 1).

Table 1: Sidewalk satisfaction correlation with social variables

	Number of known neighbours	**Number of close relationships**	**Frequency of chatting to neighbours**
Satisfaction with the sidewalks	0.227	0.201	0.198
	0.000	0.002	0.002

The interview analysis revealed intervening factors that affected sidewalk use – such as the season, distance, and destination. The quotes below concern walking patterns and the influence of the neighbourhood's physical quality:

> *'I used to walk to the grocery store and the health centre, but now I am afraid of falling as the road has been dug up. So, I use the car' (female, 50s, semi-gridded layout).*

> *'The main daily destination is the mosque. I walk in the neighbourhood, especially after sunrise. My path depends on what is the shortest and the quickest. Sometimes in winter, puddles make me avoid some paths' (male, 60s, owner-designed dwelling).*

The physical environment condition mapping revealed that the sidewalks in most neighbourhoods were used for parking spaces (Fig. 1 and Fig. 2). The elderly and families with young children used the sidewalks less often than other populations. The neighbourhood observation confirmed that the walking population was primarily young men. Additionally, parked cars reduced the visual field, which reduced visibility and limited casual interaction between neighbours.



Fig. 1: Sidewalk condition in Khulaifat neighbourhood



Fig. 2: Sidewalk used as a parking space

Vehicle

The observational survey data illustrated the impact of the public spaces' location and quantity on pedestrian movement. Distinct pedestrian distribution and movement can be seen across neighbourhoods. For instance, the pedestrian movement was more widely distributed in Khulaifat neighbourhood, which has several small shops (Fig. 3), whilst in Dahil Alhamam neighbourhood, it was concentrated around a large grocery store (Fig. 4). Moreover, neighbourhoods with fewer communal spaces – such as Duhail – were found to have less pedestrian movement.

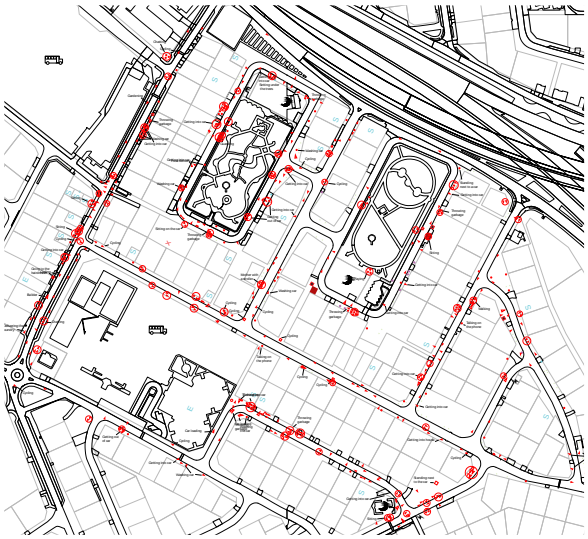


Fig. 3: Khulaifat neighbourhood

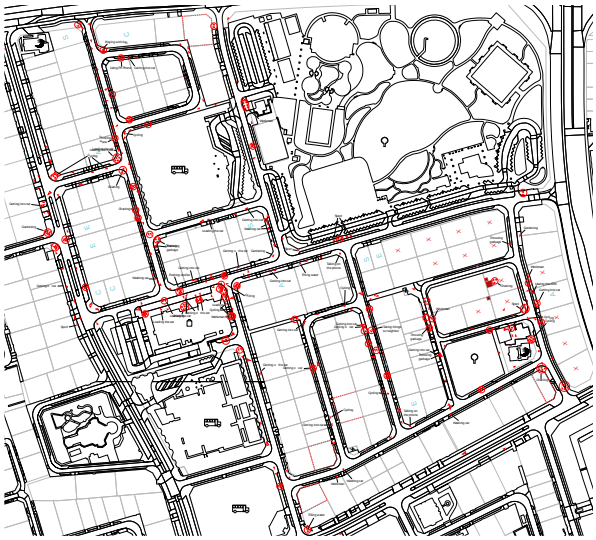


Fig. 4: Dahil Alhamam neighbourhood

S Shop E Educational A Authority C Clinic X Empty land Pedestrian movement

The behavioural observation survey and the spatial analysis of the neighbourhood layouts suggest that visually integrated spaces have higher levels of pedestrian movement. Nevertheless, some of the spatial uses located in a low visual integration street attracted inhabitants (Fig. 5).

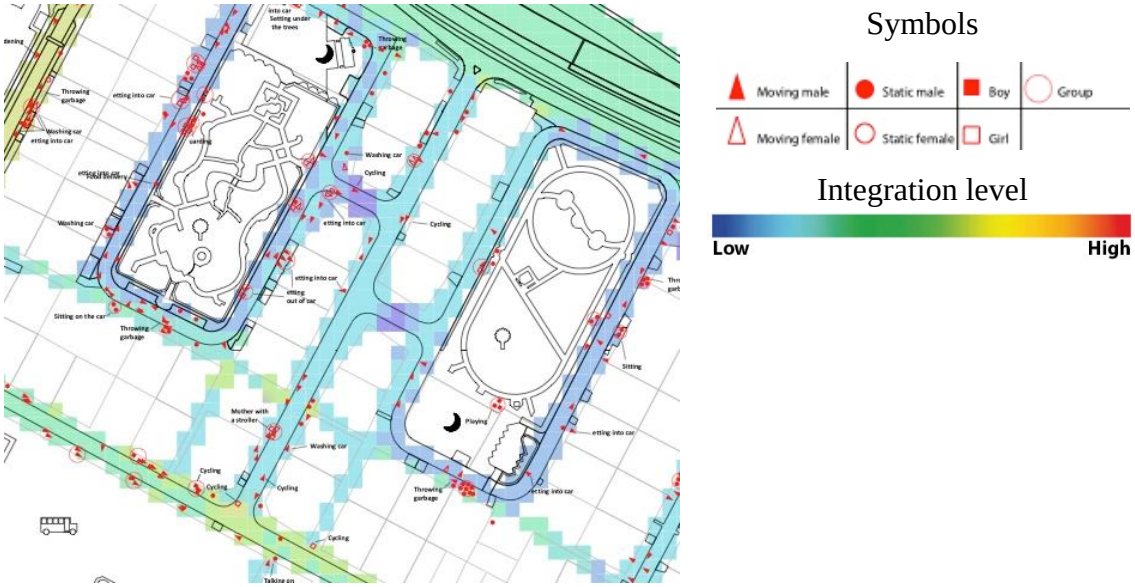


Fig. 5: Observed movement around public spaces, overlaid with the visual integration analysis

Public parks

Previous research has extensively explored the impact of public parks on residents' physical, mental, and social wellbeing. The weather conditions in Doha are an obvious limitation on inhabitants' use of outdoor spaces. In addition, the thematic analysis found that the size of the park was an obstacle, limiting the activities that could be practised there and restricting the use of the park by both sexes at the same time. In this cultural context, the distance between men and women is crucial for maintaining personal privacy. Therefore, inhabitants tend to use the park at different times to maintain cultural norms. Many interviewees reported that they avoided using the park in case privacy was not possible.

> *'I go to many parks – not only the one in our neighbourhood. I use the park approximately every week. Sometimes I find the park full of women, so I go to another park; if the park is small, I don't use it. I go to Al Rayan park and Aspire park once or twice a week to do my exercise there' (male, 50s, loop layout).*

> *'My neighbours walk as a group during the night, but I don't join them. They walk in the park and they ask me to turn off the house lights so they have their privacy when exercising. When my children were young, they used to go to the park. I used to watch them from my room window. Only during summer, when it is very humid, we don't want to go to outdoor spaces. My husband and the neighbours (men) who are retired gather in the park after the Fjeer prayer. Also, they gather during the weekend to work out in the park. Women use the park during the night. Kids always play football in the park. During the weekends, some strangers come to use the park, as Dhal Alhamam park gets crowded' (female, 50s, semi-gridded layout).*

The investigation found that the park was used for certain activities by specific populations. Inhabitants with young children or grandchildren tended to use the park more frequently than others. The statistical analysis revealed the importance of public parks as family spaces within the neighbourhood for children's safety (Spearman correlation coefficient of 0.503, p-value 0.000). The senior population used the park for exercise, whilst the younger generation preferred the large national parks in the city.

3.2 Indoor Public Spaces and Social Interaction

The thematic analysis of the interviews found that some public buildings had more positive social influence than others in Doha's neighbourhoods. Almost all the male participants mentioned the mosque as a regular location for meetings and interactions between neighbours. However, few said they also met with neighbours in other public buildings, such as the grocery store. In contrast, women reported seasonal use of the mosque during the holy month of Ramadan for Tarawih prayer. But they did not report the use of any public buildings for regular interaction with their neighbours. Shopping facilities, for example, had a statistically significant correlation with social interaction and networks for men, but not for women (Table 2). In addition, the behavioural observation documented more men than women interacting in communal spaces.

Table 2: Sex and interaction with neighbours in communal spaces

	Gender	**Number of known neighbours**	**Number of close relationships**	**Number of recognised neighbours**
Satisfaction with	Female	0.0132	0.139	0.210
shopping		0.133	0.113	0.016
facilities	Male	0.2940	0.378	0.096
		0.002	0.000	0.322

Interviewees indicated the importance of the mosque for initiating social interaction between neighbours:

> *'I meet the neighbours at home. My mum sometimes meets her neighbours in the park, but not me. We also meet at the mosque during Ramadan' (female, 20s, cul-de-sac layout).*

> *'As men, mostly we meet in the mosques. We have visits to neighbours' Majles, we know people who come to masque. We used to have a public Majles next to the mosque. It was supposed to be for us (neighbours), but they took it and gave it to "Mowater Qatar" – a centre under the Ministry of Youth and Sports. We need a common Majles for happy and sad occasions. I saw this idea in Oman; they have big halls next to the mosque' (male, 60s, cul-de-sac layout).*

Whilst people met at their neighbours' Majles, many – male and female – stated the need for communal Majles for the neighbourhood. They said this would expand their social networks, as it would resolve some constraints, such as the need to know the Majles' owner and the location of the Majles frequently used for gatherings with neighbours.

The women had other non-spatial methods for initiating and maintaining relationships, as they did not meet regularly in person. The first method involved sharing food with their neighbours. This practice increased during the holy month of Ramadan. Although this behaviour was not a kind of social support in this context, the women reported sharing food to initiate social contact with new neighbours and to maintain relationships with old neighbours. Another method involved 'virtual communication' via social media. Many of the neighbours are members of a WhatsApp group. Here are some quotes from the inhabitants:

> *'We talk to each other on the phone and via WhatsApp. During Ramadan, we interact more and we send food to each other. Our neighbour at the back – we share a wall – we pass things over the wall' (female, 50s, cul-de-sac layout).*

> *'The most interesting thing in our neighbourhood is that even if we do not socialise regularly, we communicate through food. We always share food' (female, 40s, loop layout).*

Although the use of social media for communication between neighbours is common worldwide these days, sharing food is a characteristic method of communication in this cultural context. The difference between the two methods is that a new neighbour needs to know a group member before they can join the virtual network. In contrast, food-sharing gives individuals a chance to form a network themselves.

In contrast, some interviewees expressed dissatisfaction with some uses that they said caused disturbance, including noise, traffic, and infringement on private property. For example, schools, embassies, and parks have been associated with annoyance of the local inhabitants. Below are some comments from inhabitants who live near schools:

> *'I don't think that there is better than this neighbourhood. It is very tidy, the park is nearby, the only noise is this school. It should be illegal to open a school in the middle of a neighbourhood. There should only be a nursery. They park cars in our private parking area. The school should have its own parking area' (female, 60s, cul-de-sac layout).*

> *'The condition of the street changes depending on the time of the day. For example, you will hate it in the morning. If you want to get out using your car, you need an hour because of the school traffic. There are more than five schools near the house' (female, 30s, loop layout).*

Although previous studies have shown public buildings to have a positive impact on inhabitants' social interaction, in this context, they were found to have other impacts such as negative impact or no impact. When inhabitants were asked where they usually met and talked to their neighbours, the Majles was the most common response from the male participants, with female participants citing private dwellings. Visitor spaces are essential in this cultural context, as they facilitate social interaction with the wider community, ensure both household and visitor privacy, and consequently enhance overall social wellbeing. The spatial analysis of the dwelling designs found that the dwellings had at least two spaces dedicated to hosting guests (*Majles* and the dining space) in a strategic location that ensured family privacy and connectivity to the neighbourhood.

4 The Influence of Demographic Factors on Using Communal Spaces

The statistical analysis found that gender is a significant intervening factor that affects social interaction location and frequency. Men have more frequent interactions than women (Table 1). Male interviewees reported more frequent meetings with neighbours, and interacting in the mosque after prayers:

> *'We always gather in my neighbour's Majles. Also, we meet at the mosque or when we are walking to or from the mosque' (male, 50s, cul-de-sac layout).*

Table 4: Gender and frequency of gatherings between neighbours

Gender		**Male**	**Female**
Frequency of gatherings within the neighbourhood	Never	3	9
	Occasionally	21	38
	Once a month	8	14
	Once a week	16	21
	Twice a week or more	37	16
Pearson chi-square	0.001		

Another demographic factor found to affect the frequency of interaction between neighbours was the presence of children. The interviewees reported more frequent interaction with neighbours who had young children, confirming that they came to know other people through their children, who went to the same school or played in the park as their own children. The statistical analysis confirmed that the frequency of meeting with neighbours was positively correlated with the number of children in the household (Spearman correlation coefficient of 0.174, p-value 0.006). Below are some examples of interviewees mentioning the influence of children on their relationships with neighbours:

> *'I know people who come to the mosque and people whose children go out with my children' (male, 50s, loop layout).*
>
> *'We do not have young children. Maybe that is why there is no interaction with our neighbours' (female, 30s, loop layout).*
>
> *Other differences in social interaction associated with spatial use are discussed in the following sections.*

Although children were found to be a link between neighbours, a common view amongst the interviewees was that children were at risk of road accidents. Parents or grandparents were asked whether they allowed their children to independently play in or move around the immediate

neighbourhood (i.e., the street in which they lived), which negatively influenced social interaction between neighbours. One interviewee answered:

> *'My grandchild plays in the outdoor space only. He is not allowed to play beyond the fence of the dwelling. I am afraid of crazy people who drive very fast. And I want them to place speed bumps to reduce the cars' speed' (female, 50s, loop layout).*

5 Conclusion

This study found that patterns of use of spaces have different impacts on inhabitants' social wellbeing. A key finding that emerges from the analysis is that Doha's harsh weather conditions result in many people using indoor public spaces more frequently than outdoor spaces. Furthermore, the use of public space is influenced by the users' gender. This research presented evidence of the vitality of mosques as public spaces for social interaction, especially for men. Most of the men's social contacts are formed in public spaces, whilst women's social contact with their neighbours is less influenced by public spaces, relying instead on non-spatial forms of communication for initiation and maintenance. The relationships that were formed within the neighbourhood were maintained in an indoor privet space – Majles.

Services and facilities in the neighbourhood were shown to increase residential tenure and, therefore, stability. Similarly, a considerable number of the participants cited their extended families and social ties within the neighbourhood as the key reasons for their choice to remain within the neighbourhood

References

Abu-Ghazzeh, T. M. (1999) Housing layout, social interaction, and the place of contact in Abu-Nuseir, Jordan. *Journal of Environmental Psychology 19*(1): 41–73. DOI: 10.1006/jevp.1998.0106.

Bakar, A. A., Osman M. M. & Bachok, et al. (2015) Modelling economic wellbeing and social wellbeing for sustainability: A theoretical concept. *Procedia Environmental Sciences 28*: 286–296. DOI: https://doi.org/10.1016/j.proenv.2015.07.037.

Bonaiuto, M. (2004) Residential Satisfaction and Perceived Urban Quality. In: Spielberger CDBT-E of AP (ed.) Encyclopedia of Applied Psychology, Three-Volume Set. New York: Elsevier, pp. 267–272. doi: 10.1016/B0-12-657410-3/00698-X.

Bonaiuto, M. & Alves, S. (2012) *Residential places and neighborhoods: Toward healthy life, social integration, and reputable residence*. The Oxford Handbook of Environmental and Conservation Psychology. Oxford University Press.

Brown, S. C. & Lombard, J. (2014) Neighborhoods and social interaction. In: Wellbeing. John Wiley & Sons, Ltd. doi: 10.1002/9781118539415.wbwell059.

Cooper, R. (2014). Wellbeing and the environment. In: Wellbeing. John Wiley & Sons, Ltd. doi: 10.1002/9781118539415.wbwell055.

Creswell, J. W. & Creswell, J. D. (2018) Research Design : Qualitative, Quantitative & Mixed Methods Approaches . Fifth edit. Los Angeles ; Sage.

Finlay, J., Esposito, M. & Kim, et al. (2019) Closure of 'third places'? Exploring potential consequences for collective health and wellbeing. Health & Place 60: 102225. doi: https://doi.org/10.1016/j.healthplace.2019.102225.

Földi Z (2006) Neighbourhood Dynamics in Inner-Budapest-A Realist Approach. Utrecht University.

Francis, J., Giles-Corti, B. & Wood, et al. (2012). Creating sense of community: The role of public space. *Journal of Environmental Psychology 32*(4). Elsevier Ltd: 401–409. doi: 10.1016/j.jenvp.2012.07.002.

Gregar, J. (1994) *Research design (qualitative, quantitative and mixed methods approaches)*. Book published by SAGE Publications 228.

Hanson, W. E., Creswell, J. W. Clark, et al. (2005) Mixed methods research designs in counseling psychology. *Journal of counseling psychology 52*(2). American Psychological Association: 224.

Jackson, L. E. (2003) The relationship of urban design to human health and condition. *Landscape and Urban Planning 64*(4): 191–200. doi: https://doi.org/10.1016/S0169-2046(02)00230-X.

Karuppannan, S. & Sivam, A. (2011). Social sustainability and neighbourhood design: An investigation of residents' satisfaction in Delhi. *Local Environment 16*(9): 849–870. DOI: 10.1080/13549839.2011.607159.

Ministry of Housing Communities and Local Government (2021). National design guide. London. Available at: www.gov.uk/mhclg.

Montford, J. E. (2013) Mental wellbeing and the built environment.

Mortada, H. (2003) Traditional Islamic Principles of Built Environment. Abingdon, Oxon: Abingdon, Oxon: Taylor and Francis. doi: 10.4324/9780203422687.

Mouratidis, K. (2018) Built environment and social well-being: How does urban form affect social life and personal relationships? Cities 74(October 2017). Elsevier: 7–20. doi: 10.1016/j.cities.2017.10.020.

Muzayanah, I. F. U., Nazara, S. & Mahi, et al. (2020) Is there social capital in cities? The association of urban form and social capital formation in the metropolitan cities of Indonesia. *International Journal of Urban Sciences 24*(4). Taylor & Francis: 532–556.

Ozbil, A., Peponis, J. & Stone, B. (2011) Understanding the link between street connectivity, land use and pedestrian flows. *Urban Design International 16*(2). Springer: 125–141.

Rezvani, M. R., Mansourian, H. & Sattari, M. H. (2013) Evaluating quality of life in urban areas (case study: Noorabad City, Iran). *Social indicators research 112*(1). Springer: 203–220.

Small, M. L. & Adler, L. (2019) The role of space in the formation of social ties. Annual Review of Sociology 45. Annual Reviews: 111–132.

Stevenson, M., Thompson, J. & de Sá, et al. (2016) Land use, transport, and population health: estimating the health benefits of compact cities. The Lancet 388(10062). Elsevier: 2925–2935.

Wickes, R., Zahnow, R. & Corcoran, et al. (2019) Neighbourhood social conduits and resident social cohesion. *Urban studies 56*(1). Sage Publications Sage UK: London, England: 226–248.

Williams, J. (2006). Designing neighbourhoods for social interaction: The case of cohousing. *Journal of Urban Design 10*(2): 195–227. doi: 10.1080/13574800500086998.

Zhu, Y. & Fu, Q. (2017) Deciphering the civic virtue of communal space: Neighborhood attachment, social capital, and neighborhood participation in urban China. *Environment and Behavior 49*(2): 161–191. doi: 10.1177/0013916515627308.

Cite as: A Janahi H. Y., "The Impact of Land Mix-use on Inhabitants' Social Wellbeing in the Qatari Neighbourhoods", *The 2nd International Conference on Civil Infrastructure and Construction (CIC 2023)*, Doha, Qatar, 5-8 February 2023, DOI: https://doi.org/10.29117/cic.2023.0147

Building Information Modeling (BIM) for Energy Efficiency Awareness in Gulf Countries

Ali Hussain Alhamami
Civil Engineering Department, College of Engineering, Najran University,
Najran, Kingdom of Saudi Arabia
ahalhamami@nu.edu.sa

Mohammed Awad Abuhussain
Architectural Engineering Department, College of Engineering, Najran University,
Najran, Kingdom of Saudi Arabia
maabuhussain@nu.edu.sa

Yakubu Aminu Dodo
Architectural Engineering Department, College of Engineering, Najran University,
Najran, Kingdom of Saudi Arabia
yadodo@nu.edu.sa

Abstract

Energy efficiency in the built environment has been adopted through several initiatives depending on the context of implementation; this paper further assesses Building Information Modelling (BIM) as a toolkit designed to tackle energy-related concerns in buildings. The paper leverages energy efficiency program cases of the gulf countries' level of BIM adoption. This case study design was qualitatively approached in which literature and authoritative contents were reviewed to ascertain the region's adoption of the technology as a body Gulf Cooperation Council. (GCC) and independently as a country (member states). It was identified that only Saudi Arabia and the UAE have BIM tied to their energy efficiency programs, unlike other member states that have energy efficiency programs with little or no trace of BIM. The GCC management committee is therefore saddled with the responsibility of implementing BIM. Utilizing BIM for sustainability will lead to significant savings through a combination of accurate energy monitoring, immediate decision support systems, actuators, and consumption form recognition.

Keywords: BIM; Carbon rates; Energy efficiency; Awareness; Gulf countries; Gulf Cooperation Council

1 Introduction

At the national and European levels, tight laws and regulations have taken into account the necessity of reducing energy use and carbon emissions (Alhamami, et al., 2020). Along with energy use, the building industry also contributes to greenhouse gas emissions, which in 2035 would total 42.2 billion tons, with 288 million tons produced annually in the UAE alone (British Petroleum Company, 2020).

The construction industry can help reduce low energy usage and make the process of global decarbonization as easy as possible. As a building or facility is designed, repurposed, built, and operated, numerous new professions in fields like energy and the environment are employed in addition to the traditional specialties and BIM, which refers to the process of collecting and managing data and knowledge about the building envelope all through the life cycle, from design concept to decommissioning, is one of the notable initiatives for reducing energy usage (Rezqui & Miles, 2011). This research is combined with the knowledge bank of the Gulf States to determine their energy

efficiency policies and whether or not Building Information Modeling (BIM), a crucial tool for efficiently regulating energy use and lowering energy costs is implemented.

2 Conceptual Review

2.1 Building Information Modelling (BIM)

BIM is a tool that can be used to effectively work in terms of collaboration among the construction stakeholders. In essence help in managing energy. This modeling can significantly reduce energy use. BIM may complement how architectural design artifacts are formed and can significantly alter the collaborative process involved in the building. It also has a number of socio-technical benefits at both the process and technological levels. Utilizing the data produced throughout the facility life cycle and a uniform system is a technique for boosting output and effectiveness in the building industry (Choi, Shin, Kim & Kim, 2016).

BIM is described by PAS 1192-2:20131 as the "process of designing, constructing, or running a building or infrastructure asset utilizing computerized object-oriented information." BIM is now defined by the succeeding BS EN ISO 196502 as "the use of a shared digital model of a constructed asset to facilitate design, cost construction operation." Buildings, bridges, roads, and manufacturing facilities are examples of built assets. With this extra description, it is made clear that BIM is a help in sharing information amongst stakeholders in a visual manner Figure 1 shows some benefit of BIM in construction (Stannard, 2021).



Fig. 1: Benefit of BIM in Construction. Source: (Stannard, 2021)

BIM is one strategy for putting the challenge into practice (Seyis, 2020). One of the best methods for integrating building data and facilitating its administration over the whole building lifecycle is the BIM concept (Lu, et al. 2020). All project stakeholders, as well as the architectural, engineering, and construction (AEC) teams, may communicate and share information more simply with the use of building information modelling. NBS National BIM survey shows that 60% of those who responded to the survey thought that BIM cuts the life-cycle phase of construction by 50% (Wong et. al, 2015).

2.2 BIM for Energy Efficiency

By using BIM, it is possible to lessen greenhouse gas emissions, the amount of trash generated, and the energy used to create and operate buildings. Observable carbon dioxide emissions (Xu et al., 2020). BIM also includes specific elements that support energy efficiency goals from the design to field phases of construction, such as covering all aspects of the construction phases, especially the whole life circle (Soroush & Amani, 2011). Numerous features of BIM technology include visual analysis, collision checking, construction timeline simulation, and the development of practical construction design plans and scientific lighting techniques (Zhenshuang, Liguo, Ping & Xiaobo, 2015).

2.3 BIM Level of Details or Development (LOD)

The American Institute of Architects has identified six distinct levels of development (AIA). LOD explains the design parameters at each step, according to (AIA, 2019). In order to represent an element's existence at LOD 100, that is the pre-design stage, the model utilizes 2D symbols and masses. By describing the elements' approximative quantity, size, shape, and placement at LOD 200, they are partially specified. The elements are precisely defined by LOD 300. accuracy is reinforced by measurements and their relative locations. LOD 350 specifies an element's relationship to and relationship with other components as well as precisely describes an element's information. The fundamental details of the creation of various elements are described at the LOD 400 level. By LOD 500, the model starts to depict the actual uses of components in a real building.

2.4 BIM Dimensions

For use cases, also known as predefined special purposes, a BIM model can be applied. Control parameters are added to the data already present in BIM based on the project complexity and project stage requirements. BIM dimensions could be used to express these enhancements of pre-established utilised situations. With the help of these dimensions, data from a model can be improved in order to share a deeper understanding of a construction project. Each of the BIM dimensions—3D, 4D, 5D, 6D, and 7D—has a specific usage and is helpful for determining the cost, schedule, completion date, and sustainability of a project (United BIM, 2019), in addition Figure 2 shows BIM dimension to 10D (Patel, 2020).

2.5 BIM and Digital Twin

Digital twins are the key to controlling smart buildings, which are constructed using BIM. Because each of these intelligent platforms constitutes a digital reconstruction of the structure, there is some confusion between them. Their ability to support it is what distinguishes them from one another. BIM keeps design-build on schedule, within budget, and true to form. A well-designed structure can achieve and even surpass its goals with the aid of digital twins. Because smart buildings are only going to get smarter, they need intelligent software to support them over their entire life cycle. Together, BIM and digital twins can meet this demand, with each technology playing a crucial part in the build's planning, execution, and numerous subsequent uses (Spaceiq, 2022).

2.6 Gulf Countries/Gulf Corporation Council

The Gulf Cooperation Council is made up of six nations: the United Arab Emirates, Saudi Arabia, Oman, Bahrain, and Kuwait (GCC). There are 25 percent of the world's natural gas reserves and 29.4 percent of the world's oil reserves (British Petroleum Company, 2020). The GCC countries' increased primary energy consumption, which has overtaken Africa's total primary energy consumption despite having just one-twentieth the population of that continent, is clearly a reflection of this increase in

population. Between 1971 and 2011 the primary energy usage in the various GCC indicate that the United Arab Emirates is followed by Kuwait, while Saudi Arabia has the greatest share and GCC demographic shift, June 2012 (Doukas, Patlitzianas, Kagiannas & Psarras, 2005 & IEA, 2014).

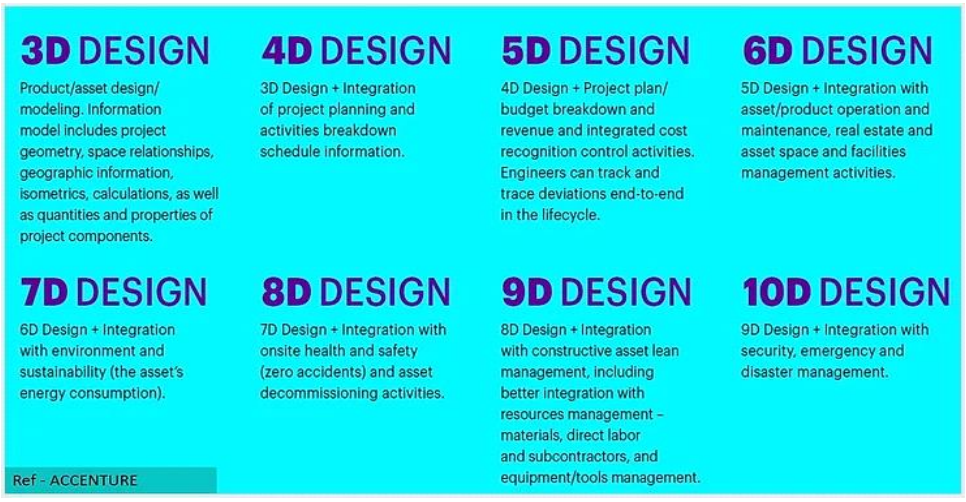


Fig. 2: BIM Dimensions. Source: (Patel, 2020)

3 Methods

This paper adopts a qualitative methodology of research to elicit data related to the variables of the study. This was done through in-depth desk reviews of relevant pieces of literature and contents related to understanding Golf Countries' energy efficiency awareness and the incorporation of BIM in its building and construction practices. The content review clusters the GCC based on the countries which were initially complimented with a holistic analysis of the GCC energy program as a body. Below is a tabulated illustration of the literature reviewed per GCC country to elicit their level of adoption of energy efficiency initiatives proposed and deployed.

Table 1: A Comparative Review of BIM for Energy Efficiency Awareness in Gulf Countries

GCC Country	Literatures Reviewed	Year of publication	Author
Bahrain	National Energy Efficiency Action Plan	2017	NEEAP
Kuwait	Country's Data: Statistics & Balances.	2014	International Energy Agency
	Energy Efficiency Program for the State of Kuwait	2020	Al-Mulla, A
Oman	The status of renewable energy in the GCC countries.	2011	Alnaser, W. E., & Alnaser, N. W.
	Renewable Energy Technologies: Cost Analysis Series	2020	IRENA
Qatar	The status of renewable energy in the GCC countries.	2011	Alnaser, W. E., & Alnaser, N. W.
Saudi Arabia	A literature review of the factors limiting the application of BIM in the construction industry	2017	Sun C, Jiang S, Skibniewski MJ, Man Q, Shen L
	Exploring the challenges in utilization of BIM in maintenance management of mosques.	2016	Sodangi, M., Salman, A.F, Shaawat, M.E
	Saudi's strategic vision for 2030.	2016	Hashmi, N.
United Arab Emirates	Renewable Energy Technologies: Cost Analysis Series	2020	IRENA
	Energy efficiency in the UAE Aiming for sustainability	2020	(Karlsson, Decker, & Moussalli, 2020).

4 Results and Discussion

4.1 Gulf Cooperation Council: Energy Overview, Energy Efficiency and (BIM)

Only Oman has access to sufficient water resources to suit its needs throughout the year; the other GCC nations primarily desalinate seawater to produce drinkable water. As a result, water is more valuable than hydrocarbons and is more expensive per ton than oil (Aidrous, August 2014). There have been indications of a slowdown in demand growth since the GCC countries ratified the Kyoto agreement in (2005 and 2006), which called for legislative efforts to control GHG rise. However, efficiency gains outside the OECD region surged between 1995 and 2010. Energy demand increased by just 3.8% p.a. despite the economy expanding by 5.6% p.a., suggesting that energy intensity decreased on average by 1.7% p.a.

4.2 Case Study Findings: Gulf Countries Focus

4.2.1 Bahrain

The kingdom of Bahrain still uses a very modest amount of renewable energy in its energy mix, similar to the majority of GCC countries. Though no project has yet been built, the government expresses interest in renewable energy, particularly solar. For instance, Bahrain consumes around three times as much energy per person as the typical country, making it one of the top energy consumers in the world. Bahrain's power consumption varies significantly from season to season; from May to October, when temperatures are at their highest, consumption rises significantly. This is mostly because air conditioners are used heavily, using 60 to 65 percent of the country's electricity. The Bahraini government created the National Energy Efficiency Action Plan (NEEAP, 2017), which is one of the most significant steps the nation has taken toward more efficient energy consumption. The plan builds on previous successes and includes a wide range of initiatives to maximise future energy efficiency potential in the Kingdom.

4.2.2 Kuwait

In 2010, Kuwait's Total Primary Energy Supply (TPES) was around 23158 ktoe, natural gas accounts for the remaining 43% of the total. Crude oil accounts for 57% of this supply. In Kuwait, the summers are unusually long and the temperatures are very high. This has necessitated the use of air conditioning as a requirement for all kinds of structures, resulting in higher annual electricity consumption (kWh/year). A/C and lighting account for 85% of annual peak load and 65% of annual electricity consumption, and consumers pay about 5% of the actual cost of energy. The government has implemented several strategies in order to further establish a Kuwait that is energy efficient. These programs include the Energy Conservation Code of Practice (ECCP) and Energy Efficiency Technologies (EET) programs, which are noteworthy. While maintaining people's quality of life, the EET initiatives look for novel ways to reduce per capita energy consumption through the use of energy efficiency technologies in homes, companies, and power plants. With the help of the software, both new and ancient building constructions used less energy (Al-Mulla, 2020).

4.2.3 Oman

Looking at Oman's energy balance reveals that the country's main energy source is natural gas, which accounts for 73% of the Total Primary Energy Supply (TPES) and 27% of crude oil. Roughly 9218 ktoe, or 60% of Oman's total final consumption (TFC), was consumed by the industry sector in 2010. Transport used 2823 ktoe, or 18%, non-energy used around 12%, and other sectors including residential and services used the remaining 10% (Sweetnam, 2014). Large-scale renewable energy projects haven't been started in Oman yet. Despite a 100-200 MW solar project being announced by

the Omani government, nothing has yet to be implemented (IRENA, 2012). The closest thing to implementation is a nine-month scoping project that has improved our comprehension of how energy is used in Oman and proposed a framework effective utilization of energy in a sustainable manner

4.2.4 Qatar

Like the other GCC countries, Qatar has considerable solar energy potential (Alnaser & Alnaser, 2011). Oil makes up the remaining 19% of the Total Primary Energy Supply (TPES), with natural gas making up the majority (81%). On the other hand, when examining energy consumption by industry, transportation and industry sectors account for about 60% of Total Final Consumption (TFC), while residential, commercial, and public services as a whole account for only about 8% of TFC and non-energy sectors account for the remaining consumption.There hasn't been a thorough investigation of how much energy is used in Qatari structures. However, building owners find it challenging to put even basic measures into practice due to a lack of specialists, such as trained operating engineers, materials, and energy-saving goods. Reducing the energy intensity of power use through the application of best practices in sustainable building for Qatar is one of the objectives of Qatar's Vision 2030 and Qatar National Development Strategy 2011-2016.

4.2.5 Saudi Arabia

Even though BIM is used in Saudi Arabia, it is still in its infancy and the country's building industry only occasionally uses it (Asif, 2016). This is because some business owners began to recognise the many advantages of utilizing BIM, such as the ability to enable a wide range of options for structures, the ability to run a wide range of tests on a model, and the ability to enable the early detection of deliberate mistakes to prevent costly rebuilds. A small number of significant firms use BIM mostly in Saudi Arabia's construction industry, which has a relatively underdeveloped subcontracting industry (Sodangi et al., 2016). BIM usage in Saudi Arabia is limited to a select few of the country's large enterprises, and the subcontracting sector there is dominated by small and medium-sized construction companies, thus it is necessary to develop methods that would certify the industry's adoption of BIM (Sun et al., 2017).

4.2.6 United Arab Emirates

The UAE has implemented a number of building efficiency initiatives. For instance, a program in Abu Dhabi called Estidama, which is the Arabic for "sustainability," supervises the planning, development, and use of structures through a series of licenses. In order to evaluate the sustainability performance of villas, buildings, and communities, Estidama also employs a rating system known as the "Pearl Rating System." The government of Dubai has released a set of green construction guidelines and specifications that include planning, resource use, material use, and waste. Notably, the standards aim to enhance the sustainability performance of buildings at every stage of their lifespans, from design through construction, use, and eventual demolition. Various programs and strategies have been introduced in the United Arab Emirates around 2011 (Karlsson, Decker, & Moussalli, 2020).

5 Conclusion

This paper identified the establishment of energy efficiency programs independently in Gulf countries but sees the absence in the adoption of BIM except in Saudi Arabia and some traces in the UAE. Although other countries in the council have interrelated programs, projects, and initiatives and are growing fast in reducing carbon rates based on their contextual approaches. The GCC should

therefore lead the establishment of region-wide energy efficiency initiatives taking in cognizance of member countries' areas of milestones for sub-coordination at the regional level (Alhamami, Rezgui, & Petri, 2021).

Lessons should be drawn for the development of the BIM sub-sector in Energy Efficiency and further implemented in member states to ensure a uniform carbon rate reduction. The use of BIM for energy efficiency will lead to energy savings by fusing precise energy observation, real-time decision support systems, actuators, and pattern recognition. Additionally, (a) the application of a semantic method, such as (BIM, real-time data analysis, behaviour modelling), etc., (b) improved energy flows and use supervision in buildings, and (c) new collaborations between energy managers, energy equipment suppliers, energy distributors, and technology (including smart software tools), will help energy managers make the best decisions regarding the development of energy use in buildings and result in a quantifiable decrease in energy consumption in the GCC. The study also suggests that all GCC member nations adopt the strategy to fully utilize BIM, particularly to meet sustainability standards, with special consideration to energy efficiency in construction.

Acknowledgements

The authors are thankful to the deanship of scientific research at Najran University for funding this work, under the general research funding program grant code (NU/IFC/2/SERC/-/14).

References

AIA (2019). Architect's Guide to Building Performance: Integrating performance simulation in the design process. 1735 New York Ave NW, Washington, DC 20006-5292. Retrieved via https://content.aia.org/sites/default/files/2019-06/AIA_BPSGuide_2019_FINAL.pdf

Aidrous, I. A. (2014). How to Overcome the Fresh Water Crisis in the Gulf. Moscow: Russian International Affairs Council.

Alhamami, et. al (2020). Promoting Energy Efficiency in the Built Environment through Adapted BIM Training and Education. *Energies 2020*, 13, 2308; doi:10.3390/en13092308.

Alhamami, A., Rezgui, Y. & Petri, I. (2021). BIM for Energy Efficiency Training Requirements in the Context of a Developing Country: The Case of Saudi Arabia. In 2021 IEEE International Conference on Engineering, Technology and Innovation (ICE/ITMC) (Proceeding) Alhamami, A., Petri, I. and Rezgui, Y., 2018, September.

Al-Mulla, A. (2020). Energy Efficiency Program for the State of Kuwait, Energy Efficiency Technologies Program Energy and Building Center Kuwait Institute for Scientific Research.

Alnaser, W. E. & Alnaser, N. W. (2011). The status of renewable energy in the GCC countries. *Elsevier*, 25.

Asif, M. (2016). Growth and sustainability trends in the buildings sector in the GCC region with particular reference to the KSA and UAE. Renew Sustain Energy Rev 55:1267–1273

BigRentz (2021). What is BIM? Building Information Modelling Explained

British Petroleum Company. (2020). BP statistical review of world energy. doi:10.2307/3324639

Choi, et al. (2016). "Development of open BIM-based energy analysis software to improve the interoperability of energy performance assessment," Automation in Construction, vol. 72, pp. 52–64.

Doukas, et al. (2005). Renewable energy sources and rationale use of energy development in the countries of GCC: Myth or reality? Elsevier.

IEA. (2014). (International Energy Agency). Country's Datat: Statistics & Balances. Retrieved from http://www.iea.org/stats/index.asp

IRENA. (2012). Renewable Energy Technologies: Cost Analysis Series – Solar Photovoltaics. Bonn: IRENA.

Karlsson, P-O, Decker, C. & Moussalli, J (2020) Energy efficiency in the UAE Aiming for sustainability. Strategy & formerly Booz and Company retrieved on 7th August, 2023 available @ https://www.strategyand.pwc.com/m1/en/reports/energy-efficiency-in-the-uae.pdf

Lu, W., Xu, J. & Söderlund, J. (2020). Exploring the effects of building information modeling on projects: Longitudinal social network analysis. *Journal of Construction Engineering and Management, 146*(5), 04020037.

NEEAP (2017). National Energy Efficiency Action Plan (NEEAP) (2017),

Patel, Y. (2020). #20 - BIM Dimensions. BIM Training: Laern Better and be Batter. Retrieved via https://www.bimtraining.in/post/bim-dimensions

Rezgui, Y. & Miles, J.C. (2011). *Harvesting and Managing Knowledge in Construction: From Theoretical Foundations to Business Applications*; Taylor & Francis Group Ltd: Oxford, UK; ISBN 9780415545952.

Seyis, S. (2020). Mixed method review for integrating building information modeling and life-cycle assessments. *Building and Environment, 173*(106703), 106703.

Sodangi, M., Salman, A. F. & Shaawat, M. E. (2016). Exploring the challenges in utilization of BIM in maintenance management of mosques. In Proceedings of the first international conference on mosque architecture. p 31–48

Soroush, A. R. & Amani, N. (2011). IM-Based Optimum Design and Energy Performance Assessment of Residential Buildings. Research Article, *Journal of Energy Management and Technology (JEMT)* Vol. 5, Issue 2 64

Spaceiq (2022). Digital Twin Vs. BIM. Retrieved via https://spaceiq.com/blog/digital-twin-vs-bim/

Stannard, L. (2021). What is BIM? Building Information Modeling Explained Retrieved on 7th August, 2023 available @ https://www.bigrentz.com/blog/what-is-bim

Sun, et al.(2017). A literature review of the factors limiting the application of BIM in the construction industry. *Technol Econ Dev Econ 23*(5):764–779

Sweetnam, T. (2014). Residential Energy Use In Oman: A Scoping Study. Project Report.

United-Bim (2019). BIM Level of Development. Retrieved via https://www.united-bim.com/wp-content/uploads/2019/12/BIM-Level-of-Development-Explained-LOD-100-200-300-400-500.pdf

Wong, J. K. W. & Zhou, J. (2015). Enhancing environmental sustainability over building life cycles through green BIM: A review. *Automation in Construction*, 57, 156–165.

Xu, X., Mumford, T. & Zou, P. X. W. (2020). Life-cycle building information modelling (BIM) engaged framework for improving building energy performance. Energy and Buildings, (110496).

Zhenshuang, et al. (2015). Research on green building materials management system based on BIM technology. *Building Economy*, 2015(4):83-86.

Cite as: Alhamami A., Abuhussain M.A. & Dodo Y.A., "Building Information Modeling (BIM) for Energy Efficiency Awareness in Gulf Countries", *The 2nd International Conference on Civil Infrastructure and Construction (CIC 2023)*, Doha, Qatar, 5-8 February 2023, DOI: https://doi.org/10.29117/cic.2023.0148

Cultural Heritage Tourism as a Catalyst for Urban Regeneration: Case of the Doha Historic Center in Qatar

Djamel Boussaa
Department of Architecture and Urban Planning, College of Engineering, Qatar University, Doha, Qatar
DjamelB60@qu.edu.qa

Abstract

Heritage and tourism have become during the last two decades dynamic areas of development in the world. The idea of heritage is crucial to the critical decision-making process as to how irreplaceable resources are to be utilized by people of the present or conserved for future generations in a fast changing world. In view of the importance of 'heritage' to the development of a tourist destination the emphasis on developing appropriate adaptive reuse strategies cannot be overemphasized. In October 1999, the 12th general assembly of the ICOMOS in Mexico stated, that in the context of sustainable development, two interrelated issues need urgent attention, cultural tourism and historic towns and cities. Without adequate rehabilitation actions to ensure a sustainable future for these historic resources, may lead to their complete vanishing. According to the World Tourism Organization, natural and cultural heritage resources are and will remain motivating factors for travel in the near future. According to the experts, people choose travel destinations where they can learn about traditional and distinct cultures in their historic context. Historic centers in the Gulf are now being recognized as valuable resources for sustainable development. This paper focuses on the role of heritage tourism and its implications for urban regeneration in the context of Doha in Qatar and Jeddah in Saudi Arabia. Therefore, in order to use heritage wisely, it will be necessary to position heritage as an essential element of sustainable development, giving particular attention to heritage tourism.

Keywords: Cultural heritage tourism; Urban regeneration; Development; Sustainability; Historic centres

1 Introduction

The world's urban population is expected to reach 61% by 2030. Tourism generates foreign exchange that can be used to contribute in the local economic development of cities. International records show that tourist arrivals exceeded 800 million in 2005 while generating revenues estimated at 680 billion $ (UNWTO, 2006). Non-tourist areas can also benefit indirectly from tourism through an equitable distribution and share of the wealth generated. In many developing countries, travel emerged as an important source of growth and prosperity, which directly and indirectly affects related tourism activities. The World Tourism Organization (2004) stated that tourism doubled between 1995 and 2005 and has become a major source of foreign exchange for some small and medium-sized countries such as Qatar, thus contributing significantly to their national economic growth (Kim, Chen & Jang, 2006).

With the rapid expansion of globalization, as well as the development of transportation and communication, the attention of many city stakeholders and local government officials has been directed to tourism as a strategic catalyst for urban regeneration. Cultural heritage is a valuable asset for both the local and global visitors to a particular area. Visitors to such sites provide significant revenues that can be used to regenerate the resilient historic cities in the Gulf. Tourism can be more efficient when the host community is the first beneficiary of the financial returns.

Tourism is a major contributor to foreign exchange, but if not carefully managed, it can have many negative consequences. Tourists make extensive use of the historic center and practice a variety of cultural activities during their visits, which often overlap with the pursuit of locals for their daily activities. In compact historic cities such as Old Doha, the increase in visitors if not properly controlled may lead to overcrowding, mobility and parking problems and queues of people in malls, cafes and restaurants. Mass tourism can give rise to the perception of congestion, but visitors can see it as a normal aspect of tourist destinations (Popp, 2012).

2 Cultural Heritage Tourism and Urban Regeneration

Cultural heritage, historical landscapes, recreation and tourism are interrelated phenomena; Timothy (2011) argues that there is very little difference between cultural and heritage tourism. Cultural heritage resources are largely seen as powerful tools in social and economic dimensions, a means towards urban regeneration and a positive asset for innovation (Timothy, 2011). Therefore, historic cities and centres can stimulate urban regeneration, provide new experiences and enrich the tourism experience. Urban regeneration often underestimates the value of culture to the people of a place. In historic cities of the Gulf "respect of local traditions" is a very sensitive issue, which should not be excluded when initiating any tourism led regeneration strategy. The main concern is to preserve the local cultural identity while reusing the history city or district for tourism (Boussaa, 2014 a, Boussaa, 2014b, Boussaa 2018 & Boussaa, 2020).

Ashworth and Page (2011) pointed out an important issue: "the more unique the urban attraction is, the less likely is the visit to be repeated and will tend to be a once-in-a-life-time experience". They further conclude, "a more generalized way of selling an ambiance or 'way of life' (Paris, Vienna, New York) is likely to generate more repeat visits than a specific attraction". It is thus important to consider this when applying a regeneration approach for the resilient historic cities in the Gulf to be constantly revisited as a way to sustain their liability.

Tourism led regeneration should not only focus on spatial regeneration to provide benefits to its users, it should aim to improve the socio-economic conditions of the local inhabitants, who are the real custodians of the area. Moreover, tourism led regeneration may provide a solution to the problem of social marginalization of the low income inhabitants. This can happen by strengthening the relations between residents of the area, tourists and also between its residents and public authorities, as will be explored in the historic city of Doha. Achieving sustainability in historic areas requires meeting various needs and balancing the economic, social and environmental dimensions (Wall, 2009).

Low-income people inhabit most of the historic cities in the Gulf. The latter have replaced the original owners, who moved out to live in more laborious villas and apartments at the periphery. Since the current tenants cannot afford to restore or maintain their dilapidated houses, there is a need to seek for an urgent regeneration strategy. The surviving historic cities are mainly residential, with some few public facilities, like souks, mosques and forts. The latter have been converted into museums and cultural centers. Therefore, what should be done with the surviving houses in the remaining historic neighbourhoods, which are is a desperate situation? This paper aims to explore the concept of "cultural heritage tourism" as a vector to regenerate these historic cities.

This paper utilises an exploratory case study approach to discover the key tourism issues in the city of Doha. The study of these two cities aims to generate lessons that will be the basis to develop strategies that can be adopted to revive them as well as other historic cities in the Gulf and the Arab world. This research uses of a variety of data sources, including publicly available relevant documents, websites, presentation reviews, field observations and follow-up communication by phone and email.

3 Historic Cities and Tourism

Many historic sites in the Gulf disappeared because local authorities were not aware of their potential economic value. With the involvement of UNESCO to discover potential sites for inclusion on the world heritage list, many countries are striving to include their historical cities on that list. This will increase people's pride towards their localities while hosting their international and local visitors' home. Regeneration of historic districts tends to attract a variety of economic activities and competition, therefore encouraging both new inhabitants and visitors to visit and discover these areas. In addition, upgrading the physical built environment, social fabric and urban spaces within the historical urban structure all contribute towards increasing their adoption as places for local-global tourist's integration.



Fig. 1: Pressures of economic forces resulting in the erosion of many historic districts, leaving only a few patches in old Doha

The challenge for regeneration is to develop strategies, which not only ensure the continuing contribution of heritage to the present and the future, however it should be responsive to the historic environment and collective needs. Such strategies will lead to more equitable and sustainable solutions to the problems currently faced by the historic quarters in the Gulf. Many strategies for the manipulation and exploitation of culture inside the historical cities can be found. These may include funding for facilities of the arts; investment in public spaces; recreation and refurbishment of distinctive settings as waterfronts and historic districts. Other kinds of intervention may comprise the expansion and improvement of museums and the conservation of historical landmarks, which are needed to promote tourism. Working to be competitive within a global world, many places have tried to increase their distinctiveness and character to attract flows of tourists and visitors.

In many historical cities, a "local fatigue" may result from over-consumption of local infrastructure, and fragile historical buildings. These issues are pertinent in the Gulf, where the conflict between conservation and development is at its apex, and a need to create a balance between these two forces is crucial for a sustainable future of the historical city. Therefore, to sustain the surviving historical cities, enough modernization of the urban fabric should be provided to avoid disrupting the community life.

The economic role tourism plays in the industry and global growth is highly important. Historic cities

and urban centers attract skillful occupants, as they are the core of economic activities, which creates an agglomeration of diverse cultural and socioeconomic backgrounds triggering fragmentation of the social fabric, and bonds, which are essential for cultural sustainability. From that sense, cultural heritage tourism finds a fertile ground to grow as means to salvage cultural identity and generating adequate products and services for the demand in these growing city cores. This cycle in return increases the diversity of occupants and visitors in the area, which plays a significant role towards a local-global integration (Madanipour et al., 2013), (Sharpley & Telfer, 2014).

Countries such as in the gulf area have had rapid development booms resulting in less sustainable decision making towards the conservation of valuable heritage sites undermined or destroyed during the process of modernization, development and physical growth of the cities fabric. As planning becomes a tool to sustain cultural heritage whilst ensuring the continuity of financial security needed to conserve and regenerate heritage destinations, identification of urban physical characteristics and the cohesive collaboration of multidisciplinary professionals involved in establishing these features is measured crucial.

Tourism introduces many values within its context; the value chain involves direct and indirect contributors and beneficiaries in the process. These include social values through exposure to norms and standards of diverse cultures, exploration, knowledge sharing and reference to the past layers of physical and cultural lifestyles. The economic value of tourism is considerably dominant in directing the approach to development. According to UNWTO, tourism will face a 43million/3.3percentage increase yearly. Despite the growing cost of transportation and travel in the past decade compared to earlier periods, international tourist activities are expected to range at 1.8 billion in 2030, a considerable 80% growth in the coming 2 decades ranking MENA region as most visited region worldwide (Beyer, 2014).

4 Doha; Rapid Growth and Globalization

Doha, the capital of Qatar is the largest city, with over 80% of the nation's population residing in Doha and its suburbs. It is also the administrative and economic centre of the country with a population of 2,718,227 persons in August 2023 (https://worldpopulationreview.com/countries/qatar-population). Every year thousands of people migrate to Qatar, inciting an explosive growth rate in population. Prior to 1950, Doha was a small fishing and pearling village, today, it has become well known for its mega sports, conferences, and exhibition events. Prior to reaching this strategic, place in the region, Doha experienced a staggering rapid urban growth since the discovery of oil in 1940 and the beginning of its exportation in 1950.



Fig. 2: Location of Souk Waqif and Msheireb (Heart of Doha) in old Doha

Oil exports and payments for offshore rights started in early 1950s, and marked a major shift in Qatar's future. In parallel to oil exportation, the year 1949 saw the importation for the first time of the cement as a new building material. Cement provoked a major shift in construction trends from reliance on local building materials such as coral stones, and *Danchal* to the introduction of new materials based on cement. In order to meet the rising demand for housing, education facilities, shopping areas that followed the discovery of oil, large areas had to be prepared in the downtown area. Consequently, the bulldozer cleared away several historic areas, which usually contained significant heritage landmarks.

Due to the complex process of land expropriation that involved high costly compensations, planning started to move from downtown to the sea through land reclamation. This new trend left the old town with large empty areas to be used for informal parking and gathering areas for the low-income workers especially during weekends. During the period 1978-1981, the West bay was being prepared to become the new modern district in Doha, where a number of iconic towers started to emerge. The Sheraton hotel as a main landmark in the west bay of Doha was the first modern structure to be built during 1982-83. While the West bay has been given continuous consideration and attention by the development of "star-architecture" towers, designed by international consultants and famous architects such as Jean Nouvel, old Doha has been left to die slowly, through neglect, overcrowding, isolation and lack of active regeneration actions.

In 1980, the Government of Qatar established the first conservation law to preserve the archaeological and cultural heritage of the country. Since, then only piecemeal restoration work was implemented. A number of single monuments were restored such as the Zubarah fort which was added on the world heritage list in 2013 and the Mohamed said Nasrallah house; the only remaining wind-tower house in Doha. The first historic district to be rehabilitated in Doha and Qatar is Souk Waqif during the period 2004-2010.

5 Tourism Led Regeneration in Souk Waqif

The souk contains about 500 shops varying between pottery, traditional swords, daggers, handcrafts, jewellers and copper utensils. Entering the old Souk from the northern side, is accompanied with the oriental experience of smells, colours and the journey starts in Souk ―Al Etem (darkness). Gold, wholesale, clothes, and the animals' souk are specialized and unique as much as the spices' market. Amenities have been distributed within two major areas, the old souk accessed from Abdullah Bin Thani Street and Grand Hamad Street. The new restaurants take place along Al Kharis Street in Al Najada area.

After long years of dilapidation and neglect the beginning of the 21st century, the souk fell into disrepair and decay. Moreover, the souk was intruded by unsympathetic buildings, of dense shops frontage, crowded entrances and clash of functions, leading to a hybrid environment of modern and old structures. The upgrading process was randomly done by the shopkeepers due to the absence of a common strategy of maintenance during that time. Alleyways were covered with temporary metal sheets as a quick and cheap solution to provide shade for the shoppers. The use of these metallic roofs increased heat gain and solar absorption, thus creating a condensed humid air and unpleasant spaces for the visitors and users of the souk.



Fig. 3: Picture is showing the state of the Souk before the beginning of restoration in 2004

Due to this critical situation, the Emir of Qatar, HH Sheikh Hamad Bin Khalida the present Emir's father asked the Art designer Mohamed Ali Abdulla to implement the rehabilitation of Souk Waqif. Before starting, Mohamed Ali Abdulla took his time to undertake research of the gulf architecture by visiting most of the Gulf countries and South of Iran. Based on his fieldwork and research he set up a challenge to achieve the following objectives:

- "Reconstruct the lost image of historic Doha through the rehabilitation of its authentic Souk Waqif,
- Protect the area of the souk and its surroundings from real estate development,
- Create an open-air public area totally pedestrianized,
- Establish a vibrant souk with its original layout and goods."



Fig. 4: Showing the main areas in the Souk

This urban regeneration project had to resolve the following issues:

- "Augment the human dimension and users' experience,
- Conserve the activities of the souk and distribution of its specialized areas,
- Activate the social memory,
- Update and modernize its services,
- Maintain an authentic environment,
- Restore the dilapidated buildings,
- Remove alterations and random additions,
- Reconstruct the lost parts,
- Create organic pathways and alleys,
- Provide maximum shaded area" (Radoine, 2010).

After complementing the restoration work and a comprehensive adaptive reuse program was implanted in Souk Waqif. The traditional crafts and activities deserve a special attention, as they need to be sustained for the future generations. Competing with the spacious shopping malls Souk Waqif offers a unique outdoor living heritage environment in Doha, which is used by the local inhabitants and visitors.

All services are distributed within a walking distance where vehicular circulation is prohibited. The parking area, which was a main issue witnessed several extensions since the souk started to be rehabilitated, it has changed several times with different extensions the parking capacity increased from 410 parking lots in 2003, to 440 in 2007 and 590 parking spaces, distributed in two parts in 2009. In addition, the parking roof enabled the creation of a green area facing the corniche, as an additional outdoor space facing the corniche for gatherings and recreation.

Local and global visitors come frequently to Souk Waqif, especially during weekends and holidays. Nowadays and after six years from the completion of the rehabilitation, Souk Waqif has been transformed from a derelict souk to a living environment in the present yet with a spirit of the past. This has been noticed during the recent FIFA world cup where Souk Waqif became one of the most attractive places for fans. During the year 2009/10 a comprehensive survey of 100 people chosen randomly, was undertaken to express what was missing in Souk Waqif. Furthermore, a series of informal interviews and discussion were held with a number of decisions makers from Qatar Museums, the Private Engineering Office and Msheireb Properties. The outcome of the survey and discussions enabled to highlight some recommendations to further enhance life in the Souk:

- A branch for the Qatari Ministry of Culture, Arts and Heritage to be approached easily by the public. This institution would provide people with cultural insights and events happening in Doha on a monthly and annual basis, as well as using Souk Waqif as a station to host these events.
- A Library specialized for historical records, archives, manuscripts retaining the history, emergence and development of Qatar's heritage in general, Doha and Souk Waqif in particular.
- A Community Centre providing the public with classes and workshops about old Qatari handicrafts, pottery, bronze and metalwork.

- A Cultural centre specialized for creative and interactive events such as fashion shows for Qatari costumes, storytelling of pearl diving, different ways of city and Bedouin traditional ways of life;
- Exhibition spaces that are both stationary and travelling that help narrate the history of Doha and Souk Waqif.
- Children‘s Centre: a corner that might be designed as a courtyard house where old Qatari games can be practiced and revived.

One of the major drawbacks of the rehabilitation strategy in Souk waqif is the absence of housing in the adaptive reuse program as this prevented the souk from being active 24 hours a day living environment. However, this deficiency was reduced by the development of a number of boutique hotels. Souk Waqif has become a major attraction for both the local and global visitors. Despite a lack of authenticity in the way, a number of historic buildings have been restored; their adaptive reuse enabled the creation of a vibrant living environment to the once derelict area, and thus overshadowed the inauthentic physical additions.



Fig. 5: Souk Waqif; the restaurants’ area provides a bustling life day and night

A combination of modern and traditional crafts has contributed greatly to the revival of the souk, thus in creating a destination that combines the past and present of Doha. Following the successful regeneration of Souk Waqif experience, it can be noticed that a wise adaptive reuse program was the main catalyst in establishing a sustainable urban conservation approach in the souk. Ultimately, this project layered the foundations to other conservation initiatives to take place in the adjacent districts such as Msheireb during the period 2008-2020.

6 Conclusion

In a growing world, fierce competition between cities is a driving force in promoting strategies to improve the operational performance of a city to attract more tourists and ensure their satisfaction. The emergence of the concept of tourism led regeneration has drawn the attention of tourists to the need to protect them from the negative effects of touristification such as gentrification. Developing

resource-based attractions, especially heritage sites, requires effective management systems and the development of an appropriate planning process to avoid mass tourism and gentrification.

This study has shown that a successful tourism cannot rely only on the primary cultural heritage attractions. A provision of secondary resources such as accommodation for tourists as was developed in Souk Waqif can help attract more visitors to stay in the historic city. In this way, more money can be generated to improve the local inhabitants' derelict living conditions. Consequently, more jobs can be created especially for the youth, who will be encouraged to contribute in sustaining life in their historic city. As an outcome of all these efforts, the historic centers will shift from being redundant to living heritage areas, where people can live, work, enjoy their time and most of all be proud of their old city.

Successful strategies for tourism development should not be evaluated solely in terms of increasing the number and income of tourists. Tourism must also be evaluated primarily in terms of its role in improving the overall quality of life of the host community. Too much emphasis on tourism can put new services and related development at risk, often at the detriment of the locals. Therefore, it is important to carefully manage and control tourism potential according to the local potentialities.

Cultural heritage tourism led regeneration is now a widely spread idea in the world. A city that values its cultural heritage gives itself the means to better prepare its future and recreates an idealized past. Theoretically, historic cities have all the means to develop a sustainable cultural heritage tourism, responsive first to the needs of their inhabitants and then for the visitors. Therefore, cultural heritage tourism remains a potential changing living space and a perfectible niche to explore. In this way, cultural heritage tourism led regeneration can form a blessing and not blight the resilient historic centers and their inhabitants, in the Gulf and worldwide.

References

Ashworth, G., J. & Page, S. J. (2011). Urban tourism research: Recent progress and current paradoxes. *Tourism Management, 32*(1), 1- 15.

Beyer, M. (2014). Tourism Planning in Development Cooperation: A Handbook; Challenges-Consulting Approaches-Practical Examples-Tools, GIZ.

Boussaa, D. (2014a). Urban Heritage and Tourism in the Gulf: The Case of Dubai in the UAE; *Journal of Tourism, 2*(4), 174-181.

___ (2014b). "Rehabilitation as a Catalyst of Sustaining a Living Heritage: The Case of Souk Waqif in Doha, Qatar." *Art and Design Review* 2(3): 62–71. doi:10.4236/adr.2014.23008.

___ (2018). "Urban Regeneration and the Search for Identity in Historic Cities." *Sustainability 10, 48*(1): 1–16. MDPI. www.mdpi.com

___ (2020). The past as a catalyst for cultural sustainability in historic cities; the case of Doha, Qatar, *International Journal of Heritage Studies*, doi: 10.1080/13527258.2020.1806098. https://doi.org/10.1080/13527258.2020.1806098.

https://worldpopulationreview.com/countries/qatar-population

Kim, H. J., Chen, M. H. & Jang, S. S. (2006). Tourism Expansion and Economic Development: The Case of Taiwan. Tourism Management 27: 925–933.

Madanipour, et al. (2013). *Public space and the challenges of urban transformation in Europe*, Routledge.

Popp, M. (2012). Positive and negative urban tourist crowding: Florence, Italy. Tourism Geographies, 14, 50–72.

Radoine, H. (2010). "Onsite Review Report, Souk Waqif, Doha, Qatar." Accessed 1 June 2015. http://www.akdn.org/architecture/project

Sharpley, R. & Telfer, D. J. (2014). *Tourism and development: concepts and issues*, Channel View Publications.

Timothy, D. J. (2011). Cultural Heritage and Tourism: An Introduction (Vol. 4). Bristol: Channel View Publications.

UNWTO. (2006). https://www.e-unwto.org/doi/book/10.18111/9789284413492 (Accessed; 25-07-2020).

Wall, G. (2009). Tourism and Development: Towards Sustainable Outcomes, In Fusco Girard, L. & Nijkamp, P. (Eds.) Cultural Tourism and Sustainable Local Development (pp.31-47). Farmhand: Ash gate.

Cite as: Boussaa D., "Cultural Heritage Tourism as a Catalyst for Urban Regeneration: Case of the Doha Historic Center in Qatar.", *The 2nd International Conference on Civil Infrastructure and Construction (CIC 2023)*, Doha, Qatar, 5-8 February 2023, DOI: https://doi.org/10.29117/cic.2023.0149

Theme 4:

Water, Environment, and Climate Change

Efficient Reservoir Operation in an Arid Region with Extreme Hydrologic Flows: A Case Study, Oman's Largest Dam

Akbar Karimi
Department of Civil Engineering, National University of Science and Technology, Muscat, Oman
akbarkarimi@nu.edu.om

Banafsheh Nematollahi
Department of Civil Engineering, National University of Science and Technology, Muscat, Oman
b.Nematollahi@shirazu.ac.ir

Mohammad Reza Nikoo
Department of Civil and Architectural Engineering, Sultan Qaboos University, Muscat, Oman
m.reza@squ.edu.om

Abstract

Wadi Dayqah dam (WDD) is still not operating, and its operation targets are not yet fixed. Arid hydrology and the presence of new users require a new look at this dam's operation plan. The updated and optimal operation plan of WDD is the central research gap about this dam. In this study, to fill this gap, Water Evaluation and Planning (WEAP) is used to model the system and six scenarios, including the reference target of 35 MCM per year suggested goal that considers different operation targets as well as a modification to water system configuration by the addition of an upstream dam is suggested. This model is validated and used for 37 years of historical flow. Results show that the reference scenario is less than 55%, and an annual goal of 15 MCM has a maximum of 85% supply reliability. Adding a 20 MCM upstream dam can increase reliability by 5%. It is recommended that to enhance the economic aspects of the dam, suitable energy generation schemes are studied with unique configurations, such as pumped-storage hydro, as well as studying the other sizes of upstream dams that can contribute more to water distribution and energy generation.

Keywords: WEAP model; Wadi Dayqah dam (WDD); Optimal reservoir operation; Water resources planning; Variable hydrology

1 Introduction

Wadi Dayqah dam (WDD), since its completion in 2009, is still not operational, and its initial suggested water demand target of 35 MCM may be exposed to modifications according to the existing hydrologic and water demands development conditions. The extreme and ephemeral nature of the Wadi Dayqah basin hydrology brings up this critical question to decision-makers: What is this dam's reliable capability for water supply to downstream demands. Optimal dam reservoir water resource allocation is essential for efficient and sustainable environmental health and development (Agarwal et al., 2018; Nematollahi et al., 2021). The capability of adequate water resources management requires correctly understanding the physical system and the inclusion of hydrological procedures (Mustafa & Yusuf, 2012; Yazdandoost et al., 2021; Nematollahi et al., 2022). Climate change is an essential factor affecting the efficiency of water resource systems (Hong et al., 2016). Modelling is capable of providing an integrated and comprehensive framework for assessing water resources and policy-making for them, including the dams. Water Evaluation

and Planning (WEAP) software is successfully applied worldwide in many water resource systems with different hydrologic conditions. To establish modelling for efficient water resources management and allocation in extreme hydrological situations, the WEAP software can be considered a powerful tool.

The WEAP model has been extensively utilized for managing water resources, particularly in extreme hydrological conditions such as drought and flood (Yates et al., 2005; Roberto & Matthew, 2007). The WEAP model has been used in the literature to study the models of the saline lake (Raskin et al., 1992), river basins (Levite et al., 2003), groundwater and surface water (Yates et al., 2005), reservoirs (Hagan, 2007), and dams (Mounir et al., 2011). These applications have revealed that the WEAP model is an effective tool for water, agricultural, and municipal systems modelling for single and multiple catchments networks to handle water resources in different hydrological conditions (Daniyal et al., 2017; Suryadi et al., 2018). Hence, applying the WEAP modelling for water allocation in extreme hydrological conditions can be considered a significant advancement in each water system.

Several studies have been proposed in the literature on hydrological modelling using the WEAP model to simulate the catchment procedures. For this purpose, different WEAP models have been generated corresponding to different study areas such as Krishna, India (Bharati et al., 2008), Seybouse valley, Algeria (Berredjem & Azzedine, 2017), Mara river basin, Kenya (Metobwa et al., 2018). However, although the Wadi Dayqah dam (WDD) reservoir exists in Oman, its operation plans and water supply targets are not decided yet. Furthermore, the hydrological flow to this dam has an ephemeral nature with extreme conditions varying between 3.15 to 467 MCM. In such conditions obtaining an optimal reservoir operation plan based on highly varying hydrological conditions can be well modelled and analysed by well-developed tools such as the WEAP software.

In this study, WEAP software is used to model the optimal monthly operation of the WDD and find the optimized water demands that maximize the reservoir operations efficiency in terms of water supply reliability. In sum, the main goals of this study were delineated as the following:

(1) Modelling the WDD reservoir operation by the WEAP model,

(2) Statistical analysis of annual Wadi Dayqah (WD) catchment flow,

(3) Defining the water allocation scenarios for WDD with the WEAP model,

(4) Obtaining reservoir operational rule curves for the WDD.

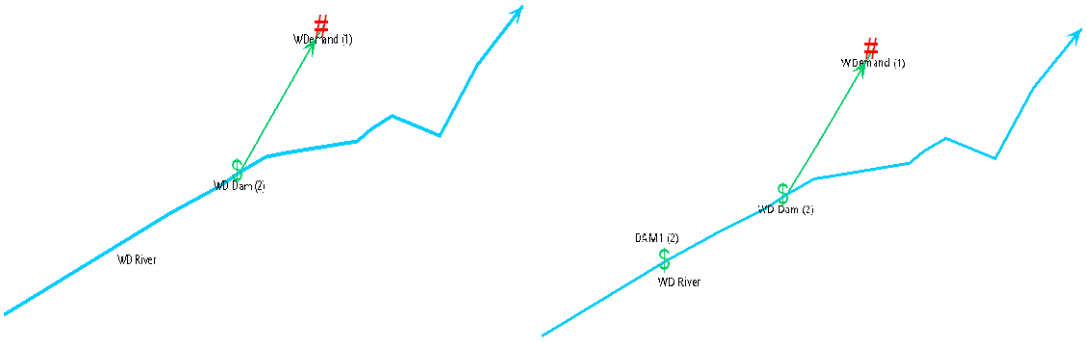
2 Methodology

The proposed methodology endeavoured to address several concerns related to the WDD operations through modelling by the WEAP:

- In the current condition, how is the efficiency of the WDD in fulfilling its operation?
- How could the WDD operational efficiency be improved by modifying the water demands or water system configuration, such as adding an upstream dam?
- What are the contributions of the effective reservoir operations for the WDD in the current and modified conditions?
- How much demand is achievable with good reliability in the current and future conditions?

2.1 WEAP Modelling

Figure 1 illustrated a schematic view of the WDD reservoir and its operational zones in the WEAP. This figure showed the WDD reservoir operation model, wherein monthly reservoir operation was modelled. In this study, all the priorities were assumed as one during modelling for the dam and demand for the WDD and the WD two dams' system except the priority of filling the WDD for the two dams' system to avoid filling water without a specific requirement. In addition, it was hypothesized that the consumption for the demand was 100%. Moreover, the total capacity of 100 and 20 MCM were assumed for the WDD and upper dam. In addition, in modelling the WEAP model for the WDD, the normal water year was assumed for the dam with the storage capacity of 100 MCM, considering the initial storage of 25 MCM in 1983. Finally, the maximum flow in the transmission links was hypothesized as 3.55 MCM in the presented model.



(a) **(b)**

Fig. 1: Schematic view of the Wadi Dayqah reservoir and its operational zones in the WEAP for **(a)** the WDD and **(b)** the WD and upstream dams' system

2.2 Problem Statement

Wadi Dayqah is a multi-purpose reservoir in Oman, and its primary objectives are flood management and water supply. The capability of the WDD to satisfy its future water requirements is essential to plan wisely for water resource allocation. To this extent, the modelling tools coupled with the scenario analysis approach can be essential for effective management strategies considering different hydrological situations. Therefore, applying the WEAP model as a robust modelling technique in conjunction with a scenario analysis technique results in an applicable water resources management for the WDD.

This study endeavoured to obtain the optimal reservoir operations for the WDD under different hydrological conditions based on the WEAP modelling. This paved the road for the reservoir planners to assess the effects of various possible future management approaches for the optimum releases from the dam, considering the constraints and priorities in extreme conditions.

Scenarios

Through this modelling, the scenarios were defined to determine the most reliable water level to fulfil the water demand requirements, considering the variations in the safe yield of the reservoir due to different inflow. These scenarios could be noted as follows:

(1) Reference scenario: Simulating the existing design of the dam considering the main

application of water supplying as 15, 20, 30, and 35 MCM per month,

(2) Increasing demand scenario: Considering the increase in the demand resulting in rising hydraulic releases of up to 45 and 55 MCM per month,

(3) Upstream dam construction scenario: Hypothesizing an upstream dam building to increase the performance of the WDD to enhance the water supply reliability (This scenario became critical if the water supply reliability was very low in a reference scenario).

2.3 Water Demand

The water demand requirement for domestic utilization, hydropower generation, environmental demands, and irrigation allocations should be defined in this model (Figure 2). Annual water demand scenarios are considered as 15, 20, 30, 35 (reference scenario), 45, and 55 MCM with the same monthly distribution as the reference scenario. This range of water demands helps to understand the safe annual yield of WDD and if there is any possibility to develop the water demands to higher values.

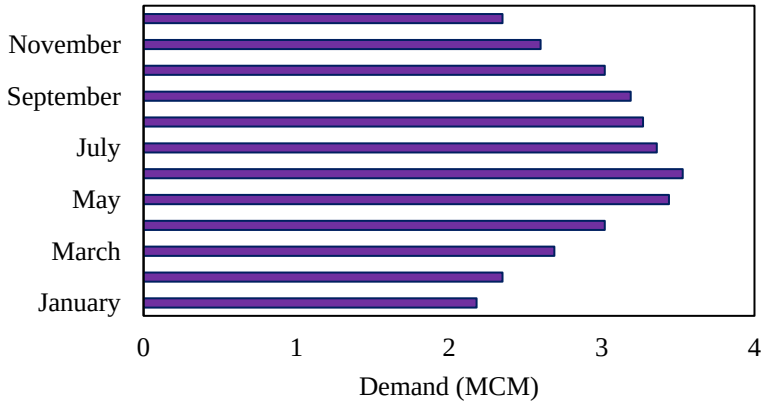


Fig. 2: Monthly demand for the Wadi Dayqah dam

3 Study Area

The WD catchment is located in the Al Hajar Ash Sharqi Mountains, wherein the wadi flows from the village of Tul down to Daghmar, and discharges to the coastal alluvial catchment (Figure 3). The WDD, built on 2010, is the principal flood controller for the WD flows while supplying drinking water for Quriyat and Muscat in Oman, which water supply system is still under construction (Figure 3). The average surface flow through the Wadi Dayqah from 1978 to 2005 was 50.97 million m^3 per year, so a reliable water yield of 35 MCM per year was assumed for the WDD.

The WDD reservoir has a volume of 100 million m3, equal to two years of average flow. This reservoir has an area of 350 hectares, a gross yield of 35 Mm3 per year, and an average stream flow of 50.97 MCM per year. The WDD water supply system consists of modern water treatment and supply system. This water allocation system takes water from the WDD reservoir to Quriyat Wilayat and other Wilayats of Muscat (Wadi Dayqah dam book, 2006).



Fig. 3: The Wadi Dayqah dam's location

4 Results and Discussion

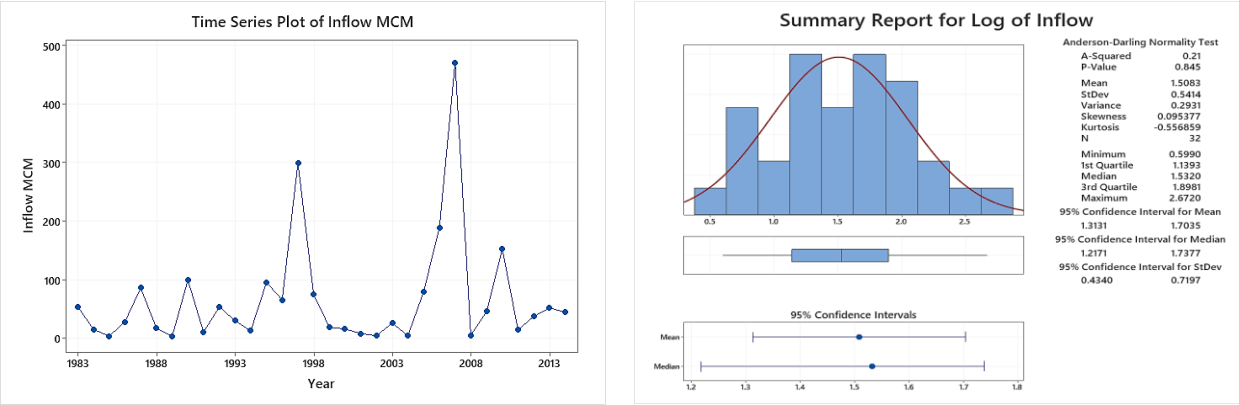
In the proposed WEAP model, the reference scenario could be utilized to validate the model considering the:

- Inflow statistical properties and downstream flow must be related.
- If water demand is low, the reliability of the water supply must be high.

4.1 Statistical Analysis of Inflow

In the proposed The statistical behaviour of flows to clarify that in arid or semi-arid catchments, the routine method of dam reservoir design may not apply was delineated in the following using Minitab. Figure 4 (a) was the time series of annual flows, including high and low amounts. This analysis indicated that Log(Mean) = 1.5083. This value revealed that the Mean was equal to 32 MCM, which was different from the arithmetic mean, 52 MCM by data of 1978-2003 or 66 MCM by data of 1978 – 2014.

Figure 4 (b) indicated that flow followed a log-normal distribution. According to this statistical analysis, the Median was 1.532; that was the Log(Q), so that Q = 34 MCM. In addition, when the Mean was 1.5083, Q = 32.2 MCM, much less than the considered Q-ave = 50 MCM for the dam design.

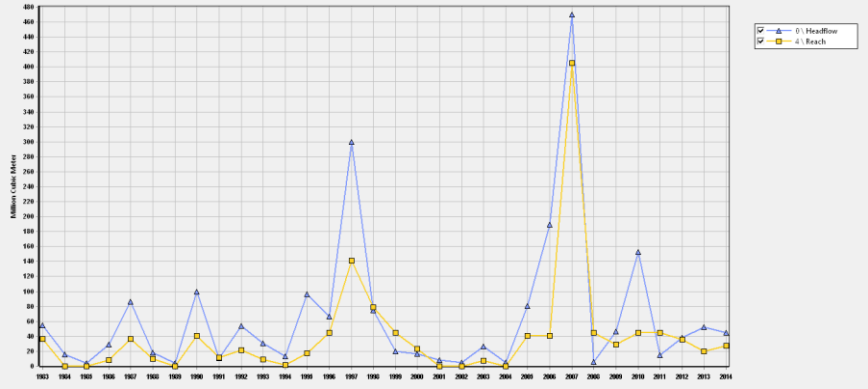


(a) (b)

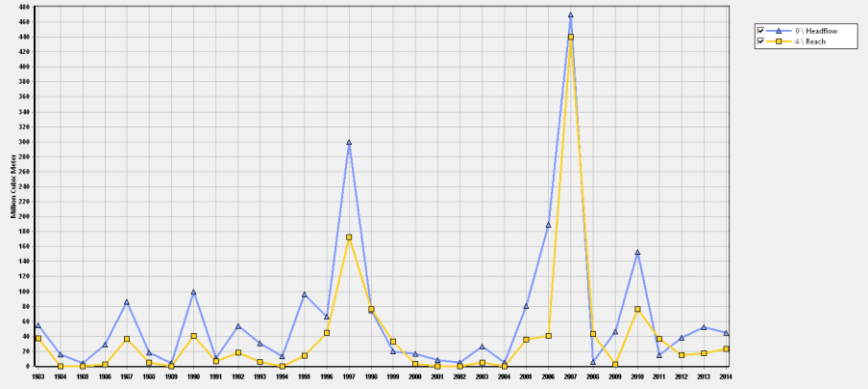
Fig. 4: Statistical analysis of WD catchment flow at Dagmer Station, **(a)** Time-series plot (MCM), **(b)** Log of inflow

4.2 Head Flow

Figure 5 showed the head flow after the WDD downstream. Some changes in flow were generally addressed as reservoirs regulating the flow. However, the statistical properties of both flows, such as the mean, were different due to water consumption. On the other hand, the other properties did not change meaningfully, which can be an indicator of model validity since the statistical properties of both head flow and downstream flow were within the range of head flow used as a validation for this model. Figure 6 indicated that the Wadi release to the sea was reduced and could be consumed for different purposes through the WDD and its upstream dam.



(a)

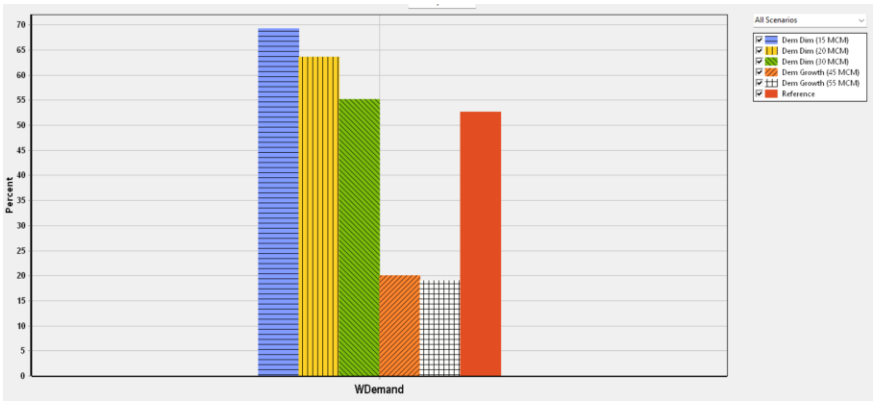


(b)

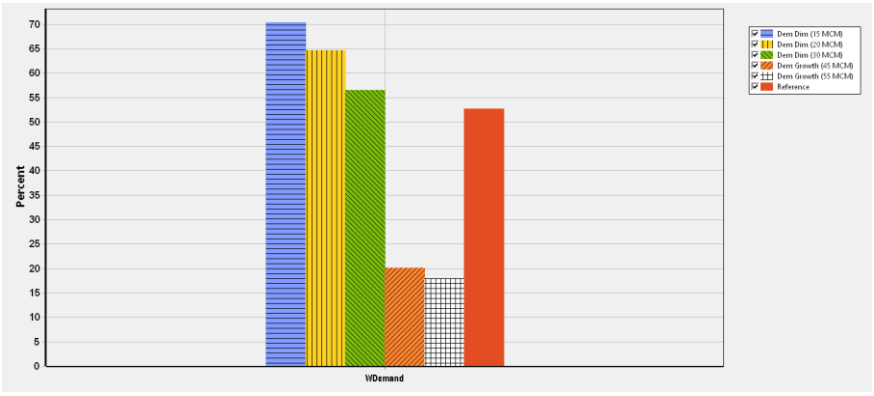
Fig. 5: Headflow at WDD downstream for **(a)** the WDD and **(b)** the WD two dams' system

4.3 Demand Analysis

Figure 6 showed the reliability of water demand supply since the reliability of water supply to demands is the primary measure of the efficiency of the WDD system. This figure approved that higher reliability was achieved with less demand, which was logical as another confirmation for model validity and validation. Therefore, this figure proved the effectiveness of the present modelling in meeting the water demand requirements.



(a)



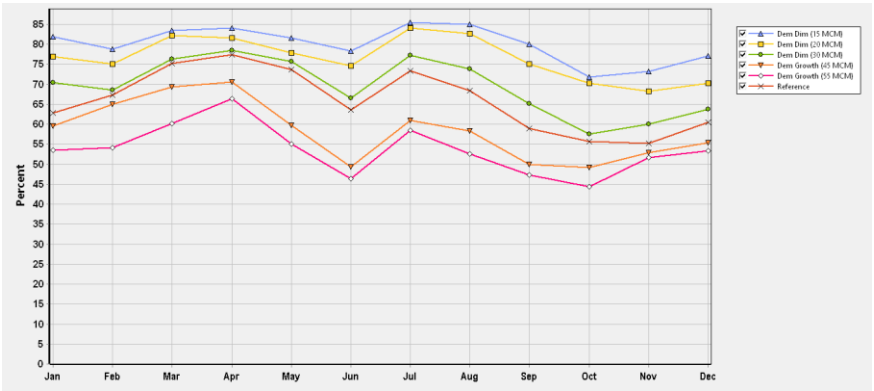
(b)

Fig. 6: Upstream optimal reservoir storage for **(a)** the WDD and **(b)** the WD two dams' system

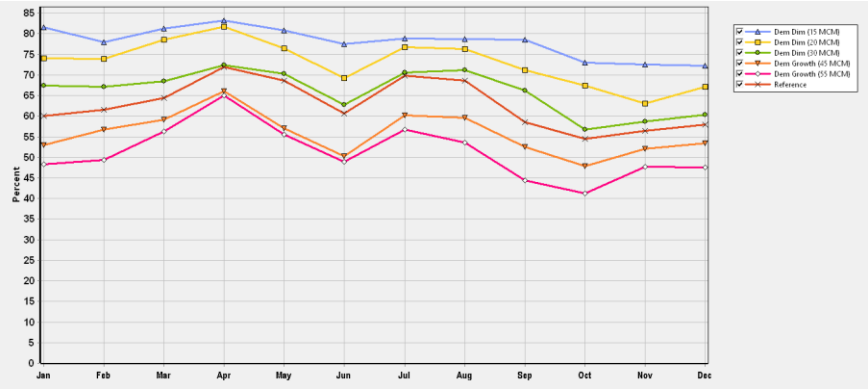
Notably, adding an upstream dam increased the water supply reliability by 5% maximum. However, to determine whether this 5% was meaningful, an economic analysis of the water supply that included the value of water was required to determine that this 5% increase justified the consideration of the upstream dam as a serious suggestion.

4.4 Water Supply

Figure 7 illustrated the percentage of water supply each month, showing that each month for each scenario met a considerable percentage of demand from the reservoir. The annual demand of 15 MCM had the highest reliability of 85%, while the annual demand of 55 MCM had the lowest reliability of 45%.



(a)



(b)

Fig. 7: Water Supply **(a)** the WDD and **(b)** the WD two dams' system

5 Conclusion

In this study, optimal operational rules have been determined considering present and future optimal water allocations from the WDD using the WEAP model. Model analysis showed that water demands in the range of 15 to 55 MCM could not be supplied with 100% reliability, and maximum reliability belonged to 15 MCM with 85% reliability. Furthermore, this study showed that adding an upstream 20 MCM dam on the main Wadi drainage at 2 Km upstream could increase the water supply reliability by 5% maximum.

It is recommended that economic energy generation alternatives be added to this system to make the reservoir operation more economical by the special scheme for upstream dam suggested with a power plant located at WDD Lake to provide high net head or inclusion of pumped-storage dams at high elevations.

References

Agarwal, et al. (2018). "A review on WEAP21 model for managing water resources". *J. Indian Water Resour. Soc. 38*(4).

Berredjem, A. F. & Azzedine, H. (2017) "Modelling current and future supply and water demand in the northern region of the Seybouse valley". *Journal of Water and Land Development 33*(IV-VI):31-38 PL ISSN 1429-7426.

Bharati, L., Anand, B. K. & Smakhtin, V. (2008) "Analysis of the Inter-basin water transfer scheme in India: a case study of the Godavari-Krishna link". Strategic Analyses of the National River Linking Project (NRLP) of India Series 2: 63.

Daniyal, et al. (2017) "Modeling water demand and supply for future water resources management". *International Journal of Scientific and Engineering Research 8*(5): 1747.

Hagan, Isaac. (2007) "Modelling the impact of small reservoirs in the upper east region of Ghana". Master Thesis, TVVR 07/5008, Division of Water Resources Engineering, Lund University, Sweden.

Hong, et al. (2016) "Evaluating water supply risk in the middle and lower reaches of Hanjiang river basin based on an integrated optimal water resources allocation model". Water 8: 364.

Levite, H., Hilmy, H. & Julien, C. (2003) "Testing water demand management scenarios in a water stressed, basin in South Africa: Application of the WEAP model". Physics and Chemistry of the Earth, Parts A/B/C 28(20-27): 779-786.

Metobwa, M. G. O., Khaldoon, A. M. & Lars, R. (2018) "Water demand simulation using WEAP 21: A case study of the Mara river basin, Kenya". *International Journal of Natural Resource Ecology and Management 3*(1): 9-18. https://doi.org/10.11648/j.ijnrem.20180301.12.

Mounir, M. Z., Ma, M. C. & Amadou, I. (2011) "Application of Water Evaluation and Planning (WEAP): A model to assess future water demands in the Niger River (In Niger republic)". *Modern Applied Science 5*(1).

Mustafa, S. & Yusif, M. I. (2012) "*A Textbook of Hydrology and Water Resources*". Publishing Company Abuja Nigeria, 1-2.

Nematollahi, B. Niazkar, M. & Talebbeydokhti, N. (2021) "Analytical and numerical solutions to level pool routing equations for simplified shapes of inflow hydrographs". *Iran J Sci. Technol. Trans. of Civ. Eng.* https://doi.org/10.1007/s40996-021-00757-x.

Nematollahi, et al. (2022) "A stochastic conflict resolution optimization model for flood management in detention basins: Application of fuzzy graph model". *Water 14*(5):774, https://doi.org/10.3390/w14050774.

Raskin, et al. (1992) "Simulation of water supply and demand in the Aral Sea Region". *Water International 17*(2): 55-67.

Roberto, A. & Matthew, M. (2007) "Application of the Water Evaluation and Planning (WEAP) model to assess".

Suryadi, et al. (2018) "Study on water resources allocation for Kertajati, Jatitujuh, and Ligung sub-districts to support the development of West Java International Airport (BIJB) and Kertajati Aerocity area". MATEC Web of Conferences, 147: 1-6.

Wadi Dayqah dam book (2006). "Wadi Dayqah dam and water supply scheme to Muscat and Quriyat book". Sultanate of Oman.

Yazdandoost, F., Razavi, H. & Izadi, A. (2021) "Optimization of agricultural patterns based on virtual water considerations through integrated water resources management modeling". *International Journal of River Basin Management*. 1-22. https://doi.org/10.1080/15715124.2021.1879093.

Cite as: Karimi A., Nematollahi B. & Nikoo M.R., "Efficient Reservoir Operation in an Arid Region with Extreme Hydrologic Flows: A Case Study, Largest Oman's Dam", *The 2nd International Conference on Civil Infrastructure and Construction (CIC 2023)*, Doha, Qatar, 5-8 February 2023, DOI: https://doi.org/10.29117/cic.2023.0150

Numerical Simulation of Climate Change Impacts on the Coast of Oman

Talal Etri
Sultan Qaboos University, College of Engineering, Muscat, Oman
t.etri1@squ.edu.om

Ghazi Al-Rawas
Sultan Qaboos University, College of Engineering, Muscat, Oman
ghazi@squ.edu.om

Ahmad Sana
Sultan Qaboos University, College of Engineering, Muscat, Oman
sana@squ.edu.om

Mohammad Reza Nikoo
Sultan Qaboos University, College of Engineering, Muscat, Oman
m.reza@squ.edu.om

Abstract

It is well known that there is an apparent increase in the intensity and frequency of extreme weather events, such as tropical cyclones (IPCC, 2023). This will lead to a significant effect not just on the infrastructure and the economic activities but also on the coastal environments. On the other hand, an increase in the population along the coastal areas in such a country as the Sultanate of Oman will also increase the risk and the hazard. It has been noticed extremely heavy rainfall during the most recent tropical cyclone, Shaheen (October 3 2021). It is also recorded along the Omani coast's extremely high waves during this storm event. Some other tropical cyclones in the past also indicated an essential effect on the Omani coast (Shawky et al., 2021). In this regard, the development of a fundamental understanding of the hydrodynamic behaviour along the coastal system during these events has been necessary. Moreover, the tropical cyclone track and wind speeds have been recorded only for a few temporal spans. This leads to better reliable estimations of such a kind of event. The state-of-the-art process-based numerical model will be utilized to hind cast the hydrodynamic developments from several tropical cyclone events along the Omani coast. A well-calibrated and validated flow model has been set up using Deft3D, a world leader's software (Lesser et al., 2004). Furthermore, the impact of wind-induced waves has been investigated using the SWAN wave model (Booij et al., 1999; Ris et al., 1999). In this paper, four well-known tropical cyclones in the Indian Ocean will be simulated. The four tropical cyclones were selected due to their historical significance and the amount of destruction they caused on the Omani coast. The investigation results showed significant tropical cyclones' effects on the Omani coasts due to their intensity and the cyclones' pattern. Overall, the numerical models that are showing good descriptions of climate change can be valuable tools for comprehending and predicting the influences of climate change on the Omani coast and can be employed to support in the decision-making.

Keywords: Sultanate of Oman; Numerical models; Tropical cyclones

1 Introduction

Many researchers and scientists declared that the climate is changing, leading to climate-related hazards like rising sea levels and increases in the intensity and frequencies of tropical cyclones (TC)

and storm surges (IPCC, 2023). According to the world meteorological organization (WMO), between 1970 and 2019, globally, about 11072 disaster events have been imputed only to weather, climate and water-related (WMO, 2020). Over the last 50 years, the recorded weather, water, and climate hazard events showed about 79%, 56% of deaths and about 75% of economic losses. Moreover, it has been recorded in the last ten years, i.e. between 2010 and 2019, there is an apparent increase in the tendency of disasters associated with weather, climate, and water by 9% compared to the previous decade and almost 14% between 1991 and 2000 (WMO, 2020).

Intense cyclones, tropical storms and hurricanes often hit the coast of Oman. This kind of weather phenomenon is called a sea hurricane. Storm surge-driven waves travelling off the shore cause significant damage in erosion phenomena. Besides destroying forests, buildings and coastal infrastructure, it also causes widespread pollution of drinking water sources and flooding (WMO, 2020). Moreover, Oman has a coastal line about 3165 km in length connecting the Arabian/Persian Gulf, the Sea of Oman and the Arabian Sea (Shawky et al., 2021). Therefore, Oman's location is more exposed to TCs, especially when about 7% of the global TCs are from the Indian Ocean (Leijnse et al., 2022).

Many researchers studied the effect of the TCs, based on remote sensing analysis and assessments, on the coast of Oman. Besides, the most recent studies cover mainly local regions of the Omani coast due to the need for more available data. Fritz et al. (2010) modelled the storm surge of Gonu using the Advanced Circulation Model (ADCIRC). The study has been conducted for non-spatial analysis (Fritz et al., 2010). Shawky et al. (2019) utilized geospatial techniques to model cyclone risk on the southern coasts of Oman. Hereher et al. (2020) recounted cyclones and tsunamis using the coastal vulnerability index (CVI). Likewise, Shawky et al. (2021) described a single risk index using a geospatial modelling technique. As it is known, the CVI assessment estimates a simplified index as one number indicating the coastal lines' vulnerability to the impact of climate changes. Mainly six physical processes, geomorphology, coastal slope, rate of relative sea-level rise, rate of shoreline erosion/accretion, mean tide range and mean significant wave heights are used to estimate CVI ranked from 1 (low) to 5 (high) (Al-Sariri, T., 2014). On the one hand, previous studies mentioned could help decision-makers and governors quantify the risk. On the other hand, these index numbers still need to describe the weather-related risks adequately. It will be challenging to use them in many engineering applications depending on water levels or wave parameters due to TCs.

In this study, a state-of-the-art hydrodynamics model developed by Deltares in Delft, Netherlands (Lesser et al., 2004) coupled with the wave model SWAN (Booij et al., 1999; Ris et al., 1999) is used to simulate storm surge, and wave conditions due to several TCs happened in the past. In particular, a good description of the sea state (tides and wave conditions) using well-calibrated numerical models will improve the estimation of the CVI.

2 Area of Study

The study area covers the entire Omani coastal line. The Sultanate of Oman is the third country located in the south-eastern quarter of the Arabian Peninsula, covering about 309000 km^2 (Hereher et al., 2020). The coastline stretches out over a distance of about 3165 km, from the Strait of Hormuz to the border with Yemen (Al-Sariri et al., 2014). Oman is classified as hyper-arid, with less than 100 mm rainfall, from the arid desert climate, 100 to 200 mm rainfall, to semi-arid, with 250-500 mm rainfall in different parts of the country (Al-Sariri et al., 2014).

The unique location of Oman (Fig. 1) during Tropical Cancer makes the climate conditions vary

throughout the country. Nevertheless, two main seasons occur, winter from November to April and Summer from May to October; the wind speed leans moderate (Hereher et al., 2020). For low-land regions, the wind speed is generally between 2 and 3 m/s (2 m above the ground). In general, the wind speed is not varying too much during the year, excluding some tropical cyclones generated in the Indian Ocean. Moreover, a strong wind along the Arabian Sea during the Monsoon also leads to tropical cyclones (Dibajnia et al., 2010). In the study area, it has been observed since 1945 about 29 tropical cyclones storms (Sarker, 2017). Most of the tropical cyclones occurred, namely pre-monsoon (May) and post-monsoon (October to November), and in some cases, TC events were also recorded between June and September (Evan et al., 2011; Fritz & Okal, 2008).

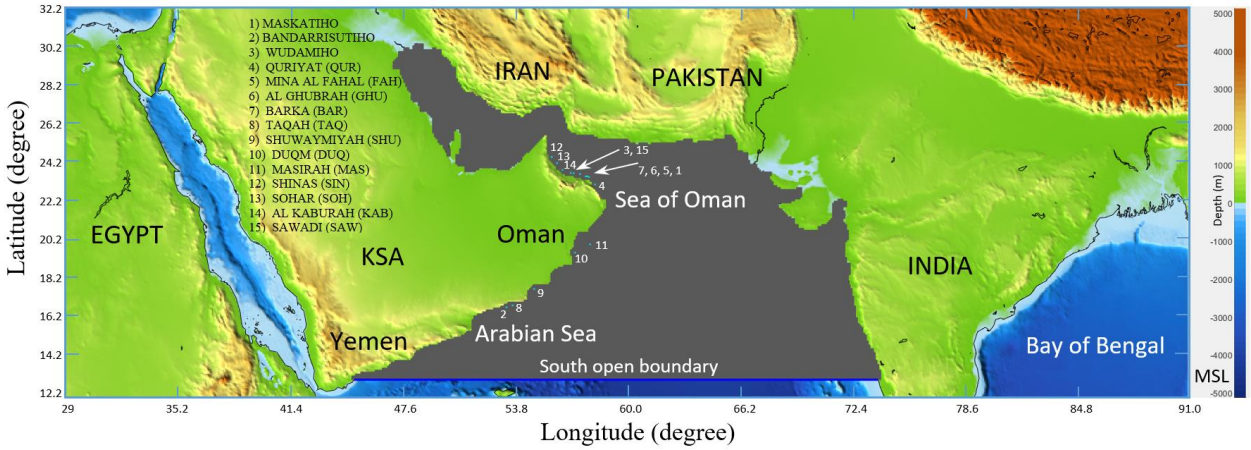


Fig. 1: Area of study (models' grid, open boundary, and observation points)

3 Purpose and Methodology of the Present Study

Studies of the TC and their effects on the coastal regions along the Omani coast have been exploratory, and a detailed study is required. Therefore, this paper presents a 2DH model for flow based on Delft3D software developed by Deltares coupled with SWAN wave models. The flow model was used to compute current velocities and water levels at several locations along the Omani coast. The flow model was set up for astronomical conditions, calibrated and validated using relevant tide gauge measurements at different locations in the area. Moreover, the current-induced wind has been intensively studied. The wave and flow models were then coupled to study only the wave-induced wind due to TC's without considering the swell waves. The methodology which has been pursued, the flow and wave model's setup and TC's events, can be described in the way that the wind and pressure fields are used from ERA5 (Hersbach et al., 2018) data sets to force the hydrodynamics and wave models. The results for the wave heights extracted from these models are evaluated using several statistical techniques, which will confirm the effects of the selected TCs on the coastal regions. Additionally, the two models, when completed, should help arrive at decisions about the coastal protection (long-term) and contingency and evacuation plans (short-term) due to TC's events.

4 Tropical Cyclone Hazards

It is well known that the tropical Indian Ocean is mainly described by surface warming more than other tropical cyclones in the northeast Pacific and north Atlantic. Moreover, TCs in the Indian Ocean are highly possible due to global warming (Charabi, 2010). Therefore, the TCs in the Indian Ocean have gotten more attention from researchers since 2007, since it has been observed that about 2 to 4 TCs per year (Bakker et al., 2022).

In a recent paper, the IBTrACS data set (The International Best Track Archive for Climate

Stewardship), which was developed by National Climatic Data Center (NCDC) from National Oceanic and Atmospheric Administration (NOAA) and World Data Center for Meteorology from World Meteorological Organization (WMO) is used for the TC's tracks and intensity (Knapp et al., 2018). In June 2007, the TC Gonu was one of the strongest cyclones that attacked the coast of Oman and the whole Indian Ocean. However, it only caused significant damage and about 50 deaths in Oman and has been described as the worst national disaster (Charabi, 2010). According to the Indian Meteorological Department, cyclone Gonu developed from a lasting area with high sea surface temperatures east of the Arabian Sea. The maximum wind speed recorded was about 270 km/h (June 1), and then it changed its direction toward the north entering the Gulf of Oman and dispersing on June 7. In 2007, Gonu was the second named TC in the Indian Ocean and categorized as Category 5 according to the Saffir–Simpson hurricane wind scale (SSHWS) (Saffir, 1973; Mohanty et al., 2014).

In June 2010, almost 3 years after Gonu, the Phet cyclone developed between the Arabian Sea and the Indian Ocean. It was the third described TC in the region, with a maximum wind speed of about 155 km/h (June 2). It started as a thunderstorm off the southwest of the Indian coast in the south-eastern Arabian Sea (Mohanty et al., 2014).

In October 2019, the super TC Kyarr developed (October 24) from a low-pressure region close to the Equator. The TC Kyarr showed an extremely strong TC in the North of the Indian Ocean and was denoted as the first strong TC after Gonu in 2007. The maximum wind speed that has been recorded was about 250 km/h. It has been noted that Kyarr did not cause severe damage because its path is offshore and almost parallel to the coastal lines along the affected areas. Moreover, Kyarr was merged with another TC (Maha), which makes for the first time two simultaneous TCs in the Arabian Sea (Mohanty et al., 2014). After two years since Kyarr occurred, the most recent TC Shaheen impacted the Omani coast in October 2021. Shaheen was named the fourth TC during the cyclone season in the Indian Ocean. Although the maximum wind was recorded at about 110 km/h, it caused great damage, especially along the Omani coast. It can be noted that the track of Shaheen starts from the east-central Bay of Bangel (it is named TC Gulab) towards the west of the Arabian Sea (named Shaheen). Additionally, Shaheen delivered extreme rainfall exceeding normal records. As a result, it caused flooding across many regions in Oman and High waves along the coastlines (Mohanty et al., 2014).

5 Flow and Wave Models Set Up

Due to the tropical cyclones, coupled 2DH flow and wave models are used to simulate the climate change impacts on the coast of Oman. Delft3D model is used in this study that Deltares, Netherlands have developed (Deltares, 2018). The model can solve the two- and three-dimensional unsteady shallow water equations by implementing a hydrostatic pressure approximation. The flow model is also able to simulate unsteady flow resulting from tides only, tidal and metrological forcing (wind-driven flow), wind shear, wave forces, density-driven flow, and atmospheric pressure changes in coastal regions, rivers, and estuarian areas (Lesser et al., 2004; Deltares, 2018). Moreover, the model is designed to solve the numerical equations for Cartesian or spherical unstructured grids using Generalized Lagrangian Mean (GLM) or Eulerian equations (Lesser et al., 2004). All the numerical formulations can be found in detail in the paper from (Lesser G.R. et al., 2004) or in a short description in the paper from Talal et al., 2022 (Etri et al., 2022). To include the effects of the waves on the hydrodynamics of the coastal processes, the SWAN wave model is coupled with the flow model. The well-known SWAN model is designed to simulate the sea state by calculating the wave action density (Booij, et al., 1999; Ris et al., 1999). The great benefit of coupling Delft3D flow and SWAN wave models is that the wind included in the simulation is only a result of the TCs. On the one hand, this

goal can be achieved by controlling the hydrodynamic inputs of the wave model under the Delft3D platform, which would be difficult to do under a standalone SWAN model. On the other hand, no wave conditions were applied along the open boundaries of the wave model.

For the flow and the wave models, an unstructured grid with a resolution of about 2 km (about 0.018^o) has been used (Figure 1). The setup of the models has been done using the tool Delft Dashboard (DDB) from Deltares. The DDB is mainly a MATLAB-based tool using several open-source datasets (Van Ormondt et al., 2020). Three of the most important input parameters are the bathymetry, astronomical tides, and wind of the TCs. Therefore, the available GEBCO08 gridded bathymetry data set is utilized (IHO, 2018). The grid resolution for this data set is about 30 arc seconds (1 km) which consists of the proposed grid (2 km) for flow and wave models. For the astronomical tides, DDB provides complete data from the International Hydrographic Organization (IHO) and the Intergovernmental Oceanographic Commission (IOC) of UNESCO (Van Ormondt et al., 2020). In addition, ERA5 hourly data on single levels from 1959 to the present has been imposed for the wind inputs for both the flow and the wave models. ERA5 wind and wave data set is the 5th version of ECMWF reanalysis, not only for the wind and wave but also for the global climate and weather for the last 4 to 7 decades. The data covers a period from 1950 to the present and a horizontal resolution of 0.25^o and 0.5^o for the atmosphere and ocean waves, respectively (Hersbach et al., 2018). For the flow model, the open boundaries were selected to be only one open boundary as astronomical tide components are imposed at the south of the domain with enough distance to avoid any numerical instability close to the Omani coast (Figure 1).

6 Results and Discussions

To determine whether the results of the flow and wave models are showing good descriptions for climate change and to reach a high degree of confidence in the results of the models, an extensive study was conducted for sensitivity, calibration, and validation. In these stages, acceptable numerical and physical parameter settings were reached, as shown in Table 2. Also, to guarantee an independent evaluation of the model results from the TC's events, the period in December 2018 is used. For this purpose, 15 observation points along the Omani coast have been used.

Table 2: Flow and wave model settings

Parameter	Value	Description
Δt_{Flow}	5	Flow computational time step (minute)
Δt_{Wave}	60	Wave computational time step (minute)
C_d	0.0025 to 0.005	Wind drag coefficient
NDir	36	Directional bins
FreqMin and FreqMax	0.033 to 0.5	Frequency ranges (Hz)
NFreq	30	Frequency bins
BedFricCoef (jonswap)	0.067	Bottom friction (m^2s^{-3})

As seen in Table 2, using a frequency range from 0.033 to 0.5 Hz will allow wave periods from 2 to 33.3 s. One important point should be mentioned that due to the grid resolution (about 2 km), the wave model cannot represent nearshore wave conditions like wave shoaling, refraction, and wave breaking. Because of this, the observation points and the wave analysis have been extracted for water

depths not less than 30 m, as proposed by (Leijnse et al., 2022). This is valid since the effects of the local wind-induced setup are not significant on such a large simulation scale.

Usually, the flow model simulations' quality is evaluated using the mean square error (MSE) and mean absolute error (MAE). In this study, it is highly recommended to use the MAE, which is more suitable and practical for evaluating the hydrodynamic models (Sutherland et al., 2004). For the quality of the wave model, the evaluation using the qualification proposed by Van Rijn et al. (2003), will be implemented (Van Rijn et al., 2003). It can be noted that the proposed qualification is converting the values of the root mean absolute error (RMAE) of the significant wave heights into qualification categories from Bad to Excellent.

The flow model results showed a good performance for the astronomical Semi-diurnal (M2, S2, N2, and K2) and diurnal components (K1, O1, P1, and Q1) in terms of amplitude and phase. In this regard, simulations for one year (2018) have been carried out. The comparison between the modelled and the estimated tidal components in the observation points showed differences between less than 1cm to 23cm for the amplitude and from 42 to 270o for the phase. Therefore, it can be confirmed that the astronomical tides imposed along the open boundary represent the tide conditions reasonably. Since this paper focuses on the TC's effects, further improvements in the tide conditions will not significantly change the wave conditions. In addition to the tidal analysis, a time series analysis for the tide with the wind as a driven force of the flow model has been carried out in December 2018. It is crucial to evaluate the flow model preference under the wind effect since the hydrodynamic conditions from the flow model will be used as input for the wave model. Since the area of interest is located along the Omani coast, only four stations are used to analyse the wind effects on the water level of the flow model results. The selection is based on the available water level measurements from the previously mentioned IHO tide observation points. The four stations (QURIYATIHO, MASKATIHO, BANDARRISUTIHO, and WUDAMIHO) cover a significant part of the south-eastern to the north-western coastline in the area of interest. The water levels in the four stations showed a good agreement between the measured and the modelled flow by using the wind from ERA5 wind datasets as driven forces. The calculated MAE in the four stations varies from 1 to 6 cm. Moreover, the results showed an excellent agreement in the phase without having any phase lag in any of the four stations.

The encouraging results from the flow model will reflect positively on the wave model, especially since the wave model is considered an essential element in studying the impact of hurricanes along the coasts of Oman. As the flow model was simulated in December 2018, the wave model was carried out for the same period. The wave model runs only using the hydrodynamics from the flow model (online coupling), including the wind speed and direction, without imposing any wave conditions at the open boundaries. In this way, the results from the wave model will only illustrate the effects of the TCs without any interaction with the swell waves. As mentioned before, the qualification proposed by (Van Rijn et al., 2003) will be used to evaluate the wave model preference. A comparison between the modelled and the measured wave data has been made using the ERA5 dataset. Although the ERA5 wave dataset is too coarse in terms of spatial (0.5o by 0.5o) and temporal (3 hours) resolution, it can be used for such analysis. Therefore, significant wave heights analysis took place in the 15 observation points, which showed RMAE values between 0.01 and higher than 0.3 (Bad to Excellent). It should also be clear that the high RMAEs are mainly observed at the shallow observation points depths where the ERA5 dataset accuracy is low (ocean waves).

For the quality of the simulations from the coupled flow and wave models, the effects of the TCs on

the Omani coast can now be described with high confidence using the ERA5 wind dataset. For this purpose, four simulations of the selected TCs have been executed. Initially, time series analysis of the wave model results from the four TCs will cover the significant wave heights and wave peak periods at 15 observation points. Here, the simple analysis will take place by plotting the significant wave heights (Hs) vs the time in terms of days, neglecting the months and the years. This way, it will be possible to compare all the TC's effects on the Hs at the 15 observation points. Moreover, water levels from the flow model will be used for the same TCs at the 15 stations to describe the tide conditions (Neap-Spring). The model results showed that Gonu, Phet, and Shaheen mainly occurred during the spring tide in contrast with Kyarr, which occurred during the neap tide.

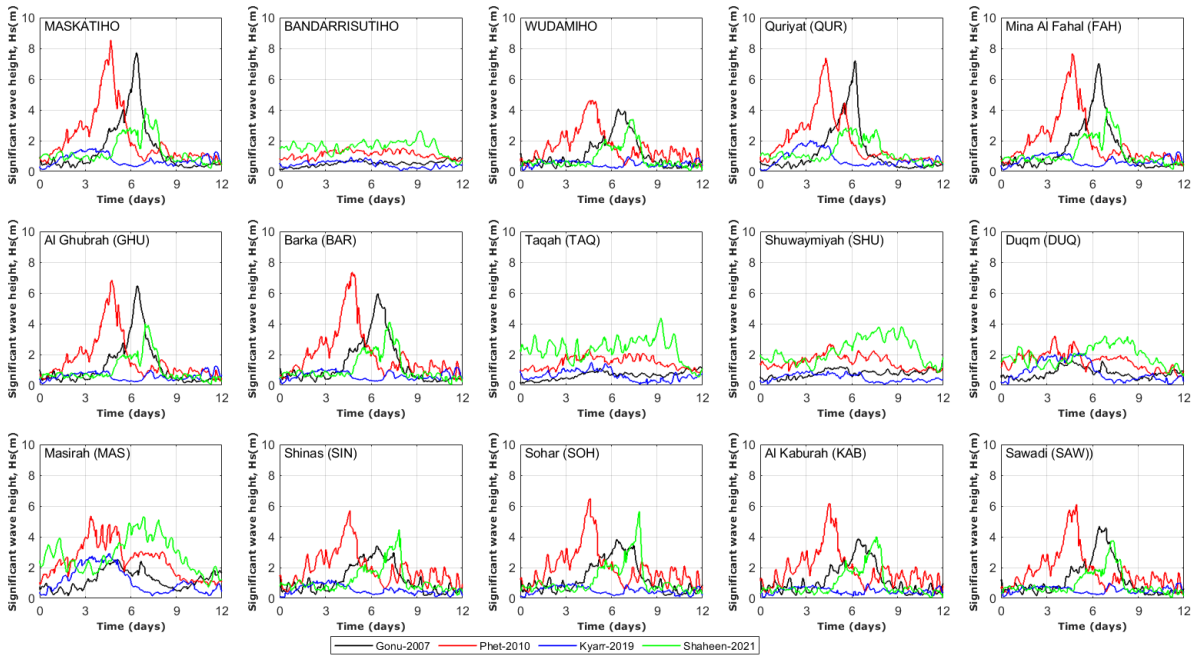


Fig. 2: Significant wave heights (Hs) in meters for the four TCs

Figure 2 shows the significant wave heights (Hs) from the wave model results in the 15 observation points. It can be seen clearly that the effects of the TCs on the Hs can be divided into 3 patterns. Pattern 1, low effects along the Arabian Sea, at the most south-western part of the Omani coast (BANDARRISUTIHO, TAQAH (TAQ), and SHUWAYMIYAH (SHU)). Pattern 2, medium effects at DUQM (DUQ) and MASIRAH (MAS). Pattern 3, significant effects at the rest of the 15 observation points along the Sea of Oman. This is valid for Gonu 2007, Phet 2010, and Shaheen 2021 TCs. It can be seen that Gonu 2007 and Phet 2010 caused extreme wave conditions (between 4 and 8m) in pattern 1 observation points. The observation of the Hs results from Gonu, and Phet TCs showed similar wave heights and event duration behaviour. It can be seen that both of the TCs reached 8m wave heights for a duration of 3 to 4 days. This will lead to more pressure due to events on the coastal structures. The more important point can be added that the Phet TC can be compared, even worse than the well-known TC Gonu. On the other hand, the TC Kyarr 2019 showed fewer effects on the Hs. However, a high wind speed is recorded, which could be mainly due to the cyclone's path following parallel to the Omani coast and in conjunction with neap tidal conditions. This leads to wave heights of less than 2 m at the 15 observation points. The Hs model results reveal the most critical effects due to TC Shaheen almost along the Omani coast from the north to the south. In pattern 1 region, the Hs can be recorded in the order of 4m. In pattern region 2 the wave heights were recorded between 2 and less than 4m, and in pattern 3 region about 2 m. It can be noted that the durations of

the extreme wave conditions in all regions take from 4 to 5 days. In this case, the TC Shaheen can be considered the most severe event of the four simulated TCs. This is not due to high wind speed but to the path that the wind is following, the duration of the event and, additionally, the spring tidal conditions.

7 Conclusion

A 2DH flow model from Deltares and a wave from the SWAN model were set up along the Omani coast. The two models simulations have accounted for the tides for the hydrodynamics and wind for the wave models. The two models were calibrated in December 2018, and the model results showed that the models are capable of predicting wave conditions with acceptable accuracy. Four TCs, namely, Gonu 2007, Phet 2010, Kyarr 2019, and the most recent cyclone Shaheen 2021, have been simulated. The wave results clearly described the TC's events and their effects along the Omani coast. The results showed a clear tendency to increase the intensity of the TCs in the last two decades. Moreover, it has also been confirmed that the duration and the path of the TC event play an important role in studying the TCs. Additionally, the model's results showed a significant effect due to neap-spring tides on the wave conditions along the coast of Oman. The model's results improve the understanding of the TC's effects on the most exposed regions along the Omani coast. It can also be seen that not only the well-known TCs with 4 or 5 SSHWS categories (Gonu, Phet, and Kyarr) reveal extreme wave conditions but also TCs with 1 SSHWS category (Shaheen).

Although it has been found that the flow and the wave models, in general, are appropriate for describing the wave conditions due to TC's improvements, using field measurements is recommended. It is also highly recommended to generate reliable synthetic TCs using wind and pressure estimations to be used with flow and wave models.

References

2020 State of Climate Services: Risk Information and Early Warning Systems (2020). World Meteorological Organization (WMO), WMO- No. 1252.

Al-Sariri, T. (2014). "Coastal Zone and Climate Change Management in Oman". PhD Dissertation, Centre for Environmental Strategy, Faculty of Engineering and Physical Science, ProQuest LLO (2019), UK.

Bakker, et al. (2022). "Estimating tropical cyclone-induced wind, waves, and surge: A general methodology based on representative tracks". Coastal Engineering, Vol. 176. https://doi.org/10.1016/j.coastaleng.2022.104154.

Booij, N., Ris, R.C. & Holthuijsen, L. H. (1999). "A third-generation wave model for coastal regions, Part I, Model description and validation". *J. Geophys. Res. C4, 104*, 7649-7666.

Charabi, Y. (2010). "Indian Ocean Tropical Cyclones and Climate Change". Proceeding of the International Conference on Indian Ocean Tropical Cyclones and Climate Change, Muscat, Oman. Springer Dordrecht Heidelberg London New York, https://doi.org/10.1007/978-90-481-3109-9.

Deltares (2018). "Delft3D-Flow Simulation of multi-dimensional hydrodynamic flows and transport phenomena, including sediments". User Manual.

Dibajnia, et al. (2010). "Cyclone Gonu: The Most Intense Tropical Cyclone on Record in the Arabian Sea". Y. Charabi (ed.), Indian Ocean Tropical Cyclones and Climate Change, pp. 149-157. Springer Dordrecht Heidelberg London New York, https://doi.org/10.1007/978-90-481-3109-9.

Etri, T., Abugdera, A. F. & Elata, A. (2022). "A Tidal Flow Model of The Western Coast Of Libya". *Journal of Engineering Research*, Vol. 19, Issue 1. pp. 54–62. https://doi.org/10.53540/tjer.vol19iss1pp54-62.

Evan, et al. (2011). "Arabian Sea tropical cyclones intensified by emissions of black carbon and other aerosols". *Nature*,

479(7371):94–7. https://10.1038/nature10552. PMID: 22051678.

Fritz, H. M. & Okal, E. A. (2008). "Socotra Island, Yemen: field survey of the 2004 Indian Ocean tsunami". *Nat Hazards 46*(1):107–117. https://doi.org/10.1007/s11069-007-9185-3.

Fritz, et al. (2010). "Cyclone Gonu Storm Surge in the Gulf of Oman". Proceeding of the International Conference on Indian Ocean Tropical Cyclones and Climate Change, Muscat, Oman. Springer Dordrecht Heidelberg London New York, https://doi.org/10.1007/978-90-481-3109-9.

Hereher, et al. (2020). "Assessment of coastal vulnerability to sea level rise: Sultanate of Oman". *Environmental Earth Sciences* 79:369. https://doi.org/10.1007/s12665-020-09113-0.

Hersbach, et al. (2018): ERA5 hourly data on single levels from 1959 to the present. Copernicus Climate Change Service (C3S) Climate Data Store (CDS). (Accessed on 14-NOV-2022), 10.24381/cds.adbb2d47.

International Hydrographic Organization, Intergovernmental Oceanographic Commission (2018). "The IHO-IOC GEBCO Cook Book". IHO Publication B-11, Monaco, 416 pp - IOC Manuals and Guides 63.

Intergovernmental Panel on Climate Change (IPCC). (2023). Climate Change 2021 – The Physical Science Basis: Working Group I Contribution to the Sixth Assessment Report of the Intergovernmental Panel on Climate Change. Cambridge: Cambridge University Press. https://doi:10.1017/9781009157896.

Knapp, et al. (2018). International Best Track Archive for Climate Stewardship (IBTrACS) Project, Version 4.00. NOAA National Centers for Environmental Information. https://doi.org/10.25921/82ty-9e16.

Leijnse T., Giardino A., Nederhoff, K. & Caires, S. (2022). "Generating reliable estimates of tropical-cyclone-induced coastal hazards along the Bay of Bengal for current and future climates using synthetic tracks". *Natural Hazards Earth Systems Science*. Vol. 22, Issue 6. https://doi.org/10.5194/nhess-22-1863-2022.

Lesser, et al. (2004). "Development and validation of a three-dimensional morphological model". *Coastal Engineering*, (51), 883-915.

Mohanty, et al. (2014). "Monitoring and Prediction of Tropical Cyclones in the Indian Ocean and Climate Change". Springer, pp.428, https://doi.org/10.1007/978-94-007-7720-0

Ris, R.C., Booij, N. & Holthuijsen, L. H. (1999). "A third-generation wave model for coastal regions, Part II, Verification". *J. Geophys. Res. C4, 104*, 7667-7681.

Saffir, H. S. (1973). "Hurricane Wind and Storm Surge, "The Military Engineer, Vol. 423, 1973, pp.4-5

Sarker, M. (2017). "Numerical Modelling of Major Cyclonic Waves and Surge at Duqm (Oman) since 1945". World Port Development. Engineering Numerical Modeling. Pp. 38–40. Technical report from Royal HaskoningDHV.

Shawky M. (2019). "Geospatial modelling of tropical cyclone risks to the southern Oman coasts". *International Journal of Disaster Risk Reduction*. Vol. 40, 101151. https://doi.org/10.1016/j.ijdrr.2019.101151.

Shawky, et al. (2021). "Geospatial modelling of tropical cyclone risk along the northeast coast of Oman". Marine hazard mitigation and management policies, Marine Policy, Vol. 129, 104544.

Sutherland, J., Peet, A. H. & Soulsby R. L. (2004). Evaluating the performance of morphological models, *Coastal Engineering*, (51), 917–939.

Van Ormondt, M., Nederhoff, K. & van Dongeren, A. (2020). "Delft dashboard: a quick setup tool for hydrodynamic models". *Journal of Hydroinformatics*, (22), 510-527.

Van Rijn, et al. (2003). The predictability of cross-shore bed evolution of sandy beaches at the time scale of storms and seasons using process-based Profile models, Coastal Engineering, Volume 47, 295-327.

Cite as: Etri T., Al-Rawas G., Sana A. & Nikoo M.R., "Numerical Simulation of Climate Changes Impacts on The Coast of Oman Sea", *The 2nd International Conference on Civil Infrastructure and Construction (CIC 2023)*, Doha, Qatar, 5-8 February 2023, DOI: https://doi.org/10.29117/cic.2023.0151

The Dependent Clogging Dynamics and Its Impact on Porous Media Permeability Reduction

Ahmed Elrahmani
Department of Civil and Environmental Engineering, Qatar University, Doha, Qatar
ae1304061@qu.edu.qa

Riyadh I. Al-Raoush
Department of Civil and Environmental Engineering, Qatar University, Doha, Qatar
riyadh@qu.edu.qa

Abstract

The dynamics of fine particle entrapment, transport, and deposition within pore systems, particularly the ability of mobile fines to impair permeability within porous media, are critical to a variety of natural and manmade phenomena, impacting oil and gas recovery, slope stability, filter capacity, and the efficiency of lab-on-chip diagnostics in medical disciplines. According to the research, clogging of pore throats in the porous media is not a random process; clogged throats, in particular, modify flow conditions and promote subsequent clogging nearby which is called dependent clogging. Over the last several decades, significant efforts have been made to identify and parameterize the role of dependent clogging in permeability reduction, with studies applying a combination of physical investigation and numerical simulation to this objective. In this work, we deploy a coupled computational fluid dynamics-discrete element method-based framework to investigate fines migration and consequent pore-throat clogging within a geologically realistic pore system extracted from an x-ray microtomographic image of a sand pack. The analysis of the simulation results revealed a spatial correlation between the clogged throats, implying that throats in close proximity became clogged dependently around the same time. Furthermore, dependent clogging was observed to be more frequent than independent clogging and it impacts system permeability more efficiently. This suggests that the distribution of clogged throats has a significant impact on the system's permeability reduction other than the total number of clogged throats.

Keywords: Fine migration; Pore-throat dependent clogging; Permeability reduction; CFD-DEM simulations

1 Introduction

Many researchers have lately focused on the transport and fate of fine particles in porous surfaces due to their significance in a variety of industrial and environmental applications (Han et al., 2019; Jang et al., 2018; Jarrar et al., 2020). Fine migration can induce physical damage to the pore structure, such as clogging and permeability reduction (Frimmel et al., 2007). Clogging in porous media has an influence on a wide range of industrial applications, including water filtration, inkjet printing, and oil recovery (Tavakkoli et al., 2015). Clogging dynamics are also significant in a range of suspension flow in porous media applications, ranging from biophysical systems to filters and sensors, as well as fractured rocks (Bächer et al., 2017; Huang et al., 2014; Pang et al., 2015). In general, three main processes for fines migration in porous media are defined: piping, which occurs when there is no contact between fines and grain particles, bridging, which is the process of pore-filling or the start of clogging, and complete clogging (Kartic and H. Scott, 1998).

Clogging in porous media is not a random process; clogged pores modify flow conditions and promote more clogging nearby. According to pore network model simulations in the literature, dependent clogging reduces the permeability of the porous medium more efficiently than independent clogging (Liu et al., 2019). Clogging is classified as a dependent when one or more of the neighbouring pore throats are already clogged. This classification is developed for the symmetrical homogenous geometry that was used in the research; however, this is not the case with a heterogeneous pore geometry where the range of influence of each clogged throat must be established. (Sauret et al., 2018) used parallel micro-channels to conclude that the distribution of clogged pore throats has a substantial impact on the reduction in permeability of porous media. Despite this, the study's use of parallel microchannels restricts its ability to mimic the natural behaviour of true porous media. Furthermore, the assumption that the flow rate in a microfluidic channel is equal to zero when it is obstructed by only one particle is exceedingly restricting. (Liot et al., 2018) used parallel microchannels in a microfluid experiment, as well, and determined that the presence of a clogged throat can shift flow to neighbouring channels, increasing their chances of being clogged as well. This leads to complex clogging dynamics described in the literature as a "cross-talk" interaction (Liot et al., 2018; Sauret et al., 2018; van Zwieten et al., 2018).

The dependent clogging, also known as cross talking, mechanism and the range that defines dependent clogging for a realistic, non-homogeneous, and non-symmetrical porous media geometry were not covered in any of the studies published in the literature. Furthermore, the dynamic influence of dependent clogging on the lowering of permeability in realistic porous media has received little attention. In this research, we examine the dependent clogging behaviour in natural porous media using Computational Fluid Dynamics (CFD) combined with Discrete Element Methods (DEM) numerical models for a geologically realistic pore system extracted from an x-ray microtomographic image of a sand pack. The goal of this study is to examine the correlation between clogged pores in natural porous media, determine the likelihood of dependent clogging and its different behaviour and determine the effect of the dependent clogging behaviour on the permeability reduction.

The structure of this paper is as follows, implementation details of the coupled CFD-DEM modelling framework and the used porous media geometry are presented in section 2. The clogging dependency range and ratio as well as their effects on permeability reduction are presented and discussed in section 3. Finally, the main results and conclusions are drowned out in section 4.

2 Methodology

2.1 Numerical Model

A CFD-DEM architecture connected with IBM is used to model fine particle migration, attachment, and detachment. The coupled framework is capable of modelling a high content of fine particles traveling in realistic pore geometries generated from computed tomography 3D images. The model is designed to operate in parallel to simulate a large concentration of fine particles within the pore space by splitting the simulation domain among processors and utilizing MPI for communication. The model was validated against a micro-model experiment to ensure its ability to capture complex behaviour (Elrahmani et al., 2022). The framework's CFD component solves the fluid velocity and pressure field for an incompressible fluid. The open-source toolkit OpenFOAM was used to solve the Navier-Stokes equations and the continuity equation, Eq. 1a and 1b, for single-phase fluid flow. (Weller et al., 1998).

$$\frac{\partial}{\partial t}(\rho u) + \nabla \cdot (\rho u u) = \nabla p + \left[\nabla \cdot \left(\mu(\nabla u + \nabla u^T)\right)\right] + F_{sa} \quad (1a)$$

$$\nabla \cdot u = 0 \quad (1b)$$

Within each simulation, the Discrete Element Method (DEM) was employed to compute the trajectory of individual particles. The trajectory of a specific particle I was computed by accounting for its interactions with other particles and/or the pore walls around it (Goniva et al., 2012). The open source solver LIGGGHTS solved the following equations, Eq. 2a, and 2b, that were derived from Newton's equations of translational and rotational motion, respectively, and provide a foundation for describing particle motion inside the system.

$$m_i \frac{dv_i}{dt} = m_i g + \sum_{N_p} F_i^{p-p} + \sum_{N_w} F_i^{w-p} + F_i^{f-p} \quad (2a)$$

$$I_i \frac{d\omega_i}{dt} = \sum_{N_p} r_{ic} \times F_i^{p-p} + \sum_{N_w} r_{ic} \times F_i^{w-p} + T_i^{f-p} \quad (2b)$$

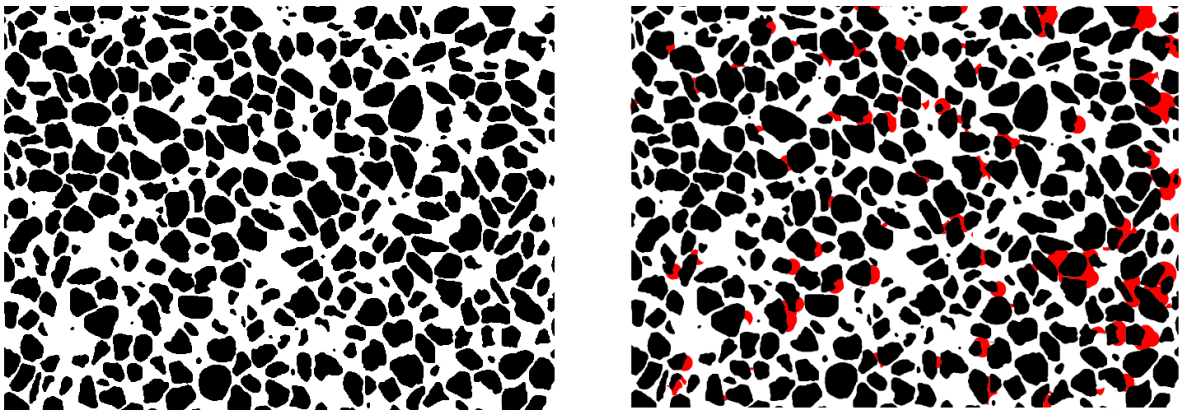
The CFD-DEM model takes into account both fluid-particle and particle-particle interactions, yielding a four-way coupling system. To enable coupling, the Eulerian-Lagrangian technique is adopted in the model, with the addition of a volume fraction term, accounting for the granular phase, inside the Navier-Stokes equations (Goniva et al., 2012; Zhou et al., 2010). The Immersed Boundary Method is used to incorporate the influence of a flowing particle on the system into the simulation (IBM). The pressure and velocity field from the previous time step t_{n-1} are utilized within the DEM to update the particle's position, velocity, and associated properties for each time step t_n. Following that, the Navier-Stokes equations for pressure and velocity are calculated while accounting for the volume fraction of the solid phase. The pressure and velocity of the fluid are then rectified using a neighbourhood of cells to represent each mobile particle. These procedures are repeated for each iteration until the simulation is finished (Goniva et al., 2011; Hager et al., 2014).

2.2 Porous Media Geometry

The geometry of the porous media utilized in the study was extracted from Argonne National Laboratory (ANL) synchrotron x-ray micro-computed tomographic image of a sand pack (Jarrar et al., 2020). The sand pack was scanned in 3D computed tomography using the ANL synchrotron facility. The photos were binarized using global thresholding, and grain boundaries were reconstructed and converted into lines that were converted into polylines in AutoCAD after a morphological opening was done. The geometry has 6700x5000μm lateral dimensions and a channel depth of 40μm. The details of the image processing as well as the mesh generation followed the procedure described in (Elrahmani et al., 2022).

The pore system used in this research, presented in Figure 1a, had geometrical parameters of (4.28μm^2 permeability, 0.483 porosity, 79μm median grain radius, 33.1μm median pore radius, 1.33 tortuosity, and 2.82 coordination number). The pore system was subjected to four CFD-DEM simulations using various monodisperse suspensions with particle sizes of 5, 7, 10, and 15μm. The density of the fine particles was 1.05 g/cm^3. For all simulated situations, the flow velocity was constant (0.06 cm/min), and the initial particle content was 2% by volume.

Clogging events in the modelled porous medium were discovered in this study by binarizing the simulation grid so that cells inside the flow domain with zero velocities were set to true and no-zero cells were set to false, shown in Figure 1b. It is worth mentioning that this method defines clogging as a total blockage of water passage through the cells. The pore-throat size distributions of the examined porous media were then determined using the technique proposed by (Rabbani et al., 2016). This made it possible to count the number of clogged throats in each time step by comparing the number of throats in the picture at time t_n to the original geometry at time t_0.



a) After 1 Pore Volume Injection **b)** After 15 Pore Volume Injection

Fig. 1: Illustration of clogging after injecting 15µm diameter fine particles (the clogged fluid cells with zero flow velocity are coloured in red)

3 Results and Discussion

3.1 Dependent Clogging Parameters

Since the semi-variogram is defined as a measure of spatial variability, it could be utilized to assist in the spatial autocorrelation of clogged throats and to determine the range of dependency (Kigobe and Kizza, 2006; Olea, 1999). The premise here is that throats next to one other are expected to clog around the same time, compared to throats separated by larger distances. The experimental semi-variogram was calculated using Eq. 3, where $N(h)$ is the number of clogged throats separated by h distance. T_i and T_j are the time steps when the throats i and j clogged. The value of h was set to increase by an increment that equals to the median pore radius of the analyzed geometry.

$$\gamma(h) = \frac{1}{2\,N(h)} \sum_{i,j \in N(h)} \left(T_i - T_j\right)^2 \tag{3}$$

The algorithms proposed by Schwanghart were used in computing and the experimental semi-variogram and fit its thermotical model as shown in Figure 2a (Schwanghart, 2023). The practical range is defined as the distance for which the value of the model is 95% of the sill, which is the value of the variation chart (Mendes and Lorandi, 2006). From the point of the range and forward, it is safe to assume no more spatial dependence between the clogged throats, hence it is mentioned as the dependency range in this study.

The dependently clogged throats could be quantified using the stated dependency range. Clogged throats that are less than or equal to the dependence range away from an initially clogged throat are classified as dependently clogged. Figure 2b illustrates the separation of the overall clogged fraction, the number of clogged throats at any time t over the total number of throats, into independent and dependent clogged fractions. Figure 7b shows a linear trend for the dependent vs independent clogged fraction, with the slope of the line representing the dependency ratio. The dependency ratio is a measure of how many throats are impacted by clogging one throat, while the dependency range is a numerical quantity indicating how far a clogged throat would affect other throats.

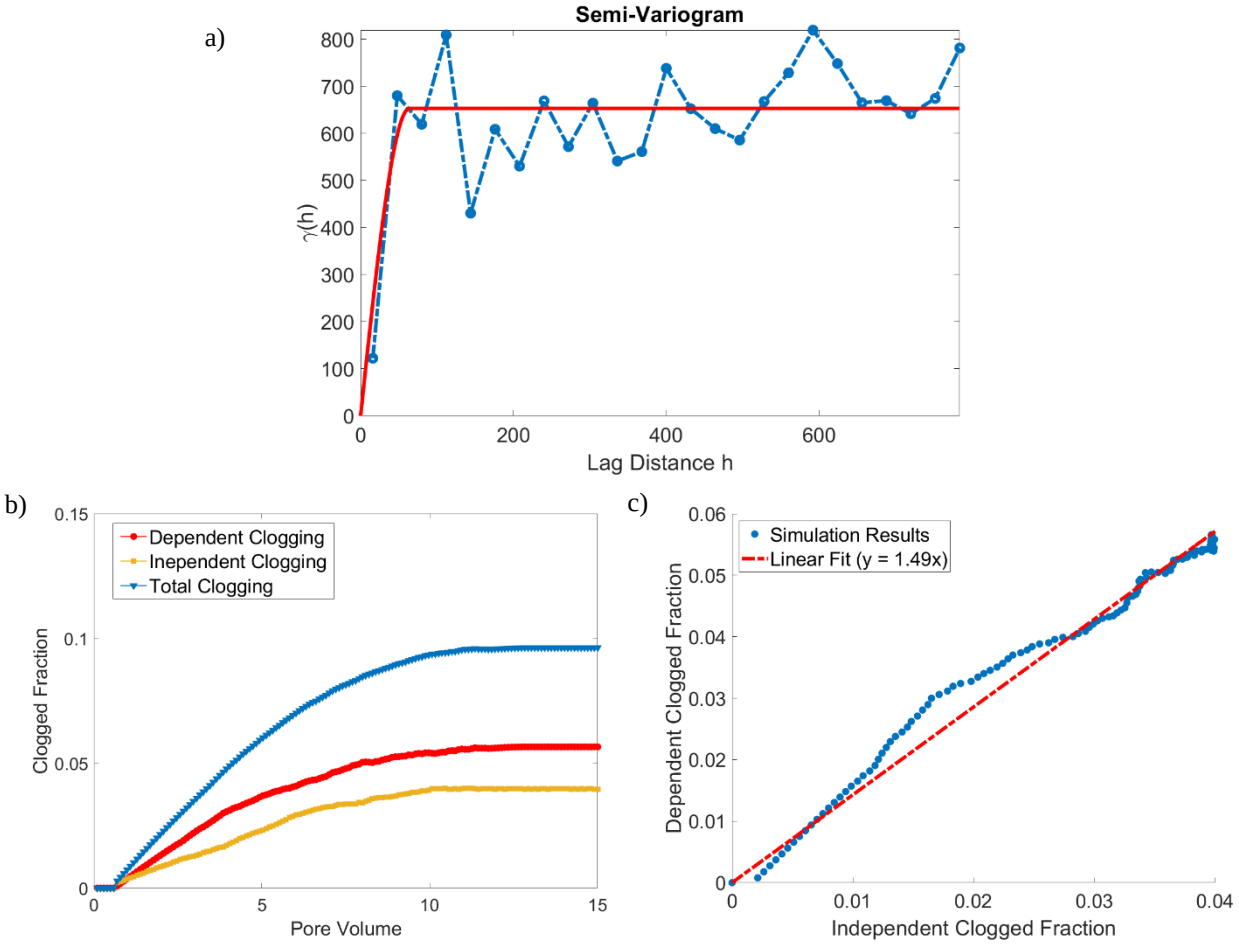


Fig. 2: a) The experimental semi-variogram for the clogged throats and its spherical model fit, **b)** the dependent, independent, and total clogged fractions, **c)** the dependent against independent clogged fractions (dependency ratio 1.49) after 15-pore volume injection of 5-micron fines

3.2 Dependent Clogging Behaviours

As shown in Figure 3, the dependency ratio is found to be more than one for all the simulated cases, which indicates that the dependent clogging is more frequent than the independent clogging. Moreover, the trend for the dependency ratio was increased by increasing the injected fine sizes, since larger particles can clog more throats. Furthermore, increasing the injected fine sizes improved the tendency for the dependency ratio, since bigger particles potentially clog more throats. The trend for the dependency range, on the other hand, experienced a sharp decline when the system was injected with 10-micron fine particles. A closer look at the simulation data revealed that the rapid shift in the dependency range is caused by a change in the dependent clogging mechanism. The simulations revealed two types of dependent clogging behaviours. The first behaviour is dependent clogging due to flow path change; this occurs when one throat is clogged, causing the flow streams around it to shift, leading particles to change their flow path and clog other throats. As illustrated in Figure 4a, independent clogging of the throat circled in blue prompted the flow to modify its direction and clog the throat circled in green dependently. The other type is dependent clogging due to pore filling, which happens when one throat is clogged and the inertia of the flowing particles is significant, so their flow direction does not change, causing fine particles to accumulate in the pore and clogging the throats linked to the pore as well. This is seen in Figure 4b, where the independent clogging of the throat circled in blue caused fine particles to accumulate in the pore, causing the throats connected to the pore to clog as a dependent clogging, circled in green.

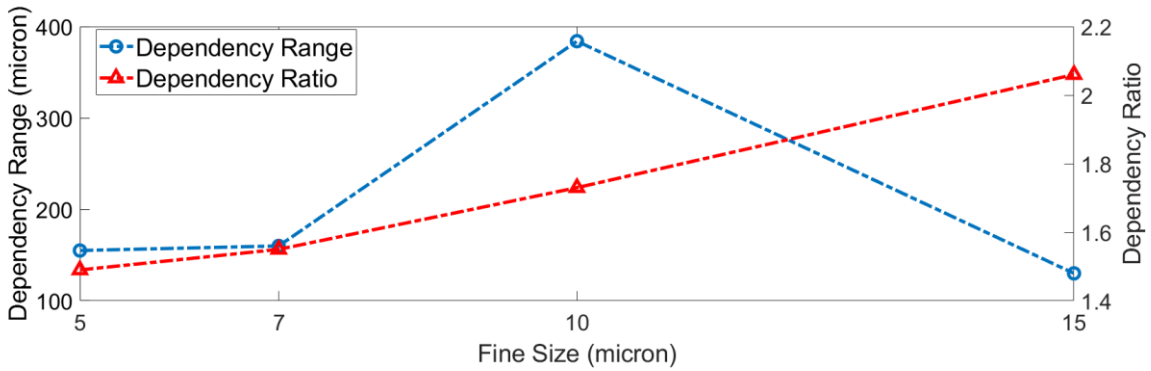
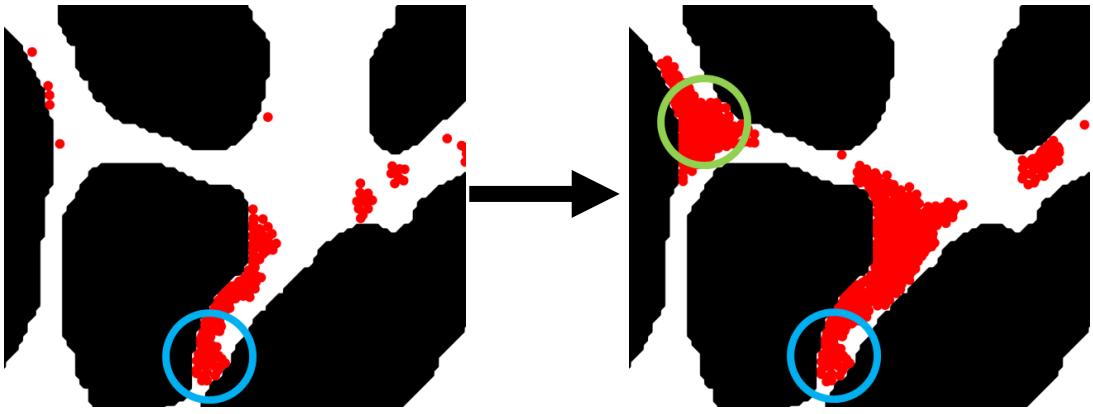


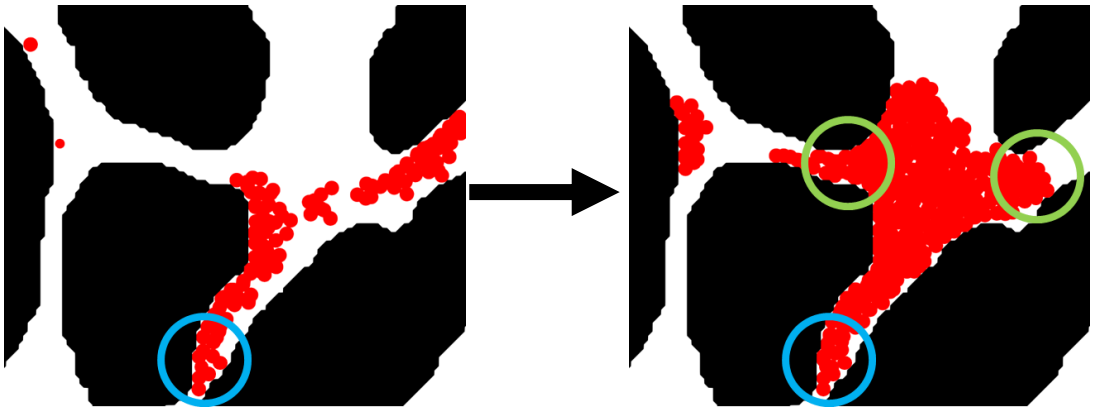
Fig. 3: The dependency range and ratio against the size of the injected fine particles after 15 pore volume injection

a)



Independent Clogging Change of Flow Path Dependent Clogging

b)



Independent Clogging Pore Filling Dependent Clogging

Flow Direction

Fig. 4: Illustration from the simulation results with fine sizes **a)** 10-microns and **b)** 15-microns showing the behaviours of dependent clogging. The independent clogging is circled in blue, and the dependent clogging is in green

3.3 Permeability Reduction

Clogging of throats creates a disruption and restriction in the flow channels, resulting in a decrease in the system's initial permeability. Figure 5a displays the results for the 5-micron case, whereas

Figure 5b shows the results for the 15-micron. As shown, the overall clogged fraction is extremely close in both cases, around 0.1. However, there is a significant variation in the permeability ratios, which are 0.18 and 0.63 for the 5 and 15-micron examples, respectively. This discrepancy might be attributed to the dependency ratios, which are 1.49 and 2.06 for the 5 and 15-micron cases, respectively, resulting in more dependent clogs in the 15-micron example. This demonstrates that having a greater dependency ratio causes more clogging in throats close to one other, which affects system permeability more efficiently than the overall number of clogged throats.

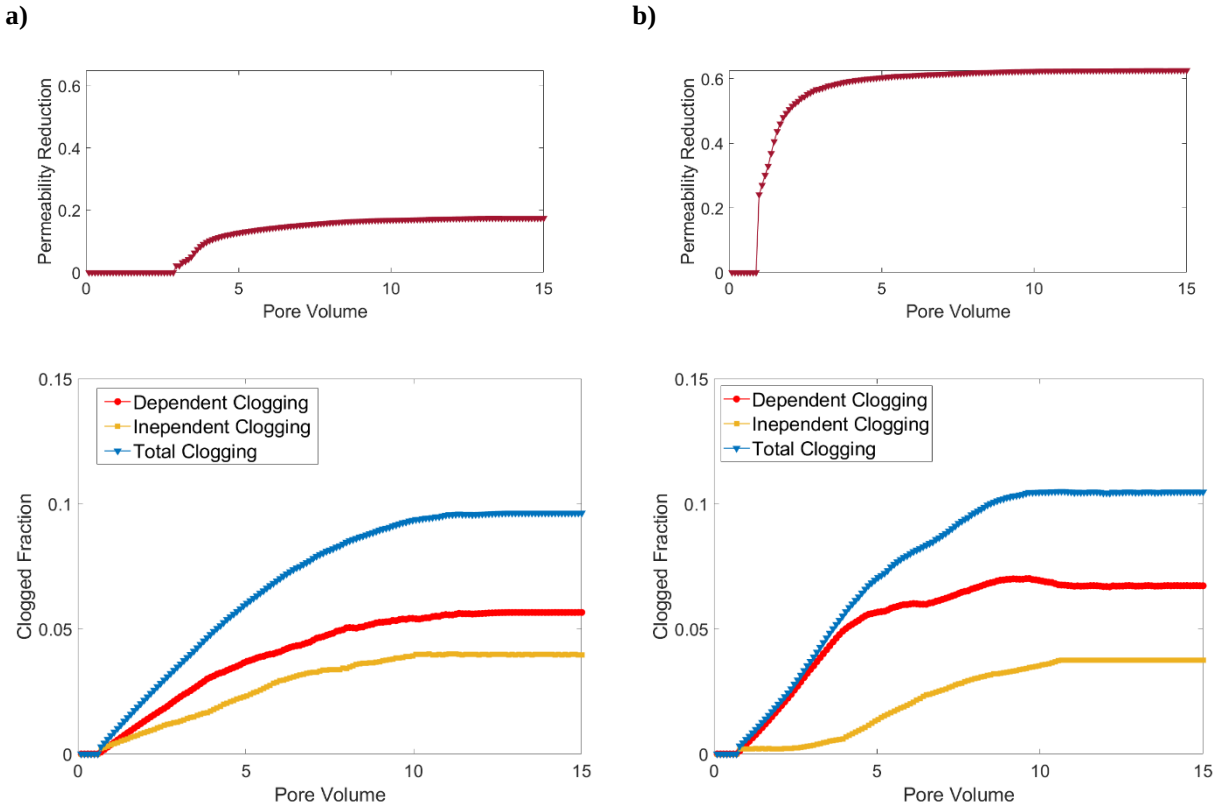


Fig. 5: Permeability reduction and clogged fractions for fine sizes **a)** 5 microns (dependency ratio of 1.49), **b)** 15 microns (dependency ratio of 2.06)

4 Conclusion

In this study, we utilize CFD-DEM coupled simulations to examine the dependent clogging behaviour in a realistic porous media for fine particle sizes. The purpose of this study was to investigate the correlation between clogged pores in natural porous media, to estimate the probability of dependent clogging and its different behaviours, and to assess the influence of dependent clogging behaviour on permeability reduction. The study took into account actual pore geometry determined by computed tomography. CFD-DEM simulations were run on the geometry four times, with the injected fine particle size ranging from 5 to 15 microns. The following are the key findings of the study:

- A spatial correlation between clogged throats was demonstrated, implying that throats near each other became clogged around the same time because of the effect of clogging one throat on the nearby ones.
- Dependent clogging was discovered to be more common than independent clogging in porous media with a dependency ratio higher than one.
- Two kinds of dependent clogging behavior were explored: dependent clogging which is

caused by a change in the flow path, as well as dependent clogging which is caused by the accumulation and pore filling.

- The higher dependency ratio demonstrates a higher dependent clogging probability causing throats close to each other to clog. This affects the system permeability more effectively than the total number of clogged throats.

Acknowledgement

This publication was supported by Qatar University Grant (QUHI-CENG-22/23-517). The findings achieved herein are solely the responsibility of the authors.

References

Bächer, C., Schrack, L. & Gekle, S. (2017). Clustering of microscopic particles in constricted blood flow. *Phys. Rev. Fluids*. https://doi.org/10.1103/PhysRevFluids.2.013102

Elrahmani, et al. (2022). Pore-scale simulation of fine particles migration in porous media using coupled CFD-DEM. *Powder Technol. 398*, 117130. https://doi.org/https://doi.org/10.1016/j.powtec.2022.117130

Frimmel, et al. (2007). Colloidal Transport in Porous Media.

Goniva, et al. (2011). A multi-purpose open source CFD-DEM approach, in: The 8th Int. Conf. on CFD in the in the Oil & Gas, Metallurgical and Process Industries, Trondheim, Norway 21-23 June 2011.

___. (2012). Influence of rolling friction on single spout fluidized bed simulation. *Particuology 10*, 582–591. https://doi.org/10.1016/j.partic.2012.05.002

Hager, et al. (2014). Parallel Resolved Open Source CFD-DEM: Method, Validation and Application. J. Comput. Multiph. Flows 6, 13–27. https://doi.org/10.1260/1757-482X.6.1.13

Han, et al. (2019). Fines migration and pore clogging induced by single- and two-phase fluid flows in porous media: From the perspectives of particle detachment and particle-level forces. Geomech. *Energy Environ. 23*, 100131. https://doi.org/10.1016/j.gete.2019.100131

Huang, et al. (2014). Highly sensitive enumeration of circulating tumor cells in lung cancer patients using a size-based filtration microfluidic chip. Biosens. Bioelectron. https://doi.org/10.1016/j.bios.2013.07.044

Jang, et al. (2018). Impact of Pore Fluid Chemistry on Fine-Grained Sediment Fabric and Compressibility. *J. Geophys. Res. Solid Earth* 0, 5495–5514.

Jarrar, et al. (2020). 3D synchrotron computed tomography study on the influence of fines on gas driven fractures in Sandy Sediments. Geomech. *Energy Environ. 23*, 100105. https://doi.org/https://doi.org/10.1016/j.gete.2018.11.001

Kartic, C. K. & Scott, F. (1998). Migrations of Fines in Porous Media. Kluwer Academic Publishers.

Kigobe, M. & Kizza, M. (2006). Dealing With Spatial Variability Under Limited Hydrogeological Data. Case Study: Hydrological Parameter Estimation in Mpigi-Wakiso, in: Mwakali, J.A., Taban-Wani, G.B.T.-P. from the I.C. on A. in E. and T. (Eds.). Elsevier Science Ltd, Oxford, pp. 211–220. https://doi.org/https://doi.org/10.1016/B978-008045312-5/50024-8

Liot, et al. (2018). Pore cross-talk in colloidal filtration. Sci. Rep. 8, 12460. https://doi.org/10.1038/s41598-018-30389-7

Liu, Q., Zhao, B. & Santamarina, J. C. (2019). Particle Migration and Clogging in Porous Media: A Convergent Flow Microfluidics Study. *J. Geophys. Res. Solid Earth* 124, 9495–9504. https://doi.org/https://doi.org/10.1029/2019JB017813

Mendes, R. M. & Lorandi, R. (2006). Indicator kriging geostatistical methodology applied to geotechnics project planning. IAEG2006 Pap. 527, 1–12.

Olea, R. A. (1999). The Semivariogram BT - Geostatistics for Engineers and Earth Scientists, in: Olea, R.A. (Ed.), . Springer US, Boston, MA, pp. 67–90. https://doi.org/10.1007/978-1-4615-5001-3_5

Pang, et al. (2015). Deformability and size-based cancer cell separation using an integrated microfluidic device. Analyst. https://doi.org/10.1039/c5an00799b

Rabbani, et al. (2016). Estimation of 3-D pore network coordination number of rocks from watershed segmentation of a single 2-D image. Adv. Water Resour. 94, 264–277. https://doi.org/https://doi.org/10.1016/j.advwatres.2016.05.020

Sauret, et al. (2018). Growth of clogs in parallel microchannels. *Phys. Rev. Fluids* 3, 104301. https://doi.org/10.1103/PhysRevFluids.3.104301

Tavakkoli, et al. (2015). Indirect method: A novel technique for experimental determination of asphaltene precipitation. Energy and Fuels. https://doi.org/10.1021/ef502188u

van Zwieten, et al. (2018). From cooperative to uncorrelated clogging in cross-flow microfluidic membranes. Sci. Rep. 8, 5687. https://doi.org/10.1038/s41598-018-24088-6

Weller, et al. (1998). A tensorial approach to computational continuum mechanics using object-oriented techniques. Comput. Phys. 12, 620–631. https://doi.org/10.1063/1.168744

Wolfgang Schwanghart (2023). Experimental (Semi-) Variogram (https://www.mathworks.com/matlabcentral/fileexchange/20355-experimental-semi-variogram), MATLAB Central File Exchange. Retrieved February 6, 2023.

Zhou, et al. (2010). Discrete particle simulation of particle–fluid flow: model formulations and their applicability. *J. Fluid Mech*. 661, 482–510. https://doi.org/DOI: 10.1017/S002211201000306X

Cite as: Elrahmani A. & Al-Raoush R., "The Dependent Clogging Dynamics and Its Impact on Porous Media Permeability Reduction", *The 2nd International Conference on Civil Infrastructure and Construction (CIC 2023)*, Doha, Qatar, 5-8 February 2023, DOI: https://doi.org/10.29117/cic.2023.0152

Environmental, Social and Governance-related Challenges in the Construction Industry (CIC 2023)

Khalil Roukoz
Mott Macdonald, Doha, Qatar
khalil.roukoz@mottmac.com

Dila Ersenkal
Mott Macdonald, Doha, Qatar
dila.ersenkal@mottmac.com

Abstract

The construction industry is faced with several Environmental, Social and Governance (ESG) challenges and opportunities that include, but are not limited to, a massive carbon footprint, the physical impacts of climate change, green building certifications, supply chain, innovative product design, pollution control, health and safety, diversity and inclusion, community development, business ethics, and biodiversity. With these ESG issues front and centre in daily headlines, investors, shareholders and all other stakeholders are demanding greater transparency in relation to the construction industry's interaction with the environment and the society in which they operate and upon which they depend for long-term business continuity. ESG factors are becoming fundamental nonfinancial information for the long-term valuation of a company, for the investment decision-making process and in determining capital allocations. All the key players in the construction industry, including engineering and construction services firms, manufacturers and distributors of construction materials, buildings products and furnishing companies, real estate developers, and real estate services companies, need to convince stakeholders that they are delivering optimal outcomes when it comes to the triple bottom line of people, planet and profit. In this paper, we will address and discuss the following questions: What are the key ESG challenges and opportunities that construction industry is facing? How are these key ESG challenges identified and acted upon? What are the enablers used by the construction industry to address and manage ESG factors? Among these enablers, we will look in details at the Global Sustainability Assessment System (GSAS) and its capability to satisfy the investors ESG disclosures needs.

Keywords: ESG; Climate change; Construction industry; Disclosure; Investors; Green Certifications; GSAS; Financial impact

1 Introduction

In this paper we will look at the ESG challenges and opportunities of the construction sector be it the construction companies, engineering firms, real estate developer, real estate service providers and construction material manufacturers. The key idea of this paper is to explore these ESG topics from an investors point of view. What information investors are expecting on ESG topics in order to make investment decisions about a project or a company operating in the construction sector. First, we will start with a high-level overview of the common ESG topics of the construction industry and then we will look more closely on how companies identify those topics. We will then focus on the ESG topics that are of interest to investors basing our selection on the Sustainable Accounting Standards Board (SASB) of the

International Financial Reporting Standards Foundation (IFRS). We will then discuss the efficiency of using green certifications by the construction sector in meeting the investors' expectations (focusing specifically on the Global Sustainability Assessment System – GSAS certification scheme). We will identify where the GSAS certification comply and where it does not comply with investors' expectations and information needs such as reputational, legal, operational, market, climate change and social risks, as well as ESG opportunities and financial integration of ESG information.

Section 2 will cover the most common ESG opportunities and challenges of the construction sector, while section 3 will touch on ESG identification and planning. Section 4 will zoom in on the investors ESG expectation and material topics. Finally, Section 5 will discuss GSAS versus the investors ESG expectations and section 6 will conclude the paper.

2 Key ESG Challenges and Opportunities

2.1 ESG Challenges

2.1.1 Environmental Challenges

According to the World Green building Council (2019), the building and construction industry is responsible for 39 % of the global GHG emissions where 28% comes from operations and 11% from construction and materials manufacturing and transportation. It is estimated that the Iron and Steel manufacturing energy use generate approximately 6.1 % of global carbon emissions and the cement industry is responsible for 3.4% of the global GHG emissions (World Resources Institute, 2022).

With the global fight on climate change, the construction sector find itself challenged to reduce its carbon footprint. In addition to being a key contributor to the global carbon emissions finds, the construction sector finds itself at risk from the physical impacts of climate change. These include extreme weather events resulting in the disruption of the construction materials supply chain and subsequently delays and increase in prices for the construction process. Temperature and sea level rise due to global warming will respectively cause an increase of operations costs (maintenance, heating and cooling) and physical damage to the built environment structure caused by flooding and water submersion.

In addition to climate change, the negative impacts of the construction industry on the environment are numerous. It starts with the pollution caused by the raw materials extraction required for the construction of an asset all the way through the negative impacts of the construction activities and the pollution generated by the operations of the built environment. This pollution is linked to the outputs of a manufacturing plant during the production process such as wastewater, solid waste, hazardous waste, air emissions (GHG emissions and key pollutants such as dust, NOx, SOx, Ozone, Sulphur) and it can be also linked to the transportation of the produced material.

The construction phase produces very similar pollution types including wastewater (dewatering and sewage), dust, emissions from construction equipment, construction waste, hazardous waste, domestic waste and can also cause a risk of pollution to the soil and ground water via the excavation and drilling activities. The built environment also can be a risk of pollution from the generation of wastewater and domestic waste and a risk to the indoor air quality from chemical products used in the building finishing process.

Water management is another important issue for the construction sector as the production of construction materials, in addition to being energy intensive; it also requires substantial volumes of water. Water scarcity can affect construction material manufacturers by affecting day-to-day

operations, increasing the cost of water acquisition, and facing tightening regulations and possible fines. Water scarcity is an environmental and a social challenge for the construction industry as companies will have to respect the communities' needs for water access and operate in an environment with high competition on water resources.

Water management is also an important topic for the construction sector during the construction phase where contractors need to use water for the construction activities and dewater for excavations and foundation laying purposes.

On the biodiversity front, infrastructure projects and large real estate developments present a significant risk especially when they are located in an ecologically sensitive area. Developers should avoid if possible, building in sensitive areas and find ways to protect/restore those areas. With biodiversity as a top item on the agenda of United Nations and the Conference of Parties, the construction industry will be faced with more pressure to look after biodiversity by conserving, protecting, restoring and managing sustainably ecosystems for the coming decades.

2.1.2 Social Challenges

The health and safety issues has been and will remain a high priority for engineering and construction firms as a well as for the construction materials manufacturing. Even though incidence rates and nonfatal injuries are significantly lower than what they used to be a 100 years ago, fatality and injury rates in these sectors are high compared with other industries as a result of workforce's exposure to powered haulage and heavy machinery accidents, fall accidents and exposure to hazardous chemicals.

Beyond the construction phase, engineering and construction firms should ensure the safety and integrity of their work by avoiding errors or inadequate quality in the project design and construction phases. If companies perform poorly on that front, they can face high costs to redesign, repair work and legal liabilities, reputational damage. Moreover, when designing, the impact of climate change, which might affect structural integrity and must be taken into account. In this instance, compliance with minimal applicable codes might not be sufficient.

2.1.3 Governance Challenges

The construction industry is perceived as a male white dominated sector and is now expected to promote the inclusion of women in leading roles and to increase ethnic diversity. Gender and diversity are becoming important competitive differentiator.

In addition, companies in the construction industry must deal with risks related to bribery, corruption and anti-competitive practices. The fact that several companies in the construction sector have international reach makes the ethics issue more complex to manage especially when it comes to cultural differences and different ways of doing business between geographical locations. Ethical breaches can have serious consequence on companies such as large fines and reputational damage.

2.2 ESG Opportunities

It is well proven these days, that while green buildings can cost more than conventional buildings, they outperform them on many fronts such as operation cost, staff productivity, return on investment and attracting capital.

In the same direction, the construction industry is focusing on sustainable building materials innovation to manufacture and use materials and processes that are more resource efficient and that protect the health of the construction workers as well as the buildings users. This is a business driver for construction

materials companies because it is a way to increase revenues but also to decrease production costs as some materials will require less raw material and energy in their production process.

Real estate developer/owner need to play a role in influencing tenants' sustainability behaviour by the way they structure their agreements, contracts and relationships with tenants. By managing the sustainability of their tenants, they can manage the overall sustainability impacts of their assets. By managing upstream, the impacts of tenants they can align their financial interests with the ones of their tenants. This can drive asset value appreciation, increase tenant demand and satisfaction, decrease operation costs and risks related to buildings codes and regulations.

Real estate services provider can contribute to the sustainability of the buildings they service by reducing the sustainability impacts of a built environment through data management, energy procurement, energy and water benchmarking, resource efficiency improvement and activities related to green certifications. They can also contribute further by arranging leases that incentivize both the owner and tenants to enhance sustainability performance while resulting in a better financial performance for both parties. These services can increase revenues, client retention, tenant demands, and improve asset values; also, it can decrease operating costs and improve tenant experience.

Finally, studies have shown that there is a high correlation between corporate diversity and business performance. A study by McKinsey (2019) showed that there is a positive correlation between companies that commit themselves to diverse leadership and business success. They seem better in winning talent; improve their customer orientation and employee satisfaction.

3 ESG Identification and Planning

Identification of ESG issues, integrating them in the business model and disclosing to meet the expectations of stakeholders is becoming a challenging but very important task for all companies. With the ever-changing ESG landscape, it is getting difficult for companies to pin down their ESG scope. When it comes to ESG, Companies must answer strategic questions. Those questions not only look at the influence of ESG factors on the business, but they also address the influence of the business on the ESG aspects. In other words, a company's board and shareholders need to understand how the environmental, social and governance factors can influence the organisation's financial performance, operations and capacity for creating long-term value, at the same time; they must understand the company's activity impacts on the environment, the society and the local/regional economy. This is what a lot of ESG reporting frameworks is calling these days double materiality.

Like mentioned above, the EGS landscape is not easy to navigate. Identifying what ESG topics can drive business value is not always evident for companies. Companies in the construction industry, like all other sectors, will look at the global ESG or sustainability disclosure frameworks to identify their material ESG topics (whether to understand which ESG topics are material to the sector or what is the materiality assessment process they need to undertake) and then they will start collecting data on the identified ESG topics and try to build a sustainability vision and strategy based on the collected data.

The data collection process is usually an eye-opener for companies going through the materiality process as it can reveal the strength and weakness of a company when it comes to ESG and help them identify the material ESG topics to their business.

The ESG topics we have described earlier in section 4, although they are the most common themes within the construction industry, are not applicable to all companies operating in the sector. This is why ESG reporting frameworks advice companies to go through the ESG materiality process and

identify the topics that are company specific based on accurate and timely data collection, companies' activities, geographical location and stakeholders' expectations.

The construction industry and more specifically the companies involved in design, construction and operations of the built environment often reduce the above process to simply getting their projects/assets certified under the globally recognized green certifications schemes such as GSAS, LEED, BREEAM, CEEQUAL, ENVISION, WELL. Although, these certification schemes are efficient in making the built environment significantly more sustainable they do not always offer the best solutions to a full ESG strategy, implementation and disclosure. These schemes do not often cover all the ESG material topics and are not 100% aligned with the expectations of the investors.

4 ESG Expectations of Investors

As we mentioned in the previous section, even though companies within the same sector have ESG common themes, each company will approach the identification of its ESG material issues uniquely based on their sector and business model specifics as well as geographical context and the expectations of the stakeholders. According to Sustainability Accounting Standards Boards (SASB), investors are interested to understand the financial impact of ESG on companies. A CFA Institute survey showed that 76% of institutional investors and 69% of retail investors expressed interest in ESG as a way to contribute to more holistic financial analysis (CFA ESG Certificate Training Material, 2021). Particularly, when it comes to the construction industry, investors would like to focus on the following ESG common topics that are considered to have a financial impact on organizations operating on the construction sector:

Table 1: ESG Construction Industry Common topics (as per the SASB standards)

E	S	G
• Energy and water Management • Air Quality • Climate Change adaption • Sustainability services • Environmental Impacts of Project Development • Lifecycle Impacts of Buildings & Infrastructure • Wood Supply Chain Management	• Structural Integrity & Safety • Workforce Health and Safety • Chemicals in Construction Products	• Management of tenant • Sustainability Impacts • Competitive Behaviour (Pricing Integrity and Transparency • Business Ethics • Diversity and Inclusion • Product Innovation • Climate Impacts of Business Mix

According to SASB, the above ESG factors are among the most common topics shared by companies in the construction industry. A study by Guggenheim Investments, WWF, KPMG, Mott MacDonald (2020) describe what investors are looking to understand when it comes to ESG factors and companies involved in delivering infrastructure projects: reputational risk, regulatory risk, operational risk, market risk, physical and climate risk, social risk, opportunity insights, social impact, financial integration of the ESG factor. ESG factors can have a financial impact on the companies whether through being a risk or an opportunity, which is crucial information for investors in their investment decision-making process.

5 GSAS and ESG Investors Expectations

This section will focus on the Global Sustainability Assessment System of the Gulf Organisation for Research and Development (GORD) that is used in Qatar for green buildings and infrastructure in attempt

to understand how this rating system satisfy the investors ESG expectations and how it falls short of providing investors the information they need. The GSAS criteria will be assessed against the ESG factors for the construction sector that were identified and described in the previous section by identifying whether they are covered by GSAS. Following that we will also discuss whether GSAS can be in effective tool for investors to make a decision to whether to invest in a project or a company in the construction sector or not. First, we will start by presenting a high-level description of each GSAS categories that we will consider. As per the GSAS Design & Build Assessment Manual (2019) and the GSAS Construction Management Assessment Manual for building and infrastructure (2019), and GSAS Operations the rating system has eight (8) categories of sustainable criteria which are as follow:

a. [The Urban Connectivity category is concerned with the design of the proposed development having a direct impact on the adjacent buildings, properties, neighbourhood and the larger urban community…] it contains six (6) criteria: proximity to infrastructure, proximity to amenities, load on local traffic conditions, public transportation, green transportation and neighbouring acoustics.

b. [The Site category is concerned with the design of the proposed development having a direct impact on both the site of the development itself as well as any adjacent sites…] it contains 15 criteria: land preservation, waterbody preservation, biodiversity preservation, vegetation, drain and storm water contamination, rainwater runoff, heat island effect, shading, accessibility, external lighting, light pollution, noise pollution, eco-parking, mixed use, and construction practices.

c. [The Energy category is concerned with improving the design and energy performance of the development having a direct and positive impact on both the consumption of resources and environmental quality including climate change, fossil fuel depletion, air pollution and human comfort, health and well-being…] it contains six (6) criteria: thermal energy demand performance, energy use performance, CO_2 emission, energy sub-metering and renewable energy.

d. [The Water category is concerned with water conservation for indoor and outdoor use…] it contains three (3) criteria: water demand performance, water reuse performance and water sub-metering.

e. [The Materials category is concerned with the conservation of natural resources and the use or reuse of materials and structure to have the least environmental impact…] it contains seven (7) criteria: locally sourced material, materials eco-labelling, recycle content of materials, materials reuse, existing structure reuse, design for disassembly, responsible sourcing of materials.

f. [The outdoor and indoor environment concerned with the quality of the indoor and outdoor environment for the comfort, health and well-being of workers, occupants and users...] It has twelve criteria: dust control, noise and vibration control, thermal comfort, natural ventilation, mechanical ventilation, lighting, daylight, glare, views, acoustics, low-VOC materials and airborne contaminants.

g. [The Culture & Economic Value category is concerned with the cultural impacts in the design of the built environment and support of the national economy…] it contains two (2) criteria: heritage and cultural identity and support of national economy.

h. [The Management & Operations category is concerned with the design of the development for use during the operational phase and for the management and operations of the construction activities. The development should plan for and implement sustainable and effective building management and operations practices…] it contains nine (9) criteria: system commissioning, waste management, welfare facilities, construction health and safety, workers accommodation, facility management, leak detection systems, automated control system, and transportation systems in building.

The below tables 2 to 5 identify what construction sector specific ESG factors the GSAS scheme covers and how does it satisfy the need for information and analysis for investment decision making. Tables 2 to 4 list the ESG factors versus GSAS coverage while table 5 takes is a deeper dive into the ESG metrics

that investors can use in their evaluation of companies versus GSAS coverage. The checkmarks indicate GSAS contribution to investors' requirements and the blanks indicates no contribution.

Table 2: GSAS coverage of the Environmental Factors in ESG

GSAS Categories / ESG	Energy	Air Quality	Water	Climate Change adaption and Carbon footprint	Sustainability services	Environmental Impacts of Project	Lifecycle Impacts of Buildings & Infrastructure	Wood Supply Chain
Urban Connectivity/Considerations		✓		✓	✓			
Site		✓	✓			✓		
Energy	✓			✓			✓	
Water			✓					
Materials						✓	✓	✓
Outdoor/Indoor Environment		✓			✓			
Cultural and Economic Value								
Management and Operations	✓	✓	✓		✓		✓	

Table 3: GSAS coverage of the Social Factors in ESG

GSAS Categories / ESG	Structural Integrity & Safety	Workforce Health and Safety	Chemicals in Construction Products
Urban Connectivity/Considerations			
Site			
Energy			
Water			
Materials			✓
Outdoor/Indoor Environment		✓	✓
Cultural and Economic Value			
Management and Operations			

Table 4: GSAS coverage of the Governance Factors in ESG

GSAS Categories / ESG	Management of tenant Sustainability Impacts	Competitive Behaviour (Pricing	Business Ethics	Diversity and Inclusion	Product Innovation	Climate Impacts of Business Mix
Urban Connectivity/Considerations	✔					
Site						
Energy	✔					
Water	✔					
Materials					✔	
Outdoor/Indoor Environment	✔					
Cultural and Economic Value						
Management and Operations	✔					

An initial look at the above tables indicates that GSAS seems to cover all of the E and 2 out of 3 of the S factors that are potentially material to investors while it falls short in covering most of the G factors (covering only 2 out 6). As a general note, GSAS is project oriented, and it is not unusual for a certification scheme not to be informative on and/or not to have criteria that address corporate level requirements. As such, important G topics are not addressed by the GSAS scheme as it does not inform investors on whether the company in question is conducting business with integrity and transparency while not engaging in unethical behaviour such as bribery, child labour or whether a company encourage diversity and inclusion in the workplace. Finally, the scheme does not inform investors on the business mix (hydrocarbons related projects/assets versus renewable energy projects/assets) and the risk of a company of having cancelled projects or stranded assets because if high carbon intensity and regulations that are getting more stringent on carbon emissions.

A deeper dive into the metrics to be disclosed in relations to the ESG topics (table 5 below), shows that while GSAS seems to cover most of the E factors, it only provides 25 out of 38 corresponding E metrics that can be useful to investors. Metrics such as scope 1 GHG emissions, strategy to manage scope 1 GHG emissions, percentage of GHG emissions under emissions-limiting regulations, air pollutants, percentage of water withdrawal in high or extremely high baseline water stress locations, environmental policies, and water management policies are not covered by GSAS. The metrics gap gets bigger when we look at the Social and Governance side where GSAS provide only 1 out of 7 and 5 out of 21 of the S and G topics respectively. Metrics that helps investors get a sense of the social and financial risks or on how the board and upper management manage and oversee those risks are mostly what is lacking from the GSAS schemes. These include metrics such as the potential revenue from capturing more market share of a certain sustainable product or practice versus the actual market share, monetary losses due to legal proceedings, conducting business in countries scoring low on the transparency International's Corruption perception index, contractual agreements with tenants when it comes to sustainable requirements, policies and practices on bribery and human rights, the diversity and inclusion practices and so on as listed in the below table.

Table 5: ESG metrics for investors (as per the SASB standards)

	Metrics	GSAS Coverage
E	Total Energy Consumed	✔
	Percentage of grid Electricity	✔
	Percentage of Renewables	✔
	Energy consumption data coverage as a percentage of total floor area by property subsector	✔
	Total Energy consumed by portfolio area with data coverage by property subsector	✔
	Percentage of eligible portfolio that has an energy rating	✔
	Percentage of eligible portfolio that is certified to energy star	
	Like-for-like percentage change in energy consumption for the portfolio year-on-year	✔
	Weight of end-of-life material recovered	✔
	Percentage of recovered materials recycled	✔
	Total weight of wood fibre materials purchased	✔
	Percentage of wood fibre from third-party certified forestlands	✔
	Percentage of wood fibre per certification standards	✔
	Percentage of wood fibre not certified by a third party	
	Gross global scope 1 emissions	
	Percentage of Scope 1 Emissions covered under emissions-limiting regulations	
	Air emissions of the following pollutants: NO_x, SO_x, PM_{10}, Dioxins/Furans, VOCs, PAHs, Heavy Metals	
	Total fresh water withdrawn	✔
	Recycled percentage of fresh water used	✔
	Water consumption data coverage as a percentage of floor area	✔
	Water consumption data coverage as a percentage of floor area in regions with high or extremely high baseline water stress by property subsector	
	Total water withdrawn by portfolio area with data coverage	✔
	Total water by portfolio area with data coverage in regions with high or extremely high baseline water stress	
	Amount of waste generated	✔
	Percentage of waste that is hazardous	✔
	Percentage recycled	✔
	Terrestrial acreage disturbed	✔
	Percentage of impacted area restored	✔
	Number of environmental incidents	✔
	Number of commissioned projects certified under a green certification scheme	✔
	Area of properties located in 100-year flood zones	✔
	Floor area and number of buildings under management that obtained energy rating	
	Long-term and short-term strategy to manage scope 1 emissions, analysis of performance against those targets	
	Description of water management risk and mitigation measures	
	Environmental management policies and practices	
	Discussion of processes to assess and manage environmental risks	
	Description of effort to manage product lifecycle impacts and meet demand for sustainable products	
	Management and assessment process of risks and hazards associated with chemicals in products	

	Metrics	GSAS Coverage
S	Percentage of eligible products meeting VOC emissions and content standards	✓
	Amounts of defect and safety relate work costs	
	Percentage of fresh water withdrawn from regions with high or extremely high baseline water stress	
	Total recordable incident rate	
	Near miss frequency rate	
	Full time employees	
	Contract employees	
G	Description of how building energy management considerations are integrated into property investment analysis	
	Percentage of products that qualify for credits in green certifications	✓
	Potential revenue from capturing 100 % of a market share of a given sustainability product category	
	Current market share compares to the potential revenue at 100% market share	
	Amount of monetary loss as a result of legal proceedings associated with integrity and transparency	
	Total amount of monetary losses due to defects and safety-related issues	
	Number of active projects	✓
	Number of commissioned projects	✓
	Total backlog (value of projects not completed as of close of reporting year)	
	Amount of backlog for hydrocarbon related projects	
	Amount of backlog for renewal projects	
	Amount for backlog for projects associated with climate change mitigation	
	Active projects in countries of 20 lowest rankings in Transparency International's Corruption perception index	
	Backlog in countries of 20 lowest rankings in Transparency International's Corruption perception index	
	Total amount of legal proceedings monetary for bribery or corruption or anti-competitive practices	
	Policies for prevention of bribery, corruption and anti-competitive practices	
	Number of assets by property sub-sector	✓
	Number of new leases that has a cost recovery clause for resource efficiency	
	Percentage of tenants that are separately metered for grid electricity and water withdrawals	✓
	Revenue from energy and sustainability services	
	Floor area and number of buildings under management that are provided with sustainability services	

This been said, we will discuss in Table 6 using the above ESG factors and metrics how GSAS contribute or does not contribute to providing the information investors need to obtain on a company operating in the construction sector as well as what practices they would want to see.

Table 6: Summary of GSAS versus investor's ESG expectations

Reputational Risk	In general, green buildings and infrastructure have a good reputation when it comes to ESG factors, and it is the case for GSAS certified buildings, infrastructure and real estate developments projects. Green certifications build trust in the asset when it comes to water and energy consumption (both environmentally friendly and cost saving, to the indoor quality of the built environment, the site selection and preservation process, etc.) in the health and safety compliance during construction. This attracts both investors and tenants. GSAS certification like many other green certifications is a good tool to ensure investors that there is no reputational risk linked to a proposed or an existing building, community and infrastructure. As seen in the above tables GSAS contributes to the management of the tenant's sustainability, the quality of the indoor environment, to management and operations and to the energy and water consumption as well as to ensure that a project's environmental impacts are minimized and mitigated. Nevertheless, GSAS does not provide insights to investors on social risks and governance practices that might be linked to assets owned or under construction by a company or on the corporate level. GSAS does not cover an important S topic, which is the structural integrity of a built assets that does not give investors insights on whether a company is protected against bad reputation associated to structural failure that can put lives in danger and might weight heavily on the company's financials in the form of financial compensation and repair cost. GSAS also does not provide investors with a sense of how companies are governed when it comes to bribery, competitive behaviour, business ethics and diversity and inclusion. In the world of social media, companies' reputation can take a big hit due to failure on any of those aforementioned topics. A look at the metrics gives us a more in depth understanding on how GSAS can contribute to the reputation protection of a company. GSAS can either provide directly or help to provide to investors metrics such as comparison on year-to-year basis on how energy consumption is evolving which gives investors a solid understanding on the performance of those companies when it comes to energy consumption reduction. GSAS also can help companies provide investors information on how much of their portfolio is monitored and how well it is managed when it comes to energy and water consumption. GSAS can also help provide to investors insights on how waste is managed and what is a certain company portfolio is performing on the recycling front. Looking at the social and governance metrics, GSAS does not seem to contribute to informing investors on reputational risks that can be assessed by knowing how much revenue a company makes from hydrocarbons related projects or from working in corrupted countries.
Regulatory/Legal Risk **Regulatory/Legal Risk**	GSAS does not help investors understand the legal compliance risk of a development or of a company operating in the construction industry. As we see in table 4 above, GSAS does not have criteria when it comes to business ethics or competitive behaviour, which are Governance (G) factors that can pose a significant legal risk on companies operating in the construction industry. GSAS does not provide information to investors on how a company, or a project is protecting themselves against potential fines or lawsuits from structural failures and incidents related to their assets (see Table 3). Being GSAS certified does not provide the investors with information to decide whether his investments or potential investment are protected against structural integrity failures and safety accidents. Looking closer at the metrics, it is clear that GSAS does not help investors getting information such as the amount of monetary losses due to legal proceedings or defects and safety-related issues. Companies will not be able to inform investors by using GSAS on how they are managing anti-bribery and corruption and uncompetitive behaviour or their GHG emissions under emissions-limiting regulations.
Operational Risk	GSAS does provide insights on operational phase of a project/development as it considers the Environmental (E) and Social (S) risk during operations but when it comes to Governance (G)

	it does not provide information to the investors on the project governance itself or on the governance of the companies operating in the construction industry. GSAS being a project-oriented scheme, companies cannot expect to meet investors' expectations by only getting their projects certified under GSAS or any other green building/infrastructure certification scheme. They will miss providing investors information they need on the governance project and management practices. Policies and processes on how carbon emissions, environmental impacts, energy and water consumption, product lifecycle and all other ESG related operational risks are not required by GSAS while investors need to understand how these issues are governed within a company. In addition, investors need to get insights on how a company is managing their tenants from a contractual point of view and from operational cost and maintenance point of view. Metrics such as the percentage of tenant metered for energy and water, the number of leases that contains a cost recovery clause for resource efficiency, revenue from sustainable services and green buildings versus from other services and built assets that do not have a good ESG performance can give an investors insight on how companies are performing or can perform when it comes to suitability performance during operations. GSAS does not provide such information to the investors.
Market Risk	GSAS does not provide insights on the climate impact of a company's business mix and on how much a company might be affected by a changing market lead by a change of consumers and social preferences linked to ESG topics. GSAS is silent on the supply chain risks even though it indirectly mitigates the impacts of supply chain interruption of individual projects of a company by requiring local sourcing of material, when possible, through the "Materials" category. It also, indirectly speaks to the evolving consumers preferences (especially among the young generation) that are leaning towards green buildings. GSAS does not provide information for investors on tenants' management and on how a real estate development that was designed to be green will be managed to ensure that sustainability requirements are implemented and maintained during operations specifically through tenants' management and contractual measures. A closer look at the metrics shows that GSAS does not provide information on a metrics related to company's current market share of green products/services/buildings and on the potential revenue from capturing more of that market share. This is an important information to investors as it helps evaluate how flexible a company is to profit from the ESG opportunities and on its capability to continue creating value within a market and consumers preference shift towards sustainable and green built environment. Another metrics that is important to investors and not provided by GSAS is a company's backlog for hydrocarbons related projects versus renewable energy related projects as well as backlog of projects associated to climate change mitigation.
Physical and Climate Risk	Certain categories of GSAS address Energy, Carbon emissions, water consumption, renewable energy, water demand and water reuse, nevertheless, it does not address the physical impact of climate change on the built environment such sea level rise and rise/drop in temperatures. It also does not inform the investors on the financial implications of climate change transitional risks (stranded assets because of stingiest emissions regulations) or of climate change physical impacts (such as sea level rise and rise or drop in temperatures. Finally, GSAS does not provide investors information of the future climate risks so they can assess whether a company or a project would continue to be able to provide value on the long run.
Social Risk	GSAS does address community planning via the Urban connectivity and Cultural and Economic value categories encompassing many social issues related to the built environment and to communities such the quality of life, access to amenities and public transportation, indoor environment quality, green transportation, pedestrian access. By integrating these social aspects to the design and construction of the built environment, GSAS reduce the social risks during operations and can give investors assurance that a given project or company are

	mitigation the social impacts of developments. Nevertheless, besides cultural and heritage sites preservation, GSAS does not provide insight on social issues pre-development or on social issues that might rise post-development.
Opportunities	GSAS helps construction projects and companies developing those projects make the most of the ESG opportunities or being future ready to profit of potential ESG opportunities such advancement in renewable energy, better staff retention, attractiveness to younger investors, lower costs, and tighter regulations, green bonds. Nevertheless, investors need to understand how these opportunities can financially affect a project or a company operating in the construction sector. GSAS operations phase certification could be a very interesting tool to inform investors on the performance of certified assets on the energy, water savings front, maintenance cost, satisfaction of tenants in real time during the life of the building and thus provide backed financial implications of the green building's performance.
Material ESG coverage	GSAS seems to cover all of the E and 2 out of 3 of the S factors that are potentially material to investors while it falls short in covering most of the G factors (covering only 2 out 6). As a general note, GSAS is project oriented, and it is not unusual for a certification scheme not to be informative on and/or not to have criteria that address corporate level requirements. As such, important G topics are not addressed by the GSAS scheme as it does not inform investors on whether the company in question is conducting business with integrity and transparency while not engaging in unethical behaviour such as bribery, child labour or whether a company encourages diversity and inclusion in the workplace. Finally, the scheme does not inform investors on the business mix (hydrocarbons related projects/assets versus renewable energy projects/assets) and the risk of a company of having cancelled projects or stranded assets because if high carbon intensity and regulations that are getting more stringent on carbon emissions. A deeper dive into the metrics to be disclosed in relations to the ESG topics (table 5 below), shows that while GSAS seems to cover most of the E factors, it only provides 25 out of 38 corresponding E metrics that can be useful to investors. The metrics gap gets bigger when we look at the Social and Governance side where GSAS provide only 1 out of 7 and 5 out of 21 of the S and G topics respectively. Metrics that helps investors get a sense of the social and financial risks or on how the board and upper management manage and oversee those risks are mostly what is lacking from the GSAS schemes. These include metrics such as the potential revenue from capturing more market share of a certain sustainable product or practice versus the actual market share, monetary losses due to legal proceedings, conducting business in countries scoring low on the transparency International's Corruption perception index, contractual agreements with tenants when it comes to sustainable requirements, policies and practices on bribery and human rights, the diversity and inclusion practices and so on as mentioned in previous sections.
Financial Integration of ESG	GSAS like many of the other green certification schemes does not provide information to the investors that can be used in financial analysis. This is supported by the fact that GSAS does not provide information on the following metrics: • Like-for-like percentage change in energy consumption for the portfolio year-on-year • Number of commissioned projects certified under a green certification scheme • Amounts of defect and safety relate work costs • Potential revenue from capturing 100 % of a market share of a given sustainability product category • Current market share compares to the potential revenue at 100% market share • Amount of monetary loss as a result of legal proceedings associated with integrity and transparency • Total amount of monetary losses due to defects and safety-related issues • Number of active projects

	• Number of commissioned projects • Total backlog (value of projects not completed as of close of reporting year) • Amount of backlog for hydrocarbon related projects • Amount of backlog for renewal projects • Amount for backlog for projects associated with climate change mitigation • Number of new leases that has a cost recovery clause for resource efficiency • Revenue from energy and sustainability services The above metrics can be easily integrated in the company evaluation exercise for investors to understand what financial liabilities a company have because of ESG risks and what are the potential financial advantages that can be potentially generated by ESG opportunities.

The investors' expectations used in the table are extracted from the study by Guggenheim Investments, WWF, KPMG, Mott MacDonald (2020)

6 Conclusion

ESG topics are growing in importance in the investment community and investors' decisions will require the integration of ESG information in the financial analysis whether to decide to invest in a company or in the built environment. Investors expect companies in the construction sector to provide ESG information that is helpful in the decision-making process and companies operating in the construction sector will need to provide that information to investors as a way to prove that they are integrating ESG factors in their business model. This integration must prove to the investors the company's ability to create value on the long-term by being future ready to mitigate ESG risks or to ride the wave of ESG benefits.

As mentioned previously, GSAS seems to cover all of the E and 2 out of 3 of the S factors that are potentially material to investors while it falls short in covering most of the G factors (covering only 2 out 6). As a general note, GSAS is project oriented, and it is not unusual for a certification scheme not to be informative on and/or not to have criteria that address corporate level requirements. As such, important G topics are not addressed by the GSAS scheme as it does not inform investors on whether the company in question is conducting business with integrity and transparency while not engaging in unethical behaviour such as bribery, child labour or whether a company encourages diversity and inclusion in the workplace. While GSAS seems to cover most of the E factors, it only provides 25 out of 38 corresponding E metrics that can be useful to investors.

The metrics gap gets bigger when we look at the Social and Governance side where GSAS provide only 1 out of 7 and 5 out of 21 of the S and G topics respectively. Metrics that helps investors get a sense of the social and financial risks or on how the board and upper management manage and oversee those risks are mostly what is lacking from the GSAS schemes.

By counting mostly on green certification, such as GSAS, companies can make buildings and the built environment more sustainable and compliant with most ESG factors. Nevertheless, companies must embrace a more holistic ESG strategy where green certification is one of the tools towards a better sustainability performance. Reporting frameworks such as the Global Reporting Initiative (GRI), the Sustainable accounting Standards (SASB), the Task Force on Climate-related Financial Disclosures (TCFD), can be used by companies to make sure they identify their material topics especially ones that are not covered by green as mentioned above. Reporting frameworks such as SASB and TCFD and the upcoming International Sustainability Standards Boards (ISSB) can help companies operating in the construction by providing ESG information that are useful for investors.

References

CFA Society of the UK (2021). "*ESG investing official training Manual Edition 3*." ISBN 978-1-9164496-8-8

Guggenheim, World Wildlife Fund, KPMG and Mott MacDonald Report (2020). "Measuring Sustainability in Infrastructure Investment: A case study Assessment of Selected Standards and Tools", 75 pages.

Gulf Organisation for Research and Development (2022). Global Sustainability Assessment System. Categories and criteria. Categories & Criteria – GSAS Trust (gord.qa)

Gulf Organisation for Research and Development (2022). "Global Sustainability Assessment System (2019), Technical Guidance" Issue 2. All rights reserved to Gulf Organization for Research & Development. GSAS Technical Guide 2019 (gord.qa)

Gulf Organisation for Research and Development (2022). "Global Sustainability Assessment System (2019) Design and Build Guidelines: for building typologies", 4th of Edition. All rights reserved to Gulf Organization for Research & Development. GSAS 2019 Design & Build Assessment Manual - For Building Typologies (gord.qa)

Gulf Organisation for Research and Development (2022). "GSAS 2019 Construction Management guidelines Manual: For Building and Infrastructure", 4th Edition. All rights reserved to Gulf Organization for Research & Development. GSAS 2019 Construction Management Guidelines Manual - For Buildings And Infrastructure (gord.qa)

Gulf Organisation for Research and Development (2022). "GSAS 2019 Operations: Assessment and Guidelines Manual for Existing Buildings: 4th Edition – Issue 2. All rights reserved to Gulf Organization for Research & Development. GSAS 2019 Operations Assessment & Guidelines Manual - For Existing Buildings (gord.qa)

International Financial Reporting Standards - Sustainability Accounting Standards Board (2018). Building Products and Furnishing, Construction Material Sustainability, Engineering Construction Services, Real Estate Services Sustainability Accounting Standards. https://sasb.org/standards/download/

McKinsey & Company (January 2015). Why Diversity matters. Copyright © 2015 McKinsey & Company. All rights reserved. why diversity matters.pdf (mckinsey.com)

World Green Building Council (2019). "Bringing embodied carbon upfront: Coordinated Action for the building and construction sector to tackle embodied carbon", Report written in collaboration with Ramboll and C40 Cities, 67 pages.

World Resources Institute (June 2022). "World Greenhouse Gas Emissions in 2019 per sector". Climate Watch, based on raw data from IEA (2021), GHG Emissions from Fuel Combustion, www.iea.org/statistics; modified by WRI. World Greenhouse Gas Emissions: 2019 | World Resources Institute (wri.org)

Cite as: Roukoz K., Porter F., Terry L. & Ersenkal D., "Environmental, Social and Governance in the Construction Industry", *The 2nd International Conference on Civil Infrastructure and Construction (CIC 2023)*, Doha, Qatar, 5-8 February 2023, DOI: https://doi.org/10.29117/cic.2023.0153

Diffuser Bed Construction Challenges on the Musaimeer Pump Station and Outfall Project

Gary Peach
Mott MacDonald, Doha, Qatar
gary.peach@motmac.com

Saad Zayed Al-Marri
Public Works Authority, Doha, Qatar
smarri2@ashghal.gov.qa

Hernan Vigil Fernandez
HBK-PORR JV, Doha, Qatar
hernan.vigil@auccqatar.com

Abstract

Musaimeer Pump Station and Outfall project (MPSO) is a strategically important drainage asset initiated, developed, and completed by Ashghal in 2022. This project accommodates ground and storm water received from the drainage networks of 270 km2 of urban areas in southern Doha, along with storm protection for four soccer stadiums used during the FIFA 2022 World Cup. The key elements of this project were a pump station with a capacity of 19.7 m^3 / s, one of the longest ground and storm water tunnels in the world with a total length of 10.2 km and the diffuser bed structure measuring 194 m x 40 m. The diffuser bed structure is connected to the outfall tunnel by a riser shaft and is the structure used to disperse the ground and storm water in a controlled manner and in accordance with environmental standards. This technical paper will detail the entire process from dredging and material stockpiling, riser shaft drilling and construction, diffuser bed fabrication onshore, transportation to final location, installation on the sea floor, backfilling and protection works and finally commissioning of the entire project.

Keywords: Diffuser bed structure; Riser shaft; Outfall tunnel

1 Introduction

The Musaimeer Pumping Station project is governed by the Qatar Construction Specifications (QCS, 2014). The Public Works Authority (PWA) have engaged in two contracts. Firstly Mott MacDonald Ltd., which is the Project Management Consultant (PMC) company, and HBK-PORR JV, which is the Design, Build, Operation and Maintain Contractor for the construction of the MPSO Project, which is the final receiver of the upstream drainage system and located at the end of the Abu Hamour Tunnel, immediately south of the Hamad International Airport (HIA). The outfall tunnel extends from the pump station, 10.2 km offshore discharging the flows into the Arabian Gulf. The discharging will be performed through a vertical riser shaft and a marine outfall diffuser field. Figure 1 shows the project location.



Fig. 1: Project Location

2 Design

The marine diffuser field structure is shown in Fig. 2. The central manifold is located directly on top of the riser shaft and is a concrete structure measuring 4 m x 4 m x 4 m and weighing 120 Tons. Connected the main manifold are 6 radial arm structures which either directly connect to the manifold or are connect by short secondary manifolds. Each arm is 147 m long and is separated from the adjacent arm by 20 m. This makes the entire structure outline 294 m x 40 m. The secondary manifolds and 6 arms are manufacture out of High-Density Polyethylene (HDPE) pipe and are of various diameters 2000,1400, 1200 and 710 mm to ensure an even flow throughout the various arms under varying flow rates from the pump station. The discharge from the structure to the sea is via 84 duck bill valves located equal spacing along the 6-arm structure.

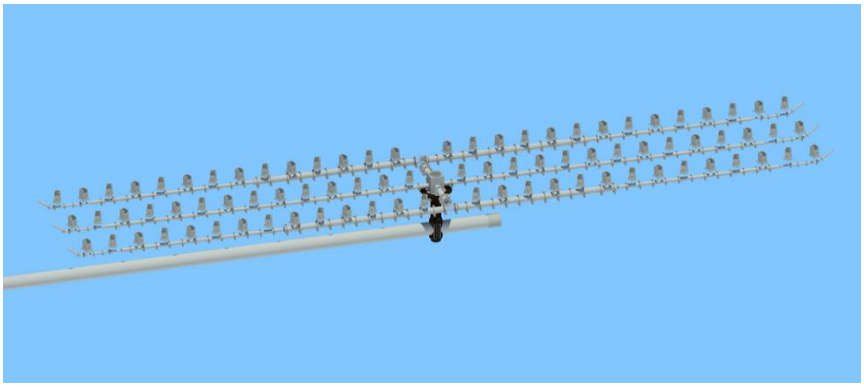


Fig. 2: Marine diffuser field structure, riser shaft and TBM outfall tunnel

3 Derdging and Material Stockpiling

The dredging was carried out by a Cutter Suction Dreger (CDS), which consists of a cutter mechanism mounted upon a barge and is capable of being lowered and raised from the seabed allowing excavation of the diffuser field pocket, which was 300 m long, 60 m wide and 5 m deep. The total matter excavated was 65,000 m^3. The excavated material was placed in a stockpile located 50 m away and transportation of material was via a floating discharge pipe. All excavated material was later reused for back filling purposes, significantly reducing the environmental impact of the marine works

4 Riser Shaft Construction

The riser shaft is the structure which connects the TBM outfall tunnel to the marine diffuser bed. The invert of the outfall tunnel is 14.5 m below the seabed and the depth of the sea at this location is 15.5 m. The specialist Contractor engaged for the section of the work by HBK PORR JV was MIC

(W.L.L). The first stage in the construction is carried out by a dredger which on average removes 2.5 m of the loose sediments located on the seabed. Near the riser shaft a further 2 m is excavated to ensure competent strata is exposed which will improve the drilling operation required to construct the riser shaft.



Fig. 3

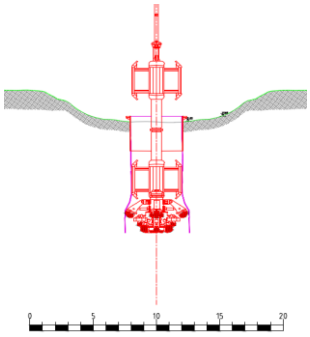


Fig. 4



Fig. 5

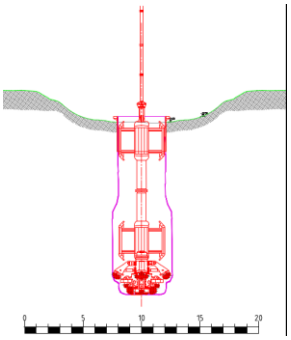


Fig. 6

With the dredging complete the next stage of the construction is carried out from a jack-up rig which is located direct adjacent to the centre line of the riser shaft. A cantilever frame is then installed to the side of the jack-up rig, this is the location the drilling equipment will be installed. The drilling rig or Bottom Hole Assembly (BHA) is shown in Figure 3. The BHA is lowered down to the correct location and commences to drill the rise shaft, shown in Figure 4 and 5. The BHA can dill various diameter holes from 4 to 5.3 m by use of extending hydraulically activated arms to suit the desired diameter of shaft. In this case the first section was drilled at 4 m diameter and then the arms are extended out, as shown in Figure 6 to the 5.3 m settings. The 5.3 m section is the location through which the TBM will excavate, giving a clearance of 500 mm each side of the TBM, which has an outer diameter of 4. 3 m.

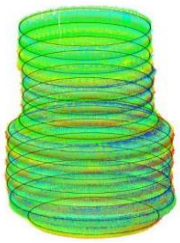


Fig. 7

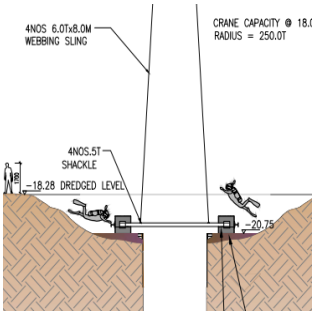


Fig. 8



Fig. 9

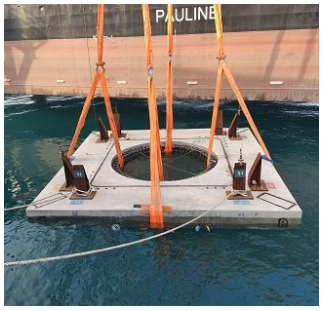


Fig. 10

On completion of the riser shaft drilling the BHA is then removed, and a three-dimensional survey carried out to determine the exact dimensions and position of the riser shaft, shown in Figure 7. The next stage shown in Figure 8 is to install a steel casing into the top 3 m of the riser shaft, to provide stability and prevent collapsing of the shaft inwards. Four Concrete manifold foundation blocks are then positioned and levelled into the correct position and connected to the steel casing, these activities are shown in Figures 8 and 9. A manifold concrete base slab (Figure 10) is then positioned on top manifold foundation blocks as shown in Figure 11.

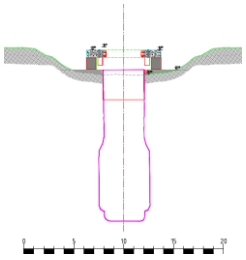


Fig. 11



Fig. 12

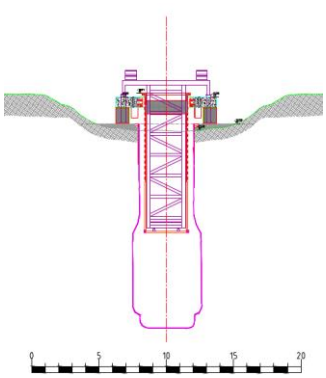


Fig. 13

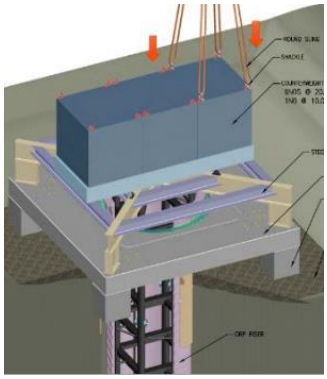


Fig. 14

The riser shaft internal lining protects downwards from the base of the concrete manifold to 500 mm above the TBM outfall tunnel and is made from Glass Reinforced Plastic (GRP). This is a cylindrical shape with a fixed end at the lowest end and a removable flange at the other end. A temporary steel support frame is installed within the GRP cylinder, refer to Figure 12. The GRP cylinder and steel frame are then installed into the riser shaft as shown in Figure 13 and positioned centrally within the riser haft and connected to the base slab. At this point the riser shaft is still full of sea water. Figure 14 shows the temporary Kentledge, which is then placed on top of the whole structure to prevent uplift during the grout placement.

The void between the GRP cylinder and the whole of the lower portion is then installed with a grout mixture, which fills the void in a controlled manner, slowly displacing the seawater. The grouting is shown by the blue colour in Figure 15.

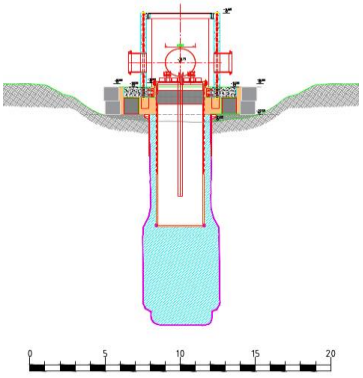


Fig. 15

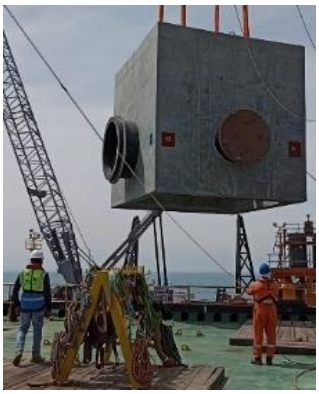


Fig. 16

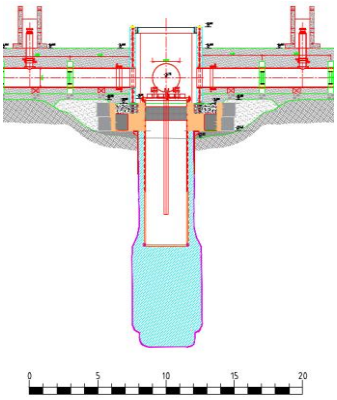


Fig. 17

When the grout has cured, the kentledge is removed along with the internal steel frame and the upper flanged is secured and sealed to the top of the GRP cylinder. Both top and bottom ends of the GRP cylinder have a series of installed valves which allow venting of air or water. The upper valves are then used in connection with compressed air to remove all the seawater within the GRP cylinder and leave only air within the GRP cylinder.

The central manifold which collects the combined ground and storm water from the outfall tunnel and then distributed evenly to the diffuser structure, was constructed on shore, and weighed 120 tons. The concrete manifold is shown in Figure 16 and is then lowered and positioned on top of the riser shaft and connected to the manifold base slab as shown in Figure 17.

In due course all the diffuser field structure is connected piece by piece to the central manifold until

the full diffuser bed structure is installed and covered with back fill material and then a final layer of scour protection installed and covering the entire diffuser bed structure, this shown in Figure 17. At this point the riser shaft structure is ready to receive the TBM constructing the outfall tunnel.

5 Onshore Fabrication

All the major components of the offshore diffuser bed structure were manufactured at two onshore locations in the Doha area. The major components include pipe work in

- HDPE Pipe and Connections.
- Concrete Manifold.
- Concrete Protection box.
- Concrete collars.

The main fabrication site was located a Milaha port south of Wakra. In this site all the above except the concrete collars were fabricated and assembled. These are shown in Figure 18. To ensure an equal flow through the entire length of each of the six arms each start at 2000 mm diameter and then reduced to 1400 mm and then finally 1200 mm.



Milaha Port site



HDPE pipework being assembled



HDPE pipework transition

Fig. 18: Onshore fabrication works

6 Transportation

When each section of the diffuser field pipe structure was complete it was then assembled on shore, the end is than capped with a blank flange to ensure water does not end the inside of the pipe. The pipe is then launched onto the sea, the structure then towed out to the diffuser bed location. Figure 19 shows a pipe structure in process of being towed out to the diffuser bed location. The Concrete manifold was transported separately by barge.



On-shore to Off-shore launching



Pipe section ready for towing



Pipe section with concrete collars

Fig. 19: Launching of pipe elements from onshore to the sea

7 Installation of Disfusser Structure

After the various elements of the diffuser structure have been transported to the final location, they are anchored and stored ready for installation. The main barge is positioned in line with the final seabed location. The individual sections are then manoeuvred into position and then the central manifold sections are lowered first using a barge mounted crane. Final under water positioning is carried out by specialist divers. The first sections installed are the ones which connect to the central manifold, then followed by sections moving out from the central manifold. The pipe section is manoeuvred into position and buoyancy aids attached the full length of the pipe. Water acting as ballast is slow allowed to enter the pipe section resulting in the structure submerging in a controlled manner to the seabed, refer to figure 20. The final positioning is carried out by specialist divers and secured to the already installed elements.



Central manifold



Pipe section with buoyancy aids



Submerging the pipe

Fig. 20: Launching of pipe elements from onshore to the sea

The whole structure is then assembled section by section in this manner until the full diffuser arrangement is completed.

8 Backfilling and Scour Protection

On completion of the diffuser bed structure the next sequence of work is to back fill the structure for stability and then install scour protection for the whole installation along with specially designed concrete protection boxes for each of the 84 duck bill valves. Back filling activity is shown in Figure 21



Backfilling barge and excavator



Reused back filling material



Backfilling in process

Fig. 21: Backfilling of the diffuser bed structure

9 Connection to Outfall Tunnel

The programme for the overall project required the diffuser bed structure to be completed prior to the arrival of the TBM, this was achieved. The TBM excavated to within 5 m of the riser shaft shown in Figure 23 and depressurizes the cutter head and monitors the situation for any water inflow over 8 hours. This was to test if the riser shaft was watertight to ensure the future connection works to be carried out in a safe manner. In this case there was no water inflow and thus the TBM excavates through the lower portion of the riser shaft and stops 25 m beyond the riser shaft as shown in Figure 23.

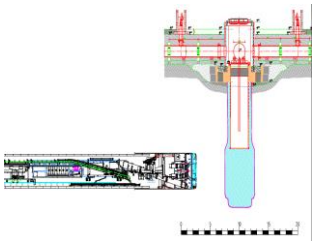


Fig. 22

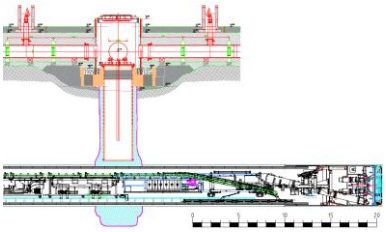


Fig. 23

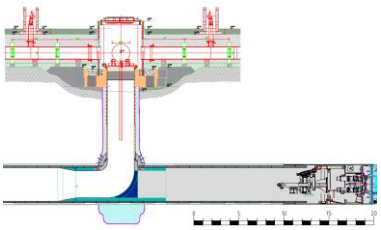


Fig. 24

The TBM and associated plant and equipment is then dismantled and removed back through the outfall tunnel and at the pump station location removed to the surface. The 25 m tunnel beyond the riser shaft is filled with concrete, refer to Figure 14, and then there follows very intricate and complex series of construction activities requiring precise logistical planning and execution to complete the connection of the outfall tunnel to the riser shaft and installation of the permanent works all of which is carried out 10.2 km offshore.

10 Commissioning

With the connection to the outfall tunnel complete the final element of the work is to fill the entire system with water from the inland tunnels. This is a slow process in which the filling is controlled to ensure all the air is removed from the system and the system is then ready for operation. This process went to plan and the project was commission on the due date and is now in full time operation.

11 Conclusion

This was the first of three possible outfall projects planned by Ashghal for the long-term management of rising ground water level and storm events, which will bring significant benefits to the population of Doha and surround areas. There were many lessons learned from the project and these have all been categorized and been considered by Ashghal for future projects. The project was a significant success and appreciation is extended to all parties involved in coming together and working to achieve the successful completion of this project.

References

Karagkounis, et al. (2016). Geology and geotechnical evaluation of Doha rock formations. *ICE Geotechnical Research UK*, *3*(3), pp. 120-121.

Sadiq, A.M. & Nasir, S. J. (2002). Middle Pleistocene Karst Evolution in the state of Qatar, Arabian Gulf. *Journal of cave and Karst studies*, pp. 137-139.

Poulos, H.G. (2018). A review of geological and geotechnical features of some Middle Eastern countries – Innovative Infrastructure solutions, Springer, pp. 6-8.

Cite as: Peach G., Fernandez H.V. & Al-Marri S.Z., "Diffuser Bed Construction Challenges on the Musaimeer Pump Station and Outfall Project", *The 2nd International Conference on Civil Infrastructure and Construction (CIC 2023)*, Doha, Qatar, 5-8 February 2023, DOI: https://doi.org/10.29117/cic.2023.0154

Assessment of Ablution Water Consumption in Mosques

Aliya Ali Said Al Alawi
University of Technology and Applied Sciences, Muscat, Sultanate of Oman
aliya.alalawi@utas.edu.om

Parameswari K.
University of Technology and Applied Sciences, Muscat, Sultanate of Oman
parameswari.k@utas.edu.om

Gopalakrishnan Kumarasamy
University of Technology and Applied Sciences, Muscat, Sultanate of Oman
gopalakrishnan.kumarasamy@utas.edu.om

Khoula Said Al Kaabi
University of Technology and Applied Sciences, Muscat, Sultanate of Oman
khoula.alkaabi@utas.edu.om

Abstract

In Muslim majority countries, like those of the Gulf Cooperation Council (GCC), ablution is a necessary component to fulfil religious commitments of prayer, thus a significant amount of water is consumed on daily basis with minimal efforts and measures to manage or conserve that water use. This study aims to highlight the importance of redesigning the appliances in the Mosque for ablution purposes to save scarce water. The study assesses the water usage during ritual ablution (wudu-following Prophet Muhammad's (PBUH) way) in the Mosques of Oman. The findings from this study can have a global impact, as it can set an example for GCC countries as well as other countries all over the world where ablution is being practiced. Total consumption per capita for performing ritual ablution was measured using the normal tap, sensor tap, and pot. The study found that 7 L is being used while using normal and sensor taps of water per ablution while it could be done with 0.6 L of water. The major conclusion of the study is that current water consumption for ablution in Oman is around 8 times more than that of following Prophet Muhammad's (PBUH) way–during ablution. Special taps that conserve water and suit the purpose of ablution have to be designed.

Keywords: Ablution; Water; Mosques; Management; Conservation

1 Introduction

Water is a precious natural resource that has to be managed efficiently in all the sectors such as domestic, industrial, agricultural, and commercial consumption and usage in public buildings such as mosques, government offices etc. Because of urbanization and modernization advanced appliances have been introduced in the water usage sector without serving water management for different purposes. In the present study, water usage in mosques has been considered. In mosques, the major amount of water is used for ablution which is a ritual performance before the prayer. The ritual ablution is known as 'Wudu', which means cleaning the different exposed parts of the body before performing the prayer in the mosques. The 'Wudu' process is washing hands up to wrists, rinsing the mouth and nose, the entire face and arms to the elbows, then wiping the head and ears and washing the feet to the ankles and, as shown in Figure 2.4 (Abu-Rizaiza, 2002). Presently either manual tap or sensor tap is being used for ablution.



Fig. 1: Steps in the ablution process for prayer (Abu-Rizaiza, 2002)

Previous literature studies claimed that about 90% of the water consumed in mosques is used for performing the ritual ablution (Suratkon et al., 2014; Rahman et. al, 2016; Prathapar et al., 2005). Once the water is used for ablution, it is allowed to run and drain away as waste water without any other usage. As quoted in the Hadith (Ibn Majah – Book 2, Hadith 425), Prophet Muhammad reminded Muslims to avoid wastage of water, even when performing the cleansing ritual of ablution before prayer. A recent study in a university mosque in Malaysia (Utaberta, 2014) and another study in a university mosque in Oman by Prathapar et al. (2005) and Aliya et al. (2021) assessed the amount of grey water produced from ablution. The study reveals recycling and reuse of this significant quantity of greywater and water demand management especially in mosques is very limited; hence, an investigation into this aspect is the need of the hour to save the precious resource. The present study aims to enable the management of required water demand in public buildings, especially the mosques in the Sultanate of Oman. The existing appliances such as manual and sensor taps are used for ablution consuming the maximum quantity of water. The major amount of consumed water is not efficiently used for ablution. While performing the 'Wudu' if it is a manual tap, people open the tap and it will not be closed until performing the full ablution. Similarly, in a sensor tap which have an automatic on-and-off process, it takes a few seconds to arrest the water flow which is not considered to be an efficient way from a water management perspective mainly for ablution purpose. The research study enhances the saving potential of water by considering the religious policies which can promote the invention of suitable appliances and techniques which suits the mosques.

2 Methodology of the Study

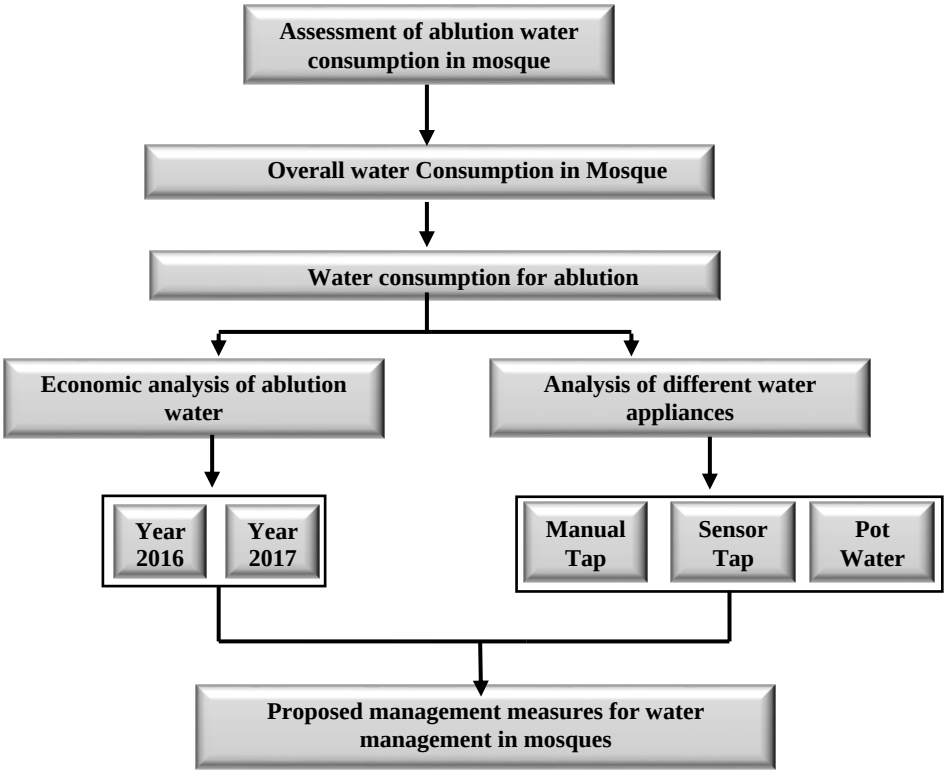


Fig. 2: Framework of the study

In this study, qualitative and quantitative analysis have been made by collecting data from various government sectors. The overall water consumption data has been collected from PAEW (Public Authority for Electricity and Water) Oman's annual report. Information regarding the various water dispensing systems such as types of taps, toilet systems employed in the mosques have been collected from the Ministry of Regional Municipalities and Water Resources and by interviews and observations. From this data, the types of taps used in the different mosques were identified and the consumption rate for the different taps was calculated. The research included both types of of mosques, the Jama (big mosque) and Masjid (small mosque). Additionally, qualitative data has been collected through the questionnaire survey. The main reason for the qualitative survey was to assess the behaviors of the users and the social acceptance of reusing the ablution water. The qualitative survey data has been collected from engineers of PAEW, Mosque management, the public who performs the prayer in the mosques, and the policymakers. For the quantitative study, a total of 120 users were identified from different mosques and the per capita water consumption was recorded. A special device for measuring the discharge is found and it was fitted into the mosque taps. Different taps were identified in the different mosques and the discharge measuring device has been attached and the per capita rate has been collected while performing the ritual ablution. The researcher informs the users about the presence of a discharge measuring device and asks them to perform as usual ritual ablution. At the same time, the majority of the persons who perform the prayer in the mosque are not willing to use the pot-type method of ablution. For identifying the quantity of water required for ablution by pot method, the researcher collected the data at the local level from home. Finally, the data collected from various places and methods are analysed and identified for further processing.

3 Water Consumption for Ablution

3.1 Overall Water Consumption in the Mosque

In this research, the water consumption in Oman mosques was analyzed and compared for the years 2016 and 2017. The total number of mosques considered for the study is 688. For the year 2016, 11 months of water consumption data are only available. But for the year 2017, 12 months of water consumption data were available. During the year 2016, the total water consumption in the mosques was quantified as 158,339,867 gallons which is equal to 712,529,401 litres. Similarly, the water consumption for the year 2017 was quantified as 217,901,095 gallons which are equal to 980,554,927 litres. The drastic increase in water consumption is mainly due to an increase in population and 12 months of data were considered here. To maintain uniformity between the years, 11 months of data were considered.

3.2 Ablution Water Consumption

Most of the literature quoted that around 90% of the water used in mosques are for ritual ablution purpose (Suratkon et al., 2014; Rahman et. al, 2016; Prathapar et al., 2005). The per capita average total water consumption includes toilet flushing and usage of taps in the toilet, along with ablution consumption is shown in Table 1. The present study shows that only 25% to 35% of the overall consumption is being used for ablution as shown in the table. The water consumption data for ablution is measured from Jama and Masjid using sensor and manual taps respectively. As per the present study, 50% of the current ablution water consumption serves the need for ritual ablution.

Table 1: Ablution water consumption

	Average total Consumption in litres	**Ablution Consumption in litres**	**Percentage variation**
Jama	24.7	7.5	30
Masjid	9.7	2.5	26

4 Economic Analysis of Ablution Water

4.1 Economic Analysis of Water Bills for the year 2016

The overall consumption of water and its cost for 688 mosques for the duration of 11 months (January to November) for the year 2016. Overall water consumption in the mosque during this period was 158,339,867 gallons (712,529,401 litres). In 2016 for the initial two months (January and February) the rate of water per gallon in Oman was 0.0025 baisa. Later the month of March the rate changed to 0.0035 baisas. The water consumption bill was calculated using 0.0025 baisas for the initial period, for the rest of the period the rate has been considered as 0.0035 baisa. The overall cost consumed for 688 mosques over a period of 11 months is around 511,787 OMR.

4.2 Economic Analysis of Water Bills for the year 2017

The water consumption data from January to December for 688 mosques were collected. Overall water consumption during 2017 was 217,901,095 gallons (980,554,927 litres). The tariff per gallon of water was 0.0035 baisa in Oman. The total cost for the year 2017 was estimated at 763,974 OMR. The aforementioned data includes 12 months in 2017, whereas, for the year 2016, only 11 months of data were available.

Presently for the year 2017, the water consumption and its respective rates were analyzed and

compared for 11 months period (January to November). Overall consumption of water for the year 2017 was 198,807,075 gallons (894,631,837 litres). The overall cost consumed for 688 mosques over 11 months is around 697,145 OMR.

In comparison between 2016 and 2017 data shows a drastic increase in the quantity of water and thereby consumption cost increases. It may be due to an increase in population and also variation in the rate used for per capita consumption. Lifestyle is an important parameter that contributes to the increase in water consumption.

5 Analysis of Different Techniques in Existing Water Supply Appliances

General observation on current water flow for ablution can be reduced to 50% of the existing water consumption. This can be effectively achieved by selecting appropriate water appliances for ablution purposes. Previous literature on water demand management (Jamrah et al., 2008; Kayaga & Smout, 2007; Jamrah et al., 2006; Prathapar et al., 2005) shows that around 50% of water could be saved by changing the appliances. The average overall consumption per capita using the modern tap (sensor tap) with timer is 18L and 4.5L for ablution per capita. While the overall consumption per capita using the manual tap is 9L and 3.1L for ablution per capita. The analysis clearly shows that the modernization of the existing manual tap doesn't serve the purpose of water saving in regards to ablution. The results show the necessity of redesigning special taps for ablution.

As per the water consumption in the year 2016, the water bill with government support is 511787 OMR. Adopting the changes in the water appliances can save 50% of the water bill which is around 255,894 OMR. The water bill without government support is around 1,108,379 OMR in the year 2016. While adopting the proposed changes, about 50% of this water bill comes to 554,189 OMR can be saved. As per the water consumption in the year 2017, the water bill with government support is 697,145 OMR. Adopting the changes in the water appliances can save up to 50% of the water bill which is around 348,572 OMR. The water bill without government support is around 1,391,649 OMR in the year 2017. While adopting the changes about 50% of this water bill comes to 695,824 OMR can be saved.

6 Percentage Saving by Changing the Ablution Device Method to Using A Pot

The actual quantity of water traditionally required for ablution is measured by using a suitable pot with a measured quantity of water. The quantity of water required traditionally has been compared with the quantity consumed by normal and sensor taps. The average overall pot consumption per capita is around 0.6 L for ablution. It saves almost 80% of total water consumption used for ablution using sensors and manual taps. If the population is around 2.04 billion and considering ablution and praying 5 times a day with a consumption rate of 0.6 L will come to around 6.12 billion L of water consumption. By introducing the specifically designed taps for ablution with minimal water consumption, both the natural and financial resources can be saved by 80%.

7 Conclusion

In this present study, different water supply appliances such as sensor taps, manual taps and pots were considered for measuring the water consumption for ablution in the mosques. The study reveals that different appliances have varied discharge rates and the consumption cost were varying as per the discharge rate. The different appliances used in the mosque satisfy the purpose of ablution but are not efficient from the water management perspective. Most of the mosques were equipped with sensors and manual taps in Oman. While considering the sensor and manual tap, about 4.5 L and 3.1 L of

water per capita are required for performing the ritual ablution respectively. At the same time, the ritual ablution is performed by using a pot means about 0.6 L of water would be sufficient. This phenomenon indicates that about 80% of water can be saved when compared to its current usage. In Oman, the annual consumption of water in mosques is around 894,631,837 L at 697,145 OMR. Every year, the consumption of water has increased with respect to the population growth and standard of living. As per the research, a new device has to be designed with the same discharge rate as the pot which reduces 80% of the present water consumption. The newly designed appliances will also save natural resources and be helpful for saving the economy of the country. Apart from economic benefits and water-saving concepts, the ablution water can be recycled and reused since it has less amount of contamination. The recycled water cannot be used again for ablution though it meets the potable standards due to religious constraints. However, it can be reused for flushing toilets, cleaning purposes, and irrigating the landscape around the mosques which may benefit a considerable amount in the water bills.

References

Abu-Rizaiza, O. S. (2002). Ablution water: prospects for reuse in flushing of toilets at mosques, schools, and offices in Saudi Arabia. *Engineering Sciences*, *14*, 3-28.

Aliya, et al (2021). Water management in Mosques of Oman. *Sustainable Water Resources Management*, 7(6).

Ibn Majah. (2007). English Translation of Sunan Ibn Majah. *Translated by Nasiruddin al-Khattab, Darussalam Publications*, Vol. 1, Book 2, Hadith 425.

Jamrah, et al. (2006). Assessment of availability and characteristics of greywater in Amman. *Water international*, *31*(2), 210-220.

Jamrah, et al. (2008). Evaluating greywater reuse potential for sustainable water resources management in Oman. *Environmental monitoring and assessment*, *137*(1-3), 315.

Kayaga, S. & Smout, I. (2007). Water demand management: A key building block for integrated resource planning for the city of the future. In First SWITCH Scientific Meeting, Univ. of Birmingham, UK.

Prathapar, et al. (2005). Overcoming constraints in treated greywater reuse in Oman. *Desalination*, *186*(1-3), 177-186.

Rahman, et al. (2016). ReWudhuk: A Sustainable Device to Reuse Musta'mal Water for Ablution Purpose. *Advanced Science Letters*, *22*(9), 2170-2173.

Suratkon, et al. (2014). Smart WUDHU': Recycling Ablution Water for Sustainable Living in Malaysia. *Journal of Sustainable Development*, *7*(6), 150.

Utaberta, N. & Handryant, A. N. (2014). Greywater treatment system in universiti kebangsaan malaysia mosque: utilizing filter wells as an alternative sustainable innovation, *Journal of Islamic Architecture*, *3* (1), 19-24.

Cite as: Al Alawi A.A.S., Parameswari K., Kumarasamy G. & Al Kaabi K.S., "Assessment of Ablution Water Consumption in Mosques", *The 2nd International Conference on Civil Infrastructure and Construction (CIC 2023)*, Doha, Qatar, 5-8 February 2023, DOI: https://doi.org/10.29117/cic.2023.0155

Review on Decarbonizing the Building Sector in Oil and Gas Countries: The Case of Qatar

Reem Al-Mohammed
Department of Architecture and Urban Planning, Qatar University, Doha, Qatar
200753670@qu.edu.qa

Djamal Ouahrani
Department of Architecture and Urban Planning, Qatar University, Doha, Qatar
djamel@qu.edu.qa

Abstract

Climate change is a serious international issue, and nations must move to carbon reduction to mitigate this problem. Therefore, Qatar is building strategies, towards energy transitions and decarbonization. Whereas, energy transitions from hydrocarbons to renewable energy is challenging, since Qatar is a gas producing country. Thus, decarbonization in energy-based countries is challenging, due to their economic development dependence on fossil-fuel by exporting oil and gas, and generating energy and electricity. However, most of the global carbon emissions are caused by buildings. Hence, the challenge of energy demand reduction in buildings in hot climate regions such as Qatar, is due to using air conditioning systems. Therefore, the research aims to investigate the decarbonization strategies implemented in the building sector in oil and gas countries, where electricity bills are subsidised by the government. In order to tailor decarbonization strategies for Qatar, according to the country's context and social status.

Keywords: Decarbonization; Buildings; Energy; Qatar

1 Justification of the Study

Buildings account for 48% of the global emissions. Furthermore, 40% is caused by the energy consumption in the building operating phase such as cooling (Lechner, 2015). Therefore, there is a high potential in decarbonizing the building sector, by reducing greenhouse gas (GHG) emissions by 2050 up to 85–95% (Kranzl et al., 2019). Accordingly, many international building codes have been established, to minimize energy consumption and to reduce GHG emissions (Lechner, 2015), such as the Global Sustainability Assessment System (GSAS), which was developed to improve sustainability in the built environment for Qatar and the MENA region countries (Khater, 2013). This work addresses the challenges of decarbonizing the building sector in oil and gas countries, and showcasing global case studies, to study the decarbonization strategies in the building sector in oil and gas countries such as Qatar, where electricity bills are subsidized by the government. It is significant to identify the decarbonization strategies

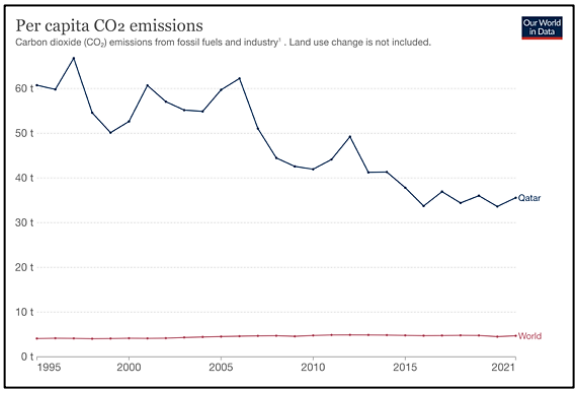


Fig. 1 : Per Capita CO2 emissions in Qatar - Our world in data based on Global Carbon Project (2022).

implemented in the oil and gas countries, including buildings energy efficiency measures, based on the current research context. In order to accelerate the process of decarbonization in Qatar .

Qatar is a gas exporter country, and one of the highest income per capita, and the highest energy consumers in the world with high Gross Domestic Product (GDP) (KAHRAMAA, 2020). The state of Qatar has the highest per capita CO_2 emissions in the world (Figure 1). According to KAHRAMAA annual statistics report (2018), as illustrated in (Figure 2) the residential sector consumes more electricity than the industrial sector (KAHRAMAA, 2020). Moreover, 80% of the electricity used in the Qatari buildings is consumed in air conditioning; which is the highest consumption globally (Meier et al., 2013). However, electricity bills are subsidised by the government for the local population in Qatar. Therefore, assessing the efficiency of decarbonizing the building sector, accelerates and improves the decarbonization process in the country.

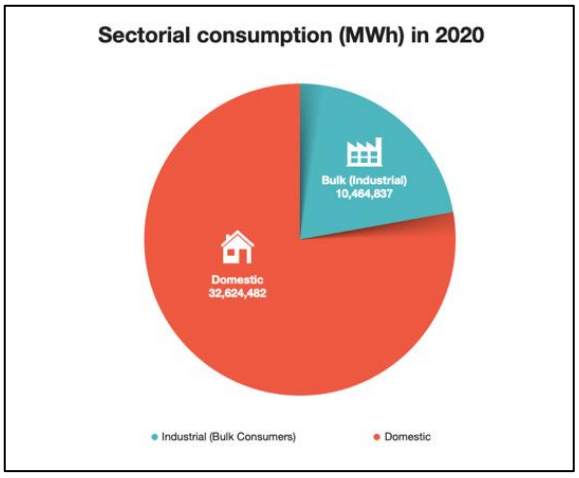


Fig. 2: Sectoral Consumption in 2020, MWH in Qatar, (Kahramaa annual statistics report, 2020)

2 Case Studies

The following global case studies review the different decarbonization methods implemented in different cities and countries.

2.1 Oil and Gas Exporter City:

2.1.1 Oslo, Norway

Oslo has the largest economic, and knowledge hub in the country (Eriksson et al., 2016). Therefore, the City of Oslo has implemented measures to reduce CO2 emissions by 41% compared to 2009 levels by 2020, 50% by 2022 and by 95% in 2030, in order to reach carbon neutrality by 2050 (Figure 3) (City of Oslo, 2020). The majority of the reduction achieved after 2013 proves that GHG emissions in large cities can be rapidly reduced by targeted measures through buildings and construction. However, there was a difficulty to meet Oslo's 41% climate target for 2020. The decreased use of oil for heating is a result of the ban on using mineral oil to heat buildings, which has resulted in a significant decrease in emissions from fossil heating. Moreover, several zero-emission options, such as zero-emission automobiles and fossil-free district heating, have been phased out in Oslo. The building energy efficiency strategies undertaken in the city of Oslo are listed in Table 1.

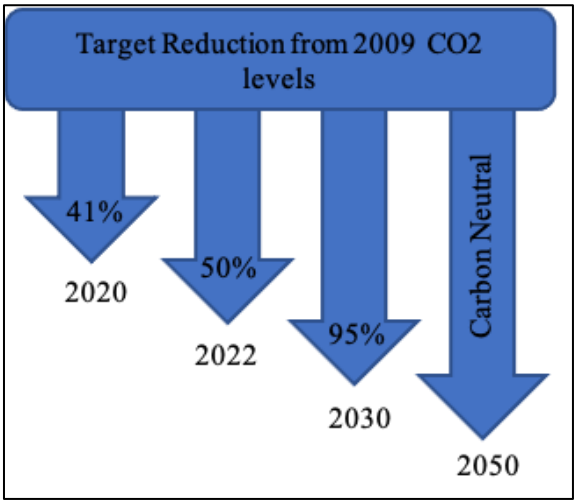


Fig. 3: Target Reduction from 2009 CO2 levels

Table 1: Building Energy Efficiency Strategies in Exporting Country: Norway

City	Carbon Reduction targets	Building energy efficiency strategies
1) Oslo, Norway	**Target:** 50% by 2030, and 100% by 2050 (100% fossil fuel-free)	1- electricity supplies are 100% carbon neutral . 2- city cooperation with citizens, business communities and organizations. 3- annual fund to promote research and development. 4- **prioritized emissions reduction goals** and annual progress **reports.** 5- Oslo's Climate Budget highlights the measures Oslo will apply to reduce CO_2 emissions (*Climate Budget 2019*, 2019). 6- The successful development of the Climate Budget depends on: **Governance and commitment, Communication and collaboration** of the population, and business communities, **cross-sectoral commitment** from public and private organizations, and **City agencies** involved in the design process. 7- The transparency of the Climate Budget enables the budget to be easily understood by stakeholders and **promote trust** in the process. 8- Statistic Norway records **Emissions statistics** to achieve the aims of the Climate Budget. 9- **Oslo has chosen 16 areas as a priority, which reflects strategic and long-term decisions** (*Climate Strategy for Oslo towards 2030*, 2020)(Climate Strategy for Oslo towards 2030, 2020).Some of them are: • construction activities and buildings in Oslo will be fossil-free and emission-free by 2030. • The greater source of energy in Oslo will be generated locally. • The buildings in Oslo will utilize electricity efficiently and decrease the consumption of energy. • low greenhouse gas emissions construction materials.

2.2 Oil and Gas Importer Cities

2.2.1 Stockholm , Sweden

Stockholm has stated its intention to be fossil-fuel-free by the year 2050. The Environment and Public Health Committee was commissioned in the 2012 budget with developing a roadmap to show how this target can be achieved. This roadmap is based on indicators that have been monitored since 1995 and are reported to the Environment and Public Health Committee on an annual basis. The calculations indicates the emissions produced from energy for heating uses, transportation, and for gas and electricity uses (Lönngren & Nilson, 2014). (Figure 4) shows significant carbon reduction per capita after 2012 in sweden. Emisssions reduction in Stocholm from 1990 is 49% in 2019, and economic growth has increased by 100% , and 33% of the emissions is from buildings (Stockholm - Sweden, 2022).

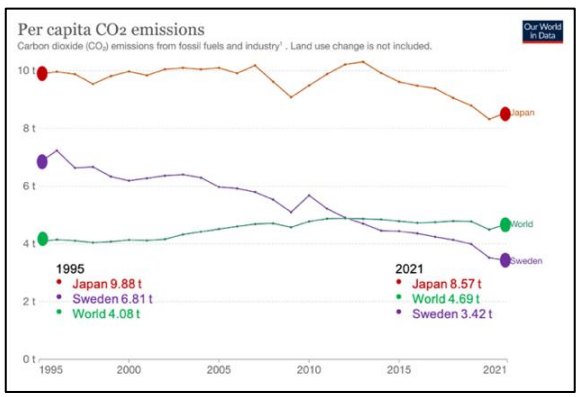


Fig. 4: Per capita CO2 emissions in Sweden and Japan, our world in data (2022)

2.2.2 Yokohama, Japan

As SDGs FutureCity Yokohama (chosen, 2018), the city constructs local and worldwide alliances and promotes innovative measures that simultaneously tackle environmental, economic, and social challenges in order to contribute to the achievement of the world's agreed upon Sustainable Development Goals (SDGs) ("SDGs Future City Yokohama," 2019). The greenhouse gas emissions in 2020 were 17.13 million t-CO2, 20.6% less than 2013 level (Figure 5). Moreover, 46% of the electricity is generated from gas and 20% is from nuecleare (Yokohama - Japan, 2022).

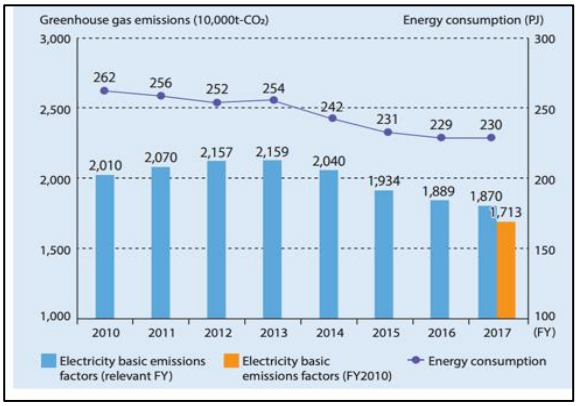


Fig. 5: Greenhouse gas emissions and energy consumption in Yokohama (Yokohama's Climate Change Countermeasures / SDGs FutureCity Yokohama, 2020)

Table 2: Building Energy Efficiency Strategies in Importing Countries: Sweden & Japan

City	Carbon Reduction targets	Building energy efficiency strategies
1) Stockholm, Sweden	**Target:** 100% by 2050 (100% fossil fuel-free)	1- target to become "fossil-fuel free by 2050." 2- The city assessed 50 potential measures to reduce carbon, according to four criteria: reduction potential, impact achievement speed rate, level of city control, and cost efficiency (Lönngren et al., 2010). 3- Finance climate change concepts. 4- The city predicted a 40% growth in population from 2012 to 2050, creating a demand for 5,000 new residential buildings annually, and 190,000 new homes by 2050. consequently, the total energy demands are expected to increase by 40% .
2)Yokohama, Japan	**Target:** 25% by 2020, 80% by 2050	1- The city's integrated Building Energy Management System (BEMS) has a control on a 29 separated BEMS's in Yokohama's amenities, which has reduced the peak demand by 22.8% ("SDGs Future City Yokohama," 2019). 2- In the summer of 2013, the city tested the energy management systems in around 3,500 residential buildings, and discovered that the power peak demand dropped up to 15.2% .

3 Conclusion

One of the primary components of city climate action plans to measure carbon emissions on regular basis, by setting benchmarks to annually track and report the progress. In order to assess the strategies and actions on carbon reduction, and to conduct comparison of potential costs and impacts of employing carbon reduction technologies. Moreover, the five-milestone framework for implementing the climate action plan are as follow: 1) Decarbonation and carbon mitigation starts with collecting data and analysing the existing emissions in order to predict future emissions; 2) Emission reduction targets should be set; 3) The development of a community action plan, according to the targets; 4) The implementation of the action plan; 5) To regularly monitor and record the progress of implementing the climate action plan. The successful development of decarbonization strategies relies on the government commitment and collaboration, targeting measures and benchmarks, enforced regulations, transparency, and reporting.

There are two decarbonization methods in the oil-exporter countries such as Qatar and Oslo 1) the implementation of carbon capture within the production of oil and gas, to sustain the industry and the

environment, and 2) to reduce energy consumption, by the implementation of energy efficient processes and sustainable buildings, and moving to renewable energy, which are the processes implemented by both oil-exporters and non-exporters countries. Therefore, the decarbonization methods that should be adopted will be according to how the energy is consumed in existing buildings in oil and gas countries.

The cities have set the reduction targets according to the country's capability to reach that target. Some cities have reached their targets such as the City of Stockholm, due to the high awareness in Sweden. Therefore, Sweden has set 100% achievable target to be reached by 2050. This is achieved by setting benchmarks and milestones, annual monitoring and reporting. However, some cities have set targets less than 100% , because they are not capable to reach it such as Yokohama. The city has formulated a medium and long-term strategy extending to 2050 and policies to be implemented by phases with priority during the years. On the other hand, the city of Oslo had a difficulty to meet the targets. Therefore, to accelerate the decarbonization process in the state of Qatar, measurable targets and milestones should be set, to reduce CO2 emissions from 2010 levels (Figure 6).

The decarbonization process was established according to the decarbonization purposes of the countries in each category. In the oil and gas exporting countries, decarbonization strategies were implemented mainly for environmental purposes. Since they have ample resources, their main purpose of the decarbonization process is to sustain the environment, due to the high level of awareness. On the other hand, the decarbonization strategies in the oil and gas importing countries, were implemented for environmental and economical purposes. Since they have to move to renewable energies.

Awareness is the key to accelerate the decarbonization process in Qatar. It is essential to establish an awareness campaign, to increase the awareness and involve the people in the decarbonization process. This might be the most appropriate strategy to decarbonize Qatar. Thus, it is essential to collect the energy consumption data in the building sector in Qatar. In order to investigate the energy consumption in the residential sector. This is to create mechanisms to encourage people to retrofit their houses with sustainable building materials, which leads to a whole economical green industry that support the decarbonization process in Qatar.

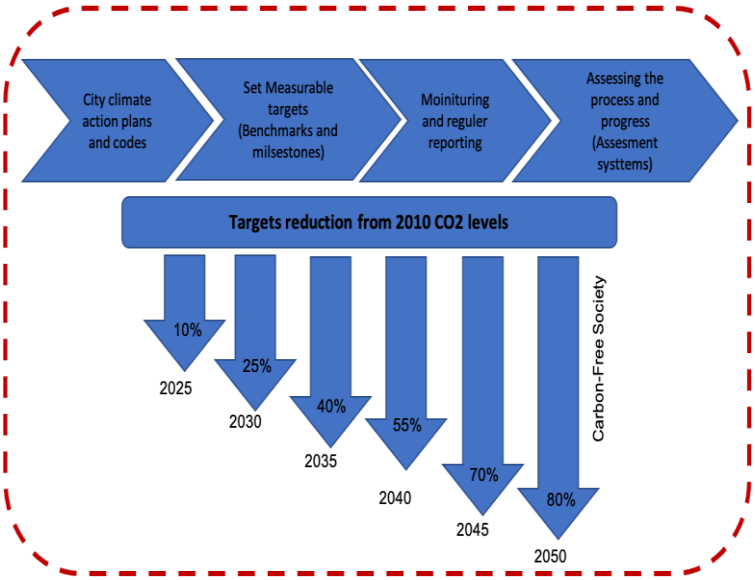


Fig. 6: Accelerating the decarbonization process in Qatar

The oil and gas industry is out of the context and excluded from this study, since the state of Qatar is exporting the oil and gas globally, and it is not used for local purpose only. However, the oil and gas countries need to measure and monitor the annual CO_2 consumption from buildings in kWh/sq^2. Such as

the case in Sweden the electricity demand is declining, due to retrofitting and buildings regulations. Therfore, the consumption per square meters is declining.

The electricity bill is 100% subsidized by the state of Qatar for the local population. Therefore, it is essential to encourage the local population to reduce the electricity consumption. This is achieved by 1) increasing the awareness within the local population, without removing the subsidies; 2) calculating the average electricity consumption for the local residential sector in kWh/sq^2 ; 3) to set a reasonable and reachable benchmark according to the average local population electricity consumption; 4) to set financial rewards for individuals based on the reduced amount of electricity consumption; 5) to measure, monitor and report the electricity consumption reductions on annual basis; 6) government subsidise a percentage of the energy efficient retrofits and materials for residential buildings. This is a proposed draft of the decarbonisation strategy in oil and gas countries, where the electricity subsidized by the country.

There should be more studies on developing the carbon emissions reduction measures and policies in the building sector, to achieve a non-carbon-based society by 2030, and a zero-emission society by 2050 in Qatar. Moreover, setting milestones requires a deeper understanding on how the energy is consumed, to be able to set up achievable goals, and develop long-term efficient decarbonizing strategies for the building sector in Qatar. In order to accelerate the process of decarbonization in the country.

References

City of Oslo. (2020). *Climate budget 2020. Chapter 2, Oslo City Government's budget proposal 2020 with appendix*. https://www.klimaoslo.no/wp-content/uploads/sites/88/2022/03/Climate-Budget-2022-with-appendix.pdf

Climate Strategy for Oslo towards 2030. (2020).

Eriksson, et al. (2016). Oslo : TU1206 COST Sub-Urban WG1 Report. In *Proceedings of the 25th International Symposium on Urban Data Management UDMS 2006 in Aalborg, Denmark, 15-17 May 2006*.

IPCC (2018). *Global Warming of 1.5°C. An IPCC Special Report on the impacts of global warming of 1.5°C above pre-industrial levels and related global greenhouse gas emission pathways, in the context of strengthening the global response to the threat of climate change*.

KAHRAMAA. (2020). *KAHRAMAA : ANnual Statistics Report* (Vol. 1, Issue 1).

Khater, I. (2013). *Certification Systems as a Tool for Sustainable Archiecture and Urban Planning Case Study : Estidama*. Abu Dhabi: HafenCity University.

Kranzl, et al. (2019). Are scenarios of energy demand in the building stock in line with Paris targets? *Energy Efficiency*, *12*(1), 225–243. https://doi.org/10.1007/s12053-018-9701-1

Lechner, N. (2015). *Heating, cooling, lighting : sustainable design methods for architects* (fourth edi). Wiley.

Lönngren, Ö. & Nilson, L. A. (2014). *Roadmap for a fossil fuel-free Stockholm 2050* (Vol. 1, Issue 1).

Lönngren, Ö., Hedvik, C. & Musabasic, A. (2010). Stockholm action plan for climate and energy 2010 – 2020. In *Energy*.

Meier, A., Darwish, M. & Sabeeh, S. (2013). Complexities of saving energy in Qatar. *ECEEE 2013 Summer Study Proceedings*, 41–46. http://www.eceee.org/

SDGs Future City Yokohama. (2019). In *SDGs FutureCity Yokohama*.

Stockholm-Sweden. (2022). Retrieved from CNCA: carbon neutral cities: https://carbonneutralcities.org/cities/stockholm/

Cite as: Al-Mohammed R., & Ouahrani D., "Review on Decarbonizing the Building Sector in Oil and Gas Countries: The Case of Qatar", *The 2nd International Conference on Civil Infrastructure and Construction (CIC 2023)*, Doha, Qatar, 5-8 February 2023, DOI: https://doi.org/10.29117/cic.2023.0156

Estimation of Blue and Green Water Potentials of Türkiye under Global Climate Change Effects

Ali Erturk
Freshwater Biology Department, Faculty of Aquatic Sciences, Istanbul University, Istanbul, Turkiye
erturkali@istanbul.edu.tr

Gokhan Cuceloglu, Alpaslan Ekdal, Mehmet Kalfazade, Salim Yaykiran, Aslı Ozabalı Sabuncugil, Aysegul Tanik, Izzet Ozturk
Environmental Engineering Department, Faculty of Civil Engineering, Istanbul Technical University, Istanbul, Turkiye
cuceloglu@itu.edu.tr, ekdala@itu.edu.tr, kalfazade@itu.edu.tr, salimyaykiran@gmail.com, asliozabali@yahoo.com, tanika@itu.edu.tr, ozturkiz@itu.edu.tr

Abstract

This study analyzed the impact of global climate change scenarios on the water resources of Turkiye by means of various climate and hydrological simulations projected for this century. An integrated approach was used by coupling regional climate models and a semi-distributed hydrologic model to assess the climate change impacts. A regional climate model, that is the output of 3 global models (HadGEM2-ES, MPI-ESM-MR and CNRM-CM5.1), has been conducted with RCP4.5 & RCP8.5 emission scenarios for whole the country at the watershed-scale with a resolution of 10x10 km. Hydrological simulations were conducted by using the Soil and Water Assessment Tool (SWAT) Model to determine the variation of surface and groundwater resources based on climate change projections. Blue water flow (water yield + deep aquifer recharges), green water storage (soil water), and water surplus/deficit projections have been conducted considering the current and projected status for water-consuming sectors of domestic, industry, agriculture, and ecosystem services. Results attained were further evaluated through statistical methods regarding blue water flow and green water storage potential of the country. The main purpose of the study was to aid the legal authorities, and decision-makers in prioritizing the environmental measures to be taken for mitigation of climate change impacts on Turkiye in the long- run. The work was the first country-wide hydrological modelling study through globally accepted climate change scenarios.

Keywords: Turkiye; Hydrology; Water budget; Climate change; Mediterranean Region

1 Introduction

Based on the existing monitoring data and climate projections, scientists highly agree on the fact that water resources have the potential to be strongly affected by climate change in the long-run (Arnell, 2004; Arnell et al., 2011; IPCC, 2013). Meeting water resource requirements for various water-dependent sectors has become a crucial challenge especially in arid and semi-arid regions of the world (Shamir et al., 2015) due to the increased water demand in connection with population growth. Therefore, the quantitative representation of water resources under the changing environment is an essential tool towards selecting the appropriate sectoral-based mitigation measures regarding climate change adaptation efforts. Mediterranean Region has been identified as one of the hot-spot regions of the world suffering from water scarcity and irregular water availability (Giorgi, 2006; Hoerling et al.,

2012; Lionello, 2012). Besides, future climate simulations raise a concern regarding the substantial changes in the regime of climatic variables and water availability (Kundzewicz et al., 2008; Shen et al., 2010; Koutroulis et al., 2018). Blue and green water terminology approach put forth initially by Falkenmark and Rockström (2006) is considered as one of the convenient paradigms of water resource management (Veettil & Mishra, 2016). Blue water is defined as the amount of flow that is stored in lakes, reservoir or aquifers, whereas the water stored in soil and vegetation canopy is classified as green water (Falkenmark & Rockström, 2006; Rockström et al., 2009). Blue water supplies the demand for human consumption (Rodrigues et al., 2014), and green water is critical for crop yield (Liu et al., 2009), especially in rain-fed agriculture (Schuol et al., 2008). Blue and green water paradigm has been used to quantify water resources in numerous climate change modelling studies considering its importance for water resource planning extending from regional to global scale. For example, Gerten and Heinke (2011) compared water availability and water requirements for food production in terms of green water at a global scale. Huang et al. (2019) also evaluated the global green water consumption under climate change impacts. Faramarzi et al. (2013) and Chiarelli et al. (2016) have built a continental-scale model to evaluate both blue and green water of Africa. Moreover, numerous studies were conducted on regional-scale to predict the blue and green water under climate change in the Black Sea Catchment (Rouholahnejad-Freund et al., 2017), the Ratiran River Basin, USA, (Giri et al., 2018), the Upper Narmada Basin, India (Pandey et al., 2019). Along with the changing climate, quantifying a country's water resources has become crucial for the long-term strategic planning. In this context, plenty of country-wide water availability modeling studies was conducted. Abbaspour et al. (2009) assessed the freshwater availability of Iran as a semi-arid country. White et al. (2015) utilized the SWAT model to predict the hydrologic budgets for the USA, and the usage of blue and green water resources by four commodity crops. The future food security of China was evaluated by means of the green and blue water approach by Huang et al. (2015).

Turkiye is a trans-continental country located in the Mediterranean Region on both continents of Asia and Europe. The semi-arid country has a total area of ~780,000 km^2 with a population of ~85 million as of year 2021. It has considerably high environmental gradients; such as changes in elevation, biogeographical diversity, and several climate zones that differ distinctly. Reservoirs mostly filled by surface water are used to supply the water demand from all water-using sectors such as domestic, agricultural, industrial, and ecosystem services. Managing water resources in such a diverse geography requires a more holistic approach. Therefore, considering the impacts of climate change on the blue and green water along with sectoral water demands is a key issue to be considered in detail towards sustainable water management in Turkiye. Climate change has so far been studied over the country in numerous studies with different contexts and aims. Regional climate models were used by scientists and academicians (Onol & Semazzi, 2009; Bozkurt et al., 2012; Ozturk et al., 2013; Onol & Unal, 2014) in order to analyze the temperature and precipitation regimes under climate change impacts at a national-scale. Another country-wide study conducted over Turkiye by Sen et al. (2015) indicated a decrease in precipitation that will result in a reduction in the water resources, which will in turn, negatively affect the amount of useable water in the coming decades. Numerous studies have also been conducted to evaluate the impacts of climate change at regional-scale throughout the country (Bozkurt & Sen, 2013; Selek & Tuncok, 2014; Yürekli, 2015; Sen, 2019; Yilmaz et al., 2019; Gorguner et al., 2019). These studies made valuable and significant contributions to climate change impacts on hydro-climatic conditions in Turkiye.

The work holds valid to be the initial hydrological modelling study covering all of Turkiye through globally accepted climate change scenarios with the estimation of blue and green water availability.

Even though the current literature provides valuable information on basin-scale water management strategies, climate change impacts with respect to different aspects of sectoral water use throughout the country or inter-basin water transfers are still lacking. This study is the first attempt conducted to fill this important gap in literature. It also provides a comprehensive overview on the current water resources of Turkiye. The main goal of this study is to evaluate the changes in blue water flow and green water storage potential of Turkiye in connection to climate change projections, and water requirements of domestic, agricultural, industrial, and ecosystem sectors. In order to fulfil this purpose, an integrated approach is used by coupling regional climate models and a semi-distributed hydrologic model in order to assess the climate change impacts as a whole.

2 Material and Methods

2.1 Study Area

Turkiye (Figure 1) is distributed into 25 hydrological river basins (watersheds). Table 1 compares the gross/net and sectoral water distribution condition of the country as of year 2015.

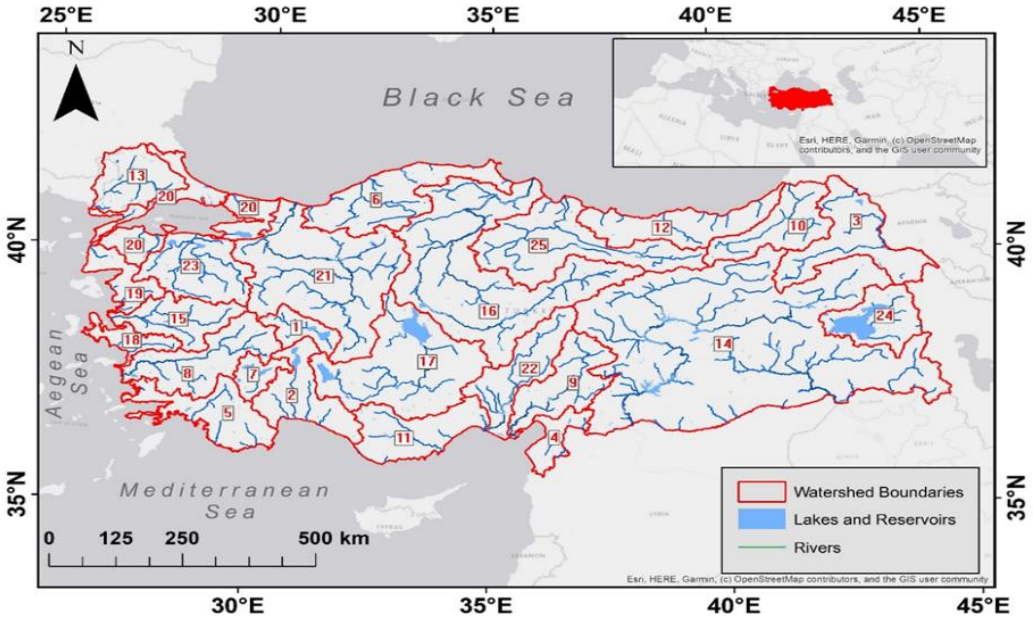


Fig. 1: Watersheds and mainstream networks of Turkiye

Table 1: Total Water Distribution Of Turkiye (2015)

Water Distribution	Turkiye (25 Watersheds)		
	Groundwater	Surface Water	Total
Gross Water Potential (million m^3/year)	19,447	186,050	205,497
Net Water Potential* (million m^3/year)	14,757	93,480	108,237
Drinking Water Allocation (million m^3/year)	2,914	7,284	10,198
Industrial Water Allocation (million m^3/year)	2,195	668	2,863
Agricultural Water Allocation (million m^3/year)	7,562	22,531	30,093
Total Water Allocation (million m^3/year)	12,671	30,483	43,154
Drinking Water Distribution (%)	23		
Industrial Water Distribution (%)	7		
Agricultural Water Distribution (%)	70		
Water Surplus (million m^3/year)	(+) 65,082		

* Technically and economically available water amount

2.2 Modelling Network

Within the scope of climate projections, outcomes of 3 global models selected from CMIP5 archive and RCP4.5 and RCP8.5 release scenarios and RegCM4.3 regional climate model forming the basis of the 5th Evaluation Report of Intergovernmental Panel on Climate Change (IPCC, 2014) were studied. A total of 8 parameters and 17 climate indices representing extreme (weather) conditions were conducted at basin-scale through model simulations covering all the watersheds of Turkiye until 2100. The studied parameters were projected as seasonal and annual averages for 10 and 30-year intervals based on the reference period accepted as of 1971-2000. Climate change simulations at 10x10 km resolution has been obtained by using start and limit conditions (ERA-40 reanalysis data) (Uppala et al., 2005) for the reference period. Followingly, the reference period climate simulations were performed with 10x10 km resolution of HadGEM2-ES, MPI-ESM-MR and CNRM-5.1 global climate models. Comparisons were made among the simulations performed with regards to the observation data of the reference period, and the simulations of the global model in order to determine the bias level of the global model. Simulations based on RCP4.5 and RCP8.5 representational concentration routes for 3 global models, and climate simulations with RegCM4.3 regional climate model for the projection period of 2015-2100 have been obtained (CCIWRT, 2016).

In the study, the Soil and Water Assessment Tool (SWAT) (Arnold et al., 1998) has been used as a precipitation-runoff model to simulate hydrological process as well as to estimate blue and green water budget of Turkiye. SWAT model, which is developed by Texas University Department of Agricultural Engineering, is a continuous-time and physically based semi-distributed model (Neitsch et al., 2011). In the model, the hydrological balance is calculated as:

$$SW_t = SW_0 + \sum_{i=1}^{t} (R_{day} - Q_{surf} - E_a - w_{seep} - Q_{gw}) \quad (1)$$

SW_t is the soil water content at time t ($mm \cdot H_2O$)

R_{day} is the precipitation on day I ($mm \cdot H_2O$)

Q_{surf} is the surface runoff on day i ($mm \cdot H_2O$)

E_a is the evapotranspiration on day i, ($mm \cdot H_2O$)

w_{seep} is the amount of the seepage to the vadose zone from soil profile on day i ($mm \cdot H_2O$)

Q_{gw} is the amount of return flow on day i ($mm \cdot H_2O$)

SW_0 is the initial soil water content

Building a hydrological model for an entire country with an area of 783,562 km^2 is a complex task that needs extensive data. In the study, the topography of the country was obtained from Space Radar Topography Mission (SRTM) data sets, where 90x90 m resolution Digital Elevation Model (DEM) was used. Land use data were obtained from the CORINE 2012 database, while the soil data was compiled from the Food and Agricultural Organization (FAO) global data sets. Meteorology data were obtained from the weather database (http://globalweather.tamu.edu/). The National Centers for Environmental Prediction (NCEP) Climate Forecast System Reanalysis (CFSR) was completed over the 31-year period from 1979 through 2009 for the meteorological data. The ArcSWAT interface was used to delineate a total of 25 river basins in Turkiye, and their sub-basins generate the necessary input files, whereas independent MATLAB based scripts were developed and used to manipulate the SWAT inputs for fine-tuning and for processing the model outputs.

Hydrogeology and irrigation areas for hydrological response unit (HRU) generation as well as irrigation and surface water-groundwater interaction were thoroughly considered to be spatially accurate. Since most of the data (such as crops, water supply, and irrigation) have been based on

administrative units (mostly provinces in Turkiye), provinces were also used to generate the HRUs. Moreover, 925 aquifers throughout the country were identified with their real attributes (such as static storage, dynamic storage as deep aquifer recharge), the ratio of confined to unconfined aquifer components, aquifer depth, etc. were identified based on 1/500,000 scaled geological and hydrogeological maps of Turkiye. The related HRU parametrization was carried out based on this information. In addition, irrigation estimates on major irrigated areas of Turkiye (more than 2,400 areas covering ~55,000 km^2) were led and utilized as well. The simulations were set up for the period of 1979-2009, where the years between 1979-1989 (end of years) were considered as the warm-up period of the model. The simulation results for 1990-2009 were averaged over time, and compared with the water budget of Turkiye obtained from State Hydraulic Works (DSI). A general overview of the modelling scheme is depicted in Figure 2 in order to summarize the models and data used.

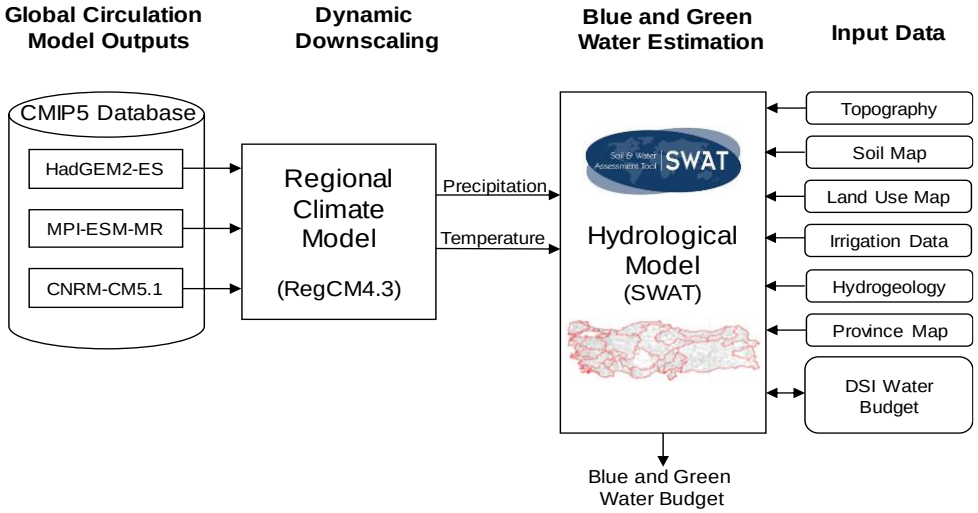


Fig. 2: Blue and green water estimation framework used in the study

At the time of this study, parallel versions of SWAT utilizing multiple CPU power were not available. The feasible solution was to divide the large Turkiye model on SWAT to 25 smaller intergrated watershed models. This was conducted enhancing the MATLAB based tool (Cerkosova et al., 2018). SWAT process results the surface water (water yield), and groundwater (deep aquifer recharge) potentials of all 25 river basins were calculated and compared at the end of the calibration process with the datasets obtained from DSI (Table 2). The two most significant components of the water budget, total flow (water yield) and groundwater potential (deep aquifer recharge), as the two most significant components of the water budget, both showed a relative deviation of + 2.3% from the reference period (1971-2000) of the SWAT model projections for Turkiye (Table 2). It has proven that the hydrological model can be used safely and accurately in climate change projections regarding all 25 river basins as well as the overall country.

Table 2: Comparison of hydrologic model estimates with the reference period for Turkiye

Water Potential Component	**Reference Period (1971-2000) Existing Data (million m^3/year)**	**Hydrologic Model Estimates for the Reference Period (million m^3/year)**	**Relative Error (%)**
Water Yield	186,050	190,383	+2.33
Deep Aquifer Recharge	19,717	20,141	+2.15
Total Blue Aquifer Flow	205,767	210,524	+2.31

3 Results and Discussions

Within the scope of this study that is based on the reference period observation data obtained from DSI (1971-2000), the blue water potential and its components have been provided as summarized in Table 3. Accordingly, Turkiye's blue water potential as calculated for the reference period with the hydrological model is given as 108.5 km^3 (instead of the total 112 km^3). Wherein the groundwater reserve gross-to-net ratios have been taken within the range of 45-99%, each taken specific to the watershed (country average: 75%) in order to calculate the groundwater potential (net deep aquifer recharge) for the overall country.

On the other hand, the gross-to-net ratio for river flows is taken as 50% for all the watersheds as Turkiye's average, in order to estimate the total surface water potential (net blue water yield). It should be noted the net amount is the technically and economically available water amount that can be retrieved from the natural resources.

Table 3: Water potential values of Turkiye obtained through hydrological modelling for the reference period

Components	**Values (km^3)**
Gross Water Yield (River Flows)	186,050
Net Water Yield	93,480
Gross Deep Aquifer Recharge	19,447
Net Deep Aquifer Recharge	14,757
Total Gross Blue Water Flow	205,497
Total Net Blue Water Flow	108,237

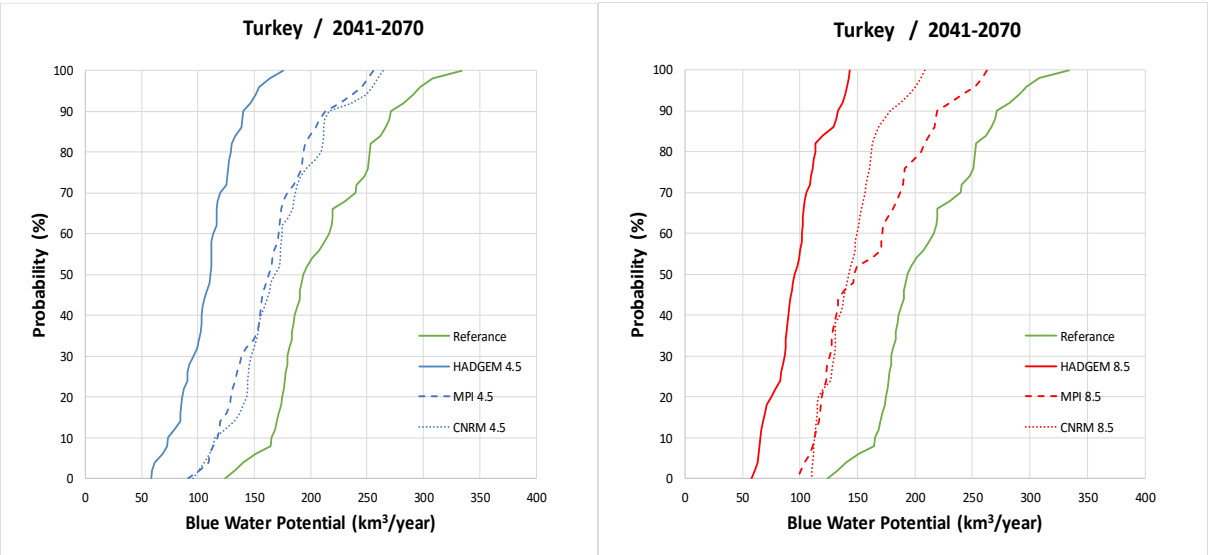
The water potential is distributed among four main water-demanding sectors (water intended for human domestic need, industry water, agricultural/irrigation water, and environmental flow). Along with the population estimations, municipal, industrial and agricultural activities specifically distinct to each watershed have been taken into consideration. The drinking and utility water (domestic/municipal water) water component takes up 23% of the total water requirement in Turkiye. Equivalent net water consumption of within the range of 100-200 L/capita-day is taken with respect to the social and economic structure of population in the basins. Watershed-based urban and rural population projections were finalized through comparison of estimates made in various national and international data sources for Turkiye. Assuming the overall water transmission network (water pipelines and distribution equipment's appurtenances) will be mostly be leak-proof over time, the decrease in water requirement due to eliminated losses has also been considered in the calculations. Agricultural water component equals to almost 70% of the total current water consumption in Turkiye. It was accepted that agricultural (mainly irrigation) water requirement will change as all areas that can be irrigated will gradually be provided with irrigation water by 2030. On the other hand, new methods and technologies, such as transition from the conventional irrigation systems to modern irrigation techniques that require less and efficient water use to provide for the same level of crop yield, and the selection of locally and environmentally suitable crop pattern is considered to be fully established by 2030. Although the water requirement of the industrial sector varies significantly among watersheds, the total of industrial water constitutes only 7% of the total water demand of the country. It should also be noted that the technically and economically unavailable water should be sufficient for the environmental flow requirements. DSI requires at least 10% of natural flow to be enabled at water structures.

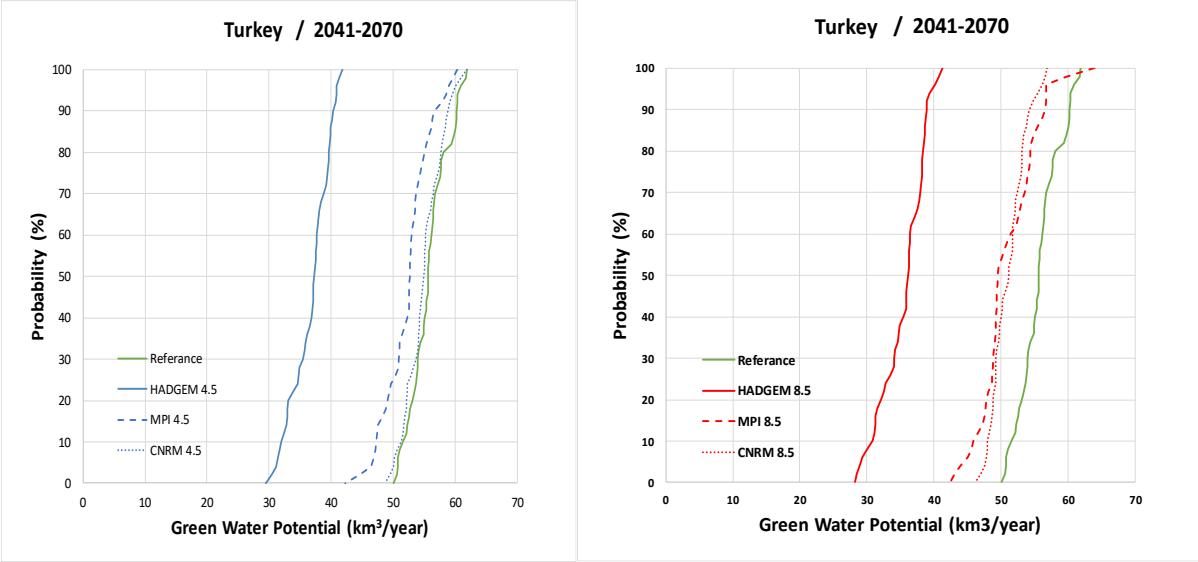
The highest water deficit throughout the century was observed in the results of both scenarios of the HadGEM2-ES model, while the other two models produced generally similar results for both scenarios with certain exceptions. In particular, it can be stated that the water deficit may become even more pronounced regarding all models and scenarios from 2050s onwards.

The water budget components estimated through hydrological modelling for 3 different global climate models and 2 emission scenarios (RCP4.5 & RCP8.5) were compared with the DSI data for the reference period within the scope of the study. Total water yield (blue water yield or surface water potential), along with groundwater supply (deep aquifer recharge), as being the most important components of water budget, showed a limited deviation (± 2.3%) relative to the reference period values according to SWAT model estimates (Table 2). The hydrological model also revealed that the relative deviation for all of the 25 watersheds of Turkiye, obtained through the same way with respect to DSI data, range from a minimum of 0.24% to a maximum of 8.90%, confirming the condition that all should be within the <10% range. Thus, it is shown that the hydrological model projections are to be safely used for both the watershed-scale and the country-scale.

In the next stage of the hydrological modelling study, the calibrated hydrological model has been re-run for the 2015-2100 period with the meteorological time series derived from the outputs of global climate models in order to finalize the hydrological projections. Projections of blue and green water obtained for 2 scenarios (RCP4.5 and RCP8.5) and for 3 different climatic climate models were analyzed in 3 consecutive (~30 year) intervals for the century. For all intervals, each model output has been accepted as an independent statistical sample belonging to the same population, and median (X0.50: 50th percentile) and 90th percentile (X0.90) values were determined by means of cumulative probability distributions (S-curves).

Figure 3 presents the blue and green water potential trends (S-curves) of Turkiye with respect to 3 models x 2 scenarios respectively for the 2nd projection period of 2041-2070 selected as the main example. While the same efforts were also given to the other projection periods, further statistical analyses have been conducted with the basic aim of validating the model outputs in the medium term, and for comparing the projected water potentials with regards to the reference values. During the 2041-2070 period where the effects of climate change in the watershed were expected to emerge clearly, the decreases in the median blue water yield with respect to the median values of the reference period are were calculated as (-)43%, (-)16%, (-)13% for the relatively optimistic (RCP4.5) scenario, and as (-)51%, (-)24%, (-)27% for the pessimistic scenario (RCP8.5), respectively for HadGEM2-ES, MPI-ESM-MR, and CNRM-CM5.1 models.





(a) **(b)**

Fig. 3: Blue and green water potential S-curves of Turkiye in 2041-2070 period for climate change scenarios of **(a)** RCP4.5, **(b)** RCP8.5

4 Conclusions

In this study, the impacts of global climate change on the blue and green water potentials of Turkiye were investigated. The hydrological modelling has been conducted for the first time in terms of the whole country-scale, where the hydrological model of SWAT has been configured based on all 25 watersheds and a total of 2480 sub-basins of Turkiye, calibrated through river flows (water yields) and deep aquifer recharges for the reference period of 1971-2000. The hydrological modelling outcomes indicated that the global climate change impacts on Turkiye's blue and green water potential will be significantly apparent especially after year 2040 (2041-2100 period).

The possible negative impacts of global climate change on blue and green water potentials of Turkiye indicate that the water demand projections of water-related sectors -particularly agriculture- needs to be reconsidered and revised further. In this context, pro-active measures that include modern irrigation methods to be expanded, measurement and pricing of irrigation water to be made accurately and accordingly, regulation of crop pattern with respect to water supply ("agriculture according to water") should be utilized for reducing the agricultural water demand, especially where critical. In watersheds that will be subjected to relatively high impacts of global climate change, it is required that sectoral water allocation planning to be made for effective and efficient management of water resources under the light of increasing climate change resilience with emphasis on water recovery and reuse. The expected 30% reduction in river flows requires the development of some water resources that are currently regarded as technically and economically unavailable (non-feasible for retrieval). The reduction of 40% in aquifer recharges reveals the need to manage underground water reserves while maintaining the sustainability of natural recharges and water balance. Similarly, the expected ~15% reduction in soil humidity (green water) may negatively affect the dry (precipitation-fed) agricultural activities along with and natural vegetation.

Such hydrological modelling studies and simulations of various scenarios may lead to further evaluations that may help the scientists working in the field of climate change and hydrology.

Projections and the outcomes derived from these studies particularly take the attention of various disciplines, such as meteorologists and environmental engineers as well as the policy-makers at both local, regional, and national levels dealing with different levels of climate change adaptation policies.

Acknowledgements

The authors would like to express their gratitıde to all scientists, academicans and policy-makers who have taken part in the "Climate Change Impacts on the Water Resources of Turkiye" Project that has been realized under the auspices of the former Ministry of Forestry and Water Affairs (MoFWA) led by a multi-disciplinary team comprised of Istanbul Technical University (ITU) members in the study period of 2013-2016.

References

Abbaspour, et al. (2009). Assessing the impact of climate change on water resources in Iran. *Water Resources Research, 45*(10). https://doi.org/10.1029/2008WR007615

Arnell, N. W. (2004). Climate change and global water resources: SRES emissions and socio-economic scenarios. *Global Environmental Change, 14*(1), 31-52. https://doi.org/10.1016/j.gloenvcha.2003.10.006

Arnell, N.W., van Vuuren, D.P. & Isaac, M. (2011). The implications of climate policy for the impacts of climate change on global water resources. Global Environmental *Change, 21*(2), 592–603.

https://doi.org/10.1016/j.gloenvcha.2011.01.015

Arnold, et al. (1998) Large area hydrologic modeling and assessment part I: Model development. *Journal of the American Water Resources Association, 34*(1), 73-89. https://doi/10.1111/j.1752-1688.1998.tb05961.x

Bozkurt, D. & Sen, O.L. (2013). Climate change impacts in the Euphrates-Tigris Basin based on different model and scenario simulations. *Journal of Hydrology, 480*, 149-161. https://doi.org/10.1016/j.jhydrol.2012.12.021

Bozkurt, et al. (2012). Downscaled simulations of the ECHAM5, CCSM3 and HadCM3 global models for the eastern Mediterranean-Black Sea region: Evaluation of the reference period. C*limate Dynamics, 39*(1-2), 207-225. https://doi.org/10.1007/s00382-011-1187-x

Cerkasova, N., Umgiesser, G. & Ertürk, A. (2018). Development of a hydrology and water quality model for a large transboundary river watershed to investigate the impacts of climate change – A SWAT application. *Ecological Engineering, 124*, 99-115. https://doi.org/10.1016/j.ecoleng.2018.09.025

Chiarelli, et al. (2016). Climate change and large-scale land acquisitions in Africa: Quantifying the future impact on acquired water resources. *Advances in Water Resources, 94*, 231-237. https://doi.org/10.1016/j.advwatres.2016.05.016

CCIWRT (2016). Climate Change Impacts on the Water Resources of Turkiye., Turkish Ministry of Agriculture and Forestry, General Directorate of Water Management, http://iklim.ormansu.gov.tr/Eng/ (accessed October 20th, 2022)

Falkenmark, M., Rockström, J. (2006). The new blue and green water paradigm: Breaking new ground for water resources planning and management. *Journal of Water Resources Planning and Management, 132*(3), 129-132. https://doi.org/10.1061/(ASCE)0733-9496(2006)132:3(129)

Faramarzi, et al. (2013). Modeling impacts of climate change on freshwater availability in Africa. *Journal of Hydrology, 480*, 85-101. https://doi.org/10.1016/j.jhydrol.2012.12.016

Gerten, et al. (2011). Global water availability and requirements for future food production. *Journal of Hydrometeorology, 12*(5), 885–899. https://doi.org/10.1175/2011JHM1328.1

Giorgi, F. (2006). Climate change hot-spots. *Geophysical Research Letters, 33*(8), L08707. https://doi.org/10.1029/2006GL025734

Giri, S., Arbab, N.N. & Lathrop, R.G. (2018). Water security assessment of current and future scenarios through an

integrated modeling framework in the Neshanic River Watershed. *Journal of Hydrology, 563*, 1025-1041. https://doi.org/10.1016/j.jhydrol.2018.05.046

Gorguner, M., Kavvas, M.L., Ishida, K. (2019). Assessing the impacts of future climate change on the hydro climatology of the Gediz Basin in Turkiye by using dynamically downscaled CMIP5 projections. Science of the Total Environment, 648, 481-499. https://doi.org/10.1016/j.scitotenv.2018.08.167

Hoerling, et al. (2012). On the increased frequency of Mediterranean drought. *Journal of Climate, 25*(6), 2146–2161. https://doi.org/10.1175/JCLI-D-11-00296.1

Huang, et al. (2015). China's water for food under growing water scarcity. *Food Security, 7*, 933–949. https://doi.org/10.1007/s12571-015-0494-1

Huang, et al. (2019). Global agricultural green and blue water consumption under future climate and land use changes. *Journal of Hydrology, 574*, 242-256. https://doi.org/10.1016/j.jhydrol.2019.04.046

IPPC (2013). Working Group I Contribution to the IPCC Fifth Assessment Report, Climate Change 2013: The Physical Science Basis. https://www.ipcc.ch/site/assets/uploads/2017/09/WG1AR5_Frontmatter_FINAL.pdf

IPCC (2014). Fifth Assessment Report, AR5 Synthesis Report: Climate Change 2014. https://www.ipcc.ch/assessment-report/ar5/

Koutroulis, et al. (2015). Exploring the ability of current climate information to facilitate local climate services for the water sector. Earth Perspectives, 2, Article number: 6. https://doi.org/10.1186/s40322-015-0032-5

Koutroulis, et al. (2018). Freshwater vulnerability under high end climate change. A pan-European assessment. *Science of the Total Environment*, 613-614, 271-286. https://doi.org/10.1016/j.scitotenv.2017.09.074

Kundzewicz, et al. (2008). The implications of projected climate change for freshwater resources and their management. *Hydrological Sciences Journal, 53*(1)3-10. https://doi.org/10.1623/hysj.53.1.3

Lionello, P. (edt.) (2012). The Climate of the Mediterranean Region, From the past to the future. ISBN 978-0-12-416042-2. https://doi.org/10.1016/C2011-0-06210-5

Liu, J., Zehnder, A. J. B. & Yang, H. (2009). Global consumptive water use for crop production: The importance of green water and virtual water. *Water Resources Research, 45*(5), W05428. https://doi.org/10.1029/2007WR006051

Neitsch, et al. (2011) Soil and Water Assessment Tool Theoretical Documentation. Temple, Texas 76502: USDA-153 ARS Grassland Soil and Water Research Laboratory, and Texas A&M University, Blackland Research and Extension Center.

Onol, et al. (2014). Evaluation of the twenty-first century RCM simulations driven by multiple GCMs over the Eastern Mediterranean-Black Sea region. *Climate Dynamics, 42*, 1949-1965. https://doi.org/10.1007/s00382-013-1966-7

Onol, B. & Semazzi, F. H. M. (2009). Regionalization of climate change simulations over the eastern Mediterranean. *Journal of Climate, 22*, 1944–1961. https://doi.org/10.1175/2008JCLI1807.1

Onol, B. & Unal, Y. S. (2014). Assessment of climate change simulations over climate zones of Turkiye. *Regional environment Change, 14*, 1921–1935. https://doi.org/10.1007/s10113-012-0335-0

Ozturk, I., Gürel, M. & Erturk, A. (2013). Effects of Climate Change on Water Resources in Turkiye, In the Proceedings of AASSA Regional Workshop, August 19-23, 2013, pp. 93-118 Barnaul, Russia

Pandey, et al. (2019). Climate change impact assessment on blue and green water by coupling of representative CMIP5 climate models with physical based hydrological model. *Water Resources Management, 33*, 141–158. https://doi.org/10.1007/s11269-018-2093-3

Rockström, J., et al. (2009). Future water availability for global food production: The potential of green water for increasing resilience to global change. *Water Resources Research, 45*(7), W00A12. https://doi.org/10.1029/2007WR006767

Rodrigues, D. B. B., Gupta, H. V. & Mendiondo, E. M. (2014). A blue/green water-based accounting framework for assessment of water security. *Water Resources Research, 50*(9), 7187-7205. https://doi.org/10.1002/2013WR014274

Rouholahnejad-Freund, E., Mikayilov, F. & Lehmann, A. (2017). Water resources of the Black Sea Catchment under future climate and landuse change projections, *Water 9*(8), 598. https://doi.org/10.3390/w9080598

Schuol, et al. (2008). Modeling blue and green water availability in Africa. *Water Resources Research, 44*(7), W07406. https://doi.org/10.1029/2007WR006609

Selek, B. & Tuncok, I.K. (2014). Effects of climate change on surface water management of Seyhan Basin, Turkiye. *Environmental and Ecological Statistics, 21*, 391–409. https://doi.org/10.1007/s10651-013-0260-5

Sen, Ö.L., Göktürk, O.M. & Bozkurt, D. (2015). Changing climate: a great challenge for Turkiye. *Journal of Black Sea/Mediterranean Environment*, Special Issue, 97-103. https://www.researchgate.net/publication/308406233_Changing_climate_a_great_challenge_for_Turkiye

Sen, Z. (2019). Climate change expectations in the upper Tigris River basin, Turkiye. Theoretical and Applied *Climatology, 137*, 1569–1585. https://doi.org/10.1007/s00704-018-2694-z

Shamir, et al. (2015). Climate change and water resources management in the Upper Santa Cruz River, Arizona. *Journal of Hydrology, 521*, 18–33. https://doi.org/10.1016/j.jhydrol.2014.11.062

Shen, et al. (2008). Projection of future world water resources under SRES scenarios: *Water withdrawal Hydrological Sciences Journal, 59*(10), 11-33. https://doi.org/10.1623/hysj.53.1.11

Uppala, et al. (2005). The ERA-40 re-analysis. *Quarterly Journal of the Royal Meteorological Society, 131*(612), 2961-3012. https://doi.org/10.1256/qj.04.176

Veettil, A. V. & Mishra, A. K. (2016). Water security assessment using blue and green water footprint concepts. *Journal of Hydrology, 542*, 589-602. https://doi.org/10.1016/j.jhydrol.2016.09.032

White, et al. (2015). Regional Blue and Green Water Balances and Use by Selected Crops in the U.S. *Journal of the American Water Resources Association, 51*(6), 1626-1642. https://doi.org/10.1111/1752-1688.12344

Yilmaz, Y. A., Sen, O. L. & Turuncoglu, U. U. (2019). Modeling the hydroclimatic effects of local land use and land cover changes on the water budget in the upper Euphrates–Tigris Basin. *Journal of Hydrology, 576*, 596-609. https://doi.org/10.1016/j.jhydrol.2019.06.074

Yurekli, K. (2015). Impact of climate variability on precipitation in the Upper Euphrates-Tigris Rivers Basin of Southeast Turkiye. *Atmospheric Research, 154*, 25-38. https://doi.org/10.1016/j.atmosres.2014.11.002

Cite as: Erturk A., Cuceloglu G., Ekdal A., Sabuncugil A.O., Kalfazade M., Yaykiran S. Tanik A., & Öztürk I., "Estimation of Blue and Green Water Potentials of Türkiye under Global Climate Change Effects", *The 2nd International Conference on Civil Infrastructure and Construction (CIC 2023)*, Doha, Qatar, 5-8 February 2023, DOI: https://doi.org/10.29117/cic.2023.0157

Efficient Turbidity Removal Using a New Gel Filtration Process

Mohammed Talhami
Department of Civil and Architectural Engineering, Qatar University, Doha, Qatar
mt1601242@qu.edu.qa

Wardan Al-Khatib
Department of Civil and Architectural Engineering, Qatar University, Doha, Qatar
wk1602800@qu.edu.qa

Obadah Dahdal
Department of Civil and Architectural Engineering, Qatar University, Doha, Qatar
od1704656@student.qu.edu.qa

Mohammad K. Hassan
Center of Advanced Materials, Qatar University, Doha, Qatar
mohamed.hassan@qu.edu.qa

Alaa H. AlHawari
Department of Civil and Architectural Engineering, Qatar University, Doha, Qatar
a.hawari@qu.edu.qa

Abstract

The removal of turbidity is a prime objective in the treatment of seawater, especially in the production of potable water. The water turbidity exists because of the colloidal particles or large-weight molecules that remain in suspension in the untreated solution. This study investigated the performance of a new gel layer for the treatment of highly turbid seawater. Based on the periodic turbidity values in the Arabian Gulf over the year, the chosen seawater samples had the turbidity values of 4.8 NTU, 76.1 NTU, and 99.7 NTU. The gel filtration layer showed promising adsorption capabilities and its physical appearance achieved a cohesive matrix form, which resulted in good mechanical strength. The proposed gel filter was effective enough for the removal of turbidity from the selected seawater samples with more than 98.5% efficiency.

Keywords: Hydrogels; Turbidity removal; Seawater; Gel filtration; Water treatment

1 Introduction

Water scarcity and contamination are worldwide concerns because of the limited freshwater resources. 97% of the available water on earth is considered saline water and only around 0.8% of the available water on earth is potable water which can be found in rivers, lakes, and underground aquifers (Gleick, 1993). The demand for freshwater is expected to increase by 20% to 30% by 2050 due to the rapid population growth and the large economic development (Boretti & Rosa, 2019). Thus, it is imperative that the focus is directed towards the innovation of strategies to obtain pure water at a low cost. One of the main impediments to desalinating seawater is the presence of organic, inorganic, and colloidal matter in the untreated water. These large-weight molecules and suspended colloidal particles are responsible for increasing the turbidity of the water. Water is defined as turbid when it is visually muddy or cloudy owing to the solid particles that remain suspended in the solution (Omar & MatJafri, 2009). More specifically, the turbidity of water is an optical property that causes

the scattering and absorbance of light rather than transmitting through the solution without changing its direction (Malik, 2018).

The most widely used technologies for the removal of turbidity today remain to be sand filtration, coagulation-flocculation, and electrocoagulation (Shaikh et al., 2021). The coagulation processes induce the formation of flocks, leading the small particles to become larger and therefore settle down in the bottom of the reactor (Palta et al., 2014). However, the filtration process allows the selective permeation of water, whereas the large and colloidal particles get rejected (Nkwonta et al., 2010). Another reliable water remediation method is adsorption which is considered an effective technique that is inherently advantageous for the removal of both inorganic and organic pollutants (Ayawei et al., 2017). The investigation for efficient adsorbents attracted immense attention in the domain of water treatment. Hydrogels have emerged as promising materials with remarkable adsorption capabilities perceived by their low cost and high treatment efficiency (Van Tran et al., 2018). Hydrogels are three-dimensional (3D) cross-linked polymeric networks formed through the reaction of one or more monomers (Ullah et al., 2015). Hydrogels are highly swollen in water and thereby can imbibe large amounts of aqueous solution and entrap and immobilize the water contaminants due to their three-dimensional cross-linked structure. Therefore, for the first time, this work proposes a gel filtration layer for the treatment of highly turbid seawater.

2 Methodology

2.1 Seawater Turbidity

Seawater was collected from the bay of the Arabian Gulf in Doha, Qatar. The average turbidity values for Arabian Gulf seawater were highly variable throughout the year, and particularly low in the second half. The maximum turbidity observed was 99.7 NTU in March. Seawater possesses high turbidity values during the first quarter of the year with the average values of 3.4, 23.2, 8.3 and 4.7 NTU in the months of January, February, March, and April, respectively. Three seawater samples with different turbidity values were chosen to assess the performance of the gel filtration capabilities for the removal of turbidity. The selected samples represent the average turbidity over the year (4.8 NTU), the average of the maximum values throughout the year (76.1 NTU), and finally, the maximum turbidity value observed (99.7 NTU).

2.2 Gel Preparation and Filtration Setup

The aluminium hydroxide hydrate gel was prepared using stoichiometric ally reagents. Sodium bicarbonate and Aluminium Sulfate salts were purchased from ALPHA CHEMIKA. The following equation (1) describes the synthesis reaction of the aluminium hydroxide hydrate gel.

$$Al_2(SO_4)_3 + 6NaHCO_3 \rightarrow 3Na_2SO_4 + 2Al(OH)_3 + 6CO_2 \quad (1)$$

All chemicals were of analytical grade. At room temperature, 53.76g of sodium bicarbonate was dissolved in 560 mL of demineralized water. Additionally, 36.4g of aluminium sulphate was dissolved in 100 mL of demineralized water. The solutions were left under magnetic stirring for 45 minutes to ensure that both salts were completely dissolved. The aqueous aluminium sulphate solution was added slowly at a rate of 20 mL/min to the sodium bicarbonate solution. The reaction was given a sufficient time to assure that CO_2 was completely emitted. The gel solution was left for 14 days for polymerisation. After the 14 days passed, the water was removed and the gel was moulded in a Büchner funnel, allowing for the formation of the filtration media. As shown in Figure

1, the feed solution was then poured into the 3mm filtration layer, and the treatment was operated using gravitation energy only.

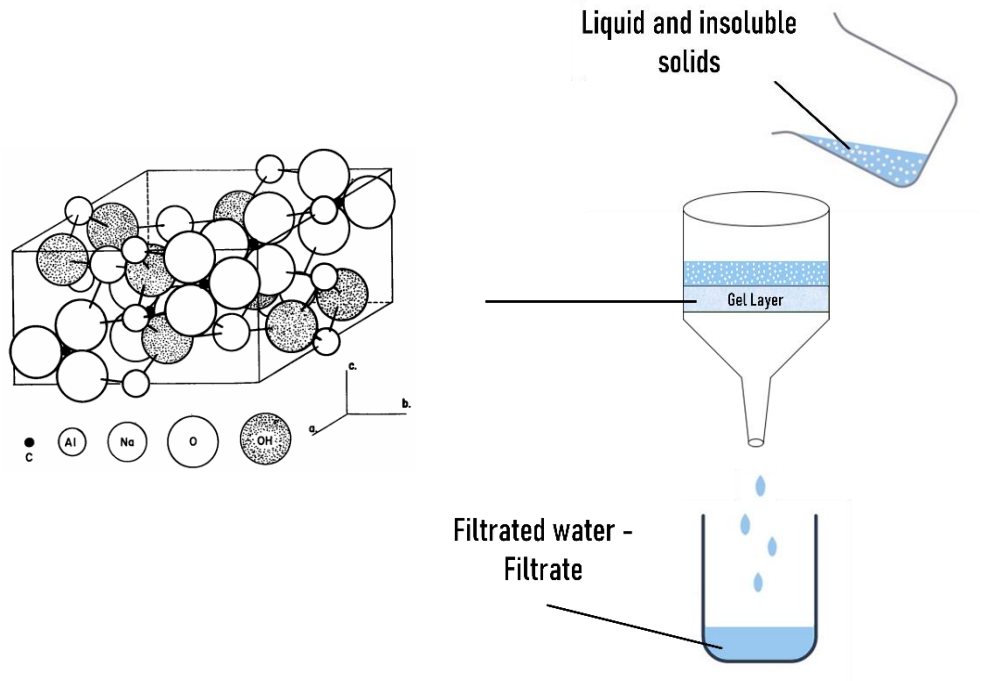


Fig. 1: Schematic drawing of the gel filtration procedure for the treatment of high turbidity seawater

3 Results and Discussion

3.1 Removal of Turbidity

After moulding the gel material in a Büchner funnel and adjusting the thickness to 3 mm, the turbid seawater was poured into the filtration layer. As mentioned previously, three seawater samples with the NTU values of 4.8, 76.1, and 99.7 were tested in the gel filtration treatment. The filtration system was operated under the gravity force only, and the filtrate of all samples was visually clear and transparent.

Table 2 shows the NTU values of the raw and treated seawater using gel filtration along with the turbidity removal percentages for the different types of feed water. The gel filtration layer showed a remarkable capacity for the elimination of turbidity to values lower than 1 NTU (>98.5% removal efficiency). The high turbidity removal potential could be attributed to the great adsorption features of the gel layer (Malekizadeh & Schenk, 2017). According to Malekzadeh et al. (2017), aluminium hydroxide hydrate gel holds great physical adsorption and mechanical straining properties.

Table 2: Turbidity Removal by gel Filtration

Feed water Sample	SW	SW	SW	Demineralized water
Before filtration	4.8 NTU	76.1 NTU	99.7 NTU	1 NTU
After filtration	0 NTU	1 NTU	1 NTU	0 NTU
% Removal	100%	98.6%	98.9%	100%

4 Conclusion

This study proposed a new gel filtration layer for the removal of turbidity from seawater. To reveal the gel filtration turbidity removal capacity, three different solutions were tested with 4.8, 76.1 and 100 NTU turbidity values. The gel filtration process removed more than 98.5% of the turbidity in the seawater, achieving 1 NTU turbidity in the filtrate. Future work includes comparing the proposed gel filtration system with other popular methods used for the removal of turbidity as well as studying the washing and recyclability aspects of the gel filtration layer.

Acknowledgement

This report was made possible by a UREP award [UREP26-012-2-006] from the Qatar National Research Fund (a member of the Qatar Foundation). The statements made herein are solely the responsibility of the authors.

References

Ayawei, N., Ebelegi, A. N. & Wankasi, D. J. J. O. C. (2017). Modelling and interpretation of adsorption isotherms.

Boretti, A. & Rosa, L. J. N. C. W. (2019). Reassessing the projections of the world water development report. 2, 1-6.

Gleick, P. H. (1993). Water in crisis. *Pacific Institute for Studies in Dev., Environment & Security. Stockholm Env. Institute, Oxford Univ. Press. 473p* 9.

Malekizadeh, A. & Schenk, P. M. (2017). High flux water purification using aluminium hydroxide hydrate gels. *Scientific reports* 7, 1-13.

Malik, Q. H. (2018). Performance of alum and assorted coagulants in turbidity removal of muddy water. *Applied Water Science* 8, 40.

Nkwonta, et al. (2010). Turbidity removal: Gravel and charcoal as roughing filtration media. 106, 1-5.

Omar, A. F. B. & MatJafri, M. Z. B. J. S. (2009). Turbidimeter design and analysis: a review on optical fiber sensors for the measurement of water turbidity, 9, 8311-8335.

Palta, S., Saroa, R. & Palta, A. J. I. J. O. A. (2014). Overview of the coagulation system, 58, 515.

Shaikh, et al. (2021). Coagulation followed by continuous sand filtration for treatment of graywater, 25, 04021032.

Ullah, et al. (2015). Classification, processing and application of hydrogels: A review, 57, 414-433.

Van Tran, et al. (2018). Hydrogel applications for adsorption of contaminants in water and wastewater treatment, 25, 24569-24599.

Cite as: Talhami M., Khatib W., Dahdal O., Hassan M. & AlHawari A., "Efficient Turbidity Removal Using a New Gel Filtration Process", *The 2nd International Conference on Civil Infrastructure and Construction (CIC 2023)*, Doha, Qatar, 5-8 February 2023, DOI: https://doi.org/10.29117/cic.2023.0158

How Efficient Would Demand-Based Water Strategies Be for Qatar?

Sophia Ghanimeh
Environmental Studies Center (ESC), Qatar University, Doha, Qatar
s.ghanimeh@qu.edu.qa

Abstract

Qatar is a water scarce country that heavily relies on seawater desalination. Multiple studies have concluded the need for a more resilient water planning through efficient "demand control" strategies. This study is among the very few attempts to "quantify" the actual impact of such solutions on the water sector. The purpose of this work is to generate "indicative" water usage figures to inform the (non-technical) decision makers and prove the benefits of shifting toward demand-based water strategies. A scenario-based approach was adopted, considering: maintaining status quo (scenario 1), improving the water pricing system (scenario 2), and regulating greywater reuse (scenario 3). Scenario 2 estimates the impact of water tariff increase based on Price Elasticity of Demand in neighbouring countries. Scenario 3 considers imposing on-site greywater reuse as part of the permitting process (for new constructions only). The study forecasted, up to year 2100, the impacts of demand control measures on: (1) domestic water consumption, (2) volume of desalinated water, (3) year by which additional desalination capacity is needed, and (4) year by which wastewater treatment facilities need expansion. It was shown that, by improving the water tariff system, the total domestic water consumption is reduced by up to 27% (equivalent to 16-19% reduction in total demand for desalinated water). As a result, the need to expand the water desalination facilities and the wastewater treatment infrastructure is delayed substantially: 15-20 years and 15-30 years, respectively. Also, regulating greywater reuse may reduce domestic water consumption by up to 6%.

Keywords: Demand-Side Water Management; Domestic water demand; Water tariffs; Greywater reuse

1 Introduction

Qatar suffers from acute freshwater scarcity, having renewable freshwater resources of 29 m^3/capita/year (2015), which is far below the global water poverty threshold of 1000 m^3 (Alhaj et al., 2017; Alsheyab & Kusch-Brandt, 2018). Yet, the country has one of the highest residential water consumption rates in the world. This is partially attributed to: (1) the hot weather, leading to a high need for water, and (2) high economic capacity of the country, making access to high-cost desalinated water affordable, among other factors. Considering the anticipated increase in population and living standards, and the expected changes in climate toward a hotter weather, the demand for residential freshwater in Qatar is expected to increase with further deficit in the water balance.

In fact, due to climate change, Qatar's mean annual rainfall has already fallen below its long-term average value of 84.9 mm/year and the mean annual temperature has increased by 0.3°C over the past four decades. Climatic projections predict a further increase in temperature of 2.3–5.9°C by 2100 (PSA, 2018; MDPS, 2018)

On the other hand, Qatar has the third largest natural gas reserve in the world and exports more than 20% of the world's liquefied natural gas (Kim et al., 2020). The high national income allowed Qatar

to meet domestic water demand using expensive desalination technologies and to distribute it to the consumers at a heavily subsidized rate (Baalousha & Ouda, 2017; Ibrahim & Shirazi, 2021).

With increasing water demand and limited freshwater supply, water demand control has been applied as a tool in integrated water resources management to balance demand and supply (Arfanuzzaman & Rahman, 2017; Xiao, 2017). Consequently, water-scarce countries have developed strategies and technologies for water conservation and increased water use efficiency (Liu et al., 2020). Several studies have addressed the potential of water conservation in households using water-saving plumbing fixtures, greywater, and rainwater harvesting. Also, the role of adequate water pricing as an economic tool for improved efficiency of water use has been investigated globally (e.g., Huang et al., 2010; Rinaudo et al., 2012; Rivers & Groves, 2013; Smith & Al-Maskati, 2007; Srouji, 2017).

In Qatar, projects that have been implemented to reduce domestic water consumption were limited to changing plumbing fixtures and promoting water saving and efficient use through conservation programs and awareness campaigns (Alghool et al., 2019). In addition, Qatar General Electricity and Water Corporation "KAHRAMAA" reduced the leakage of the water distribution network to 4% by 2016 (Kamal et al., 2021) and deployed 17,000 water meters in households, with plans to make them smart by 2024. These newly installed devices, however, are unlikely to monitor and bill more than 7.3% of households in 2020 (Hussein & Lambert, 2020).

In contrast, this study investigated the possibility of reducing residential water demand through: (1) improved water pricing, and (2) on-site greywater reuse. While these approaches are widely known to reduce household-level water demand, their actual impact on residential water needs in Qatar remains to be quantified. Even though water demand control strategies have been long advocated, the policy makers need to know how efficient those would be. In this respect, this study provides a high-level estimation of the extent of change expected upon applying demand-based strategies, specifically improved water pricing and enforcement of greywater reuse.

2 Materials And Methods

2.1 Water Demand Forecast

Water demand was projected up to year 2100 using multi-linear water demand regression models developed by Kamal et al. (2021) for the domestic, commercial, governmental, and industrial sectors in function of population, gross domestic product (GDP) and rainfall (Table 1). Acknowledging that other factors would also affect water demand forecasts, these models are considered adequate to illustrate the intensity of the impact of demand-side management – leading to further future investigations in this direction.

The overall water demand met by desalination was estimated as the sum of demand by each sector, adjusted to include the losses of the desalinated water distribution network (currently stabilized at 4%). In addition, the following consumption patterns were adopted: (1) 20 MCM/year of the domestic water demand are regularly supplied by groundwater abstraction from domestic and municipal wells, (2) 0.18 MCM/year of the industrial demand are met by groundwater withdrawal from industrial wells, (3) the commercial sector is fully supplied by desalination, and (4) around 60% of governmental water demand (including landscaping) is met by desalination while the rest is met by treated sewage effluent (PSA, 2018).

Next, the regression models were used to forecast (up to 2100) the water consumption volumes by sector under various demand scenarios. The United Nation's world population forecasts were

adopted, which include lower 95%, median, and upper 95% probabilistic projections (UN, 2019). Qatar's GDP growth was assumed to be 1.5% (Foure et al., 2012). Median annual precipitation forecasts were adopted from the Coupled Model Inter-comparison Project Phase 6 (CMIP6) projections for the following Shared Socioeconomic Pathways: SSP1–1.9, SSP1–2.6, SSP2–4.5, SSP3–7.0, and SSP5–8.5 (CCKP, 2021).

Table 1: Regression equations adopted to forecast water demand

SECTOR	Regression Model	Adjusted R^2	F-Statistic, ρ-Value ($\alpha < 0.05$)
HOUSEHOLD	$\mathrm{Hh} = 30.57771 + 147.53605\mathrm{Pop} - 0.07729\mathrm{GDP} - 0.40296\mathrm{Rnf}$	0.9507	65.22 ; $1.759*10^{-5}$
COMMERCIAL	$\mathrm{Cm} = -55.89256 + 81.96694\mathrm{Pop} - 0.34341\mathrm{GDP} + 0.05626\mathrm{Rnf}$	0.7077	9.071 ; 0.008269
GOVERNMENT	$\mathrm{Gv} = -103.39541 + 73.59485\mathrm{Pop} - 0.4746\mathrm{GDP} + 0.663756\mathrm{Rnf}$	0.7282	9.932 ; 0.006451
INDUSTRY	$\mathrm{In} = 4.63937 - 0.32591\mathrm{Pop} + 0.02608\mathrm{GDP} + 0.02805\mathrm{Rnf}$	0.6026	6.054 ; 0.0234

2.2 Scenario 1 – Status Quo

The future residential water consumption, under status-quo conditions, was estimated using the multi-linear regression model for household water demand (Table 1). Demand values were then distributed between expatriates and nationals, considering that annual per capita domestic water use by nationals is seven times higher than that of expatriates (Pandit & Osman, 2016). The present-day demographic constitution of the Qatari population was adopted, consisting of 88% expatriates and 12% nationals (Baalousha & Ouda, 2017). The total volume of collected wastewater was calculated as 40% of the water demand met by desalination (PSA, 2018).

2.3 Scenario 2 – Improved Water Pricing

The water tariff in Qatar is structured per block. The latter represents incremental ranges of household consumption. The first (lowest consumption) block corresponds to less than 20 m^3/cap/month, priced at 1.51 USD/m^3 of consumed water for expatriates and delivered at no-charge for Qataris. Most of the residential use in Qatar falls within that first block. To note that the actual cost of water production is estimated at 2.74 USD/m^3 (KAHRAMAA, 2021; PSA, 2018). There is no official statistical data providing the number of water users and water consumption, segregated per tariff block or nationality. Therefore, this study assumes a constant average consumption rate per capita (Alrefai, 2020).

The principle of price elasticity of demand (PED) was adopted to estimate the impact of increasing water tariffs on residential water consumption. The midpoint method for elasticity (Equation (1)) was used to detect the impact on both nationals' and expatriates' consumption (Srouji, 2017):

$$PED = \left|\frac{(Q_1 - Q_0)/(Q_1 + Q_0)}{(P_1 - P_0)/(P_1 + P_0)}\right| \qquad (1)$$

where P_0 and P_1 represent the initial and new marginal water price, respectively, Q_0 is the initial water demand value, and Q_1 is the new water demand value.

Given that the water PED has not been determined for Qatar, it was assumed equal to that of the

United Arab Emirates (UAE) – being a neighbour country with closely similar geographic, climatic, demographic and socio-economic setups. UAE imposed higher tariffs in 2015, charging expatriates near 4 times more than nationals who received water at 75% subsidy. Based on the change in residential water consumption within a year of implementing the reforms, an average PED of -0.23 for nationals and -0.33 for expatriates were reported (Srouji, 2017).

Assuming the same tariff increase in Qatar, nationals would pay 0.7 USD/m^3 of domestic water (subsidy of 75% as opposed to 100%) while expatriates would pay at least the full cost of water (2.74 USD/m^3). The household water demand was calculated accordingly. To note that this study assumes 100% collection of water bills – which is currently no more than 51% for expatriates and 8% for nationals (Hussein and Lambert, 2018).

2.4 Scenario 3 – Greywater Reuse

Separating greywater for reuse at the home or building level is considered a viable method to reduce the residential demand for freshwater. A recent survey proved that Qatari residents are willing to reuse treated greywater instead of desalinated water for landscaping (85-92%), toilet flushing (72-83%) and car washing (72-83%) (Lambert & Lee, 2018). Nonetheless, omitting the diluted fraction of the wastewater (that is greywater) presents drawbacks on the efficiency of the sewage treatment system due to higher concentrations of organic materials and settleable solids, among other factors. This would require reassessment and upgrading of operating system; but this is not considered within the scope of this study.

To estimate the impact of on-site greywater reuse, a minimum of 20% reduction (saving) in residential water demand was adopted. This is based on the findings of Alghool et al. (2019) for a prototype greywater reuse system implemented in a residential villa in Qatar. An upper limit of 50% saving in water demand was adopted. This is based on the findings of global studies, showing that residential water consumption can be reduced by 30-59% by greywater reuse (e.g., Kuwait: 30%, Syria: 35%; Kenya: 33-54%, Australia: 33-59%) (Samayamanthula et al., 2019).

Considering that retrofitting all households in Qatar would not be practically or economically viable, it was assumed that greywater reuse systems are implemented only in future constructions. This can be achieved by making greywater reuse system a mandatory requirement of the construction permit. The household construction growth rate and number of water users in new residential units was projected in function of the overall future population, based on the 2015 (latest) national census of population, housing and establishments (MDPS, 2016). The annual volume of water savings was calculated cumulatively for the new households, starting 2025.

3 Results And Discussions

3.1 Water Demand under Status Quo

Under the current conditions of water pricing in Qatar, residential water demand could reach 435-729 MCM by 2100. The volume of desalinated water required to meet total demand is projected at 598-1165 MCM by 2100, for the different population estimates. Following the median 95% population trend, total demand is anticipated to exceed the current supply capacity of the desalination plants (830 MCM/year) by 5%-11% between 2070-2100. Expanding the desalination units would then be required before 2040. As for the 95% upper population forecasts, expansion of the desalination capacity is anticipated around 2035, with demand exceeding supply by 40% in 2100 (Table 2).

Similarly, wastewater generation is expected to reach the current treatment infrastructure capacity (353 MCM/year), under the median population estimates, between 2060-2080. For the upper 95% population projections, wastewater generation could increase to 449 MCM in 2100, thus surpassing the treatment capacity by 27%. Expansion of the wastewater collection and treatment infrastructure would then be required before 2045 (Table 2).

Table 2: Impacts of maintaining status quo

	Lower 95% population forecasts *(% increase with respect to 2022)*	**Median population forecasts** *(% increase with respect to 2022)*	**Upper 95% population forecasts** *(% increase with respect to 2022)*
Residential Water Demand in 2050 (Mcm/Year)	522 (+16%)	558 (+24%)	591 (+31%)
Residential Water Demand in 2100 (Mcm/Year)	435 (-4%)	578 (+28%)	729 (+62%)
Volume of Desalinated Water Needed by 2050 (Mcm/Year)	816 (+26%)	885 (+37%)	950 (+47%)
Volume of Desalinated Water Needed by 2100 (Mcm/Year)	597 (-8%)	875 (+35%)	1164 (+80%)
Year by Which Upgrade of Desalination Capacity is Needed	None	2040	2035
Volume of Wastewater Generated by 2050 (Mcm/Year)	315 (+21%)	341 (+32%)	366 (+41%)
Volume of Wastewater Generated by 2100 (Mcm/Year)	230 (-11%)	337 (+30%)	449 (+73%)
Year by which Upgrade of Wastewater Treatment Capacity is Needed	None	2060	2045

3.2 Impact of Improved Water Pricing

Residential water demand is expected to drop by 27% following the implementation of the proposed tariff reforms, reaching 315-529 MCM by 2100 under all population projections, while the total water consumption could decrease by 16%-19% (485-977 MCM in 2100). Therefore, the current supply capacity of the desalination units is exceeded by 18% in 2100 only for the upper 95% population projections, and the desalination infrastructure should be expanded starting 2055 (Table 3).

Similarly, increasing water tariffs is expected to reduce the volume of generated wastewater to 187-376 MCM by 2100 (a drop of 16%-19%). Consequently, expanding the wastewater treatment infrastructure would not be needed before 2075 under upper 95% population forecasts (Table 3).

Hence, higher water tariffs could reduce the pressure on desalination plants by stabilizing water demand below their current supply capacity and delaying the need to expand the desalination and water supply infrastructure by 15-20 years within the time horizon 2025-2100. This would also alleviate the pressure on the wastewater treatment infrastructure by delaying the need for expansion by 15-30 years.

Table 3: Impacts of increased water tariffs

	Lower 95% population forecasts *(change with respect to status-quo)*	**Median population forecasts** *(change with respect to status-quo)*	**Upper 95% population forecasts** *(change with respect to status-quo)*
Residential Water Demand in 2050 (Mcm/Year)	379 (-16%)	405 (-10%)	429 (-5%)
Residential Water Demand in 2100 (Mcm/Year)	315 (-30%)	420 (-7%)	529 (+17%)
Volume Of Desalinated Water Needed by 2050 (Mcm/Year)	682 (+5%)	741 (+14%)	797 (+23%)
Volume Of Desalinated Water Needed by 2100 (Mcm/Year)	485 (-25%)	726 (+12%)	977 (+51%)
Year by Which Upgrade of Desalination Capacity is Needed	None	None	2055
Volume of Wastewater Generated by 2050 (Mcm/Year)	263 (+1%)	286 (+10%)	307 (+19%)
Volume of Wastewater Generated by 2100 (Mcm/Year)	187 (-28%)	280 (+8%)	376 (+45%)
Year by Which Upgrade of Wastewater Treatment Capacity is Needed	None	None	2075

3.3 Impacts of Greywater Reuse

The impact of reusing treated greywater in future households on residential water consumption was studied (Table 4). Based on the local figure of 20% reduction in residential water consumption, the total volume of recycled greywater could amount to 4-18 MCM in 2100 for the different population estimates, reducing domestic demand to 424-683 MCM. However, by achieving 50% savings in household water use, similar to global rates, the total volume of reclaimed greywater could reach 11-46 MCM. Overall, greywater reuse has the potential to save up to 6% the country's domestic water demand.

Table 4: Impacts of greywater reuse

	Lower 95% population forecasts	**Median population forecasts**	**Upper 95% population forecasts**
Freshwater Savings in 2050 (Mcm/Year)	4-11	7-17	9-24
Freshwater Savings in 2100 (Mcm/Year)	4-11	9-21	18-46
Reduction in Domestic Water Demand (%)	1% - 2.5%	1.5% - 3.7%	2.5% - 6.3%

4 Conclusions and Recommendations

Qatar is a water scarce country, relying mainly on desalination to supply the water needed for domestic usages. Reducing the demand on domestic water would reduce both the expenses and the environmental impacts of the water management system. This study revealed that increasing water

price could substantially lower residential water consumption (by up to 27%) and delay the need to expand the desalination infrastructure (past the year 2055). On the other hand, integrating greywater treatment and reuse (in new constructions only) could save up to 6% of the household water demand. Based on these findings, specific actions are recommended to transition into a more sustainable demand-side water management scheme.

The observations made in this paper are based on high-level assumptions and averaged rates. They are fairly accurate for a paradigm shift and informed strategic decisions. Yet, in order to produce high-accuracy forecasts, the following future work is recommended:

- Elaborate water metering that captures water consumption patterns, categories and variables needed to calculate location-specific PED values and forecast water demand based on socio-economic variables and climatic changes; and
- Conduct a detailed technical and social analysis to evaluate the potential of reusing greywater in various residential applications and allow spatial and temporal estimation of water savings across the country.

References

Alghool, et al. (2019). "Perspectives on dual-purpose smart water power infrastructures for households in arid regions", Electric power conversion, Găiceanu Marian, IntechOpen, London, 113–130.

Alhaj, et al. (2017). "A review of Qatar's water resources, consumption and virtual water trade", *Desalination and Water Treatment, 90*, 70–85.

Alrefai, B. Mohammad (2020). "Price elasticity and determinants of residential water consumption in Al Ain region", Master's thesis, United Arab Emirates University.

Alsheyab, Mohammad A.T. & Kusch-Brandt, Sigrid (2018). "Potential recovery assessment of the embodied resources in Qatar's wastewater", *Sustainability,10,* 9, 3055.

Arfanuzzaman, Md. & Rahman, A. Atiq (2017). "Sustainable water demand management in the face of rapid urbanization and ground water depletion for social–ecological resilience building", *Global Ecology and Conservation, 10*, 9–22.

Baalousha, H. M. & Ouda, O. K. M. (2017). "Domestic water demand challenges in Qatar", *Arabian Journal of Geosciences, 10*, 537.

CCKP. (2021). "Qatar-Climate projections". https://climateknowledgeportal.worldbank.org/country/qatar/climate-data-projections. Accessed 9 August 2022

Foure, et al. (2012). "The great shift: Macroeconomic projections for the world economy at the 2050 horizon, CEPII Working Paper No. 2012-3.

Huang, et al. (2010). "Irrigation water demand and implications for water pricing policy in rural China", Environment and Development Economics, 15, 3, 293–319.

Hussein, H. & Lambert, L. A. (2020). "A rentier state under blockade: Qatar's water-energy-food predicament from energy abundance and food insecurity to a silent water crisis", *Water, 12*, 4, 1051.

Ibrahim, A. J. & Shirazi, N. S. (2021). "Energy-Water-Environment Nexus and the Transition towards a Circular Economy: The Case of Qatar", *Circular Economy and Sustainability, 3*, 835–850.

KAHRAMAA, (2021). "Tariff". http://www.km.com.qa/customerservice/pages/tariff.aspx.

Accessed 2 September 2022

Kim, et al. (2020). "Swing suppliers and international natural gas market integration", *Energies,13*, 18, 4661.

Lambert, L. A. & Lee, J. (2018). "Nudging greywater acceptability in a Muslim country: Comparisons of different greywater reuse framings in Qatar", *Environmental Science & Policy, 89*, 93–99.

Liu, et al. (2020). "Individual Water-Saving Response Based on Complex Adaptive System Theory: Case Study of Beijing City, China", *Water, 12*, 1478.

MDPS. (2016). "Analysis of the results of population, housing and establishments census 2015", Ministry of Development Planning and Statistics, Doha, Qatar.

MDPS. (2018). "Qatar Second National Development Strategy: 2018-2022", Ministry of Development Planning and Statistics, Doha, Qatar.

Pandit, M. & Osman, Mohammed (2016). "Expats use seven times less water than Qataris", Zawya, Business. https://www.zawya.com/en/business/expats-use-seven-times-less-water-than-qataris-dab28c3l. Accessed 3 June 2022.

PSA (2018). "Water statistics in the state of Qatar 2017", Planning and Statistics Authority, Doha, Qatar.

Rinaudo, Jean-Daniel, Neverre, N. & Montginoul, M. (2012). "Simulating the impact of pricing policies on residential water demand: a Southern France case study", *Water Resources Management, 26*, 7, 2057–2068.

Rivers, N. & Groves, S. (2013). "The Welfare Impact of Self-Supplied Water Pricing in Canada: A Computable General Equilibrium Assessment", *Environmental & Resource Economics, 55*, 419–445.

Samayamanthula, D. R., Sabarathinam, C. & Bhandary, H. (2019). "Treatment and effective utilization of greywater", *Applied Water Science, 9*, 90.

Smith, M. & Al-Maskati, H. (2007). "The effect of tariff on water demand management: implications for Bahrain, Water Science & Technology: *Water Supply, 7*, 4, 119–126.

Srouji, H. (2017). "The impact of residential water price increases and subsidy reductions on elasticity of demand in Abu Dhabi city", Master's thesis, Harvard Extension School.

UN (2019). "World population prospects 2019". https://population.un.org/wpp/Download/Standard/Population/. Accessed 3 June 2021.

Xiao, Y. (2017). "Basin-wide Water Demand Management: Transfers and Compensation among Competing Users". UWSpace.

Cite as: Ghanimeh S., "How Efficient Would Demand-Based Water Strategies Be for Qatar?", *The 2nd International Conference on Civil Infrastructure and Construction (CIC 2023)*, Doha, Qatar, 5-8 February 2023, DOI: https://doi.org/10.29117/cic.2023.0159

Improvement in Environmental Management Performance in Ashghal Projects

Abdel Rahman Tariq A. Abdel Rahman
Quality & Safety Department (Environment Section), Public Works Authority (Ashghal), Doha, Qatar
aabdulrahman@ashghal.gov.qa

Maitha Al-Naimi
Quality & Safety Department (Environment Section), Public Works Authority (Ashghal), Doha, Qatar
malnaimi2@ashghal.gov.qa

Hany Mohamed A. Hussein
Quality & Safety Department (Laboratories Section), Public Works Authority (Ashghal), Doha, Qatar
hhussein66@ashghal.gov.qa

Aysegul Korur
Quality & Safety Department (Environment Section), Public Works Authority (Ashghal), Doha, Qatar
akorur2@ashghal.gov.qa

Abstract

The Public Works Authority (Ashghal) of Qatar is responsible for countrywide infrastructure and public building projects starting from their planning stages and through design, procurement, construction, operation, and maintenance stages. This includes highways, local roads, surface water drainage networks, foul sewers, treated sewage effluent systems, schools and hospitals. Considering the large number of projects with construction activities ongoing at the same time, it is a challenge to develop a unique and standardized tool for monitoring of environmental management performance of each project, each department or Ashghal wide. Being a supportive department to all other Ashghal departments, with a main role of ensuring the conformity of projects to environmental regulations and standards, Quality and Safety Department (QSD) of Ashghal has started several initiatives to improve environmental management performance of projects. This paper provides a brief information about some of those initiatives, such as a portal for monthly reporting of environmental management performance (EPMS), a unique annual award which was developed to increase awareness for sustainable practices in construction and assist in guiding minimization and/or reduction of adverse environmental impacts caused by construction projects (Ashghal Green Award); and a list of Ashghal approved third-party environmental service providers which will be used as a vendor list in all Ashghal projects. In addition, Ashghal QSD chemical and microbiological laboratories as well as mobile noise and air quality monitoring trucks serve to support projects departments to improve environmental impacts resulted from construction activities on the environmental sensitive receptors located within or nearby the project.

Keywords: Ashghal (Public Works Authority of Qatar); Environmental Management Performance; Monthly reports; Green award; Third Party Environmental Management Services

1 Introduction

In 2004, the Public Works Authority Ashghal in Qatar was given the responsibility of planning, design, procurement, construction, delivery, and asset management of all infrastructure projects and public buildings in the country. This scope includes roads, parks, cycling lanes, infrastructure such as storm water collection and groundwater lowering systems, foul sewer network, treated sewage

effluent (TSE) network as well as buildings such as public buildings, schools, and health centres. In this regard, Ashghal's Expressway Programme has developed and currently constructing some of the largest expressways in Qatar. Similarly, Ashghal's Local Areas Infrastructure Programme has a scope of delivering many roads and integrated infrastructure projects in local areas. Ashghal developed its corporate strategies in parallel with the Qatar National Vision 2030 with a vision of excellence in delivery and efficient sustainable infrastructure management. In this regard,

Ashghal is not only designs, constructs, delivers all its projects, but it is also responsible for operating and maintaining of roads and drainage networks including wastewater treatment plants, pump stations and outfalls. Effective execution of its operations and customer satisfaction are vital to Ashghal's mission.

Quality and Safety Department (QSD) of Ashghal has been developed to ensure the conformity of the projects to the specifications and technical standards as well as to develop an integrated system for environmental management and coordination between its departments.

2 Current Status and Initiatives

Ashghal is comprised of the following departments that manage several construction projects:

- *Highway Projects Department*: This department is responsible for the implementation of Expressways Programme, which is planned to complete the construction of approximately 800 km of roads with more than 40 contracts. Scope of the contract includes not only construction and development of an infrastructure network with underground utilities, but also surface water networks and intelligent transportation systems. The programme also includes beautification schemes to deliver cycling paths, and assets for pedestrians (i.e.., pedestrian tunnels and bridges).
- *Road Projects Department*: This department is responsible for the implementation of Local Roads and Drainage Programme, which includes development of specifically local roads and overall infrastructure, i.e., surface water networks, foul systems, treated sewage effluent networks of Qatar. This programme aims to raise the standard of living for all citizens and residents.
- *Drainage Networks Projects Department*: This department aims to develop and upgrade the drainage system in various areas of Qatar as well as to construct an infrastructure network in newly developed areas.
- *Buildings Projects Department*: This department of Ashghal manages and constructs public buildings for multiple sectors in Qatar and hands over those to the end-users. The building projects include educational projects, health centres, mosques, and endowments, etc.
- *The Supervisory Committee for Beautification of Roads and Public Places in Qatar*: Ashghal aims to provide a sustainable environment for the community through its Beautification Committee projects. These projects include beautification schemes all around Qatar such as public parks and beaches, street furniture, decorative lighting as well as pedestrian crossings and cycling paths.

Following the execution of above-stated programmes and projects, Ashghal completed more than 1,800 km of roads, 207 bridges and 143 tunnels in the past years. Similarly, construction of approximately 2,130 km of pedestrian and cycling paths, 16 pedestrian bridges and five pedestrian tunnels started serving the community. In order to promote environment, more than 900,000 trees were planted, and 11 parks and green places were developed.

Briefly, there are several projects managed by different departments simultaneously, which has different contractors and construction supervision consultants. In order to achieve the best practice environmental management applications and to improve environmental management performances,

the following initiatives have been developed by QSD:

- Environmental Management Performance Monitoring System (EPMS);
- Third Party Environmental Consultancy Services;
- Ashghal Green Award Programme; and
- Laboratories.

2.1 Environmental Management Performance Monitoring System (EPMS)

EPMS is a monthly questionnaire related to environmental management which includes the information (categories) to be provided about staffing, permitting, monitoring, reporting, non-conformances, waste management, recycling of construction waste, carbon footprint related to energy consumption, etc. specific to each project. Each category has its own specific question to be responded with necessary evidence. EPMS is being submitted monthly for review and approval. EPMS is available and accessible by Ashghal President, Department Managers, Project Engineers and Consultant Environment Team. As EPMS is linked to a scoring system, it allows projects to focus on the areas for improvement where the scores are low. Enhancing the performance helps in raising awareness in environment compliance, commitment to apply the best environmental practices as well as implementation of environmental control plans and mitigation measures.

2.2 Third Party Environmental Consultancy Services

Selecting the right company/service provider for a project reduces the risks associated environmental permitting and management, which will result in improved performance as well as better acceptance by the communities experiencing the project.

QSD of Ashghal started to establish a list of companies/service providers to work in environmental management and sustainability in Qatar (specifically in Ashghal projects). The eligible competent companies/service providers would be able to provide services in any Ashghal projects.

The approved list of company/service providers required for Ashghal projects will be published periodically and will be reached through Ashghal internet page. Any services related to environmental management and sustainability required for Ashghal projects will be limited with the service providers included in this list.

Purpose of this initiative is to set a level for third party qualifications, to achieve consistency in the level of service and to expediate the submissions for timely delivery of projects.

2.3 Ashghal Green Award Programme

Ashghal has developed the Ashghal Green Award Programme to promote and assess environment and sustainability management in design and construction, as well as recognize best practices and outstanding performances on an annual basis. The Green Award is a unique initiative created to increase awareness for sustainable practices in construction and assist in guiding Qatar's engineering industry to eliminate and/or reduce adverse impacts caused by construction projects. Accordingly, the Green Award is developed to directly achieve Ashghal's Strategic Objectives, Qatar's National Development Strategy 2018-2022 & 2023-2030 and accelerate the realisation of Qatar's National Vision 2030 (QNV 2030).

Core principles of the Green Award that promote the sustainable development of Qatar are Continual Improvement as well as Environmental, Economic, Social and Human Development. The purpose of the Green Award is multifaceted and encourages various sustainability objectives detailed at national, institutional, and programmatic levels.

The effort to achieve the above-mentioned objectives will be used as a mechanism to identify and tackle the various challenges encountered with all PWA's projects and achieve sustainability goals that will continually improve the industry model.

The Green Award was initiated in 2018 with applicant under Road Project Department only. In 2019 and 2020, the applicants were extended to wider Ashghal departments and finally Green Award 2022 was made open to all projects managed by Ashghal (i.e., projects in design, construction as well as operation and maintenance). The criteria of assessment included the following:

- Environmental benefit (including carbon footprint);
- Socio-economic benefit;
- Cost saving;
- Support of top management;
- Innovation;
- Possible adoption by others; and
- Submission presentation.

2.4 Laboratories

QSD has chemistry and microbiology laboratory units where water and soil tests are conducted as well as mobile air quality and noise monitoring stations. QSD uses these facilities to support engineers and projects where required. Dewatering discharge samples are being tested in chemistry and microbiology laboratory units where public complaints related to air quality and noise emissions will be assessed further with air quality and noise monitoring stations.

3 Benefits, Business Impact and Future Applications

Regarding EPMS application, centralization and standardization of environmental data and developing a database is a critical step in Ashghal since more than 150 projects are currently under construction with various scopes. Receiving environmental data in a standardized system is a critical step to develop a baseline and plan for improvements with a high number of infrastructure projects on going simultaneously. Since the establishment of EPMS in May 2022, high commitment from Ashghal's projects was evident, i.e., more than 90% of the projects were involved within three months after launching. In addition, EPMS has become one of the conditions of Construction Environment Management Plan (CEMP) approvals, i.e., acceptance of a CEMP is mandatory for all Ashghal projects before the commencement of construction activities.

EPMS will change the business culture from working as part of an insular team/department to working as one team/organization. EPMS will help project teams not only monitor their projects' environmental management performance, but also review existing resources in advance and share resources, where available. It will improve project planning in general, but it will be a great support specifically during mobilization. Database will also be used for future analysis and improvement in environmental management as well as for corporate reporting related to environmental management and sustainability.

A future improvement plan is to link the EPMS database to Ashghal's Geographic Information System (GIS). This plan will assess overcoming the challenge that Qatar is limited with its resources (e.g., site offices, water discharge locations, material storage areas, etc.). Another challenge that the GIS will simplify is the high number of infrastructure projects (i.e. more than 150) on going simultaneously. Linking EPMS to the GIS database will help to oversee existing facilities in the vicinity of projects, which

will enhance sharing of information among all Ashghal departments about the current and previous site facilities. In this regard, project departments will be able to consider utilizing the existing facilities for their projects, which will save time and resources, as well as reduce transportation costs and carbon emissions associated with transportation and construction activities.

QSD has not yet developed a list for third party service providers in environmental management and sustainability. However, the process started and it is currently on going. It was planned to have an initial list in the first half of 2023.

Ashghal Green Award was initiated in 2018, with 13 participants only from Ashghal's Road Projects Department project contractors, but it has been evolving since. In 2022, the competitiveness was enhanced, and the award was open to all Ashghal projects, which are in design and construction phases. Green Award 2022 categorized the competition entry, unlike the previous, i.e., Green Design, Green Project, Excellence in Waste Management, Excellence in Construction Materials, and Excellence in Energy Efficiency (Carbon Footprint Reduction).

Green Award Programme creates a friendly environment where a professional competition takes place. Others are promoting the best practices for adoption and lessons learnt are being shared for improvement and for a better environmental management performance. Contactors are also positive with this initiative since it is a platform for the winners to present themselves in front of the community and regional construction market.

QSD's chemistry and microbiology laboratory units as well as air quality and noise monitoring stations are being used to support Ashghal projects when required. However, QSD's plan for Year 2023 is to develop a monitoring plan to include random testing dewatering discharges and conducting air quality and noise monitoring campaigns based on the public complaints and/or departments requirements. The outcome of these studies together with QSD's recommendations for a better environmental management performance are planned to be shared with the project engineers for continuous improvement.

4 Conclusion

Ashghal has its own environmental objectives which are effectively included and implemented in its corporate strategies, i.e., to ensure on-time delivery without compromising on the quality of deliverables and improve the on-time delivery performance across the complete asset lifecycle; and to enhance sustainability, recycling, and its supply chain's resilience and environmental credentials through increased use of recycled materials. In doing so, the environmental aspect of the business is prioritized and monitored.

Improvement in environmental management performance is an on-going process and Ashghal wants to show all its support to the stakeholders through implementing several initiates, which are developed from lessons learnt throughout years and feedback, received from project partners (engineers, consultants, contractors, and stakeholders).

References

Ashghal Media Hub - http://portal/en/Media/Pages/news13112022-1.aspx

Cite as: Abdel Rahman A.R.T.A, Al-Naimi M., Hussein H.M.A. & Korur A., "Improvement in Environmental Management Performance in Ashghal Projects", *The 2nd International Conference on Civil Infrastructure and Construction (CIC 2023)*, Doha, Qatar, 5-8 February 2023, DOI: https://doi.org/10.29117/cic.2023.0160

Emerging Brine Management Approaches for Sustainable Desalination in the GCC Countries

Syed Javaid Zaidi
UNESCO Chair on Desalination and Water Treatment, Center for Advanced Materials, Qatar University, Doha, Qatar
szaidi@qu.edu.qa

Haleema Saleem
UNESCO Chair on Desalination and Water Treatment, Center for Advanced Materials, Qatar University, Doha, Qatar
haleema.saleem@qu.edu.qa

Hammadur Rahman Siddiqui
UNESCO Chair on Desalination and Water Treatment, Center for Advanced Materials, Qatar University, Doha, Qatar
h.siddiqui@qu.edu.qa

Abstract

The major technologies employed in Gulf Cooperation Council (GCC) based commercial desalination facilities are classified into two categories: the membrane-based (mostly reverse osmosis (RO)) and thermal-based (primarily multi-stage flash distillation (MSF)). Currently, the GCC nations are in a process of changing the current desalination facility completely or partly by RO technology. In desalination facilities, 40 % of the feed water is fresh water and the balance 60 % is the discharged brine. For the Arabian Gulf, the brine disposal as well as wastewater disposal are important. This work examines trend in desalination capacity and electricity consumption in GCC nations, the Unified Water Strategy in GCC as well as examine the emerging technologies that show promise from an environmental standpoint. Several new brine management technologies, including pressure retarded osmosis system, greenhouse desalination, different hybrid technologies like reverse electrodialyzed-based and electrodialysed-based hybrid systems have been examined in this study. According to the results of our study, desalination plants' innovative strategies are suitable and advantageous for reducing energy consumption as well as for environmental sustainability. On a commercial level, we recommend that more research is necessary to evaluate the effectiveness, applicability, and sustainability of these solutions. Additionally, we encourage greater research to be done on approaches that have the least negative environmental effects and the most readily available renewable energy sources in the GCC countries, such as wind and solar energy.

Keywords: Desalination; Brine Management; Pressure Retarded Osmosis; Greenhouse Desalination; Electro-dialysis

1 Introduction

Because of the growing population and the excessive use of easily accessible freshwater supplies, the reliance on desalinated water has been steadily growing. The Arabian Gulf is enclosed by desalination plants with approximately 50% of global capacity for desalinating seawater. Commercial-scale desalination plants established in the Gulf Cooperation Council (GCC) primarily use two types of technologies: membrane-based (mainly reverse osmosis) and thermal-based (mostly multi-stage flash distillation (MSF) technologies. Currently, all the GCC countries are in a process of adjusting

their existing desalination plant partially or completely by reverse osmosis (RO) process technology. Most of these desalination facilities discharge brine, or hypersaline wastewater, into the Gulf via nearshore and surface outfalls. Brine, also termed as concentrate, is the main seawater pollutant, and has an adverse effect on the surroundings because of its higher salinity and high temperature. The feed water used in desalination technologies will be converted to 40.0% potable water and the rest 60.0% discharge brine. For the Arabian Gulf, wastewater and brine disposal is crucial. The brine may also contain harmful pretreatment chemicals, heavy metals, and organics in addition to its greater salinity. Therefore, having affordable and practical brine management devices is crucial for lowering environmental pollution. This study analyzes the new technologies that show promise when taking the environment into account, as well as the trends in GCC desalination capacities, electricity consumption, and the GCC Unified Water Strategy. Several cutting-edge brine treatment technologies, including pressure retarded osmosis systems, greenhouse desalination, and various hybrid systems, including reverse electro-dialysed-based hybrid systems and electro-dialysed-based have been examined in this study.

2 GCC-Based Desalination Plants Capacity

In the GCC nations, a water shortage condition is expected with the water stress level considered as serious mainly because of the population growth rates, exhaustion of non-renewable subsurface water, high evaporation rates, low rainfall, and high industrial growth rate. The annual per capita renewable water obtainability in the GCC nations has reduced quickly during years 1962 - 2010. The stated annual per capita of renewable water changed from a lower value of 33 m^3 in Qatar, 20.0 m^3 in UAE, 7.3 m^3 in Kuwait, 92.0 m^3 in Bahrain to a greater value of 503.0 m^3 in Oman. Among the total 17346 online and contracted desalination plants across the world, 7499 of them are situated in the GCC nations. Out of the different GCC Countries, Saudi Arabia has the highest population and thus has the highest number of plants as well as total capacity followed by UAE. Figure 1 is the world and GCC desalination capacities trend during years 1985-2030. By 2030, installed desalination capacity is expected to doubled both globally and in the GCC. Figure 2 presents the GCC nations' electricity requirement trend from 2011 to 2050 in Terawatt-hour (TWh). The yearly electricity requirement in the GCC would rise from 467.0 Terawatt-hour in 2011 to almost 1,400 Terawatt-hour in 2030 and extending almost 2,000 TWh in the year 2040. Simultaneously, the requirement for potable water in the GCC would rise remarkably from 6,470 Gigaliter in 2011 to 16000 Gigaliter in 2030 as well as 21000 Gigaliter in 2040.

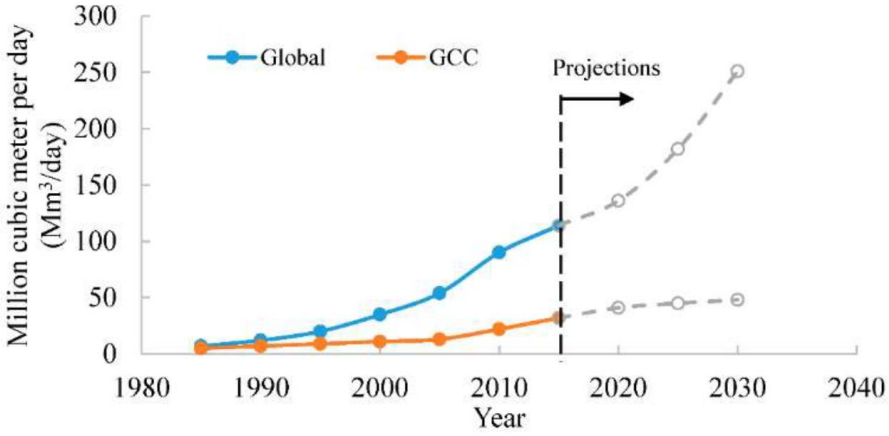


Fig. 1: World and GCC desalination capacities trend from the years 1985 to 2030

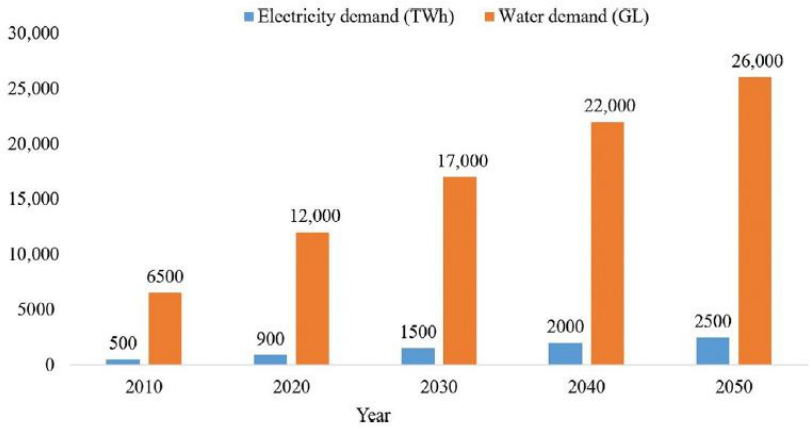


Fig. 2: Trend of GCC electricity demand in the years 2011- 2050 (TWh)

3 Unified Water Strategy in Gcc

The Gulf Cooperation Council Supreme Council and the GCC Secretariat General confirmed and endorsed a GCC Unified Water Strategy, 2016-2035, in 2016. The establishment of this strategy signifies a key breakthrough for the intricate as well as long path for dealing with the water shortage in the water stressed Gulf Cooperation Council countries. The goal of the general strategy is to launch a "sustainable water sector management system" in all the GCC nations while preserving long-term water supplies and adhering to stringent public health and environmental sustainability standards.

The programs, objectives, and policies of the strategy are steered by the succeeding principles:

- Achievement of highest international standards of service delivery in water supply as well as sanitation to the Gulf Cooperation Council growing population;
- Implementation of applicable water governance (legislation, transparency, participation, institutions, accountability and decentralization);
- Enhancing water awareness of the Gulf Cooperation Council societies;
- Implementing integrated supply as well as demand driven approach in entire water consuming sectors as well as concentrating on demand management, water efficiency, as well as conservation;
- Water valuation in the Gulf Cooperation Council nations;
- Integrating upcoming effects of climate variation by combining proper adaptation measures in water resources planning as well as management;
- Encouraging research as well as development, and groundbreaking technological solutions in the water sector;
- Employing a water, energy, and food nexus strategy to plan as well as manage the water sector;
- Improving national and institutaional human resources;
- Effective collaboration on the regional as well as global water agenda.

The Gulf Cooperation Council countries execution of the strategic objectives as well as policies set in the strategy will lead to several succeeding advantages in addition contributes to the developmental

goals of the Gulf Cooperation Council nations, will support for ensuring the consistent water supplies nowadays and for upcoming generation, and improve the overall level of water security.

4 Emerging Technologies for Brine Treatment

4.1 Greenhouse desalination

The present dependence of the GCC countries on fossil oil as well as gas is imprudent with respect to economic and environmental sustainability. The renewable energy use in the desalination field is an inspiring concept for reducing the enormous energy costs related to the desalination process. GCC countries should consider the use of renewable energy to deal with the price variations of oil and gas in the global market and for lowering the emission of greenhouse gases. The newly developed seawater greenhouse technology demonstrates a potential source of clean water for irrigation purpose in locations where just seawater or saline ground water are available. In greenhouse desalination, it is possible to decrease the brine volumes using the evaporative coolers in seawater greenhouses, therefore facilitating the high-value crop cultivation and sea salt production. The seawater greenhouse technology recreates the "hydrologic cycle" by the evaporation of water from saline water sources such as seawater and recovers it as pure water by a condensation process (Figure 3). This renewable energy based technology has experienced numerous stages of developments and exhibited a favourable practical solution in regions having a shortage of fresh water for the purpose of irrigation. In a study by Ismaili et al. (2016), the team provided an up-to-date and comprehensive review on what have been published on seawater greenhouse technology. Moreover, the study also investigated the efficiency in using the seawater greenhouse technology in Oman as a case study.

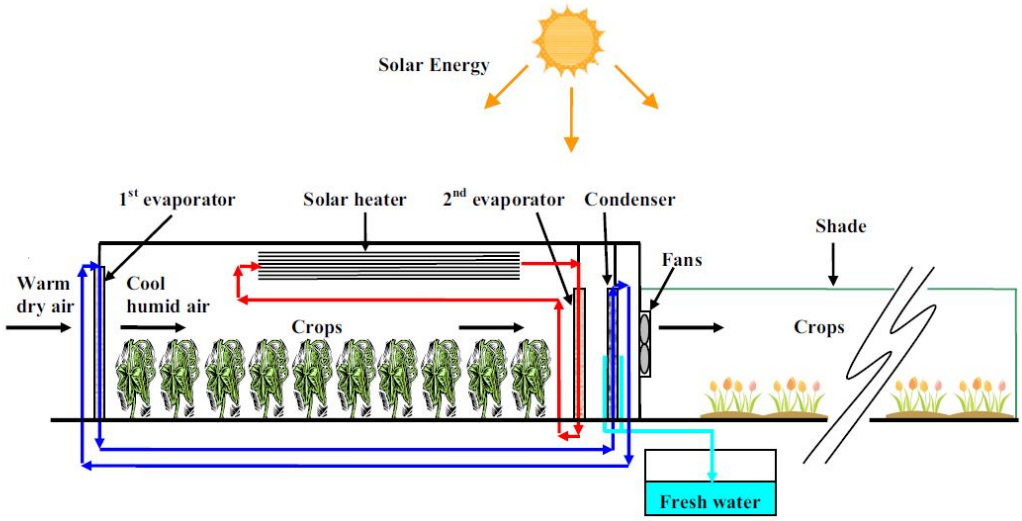


Fig. 3: Diagrammatic representation of the seawater greenhouse system in Oman

On the other hand, an obvious knowledge gap was noted in the financial attributes of seawater greenhouse because of the lack of research focus in this field. The primary trial of an understanding at the seawater greenhouse economics was performed in the work by (Ismaili et al., 2016). The major finding from the study was to decrease the capital expenses of the dehumidification units. Considering the technical aspects, the seawater greenhouse technology can be considered as a water conservational tool, due to the fact, that it decreases the water requirement of crop by practically 67.0 percent, as compared to the standard open-field cultivation. The generation of fresh water from the Oman

seawater greenhouse unit was varying between 300.0 to 600.0 Litres/day, with almost zero-salinity. Even though this quantity is considered to be half of the requirement of irrigation water, it is feasible to raise the volume of freshwater by combining with raw sea water or brackish ground water. Due to the fact that the freshwater production of seawater greenhouse unit in Oman was below the required demand and various research works confirm the prospect for progress, additional research and development works are crucial. On technical aspects, these efforts should have to be together with the efforts on the financial aspects.

4.2 Pressure Retarded Osmosis

The conventional energy production methods of using the non-renewable fossil fuels have many drawbacks. Power plants operated by fossil fuels generate greenhouse gases and cause environmental damage. For overcoming the problems associated with the standard fossil-fuel system, the requirement for eco-friendly as well as sustainable energy production systems is rising. The requirement for renewable energy sources for meeting the global energy demand and progressively substitute for fossil fuels is growing. Hence, several research studies are concentrating on developing effective alternate energy sources such as wave, tidal, solar and biomass, and are being comprehensively studied for providing sustainable and secure energy sources. However, the high installation costs, irregular availability of energy sources, or complex logistics, are still preventing these energy sources from being extensively used. Pressure retarded osmosis (PRO) is an alternate source of renewable energy presently in the advanced stage of development: and it is part of the salinity gradient energy or osmotic power sources, which employ the energy produced by salt concentrations differences between two solutions, generally freshwater and salt water. In the PRO concept (Figure 4), electrical power is generated by means of water flux brought about by the osmotic pressure difference between two different solutions.

The process employs the Gibbs' free energy of mixing of the saline solution (on the semipermeable membrane draw solution (DS) side) and the drawn solution from the feed solution (FS) (on the semipermeable membrane feed side). In this process, water will permeate through a semipermeable membrane from a lower concentration feed side into a higher concentration, moderately pressurized, brine (DS). The DS will have a lower hydraulic pressure than osmotic pressure even when it is considerably pressured. As a result, the flow of the permeate stream from the FS to the DS is still being driven by the net osmotic force. It turns out that the permeate is pressured, which weakens the DS. A turbine-generator set might then transform the energy in the pressured permeate solution into mechanical or electrical energy. Water producing from a sewage treatment facility could be used as the dilute solution (feed solution), whereas the brine discharging from a desalination facility can be employed as the concentrate (draw solution), thus being efficiently diluted before release into the sea. Correspondingly, PRO can generate energy from the salinity gradient generating from the salt concentration differences between the two different water solutions. This PRO technology is getting research attention due to its exclusive benefits:1) It will not produce hazardous waste to the environment, 2) this membrane-based packed system decreases the ecological damage caused by plant construction, 3) this is a sustainable energy production method using saline water sources, 4) PRO unit has application as a high-efficiency hybrid system, while used with commercial RO, forward osmosis (FO), and membrane distillation (MD), 5) this system has wide range of uses, in that different sources of water on the earth might be used.

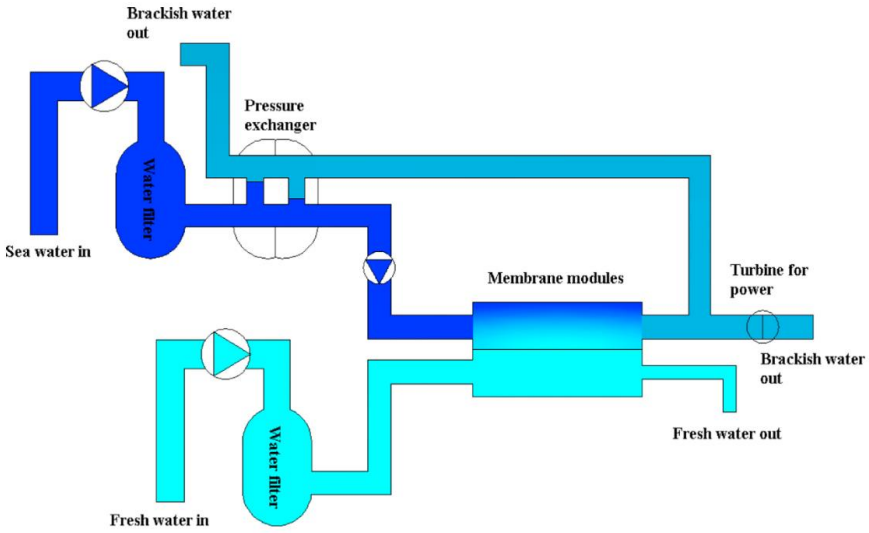


Fig. 4: Process outline for a standard osmotic power plant

The application of PRO to the seawater reverse osmosis desalination plant can simultaneously solve the issue of higher energy use and the high-salinity brine production of these plants. Subsequent to the pressure retarded osmosis process, the brine is diluted and thereby the ecological impact of the brine can be reduced. The PRO economic feasibility is extremely affected by the choice of selecting the hydroturbine or pressure exchanger for converting the resultant power to electricity. Sarp and Saththasivam recommended that employing a pressure exchanger instead of a hydroturbine for seawater reverse osmosis-PRO hybrid system might increase the rate of using the hydraulic pressure up to 97%. Therefore, this reduces the energy use of the seawater reverse osmosis desalination process by 25%. The study by Al-Anzi et al. (2018) discusses the use of 1-D analytical expressions for a parallel flow configuration in PRO exchangers by employing the real brine as well as feed TDS values from a Kuwait-based desalination facility. The results from this study confirmed that a maximal power of 2.6 kJ and 0.28 kJ could be generated by the pressure retarded osmosis system employing treated wastewater effluent or seawater as the FS, respectively. The authors confirmed that this might be definitely able to decrease the power utilization of the desalination sector in Kuwait.

4.3 Hybrid Systems

Furthermore, the hybrid systems such as electrodialysis-based and reverse electrodialysis-based hybrid systems also support in reducing the energy use and minimizing the environmental effect of the reverse osmosis brine.

4.3.1 Electrodialysis-based Hybrid Systems

Electrodialysis is an economical, feasible, as well as eco-environmentally friendly process for treating the reverse osmosis effluent, which is extensively used in water treatment. In this process, ions are carried through semipermeable membranes under the impact of an electric field driving force generated by an applied direct current (DC) voltage source. Numerous studies confirmed the capability of electrodialysis technique for treating the extremely high saline water. Casas et al. (2012) as well as Reig et al. (2014) used electrodialysis as a technical solution for recovering sodium chloride from the reverse osmosis brines, which has been subsequently employed as a raw material in the chloralkali process. In two different studies, Korngold et al. (2005, 2009) employed electrodialysis technique for reducing the reverse osmosis brine effluent volume as well as its disposal cost. In a

work by Nayar et al. (2019), the team examined the possibility of completely hybridizing reverse osmosis with electrodialysis, together with optimizing electrodialysis current densities for producing brine with a salt concentration of 120.0 g/kg. This study demonstrated that the optimization assisted for reducing the brine concentration expenses by 33.0-70.0 %, as compared to a standalone electrodialysis system. The possibility of developing salt and low salinity water by the treatment of synthetic brine was examined by Al-Anzi et al. (2021) in a pilot-scale electrodialysis-evaporator hybrid system for brine management. Presently, the desalination facilities in Kuwait release the brine effluents subsequent to combining it with seawater in which the bathymetry (bathymetry is the measurement of the depth of water in sea or rivers) is very shallow. The selected synthetic brine concentration was between 65,000–68,000 mg/L to mimic reject brine from Kuwait desalination plants. The concentrated brine effluent from electrodialysis process was taken to an evaporator for producing coarse salt with 84.75 percent salt recovery as well as less salinity water with TDS concentration of 1526 ppm. Therefore, the electrodialysis-evaporator hybrid system was noted to be a safe choice for treating the reject brine from desalination facilities.

4.3.2 Reverse Electrodialysis-based Hybrid Systems

Reverse electrodialysis is a developing membrane technology that gets electrical power from the salinity differences between two solutions. In this reverse electrodialysis technique, the fundamental ions present in the solutions will be powered by means of ion-exchange membrane by a salinity difference. In the work by Li et al. (2013), the RO and reverse electrodialysis processes have been integrated for designing an advanced hybrid process that used the synergy of reverse osmosis and reverse electrodialysis processes. From the perspective of the reverse electrodialysis process, the reverse osmosis process could offer the concentrated brine as the higher salt concentration FS for a high power density. Also, the environmental impact of the reverse osmosis brine can be reduced by reducing the salt concentration of the discharged brine by means of the reverse electrodialysis process. Conversely, the energy usage of the reverse osmosis process could be decreased by pretreating the FS by the reverse electrodialysis process; that is., the feed solution osmotic pressure will be reduced and transformed into electrical energy. Such complementary impacts turn reverse osmosis and reverse electrodialysis processes a perfect combination for low energy seawater desalination as well as brine management.

5 Discussion and Conclusion

The two important factors that influence the production of brine are the feed water type and the purification technology used in the desalination facilities. Thus, our study demonstrated that the advanced techniques analyzed here are advantageous and suitable for decreased energy utilization as well as ecological sustainability of desalination plant. Currently, due to the fact that the crude oil is a restricted energy resource, the thermal-based desalination techniques would not be practical for the prospect of the Gulf Cooperation Council nations. Majority works should be concentrated on employing the extremely accessible renewable energy in the Gulf Cooperation Council nations, like solar energy, wind energy etc., and for techniques that result in minimal influence on the ecosystem. Generally, the emergent technologies discussed in this study are very promising for the brine volume reduction of effluent volume, on the other hand, majority are just on a lab/pilot scale and it very hard to examine their applicability on a commercial scale. Several studies have confirmed that the suitable usage of extremely concentrated brine solution with diluted treated wastewater or seawater by means of PRO can not only reduce the serious environmental impacts caused by the brine discharge to the surroundings, but also can produce considerable energy output from the feed and draw salinity

gradient. The electrodialysis-based and reverse electrodialysis-based hybrid systems also proved to be ideal solutions for the brine management. Further studies are necessary on a higher scale for assessing the effectiveness and sustainability of these technologies. Numerous problems must be properly addressed for the practical application of the high salinity PRO technique for the seawater RO desalination facility. In the water sector, to ensure that the desalination processes are successfully employed and performed in a favorable manner, it is needed to have a proper structured system governed by objectives and laws. The GCC nations along with their resemblances in geography, and conditions of water constraints could be the world leaders in bringing up advanced approaches in the desalination sector.

Acknowledgement:

The authors acknolwedge the support from the project NPRP13S-0205-200263

References

Achilli, A. & Hickenbottom, K. L. (2016). Pressure retarded osmosis: Applications. In Sustainable Energy from Salinity Gradients (pp. 55-75). Woodhead Publishing.

Al-Anzi, et al. (2021). Brine management from desalination plants for salt production utilizing high current density electrodialysis-evaporator hybrid system: A case study in Kuwait. Desalination, 498, 114760.

Al-Anzi, B. S. & Thomas, A. (2018). One-Dimensional Analytical Modeling of Pressure-Retarded Osmosis in a Parallel Flow Configuration for the Desalination Industry in the State of Kuwait. *Sustainability*, *10*(4), 1288.

Al-Ismaili, A. M. & Jayasuriya, H. (2016). Seawater greenhouse in Oman: A sustainable technique for freshwater conservation and production. *Renewable and Sustainable Energy Reviews*, *54*, 653-664.

Al-Zubari, et al. (2017). An overview of the GCC Unified Water Strategy (2016–2035). *Desalination and water treatment*, *81*(s 5).

Casas, et al. (2012). Seawater reverse osmosis brines as a new salt source for the chlor-alkali industry: integration of NaCl concentration by electrodialysis. *Solvent Extraction and Ion Exchange*, *30*(4), 322-332.

Douani, et al. (2011). Modeling heat exchange in the condenser of a seawater greenhouse in Oman. *Chemical Engineering Communications*, *198*(12), pp.1579-1593.

Jia, et al. (2014). Blue energy: Current technologies for sustainable power generation from water salinity gradient. Renewable and Sustainable Energy Reviews.31: 91-100

Korngold, et al. (2005). Electrodialysis with brine solutions oversaturated with calcium sulfate. *Desalination*, *172*(1), 63-75.

Korngold, E., Aronov, L. & Daltrophe, N. (2009). Electrodialysis of brine solutions discharged from an RO plant. *Desalination*, *242*(1-3), 215-227.

Li, et al. (2013). A novel hybrid process of reverse electrodialysis and reverse osmosis for low energy seawater desalination and brine management. *Applied energy*, *104*, 592-602.

Nayar, et al. (2019). Cost and energy needs of RO-ED-crystallizer systems for zero brine discharge seawater desalination. *Desalination*, *457*, 115-132.

O. Ellabban, H. Abu-Rub & F. Blaabjerg (2014). Renewable energy resources: current status, future prospects and their enabling technology, Renew. Sustain. *Energy Rev. 39*, 748-764.

Post, et al. (2007). Salinity-gradient power: evaluation of pressure etarded osmosis and reverse electrodialysis, *J. Membr. Sci*. 288 (2007) 218-230

Reig, et al. (2014). Concentration of NaCl from seawater reverse osmosis brines for the chlor-alkali industry by electrodialysis. Desalination, 342, 107-117.

Sarp, S. & Hilal, N. (2018). Membrane Modules for Large-Scale Salinity Gradient Process Applications. In Membrane-Based Salinity Gradient Processes for Water Treatment and Power Generation (pp. 223-242). Elsevier.

Sarp, S., Li, Z. & J. Saththasivam. (2016). Pressure Retarded Osmosis (PRO): Past experiences, current developments, and future prospects. Desalination. 389: 2-14.

Shahzad, et al. (2018). Adsorption desalination—principles, process design, and its hybrids for future sustainable desalination. In Emerging technologies for sustainable desalination handbook (pp. 3-34). Butterworth-Heinemann.

Shahzad, et al. (2019). Desalination processes' efficiency and future roadmap. *Entropy*, *21*(1), 84.

Weinstein, J. N. & Leitz, F. B. (1976). Electric power from differences in salinity: the dialytic battery. *Science*, *191*(4227), 557-559.

Cite as: Zaidi S.Z., Saleem H. & Siddiqui H.R., "Emerging Brine Management Approaches for Sustainable Desalination in the GCC Countries", *The 2nd International Conference on Civil Infrastructure and Construction (CIC 2023)*, Doha, Qatar, 5-8 February 2023, DOI: https://doi.org/10.29117/cic.2023.0161

Enhancement of Polysulfone Ultrafiltration Membrane Performance for Produced Water Treatment by Incorporation of Graphene oxide/Chitosan/Silicon dioxide Nanocomposite

Ahmed. T. Yasir
Qatar University, Doha, Qatar
ay1107095@qu.edu.qa

Nadeen Alshaibi
Qatar University, Doha, Qatar
na1606783@qu.edu.qa

Nchwa Ndame
Qatar University, Doha, Qatar
nn1801822@qu.edu.qa

Alaa H. Hawari
Qatar University, Doha, Qatar
a.hawari@qu.edu.qa

Abdelbaki Benamor
Qatar University, Doha, Qatar
benamor.abdelbaki@qu.edu.qa

Abstract

Oil and gas production is accompanied by generation of large amounts of produced water as usually three barrels of produced water is generated for each barrel of oil. Membrane-based water reclamation technologies have been applied to treat produced water. However, the presence of oil content in the produced water makes its separation very complicated due to the high affinity between oil droplets and the hydrophobic polymeric membrane. This, results in low permeate flux, low oil rejection and high irreversible fouling. In this study, graphene oxide (GO) was functionalized using chitosan (CH) to synthesize GO-CH that was further functionalized with SiO_2 to produce GO-CH-SiO_2 nanocomposite. Synthesized GO-CH-SiO_2 was embedded in the polysulfone membrane matrix to modify the pristine Psf membrane and impart super-oleophobic properties to the membrane. Produced nanocomposites properties were characterized using XRD, FTIR and TEM analyses, while synthesized membranes were characterized for their porosity, pore size, membrane resistance and hydrophilicity. Different ratios of GO:CH were applied with a fixed SiO_2 loading to produce modified membranes. Performance test for the membranes modified with 0.3wt % nanocomposite with a GO:CH ratio of (2:1) showed a 271% improvement in membrane flux compared to pristine membrane while a ratio of 1:2 (GO:CH) gave the lowest total fouling.

Keywords: Graphene oxide; Chitosan; SiO_2; Produced water; Ultrafiltration

1 Introduction

The treatment of produced water generated by various industries, including the petrochemical, oil and gas sectors, has grown to be a major global concern. Untreated produced water discharge has a negative impact on the ecosystem in several ways by contaminating soil, surface water, and underground water. Methods of separation, including microfiltration (MF), ultrafiltration (UF), nanofiltration (NF), and reverse osmosis (RO), have shown considerable potential for membrane technology to treat produced

water (Shukla, Alam, Alhoshan, Dass & Muthumareeswaran, 2017; Yasir, Eljack & Kazi, 2020). A proper membrane must have a high pollution rejection rate and a stable, high-water flux at low operating pressure. The abundance of hydrophilic groups in graphene oxide (GO), including epoxy, hydroxyl, and carboxyl groups, gives GO good hydrophilicity and the potential for even further functionalization. Several chemical modification techniques have been proposed and verified to decrease the accumulation of GO on the membrane surface. One such method is creating multifactional nanocomposites of GO (Mahmoudi, Ng, Ba-Abbad & Mohammad, 2015). To improve membrane hydrophilicity, anti-fouling properties and oil removal performance of the Psf membrane, chitosan (CH) and SiO_2 can be used to functionalize GO. Chitosan (CH) is a hydrophilic polymer, with hydroxyl groups and highly reactive amino groups, which has been used widely for functionalization of GO (Xue et al., 2018). On the other hand, SiO_2 is super oleophobic and has been used extensively to improve oil removal efficiency of the polymeric membranes (Mehta & Zydney, 2005). In our previous study, addition of GO-CH nanocomposite in the membrane matrix has shown improved membrane flux due to enhanced pore radius. In this study, to improve the oil rejection of the membrane while maintaining high membrane flux, GO has been functionalized with CH and SiO_2. The synthesized nanocomposites were tested using FTIR and zeta analysis. With a constant SiO_2 loading, various GO:CH ratios were used to create customized membranes. The porosity, hydrophilicity, membrane flux, anti-fouling properties and oil removal efficiency were studied for the synthesized membranes and reported in this paper.

2 Methodology

2.1 Materials

Extra pure, fine graphite powder (99%), sodium nitrate ($NaNO_3$, 99.9%), potassium permanganate ($KMNO_4$, 99%), sulphuric acid (H_2SO_4, 98%), polysulfone pellets (99%, Mw 35,000), N-Methyl Pyrrolidone (NMP, 99.9%), Chitosan (95% deacetylation), Tetraethyl orthosilicate (TEOS, 95%) and bovine serum albumin (BSA, 99%) were all purchased from Sigma Aldrich. The oil emulsion was prepared using QALCO performance oil #64, purchased from Qatar Lubricant Company. The properties of the oil is given in Table 1.

Table 1: Properties of the oil used for preparing the water-in-oil emulsion

Flash Point	220°C
Appearance	Clear Amber Yellow
Physical State	Liquid
Vapor Density (air=1)	>1
Boiling Point	>260°C
Solubility in Water	Negligible
Specific Gravity	0.875
Viscosity	42-50 cSt
Conductivity	0 μS/cm

2.2 Synthesis of GO

The graphene oxide (GO) was synthesized following the modified Hummer's methods that has been previously used by Mahmoudi et al. (2015) (Mahmoudi et al., 2015). Initially, 115 mL sulphuric acid was taken in a round bottomed flask where 2.5g $NaNO_3$ and 5 gm graphite powder was added. The mixture was then stirred for 30 min in an ice bath until the temperature of the mixture reached 10 °C. While maintaining this temperature for 2 hours, 15 g $KMNO_4$ was added slowly. Then the temperature was increased to 35°C and maintained for 1 hour. Then, 230 mL distilled water was

added to the round bottomed flask slowly while maintaining the internal temperature of the mixture below 100ºC. The solution was then stirred for 1 hour followed by addition of 300 mL distilled water. The process was completed by adding 10 mL 30% H_2O_2 that changed the color of the mixture to brilliant yellow and reduced the residual $KMNO_4$. The mixture was then cleaned by centrifugation and washed with HCl before GO powders were obtained by freeze-drying.

2.3 Preparation of GO-CH Multifunctional Composite

A suitable quantity of GO was mixed with an aqueous solution of 2% acetic acid. To finish the functionalization process, the mixture was then given the proper amount of CH and mixed for 5 hours. Prior to vacuum drying at 60°C, the mixture was centrifuged and then rinsed with ethanol. Three distinct ratios of the multifunctional GO-CH composite (2:1, 1:1, and 1:2) have been created in this study.

2.3 Preparation of GO-CH-SiO_2 Multifunctional Composite

To prepare GO-CH-SiO_2, a mixture of ethanol and water was prepared where the ratio of ethanol to water was 5:1. The pH of this solution was increased to 9 using 25% ammonia. Then GO-CH nanocomposite and appropriate amount of TEOS was added to the solution. The obtained solution was sonicated for 15 mins and stirred at room temperature for 24 hours. The solution was then centrifuged and rinsed with water before they were vacuum dried at 60ºC to obtain the GO-CH-SiO_2 nanocomposite.

2.4 Membrane Fabrication

The phase inversion method was used to prepare the GO-CH-SiO_2 doped polysulfone membranes. The correct amount of polysulfone was added to 25 mL of the NMP solution and stirred continuously for two hours at 300 rpm and 80ºC to create the casting solution. To avoid the production of gas bubbles in the casting solution, this low stirring speed was found suitable. A suitable quantity of the GO-CH-SiO_2 multifunctional composite was dissolved in 5 mL of NMP solution in a separate beaker, and the mixture was ultrasonically agitated for 30 minutes. Then the two NMP mixtures were added together and stirred for 12 hours at room temperature. Filmography doctor blade was used to evenly spread a small amount of the prepared casting solution onto a glass plate to create the membrane film. The distance between the blade and the glass plate, which was maintained at 0.3 mm, was used to adjust the membrane thickness. After the casting solution had been evenly distributed across the glass plate, the phase inversion procedure was carried out by moving the glass plate into a bath of distilled water. The obtained membrane was removed from the glass plate and given a 30-minute rinse in distilled water. This process was used to cast 4 different membranes. Table 2 provides a summary of the elements and content of the various produced membranes.

Table 2: The membrane casting solution compositions

Membranes	NMP (wt%)	Psf (g)	GO:CH (ratio)	(GO:CH):SIO_2 (ratio)
M-0	30	6.144	-	
M-1	30	6.144	2:1	21:1
M-2	30	6.144	1:1	21:1
M-3	30	6.144	1:2	21:1

2.5 Characterization of prepared GO-CH –SiO_2 Multifunctional Composite

Using a Nicolet 6700 FTIR spectrometer, the functional groups present on the multifunctional nanocomposite were examined (Thermo Fisher Scientific Inc., MA). Additionally, utilizing XRD (Bruker D8 Advance, Germany) with CuKα radiation (1.5406 Å) in the 2 h scan range of 20–80º,

the nanocomposite's crystal phase composition was also examined.

2.6 Characterization of the Fabricated Membrane and Performance Analysis

2.6.1 Membrane Permeate Flux, Porosity, Pore Size and Resistance Analysis

The permeation tests were done by using a stirred dead-end cell, with a pressure of 4 bars. Before all studies, the membranes were compressed for 30 minutes at the same pressure. Equation 1 shows the calculations of the pure water permeate flux(J, LMH):

$$J = \frac{w_t - w_o}{A \times d_w \times \Delta t} \tag{1}$$

Where, w_o is the initial mass of the permeate water (gm), w_t is the mass of the permeate water at time t (gm), Δt is filtration time (sec), A is the surface area of the membrane (cm^2) and d_w is density of water (0.998 gm/cm^3). The porosity (ϵ) of the membrane was determined using the gravimetric method and calculated as:

$$\epsilon = \frac{\omega_1 - \omega_2}{A \times l \times d_w} \tag{2}$$

Here, ω_1, ω_2, l and d_w corresponds to weight of the wet membrane (gm), weight of the dry membrane (gm) and thickness of the membrane (cm), respectively. The pore radius (r_m) of the membranes were calculated using the porosity and Guerout–Elford–Ferry equation:

$$r_m = \sqrt{\frac{(2.9 - 1.75\epsilon)8\eta l Q}{\epsilon \times A \times \Delta P}} \tag{3}$$

Here, η, Q and ΔP corresponds to viscosity of water ($8.9 \times 10^{-4}\ Pa.s$), volume of the permeated pure water per unit time (m^3/s) and the operating pressure (Pa), respectively. The membrane resistance (R_m, m^{-1}) was calculated as:

$$R_m = \frac{\Delta P}{\mu J} \tag{4}$$

Here, μ corresponds to the dynamic viscosity of water (0.000891 $Pa.s$ at 25 °C).

2.6.2 Membrane Fouling analysis

The fouling study was conducted using a solution of 1000 ppm BSA as model foulant. For each membrane, three dynamic cycles were conducted in the dead-end setup. Initially, the pure water steady state flux (J_{w0}) was measured at 4 bars, then the feed was changed to the BSA solution where filtration was carried out for 1 hour 30 min and the permeate flux was (J_{wf}) measured at the end. After the BSA filtration stage, the membrane was washed twice with distilled water and the pure water steady state permeate flux (J_{w1}) was measured again at 4 bars. Using the data obtained at this stage, the total fouling ratio (R_t), flux recovery ratio (FRR), the reversible fouling ratio (R_r) and the irreversible fouling ratio (R_{ir}) were calculated as:

$$R_t = \frac{J_{w0} - J_{wf}}{J_{w0}} \times 100\% \tag{5}$$

$$FRR = \frac{J_{w1}}{J_{w0}} \times 100\% \tag{6}$$

$$R_r = \frac{J_{w1} - J_{wf}}{J_{w0}} \times 100\% \tag{7}$$

$$R_{ir} = \frac{J_{w0} - J_{w1}}{J_{w0}} \times 100\% \quad (8)$$

The second and third cycles were repeated following the above discussed methodology. The BSA rejection performance of the synthesized membranes were evaluated by using a UV-VIS spectrophotometer (UV-2700, Shimadzu) at 278 nm.

2.6.3 Industrial Wastewater Treatment

The industrial wastewater from Shell was treated using the dead-end cell setup. The UF process was carried out at 4 bars. The *TOC* concentration of the industrial wastewater before filtration, (TOC_i), and after filtration, (TOC_f) , was measured using AQUAfast *TOC* Colorimeter (Orion AQ2040, Thermo Scientific, US). The TOC rejection (R_{TOC}) was calculated as:

$$R_{TOC} = \frac{TOC_i - \mathrm{T}OC_f}{TOC_i} \times 100\% \quad (9)$$

For each membrane, all testes were repeated three times and their average was considered in this work while the standard deviation is indicated by the error bars.

3 Results and Discussion of the Nanoparticles

3.1.1 Surface Zeta Potential Analysis

Zeta potential measurement, as shown in Figure 3, can further confirm the surface functionalization of GO, GO-CH, GO-CH-SiO_2. The GO particles displayed negative zeta potential between the investigated pH ranges of 3 and 11.5 in the test. The functionalized GO-CH nanocomposites have a greater zeta potential than the GO nanoparticles within the studied range. As GO nanoparticles has many oxygens containing sites on its surface; whereas adding CH causes the GO surface to acquire nitrogen-containing groups, increasing the zeta potential. Moreover, for the nanoparticle with SiO_2, the zeta potential over the tested range is lower than the zeta potential of GO-CH nanocomposite due to the presence of hydroxyl group on the surface of the GO-CH-SiO_2 nanocomposite.

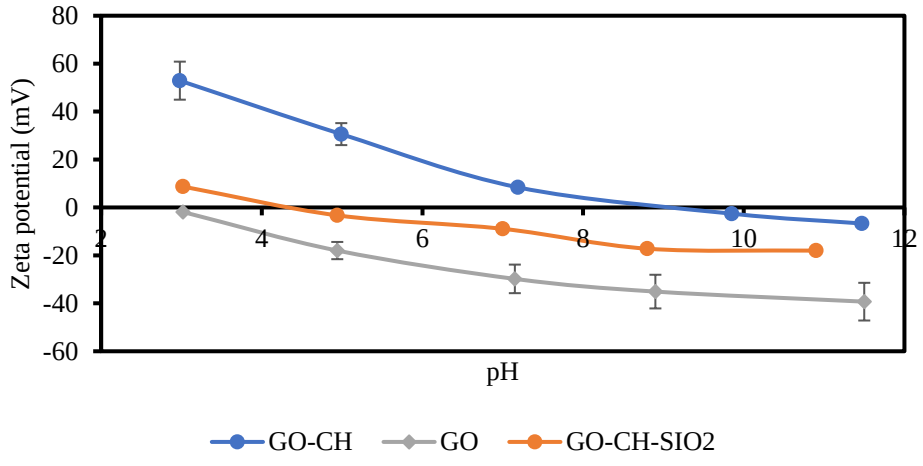


Fig. 1: Zeta potential measurement of GO, GP-CH and GO-CH-SIO2 at various pH

3.1.2 FTIR spectra of GO, CH, GO-CH and GO-CH-SiO_2

In this experiment GO, CH, GO-CH and GO-CH-SiO_2 were analyzed using fourier transform infrared (FTIR) technique that is shown below in figure.4. Due to C=C stretching vibration, there is an absorption

band at 1600 cm^{-1} as shown in figure 4. Other bands at 3400 cm^{-1} are stretching vibrations of oxygen carrying hydroxyl functional groups (OH). The absorbance bands seen along the CH curve at 1100 cm^{-1} represents the C-O-C vibration, 1600 cm^{-1} the N-H bending vibration, 2900 cm^{-1} the C-H stretching vibration, and 3450 cm^{-1} the O-H and N-H stretching vibration. Moreover, the absorbance band for the GO-CH nanocomposite demonstrates the presence of all the bands that were detected in the individual CH and GO curves. Finally, regarding GO-CH-SiO_2 nanocomposite, due to the SiO_2 it is stated that bands between 900 and 1050 cm^{-1} represent composite characteristics of Si–OH species. Therefore, the strong band at around 950 cm^{-1} is attributed to the stretching vibration of Si-OH.

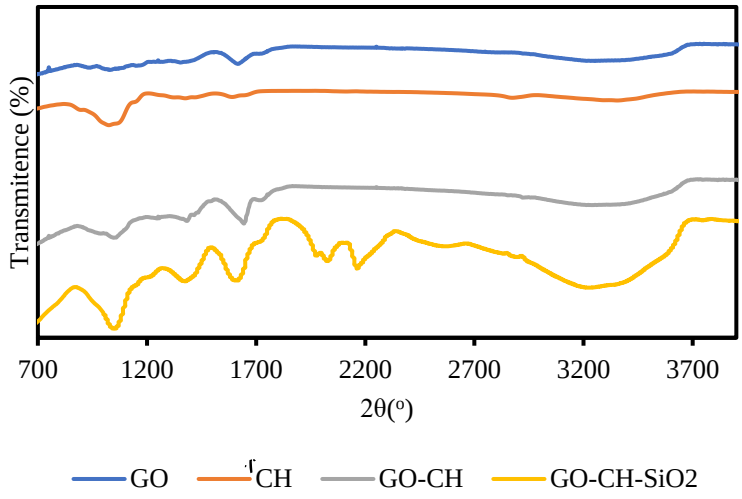


Fig. 2: FTIR spectra of GO, CH, GO-CH and GO-CH-SiO_2

3.2 Characterization of the Membranes

3.2.1 Porosity and Resistance Study

Porosity was conducted to obtain the pore size of nanocomposites at synthesized membranes. Table 3 provides the values of porosity, pore radius, membrane resistance and contact angle. As shown in Table 3, the porosity, membrane resistance pore radius and contact angle for the pristine membrane (M0) were 57.3%, 17.9, 4.2 and 87.4º, respectively. Doping the membranes with GO-CH-SiO_2 nanocomposite improves the porosity and pore radius and decreases the membrane resistance and contact angle. The presence of hydrophilic functional groups, improved affinity between polysulfone membrane and the prepared nanocomposite and increased viscosity resulted in these improvements.

Table 3: Porosity, pore radius, resistance and contact angle or the synthesized membranes

Membrane	Porosity (%)	Membrane resistance	Pore radius (nm)	Contact angle (º)
M0	57.3	17.9	4.2	87.4
M1	85.0	7.3	8.7	61.5
M2	93.3	8.1	7.5	55.8
M3	88.1	11.2	6.8	50.8

3.2.2 Pure Water Permeation Flux

Water permeation flux was determined to study the effect of CH on different concentration of GO-CH-SiO_2 nanocomposites. Figure 6 provides the flux values for each membrane. Comparing to the pristine membrane M0, M1 shows the highest flux of 23.13 LMH/bar, where porosity increased by 27.7%, pores expanded by 207%, membrane resistance decreased by 41% and contact angle reduced by 25.9°. Whereas M3 showed the lowest flux enhancement due to lower pore enlargement and the higher membrane resistance.

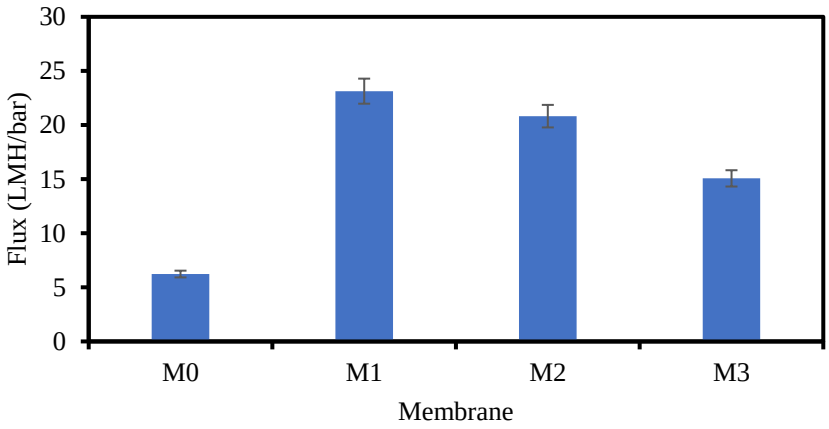


Fig. 3: Flux of GO-CH-SiO2 membranes

3.2.3 Fouling Study

The fouling study in terms of total fouling ratio (R_t), flux recovery ratio (FRR), reversible fouling ratio (R_r) and the irreversible fouling ratio (R_{ir}) was conducted according to the method discussed in section 2.6.2, where 1000 ppm of BSA solution was used as the model foulant. The results of fouling flux shown in table 4. Out of four membranes, M3 showed the lowest total fouling (%) due to its lowest contact angle. Due to improved hydrophilicity, M1, M2 and M3 showed better anti-fouling properties than the pristine M0 membrane.

Table 4: Fouling properties for GO-CH-SiO_2 membranes

Membrane	R_t(%)	FRR(%)	F_r(%)	F_{ir}(%)
M0	85.4	21.2	6.6	78.8
M1	90.7	69.3	59.9	30.7
M2	84.3	77.6	61.9	22.4
M3	47.9	74.2	22.0	25.8

3.2.4 Membrane Performance for Industrial Wastewater Treatment

Figure 8 shows the oil rejection performance of the synthesized membranes. As seen from Figure 8, all the synthesized membranes have shown greater than 99% oil rejection even at increased permeation flux. The increased pore size, as indicated by Table 3, did not affect the oil rejection performance due to the presence of super-oleophobic SiO_2 in the nanocomposite.

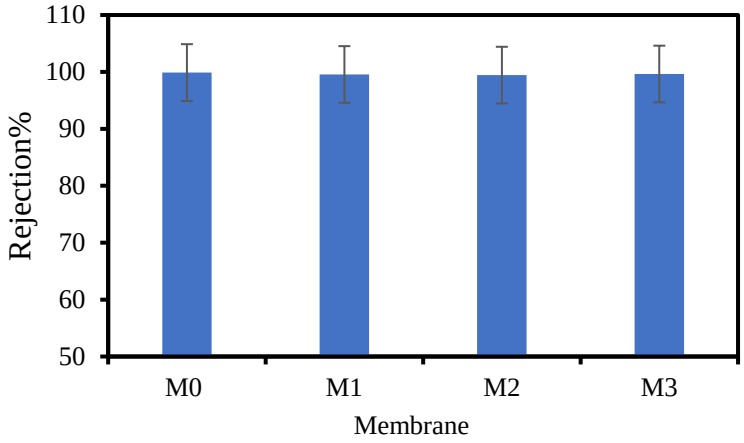


Fig. 4: Rejection percentage of GO-CH-SiO_2 membranes

4 Conclusion

This study effectively synthesized the multifunctional nanocomposite GO-CH-SiO_2 and applied it to enhance polysulfone membrane. The hydrophilic functional groups, such as hydroxyl and carboxylic acid, which were present in the produced nanoparticles, were abundant. The composition of the produced GO-CH-SiO_2 nanocomposite was verified using FTIR studies. The ratios of GO and CH were changed during the nanocomposite synthesis between 1:2, 1:1, and 2:1, while the ratio of SiO_2 remained fixed at 21:1. Results showed an increase in the flux while adding GO-CH-SiO_2 nanocomposite, which resulted in increased, porosity and pore radius and reduced membrane resistance and contact angle. Additionally, the improved hydrophilicity resulted in lower fouling rate. Finally, the presence of SiO_2 aided in high oil rejection at elevated membrane flux.

References

Mahmoudi, et al. (2015). Novel nanohybrid polysulfone membrane embedded with silver nanoparticles on graphene oxide nanoplates. *Chemical Engineering Journal, 277*, 1-10. doi:https://doi.org/10.1016/j.cej.2015.04.107

Mehta, A. & Zydney, A. L. (2005). Permeability and selectivity analysis for ultrafiltration membranes. *Journal of Membrane Science, 249*(1), 245-249. doi:https://doi.org/10.1016/j.memsci.2004.09.040

Shukla, et al. (2017). Development of a nanocomposite ultrafiltration membrane based on polyphenylsulfone blended with graphene oxide. *Scientific Reports, 7*(1), 41976. doi:10.1038/srep41976

Xue, et al. (2018). Chitosan-Functionalized Graphene Oxide for Enhanced Permeability and Antifouling of Ultrafiltration Membranes. *Chemical Engineering & Technology, 41*(2), 270-277. doi:https://doi.org/10.1002/ceat.201600709

Yasir, et al. (2020). Synthesis of water capture technologies for gas fired power plants in Qatar. *Chemical Engineering Research and Design, 154*, 171-181. doi:https://doi.org/10.1016/j.cherd.2019.12.013

Cite as: Yasir A., Alshaibi N., Ndame N., Hawari A. & Benamor A., "Enhancement of Polysulfone Ultrafiltration Membrane Performance for Produced Water Treatment by Incorporation of Graphene oxide/Chitosan/Silicon dioxide Nanocomposite", *The 2nd International Conference on Civil Infrastructure and Construction (CIC 2023)*, Doha, Qatar, 5-8 February 2023, DOI: https://doi.org/10.29117/cic.2023.0162

Adsorption of Congo Red Dye Using Activated Carbon-Fe_3O_4 Composite

Nafis Mahmud
Gas Processing Center, Qatar University, Doha, Qatar
n.mahmud@qu.edu.qa

Ludan Yasser
Gas Processing Center, Qatar University, Doha, Qatar
ladunyass@hotmail.com

Rahaf Belal Hafiz Mahmoud
Gas Processing Center, Qatar University, Doha, Qatar
rm1701572@student.qu.edu.qa

Abdelbaki Benamor
Gas Processing Center, Qatar University, Doha, Qatar
benamor.abdelbaki@qu.edu.qa

Abstract

Activated Carbon-Fe_3O_4 composites were synthesized using co-precipitation method and used in batch experiments to adsorb Congo red dyes. The effect of adsorbent dosage, temperature and initial dye concentration was investigated. Increase in the adsorbent dosage resulted in the increase of dye adsorption capacity and the optimum dose was found to be 2 g/L. Increase in temperature had slightly negative impact on the adsorption which indicated the exhothermic nature of the adsorption process. Initial dye concentration also had significant impact on the adsorption process as the adsorption capacity of the AC- Fe_3O_4 adsorbents decreased with increase in dye concentrations. Finally, the obtained adsorption data were fitted to Langmuir adsorption isotherm and the maximum adsorption capacity of Activated Carbon-Fe_3O_4 adsorbent was found to be around 129.87 mg/g. Overall, the results suggested that synthesized AC- Fe_3O_4 composites exhibit significant potential to be used as an adsorbent for the removal of organic pollutants from aqueous solutions.

Keywords: Adsorption; Congo Red Dye; Activated Carbon; Iron oxide; Isotherms; Kinetics

1 Introduction

Water pollution triggered from industrial waste discharge is an evergrowing concern for worldwide. Preservation of water is crucial for the safety and well-being of both human and aquatic life. Large volume of wastewater is being directly discharged to the water bodies without any prior treatment. A large percentage of the industrial waste consists of organic dyes due to their extensive application in textile, tannery, paper and printing industries (Harja et al., 2022). Organic dyes can inhibit the light from going into the aquatic system and disrupt the photosynthetic process (Shan et al., 2015). They are also known to be extremely harmful to human health as they are toxic and carcinogenic as well (Ahmad & Ansari, 2021; Lei et al., 2017). Therefore, it is critical to develop efficient methods to remove these harmful dyes from the industrial wastewater.

Various techniques have been employed to remove dyes from wastewater; including adsorption, photocatalysis, coagulation, flocculation, ion exchange, electro chemical method, chemical oxidation and aerobic and anaerobic degradation using microbes (Lim et al., 2016; Mahmud et al., 2021). Among these techniques, adsorption is the commonly employed technique as it is easy to operate, highly efficient and low cost compared to the others. However, the adsorption process is largely

dependent on the nature and type of the adsorbent being used. Various adsorbents like activated carbon, metal oxides, polymers and zeolites have been applied to remove dyes from wastewater (Ewis, et al., 2022a; Ba-Abbad, et al., 2022). However, the different studied adsorbents available in the open literature have several drawbacks such as low sorption capacity, high production and recovery problems. Therefore, development of easily recoverable adsorbents with high sorption capability and low cost is very crucial for their industrial application.

Recently, incorporation of iron oxide with various adsorbents for development of recoverable composites has garnered a lot of interest from the scientific community (Aryee et al., 2022; Deng et al., 2022; Ewis, et al., 2022b; Mahmud, et al., 2022; Mahmud, et al., 2023). Fe_3O_4 are environmentally benign, low cost, biocompatible and magnetically recoverable and have been widely used to modify and improve several adsorbents (Mahmud et al., 2020). Owing to these favorable properties, it is expected that incorporating Fe_3O_4 or iron oxide with activated carbon may well result in the formation of an efficient and recoverable composite (Wang et al., 2022). Therefore, in this study, magnetic Activated carbon- Fe_3O_4 composite were prepared via co-precipitation method and the adsorptive removal Congo red dye using the as-synthesized composites was investigated. Results obtained from these studies can provide useful insight on design and development of highly magnetic and iron oxide-based adsorbents that can be effectively used to remove Congo red dye and optimistically other organic pollutants from wastewater effluents.

2 Material and Methods

2.1 Chemicals

Activated carbon was purchased from Gongyi City Meiqi Industry and Company, China. While precursors for iron oxide namely; $FeCl_2.4H_2O$ and $FeCl_3.6H_2O$ both of purity 99%, 25% NH_4OH, NaOH (Purity 98%) and HCl (Purity 35-38%) were obtained from Reseachlab. Absolute Ethanol (Purity 99.9%) was purchased from Researchlab, India. Deionized water was used for preparation and cleaning of the composites throughout the experiments. All the chemicals were used as received without any further purification.

2.2 Preparation of Activated Carbon-Fe_3O_4 composite

Co-precipitation method was applied to synthesize magnetic activated carbon-Fe_3O_4 composite. The procedure consisted of firstly dissolving 0.2 g of activated carbon into 100 ml of deionized water . The solution was then sonicated for 15-20 minutes at 60 °C. After sonication, 0.87 g and of iron chloride tetrahydrate ($FeCl_2.4H_2O$) and 2.35 g iron chloride hexahydrate ($FeCl_3.6H_2O$) were added to the solution , and the mixture was stirred for 15 - 20 minutes under N_2 atmosphere. Afterwards, 20 ml NH_4OH solution was added to adjust the solution pH to 10. The temperature of the solution was then reduced to 50 ^oC and the solution was stirred for additional 60 minutes. The precipitate obtained was separated using a magnet and cleaned in multiple cycles of DI water and ethanol and dried at 80 ^oC under vacuum. Finally, the obtained magnetic activated carbon-Fe_3O_4 composite was then used for congo red adsorption studies.

2.3 Congo Red Dye Solution

A stock solution of congo red was prepared by dissolving 1 g of analytic grade congo red in deionized water to produce 1000 ppm solution. The required concentrations of working solutions were prepared from this stock solution by dilution.

2.4 Adsorption Experiments

Batch adsorption experiments were performed to investigate the effect of various operating parameters on the adsorption of the Congo red dye. The study on the effect of adsorbent dosage, temperature and initial dye concentration on the adsorption performance was carried out by varying the target parameter,

while keeping the other parameters fixed. Adsorption isotherm studies were conducted by adding 2.0 g/L of the as prepared AC-Fe_3O_4 adsorbents to a series of 50 mL conical flasks containing 50 mL Congo Red dye solutions of different concentrations (25-800 mg/L). The flasks were then sealed and stirred at 200 RPM in a Labnet air bath shaker for 24 hours at temperature of 298 K. After the completion of the adsorption experiments, the AC-Fe_3O_4 adsorbents were then separated magnetically and the Congo red dye concentrations in the supernatant was measured by determining the maximum absorbance at 498 nm using HACH UV/Vis spectrophotometer (Model: DR 3000). The amount of Congo red adsorbed by the synthesized adsorbent at equilibrium was determined using the following equation:

$$q_e = \frac{(C_o - C_e)\,V}{m} \quad (1)$$

Where, 'qe' represents the amount of Congo Red Dye adsorbed per gram of the adsorbent, the term 'V' stands for the volume of Congo red solution and 'm' represents the mass of the adsorbent. While, 'Co' and 'Ce' represents the initial and equilibrium concentrations of the Congo Red dye, respectively. While, the terms V and W stands for the volume of the solution and mass of the adsorbent. The removal efficiencies were also calculated using the following equation:

$$\text{Removal}\,\% = 100 \times \frac{(C_o - C_e)}{C_o} \quad (2)$$

3 Results and Discussion

3.1 Effect of AC-Fe_3O_4 Dosage

The effect of AC-Fe_3O_4 dosage ranging from 0.2 – 4 g/L on the removal 200 mg/L of Congo Red Dye was investigated at 298 K, a shaker speed of 200 RPM and at natural pH is shown in Figure 1. The amount of Congo red dye removed increased with the increase in AC-Fe_3O_4 dosage. This behavior can be attributed to the fact that with the increase in the adsorbent dosage, more adsorption sites became accessible, which in turn increased the adsorption surface area favoring adsorption of more Congo Red Dye (Deng et al., 2022). With the initial dose 0.2 g/L, 25 % of the Congo red dye was removed in 24 hours. A gradual increase in Congo Red adsorption (50 to 81 %) was observed between the AC-Fe_3O_4 dosage of 0.5 to 1 g/L. Almost complete removal (99 %) was obtained at adsorbent dosage of 2.0 g/L, hence, it was chosen as the optimum dosage for AC-Fe_3O_4 composites for Congo Red Adsorption experiments.

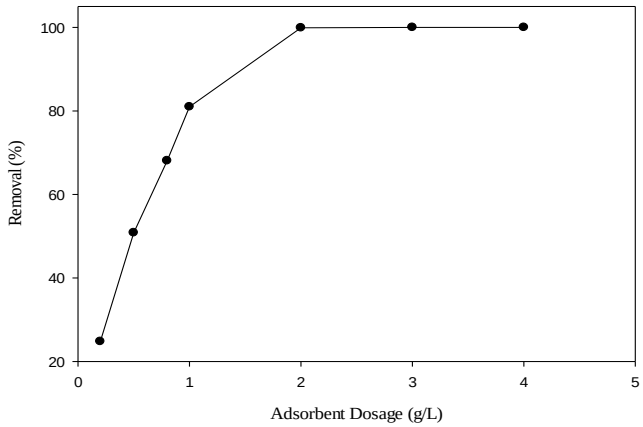


Fig. 1: Effect of Adsorbent Dosage

3.2 Effect of Temperature

The effect of temperature on adsorption of Congo red Adsorption using AC-Fe_3O_4 composites was investigated at three different temperatures (298, 308 and 318 K). Similar to the dosage experiment, the

AC-Fe_3O_4 composites dosage was varied between 0.2 – 4 g/L, while, the concentration of Congo red dye and shaker speed was kept fixed at 200 mg/L and 200 RPM, respectively. The dyes natural pH was selected to perform these experiments and obtained results after 24 hours are shown in Figure 2. At all three temperatures, the increase in adsorbent dosage resulted in increase in Congo red dye removal and complete removal of dye was observed at the maximum dosage. However, it was evident from the trends that the increase in temperature resulted in slight decrease in the adsorption capacity. This was an indication that the adsorption process was exothermic in nature (Litefti et al., 2019). Based on these results, 298 K was chosen as the optimum temperature for the dye Adsorption experiments.

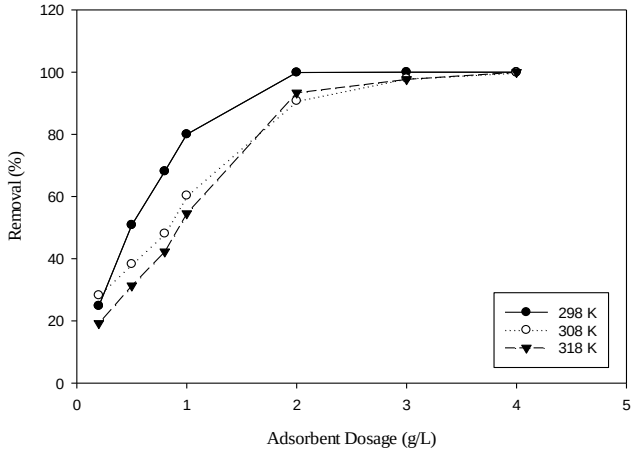


Fig. 2: Effect of Temperature

3.3 Effect of Initial Congo Red Concentration

The effect of Congo red Dye concentration on the adsorption performance was studied by varying the initial concentrations (25-800 mg/L) of the dye under the same experimental conditions (Adsorbent Dose 2.0 g.L-1, natural pH, time 24 hours, shaker speed of 200 RPM and temperature 298 K) as shown in Figure 3. It was observed that the adsorption performance is dependent on the initial dye concentration. Firstly, the complete removal of the congo red dye was observed up to the initial concentration of 200 mg/L. However, starting from initial dye concentration of 300 mg/L and beyond, removal efficiency showed a significant decrease. This phenomenon resulted from the decrease in the availability of the competitive adsorbent sites with the increase in the initial dye concentration rendering it more stable at higher concentrations which in resulted in a decrease in the removal efficiency.

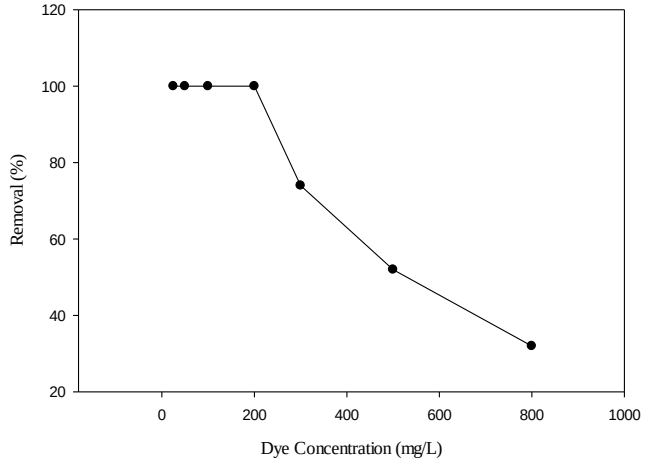


Fig. 3: Effect of Initial Dye Concentration

3.4 Adsorption Isotherm

Analysis of the adsorption isotherms is essential to understand the interactions between the surface of AC-Fe_3O_4 composites and the Congo Red molecules. The Langmuir isotherm assumes that the maximum adsorption occurs due to the formation of a monolayer by the adsorbate on the surface of the adsorbent. It further assumes that the energy required for adsorption process is constant and once the adsorbate i.e. the Congo Red molecule has occupied a site on the surface of the AC-Fe_3O_4 adsorbent, no further adsorption will occur on the same site (Langmuir, 1918). The non-linear form of the governing equation for Langmuir isotherm model is given by equation 3.

$$q_e = \frac{q_m K_L C_e}{1+q_m K_L C_e} \quad (3)$$

Here, the terms q_m and K_L stands for the maximum amount of Congo red adsorbed by the AC-Fe_3O_4 composite and Langmuir constant, respectively. Both of these terms were determined by non-linear regression. From Figure 4, it can be seen that the model could successfully depict the Congo red adsorption process using the AC-Fe_3O_4 adsorbent with a correlation coefficient, R^2 of more than 0.90. The maximum adsorption capacity of AC-Fe_3O_4 adsorbent at 298 K was be 129.87 mg.g-1. To further predict whether an adsorption process is favorable or not, (Hall et al., 1966) has proposed a dimensionless separation factor or equilibrium parameter, 'R_L' based on the obtained Langmuir constant, 'K_L' and it is given the equation 4.

$$R_L = \frac{1}{1+K_L C_e} \quad (4)$$

The adsorption process is considered to favorable when the R_L value falls between zero and unity and it is considered to be unfavorable when its greater than unity. Moreover, the adsorption is considered to be linear when R_L equals unity and irreversible when it equals to zero. The calculated values of RL was for Congo red adsorption using AC-Fe_3O_4 adsorbent was observed to be within the range 0.73 to 1, which indicates the adsorption process was favorable.

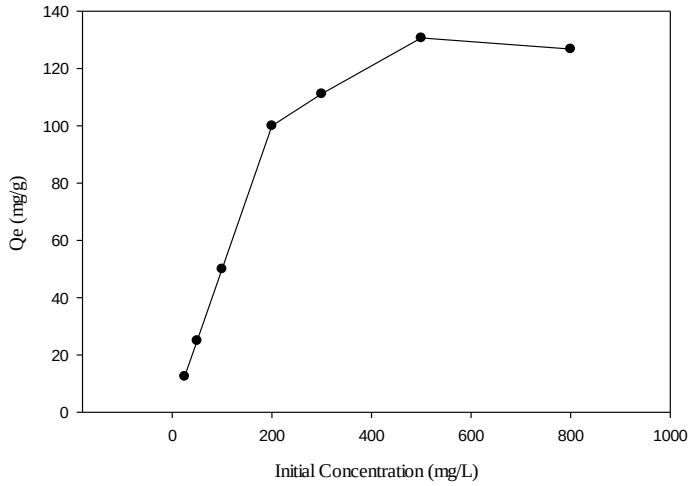


Fig. 4: Observed Isotherm for adsorption of Conge red dye using AC-Fe_3O_4 composite

4 Conclusion

This study showed that the AC-Fe_3O_4 composite is a potential adsorbent for removal of Congo red dyes from aqueous solutions. Congo red adsorption experiments were conducted using the prepared AC-Fe_3O_4 composite. Experimental parameters like adsorbent dosage and initial dye concentration were found to be have a significant effect on the Congo red adsorption process. Adsorption isotherm studies were conducted by fitting the experimental data to Langmuir, isotherm. Langmuir isotherm was found to be suitable in fitting the experimental data and the maximum adsorption capacity of the AC-Fe_3O_4 composite was found to be 129.87 mg/g. Hence, the synthesized AC-Fe_3O_4 adsorbents showed great potential to be used as an adsorbent for removal of Congo red dye as well as other organic pollutants from wastewater streams.

References

Ahmad, R. & Ansari, K. (2021). "Comparative study for adsorption of congo red and methylene blue dye on chitosan modified hybrid nanocomposite." *Process Biochemistry, 108*, 90-102. https://doi.org/https://doi.org/10.1016/j.procbio.2021.05.013

Aryee, et al. (2022). "Magnetic biocomposite based on peanut husk for adsorption of hexavalent chromium, Congo red and phosphate from solution: Characterization, kinetics, equilibrium, mechanism and antibacterial studies." *Chemosphere, 287*, 132030. https://doi.org/https://doi.org/10.1016/j.chemosphere.2021.132030

Deng, et al. (2022). "Synthesis of chitosan-modified magnetic metal-organic framework and its adsorption of Congo red and antibacterial activity." *Microporous and Mesoporous Materials, 342*, 112042. https://doi.org/https://doi.org/10.1016/j.micromeso.2022.112042

Ewis, et al. (2022a). "Adsorption of 4-Nitrophenol onto Iron Oxide Bentonite Nanocomposite: Process Optimization, Kinetics, Isotherms and Mechanism." *International Journal of Environmental Research, 16*(2), 23. https://doi.org/10.1007/s41742-022-00402-z

Ewis, et al. (2022b). "Enhanced Removal of Diesel Oil Using New Magnetic Bentonite-Based Adsorbents Combined with Different Carbon Sources." *Water, Air, & Soil Pollution, 233*(6), 195. https://doi.org/10.1007/s11270-022-05641-6

Hall, et al. (1966). "Pore-and solid-diffusion kinetics in fixed-bed adsorption under constant-pattern conditions." *Industrial & engineering chemistry fundamentals, 5*(2), 212-223.

Harja, M., Buema, G. & Bucur, D. (2022). "Recent advances in removal of Congo Red dye by adsorption using an industrial waste." *Scientific Reports, 12*(1), 6087. https://doi.org/10.1038/s41598-022-10093-3

Langmuir, I. (1918). "The adsorption of gases on plane surfaces of glass, mica and platinum." *Journal of the American Chemical society, 40*(9), 1361-1403.

Lei, et al. (2017). "Synthesis of hierarchical porous zinc oxide (ZnO) microspheres with highly efficient adsorption of Congo red." *Journal of colloid and interface science, 490*, 242-251.

Lim, et al. (2016). "Enhanced treatment of swine wastewater by electron beam irradiation and ion-exchange biological reactor." *Separation and Purification Technology, 157*, 72-79.

Litefti, et al. (2019). "Adsorption of an anionic dye (Congo red) from aqueous solutions by pine bark." *Scientific Reports, 9*(1), 16530. https://doi.org/10.1038/s41598-019-53046-z

Mahmud, et al. (2020). "Synthesis and Characterization of Fe3O4 Nanoparticles Using Different Experimental Methods." *IOP Conference Series: Materials Science and Engineering, 778*(1), 012028. https://doi.org/10.1088/1757-899X/778/1/012028

Mahmud, et al. (2021). "Effective Heterogeneous Fenton-Like degradation of Malachite Green Dye Using the Core-Shell Fe3O4@SiO2 Nano-Catalyst." *ChemistrySelect, 6*(4), 865-875.

https://doi.org/https://doi.org/10.1002/slct.202003937

Mahmud, et al. (2023). "Magnetic Iron Oxide Kaolinite Nanocomposite for Effective Removal of Congo Red Dye: Adsorption, Kinetics, and Thermodynamics Studies." Water Conservation Science and Engineering, 8(35), https://doi.org/https://doi.org/ 10.1007/s41101-023-00207-x

Shan, et al. (2015). "Highly efficient removal of three red dyes by adsorption onto Mg–Al-layered double hydroxide." *Journal of Industrial and Engineering Chemistry*, *21*, 561-568.

Wang, et al. (2022). "Effective adsorption of Congo red dye by magnetic chitosan prepared by solvent-free ball milling." *Materials Chemistry and Physics*, 292, 126857. https://doi.org/https://doi.org/10.1016/j.matchemphys.2022.126857

Cite as: Mahmud N., Yasser L., Rahaf Mahmoud R. & Benamor A., "Adsorption of Congo red dye Using Activated Carbon-Fe_3O_4 Composite", *The 2nd International Conference on Civil Infrastructure and Construction (CIC 2023)*, Doha, Qatar, 5-8 February 2023, DOI: https://doi.org/10.29117/cic.2023.0163

Implementation of Odour Control Systems for Nuisance-free and Public Friendly Environment in Qatar

Spyridon Trikis
Parsons International Limited, Doha, Qatar
Spyridon.Trikis@Parsons.com / spiros_trikis@yahoo.com

Vaibhav Sumant
Parsons International Limited, Doha, Qatar
Vaibhav.Sumant@Parsons.com / vaibhav.sumant@gmail.com

Muhammad Arshad
Parsons International Limited, Doha, Qatar
Muhammad.Arshad@Parsons.com

Anna Olliver
Public Works Authority (Ashghal), Doha, Qatar
AOlliver@ashghal.gov.qa / najder@hotmail.com

Meshaal Jarallah Abushereeda
Public Works Authority (Ashghal), Doha, Qatar
mabushereeda@ashghal.gov.qa

John Brown
Parsons International Limited, Doha, Qatar
John.Brown@Parsons.com

Abstract

The Public Works Authority (Ashghal) is contributing to the development of Qatar with the construction of first class, sustainable infrastructure with a high degree of public acceptance by utilizing best international practices. Pumping stations and sewage treatment works are traditionally constructed at the outskirts of cities, as they are generally associated with odour nuisance; however, as the cities are expanded, the facilities become part of the urban fabric and their operation becomes an issue of concern for nearby residents. To address this public concern, Ashghal has for its sewer infrastructure adopted odour emission limits as stringent as 0.5ppbV of hydrogen sulphide (H_2S) and 0.5ouE/m^3 of odour concentration, which are lower than recognisable levels by humans. Moreover, on the way to FIFA World Cup Qatar 2022™, Ashghal decided to install environmentally friendly and sustainable biological treatment units followed by activated carbon filters to ensure a nuisance-free environment at the existing Doha South Sewage Treatment Works (DS-STW) and the new Doha South Terminal Pump Station (DS-TPS). This paper presents methodologies for determining odour levels in existing and new units, available odour treatment technologies, and the selected treatment schemes for the above projects.

Keywords: Odour control; Odour treatment; Biological treatment; Sustainability; Pumping stations; Sewage Treatment Works

1 Introduction

Sewerage infrastructure is usually associated with public nuisance and health concerns due to odour emissions, the use of hazardous chemicals, increased heavy traffic load and no consideration to aesthetic appearance. This may also drastically devalue the cost of land in the adjacent areas (Arora, 2020). Consequently, sewage treatment works (STW) are typically located at the outskirts of cities.

As the development of cities progresses, STWs and pumping stations become an integral part of the urban fabric; therefore, measures must be taken to apply sustainable and economical solutions to eliminate the causes of nuisance. This paper presents overall air management and odour treatment solutions, and explains how odour can be contained, ventilated, and treated using regional Odour Control Facilities (OCF) with preference to environmentally sustainable biological treatment technologies. This has been adopted by Ashghal on two crucially important projects. The first project entails the recently completed rehabilitation of Doha South Sewage Treatment Works (STW) once considered to be in an outskirt location, to a cumulative odour treatment capacity of approx. 270,000m^3/h. The second project entails active odour extraction from the tunnels of the recently commissioned Doha South Sewer Infrastructure Project (DSSIP) and the new Doha South Terminal Pump Station (DS-TPS).

2 Odourous Compounds and Their Generation

Odours emanating from Sewage infrastructure relating to wastewater collection and treatment

facilities are composed of a mixture of various chemical compounds including hydrogen sulphide (H2S), ammonia (NH4), mercaptans, various volatile organic compounds (VOCs), etc (Baiming et. al., 2019), Odour Emission occurs at locations where the flow is turbulent, e.g., due to high velocities and where it is discharged or dissipated and cause nuisance once they are released into the atmosphere. H_2S is the most important component as it creates significant odour nuisance, is toxic and corrosive. H_2S once biochemically oxidized in the presence of moisture, it forms sulphuric acid, which is even more corrosive and detrimental to concrete.

Under laboratory conditions humans can perceive H_2S at a concentration starting at 0.5 parts per billion (ppb), which is why it is defined as the threshold odour concentration; however, nuisance concentrations are typically 5-10 times the threshold odour concentration (QSDDM, 2005).

Based on the above, Ashghal specified the following odour limits at the property line and beyond of the TPS and DS-STW which are in the close vicinity of the Al Thumama Stadium that hosted events during FIFA World Cup Qatar 2022™ (PWA, 2018 and CH2M, 2017b).

- H_2S less than or equal to 5 ppbv as a 98th percentile of the one (1) hour average concentration at all weather conditions; and
- Odour less than or equal to 5 odour units (OU) per m^3 as a 98th percentile of the one (1) hour average concentration at all weather conditions.

3 Design Stages for Odour Control Systems

According to QSDDM (2005), the preferred option should be to eliminate or at least minimize the development of uncontrolled emissions prior to select appropriate systems to treat the emissions during the design of a dour treatment system. The following design stages were therefore adopted to ascertain Odour Control system needs for DS-STW and DS-TPS:

- **Assessment of the baseline emissions.** For DS-TPS, the emission levels generated in the upstream tunnel system were estimated with the use of septicity modelling and air sampling inside sewer manholes, while the emission levels of the different facilities at the DS-STW were assessed after air sampling at different locations.
- **Assessment of the required performance of the Odour Control Units.** Air dispersion modelling was carried out to determine the maximum allowable emissions as well as the

location, the sizes, and heights of the stacks to ensure that the odour limits would not be exceeded at the property lines and beyond.

- **Selection of the Odour Treatment Scheme and determination of the capacity of the Odour Control Units.** This was based on the assessment of the emissions at the source and the desired emissions at the stack.
- **Commissioning plan of the DS-STW.** This considered minimizing the potential for septic development due to excessive storage of sludge or sewage during commissioning.
- **Operation and Maintenance Manuals of the system.** This includes description and procedures to carry out seamless and trouble-free operation by performing preventative and corrective maintenance tasks of the installed Odour Control System.

4 Assessment of Baseline Emissions

4.1 Septicity modelling for DS-TPS

A septicity model for the new sewerage conveyance system DSSIP was used to ascertain the baseline emissions for the design of DS-TPS where the three main trunks of the Main Trunk Sewer (MTS) converge before entering the coarse screen shaft at DS-TPS. Septicity model results revealed that vapour-phase H_2S levels in the tunnel could reach as high as 900ppmV while short-term spikes of up to 1700ppmV can also be expected (CH2M, 2017a). Approximately 80% of the airflow from DSSIP would be drawn off for treatment (Figure 1) while the remaining 20% would enter the coarse screen shaft and be extracted for odour control treatment (CH2M, 2017b).

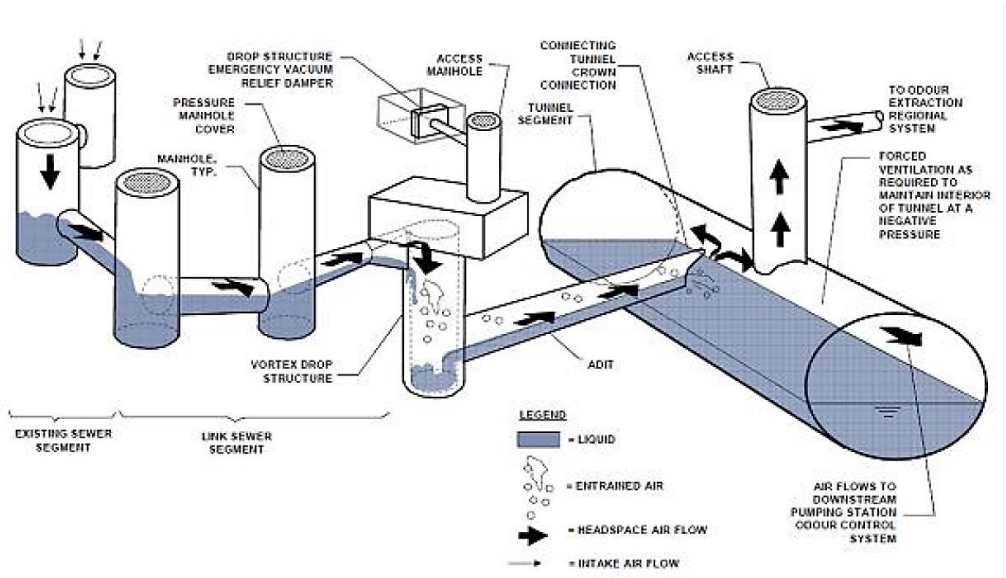


Fig. 1: Interceptor Lateral, Drop Structures and MTS Ventilation Schematic

4.2 Air Sampling at DS-STW

At DS-STW, air sampling was carried out during early morning hours, mid-day and at dusk time to capture the emissions and their concentration in different locations with the works in operation. The locations were selected after studying the STW layout and the operation conditions in order to identify the potential locations of odour development, identify the locations of major odour sources, understand, and assess the odour levels within and surrounding area, and to generate odour data sheets that would be essential for the odour modelling.

Field olfactometers, handheld H_2S detectors and a mobile meteorological station to record temperature, relative humidity, wind speed and direction (with GPS co-ordinate integration) were used to identify the odour emission sources. Air samples were collected from 19 different locations within as well as outside DS-STW, as presented in Figure 2 and Figure 3.

The highest average concentration levels of odour found at DS-STW in the morning and evening time during the study period were as follows (Wabag, 2020):

- 14,000 to 47000ouE/m^3 (100 to 500ppmV H_2S) at the Raw Sewage Handling Units.
- 500ouE/m^3 (0.5 to 2ppmV H_2S) at the existing digester area; and
- 350ouE/m^3 (50ppmV) at Sewage holding tanks area.

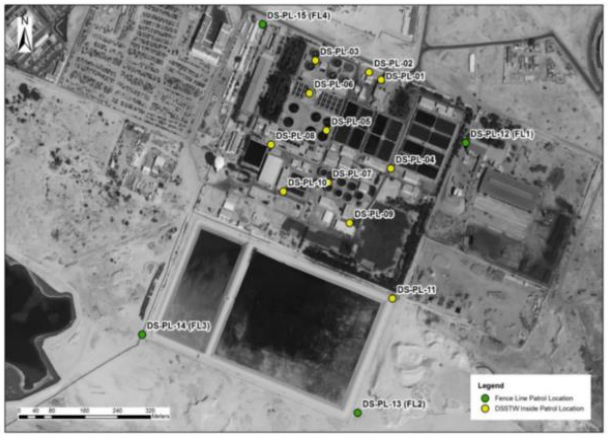


Fig. 2: Odour Sampling Locations within DS-STW



Fig. 3: Odour Sampling Locations outside DS-STW

5 Odour Impact Assessment Through Dispersion Modelling

For DS-TPS, it was assumed that a dilution ratio of 250:1 can be achieved after stack discharges. Therefore, an expected discharge concentration of 50ppbV H_2S at the stack was considered for the OCF design to meet a value of 0.20ppbV H_2S offsite (CH2M, 2017b).

For the emissions of the DS-STW, air dispersion modelling using US Environmental Protection Agency's (EPA) AERMOD algorithm (version 18081) was carried out to identify which existing and proposed sources on the DS-STW site needed to be connected to the odour control system to achieve the target levels.

Air sampling results, meteorological data for the most recent five years; and terrain and Building/Structure data of the vicinity were used as inputs to the model. The following scenarios were considered:

- ***Scenario 1***: Existing works without the implementation of Odour Control

  The dispersion model demonstrated that emissions from several existing sources such as sewage holding tanks, existing OCU stack, Thickening Building, SBR Anoxic zone, Inlet Works Building, and Septic Tank off-loading area are required to be controlled.

- ***Scenario 2***: Existing and new works without the implementation of Odour Control

  The dispersion model showed that (i) emissions from new aerobic digesters that are close to the plot limits must be controlled and (ii) H_2S emissions are exceeded at the site boundary due to the sewage holding tanks and the existing OCU stack as seen in Figure 4 and Figure 5 (Wabag, 2020).

- ***Scenario 3***: Existing and new works with Future Odour Control System

  An additional modelling scenario was run with the controlled residual emissions from the stacks of the proposed units as input to verify that with the selected scheme and when the emissions from the different sources are adequately treated, the residual odours and H_2S concentration would be less than 5ouE/m^3 and 5ppbV H_2S respectively at or beyond the site boundary as seen in Figure 6 and Figure 7 (Wabag, 2020).

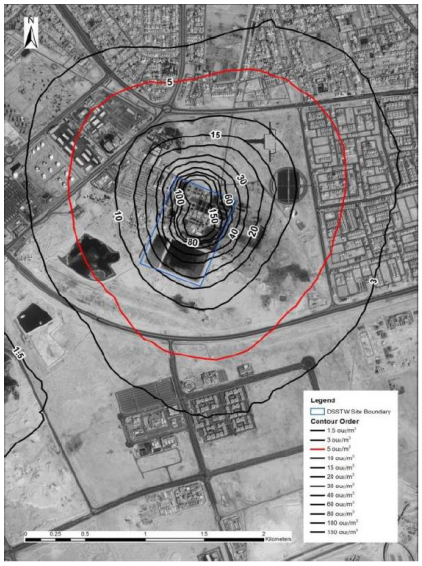


Fig. 4: Contour Plot of Scenario 2 Maximum 98th Percentile Odour Impacts (ouE/m^3)



Fig. 5: Contour Plot of Scenario 2 Maximum 98th Percentile H_2S Impacts (ppbv)



Fig. 6: Contour Plot of Scenario 3 Maximum 98th Percentile Odour Impacts (ouE/m^3)



Fig. 7: Contour Plot of Scenario 3 Maximum 98th Percentile H_2S Impacts (ppbv)

6 Selection of Odour Control Treatment Technologies

6.1 Odour Treatment Technologies

In choosing an odour control technology, several aspects need to be evaluated, such as: collection efficiency, ease of reuse or disposal of recovered material, ability of system to handle variations in gas flow and loads at required collection efficiencies, equipment reliability and freedom from operational and

maintenance attention, and initial investment and operating cost (Stanley & Muller, 2002).

There are several odour treatment technologies available on the market (WEF, 2020), which are presented and compared against each other in Table 1.

Table 1: Comparison of Odour Treatment Technologies

SN	Treatment Technology	Cost Factors	Advantages / Disadvantages
1	Packed tower wet scrubbers	Moderate capital, high operation, and maintenance (O&M) costs	**Advantages** Can be used on intermittently operated odour sources, which is often the case in bio-solids applications **Disadvantages** High chemical consumption; High O&M cost
2	Activated carbon absorbers	Cost-effectiveness depends on carbon replacement or regeneration frequency	**Advantages** Simple operation, few moving parts; Best for relatively dilute airstreams **Disadvantages** Not economical for highly concentrated streams
3	In-ground bio-filters	Low to moderate capital; low O&M	Advantages Simple operation; few moving parts; Low O&M cost Disadvantages Large footprint: Not well suited to intermittent odour sources, which is sometimes the case in bio-solids applications
4	Pre-engineered bio-filters	Moderate to high capital; low O&M	**Advantages** Low O&M cost can be very effective on bio-solids cake applications that run 24/7 **Disadvantages** Higher capital costs than in-ground bio-filters; Not well suited to intermittent odour sources
5	Bio-scrubbers, bio-trickling filters	Moderate capital; low O&M	**Advantages** High H_2S loading capacity **Disadvantages**. Little long term performance data for non-H_2S applications; Not well suited to intermittent odour sources
6	Thermal oxidizers	Very high capital and O&M (energy)	**Advantages** Effective for wide spectrum of odours and VOCs; Suitable for very complex odorous air streams **Disadvantages** Only economical for high-strength, difficult-to-treat airstreams
7	Ionization Systems	High initial capital costs, lower operational costs	**Advantages** Some systems have proven effective on complex bio-solids odours **Disadvantages** Systems suitable for small applications (51 m/s or less); Limited vendors with proven experience
8	Neutralization	Moderate capital, high operation, and maintenance (O&M) costs	**Advantages** Suitable for extend uncovered odour sources **Disadvantages** Suitable for low odour concentrations only; Limited vendors with proven experience

6.2 Odour Control Methodology at DS-TPS

To select the odour treatment scheme at DS-TPS to comply with the offsite odour limits, a multi-stage approach was selected as it reduces the risk by improving the system reliability, robustness, and overall performance. Technologies in series were evaluated based on specific set of qualitative criteria, where each technology combination was ranked for each criteria category. A combination of BTF

followed by ACF was considered the most favourable and was therefore considered as preferred option to treat the odorous air from the DSSIP tunnels and emissions at DS-TPS.

Based on the references and experience from DS-TPS, the odour treatment scheme for the Wakrah-Wukair Drainage Tunnel Project (WWDT) is in the process of being designed and constructed with the same two-stage treatment comprising of BTF followed by ACF, where dispersion modelling is used to determine the treatment efficiency of the units as well as size and height of the stack. This standalone facility to later cater for an ultimate capacity of 75,600m^3/h once it is linked with DSSIP.

6.3 Odour Control Methodology at DS-STW

Based on the Scenario 2 dispersion modelling results, a scheme of three (3) Odour Control Units (OCU) was proposed to collect emissions as indicated in Table 2. The different units were designed to reduce the H_2S levels and consequently the odour levels by >99%.

Table 2: Emission Sources and respective OCU

Odour Control Unit	Emissions Collected
OCU-1	Stack of the existing OCU for the inlet works, Screenings and Grit Skips, Sewage Holding Tanks, currently used as excess flow balancing tanks, Anoxic tanks, Thickening sludge tanks. Centrifuge centrate line for SSF, Centrifuge dewater sludge line (for new SSF)
OCU-2	SBR Anoxic zones, SBR splitting chambers
OCU-3	Existing Aerobic digesters, New covered aerobic digesters; SAS balancing tanks, Sludge tanks in the Sludge Thickening Buildings, Centrifuge centrate lines in the old Sludge Thickening Buildings, Centrifuge centrate line in the existing Dewatering Building, Sludge Thickening Buildings, Tanker unloading station

Initially, emissions from the Inlet works were treated in chemical scrubbers, which was decided to be refurbished and integrated with the new OCU-1 considering its robustness to handle the intermittent spikes. The existing unit using USFilter LO/PRO® consisted of three stage chemical scrubbers with integral sump with a rated capacity of 20,428m^3/h treating an average of 750ppmV H_2S or peak of 1000ppmV H_2S. The new OCU-1 consists of a bio-tricking (BTF) filter followed by Activated Carbon Filters (ACF) with a capacity of 47,500m^3/h. The treated gas is disposed to the atmosphere through a stack of 20m high (Figure 8).

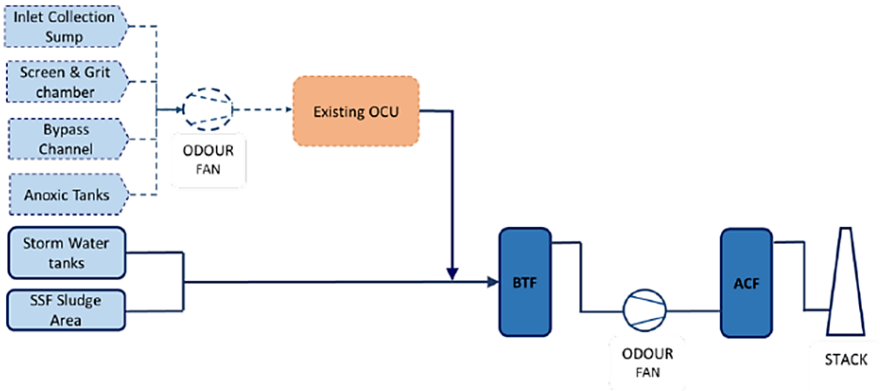


Fig. 8: Schematic Representation of OCU-1

Air from various sources identified for OCU-2 & OCU-3 has a low concentration of H_2S & Odour and pass through ACF prior to be released to the atmosphere through a 20m high stack (Figure 9 and Figure 10). OCU-2 has a treatment capacity for a flowrate of 42,200m^3/h, whereas OCU-3 has been designed for the flowrate of 182,000m^3/h.

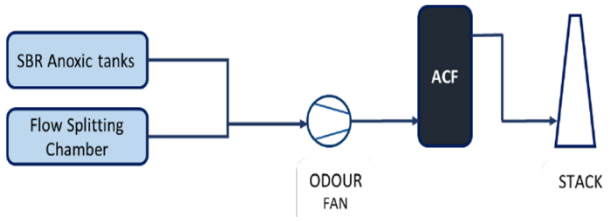


Fig. 9: OCU-2 Schematic Representation

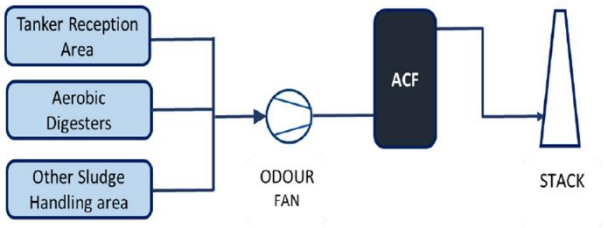


Fig. 10: OCU-3 Schematic Representation

To mitigate any observed odour emissions from large storage tanks and lagoons for sewage and TSE, SBR aeration basins and aerobic lanes which cannot be covered due to their large size, odour masking was proposed using neutralization chemicals. These chemicals consist primarily of essential oil solutions which either mask or react with the offensive odour components in the vapour phase when the solutions are atomized and sprayed as a mist around the odour source. This was the treatment strategy adopted to deal with any odorous conditions identified by the operators during the FIFA World Cup Qatar 2022™.

7 Sustainability Benefits From BTF Technologies as Primary Treament

Combination of technologies with BTF and ACF as principal treatment assures robust and reliable odour removal of a wide range of odour causing components, with limited use of chemicals. This minimizes the operation cost, and the requirements for chemical storage, handling, and the associated risks. BTF are also efficient in handling odour spikes and have relatively small footprint. In contrary, Chemical Scrubbers consume greater amounts of chemical reagents and demand higher quality potable water (preferably softened); while a portion of the solution will be wasted continuously after its reaction with the contaminants.

Finally, in a society that is increasingly committed to sustainable development, the use of biologic treatments where they can replace chemical reagents is a sustainable and environmentally preferable solution (Baiming et. al., 2019).

By selecting these technologies for odour control systems, Ashghal ensures sustainable development and provision of high standard of living for the citizens of Qatar in line with the Qatar National Vision 2030.

8 Conclusion

No odour nuisance is a key factor for public acceptance of sewerage infrastructure in residential development and Ashghal has adopted odour emission limits for its sewer infrastructure, as stringent as 0.5ppbV of hydrogen sulphide (H_2S) and 0.5ouE/m^3 of odour concentration.

From the several odour treatment technologies available, Ashghal promotes the installation of biological treatment units followed by activated carbon filters at the existing Doha South Sewage Treatment Works (DS-STW), new Doha South Terminal Pump Station (DS-TPS) and upcoming Wakrah-Wukair Drainage Tunnel Project (WWDT), as the most environmentally friendly and sustainable scheme.

The Odour Control Systems at DS-STW & DS-TPS ensured no odour nuisance at the venues of FIFA World Cup Qatar 2022™ and will continue to facilitate high living standards for the residents of Doha.

References

Arora, M. (2020). Considerations when Designing a Wastewater Treatment Plant. Water & Wastes Digest. Website accessed 20 Nov 2022. https://www.wwdmag.com

Baiming Ren, Yaqian Zhao, Nathalie Lyczko, Ange Nzihou (2019). Current Status and Outlook of Odor Removal Technologies in Wastewater Treatment Plant: Review. *Waste and Biomass Valorization, 10*(6), pp.1443-1458.

CH2M (2017a). MTS-01 Odour Modelling / Odour Load, Flow Rate, Doha South Terminal Pump Station and Regional Odour Control. Doc. No. C834-PMC-PWAP-MEM-00007, Rev. 1. Public Works Authority. Doha, p. 18.

CH2M (2017b). Terminal Pump Station OCF Study Report, Doha South Terminal Pump Station and Regional Odour Control. Doc. No. C834-PMC-PWAP-MEM-00008, Rev. 1. Public Works Authority. Doha, p. 18.

PWA (2018). Design and Built (D&B) Contract for Rehabilitation of Doha South Sewage Treatment Works (DSSTW). Doc. No. PWA/GTC/042/2017/L. Public Works Authority. Doha. Sec. E, Part 7.

Qatar Sewerage and Drainage Design Manual (QSDDM) (2005), Public Works Authority, Drainage Affairs, Qatar.

Stanley, M. B. W. & Muller, C. O. (2002). Choosing an Odour Control Technology-Effectiveness and Cost Considerations. Proceedings of Odour and Toxic Air Emissions, WEF, Albuquerque, NM, pp. 259-276.

Wabag (2020). Odour Control System Study. Doc. No. CP837-REP-PRO-0011, Rev 10. Public Works Authority. Doha, pp. 48-56.

Water Environment Federation (WEF) (2020). Odor Emissions and Control for Collection Systems and Water Resource Recovery Facilities. Manual of Practice No. 25. Alexandria, VA: Water Environment Federation.

Cite as: Trikis S., Sumant V., Muhammed A., Olliver A., Abushereeda M. & Brown J., "Implementation of Odour Control Systems for a Nuisance-free and Public Friendly Environment in Qatar", *The 2nd International Conference on Civil Infrastructure and Construction (CIC 2023)*, Doha, Qatar, 5-8 February 2023, DOI: https://doi.org/10.29117/cic.2023.0164

Study of Turbulence in Open Channels Using Two-Equation Models

Ahmad Sana
Sultan Qaboos University, Muscat, Sultanate of Oman
sana@squ.edu.om

Ghazi Al-Rawas
Sultan Qaboos University, Muscat, Sultanate of Oman
ghazi@squ.edu.om

Talal Etri
Sultan Qaboos University, Muscat, Sultanate of Oman
t.etri1@squ.edu.om

Abdullah Al-Mamun
Sultan Qaboos University, Muscat, Sultanate of Oman
aalmamun@squ.edu.om

Abstract

Prediction of the sediment transport in streams requires an accurate estimation of bed shear stress (for bed load) and eddy viscosity (for suspended load). In general, shallow water models employ empirical relationships to estimate the bottom shear stress. However, with the advancement of computing systems, the utilization of advanced turbulence models is getting common. In this paper, a number of model versions are reviewed based on their predictive abilities against the well-known bottom boundary layer properties in open channels and computational economy. Qualitative and quantitative comparisons have been made to infer that the choice of model versions should be based on the field application. For example, the bottom shear stress is very well predicted by the k-ε model whereas the cross-stream velocity profile and turbulent kinetic energy are predicted more efficiently by k-ε model versions. This study may be useful for researchers and practicing engineers in selecting a suitable two-equation model for calculating various bottom boundary layer properties.

Keywords: Turbulence model; Open channel; Bottom roughness; Bed shear stress; Turbulent flow; k-ε model; k-ω model

1 Introduction

The transport of sediment and pollutants in open channels essentially depend on the turbulence phenomenon among other factors. Being the most complex phenomenon to fully comprehend and estimate, turbulence computations have been the most challenging part of engineering calculations. A number of analytical and empirical models have been in vogue, prior to the widespread availability of powerful computing facilities, to estimate turbulent boundary layer properties. However, this practice changed approximately four decades ago when a number of turbulence models started to emerge and initially gained popularity among the researchers and then among the practicing engineers. Almost all the present day commercial models, used for engineering calculations for rivers and estuaries include some of these turbulence models. Nonetheless, many engineering calculations are based on empirical models or a combination of turbulence and empirical models yet. As usual, turbulence models used in research are far more complex and computationally expensive than the ones used in the field applications.

The velocity and pressure in a flowing fluid are expressed using Navier–Stokes equations. However, exact solutions of these equations are possible only for very simple flow phenomena. Most of the practical fluid flows including open channel flow are complex and classified as turbulent flows. Osborne Reynolds (1842-1912) proposed that each of the flow quantities (velocities and pressures) may be decomposed into mean and fluctuating components. Reynolds obtained what we know today as Reynolds-averaged Navier–Stokes (RANS) equations. However, even after averaging the Navier-Stokes equations, the fluctuating components remained in the RANS equations. These fluctuating components are there in the form of so-called Reynolds Stresses. Further research showed that if we try to express these Reynolds stresses in 'exact' quantities using more equations, more nonlinear terms will appear such that the number of unknowns will remain more than the available equations. This situation is termed as the '*closure problem*' which can be stated as '*total statistical description of turbulence requires an infinite set of equations*'. Later Boussinesq (1903) used the concept of eddy viscosity to define Reynolds stress in terms of the eddy viscosity and velocity gradient. Ludwig Prandtl (1875-1953) proposed the concept of mixing length to define the eddy viscosity using length and velocity scales. These developments later became the basis of the present-day turbulence models. The length and velocity scales can be represented by turbulent quantities that are expressed by turbulent transport equations.

Some studies on open channels based on Direct Numerical Simulation (DNS), Large Eddy Simulation (LES) and Reynolds Stress models have been carried out in the past. However, two-equation turbulence models have gained popularity among researchers as well as practicing engineers because of their reasonable accuracy with computational economy. Several versions of such models are reported in the literature; however, k-ε and k-ω have been the most popular two-equation models.

Jones and Launder (1972) proposed k-ε model for steady flow phenomena. However, this model has been applied to unsteady flow problems as well. Later a number of modifications were proposed in the model parameters by several researchers and some of them became popular among the engineering researchers such as Myong and Kasagi (1990) (MK), Nagano and Tagawa (1990) (NT) and Yang and Shih (1993) (YS). Sana and Tanaka (2000) reviewed some of the model versions for oscillatory boundary layers on smooth beds. Sana et al. (2007) proposed modifications in MK and NT models, which are referred in this paper as MKM and NTM, respectively. The modelling of rough surface flows has been a challenge using k-ε model. Many researchers have tried several methods, but all these methods have their shortcomings. One the other hand k-ω model, which was proposed by Wilcox (1988), can be easily used for rough as well as smooth surfaces using simple boundary conditions. it is believed that this model performs better than k-ε model near the bed. This fact motivated Menter (1994) to propose a blended k-ω model in which near the wall k-ω and far from the wall k-ε model is employed. Sana and Shuy (2002) reviewed some k-ω model versions for oscillatory boundary layers on a smooth bed and Sana et al. (2009) tested the blended k-ω model versions on a rough bed.

In the present study some popular versions of k-ε and k-ω model are used to simulate steady flow in a wide open channel having smooth or rough bed. The k-ε model versions have been used for smooth surfaces only, whereas k-ω model has been applied to all types of channel beds.

2 Theoretical Background

The turbulence models are classified based on the number of transport equations used in the model. For example, a model, which is not based on a transport equation, is termed as zero-equation model;

the ones using one and two transport equations are called one-equation and two-equation turbulence models, respectively. More advanced models like Reynolds Stress or Flux transport models utilize the transport equations for Reynolds stresses, fluxes and length scale. Another category of advanced models resolve large eddies exactly and model small eddies using a modelling assumption are called as Large Eddy Simulation models. In the present study two-equation models, namely *k*-ε and *k*-ω model versions were used for the simulation of turbulent flow in a wide-open channel (one-dimensional flow) having smooth and rough bed.

2.1 Governing Equations

The governing equations of the *k*-ε model (Eq. 1 to Eq. 4) are as follows:

$$\frac{\partial u}{\partial t} = \frac{\partial p}{\partial x} + \frac{\partial \tau}{\partial y} = \frac{dp}{dx} + \frac{\partial}{\partial y}\left\{(\nu + \nu_t)\frac{\partial u}{\partial y}\right\} \quad (1)$$

$$\nu_t = C_\mu f_\mu \frac{k^2}{\tilde{\varepsilon}} \quad (2)$$

$$\frac{\partial k}{\partial t} = \frac{\partial}{\partial y}\left\{\left(\nu + \frac{\nu_t}{\sigma_k}\right)\frac{\partial k}{\partial y}\right\} + \nu_t\left(\frac{\partial u}{\partial y}\right)^2 - \tilde{\varepsilon} - D \quad (3)$$

$$\frac{\partial \tilde{\varepsilon}}{\partial t} = \frac{\partial}{\partial y}\left\{\left(\nu + \frac{\nu_t}{\sigma_\varepsilon}\right)\frac{\partial \tilde{\varepsilon}}{\partial y}\right\} + C_1 f_1 \nu_t \frac{\tilde{\varepsilon}}{k}\left(\frac{\partial u}{\partial y}\right)^2 - C_2 f_2 \frac{\tilde{\varepsilon}^2}{k} + E \quad (4)$$

Where *u* is the flow velocity at y, *x* and *y* are coordinate axes, ν and ν_t are molecular and eddy viscosity, respectively, *dp*/*dx* is the pressure gradient and considered to be constant over the channel cross-section, turbulent kinetic energy, $k = \left(\overline{u'^2} + \overline{v'^2} + \overline{w'^2}\right)/2$, turbulent kinetic energy dissipation rate, $\varepsilon = \nu\overline{\frac{\partial u_i'}{\partial x_k}\frac{\partial u_i'}{\partial x_k}}$, $\tilde{\varepsilon} = \varepsilon - D$ and *D*, *E*, $C\mu$, $f\mu$, C_1, C_2, f_1 and f_2 are model parameters.

The blended *k*-ω model equations as given by Menter (1994) are shown as Eq. (5) and Eq. (6):

$$\frac{\partial k}{\partial t} = \underbrace{\frac{\partial}{\partial y}\left\{(\nu + \nu_t\sigma_{k\omega})\frac{\partial k}{\partial y}\right\}}_{\text{Diffusion}} + \underbrace{\nu_t\left(\frac{\partial u}{\partial y}\right)^2}_{\text{Production}} - \underbrace{\beta^*\omega k}_{\text{Dissipation}} \quad (5)$$

$$\frac{\partial \omega}{\partial t} = \frac{\partial}{\partial y}\left\{(\nu + \nu_t\sigma_\omega)\frac{\partial \omega}{\partial y}\right\} + \gamma\frac{\nu+\nu_t}{\nu_t}\left(\frac{\partial u}{\partial y}\right)^2 - \beta\omega^2 + 2(1-F_1)\sigma_{\omega 2}\frac{1}{\omega}\frac{\partial k}{\partial y}\frac{\partial \omega}{\partial y} \quad (6)$$

Where, ω is the turbulent kinetic energy dissipation function. This blended model has been used in various types of boundary layer flows. The model parameters are given in the respective references listed in Table 1.

Table 1: Model versions used in the present study

***k*-ε model**		***k*-ω model**	
Acronym	Reference	Acronym	Reference
JL	Jones and Launder (1972)	WL	Menter (1994)
MKM	Sana et al. (2007)	BSL	Menter (1994)
NTM	Sana et al. (2007)	SST	Menter (1994)
YS	Yang and Shih (1993)		

2.2 Solution Procedure

The governing equations were converted into dimensionless form using the average velocity, U_0 distance from the bed to the axis of symmetry y_h (free-surface with no external forces) and mass density of the fluid. These dimensionless equations require only Reynolds number $Re = U_0 y_h/\nu$ and

$k_s^* = k_s/y_h$ (k_s : Nikuradse's equivalent roughness height) as input. A Crank-Nicolson type implicit finite difference scheme was used. The grid spacing was varied exponentially for better accuracy near the bottom. In cross-stream direction 100 grid points were used. Time marching scheme was used to run the simulations. The convergence was based primarily on velocity, k and ε (or ω) and then on bottom shear stress (τ_0). The convergence limit for both the steps was set to 1×10^{-6}.

3 Results and Discussion

3.1 Smooth Bed

For smooth open channels the velocity profile was predicted using k-ε model versions by JL, MKM, NTM and YS (as describe in Table 1) in Figure 1. The experimental data of two tests (Test 3: Re = 21,620, Test 11: Re = 144180) from Kirkgoz (1989) was used for comparison. It is interesting to note that JL model predicts the velocity better than the newer versions for both the tests in the logarithmic layer. However, MKM model shows better agreement in the viscous sublayer and buffer layer (Test 3).

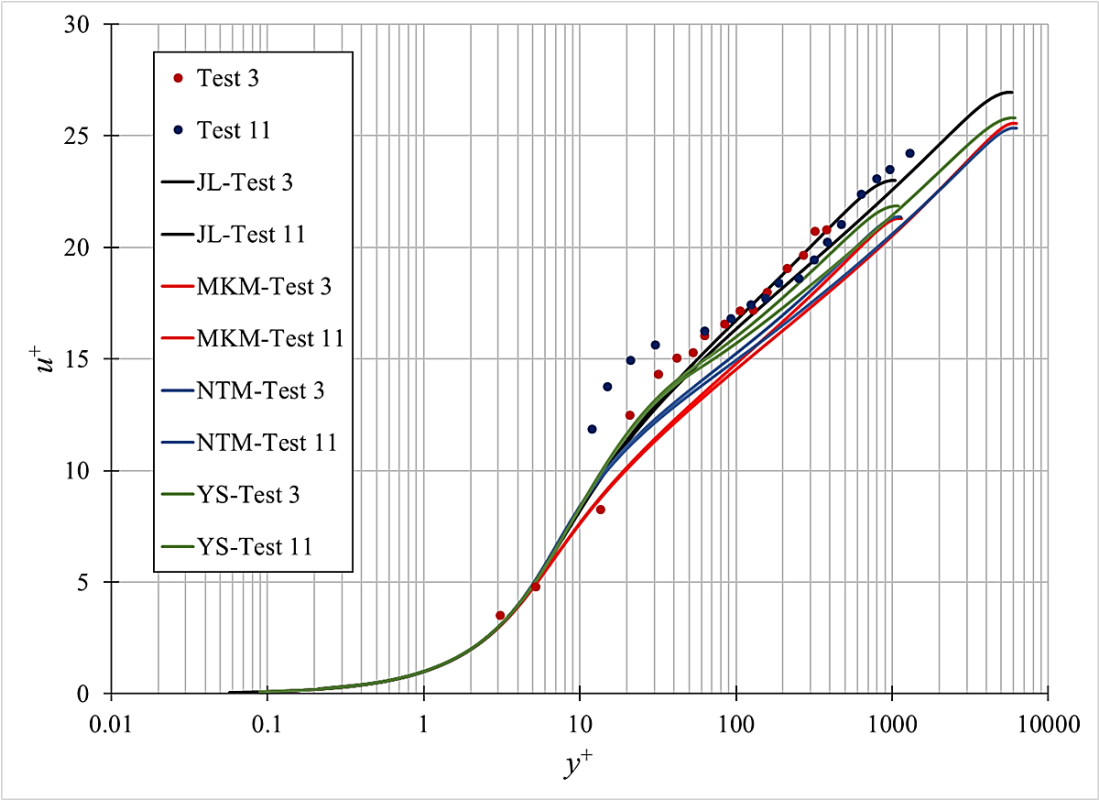


Fig. 1: Comparison of the velocity profiles between model predictions and experimental data by (Kirkgoz, 1989)

The friction factor ($f = 2\tau_0/\rho U_0^2$) is another important parameter used to calculate the bottom shear stress from the average velocity. Figure 2 shows a comparison between JL model and the relationships by Nikuradse (1933) and Colebrook (1939) who developed their relationships for pipe flow. Here these relationships are transformed for open channel using the hydraulic radius. The model shows an excellent agreement with the experimental relationships. The friction factor by Balsius (1913) and derived from logarithmic velocity profile along-with the friction factor from laminar flow ($f = 64/Re$) are also shown. The model could predict the friction factor for the whole range of flows from laminar to turbulent with precision. This characteristic of the turbulence model proves the importance of the usage of such models where it is not required to check the type of flow before applying an empirical relationship for a certain type of flow.

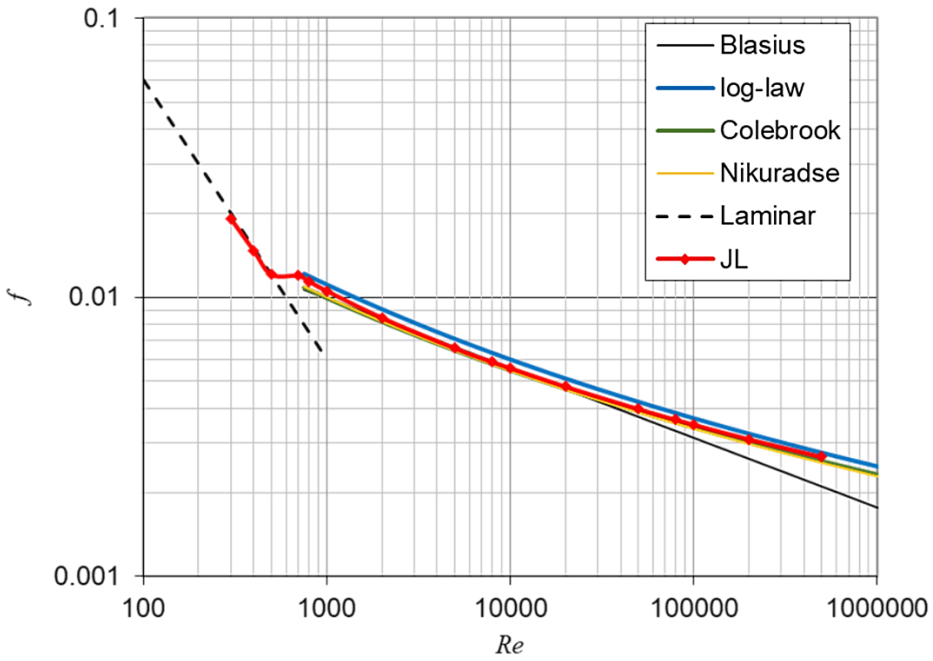


Fig. 2: Friction factor for smooth-bed open channel

3.2 Rough Bed

As mentioned before the application of k-ε model for flow over rough surfaces is extremely difficult. Various techniques have been used among which the wall function method is the most popular. This method employs the logarithmic relationship to specify the wall boundary condition. However, the location of the point where the boundary condition has to applied cannot be fixed because of its dependence on the roughness height. Besides, the shear stress has to be known for the application of the wall function. In other words, iterations have to be performed to find appropriate location for the boundary condition. On the other hand, the surface roughness can be easily described by a simple function of the value of ω at the location of the bed in case of k-ω model. Therefore, in the present computations only k-ω model is utilized for rough-bed open channels. Figure 3 shows the model parameter S_R that controls the effect of the surface roughness in k-ω model. Sana et al. (2009) proposed a single relationship for the whole range of roughness values, which is also shown in Figure 3.

Considering the rough surface classification, three cases were simulated, and velocity profiles and turbulence kinetic energy profiles are shown in Figure 4 and Figure 5, respectively. The velocity profiles show the fact that higher the roughness, larger is the logarithmic region. This is due to higher rate of turbulent kinetic energy transfer to the outer layer due to higher roughness. As a result, the velocity at the axis of symmetry is lesser than the case of a smaller roughness and the same Reynolds number. Moreover, the thickness of the viscous sublayer decreases with an increase in the wall roughness. All these characteristics of a rough-turbulent flow are shown efficiently by SST k-ω model proposed by Menter (1994). Figure 5 shows a higher production of turbulent kinetic energy for higher roughness values. Moreover, the comparison between the flow over low roughness (hydraulically smooth) and transitional roughness showing the production of turbulent kinetic energy near the wall. The model could predict all the key features of rough-bed open channel in an immaculate manner qualitatively. Further investigation using experimental or DNS data is required to judge the capabilities of the model in this regard.

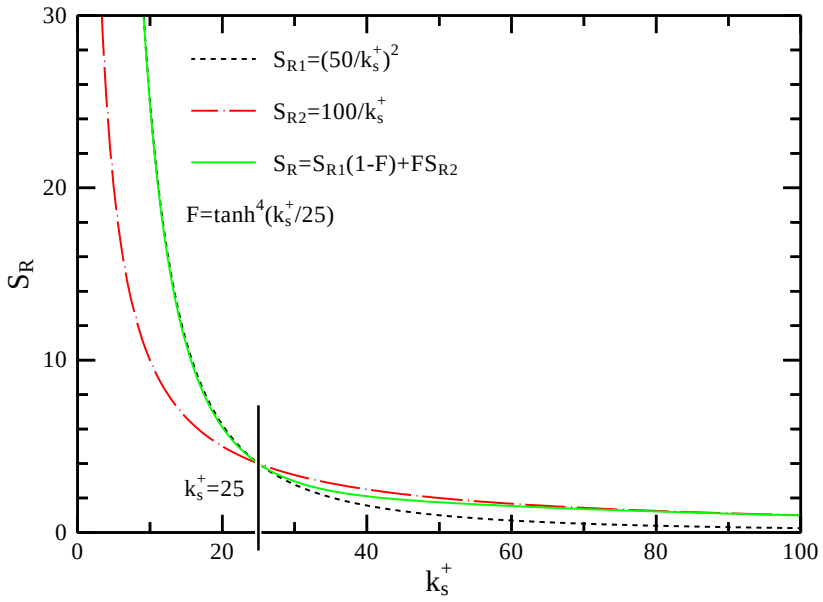


Fig. 3: Model parameter S_R in k-ω model to describe bed roughness

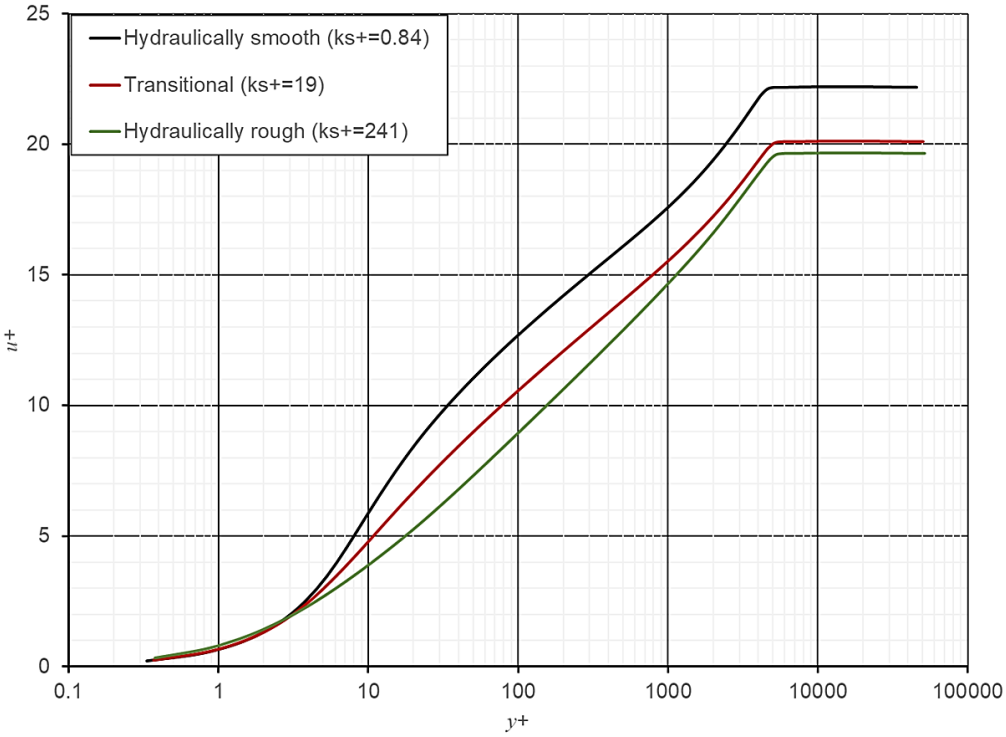


Fig. 4: Velocity profiles in a rough-bed open channel by SST k-ω model

3.3 Friction Factor

In case of smooth surface (laminar, transitional and turbulent flow) the friction factor is mainly a function of Reynolds number whereas for the flow over a rough surface the friction factor depends on $k_s^+ (= k_s/\nu)\sqrt{\tau_0/\rho}$ (τ_0: bottom shear stress, k_s : Nikuradse's equivalent roughness height, ρ: fluid mass density). The friction factor from full-range equation derived from Tanaka and Thu (1994), Colebrook (1939) and Nikuradse (1933) are also shown in comparison with the results of SST k-ω model. Over the full-range of flow types, the model performs very well in predicting the friction factor.

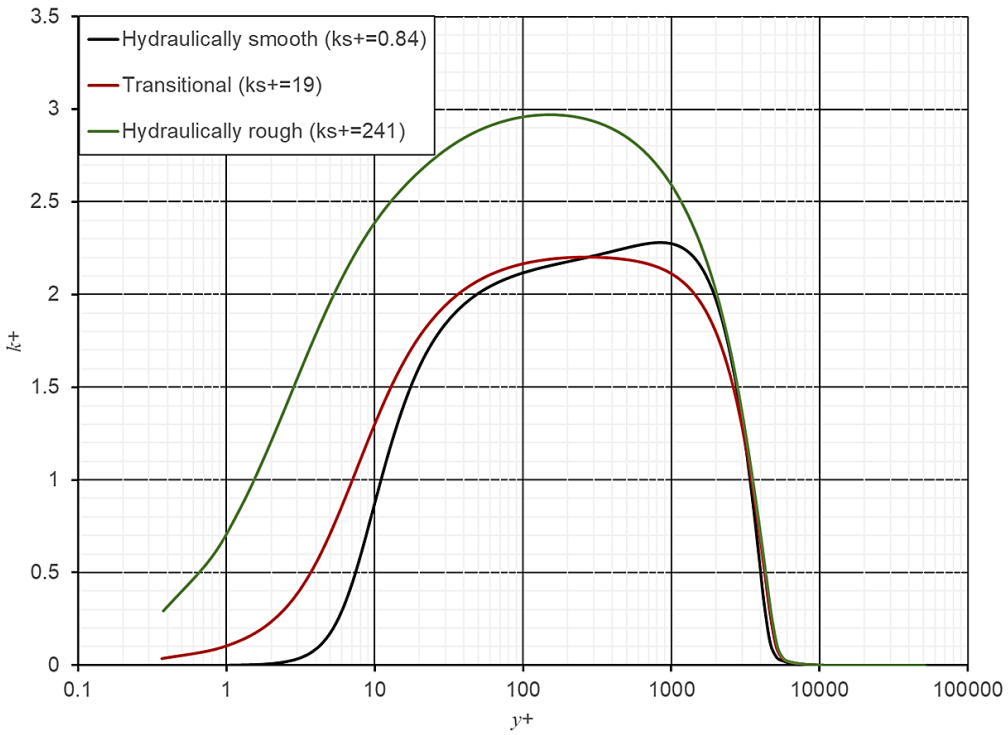


Fig. 5: Turbulent kinetic energy profiles in a rough-bed open channel by SST *k-ω* model

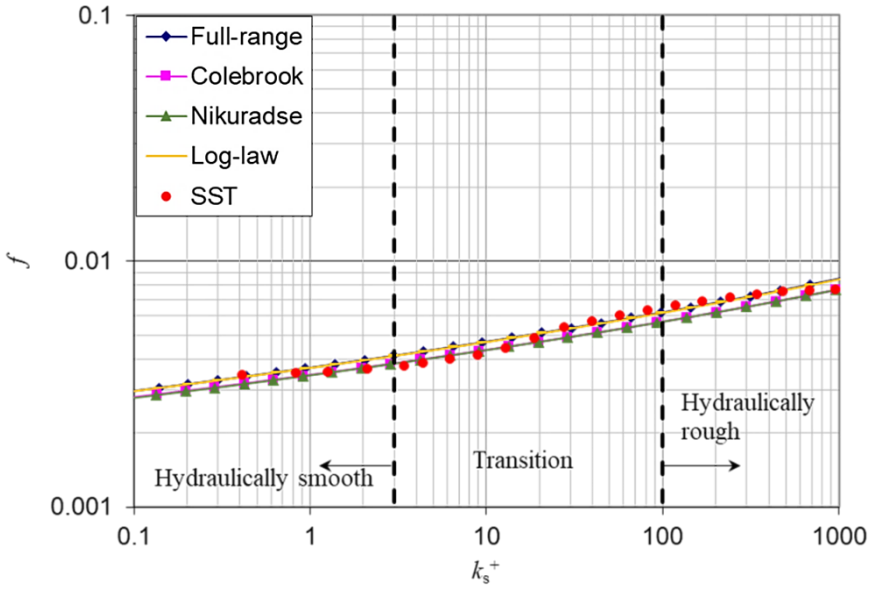


Fig. 6: Friction factor for an open channel

4 Conclusion

Two-equation turbulence models can be effectively used to analyse the whole range of laminar, transitional and turbulent flows over smooth and rough surfaces. Although it is difficult to express the roughness height in case of a *k-ε* model, the use of *k-ω* model for rough flows is rather straightforward. The original *k-ε* model (proposed by Jones and Launder, 1972) performed the best for open channel flow on a smooth surface. For rough-bed, open channel flow SST k-w model was found to be very efficient in predicting velocity, turbulent kinetic energy and friction factor. This model can be utilized for the open channel flow over the smooth as well as rough surface efficiently for the determination of fundamental

flow characteristics. The information obtained from the model results can be used to estimate the sediment transport and mixing of pollutants in an open channel over a range of surfaces. This study is useful for the practicing engineers and researchers working on the boundary layer properties, sediment movement and turbulent mixing in open channels. Further investigations using experimental data is required to judge the capabilities of the turbulence models in open channel flows.

References

Blasius, H. (1913). Das Aehnlichkeitsgesetz bei Reibungsvorgängen in Flüssigkeiten. In: Mitteilungen über Forschungsarbeiten auf dem Gebiete des Ingenieurwesens. Mitteilungen über Forschungsarbeiten auf dem Gebiete des Ingenieurwesens, vol 131. Springer, Berlin, Heidelberg. https://doi.org/10.1007/978-3-662-02239-9_1

Colebrook, C. (1939) Turbulent Flow in Pipes, with Particular Reference to the Transition Region between the Smooth and Rough Pipe Laws. *Journal of the Institution of Civil Engineers, 11*, 133-156. https://doi.org/10.1680/ijoti.1939.13150

Jones, W. P. & Launder, B.E., (1972). The prediction of laminarization with a two-equation model of turbulence. *International Journal of Heat and Mass Transfer 15*, 301–314.

Kirkgoz, M.S. (1989). Turbulent Velocity Profiles for Smooth and Rough Open Channel Flow, *Journal of Hydraulic Engineering*, Vol. 115, No. 11, 1543-1561

Menter, F. R. (1994). Two-equation eddy-viscosity turbulence models for engineering applications. *AIAA Journal 32*(8), 1598–1605.

Myong, H. K. & Kasagi, N. (1990). A new approach to the improvement of k–e turbulence model for wall-bounded shear flows. *JSME International Journal Series II 33*(1), 63–72.

Nagano, Y. & Tagawa, M. (1990). An improved k–e model for boundary layer flows. *Journal of Fluids Engineering—ASME 112*, 33–39.

Nikuradse, J. (1933) Stromungsgesetze in Rauhem Rohren. (Laws of Turbulent Pipe Flow in Smooth Pipes.) VDI-Forschungsheft: Germany) 361. (in German) (Translated in NACA Tech. Memo. No. 1292, 1050).

Sana A., Ghumman, A. R. & Tanaka, H. (2007). Modification of the damping function in the k–ε model to analyze oscillatory boundary layers. *Ocean Engineering, 34*(2), 320–326.

___. (2009). Modeling of a rough-wall oscillatory boundary layer using two-equation turbulence models. *J. Hydr. Eng., 135*, 60–65.

Sana, A. & Shuy, E. B. (2002). Two-equation turbulence models for smooth oscillatory boundary layers. *J. Waterway, Port, Coastal, Ocean Eng., 128*(1), 38–45.

Sana, A. & Tanaka, H. (2000). Review of k–e model to analyze oscillatory boundary layers. *Journal of Hydraulic Engineering—ASCE 126*(9), 701–710.

Tanaka, H. & Thu, A. (1994). Full-range equation of friction coefficient and phase difference in a wave-current boundary layer. *Coast. Eng. 22*, 237–254.

Wilcox, D. C. (1988). Reassessment of the scale-determining equation for advanced turbulence models. *AIAA J., 26*(11), 1299–1310.

Yang, Z. & Shih, T. H. (1993). New time scale based k2e model for near-wall turbulence. *AIAA J., 31*(7), 1191–1198.

Cite as: Sana A., Al-Rawas G., Etri T. & Al-Mamun A., "Study of Turbulence in Open Channels Using Two-Equation Models", *The 2nd International Conference on Civil Infrastructure and Construction (CIC 2023)*, Doha, Qatar, 5-8 February 2023, DOI: https://doi.org/10.29117/cic.2023.0165

Development of Climate Data Inputs Towards the Implementation of Mechanistic-Empirical Pavement Design in the UAE

Waleed Zeiada
University of Sharjah, Sharjah, UAE; Mansoura University, Mansoura, Egypt
Wzeiada@Sharjah.Ac.Ae; Wzeiada@Mans.Edu.Eg

Sham Mirou
University of Sharjah, Sharjah, UAE
U19104388@Sharjah.Ac.Ae

Ayat Ashour
University of Sharjah, Sharjah, UAE
U21200308@Sharjah.Ac.Ae

Reem Hassan
University of Sharjah, Sharjah, UAE
U19104079@Sharjah.Ac.Ae

Muamer Abuzwidah
University of Sharjah, Sharjah, UAE
Mabuzwidah@Sharjah.Ac.Ae

Abstract

The current state of practice in the UAE is to use AASHTO 1993 for pavement designs, yet this method is empirical and has several limitations. The local traffic characteristics, climate conditions, and materials properties must be incorporated in more explicit and mechanistic ways. This study is part of ongoing local research efforts to move towards the implementation of the Mechanistic-Empirical Pavement Design Guide, known as MEPDG, which depends on fundamental material properties, integrated climate conditions, and real traffic characteristics. The main objective of this study is to develop the historical climate data files and climate inputs for 20 different automatic and airports stations covering the entire UAE. These weather stations were divided into four geographical regions: desert area, urban area, coastal area, and mountainous area. In addition, the study investigates the impact of local climate conditions on the simulated asphalt pavement performance using the AASHTOWare Pavement ME Design. This study showed that, however, UAE is a small country yet there are some differences between the climate records of the different weather stations, which is expected to affect pavement design and performance depending on the project site location. For example, the warmest weather station has 36% higher temperature than the coldest weather station at Jabal Jais. This in turn displayed up to 40% and 23% differences in the asphalt concrete (AC) rutting and total rutting, respectively between these extreme weather stations. These findings and many other emphasize the crucial need to consider the climate data inputs at the project level bases, where a single climate data file cannot represent the entire UAE.

Keywords: AASHTOWare; MEPDG; Climate; Pavement Performance; Distress

1 Introduction

Road infrastructure is integral to any country's economic and social development. Pavement design should consider the daily loads under the local climate conditions to ensure the level of serviceability that is required (Abu Dabous et al., 2021). The pavement performance is directly affected by the climate condition, especially temperature and moisture (Hemed et al., 2020). Low temperatures can

cause asphalt to harden and crack in layers, and extremely low temperatures can cause it to crack due to thermal and fatigue stresses. In contrast, asphalt becomes softer and more viscous at high temperatures, causing more rutting (Kodippily et al., 2020). An empirical design method was developed by AASHTO for rigid and flexible pavements in 1972. It has been updated several times over the years, the last time in 1993, and has been implemented by many countries (El-Badawy et al., 2011). Due to its empirical nature, several limitations affect the reputation of thickness layers formed by the process. Additionally, the empirical drainage layer coefficients for expressing the influence of moisture on the unbound layers are a significant limitation. There is only one environmental consideration in this method, which is the seasonal variation of the roadbed resilient modulus and the coefficients of the drainage layer (Elshaeb et al., 2014).

As part of the Mechanistic-Empirical Pavement Design Guide (MEPDG), AASHTO published a temporary version in 2008. MEPDG criteria provide an advanced approach to pavement development (Li et al., 2011). In contrast to AASHTO (1993), the MEPDG predicts several performance metrics and considers material properties, structural design, climate conditions, traffic levels, and paving systems (El-shaib et al., 2017; Justo-Silva et al., 2022). It is an advanced tool used to design and analyze new and rehabilitated flexible and rigid pavement structures (Gkyrtis et al., 2022). Mulandi et al. (2006) compared between AASHTO 1993 and MEPDG, and they concluded that the AC section of the MEPDG produced better results than the AC sections derived from the 1993 AASHTO design guidelines because real traffic loads and different climate factors have been considered. Many research investigated the effect of using climate files to evaluate pavement distresses. (Elshaeb et al., 2014) developed a climate data to assist the implementation of pavement ME design in Egypt and to investigate its influence on flexible pavement performance. The research reported that the warm climate conditions result in higher predicted AC rutting and total rutting. Another study was conducted by (Qiao et al., 2013) to prepare a climate file including (temperature, precipitation, wind speed, sunshine, and groundwater level) to evaluate pavement performance in Virginia City, USA using MPDG. Furthermore, (Saha et al., 2014) used a mechanistic-empirical pavement design guide (MEPDG) to investigate the quality of the recently developed Canadian climatic database. According to the study, asphalt concrete, total pavement rutting, and the international roughness index are sensitive to the climate. (Ankit et al. (2011) investigated the impact of different environmental factors in India on flexible pavement performance modeling. Some models have been used to correlate different environmental variables and their structural characteristics. These models involved different environmental parameters, such as precipitation, wind speed, air temperature, relative humidity, and solar radiation.

Flexible pavement design in the UAE is currently based on the AASHTO 1993, which doesn't take into account the local climate conditions in the UAE (Hassan et al.,2022 ; Ashour et al., 2022) Therefore, the primary goal of this research is to create the climatic data inputs necessary for structural pavement design in the UAE as a first step toward implementing the MEPDG, known as AASHTOWare ME Pavement Design in the UAE.

2 Study Area

United Arab Emirates, a federation comprising seven emirates along the Arabian Peninsula's eastern coast. The largest emirate is Abu Dhabi, which accounts for more than three-fourths of the total land area of the federation. Followed by Dubai, which is situated at the base of the rocky Musandam Peninsula. The Peninsula is also occupied by the smaller emirates of Sharjah, Ajman, Umm Al-Quwain, and Ras al-Khaimah. Fujairah, the federation's seventh member, confronts the Gulf of Oman. This study was conducted over the entire area of UAE, which is located at latitude 23.4 and longitude 53.8. Figure 1 shows the locations of the 20 weather stations considered in this study, including 14 automatic weather stations and 6 airports weather stations.

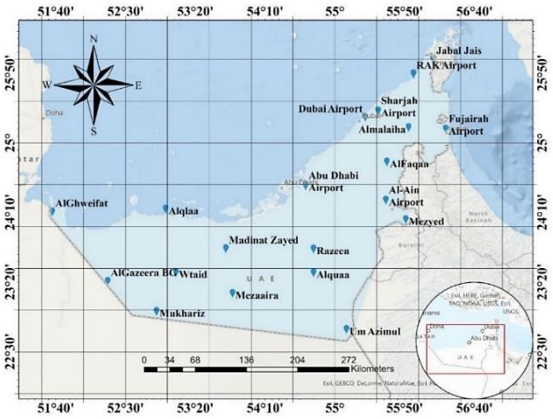


Fig. 1: Location of weather stations and airports

3 Methodology

To assess and compare the impact of climate across different climate zones in the UAE, a three-phase methodology was developed. These three phases are: data acquisition, data processing, and data analysis. The first phase includes data collection that involves historical climate data from 14 local and 6 International airports weather stations. The second step is the development of climate files and inputs needed for MEPDG considering five climate factors: Air Temperature, Precipitation, Wind Speed, Sunshine, and Relative Humidity. The third phase comprises investigating the impact of the climate files of different weather stations on simulated pavement performance using AASHTOware Pavement ME Design software in terms of five distresses (AC Rutting, Total Rutting, and Bottom-Up Fatigue Cracking, and International Roughness Index (IRI)).

3.1 Historical Weather Stations Data Acquisition

The AASHTOware Pavement ME Design software uses hourly records of air temperature, wind speed, sunshine, precipitation, and relative humidity to implement the analysis. Historical data for the main five climate factors were collected from the National Center of Meteorology. The duration of climatic data measurement is 15 minutes, which is appropriate for MEPDG implementation. The 14 weather station data involves 17 years (2004-2020) and 32 years for the airport weather station (1989-2020).

3.2 Development of Climate Files and Inputs for MEPDG

The MEPDG aims to define the physical causes and calibration of the restrictions on the design of the roadways with the performance of the pavement. In order to use the EICM model, climate information includes hourly air temperature, precipitation, wind speed, sunshine, and relative humidity. The climate data files should be prepared in the format acquired by the software. The modification of the climate data files to the required software format was conducted using initially Excel spreadsheets. In the Excel spreadsheets, climate data obtained initially have been translated into CSV files (Comma Delimited). The CSV files were first opened as text files, then saved as a text file in which the *. hcd extension for each text file was manually added. Each climatic file contains the following information in order: date (YYYY/mm/dd/hr), air temperature (ºF), wind speed (mile/h), sunshine (percentage), precipitation (in), and relative humidity (percentage).

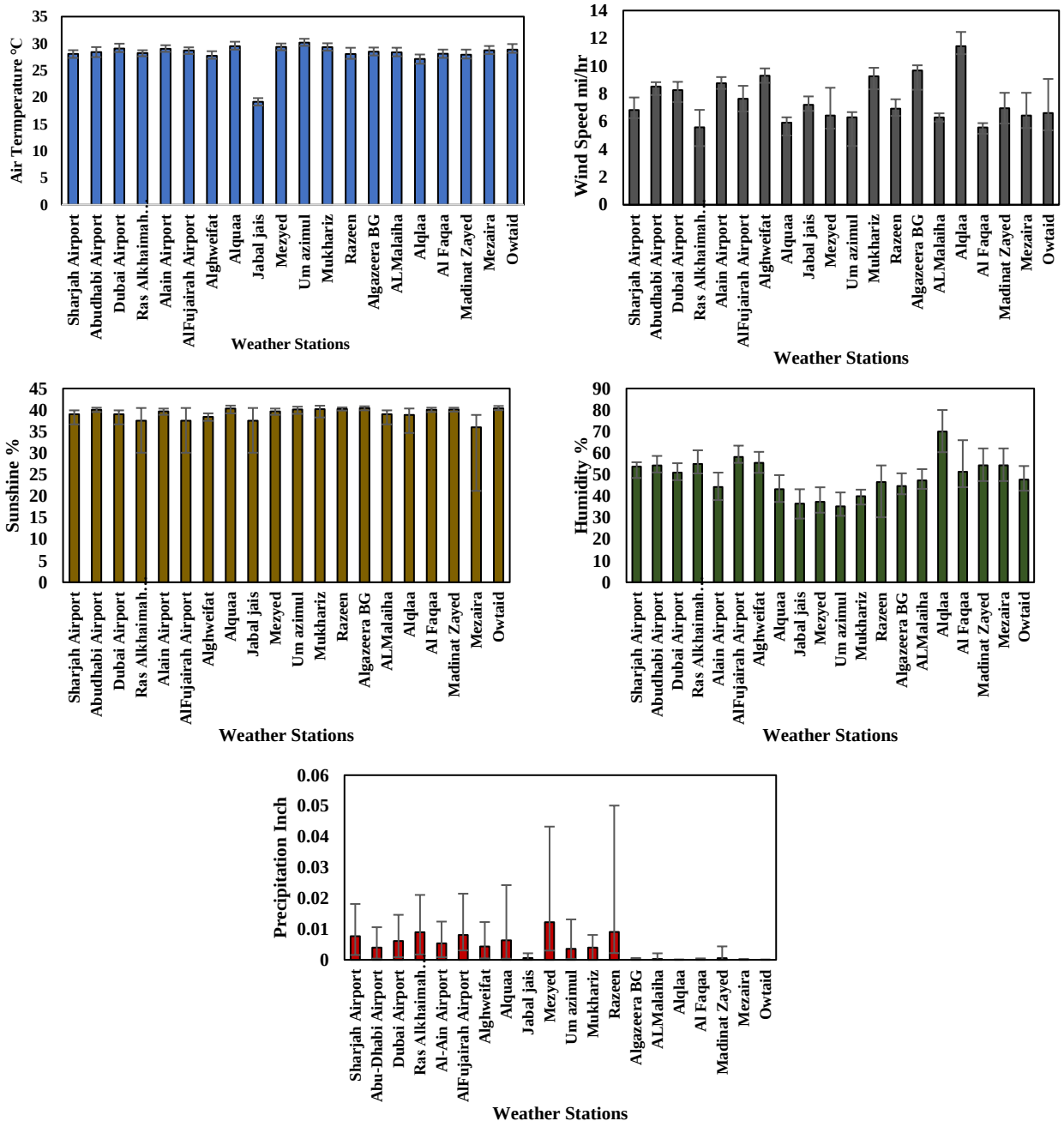
3.3 Impact of Climate Files and Inputs on Simulated Pavement Performance

The primary research tool to evaluate the climate impacts on pavement performance considering different weather stations in the UAE was the AASHTOWare Pavement ME Design software. MEPDG is an iterative method for pavement design according to paving distresses and smoothness. Several site circumstances should be taken into consideration such as traffic, climate, subgrade, and current pavement requirements for rehabilitation. The sufficiency against user input, performance criteria, and reliability values would then be assessed through the output for both predicting distress

and smoothness. If the specification does not fulfil the reliability performance requirements, it will be reviewed, and the assessment process will be replicated as required. This ME approach allows for the optimization of the design and ensures that some kinds of distress are reduced to values less than the failure criterion in the paving structure's design life.

4 Visualization of Historical Climate Factors Data in the UAE

Adaptation and climate impact evaluations have been grown in number, consistency, and importance over the last few decades. Asphalt pavement performance is significantly affected by air temperature. Temperature, precipitation, wind speed, sunshine, and relative humidity are the climate factors taken from the different 20 weather stations as shown in 1Fig. 2. Although the weather stations are close to each other, there are remarkable differences between different climate factors measured at different locations of the weather stations. These differences are expected to induce differences in simulated pavement distresses including, bottom-up fatigue cracking, and total and AC rutting.



1Fig. 2: Historical Annual Average **(a)** Air Temperature, **(b)** Wind Speed, **(c)** Sunshine, **(d)** Relative Humidity and **(e)** Precipitation for Weather Stations.

5 Influence of Climate Data on Pavement Performance

The main aim of this section is to determine the impact of changes in climate conditions measured at different locations on the simulated pavement performance and corresponding pavement service life. If the simulated pavement performance at different locations varies remarkably across the UAE, this will indicate that using the project site climate conditions is a must as part of pavement design and performance. The AASHTOWare Pavement ME Design calculates the cumulative values of various distresses as a function of pavement age till the end of the pavement design life. Fig. **3** (a) illustrates the AC rutting value for the 20 weather stations that cover the entire UAE. The highest AC rutting recorded was 0.60 inches, whereas the lowest AC rutting was 0.36 inches. Fig. **3** (b) demonstrates the total rutting value, where the highest total rutting was recorded at 1.06 inches and the lowest total rutting was recorded at 0.83 inches. The southern region showed more AC and total rutting compared to the northern region due to elevated temperatures at the southern region. Fig. **3** (c) shows the IRI values across the entire UAE. IRI is an indicator to assess the smoothness of a road surface. The lower the IRI value, the smoother the road surface. It is commonly used to evaluate the condition of a pavement and to identify areas that may require maintenance or rehabilitation. As rutting and cracking develop, it can increase the roughness of the pavement surface, which will be reflected in a higher IRI value. Many transportation agencies around the world have developed IRI criteria for different maintenance and rehabilitation activities (Guidelines IRI, 2018; Baladi et al., 2017). The highest IRI value was 175 inches/mile, whereas the lowest IRI value was 161 inches/mile. The IRI differences between the different weather stations varied between 0% to 9.1%. The IRI result showed the same trend of AC rutting results across the UAE which indicate the relation between them. The bottom-up fatigue cracking values are shown in Fig. **3** (d). The highest bottom-up fatigue cracking value was 2.5% and the lowest bottom-up fatigue cracking was 2.2%. The bottom-up fatigue cracking values were so low as expected in warm climate regions with a percent difference between weather stations up to 15%.

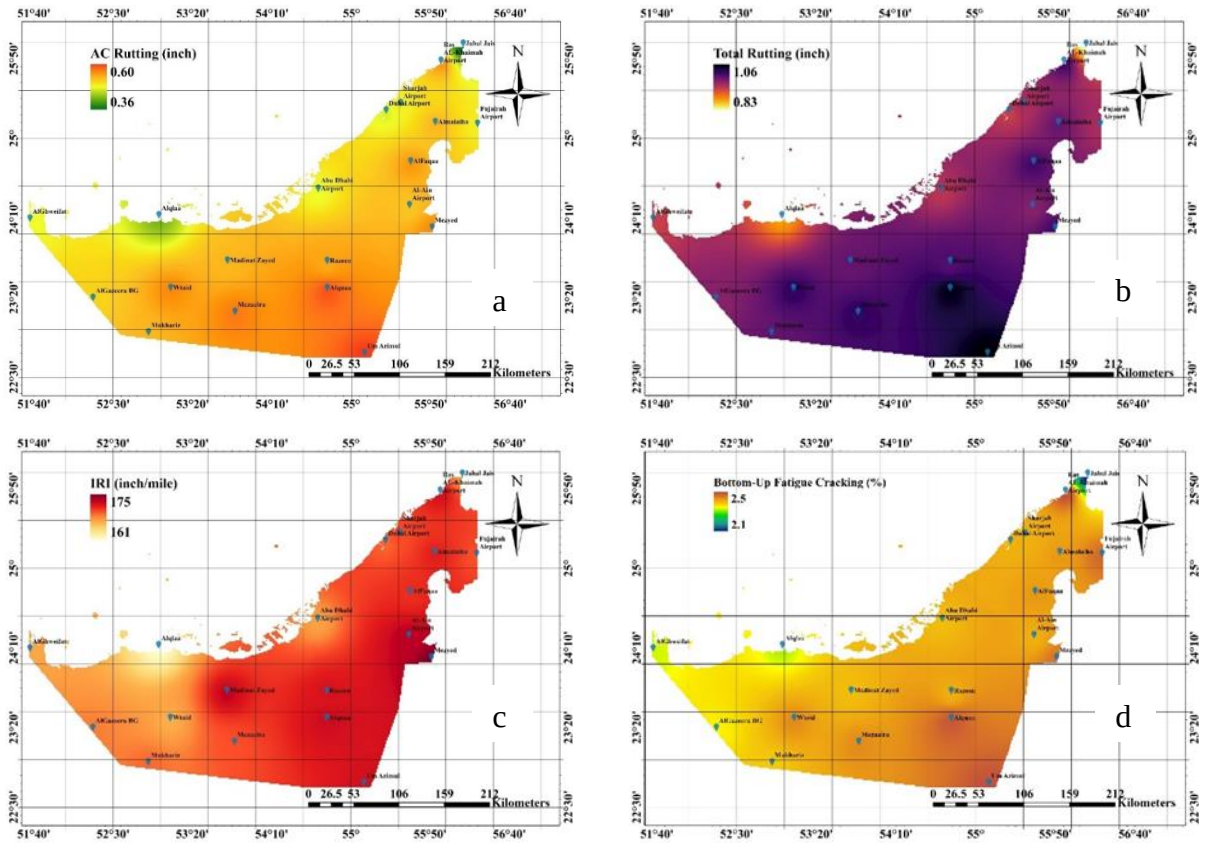


Fig. 3: Simulated **(a)** AC Rutting; **(b)** Total Rutting; **(c)** Terminal IRI; and Bottom-Up Fatigue Cracking Maps

Figure 4 shows the performance results and corresponding pavement service life of both AC and total rutting since rutting was the most significant distress leading to pavement failures. The percentage changes in AC Rutting between different weather stations varied between 0% to 42.9%. For the pavement age calculated corresponding to AC rutting of 0.25 inches, the difference in AC rutting age was found to range from 0-11 years. These differences in AC rutting and corresponding pavement life were due to the significant variation in temperatures between the northern and southern regions. Similarly, the total rutting values varied between different weather stations with up to 22.6%, causing differences in corresponding pavement lives 13 years. Since the simulated pavement performance and corresponding pavement service life reviled different results, which are expected to remarkably affect the construction and maintenance costs, it is therefore critical to consider the local climate conditions at a project level as part of the pavement design and rehabilitation. This surely will not be attained using the 1993 AASHTO design method, yet it could be achieved by implementing more updated and accurate pavement design methods such as the MEPDG.

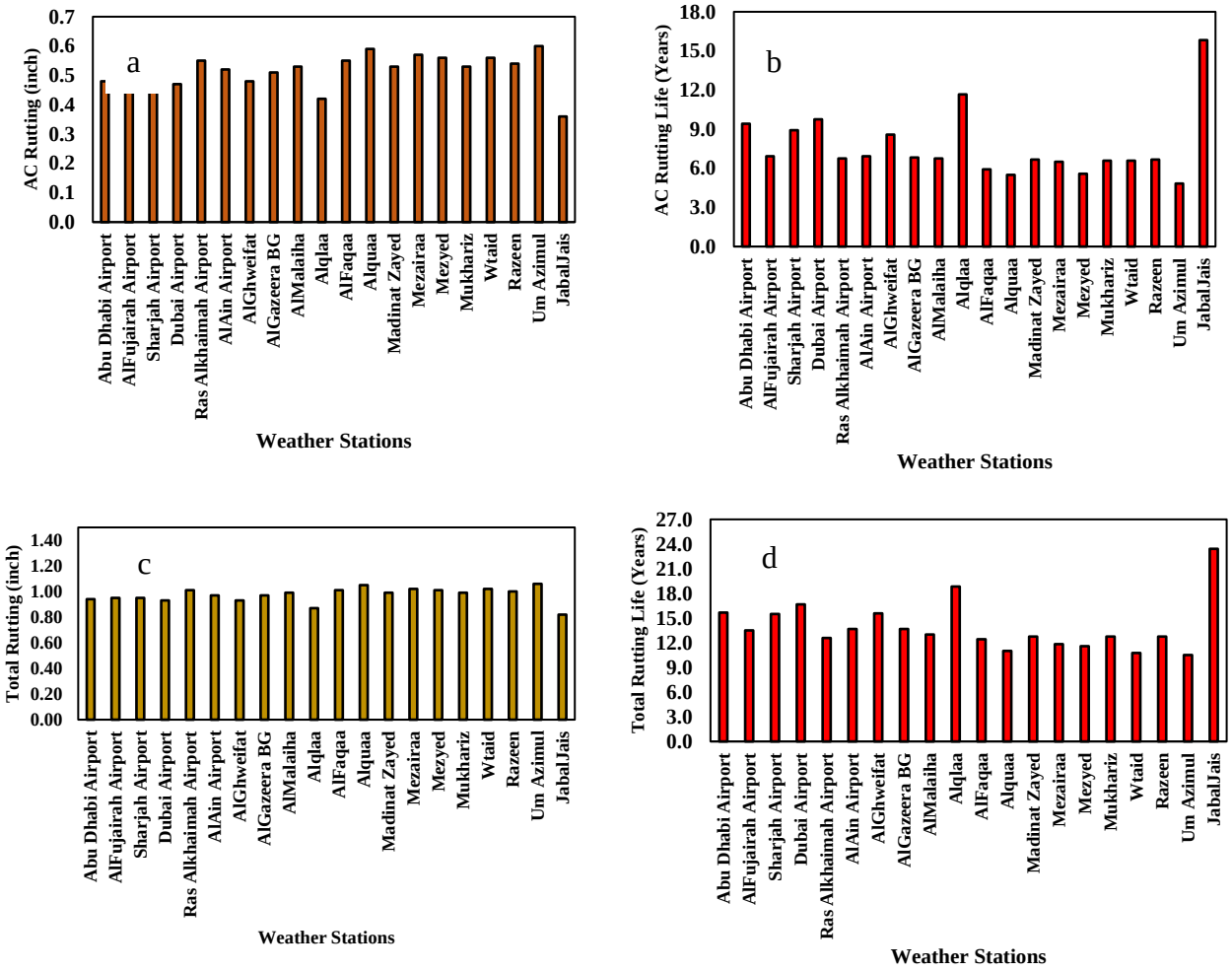


Fig. 4: Simulated **(a)** AC Rutting; **(b)** AC Rutting Life; **(c)** Total Rutting; and **(d)** Total Rutting Life for Different Weather Stations

6 Conclusion

MEPDG is the latest and state-of-the-art design methodology that offers an integrated platform to consider local climate conditions more preciously. In UAE, the MEPDG has not been yet implemented for structural pavement design, where the current pavement design practice is based on AASHTO 1993 design method. The main objective of this study is to develop the climate data files

and inputs for the UAE as an initial step towards the implementation of the MEPDG in the UAE. The predicted pavement performance using 20 climate files representing different locations in the UAE was analysed to assess the impact of climate factors on simulated pavement performance. The following conclusions were drawn from this research effort.

- 20 different climate data files were successfully developed for the implementation of MEPDG in UAE using historical hourly data records collected from different weather stations across the country.
- The climate data files were incorporated and described successfully in the AASHTOWare pavement ME design software without any detected errors.
- AC rutting was significantly affected by the climatic zone ranging between 0% to 42.9%.
- The highest AC rutting recorded was 0.60 inches at Um Azimul weather station, whereas the lowest AC rutting was 0.36 inches in Jabal Jais.
- AC rutting life was decreased consequently with the increase in AC rutting values and the difference in AC rutting life between different stations was up to 11 years.
- Total rutting recorded 1.06 inches as the higher value and 0.83 inches as the lower value.
- There was a variation of up to 22.6% in the total rutting values among different weather stations.
- This results in pavement life differences of up to 13 years between weather stations.
- A maximum value of 2.5% was observed for bottom-up fatigue cracking, while the lowest value was 2.2%.
- In warm climate regions, fatigue cracking values are so low, with a percent difference of up to 15% between weather stations.
- In terms of IRI values, 175 inches/mile was the highest and 161 inches/mile was the lowest. It was found that the IRI differences between the various weather stations ranged as high as 9.1%.
- In this study, the impact of climate conditions at different locations across the UAE on pavement on pavement design and performance was investigated using the MEPDG. Impacts of materials selection and local traffic characteristics should be also investigated in future research work.

Acknowledgment

To complete this research project, the authors are grateful to the Emirates National Centre of Metrology and the Ministry of Energy and Infrastructure for providing climate data and funding research project No. 130169.

References

A. Elshaeb, M., M. El-Badawy, S. & A. Shawaly, E. S. (2014). Development and Impact of the Egyptian Climatic Conditions on Flexible Pavement Performance. *American Journal of Civil Engineering and Architecture*, *2*(3), 115–121. https://doi.org/10.12691/ajcea-2-3-4

Abu Dabous, et al. (2021). Distress-based evidential reasoning method for pavement infrastructure condition assessment and rating. *International Journal of Pavement Engineering*, *22*(4), 455–466.

https://doi.org/10.1080/10298436.2019.1622012

Ankit, G., Kumar, P. & Rastogi, R. (2011). Effect of Environmental Factors on Flexible Pavement. *8th International Conference on Managing Pavement Assets*, *3*.

Ashour, et al. (2022). Assessment of Potential Temperature Increases in The UAE due to Future Global Warming. *2022 Advances in Science and Engineering Technology International Conferences, ASET 2022*. https://doi.org/10.1109/ASET53988.2022.9734915

Baladi, et al. (2017). Pavement Performance Measures and Forecasting and the Effects of Maintenance and Rehabilitation Strategy on Treatment Effectiveness (Revised). *Fhwa-Hrt-17-095*, *September*, 1–329. https://www.fhwa.dot.gov/publications/research/infrastructure/pavements/ltpp/17095/17095.pdf

El-Badawy, et al. (2011). Comparison of Idaho pavement design procedure with AASHTO 1993 and MEPDG methods. *T and DI Congress 2011: Integrated Transportation and Development for a Better Tomorrow - Proceedings of the 1st Congress of the Transportation and Development Institute of ASCE*, *41167*(October), 586–595. https://doi.org/10.1061/41167(398)56

El-shaib, et al. (2017). Comparison of AASHTO 1993 and MEPDG considering the Egyptian climatic conditions. *Innovative Infrastructure Solutions*, *2*(1). https://doi.org/10.1007/s41062-017-0067-6

Gkyrtis, K., Plati, C. & Loizos, A. (2022). Mechanistic Analysis of Asphalt Pavements in Support of Pavement Preservation Decision-Making. *Infrastructures*, *7*(5). https://doi.org/10.3390/infrastructures7050061

Guidelines for Routine Road Maintenance Using IRI. (2018). *February*.

Hassan, et al. (2022). Investigation of Historical and Future Air Temperature Changes in the UAE. *In International Road Federation World Meeting & Exhibition (pp. 1148-1166). Springer, Cha*m.

Hemed, et al. (2020). Impact of climate change on pavements. *E3S Web of Conferences*, *150*(20 20). https://doi.org/10.1051/e3sconf/202015001008

Justo-Silva, R., Simões, F. & Ferreira, A. (2022). Mechanical-Empirical Pavement Design Guide Applied to Portuguese Pavement Structures. *Applied Sciences (Switzerland)*, *12*(11). https://doi.org/10.3390/app12115656

Kodippily, et al. (2020). Effects of extreme climatic conditions on pavement response. *Road Materials and Pavement Design*, *21*(5), 1413–1425. https://doi.org/10.1080/14680629.2018.1552620

Li, et al. (2011). Mechanistic-empirical pavement design guide (MEPDG): a bird's-eye view. *Journal of Modern Transportation*, *19*(2), 114–133. https://doi.org/10.1007/bf03325749

Mulandi, et al. (2006). Comparison of pavement design using AASHTO 1993 and NCHRP mechanistic- empirical pavement design guides. *Proceedings of the 2006 Airfield and Highway Pavement Specialty Conference*, *2006*, 912–923. https://doi.org/10.1061/40838(191)77

Qiao, et al. (2013). Examining effects of climatic factors on flexible pavement performance and service life. *Transportation Research Record*, *i*(2349), 100–107. https://doi.org/10.3141/2349-12

Saha, et al. (2014). Evaluation of the effects of Canadian climate conditions on the MEPDG predictions for flexible pavement performance. *International Journal of Pavement Engineering*, *15*(5), 392–401. https://doi.org/10.1080/10298436.2012.752488

Cite as: Zeiada W., Mirou S., Ashour A., Hassan R. & Abuzwidah M., "Development of Climate Data Inputs Towards the Implementation of Mechanistic-Empirical Pavement Design in the UAE", *The 2nd International Conference on Civil Infrastructure and Construction (CIC 2023)*, Doha, Qatar, 5-8 February 2023, DOI: https://doi.org/10.29117/cic.2023.0166

Impact of Pore Morphology on Colloid Migration at Variable Saturation Levels of Natural Porous Media

Mhd. Taisir Albaba
Qatar University, Doha, Qatar
ma1609536@qu.edu.qa

Jamal Hannun
Qatar University, Doha, Qatar
jh1300283@student.qu.edu.qa

Riyadh Al-Raoush
Qatar University, Doha, Qatar
riyadh@qu.edu.qa

Abstract

The migration of colloids within porous media has a critical impact on many important industrial processes such as oil production and groundwater recharge. Colloids can clog the pore space and hence impair the permeability of fluids which adversely impacts the efficiency of fluids movement through such media. Therefore, understanding the mechanisms of pore clogging at the pore-scale is critical to develop efficient remediation methodologies for permeability reduction at different physio-chemical conditions. To study pore clogging at a pore-scale, microfluidic chips were fabricated to mimic geometries of natural porous media extracted from tomographic scans of sand packs. A colloidal suspension was injected in three phases into the system. The phases consisted of an initial imbibition of the suspension, followed by drainage of the suspension from the system, and finally, a second imbibition. During each phase, a series of images are taken of a section of the porous media. Findings reveal that pore-clogging considerably impairs saturation levels of the porous media through blocking the flow from reaching the gas phase within the system. Considerably increasing the time the gas is trapped in the pore-space, which in turn develops higher irreducible water saturation. This was also observed in the case of drainage of the colloidal suspension from the pore-space where colloids blocked pathways of the gas phase and prevented its migration through the pore space. In contrast, the migration of colloids was also impacted by the presence of the gas phase. Gas provided a clogging surface while forcing colloids to migrate through the pore space and accumulate at other pores. This implies that gas phase presence within a low porosity system can increase pore clogging at a significant rate. This is also supported by the short period between the clogging of two pores and the clogging of a dozen pores within the observed system.

Keywords: Colloid; Pore-scale; Pore-clogging; Saturation; Multiphase

1 Introduction

A multitude of highly impactful industries are impacted by colloid migration in porous media. These industries include CO_2 injection and sequestration (Yusof et al., 2020, 2021; Yusof et al., 2022), groundwater recharge (Akhtar et al., 2021; Reddi et al., 2000)(Akhtar et al., 2021; Reddi et al., 2000), and oil production (Khilar & Fogler, 1983; Liu et al., 2019). This is because colloids can clog the pore throats of the media by accumulating at those throats and thereby reduce the permeability of the

media itself (Yusof et al., 2022). Permeability reduction as a consequence of pore clogging was also observed by (Hannun et al., 2022) and (Prempeh et al., 2020), where the latter study additionally reported non-monotonic permeability reduction relative to clay content due to the residual gas phase blocking flow paths. While (Han et al., 2020) observed pore clogging at velocities beginning from over 25 mm/s and 5 mm/s for single and two-phase flows respectively using a semi-circular cylinder to examine colloid transportation under both single and two-phase flows. The studies by Prempeh et al. and Han were not visually observed at a pore-scale, which may have yielded more information on how the mechanics of pore clogging interact with colloid migration in a multiphase system. On the other hand, (Cao et al., 2019) performed experiments using a PDMS micromodel chip with homogeneous circular grains with pore throat widths ranging from 20 to 100 μm, on clogging behaviour of sediment fines that were sieved to be under 75 μm. The study found that the presence of a gas phase along the model enhances clogging of pores irrespective of particle types or solution salinity. (Bate et al. (2022) also made use of PDMS microchips to investigate the flow of Montmorillonite and Kaolinite particles in a multiphase system. The PDMS chips were contained homogeneous micro-pillars to simulate grains in porous media. Clogging was found to occur more easily at the throats within a multiphase flow. Additionally, (Jung et al., 2018) performed pore-scale experiments using a micromodel with homogeneous circular grains under both saturated and unsaturated conditions to investigate clogging due to effect of AWI. The throat width was ranged from 50, 100, 300, and 700 μm. the colloids used in the experiment were PS particles with an average diameter of 19 μm. And from the obtained results, they concluded that bridging and clogging occurred due to accumulation of fines on the gas interface, which is then followed by depositing the colloids onto pore throats upon the gas phase passing through that throat. This differs from the conclusions by (Prempeh et al., 2020) possibly due to the differentiation between a multiphase system and residual phases. While the previous studies were visually observed at a pore-scale, the model of the microchips does not accurately simulate the heterogeneity of actual porous media as they used homogeneous micro-pillars instead of modelled grains.

The structure of the porous media itself plays an important role in colloid migration, and this was confirmed by (Li & Prigiobbe, 2018) in their numerical simulation of the migration of 4 particles within actually simulated porous media. And they found that the media structure plays a dominant role in determining colloid migration. (Rod et al., 2018) examines the impact of media heterogeneity using glass bead columns in place of actual media. Where the heterogeneity was obtained through mixing different sized beads into a column, which would be compared with a homogeneous column filled with same-sized glass beads. The study found that heterogeneity would retard transport of colloids more than homogeneity. Though the study does not allow for visual analysis on how the retardation occurred. To that end, (Kokubun et al., 2019) used a numerical model to simulate transport of colloids in both hetero and homogeneous porous media in single-phase conditions. The media itself was made up of circular pillars, where heterogeneity was achieved through changing the diameter of some of the pillars along the flow path. The results show that heterogeneous media accumulated at low and high velocities, while homogeneous media only showed accumulation for low velocities. Furthermore, the study found that accumulation at high velocity regions leads to clogs forming. This shows that heterogeneous media has a higher likelihood of pore-clogging. Other studies have examined specific features of pore throats such as the angle of convergence (Mondal et al., 2016)and the shape of the throat itself (Dersoir et al., 2015). And while studying such specifics can help in developing future equations and formulae, observing how these effects impact pore clogging on a larger scale can lead to other discoveries. One such discovery is how clogged pores can affect the

clogging of other pores around them in a phenomenon called dependent clogging. Liot et al. (2018) studied this phenomenon using 10 adjacent micro-channels with a width, length, and depth of 5, 50, and 0.83 µm, respectively. And injecting polystyrene particles with a diameter of 250 nm. The results from the experiments showed an increase of clog growth rate as the number of clogged channels increased. (Liu et al., 2019) expanded on this concept using homogeneous porous media simulated through a PDMS micromodel under single-phase convergent radial flow conditions. Where dependent clogging was attributed to any clogs that occur adjacent to an already clogged pore throat. The study then concluded that dependent clogging is more effective in lowering permeability than independent clogging. Though considering adjacency alone in determining dependence can be inaccurate. This is because an important factor to consider in dependent clogging is tortuosity. (Shen & Ni, 2017) studied the relation between clogging and tortuosity using column experiments with glass beads as the media and concluded that clogging increases tortuosity and causes particles to travel in transverse paths for longer periods. In addition to that, the remaining open pores experience an increase in pressure as the number of clogged pores increases. Parvan et al. (2020) confirms Shen and Ni's conclusion regarding how clogging increases tortuosity through numerically investigating colloid flow within models based on actual porous media. Bacchin et al. (2014) shows how this relation is reciprocal in that they found an increase in clogged pores in more tortuous paths. The conclusion reached from the examination of the previous papers is the accumulative effect of dependent clogging in terms of increased tortuosity, which in turn promotes pore clogging. Therefore this paper suggests that tortuosity can be used to examine dependent pore clogging on a scale that is not confined with adjacency.

With an increased interest in examining the reciprocal relationship between pore clogging and saturation degradation, this paper presents the following objectives:

1- Visually investigate how residual gas phases impact colloid migration and pore clogging.

2- Visually investigate how colloid-clogged pores impact desaturation on porous media.

3- Visualize the link between dependent clogging and tortuosity and flow paths.

2 Methodology

2.1 The Microchip

A hydrophobic PDMS microchip was with a surface area of **6.7x5 mm^2** and having a depth of 20 µm (Micronit Micro Technologies) was etched with a geometry based on actual porous media. The geometry was extracted using synchrotron x-ray micro-computed tomographic images from sand packs. These images were taken at the Argonne National Laboratory (ANL) synchrotron facility. Using global threshold, the tomographic images were binarized. Additionally, grain boundaries were determined through the construction of line segments with a non-zero gradient value between adjacent pixels. The characteristics of the geometry used in the experiment are presented in table, with the symbols explained in table.

Table 1: Geometry characteristics

Φ	R_{Throat} (µm)	R_{Pore} (µm)	R_{Pore}/ R_{Throat}	Ψ_{Grains}	θ_{Grains} (Degree)	τ	K (µm^2)
0.526	22.6	53.9	2.38	0.586	43.87	1.32	5.99

Table 2: meaning of geometry characteristics symbols

Φ: Porosity	R_{Throat}: Median Throats Radius
R_{Pore}: Median Pore Radius	$R_{Pore/}$ R_{Throat}: Pore Aspect Ratio
Ψ_{Grains}: Median Grains Sphericity	θ_{Grains}: Median Grains Orientation
τ: Tortuosity	k: Permeability

2.2 Colloid Suspension

Two 10% stock colloid solutions were used to construct the suspension employed during the experiment. The two stock solutions were hydrophobic Polystyrene (PS) and hydrophilic Carboxylate Modified Polystyrene (CMPS). With both having a mean diameter of 5µm and a density of 1.05 g/cc. The suspension was made through mixing 50 µl of the CMPS solution and 50 µl of the PS solution together inside a beaker and using deionized water to fill the beaker up to 10 ml. Prior to commencing the experiment, the colloid suspension was sonicated with an ultrasonic processor (SONICS, Vibra cell) for one minute in a cold bath to achieve adequate monodispersing of the colloids.

2.3 Experimental Setup

The setup for the experiments included a microscope stage (Leica Z6 APO) (Nishad & Al-Raoush, 2021), where the microchips would be placed, and fastened using tape during each experimental run. The microscope stage is equipped with a precise moving stage that can move the micromodel with an accuracy of 1 µm. The micromodel is connected to a precision syringe pump (Kats Scientific, NE-1010) at the inlet for the sake of injecting the colloid suspensions into the model. The connection is via a tube with an outer diameter of approximately 1.5875 mm, and an inner diameter of 0.25 mm. While another tube was connected to the outlet and left hanging over an empty beaker to simulate atmospheric pressure. The Leica camera was used for image and video acquisition purposes during each injection phase with no shading and robust sharpening. The settings on the camera for exposure, gain, gamma, saturation, and resolution were 16.5 ms, 2.0x, 0.80, 103.00, and 2592x1944 respectively.

2.4 Procedure

The chips are cleaned with ethanol, followed by deionized water by manually injecting them into the media using syringes for several pore volumes. Afterwards, a syringe filled with air is inserted into the system and air is injected into the media until saturation reaches or is close to 0% of the void space.

The experiment consists of three distinct injection phases, the first imbibition (IMB1), drainage (DRN), and the second imbibition (IMB2). Where in (IMB1), the colloidal suspension is injected into the microchip at a velocity of 3 µl/min using the syringe pumps. This is done until the gas phase within the media is completely gone or the saturation reaches at least 75% of the total void space pictured within the chosen area to be investigated. During the IMB1 phase. In the DRN phase, the geometry is drained by setting the pump to the withdraw function at the velocity of 3 µl/min. The third stage involves a second imbibition IMB2 of the suspension into the geometry once again at the same velocity. The outlet is connected to open air using a tube hanging over an empty beaker to collect the suspension during the experimental run. During each phase, images are acquired continuously at a zoom level of 2.5 on the middle left portion of the geometry, which is facing the inlet.

3 Results

3.1 IMB1 Phase

Figure 1 demonstrates the accumulative effect of pore clogging in the IMB1 phase. As it shows clogging events developed over a small period of time. Some of the clogging events documented in the figure can be taken as a result of residual gas bubbles dissolving, resulting in opening more pathways for the colloids to migrate through. The impact of clogged pores on the clogging of surrounding pores remains apparent, especially going from Figure [1, c] to [1, d]. From examining figures [1, c] and [1, d], the change in the tortuosity of the colloid pathways becomes clear. Wherein the colloids are forced into more tortuous paths that lead to a higher amount of clogged pores. This is exemplified in the 23rd and 24th clogging events documented in Figure [1, d], as prior to the lower clogging events, the upper middle area of the recorded geometry was not under much pressure from the migration of colloids compared to its latest state. The dependency of these clogging events becomes more apparent when considering that clogging events 5, 6, and 9 in blue, and 18, 19, and 20 in red block the direct pathways towards clogging events 23 and 24. This proves that the lower clogging events caused alterations in the flow paths of the colloids and moved them upwards.

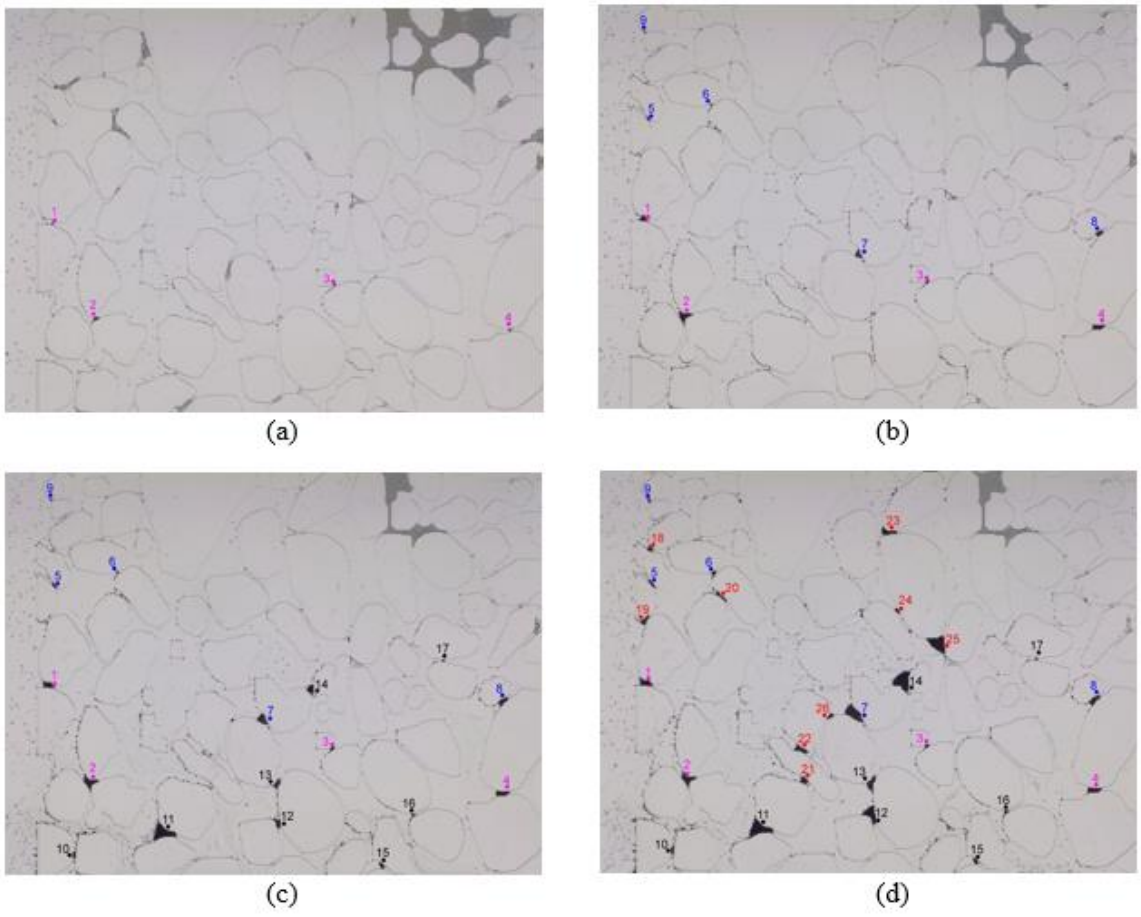


Fig. 1: Accumulative clogging through developing pathways. (a) was acquired at 10:46, (b) was acquired at 10:51, (c) was acquired at 10:53, and (d) was acquired at 10:54. The colors indicate when each clogging event occurred. The colours of purple, blue, black, and red indicate clogging developments for images (a) through (d)chronologically, respectively.

Figure 2, on the other hand, shows the blocking effect of residual gas bubbles within the media on colloid migration and pore clogging. In that in the five highlighted clogging events, colloids do not

even approach nor attach around residual gas bubbles that block pore throats. This is indicative of the effect that residual gas has on colloid migration and pore clogging through lowering the number of throats that colloids can pass through. Thereby forcing them to accumulate instead of branching out in multiple pathways. This visually confirms the findings of (Prempeh et al., 2020) with regard to residual gas lowering permeability.

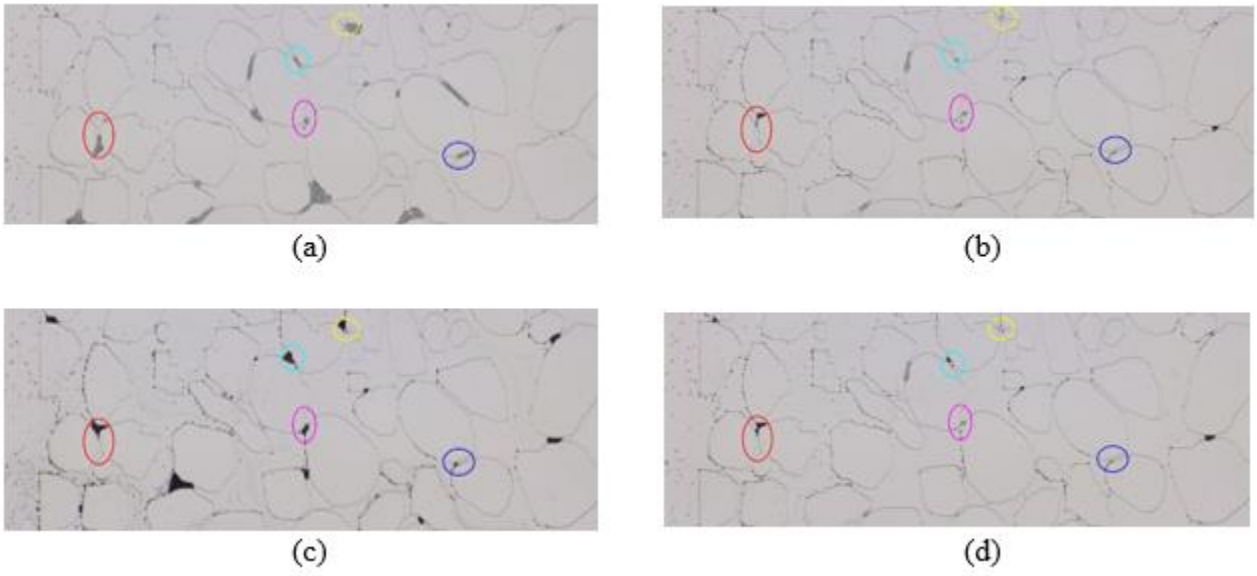


Fig. 2: Residual gas bubbles blocking colloid attachment and pore clogging prior to dissolving.
Images **(a)** through **(d)** are ordered chronologically, with **(a)** being acquired first, and **(d)** being acquired last

3.2 DRN Phase

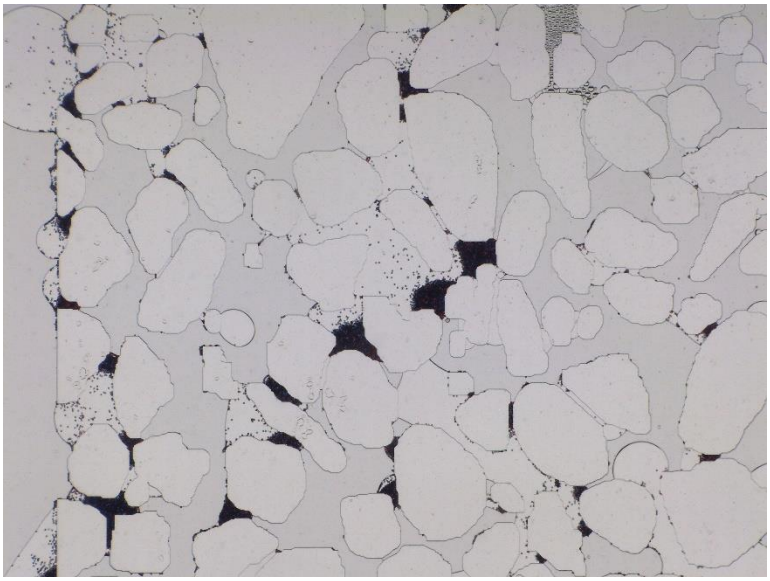


Fig. 3: Clogged pores successfully blocking gas phase from expanding

Figure 3 from the drainage phase clearly displays how the pores that were clogged by the accumulation of colloids successfully block the gas phase in the recorded region from escaping or expanding further. The loose gas phase on the right side of the image is most likely a result of unclogged pores from above and below the recorded area. And while there was some dispersion of the clogging colloids during the beginnings of the DRN phase, most of the colloids remained clogging the pore throats.

3.3 IMB2 Phase

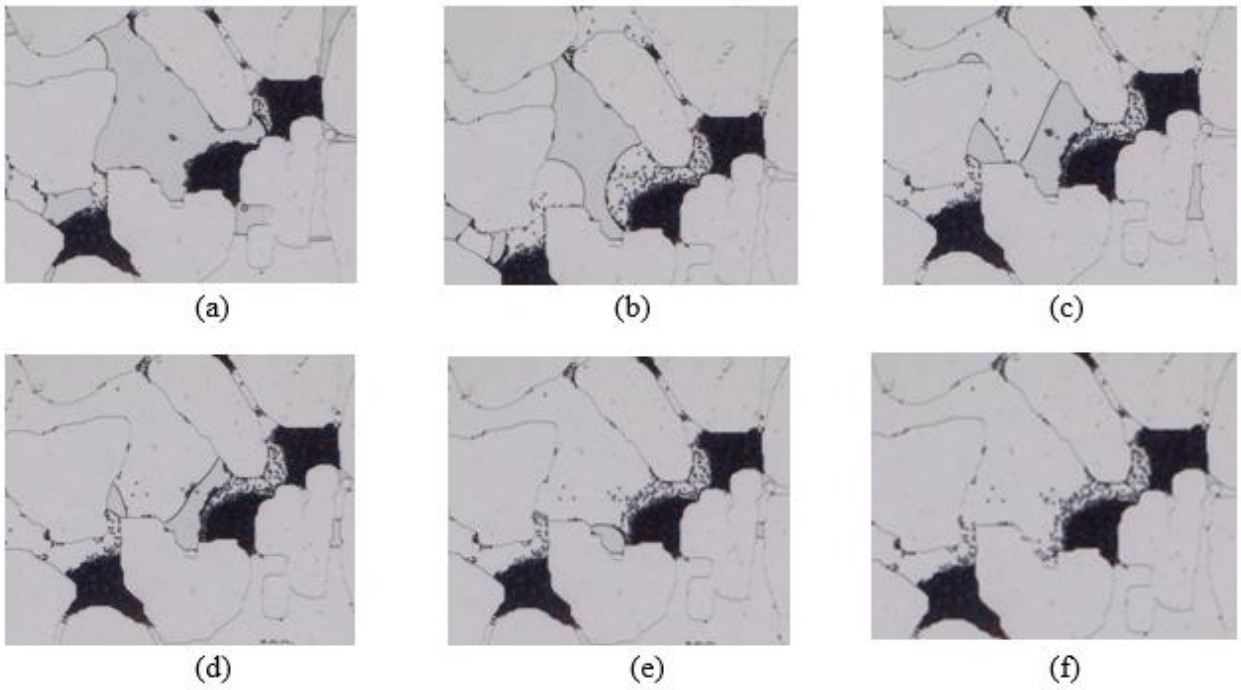


Fig. 4: Dissolved bubble blocked from protruding into geometry.
The images are ordered chronologically from **(a)** to **(f)**

The series of images from Figure 4 show that the clogged pores also block gas bubbles from moving throughout the geometry, and trap them in place. This, along with the injection of the colloidal solution during this phase leaves no option for the trapped gas bubbles adjust to the applied pressure other than dissolving. It is also notable that these trapped gas bubbles cannot carry colloids with them throughout the system like the case mentioned in (Nishad & Al-Raoush, 2021). This can be safely attributed to the lower porosity and smaller throat sizes of this geometry compared to the one used in that study.

4 Conclusion

This study has managed to visualize the relation between dependent clogging and flow paths within a geometry modelled after actual porous media. This is an important observation when studying dependent clogging, as it was mostly studied based on adjacency alone as done previously by (Liot et al., 2018; Liu et al., 2019). The paper also shows the concurrent impact that the residual gas phase and colloids have on each other. As clearly shown with the case of the residual gas bubbles blocking colloids from approaching certain throats that they occupy. And with the case of colloid-clogged throats trapping the gas bubbles within them. Preventing them from expanding and migrating throughout the system, and forcing them to dissolve.

Acknowledgement

This publication was supported by Qatar University Grant (QUHI-CENG-22/23-517). The findings achieved herein are solely the responsibility of the authors.

References

Akhtar, M. S., Nakashima, Y. & Nishigaki, M. (2021). Clogging mechanisms and preventive measures in artificial recharge systems. *Journal of Groundwater Science and Engineering*, *9*(3), 181–201. https://doi.org/10.19637/j.cnki.2305-7068.2021.03.002

Bacchin, et al. (2014). Clogging of microporous channels networks: role of connectivity and tortuosity. *Microfluidics and Nanofluidics*, *17*(1), 85–96. https://doi.org/10.1007/s10404-013-1288-4

Bate, et al. (2022). The Migration and Deposition Behaviors of Montmorillonite and Kaolinite Particles in a Two-Dimensional Micromodel. *Materials*, *15*(3), 855. https://doi.org/10.3390/ma15030855

Cao, et al. (2019). 2D micromodel study of clogging behaviour of fine-grained particles associated with gas hydrate production in NGHP-02 gas hydrate reservoir sediments. *Marine and Petroleum Geology*, *108*, 714–730. https://doi.org/10.1016/j.marpetgeo.2018.09.010

Dersoir, et al. (2015). Clogging of a single pore by colloidal particles. *Microfluidics and Nanofluidics*, *19*(4), 953–961. https://doi.org/10.1007/s10404-015-1624-y

Kokubun, et al. (2019). A pore-scale study of transport of inertial particles by water in porous media. *Chemical Engineering Science*, *207*, 397–409. https://doi.org/10.1016/j.ces.2019.06.036

Han, et al. (2020). Fines migration and pore clogging induced by single- and two-phase fluid flows in porous media: From the perspectives of particle detachment and particle-level forces. *Geomechanics for Energy and the Environment*, *23*, 100131. https://doi.org/10.1016/j.gete.2019.100131

Hannun, et al. (2022). Fines effect on gas flow in sandy sediments using μCT and pore networks. *Journal of Natural Gas Science and Engineering*, *108*, 104834. https://doi.org/10.1016/j.jngse.2022.104834

Jung, et al. (2018). A microfluidic pore model to study the migration of fine particles in single-phase and multi-phase flows in porous media. *Microsystem Technologies*, *24*(2), 1071–1080. https://doi.org/10.1007/s00542-017-3462-1

Khilar, K. C. & Fogler, H. S. (1983). Water Sensitivity of Sandstones. *Society of Petroleum Engineers Journal*, *23*(01), 55–64. https://doi.org/10.2118/10103-PA

Li, Q. & Prigiobbe, V. (2018). Numerical Simulations of the Migration of Fine Particles Through Porous Media. *Transport in Porous Media*, *122*(3), 745–759. https://doi.org/10.1007/s11242-018-1024-3

Liot, et al. (2018). Pore cross-talk in colloidal filtration. *Scientific Reports*, *8*(1). https://doi.org/10.1038/s41598-018-30389-7

Liu, Q., Zhao, B. & Santamarina, J. C. (2019). Particle Migration and Clogging in Porous Media: A Convergent Flow Microfluidics Study. *Journal of Geophysical Research: Solid Earth*, *124*(9), 9495–9504. https://doi.org/10.1029/2019JB017813

Mondal, S., Wu, C. H., & Sharma, M. M. (2016). Coupled CFD-DEM simulation of hydrodynamic bridging at constrictions. *International Journal of Multiphase Flow*, *84*, 245–263. https://doi.org/10.1016/j.ijmultiphaseflow.2016.05.001

Nishad, S. & Al-Raoush, R. I. (2021). Colloid retention and mobilization mechanisms under different physicochemical conditions in porous media: A micromodel study. *Powder Technology*, *377*, 163–173. https://doi.org/10.1016/j.powtec.2020.08.086

Parvan, et al. (2020). Insight into particle retention and clogging in porous media; a pore scale study using lattice Boltzmann method. *Advances in Water Resources*, *138*, 103530. https://doi.org/10.1016/j.advwatres.2020.103530

Prempeh, et al. (2020). Effects of the capillary-entrapped phase on fines migration in porous media. *Journal of Natural Gas Science and Engineering*, *73*, 103047. https://doi.org/10.1016/j.jngse.2019.103047

Reddi, et al. (2000). Permeability Reduction of Soil Filters due to Physical Clogging. *Journal of Geotechnical and Geoenvironmental Engineering*, *126*(3), 236–246. https://doi.org/10.1061/(ASCE)1090-0241(2000)126:3(236)

Rod, et al. (2018). Effect of chemical and physical heterogeneities on colloid-facilitated cesium transport. *Journal of Contaminant Hydrology*, *213*, 22–27. https://doi.org/10.1016/j.jconhyd.2018.03.012

Shen, J. & Ni, R. (2017). Experimental investigation of clogging dynamics in homogeneous porous medium. *Water Resources Research, 53*(3), 1879–1890. https://doi.org/10.1002/2016WR019421

Yusof, et al. (2020). Petrophysical Changes of Sandstone Due to Salt Precipitation and Fines Migration During Carbon Dioxide Injection. *Journal of Computational and Theoretical Nanoscience*, *17*(2), 1207–1213. https://doi.org/10.1166/jctn.2020.8791

___. (2021). Influence of Brine–Rock Parameters on Rock Physical Changes during CO2 Sequestration in Saline Aquifer. *Arabian Journal for Science and Engineering*. https://doi.org/10.1007/s13369-021-06110-8

___. (2022). Experimental study of CO2 injectivity impairment in sandstone due to salt precipitation and fines migration. *Journal of Petroleum Exploration and Production Technology*. https://doi.org/10.1007/s13202-022-01453-w

Cite as: Albaba M.T., Hannun J. & Al-Raoush R., "Impact of Pore Morphology on Colloid Migration and Pore Clogging at Variable Saturation Levels in Microfluidics of Natural Porous Media", *The 2nd International Conference on Civil Infrastructure and Construction (CIC 2023)*, Doha, Qatar, 5-8 February 2023, DOI: https://doi.org/10.29117/cic.2023.0167

A Strategic Design Approach for Implementing Rainwater Management System Using an Integration of GIS and BIM Tool

Deshbhushan Patil
Birla Institute of Technology and Science, Pilani, India
p20200061@pilani.bits-pilani.ac.in/ deshbhushanpatilp@gmail.com

Raghavendra Kumar Raya
Nirma University, Ahmedabad, India
raya.kumar@nirmauni.ac.in

Abobakr Al-Sakkaf
Concordia University, Montreal QC, Canada
abobakr.alsakkaf@concordia.ca

Ashutosh Bagchi3
Concordia University, Montreal QC, Canada
ashutosh.bagchi@concordia.ca

Rajiv Gupta
Birla Institute of Technology and Science, Pilani, India
rajiv@pilani.bits-pilani.ac.in

Abstract

An increase in urbanization and uncontrolled development has resulted in a water stress situation, which necessitates the exploration of alternate water sources. Rainwater has proven to be a prominent alternate water source after being efficiently harvested. On-ground implementation of the Rainwater Harvesting System (RWHs) at a community level in urban areas has always been challenging and requires technological advancement. To facilitate the implementation of RWHs, the proposed study provides a comprehensive methodology by integrating the Geographical Information System (GIS) and the Building Information Modeling (BIM) tools. Initially, the hydro-spatial analysis was performed with a GIS tool to obtain an optimized rainstorm collection network and to aid in establishing the geometrical properties of RWHs. Further, an outcome from the analysis was utilized to develop a visualization model using the BIM tool. The proposed methodology is implemented as a case study in the municipality of Jaipur (India). The developed multidimensional BIM contributes to the sustainability of the project in terms of resources, economy, and efficiency over the life cycle. As an outcome, the proposed study provides a comprehensive methodology for effectively utilizing rainwater to cope with the growing water demand and contribute to flood mitigation in urban regions.

Keywords: Water; Sustainability; Rainwater Harvesting; Geographical Information System; Building Information Modeling

1 Introduction

With the increase in population and urbanisation, meeting water demand has become a primary concern in most urban areas (Sitzenfrei et al., 2017). Over half of the world's population would face extreme water scarcity by 2050 (Marzouk & Othman, 2020). To address water-related challenges, various initiatives have been enforced to build sustainable water management practices which aids in conserving and utilizing water resources (Słyś & Stec, 2020). In most regions Rainwater Harvesting (RWH) has been implemented to alleviate water scarcity by serving as an alternate water source (Gwenzi & Nyamadzawo,

2014). Rainwater serve as the primary source for numerous utilities, including drinking, residential use, everyday life activities, agriculture, animal management, reservoir storage, groundwater recharge after being effectively collected and stored (Kimbonguila et al., 2019).

Along with traditional RWH practices, modern RWH practices such as bio-swales, rain gardens, pervious pavements, and green roofs are often designed and implemented in developed regions by simulating natural hydrological responses and to percolate urban rainstorms through soil infiltration, stormwater retention, storage, purification, groundwater recharge to reduce the risk of the flood (Everett et al. 2016). On the other hand, the design and implementation of the RWHs in urban areas have a substantial impact on society's environmental and economic consequences while serving as an alternate water source (Amos, Rahman & Gathenya, 2016). Strategic planning, identification of RWH sites, and design considerations play an important role to create efficient RWHs (Raya & Gupta, 2020; Patil et al., 2022). While designing and planning for the centralized RWHs numerous statical methods, water balance methods, non-dimensional design methods, and detailed design approaches were applied (Patil & Gupta, 2022; Semaan et al., 2020). Along with these approaches, modern tools such as STORM and SWMM have been applied to analyse and manage the urban drainage network (Wang, Pan & Luo, 2019a).

However in numerous instances, designing the centralized RWHs in urban areas are critical, due to the presence of on-ground components such as power and communication lines, potable water networks, gas pipes, and ground gradients (Li & Matthew, 1990). In such a case, computer models and mapping tools, such as Geographical Information System (GIS), have proved extremely useful in incorporating multiple parameters at a single point by digitizing the maps and performing the spatial analysis (Mustajoki & Marttunen, 2017). In addition to GIS tool, to assess and improve the drainage network management, interface method or multiple developed tools aid in enhancing optimal placement of model element or system controllers have been used (Leitão et al., 2018).

Very few studies focused on GIS-based management applications that accommodate varied data resources, such as BIM data, CAD data, and simulation results, to promote data fusion and increased decision-making on GIS-based platforms (Zhang et al., 2020). Moreover, the visualization of the analysed data from the GIS could be employed using a proven effective tool, i.e., BIM, since it focuses on the implementation of digital modelling and informatics management throughout the entire construction project life cycle (Eastman et al., 2011). Representation of the 3D model for stakeholder involvement, environmental impact studies, collision testing with existing infrastructure, energy consumption behaviour monitoring at both the building and community levels, heritage preservation, urban emergency response, and updating the topographic information system after completing the structure is performed by integrating the GIS and BIM tool (Amirebrahimi et al., 2015; Wang, Pan & Luo, 2019b).

Although the previously used approaches provide the visualization of simulations by allowing multiple mathematical analyses, which consumes a significant amount of precise data and needs technological improvement, which restricts its application in developing countries. The applied household approaches necessitate a significant capital investment and area, which is not realistically possible for low and middle-income groups. To facilitate the implementation of RWHs and to cover this significant knowledge gap, the current study provides an alternate way to develop the rainstorm collection network and estimates the geometrical properties of the centralised RWHs over the region using the integration of ArcGIS and BIM tools. The municipality area of Jaipur (India) is considered as a case study to validate the proposed methodology.

2 Methodology

The proposed study's methodology is categorized into three components: hydro-spatial analysis, design, and visualization, as illustrated in figure 1. To begin, a hydro-spatial analysis of the developed

digital elevation model (DEM) and the acquired satellite data is required to establish a relationship between the topography and hydrological parameters of the region. Later, at the design stage, the results obtained from the hydro-spatial analysis assist to determine the geometrical characteristics of the RWH components in accordance with Indian standard codes and design guidelines. Finally, the visualization of the RWHs is created using the BIM tool, enhancing information sharing among stakeholders across different project phases.

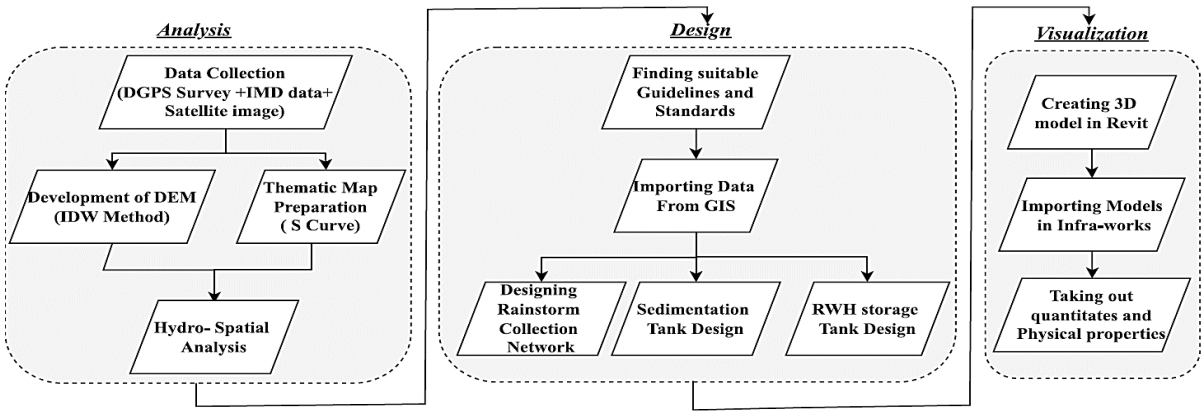


Fig. 1: Proposed Methodology

2.1 Hydro-spatial Analysis

A DEM is required to perform the hydro-spatial analysis over the study region. The data from the Differential Global Positioning System (DGPS) survey must be collected in the WGS-84 coordinate system for creating the DEM. The z-coordinate values from the data were incorporated for creating a DEM using an inverse distance weighted (IDW) interpolation method in the ArcGIS environment. The generated (DEM) was processed for creating the flow accumulation map in identifying RWH locations and establishing the drainage network. The flow accumulation raster is generated by pre-processing the DEM (Fill DEM) and developing the Flow direction raster, which was consecutively consumed as raw data. Finally, the stream order tool provides a stream order with threshold values for the flow accumulation map. The generated flow accumulation map provides the flow path and locations where the maximum flow would occur.

Further, multiple spatially referenced thematic maps are required to be generated from the acquired raw data for determining the hydrological characteristics of the region. Eventually, for estimating the amount of runoff, the SCS-CN (Soil Conservation Service-Curve Number) approach (SCS Engineering Division, 1986) was used. Raster maps for land use/land cover and soil hydrologic group were utilized to create the CN (Curve number) raster, which was then used to create the first soil abstraction raster. Finally, the runoff raster was created by combining the rainfall and initial soil abstraction rasters. The conditional tool (Con) and Raster Calculator tools have been used in the ArcGIS environment to create the runoff raster.

2.2 Design

The geometrical characteristics of RWHs components were determined using the outcomes hydro-spatial analysis. The runoff values from the stream order were used to determine the size of the rainstorm collection network. After collecting rainstorm water, a provision of a sedimentation tank near the RWH storage tank is necessary to remove silt before storing the water in a tank. Henceforth, the design of the sedimentation tank is performed using the guidelines stated in IS 10261(1982). After the primary treatment, water must be stored in a tank for future use. A 10-day design period is considered while determining the underground tank size.

2.3 Visualization

After determining the geometrical characteristics, the multidimensional visualization model is required to share the data among the stakeholders. The three main parts of the 3D model are the surface model, existing building, and pipe system modeling. To create the 3D model, all the data was organized into layers and imported into multiple BIM tools. The determined drain path in Shapefile (.*SHP format) was directly imported as a pipeline in the InfraWorks tool. Whereas in the case of the sedimentation tank and storage tank, a 3D model is required to prepare in the Autodesk Revit tool that could be imported into the InfraWorks tool with georeferencing.

3 Implementation

The municipal region of Jaipur (India) is considered as a case study to validate the practical applicability of the proposed methodology. The municipality boundaries of Jaipur spread from 26° 46’ to 27° 01’ north and 75° 37’ to 76° 57’ east. The administration of the city is overseen by the Jaipur Municipal Corporation (JMC), which encompasses the 467 square kilometers and is divided into two municipal corporations: the Greater Jaipur Municipal Corporation and the Jaipur Heritage Municipal Corporation, with 150 and 100 wards, respectively. To conduct the proposed study, ward number 06 of Greater Jaipur Municipal Corporation falls under the Jamna Puri area, is considered. The ward is located on the Northwest side of the city at latitude 26°59’09.88 "N to 26°59’53.37 "N and Longitude 75°45’11.54"E to 75°44’11.02"E and having an area of about 1.6462 sq. km.

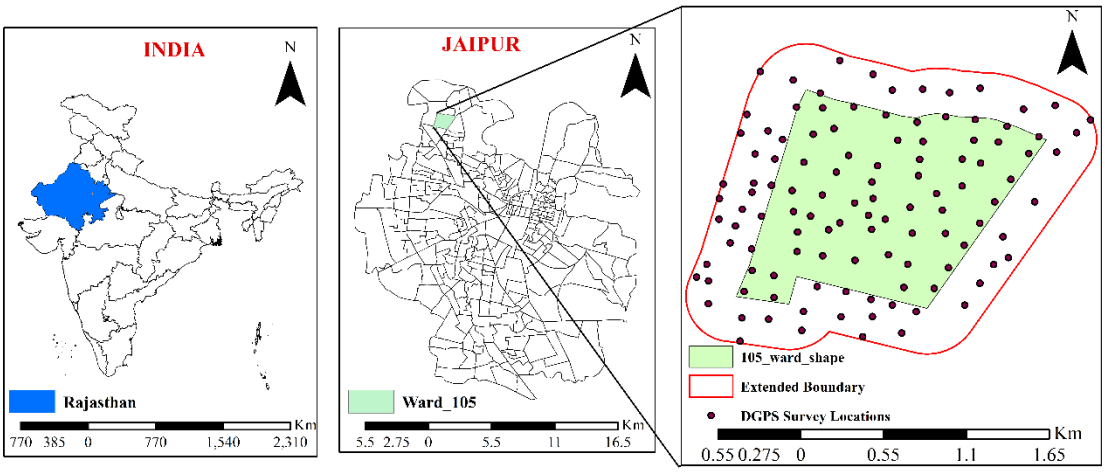


Fig. 2: Study area map

3.1 Data Collection and Preparation

A Differential Global Positioning System (DGPS) survey was conducted over the study area to collect three-dimensional coordinates in the WGS-84 coordinate system. The raw data was pre-processed with GNSS software (Trimble Survey Division, 2013) for removing inaccuracies and calibrating the readings to centimeter precision. The processed data ground data were imported into the ArcGIS environment and plotted as a shape file. Over the study area total of 115 three-dimensional coordinates were collected by considering a 500 m buffer area. The satellite images of IRS (Indian Remote Sensing) Resourcesat LISS-4 with the scene specifications 95-52-D, captured on 9/10/2019, having a spatial resolution of 5 m, have been procured from National Remote Sensing Centre, India. Daily rainfall data for Jaipur from the year 2011 to the year 2021 has been acquired from the Climate Data Service Portal of IMD (Indian Meteorological Department), Pune. The single rainfall raster was created for 2011 to 2021 and clipped within the study area. The study compromises two soil types, C

and D, which were downloaded from the United Nations FAO (Food and Agricultural Organization) soil map (FAO, soil map) (Neitsch et al., 2011; FAO Map Catalog, n.d.).

3.2 Hydro-spatial Analysis

Importing the DGPS survey data in the ArcGIS tool led to the preparation of DEM raster by using the IDW interpolation method. The created DEM was used further to create a flow accumulation raster by performing hydro-spatial analysis. The created accumulation raster for the region was multiplied by the per-hr. rainfall value of 0.1693 mm/hr. (i.e., average rainfall value for the rainy season) to create the runoff raster. The created runoff raster provides the volume of water along the drainage path in the form of the cell value. The maximum and minimum values of the runoff raster were used in determining the drain size. The maximum peak runoff values at the end of the ward were used for estimating the geometrical properties of the RWH tank by considering 10 days of average rainfall. Figure 3. shows the maps created while performing hydro spatial analysis.

3.3 Drainage Mapping

The generated runoff raster was required to classify using the peak runoff value to design the economic drainage network over the area. By understanding the maximum and minimum runoff values, the standard drain size of depths 0.5m, 1.5m, 2m, and 2.75m was considered for classifying the runoff raster. Based on the calculated peak runoff values, the runoff raster was classified as 1.702m^3/hr., 31.86 m^3/hr., 68.68m^3/hr., and 148.74 m^3/hr., and the new runoff raster was created. The created runoff raster was converted to polyline features for quantifying the geometric characteristics of flow lines. The acquired LISS-4 image was used as a base map for aligning the drainage network, and digitization was performed. Depending on the size, the created shapefile files were classified as lateral, sub-mains, main, and outfall drains. The runoff values generated by considering 10 days of average rainfall were used to determine the geometrical characteristics of the storage tank.

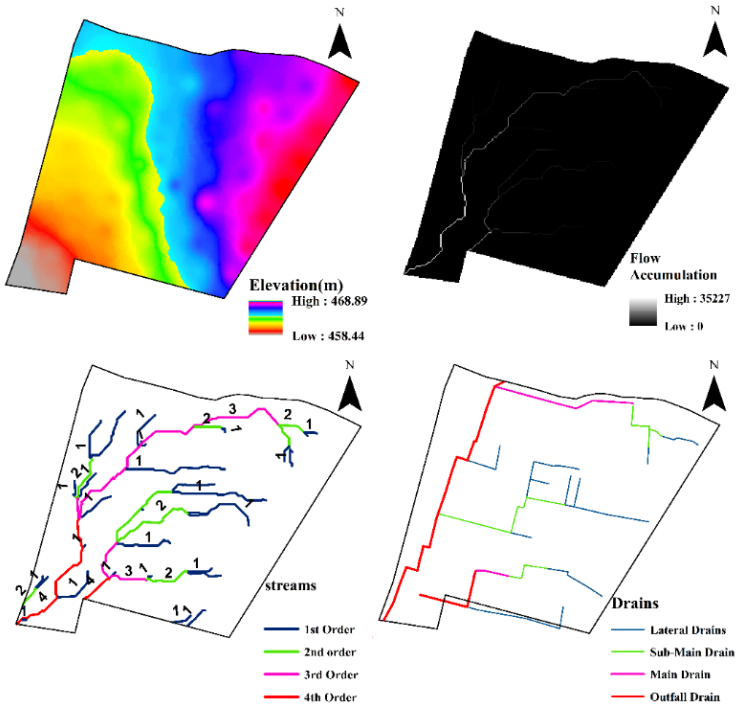


Fig. 3: Hydro Spatial Analysis

3.4 Visualization

A 3D model for the storage tank and sedimentation tank was created in the Autodesk Revit tool directly imported into InfraWorks. The created georeferenced shapefiles for the drainage network

were imported directly in InfraWorks as the pipelines. The visualizations involved the development of the real-time scenario in the study region, integrating features like roads, vegetation, and boundary limits. The model builder feature in the Infraworks help in incorporating the on-ground objects.

4 Results and Discussion

The selection of suitable sites and their technological design are key factors in the success of RWHs (Al-Adamat et al., 2012). Numerous design techniques and modern tools were implemented to increase the sustainability and efficiency of the RWHs. Most researchers integrated the multicriteria analysis (MCA) and GIS to provide a rational, objective, and unbiased technique for identifying potential regions for RWH creation by utilizing the ground survey data (Alwan, Aziz & Hamoodi, 2020). Multiple simulations and mathematical models were implemented along with the MCA to perform the micro-level planning (Patil & Gupta, 2022).

Considering past research, the proposed methodology provides a strategic approach for creating community RWHs. The performed hydro-spatial analysis over the study area comes out with designing a rainstorm collection network and establishing the geometrical characteristics of RWHs components. The detailed characteristics of the classified drains are mentioned in Table 1.

Table 1: Drain Characteristics

Drain Name	Drain Depth (m)	Drain Width (m)	Perimeter (m)	Area (m^2)	Total Length (m)	Peak Runoff (m3/hr)
Lateral Drain	0.5	1	2	0.5	3114.767	1.702
Sub Main Drain	1.5	3	6	4.5	1535.113	31.86
Main Drain	2	4	8	8	975.5422	68.68
Outfall Drain	2.72	5.44	10.88	14.8	3681.807	148.74

After designing the collection network, the sedimentation tank and storage tank design were performed using the obtained runoff values. The visual model is prepared using Autodesk Revit and integrating with the InfraWorks tool by incorporating multiple information layers of buildings, roads, and topography. The properties of the designed model were extracted and mentioned in Table 2.

Table 2: RWHs components Characteristics

RWH Component	Area (m^2)	Volume(m^3)	Dimensions
Sedimentation Tank	195	1072.5	30*6.5*5.5
Storage Tank	1912	17121.1	40*47.80*37.80*10

The identified location of the starting and ending node of the drain during execution for placing the drainage network without any clashes and misalignment issues. BIM helps to visualize the present drainage network by incorporating multiple information layers of buildings, roads, topography, and drainage network characteristics. The Figure 4 a, b, c) represents the different information layers for the RWH system and collection network which integrated in Infraworks model, respectively. The created visual model for the entire RWHs increases the information sharing among the stakeholders and aids the planner in estimating the resource at the initial planning phase. The study uses the rectangular open-drain section, which could be modified with alternate materials and shapes based on requirements and present locations.

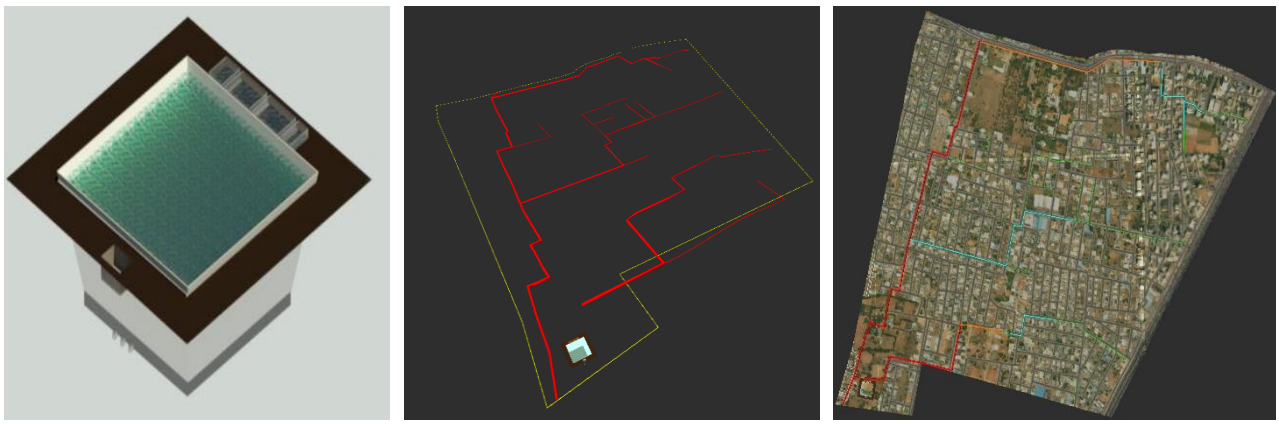


Fig. 4: a) RWH tank visualization **b)** Drainage Network visualization **c)** InfraWorks Visualization

5 Conclusion

Exploration of alternate water sources is essential to meet the global water demand rise. Strategic planning, advancement in technology, and design considerations are required for enhancing the efficiency of rainwater harvesting system (RWHs). The suggested methodology in the study integrates Geographical Information System (GIS) and Building Information Modelling (BIM) tools to provide a strategic approach for creating a community RWHs over a region. The methodology was applied to a municipality ward of Jaipur city, India, as a case study. The performed hydro-spatial analysis aids in determining the geometrical characteristics of RWHs components such as drain size, sedimentation tank size, and storage tank design spread over the wards. In addition, created visualization using the determined geometrical characteristics enhance the information sharing among the stakeholders by incorporating topographic information such as the location of roads, buildings, and important structures, conflict's resolution during the execution. Further detailed design of the RWH structure over the distributed locations would increase the study's feasibility by creating a continuous chain of RWHs along the periphery of the municipality, which could be incorporated in a future study.

Acknowledgement

The work is partially funded by the Department of Science and Technology India, and Mr. Cuckoo Kochar (President & CEO, DCR Phoenix Group) & Indian Council of Cultural Relations for GNDJ initiative (Guru Nanak Dev Ji Academic and Research Initiative).

References

Al-Adamat & Rida et al. (2012). "The Combination of Indigenous Knowledge and Geo-Informatics for Water Harvesting Siting in the Jordanian Badia." *Journal of Geographic Information System 2012*(04): 366–76. http://www.scirp.org/journal/PaperInformation.aspx?PaperID=22156 (February 21, 2022).

Alwan, et al. (2020). "Potential Water Harvesting Sites Identification Using Spatial Multi-Criteria Evaluation in Maysan Province, Iraq." *ISPRS International Journal of Geo-Information 9*(4).

Amirebrahimi, et al. (2015). "A Framework for a Microscale Flood Damage Assessment and Visualization for a Building Using BIM–GIS Integration." http://dx.doi.org/10.1080/17538947.2015.1034201 9(4): 363–86.

Amos, C. C., Rahman, A., & Gathenya, J. M. (2016). "Economic Analysis and Feasibility of Rainwater Harvesting Systems in Urban and Peri-Urban Environments: A Review of the Global Situation with a Special Focus on Australia and Kenya." Water 2016, Vol. 8, Page 149 8(4): 149. https://www.mdpi.com/2073-4441/8/4/149/htm (May 12, 2022).

André et al. (2019). "Effect of Physical Treatment on the Physicochemical, Rheological and Functional Properties of Yam Meal of the Cultivar 'Ngumvu' From Dioscorea Alata L. of Congo." *International Journal of Recent Scientific Research 10*: 30693–95.

Deshbhushan, P. & Gupta, R. (2022). "GIS-Based Multi-Criteria Decision-Making for Ranking Potential Sites for Centralized Rainwater Harvesting." *Asian Journal of Civil Engineering* 2022: 1–10. https://link.springer.com/article/10.1007/s42107-022-00514-z (November 8, 2022).

Deshbhushan, et al. (2022). "A Systematic Basin-Wide Approach for Locating and Assessing Volumetric Potential of Rainwater Harvesting Sites in the Urban Area." *Environmental Science and Pollution Research 1*: 1–15. https://link.springer.com/article/10.1007/s11356-022-23039-z (October 7, 2022).

Eastman, et al. (2011). "BIM Handbook, a Guide to Building Information Modelling 2nd Ed." John Wiley & Sons, Inc, Hoboken: 1–650.

Everett, et al. (2016). "Sustainable Drainage Systems: Helping People Live with Water." Proceedings of the Institution of Civil Engineers: Water Management 169(2): 94–104. http://dx.doi.org/10.1680/wama.14.00076 (November 8, 2022).

"FAO Map Catalog."https://data.apps.fao.org/map/catalog/srv/eng/catalog.search?id=14116#/metadata/446ed430-8383-11db-b9b2-000d939bc5d8 (May 4, 2022).

Gwenzi, W. & Nyamadzawo, G. (2014). "Hydrological Impacts of Urbanization and Urban Roof Water Harvesting in Water-Limited Catchments: A Review." *Environmental Processes 1*(4): 573–93. https://link.springer.com/article/10.1007/s40710-014-0037-3 (May 12, 2022).

Jyri, M. & Marttunen, M. (2017). "Comparison of Multi-Criteria Decision Analytical Software for Supporting Environmental Planning Processes." *Environmental Modelling & Software 93*: 78–91.

Leitão, et al. (2018). "Identifying the Best Locations to Install Flow Control Devices in Sewer Networks to Enable In-Sewer Storage." *Journal of Hydrology 556*: 371–83.

Li, G. & Matthew, R. G. S. (1990). "New Approach for Optimization of Urban Drainage Systems." *Journal of Environmental Engineering 116*(5): 927–44. https://ascelibrary.org/doi/abs/10.1061/%28ASCE%290733-9372%281990%29116%3A5%28927%29 (November 8, 2022).

Mohamed, M. & Ahmed, O. (2020). "Planning Utility Infrastructure Requirements for Smart Cities Using the Integration between BIM and GIS." *Sustainable Cities and Society* 57: 102120. https://doi.org/10.1016/j.scs.2020.102120.

Mary et al. (2020). "Optimal Sizing of Rainwater Harvesting Systems for Domestic Water Usages: A Systematic Literature Review." Resources, Conservation & Recycling: X 6: 100033.

Neitsch, et al. (2011). "College of Agriculture and Life Sciences Soil and Water Assessment Tool Theoretical Documentation Version 2009."

Raya, R. K. & Gupta, R. (2020). "Rural Community Water Management through Directional Tunnelling: Visual Modelling of Rainwater Harvesting System." *Water Practice and Technology 15*(3): 734–47. http://iwaponline.com/wpt/article-pdf/15/3/734/745316/wpt0150734.pdf (June 26, 2022).

Sitzenfrei, et al. (2017). "Impact of Hybrid water Supply on the Centralised Water System." *Water (Switzerland) 9*(11).

Słyś, D., & Stec., A. (2020). "Centralized or Decentralized Rainwater Harvesting Systems: A Case Study." Resources 2020, Vol. 9, Page 5 9(1): 5. https://www.mdpi.com/2079-9276/9/1/5/htm (January 28, 2022).

Sherong et al. (2020). "Integrating and Managing BIM in 3D Web-Based GIS for Hydraulic and Hydropower Engineering Projects." *Automation in Construction 112*: 103114. https://doi.org/10.1016/j.autcon.2020.103114.

Wang, H., Pan, Y. & Luo, X. (2019a). "Integration of BIM and GIS in Sustainable Built Environment: A Review and Bibliometric Analysis." *Automation in Construction 103*: 41–52.

(2019b). "Integration of BIM and GIS in Sustainable Built Environment: A Review and Bibliometric Analysis." Automation in Construction 103(March): 41–52. https://doi.org/10.1016/j.autcon.2019.03.005.

Cite as: Patil D., Raya R.K., Al-Sakkaf A., Bagchi A. & Gupta R., "A Strategic Design Approach for Implementing Rainwater Management System Using an Integration of GIS and BIM Tool", *The 2nd International Conference on Civil Infrastructure and Construction (CIC 2023)*, Doha, Qatar, 5-8 February 2023, DOI: https://doi.org/10.29117/cic.2023.0168

The Influence of Urbanization on Natural Overland Flow Paths

Amna Mohammed Al-Sayed
Planning Engineer – 2**,** Public Works Authority **(**Ashghal**),** Doha, Qatar
aalsayed@ashghal.gov.qa

Mohammed Amer Younus Al-Shaheen
GIS Senior Engineer**,** Public Works Authority **(**Ashghal**),** Doha, Qatar
moalshaheen@ashghal.gov.qa

Abstract

This paper studies the influence of urbanization on the natural overland flow paths on topography. The main objectives of this study are to: measure the effectiveness of drainage networks, study the influences of urban structure, compare the pre-and post-urban overland flow paths, and provide recommendations for flood prevention. The study was conducted on a catchment (81 km2) in Qatar that lies between Doha and Al-Rayan. Land cover, soil data, rain data, and digital elevation model (DEM) were the main inputs of the study to obtain run-off depths, time of concentration, and peak flows. The Soil Conservation Service (SCS) method was applied, where Curve Numbers (CNs) were identified for each land cover based on soil groups concerning the infiltration rate. A geographic information system (GIS) integration has provided better results. ArcMap tools have been used to study flow changes such as flow direction, flow accumulation, and stream definition. The result of the study shows that urbanization has a significant effect on the characteristics of the flow path as it causes the time of concentration to decrease, resulting in increased run-off depth and peak flow.

Keywords: Urbanization; GIS; Flood; Overland; Drainage

1 Introduction

The natural and unnatural flow of water can cause problems for infrastructure (Graham, 2010; Koval et al., 2021; Wahyudi et al., 2012). This could be due to an unnatural flood caused by rainfall in an area upstream of an area, which increases water flow in a short period of time. The same phonemena can also be caused by intense rainfall in a particular area where the systems designed to flush the water (through the storm-water collection system or through the designed or natural percolation) become overwhelmed. Thus the water is contained in an area where the soil is too dense or when there is direct precipitation on saturated areas (DPSA) (Steenhuis et al., 2005).

A high level of water absorption during rainfall or a high groundwater table can cause an area to become saturated (Ahuja, 2022; Azarnivand et al., 2020; Szabó et al., 2022). To assess such an accumulation of water in an area, many parameters, such as slope, soil structure, vegetation, flow velocity, channel density, intensity, and duration of rainfall, should be considered (Abuzied & Pradhan, 2021; Bai et al., 2022; W. Liu et al., 2021).

Different modeling techniques shall be used to understand the impact of such water clogging not only in a particular area but also in upstream and downstream areas. For such purposes, two-dimensional mapping, rainfall modeling, contour-based water passage, and volume modeling can be applied (Ornelas et al., 2017). These types of models can also be integrated in a suitably organized geographic

information system (GIS) for the concerned area. The Soil Conservation Service Curve Number (SCS-CN) method is one of the best and most traditional methods for studying water overflow using GIS (Soulis, 2021). SCS mainly depends on four key factors: land cover, soil, treatment, and hydrologic conditions. In this method, the CN is identified for each land use. The CN is about the soil and is divided into four groups based on how well the soil drains. When the SCS method is used with GIS, the overflow in a catchment can be shown and analyzed in a complete way.

Urban development of many structures like buildings, roads, drainage systems, etc. has a great effect on topography and land characteristics (Zhai et al., 2021). Runoff water impacting urban areas should be discharged through a drainage system that is designed to handle the clogging volumes of overland water and is aligned to use natural terrains to flush water. Identifying the natural overland flow before urbanization should be part of urban planning, and drainage design engineers should think about using these flow paths as a basis for designing the drainage network (Zheng et al., 2018).

The study of water flow and water clogging on urbanization is important to design an efficient and effective water flushing system (T. Liu et al., 2021; Zhou et al., 2021). Due to the increased urbanization and increased population density in those areas, any water clogging or high-volume overland water flow can cause social, economic and environmental problems.

Ultimately, the analysis of the flow and the capacity of the infrastructure may consider various parameters on a spatial information system can help the planner to visualize the problem and design systems that will minimize the impact. The objective of the study is to measure the effectiveness of the drainage network in the catchment area. Then, to study the influence of the urban structure on the overland flow paths in the catchment area and compare the overland flow paths before and after urbanization. Ultimately, the study is going to provide recommendations to minimize the impact of intense rainfall in the area.

2 Methodology

An integration of SCS and GIS system is used to model water flow and water clogging in a catchment that lies between Doha and Al-Rayan (81 km^2), which is a thickly populated urban area in Qatar (Figure 1).

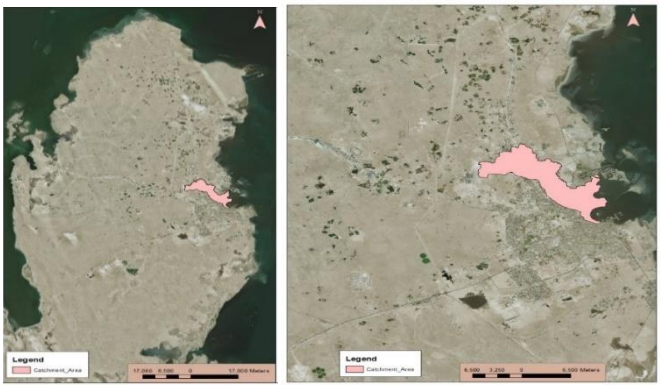


Fig. 1: Catchment Location on Qatar Map

The studied area is a catchment between Doha and Al-Rayan, located in the eastern part of the country.

The area is urbanized with many residential properties though there are few parts that are non-urbanized. The study area is about 81 km^2. Doha's recent land use statistics indicate that its open

spaces have reduced from 76.81% to 25.3% (Koch, 2019). There are three reasons for selecting this area are:

1. The catchment consists of different elevations where flow paths can be studied more efficiently.
2. The catchment is mainly urbanized and has non-urbanized spots where the influence of urbanization can be compared comprehensively Figure 2.
3. The capacities of the drainage systems in the urbanized area can be studied and compared with the amount of run-off water.

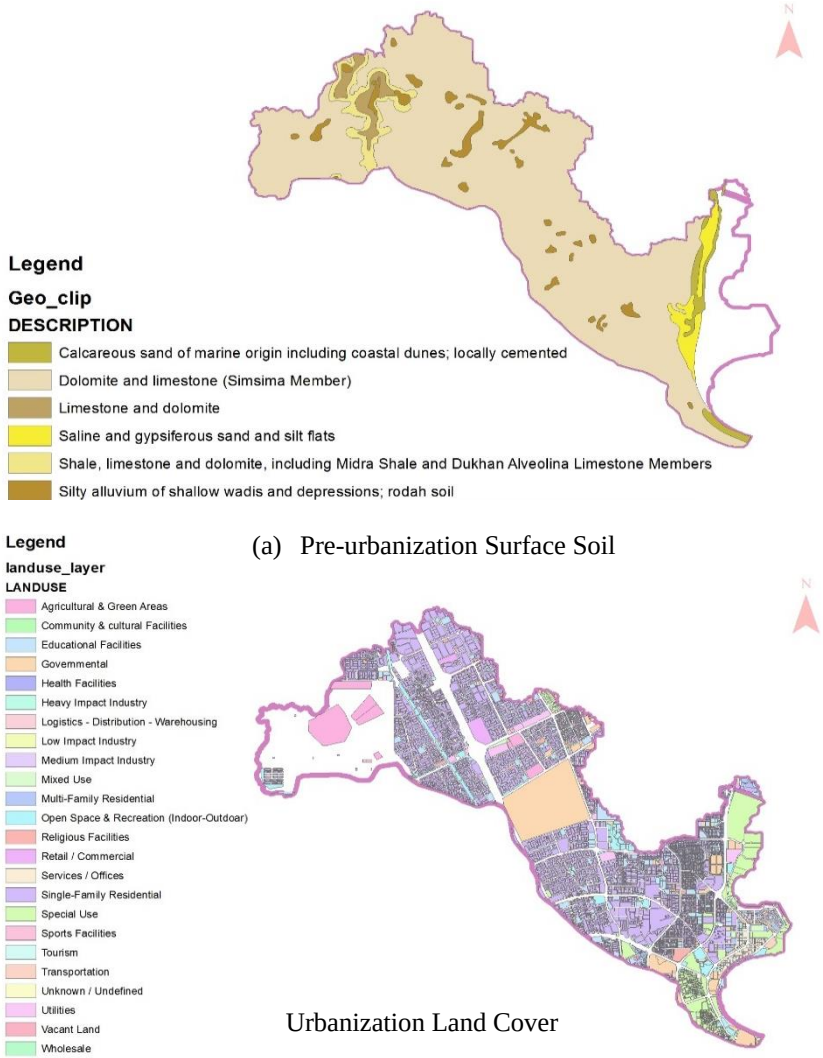


Fig. 2: (a) Pre-urbanization Surface Soil Cover **(b)** Post-urbanization Land Cover

The methodology applied in this project comprised two parts: mathematical model and GIS model. Both models were integrated to obtain run-off volumes and peak flow as represented in **خطأ! لم يتم العثور على مصدر المرجع.** Page 4. SCS mathematical model was applied using soil and land use maps to identify the CN to obtain the potential maximum soil retention based on that value. Run-off value calculated using initial abstraction, total precipitation, area and soil retention. For the GIS model, DEM data were created by integrating buildings footprints and heights. A sequence of ArcMap tools were applied to obtain the time of concentration where CN was an input to longest path. Finally, to integrate both models to calculate the peak flow. The limitation of modelling accuracy with CN decreases when historical data are used.

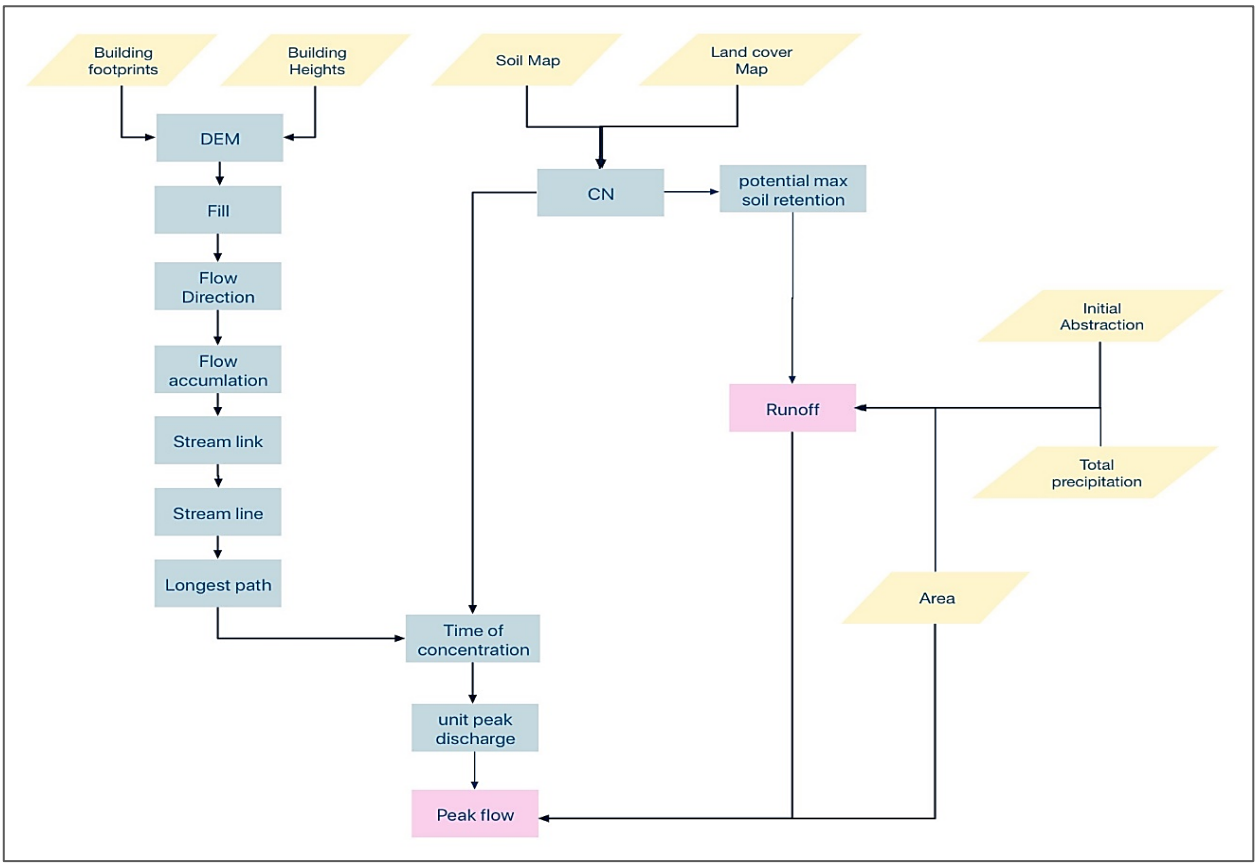


Fig. 3: Methodology Diagram

2.1 Factors

A list of factors have been identified as part of this study, summarised in **Table 1:** Summary of the Study Factors.

Table 1: Summary of the Study Factors

Factor	Description
Curve number	CN is related to soil type, infiltration, land use and water table level where soil is categorized into four soil groups based on the infiltration rates.
Land use	Classified based on usage, such as residential, commercial and open places. The cover type and condition impact the run-off volume by influencing the infiltration.
Rainfall data	The rainfall data were provided by the drainage design department in Ashghal using a 10-year rainfall event of 24 hours.
Digital elevation model	Spatially distributed hydrological attributes used to generate DEMs using LiDAR data for the whole of Qatar.
Drainage capacity	In this catchment, two pumping stations were available: • SW 3, which actually drains most of the catchment and has a capacity of 6.3 m3/s. • SW 4, which actually drains a small part of coastal area; pearl etc. and has a capacity of 0.8 m3/s. This gives a total pumping station capacity of 7.1 m3/s.

2.2 SCS-CN Method

SCS-CN method was implemented to predict direct run-off volumes in the studied area for a 10-year rainfall event depending on four important factors, among which soil type and land cover were important. The following three equations were used to calculate run-off volume generated, as attained from Ashghal's Drainage Design Manual (chapter 4)(PWA, 2006).

$$Q = \frac{(P-I_a)^2}{P-I_a+S} \quad (1)$$

$$S = \frac{1000}{CN} - 10 \quad (2)$$

$$CN_w = \frac{\sum_1^n CN_i A_i}{\sum_1^n A_i} \quad (3)$$

Where,

Q = Run-off generated (in).

P = Total precipitation (in).

S = Potential maximum soil moisture retention after run-off begins (in).

$\mathbf{I_a}$ = Initial abstraction (in) or infiltration or rainfall interception from Table A.2 -Appendix (A).

$\boldsymbol{CN_i}$ = The CN for particular land from Table A.1- Appendix (A).

$\boldsymbol{A_i}$ = Area of each land use.

2.3 Determine Peak Flow

Peak flow is the rate of the maximum discharge of run-off in a storm event. Peak flow depends on time of concentration and unit peak discharge. To calculate the peach flow, the equations below were obtained from the Urban Hydrology for Small Watersheds Manual published by the United States Department of Agriculture (Technical Relase55).

$$t_c = 0.0136 \times L^{0.8} \times (\frac{1000}{CN} - 9)^{0.7} H^{-0.5} \quad (4)$$

$$H = \frac{\text{highest elevation} - \text{lowest elevation}}{L} \quad (5)$$

$$q_u = 10^{[C_0 + (C_1)(logt_c) + (C_2)(logt_c)^2]} \quad (6)$$

Peak flow= q_u*A*Q (7)

Where,

t_C = Time of concentration in (hr)

L = Hydraulic watershed length (m)

CN = Hydrologic area-weighted CN

H = Average watershed land slope (m/m)

A = Area of catchment (km^2)

q_u = Unit peak discharge (csm/in)

Q = Run-off (in)

$C0$, C_1, C_2 = Dimensionless coefficient for rain type II listed in Table A.4 - Appendix (A).

2.4 SCS Implementation

The results show that an urban area has a higher run-off depth than a rural area because Q is bigger, as shown in Table 2 page 6. This difference results from the changes in the characteristics of the topography due to urbanization, where the infiltration rates and precipitation decreases and land cover change and results in higher run-off depth.

Table 2: SCS Calculation of Q

	Post-urbanization	Pre-urbanization
CN weighted	92	67
Ia	0.174	0.41
P	1.984	1.984
Ia/P	0.088	0.207
S	0.915	4.927
Q	**1.202**	**0.381**

2.5 GIS Implementation

The The following steps are applied by sequencing the use of GIS tools to generate the flow stream in ArcMap and then calculating the peak flow using the stream create:

- Generate DEM of the Catchment Area.
- Fill Tool Applied to the Catchment Area.
- Flow Directions defined of the Catchment Area.
- Flow Accumulation of the Catchment defined.
- Stream Link Applied to the Catchment Area.
- Stream Lines Identified in the Catchment Area.
- Longest Path Identified in the Catchment Area.

2.6 Peak Flow and Drainage Capacity

Two scenarios are discussed for the post-urbanization. First, all run-off water (including water accumulated on buildings, etc.) is considered and flash to the drainage. Second, only water from the Right of Way is considered and flash to the drainage. The time of concentration, qu, peak flow and all related parameters are calculated and represented in Table 3.

Table 3: Peak Flow Calculations

Parameters	Post-urbanization	Post-urbanization (RoW)	Pre-urbanization
CN weighted	92	92	67
L (m)	22,620	22,620	30500
Lowest elevation (m)	1.2	1.2	2
highest elevation (m)	23	23	31
H (m/m)	0.00096	0.00096	0.00095
Tc (hr)	34.5	34.5	98.8
I_a (in)	1.174	0.174	0.410
P (in)	1.98	1.98	1.98
I_a/P	0.6	0.1	0.2
C_0	2.55	2.55	2.509
C_1	–0.615	–0.615	-0.619
C_2	–0.164	–0.164	-0.141
q_u ($m^3/s/in/km^2$)	0.18	0.18	5.2
A (km^2)	81	29	0.06
Q (in)	1.20	1.20	0.38
Peak Flow (m^3/s)	**17.6**	**6.3**	**1.8**

It is observed that the post-urbanization time of concentration (tc) for both scenarios is less than the post-urbanization time, which means that more water will accumulate in less time, causing the run-off depth (Q) to increase. The peak flow of the post urbanized catchment has the highest value in comparison with the other values with a significant difference.

Because the capacity of pumping stations is 7.1 m3/s, the capacity of the pumping station will be able to discharge the total amount of ROW run-off for a 10-year rainfall event intensity. If run-off water falls into the stream from other sources (e.g. building roofs), the drainage capacity will not be able to discharge these amounts, thereby resulting in the flooding of the urban area and harm to the residents.

3 Results and Findings

3.1 Influence of Urbanization on Flow Paths

The results show that overrun characteristics vary due to changes in land use, geology, topography and more. It can be observed that urban development of the catchment has a notable effect on the hydrological response based on the amount of change by human activities. As the land is covered by roads, buildings, etc., it will have a smaller capacity to store water, causing flood risk mainly in areas with dense population. Due to storage capacity, urban flow rises quickly with higher peak discharge rates of 17.6 m3/s, whereas it is only 3 m3/s for rural area.

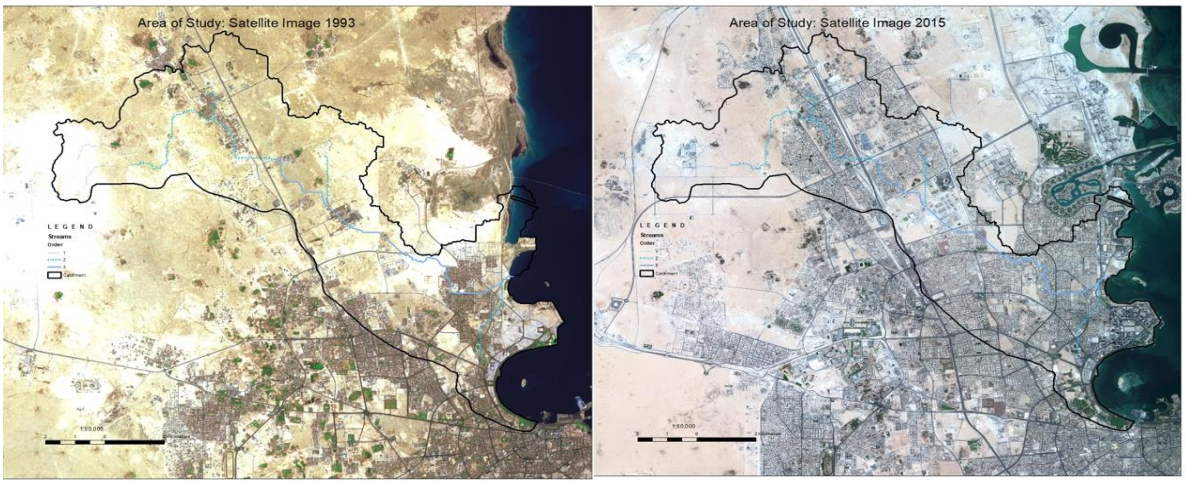


Fig. 4: Satellite Images for Years 1993 and 2015

This shows a significant raising of peak flows due to human activities where water is blocked by structures and forced to change the flow, causing accumulation of water in urban areas. Figure 4 shows the urban development difference in the catchment area pre- and post-urbanization. Moreover, urbanization causes reduction in evapotranspiration and percolation of water. This results in the acceleration in run-off and accumulation of water in various areas. In addition, there is the material covering the soils, which reduce the amount of water that may be infiltrated by soil and increase the run-off rate.

3.2 Analyse Drainage Design Capacity

Urbanization causes a loss of natural flood storage that should be replaced by artificial drainage networks. When the drainage capacity is inadequate, run-off occurs in urban areas. The results show the drainage network in the catchment will be able to discharge the amount of rain considering only ROW run-off. Due to the improper commitment to the standards considered whilst designing the drainage network, for this catchment, most of water from building rooftops and other sources also run into the ROW, causing high flood level.

The amount of water falling into the stream from sources other than ROW has been studied based on the land cover map. Different area percentage of these sources are added gradually to show how much the drainage network can actually discharge before causing a flood in the area. Table 4 shows the peak flows for different percentages.

Table 4: Flow Peaks of Adding Different Area Percentages

Percentage (%)	Area other than ROW% (km^2)	Total area (km^2) [ROW + non-ROW%]	Peak flow (m^3/s)	Peak flow difference
10%	5	34	7.36	4%
20%	10	39	8.47	19%
30%	16	44	9.59	35%
40%	21	50	10.71	51%
50%	26	55	11.82	67%
60%	31	60	12.94	82%
70%	36	65	14.05	98%
80%	41	70	15.17	114%
90%	47	75	16.29	129%
100%	52	81	17.40	145%

These results show the drainage can handle the water accumulated in the stream only for 8% of other areas. If that percentage increases, it will result in increasing the amount of peak flow to cause flooding of the catchment. This is because the excess amount of water is not considered in the design of the drainage network. For this catchment, the area was urbanized where the drainage network was constructed between 2000 and 2014, whilst few ones were newly constructed between 2016 to 2018. This may impact the condition of the drainage network, where it will not be able to flash the run-off water volumes. Moreover, part of the drainage network in that catchment is negative and part is positive. Negative networks are constructed but not connected to the main network, whilst positive networks are connected.

These negative networks are flushed in soakaways or sub-tanks where water will evaporate. This means that some portion of the run-off water will not be discharged through the pump station where it will be discharged in the ground, resulting in an increased water table level if the soakaway cannot handle the amount of water causing the soil to be saturated anot able to absorb the water. Compared with the flood history in the catchment for the year 2017, the catchment had slight floorings for the past years, which can be considered proof for the results obtained from this study, as shown in Figure 5.

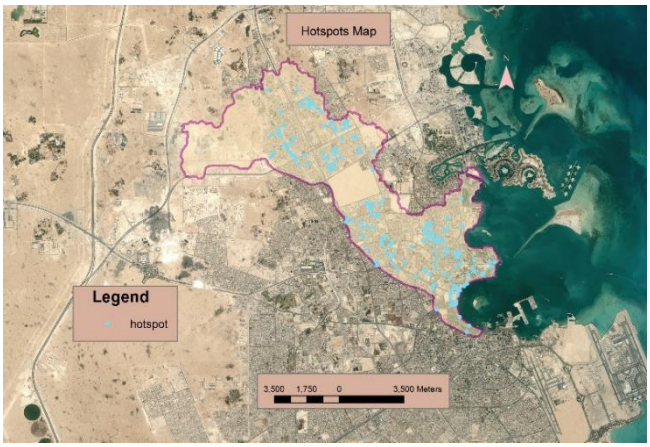


Fig. 5: Flooding History of the Catchment

3.3 Compare Flow Paths

It is observed the pre-urbanized stream had one continuous flow with many branches, whilst the post-urbanization split into two streams with less branches, thus causing the stream length to be shorter. Furthermore, the longest path of the pre-urbanized stream is around 31 km, whilst the longest path of the post-urbanized stream is only 22 km. This is due to the build-up of roads and other structures that lead the water to flow in a certain and defined path instead of running naturally along the topography Figure 6.

The amount water in urban areas is accumulated in a stream with a shorter length for the post-urbanized than the pre-urbanized, which is much longer and causes the water accumulation depth to increase from 0.3 in to 1.3 in for the post urban. On the other hand, the time of concentration for the post-urbanization is reduced due to the reduction in the flow length, which can be observed from the calculation results in Table 3 Page 6 as both have a directly proportional relationship.

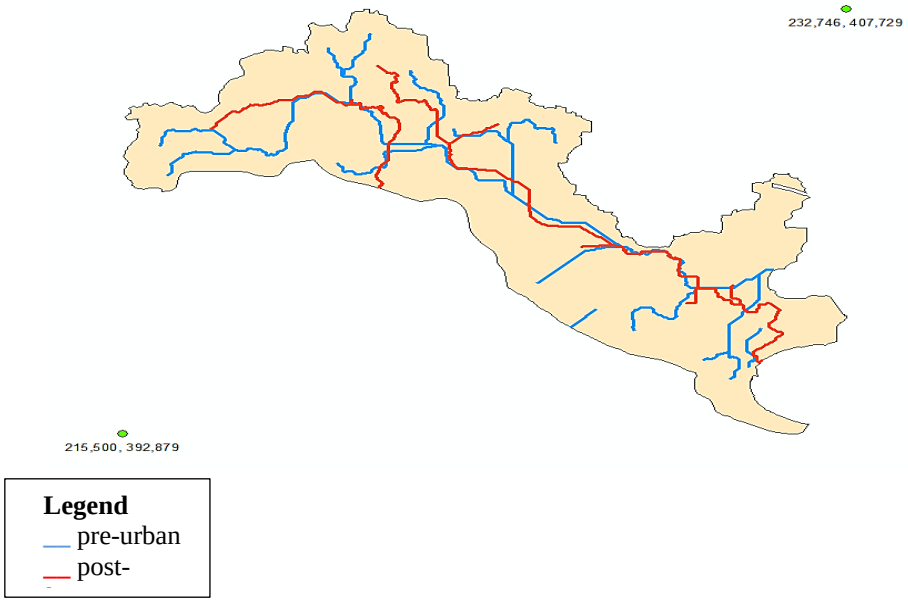


Fig. 6: Comparison of Pre- and Post-urbanized Streams

4 Conclusion and Recomendations

In this study, the influence of urban structure on natural flow paths of water is presented. Due to the increase of population density and urbanization, high volumes of water flow accumulated and caused floods. The project was conducted for an 81 km2 catchment that lies between Doha and Al-Rayan in Qatar. The analysis measured the catchment's drainage capacity for a 10-year rainfall event of 24 hours where all run-off water was assumed to be discharged through the pump station.

Parameters such as soil data, land cover, and rain fall data are considered in this project. As more factors were considered, the efficiency of the model improved and became more accurate. The SCS method was applied for this study, where soil type was the main factor to identify the CN for each land use. GIS was integrated to represent flow directions and accumulations and to identify stream flow where DEM was used as an input to asses pre- and post-urbanization flow.

The results of the study showed that urbanization increased the run-off volume in the catchment and the peak flow by reducing the time of concentration. The characteristics of the flow paths has been changed due to human activities in the catchment, causing the flow path length to decrease. The

techniques applied in this project were useful where changes in flow paths pre- and post-urbanization were expressed in an efficient way.

Studying flow paths requires knowledge of several areas—GIS, geology and hydrology—to conduct a more accurate study. Understanding the natural flow of water is an important aspect for planners, and designers need to consider it to have a proper drainage design and to prevent flooding. From this study, it is recommended that the following actions be considered to prevent flooding:

1. Drainage systems should be expanded to increase their capacity for high stream flows in order to prevent flooding in case the amount of water if runoff increased to be more than 8% from other areas in addition to the ROW.
2. the status of existing drainage should be studied and periodicaly monitored to prevent any network blocking. This will make the drainage network more efficient and capable of discharging the amount of water that it is designed for.
3. Accumulated water in areas rather than ROW should be drained in places other than the road as it impacts the other land features.
4. Infiltration should be considered for water storage in the soil, such as in infiltration trenches, sokaways and permeable pavements.
5. In order to reduce the amount of runoff water and increase the value of CN, planting more vegetation in streets, schools and hospitals and encouraging people to plant in their backyards can help decrease run-off as green areas and vegetation increase the possibility of water aborbtion.

References

Abuzied, S. M. & Pradhan, B. (2021). Hydro-geomorphic assessment of erosion intensity and sediment yield initiated debris-flow hazards at Wadi Dahab Watershed, Egypt. *Georisk: Assessment and Management of Risk for Engineered Systems and Geohazards*, *15*(3), 221-246.

Ahuja, L. R. (2022). Water and Chemical Transport in the Soil Matrix and Macropores. *Modeling Processes and Their Interactions in Cropping Systems: Challenges for the 21st Century*, 1-32.

Azarnivand, et al. (2020). Simulated response of an intermittent stream to rainfall frequency patterns. *Hydrological Processes*, *34*(3), 615-632.

Bai, et al. (2022). Flow-slide characteristics and failure mechanism of shallow landslides in granite residual soil under heavy rainfall. *Journal of Mountain Science*, *19*(6), 1541-1557.

Graham, S. (2010). When infrastructures fail. In *Disrupted cities* (pp. 13-38). Routledge.

Koval, et al. (2021). Ecosystem of environmentally sustainable municipal infrastructure in Ukraine. *Sustainability*, *13*(18), 10223.

Liu, et al. (2021). Low impact development (LID) practices: A review on recent developments, challenges and prospects. *Water, Air, & Soil Pollution*, *232*(9), 1-36.

Liu, W., Yang, Z. & He, S. (2021). Modeling the landslide-generated debris flow from formation to propagation and run-out by considering the effect of vegetation. *Landslides*, *18*(1), 43-58.

Ornelas, et al. (2017). Two-Dimensional Hydraulic Modeling and Geotechnical Analysis of Earthen Regulation Dams Located at Arroyo Las Viboras Watershed in a Major Transboundary Mexico-USA Metroplex: How an Ordinary Rain Event Caused Major Damage Related to Extraordinary Flooding. In. InTech. https://doi.org/10.5772/intechopen.68853

PWA. (2006). *Qatar Sewerage and Drainage Design Manual*. Doha -Qatar: Ashghal.

Soulis, K. X. (2021). Soil conservation service curve number (SCS-CN) Method: Current applications, remaining challenges, and future perspectives. In (Vol. 13, pp. 192): MDPI.

Steenhuis, et al. (2005). Overland Flow. In D. Hillel (Ed.), *Encyclopedia of Soils in the Environment* (pp. 130-133). Elsevier. https://doi.org/https://doi.org/10.1016/B0-12-348530-4/00568-3

Szabó, et al. (2022). The soil moisture regime and groundwater recharge in aged forests in the Sand Ridge region of Hungary after a decline in the groundwater level: an experimental case study. *Journal of Hydrology and Hydromechanics*, *70*(3), 308-320.

Wahyudi, et al. (2012). Problems, causes and handling analysis of tidal flood, erosion and sedimentation in northern coast of Central Java: review and recommendation. *International Journal of Civil & Environmental Enginering*, *12*(04), 65-69.

Zhai, et al. (2021). Multiscale watershed landscape infrastructure: Integrated system design for sponge city development. *Urban Forestry & Urban Greening*, *60*, 127060.

Zheng, et al (2018). Identifying important ecological areas for potential rainwater harvesting in the semi-arid area of Chifeng, China. *PloS one*, *13*(8), e0201132.

Zhou, et al. (2021). Novel perspective for urban water resource management: 5R generation. *Frontiers of Environmental Science & Engineering*, *15*(1), 1-13.

Appendix A: Construction Contract Administration Framework

Table A.1: Runoff Curve Number for Urban Areas

Cover Description		Curve numbers for hydrologic soil group			
Cover type and hydrologic condition	Average percent impervious area [2]	A	B	C	D
Fully developed urban areas (vegetation established)					
Open space (lawns, parks, golf courses, cemeteries, etc)[3]:					
Poor condition (grass cover < 50%)		68	79	86	89
Fair condition (grass cover 50% to 75%)		49	69	79	84
Good condition (grass cover > 75%)		39	61	74	80
Impervious areas					
Paved: parking lots, roofs, driveways, etc. (excluding right-of-way)		98	98	98	98
Streets and roads:					
Paved: curbs and storm sewers (excluding right of way)		98	98	98	98
Paved; open ditches (including right-of-way)		83	89	92	98
Gravel (including right-of-way)		76	85	89	91
Dirt (including right-of-way)		72	82	87	89
Western desert urban areas:					
Natural desert landscape (pervious areas only)[4]		63	77	85	88
Artificial desert landscaping (impervious weed barrier, desert shrub with a 1 to 2 inch sand or gravel mulch and basin boarders)		96	96	96	96
Urban districts:					
Commercial and business	85	89	92	94	95
Industrial	72	81	88	91	93
Residential districts by average lot size:					
1/8 acre or less (town houses]	65	77	85	90	92
1/4 acre	38	61	75	83	87
1/3 acre	30	57	72	81	86
1/2 acre	25	54	70	80	85
1 acre	20	51	68	79	84
2 acres	12	46	65	77	82
Developing urban areas					
Newly graded areas (pervious areas only, no vegetation)[5]		77	86	91	94
Idle lands (CN's are determined using cover types similar to those in Table 10.2c).					

Table A.2: Ia value for runoff CN

Curve number	I_a (in)	Curve number	I_a (in)
40	3.000	70	0.857
41	2.878	71	0.817
42	2.762	72	0.778
43	2.651	73	0.740
44	2.545	74	0.703
45	2.444	75	0.667
46	2.348	76	0.632
47	2.255	77	0.597
48	2.167	78	0.564
49	2.082	79	0.532
50	2.000	80	0.500
51	1.922	81	0.469
52	1.846	82	0.439
53	1.774	83	0.410
54	1.704	84	0.381
55	1.636	85	0.353
56	1.571	86	0.326
57	1.509	87	0.299
58	1.448	88	0.273
59	1.390	89	0.247
60	1.333	90	0.222
61	1.279	91	0.198
62	1.226	92	0.174
63	1.175	93	0.151
64	1.125	94	0.128
65	1.077	95	0.105
66	1.030	96	0.083
67	0.985	97	0.062
68	0.941	98	0.041
69	0.899		

Table A.3: Coefficients for SCS discharge method

Rainfall Type	I_a/P	C_0	C_1	C_2
I	0.10	2.30550	−0.51429	−0.11750
	0.20	2.23537	−0.50387	−0.08929
	0.25	2.18219	−0.48488	−0.06589
	0.30	2.10624	−0.45695	−0.02835
	0.35	2.00303	−0.40769	0.01983
	0.40	1.87733	−0.32274	0.05754
	0.45	1.76312	−0.15644	0.00453
	0.50	1.67889	−0.06930	0.0
IA	0.10	2.03250	−0.31583	−0.13748
	0.20	1.91978	−0.28215	−0.07020
	0.25	1.83842	−0.25543	−0.02597
	0.30	1.72657	−0.19826	0.02633
	0.50	1.63417	−0.09100	0.0
II	0.10	2.55323	−0.61512	−0.16403
	0.30	2.46532	−0.62257	−0.11657
	0.35	2.41896	−0.61594	−0.08820
	0.40	2.36409	−0.59857	−0.05621
	0.45	2.29238	−0.57006	−0.02281
	0.50	2.20282	−0.51599	−0.01259
III	0.10	2.47317	−0.51848	−0.17083
	0.30	2.39628	−0.51202	−0.13245
	0.35	2.35477	−0.49735	−0.11985
	0.40	2.30726	−0.46541	−0.11094
	0.45	2.24876	−0.41314	−0.1150°
	0.50	2.17772	−0.36803	−0.09525

Cite as: Al-Sayed A.M. & Al-Shaheen M., "The Influence of Urbanization on Natural Overland Flow Paths", *The 2nd International Conference on Civil Infrastructure and Construction (CIC 2023)*, Doha, Qatar, 5-8 February 2023, DOI: https://doi.org/10.29117/cic.2023.0169

Potential Application of Porous Membrane from Blends of Homopolymer for Industrial Water Treatment

Rayane Akoumeh
Center for Advanced Materials, Qatar University, Doha, Qatar
Rayane.akoumeh@qu.edu.qa

Tamara Elzein
National Council for Scientific Research, Lebanon
tamara.elzein@cnrs.edu.lb

Juan Rodríguez-Hernández
Instituto de Ciencia y Tecnología de Polímeros, Madrid, Spain
jrodriguez@ictp.csic.es

Mohammad K. Hassan
Center for Advanced Materials, Qatar University, Doha, Qatar
Mohamed.hassan@qu.edu.qa

Abstract

The self-organization of matter has been extensively explored in recent years, and significant advancements have been made in the field of porous ordered films produced by the auto-assembly of different polymer materials, being block of copolymers, blends of homopolymers or amphiphilic polymers. The hierarchical ordering in micro-organized films, known also as Honeycomb (HC) structure, generates a significant increase of specifics characteristics enhancing certain properties of the materials. The preparation of self-assembled porous membrane is done by different approaches. We use hereby the bottom-up microporous structuring method specifically the breath figure (BF) approach to prepare highly-organized membrane from polymer blends. The foremost motives for using the BF are the simplicity of implementation and the adaptability to multiple systems which make it a robust and inexpensive technique for the production of structured surfaces. The honeycomb (HC) structures formed by the BF is a potential candidate for water treatment as a filtration membrane to treat stable oil-water emulsions encountered in the oil and gas industry. The use of homopolymer blends improves the selectivity, permeability and anti-fouling properties comparing to the commercial homopolymer membrane. This presentation will highlight the preparation of self-assembled blends of homopolymers membrane by BF and their performance for cleaning of industrial wastewater and the fouling/re-use potential.

Keywords: Microporous surfaces; Polymer blends; Breath figures; Water treatment

1 Introduction

Qatar National Vision 2030 strives to build an advanced society providing a high standard living for its citizens, the vision faces various concerns among them the environmental challenge. Recently the advancement in urbanization and industrialization caused alarming challenges for wastewater treatment. Indeed, Oil, gas, generated water, and solid particles are all components of the (crude oil) that comes from the oil wells. Well-defined layers of gas, crude oil, and process water are produced after transferring the mixture into primary gravity separators (Yu, Han et al., 2017). One of the utmost techniques for treating wastewater on an industrial scale is membrane filtration. Numerous processing

aspects, including easy cleaning, the capacity to recycle the membrane, and pure permeate, encourage the use of a porous membrane in industry. Membrane separation is predominantly cantered on a size-sieving mechanism. The morphology of the membrane (size, porosity, thickness, and surface chemistry of pores) has a high impact on the membrane performance in filtration. In wastewater treatment, four types of membranes, specifically, microfiltration (MF), ultrafiltration (UF), nano-filtration (NF) and reverse osmosis (RO) are used in the separation process (Strathmann 2001). While the MF membrane rejects particles of microns' size and microorganisms, the UF additionally excludes bacteria and soluble macromolecules. On the other hand, the RO membrane rejects small particle-size ion salts, whereas NF's performance resides between RO and UF membranes (Sagle and Freeman 2004). The Fig. **1** shows the pores' size range of the aforementioned membrane.

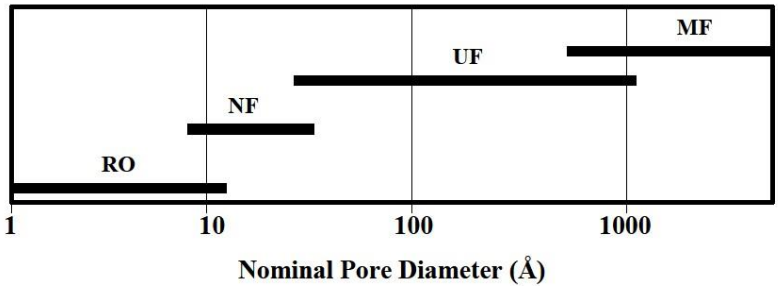


Fig. 1: Pore size scale of the industrial membrane (reproduced with permission from Sagle et al. 2004).

All developed membranes present an intrinsic trade-off between permeability and selectivity, particularly, how fast the molecules go through the membrane and the rejection of certain molecules from the rest (Park, Kamcev et al., 2017). The filtration by size exclusion approach is directly linked to the pore size and thus to the membrane selectivity (Werber, Osuji et al., 2016). The distinctive capability of amphiphilic polymer (homopolymer, blends of polymer, and block copolymer) to be self-organized in hierarchically porous domains has urged researchers to explore the usefulness of these materials in membrane filtration (Xu, Stevens et al., 2003; Yang, Ryu et al. 2006; Jackson & Hillmyer, 2010). The self-organization of matter is extensively studied in recent years, this attention is motivated by the adaptability, easiness of implementation for different applications (e.g. microelectronic, optoelectronic, photonic, sensors, catalyst, and scaffolds) (De Rosa, Park et al., 2000, Cho & Ihm, 2002, Yabu & Shimomura, 2005), and the possible applicability to large-scale.

The surface properties including, among others, the chemical composition or micro/nano-structuring play a key role in their final application (Jeon, Simon Jr et al., 2014). Considering the surface properties, for instance, superhydrophobic surfaces (Bolognesi, DiGianvincenzo et al. 2008, de León, del Campo et al., 2012), biocompatible surfaces for cell culture and adhesion (Tsuruma, Tanaka et al., 2005, Yabu, Hirai et al., 2008), active layers for magnetic, optical and conductive fields (Fukuhira, Ito et al., 2008), (Jiang, Zhang et al., 2012), (Kurono, Shimada et al., 2002), and smart systems (Connal, Franks et al., 2010), these hierarchically porous membranes have been elaborated using different approaches (Akoumeh, Elzein et al. 2020). Among these approaches, those based on surface instabilities have attracted special attention.,(Rodríguez-Hernández & Drummond, 2015) the bottom-up microporous structuring specifically, the Breath figure approach has been largely employed for the preparation of Honeycomb structures with variable pore sizes, and chemical distribution.(Escalé, Rubatat et al., 2012, Heng, Wang et al., 2013, Muñoz-Bonilla, Fernández-García et al., 2014, Dou, Jin et al., 2015, Bormashenko, 2017, Calejo, Ilmarinen et al., 2018, Yabu, 2018). Bunz et al. explained the breath figure (BF) phenomenon that occurs when water droplets condense on a cold surface (due to evaporation of the highly volatile solvent). The imprint of the water droplets left in the polymer

matrix after solvent evaporation acts as the template during the formation of the microporous surfaces called honeycomb (HC) (Bunz et al. 2006, Beattie, Wong et al., 2006). Membranes prepared using star polymers, amphiphilic copolymers, block copolymers but also polymer blends are well known for their directed hierarchical self-assembly in honeycomb structures (Bertrand, Bousquet et al., 2016, Akoumeh, Elzein et al., 2020).

In this work, we discuss the elaboration of a porous stand-alone membrane by breath figure approach using a blend of biodegradable polymers: Polycaprolactone (PCL) and Polylactic acid (PLA). The choice of these two polymers is justified by multiple reasons. First of all, PCL addition to PLA shows a significant improvement in the ductility and toughness of PLA (Kawano, Sato et al., 2014). Second, the PLA might exhibit reversible pH-responsive wettability due to the presence of carboxylic groups. Thus, hydrophobic and hydrophilic characteristic in membranes provides a better fouling resistance (Banerjee, Pangule et al., 2011). Both the morphology of the prepared micro-structured membrane and the chemical distribution on the surface is thoroughly studied.

2 Materials and Methods

2.1 Materials

Poly (ε-caprolactone) (PCL) (PBI 010) and poly(lactic acid) (PLE 003) were purchased from Natureplast. All other solvents were employed as received without further purification and purchased from Sigma Aldrich.

2.2 Characterisation Technique

Scanning electron microscopy (SEM) micrographs were taken using a Philips XL30 with an acceleration voltage of 25 kV. The samples were coated with gold prior to scanning.

Confocal RAMAN imaging was done using the WITec alpha 300RA+ Raman microscope, which was equipped with Frequency Doubled Nd: YAG 532 nm laser and a CCD detector (cooled to −65 degree). A 50 X Objective from Zeiss LD Epiplan Naofluar 50X DIC; working distance: 9.1mm; Numerical Aperture: 0.55 NA was used for this measurement. For each image, a surface of 50×50 μm^2 was analysed, and an integration time of 0.5s was used. Confocal RAMAN data analysis was performed using WITec Project 4.10 software. Raman images were generated based on the integrated intensity of marker bands and were calculated without pre-processing. Cluster analysis was carried out after cosmic ray removal and background subtraction.

Contact Angle: The wettability of the surface was characterized by contact angle measurement with an OCA35 from Dataphysics instruments. All of the measurements were performed at room temperature.

2.3 Elaboration of Micro-Structured Membrane

Polymer blend with a composition of 85/15 (PLA/PCL) was prepared by dissolving homopolymer pellets in the appropriated amount of chloroform. The polymer solution, with a concentration of 100 mg/mL, was evaporated using a circular glass cell culture dish as support. The relative humidity was maintained constant for all the experiments to 90%.

3 Results and Discussion

Elaboration of micro-structured Honeycomb stand-alone membrane. The used approach allows the preparation of large micro-structured stand-alone membrane (dm^2) without the use of any extensive materials or equipment such as dip or spin coaters

*Micro structuring and morphology of the Honeycomb films. A*s evidenced in the SEM images, the pores' size is between 10 to 18 microns, and the porosity was observed over the entire membrane indicating homogeneous evaporation and a convenient water vapour condensation.

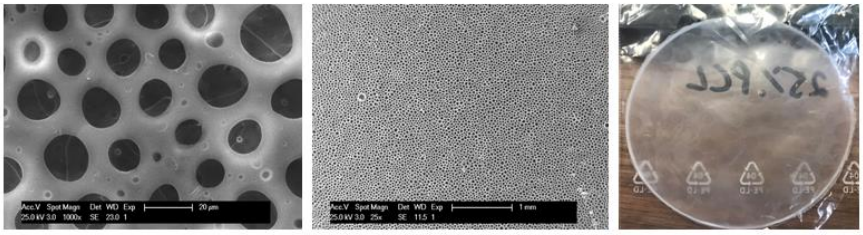


Fig. 2: SEM images of the PCL-PLA membrane scale 20µm (left) , 1mm (middle), real photograph of the membrane (right)

Analysis of the surface chemistry and evaluation of the functional group distribution: Contact angle measurement provides information about the wettability of a given surface, and consequently an idea about the chemical aspect of the analysed surface at the macroscopic scale. The Honeycomb membrane was first treated with a basic buffer solution (pH=12). The contact angle measurement shows a decrease in the contact angle from 80° to 60° after the treatment referring to the ionization of the PLA, as the base attack the hydrogens at the alpha position which is fairly acidic forming enolates (Fig. **3**).

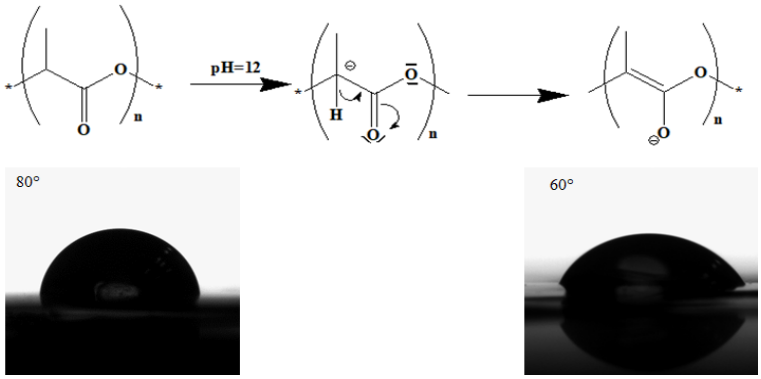


Fig. 3: Represents the shape of a water droplet on the untreated and treated HC membrane and the possible reaction of forming the enolates

To understand the phase separation, and the chemical distribution of both PCL and PLA on the surface, Raman Confocal was employed. The characteristic peaks of both PCL and PLA were defined as per previous work (Akoumeh, Elzein et al., 2020). In particular, peaks at 1723 cm^{-1} and a shoulder peak at 2869 cm^{-1} are characteristic of PCL, and peaks at 868 cm^{-1} and 2999 cm^{-1} are characteristic of PLA. The presented images in (Figure 4) were generated from the aforementioned peaks.

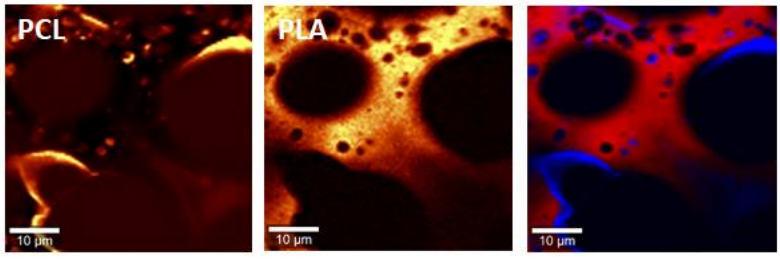


Fig. 4: Raman Imaging of PCL (left), PLA (middle), and an overlay of both component (right)

The Raman imaging proved that micrometre-scale PCL domains are randomly distributed in the wall of the pores while the rest of the porous structure is formed by a continuous PLA matrix. The role of water condensation on phase separation has been emphasized in previous studies. The formation of macrophase separation is avoided and reduced to microphase separation under humidity and water condensation

4 Conclusion

In this article, a large micro-structured stand-alone membrane formed from blends of two commercial homopolymers PLA and PCL was successfully prepared. The chosen homopolymers used to prepare honeycomb-like membranes were thoroughly characterized to investigate the topography, the chemistry, and subsequently the miscibility of the blend. The wettability measurement shows a pH-responsive surface. Further experimental works should be conducted to study the efficiency of these membranes in water filtration.

References

Akoumeh, et al. (2020). "Fabrication of porous films from immiscible polymer blends: Role of the surface structure on the cell adhesion." *Polymer Testing 91*: 106797.

Banerjee, I. R. C. Pangule & R. S. Kane (2011). "Antifouling coatings: recent developments in the design of surfaces that prevent fouling by proteins, bacteria, and marine organisms." *Advanced materials 23*(6): 690-718.

Beattie, et al. (2006). "Honeycomb-Structured Porous Films from Polypyrrole-Containing Block Copolymers Prepared via RAFT Polymerization as a Scaffold for Cell Growth." *Biomacromolecules 7*(4): 1072-1082.

Bertrand, et al. (2016). "Hierarchically porous bio-inspired films prepared by combining "breath figure" templating and selectively degradable block copolymer directed self-assembly." *Chemical Communications 52*(61): 9562-9565.

Bolognesi, et al. (2008). "Polystyrene functionalized with EDOT oligomers." *European Polymer Journal 44*(3): 793-800.

Bormashenko, E. (2017). "Breath-figure self-assembly, a versatile method of manufacturing membranes and porous structures: Physical, chemical and technological aspects." *Membranes 7*(3): 45.

Bunz, U. H. F (2006). "Breath Figures as a Dynamic Templating Method for Polymers and Nanomaterials". Advanced Materials 18: 973-989.

Calejo, et al. (2018). "Breath figures in tissue engineering and drug delivery: State-of-the-art and future perspectives." *Acta Biomaterialia 66*: 44-66.

Cho, C. H. & Ihm, S. K. (2002). "Development of new vanadium-based oxide catalysts for decomposition of chlorinated aromatic pollutants." *Environmental science & technology 36*(7): 1600-1606.

Connal, L. A., G. V. Franks & Qiao, G. G. (2010). "Photochromic, metal-absorbing honeycomb structures." *Langmuir 26*(13): 10397-10400.

de León, et al. (2012). "Hierarchically Structured Multifunctional Porous Interfaces through Water Templated Self-Assembly of Ternary Systems." *Langmuir 28*(25): 9778-9787.

De Rosa, et al.. "Microdomain patterns from directional eutectic solidification and epitaxy." *Nature 405*(6785): 433-437.

Dou, et al. (2015). "Breath figure method for construction of honeycomb films." *Membranes 5*(3): 399-424.

Escalé, et al. (2012). "Recent advances in honeycomb-structured porous polymer films prepared via breath figures." *European Polymer Journal 48*(6): 1001-1025.

Fukuhira, et al. (2008). "Prevention of postoperative adhesions by a novel honeycomb-patterned poly (lactide) film in a rat experimental model." *Journal of Biomedical Materials Research Part B: Applied Biomaterials: An Official Journal of The Society for Biomaterials, The Japanese Society for Biomaterials, and The Australian Society for Biomaterials and the Korean Society for Biomaterials 86*(2): 353-359.

Heng, et al. (2013). "Advances in fabrication materials of honeycomb structure films by the breath-figure method." *Materials 6*(2): 460-482.

Jackson, E. A. & M. A. Hillmyer (2010). "Nanoporous membranes derived from block copolymers: from drug delivery to water filtration." *ACS nano 4*(7): 3548-3553.

Jeon, H., C. G. Simon Jr. & G. Kim (2014). "A mini-review: cell response to microscale, nanoscale, and hierarchical patterning of surface structure." *Journal of biomedical materials research Part B: applied biomaterials 102*(7): 1580-1594.

Jiang, et al. (2012). "Bacterial adhesion on honeycomb-structured poly (L-lactic acid) surface with Ag nanoparticles." *Journal of Biomedical Nanotechnology 8*(5): 791-799.

Kawano, et al. (2014). "Honeycomb-shaped surface topography induces differentiation of human mesenchymal stem cells (hMSCs): Uniform porous polymer scaffolds prepared by the breath figure technique." *Biomaterials science 2*(1): 52-56.

Kurono, et al. (2002). "Fabrication and optical property of self-organized honeycomb-patterned films." *Molecular Crystals and Liquid Crystals 377*(1): 285-288.

Muñoz-Bonilla, A., Fernández-García, M. & Rodríguez-Hernández, J. (2014). "Towards hierarchically ordered functional porous polymeric surfaces prepared by the breath figures approach." *Progress in Polymer Science 39*(3): 510-554.

Park, et al. (2017). "Maximizing the right stuff: The trade-off between membrane permeability and selectivity." *Science 356*(6343): eaab0530.

Rodríguez-Hernández, J. & Drummond, C. (2015). Polymer surfaces in motion: Unconventional patterning methods, Springer.

Sagle, A. & Freeman, B. (2004). "Fundamentals of membranes for water treatment." *The future of desalination in Texas 2*(363): 137.

Strathmann, H. (2001). "Membrane separation processes: current relevance and future opportunities." A*IChE Journal 47(5)*: 1077-1087.

Tsuruma, et al. (2005). "Morphological changes in neurons by self-organized patterned films." *e-Journal of Surface Science and Nanotechnology 3*: 159-164.

Werber, J. R., Osuji, C. O. & Elimelech, M. (2016). "Materials for next-generation desalination and water purification membranes." *Nature Reviews Materials 1*(5): 1-15.

Xu, et al. (2003). "Block copolymer surface reconstuction: A reversible route to nanoporous films." *Advanced Functional Materials 13*(9): 698-702.

Yabu, H. (2018). "Fabrication of honeycomb films by the breath figure technique and their applications." *Science and Technology of Advanced Materials 19*(1): 802-822.

Yabu, et al. (2008). "Surface properties of honeycomb and pincushion structures of various hydrophobic polymer materials prepared by self-organization." *Journal of Adhesion Science and Technology 22*(3-4): 277-284.

Yabu, H. & Shimomura, M. (2005). "Single-step fabrication of transparent superhydrophobic porous polymer films." *Chemistry of materials 17*(21): 5231-5234.

Yang, et al. (2006). "Nanoporous membranes with ultrahigh selectivity and flux for the filtration of viruses." *Advanced materials 18*(6): 709-712.

Yu, L., Han, M. & He, F. (2017). "A review of treating oily wastewater." *Arabian Journal of chemistry 10*: S1913-S1922.

Cite as: Akoumeh R., Elzein T., Rodriguez-Hernandez J. & Hassan M.K., "Potential Application of Porous Membrane from Blends of Homopolymer for Industrial Water Treatment", *The 2nd International Conference on Civil Infrastructure and Construction (CIC 2023)*, Doha, Qatar, 5-8 February 2023, DOI: https://doi.org/10.29117/cic.2023.0170

Recycling of Tetra Pak for Space and Water Heating by Blending with Phase Change Materials

Safna Nishad
Center for Advanced Materials, Qatar University, Doha, Qatar
sn1518223@qu.edu.qa

Igor Krupa
Center for Advanced Materials, Qatar University, Doha, Qatar
igor.krupa@qu.edu.qa

Abstract

A rapid rise in demands for thermal comfort in the building sector necessitates higher energy consumption for air conditioning, ventilation, space, and water heating systems. Recently, phase change materials (PCMs) have gained much attention from researchers for passive heating/cooling of space and water. PCM can store/release thermal energy as latent heat during its phase change process isothermally. Moreover, PCM facilitates solar energy harvesting by photothermal conversion and storage. However, major limitations of PCM include low thermal conductivity, leakage during phase change, and lack of photoabsorbance. Therefore, in this study, the shape-stabilized phase change composites were prepared by melt blending of Paraffin Wax (PW), Tetra Pak (TP), and expanded graphite (EG). PW is an organic PCM, widely being studied due to its high enthalpy, availability at various melting points, and chemical and thermal stability. In addition to providing shape stability and thermal conductivity enhancement of PCM, the usage of TP promotes the recycling of TP waste into useful products. The addition of EG contributes to the thermal conductivity increase of 3.6 times that of pure PW. Moreover, the excellent photoabsorption of EG and TP effectively converted the photo energy to thermal energy and stored it as latent heat by PW in the composite. Two types of composites using PW of melting points 44 ℃ and 64 ℃ were exhibited a photothermal conversion and storage efficiency of 80 and 55 %, respectively and which is promising for solar water heating applications.

Keywords: Tetra Pak; Phase change material; Space and water heating; Recycling; Photothermal conversion

1 Introduction

Recently, the global energy demand in the building sector has increased with the rapid social and economic development of society. Heating, ventilation, and air conditioning systems are often used for thermal comfort in buildings that consume conventional energy resources. In order to deal with environmental concerns and the depletion of conventional energy resources, the development of efficient and renewable sources of energy is essential. Solar energy is an important renewable energy source due to its endless reserves (Kannan & Vakeesan, 2016; Shahsavari & Akbari, 2018). Studies on the efficient utilization of solar energy have gained much attention due to its carbon-neutral and renewable characteristics. Solar energy is often transformed into electrical and thermal energy by photovoltaic and photothermal conversion techniques (Boldoo et al., 2020; Rawat et al., 2017). Photothermal conversion is the most efficient and simple solar energy utilization technique for space

and water heating (Arunkumar et al., 2020; Tyagi et al., 2012; Vengadesan & Senthil, 2020), power generation (Zhanget al., 2018b), desalination (Wang, 2018), etc. However, thermal energy storage (TES) systems are required for a continuous supply of heat energy due to the intermittent properties of solar energy. Phase change materials (PCMs) are widely adopted for TES systems to store thermal energy isothermally (Chaturvedi et al., 2021). Among various types of PCMs, paraffin waxes are usually used in practical applications due to the commercial availability of various grades having different phase change temperatures and latent heat, non-corrosiveness, and negligible supercooling (Gulfam et al., 2019). However, low thermal conductivity, shape instability, and poor photoabsorption are the major drawbacks of paraffin in practical applications of energy conversion and storage (Karkri et al., 2015).

There are different strategies adopted to overcome the above limitations, including microencapsulation in the polymeric matrix (Maithya et al., 2021; Yuan et al., 2020; Zhang et al., 2018a), PCMs impregnated in porous materials(Maleki et al., 2019; Umair et al., 2019; Yang et al., 2016), and blending with polymers (Chriaa et al., 2021; Hu, 2020; Mochane & Luyt, 2015a, 2015b; Sobolčiak et al., 2021). Recently, polymeric phase change composites have attracted researchers due to their (i) cost-effectiveness, (ii) high mechanical strength, (iii) efficiency in leakage prevention and heat storage capacity enhancement, (iv) lightweight characteristics with a high strength/weight ratio, and (v) abundance and availability.

Among various polymeric phase change composites, polyethylene and paraffin wax blends have attracted much attention due to their chemical and structural similarities (Hu, 2020; Krupa et al., 2007). They provide good processability, are lightweight, and are low-cost. Krupa et al. (Krupa et al., 2007) examined the energy storage capabilities of low-density polyethylene blends (LDPE) with paraffin wax. The LDPE base provides a compact shape to the composite, while the paraffin wax stores latent heat during melting. The usage of recycled polymer waste in the composite preparation not only improved the thermophysical properties but also provided their sustainable application. Similarly, the tetra Pak waste has gained much attention from researchers to provide an efficient reuse application. Therefore, in this study, PCM composites were prepared by blending PW with recycled tetra Pak and expanded graphite to enhance the PCM shape stability, thermal conductivity, and photo absorbance.

2 Experimental

2.1 Materials

Paraffin wax RT44 and RT64 ((Rubitherm® Technologies GmbH, Germany), and expanded graphite (EG, average particle size of 200 µm, SIGRATHERM®, SGL Carbon, Germany), Tetra Pak (TP) waste consist of 20 % aluminum and 80 % low-density polyethylene (Zlin, Czech Republic) were used for the preparation of the PCM composite.

2.2 Composite Preparation

The components in the required weight fraction were mixed in a Brabender® Plastograph® EC W50 PLE 331 (Duisburg, Germany). The components were melted at 160 °C and mixed at a speed of 35 rpm for 10 minutes (Figure 1). The composite was then hot-pressed at 160 °C for 3 minutes using a hydraulic mounting machine at 3-ton force.

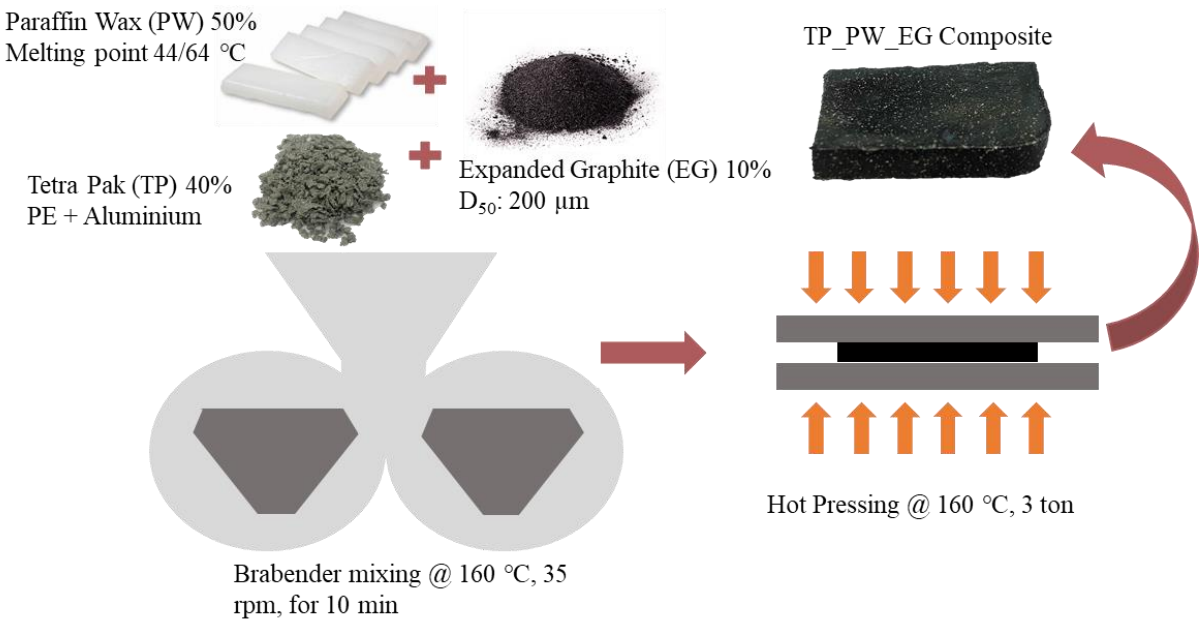


Fig. 1: Schematic representation of TP_PW_EG composite preparation

2.3 Material Characterization

The thermal conductivity of the TP_PW_EG composite was measured on a cylindrical sample of size 7 cm diameter and 9 mm height using the ISOMET apparatus (Applied Precision, Slovakia). The thermal flow in the material was measured using a flat probe at 20 °C. The thermal conductivity measurements were reproducible with an accuracy of 5 % of reading.

The leakage of PW from the composite was measured when the TP_PW_EG composite was placed in an oven at a temperature of 80 °C. The strips of sample specimens with size 60x60x1 mm were placed in the oven for 14 days and the sample weight loss was noted using an analytical balance. The percentage of the PW weight loss in the composite was calculated from the equation:

$$Weight\ loss = \frac{(m_0 - m)}{m_0 \times w} \times 100\ (\%) \qquad (1)$$

The thermophysical properties of the composite were measured using differential scanning calorimetry (DSC 8500, Perkin Elmer, USA) at a rate of 10 °C/min. The latent heat and phase transition temperatures were obtained from DSC and the average values at the second heating cycle are presented with an accuracy of ±0.05 °C for the temperature and 0.2 % for the heat flow.

2.4 Photothermal Conversion Testing

The photothermal conversion and storage capacity of the composite were tested under simulated sunlight of intensity 1000 W/m^2 using a solar simulator (Sunlite, ABET Technologies). The changes in the sample top and bottom temperature and heat flux during the energy conversion and storage process were measured using an infrared thermometer (Testo 845, Germany), a T-type thermocouple, and a heat flux sensor (Captec, France), respectively. The data collection and analysis were carried out using a CR1000X datalogger (CampBell Scientific, USA). A schematic of the photothermal conversion test system is shown in Figure 2.

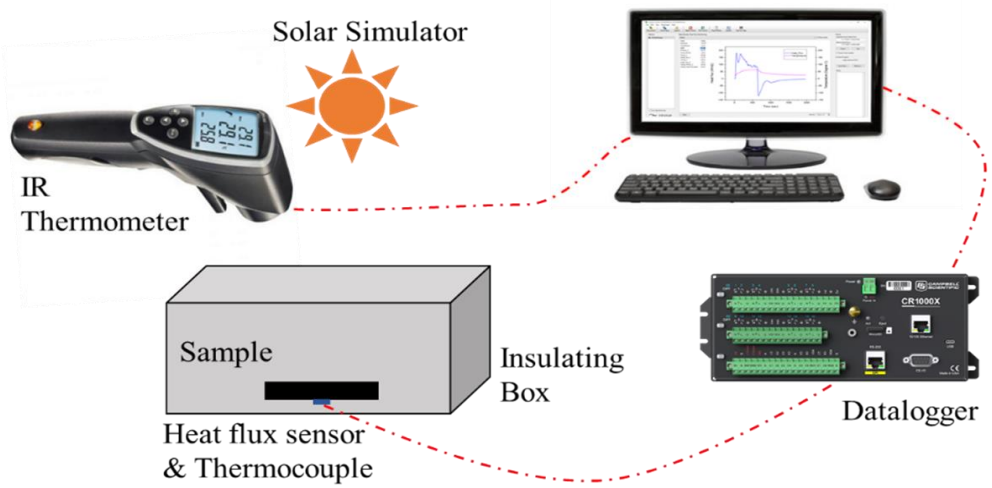


Fig. 2: Schematic representation of photo-thermal energy conversion and storage performance measuring system

3 Results and Discussion

3.1 Thermal Conductivity

The pure TP, RT44, RT64, TP_RT44_EG, and TP_RT64_EG showed thermal conductivities of 0.48, 0.20, 0.19, 0.71, and 0.70 W/m. K, respectively. The introduction of TP and EG into the PW enhanced the thermal conductivity of the TP_PW_EG composite by around 3.6 times that of pure PW.

3.2 Shape Stability

The PW leakage from the TP_PW_EG composite determines the shape stability of the composite. The mass loss of composite over 14 days in the oven at 80 ℃ was less than 7 %. These results show that the TP matrix effectively encapsulates the PW to prevent the leakage of PW even after melting for a long time. In addition, the porous configuration of EG prevents the leakage of infiltrated PW via the capillary and surface tension forces.

3.3 Thermophysical Properties

The phase change enthalpy and temperatures of pure PWs (i.e., RT44 and RT64) and TP_PW_EG composites attained from DSC analysis are shown in Figure 3. The thermal characteristics estimated from the DSC curves are shown in Table 1. It can be observed from the DSC curves (Figure 3) that RT44, RT64, and their composites have two exothermic and endothermic peaks during the heating and cooling due to an intermediate solid-solid phase change. The temperatures of solid-solid and solid-liquid phase transition processes are close during melting for RT44, RT64, and their composites as seen in Figure 3. However, two distinct peaks for liquid-solid and solid-solid phase change are observed during the crystallization process as shown in Figure 3. The solid-liquid transition peak of the composites (i.e., T_m) was slightly varied from pure PW as shown in Table 1 and Figure 3. However, the liquid-solid transition peak (i.e., T_c) was decreased by 1.8-2.3 ℃ in the composite than pure PW. This reduced phase change temperature of the composites than pure PW is due to the confinement of PW in the microscopic pores of TP and EG, which prevents molecular motion during the phase transition process (Li et al., 2020).

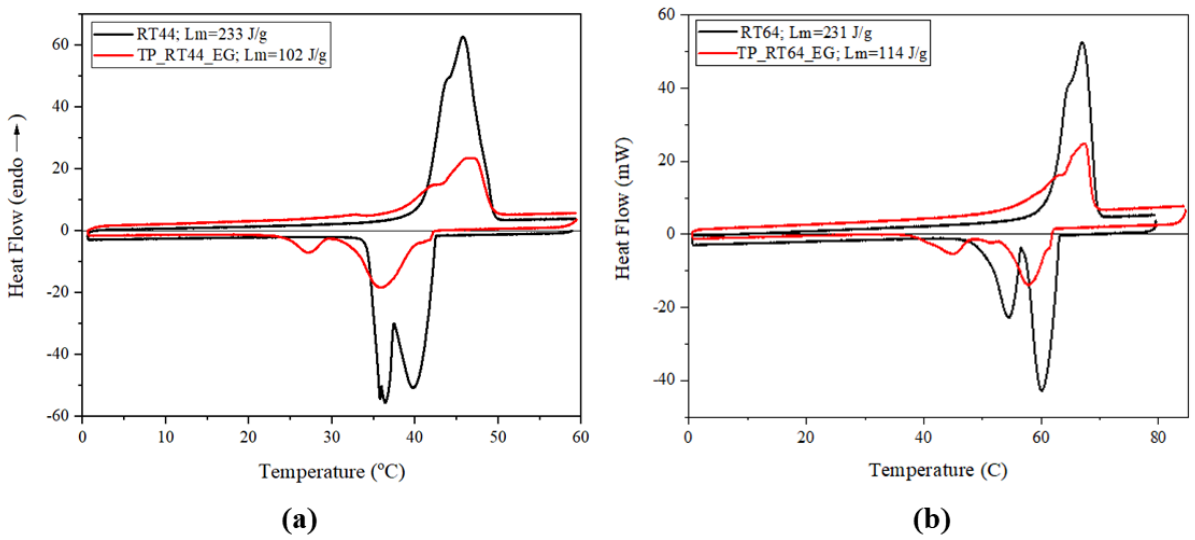


Fig. 3: DSC curves of pure PW and TP_PW_EG composites; (a) RT44, and (b) RT64

Table 1: Thermal properties of PW and TP_PW_EG composites from DSC
(Standard deviations from three samples are shown in parenthesis)

Sample	Heating			Cooling		
	$T_{s\text{-}s}$ (°C)	T_m (°C)	ΔH_m (J/g)	$T_{s\text{-}s}$ (°C)	T_c (°C)	ΔH_c (J/g)
RT44	43.7	45.7	233 (0.1)	36.1	39.5	231.3 (0.1)
TP_RT44_EG	41.9	46.4	102 (0.2)	27	35.7	100.5 (0.1)
RT64	64.5	67.0	231 (0.2)	54.3	60.2	225.9 (0.1)
TP_RT64_EG	62.8	67.2	114 (0.4)	45.1	57.9	112.8 (0.3)

3.4 Photothermal Conversion

Figure 4 shows the sample top and bottom temperature and heat flux evolution plots of the TP_RT44_EG and TP_RT64_EG composites under the simulated solar irradiation of 1000 W/m^2 for 20 or 30 minutes. The sample was placed in an insulation box to avoid heat loss from the bottom and sides of the composite.

As shown in Figure 4, the temperature and heat flux of the composite increase with time during solar irradiation indicating the photothermal conversion capacity of the composite. The heat flux decreases or stabilizes during the phase transition. The conductive heat flux passing through the composite was partially absorbed for the melting of PW which decreases the temperature rise. Therefore, the temperature evolution curve shows a plateau in the PW melting range. After the completion of the phase transition, the heat flux and temperature started to increase rapidly. The time taken for the phase transition of the RT64 composite was higher than the RT44 composite .

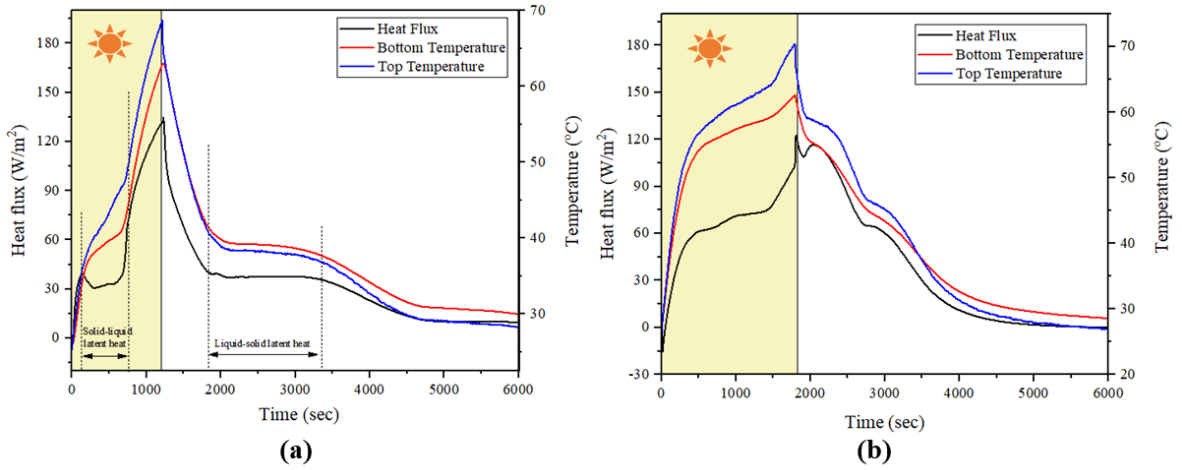


Fig. 4: Temperature and heat flux-time evolution curves of TP_PW_EG composites; **(a)** TP_RT44_EG, and **(b)** TP_RT64_EG

The photothermal conversion and storage efficiency (η_p) was calculated by the ratio of the latent heat of the paraffin to the energy of simulated solar light during a phase change Therefore, the storage efficiency is,

$$\eta_p = \frac{m\Delta H}{PS\Delta t} \tag{3}$$

considering all the paraffin in the composite undergone phase transition.

where m is the mass of the composite, ΔH is the latent heat enthalpy, P is the intensity of the light source, S is the surface area of the composite and Δt is the time taken for phase change.

The efficiencies of the composites with RT44 and RT64 were 80 and 55 %, respectively. The reduced efficiency of the TP_RT64_EG composite was due to the increase in time taken for phase change as shown in Figure 4b. This could be due to the increased convective heat loss from the sample surface with the rise in temperature.

4 Conclusion

In this study, a shape-stabilized phase change composite was fabricated by the physical blending and hot pressing of TP, PW, and EG. The integration of TP and EG into the composite significantly enhanced the thermal conductivity and reduced the PCM leakage of the composite. The composite with 10 wt.% EG has a thermal conductivity of 0.71 W/m.℃, which was 3.6 times higher than that of pure PW. The latent heat of the composite varied in the range of 102-112 J/g. The TP provided shape stability to the composite and reduced PW leakage during phase change. In addition to the enhanced physical properties of the composite, usage of TP provides an application for recycled TP from Tetra Pak waste. Two types of composites using PW of melting points 44 ℃ and 64 ℃ were exhibited a photothermal conversion and storage efficiency of 80 and 55 %, respectively. The excellent photothermal conversion capacity of the composite can be effectively utilized for solar thermal energy conversions and used for space and water heating applications in the building industry.

Acknowledgement

This work was supported by the Qatar National Research Fund through the award NPRP13S-0127-200177. The statements made herein are exclusively the accountability of the authors.

References

Arunkumar, H. S., Vasudeva Karanth, K. & Kumar, S. (2020). Review on the design modifications of a solar air heater for improvement in the thermal performance. *Sustainable Energy Technologies and Assessments*, *39*, 100685. https://doi.org/10.1016/J.SETA.2020.100685

Boldoo, et al. (2020). Review of the Photothermal Energy Conversion Performance of Nanofluids, Their Applications, and Recent Advances. *Energies 2020, Vol. 13, Page 5748*, *13*(21), 5748. https://doi.org/10.3390/EN13215748

Chaturvedi, R., Islam, A. & Sharma, K. (2021). A review on the applications of PCM in thermal storage of solar energy. *Materials Today: Proceedings*, *43*, 293–297. https://doi.org/10.1016/J.MATPR.2020.11.665

Chriaa, et al. (2021). The performances of expanded graphite on the phase change materials composites for thermal energy storage. *Polymer*, *212*, 123128. https://doi.org/10.1016/J.POLYMER.2020.123128

Gulfam, R., Zhang, P. & Meng, Z. (2019). Advanced thermal systems driven by paraffin-based phase change materials – A review. *Applied Energy*, *238*, 582–611. https://doi.org/10.1016/J.APENERGY.2019.01.114

Hu, H. (2020). Recent advances of polymeric phase change composites for flexible electronics and thermal energy storage system. *Composites Part B: Engineering*, *195*, 108094. https://doi.org/10.1016/J.COMPOSITESB.2020.108094

Kannan, N. & Vakeesan, D. (2016). Solar energy for future world: - A review. *Renewable and Sustainable Energy Reviews*, *62*, 1092–1105. https://doi.org/10.1016/J.RSER.2016.05.022

Karkri, et al. (2015). Improvement of thermal conductivity of paraffin by adding expanded graphite: *Http://Dx.Doi.Org/10.1177/0021998315612535*, *50*(19), 2589–2601. https://doi.org/10.1177/0021998315612535

Krupa, I., Miková, G. & Luyt, A. S. (2007). Phase change materials based on low-density polyethylene/paraffin wax blends. *European Polymer Journal*, *43*(11), 4695–4705. https://doi.org/10.1016/J.EURPOLYMJ.2007.08.022

Li, C., Zhang, B. & Liu, Q. (2020). N-eicosane/expanded graphite as composite phase change materials for electro-driven thermal energy storage. *Journal of Energy Storage*, *29*, 101339. https://doi.org/10.1016/J.EST.2020.101339

Maithya, et al. (2021). High-energy storage graphene oxide modified phase change microcapsules from regenerated chitin Pickering Emulsion for photothermal conversion. *Solar Energy Materials and Solar Cells*, *222*, 110924. https://doi.org/10.1016/J.SOLMAT.2020.110924

Maleki, et al. (2019). Development of graphitic domains in carbon foams for high efficient electro/photo-to-thermal energy conversion phase change composites. *Chemical Engineering Journal*, *362*, 469–481. https://doi.org/10.1016/J.CEJ.2019.01.032

Mochane, M. J. & Luyt, A. S. (2015a). The effect of expanded graphite on the thermal stability, latent heat, and flammability properties of EVA/wax phase change blends. *Polymer Engineering & Science*, *55*(6), 1255–1262. https://doi.org/10.1002/PEN.24063

___. (2015b). The effect of expanded graphite on the flammability and thermal conductivity properties of phase change material based on PP/wax blends. *Polymer Bulletin*, *72*(9), 2263–2283. https://doi.org/10.1007/S00289-015-1401-9/FIGURES/17

Rawat, R., Lamba, R. & Kaushik, S. C. (2017). Thermodynamic study of solar photovoltaic energy conversion: An overview. *Renewable and Sustainable Energy Reviews*, *71*, 630–638. https://doi.org/10.1016/J.RSER.2016.12.089

Shahsavari, A. & Akbari, M. (2018). Potential of solar energy in developing countries for reducing energy-related emissions. *Renewable and Sustainable Energy Reviews*, *90*, 275–291. https://doi.org/10.1016/J.RSER.2018.03.065

Sobolčiak, et al. (2021). Foamed Phase Change Materials Based on Recycled Polyethylene/Paraffin Wax Blends. *Polymers 2021, Vol. 13, Page 1987*, *13*(12), 1987. https://doi.org/10.3390/POLYM13121987

Tyagi, et al. (2012). Review on solar air heating system with and without thermal energy storage system. *Renewable and Sustainable Energy Reviews*, *16*(4), 2289–2303. https://doi.org/10.1016/J.RSER.2011.12.005

Umair, et al. (2019). A novel flexible phase change composite with electro-driven shape memory, energy conversion/storage and motion sensing properties. *Journal of Materials Chemistry A*, *7*(46), 26385–26392.

Vengadesan, E. & Senthil, R. (2020). A review on recent development of thermal performance enhancement methods of flat plate solar water heater. *Solar Energy*, *206*, 935–961. https://doi.org/10.1016/J.SOLENER.2020.06.059

Wang, P. (2018). Emerging investigator series: The rise of nano-enabled photothermal materials for water evaporation and clean water production by sunlight. *Environmental Science: Nano*, *5*(5), 1078–1089. https://doi.org/10.1039/C8EN00156A

Yang, et al. (2016). An ice-templated assembly strategy to construct graphene oxide/boron nitride hybrid porous scaffolds in phase change materials with enhanced thermal conductivity and shape stability for light–thermal–electric energy conversion. *Journal of Materials Chemistry A*, *4*(48), 18841–18851. https://doi.org/10.1039/C6TA08454K

___. (2020). Crafting visible-light-absorbing dye-doped phase change microspheres for enhancing solar-thermal utilization performance. *Solar Energy Materials and Solar Cells*, *218*, 110759. https://doi.org/10.1016/J.SOLMAT.2020.110759

Zhang, et al. (2018a). Solar-driven phase change microencapsulation with efficient Ti4O7 nanoconverter for latent heat storage. *Nano Energy*, *53*, 579–586. https://doi.org/10.1016/J.NANOEN.2018.09.018

Zhang, et al. (2018b). Ultrafast and efficient photothermal conversion for sunlight-driven thermal-electric system. *Chemical Engineering Journal*, *344*, 402–409. https://doi.org/10.1016/J.CEJ.2018.03.098

Cite as: Nishad S. & Krupa I., "Recycling of Tetra Pak for Space and Water Heating by Blending with Phase Change Materials", *The 2nd International Conference on Civil Infrastructure and Construction (CIC 2023)*, Doha, Qatar, 5-8 February 2023, DOI: https://doi.org/10.29117/cic.2023.0171

Design Considerations of MPSO Marine Outfall and Diffuser Field

Panagiotis Verros
Public Works Authority (PWA), Doha, Qatar
panosverros@gmail.com

Saad Zayed Al-Marri
Public Works Authority, Doha, Qatar
smarri2@ashghal.gov.qa

Alexios Kyriakopoulos
HBK-PORR, Doha, Qatar
alexios.kyriakopoulos@phm-jv.com

Lefteris Alvanitopoulos
HBK-PORR, Doha, Qatar
lefteris.alvanitopoulos@mottmac.com

Abstract

The purpose of the Musaimeer Pump Station and Outfall (MPSO) project is to receive storm water runoff and groundwater flows from the Abu Hamour Tunnel and to provide a pumping station, a marine outfall tunnel and a diffuser field to dispose of the flows into the sea. Musaimeer outfall tunnel is one of the longest storm water tunnels in the world with a total length of 10.2 km. The tunnel is connected via a drop shaft to the main pump station. This system will accommodate surface and storm water received from the drainage networks of 190 km^2 of urban areas in southern Doha. The outfall tunnel comprised precast segmental lining with internal diameter of 3700 mm sloped at 0.05% upward to the riser shaft. The riser shaft, which is located at the end of the outfall tunnel, is connected to a diffuser field positioned on the Arabian Gulf seabed. This paper will focus on the design considerations and recommendations related Marine outfall riser shaft, distribution manifolds and diffuser field. to The MPSO marine outfall was designed in two phases, first comprising installation of riser shaft, primary and secondary manifolds, 3 lines of HDPE piping with variable internal diameter, 84 diffuser duckbill valves, 84 diffuser protection boxes and scour protection. The diffuser is laid in an area of 280mX40m 15m beneath the sea water level. Second phase of marine outfall design included the meticulous connection works between GRP riser shaft and 10.2km TBM tunnel 15m beneath the seabed. Design considerations and final conclusions of such marine design works will be presented.

Keywords: Marine outfall Design; Riser shaft; Scour protection; Diffuser field; Duckbill valves

1 Introduction

Southern and Western Doha has been experiencing a rapid expansion and growth in recent years. Consequently, the need to increase drainage capacity to accommodate additional storm runoff and construction activities has become critical. In response, Drainage Networks Projects Department of the Public Works Authority (PWA) has undertaken significant studies and developed numerous projects that will provide an integrated approach for existing and future drainage systems for this area. One such project is Musaimeer pumping station and outfall, which provides for the installation of a collection tunnel, pumping station and marine outfall to discharge storm and groundwater

drainage into the Arabian Gulf. PWA has successfully completed the Musaimeer Pumping station and Outfall tunnel project on Sep 2022 enabling the effective discharge to the sea. One of the most challenging parts of design and installation works included the integrated Marine outfall design which is presented in this paper.

2 Overview of the MPSO Marine Outfall

The project site is located immediately south of the land that was reclaimed for the newly constructed Hamad International Airport (HIA) at the eastern terminus of the Abu Hamour Tunnel which forms a link to allow discharge of storm flows collected in the southern and western parts of the Doha over a total catchment area of approximately 190 km^2. Hydraulic Design was implemented considering all sections of works from Abu Hamour tunnel up to Marine discharge in 10km distance from shoreline. The design high water level (surge tide) of 2.00m QNDH takes into consideration climate change effects to the year 2060.

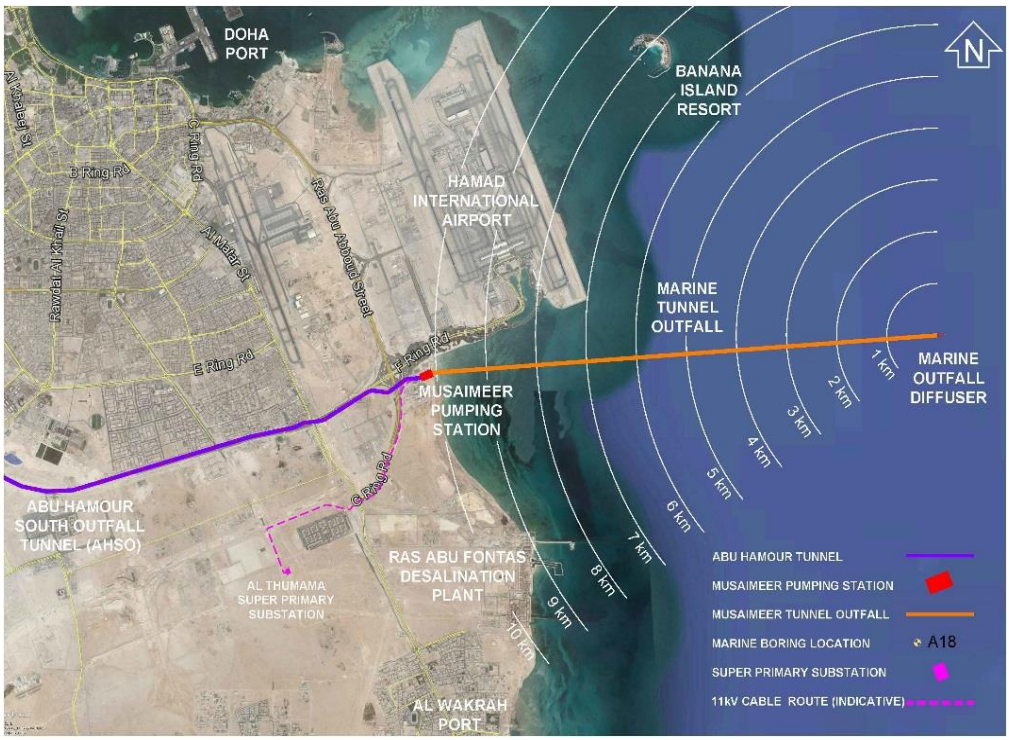


Fig. 1: Location plan for MPSO project

According to Hydraulic Design, the received flows shall be pumped to the Outfall Chamber and will flow by gravity to the subsea outfall tunnel and the diffuser field. Gravity flow system includes the outfall chamber and drop shaft, the 10km, 3.7m I.D. SFRC lining tunnel as well as marine discharge system, riser shaft, manifold, and diffuser field (figure 3). In order to avoid negative environmental impacts to potential key receptors, namely the Banana Island Resort and RAF Water Plant, based on the modelling results of the Preliminary EIA Report and Additional Environmental Studies, the outfall for the storm water discharge is approximately 10.0 km long. A multiple port outfall diffuser provides the necessary dispersion in the marine hydrodynamic environment. Rubber (duckbill) check valves were designed and installed for the Musaimeer Outfall. The outfall diffuser layout is shown on figure 4 &5. The conceptual design includes 84 diffuser ports. Qatar Construction Standards 2014 shall be followed when selecting materials to meet set design life. Materials including duplex or super duplex grades of stainless steel are recommended to be utilised within the aggressive marine environment. High durability concrete with appropriate additional protection for the tunnel and

underground structures was used to minimize the effect of the corrosive nature of conveyed flows and the surrounding environment.

3 Parameters Defining the Location and Arrangement of Diffuser

Ministry of Environment and Climate Change (MoECC), in conjunction with Ashghal, agreed that a marine outfall tunnel should be added so that the discharge could be extended offshore, well into the Gulf, to alleviate any negative environmental impacts to potentially sensitive receptors. The environmental studies during preliminary design phase, included preparation of marine and land based environmental baseline surveys, a marine bathymetric survey for the proposed outfall alignment, performing water and soils sampling and testing programme, and completion of a 3-D hydrodynamic model for nearfield, far field, and water quality standards for discharge and environmental impact. The results of these studies have been included in the Preliminary Environmental Impact Assessment (EIA) Report for MoECC review and approval and subsequent Additional Environmental Studies Report. The coastline is generally shallow in depth and, as such, areas of mud and sand flats are exposed at low tide. This part of the coastline is not used for recreation, which is concentrated in areas such as Doha Bay to the north and Al Wakrah to the south. There are no protected areas or special areas of conservation within or near the project area. The outfall tunnel alignment passes beneath extensive sea grass beds, which are regarded as sensitive habitat (project's sensitive receptor). The existence of the sea grass beds was considered as an environmental constraint in selecting the type of outfall and they were considered when developing construction methods. A multiple port outfall diffuser is necessary to obtain the necessary dispersion in the marine environment. There are a variety of outfall diffusers including open port (free discharge) and duckbill rubber check valves, and for the reasons discussed below the rubber check valve was recommended for the Musaimeer Outfall.

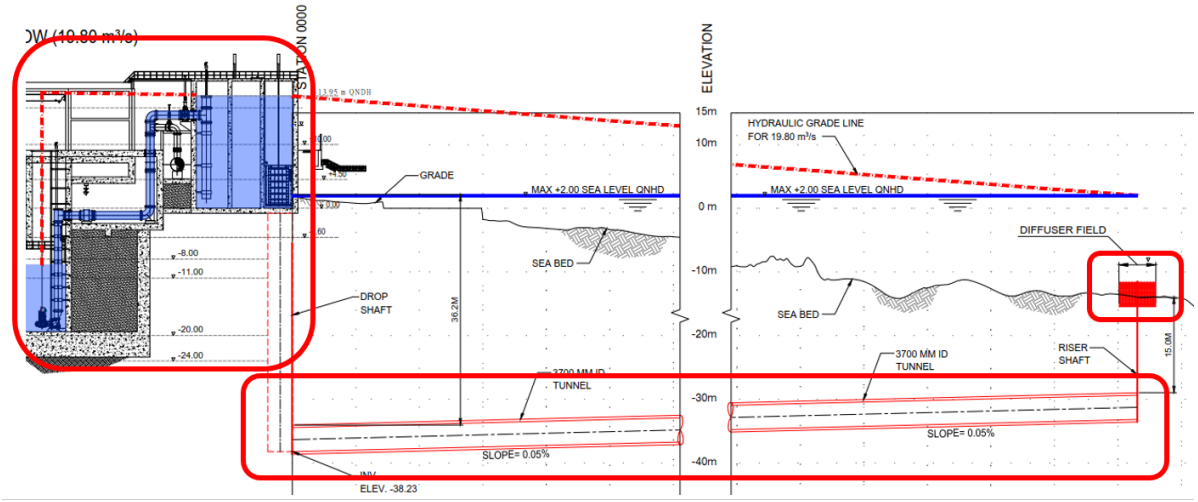


Fig. 2: Gravity flow system

3.1 Seawater Intrusion

Seawater can intrude into the diffuser and outfall pipe if the flow rate from the pump station is low. Salt water is typically 2% heavier (about 4% heavier in the Gulf) than fresh water and if allowed to intrude into the outfall pipe can cause a saline wedge that can impair system hydraulics and diffuser effectiveness and dilution. Additionally, water pressure may be significantly greater under a wave crest, as opposed to the trough, so "duckbill" check valves are recommended to prevent the intermittent entrance of seawater into the outfall pipeline. Due to the intermittent operation of the storm water outfall the prevention of seawater intrusion into this outfall over the long off-line periods is impractical, so hydraulic design has

accounted for seawater intrusion. However, base flows are expected to be continuous and diffuser design should mitigate seawater intrusion and consider the use of a check valve.

3.2 Sediment Intrusion

Suspended solids in the Arabian Gulf water are relatively high, which increase during high winds that occur throughout the year. The sea floor and diffuser are shallow leading to re suspension of sand and sediment during high wave activity. The suspended solids (sediment) can enter through the diffuser port during low or no flow and accumulate inside the outfall pipe. Ambient sediment transport along the sea floor can carry bottom material and suspended material into the diffuser, and sand dunes that naturally move across the seabed can transport material into the diffuser orifice and potentially bury the diffusers. Because flow through the storm pipe will not be continuous in the future, there is a risk of sediment intrusion; to mitigate the clogging of the diffuser and outfall pipes with sediment during extended periods of little or no flow, diffusers are equipped with check valves (duckbill valves).

Discharges into shallow oceans can attain sufficient near field dilution when specific requirements are followed. Initial dilution should be maximized by implementing a diffuser field with the maximum possible length, installing the diffuser axis at 90 degrees to the predominant current and Orifices to be discharging horizontally. Diffuser spacing should allow the plumes to merge just below the surface by using the smallest feasible port diameter. Port spacing shall be $s/H > 0.3$ for un-stratified water, where s is the port spacing along the diffuser and H is the water depth. At 10,000m from the shoreline, the water depth is 15m and therefore the minimum diffuser spacing should be 4.5m. The selected size of port is 300mm port size installed in a spacing of 10m.

All diffuser ports should be the same size and depth. The sea floor and the outfall pipe can and should slope, however the diffuser check valves shall all be at the same elevation. Head loss through the diffuser should be small and the diffuser pipe will be buried so each diffuser port will require a riser pipe with an elbow on top to discharge flow to either side of the diffuser pipe. The diffuser should detach (bolted connection) from the riser for maintenance access. Check valves can resist the design head due to tidal effects and prevent inversion of the rubber check valve. Selected dimension of the diffuser field is approximately 280m x 40m.

4 Hydraulic Analysis of Diffuser Field

Following preliminary hydraulic calculations, a 3m Diameter of the 10km tunnel is selected and a 3.7m diameter GRP riser shaft is proposed at the end of the tunnel. The end of the tunnel and riser shaft diameter is smaller than the tunnel diameter to provide higher velocities that will help ensure re suspension of any sediment that has travelled along the tunnel invert. Riser shaft is connected with the main manifold and through the primary and secondary manifolds, 6 HDPE pipe branches are developed in the sea bottom. The Riser Shaft will also serve as an exit point for remotely operated maintenance vehicles during tunnel inspections so appropriate access covers will be required to allow the shaft to be opened for recovery of remotely operated vehicles. The access covers should prevent discharge from the riser shaft but be removable by divers. It is not envisaged that the tunnel will be drained down at any time during its design life and therefore the access covers do not need to provide a drop tight seal. Access to the Riser Shaft for divers should also be provided.

The assessment of hydraulic properties of the system including drop shaft, marine outfall tunnel and diffuser field, was implemented through a one-dimensional hydraulic model using Wanda Version 4.5 software. The purpose of the assessment was to calculate the required free surface levels inside the MPSO outfall chamber add drop shaft located onshore in order to provide the conveyance of design flows related

to both to both wet and dry weather discharge of MPSO. Through the analysis, the final arrangement of diffuser field was also selected and verified which will be further presented herewith. The major criteria which shall be complied is to ensure balanced flow out of discharge ports for both dry and wet weather flow. Grit conveyance shall also be ensured if flow velocities in diffuser pipes are higher than outfall tunnel velocities. For this purpose, a varying diameter sizing is implemented for both piping and diffuser header system. Short-term and long-term hydraulic roughness (k factor) for concrete liner, GRP riser shaft, main diffuser header/manifold, fittings and riser pipes is implemented. Design high water level in the recipient is 2.00mQNHD, which takes into consideration climate change effects of the year 2060. 300mm Tideflex rubber duckbill valves were selected the hydraulic characteristics of which are presented in Figure 3.

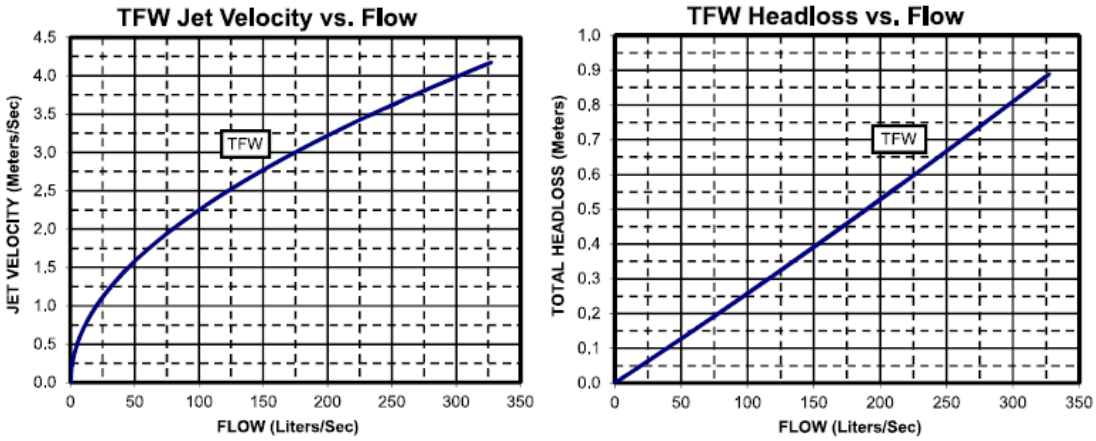
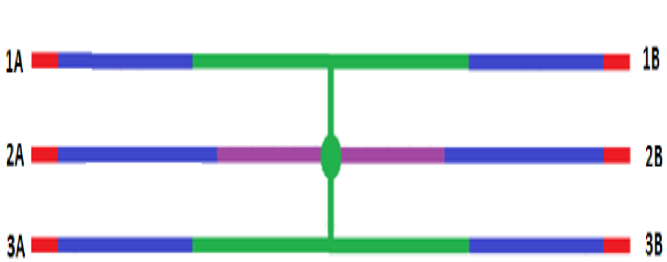


Fig. 3: Duckbill valve charts - Jet velocity vs Flow Rate and Head loss vs Flow Rate (courtesy of Tidelfex)

4.1 Results

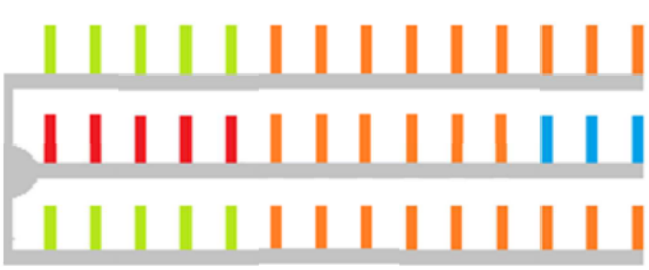
Hydraulic assessment included 3 scenarios for dry weather flow (1.9m^3/s), wet weather flow (19.7m3/s) and tunnel flushing. Based on model outputs it was concluded that under most onerous hydraulic conditions, a water level of 13.56mQNHD in the drop shaft is required to ensure delivery of the wet weather flow (19.7m^3/s) to diffuser field. This value was derived during the simulation for the worst operational scenario with the incoming flow of 19.7m^3/s, high tide level of +2m QNHD and long-term concrete roughness value. Duckbill valves of integral bend of 45° maximum head loss reaches 0.8m under flushing scenario. As per manufacturer's data, capacity of the 84 duckbill valves is sufficient to withstand maximum theoretical flow of 27.3m^3/s whereas maximum flow delivered to duckbill valves during flushing procedure is 24.64m^3/s. Flow distribution along lateral lines was calculated with a 5% variation which falls within acceptable limits. The piping configuration has been developed and adjusted to minimize the flow variation. Finally, it is confirmed that velocities within the diffuser field do not fall below the Qatar Surface and Ground Water Drainage manual threshold of 0.7m/s during the wet weather flow.



Color Code	Material	OD [mm]	ID [mm]
	HDPE	2000	1,847.20
		1400	1,293.00
		1200	1,108.20
		710	655.60

Fig. 4: Diffuser field piping arrangement and size

The finally implemented arrangement following the above-mentioned requirements is depicted in Figures 4, 5 & 6. Diameter of HDPE piping is varying from 2000mm to 710mm, and diameter of raisers are also varying between 560 to 710mm. It is noticed that starting from connections with the main manifold pipe diameters are reduced while raiser diameters are gradually increased. This proposal ensures equalization of flows throughout the whole length of the diffuser.



Color Code	Material	OD [mm]	ID [mm]
	HDPE	560	517.20
		630	581.80
		500	461.80
		710	655.60

Fig. 5: Diffuser field piping arrangement and size

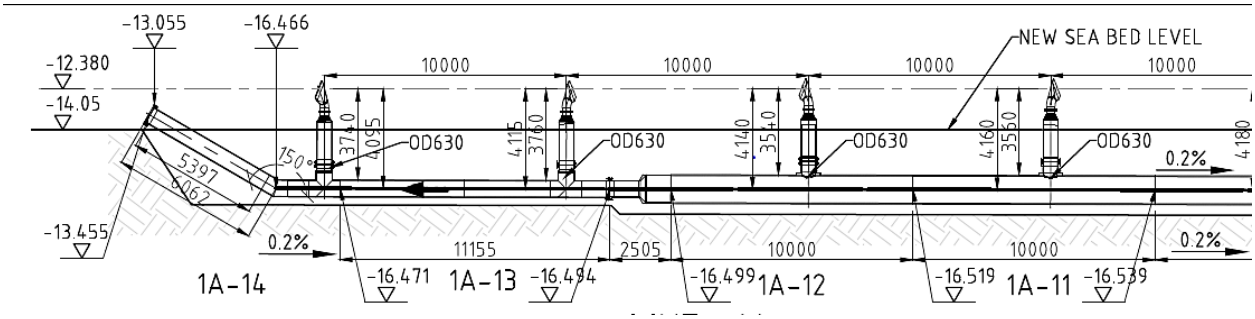


Fig. 6: Longitudinal section of diffuser pipes and ports

5 Design Criteria for Marine Works

Design criteria related to Marine works of the projects were set out in the initial stage of the project in accordance with Contractual requirements and international codes and practices. The major challenges included the selection of the proper marine grade materials as well as the Design of prefabricated part of works. The selected materials shall be able to withstand the aggressive corrosive environment of seawater complying at the same time with project's demanding service life requirements. Material selection for all Marine installation works was implemented in line with durability Assessment report meeting the required service design life of all permanent structures within the marine environment. The concrete mix design also met the durability requirements to achieve the required design life for all structures. Concrete material properties, cover to reinforcement, waterproofing requirements, exposure classes for reinforcement corrosion, surface finish, concrete mix design, grade of concrete, crack-width criteria, achieving design life of structure in accordance with Durability Assessment Report requirements.

Another challenging part is the meticulous design of prefabricated and precast sections of work ensuring transportation and installation safety during adverse weather conditions as well as during operational period.

6 Sequence of Marine Works

Installation of the marine outfall tunnel and diffuser system was performed in a safe and environmental sensitive manner, following best practices, while complying with Qatari regulations,

Environmental permit requirements and international maritime regulations. The Main Contractor was responsible for design and Construction of all Marine related activities. Marine activities and respective requirements are listed in Table 1.

Table 1: Construction sequence and requirements

Construction sequence	Requirements
Dredging works	Bathymetric surveys prior and as built, ensure dredgability of the diffuser area, minimize impact on marine environment during dredging works, safe deposition of dredged material
Riser shaft construction	Selection of appropriate offshore drilling rig
Riser shaft permanent grp (glass reinforced plastic) pipe and main distribution header	Ensure structure installation within acceptable tolerances
Pipeline fabrication onshore and transportation offshore	Material selection as per durability requirements, safe transportation under any adverse weather conditions
Connection between the outer diffuser lines and the main distributor of the riser shaft	Diffuser trench and pipelines shall be adequately protected to prevent trench erosion by sea conditions, wind, waves, tides, and currents.
Installation of flanges, covers, manifolds gaskets	Installation to ensure water tightness/sea water intrusion
Diffuser pipes/raisers and duckbill valves	Installation to ensure water tightness/sea water intrusion
Backfilling of diffuser field	Ensure stability during backfilling operations, environmental impact to be minimized
Protection collar and protection boxes	Ensure stability during installation, ensure proper anchorage of protection boxes
Scour protection	Ensure stability during backfilling operations, environmental impact to be minimized
Connection of riser shaft with Outfall tunnel	Cast in situ works with proper concrete quality, removal of segments and excavate in dry conditions, waterproofing installation



Fig. 7: Various stages of Marine Construction activities

The diffuser field pipes were manufactured with openings in accordance with the hydraulically calculated diameter of the diffuser risers in equal distance between the 84 diffusers positioned in the

diffuser pipes. The diffuser raisers were fixed by thermal butt fusion welding according to the standards. On the diffuser raisers, the duckbill valves of 300mm will be fixed by flange connection. The duckbills valves were flanged with the diffuser risers using a gasket considering the standard requirements. The entire horizontal pipelines, primary and secondary manifolds were backfilled re-using the previously dredged material for sustainability purposes. Following the installation of concrete collars-ballasts and protection boxes for duckbills scour protection layers were applied throughout the whole layout of the diffuser field. The final step of sequence involved the critical connection activities between riser shaft and TBM tunnel, which ensured the final hydraulic connection of the whole gravity system as, depicted in figure 8. During operational tests for the stormwater discharge through the diffuser field, system design parameters such as head losses and flow conditions had been cross verified and confirmed.

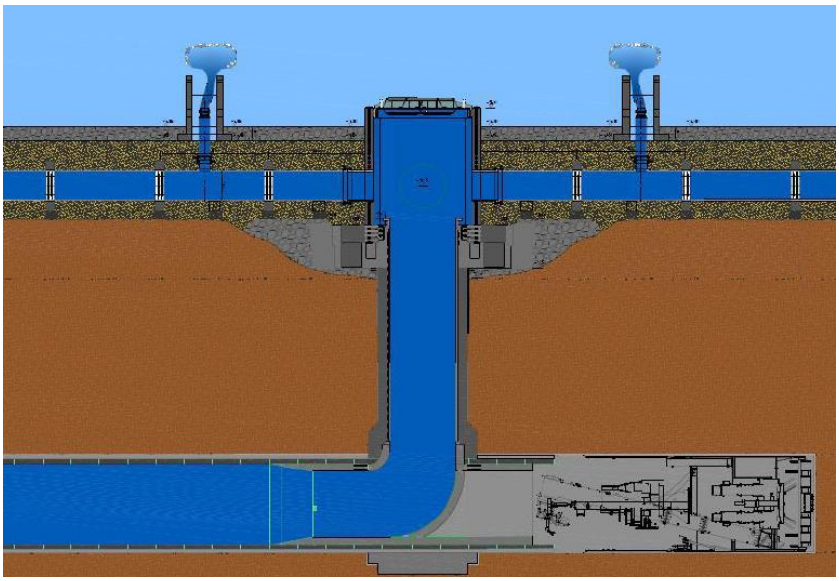


Fig. 8: Final stage of diffuser field section-Operational phase

7 Conclusions

Musaimeer pumping station Marine outfall design considerations included several challenging aspects. Gravity system shall ensure full flow conveyance of dry weather and storm weather flow through the 10km tunnel ensuring homogenous flow through the diffuser field-duckbill valves to the marine environment. All the design values, parameters and results have been cross verified and confirmed during the first 5-month operational period of the pumping station and outfall. Marine related construction activities shall be implemented with increased factors of safety compared with onshore activities, maximizing prefabrication structures, and allowing only installation works mainly to be implemented offshore.

Acknowledgments

The authors would like to thank Ashghal and HBK-PORR JV for their permission to publish this article. Credits are also given to HBK PORR JV, Design Consultant COWI as well as Project Management Consultant Mott Mac Donald for the successful project delivery.

References

COWI. (2021). Hydraulic Design of MPSO.

Public Works Authority (2017). Contract Documents for Design, Build, Operate and Maintain of Musaimeer Pumping Station and Outfall, PROJECT ID: IA 14/15 C 015 G, Contract Number: C2017/109.

Public Works Authority (2008). Qatar Sewerage and Drainage Manual.

Qatar Construction specification (2014). - QCS 2014.

Cite as: Verros P., Al-Marri S.Z., Kyriakopoulos A. & Alvanitopoulos L., "Design Considerations of MPSO Marine Outfall and Diffuser Field", *The 2nd International Conference on Civil Infrastructure and Construction (CIC 2023)*, Doha, Qatar, 5-8 February 2023, DOI: https://doi.org/10.29117/cic.2023.0172

Challenging Hydraulic Aspects of MPSO Project, Qatar's Showcase for Storm Water Outfall

Panagiotis Verros
Jacobs, Doha, Qatar
panosverros@gmail.com

Joao Carlos Henriques Miranda
Public Works Authority, Doha, Qatar
jmiranda@ashghal.gov.qa

Nikola Manojlovic
COWI, Doha, Qatar
namc@cowi.com

Alexios Kyriakopoulos
HBK-PORR, Doha, Qatar
alexios.kyriakopoulos@phm-jv.com

Abstract

The purpose of the Musaimeer Pump Station and Outfall (MPSO) project is to receive storm water runoff and groundwater flows from the Abu Hamour Tunnel and to provide a pumping station, a 10 km marine outfall tunnel and a diffuser field to dispose of the flows into the sea. The project site is located immediately south of the land that was reclaimed for the newly constructed Hamad International Airport (HIA) at the eastern terminus of the Abu Hamour Tunnel which forms a link to allow discharge of storm flows collected in the southern and western parts of the Doha over a total catchment area of approximately 190 km^2. Hydraulic Design for MPSO (Musaimeer pumping station and outfall) was implemented for dry weather flow of 1.9m^3/sec and wet weather flow of 19.7m^3/sec. The system was designed with increased operational redundancy including 2 screen channels, bar screens and grab rakes, each channel being able to handle the maximum design flow, 2 wet wells with grit removal and oil and grease removal system, 10 submersible pumps (9 duty+1 standby), outfall chamber, drop shaft, 10 km marine outfall tunnel and diffuser field comprising of 6 HDPE pipe branches and 84 non return diffuser ports-duckbill valves. Hydraulic Design calculations were cross verified by CFD modelling, physical modelling in 1:9 scale and surge analysis results concluding on final hydraulic design conclusions and recommendations. Hydraulic Design parameters presented in this paper were verified during operation and maintenance period of the project and will be demonstrated herewith.

Keywords: Hydraulic Design; CFD; Physical modelling; Bar screens; Diffuser field

1 Introduction

Southern and Western Doha has been experiencing a rapid expansion and growth in recent years. Consequently, the need to increase drainage capacity to accommodate additional storm runoff and construction activities has become critical. In response, Drainage Networks Projects Department of the Public Works Authority (PWA) has undertaken significant studies and developed numerous projects that will provide an integrated approach for existing and future drainage systems for this

area. One such project is Musaimeer pumping station and outfall which provides for the installation of a collection tunnel, pumping station and marine outfall to discharge storm and groundwater drainage into the Arabian Gulf. The plan encompasses a drainage catchment area of approximately 190 km^2. PWA has successfully completed the Musaimeer Pumping station and Outfall tunnel project on Sep 2022 enabling the effective discharge to the sea. The most challenging part of Design Works included the integrated Hydraulic Design which is presented in this paper.

2 Overview of the Project

The project site is located immediately south of the land that was reclaimed for the newly constructed Hamad International Airport (HIA) at the eastern terminus of the Abu Hamour Tunnel which forms a link to allow discharge of storm flows collected in the southern and western parts of the Doha over a total catchment area of approximately 190 km^2. Hydraulic Design was implemented considering all sections of works from Abu Hamour tunnel up to Marine discharge in 10km distance from shoreline. Abu Hamour tunnel, MPSO pumping station, MPSO tunnel and marine outfall diffuser field are presented in the location plan in Figure 1. The pumping station plot is 100m x 160m with its eastern boundary at approximately elevation zero Qatar National Height Datum (QNHD). The site was graded to generally have a final elevation between 2.6m at its westerly boundary to 4.5m at its easterly boundary. The design high water level (surge tide) of 2.00m QNDH takes into consideration climate change effects to the year 2060.

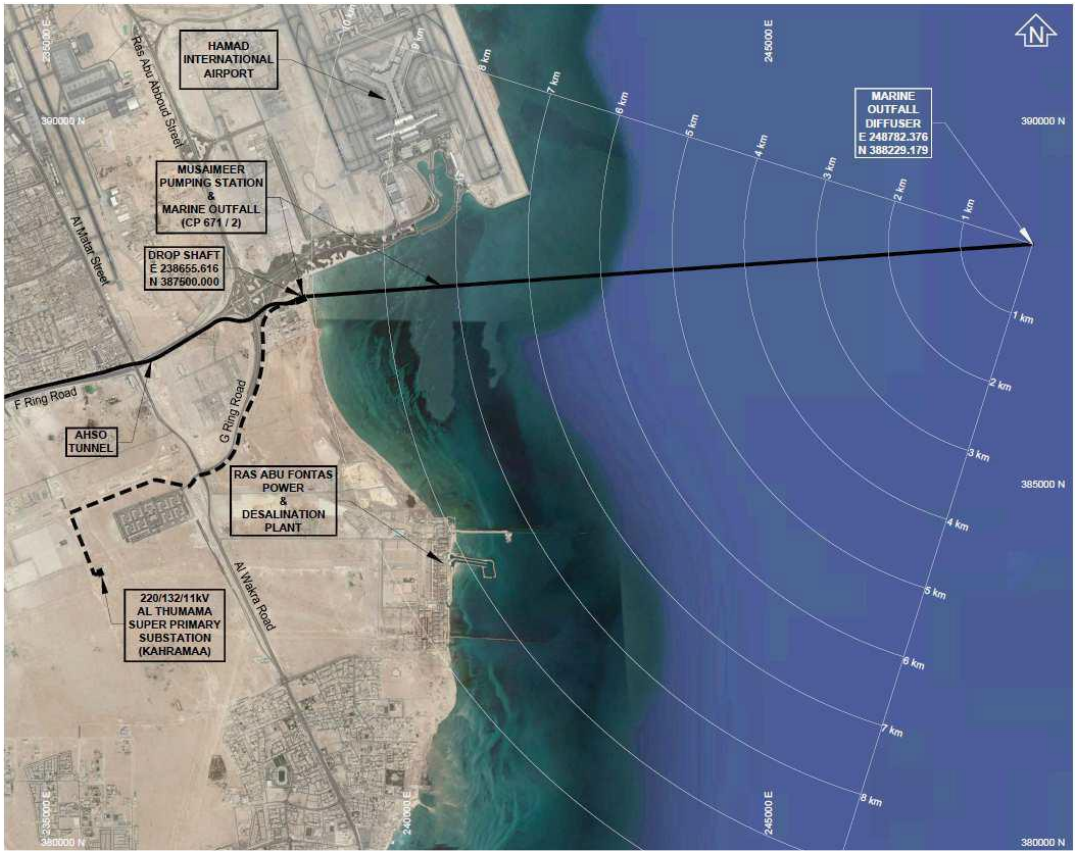


Fig. 1: Location plan for MPSO project

Pumping station comprise of overflow chamber, inlet, screen & outlet chambers, wet wells, delivery lines & valves and outfall chamber (Figure 2 & 3). The Pumping Station shall receive ground water and storm water from the Abu Hamour Storm Outfall (AHSO) Tunnel. Subsequently, the received flows shall be pumped to the Outfall Chamber and will flow by gravity to the subsea outfall tunnel

and the diffuser field. Gravity flow system includes the outfall chamber and drop shaft, the 10km, 3.7m I.D. SFRC lining tunnel as well as marine discharge system, riser shaft, manifold and diffuser field (Figure 4).

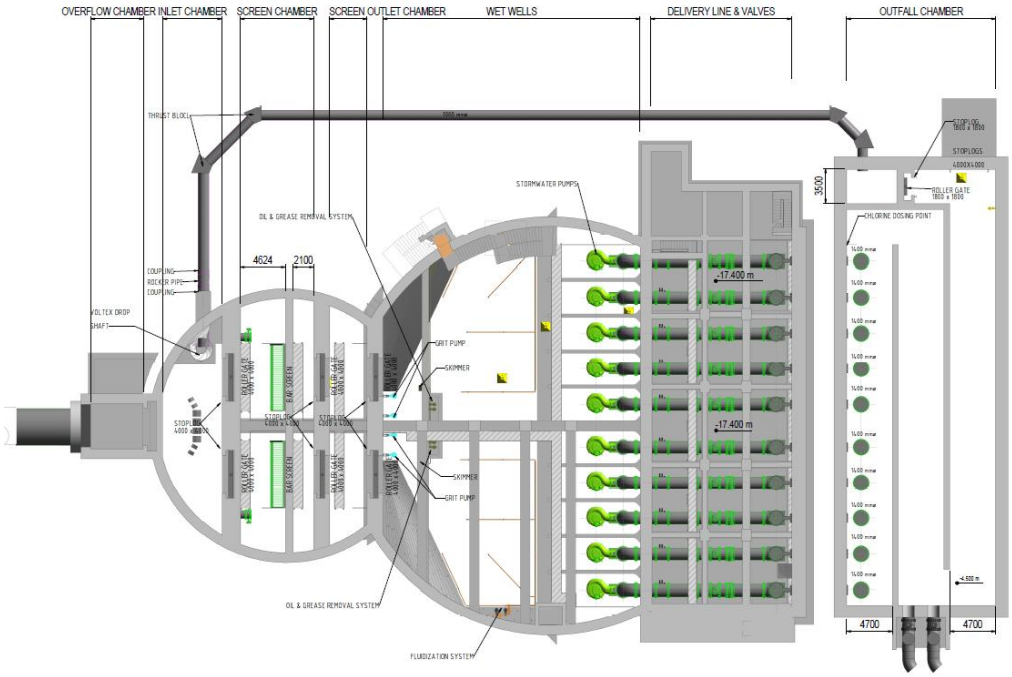


Fig. 2: Pumping station layout

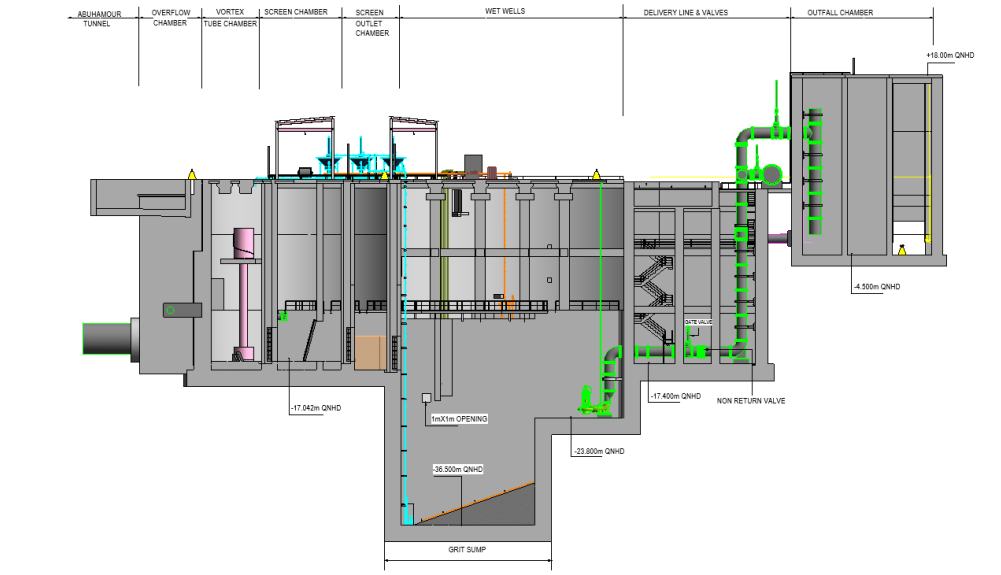


Fig. 3: Hydraulic profile of pumping station

The (upstream) water level in drop-shaft required to drive both dry and wet weather discharge flow was calculated by taking into consideration the pressure head-losses through the system and corresponding hydrostatic head for both normal and high-tide sea level scenarios. Apart from stability and durability of the system, the main concerns of design are flow distribution in manifold pipes and duckbill valves as well as the maintenance requirements.

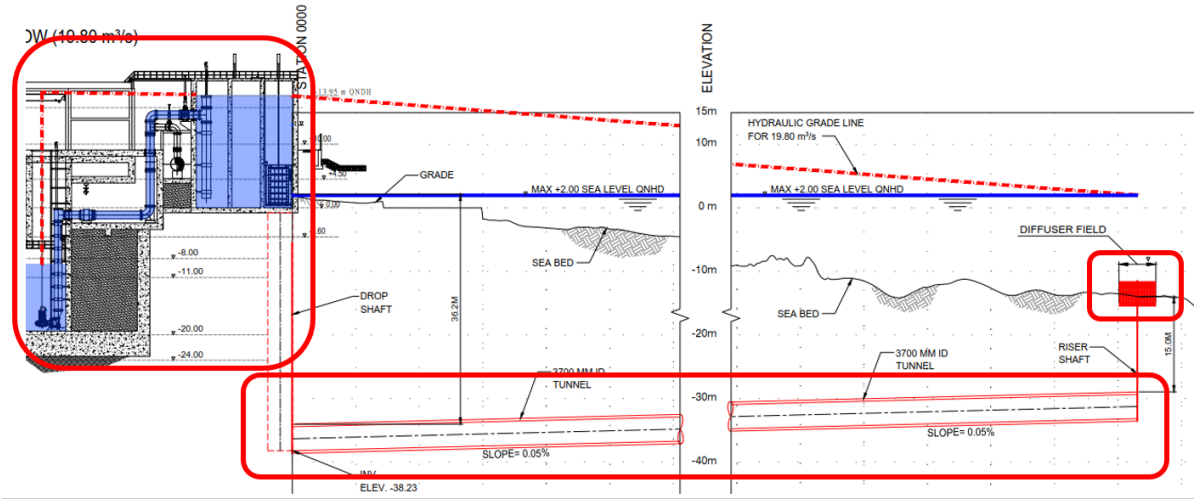


Fig. 4: Gravity flow system

3 Hydraulic Design Parameters & Scenarios

Major hydraulic design criteria were set out by the client (Public Works Authority) in contract documents during the preliminary/tender design stage and after coordination with various stakeholders regarding the extent of the catchment area, the upstream surface and groundwater collection system as well as the discharge location into the marine environment.

Table 1: General Design Parameters

Parameter	Value	Unit
Design Storm flow	19.70	[m^3/s]
Dry weather flow	1.90	[m^3/s]
Pumps (duty/standby)	9+1	N/A
Flow per pump	2.20	[m^3/s]
Min. number of duty screens	2	N/A
Screen Bar width	20	mm
Spacing between Screen Bars	30	mm
Bar screen redundancy	One screen 50% blinded	N/A
Estimated grit quantity (1:25-years storm, 4 hours duration):	244	[metric tons]:

Pump station shall maintain continuous operation under all flow conditions including discharge to the Outfall Chamber during different ground and storm water flow conditions, discharge to the re-use areas, and operation under emergency conditions (either overflow at overflow chamber or overflow at outfall chamber). Based on the above, a number of defined operating scenarios presented in table 2 were analyzed in order to evaluate hydraulic performance of pump station and its related components under the relevant flow conditions.

Table 2: MPSO Operating Scenarios

S/N	Hydraulic scenario	Case 01	Case 02
1	Dry Weather Flow	Both bar screen channels in duty	One 50% blinded bar screen channel in duty
2	Wet Weather Flow	Both bar screen channels in duty	One 50% blinded bar screen channel in duty
3	Re-Use Flow	Both bar screen channels in duty	One 50% blinded bar screen channel in duty

4	Pump Station Maximum Level/Flooding	Both bar screen channels in duty	One 50% blinded bar screen channel in duty
5	Flow Through Outfall Chamber Overflow Weir	Both bar screen channels in duty	One 50% blinded bar screen channel in duty

4 Hydraulic Design Calculations

All hydraulic systems, pumps, wet wells, and pipes were designed in accordance with best practices worldwide for conveying of storm water. Proposed hydraulic designs are suitable for the full range of flow and operating conditions followed by criteria such as a minimum freeboard of 0.50m to be maintained under all flow and operating conditions and flow velocities were designed to keep grit in suspension in pipes and conduits and allow grit to settle at the grit sump. The requirement of selected design scenarios was to analyze Hydraulic flow performance through Musaimeer Pump Station compartments, performance of bar screens and performance of submersible storm water pumps.

4.1 Inlet, Outlet and Forced Flow System

The objective of the Hydraulic Design calculations was to describe the investigations, analyses, calculations, conclusions and recommendations for the pumping system and outfall. In particular it included analysis of AHSO discharge level (to the PS Intake Works) under given design flows and all operating conditions, definition and analysis of relevant hydraulic scenarios where flows, levels and velocities may affect the required performance of the Pumping Station and Outfall System. Provision of hydraulic design calculations for the defined scenarios where Musaimeer Pump Station is either under normal operation (dry and wet weather flows) with both screen channels in operation or one of the screen channels is out of service as per Qatar Sewerage and Drainage Manual recommendations. Defining Wet Well operating levels for each of the specified scenarios and analysis of required level of outfall chamber. Hydraulic calculations were based on the table 3 formulas according to international practice:

Table 3: Hydraulic Design formulas

S/N	Design section	Applicable formula
1	Pipeline losses	Darcy Weisbach formula
2	Rectangular weir losses	Sharp and Broad-crested Weirs formula
3	Opening losses	Submerged Orifice formula
4	Sloped channel losses	Chezy formula
5	Partially full pipe	Manning formula
6	Head losses through screens	Coarse screen head loss formula
7	Main pipework head losses	Stringent value from friction loss theory by Miller, theory of Thorley and manufacturer's data

Validation of the suitability of the proposed pumps for MSPO was implemented by the Designer performing calculations of minor losses in the rising main using three different methods (item 7 of table 3). Pumps are required to achieve a duty of 2.2 m^3/sec under maximum friction for a calculated total static head of 30.3m. The performed analysis and comparison between different calculations methods identified that the theoretical head losses calculations on the piping system is 1.63m and the

pumps would be able to deliver a total head of 31.93m meeting the project's requirements. All the above values have been cross checked and verified during main pumps testing and commissioning procedure.

4.2 Gravity Flow System

The MPSO outfall tunnel is designed for the gravity flow regime being driven by the difference of (free surface) water levels between the drop-shaft and the recipient (the sea) as illustrated in Figure 4. The drop-shaft is vertical, cylindrical RC concrete structure with the internal diameter of 10.00m which receive the storm water from MPSO discharge chamber by gravity. The anticipated bottom of drop-shaft is at level -40.0 mQNHD. The marine outfall is proposed as the approximately 10 km long, 3.7m internal diameter stell fibre RC concrete subsea tunnel. At its downstream end, the tunnel is equipped with a 3000mm diameter riser shaft and diffuser (manifold) system which includes 84 duckbill diffuser nozzles connected to HDPE pipes arranged in three parallel lines.

Regarding the assessment of hydraulic performance of the outfall chamber, drop shaft, marine outfall tunnel and diffuser field at the downstream end, a one-dimensional hydraulic model was created using WANDA software Version 4.5. The purpose of the assessment was to calculate the required free surface levels inside the MPSO outfall chamber and drop-shaft to provide the conveyance of the design flows related to both wet and dry weather discharge. Balanced flow criterion was prioritized considering acceptable flow balancing deviation of ±10.00 % during dry weather flow conditions and ± 5.00 % during wet weather flow conditions.

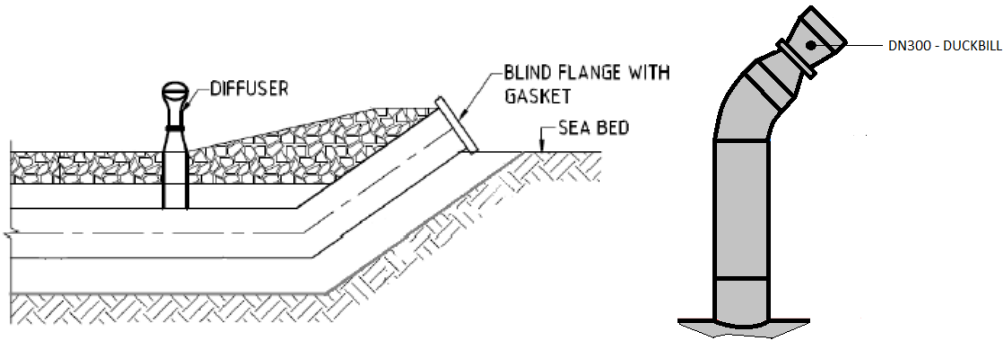


Fig. 5: Diffuser Field Pipe Section and Duckbill Arrangement

5 CFD Modelling

Computational Fluid Dynamics (CFD) analysis for MPSO project was conducted from COWI and BHR Group as approved vendors from client's (Ashghal) vendor list. CFD objective is to assess the overall flow patterns through the Pumping Station intake and predict if physical modelling will demonstrate the conformance with ANSI/HI 9.8 standards as per contractual requirements (1). The analysis focused on presenting the flow characteristics such as contours and vectors of the velocity at various sections of the structures, presence of dead zones (low velocity zones) and recirculation zones, identification of potential separation and flow instabilities, detection of high vorticity regions, determination of pump-pre-swirl angles and illustration of zones with highest tendency for sedimentation. The model was presented with colour coded graphics showing insight into a detailed flow pattern and velocities which helped to visualise the flow patterns through the structure and into the pumps.

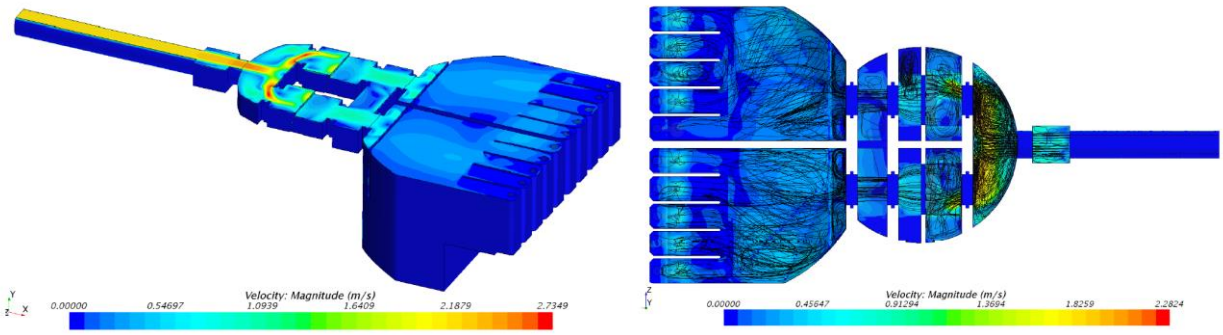


Fig. 6: Velocity magnitude contours and velocity streamlines

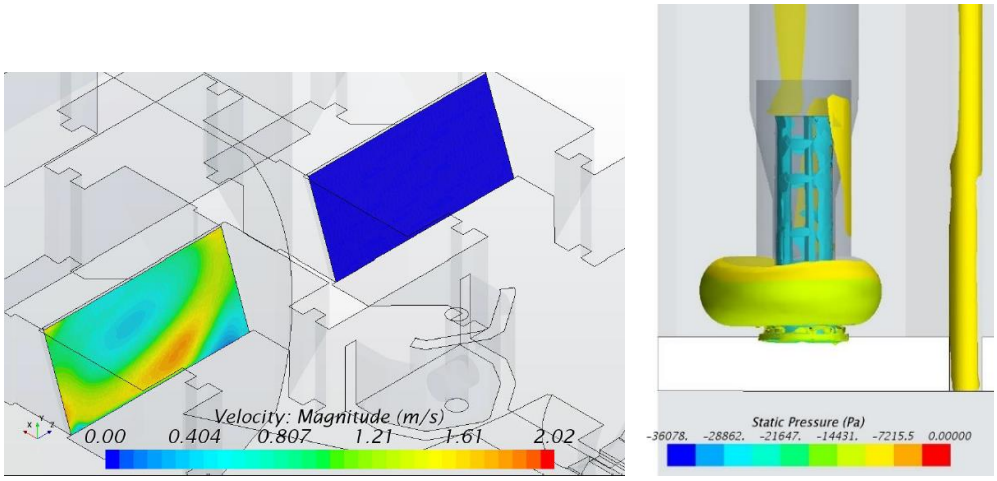


Fig. 7: Velocity distribution across bar screens and pump intake hydraulics

Scenarios studied under CFD analysis are a subset of the set of operating conditions, and the results obtained, regarding flow patterns, vorticity, swirl, etc., may differ for other conditions. Therefore, a broader range of operations was tested on the physical model of the pumping station to confirm its performance.

6 Physical Modelling

MPSO Physical Model Study was conducted by the Ashghal approved specialist BHR Group, UK. Each of the scenarios, have been analyzed based on the worst hydraulical conditions specified under table 2. Major observations and measurements made during the final testing on the Musaimeer Pumping Station physical model are presented herewith. The sufficient length of the inlet pipe was modelled to ensure representative flow conditions. The model extended to a level of -11.00mQNHD, with the overflow chamber walls rising to this height. This allowed for testing up to the normal maximum operating level.



Fig. 8: Model overview and angled jet impinging on the screen

Upstream water levels were not observed to be backed up, with the tunnel remaining un-surcharged under all test conditions and below the maximum available level even with a single screen operating partially clogged at the maximum station design flowrate. Minor settlement was observed at several locations under low flow conditions. This material was largely swept clear under higher test conditions. Settlement at the maximum flow was limited to one side of the forebay area around the vortex plunge pool and the edges of the screen distribution chamber. The distribution chamber was swept clear at lower flowrates due to reduced water levels. No coarse material was carried past the grit traps. Conditions in the forebay area were highly energetic. At flowrates below half the station maximum baffle blocks in the forebay area conditioned flow to the screen chambers; at higher flows, flow to the screens retained a significant angle. Approach flow to the screens had a center bias, but average velocity was below industry maximum for bar screens. The change in flow patterns local to the screens and pumps that were shown in the CFD study, were found to be minimal. Changeable conditions in the pump bays were resolved by modifications local to the pumps. All pump swirl angles were measured well below the maximum of 5 degrees and no detrimental surface or submerged vortices were observed.

As a result of the combined studies from Hydraulic design calculations, CFD analysis and physical modelling several adjustments to the original design have been implemented such as peripheral benching along the walls of the distribution chamber feeding the settling basins and corner fillet downstream of the screens to minimize solid settlement. Installation of baffle wall within the settling basin for the purpose of minimizing flow velocities and solids carryover as well as installation of benching and cone arrangement in pump intake. Adjustments in the diffuser field arrangement such as varying diameter of HDPE pipework also ensured homogenous flow distribution through duckbills.

7 Conclusions

Musaimeer pumping station Hydraulic Design considered various challenging aspects such as full operational capability with only one bar screen in operation partially clogged, minimization of grit accumulation throughout the inlet and outlet works, avoidance of grit conveyance through the piping system and adequately sized pipework system for 19.7m^3/s for 32m approximately available head. Finally, gravity system shall ensure full flow conveyance of dry weather and storm weather flow through the 10km tunnel ensuring homogenous flow through the diffuser field-duckbill valves to the marine environment. All the design values, parameters and results have been cross verified and confirmed during the first 5-month operational period of the pumping station and outfall.

The above-mentioned studies and tests ensure the uninterrupted operational efficiency of this unique project for Qatar as well as increased redundancy against current and future extreme rainfalls events.

Acknowledgments

The authors would like to thank Ashghal and HBK-PORR JV for their permission to publish this article. Credits are also given to HBK PORR JV, Design Consultants COWI and BHR group as well as Project Management Consultant Mott Mac Donald for the successful project delivery.

References

COWI (2021). Hydraulic Design of MPSO.

Public Works Authority (2008). Qatar Sewerage and Drainage Manual.

Public Works Authority (2017). Contract Documents for Design, Build, Operate and Maintain of Musaimeer Pumping Station and Outfall, PROJECT ID: IA 14/15 C 015 G, Contract Number: C2017/109.

Cite as: Verros P., Miranda J.C.H., Manojlovic N. & Kyriakopoulos A., "Challenging Hydraulic Aspects of MPSO Project, Qatar's Showcase for Storm Water Outfall", *The 2nd International Conference on Civil Infrastructure and Construction (CIC 2023)*, Doha, Qatar, 5-8 February 2023, DOI: https://doi.org/10.29117/cic.2023.0173

Automated Calibration of the EPA-SWMM Model for an Impact of Land Use and Land Cover Changes on Peak Discharge for a Sub-Urban Catchment of Delhi

Ved Prakash
Department of Civil Engineering, Indian Institute of Technology Guwahati, Guwahati, Assam, India
ved174104112@iitg.ac.in

Dhruba Jyoti Sarmah
Department of Civil Engineering, Indian Institute of Technology Guwahati, Guwahati, Assam, India
dhrubajyotisarmah3@gmail.com

Rajib Kumar Bhattacharjya
Department of Civil Engineering, Indian Institute of Technology Guwahati, Guwahati, Assam, India
rkbc@iitg.ac.in

Abstract

The Environmental Protection Agency's (EPA) Storm Water Management Model (SWMM), USA is a dynamic hydrologic-hydraulic model that simulates the amount and quality of runoff from urban areas. It is broadly used for planning, analysing, and designing storm water runoff, combined and sanitary sewers, and other urban drainage systems. SWMM can solely be used to do the modelling of urban drainage systems. However, SWMM can be automated and convert model files to and from GIS data using R programming, allowing for more in-depth analysis and visualization. Automatic calibration is also a promising alternative, ideally supporting a user-independent and time-efficient method for estimating model parameters. This study investigates the impact of Land Use and Land Cover (LULC) variation on peak discharge at the outfall of the Najafgarh-Mahipalpur drain during rapid urbanization from 2005 to 2022. The findings show that the historical LULC fluctuation for seventeen years resulted in a nearly 28% rise in the peak flow rate at the outfall, according to SWMM simulation. The findings of this study could serve as a guide for planning and managing urban flooding in cities that are rapidly expanding, particularly in developing countries.

Keywords: Urban drainage modelling; SWMM; R; Automated calibration; LULC

1 Introduction

Natural disasters, such as flash floods caused by severe storms, can have devastating effects on human life and society, especially in densely populated urban areas (Gülbaz et al.). Numerous scholars have investigated flash floods, their driving mechanism, their simulation, and their local and regional prediction (Jiang et al.). Concerned City officials have been working on a new system to better handle flooding from heavy rainfall. An abundance of lumped and distributed software packages was applied to construct stormwater drainage systems, propagate flood throughout the landscape, and model the rainfall-runoff process. One of these models that are frequently utilized is the Storm Water Management Model (SWMM). It allows for modelling surface water processes, sewage system flows, and stormwater quality. The variety of modelling approaches now accessible is expanding their use in the actual design of drainage networks and assessing urban runoff and loads (Mehr et al.).

Creating and applying automatic calibration processes for estimating model parameters could be a viable option, resulting in timesavings and a more user-independent approach. (Perin et al.). To evaluate the

performance achievable by automated calibration tools, in this paper, we automated EPA-SWMM. A SWMM model calibration for a runoff time series can be carried out using the current R code SWMMR (Leutnant, 2019). However, RSWMM is primarily concerned with calibration and output generation; it does not account for the curved drainage line geometry and the irregular cross-section of the drain.

We converted model files to and from GIS (Geographic Information System) data using R programming, allowing for more in-depth analysis and visualization. It is demonstrated that integration of GIS using R programming in SWMM models, in addition to the automated analysis of output, significantly improves the efficiency of modelling tasks. A workable option that could result in timesavings and a more user-independent method is the creation and usage of automatic calibration procedures for estimating model parameters. The goal of automatic calibration techniques is to automate the input data curve number based on the LULC change and get the discharge variation at the outfall as a runoff. This is accomplished through a self-driven search in the parameter space of the model.

Changes in Land Use and Land Cover (LULC) as well as climate alteration, have far-reaching impacts on the hydrological cycle, influencing variables like precipitation, infiltration, and evapotranspiration in significant ways, thus affecting the rainfall-runoff processes and the quantity of accessible water resources. Therefore, a study on runoff response to LULC modification and climate change is crucial for planning and managing water resources. Therefore, research on runoff response to LULC modification and climate change is crucial for planning and managing water resources (Umukiza et al.).

This study uses the Automated calibration of the EPA-SWMM model to assess hydrological changes in an urbanizing catchment. The study assessed the impact of Land Use and Land Cover (LULC) change on peak discharge at the outfall of the Najafgarh-Mahipalpur drain. Analyze the peak discharge and flow volume under various LULC projections based on a diachronic analysis of satellite images from 2005, 2010, 2015, and 2022.

2. General Overview of the Study Area

The total area of the catchment is about 47.14 km^2 covering the outfall of the Najafgarh-Mahipalpur drain, including a part of the Indira Gandhi International Airport (IGIA), Delhi. It is located between latitude 28°30′ N and 28°34′N and longitude 77°2′ E and 77°8″ E (Fig. ***1***). About 74.91 km parts of major roads were considered for this study. The runoff from this land parcel outflows at the southern outfall and finally flows to the Najafgarh Nallah. This drain carries stormwater runoff from Mahipalpur, part of Indra Gandhi International Airport, Kapashera, Pushpanjali, Bharthal, and their adjacent areas.

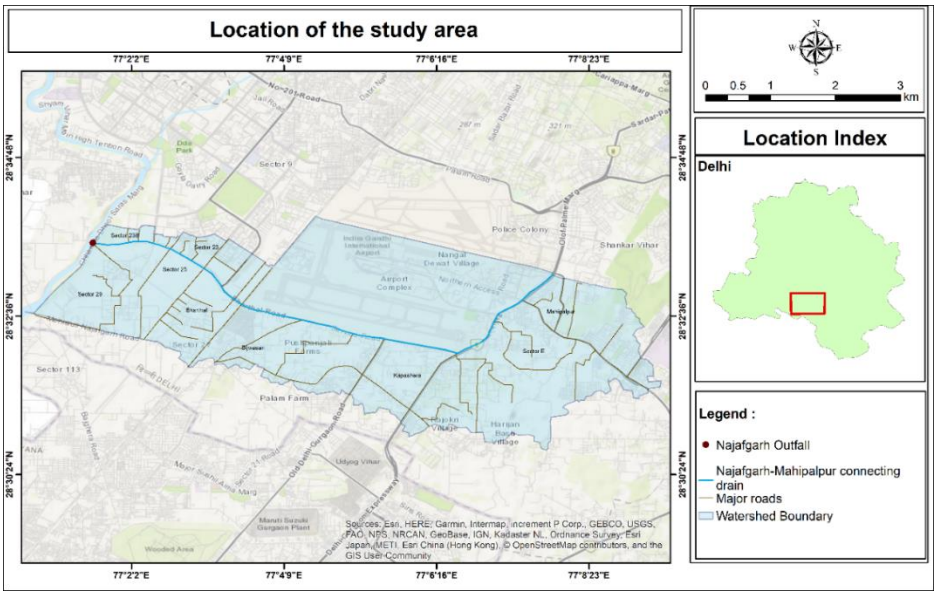


Fig. 1: Location map of the study area

3. Data and Methodology

The EPA SWMM simulates the urban catchment's hydrological response to rainfall events. SWMM is a dynamic hydrology-hydraulic water quality simulation model that can be used to simulate runoff quantity and quality from most metropolitan regions over a single event or over a long period (Continperiodan, 2010). R is compatible with most operating systems, was chosen for this study to create input files, and could execute SWMM simulations. An existing R code known as RSWMM was used for reading output generated from the SWMM for the peak flow hydrograph.

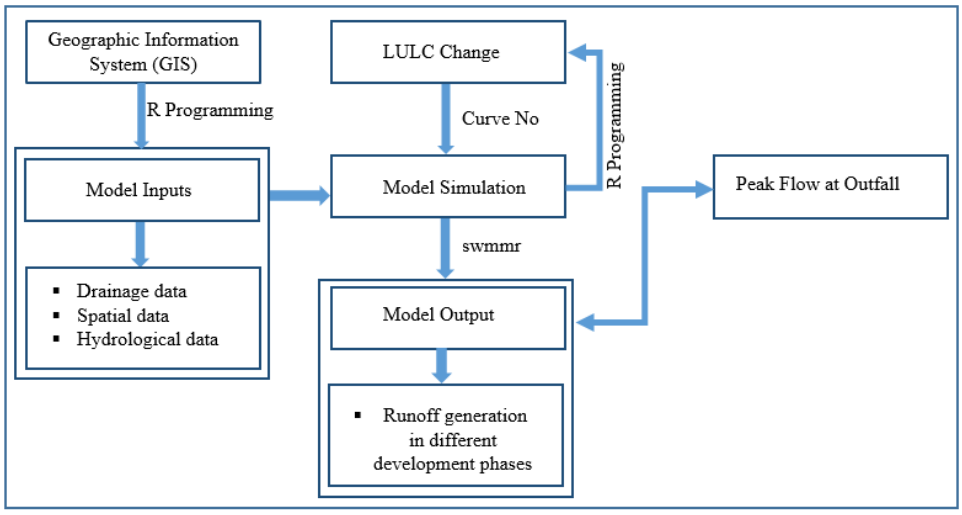


Fig. 2: Workflow for automation

One of the most challenging tasks when modeming an urban rainfall-runoff model using the SWMM GUI interface is to design a large number of drains, sub-catchments, and nodes over a sizeable urban drainage network design. GIS is the best available resource for drawing shape files such as lines, points, and polygons, corresponding to links, nodes, and sub-catchments. The shape files can be converted to input files using SWMMR, but limitation of the existing SWMMR module is that it does not consider the curvature drainage line and its irregular cross-section, which is quite reverent in the real world. In order to create the different scenario of development based on LULC change, curve number is automated for each sub catchment through R programming as shown in Fig. ***2*** and Fig. ***3***.

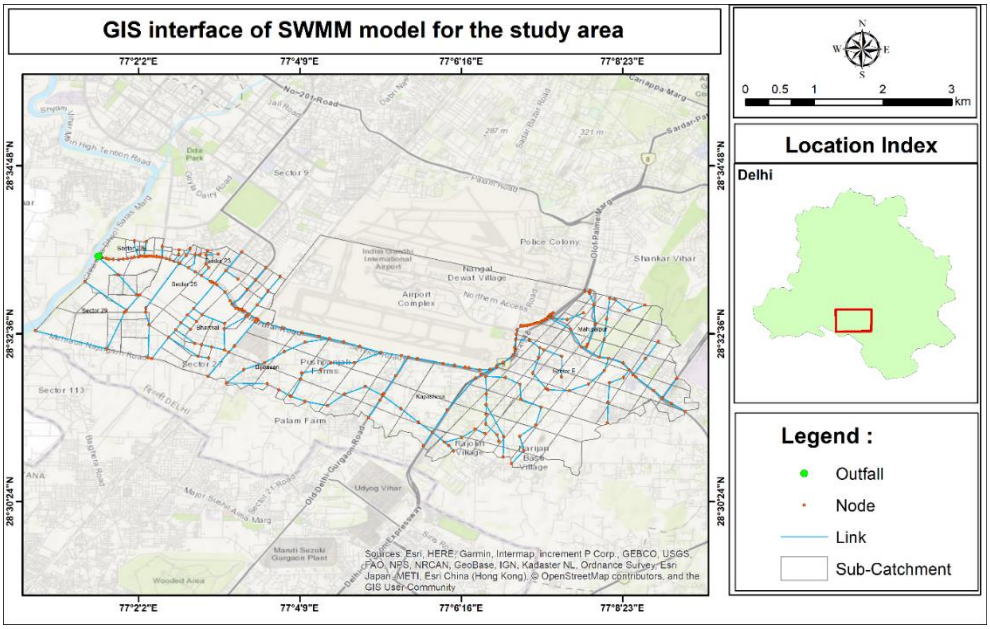


Fig. 3: Workflow for automation

The road networks of the study area were digitized from the street base map and added in Arc GIS software from the Google Earth satellite imagery. It is assumed that all the external drains are parallel to existing major roads as the actual drainage network is unavailable. The drains' size and shape are assumed so that there is no flooding in the assumed external drains. Invert levels of the drains are provided based on SRTM data.

The Curve Number (CN) is a dimensionless quantity representing the drainage basin runoff response characteristics. CN of the catchments are considered based on the past and present Land Use Land Cover (LULC) data and the tables provided in Table 2-2a (Cronshey, 1986). A synoptic view of Land Use and Land Cover changes was obtained from different multi-temporal satellite images of the last 17 years from 2005 to 2022, as shown in **Table *1***.

Table 1: Details of satellite imageries used in this study

Type of Data	Year	Source
LANDSAT_5(TM)	2005 and 2010	https://earthexplorerusgs.gov
LANDSAT_8(OLI_TIRS)	2015 and 2022	https://earthexplorerusgs.gov

Quantitative analysis of Land Use Land Cover (LULC) changes maps have been prepared over the study period by using a supervised classification technique using ESRI ArcGIS 10.8 software. The final SWMM model setup for the study area is shown in Fig. ***4***.

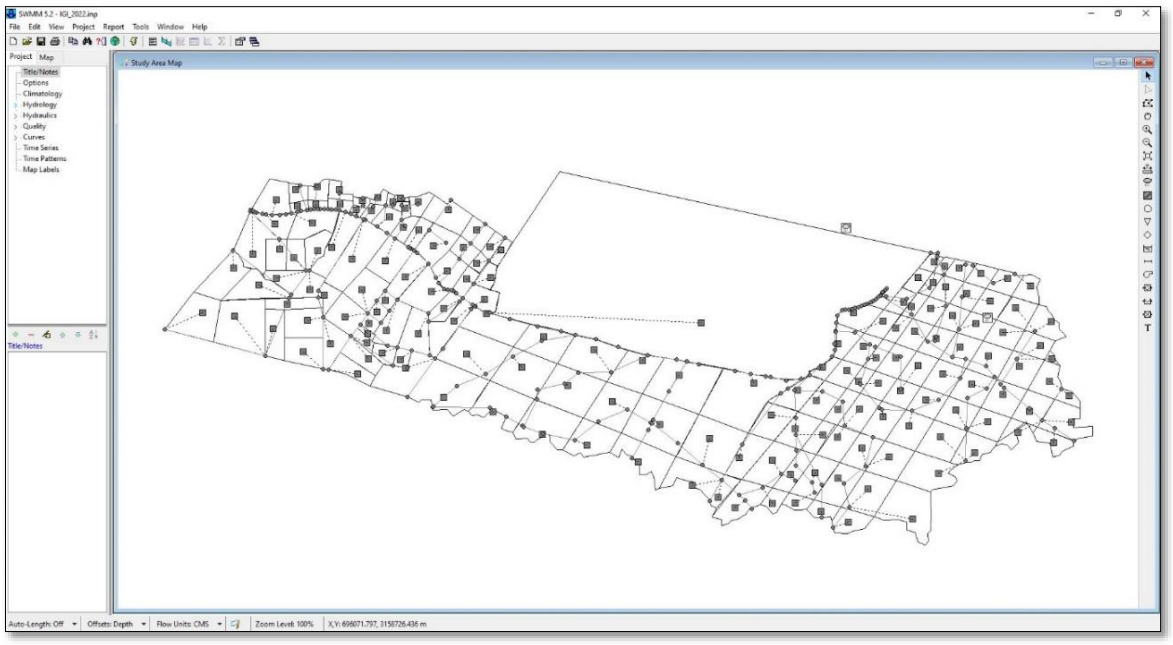


Fig. 4: SWMM model interface for the study area

4. Results and discussion

4.1. Land Use and Land Cover Change Analysis

This study demonstrates the extent of urbanization in terms of built-up areas. Rapidly development outward from the early urban establishments viz. in IGA Airport, Sector 25, Sector 23, Bharthal, Kapashera, Sector E, Mahipalpur, and their adjacent areas can be noted over the years and are still providing evidence of ongoing growth. Results of LULC changes in the study area are presented in Table 2 and Figure 5.

Table 2: Area (km^2) and percentage of Land Use and Land Cover classifications for various years (2005, 2010, 2015, and 2022) of the study area

LULC Cover Categories	CN	2005		2010		2015		2022	
		Area (km^2)	Area (%)	Area (km^2)	Area (%)	Area (km^2)	Area (%)	Area (km^2)	Area (%)
Built-up	90	6.22	13.04	21.39	44.85	26.56	55.71	33.89	71.07
Bare soil/Sparse vegetation	79	19.88	41.69	10.97	23.01	7.39	15.49	4.06	8.52
Shrub land	79	13.18	27.65	8.50	17.83	7.23	15.16	4.36	9.14
Trees/Grassland	61	8.03	16.84	6.54	13.73	6.26	13.13	5.13	10.76
Waterbody		0.37	0.78	0.28	0.58	0.24	0.50	0.24	0.50
Total		47.68	100.00	47.68	100.00	47.68	100.00	47.68	100.00

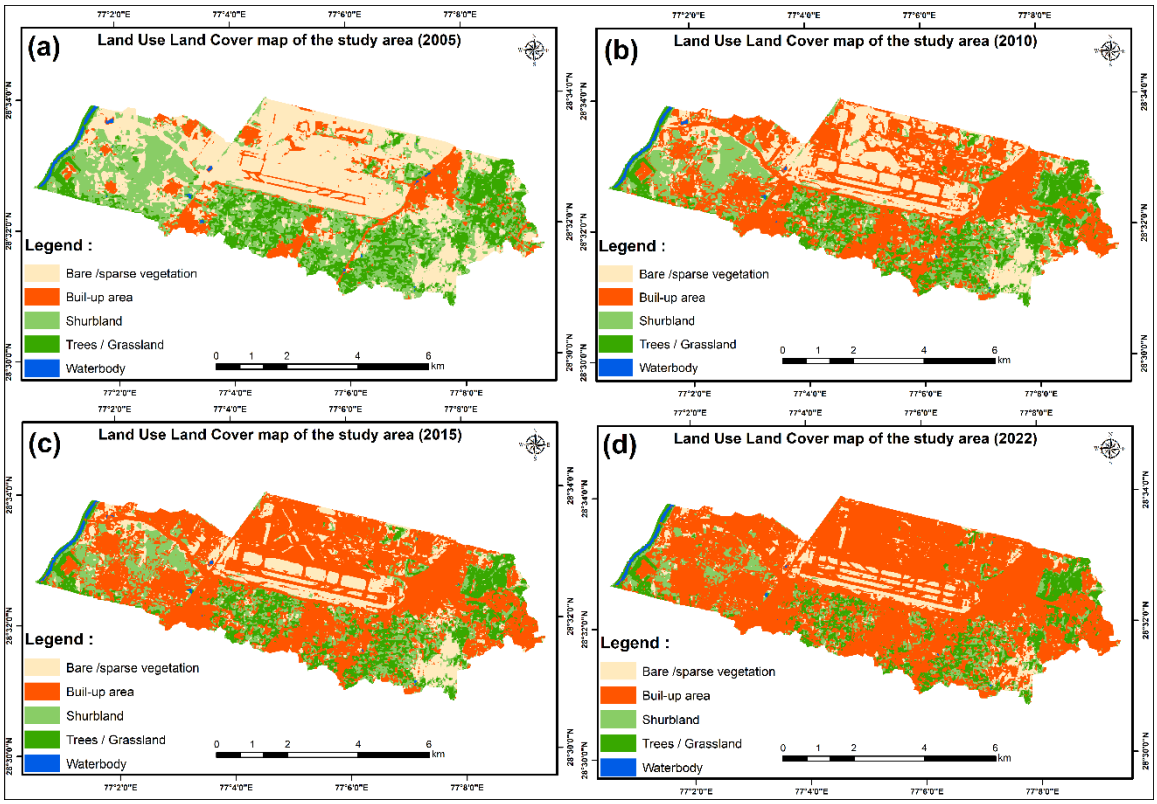


Fig. 5: Changing pattern of Land Use and Land Cover over the study area for the years (a) 2005 (b) 2010 (c) 2015 (d) 2022

It can be seen that the highest area of the built-up area has grown over time in 17 years, from 13% to 71% from the year 2005 to 2022. The area covering bare soil/sparse vegetation and trees/grassland decreased during the study period and converted to built-up areas. There is also decreasing trend of waterbodies from 0.37% to 0.24% from 2005 to 2022.

4.2 Evaluation of the Flow Contribution of the Najafgarh-Mahipalpur Drain from Different Regions Considering Different LULC Scenarios

The developed SWMM model is run for the southern outfall basin considering different LULC

scenarios (2005, 2010, 2015, 2022). **Table 3** shows the change in peak discharge in percentage, considering 2005 as the base period.

Table 3: The peak flow generated for different LULC scenarios

LULC (Yrs)	2005	2010	2015	2022
% Flow change	0	3.43	22.90	27.73

According to the SWMM simulations, the historical LULC changes in seventeen years resulted in a nearly 28 % rise in the peak flow rate at the outfall. Figure 6 shows the relative change in the peak flow since 2005.

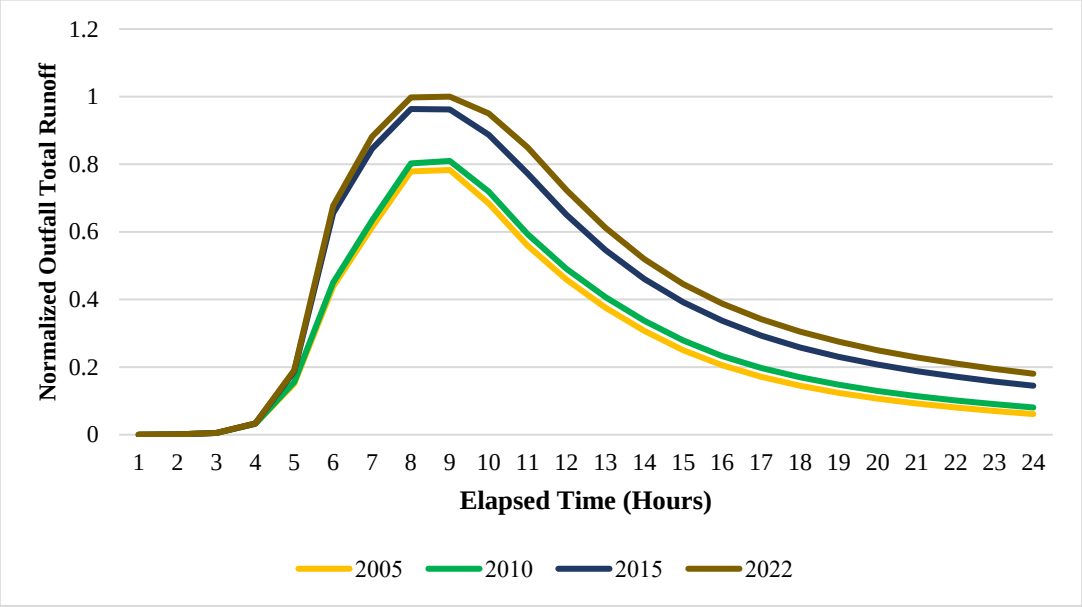


Fig. 6: The peak flow generated for different LULC scenarios

5. Conclusions

The stormwater management model (SWMM) with R, bridges the gap between modelling and advanced model analytics. Integration with Geographic Information System (GIS) and SWMM model using R, improved the automation capability and visualization the real-world problems. In this study, we examined the implementation of GIS and R programming for the automatic calibration of runoff at the outfall for the different scenarios of LULC change. The catchment covering the IGI Airport, Delhi, was examined considering the varied situations of land use/land cover (LULC), based on an assumption made after a diachronic examination of satellite imageries displaying the LULC alterations that took place during the period 2005–2022. The findings validated and demonstrated that LULC significantly affects designed systems' peak discharge and flow volumes. As a result of this analysis, the following points become clear: Sustainable land conservation techniques at a watershed scale should be paired with urban growth. Implementing strategic countermeasures that do not increase the area susceptibility is necessary if a rise in built-up areas is undertaken. The results can be used for urban runoff management plans that are appropriate for the local climate.

References

Cronshey, R. (1986). Urban hydrology for small watersheds. US Dept. of Agriculture, Soil Conservation Service, Engineering Division.

Jiang, L. E. I., Chen, Y. A. N. G. B. O., & Wang, H. U. A. N. Y. U. (2015). Urban flood simulation based on the SWMM model. Proceedings of the International Association of Hydrological Sciences, 368, 186-191.

A. D. & Akdegirmen, O. (2021). Estimation of urban imperviousness and its impacts on flashfloods in Gazipaşa, Turkey. *Knowledge-Based Engineering and Sciences, 2*(1), 9-17.

Gülbaz, S. (2019). Water quality model for non-point source pollutants incorporating bio-retention with EPA SWMM. Desalination and Water Treatment, 164.

Perin, et al. (2020). Automated calibration of the EPA-SWMM model for a small suburban catchment using PEST: a case study. *Environmental Monitoring and Assessment, 192*(6), 1-17.

Umukiza, et al. (2021). Impacts of land use and land cover changes on peakdischarge and flow volume in kakia and esamburmbur sub-catchments of narok town, kenya. *Hydrology, 8*(2), 82.

Utnant, D., Döring, A. & Uhl, M. (2019). Swmmr-an R package to interface SWMM. *Urban Water Journal, 16*(1), 68-76.

Cite as: Ved Prakash., Sarmah D.J. & Bhattacharjya R.K., "Automated Calibration of the EPA-SWMM Model for an Impact of Land Use and Land Cover Changes on Peak Discharge for a Sub-Urban Catchment of Delhi", *The 2nd International Conference on Civil Infrastructure and Construction (CIC 2023)*, Doha, Qatar, 5-8 February 2023, DOI: https://doi.org/10.29117/cic.2023.0174

Advanced Block Copolymer Membranes for Oily Industrial Wastewater Treatment

Mohammad K. Hassan
Center for Advanced Materials, Qatar University, Doha, Qatar
mohamed.hassan@qu.edu.qa

Shifa Shaikh
Center for Advanced Materials, Qatar University, Doha, Qatar
sshaikh@qu.edu.qa

Moustafa Zagho
School of Polymer Science and Engineering, University of Southern Mississippi, Hattiesburg, MS, US
Moustafa.Zagho@usm.edu

Mustafa Nasser
Gas Processing Center, College of Engineering, Qatar University, Doha, Qatar
m.nasser@qu.edu.qa

Xiaodan Gu
School of Polymer Science and Engineering, University of Southern Mississippi, Hattiesburg, MS, US
xiaodan.gu@usm.edu

Sergei Nazarenko
School of Polymer Science and Engineering, University of Southern Mississippi, Hattiesburg, MS, US
sergei.nazarenko@usm.edu

Alamgir Karim
Department of Chemical and Biomolecular Engineering, University of Houston, Houston, TX, US
akarim3@Central.UH.EDU

Abstract

Tremendous amounts of oily wastewater are produced daily from industrial processes, including petrochemical, textile, leather, and steel processing. This wastewater is a huge challenge to the environment and industry uses multiple approaches to separate the water from oil including oil-absorbing materials, gravity separation, flocculation, and coagulation. However, these concepts are ineffective in separating oily water emulsions where the oil droplets are smaller than 20 µm in size and do not perform well upon incorporating chemicals or using an electric field. Membrane filtration is one of the best strategies to handle such emulsions, especially the surfactant-stabilized ones, as they yield highly pure water permeate via simple filtration process and they can be cleaned re-used for multiple times at large-industrial scales. This presentation will give an overview of novel polystyrene-based copolymer membranes developed and tested at Qatar University in collaboration with the University of Southern Mississippi. The newly developed membranes display substantial enhancement in separating oil from water in tight emulsions while demonstrating remarkably high resistance to fouling over five runs in comparison to the commercial membranes that get fouled within only two emulsion runs. The presentation will outline the membranes' oil rejection efficiency, chemical, morphological, and mechanical stability after cycles of cleaning and reuse. Finally, the membranes were tested using synthetic oily water and real-field samples and testing protocols from the oil & gas companies in Qatar.

Keywords: Ultrafiltration; Block Copolymers composite membranes; Oil/water separation; Roll to Roll; Fouling resistance

1 Introduction

1.1 Membrane Separation

A significant breakthrough in membrane science would have profound economic and environmental impacts that ripple from increasing chemical production efficiency. Membrane separation is predominantly based on a size-sieving mechanism. Membrane performance is dictated by size, size distribution, porosity, pore geometry and the surface chemistry of pore walls. All membranes have an inherent tradeoff between membrane permeability (i.e., how fast molecules pass through a membrane material) and selectivity (i.e., to what extent the desired molecules are separated from the rest). For size-sieving based membrane filtration, pore size distribution directly determines the rejection rate of solutes present in a feed solution and thus membrane selectivity. To completely separate a mixture of solutes, membrane pores must be smaller than the smallest solute that is to be retained, and larger than the solutes to separate. Currently, the dominant technology for nano-filtration (pore size < 1 nm) and ultrafiltration (1 nm < pore size < 100 nm) is based on polymeric membranes made by phase inversion. Such membranes suffer from poor selectivity due to irregular pore openings and tortuous pore structure through the membrane. Such ill-defined pore structures impair both selectivity and fouling properties, causing a performance drop over the membrane's lifetime (Banerjee et al., 2010, Rana et al., 2010, Krishna et al., 2008). Surface modification with hydrophilic polymers (i.e. polyethylene-glycol (PEG) and zwitterion containing copolymers) onto polymer membranes have played an important role in improving membrane fouling performance (Li et al., 2015). Membrane fouling solutions remain urgently needed and are highly sought after. Despite their poor selectivity and fouling tendencies, polymeric membranes continue to dominate the market due to low material and manufacturing cost.

1.2 Self-assembled Isoporous Membranes

Block copolymers (BCPs) consist of two chemically distinct polymers that are covalently linked at one end. The unfavorable block-block interactions in tandem with the inherent, due to long-chain nature of the BCPs, entropic factor results in the separation of blocks into highly uniform microdomains with the size scale ranging from a few to tens of nanometers depending on the chain lengths used (Bates et al. 1990, Bates et al. 2017). The unique capability of BCPs to self-assemble into uniform microdomains has spurred researchers to investigate the possibility to use them in membrane filtration (Jackson et al., 2010, Xu et al., 2003, Yang et al., 2006). Two routes have been used to incorporate the ordered BCP domains into porous membranes. The composite BCP membrane approach involves-a composite membrane consisting of an isoporous BCP membrane layer (>80 nm) which serves as a sieve sits on top of a thick layer (~100 μm) of macroporous material serving as mechanical support (Yang et al. 2010). It has been demonstrated that the composite membrane shows high flux and selectivity for separating viruses from healthy cells (Yang et al., 2006, Yang et al., 2008). However, poor mechanical integrity of thin porous BCP films limits the maximum of allowable pressure for separation (2 bar) (Yang et al., 2008). In an alternative way to generate isoporous membranes, the BCP self-assembly has been combined with non-solvent phase inversion process (Peinemann et al., 2007; Wang et al., 2013). A brief description of the membrane fabrication process is as follows. After the BCP film is cast from solution, polymer concentration gradient is formed in the membrane due to solvent evaporation. The top layer of the membrane is high in polymer concentration while the bottom layer of the membrane is low in polymer concentration. Thus, the BCP chains in the top of the membrane would pass the disorder to order transition and form an ordered domain, while the BCP chains in the bottom of the membrane are still in the disordered state, which later become macroporous pores through the phase inversion.

1.3 Challenges for Isoporous Polymeric Membranes

Using the isoporous structure from BCP self-assembly is not an entirely new concept, yet through the past ten years of research the path to commercialization has yet to be realized. Two key factors limit using isoporous membranes manufactured by phase inversion. First, tight processing restrictions are required to order the top domain, which complicates the membrane manufacture process. Too short drying time results in no pore formation, while too long drying time make pores too wide. Additionally, phase inversion process is limited with respect to high molecular weight BCPs (>100 kDa) since ordered microdomains near the disorder to order transition are required while in solution. Smaller pore size (5 nm) requires lower molecular weight BCP (i.e. < 20 kDa), which do not tend to order in dilute solutions, limiting their use in the BCP based asymmetric membranes (Sutisna et al., 2016). Secondly, phase inversion of bulk BCP membranes consume large quantities of expensive block copolymers and thus are not ready for mass production despite the improvement in separation efficiency. Current homopolymer filtration membranes are based on low-cost polysulfone, polyethersulfone (PES), polyvinylidene fluoride (PVDF), and similar polymeric materials. Those commodity polymers are easy to synthesize in an industrial scale (> tons). While the cost of the block copolymer remains high.

1.4 Oil and Water Separation

The “crude oil” from the oil wells contain oil, gas, produced water and solid particulates. In the oil and gas extraction processes, the first step is to transfer this mixture to primary gravity separators to produce well defined layers of gas, oil and water. Thereafter, the separator outputs three major components: crude oil, process water (emulsion) and gas. There are many techniques for the separation of emulsions, yet all show major disadvantages. Membrane filtration is one of the best methods for large-scale separation of oily wastewaters. Their use in industry is encouraged due to many processing factors, such as simplicity washing, recyclability of throughput material in cross-flow membrane assemblies, and highly pure permeate. There is a significant difference in membrane properties depending on their surface properties. Thus, hydrophobic and hydrophilic membranes are prepared in various ways to provide better fouling resistance.

There are four membrane separation processes in water and wastewater treatment, namely, microfiltration (MF), ultrafiltration (UF), nano-filtration (NF), and reverse osmosis (RO). Based on membrane structure and function they can additionally be divided into a) Symmetric (MF/UF), b) Asymmetric (MF/UF), c) Thin film composite (RO/NF), and d) Skinned (MF/UF) (Nunes, 2006; Strathmann, 2001). Of specific interest in this study is the multilayer composite or thin film membrane and its typical structure. The composite membrane consists of very thin top filtration layer with a thickness typically less than 100 nm sitting on a top of porous support and backing polymer layer or layers. By having such structure, one can have the best of both worlds for flux, selectivity and cost.

1.5 Knowledge Gap and Advantage of our Approach

Non-solvent induced phase separation (NIPS) is the predominate method of manufacturing membranes, producing a thick network of interconnected pores (Peinemann et al., 2007). Selectivity and permeability of NIPS membranes are acceptable, but the reason this manufacturing method has been so widely adopted is that it is inexpensive, and these membranes can be produced substantially cheaper than better performing membranes. Block copolymer (BCP) membranes have been studied for years due to their ability to phase separate into highly regular pores and have been shown to have increased permeability and selectivity compared with NIPS membranes (Abetz, 2014, Nunes, 2016). Sadly, block-copolymer synthesis cost has been hindering the marketability of such membranes. Our work bridges the technological gap, i.e., superior block copolymer-based membranes can be made in a manner that their cost will become comparable with that of traditional NIPS membranes.

2 Methodology and Results

2.1 Membrane Preparation Methods

Various annealing methods were tested to fabricate a range of BCP membranes for oil-water separation in this work. Cold zone annealing (CZA), a dynamic and roll-to-roll compatible method for continuous membrane production, and UV etching were chiefly selected to synthesize BCP membranes. Asymmetric membranes comprised of a 100 nm thick nanoporous selective thin film layer with vertically oriented nano-pores, and templated by block copolymer self-assembly. A conventional PES microfiltration membrane provides mechanical support. In one piece of work, we used the CZA technique to fabricate thin-film membranes based on the PS-b-PMMA (57k-b-25k) block copolymer system. The BCP samples were mixed with different percentages of the PMMA (25 kDa) homopolymer. PMMA was able to swell only the PMMA blocks in the BCP and therefore help to achieve higher extents of phase separation between the two blocks. This method enabled us to control the cylinder size, therefore the pore size, by blending different percent of the homopolymers with a great degree of tune ability as shown in Figure 1. The membranes obtained have a thickness of around 100 nm and fabricated using zone annealing at 210°C with a speed of 10 µm/s.

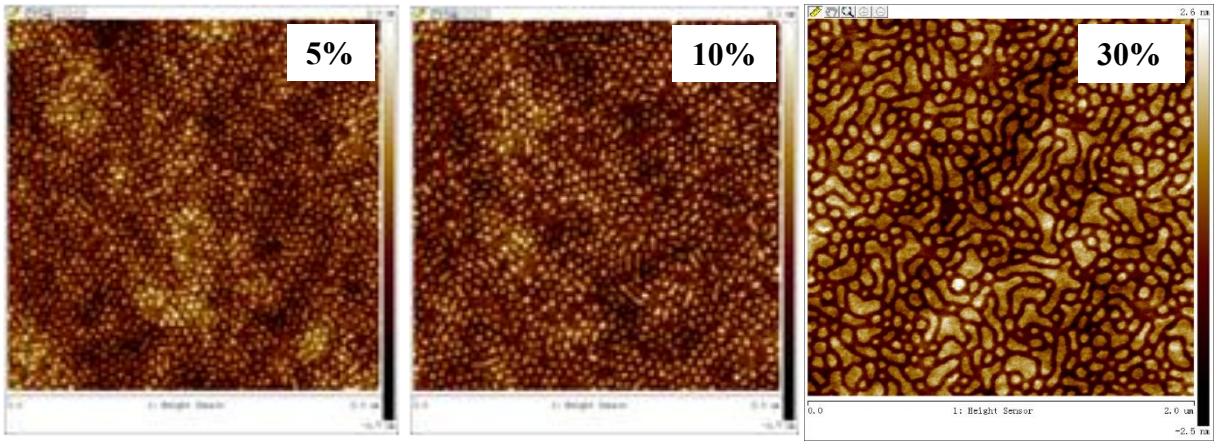


Fig. 1: Membranes based on PS-b-PMMA (57k-b-25k) swollen with different percentage of the PMMA homopolymer (25 kDa)

2.2 Membrane Filtration Efficiency

A bench scale setup incorporating an Amicon Ultrafiltration stirred cell (50 mL capacity, membrane diameter of 44.5 mm, actual filtration area 13.5 cm^2) was applied for testing flat sheet BCP membranes at pressures ranging from 1 to 5 bar. The filtration cell was placed on a magnetic stirring plate to ensure homogeneity of the produced water feed. The filtered water was collected in a glass beaker placed on a digital balance to weigh the permeate. The membrane water flux was then monitored.

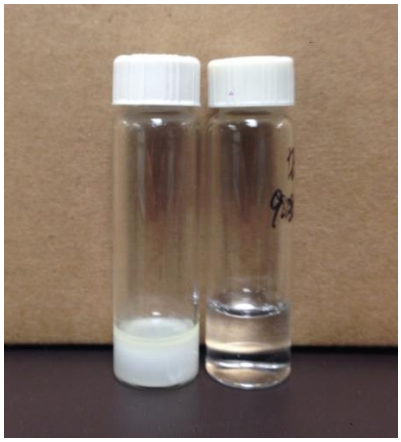


Fig. 2: Oil/water separation performance exhibited by fabricated BCP membranes

3 Conclusion

A wide range of nano-porous BCP membranes were synthesized and tested for effective separation of oil from produced water in this project. Various solvent annealing processes were assessed for directing self-assembly on BCP layer fabrication on conventional microfiltration membranes serving as a support layer. BCP membrane are being tested for their oil-water separation performance with promising results. Well-ordered BCP membranes displays high potential for upscaling and subsequent application in large scale produced water treatment.

Acknowledgement

This project was made possible by NPRP grants # NPRP12S-0306-190247 and NPRP10-0127-170269 from the Qatar National Research Fund (a member of Qatar Foundation). The statements made herein are solely the responsibility of the authors.

References

Abetz, V. *Macromolecular Rapid Communications* 2014, *36*(1), 10–22.

Banerjee, I., Pangule, R. C. & Kane, R. S. (2010). *Adv. Mater*, *23*(6), 690–718.

Bates, F. S. & Fredrickson, G. H. (1990). *Annu. Rev. Phys. Chem.*, *41* (1), 525–557.

Bates, C. M. & Bates, F. S. (2017). *Macromolecules*, *50*(1), 3–22.

Jackson, E. A. & Hillmyer, M. A. (2010). *ACS Nano*, *4*(7), 3548–3553.

Krishnan, S., Weinman, C. J. & Ober, C. K. (2008). *J. Mater. Chem*, *18*(29), 3405–3409.

Li, et al. (2015). *J. Appl. Polym. Sci.* 2015, *132*(21), n/a–n/a.

Nunes, S. P. & Peinemann, K. V. (2006). *Membrane Technology*; Nunes, S. P., Peinemann, K.-V., Eds.; John Wiley & Sons: Weinheim, FRG.

Nunes, S. P. (2016). *Macromolecules*, *49* (8), 2905–2916.

Peinemann, K. V., Abetz, V. & Simon, P. F. W. (2007). *Nat Mater*, *6*(12), 992–996. NPRP12S-0306-190247.

Rana, D. & Matsuura, T. (2010). *Chem. Rev.*, *110*(4), 2448–2471.

Strathmann, H. (2001). *AIChE J.*, *47*(5), 1077–1087.

Sutisna, et al. (2016). *Molecular Systems Design & Engineering*, *1*, 278–289.

Wang, D. M. & Lai, J. Y. (2013). *Current Opinion in Chemical Engineering*, *2*(2), 229–237.

Xu, et al. (2003). *Adv. Funct. Mater.*, *13*(9), 698–702.

Yang, et al. (2006). *Adv. Mater. 18*(6), 709–712.

___. (2008). *Adv. Funct. Mater.*, *18*(9), 1371–1377.

___. (2010). *ACS Nano*, *4*(7), 3817–3822.

Cite as: Hassan M., Shaikh S., Zagho M., Nasser M., Gu X., Nazarenko S., & Karim A., "Advanced Block Copolymer Membranes for Oily Industrial Wastewater Treatment", *The 2nd International Conference on Civil Infrastructure and Construction (CIC 2023)*, Doha, Qatar, 5-8 February 2023, DOI: https://doi.org/10.29117/cic.2023.0175

Rainfall Change Projections under Different Climate Change Scenarios in UAE

Muamer Abuzwidah
University of Sharjah,Sharjah, United Arab Emirates
mabuzwidah@sharjah.ac.ae

Ahmed Elawady
University of Sharjah,Sharjah, United Arab Emirates
u19104273@sharjah.ac.ae

Waleed Zeiada
University of Sharjah,Sharjah, United Arab Emirates
wzeiada@sharjah.ac.ae

Tala Abushukair
Ministry of Energy & Infrastructure,United Arab Emirates
tala.abushukair@moei.gov.ae

Rafeeah Al Ali
Ministry of Energy & Infrastructure,United Arab Emirates
Rafeeah.AlAli@moei.gov.ae

Soughah Al Samahi
Ministry of Energy & Infrastructure,United Arab Emirates
Soughah.AlSamahi@moei.gov.ae

Habiba Aflatoon
Ministry of Energy & Infrastructure,United Arab Emirates
Habiba.Aflatoon@moei.gov.ae

Abstract

The increase of greenhouse gases in the atmosphere due to human activities is predicted to have significant and lasting effects on the global climate throughout the 21st century. The resulting warming over the past decades has caused various hydrologic and landscape reactions, which may continue and accelerate without proper strategies to reduce greenhouse gas emissions. Climate changes due to greenhouse gases have been observed across the world, including in the United Arab Emirates (UAE) and the Arabian Gulf region. Changes in precipitation patterns can have severe consequences for natural and human systems as precipitation is a crucial part of the hydrological cycle. As the UAE is highly susceptible to climate change, it is necessary to investigate potential local impacts in-depth to develop sustainable adaptation strategies. This study assesses the future changes in precipitation patterns in the UAE under different climate change scenarios, using statistically downscaled results from global climate models (GCMs) and considering two representative concentration pathways (RCPs): RCP4.5 and RCP8.5. The study period ranges from 2021 to 2100 and compares it to the observed historical period of 1982 to 2011. The analysis examines precipitation changes at monthly and annual scales. Based on selected GCMs under the two RCPs, the average annual rainfall in the UAE is expected to change by -61% to 88%. This study emphasizes the importance of assessing potential impacts of climate change on precipitation patterns in vulnerable regions such as the UAE and the need to develop adaptation strategies to mitigate these potential impacts.

Keywords: Climate change; Precipitation; Projection; Climate models; Downscaling; RCP

1 Introduction

The 21st century is projected to witness significant, persistent shifts in the climate globally because of the substantial increases in atmospheric greenhouse gas concentrations attributable to human activities. Observations indicate that warming has already persisted for several decades, accompanied by diverse hydrologic and landscape responses, which are predicted to escalate unless greenhouse-gas emissions are effectively reduced or reversed. Climate change projection is subject to considerable uncertainty; Despite the fact that forecasting the future impact of climate change is a complex challenge, modern numerical models of the global climate can provide useful predictions to help determine potential vulnerabilities in sediment, nutrient, hydrologic and systems (Costa-Cabral et al., 2013; Samuels et al., 2010). Considering the growing apprehension regarding impending climate change, evaluations of regional and local resource systems are being conducted across the globe. In response, assessment policies and scenarios have been developed and are being employed for preliminary evaluations (Dixon et al., 2016; Gebrechorkos et al., 2019a, 2019b).

In recent decades, global climate change has had widespread effects on both natural and human systems, affecting regions across all continents and oceans (Stocker, 2014). The United Arab Emirates (UAE) and the surrounding Arabian Gulf region have also been impacted by climate change, given the country's large coastal area, numerous islands, and rapid economic growth resulting in significant urban development. The UAE is particularly vulnerable to climate change given its susceptibility to abnormal rainfall events, rising population, and changes in atmospheric CO2 and temperature.

It is anticipated that climate change will have significant effects on global precipitation patterns, resulting in both increases and decreases in rainfall across different regions. The degree of warming experienced by the Earth is a primary determinant of future precipitation patterns. Increased atmospheric temperature can hold more moisture, potentially leading to enhanced rainfall in certain areas. Conversely, in other areas, increased evaporation due to warming can lead to a decrease in precipitation. Additionally, changes in atmospheric circulation patterns, specifically in the strength and position of the jet stream, are also important factors affecting precipitation. Climate models are utilized to predict precipitation changes under varying climate scenarios, accounting for the factors mentioned above as well as other factors such as aerosol emissions and land use modifications.

Industries have been assessed for their potential susceptibility to climate change utilizing General Circulation Models (GCMs). GCMs are typically employed to predict future climates using energy and mass balance equations (Adhikari et al., 2015; Chiew et al., 2009) , and their effectiveness in accurately describing physical processes in the climate system such as the, ocean land , and atmosphere is well-established (Cooper et al., 2008). Yet, the limited resolution of current GCMs impedes their ability to factor in local features like topography and convective clouds, potentially compromising the accuracy of projections (Donat et al., 2016).

In order to investigate weather dynamics regionally and locally, global models are often downscaled using dynamical downscaling methods. This process involves using a set of coarse-resolution large-scale meteorological fields, typically derived from a GCM or global reanalysis data, to provide the preliminary, lateral, and surface boundary conditions for a regional climate model. Various approaches are used for dynamical downscaling, including GCM anomaly smoothing and interpolation, statistical modelling, machine learning, and regional dynamical climate modelling, which vary in terms of precision, resolution of the output, processing demands, and scientific resilience (Rummukainen, 2010; Tabor & Williams, 2010). The two most commonly used methods for downscaling GCMs for climate change impact research

are dynamic and statistical downscaling. Bias-correction, on the other hand, involves applying statistical techniques to improve the realism and spatial resolution of climate model outputs, especially when high-resolution observations are available (Ehret et al., 2012; Hawkins et al., 2013).

Several studies have utilized GCMs to generate future climate projections under different GHG emission scenarios. For instance, Alexander and Arblaster utilized the CMIP5 models to evaluate the impacts of projected precipitation and temperature extremes in Australia (Alexander & Arblaster, 2017). They discovered that cold temperature extremes would decrease significantly while warm temperature extremes would increase significantly by the end of the century. They also found that that dry periods are projected to increase while the frequency of the most severe precipitation extremes is expected to significantly rise. Similarly, Ishida et al. investigated the impact of climate change on precipitation at the watershed scale, utilizing dynamically downscaled CMIP5 future climate projections for Northern California. However, their analysis found no major trend in the yearly accumulated precipitation amount (Ishida et al., 2017). Meanwhile, Hussain et al. (2017) projected future precipitation and air temperature values in Sarawak, Malaysia, based on CMIP5 scenarios, and projected that by 2100, the lowest air temperature would increase by 0.83°C to 2.08°C, maximum air temperatures would rise by 0.78°C to 0.94°C, and precipitation would increase by 4.5% to 10.5%, depending on the scenario (Hussain et al., 2017). Wambura et al. (2014) conducted an investigation of climate change for Tanzania utilizing 20 GCMs and the CMIP5-established RCP 8.5. Their findings indicate that temperatures are expected to rise by 0.9°C, while there will be an increase in rainfall, particularly during the month of April (Wambura et al., 2014).

However, to the best of our understanding, no research has projected future precipitation for the United Arab Emirates (UAE). Additionally, no UAE climate estimates have been produced using CMIP5, the most recent GCM platform used by the Intergovernmental Panel on Climate Change (IPCC). To address this gap, this study employs a multi-ensemble CMIP5 GCMs to provide monthly rainfall estimates for the near (2020–2050) and far (2051-2100) futures in the UAE. A trend analysis is then carried out to identify patterns in projected future precipitation for the UAE. The objective of this research is to contribute to future climate change impact studies in the UAE and to assist policymakers in developing climate change adaptation policies.

2 Study Area

UAE is located at the eastern end of the Arabian Peninsula between 22°50′ and 26° north latitude and between 51° and 56°25’ east longitude with an area coverage of 83,600 km2. The coastline of UAE spans roughly 1,318 kilometers along the Persian Gulf and the Gulf of Oman. Along the southern coast of the Persian Gulf are several saltpans that extend deep into the inland. UAE is primarily an arid area with enormous sand deserts, but it also contains sand dunes, oasis, rock mountains, valleys, marshes, mangroves, and salt plains. The majority of oasis are found in the emirate of Abu Dhabi, which is dominated by date palms. It is mainly located in a hot, arid environment with average temperatures between 26°C to 33.5°C. The UAE's rainy season normally runs from December to March, with average annual precipitation ranging from 140 to 200 millimeters and mountainous regions receiving up to 350 millimeters. The UAE is also susceptible to strong dust storms, known locally as shamal winds.

3 Methodology

3.1 Data Collection and Preparation

As shown in Figure 1, this research utilized 35 years (1985-2020) of precipitation data from 21 weather stations in different climate zones in the UAE. The data were obtained from the National Meteorology

Centre (NMC) and were collected in an appropriate format for further analysis. The completeness, accuracy, and representativeness of the data were evaluated to ensure their reliability in the study. The Normal Ratio Approach and Inverse Distance Method were employed to complete missing data.

The data utilized in this study were gathered from various weather locations situated throughout the United Arab Emirates (UAE). Furthermore, the future GCMs datasets were procured from the CMIP5 platform, which is accessible through the Earth System Grid Federation (https://esgf-node.llnl.gov/search/esgf-llnl/). The study includes three distinct scenario periods: historical, near future (2021-2050), and far future (2050-2100). Each GCM generates data for four representative concentration pathways (RCPs) scenarios, which were developed in the CMIP5 project. The RCPs in question include RCP2.6, RCP4.5, RCP6, and RCP8.5 where RCP2.6 represents the scenario with the lowest GHG emissions, while RCP8.5 indicates the scenario with the highest greenhouse gas emissions. In this study, a multi-model ensemble comprising 19 GCM models was employed. The precipitation scenarios of the selected models under two RCPs, namely RCP 4.5 and RCP 8.5, were utilized.

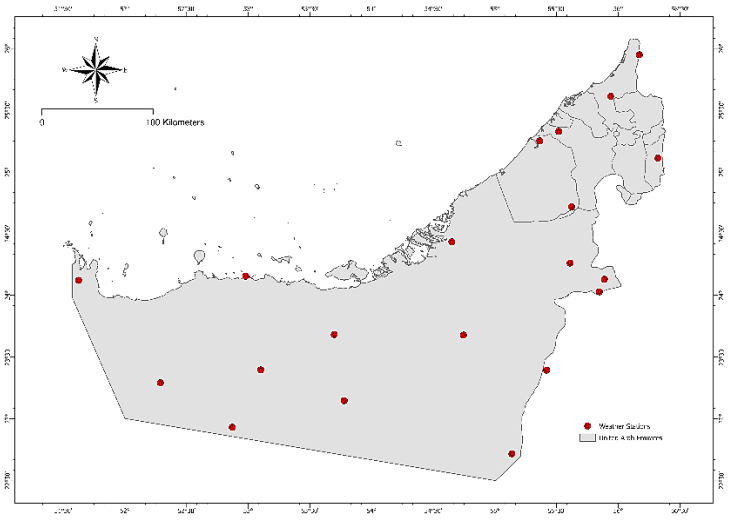


Fig. 1: Distribution of the weather stations in UAE

3.2 Bias Correction

The climate models have data that is available as a function of latitude and longitude along predetermined grid lines to cover every area on Earth. Scaling down data for UAE weather stations required interpolation or extrapolation for each model. Interpolation is the process of predicting data from a dataset using the available data. Extrapolation is the process of making predictions that go beyond the data set. Three different forms of interpolation are used to clarify the precise rainfall or temperature for each area in accordance with the station's placement within the grids of each model. When a station was between two points, interpolation between those two points was needed, and when it was in the middle of a square between four points, interpolation between those four points was required. In this study, bias correction using delta approach was used. The delta change approach is a technique that makes the output of GCMs usable for hydrological modelling and watershed scale study (which means that the GCM outputs are used indirectly). The average monthly precipitation and temperature are determined based on 35 years of records (1985 to 2020) is used to calculate the delta correction factors in this study. All data from various RCPs (RCP 4.5 and RCP 8.5) are corrected using delta approach. The delta factor can be calculated using the following equation:

$$\Delta\, month\ i = \frac{\text{Future average monthly precipitation for month i (from model used)}}{\text{Historical average monthly precipitation for month i (from a model used)}} \quad (1)$$

3.3 Trend Analysis

The examination of trends in climatological data records at selected stations is a critical component of climate change research. To unveil trends, unfiltered data is subjected to analysis using a simple linear regression method. However, it is worth noting that the authentic trend may not manifest as a linear relationship and could be obscured by the data's noise. In the present study, the precipitation data from 20 stations were utilized to illustrate trend analysis.

4 Results and Discussion

Figure 2 presents the annual precipitation time series for the different weather zones analyzed in the investigation, which involved a comprehensive evaluation of the annual and monthly precipitation data to identify discernible trends. The results indicated a modest declining trend in annual precipitation, as evidenced by the negative slope of the regression line and a correlation coefficient of approximately 0.3.

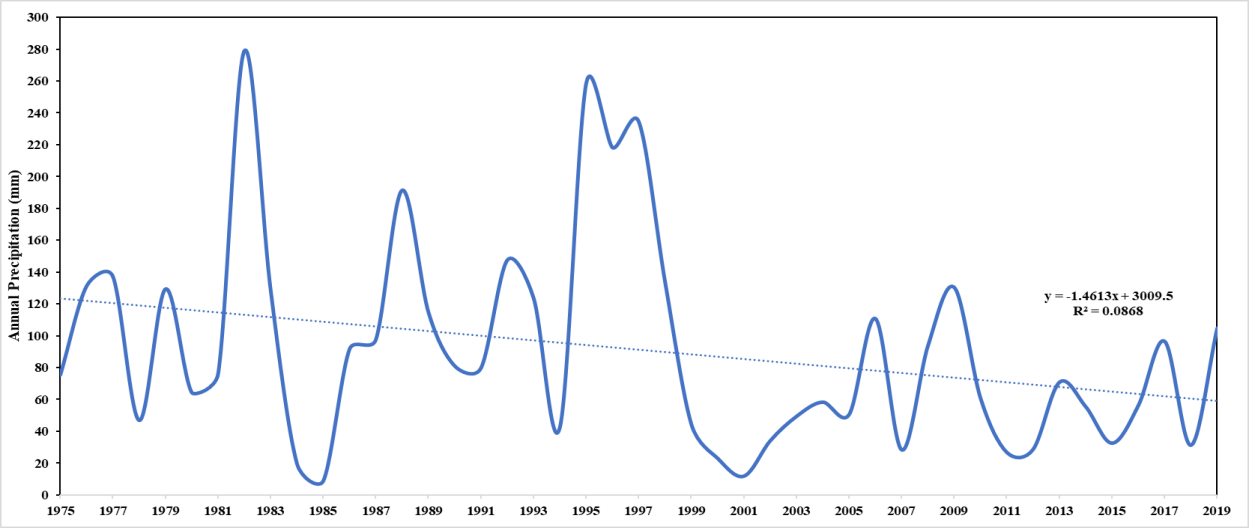
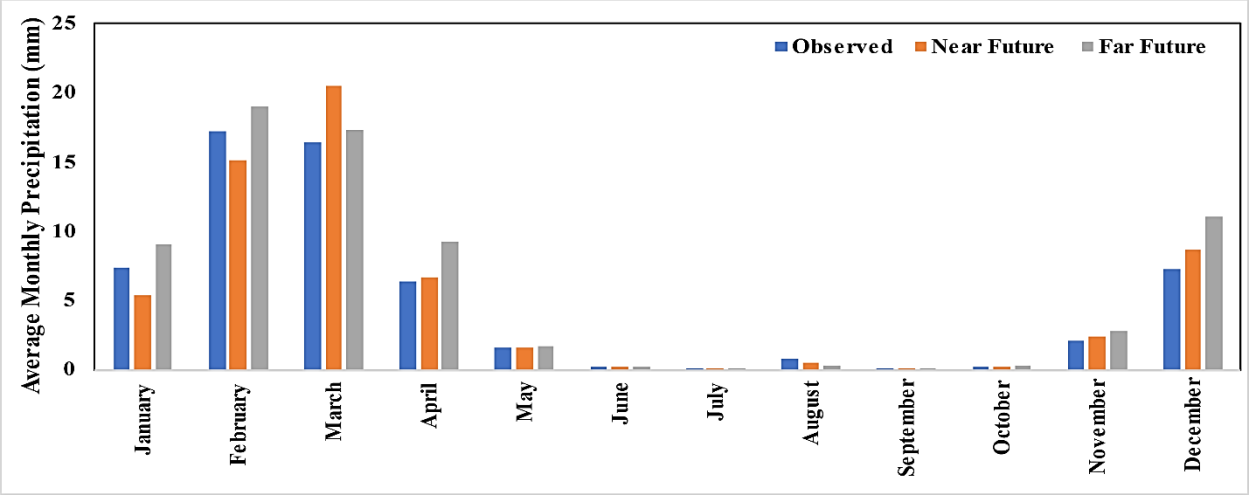


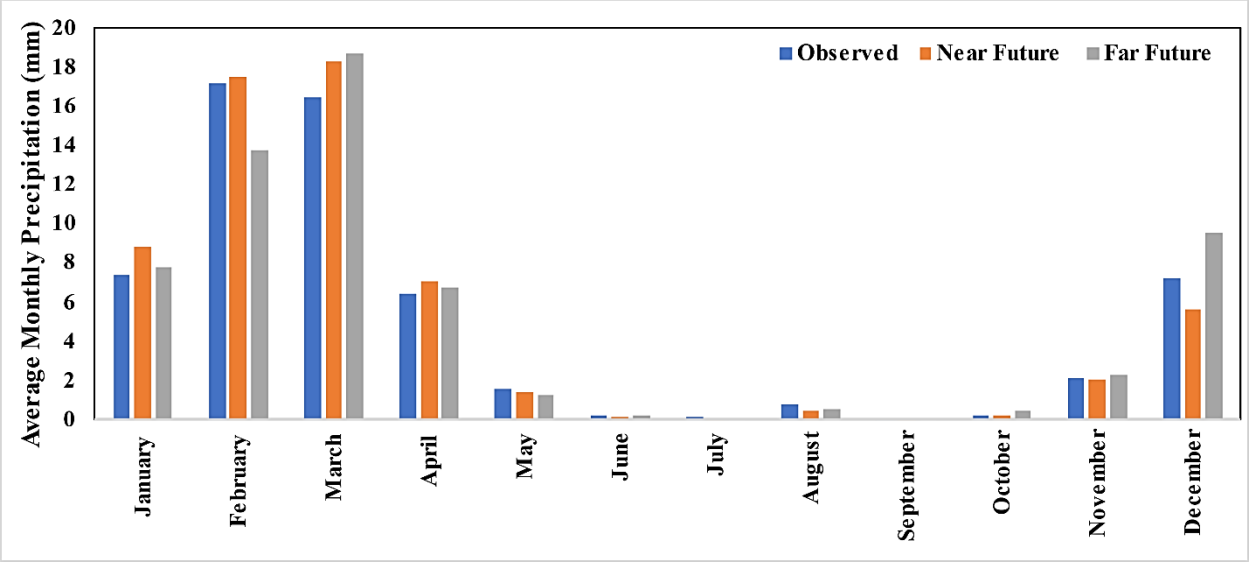
Fig. 2: Historical Annual Precipitation

Fig. 3 shows the average monthly precipitation for the near and far futures under RCP 4.5 and RCP 8.5 scenarios for UAE, respectively. There will be mainly a decrease in precipitation in almost all the months except for March, April, and December in the near future compared to the observed precipitation for RCP 4.5. However, all the months have an increase in precipitation except for July and August. In general, there will be a change in precipitation from -30% to 25% and -61% to 52% depend on the month in near and future, respectively, for RCP 4.5. Moreover, precipitation is expected to decrease in the near future for RCP 8.5 compared to the observed precipitation in almost all months except winter months (from January to April). On the other hand, the far future RCP 8.5 demonstrated mixed results where half of the months showed an increase (January, March, April, June, October, November, and December) and the other half had a decrease. Precipitation changes are expected to range from -41% to 20% and -34% to 88% depending on the month in the near future and the far future for RCP 8.5, respectively. Overall, Highest average precipitation value for RCP 4.5 and RCP 8.5 are 20.5 mm (March) and 18.3 mm (March), respectively, for the near future. In the far future, the highest values are 19 mm (February) and 18.7 mm (March) for RCP 4.5 and RCP 8.5, respectively. **Fig. 4** and **Fig. 5** show the heat maps for change in precipitation every 10 years for RCP 4.5 and RCP 8.5, respectively.

The study reports that under the RCP 4.5 scenario, the UAE is expected to experience a decrease in precipitation in most months of the year, except for March, April, and December, in the near future. On the other hand, all months are expected to see an increase in precipitation except for July and August. Similarly, under the RCP 8.5 scenario, the UAE is expected to experience a decrease in precipitation in most months, except for the winter months (from January to April) in the near and far future. In contrast, the future RCP 8.5 scenario demonstrated mixed results where half of the months showed an increase, and the other half had a decrease in precipitation.



(a)



(b)

Fig. 3: Precipitation for UAE for the near and far futures under **(a)** RCP 4.5 and **(b)** RCP 8.5 scenarios

Under scenario RCP 4.5, the potential change in precipitation varies from less than -1.23 mm to about 0.62 mm between 2020 and 2050, whereas the potential change in precipitation varies from –1.62 mm to 1.54 mm between 2051 and 2100. Under scenario RCP 8.5, the possible precipitation varies from less than -0.57 mm to about 0.42 mm between 2020 and 2050, whereas the potential precipitation changes ranges from -1.17 mm to 0.97 mm between 2051 and 2100.

The potential changes in precipitation between 2020 and 2050 are relatively small compared to the

changes expected between 2051 and 2100. This suggests that the changes in precipitation patterns will become more pronounced as we move further into the future, and the impact of climate change on precipitation patterns in the UAE will be more significant in the long term. It is also interesting to note that the range of potential changes in precipitation is broader under the RCP 8.5 scenario than under the RCP 4.5 scenario. This is likely because the RCP 8.5 scenario represents a more severe emissions scenario than the RCP 4.5 scenario, leading to more significant changes in climate variables such as precipitation.

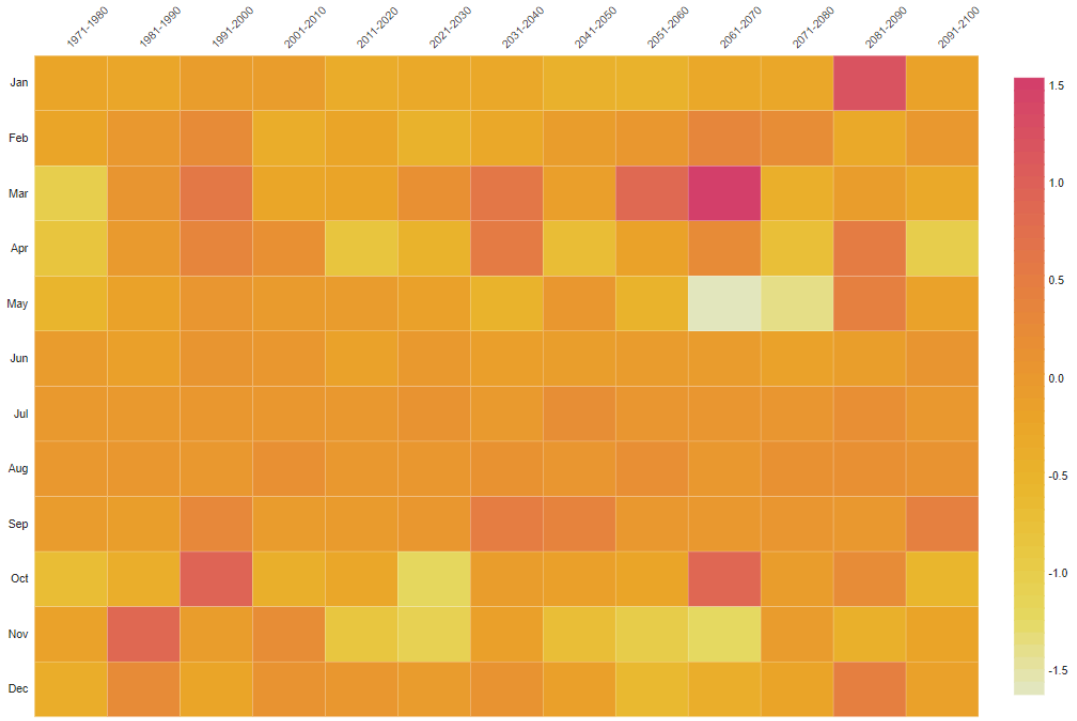


Fig. 4: Projected precipitation anomaly under RCP 4.5

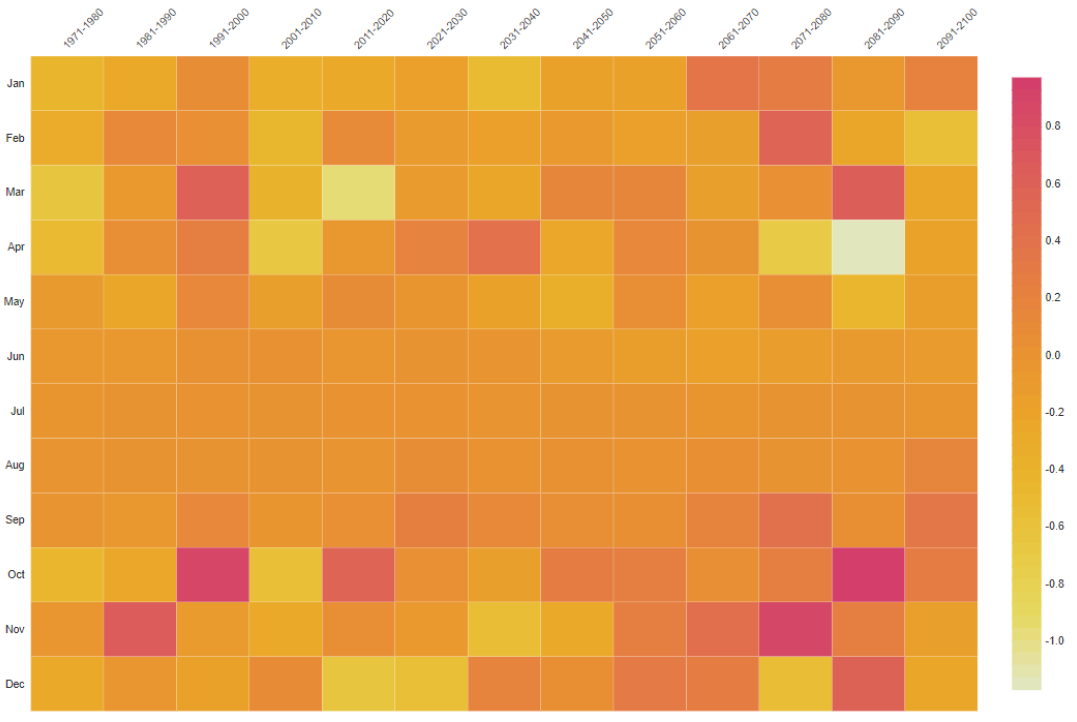


Fig. 5: Projected precipitation anomaly under RCP 8.5

5 Conclusion

In this research, a combination of 19 GCM models were utilized to produce future precipitation projections at 20 meteorological stations in UAE under RCP 4.5 and RCP 8.5 scenarios for both near and far future periods. The principal findings of this study were that the UAE has experienced a reduction in precipitation over the years, according to historical data. Furthermore, based on the GCM models and RCPs selected, it is anticipated that average annual precipitation in the UAE will vary between-61% and 88% by the end of the century. Analyses also revealed that the most significant decreases in precipitation occurred in January and February for RCP 4.5 and RCP 8.5, respectively, while the greatest increases were observed in March and October under the respective RCPs. This research suggests that the UAE is likely to continue experiencing a decline in precipitation, similar to other climate change studies conducted in the region. Given the UAE's location in a water-scarce region, continued drought could have severe consequences for the country. As such, it is crucial to conduct impact assessments of climate change using the projected precipitation values from this study, as well as those from other climate change projection studies in the UAE, and to develop and implement adaptation policies based on the results of hydrological impact studies.

References

Adhikari, U., Nejadhashemi, A. P. & Woznicki, S. A. (2015). *Climate change and eastern Africa: a review of impact on major crops. Food Energy Secur 4:* 110–132.

Alexander, L. V & Arblaster, J. M. (2017). Historical and projected trends in temperature and precipitation extremes in Australia in observations and CMIP5. *Weather and Climate Extremes*, *15*, 34–56.

Chiew, et al. (2009). Estimating climate change impact on runoff across southeast Australia: Method, results, and implications of the modeling method. *Water Resources Research*, *45*(10).

Cooper, et al. (2008). Coping better with current climatic variability in the rain-fed farming systems of sub-Saharan Africa: An essential first step in adapting to future climate change? *Agriculture, Ecosystems & Environment*, *126*(1–2), 24–35.

Costa-Cabral, M.et al. (2013). Climate variability and change in mountain environments: some implications for water resources and water quality in the Sierra Nevada (USA). *Climatic Change*, *116*(1), 1–14.

Dixon, et al. (2016). Evaluating the stationarity assumption in statistically downscaled climate projections: is past performance an indicator of future results? *Climatic Change*, *135*(3), 395–408.

Donat, et al. (2016). More extreme precipitation in the world's dry and wet regions. *Nature Climate Change*, *6*(5), 508–513.

Ehret, et al. (2012). HESS Opinions" Should we apply bias correction to global and regional climate model data?". *Hydrology and Earth System Sciences*, *16*(9), 3391–3404.

Gebrechorkos, S. H., Hülsmann, S. & Bernhofer, C. (2019a). Changes in temperature and precipitation extremes in Ethiopia, Kenya, and Tanzania. *International Journal of Climatology*, *39*(1), 18–30.

Gebrechorkos, S. H., Hülsmann, S. & Bernhofer, C. (2019b). Statistically downscaled climate dataset for East Africa. *Scientific Data*, *6*(1), 1–8.

Hawkins, et al. (2013). Calibration and bias correction of climate projections for crop modelling: an idealised case study over Europe. *Agricultural and Forest Meteorology*, *170*, 19–31.

Hussain, et al. (2017). Projected changes in temperature and precipitation in Sarawak state of Malaysia for selected CMIP5 climate scenarios. *International Journal of Sustainable Development and Planning*, *12*(8), 1299–1311.

Ishida, et al. (2017). Trend analysis of watershed-scale precipitation over Northern California by means of dynamically-downscaled CMIP5 future climate projections. *Science of the Total Environment*, *592*, 12–24.

Rummukainen, M. (2010). State-of-the-art with regional climate models. *Wiley Interdisciplinary Reviews: Climate Change*, *1*(1), 82–96.

Samuels, et al. (2010). Climate change impacts on Jordan River flow: downscaling application from a regional climate model. *Journal of Hydrometeorology*, *11*(4), 860–879.

Stocker, T. (2014). *Climate change 2013: the physical science basis: Working Group I contribution to the Fifth assessment report of the Intergovernmental Panel on Climate Change*. Cambridge university press.

Tabor, K. & Williams, J. W. (2010). Globally downscaled climate projections for assessing the conservation impacts of climate change. *Ecological Applications*, *20*(2), 554–565.

Wambura, et al. (2014). *Tanzania CMIP5 climate change projections*.

Cite as: Abuzwidah M., Elawady A., Zeiada W., Abushukair T., Al Ali R., Al Samahi S. & Aflatoon H., "Rainfall Change Projections under Different Climate Change Scenarios in the UAE", *The 2nd International Conference on Civil Infrastructure and Construction (CIC 2023)*, Doha, Qatar, 5-8 February 2023, DOI: https://doi.org/10.29117/cic.2023.0176

Retention of Hydrophobic Colloids in Unsaturated Porous Media using Microfluidics

Jamal Hannun
PhD Candidate, Department of Civil and Architectural Engineering, Qatar University, Doha, Qatar
jh1300283@qu.edu.qa

Riyadh Al-Raoush
Professor, Department of Civil and Architectural Engineering, Qatar University, Doha, Qatar
riyadh@qu.edu.qa

Abstract

Water recharge wells can provide a solution for 3.5 billion people, living in regions suffering from water scarcity. Due to fines migration, freshwater wells that are used to recharge aquifers, often experience expedited deterioration. Colloidal clay fine particles can be mobilized from within aquifers due to hydrodynamic forces or the sweeping of gas-water interface (GWI). The released colloids concentration increases then starts to retain and clog at the pores within the aquifer formation. Although fines migration is responsible for decommissioning many recharge wells, yet there is a lack of pore scale observations that uncover clogging mechanisms within porous media. Thus, this study utilizes wide-field optical macroscopy and microfluidic models with pore morphology of sandstone, to investigate the clogging mechanisms of hydrophobic colloids. The aim is to discover how interfacial surfaces within porous media retain colloids. Hence imbibition and drainage of colloidal suspension were carried to vary water saturation. Flow experiments were imaged at a resolution of 1µm/pixel, while colloids diameter was 5 µm. Images were segmented into solid, water, gas and colloids. Then the amount of colloids retained on each interface was quantified. Findings revealed that hydrophobic colloids retained mainly on the GWI. For colloids suspension in deionized water, affinity of colloids to GWI was high enough to cause bubble stabilization. In both hydrophobic and hydrophilic porous media, colloids disconnected the gas phase to create larger GWI surface. More than 90% of hydrophobic colloids were cleaned from the media after drainage, uncovering an efficient remediation technique for water aquifer.

Keywords: Fines clogging; Unsaturated Porous Media; Microfluidic; Hydrophobicity; Colloid retention

1 Introduction

Managed or artificial water recharge is the practice of using groundwater wells to pump surplus water into aquifers, to be used during water shortages, or to support overexploited aquifers (“Ground Water Recharge Using Waters of Impaired Quality,” 1994). Nearly two thirds of earth population live in regions suffering from severe water scarcity during drought periods (Mekonnen & Hoekstra, 2016). The recharge of water aquifers can provide a cost effective and a sustainable solution for this problem. Kim et al. (2021) assessed that there is a growth in the practice of collecting rainwater in order to recharge groundwater aquifers. Specially in arid regions, where rainwater is the primary renewable water source (Edmunds, 2003). This is because naturally trivial segment of rainwater reaches to groundwater aquifers (Baalousha et al., 2018). Thus, artificial

geological water recharge (AGWR) is an environmental, sustainable and an economic solution, for many water-stressed populations around the globe. AGWR can raise the recovery ratio of rainwater by 1000% (Mohieldeen et al., 2021).

However, due to fines migration, freshwater wells that are used to recharge aquifers, often experience expedited deterioration. Fines colloidal clay particles are released from within the porous media of sediments that compose the structure of aquifers, this is due to either the hydrodynamic forces, or the sweeping of gas-water interface (GWI) between the pores (Hannun et al., 2022). As the concentration of the released colloids increases within the pores, the colloids then start to retain and clog within the formation of the aquifer (Hannun et al., 2020), radially outward of an injection well, around the well formation (Jarrar et al., 2020). Even though fines migration and the subsequent clogging are responsible for the early decommissioning of many recharge wells, yet there is a lack of pore scale observations that reveal clogging mechanisms within porous media, especially during multiphase flow of gas and water. Other than groundwater recharge, progress in numerous environmental, hydrological and industrial applications is restricted, due to a knowledge gap on how the hydrophilicity of the porous media, affects retention and clogging of colloids (Wang et al., 2020).

The target of this paper is to explore the influence of hydrophilicity of porous media on colloids retention at the different interfaces within a porous media, and to connect colloids retention with different flow conditions such as drainage and imbibition. To capture the release and retention of colloids at each interface. Hence developing the ability to use microscopic images of micromodels to quantify water saturation, volume of colloids in pores and at the interfaces. With the aim to discover how interfacial surfaces within porous media retain colloids, and how the hydrophilicity of the porous media influences the distribution of colloids on interfaces.

2 Methodology

2.1 Materials Experimental Setup

Table 1 details the parameters of the microfluidic flow experiments. The two glass porous media with pore geometry of sandstone were used to compare how the media hydrophilicity will affect colloids retention on the solid collector surfaces. One chip was made of normal glass which is hydrophilic, while the other was made with glass that is coated with a hydrophobic material. The contact angle of a water droplet under atmospheric pressure was 37° for the hydrophilic chip, and 75° for the hydrophobic chip, measured from solid to air through water. The colloids used were water unfavourable polystyrene latex microspheres, which is naturally hydrophobic. Both imbibition and drainage of the colloidal suspension were carried out to vary water saturation and test how changing flow condition alters the distribution of colloids at the interfaces. The macroscope was used to collect coloured images, where the water saturation was varied to capture four steps per flow condition.

Table 1: Experimental test matrix

Property	**Parameters**	
Collector hydrophilicity	Hydrophobic (75°)	Hydrophilic (37°)
Colloids water favorability	Water unfavorable	
Flow condition	Drainage	Imbibition
Saturation steps	4 steps at each flow condition, a total of 8	

2.2 Experimental Setup

The experiment employed a widefield macroscope with microfluidic chips that resemble the pore morphology of sandstone rock samples. To study, the mechanisms of hydrophobic colloids retention and subsequent clogging (Hannun et al., 2019). The microfluidic flow experiments were captured using 5 MP images at a spatial resolution of 1µm/pixel. The sandstone media have a well-connected porous media, with pore and throat sizes ranging between 500 µm to 50 µm.

The chips are cleaned by pumping multiple pore volumes of deionized water and ethanol as per the procedure of Nishad & Al-Raoush (2021). Then a water-colloid suspension is prepared by mixing the polystyrene latex microspheres with deionized water (0.5% colloids and 99.5% water). The suspension is then sonicated to uniformly disperse the colloids after that placed into a syringe. The microspheres have a diameter of 5 µm, ten times smaller than the narrowest throat. The syringe is placed in a syringe pump and connected to one inlet of the microfluidic chip. The chip has an outlet that is open to the atmosphere. The experiment starts with the micromodel fully saturated with water-colloid suspension, then the pump actuates the syringe to force drainage and imbibition. The chips are imaged during the flow experiments to collect coloured microscopic observations.

2.3 Analysis

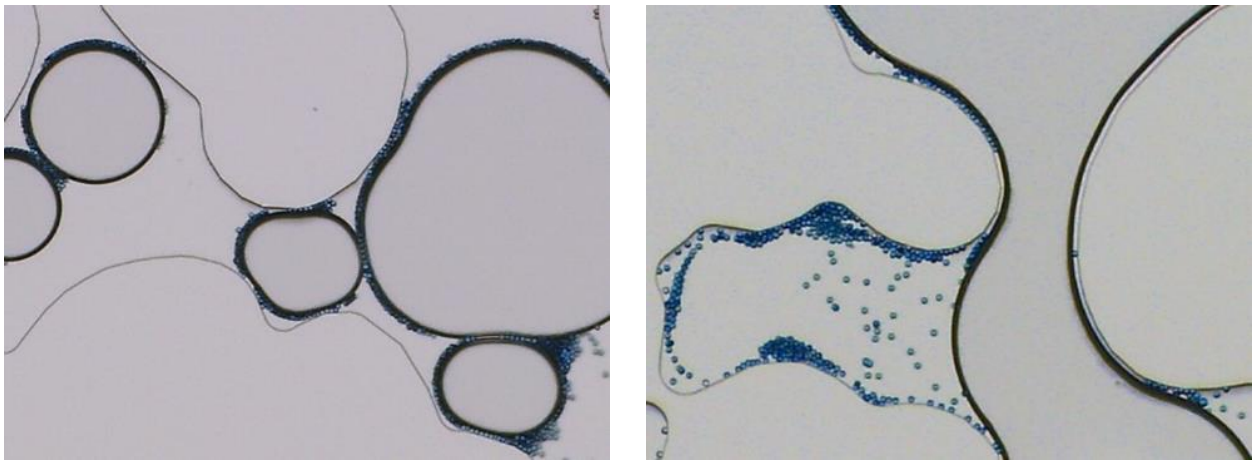
Images were segmented into gas, water, solid and colloids using computer vision algorithms (Al-Raoush et al., 2019), allowing the quantification of porosity, water saturation and colloidal fines content (Jarrar et al., 2021). Next edge detection was used to extract the interfaces of GWI, Gas-Solid interface and Water-Solid interface; permitting the measurements of each interfacial area. Then the amount of colloids retained on each interface was quantified, to study the location and quantity of colloids retention at the interfaces.

3 Results

In the hydrophilic micromodel that resembles a sandstone porous media, drainage was carried from a fully saturated media to an irreducible water saturation of 25%. Gas entered the micromodel mobilizing the colloids retained within the pores and at the solid interface, of the collector media, GWI started to sweep and retain the colloids. While the gas front progressed through the media, the colloids attached to the GWI started to disconnect the front, leaving detached bubbles throughout the media. Figure 1 (A) shows how the colloids are responsible for bubble stabilization.

In the hydrophobic micromodel, drainage was carried from full saturation to an irreducible water saturation of 18%. As gas invaded the media, colloids started to retain within the pores, at the water-solid interface and at the GWI, as shown in Figure 1 (B). Compared to hydrophilic media, colloids in hydrophobic media are more distributed over the different interfaces during drainage.

Figure 2 (I) displays a microscopic image of hydrophilic porous media during drainage, at a water saturation of 58%; the image was segmented into labels that were quantified to measure the amount of colloids retained on each interface. Figure 2 (II) demonstrates that the ratio of colloidal fines retained on the GWI to the media volume, increases with drainage up to 58% water saturation. This increase is caused by the separation of the gas front into disconnected bubbles, where the colloids expand the GWI surface area to allow for more retention. This reveals that water unfavourable colloids can be swept out of a hydrophilic porous media under drainage.

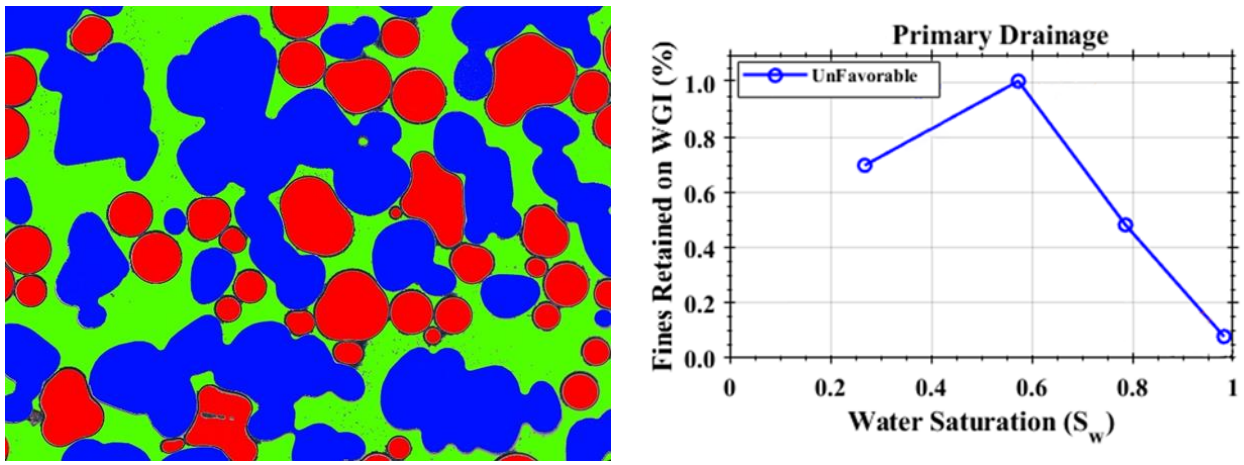


(a) **(b)**

Fig. 1: Microscopic images showing the first flow condition of air drainage, mobilizing the colloids-water suspension from the porous media, **(a)** hydrophilic collector model with water unfavourable colloids. Similarly **(b)** hydrophobic collector model with water unfavourable colloids

The second part of the experiment test the flow condition of imbibition, colloids were distributed more evenly within the pores and over the interfaces of the porous media, compared to drainage. This shows that the flow condition is responsible for generating hydrodynamic forces and an invading pattern that can change the distribution of colloids retention locations and quantities.

The breakthrough of this work is connecting quantitative measurements of colloidal fines with microscopic visual observations, of colloids retention at the interfaces within a porous media. Visual and quantitative evidence demonstrates that unfavourable colloids undergoing drainage in a hydrophilic micromodel, mainly retain on GWI causing a disconnected flow regime due to bubble stabilization.



(I) **(II)**

Fig. 2: (I) shows a segmented microscopic image of hydrophilic porous media with water unfavourable colloids, phases of gas, water, solid and colloids, are labelled as red, green, blue and grey, respectively. (II) is the measured ratio of colloidal fines retained on GWI to the volume of the porous media, versus water saturation during drainage.

4 Conclusion

Findings revealed that:

1- Hydrophobic colloids (5µm diameter latex spheres), have higher retention at the GWI, compared to other interfaces or the pores within the porous media.

2- In a deionized water medium, a suspension of hydrophobic colloids can cause bubble stabilization within the porous media, because of the high affinity of colloids toward GWI.

3- Retention of colloids at the GWI, disconnected the invading gas phase during drainage, increasing the GWI surface area, noticeably more in hydrophilic compared to hydrophobic porous media.

4- Drainage removed over 90% of hydrophobic colloids from the porous media, uncovering an efficient method for the remediation of water aquifers, which can utilize the drainage of water and air bubbles to clean a contaminated porous media within an aquifer.

5- During water imbibition, the hydrophobic colloids are distributed over all the interfaces in the porous media, unlike drainage where the majority is swept by the GWI.

References

Al-Raoush, et al. (2019). Impact of fines type on gas flow using 3D micro-computed tomography. *Society of Petroleum Engineers - SPE Kuwait Oil and Gas Show and Conference 2019, KOGS 2019*. https://doi.org/10.2118/198106-ms

Baalousha, et al. (2018). Groundwater recharge estimation and its spatial distribution in arid regions using GIS: a case study from Qatar karst aquifer. *Modeling Earth Systems and Environment*, *4*(4), 1319–1329. https://doi.org/10.1007/S40808-018-0503-4/TABLES/8

Edmunds, W. M. (2003). Renewable and non-renewable groundwater in semi-arid and arid regions. *Developments in Water Science*, *50*(C), 265–280. https://doi.org/10.1016/S0167-5648(03)80023-0

Ground Water Recharge Using Waters of Impaired Quality (1994). *Ground Water Recharge Using Waters of Impaired Quality*. https://doi.org/10.17226/4780

Hannun, et al. (2022). Fines effect on gas flow in sandy sediments using µCT and pore networks. *Journal of Natural Gas Science and Engineering*, *108*, 104834. https://doi.org/10.1016/J.JNGSE.2022.104834

Hannun, et al. (2019). *Pore Networks to Characterize Formation Damage Due to Fines at Varied Confinement and Sand Shape*. https://doi.org/10.3997/2214-4609.201903116

Hannun, et al. (2020). *Use of 3D Images to Evaluate Formation Damage Induced by Montmorillonite Fines in Porous Media Systems*. 644–648. https://doi.org/10.29117/cic.2020.0082

Jarrar, et al. (2021). New model for estimating geometric tortuosity of variably saturated porous media using 3D synchrotron microcomputed tomography imaging. *Soil Science Society of America Journal*, *85*(6), 1867–1879. https://doi.org/10.1002/saj2.20289

Jarrar, et al. (2020). 3D synchrotron computed tomography study on the influence of fines on gas driven fractures in Sandy Sediments. *Geomechanics for Energy and the Environment*, *23*, 100105. https://doi.org/10.1016/J.GETE.2018.11.001

Kim, et al. (2021). Assessment of the need and potential for groundwater artificial recharge based on the water supply, water demand, and aquifer properties in a water shortage region of South Korea. *Environmental Earth Sciences 2021 80:3*, *80*(3), 1–15. https://doi.org/10.1007/S12665-021-09445-5

Mekonnen, M. M. & Hoekstra, A. Y. (2016). Sustainability: Four billion people facing severe water scarcity. *Science Advances*, *2*(2). https://doi.org/10.1126/SCIADV.1500323/SUPPL_FILE/1500323_SM.PDF

Mohieldeen, Y. E., Elobaid, E. A. & Abdalla, R. (2021). GIS-based framework for artificial aquifer recharge to secure sustainable strategic water reserves in Qatar arid environment peninsula. *Scientific Reports 2021 11:1*, *11*(1), 1–13. https://doi.org/10.1038/s41598-021-97593-w

Nishad, S. & Al-Raoush, R. I. (2021). Colloid retention and mobilization mechanisms under different physicochemical conditions in porous media: A micromodel study. *Powder Technology*, *377*, 163–173. https://doi.org/10.1016/J.POWTEC.2020.08.086

Wang, et al. (2020). Colloid transport through soil and other porous media under transient flow conditions—A review. *Wiley Interdisciplinary Reviews: Water*, *7*(4), e1439. https://doi.org/10.1002/WAT2.1439

Cite as: Hannun J., Al-Raoush R., "Retention of Hydrophobic Colloids in Unsaturated Porous Media using Microfluidics", *The 2nd International Conference on Civil Infrastructure and Construction (CIC 2023)*, Doha, Qatar, 5-8 February 2023, DOI: https://doi.org/10.29117/cic.2023.0177

Geotechnical Challenges for Underground Infrastructure in Qatar: Hydrogeological Assessment for Dewatering and Deep Excavation Works: South of Wakrah Pumping Station and Outfall (SWPSO) Project

Enric Vázquez-Suñé
Institute of Environmental Assessment and Water Research (IDAEA/CSIC), Barcelona, Spain
enric.vazquez@idaea.csic.es

Ignacio Bulboa
Institute of Environmental Assessment and Water Research (IDAEA/CSIC), Barcelona, Spain
ic.bulboa@gmail.com

Ilayaraja Kumba Krishnamurthi
Public Works Authority (Ashghal), Doha, Qatar
ikrishnamurthi@ashghal.gov.qa

Andres E. Pinto Candia
Stantec UK Limited,Doha, Qatar
Andres.pinto@stantec.com

Abstract

The evaluation of hydrogeological conditions and groundwater inflows, as part of the geotechnical risk assessment, poses one of the key challenges during the design and construction of major infrastructure projects and underground works. This paper presents an example of a recently developed geotechnical and hydrogeological investigation program for the Pre-Tender design of the South of Wakrah Pumping Station and Outfall project in Qatar, where a comprehensive hydrogeological study was carried out to characterize heterogeneous hydrogeological conditions along the project area and to determine potential impacts on the groundwater levels drawdown and groundwater inflows during excavation and dewatering activities. The results of the hydrogeological evaluation concluded that a proper groundwater management approach and mitigation measures are required at an early stage of the project to minimize the impact on dewatering, groundwater inflows and groundwater levels drawdown for construction works. A similar approach can be adopted for future infrastructure projects to support the geotechnical risk assessment and to minimize the impact of construction activities on the environment.

Keywords: Hydrogeological assessment; Permeability; Dewatering; Deep excavations; Groundwater management

1 Introduction

In Qatar, the Vision for efficient mass transit and resilient urban drainage infrastructure, with recent rapid urbanization and extreme weather events, motivated a massive increase in the construction of underground infrastructure projects in a short span of time. Given unknown ground conditions, the pioneering tunnelling and underground projects like the Doha Metro, the Inner Doha Resewerage Implementation Strategy (IDRIS) and most recently the Doha South Terminal Pumping Station (DSTPS) and the Musaimeer Pumping Station and Outfall (MPSO) faced challenges to identify and quantify the geotechnical risks and to develop an appropriate risk mitigation approach for underground works, to guarantee the completion of the projects on time and within budget.

Although the extensive experience gained during the execution of these major infrastructure projects in Qatar has led to a better understanding of the geotechnical risks, the role of hydrogeological conditions in geotechnical risk assessment is still one of the key challenges during engineering design and construction stages. The assessment of karst environment and associated groundwater inflows and dewatering requirements for the construction of deep underground works require a considerable amount of time and resources against the tight schedules of the projects.

Thus, it is of paramount importance to carry out a detailed hydrogeological risk evaluation during the early stages of the project to minimize the impact of unknown ground and groundwater conditions. This paper presents an example of a recently developed geotechnical investigation program for the pre-tender design of the South of Wakrah Tunnels, Pumping Station and Outfall project, where a comprehensive hydrogeological study was carried out to characterize heterogeneous hydrogeological conditions along the tunnel, shafts and pumping station areas and to be able to determine potential impacts on: (1) the environment (e.g., expected groundwater levels drawdown, barrier effect and groundwater resources discharge), and (2) the project (groundwater inflows, dewatering, ground improvement requirements). As a result, we assessed the mitigation measures for the future excavation of pumping station and screening shafts and propose a groundwater management approach to support the geotechnical risk assessment and to minimize the impact of construction activities for future infrastructure projects.

2 Project Background

2.1 Ground Investigations

The South of Wakrah Pumping Station and Outfall project is one of the key capital projects in the State of Qatar, whose major goal is to provide a long-term optimum strategic drainage system for stormwater and groundwater in the catchment area. Most of the project challenges come from the construction of deep underground structures (i.e., tunnels and shafts), with variable groundwater conditions and presence of karstic deposits.

The geology of the project area comprises thin Quaternary deposits (<2m thick), followed by a sequence of horizontally layered sedimentary rocks with Simsima Limestone, Midra Shale and Rus Formations reaching the full depth of the projected civil works. The main geotechnical hazards identified for the construction of the underground works are: (i) the presence of karstification, cavities and caverns and (ii) shallow groundwater levels, presence of underground channels and potential high groundwater inflows.

Due to the large size of the underground works (i.e., pumping station of approximately 80 metres diameter and 60 metres depth and tunnel diameters ranging from 4.5 to 8.5metres ID), with the associated risks, it was required to carry out a comprehensive hydrogeological assessment to quantify the expected groundwater inflows for dewatering requirements and to evaluate the impact of potential groundwater levels drawdown during construction activities. The executed ground investigation works for the pumping station area included the drilling of 33 boreholes (60-80metres deep), together with 120 packer permeability tests and a pumping test tomography to test both shallow and deep aquifers. In addition, 12 observation wells and 6 standpipe piezometers were utilized to monitor groundwater levels during the execution of the in-situ testing program.

2.2 Geological Model

The geotechnical and hydrogeological model was prepared based on the findings of the ground

investigations program. The following general geological sequence and main description has been defined for the 3D geological model (Figure 1):

- Quaternary Deposits (QD): Superficial layers of sand fill with material as light brown silty, gravelly to very gravelly, fine to medium sand.
- Simsima Limestone (SL): In the conceptual model corresponds to the Upper aquifer, typically described as a buff to pale brown chalky crystalline limestone with siltstone inclusions, variably dolomitic.
- Midra Shale (MS): Aquitard unit, typically described as yellow-brown laminated occasionally fissile shale, fossiliferous with limonite and phosphatic nodules, with thin bands of limestone. Its lateral continuity is variable, and its thickness is considerably reduced in some areas of the domain.
- RUS Limestone (RL): Lower aquifer, cyclic deposition of weak carbonate marls, siltstones, thin limestones and chalk.
- RUS Gypsum (RG): Lower Aquifer, typically described as anhydrite and gypsum with marl and thin limestone

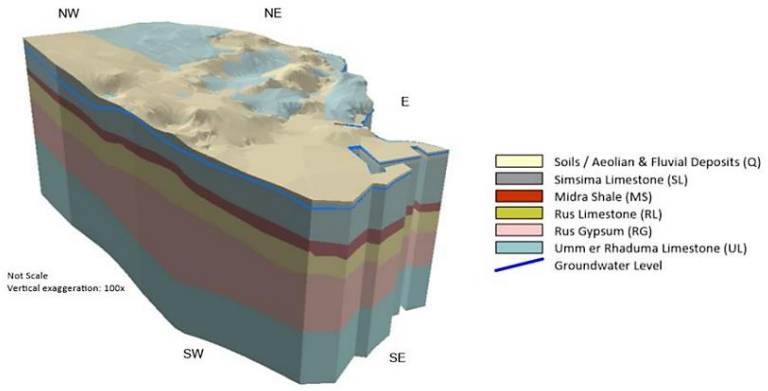


Fig. 1: 3D Geological Model South of Wakrah Project Area

3 Results and Project Implementation

3.1 Hydrogeological Modelling Strategies

Based on the compilation of previous information, and the new geological and geotechnical data, we defined the hydrogeological conceptual model (CM) of the study area. This CM consist of a saturated medium, which considers the groundwater level variations in the aquifers of South Al Wakrah, due to natural processes and the drawdowns induced by pumping in the industrial sector and the dewatering preformed during the construction of tunnels and pumping stations. Various sources of information have been consulted for the development of technical reports and the groundwater numerical model proposal. Once the CM is defined, it is possible to develop Numerical Models (NM) capable of quantifying the hydrogeological processes of interest. To define the expected models it is necessary, to have a proper assessment of the hydrogeological conditions of the area of study, by adopting the following methodology:

- Conduct a desktop survey of the project's available data; collect background geological and hydrogeological information outlining the characteristics of the major aquifers and aquitards,

existing groundwater levels and permeability values, to establish an initial 3D hydrogeological CM.

- Design the packer permeability and pumping tests at each location of interest (i.e., location, depth, flowrates).
- Technical review of the permeability tests and procedures implemented during drilling, collation, and processing of the pumping test data to derive the aquifers' parameters, required as input data for the dewatering modelling.
- Assessment of local and catchment Hydrogeological NM at each location of interest followed by the calibration of the models with the available short-term data.
- Complete the simulations of the various dewatering scenarios, provide conceptual groundwater control measures, provide estimates of groundwater inflows and surrounding impacts, and produce a dewatering schedule for design and construction purposes.

In order to implement the proposed methodology, three different kinds of modelling procedures are required: (1) to process the pumping test data to derive the aquifers' parameters, required as input data for the dewatering modelling; (2) to quantify the dewatering requirements and predict the characteristics of the drawdown (estimate pumping flow rate, maximum drawdown, radius of influence, etc.); and (3), to simulate the various dewatering scenarios for shafts and tunnels (both, during the construction and in their final stage), providing conceptual groundwater control measures, estimates of groundwater inflows and surrounding impacts, and developing a dewatering schedule for design and construction purposes.

3.2 Numerical Models for Processing the Pumping Test Data

Pumping tests design: To design an effective drainage system, it is essential to know the permeability (hydraulic conductivity) and storage coefficient of the different geological layers involved. This requires the execution and later interpretation of pumping tests. The interpretation of the pumping tests is based on monitoring the evolution of the piezometric level (drawdown) produced by a determined pumping flow rate. Various methods of quantification of hydraulic parameters can be used depending on the type of test and the heterogeneity of the terrain. If the terrain is homogeneous and the well and piezometers are totally penetrating the hydrological units, conventional analytical formulas can be applied (i.e.: Theis or Jacobmethods) using common pumping test interpretation software. By contrast, when the terrain is heterogeneous and the wells or piezometers are partially penetrating, the analytical formulas are not applicable, and it is necessary to use numerical flow models to calibrate and estimate the values of the parameters.

In the area of South Wakrah Pumping Station, the terrain has a high degree of heterogeneity. This largely determines the specific design of the drainage system. Thus, it is necessary to establish the specific design elements required for the execution of pumping tests (number of pumping wells and observation piezometers), their specific characteristics, and a proposal of activities to measure piezometric levels in wells and piezometers, as well as pumping rates. In this project, the pumping tests general proposal consist of one or two pumping wells, and six to nine piezometers to measure the evolution of the drawdown and recovery of the piezometric levels. An example of the pumping test configuration at the pumping station area is presented in Figure 2.

From the six piezometers, two of them will be open (slotted sections) in Simsima Limestone

Formation, two in Rus Formation, two in Rus Gypsum Formation, and the other two all along their length, in the same way, that their corresponding pumping well. It is important to define a clear protocol that reflects the important tasks to be carried out before, during, and after the test, as well as the solution to possible problems that may arise during the pumping test. Despite some additional tests (i.e. Step Drawdown Test), the pumping test will consist of three days of pumping and, at least, the same period for recovery. Measuring the groundwater heads and the flow measurements are crucial in the interpretation of the pumping test, at an acceptable frequency defined in the protocol. All these measurements are performed by, both, manual and data logger procedures in order to have a highly consistent and error-free measurements data set. Three different areas were selected for the pumping test deployment in order to be representative of the whole study area. These areas are (1) inland; (2) pumping station; and (3) coastal area.

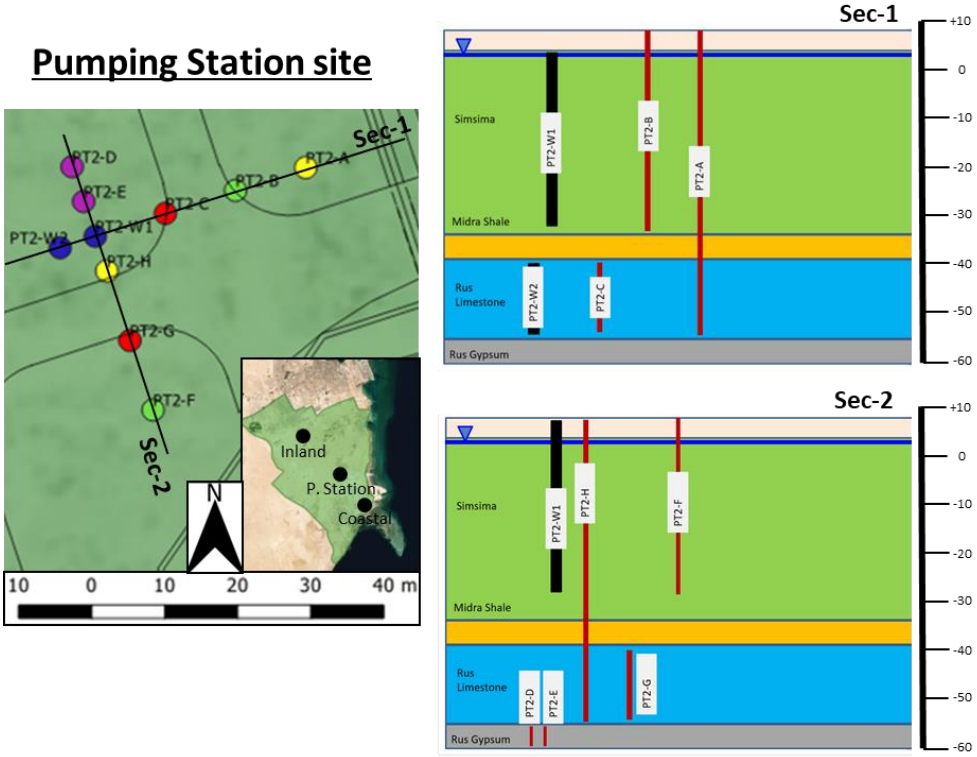


Fig. 2: Pumping test design at Pumping Station site

Pumping test interpretations: The aquifer characteristics which are evaluated by most aquifer tests are: Permeability; Specific storage or Storativity; and transmissivity. Additional aquifer characteristics are sometimes evaluated, depending on the type of aquifer, including: Specific yield; Leakage coefficient and the presence of aquifer boundaries. In this case, as a general procedures in each pumping test interpretation, it was necessary to provide: (1) Conceptual Model (CM): CM definition and constrains in each aquifer test site previous to perform Pumping Test (PT) interpretation; (2) Methods: The use of the selected pumping test interpretation methods, and its related assumptions, has to be properly justified and documented; and (3) Results: Once the interpretation is finished all information related the pumping test interpretation results have to be clearly provided.

Within the framework of this project and to have great guarantees that the results are of high quality and representative of the properties of the site, various methods have been applied for pumping test interpretation with respect to each parameter:

1. The following analytical methods were utilized to provide the Equivalent Hydraulic parameters of all hydrogeological sections:
    - Conventional Jacob adjustment method: applied to constant rate pumping test.
    - Pumping test software interpretation: applied to constant rate pumping test and step pumping test.
2. The following three numerical models were performed to provide the specific Hydrogeological Unit Hydraulic parameters:
    - Multilayer plan view model (Constant Rate Pumping test).
    - 2D axisymmetric model (Constant Rate Pumping test).
    - 2D axisymmetric model (Step Pumping test).

The hydraulic parameters obtained by the four pumping test in the three sites are consistent, with significant differences, as summarized in Table 1.

Table 1: HU hydrogeological parameters at each pumping test site

	Permeability - K(m/d)			**Storativity - S**		
Hydrogeological Units (HU)	**Inland PT**	**Pumping Station PT (x2 tests)**	**Coastal PT**	**Inland PT**	**Pumping Station PT (x2 tests)**	**Coastal PT**
QUATERNARY			2.73			4.00E-02
W. SIMSIMA			0.76			3.80E-05
SIMSIMA	8.4	155	44	0.017	0.045	2.78E-05
MIDRA	0.0014	1.7	0.24	9.20E-06	4.40E-03	3.32E-05
RUS	0.034	1.9	0.3	5.54E-06	3.70E-04	4.05E-05
RUS GYPSUM		0.008			2.85E-06	

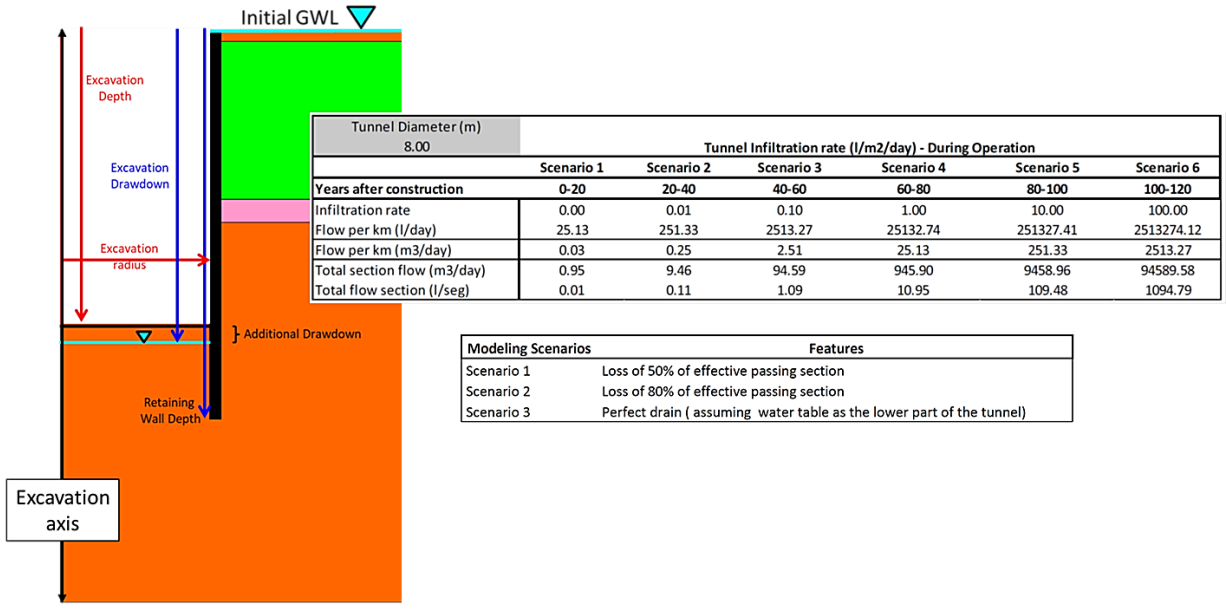
The models' results provided by different methods and models in each site are very consistent. Adjustments results statistics and validation indicators are very good. The results provide confident parameters. Simsima Unit is the most permeable HU in the three sites (44-155 m/d) and constitutes the main aquifer. Midra, Rus and Rus gypsum have very low permeability (0.001 - 2 m/d) and both are considered aquitards. The less permeable area is the inland site; the most permeable (2 orders of magnitude higher) is the pumping station area. These results are consistent with the observed intense karstic development in the Pumping Station area. This intense karst development was identified by means of a comprehensive geological and geophysical works carried out in this area.

3.3 Numerical Models to Quantify the Dewatering Requirements

For the execution of the shafts of South Wakrah Pumping Station and Outfall, it is planned to excavate below the groundwater table. Excavation needs to be done in safe and drained conditions. To design an effective dewatering system, it is essential to know the permeability, storativity and boundary conditions of the different geological layers involved. Once these parameters are appropriately quantified by means of pumping test interpretation, it is possible to quantify the groundwater flow rates required for the shaft dewatering purposes and the groundwater level drawdown (magnitude and extension) caused by the dewatering pumping rates. The objective is to quantify the dewatering

requirements and predict the characteristics of the drawdown (estimate pumping flow rate, maximum drawdown, radius of influence, etc.). This requires adequate simulation and dewatering quantification in each required shaft by means of groundwater modeling. Various dewatering simulations have been performed related to the selected examples: Inland Shaft; Pumping Station screen and pumping Shafts; and a Coastal Shaft.

Two different dewatering modelling procedures are performed: (1) Multilayer Plan View model and (2) Cross Section models. In both cases, aquifers are considered isotropic (Kv=Kh) and anisotropic (Kv=10·Kh) for the different hydrogeological units. All these models are based on those performed for pumping test interpretations and include all layers defined in each site, with their corresponding geometry, depth, thickness, hydraulic properties, etc. Additionally, we apply design conditions for dewatering quantification as; (1) Excavation depth; (2) Shaft Diameter; (3) Retaining walls; etc. The basic design parameters are summarized in Figure 3.



Tunnel Diameter (m) 8.00	Tunnel Infiltration rate (l/m2/day) - During Operation					
	Scenario 1	Scenario 2	Scenario 3	Scenario 4	Scenario 5	Scenario 6
Years after construction	0-20	20-40	40-60	60-80	80-100	100-120
Infiltration rate	0.00	0.01	0.10	1.00	10.00	100.00
Flow per km (l/day)	25.13	251.33	2513.27	25132.74	251327.41	2513274.12
Flow per km (m3/day)	0.03	0.25	2.51	25.13	251.33	2513.27
Total section flow (m3/day)	0.95	9.46	94.59	945.90	9458.96	94589.58
Total flow section (l/seg)	0.01	0.11	1.09	10.95	109.48	1094.79

Modeling Scenarios	Features
Scenario 1	Loss of 50% of effective passing section
Scenario 2	Loss of 80% of effective passing section
Scenario 3	Perfect drain (assuming water table as the lower part of the tunnel)

Fig. 3: Basic design parameters for dewatering simulations modelling – Top table: Simulation scenarios for different infiltration rates. Bottom Table: Simulation scenarios for barrier effect

Note that for Retaining walls design, some considerations and challenges could arise. In this case, it is recommended the use of cut-off walls, mostly without any load-bearing function, that basically consist of a vertical slurry wall with very low water permeability to minimize the groundwater flow. In this regard, the following cut-off wall types can be implemented: (1) Cut-off walls constructed using diaphragm wall techniques; (2) Secant pile walls from concrete of slurry; (3) Thin slurry walls; (4) Grout Injection walls; and (5) Freezing walls. As these last details are not defined in this stage of the project, here the quantification of the dewatering flow rate and related effects are performed taking into consideration a wide range of possibilities. These different scenarios correspond to:

- No Retaining walls.
- Moderate permeability Retaining walls (equivalent permeability: 0.1 to 0.01 m/d).
- Low permeability Retaining walls (equivalent permeability 0.001 to 0.00001 m/d).
- Very low permeability Retaining walls equivalent permeability < 10e-7 m/d).

“Equivalent permeability (K)” refers to the final permeability of the Cut-off wall once it is implemented. This means the integrated permeability includes: construction method, materials, width, execution quality (joints, defects, etc.). During the implementation of the projects a design equivalent permeability must be guaranteed, which must be defined according to the dewatering requirements.

In the performed scenarios the necessary pumping rates and the impact of the drawdown have been calculated based on the “equivalent permeability”, and 6 different scenarios have been simulated in each case. As a result, the relationship between the equivalents K of the retaining walls related the required flow rate can be defined according to a graphic function. The application of all this modelling methods shows that the differences between Plan View and X-Section models are very little and are caused by the slight differences between the models. Furthermore, differences between isotropic and anisotropic results are also very few. In the case of anisotropic model, flow rate results are slightly lower. This is due that in the bottom of the shaft the flow is essentially vertical. In Table 2 it is possible to observe the relationship between the equivalents K of the retaining walls related the required flow rate corresponding Pumping Station Shaft. This function will be useful for assigning the “equivalent permeability” requirements in the project. Furthermore, the expected drawdown produced by the dewatering in the entire domain of the model has been calculated. As an example, the Table 2 summarizes the drawdown calculated on the outside of the Cut-off wall corresponding Pumping Station Shaft site. In all cases the implementation of Cut-off walls greatly reduces the drawdown outside the excavation.

Table 2: Dewatering scenarios in the Pumping Station Shaft.
Left: dewatering pumping rates. Right: Outside Cut-off wall drawdown

Retaining wall K(m/d)	Q(L/s)
NO Ret. wall	5272
1.0E-01	611
1.0E-02	80
1.0E-03	9
1.0E-05	0.90
1.0E-07	0.81

Retaining wall K(m/d)	Outside Retaining Wall Drawdown (m)
NO Ret. wall	52.2
1.0E-01	5.8
1.0E-02	0.8
1.0E-03	0.09
1.0E-05	0.02
1.0E-07	0.01

According to the results presented in Table 2, it is important to highlight that:

- Inland Access shat pumping rates are low (< 60 L/s). It is possible to dewater the shaft without considering cut-off walls.
- In the Pumping Station area (Screen Shaft and Pumping Shaft) very high flow rates are expected. It will be very difficult to dewater these shafts without considering cut-off walls.
- In the Coastal Area high flow rates are expected. It will be difficult to dewater these shafts without considering cut-off walls. The moderate permeability of the bottom of the excavation (Rus Unit) produces considerable up flow to the dewatering excavation bottom. Significant both, pumping rates and drawdown, will be produced, even considering low permeability retaining wall values.

3.4 Numerical Models to Determine Potential Impacts

For the execution of the shafts of South Wakrah Pumping Station and the construction of the tunnel, it is planned to excavate below the groundwater table. These actions could modify the original

geological settings of the layers, causing possible impacts on the distribution of the water table and flow direction. The main objective of these numerical models is to understand the steady-state and transitory conditions of the aquifers in the area to help assess the construction of the South Wakrah Pumping Station and Sea Outfall Project.

This Project is located in the southern sector of Al Wakrah (Qatar), and the model area covers a total area of 552 square kilometres. The area is limited to the East by the sea and to the west by a groundwater contour line. The North and South limits are defined by the flow directions lines. As mentioned before, the limits of the domain have been defined considering the project area and according to hydrogeological criteria, the reason why the final area of the model is greater than the one initially defined in the project (Figure 4). The numerical model was built using the finite element code FEFLOW v.7.4, which solves the flow equation in a saturated underground medium. FEFLOW allows the adaptation to complex geometries and the incorporation of geological structures through unstructured meshing.

Discretization involves dividing the modelling domain into a series of individual elements. The finite element method solves the groundwater flow equation at the vertices of mentioned elements and/or within each of them. The limits of the domain of the numerical model are conditioned by the geometry and extension of the aquifers, so its discretization must be adapted to these characteristics and to the existing singular elements. To achieve optimal discretization, it is especially important to consider the areas that are most sensitive to flow and those areas in which the greatest hydraulic gradients are expected, since only with a good distribution of elements can they be reproduced mathematically with a minimum error. The 3D domain has been divided into 371,810 elements and 223,818 nodes (Figure 4). The different hydrogeological units (UH) are represented by using five layers in the model, which have been described in the previous sections (Figures1 and 4):

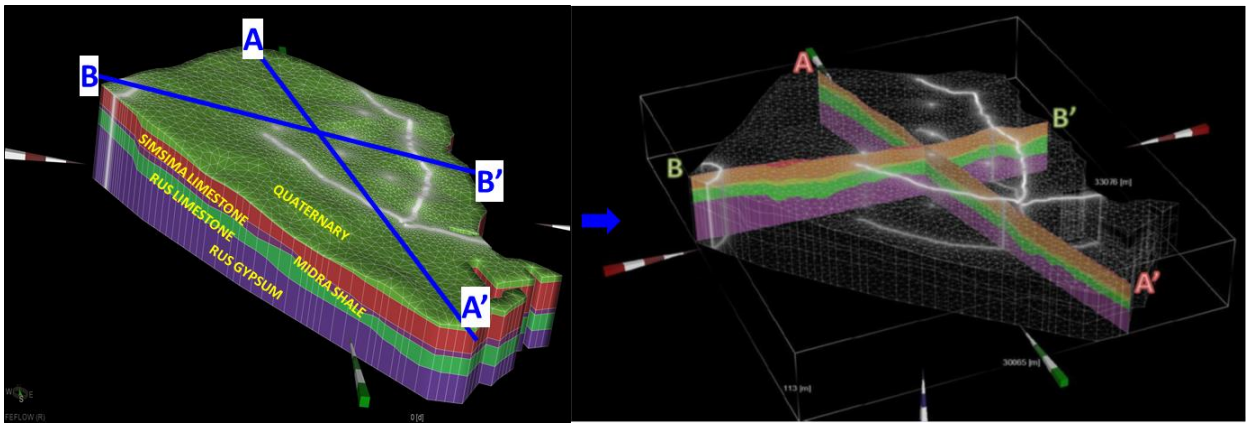


Fig. 4: 3D hydrogeological model domain, discretisation and cross sections examples

The hydrogeological **parameters** assigned to the aquifer units are considered as a basis for the calibration process. The interpretation of these pumping tests provided information on permeability and storativity, these values oscillate considerably depending on their geographic positions due to the high grade of heterogeneity and karstification features. For the reason mentioned before, an approximation was made to obtain the general value for the different layers, with the objective of representing the general distribution of the water levels in the model.

Different **boundary conditions** were implemented (Figure 5): The no flux condition is intended to impose an impervious boundary. It has been considered null flow in all those contours of the model

in which there is no exchange of water between the modelled domain and the outside (or is negligible). This condition has been considered for (1) the basal surface: represents the lower limit, the contact between the aquifer unit with the basement is considered hydraulically impervious; and (2) the lateral contours: the south and north limits are defined and determined by the flow direction, where the northern limit corresponds to a watershed and on the other hand the southern limit corresponds to a line parallel to the flow direction. The prescribed level condition corresponds to levels that are well known during the modeled period. Based on this, two prescribed level limits were defined: (1) Sea: This boundary condition is defined throughout the eastern limit and corresponds to the coastline; and (2) Sinkholes: It is applied to the westernmost part of the model and corresponds to the average of the water table in the sinkhole. The prescribed flux boundary conditions are implemented to represent the piezometric dynamics and water level distribution in the numerical model due to the anthropic effects, example; the effects of the drawdowns produced by the pumping wells and infiltration rates of the tunnel: (1) Current extraction wells and their pumping rates were defined based on previous studies of the area; (2) Tunnel drain rate: The tunnel drain rate is related with the surface of the tunnel and their infiltration rates, the infiltration rates increase as the years pass, according to the design, the life of the tunnel is 120 years. The drain rate was calculated for the whole tunnel section.

After reviewing and filtering the last updated database of observed hydraulic heads we have selected a total of 138 **observation points** that have been used to calibrate the model in a stationary state and to estimate the general hydraulic parameters (Figure 5). Once the model is calibrated, it is possible to implement the various simulation scenarios

The modelling of the **simulation's scenarios** consisted of (1) a steady-state model to determine the initial conditions and previous hydrogeological conditions before the construction works; and (2) quantifying tunnel hydrogeological impacts under different scenarios, including, both, tunnel infiltration and barrier effect simulations.

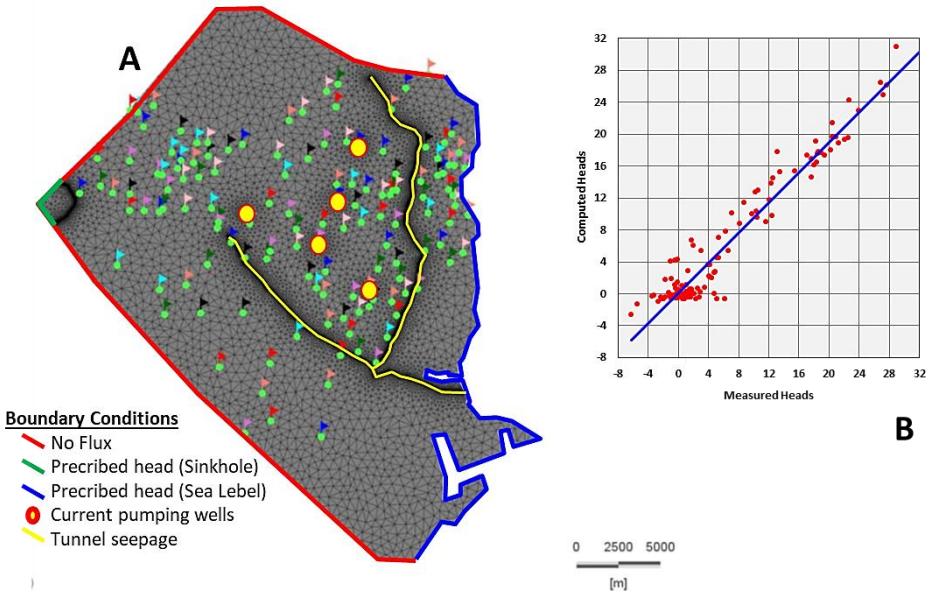


Fig. 5: A: Plan view of geographical location of the boundary conditions for the Simulations models. B: Stationary Model calibration results, observed vs. simulated levels

Tunnel infiltration simulations: Given that the construction level of the tunnel is below the water table, there is the possibility that this structure acts as a drain. Considering that the tunnel will be a precast segmental lining and that there will be an increase in infiltration rates as the years pass (design

life is 120 years), the following infiltration rates scenarios for a tunnel of 8 metres of diameter are suggested (Figure 6, Table 4):

Barrier effect simulations: As a result of the construction of the tunnel, there is a loss of the effective passage section for groundwater, which will result in a rise or fall of the water table in the vicinity of the tunnel. The possible ascent/descent will be proportional to the loss of the effective passage section as well as to the direction of the flow. To represent the possible barrier effect different scenarios are proposed (Figure 6, Table 3).

Table 3: Calculated Flow Rates and Drawdowns corresponding the simulated scenarios

	Scenario 1	Scenario 2	Scenario 3	Scenario 4	Scenario 5	Scenario 6
Years after construction	0-20	20-40	40-60	60-80	80-100	100-120
Infiltration rate	0.00	0.01	0.10	1.00	10.00	100.00
Flow per km (l/day)	25.13	251.33	2513.27	25132.74	251327.41	2513274.12
Flow per km (m3/day)	0.03	0.25	2.51	25.13	251.33	2513.27
Total section flow (m3/day)	0.95	9.46	94.59	945.90	9458.96	94589.58
Total flow section (l/seg)	0.01	0.11	1.09	10.95	109.48	1094.79
Maximum Drawdown (m)	0.00028	0.00280	0.02841	0.28816	2.88116	28.81000

Modeling Scenarios	Features	Maximum water table rise (m)	Maximum water table drawdown (m)
Scenario 1	Lose of 50% of efective passing section	0.01	0.004
Scenario 2	Lose of 80% of efective passing section	0.04	0.02
Scenario 3	Perfect drain (assuming water table as the lower part of the tunnel)	-	42.04

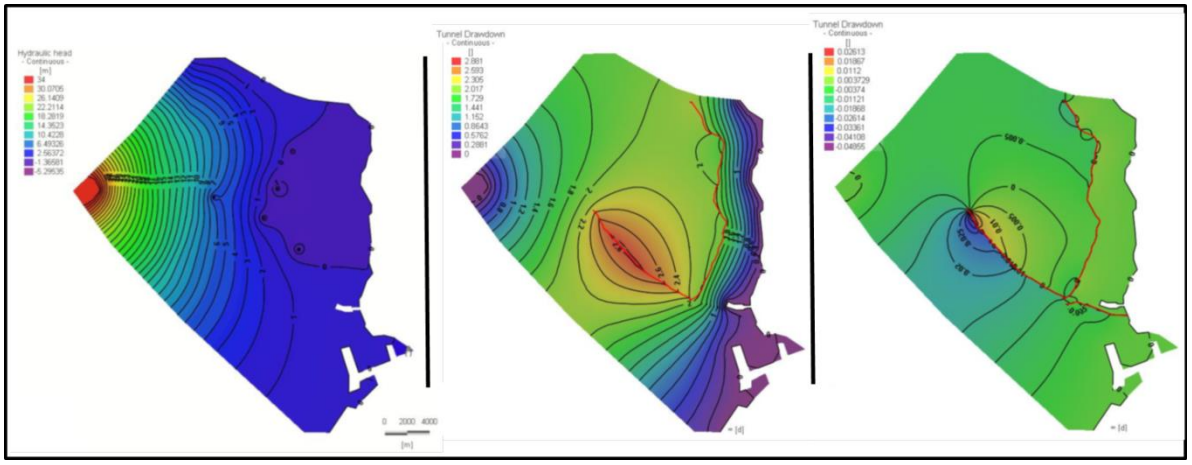


Fig. 6: Model results corresponding to: **(a)** current steady state piezometry; **(b)** tunnel infiltration scenario 5; **(c)** tunnel barrier effect scenario 2

4 Conclusion

This paper presents an example of a recently developed geotechnical investigation program for the pre-tender design of the South of Wakrah Pumping Station and Outfall project. A comprehensive hydrogeological study was carried out to characterize heterogeneous hydrogeological conditions along the project area and to be able to determine potential impacts on the environment and on the project. Complete geological and geotechnical data has been utilized to define the hydrogeological conceptual model of the study area, which made it possible to develop numerical models capable to quantify the hydrogeological processes of interest.

Three different kinds of modelling procedures were required: (1) for processing of the pumping test data to derive the aquifers' parameters, required as input data for the dewatering modelling; (2) to quantify the dewatering requirements and predict the characteristics of the drawdown; and (3), simulations of the various dewatering scenarios related shafts and tunnels.

As a result, we assessed the mitigation measures for future excavation of pumping station and screening shafts and propose a groundwater management approach to support the geotechnical risk assessment and to minimize the impact of construction activities for future infrastructure projects. In consequence, we propose a groundwater management approach to support the geotechnical risk assessment and to minimize the impact of construction activities for future infrastructure projects.

References

Botey-Bassols, J. et al. (2021) D-InSAR monitoring of ground deformation related to the dewatering of construction sites. A case study of Glòries Square, Barcelona, *Engineering Geology* (2021), https://doi.org/10.1016/j.enggeo.2021.106041

Criollo, et al. (2016). An integrated GIS-based tool for Aquifer Test Analysis. *Environmental Earth Sciences*, (2016) 75:1-11. doi: 10.1007/s12665-016-5292-3

Font-Capo, et al. (2015). Assessment of the barrier effect caused by underground constructions on porous aquifers with low hydraulic gradient: A case study of the metro construction in Barcelona, Spain. *Engineering Geology 196* (2015) 238–250, doi: 10.1016/j.enggeo.2015.07.006

Pujades, et al. (2015). Hydrogeological impact assessment by tunnelling at sites of high sensitivity. *Engineering Geology 193*(2015) 421-434, doi: 10.1016/j.enggeo.2015.05.018

Vázquez-Suñé, et al. (2016). A geological model for the management of subsurface data in the urban environment of Barcelona and surrounding area. *Solid Earth, 7*, 1317-1329, doi: 10.5194/se-7-1317-2016

Cite as: Vázquez-Suñé E., Bulboa I., Krishnamurthi I.K. & Candia E.A.P., "Geotechnical Challenges for Underground Infrastructure in Qatar: Hydrogeological Assessment for Dewatering and Deep Excavation Works: South of Wakrah Pumping Station and Outfall (SWPSO) Project", *The 2nd International Conference on Civil Infrastructure and Construction (CIC 2023)*, Doha, Qatar, 5-8 February 2023, DOI: https://doi.org/10.29117/cic.2023.0178

UV Induced Photodegradation of Direct Green dye by Tb-doped $La_{10}Si_6O_{27}$ Catalyst

Rajender Boddula
Center for Advanced Materials (CAM), Qatar University,Doha, Qatar.
rajender.boddula@qu.edu.qa

Ramachandra Naik
Department of Physics, New Horizon College of Engineering,Bangalore, India.
rcnaikphysics@gmail.com

Naveen Kumar A
Department of Physics, South East Asian College of Engineering and Technology, VTU,Bangalore, Karnataka, India
naveenphysics12@gmail.com

Ramyakrishna Pothu
College of Chemistry and Chemical Engineering, Hunan University,Changsha, China
research.ramyakrishna@gmail.com

Ahmed Bahgat Radwan
Center for Advanced Materials (CAM), Qatar University,Doha, Qatar
ahmedbahgat@qu.edu.qa

Noora Al-Qahtani
Center for Advanced Materials (CAM), Qatar University,Doha, Qatar
noora.alqahtani@qu.edu.qa

Abstract

Due to the expansion of industry, the world's population growth has led to increased air and water contamination. Because they are poisonous and non-biodegradable, organic dyes are a significant source of this contamination. Studies have concentrated on photocatalysts to transform organic dyes into innocuous compounds in order to lessen the harm that organic colours cause. In this study, solution combustion technique was employed to prepare rare-earth metal (terbium (Tb)) doped lanthanum silicate phosphor ($La_{10}Si_6O_{27}$) using lanthanum nitrate and fumed silica were utilized as precursors, oxalyldihydrazide was used as fuel, and terbium nitrate was used as a dopant. The photocatalytic activities for the Direct Green-23 (DG23) dye degradation under UV irradiation were studied and found that 59.05% of dyes degraded at 120 min. These findings shows that, $La_{10}Si_6O_{27}$ is a promising material for industrial dye degradation since 59.05% of the dyes were absorbed by the material in 120 min.

Keywords: Water treatment; Photodegradation; Direct Green-23 (DG23) dye; Toxic pollutant; Nanophosphors

1 Introduction

Dyes have been used in many trades to colour their articles, in textiles, food, paper, plastics, elastic, carpet and beauty care products. Amid the generation and utilization of distinctive coloration matters, until 10% of utilized colours are released as wastewater, making an assortment of natural and wellbeing issues. Colouring wastewater stemming is popular as deeply adulterated wastewaters because it holds complete colour, exaggerated chemical oxygen demand/synthetic oxygen request (COD), sour pH, harmful overpowering metals, and different harmful contaminants. The most

necessary and largest shade forged inside the manufacturing is the azo colour draw, that are acknowledged apiece posture of azo-groups (–N = N–) in relationship accompanying fragrant rings (naphthalene and/or benzene). Direct green 23 (DG23) dye (molecular formula: $C_{45}H_{33}N_7Na_4O_{16}S_4$; Figure 1) is one of the azo colours, which is recognized as one of the foremost hazardous banner since of their long career in water. This applies in specific to organic azides that have existed stimulated for one growth of mineral salts or dependable acids. Poisonous gasses are formed by mixing matters concerning this course accompanying acids, aldehydes, amides, carbamates, cyanides, not organic fluorides, halogenated organics, isocyanates, ketones, metals, nitrides, peroxides, phenols, epoxides, acyl halides, and hard oxidizing or lessening controllers.

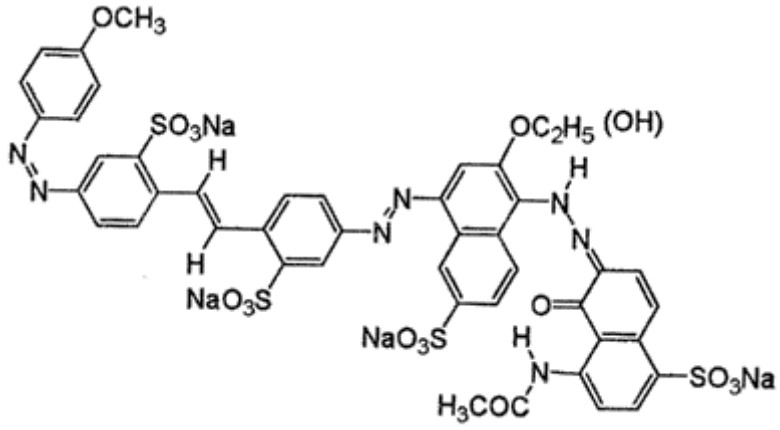


Fig. 1: Chemical structure of DG23 dye

Combustible gasses are formed by mixing matters in this place bunch accompanying being basic metals. Dangerous consolidation can occur with something complete oxidizing professionals, ingot salts, peroxides, and sulphides. As recently, all governments are disturbed be following accurate to halt this in a way color wastewater to the open waterways, except that it is medicated suitably. The primary objective of wastewater treatment features is to ensure people and the biological system from destructive and harmful components found in wastewater (Saeed et al. (2018); Maavia et al. (2019)). Water treatment facilities were planned to speed up the normal prepare of filtering water since the common prepare is over-burden. These facilities are utilized to treat the wastewater in different ways and after that send the filtered water back into the environment. Heterogeneous photocatalysis is considered an emerging destructive innovation that leads to the entire mineralization of assorted natural contaminants, in which the degradation of the sullying compound broken up in water happens by the activity of semiconductor materials illuminated by light, primarily bright (Nagaraj et al. (2021); Priya et al. (2020)). A few of the foremost used photocatalyst metallic semiconductor materials are TiO_2, ZnO, Fe_2O_3, WO_3, BiOCl, and g-C_3N_4, as well as a few blends of these have been examined (Nemiwal et al. (2021); Aslam et al. (2019a) (2019b); Farooq et al. (2019); Michael et al. (2019)). Nowadays, rare-earth doped metal oxide nanocomposites were gotten to be exceptionally one of a kind and tend to appear plenteous execution in all sorts of areas such as biological, electrochemical, and photocatalytic, etc (Naveen Kumar et al. (2020) and (2021)).

Lanthanum silicate ($La_{10}Si_6O_{27}$) nanophosphor is demonstrated to be an amazing multifunctional material for photoluminescence, photocatalytic and electrochemical applications. Its precious stone structure is hexagonal oxy-apatite with a space bunch P63/m, and shaped due to covalent and confined silicate tetrahedra (SiO_4). There are two locales named 6h which obliges seven La cations 4f which

obliges nine-coordinated locales. NMR spectroscopy and Raman spectroscopy have illustrated that the interstitial oxide particles in $La_{10}Si_6O_{27}$ contribute to expanded conductivity. Tb^{3+} particles have demonstrated to be incredible activator for doping into the cross section of $La_{10}Si_6O_{27}$ which comes about within the upgraded execution as a multifunctional material. To date, a composition of material, synthetic and natural means have happened itemized to empty colour from wastewater. Distinctive methods were checked for the banishing of various sorts of poisons from water to a degree advanced corrosion for effluents situation of material banner, blend of various composites for situation of water holding hurtful metals and taking advantage of nanomaterials as a stimulant for photodegradation of material effluents.

In this manner, the point of the show think about was to test Tb^{3+} doped $La_{10}Si_6O_{27}$ by the joining of 5 mol% Tb^{3+} for improved photocatalytic application for the evacuation of a material anionic DG23 dye from wastewater was performed beneath UV light for the length of 120 min to explore the photocatalytic action of $La_{10}Si_6O_{27}$:Tb^{3+} (5 mol%). This report demonstrates 5 mol% Tb^{3+} doped $La_{10}Si_6O_{27}$ may be a UV photocatalyst for wastewater treatment.

2 Experimental

Stoichiometric sums of crude materials required for the planning have been procured from Sigma Aldrich with 99% immaculateness and analytical reagent grade. Terbium nitrate (Tb $(NO_3)_3$) as a dopant, lanthanum nitrate (La $(NO_3)_3 \cdot 6H_2O$) as an oxidizer, smouldered silica and oxalyldihydrazide ($C_2H_6N_4O_2$) as a fuel were broken up in refined water taken in a container. 5 mol % Tb^{3+} doped lanthanum silicate ($La_{10}Si_6O_{27}$:Tb^{3+}) have been arranged as per the stoichiometric proportions and by keeping up the fuel to oxidizer proportion solidarity by arrangement combustion method. Container was kept in pre-warmed suppress heater of temperature 450 ºC where combustion takes put. Lack of hydration and seething of the response blend happens with the freedom of gigantic sum of vaporous items coming about in arrangement of the specified Tb^{3+} doped $La_{10}Si_6O_{27}$ nanomaterials by the substitution of La/Si destinations by Tb^{3+} particles. Last item gotten have been crushed and collected in an discuss tight holder.

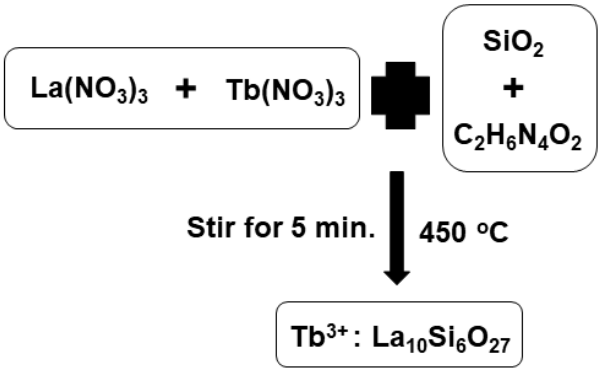


Fig. 2: Synthesis procedure of Tb^{3+} doped $La_{10}Si_6O_{27}$ material

The chemical responses for the union of have and one of the mole rates of Tb doped as appeared underneath.

$$10\,La(NO_3)_3.6H_2O + 6\,SiO_2 + 15\,C_2H_6N_4O_2 + 5\,Tb(NO_3)_3.6H_2O \rightarrow La_{9.95}Si_6O_{27}Tb_{0.5} + 105\,H_2O + 30\,CO_2 + 45\,N_2$$

3 Results and Discussion

Tb^{3+} doped $La_{10}Si_6O_{27}$ nanophosphors are characterized by FT-IR, XRD, UV-DRS, and TEM techniques (Naveen Kumar et al., 2021). Photocatalytic exercises were completed activity resorting

to the UV–Visible spectrophotometer show 2600 from Shimadzu. In arrange to debase the DG23 dye color within the nearness of UV radiation, a photocatalytic explore was completed activity on the devised 5 mol% Tb^{3+} doped test. A 250 ml color arrangement containing 20 ppm of the dye colors was made as the stock arrangement. In a circular glass reactor, catalyst measurements of 0.06 g were connected to the color arrangement. The response blend was attractively unsettled and uncovered to a 400W mercury light with a 254 nm wavelength whereas being lit up by UV radiation. A pyrex glass container was utilized for the tests. The response blend was exposed to UV radiation within the open discuss for to 120 min, and 5 ml of the sample arrangement were taken out and observed within the UV–Visible extend of 200–800 nm at 15 min interims.

The photodegradation of DG23 dye solution was utilized to gage the photocatalytic movement of 5 mol% Tb^{3+} doped test beneath UV light. It was taken in a circular glass reactor, kept underneath the UV source of mercury vapor light by keeping up the separate of 23 cm to maintain a strategic distance from the warm on a test (Satish Kumar et al. (2009)). Firstly, the explore was conducted in dim condition for DG23 color. No alter was watched as the color did not experience any degradation (Shams et al. (2019)). This was ascribed to the characteristic of the catalyst, which has less crystallite estimate, great charge transport capacity, and a more noteworthy number of oxygen opportunities due to doping. These properties make the material potential for photocatalytic applications (Shahbazi et al. (2017)). Figure 3 appears its absorbance spectra which shows most extreme retention at 621 nm. It appears rate degradation with regard to time up to 120 min. It was watched from the chart that; rate debasement is about 59.05% after 120 min of light.

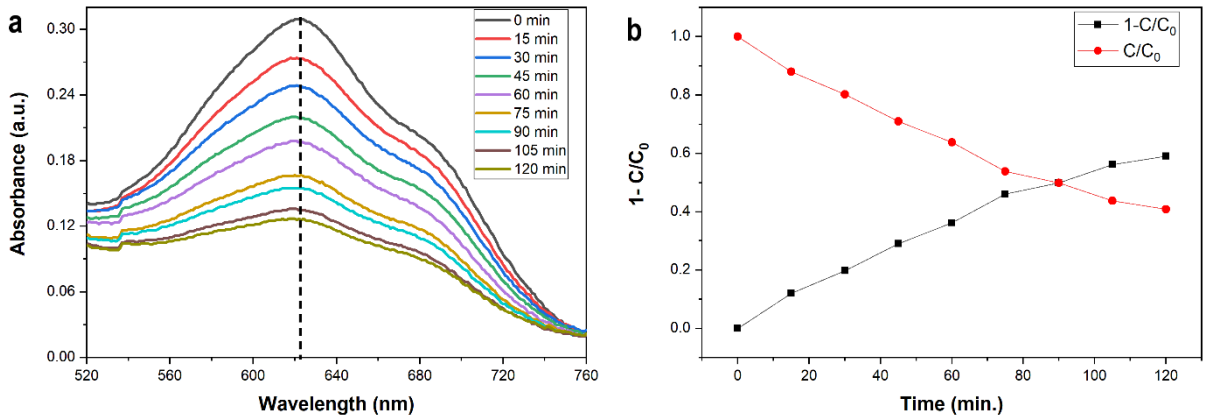


Fig. 3: a) DG23 dye degradation and **b)** time span vs 1-C/C_0 for the DG23 dye decolorization over Tb^{3+} doped $La_{10}Si_6O_{27}$ UV photo catalyst

Table 1 appears the nitty gritty investigation of debasement handle beneath UV light. Rate degradation was calculated utilizing the condition (i),

$$\% D = \frac{C_o - C}{C_o} \times 100 \qquad (i)$$

Where, C_o is the introductory colour concentration and C is the colour concentration after photo decolorization with regard to time. It presents C/C_o for the decolorization of DG23 dye with UV light, which clearly appear that, the degradation has been moved forward with time and achieved most extreme for 120 min. In arrange to decide the arrange of energy, log C/C_o have been assessed utilizing the condition (ii).

$$log\frac{C}{C_o} = -Kt \qquad (ii)$$

Where, K=first arrange rate steady, C_o = color concentration at t = min and C = color concentration amid testing (Prathap Kumar et al. (2021)). The linearity between log C/C_o and K was watched, which appears the primary arrange energy. The esteem of K was found to be 0.007419 min^{-1} for DG23 appeared within the Table 1.

Table 1: DG23 degradation percentage over 5 mol% Tb^{3+} doped $La_{10}Si_6O_{27}$ photocatalyst under UV light (20ppm DG23 + 0.06 g of photocatalyst + UV light, slope rate = 0.007419 min^{-1})

t	C	C/C_o	log C/C_o	-log C/C_o	%D
0	20	1	0	0	0
15	17.6	0.88	-0.055517328	0.055517328	12
30	16.06	0.803	-0.095284455	0.095284455	19.7
45	14.19	0.7095	-0.1490476	0.1490476	29.05
60	12.77	0.6385	-0.194839098	0.194839098	36.15
75	10.77	0.5385	-0.268814292	0.268814292	46.15
90	10	0.5	-0.301029996	0.301029996	50
105	8.77	0.4385	-0.358030402	0.358030402	56.15
120	8.19	0.4095	-0.387746094	0.387746094	59.05

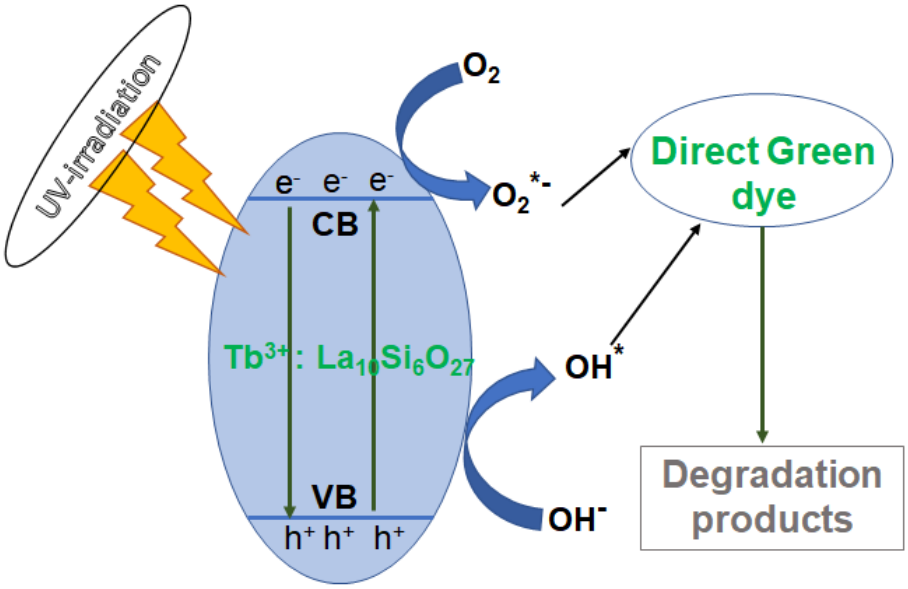


Fig. 4: Mechanism of DG23 dye degradation over 5 mol% Tb^{3+} doped $La_{10}Si_6O_{27}$ photocatalytic activity under UV light illumination

Figure 3b appears the analysed debasement half-life in which 50% color debasement has been recognized in 90 min. From these comes about, it can be concluded that 5 mol% Tb^{3+} doped $La_{10}Si_6O_{27}$ could be a potential photocatalyst for DG23 dye decolorization with more photo-decolorization capacity due to electron gap recombination, era of hydroxyl and superoxide radicals. In expansion, dynamic photo energized electrons and holes too degrades the color particles as appeared in Figure 4. When 5 mol% Tb^{3+} doped $La_{10}Si_6O_{27}$ was uncovered to the radiation, electrons

from valence band hops to conduction band and gaps are made in valence band (Naveen Kumar et al. (2021)). These electrons will move towards surface and produces anion radicals (O_2*−) from atomic oxygen, while gaps will oxidize the color or deliver hydroxyl radicals (OH*) from adsorbed water atoms. The adsorbed color atoms are oxidized by these dynamic radicals.

4 Conclusion

In summary, we have successfully synthesized a 5 mol% Tb doped $La_{10}Si_6O_{27}$ nanophosphor by combustion method. To examine the photocatalytic degradation of DG23 dye over nanophosphor beneath UV light. DG23 photodegradation over 5 mol% Tb doped $La_{10}Si_6O_{27}$ catalyst exhibited superior photocatalytic efficiency and found to be first-order rate reaction with rate constant is 0.007419 min^{-1}. 50% DG23 dye degradation half-life has been detected in 90 min and 59.05% after 120 min of UV light. These findings are very useful for cleaning the industrial wastewater applications.

Acknowledgements

This work was supported by Qatar University through a National Capacity Building Program Grant (NCBP), [QUCP-CAM-2022-463]. The publication of the article was funded by Qatar National Library. Statements made herein are solely the responsibility of the authors.

References

Aslam, et al. (2021). Synthesis of Non-Toxic Fe2 (WO4) 3 Photocatalyst with Efficient Performance. *Current Analytical Chemistry, 17*(5), 628-639.

Aslam, et al. (2019a). Synthesis of novel g-C3N4 microrods: A metal-free visible-light-driven photocatalyst. *Materials Science for Energy Technologies, 2*(3), 401-407.

Aslam, et al. (2019b). Synthesis of WO3· H2O spherical particles for efficient photocatalytic properties under visible light source. Materials Science for Energy Technologies, 2(2), 187-193.

Farooq, et al. (2019). Improved photocatalytic performance of reduced zinc oxide (ZnO) novel morphology of astray like microstructure under solar light irradiation. *Materials Science for Energy Technologies, 2*(2), 181-186.

Maavia, et al. (2019). Facile synthesis of g-C3N4/CdWO4 with excellent photocatalytic performance for the degradation of Minocycline. *Materials Science for Energy Technologies, 2*(2), 258-266.

Micheal, et al. (2019). Assembled composite of hematite iron oxide on sponge-like BiOCl with enhanced photocatalytic activity. *Materials Science for Energy Technologies, 2*(1), 104-111.

Nagaraj, et al. (2021). A Facile synthesis of anatase Ni2+ doped TiO2 nanorods with highly improved visible-light photocatalytic performance. *Current Analytical Chemistry, 17*(2), 279-284.

Nantharak, et al. (2017). Effect of local structure of Sm3+ in MgAl2O4:Sm3+ phosphors prepared by thermal decomposition of triethanolamine complexes on their luminescence property, *Journal of Alloys and Compounds, 701*, 1019-1026.

Naveen et al. (2020). Photoluminescence and electrochemical performances of Eu3+doped La10Si6O27 nanophosphor: Display and electrochemical sensor applications, *Applied Surface Science Advances 1*, 100026.

Naveen et al. (2021a). La10Si6O27:Tb3+ nanomaterial; its photocatalytic and electrochemical sensor activities on Disperse Orange and Fast Blue dyes, *Sensors International, 2*, 100076.

Naveen, et al. (2021b). Photoluminescence, photocatalytic and electrochemical performance of La10Si6O27:Sm3+ nanophosphor: It's applications in display, photocatalytic and electrochemical sensor, *Applied Surface Science Advances, 4*, 100070.

Nemiwal, M., Zhang, T. C. & Kumar, D. (2021). Recent progress in g-C_3N_4, TiO_2 and ZnO based photocatalysts for dye degradation: Strategies to improve photocatalytic activity, *Science of The Total Environment, 767*, 144896.

Pratapkumar, et al. (2021). Structural, photocatalytic and electrochemical studies on facile combustion synthesized low-cost nano chromium (III) doped polycrystalline magnesium aluminate spinels, *Journal of Science: Advanced Materials and Devices, 6*(3), 462-471

Priya, et al. (2020). A study of photocatalytic and photoelectrochemical activity of as-synthesized WO3/g-C3N4 composite photocatalysts for AO7 degradation. *Materials Science for Energy Technologies, 3*, 43-50.

Saeed, et al. (2018). Ag@Mn_xO_y: an effective catalyst for photo-degradation of rhodamine B dye. Environmental chemistry letters, 16(1), 287-294.

Sathish et al. (2009). Visible light assisted photocatalytic degradation of acid red 88 using Au-ZnO nanophotocatalysts, *Water Science and Technology*, *60*(6), 1589–1596.

Shahbazi, H., Shokrollahi, H. & Alhaji, A. (2017). Optimizing the gel-casting parameters in synthesis of MgAl2O4 spinel, *Journal of Alloys and Compounds, 712*, 732-741.

Shams, et al. (2019). Facile and Eco-Benign Synthesis of Au@Fe_2o_3 Nanocomposite: Efficient Photocatalytic, Antibacterial And Antioxidant Agent, *Journal of Photochemistry and Photobiology B: Biology*, *199*, 111632.

Cite as: Boddula R., Naik R., Kumar A.N., Pothu R., Radwan A.B. & Al-Qahtani N., "UV Induced Photodegradation of Direct Green dye by Tb-doped $La_{10}Si_6O_{27}$ Catalyst", *The 2nd International Conference on Civil Infrastructure and Construction (CIC 2023)*, Doha, Qatar, 5-8 February 2023, DOI: https://doi.org/10.29117/cic.2023.0179

Sustainable Urban Drainage Master Plan for Al Khor Municipality

Hassan Qasem
Lead Infrastructure Engineer/ Ministry of Municipality Infrastructure Planning Department,Doha, Qatar
HQasem@mm.gov.qa

Mohsin Mahmood
Senior Hydraulic Modeller, Ministry of Municipality Infrastructure Planning Department,Doha, Qatar
mmahmood@mm.gov.qa;

Abstract

It is of upmost importance that the type of hydrological basin of the region should be established before developing its drainage strategy. Unlike exhoric basin which is characterised by well-defined pattern of streams and rivers ultimately discharging into the sea, Qatar's topography exhibits mix of arheic, and predominantly endorheic basin features i.e., rainwater drains to inland depressions to form temporary water bodies. Keeping drainage basin type in view, Al Khor drainage master is developed which function sustainably with the nature with aim to utilize drainage water to achieve Qatar National Vision 2030 and Qatar Water Strategy goals.

Keywords: Al Khor SUDS; Drainage strategy; Stormwater; Drainage water management and reuse in endorheic basin

1 Introduction

Al Khor Municipality Sustainable Urban Drainage Masterplan is a project of national importance that will not only transform current drainage water management approach from rejection to utilization but more importantly, shall provide an infrastructure platform to help achieve targets and goals envisioned in Qatar Water Strategy based on Qatar National Vision 2030.

2 Sustainable Urban Drainage System

The foremost objective of this project is to solve drainage problems in a sustainable manner i.e., working in line with natural hydrological pattern of the region to control flooding, in addition to achieving long term benefits in terms of environmental, social, and economic fronts. This project is envisioned to manage stormwater using natural hydrology of the project area. The hydrological pattern of a typical watershed in the project area consists of flat terrain and local depressions. Most of the undeveloped watersheds in the project area retain and store stormwater runoff within depression areas. A wadi (natural stream/ channel) is very rarely observed conveying water from one watershed to another. However, the current stormwater drainage strategy in the urban areas completely overlook the natural hydrological pattern of the watersheds. It is based on design approach to collect, convey, and dispose stormwater into the sea via tunnels and outfalls. Consequently, in the event of rainfall exceeding design capacity of the stormwater system, the excess runoff follows the natural hydrological pattern of the urban watershed and accumulates in the low laying depression areas causing flooding of properties and facilities located therein. Likewise, surficial groundwater generated due to human activities (leakage from wet utility pipes, excess landscape, and agriculture

irrigation etc.) also appear at the low-lying areas in the watersheds. Therefore, it is prudent that watershed topography and hydrological characteristics should be considered thoughtfully while planning and designing infrastructure facilities for the development. Accordingly, the roads and drainage system should follow natural topography of the watershed enabling roads to facilitate conveyance of excess runoff in the form of sheet flow from overwhelmed drainage system to lowest areas in the watershed reserved as stormwater storage and treatment facilities. This design approach will not only provide a reliable and resilient drainage strategy but will also result in much cheaper infrastructure to cater for stormwater system.

The design philosophy of the project is developed using MME-IPD flood portal, which employs 2D runoff model of the watershed in identifying watershed hydrological characteristics.



Fig. 1: Natural Hydrology of Al Khor

Figure 1 shows model results highlighting sporadically distributed flooding in depression areas. The runoff from two wadies i.e., Wadi Al Jalta and Al Jalat also shown to be obstructed by current and future developments as more prominently shown in figure below by overlapping with land use policy plan.

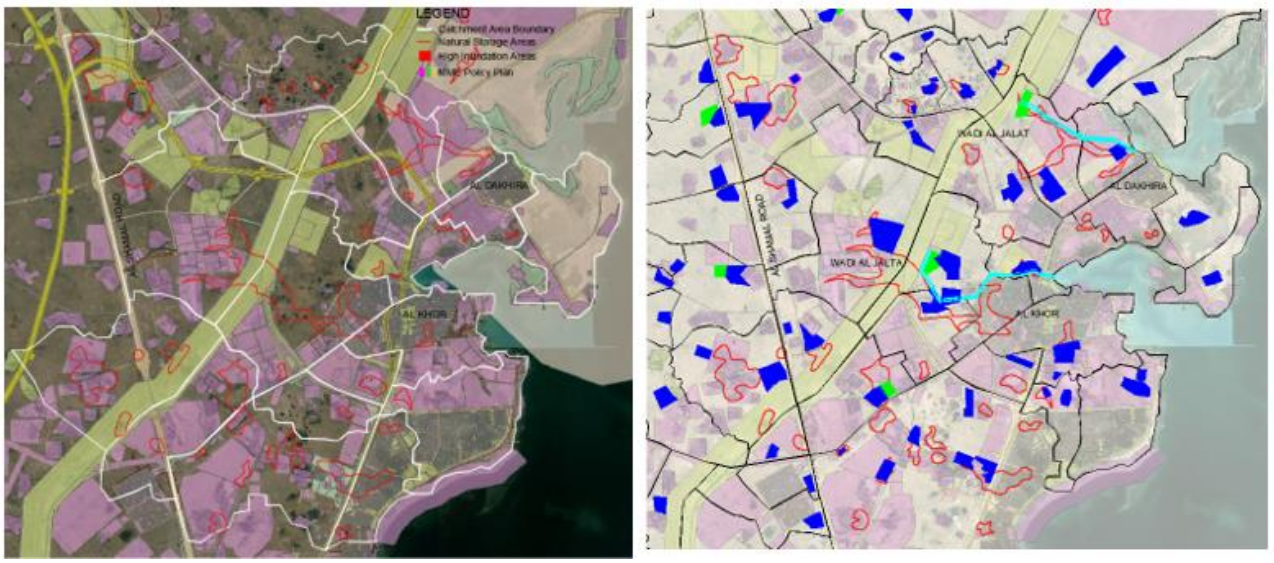


Fig. 2: Natural Hydrological Pattern, Land Use Policy Plan & Proposed SUDS

From left part of figure 2 it can be observed that current and future developments are at the risk of inundation due to natural hydrological characterises of watershed conflicting with land use policy plan. Ideally low laying depression areas in watersheds should be allocated for storing and managing rainfall runoff, however due to land already taken by existing and future developments suitable adjacent areas are proposed to be allocated for managing drainage waters in the watersheds as shown in the right part of Figure 2. The proposed rainfall storage lagoons are shown as blue polygons designed to cater for 100mm rainfall event which exceeds 100-year return period. The wadis are restored as channels following natural wadi alignment shown in as cyan lines. The green polygons are areas dedicated as wetlands for treatment of groundwater.

The vision of Qatar Water Strategy is based on sustainable and integrated management of all water resources. The strategy elements warrant for the development of smart infrastructure capable to manage seasonal rainwater and rising groundwater levels. The water strategy policy elements demand harvesting and treatment of rainwater to recharge groundwater aquifers and development of new sources of water by treating groundwater and storm water to enable maximum reuse potential. In this context, the depressed areas of the watershed in the drainage strategy of this project as shown in blue polygons in Figure 2 will serve to store rainwater. The stored rainwater will be treated to suitable standards for recharging of shallow groundwater aquifers or to be used for agriculture irrigation. The stormwater system for the project area shall be designed with integrated groundwater lowering system. This will not only benefit in lowering the surficial groundwater table level but will also provide a perennial source of water which can be treated for recycle use. During wet season the major volume of water collected by the drainage system will be rainwater which shall be stored in the depression areas. However, during dry season the drainage system will collect groundwater which will be pumped to wetlands located in designated areas as shown in green polygons of figure 2 for treatment and reuse. The groundwater treated in the wetlands will be used to help meet economic and environmental objectives of Qatar national programs.

Economic and environmental development are two of the four pillars of Qatar National Vision 2030. One of the goals for the economic development is to develop world class infrastructure and diversification of economy. Whereas environmental development requires using the resource wisely and managing the environment in harmony with economic growth, social development, and environmental protection. This project supports Qatar National Vision 2030 by providing new avenues for economic diversification and environmental protection and development objectives. The drainage water collected, stored, and treated in wetlands and EFAs will be used for urban resilience programs, sports/ outdoor activities, commercial, research and edutainment programs. The objectives of drainage master plan reinforce Al Khor City Master Plan 2032 vision seeking to develop verdant coastal garden city that blends traditional Qatari culture, maritime heritage, and innovative family attractions to create a thriving green and blue crescent community. Figure 3 shows recommended development master plan for Al Khor which amplifies the development of green city-wide network by utilizing drainage masterplan element to create green urban designs such as wadi channels alignment to create wadi and spring meadow parks in a form of naturalistic park setting for active leisure and nature intermigration using wider landscape setting with planting density and species carefully considered to enhance natural environment. Drainage water captured shall be used to support Green Oasis program which aims to plant 115, 000 trees to lower city daytime temperatures upto 9°C.

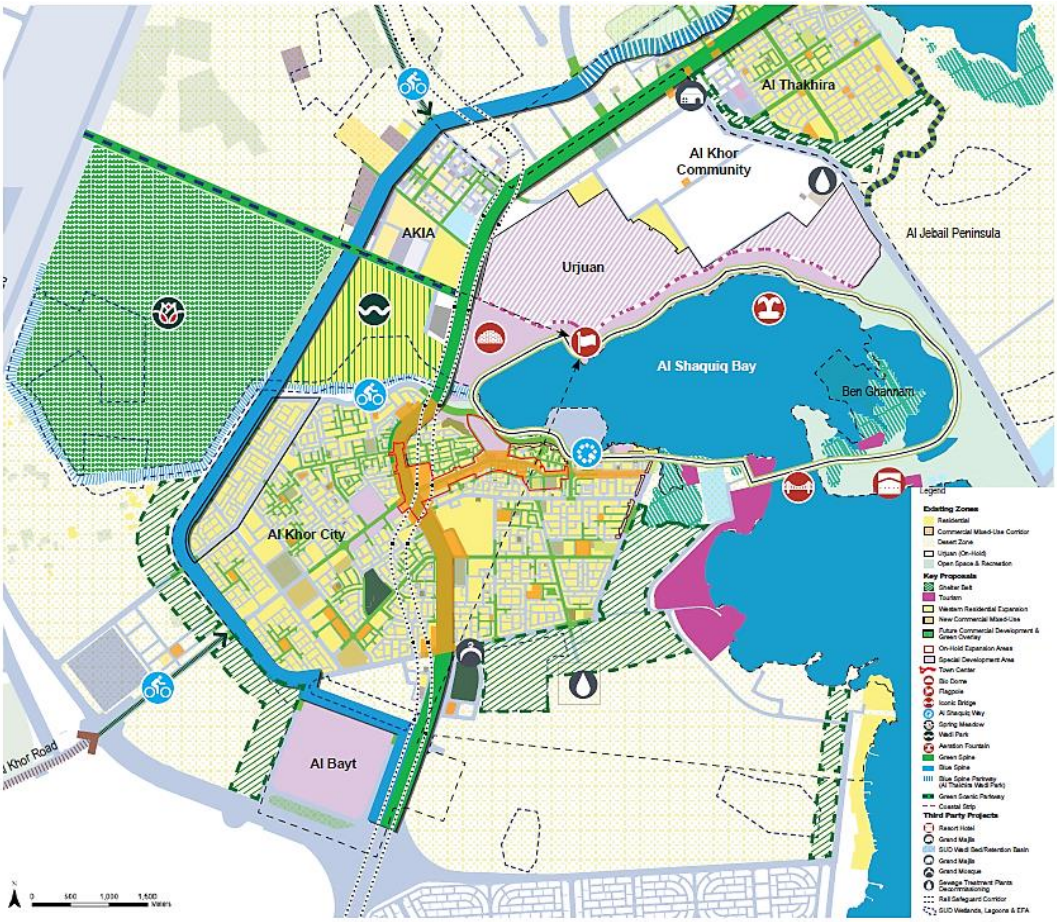


Fig. 3: Al Khor City Master Plan

3 Conclusion

The effects of global warming are noticeably changing weather patterns resulting in erratic storm events and pronounced flooding in gulf region. The climate change is also impacting natural environment and is causing desertification, biodiversity loss, pollution in marine and coastal areas, air pollution, and water scarcity and quality. The planning and development for the future warrant addressing solutions to these challenges and drainage water planning strategies are no exception. Keeping these challenges in view Al Khor drainage master plan is prepared which not only supports environment challenges but also provides a reliable and resilient drainage solution to manage flooding for current and future development conditions.

References

Ministry of Municipality, Infrastructure Planning Department (2017). Flood Mapping Portal. https://aldeera.gisqatar.org.qa/mmeflood/

Ministry of Municipality, Infrastructure Planning Department (2014). Utilities Planner Portal. https://swprupfs.mmaa.gov.qa/javaapps/mapviewer2/

Ministry of Municipality, Infrastructure Planning Department (2017). Qatar Rainfall and Runoff Characteristics. https://www.mme.gov.qa/webcenter/portal/MM

Ministry of Municipality, Urban Planning Department (2022). Al Khor City Master Plan.

Public Works Authority 'Ashghal', Design Department (2017). Qatar Integrated Drainage Master Plan.

Cite as: Qasem H. & Mahmood M., "Sustainable Urban Drainage Masterplan for Al Khor Municipality", *The 2nd International Conference on Civil Infrastructure and Construction (CIC 2023)*, Doha, Qatar, 5-8 February 2023, DOI: https://doi.org/10.29117/cic.2023.0180

The Importance and Evaluation of Environment-Friendly Megaprojects - As Perceived By Users

Ágnes Csiszárik-Kocsir
Keleti Károly Faculty of Business and Management, Óbuda University, Budapest, Hungary
kocsir.agnes@uni-obuda.hu

János Varga
Keleti Károly Faculty of Business and Management, Óbuda University, Budapest, Hungary
varga.janos@uni-obuda.hu

Abstract

The environmental degradation of our time, the environmental devastation of previous years and global warming have presented the world with new and novel challenges that were not experienced in previous decades. Rising sea levels, increasing energy demand and the explosion in energy prices have created new focal points in the thinking of all spheres of economic life. The environmental degradation of fossil fuels has led to an increasing focus on renewable energy sources and innovative solutions. The aim of this paper is to examine the main issues outlined above through the examples of two flagship megaprojects. The study will examine the Maldivian floating city and the European Energy Island project from a user perspective, specifically in terms of their environmental and visionary messages. In this study, we will examine the two flagship projects through the results of a primary research, formulating the main messages for the design of the future projects. The aim of the study is to demonstrate the importance of environmental considerations in the definition of project scope, in order to give a starting point for projects with similar objectives, and to give ideas for their design and implementation. The acceptance of any project by its users is a key success factor, as the two projects under review are intended to demonstrate.

Keywords: Change; Environment; Project; User evaluation

1 Introduction

It is a well-known fact that the impacts of environmental and climate change are extremely wide-ranging. Not only our quality of life, but also our health and future are determined by global processes that can be linked to changes in the natural environment (WHO, 2015; Costello et al., 2009). We can hardly be independent of environmental change. There are very few economic actors that are not directly or indirectly affected by some external environmental change. The environment in which economic actors operate has undergone significant changes in recent decades. Whereas in the past the pace of change was slower and the economic systems were not so extensive, these actors could operate in a much simpler, so-called static environment. In such an environment, the pace and speed of change was not so rapid that it would have placed a significant strain on the day-to-day functioning of economic agents. However, recent decades have changed this situation. After the Second World War, the world economy started to grow intensively, if we only look at GDP or world trade. Population growth has also been unprecedented in our history. It is practically impossible to list all the factors that have made the economic system of our time so complex and changeable. Yet the

effects of globalisation, the development of telecommunications and the spread of the internet (digitalisation), the emergence of new consumer awareness, the easier availability of resources, the proximity of distant markets, etc., are very often highlighted, as are new trends such as sustainability. The reasons for the slow shift from a static environment to a turbulent global environment are almost endless. Of course, this does not mean that all areas of life have the same environmental conditions. But we can say that most economic actors are experiencing an acceleration of events and that these changes require us to respond in some way. We can relate climate variability in the natural environment to sudden and irreversible changes in ecosystems (Malhi et al., 2019). This paper also focuses on changes in the natural environment as a primary focus of environmental change and presents examples of good responses to such challenges.

It was mentioned in the introduction that for most economic actors the world has accelerated and events are becoming more intense and varied, impacting on our daily lives (Russell-Jones, 2005). The complexity of economic globalisation and the increased dynamism of business have also led to a surge in unexpected events and changes. These come from our immediate environment and have an impact on our daily lives. Among the most significant environmental changes of our time are digitalisation, sustainability and the green transition, technological advances, the COVID-19 crisis, the Russian-Ukrainian conflict, the energy crisis and, last but not least, the environmental degradation that has been observed for decades, or the impact of global warming. There are common points and differences. The common point is that they all affect a large number of economic actors, while there is also a fundamental difference.

Part of the environmental change is taking place in the natural environment, which we can only influence indirectly, while the other part is taking place in the social environment. Global environmental change is a topic that is increasingly discussed in the literature (Pyhälä et al., 2016). Changes in the natural environment include global warming, the green transition or resource scarcity. Changes in these areas could be caused or triggered by human activity, but it is essentially the natural environment itself that is driving the change process. In the social environment, on the other hand, it is humanity, the economic actors, who cause the change and who carry out the change. Digitalisation or the conflict between Russia and Ukraine are clearly changes caused by humanity and are also being carried out by people themselves. Human activity, which is mostly a feature of the social environment, is changing many of the world's natural systems, including the climate system (McMichael et al., 2008).

Global environmental change is challenging both natural and social scientists to better understand. Global environmental change offers a strategy for combining the efforts of natural and social scientists to better understand how our actions affect global changes and how these changes affect us (NRC, 1992). Whatever the environment in which the change takes place, it will affect a narrow or broad range of actors. Each of the processes identified above has affected economic actors and people more broadly, so that none of the events has not been an epoch-shaping factor in recent years (Shi, 2018). Of the environmental changes, changes in the natural environment are the main focus. Among the changes in the natural environment, climate change is one of the most significant challenges (Lenton et al., 2019). It is a proven fact that climate change has negative impacts on people's lives (Stern, 2006).

In terms of concrete economic impacts, this is reflected in the deterioration of access to adequate drinking water, the negative impact on food production, and the deterioration of people's health and the quality and condition of the environment. Environmental change can only be considered in a

complex, even global, way (Norgaard-Bode, 1998). This is because ecological change cannot be limited to a narrow geographical context. Global warming or resource scarcity does not stop at national borders and does not discriminate between people and people. What is more, the effects of changes in the natural environment spill over into the social environment, where they have their real impact. Changes in the natural environment can all affect the lives of societies more widely, but this is not always the case in the social environment, where, for example, the closure of an economic organisation that did not have a large market share anyway may not affect the lives of many people. In the natural environment, there are fewer changes that are concentrated in a narrow segment of society, if only because, for example, natural disasters do not happen every day, but in the economy, new products may be released on a daily basis, causing changes in some consumers. The social environment is more likely to generate a number of changes, but not all of them are comprehensive. In the natural environment, we see fewer changes, but most of them have a knock-on effect on several people or economic actors.

The drive for sustainability, which has also become a dominant trend today and is linked to the natural environment, can also be seen as a response to changes in the natural environment. The concept of sustainability dates back to the 1960s, although its roots go back even further (McKenzie, 2004; Engelman, 2013). The underlying causes of sustainability can be highlighted as societal environmental changes, such as globalisation, market liberalisation, international factor mobility or the emergence of economic integration. These have been created by the social environment and have had an impact on the natural environment.

This has led to adverse processes in the natural environment, and nature has reacted in its own way. Climate change is now an alteration of the natural environment, the effects of which feed back into the environment that actually caused it, which was none other than our social environment. The consequences can be unforeseeable. Rising sea levels, rising average annual temperatures, water scarcity, drought, energy shortages, while our continuing population growth will only place greater demands on the planet's resources, which are in turn becoming increasingly scarce and scarce. Fossil fuels are extremely polluting, and we must take significant steps to keep our air and water clean. Climate change is a threat to vulnerable societies.

It can cause heat waves, floods, tornadoes, hurricanes, droughts, fires and the disappearance of glaciers (Cianconi et al., 2020; Church et al., 2013). We need new thinking and new awareness to protect the values of the natural environment. We need to implement projects and investments that are sufficiently innovative and green to mitigate or possibly prevent negative impacts on the natural environment and adverse changes in the natural environment. Understand the ecological dynamics of climate impacts, identify vulnerabilities and points of resilience. Identify intervention steps that can help build resilience of the biosphere to climate change. At the same time, ecosystems can also help mitigate and adapt to climate change. The mechanisms, opportunities and constraints of climate change solutions need to be explored and quantified as clearly as possible. Environmental problems are more common in developing countries and less developed countries need more money and investment to become more sustainable.

Developing countries need to invest more in promoting environmentally friendly activities and responding to the risks of climate change (Ahmed et al., 2018). However, there is no question that responding to environmental challenges requires funding and targeted investments, projects and development (Varga – Csiszárik-Kocsir, 2019; Dobos et al., 2022). Some people need to spend more

and others less, but we are talking about something that is a common concern for all. We have talked about global environmental change, which includes the word global.

2 Material and Method

The megaprojects presented in this study are included in the list of the top 50 projects published by the Project Management Institute (PMI, 2021). The questionnaire on which this study is based was completed in April 2022 by the survey respondents. The questionnaire included 14 megaprojects that were on the priority project list published by PMI. The projects included in the survey were selected on the basis of their relevance to the challenges of the 21st century, and thus projects with an environmental, innovation or digital aspect were selected for the survey. The survey was conducted using an online questionnaire with the survey facilitator present throughout. The projects were presented first and then the questionnaire on which the evaluation was based was completed. For each of the characteristics of the project scope, an effort was made to provide clear and general characteristics. Where the meaning of a characteristic was not clear to respondents, they were given the opportunity to clarify its meaning. The research was conducted as a pilot programme and is not intended to be repeated for the present projects. However, we intend to measure the priority projects on the 2022 project list on a larger sample of projects with similar criteria. The results obtained are intended to provide a basis for the design of future projects, in order to define similar project ideas and provide an external reference point for defining them.

The study presents two projects that address contemporary environmental problems, meet the requirements of environmental protection and conservation, and are considered to be important and interesting from a user perspective. The two selected projects (Energy Island, Maldives Floating City) were evaluated from the perspective of ordinary people as users, i.e. there was no educational background or previous project management experience as a prerequisite for inclusion in the sample, so the questionnaire on which the evaluation was based could be completed by anyone. Respondents were asked to rate the selected projects according to some factors of project scope. Respondents rated the factors on a scale of 1 to 4, with a value of 1 indicating a very weak factor and a value of 4 indicating a very strong factor. We then examined how respondents rated the project overall on a scale of 1 to 5, where 1 was the weakest and 5 the best, and then used significance analysis to see if there was a correlation between the specific scope characteristic and the overall rating of the project. There were 172 evaluable responses to the questions. Of the sample respondents, 39.5% had a tertiary education and 60.5% had a secondary education. 12.2% of the respondents are Generation Y, 23.3% are Generation X and 64.5% are Generation Z. The survey was conducted in April and May 2022.

3 Results

3.1 User Evaluation of the Maldives Floating City project

The 24th ranked Maldivian floating city project looks like a utopia at first glance. But the problem it seeks to solve is very real. The island nation will be one of the biggest victims of global warming in the near future. It is estimated that sea levels could rise by as much as half a metre by 2100, which means that 77% of the island group will be covered by water. That is why decision-makers have tried to run ahead and find a solution to the looming problem. The project itself would be built in a warm-water lagoon not far from the Maldivian capital. The project would provide homes for thousands of families, in addition to hospital and school facilities and commercial property. The floating city would rely entirely on renewable energy to protect the environment. The floating city would be both flexible and stable, following the geometric pattern of the local coral. If successful, the project could be a

model for all countries involved, as it would be the world's first and largest floating structure, with 5,000 floating houses. Construction was scheduled to start in 2022, which is estimated to take 5 years (PMI, 2021).

Respondents gave the project the highest average rating of interest and a very high rating of novelty, above 3.5. The uniqueness of the project and its future focus also received a high rating, with an average of over 3.4. In addition, the project design presented was considered by many to be useful, usable, of public interest and feasible. However, the respondents felt that the environmental, profit orientation, and cost saving aspects of the project were less dominant. Thus, many fear that the project will be implemented with a very high budget, which will be a problem in terms of usability and utilisation, i.e. poorer people, who are more in need, will not be able to benefit from this solution.

Table 1: Scope assessment of the Maldives floating city based on means and standard deviations

	Mean	**St. dev.**
Novelty	3,512	0,662
Usefulness	3,198	0,821
Interesting	3,558	0,594
Future Focus	3,465	0,737
Sustainability	2,971	0,812
Relevance	2,930	0,835
Feasibility	3,000	0,692
Usability	3,174	0,752
Public Interest	3,140	0,887
Profit Orientation	2,721	1,067
Uniqueness	3,494	0,662
Cost-Effectiveness	2,320	0,903
Environmental Awareness	2,860	0,881

When looking at the overall rating of the project, it was rated very highly by the respondents. Overall, they rated the project 3.98 on a five-point scale. The overwhelming majority of the ratings were in the positive direction, with only three respondents rating it as unsatisfactory, which clearly indicates acceptance and positive reception of the project idea.

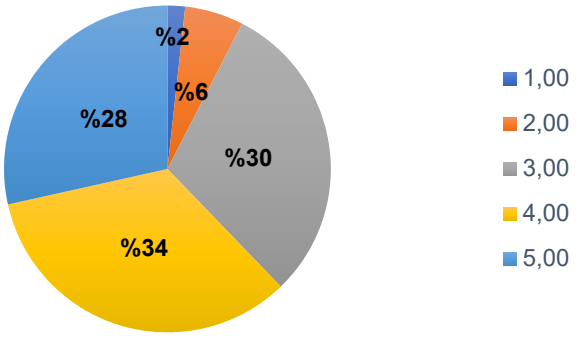


Fig. 1: Average rating of the Maldives Floating City project

We also wanted to find out whether the overall perception of the project is related to certain characteristics of the project scope. As shown in the Anova table below, a correlation was found for almost all characteristics, as the significance value was below 5% for all characteristics tested. This suggests that respondents who rated positively all the characteristics of the scope also rated the project itself highly. This shows that the project design presented a positive picture from the users' point of view, i.e. its innovativeness and novelty is certainly exemplary and should be followed if the project is successful.

Table 2: Correlation of the Maldivian Floating City scope elements with the project evaluation

	F	**Sig.**
Novelty	9,239	0,000
Usefulness	17,390	0,000
Interesting	12,740	0,000
Future Focus	25,109	0,000
Sustainability	10,214	0,000
Relevance	13,206	0,000
Feasibility	5,616	0,000
Usability	9,293	0,000
Public Interest	10,714	0,000
Profit Orientation	5,385	0,000
Uniqueness	4,206	0,003
Cost-Effectiveness	3,340	0,012
Environmental Awareness	9,985	0,000

3.2 Evaluation of the Energy Island Project from the User Perspective

The project ranked 9th in the PMI Top 50. Thirty years after Denmark built its first offshore wind farm, it is now embarking on another gigantic project to secure the country's entire energy supply from renewable sources. To do this, they want to create an artificial offshore island capable of collecting, storing and delivering the energy generated by the surrounding wind farms to where it is needed. The surplus energy that they plan to produce will be sold to other parts of Europe, providing part of their electricity supply from renewable energy sources. The project is scheduled to come on stream in 2023, and will be defined as one of the largest construction projects in the country's history in terms of budget. The gigantic scale of the project could once again serve as a model for other coastal countries, offering an alternative to renewable energy projects that take up land (PMI, 2021).

For some characteristics of the project coverage, it can be seen that, in contrast to the Maldives Floating City, there was a much higher proportion of characteristics above 3.5. The future focus of the project was ranked first, practically the highest on the scale, but utility, environmental awareness, public interest, sustainability and usability of the project were also highly rated (in descending order). The lowest score for each of the scope characteristics was for the profit orientation of the project, which was the only characteristic below 3 for the factors studied. At the very end of the list, in addition to profitability, were feasibility and cost-effectiveness. Overall, it can be said that the purpose of the project was clearly appreciated by the respondents.

Table 3: Assessment of the scope of the energy island based on means and variances

	Mean	St. dev.
Novelty	3,465	0,687
Usefulness	3,767	0,566
Interesting	3,465	0,737
Future Focus	3,831	0,460
Sustainability	3,593	0,628
Relevance	3,331	0,710
Feasibility	3,180	0,715
Usability	3,523	0,653
Public Interest	3,651	0,636
Profit Orientation	2,645	0,983
Uniqueness	3,285	0,806
Cost-Effectiveness	3,093	0,818
Environmental Awareness	3,698	0,603

If we look at the average project rating, it is much higher than for the previous project. Respondents rated the project above 4.4 on a five-point scale, which is a very high level of acceptance. Almost 60% of respondents gave the project a rating of 5, the highest on the scale. Among the ratings, there is no score of one, and only 3 out of 2. This shows that respondents were positive about the project plan to tackle the energy crisis, and that the success of the project could be an example for other countries to follow in responding to the increasingly serious energy issue of today.

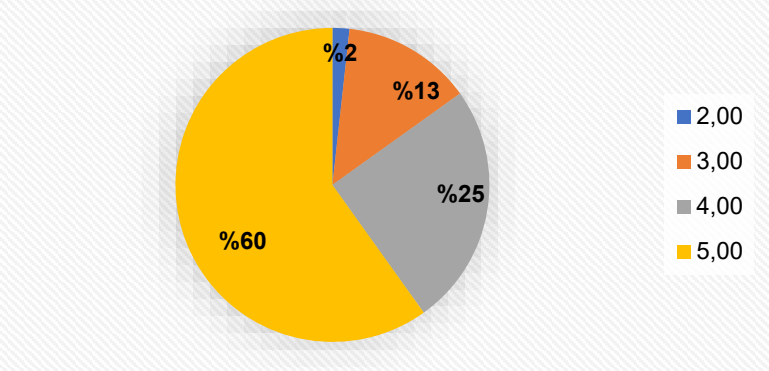


Fig. 2: Average evaluation of the Energy Island project

As with the previous project, we were interested to see if there was a significant relationship between the rating of each feature of the project scope and the overall rating of the project. In this case, too, this relationship was found for the vast majority of the individual characteristics. Only project orientation and uniqueness did not show a significant correlation with the users' perception of the project, i.e. it can be stated that there is a clearly detectable relationship between those who positively evaluated the project and the overall acceptance of the scope.

Table 4: Correlation of energy island scope elements with project evaluation

	F	Sig.
Novelty	7,732	0,000
Usefulness	22,470	0,000
Interesting	7,665	0,000
Future Focus	21,391	0,000
Sustainability	10,402	0,000
Relevance	9,196	0,000
Feasibility	2,692	0,048
Usability	16,390	0,000
Public Interest	19,501	0,000
Profit Orientation	0,456	0,714
Uniqueness	1,262	0,289
Cost-Effectiveness	5,479	0,001
Environmental Awareness	3,725	0,013

4 Conclusion

Today's increasingly serious environmental problems call for new and innovative solutions. The challenges that have arisen from the environmental degradation of previous years cannot be tackled by traditional means because our existing knowledge is finite. That is why only innovation can provide solutions. The two projects presented in this study are highly regarded for their innovation. Both projects aim to address acute problems that could become serious in the decades ahead. Rising sea levels, the increasing depletion of conventional energy sources and the environmental damage they are causing are problems that must be addressed. The project plans presented in this study can only be described as pilot programmes for the time being, but their success will provide solutions to the problems described above. The positive nature of the projects has been demonstrated by the present non-representative research and can be used as a model for future similar projects in order to provide more workable solutions to the challenges of environmental degradation. We intend to continue this research in the future, especially during the implementation phase of the projects, in order to provide a starting point for future projects with similar objectives.

Acknowledgement

The paper was prepared with the support of Széll Kálmán Public Finance Research Group of the University of Public Service.

References

Ahmed, N., Khan, I. & Augustine, A. (2018) Climate change and environmental degradation: a serious threat to global security. *European Journal of Social Sciences Studies*. doi:http://dx.doi.org/10.46827/ejsss.v0i0.394

Church, et al. (2013) *Sea Level Change*. Cambridge University Press Cambridge, United Kingdom.

Cianconi, P., Betró, S. & Janiri, L. (2020) The Impact of Climate Change on Mental Health: A Systematic Descriptive Review. Frontiers in Psychiatry. 06 March 2020 https://doi.org/10.3389/fpsyt.2020.00074

Costello, et al. (2209) Managing the health effects of climate change. Lancet. 2009:373:1693–733.

Dobos, et al. (2022) How Generation Z managers think about the agility in a world of digitalization. In: Szakál, Anikó (ed.) IEEE 20th Jubilee World Symposium on Applied Machine Intelligence and Informatics SAMI (2022): Proceedings, Poprad, Slovakia, pp. 207-212.

Engelman, R. (2013) *Beyond Sustainable Instate of the World: Is Sustainability Still Possible*? Washington DC: Island Press.

Lenton, et al. (2019) Climate tipping points - too risky to bet against. Nature 575, pp. 592-595. doi:10.1038/d41586-019-03595-0

Malhi, et al. (2020) Climate change and ecosystems: threats, opportunities and solutions. Phil. Trans. R.S. https://doi.org/10.1098/rstb.2019.0104

McKenzie, S. (2004). Social sustainability: towards some definitions. Hawke Research Institute. Working Paper Series. No. 27. University of South Australia. 2004.

McMichael, A. J., Friel, S., Nyong, A. & Corvalan, C. (2008) Global environmental change and health: impacts, inequalities, and the health sector. BMJ. 2008 Jan 26; 336 (7637):191-4. doi: 10.1136/bmj.39392.473727

National Research Council (NRC). (1992) Division of behavioral and social sciences and education; Board on environmental change and society; Committee on the Human Dimensions of Global Change.

Norgaard, R. B. & Bode, C. (1998) Next, the value of God, and other reactions. *Ecological Economics*, 25, 1, pp. 37-39.

Pyhälä, et al. (2016) Global environmental change: local perceptions, understandings, and explanations. *Ecology and Society 21*(3):25. http://dx.doi.org/10.5751/ES-08482-210325

Russell-Jones, N (2005) Change management. Manager Ltd. Budapest.

Shi, Z. (2018) Impact of climate change on the global environment and associated human health. *Open Access Library Journal*, 5, 1-6. doi: 10.4236/oalib.1104934.

Stern, N. (2006). *Stern review on the economics of climate change*. Cambridge University Press, New York. (Internet: http://www.hm-treasury.gov.uk)

Varga, J. & Csiszárik-Kocsir, Á. (2019) Redefining the Role of Project Leader for Achieving a Better Project Result. *PM World Journal*, 8: 8 pp. 1-18.

World Health Organization (2015). WHO calls for urgent action to protect health from climate change-sign the call http://www.who.int/globalchange/global-campaign/cop21/en/

Cite as: Csiszárik-Kocsir Á. & Varga J., "The Importance and Evaluation of Environment-Friendly Megaprojects - As Perceived By Users", *The 2nd International Conference on Civil Infrastructure and Construction (CIC 2023)*, Doha, Qatar, 5-8 February 2023, DOI: https://doi.org/10.29117/cic.2023.0181

A Multi-Criteria Decision-Making Approach for Selection of Wave Energy Converter Optimal Site

Alireza Shadmani
Department of Maritime Engineering, Amirkabir University of Technology (Tehran Polytechnic), Tehran, Iran
alireza.shadmani@aut.ac.ir

Mohammad Reza Nikoo
Department of Civil and Architectural Engineering, College of Engineering, Sultan Qaboos University, Muscat, Oman
m.reza@squ.edu.om

Amir H. Gandomi
Faculty of Engineering and Information Technology, University of Technology Sydney, Ultimo, Australia; University Research and Innovation Center (EKIK), Óbuda University, Budapest, Hungary
gandomi@uts.edu.au

Ghazi Al-Rawas
Department of Civil and Architectural Engineering, College of Engineering, Sultan Qaboos University, Muscat, Oman
ghazi@squ.edu.om

Abstract

Ocean wave energy is an essential source of renewable power for coastal communities. Choosing the optimal site for the wave energy converter (WEC) deployment depends on a number of criteria. The characteristics of the WEC must be taken into account in the prediction power supply, whereas the local sea state is connected to elements like wave condition (as a representation of construction budget) and energy output as well as the influence of the exploitable storage of wave energy and its trend. As a result, this research provides a multi-criteria decision-making (MCDM) strategy for considering several factors simultaneously to choose the best possible site. The suggested MCDM technique incorporates two primary factors, i.e., exploitable storage of wave energy and energy production, into a single metric that takes into account both WEC efficiency of a particular type, WEPTOS, and sea state to aid decision-makers in the development of a pilot project. The method was then used to analyse the waves at two locations that had been identified as promising sites for harvesting wave energy along the coast of Oman. To further assess a site's potential upcoming pilot project and select the most efficient WEC, we compared the MCDM results at the stations with certain WEC types. In conclusion, optimal sites for placement of the WEPTOS WEC along the coast of Oman were identified considering the highest annual energy production and exploitable energy storage. Through solving the MCDM technique, 17 sites were pinpointed, and only 6 points were picked up.

Keywords: Ocean wave energy; Wave energy converter; Optimal site; Multi-Criteria Decision-Making

1 Introduction

The use of fossil fuels has resulted in detrimental climate change and global warming. Due to their scarcity, research and industrial initiatives have shifted their focus toward finding sustainable alternatives, and renewable energy has emerged as a focal point in the recent development plans of the majority of industrialized and some emerging countries. Solar, wind, hydropower, and marine (tide and wave) energy

are only a few renewable energy sources that might be used to meet the world's clean energy needs in the future. While solar and wind power are both widely available, marine power is still in the prototyping phase, and advancement in wave energy converter technology (WEC) into economically sustainable accomplishments has been gradual, even in regions with high wave activity. However, research into the criteria for choosing the ideal site for a certain WEC is irreversible. Recently, Portilla et al. (2013) found that it is more effective to gather wave energy in locations with minimum power but temporally stable settings. As described by Dunnet and Wallace (2009), locations with a higher mean annual wave power were chosen for wave energy harvesting and device efficiency analysis.

Existing resource stability and viability must be taken into account while formulating a strategy for long-term growth. When compared to other forms of renewable marine energy, wave power has a higher energy density, making it more practical for large-scale energy extraction in places bordering open sea bodies. WECs have a potential economic benefit due to their relatively cheap capital costs, which are expected to fall further when new, specialized businesses for WEC components and subcomponents arise. WECs are equally visually intrusive to neighbouring homes as wind turbines or solar panels, despite their modest profile. Furthermore, unlike other renewable energy sources such as wind and solar, wave energy can be predicted with greater accuracy. Technically, WEC's key benefit is its predictability, which distinguishes it from other renewable energy sources that might experience abrupt and unpredicted variations in output. WECs may also be utilized as coast protection measures, according to recent research by (Mendoza et al., 2014). Because of these benefits, wave energy is a good fossil fuel replacement for seaside communities where some energy needs are met. Preserving the WECs for the future, particularly in the face of harsh weather, is one of the key technological difficulties that have to be explored, as stated by Leijon et al. (2006), Pontes (1998), Cornett (2009), Arinaga and Cheung (2012). Optimizing the system's efficiency is yet another issue that may be considered in terms of structural and economic considerations. Therefore, for planning and adjusting the WECs, wave power must be accessible and available, as well as an accurate forecast of energy generation, (Shadmani et al., 2022). Additionally, uncertainty surrounding wave energy assessment and site selection, which must consider climatic unpredictability, contributes to the industry's delayed development. Additionally, recent research has shown that regions with a reduced power source but more constant weather are more suitable and trustworthy for harvesting wave energy, (Morim et al., 2014; Monteforte et al., 2015).

Initially, it has been shown that the potential energy output is one of many factors in deciding where to collect wave energy. Second, determining the optimal site to analyse WEC performance has been done using a variety of parameters. Because of this, this research will present a multi-criteria decision-making (MCDM) method based on exploitable energy storage and energy production for selecting the optimal site, one that considers device performance alongside wave condition and resource sustainability. In order to determine the optimal sites for a particular WEC type, WEPTOS, we will use wave power characteristics from two locations, each of them situated in a separate water depth.

2 Methodology

Several criteria and circumstances determine the optimal site for harvesting wave energy. Key criteria in WEC installation include the features of exploitable and total wave energy storage, accessibility, availability, monthly and yearly energy output, monthly variability index, and design wave height, (Kamranzad et al., 2020). Evaluating the aforementioned factors will reveal the optimal site and best equipment to use under certain circumstances. To take into account all relevant factors, we propose a multi-criteria decision-making (MCDM) technique based on the above parameters.

On the basis of the authors' prior research in the seas near the borders of Oman, namely the Gulf of Oman, we will make estimates of the relevant parameters at two regional sites to examine the efficacy of the

suggested technique. This research provides a useful application for the findings of prior research and reaches a judgement that can be used by decision-makers regarding which of the stations as far discussed is best situated to provide some of the energy needs through wave power. The dataset is briefly explained in the next section, followed by a description of the selected stations.

2.1 Wave Energy Resource

Incorporating a large-scale collection of waves modelled numerically across time, wave energy resources have been explored in the waters around Oman, the Gulf of Oman border. The potential of wave energy in the Gulf of Oman has been assessed for two stations using the wave data collected from the offshore buoys, as shown in Figure 1. The present study's major criteria for selecting hotspots were the availability of energy and the suggested criteria for taking into account the sustainable and long-term consistency of the resources. While this paper proposes a technique for evaluating WEC performance, such evaluation has not yet been conducted thoroughly.

The wind and wave conditions in each of these water bodies vary seasonally and annually. For instance, the fall is when the Gulf of Oman's wave environment is at its peak. Due to its proximity to the Indian Ocean, the Gulf of Oman has summer monsoons that significantly influence the wave environment, causing southern waves to predominate throughout the monsoon season. For further information on wave modelling and wave energy estimate in the Gulf of Oman. SWAN (Simulating Waves Nearshore) model has been used to simulate the wave field. The ECMWF's modified ERA5 product, localized and adjusted in each research region, served as the forcing. Each wind component has had its wind field modified to accommodate changes in the wind's direction and magnitude. Mazaheri et al. (2013) provides further information regarding the influential variables derived from the used wind domain. The wave strength was then determined, and its spatiotemporal fluctuation in each location was assessed using the dataset of wave characteristics in long-term that had been created. The equation ($P = 0.49H_s^2 \times T_e$) was used to determine the wave power (P) for deep sea circumstances, where H_s is significant wave height and T_e is the energy period ($T_e = m_{-1}/m_0$).

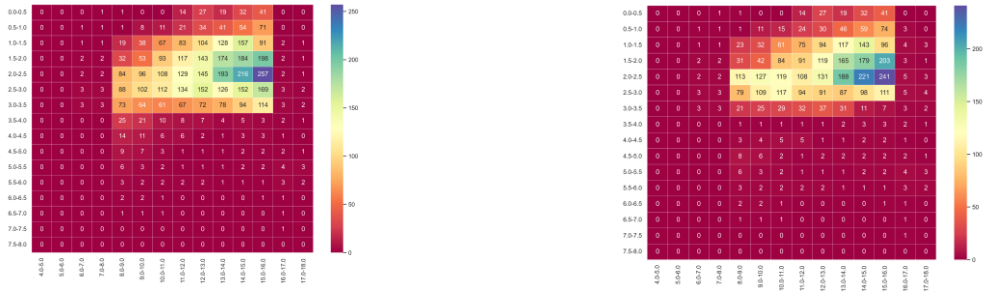
In order to generate the wave features in the more promising places, noticeably higher-resolution local models were constructed using the boundary condition generated from the master versions. The spatio-temporal wave energy variability was then investigated using refined wave data, and the best position was chosen while considering the local resources' sustainability. Last but not least, the best position within each body of water was chosen based on various variables, such as the amount of energy, unpredictability, and frequency of wave power over a specific threshold, and the depth at which WECs may be deployed. Figure 1 displays the chosen sites in the Gulf of Oman (Barka and Quriyat). According to a regional assessment of wave energy capacity, the aforementioned two stations not only have the greatest promise, but also are the best fit in terms of sustainability.



Fig. 1: Selected sites along coast of Oman

2.2 Wave Energy Converter Type

Since the wave characteristics significantly influence the WEC's efficiency, it is different from several forms of renewable energy because there are several proven technologies to produce energy. As a result, the most suitable WECs are often most effective within the typical parameters of the considerable wave heights and times. A power wave resource evaluation is necessary to calculate the amount of usable electricity produced by a certain WEC device at a given location. The total electric output may be obtained towards this end when the device's power matrix is multiplied by the wave resource matrix (the probability of occurrences), a more accurate prediction may be made (i.e., the electric production for various sea conditions) (Margheritini et al., 2009). Figure 2 depicts the wave resource matrix at two considered stations, Barka and Quriyat.



(a) **(b)**

Fig. 2: Probability of occurrence of different wave conditions at **(a)** Barka station and **(b)** Quriyat station

Despite the numerous devices for collecting wave energy, WEPTOS WEC, a new and innovative one, is considered in this research, presented by (Pecher et al., 2012). With a smart structure that can adjust the amount of incoming wave energy and minimize loads in harsh wave environments, the WEPTOS WEC is a unique device that combines a well-known and influential wave energy absorption mechanism. This novel WEC type, as seen in Figure 3, might be deployed strategically to maximize wave energy extraction. Through various rotor modes, this movable A-shaped, slack-moored, floating structure absorbs the energy of the waves. The rotors on each leg pivot around a single axle, which allows them to send the absorbed power to a single power take-off (PTO) mechanism. In order to capture wave energy in a brand-new and creative way, the WEPTOS WEC uses an established technique. The WEPTOS structure's survival capacity has been crucial since its conception.



Fig. 3: WEPTOS WEC structure

The primary features of the devices under consideration are listed in Table 1 after being compiled from the appropriate sources. Energy output will be studied annually and monthly timescales to account for the effects of climatic variability on the devices' operation.

Table 1: Main characteristics of WEPTOS WEC

Technology	Rated Power (kW)	Classification	Matrix resolution
			$(H_s \times T_e)$
WEPTOS	3587	Attenuator	$0.5\ m\ \times 1.0\ s$

2.3 Total Exploitable Storage and Energy Production

Total and exploitable wave energy per unit area (E_t and E_e, respectively) were determined as part of an effort to look at the viability of using WECs in various stations:

$$E_t = P_{mean} \times t \quad (1)$$

$$E_e = P_{mean} \times t_e \quad (2)$$

Where, t is the sum of all hours in a year (=8760 h), t_e is the sum of all hours that correspond to wave power higher than a threshold (2 kW/m) and P_{mean} represents the mean wave power. Energy output (E_0) was determined using the following equations to compare the effectiveness of each WEC at various sites:

$$E_0 = \sum_{i=1}^{n_T} \sum_{j=1}^{n_H} p_{ij} P_{ij} \quad (3)$$

where $\boldsymbol{p_{ij}}$ is the proportion of periods a certain sea state occurs, as specified by significant wave height ($\boldsymbol{H_s}$) and energy period ($\boldsymbol{T_e = m_{-1}/m_0}$). WEC's electrical power output, denoted by $\boldsymbol{P_{ij}}$, corresponds to an identical energy bin. Monthly energy output was computed using the power matrix of the WEPTOS WEC, as illustrated in Figure 4.

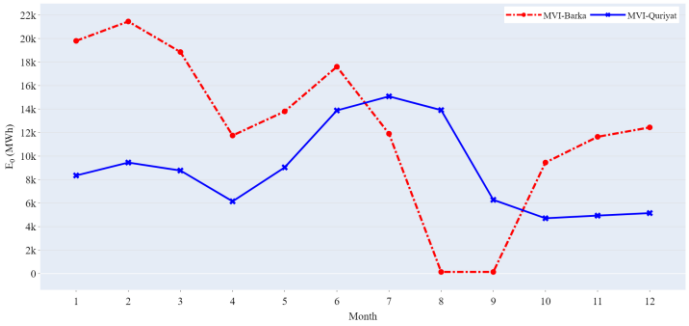


Fig. 4: Monthly variability of energy output at two considered stations

2.4 Multi-criteria Decision-making Approach

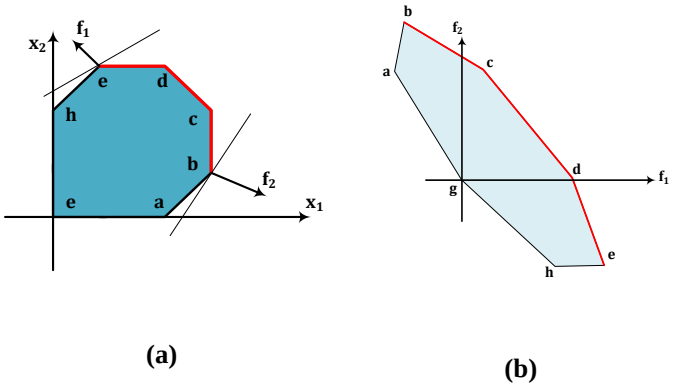
Multi-criteria decision-making (MCDM), often referred to as multiple criteria decision analysis (MCDA), is a study topic that examines numerous options in a circumstance or research subject that encompasses ordinary activities, social sciences, engineering, medicine, and many other disciplines. MCDM is one of the most prominent decision-making strategies applied in numerous domains (Bruno & Genovese, 2018).

MCDM assesses the criteria to evaluate if each criterion is a desirable or undesirable decision for a given application. It also tries to evaluate this criterion, depending on the specified criteria, against

every other accessible choice in an effort to aid the decision maker in picking an alternative with the lowest tradeoff and greatest benefits. The factors utilized in assessing these criteria might be either deductive or inductive. There are many methods available for solving MCDM problems, such as Analytic Hierarchy Process (AHP), Technique for Order of Preference by Similarities to Ideal Solution (TOPSIS), Elimination Et Choix Traduisant la Realite (ELECTRE), Preference Ranking Organization Method for Enrichment of Evaluations (PROMETHEE), ViseKriterijumska Optimizcija i Kaompromisno Resenje (VIKOR), and Data Envelopment Analysis (DEA). In this study, a TOPSIS method is used to evaluate the model.

TOPSIS is a valuable MCDM technique. This is an alternate method that uses parameter weights to normalize score distributions and identify the best possible solution, which meets all criteria. For best results, it employs a straightforward mathematical technique. TOPSIS's guiding principle is to choose the option that is geometrically closest to the positive ideal solution and farthest from the negative ideal solution, as measured by the Euclidean distance. By adding together, the greatest possible results for each option, we get the positive ideal solution (X_+). The negative ideal solution (X_-) incorporates all the lowest possible values for each feasible choice. Both answers are speculative and derived from this procedure. This approach does this by determining how close a given value is to the positive ideal solution. In light of the evaluation and computation, we decide on a different priority (γ), as shown in Figure 4. This MCDM approach is often used to address practical issues. It is a simple method that can efficiently compute and evaluate the relative merits of several possibilities for making a decision.

Therefore, our proposed approach for locating optimal sites for deployment of WECs is illustrated in Figure 5, which is integrated with the wave generation model, SWAN.



(a) **(b)**

Fig. 4: Demonstration of **(a)** decision space and **(b)** solutions in the criterion space

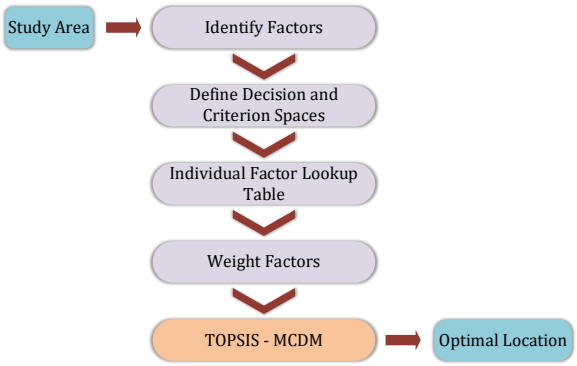


Fig. 5: Proposed methodology

3 Results

In summary, this study performs an MCDM approach to locate the optimal sites along the coast of Oman for emplacing the WECs. Two primary factors have been employed in this approach: exploitable energy storage of wave energy and energy production, which carry out the decision-making process through the TOPSIS-based MCDM approach. In addition, the best locations are found on the basis of WEPTOS WEC deployment, which is a novel WEC type. As a result of examining these two items, it is possible to quickly and easily evaluate the relative merits of several stations.

Comparing the chosen stations revealed that, while being shallower, the Barka station had larger exploitable storage of wave energy (E_e), reaching around 3212 kWh/m. where wave heights are greater, and the environment is harsh in certain seasons, with monsoon predominating in summer. Quriyat, which is east of Muscat, has the second-highest wave energy storage that may be used. This region is subject to swells in pre-monsoon and locally produced high waves during the monsoon. E_e/E_t, a measure of the exploitable storage of wave energy, shows that Barka has the highest value (19.8%). The percentage at Quriyat, where 13.1% of the total wave energy (E_t) storages are exploitable, is the second highest. Accordingly, Quriyat seems to be the greatest place for wave energy extraction despite Barka having a large ratio of wave energy that may be exploited for overall wave energy storage.

Table 2: Wave energy properties in each station along the coast of Oman

Station:	$P_{mean}\ (kW/m)$	$t_e\ (hr)$	$E_t\ (kWh/m)$	$E_e\ (kWh/m)$	E_e/E_t (%)
Barka	1.85	1736.4	16206	3212.3	19.8%
Quriyat	1.2	1149.3	10512	1379.2	13.1%

Based on the results presented in Table 3, Barka provides higher annual mean energy production, while Quriyat produce the least energy. The concentration of optimal sites is near the Barka station, where WEPTOS can generate the highest annual mean energy production with considerable amounts.

In the wave energy map, 17 sites (PO1, …, PO17) were positioned as shoreline sites based on the most relevant patterns for the spatial variability of the wave energy, which correspond to the energy conditions in an average year (Figure 6). The reddish colours dominating the colour scale show that the average wave energy is comparable for all the nearshore places shown, with values around 23460 MWh. Finding the optimal site to deploy the WEC is not simple at first glance. It will depend on each sea state's contribution to each research site. The existence of two further offshore locations (PO11 and PO12) can be seen on the wave energy map and would be useful for future energy studies about the potential building of an offshore wave farm.

Table 3: Annual mean energy production in each station

	Barka $E_0\ (MWh)$	Quriyat $E_0\ (MWh)$
WEPTOS	3248	2135

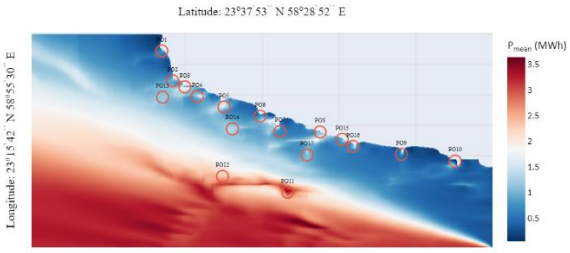


Fig. 6: Optimal sites selected based on the MCDM approach

Figure 7 shows a map of the predicted energy production from a WEPTOS WEC pilot project along the shore. The nearshore zone, which includes sea depths between 9 and 15 m, is shown on this map with its geographic variations. By mapping the wave energy map with the wave energy of WEPTOS, a reduction in the number of potential sites for the WEC installation from the previously specified 17 points to only six (PO3, PO5, PO6, PO7, PO8, PO16) has been determined. The six locations pinpointed in Figure 7 produce energy at yearly production levels of around 34868 MWh. It is essential to note the emergence of additional exploitation-prone regions that were not initially anticipated as locations that would produce energy at levels near 26770 MWh. The aforementioned situations cause the incidence of sea states relapsing inside the ranges of greater efficiency.

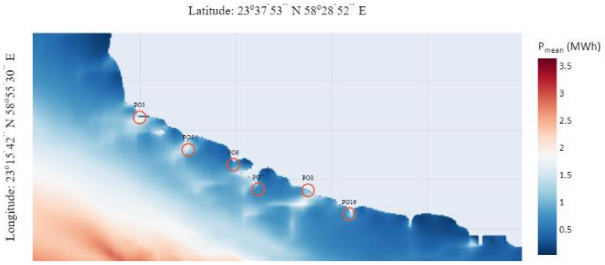


Fig. 7: Mapped wave energy from WEC along the coast of Oman between 9 and 15 m water depth

4 Conclusion

Finding the coastal regions where the process of refraction or shoaling focuses solely on the wave energy into the so-called spots or locations with the most energy is one of the main goals of any evaluation of the wave resource. In terms of where wave farms may be located, these nearshore areas are particularly intriguing. In this research, wind data from the ECMWF were combined with wave data from offshore buoys. In addition, two key criteria—exploitable energy storage and energy production for a specific WEC type, WEPTOS—were taken into account for determining the best locations using a TOPSIS-based MCDM technique. 17 sites were identified as a consequence of the propagation of these instances using a wave model from offshore conditions to the shoreline. Given that Oman's coastline is devoid of any other WEC plants and that the study zone is one of the most active ones, the locations spotted here seem to be valuable sites that may be tapped in future.

Conclusively, it should be noted that these two components are not the only ones that should be taken into consideration. The location of a future wave farm installation may be influenced by other components, such as the effects of local and national development, availability, accessibility, and the monthly variability index. Even in such situation, MCDM may be used to rank the possibilities since it gives the necessary details about the viability of various device-station combinations for future sustainable growth based not only on the amount of electricity generated but also on the unpredictability of the output.

References

Arinaga, R. A. & Cheung, K. F. (2012), "Atlas of global wave energy from 10 years of reanalysis and hindcast data", *Renewable Energy*, *39*(1), pp. 49-64. https://doi.org/10.1016/j.renene.2011.06.039

Bruno, G. & Genovese, A. (2018), "Multi-Criteria Decision-Making: advances in theory and applications—an introduction to the special issue", *Soft Computing*, *22*, 7313-7314. https://doi.org/10.1007/s00500-018-3531-0

Cornett, A. M. (2009), "A global wave energy resource assessment", Proceeding of the Eighteenth International Offshore and Polar Engineering Conference, Vancouver, Canada, *50*, pp. 59-64.

Dunnet, D. & Wallace, J. S. (2009), "Electricity generation from wave power in Canada", *Renewable Energy*, *34*(1), pp. 179-195. https://doi.org/10.1016/j.renene.2008.04.034

Kamranzad, B. & Hadadpout, S. (2020), "A multi-criteria approach for selection of wave energy converter/location", *Energy*, *204*, 117924. https://doi.org/10.1016/j.energy.2020.117924

Leijon, et al. (2006), "An electrical approach to wave energy conversion", *Renewable Energy*, *31*(9), pp. 1309-1319. https://doi.org/10.1016/j.renene.2005.07.009

Margheritini, L., Vicinanza, D. & Frigaard, P. (2009), "SSG wave energy converter: Design, reliability and hydraulic performance of an innovative overtopping device", *Renewable Energy*, *35*(5), pp. 1371-1380. https://doi.org/10.1016/j.renene.2008.09.009

Mazaheri, S., Kamranzad, B. & Hajivalie, F. (2013), "Modification of 32 years ECMWF wind field using QuikSCAT data for wave hindcasting in Iranian Seas", *Journal of Coastal Research*, *65*, pp. 344-350. https://doi.org/10.2112/SI65-059.1

Mendoza, et al. (2014), "Beach response to wave energy converter farms acting as coastal defence", *Coastal Engineering*, *87*, pp. 97-111. https://doi.org/10.1016/j.coastaleng.2013.10.018

Monteforte, M., Lo Re, C. & Ferreri, G.B. (2015), "Wave energy assessment in Sicily (Italy)", *Renewable Energy*, *78*, pp. 276-287. https://doi.org/10.1016/j.renene.2015.01.006

Morim, et al. (2014), "A review of wave energy estimates for nearshore shelf waters off Australia", *International Journal of Marine Energy*, *7*, pp. 57-70. https://doi.org/10.1016/j.ijome.2014.09.002

Pecher, A., Kofoed, J. P. & Larsen, T. (2012), "Design Specifications for the Hanstholm WEPTOS Wave Energy Converter", *Energies*, *5*, pp. 1001-1017. https://doi.org/10.3390/en5041001

Pontes, M. T. (1998), "Assessing the European Wave Energy Resource", *J. Offshore Mech. Arct. Eng*., *120*(4), pp. 226-231. https://doi.org/10.1115/1.2829544

Portilla, J., Sosa, J. & Cavaleri, L. (2013). "Wave energy resources: Wave climate and exploitation", *Renewable Energy*, *57*, pp. 594-605. https://doi.org/10.1016/j.renene.2013.02.032

Shadmani, et al. (2022), "The optimal configuration of wave energy conversions respective to the nearshore wave energy potential", *Energies*, *15*(20), 7734, https://doi.org/10.3390/en15207734

Cite as: Shadmani A., Nikoo M.R., Gandomi A.H. & Al-Rawas G., "A Multi-Criteria Decision-Making Approach for Selection of Wave Energy Converter Optimal Site", *The 2nd International Conference on Civil Infrastructure and Construction (CIC 2023)*, Doha, Qatar, 5-8 February 2023, DOI: https://doi.org/10.29117/cic.2023.0182

Physico–mechanical Properties of Sustainable Building Material Based Gypsum and Recycled Polyethylene Waste

Djoudi Amina
Laboratory of Civil Engineering Research (LRGC), Faculty of Civil engineering and architecture,
University of Amar Thelidji, Laghouat, Algeria
aminag0012@yahoo.fr

Abstract

The economic focus in the building sector is on lightweight materials. Recycled polyethylene particles coming from plastic botteles waste can ensure this lightness and can solve not only technical problems, but also produce economic and environmental benefits. Different polyethylene particle proportions of 5,10,15,20 and 25% were introduced in gypsum mortar in order to characterize its physical and mechanical properties. Results proved the positive effect of the introducing of PET particles in the matrix of gypsum mortar, the lightening of this material but a decrease of mechanical properties was recorded comparing in to reference without polyethylene particles. This new material with promising functional properties can be used as a masonry element in a new construction or in the rehabilitation of the old building.

Keywords: Gypsum; Plaster; Waste; Polyethylene; Mechanical strength; Microstructure

1 Introduction

The present day construction industry mainly focuses on the reduction of waste accumulation by effective utilization of wastes and by-products in the production of high value building units (Sophia & Sakthieswaran, 2019). Ouakarrouch et al. (2019) shows that the addition of waste chicken feathers to the plaster leads to a remarkable reduction in apparent density of about 12.3%. The results of Markssuel et al. (2020) proved the feasibility of using the waste in renderings to repair the studied buildings, namely when 25% of sand was replaced with waste. With this composition, flexural strength increased from 0.91 MPa to 1.33 MPa and compressive strength from 1.89 MPa to 3.18 MPa. Jiménez Rivero et al. (2014) and in view of their experimental results, the mechanical strength of plaster decreases with an increase in waste rubber addition. In the present study, taking into account the proportions of recycled polyethylene particles on the physical and mechanical effectiveness of gypsum mortar after hardening. The mechanical and physical properties obtained from the experiments were compared with theoretical evaluations.

2 Materials and Methods

The plaster used in this study is a product of commercial available gypsum. Natural quartz sand 0/2 mm with continuous granulometry and polyethylene terephthalate (PET) particles of plastic recycled bottles waste were used in this study (Fig. 1). Aerial lime is selected in this reasearch as a setting retarder of the plaster because it is liable to decrease its solubility and to increase its time of use.



Fig. 1: Polyethylene terephthalate (PET) particles of plastic recycled bottles

For the formulation of the studied gypsum mortar, the recommendations given by CNERIB (National Centre for Studies and Researches Integrated to Building) have been used:

First, we fixed the Water/Plaster ratio (W/P= 0.60) equal to the saturation mixing ratio. We fix the plaster/sand ratio (P/S = 0.50) by weight (also recommended by the CNERIB (1993) because, according to CNERIB's recommendations (1993), an excess in the sand quantity reduces the mechanical properties of the plaster-based materials.

Regarding the lightweight aggregates, the polyethylene terephthalate (PET) particles were incorporated in a matrix consisting of 'plaster + sand'; the percentages by weight of polyethylene terephthalate (PET) particles varied from 5 to 25% with steps of 5%. The density of the studied composites was determined by measuring the weight and the volumes of samples. The flexural strength was measured on 4x4x16cm^3 prisms and the compressive strength on 4x4x4cm^3 cubes using a universal press of type ''Controls'' (EN196-1).

3 Results and Discussion

Fig. 2 shows that the density of gypsum mortar decreases with the increase of the quantity of the polyethylene terephthalate (PET) particles. this can be attributed to the low density of the PET aggregates used (257 kg/m^3) hence the beneficial effect of the lightening of the the elaborate material. Our results are concurs with the works of (Laoubi et al., 2018).

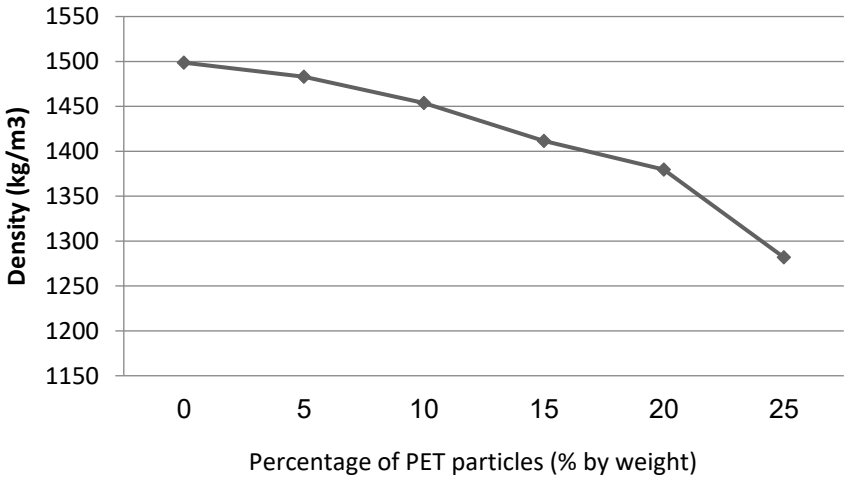


Fig. 2: Variation of the density of gypsum mortar according to the percentage by weight of PET particles

Fig. 3 presents the variation of the porosity of gypsum mortar according to the percentage of PET particles. It is clear that the porosity of the composite decreases compared to plaster alone but it increase slightely with the increase of the quantity of PET particles.

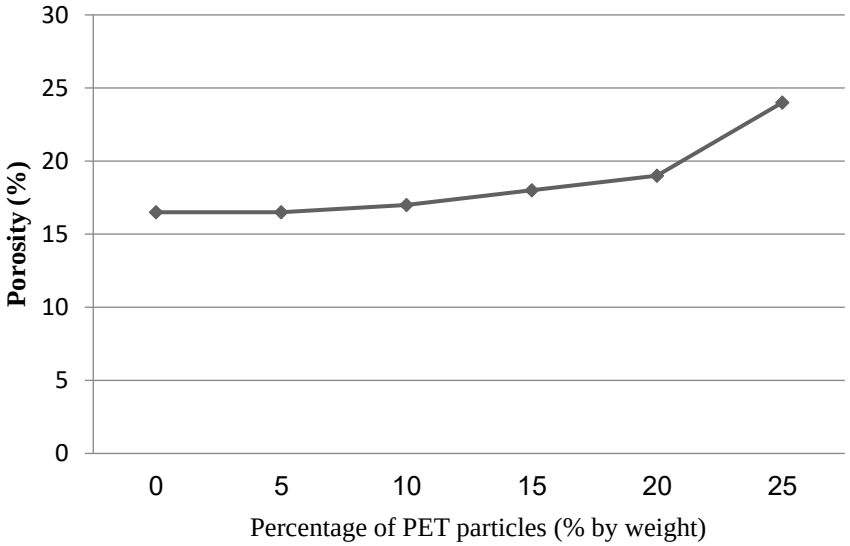


Fig. 3: Variation of the porosity of gypsum mortar according to the percentage by weight of PET particles

Table 1 summarizes the results of the variation of the mechanical properties of gypsum plaster according to the proportions of PET particles.

Table 1: Variation of the mechanical properties of gypsum according to the percentage by weight of PET particles

Compositions	Compressive strength(MPa)	Flexural strength(MPa)
Gypsum mortar (0% of PET particles)	8,13	3,28
Gypsum mortar (5% of PET particles)	6.78	3,02
Gypsum mortar (10% of PET particles)	7,01	2
Gypsum mortar (15% of PET particles)	7,27	3,51
Gypsum mortar (20% of PET particles)	7,49	4
Gypsum mortar (25% of PET particles)	6,88	3,75

According to the Table 1, it is clear that the mechanical strengths decrease with the increase of the content of the PET particles compared to the gypsum mortar (0% by weight of PET particles), this can be attributed to the disturbance of the mineral skeleton of the plaster mortar by the addition of PET particles. An increase is recorded for both properties, compressive and flexural strength, for the content 20% of the PET particles after it falls for the percentage 25% and this is due to a loss of maneuverability.Our results are in agreement with the studies of (Saikia & Brito, 2014; Yazoghli et al., 2006).

Fig. 4 shows the porous microstructure of the gypsum matrix. According to the Fig. 5, it is clear that the grains of sand fill the existing voids in the porous gypsum matrix . The Figs. 6 and 7 give the random distribution of PET particles

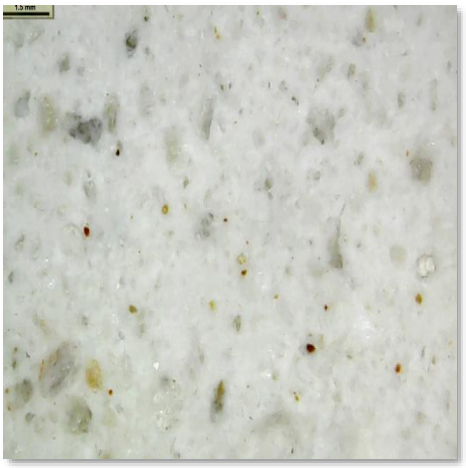


Fig. 4: Gypsum matrix

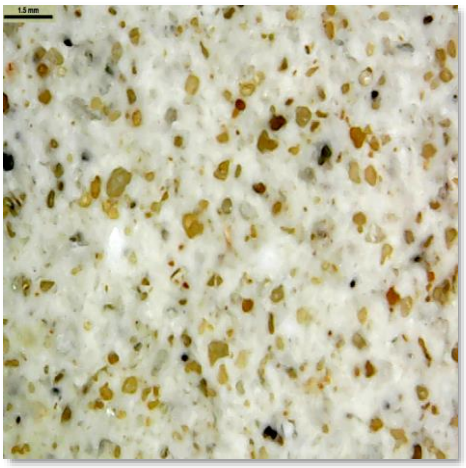


Fig. 5: Mortar based gypsm Matrix

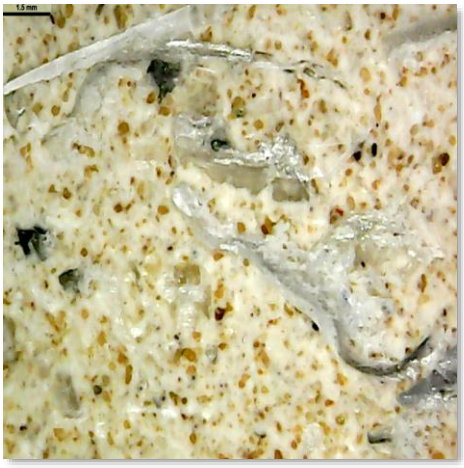


Fig. 6: Mortar based gypsm + 5% of PET particles



Fig. 7: Mortar based gypsm + 10% of PET particles

According to the Figs. 8 and 9 , We notice the different dispositions of PET particles in the mortar based gypsum matrix. Finally Fig 10 shows the good adhesion between the matrix and the PET particles.

Different dispositions of PET particles

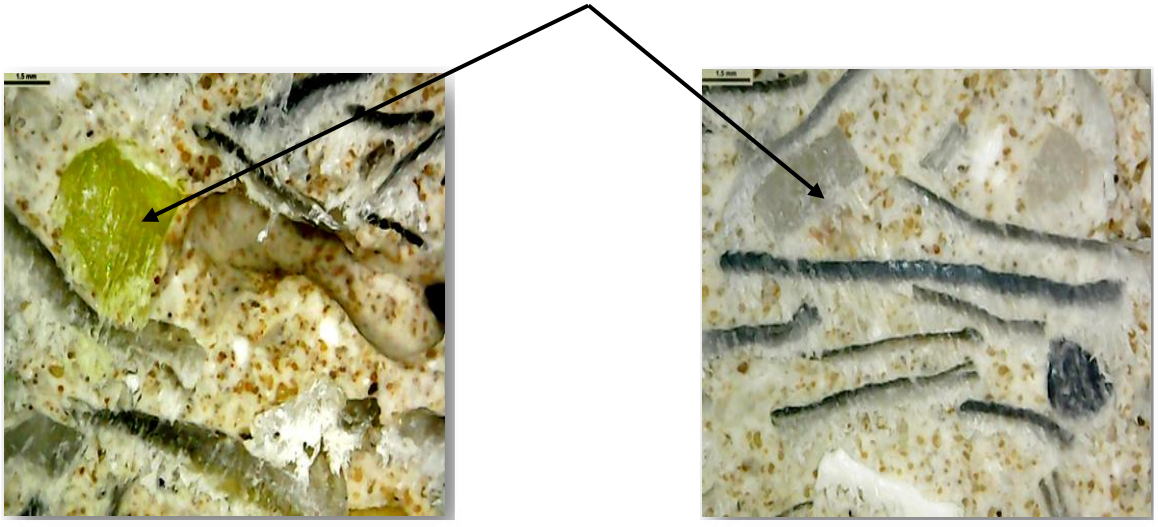


Fig. 8: Mortar based gypsm + 15% of PET particles

Fig. 9: Mortar based gypsm + 20% of PET particles



Fig. 10: Mortar based gypsm + 25% of PET particles

4 Conclusion

The present study has shown the possibility of using mortar based gypsum with the PET particles in several construction areas, given their satisfactory mechanical properties. The incorporation of PET plastic waste in mortar based gypsum is beneficial from the point of view of lightweighting. It was possible to reduce the density from 1498.67 to 1281.87 Kg / m^3 for The mortar based gypsum. An increase in the porosity was recorded of about 31.25%.Depending on the proportion of the PET particles introduced, a clear improvement of the flexural strength was obtained for the gypsum mortar with 20% of the PET particles (4 MPa) and this is due to the good adhesion between gypsum mortar and the PET particles. The addition of PET plastic waste has reduced compressive strength from 8,13 to 6,78 MPa for the mortar based gypsum with 5% of the PET particles. According to the ACI21-213R-87 Guide, the best compressive strength for this new composite is included in the range of 7 to 17 MPa with densitiy included in the range of 800 to 1350 Kg/m3, which allows us to classify it in the class of concrete of medium strength. Moreover, a microscopy study has shown a good interaction between the mortar based gypsum matrix and the the PET particles.

References

AnaJiménez, R., Guzmán Báez, A. & JustoGarcía, N. (2020). New composite gypsum plaster-ground waste rubber coming from pipe foam insulation, *Construction and Building Materials, 55*, pp. 146-152.

CNERIB (1993). Recommandations pour la construction en plâtre, Ministère de l'habitat,Algeria.

D. N. Saika, & Brito, J. (2014). «Mechanical properties and Abrasion behaviourof concrete containing shredded PET bottle waste as a partial substitution of natural aggregate, *Construction and Building Materials, 52*(15), pp. 236-244.

Laoubi, et al. (2018). Study of a New Plaster Composite Based on Dune Sand and Expanded Polystyrene as Aggregates, *The Open Civil Engineering Journal,12*, pp. 401-412.

Markssuel et al. (2020). Gypsum plaster using rock waste: A proposal to repair the renderings of historical buildings in Brazil, Construction and Building Materials, *250*, 118786.

Ouakarrouch, M., Laaroussi, N. & Garoum, M. (2020). Thermal characterization of a new bio-composite building material based on plaster and waste chicken feathers, *Renewable Energy and Environmental Sustainability, 5*(2), number of pages 7.

Sophia, M. & Sakthieswaran, N. (2019). Waste shell powders as valuable bio- filler in gypsum plaster – Efficient waste management technique by effective utilization, *Journal of Cleaner Production, 220*, pp. 74-86.

Yazoghli Marzouk, O., Dheilly, R. M. & Queneudec, M. (2007). Valorization of post-consumer waste plastic in cementitious concrete composites, *Waste Management, 27*(2), pp. 310-318.

Cite as: Amina D., "Physico–mechanical Properties of Sustainable Building Material Based Gypsum and Recycled Polyethylene Waste", *The 2nd International Conference on Civil Infrastructure and Construction (CIC 2023)*, Doha, Qatar, 5-8 February 2023, DOI: https://doi.org/10.29117/cic.2023.0183

Biogas Production from Cow Manure Using an Anaerobic Digestion Technique

Abdul Rahim Al Umairi
Department of Civil and Architectural Engineering, College of Engineering and Technology,
University of Technology and Applied Sciences, Muscat, Oman
abdulrahim.alomairi@utas.edu.om

Hatem Al Amri, Abdullah Al Kalbani, Al Hussain Al Hadidi, Marwan Al Hashami
Department of Civil and Architectural Engineering, College of Engineering and Technology,
University of Technology and Applied Sciences, Muscat, Oman

Abstract

The world is suffering from limited sources of energy thus finding a renewable and sustainable source is very crucial. Cow manure is an unexploited treasure and is expected to have a high potential for energy recovery. This study aimed to evaluate biogas production from cow manure (CM) under an anaerobic condition. The cow manure was collected from a local farm in Oman and diluted with a ratio of 1:3 (dry CM/Water). The diluted cow manure (DCM) was characterized and found to have pH 7.9, total solids (TS) 8930 mg/L, total dissolved solids (TDS)1390 mg/L, dissolved organic carbon (DOC) 8160 mg/L and electrical conductivity (EC) 2730 µS/cm. The used anaerobic reactor (20 litres, black) was fed with DCM (15 litres) and operated at atmospheric mesophilic conditions (40 to 45°C). The gas was measured by the water displacement method. The results revealed that the biogas was generated in low amounts after three days (119 mL) and achieved more than 20 litres after nine days. The percentage of volatile solids to total solids was found to be 71% and the production of the biogas was calculated as 131 L/kg VS. This study is believed to pave the way for reducing the pressure on landfills and converting an environmental burden into a product of added value serving the circular economy theme.

Keywords: Cow manure; Biogas; Renewable energy

1 Introduction

The improper management of animal manure in the open area causes various environmental concerns namely: soil nutrient saturation, water eutrophication and greenhouse gas emission (Díaz-Vázquez et al., 2020). Soil nutrient saturation results in the uncontrolled growth of microorganisms including pathogens infection. During heavy rain seasons, the runoffs will transport soil nutrients to the nearby water body. This eventually will cause water eutrophication due to the accumulation of nitrogen and phosphorus content. Consequently, that will lead eventually to rapid algal blooms disturbing the aquatic life's biodiversity. Greenhouse gases also are emitted by livestock waste such as ammonia, nitrous oxide and methane. The contribution of the livestock sector to global greenhouse emissions is counted as 7.1 Gigatonnes of CO_2 equivalent/ year representing 14.5% with 65% attributed to cattle (FAO, 2022).

However, utilizing animal manure by using an anaerobic technique is expected to mitigate greenhouse gas emissions and also provide a renewable energy source (Liebetrau et al., 2021).

Indeed, anaerobic digestion (AD) is a well-established technique (in Europe there are more than 17,000 biogas plants) which is used to digest organic waste collected from different sectors (food, agriculture, animal manure, sewage sludge) (Tampio et al., 2019). The composition of the biogas produced is 50 to 70% methane, 30 to 40 % carbon dioxide and the remaining are trace gases such as hydrogen, oxygen and nitrogen (Cheremisinoff NP, 1980).

AD process is a microbial-assisted sequential biodegradation process that involves different stages: hydrolysis, acidogenesis, acetogenesis, and methanogenesis (Jomnonkhaow et al., 2021). In the first step, the complex compounds: proteins and carbohydrates are hydrolyzed into monomers like compounds: amino acids, long-chain fatty acids and sugar. Then the generated compounds are fermented into fatty acids (lactic, propionic and butyric acids). Then the VFAs are consumed to generate acetic acid, carbon dioxide and hydrogen followed by methane production which is the final step (Haryanto et al., 2018).

AD generates intermediate products: volatile fatty acids (VFA) and biogas (e.g. hydrogen, CO2, methane). Both VFA and methane are valuable products that are classified as products of added value and may act as major elements in the circular economy. Indeed, VFA can be utilized for the production of bioplastic and biodiesel (Cavinato et al. (2017); Jomnonkhaow et al., (2021)). On the other hand, methane recovery from AD is more viable and feasible. In a comparative study, it was reported that food waste could produce twice the amount of methane compared to that produced by cow slurry (Tampio et al., 2019). That being said, the feasibility depends highly on the availability of raw wastes. Furthermore, biogas production from biomass is much easier than the extraction of the VFA for industrial applications. The methane potential from dairy cattle is 0.24 m^3 CH_4/ kg of VS (Liebetrau et al., 2021). In line with this study, it was reported that the highest methane yield was obtained from sheep dung while cow dung is the second and the least from chicken dung and tomato wastes (Adamu, 2014).

In German, the total production of fresh matter (cattle manure) is approximately 115 mt and 33% of that is used for biogas production. The production of electricity from the produced methane is calculated based on the below model (1) (Liebetrau et al., 2021):

$$9.32\text{t FM}*\text{yr}^{-1}\text{r per cow} * 10\%\text{TS} * 80\%\text{ VS} * \text{biogas yield of } 380\ \text{l}*\text{kgVS}^{-1} * 5.3\ \text{kWh}*\text{m}^3 * 35\%\ \text{electrical efficiency} * (365\text{days} * 24\text{hours})^{-1} = 0.06\ \text{kW}_\text{e}\ \text{per cow} \quad (1)$$

Therefore, for the production of 100 kWe (the typical size of the biogas plant), 1666 cows are required.

The Gulf Cooperation Council (GCC) countries produce one-third of the crude oil in the world and have one-fifth of the gas reserve (Al-Badi et al., 2019). The total energy consumption in GCC countries was 536 TWh (Terra Watt-hour) and that is expected to increase to 2000 TWh by 2040. In 2018, the contribution of renewable energy (solar, wind, bioenergy) to electricity generation is the highest in UAE reaching 600 MW and around 140 MW in Saudi Arabia while it is nearly 40 MW for Kuwait and Qatar whereas it is less than 10 MW for Oman and Bahrain (Basha, et al., 2021). The GCC countries plan to increase the contribution of renewable energy to the total electricity produced. In particular, Oman and Bahrain 10% and 5% respectively by 2025, Saudi Arabia and Kuwait aim for 30% and 15% respectively by 2030, and UAE aims for 44% by 2050 (Atalay et al., 2016). In the GCC countries, the contribution of bioenergy to the total renewable energy is expected to be 2% by 2030 while the solar energy sector contributes 75%. Indeed, the biomass generated from municipal solid waste and animal waste reach 19.5 Mtpa and 25.52 Mtpa respectively. Therefore, the bioenergy potentials in biomass could secure 23% of the total electricity demand in the GCC countries (Welfe & Al Awadhi, 2021).

Currently, most of the biomass is sent to landfills and minimal is utilized. However, there are a few pioneer projects in the region utilizing biomass for bioenergy production such as Sharjah using sewage sludge and Ras Al Kaimah using camel manure (Basha et al., 2021).

The aim of this study was to assess the potential of biogas production using cow manure treated anaerobically. The reaction was conducted under ambient temperature (35 to 40 ºC) for 10 days and the gas volume was measured using the water displacement method. This project is expected to pave the way for more research in this area.

2 Methodologies

2.1 Sample Collection

The cow manure (CM) (4 kg, fresh) was collected from a local farm in Oman and placed in a plastic container. The CM was diluted with deionized water (DI): 1:3 (CM: DI) to assure good microbial activities. The characterization of the sample was conducted before starting the treatment.

2.2 The Operation Condition of the Reactor

The reactor was made of high-density polyethylene (HDPE) material and provided with the required fittings (Figure 1). The reactor was placed in an open area (campus of the University of Technology and Applied Sciences-Muscat). The size of the reactor is 30 litres, painted with a black colour to prevent the photosynthesis process. The reactor was provided with two outlets: the first for gas sampling (at the top) and the second for biowaste sample collection (5 cm from the bottom). Two third of the reactor volume was filled with the diluted CM (total 20 litres). The ambient temperature was in the range of 35 to 40 ºC which was within the range of mesophilic conditions 20 to 45 ºC and that proved to be ideal for anaerobic digestion.



Fig. 1: Reactor arrangement (HDPE container, 30 litres size)
with stainless steel valve (bottom) sampling outlet, gas outlet (top)

2.3 Characterization of Sample

The diluted cow manure was characterized before and after the anaerobic digestion. pH, total dissolved solids TDS, and electrical conductivity were measured using a digital meter. The total solids content was measured as per the standards method (2540). For the dissolved organic carbon, prior to the measurement, the sample was filtered through a cellulose membrane filter with pore sizes of 0.45 microns. Then the measurement was conducted using Sievers InnovOx ES Laboratory TOC Analyzers (conditions: 1% 6M phosphoric acid and 15% oxidizer (30% Sodium persulphate solution).

2.4 Gas Measurement

The reactor was operated for more than 10 days, and gas samples were collected using a well-established method called the water displacement method (Figure 2). The gas outlet from the reactor was connected via a hose (3/4 inch) to an inverted graduated cylinder (1000 mL) filled with water. Upon opening the gas valve, the water will be displaced by the biogas and the difference in the water height will be recorded.



Fig. 2: Water displacement method setup for measuring gas volume

3 Results and Discussion

Samples of the cow manure (CM) were analysed before and during the anaerobic digestion (AD) process (Table 1). The results revealed that the pH of CM before the AD process was 7.9 and reached 6.1 on the 9th day. The drop in pH value might be explained by referring to the mechanism of the AD in which it is expected to generate higher quantities of acetic acids. This indeed came in line with another study which also reported a similar observation (Tampio et al., 2019). The EC values also increased aligned with the progress of the AD process which may be attributed to the accumulation of the ions in the digested biosolids.

The initial VS/TS ratio was 64% and it reached 74% after 9 days which is comparable to what was reported by (Baek et al., 2020; Haryanto et al., 2017). The VS/TS is a very good indicator of biomass biodegradability. That increment in VS content might be attributed to the acidogenesis stage of the AD process where most long-chain acids are converted to volatile fatty acids. Moreover, VS content in CM might change from one country to another depending on the feeding system, bedding material in the pens floor and method of manure collection.

Table 1: The characteristics of the diluted cow manure (CM) at different time intervals

Day	pH	EC (µS/cm)	VS/TS %
0	7.9	2730	64
3	7.5	2555	74
4	7.4	2460	72
5	6.6	2350	72
7	6.0	4810	70
9	6.1	4815	74

DOC levels fluctuated during the period of observation (Figure 3). In the beginning, the apparent sudden increment in the DOC within the first three days might be attributed to the hydrolysis process where most of the organic complex compounds are converted into more soluble compounds. Then, in the following seven days the DOC level remained constant and then drop to 7.5 g/L on the ninth day. That behaviour was expected due to the production of the biogas at the final stage where acetic acids (DOC) were converted into biogas (Tampio et al., 2019).

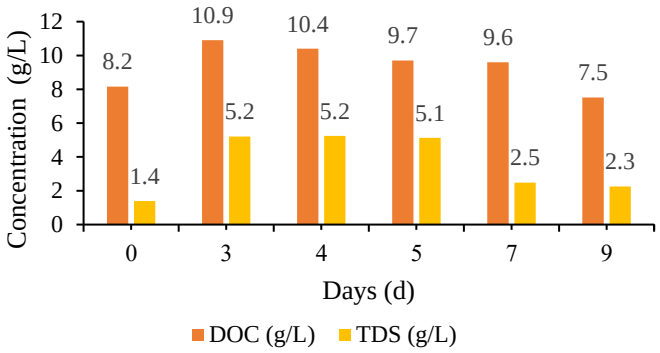


Fig. 3: The concentration of DOC and TDS during anaerobic digestion of the diluted cow manure

Interestingly, the production of biogas was observed since the third day (Figure 4). The methane content is expected to be between 65% to 70% of the total biogas produced (Adamu et al., 2014; Vazquez et al., 2020; Haryanto et al., 2017). The accumulated produced biogas after 9 days was 47 biogas L/kg VS which is equivalent to 30.6 CH_4 L/ kg of VS (considering CH_4 is 65%). That indeed is very comparable to the value of 40 CH_4 L/ kg of VS reported by Baek et al. (2020) after 10 days. Nevertheless, Tampio et al. (2019) reported higher production of methane at 200 L/kg VS. The discrepancy in the previously mentioned study might be attributed to the dilution factor used, and the characteristics of CM.

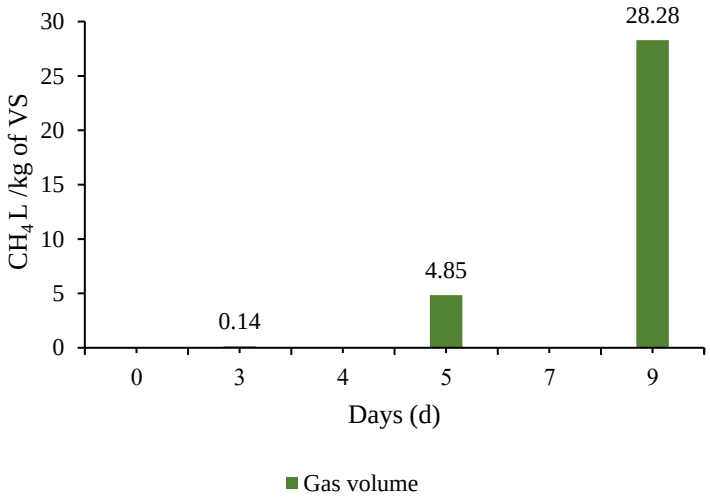


Fig. 4: Gas volume production during anaerobic digestion of the diluted cow manure

4 Oman Implications

In Oman, the total number of cows is around 421,000 cows (National Centre for Statistics and Information, 2021). The total annual national natural gas consumption was 46642.5 million m^3 in 2019. Using the AD technique will be able to provide as per this study 0.003 m^3 of CH_4/kg VS/day. The total production of the CM/year/cow is 9320 kg. Consider the total solid content 20% and VS

64%. Therefore, the total VS content equals 1192.96 kg VS/cow/year. Therefore, the total production of methane in Oman can be predicted by the model below:

CH_4 m^3 / year= 1192.96 kg Vs/cow *0.003 m^3 of CH_4/kg VS/day*365 day/year* 421,000 cow =

550 million m^3 CH_4/ year

The calculated amount of methane represents around 1.2% of the total natural gas consumed in Oman. This can be extended if other sources of biomass are considered such as municipal wastes and sewage sludge and other animal waste (horse, camel, chicken). In fact, a detailed study is required to address the unexplored potentials of this sector and what is the best way to manage this huge sector.

5 Conclusion

This study successfully achieved the main objective by evaluating the potential of biogas production from cow manure using an anaerobic digestion technique. This study found that, under the experimental conditions (mesophilic, 10 days of reaction), the total amount of the biogas produced was 20 litres which is corresponding to 3 L of CH_4/kg of VS/day. The mentioned value came aligned with what was reported in the literature. This study predicted that the total amount of cow manure in Oman could produce 1.2% of the total natural gas consumption in the country. Nonetheless, a comprehensive study is required to address the potential of bioenergy utilizing different sources of biomass including animal wastes, municipal wastes, and sewage sludge. This study is expected to pave the way for more studies to evaluate this sector from different perspectives.

References

Adamu, A. A. (2014). Effect of substrate on biogas yield, *Global Journal of Engineering Research, 13*, 35-39

Al-Badi, A. & Al Mubarak, I. (2019). Growing energy demand in the GCC countries. *Arab. J. Basic Appl. Sci., 26*, 488–496.

Atalay, Y., Biermann, F. & Kalfagianni, A. (2016). Adoption of renewable energy technologies in oil-rich countries: Explaining policy variation in the Gulf Cooperation Council states, *Renew. Energy*, *85*, 206–214.

Baek, et al. (2020). Treatment of Cattle Manure by Anaerobic Co-Digestion with Food Waste and Pig Manure: Methane Yield and Synergistic Effect, *Int. J. Environ. Res. Public Health*, *17*, 4737.

Basha, et al. (2021). Review Potential of Utilization of Renewable Energy, Technologies in Gulf Countries. *Sustainability*, *13*, 10261.

Cavinato, et al. (2017). Volatile fatty acids production from organic waste for biorefinery platforms, In 5th International Conference on Sustainable Solid Waste Management, Athens, Greece, 21–24 June 2017.

Cheremisinoff, N. P. (1980). Biomass Application. In: Technology and Production. Marcel Dekkar Inc, USA.

Díaz-Vázquez, D.et al. (2020). Evaluation of Biogas Potential from Livestock Manures and Multicriteria Site Selection for Centralized Anaerobic Digester Systems: The Case of Jalisco, México, Sustainability, 12, 3527.

FOA (Food and Agriculture Organization) (2022). https://www.fao.org/news/story/en/item/197623/icode, (Accessed December 17, 2022).

Haryanto, et al. (2018). Biogas production from anaerobic co-digestion of cow dung and elephant grass (Pennisetum Purpureum) using batch digester, IOP Conf. Series: Earth and Environmental Science, 141, 012011.

Jomnonkhaow, et al. (2021). Membrane bioreactor-assisted volatile fatty acids production and in situ recovery from cow manure, *Bioresource Technology*, *321*, 124456

Liebetrau, et al. (2021). Potential and utilization of manure to generate biogas in seven countries, Murphy, J.D. (Ed.) IEA Bioenergy Task 37, 2021:6.

National Centre for Statistics and Information (NCSI), 2021. https://www.ncsi.gov.om/Pages/AllIndicators.aspx, (Accessed December 17, 2022).

Onwuliri, F. C., Onyimba, I. A. & Nwaukwu, I. A. (2013). Generation of Biogas from Cow Dung, *J Bioremed Biodeg*, S18, 002.

Tampio, et al. (2019). Volatile fatty acids (VFAs) and methane from food waste and cow slurry: Comparison of biogas and VFA fermentation processes, GCB Bioenergy, 11, 72–84.

Welfle, A. & Alawadhi, A. (2021). Bioenergy opportunities, barriers and challenges in the Arabian Peninsula—Resource modelling, surveys & interviews, *Biomass Bioenergy, 150*, 106083.

Cite as: Al Umairi A., Al Amri H., Al Kalbani A., Al Hadidi A. & Al Hashami M., "Biogas Production from Cow Manure Using an Anaerobic Digestion Technique", *The 2nd International Conference on Civil Infrastructure and Construction (CIC 2023)*, Doha, Qatar, 5-8 February 2023, DOI: https://doi.org/10.29117/cic.2023.0184

Statistical Analysis of the Effect of Water Table Fluctuation and Soil Layering on the Distribution of BTEX on Soil and Groundwater Under Anaerobic Condition

Reem Ismail
Department of Civil and Architectural Engineering, Qatar University, Doha, Qatar
ri1607496@qu.edu.qa

Riyadh I. Al-Raoush
Department of Civil and Architectural Engineering, Qatar University, Doha, Qatar
riyadh@qu.edu.qa

Abstract

Crude oil, gasoline, and diesel fuel spills pollute groundwater in many coastal areas. BTEX is a hydrocarbon of concern due to its high-water solubility, which allows it to spread widely in the subsurface environment. The mobile phase of LNAPLs percolates through porous soil and accumulates above the water table. Subsurface geological, pollutant morphology, and hydrogeologic site features make natural attenuation difficult to understand. Texture and vertical spatial variability affect soil hydraulic properties and water and contaminant distribution in soil profiles. Changes in rainfall strength and frequency and increased water demand may increase groundwater level oscillations in the next century. Five sets of columns, including one soil column and one equilibrium column, were operated for 150 days. One of the columns was operated under a steady state condition (S), and four columns under transient water table condition. The stable column (S), and the Fluctuating column 1 (F1) contain homogenized soil, while the fluctuating columns 2, 3, and 4 contains heterogenous soil. ORP values at the middle of the columns varied cyclically with WTF. EC values affected greatly by fluctuation and temperature and the statistical test p-value $3.119e^{-10} < 0.05$ implying that there are statistical differences between EC values of these columns. On the other hand, pH for the five columns were fluctuated in the same range (P-value $0.3694 > 0.05$). Soil layering affects the attenuation of BTEX, as the peak concentrations for benzene occurred at second imbibition cycle for the homogeneous soil, while for the heterogeneous soil occurred between second and fourth imbibition cycles.

Keywords: BTEX; Groundwater; Water table fluctuations; soil hydrogeochemistry

1. Introduction

Groundwater pollution is common in coastal areas and it is caused by the accidental spilling of petroleum products such as crude oil, gasoline, and diesel fuel (Huang et al., 2021). Certain compounds in LNAPL, such as benzene, have a negative impact on the environment and human health. (Cavelan et al., 2022; Sookhak Lari et al., 2018). Because of this, BTEX is among the hydrocarbons of highest concern (Chompusri et al., 2002). After LNAPL spilled, the mobile phase infiltrates through the soil and collects at the top of the water table. A considerable fraction of pollutants may be residualized as LNAPL ganglia by capillary pressures or sticking to soil grains (Cavelan et al., 2021). When the water table decreases,

the mobile LNAPL goes down with it, which results in a redistribution of the LNAPL and a rearrangement of the partitioning of LNAPL components across various phases (Cavelan et al., 2022).

Remediation strategies for polluted aquifers and the natural attenuation mechanisms of hydrocarbons in the source zone and groundwater plumes have been studied extensively (Sihota et al., 2016). Due to factors such as subsurface geological and microbiological heterogeneity, pollutant morphology and type, and hydrogeologic features of a site, all of which influence the amount and rate of NSZD depletion (Sookhak Lari et al., 2018; Van De Ven et al., 2021; Zanello et al., 2021). Texture and vertical spatial heterogeneity affect soil hydraulic properties and water and pollutant distribution in soil profiles. Depending on soil hydraulic properties, the hydraulic relationship between surface soil and groundwater can fluctuate while the water table depth remains constant (Li et al., 2014).

Subsurface biogeochemical cycling and pollutant and nutrient are regulated by soil hydrological oscillations (Zhang & Furman, 2021). Dissolution, volatilization, and transverse migration of dissolved LNAPL components are restricted in stable water table conditions due to the slow vertical dispersion and diffusion of dissolved LNAPL compounds (Cavelan et al., 2022; K. Gupta et al., 2019). The movement of water table results in the movement and distribution of LNAPLs, particularly in the vertical direction (Alazaiza et al., 2021). Moreover, successful remediation planning is heavily reliant on our understanding of the aquifer's structure (i.e., porosity and permeability) (Di Palma et al., 2017). Temperature variations, pH fluctuations, changes in water table dynamics, and changes in soil moisture content are often what distinguish difficult contaminated areas (Haberer et al., 2015).

Few studies have been conducted to investigate the mass transfer of NAPLs in the capillary fringe in the presence of dynamic boundary conditions; however, these studies are uncommon. There is a lack of research that focuses on the alteration of redox conditions and the soil geochemical properties under these conditions (J. Y. Lee et al., 2001; Rühle et al., 2015; Zhou et al., 2015). In this experiment, the distributions of hydrocarbon pollutants and hydrogeochemical parameters were investigated in five columns polluted with petroleum hydrocarbons (BTEX) under anaerobic conditions, and the analysis carried out using Kruskal wallis test for the individual parameters and Kendall correlation to find if there any connection between the hydro-chemical properties and BTEX concentrations in the columns.

2. Materials and Methods

Five sets of columns, including one soil column and one equilibrium column, were built. One of the columns was operated under a steady state condition (S), and four columns were operated under transient water table condition in a range of soil surface (0 cm) to -40 cm. The stable column (S), and the Fluctuating column 1 (F1) contain homogenized soil, while the fluctuating columns 2, 3, and 4 (i.e., F2, F3, and F4) contains heterogenous soil. Moreover, the fluctuating columns 3 and 4 (i.e., F3, and F4) has higher temperature to represent groundwater temperature in the state of Qatar (Ahmad et al., 2020; Ngueleu et al., 2018).The water level in the equilibrium columns was used to manage the imposed water regime, and the water level in the equilibrium column was determined by pump channel. The soil for this study was collected from Sumaysima beach in Qatar's eastern suburb of Doha (25°34'26.4"N 51°29'15.7"E). This location demonstrates the ongoing interplay between seawater and groundwater, as seen by the oscillation of the water table (Ngueleu et al., 2019). The synthetic influent solution was prepared by mixing Milli-Q water with background nutrients such as $MgCl_2$ (89 mg L-1), KCl (24 mg L-1) Calcium chloride (243 mg L-1) and NaCl (1300mg L-1). During the first 24 hours of the experiment,

the pump channel A was used to fill the equilibrium columns with the synthetic groundwater. 2 L Tedlar bags filled with argon gas was connected to the equilibrium columns to offer hydraulic elements of water fluctuation and collect gas samples. The anaerobic conditions were achieved by continuously purging the equilibrium columns to a DO concentration < 0.8 mg L-1.

3. Results and Discussion

3.1 Hydro-chemical properties

The average porosity of the soil in the groundwater level column, S, F1, and F2 were 22%, 22%, and 22%, respectively. ORP values at the middle of the columns fluctuated during the experiment, while for the bottom of the columns a drop in ORP values occurred in F1, F2, and F3 between 30 and 40 days, and for S and F4, the decrease in ORP values occurred at 70 and 150 days, respectively. This suggests that circumstances conducive to anaerobic respiration have developed in each and every soil column (Ismail et al., 2020; Shafieiyoun et al., 2020; Meng et al., 2021). The results of the statistical test for the middle of S, F1, and F2 showed that the p-value is equal to 0.6771 which is > 0.05, which implies that there is no significant difference between the ORP values, while the p-value for ORP values at the bottom of the columns is equal to 0.0649 which is > 0.05 implies that there is no statistical difference between the columns. This finding implies that ORP values statistically didn't change either with water table fluctuations or due to soil heterogeneity. Haberer et al., (2012), Rezanezhad et al., (2014), Wang et al., (2014), and Meng et al., (2021), they demonstrated that the ORP measured at a particular depth varies cyclically with the fluctuations of the water level.

At the middle of the columns, EC for the stable column S was fluctuated in a lower range than F1, while F1 started at 5000 mS cm^{-1} and decreased to ~ 4000 by the end of the experiment. while comparing the fluctuating columns F1 and F2 to observe the influence of soil layering, these two columns have an inverse effect on the EC values as F1 started at higher concentration and decreased, while F2 started at a lower concentration and increased. The p-value for the EC values at the middle of the columns is equal to $1.7971e^{-05}$ which < 0.05 implying that there are statistical differences between EC values at the middle of these columns. Atekwana and Atekwana (2010) reported that changes in pore fluid conductivity can be caused by both hydrologic and microbiological process. The hydrological process such as advective flow due to water table fluctuation.

The initial sulfate concentrations at the middle of all columns are 100, 282, and 134 mg L^{-1} for S, F1, and F2, respectively. For the stable column S no change in sulfate concentration were detected during the experiment, while for the fluctuating column F1, the concentration of sulfate increased with the first imbibition cycle and by the end of the experiment decreased by 75% of the initial concentration. Moreover, for the fluctuating columns F2, the concentration of sulfate increased after the second imbibition cycle and decreased by 34% of the initial concentration. The increase in sulfate concentration occurs due to the movement of sulfate to the middle of the column with the water table.

The effect of water table fluctuation is observed by comparing the columns S and F1, significant reduction occurs in F1 as compared with S. Comparing the columns F1 and F2 would provide insight into the effect of soil layering, as the reduction in sulfate concentration is greater in F1 than in F2. The p-value for at the middle of the columns S, F1, and F2 is found to be equal to $2.2516e^{-04}$ which < 0.05 implying that there are statistical differences between sulfate concentrations during the experiment between the columns and the water table fluctuations and soil heterogeneity has effects on sulfate concentrations.

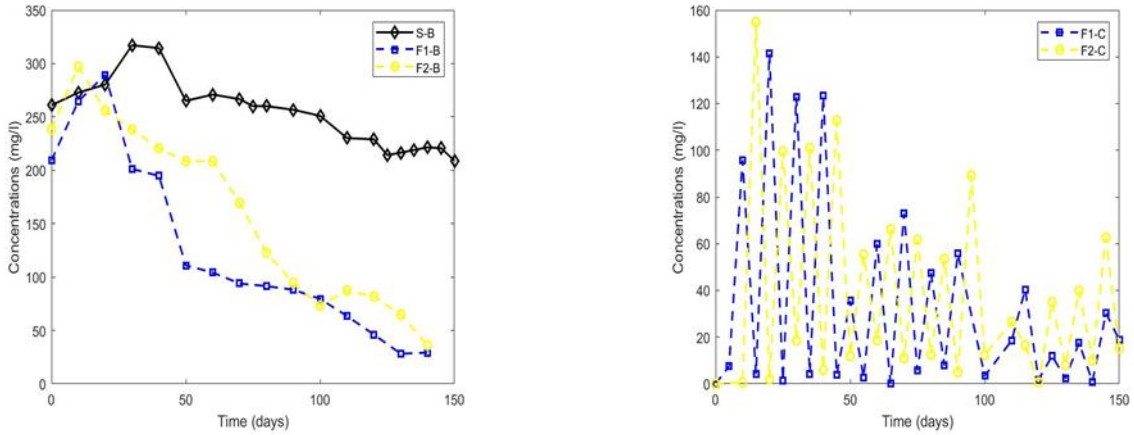


Fig. 1: Benzene concentrations at the middle and the bottom of the columns S, F1, and F2

3.2 Correlation between the Hydro-chemical Parameters of Dissolved Organics

For the experimental condition, LNAPLs which refer to benzene and toluene were under completely saturated condition in the stable column (S). Whereas the conditions of the LNAPLs in the fluctuating columns (F1& F2) were continuously cycling between being saturated and unsaturated. The Kendall tau correlation test is used to test the correlation between the concentration of hydro-chemical indicators (ORP, EC, and sulfate concentrations) and the concentration of benzene and toluene.

The concentrations of benzene and toluene are found in Figure 1 and figure 2. For ORP, both S and F1 columns have positive moderate correlation with benzene, while for toluene, it is a positive weak correlation. It implies that water table fluctuations didn't affect the ORP values between the two homogenized soil columns in the presence of LNAPLs. For EC, benzene and toluene correlation in the column S in not statistically significant, while in the column F1, the correlation is positive strong and moderate, for benzene and toluene, respectively. For the sulfate concentrations with benzene between stable and fluctuating homogenized soil, the correlation is positive strong and very strong in the columns S and F1, respectively. For toluene, the correlation is weak and strong in S and F1, respectively. These differences occurred as a result of BT dissolution due to water table fluctuation while at the same time sulfate is accumulated at the middle (depth B) of the column by the moving synthetic groundwater from the bottom of the columns to the top due to sampling. This argument can be supported by the decrease in sulfate concentrations at the bottom (depth C) of the stable column. It may be validated by examining the sulfate concentration pattern in the stable column with the concentrations of Ca^{2+} and Mg^{2+} concentration patterns. In a study that was quite similar to this one, Rezanezhad et al., (2014) found that the solid-phase concentrations of elements such as iron, manganese, and others are higher in the first 30 centimeters of the stable column, but decrease with increasing depth. The increase in benzene concentration can be a result of its high dissolution rate and higher solubility in water (Kim et al., 2008; Njobuenwu et al., 2005), which occurs due to increase contact time. This correlation may possibly be a consequence of increased biodegradation and natural attenuation at this location of the column, particularly when it is accompanied with a positive correlation with ORP and a negative correlation with DIC.

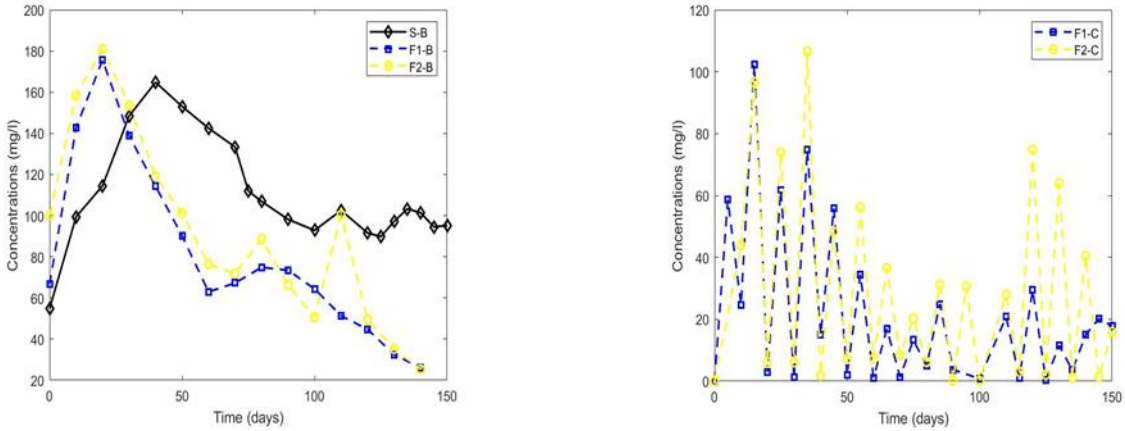


Fig. 2: Toluene Concentrations at the middle and the bottom of the columns S, F1, and F2

Between the two fluctuating columns, F1 and F2, for ORP in both F1 and F2 has positive moderate correlation with benzene and toluene. This may imply that soil heterogeneity didn't affect ORP values. For EC, benzene has strong positive correlations in F1, while it is negative strong in F2. Same for toluene, the correlation with EC, is moderate positive in F1, but it is moderate negative in F2. The correlations between Benzene and sulfate concentrations are positive, very strong and positive moderate, respectively. For toluene, it is strong and moderate for F1 and F2, respectively. Soil homogeneity varies between the two columns, with homogenized soil found in F1 and heterogeneous soil in F2. By comparing solely homogeneous and heterogeneous soil (F1, and F2), it can be observed that homogeneity has a greater impact on the dissolution of benzene and toluene and the flow of sulfate through the column, particularly in the layered column F2 where injected layer has a low permeability. Johnston and Trefry (2009) demonstrates that the layer variability has an influence on the initial vertical distribution of LNAPL, while the source zone layer does not have such a significant influence on the LNAPL recovery rate. Rather, the most influential factors are media properties around the water table that are farther from the well.

The soil texture and vertical spatial variability is significantly impact soil hydraulic characteristics and the distribution of water and contaminants throughout the soil profile (Johnston & Trefry, 2009; Li et al., 2014). When the fluctuating water table moved to the upper and lower portions of the column during the imbibition and drainage cycles, it redistributed LNAPLs and sulfate vertically, which explains their concentration increase at the second and third imbibition cycles for the fluctuating columns. Kehew and Lynch (2011) stated that sulfate can be carried as far as 1.75 meters below the water table. Numerous scholars have explained how variations in groundwater level affect the vertical mobility and spatial distribution of NAPLs within an aquifer (Alazaiza et al., 2020; Kehew & Lynch, 2011; Lee et al., 2001; Van De Ven et al., 2021).

4. Conclusion

ORP values in the middle columns varied cyclically with WTF and promoting reducing conditions, but statistically it has similar correlation in term of water table fluctuations and soil heterogeneity. EC values was affected greatly by water table fluctuation, as well as soil heterogeneity in the presence of benzene and toluene. The sulfate concentrations reduction in homogenized soil is greater than layered soil, and it reduces the correlation between LNAPLs and sulfate concentrations. The association between BTEX and sulfate concentrations, when combined with a positive correlation with ORP and a negative correlation with DIC, may indicate an increase in natural attenuations in the fluctuating columns.

References

Ahmad, et al. (2020). Hydrogeochemical characterization and quality evaluation of groundwater suitability for domestic and agricultural uses in the state of Qatar. *Groundwater for Sustainable Development*, *11*(April), 100467. https://doi.org/10.1016/j.gsd.2020.100467

Alazaiza, et al. (2021). Assessing the impact of water infiltration on LNAPL mobilization in sand column using simplified image analysis method. *Journal of Contaminant Hydrology*, *238*(June 2020), 103769. https://doi.org/10.1016/j.jconhyd.2021.103769

Alazaiza, et al. (2020). LNAPL saturation distribution under the influence of water table fluctuations using simplified image analysis method. *Bulletin of Engineering Geology and the Environment*, *79*(3), 1543–1554. https://doi.org/10.1007/s10064-019-01655-3

Atekwana, E. A. & Atekwana, E. A. (2010). Geophysical signatures of microbial activity at hydrocarbon contaminated sites: A review. *Surveys in Geophysics*, *31*(2), 247–283. https://doi.org/10.1007/s10712-009-9089-8

Cavelan, et al. (2021). A critical review of the influence of groundwater level fluctuations and temperature on LNAPL contaminations in the context of climate change. *Science of The Total Environment*, *806*, 150412. https://doi.org/10.1016/j.scitotenv.2021.150412

Chompusri, S., Rivett, M. O., & Mackay, R. (2002). LNAPL redistribution on a fluctuating water table: Column experiments. *IAHS-AISH Publication*, *275*, 225–234.

Di Palma, et al. (2017). Pore-scale simulations of concentration tails in heterogeneous porous media. *Journal of Contaminant Hydrology*, *205*(July), 47–56. https://doi.org/10.1016/j.jconhyd.2017.08.003

Dobson, R., Schroth, M. H., & Zeyer, J. (2007). Effect of water-table fluctuation on dissolution and biodegradation of a multi-component, light nonaqueous-phase liquid. *Journal of Contaminant Hydrology*, *94*(3–4), 235–248. https://doi.org/10.1016/j.jconhyd.2007.07.007

Gupta, P. K., Yadav, B., & Yadav, B. K. (2019). Assessment of LNAPL in Subsurface under Fluctuating Groundwater Table Using 2D Sand Tank Experiments. *Journal of Environmental Engineering*, *145*(9), 04019048. https://doi.org/10.1061/(asce)ee.1943-7870.0001560

Gupta, P., & Yadav, B. (2017). Bioremediation of Nonaqueous Phase Liquids (NAPLs)-Polluted Soil-Water Resources. *Environmental Pollutants and Their Bioremediation Approaches* , *July*, 241–256. https://doi.org/10.1201/9781315173351-9

Haberer, et al. (2015). Diffusive-Dispersive and Reactive Fronts in Porous Media: Iron(II) Oxidation at the Unsaturated-Saturated Interface. *Vadose Zone Journal*, *14*(5), vzj2014.07.0091. https://doi.org/10.2136/vzj2014.07.0091

Haberer, et al. (2012). Oxygen Transfer in a Fluctuating Capillary Fringe. *Vadose Zone Journal*, *11*(3), vzj2011.0056. https://doi.org/10.2136/vzj2011.0056

Huang, et al. (2021). Simulated groundwater dynamics and solute transport in a coastal phreatic aquifer subjected to different tides. *Marine Georesources and Geotechnology*, *39*(6), 719–734. https://doi.org/10.1080/1064119X.2020.1754975

Johnston, C. D., & Trefry, M. G. (2009). Characteristics of light nonaqueous phase liquid recovery in the presence of fine-scale soil layering. *Water Resources Research*, *45*(5), 1–20. https://doi.org/10.1029/2008WR007218

Kehew, A. E., & Lynch, P. M. (2011). Concentration trends and water-level fluctuations at underground storage tank sites. *Environmental Earth Sciences*, *62*(5), 985–998. https://doi.org/10.1007/s12665-010-0583-6

Kim, et al. (2008). Influence of soil components on the biodegradation of benzene, toluene, ethylbenzene, and o-, m-, and p-xylenes by the newly isolated bacterium Pseudoxanthomonas spadix BD-a59. *Applied and Environmental Microbiology*, *74*(23), 7313–7320. https://doi.org/10.1128/AEM.01695-08

Lee, et al (2001). Attenuation of Petroleum Hydrocarbons in Smear Zones: A Case Study. *Journal of Environmental Engineering*, *127*, 639–647.

Lee, et al. (2001). Factors affecting the distribution of hydrocarbon contaminants and hydrogeochemical parameters in a shallow sand aquifer. *Journal of Contaminant Hydrology*, *50*(1–2), 139–158. https://doi.org/10.1016/S0169-7722(01)00101-2

Li, X., Chang, S. X., & Salifu, K. F. (2014). Soil texture and layering effects on water and salt dynamics in the presence of a water table: A review. *Environmental Reviews*, *22*(1), 41–50. https://doi.org/10.1139/er-2013-0035

Meng, et al. (2021). Response of the redox species and indigenous microbial community to seasonal groundwater fluctuation from a typical riverbank filtration site in Northeast China. *Ecological Engineering*, *159*(October 2020), 106099. https://doi.org/10.1016/j.ecoleng.2020.106099

Ngueleu, et al. (2019). Biodegradation Kinetics of Benzene and Naphthalene in the Vadose and Saturated Zones of a (Semi)-Arid Saline Coastal Soil Environment. *Geofluids*, *2019*(December). https://doi.org/10.1155/2019/8124716

Ngueleu, et al. (2018). Sorption of benzene and naphthalene on (semi)-arid coastal soil as a function of salinity and temperature. *Journal of Contaminant Hydrology*, *219*(May 2019), 61–71. https://doi.org/10.1016/j.jconhyd.2018.11.001

Njobuenwu, D. O., Amadi, S. A., & Ukpaka, P. C. (2005). Dissolution rate of BTEX contaminants in water. *Canadian Journal of Chemical Engineering*, *83*(6), 985–989. https://doi.org/10.1002/cjce.5450830608

Rezanezhad, et al. (2014). Water table fluctuations and soil biogeochemistry: An experimental approach using an automated soil column system. *Journal of Hydrology*, *509*, 245–256. https://doi.org/10.1016/j.jhydrol.2013.11.036

Rühle, et al. (2015). Response of Transport Parameters and Sediment Microbiota to Water Table Fluctuations in Laboratory Columns. *Vadose Zone Journal*, *14*(5), vzj2014.09.0116. https://doi.org/10.2136/vzj2014.09.0116

Sihota, et al. (2016). Seasonal Variability in Vadose Zone Biodegradation at a Crude Oil Pipeline Rupture Site. *Vadose Zone Journal*, *15*(5), vzj2015.09.0125. https://doi.org/10.2136/vzj2015.09.0125

Sookhak Lari, et al. (2018). Field-scale multi-phase LNAPL remediation: Validating a new computational framework against sequential field pilot trials. *Journal of Hazardous Materials*, *345*, 87–96. https://doi.org/10.1016/j.jhazmat.2017.11.006

Van De Ven, et al. (2021). Impacts of water table fluctuations on actual and perceived natural source zone depletion rates. *Journal of Contaminant Hydrology*, *238*(July 2020), 103771. https://doi.org/10.1016/j.jconhyd.2021.103771

Wang, et al. (2014). Shallow groundwater dynamics and its driving forces in extremely arid areas: A case study of the lower Heihe River in northwestern China. *Hydrological Processes*, *28*(3), 1539–1553. https://doi.org/10.1002/hyp.9682

Yadav, B. K., Shrestha, S. R., & Hassanizadeh, S. M. (2012). Biodegradation of toluene under seasonal and diurnal fluctuations of soil-water temperature. *Water, Air, and Soil Pollution*, *223*(7), 3579–3588. https://doi.org/10.1007/s11270-011-1052-x

Zanello, V., Scherger, L. E., & Lexow, C. (2021). Assessment of groundwater contamination risk by BTEX from residual fuel soil phase. *SN Applied Sciences*, *3*(3), 1–20. https://doi.org/10.1007/s42452-021-04325-w

Zhang, Z., & Furman, A. (2021). Soil redox dynamics under dynamic hydrologic regimes - A review. *Science of the Total Environment*, *763*, 143026. https://doi.org/10.1016/j.scitotenv.2020.143026

Zhou, et al. (2015). Response of the microbial community to seasonal groundwater level fluctuations in petroleum hydrocarbon-contaminated groundwater. *Environmental Science and Pollution Research*, *22*(13), 10094–10106. https://doi.org/10.1007/s11356-015-4183-6

Cite as: Reem Ismail R. & Al Raoush R., "Statistical Analysis of the Effect of Water Table Fluctuation and Soil Layering on the Distribution of BTEX on Soil and Groundwater Under Anaerobic Condition", *The 2nd International Conference on Civil Infrastructure and Construction (CIC 2023)*, Doha, Qatar, 5-8 February 2023, DOI: https://doi.org/10.29117/cic.2023.0185

Eco-friendly Concrete Using Waste Plastic Bottles as Aggregate: A Case Study from Oman

Abdul Rahim Al Umairi
abdulrahim.alomairi@utas.edu.om
Department of Civil and Architectural Engineering, College of Engineering and Technology,
University of Technology and Applied Sciences, Muscat, Oman

Nawf Al Mahrouqi, Maryam Al Wahaibi, Maryam Al Hooti,
Fatemah Al Nabhani, Hiba Al Mammari
Department of Civil and Architectural Engineering, College of Engineering and Technology,
University of Technology and Applied Sciences, Muscat, Oman

Abstract

Waste plastic bottles (WPB) (polyethylene terephthalate (PET)) type are used widely for water storage and eventually become environmental burden. This study investigated an innovative application of the WPB to partially replace the fine aggregate in concrete nonstructural element. This research evaluated the effect of plastic content on concrete mechanical and physical properties. The WPBs were ground into < 5 mm in size equal to the fine aggregate size. Therefore, different percentages of WPB were used namely 10, 20 and 30%. The results revealed that 20% of the WPB showed the best results to produce light weight concrete. The compressive strength was reduced by 20% only with 20% of WPB which it declined by 42% with higher WPB content. Moreover, concrete with 20% of WPB content achieved ultrasonic pulse velocity (UPV) of 3 km/s which indicated a satisfactory level of concrete integrity. This indeed clearly indicated that the plastic content should be carefully selected before full applications. This study suggested that each cubic meter of concrete can accommodate around 100 kg of WPB. Indeed, that will reduce the pressure on landfills and the environment by having this innovative application.

Keywords: Recycling; Concrete; PET; Environment

1 Introduction

The word plastic is derived from “pliable” which means “easily shaped”. Plastic is basically polymers or monomers with long chains. It was successfully synthesized since the end of the nineteen century (Gilbert et al., 2017). Nowadays, the plastic become a prominent content of many items in our daily life (e.g. plastic bags, furniture, cars, toys etc.). Annual world production of plastic reached 370 Mt tons in 2019 and expected to reach 800 Mt by 2035 and 1600 Mt by 2050 (Alagha et al., 2022; Ali et al., 2021). Globally, around 72% of plastic is wasted (40% landfills, 34% released to the environment), 14% incinerated while only 14% is recycled (Evode et al., 2021). The sea receives annually 8.3 Mt which cause death of 1.5 million marine animal per year. The plastic is decomposed into small particles called microplastic which transferred easily to different receptors (animal, human beings) though air, water, and food chains. Recent studies revealed that microplastics presents in table salt, sugar, honey, bottled water etc. (Cooc et al., 2020). That alarmed the researchers and decision makers to implement new methods to mitigate the effect of the

plastic in our daily life. Furthermore, plastic manufacturing processes released wide variety of harmful gases to the atmosphere including hydrogen cyanide, carbon monoxide, dioxins, nitrogen oxides (Ali et al., 2021)

Plastic can be categorized into different types: polyethylene (PE), polyvinyl chloride (PV), polystyrene (PS), High density polyethylene (HDPE), polyethylene terephthalate (PET), polypropylene (PP) and polyurethane (PU) (Evode et al., 2021; Ali et al.,2021). PET and PU represent 18% of the total plastic production. PET is produced from fossil feedstock since 1940s and used mainly for manufacturing of plastic bottles. Most of the PET end up to the environment.

Plastic wastes can be used effectively in different construction materials such as aggregate, insulator, or filler compound, road pavement. Lightweight concrete can be produced by replacing aggregate content with light weight material. Plastic became the best candidate due to its abundance and good mechanical properties. Many studies reported the efficacy of reducing unit weight of the concrete by partially replacing the sand or aggregate contents by plastic (Almeshala et al., 2020; Ayewera & Adesina, 2020). The lightweight concrete can provide better heat insulation features, more cost effective and less manpower. Moreover, using plastic in construction materials partially will reduce sand consumption and preserve the natural resources. Plastic application should be limited to non-structural elements as the compressive strength is reduced significantly. That mainly attributed to vulnerable bonding between plastic and cement and small unit weight of plastic. Nonetheless, studies showed that using plastic fiber in concrete reduce shrinkage effects and improved the thermal properties of the cementitious materials (Ochi et al, 2007; Silva et al., 2005). Using plastic content as base and subbase materials in road construction showed betterment in the stiffness, shear and bearing capacity of the road (Benson & Khire, 1994).

Gulf Cooperation Council (GCC) countries generate nearly 11.9 Mt of municipal solid waste(MSW), of which 25±15 % is recycled (Alagha, et al., 2022). In Particular, United Arab Emirates (UAE) accounted for higher percentage (37%) of MSW followed by Kuwait and Saudia Arabia with 20%, then Oman 17% (2 Mt/year) and the lowest Qatar (10%) and Bahrin 8% (Beah, 2022 and Alagha et al., 2022). The plastic waste represents around 14% of the total generated MSW. In Qatar, around 14% of plastic waste is recovered of which 40% is recycled (8.6 kt) the remaining either discarded to landfills or incinerated in open area (Alagha et al., 2022).

GCC countries have few initiatives to mitigate the effects of plastic waste by reducing the waste production and promoting recycling practices. In Oman, the government recently banned the single-use plastic shopping bags and promote the use of textile reusable bags (Environment Authority, 2022). That indeed is expected to reduce the plastic waste generation significantly. In Saudi Arabia, recycling and energy recovery from plastic waste is still underdevelopment with up to 15% of plastic waste recovery (Alagha et al., 2022).

The main aim of this study was to find ecofriendly solution for wasted plastic bottles (WPB) by using in concrete blocks with partial replacement of the fine aggregate. This is expected to have dual benefits to protecting the environment from hazardous materials and secondly protecting the natural sources. WPBs were collected and shredded to the size range of the fine aggregated and used in concrete block with different ratios. Different tests were conducted to evaluate the effect of the plastic content on the mechanical and physical properties of the concrete. In connection to this, the current study also provided a data related to the plastic consumption rate per capita per day in

Oman based on field study with 70 participants over 4 weeks. It is suggested that the outcomes of this study will trigger the research in this area and provide more insights on plastic waste management using ecofriendly technology.

2 Methodologies

The plastic water bottles were collected from homes with different sizes 250 ml to 500 ml. The bottle caps and plastic labels were removed. Then the bottles were sent to be shredded using shredding machine. The shredded particle sizes less than 4.7 mm equivalent to the size of the fine aggregate. Three different plastic percentages (10, 20 and 30%) were used in this study to partially replace the fine aggregate. Control sample without plastic content was examined to observe the effect of the plastic contents

2.1 Concrete Mix Design

The concrete mix was designed as per the Department of Environment (DOE) method. The design outputs summarized in the table below (Table 1). The type of cement used is ordinary Portland cement (OPC), crushed aggregate. The sieving analysis was performed to assure aggregate fit within the range of coarse aggregate (20 mm to 10 mm) and fine aggregate (4.75 mm to 150 micron).

Table 1: Concrete mix design as per DOE

Parameter	**Value**	**Parameter**	**Value**
Target mean strength N/mm^2	36.68	Coarse aggregate (kg/m^3)	505
Water cement ratio	0.47	Fine aggregate (kg/m^3)	1238
Cement (kg/m^3)	447		

2.2 Mechanical and Physical Properties of the Concrete

Different tests were conducted to evaluate mechanical and physical properties of the concrete with and without plastic content. To evaluate the workability of the concrete slump test was performed as per the standard method (BS 1881: Part 102). The mechanical properties were evaluated by conducting compressive strength test (BS 1881: Part 116:1983) (Brand ELE International ADR Touch Mod:36-3280/01). The cube sizes 100x100x100 mm. The curing time of the concrete was 7 and 28 days in which the compressive strength was conducted. Ultrasonic is non-destructive test performed to evaluate the integrity of the hardened concrete (Brand MATEST Mod:C372N). The velocity is calculated by dividing the length of the specimen by the required time to pass a sound wave through the specimen.

2.3 Waste Plastic Bottle Field Survey

Field quantification of the waste plastic bottle (WPB) which are used for water storage (200 to 500 ml) was performed over 4 weeks. The number of the family involve in this study was 12 families with total number of 69 person. The WPB is categorized as the polyethylene terephthalate (PET). The number of WPB generated by each family were quantified and the weight is measured. The generation rate was calculated as kg/capita/day.

3 Results and Discussion

3.1 Waste Plastic Bottle (WPB) Survey

The table below showed the details of the field survey (Table 2). The total production of the plastic bottle from the participants was 67143.5 g over 28 days equals 0.035 kg/capita/day.

Table 2: The plastic water bottle production involving 12 families (69 person) over four weeks (28 day) in Muscat, Oman

Sr. No	No. Member	No. Bottles	Size of the bottle (ml)	Weight / bottle (g)	Total weight (g)
1	7	410	500	11.5	4715
2	5	299	500	11.5	3438.5
3	7	760	200	8.5	6460
4	4	111	250	10	1110
5	2	224	250	10	2240
6	9	1440	250	10	14400
7	7	924	250	10	9240
8	5	380	250	10	3800
9	7	255	250	10	2550
10	5	695	250	10	6950
11	7	816	250	10	8160
12	4	408	250	10	4080
total	69				67143.5

3.2 Effects of Plastic Content on the Mechanical and Physical Properties of the Concrete

The concrete fresh mix was tested for the workability using slump test as an indicator. The results revealed that the plastic content reduced the workability of the concrete (Figure 1). That might be attributed to lessening of the homogeneity of the concrete due to plastic addition. Similar observation was reported in other studies (Akinyele et al., 2018; Almeshal et al., 2020; Mustafa et al., 2019).

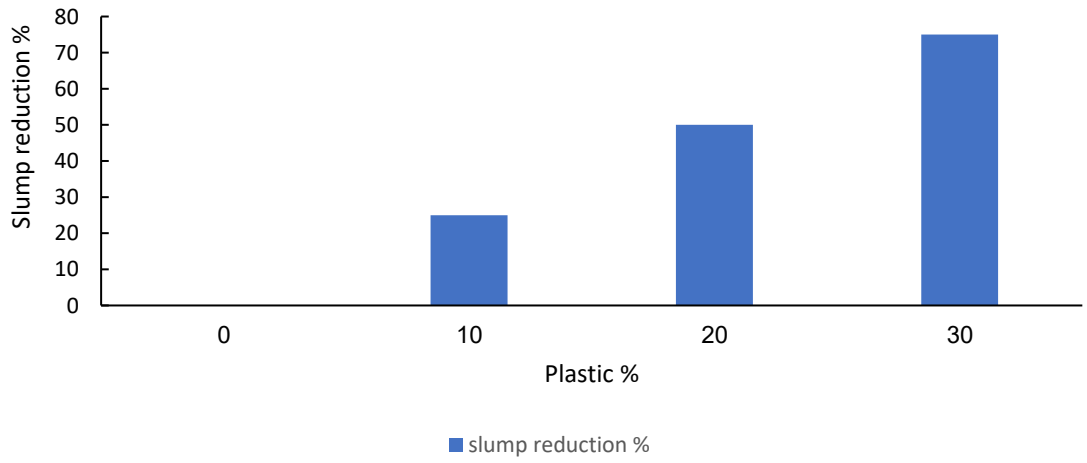


Fig. 1: The effect of the plastic percentage (replacing fine aggregate) on workability of concrete (slump value)

The result compressive strength of the casted cubes with different plastic contents were tested for 7 and 28 days. The results revealed that the plastic contents are reducing the compressive strength of the concrete (Figures 2 & 3). The compressive strength was reduced by 20% with plastic content of 20% while reached 42% with 30% of replacement. These finding came in line with what reported by (Almeshal et al. 2020). This concluded that, the optimum percentage of replacement is 20%. The observed reduction in the compressive strength is mainly attributed to the reduction in the bulk density of the specimen. Moreover, the plastic at high content will lose the bonding with cement and reduce the integrity of the specimen which clearly reflected by Ultrasonic pulse velocity results (Figure 4). The integrity of the concrete was affected positively by the plastic content of 20% with corresponding UPV of 3.1 km/s compared to 2.6 km/s with zero plastic content. That might be attributed to role of small particles of plastic acting as a filler material. In general, values greater than or equal to 3 km/s indicate satisfactory level of concrete integrity.

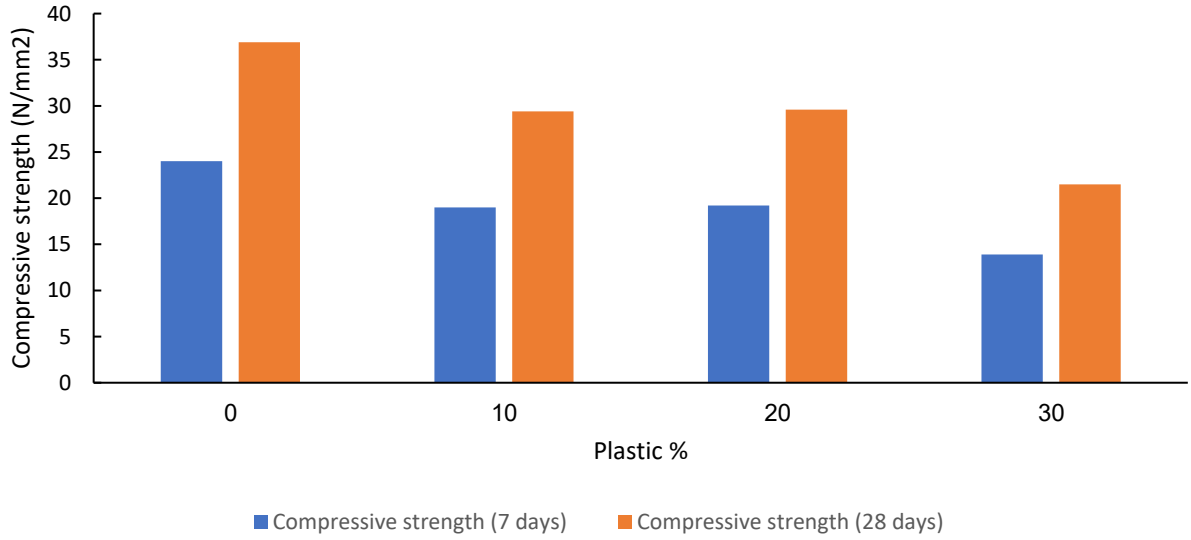


Fig. 2: The effect of the plastic percentages (replacing fine aggregate) on the concrete compressive strength (N/mm^2) after 7 and 28 days

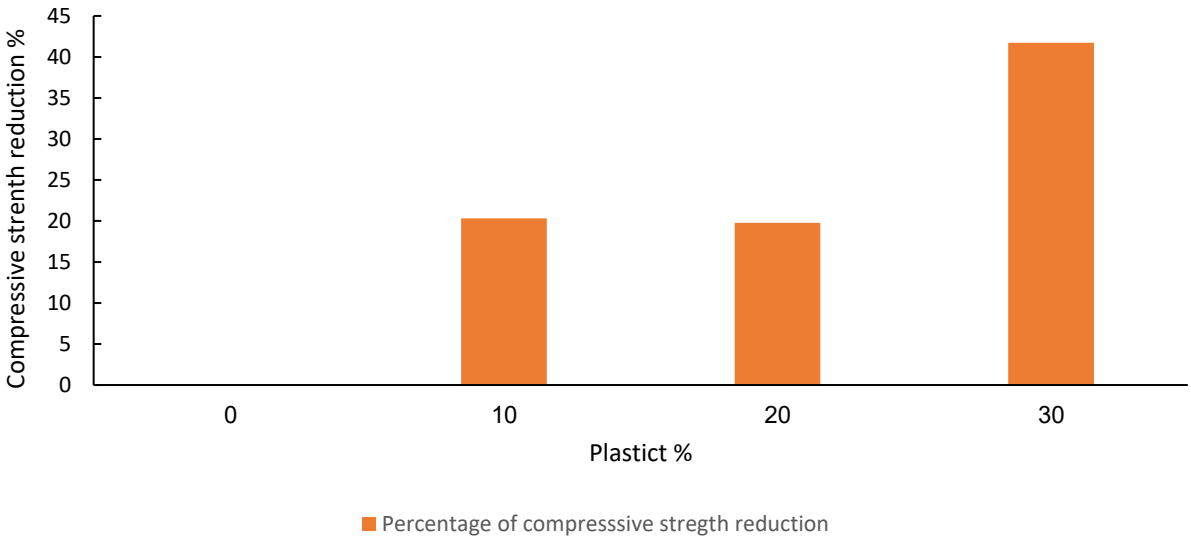


Fig. 3: Reduction on the compressive strength due to plastic percentages after 28 days

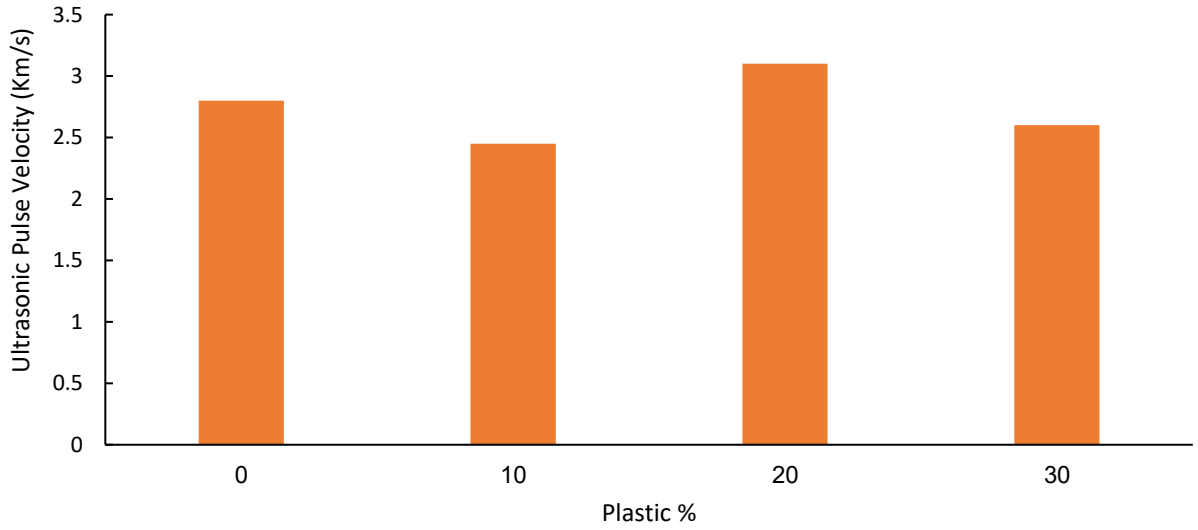


Fig. 4: Ultrasonic pulse velocity (km/s) for different plastic percentages

4 Conclusion

This study concluded that using waste plastic bottles in non-structural concrete (lightweight concrete) was successfully achieved. The optimum plastic content was 20% in partial replacement of fine aggregate. The compressive strength of the produced lightweight block was 30 N/mm^2 compared to 37 N/mm^2 of the control mix (0% plastic). That being said, more investigation is required to address the feasibility of this option. Indeed, using WPB in construction will be reduced tremendously the land size required for landfills and will mitigate the environmental risks associated with plastic waste. This study suggested that each cubic meter of light weigh concrete could accommodate 200 kg of plastic waste.

References

Akinyele J.O. & Ajede A. (2018). "The use of granulated plastic waste in structural concrete". *African J Sci Technol Innov. Dev., 10*(2):169–75.

Ali, et al. (2021). "Degradation of conventional plastic wastes in the environment. A review on current status of knowledge and future perspectives of disposal", *Sci. Total Environ*. 144719.

Almeshala, et al. (2020). "Eco-friendly concrete containing recycled plastic as partial replacement for sand", *Journal of mater res technol., 9*(3):4631–4643

Beah Oman environmental services holding company. https://www.beah.om, Accessed December 2022.

Benson, C.Y. & Khire, M. V. (1994). "Reinforcing sand with strips of reclaimed high-density polyethylene", *J. Geotech. Eng*. 120 838–855.

Cook, C. R. & Halden, R. U. (2020)." Ecological and health issues of plastic waste, in: Plastic Waste and Recycling", Academic Press, pp. 513–527.

Environment Authority, Sultanate of Oman, 2020. https://www.ea.gov.om, Accessed December 20, 2022.

Gilbert, M. (2017). "Plastics materials: introduction and historical development, in: Brydson's Plastics Materials", Butterworth-Heinemann, pp. 1–18.

Mustafa, et al. (2019). "Effect of partial replacement of sand by plastic waste on impact resistance of concrete: experiment and simulation", Structures; 20: 519–26.

Ochi, T., Okubo, S. & Fukui, K. (2007). “Development of recycled PET fiber and its application as concrete-reinforcing fiber”, *Cem. Concr. Compos. 29*(2007)448–455,

Silva, D et al. (2005). “Degradation of recycled PET fibers in Portland cement-based materials”, *Cem. Concr. Res. 35*(2005) 1741–1746.

Cite as: Al Umairi A., Al Mahrouqi N., Al Wahaibi M., Al Hooti M., Alnabhani F. & Al Mamri H., “Eco-friendly Concrete Using Waste Plastic Bottles as Aggregate: A Case Study from Oman”, *The 2nd International Conference on Civil Infrastructure and Construction (CIC 2023)*, Doha, Qatar, 5-8 February 2023, DOI: https://doi.org/10.29117/cic.2023.0186

Watermain Breaks in Hong Kong: Causes and Consequences

Tayyab Ahmad
Department of Civil and Architectural Engineering, Qatar University, Doha, Qatar
tayyab@qu.edu.qa

Ibrahim Shaban
Mechanical and Aerospace Engineering Department, UAE University, Al Ain, United Arab Emirates
ibrahim.shaban@uaeu.ac.ae

Tarek Zayed
Department of Building and Real Estate, Polytechnic University Hong Kong, Hung Hom, Hong Kong
tarek.zayed@polyu.edu.hk

Abstract

Watermain failure is a complex problem associated with significant socio-economic and environmental impacts. The complexity of this problem originates from many factors of physical, operational, and environmental nature. These aspects have varying contribution towards watermain breaks depending on the regional context. This, therefore, requires specialized studies for each individual region. This study aims at adopting the text mining approach to investigate the aspects contributing to the failure of watermains in Hong Kong (HK) and the socio-economic and environmental consequences of these failures. In this regard, a sum of 94 media articles discussing HK-based watermain failures from 1984 onwards are studied. The findings showed that the aging pipes, hilly terrain, ground settlement, excavation works, and high-water pressure, are the most repeated failure causes in the media. The watermain bursts in HK are found to result in traffic disruptions and incidents, loss of water supply, loss of business activity, flooding inside buildings, cave-in incidents, etc. The inquiry has resulted in a network of interrelationships among consequences of main breaks indicating that these breaks are complex occurrences where chains of events lead to significant socio-economic and environmental impacts. This demonstrates the need of resilient Water Distribution Network (WDN) in HK and also the need of rigorous risk management to deal with the threats related to main failures. The causes behind breaks identified in this study can lead to the modelling of HK-based WDN helping forecast the occurrence of such events. The consequences of breaks identified in this study can help formulate risk management frameworks for HK-WDN.

Keywords: Water Distribution Network; Hong Kong; Break; Media report; Causes; Consequences

1 Introduction

Owing to the critical use of freshwater in daily life, well-conditioned watermains are needed to address the basic needs of society. Watermain failures lead to a multitude of problems, such as water supply disruptions, water waste, damage to nearby utilities, traffic gridlocks, and high maintenance expense from taxpayers' money. Hong Kong City, popular for its highest population density worldwide, has over 1,000,000 watermain assets (i.e., the number of pipes). Approximately, 85% of these assets transmit freshwater for drinking uses, and 15% are used to carry salt water for toilet flushing purposes. Although, the Water Supplies Department of Hong Kong (WSD-HK) pays reasonable attention to reducing the water losses from watermain leakages and breaks, at least until

2018, a high amount of water wastage from main failures was reported. In 2018, a Hong Kong-based watchdog claimed that the WSD-HK spent almost HK $530 million to control the frequent leakage incidents around the city. Over the last two decades, news media has actively reported the occurrences of main breaks across Hong Kong indicating socio-economic and environmental impacts of such failures.

Watermain failure studies are highly contextual primarily because of the different ages, materials, and environmental conditions of watermains. Studies have been conducted before to investigate the watermain failure in other regions such as Canada, USA, and the Netherlands; however, there is a general lack of such studies for HK-based WDN. Owing to the contextual nature of these studies, the practical application of these studies is often limited to their subject regions. The lack of research on HK-WDN needs attention.

With the focus on Hong Kong, the aim of this study is to help improve the resilience of HK-WDN and reduce the damages resulting from its failures. Accordingly, two key objectives are proposed. First, to study the causes of watermain failure in Hong Kong. Secondly, to study the consequences of watermain failure in Hong Kong. To achieve these objectives, text mining approach is used to analyse HK-based media and governmental reports.

Achieving the study's aim has significant theoretical and practical implications. Theoretically, the study will inform the factors contributing to main failure. These factors can further be employed in future studies for modelling the main failure. Also, a detailed account of the consequences of main failure will be useful in practice, to develop risk management measures which can be employed for HK-WDN.

The organization of this paper is such that, first a brief account of previous studies is provided in the literature review. This is followed by an explanation of the methodology employed, which will be followed by a detailed account of findings. Lastly, the study is concluded with an account of its limitations and directions for future studies.

2 Literature Review

The review of relevant studies indicates that the failure factors for watermains can be broadly categorized as pipe, soil, operational, and environment-related (see **Table 1**). The pipe-related factors are diameter, material, length, age, manufacturing defects, thickness, connection methods, and installation methods. Soil-related factors include bedding condition, soil properties, backfilling material, buried depth, and external protection. Operation-related factors include pressure head, water use rate, water quality, and internal corrosion. Lastly, environment-related factors include ground water level, precipitation, rain deficit, temperature, humidity, frost load, number of road lanes, location, population density, and street block length. Depending on the regional context of a WDN, some of these factors contribute more towards the failure of watermains than others.

Few studies have been conducted with attention towards watermain failure in Hong Kong. Shi, Zhang, and Ho (2013) conducted a spatial analysis of watermain failure in Hong Kong. The study revealed quantitative relationships between failure rate and pipe diameter, pipe age, material and temperature. Zhou, Ng, Yang, and Xu (2020) provided an approach to mine news articles to delineate infrastructure failure interdependencies and associated stakeholders. In this study, interdependencies in HK's watermain failure were identified and 25 associated stakeholders were also identified.

Table 1: Factors frequently associated with watermain failure

Reference	Kabir, Tesfamariam, Loeppky, and Sadiq (2016)	Fares and Zayed (2010)	Jafar, Shahrour, and Juran (2010)	Najjaran, Sadiq, and Rajani (2006)	Tesfamariam, Rajani, and Sadiq (2006)	B Rajani and Tesfamariam (2005)	Park (2004)	Balvant Rajani and Makar (2000)	Fan, Wang, Zhang, and Yu (2022)	Le Gat and Eisenbeis (2000)	Al-Barqawi and Zayed (2008)	Yannopoulos and Spiliotis (2013)	Rezaei, Ryan, and Stoianov (2015)
Diameter	x	x	x		x	x	x	x	x	x	x	x	x
Material	x	x	x	x	x	x	x	x	x		x	x	x
Length	x	x	x		x	x		x	x			x	
Age	x	x	x	x	x	x		x	x		x	x	x
Manufacturing defects	x												
Thickness					x	x							
Connection method												x	
Installation method													x
Bedding condition		x	x	x	x	x	x	x					
Soil properties	x	x	x	x	x	x	x	x	x	x			x
Backfilling material		x	x	x	x	x	x						
Buried depth	x	x	x	x	x	x	x						
External protection		x					x				x		
Pressure head		x	x	x	x	x		x			x	x	
Water use rate		x											
Water quality		x					x						
Internal corrosion		x	x		x	x							
Ground water level											x		
Precipitation	x												
Rain deficit	x												
Temperature	x			x	x	x		x	x				x
Humidity										x			
Frost load	x						x	x					
Number of road lanes											x		
Location	x	x	x	x	x	x					x		
Population density									x				
Street block length	x												

Some studies are also conducted regarding the consequences, damages or risks associated with watermain failure in different regional contexts. Pietrucha-Urbanik and Studziński (2019) conducted qualitative risk analysis of watermain failure in terms of water supply safety for a city in southern Poland. Fluctuations in the water supply was considered as the key consequence of main failure. In a study conducted by Laakso, Ahopelto, Lampola, Kokkonen, and Vahala (2017), the consequences of water and wastewater pipe failure were estimated for Helsinki region. In a study conducted for main breaks in the US, some of the significant consequences of main breaks were analyzed including property damage, health risks, and water losses (Yerri et al., 2017). Similar to the factors contributing to main failure, the consequences associated with main failure also vary from region to region, necessitating a specialized inquiry for Hong Kong region.

3 Methodology

The study employs a qualitative methodology where the causes and consequences of main failure are identified and analysed using text-mining of news media articles. The collection process of media reports is about selecting suitable media sources, determining relevant keywords for search process, and extracting the articles. Two key factors influencing the selection of media and news sources are reliability (i.e., need of verifying legitimacy of the sources) and collection burden (i.e., sources and efforts required to collect and store data through news sources) (Nam & Seong, 2019; Zhou et al., 2020). Integrated news engines such as Google News, Wise News, and Factiva are less time-consuming to retrieve than the news reported in individual newspapers. Accordingly, for this study, media and news articles are searched on 'Factiva' database. The search was constrained to Hong Kong region and English articles, however, no constraint on the publication time was applied.

Keyword logic used to search for articles: ("Watermain" OR "Water pipe" OR "Water infrastructure" OR "Water distribution network") AND ("failure" OR "break" OR "deterioration" OR "burst" OR "leak")

As a result of the preliminary search, 320 articles were obtained which were subjected to content analysis in NVIVO-12 application, where 94 articles met the criteria of relevance. The shortlisted articles are mostly published in 'South China Morning Post', 'The Standard', 'China Daily', 'Hong Kong Government News', 'Foreign Affairs', and 'XNEWS'.

The shortlisted articles were thoroughly reviewed and based on inductive and deductive thinking, 2 key themes were developed. The themes emerging from these shortlisted articles are about (1) causes of watermain failure and (2) sequence of damages from main failures. These themes are discussed in the next section.

4 Results and Discussion

4.1 Watermain Failure trends in Media reports

Watermain failures can be categorized as bursts and leaks. A leakage is a minor failure that needs tools and equipment to locate. On the contrary, burst are breaks in the mains resulting in flooding of water.

Upon analyzing the media reports extracted from Factiva database, it was found that the discussion on watermain failures have been covered only from 1984 onwards (Fig. **1**). Until 2003, very few articles reported main breaks and only from 2004 onwards multiple breaks have been reported in news articles each year. However, after year 2016, the number of such reports per year has, subsided.

The trends in bursts and leaks of HK-WDN are plotted (see Fig. **2**) in accordance with the data publicly shared by WSD (WSD, 2022a). When compared to the peak number of main leaks for year 2000 (number of leaks=22,428) and 2002 (n=23,729), the leaks have significantly reduced since 2016. Similar trends are also observed in terms of the number of bursts. This reduction in leaks and bursts can be associated with the regional attempts to repair and replace 3000 km of aged watermains to avoid the risk of failure (WSD, 2022b).

Five or less than five main failures reported in media for each year are insignificant compared to the actual number of main failures each year. This can be attributed to the fact that media reports cover the disruptive failures only (i.e., failures that cause either socio-economic or environmental impacts). This indicates that very few of the main failures in HK WDN are associated with noteworthy damages to property and service disruptions.

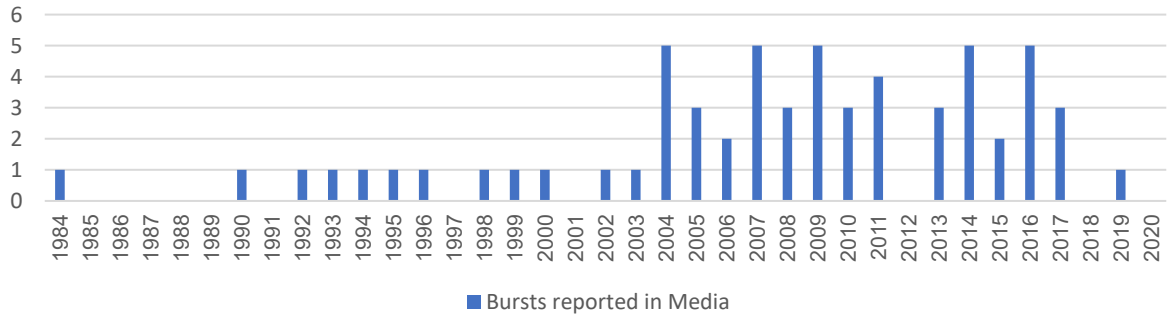


Fig. 1: Temporal trend of watermain breaks reported in news articles

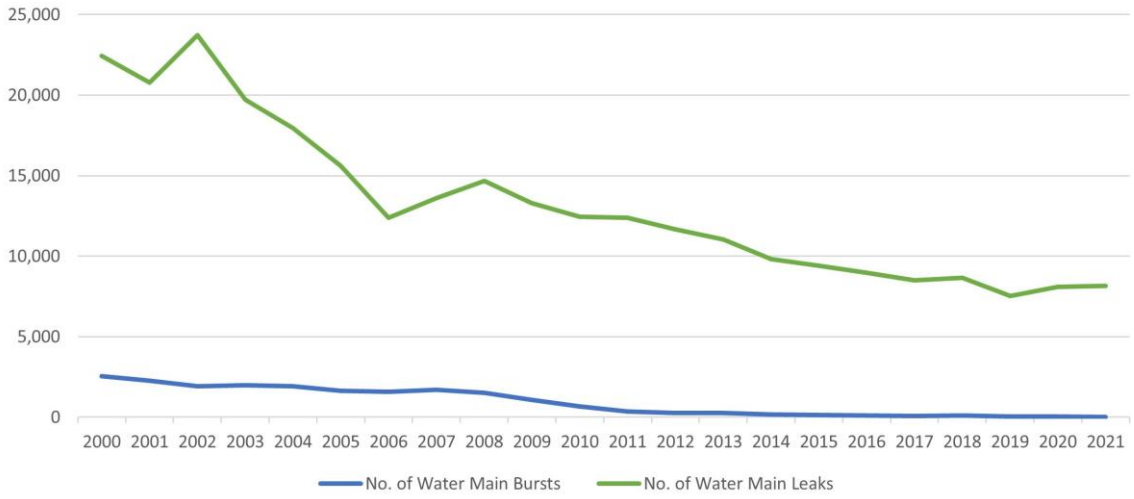


Fig. 2: Temporal trend of watermain breaks in Hong Kong

4.2 Causes of Watermain Failure in Hong Kong

As identified from news articles, the main causes of watermain breaks in Hong Kong include 'Aging watermains' (number of occurrences in media reports=9), 'Hilly terrain of Hong Kong' (n=2), 'Ground settlement' (n=2), 'Damage from excavation works' (n=2), 'High water pressure' (n=2), 'Road traffic' (n=1), 'Pressure from human crowd' (n=1), 'Frequent roadworks' (n=1), 'External loading and vibration' (n=1), 'Deformation of building foundations' (n=1), and 'Lack of coordination between Water Supplies Department and Transport Department' (n=1).

Some of the causes of main breaks are interlinked and are specific to Hong Kong because of its geography. Hong Kong's WDN has been developing according to demand. The system is massive and complex, measuring about 7,800 kilometers in total length. The hilly terrain of Hong Kong leads to relatively high-water supply pressure. For optimal use of scarce land resources in Hong Kong, service reservoirs are typically built at high level. The high-water pressure resulting from hilly terrain of Hong Kong contributes to main failure. While reporting about this issue, an article stated, "given the hilly terrain of Hong Kong, the water pressure of our water supply networks generally ranges from 60 to 80 meters, higher than the 40 meters or so of Singapore and other places by a margin of 50 per cent to 100 percent. High water pressure increases the risk of watermain bursts."

A significant area in Hong Kong is comprised of artificial islands. Ground settlement in such a topography can be more intense and frequent which according to an article has resulted in main breaks. Since WDN in Hong Kong is mostly occurring underneath the road network, the coordination between WSD and Transport Department seems immensely important. More so, as the lack of coordination between these two departments is reported as a cause of main breaks. Road and basement excavations in two reports are

found to be directly responsible for main breaks. Roadworks also indirectly affect the vulnerability of watermains as they add to the external loading and vibrations which can lead to main failure.

Some of the watermains bursting in Hong Kong are more than 30 years old. Monitoring the health of watermains and replacing old mains in Hong Kong is challenging because of its complex urban development. As reported in a news article, "improving the buried infrastructure in a dense environment like Hong Kong is sometimes like threading the eye of a needle. You do not have the luxury of simply opening up the road and laying a new pipe to replace the old."

These causes of main failure in Hong Kong indicate the context-specific nature of this problem. The high population density, land scarcity, and hilly terrain of the region are unique challenges which contribute towards the failure incidents of HK-WDN. Previous studies conducted in different regional contexts have also indicated age, water pressure, road traffic, and population density as factors contributing to main failure (Fan et al., 2022; Rifaai, Abokifa, & Sela, 2022; Shirzad, Tabesh, & Farmani, 2014). The damages resulting from the myriad of failure causes have severe impact on society and economy as explained in the next section.

4.3 Sequence of Damages from Watermain breaks

A key theme resulting from the analysis of news articles is about the sequence of damages and disruptions resulting from watermain failure in Hong Kong. Considering the content of news articles, this is the most important theme as articles have been mostly focused on the socio-economic losses and disruptions resulting from watermain breaks. **Fig. 3** indicates the damages and disruptions resulting from watermain failure in Hong Kong. The thickness of links (i.e., network edges) among different factors indicates the number of news articles indicating a certain sequence of events. For instance, many of the news articles (n=28) have indicated that 'watermain break' leads to 'traffic disruption', however, few articles (n=4) have discussed 'watermain break' leading to 'gas pipe rupture'. The mutual association of the factors (see **Fig. 3**) indicates that watermain breaks in Hong Kong lead to complex socio-economic problems.

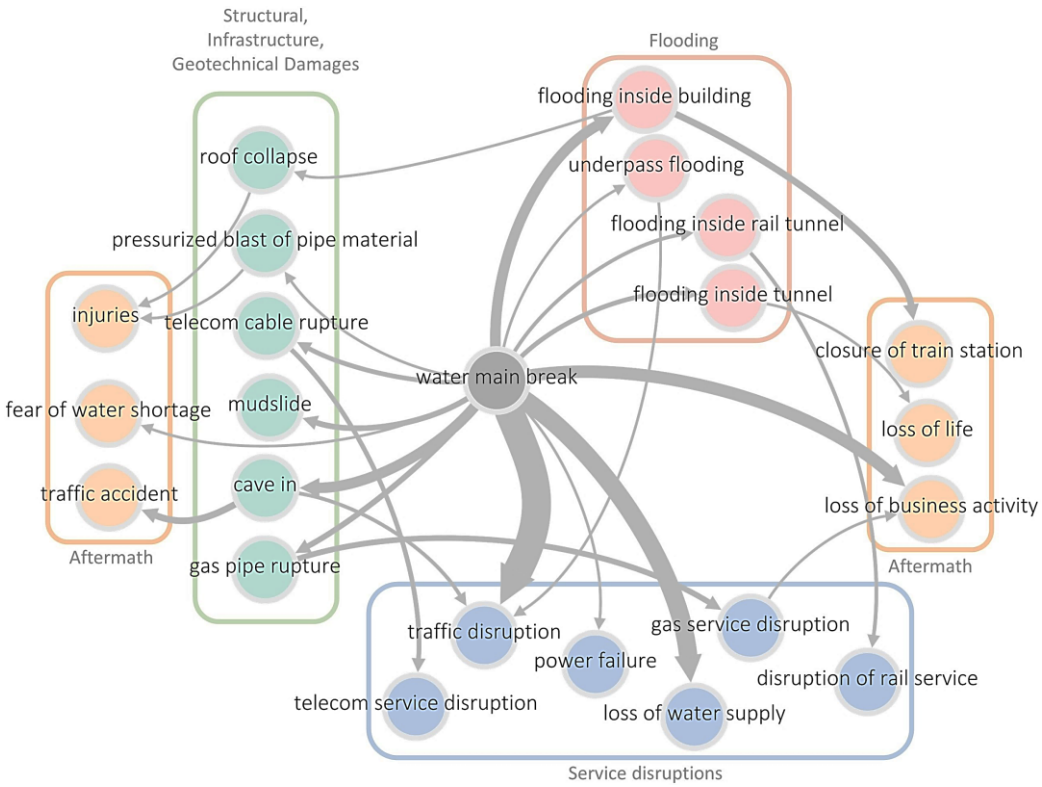


Fig. 3: Sequence of damages and disruptions from watermain breaks

The events resulting from main breaks and their subsequent effects on other events have been classified into four groups as shown in **Fig. 3**. The most frequent mention in news articles is that of service disruptions including traffic, railway, and utility disruptions. Traffic disruptions have single-handedly attracted most attention from news articles. Several structural, infrastructure, and geotechnical damages have also been reported in articles. These damages are a significant cause of service disruptions, as typically the former leads to later.

Flooding of buildings, underpasses, and tunnels from main breaks have also been largely reported. Watermain breaks either directly or by subsequent damages and disruptions lead to socio-economic losses such as injuries, casualties, panic, loss of business, and traffic accidents. Most of the reported damages are of built assets and surprisingly very few articles have indicated the occurrence of main bursts leading to injuries and deaths. Even in such accounts there are very few instances when the pressurized blast of pipe material leads to injuries. Most of the injury and casualty accounts are associated with roof collapses and flooding from main failures. Unsurprisingly, most of the damages and disruptions from main breaks are to road infrastructure or the utilities underneath roads. This is because Water Distribution Network in Hong Kong is mostly buried underneath the road infrastructure.

For Hong Kong, the average duration of fresh water supply interruption caused by main bursts in 2016 is 4.3 hours and in 2020 is 9 hours. The quantity of fresh water drained away because of main leaks in 2019 and 2020 was about 0.02% of the total annual water supplied (ENB, 2021). This indicates a significant environmental damage resulting from main breaks. In a study conducted for main breaks in US, some of the significant consequences of main breaks were also indicated as travel delays, property damage, health risks, and water losses (Yerri et al., 2017).

5 Conclusion

This study reviewed the media reports to identify the causes and consequences of watermain breaks in HK-based Water Distribution Network (WDN). Over the last two decades, Hong Kong news media has repeatedly reported the loss of life, injuries, loss of business activities, traffic disruptions and disruption of utilities (freshwater, telephone, and power) because of watermain failures. These losses are outcomes of mudslides, cave-in, and structural collapses resulting from main breaks.

Media reports are particularly useful when reporting the sequence of damages. Large scale and multi-regional studies conducted using the media reports can provide a high-resolution understanding of the damages from the main breaks and how they are interrelated. Studying such networks using the complexity theory can help develop effective risk management measures.

The limitations of this study lie within the data source used i.e., media reports. Damages which are not of socio-economic significance are typically not found in the media reports. Similarly, many deteriorating factors which are investigated in previous studies are not reported as failure causing factors in media reports. Hence, the news media seems to uncover some causes and consequences of main failure, yet leave the others unaddressed. Future studies regarding HK-WDN need to account for the limitations of this study by also resorting to other means of factor identification. The causes of main breaks identified in this study can help develop failure models of HK-based WDN helping forecast the occurrence of such events. The consequences of breaks identified in this study can help formulate risk mitigation measures for HK-WDN.

References

Al-Barqawi, H., & Zayed, T. (2008). Infrastructure management: Integrated AHP/ANN model to evaluate municipal water mains' performance. *Journal of Infrastructure Systems, 14*(4), 305-318.

ENB. (2021). *Examination of Estimates of Expenditure 2021-22*. Retrieved from https://www.isd.gov.hk

Fan, X., Wang, X., Zhang, X., & Yu, P. A. X. B. (2022). Machine learning based water pipe failure prediction: the effects of engineering, geology, climate and socio-economic factors. *Reliability Engineering & System Safety, 219*, 108185.

Fares, H., & Zayed, T. (2010). Hierarchical fuzzy expert system for risk of failure of water mains. *Journal of Pipeline Systems Engineering and Practice, 1*(1), 53-62.

Jafar, R., Shahrour, I., & Juran, I. (2010). Application of Artificial Neural Networks (ANN) to model the failure of urban water mains. *Mathematical and Computer Modelling, 51*(9-10), 1170-1180.

Kabir, G., Tesfamariam, S., Loeppky, J., & Sadiq, R. (2016). Predicting water main failures: a Bayesian model updating approach. *Knowledge-Based Systems, 110*, 144-156.

Laakso, T., Ahopelto, S., Lampola, T., Kokkonen, T., & Vahala, R. (2017). Estimating water and wastewater pipe failure consequences and the most detrimental failure modes. *Water Supply, 18*(3), 901-909. doi:10.2166/ws.2017.164

Le Gat, Y., & Eisenbeis, P. (2000). Using maintenance records to forecast failures in water networks. *Urban water, 2*(3), 173-181.

Najjaran, H., Sadiq, R., & Rajani, B. (2006). Fuzzy expert system to assess corrosion of cast/ductile iron pipes from backfill properties. *Computer-Aided Civil and Infrastructure Engineering, 21*(1), 67-77.

Nam, K., & Seong, N. (2019). Financial news-based stock movement prediction using causality analysis of influence in the Korean stock market. *Decision Support Systems, 117*, 100-112.

Park, S. (2004). Identifying the hazard characteristics of pipes in water distribution systems by using the proportional hazards model: 1. Theory. *KSCE Journal of Civil Engineering, 8*(6), 663-668.

Pietrucha-Urbanik, K., & Studziński, A. (2019). Qualitative analysis of the failure risk of water pipes in terms of water supply safety. *Engineering Failure Analysis, 95*, 371-378. doi:https://doi.org/10.1016/j.engfailanal.2018.09.008

Rajani, B., & Makar, J. (2000). A methodology to estimate remaining service life of grey cast iron water mains. *Canadian Journal of Civil Engineering, 27*(6), 1259-1272.

Rajani, B., & Tesfamariam, S. (2005). Estimating time to failure of ageing cast iron water mains under uncertainties, ICE Water Manag. *J, 160*(2), 83-88.

Rezaei, H., Ryan, B., & Stoianov, I. (2015). Pipe failure analysis and impact of dynamic hydraulic conditions in water supply networks. *Procedia engineering, 119*, 253-262.

Rifaai, T. M., Abokifa, A. A., & Sela, L. (2022). Integrated approach for pipe failure prediction and condition scoring in water infrastructure systems. *Reliability Engineering & System Safety, 220*, 108271.

Shi, W. Z., Zhang, A. S., & Ho, O. K. (2013). Spatial analysis of water mains failure clusters and factors: A Hong Kong case study. *Annals of GIS, 19*(2), 89-97. doi:10.1080/19475683.2013.782509

Shirzad, A., Tabesh, M., & Farmani, R. (2014). A comparison between performance of support vector regression and artificial neural network in prediction of pipe burst rate in water distribution networks. *KSCE Journal of Civil Engineering, 18*(4), 941-948.

Tesfamariam, S., Rajani, B., & Sadiq, R. (2006). Possibilistic approach for consideration of uncertainties to estimate structural capacity of ageing cast iron water mains. *Canadian Journal of Civil Engineering, 33*(8), 1050-1064.

WSD. (2022a). Number of Water Main Bursts/Leaks. Retrieved from https://www.wsd.gov.hk/en/core-businesses/major-infrastructure-projects/risk-based-improvement-programme-of-water-mains/number-of-cases-includes-damage-by-other-parties-/index.html

WSD. (2022b). Replacement and Rehabilitation Programme of Water Mains. Retrieved from https://www.wsd.gov.hk/en/core-businesses/major-infrastructure-projects/r-r-projects/index.html

Yannopoulos, S., & Spiliotis, M. (2013). Water distribution system reliability based on minimum cut–set approach and the hydraulic availability. *Water resources management, 27*, 1821-1836.

Yerri, S. R., Piratla, K. R., Matthews, J. C., Yazdekhasti, S., Cho, J., & Koo, D. (2017). Empirical analysis of large diameter water main break consequences. *Resources, Conservation and Recycling, 123*, 242-248. doi:https://doi.org/10.1016/j.resconrec.2016.03.015

Zhou, S., Ng, S. T., Yang, Y., & Xu, J. F. (2020). Delineating infrastructure failure interdependencies and associated stakeholders through news mining: The case of Hong Kong's water pipe bursts. *Journal of Management in Engineering, 36*(5), 04020060.

Cite as: Ahmad T., Ibrahim Shaban I. & Zayed T., "Watermain Breaks in Hong Kong: Identifying Causes and Consequences", *The 2nd International Conference on Civil Infrastructure and Construction (CIC 2023)*, Doha, Qatar, 5-8 February 2023, DOI: https://doi.org/10.29117/cic.2023.0187

Performance Criteria Priorities in Green Buildings: A Proof-of-Concept Study

Tayyab Ahmad
Department of Civil and Architectural Engineering, Qatar University,
Doha, Qatar
tayyab@qu.edu.qa

Abstract

Green Buildings (GBs) are becoming increasingly popular as an alternative to resource-intensive traditional buildings. Like any other construction project, GB projects are subject to project management-related criteria, including cost, quality, and schedule performance. In addition to these criteria, GBs also include sustainability performance criteria. As a GB is being developed, some criteria may be prioritized over others. To understand the development and sustainability performance of GB projects, it is necessary to understand the priorities given to different performance criteria and the factors resulting in such priorities. Using the findings from an online survey of 46 GB professionals based in Australia and some Asian countries, it is realized that project management criteria are typically ranked higher in GB projects compared to sustainability performance criteria. The survey has also revealed that these priorities of performance criteria are driven by the choice of owner/developer, obligations from state development authorities, developer's market position, investor requirements, etc. Performance criteria priorities in GBs are also found to be associated with regional factors such as climate, availability of natural resources, regulations, and culture. The findings of this study will support the theoretical development in the field of GB project management by leading to in-depth inquiries in this area.

Keywords: Green Buildings; Performance criteria; Online survey; Sustainability; Project management

1 Introduction and Literature Review

Buildings are an essential part of the built environment owing to their critical role in human lives. Typically, the construction and operation of buildings associates with large amounts of resources. To mitigate these environmental issues, Green Buildings (GBs) are being developed which are usually more environment-conscious, socially habitable and even economically affordable in long terms. While the GB sector is still a niche sector of the construction industry, the knowledge associated with the management and development of GB projects is evolving.

1.1 Performance Criteria in Green Building projects

The conventional performance measures of time, cost, and quality have dominated the construction project and these terms have been collectively termed as the 'iron triangle' by (Atkinson, 1999). Although, for a number of recent decades, the iron triangle has found wide-spread usage, this triad of performance criteria is constrained to project management performance only. While not as widely followed as the iron triangle, the criteria of sustainability and safety are also critical in determining project success. The success of infrastructure and buildings in the future will be determined on the

basis of the well-being of end-users, sustainability, energy efficiency, as well as the flexibility and maintainability of developments (Toor & Ogunlana, 2010). While sustainability as a performance criterion is expected to become *modus operandi* in a typical construction project development in future, usually it is not considered a performance criterion in developments other than sustainable construction projects.

In GBs, project success or project performance is inherently dependent on sustainability criteria alongside project management criteria. The term "project management-related criteria" as informed by Cooke-Davies (2002) is used in this study to collectively address time, cost, and quality performance. There is a general lack of studies inquiring performance criteria in Green Building projects. A notable study in this regard was conducted by Ahmad, Aibinu, Stephan and Chan (2019) in which the associations among project management-related criteria and sustainability performance criteria were inquired for GB projects. While studies have been conducted which individually address cost, schedule, and quality performance in GBs, studies collectively considering performance criteria for GBs are generally lacking.

While GB projects continue to be developed under conventional project development and management practices, it becomes imperative to compare the priorities towards sustainability criteria and priorities towards project management-related criteria. Although the need of including sustainability as a performance criterion in construction projects is proposed in the literature, to date, no study is found that compares the priorities of sustainability performance criteria alongside project management-related criteria. Regarding the priorities of performance criteria for GB projects, a research gap exists which needs to be filled for contributing to the theory of GB project development and management. Accordingly, the objectives of this study are: (1) to determine how the project management-related and sustainability-related performance criteria are prioritized in GB projects; and (2) to investigate the factors influencing priorities of performance criteria in GB projects.

2 Methodology

With the scope of this study limited to Green Office Building projects, the study objectives are addressed by the findings from an online survey. Findings from three semi-structured interviews are also used to support the survey findings. To address the study objectives, the online survey posed three key questions: (1) Respondents to specify the priorities of performance criteria for actual Green Office projects in their regions of belonging, (2) Respondents to rank the factors influencing priorities of performance criteria, and (3) Respondents to indicate if regional context affects priorities of GB performance criteria.

For the first question, survey respondents were provided with the list of seven criteria and they could indicate the priorities of those criteria based on their previous experiences of GB projects. To inquire factors affecting performance criteria priorities, a question regarding this was included in the survey. The organization of inquiry was such that, first the survey participants were questioned about the ranks of performance criteria, and subsequently presented with a list of factors responsible for the priorities of performance criteria. When asked to rank the factors in the order of their impact on performance criteria priorities, 44 responses were obtained.

The question was asked in a way that an initial list comprised of 8 factors was presented to the respondents. The factors in the list were basically solicited from literature and through interviews with two Australia-based GB professionals who both had the experience of being involved in more than 20 green office projects during their professional careers. The respondents of online survey were

asked to rank the factors in the list from Rank-1 (Most important) to Rank-8 (Least important), and also had the option to declare if they found a factor in the list as irrelevant to the question, by selecting the NA (Not Applicable) option. Further, the respondents also had the option to mention factors in addition to those already listed, in case they found it necessary.

To conduct the survey, a list of GB professionals was compiled using the information available on online databases of the GB certification systems i.e., United States Green Building Council (USGBC), Green Building Council of Australia (GBCA), and Singapore Green Building Council (SGBC). The professionals experienced in GB development were contacted to participate and overall, 46 participants from Australia and some Asian countries contributed to the survey. The findings of the survey were supported by three semi-structured interviews conducted with GB professionals in the UK. All these interview participants had both the experience of Sustainability and Design consultancy. The interview participants were highly experienced building professionals with a minimum of 6-year experience in GB projects.

3 Results and Discussion

3.1 Performance Criteria Priorities in Green Office Buildings

In the online survey, 46 respondents provided the priorities/ranks of different performance criteria of GB projects (see Fig. **1**). Resulting from the provision in online survey, most respondents (87%; n=40) highlighted the performance criteria priorities according to different regions while agreeing with the assumption that the regional context affects these priorities. However, the rest of the participants (13%; n=6) did not agree with this assumption and provided their response according to the majority of projects they had worked on.

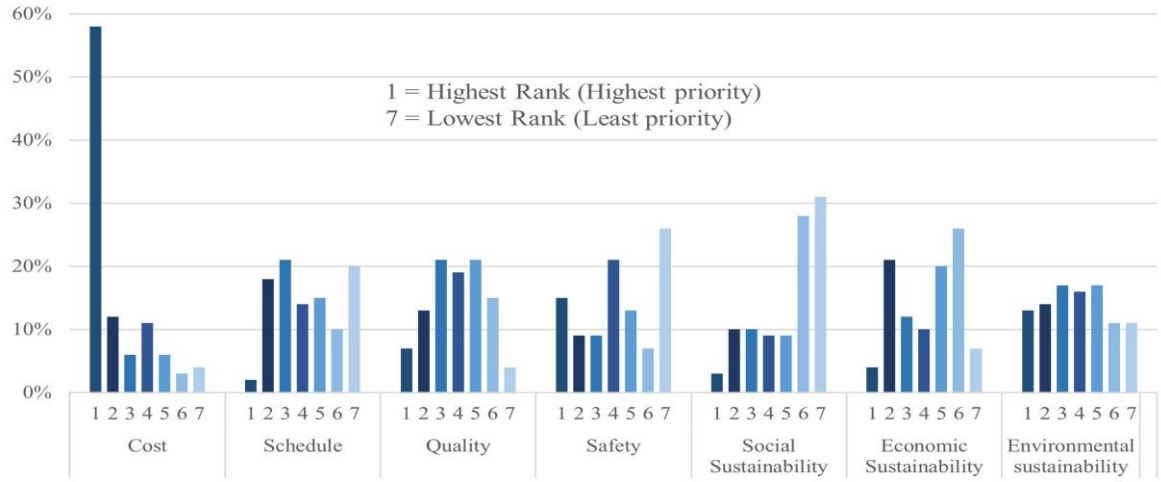


Fig. 1: Overall ranks of performance criteria in green building projects

Table 1: Descriptive statistics relating to performance criteria findings

Performance criterion	Mode	N (%) for mode	Mean	St. Dev	Skewness	Ranks
Cost	1	59	2.13	1.72	1.51	1
Quality	3, 5	22	3.91	1.55	-0.11	2
Environmental sustainability	3, 5	17	3.85	1.90	0.11	2
Schedule	3	22	4.33	1.85	0.13	3

Performance criterion	Mode	N (%) for mode	Mean	St. Dev	Skewness	Ranks
Safety	7	26	4.33	2.13	-0.17	3
Economic sustainability	6	26	4.28	1.73	-0.19	3
Social sustainability	7	30	5.17	1.84	-0.74	4
Note: Arithmetic mean values calculated by dividing the sum of sampled values by the number of items						

Based on the analysis of findings it can be seen that some criteria have clear trends such as cost, quality, social sustainability, and environmental sustainability while other criteria exhibit multiple trends requiring the use of descriptive analysis (see **Table 1**). For assigning relative ranks to the performance criteria, mean value technique is used. This technique is often used when key factors have to be highlighted amongst a number of factors (Moungnos & Charoenngam, 2003). In this study, small mean-rank values imply higher importance given to a performance criterion, while the large mean values imply lower importance given to a performance criterion. Since quality and environmental sustainability had similar mean values, they can be assigned the same rank i.e., "2". Furthermore, as schedule, safety, and economic sustainability had similar mean values, they can also be assigned the same rank i.e., "3".

Skewness is a measure of the asymmetry of a variable about its mean. In Table 1, a large negative skewness value suggests a relatively higher number of respondents opting for a low priority of a performance criterion and vice versa. The highest positive and highest negative skewness values are noticed in case of cost and social sustainability, respectively.

While the mean values provide overall ranks, they may not respond to the dispersions in data distribution. Unlike the case of cost and social sustainability (Fig. **1**) with singular trends, schedule, safety, and economic sustainability seem to have multiple trends as can be seen in terms of multiple mode values shown in Table 1.

The multiple trends in dataset for some performance criteria mean that these criteria may have low priorities in some projects while high priorities in some other projects. For instance, schedule, social, and economic sustainability performance have a mix of low and high ranks according to different respondents. The data analysis shows that cost performance is the most highly ranked (R-1) performance criterion according to mean value and its data distribution resembles a Pareto distribution with highly positive skewness. Quality performance curve has a normalized distribution and based on mean value it is ranked second. However, the multiple mode values for this criterion (i.e., 3 and 5) suggest that it can take multiple priorities depending on the project context. In case of schedule performance, the distribution of survey responses is such that either it is highly prioritized, or it has low priority. It is ranked 3rd based on the mean value. The data distribution in case of the safety criterion suggests that it could be a high, medium, or a low priority criterion. Safety is also ranked third based on the mean value. The data in case of environmental sustainability is evenly distributed, suggesting a high to medium priority for this criterion. Based on mean value, it is ranked 2nd. In case of the economic sustainability, the data has multiple peaks, suggesting both, a high as well as a low priority. Based on mean value, it is ranked 3rd. In terms of social sustainability performance criterion, data distribution is strikingly right skewed, suggesting a low priority. Based on mean value, it is ranked 4th.

It can be argued that the overall project management-related criteria comprised of cost, quality, and schedule have relatively higher priorities as they are ranked 1st, 2nd, and 3rd respectively. However,

sustainability criteria in comparison have relatively lower priorities as 2nd, 3rd, and 4th ranks are given to environmental, economic, and social sustainability respectively. Within the sustainability criteria, social sustainability has relatively lower priority than other criteria.

A variation in the priorities towards performance criteria is not surprising, as even within a region, projects are developed with different considerations and different priorities for performance criteria. While underperformance on a criterion can be acceptable for one project, it may be considered an absolute failure in another project. For instance, a schedule delay of 5 days to deliver better functionality in a particular IT project may not be given much attention. However, similar delay in developing an Olympic village, can be considered a serious setback (Müller & Turner, 2007).

A potential reason for the sustainability performance criteria to be ranked lower than the project management criteria is because sustainability is often perceived in the construction industry as an added value, and not as an intrinsic requirement. As evident from survey responses, managing the allocated project budget remains the top priority for every project to safeguard the interest of stakeholders. For a project, the schedule, built quality and safety cannot be compromised. Sustainability is prioritized if compliance is required for the issuance of building permits, in case the project is located in a country with strict legislations. Otherwise, sustainability is an added value to seek the interest of multi-national companies, with stringent set of corporate social responsibilities, such as CISCO, Google, Unilever or Citibank. These priorities identified from the survey were corroborated by another interview participant (UK-M-5), according to whom, the criteria receiving the most attention is the project cost, and it is always hard to maintain a balance between schedule, cost and quality. Following cost, reducing time on construction site is a priority, followed by quality performance, notably to reduce ongoing maintenance. Although safety receives greater attention than sustainability, it is often compromised when cost is an issue. Projects can be approved even with the minimum safety requirements. The reason why sustainability sometimes becomes a priority is because certain sustainability thresholds need to be satisfied to meet regulatory requirements. This reasoning provided by the interview participant also points to the fact that project management-related criteria often lead to direct and immediate benefits for project sponsor and project team, while sustainability and safety performance criteria may not offer tangible benefits and may only be pursued for regulatory purposes.

During the development of a GB project, the priorities towards performance criteria may also shift during different stages. As mentioned by an interview participant (UK-M-6), in the early stages of most GB projects there is a strong desire to achieve a sustainable building. However, when the project starts and as the client starts to pay the bills, cost becomes a key focus. When the project is being executed on site, schedule becomes the prime concern. Once the project is near completion, the client begins to notice quality issues, for instance those resulting from employing cheaper contractor. Years after project completion, the schedule delays incurred in development become insignificant and the sustainability and quality of project become a concerning matter. This argument by the interview participant indicates that the project management criteria that are more prioritized are usually short-lived and last up to project delivery. Other criteria such as sustainability performance are significant throughout the project's life. However, lack of priority towards sustainability criteria during the project development results in overlooking such core project aspects which are difficult and costly to address once a project becomes operational and the need of sustainability is felt.

An overwhelming focus towards cost and schedule performance in a GB project development, may have adverse effects on sustainability performance. According to an interview participant (UK-M-1),

"The thing which matters most in projects is the timely delivery of design and construction. Both the schedule and cost matter a lot in GB projects. It is always hard to maintain a balance between schedule, cost and quality. It's very difficult to keep up the sustainability performance in case speed of project delivery is the focus. Normally when focussed on project delivery time, the project team forgets the timeliness of sustainability consultants. Sustainability is ignored when the sustainability consultants are not kept on-board while the schedules are being established. This doesn't happen all the times, but it happens once in 10 times." Hence, it can be argued that a focus on time and cost performance instead of sustainability performance can have negative effects for building sustainability.

3.2 Factors Influencing Priorities of Performance Criteria

The factors which affect the priorities of performance criteria, can be considered as the driving factors of project development. It is important to account for such driving factors as they are the underlying reasons of GB project priorities. Upon analysing the responses (shown in Fig. 2), it was realized that the ranks provided to some of the factors including *Owner/Developer's choice*, and *Obligations from state development authorities/Government planning approvals* had relatively clear trends and both these factors were ranked high (R-1 to R-3) in terms of significance by the majority of respondents. The high ranks of these factors imply that they indeed influence performance criteria priorities in GBs. *Investor requirements*, and *Developer's market position* also had trends similar to each other and were left-skewed with most responses for the 4th rank. The responses in case of the factor of *Design team's advocating* were majorly skewed towards right suggesting a 5th to 6th rank for it. Two other factors i.e., *Life Cycle Cost (LCC)* and *State incentives* had multiple peaks for the extreme ranks (i.e., R-2 and R-8) and a trough in between, suggesting that in some cases these factors can become very important while in some other cases they can become least important in affecting performance criteria priorities. The factor of *user requirements*, however, was found to have no trend at all and had a spread of responses between R-2 and R-6. Based on overall analysis, it can be concluded that all the ranked factors are highly relevant in affecting performance criteria priorities of GB office projects.

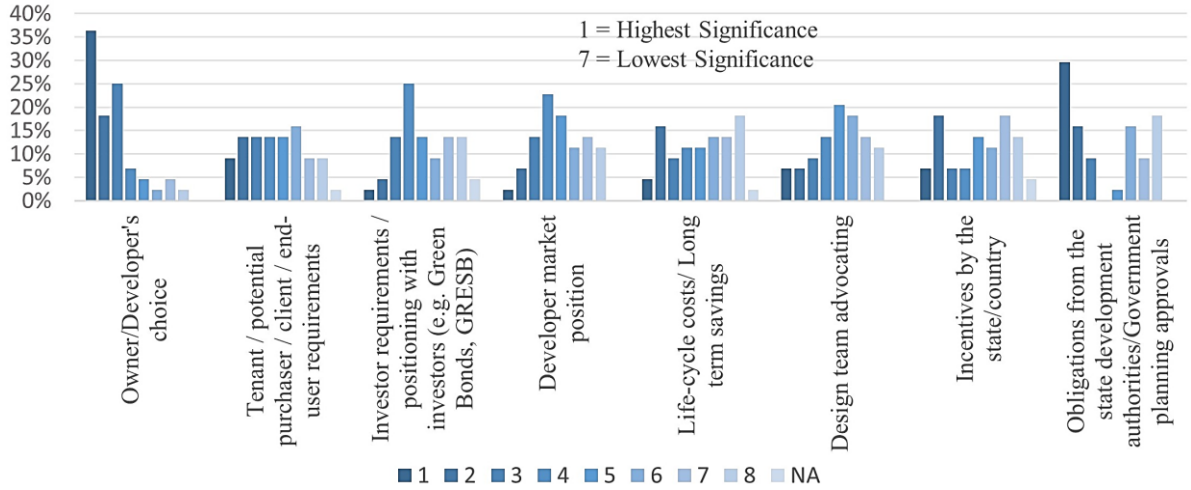


Fig. 2: Ranks of factors influencing priorities of performance criteria in GB projects

In addition to the list of factors provided in the online survey, some other factors were also mentioned by respondents that can influence the choice and priorities of performance criteria in Green Office projects. These additional factors include company brand and ability to attract talent, GB consultant's

advocating, total investment cost, technology and workmanship, corporate image, marketing, and culture. The preselected factors (provided in closed-ended question in survey) and the new factors (identified in the open-ended question in survey) are compared with each other (see Fig. 3). Their cross-comparison shows that the list of factors presented to participants for ranking purpose was reasonably exhaustive.



Fig. 3: List of participant-proposed factors and their resemblance with preselected factors

3.3 Regional Factors Affecting Priorities of Performance Criteria

The difference in priorities of GB project-related performance criteria is governed by the regional context, to some extent. For instance, delivery speed may be a major concern in a region because of the overall fast-paced market there, while for some other regions delivering sustainability may be a more pressing issue because of the regional regulations for it. A question regarding this aspect was responded by 46 survey participants. According to most of the respondents (87%), green office projects **definitely** have differences in priorities of performance criteria resulting from regional differences. According to some respondents (9%), the difference in priorities is **probably** due to regional differences while a small percentage of respondents (4%) **totally disagree** that the regional context affects performance criteria priorities.

For the majority of respondents (87%), performance criteria priorities are influenced by Geo-Specific factors. When asked to provide reasons why priorities of performance criteria in green office projects depend on the difference in regional context, the respondents provided a variety of reasons. The responses found in case of this open-ended question were analysed and a repetition was found in the factors mentioned by respondents. The reasons why performance criteria priorities depend on regional context include climate (number of survey participants indicating this reason=14), natural resource availability (n=11), regulations (n=9), culture (n=7), knowledge and awareness of sustainability (n=6), regional economy (n=5), market demand and maturity (n=3), maturity and innovation in construction methods (n=2), and building product availability (n=1).

3.3.1 Climate

Each region has unique climatic conditions and since building design is highly influenced by ambient conditions, a difference in performance criteria priorities of GB projects can be expected for different regions. According to survey findings, outside conditions impact the extent of energy efficiency and occupant comfort. Highly energy-efficient natural ventilation strategies can be adopted in areas with pleasant climate than in areas with extremely high or low temperatures. Furthermore, heat recovery performances vary in different regions, for instance in Singapore, the sensible heat recovery is not as efficient as compared to enthalpy recovery.

3.3.2 Regulations

Different regions can have different regulations, policies, and statutes for built environment which need to be complied with, resulting in a difference of performance criteria priorities. According to survey findings, while some countries require green development by law, this is voluntary in some other countries. Furthermore, different states and councils provide different incentives and benchmarks for different areas resulting in a difference in performance criteria priorities.

3.3.3 Natural Resource Availability

Different regions are associated with different levels of natural resource availability, therefore resulting in a difference in performance criteria priorities of GB projects. According to survey findings, while some regions have abundance of some natural resources they lack in other aspects. For instance, Hong Kong has a huge waste issue, but energy is not a problem for it.

3.3.4 Building Product Availability

Different regions are associated with different availability of building products, particularly sustainable building materials and systems, which can result in variations of delivery time and cost. This can result in a difference in performance criteria priorities.

3.3.5 Maturity and Innovation in Construction Methods

Different regions are associated with varying levels of maturity and innovation in construction methods, which affects performance criteria priorities of GB projects.

3.3.6 Regional Economy

Regional economy has a strong impact on the construction industry and on all its allied disciplines and niche areas. Different regions have varying economic conditions resulting in a difference in performance criteria priorities for GB projects.

3.3.7 Knowledge and Awareness of Sustainability

Different regions are associated with varying levels of knowledge and awareness regarding built environment sustainability. Since such awareness is instrumental in motivating project stakeholders for developing GBs, it also results in difference of performance criteria priorities. According to some survey participants, awareness of the availability of resources is an important factor that motivates people towards resource conservation. For instance, in case of sustainability awareness, the difference between Sydney and Melbourne would be less. However, if a comparison of these cities is made with Adelaide or Hobart, awareness could be a significant factor, because Sydney and Melbourne are major business centres while Adelaide or Hobart are small capital cities. They may be aware of more established green building schemes or energy efficiency, but less aware of the formal side of sustainability.

3.3.8 Culture

Difference in regional cultures influence end-user perceptions, tolerances, and priorities, therefore resulting in a difference in performance criteria priorities for GB projects. While reflecting on this, a survey participant opined that end-user habits impose different design criteria.

3.3.9 Market Demand and Maturity

Different regions are associated with varying built environment related market demands. Some markets can provide better Return on Investment (ROI) than others, therefore resulting in a difference

in performance criteria priorities for GB projects. According to some survey participants, some markets are more mature than others and can go beyond conventional performance.

4 Conclusion

Based on the findings of online survey, it is realized that in GBs, project management performance is prioritized over sustainability performance. The most importance performance criterion considered is cost performance and the least prioritized criterion is social sustainability performance. Such lack of attention towards sustainability performance criteria becomes a matter of much concern when performance on one criterion such as environmental sustainability needs to be sacrificed to achieve high performance on a highly prioritized criterion such as cost performance. The priorities of performance criteria are decided by the owner/developer, obligations from state development authorities, developer's market position, and investor requirements. Performance criteria priorities in GBs are also associated with regional factors such as climate, availability of natural resources, regulations, and culture. Owing to the limited number of survey responses, some of the findings of this study can only be used as a proof of concept. Studies with large sample sets need to be conducted to understand the priorities of performance criteria in further detail.

Also, the lack of priority of sustainability performance criteria compared to project management criteria is a matter requiring debate among academics and industry stakeholders to assess the outcomes of such a practice and to provide mitigation measures. In addition, this study has lead to some questions which need to be addressed by future research. For instance, (1) what are the scenarios in which preferences towards project management criteria has adverse effects on the sustainability performance criteria? Also, how critical can those adverse effects become? (2) which stakeholders are typically responsible for the prioritization of project management criteria and how a relatively balanced attention towards different performance criteria can be ensured?

References

Ahmad, et al. (2019). Investigating associations among performance criteria in Green Building projects. *Journal of Cleaner Production, 232*, 1348-1370. doi:https://doi.org/10.1016/j.jclepro.2019.06.013

Atkinson, R. (1999). Project management: cost, time and quality, two best guesses and a phenomenon, its time to accept other success criteria. *International journal of project management, 17*(6), 337-342.

Cooke-Davies, T. (2002). The "real" success factors on projects. *International journal of project management, 20*(3), 185-190.

Moungnos, W. & Charoenngam, C. (2003). Operational delay factors at multi-stages in Thai building construction. *International Journal of Construction Management, 3*(1), 15-30.

Müller, R. & Turner, R. (2007). The influence of project managers on project success criteria and project success by type of project. *European management journal, 25*(4), 298-309. doi:10.1016/j.emj.2007.06.003

Toor, S. U. R. & Ogunlana, S. O. (2010). Beyond the 'iron triangle': Stakeholder perception of key performance indicators (KPIs) for large-scale public sector development projects. *International journal of project management, 28*(3), 228-236. doi:https://doi.org/10.1016/j.ijproman.2009.05.005

Cite as: Ahmad T., "Performance Criteria Priorities in Green Buildings: A Proof-of-Concept Study", *The 2nd International Conference on Civil Infrastructure and Construction (CIC 2023)*, Doha, Qatar, 5-8 February 2023, DOI: https://doi.org/10.29117/cic.2023.0188

New Technique for Flood Risk Assessment of Sub-Networks in Large Networks Using InfoWorks ICM: A Case Study of Qatar's Full Storm Water Network

Yahia Alabbasi
Seero Engineering Consulting LLC, Doha, Qatar
yahia.alabbasi@seeroeng.com

Khaled Aboelenen
Seero Engineering Consulting LLC, Doha, Qatar
khaled.aboelenen@seeroeng.com

Mohammed Sadeq
Seero Engineering Consulting LLC, Doha, Qatar
mohammed.sadeq@seeroeng.com

Abstract

The elements of the storm water network are made to safely drain most water during a heavy rainstorm. Flood risk modelling (mathematical modelling) with hydraulic software is a good way to check the network's level of service, especially now that technology has changed. Flood risk modelling is an essential method for checking the network sufficiency and adequacy for different kinds of rain. Modelling flood risk should be done for the whole network to ensure that flows are connected and get accurate results. In this study, one-dimensional flood risk modelling is needed for a sub-network that is part of Qatar's full storm water network. The flood risk modelling is conducted using InfoWorks ICM software. Running the whole model takes a lot of computational data processing. Splitting the entire stormwater network to the concerned sub-network without considering the hydraulic effects of upstream and downstream flows at the boundary conditions of the sub-network will lead to erroneous conclusions. In this research, a new method for hydraulically dividing the network into sub-networks is presented, taking into account the characteristics of the boundaries. This method increases the efficiency and viability of hydraulic modelling for sub-networks in big networks. For purposes of validation, the results of the reduced model in terms of flood depths and volumes are compared with those of the full model. The results of the split model are in good agreement with the entire model.

Keywords: Flood Risk Assessment; InfoWorks ICM; Flood Modelling; Qatar; Storm water

1 Introduction

As per Qatar 2030 Vision and readiness for FIFA World Cup 2022, the state of Qatar has been witnessing enormous development and improvement in the roads and infrastructures sector for urban and rural areas. This includes roads, utilities, landscape, and road furniture. One of the main significant enhancements was in the stormwater networks, where a number of projects have been initiated and finalized to improve the sustainability, resiliency, and readiness of Qatar's storm water network, especially prior to FIFA World CUP 2022.

The State of Qatar by nature encounters variable rainfall, where annual rainfall varies from 0 mm to more than 250 mm. For 24-hour storm duration, a maximum of 136 mm rainfall was recorded in

Umm Al Faye in March 1995, and a maximum of 36 mm for 3 hours storm. Thunderstorms with high rainfall intensity and short storm duration are severe and limited to a certain geographical extent within the State of Qatar.

The main function of storm water management is to safely discharge the surface runoff and raised level groundwater table during and after the rainfall event. Qatar's government represented by Public Works Authority (PWA) has obligated engineers to carry out flood risk modelling for the stormwater network before construction; to check the network's level of service (adequacy), assess the flood risks, and provide proper mitigation measures. The flood modelling of the stormwater network should be done for the design and exceedance of rainfall events under different storm durations. InfoWorks ICM is one of the prescribed mathematical flood modelling software that has been used in flood modelling of any proposed stormwater sub-network connected to the existing full stormwater network. This is to ensure that the additional flows discharging from the proposed sub-networks into the existing full network will not cause it to fail. Flood modelling should be done for the entire stormwater to ensure flow connectivity and results' accuracy. However, computational time including running time and pre/post data processing is dependent on the network's size. This paper presents an industrial case study in Qatar where a new approach is used to accurately conduct flood modelling for sub-network in large networks using InfoWorks ICM with reduced computational time, and without affecting the flow connectivity and accuracy of results.

2 Project Brief

The project comprises the construction of roads and infrastructure in Al Mearad and Southwest of Muaither-Doha West-Zone 44-Package 06 (DW044-P06) with a project value of almost 420 million Qatari Rial. The project location and surroundings are shown in **Fig. 1**. The proposed Stormwater network consists of almost 700 manholes and 1400 m pipe length. Moreover, the proposed stormwater network has inflows from surrounding packages 04 and 05 and discharges into the existing network. The tie-in with the existing network is in the southeast direction of the network at DW082 P00MT-2027. The proposed stormwater network is shown in **Fig. 2**.

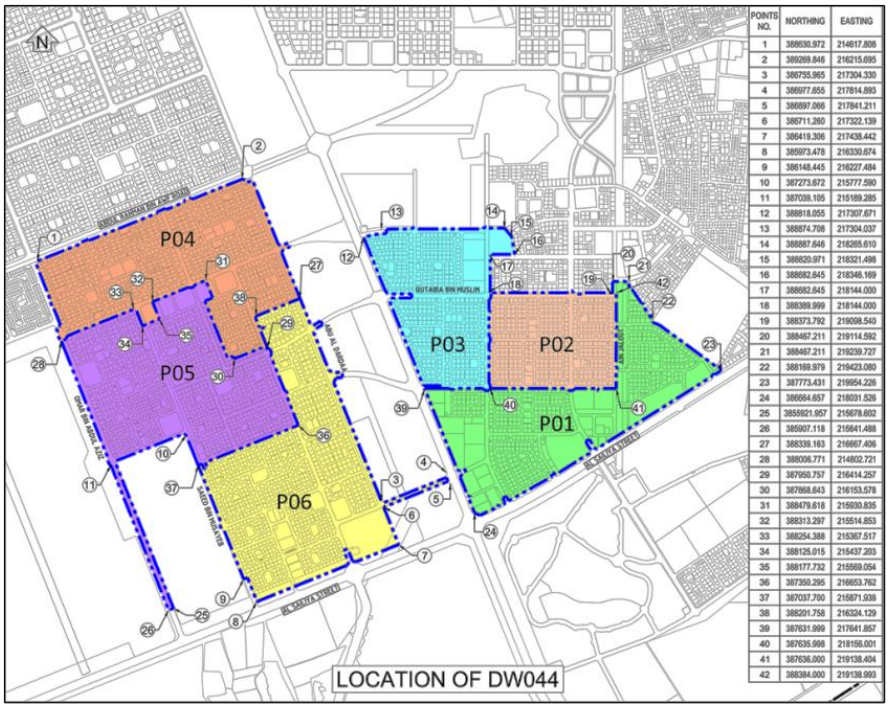


Fig. 1: Location of DW022-P06 and surroundings

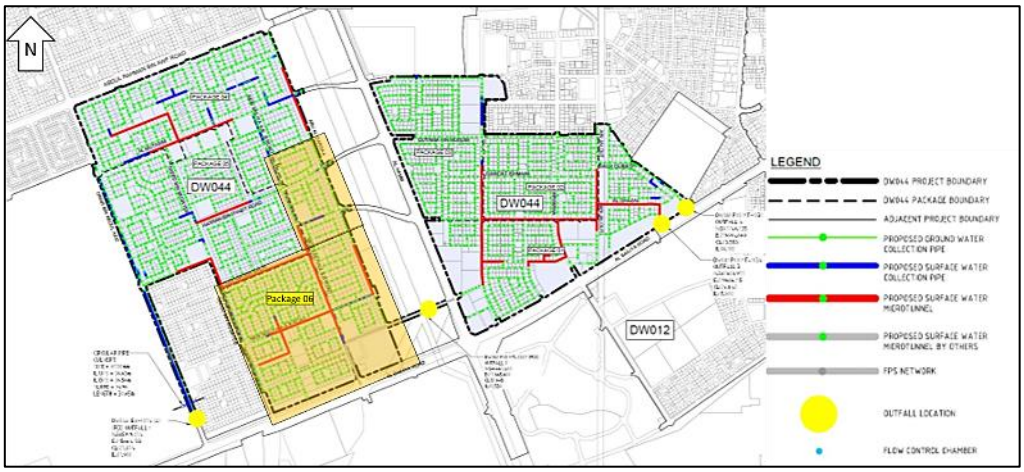


Fig. 2: Stormwater network of DW044-P06

During construction, challenges were encountered in executing the approved stormwater trench design in different project areas due to site constraints, where stormwater trenches are close to the property/boundary wall of the public villas, especially for local urban roads with right of way less than or equal to 12m.

The excavation activity and the related logistics requirements of those trenches were difficult and consumed more resources than planned. Therefore, optimized trench sizes were proposed to maintain the trench volume capacity. In other words, the trench width is reduced, and depth is increased with maintaining the trench cross-sectional area.

3 Modelling Challenges

The full hydraulic model of Qatar's storm water network consists of almost 34,000 manholes (nodes) and 53,000 pipes (conduits) as shown in **Fig. 3**. Almost 33,500 manholes (nodes) and 52,700 pipes (conduits) including the proposed DW044-P06 stormwater network are connected (i.e., having the same outfall/discharge points).

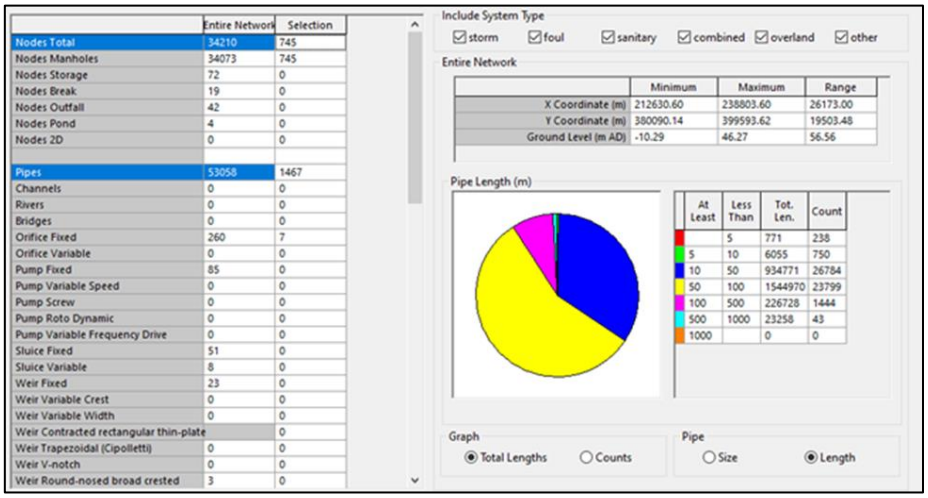


Fig. 3: Qatar's full storm water network information

Nevertheless, the storm water network of the DW044-P06 is much smaller as highlighted in red in **Fig. 4**. The stormwater network of the DW044-P06 is connected to the full network from upstream and downstream directions. At the upstream condition, there are inflows from other projects' networks, and from the downstream condition DW044-P06 network discharges to other networks.

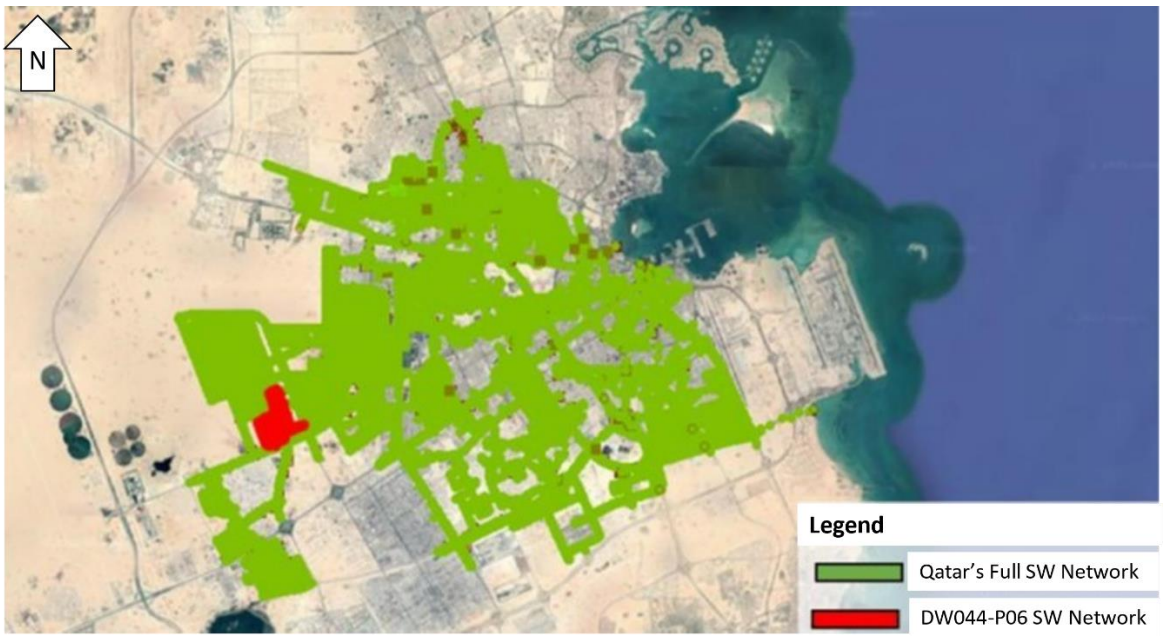


Fig. 4: Qatar's full storm water network

The size of the network in terms of manhole (nodes) and pipe (conduits) numbers affects the computational, data pre-processing, and post-processing times. The full model for the design rainfall event (1 in 5 years return period) and exceedance rainfall event (1 in 10 years return period) for 7 storm durations (15 min, 30 min, 60 min, 2hrs, 6 hrs, 12 hrs, 24 hrs) corresponds to 14 model runs. The estimated running computation time for one full model is 8 hours. Thus, running 14 full models about 5 to 6 days, excluding the time required in the pre-processing stage (updating trench width based on the optimized dimensions), post-processing stage (results analysis), and work contingency in case of model/software malfunctions. Long computational time significantly affects the validity of the modelling exercise, the project's cost, and the baseline. Accordingly, reducing the computational time and expediting the exercise time is required. Splitting the full network into smaller portions without considering the flows from the upstream and downstream of the network impacts the network's hydraulic calculations and outcomes. Therefore, the best practice approach is to hydraulically split the large network into smaller portions to concentrate the study on the required sub-network, thus reducing the computational time. A new approach is used to hydraulically split the model while taking into consideration the flow connectivity from the storm water network's boundaries.

4 Methodology

The main concept of hydraulically splitting the network is to ensure that all the flows from the upstream and downstream boundary conditions are included after the splitting. This can be done by knowing the flow hydrographs (the incoming flow per time) of each boundaries manholes for each storm duration.

First, the boundary conditions of the network are defined as shown in **Fig. 5**. Secondly, the flow hydrograph (Profile file from InfoWorks ICM) is exported from the full model for each storm duration for each boundary manhole. Third, exclude the DW044-P06 stormwater network from its scope. Finally, import the flow hydrographs and assign them to the boundary manholes. A hydraulically Split model of the stormwater network for DW044-P06 is done as shown in Fig. 7. The procedure for hydraulically splitting the stormwater model is summarized in **Fig. 7**.

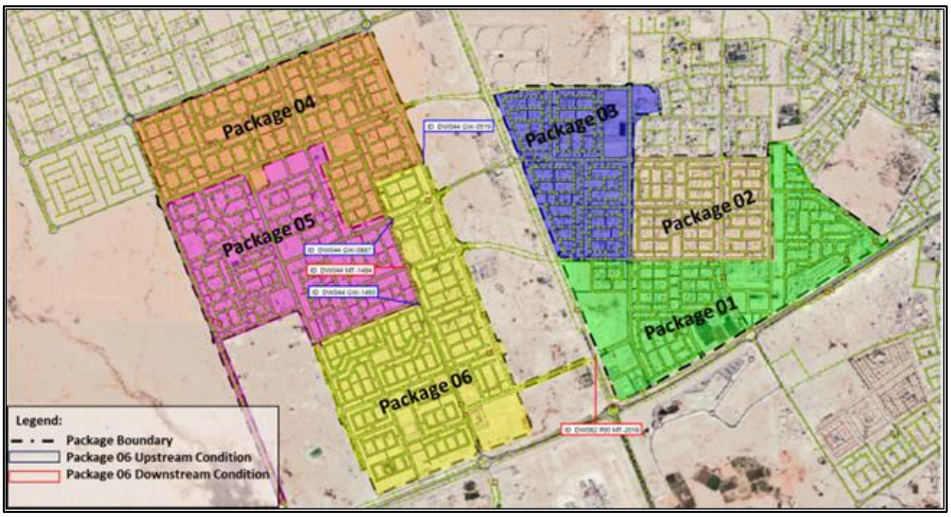


Fig. 5: Boundaries manholes for the stormwater network of DW044-P06 project



Fig. 6: Split model-screenshot from InfoWorks ICM

1.Step 1
- Defining the most representative boundaries manholes in InfoWorks

1.Step 2
- Exporting the flow hydrograph of the boundaries manholes for each rainfall design event and storm duration from the full models to be used in splitted model.

1.Step 3
- Omit the other networks elements.

1.Step 4
- Importing the flow hydroghrpahs files in the splitted model for boundaries manholes for each rainfall design event and storm duration.

Fig. 7: Hydraulic Splitting Model Steps

The computation time for each split model is two hours, thus, the computational time for the 14 simulations is almost one day. The new approach of splitting the full model reduced the computational time of the full exercise by almost 80%, which positively contributes to the practicality and efficiency of the entire modelling exercise. Fig. 8 shows a graphical comparison between both models' run times.

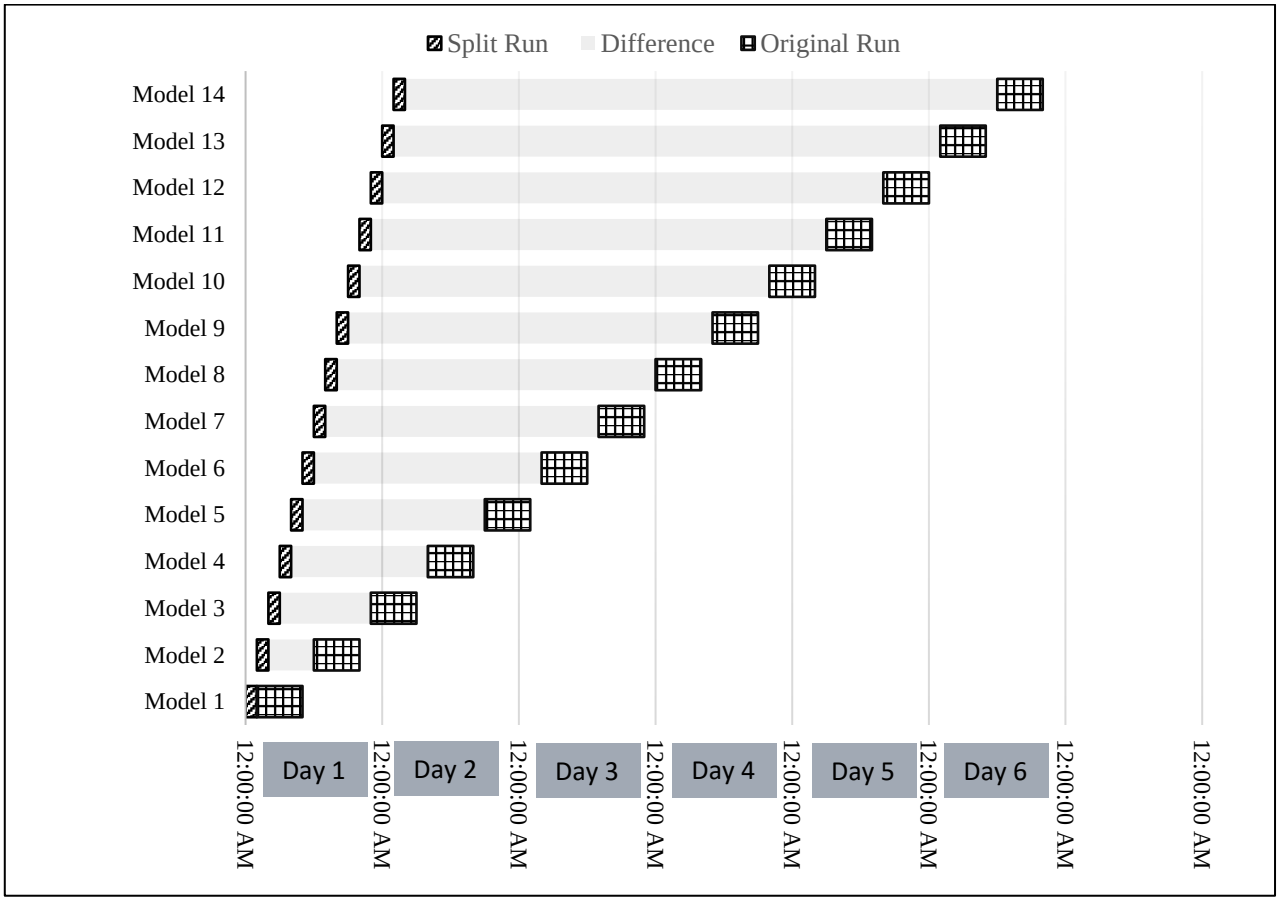


Fig. 8: Shows a graphical comparison between the original and split model run times

5 Approach Verification

After splitting the full model, it is essential to verify the split models. This is done by comparing the results (e.g., maximum flood depth) of the full network with the split network for each rainfall event and storm duration. In this paper, the maximum flood depths both models was compared in the 1 in 5 and 10 years return periods, through the 6, 12 and 24 hours storm duration as shown in **Fig. 9** (presented in the next page). Furthermore, a t-test was carried out, and no significant difference was observed between the two models as shown in **Table 1** below.

Table 1: Comparison of t-test results

Return period (years)	Duration (hour)	T-stat	T-critical (two-tails)	Significance
1 in 5	6	-0.100	1.961	no significant difference
	12	0.324	1.961	no significant difference
	24	0.618	1.961	no significant difference
1 in 10	6	0.038	1.961	no significant difference
	12	0.091	1.961	no significant difference
	24	0.416	1.961	no significant difference

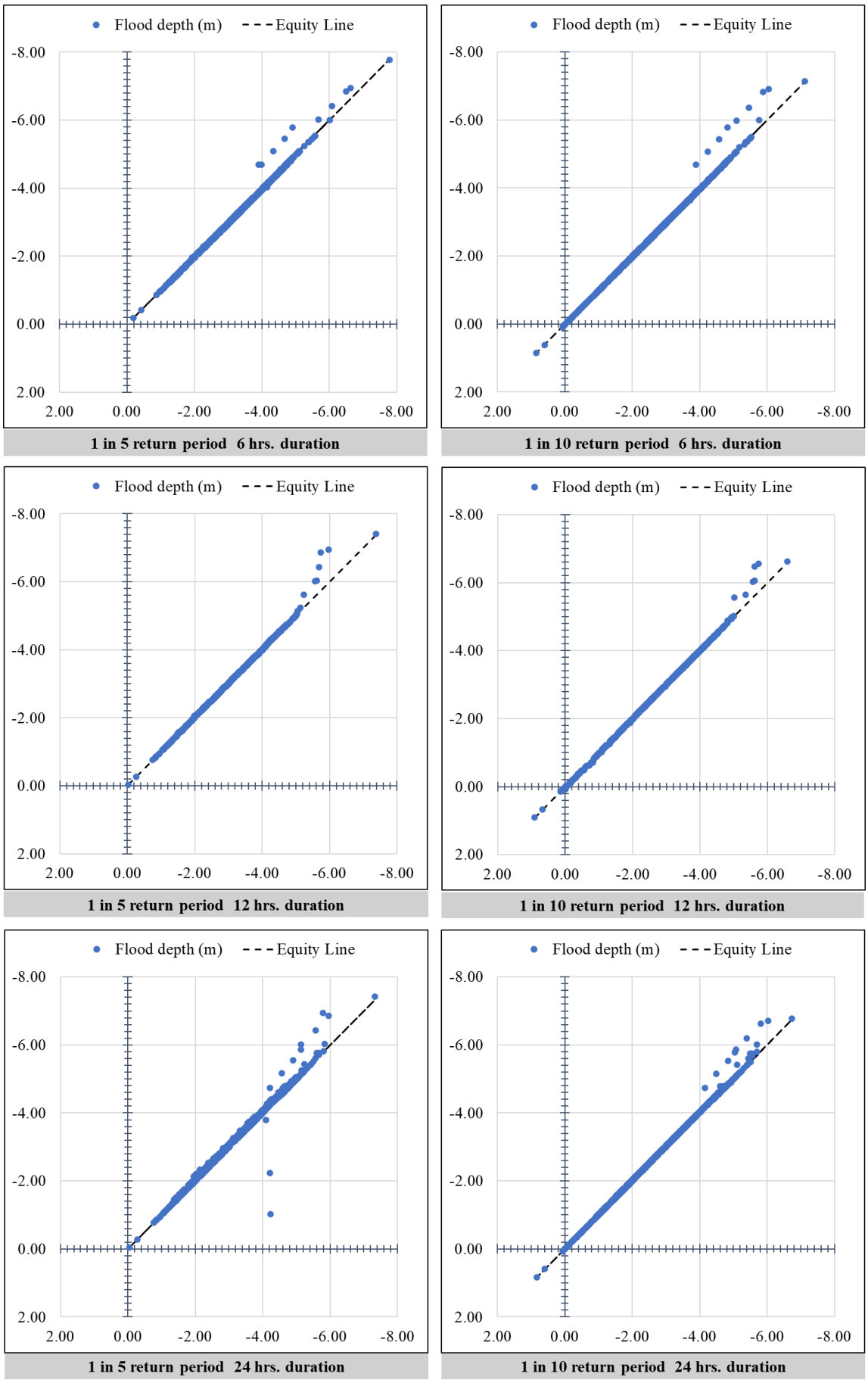


Fig. 9: Comparison between the max flood depth of the 1 in 5 and 1 in 10 years return period – for 6, 12 & 24 hours storm of the full and split models

The results of the full model and the split model are nearly identical, as previously shown in Fig. 9. Furthermore, the results of the split model were acquired in a considerably less amount time than those of the whole model as previously shown in **Fig. 8**.

This new approach was acknowledged by Autodesk and highlighted in their website as a case study in Qatar and considered the first highlighted case study in the Middle East.

6 Conclusion

The State of Qatar went through major enhancement of infrastructure and roads network in the last 10 years. The enhancement of the stormwater network is one of Qatar's significant infrastructure improvements. Qatar government represented by Public Works Authority mandate the investing of technology to deliver safe and adequate engineering drainage solutions. As an example, flood mathematical modelling by InfoWorks ICM.

Flood modelling under various rainfall events and storm durations is an obligatory step prior to construction, this applies also to any new sub-network ties-in with the Qatar's full network. Modelling the full network is a time expensive activity. Splitting the network without taking into consideration the flow connectivity leads to wrong hydraulic calculations and results.

This industrial case study presented and verified a new approach to hydraulically split the full model to the concerned area, taking into consideration flow connectivity and results' accuracy with efficient computational time (80% computational time saving relative to full model running).

References

"Interim Advice Note Section Design Status Final Interim Advice Note LRDP 013-Guidance on the use of current design standards for the design of surface water and ground water systems." (2014).

"Qatar Rainfall and Runoff Characteristics." (2018). [Online]. Available: http://www.mme.gov.qa

Public Works Authority (PWA) (2005). "State of Qatar-PWA Drainage Affairs Stormwater drainage manual."

Suesz, E. (2022). "SEERO: growing their use of InfoWorks ICM as they grow their business - One Water blog," *One Water blog*, Oct. 24, 2022. https://blogs.autodesk.com/innovyze/2022/10/24/seero-growing-their-use-of-infoworks-icm-as-they-grow-their-business/ (accessed Dec. 20, 2022).

Cite as: Alabbasi Y., Aboelenen K. & Sadeq M., "New Technique for Flood Risk Assessment of Sub-Networks in Large Networks Using InfoWorks ICM: A Case Study of Qatar's Full Storm Water Network", *The 2nd International Conference on Civil Infrastructure and Construction (CIC 2023)*, Doha, Qatar, 5-8 February 2023, DOI: https://doi.org/10.29117/cic.2023.0189

وقائع المؤتمر الدولي الثاني للبنية التحتية والتعمير (CIC 2023)

5-8 فبراير 2023، جامعة قطر، الدوحة-قطر

هذا الكتاب يضم بين دفتيه وقائع المؤتمر الدولي الثاني للبنية التحتية والتعمير (CIC 2023)، الذي عقد في جامعة قطر بالدوحة، في الفترة من 5 إلى 8 فبراير 2023. وقد نظمته جامعة قطر، بالتعاون مع عدد من المؤسسات القطرية، ومنها وزارة البلدية، ووزارة البيئة والتغير المناخي، وهيئة الأشغال العامة، كان هذا المؤتمر بمثابة حلقة وصل لمجموعة متنوعة من المشاركين، امتدت إلى ما وراء الأوساط الأكاديمية لتشمل المهنيين وصانعي السياسات ومتخذي القرار وأصحاب الرؤى.

من أبرز أهداف هذا المؤتمر؛ تهيئة بيئة مواتية لتبادل المعرفة والخبرات والحلول في مجالات البنية التحتية والتعمير الرائدة. فالموضوعات التي تم استكشافها في هذا الكتاب تُظهر مجموعة واسعة من المناقشات التي تم الكشف عنها خلال المؤتمر، بدءًا من رصد التحديات في هندسة وإدارة البناء، إلى الخطوات الكبيرة التي أُحرزت في مجال استدامة البنية التحتية وتجديدها ومراقبتها. كما كان هناك تركيز قوي على التخطيط والتصميم الحضري لرفاهية المجتمع، بالإضافة إلى المسائل والقضايا المتعلقة بالمياه والبيئة وتغير المناخ.

ونحن، إذ نقدم للقراء هذا المحتوى العلمي، نتقدم بالشكر إلى المتحدثين الرئيسيين المتميزين، والمهنيين المحترمين، وجميع المشاركين والمؤلفين المتفانين، الذين جعلوا هذا المؤتمر نابضًا بالحياة بأفكارهم.

كما لا يسعنا إلا أن نزجي وافر الامتنان للدعم القوي الذي تلقيناه من رعاة المؤتمر، وشركائنا المهنيين. ونخص بالشكر الجزيل اللجان التنظيمية والعلمية والتقنية للمؤتمر لالتزامهم الراسخ، وتفانيهم الذي كان له أثره في نجاح هذا الحدث. ولا يفوتنا أن نتقدم بجزيل الشكر إلى دار نشر جامعة قطر، وفريقها المميز على ما بذلوه من جهد في كافة مراحل إنتاج الكتاب؛ تحريرًا وتدقيقًا وتصميمًا ونشرًا، حتى خرج للقراء في هذا الثوب القشيب، المتميز شكلا ومضمونًا.

ونرجو أن تكون العلوم والمعارف التي نشاركها عبر هذه الصفحات مصدر إلهام وتوجيه للباحثين والممارسين وصانعي السياسات في جهودهم المستمرة؛ لبناء مجتمعات مرنة ومستدامة ومزدهرة.

د. وائل النحال

رئيس التحرير



Print ISSN: 2958-3128





Platinium Sponsor

Research Council Sponsor

Silver Sponsors

Professional Partners